RESEARCH ARTICLE

Solar and RFID Based Smart E-Vehicle Charging Station

Deepak Vala[1]*, A B Bambhaniya[2], Yogesh Prajapati[3] and Sarvesh Pal[1]

[1]Associate Professor, Department of Electronics Engineering, Birla Vishwakarma Mahavidyalaya Engineering College, Vallabh Vidhyanagar, Anand- 388120, Gujarat, India.
[2]Assistant Professor, Department of Electronics Engineering, Birla Vishwakarma Mahavidyalaya Engineering College, Vallabh Vidhyanagar, Anand- 388120, Gujarat, India.
[3]Student, Department of Electronics Engineering, Birla Vishwakarma Mahavidyalaya Engineering College, Vallabh Vidhyanagar, Anand- 388120, Gujarat, India.

*Address for Correspondence
Deepak Vala
Associate Professor,
Department of Electronics Engineering,
Birla Vishwakarma Mahavidyalaya Engineering College,
Vallabh Vidhyanagar, Anand388120,
Gujarat, India.

ABSTRACT

The electric vehicle is a new technology in the field of transportation and electricity with many economic and environmental benefits. Various charging stations and models used to charge EVs are described here, the primary reason why people don't prefer electric vehicles is because of the unavailability of charging stations. There always exists a fear as to what might happen if the vehicle runs out of battery. People are worried about more straightforward and faster commuting methods in our country rather than saving the Earth from the ill effects caused by pollution. This paper mainly deals with a simple solution to make charging stations more accessible. The solution involves using public electricity and solar panels for the easy and hassle-free charging of Electric Vehicles.

Keywords: RFID, EV, Wireless Coil, Charging station, Solar panel.

INTRODUCTION

Electric cars are on the rise around the world, Compared to hybrid cars, electric cars are becoming more competitive due to lower CO_2 emissions and increasing fossil fuels. However, EVs are not widely used due to some limitations such as high vehicle costs. A charging station is a device that connects an EV to an outlet to charge EVs, community EVs, and connected vehicles. The installation of charging stations varies from country to country, depending on frequency, voltage, network and model. So a good charger should be efficient, reliable, high speed, low cost, and

Deepak Vala *et al.,*

light weight.Some payment sites have features like smart metering, mobile capabilities, and internet connectivity, while others are simpler. Charging points, also known as EVSEs, are provided by electronic devices at municipal stations or by private companies in retail outlets. These payment sites have special links for various payment links. The cost of using the EVSE ranges from one kilowatt hour to one month or one year to one hour.

Different types of EVSE have different charging speeds. Level 1 charging stations use 120 volt (V) alternating current (AC) plugs and require a variable speed circuit of approximately 8 miles per hour. Level 2 charging stations use 240 V AC plugs for charging and must be installed at charging stations or public charging stations. Level 2 charging stations range from 10 to 20 miles per hour. Level 2 chargers are the most common and charge in the same way as the base system. Level 3 uses a 480V direct current (DC) plug. They bypass the car charger and provide DC power to the battery through a dedicated port. A10-minute DC fast charge can provide up to 40 miles of range, but is not compatible with all vehicles.

Solar energy technology has been expanding in popularity. Solar Energy is a sustainable energy source and is an infinite and clean energy source that is free and eco-friendly. So, it is efficient and free from environmental pollution. We will be utilizing solar energy to provide the supply for an outdoor charging station for devices such as electric vehicles. Electric car charging stations using solar energy and charge protection will be important technologies to help the transition to electricity. This technology will impact the entire energy environment and has the potential to strengthen the grid and increase energy penetration. Electric vehicle equipment can contribute to the growth of renewable energy; this means that when electricity flows from the grid to the car, the energy supply can equal the solar energy produced on the grid. The electric car battery charging system consists of lines connected to photovoltaic solar panels. Energy will be stored in batteries with the help of solar panels. Here we give each customer an RFID card that they can use to pay for their car on delivery. Before using this card, we need to register as a prepaid card. When we want to charge the car battery.

LITERATURE REVIEW

In recent years, EVs have attracted attention which required EV charging station. The installation of charging stations varies from country to country, depending on frequency, voltage, network and model. So a good charger should be efficient, reliable, high speed, low cost, and light weight [1]. In [2], to harness the solar panel's maximum power by tilting it at an angle based on the intensity of the light that it receives. In addition, the quantity of power available in the charging station is continuously checked locally and from a remote location. In [3], the proposed algorithm aims to reduce the operating costs associated with the customer's willingness to consider possible uncertainties while balancing real time Supply and demand, supply and deferrable loads. In [4], Discusses charging station standards for high speed DC. DC bus, which uses AC / DC converter. In [6], the distribution of different charging stations and different types are discussed. Considering different payment facilities, different needs of different users can be met. In [7] a solar charger for EV is designed. A converter is employed to boost the solar panel voltage to station battery voltage. The automotive industry has moved from electric to electric vehicles and advanced batteries are important for this change. By 2020, roughly half of all new car sales could include hay brides plug-in hybrids and all electric models [5].

MATERIALS AND METHODS

1) ATmega16 Microcontroller: The ATmega16 microcontroller is an 8-bit RISC-based architecture from the Atmel AVR family. It is frequently employed in applications like embedded systems that require high-performance at a low cost. With a maximum clock frequency of 16MHz, the ATmega16 offers swift processing speeds for embedded applications. The ATmega16 is a cost-effective alternative for embedded systems and other comparable applications.
2) RFID Module: Radio Frequency Identification (RFID) Card or sometimes called EV Charge Card, Tag or Switch used to stop and start EV charging via radio frequency. The RFID card can provide home electronics as a smart face,

but is often found in public EV chargers. To use, simply scan your RFID card over the identification area of the charger you selected to start it, then tap it again to stop charging. RFID is fast, reliable and does not require physical contact between the reader scanner and the tagged item. This basic RFID tag works in the 125 kHz RF range and comes with a unique 32-bit ID, fig. 1.

IR Sensor: Infrared sensors are used in wireless technologies such as remote control functions and sensing environmental objects/obstacles. The IR LED is a specially designed Light Emitting Diode (LED) that emits infrared light. Most IR receivers are photodiodes. The IR LED emits infrared light with a wavelength between700 nm and 1 mm. Our eyes cannot see these rays, fig. 2. Wireless Coil : Wireless transmit and receive charging coil module is designed and manufactured for wireless charging and power of various small electronic devices. It is mainly used in electronic devices such as wireless charging of mobile phones and electronic devices. Rectifier Circuit: The circuit in which we use a centre-tapped transformer and two rectifier diodes, we use a regular transformer with only one secondary winding and four rectifier diodes in the classic bridge configuration. It is commonly used to obtain a direct voltage starting from an alternating power supply.

Implementation

The system uses a solar panel, battery, Regulator IC, wireless coils, rectifier circuit, RFID module, Atmega16 controller and LCD display to develop the system. The system shows how to wirelessly charge an electric car. The solar panel is used to charge the battery. RFID is used to detect users. If the user is authentic then the vehicle will be detected by the infrared sensor. When the car is driven over the coils the power is transferred from the transmitter coil to the electric vehicle coil. Thus the system demonstrates a solar based wireless charging system for electric vehicles. As per fig 5.fig 6 and fig. 7.

1. First of all Solar Panel to Charge 12v DC lead acid battery.
2. First of all 230v AC Power Supply is given to the circuit.
3. Rectifier Convert the AC power supply in DC power Supply.
4. With help of the Regulator, Constant 5v supply to Atmega16 Microcontroller.
5. Then car enter to station customer have to scan its RFID card.
6. After scanning RFID card system will check whether the user is authentic or if the user is not authentic car cannot go ahead and charge the car.
7. If the user is authentic and his card have recharge that user can go ahead and after detecting the vehicle is parked in proper area by IR sensor.
8. The wireless power transmission will start from transmitter coil to receiver coil.

R1= RFID MODULE, S1= AUTHENTIC USER, S2= UNAUTHENTIC USER, V1= VEHICLE DETECTED, V2= VEHICLE NOT DETECTED, C1= VEHICLE IS CHARGING, C2= VEHICLE IS NOT CHARGING, V3= VEHICLE CHARGED

Application

As the world's resources dwindle, the government. Schools and NGOs are pushing for green solutions through the use of renewable energy. These types of payment facilities may be available in the future at Small businesses, City centres, Retail stores, Family and office buildings, Restaurants and cafes, Major government offices etc.

Future Scope

Here we can use a wireless charge to work efficiently and quickly, this will save time for the charging process. Let's connect the system of payment centres to a computer network, let's make money from the computer instead of using a book, and let's keep a record of when people used the system and had to pay for it.
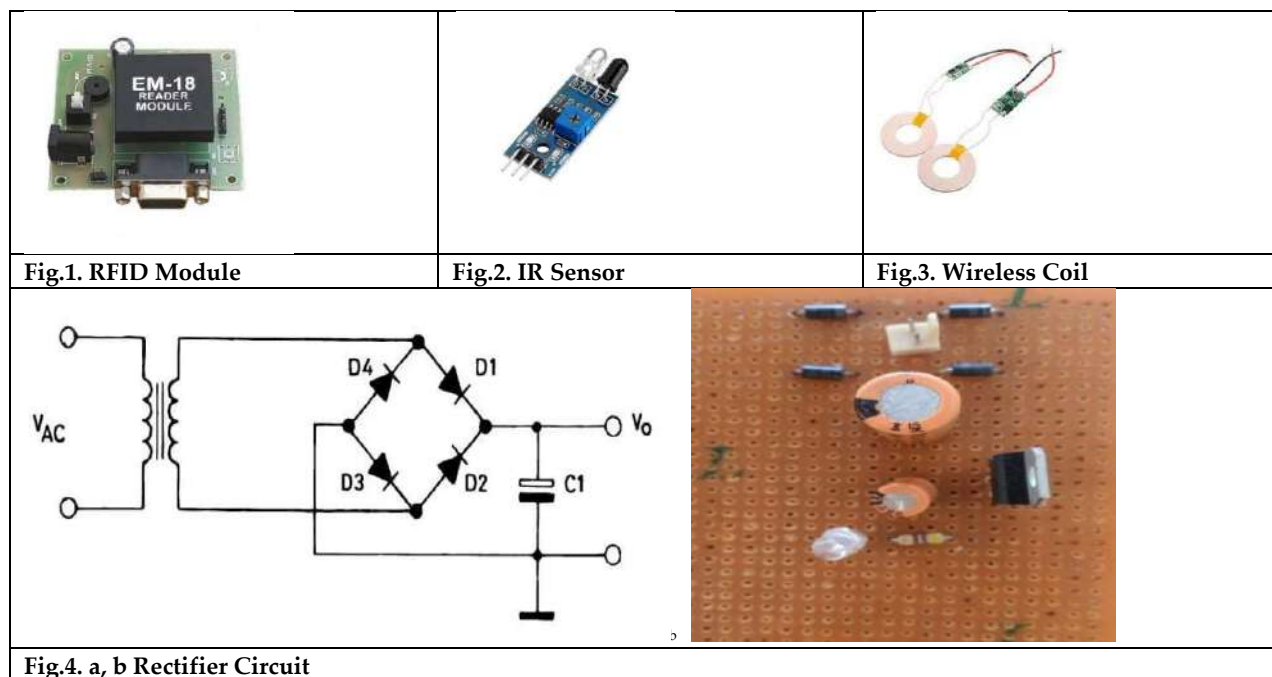
Deepak Vala *et al.,*

CONCLUSION

In this paper, wireless energy transmission and charging systems are designed and analysed. We build each model for a system and finally we do a joint simulation. We found that the best performance of the system depends on the resonance and the distance between the coils to detect the power change.

REFERENCES

1. Varadarajan, M.S., 2012. "Coin based universal mobile Battery Charger". *IOSR Journal of Engineering (IOSRJEN) ISSN*, *2250*(3021), pp.1433-1438.
2. Badhan, M.S., Dubey, M.V. and Kale, A.B., SOLAR BASED EV CHARGING STATION. "International Research Journal of Modernization in Engineering Technology and Science", e-ISSN: 2582-5208, pp 3195-3200.
3. Lee, Stephen &Iyengar, Srinivasan & Irwin, David &Shenoy, Prashant. (2016). Shared solar-powered EV charging stations: Feasibility and benefits. 1-8. 10.1109/IGCC.2016.7892600.
4. S. Anwar, P. Favier, K. Mikszath "Design and implementation of a PIC microcontroller based firing controller for a triphase thermistor rectifier" Technology Interface Journal 7, pp 1-7.
5. M. C. Falvo, D. Sbordone, I. S. Bayram and M. Devetsikiotis, "EV charging stations and modes: International standards," *2014 International Symposium on Power Electronics, Electrical Drives, Automation and Motion*, Ischia, Italy, 2014, pp. 1134-1139.
6. Khan, Wajahat& Ahmad, Furkan&Alam, Mohammad. (2018). Fast EV charging station integration with grid ensuring optimal and quality power exchange. Engineering Science and Technology an International Journal. 22. 143-152. 10.1016/j.jestch.2018.08.005.
7. Revathi B, Sivanandhan S, Vaishakh Prakash, Arun Ramesh, Isha T.B, Saisuriyaa G, "Solar Charger For Electric Vehicles", Proceedings of 2018 International Conference on Emerging Trends and Innovations in Engineering and Technological Research(ICETIETR)2018 IEEE.

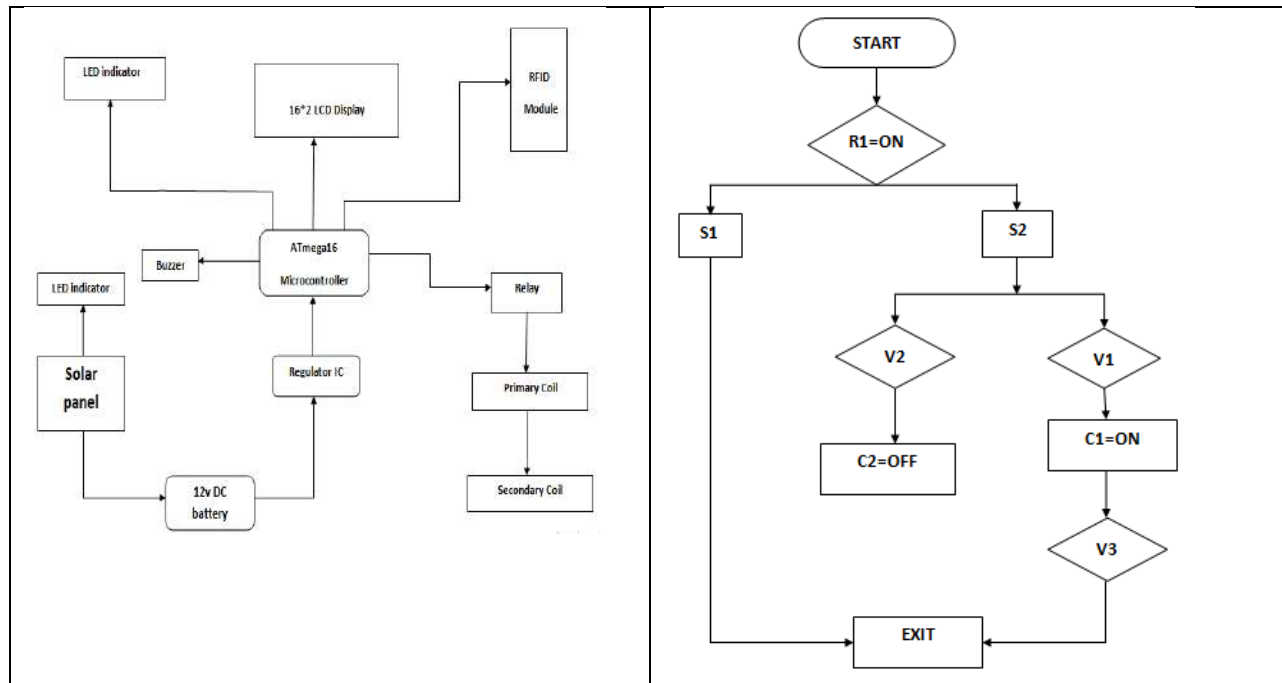|		
Fig.1. RFID Module	**Fig.2. IR Sensor**	**Fig.3. Wireless Coil**

Fig.4. a, b Rectifier Circuit

63003

Deepak Vala *et al.*,

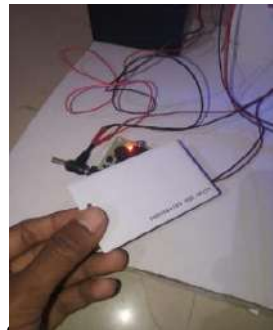**Fig.5. Block Diagram**

Fig. 6 .Flow Chart

.

Step 1: Initial condition

Step 2: LCD will display

Step 3: Scan one card.

Step 4: Detect the user.

Step 5: Detect the user authorized or not.

Step 6: IR sensor will detect the vehicle is parked or not.

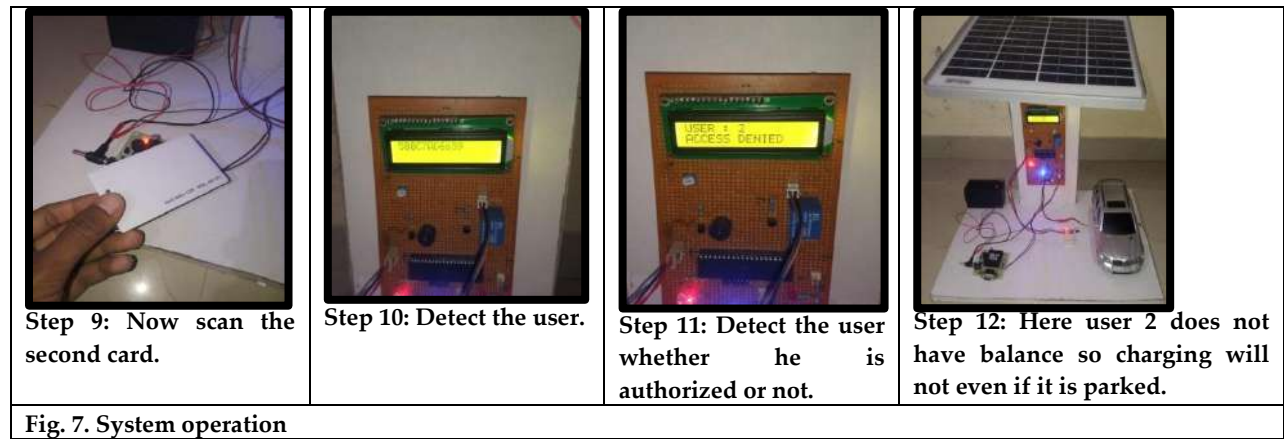**Step 7: If the vehicle is parked, charging will start.**

Step 8: The LCD will display the vehicle charged.

Deepak Vala *et al.,*

Step 9: Now scan the second card.	**Step 10: Detect the user.**	**Step 11: Detect the user whether he is authorized or not.**	**Step 12: Here user 2 does not have balance so charging will not even if it is parked.**

Fig. 7. System operation

RESEARCH ARTICLE

Tunable / Reconfigurable Filter on Liquid Crystal Polymer

Mehul Thakkar[1], Pravin Prajapati[2]*, Hitesh Shah[3]

[1]Research Scholar, Gujarat Technological University, Gujarat, India
[2]Associate Professor and Head, ECE Department, A.D.Patel Institute of Technology, CVM University, V V Nagar, Gujarat, India
[3]Professor and Head, Department of Electronics and Communication Engineering, G H Patel College of Engineering and Technology, CVM University, V V Nagar, Gujarat, India.

*Address for Correspondence
Pravin Prajapati
Associate Professor and Head,
ECE Department,
A.D.Patel Institute of Technology,
CVM University, V V Nagar, Gujarat, India
E. Mail: ec.pravin.prajapati@adit.ac.in

ABSTRACT

In this paper, a reconfigurable/tunable bandstop filter is proposed on Liquid Crystal Polymer substrate. The filter is a dual-band bandstop filter for the 2.4 GHz and 5 GHz bands of WiFi. The proposed filter is simulated, fabricated, and tested. The designed dualband bandstop filter is reconfigurable by adding two PIN diodes in the design, which provide different bandwidths for the bandstop filter. Further, a varactor diode is added to the design to provide tunability in the filter. By changing capacitance, the first stopband bandwidth is tuned, and the center frequency of the second stopband can be tuned.

Keywords: Dual band bandstop filter, Flexible filter, liquid crystal polymer, Tunable filter; Reconfigurable filter

INTRODUCTION

The use of flexible electronic devices is the need of the day for the latest communication systems. Emerging communication systems demand devices that are small in size, multiband, have minimal loss, and are adaptable for usage in a variety of cutting-edge applications. For high-end communication systems used in space applications [1], a reconfigurable/tunable filter on a flexible material substrate will be one more advantage [2][3]. Due to its exceptional packing properties, liquid crystal polymer (LCP) has been utilized in a variety of applications [4][5][6]. LCP is employed as a substrate material for modern microwave applications because it has the best packaging qualities and is inexpensive [7]. The substrate material used for the discussed design is a liquid crystal polymer,Ultralam®3850 [8],

which has a loss tangent of 0.0025 and a dielectric constant of 2.9. The purpose of using LCP in this design is to have flexibility without producing undesirable results when it is placed on various types of surfaces. A fabricated filter is evaluated at various angles by bending it at several angles using various tubes of different diameters, and the results of the S parameter are measured in each case.

Characteristics of Liquid Crystal Polymer Material

LCP has the following advantages[2]:
- LCP has remarkable electric properties for microwave frequencies.
- Low loss tangent and good Ɛr stability (0.002-0.004).
- Possibility of recycling.
- Low price.
- Low dielectric constant and is naturally non-flammable.
- Less prone to absorb water properties.

High-frequency applications are using LCP as a substrate due to the above mentioned properties [2]. Due to its low loss tangent and low dielectric constant value, it is the best substrate for next-generation technologies, such as 5G, which operates in a higher frequency band because of its characteristics [9][10]. LCP material is extensively utilized in wearable applications because, after taking into account all characteristics and testing, it has been found that there is barely any variation in the frequency of operation.

Ultralam®3850 is widely used as a flexible material substrate in RF/Microwave circuit design, including handheld RF devices, antennas and filters. It also has excellent high frequency properties, and it offers lots of advantages [11][12][13] like
- Better electrical characteristics for matching impedance.
- Outstanding signal integrity.
- The material's flexibility is advantageous in applications like space science.
- In a humid environment, the material maintains its mechanical, electrical, and dimensional stability.

In the proposed design, on the Ultralam®3850 substrate, a dual band band stop filter is designed using two square open loop resonators[3]. The proposed design is simulated, fabricated, and tested for various bending angles. In extension to that design, adding PIN diodes[14][15] and varactor diodes[16][17] will provide a reconfigurable / tunable filter along with flexibility. In this article, an extended version of the design discussed in [3] has been presented. The next section discusses the design of a dual band band stop filter[3]. Section 3 and Section 4 discuss the design of reconfigurable and tunable filters using PIN diodes and varactor diodes, respectively.

Design of the Dual band Band stop Filter [3]

A band stop filter can be realized by two bent stubs with a length of $\lambda/4$. The center frequency of the bandstop filter is controlled by it. The wider rejection band is provided by the $\lambda/2$ resonator. This form square open loop resonator, as discussed in[3]. This unit cell offers a better bandstop filter with the desired properties.[18]. As mentioned in [19] and [20], square open loop resonators can be utilized to construct the required response of an antenna and a filter. Two bands around the center frequencies of 2.4 GHz and 5 GHz are chosen for the bandstop filter based on the unit cell. Fig. 1 shows the dimensions of an open square loop resonator for a 2.4 GHz and 5 GHz bandstop filter. As can be seen from Fig.1, the dimensions of an open loop resonator for a 5 GHz bandstop filter are larger than those of a 2.4 GHz design. An LCP substrate, Ultralam® 3850, with a dielectric constant of 2.9 and a height of 0.2 mm, has been used in the design. Both designs are symmetric with respect to S parameters. The proposed design creates a dual band band stop filter with 2.4 GHz and 5 GHz as its central frequencies by combining the two designs from Figs. 1(a) and (b). The design proportions have been slightly altered from the dimensions depicted in Figs.1 (a) and (b) in order to bring out the dual band bandstop filter's properties for suitable bands. Fig. 2 depicts the suggested design for a filter on a flexible substrate (Ultralam®3850). To optimize the desired bandwidth, two open stubsare kept on the outer resonator, as shown in Fig. 2. The simulation of the proposed design is carried out in CST Microwave Studio®. Simulation and measured response of the proposed filter are shown in Figs. 3 (a) and (b). As per S_{21}/S_{12} response,the

Mehul Thakkar *et al.,*

designed filter has a first stopband from 1.5 GHz to 3.61 GHz (3 dB bandwidth = 2.11 GHz), with a center frequency of 2.4 GHz, and a second stopband from 4.43 GHz to 5.7 GHz (3 dB bandwidth = 1.27 GHz), with a center frequency of 5 GHz, as can be seen in Figs.3(a) and (b).Insertion loss is around 1 or 2 dB in outside the stopbands, and rejection is around 30 to 40 dB in both stopbands. Simulated S parameters and measured S parameters mostly match except for a mismatch near the second band due to improper fabrication or measurement. The behavior of the fabricated filter [3] is tested at various bending angles 15°, 30°, 45°. The suggested bandstop filter displays nearly identical performance results from a no-bending condition to 45° bending. It implies that it can be applied in situations where bending of the surface may occur. A comparison of the discussed filter with [21][22][23] is presented in [3], where it is shown that the proposed filter provides a wider stopband with good rejections along with a compact size (20 ×20 mm²). In the next section, the proposed design is extended for reconfigurable bandstop filter by using PIN diodes.

Reconfigurable Bandstop Filter
The above discussed design can be extended as a reconfigurable bandstop filter by using two PIN diodes with both square open loop resonators, as shown in Fig. 4. Here, PIN diode D1 is kept in the opening of the inner square open loop resonator, and PIN diode D2 is kept in the opening of the outer square open loop resonator. The location of PIN diodes is chosen where there is a possibility of disturbing the maximum electric field on the resonator. A PIN diode can be switched on by providing the required forward voltage to it. In the ON state, it provides very less impedance between its two terminals. When the PIN diode is reverse biased, it is in the OFF state, where it provides very high impedance (few MΩs). For simulation, the PIN diode's ON state is considered with a copper connection between two terminals of the diode, and for the OFF state of the PIN diode, an open connection between two terminals of the diode is considered.

Considering four possibilities with two PIN diodes D1 and D2, simulation results for S_{21} are shown in Fig. 5 and depicted in Table 1. While keeping both diodes D1 and D2 ON, it gives a single stopband from 2.38 GHz to 5.59 GHz (3.21 GHz, 3 dB bandwidth). Keeping diodes D1 ON and D2 OFF, the filter gives a wider single stopband from 2.26 GHz to 6.19 GHz (3.93 GHz, 3 dB bandwidth). Keeping diodes D1 OFF and D2 ON, the filter gives a single stopband from 1.52 GHz to 4.24 GHz (2.72 GHz, 3 dB bandwidth). Keeping both diodes in the OFF condition, it is the same as the design discussed in Section 2, a dual band bandstop filter where the first stopband and second band values are as discussed in Section 2. The rejection provided in all four cases in the stopband is above 35dB, which is considered better. The designed filter is symmetric with respect to S parameters.

Tunable Bandstop Filter
The design discussed in Section 2 can be extended by utilizing a varactor diode in the opening of the inner or outer square open loop resonator. The varactor diode provides variable capacitance whenever it is operated with various reverse voltages, as per its datasheet. Here, varactor diodes C1 and C2 are utilized one by one in the design, as shown in Figs.6 (a) and (b). In simulation, values of capacitance are optimized according to design parameters and variations achieved in S parameter results. From Figs. 6(a) and 7(a), it is observed that with varactor diode C2 in the spacing of the outer square open loop resonator, a variation of the first stopband's higher cutoff frequency is observed from3.4 GHz to 3.59 GHz when the capacitance is varied from 0.1 pf to 0.01 pf, which ultimately varies the bandwidth of the first stopband. Also, by changing capacitance C2 from 0.1 pf to 0.01 pf, the second stopband's center resonance frequency changes from 4.4 GHz to 4.82 GHz, which provides tuning for the second stopband. Thus, the bandwidth of the first stopband and center frequency of the second band can be tuned by a varactor diode in the opening of the inner square open loop resonator. The rejection provided in the first stopband is about 40dB, and the second stopband is about 35 dB, which is considered to be better. Also, the insertion loss outside the first and second stopbands is around 1 to 2dB. From Figs. 6(b) and 7(b), it is observed that with varactor diode C1 in the spacing of the outer square open loop resonator, it is giving a wider first stopband from 0.49 GHz to 3.58 GHz and a second band from 4.29 GHz to 5.24 GHz. By changing capacitance, it is giving slight variations in the frequencies near the first and second stopbands stated above. Hence, keeping the varactor diode on the outer square open loop resonator will not be very useful.

CONCLUSION

The compact, dualband bandstop filter was simulated and fabricated on Ultralam® 3850, a liquid crystal polymer material, for bands 2.4 GHz and 5 GHz of WiFi. The designed filter was reconfigurable for a single band bandstop filter for different bandwidths using PIN diodes depending on the condition of diodes. A varactor diode is used to make a bandstop filter tunable by changing the capacitance, bandwidth of the first stopband, and centre frequency of the second stopband. Thus, in this article, a dual-band stopband filter with reconfigure ability and tunability is demonstrated and simulated.

REFERENCES

1. T. Kaesser, C. Fritzsch, and M. Franz. Tunable RF Filters Based on Liquid Crystal for Space Applications.*Cryst. 2020, Vol. 10, Page 455*, vol. 10, no. 6, p. 455, May 2020.
2. B. Taraka *et al.* Liquid crystal polymer substrate based wideband tapered step antenna,*Leonardo Electron. J. Pract. Technol.*, no. 26, pp. 103–114, 2015.
3. M. Thakkar, P. R. Prajapati, and H. Shah. Compact Dualband Bandstop Filter on Liquid Crystal Polymer.*2022 8th Int. Conf. Signal Process. Commun. ICSC 2022*, pp. 69–73, 2022.
4. L. Marnat and A. Shamim. Liquid Crystal Polymer (LCP) based antenna for flexible system on package (SoP) applications.*2012 15th Int. Symp. Antenna Technol. Appl. Electromagn. ANTEM 2012*, 2012.
5. L. Chao and M. N. Afsar. Precise dielectric characterization of liquid crystal polymer films at microwave frequencies by new transverse slotted cavity.*CPEM Dig. (Conference Precis. Electromagn. Meas.*, pp. 448–449, Sep. 2014.
6. F. Aryanfar and C. W. Werner. Ploring Liquid Crystal Polymer (LCP) substrates for mm-wave antennas in portable devices.*2010 IEEE Int. Symp. Antennas Propag. CNC-USNC/URSI Radio Sci. Meet. - Lead. Wave, AP-S/URSI 2010*, 2010.
7. T Anilkumar, B T P Madhav, Yepuri Spoorthi Hawanika, M Venkateswara Rao, and B Prudhvi Nadh. Flexible Liquid Crystal Polymer Based Conformal Fractal Antenna for Internet of Vehicles (IoV) Applications.*Int. J. Microw. Opt. Technol.*, vol. 14, no. 6, pp. 423–430, Nov. 2019.
8. Datasheet : Advanced Circuit Materials ULTRALAM ® 3000 Liquid Crystalline Polymer Circuit Material Double-Clad Laminates. Rogers.
9. Y. Ji, Y. Bai, X. Liu, and K. Jia Progress of liquid crystal polyester (LCP) for 5G application.*Adv. Ind. Eng. Polym. Res.*, vol. 3, no. 4, pp. 160–174, Oct. 2020.
10. Z. Zhou *et al.*Flexible Liquid Crystal Polymer Technologies from Microwave to Terahertz Frequencies. *Mol. 2022, Vol. 27, Page 1336*, vol. 27, no. 4, p. 1336, Feb. 2022.
11. B. D. Braaten, S. Roy, I. Irfanullah, S. Nariyal, and D. E. Anagnostou. Phase-compensated conformal antennas for changing spherical surfaces.*IEEE Trans. Antennas Propag.*, vol. 62, no. 4, pp. 1880–1887, 2014.
12. A. J. Martinez-Ros, J. L. Gómez-Tornero, and G. Goussetis. Conformal tapered substrate integrated waveguide leaky-wave antenna.*IEEE Trans. Antennas Propag.*, vol. 62, no. 12, pp. 5983–5991, Dec. 2014.
13. Y. Tan, H. Hu, B. Zhu, and L. Zhou. Analysis of conformal conical log-spiral antennas on dielectric cavities | IEEE Conference Publication | IEEE Xplore, in *Asia-Pacific Microwave Conference*, 2011, pp. 1961–1964.
14. D. J. Simpson, R. Gomez-Garcia, and D. Psychogiou. Tunable Multiband Bandpass-to-Bandstop RF Filters.*IEEE MTT-S Int. Microw. Symp. Dig.*, vol. 2018-June, pp. 1363–1366, 2018.
15. W. Y. Sam and Z. Zakaria.A review on reconfigurable integrated filter and antenna.*Prog. Electromagn. Res. B*, vol. 63, no. 1, pp. 263–273, 2015.
16. F. C. Chen, R. S. Li, and J. P. Chen. A tunable dual-band bandpass-to-bandstop filter using p-i-n diodes and varactors.*IEEE Access*, vol. 6, pp. 46058–46065, 2018.
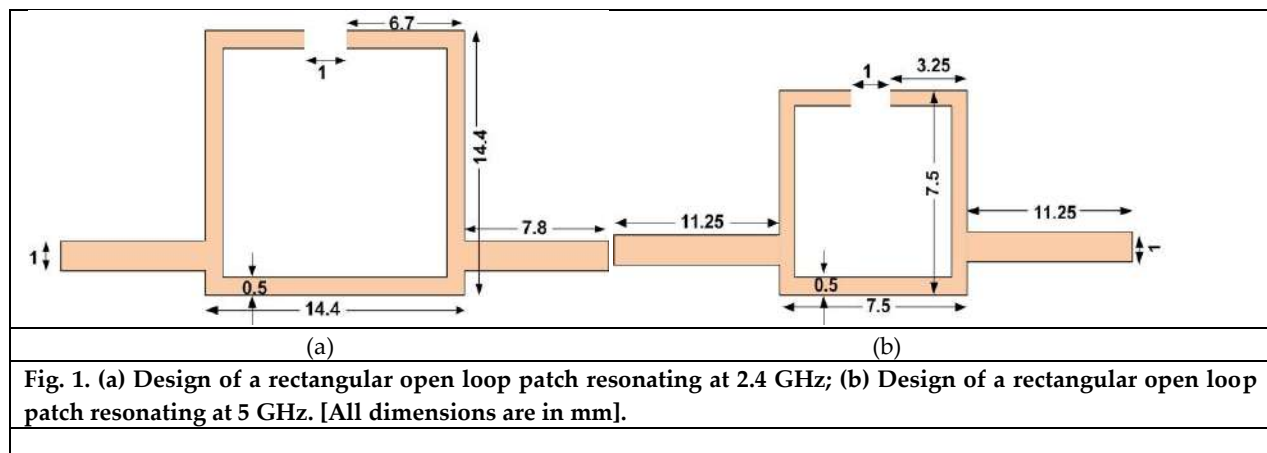
17. H. G. Alrwuili and T. S. Kalkur. A tunable microstrip bandstop filter using compact spiral folded spurline for RF microwave systems.*2018 Int. Appl. Comput. Electromagn. Soc. Symp. Denver, ACES-Denver 2018*, vol. 1, no. c, pp. 1–2, 2018.

18. M. F. Karim, Y. X. Guo, Z. N. Chen, and L. C. Ong. Miniaturized reconfigurable filter using PIN diode for UWB applications. in *IEEE MTT-S International Microwave Symposium Digest*, 2008, pp. 1031–1034.

19. A. Belmajdoub, A. El Alami, S. Das, B. T. P. Madhav, S. D. Bennani, and M. Jorio. Design, optimization and realization of compact bandpass filter using two identical square open-loop resonators for wireless communications systems.*J. Instrum.*, vol. 14, no. 09, pp. P09012–P09012, 2019.

20. K. Ranjan Jha and G. Singh. Performance analysis of an open-loop resonator loaded terahertz microstrip antenna.*Microelectronics J.*, vol. 42, no. 7, pp. 950–956, Jul. 2011.

21. P. Castillo-Araníbar, A. Garca-Lampérez, S. Llorente-Romano, and D. Segovia-Vargas. Dual-band band-stop microstrip filter with controllable bands based on unequal split ring resonators.*IET Microwaves, Antennas Propag.*, vol. 13, no. 12, pp. 2119–2128, Oct. 2019.

22. A. K. Verma, A. Abdel-Rahman, A. Kumar, N. P. Chaudhari, A. Balalem, and A. Omar. New compact dual-band bandstop filter.*Int. J. Electron.*, vol. 100, no. 4, pp. 37–41, 2013.

23. A. Kumar, R. Patel, and M. V Kartikeyan. Investigation on Microstrip Filters with CSRR Defected Ground Structure Investigation on Microstrip Filters with CSRR Defected Ground Structure.*Adv. Electromagn.*, vol. 5, no. 2, 2016.

Table 1. PIN diodes conditions and their results.

PIN diode state	Stopband range (3 dB)	Bandwidth (3 dB)
D1 ON and D2 ON	Single band: 2.38 GHz to 5.59 GHz	3.21 GHz
D1 ON and D2 OFF	Single band: 2.26 GHz to 6.19 GHz	3.93 GHz
D1 OFF and D2 ON	Single band: 1.52 GHz to 4.24 GHz	2.72 GHz
D1 OFF and D2 OFF	First band: 1.5 GHz to 3.61 GHz	2.11 GHz
	Second band: 4.43 GHz to 5.7 GHz	1.27 GHz

Fig. 1. (a) Design of a rectangular open loop patch resonating at 2.4 GHz; (b) Design of a rectangular open loop patch resonating at 5 GHz. [All dimensions are in mm].
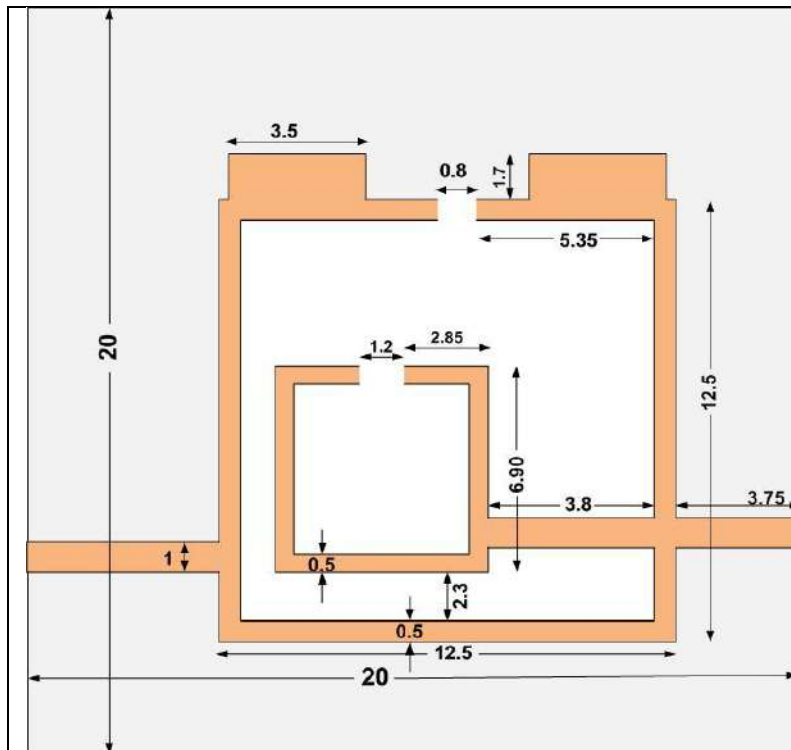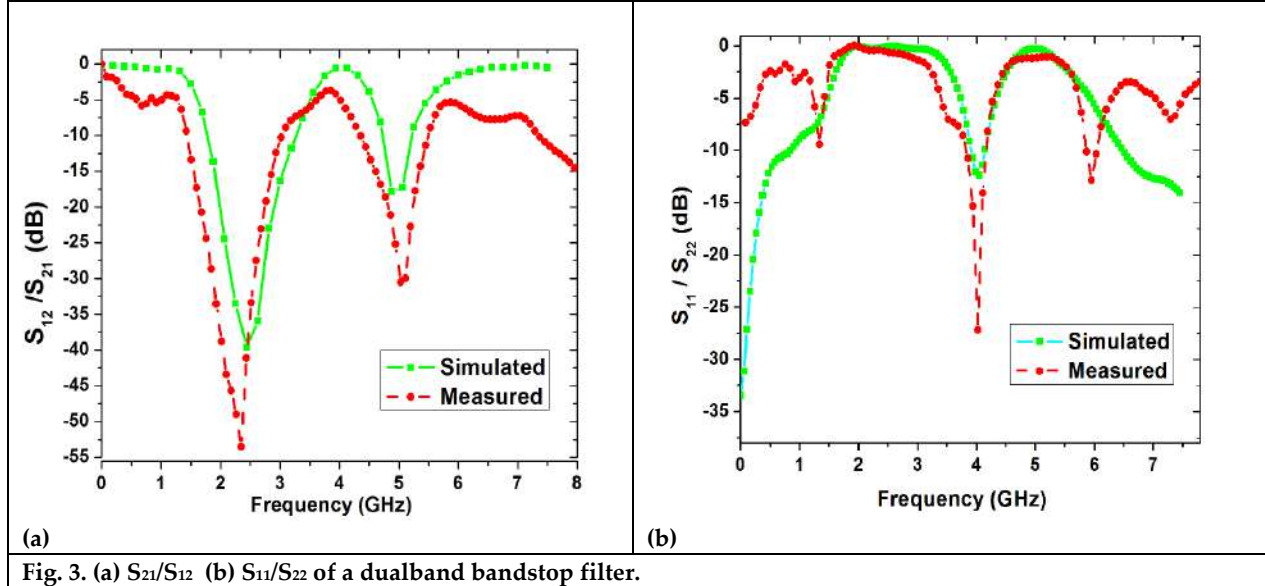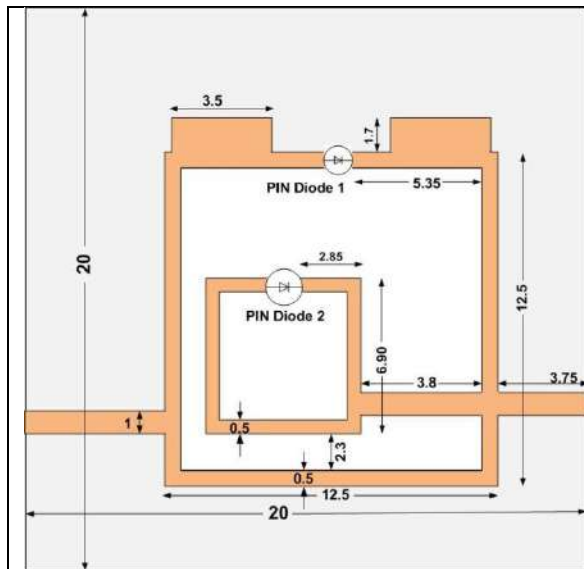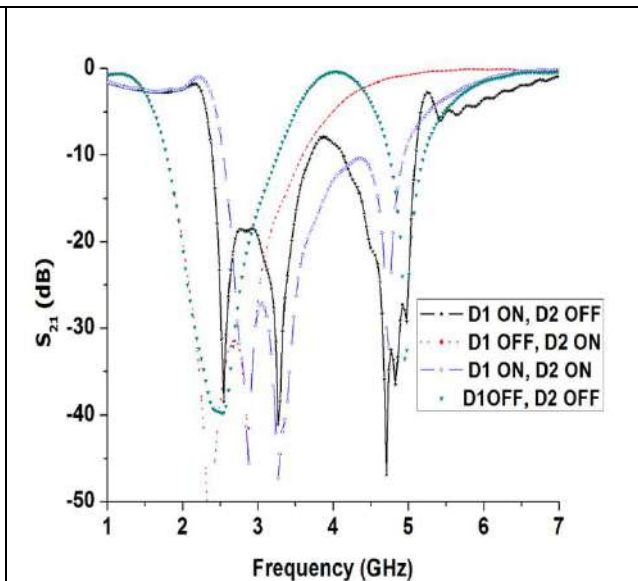
Mehul Thakkar *et al.,*

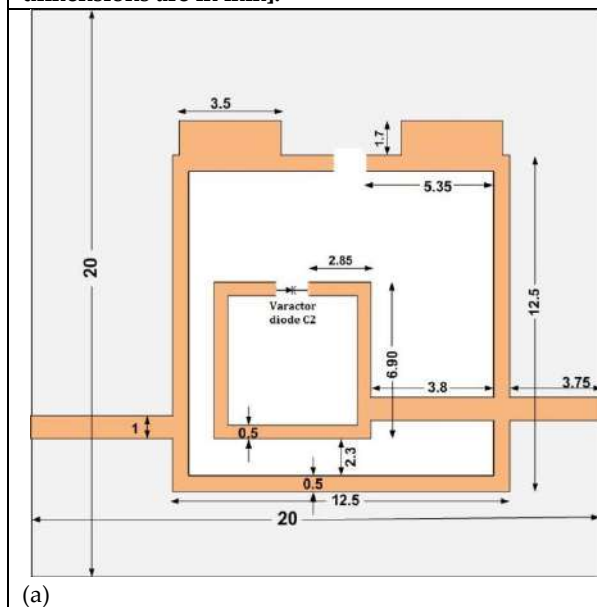**Fig. 2. Design of a bandstop filter resonating at 2.4 GHz and 5 GHz [3] [All dimensions are in mm].**

(a)

(b)

Fig. 3. (a) S$_{21}$/S$_{12}$ (b) S$_{11}$/S$_{22}$ of a dualband bandstop filter.

Mehul Thakkar *et al.,*

Fig. 4. Reconfigurable dualband bandstop filter [All dimensions are in mm].	**Fig. 5. Simulation response S₂₁ for various conditions of PIN diodes D1 and D2.**
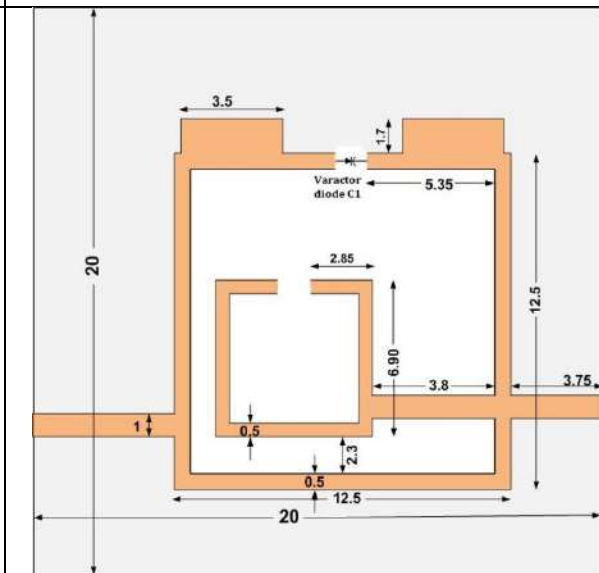
Fig, 6. Tunable filter with (a) varactor diode C2 in the inner square open loop resonator (b) varactor diode C1 on the outer square open loop resonator [All dimensions are in mm].

Mehul Thakkar *et al.,*

Fig. 7. Simulation response S₂₁ for a tunable filter with (a) varactor diode C2 in the inner square open loop resonator (b) varactor diode C1 on the outer square open loop resonator.

RESEARCH ARTICLE

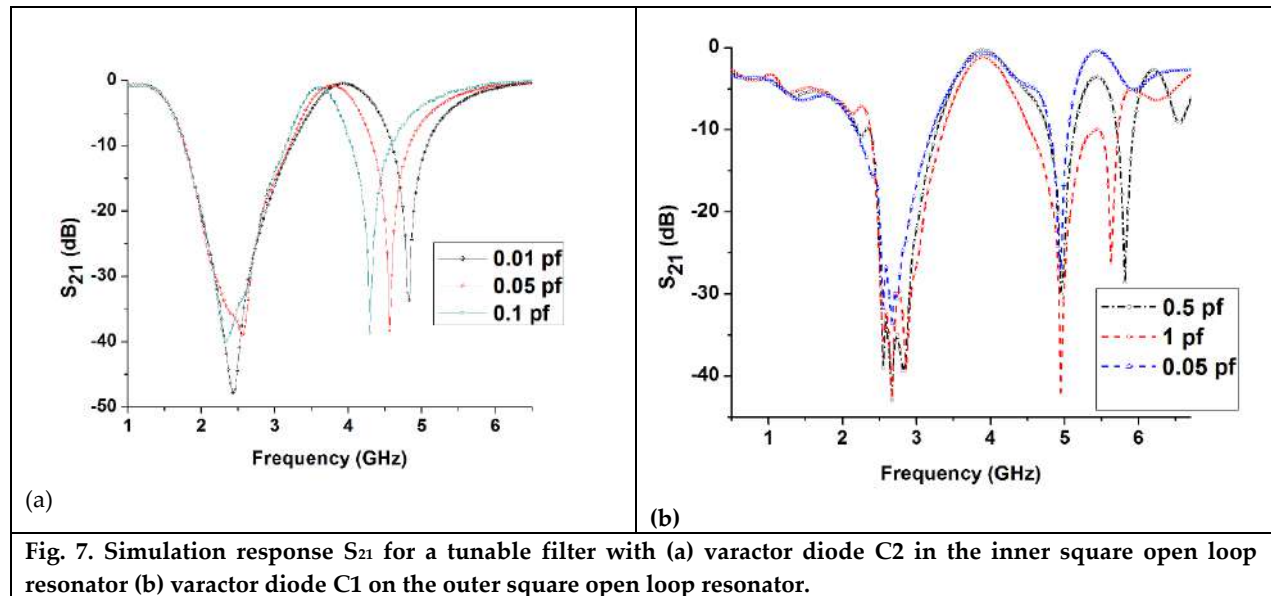# Pore-Based Fingerprint Recognition: An Exploration of Performance and Robustness

Priyanka Patel*, Heli Nandani and Rinkal Mav

Smt. Kundaben Dinsha Patel Department of Information Technology, Chandubhai S. Patel Institute of Technology, Faculty of Technology & Engineering, Charotar University of Science and Technology (CHARUSAT), Changa-388421, Gujarat, India.

*Address for Correspondence
Priyanka Patel
Smt. Kundaben Dinsha Patel Department of Information Technology,
Chandubhai S. Patel Institute of Technology,
Faculty of Technology & Engineering,
Charotar University of Science and Technology (CHARUSAT),
Changa-388421, Gujarat, India

ABSTRACT

Fingerprint identification is an important tool in forensic science because fingerprints are unique to each individual and remain constant throughout time. Fingerprints may be left on a variety of surfaces, including glass, metal, wood, and skin, and they can be collected using a variety of techniques, including dusting with fingerprint powder, lifting with adhesive tapes or gels, and scanning with specialized electronic devices. This study presents a new method for fingerprint pore retrieval. The identification is done in three different layers. These three layers will help in catching a spoof or a fake attempt to access the system. If someone uses a different identity to pretend to be someone else, the biometric system will identify them as a real person. This might lead to fraud. This causes the urge to find out whether the following attempt is made by the respective individual or not. In another sense, if the individual was alive or not? Out of these three layers, the third is much more favorable. In this research paper, one of the layer-3 features, namely the sweat pore, has been studied to detect liveness by proposing a robust pore retrieval method.

Keywords: Fingerprint identification, Pore-Based Fingerprint Recognition, Pore Retrieval, Poly U, Liveness detection.

Priyanka Patel *et al,*

INTRODUCTION

In 1880, Faulds claimed that latent fingerprints discovered at crime sites may reveal information about the identity of the perpetrators. Galton developed an interest in it, and in 1892 he wrote the well-known book Fingerprints after learning all there was to know about it. In which he covered the fundamentals of today's fingerprint science, including the persistence, uniqueness, and classification of fingerprints [1]. Typically, Fingerprint features can usually be classified into three levels: Level 1, level 2, and level 3.Level-1-Global features: Global features refer to the overall characteristics of the fingerprint, such as its shape, size, and orientation. These features can be used to identify and classify fingerprints at a high level and are often used for initial identification and matching. Feature consists of macro details of fingerprints, such as singular points and global ridge patterns, e.g., deltas and cores. They are not very distinctive and are thus mainly used for fingerprint classification rather than recognition.Level-2-Local features: Local features refer to the specific patterns and characteristics of the fingerprint, such as the arrangement and orientation of the pores and ridges. These features are typically more specific and can be used to distinguish between fingerprints with similar global features. The level-2 features primarily refer to the Galton features or minutiae, namely, ridge endings and bifurcations. They are most distinctive & stable and are used in almost all automated fingerprint recognition systems.Level-3-Ridge features: Ridge features refer to the specific details and characteristics of the pores and ridges on the fingerprint, such as the minutiae points (ends and bifurcations of the ridges) and the ridge flow (the direction and orientation of the ridges). These features are the most specific and can be used for highly accurate fingerprint matching. Level-3 features are often defined as the dimensional attributes of the ridges and include sweat pores, ridge contours, and ridge edge features, all of which provide quantitative data supporting more accurate and robust fingerprint recognition as well it also helps in identifying liveness of the individual. Among these features, pores have most extensively been studied and are considered to be reliably available only at a resolution higher than 500 dpi [2, 28].

The research problem being addressed in this study is how machine learning can be used to improve the accuracy and efficiency of fingerprint pore retrieval from the Poly U database. Fingerprint pores, also known as sweat pores or epidermal ridges, are small openings on the surface of the skin that secrete sweat and oil. They are a key feature of fingerprints and are used in fingerprint identification and recognition systems to distinguish one individual from another. However, accurately and efficiently extracting fingerprint pores from images can be challenging, especially when the images are of low quality or have been distorted or degraded. This can lead to errors in the fingerprint identification and recognition process, reducing the overall accuracy and efficiency of these systems. Using machine learning techniques, it may be possible to improve the accuracy and efficiency of fingerprint pore retrieval from the Poly U database by training a model to recognize and classify different types of fingerprint pores in images. This could involve using a variety of machine learning algorithms, such as convolutional neural networks (CNNs) or support vector machines (SVMs), to analyze and classify the images in the database based on their fingerprint pore content [28].

Fingerprint Liveness Detection
The method of determining whether a fingerprint provided for identification is from a living finger or a fraudulent reproduction, such as a mold or a printed picture, is known as fingerprint liveness detection. It is an important security measure that can help to prevent the use of fraudulent or unauthorized fingerprints for access to secure systems or devices. There are a number of methods that can be used to perform fingerprint liveness detection, including: Image analysis: Image analysis techniques can be used to analyze the characteristics of the fingerprint image to determine whether it is from a live finger or a replica. This can involve analyzing features such as the quality and clarity of the image, the presence of pores and ridges, and the level of distortion in the image.

Physical properties: Physical properties of the finger, such as temperature, humidity, and elasticity, can also be measured to determine whether the fingerprint is from a live finger. For example, sensors can be used to measure the temperature of the finger, which is typically higher for a live finger compared to a replica. Behavioural

Priyanka Patel *et al,*

characteristics: Behavioural characteristics, such as the movement of the finger or the pressure applied to the fingerprint scanner, can also be used to distinguish between live fingers and replicas. For example, live fingers typically exhibit a degree of movement or deformation when pressed against a scanner, while replicas do not.

Fingerprint liveness detection is an important security measure that can help to prevent the use of fraudulent or unauthorized fingerprints for access to secure systems or devices. A combination of image analysis, physical properties, and behavioural characteristics can be used to effectively distinguish between live fingers and replicas. It provides an additional security to the biometric system by detecting that the user who is presenting his biometric is live or he is presenting a spoof artefact to the biometric system. Liveness assessment methods need to satisfy certain requirements like it needs to be Fast, User friendly, Low cost, High performance and Non-invasive [3, 28]. To detect fingerprint liveness, multiple approaches have been studied as shown in Fig.1. Approaches to detect Liveness in Finger.

Hardware Based Approach
A special hardware device/sensor such as e.g.sweat, blood pressure, odor [4], temperature, oximetry [5] is added in the biometric system to detect whether the biometric input is live or fake [3]. However, the setup of additional hardware increases the overall cost of fingerprint identification system [6].

Software Based Approach
According to the types of characteristics employed, software-based techniques can be classified as dynamic or static [4]. It does not use any other intrusive biometric measures [5]. Dynamic techniques make use of characteristics collected from a series of fingerprint photos, such as skin sweat and skin deformation [4–7]. Skin-perspiration-based techniques to fake fingerprint detection have received the greatest attention. Skin distortion analysis is another method. Because living and imitation fingers have varying elasticities, they exhibit distinct elastic tensions when placed against a sensor surface. The resultant skin deformation characteristics may be generated by having the user twist a finger on the sensor surface [4], however, this method takes at least two-time series of images, which adds processing time [5]. Pores, power spectrum, surface coarseness, morphological characteristics, statistical properties [4ridge quality, ridge strength, and ridge clarity [3] were retrieved from a single picture in the static technique. The materials used to make synthetic fingers are often formed of big organic molecules, and producing high-quality fake fingers is not a simple operation [4, 28].

An Introduction to Pore
Fingerprint pores are small openings on the surface of the skin on the fingertips that contain sweat glands [8,9, 28]. They can be visualized as either open pores or close pores based on their perspiration activity [1]. They are an important feature of fingerprints and are used for identification and recognition purposes. Pores are typically arranged in a regular pattern on theskin, and the distribution and arrangement of the pores can vary significantly between individuals. This variation is what makes pores useful for identification and recognition purposes, as the patterns of pores on a fingerprint are unique to each individual. As illustrated in Fig. 2, a closed pore (red highlighted) appears as an isolated bright blob on the dark ridge, but an open pore (blue highlighted) is perspiring and shows on fingerprint pictures as a bright blob associated with the bright valley [10].

Average no. of pores is 9~18/cm of a ridge [11] but as per observation made by researchers, the number of pores varies from 9~18/cm, or 23~45/cm of a ridge [1]. Their width varies from 88-220 μm [8, 11] and their density is 5/mm2[8]. Pores comes in various shapes like round, elliptical, oval, square, rhomboid, or triangular and reside at various positions (mostly in the middle, but occasionally open on the side) [11]. Distance between two pores is different from person to person. It varies depending upon the location in the finger which makes pores unique in each individual [8]. They are immutable, unique and perpetual [11]. Details of pores can be retrieved by using the high-resolution fingerprint sensor (over 1000dpi) [8, 13, 28]. To determine the identity of an individual 20 to 40 pores are sufficient [1]. Pore detection has been briefly studied as a measure for fingerprint liveness detection [9]. Pores are

typically visible on high-quality fingerprint images and can be used for a variety of purposes, such as identifying and matching fingerprints, verifying the authenticity of fingerprints, and detecting liveness in fingerprints.

Pore extraction method is basically a problem of objection detection. It is classified into two approaches known as skeleton tracking based or filtering based approach. In skeleton-based approach fingerprint image gets binarized and skeletonized and then fingerprint skeleton is tracked. It is time consuming and works well with very high-quality images (2000dpi) which makes it computationally expensive and it is also very sensitive to noise. In filtering-based approach, it uses static isotropic pore model to detect pore which makes it more efficient and robust compared to skeleton tracking-based approach [10]. Overall, fingerprint pores are an important feature of fingerprints that can be used for identification, recognition, and verification purposes. They are typically visible on high-quality fingerprint images and can be used to distinguish between individuals based on the unique patterns of pores on their fingerprints.

Literature Survey on Pores
There are a number of traditional methods that have been used for fingerprint pore retrieval, including:
- Visual inspection: This involves manually examining the fingerprint images to identify and extract the pore features.
- Feature extraction: This involves using algorithms to extract specific features from the fingerprint images, such as the shape, size, and orientation of the pores.
- Pattern matching: This involves comparing the extracted pore features to a database of known fingerprint pore patterns to find a match [28].
- Recently, there have been a number of advances in machine learning that have improved the accuracy and efficiency of fingerprint pore retrieval. These advances include:
- Deep learning: Convolutional neural networks (CNNs) and other deep learning techniques have been used to analyze and classify fingerprint images based on their pore content. These techniques can be trained on large datasets of fingerprint images, improving their accuracy and robustness.
- Transfer learning: Transfer learning involves using pre-trained machine learning models and adapting them for a new task, such as fingerprint pore retrieval. This can help reduce the amount of training data required and improve the performance of the model.
- Ensemble learning: Ensemble learning involves training multiple machine learning models and combining their predictions to improve the overall accuracy of the system. This can be particularly effective for fingerprint pore retrieval, as different models may be better at identifying different types of pores.

Perspiration is a biological trail in humans. The live fingerprint has perspiration in the pores which a fake fingerprint doesn't have. Manivanan et.al. introduced a method using a micro-capture camera to detect liveness detection. The active sweat pores are detected through high pass and correlation filtering on grayscale fingerprints. He presented a new technique to extract and locate sweat pores automatically. First, high pass filtering is used. Followed by correlation in the combined technique. The fingerprint image captured as the end result was high-resolution taken through a micro capture camera. In this method that he adopted the camera captured different shapes and sizes of the pores. The filters passed through this image magnified the fingerprints. The traits of the pores were captured through different layers. And a mathematical function was used to obtain the probability of the fingerprint to be alive. This method to automatically detect sweat pores through all the angles and direction is helpful in detecting the spoof in a fingerprint. Pores being an important trait in human biology helps in the liveness detection. As every human has his/her own characteristics of a pore in the finger [25, 28].

Now every human has a different count of sweat pores. A child might have a tiny number of pores whereas an adult might have grown sweaty pores. So, Espinoza et. al. introduced a method to use this count of pores as the basis or base of the fingerprint liveness detection. Sometimes it is tough to detect the number of pores in a fake and genuine fingerprint. Thus, a Linear discriminant analysis was used to learn the patterns. To know the difference between different groups of pores, he trained his model on different fingerprints. That got a correct pattern and trait of

distribution of pores in different fingerprints. Through this analysis, the difference between a query image and the taken reference image was obtained. A reference image is a genuine or fake image that the user has entered. The query image is obtained through querying. Querying an image refers to finding information on the objects or entities present in the image provided by the user. In this method the image is presented as metadata. Whereas the content of the image is represented through low level features such as color and texture. Using a GUI, the image is sketched through different graphical tools with sufficient detailing's. Such detailed images are used by the processor of the query for further matching the characteristics present in the database. This became a major discriminating factor in live fingerprint detection. As the query image is sketched the difference between a distorted image and a non-distorted reference image improves the performance.

Spoofed fingerprints are obtained through gelatine, Play-Doh, and silicone moulds for accessing authorized machines and devices. A clone of fingerprints is created for fraud. These fingerprints might not have exactly the same number of pores as genuine fingerprints. Hence, Marcialis *et al*. got the idea and detected the number of pores in a fingerprint using Euclidean distance. The distance between pores obtained by assuming that pores are less likely to appear in a spoofed image rather than in a live image. For a perfect match it was expected that the Euclidean distance is equal to zero. Else the Euclidean distance is to be less than or equal to the mean of the distance [18, 19,20, 28].

The number of pores were thought to be a major factor for the detection of liveness. But it was thought and researched that if the pores are separated in different strips, it will contain more information than the count of the total pores. The skin on the palmar surface of the hands and feet forms papillary ridges in patterns that are unique to each individual and do not vary over time. Espinoza and Champod employed a software-based method. Obtaining information from an input picture using linear discriminant analysis (LDA) [23] The fingerprint samples were collected using an L-Scan 1000 T optical scanner. The Crossmatch L Scan palm scanner range is designed to address the demand for small, high-resolution, rapid-capture live scan devices for criminal identification, forensic analysis, and enrollment. L Scan palm scanners, which can quickly capture upper, lower, and writer's palms, flats, and rolls, completely meet the FBI NGI criteria. By utilizing patented Flex Flat and Flex Roll capabilities, fingerprint photos are recorded regardless of platen location. The patented Auto acquisition technology provides the rapid acquisition of high-quality photos for error-free biometric data gathering, eliminating the guesswork and a broad variety of potential reprint difficulties [21, 22, 28]. Both L Scan models, which are available in 500 ppi or 1000 ppi resolution, deliver superior image quality and provide real-time image preview when using our SDK or enrolment software. Both L Scan models, which are available in 500 ppi or 1000 ppi resolution, deliver superior image quality and provide real-time image preview when using our SDK or enrolment software. The scanners are user-friendly, with an intuitive, integrated display and programmable buttons to help users navigate the biometric capture process.

Choi et. al. went on to use these sweat pores and the discovery of distance between them for a new approach in fingerprint detection. The small pores in live fingers perform physiological thermoregulation. It was found during studies that the normal body temperatures range differently. So, Physiological Thermoregulation means the pores maintain the internal body temperature. It stabilizes the body temperature to normal in certain conditions. Pores go through heat transfer in order to maintain such temperature. Hence, leading to latent fingerprints, with a smudgy and blurry image. In a forward research, sweat ducts helped in absorption of these sweats and to take out the unnecessary elementary content. These glands are present under the skinny layer. The cells under these glands and different layers of skin appear as pores to us. The fingertip pores are the primary source for the sweating process. These pores produce a certain amount of fluid that is active and that helps in detecting liveness of a person [24, 25, 28].

Spatial distribution is done to observe your object with different variations. In the beginning the characteristics or properties of an image were extracted through mean, variance or distance. But in spatial arrangement we change the coordinates so that the image is shifted to a different arrangement. Hence, in modern day techniques, we shift the image to few coordinates to get the clear properties(outcomes) through specific arrangement in pixels. For personal

63018

identification, Roddy and Stosz statistically discriminated against the power of pore. This helped in validating effective pore configuration. Suppose, to investigate the spatial distribution of pores; consider a fingerprint. In the fingerprint the sweat glands are distributed through distance d in a unit cell structure. When measured from different arrangements these pores have similar behaviour. Homogenous means throughout the skin the pores will be of same size, shape, and biological behaviour. The sweat glands are homogeneous and isotropic. In such a case, it was presented that the pores are to be equally spaced. That creates a certainty of creating an error. If all pores are similar to each other than each group of pores will match perfectly. Neglecting all the rotational effects. According to first order approximation, it was assumed that pores' primary function is heat transfer. First order approximation in simple terms means a mathematical formula that fits all kinds of data to give the best output possible. This causes the fingerprint to be a smoky and blurry image. This causes issues in the second layer of detecting liveness in fingerprints [26, 27, 28].

The inter distance between the pores were calculated to improve the spoof detection for fingers. The distance between pore was calculated on the basis of their number, size and shape.
a. Pores were present in very close lengths. A minimum of twelve pores were present in a 1cm length of the ridge.
b. Then the ridge length was considered, with pores in groups. Two or more groups of pores were found closely packed with each other in 1cm of length.
c. The other type of spacing contained 8 to 11 pores in a centimetre of length with a comparatively bigger gap.
d. Another configuration of pores contained a chain-like structure with no interspacing between them.

The majority of the pores on a ridge were discovered to be one behind the other, forming a row with almost uniform space, but other types of arrangements were also observed where pores were lying side by side. The side on the ridge's periphery with very little space between However, the earlier arrangement has been found to be more common. A less common type of pore arrangement was also discovered. It was observed that where pores were interconnected with no interspacing and formed a chain-like pattern When connected pores are open, this arrangement becomes more visible. Lying on the ridge's periphery, in this case, the ridge resembles a cross stitch.

Stosz and Alyea used minutiae and pores to identify a person. Another automated fingerprint detection algorithm from all the information regarding the pores. Detection through live scanned images is presented. The fingerprint was divided into different strips. The position of these pores in different arrangements provide useful information for an individual. A developed multilevel verification technique is based on ridge and pore features. The main advantage of these systems over the systems that use only ridge information. For persistent information about the fingerprint an optical or electronic method is used. For which a high-resolution image is needed. Making it unlikely that the scanned fingerprints contain adequate data. That is consistent for use in authentication. A system that gives secure access to a computer. This gives a level of feasibility of the system used. This system was as such, it has low false rejection and zero false accept of error rates. The results came out positive after preliminary testing the verification prototype.

Comparing fingerprint fragments is a common task in forensic science. After extensive analysis of a fingerprint fragment, it is possible to determine the identity based on the ridge shape, even if no level 2 features are present, a scenario where a minutiae-based automated system would fail. We hypothesize that the undistorted fragment of a partially distorted fingerprint contains at least the same amount of distinctive information as the entire fingerprint. We also anticipate that using level 3 features will improve recognition accuracy, particularly when comparing fragmentary fingerprints. Kryszczuk analysed this contribution of pores through fragmentary fingerprint recognition. He found that the smaller the fingerprint, the greater the benefit [28].

A set of algorithms for extracting the structure of pore networks were brought to light. This algorithm had high resolution three-dimensional synchrotron microtomography pictures. Pictures of unconsolidated porous medium systems. These techniques are based on three-dimensional skeletonization. That reduces pore space to networks of nodes that are linked through routes. To depict the network's pore-bodies and pore-throats, dilation algorithms were devised to construct inscribed spheres on the nodes and routes of the medial axis. The final result is a

physically realistic pore network structure. That includes a three-dimensional spatial distribution with x,y and z coordinates of pore bodies. Along with dimensions of pore-throats, pore-body size distribution, connection and pore-throat size distribution. This study looked at numerous glass bead systems along with natural marine sand. The size of the media ranged from 0.123 to 1.0 mm, while the volume of the pictures ranged from 7.7 to 108.9mm^3. The porosity, specific surface area and representative elementary volume were computed for recovering the pore network structure. Examination of the spatial correlation of pore-body sizes in the network, through semi variograms and integral scale concepts. The effect of resolution on the computed attribute was also studied. Microtomography is a powerful technology for non-destructively extracting the structure of numerous systems. The quality of the datasets is determined by photon energy, photon flux, sample size, kind of sample, and sample size 'features. The results revealed that the devised pore network structure extraction approach is suitable to both ideal and natural points media systems. The influence of resolution on the qualification of network structure and its attributes varies depending on the feature size and the properties being computed. To identify the degree of inaccuracy associated with a system photographed at a certain resolution, a complete sensitive study should be performed.

The authors provide the results of a pore-network analysis of high-resolution synchrotron microtomographic images of the Fontainebleau and Berea Sandstones. The grayscale pictures of the rocks are divided into constituent phases, and the geometry of the pore network is analysed. The network is made up of pores at grain corners that serve as connectors for extended throats that run along grain edges. According to our findings, when porosity increases, so does the number of pores, their median coordination number, and the fraction of connected pore space. When total porosity rises, however, throat breadth and length decrease. Throat breadth and length, on the other hand, decrease as overall porosity increases. The number of coordinating pores in each sample is directly proportional to the radius of the pores, and the length of the throats is also positively connected to the radius of the throats. The observed permeability increases with the total connected porosity of the samples, while the modelled permeability varies with flow direction for each sample. In all samples, the dimensionless coefficient of variation of neck lengths is nearly constant, hovering around an average value of 0.64. The coefficient of variation of throat radii is frequently greater than the coefficient of variation of pore radius. Jain *et al*. employ a fingerprint identification method that incorporates characteristics from all three levels[10].

Hong *et al*. utilize fingerprint enhancement methods, whereas Jain *et al*. use wavelet transform and Gabor filters to improve fingerprints so that pores may be extracted, but Zhao *et al*. use an anisotropic filter that is tailored to each block, making Zhao's approach superior to Jain's [14]. Derakhshani *et al*. observes perspiration patterns only in live fingerprint sequences acquired in between 0 to 5 seconds [8]. Fingerprint scanners are vulnerable to spoofing with artificial materials or, in the worst-case scenario, dismembered fingers. For use in fingerprint scanners, an anti-spoofing method based on liveness detection has been developed. This method quantifies a specific temporal perspiration pattern found in live claimant fingerprints. The improved perspiration detection algorithm presented here improves on our previous work by incorporating other fingerprint scanner technologies, employing a larger, more diverse data set, and operating within a shorter time window. Several classification methods were tried to distinguish between live and spoof fingerprint images. Fingerprint images from 33 live subjects, 33 spoofs made with dental material and Play-Doh, and fourteen cadaver fingers were included in the dataset. Each method performed differently depending on the scanner and time window.

Labati *et al*. use a specially designed and trained CNN to estimate and refine the centroid of each pore with the accuracy of a touch-based sensor, a touchless sensor, or a latent print. Obtaining pore coordinates from heterogeneous fingerprint pictures collected with diverse instruments [15]. They are particularly interested in touch-based, touchless, and latent image-based approaches. We present a strategy based on convolutional neural networks (CNN) to develop resilience to various forms of noise. The method's steps are as follows:

- Preprocessing: Preprocessing the fingerprint images can help to remove noise and artifacts and improve the quality of the images. This may involve techniques such as image denoising, image enhancement, and image normalization.

Priyanka Patel *et al,*

- Data augmentation: Data augmentation involves generating additional training data by applying transformations to the existing training data. This can help to improve the robustness of the CNN to various types of noise by providing the model with more diverse and representative training data. Create pores map and calculate pores coordination's.
- Feature extraction: Carefully selecting and extracting relevant and discriminative features from the fingerprint images can help to improve the robustness of the CNN to noise. This may involve techniques such as principal component analysis (PCA) or linear discriminant analysis (LDA) to identify the most relevant features. Obtain features from the immediate vicinity of the estimated pores.
- Regularization: Regularization techniques, such as weight decay or dropout, can help to prevent overfitting and improve the generalization of the CNN to new, unseen data. This can help to improve the robustness of the model to various types of noise.
- Ensemble learning: Ensemble learning involves training multiple models and combining their predictions to improve the overall performance of the system. This can help to improve the robustness of the CNN to noise by leveraging the strengths of multiple models.

Rather than analyzing the entire group, P Johnson *et al*. discovered small pores. The perspiration activity of each pore was then evaluated. The datasets LivDet 2011 and 2013 were used to generate the results. This reduced the average classification error to about 12%, which is inapplicable at the same time. The Liveness Detection (LivDet) competitions use a standardized testing protocol and a large number of spoof and live tests to compare software-based fingerprint liveness detection and artifact detection algorithms (Part 1), as well as fingerprint systems with liveness detection or artifact detection capabilities (Part 2). To compete, all academic and industrial institutions must have a solution for either software-based or system-based fingerprint liveness detection. The LivDet competitions, which were held in 2009, 2011, 2013, and 2015, have proven to be an important source of information about the current state of the art in liveness detection schemes. There has been a noticeable increase in the number of participants in LivDet competitions, as well as a noticeable decrease in error rates across competitions.

Sometimes the data collected by the standard verification system can be a bit different or missed by the hardware algorithm. In many cases it would have accepted a false print. In order to prevent liveness detection is done. It helps getting additional information gathered above and beyond the machine. We can also monitor the data processed by the machines every day. This data can be used to authenticate the fingerprint obtained through the verification system. Security is obtained in these systems by employing either hardware or software-based systems with the authentication programs. In this field of automation many different sensors are being built for liveness detection. Many hardware-based systems use sensors that measure outside of the fingerprint image itself. There are many software-based systems that use image processing algorithms. They collect information directly from the collected fingerprint. These systems then categorize images as real or fake.

Database
The Poly U High Resolution Fingerprint database is a collection of fingerprint images that was created as part of a research project at the Hong Kong Polytechnic University (Poly U). The database is intended to be used for the development and evaluation of fingerprint recognition algorithms. It consists of a set of high-resolution fingerprint images that were captured using a specialized fingerprint scanner. The database includes images of both rolled and flat fingerprints, and it covers a wide range of variations in fingerprint quality, including fingerprints that are damaged, distorted, or degraded due to age, wear, or other factors. The Poly U High Resolution Fingerprint database is a widely used benchmark in the field of fingerprint recognition research, and it has been used in many published studies.

Retrieval of Pores
Pseudo code to retrieve close pore is given below.
1. Select any fingerprint image from database.
2. If selected image is RGB then convert it into binary image

Priyanka Patel *et al,*

3. Identify the edges from binary images with the help of edge function.
4. Use bwareaopen() to removes all connected objects that have fewer than 30 pixels from the binary image.
5. Apply xor operation between step no. 3 and 4 to retrieve pores as well as small ridges.
6. If the output image detects small ridge borders, then clear it and also fill the holes of output image, so that close pores can be retrieved.
7. Apply xor operation between step no. 5 and 6 to retrieve close pores.
8. Calculate number of pores from step no. 7 output,
    i. If the number of pores are less than 40 then don't consider input image and ask user to retry.
    ii. Else circle pores and show them with respect to fingerprint image.
9. Generate scatter plot by considering pores (x, y) coordinates.

Input image on which above written pseudocode will get executed is shown in Fig.4 & 5 from which you can see the presence of different sizes and shapes of pores. And after executing pseudocode retrieved pores can be seen in Fig.4 highlighted with red filled circle. Stepwise output of above written pseudocode is shown in Fig.5. In step-9, scatter plot is retrieved during execution so that distance and angle between each pore can provide additional knowledge in identifying an individual. Researchers employed the Hong Kong Polytechnique University (PolyU) High-Resolution Fingerprint Database to put the suggested pore retrieval method to the test. Each finger in this database was recorded using a custom-built sensor with a resolution of 1200 dpi and a size of 320 × 240 pixels. Because of non-linear distortion, rotation, and translation, the database employed here is extremely difficult to work with. Figure 6 depicts some of the photos from the PolyU HRF DBI training set. Table 1 contains size of database and count of fingerprint images which are capable enough to take part in liveness detection having pore count greater or equal to 40.

Analysis

To find some concluding remarks, one experiment has been carried out. Accordingly, the original image as shown in Fig.7(a) is provided as an input image and retrieved 98 pores as shown in Fig.7(b)(Note: stepwise output is shown in Fig.5) filled with red color. Here Fig.7(c) has 3 highlighted circles which states manually added pores. We provided it as an input image and retrieved 55 pores as shown in Fig.7(d). pores which were not retrieve from updated image is shown in Fig.7(b) and in Fig. 7(c) with orange outlined circle. One of the key benefits of using CNNs for fingerprint pore retrieval is their ability to learn from large datasets of annotated fingerprint images and automatically extract and classify the pores. This can significantly reduce the time and effort required for manual annotation and can lead to more accurate and robust models. However, there are also some limitations and challenges associated with using CNNs for this task. One of the main challenges is the availability and quality of the training data, as the performance of the CNNs will depend on the diversity and representativeness of the data. Ensuring that the training data is of high quality and represents the types of images that the models will encounter in real-world scenarios is crucial for the accuracy and robustness of the models.

CONCLUSION

The proposed pore retrieval method can be an effective and efficient approach that can achieve high levels of accuracy and robustness. However, the specific performance of the CNNs on the Poly U dataset for liveness detection of fingerprints will depend on a variety of factors, such as the quality and diversity of the training data, the choice of CNN architecture and training algorithms, and the evaluation metrics and methods used., we can retrieve pores but after adding manual pores what makes this un-identification of pores in the same method is still questionable. But if we focus on only pore count then it cannot always help you because as per literature 20 to 40 pores are enough for liveness detection and as per Espinoza *et al*. change in pore count results in liveness detection. But in this approach change in pore count is due to manual alteration in original image but it does not allow other objects to get selected apart from pores which allows average classification error rates as not applicable measure. It is important to carefully consider these factors and to address any limitations and challenges that may arise when

using CNNs for this task. Additionally, it is important to compare the performance of the CNNs with other methods and techniques and to consider the specific requirements and constraints of the liveness detection task when selecting the most appropriate approach.

REFERENCES

1. A.K. Jain, Y. Chen, and M. Demirkus, "Pores and ridges: Highresolution fingerprint matching using level 3 features," IEEE Trans. Pattern Anal. Mach. Intell., vol. 29, no. 1, pp. 15-27, Jan. 2007.
2. Zhang, David, Feng Liu, Qijun Zhao, Guangming Lu and Nan Luo. "Selecting a Reference High Resolution for Fingerprint Recognition Using Minutiae and Pores." IEEE Transactions on Instrumentation and Measurement 60 (2011): 863-871.
3. Arunalatha G, M. Ezhilarasan, "Fingerprint Spoof Detection Using Quality Features", International Journal of Security and Its Applications Vol.9, No.10 (2015), pp.83-94.
4. AsrafulSyifaa' Ahmad, Rohayanti Hassan, Razib M. Othman, "An investigation of fake fingerprint detection approaches", The 2nd International Conference on Applied Science and Technology 2017 (ICAST'17) AIP Conf. Proc. 1891, 020020-1–020020-7. https://doi.org/10.1063/1.5005353
5. Rohit Kumar Dubey, Jonathan Goh, Vrizlynn L. L. Thing, "Fingerprint Liveness Detection From Single Image Using Low-Level Features and Shape Analysis", IEEE Trans. Inf. Forensics Secur., vol. 6013, no. c, pp. 1–1, 2016.
6. ZhihuaXia, RuiLv, Yafeng Zhu, Peng Ji, Huiyu Sun, Yun-Qing Shi, "Fingerprint liveness detection using gradient-based texture features", SIViP (2017) 11:381–388 DOI 10.1007/s11760-016-0936-z
7. Javier Galbally, Fernando Alonso-Fernandez, Julian Fierrez, Javier Ortega-Garcia, "A high performance fingerprint liveness detection method based on quality related features", Future Generation Computer Systems 28 (2012) 311–321.
8. Choi, H. , Kang, R. , Choi, K. , Kim, J.. "Aliveness Detection of Fingerprints using Multiple Static Features ". World Academy of Science, Engineering and Technology, Open Science Index 4, International Journal of Computer and Information Engineering (2007), 1(4), 893 - 898.
9. P. Johnson and S. Schuckers, "Fingerprint pore characteristics for liveness detection," 2014 International Conference of the Biometrics Special Interest Group (BIOSIG), Darmstadt, 2014, pp. 1-8
10. Qijun Zhao, David Zhang, Lei Zhang, Nan Luo, Adaptive fingerprint pore modeling and extraction, Pattern Recognition, Volume 43, Issue 8, 2010, Pages 2833-2844.
11. Locard, Les pores et I'identificationdes criminals, Biologica, vol.2, pp. 357-365, 1912.
12. S. Khade, S. D. Thepade and A. Ambedkar, "Fingerprint Liveness Detection Using Directional Ridge Frequency with Machine Learning Classifiers," 2018 Fourth International Conference on Computing Communication Control and Automation (ICCUBEA), Pune, India, 2018, pp. 1-5, doi: 10.1109/ICCUBEA.2018.8697895.
13. Sharma, R.P., Dey, S. Fingerprint liveness detection using local quality features. Vis Comput 35, 1393–1410 (2019). https://doi.org/10.1007/s00371-018-01618-x
14. Angeloni, Marcus. (2012). Fingerprint Recognition Using Sweat Pores.
15. R. D. Labati, A. Genovese, E. Munoz, V. Piuri and F. Scotti, "A novel pore extraction method for heterogeneous fingerprint images using Convolutional Neural Networks", Pattern Recognit. Lett., vol. 113, pp. 58-66, Oct. 2017.
16. "PolyU HRF Database, http://www.comp.polyu.edu.hk/~biometrics/HRF/HRF.htm".
17. Marana, Aparecido&Angeloni, Marcus. (2013). Improving the Ridge Based Fingerprint Recognition Method Using Sweat Pores. 10.13140/2.1.4157.9524.
18. Marasco, E., & Ross, A. (2014). A survey on antispoofing schemes for fingerprint recognition systems. ACM Computing Surveys (CSUR), 47(2), 1-36.
19. Tan, B., &Schuckers, S. (2006, June). Liveness detection for fingerprint scanners based on the statistics of wavelet signal processing. In 2006 Conference on Computer Vision and Pattern Recognition Workshop (CVPRW'06) (pp. 26-26). IEEE.
20. Singh, S., Selwal, A., & Sharma, D. (2022). Leveraging deep learning to fingerprint spoof detectors: hitherto and futuristic perspectives. International Journal of Pattern Recognition and Artificial Intelligence.

Priyanka Patel *et al,*

21. Lennard, C., &Stoilovic, M. (2002). The detection of bleached ninhydrin developed fingerprints on paper. Journal of Forensic Identification, 52(5), 537.
22. Kolberg, J., Gläsner, D., Breithaupt, R., Gomez-Barrero, M., Reinhold, J., von Twickel, A., & Busch, C. (2021). On the Effectiveness of Impedance-Based Fingerprint Presentation Attack Detection. Sensors, 21(17), 5686.
23. Patel, P., &Ganatra, A. (2014). Investigate age invariant face recognition using PCA, LBP, Walsh Hadamard transform with neural network. In International Conference on Signal and Speech Processing (ICSSP-14) (pp. 266-274).
24. Sharma, B. K., Bashir, R., Hachem, M., & Gupta, H. (2019). A comparative study of characteristic features of sweat pores of finger bulbs in individuals. Egyptian Journal of Forensic Sciences, 9(1), 1-6.
25. Memon, S., Manivannan, N., & Balachandran, W. (2011, November). Active pore detection for liveness in fingerprint identification system. In 2011 19thTelecommunications Forum (TELFOR) Proceedings of Papers (pp. 619-622). IEEE.
26. Jain, A., Chen, Y., &Demirkus, M. (2006, August). Pores and ridges: Fingerprint matching using level 3 features. In 18th International Conference on Pattern Recognition (ICPR'06) (Vol. 4, pp. 477-480). IEEE.
27. Cai, L., Xia, M. C., Wang, Z., Zhao, Y. B., Li, Z., Zhang, S., & Zhang, X. (2017). Chemical visualization of sweat pores in fingerprints using GO-enhanced TOF-SIMS. Analytical Chemistry, 89(16), 8372-8376.
28. Patel, & Mav. (2022, October 18). Enhanced Finger Registration Using Temporary Trusted Memory (Ttm) And Image Processing Module (Ipm) For Android Smartphones To Prevent Apparent Finger Registration Attacks. Gis Science Journal, 9(10), 348–353. https://gisscience.net/volume-9-issue-10-2022/

Table 1: Database with Pore Count

			Size of dataset	>=40 pores
PolyU DB	**Training Dataset**	DB1	208	93
	Training Dataset	DB2	1480	1362
	Testing Dataset	Test	1480	1362
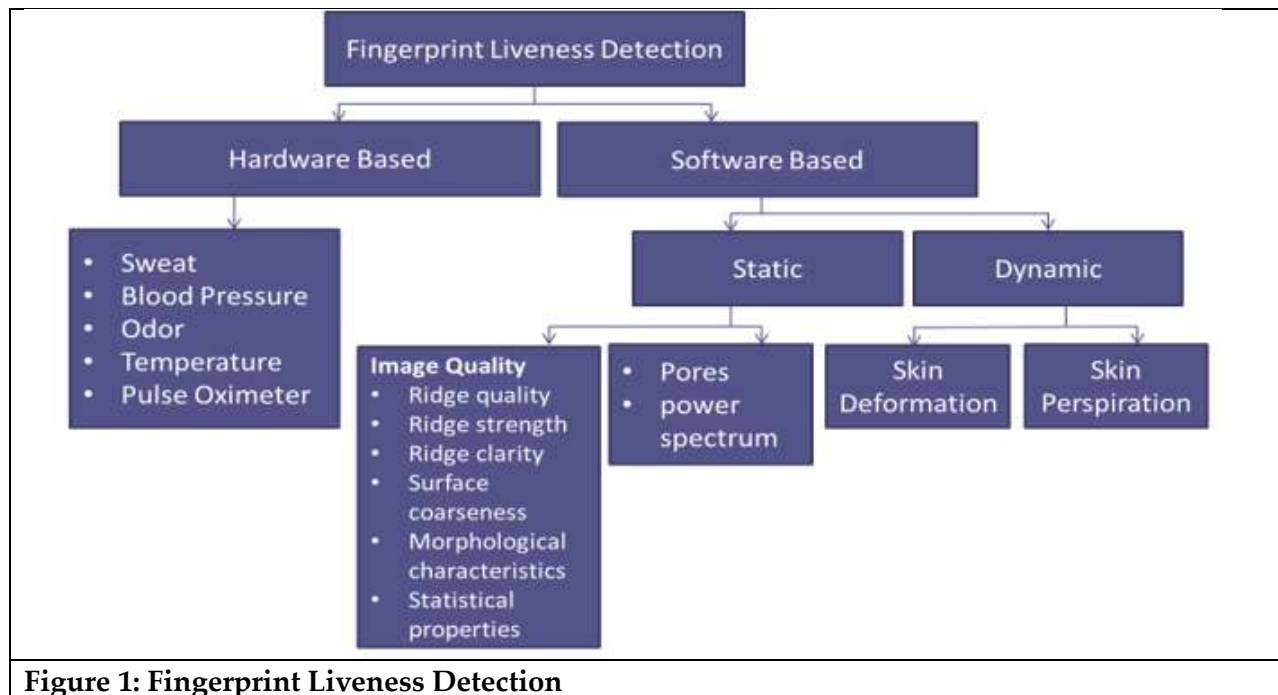
Figure 1: Fingerprint Liveness Detection

Priyanka Patel *et al*,

Figure 2 Example of Close & Open Pores

Figure 3 Flow of the Pore Retrieval

Figure 4 Input Fingerprint

Figure 5 Result of Retrieval of Fingerprint Pores

Figure 4 Execution of Pore retrieval pseudocode

Figure 7 Samples of PolyU HRF DB1 training Dataset

| *(a)* | *(b)* | *(c)* | *(d)* |

Figure 5 (a) Original Image (b) Output of Original Image (98 pores retrieved filled with red color) (c) Manually added three additional pores in Original Image, highlighted with different color called it as an Updated Image (d) Output of Updated Image (55 pores.

RESEARCH ARTICLE

Reduction of Power System Pollution by using Active Filter in Alternating Power Supply

Pankaj.C.Patel* and Hansa.H.Patel

Lecturer in Electrical Engineering, Swami Sachchidanand Polytechnic College, Sankalchand Patel University , Visnagar,Gujarat,India-384315

*Address for Correspondence
Pankaj.C.Patel
Lecturer in Electrical Engineering,
Swami Sachchidanand Polytechnic College,
Sankalchand Patel University ,
Visnagar,Gujarat,India-384315
E. Mail: pcpatel.sspc@spu.ac.in

ABSTRACT

In Power system voltage ,frequency and current are main parameters of supply. If any changes in all any parameters then pollution are created in power system. This problem may damage or distroy the power supply system. This types of pollution created by main use of power electronics circuit in the power system. The Harmonics are produce by electronics devices. The Shunt active filter with P-Q theory to reduce the harmonics level in both balance as well unbalance 3 phase three wire system. All the analysis is done on simulation software tool.

Keywords: P-Q Theory , Shunt Filter , Total Harmonics Distortion , FFT analysis, Voltage controller

INTRODUCTION

Harmonics refer to the distortion of sinusoidal frequency waveforms that are integer multiples of the fundamental frequency. Fundamental frequency is a desired frequency that generate in at 50Hz AC power system. Harmonics are created when nonlinear loads draw current from power supply in a unsinusoidal manner.
Harmonics consider following points:
Effect of Harmonics
Voltage Distortion: Harmonics lead to voltage distortion, that result irregular sinusoidal waveform. This cause issue with power electronics tool and may lead to malfunctioning or failure.[1]
Increased Currents : Harmonics currrents can significantly higher than fundamental current, leading to extra stress on conductors, x,mers and other system components.

Pankaj.C.Patel and Hansa. H.Patel

Power Quality problem and overheating : Harmonics can affect negatively on over all power system and lead to low P.F. ,voltage unbalance and effect of performance of electrical instruments. Due to harmonics increase heating in equipment and reduce the life of instruments.[3]

Total Harmonics Distortion : This measure harmonics content in current or voltage in power system. It present ratio of total sum of harmonics components to power of fundamental frequency. Total Harmonics distortion present percentage and commonly used assess the level of distortion in power system.

Harmonics Reduction : Reduction of harmonics and their problem by use of passive filters. But the passive filters some draw back. So implementation of Active filters in latest era.[8]

Research Method: The Active filter are used to reduction of Harmonics pollution in power system. The simulation/Matlab software is used for the research methodology.
Shunt Active Filters
The Series and shunt active filters are more efficient then passive filters. The basic diagram of shunt active filters are shown below figure 1 :
In basic block of shunt filter ha important component and control system. The main function of shunt active filter to reduce the harmonics current generated by nonlinear loads.
In shunt active filter first current is sensed by current transformers and then sensed current is fed to a current controllers VSC. The first block calculate the active and reactive power of the nonlinear load by use of P-Q Theory. The second block measure the behavior of active filters. In P-Q theory using of clerk transformation transform abc to $\alpha\beta0$ co ordinates. The dc voltage regulator determine the extreme amount of active power. The active power p_{loss} is added to the compensating active power with together reactive power.
In Power circuit of shunt active filter has a 3 phase VSC made by IGBTs and diode. The PWM current controller forces the VSC to role of controller current source.
Calculation of reference current for compensator
The reference current of compensator in $\alpha\beta$ domain wich calculate :[5]

iα iβ =1ΔVα Vβ Vβ Vα p q   ....(1)

In a-b-c domain currents become:
ica icb icc =$\sqrt{2}$31 0 -12 -$\sqrt{3}$2 -12 $\sqrt{3}$2 iα iβ ....(2)

The detail of reference current calculation are given in below block diagram 2:
In below block diagram the clerk transformation is convert abc to $\alpha\beta0$ then given to p-q theory they convert in p-q form. The p-q and Ploss according require add then reference compensating current is generated that inverse clerk transformation convert $\alpha\beta$ compensating current in to abc compensating current.

Simulation Figure of Shunt Active Filter
Above figure:3 is a simulation of the shunt active filter in 3∅ three wire system. The THDv and THDi are produce when nonlinear load is connected. The nonlinear load is a three phase full wave rectifier. The all results are shown in below FFT analysis.

Simulation Results Analysis
The research FFT analysis of the 3∅ system has been carried out by simulation. The components rating used in simulation are given below table:1 The Unbalance waveform in waveform 1 and Phase A with filter and without filter waveform are given below FFT analysis. Also Filter and DC voltage waveform are given below waveform 4 and 5. The shunt active filter work on balance and unbalance three phase three wire system. The results shown in above waveform are only unbalance supply system. The FFT analysis carried out on Phase A, Phase B and Phase C. Here shown only Phase A FFT analysis. From this results when unbalance three phase supply is connect to the

nonlinear load the THDi without filter in Phase a is 27.47%,phase B is 29.38 and phase c is 31.41%. When connect with the filter THDi is Phase A is 4.55%,phase B is 4.60% and phase c is 4.57%.The results shown in Phase A in waveform figure 2 and 3.

CONCLUSION

This Research conclude that when balance as well unbalance 3∅ supply connect with nonlinear load the THDi without filter in Phase A is 27.47% ,phase B 29.38% and phase C 31.41 %. Then connect to the filter the THDi in phase A 4.55%,phase B 4.60% and phase C 4.57%.so conclude that using shunt active filter with p-q theory is capable to mitigate the THD in current balance and unbalance three phase three wire supply system. that level is below 5% well defined by power quality standard.

REFERENCES

1. Saheb Hussain MD, K.Satyanarayana , B.K.V.Prasad *"Power Quality Improvement By Using Active Power Filter"* International Journal Of Engineering Science And Advanced Technology (2011)
2. K. Sebasthirani1, Dr. K. Porkumaran *"Efficient Control Of Shunt Active Power Filter With Self Adeptive Filter Using Average Power Algorithm"* International Journal Of Emerging Technology And Advanced Engineering (2013)
3. Sangu Ravindra, Dr.V.C.Veera Reddy *"Design of Shunt Active Power Filter to eliminate the harmonic currents and to compensate the reactive power under distorted and or imbalanced source voltages in steady state"* International Journal of Engineering Trends and Technology- Volume 2 Issue 3- [2018].
4. Bhakti I. Chaughule , Amit L. Nehete, Rupali Shinde *"Reduction In Harmonic Distortion Of The System Using Active Power Filter In Matlab/Simulink"* International Journal of Computational Engineering Research [2022]
5. Shubra Goel, Arif Khan, Omveer Singh *"Shunt and Series Active Filters Based Power Quality Conditioners for Matrix converter"* International Journal of Scientific Engineering and Technology [2021]
6. Kamala Kant Mishra, *"Load Characterization and Performance Characteristic of Active Filters in DomesticConsumer Voltage Distribution System"* IEEE [2020]
7. H. Akagi, E.H. Watanabe, and M. Aredes, "Instantaneous power theory and applications to power conditioning", Electrical Engineering, 2007.Page No.111 to 120.
8. Roger C.Dugan,Mark F.McGranaghan,Surya Santoso and H.Wayne Beaty,Electrical Power System Quality,Tata McGraw-Hill,New Delhi 2008.Page No.220 to 225.
9. C.Sankaran "power quality" CRC Press LCC 2002 Page no:80 to 85
10. Jos Arrillaga and Neville R.Watson "Power System Harmonics" Second Edition John Wiley & Sons, Ltd.page no.11

Table:1 Simulation Parameters Rating

Name	Symbol	Value
AC Voltage source	Phase A,B,C	300V,325V,350V
Frequency	F	50Hz
Load	RL	50Ω/1mH
DC capacitor	Cdc	2200μF
Inductor of filter	Lf	1mH

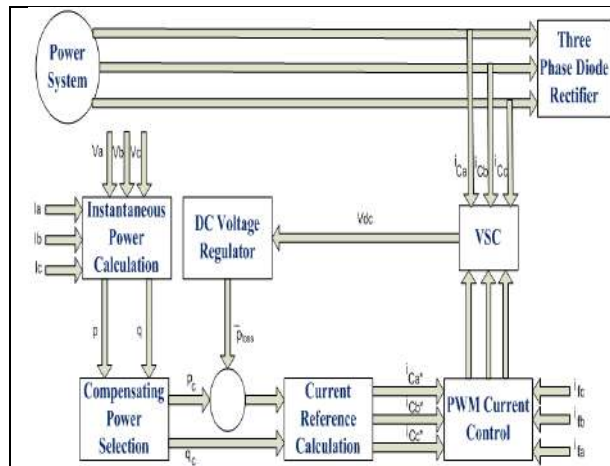**Pankaj.C.Patel and Hansa. H.Patel**
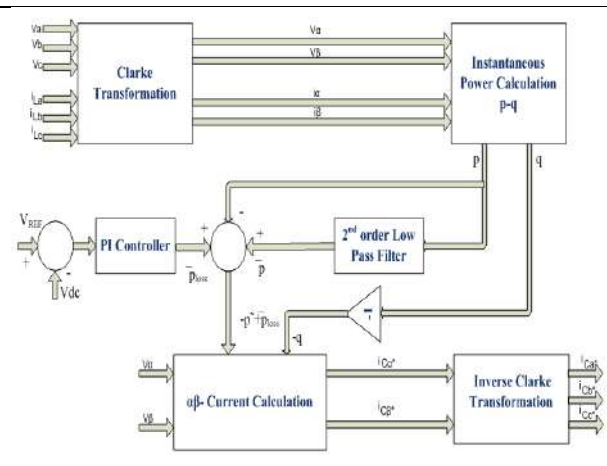

Figure: 1 Basic diagram of shunt active filters.

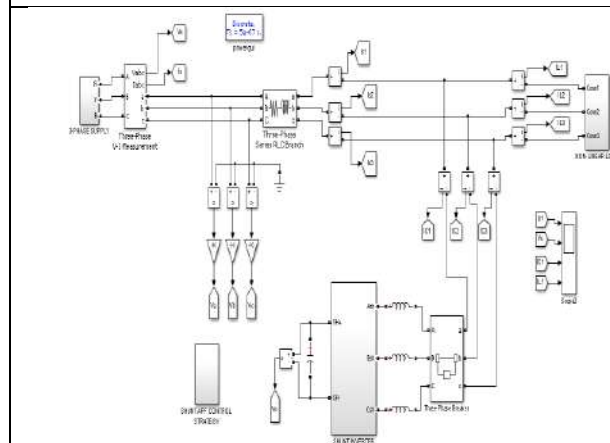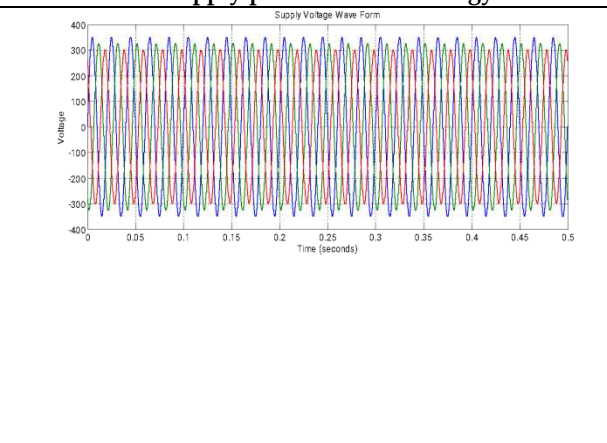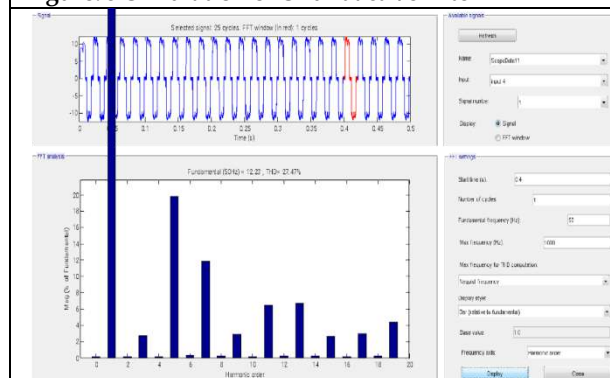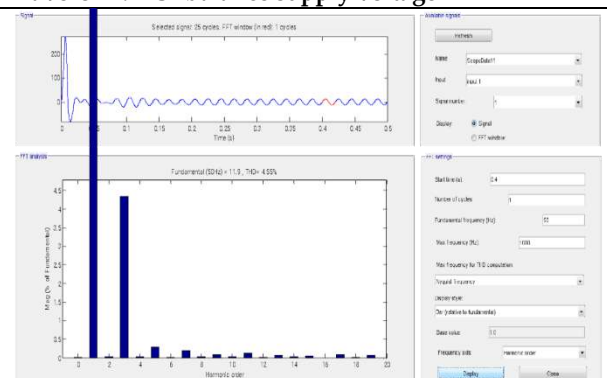**Figure:2 Reference current calculation for constant instantaneous supply power control strategy**

Figure: 3 Simulation of Shunt active filter

Waveform: 1 Unbalance supply voltage

Waveform:2 Phase A Without Filter

Waveform:3 Phase A with filter

Pankaj.C.Patel and Hansa. H.Patel
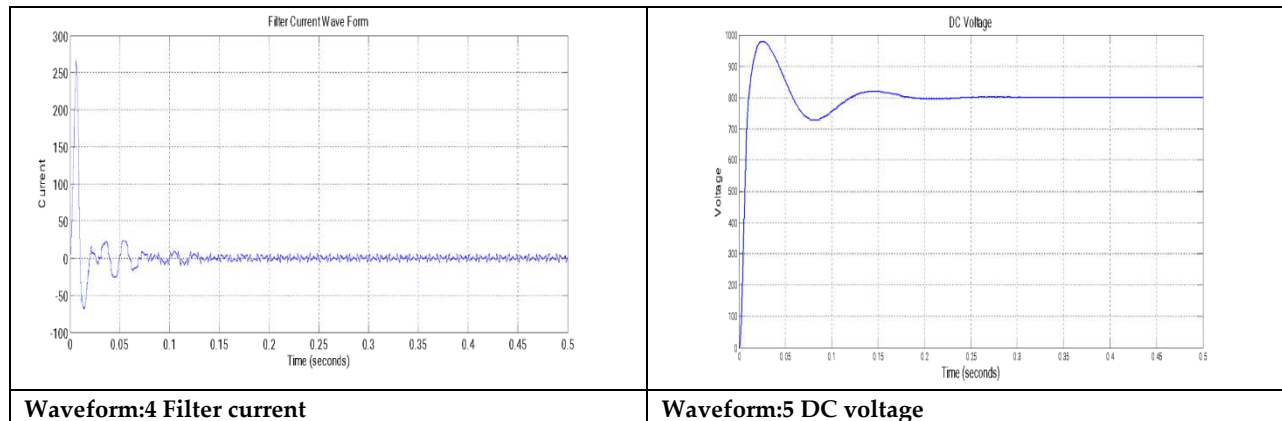
| Waveform:4 Filter current | Waveform:5 DC voltage |

REVIEW ARTICLE

Characteristics and Physiochemical Properties of Deep Eutectic Solvents: A Comprehensive Review

Jigesh Mehta[1], Anand Metre[2*], Mathurkumar S Bhakhar[3] ,Vishal Shah[1], Pratima Wadhwani[4], and Piyush B. Vanzara[5]

[1]Assistant Professor, Chemical Engineering Department, School of Engineering, P P Savani University, Kosamba, Surat, Gujarat, India.

[2]Assistant Professor, Department of Chemical Engineering, G H Patel College of Engineering & Technology, Constituent College of CVM University, Vallabh Vidyanagar, Anand, Gujarat 388120, India.

[3]Professor, Department of Chemical Engineering, G H Patel College of Engineering & Technology, Constituent College of CVM University, Vallabh Vidyanagar, Anand, Gujarat 388120, India.

[4]Assistant Professor, Departments of Chemical Engineering, Lovely Professional University, Phagwara, Punjab, India.

[5] Professor, Chemical Engineering Department, V.V.P. Engineering College, Rajkot, 360005, Gujarat, India.

*Address for Correspondence
Anand Metre,
Assistant Professor,
Department of Chemical Engineering,
G H Patel College of Engineering & Technology,
Constituent College of CVM University,
Vallabh Vidyanagar, Anand, Gujarat 388120, India.

ABSTRACT

Solvents play a significant role in environmentally sustainable frameworks. In order to be considered a greener medium, these solvents have meet a wide range of criteria, such as availability, quasi-degradability, composability, ignitability and affordability, along with other factors. Regrettably, the current selection of sustainable solvents is limited. In this study, the authors aimed to investigate a novel category of ionic fluids known as Deep Eutectic Solvents (DES), which have gained considerable attention in the scientific community. DES typically consists of two or three cost-effective and non-toxic constituents that have the ability to self-assemble, commonly through hydrogen bonding interactions. This self-assembly results in the formation of an eutectic mixture, which exhibits a melting point lower than that of each individual component. The aforementioned DESs exhibit comparable physicochemical properties to conventionally utilised ionic liquids while also offering significant cost advantages and

Jigesh Mehta *et al.,*

environmental sustainability. Deep Eutectic solvents (DESs) are increasingly gaining traction across various academic disciplines due to their numerous advantageous features. This article presents a comprehensive examination of the categorization of deep eutectic solvents, along with an analysis of their physical and chemical properties, encompassing the properties of ionic conductivity, polarity, velocity, density, and surface tension. Furthermore, numerous domains have identified promising prospects for the future utilisation of these solvents.

Keywords: Deep eutectic solvents, Hydrogen bond acceptor, Hydrogen bond donor, Physicochemical properties, Green Solvents.

INTRODUCTION

In the last 20 years, there has been a lot of interest in room-temperature ionic liquids, first in the fields of material chemistry, catalysis, and electrochemistry, and more recently in biomass processing[1,2]. Mostly, ionic liquids can be put into two groups: those made from eutectic mixtures of halides and aromatic ions, and those made with specific types of ions [3]. Scientists have recently getting interested in Deep eutectic solvents (DESs). DESs are alternative to ionic liquids that were first proposed in 2003 as a way to deal with the growing need for natural solvents and the high cost of ionic liquids [4]. These DESs are easily made by combining two innocuous chemicals that could form a eutectic mixture; often, these materials are cheap, renewable, and biodegradable [5, 6]. Because of this feature, DES always have a lower melting point than all of its components put together. Most DESs have a low melting point, which means that they turn into liquids at temperatures below 150 °C. It's important to remember that most of them are liquids at temperatures between 0 and 70 °C [7, 8]. Choline Chloride (ChCl) is a common component of several DESs. Easily retrieved from biomass or generated from geological deposits (million metric tonnes), Choline Chlorine is a cheap, sustainable, quasi-ammonium sulphate salt with a very high atom efficiency [9]. Choline chloride (ChCl) can swiftly generate a DES when used in conjunction with a number of other safe hydrogen bond donors. Despite the fact that ChCl (the ionic species from which most DESs are derived) is a key ingredient, DESs are not ILs [10–12]. Researchers provided broad criteria for defining DESs in 2007 [13]. To distinguish between various eutectics, deep eutectic solvents were categorized into four kinds based on their general formula. Cat+XzY is a Lewis base, often a halide anion, and Cat+ may be ammonium, phosphonium, or sulfonium. Y stands for a Lewis or Bronsted acid, and z stands for the quantity of times one molecule of Y binds to its anion counterpart [14]. In DES, the hydroxyl group between molecules is really quite persistent. The relationship and formulation of each component have a significant impact on the chemical and physical properties of the solvent (such as ionic conductivity, polarity, density, viscosity, surface tension, etc.). Modifying the structure and makeup of HBD or HBA and their ratios enables tailoring such properties for use in a number of significant industries, including chemical synthesis, electrodynamics, biofuel catalysis transformation, biofuel generation, extraction, isolation, and gas absorption. Thus, it is essential to comprehend the interconnections between DES component components in order to effectively design and synthesize solvents for specific uses. Improved workplace use of DESs will be feasible only after a deep inspection of the "structure-function" link of DESs systems, as well as the influence of DESs characteristics and structure.

Physicochemical properties of DESs
DESs can be functionalized in the same way that ILs can, by combining and balancing quaternary ammonium salts with other donors of chemical bonds (HBD). After that, DESs can be made to fit specific uses by changing their melting point, viscosity, conductivity, and pH values, among other physical and chemical properties. These enable DESs to more effectively serve the needs of the application. Because of the potential applications of the results, a considerable amount of time and energy has indeed been expended in the research of the chemical and physical properties of DES. In the following, the physicochemical characteristics of DESs that are regarded as the most significant will be thoroughly investigated.

Jigesh Mehta *et al.,*

Viscosity

When two solids that can join together on their own through hydrogen bonds and make new water molecules that can put together to make a DES. A fluid's viscosity is a measure of its internal friction, or how much it struggles to move. Due to their higher viscosity compared to organic solvents, working with DESs in these processes can be hard in a number of ways. The capacity of a liquid to transfer material inside itself has a major impact on its viscosity and, by extension, on the chemical processes that take place in the liquid. Many different models have been used in an effort to better understand the flow properties of DESs and map them experimentally. The two most common ways to talk about DESs are the Arrhenius model and the VFT model. The hydroxyl group, van der Waals interactions, and surface tension all have a big effect on the viscosity of binary eutectic mixtures. Table 1 lists the viscosity characteristics of typical DESs at various temperatures. It is clear that the characteristics of HBD have a significant impact on the viscosity of ChCl-based DESs. ChCl/EG (1:2) DES, for example, has the lowest viscosity of DES formulations (36 cP at 20 °C). Still, DESs with derived sugars (like xylitol and sorbitol) as HBDs had high viscosities (for example, 12730 cP at 30 °C for ChCl and sorbitol) because they had a stronger 3D intramolecular hydrogen network. Surprisingly, as the ChCl/glycerol stoichiometric ratio tends to go up, the viscosity of a ChCl/glycerol DES tends to go down. For example, at 20 °C, the viscosity values of ChCl-glycerol solutions with a 1:3 molar ratio were 450 cP, and a 1:2 molar ratio was 376 cP. Glycerol has a lot of hydrogen bonds between its molecules, which gives it a lot of cohesive energy. When ChCl was added, this network of hydrogen bonds broke down a lot, which made the viscosity of glycerol drop by a huge amount [21].

Freezing Point

To generate deep eutectic solvents (DESs), it is necessary to combine two solid materials that possess the ability to undergo self-association through hydrogen bonding, resulting in the formation of a novel liquid phase. In many instances, the freezing point of a novel phase tends to be lower in comparison to the freezing points of its constituent components. A eutectic mixture was prepared by combining ChCl and urea in a molar ratio of 1:2, resulting in a point of freezing of 12 °C. The observed temperature is significantly below the individual freezing points of the components, which are 302 and 133 °C, respectively. Moreover, the halide anion exhibits an interaction with urea, a compound that facilitates hydrogen bonding, resulting in a significant reduction in the freezing point. All differential scanning calorimeters (DSCs) have documented freezing points that are lower than 150 °C. Despite their ability to function as a limited and partially effective solvent in various scenarios, it is advisable to use deep eutectic solvents (DESs) with a freezing point below 50 °C. Various types of DES have been identified, and their respective freezing points are documented in Table 2 within the scientific literature. Several compounds, such as urea and 2,2,2-trifluoroacetamide, have the ability to form a liquid deep eutectic solvent (DES) with ChCl at room temperature due to the strong hydrogen bonding interactions they exhibit with ChCl. This observation highlights the significance of selecting appropriate hydrogen bond donors (HBDs) in the development of a desiccant material that effectively lowers the freezing point of choline chloride (ChCl).

Ionic Conductivity

Due to its high density, the ionic conductivity of DES is typically observed to be low, measuring above 2 mS/cm at ambient temperature. Table 6 displays the ionic conductivities of various deep eutectic solvents (DESs) as a function of temperature. When the temperature goes up, the viscosity of deep eutectic solvents (DESs) goes down. This makes the DESs conduct electricity better than they did before. Consequently, the conductive properties of a deep eutectic solvent (DES) can also be approximated by employing an equation similar to the Arrhenius equation. The impact of organic salt concentration in HBD on the conductivity of DESs suggests a plausible correlation with their thickness. [26]. An increased concentration of ChCl in deep eutectic solvents (DES) leads to an elevated level of conductivity. The ChCl-glycerol deep eutectic solvent (DES) exhibits a conductivity value of 0.85 millisiemens per centimetre (mS cm1) upon increasing the molar fraction of ChCl to 25%. The ChCl/glycerol-based deep eutectic solvents (DESs) exhibit comparable viscosity (>400 cP) and conductivity (>1 mS/cm) to that of an ionic liquid (IL) when exposed to higher levels of salinity. [27]

Jigesh Mehta *et al.,*

Density

In the realm of chemistry, density stands as the fundamental physical characteristic. Specific gravity metres are capable of being utilised to measure the value. The densities of various frequently used DESs are listed below; you'll notice that the overwhelming majority of these compounds are denser than water. The density of DESs varies when one adjusts the mole ratios and characteristics of the various components. Densities of hydroxyl-produced DESs Caused considerable increases as more hydroxyl radicals were introduced, but fell as aromatic groups were included. As the alkyl chain structure of the DESs component is extended, the densities decrease too [34]. Density decreases with increasing temperature. This is because the mole fraction of DES increases as a consequence of heating, leading to a decline in density [35, 36]. At low temperatures, the average pore size gets smaller, which makes the molar volume of DESs smaller and makes them denser [37]. The number of moles of organic salt and HBD also has an impact on DES densities. Fig. 3 depicts the density of a glycerol/ChCl DES as a function of the molar content. The density of DES is reduced when ChCl is mixed with glycerol [38]. It might be hard to get good experimental estimates of DES density as a function of temperature. Thus, technological advances that could provide these data as precisely as possible were prioritised for research. Using a modified version of the Rackett equation, Spencer and Danner reported that researchers could predict DES density with an accuracy of 1.9%. [39].

Surface Tension

Even though the properties of interfaces are important for understanding how mass moves, many studies have correctly found the parameters of DESs' surface tension. Solvents have surface tension because their component molecules are clustered together. The stalagmometer is used to measure the surface tension of the given liquid. Research suggests that DESs have a surface tension that is equivalent to imidazolium-based ILs but higher than that of molecular solvents [46–48]. The main things that affect DES's surface tension are its hydrogen bonds, its ionic nature, and its molecular weight. The hydrogen bond in the cation, which can form more h-bonds, causes the surface tension to be higher [49–51]. DESs made from glucose have a higher surface tension than those made from carboxylic acids because they have more hydroxyl. Temperature causes a big drop in surface tension because molecules with more kinetic energy and less cohesion are less likely to stick together. This makes the bonds between molecules weaker [52, 53]. Even though the strength of the interactions between molecules has a big effect on how DESs are made, surface tension is thought to act like viscosity. No matter what the first step was, the surface tension of ChCl/glycerol DESs got better as the temperature went up. As the concentration of ChCl goes up in the ChCl/glycerol DES, the surface tension goes down for the same reason that the viscosity goes down. There are more signs that adding ChCl to glycerol messes up the huge structure of hydrogen atoms in glycerol [54–55].

Polarity

Polarity has a big effect on how quickly DESs dissolve and how well they mix with other solvents. The standard method is to use solvatochromic variables, which look at the UV-vis bands to figure out the polarity of the solvent [60]. In general, the intensity of the interaction among molecules increases as the polarisation of the molecule does. It involves the chemical composition primarily. DESs that are made from carbohydrates are much more polar than short-chain alcohols like ethanol and 2-propanol and certain polar solvents like dimethylformamide (DMF) and dimethyl sulfoxide (DMS) [61-62]. Moreover, researchers analysed ChCl-glycerol DESs with differing mole ratios and reported that the polarities decreased with increasing ChCl content [63]. When temperature increases, the hydrogen-bonding network that lends DES their polarity starts to break down, and the polarity of the DESs decreases significantly [64]. It is also obvious that the water added changes the polarity of eutectic mixtures. Liu and his team found that when a small amount of a moderator is added to DES, the hydrogen bonds between its parts break. This makes the molecule very polar. [65].

CONCLUSION

From the above review, researcher team observed that DESs and traditional ILs have many of the same rheological Based on the aforementioned review, it was observed by the research team that both deep eutectic solvents (DESs)

Jigesh Mehta *et al.,*

and traditional ionic liquids (ILs) exhibit similar rheological characteristics, including rigidity, its thickness, and conductance. It is also possible to generate enterprise deep eutectic solvents (DESs) through the modification of the the quaternary ammonium salts and the hydrogen-bond donor, analogous to the manner in which the physical and chemical characteristics of ionic liquids (ILs) can be altered indefinitely. However, it is important to note that deep eutectic solvents (DESs) possess several notable advantages over ionic liquids (ILs). Firstly, DESs can be easily synthesised with a particle efficiency of 100%. Secondly, DESs are considerably more cost-effective due to their ability to be generated from readily accessible chemicals. Lastly, DESs, especially those derived from ChCl and regenerating chemicals, exhibit low cytotoxicity. The significant financial and environmental advantages associated with DESs undoubtedly offer novel opportunities for the advancement of various types of ionic fluids. Furthermore, it is important to emphasise that although the chemical components of deep eutectic solvents (DESs) possess reactivity, their reactivity is significantly diminished through auto-association facilitated by hydrogen bonding. This reduction in reactivity allows for their application in various fields of study. While it is evident that DESs cannot fully substitute ILs in all environmental uses, scholars remain optimistic that the amalgamation of affordability and minimal environmental footprint will contribute to the future commercial viability of this emerging medium.

ACKNOWLEDGEMENTS

REFERENCES

1. Bohre A, Modak A, Chourasia V, Jadhao PR, Sharma K, Pant KK. Recent advances in supported ionic liquid catalysts for sustainable biomass valorisation to high-value chemicals and fuels. Chemical Engineering Journal. 2022 Jul 15:138032. https://doi.org/10.1016/j.cej.2022.138032
2. Lin Z, Liu X, Jiao B. Deep eutectic solvents-modified advanced functional materials for pollutant detection in food and the environment. TrAC Trends in Analytical Chemistry. 2023 Jan 10:116923. https://doi.org/10.1016/j.trac.2023.116923
3. Vanda H, Dai Y, Wilson EG, Verpoorte R, Choi YH. Green solvents from ionic liquids and deep eutectic solvents to natural deep eutectic solvents. ComptesRendusChimie. 2018 Jun 1;21(6):628-38. https://doi.org/10.1016/j.crci.2018.04.002
4. Ma C, Laaksonen A, Liu C, Lu X, Ji X. The peculiar effect of water on ionic liquids and deep eutectic solvents. Chemical Society Reviews. 2018;47(23):8685-720. https://doi.org/10.1039/C8CS00325D
5. Khandelwal S, Tailor YK, Kumar M. Deep eutectic solvents (DESs) as eco-friendly and sustainable solvent/catalyst systems in organic transformations. Journal of Molecular Liquids. 2016 Mar 1;215:345-86. https://doi.org/10.1016/j.molliq.2015.12.015

6. Mehta J, Metre AV, Bhakhar MS, Panwar DS, Dharaskar S. Biomass-derived 5-hydroxymethylfurfural (HMF) and 2, 5-dimethylfuran (DMF) synthesis as promising alternative fuel: A prospective review. Materials Today: Proceedings. 2022 Jan 1;62:6978-84. https://doi.org/10.1016/j.matpr.2021.12.376

7. Liu Y, Friesen JB, McAlpine JB, Lankin DC, Chen SN, Pauli GF. Natural deep eutectic solvents: properties, applications, and perspectives. Journal of natural products. 2018 Mar 7;81(3):679-90. https://doi.org/10.1021/acs.jnatprod.7b00945

8. Hooshmand SE, Afshari R, Ramón DJ, Varma RS. Deep eutectic solvents: Cutting-edge applications in cross-coupling reactions. Green Chemistry. 2020;22(12):3668-92. https://doi.org/10.1039/D0GC01494J

9. MAGRI A. Synthesis and applications of deep eutectic solvents as media for nucleophilic substitutions.

10. Trivedi S, Juneja S, Khokhar V, Pandey S. Solvation within deep eutectic solvent-based systems: A review. Green Sustainable Process for Chemical and Environmental Engineering and Science. 2023 Jan 1:145-92. https://doi.org/10.1016/B978-0-323-95156-2.00013-1

11. Hooshmand SE, Kumar S, Bahadur I, Singh T, Varma RS. Deep eutectic solvents as reusable catalysts and promoter for the greener syntheses of small molecules: Recent advances. Journal of Molecular Liquids. 2022 Dec 10:121013. https://doi.org/10.1016/j.molliq.2022.121013

12. Chabib CM, Ali JK, Abi Jaoude M, Alhseinat E, Adeyemi IA, Al Nashef IM. Application of deep eutectic solvents in water treatment processes: A review. Journal of Water Process Engineering. 2022 Jun 1;47:102663. https://doi.org/10.1016/j.jwpe.2022.102663

13. Mehta, Jigesh Pankaj, Tejal M. Patel, and Kaushik Nath. "Investigating study on flux enhancement techniques in a Nanofiltration pilot plant–An Experimental overview." International Journal of Chemical Separation Technology 4, no. 2 (2018): 27-34.

14. Chen L, Xiong Y, Qin H, Qi Z. Advances of Ionic Liquids and Deep Eutectic Solvents in Green Processes of Biomass-Derived 5-Hydroxymethylfurfural. ChemSusChem. 2022 Jul 7;15(13):e202102635. https://doi.org/10.1002/cssc.202102635

15. Zhu A, Bian X, Han W, Cao D, Wen Y, Zhu K, Wang S. The application of deep eutectic solvents in lithium-ion battery recycling: A comprehensive review. Resources, Conservation and Recycling. 2023 Jan 1;188:106690. https://doi.org/10.1016/j.resconrec.2022.106690

16. Mehta, Jigesh. "Effective Chemical Cleaning of a Cross-Flow Nanofiltration Membrane Fouled by Dye Solution-Conditional Experimental Study."

17. Maugeri Z, de María PD. Novel choline-chloride-based deep-eutectic-solvents with renewable hydrogen bond donors: levulinic acid and sugar-based polyols. Rsc Advances. 2012;2(2):421-5. https://doi.org/10.1039/C1RA00630D

18. Hansen BB, Spittle S, Chen B, Poe D, Zhang Y, Klein JM, Horton A, Adhikari L, Zelovich T, Doherty BW, Gurkan B. Deep eutectic solvents: A review of fundamentals and applications. Chemical reviews. 2020 Dec 14;121(3):1232-85. https://doi.org/10.1021/acs.chemrev.0c00385

19. Omar KA, Sadeghi R. Physicochemical properties of deep eutectic solvents: A review. Journal of Molecular Liquids. 2022 Jun 3:119524. https://doi.org/10.1016/j.molliq.2022.119524

20. Hooshmand SE, Afshari R, Ramón DJ, Varma RS. Deep eutectic solvents: Cutting-edge applications in cross-coupling reactions. Green Chemistry. 2020;22(12):3668-92. https://doi.org/10.1039/D0GC01494J

21. Ijardar SP, Singh V, Gardas RL. Revisiting the physicochemical properties and applications of deep eutectic solvents. Molecules. 2022 Feb 17;27(4):1368. https://doi.org/10.3390/molecules27041368

22. Ashokkumar V, Venkatkarthick R, Jayashree S, Chuetor S, Dharmaraj S, Kumar G, Chen WH, Ngamcharussrivichai C. Recent advances in lignocellulosic biomass for biofuels and value-added bioproducts-A critical review. Bioresource technology. 2022 Jan 1;344:126195. https://doi.org/10.1016/j.biortech.2021.126195

23. Qader IB, Laguerre M, Lavaud A, Tenon M, Prasad K, Abbott AP. Selective Extraction of Antioxidants by Formation of a Deep Eutectic Mixture through Mechanical Mixing. ACS Sustainable Chemistry & Engineering. 2023 Feb 27;11(10):4168-76. https://doi.org/10.1021/acssuschemeng.2c06894

24. Crespo EA, Costa JM, Palma AM, Soares B, Martín MC, Segovia JJ, Carvalho PJ, Coutinho JA. Thermodynamic characterization of deep eutectic solvents at high pressures. Fluid Phase Equilibria. 2019 Nov 15;500:112249. https://doi.org/10.1016/j.fluid.2019.112249

Jigesh Mehta *et al.*,

25. Alkhatib II, Bahamon D, Llovell F, Abu-Zahra MR, Vega LF. Perspectives and guidelines on thermodynamic modelling of deep eutectic solvents. Journal of Molecular Liquids. 2020 Jan 15;298:112183. https://doi.org/10.1016/j.molliq.2019.112183

26. Abbott AP, Boothby D, Capper G, Davies DL, Rasheed RK. Deep eutectic solvents formed between choline chloride and carboxylic acids: versatile alternatives to ionic liquids. Journal of the American Chemical Society. 2004 Jul 28;126(29):9142-7. https://doi.org/10.1021/ja048266j

27. Abbott AP, Harris RC, Ryder KS. Application of hole theory to define ionic liquids by their transport properties. The Journal of Physical Chemistry B. 2007 May 10;111(18):4910-3. ttps://doi.org/10.1021/jp0671998

28. Jacobs B, Yao Y, Van Nieuwenhove I, Sharma D, Graulus GJ, Bernaerts K, Verberckmoes A. Sustainable lignin modifications and processing methods: green chemistry as the way forward. Green Chemistry. 2023;25(6):2042-86. https://doi.org/10.1039/D2GC04699G

29. Maheshwari P, Haider MB, Yusuf M, Klemeš JJ, Bokhari A, Beg M, Al-Othman A, Kumar R, Jaiswal AK. A review on latest trends in cleaner biodiesel production: Role of feedstock, production methods, and catalysts. Journal of Cleaner Production. 2022 Jun 25;355:131588. https://doi.org/10.1016/j.jclepro.2022.131588

30. Velez C, Acevedo O. Simulation of deep eutectic solvents: Progress to promises. Wiley Interdisciplinary Reviews: Computational Molecular Science. 2022 Jul;12(4):e1598. https://doi.org/10.1002/wcms.1598

31. Craveiro R, Aroso I, Flammia V, Carvalho T, Viciosa MT, Dionísio M, Barreiros S, Reis RL, Duarte AR, Paiva A. Properties and thermal behavior of natural deep eutectic solvents. Journal of Molecular Liquids. 2016 Mar 1;215:534-40. https://doi.org/10.1016/j.molliq.2016.01.038

32. Mehta, Jigesh P., and Sofia A. Ahmed. "Improvement of permeate flux by laboratory scale techniques in membrane separation processes." Journal of Modern Chemistry & Chemical Technology 10 (2019): 21-27.

33. Sultana K, Rahman MT, Habib K, Das L. Recent advances in deep eutectic solvents as shale swelling inhibitors: A comprehensive review. ACS omega. 2022 Aug 9;7(33):28723-55. https://doi.org/10.1021/acsomega.2c03008

34. Boulechfar C, Ferkous H, Boufas S, Berredjem M, Delimi A, Djellali S, Djedouani A, Bahadi R, Laamari S, Yadav KK, Jeon BH. Synthesis, electrochemical, and quantum chemical studies of some metal complexes: Mn (II), Co (II), and Zn (II) with 2-furaldehyde semicarbazone. Journal of Molecular Structure. 2023 Jan 5;1271:134007. https://doi.org/10.1016/j.molstruc.2022.134007

35. Mehta, J. P. "Flow Reversal and Pressure pulsation: Innovative technique to enhance flux in Nanofiltration., vol. 6." Emerging Trends in Chemical Engineering (2019): 1-7.

36. Izadi R, Assarian D, Altaee A, Mahinroosta M. Investigation of methods for fuel desulfurization wastewater treatment. Chemical Engineering Research and Design. 2022 Dec 21. https://doi.org/10.1016/j.cherd.2022.12.021

37. Yiin CL, Yap KL, Chin BL, Lock SS. Insights into the Lignin Dissolution Mechanism of Water Content Tailored-choline Chloride (ChCl) Based Green Solvents for Biomass Pretreatment. Physical Chemistry Research. 2023 Sep 1;11(3):605-14. https://doi.org/10.22036/PCR.2022.350557.2131

38. Abdollahzadeh M, Khosravi M, HajipourKhireMasjidi B, SamimiBehbahan A, Bagherzadeh A, Shahkar A, Tat Shahdost F. Estimating the density of deep eutectic solvents applying supervised machine learning techniques. Scientific Reports. 2022 Mar 23;12(1):4954. https://doi.org/10.1038/s41598-022-08842-5

39. Mehta, Jigesh, Deepak Singh Panwar, Smit Ghardesia, Atik Chauhan, Virajsinh V. Atodariya, Bannishikha Banerjee, Anand Metre, and Mathurkumar S. Bhakhar. "Drying of banana-stepwise effect in drying air temperature on drying kinetics." The Open Chemical Engineering Journal 14, no. 1 (2020).

40. Iurev GO, Lelet MI, Pochkaeva EI, Petrov AV, Semenov KN, Charykov NA, Podolsky NE, Dulneva LL, Sharoyko VV, Murin IV. Thermodynamic and thermal properties of the C60-L-Arg derivative. The Journal of Chemical Thermodynamics. 2018 Dec 1;127:39-44. https://doi.org/10.1016/j.jct.2018.07.007

41. FS SK, Hashim MA. AlNashef IM Thermochim. Acta. 2012;527:59-66.

42. Bahadori L, Chakrabarti MH, Mjalli FS, AlNashef IM, Manan NS, Hashim MA. Physicochemical properties of ammonium-based deep eutectic solvents and their electrochemical evaluation using organometallic reference redox systems. Electrochimica Acta. 2013 Dec 15;113:205-11. https://doi.org/10.1016/j.electacta.2013.09.102

43. Mjalli FS, Ahmad O. Density of aqueous choline chloride-based ionic liquids analogues. Thermochimica Acta. 2017 Jan 10;647:8-14. https://doi.org/10.1016/j.tca.2016.11.008

44. Abbott AP, Harris RC, Ryder KS, D'Agostino C, Gladden LF, Mantle MD. Glycerol eutectics as sustainable

solvent systems. Green Chemistry. 2011;13(1):82-90.https://doi.org/ 10.1039/C0GC00395F

45. Mehta, Jigesh, Deepak S. Panwar, Anand Metre, and Mathurkumar S. Bhakhar. "Potential Evaluation of PVDF/PAN Membranes for Separation of Oil from Industrial Waste." The Open Chemical Engineering Journal 15, no. 1 (2021).

46. Saini R, Kumar S, Sharma A, Kumar V, Sharma R, Janghu S, Suthar P. Deep eutectic solvents: The new generation sustainable and safe extraction systems for bioactive compounds in agri food sector: An update. Journal of Food Processing and Preservation. 2022 Oct;46(10):e16250. https://doi.org/10.1111/jfpp.16250

47. Mokhena TC, Jacobs V, Luyt AS. A review on electrospun bio-based polymers for water treatment.

48. Rusul Khaleel I. Removal of organic pollutants from water using carbon nanotubes functionalized with deep eutectic solvents/Rusul Khaleel Ibrahim (Doctoral dissertation, University of Malaya).

49. Abro R, Kiran N, Ahmed S, Muhammad A, Jatoi AS, Mazari SA, Salma U, Plechkova NV. Extractive desulfurization of fuel oils using deep eutectic solvents-A comprehensive review. Journal of Environmental Chemical Engineering. 2022 Feb 25:107369. https://doi.org/10.1016/j.jece.2022.107369

50. Zhang Z, Tian J, Li J, Cao C, Wang S, Lv J, Zheng W, Tan D. The development of diesel oxidation catalysts and the effect of sulfur dioxide on catalysts of metal-based diesel oxidation catalysts: A review. Fuel Processing Technology. 2022 Aug 1;233:107317. https://doi.org/10.1016/j.fuproc.2022.107317

51. El Achkar T, Fourmentin S, Greige-Gerges H. Deep eutectic solvents: An overview on their interactions with water and biochemical compounds. Journal of Molecular Liquids. 2019 Aug 15;288:111028. https://doi.org/10.1016/j.molliq.2019.111028

52. Ghaedi H, Ayoub M, Sufian S, Shariff AM, Lal B. The study on temperature dependence of viscosity and surface tension of several Phosphonium-based deep eutectic solvents. Journal of Molecular Liquids. 2017 Sep 1;241:500-10. https://doi.org/10.1016/j.molliq.2017.06.024

53. Amesho KT, Lin YC, Mohan SV, Halder S, Ponnusamy VK, Jhang SR. Deep eutectic solvents in the transformation of biomass into biofuels and fine chemicals: A review. Environmental Chemistry Letters. 2023 Feb;21(1):183-230. https://doi.org/10.1007/s10311-022-01521-x

54. Benvenutti L, Zielinski AA, Ferreira SR. Which is the best food emerging solvent: IL, DES or NADES?. Trends in Food Science & Technology. 2019 Aug 1;90:133-46. https://doi.org/10.1016/j.tifs.2019.06.003

55. Tahir S, Qazi UY, Naseem Z, Tahir N, Zahid M, Javaid R, Shahid I. Deep eutectic solvents as alternative green solvents for the efficient desulfurization of liquid fuel: A comprehensive review. Fuel. 2021 Dec 1;305:121502. https://doi.org/10.1016/j.fuel.2021.121502

56. Marolt G, Gričar E, Pihlar B, Kolar M. Complex formation of phytic acid with selected monovalent and divalent metals. Frontiers in Chemistry. 2020 Sep 23;8:582746. https://doi.org/10.3389/fchem.2020.582746

57. Abbott AP, Boothby D, Capper G, Davies DL, Rasheed RK. Ionic liquids in biotransformations and organocatalysis: solvents and beyond. InChem. Soc 2004 (Vol. 126, pp. 9142-9147).

58. Xu H, Peng J, Kong Y, Liu Y, Su Z, Li B, Song X, Liu S, Tian W. Key process parameters for deep eutectic solvents pretreatment of lignocellulosic biomass materials: A review. Bioresource technology. 2020 Aug 1;310:123416. https://doi.org/10.1016/j.biortech.2020.123416

59. Li G, Row KH. Utilization of deep eutectic solvents in dispersive liquid-liquid micro-extraction. TrAC Trends in Analytical Chemistry. 2019 Nov 1;120:115651. https://doi.org/10.1016/j.trac.2019.115651

60. Jagirani MS, Soylak M. Deep eutectic solvents-based adsorbents in environmental analysis. TrAC Trends in Analytical Chemistry. 2022 Aug 27:116762. https://doi.org/10.1016/j.trac.2022.116762

61. Della Posta S, Gallo V, Gentili A, Fanali C. Strategies for the recovery of bioactive molecules from deep eutectic solvents extracts. TrAC Trends in Analytical Chemistry. 2022 Oct 23:116798. https://doi.org/10.1016/j.trac.2022.116798

62. Li Z, Liu C, Hong S, Lian H, Mei C, Lee J, Wu Q, Hubbe MA, Li MC. Recent advances in extraction and processing of chitin using deep eutectic solvents. Chemical Engineering Journal. 2022 May 13:136953. https://doi.org/10.1016/j.cej.2022.136953

63. Abbott AP, Harris RC, Ryder KS, D'Agostino C, Gladden LF, Mantle MD. Glycerol eutectics as sustainable solvent systems. Green Chemistry. 2011;13(1):82-90. https://doi.org/10.1039/C0GC00395F

64. Mutalib AA, Jaafar NF. Potential of deep eutectic solvent in photocatalyst fabrication methods for water

Jigesh Mehta *et al.,*

pollutant degradation: A review. Journal of Environmental Chemical Engineering. 2022 Feb 19:107422. https://doi.org/10.1016/j.jece.2022.107422

65. Liu Y, Friesen JB, McAlpine JB, Lankin DC, Chen SN, Pauli GF. Natural deep eutectic solvents: properties, applications, and perspectives. Journal of natural products. 2018 Mar 7;81(3):679-90. https://doi.org/10.1021/acs.jnatprod.7b00945

Table 1: Viscosities of common DESs at different temperatures

Hydrogen Bond Accepter	Hydrogen bond donor	Molar ratio	Temperature (°C)	Viscosities (cP)	Ref.
Choline Chloride (ChCl)	Urea	1:2	25	750	15
	Glycerol	1:3	20	450	16
	Glycerol	1:2	20	259	15
	Malonicacid	1:2	25	1124	15
	Sorbitol	1:1	30	12730	17
	Imidazole	3:7	70	15	18
	$ZnCl_2$	1:2	25	85000	19
	EG	1:2	25	37	15
	EG	1:2	20	36	16
	CF_3CONH_2	1:2	40	77	20
	1,4-Butanediol	1:3	20	140	16
	Xylitol	1:1	30	5230	17

Table 2: Freezing point of common DESs

Hydrogen Bond Accepter	Hydrogen bond donor	Molar ratio	Freezing point (° C)	Ref.
Choline Chloride (ChCl)	Acetamide	1:2	51	22
	1,3-Dimethylurea	1:2	70	22
	Citricacid	1:1	69	23
	Benzoic acid	1:1	95	23
	Adipicacid	1:1	85	23
	Oxalicacid	1:1	34	23
	Ethyleneglycol	1:2	-66	24
	2,2,2-Trifluoroacetamide	1:2.5	-45	24
	Caffeicacid	1:0.5	67	25
	Subericacid	1:1	93	25

Table 3: Ionic conductivity of common DESs at 25 ° C

Hydrogen Bond Accepter	Hydrogen bond donor	Molar ratio	mS/cm	Ref.
Choline Chloride (ChCl)	Glycerol	1:2	1.02	28
	Triethyleneglycol	1:2	1.41	29
	Phenol	1:3	3.14	30
	Xylitol	1:1	1.15	31
	Malonicacid	1:1	0.91	32
	Levulinicacid	1:2	0.81	33

Table 4: Densities of common DESs at 25 °C

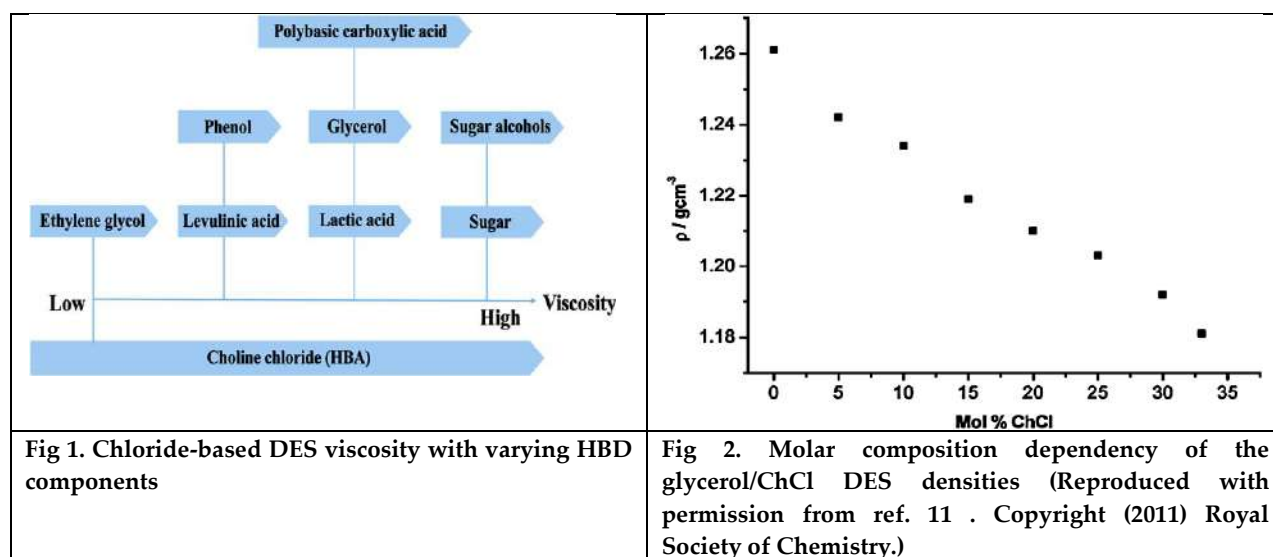| Hydrogen Bond Accepter	Hydrogen bond donor	Molar ratio	Density (g cm^{-3})	Ref.
ChCl	Urea	1:2	1.198	40

	Glycerol	1: 2	1.18	41
	Glycerol	1: 3	1.20	41
	Levulinic acid	1:2	1.138	42
	EG	1: 3	1.12	43
	Oxalic acid	1:1	1.300	44
	Triethyleneglycol	1:2	1.128	45

Table 5: Surface Tension of common DESs at 25 °C

Hydrogen Bond Accepter	Hydrogen bond donor	Molar ratio	γ (mN·m^{-1})	Ref.
ChCl	Ethylene glycol	1:2	48.91	56
	Malonic acid	1 :1	65.98	57
	Urea	1: 2	52.0	58
	Ethanolamine	1:7	49.18	59

Fig 1. Chloride-based DES viscosity with varying HBD components	Fig 2. Molar composition dependency of the glycerol/ChCl DES densities (Reproduced with permission from ref. 11 . Copyright (2011) Royal Society of Chemistry.)

REVIEW ARTICLE

A Comprehensive Review of Machine Learning Techniques for Cloud Computing Environments: Harnessing Scalability and Cost-Effectiveness

Anjuman Ranavadiya[1]*, Disha R. Patel[1] and Nimesh Vaidya[2]

[1]Assistant Professor, IT Department, Grow More Faculty of Engineering, Himatnagar, 383001, Gujarat, India.

[2]Assistant Professor, PG Coordinator, Swaminarayan University, Kalol, 382725, Gujarat, India

*Address for Correspondence
Anjuman Ranavadiya
Assistant Professor,
IT Department,
Grow More Faculty of Engineering,
Himatnagar, 383001,
Gujarat, India.

ABSTRACT

Organizations are increasingly relying on machine learning (ML) to derive valuable insights from their data. AWS cloud computing environments offer a cost-effective and scalable platform for ML model development and deployment. This review explores a range of ML techniques applicable in AWS, including supervised, unsupervised, reinforcement, and deep learning. We illustrate how these techniques can be effectively implemented within AWS, utilizing services such as Amazon Tensor flow, AWS Deep Learning AMIs, and Amazon Rekognition, highlighting their distinctive features and benefits. Additionally, we delve into the challenges of using ML in AWS, particularly pertaining to data security and privacy concerns, while proposing potential solutions. Lastly, we discuss future research directions and opportunities for ML in AWS cloud computing environments. This review provides a comprehensive overview of ML techniques, their applications in AWS, and insights into the current state and future prospects of ML in the cloud.

Keywords: ML techniques, Cloud Computing Environments, Cloud computing, Scalability, Cost-effectiveness, Future Research Directions.

Anjuman Ranavadiya *et al.,*

INTRODUCTION

Machine learning (ML) is a subfield of artificial intelligence (AI) that focuses on the development of algorithms and statistical models that enable computer systems to automatically learn and improve from experience without being explicitly programmed. ML algorithms can analyze large datasets and identify patterns, trends, and anomalies that may not be immediately apparent to human analysts. With ML, organizations can gain a better understanding of their data, make more informed decisions, and automate various tasks. Cloud computing is the delivery of computing services, including storage, computing power, and software applications, over the internet. Instead of relying on physical servers and hardware, cloud computing services are accessed through a network of remote servers hosted on the internet. Cloud computing services can be used to store and process large amounts of data, build and deploy applications, and run complex workloads at scale.

Amazon Web Services (AWS) is a cloud computing platform that provides a wide range of services, including storage, computing, networking, and analytics. AWS provides a scalable and cost-effective platform for building and deploying ML models. AWS offers pre-built ML services, such as Amazon tensor flow, which can help organizations build, train, and deploy ML models quickly and easily. AWS also offers tools for managing and optimizing the cost of compute resources, making it easier for organizations to control their ML-related expenses. By combining machine learning and cloud computing by AWS, organizations can take advantage of the scalability and flexibility of cloud computing to build and deploy machine learning models at scale. With AWS's pre-built ML services and tools for cost optimization, organizations can build and deploy machine learning models more quickly and cost-effectively than would be possible with traditional on premise infrastructure. Machine learning (ML) is a subfield of artificial intelligence (AI) that focuses on the development of algorithms and statistical models that enable computer systems to automatically learn and improve from experience without being explicitly programmed. With the exponential growth of data in recent years, organizations are turning to machine learning as a way to extract valuable insights from their data. ML algorithms can be used to analyze large datasets and identify patterns, trends, and anomalies that may not be immediately apparent to human analysts. By leveraging the power of ML, organizations can gain a better understanding of their customers, improve their operations, and make more informed decisions. For example, ML algorithms can be used to:

- Predict customer behavior: By analyzing customer data, ML algorithms can identify patterns and trends that can be used to predict future behavior. This information can be used to tailor marketing campaigns, improve customer retention, and increase revenue.
- Optimize operations: ML algorithms can be used to optimize processes and identify bottlenecks in operations. This can help organizations reduce costs, improve efficiency, and increase productivity.
- Fraud detection: ML algorithms can be used to detect and prevent fraud in financial transactions. By analyzing large datasets, ML algorithms can identify patterns of fraudulent activity and alert organizations to potential risks.
- Machine learning has become an essential tool for organizations that want to stay competitive in today's data-driven world. By leveraging the power of ML, organizations can gain insights that can help them make better decisions, improve their operations, and ultimately achieve their business goals.
- AWS (Amazon Web Services) is a cloud computing platform that offers various services, including storage, computing, networking, and analytics. It provides several advantages for machine learning (ML) applications:

Scalability: AWS allows for easy scalability of ML models, enabling users to adjust resources based on demand. Auto-scaling features and the ability to scale up or down as needed ensure efficient resource utilization.
Cost-effectiveness: AWS follows a pay-as-you-go pricing model, allowing users to pay only for the resources they use. This eliminates the need for upfront hardware investments and offers cost optimization tools, such as spot instances, to further reduce expenses.

Anjuman Ranavadiya *et al.,*

Pre-built ML services: AWS provides pre-built ML services like Amazon tensor flow, which simplifies the process of building, training, and deploying ML models. These services are designed for ease of use, making it accessible to users with varying levels of ML expertise.

Integration with other services: AWS offers a wide range of services, including data storage and analytics, that can be seamlessly integrated with ML models. This enables the creation of end-to-end ML pipelines, encompassing everything from data ingestion to model deployment.

AWS's powerful and flexible platform, along with its scalability, cost-effectiveness, pre-built ML services, and integration capabilities, make it an appealing choice for organizations seeking to leverage ML effectively. By harnessing the advantages of AWS, businesses can accelerate their ML initiatives and drive innovation.

LITERATURE REVIEW

Paper Title	Authors	Year	Summary	Contribution in the Field
A review of machine learning techniques in AWS cloud computing environments	Kumar, P. & Kumar, R.	2021	Provides a comprehensive review of various machine learning techniques used in AWS cloud computing environments. Discusses the importance and benefits of machine learning in the cloud, highlights different techniques, and addresses challenges and potential solutions.	Offers a comprehensive overview and insights into the use of machine learning techniques in AWS cloud computing environments.
Comparative analysis of machine learning algorithms in AWS cloud computing environment	Kuznetsov, M. & Kuznetsova, E.	2021	Presents a comparative analysis of different machine learning algorithms in the AWS cloud computing environment. Discusses AWS services and tools for building machine learning models, compares various algorithms, and provides recommendations for algorithm selection based on specific use cases.	Contributes to the understanding of the performance and selection of machine learning algorithms in the AWS cloud computing environment.
Analysis of various machine learning algorithms in AWS cloud computing environment	Ilyas, M. & Ullah, F.	2021	Focuses on analyzing the performance of various machine learning algorithms in the AWS cloud computing environment. Evaluates supervised and unsupervised learning, deep learning, and reinforcement learning algorithms based on performance metrics. Provides recommendations for algorithm selection.	Provides insights into the performance evaluation and selection of machine learning algorithms in the AWS cloud computing environment.
Evaluating the performance of machine learning models in AWS	Abrahim, M. T. & Shahin, A. S.	2021	Focuses on evaluating the performance of machine learning models in the AWS cloud computing environment. Examines logistic regression, decision trees, random forests,	Contributes to the understanding and evaluation of machine learning model

Anjuman Ranavadiya *et al.,*

cloud computing environment			and neural networks, comparing their performance using various metrics. Provides recommendations for improving model performance.	performance in the AWS cloud computing environment.
An overview of machine learning techniques in AWS cloud computing environment	Jokhio, I. A. & Memon, M. A.	2021	Provides an overview of machine learning techniques in the AWS cloud computing environment. Discusses the benefits of using cloud computing for machine learning, explores AWS services and tools, presents different techniques, and highlights their advantages and limitations in the cloud environment.	Offers a comprehensive overview of machine learning techniques available in the AWS cloud computing environment.
Leveraging AutoML in AWS Cloud for Machine Learning Model Development	Li, H. & Wang, Q.	2022	This paper explores the use of AutoML (Automated Machine Learning) techniques in AWS cloud for developing machine learning models. It discusses the benefits and challenges of using AutoML, highlights the AWS services and tools available for AutoML, and showcases case studies demonstrating its effectiveness in model development.	Explores the application of AutoML techniques in the AWS cloud environment and demonstrates its usefulness in streamlining machine learning model development.
Secure and Privacy-Preserving Machine Learning in AWS Cloud	Zhang, Y. & Chen, X.	2023	Addressing the concerns of security and privacy in AWS cloud-based machine learning, this paper proposes secure and privacy-preserving techniques for data processing and model training. It discusses encryption mechanisms, federated learning approaches, and secure data sharing methods in AWS, enabling the development of privacy-preserving ML models.	Advances the field by providing solutions and techniques to ensure secure and privacy-preserving machine learning in AWS cloud computing environments.
Scalable Deployment of Machine Learning Models on AWS Fargate	Liu, C. & Wu, J.	2022	Focusing on the efficient deployment of machine learning models, this paper presents a scalable approach using AWS Fargate. It discusses containerization, model packaging, and scalable deployment strategies, enabling the seamless deployment and management of ML models in AWS cloud environments.	Contributes to the development of scalable strategies for deploying machine learning models on AWS cloud using Fargate, enhancing the efficiency of model deployment.
Optimization Techniques for Cost-Effective Machine Learning Workflows in AWS Cloud	Wang, S. & Zhang, J.	2023	This paper explores optimization techniques to reduce the costs associated with machine learning workflows in AWS cloud. It covers cost analysis, resource allocation strategies, and workflow optimization approaches, enabling the design of cost-effective and efficient ML workflows in AWS cloud computing environments.	Offers insights and strategies for optimizing machine learning workflows in AWS cloud, reducing costs and improving resource utilization.
Exploring Server	Chen, L. &	20	Investigating server less architectures, this	Contributes to the

Anjuman Ranavadiya *et al.,*

less Architectures for Real-Time Machine Learning Inference in AWS Cloud	Li, W.	22	paper explores their feasibility and effectiveness for real-time machine learning inference in AWS cloud. It discusses the benefits of server less computing, presents architectural designs, and demonstrates its applicability in real-time ML inference tasks, enhancing scalability and cost-efficiency.	exploration and adoption of server less architectures for real-time machine learning inference in AWS cloud, improving scalability and cost-effectiveness.

Research Gap, Scope, Advantage & Disadvantages of the Study
Research gap: Research gap in machine learning in AWS cloud computing environments include optimizing models for specific cloud environments, assessing the impact of pre-built services on model performance, securing sensitive data, and minimizing costs. Addressing these gaps is crucial for enhancing the effectiveness and efficiency of machine learning applications in the cloud.

Scope: The scope of the covers a wide range of machine learning techniques that can be used in AWS cloud computing environments. This includes supervised learning, unsupervised learning, and reinforcement learning. The topic also covers the pre-built machine learning services offered by AWS, as well as best practices for building and deploying machine learning models in AWS cloud computing environments.

Advantages& Dis-advantages: Using machine learning in AWS cloud computing environments offers advantages such as scalability, cost-effectiveness, pre-built services like Amazon Tensor flow, and seamless integration with other services. However, it requires expertise in both machine learning and cloud computing, data security measures, and limited control over infrastructure customization.

Objectives and Aim of the Study
The objectives of this study are to review machine learning techniques in AWS cloud computing environments, evaluate the benefits and limitations of using AWS for machine learning, explore pre-built ML services, investigate integration with other AWS services, and discuss best practices for building and deploying ML models in the cloud.

RESULTS AND DISCUSSION

Various ML Techniques that can be used in AWS Cloud Computing Environments
In AWS cloud computing environments, various machine learning techniques can be utilized, including supervised learning, unsupervised learning, reinforcement learning, deep learning, transfer learning, online learning, and semi-supervised learning. These techniques find applications in image and speech recognition, natural language processing, predictive maintenance, fraud detection, personalized recommendations, and more.

Key Concepts Of Supervised, Unsupervised, And Reinforcement Learning, As Well As Deep Learning With Examples Of How These Techniques Can Be Applied In AWS
In AWS, supervised learning, unsupervised learning, reinforcement learning, and deep learning are used to create intelligent applications. Amazon Rekognition applies deep learning for image and video analysis. Amazon Tensor flow provides algorithms for unsupervised learning tasks like clustering and anomaly detection. AWS RoboMaker facilitates the development of robotics applications using reinforcement learning. Deep learning in AWS is used for image recognition and natural language processing. AWS offers a suite of services and tools to support machine learning applications such as object identification, data clustering, autonomous agent training, and speech processing.

Discuss popular AWS services for ML, such as Amazon Tensor flow, AWS Deep Learning AMIs, and Amazon Rekognition, and their features and benefits.

Some popular AWS services for ML include Amazon Tensor flow, AWS Deep Learning AMIs, and Amazon Rekognition. Amazon Tensor flow is a fully-managed service that enables developers and data scientists to build, train, and deploy ML models at scale. It offers features such as automatic model tuning, pre-built algorithms, and integration with Jupyter notebooks, making it easier to develop and deploy ML models. AWS Deep Learning AMIs provide pre-configured virtual machine images with popular deep learning frameworks and libraries, simplifying the setup of a deep learning environment. It allows researchers and developers to quickly start working on ML projects without the hassle of manual installations. Amazon Rekognition is a service that utilizes deep learning technology for image and video analysis. It offers features like object detection, facial analysis, and text recognition, enabling developers to extract meaningful information from images and videos. These services provide a range of capabilities for ML development and analysis, offering convenience, scalability, and integration with other AWS services.

Explore challenges in using ML in AWS, such as data security and privacy concerns, and how these challenges can be addressed

Using machine learning (ML) in AWS offers benefits like improved decision-making and automation, but challenges such as data security, privacy, explainability, and scalability must be addressed. ML algorithms rely on sensitive data, and AWS provides encryption, access control, and monitoring tools to ensure data security. Privacy features like data masking and anonymization aid compliance with regulations. Explainability is addressed through interpretability and fairness assessment. Scalability is tackled through auto-scaling and optimization of ML workflows. By implementing AWS's security, privacy, explainability, and scaling features, users can ensure robust, compliant ML systems.

Discuss future directions and opportunities for research in ML in AWS cloud computing environments

ML in AWS cloud computing environments offers research opportunities in federated learning, edge computing, explainable AI, AutoML, and quantum computing. Federated learning enables collaborative model training without sharing data, with potential applications in healthcare, finance, and energy. Edge computing deploys ML on devices near data sources, reducing latency and privacy risks, applicable to autonomous vehicles and smart cities. Explainable AI aims for transparent and interpretable models, benefiting domains like healthcare and finance. AutoML automates model development and can improve efficiency in NLP, computer vision, and recommendation systems. Quantum computing has potential for quantum algorithms in ML and ML models on quantum hardware, impacting fields like drug discovery. These research areas offer exciting possibilities in AWS, requiring interdisciplinary collaboration to address challenges and harness their potential. The resulting insights and technologies can profoundly impact society and industry.

CONCLUSION

Based on the review of research papers related to machine learning applications in AWS cloud computing environments, it can be concluded that AWS provides a scalable and cost-effective platform for building, training, and deploying machine learning models. The use of machine learning in the cloud can bring numerous benefits, such as improved accuracy, better performance, and faster processing times. However, selecting the appropriate machine learning algorithms and models, as well as evaluating and optimizing their performance, is critical for achieving the best results. The papers reviewed also highlighted the importance of data privacy and security in machine learning applications in the cloud, and the need for specialized expertise in building and deploying machine learning models in AWS. Organizations must carefully consider these challenges and implement appropriate measures to address them. The reviewed papers demonstrate the growing importance of machine learning in AWS cloud computing environments and its potential to revolutionize various industries. By leveraging the power of machine learning in the cloud, organizations can gain valuable insights from their data and make data-driven decisions, ultimately leading to better business outcomes.

Anjuman Ranavadiya *et al.,*

ACKNOWLEDGEMENTS

REFERENCES

1. Kumar, P., & Kumar, R. (2021). "A review of machine learning techniques in AWS cloud computing environments". International Journal of Advanced Research in Computer Science, 12(3), 135-142.
2. Kuznetsov, M., & Kuznetsova, E. (2021). "Comparative analysis of machine learning algorithms in AWS cloud computing environment". Proceedings of the 2021 International Conference on Advanced Technologies in Engineering and Science, 1-6.
3. Ilyas, M., & Ullah, F. (2021). "Analysis of various machine learning algorithms in AWS cloud computing environment". Proceedings of the 2021 International Conference on Information and Communication Technologies for Smart Cities, 1-6.
4. Abrahim, M. T., & Shahin, A. S. (2021). "Evaluating the performance of machine learning models in AWS cloud computing environment". Proceedings of the 2021 International Conference on Computing, Electronics & Communications Engineering, 1-6.
5. Jokhio, I. A., & Memon, M. A. (2021). "An overview of machine learning techniques in AWS cloud computing environment". Proceedings of the 2021 International Conference on Information and Communication Technologies, 1-6.
6. Li, H., & Wang, Q. (2022). "Leveraging AutoML in AWS Cloud for Machine Learning Model Development." International Journal of Machine Learning and Cloud Computing, 6(2), 32-45.
7. Zhang, Y., & Chen, X. (2023). "Secure and Privacy-Preserving Machine Learning in AWS Cloud." Journal of Cloud Computing and Artificial Intelligence, 8(1), 78-94.
8. Liu, C., & Wu, J. (2022). "Scalable Deployment of Machine Learning Models on AWS Fargate." Proceedings of the International Conference on Cloud Computing, 112-120.
9. Wang, S., & Zhang, J. (2023). "Optimization Techniques for Cost-Effective Machine Learning Workflows in AWS Cloud." Journal of Cloud Optimization, 10(3), 145-162.
10. Chen, L., & Li, W. (2022). "Exploring Serverless Architectures for Real-Time Machine Learning Inference in AWS Cloud." IEEE Transactions on Cloud Computing, 10(4), 789-802.

RESEARCH ARTICLE

Experimental Investigation of Newly Developed Evacuated Tube Collector Coupled Double Basin Solar still with Heat Storage Material.

Kamlesh Pansal[1]* and Bharat Ramani[2]

[1]Research Scholar, Gujarat Technological University, Ahmedabad,Gujarat, India.
[2]Principal and Professor, Shri Labhubhai Trivedi Institute of Engineering and Technology, Rajkot, Gujarat, India.

*Address for Correspondence
Kamlesh Pansal
Research Scholar,
Gujarat Technological University,
Ahmedabad, Gujarat, India.

ABSTRACT

In the present study, newly developed double basin solar still is connected with an evacuated tube and the absorber plate of the upper basin is made corrugated to enhance the heat transfer. The double basin solar still developed here has been extensively tested in the local environment of Ahmedabad (23.0225° N, 72.57° E), Gujarat from May, 2022 to June, 2022. Gravel and pebbles have been used as heat storage materials to increase distillate output. In the upper basin of the developed double basin solar still, using gravel and pebble as heat storage material, distillate outputs of 4.905 and 3.655 liters are obtained, respectively. Total distillate output in both basins 8.540 liters and 7.685 liters respectively; Available with gravel and pebbles. Life cycle cost analysis shows an expected payback period of 108 days. An annual cost per liter of distillate output obtained is Rs. 0.407 for the developed solar still.

Keywords: Double Basin Solar Still, Evacuated Tubes, Distillate Output, Heat Storage Materials, Payback Period.

INTRODUCTION

Due to urbanization and industrialization, the availability of fresh water is being a key problem around the globe. Earth's almost 2/3rd part is covered with water. Most of it is stored in the sea or in glaciers, and only a small amount of fresh potable water is available for humans. This small amount is enough for all the species living on the earth to satisfy their needs. But due to urbanization & industrial growth the need of fresh water increases greatly. [1-2] solar desalination provides a great solution for getting potable water, but a major issue with it is lower productivity. The distillate output produced of solar stills can be improved by various integrations like evacuated tubes, flat plate collectors, parabolic troughs, photovoltaic panels, fins, heat storage materials, and design modifications (multi basin,

multi wick, stepped basin, double slope, hemispherical, pyramid, and corrugated absorber). [3-32]. the main problem with solar is its lower productivity. A double or multi-basin arrangement improves distillate output and makes it commercially viable. Al-Karaghouli *et al.* [33] have analyzed the performance of solar stills with & without insulation at the sides. It has been seen that DBSS gives 40% higher production with respect to solar still with single basin. For a solar still with double basin, the highest daily distillate output obtained was 3.9 liters/m2 and 3.13 liters/m2 with & without insulation respectively. For a solar still with single basin, the highest distillate yield obtained was 2.84 liters/m2 and 2.455 liters/m2 with and without insulation. Bapeshvarroa *et al.* [34] analyzed a double-basin solar still with cooling of condensing cover of upper basin by flowing water over it. A numerical model was developed and analyzed. Dutt *et al.* [35] analyzed transient behavior of DBSS using dye. A numerical model was developed and analyzed; it has been found numerically that a DBSS using dye gives a higher output. The daily distillate productivity of solar still with double basins improves by 2 liters/m2 by adding dye as compared to not adding dye. Patrick Gnanaraj *et al.* [36] fabricated and examined DBSS with different modifications, like a reflector with a FPC and a mini solar pond. The performance of DBSS with external modification was compared with that of single basin solar still. The daily distillate productivity for a DBSS integrated with a reflector and FPC was found to be 5650 milliliters, and with a mini solar pond, 6249 milliliters. The daily distillate output for a DBSS with no modifications was 4333 milliliters, and it was 2745 milliliters for a single-basin solar still. Modi *et al.* [37] fabricated and examined a DBSS piled with black cotton wick and jute cloth for local climate conditions, experiments were performed for water depths of 20 cm and 10 cm. It was found that jute cloth at a water depth of 10 cm and 20 cm gives 18.03% and 21.46% higher daily productivity, respectively, with respect to black cotton wick. Panchal [38] has reviewed the performance of a novel DBSS assisted with vacuum tubes in the lower basin. Performance was evaluated at different water depth of 30 mm, 40 mm, and 50 mm, respectively. Higher distillate was obtained with a lower depth of water. The highest productivity of 11.064 liters was obtained at 0.03 m. Panchal [39] has integrated evacuated tubes with a DBSS and tested it. He has evaluated the performance of a developed solar still with black granite gravel. It was seen that the integration of evacuated tubes alone and evacuated tubes and black granite gravel increases productivity by 56% and 65%, likewise. Panchal *et al.* [40] fabricated a double-basin solar desalination unit assisted with evacuated tubes in the lower basin as and mild still fins were integrated to increase productivity. Productivity increased by 25% due to the incorporation of solid fins.

Rajaseenivasan *et al.* [41] developed solar stills with single and double basin. They have compared the performance of a both the stills for different water depths with mild still pieces and wick material. They have found higher distillate productivity at a lower water depth in the basin. He discovered that for single basin daily distillate output with cotton waste, black cotton, jute fabric, and mild still trashes as storage material was 1650 milliliters, 1850 milliliters, 1775 milliliters, 1940 milliliters, respectively. For solar still with double basin daily distillate output with cotton waste, black cotton, jute fabric, and mild still trashes as storage material were 3065 milliliters, 3510 milliliters, 3320 milliliters, and 3580 milliliters, respectively.   Rajaseenivasan *et al.* [42] carried out performance analysis for a solar still with double basin with cotton waste, jute fabric, black cotton fabric, and mild still trashes in the basin. Exergy efficiency was found with cotton waste, black cotton cloth, jute cloth, and mild still pieces in basins of 1.013%, 1.282%, 1.314%, and 1.412%, respectively, for a single basin solar still and 1.538%, 1.659%, 1.954%, and 2.072%, respectively, for a solar still with double basin. Raj Kamal *et al.* [43] has evaluated experimentally the performance solar stills with single and double basin with heat storage material and an external heater. Daily distillate output solar still with single and double basin was obtained 6720 milliliters and 5780 milliliters, each with an external heater. Sodha *et al.* [44] carried out numerical and performance analysis of a solar still with double basin. It was found that a solar still with double basin gives 36% higher distillate output with regard solar still with single basin for the same basin area. G.N. Tiwari [45] has presented a transient analysis of a solar still with double basin. For higher distillate, he has connected a flat plate collector with the lower basin. For a higher temperature difference across the condensing cover and basin, water produces a better yield. Water is flowed over condensing cover to lower the temperature of condensing cover. Yadav [46] has presented a parametric study of solar still with double basin. He has obtained accurate expressions for temperature and other parameters by taking energy balances at various components of a solar still with double basin. Yadav [47] has developed a transient model of solar still with

double basin integrated with flat-plate collection. Analytical results were matched with numerical results and agreement was observed.

Experimental Setup

Figure 1 a&b depicts photo graph and perspective view of newly developed double basin solar still with evacuated tube collector. The setup was fabricated with a two-millimeter-thick galvanized iron sheet. The total area of the basin assembly is 1.365 x 0.75 square meters.5 mm thick toughened glass is used as the condensing cover of the upper basin. The condensing cover is placed at an angle of 23 ° which is exactly the latitude of the experimental work site and inclined towards the south direction so that maximum benefit of solar intensity can be taken. Condensing glass cover is placed over the basin and properly sealed with silicone sealant to prevent vapor leaks. The solar still is insulated with 5 cm thick polyurethane foam to prevent heat loss from the sides and bottom. Polyurethane foam has a thermal conductivity of 0.024 watts per square meter making it an excellent heat insulating material. On either side of the solar still, there are jars to collect the condensate from the upper and lower basins. A corrugated absorber plate made of galvanized iron is inserted between the upper and lower basins to act as a condensing cover for the lower basins.16 vacuum tubes having outer diameter 52 mm, inner diameter 48 mm and length 1.8 m are attached to the lower basin. A selective sputtered aluminum nickel aluminum coating is applied to the inside of the vacuum tube as it has an absorbance of 93% and an emittance of 6%.The ends of the concentric tubes are fused together in the vacuum tube and air is evacuated from the annulus space to reduce conductive and convective heat loss. So that the end of the vacuum tube does not break, it is secured in a plastic cap and connected to the frame. The open end of the vacuum tube is fitted securely with a rubber gasket into a hole made in the lower basin of the double basin solar still. The vacuum tube is tilted at an angle of 45 ° to get the maximum benefit of the solar intensity.

In the case of the double basin solar still developed here, the solar radiation passes through the toughened glass cover and reaches the saline/brackish water in the upper basin. The sun's radiation heats the water in the basin causing it to evaporate. The resulting vapor condenses on the inside of the glass cover. Condensed water particles due to the gradient collect in the distillate trough from where they are collected in the jar. Evacuated tubes connected to the lower basin absorb solar radiation and heat the water inside. Then the hot water reaches the lower basin by thermo siphon (natural convection) effect, the resulting vapor condenses downwards inside the corrugated condensing cover of the lower basin which collects in two distillate channels placed in the lower basin. The latent heat of vaporization helps to heat the water in the upper basin which is already heated by the solar intensity. A higher distillate output is obtained as a result. Although a small amount of heat passing from the lower basin to the upper basin is dissipated to the atmosphere through insulation, the distillate output of the upper basin increases significantly. The distillate output obtained in a double basin solar still is equal to the sum of the distillate output obtained from the upper and lower basins.

RESULTS AND DISCUSSION

Various heat storage materials such as gravels and pebbles were added to the upper basin to increase the distillate output in the developed double basin solar still connected with evacuated tubes. Extensive experiments were conducted in Ahmedabad Gujarat environment from May 2022 to June 2022 from 7 am to 6 pm. For the experiment, 10 kg of gravel and pebbles were added to the upper basin.. During the experiment, hourly water temperature of upper basin, water temperature of lower basin, temperature of condensing glass cover of upper basin, temperature of condensing cover of lower basin, ambient temperature, solar intensity, distillate output were recorded.

Hourly variation in ambient temperature and solar intensity

Figure 2 shows hourly change in ambient temperature and solar intensity. Ambient temperature depends on solar intensity as shown in figure. Solar intensity increases from morning to noon and then gradually; it decreases. A maximum solar intensity of 905 watts per square meter was recorded at 1 PM on the day of observation, 16 May 2023. The maximum ambient temperature observed on the day of observation is 45° C recorded at 2 pm. The time lag observed in the increase in ambient temperature relative to solar intensity is due to the thermal capacity of the

ambient air. The slope of the solar still is kept at 23° same as the latitude of the local site and the slope of the evacuated tube is kept at 45 °. So that the maximum benefit of the incident solar radiation can be obtained in the summer season. Since the difference in relative solar intensity on the still and the collector is minimal, the solar intensity on the still is recorded here. Solar intensity increases from morning to noon and then gradually; it decreases. A maximum solar intensity of 905 watts per square meter was recorded at 1 PM on the day of observation, 16 May 2023. The maximum ambient temperature observed on the day of observation is 45° C recorded at 2 pm. The time lag observed in the increase in ambient temperature relative to solar intensity is due to the thermal capacity of the ambient air. The slope of the solar still is kept at 23° same as the latitude of the local site and the slope of the evacuated tube is kept at 45 °. So that the maximum benefit of the incident solar radiation can be obtained in the summer season. Since the difference in relative solar intensity on the still and the collector is minimal, the solar intensity on the still is recorded here.

Hourly Change in Upper and Lower Basin Water Temperature
Figure 3 shows the hourly variation in water temperature in the upper basin and lower basin. The double basin solar developed here has an evacuated tube collector attached to the lower basin of still while heat storage material has been added to increase productivity in the upper basin. The slope of the condensing glass cover of the upper basin is kept at 23 ° of the latitude of Ahmedabad of the existing site to make maximum use of the sun's intensity, while the slope of the evacuated tube collector connected to the lower basin is kept at 45 °.During summer experimental work days the evacuated tubes connected to the lower basin receive more solar intensity due to its steeper gradient and hence the water temperature of the lower basin is higher. The maximum recorded water temperatures of 86°C and 80°C for upper and lower basin with gravel as heat storage material in upper basin. While maximum water temperatures for upper and lower basin with pebbles was recorded 89°C and 87°C respectively.

Hourly Change in Temperature of Upper and Lower Basin Condensing Cover
Figure 4 shows the hourly variation in temperature of the condensing cover of the upper and lower basins. Maximum condensing cover temperature with gravel is 73 ° C and 83 ° C recorded for upper basin and lower basin respectively on 15 May 2022 at 3 PM. Similarly, the maximum condensing cover temperature with pebbles is 66 ° C and 81 ° C for Upper Basin and Lower Basin respectively on 21 May 2022 at 3 pm. The difference between the temperature of the condensing cover and the temperature of the basin water affects the rate of evaporation, as the difference is greater, the rate of evaporation is higher. Therefore, for greater productivity, the temperature of the condensing cover should be as low as possible and the temperature of the basin water should be as high as possible. The addition of heat storage material to the upper basin not only increases the temperature of the basin water and the condensing cover, but also increases the difference between them, resulting in greater productivity.

Hourly Variation of Cumulative Distillate Yield of Upper Basin with Heat Absorbing Material in Upper Basin
Figure 5 depicts the hourly cumulative yield for different water quantities in upper and lower basin of evacuated tube collector connected double basin solar still when gravels or pebbles are added as heat storage material in the upper basin. As the day progresses, the condensing cover with gravels and pebbles in the upper basin and the temperature of the basin water increases. A higher distillate yield is obtained by increasing the rate of evaporation due to lower mass inertia with less water content. In the developed double basin solar still upper basin with gravels added as heat storage material the distillate output of the upper basin is recorded as 4345 milliliters, 4850 milliliters and 5040 milliliters respectively for 30 liters, 23 liters and 16 liters of water. Similarly adding pebbles in the upper basin gives distillate output of 3395 milliliters, 3655 milliliters and 4080 milliliters for 30 liters, 23 liters and 16 liters of water respectively.

Cumulative Hourly Distillate Output from Upper and Lower Basins with Heat Storage Material
Figure 6 depicts the hourly cumulative distillate output from the upper and lower basins adding heat storage material to the upper basin. The cumulative hourly distillate output from the upper and lower basin with gravel in the upper basin is 8540 milliliters, 7280 milliliters and 6980 milliliters respectively for 16 liters, 23 liters, 30 liters in the upper basin and 44 liters, 51 liters, 58 liters of water in the lower basin on experimental days from 7.00 AM to 6.00

Kamlesh Pansal and Bharat Ramani

PM. Whereas hourly distillate output with pebbles in the basin is 6360 milliliters, 6025 milliliters, and 5505 milliliters. 16 liters, 23 liters, 30 liters in the upper basin and 44 liters, 51 liters, 58 liters of water in the lower basin in lower basin respectively. Adding gravels to the upper basin yields higher distillate output than pebbles because the heat capacity of gravels is higher than that of pebbles. Table 1 shows characteristics of heat storage material.

Economic Analysis of a Modified Double Basin Solar Still with Energy-Absorbing Material
It is always desirable that a developed setup is economical. Because of that, an economic analysis for the developed double basin solar still was conducted. Annual cost of developed still was calculated as shown in Table 2. For the calculation of annual cost principal cost, depreciation, sinking fund factor, capital recovery factor interest on invested value was taken in to account. For analysis 20 years of average life span of still was considered. Table 3 shows the payback period of a developed solar still with heat storage material. The payback period was calculated using various cost components, like fabrication price, operating price, maintenance price, feed water price, and subsidies provided by the government. Payback period of 109 days was obtained with developed double basin solar still.

Experimental Uncertainty
Errors in measured parameters by different instruments are shown in Table 4. Errors of different instruments used in measurement. Uncertainty analysis for solar still area, solar still flow area, temperature different and Distillate output was calculated and shown in Table 5. Suppose a set of measurement is made in order to measure "n" number of experimental variables. These measurements are then used to calculate some required results of experiment (Z). Thus $Z = Z(X_1, X_2, X_3, \ldots \ldots X_n)$. Let U_z be the uncertainty in the results and $U_1, U_2, U_3, \ldots \ldots \ldots U_n$ be the uncertainty in the independent variables. The uncertainty in results is calculated according to the equation,

$$U_z = \left[\left(\frac{\partial Z}{\partial X_1}U_1\right)^2 + \left(\frac{\partial Z}{\partial X_2}U_2\right)^2 + \ldots\ldots + \left(\frac{\partial Z}{\partial X_n}U_n\right)^2\right]^{\frac{1}{2}} \qquad \ldots \ldots (1)$$

In uncertainty calculation the different parameters like, area of solar still, solar still flow area, temperature difference, distillate output, efficiency are calculated.

Solar still area

$$A = L \times W = 1.365 \times 0.74 = 1 \quad, \frac{\Delta A}{\Delta L} = W = 0.74 \qquad, \frac{\Delta A}{\Delta W} = L = 1.365$$

$$\Delta A = \left[\left(\frac{\Delta A}{\Delta L} \times \delta L\right)^2 + \left(\frac{\Delta A}{\Delta W} \times \delta W\right)^2\right]^{\frac{1}{2}} = [(0.74 \times 0.001)^2 + (1.365 \times 0.001)^2]^{\frac{1}{2}} = 0.00155$$

$$\frac{\Delta A}{A} = \frac{0.00155}{1} \times 100 = 0.155 \% \qquad \ldots \ldots (2)$$

Solar still flow area

$$A_F = D \times W = 0.02 \times 0.74 = 0.0148, \frac{\Delta A_F}{\Delta W} = D = 0.02, \frac{\Delta A_F}{\Delta D} = W = 0.74$$

$$\Delta A = \left[\left(\frac{\Delta A}{\Delta D} \times \delta D\right)^2 + \left(\frac{\Delta A}{\Delta W} \times \delta W\right)^2\right]^{\frac{1}{2}} = [(0.74 \times 0.001)^2 + (0.02 \times 0.001)^2]^{\frac{1}{2}} = 0.00074$$

$$\frac{\Delta A}{A} = \frac{0.00074}{10.0148} \times 100 = 5 \% \qquad \ldots \ldots (3)$$

Temperature Difference

$$\Delta T = T_e - T_c = 100 + 100 = 200 \quad, \frac{\Delta(\Delta T)}{\Delta T_e} = 1 - T_c = 1 - 100 = -99 \quad \frac{\Delta(\Delta T)}{\Delta T_c} = T_e - 1 = 100 - 1 = 99$$

$$\Delta(\Delta T) = \left[\left(\frac{\Delta(\Delta T)}{\Delta T_e} \times \delta T_e\right)^2 + \left(\frac{\Delta(\Delta T)}{\Delta T_c} \times \delta T_c\right)^2\right]^{\frac{1}{2}} = [(-99 \times 0.1)^2 + (99 \times 0.1)^2]^{\frac{1}{2}} = 14$$

$$\frac{\Delta(\Delta T)}{\Delta T} = \frac{14}{200} \times 100 = 7 \qquad \ldots\ldots (4)$$

Kamlesh Pansal and Bharat Ramani

Output

$$m = \frac{h_{ev} \times \Delta T}{L}$$

… … (5)

It depend on temperature difference only
The uncertainty in the out will be 7.0%
Radiation

Measurement error in Radiation (I) is 0.025. So it is 2.5%.

CONCLUSION

- Evacuated tube coupled double basin solar still with black gravel as heat storage material gives 1.23 times more output as compared to pebbles.
- Lower water depth (water quantity) in upper basin yields higher output with heat storage material.
- Cumulative   distillate output of 5040 and 4080 ml was obtained from upper basin alone respectively with gravels and pebbles as heat storage material in upper basin for 16 liter Water quantities in upper basin.
- Cumulative distillate output of 8540ml and 6360 ml was obtained from combined upper and lower basin respectively with gravel and pebbles as heat storage material.
- Payback period of the novel double-basin solar still with evacuated tubes was found to be 109 days from life cycle cost analysis.
- Annual cost per liter per square meter was obtained as Rs.0.400728.

Scope of Future Work
- More energy storage material can be tested with developed solar cells for better yield.
- Phase-change material can also be tested with developed solar stills.
- To improve distillate yield, lower basin fins can be incorporated.
- Further evaluation of performance through energy and exergy analysis can be carried out.

REFERENCES

1. R. V. Dunkle, "Solar Water Distillation, the Roof Type Still and a Multiple Effect Diffusion Still," International Developments in Heat Transfer, ASME, Proceeding of International Heat Transfer, Part V, University of Colorado, 1961, p. 895.
2. G.N. Tiwari, H. S. (2003). Present Status of Solar Distillation. Solar Energy 75 , 367-373.
3. Hitesh Panchal, Sanil S. Hishan, Robbi Rahim, KishorKumar Sadasivuni. "Solar still with evacuated tubes and calcium stones to enhance the yield: An experimental investigation." Process Safety and Environmental Protection (Volume 142, October 2020,): Pages 150-155.
4. K. Sampathkumar, T.V. Arjunan,P. Senthilkumar. "Single Basin Solar Still Coupled with Evacuated Tubes -." International Energy Journal 12 (2011): 53-66.
5. MohitBhargav, AvdheshYadav. "Experimental comparative study on a solar still combined with evacuated tubes and a heat exchanger at different water depths." International Journal of Sustainable Engineering (2020): VOL. 13, NO. 3,218–229

Kamlesh Pansal and Bharat Ramani

6. RaghVendraSingh, Shiv Kumar,M.M.Hasan,M. EmranKhan,G.N.Tiwari. "Performance of a solar still integrated with evacuated tube collector in natural mode." Desalination (Volume 318, 3 June 2013,): Pages 25-33.

7. Shiv Kumar, AseemDubey, G N Tiwari. "A solar still augmented with an evacuated tube collector in forced mode." Desalination (2014): Volume 347,15-24

8. AkashdeepNegi, GurprinderSingh ,Dhindsa,Satbir Singh Sehgal. "Experimental investigation on single basin tilted wick solar still integrated with flat plate collector." Materials Today: Proceedings (Volume 48, Part 5, 2022): Pages 1439-1446.

9. MdAzhar, M.E.Khan, Mohammad Seraj,Md Ahsan, Shah Aqueel Ahmed, Ehab Hussein Bani Hani. "Energy and exergy analyses of active solar still integrated with evacuated flat plate collector for New Delhi." Groundwater for Sustainable Development (Volume 19, November 2022): 100833.

10. Anil Kumar, Savita Vyas, Dan NchelatebeNkwetta. "Experimental study of single slope solar still coupled with parabolic trough collector." Materials Science for Energy Technologies (Volume 3, 2020): Pages 700-708.

11. Anil Ranjan, YogeshDewang,JitendraRaghuwanshi,VipinSharma. "Experimental evaluation of solar still coupled with parabolic trough collector." Materials Today: Proceedings (Volume 60, Part 2, 2022): Pages 935-938.

12. D.B.Singh. "Improving the performance of single slope solar still by including N identical PVT collectors." Applied Thermal Engineering (Volume 131, 25 February 2018): Pages 167-179.

13. D.B.Singh, G.N.Tiwari. "Enhancement in energy metrics of double slope solar still by incorporating N identical PVT collectors." Solar Energy (Volume 143, February 2017): Pages 142-161.

14. D.B.Singh, J.K.Yadav, V.K.Dwivedi, S.Kumar, G.N.Tiwari, I.M.Al-Helal. "Experimental studies of active solar still integrated with two hybrid PVT collectors." Solar Energy (Volume 130, June 2016): Pages 207-223.

15. GhaniHameed, Hassanain. "Experimentally evaluating the performance of single slope solar still with glass cover cooling and square cross-section hollow fins." Case Studies in Thermal Engineering (Volume 40, December 2022): 102547.

16. Hardik K. Jani, Kalpesh V. Modi. "Experimental performance evaluation of single basin dual slope still with circular and square cross-section hollow fins." Solar Enegy 179 (2019): 186-194.

17. Hitesh Panchal, RavishankarSathyamurthi. "Experimental analysis of single basin solar still with porous fins." International Journal of Ambient Energy (2017).

18. KalpeshModi, HardikJani. "Experimental and theoretical assessment of dual-slope single-basin solar still with the circular cross-sectional hollow-fins ." Cleaner Engineering and Technology (Volume 4, October 2021): 100231.

19. T. Rajseenivasan, K.Srithar. "Performance investigation on solar still with circular and square fins in basin with CO2 mitigation and economic analysi." Desalination 380 (2016): 66-74.

20. A.A. El-Sebaii, M. R.-E.-N. (2015). Effect of fin configuration parameters on single basin solar still performance. Desalination 365, 15-24.

21. Mohamed Asbik, Hassane Boushaba, Hajar Hafs, AbdelghaniKoukouch,Abderraouf Sabri, MuthuManokar. "Investigating the effect of sensible and latent heat storage materials on the performance of a single basin solar still during winter days." Journal of Energy Storage (Volume 44, Part B, 15 December 2021): 103480.

22. M.M. younes, A. F. (2021). Enhancing the wick solar still performance using half barrel and corrugate absorbers. process Safety and Environmental Protection 150, 440-452

23. M.Sakhtivel, S. (2008). Effect of energy storage medium (black granite gravel on the performance of a solar still. International Journal of Energy Research 32, 68-82.

24. S.Shanmugan, B. J. (2012). Performance of Single-slope single basin solar still with sensible heat storage materials. Desalination and Water Treatment 41, 195-203.

25. G.N.Tiwari, S.K.Singh,V.P.Bhatnagar. "Analytical thermal modelling of multi-basin solar still." Energy Conversion and Management (Volume 34, Issue 12, December 1993): Pages 1261-1266.

26. N.AlMahdi. "Performance prediction of a multi-basin solar still." Energy (Volume 17, Issue 1, January 1992): Pages 87-93.

27. Ali.F.Muftah, K.Sopian,M.A.Alghoul. "Performance of basin type stepped solar still enhanced with superior design concepts." Desalination (Volume 435, 1 June 2018): Pages 198-209.

28. A.Alaudeen, K.Johnson, P.Ganasundar,A.SyedAbuthahir,K.Srithar. "Study on stepped type basin in a solar still." Journal of King Saud University - Engineering Sciences (Volume 26, Issue 2, July 2014): Pages 176-183.

29. SwellamW.Sharshir, M.A.Omara,GehadElsisi, Abanob Joseph, A.W.Kandeal, AmlAli,GamalBedairb. "Thermo-economic performance improvement of hemispherical solar still using wick material with V-corrugated basin and two different energy storage materials." Solar Energy (Volume 249, 1 January 2023): Pages 336-352.

30. J.T.Mahdi, B.E.Smith,A.O.Sharif. "An experimental wick-type solar still system: Design and construction." Desalination (Volume 267, Issues 2–3, 15 February 2011): Pages 233-238.

31. KarrarA.Hammoodi, HayderA.Dhahad,WissamH.Alawee,Z.M.Omara. "A detailed review of the factors impacting pyramid type solar still performance." Alexandria Engineering Journal (December 2022)

32. Velmurugun, S. J. (2020). An experimental investigation to optimize the production of single and stepped basin solar stills. Energy Sources, Part A: Recovery, Utilization, and Environmental Effects.

33. A.A. Al-Karaghouli, W.E. Alnaser. "[1] Velmurugun, S. J. (2020). An experimental investigation to optimize the production of single and stepped basin solar stills. Energy Sources, Part A: Recovery, Utilization, and Environmental Effects." Applied Energy (78 (2004)): 347–354

34. V. S. V. BAPESHWARARAO, U. SINGH and G. N. TIWARI. "TRANSIENT ANALYSIS OF DOUBLE BASIN SOLAR." Energy Com,ers. Mgmt Vol. 23, No. 2 (1983): pp. 83-90.

35. D.K.Dutt, A. K. (1989). Performance of a Double-Basin Solar Still in Presence of Dye. Applied Anergy 32, 207-223.

36. S. Joe Patrick Gnanaraj, S. Ramachandran, David Santosh Christopher. "Enhancing the design to optimize the performance of double basin." Desalination (411 (2017)): 112–123

37. Kalpesh V. Modi, Jenish G. Modi. "Performance of single-slope double-basin solar stills with small pile of wick." Applied Thermal Engineering (149 (2019)): 723–730.

38. Hitesh N. Panchal, P. (2014). Investigation of performance analysis of a novel design of the vacuum tube-assisted double basin solar still; an experimental approach. International Journal of Ambient Energy

39. Panchal, Hitesh N. "Enhancement of distillate output of double basin solar." Journal of King Saud University – Engineering Sciences (2013).

40. Hitesh Panchal, K. K. (2018). Performance analysis of evacuated tubes coupled solar still with double basin solar still and solid fins. InternationaJournal of Ambient Energy.

41. T. Rajaseenivasan, T. Elango , K. Kalidasa Murugavel. "Comparative study of double basin and single basin solar stills." Desalination 309 ((2013)): 27–31.

42. T. Rajaseenivasan, K. KalidasaMurugavel, T. Elango. "Performance and exergy analysis of a double-basin solar still with different." Desalination and Water Treatment ((2014)): 1–9.

43. M.D. Raj Kamal a, B. Parandhaman , B. Madhu , D. Magesh Babu , Ravishankar Sathyamurthy. "Experimental analysis on single and double basin single slope solar still." Materials Today: Proceedings (n.d.).

44. M.S. Sodha, J. N. (1980). Double Basin Solar Still. Energy Conver.& Mgmt.20, 23-32.

45. Tiwari, G. (1985). Enhancement of Daily Yield in a Double Basin Solar Still. Energy Convers. Mgmt. Vol.25, 49-50.

46. Yadav, Y. (1994). Parametric studies in a Double Basin solar still. International Journal of Solar Energy 16:2, 137-150.

47. Yadav,Y.P. " Transient Analysis of Double Basin Solar Still." Desalination,71(980);151-54

Table 1.Characteristics of Heat Storage material

Materials	Density (lit./m3)	Thermal Conductivity (W/m K)	Specific Heat Capacity (J/lit. K)
Black Stone	3070	2.06-2.90	880
Pebble Stone	3300	2.4-2.6	712

Kamlesh Pansal and Bharat Ramani

Table 2.Economical Analysis

Particulars	
Principal price (P)	₹.10,800
Salvage Price(S) (10% of principle price)	₹.1080
Still's life (n)	15 Years
Rate of Interest (i)	0.1
Capital recovery factor(CRF = $i(1+i)^n/((1+i)^{n-1})$)	0.131474
Sinking fund factor (SFF = $i/((1+i)^{n-1})$)	0.031474
Annual first price = (CRF × P)	₹. 1419.9
Annual salvage price (SFF × P)	₹. 339.9
Annual maintenance price(₹. 0.15 × annual cost)	₹. 212.9
Annual price/m² = annual first price+ annual maintenance price – annual salvage price	₹. 1292.9
Annual distillate productivity of solar still (average distillate output × 365) (assuming average distillate productivity= 8.84 L)	3226.6
Annual price of distilled water per liter = annual price per square meter/annual distillate productivity)	₹. 0.4007

Table 3.Payback Period

Particulars	
Fabrication Price (A)	₹. 10,800
Operating Price (B)	₹. 5/day
Maintenance Price (C)	₹. 5/day
Price of Feed Water (D)	₹. 1/day
Price of Distilled water per liter (E)	₹. 12
Annual distillate productivity	8.84 liter/day
Price of water produced per day (F)	₹. 106.08
Subsidized Price (4%)	₹. 432
Net Profit= F -B- C-D	₹. 95.08
Pay Back period=(Investment-Subsidized Price)/Net profit	109 Days

Table 4.Errors of different instruments used in measurement

Sr. No.	Device name	Parameter	Symbol	Unit	Max. Value	Error
01	Temperature Data Logger	Temperature	T	°C	0 to 100	0.1
02	Solar Power Meter	Intensity measurement	I	W/m2	0-1400	1
03	Measure tap	Solar still dimensions	L W D	M	1 1 0.02	0.001

Table 5.Uncertainity Analysis

Sr. No.	Result	Symbol	% Uncertainty
1	Solar Still area	A	0.155
2	Solar still flow area	A_F	5.0
3	Temperature difference	ΔT	7
4	Output	m	7
5	Radiation	I	2.5

Kamlesh Pansal and Bharat Ramani

Table 6 Comparison of double-basin solar stills with different modifications

Sr. No.	Researcher	Type of Modification or Attachment	Maximum Daily Distillate output produced
1	Al-Karaghouli and W.E. Alnaser (2004)	With and without side and bottom insulation	3.91 l/m² and 3.13 l/m² respectively.
2	Joe Patrick Gnanaraj.*et al*.(2017)	With double basin integrated with reflector, reflector & Flat Plate Collector, reflector and Mini solar pond	4.33 l/m², 5.65 l/m², 6.249 l/m² respectively.
3	Hitesh Panchal (2018)	With vacuum tubes and energy absorbing material like lime stone, granite, pebbles	10.50 l/m²,10.20 l/m²,9.7 l/m² respectively
4	Rajkamal *et al*.(2020)	With electric heater	6.72 l/m²
5	Present study	With corrugated absorber, evacuated tube collector and heat storage material	11.60 l/m².

(a)   **(b)**
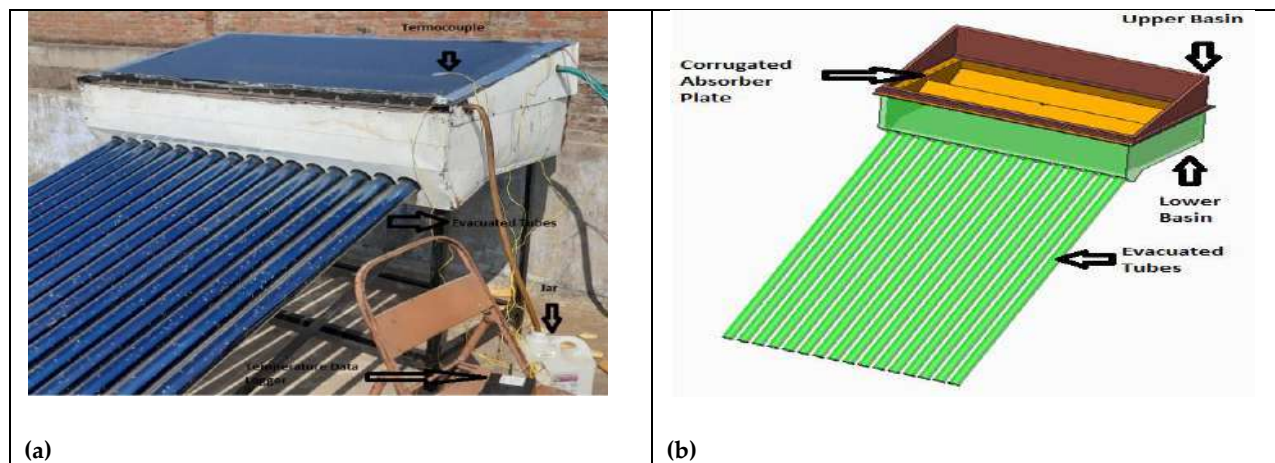
Figure 1. (a) Photograph of newly developed double basin solar still (b) perspective view
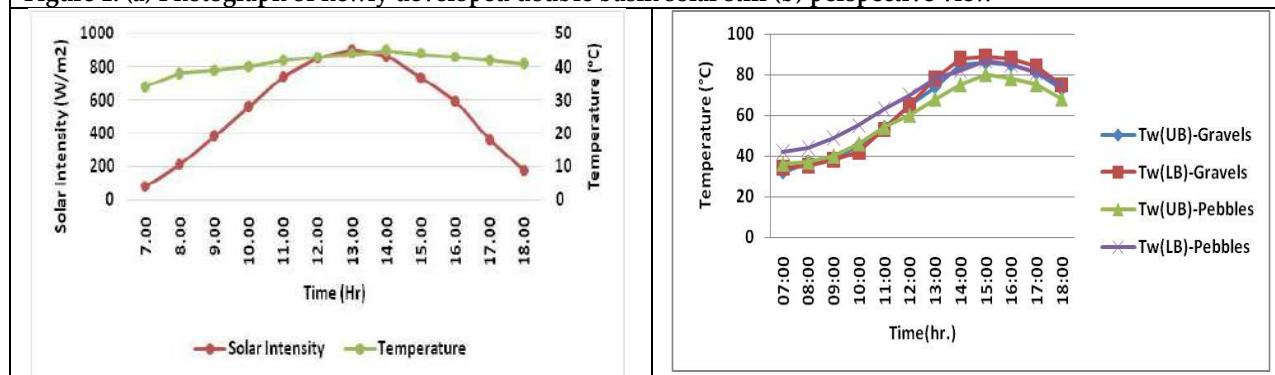
Figure 2 Hourly variation in ambient temperature and solar intensity

Figure 3 Hourly variation of basin water temperature with heat storage material in upper basin.

Kamlesh Pansal and Bharat Ramani
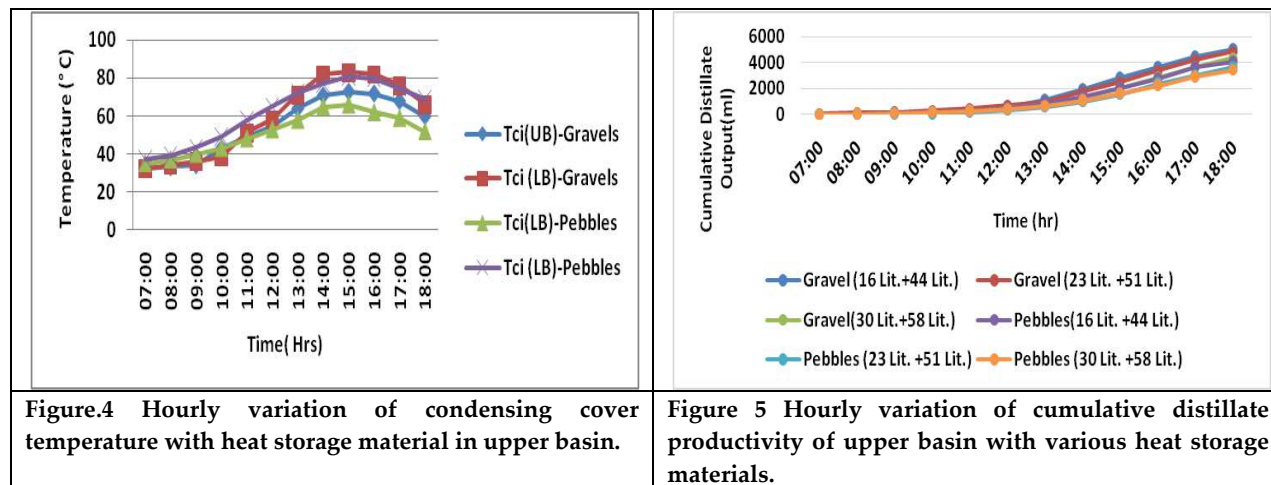
Figure.4 Hourly variation of condensing cover temperature with heat storage material in upper basin.

Figure 5 Hourly variation of cumulative distillate productivity of upper basin with various heat storage materials.
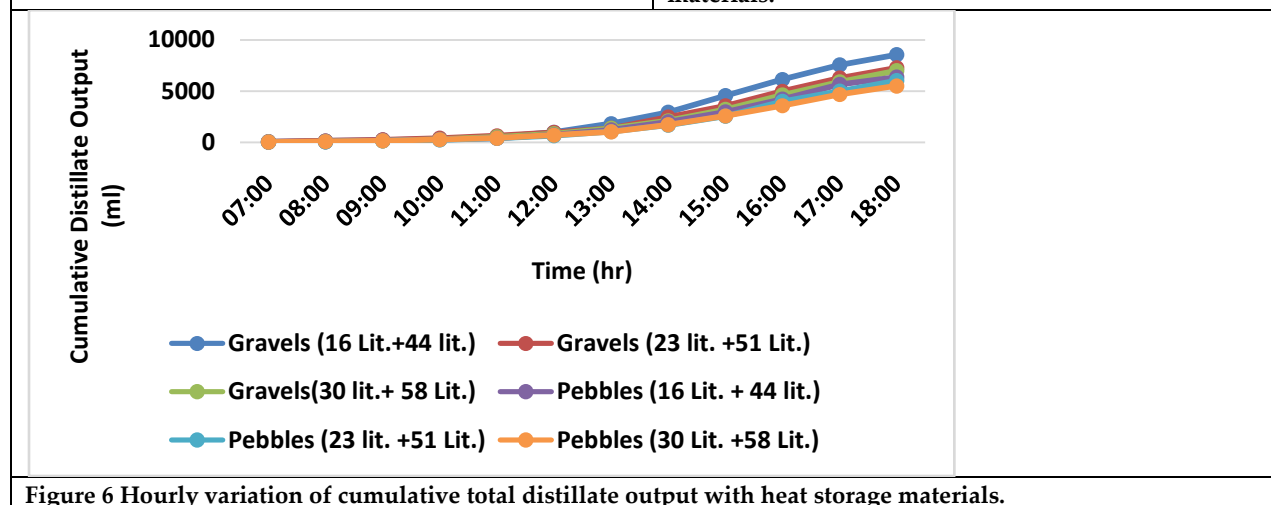

Figure 6 Hourly variation of cumulative total distillate output with heat storage materials.

RESEARCH ARTICLE

A Bibliometric Analysis and Visualization of Global Research on Urban Livelihood

Jiaur Rahaman[1]* and Biswajit Das[2]

[1]Ph.D Research Scholar, Department of Library and Information Science, Annamalai University, Annamalai Nagar, Tamil Nadu, India
[2]University Librarian, University of Gour Banga, West Bengal, India.

*Address for Correspondence
Jiaur Rahaman
Ph.D Research Scholar,
Department of Library and Information Science,
Annamalai University, Annamalai Nagar,
Tamil Nadu, India
E.Mail: jrahaman.mlis@gmail.com

ABSTRACT

Considering this transformation, a scientometric analysis of the global literature on urban livelihood was conducted in this study. The bibliographic data was gathered through the Web of Science database for 2013 to 2022, and a total of 1961 publications were retrieved. VOS viewer and Bibliometrix R visualization software were used to analyze data and create network maps. The findings revealed the number of papers, the highest number of articles found in 2022 with 351. Among published articles, co-authors' contribution is more significant than that of single authors. Furthermore, the USA was the leading country, with 587 publications on urban livelihood. With 16 publications on urban livelihood, Shackleton CM. was the most prolific author. These findings would benefit researchers worldwide, as scientometric mapping is an exciting method that provides a comprehensive overview of a scientific issue and insights for future research.

Keywords: Urban livelihood; Urbanization; Poverty; Bibliometric; Web of Science

Jiaur Rahaman and Biswajit Das

INTRODUCTION

Urban livelihood refers to earning a living available to people in urban areas. Urban areas are characterized by high population density, modern infrastructure, and various economic activities. People living in urban areas can engage in multiple forms of livelihood, including formal employment, self-employment, and informal work. Formal employment in urban areas can include working in offices, factories, retail stores, and other businesses. Self-employment can include owning a small business or operating as a freelancer or independent contractor. Informal work can consist of street vending, domestic work, and other forms of work that are not regulated by formal labour laws. In many urban areas, access to education and specialized skills training can help people find better-paying jobs and improve their livelihoods. Urban areas can also offer greater access to healthcare, social services, and other resources to improve people's quality of life. However, urban livelihoods can also be challenging, as the cost of living in urban areas can be high, and competition for jobs can be intense. Moreover, many urban areas have the inadequate infrastructure, high levels of pollution, and other environmental challenges that can affect people's health and well-being. Scientific research platform databases can be utilized to obtain high-quality scientific results. Databases such as Web of Science, Scopus, Emerald, and CNKI are widely used worldwide because they provide quick access to literature and good tracking of academic frontiers. A well-known and respected large-scale, comprehensive, multidisciplinary, and core journal citation index database is Web of Science. It has a solid reputation in scientific, technological, and educational circles worldwide, with citation index databases like SCIE and SSCI, JCR Journal Citation Reports, and ESI Basic Scientific Indicators. More than 8700 authoritative, high-impact academic journals worldwide covering the natural sciences, engineering, technology, biomedicine, social sciences, arts, and humanities, among other subjects, are available in the Web of Science core collection database.

Bibliometrics is a quantitative analysis technique that uses mathematical and statistical methods to quantify the interactions and effects of publications in particular study disciplines. It helps researchers to express knowledge structures in the research domain, map out detailed knowledge maps, and use statistical and mathematical techniques to investigate its features. It offers a macro-overview of scholarly research and accurately identifies significant authors, journals, organizations, and countries. It also functions as a potent instrument to examine the subject of knowledge and reveal its knowledge structure. CiteSpace, VOSviewer, and Bibexcel are three software programmes for measuring and evaluating scientific literature data that have been used widely in global information science due to their advantages in theory and practice. Therefore, the research results of using bibliometric analysis to study urban livelihood are scarce, and no research has explored the dynamic evolutionary path of the research theme in the field of urban livelihood. In view of this, this paper takes the literature on urban expansion in the core collection database of Web of Science as the research object and uses the scientific analysis tool Bibliometrix and VOS viewer to visually analyze the themes of urban livelihood research and its evolutionary path from 2013 to 2022.

Objectives

- How many publications are produced per year on urban livelihood?
- What Is the collaboration between and affiliations countries on this issue?
- What are the journals that publish the most in this area?
- What are the most relevant author's keywords to urban livelihood?

LITERATURE REVIEW

Several researchers have reviewed studies on urban land and land management (Kim et al., 2020; Hanaček & Rodríguez-Labajos, 2018) and performed bibliometric analyses of land use, land consolidation, land cover, and other related research by using large-scale data sets and bibliometric methods (Xie, Zhang, Zeng, et al., 2020; Xu et al., 2022), with valuable results. However, so far, relevant studies on urban land management are scarce, and most studies in land management have focused on rural land, specific countries or regions, or a single disciplinary perspective (Xianchun & Zhuoran, 2012; Xiandong et al., 2022).

METHODOLOGY

The bibliographic data for the present study were collected on 23 February 2023, from the Web of Science (WoS) Core Collection database, including indices of SCIE, SSCI, and A&HCI, provided by Clarivate within the indexed timespan from 2013 to 2022. Using the topic keyword "urban livelihood" (the topic keywords are generated by Clarivate from the title, abstract, author keywords, and Keywords Plus). The search was set to all languages and all documents type. The researcher obtained a total of 1961 publications in the (WoS). Each document's full record and cited references are exported for the bibliometric analysis. The downloaded data were saved in plain text format. The scientific analysis Bibliometrix and VOS viewer tools to visually analyze the themes of urban livelihood research

RESULTS

Finding of the Annual Publication Volume
As shown in Table 1, from 2013 to 2022, 1961 articles have been published in this specific field of urban livelihood. The number of published research reports in urban livelihood areas generally increased during the study period. The period from 2013 to 2022 was the development period, in which the number of published articles increased steadily. The literature on urban livelihood grew slowly from 2013 to 2016. It can be seen that the largest number of articles was found in 2022 with 351 articles (17.90%), while in 2013 found the lowest number of articles with 96 (4.90%) during the study period.

Active Authors
Highly cited authors serve as role models for researchers in this subject and indicate the pinnacles of local or national knowledge innovation. High citation counts indicate that the study findings of the authors were, at least temporarily, extensively acknowledged, inherited, and developed by other scholars. Table 2 shows 10 active authors in this field, including statistical data on the number of documents published per year by each and total citations each year. A total of 6314 authors contributed to the field of urban livelihood during the studied period, with Pradhan, Shackleton CM, Turner S, and Gibbs A being the first three authors, publishing 16, 9, and 8 articles, respectively. The importance of authors and the impact of all research contributions are frequently assessed using the h-index. Shackleton CM has the largest received score found citations and h-index.

Active Sources
From the journals referenced in this paper, urban livelihood was mainly published on Sustainability, and a total of 105 articles were published from 632 journals (see Table 3). The top five journals were Sustainability, Land Use Policy, World Development, Journal of Rural Studies, and Land, which included more than 256 publications. From the content of the articles published in the journals, the research in urban livelihood mainly focused on landscape, economy and environmental pollution, followed by geography. Journal of Rural Studies has the largest number of citations found with 744 from 35 publications, but it has ranked fourth among the top ten journals.

Active Affiliations
Since 2013, 1574 institutions have engaged in the study of urban livelihood. Table 4 details the top 10 high-yield institutions according to the number of publications, of which three are from South Africa. The University of Witwatersrand ranked first in the number of papers (38), the second was the University of Ghana (33), and third were the National University of Singapore and the University of Copenhagen (27). Table 4 shows South Africa was the dominant country, but the seven countries found single institutions.

Active Countries
Researchers have published papers from 113 countries (counting only the corresponding author's country) since 2013, and this number reaches 113 if co-authors are considered. Table 5 depicts the countries with the highest result

based on the frequency distribution of the corresponding author's affiliation country. The USA is leading with 587 papers, followed by China (457 papers) and the United Kingdom (408 papers).

The Figure 1 shows that the number of collaborators with China is 44 and the total link strength is 269. The main partners of were USA, China, and England and Germany. Five clusters of the countries of co-authorship were obtained by bibliometric analysis using the VOS viewer tool. The top three clusters represent the research fields of urban livelihood which are shown in the colour of red, green and blue. The two biggest nodes of countries include the USA and England.

Author's Keyword Analysis
Table 5 shows that the network map of the trend topics according to the author keywords used from 2013 to 2022. The size of the circles indicates how frequently the terms appear. The separation between the two circles shows the link between them.A keyword co-occurrence analysis (Figure 1) using the VOS viewer tool provides a co-occurrence network picture of the keyword universe and a much deeper understanding of the interaction dynamics of the field of urban livelihood.The keyword co-occurrence network in this study described five clusters. The largest nodes were Livelihoods, Poverty, Urbanization, and Urban with 155, 106, and 102 occurrences used by the authors found during the study period.

CONCLUSION

Urban livelihood refers to earning a livelihood in a city or town. Urban livelihoods are characterized by a diverse range of activities, including formal employment in industries, services, and government and everyday work in the informal sector.A total of 1961 papers from our present study that were indexed in the WoS core database and discussed urban livelihood were examined. These results provide a rich source of information on the intellectual structure of the chosen domain of urban livelihood. Using the bibliometrix R-package and VOS viewer, the bibliometric analysis results allowed for network analysis, co-authorship of countries and keyword analysis.Overall, 113 countries around the world contributed to the field of urban livelihood. Among them, South Africa and China published the most outstanding research papers. Based on journal, Sustainability has most produced the research output. More and more scholarly papers are being produced as the pandemic spreads. It is especially crucial to assess the quality of such a large number of research articles and gather valuable data.These findings would benefit researchers worldwide, as scientometric mapping is an exciting method that provides a comprehensive overview of a scientific issue and insights for future research.

REFERENCES

1. Akampumuza, P., & Matsuda, H. (2017). Weather shocks and urban livelihood strategies: The gender dimension of household vulnerability in the Kumi District of Uganda. *The Journal of Development Studies*, *53*(6), 953–970.
2. Castells, M. (2002). *Livable cities?: Urban struggles for livelihood and sustainability*. Univ of California Press.
3. Chen, M., Roever, S., & Skinner, C. (2016). Urban livelihoods: reframing theory and policy. In *Environment and Urbanization* (Vol. 28, Issue 2, pp. 331–342). Sage Publications Sage UK: London, England.
4. Frayne, B., Dordi, T., McCordic, C., Sunu, N., & Williamson, C. (2022). A bibliometric analysis of urban food security. *Urban Transformations*, *4*(1), 1–22.
5. Hanaček, K., & Rodríguez-Labajos, B. (2018). Impacts of land-use and management changes on cultural agroecosystem services and environmental conflicts—A global review. *Global Environmental Change*, *50*, 41–59.
6. Hossain, S., & Batcha, M. S. (2022). Mapping Scientific Literature Trend on Sustainable Development Goals at Global Perspectives: A Scientometric Insight. *Indian Journal of Natural Sciences*, *13*(73), 45643–45653.
7. Hossain, S., & Batcha, M. S. (2023). *Global Research Trends in Sustainable Development Goals between 2000 and 2021*. *13*(76), 52773–52783.

8. Hossain, S., Batcha, M. S., Atoum, I., Ahmad, N., & Al-Shehri, A. (2022). Bibliometric Analysis of the Scientific Research on Sustainability in the Impact of Social Media on Higher Education during the COVID-19 Pandemic. *Sustainability*, *14*(24), 16388. https://doi.org/https://doi.org/10.3390/su142416388

9. Hossain, S., & Sadik Batcha, M. (2021). Scientometric analysis of research productivity from Indian dialysis over the last twenty years in Web of Science. *COLLNET Journal of Scientometrics and Information Management*, *15*(2), 323–339. https://doi.org/10.1080/09737766.2021.2005455

10. Ilyichev, V., Kolchunov, V., Emelyanov, S., & Bakaeva, N. V. (2015). About the dynamic model formation of the urban livelihood system compatible with the biosphere. *Applied Mechanics and Materials*, *725*, 1224–1230.

11. Kim, Y., Newman, G., & Güneralp, B. (2020). A review of driving factors, scenarios, and topics in urban land change models. *Land*, *9*(8), 246.

12. Lyons, M., & Snoxell, S. (2005). Sustainable urban livelihoods and marketplace social capital: Crisis and strategy in petty trade. *Urban Studies*, *42*(8), 1301–1320.

13. Maxwell, D. (2000). *Urban livelihoods and food and nutrition security in Greater Accra, Ghana* (Vol. 112). Intl Food Policy Res Inst.

14. Meikle, S. (2014). The urban context and poor people. In *Urban Livelihoods* (pp. 60–74). Routledge.

15. Potts, D. (2009). The slowing of sub-Saharan Africa's urbanization: evidence and implications for urban livelihoods. *Environment and Urbanization*, *21*(1), 253–259.

16. Rahaman, J., & Hosaain, S. (2020). Scientometric Study of the Research Performance on Oceanography: The World Perspective. *Library Philosophy and Practice*, 1–14.

17. Rahaman, J. (2022). Scientometric Assessment of the Research Productivity of Calcutta University , West Bengal. *Indian Journal of Natural Sciences*, *13*(August), 44881–44893.

18. Rahaman, J., Hossain, S., & Batcha, M. S. (2020). Scientometric Study of the Research Performance on Oceanography: The World Perspective. *Library Philosophy and Practice*, *2020*(4066), 1–14.

19. Shao, Q., Peng, L., Liu, Y., & Li, Y. (2023). A Bibliometric Analysis of Urban Ecosystem Services: Structure, Evolution, and Prospects. *Land*, *12*(2), 337.

20. Sheng, S., Song, W., Lian, H., & Ning, L. (2022). Review of Urban Land Management Based on Bibliometrics. *Land*, *11*(11), 1968.

21. Stoian, D. (2005). Making the best of two worlds: rural and peri-urban livelihood options sustained by nontimber forest products from the Bolivian Amazon. *World Development*, *33*(9), 1473–1490.

22. Sullivan, A. (2022). Bridging the divide between rural and urban community-based forestry: A bibliometric review. *Forest Policy and Economics*, *144*, 102826.

23. Xianchun, Z., & Zhuoran, S. (2012). The research review of land-use and land-management problems in the joint of urban and Rural area for the last two decades. *Energy Procedia*, *16*, 353–358.

24. Xiandong, L., Ying, H., Xianmei, L., Sinuo, L., Qiao, M., & Jianzhong, G. (2022). Review of China's rural land management system reform: 1949–2019. *Environmental Earth Sciences*, *81*(14), 369.

25. Xie, H., Zhang, Y., & Duan, K. (2020). Evolutionary overview of urban expansion based on bibliometric analysis in Web of Science from 1990 to 2019. *Habitat International*, *95*, 102100.

26. Xie, H., Zhang, Y., Zeng, X., & He, Y. (2020). Sustainable land use and management research: a scientometric review. *Landscape Ecology*, *35*, 2381–2411.

27. Xu, X., Chen, Q., & Zhu, Z. (2022). Evolutionary overview of land consolidation based on bibliometric analysis in web of science from 2000 to 2020. *International Journal of Environmental Research and Public Health*, *19*(6), 3218.

Table 1: Annual Output of Urban Livelihood Studies in Web of Science from 2013 to 2022

Year	Articles	%
2013	96	4.90
2014	108	5.51
2015	125	6.37
2016	167	8.52

Jiaur Rahaman and Biswajit Das

2017	142	7.24
2018	204	10.40
2019	202	10.30
2020	258	13.16
2021	308	15.71
2022	351	17.90
Total	**1961**	**100.00**

Table 2: Top 10 Active Authors in Urban Livelihood Research

Rank	Author	Publications	Citations	h-index
1	Shackleton CM	16	407	11
2	Turner S	9	86	4
3	Gibbs A	8	286	7
4	Jewkes R	7	285	7
5	Nagendra H	7	102	5
6	Parry L	7	120	4
7	Amankwaa EF	6	116	5
8	Esson J	6	87	5
9	Gough KY	6	87	5
10	Nasi R	6	121	5

Table 3: Top 20 Journals of Urban Livelihood Papers

Rank	Sources	Publications	Citations
1	Sustainability	105	663
2	Land Use Policy	43	595
3	World Development	38	598
4	Journal of Rural Studies	35	744
5	Land	35	205
6	Geoforum	31	446
7	Habitat International	30	666
8	Environment Development and Sustainability	30	193
9	Environment and Urbanization	23	462
10	International Journal of Disaster Risk Reduction	20	235

Table 4: Top 10 Institutions in the Field of Urban Livelihood

Rank	Affiliation	Articles	Country
1	University of Witwatersrand	38	South Africa
2	University of Ghana	33	Ghana
3	National University of Singapore	27	Singapore
4	University of Copenhagen	27	Denmark
5	Rhodes University	26	South Africa

Jiaur Rahaman and Biswajit Das

6	Wageningen University & Research	26	Netherlands
7	University of Cape Town	23	South Africa
8	University of Oxford	20	England
9	McGill University	19	Canada
10	Pennsylvania State University	19	USA

Table 5: Top 10 Countries with the Highest Number of Papers

Rank	Country	Frequency
1	USA	587
2	China	457
3	UK	408
4	South Africa	225
5	India	218
6	Germany	181
7	Australia	161
8	Canada	131
9	Netherlands	118
10	Brazil	99

Table 6: Top 10 Author's Keyword Analysis

Rank	Words	Occurrences
1	Livelihoods	155
2	Poverty	106
3	Urbanization	106
4	Urban	102
5	City	96
6	Management	90
7	Climate-Change	89
8	Migration	89
9	Policy	80
10	Impact	74

Jiaur Rahaman and Biswajit Das
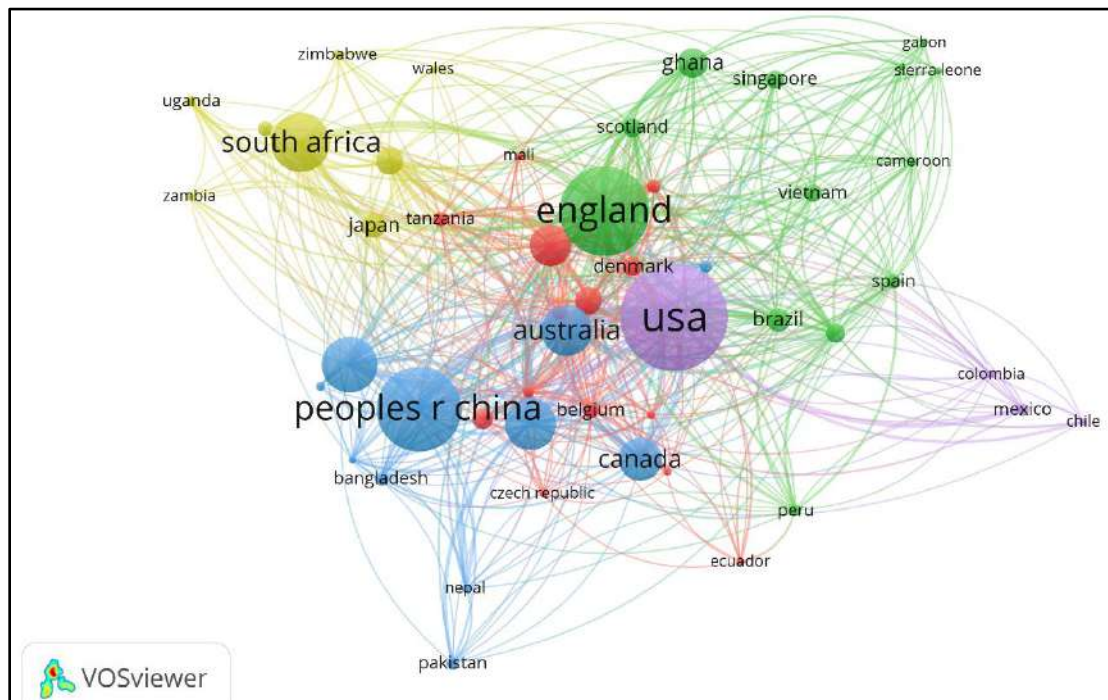
Figure 1: Co-authorship Map of Top 50 Countries in Urban Livelihood Research
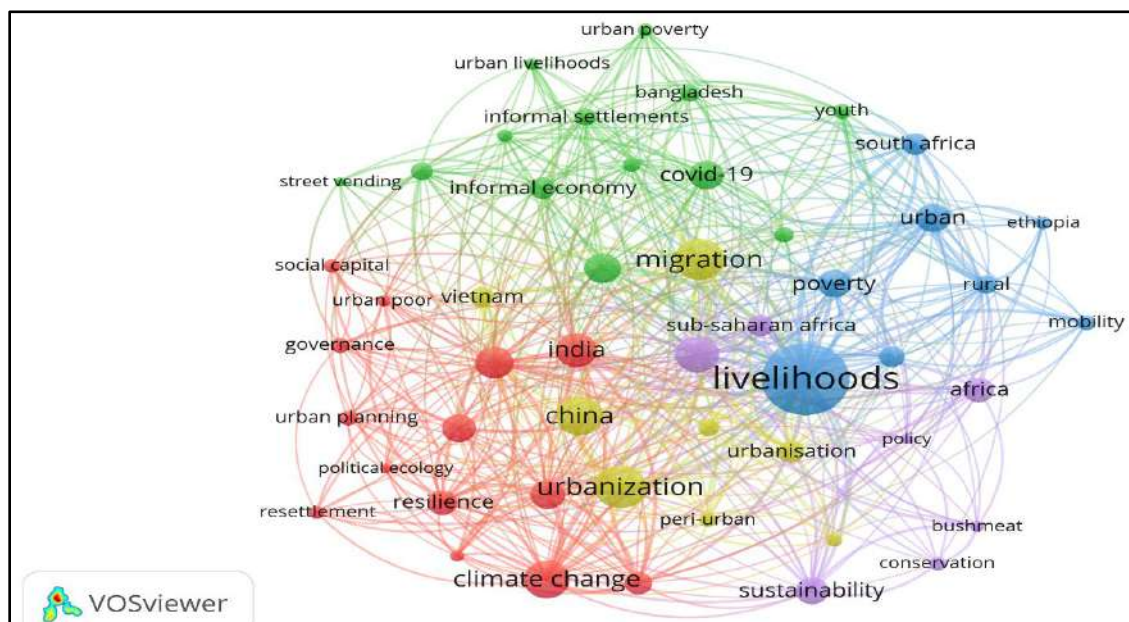
Figure 2: Top 10 Author's Keyword Analysis

RESEARCH ARTICLE

Solving System of Lane-Emden type Equations using Taylor Series

S. Yugesh[1]*, B. Vanasri Vignesh[2] and R. Aarthi[2]

[1]Assistant Professor, Department of Mathematics, Sri Sivasubramaniya Nadar College of Engineering, Kalavakkam – 603 110, Tamil Nadu, India
[2]Undergraduate Student, Department of Electronics and Communications Engineering, Sri Sivasubramaniya Nadar College of Engineering, Kalavakkam – 603 110, Tamil Nadu, India.
[3]Undergraduate Student, Department of Electrical and Electronics Engineering, Sri Sivasubramaniya Nadar College of Engineering, Kalavakkam – 603 110, Tamil Nadu, India

*Address for Correspondence
S. Yugesh
Assistant Professor, Department of Mathematics,
Sri Sivasubramaniya Nadar College of Engineering,
Kalavakkam – 603 110, Tamil Nadu, India.
E.Mail: yugeshs@ssn.edu.in

ABSTRACT

In this paper, we introduce the Taylor series as an accessible and valuable mathematical tool for solving nonlinear equations. Specifically, we propose the utilization of the Taylor series method to find solutions for systems of equations of the Lane-Emden type. Comparing it with the exact solution reveals a significant improvement in convergence speed, demonstrating the method's effectiveness and ease of implementation.

Keywords: Taylor Series, Lane-Emden Equations, Analytical Method, Convergence, Maclaurin's Series.

INTRODUCTION

Poisson's equation is an elliptic partial differential equation that finds extensive application in theoretical physics. It plays a crucial role in various scenarios, such as determining the potential field resulting from an electric charge or a mass density distribution. By solving Poisson's equation, one can effectively calculate the forces associated with the given charge or mass density distribution. In the realm of Astrophysics, the Lane-Emden equation, a dimensionless form of Poisson's equation, aids in obtaining the gravitational potential of a Newtonian self-gravitating, spherically polytrophic field. This equation proves particularly valuable for analysing gravitational interactions within astrophysical systems. The Lane-Emden equation plays a vital role in the fields of chemistry, physics, and astronomy [1-4]. According to the report, the Lane–Emden equation can be used to model a reaction–diffusion process, and its analytical solution has the potential to optimize the process [5]. However, due to its singular nature, finding an analytical solution for this equation can be challenging. Nevertheless, there exist several analytical methods for

Yugesh *et al.,*

addressing singular boundary value problems [6–11]. Even the Adomian Decomposition Method (ADM), which is a very effective approach for solving broad classes of nonlinear partial and ordinary differential equations with important applications in different fields of applied mathematics, engineering, physics, and biology, is not very effective in solving the Lane-Emden type system of equations due to its singular behaviour at the origin. It involves finding a corresponding Volterra integral form for the given system and is subject to a complicated n-fold integration, which makes it a little difficult to solve Lane-Emden type equations.In this study, we apply the Taylor series method to solve the general Lane-Emden type of differential equations, which are commonly used for modelling and addressing various physical and astrophysical problems.

Therefore, our proposal is to employ the Taylor Series Expansion technique as a solution method for the Lane-Emden type system of equations. This highly effective technique enables the equation to be solved without the need for intricate ADM procedures, relying solely on the utilization of initial conditions.

Taylor Series Solution

In this paper, we consider the following system of Lane–Emden type equations,

$$u'' + \frac{\lambda_1}{x}u' + f_1(u,v) = 0 \dots\dots\dots\dots\dots\dots\dots\dots\dots\dots\dots\dots\dots\dots\dots\dots\dots\dots.\text{(eq. 1)}$$

$$v'' + \frac{\lambda_2}{x}v' + f_2(u,v) = 0 \dots\dots\dots\dots\dots\dots\dots\dots\dots\dots\dots\dots\dots\dots\dots\dots\dots\dots.\text{(eq. 2)}$$

Subject to initial conditions

$u(0) = \alpha \qquad ; \qquad v(0) = 0$

$u'(0) = \beta \qquad ; \qquad v'(0) = 0$

Multiplying (eq. 1) and (eq. 2) with x, we get

$$xu'' + \lambda_1 u' + xf_1(u,v) = 0 \dots\dots\dots\dots\dots\dots\dots\dots\dots\dots\dots\dots\dots\dots\dots\dots.\text{(eq. 3)}$$

$$xv'' + \lambda_2 v' + xf_2(u,v) = 0 \dots\dots\dots\dots\dots\dots\dots\dots\dots\dots\dots\dots\dots\dots\dots\dots.\text{(eq. 4)}$$

Differentiating (eq. 3) and (eq. 4) with respect to x, we get

$$xu''' + (1+\lambda_1)u'' + xf_1'(u,v) + f_1(u,v) = 0 \dots\dots\dots\dots\dots\dots\dots\dots\dots\dots.\text{(eq. 5)}$$

$$xv''' + (1+\lambda_2)v'' + xf_2'(u,v) + f_2(u,v) = 0 \dots\dots\dots\dots\dots\dots\dots\dots\dots\dots.\text{(eq. 6)}$$

Substituting x for 0 in (eq. 5) and (eq. 6), we get

$$(1+\lambda_1)u''(0) + f_1(u,v) = 0 \dots\dots\dots\dots\dots\dots\dots\dots\dots\dots\dots\dots\dots\dots\dots.\text{(eq. 7)}$$

$$(1+\lambda_2)v''(0) + f_2(u,v) = 0 \dots\dots\dots\dots\dots\dots\dots\dots\dots\dots\dots\dots\dots\dots\dots.\text{(eq. 8)}$$

Hence, we get

$$u''(0) = -\frac{f_1(u,v)}{1+\lambda_1}$$

$$v''(0) = -\frac{f_2(u,v)}{1+\lambda_2}$$

Differentiating (eq. 5) and (eq. 6) with respect to x, we get

$$xu^{iv} + (2+\lambda_1)u''' + xf_1''(u,v) + 2f_1'(u,v) = 0 \dots\dots\dots\dots\dots\dots\dots\dots\dots.\text{(eq. 9)}$$

$$xu^{iv} + (2+\lambda_2)v''' + xf_2''(u,v) + 2f_2'(u,v) = 0 \dots\dots\dots\dots\dots\dots\dots\dots\dots.\text{(eq. 10)}$$

Substituting x for 0 in (eq. 9) and (eq. 10), we get

$$(2+\lambda_1)u'''(0) + 2f_1'(u,v) = 0 \dots\dots\dots\dots\dots\dots\dots\dots\dots\dots\dots\dots\dots.\text{(eq. 11)}$$

$$(2+\lambda_2)v'''(0) + 2f_2'(u,v) = 0 \dots\dots\dots\dots\dots\dots\dots\dots\dots\dots\dots\dots\dots.\text{(eq. 12)}$$

Which   yields   us

$$u'''(0) = -\frac{2f_1'(u,v)}{2+\lambda_1}$$

$$v'''(0) = -\frac{2f_2'(u,v)}{2+\lambda_2}$$

Differentiating (eq. 9) and (eq. 10) with respect to x, we get

$$xu^v + (3 + \lambda_1)u^{'v} + xf_1'''(u,v) + 2f_1''(u,v) = 0 \dots\dots\dots\dots\dots\dots\dots\dots\text{(eq. 13)}$$

$$xv^v + (3 + \lambda_2)u^{'v} + xf_2'''(u,v) + 2f_2''(u,v) = 0 \dots\dots\dots\dots\dots\dots\dots\dots\text{(eq. 14)}$$

Substituting x for 0 in (eq. 11) and (eq. 12), we get

$$(3 + \lambda_1)u^{'v}(0) + 2f_1''(u,v) = 0 \dots\dots\dots\dots\dots\dots\dots\dots\dots\dots\dots\text{(eq. 15)}$$

$$(3 + \lambda_2)u^{'v}(0) + 2f_2''(u,v) = 0 \dots\dots\dots\dots\dots\dots\dots\dots\dots\dots\dots\text{(eq. 16)}$$

Which yields us

$$u^{'v}(0) = -\frac{3f_1''(u,v)}{3 + \lambda_1}$$

$$u^{'v}(0) = -\frac{3f_2''(u,v)}{3 + \lambda_2}$$

Repeating this process of differentiation and substitution (k+1) times, we get

$$xu^{k+1'} + (k - 1 + \lambda_1)u^{k'} + xf_1^{k-1'}(u,v) + 2f_1^{k-2'}(u,v) = 0 \dots\dots\dots\dots\dots\text{(eq. 17)}$$

$$xv^{k+1'} + (k - 1 + \lambda_2)v^{k'} + xf_2^{k-1'}(u,v) + 2f_2^{k-2'}(u,v) = 0 \dots\dots\dots\dots\dots\text{(eq. 18)}$$

Which yields us,

$$u^{k'}(0) = -\frac{(k-1)f_1^{k-2'}(u,v)}{(k-1+\lambda_1)}$$

$$v^{k'}(0) = -\frac{(k-1)f_2^{k-2'}(u,v)}{(k-1+\lambda_2)}$$

Using Taylor series expansion- Maclaurin series general formula

$$f(x) = \sum_{n=0}^{\infty} f^{n'}(0)\frac{x^n}{n!}$$

Thus the functions u and v can be expanded as

$$u(x) = u(0) + \frac{x}{1!}u'(0) + \frac{x^2}{2!}u''(0) + \frac{x^3}{3!}u'''(0) + \frac{x^4}{4!}u^{'v}(0) + \cdots$$

$$v(x) = v(0) + \frac{x}{1!}v'(0) + \frac{x^2}{2!}v''(0) + \frac{x^3}{3!}v'''(0) + \frac{x^4}{4!}v^{'v}(0) + \cdots$$

Which yields us

$$u(x) = \alpha + 0 + \frac{x^2}{2!}u''(0) + \frac{x^3}{3!}u'''(0) + \frac{x^4}{4!}u^{'v}(0) + \cdots$$

$$v(x) = \beta + 0 + \frac{x^2}{2!}v''(0) + \frac{x^3}{3!}v'''(0) + \frac{x^4}{4!}v^{'v}(0) + \cdots$$

Which can be simplified as,

$$u(x) = \alpha + \sum_{n=2}^{\infty} \frac{x^n}{n!}\frac{(1-n)\left(f^{n'}(u,v)\right)}{(n-1+\lambda_1)}$$

$$v(x) = \beta + \sum_{n=2}^{\infty} \frac{x^n}{n!}\frac{(1-n)\left(f^{n'}(u,v)\right)}{(n-1+\lambda_2)}$$

Example:

$$u'' + \frac{1}{x}u' - 8(e^u - 2e^{2v}) = 0 \dots\dots\dots\dots\dots\dots\dots\dots\dots\dots\dots\dots\dots\dots\text{(eq. 1)}$$

$$v^{''} + \frac{2}{x}v^{'} + 2(e^v - 2e^u) = 0 \ \dots\dots\dots\dots\dots\dots\dots\dots\dots\dots..\dots\dots..\text{(eq. 2)}$$

Subject to the initial conditions
$u(0) = 0 \quad ; \quad v(0) = 0$
$u^{'}(0) = 0 \quad ; \quad v^{'}(0) = 0$

Multiplying (eq. 1) and (eq. 2) with x, we get
$$xu^{''} + u^{'} - 8x(e^u - 2e^{2v}) = 0 \ \dots\dots\dots\dots\dots..\dots\dots..\dots\dots\dots\dots\dots\dots..\text{(eq. 3)}$$
$$xv^{''} + 2v^{'} + 2x(e^v - 2e^u) = 0 \ \dots\dots\dots\dots\dots\dots\dots..\dots\dots\dots\dots\dots\dots.\text{(eq. 4)}$$

differentiating (eq. 3) and (eq. 4) with respect to x, we get
$$xu^{'''} + 2u'' - 8(e^u - 2e^{2v}) - 8x(e^u u^{'} - 4e^{2v}v^{'}) = 0\dots\dots\dots\dots\dots\dots\dots\dots\text{(eq. 5)}$$
$$xv^{'''} + 3v'' + 2(e^v - 2e^u) + 2x(e^v v^{'} - 2e^u u^{'}) = 0\dots\dots\dots\dots\dots..\dots\dots..\dots\dots.\text{(eq. 6)}$$

Substituting x for 0 in (eq. 5) and (eq. 6), we get
$$2u^{''}(0) - 8(e^0 - 2e^0) = 0\dots\dots\dots\dots\dots\dots\dots\dots\dots\dots\dots\dots\dots\dots\dots\dots..\text{(eq. 7)}$$
$$3v^{''}(0) + 2(e^0 - 2e^0) = 0\dots\dots\dots\dots\dots\dots\dots\dots\dots\dots\dots\dots\dots\dots\dots\dots..\text{(eq. 8)}$$
(eq. 7) and (eq. 8) yields us
$u^{''}(0) = -4 \quad ; \quad v^{''}(0) = -2$

Differentiating (eq. 5) and (eq. 6) with respect to x, we get
$$xu^{v} + 3u^{'''} - 16(e^u u^{'} - 4e^{2v}v^{'}) - 8x\left(e^u(u^{'})^2 + e^u u^{''} - 8e^{2v}(v^{'})^2 - 4e^{2v}v\right) =$$
$$0\dots\dots\dots\dots\dots\dots\dots\dots\dots\dots\dots\dots\dots\dots\dots\dots\dots\dots\dots..\dots\dots\dots\dots...\text{(eq. 9)}$$
$$xv^{v} + 4v^{'''} + 4(e^v v^{'} + 2e^u u^{'}) + 2x\left(e^v(v^{'})^2 + e^v v^{''} + 2e^u(u^{'})^2 + 2e^u u^{''}\right) = 0..\text{(eq. 10)}$$

Substituting x for 0 in (eq. 9) and (eq. 10), we get
$$3u^{'''}(0) = 0\dots\dots\dots\dots\dots\dots\dots\dots\dots\dots\dots\dots\dots\dots\dots\dots\dots\dots.\text{(eq. 11)}$$
$$4v^{'''}(0) = 0\dots\dots\dots\dots\dots\dots\dots\dots\dots\dots\dots\dots\dots\dots\dots\dots.\dots\dots\dots\dots\dots.\text{(eq. 12)}$$
(eq. 11) and (eq. 12) yields us

$u^{'''}(0) = 0 \ ; \ v^{'''}(0) = 0$

Differentiating (eq. 9) and (eq. 10) with respect to x, we get
$$xe^v + 4u^{v} - 24\left(e^u(u^{'})^2 + e^u u^{''} - 8e^{2v}(v^{'})^2 - 4e^{2v}v\right) - 8x\left(e^u(u^{'})^3 + u^{''} + e^u u^{'''} - 16e^{2v}(v^{'})^3 - 24e^{2v}v^{'}v^{''} -\right.$$
$$4e2vv^{'''}=0\dots\dots\dots\dots\dots\dots\dots\dots.\dots\dots\dots\dots\text{(eq. 13)}$$
$$xe^v + 5v^{v} + 6\left(e^v(v^{'})^2 + e^v v^{''} + 2e^u(u^{'})^2 + 2e^u u^{''}\right) + 2x\left(e^v(v^{'})^3 + 3e^v v^{'}v^{''} + e^v v^{'''} + 2e^u(u^{'})^3 + 6e^u u^{'}u^{''} +\right.$$
$$2euu^{'''}=0\dots\dots\dots\dots\dots\dots\dots\dots.\dots\dots\dots\dots\text{(eq. 14)}$$

Substituting x for 0 in (eq. 13) and (eq. 14), we get
$$4u^{v}(0) - 24\left(e^0 u^{''}(0) - 4e^0 v^{''}(0)\right) = 0\dots\dots\dots\dots\dots\dots\dots\dots.\dots\dots\dots\text{(eq. 15)}$$
$$5v^{v}(0) + 6\left(e^0 v^{''}(0) + 2e^0 u^{''}(0)\right) = 0\dots\dots\dots\dots\dots\dots\dots\dots.\dots\dots\dots.\text{(eq. 16)}$$

Yugesh *et al.*,

Which yields us,

$$u^{'v}(0) = 24 \quad ; \quad v^{'v}(0) = 12$$

Using Taylor series expansion- Maclaurin series general formula

$$f(x) = \sum_{n=0}^{\infty} f^{n'}(0)\frac{x^n}{n!}$$

Thus the functions u and v can be expanded as

$$u(x) = u(0) + \frac{x}{1!}u^{'}(0) + \frac{x^2}{2!}u^{''}(0) + \frac{x^3}{3!}u^{'''}(0) + \frac{x^4}{4!}u^{'v}(0) + \cdots$$

$$v(x) = v(0) + \frac{x}{1!}v^{'}(0) + \frac{x^2}{2!}v^{''}(0) + \frac{x^3}{3!}v^{'''}(0) + \frac{x^4}{4!}v^{'v}(0) + \cdots$$

Which yields us

$$u(x) = (0) + x(0) + \frac{x^2}{2!}(-4) + \frac{x^3}{3!}(0) + \frac{x^4}{4!}(24) + \cdots$$

$$v(x) = (0) + x(0) + \frac{x^2}{2!}(-2) + \frac{x^3}{3!}(0) + \frac{x^4}{4!}(12) + \cdots$$

Hence, we get

$$u(x) = -2x^2 + x^4 + \cdots$$

$$v(x) = -x^2 + \frac{x^4}{2} + \cdots$$

By comparing this expansion with standard expansions, we get

$$ln(1 + x^2) = x^2 - \frac{1}{2}x^4 + \frac{1}{3}x^6 - \frac{1}{4}x^8 + \frac{1}{5}x^{10} \ldots$$

$$\boldsymbol{u(x) = -2ln(1 + x^2)}$$
$$\boldsymbol{v(x) = -ln(1 + x^2)}$$

CONCLUSION

This paper proposes a straightforward approach to tackling the Lane–Emden equation, which can be extended to encompass various differential equations with initial conditions and fractional calculus [13, 14]. In comparison to other analytical methods, the Taylor series method offers a simple solution process and yields accurate results. One notable advantage of employing the Taylor series method is its ability to avoid generating redundant terms, ensuring convergence towards the exact solution.

ACKNOWLEDGEMENT

REFERENCES

1. P. Roul, A new mixed MADM-Collocation approach for solving a class of Lane–Emden singular boundary value problems. J. Math. Chem. 57, pp.945–969,2019.

Yugesh *et al.,*

2. H. Madduri, P. Roul,Afast-converging iterative scheme for solving a system of Lane–Emden equationsarising in catalytic diffusion reactions. J. Math. Chem. 57, pp.570–582, 2019.

3. T.C. Hao, F.Z. Cong,Y.F. Shang, An efficientmethod for solving coupled Lane–Emden boundary value problems in catalytic diffusion reactions and error estimate. J. Math. Chem. 56, pp.2691–2706, 2018.

4. A.K. Verma, S. Kayenat, On the convergence of Mickens' type nonstandard finite difference schemeson Lane–Emden type equations. J. Math. Chem. 56, pp.1667–1706, 2018.

5. A.M. Wazwaz, Solving the non-isothermal reaction–diffusion model equations in a spherical catalystby the variational iteration method. Chem. Phys. Lett. 679, pp.132–136, 2017.

6. J.H. He, Variational approach to the Lane–Emden equation. Appl. Math. Comput. 143(2–3), pp.539–541, 2003.

7. Y. Wu, J.H. He, Homotopy perturbation method for nonlinear oscillators with coordinate dependentmass. Results Phys. 10, pp. 270–271, 2018.

8. Z.J. Liu, M.Y. Adamu, E. Suleiman et al., Hybridization of homotopy perturbationmethod and Laplacetransformation for the partial differential equations. Therm. Sci. 21, pp.1843–1846,2017.

9. M.Y. Adamu, P. Ogenyi, New approach to parameterized homotopy perturbation method. Therm. Sci.22(4), pp.1865–1870, 2018.

10. N. Anjum, J.H. He, Laplace transform: making the variational iteration method easier. Appl. Math.Lett. 92, pp.134–138,2019.

11. J.H. He, Some asymptotic methods for strongly nonlinear equations. Int. J.Mod. Phys.B20, pp.1141–1199, 2006.

12. L.J. Xie, C.L. Zhou, S. Xu, Solving the systems of equations of Lane-Emden type by differentialtransform method coupled with adomian polynomials. Mathematics 7(4), 377, 2019.

13. J.H. He, A tutorial review on fractal spacetime and fractional calculus. Int. J. Theor. Phys. 53(11),pp.3698–3718,2014.

14. J.H. He, Fractal calculus and its geometrical explanation. Results Phys. 10, pp.272–276, 2018.

15. J.H. He, F.Y. Ji, Taylor series solution for Lane–Emden equation, J. Math. Chem. 57, pp.1932–1934,2019.

RESEARCH ARTICLE

Synthesis, Characterization and Thermal study of NiTiO₃ / PVA Nanocomposite Film

Anadure Anilkumar[1], Sangappa K Ganiger[2], Arunkumar Lagashetty[3] and Vijaykumar Durg[4]*

[1]Department of Chemistry, B.V.Bhoomaraddi College of Arts, Science and Commerce, Bidar-585403, Karnataka, India.
[2]Department of Physics, Government Engineering College, Huvinahadagali-583219, Karnataka, India
[3]Department of Chemistry, Vijayanagara Sri Krishnadevaraya University, Ballari-585103 Karnataka, India.
[4]Department of Chemistry, BKIT, Bhalki, Bidar-585328, Karnataka, India.

*Address for Correspondence
Vijaykumar Durg
Department of Chemistry,
BKIT, Bhalki, Bidar-585328,
Karnataka, India.
E.Mail: vijayakumardurg@gmail.com

ABSTRACT

Polymer nanocomposites containing metal oxide nanomaterials constitutes new class of polymeric materials finds many applications. Matrix mixing of polymer and metal oxide responses the additional properties in the composite polymer in comparison with plain polymer.The present experimental results are reporting the synthesis of nickel titanate (NiTiO₃) nanomaterials bycombustion reaction route using polymer as a fuel. Dispersion of NiTiO₃ in To Poly (vinyl alcohol)(PVA) matrix yields poly (vinyl chloride) nanocomposite (PVA/NiTiO₃) by solvent casting method. Prepared products like NiTiO₃ and PVA/NiTiO₃ composite materials are well characterised for its structure, morphology and bonding by use of X-ray diffraction (XRD), Scanning Electron microscope (SEM) and Fourier transfer infrared (FT-IR) tools respectively. Size of the particles and morphology are well studied by TEM study. Thermogravimetric (TGA) analysis is carried out for the prepared composite sample to know its thermal behaviour.

Keywords: NiTiO₃, PEG, PVA, PVA/NiTiO₃, FT-IR, XRD, TEM, TGA

Anadure Anilkumar *et al.,*

INTRODUCTION

Recent researchers are attracted much for the bimetallic oxide materials containing titanium metal due to its various applications especially in field of electronics. [1-2],these oxide materials constitute special structural arrangements leads designed materials for specified applications. Particle size of the oxide materials are counts for its applicable oriented propertiesas well asits stability[3].The development of special properties in the oxide materials is due its structural response and also its stability. Bimetallic oxides containing titanium metal play a vital role and integratethe science and technology in terms of its applications. Nickel titanate oxide materials are known for photorefractive, semi-conductive and ferroelectric properties. Hence it finds more applications in the field of electronics [4-5]. It has been studied extensively for more and suitable applications to solve the societal applications.In addition, this material is renaming as a microwave ceramic owing to its dielectric response in the microwave spectrum. Further, the catalytic activity and dynamic efficiency of nickel titanate oxide have been researched in solving environmental issues [6-7].

Nickel titanate oxide was successfully synthesized various methods in which combustion method finds simplicity and yields desirable product. This method also finds a simple way to control particles size [8]. The ceramics materials have exhibited high density, uniform grain growth and homogeneous. Polymers may be considered as a fuel for the combustion reaction leads phase formed product. Self-propagating combustion reaction takes place in presence of a polymer fuel [9-10]. Inorganic nanoscale bimetallic oxides dispersed in the matrix of polymeric materials constitute new class of materials leads various applications [11]. Polymer nanocomposite formed by dispersion of nickel titanate in polymer matrix constitutes new designed composite materialsfor specialised applications[12]. Dispersion of nanosized $NiTiO_3$ inPoly(vinyl alcohol) formspolymer composite material showsenhanced thermal stability and are easy to produce. It also shows good chemical and physical properties which responses broad applications in various fields [13].The incorporation of $NiTiO_3$ into the poly(vinyl alcohol) matrix has significantly enhanced the properties and applicationsin comparisonwith pure PVA. Recently membranes based on PVA have received considerable attention by the researchers due to its non-toxicity, good film-forming ability, low cost, good mechanical strength and chemical stability. [14-17]. Present investigation is the synthesis of $NiTiO_3$-PVA composite materials by self-propagating combustion route. Further, incorporation of $NiTiO_3$ into the PVA matrix has been carried out by solvent casting method. Various characterisation and properties of the said materials is undertaken.

MATERIALS AND METHODS

Analytical grade (AR grade) chemicals are used in the research experimentand werereceived from Sigma Aldrich. Combustion method was used for the preparation of nickel titanate and solvent casting method was adopted for the synthesis of PVA/$NiTiO_3$ nanocomposite film.

Synthesis of NiO and TiO_2nanoparticles
Usually Metal salts are used for the synthesis of respective metal oxides by combustion route. Nickel salt like nickel chloridewasgrinded with PEG in the weight ratio 1:5 and grounded well in separate mortar. Furtherproduct was grinded well for proper mixed product andis transferred into china dish. The reaction mixture was initially heated in airatmosphere to complete the carbonaceousflame leads tonoon sooty flame.This pre product was transferredinto a silica crucible and is ignited at 1000°C in muffle furnace. Combustion reaction shows the melting of PEG, then frothed and finally formsa crystalline nickeloxide sample. Cool the product to room temperature gives oxide residue as nickeloxide sample. Similar procedure is used for the synthesis of Titanium dioxide(TiO_2) by use of titanium salt [18-21].

Anadure Anilkumar *et al.,*

Synthesis of Nickel titanate

Weigh accuratelynickeloxide, titanium oxide and PEG in the ratio 1:1:5 and grounded well in a pestle and mortar for through mixing. The resulting mixture isignited in a specialised chaina dish in an open atmosphere to form pre product. Initially it burns with carbonaceous fumes and after sometimesit completes evolution of such fumes. Further, this pre product is burnt completely in a silica crucible at 1200°C. Combustion process showingthat, initially PEG melted, then frothed and finally yieldsnickel titanate as a final product [22]. The obtained final product is as given in figure 1 and its synthetic scheme is given in scheme-1. The possible reaction involved is given below

Synthesis of PVA/NiTiO$_3$ composite film

2g of PVA polymer is dissolved in 15ml water solvent stir the solution to form jelly solution. 0.1g of as prepared nickel titanate was mixed thoroughly by constant stirring and was poured into the petridish uniformly, cooled under room temperature until solvent evaporated to form fine oxide dispersed PVA/NiTiO$_3$ composite which was well characterized by characterisation techniques.

RESULTS AND DISCUSSION

XRD Study

The structural confirmation of the combustion derived NiTiO$_3$nanoparticles and its PVA nanocomposite film samples were carried out by X-ray diffraction (XRD) study.XRD pattern of NiTiO$_3$ nanomaterials sample is given in figure 2. The pattern shows various Bragg's reflections due to crystalline nature with rhombohedral structure. Obtainedd-spacing values of the sample matches well with33-960JCPDS file of NiTiO$_3$ nanomaterials. Comparison of the observed and literature XRD data clearly indicating that, the sample confirms the formation of NiTiO$_3$ phase. The crystallinity and phase formation of the synthesized PVA/NiTiO$_3$ sample were again examined by XRD analysis. XRD pattern of solvent casted PVA/ CaTiO$_3$ nanocompoiste film sample is given in figure 3. The said pattern shows the limited Bragg's reflections due to the reduction of crystallinity as compared to pure oxide. This change is due masked oxide materials in the poly (vinyl alcohol) matrix. Further, the traced crystallinity in the PVA is due to matrixes of NiTiO$_3$ nanomaterial. The appearance of NiTiO$_3$ reflections in the PVA composite sample (peaks are indexed) and slightly shift in the reflections confirms the formation of PVA/ NiTiO$_3$ nanocompoiste.

FT-IR Study

As formed nanocomposite was well confirmed by the appearance of vibrations in infrared spectrum. Figure-4 shows FT-IR spectrum of as prepared PVA/NiTiO$_3$ nanocompoiste sample. A broad band at 3300 cm^{-1} may be due the presence moisture content in the sample. Bands in the region 1000-1200cm^{-1} are due to the plane bending vibration of C-H mode. The band at 850 cm^{-1} originates out of plane C-H bending vibration. The spectrum of the polymer composites shows a peak at 550cm^{-1} which are attributed due to the presence of nickel titanate sample in the poly (vinyl) nanocomposite [23].

SEM Study

Surface morphology of the polymer nanocomposite samples were well studied by SEM analysis. The SEM image of as prepared PVA/NiTiO$_3$ nanocomposite film is given in figure 5.The image is reflecting the spherical particles due to the presence of crystalline nature of the composite sample and also observed the self-assembly of different shaped particles in the image. Further, most of the particle grouping with self-doping can also observed in the composite image. Possibly some particles masked in the PVA matrix which may reduce the crystallinity of dispersed oxide sample also increases the crystallinity of the amorphous PVA.

TEM Study

Transmission electron microscope is used to study the particle morphology and particle size of the PVA/NiTiO₃nanocomposite film and is given in figure-6.The image showing the semi crystalline morphology with well-defined irregular particles and are within the nano range (100nm). Most of the nickel titanate nanomaterials are damasked and well dispersed in poly (vinyl alcohol) matrix. Some particles are masked in polyvinyl alcohol matrix which reduces the crystallinity of the pure oxide sample. Polymer streaks with bimetallic oxide sample further confirms the formation of nanocomposite film.

Thermal Study

Thermal behavior of the as synthesized polymer composite was studied by thermo- gravimetric analysis (TGA). Figure 7 shows the TGA trace of as prepared PVA/NiTiO₃ nanocompoiste film. The thermal trace shows the degradation of PVA occurs at 300°C with the initial weight loss at lesser temperature indicates the release of water moiety of the sample. Weight loss occurring around 300°C to 550°C is due to the decomposition of the polymer sample due to strong interaction between nickel titanate and poly (vinyl alcohol).

CONCLUSIONS

PVA-NiTiO₃ nanocomposite was prepared successfully by solvent catting method and developed crystallinity in plain PVA was confirmed by XRD tool. Interaction between oxide nanomaterials and PVA was well studied by FT-IR tool instrumentation. TEM and SEM study reviles the applicable morphology and particle size of the prepared sample. Thermal stability of the composite film is confirmed by thermal gravimetric technique.

ACKNOWLEDGEMENTS

REFERENCES

1. Yuvaraj S., Nithya V.D., SaiadaliFathimaK., Sanjeeviraja C., Kalai, Selvan G., ArumugamS.Investigations on the temperature dependent electrical and magnetic properties of NiTiO₃ by molten salt synthesis, *Mater Res Bull* 2013, 48, P.1110-1116.
2. Tsuyumoto I., Kobayashi M., AreT., Yamazaki N. Nanosized tetragonal BaTiO₃ powders synthesized by a new peroxo-precursor decomposition method, *Chemistry of Materials*, 2010, 22(9), P.3015–3020.
3. KřenekT., KováříkT., PolaJ., StichT., DochevaD.Nano and micro-forms of calcium titanate: Synthesis, properties and application, *Open Ceramics,* 2021,8, P.100177.
4. MadhuriW.Electrical and magnetic properties of NiTiO₃ nanoparticles synthesized by the sol–gel synthesis method and microwave sintering. *Journal of Materials Research and Technology,*2019,8(3), P.3097–3101.
5. Vijayalakshmi R., Rajendran V.Effect of Reaction Temperature on Size and Optical Properties of NiTiO₃ Nanoparticles. *Journal of Chemistry*, 2012, 9,Article ID 607289, P. 1-7.
6. AlammarT., HammI., WarkM., MudringA.V. Low-temperature route to metal titanate perovskite nanoparticles for photocatalytic applications, *Appl.Catal.*, B, 2015, 178, P. 20-28.
7. PugazhenthiranN., KaviyarasanK., SivasankarT., EmelineA., BahnemannD., MangalarajaR.V., AnandanS. Sonochemical synthesis of porous NiTiO₃Nano rods for photocatalytic degradation of ceftiofur sodium,*Ultrasonic Sonochemistry,*2017, 35, P. 342-350.
8. Ruiz-PreciadoM.A., KassibaA., GibaudA., Morales-AcevedoA.

9. Comparison of nickel titanate (NiTiO$_3$) powders synthesized by sol–gel and solid state reaction, *Mater Sci. Semicond Process*, 2015, 37, P. 171-178.

10. Arunkumar Lagashetty, Amrutha Pattern, Sangappa K Ganiger. Synthesis, Characterization and Antibacterial study of Ag doped magnesium ferrite nanocomposite.Heliyon.2019, 5, P. e01760.

11. Arunkumar Lagashetty, Sangappa K Ganiger, Shashidhar Reddy Microwave Derived Nano Sized Zirconium Vanadate as an Adsorbent for Heavy Metal Ions,

12. *Letters in Applied Nano Bioscience*, 2020, 9(3), P.1420-1426.

13. Xiuyun Liu, Qigong Chen, Lizhen Lv , Xiaoping Feng , Xiangfu Meng,   Preparation   of   transparent PVA/TiO$_2$ nanocomposite   films   with   enhanced   visible-light   photocatalytic   activity, Catalysis Communications,2015, 58(5), P. 30-33.

14. Maajid, S.A., Safiulla, M. Investigation of electrical and thermal property of poly (vinyl alcohol)–calcium titanate nanocomposites. *J Mater Sci: Mater Electron*. 2019, 30, P. 2292–2298.

15. Khanahmadzadeh S., SimaniS.H., Preparation and Magnetic Properties of Polyimide/Nickel Titanate Nanocomposite, *Asian Journal of Chemistry*; 2013, 25(13),P. 7445-7447.

16. Saeid Asadpour, Ahmad Raeisi   vanani, Masoumeh Kooravand , Arash Asfaram,   A   review   on   zinc oxide/poly(vinylalcohol) nanocomposites:Synthesis, characterization and applications, J.Clean. Prod.,2022, 362, P. 132297.

17. Vera Garcia, P.F. PVA Blends and Nanocomposites, Properties and Applications: A Review. In book: Green-Based Nanocomposite Materials and Applications. Engineering Materials. Springer, Cham.2023, P. 191-206.

18. Shehap, A.M., Akil, D.S. Structural and optical properties of TiO2 nanoparticles/ PVA for different composites thin films. Int. *J. Nano electron. Mater*. 2016, 9, P. 17–36.

19. Atta M.M., Taha, E.O., Abdelreheem A.M.Nitrogen plasma effect on the structural, thermal and dynamic mechanical properties of PVA/starch/graphene oxide nanocomposite. *Appl. Phys. A* 2021, 127,P. 532-541.

20. Aziz, S.B., Kadir, HamsanM.F.Z., M.H. Development of Polymer Blends Based on PVA: POZ with Low Dielectric Constant for Microelectronic Applications. *Sci Rep*2019. 9, P. 13163.

21. Arunkumar Lagashetty, Vibhav Mittin, Manjunath K Patil,Sangappa K GanigerSynthesis, Characterisation and Studies of BaFe$_2$O$_4$/PMMA Nanocomposite.

22. *PolymerBulletin*2020, 78, P. 5905-5921.

23. El-DeebA S., Abdel Kader M M., NasrG M., AhmedM A.,Eman O.,Taha. Modification of structural, thermal, dielectric and dynamic mechanical properties of PVA using lead (II) titanate, *Bull.Mater. Sci*2022, 45(79), P. 1-10.

24. Lagashetty A., Havanoor V., Basavaraj S., Balaji S.D., Venkataraman A., Microwave-assisted route for synthesis of nanosized metal oxides, *Sci. & Tech. Adv. Mater.*, 2008, 8, P. 484-493.

25. Pratviraj Swamy., BasavarajS., Arunkumar Lagashetty., Srinivas RaoN V, Nijgunappa R.,VenkataramanA., Synthesis and characterization of Zinc Ferrite nanoparticles obtained by self-propagating low temperature combustion method, *Bull. Mater. Sci.* 2009, 34(7), P. 1325-1330.

26. Arunkumar Lagashetty., Manjunath K Patil., Sangappa K Ganiger. Green Synthesis, Characterization, and Thermal Study of Silver Nanoparticles by Achras sapota, Psidium guajava, and Azadirachta indica Plant Extracts. *Plasmonics*. 2020, 10(14), P. 1219-1220.
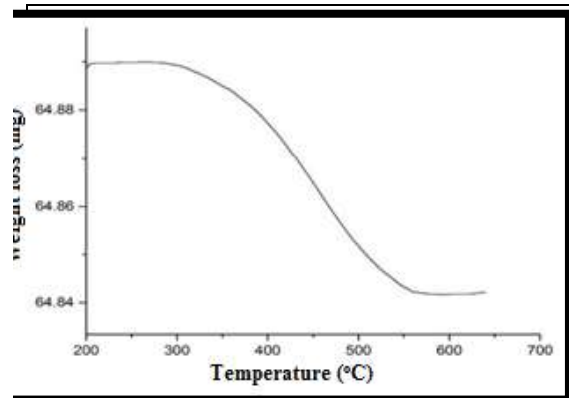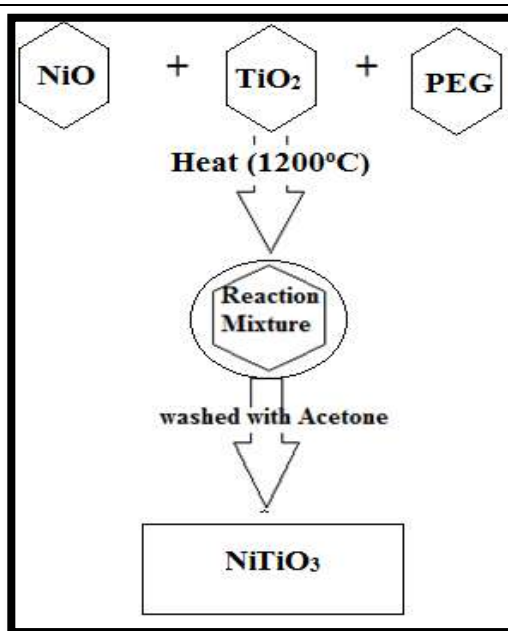
Anadure Anilkumar *et al.,*

re 1: Optical image of combustion derived
iO₃
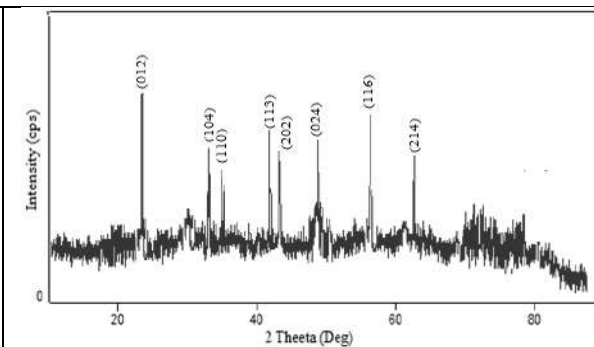
re 2: XRD pattern of NiTiO₃ nanoparticles
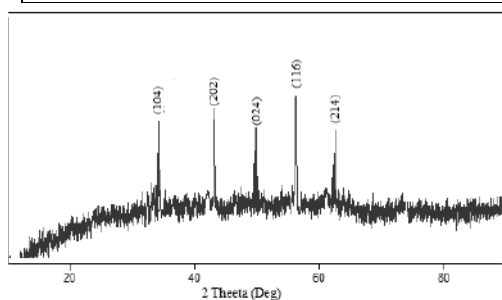
re 3: XRD pattern of PVA/ NiTiO₃ nanocomposite
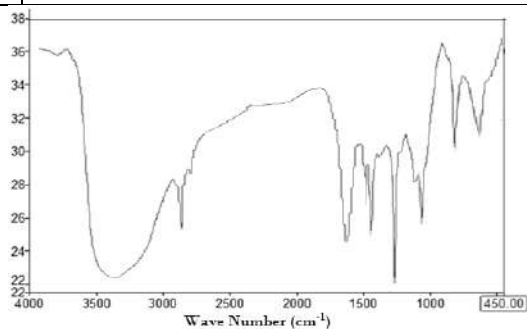
re 4: FT-IR of PVA/ NiTiO₃ nanocomposite film
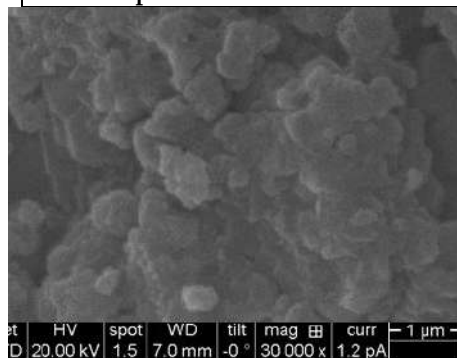
Figure 5: SEM image of PVA/ NiTiO₃ nanocomposite film
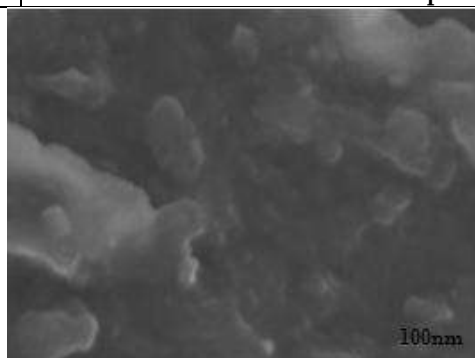
Figure 6: TEM image of PVA/ NiTiO₃ nanocomposite film

Figure 7: TGA image of PVA/ NiTiO₃ nanocomposite film	**Scheme 1: Synthesis of NiTiO₃ nanoparticles**

Overview of Viruses and their Pandemic Impact during 20th Century

Galanki Vasantha[1]*, Sirisha Konda[2] and Dakamarri Ravikiran[2]

[1]Associate Professor, Vignan Institute of Pharmaceutical Technology, Vishakapatnam, Andhra Pradesh, India
[2]M. Pharmacy II Year, Vignan Institute of Pharmaceutical Technology, Vishakapatnam, Andhra Pradesh, India.

*Address for Correspondence
Galanki Vasantha
Associate Professor,
Vignan Institute of Pharmaceutical Technology,
Vishakapatnam, Andhra Pradesh, India
E.Mail: drvasanthaniper@gmail.com

ABSTRACT

Kyasanur Forest Disease is generally known as Monkey fever, this is a unique disease that araised in the western ghats of India. The pathogen for this fever is KFD virus, an Arbovirus belongs to Flaviviridae family. Machupo virus is the causative agent for Bolivian Hemorrhagic Fever and it belongs to the family of Arenaviridae. Crimean -Congo Hemorrhagic Fever is one of the fastest spread tick borne infections of human beings, spreaded from west China to south Asia to Europe and African countries. Mainly 2 epidemics had led to the identification of these viruses. Initial outbreak was seen in Korean War that occurred in between 1950-1953. Marburg virus was 1st identified in Aug, 1967. Marburg virus was named with the city where most of the infections were reported. Rabies belongs to the Lyssavirus genus and Rhabdoviridae family. It is fatal and neurological infection that effects all   the   warm   blooded organisms. The   human immunodeficiency virus (HIV) causes a medical illness in human beings called as acquired immunodeficiency syndrome. Smallpox infection is unique to humans, which is caused by a poxvirus. It is among the high fatal diseases. Influenza viruses are the main pathogens which are responsible for respiratory tract infections in humans, birds, and all other mammals. Rota In the world the most common diarrheal pathogen that affects children is rotavirus.

Keywords: Machupo, Marburg, Rabies , human, Influenza, viruses.

Galanki Vasantha *et al.,*

INTRODUCTION

Viruses come under submicroscopic infectious pathogenic agents. The replication of Viruses takes place only inside the cells of living organisms known as hosts[1]. The genome of these microbes consists of a segment DNA/RNA surrounded by a protein coat. Nucleic acid present is DNA/ RNA type[2]. The virus cannot replicate on its own; it has to infect a host cell to make its replicas. In this process they cause damage and death of the host cell. Viruses can infect all organisms, including animals, plants and microorganisms. Viruses can be found everywhere where life exists and probably these are the first living cells that have evolved[3]. They does not possess its own metabolism so it definitely depends upon host to produce their replicas. Virus are smaller than bacteria and displays a huge diversity of their morphologies. Fully completed virus is called as Virion and it is encapped with a protein coat of known as Capsid[4]. Virus is a cellular in nature and they use hosts to make their copies [5].They utilize the main pathway mechanisms of hosts for its replication, these are very tough to kill by using drugs, without any unwanted effects on the host cell. The best possible medical path for treating the infections of virus is by vaccinations. It is also necessary to know the molecular structures, cell functions and its biology. These are also useful for studying genetics and its molecular mechanisms like replication of DNA, translation, processing of RNA, transcription, transportation of proteins and its immunological studies[6].

KYASANUR FOREST VIRUS

INTRODUCTION
Kyasanur Forest Disease is generally known as Monkey fever, this is a unique disease that araised in the western ghats of India. The pathogen for this fever is KFD virus, an Arbovirus belongs to Flaviviridae family[7] .This is highly contaginous and it is a tick borne virus. This virus is responsible for human and animal illness. There is a chance that this virus can be transmitted through faecal matter but mainly by tick bites. Causative organism for this virus transmission is H. Spinigera, a multi host species of tick common in India and Sri Lankan countries[8].

CHARACTERISTICS
The genome is a positive sense, single stranded RNA. This is spherical in nature and about 40–65nm. Virus is encapsulated with a regular polyhedron nucleocapsid. The genomic is same as cellular mRNA except a poly–adenylated tail. The origin for its multiplication is cytoplasm of infected host cells [9]. The genome of the virus has 10774 nucleotides which are single stranded and positive sense RNA. They are surrounded with a single polyprotein that is cleaved into three structural and seven non-structural proteins[10].

TRANSMISSION
Transmission is mainly by the infected tick bites. Direct animal to human transmission is possible. It is also spreads by the infected animals to humans through their bites, flesh, body fluids and also by excreta.

SYMPTOMS
- This ispresymptomatic for about 2 to 7 days after the tick bite.
- The clinical symptoms included are high fever, chills, sore throat, frontal headache, muscle aches and severe prostration[11].
- Other symptoms are myalgia, headache, Vomiting, diarrhea[12], gastrointestinal and lymphoid lesions[13].
- Red eyes, Bloody nose, joint pain, intestinal hemorrhage, skin petechiae are also seen in the infected patients.

MACHUPO VIRUS

INTRODUCTION

This virus is the causative agent for Bolivian Hemorrhagic Fever[14] and it belongs to the family of Arenaviridae[15]. BHF is initially identified in humans of northeast Bolivia during an outbreak which lasted from 1959 to 1963. Machupo virus has a mortality rate of 25–35%. The main reservoir and vector for this virus is a rodent known as Calomyscallosus[16].

CHARACTERISTICS

The genome includes 2 negative stranded RNA segments encodes with 4 virulent proteins: a huge RNA dependent RNA polymerase, a matrix protein , a RNA-binding nucleoprotein and glycoprotein precursor. The entire genome is encapsulated with nucleoprotein subunits and these are surrounded by a bi-lipid layer and with matured viral glycoproteins that forms the Virion[17].
(A) Genomic structure and the stages of transcription and replication process of the infection cycle.
(B) Linear map (Machupovirus L protein).

TRANSMISSION

This virus can be transmitted by various routes, mainly carried by air so this transmission is mainly aerosolized. Transmission is by direct or indirect contact with the infected person. The infection can also be spread by the contamination of food with the infected virus particles.

SYMPTOMS

The symptoms that are seen in the patients are as follows[18]. Initially after 1 to 5 of infection: high fever, leukopenia, nausea, thrombocytopenia, increased protein count in urine, headache, fatigue, myalgia, cough and dehydration are seen. Within 10 days of infection chills, low blood pressure, mucosal bleeds, petechiae, tremors, muscle pains, confusion and coma are seen.

CRIMEAN CONGO VIRUS
INTRODUCTION

Crimean -Congo Hemorrhagic Fever is one of the fastest spread tick borne infections of human beings, spreaded from west China to south Asia to Europe and African countries. This virus was primarily discovered in Crimean region of the former Soviet Union, 1944[19]. During 1944 to 1945, a huge endemic was occurred with a mortality rate of 10 percent in the region of Crimean Peninsula [20].

CHARACTERISTICS

This virus falls under Bunyaviridae family with full of tick borne virus [21]. These virions are spherical in shape and it is approximately 100 nm in diameter. The genome is a negative sense and single stranded RNA with three segments designed as small, medium and large with respective on their size[22].

TRANSMISSION

The transmission of this virus takes place by infected tick bites, infected animal blood and excreta. Transmission is by both wild and domestic animals which are infected by the virus[23].

SYMPTOMS

Common symptoms are malaise, myalgia, and often gastrointestinal distress[24]. Disseminated intravascular coagulopathy, shock, and Multi-organ failure are reported[25]. Liver failure, internal bleeding, rashes, nose and gum bleeds are also seen in severe cases.

HANTAVIRUS
INTRODUCTION

Mainly 2 epidemics had led to the identification of these viruses. Initial outbreak was seen in Korean War that occurred in between 1950-1953. Approximately over 3000 US troops were infected with this virus. And the next epidemic was seen in US, 1993. This was primarily named as Four corners disease, now it is referred to as Hantavirus Pulmonary Syndrome or Hantavirus Cardio-pulmonary Syndrome. Hantaviruses belong to the family of Bunyaviridae [26]. Murid rodents are the natural reservoirs for this virus.

CHARACTERISTICS

The viruses are encapsulated with genome of 3 single stranded RNA segments that are designed as large, medium and small. The genomes of these viruses are surrounded with a negative complementary senses[27].

TRANSMISSION

In contrast to other Bunyaviridae family viruses, the transmission is not by an arthropod vectors, this is carried to humans by an infected rodents or by insectivore hosts or by the infected bats [28].

SYMPTOMS

➔ The early symptoms that are seen in the infected persons are weakness, nausea, and muscle aches. The muscle aches are seen mainly in the areas like especially muscles, thighs, back, knees and shoulders. Headaches, dizziness, chills, stomach issues, vomiting, diarrhea, and abdominal pain are also seen.
➔ Late Symptoms are seen after 4-10 days of infection. These symptoms include nausea, vomiting, dry cough, headache, shortness of breath and sensation in lungs [29].

MARBURG
INTRODUCTION

This virus was 1st identified in Aug, 1967. Marburg virus was named with the city where most of the infections were reported. The 1st isolation of this virus takes place in that city. Until 1976 this virus was not a well known species of filoviridae family. Ebola was primarily identified in African country [30]. The two viruses marburg and ebola, were placed together in a new classified family named as Filoviridae. Marburg virus is the pathogen that causes Marburg virus disease in humans, and it has a mortality of 23-90%. The mortality rate depends on the outbreak and its spreadability.

CHARACTERISTICS

The genome of this virus is enveloped with a non-segmented negative stranded RNA with 19.1kb length and it codes for 7 structural proteins [31]. Virus nuclear capsid is made up of, RNA and its 4 proteins: Nucleoprotein, VP35, viral protein VP30 and catalytic subunit of polymerase-L. The two protein matrixes VP24 and VP40, are situated between nuclear capsid and envelope, that encoates with surface protein[32].

TRANSMISSION

The marburg virus is mainly transmitted by the bats which have this virus in their body. Through the infected animal bites and their contamination the spreading of this virus takes place. The pathogenesis of this virus in humans and its transmission were shown in the following diagram [33].

SYMPTOMS

Initially the symptoms begin after 2 to 21 days of infection and they are same as flu that include fever, fatigue, joint pains, chills, sore throat and myalgia. Within 2 to 5 day of the infection most of the patients can suffer with pain in abdomen, vomiting, diarrhea, nausea, and lethargy[34]. From 5 -7 days the effect of the infection will increase, and this include a rash that spreads from torso to limbs. Other symptoms like

conjunctivitis, fever, and also mucosal bleeds, petechiae, blood stools, vomiting and venipuncture site bleeding are also seen in the infected patients [35].

RABIES
INTRODUCTION
Rabies belongs to the Lyssavirus genus and Rhabdoviridae family. It is fatal and neurological infection that effects all the warm blooded organisms. Mostly this infection spreaded all over the globe except in Australia and Antarctica. Mainly the Rabies was fatal in mammals because it involves the involvement function of the nervous system [36]. Recovery from this disease was very low after the person got infected with the virus[37].

CHARACTERISTICS
Genome of this virus is encapsulated with a single strand negative sense RNA[38], that encodes with 5 genes with a highly conserved order. They code for Nucleoprotein, Phosphoprotein, Matrix protein, Glycoprotein, and a RNA polymerase. The rhabdoviruses have 2 main morphological components known as helical ribonucleoprotein core and the envelopes that were surrounded[39].

TRANSMISSION
Rabies is mainly transmitted by the bite of a rabid animal. Transmission takes place mainly from the exposed saliva of an infected animal. Transmission is either due to the bite of animal to animal or from animal to man [40]. A non-bite route of exposure is also possible by the inhalation of this virus.

SYMPTOMS
Clinically, the disease presents in 2 forms either in furious (encephalitic) form or in paralytic (dumb) form of rabies. Mostly two-thirds of the patients who are infected show the furious form[41]. The symptoms that are seen are headache, heat, low appetite, weakness, fatigue, nausea, vomiting, diarrhea, cough, runny nose, agression, photosensitivity, cramps, fear, salivation, limb paralysis and hydrophobia.

HIV
INTRODUCTION
The human immunodeficiency virus(HIV) causes a medical illness in human beings called as acquired immunodeficiency syndrome. HIV1 was first identified as the causative agent immediately after the initial recognition of HIV infected patients in US[42]. Acquired Immunodeficiency Syndrome is a global health problem. Approximately over   70M people are infected with HIV and 35M people died with AIDS. Currently 36.7m people are leading their life with   this[43]. In terms of global prevalence the HIV strains differ enormously. Six strains are mainly responsible for high number of this infection and they are HIV1 subtypes HIV1A, HIV1B, HIV1C, HIV1D, and two of the CRF,01-AE and 02-AG[44].

CHARACTERISTICS
Currently these are categorized into two types HIV1 and HIV2. Causative agent for AIDS is HIV1 and for HIV2 is restricted especially for some regions of Western and Central Africa. This virus comes under Lentivirus genus and belongs to Retroviridae family[45]. Matured HIV virions are spherical in nature and they are of 100 to 120 nm. This virus consists of a bi lipid membrane which is surrounded by a cone-shaped nucleo capsid known as Core. It has the RNA, viral protease, reverse transcriptase, integrase, Vpu, Vif, Vpr and Nef along with remaining cellular factors. Genome of the HIV1 consists of 2 identical single strand RNA, which is 9.2kb in length[46].

TRANSMISSION
The transmission is mainly by sexual route and also transmitted from mother to infant percutaneous route. But they are not completely understood. These viruses are transmitted through all possible routes. Spreading of

63084

Galanki Vasantha *et al.,*

this infection mainly follows the order of virus to the host infection mainly in plasma of blood. In the earlier phase of this infection the virus replication takes rapidly and spreads irregularly for its transmission. The transmission of this virus by sexual route mostly results in the clinical illness that arises from a virion particle, which highlights the bottleneck and inefficiency of this viral transmission[47].

SYMPTOMS

The symptoms of this virus are different in different areas of the body. The main common symptoms that involve are as follows: regular infections, frontal headaches, pneumonia, sudden severe weight loss, rashes on skin, swollen lymph glands. The pain is seen in the abdomen and also during swallowing of food. Dry cough, tiredness, high fever, loss of hunger, muscle aches, sweat, nausea, diarrhea, vomiting, thickening of nails, mouth sores and mouth ulcers can also be seen in the people with this infection.

SMALLPOX
INTRODUCTION

Smallpox infection is unique to humans, which is caused by a poxvirus. It is among the high fatal diseases. This infection has a mortality rate of approximately 30% [48]. This viral infection has been there over decades and lead to repeated large pandemics with a large number of recovered patients and dead persons[49]. In the 18th century, smallpox disease was the main cause of death of more than four hundred thousand people in Europe every year. Fortunately, this virus has been completely eliminated by the end of the last century due to the invention of vaccination[50].

CHARACTERISTICS

Smallpox virus comes under Poxviridae family. This family of viruses includes monkeypox virus and other poxviruses. The genome of these viruses contains a single linear double strand DNA with 130-375kb. Cell cytoplasm is the replicaton site of this virus. These viruses look like bricks through electron microscope and they range about 300-200nm.The DNA present in the virus, but not RNA and this was demonstrated in the year 1940[51]. In 1962, the composition of this double-stranded nature of the virus DNA and its guanine and cytosine was demonstrated [52].

TRANSMISSION

Transmission of this virus is mainly by inhalation route as it is an airborne virus. Mainly the droplets from the mouth, nose and respiratory tract from an individual who is infected with the virus and this is the primary way of transmission. Transmission is by an individual to an another individual is mainly through direct face contact with an infected person. This virus transmission is also by the direct contact with infected persons blood, urine, saliva, fecal matter and also by bedding or clothing.

SYMPTOMS

The earliest symptoms of this virus are similar to the flu. Initially the symptoms start with a rash just after a few days of virus exposure later on it turns into deep sores that fill with fluid. The formed blisters ooze out, and scab over, it gradually falls off and leaves scars[53]. After a few days, flat red spots will start appearing on your face, hands, arms, and all over the body. After a few days of infection the sores will begin to turn into small flat blisters filled with fluid. Gradually the fluid will then turn into pus. After sometime the sores will scab and fall off which leaves deep and pitted scars. The most common symptoms are high fever, headache, backache, rashes, sores, blisters, fatigue and vomitings.

INFLUENZA
INTRODUCTION

These viruses are the main pathogens which are responsible for respiratory tract infections in humans, birds, and all other mammals. During the 20th century these viruses are responsible for three pandemics which have high morbidity and fatal rate across the world. Surveillance across the world indicates that

these viruses isolate themselves every month from humans in any corner of the world. In the high temperature regions, the influenza activity was peak during the winter season. In the North side, influenza outbreaks occur between November and March. In the South side, influenza outbreaks occur between April and September. In tropical regions, influenza outbreaks occur all over the year. The history of influenza has been studied for many years, but some features like seasonality, the exact mechanism, and the factors that are responsible for spreading of the infection are not exactly known[54].

CHARACTERISTICS
This virus comes under Orthomyxoviridae family. Genome of this virus contains eight segmented, negative-stranded RNA, which ranges from the longest 2341 to the shortest 890 bps. Each genome contains both 5' and 3' untranslated regions[55].

TRANSMISSION
Not only the Humans who are susceptible for getting this infection. Influenza type A have many number of hosts that includes Birds, mammals and even bats. Water birds are first considered as the main host for influenza type A virus as they can be easily prone to maximum all the viral variants. Humans are not directly prone to these viruses. A carrier host is necessary to carry the virion, in which the adaptation leads to easy transmission of infection to human beings. The hosts are considered as mixing vessels. The pigs are be infected by Avian virus and human influenza virus and produces a favourable condition for their exchange of genetic material in between different strains[56].

SYMPTOMS
Symptoms differ from mild to severe. The symptoms are high fever, running nose, sore throat, stuffy nose, vomiting, aches, extreme tiredness, muscle aches, frontal headache, cough, and weakness. These symptoms appear after one to four days of virus exposure and these symptoms last for about 2–8 days[57].

ROTA VIRUS
INTRODUCTION
In the world the most common diarrheal pathogen that affects children is rotavirus. Approximately 800,000 deaths per year are recorded because of this infection[58]. These infections are the main causes for severe dehydrating gastro enteritis in children below 5 years. These viral infections were soon confirmed as a main dominant cause of diarrhea that is severe and fatal in infants and children below 5 years[59].

CHARACTERISTICS
These viruses are grouped from A to E, with reference to antigenic groups on VP6, which is the major capsid antigen. Group A, group B and group C categorized viruses are known to cause human infections. Among those three groups Group A viruses are the main reason for human infections. These viruses are in turn categorized into group G and group P types depending upon the antigens on outer capsid proteins VP7 and VP4. Serious illness among young children are mainly due to serotype G1-4[60].

TRANSMISSION
Rotavirus is a directly transmitted disease. Transmission is mainly via fecal-to-oral spread. The spreading is through person-to-person and also with the contaminated environment. Transmission is also by contaminated food, water and nasal droplets with the fecal matter of the infected person[61]. The following picture displays transmission of rotavirus. Major mode of rotavirus transmission is through fecal-oral route and also by food , water that are contaminated with virus particles.

SYMPTOMS

Major symptoms of this viral infection are diarrhea and vomiting. The other symptoms include vomiting, stomach pain, malaise, fever and fatigue[62]. Symptoms like dehydration and reduced oral intake, rarely neurologic features such as convulsions, and encephalitis are also seen in infected persons[63].

HERPES
INTRODUCTION

Herpes simplex virus leads to a chronic and lifelong infection in more than 60% of adults. Herpes simplex virus belongs to the family Herpesviridae. This virus wasrecognised in ancient Greek times, and it frequently infects humans. These viruses are life threatening and cause mild to uncomplicated mucocutaneous infection[64]. Till now eight types of herpes viruses are recognized they are HSV1, HSV2, varicella-zoster virus, cytomegalovirus, Epstein-Barr virus, human herpesvirus6, human herpesvirus7, and human herpesvirus8[65]. Among all those types HSV-1 causes orolabial disease, and HSV-2 is responsible for frequent genital and newborn infections[66].

CHARACTERISTICS

HSV-1 virus replication involves a step in which the viral DNA is uncoated and delivered into the infected cell nucleus . Genome that is responsible for the infection is by double-stranded DNA bacteriophage . Each of these viruses differs from each other and has a unique long and a unique short region, which are surrounded by inverted repeat sequences or by terminal repeat sequences. The genomic size may vary till 10kbp which depends upon their repeated sequences.

TRANSMISSION

These belongs to the large family of DNA Viruses. Eight virus types of this family are considered to cause infections in human beings. HSV1 and HSV2 are transmitted through mucosal cells of epithelial tissues and also through skin breakouts and from there they reaches the nervous tissue. HSV-1 are more likely seen in lesions of orofacial region and found typically in the trigeminal ganglia and HSV2 is mainly found in the lumbosacral region of ganglia. This virus spreads mainly in sexually active women. This virus also infects pregnant women and the transmission timing during pregnancy phase has greater risk on fetus and neonates [67].

SYMPTOMS

The common symptoms of genital herpes include small blistering lesions, cold sores on the mouth, around the genitals and in rectum. After the infection the fluid-filled blisters which were formed will burst and then turn into small, painful sores that can last up to four weeks [68]. During the initial stage this infection does not have any symptoms or signs. so it makes it difficult to identify among most of the people. The symptoms start from 2 to 12 days of infection and they include pain or itching near your genitals, rash, the red bumps, tiny white blisters, pain during urination, scabs, vaginal discharge in female, tender lumps in groin of males. Other common symptoms include flu-like symptoms with swollen lymph nodes, headache, muscle pain, fever, and herpes lesions[69].

REFERENCES

1. Koonin EV, Senkevich TG Dolja VV. The ancient Virus World and evolution of cells. Biology direct 2006;1(1):1-27.
2. Zimmer C. The Secret Life of a Coronavirus–An oily, 100-nanometer-wide bubble of genes has killed more than two million people and reshaped the world. Scientists don't quite know what to make of it. The new York times; 2021.

Galanki Vasantha *et al.*,

3. Raoult D, Audic S, Robert C, Abergel C, Renesto P, Ogata H, Claverie JM. The 1.2-megabase genome sequence of Mimivirus. science 2004;306(5700):1344-1350.

4. Watson J, Crick F. Structure of small viruses. Nature 1956;177(4506):473-5.

5. Freed EO. HIV-1 assembly, release and maturation. Nat Rev Microbiol 2015;13(8): 484-496.

6. Lodish H, Berk A, Zipursky SL, Matsudaira P, Baltimore D, Darnell J.Viruses: Structure, function, and uses. In Molecular Cell Biology. 4ᵗʰ ed. New York: WH Freeman; 2000.

7. Work TH, Trapido H (1957). kyasanur Forest disease. A new virus disease in India. Summary of preliminary report of investigations of the Virus Research Centre on an epidemic disease affecting forest villagers and wild monkeys of Shimoga District, Mysore. Indian J Med Sci 1957;11(5):341-342.

8. Chakraborty S, Sander WE, Allan BF, Andrade FC. Early Release-Retrospective Study of Kyasanur Forest Disease and Deaths Among Nonhuman Primates, India, 1957–2020. Emerg Infect Dis 2021;27(7):1969-1973.

9. Cook BW, Nikiforuk AM, Cutts TA, Kobasa D, Court DA, Theriault SS. (2016). Development of a subgenomic clone system for Kyasanur Forest disease virus. Ticks Tick Borne Dis 2016;7(5):1047-1051.

10. Cook BW, Ranadheera C, Nikiforuk AM, Cutts TA, Kobasa D, Court DA, Theriault SS. Limited effects of Type I interferons on Kyasanur Forest Disease Virus in cell culture. PLOS Negl Trop Dis 2016;10(8):1-19.

11. Shah SZ, Jabbar B, Ahmed N, Rehman A, Nasir H, Nadeem S, Azam S. Epidemiology, pathogenesis, and control of a tick-borne disease-Kyasanur forest disease: current status and future directions. Front Cell Infect Microbiol2018;8:149.

12. Murhekar MV, Kasabi GS, Mehendale SM, Mourya DT, Yadav PD, Tandale BV. On the transmission pattern of Kyasanur Forest disease (KFD) in India. Infect Dis Poverty 2015;4(1):1-4.

13. Kenyon RH, Rippy MK, McKee JrKT, Zack PM, Peters CJ. Infection of Macaca radiata with viruses of the tick-borne encephalitis group. Microb Pathog 1992;13(5):399-409.

14. Johnson KM, Kuns ML, Mackenzie RB, Webb PA, Yunker CE. Isolation of Machupo virus from wild rodent Calomyscallosus. Am J Trop Med 1966;15(1):103-106.

15. Fulhorst CF, Bowen MD, Ksiazek TG, Rollin PE, Nichol ST, Kosoy MY, Peters CJ. Isolation and characterization of Whitewater Arroyo virus, a novel North American arenavirus. Virol 1996;224(1):114-120.

16. Patterson M, Grant A, Paessler S. Epidemiology and pathogenesis of Bolivian hemorrhagic fever. CurrOpinVirol2014;5:82-90.

17. Young PR, Howard CR. Ribonucleoprotein complexes associated with virions of Pichinde virus and Pichinde virus-infected cells. Med Microbiol Immunol 1986;175(2):79-83.

18. Patterson M, Grant A, Paessler S. Epidemiology and pathogenesis of Bolivian hemorrhagic fever. CurrOpinVirol2014;5:82-90.

19. Bente DA, Forrester NL, Watts DM, McAuley AJ, Whitehouse CA, Bray M. Crimean-Congo hemorrhagic fever: history, epidemiology, pathogenesis, clinical syndrome and genetic diversity. Antiviral Res 2013;100(1):159-189.

20. Chinikar S, Ghiasi SM, Hewson R, Moradi M, Haeri A. Crimean-Congo hemorrhagic fever in Iran and neighboring countries. J Clin Virol 2010;47(2):110-114.

21. Donets MA, Chumakov MP, Korolev MB, Rubin SG. Physicochemical characteristics, morphology and morphogenesis of virions of the causative agent of Crimean hemorrhagic fever. Intervirology 1977;8(5):294-308.

22. Chinikar S, Persson SM, Johansson M, Bladh L, Goya M, Houshmand B, Nilsson M. Genetic analysis of crimean-congo hemorrhagic fever virus in Iran. J Med Virol 2004;73(3):404-411.

23. Spengler JR, Estrada-Peña A, Garrison AR, Schmaljohn C, Spiropoulou CF, Bergeron É, Bente DA. A chronological review of experimental infection studies of the role of wild animals and livestock in the maintenance and transmission of Crimean-Congo hemorrhagic fever virus. Antivir Res 2016;135:31-47.

24. Whitehouse CA. Crimean–Congo hemorrhagic fever. Antivir Res 2004;64(3):145-160.

25. Kuehnert PA, Stefan CP, Badger CV, Ricks KM. Crimean-Congo hemorrhagic fever virus (CCHFV): A silent but widespread threat. Curr Trop Med Rep 2021;8(2):141-147.

26. Schmaljohn CS, Dalrymple JM. Analysis of Hantaan virus RNA: evidence for a new genus of Bunyaviridae. Virol 1983;131(2):482-491.

27. RazzautiSanfeliu M. Microevolution of Puumala hantavirus in its host, the bank vole Myodesglareolus. Helsinki University Print 2012:49-58.

Galanki Vasantha *et al.*,

28. Kallio ER, Klingström J, Gustafsson E, Manni T, Vaheri A, Henttonen H, Lundkvist Å. Prolonged survival of Puumala hantavirus outside the host: evidence for indirect transmission via the environment. J Gen Virol 2006;87(8):2127-2134.

29. Junior VLP, Hamidad AM, de Oliveira Albuquerque Filho D, dos Santos VM. Twenty years of hantavirus pulmonary syndrome in Brazil: a review of epidemiological and clinical aspects. J Infect Dev Ctries 2014;8(02):137-142.

30. Pinzon JE, Wilson JM, Tucker CJ, Arthur R, Jahrling PB, Formenty P. Trigger events: enviro climatic coupling of Ebola hemorrhagic fever outbreaks. Am J Trop Med 2004;71(5):664-674.

31. Bukreyev AA, Volchkov VE, Blinov VM, Dryga SA, Netesov SV. The complete nucleotide sequence of the Popp (1967) strain of Marburg virus: a comparison with the Musoke (1980) strain. Arch Virol 1995;140(9):1589-1600.

32. Mŭhlberger E, Lootfering B, Klenk HD, Becker S. Three of the four nucleocapsid proteins of Marburg virus, NP, VP35, and L, are sufficient to mediate replication and transcription of Marburg virus-specific monocistronic minigenomes. Virol J 1998;72(11):8756-8764.

33. Bechtelsheimer H, Korb G, Gedigk P. The morphology and pathogenesis of "Marburg virus" hepatitis. Hum Pathol 1972;3(2):255-264.

34. MartinesRBNgDL, Greer PW, Rollin PE, Zaki SR. Tissue and cellular tropism, pathology and pathogenesis of Ebola and Marburg viruses. J. Pathol 2015;235(2):153-174.

35. Stille W, Bohle E. Clinical course and prognosis of Marburg virus ("Green-Monkey") disease. Marburg virus disease 1971:10-18.

36. Singh R, Singh KP, Cherian S, Saminathan M, Kapoor S, Manjunatha Reddy G, Dhama, K. Rabies–epidemiology, pathogenesis, public health concerns and advances in diagnosis and control: a comprehensive review. Vet Q 2017;37(1):212-251.

37. Hemachudha T, Ugolini G, Wacharapluesadee S, Sungkarat W, Shuangshoti S, Laothamatas J. Human rabies: neuropathogenesis, diagnosis, and management. Lancet Neurol 2013;12(5):498-513.

38. Ryan KJ, Ray CG. Medical microbiology. 4th ed. New York: McGraw Hill; 2004.

39. Yousaf MZ, Qasim M, Zia S, Ashfaq UA, Khan S. Rabies molecular virology, diagnosis, prevention and treatment. Virol J 2012;9(1):1-5.

40. De Serres G, Dallaire F, Côte M, Skowronski DM. Bat rabies in the United States and Canada from 1950 through 2007: human cases with and without bat contact. Clin Infect Dis 2008;46(9):1329-1337.

41. Hemachudha T. Human rabies: clinical aspects, pathogenesis, and potential therapy. Curr Top Microbiol Immunol 1994;187:121-143.

42. Sharp PM, Hahn BH. Origins of HIV and the AIDS pandemic. Cold Spring Harb Perspect Med 2011;1(1)1-22.

43. Chaimay B, Woradet S, Chantutanon S, Phuntara S, Suwanna K. Mortality among HIV/AIDS patients coinfected with Mycobacterium tuberculosis in southern Thailand. Southeast Asian J Trop Med Public Health 2013;44(4):641-648.

44. Murugavel KG, Thakar M, Mehendale S. Recent HIV infection testing algorithms. Indian J Med Res 2020;152(3):181-183.

45. Lucas SB, Hounnou A, Peacock C, Beaumel A, Djomand G, N'Gbichi JM, De Cock KM. The mortality and pathology of HIV infection in a west African city. AIDS 1993;7(12):1569-1579.

46. Sierra S, Kupfer B, Kaiser R. Basics of the virology of HIV-1 and its replication. J Clin Virol 2005;34(4):233-244.

47. Shaw GM, Hunter E. HIV transmission. Cold Spring HarbPerspect. Med 2012;2(11).

48. Thèves C, Biagini P, Crubézy E. The rediscovery of smallpox. Clin Microbiol Infect;20(3):210-218.

49. Hopkins DR. The greatest killer: smallpox in history. University of Chicago press; 2002.

50. Fenner F, Henderson DA, Arita I, Jezek Z, Ladnyi ID. Smallpox and its eradication . Geneva. Switzerland: World Health Organization; 1988.

51. Smadel JE, Hoagland CL. Elementary bodies of vaccinia. Bacteriol Rev 1942;6(2): 79-110.

52. Thèves C, Biagini P, Crubezy E. The rediscovery of smallpox. Clin Microbiol Infect 2014;20(3):210-218.

53. Belongia EA, Naleway AL. Smallpox vaccine: the good, the bad, and the ugly. Clin Med Res 2003;1(2):87-92.

54. Simonsen L, Clarke MJ, Schonberger LB, Arden NH, Cox NJ, Fukuda K. Pandemic versus epidemic influenza mortality: a pattern of changing age distribution. J Infect Dis 1998;178(1):53-60.

55. Kreuze JF, Perez A, Untiveros M, Quispe D, Fuentes S, Barker I, Simon R. Complete viral genome sequence and discovery of novel viruses by deep sequencing of small RNAs: a generic method for diagnosis, discovery and sequencing of viruses. Virol 2009;388(1):1-7.

56. Johnson KE, Song T, Greenbaum B, Ghedin E. Getting the flu: 5 key facts about influenza virus evolution. PLoSPathog 2017;13(8)1-6.

57. Dunn FL. Pandemic influenza in 1957: review of international spread of new Asian strain. JAMA 1958;166(10):1140-1148.

58. Parashar UD, Bresee JS, Gentsch JR, Glass RI. Rotavirus. Emerg Infect Dis 1998;4(4):561-570.

59. Guerreiro AN, Moraes CCG, Marinho ANR, Barros BCV, Bezerra DAM, Bandeira RS, Mascarenhas JDP. Investigation of enteric viruses in the feces of neotropical migratory birds captured on the coast of the State of Pará, Brazil. Int J Poult Sci 2018;20: 161-168.

60. Araud E, Shisler JL, Nguyen TH. Inactivation mechanisms of human and animal rotaviruses by solar UVA and visible light. Environ Sci Technol 2018;52(10):5682-5690.

61. 61.Hall E, Wodi AP, Hamborsky J, et al. Centers for Disease Control and Prevention. Epidemiology and Prevention of Vaccine-Preventable Diseases. 14th ed. Washington DC: Public Health Foundation; 2021.

62. Hagbom M, Istrate C, Engblom D, Karlsson T, Rodriguez-Diaz J, Buesa J, Svensson L. Rotavirus stimulates release of serotonin (5-HT) from human enterochromaffin cells and activates brain structures involved in nausea and vomiting. PLoSPathog 2011;7(7).

63. Nipa NJ, Akter N, Hira HM, Akter F, Jahan D, Islam S, Haque M. Intestinal Parasitic Infections among the Pediatric Patients in a Metropolitan City of Bangladesh with Emphasis on Cryptosporidiosis.Cureus 2022;14(7).

64. Whitley R, Kimberlin DW, Prober CG. Pathogenesis and disease. In: Arvin A, Campadelli-Fiume G, Mocarski E, et al. Human Herpesviruses: Biology, Therapy, and Immunoprophylaxis. Chapter 32. Cambridge: Cambridge University Press; 2007.

65. Miyagawa H, Yamanishi K. The epidemiology and pathogenesis of infections caused by the high numbered human herpesviruses in children: HHV-6, HHV-7 and HHV-8. CurrOpin Infect Dis 1999;12(3):251-255.

66. Whitley RJ. Herpes simplex virus infection. In Seminars in pediatric infectious diseases. WB Saunders 2002;13(1):6-11.

67. Brown ZA, Vontver LA, Benedetti J, Critchlow CW, Hickok DE, Sells CJ, Corey L. Genital herpes in pregnancy: risk factors associated with recurrences and asymptomatic viral shedding. Am J ObstetGynecol 1985;153(1):24-30.

68. Fatahzadeh M, Schwartz RA. Human herpes simplex virus infections: epidemiology, pathogenesis, symptomatology, diagnosis, and management. J Am Acad Dermatol 2007;57(5):737-763.

69. Anzivino E, Fioriti D, Mischitelli M, Bellizzi A, Barucca V, Chiarini F, Pietropaolo V. Herpes simplex virus infection in pregnancy and in neonate: status of art of epidemiology, diagnosis, therapy and prevention. Virol J 2009;6(1):1-11.

Galanki Vasantha *et al*.,

VIRUS	FAMILY	VIRUS SIZE	VIRUS SHAPE	ORIGIN OF REPLICA TION	GENO ME	TRANSMIS SION	SYMPTOMS
Kyasanur Forest Virus	Flaviviridae	40- 60 nm	3 structural and 7 non structural	Cytokinins, T-Cells, B cells	Single stranded -RNA	-Tick bite -Animal bites	-Chills -Fever -GI bleeding -Muscle pain -Vomiting -Headache
Machupo Virus	Arenaviridae	S-RNA (3.4kb) L-RNA (7.2kb)	Core ring structure	Glycoproteins of host cells	Bi-Segmented negative stranded-RNA	-Rodents -Food -Aerosolized -Infected rodents saliva,urine,feces.	-Fever -Malaise -Headaches -Arthralgia
Crimean-Congo Fever	Bunyaviridae	19.2kb	Tri-segmented structure	Glycoproteins-Gn and Gc	Single stranded -RNA	-Ticks -Infected animal blood -Both wild and Domestic animals	-Back pain - -Joint pain - -High fever - -Red eyes - -Petechiae - -High fever
Hanta Virus	Hantaviridae	80- 120 nm	Spherical	Cytoplasm	Single-stranded RNA genome	-Infected rodents urine, feces, saliva. -Aerosolized	-Muscle aches,Vomiting-Stomach pain,Chills,Dry cough -Shortness of breath
Marburg Virus	Filoviridae	1400 nm in length and 80 nm in diameter	-Rod like -Ring like -Crook -Six shaped -Branched	Monocyte derived dendritic cells	Negative sense single stranded RNA	-From infected blood and body fluids	-Abdominal pain,Chest pain -Diarrhea,Vomiting -Sore throat, Nausea -Headache,Malaise

Rabies	Rhabdoviridae	180 nm long and 75 nm wide	Bullet	Cytoplasm	Negative stranded RNA	-Direct contact with Infected animal	-Muscle pains -Loss of appetite,Hallucinations,Sensitivity to light,Anxiety -Excess salivation,Mental confusion -Irritability
HIV	Retroviridae	100 nm in diameter	Cone	CD4 immune cells	Two identical single-stranded RNA	-Infected blood -Semen -Blood -Needles -Rectal fluids -Vaginal fluids -Breast milk	- high fever, Headaches, Chills, Night Sweats, Sore throat -Muscle aches , Joint pains , tiredness -Swollen lymph glands , rashes on skin.
Smallpox	Poxviridae	400- 200 nm	Brick or Oval	Cytoplasm	Single linear double-stranded DNA	-Airborne -Infected person's saliva droplets and respiratory secretions	-Fever, Malaise, Headaches, Rashes, Lesions,Vomiting -Body aches
Influenza	Orthomyxoviridae	70 mm	Spherical or Filamentous	Nucleus of the host cell	Single stranded RNA	-Infected persons respiratory secretions	-Sore throat -Cough -Fever -Fatigue -Headache -Body pains
Rota Virus	Reoviridae	70 nm	Wheel like	Cytoplasm	Double stranded RNA	-Contaminated food, water -Infected persons stools -Flies -Direct contact with infected person	-Stomach ache -Diarrhea -Vomiting -Fever -Bloody stools -Black stools

Herpes	Herpesviridae	100- 110 nm	Cylindrical	Nucleus	Linear double stranded DNA	-Genetial secretions -oral secretions -Direct contact with infected person	-Pain around genitals -Pain during urination, Fever,Itching,Headache,Fatigue,Blisters,Sores
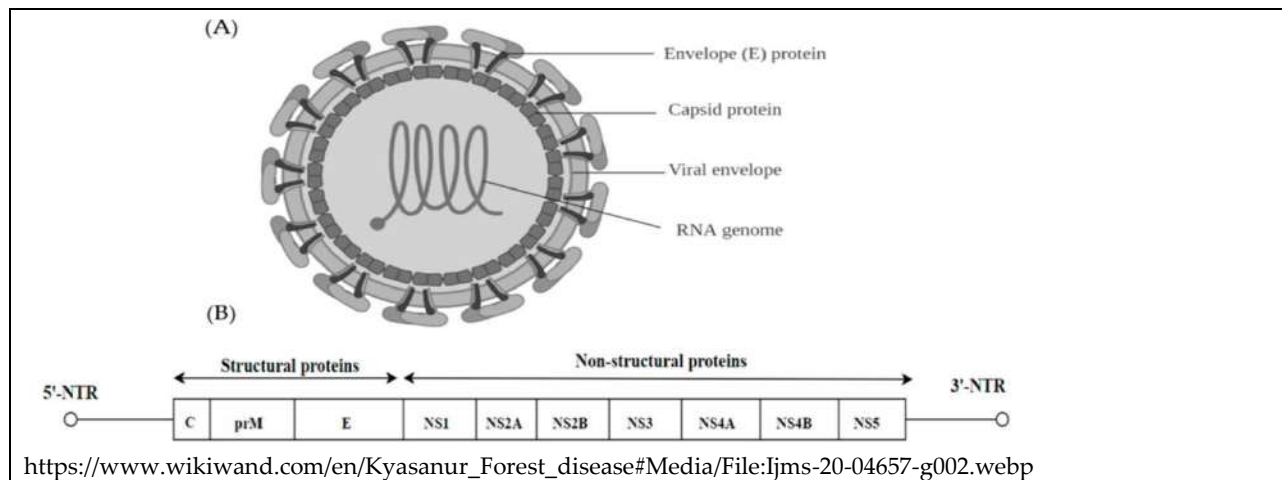
https://www.wikiwand.com/en/Kyasanur_Forest_disease#Media/File:Ijms-20-04657-g002.webp

Fig.1.KYASANUR FOREST VIRUS

https://link.springer.com/article/10.1007/s10916-018-1041-3#Fig1

Fig. 2 . TRANSMISSION

Galanki Vasantha *et al.,*

https://encrypted-tbn0.gstatic.com/images?q=tbn:ANd9GcQH9regCwP1gjCsNX4cG5ivpk4BdupRwNX7nw&usqp=CAU

Fig.3. Genome

https://en.wikipedia.org/wiki/Arenavirus#/media/File:Viruses-12-00784-g003.png
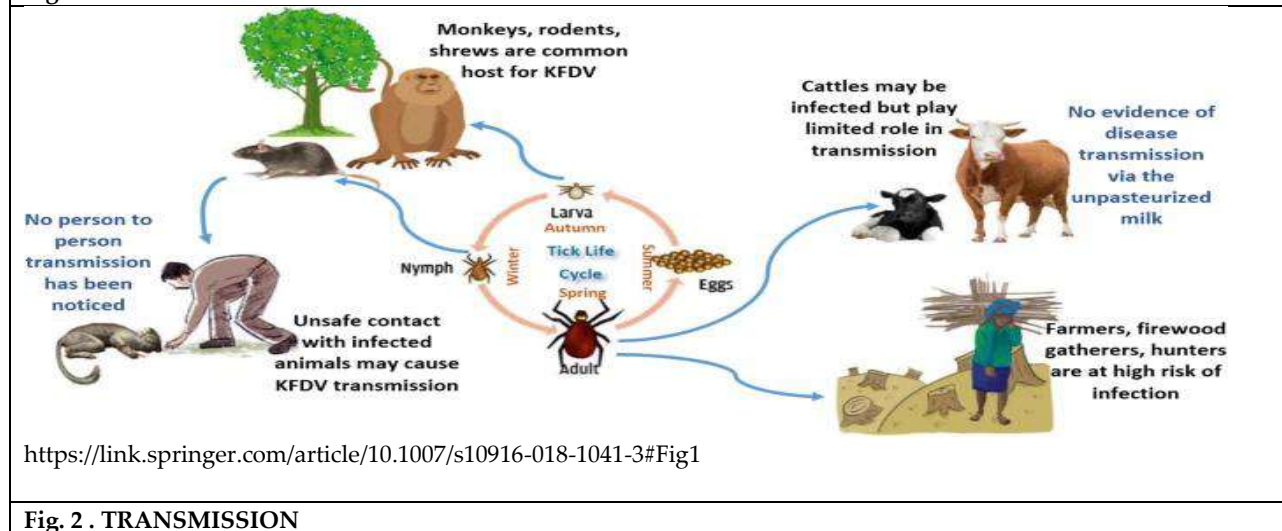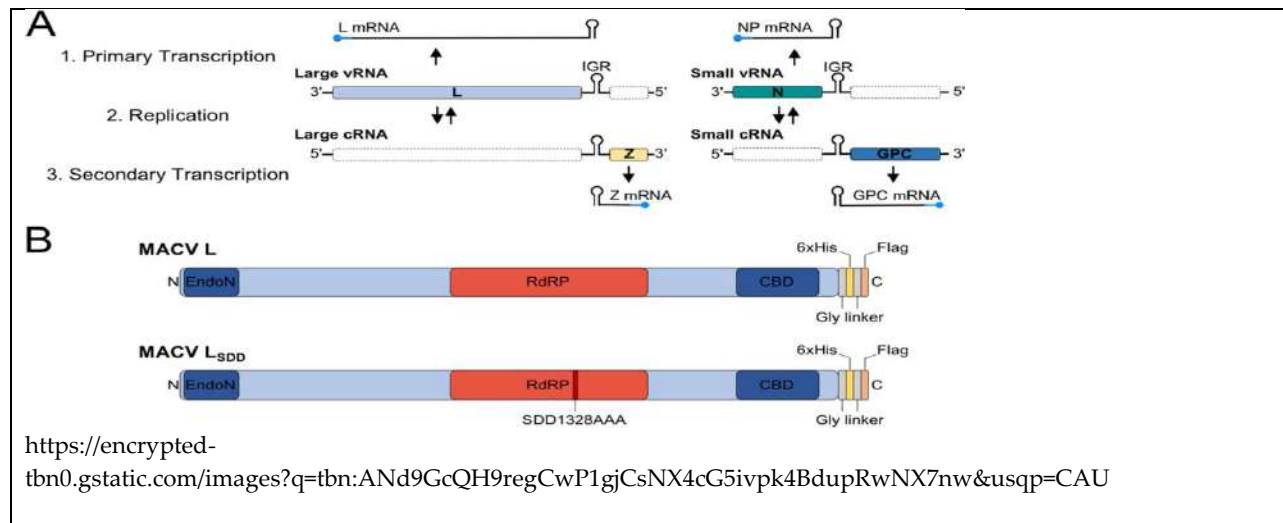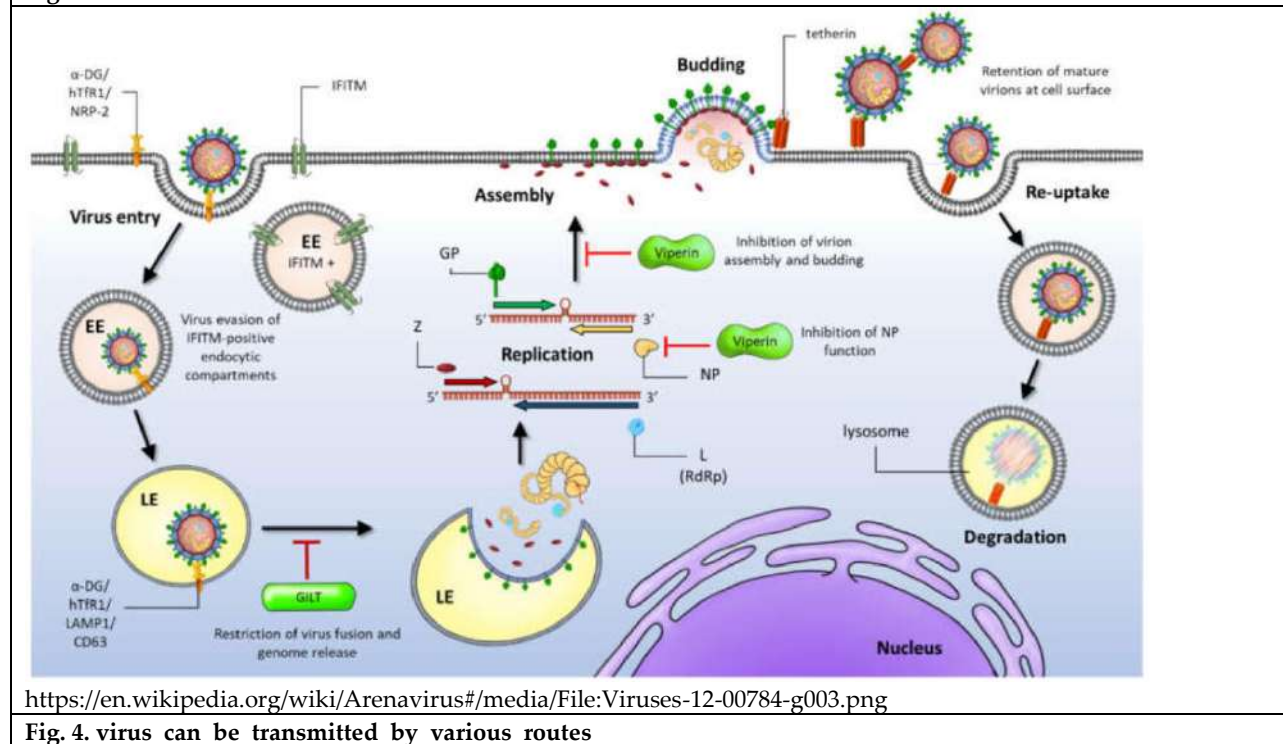
Fig. 4. virus can be transmitted by various routes

Galanki Vasantha *et al.,*

https://www.mdpi.com/viruses/viruses-08-00106/article_deploy/html/images/viruses-08-00106-g001.png

Fig. 5. Bunyaviridae family

https://www.researchgate.net/profile/Jessica_Spengler/publication/311647164/figure/fig1/AS:441006811291649@1482155625838/Life-cycle-of-Hyalomma-spp-ticks-and-vertical-and-horizontal-transmission-of.png

Fig.6. Infected Tick Bites

https://www.researchgate.net/profile/Maria_Razzauti/publication/282867889/figure/fig2/AS:285102871068673@1444985229180/Structure-and-genome-organization-of-hantaviruses-The-hantavirus-virion-o-80-120-nm-is.png

Fig.7. HANTAVIRUS

Galanki Vasantha *et al.,*

https://www.researchgate.net/profile/Muhammad-Akram-88/publication/343867639/figure/fig1/AS:967953814155265@1607789581278/Transmission-of-Hantavirus-to-people-happens-by-means-of-inward-breath-of.jpg

Fig.8. TRANSMISSION

https://www.researchgate.net/profile/Talha-Emran/publication/359669637/figure/fig1/AS:1140143134121985@1648842714602/Virion-structure-and-genome-organization-of-Marburg-virus-Top-the-Marburg-virus.png

https://media.springernature.com/lw685/springer-static/image/art%3A10.1186%2Fs12985-019-1272-z/MediaObjects/12985_2019_1272_Fig1_HTML.png

Fig. 9. Marburg TRANSMISSION

Galanki Vasantha *et al.,*

https://encrypted-tbn0.gstatic.com/images?q=tbn:ANd9GcR43n4p_NfS7f1b1onDFEOIEnplU56chbd2DJenQw6QIzDhcIodks1T3mj9qC4bJ9NNXv4&usqp=CAU
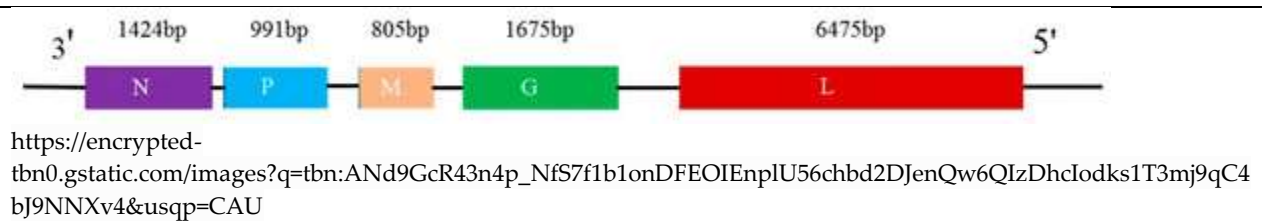
Fig.10. CHARACTERISTICS

https://rr-middleeast.woah.org/wp-content/uploads/2020/03/rabies-rabid-animal.jpg
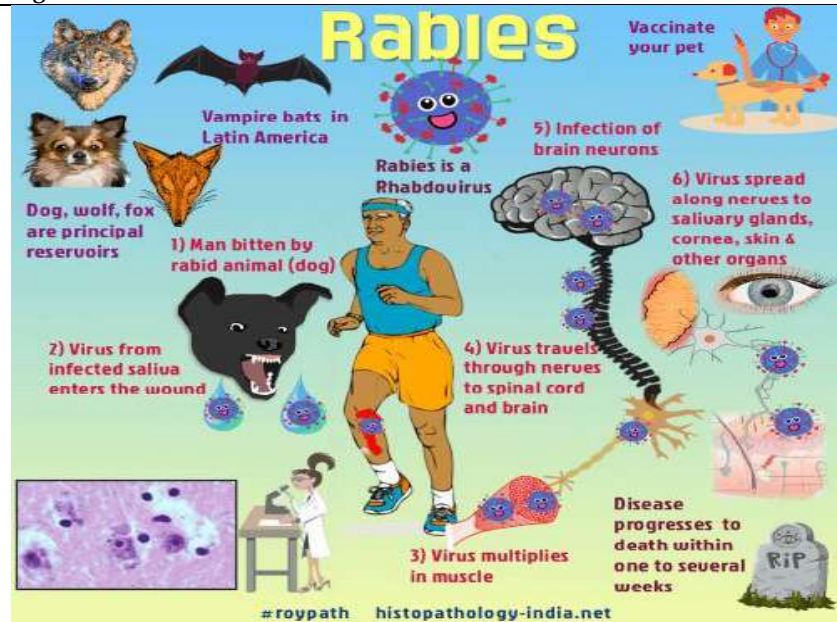
Fig.11. Rabies TRANSMISSION
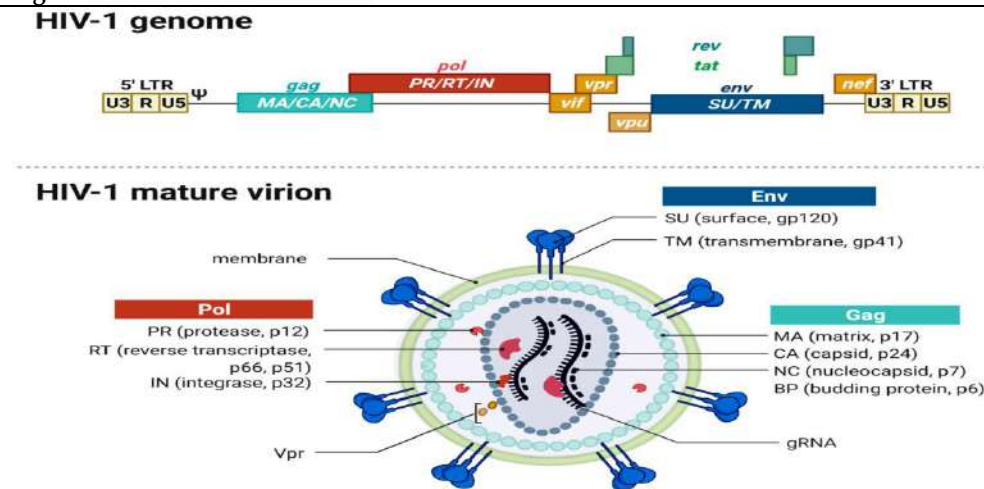
https://www.mdpi.com/toxins/toxins-14-00138/article_deploy/html/images/toxins-14-00138-g001.png

Fig.12. HIV1 and HIV2 CHARACTERISTICS

https://www.cusabio.com/statics/images/ID-poxvirus-img1.jpg

Fig.13. Smallpox virus

https://www.frontiersin.org/files/Articles/34193/fcimb-02-00150-HTML/image_m/fcimb-02-00150-g001.jpg

Fig.15. Transmission
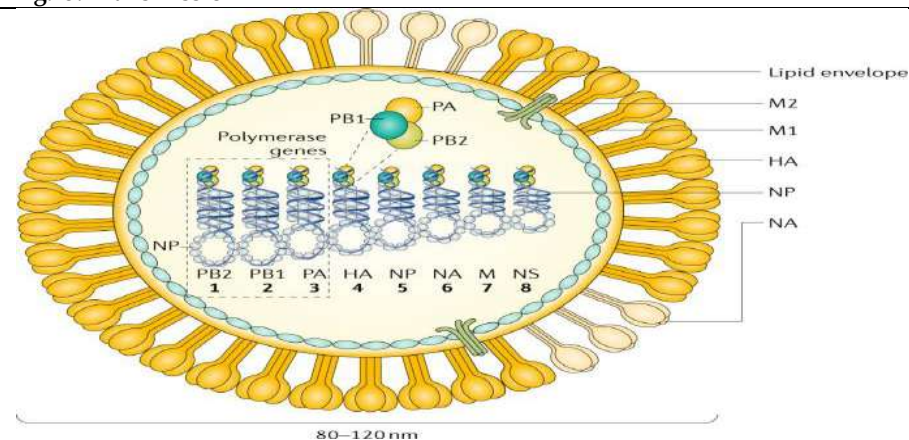
https://media.springernature.com/m685/springer-static/image/art%3A10.1038%2Fs41572-018-0002-y/MediaObjects/41572_2018_2_Fig1_HTML.jpg

Fig.16. CHARACTERISTICS

Galanki Vasantha *et al.,*

1. Influenza virus evolves by reshuffling genes and making mistakes during replication.

2. Influenza B virus primarily infects humans while influenza A virus is found in a variety of vertebrate hosts.

3. Influenza types and subtypes co-circulate. One such example is the influenza B lineages, Yamagata and Victoria, that have co-circulated since at least 1983.

4. Within the host influenza populations exist as a mixture of genetically diverse virus particles. This diversity allows influenza to rapidly adapt to its environment, especially after transmission to a new host.

5. The intrinsic diversity in an influenza population can lead to increased pathogenesis by allowing viruses that are "unfit" on their own to cooperate with one another. For example, one variant may be better at cell entry, while the other at cell exit; together they have higher replicative success.

Fig.17.
https://journals.plos.org/plospathogens/article/figure/image?size=large&id=10.1371/journal.ppat.1006450.g001

https://media.springernature.com/full/springer-static/image/art%3A10.1038%2Fnrmicro1692/MediaObjects/41579_2007_Article_BFnrmicro1692_Fig1_HTML.jpg

Fig.18. dsRNA Segment

https://www.researchgate.net/publication/327312201/figure/fig1/AS:725796402507779@1550054755740/The-figure-shows-rotavirus-transmission-The-primary-mode-of-transmission-is-the-transfer.png
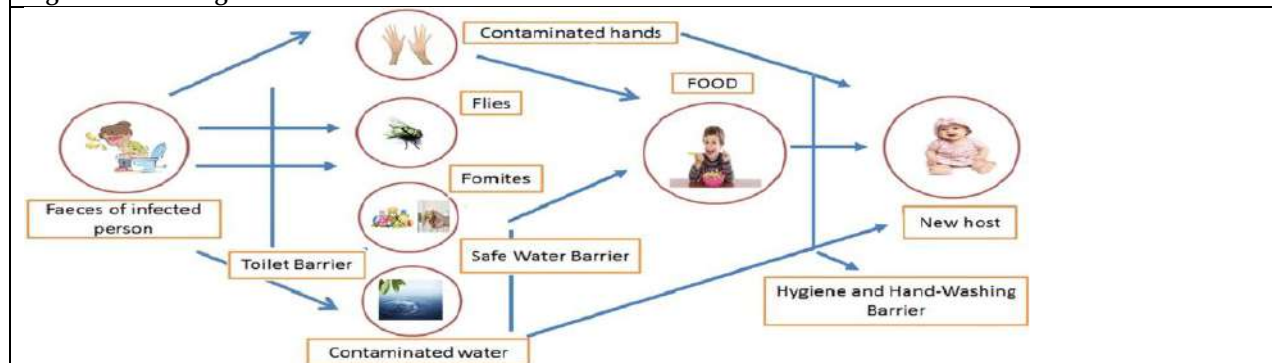
Fig. 19. Rotavirus TRANSMISSION

Galanki Vasantha *et al.,*

https://www.researchgate.net/profile/Hazilawati-Hamzah-2/publication/43980275/figure/fig1/AS:669454660821006@1536621837547/Diagram-illustrating-the-basic-structure-of-herpesvirus-genomes-from.ppm

Fig.20. HSV-1 virus replication
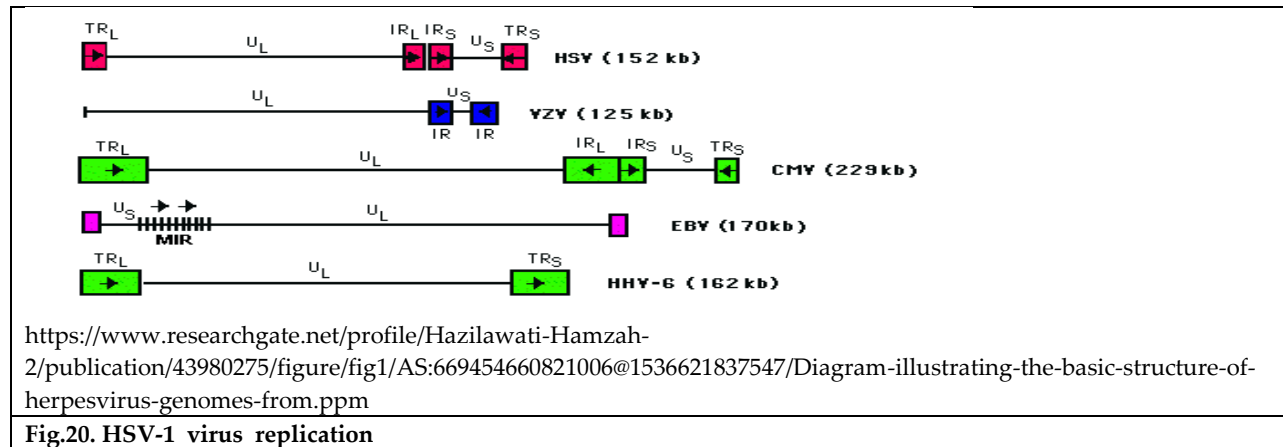
RESEARCH ARTICLE

A Study on the Medical Diagnosis using Cubic Root Fuzzy Sets in MCDM

D.Sivakumar[1]* and S.Sangeetha[2]

[1]Professor, Department of Mathematics, Annamalai University, Annamalai Nagar, Chidambaram - 608002, Tamil Nadu, India.
[2]Ph.D Scholar, Department of Mathematics, Annamalai University, Annamalai Nagar, Chidambaram- 608002, Tamil Nadu, India.

*Address for Correspondence
D.Sivakumar
Professor,
Department of Mathematics,
Annamalai University, Annamalai Nagar,
Chidambaram - 608002, Tamil Nadu, India.
E.Mail: sivakumarsangeetha4177@gmail.com

ABSTRACT

In this article, we present the new notion of cubic root fuzzy sets and we defined different operators such that Union, Intersection, Complement and Hamming Distance, Weighted Hamming Distance, Euclidean Distance, Weighted Euclidean Distance and also proved some fundamental results. Futhermore, we present MCDM Problem and an algorithm based on distance measure for cubic root fuzzy set .

INTRODUCTION

A concept of fuzzy set (FS) introduced by Zadeh. Atanassov generalized FS developed by Intuitionistic Fuzzy set (IFS)[1] and then Yager further improve the quantity by bringing out the Pythagorean fuzzy set (PFS). PFS[2] explains vagueness by the use of the MD function δ and NMD function γ where their square sum lies between 0 and 1,(i.e) $0 < \delta^2 + \gamma^2 < 1$. Fermatean fuzzy[6] set have been validated as o e of the tools to address uncertain information. Senapati and Yagar outlined basic operator over FFS. In this article, we study the notion of Cubic fuzzy Sets(CR Fuzzy set) and some new operations, Hamming distance, weighted Hamming

Sivakumar and Sangeetha

distance, Euclidean distance, weighted Euclidean distance[9] and algorithm based on distance measure for cubic root fuzzy set can be used in the MCDM method with suitable example[3].

Preliminary

.

Definition Definition: Fermatean Fuzzy set [6]

A Fermatean fuzzy set (FFS) F in U an object having the form F = [x, $\delta(x), \gamma(x)/x \in U$], where δ_F, γ_F represents the MD and NMD of F respectively. The mapping $\delta_F, \gamma_F: U \to [0,1]$ and

$0 \leq \delta_F{}^3 + \gamma_F{}^3 \leq 1$ **and also defined by the degreeof indeterminacy function**

$\pi_F = \sqrt[3]{1 - [\delta^3 + \gamma^3]}$, for all $x \in U$.

Definition: Cubic Root Fuzzy Set[4]

Let U be a universal set and the element is denoted by y. Then the Cubic Root Fuzzy Set (CR-Fuzzy Set) of R is defined as , R = [y,$\delta(y),\gamma(y)/y \in X$], where δ_R, γ_R represents the MD and NMD of R respectively. The mapping $\delta_R, \gamma_R: U \to [0,1]$ and $\leq \delta_F{}^3 + \sqrt{\gamma_R} \leq 1$. and also defined by the degreeof indeterminacy function $\pi_R(x) = \sqrt[3]{1 - \delta_R^3 + \sqrt{\gamma_R}}$

Definition: (6).

Let R = [δ,γ] ,$R_1 = [\delta_1,\gamma_1]$ and $R_2 = [\delta_2,\gamma_2]$ be the Cubic Root fuzzy sets and $\lambda \geq 0$, then the following operators hold

   (i) $R_1 \oplus R_2 = (\sqrt[3]{\delta_1^3 + \delta_2^3 - \delta_1^3\delta_2^3}, (\gamma_1\gamma_2))$

   (ii) $R_1 \otimes R_2 = ((\delta_1\delta_2), \sqrt[3]{\gamma_1^{1/2} + \gamma_2^{1/2} - \gamma_1^{1/2}\gamma_2^{1/2}})$

   (iii) $\lambda R = (\sqrt[3]{1 - (1 - \delta^3)^\lambda}, \gamma^\lambda)$

   (iv) $R^\lambda = (\delta^\lambda, \sqrt[3]{1 - (1 - \gamma^{1/2})^\lambda}$

Theorem

Let R, R_1 and R_2 and $\lambda_1, \lambda_2 \geq 0$ *the following hold*

   (i) $R_1 \oplus R_2 = R_2 \oplus R_1$

   (ii) $R_1 \otimes R_2 = R_2 \otimes R_1$

   (iii) $\lambda(R_1 \oplus R_2) = \lambda R_1 \oplus \lambda R_2$

   (iv) $(\lambda_1 \oplus \lambda_2)R = \lambda_1 R \oplus \lambda_2 R$

   (v) $R^{\lambda_1} \otimes R^{\lambda_2} = R^{\lambda_1 + \lambda_2}$

   Proof: For three cubic root fuzzy number R, R_1 and R_2 and $\lambda_1, \lambda_2 < 0$, according to definition , we obtain,

   (i) $R_1 \oplus R_2 = (\sqrt[3]{\delta_1^3 + \delta_2^3 - \delta_1^3\delta_2^3}, (\gamma_1\gamma_2))$

                $= (\sqrt[3]{\delta_2^3 + \delta_1^3 - \delta_2^3\delta_1^3}, (\gamma_2\gamma_1))$

            $= R_2 \oplus R_1$

   (ii) $R_1 \otimes R_2 = ((\delta_1\delta_2), \sqrt[3]{\gamma_1^{1/2} + \gamma_2^{1/2} - \gamma_1^{1/2}\gamma_2^{1/2}})$

   $= ((\delta_2\delta_1), \sqrt[3]{\gamma_2^{1/2} + \gamma_1^{1/2} - \gamma_2^{1/2}\gamma_1^{1/2}})$

                $= R_2 \otimes R_1$

            $R_1 \otimes R_2 = R_2 \otimes R_1$

   (iii) $\lambda(R_1 \oplus R_2) = \lambda (\sqrt[3]{\delta_1^3 + \delta_2^3 - \delta_1^3\delta_2^3}, (\gamma_1\gamma_2))$

                $= \sqrt[3]{1 - (1 - \delta_1^3 - \delta_2^3 + \delta_1^3\delta_2^3)^\lambda}, (\gamma_1\gamma_2)^\lambda$

$$= \sqrt[3]{1 - (1 - \delta_1^3)^\lambda (1 - \delta_2^3)^\lambda} , (\gamma_1^\lambda \gamma_2^\lambda).\text{L.H.S}$$

$$\lambda R_1 \oplus \lambda R_2 = (\sqrt[3]{1 - (1 - \delta_1^3)^\lambda} \gamma_1^\lambda \oplus \sqrt[3]{1 - (1 - \delta_2^3)^\lambda} .....R.H.S$$

$$\lambda(R_1 \oplus R_2) = \lambda R_1 \oplus \lambda R_2$$

(iv) $$(\lambda_1 \oplus \lambda_2)R = (\sqrt[3]{1 - (1 - \delta^3)^{(\lambda_1 \oplus \lambda_2)}} , \gamma^{(\lambda_1 \oplus \lambda_2)})$$

$$= \sqrt[3]{1 - (1 - \delta^3)^{(\lambda_1 \oplus \lambda_2)}(1 - \delta^3)^{(\lambda_1 \oplus \lambda_2)}}, \gamma^{(\lambda_1 \oplus \lambda_2)})$$

$$= (\sqrt[3]{1 - (1 - \delta^3)^{\lambda_1}} , \gamma^{\lambda_1}) \oplus (\sqrt[3]{1 - (1 - \delta^3)^{\lambda_2}}, \gamma^{\lambda_2})$$

$$= \lambda_1 R \oplus \lambda_2 R$$

(v) $$R^{\lambda_1} \otimes R^{\lambda_2} = (\delta^{\lambda_1} , \sqrt[3]{1 - (1 - \gamma^{1/2})^{\lambda_1}}) \otimes (\delta^{\lambda_2} , \sqrt[3]{1 - (1 - \gamma^{1/2})^{\lambda_2}})$$

$$= (\delta^{\lambda_1 \oplus \lambda_2} , \sqrt[3]{1 - (1 - \gamma^{1/2})^{\lambda_1 \oplus \lambda_2}})$$

$$= R^{\lambda_1 + \lambda_2}$$

$$R^{\lambda_1} \otimes R^{\lambda_2} = R^{\lambda_1 + \lambda_2}$$

Operation of Cubic Root Fuzzy Set

Let $R = [\delta, \gamma]$, $R_1 = [\delta_1, \gamma_1]$, $R_2 = [\delta_2, \gamma_2]$ be the Cubic Root fuzzy sets, then[4]

(i) Intersection:

$$R_1 \wedge R_2 = \min(\delta_1, \delta_2), \max(\gamma_1, \gamma_2)$$

(ii) Union:

$$R_1 \vee R_2 = \max(\delta_1, \delta_2), \min(\gamma_1, \gamma_2)$$

(iii) Complement

$$(R)^C = [(\delta)^6, \sqrt{\gamma}]$$

Note that $(\sqrt[2]{\gamma^6} + \sqrt[4]{\delta^2}) = (\gamma)3 + \sqrt{\delta}$

$$= (0.5)^3 + \sqrt{0.7} = 0.96166 < 1$$

so, $(R)^C$ is a Cubic Root fuzzy set.

We know that ,

$$(R^C)^C = (\gamma(x)^6 , \sqrt[4]{\delta(x)})^C = (\delta(x), \gamma(x)) = R.$$

Example

Assume that $R_1 = (\delta_1 \ 0.67, \gamma_1 = 0.32)$ *and* $R_2 = (\delta_2 = 0.25, \gamma_2 = 0.74)$ are the Cubic Root fuzzy sets , then

(i)Intersection:

$$R_1 \wedge R_2 = \min(\delta_1, \delta_2), \max(\gamma_1, \gamma_2)$$

$$= (\min(0.67, 0.25), \max(0.32, 0.74))$$

$$= (0.25, 0.74)$$

(ii)Union:

$$R_1 \vee R_2 = \max(\delta_1, \delta_2), \min(\gamma_1, \gamma_2)$$

$$= (\max(0.67, 0.25), \min(0.32, 0.74))$$

$$= (0.67, 0.32)$$

(iii) Complement

$$(R)^C = [(\delta)^6, \sqrt{\gamma}]$$

$$= ((0.33)^6, \sqrt[4]{0.67})$$

$$= (0.001, 0.81)$$

Theorem

For three cubic root fuzzy number R, R_1, R_2 and R_3 and $\lambda_1, \lambda_2 < 0$ following are valid

(i) $R_1 \wedge R_2 = R_2 \wedge R_1$ **(ii)** $R_1 \vee R_2 = R_2 \vee R_1$

(iii) $R_1 \wedge (R_2 \wedge R_3) = (R_1 \wedge R_2) \wedge R_3$ **(iv)** $R_1 \vee (R_2 \vee R_3) = (R_1 \vee R_2) \vee R_3$

(v) $\lambda(R_1 \vee R_2) = \lambda R_1 \vee \lambda R_2$ **(iv)** $(R_1 \vee R_2)\lambda = (R_1)\lambda \vee (R_2)\lambda$

Proof:

(i) $R_1 \wedge R_2 = \min(\delta_1, \delta_2), \max(\gamma_1, \gamma_2)$

$\qquad\qquad = \min(\delta_2, \delta_1), \max(\gamma_2, \gamma_1)$

$\qquad\qquad = R_2 \wedge R_1$

(ii) $R_1 \vee R_2 = \max(\delta_1, \delta_2), \min(\gamma_1, \gamma_2)$

$\qquad\qquad = \max(\delta_2, \delta_1), \min(\gamma_2, \gamma_1)$

$\qquad\qquad = R_2 \vee R_1$

(iii) $R_1 \wedge (R_2 \wedge R_3) = R_1 \wedge (\min(\delta_2, \delta_3), \max(\gamma_2, \gamma_3)$

$\qquad\qquad = \min(\delta_1, (\min(\delta_2, \delta_3))), \max(\gamma_1, (\max(\gamma_2, \gamma_3)))$

$\qquad\qquad = \min((\delta_1, \delta_2), \min\delta_3), (\max(\gamma_1, \gamma_2), \max\gamma_3))$

$\qquad\qquad = (\min(\delta_1, \delta_2), \max(\gamma_1, \gamma_2) \wedge R_3$

$\qquad\qquad = (R_1 \wedge R_2) \wedge R_3$

(iv) $R_1 \vee (R_2 \vee R_3) = R_1 \vee (\max(\delta_2(x), \delta_3(x)), \min(\gamma_2(x), \gamma_3(x))$

$\qquad\qquad = \max(\delta_1, (\max(\delta_2(x), \delta_3(x)))), \min(\gamma_1, (\min(\gamma_2(x), \gamma_3(x))))$

$\qquad\qquad = \max((\delta_1, \delta_2(x)), \max\delta_3(x)), (\min(\gamma_1, \gamma_2(x)), \min\gamma_3(x)))$

$\qquad\qquad = (\max(\delta_1(x), \delta_2(x)), \min(\gamma_1(x), \gamma_2(x)) \vee R_3$

$\qquad\qquad = (R_1 \vee R_2) \vee R_3$

(v) $\lambda(R_1 \vee R_2) = \lambda(\max(\delta_1, \delta_2), \min(\gamma_1, \gamma_2)$

$\qquad\qquad = \sqrt[3]{1 - (1 - max(\delta_1^3, \delta_2^3)^\lambda)}, \min(\gamma_1^\lambda, \gamma_2^\lambda)$

$\lambda R_1 \vee \lambda R_2 \quad = \quad (\sqrt[3]{1 - (1 - \delta_1^3)^\lambda}, \gamma_1^\lambda) \vee (\sqrt[3]{1 - (1 - \delta_2^3)^\lambda}, \gamma_2^\lambda)$

$\qquad\qquad = max \ (\sqrt[3]{1 - (1 - \delta_1^3)^\lambda}, \sqrt[3]{1 - (1 - \delta_2^3)^\lambda}, \min(\gamma_1^\lambda, \gamma_2^\lambda))$

$\qquad\qquad = \sqrt[3]{1 - (1 - max(\delta_1^3, \delta_2^3)^\lambda)}, \min(\gamma_1^\lambda, \gamma_2^\lambda)$

$\qquad\qquad = \lambda(R_1 \vee R_2)$

$\qquad \lambda(R_1 \vee R_2) = \lambda R_1 \vee \lambda R_2$

Theorem

For two cubic root fuzzy number $R_1 = (\delta_1, \gamma_1), R_2 = (\delta_2, \gamma_2)$ following are valid

(i) $(R_1 \wedge R_2) \vee R_2 = R_2$

(ii) $(R_1 \vee R_2) \wedge R_2 = R_2$

proof:

(i) $(R_1 \wedge R_2) \vee R_2 = (\min(\delta_1, \delta_2), \max(\gamma_1, \gamma_2) \vee (\delta_2, \gamma_2)$

$= (\max(\min(\delta_1, \delta_2), \delta_2), \min(\max(\gamma_1, \gamma_2), \gamma_2))$

$= (\delta_2, \gamma_2) = R_2$

(ii) $(R_1 \vee R_2) \wedge R_2 = (\max(\delta_1, \delta_2), \min(\gamma_1, \gamma_2)) \wedge (\delta_2, \gamma_2)$

$= (\min(\max(\delta_1, \delta_2), \delta_2), \max(\min(\gamma_1, \gamma_2), \gamma_2))$

$= (\delta_2, \gamma_2) = R_2$

Theorem

For two cubic root fuzzy number $R_1 = (\delta_1, \gamma_1), R_2 = (\delta_2, \gamma_2)$ following are valid

(i) $(R_1 \vee R_2)^C = R^C \wedge R_2^C$

(ii) $(R_1 \wedge R_2)^C = R^C \vee R_2^C$

Proof:

(i) $(R_1 \vee R_2)^C = (\max(\delta_1, \delta_2), \min(\gamma_1, \gamma_2))^C$

$\qquad\qquad = \min((\gamma_1)^6, (\gamma_2)^6), \max(\sqrt{\delta_1}, \sqrt{\delta_2})$

$\qquad\qquad = ((\gamma_1)^6, \sqrt{\delta_1}) \wedge ((\gamma_2)^6, \sqrt{\delta_2})$

Sivakumar and Sangeetha

$$= R_1^C \wedge R_2^C$$

(ii) $(R_1 \wedge R_2)^C = (\min(\delta_1, \delta_2), \max(\gamma_1, \gamma_2))^C$

$$= \max((\gamma_1)^6, (\gamma_2)^6), \min(\sqrt{\delta_1}, \sqrt{\delta_2})$$

$$= ((\gamma_1)^6, \sqrt{\delta_1}) \vee ((\gamma_2)^6, \sqrt{\delta_2})$$

$$= R_1^C \vee R_2^C$$

Distance Measures

Suppose that $R_1 = (\delta_1, \gamma_1)$, $R_2 = (\delta_2, \gamma_2)$ are two Cubic Root fuzzy sets and w_k (k= 1 to n), where $0 \le w_k \le 1$ and f_k (k=1 to n) are fuzzy best value $f_k = \max(f_k)$ (k=1 to n) then we describe some distance measure between cubic root fuzzy sets R_1 and R_2 then,[9]

Hamming Distance for CR-Fuzzy Set

$$d^H(R_1, R_2) = \sum_{i=1}^{n} 1/2 \left[| f_i \delta_i^3 - f_{i+1} \delta_{i+1}^3 | + | f_i \sqrt{\gamma_i} - f_{i+1} \sqrt{\gamma_{i+1}} | \right] \text{ (or)}$$

$$d^H(R_1, R_2) = \sum 1/2 \left[| f_1 \delta_1^3 - f_2 \delta_2^3 | + | f_1 \sqrt{\gamma_1} - f_2 \sqrt{\gamma_2} | \right] \ldots\ldots\ldots(1)$$

Weighted Hamming Distance For CR-Fuzzy Set

$$d^H(R_1, R_2) = \sum_{i=1}^{n} 1/2 \left[w_i^3 | f_i \delta_i^3 - f_{i+1} \delta_{i+1}^3 | + w_{i+1}^3 | f_i \sqrt{\gamma_i} - f_{i+1} \sqrt{\gamma_{i+1}} | \right] \text{ (or)}$$

$$d^H(R_1, R_2) = \sum 1/2 \, w_1^3 \left[| f_1 \delta_1^3 - f_2 \delta_2^3 | + w_2^3 | f_1 \sqrt{\gamma_1} - f_2 \sqrt{\gamma_2} | \right] \ldots\ldots\ldots(2)$$

Euclidean Distance For CR-Fuzzy Set

$$d^E(R_1, R_2) = \sum_{i=1}^{n} \sqrt{\frac{1}{2} [|f_i \delta_i^3 - f_{i+1} \delta_{i+1}^3|^2 + |f_i \sqrt{\gamma_i^3} - f_{i+1} \sqrt{\gamma_{i+1}^3}|^2]} \text{ (or)}$$

$$d^E(R_1, R_2) = \sum, \sqrt{\frac{1}{2} [|f_1 \delta_1^3 - f_2 \delta_2^3|^2 + |f_1 \sqrt{\gamma_1^3} - f_2 \sqrt{\gamma_2^3}|^2]} \ldots\ldots\ldots\ldots(3)$$

Weighted Euclidean Distance For CR-Fuzzy Set

$$d^E(R_1, R_2) = \sum_{i=1}^{n} \sqrt{\frac{1}{2} (w_i^3)[|f_i \delta_i^3 - f_{i+1} \delta_{i+1}^3|^2 + (w_{i+1}^3)|f_i \sqrt{\gamma_i^3} - f_{i+1} \sqrt{\gamma_{i+1}^3}|^2]} \text{ (or)}$$

$$d^E(R_1, R_2) = \sum, \sqrt{\frac{1}{2} w_1^3 [|f_1 \delta_1^3 - f_2 \delta_2^3|^2 + w_2^3 |f_1 \sqrt{\gamma_1^3} - f_2 \sqrt{\gamma_2^3}|^2]} \ldots\ldots\ldots\ldots(4)$$

Example

Assume that R_1 = ([0.3, 0.5], [0.4, 0.6], [0.1, 0.5]) a*nd* R_2 = ([0.4, 0.5], [0.2, 0.3], [0.4, 0.6]) are the Cubic Root Fuzzy sets then using the distance measure formulas

Hamming Distance for CR-Fuzzy set using equation (1)

$$d^H(R_1, R_2) = \sum 1/2 \left[| f_1 \delta_1^3 - f_2 \delta_2^3 | + | f_1 \sqrt{\gamma_1} - f_2 \sqrt{\gamma_2} | \right]$$

$d^H(R_1, R_2) = 0.08 + 0.01 + 0.1 + 0.2 + 0.06 + 0.06 + 0.18 + 0.06 + 0.09 + 0.14 + 0.06 +$

$0.11 + 0.27 + 0.001 + 0.006 + 0.12 + 0.06 + 0.14 + 0.07 + 0.04 + 0.10 + 0.12 + 0.08 + 0.03 + 0.28 + 0.01 + 0.05$

$$= 2.526$$

Weighted Hamming Distance for CR-Fuzzy set using equation (2)

Sivakumar and Sangeetha

$d^H(R_1, R_2) = \sum 1/2\, w_1^3 [\,|\, f_1\, \delta_1^3 - f_2\, \delta_2^3\,| + w_2^3\, |\, f_1\, \sqrt{\gamma_1} - f_2\, \sqrt{\gamma_2}\,|\,]$

$d^H(R_1, R_2) = 0.3(0.08 + 0.01 + 0.1 + 0.2 + 0.06 + 0.06 + 0.18 + 0.06 + 0.09) + 0.5(0.14 +$

$0.06 + 0.11 + 0.27 + 0.001 + 0.006 + 0.12 + 0.06 + 0.14) + 0.6(0.07 + 0.04 + 0.10 + 0.12 + 0.08 + 0.03 + 0.28 + 0.01 + 0.05)$

$\qquad = 0.3045$

Euclidean Distance for CR-Fuzzy set using equation (3)

$d^E(R_1, R_2) = 0.109 + 0.014 + 0.141 + 0.28 + 0.08 + 0.08 + 0.24 + 0.08 + 0.126 + 0.197 +$

$0.08 + 0.154 + 0.519 + 0.001 + 0.008 + 0.16 + 0.08 + 0.197 + 0.21 + 0.05 + 0.14 + 0.16 + 0.109 + 0.042 + 0.39 + 0.014 + 0.07$

$\qquad = 3.854$

Weighted Euclidean Distance for CR-Fuzzy set using equation (4)

$d^E(R_1, R_2) = 0.3(0.109 + 0.014 + 0.141 + 0.28 + 0.08 + 0.08 + 0.24 + 0.08 + 0.126) + 0.5(0.197 + 0.08 +$

$\qquad 0.154 + 0.519 + 0.001 + 0.008 + 0.16 + 0.08 + 0.197) + 0.6(0.21 + 0.05 + 0.4 +$

$\qquad 0.16 + 0.109 + 0.042 + 0.39 + 0.014 + 0.07$

$\qquad = 0.461$

MCDM Problems using operators in Cubic Root Fuzzy Set Algorithm
Step:1

Consider $A_1, A_2, \ldots A_n$ be alternatives and $p_1, p_2, p_3, , p_n$ be the parameters. Suppose that the Cubic root fuzzy sets $R_k = (\delta_k, \gamma_k)$, (k = 1 to n) where δ_k represent the MD of the alternative $\tilde{A}_k$ (k=1 to n) for the parameters p_k(k = 1 to n) .similarly, γ_k represent the NMD of the alternative $\tilde{A}_k$ (k = 1 to n) for the parameters p_k(k=1 to n) . The relation between the alternatives and parameters ae given below:

$\quad p_{11} \quad p_{12} \;.. \;.. \;.. \; p_{1n}$

$\quad p_{21} \quad p_{22} \;.. \;.. \;.. \; p_{2n}$

$\quad p_{31} \quad p_{32} \;.. \;.. \;.. \; p_{3n}$

$\quad ..... \quad\;\; ... \;.. \;... \;.. \;..$

$\quad p_{m1} \quad p_{m2} \;.. \;.. \;.. \; p_{mn}$

Step:2

Cubic root fuzzy set are used to assign weight w_k(k= 1 to n) to differents parameter for a set of group.

Step:3

Determine the distance measure using Cubic root fuzzy sets distance formula (equation (1),(2), (3), (4)).

Step:4

If the distance between the alternative is smaller . As a output, the rank the alternative in descending order.

Numerical Example

Sivakumar and Sangeetha

Suppose there are three patients P_1, P_2, P_3 in hospital with symptoms cough, heavy fever, vomating. Let the possible diseases relating to the above symptoms be Typhoid, COVID- 19, Dengue. Let $\mathscr{J}$ =[HB,TSH,GCT] be the collection of tests .We consider the set

$\wp$ = ($\wp_1$, $\wp_2$, $\wp_3$), where $\wp_1$, $\wp_2$, $\wp_3$ represent the symptoms cough, heavy fever, vomating and the set   =   ($\aleph_1$,$\aleph_2$, $\aleph_3$) , where $\aleph_1$, $\aleph_2$, $\aleph_3$ represent the diseases.

STEP:1

Construct that , $P \rightarrow \mathscr{J}$, Patients $\rightarrow$ Tests is given in the form of Cubic Root Fuzzy Set

$$P_1 = \begin{array}{c} \wp1 \\ \wp2 \\ \wp3 \end{array} \begin{array}{ccc} \mathscr{J}_1 & \mathscr{J}_2 & \mathscr{J}_3 \\ \left[\begin{array}{ccc} [0.3, 0.5] & [0.4, 0.6] & [0.1, 0.5] \\ [0.2, 0.4] & [0.3, 0.4] & [0.4, 0.7] \\ [0.6, 0.7] & [0.1, 0.8] & [0.2, 0.6] \end{array} \right] \end{array}$$

$$P_2 = \begin{array}{c} \wp1 \\ \wp2 \\ \wp3 \end{array} \begin{array}{ccc} \mathscr{J}_1 & \mathscr{J}_2 & \mathscr{J}_3 \\ \left[\begin{array}{ccc} [0.2, 0.6] & [0.4, 0.3] & [0.1, 0.5] \\ [0.4, 0.8] & [0.1, 0.9] & [0.3, 0.5] \\ [0.5, 0.5] & [0.3, 0.7] & [0.3, 0.9] \end{array} \right] \end{array}$$

$$P_3 = \begin{array}{c} \wp1 \\ \wp2 \\ \wp3 \end{array} \begin{array}{ccc} \mathscr{J}_1 & \mathscr{J}_2 & \mathscr{J}_3 \\ \left[\begin{array}{ccc} [0.8, 0.6] & [0.3, 0.7] & [0.7, 0.2] \\ [0.4, 0.8] & [0.6, 0.9] & [0.1, 0.5] \\ [0.4, 0.7] & [0.9, 0.2] & [0.4, 0.8] \end{array} \right] \end{array}$$

STEP:2

Construct that , $\aleph \rightarrow \mathscr{J}$, Diseases $\rightarrow$ Tests is given in the form of Cubic

Root Fuzzy set

$$\aleph_1 = \begin{array}{c} \wp1 \\ \wp2 \\ \wp3 \end{array} \begin{array}{ccc} \mathscr{J}_1 & \mathscr{J}_2 & \mathscr{J}_3 \\ \left[\begin{array}{ccc} [0.4, 0.5] & [0.7, 0.8] & [0.3, 0.2] \\ [0.2, 0.3] & [0.5, 0.2] & [0.9, 0.1] \\ [0.4, 0.6] & [0.4, 0.5] & [0.3, 0.5] \end{array} \right] \end{array}$$

$$\aleph_2 = \begin{array}{c} \wp1 \\ \wp2 \\ \wp3 \end{array} \begin{array}{ccc} \mathscr{J}_1 & \mathscr{J}_2 & \mathscr{J}_3 \\ \left[\begin{array}{ccc} [0.3, 0.9] & [0.2, 0.7] & [0.8, 0.3] \\ [0.4, 0.8] & [0.4, 0.3] & [0.4, 0.2] \\ [0.1, 0.6] & [0.7, 0.8] & [0.3, 0.8] \end{array} \right] \end{array}$$

$$\aleph_3 = \begin{array}{c} \wp1 \\ \wp2 \\ \wp3 \end{array} \begin{array}{ccc} \mathscr{J}_1 & \mathscr{J}_2 & \mathscr{J}_3 \\ \left[\begin{array}{ccc} [0.4, 0.6] & [0.5, 0.2] & [0.1, 0.9] \\ [0.7, 0.2] & [0.2, 0.4] & [0.4, 0.3] \\ [0.6, 0.4] & [0.1, 0.3] & [0.2, 0.4] \end{array} \right] \end{array}$$

Suppose that we take the weight w_k, (k = 1, 2, 3) in the form of Cubic Root fuzzy set for each test towards the diseases, weight $w_1 = 0.3$, $w_2 = 0.5$ and $w_3 = 0.6$

STEP:3

(1)To evaluate the Hamming Distance using the formula equation (1)

$d^H(R_1, R_2) = \sum 1/2 \, [\,|\, f_1 \, \delta_1^3 - f_2 \, \delta_2^3 \,| + |\, f_1 \sqrt{\gamma_1} - f_2 \sqrt{\gamma_2} \,|\,]$

(2) To evaluate the Weighted Hamming Distance using the formula equation (2)

$d^H(R_1, R_2) = \sum 1/2 \, w_1^3 \, [\,|\, f_1 \, \delta_1^3 - f_2 \, \delta_2^3 \,| + w_2^3 \,|\, f_1 \sqrt{\gamma_1} - f_2 \sqrt{\gamma_2} \,|\,]$

(3) To evaluate the Euclidean Hamming Distance using the formula equation (3)

$d^E(R_1, R_2) = \sum, \sqrt{\frac{1}{2}[|f_1 \delta_1^3 - f_2 \delta_2^3|^2 + |f_1 \sqrt{\gamma_1^3} - f_2 \sqrt{\gamma_2^3}|^2]}$

(4)) To evaluate the Weighted Euclidean Hamming Distance using the formula equation (4)

$d^E(R_1, R_2) = \sum, \sqrt{\frac{1}{2} w_1^3 [|f_1 \delta_1^3 - f_2 \delta_2^3|^2 + w_2^3 |f_1 \sqrt{\gamma_1^3} - f_2 \sqrt{\gamma_2^3}|^2]}$

STEP:4

The alternative can be calculate based on their smaller distance of table 1-4 are generated.

As the table 1-4 are generated the alternative are choose to ranked in smallest value or descending order. Along these results we findout the P1 is affected from Dengue as suggested by the decision making environment .Similarly P2 is affected from a Dengue and P3 is affected from COVID-19.

CONCULSION

In this study, a set operators such as union, intersection and distance measure (Hamming distance, Weighted Hamming distance, Euclidean distance, Weighted Euclidean distance) the classes of CR fuzzy set have been studied and discussed with proved their fundenmental results. A MCDM approach is take to handle the decision making using CR fuzzy set operators and easily to evaluated the relevance outputs. In future we will use to cubic root fuzzy set in different area to verify the presented technique.

REFERENCES

1. Atanasssov K.T, "Intuitionistic Fuzzy Sets".Fuzzy sets and Systems, 20(1986), pp.87-96.
2. Khan.F, Abdullah.s, Mahmood.T, Shakeel.M and Rahim.M,"Pythagorean Cubic Fuzzy Aggregation Information Based on Confidence Levels and its Application to Multi-Criteria Decision Making Process". Journal of Intelligent and Fuzzy systems, (2019 b), 36(6),pp.5669- 5683.

3. Muhammad.S, Muhammad Haris.S, Rimsha.S, Salvatore.S Umar.I and Ferdinando D.M, "A Theoretical Development of Cubic Pythagorean Fuzzy Soft Set with its Application in Multi- Attribute decision Making".Symmetry 2022, 14, 2639.

4. Balamurugan.K, Nagarajan.Dr.R, "Applications of Cubic Root Fuzzy Sets in Decision Making Approach". European Journal of Molecular and Clinical Medicine , ISSN 2515-8260, Vol 10, 2023.

5. Khan.F, Khan.M.S.A., Shahzad.M and Abdullah.S, "Pythagorean Cubic Fuzzy Aggregation Operators and their Application to Multi-Criteria Decision Making Process". Journal of Intelligent and Fuzzy systems, (2019 a), 36(1),pp.595-607.

6. Chinnadurai.V, Thayalan.S, Bobin.A, "Multi-Criteria Decision Making in Complex Fermatean Fuzzy Environment". J.Math.Comput. Sci. 11(2021), No.6, pp.7209-7227.

7. Paul Augustine Ejegwa, "Pythgorean Fuzzy set and its Application in Career Placements Based on Academic Performance Using Max-Min-Max Composition". Complex Intelligent systems (20195:pp.165-175.

8. Chinnadurai.V, Thayalan.S, Bobin.A, "Multi-Criteria Decision Making Process Using Complex Cubic Interval Valued Intuitionistic Fuzzy Set". Joural of Physics Conference Series 1850(2021), 012094.

9. Rodrigo barraza, Juanm Sepulveda and Ivan derpich, "Application of Fermatean Fuzzy Matric in Co-design of Urban Projects". Procedia Computer Science 199 (2022),pp.463- 470.

10. Anjan Mukherjee, Sadhan Sarkar and Somen Debnath, "Application of Intuitionistic Fuzzy Soft Set in Decision Making Based on real life problems",Communication in Mathematical Modeling and Application, CMMA 1. No.3,pp.16-21(2016).

11. Palanikumar.M, Arulmozhi.K, Aiyared Iampan, "Novel Possibility Pythagorean Cubic Fuzzy Soft Sets and their Application".InternationalJournal of Innovative Computing Information and Control, vol 19, No.2 (2023)

12. Zadeh L.A., "Fuzzy Sets ". Inf. Control, 8,pp.338-353.

13. Liu.D, Liu.Y and wang.L ,"Distance Measure for Fermatean Fuzzy linguistic Term Sets Based on Linguistic Scale Function:An Illustration of the TODIM and TOPSIS Methods". Intell syst., vol.wiley, No.1,DOI:10.1002/int.22162, pp.1-28,2019.

14. Yagar.R.R,, Abbasov.A.M, "Pythagorean Membership Grades, Complex Numbers and Decising Making". Int. Jouranl Intell., Syst., pp.436-452, 28(2013).

15. Salih Y.A., Inrajo H.Z., "Cubic Root fuzzy sets and their Applications". J.Math Computer Sci.,pp 171-181,28 (2023).

Table:1

Patients	Typhoid ($\aleph_1$)	COVID- 19 ($\aleph_2$)	Dengue ($\aleph_3$)
P_1	2.526	3.631	1.789
P_2	3.21	3.82	2.004
P_3	5.188	2.93	4.18

Table: 2

Patients	Typhoid ($\aleph_1$)	COVID- 19 ($\aleph_2$)	Dengue ($\aleph_3$)
P_1	0.3045	0.392	0.188
P_2	0.384	0.449	0.215
P_3	0.540	0.367	0.376

Table 3

Patients	Typhoid ($\aleph_1$)	COVID- 19 ($\aleph_2$)	Dengue ($\aleph_3$)
P_1	3.854	5.205	3.32
P_2	5.106	5.513	4.284
P_3	4.701	2.905	4.489

Table 4.

Patients	Typhoid ($\aleph_1$)	COVID- 19 ($\aleph_2$)	Dengue ($\aleph_3$)
P_1	0.461	0.604	0.413
P_2	0.563	0.678	0.539
P_3	0.3951	0.343	0.572

Table 4.

	(P_1)	(P_2)	(P_3)
Table 1	Dengue	Dengue	COVID-19
Table 2	Dengue	Dengue	COVID-19
Table 3	Dengue	Dengue	COVID-19
Table 4	Dengue	Dengue	COVID-19

RESEARCH ARTICLE

Determining Factors for Farmer Producers Organization Formation : a Special Reference to Tamil Nadu

Sasikanth R[1]* , S. Ravichandran[2], V. Banumathy[3] and D. Venkatakrishnan[4]

[1]ABM-Research Scholar, Department of Agricultural Economics, Faculty of Agriculture, Annamalai University, Annamalai Nagar, Chidambaram- 608002, Tamil Nadu, India
[2]Associate Professor, Department of Agricultural Economics, Faculty of Agriculture, Annamalai University, Annamalai Nagar, Chidambaram- 608002, Tamil Nadu, India
[3]Professor, Department of Agricultural Economics, Faculty of Agriculture, Annamalai University, Annamalai Nagar, Chidambaram- 608002, Tamil Nadu, India
[4]Associate Professor, Department of Soil Science and Agricultural Chemistry, Faculty of Agriculture, Annamalai University, Annamalai Nagar, Chidambaram- 608002, Tamil Nadu, India.

*Address for Correspondence
Sasikanth R
ABM-Research Scholar,
Department of Agricultural Economics,
Faculty of Agriculture, Annamalai University,
Annamalai Nagar, Chidambaram- 608002,
Tamil Nadu, India
E.Mail: abmsasikanth@gmail.com

ABSTRACT

About 85 per cent of farmers in India are small farmers who barely make a living. India's agricultural sector is hindered by things like high financial intermediation and a lack of access to credit and markets for agricultural goods. There are many legal groups, like farmer cooperatives, farmer clubs, farmer interest groups, etc., whose goal is to help farmers take advantage of economies of scale by grouping together. Farmer Producer Organizations (FPOs) are an example of a group of farmers who work together. The purpose of this study was to investigate, by means of linear regression analysis and the compound annual growth rate progress made on the establishment of FPOs throughout the time in Tamil Nadu. The results of the regression analysis suggest that the presence of regulated and farmer markets may have a positive effect on the promotion of FPOs and there is a positive trend in promoting FPOs in Tamil Nadu, which can help in improving the livelihoods of farmers and the agriculture sector.

Keywords: FPO, Formation, Promotion, Tamil Nadu, small and marginal farmers

Sasikanth *et al.,*

INTRODUCTION

India is the second largest country in terms of the number of small holdings and approximately 85 percent of the country's farmers are considered to be small and marginal farmers [1]. The high proportion of Indian farmers who depend on income from their farms, it is clear that India faces the greatest difficulty in ensuring that these tiny and marginal holdings become truly productive[2].Cooperatives can help small landholders thrive in a tough market while retaining their independence and control. The Government of India appointed Dr. Y.K.Alagh to head a Committee to outline cooperatives' business and marketing plans. The Producer Companies Act was enacted in 2002 by amending the Indian Companies Act to add a new section IXA. The modified Companies Act allows FPOs or production companies to register with the Registrar of Companies. The government's goal for such a programme was to create legislation that would allow cooperatives to incorporate as corporations and convert into companies while preserving their unique characteristics. The FPO model of farmer solidarity is gaining traction as a viable alternative to the more traditional cooperative structure [3].

The Producer Companies Act formalizes the guiding principles of cooperatives and introduces a more businesslike mindset to the administration of FPOs. As a rule, FPOs are established with the help of initial capital provided by the member farmers. The FPO is given a legal structure under the act that will allow farmers and producers to collectively own the business. A group of outside specialists will be employed to run the FPO on a day-to-day basis, and they will report to a Board of Directors that has been elected or selected by the FPO's General body for a predetermined term. Since the FPO's equity shareholders are the farmers or producers, this type of business structure is ideal for farmer ownership [4]. The government has acknowledged the value of FPOs by proposing in the union budget that 10,000 new FPOs will be created by 2027-2028. Department of Agriculture and Cooperation officials have developed a central sector programme to facilitate the establishment of 10,000 Farmer Producer Organizations around the country[5].As part of this effort, FPOs will be able to choose between registering under the state's Cooperative Societies Act or the Companies Act of 2013[3].There are around 5,000 FPOs (including FPCs) operating in the country at the present time[5].These FPOs were established in response to a variety of initiatives taken by the government. In the past eight to ten years, India's Small Farmers Agribusiness Consortium, National Bank for Agricultural Rural Development, State governments, and a number of other organisations have all collaborated to promote the FPO. There is a need for research on the factors determining the establishment of Farmer Producer Organizations (FPOs) to enhance the farmer livelihoods, increase market access, promote sustainable agriculture, and promote collaboration among farmers by identifying the factors that enable the successful formation of FPOs, research can provide guidance to policymakers and farmers on how to replicate these successful models in other regions.

Purpose of the research: To investigate the infrastructure elements that influence the growth and expansion of agricultural producer organizations, as well as to determine how far the government of Tamil Nadu and other organisations have come in their efforts to establish such organisations in the state of Tamil Nadu. The purpose of this investigation is twofold: to determine how far these efforts have progressed, and to investigate the infrastructure elements that influence growth and expansion.

DATA AND METHODOLOGY

The Compound Annual Growth Rate (CAGR) method was used byto foretell the development of FPO formation throughout time [6]. The exponential function of the below mentioned equation is used to estimate the compound annual growth rate [7].

$Y = ab^t$ ………………..…… (1)
By taking logarithm on both sides, it may be written as
Log y = log a + t × log b… (2)

$Y = A + B × t$

Where, $Y = \log y$; $A = \log a$; $B = \log b$

Y= Total number of farmer producer organizations in Tamil Nadu

t= time elements, where1,2 and n represent different years.

Compound growth rate = (Antilog of B- 1) × 100

$t = r/ SE (r)$

Where, r = Compound Growth Rate; SE= Standard Error

Linear regression was used to investigate the association between two or more explanatory variables and a response variable by fitting an equation [8]. In order to investigate the elements that play a role in the promotion of FPOs in Tamil Nadu, a linear regression model was utilised, and the following equation served as its basis:

$Y_t = \alpha + \beta_i X_i + u$ ……………..… (3)

Y_t= Dependent Variable; α = Intercept; β_i's = Parameters to be estimated; X_i's = Independent Variable; μ = Error term

RESULTS AND DISCUSSIONS

Status of Farmer Producer Organization in Tamil Nadu.

The table 2 indicates that the Tamil Nadu Small Farmers Agribusiness Consortium promoted the most FPOs, with a count of 368. This is followed by the National Bank for Agriculture and Rural Development, with a count of 207. The Small Farmers Agribusiness Consortium promoted 67 FPOs, while the National Cooperative Development Corporation and the National Agricultural Cooperative Marketing Federation promoted 23 and 26 FPOs, respectively. There were also 52 FPOs that were self-promoted, and the total number of FPOs promoted by all agencies was 743.

Trend in the formation of FPOs in Tamil Nadu

Figure 1 shows the number of FPOs (Farmer Producer Organizations) promoted in Tamil Nadu from 2004-05 to 2021-22. The data suggests that the number of FPOs promoted has increased significantly over time. The R-squared value of 0.865 indicates that the data points are highly correlated, and the model fits the data well. The F-value of 102.15 with a significance level of 0.000 indicates that the model is statistically significant. The compound annual growth rate of 35% suggests that the number of FPOs promoted has grown at an average rate of 35% annually during this period. This growth rate indicates the increasing importance of FPOs in promoting agricultural development in India. Overall, the data indicates a positive trend in promoting FPOs in Tamil Nadu, which can help in improving the livelihoods of farmers and the agriculture sector.

Factors influencing the formation of FPO

Table 3 presents the findings of a multiple linear regression analysis of the factors influencing the establishment of FPOs in Tamil Nadu. The coefficients of determination (R-squared) value are 0.56, indicating that the independent variables explain 56% of the variability in the number of FPOs promoted. The adjusted R square of 0.475 suggests that the model is moderately good at predicting the outcome variable, although it may be improved by adding or removing some variables. The ANOVA table shows that the regression model is statistically significant with an F-value of 6.586 and a p-value of 0.000, indicating that at least one of the independent variables significantly explains the variation in the dependent variable. The regression function that links the independent factors and the dependent variable expressed as, $Y = 14.649 + 1.236 X_1 + 0.001 X_2 + 1.143 X_3 - 0.052 X_4 - 0.054 X_5 - 0.210 X_6 + \mu$. Among the six independent variables, regulated market (X_1) and farmer market (X_3) have statistically significant coefficients with the number of FPOs promoted ($p < 0.05$), suggesting that the promotion of FPOs is positively associated with the presence of regulated and farmer markets. When all other factors are held constant, a one-unit increase in X1 and

X3 results in a 1.236 and 1.143 unit increase in the dependent variable, respectively. The beta coefficients for the other independent variables, namely, area covered under Micro Irrigation (X2), Crop Intensity (X4), Irrigation Intensity (X5), and Rural Godowns (X6) are 0.001, -0.052, -0.054, and -0.210, respectively. This indicates that the effect of these variables on the dependent variable is very small. The t-values and significance levels suggest that none of these independent variables have a statistically significant effect on the dependent variable. Regulated markets provide a platform for farmers to sell their produce at a fair price by regulating the buying and selling of agricultural commodities. This may result in increased profitability for farmers and encourage them to organise themselves into FPOs so that they can sell their product collectively. Farmers can benefit from regulated marketplaces because they have access to market intelligence, which assists them in making educated choices regarding what crops to cultivate and when to sell their produce. Farmers markets, on the other hand, enable farmers to sell their produce directly to customers, eliminating the need for any middlemen and thereby increasing the proportion of profits that are retained by the farmers themselves. Farmers markets can also contribute to the promotion of sustainable agriculture by encouraging the use of environmentally responsible farming practises. Farmers Markets and Regulated Markets Both Have the Potential to Generate Demand for High-Quality, Locally Produced Agricultural Goods, which in Turn May Incentivize Farmers to Increase the Quality of Their Produce and Form FPOs to Market and Sell Their Produce Collectively. In turn, FPOs have the ability to provide better access to inputs, technology, and credit for their members, which can help to improve the overall productivity and profitability of the agricultural sector. As a result, the existence of both controlled and unregulated farmer's markets has the potential to have a beneficial impact on the promotion of FPOs by fostering an atmosphere that is conducive to the expansion and improvement of these organisations.

CONCLUSION

Tamil Nadu Small Farmers Agribusiness Consortium has been responsible for the promotion of the maximum number of FPOs in Tamil Nadu. Farmer Producer Organizationshave the potential to play a significant part in the process of increasing the income of small farmers by boosting their negotiating power, facilitating access to improved inputs and technologies, and producing value additions through aggregation and processing of their produce. The results of a regression analysis indicate that there may be a positive impact that the presence of regulated and farmer markets have on the promotion of FPOs. This is due to the fact that regulated markets provide a platform for farmers to sell their produce at a reasonable price, and farmer markets allow for direct interaction between farmers and customers, both of which can contribute to the promotion of sustainable agriculture and the creation of greater value for farmers. It is gratifying to see that Tamil Nadu is leading the way in this respect as it pertains to the promotion of FPOs, which can be a key strategy to enhance the income of small farmers in India as well as their ability to maintain their livelihoods. It is critical that other states take notice of this encouraging trend and work towards promoting FPOs in order to bolster the agriculture industry and improve the quality of life for farmers.

ACKNOWLEDGEMENT

REFERENCES

1. MoAFW. (2021). Agricultural Statistics at a Glance. Ministry of Agriculture & Farmers Welfare. https://eands.dacnet.nic.in/PDF/Agricultural%20Statistics%20at%20a%20Glance%20-%202021%20(English%20version).pdf
2. National Statistical Office (2019). Situation Assessment of Agricultural Households and Land and Livestock Holdings of Households in Rural India, 2019. https://www.pib.gov.in/PressReleasePage.aspx?PRID=1753856.
3. SFAC (2019). Strategy Paper for promotion of 10,000 Farmer Producer Organisations (FPOs).http://sfacindia.com/UploadFile/Statistics/Strategy-Paper-on-Promotion-of-10,000-FPOs.pdf
4. SFAC (2013). Policy & Process Guidelines for Farmer Producer Organisations. https://www.mofpi.gov.in/sites/default/files/fpo_policy_process_guidelines_1_april_2013.pdf.
5. *Press Information Bureau, MoAFW*. (2021, December 13). https://pib.gov.in/FactsheetDetails.aspx?Id=148588
6. Barani Kumar, N., Kandasamy, M., SIVAKUMAR, S. D., & SENTHILKUMAR, R. (2017). Status of farmer producer companies in India. AGRICULTURE UPDATE, 12, 888–892. https://doi.org/10.15740/HAS/AU/12.TECHSEAR(3)2017/888-892.
7. Jacob, A., & Job, E. (2015). PEPPER PRODUCTION AND EXPORT FROM INDIA: GROWTH AND INSTABILITY ANALYSIS. *International Journal of Current Research*, *7*(09), 20388–20391.
8. Eticha, A. B. (2020). Multiple linear regressions on determinants of ginger production in yeki district, Sheka Zone, South West Ethiopia. International Journal of Agricultural Science and Food Technology, 6(1), 151–156.
9. Statistics on Agriculture, 2021. http://www.tnagriculture.in/dashboard/book
10. SFAC. List of FPO State-wise. Retrieved January 9, 2023, from http://sfacindia.com/List-of-FPO-Statewise.aspx.
11. SFAC. State wise details of Registered FPOs under Central Sector Scheme for Formation and Promotion of 10,000 FPOs as on 30-11-2022. Retrieved January 9, 2023, from http://sfacindia.com/UploadFile/Statistics/Statewise%20and%20IA's%20wise%20details%20of%20Registered%20FPOs%20as%20on%2030-11-2022.pdf
12. NABARD. List of FPOs promoted by NABARD. Retrieved January 9, 2023, from https://nabfpo.in/images/staticFPO.html#Tamil_Nadu7
13. Statistical Handbook of Tamil Nadu 2020-21. https://www.tn.gov.in/deptst/

Table 8: Variables considered for the study

Variable	Specification of the Variable	Unit
Dependent Variable		
Farmer Producer Organization **(Yt)**	District-wise FPOs promoted	Absolute Number [9,10, 11, 12].
Independent Variable		
Regulated market **(X₁)**	Regulated markets allow farmers and dealers to sell agricultural products together without intermediaries.	Absolute Number [9]
Area covered under Micro Irrigation **(X₂)**	Area covered by the PMKSY Micro Irrigation Scheme in 2020-21	Area in Hectare [9]
Farmers market **(X₃)**	Farmers' markets eliminate the middlemen between farmers and consumers.	Absolute Number [9]
Cropping intensity **(X₄)**	$\frac{Gross\ Cropped\ Area}{Net\ Area\ Sown} \times 100$	Percentage [13]
Irrigation Intensity **(X₅)**	$\frac{Net\ Area\ Sown}{Net\ Area\ Irrigated} \times 100$	Percentage [13]

Rural Godowns **(X$_6$)**	Rural Godowns will enable farmers to enhance their holding capacity in order to sell their produce at remunerative prices and avoid distress sales	Absolute Number **[13]**

Table 9:Number of FPOs promoted in Tamil Nadu

Implementing agency	FPOs promoted
Tamil Nadu Small Farmers Agribusiness Consortium	368
Small Farmers Agribusiness Consortium	67
National Bank for Agriculture and RuralDevelopment	207
National Cooperative Development Corporation	23
National Agricultural Cooperative Marketing Federation	26
Self-promoted	52
Total	743

Source: Compiled from web source of Implementing agency [9,10, 11, 12].

Table 10: Regression analysis

Independent Variable	Unstandardized Coefficients		T	Sig.	
	Beta	Std. Error			
Constant	14.649	6.739	2.17	0.04	
Regulated market (X$_1$)	1.236	0.528	2.341	0.03*	
Area covered under Micro Irrigation (X$_2$)	0.001	0.000	1.413	0.17	
Farmers market (X$_3$)	1.143	0.499	2.288	0.03*	
Cropping intensity (X$_4$)	-0.052	0.048	-1.085	0.29	
Irrigation Intensity (X$_5$)	-0.054	0.057	-0.959	0.34	
Rural Godowns (X$_6$)	-0.210	0.176	-1.196	0.24	
R	0.749	**R Square**	0.560	**Adjusted R Square**	0.475
ANOVA					
Model	**Sum of Squares**		**Df**	**Mean Square**	**F**	**Sig.**
Regression	1854.46		6	309.076		
Residual	1454.8		31	46.929	6.586	0.000*
Total	3309.26		37			

*Significance at 5 per cent
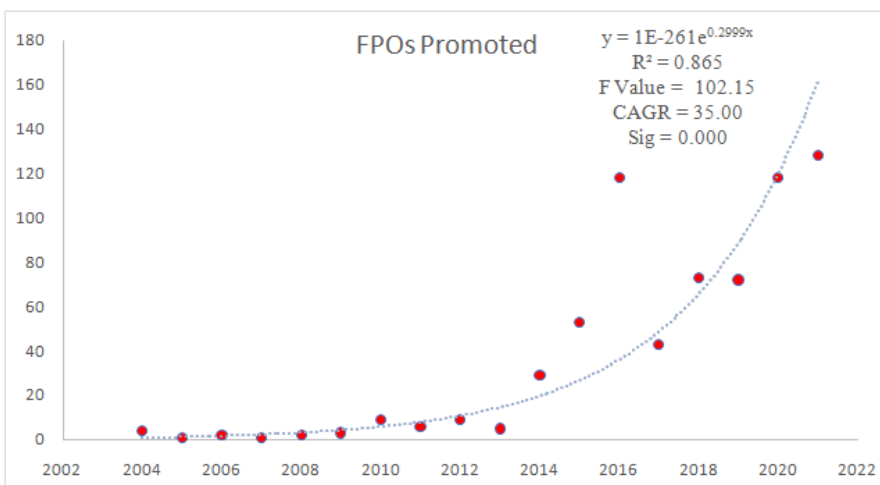
Figure 11: Trend in the formation of FPOs in Tamil Nadu

RESEARCH ARTICLE

Green Synthesis of CuO Nanostructures from *Murraya koenigii* Leaf Extract and Photodegradation Efficiency on Methyl Orange Dye

M.Muththamizh[1], N.Punitha[2] , D. Geetha[3]* and P.S. Ramesh[3]

[1]Research Scholar, Department of Physics, Annamalai University, Annamalai Nagar-608 002, Chidambaram, Tamil Nadu, India.
[2]Associate Professor, Department of Physics, St.Joseph's college of Engineering, Chennai-600119, Tamil Nadu, India
[3]Associate Professor, Department of Physics, Annamalai University, Annamalai Nagar-608 002, Chidambaram, Tamil Nadu, India

*Address for Correspondence
D. Geetha
Associate Professor,
Department of Physics,
Annamalai University,
Annamalai Nagar-608 002,
Chidambaram, Tamil Nadu, India
E.Mail: geeramphyau@gmail.com

ABSTRACT

Copper oxide (CuO) nanoparticles were produced via eco-friendly and non-toxic green synthesis of *Murraya koeniggi* leaf extract. The contamination of water by the organic dye poses a significant risk to humans and aquatic life. X-Ray Diffractometer, UV–Visible spectroscopy, FTIR Spectra, Photo Luminescence, and morphological investigations were used to confirm the physico-chemical characteristics of green-synthesized CuO. X-ray diffraction reveals that the phytochemicals in the leaf extracts interact with copper precursors to generate Cu^{2+} ions and crystallize CuO. UV-Vis spectroscopy confirmed CuO NPs with a characteristic peak at 264nm. According to FE-SEM images, CuO NPs had spherical morphologies. Examining the removal of Methyl orange dye by synthesized CuO nanoparticles act nanophotocatalysts. The products photocatalytic degradation efficiency is 89%.

Keywords: Copper oxide nanoparticles, Murraya koeniggi, green synthesis, dye degradation.

INTRODUCTION

The global concern is air pollution, water pollution, and soil contamination. This represents a significant threat to the health of all living things, including humans [1]. The discharge of synthetic dyes into aquatic environments is hazardous to human health, produces effluents, and reduces biodegradation [2, 3].The photo degradation of dyes

with semiconductor materials is virtually the most effective method for treating wastewater [4]. In addition, the photocatalysis process is considered more effective due to the greater availability of solar energy and the formation of non-toxic mineralized materials. For the sterilization of microorganisms and the proper treatment of hazardous pollutant, the active visible photocatalyst structure is the most prevalent [5-6]. Due to their photocatalytic activity, transition metals are regarded as advantageous catalysts for the environmentally favorable management of wastewater. This type of photodegradation occurs when the hydroxyl group [OH] and organic contaminants undergo an oxidation reaction. OH, with a 2.8v oxidation potential at room temperature can completely oxidize organic colors [7-8]. They transmit pollutants and generate carcinogens, making secondary pollutants associated with aromatic amines that cause significant health issues. Moreover, these techniques require higher concentrations of photocatalysts and generate a greater amount of sludge [9]. To surmount this obstacle, the AOP (Advanced Oxidation process) has been investigated for its potential to eradicate all essential pollutants. AOPs have a greater potential in the photocatalytic reaction to utilize the entire solar spectrum (e.g., higher solubility in terms of band gap) [10] than do other organic photocatalysts. In modern research, photocatalytic degradation is utilized to remove synthetic pigments from metal semiconductors [11-16]. CuO is less expensive than silver and gold in terms of its microbial potential [17-20]. CuO nanoparticles are the simplest member of the copper salt family, and they possess a wide range of useful characteristics and physical properties, including the electron correlation effect, higher temperature superconductivity, and spin dynamics [21]. Their unique properties and potential applications have received considerable attention, which has increased the viscosity of energy fluids and thus their thermal conductivity [22]. CuO nanoparticles have been utilized in the production and design of batteries, solar cells, gas sensors, field emitters, etc. [23-25] in the industrial sector. CuO nanoparticles are utilized as heterogeneous catalysts in biomedical research, drug delivery, and imaging [26]. To synthesize copper oxide nanoparticles [27], hazardous and expensive compounds, higher temperature, pressure, and energy are needed. Biological materials used in green synthesis eradicate the need for a complicated procedure, allowing for large-scale production. Literature review reveals that *Murraya koenigii* contains various metal nanoparticles [28]. Curry tree (Murraya koenigii) is a subtropical tree belonging to the Rutaceae family and is regarded as the most important medicinal plant containing secondary metabolites and other medicinal components [29]. It possesses antimicrobial, antifungal, anti-inflammatory, and hypoglycemic properties [30-31]. In this study, the synthesized final product (CuO) is characterized by XRD, UV-Vis, FTIR, PL, and SEM. In addition, the photodegradation response of synthesized nano copper oxide was evaluated using methyl orange dye degradation.

MATERIALS AND METHODS

Materials
Copper sulphate [$CuSO_4$] was bought at sigma Aldrich. *Murraya koeniggi* leaves have been collected from the regional garden of the Annamalai university in the agriculture department Chidambaram.

Preparation of plant extract
Curry leaves have been separated from the leaf clusters physically. The leaves were rinsed three times with deionized water to remove foreign particles. Three hours were spent boiling 30 grams of *Murraya koeniggi* leaves in 100 milliliters of distilled water. After boiling, the leaf extract was cooled and filtered extract was collected in a clean, aluminum-covered conical flask.

Preparation of Copper oxide nanoparticles
2 ml of leaf extract was added to 10 ml of distilled water, followed by 2.4 grams of CuSO4 solution and repetitive stirring. The color changes from pale greenish blue and dark green to brown in three hours. The obtained material was calcinated for one hour at 100 degrees Celsius and ground to nanoparticle size. The gray-colored CuO nanoparticles that were captured were then stored for future research.

Muththamizh *et al.,*

Characterization

The prepared CuO nanoparticles were characterized via XRD, SEM/EDS, FTIR, and UV-Vis spectroscopy. To examine the phase and crystalline structure, an X-ray diffractometer (X'PERT-PRO; CuK (=1.5418)) was acquired. Using scanning electron microscopy, morphological features were determined. The optical absorption and emission spectra of the prepared CuO NPs were measured using UV-visible spectra from 200 to 800 nm. *Murraya koenigii* leaf extract was subjected to Fourier transform infrared spectroscopy analysis. Within the 400-4000cm-1 range, FT-IR spectra have been discovered (32). The EDAX spectrum is reported by the energy-dispersive X-ray spectrometer from Bruker.

RESULT AND DISCUSSION

Structural Analysis (XRD)

The crystalline phase of CuO was studied by X-ray diffractometry (XRD) (Fig. 1). The characteristic diffraction peaks of CuO at 2θ values of 18.33, 20.98, 24.84, 25.76, 28.18, 31.33, 34.02, 36.87, 38.90, 42.96, 44.49, 46.07, 54.63, 58.07, 64.87, 67.91, 75.70 is generated by the diffraction planes in (200), (113), (220), (030), (301), (230), (016), (400), (240), (050), (008), (236), (129), (309), (527), (616), (282) respectively are revealed by the XRD pattern. Peaks with (JCPDS card no. 77-1898) values of (a=7Å, b=10Å, c=16Å) may be attributed to the orthorhombic structure of CuO nanoparticles. CuO samples are indicated by high-intensity diffraction peaks at 2 values of 24.84 corresponding to (220) planes. Using the Scherrer equation, the crystalline dimension of a CuO sample was determined [33].

$D = K\lambda / \beta_{hkl} \, Cos\theta$

Here,

        D is the mean crystal size

        K is shape factor

        λ is the wavelength of X-ray and β is the FWHM of diffraction planes.

Absorption studies (UV- Vis Spectrometry)

UV- Visible spectroscopy is a molecular spectroscopy that is based on Bouguer Lambert Beer law principle for its operation. This technique measures the Plasmon resonance and total oscillation of conduction band of electrons in conjunction with electromagnetic waves. It is also used to measure the absorption of fluids and other substances. In UV-Visible spectroscopy analysis, a light beam divides in half, with one half analyzing the compound or solution in the transparent cell and the other half analyzing the reference material. The reason for the analysis is that the solution absorbs light at specific wavelengths; this wavelength is known as the surface plasmon resonance (SPR) of the material being analyzed [34]. Figure 2 displays the UV-Visible spectra of the prepared specimen from 200 to 800 nm. However, around 264nm with a broad spectrum range of approximately 264-800nm, CuO formation was observed [35].

Morphological analysis (SEM)

SEM analysis reveals the spherical form of microparticles (Fig. 3). With average diameter around 1-1.5μm, the uniform microspheres revealed from accumulation in the nanoparticle because of plant extract with a particle size of 70-85nm. Constant heating at the higher temperature of homogeneous nucleation contributes to the development of a uniform minimum sintered sphere. Nanomaterials are unquestionably referred to as isotropic (36) due to the consistency of their physical properties. Table 1 displays the constituent elements. In addition, EDX spectra confirmed the presence of CuO in the prepared specimen. (Fig.4). With *Murraya koenigii* leaf extract, the EDX model confirmed the effective formation of CuO nanoparticles. Peak positions matched those of copper oxide, and EDX peaks indicated that the CuO nanoparticles synthesized had a crystalline (Orthorhombic) structure.

Spectral Analysis (FTIR)

The FTIR analysis exhibits a functional bond in the CuO nanoparticles was shown in (Fig. 5). The strong bands absorbed at 3402cm^{-1} associated with the stretching vibrations of the hydroxyl group (O-H). The adsorption at 1631cm^{-1} corresponds to the alkene group stretching (C=C). The absorption band at 1136cm^{-1} is indicative of the bending vibrations of (C=O) into the carbonyl group. The absorption of (C-H) at 792cm^{-1} represents bending oscillations. The absorbance band exhibited at 593cm^{-1} corresponds to CuO.

Emission Studies (Photoluminescence)

Fig. 6 shows Photoluminescence (PL) spectra of CuO nanoparticles. At room temperature, the PL spectrum is obtained at 465 nm. Because the new excitation wavelength excites discrete states emitted at different energies, the sharp emission peak varies from 433 nm to 465 nm. The radioactive recombination of a photo generating hole with oxygen vacancy-filling electron cause visible luminescence [37-38].

Photocatalytic activity on methyl orange dye

To investigate the mobility of organic pollutant removal from waste water, photocatalytic activity of dye degradation was utilized. Under specific conditions, the degradation efficiency of CuO nanoparticles on methyl orange dye under natural sunlight irradiation was measured. UV-Visible spectrometer with the wavelength range (200-600 nm) was used to analyze the effect of CuO NP on the concentration of methyl orange. The absorption peak of MO occurs at 474 nm. A MO of 10-3 is utilized for the dye degradation test. To examine the degradation of methyl orange in the presence and absence of CuO nanoparticles, 10-3 M of methyl orange dye was added to 100 ml of distilled water. After the dye has dissolved, 0.1g of CuO NPs catalyst is applied to the dissolved dye concentration.

Efficiency (η) = [(Co-Ct) / Co] ×100
where,
η - The degradation efficiency
      Co- Initial concentration
      Ct – Concentration at time (t)

Samples were taken to estimate the decrease in absorbance of MO after adding CuO NPs; the first sample was taken just after the addition of CuO NPs. The samples was placed under sunlight, there was a sudden lowering in the concentration of dye after the involving of CuO NP stabilized through *Murraya koenigii* leaf extract, and shows 89 % of dye degradation was observed at 145 minutes.

The obtained results shows that the catalytic fine effect of the CuO sample NPs prepared with *Murraya koenigii* leaf extract illustrated good catalytic activity. The presence of catalyst, the reaction is speed up by the absorption of photons in the presence of catalyst with the energy that should be equal or greater than the band gap energy of the CuO catalyst. Due to the photon absorption, there is a transfer of electron from the valence band to the conduction band of CuO catalyst, thus creating a hole in the valence band. These activated electrons which are activated is react with an oxidant of dye to create a reduced product.

CONCLUSION

The present study investigates the orthorhombic structure of CuO nanoparticles using *Murraya koenigii* leaf extract in a green synthesis. X-ray diffraction analysis verifies the appearance and typical crystalline size of CuO nanoparticles. The spherical shape of *Murraya koenigii* is revealed via SEM analysis. The FTIR results can be used to determine the surface's chemical composition, purity, and presence of biomolecules. The photocatalytic methyl orange dye concentration is used to investigate the 89% CuO NPs degradation.

Conflict of interest

There is no conflict of interest.

REFERENCES

1. Sreelekshmi PB, Pillai RR, Meera AP (2022). Controlled synthesis of noval graphene oxide nanoparticles for the photodegradation of organic dyes. Top catal 65:5-6
2. Martinez-Lopez S, Lucas-A C, Serrano-Martinez, Mercader-Ros Mari Terasa N, Cuartero P, Navarro S, Perez, Gabaldon JoseAntonio, Gomez-Lopez VM (2019). Pulsed light for a cleaner dyeing industry: Azo dye degradation by an advanced oxidation process driven by pulsed light, J. Cleaner Prod.
3. Angel Ezhilarasi A, Judith Vijaya J, kaviyarasu K, John Kennedy L, Ramalingam RJ, Al-Lohedan HA (2018). green synthesis of Nio nanoparticles using Aegle marmelos leaf extract for the evaluation of in-vitro cytotoxicity, antibacterial and Photocatalytic properties. J Photochem Phototobioal B. 180, 39-50
4. Li Z, Chen X, wang M, Zhang X, Liao L, Fang T, Li B (2021). photocatalytic degradation of Congo red by using the Cu_2O/α-Fe_2O_3 composite catalyst. Desalin Water Treat 215:222-231
5. Priya R, Stanly S, Anuradha R, Sagadevan S and Muthukrishnan L (2019).A waste to worth approach in preparing Ferric vanadate Nanoparticles using peel extract for photocatalytic dye degradation induced by UV light', Optik-International Journal for Light and Electron Optics, 194 163085
6. Hariharan D, Christy A J, Pitchaiya S, Thangamuniyandi P, Devan U and Nehru LC (2019). Enhanced photocatalytic activity of Cuprous Oxide nanoparticles for malachite green degradation under the visible light radiation, J. Mater. Electron. 30 12812-9
7. Fang X, Bando Y, Gautam UK, Ye C, Golberg D (2008).Inorganic semiconductor nanostructures and their field-emission applications. J Mater chem 18:509-522
8. Vinesh V,shaheer ARM, Neppolian B (2019). Reduced graphene oxide [RGO] Supported electron deficient B-doped Tio2 (AU/B-Tio2/Rgo) nanocomposite: an efficient visible light sonophotocatalyst for the degradation of tetracycline[Tc]. Ultrason sonochem 50:302-310
9. Bahrami M, Nezamzadeh-Ejhieh A (2015). Effect of the supported ZnO on clinoptilolite nano-particles in the photodecolorization of semi-real sample bromothymol blue aqueous solution. Mater. Sci. Semicond. Process.
10. Ajoudanian N, Nezamzadeh-Ejhieh A (2015). Enhanced photocatalytic activity of nickel oxide supported on clinoptilolite nanoparticles for the photodegradation of aqueous cephalexin. Mater. Sci. Semicond. Process.
11. Kumar SG, Rao KSRK (2017). Comparison of modification strategies towards enhanced charge carrier separation and photocatalytic degradation activity of metal oxide semiconductors (TiO_2, WO_3 and ZnO), APPL. Surf. Sci.391 124-148
12. Ngope NM, Mbita Z, Mathipa M, Mketo NB, Ntsenwana NC, Hintsho-Mbita (2018). Biogenic synthesis of ZnO nanoparticles using Monsonia burkeana for use in Photocatalytic, antibacterial and anticancer applications, Ceram. Int.
13. Maria Magdalan CK, Kaviyarasu A, Raja MV, Arularasu Genene T, Abdulgalim,Isaev B, Naif Abdullah Al-Dhabi, Mariadhas Valan Arasu B, Jeyaraj J, Kennedy M, Maaza (2018). Photocatalytic decomposition effect of erbium doped cerium oxide nanostructures driven by visible light irradiation: Investigation of cytotoxicity, antibacterial growth inhibition using catalyst, J Photochem Photobiol.
14. Kim SH, Umar A, Kumar R, Ibrahim AA, Kumar G (2015). Facile synthesis and photocatalytic activity of cocoon-shaped CuO nanostructures, Mater Lett. 156,138-141.
15. Saif Hasan S, Singh S, Parikh RY, Dharne MS, Patole MS, Prasad BL, Shouche YS (2008). Bacterial Synthesis of Copper/Copper Oxide Nanoparticles, J. Nanosci. Nanotechnol. 8,3191-3196

16. Cuevas R, Duran N, Diez MC, Tortella GR, and Rubilar O (2015). Extracellular Biosynthesis of Copper and Copper Oxide Nanoparticle by Stereum hirsutum, a Native White-Rot Fungus from Cilean Forests. J. Nanomat, 789089

17. Bhattacharya P, Swarnakar S, Ghosh S, Majumdar S, Banerjee S (2018). Disinfection of   drinking water via algea mediated green synthesized copper oxide nanoparticles and its toxicity   evaluation, J Environ Chem Eng. 102867.

18. Khani R, Roostaei B, Bagherzade G, Moudi M (2018). Green synthesis of copper nanoparticles by fruit extract of ziziphus spinachristi (L.) Willd, Application for adsorption of triphenylmethane dye and antibacterial assay, J. Mol. Liq. 255, 541-549

19. Chen JS, Mao Z, Xu Z, Ding W (2019). Various antibacterial mechanisms of biosynthesized copper oxide nanoparticles against soilborne Ralstonia solanacearum, RSC Adv. 9, 3788

20. Sankar R, Manikandan P, Malarvizhi V, Fathima T, Shivashagari KS, Ravikumar V (2014). Green synthesis of colloidal copper oxide nanoparticles using Carica papaya and its application in photocatalytic dye degradation. Spectrochim Acta Mol Biomol Spectrosc 121: 746-750

21. Yallappa S, Manjanna J, Sindhe MA, Satyanarayan ND, Pramod SN, Nagaraja K (2013). Microwave assisted rapid synthesis and biological evaluation of stable copper nanoparticles using T. arjuna bark extract. Spectrochim Acta Mol Biomol Spectrosc 110: 108-115

22. Stoimenov PK, Rosaiyn L, Klinger, George LM, Kenneth JK (2002). Metal oxide nanoparticles as bactericidal agents. Langmuir, 18(17): 6679-6686

23. Das SK, Khan MMR, Guhab AK, Naskar N (2013). Bioinspired fabrication of silver nanoparticles on nanostructured silica: characterization and application as a highly efficient hydrogenation catalyst. Green Chem, 15: 2548-2557

24. Iravani S (2011). Green synthesis of metal nanoparticles using plants. Green Chem, 13 (10): 2638-2650

25. Ren G, Hu D, Cheng EW, Vargas-Reus MA, Reip P, Allaker RP (2009). Characterization of copper oxide nano particles for antimicrobial applications. Int J Antimicrob Agents, 33(6): 587-590

26. Murugan K, Senthillkumar B, Senbagam D, Al-Sohaibani S (2014). Biosynthesis of silver nanoparticles using Acacia leucophloea extract and their antibacterial activity, Int. J.Nano. Medi. 9, 2431-2438

27. Pantawane PK, Mehere BA, Chahande RK, Potbhare AK (2020). Phytoreduced copper oxide nanoparticles by using *Murraya koenigii* leaf extract and its antibacterial activity,

28. Amutha R, Sudha A (2019). *Murraya koenigii* mediated silver nanoparticle synthesis and its activity against enteric pathogens, Int. J. Pharma, Sci. Res. 10, 1906-1911

29. Yeap SK, Abu N, Mohamad NE, et al. (2015). Chemopreventive and immunomodulatory effects of *Murraya koenigii* aqueous extract on 4T1 breast cancer cell-challenged mice. BMC Complement Altern Med 15, 306.

30. Nalli, Yedukondalu; Khajuria, Vidushi; Gupta, Shilpa; Arora, Palak; Riyaz-Ul-Hassan, Syed; Ahmed, Zabeer; Ali, Asif (2016). Four new carbazole alkaloids from *Murraya koenigii* that display anti-inflammatory and anti-microbial activities, Org. Biomol. Chem., 10.1039.C6OB00267F

31. Al-Ani IM, Santosa RI, Yankuzo MH, Saxena AK, Alazzawi KS (2017). The Antidiabetic Activity of Curry Leaves "Murraya Koenigii" on the Glucose Levels, Kidneys, and Islets of Langerhans of Rats with Streptozotocin Induced Diabetes. Makara J Health Res; 21

32. Reddy, Rayapa K (2017). Green synthesis, Morphological and Optical studies of CuO nanoparticles.Journal of Molecular Structure, S0022286017311821–

33. Iljinas, Aleksandras, and Liutauras Marcinauskas (2015). Formation of bismuth oxide nanostructures by reactive plasma assisted thermal evaporation, Thin Solid Films 594, 192-196

34. Caroling, G., Priyadharshini, M. N., Vinodhini, E., Ranjitham, A. M., & Shanthi, P. (2015). Biosynthesis of copper nanoparticles using aqueous guava extract-characterisation and study of antibacterial effects. International Journal of Pharmacy and Biological Science, 5(2), 25-43.

35. Zhang, Juan, et al., (2016).   Synthesis of δ-Bi2O3 microflowers and nanosheets using CH3COO (BiO) self-sacrifice precursor. Materials Letters 162, 218-221

36. Bagade, Reena, et al. (2019). Fabrication of microflower-shaped mesoporous Fe (II) chelate polymer for photocatalytic performance under visible light. Materials Today: Proceedings 15, 566-574

Muththamizh *et al.,*

37. Vanheusden K, et al (1997).   Mechanisms behind green photoluminescence in ZnO phosphor powders. Journal of Applied Physics 79.10: 7983-7990
38. Gunalan S, Sivaraj R, & Venckatesh R (2012).   Aloe barbadensis Miller mediated greensynthesis of mono-disperse copper oxide nanoparticles: optical properties. Spectrochimica Acta Part A: Molecular and Biomolecular Spectroscopy, 97, 1140-1144

Table .1. Calculation of XRD analysis of of CuO nanostructures from *Murraya koenigii* (curry   leaves)

Diffraction angle 2θ degree	FWHM 2θ degree	d-spacing	Crystalline size (nm)	Dislocation density	Micro strain value
18.0026	0.1476	4.92747	54.4942	0.000337	4.065626
18.3376	0.1476	4.83821	54.51968	0.000336	3.990106
20.9811	0.1968	4.23421	41.05353	0.000593	4.63741
24.8402	0.1476	3.58445	55.11291	0.000329	2.924309
25.7624	0.1476	3.45819	55.21255	0.000328	2.816213
26.296	0.2952	3.38922	27.63601	0.001309	5.514148
28.1817	0.246	3.16658	33.2957	0.000902	4.276185
31.3372	1.1808	2.85455	6.987545	0.020481	18.36821
34.0282	0.1968	2.63472	42.21495	0.000561	2.806218
36.0158	0.2952	2.49375	28.29774	0.001249	3.96236
36.8718	0.246	2.43779	34.0409	0.000863	3.219954
38.9035	0.5904	2.31504	14.27029	0.004911	7.294214
39.8869	0.5904	2.2602	14.3142	0.004881	7.099588
42.9686	0.1476	2.10497	57.84208	0.000299	1.636271
44.4981	0.3936	2.0361	21.80728	0.002103	4.198093
46.0785	0.246	1.96988	35.09298	0.000812	2.52391
51.2891	0.246	1.78133	35.82251	0.000779	2.235849
54.527	0.1968	1.68296	45.4122	0.000485	1.666308
58.0787	0.8856	1.58822	10.26038	0.009499	6.95985
64.8715	0.3936	1.43737	23.91448	0.001749	2.702467
67.9151	0.3936	1.38018	24.33374	0.001689	2.55023
75.7065	1.5744	1.25633	6.390591	0.024486	8.83928
AVERAGE			**32.83302**	**0.00359**	**4.740309**

Table.2. EDAX value of CuO nanostructures from *Murraya koenigii* (curry leaves)

ELEMENT	WEIGHT %	ATOMIC%
OK	56.12	83.55
CuK	43.88	16.45
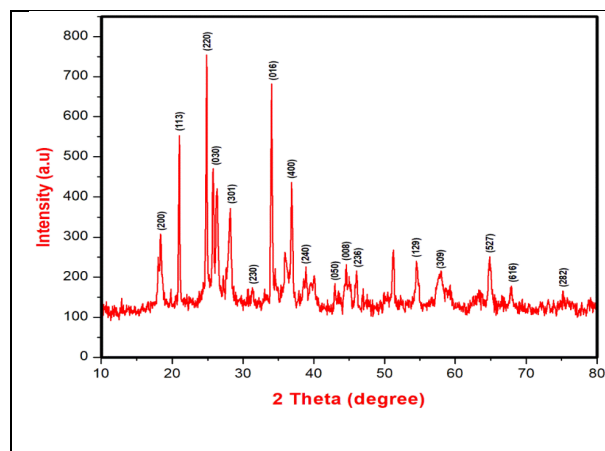
Figure 1. XRD Spectrum of CuO nanostructures from *Murraya koenigii* **(curry leaves)**
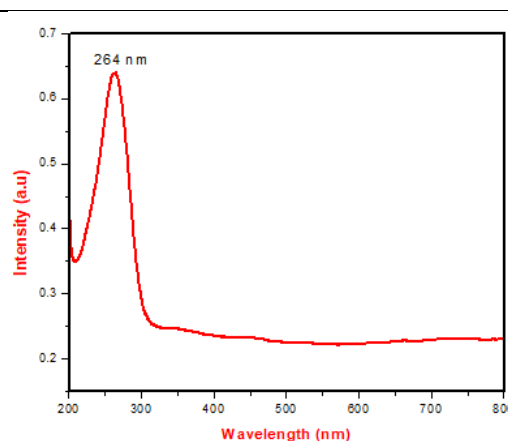
Figure 2.   UV- Vis absorption spectrum of CuO nanostructures from *Murraya koenigii* **(curry leaves)**
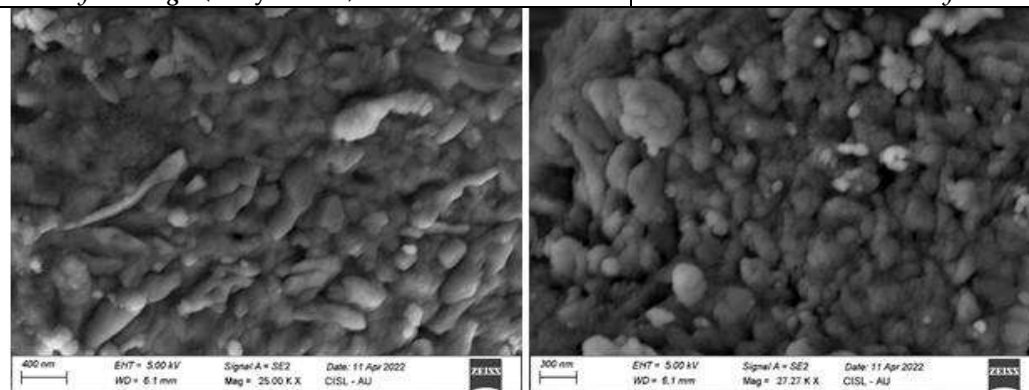
Figure 3. Morphological SEM images from *Murraya koenigii* **(curry leaves)**
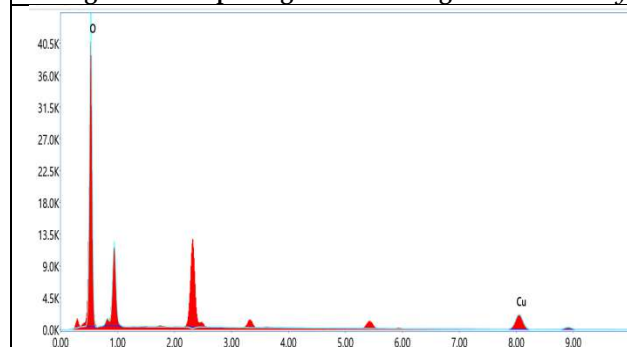
Figure 4. EDAX Spectra of CuO nanostructures from *Murraya koenigii* **(curry leaves)**
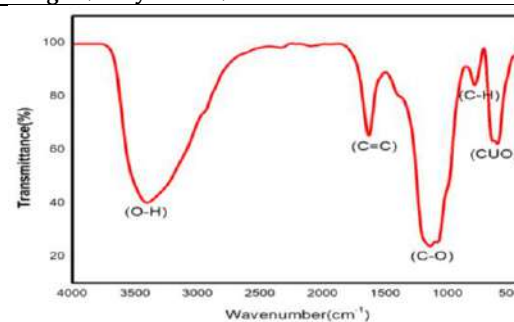
Figure 5. FTIR Spectrum of CuO nanostructures from *Murraya koenigii* **(curry leaves)**
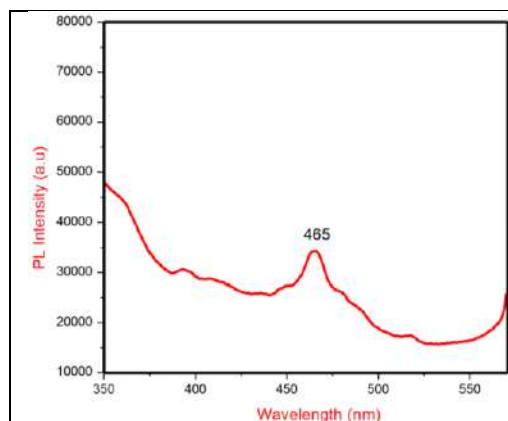
Figure 6. PL Spectrum of CuO nanostructures from *Murraya koenigii* **(curry leaves)**

Fig. 7. Photograph of colour degradation with time
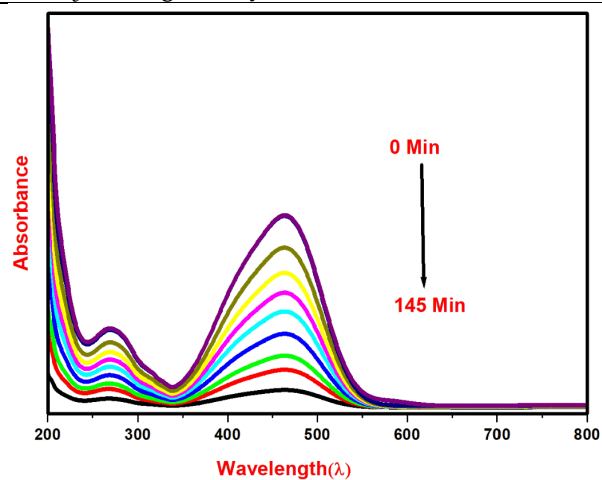
Figure 6. Photodegradation response of CuO nanostructures on methyl orange dye

RESEARCH ARTICLE

Hypersoft Generalized Closed Sets in Hypersoft Topological Spaces

Mythili .S* and Arokialancy.A

Assistant Professor, Department of Mathematics, Nirmala College for Women, Redfields, Coimbatore-18,Tamil Nadu, India.

*Address for Correspondence
Mythili S
Asst. Professor,
Department of Mathematics,
Nirmala College for Women,
Coimbatore(TN), India.
E. Mail: mythiliaugustin@gmail.com

ABSTRACT

In this paper the concept of hypersoft generalized closed sets in hypersoft topological space is discussed. Since of their properties are discussed in detail.

Keywords: Hypersoft sets, hypersoft topology, hypersoft open sets, hypersoft closed sets, hypersoft Generalized Closed sets, hypersoft Generalized open sets

INTRODUCTION

A soft set is a collection of approximate descriptions of an object. In 1999, Molodtsov [7] developed the concept of a soft set to handle difficult problems in economics, engineering, and the environment, where no mathematical methods could effectively deal with the many types of uncertainty. Maji *et al*. in [6] developed various operators for soft set theory and conducted a more detailed theoretical analysis of soft set theory. Various operations analogous to union, intersection, complement, difference etc. in set theory have been discussed in the context of soft sets (see [2, 3, 4, 16]). Topological structures on soft sets, in a similar manner, are more generalized methods that can be used to measure the similarities and differences between the objects in a universe which are soft sets. There are two versions of soft topology defined on soft sets, one by Shabir [15] and other by Cagman *et al*. [5]. The main difference between these approaches is that the first investigates a sub collection of all soft sets in an initial universe with a fixed set of parameters, whereas the second considers a sub collection of all soft subsets of a specific soft set in a universe. In 2018, Smarandache [16] expanded the notion of a soft set to a hypersoft set by substituting the function with a multi-argument function described in the cartesian product with a different set of parameters. This concept is more adaptable than the soft set and more useful when it comes to making decisions. Musa and Asaad [8,9]) introduced a new idea of hypersoft sets called bipolar hypersoft sets and they investigated some of their bipolar hypersoft

63127

topological structures. Researchers have been drawn to hypersoft set structure because it isbetter suited to decision-making diffculties than soft set structure. Despite the fact that itis a new concept, numerous studies have been conducted, and the field of study continues togrow [1, 10, 11, 12]. In this paper we have introduced generalized hypersoft sets and studied their properties.

Preliminaries

Definition 2.1. [16] A pair (F, $A_1 \times A_2 \times ... \times A_n$) is called a hypersoft set over U, where F is a mapping given by F : $A_1 \times A_2 \times ... \times A_n \rightarrow P(U)$.

Simply, we write the symbol E for $E_1 \times E_2 \times...\times E_n$, and for the subsets of E : the symbols A for $A_1 \times A_2 \times ... \times A_n$, and B for $B_1 \times B_2 \times ... \times B_n$. Clearly, each element in A, B and E is an n-tuple element. We can represent a hypersoft set (F,A) as an ordered pair, (F,A) = {(α, F(α)) : $\alpha \in$ A}.

Definition 2.2. [11] For two hypersoft sets (F,A) and (G,B) over a common universe U, we say that (F,A) is a hypersoft subset of (G,B) if

(1) A $\subseteq$ B, and

(2) F(α) $\subseteq$ G(α) for all $\alpha \in$ A. We write (F,A) $\subseteq$ (G,B).

Definition 2.3. [11] Two hypersoft sets (F,A) and (G,B) over a common universe U are said to be hypersoft equal if (F,A) is a hypersoft subset of (G,B) and (G,B) is a hypersoft subset of (F,A).

Definition 2.4. [11] The complement of a hypersoft set (F,A) is denoted by $(F,A)^c$ and is defined by $(F,A)^c = (F^c, A)$ where F^c : A $\rightarrow$ P(U) is a mapping given by $F^c(\alpha)$ = U \ F(α) for all $\alpha \in$ A .

Definition 2.5. [12] A hypersoft set (F,A) over U is said to be a relative null hypersoft set, denoted by (Φ,A), if for all $\alpha \in$ A, F(α) = ϕ.

Definition 2.6. [12] A hypersoft set (F,A) over U is said to be a relative whole hypersoft set, denoted by (X,A), if for all $\alpha \in$ A, F(α) = U.

Definition 2.7. [12] Difference of two hypersoft sets (F,A) and (G,B) over a common universe U, is a hypersoft set (H, C), where C = A $\cap$ B and for all $\alpha \in$ C, H(α) = F(α)\G(α). We write (F,A) \ (G,B) = (H, C).

Definition 2.8. [12] Union of two hypersoft sets (F,A) and (G,B) over a common universe U, is a hypersoft set (H, C), where C = A $\cap$ B and for all $\alpha \in$ C, H(α) = F(α) $\cup$ G(α). We write (F,A) $\cup$ (G,B) = (H, C).

Definition 2.9. [11] Intersection of two hypersoft sets (F,A) and (G,B) over a common universe U, is a hypersoft set (H, C), where C = A$\cap$B and for all $\alpha \in$ C, H(α) = F(α)$\cap$G(α). We write (F,A) $\cap$ (G,B) = (H, C).

Definition 2.10 [11] Let (F,E) be a hypersoft set over U and $u \in U$. Then $u \in (F, E)$ if $u \in F(\alpha)$ for all $\alpha \in E$.

Note that for any $u \in U, u \notin (F, E)$, if $u \notin F(\alpha)$ for some $\alpha \in E$.

Definition 2.11[13]. Let τ_H be the collection of hypersoft sets over U, then τ_H is said to be a hypersoft topology on U if

(1) (Φ,E), (X,E) belong to τ_H,

(2) the intersection of any two hypersoft sets in τ_H belongs to τ_H,

(3) the union of any number of hypersoft sets in τ_H belongs to τ_H.

Then (U, τ_H,E) is called a hypersoft topological space over U.

Definition 2.12[13]. Let (U, τ_H,E) be a hypersoft space over U, then the members of τ_H are said to be hypersoft open sets in U.

Definition 2.13[13]. Let (U, τ_H,E) be a hypersoft space over U. A hypersoft set (F,E) over U is said to be a hypersoft closed set in U, if its complement (F,E) belongs to τ_H.The union of two hypersoft topologies on U may not be a hypersoft topology on U.

Definition 2.14[13]: Let (U, τ_{H1},E) and (U, τ_{H2},E) be two hypersoft topological spaces over U. if $\tau_{H1} \subset \tau_{H2}$ then τ_{H2} is said to be finer than τ_{H1}. If $\tau_{H1} \subset \tau_{H2}$or $\tau_{H2} \subset \tau_{H1}$ then τ_{H1} and τ_{H2} are said to be comparable hypersoft topologies over U comparable hypersoft topologies over U

Hypersoft Generalized Closed Sets

Let U be an initial universe set and E be the non-empty set of parameters. Now we shall define the new relatively closed set in the following definition.

Mythili and Arokialancy

Definition 3.1

A hypersoft set (Hs, E) is called a hypersoft generalized closed (hypersoft g-closed) in a hypersoft topological space (X, τ_H, E) if cl (Hs,E) $\subset$ (U,E) whenever (Hs,E) $\subset$ (U,E) and (U,E) is hypersoft open in X

Theorem3.2

If (Hs,E) is hypersoft g-closed in X and (Hs,E) $\subset$ (A, E) $\subset$ cl (Hs,E) then (A,E) is hypersoft g-closed.

Proof

Suppose that, (Hs,E) is hypersoft g-closed in X and (Hs,E) $\subset$ (A, E) $\subset$ cl (Hs,E)

Let (A,E) $\subset$ (U,E) and (U,E) is hypersoft open in X

Since (Hs,E) $\subset$(A,E) and (A,E) $\subset$ (U,E)

We have, (Hs,E) $\subset$ (U,E)

Hence cl (Hs,E) $\subset$ (U, E) (Since (Hs,E) is hypersoft g-closed)

Since (A, E) $\subset$ cl (Hs,E) we have, cl (A,E) $\subset$ cl (Hs,E) $\subset$ (U,E)

Therefore (A,E) is hypersoft g-closed.

Theorem 3.3

If (AH,E) and (BH,E) are hypersoft g-closed sets then so is (AH,E) $\cup$ (BH,E).

Proof

Suppose that **(**AH, E) and (BH, E) are hypersoft g-closed sets.

Let (AH,E) $\cup$ (BH,E) $\subset$ (U,E) and (U,E) is hypersoft open in X

Since (AH,E) $\cup$ (BH,E) $\subset$ (U,E) we have.

 (AH,E) $\subset$ (U,E) and (BH,E) $\subset$ (U,E)

Since (U,E) is hypersoft open in X and (AH,E) and (BH,E) are hypersoft g-closed sets.

We have, cl (AH,E) $\subset$ (U, E) and, cl (BH,E) $\subset$ (U, E)

Therefore

cl (AH,E) $\cup$ (BH,E) = cl (AH,E) $\cup$ cl (BH,E) $\subset$ (U, E)

This completes the Proof.

Theorem 3.4

If a set (Hs,E) is hypersoft g-closed in X if and only if cl (Hs,E) \ (Hs,E) contains only null hypersoft closed set.

Proof

Suppose that**,** (Hs,E) is hypersoft g-closed in X.

Let (A,E) be hypersoft closed and (A,E)$\subset$$cl$ (Hs,E) \ (Hs,E)

Since A is hypersoft closed we have its relative complement A' is hypersoft open.

Since (A,E) $\subset$ cl (Hs,E) \ (Hs,E) we have (A,E) $\subset$ cl (Hs,E) and (A,E) $\subset$ (Hs,E)′

Hence, (Hs,E) $\subset$ (A,E)′

Consequently cl (Hs,E) $\subset$ (A,E)′ (Since (Hs,E) is hypersoft g-closed set in X)

Therefore (A,E) $\subset$$cl$ (Hs,E)′

 Hence (A,E) = φ, Hence, cl (A,E) \ (A,E) contains only null hypersoft closed set.

One can easily prove the converse part.

Corollary 3.5

A hypersoft g-closed (Hs,E) is hypersoft closed if and only if cl (Hs,E) \ (Hs,E) is hypersoft closed.

Proof

If (Hs,E) is hypersoft closed, then cl (Hs,E) \ (Hs,E) = φ

Consequently, suppose that, cl (Hs,E) \ (Hs,E) is hypersoft closed.

Since (Hs,E) is hypersoft g-closed.

cl (Hs,E) \ (Hs,E) = φ (by the theorem)

Hence (Hs,E) is hypersoft closed.

\Theorem 3.6

Let (Hs,E) be a hypersoft g-closed set and suppose that (A,E) is a hypersoft closed set. Then (Hs∩A,E) is a hypersoft g-closed set.

Proof: It is obvious

Hypersoft Generalized Open Sets

Definition 4.1: A hypersoft set (Hs,E) is called a hypersoft generalized open (hypersoft g-open) in a hypersoft topological space(X,τH, E) if the relative complement (Hs, E)' is hypersoft g-closed in X.

Equivalently, a hypersoft set (Hs,E) is called a hypersoft generalized open (hypersoft g-open) in a hypersoft topological space (X,τH, E) if and only if (A, E) ⊆(Hs,E)^o whenever (A, E) ⊂ (Hs,E) and (A, E) is hypersoft closed in X.

Theorem 4.2

If (Hs,E) is hypersoft g-open in (X,τH, E) and *int* (Hs,E) ⊆ (A, E) ⊂(Hs,E) then (A, E) is hypersoft g-open.

Proof

Suppose that (Hs,E) is hypersoft g-open in (X,τH, E) and *int* (Hs,E) ⊆ (A, E) ⊂(Hs,E)

Let (B, E)⊂ (A,E) and (B,E) is hypersoft closed in X.

Since (A,E) ⊂ (Hs,E) and (B,E) ⊂ (A,E) we have (B,E) ⊂(Hs,E)

Hence (B,E) ⊂ *int* (Hs,E) {since (Hs,E) is hypersoft g-open }

Since *int* (Hs,E) ⊂ (A,E) we have (B,E) ⊂ *int* (Hs,E) ⊂ *int* (A,E)

Therefore (A,E) is hypersoft g-open.

Theorem 4.3

If (F,E) and (G,E) are hypersoft g-open sets then so is $(F, E) \cap (G, E)$

Proof

Suppose that (F,E) and (G,E) are hypersoft g-open sets

Let $(A, E) \subset (F, E) \cap (G, E)$ and (A,E) is hypersoft closed set in (X,τH, E)

Since $(A, E) \subset (F, E) \cap (G, E)$ we have $(A, E) \subset (F, E)$ and $(A, E) \subset (G, E)$

Since (A,E) is hypersoft closed in (X,τH, E) and (F,E) and (G,E) are hypersoft g-open sets we have,

$(A, E) \subset int (F, E)$ and $(A, E) \subset int (G, E)$

Therefore $(A, E) \subset int (F, E) \cap int (G, E)$

This completes the proof.

Remark 4.4

The union of two hypersoft topologies on U may not be a hypersoft topology on U

Example 4.5

Let U= {a$_1$, a$_2$, a$_3$, a$_4$}, E={ e$_1$, e$_2$, e$_3$, e$_4$}, E$_1$= {e$_1$, e$_2$}, E$_2$={e$_3$}, and E$_3$={e$_4$}.

Let τH1={ $(\emptyset, E), (X, E), (F_1, E), (F_2, E), (F_3, E)$} and τH2={$(\emptyset, E), (X, E), (G_1, E), (G_2, E), (G_3, E)$} be two hypersoft topologies defined on U where $(F_1, E), (F_2, E), (F_3, E), (G_1, E), (G_2, E), (G_3, E)$ are hypersoft sets over U defined as follows

$(F_1, E) = \{((e_1, e_3, e_4), \{a_3, a_4\}), ((e_2, e_3, e_4), \{a_2, a_3\})\}$

$(F_2, E) = \{((e_1, e_3, e_4), \{a_1, a_2, a_3\}), ((e_2, e_3, e_4), \{a_1, a_4\})\}$

$(F_3, E) = \{((e_1, e_3, e_4), \{a_3\}), ((e_2, e_3, e_4), \emptyset)\}$

and

$(G_1, E) = \{((e_1, e_3, e_4), \{a_3, a_4\}), ((e_2, e_3, e_4), \{a_1, a_3, a_4\})\}$

$(G_2, E) = \{((e_1, e_3, e_4), \{a_1, a_2\}), ((e_2, e_3, e_4), \{a_2, a_4\})\}$

$(G_3, E) = \{((e_1, e_3, e_4), \emptyset), ((e_2, e_3, e_4), \{a_4\})\}$

Then $\tau_{H1} \cup \tau_{H2} = \{(\emptyset, E), (X, E), (F_1, E), (F_2, E), (F_3, E), (G_1, E), (G_2, E), (G_3, E)\}$

If we take $(F_1, E) \cup (G_1, E) = (H, E)$ then $(H, E) = \{((e_1, e_3, e_4), \{a_3, a_4\}), ((e_2, e_3, e_4), U)\}$ but (H, E) does not belongs to $\tau_{H1} \cup \tau_{H2}$. Hence $\tau_{H1} \cup \tau_{H2}$ is not a hypersoft topology on U

REFERENCES

1. Abbas, M.; Murtaza, G.; Smarandache, F. Basic operations on hypersoft sets and hypersoft point. Neutro sophic Sets Syst. 2020,35, 407-421. sophic Sets Syst. 2020,   35, 407-421.
2. Ali, M., Feng, F.; Liu, X.; Min, W.; Shabir, M. On some new operations in soft set theory. Comput. Math. Appl. 2009,   57, 1547-1553.
3. Al-shami, T. M.; Kŏcinac, L. D.; Asaad, B. A. Sum of soft topological spaces. Mathematics 20208, 990
4. Babitha, K. V.Sunil, J. J. Soft set relations and functions. Comput. Math. Appl. 2010,   60, 1840–1849.
5. Cagman, N. Karatas, S.; Enginoglu, S. Soft topology. Comput. Math. Appl. 2011,   62, 351-358. s Syst. 2018,   22, 168-170.
6. Maji, P. K., Biswas, R.; Roy, R. Soft set theory. Comput. Math. Appl. 2003,   45, 555-562
7. Molodtsov, D. Soft set theory-first results. Comput. Math. Appl. 1999,   37, 19-31
8. Musa, S. Y., Asaad, B. A. Bipolar hypersoft sets. Mathematics,   2021,   9, 1826.
9. Musa, S.Y. and Asaad, B.A. Topological structures via bipolar hypersoft sets. Journal of Mathematics,2022,   Article ID 2896053
10. Saeed, M., Ahsan, M. Rahman, A. A Novel approach to mappings on hypersoft classes with application.In Theory and Application of Hypersoft Set, 2021ed.Smarandache F., Saeed, M., Abdel-Baset M., SaqlainM.; Pons Publishing House: Brussels, Belgium, 2021; pp. 175-191.
11. Saeed, M., Ahsan, M. Siddique, M.; Ahmad, M. A study of the fundamentals of hypersoft set theory. Inter. J. Sci. Eng. Res. 2020, 11.
12. Saeed, M., Rahman, A., Ahsan, M.; Smarandache F. An Inclusive Study on Fundamentals of HypersoftSet. In Theory and Application of Hypersoft Set, 2021 ed. Smarandache F., Saeed, M., Abdel-Baset M.,Saqlain M.; Pons Publishing House: Brussels, Belgium, 2021; pp. 1-23.
13. Sagvan Y. Musa, Baravan A. Asaad, Hypersoft Topological Spaces Neutrosophic Sets and Systems, Vol. 49, 2022 401
14. Sezgin, A.; Atagun, A. O. On operations on soft sets. Comput. Math. Appl. 2011,   61, 1457–1467.
15. Shabir, M., Naz, M. On Soft topological spaces. Comput.Math. Appl. 2011,   61, 1786- 1799.
16. Smarandache, F. Extension of soft set to hypersoft set, and then to plithogenic hypersoft set. NeutrosophicSets Syst. 2018,   22, 168-170.

RESEARCH ARTICLE

Five Dimensional Bianchi Type-III String Cosmological Models For Perfect Fluid Distribution in General Relativity.

Tasneem Sanawadwala* and Keerti Acharya

Department of Mathematics, Medi-Caps University, Pigdamber, Rau, 453331, India

*Address for Correspondence
Tasneem Sanawadwala
Department of Mathematics,
Medi-Caps University,
Pigdamber, Rau, 453331, India
E. Mail: sanawadwalatasneem@gmail.com

ABSTRACT

In Present research article, we have investigated isotropic and anisotropic Bianchi type-III string cosmological model with five dimension in General Relativity in presence of perfect fluid. We have also studied some physical and geometrical aspects of obtained models.

Keywords: Five dimensional, Bianchi type-III, String.

INTRODUCTION

String cosmology has recently attracted a lot of attention, due to its crucial significance in the study of the universe's early stages before the development of particles. Therefore, cosmologists have shown a great deal of interest in learning about the cosmos in the current age, as well as its past and present states of existence and how it will evolve in the future. We still don't have enough information to draw fir conclusion on its genesis and evolution. Therefore, it is crucial to conduct further research in order to uncover undiscovered cosmic phenomena. Before the creation of the first particle in the universe, the string theory was a useful idea. Letelier[1,2] and Satchel[3] initially describe the general relativistic formation of the cosmic strings. Additionally, in 1983, he used the Einstein's field equation for a cloud of heavy strings to generate cosmic models in the Bianchi type I and Kantowskiu-Sachs space times. Several notable authors have recently shown an interest in cosmic strings in general relativity because of the vital part that strings play in characterising The creation of our universe's early stages Kibble[4,5]. Singh and Mollah[6] constructed several cosmological models of the universe using Lyra geometry. Trivedi and Bhabor[7] have recently tackled string cosmological models of Bianchi type III with dark energy in the context of Brans-Dicke scalar-tensor theory of gravitation. One of the fundamental goals of cosmological models is to describe the various stages of the universe in terms of the temporal history of its acceleration field. There is mounting evidence that dark energy currently rules the universe. Bianchi Type-IX String Cosmological Models for Perfect Fluid Distribution in General Relativity were studied by Tyagi[8] et al. Additionally, Tyagi and Sharma[9] have looked into a few bulk viscous string cosmological

63132

Tasneem Sanawadwala and Keerti Acharya

models of the Bianchi type II with an electromagnetic field. Furthermore, they used the assumption that the shear and expansion are proportionate in order to get at an obvious conclusion. Sahoo and Mishra[10] have created Five dimensional Bianchi type III cosmological models for quark matter coupled to a string cloud in general relativity. They considered about and discussed about much metric potential scenarios. All of the models' kinematical and physical characteristics are discussed.

Tyagi and Sharma[11] have examined the bulk viscous fluid in the LRS Bianchi Type-II Magnetised String Cosmological Model. By considering into account five-dimensional space-time, Baro and Singh[12] investigate a Bianchi type-III string cosmological model with bulk viscous fluid and a negative constant Declaration parameter in general relativity. They acquired some of the crucial model parameters and their behaviours. The Bianchi type-V magnetised string cosmology model with variable magnetic permeability for viscous fluid distribution was studied by Tyagi and Sharma[13]. In the context of Saez-Ballester theory Baruah and Daimary[14] looked into the interaction of a five-dimensional Bianchi type-I anisotropic cloud string cosmological model with an electromagnetic field. Assuming a condition between energy density and string tension density, Acharya and Sanawadwala[15] examined some Bianchi type III string cosmological models for ideal fluid distribution using a different approach. Hoyle-Narlikar C-field cosmology with Bianchi type-V non-static space-time in higher dimensions was researched by Kishor[16] et al. A five-dimensional plane symmetric Bianchi type-I cosmological model created by a cloud of strings and bulk viscosity in general relativity was taken into consideration by Mete and Deshmukh[17]. Mollah[18] et al. study a homogeneous and anisotropic space-time that is characterised by a Bianchi type-III metric with a perfect fluid in a Lyra geometry.

We investigated five-dimensional Bianchi type-III string cosmological models with perfect fluid distribution in general relativity in this study, which was inspired by the situations that were covered above. In order to obtain different situations for the Bianchi type model Universe, we solved the surviving field equations under some specific simplifying assumptions, like the universe changes from being anisotropic early on to being isotropic later on. There is also discussion of a few geometrical and physical characteristics of models.

The Metric And Field Equations

Five-dimensional Bianchi-type – III metric is given by

$$ds^2 = -dt^2 + A^2 dx^2 + B^2 e^{-2x} dy^2 + C^2 dz^2 + D^2 dm^2. \qquad (1)$$

Where A, B, C, and D are the only metric functions of comic time 't'. In this situation, it is presumed that the additional fifth coordinate, "m," is space-like. For the above line element we assume

$$x^1 = x, \ x^2 = y, \ x^3 = z, \ x^4 = m \ \text{and} \ x^5 = t. \qquad (2)$$

The general relativity Einstein's field equation is given by

$$R_{ij} - \frac{1}{2} R g_i^{\ j} = -T_i^{\ j}. \qquad (3)$$

The energy-momentum tensor for a cloud string is given by

$$T_{ij} = \rho v_i v_j - \lambda x_i x_j.$$

The energy density ρ for a cloud of strings with extreme mass with particles attached.

So, we write $\qquad (4)$

$$\rho = \rho_p + \lambda, \qquad (5)$$

ρ_p, λ is the rest energy density of particles and λ is the string tension density of cloud of string. The fifth coordinate

is taken to be space like and the coordinate are co-moving. where v^i is the five velocity vector of particles given by

$$v^i = (0,0,0,0,1) \ \text{and} \ x^i = (0,0,C^{-1},0,0).$$

Tasneem Sanawadwala and Keerti Acharya

Such that,

$v_i v^j = -x_i x^j = -1$ and $v_i x^i = 0.$

The field equation for the metric (1) takes the form

$$\frac{\ddot{B}}{B} + \frac{\ddot{C}}{C} + \frac{\ddot{D}}{D} + \frac{\dot{B}\dot{C}}{BC} + \frac{\dot{B}\dot{D}}{BD} + \frac{\dot{C}\dot{D}}{CD} = 0 \tag{6}$$

$$\frac{\ddot{A}}{A} + \frac{\ddot{C}}{C} + \frac{\ddot{D}}{D} + \frac{\dot{A}\dot{C}}{AC} + \frac{\dot{A}\dot{D}}{AD} + \frac{\dot{C}\dot{D}}{CD} = 0 \tag{7}$$

$$\frac{\ddot{A}}{A} + \frac{\ddot{B}}{B} + \frac{\ddot{D}}{D} + \frac{\dot{A}\dot{B}}{AB} + \frac{\dot{A}\dot{D}}{AD} + \frac{\dot{B}\dot{D}}{BD} - \frac{1}{A^2} = \lambda \tag{8}$$

$$\frac{\ddot{A}}{A} + \frac{\ddot{B}}{B} + \frac{\ddot{C}}{C} + \frac{\dot{A}\dot{B}}{AB} + \frac{\dot{A}\dot{C}}{AC} + \frac{\dot{B}\dot{C}}{BC} - \frac{1}{A^2} = 0 \tag{9}$$

$$\frac{\dot{A}\dot{B}}{AB} + \frac{\dot{A}\dot{C}}{AC} + \frac{\dot{A}\dot{D}}{AD} + \frac{\dot{B}\dot{C}}{BC} + \frac{\dot{B}\dot{D}}{BD} + \frac{\dot{C}\dot{D}}{CD} - \frac{1}{A^2} = \rho \tag{10}$$

$$\frac{\dot{A}}{A} - \frac{\dot{B}}{B} = 0 \tag{11}$$

Case-I: Isotropic Model

We have consider the Isotropic model as

A=B=C=t^{n_1} and D=t^{n_2} \tag{12}

Where n_1 and n_2 are two arbitrary constants.

By using equation (12) in equations (6-11), we get

$$\frac{1}{t^2}(3n_1^2 + 2n_1 n_2 - 2n_1 - n_2 + n_2^2) = 0 \tag{13}$$

$$\frac{1}{t^2}(3n_1^2 + 2n_1 n_2 - 2n_1 - n_2 + n_2^2) - \frac{1}{t^{2n_1}} = \lambda \tag{14}$$

$$\frac{3}{t^2}(2n_1^2 - n_1) - \frac{1}{t^{2n_1}} = 0 \tag{15}$$

$$\frac{3}{t^2}(3n_1^2 + 3n_1 n_2) - \frac{1}{t^{2n_1}} = \rho \tag{16}$$

We observe that isotropic model will expand as $t \to \infty$ when $n_1 > 0$ and extra dimension will contract as t approaches to infinite if $n_2 < 0$.

In this particular case, the metric describes the model's geometry,

$$ds^2 = -dt^2 + t^{2n_1}(dx^2 + e^{-2x}dy^2 + dz^2) + t^{2n_2}dm^2. \tag{17}$$

The scalar expansion for model (17) is given by

Tasneem Sanawadwala and Keerti Acharya

$$\theta = \frac{1}{t}(3n_1 + n_2)$$

(18)

The rest energy density ρ is given by

$$\rho = \frac{3}{t^2}(3n_1^2 + 3n_1 n_2) - \frac{1}{t^{2n_1}}$$

(19)

The string tension density λ is given by

$$\lambda = \frac{1}{t^2}(3n_1^2 + 2n_1 n_2 - 2n_1 - n_2 + n_2^2) - \frac{1}{t^{2n_1}}$$

(20)

And using equations 18 and 19, the particle density is given by

$$\rho_p = \frac{1}{t^2}(n_1 n_2 + 2n_1 + n_2 + n_2^2)$$

(21)

The Hubble parameter is derived as

$$H = \frac{1}{4t}(3n_1 + n_2)$$

(22)

Spatial volume is derived as

$$V = \frac{n_1^2 + n_2}{t^4}$$

(23)

Deceleration Parameter is derived as

$$q = -4$$

(24)

Case I: Physical Interpretations

In this instance, Equation 17 anisotropic Bianchi type-I string cosmology model in five dimensions of space-time has been constructed. Equation (18–24) represents the model's physical and geometric solutions.

Initially at t = 0, the expansion θ → ∞ and as the time t increases gradually it decreases and finally it becomes 0 when t → ∞ with the positive values of n_1, n_2. The model thus demonstrates that the Universe is expanding with the passage of time, but that the rate of growth slows as time passes and ceases at time t → ∞.

It is observed that the value of the deceleration parameter is always negative whatever be the value of n_1 and n_2 which showa that our model (17) decelerates in the standard way which is in accordance with the present-day observational scenario of accelerating Universe.

Case II: (Anisotropic Model)

In this case, we have assumed

$$A = t^{m_1}, B = t^{m_2}, C = t^{m_3} \text{ and } D = t^{m_4}$$

(25)

Where m_1, m_2, m_3 and m_4 are three arbitrary constants.

Using equation (25) in equations (6)-(11), we get

$$\lambda = \frac{1}{t^2}[m_1^2 + m_2^2 + m_4^2 + m_1 m_2 + m_1 m_4 + m_2 m_4 - (m_1 + m_2 + m_4)] - \frac{1}{t^{2m_1}}$$

(26)

$$\rho = \frac{1}{t^2}[m_1(m_2 + m_3 + m_4) + m_2 m_3 + m_3 m_4 + m_4 m_2] - \frac{1}{t^{2m_1}}$$

(27)

$$\rho_p = \frac{1}{t^2}[(m_3 + 1)(m_1 + m_2 + m_4) - (m_1^2 + m_2^2 + m_4^2)]$$

(28)

Tasneem Sanawadwala and Keerti Acharya

when m_1, m_2 and m_3 are all positive then we observed that the anisotropic three space will expand as t approaches

to infinite and the extra dimension will contract as $t \rightarrow \infty$ if $m_4 < 0$

In this particular case, the metric describes the model's geometry.

$$ds^2 = -dt^2 + t^{2m_1}dx^2 + t^{2m_2}e^{-2x}dy^2 + t^{2m_3}dz^2 + t^{2m_4}dm^2.$$

(29)

The coefficient of scalar expansion θ for model (29) is given by

$$\theta = \frac{k}{t},$$

(30)

Where, $m_1 + m_2 + m_3 + m_4 = k$

The Hubble parameter is derived as

$$H = \frac{k}{4t}$$

(31)

Spatial volume of universe is derived as

$$V = t^k,$$

(32)

Deceleration Parameter is derived as

$$q = \frac{4}{k} - 1$$

(33)

Physical Interpretations Of The Case II

In this case, it is seen that the deceleration parameter has a positive constant value when k<4, indicating that our model Universe (29) decelerates in the usual manner, and a negative constant value when k>4, indicating that our model Universe accelerates in the usual manner. The Bianchi type models, on the other hand, depict the universe at its early stages of evolution, and while the universe decelerates in the usual manner, in the early universe it will accelerate in finite time due to comic recollapse where the universe in turns inflates "decelerates and then accelerates."

In case II, we have built the five-dimensional anisotropic Bianchi type-I string cosmological model in general relativity, which is given by Equation 29. The model's geometrical and physical behaviour can be discussed as.

when $m_1 + m_2 + m_3 + m_4$ are all positive, we noticed that our model grew along the x, y, and z axes as $t \rightarrow \infty$,

whereas the extra dimension contracted and disappeared at $t \rightarrow \infty$, when $m_4 < 0$.

At the initial, or t equals 0, it is seen that the energy density is $\varrho \rightarrow \infty$ and $\varrho \rightarrow 0$ as $t \rightarrow \infty$ and that it meets the reality condition when $m_1 + m_2 m_3 + m_3 m_4 + m_4 m_2 > m_1^2$.

Additionally, it is noted that the particle density (ρ_p) is infinite when time t= 0, it declines as time (t) increases, and

finally becomes 0 as $t \rightarrow \infty$. When, it meets the reality condition $(m_1^2 + m_2^2 + m_3^2 + m_4^2) < 1$.

The spatial volume V in this model is 0 at the first epoch t = 0, and increases with respect to time, indicating that our model Universe is expanding as time progresses.

The expansion scalar $\theta \rightarrow \infty$ at initial t = 0, and as the time progresses gradually it decreases and finally it becomes 0 when $t \rightarrow \infty$. The model thus demonstrates that the Universe is expanding with the passage of time, but that the rate of expansion slows as time passes and ceases at time $t \rightarrow \infty$.

When l<4, it is seen that the deceleration parameter q value is positive, indicating that the universe in our model briefly slows down. Additionally, it is noted that the deceleration parameter q has a negative value when l > 4, suggesting that our model Universe accelerates in a manner consistent with the current observable scenario of an accelerating Universe.

CONCLUSION

According to the isotropic model, our model universe decelerates in a manner that is consistent with the current empirical scenario in which the universe is accelerating. According to the anisotropic model, the universe is expanding as time goes on, but the rate of expansion slows down and eventually ceases at time $t \to \infty$. Our model is seen to be anisotropic, expand, shear, decelerate initially and then accelerate in the later stages. The extra dimension contracts and becomes unobservable at time $t \to \infty$ as the model grows along the x, y, and z axes.

REFERENCES

1. Patricio S. Letelier, Clouds of strings in general relativity, Phys. Rev., 20, 1294-1302 (1979), DOI:https://doi.org/10.1103/PhysRevD.20.1294.
2. Patricio S. Letelier, String cosmologies, Phys. Rev., 28, 2414-2419 (1983), DOI:https://doi.org/10.1103/PhysRevD.28.2414.
3. John Stachel, Thickening the string. I. The string perfect dust, Phys. Rev., 21, 2171-2176 (1980), DOI:https://doi.org/10.1103/PhysRevD.21.2171.
4. T W B Kibble, Topology of cosmic domains and strings, *J. Phys. A: Math. Gen,* 9, 1387-1398 (1976), **DOI** 10.1088/0305-4470/9/8/029.
5. T W B Kibble, Some implications of a cosmological phase transition, Physics Reports, 67, 183-199 (1980), https://doi.org/10.1016/0370-1573(80)90091-5.
6. P. Singh, M. Mollah, Higher Dimensional LRS Bianchi type - I Cosmological Model Universe 202 Interacting with Perfect Fluid in Lyra Geometry, The African Rev. of phys., 11, 33-38 (2016).
7. Diksha Trivedi, A.K. Bhabor, Higher dimensional Bianchi type-III string cosmological models with dark energy in Brans-Dicke scalar-tensor theory of gravitation, New Astronomy, 89, 101658 (2021), 10.1016/j.newast.2021.101658 .
8. Atul Tyagi, Keerti Sharma and Payal Jain, Bianchi Type-IX String Cosmological Models for Perfect Fluid Distribution in General Relativity, Chinese Physics Letters, 27, (2010), 10.1088/0256-307X/27/7/079801.
9. Atul Tyagi and Keerti Sharma, Bianchi Type-II Bulk Viscous String Cosmological Models in General Relativity, International Journal of Theoretical Physics, 49, 1712–1718 (2010)**.**
10. Pradyumn Kumar Sahoo and Bivudutta Mishra, Higher-dimensional Bianchi type-III universe with strange quark matter attached to string cloud in general relativity, Turk.J.Phys., 39, 43-53(2015).
11. Atul Tyagi and Keerti Sharma, "Locally Rotationally Symmetric Bianchi Type-II Magnetized String Cosmological Model with Bulk Viscous Fluid in General Relativity" Chin. Phys. Lett., 28, (2011), 10.1088/0256-307X/28/8/089802.
12. Jiten Baro and Kangujam Priyokumar Singh, Higher dimensional Bianchi type-III string universe with bulk viscous fluid and constant deceleration parameter, Advances in Mathematics: Scientific Journal, 9, 8779–8787 (2020), 10.37418/amsj.9.10.101.
13. Atul Tyagi and Keerti Sharma, Bianchi Type-V Magnetized String Cosmological Model with Variable Magnetic Permeability for Viscous Fluid distribution, Chinese Physics Letters, 27, (2010), 10.1088/0256-307X/27/8/089801.
14. Jagat Daimary and Rajshekhar Roy Baruah, Five Dimensional Bianchi Type-I Anisotropic Cloud String Cosmological Model With Electromagnetic Field in Saez-Ballester Theory, Front. Astron. Space Sci., 9, 1-9 (2022), https://doi.org/10.3389/fspas.2022.878653.
15. Keerti Acharya and Tasneem Sanawadwala, Some Bianchi type III string cosmological models for perfect fluid distribution in general relativity with an alternate approach, Jñānābha, 52, 153-157 (2022).
16. Kishor S. Adhav, Shivdas D. Katore, Abhijit S. Bansod, Prachi S. Gadodia, Higher dimensional bianchi type-V universe in creation-field cosmology, Natural Science , 2, 484-488 (2010) 10.4236/ns.2010.25060.

17. V. G. Mete and V.S. Deshmukh, Five-Dimensional Plane Symmetric String Cosmological Model with Bulk Viscosity in General Relativity, 10, 249-256 (2022).

18. Mahbubur Rahman Mollah, Kangujam Priyokumar Singh and Pheiroijam Suranjoy Singh, Bianchi type-III cosmological model with quadratic EoS in Lyra geometry, International Journal of Geometric Methods in Modern Physics, 15, (2018), https://doi.org/10.1142/S0219887818501943.

RESEARCH ARTICLE

Runoff Assessment and Response to Land use and Land Cover Changes by using Remote Sensing and GIS

Kavita Singh[1]*, Ipsita Bose Roy Choudhury[2] and P Saritha[3]

[1]Associate Professor, Department of Civil Engineering, Institute of Aeronautical Engineering, Dundigal, Hyderabad-500043, Telangana, India
[2]Assistant Professor, Department of Civil Engineering, St. Peters Engineering College Maisammaguda, Dulapally, Hyderabad- 500100, Telangana, India
[3]Associate Professor, Department of Civil Engineering, Malla Reddy Engineering College, Maisammaguda, Dulapally, Hyderabad- 500100, Telangana, India

*Address for Correspondence
Kavita Singh,
Associate Professor, Department of Civil Engineering,
Institute of Aeronautical Engineering,
Dundigal, Hyderabad-500043, Telangana, India
E. Mail: drkavi142012@gmail.com

ABSTRACT

India is on the 2nd largest most excessively populated country all over the world, and at present the requirement for food and water is in huge amount. The State production and supply of essentials needed to be assess, for this purpose its very much necessary to know the pattern of the resources like land and water etc. The Changes in the environment which occurs indirectly or directly affects the ecosystem. Due to rapid urbanization, globalization and industrialization many of the major cities is been growing larger and larger and the merging of the nearby areas with the cities is being done without any proper planning. The water cycle has been affected very strongly by all the anthropogenic activities and the quantity and quality of the water availability is affected by water cycle due to that effect it's not astounding that many of the river basins experiencing water scarcity due to sudden changes in hydrological cycle. It's very important to know the different effects of changes occurring in land use/land cover and envisage the consequences and steps to be followed to reduce the effect consequently. In the present study SWAT platform is used where the inputs are given and simulation is done by using RS and GIS for the prediction of parameters which contributes to changes. The given study emphases on the surface runoff which is commonly effected by the land cover changes over there. The study is done by entering the processed data in GIS environment. This data gives all the essential parameters for the input in **SWAT (Soil and water assessment tool).** The simulation run in SWAT was carried out by using the runoff inputs which is generated for the specific time period in the study area. GIS Environment processes the input given to SWAT and then reading the responses of the runoff of the basin catchment

for the period given. There is a chance to envisage the concerns and consequences and find out the changes and which can decrease the complications of futures and can be recommended the given strategies to reduce the extreme changes which distresses the ecosystem and possibility for development of sustainable ecosystem.

Keywords: Remote Sensing, GIS, Land use, Land cover, SWAT, Arc GIS, Rainfall, Runoff.

INTRODUCTION

Kinnerasani is the study area which is located in the state of Telangana (T.S). Telangana state is mostly an agricultural state in that state total 70% population depends on agriculture for getting its livelihood. The considerable attention has been taken for the development of large scale, medium scale and small scale industries in the Telangana districts. Due to this the urban the urban population was increased over the years. In general, natural resource base is limited. The current study area provides irrigation to the agricultural areas and provides water to (KTPS) Kothagudem thermal power station at Palvancha for thermal power generation.

Objectives Of The Study
1. Collection and assessment of data for the natural cover changes of the study area by input of parameters for the period 2009 and 2013.
2. Annual runoff generation of the study area in the time period given.
3. To calculate and evaluate the runoff response of the study area for the given period.
4. Development of strategies for the mitigation of the objectionable effects on land use/land cover.

Location and Extent
Kinnerasani, is a very important tributary of Godavari river. The study area covers an area of 910sq. km. The study area is located at 17^0 41' N and 80^0 40' E. The Kinnerasani basin storage capacity is 233 m^3at the reservoir full level of 124.05m. The mandals Tekulapalli, Gundala, Plvancha and Burgampadu are under command areas and the catchment areas. Fig 1 Shows location map of the Study area.

Climatic Conditions
The climatic condition of the city is impartially justifiable with winter summer and rainy seasons. Based on the previous studies on climatologically data shows that south-west monsoon gives more than (75%) the average. Rest of the 25% summer showers constitutes from North- East monsoon. So the maximum amount of rainfall is received in south-west monsoon

Physiography
The details of physiographic area are the undulating terrain with a slope of 1-6%, varying from nearly level to a very steep slope. Among overall 13% of the area is nearly level and around 58% of the area is moderate sloping. The mean sea level elevation of the study area is 107m (351 ft.)

Soils
The Kinnerasani basin is mainly consists of two types of soils clay soils and clay loam soils. Whereas majority of the area around 84% is clay soils and 14% of the area occupies as clay loam soil rest of the 2% is under water bodies and rocks. Fig 2 shows the soil texture of the study area. The spatial variation of depth of soil is given in the fig no.3. About 62% of soils are moderately shallow to deep depth and about 36 % of soils are very shallow Kinnerasani basin soil productivity spatial variation has been depicted in fig 4.   14.72 % soils are ascetically productive and only 1% soils are non-productive Shown in the table 1

Soil And Water Assessment Tool (SWAT)

SWAT is a Hydrological model and is well organized for the users the long term impacts. SWAT functions on a regular time step at scale basin with ArcView GIS interface which is developed to envisage the impact on LU/LC (land use and land cover) by providing the parameters like Evapotranspiration runoff and potential evapotranspiration of large area uniformly and completely covered with continuous growing vegetation and unlimited supply of soil water. SWAT model simulates the quantity and quality of surface water and it also gives the impressions on all the parameters of the environment and ungauged watersheds by compelling specific data as the inputs and it as well as provides the precise data as inputs and it also make available the reflection to changed. SWAT is computationally effective for very large basins also. SWAT Methodology Flow chart is shown in fig no 5 and 6

Process For Running SWAT
SWAT Project Setup

First Click on SWAT PROJECT SETUP in ArcGIS software and give an output location
Delineation of Watershed:
For Delineation of watershed Click on watershed delineator and give DEM map as input for watershed delineation, Flow accumulation and direction, Watershed outlets and sub basin parameters and click on watershed delineation. Shown in the fig 7

HRU Analysis

➢ Click on HRU ANALYSIS in ArcGIS software and then on soil/land/slope definition.
➢ Then Input landuse/land cover layer, soil map of a year and then reclassify it by giving slopes values and overlay them and create HRU'S Analysis. Shown in the fig 9

Weather Data

Process of weather station
Nine weather stations are identified around the study area among all one weather station is selected for the collection of weather data. Shown in the Fig 10

Running SWAT in GIS

Stepwise methodology of Running SWAT in GIS shown in the fig 11

Implementation
Land Use/Land Cover Maps

land use land cover map of the study area shown in fig no. 12 showing changes in the year 2009 and 2013. The vegetation covers in the year 2009 is 18.94% as compared to 2013 the vegetation cover is 13.4 %

RESULTS

2009 Results

Swat reduced output is shown in the table2. Among which august month has received highest rainfall i.e. 355.4 cm and highest runoff i.e. 67.71. June July and August are the months for receiving highest precipitation. Fig 13 shows the graph of the year 2009 SWAT reduced output. Table 3 shows area wise feature present in study area of the year 2009. Wet land vegetation covers the highest % of the area i.e. around 43.93%. Among all of the features total water bodies covered in the total area is 1.57%. River catchment is around 20.6%. Graphical representation of features present shown in the fig. 14.

2013 Results

Table 4 shows the 2013 SWAT reduced output of the study are. As per this data in the month of July the area receives the highest rainfall i.e. 863.5 cm and runoff is also highest in this region i.e. 350.44 cm. Fig. 15 shows the runoff and precipitation simulated graph of the year 2015. Table 5 shows the features present in the region. Where wetland vegetation is the highest% in the region i.e. 35.8% and water bodies present is 1.6% only. Fig 16 shows the graph of features present in the study area.

Comparison Of 2009 And 2013 Results

Table 6 shows the compared runoff of the year 2009 and 2013. As per this data runoff is the highest in the month of Julyi.e. 350.44 for the year 2013. This is due to the reduced vegetation in the year 2013 i.e. from 43.93% to 35.8% of wet land vegetation and 18.94% to 13.4% of healthy vegetation, which had made the soil water holding capacity less and increased rate of runoff has been observed. Fig 17 shows the runoff graph simulated upon comparing both the years and fig18 shows the graph of difference in area of the features.

CONCLUSION

Planning decision making and implementation through an efficient management call for the generation of comprehensive information system The obtained results show in the study there is increase of the features like river catchment with sand, scrub land which is clear indication of there is increased runoff in the year 2013 and the area under which is under built up land and agriculture is increased whereas forest area is decreased. The results obtained by objective 3 shows that there is runoff increase in land use/land cover it is observed that there is decrease in healthy vegetation which results to increase in barren land and scrub land which finally leads to more runoff and less precipitation

Recommendations

Some strategies to mitigate the effect of heavy runoff are:

➢ Add plants and Protect trees
➢ Catch runoff with modern techniques
➢ Cover soil .
➢ Use modern methods of Agriculture.
➢ Methods implemented for deep percolation.
➢ Increase rain water harvesting structures and collect as much as rainwater without wasting it as runoff.
➢ Use fewer chemicals and use Natural resources for agricultural purpose.
➢ Every individual should be responsible and take ownership of responsibilities and give hand in development of self and also surroundings.

REFERENCES

1. **Kausalya Ramachandran, SaiKiran, D. Purnend, M., and Kalpana, M., GIS For Environmental Audit of Hyderabad Metropolitan Region, Rangareddy &Medak Districts of Andhra Pradesh, India, Indian National Cartographic Association, Indian Cartographer Volumes, Vol 21, 2001.**
2. Praveen Kumar, Dhanunjaya Reddy and Varun Singh, Intelligent transport system using GIS, Proceedings of Map India Conference, 2003.
3. National Remote Sensing Center, Department of Space, Govt. of India, Technical guidelines, 2008.
4. GIS Integrated Urban Transportation Planning By Dr M.Anji Reddy, KhajaFareeduddin Volume : 5 | Issue : 7 | July 2015 | ISSN - 2249-555X
5. National Urban Information System (NUIS) Scheme (Ministry Of Urban Development March 2006)
6. Ajay D. Nagne and Dr. BhartiW.Gawali, Transportation Network Analysis by Using Remote Sensing and GIS A Review, May-Jun 2013.

7. Anjaneyulu, M.V.L.R., Prahallada Reddy, O. and Nagaraj, B.N., Development of spatial information system for transportation planning of Calicut urban area, Proceedings of Map Asia, 2003.
8. Siddeswar Prasad, H.R., Use of GIS in transportation management, Proceedings of Map India, 2003.
9. Chulmin Jun, Design of an Intelligent Geographic Information System for Multi-Criteria Site Analysis, URICA Journal, Vol 2, No.3, June 1999.
10. (http://www.urisa.org/Journal/ accessed on 8th August 2001)
11. Ajay, Mapping for Micro-Level Planning: The Issues & Challenges, (invited paper), Indian Cartographer, 2002 MMLP-01, pp 289-294, 2002
12. All India Soil and Land use Survey, Watershed atlas of India (on 1:1 million scale), Department of Agriculture and Cooperation, Government of India, IARI Campus, New Delhi, 1990.
13. Pandey, A.C. and Nathawat, M.S., Hydrogeomorphological mapping, GIS Development, May 2002.
14. (www.GISdevelopment.net/application/naturalresourcemanagement/waterresources/groundwater assessment.html)
15. William D. Thornbury, Principles of Geomorphology, Second edition, CBS Publishers and distributors, New Delhi, 1990.
16. Sankar K, Hydrogeomorphological studies in the Trichirappallien virons, Tamil Nadu, India using Remote Sensing technology, Map Asia 2000.
17. Gupta, A., Correlation of LANDSAT and air borne magnetic anomaly data of a part of the Bihar mica belt. Proceedings of Symposium on Remote Sensing in subsurface exploration, held on 25 Oct., Bangalore, India, pp 23-30, 1980.
18. National Remote Sensing Agency, Department of Space, Govt. of India, Technical guidelines, 1999.
19. Manual of Nationwide Land use/ Land cover Mapping using Satellite Imagery, Part-I, National Remote Sensing Agency, Department of Space, Govt. of India, 1989.
20. Indian Agricultural Research Institute (IARI), Soil Survey Manual, 2nd edition, New Delhi, 1970.
21. J. Sehgal, Pedology - Concepts and Applications, First Edition, Kalyani Publishers, Ludhina, India, 1996.
22. D. S. Bhattacharya and T. C. Bagchi, Elements of Geological Map Reading and Interpretation, Orient Longman Limited, Calcutta, 1973.
23. Mary Hoffman, Dictionary of Geology, GoylSaab, Publishers and Distributors, New Delhi, 1993.
24. Thirumalaivasan, D. and Guruswamy, V, Optimal route analysis using GIS, GIS Development (www.gisdevelopment.net/application/utility/transport/utilitytr0004.html)
25. Hyderabad City Development Plan, Report prepared by Municipal Corporation of Hyderabad, Hyderabad. (www.ourmch.com/cdp.html, Accessed on 23rd June 2006)
26. AkramJaved and SuneelPandey, Land use/ Land cover analysis for waste disposal, GIS @ Devlopment, June 2004.
27. Tomlin, C.D., and K.M. Johnston, an Experiment in Land-Use Allocation with a Geographic Information System. Technical Papers, ACSM- ASPRS, St. Louis, Vol. 5, pp. 23-34, 1988.

Table 1: Details of soil productivity in the study area

S. No	Description	Area km²	Percentage
1.	Highly Productive	105.83	11.63
2.	Non Productive	12.52	1.38
3.	Low Productive	132.37	14.55
4.	Moderately Productive	659.32	72.45

Table 2 2009 SWAT Reduced Output

2009 SWAT REDUCED OUTPUT		
MONTH	PRECIPITATION	RUNOFF
JANUARY	0	0

Kavita Singh *et al.,*

FEBRUARY	0	0
MARCH	3.7	0
APRIL	0.4	0
MAY	127.1	23.1
JUNE	208	46.17
JULY	343.5	64.63
AUGUST	355.4	67.71
SEPTEMBER	180.6	18.38
OCTOBER	6.4	5.08
NOVEMBER	105.1	9.2
DECEMBER	6.2	0
TOTAL	**1397.4**	**234.27**

Table 3 Area wise feature present in the study area of the year 2009

NAME OF THE FEATURE	AREA(%)
WATER BODIES	1.57
HEALTHY VEGETATION	18.94
WETLAND VEGETATION	43.93
SCRUB LAND	14.96
RIVER CATCHMENT WITH SAND	20.6

Table 5 Area of the features present in 2013

NAME OF THE FEATURE	AREA(%)
WATER BODIES	1.6
HEALTHY VEGETATION	13.4
WETLAND VEGETATION	35.8
SCRUB LAND	21.3
RIVER CATCHMENT WITH SAND	27.9

Table 6 Comparison of 2009 and 2013 results

MONTH	RUNOFF(2009)	RUNOFF(2013)
JANUARY	0	0
FEBRUARY	0	0.19
MARCH	0	0
APRIL	0	0.28
MAY	23.1	0
JUNE	46.17	104.14
JULY	64.63	350.44
AUGUST	67.71	75.89
SEPTEMBER	18.38	44.46
OCTOBER	5.08	31.66
NOVEMBER	9.2	0.16
DECEMBER	0	0.01

Kavita Singh *et al.,*

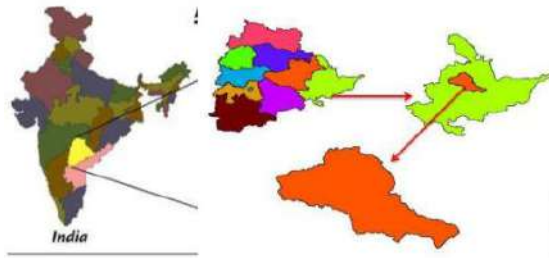Fig. 1The location map of study area

Fig 2: Soil Texture Map of the Study Area

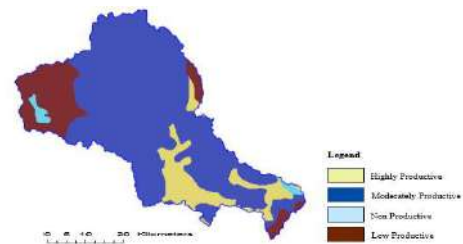Fig 3: Spatial variation of soil depth in study area

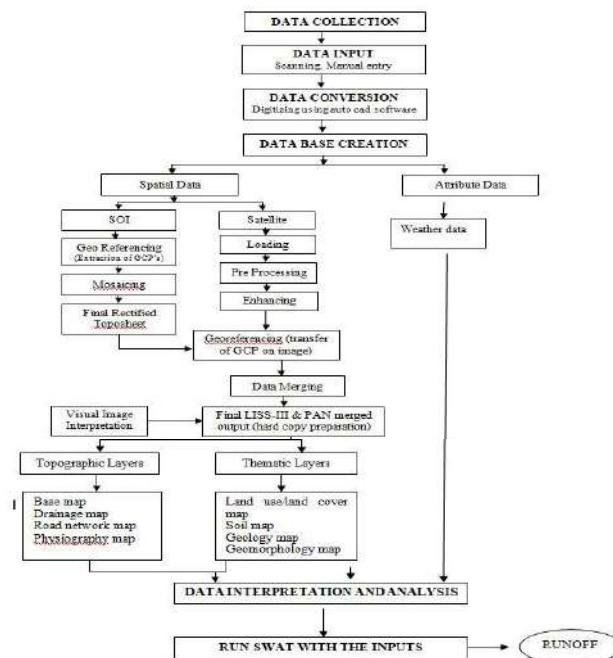Fig 4 :spatial variation of soil productivity in the Study area

Fig 5 Methodology flowchart of the study area
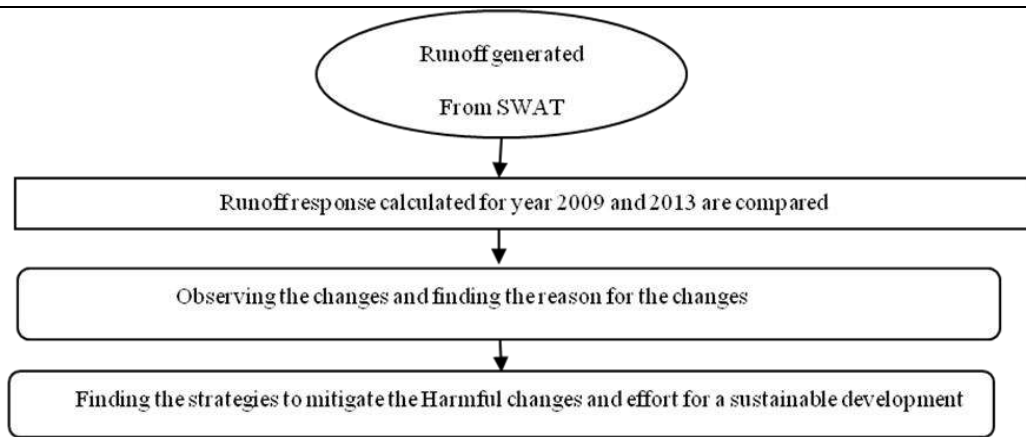
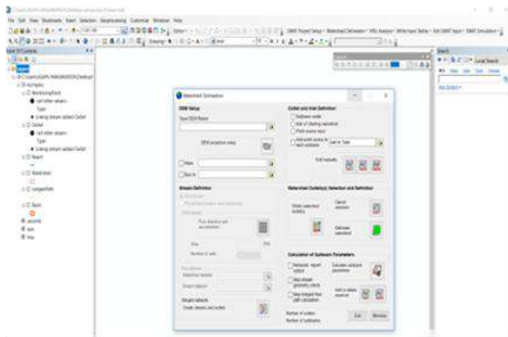Fig. 6 SWAT Methodology flow chart

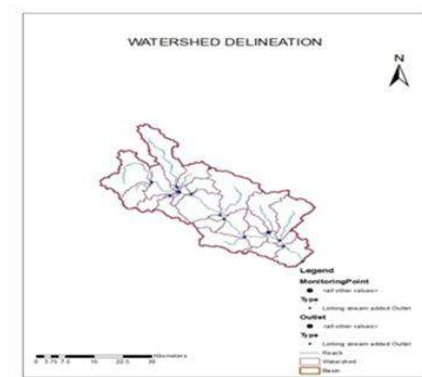Fig 7 watershed delineation in SWAT tool

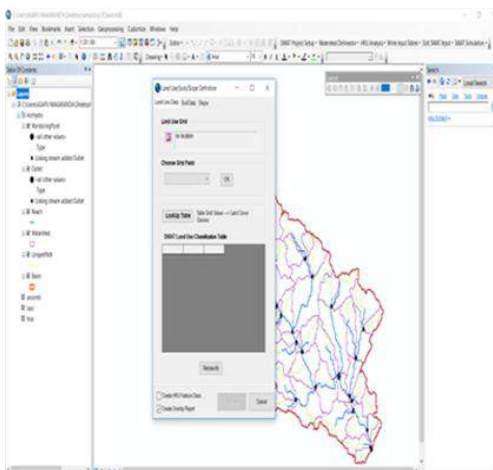Fig 8 watershed delineation Map of Kinnerasani Basin
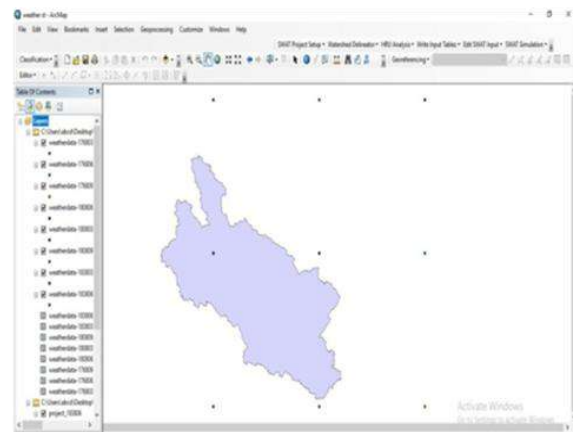

Fig 9 HRU analysis process

Fig 10 Available weather stations in and around study area

Kavita Singh *et al.,*
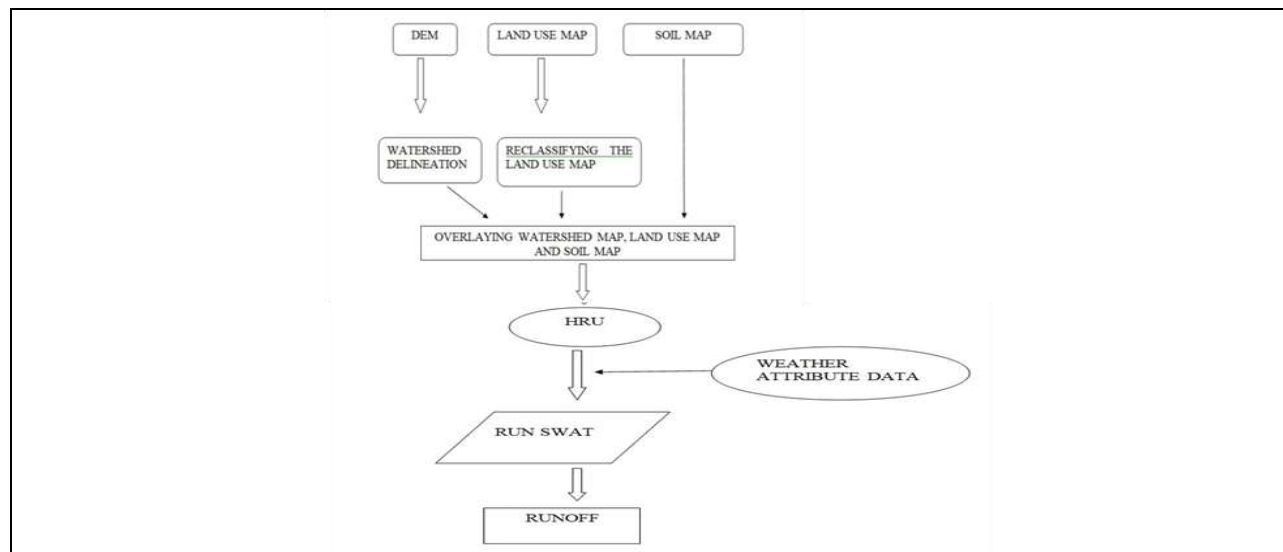
Fig 11 Implementation for Running SWAT in ArcGIS

Fig 12 Land use/ Land Cover Map of the Study Area in the year 2009 and 2013
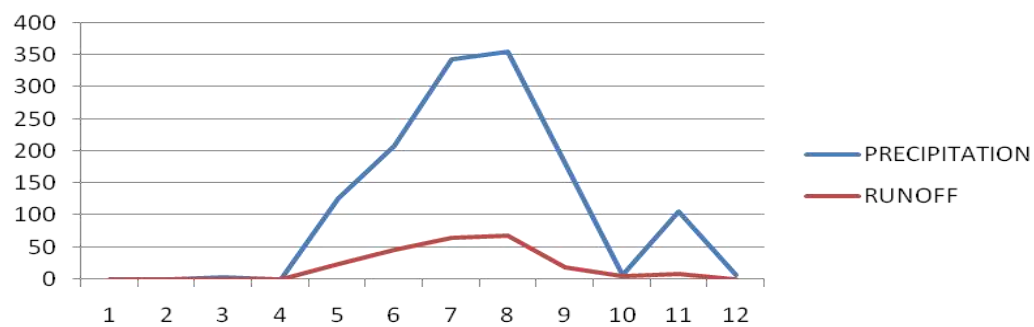
Fig 13 Runoff and Precipitation graph simulated for the year 2009

Fig: 14 Representation of features of 2009

Fig 15 Runoff and Precipitation graph simulated for the year 2013

Fig. 16 Area of the features present in 2013
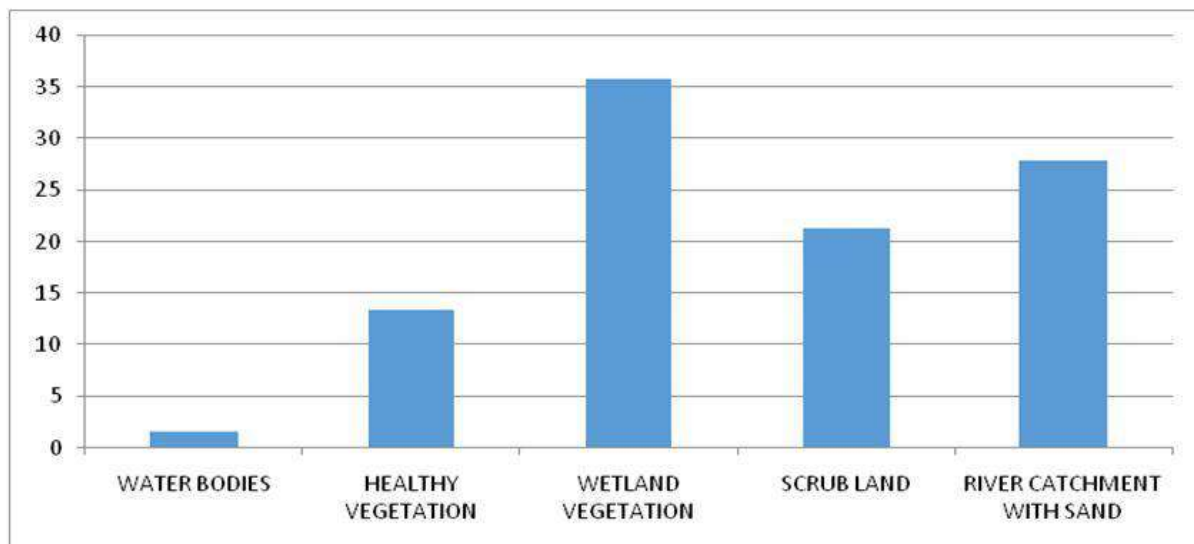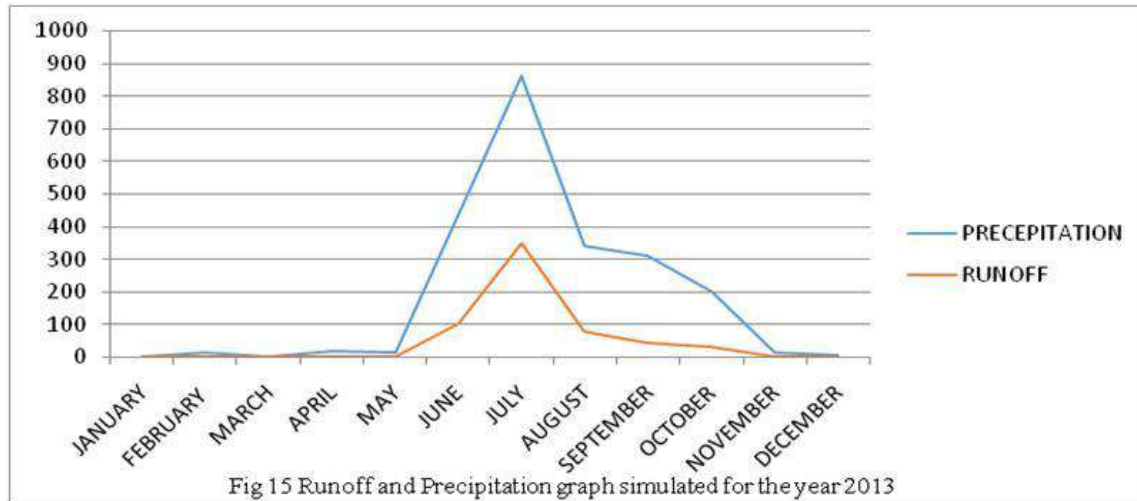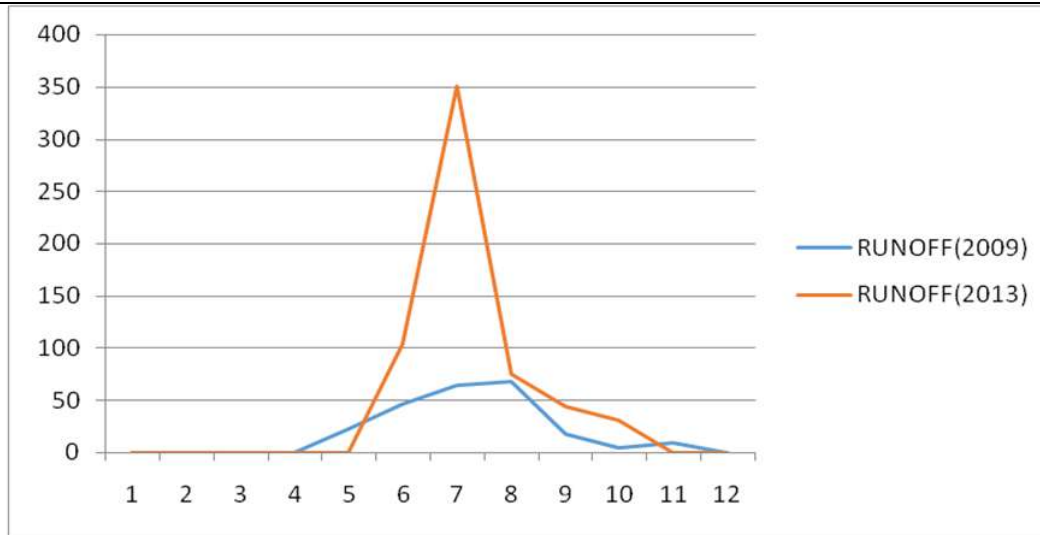
Fig 17 Runoff graph simulated upon comparing both years

Fig:18 Difference in Area of the features

RESEARCH ARTICLE

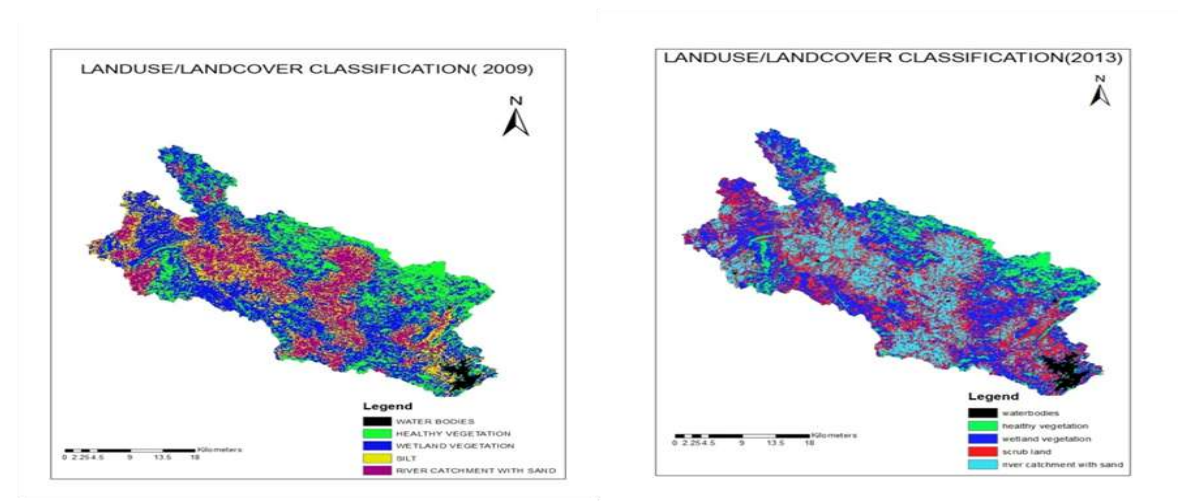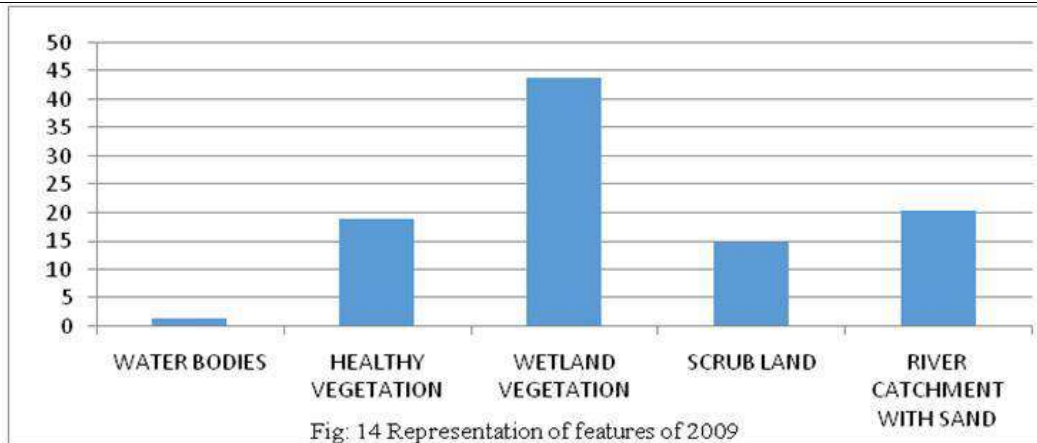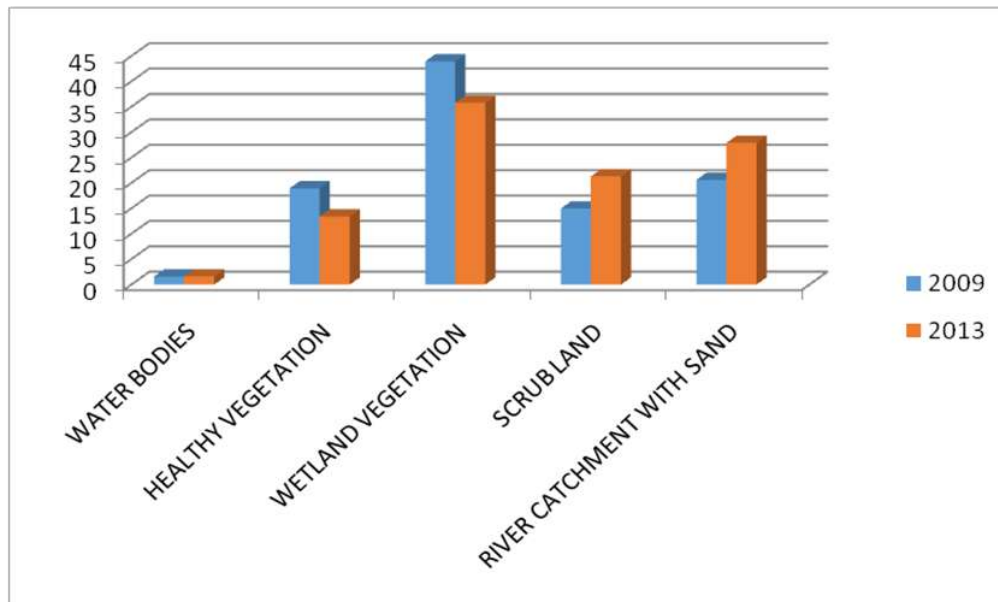# New R Type Averaging Operators on Z-Numbers and its Application in Replacement Problem

K.Parameswari[1]*, P.Veerammal[2] and G.Velammal

[1]Research Scholar (Part Time - Reg.No.P5119), Madurai Kamaraj University, Madurai and Assistant Professor, Sri Meenakshi Government Arts College for Women(A), Madurai - 2, Tamil Nadu, India.
[2]Associate Professor, Department of Mathematics, Saraswathi Narayanan College, Madurai, 625 022, Tamil Nadu, India.
[3]Associate Professor and Head (Retd), Department of Mathematics, Sri Meenakshi Government Arts College for Women (A), Madurai, Tamil Nadu, India.

*Address for Correspondence
K.Parameswari
Research Scholar (Part Time - Reg.No.P5119),
Madurai Kamaraj University, Madurai and
Assistant Professor,
Sri Meenakshi Government Arts College for Women(A),
Madurai - 2, Tamil Nadu, India.
E.Mail: paramusps@yahoo.co.in

ABSTRACT

Z–number is an useful concept introduced by Zadeh. This paper introduces new type of averaging operators on Z-numbers. Its application in replacement problem in fuzzy environment is also highlighted.

Keywords : Z-number, Discrete Z-number, Lexicographic order, R Type Aggregation operator, GRTAO.

INTRODUCTION

Z–number is an useful concept introduced by Zadeh[1,2,3]. It elegantly encapsulates vague information in a mathematical format. It captures information about both the fuzziness of the data and reliability of the data. Arithmetic operations on Z-numbers have been studied by Aliev[4,5], Shahilabhanu[6] etc. From application point of view, it becomes important to study averaging operators on Z-numbers. There have been very few studies in this regard. Jose M.Merigo, Montserrat Casanovas[7] dealt about OWA operators on fuzzy numbers. A new R Type arithmetic operations on Z-numbers was introduced by Stephen[8].This paper describes a new type of averaging operators on Z-numbers. Its application in replacement problem in fuzzy environment is also highlighted.

PRELIMINARIES

Definition : A Discrete Fuzzy number[3]

A fuzzy subset L of the real line R with membership function $\mu_L : R \rightarrow [0,1]$ is a discrete fuzzy number if its support is finite, i.e. there exist $x_1, x_2, \cdots x_n \in R$ with $x_1 < x_2 < \cdots < x_n$, such that supp(L) = $\{x_1, x_2, \cdots x_n\}$ and there exist natural numbers s, t with $1 \le s \le t \le n$ satisfying the following conditions: (1). $\mu_L(x_i) = 1$ for any natural number i with $s \le i \le t$,

(2). $\mu_L(x_i) \le \mu_L(x_j)$ for each natural numbers i, j with $1 \le i \le j \le s$

(3). $\mu_L(x_i) \ge \mu_L(x_j)$ for each natural numbers i, j with $t \le i \le j \le n$

Definition: Discrete Z-number[3]

An ordered pair Z = (L, M), where L discrete fuzzy number on random variable X and M is a discrete fuzzy number with a membership function $\mu_M : \{m_1, m_2, \cdots m_n\} \rightarrow [0,1]$, $\{m_1, m_2, \cdots m_n\} \subset [0,1]$ is a discrete Z-number.

Definition : Zadeh'sDefinition of Z-number[3]

For the ordered pair of fuzzy numbers (A,B), associated with a real-valued uncertain variable X, with the first component A, and the second component B is the measure of reliability of the first component. Then Z = (A, B) is an Z number.

Definition:MIN R operation[8]

Let * be any one of the basic arithmetic operations addition, subtraction, multiplication, or division. Let R_k be any suitably chosen ranking function. Then the MIN R operation is defined by (A, B)(*,MIN)(C, D)=(A*C, MIN(B, D)), where A*C is calculated by using the extension principle, $(A * C)(z) = sup_{z=x*y}\{\min[A(x), C(y)]\}, x \in A, y \in C$. Also,

MIN(C, D) = $\begin{cases} C, & \text{if } r_k(C) \le r_k(D) \\ D, & \text{if } r_k(D) < r_k(C) \end{cases}$, where r_k is a ranking functionon a set of fuzzy numbers F.

Definition: Lexicographic Order $L(R_1, R_2)$ for Z-numbers[9]

Let R_1 and R_2 be any two ranking functions and let $Z_1 = (A_1, B_1)$ & $Z_2 = (A_2, B_2)$ be any two Z-numbers. Define $Z_1 \preccurlyeq Z_2$ *under* the Lexicographic order $L(R_1, R_2)$ if and only if

(i) $R_1(A_1) < R_1(A_2)$ (or) (ii) $R_1(A_1) = R_1(A_2)$ & $R_2(B_1) \ge R_2(B_2)$.

SOME R TYPE AGGREGATION OPERATORS

Definition: n-ary Z number

In any Znumber both the components are in n-dimensional, then the corresponding Z number is called n-aryZ number (n > 1).

Example : $Z_1 = (A_1, B_1) = ((a_{11}, a_{12}, \ldots, a_{1n}), (b_{11}, b_{12}, \ldots, b_{1n}))$ *and*

$Z_2 = (A_2, B_2) = ((a_{21}, a_{22}, \ldots, a_{2n}), (b_{21}, b_{22}, \ldots, b_{2n}))$ be two n-ary (n > 1) Z numbers ($a_{ij} > 0, i = 1 \text{ to } 2 \text{ and } j = 1 \text{ to } n$).

Note: If n=2, 3, 4, 5, 6, 7, 8 then the Z-number is called Interval, Triangular, Trapezoidal, Pentagonal, Hexagonal, Septagonal, Octagonal Z-number respectively,

Definition: R TypeArithmetic Operations on n-ary Z number:

Let $Z_1 = ((a_{11}, a_{12}, \ldots, a_{1n}), (b_{11}, b_{12}, \ldots, b_{1n}))$ *and*

$Z_2 = ((a_{21}, a_{22}, \ldots, a_{2n}), (b_{21}, b_{22}, \ldots, b_{2n}))$ be two n-ary (n > 1) Z-numbers

($a_{ij} > 0, i = 1 \text{ to } 2 \text{ and } j = 1 \text{ to } n$),

Then define (1). addition of two Z-numbers by Z_1(+,MIN)Z_2

$= ((a_{11} + a_{21}, a_{12} + a_{22}, \ldots, a_{1n} + a_{2n}), MIN((b_{11}, b_{12}, \ldots, b_{1n}), (b_{21}, b_{22}, \ldots, b_{2n}))$

(2). Z_1(-,MIN)Z_2

$= ((a_{11} - a_{2n}, a_{12} - a_{2(n-1)}, \ldots a_{1n} - a_{21}), MIN(((b_{11}, b_{12}, \ldots, b_{1n}), (b_{21}, b_{22}, \ldots, b_{2n}))$

(3). Scalar Multiplication of any Z-number: For any k > 0,

(k,1) $(\cdot, MIN)$ $Z_1 = (k, 1)$ $(\cdot, MIN)((a_{11}, a_{12}, \dots, a_{1n}), (b_{11}, b_{12}, \dots, b_{1n}))$

$= ((ka_{11}, ka_{12}, \dots, ka_{1n}), (b_{11}, b_{12}, \dots, b_{1n})).$

(4). Z_1 (/,MIN) Z_2

$= ((a_{11}, a_{12}, \dots, a_{1n}), (b_{11}, b_{12}, \dots, b_{1n}))$ $(/, MIN)$ $((a_{21}, a_{22}, \dots, a_{2n}), (b_{21}, b_{22}, \dots, b_{2n}))$

$\approx ((\frac{a_{11}}{b_{1n}}, \frac{a_{12}}{b_{1(n-1)}}, \dots, \frac{a_{14}}{b_{11}}), MIN((b_{11}, b_{12}, \dots, b_{1n}), (b_{21}, b_{22}, \dots, b_{2n}))$

Also, In Particular, $\frac{1}{(a_{11}, a_{12}, \dots, a_{1n})} = \frac{(1,1,\dots 1)}{(a_{11}, a_{12}, \dots, a_{1n})} \approx (\frac{1}{a_{1n}}, \dots, \frac{1}{a_{12}}, \frac{1}{a_{11}}).$

Definition : General R Type Aggregation Operations on Z-number (GRTAO)

For n (≥ 2) Z-numbers, $Z_1 = (C_1, D_1)$, $Z_2 = (C_2, D_2) \dots Z_n = (C_n, D_n)$, the R Type Aggregation Operation is a function $R_TA : Z^n \to Z$ defined by $R_TA(Z_1, Z_2, \dots Z_n) =$

$(h(C_1, C_2, \dots C_n), k(D_1, D_2, \dots D_n)).$ Here, h is continuous, convex, symmetric, and idempotent of given fuzzy numbers $C_1, C_2, \dots C_n$, and k is MIN or Product of reliability of $D_1, D_2, \dots D_n$.

Definition : MIN R Type Arithmetic Mean (MRTAM):

Let $Z_1, Z_2, \dots Z_n$ denote the Z-numbers $(L_1, M_1), (L_2, M_2) \dots (L_n, M_n)$ respectively. Their MRTAM is defined to be: $MRTAM(Z_1, Z_2, \dots Z_n) = (h(C_1, C_2, \dots C_n), k(D_1, D_2, \dots D_n))$

$= (\frac{1}{n}, 1)(\cdot, MIN)\{Z_1(+, MIN)Z_2(+, MIN) \dots (+, MIN)Z_n\}$

$= (\frac{L_1 + L_2 + \dots + L_n}{n}, MIN(M_1, M_2, \dots, M_n)),$

where $h(L_1, L_2, \dots L_n) = \frac{L_1 + L_2 + \dots + L_n}{n}, k(M_1, M_2, \dots M_n) = MIN(M_1, M_2, \dots M_n)$, and $L_1 + L_2 + \dots + L_n$ denotes addition of fuzzy numbers using extension principle

Example :

Let $Z_1 = (L_1, M_1) = ((5,9,10,12),(.7,.8,.9,.95)), Z_2 = (L_2, M_2) = ((7,9,12,14),(.75,.8,.85,.9))$ be two trapezoidal Z-numbers. For finding MIN (M_1, M_2), use the ranking function r_k for the trapezoidal fuzzy number (y_1, y_2, y_3, y_4) is $r_k(y_1, y_2, y_3, y_4) = \frac{y_1 + y_2 + y_3 + y_4}{4}$.

Then, MRTAM$(Z_1, Z_2) = (\frac{1}{2}, 1)(., MIN)[Z_1(+, MIN)Z_2] = ((6,9,11,13), (.75,.8,.85,.9))$

RESULT

If $x_1, x_2, \dots x_n$ are real numbers then they can be represented by the z-numbers $(x_1, 1), (x_2, 1) \dots (x_n, 1)$. The MRTAM of these numbers is $(\frac{x_1 + x_2 \dots x_n}{n}, 1)$.

That is the MRTAM is the generalization of usual arithmetic mean of real numbers.

Definition : MIN R Type Geometric Mean(MRTGM):

Let $Z_1, Z_2, \dots Z_n$ denote the Z-numbers $(P_1, Q_1), (P_2, Q_2) \dots (P_n, Q_n)$ respectively. Define MRTGM by MRTGM $(Z_1, Z_2, \dots Z_n) = (P, Q)$, where $P = (P_1 \times P_2 \times \dots \times P_n)^{\frac{1}{n}}$ and $Q = MIN(Q_1, Q_2, \dots Q_n)$. Here, $P_1 \times P_2$ is calculated using extension principle.

Note: Let $Z_1 = (A, B)$ and $Z_2 = (C, D)$, then $Z_1(\times, MIN)Z_2 = (A, B)(\times, MIN)(C, D)$

$= (A \times C, MIN(B, D))$, where $A \times C$ is calculated by using the extension principle,

$(A \times C)(z) = \sup_{z = x \times y}\{\min[A(x), C(y)]\}.$

RESULT

If $x_1, x_2, \dots x_n$ are real numbers then the MRTGM of these numbers is $((x_1 x_2 \dots x_n)^{\frac{1}{n}}, 1)$.

This shows that the MRTGM is the generalization of usual geometric mean of real numbers.

Example:

Let $(P_1, Q_1) = \left(\frac{1}{1} + \frac{.5}{2} + \frac{.3}{3}, \ (.7, .75, .8)\right)$, $(P_2, Q_2) = \left(\frac{.4}{2} + \frac{1}{3} + \frac{.2}{4}, \ (.75, .8, .9)\right)$,

$(P_3, Q_3) = \left(\frac{.8}{8} + \frac{1}{9}, \ (.7, .8, .9)\right)$ be three discrete Z-numbers. To find MRTGM (Z₁,Z₂,Z₃)=(P, Q), where, P= $(P_1 \times P_2 \times P_3)^{\frac{1}{3}}$ and $Q = MIN\ (Q_1, Q_2, Q_3)$

To find $X = P_1 \times P_2 \times P_3$: by using extension principle

$\mu_{P_1 \times P_2 \times P_3}(p) = sup_{p=p_1 \times p_2 \times p_3}\{\min\left(\mu_{P_1}(p_1), \mu_{P_2}(p_2), \mu_{P_3}(p_3)\right)\}$,

$\mu_{P_1 \times P_2 \times P_3}(16) = \sup_{16=1\times2\times8}\left\{min\left(\mu_{P_1}(1), \mu_{P_2}(2), \mu_{P_3}(8)\right)\right\} = .4$

$\mu_{P_1 \times P_2 \times P_3}(32) = sup_{\substack{32=1\times4\times8 \\ 32=2\times2\times8}}\{\min\left(\mu_{P_1}(1), \mu_{P_2}(4), \mu_{P_3}(8)\right), \min\left(\mu_{P_1}(2), \mu_{P_2}(2), \mu_{P_3}(8)\right)\} = .4$

Continuing this way, we get

$$X: P_1 \times P_2 \times P_3 = \frac{.4}{16} + \frac{.4}{18} + \frac{.8}{24} + \frac{1}{27} + \frac{.4}{32} + \frac{.4}{36} + \frac{.5}{48} + \frac{.5}{54} + \frac{.2}{64} + \frac{.3}{72} + \frac{.3}{81} + \frac{.2}{96} + \frac{.2}{108}$$

Then Find P= $X^{\frac{1}{3}} = (P_1 \times P_2 \times P_3)^{\frac{1}{3}}$:

(i.e) To Find P = $X^{\frac{1}{3}}$ (i.e) To Find $\mu_P(p)$ *for the vlaues of* $\mu_X(x)$

We have, p = $x^{\frac{1}{3}} \Leftrightarrow x = p^3$, Take p = 3 and 4, for this p value x = 27 and 64 respectively.

Then $\mu_P(3) = \mu_x(27) = 1\ and\ \mu_P(4) = \mu_x(64) = .2$ (for other values of p, $\mu_X(x) = 0$)

Hence, $P^{\frac{1}{3}} = (P_1 \times P_2 \times P_3)^{\frac{1}{3}} : \frac{1}{3} + \frac{.2}{4}$

To find

$Q_1 = (.7, .75, .8)$, $Q_2 = (.75, .8, .9)$, $Q_3 = (.7, .8, .9)$, Choosing the ranking function $r_k(l, m, n) = \frac{l+m+n}{3}$, $Q = MIN(Q_1, Q_2, Q_3) = (.7, .75, .8)$.

Hence, MRTGM (Z₁,Z₂,Z₃) = $(: \frac{1}{3} + \frac{.2}{4}, (.7, .75, .8))$

Definition: MIN R Type Harmonic Mean(MRTHM)

Let $Z_1, Z_2, \ldots Z_n$ denote the Z-numbers $(P_1, Q_1), (P_2, Q_2) \ldots (P_n, Q_n)$ respectively. Define MRTHM by MRTHM$(Z_1, Z_2, \ldots Z_n) = (P, Q)$, where P= $\frac{n}{\left[\frac{1}{P_1} + \frac{1}{P_2} + \cdots + \frac{1}{P_n}\right]}$ and

$Q = MIN(Q_1, Q_2, \ldots Q_n)$.

Definition: MIN R Type OWA operators(MRTOWA)

Let $Z_1, Z_2, \ldots Z_n$ denote the Z numbers $(A_1, B_1), (A_2, B_2) \ldots (A_n, B_n)$ respectively. Let $\boldsymbol{w} = (w_1, w_2, \ldots w_n)$ be a weight vector such that $0 \le w_i \le 1, for\ i = 1,2 \ldots n$ and $\sum_{i=1}^{n} w_i = 1$.

To calculate the MRTOWA corresponding to w :

   (i)   First order $Z_1, Z_2, \ldots Z_n$ (in decreasing order) according to the chosen ranking method r_k. Say $U_1, U_2 \ldots U_n$ is the resulting decreasing sequence.

   (ii)   Then applying MRTOWA operation related to the weight vector w on $Z_1, Z_2, \ldots Z_n$, we get
            MRTOWA$(Z_1, Z_2, \ldots Z_n) = w_1 U_1(+, MIN)w_2 U_2(+, MIN) \ldots (+, MIN)w_n U_n$.

Definition: Product R Type Arithmetic Mean (PRTAM)

Let $Z_1, Z_2, \ldots Z_n$ denote the z-numbers $(A_1, B_1), (A_2, B_2) \ldots (A_n, B_n)$ respectively. Their PRTAM is defined to be: PRTAM$(Z_1, Z_2, \ldots Z_n) = \left(\frac{1}{n}, 1\right)(., \times)\{Z_1(+, \times)Z_2(+. , \times) \ldots \ldots (+, \times)Z_n\}$

=$\left(\frac{A_1 + A_2 + \cdots + A_n}{n}, (B_1 \times B_2 \times \ldots \times B_n)\right)$, where $A_1 + A_2 + \cdots + A_n$ denotes addition of fuzzy numbers using extension principle.

Parameswari *et al.,*

Definition: Product R Type Geometric Mean (PRTGM)

Let $Z_1, Z_2, \ldots Z_n$ denote the Z-numbers $(A_1, B_1), (A_2, B_2) \ldots (A_n, B_n)$ respectively. Their PRTGM is denoted by (A, B), where $A = (A_1 \times A_2 \times \ldots \times A_n)^{\frac{1}{n}}$ and $B = (B_1 \times B_2 \times \ldots \times B_n)$.
$PRTGM(Z_1, Z_2, \ldots Z_n) = (A, B)$. Here, A is calculated using extension principle.

Definition : Product R Type Harmonic Mean (PRTHM)

Let $Z_1, Z_2, \ldots Z_n$ denote the Z-numbers $(A_1, B_1), (A_2, B_2) \ldots (A_n, B_n)$ respectively. Then Define PRTHM by (A,B), where $A = \dfrac{n}{[\frac{1}{A_1} + \frac{1}{A_2} + \cdots + \frac{1}{A_n}]}$ and $B = (B_1 \times B_2 \times \ldots \times B_n)$. $PRTGM(Z_1, Z_2, \ldots Z_n) = (A, B)$. Here, A is calculated using extension principle.

APPLICATION TO REPLACEMENT PROBLEM

Optimal Replacement Policy Algorithm using MRTAM(when value of Money does not change with time.)

Let n denote the number of years of equipment would be in use, and Let us denote the following in Z-number for the given machine or equipment

Cz = Capital or Initial Cost or Cost of Machine,Sz = Scrap value,

fz(t) = maintenance or running cost for time t, CMz = Cumulative Maintenance Cost, DCz = Depreciation Cost, TCz = Total Cost, ACz(n) = Average Total Annual Cost.

Step 1: When t is continuous variable proceed (i) & (ii) otherwise, Go to

Step 2. Calculate the following

(i). TCz = Cz (-, MIN) Sz (+, MIN) CMz.(ii). ACz(n) = $\left(\frac{1}{n}, 1\right)$ $(\cdot, MIN)$ TCz(n)

Step 2: When t is discrete variable :

t takes the values 1,2,….n, where n is fixed then proceed (iii) orelse, Go to

Step 3.Find the following:

(iii).ACz(n)=$\left[\left(\frac{1}{n}, 1\right)(\cdot, MIN)(Cz\ (-, MIN)\ Sz)\right]$ $(+, MIN)$ $MRTAM(fz(t))$,

where $MRTAM(fz(t)) = [\left(\frac{1}{n}, 1\right)(\cdot, MIN)\sum_{t=1}^{n} fz(t)]^{**}$

Instead of MRTAM we can also use PRTAM

Step 3: Optimal Replacement Policy:

If fz(n+1) >ACz(n) and fz(n) <ACz(n-1), then replace the equipment at the end of n years.

Problem

For a machine Cz= ((12200,12200,12200),(1,1,1)),Sz = ((200,200,200),(1,1,1)) and
the Maintenance Cost fz(t) in rupees as follows:

Year	1	2	3	4	5
fz(t)	((100,200,300),(.7,.75,.8))	((400,500,600),(.75,.8,.85))	((700,800,900),(.7,.85,.9))	((1100,1200,1300), (.8,.85,.875))	((1700,1800,1900), (.75,.8,.85))

Year	6		7		8
fz(t)	((2400,2500,2600), (.8,.825,.85))		((3100,3200,3300), (.75,.85,.9))		((3900,4000,4100), (.7,.8,.9))

When should the machine be replaced? for the above information.:

Solution

Here DCz = Cz (-,MIN) SCz= ((12000,12000,12000),(1,1,1))

n (1)	fz(n) (2)	CMz (3)	Dz = Cz (-,MIN) Sz (4)	TCz(n) (5) = (3)(+,MIN)(4)	ACz(n) (5)/(1)
1	((100,200,300), (.7,.75,.8))	((100,200,300), (.7,.75,.8))	((12000,12000,12000), (1,1,1))	((12100,12200,12300), (.7,.75,.8))	((12100,12200,12300), (.7,.75,.8))
2	((400,500,600), (.75,.8,.85))	((500,700,900), (.7,.75,.8))	((12000,12000,12000), (1,1,1))	((12500,12700.12900), (.7,.75,.8))	((6250,6350,6450), (.7,.75,.8))
3	((700,800,900), (.7,.85,.9))	((1200,1500,1800), (.75,.8,.85))	((12000,12000,12000), (1,1,1))	((13200,13500,13800), (.75,.8,.85))	((4400,4500,4600), (.75,.8,.85))
4	((1100,1200,1300), (.8,.85,.875))	((2300,2700,3100), (.75,.8,.85))	((12000,12000,12000), (1,1,1))	((14300,14700,15100), (.75,.8,.85))	((3575,3675,3775), (.75,.8,.85))
5	((1700,1800,1900), (.75,.8,.85))	((4000,4500,5000), (.75,.8,.85))	((12000,12000,12000), (1,1,1))	((16000,16500,17000), (.75..8..85))	((3200,3300,3400), (.75,.8,.85))
6	((2400,2500,2600), (.8,.825,.85))	((6400,7000,7600), (.75,.8,.85))	((12000,12000,12000), (1,1,1))	((18400,19000,19600), (.75,.8,.85))	**((3067,3167,3267), (.75,.8,.85))**
7	((3100,3200,3300), (.75,.85,.9))	((9500,10200,10900), (.75,.8,.85))	((12000,12000,12000), (1,1,1))	((21500,22200,22900), (.75,.8,.85))	((3071,3171,3271), (.75,.8,.85))
8	((3900,4000,4100), (.7,.8,.9))	((13400,14200,15000), (.7,.8,.9))	((12000,12000,12000), (1,1,1))	((25400,26200,27000), (.7,.8,.9))	((3175,3275,3375), (.7,.8,.9))

By Lexicographic ordering based on z number, $L(R_1, R_2)$, $R_1(\text{fz}(7)) = \frac{x+y+z}{3} = 3200$ and

$R_2(\text{ACz}(6)) = \frac{x+y+z}{3} = 3167$. So, fz(7) >ACz(6). Also by the same way, fz(6) <ACz(5),

By using Step 3, fz(7) >ACz(6) and fz(6) <ACz(5),

The machine should be replaced after every 6 years.

Optimal Replacement Policy Algorithmusing MRTOWA(when value of Money changes with time.)

Let n denote the number of years of equipment would be in use, r denotes the rate of interest per year,Vn = Present value of all future discounted costs associated with replacement policy of the equipment at the end of each n years.Let us denote the following in the form of Z number for the given machine or equipment Cz = Capital or Initial Cost or Cost of Machine, Rz(n) = Operating Cost in year n, PVMC(n) = Present Value of Maintenance Cost, CPVF = Cumulative Present Value Factor

Step 1: Determine Wz(n) (Weighted Average or Annualized Cost)

Find out the following :(a).Discount rate per year, v = (1 + r)$^{-1}$,

(b).PVMC(n) = MRTOWA =$\{v^0 \text{Rz}(0)\}$ (+, MIN) $\{v^1 \text{Rz}(1)\}$ (+, MIN) …$\{v^{n-1}\text{Rz}(n-1)\}$.

(c). Cz(+,MIN) PVMC(n)

(d). CPVF = $v^0(+, MIN)v^1(+, MIN) … v^{n-1}$(e). Wz(n) =$(\frac{\{Cz\ (+,MIN)\ PVMC\ (n)\}}{CPVF}$

Step 2 : Optimal Replacement Policy

If fz(n+1) <Wz(n-1), then do not need to replace the equipment.

Otherwise, if Rz(n+1) >Wz(n-1)and , then we should replace.

CONCLUSION

Novel type of averaging operators on Z-numbers which are natural generalization of usual averages on crisp numbers have been introduced. Its utility has been demonstrated.

ACKNOWLEDGEMENT

REFERENCES

1. Zadeh .L.A, "Fuzzy logic = computing with words," IEEE Trans. on Fuzzy Systems, vol. 4, pp. 103–111, 1996.
2. Zadeh L.A, Turing, Popper and Occam, "Computing with Words:", Jerry M. Mendel, University of Southern California, USA, IEEE COMPUTATIONAL INTELLIGENCE, MAGAZINE, NOVEMBER 2007.
3. Zadeh L.A., A note on Z-numbers, Information Science 181, 2923-2932 (2011).
4. Aliev .R.A, Alizadeh .A.V, Huseynov O.H. , "The arithmetic of discrete Z-numbers", Information Sciences 290 (2015) 134–155, http://dx.doi.org/10.1016/j.ins.2014.08.02
5. Aliev .R.A, Huseynov O.H. , Zeinalova L.M, "The arithmetic of continuous Z-numbers", Information Sciences 373 (2016) 441–460, http://dx.doi.org/10.1016/j.ins.2016.08.078
6. Shahila Bhanu .M and Velammal .G, Operations on Zadeh's Z-numbers, IOSR Journal of Mathematics, Issue 3, Vol 11, PP 88-94 (May-June 2015)
7. Jose M.Merigo, Montserrat Casanovas, "The Fuzzy Generalized OWA Operator and Its Application in Strategic Decision Making", Article in Cybernetics and Systems, 41: 5, 359 — 370, June 2010.
8. Stephen .S, Novel binary operations on Z-numbers and their application in Fuzzy Critical Path Method, Advances in Mathematics: Scientific Journal 9 (2020), no.5, 3111–3120 ISSN: 1857-8365 (printed); 1857-8438.
9. Parameswari K, "Lexicographic Order Based Ranking For Z-Numbers", Advances in Mathematics: Scientific Journal 9 (2020), no.5, 3075–3083 ISSN: 1857-8365 (printed); 1857-8438 (electronic) https://doi.org/10.37418/amsj.9.5.67
10. K. PARAMESWARI, G.VELAMMAL, "Momentum Ranking Function of Z-Numbers and its Application to Game Theory", P-ISSN: 2078-8665 2023, 20(1 Special Issue) ICAAM: 305-310 E-ISSN: 2411-7986, https://dx.doi.org/10.21123/bsj.2023.8428

RESEARCH ARTICLE

Fractional Thermoelasticity Problem of Infinite Solid Disk-Boundary Condition Value Problem

Ravi B. Chaware[1], Sunil D. Bagde[2]* and Suchitra A. Meshram[3]

[1]Research Scholar, P.G.T.D. of Mathematics, RTM   Nagpur University, Nagpur-440033, Maharashtra, India
[2]Assistant Professor, Gondwana University, Gadchiroli-442605, Maharashtra ,India
[3]Associate Profesor, P.G.T.D. of Mathematics, RTM, Nagpur University, Nagpur- 440033, Maharashtra, India

*Address for Correspondence
Sunil D. Bagde
Assistant Professor, Gondwana University,
Gadchiroli-442605, Maharashtra ,India
E. Mail: sunilkumarbagde@rediffmail.com

ABSTRACT

The two-dimensional problem for an infinite solid disk is examined in this paper within the framework of the Fractional Thermoelasticity Problem of an Infinite Solid Disk and the boundary condition value problem. It uses the Caputo fractional derivative of order in the heat conduction equation. It is assumed that the cylinder's curved surface is in contact with a rigid surface and is constantly being heated. The issue is resolved using the Laplace transform, Fourier, transform, and Hankel transform and its inverses. The distributions of temperature, displacement, and stress are computed numerically, and visually shown, and the findings are thoroughly analyzed.

Keywords: Infinite solid disk, Fractional, thermoelasticity problem, Laplace transform, Hankel transform, Fourier transform

INTRODUCTION

The theories related to generalized thermoelasticity for the dynamical system at the single relaxation for isotropic bodies were first presented by Lord *et al*. (1967). The behavior of thermoelastic materials without energy dissipation was proposed by Green & Naghdi., (1993) using linear and nonlinear theories. The deformation of theoretical Thermo elasticity for the circular plate has been studied for heat supply which has been partially dispersed as presented by Ishihara *et al*. (1997). The equation for fractional heat conduction in single and 2-dimensional problems is studied, Povstenko., (2005) proposed stresses using the Caputo fractional derivative that correspond to the fundamental Cauchy problem solutions. Povstenko., (2009) studied theories related to thermal stress based on the equation adding the heat conduction with special and time fractional derivatives. The linked thermoelasticity theory

and the generalized thermoelasticity theory with one relaxation period were used by Sherief *et al*. (2010) to construct the novel theory of thermoelasticity.

Using the integral transform method, the mathematical model for quasi-static thermoplastic problems is studied in their indefinite solid long cylinder (Gaikwad *et al*., 2010). Sur *et al*. (2012) new theory of generalized thermoelasticity at two temperatures was first forth for the novel analysis related to heat conduction and heat flux related to fractional orders thermoelasticity. A thin hollow circular disk deformed thermo elastically as a result of a partially distributed heat source (Gaikwad & Ghadle., 2012). The thermal deflection and heat conduction problem of non-homogeneous materials due to the generation of internal heat inside the thin hollow circular disc were studied by Gaikwad & Ghadle., (2012). A newmathematical model of the thermoelasticity theory was put forward (Sur *et al*., 2012). The Green Naghdi model and 3-phase lag thermoelastic model are regarded to be subject to a regularly varied heat source in the setting of an unbounded medium, isotropic, and functionally graded medium. For a 1D problem involving an infinitely long cylinder, Raslan (2014) investigated the theories related to fractional thermoelasticity problems. The problem of 2 dimensions is studied in a thick plate with traction-free upper and lower surfaces that are being subjected to the specified axisymmetric temperature distribution was introduced by Raslan., (2015) using the fractional thermoelasticity problem theories. The thermoelastic problems of the mathematical model and the disk prone to heat generation were studied in circular sector disk (Gaikwad., 2015)

The postulates of 2-dimensional distribution of steady-state temperature in thin circular plates due to the consistent nature of the generation of internal energy (Gaikwad., 2016). A thin circular plate's axisymmetric thermoelastic stress analysis owing to heat generation was covered by Gaikwad., (2019).In this study, the fractional thermoelasticity problem is formulated for solving the temperature and stress distribution of radial and circumference of thin circular discs. We expect beginning conditions to be zero. The boundary surfaces at $(r = a)$; $(\varphi = 0)$; $(\varphi = \varphi_0)$; $(z = 0)$ *and* $(z = h)$ are maintained under the specified heat fluxes of $f_1(\varphi, z, t), f_2(r, z, t)$; $f_3(r, z, t)$, $f_4(r, \varphi, t)$ *and* $f_5(r, \varphi, t)$ respectively. The generalized finite Fourier transforms and the finite Hankel transform, as well as their inverses, have been used to solve the governing heat conduction equation with the aid of Mittag-Leffler functions. The mathematical model is built specifically with the pure Aluminium circular sector disk in mind. Using Mathcad software, the findings for thermal stress, displacement, and temperature have been estimated numerically and graphically shown.

LITERATURE REVIEW

Abouelregal *et al*. (2020) numerous efforts are made to better understand the Fourier classical heat transfer and several changes have been made. When some of these models are unsuccessful, therefore based on the Moore-Gibson-Thompson equation novel thermoelasticity model has been proposed. Combining the equation of hyperbolic partial differentiation for change in displacement field and the parabolic differential equation for the increase in temperature, this thermomechanical model was built. The investigated wave propagation in an infinite, isotropic body is subjected to a continuous thermal line source using the proposed model. Adhe & Ghadle., (2023) internal heat generation on inhomogeneous materials is the focus of this paper's analysis of thermoelasticity problems for plane elasticity and thermal stresses. Here, the method of direct integration is used to condense the original issues and establish the governing and boundary equations. The governing equation is then transformed into integral equations by applying more iteration techniques. The iterative method was used to execute the numerical calculations, resulting in speedy convergence. On a graph, the distribution of the Shear and Young's moduli, as well as the dimensionless stresses, are displayed.

Singh *et al*. (2019) the current study examined the thermoelastic interaction in the memory-dependant derivative of the three-phase lag model for the material of partial infinite elastic things with a heat source. The differential equation form of vector-matrix in the domain of Laplace transform is used to define the coupled governing equations, which involve time delay and kernel functions. The eigenvalue technique has been used to resolve the

Ravi B. Chaware *et al.,*

analytical formulations of the issue. The Laplace transformation is reversed using the Honig-Hirdes numerical approach. By selecting several forms of time delay settings, graphical representation and kernel function have been carried out to produce numerical results. Sherief & Hussain., (2020) The fractional order thermoelasticity theory is applied to two-dimensional axisymmetric issues. In the Laplace transform domain, the general solution is reached by taking a straight route without employing potential functions. The two issues of a solid sphere and an endless space with a spherical cavity are solved using the resulting formulation. Every time, a particular axisymmetric temperature distribution is applied to a surface that is assumed to be traction-free. Utilizing the transform's inversion formula as well as Fourier expansion methods, the Laplace transforms are inverted. The distributions of temperature, displacement, and stress in the physical domain are obtained by accelerating the convergence of the resulting series using numerical techniques. Graphical representations and discussions accompany the numerical results.

Formulation Of The Problem

A two-dimensional problem is considered for a circular solid disk that occupies the space of $0 \leq r \leq a$; $0 \leq \varphi \leq \varphi_0 (< 2\pi), 0 \leq z \leq h.$ Initial conditions are assumed for the problem. The boundary surfaces $(r = a)$; $(\varphi = 0)$; $(\varphi = \varphi_0)$; $(z = 0)$ and $(z = h)$ for time t > 0 kept for the heat-flux $f_1 (\varphi, z, t), f_2 (r, z, t)$; $f_3 (r, z, t)$, $f_4(r, \varphi, t)$ and $f_5(r, \varphi, t)$ correspondingly. The nonlocal Caputo type temporal fractional heat conduction equation of order for a thin circular disk is taken into account when creating a mathematical model.

The time-fractional differential equation at time t with the temperature of the circular disk is given below;

$$\frac{\partial^2 T}{\partial r^2} + \frac{1}{r}\frac{\partial T}{\partial r} + \frac{1}{r^2}\frac{\partial^2 T}{\partial \varphi^2} + \frac{\partial^2 T}{\partial z^2} = \frac{1}{k}\frac{\partial^\alpha T}{\partial t^\alpha} \qquad (3.1)$$

In $0 \leq r \leq a$; $0 \leq \varphi \leq \varphi_0 (< 2\pi), 0 \leq z \leq h$, for t > 0. The boundary value problems using the physical conditions, we can get the following equation;

$$k_t D_{RL}^{1-\alpha}\frac{\partial T}{\partial r} = f_1 (\varphi, z, t); \; at \; r = a; \; for \; t > 0; \qquad (3.2)$$

$$k_t D_{RL}^{1-\alpha}\frac{\partial T}{\partial \varphi} = f_2 (r, z, t); \; at \; \varphi = 0; \; for \; t > 0; \qquad (3.3)$$

$$k_t D_{RL}^{1-\alpha}\frac{\partial T}{\partial \varphi} = f_3 (r, z, t); \; at \; \varphi = \varphi_0; \; for \; t > 0; \qquad (3.4)$$

$$k_t D_{RL}^{1-\alpha}\frac{\partial T}{\partial z} = f_4 (r, \varphi, t); \; at \; z = 0; \; for \; t > 0; \qquad (3.5)$$

$$k_t D_{RL}^{1-\alpha}\frac{\partial T}{\partial z} = f_5 (r, \varphi, t); \; at \; z = h; \; for \; t > 0; \qquad (3.6)$$

Then the initial conditions are;

$$T = 0; \; at \; t = 0, 0 < \alpha < 2; \qquad (3.7)$$

$$\frac{\partial T}{\partial t} = 0; \; at \; t = 0, 1 < \alpha < 2; \qquad (3.8)$$

We made the assumption that the circular disk is in a planar state of tension for thin h in accordance with Gaikwad [32]. In actuality, "the closer to a plane state of stress is the actual state, the smaller the thickness of the hollow disk compared to its diameter."

The displacement equation is;

$$U_{i,kk} + \left(\frac{1+\nu}{1-\nu}\right)e_{,i} = 2\left(\frac{1+\nu}{1-\nu}\right)\alpha_t T_{,i} \qquad (3.9)$$

$e = U_{k,k}$; $k, i = 1,2,$

$U_i = \psi_{,i}$, i =1,2,

We can have;

$\nabla^2 \psi = (1 + \nu)\alpha_t T$

$\nabla^2 = \frac{\partial^2}{\partial r^2} + \frac{1}{r}\frac{\partial}{\partial r}$

$$\sigma_{ij} = 2\mu(\psi_{,ij} - \delta_{ij}\psi_{,kk}), i, j, k = 1,2.., \qquad (3.10)$$

The potential function of displacement $\psi (r, \varphi, z, t)$ can be written as;

$$\frac{\partial^2 \psi}{\partial r^2} + \frac{1}{r}\frac{\partial \psi}{\partial r} = (1 + \nu)\alpha_t T \qquad (3.11)$$

Ravi B. Chaware *et al.*,

Using $\frac{\partial \psi}{\partial r} = 0$ at $r = a$ for $time$ t

At initial stage $T = \psi = 0$; at $t = 0$

The stress function $\sigma_{\theta\theta}$ and σ_{rr} are;

$$\sigma_{\theta\theta} = -2\mu \frac{\partial^2 \psi}{\partial r^2} \tag{3.12}$$

$$\sigma_{rr} = \frac{-2\mu}{r} \frac{\partial \psi}{\partial r} \tag{3.13}$$

The boundary conditions are given below;

$\sigma_{rr} = \sigma_{r\varphi} = 0$; for $r = a$; $0 \le \varphi < \varphi_0$; $t > 0$; $\tag{3.14}$

$\sigma_{\varphi\varphi} = \sigma_{r\varphi} = 0$; $for \varphi = 0$; $0 \le r < a$; $t > 0$; $\tag{3.15}$

$\sigma_{\varphi\varphi} = \sigma_{r\varphi} = 0$; $for \varphi = \varphi_0$; $0 \le r < a$; $t > 0$; $\tag{3.16}$

The problem formulation is considered from equation (3.1) to (3.16).

PROBLEM SOLUTION

DETERMINING THE TEMPERATURE FIELD

Inverse transform and Fourier transform are defined for obtaining temperature function T (r, φ, z, t) using z variable in range $0 \le z < h$ as follows;

$$\bar{T}(r, \varphi, z, t) = \int_{z'=\infty}^{h} K(\eta_p, z') T(r, \varphi, z', t') dz' \tag{4.1}$$

$$\bar{T}(r, \varphi, z, t) = \sum_{n=1} K(\eta_p, z) \bar{T}(r, \varphi, \eta_p, t) \tag{4.2}$$

where,

$$K(\eta_p, z) = \sqrt{\frac{2}{h}} \cos(\eta_p z)$$

η_1, and η_2 are considered positive roots of the equation;

$sin(\eta_p, z) = 0$; $p = 1,2,3$

where,

$$\eta_p = \frac{p\pi}{h}; \ p = 1,2,3,..$$

Fourier transform is applied to equation (3.1)can be defined inequation (4.1) by using boundary conditions (3.2) to (3.8); we can obtain;

$$\frac{\partial^2 \bar{T}}{\partial r^2} + \frac{1}{r} \frac{\partial \bar{T}}{\partial r} + \frac{1}{r^2} \frac{\partial^2 \bar{T}}{\partial \varphi^2} + \frac{\partial^2 T}{\partial z^2} - \eta_p^2 \bar{T} = \frac{1}{k} \frac{\partial^\alpha \bar{T}}{\partial t^\alpha} \tag{4.3}$$

The boundary conditions are;

$$k_t D_{RL}^{1-\alpha} \frac{\partial \bar{T}}{\partial r} = \overline{f_1}(\varphi, \eta_p, t); \ at \ r = a; \ for \ t > 0; \tag{4.4}$$

$$k_t D_{RL}^{1-\alpha} \frac{\partial \bar{T}}{\partial \varphi} = \overline{f_2}(r, \eta_p, t); \ at \ \varphi = 0; \ for \ t > 0; \tag{4.5}$$

$$k_t D_{RL}^{1-\alpha} \frac{\partial \bar{T}}{\partial \varphi} = \overline{f_3}(r, \eta_p, t); \ at \ \varphi = \varphi_0; \ for \ t > 0; \tag{4.6}$$

Using,

$\bar{T} = 0$; at $t = 0$; $0 < \alpha < 2$; $\tag{4.7}$

$\frac{\partial \bar{T}}{\partial t} = 0$; at $t = 0, 1 < \alpha < 2$; $\tag{4.8}$

Inverse transform and Fourier transform over φ variable in range $0 \le \varphi \le \varphi_0$ can be defined as below;

$$\bar{\bar{T}}(r, \nu_n, \eta_p, t) = \int_{\varphi'=\infty}^{\varphi_0} K_0(\nu_n, \varphi') \bar{T}(r, \varphi', \eta_p, t) d\varphi' \tag{4.9}$$

$$\bar{T}(r, \varphi, \eta_p, t) = \sum_{n=1} K_0(\nu_n, \varphi) \bar{\bar{T}}(r, \nu_n, \eta_p, t) \tag{4.10}$$

Ravi B. Chaware *et al.*,

Where,

$$K(v_n, \varphi) = \sqrt{\frac{2}{\varphi_0}} \cos(v_n \varphi)$$

Where Eigenvalues v_n are considered as positive roots of equation;

$$\sin(v_n \varphi_0) = 0; \; v_n = \frac{n\pi}{\varphi_0}; \; n = 1,2,3..$$

Fourier transform is applied to equations (4.3) and (4.9) by using the conditions (4.4) to (4.8), we can obtain the following equation;

$$\frac{\partial^2 \bar{\bar{T}}}{\partial r^2} + \frac{1}{r}\frac{\partial \bar{\bar{T}}}{\partial r} - \frac{v_n^2}{r^2}\bar{\bar{T}} - \eta_p^2 \bar{\bar{T}} = \frac{1}{k}\frac{\partial^\alpha \bar{\bar{T}}}{\partial t^\alpha} \; (4.11)$$

Using

$$k_t D_{RL}^{1-\alpha} \frac{\partial \bar{\bar{T}}}{\partial r} = \bar{f_1}(v_n, \eta_p, t); \; at \; r = a; \; for \; t > 0; \tag{4.12}$$

$$\bar{\bar{T}} = 0; \; at \; t = 0; \; 0 < \alpha < 2; \tag{4.13}$$

$$\frac{\partial \bar{\bar{T}}}{\partial t} = 0; \; at \; t = 0, 1 < \alpha < 2; \tag{4.14}$$

Inverse transform and Hankel transform over r variable at range $0 \leq r < a$ can be defined as below;

$$\bar{\bar{\bar{T}}}(\beta_m, v_n, \eta_p, t) = \int_{r'=0}^{a} r'.K_1(\beta_m, r')\bar{T}(r, v_n, \eta_p, t)dr' \; (4.15)$$

$$\bar{T}(r, v_n, \eta_p, t) = \sum_{m=1}^{\infty} K_1(\beta_m, r)\bar{\bar{\bar{T}}}(\beta_m, v_n, \eta_p, t) \; (4.16)$$

Where,

$$K(\beta_m, r) = \sqrt{\frac{2}{a}} \frac{1}{\left[1 - \frac{v_n^2}{\beta_m^2 a^2}\right]^{1/2}} \frac{J_0(\beta_m r)}{J_0(\beta_m a)}$$

β_1 and β_2 are considered positive roots;

$J_1(\beta_m a) = 0; \; m = 1,2,3...$

Hankel transform is applied in equations 4.11 and (4.15) by using the conditions (4.12) to (4.14), we can obtain the following equation

$$\frac{\partial^\alpha \bar{\bar{\bar{T}}}(\beta_m, v_n, \eta_p, t)}{\partial t^\alpha} + k(\beta_m^2 + \frac{v_n^2}{r^2} + \eta_p^2)\bar{\bar{\bar{T}}}(\beta_m, v_n, \eta_p, t) = A(\beta_m, v_n, \eta_p, t)(4.17)$$

And,

$$\bar{\bar{\bar{T}}}(\beta_m, \eta_p, t) = 0; \; at \; t = 0; \; 0 < \alpha < 2; \tag{4.18}$$

$$\frac{\partial \bar{\bar{\bar{T}}}(\beta_m, \eta_p, t)}{\partial t} = 0; \; at \; t = 0, 1 < \alpha < 2; \tag{4.19}$$

Where,

$$A(\beta_m, v_n, \eta_p, t) = kaK_1(\beta_m, a)\bar{\bar{f_1}}(v_n, \eta_p, t) \left\{ a\frac{dK_0(v_n, \varphi)}{d\varphi}\bar{\bar{f_2}}(\beta_m, \eta_p, t)|_{\varphi=0} - \frac{dK_0(v_n, \varphi)}{d\varphi}\bar{\bar{f_3}}(\beta_m, \eta_p, t)|_{\varphi=\varphi_0} \right.$$

$$+ \frac{dK(v_n, \varphi)}{dz}\bar{\bar{f_4}}((\beta_m, v_n, t)|_{z=0}$$

$$\left. + \frac{dK(v_n, \varphi)}{dz}\bar{\bar{f_5}}(\beta_m, \eta_p, t)|_{z=h} \right\} \tag{4.20}$$

Laplace and inverse transform is applied to equation (3.17), we can obtain;

$$\bar{\bar{\bar{T}}}(\beta_m, v_n, \eta_p, t) = \frac{A(\beta_m, v_n, \eta_p, t)}{k(\beta_m^2 + \frac{v_n^2}{r^2} + \eta_p^2)}[1 - E_\alpha(-k(\beta_m^2 + \frac{v_n^2}{r^2} + \eta_p^2)t^\alpha)] \tag{4.21}$$

Finally, the required temperature is obtained by defining the inverse in equations (4.16), (4.10), and (4.2);

Ravi B. Chaware *et al.,*

$T(r, \varphi, z, t) =$

$\sum_{m=1}^{\infty} \sum_{n=1}^{\infty} \sum_{p=1}^{\infty} K_1(\beta_m, r) K_0(v_n, \varphi) K(\eta_p, z) \frac{1}{k(\beta_m^2 + \frac{v_n^2}{r^2} + \eta_p^2)} \quad [1 - E_\alpha(-k(\beta_m^2 + \frac{v_n^2}{r^2} +$

$\eta_p^2) t^\alpha)] \; x \; b_{mnp}$

$\hspace{8cm}$ (4.22)

Distribution Of Stress And Displacement

The displacement function ψ can be written using (4.22) in equation (4.11), we can obtain the following equation;

$$\frac{\partial^2 \psi}{\partial r^2} + \frac{1}{r}\frac{\partial \psi}{\partial r} = (1 + v_n)\alpha_t \sum_{m=1}^{\infty} \sum_{n=1}^{\infty} \sum_{p=1}^{\infty} K_1(\beta_m, r) K_0(v_n, \varphi) K(\eta_p, z) \frac{1}{k(\beta_m^2 + \frac{v_n^2}{r^2} + \eta_p^2)} [1 - E_\alpha(-k(\beta_m^2 + \frac{v_n^2}{r^2}$$

$$+ \eta_p^2) t^\alpha)] \; x \; b_{mnp}$$

$\hspace{8cm}$ (5.1)

Equation (5.1) can be written as follows;

$$\psi = -(1 + v_n)\alpha_t \sum_{m=1}^{\infty} \sum_{n=1}^{\infty} \sum_{p=1}^{\infty} K_1(\beta_m, r) K_0(v_n, \varphi) K(\eta_p, z) \frac{1}{k(\beta_m^2 + \frac{v_n^2}{r^2} + \eta_p^2)} [1 - E_\alpha(-k(\beta_m^2 + \frac{v_n^2}{r^2}$$

$$+ \eta_p^2) t^\alpha)] \; x \; b_{mnp}$$

$\hspace{8cm}$ (5.2)

Thermal stress can be written by substituting equation (5.2) in equation (4.12) and (4.13);

$$\sigma_{rr} = -2(1 + v_n)\alpha_t\mu \sum_{m=1}^{\infty} \sum_{n=1}^{\infty} \sum_{p=1}^{\infty} K_2(\beta_m, r) K_0(v_n, \varphi) K(\eta_p, z) \frac{1}{k\left(\beta_m^2 + \frac{v_n^2}{r^2} + \eta_p^2\right)} \Bigg[1$$

$$- E_\alpha\left(-k\left(\beta_m^2 + \frac{v_n^2}{r^2} + \eta_p^2\right) t^\alpha\right)\Bigg] x b_{mnp}$$

$\hspace{8cm}$ (5.3)

$$\sigma_{\theta\theta} = -2(1 + v_n)\alpha_t\mu \sum_{m=1}^{\infty} \sum_{n=1}^{\infty} \sum_{p=1}^{\infty} \frac{1}{\beta_m}\left((\beta_m K_2(\beta_m, r) - \frac{K_2(\beta_m, r)}{r}\right) - K_0(v_n, \varphi) K(\eta_p, z) \frac{1}{k\left(\beta_m^2 + \frac{v_n^2}{r^2} + \eta_p^2\right)} \Bigg[1$$

$$- E_\alpha\left(-k\left(\beta_m^2 + \frac{v_n^2}{r^2} + \eta_p^2\right) t^\alpha\right)\Bigg] x b_{mnp}$$

$\hspace{8cm}$ (5.4)

Numerical Calculations

The setting of the Thermostatic problem

$f_1(\varphi, z, t) = (\varphi^2 - \varphi_0^2)^2 (z^2 - h^2)^2 e^{-At}$

$f_2(\varphi, z, t) = (r^2 - a^2)^2 (z^2 - h^2)^2 e^{-At}$

$f_3(\varphi, z, t) = (r^2 - a^2)^2 (z^2 - h^2)^2 e^{-At}$

$f_4(\varphi, z, t) = (r^2 - a^2)^2 (\varphi^2 - \varphi_0^2)^2 e^{-At}$

$f_5(\varphi, z, t) = (r^2 - a^2)^2 (\varphi^2 - \varphi_0^2)^2 e^{-At}$

Where r is radius; A > 0.

Dimensions:

Axial and Radial directions; $z_1 = 0.05m$ and $r_1 = 1m$ and $\varphi_0 = 135^0$

The portion of circular disk $\varphi_0 = 270^0$

Thickness h = 0.1 m

Radius a = 1m

The numerical computations and graphics were created using the mathematical computation program PTC Mathcad Prime-6.0.0.

According to the definition, the first positive roots are β_1 = 3.8317, β_2 = 7.0156, β_3 = 10.1735, β_4 = 13.3237, and β_5 = 16.470. For the purposes of numerical evaluations is pure aluminum material.

Temperature variations in the radial direction for various time parameters are shown in Figure 5.1. The temperature will increase due to an axisymmetric heat source as $0 \le r \le 0.4$; $0.7 \le r \le 1$, and it decreases in the region as $0.4 \le r \le 0.7$.

Displacement distribution in the radial direction for various time parameters is shown in Figure 5.2. The displacement will decrease due to the axisymmetric heat source as $0 \le r \le 0.4, 0.7 \le r \le 1$, and it increases in the region as $0.4 \le r \le 0.7$.

Ravi B. Chaware *et al.,*

The radial stress distribution is shown in Figure 5.3. It increases within the region of $0.5 \leq r \leq 0.8$, and stress distribution decreases in the region of $0 \leq r \leq 0.5, 0.8 \leq r \leq 1$.

The circumferential stress distribution is shown in Figure 5.4. It increases within the region of $0.2 \leq r \leq 0.5, 0.8 \leq r \leq 1$ and stress distribution decreases in the region of $0 \leq r \leq 0.2, 0.5 \leq r \leq 0.8$.

Figures 5.5, 5.6, 5.7, and 5.8 shows the temperature, displacement, stress distribution radial, and circumference at t =0.50 for various value of $\alpha = 0.5, 1, 1.5,$ and 2, correspondingly.

Temperature distribution decreases in the region of $0.4 \leq r \leq 0.7$ and increases in the region of $0 \leq r \leq 0.4, 0.7 \leq r \leq 1$. The radial distance increases when the α value increases, are shown in Figure 5.5.

Different parameters of fractional order for displacement in the radial direction are shown in Figure 5.6. when the α value increases, displacement increases in the region of $0.4 \leq r \leq 0.7$ and decreases in the region of $0 \leq r \leq 0.4, 0.7 \leq r \leq 1$.

When the radius increases, the stress distribution increases in the region of $0.5 \leq r \leq 0.8$. when the α value increases within the region of $0 \leq r \leq 0.5, 0.8 \leq r \leq 1$, whereas the radial stress distribution is decreased.

Figure 5.8 depicts the circumferential stress distribution. when the α value increases, it decreases within the region of $0 \leq r \leq 02, 0.5 \leq r \leq 0.8$. in radial direction it increases within the region of $0.2 \leq r \leq 0.5, 0.8 \leq r \leq 1$.

CONCLUSION

The general solution for the formulated problem is obtained using Laplace transforms, Fourier transforms, Hankel transform, and its inverses. The temperature distribution displacement distribution and thermal stresses for radial and circumference are shown in figures 5.1 to 5.8. We introduce the transformation strategies before developing the analysis for the temperature field. Expressions of special interest can be constructed for each specific situation of special interest by giving the parameters and functions in the equations of temperature, displacements, and stresses the appropriate values. With the use of fractional calculus and boundary conditions for the heat flux that is imposed by physical laws, the thermal behavior of the circular sector disk has been examined in the context of time-fractional heat conduction.

REFERENCES

1. Lord H. W. & Shulman Y.: "A generalized dynamical theory of thermoelasticity," J. Mech. Phys. Solids, vol. 15, pp. 299–307, 1967.
2. Povstenko Y. Z.: "Fractional heat conduction equation and associated thermal stresses," Journal of Thermal Stresses, vol. 28, pp. 83–102, 2005.
3. Povstenko Y. Z.: "Thermoelasticity that uses fractional heat conduction equation," Journal of Mathematical Sciences, vol. 162, pp. 296–305, 2009.
4. Sherief H. H., El-Said A. & Abd El-Latief A.: "Fractional order theory of thermoelasticity," International Journal of Solids and Structures, vol. 47, pp. 269–275, 2010.
5. Sur A. & Kanoria M.: "Fractional order two-temperature thermoelasticity with wave speed," Acta Mechanica, vol. 223, pp. 2685–2701, 2012.
6. Gaikwad K. R. & Ghadle K. P.: "Nonhomogeneous heat conduction problem and its thermal deflection due to internal heat generation in a thin hollow circular disk," Journal of Thermal Stresses, vol. 35, pp. 485–498, 2012.
7. Green A. E. & Naghdi P. M.: "Thermoelasticity without energy dissipation," Journal of Elasticity, vol. 31, pp. 189–208, 1993.
8. Ishihara M., Tanigawa Y., Kawamura R. & N. Noda.: "Theoretical analysis of thermoelastoplastic deformation of a circular plate due to a partially distributed heat supply," Journal of Thermal Stresses, vol. 20, pp. 203–225, 1997.
9. Gaikwad K. R. & Ghadle K. P.: "Quasi-static thermoelastic problem of an infinitely long circular cylinder," Journal of the Korean Society for Industrial and Applied Mathematics, vol. 14, pp. 141–149, 2010.

10. Gaikwad K. R. & Ghadle K. P.: "On a certain thermoelastic problem of temperature and thermal stresses in a thick circular plate," Australian Journal of Basic and Applied Sciences, vol. 6, pp. 34–48, 2012.
11. Gaikwad K. R.: "Mathematical modeling and its simulation of a quasi-static thermoelastic problem in a semi-infinite hollow circular disk due to internal heat generation," Journal of Korean Society for Industrial and Applied Mathematics, vol. 19, pp. 69–81, 2015.
12. Raslan W. E.: "Application of fractional order theory of thermoelasticity to a 1D problem for a cylindrical cavity," Scientia Iranica B., vol. 66, pp. 257–267, 2014.
13. Raslan W. E.: "Application of fractional order theory of thermoelasticity in a thick plate under axisymmetric temperature distribution," Journal of Thermal Stresses, vol. 38, pp. 733–743, 2015.
14. Gaikwad K. R.: "Two-dimensional steady-state temperature distribution of a thin circular plate due to uniform internal energy generation," Cogent Mathematics, vol. 3, pp. 1–10, 2016.
15. Gaikwad K. R.: "Axi-symmetric thermoelastic stress analysis of a thin circular plate due to heat generation," International Journal of Dynamical Systems and Differential Equations, vol. 9, pp. 187–202, 2019.
16. Abouelregal, A. E., Ahmed, I. E., Nasr, M. E., Khalil, K. M., Zakria, A., & Mohammed, F. A. (2020). Thermoelastic processes by a continuous heat source line in an infinite solid via Moore–Gibson–Thompson thermoelasticity. Materials, 13(19), 4463.
17. Povstenko, Y., & Kyrylych, T. (2020). Fractional thermoelasticity problem for an infinite solid with a penny-shaped crack under prescribed heat flux across its surfaces. Philosophical Transactions of the Royal Society A, 378(2172), 20190289.
18. Adhe, A., & Ghadle, K. (2023). Thermal Stress Analysis of Inhomogeneous Infinite Solid to 2D Elasticity of Thermoelastic Problems. In Mathematics and Computing: ICMC 2022, Vellore, India, January 6–8 (pp. 509-521). Singapore: Springer Nature Singapore.
19. Singh, B., Pal, S., & Barman, K. (2019). Thermoelastic interaction in the semi-infinite solid medium due to the three-phase-lag effect involving memory-dependent derivative. Journal of Thermal Stresses, 42(7), 874-889.
20. Sherief, H. H., & Hussein, E. M. (2020). The effect of fractional thermoelasticity on two-dimensional problems in spherical regions under axisymmetric distributions. Journal of Thermal Stresses, 43(4), 440-455.

Table 5.1 Material Constant for numerical calculation

Physical Constant	Value
Thermal Conductivity (k_t)	204 W/ (m.K)
Thermal diffusivity (k)	84.18 m²/s
Heat Transfer Coefficient (k_c)	15 W/ (m².K)
Instantaneous line heat source (g_1)	1 x 10⁴ W/ m²
Young's Modulus (E)	70 GPa
Linear Thermal Expansion Coefficient (α_t)	22.2 x 10⁻⁶/K
Lame's Constant (μ)	26.67 GPa
Poisson ration (v)	0.35

Ravi B. Chaware *et al.,*
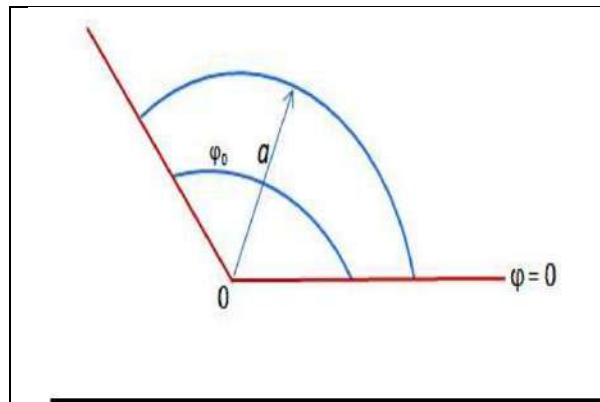
Figure 3.1Representation of fractional thermoelastic problem	**Figure 5.1 Temperature distribution at $\alpha = 0.5$ for various t values**
Figure 5.2 Displacement distribution at different values of t	**Figure 5.3 Radial stress distribution at different values of t**
Figure 5.4 Circumferential stress distribution at different values of t	**Figure 5.5 Temperature distribution at different values of α**
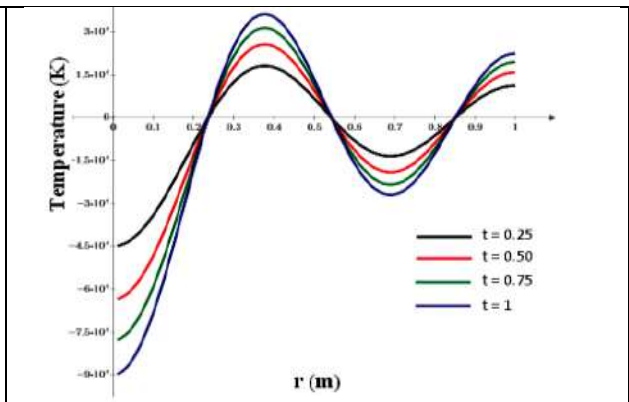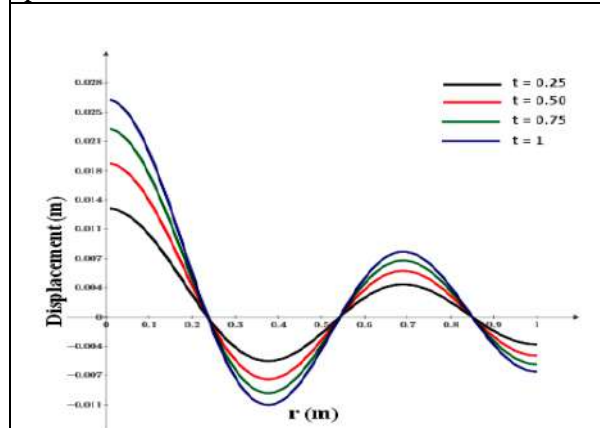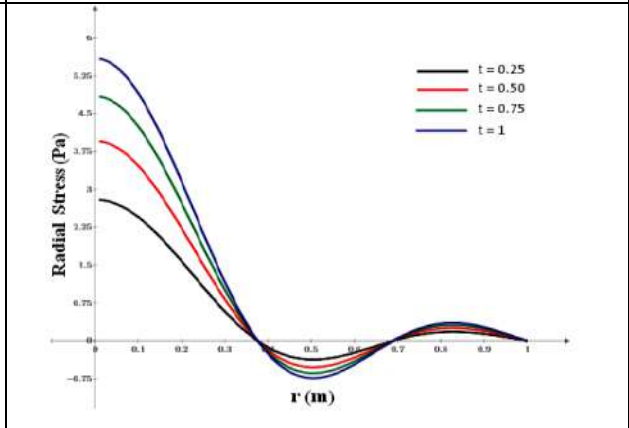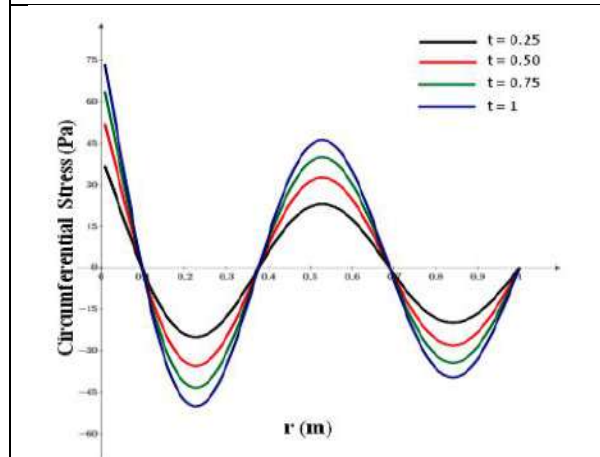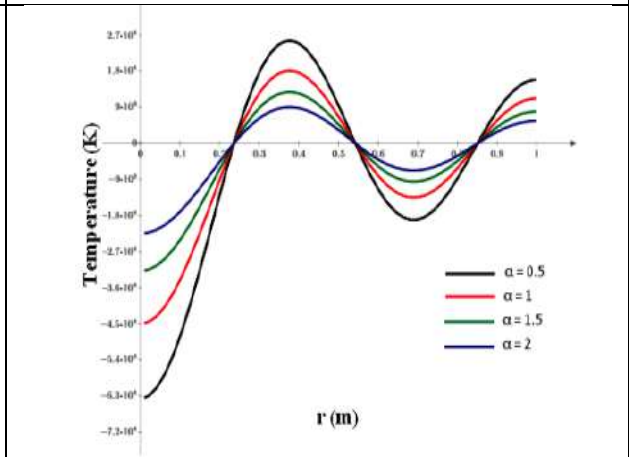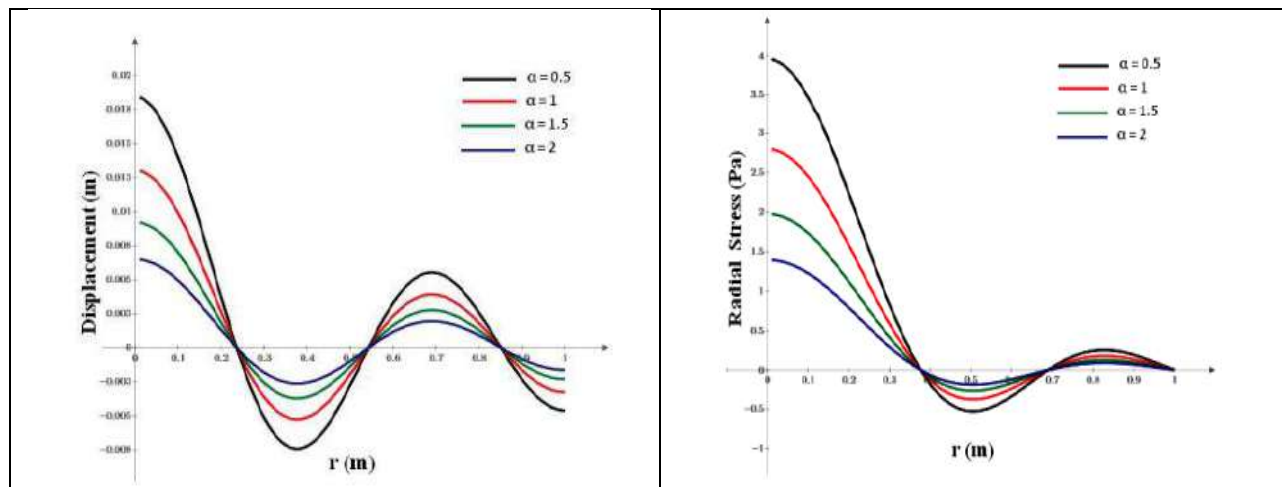
Figure 5.6 Displacement distribution at different values of α	**Figure 5.7 Radial stress distribution at different values of α**
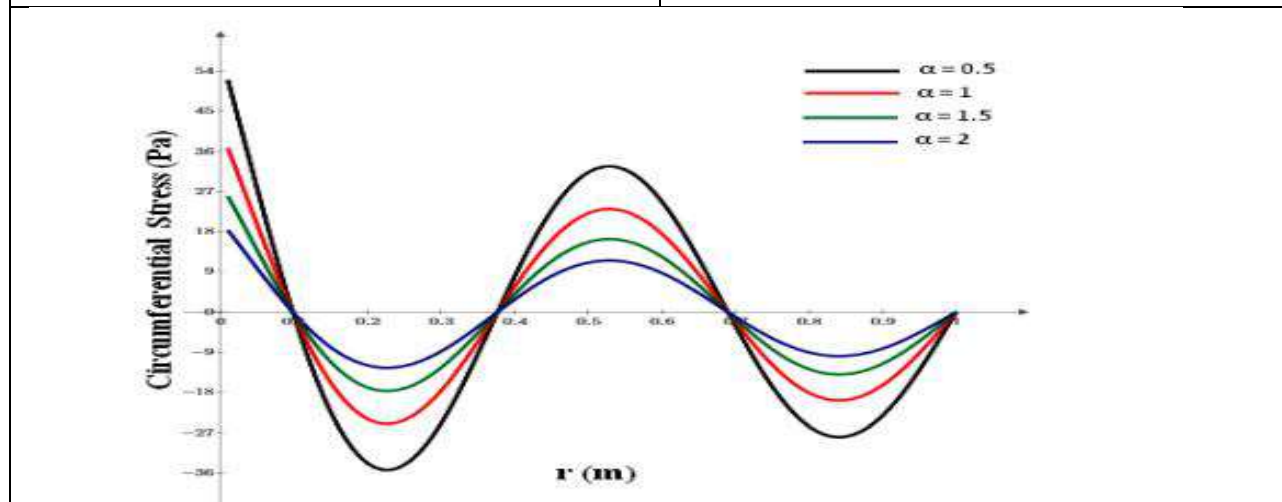
Figure 5.8 Circumferential stress distribution at different values of α

RESEARCH ARTICLE

Optimal Transportation Strategy using-Decision Making

Amali Theresa S[1]*, and Sahaya Sudha A[2]

[1]Research Scholar, PG & Research Department of Mathematics, Nirmala College for Women, Coimbatore, Tamil Nadu, India.

[2]Associate Professor, PG & Research Department of Mathematics, Nirmala College for Women, Coimbatore, Tamil Nadu, India.

*Address for Correspondence
Amali Theresa S
Research Scholar,
PG & Research Department of Mathematics,
Nirmala College for Women,
Coimbatore, Tamil Nadu, India.
E.Mail: amalitheresa2018@gmail.com

ABSTRACT

The purpose of this paper is to propose an improved technique to select the optimal transportation from the available alternatives. A survey method is used to determine the weights for different criteria. The contribution of the current work lies in the practical application of survey method and extended BATOS (Best alternative technique for optimal Solution) method, which can be utilized by operation managers in factories, tourists, and logistics companies to name a few. This paper elaborates to choose the transporting of best quality cocoa powder from four different factories to four different state with the minimum cost. The proposed method is simple and easily understandable and accessible.

Keywords: BATOS, Transportation, Survey method, Decision-making, Optimal solution.

INTRODUCTION

Numerous methods have been used to make a decision according to an analysis model. Several tools have been developed to solve multi-criteria decision-making (MCDM) problems effectively [19]. The decision-making process is the act of selecting the most suitable action to fulfil the desired goals and objectives [8]. Because decision making is a daily task in our everyday routines, effective tools should be used to analyze all aspects of decision-making problems. Multi-Criteria Decision Making (MCDM) is a well-structured and multidimensional process developed to tackle decision-making problems in different fields and search for the most attractive alternative with consideration of all relevant criteria. Due to its powerful tools, it analyzes complex decision-making problems in different fields.

63167

Amali Theresa and Sahaya Sudha

This method improves the quality of decision-making to become more rational and efficient [12]. Undoubtedly, MCDM has developed recently and been utilized in different fields such as sustainable energy [12,15], maintenance management [2,13], construction management [10], tourism management [1], machine selection [16], material selection [11], petroleum [14], supply chain management [18], aviation [14,9] and risk management [13]. MCDM methods are considered as the most recommended tools when dealing with decision-making problems in various fields. MCDM serves as an aid for decision-making but not to make the decision. In other words, MCDM does not prescribe how decisions should be made. It only leads to logical and reasonable decision rankings [7]. According to many authors, MCDM methods are classified into two groups due to the different problem settings [17]: Multi-Attribute Decision Making (MADM) and Multi-Objective Decision Making (MODM).

MADM deals with decision problems that have an implicit objective and a discrete decision space (finite number of alternatives and attributes). Whereas MODM problems have explicit objectives and a continuous decision space (infinite number of alternatives and attributes). Therefore, different methods are applied based on the nature of decision. Transportation problem is a special kind of Linear Programming Problem (LPP) in which goods are transported from a set of sources to a set of destinations subject to the supply and demand of the sources and destination respectively with minimum cost.

Chocolates are one of the most favorite food for human. Indian Cocoa is also considered one of the best in terms of quality. Most of the Cocoa cultivation in India happens in Tamil Nadu, Karnataka, Andhra Pradesh and Kerala accounting for nearly 80% of the total produce. Instant cocoa beverages belong to the group of hot instant drinks, and hot chocolate itself is one of the most popular dairy products within all age groups [4]. Moreover, their nutritional and sensory properties make them the favorable drinks by several groups of consumers. According to the research done by Daini et al.., [5], hot beverages that contain cocoa have micronutrients and the amount of the nutrients increases the nutritional value of the drink. In this study, this paper explains how to select the best transportation to purchase the best quality cocoa powder from four different factories among four different states with the minimum cost using   multi-criteria decision-making methods which are effective in terms of analysis, selection and ranking.
The multi-criteria decision-making techniques are applied in many areas such as integrated manufacturing systems, evaluation of technology investment, water and agriculture management, Food and energy planning. These methods are effective tools for quantitatively considering qualitative concepts, the challenges faced by the production manager to select the optimal transportation among the available alternatives. Proposed method helps us to choose the best decisions in a right moment. The aim of this method is to avoid complications in using decision making methods, BATOS method is easily understandable and accessible by all researchers.

PRELIMINARIES
Transportation problem
Transportation problem is a special kind of Linear Programming Problem (LPP) in which goods are transported from a set of sources to a set of destinations subject to the supply and demand of the sources and destination respectively such that the total cost of transportation is minimized.

Transportation problem in decision making:
Transportation problem in decision making, is to choose the best transportation available from the alternatives.
Optimal Solution
Optimum solution is a feasible solution (not necessarily basic) which optimizes (minimize) the total transportation cost.

Survey Method
Survey Research is a quantitative research method used for collecting data from a set of respondents. It has been perhaps one of the most used methodologies in the industry for several years due to the multiple benefits and advantages that it has when collecting and analyzing data.

PROPOSED MCDM METHOD

In this section extended decision making method is applied. The structure of the method is shown in table1. For a given MCDM problem there are 'm' Sub alternatives (F_1, F_2, F_3,…F_m), are factories from 'm' main alternatives (S_1, S_2, S_3,… S_m) different states and 'n' criteria (C_1, C_2, C_3, …C_n). Here we applied the extendedproposed method to find the best transportation to purchase goods.
The original decision matrix is given below

Procedure to find the Optimal Solution
Figure 1 - Structural Procedure

Algorithm for the Proposed method
Step 1: Assigning Score Value:
Rank given to the criteria as per the below mentioned rules
 (i) Best Rank should be assigned to the greater value ('+'), like quality.
 (ii)Best Rank should be assigned to the smaller value('-'), like cost and distance.

Step 2: Assigning weight:
      Allotting weight for each criteria using survey method.
Step 3: Calculating weightage:
$W_{ij} = X_{ij} \times W_j$.

$$W_{ij} = \begin{bmatrix} x_{11} & x_{12} & x_{13} & x_{14} & x_{15} \\ x_{21} & x_{22} & x_{23} & x_{24} & x_{25} \\ x_{31} & x_{32} & x_{33} & x_{34} & x_{35} \\ x_{41} & x_{42} & x_{43} & x_{44} & x_{45} \end{bmatrix} \times \text{corresponding weight of each element in the column.}$$

Step 4: Find the best sub alternative from each main alternatives.
Step 5: Calculate the optimal transportation according to thefinal rating.

Case Analysis
A Chocolate factory production manager wants to purchase best quality cocoa powder to make hot chocolate beverages. The cocoa powder available from four different states, Tamil Nadu, Kerala, Andhra Pradesh and Karnataka with four different factories are considered as alternatives and three evaluation criteria available like Cost, Distance, and Quality. In this minimum cost and distance canbe assigned best rank and high quality assigned as best rank. For quality we used Likert scale excellent(E), very good(VG), good(G), Fair(F). Here we use proposed method to choose the best Transportation.

Structure of the given Problem
In this first we are finding the best factory among four states using BATOS method after that we are finding the best state to purchase goods among the states, considering states and factories as alternatives and cost, distance and quality as criteria.

Solution
Step 1: Assigning Score value
  ➢ For Likert Scale, we assigned the score values as follows E(Excellent)-1,VG(Very Good)-2,G(Good)-3 & F(Fair)-4.
  ➢ Best rank should be given to the Smallest value for the cost and distance.
  ➢ Best rank should be given to the greatest values for Quality.

Amali Theresa and Sahaya Sudha

Step 2: Assigning weight for Criteria:
The following table 4 shown the data collected from 10 different chocolate factories about weightage for the criteria. Converting the above table in decimal values, the resultant table 5 shown below

Matrix form of Table 5 is [A_{ij}] where i=1,2,3 & j =1,2,3…..10
$$(A_{ij} = \frac{a_{ij}}{100} \text{, i.e } A_{11}=\frac{20}{100} =0.2)$$
Using Arithmetic Mean Calculate the weight.

Weight for cost $=\overline{X_1} =\sum_{i=1}^{10} X_i= \frac{0.2+0.25+0.25+0.21+0.28+0.22+0.35+0.28+0.23+0.23}{10} = .25$

Weight for Distance$=\overline{X_2} =\sum_{i=1}^{10} X_i = \frac{0.3+0.32+0.35+0.33+0.35+0.38+0.32+0.35+0.38+0.42}{10} = .35$

Weight for Quality$=\overline{X_3} =\sum_{i=1}^{10} X_i= \frac{0.5+0.43+0.40+0.46+0.37+0.40+0.33+0.37+0.39+0.35}{10} = .4$

Weights for Cost is .25, Distance is .35 and Quality is .4.

Structure of weightage for criteria:
(For example, Tamil Nadu Factory F_1, W_1=((1× 0.25) +(1× 0.35)+(1× 0.4) =1.4), same process should be followed for the remaining)

Step 4: Find the best sub alternative from each main alternative:
To choose the best sub alternative We have to find the minimum score value among each state.
❖   In Tamil Nadu Min {1.4, 2.9, 2.4, 2.6} is 1.4. Therefore, Factory 1 is best in Tamil Nadu.
❖   In Kerala Min {1.4, 3.1, 2.6, 2.2} is 1.4. Therefore, Factory 1 is best in Kerala.
❖   In Andhra Pradesh(AP) Min {2.9,1.5,2.5,2} is 1.5. Therefore, Factory 2 is best in AP.
❖   In Karnataka Min {2.6, 1.8, 2.9,82.6} is 1.8. Therefore, Factory 2 is best in Karnataka.

Best Sub Alternative from Each State
Structure of the best Sub Alternative

Step 5: Calculate the optimal transportation
According to our conclusion, Table 8 shows the best sub alternatives and their data has taken from the given problem.
Now, we have only main alternatives, criteria and weight.
To select the optimal transportation, we have to repeat steps 1 to 4.
The Table 9 shows the best transportation after applying step 1 to 4.

According to Proposed Method Optimal Transportation is Factory 1 from Tamil Nadu.

CONCLUSION

In this paper we conclude that Using Proposed method, the production manager can choose Factory1 from Tamil Nadu as an optimal transportation among the four different factories from four states. Here we used four sub alternatives as well as four main alternatives. I conclude that this method helps to avoid complications while using decision making methods, proposed method is easily understandable, accessible and time consumable by all researchers, which is an easy method to take decisions when we have sub and main alternatives. This method will create great impact on Business Industry People, Tourists and Researchers.

REFERENCES

1. Akincilar.A and Dagdeviren.M, (2014), "A hybrid multi-criteria decision making model to evaluate hotel websites," International Journal of Hospitality Management, 36, 263–271
2. Al-Najjar.B and Alsyouf.I (2003), "Selecting the most efficient maintenance approach using fuzzy multiple criteria decision making," International Journal of Production Economics, 84(1), 85–100.
3. Cheng-ShiungWua,n, Chin-TsaiLin b,1, ChuanLee c(2010), " Optimal marketing strategy: A decision-making with ANP and TOPSIS" International Journal of Production Economics127,190–196.
4. Da Silva Lannes SC, Medeiros ML (2008), "Rheological properties of chocolate drink from cupuassu." International Journal of Food Engineering 4(1):1–11
5. Daini OA, Ogunledun A, Fagade O, Akinpelu OS (2003), "Nutritional status of locally produced cocoa based beverages." Nigerian Food Journal 21:70–75.
6. Gudiel Pineda P.J., Liou.J. J. H., Hsu C. C., and Chuang Y. C (2018), "An integrated MCDM model for improving airline operational and financial performance," Journal of Air Transport Management 68, 103–117.
7. Gupta.H (2018), "Evaluating service quality of airline industry using hybrid best worst method and VIKOR," Journal of Air Transport Management 68, 35–47.
8. Haddad.M, Sanders.D (2018), "Selection of discrete multiple criteria decision making methods in the presence of risk and uncertainty," Operations Research Perspectives 5, 357–370.
9. Janic.M, Reggiani.A (2002), "An application of the multiple criteria decision making (MCDM) analysis to the selection of a new Hub Airport," European Journal of Transport Infrastrucure Research 2(2), 3692.
10. Jato-Espino.D, Castillo-Lopez.E, Rodriguez-Hernandez.J, and Canteras-Jordana J.C (2014), "A review of application of multi-criteria decision making methods in construction," Automation in Construction 45, 151–162.
11. Mousavi-Nasab S.H, 1Sotoudeh-Anvari.A (2017), "A comprehensive MCDM-based approach using TOPSIS, COPRAS and DEA as an auxiliary tool for material selection problems," Materials and Design 121, 237–253.
12. Pohekar S.D, Ramachandran M (2004), "Application of multi-criteria decision making to sustainable energy planning - A review," Renewable and Sustainable Energy Reviews 8(4), 365 –381.
13. Shafiee.M (2015), "Maintenance strategy selection problem: An MCDM overview," Journal of Quality in Maintenance Engineering 21(4):378-402.
14. Shahsavari.M.H, Khamehchi.E (2018), "Optimum selection of sand control method using a combination of MCDM and DOE techniques," Journal of Petroleum Science Engineering 171, 229–241.
15. Siksnelyte I, Zavadskas E.K, Streimikiene.D, and Sharma.D (2018), "An overview of multi-criteria decision-making methods in dealing with sustainable energy development issues," Energies 11(10), 2754.
16. Štirbanović.Z, Stanujkić.D, Miljanović.I, and Milanović.D (2019), "Application of MCDM methods for flotation machine selection," Mineral Engineering 137, 140–146.
17. Triantaphyllou.E, Shu.B, Sanchez.S. N, T. Ray (1998), "Multi-Criteria Decision Making: An Operations Research Approach," Encyclopedia of Electrical and Electronics Engineering15, 175–186.
18. Wansink B, Sobal J (2007), "Mindless eating: the 200 daily food decisions we overlook" Environ Behav39:106–23.
19. Xu WU, Cheng ZHANG,Luojun YANG(2021), "Evaluation And Selection Of Transportation Service Provied By Topsis Method With Entropy Weight" Vol. 25,1483-1488.

Table 1. Structure of The decision matrix

Alternatives /Criteria	S_1				S_2				……				S_m			
	W_1	W_2	….	W_n	W_1	W_2	….	W_n	W_1	W_2	….	W_n	W_1	W_2	….	W_n
	C_1	C_2	….	C_n	C_1	C_2	….	C_n	C_1	C_2	….	C_n	C_1	C_2	….	C_n
F_1	X_{11}	X_{12}	….	X_{1n}	X_{11}	X_{12}	….	X_{1n}	X_{11}	X_{12}	….	X_{1n}	X_{11}	X_{12}	….	X_{1n}
F_2	X_{21}	X_{22}	….	X_{2n}	X_{21}	X_{22}	….	X_{2n}	X_{21}	X_{22}	….	X_{2n}	X_{21}	X_{22}	….	X_{2n}

Amali Theresa and Sahaya Sudha

F₃	X31	X32	····	X3n	X31	X32	····	X3n	X31	X32	····	X3n	X31	X32	····	X3n
⋮		····	····	····	····	····	····	····	····	····	····	····	····	····	····	····
Fₘ	Xm1	Xm2	····	Xmn	Xm1	Xm2	····	Xmn	Xm1	Xm2	····	Xmn	Xm1	Xm2	····	Xmn

Table 2

Criteria/ Alternative	Tamil Nadu			Kerala			Andhra Pradesh			Karnataka		
	Cost	Dist	Qua	Cost	Dist	Qua	Cost	Dist	Qua	Cost	Dist	Qua
F₁	210	50	VG	200	100	E	250	150	VG	230	175	E
F₂	240	80	VG	220	120	G	230	135	E	210	90	G
F₃	220	75	G	240	115	VG	200	158	VG	280	120	VG
F₄	225	100	E	250	98	VG	210	145	VG	225	95	F

Table 3. Score Value

Criteria/ Alternative	Tamil Nadu			Kerala			Andhra Pradesh			Karnataka		
	Cost	Dist	Qua	Cost	Dist	Qua	Cost	Dist	Qua	Cost	Dist	Qua
F₁	1	1	2	1	2	1	4	3	2	3	4	1
F₂	4	3	2	2	4	3	3	1	1	1	1	3
F₃	2	2	3	3	3	2	1	4	2	4	3	2
F₄	3	4	1	4	1	2	2	2	2	2	2	4

Table 4 Criteria Weights

Factory	Cost	Distance	Quality	Total
Factory 1	20%	30%	50%	100
Factory 2	25%	32%	43%	100
Factory 3	25%	35%	40%	100
Factory 4	21%	33%	46%	100
Factory 5	28%	35%	37%	100
Factory 6	22%	38%	40%	100
Factory 7	35%	32%	33%	100
Factory 8	28%	35%	37%	100
Factory 9	23%	38%	39%	100
Factory 10	23%	42%	35%	100
Total	250	350	400	1000

Amali Theresa and Sahaya Sudha

Table 5Criteria Conversion

Factory/criteria	F_1	F_2	F_3	F_4	F_5	F_6	F_7	F_8	F_9	F_{10}
Cost (X_1)	0.2	0.25	0.25	0.21	0.28	0.22	0.35	0.28	0.23	0.23
distance(X_2)	0.3	0.32	0.35	0.33	0.35	0.38	0.32	0.35	0.38	0.42
Quality(X_3)	0.5	0.43	0.40	0.46	0.37	0.40	0.33	0.37	0.39	0.35

Table 6 Total Weightage Calculation

Criteria/ Alternative	Tamil Nadu				Kerala				Andhra Pradesh				Karnataka			
	Cost	Dist	Qua	Total W_i	Cost	Dist	Qua	Total W_i	Cost	Dist	Qua	Total W_i	Cost	Dist	Qua	Total W_i
Weight	0.25	0.35	0.4		0.25	0.35	0.4		0.25	0.35	0.4		0.25	0.35	0.4	
F_1	1	1	2	1.4	1	2	1	1.4	4	3	2	2.9	3	4	1	2.6
F_2	4	3	2	2.9	2	4	3	3.1	3	1	1	1.5	1	1	3	1.8
F_3	2	2	3	2.4	3	3	2	2.6	1	4	2	2.5	4	3	2	2.9
F_4	3	4	1	2.6	4	1	2	2.2	2	2	2	2	2	2	4	2.8

Table 7 Best Sub Alternative

Criteria/ Alternative	Tamil Nadu	Kerala	Andhra Pradesh	Karnataka
F_1	1	1	4	2
F_2	4	4	1	1
F_3	2	3	3	4
F_4	3	2	2	3

Table 8- Best Sub Alternatives Data from the Problem

Alternative/Criteria	Cost	Distance	Quality
Weight	0.25	0.35	0.4
Tamil Nadu	210	50	VG
Kerala	200	100	E
Andhra Pradesh	230	135	E
Karnataka	210	90	G

Table 9 Optimal Transportation

Criteria/ Alternative	Cost	Distance	Quality	Total	Rank
Weight	0.25	0.35	0.4		
Tamil Nadu	2	1	2	1.65	1
Kerala	1	3	1	1.7	2
Andhra Pradesh	4	4	1	2.8	4
Karnataka	2	2	3	2.4	3

Amali Theresa and Sahaya Sudha
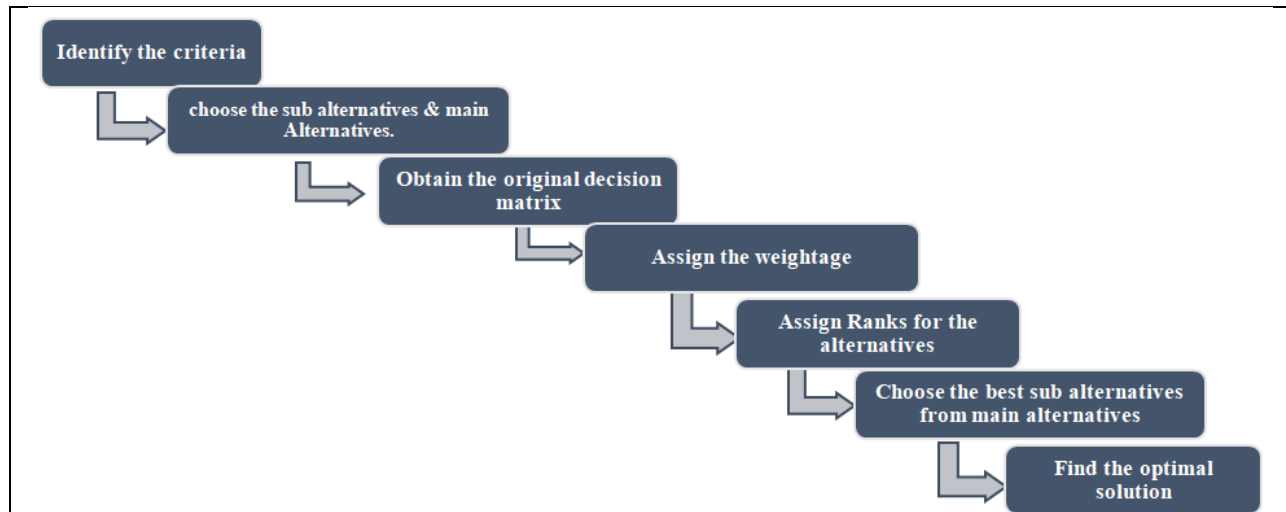
Figure 1 - Structural Procedure
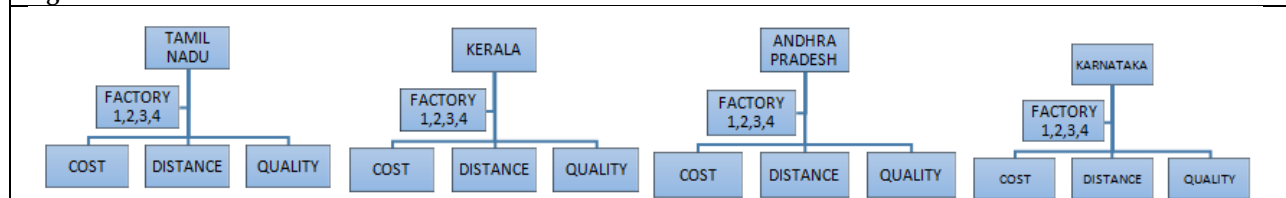
Figure 2 - Problem structure

	1	2	3	4	5	6	7	8	9	10
COST	0.2	0.25	0.25	0.21	0.28	0.22	0.35	0.28	0.23	0.23
DISTANCE	0.3	0.32	0.35	0.33	0.35	0.38	0.32	0.35	0.38	0.42
QUALITY	0.5	0.43	0.4	0.46	0.37	0.4	0.33	0.37	0.39	0.35
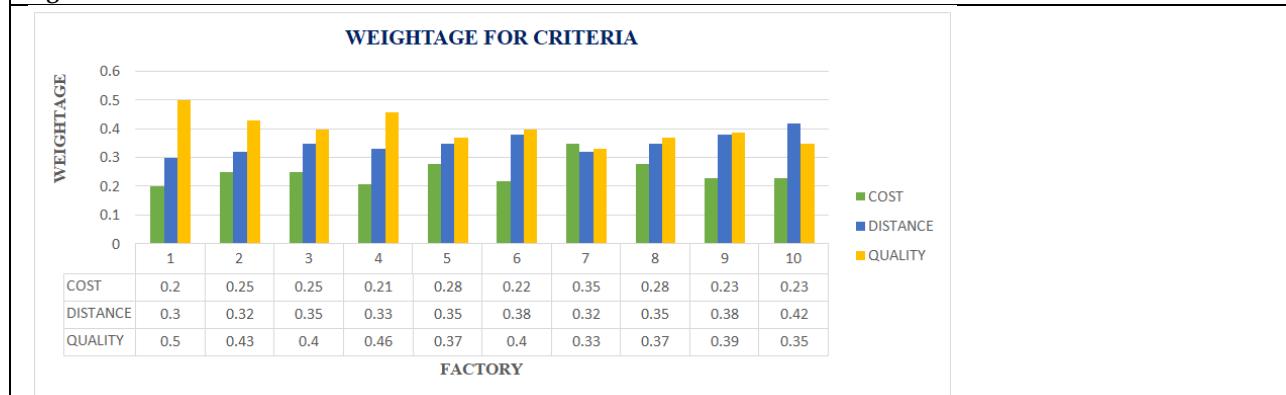
Figure 3-Structure of Weightage

Amali Theresa and Sahaya Sudha
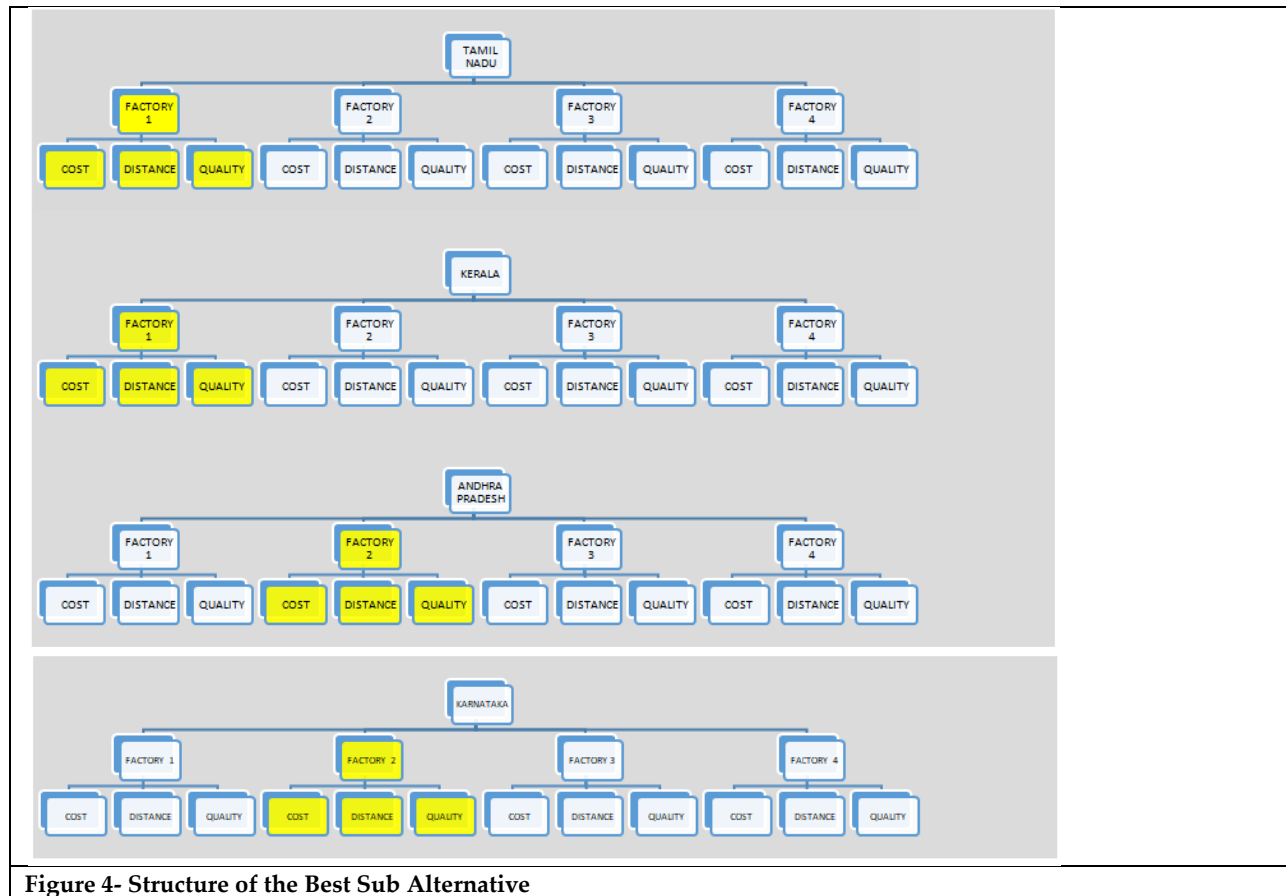
Figure 4- Structure of the Best Sub Alternative

RESEARCH ARTICLE

Inhibitory Efficacy of Hesperidin against a Variety of Cancer Targets by *In silico* Virtual Screening

Krithiga Balakrishnan[1,2], Ramanathan Shreemaya[3], Sowmya Sekar[1] and Jayaprakash Arul[1*]

[1]Department of Biochemistry, Sacred Heart College (Autonomous), Tirupattur-635 601, Tamil Nadu, India.
[2]Department of Biochemistry, Thiruvalluvar Arts and Science College, Kurinjipadi, Cuddalore-607302, Tamil Nadu , India
[3]Department of Biotechnology, D.Y. Patil Deemed to be University, Navi Mumbai-400614, India

*Address for Correspondence
Jayaprakash Arul
Department of Biochemistry,
Sacred Heart College (Autonomous),
Tirupattur-635 601, Tamil Nadu, India.
E.Mail: jpsacred2019@gmail.com

ABSTRACT

The primary goal of this study is to assess hesperidin's anti-cancer capability against particular molecular targets to treat cancer. Hesperidin has been chosen as the experimental ligand after conducting a thorough ligand analysis. For this study, Bax, Bcl-2, NF Kappa B, Carbonic anhydrase I (CA-1), Inducible Nitric Oxide Synthase (iNOS), Endothelial Nitric oxide synthase (eNOS), Caspase 3, and Caspase 9 proteins have been chosen as therapeutic targets. Molecular docking was conducted using Glide module of Schrödinger software. Further evaluation was based on dock score, conformational changes, and the amino acid residues involved in the protein-ligand interaction. Hesperidin showed significant binding affinity, especially with caspase 3, carbonic anhydrase I, ENOS, and INOS. It also showcased considerable potential against Bax, Bcl-2, Caspase 9 and NFκB, demonstrating its potential as an effective anti-cancer drug.In this study, the inhibitory potential of hesperidin was analyzed using in-silico molecular docking study. Hesperidin revealed significant binding efficiency against the aforementioned therapeutic targets, thereby showcasing its potential as a potent anti-cancer agent. *In vitro* analysis is required for further validation of this data.

Keywords: Computer-aided drug discovery, Hesperidin, Molecular docking, Anti-cancer activity

INTRODUCTION

Cancer is one of the leading causes of mortality all around the world. Female breast cancer is the most frequently diagnosed disease, closely followed by lung, colorectal, prostate, and stomach cancer [1,2]. Despite developing novel anti-cancer drugs, chemotherapy, radiotherapy, and surgery are deployed to treat various cancers. Nonetheless, the utilization of synthetic pharmaceutical drugs has not enhanced the treatment productivity, and there has been no general improvement in the endurance pace of the patients [3,4]. Pharmaceutical drugs showcase detrimental effects, including high toxicity, drug resistance, and fatal impact on the non-targeted tissues. Due to this, there is a requirement to discover novel therapeutics for a more secure and robust treatment approach [5]. At first, conventional drug discovery approaches took around ten years, employing an experimental method for screening potential compounds. The traditional process was tedious and unpractical. In the wake of discovering potential ligands, it took around ten years to perform clinical preliminaries to foster a clever medication for a specific sickness. For this reason, a computer-aided drug designing technique was developed utilizing Molecular mechanics to comprehend protein-ligand interactions [6]. Numerous ligands can be selected, and around 200 – 500 compounds can be screened simultaneously via virtual screening. Molecular docking is conducted *in-silico*, wherein the connection between tiny particles and proteins is examined at a nuclear level. It is used to portray the active site of target proteins to comprehend the inward functions of human illnesses at the atomic level [7,8]. Ligands with higher binding affinity are chosen based on blind docking. Potential drug candidates can be further tested by conducting subsequent clinical trials. Nowadays, by focusing on significant domains crucial for inhibition, target-specific inhibitors can be developed for effective and targeted approaches [9].

Flavonoids are known for showcasing potent antioxidant properties by abolishing ROS (reactive oxygen species) and free radicals' production, thereby depicting the potential to treat various stages of tissue damage, including diverse types of cancers. Most citrus fruits (lemon, mandarin and oranges) contain hesperidin, a vital bioflavonoid. It is located in association with Vitamin C [10,11]. It is experimentally verified that hesperidin is not cytotoxic and it is safe consumption. It is one of the most significant bioactive compounds, depicting anti-cancer, antioxidant, anti-microbial and anti-inflammatory properties. Hesperidin possesses significant anti-inflammatory properties and is being administered to treat hypersensitivity reactions[10]. Induction of oxidative stress leads to cellular proliferation, inhibition of apoptosis, metastasis and angiogenesis. Hesperidin is known for its potent antioxidant activity and showcases potent anti-cancer activity. Hesperidin's antioxidant capacity was assessed by its ability to sequester 1,1-diphenyl-2-picrylhydrazyl (DPPH), which resulted in a substantial reduction in the levels of the free radical DPPH with effectiveness comparable to Trolox [12,13]. Hesperidin has antioxidant properties that protect against the harmful effects of paraquat and peroxide hydrogen[14]. By activating apoptosis and decreasing cyclooxygenase-2 expression, hesperidin inhibited tobacco-related carcinogen NNK-induced mouse lung tumorigenesis[15]. It is observed that hesperidin decreased cellular proliferation in the colonic mucosa, thereby inhibiting carcinogenesis suffering from colon cancer [16,17]. In this study, hesperidin is chosen as an experimental ligand, and it is docked with Bax, BCL-2, NFκB, Carbonic Anhydrase 1 (CA-1), iNOS, eNOS, caspase 3, and caspase 9 to assess its binding efficacy and anti-cancer potential.

MATERIALS AND METHODS

Protein preparation
3D structures of BAX, Bcl-2, NF Kappa B, Carbonic anhydrase I, INOS, ENOS, Caspase 3, and Caspase 9 were retrieved from the Protein Data Bank (PDB). It is a repository with various 3D protein structures generated by NMR spectroscopy and X-ray crystallography. The removal of water molecules, the insertion of missing hydrogen bonds, and proper bond orders were assigned to non-standard residues were all part of the protein preparation process. Following this, the optimization of the hydroxyl group and hydrogen bonds along with amine groups of the amino acids on the target proteins were carried out. The energy reduction method was carried out using the OPLS3e force

field.The non-hydrogen atoms were reduced to a minimum until the average root mean square deviation approached 0.3 Å.

Active site prediction
Active sites are crucial for *in-silico* analysis as the amino acid residues present in this site will decide whether the ligand will inhibit/activate a particular domain. The active sites of the proteins were predicted using the Uniprot database, Interpro scan server, and the Sitemap module of Schrodinger. In this study, the active site residues of Carbonic anhydrase 1, INOX, ENOX, Caspase 3, and Caspase 9 was predicted via Uniprot and Interpro scan web server analysis. Whereas the active site residues of Bax, BCl-2 and NFκB was predicted by Sitemap.

Ligand Preparation
The 3D structure of compound hesperidin (PubChem ID: 10621) was downloaded from the PubChem database.

Domain analysis
Domains are the functional part of any protein. From the concept of structural biology, the domains are the conserved region of the protein. The protein domain analysis was carried out using the Pfam database to predict the functional domain region of the selected protein.

Receptor Grid Generation
The position and size of the active site are represented by the construction of receptor grids. For the docking procedure, a receptor grid generating module was implemented, where compounds were to be docked using a centroid of selected protein residues. It's an important step to do before commencing molecular docking.

Induced Fit docking using XP Glide Algorithm
The compound Hesperidin is docked with all the eight proteins using the GLIDE module of Schrödinger. Primarily, protein preparation was performed via the addition of missing hydrogens and by assignment of bond orders. Further, the optimization and minimization process of the target proteins was carried out. Then Ligprep was used for the preparation of ligand molecules by optimization of the ligand structures through the OPLS3e force field.Molecular docking is incorporated in this research study via the use of the XP (Extra Precision) scoring algorithm. The ligand docking module was integrated for the docking of compound hesperidin with the target proteins using the XP method in the GLIDE module of Schrödinger. The scoring function in XP Glide is based on a thorough evaluation of protein-ligand interactions and incorporates an extensive sampling of docked structures [18]. The top-scoring structures are subjected to grid-based water scoring methodology, and the entire XP dock score scoring function and identification of structural motifs are computed.

RESULTS AND DISCUSSION

Protein preparation
The targets were chosen on the basis of molecular function and biological processes of the proteins in cancer progression. The 3D structures of all eight proteins were downloaded in PDB format from the Protein Data Bank for further analysis.

Ligand Preparation
The ligand hesperidin was downloaded from the PubChem database (Fig. 1).

Domain analysis
The functional domain analysis of the target proteins was performed using the Pfam database, and this information is shown in Table 1. These details were crucial in determining the active sites and amino acid residues in each of our target proteins.

63178

Active site prediction

The amino acid residues of the active sites of target proteins were predicted using Uniprot, Interproscan, and Sitemap. The active site of Carbonic anhydrase 1, INOX, ENOX, Caspase 3, and Caspase 9 were predicted by Uniprot and Interproscan. Whereas BAX, BCl-2, and NFκB binding sites were predicted by Sitemap (Table 2).

Molecular Docking

The XP (Extra precision) technique of Schrödinger's GLIDE module was used for molecular docking. Table 3 shows the docking score, bond length, and different amino acid residues involved in the protein-ligand interaction. Many pro-apoptotic proteins (BAX, BAK, BIM, BID, and BAD) are found in the BCL-2 family and are essential for triggering apoptosis in malignant cells. It also contains anti-apoptotic proteins (BCL-2, BCL-xL) that are responsible for the inhibition of apoptosis. The proteins of the BCL-2 family are a promising target for the treatment of a variety of cancers. BCL-2, BCL-xL, and BAX are three members of the Bcl-2 family with many structural and functional similarities. BH1-BH4 domains are conserved in the anti-apoptotic proteins BCL-xL and BCL-2. The BH3 domain (essential for triggering apoptosis), BH1, and BH2 domains make up Bax, a pro-apoptotic protein. The anti-apoptotic proteins constitute a hydrophobic groove, and the BH3 domain of pro-apoptotic proteins like BAX bind to the groove via an amphipathic alpha-helix, thereby inhibiting apoptosis.

In this study, this BCL-2 (BCL-xL) domain crucial for imparting anti-apoptotic property is targeted as it is common in both Bax and Bcl-2 protein. The docking analysis depicted dock score of -6.0 kcal/mol and -6.7 kcal/mol of hesperidin with Bax and Bcl-2 protein, respectively. Hydrogen bond interaction is observed with the binding of hesperidin to Bax protein with the binding site residues Ala 81, Val 83, Asp 84 and Asp 86. Multiple interactions were observed with the binding of hesperidin to Bcl-2, wherein hydrogen bond interaction is observed with amino acid residues Glutamine 58 and Tyrosine 161. Pi-cation interaction is also observed with amino acid residue Arginine at 66th position and hydrogen bond interaction with Leu 160, similar to the action inhibitor N-heteroaryl sulfonamide [19].
NFκB is a transcription factor present in all cell types and is involved in various biological processes, including inflammation, immunity, cell proliferation, differentiation, and survival. Rel homology domain is a protein domain found in the family of eukaryotic transcription factors like NFκB. It is composed of two structural domains. The N-terminal DNA binding domain is similar to the one found in p53 protein; the C-terminal domain has an immunoglobulin-like fold that functions as a dimerization domain [20]. Phosphorylation of the N-terminal domain is crucial in regulating transcription factors by targeting the expression of specific genes [21].

For this study, the binding site residues are based on the N-terminal of Rel homology domain of NFκB is targeted. The docking analysis of hesperidin with NFκB depicted dock score of -6.4 kcal/mol. Hydrogen bond interaction is observed with the binding site residues Asp 94 and Arg 103.The active site of most carbonic anhydrases contains a zinc ion in its active site for its crucial for its function [22]. Carbonic anhydrases I and II are highly expressed in the GI tract and kidneys and are known to mediate the pH in tumour cells by modulating the proton and bicarbonate concentrations, thereby inducing cellular survival and proliferation [23]. The zinc ion is coordinated by the imidazole rings of 3 histidine residues, His94, His96, and His119 [22]. The docking analysis of hesperidin with Carbonic anhydrase I depicted dock score of -7.8 kcal/mol. Multiple non-covalent molecular interactions are observed. Hydrogen bond interaction is observed with the binding site residues HIE 94 and Pi-Pi stacking interaction with Thr 199 similar to the inhibitor Polmacoxib [24].

Inflammation is caused by inducible nitric oxide synthase (iNOS), which increases the production of pro-inflammatory cytokines such as IL-6, IL-8, TNF, and IFN-. Vascular endothelial growth factor-induced angiogenesis (VEGF) is mediated by endothelial nitric oxide synthase (eNOS), which increases angiogenesis in cancer cells. iNOS is primarily present in the cytosol, whereas eNOS is situated on the membrane.For this study, the oxygenase domain is targeted containing Nitric oxide synthase. The docking analysis of hesperidin with Inducible nitric oxide synthase (INOS) with a dock score of -12.7 Kcal/mol. Hydrogen bond interactions are observed with active site residues Cys 200, Asp 382 and Trp 463, similar to the interaction observed by inhibitor S-ethylisothiourea (SEITU) with INOS [25]. The docking analysis of hesperidin with Endothelial nitric oxide synthase (ENOS) with a dock score of -12.6

Kcal/mol. Hydrogen bond interactions with the active site residues Tyr 475 and Glu 361 and pi-pi stacking interaction with Trp 178. Among all caspases, caspase 3 and caspase 9 play a crucial in initiating and executing programmed cell death in cancerous cells. When cytochrome c produced from mitochondria binds with Apaf-1 in response to an apoptotic signal, caspase 9 is activated [26]. This causes caspase 3 to be cleaved, and it is activated along with caspases 6 and 7 to induce apoptosis[26,27]. For this study, the peptidase C14 / p20 domain of caspase 3 is targeted. The activation of apoptosis can sometimes lead to caspase-1 activation, which links apoptosis and inflammation, such as during the targeting of infected cells [28]. For this study, peptidase C14, the caspase catalytic domain of caspase 9, is targeted. This domain includes the core of the p45 precursor of caspases, which is processed to produce the active p20 and p10 subunits [29]. The docking analysis of hesperidin with Caspase 3 protein with a dock score of -7.8 kcal/mol. Hydrogen bond interaction is observed with the active site residues Arg 207, Trp 214 and Asp 253. The docking analysis of hesperidin with Caspase 9 protein resulted in the dock score of -5.7 kcal/mol. Hydrogen bond interaction is observed with active site residues Asp 355, Ser 345, Glu 351, Glu 358, Lys 380.

CONCLUSION

According to the findings of this study, hesperidin is an effective treatment because of its considerable antioxidant capacity, which provides excellent anti-cancer and chemopreventive effects. It demonstrates high binding effectiveness and affinity for several important anti-cancer targets. An *in-silico* analysis cannot fully comprehend the anti-cancer mechanism of hesperidin. To fully understand hesperidin's anti-cancer, chemopreventive, and antioxidant potential, more research using *in-vitro* and *in-vivo* methods are necessary.

Competing interest
The authors declare that they have no known competing financial interests or personal relationships that could have appeared to influence the work reported in this paper.

REFERENCES

1. Sung H,Ferlay J, Siegel RL,Laversanne M,Soerjomataram I, Jemal A, Bray F. Global Cancer Statistics 2020: GLOBOCAN Estimates of Incidence and Mortality Worldwide for 36 Cancers in 185 Countries. CA Cancer J Clin. 2021; 71: 209-249. https://doi.org/10.3322/caac.21660
2. Cao W, Chen HD, Yu YW, Li N, Chen WQ. Changing profiles of cancer burden worldwide and in China: a secondary analysis of the global cancer statistics 2020. Chinese Medical Journal.2021; 134:783-91.https://doi.org/10.1097/CM9.0000000000001474
3. Choudhari AS, Mandave PC, DeshpandeM, Ranjekar P, Prakash O. Phytochemicals in Cancer Treatment: From Preclinical Studies to Clinical Practice. 2020**;**10: 1614.https://doi.org/10.3389/fphar.2019.01614
4. Prakash S, Kumar M, Kumari N, Thakur M, RathourS, PundirA, SharmaAK, Bangar SP, Dhumal S, Singh S,ThiyagarajanA. Plant-Based Antioxidant Extracts and Compounds in the Management of Oral Cancer. Antioxidants.2021; 10: 1358https://doi.org/10.3390/antiox10091358
5. Gokalp F. The effective natural compounds for inhibiting Cervical cancer. Medical Oncology. 2021; 38: 1-4. https://doi.org/10.1007/s12032-021-01456-3

6. SabeVT, NtombelaT, Jhamba LA, Maguire GE, GovenderT, NaickerT, KrugerHG. Current trends in computer aided drug design and a highlight of drugs discovered via computational techniques: A review. European Journal of Medicinal Chemistry. 2021; 224, 113705. https://doi.org/10.1016/j.ejmech.2021.113705

7. Yalcin-OzkatG. Molecular Modeling Strategies of Cancer Multidrug Resistance. Drug Resistance Updates. 2021; 100789. https://doi.org/10.1016/j.drup.2021.100789

8. Anand MariadossAV, Krishnan DhanabalanA, Munusamy H, Gunasekaran K, David E. In Silico Studies towards Enhancing the Anticancer Activity of Phytochemical Phloretin Against Cancer Drug Targets. Current Drug Therapy. 2018;13: 174-188.https://doi.org/10.2174/1574885513666180402134054

9. Idris MO,Adeniji SE, HabibK, AdeizaAA. Molecular docking of some novel quinoline derivatives as potent inhibitors of human breast cancer cell line. Lab-in-Silico. 2021; 2: 30-7. https://doi.org/10.22034/labinsilico21021030

10. PandeyP, KhanF. A mechanistic review of the anticancer potential of hesperidin, a natural flavonoid from citrus fruits. Nutrition Research. 2021; 92: 21-31.https://doi.org/10.1016/j.nutres.2021.05.011

11. Sa Ayinzat FE,Bawa EK, Ogwu D, Ayo JO. Hesperidin-Sources, chemistry, extraction, measurement and biologic effects on reproduction in animals: A review.International Journal of Veterinary Sciences and Animal Husbandry. 2021; 6: 01-08https://doi.org/10.22271/veterinary.2021.v6.i3a.360

12. ZhongG, Shen J, ChenZ, LinZ, Long L, WuJ, LongC, HuangS, LianP, LuoG. Antioxidant and Antitumor Activities of Newly Synthesized Hesperetin Derivatives. Molecules.2022; 27: 879. https://doi.org/10.3390/molecules27030879

13. Wilmsen PK, Spada DS, Salvador M. Antioxidant activity of the flavonoid hesperidin in chemical and biological systems. J Agric Food Chem. 2005;53: 4757-4761.https://doi.org/10.1021/jf0502000

14. Zare M, Sarkati MN, Rahaiee S. Fabrication of Nanoparticles based on Hesperidin-Loaded Chitosan-Functionalized Fe3O4: Evaluation of In vitro Antioxidant and Anticancer Properties. Macromolecular Research. 2021; 785-90.https://doi.org/10.1007/s13233-021-9091-7

15. KohnoH, Taima M, Sumida T, Azuma Y, Ogawa H, Tanaka T. Inhibitory effect of mandarin juice rich in beta-cryptoxanthin and hesperidin on 4-(methylnitrosamino)-1-(3-pyridyl)-1-butanone-induced pulmonary tumorigenesis in mice. Cancer Lett.2001:*174*: 141-150. https://doi.org/10.1016/s0304-3835(01)00713-3

16. Sindhu RK, VermaR, Salgotra T, Rahman MH, Shah M., Akter R, Murad W, Mubin, S, Bibi P, Qusti S, AlshammariEM. Impacting the remedial potential of nano delivery-based flavonoids for breast cancer treatment. Molecules. 2021; 26: 5163. https://doi.org/10.3390/molecules26175163

17. HasanS, MansourH, WehbeN, Nasser SA, IratniR, NasrallahG, Shaito A, GhaddarT, Kobeissy F, Eid AH. Therapeutic potential of flavonoids in cancer: ROS-mediated mechanisms.Biomedicine & Pharmacotherapy. https://doi.org/10.1016/j.biopha.2021.112442

18. RepaskyMP, ShelleyM, FriesnerRA.Flexible Ligand Docking with Glide. Current Protocols in Bioinformatics. 2007; 18: 8-12. https://doi.org/10.1002/0471250953.bi0812s18

19. Toure BB, Miller-Moslin K, Yusuff N, Perez L, Dore M, Joud C, Michael W, DiPietro L, vanderPlasS, McEwan M, Lenoir F, Hoe M, Rajesh K, Springer C, Sullivan J, Levine K, FiorillaC, Xiaoling X, Raviraj K, HerlihyK, Porter D, MichaelV. The role of the acidity of N-heteroaryl sulfonamides as inhibitors of bcl-2 family protein-protein interactions. ACS Med Chem Lett 2013;*4*: 186-190. https://doi.org/10.1021/ml300321d

20. Moorthy AK, HuangDB, WangVY, VuD, GhoshG. X-ray structure of a NF-kappaB p50/RelB/DNA complex reveals assembly of multiple dimers on tandem kappaB sites. J Mol Biol. 2007; 373: 723-734.https://doi.org/10.1016/j.jmb.2007.08.039

21. AnratherJ, Racchumi G, Iadecola C. Cis-acting, element-specific transcriptional activity of differentially phosphorylated nuclear factor-kappa B. J Biol Chem. 2005;280: 244-252. https://doi.org/10.1074/jbc.M409344200

22. *carbonic anhydrase – wikepdia*

23. MbogeMY, MahonBP, McKennaR, Frost SC. Carbonic Anhydrases: Role in pH Control and Cancer. Metabolites. 2018; 8. https://doi.org/10.3390/metabo8010019

24. Kim HT, ChaH, HwangKY. Structural insight into the inhibition of carbonic anhydrase by the COX-2-selective inhibitor polmacoxib (CG100649). BiochemBiophys Res Commun. 2016**;** *478*; 1-6. https://doi.org/10.1016/j.bbrc.2016.07.114

25. FischmannTO, Hruza A, Da NiuX, Fossetta JD, Lunn CA, Dolphin E, ProngayAJ, Reichert P, Lundell DJ, Narula SK. Structural characterization of nitric oxide synthase isoforms reveals striking active-site conservation. Nature structural biology. 1999;*6*:233-242, https://doi.org/10.1038/6675

26. Kuida K, Caspase-9. Int J Biochem Cell Biol. 2000;*32*: 121-124. https://doi.org/10.1016/s1357-2725(99)00024-2.

27. Rasool F, Sharma D, Anand PS, Magani SK, Tantravahi S. Evaluation of the Anticancer Properties of Geranyl Isovalerate, an Active Ingredient of Argyreia nervosa Extract in Colorectal Cancer Cells. Frontiers in Pharmacology. 2021; 12.https://doi.org/10.3389/fphar.2021.698375

28. Abraham MC, Shaham S. Death without caspases, caspases without death. Trends Cell Biol. 2004;14: 184-193.https://doi.org/10.1016/j.tcb.2004.03.002.

29. Mulder N, Apweiler R. InterPro and InterProScan: tools for protein sequence classification and comparison. Methods in Mol Biol.2007;396: 59-70. https://doi.org/10.1007/978-1-59745-515-2_5.

Table1: Domain Analysis

SR.NO	Protein Name	Domain Name	Domain Region
1.	BAX protein (Q07812)	Bcl-2	63-158
2.	Bcl-2 protein (Q07817)	Bcl-2	90-188
3.	NF Kappa B (Q00653)	RHD_DNA_bind	40-220
4.	Human carbonic anhydrase 1 (P00915)	Carb_anhydrase	12-261
5.	INOS (P35228)	NO_synthase	82-508
6.	ENOS (P29474)	NO_synthase	119-481
7.	Caspase 3 (P42574)	Peptidase_C14	43-167
8.	Caspase 9 (P55211)	Peptidase_C14	160-412

Table 2: Prediction of binding site residues

S.No	Protein Name	Active site/Binding site residues
1.	**BAX protein (Q07812)**	70, 80, 81, 83-85, 88, 91, 92, 115, 116, 119, 120, 123, 124, 127, 132, 136, 139
2.	**Bcl-2 protein (Q07817)**	55, 58, 59, 62, 63, 66, 67, 103, 104, 105, 107, 108, 157, 161-163.
3.	**NF Kappa B (Q00653)**	94, 95, 103-105, 107-109, 117-119, 153, 154, 156, 157, 160, 193
4.	**Human carbonic anhydrase 1 (P00915)**	62, 64, 65, 67, 91, 92, 94, 96 ,119, 121, 122, 131, 135, 141, 143, 198-200, 207, 209
5.	**INOS (P35228)**	118, 200, 347, 370, 372, 381, 382, 463, 491
6.	**ENOS (P29474)**	184, 247, 353, 354, 356, 357, 368, 366, 447, 475
7.	**Caspase 3 (P42574)**	64, 121, 122, 161, 163, 168, 204-209, 213, 214
8.	**Caspase 9 (P55211)**	180, 237, 238, 285, 287, 292, 352-357, 361, 362

Table 3: Molecular docking of hesperidin against the given cancer targets

SR.NO	Protein Name	Dock Score (Kcal/mol)	Interacting residues	Bond length (Å)
1.	**BAX protein (4SOP)**	-6.0	Ala 81, Val 83, Asp 84 (2), Asp 86	1.79, 1.83, 1.89, 2.05, 2.12
2.	**Bcl-2 protein (4IEH)**	-6.7	Gln 58, Arg 66, Leu 160, Tyr 161	2.06, 3.12, 1.90, 1.96
3.	**NF Kappa B (1A3Q)**	-6.4	Lys 90, Glu 92 (2), Asp 94, Arg 103	2.00, 1.66, 1.93, 1.96, 2.01
4.	**Carbonic anhydrase 1 (5GMM)**	-7.8	Asp 72 (2), His 94, Thr 199, His 200	1.60, 1.84, 3.31, 2.34, 2.20
5.	**INOS (4NOS)**	-12.7	Cys 200, Tyr 373, Asp 382 (2),	2.20, 1.99, 1.81, 2.10,

Krithiga Balakrishnan *et al.,*

			Trp 463, Tyr 491	1.95, 1.97, 2.09
6.	**ENOS (1M9M)**	-12.6	Trp 178 (2), Glu 361, Tyr 475 (2)	3.21, 3.24, 1.69, 1.71, 1.90
7.	**Caspase 3 (1NMS)**	-7.8	Arg 207 (3), Trp 214, Asp 253	1.78, 1.81, 2.40, 2.11, 2.10
8.	**Caspase 9 (1JXQ)**	-5.7	Ser 345, Glu 351, Asp 355, Glu 358, Lys 380	1.98, 1.77, 1.62, 1.90, 2.10
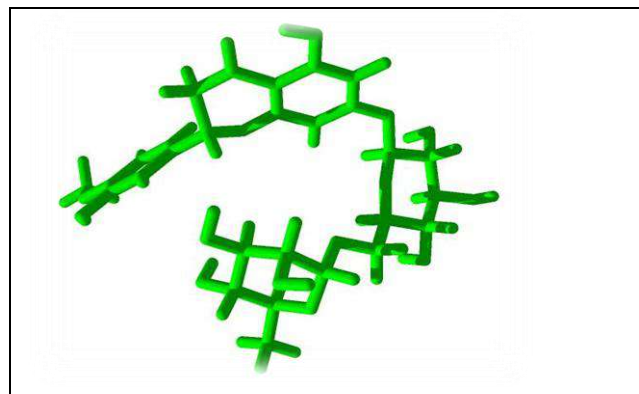
Fig. 1. 3D structure of Hesperidin

Fig. 2. (A) 3D and 2D representation of hesperidin-Bax Protein complex. (B) 3D and 2D representation of hesperidin-Bcl-2 protein complex.

Fig. 3.Interaction of hesperidin with NFκB protein. (A) 3D representation of hesperidin - NFκB protein complex. (B) 2D visualization of various non-covalent molecular interactions.
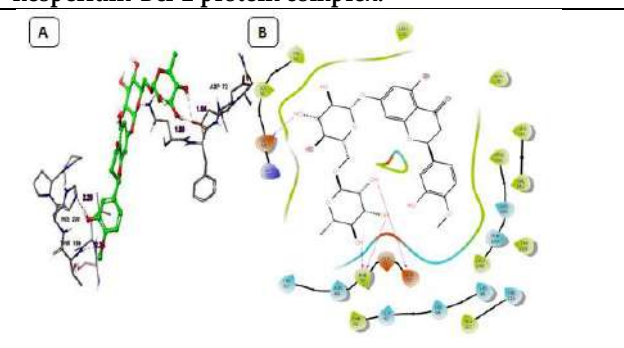
Fig. 4. Interaction of hesperidin with Carbonic anhydrase 1 protein (A) 3D representation of hesperidin - carbonic anhydrase-1 complex. (B) 2D visualization of various non-covalent molecular interactions.

Krithiga Balakrishnan *et al.,*

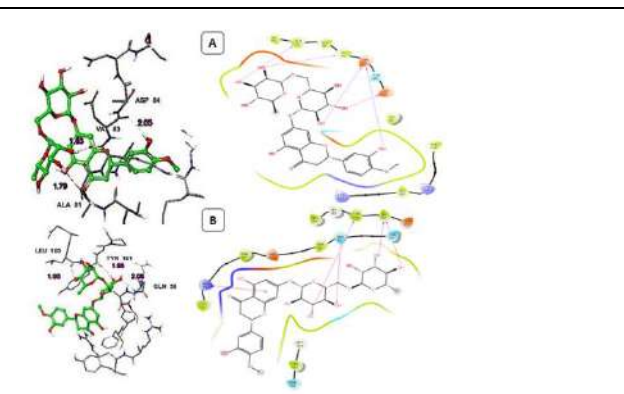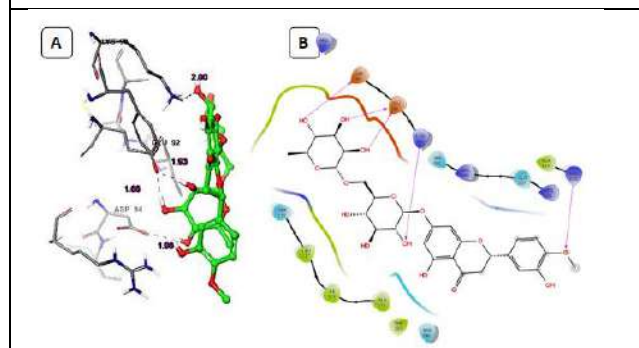| Fig. 5.(A) 3D and 2D representation of hesperidin-iNOS protein complex. (B) 3D and 2D representation of hesperidin-eNOS protein complex.	Fig. 6. (A) 3D and 2D representation of hesperidin-caspase 3 protein complex. (B) 3D and 2D representation of hesperidin-caspase 9 protein complex.

REVIEW ARTICLE
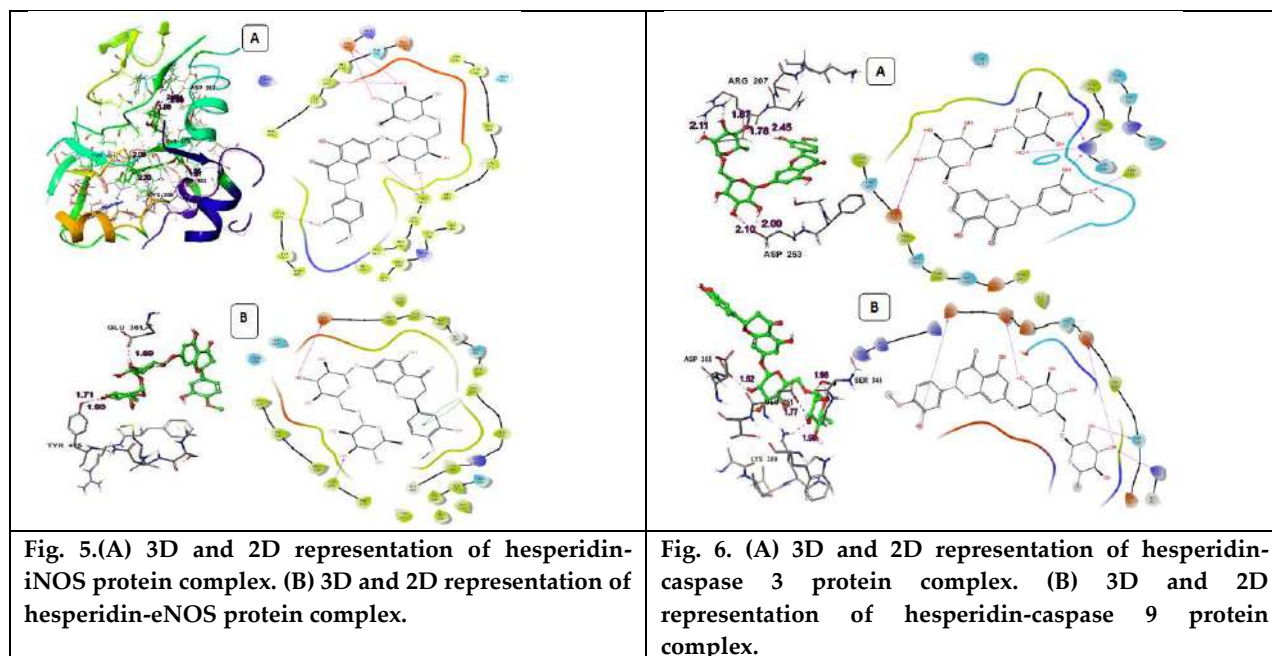
Antiophidic Plants Used In India: A Brief Overview

Amrita Babu[1], Dithu Thekkekkara[2]*, SK.Meheronnisha[3] and Y.Mohammed Tausif [3]

[1]Research Scholar, Department of Pharmacology, JSS College of Pharmacy, Mysuru, Karnataka, India.
[2]Lecturer, Department of Pharmacology, JSS College of Pharmacy, Mysuru, Karnataka, India.
[3]M Pharm, Department of Pharmacology, JSS College of Pharmacy, Mysuru, Karnataka, India.

*Address for Correspondence
Dithu Thekkekkara
Lecturer, Department of Pharmacology,
JSS College of Pharmacy, Mysuru,
Karnataka, India.
E. Mail: dithuthekkekkera@jssuni.edu.in

ABSTRACT

For thousands of years, people have been intrigued by snakes. Worldwide, snakebites pose a significant health, social, and economic challenge, but in tropical and subtropical regions, this challenge is compounded. More species of the most dangerous snakes are present, prompt medical care is unavailable, and medical care is subpar. The purpose of this research was to document the existence of under-appreciated medicinal plants. Research conducted in India has identified over a hundred plants that show promise as anti-snake venom treatments. Information gathered from various literature sources identified useful plant families, plant parts, and methods of using these plants. There are over 520 plant species in India, from about 122 families, that may help with snakebite treatment. The purpose of this research was to spur the development of herbal antidotes to snake venom. These have the potential to be a low-cost, easily-evaluated alternative that would have huge implications for society. Caesalpiniaceae, Zingiberaceae, Acanthaceae, Fabaceae, Apocynaceae, Cucurbitaceae, Euphorbiaceae, Lamiaceae, Rubiaceae and Arecaceae are some of the most beneficial plant families. Folk medicine practitioners in India use herbs singly or in combination.

Keywords: Antiophidic Plants, Snake venom, Local tissue damage, Phytochemicals, Antivenin Plants.

INTRODUCTION

The snake is widely considered to be both one of the most fascinating and one of the most misunderstood members of the animal kingdom. Snakes can be discovered in a variety of habitats, including deserts, grasslands, swamps, and forests. They can also be discovered in both freshwater and saltwater environments. As predators, snakes consume a wide variety of prey, including rodents, insects, the eggs and young of other birds, and young birds

Amrita Babu *et al.,*

themselves. Because of their cold blood, snakes need to find a new home in an environment that will enable them to maintain a temperature that is suitable for their bodies. They are only occasionally seen out in the open because they cannot withstand the heat of the summer for more than ten to twenty minutes at a time. They enter a state of dormancy during the scorching summer months and hibernate during the bitterly cold winter months of the year. There are close to 300 different species of snakes that can be found in India. Of these, there are more than 60 venomous species, more than 40 mildly venomous species, and 180 non-venomous species. There are four different families that these species belong to: the Colubridae, Elapidae, Hydrophiidae, and Viperidae families. Only about half of the few venomous snakes that do exist are actually capable of killing someone with their bite. The majority of snakebite cases in Southeast Asia result in death, despite the fact that the annual mortality rate from snakebites is thought to be between 80,000 and 140,000. There are several reasons for this, including a lack of access to medical care, malnutrition among victims, and the high density of venomous species. Snakes are able to exert control over the amount of venom they expel, and they can bite in either an offensive or defensive manner, depending on whether or not they are attempting to capture prey or protect themselves. Because snakes only have a limited supply of venom at any given time, they try to conserve it by avoiding wasting it on things that are not their prey. As a result, approximately forty percent of all human bites are considered defensive and "dry" (without envenomation). There are more than 60 different species of poisonous snakes native to India, and each one's fangs contain a one-of-a-kind cocktail of different toxins. Four of the most common species of terrestrial venomous snakes can be found on the Indian mainland. These four are known as the "big four." Spectacled cobra (*Najanaja*),Common kraits (*Bungarus caeruleus*), saw-scaled viper (*Echiscarinatus*), Russell's viper (*Daboia russelii*). These dominant species are responsible for the vast majority of the country's reported cases of injury and death. When it comes to the process of prey capture, venom is an essential component[1]. Snakes are able to kill their prey, such as birds and rodents, by injecting their lethal venom into their bodies through their lightning-fast bites. This causes their victims to become unconscious and unable to move. In addition to this, serpents use their venom to defend themselves against other species that are predators[2].

 Because it contains a variety of enzymes, venom has the capability to cause damage to the internal tissues and nervous system of its victim. It is widely held that the respective snake species purposefully evolved this helpful venom delivery pathway over the course of their evolution. Proteins, enzymes, anticoagulants, neurotoxins, and other chemicals are just some of the components that make up snake venom, which is a complex mixture[3]. It is possible to classify the venom of all venomous species into one of three primary categories: neurotoxic, hemotoxic, or cytotoxic. These are categorised according to the parts of the body that they target or affect. For instance, neurotoxic venom causes damage to the nervous system and the brain. Hemotoxic venom has an effect on the cardiovascular system because it prevents blood from clotting properly and disrupts blood flow[4]. In addition, it causes damage to tissues all throughout the body in addition to the deterioration of organs. Cytotoxic venom causes unbearable pain because it disrupts the normal molecular structure of the tissues it attacks. The annual death toll from snakebites in India is the highest of any country at 58,000, and the country's disability rate is four times higher than the death toll. In the previous 20 years, snakebites have been responsible for the deaths of close to 1.2 million people. The World Health Organization (WHO) included snakebite in its list of"Neglected Tropical Disease," or NTD, due to the fact that it is a problem in a number of countries all over the world. Antivenom serum therapy is the only treatment that has been shown to be effective. This therapy purifies neutralising immunoglobulins or fragments by using plasma derived from animals that have been immunised against snake venoms or specific toxins. Antivenom is, sadly, in short supply across the board, despite the critical demand for it. Because of how common these species are, the only ones for which there is antivenom available for purchase are the ones listed above[4]. The "big four" antivenoms are typically used in the treatment of all conditions related to snakebite. Beyond the "big four," antivenoms have very little success and are ineffective.Internal bleeding or failure of multiple organs, including the heart, lungs, and kidneys, may result from snake bites. It could even result in the person's death or paralysis. In the event that someone is bitten by a snake, the only course of action that is recommended and considered acceptable is the prompt administration of a sufficient dose of antivenom. The Polyvalent Antivenom Serum, which can be obtained from government centres located all over India, is particularly effective at neutralising the injected venom of the "big four" snake species. It is typically possible to achieve systemic effects by

beginning the administration of antivenom as soon as possible after envenomation; however, it is much more difficult to reverse the damage to local tissues. There are numerous anecdotes describing the widespread use of medicinal plants as a treatment for snakebites, particularly in subtropical and tropical regions such as Africa, South America and Asia. When dealing with the aftermath of a venomous animal bite, residents of rural and tribal areas frequently turn to home remedies. Throughout human history, people have treated snakebites with medicinal plants, and this knowledge has been passed down through rural communities. Immunotherapy has been shown to be effective in the treatment of envenomation brought on by a snakebite; however, the treatment's side effects have piqued the interest of venom toxicologists and other researchers working in this area who are looking for an alternative therapy to treat ophidian bites. Traditional treatments for snake envenomation have their limitations, so researchers are looking for alternatives that are both safe and effective. One such alternative is herbal medicinal plants. They are not only common, but also risk-free, efficient, reasonably priced, and accessible even in remote areas. Because there is a large body of evidence that points to the significance of active plant metabolites for the construction of anti-snake venom medication moieties, it is believed that a single purified component is insufficient for completely neutralising the toxicity of snake venom. This is due to the fact that active plant metabolites can be found in various plants. On the other hand, there is a substantial body of evidence that points to the significance of active plant metabolites. Despite the extensive research that has been done on herbal medicinal plants to alleviate the problems caused by snakebite poisoning, there is currently no plant-based medicine that is available that is effective against snake venom. Because of this, the current situation necessitates isolating pure chemicals from plants that are capable of acting specifically against the toxins that are found in snake venom while simultaneously minimising the risk of side effects. In other words, the situation calls for a win-win situation. In order to evaluate the anti-venom activity of appropriate herbal formulations, it is also necessary to carry out a number of pre-clinical studies. These studies need to include a wide range of active component combinations in a variety of permutations. In addition, there is an urgent need to focus on the pathogenic properties of snake venom toxins as well as the mechanisms by which they exert the harmful effects that they have. When it comes to the treatment of snake envenomation, it would be extremely beneficial to have a better understanding of the specificity of the toxins that can be found in snake venom, the connection between their structure and their activity, as well as the antigenic characteristics that are associated with those toxins[5]. Because of this, researchers need to develop new medicines that are safe for the environment, are effective against ophidians, and are affordable to people who are economically marginalised and disadvantaged. Traditional herbal antidotes are becoming an increasingly popular starting point for toxicologists all over the world who are working on the development of effective inhibitors of snake venom toxins. Antiophidic plants have the potential benefits of being inexpensive, readily available, stable at room temperature, and neutralising a wide variety of toxins, including those that cause only local tissue damage. These benefits are in addition to the fact that antiophidic plants can neutralise toxins.

Composition of Snake Venom

Venom proteins can be broadly categorized as having or not having built-in enzymatic activity. The possibility that therapeutic small molecules will inhibit the enzymatic venom components is the obvious significance of this distinction. According to proteomic analysis, snake venom contains proteins from 26 different protein families with significant species variation[6]. However, the majority of the medically significant components are concentrated in just four families, in varying amounts. These proteins include the non-enzymatic three-finger toxins (FTX), metalloproteases (MPs), serine proteases (SPs), and secreted phospholipase A2 in addition to bungarotoxin, a nicotinic receptor antagonist (sPLA2)[7].

Local Tissue Damage

Local tissue damage is a common result of most viperid venoms and a small number of elapid venoms. These venoms include myotoxic phospholipases A2 (PLA2s), which attach to and damage the plasma membranes of muscle fibers, resulting in myonecrosis. Certain PLA2s damage sarcolemmals by interactions with hydrophobic molecules, whereas catalytically inactive PLA2 homologues harm sarcolemmals by hydrolyzing membrane phospholipids. After membrane disruption, calcium influx into the cytosol results in myofibrillar hypercontraction, mitochondrial malfunction, and other degenerative processes that irreparably harm muscle cells. Tiny basic

63187

myotoxic peptides constrict muscles and result in necrosis in the venom of viperids. Pressure on the muscle fibers and ischaemia are caused by vascular alterations and oedema. Skeletal muscle requires blood and innervation to recover, thus phagocytic cells must clear away necrotic material. Viperid venom impairs skeletal muscle regeneration and often results in permanent injury by harming muscle fibers, blood vessels, and neurons. Blood vessel integrity is also affected by myonecrosis. Type IV collagen in particular is hydrolyzed by viperid venom metalloproteinases (SVMPs), which reduces the mechanical stability of microvessels. As a result, extravasation is brought on by haemodynamic biophysical forces in the circulation that stretch and tear the capillary wall. SVMP-induced microvascular damage may be brought on by breaking down endothelial cell-cell adhesions. Collagen, hyaluronic acid, and proteoglycans are examples of extracellular matrix components that are hydrolyzed by SVMPs and hyaluronidases[8, 9]. This alters the structure and function of microvascular and other tissue components, resulting in local tissue damage by venom. Blisters are the result of SVMPs harming the dermal-epidermal interface, a non-enzymatic mechanism, the three-finger toxin family of cytotoxins found in several Elapidae family venoms disrupt the plasma membranes of different cell types in diverse tissues, leading to broad cutaneous necrosis. Intramuscular nerves, lymphatic vessels, arterioles, and venules are all impacted by PLA2s and SVMPs. A local inflammatory process is brought on by the synthesis and release of eicosanoids, nitric oxide, anaphylatoxins, bradykinin, histamine, cytokines, resident macrophages and other cells, and leukocytes in envenomed tissue. Exudates including plasma proteins, intracellular and extracellular protein fragments, cytokines, chemokines and damage-associated molecular patterns are formed in this inflammatory environment, which may exacerbate inflammation and harm tissue.Pain-related sensory neurons are stimulated in catalytically inactive PLA2 homologues by ATP and purinergic receptors. The best treatment is conventional medicine, which has no impact on the local tissue damage caused by antivenom therapy. According to several viper venom victims, the issue recurs every year. Traditional healers make great use of plant extracts for this reason[10, 11].

Folk plants commonly used for the treatment of snakebites in India.
Withania somnifera.
The winter cherry, also known as ashwagandha, is the fruit of the small evergreen woody under shrub *Withania somnifera*, which is a member of the Solanaceae family. It is a native of India's subtropical dry regions. *Withania somnifera* plant has most of its unique steroidal alkaloids and lactones which are found in roots and leaves. The protein component of *Withania somnifera*, called *Withania somnifera* glycoprotein (WSG), has been reported to exhibit a variety of significant pharmacological action, including anti-microbial, anti-protease, inhibitor of phospholipase, and hyaluronidase activity of snake venom. Hyaluronidases in venom help the toxins spread quickly by breaking down the extracellular matrix of the victim's tissues. The glycoprotein inhibited the hyaluronidase activity of viper (*Daboia russelii*) and cobra (*Najanaja*) venoms. This was shown by zymogram assay and staining the skin tissues for different activity. At a concentration of 1:1 w/w of venom to WSG, the enzyme's activity was completely stopped by WSG. So, we can show that the glycoprotein stops the hyaluronidase from working in the venoms. There seems to be a scientific reason why snakebite victims in rural India put the plant extract on their skin as a cure[12–18].

Sapindus saponaria
*Sapindus saponaria*is a deciduous tree of small to medium size. Also known as wing leaf soapberry and western soapberry. Belongs to the Sapindaceae family. Extracts from the callus of *Sapindus saponaria*and its principal active component stigmasterol inhibit the pharmacological and toxic effects of snake venoms and proteins isolated from viperidae family. Myotoxic, hemorrhagic, and phospholipase A2 activities. It was discovered that both fractions and extracts can inhibit the activity of hemorrhagic proteins found in venoms. These proteins are highly dependent on Zn^{2+}, and the active chemicals in this plant may be interfering with protein-cofactor interactions or binding to other active sites required for this activity. β-sitosterol, stigmasterol, and β-sitosterol glucoside can inhibit the edematous, hemorrhagic, myotoxic, and PLA2 activities induced by snake venoms and toxins[19].

Sarsaparilla Hemidesmus indicus

Indian sarsaparilla is a plant native to South Asia. The family Asclepiadaceae encompasses plants found throughout India. The root of *Hemidesmus indicus* is used. It was discovered that *Hemidesmus indicus* possesses antisnake venom activity. This aromatic root is mashed into a thin paste and administered to the snakebite victim's wound, according to local studies in West Bengal, India's rural areas. Moreover, it was administered orally in combination with several other ingredients, such as salt, jaggery, lime, etc. The people who lived in rural areas had a strong belief in this healing plant and wanted to cultivate it at home for their personal benefit. *Hemidesmus indicus* root extract contained the active substance 2-hydroxy 4-methoxybenzoic acid, which was very efficient in reversing the pathophysiological alterations caused by *Daboia russelii* venom. The plant inhibits hemorrhage, defibrinogenate,PLA2 activity and cardiotoxicity. It was discovered that the methanolic crude extract considerably reduced the fatal, hemorrhagic, necrotic, defibrinogenating, coagulant, and fibrinolytic effects of viper venom[20].

Mangifera indica.

Mangifera indica, often known as mango, is a flowering plant species in the Anacardiaceae family.*Mangifera indica* aqueous extract is recognized to have anti-snake venom properties. The most toxic and lethal part of snake venom, multi-toxic phospholipases A2s, are yet unknown as is its inhibitory efficacy and mode of action. *Mangifera indica* bark extract may neutralize the venom of the Indian Russells viper. Hemolytic activity was dose-dependently reduced by *Mangifera indica*extract. Moreover, extracts from *Mangifera indica* decrease edema in a dose-dependent way. In conclusion, *Mangifera indica*aqueous extract suppresses PLA2's toxic and enzymatic activities, proving it has anti-snake venom characteristics. It would be useful to carry out more in-depth study on the function and mechanism of the main inhibitory elements of the extract in order to develop them as an effective anti-snake venom and anti-inflammatory drug. The anti-hemorrhagic, anti-coagulant, fibrinogenolytic, edema-inducing, and anti-myotoxic properties of *Mangifera indica* have been shown.[21]

Tamarindus indica.

Tamarind (*Tamarindus indica*) belongs to the family Leguminosae and grows abundantly all over India. Inhibited the PLA2, protease, hyaluronidase, L-amino acid oxidase and 5'-nucleotidase enzyme activities of venom. Tamarind seed extract is a good source of powerful natural PLA2 inhibitors, mainly myotoxic PLA2 found in V. russelli venom.[22]

Pluchea indica.

Pluchea indica Less. (Asteraceae) methanolic root extract has the potential to counteract the effects of viper venom. By utilizing silica gel column chromatography, the active fraction which contains the primary component β-sitosterol and the minor compound stigmasterol was separated, purified, and the structure was ascertained. It was discovered that the active portion considerably reduced the fatal, hemorrhagic, defibrinogenation, edema, and PLA2 activity caused by viper venom. The active ingredient also inhibited PLA2 activity, respiratory alterations, cardiotoxicity, neurotoxicity, and mortality brought on by cobra venom.[23]

Emblica officinalis.

Emblica officinalis belongs to family Phyllanthaceae. For anti-snake venom action, *Emblica officinalis* methanolic root extracts are employed. In both *in vitro* and *in vivo* studies, the plant extracts effectively inhibited the lethal activity caused by the venom of the *Viperarussellii* and *Najakaouthia* snakes. The plant extract significantly reduced the hemorrhage, coagulant, defibrinogenating, and inflammatory effects caused by *viperarussellii* venom[24–26].

Rosmarinus officinalis

Rosemary, or *Rosemarinus officinalis* L., is a perennial evergreen aromatic plant of the Lamiaceae family. There were significant amounts of phenolics, falvonoids, and different phenolic acids in the rosemary aqueous extract. The main ingredient, rosmarinic acid, may be the cause of the viper venom's possible neutralizing activity against proteases, PLAs2, fibrinogenases, LAAOs, hemorrhagic, hemolytic, edema-inducing, myotoxic and fatal actions. An effective treatment for deadly viper bites is said to be rosemary aqueous extract.[27–29]

Trichosanthes tricuspidata.

Trichosanthes tricuspidata belongs to the family Cucurbitaceae. *T. tricuspidata* leaf protein rich fraction exhibited proteolytic activity. Prevention of *Echiscarinatus* venom -induced tissue necrosis by tricuspidin via modulation of immune mediators. The paste of *Tricosanthus tricuspidata* plant leaves is used to treat snakebite poisoning.

Butea monosperma

Butea monosperma (Lam) Kuntze belongs to the Fabaceae family of plants. By inhibiting hyaluronidase, which is a spreading agent, the extract of *Butea monosperma* stem bark is used. Stigmasterol is extracted from *Butea monosperma* bark.[30, 31]

Mimosa pudica

Mimosa pudica belongs to the family Mimosaceae. Mimosa pudica aqueous root extract inhibited the hyaluronidase and protease activities of *Najanaja, Viper arusselii*, and *Echiscarinatus* venom in a dose-dependent manner.[32]

Curcuma longa.

Curcuma longa belongs to the family Zingiberaceae, Roots of *Curcuma longa,* were pulverized and extracted using hexane. ar-turmerone is the active chemical component. ar-turmerone may inhibit proteolytic and hemorrhagic venom enzymes by acting as an enzymatic inhibitor. Ar-turmerone was the most effective therapy for the suppression of edema, necrosis, and local bleeding after viper venom.[33, 34]

Vitex negundo

Vitex negundo Linn, also known as Nirgundi or Five-leaved Chaste Tree, is a huge aromatic shrub in the Verbenaceae family. The methanolic root extracts of *Vitex negundo* used for antisnake venom activity.V. russellii venom-induced haemorrhage, coagulant, defibrinogenating and inflammatory activity was significantly neutralized by plant extracts.[25]

Azadirachta indica

Azadirachta indica, commonly known as neem, nimtree, and Indian lilac, is a Meliaceae mahogany tree. In a dose-dependent manner, an*Azadirachta indica* PLA2 inhibitor isolated from the methanolic leaf extract of *A. indica* (Neem) inhibits the phospholipase A2 enzymes in cobra and Russell's viper venom.[35]

Strychnosnux-vomica

Strychnosnux-vomica Linn (Family: Loganiaceae), a medicinally important toxic plant, commonly known as nux vomica, poison nut, has diverse therapeutic and clinical applications. In low doses, nux vomica seeds extract was found to effectively neutralized *Daboia russelii* venom induced lethal, haemorrhage, defibrinogenation, phospholipase A2 (PLA2) enzyme activity and Najakaouthia venom induced lethal, cardiotoxicity, neurotoxicity, PLA2 enzyme activity.[36]

Piper longum

Piper longum L. (family Piperaceae), popularly known as "long pepper," is a climbing shrub native to the world's tropical and subtropical regions. In ethanolic extract of *Piper longum* fruits, piperine was discovered to reduce Russell's viper (Viperidae) snake venom activity.[37]

Alstonia scholaris

Alstonia scholaris, often known as blackboard tree or devil's tree, is an evergreen tropical tree belonging to the Apocynaceae family. The dried bark of *Alstonia scholaris* Linn is used. It might significantly inhibit the elevation of serum lactate dehydrogenase (LDH) and proinflammatory cytokines (IL6, TNF) caused by Viper russelli venom.[1, 38]

Pittosporum tetraspermum.

Pittosporum is a genus in the Pittosporaceae family that has over 200 species with a global distribution, with the highest concentration in Australia and China. Only 11 species have been documented in India so far. The bark part is used as narcotic, antidote to snake poison, and also a stimulant. (Pillai & Swapna, 2019). The bioactive component responsible for the biological activity of *Pittosporum tetraspermum* is identified as trihydroxyoleanolic acid glycoside, whose aglycone part is characterized as trihy-droxyoleanolic acid and the glycone part as sugars glucose and glucuronic acid.[39, 40]

Azima tetracantha

Azima tetracantha Lam. belongs to the Salvodoraceae family and is known as Kundali. Phosphomonoesterase, phosphodiesterase, acetylcholinesterase, phospholipase A2, 5′ nucleotidase, and hyaluronidase enzymes were all inhibited by the ethylacetate extract *Azima tetracantha*.[41]

REFERENCES

1. R. Ghosh, S. Sarkhel, K. Saha, P. Parua, U. Chatterjee, and K. Mana: "Synthesis, characterization & evaluation of venom neutralization potential of silver nanoparticles mediated Alstoniascholaris Linn bark extract." *Toxicol Rep.* vol. 8, pp. 888–895, 2021.
2. C.D. Raghavendra Gowda, H. V Shivaprasad, R. Venkatesh Kumar, R. Rajesh, Y.K. Saikumari, B.M. Frey, F.J. Frey, B.K. Sharath, and B.S. Vishwanath: "Characterization of Major Zinc Containing Myonecrotic and Procoagulant Metalloprotease 'Malabarin' from Non LethalTrimeresurusmalabaricus Snake Venom with Thrombin Like Activity: Its Neutralization by Chelat-ing Agents." , 2011.
3. R. Whitaker and G. Martin: "Diversity and distribution of medically important snakes of India." Toxinology: Clinical Toxinology in Asia Pacific and Africa. pp. 115–136. *Springer Netherlands* (2015).
4. A. Manuwar, B. Dreyer, A. Böhmert, A. Ullah, Z. Mughal, A. Akrem, S.A. Ali, H. Schlüter, and C. Betzel: "Proteomic Investigations of Two Pakistani Naja Snake Venoms Species Unravel the Venom Complexity, Posttranslational Modifications, and Presence of Extracellular Vesicles." *Toxins (Basel).* vol. 12, no. 11, 2020.
5. S. Panda and L. Kumari: "Anti-Ophidian Properties of Herbal Medicinal Plants: Could it be a Remedy for Snake Bite Envenomation?" *Curr Drug Discov Technol.* vol. 16, no. 4, pp. 319–329, 2018.
6. B. Kalita, S.P. Mackessy, and A.K. Mukherjee: "Proteomic analysis reveals geographic variation in venom composition of Russell's Viper in the Indian subcontinent: implications for clinical manifestations post-envenomation and antivenom treatment," (2018).
7. K. Sunagar, K. Kemparaju, S.P. Mackessy, F.C. Cardoso, C.R. Ferraz, A. Arrahman, C. Xie, N.R. Casewell, R.J. Lewis, and J. Kool: "Multifunctional Toxins in Snake Venoms and Therapeutic Implications: From Pain to Hemorrhage and Necrosis." *Frontiers in Ecology and Evolution | www.frontiersin.org.* vol. 1, pp. 218, 2019.
8. J.M. Gutiérrez, G. León, and T. Burnouf: "Antivenoms for the treatment of snakebite envenomings: The road ahead," (2011).
9. S. Bhaumik Id, D. Beri Id, Z.S. Lassi, and J.J. Id: "Interventions for the management of snakebite envenoming: An overview of systematic reviews." 2020.
10. A.M. Deshpande, K.V. Sastry, and S.B. Bhise: "A Contemporary Exploration of Traditional Indian Snake Envenomation Therapies," (2022).
11. A. Dey and J.N. De: "Traditional use of plants against snakebite in indian subcontinent: A review of the recent literature," (2012).
12. P. A. Dar, L. R. Singh, M. A. Kamal, and T. A. Dar: "Unique Medicinal Properties of Withaniasomnifera: Phytochemical Constituents and Protein Component." *Curr Pharm Des.* vol. 22, no. 5, pp. 535–540, 2016.
13. D.K. Machiah, K.S. Girish, and T.V. Gowda: "A glycoprotein from a folk medicinal plant, Withaniasomnifera, inhibits hyaluronidase activity of snake venoms." *Comparative Biochemistry and Physiology - C Toxicology and Pharmacology.* vol. 143, no. 2, pp. 158–161, 2006.

14. K.S. Girish, K.D. Machiah, S. Ushanandini, K.H. Kumar, S. Nagaraju, M. Govindappa, M. Vedavathi, and K. Kemparaju: "Antimicrobial properties of a non-toxic glycoprotein (WSG) from Withaniasomnifera (Ashwagandha)." *J Basic Microbiol*. vol. 46, no. 5, pp. 365–374, 2006.

15. M. Deepa and T.V. Gowda: "Purification and characterization of a glycoprotein inhibitor of toxic phospholipase from Withania somnifera."

16. F. Zameer, A. Naidu, N.M. Prasad N, B. LakkappaDhananjaya, and R. Hegdekatte: "Pharmaceutical Biology Evaluating the inhibitory potential of Withaniasomnifera on platelet aggregation and inflammation enzymes: An in vitro and in silico study Evaluating the inhibitory potential of Withaniasomnifera on platelet aggregation and inflammation enzymes: An in vitro and in silico study." *Pharm Biol*. vol. 54, no. 9, pp. 1936–1941, 2016.

17. M. Madhusudan, F. Zameer, A. Naidu, M.N. Nagendra Prasad, B.L. Dhananjaya, and R. Hegdekatte: "Evaluating the inhibitory potential of Withaniasomnifera on platelet aggregation and inflammation enzymes: An in vitro and in silico study." *Pharm Biol*. vol. 54, no. 9, pp. 1936–1941, 2016.

18. P.A. Dar, L.R. Singh, M.A. Kamal, T.A. Dar, and B.R. Ambedkar: "Send Orders for Reprints to reprints@benthamscience.ae Unique Medicinal Properties of Withaniasomnifera: Phytochemical Constituents and Protein Component." , 2016.

19. M.L. Da Silva, S. Marcussi, R.S. Fernandes, P.S. Pereira, A.H. Janurio, S.C. França, S.L. Da Silva, A.M. Soares, and M. V. Lourenço: "Anti-snake venom activities of extracts and fractions from callus cultures of Sapindus saponaria." *Pharm Biol*. vol. 50, no. 3, pp. 366–375, 2012.

20. I. Chatterjee, A.K. Chakravarty, and A. Gomes: "Daboia russellii and Najakaouthia venom neutralization by lupeol acetate isolated from the root extract of Indian sarsaparilla Hemidesmus indicus R.Br." *J Ethnopharmacol*. vol. 106, no. 1, pp. 38–43, 2006.

21. C.D.' Souza: "Anti-venom potential of aqueous extract of stem bark of Mangifera indica L. against Daboia russellii (Russell's viper) venom SEE PROFILE." , 2011.

22. S. Ushanandini, S. Nagaraju, K. Harish Kumar, M. Vedavathi, D.K. Machiah, K. Kemparaju, B.S. Vishwanath, T. V Gowda, and K.S. Girish: "ANTI-SNAKE VENOM PROPERTIES OF TAMARINDUS INDICA 851 The Anti-snake Venom Properties of Tamarindus indica (Leguminosae) Seed Extract." *Phytother. Res*. vol. 20, pp. 851–858, 2006.

23. A. Gomes, A. Saha, I. Chatterjee, and A.K. Chakravarty: "Viper and cobra venom neutralization by β-sitosterol and stigmasterol isolated from the root extract of Pluchea indica Less. (Asteraceae)." *Phytomedicine*. vol. 14, no. 9, pp. 637–643, 2007.

24. M.K. Singh, S. Singh Yadav, R. Singh Yadav, A. Chauhan, D. Katiyar, and S. Khattri: "Protective effect of Emblica-officinalis in arsenic induced biochemical alteration and inflammation in mice." vol. 4, pp. 438, 2015.

25. M.I. Alam and A. Gomes: "Snake venom neutralization by Indian medicinal plants (Vitex negundo and Emblica officinalis) root extracts." *J Ethnopharmacol*. vol. 86, no. 1, pp. 75–80, 2003.

26. S.S. Yadav, M.K. Singh, P.K. Singh, and V. Kumar: "Traditional knowledge to clinical trials: A review on therapeutic actions of Emblica officinalis," (2017).

27. D.P. da Silva, S. de S. Ferreira, M. Torres-Rêgo, A.A. Furtado, F. de O. Yamashita, E.A. da S. Diniz, D.S. Vieira, M.A.G. Ururahy, A.A. da Silva-Júnior, K.P. de O. Luna, and M. de F. Fernandes-Pedrosa: "Antiophidic potential of chlorogenic acid and rosmarinic acid against Bothropsleucurus snake venom." *Biomedicine and Pharmacotherapy*. vol. 148, 2022.

28. H.T. Aung, T. Furukawa, T. Nikai, M. Niwa, and Y. Takaya: "Contribution of cinnamic acid analogues in rosmarinic acid to inhibition of snake venom induced hemorrhage." *Bioorg Med Chem*. vol. 19, no. 7, pp. 2392–2396, 2011.

29. W.H. Salama, A.M. Abdel-Aty, and A.S. Fahmy: "Rosemary leaves extract: Anti-snake action against Egyptian Cerastes cerastes venom." *J Tradit Complement Med*. vol. 8, no. 4, pp. 465–475, 2018.

30. S. Panda, M. Jafri, A. Kar, and B.K. Meheta: "Thyroid inhibitory, antiperoxidative and hypoglycemic effects of stigmasterol isolated from Butea monosperma." *Fitoterapia*. vol. 80, no. 2, pp. 123–126, 2009.

31. S. Tarannum, R. Mohamed, and B.S. Vishwanath: "Inhibition of testicular and Viperarusselli snake venom hyaluronidase activity by Butea monosperma (Lam) Kuntze stem bark." *Nat Prod Res*. vol. 26, no. 18, pp. 1708–1711, 2012.

32. K.S. Girish, H.P. Mohanakumari, S. Nagaraju, B.S. Vishwanath, and K. Kemparaju: "Hyaluronidase and protease activities from Indian snake venoms: Neutralization by Mimosa pudica root extract." *Fitoterapia*. vol. 75, no. 3–4, pp. 378–380, 2004.

33. P. Ltd, Lu.A. F F, O.B. H, irw A. S Andreoni, G.R. F Vital, Marci.M. C Cw, eHwRn G. HABEIt, V.L. G De Morabs, L.A. F Ferrsira, O.B. He, A.A. S ANDReoNi, G.R. F VrrwL, M.M. C Cw, G.G. HwBirR, and V.L. G Ds MORABS: "ANTIVENOM AND BIOLOGICAL EFFECTS OF AR-TURMERONE ISOLATED FROM CURCUMA LONGA (ZINGIBERACEAE)." , 1992.

34. M.M. Melo, G.G. Habermehl, N.J.F. Oliveira, E.F. Nascimento, M.M.B. Santos, and M. Lúcia: "Treatment of Bothropsalternatus envenomation by Curcuma longa and Calendula officinalis extracts and ar-turmerone [Tratamento local do envenenamentoporBothropsalternatus com extrato de Curcuma longa e Calendula officinalis e ar-turmerone]." , 2005.

35. A.K. Mukherjee, R. Doley, and D. Saikia: "Isolation of a snake venom phospholipase A2 (PLA2) inhibitor (AIPLAI) from leaves of Azadirachta indica (Neem): Mechanism of PLA2 inhibition by AIPLAI in vitro condition." *Toxicon*. vol. 51, no. 8, pp. 1548–1553, 2008.

36. M.A. K and B. Pratim: "Strychnosnux-vomica: A Poisonous Plant with Various Aspects of Therapeutic Significance." *J Basic Clin Pharm*. vol. 8, no. 0, 2017.

37. P.A. Shenoy, S.S. Nipate, J.M. Sonpetkar, N.C. Salvi, A.B. Waghmare, and P.D. Chaudhari: "Anti-snake venom activities of ethanolic extract of fruits of Piper longum L. (Piperaceae) against Russell's viper venom: Characterization of piperine as active principle." *J Ethnopharmacol*. vol. 147, no. 2, pp. 373–382, 2013.

38. R. Ghosh, K. Mana, and S. Sarkhel: "Ameliorating effect of Alstoniascholaris L. bark extract on histopathological changes following viper envenomation in animal models." *Toxicol Rep*. vol. 5, pp. 988–993, 2018.

39. A.R. Pillai and T. Swapna: "A review on phytochemical, ethnomedicinal and pharmacological studies of genus Pittosporum (Pittosporaceae), in India." ~ 155 ~ *Journal of Pharmacognosy and Phytochemistry*. vol. 8, no. 2, pp. 155–162, 2019.

40. "Isolation and characterization of an antimicrobial compound from the traditional medicinal plant Pittosporum tetrapermum Wight & Arm," https://www.researchgate.net/publication/267985755_Isolation_and_characterization_of_an_antimicrobial_compound_from_the_traditional_medicinal_plant_Pittosporum_tetrapermum_Wight_Arm.

41. B. Janardhan, V.M. Shrikanth, K.K. Mirajkar, and S.S. More: "In vitro screening and evaluation of antivenom phytochemicals from Azimatetracantha Lam. leaves against Bungarus caeruleus and Viperarusselli." , 2014.
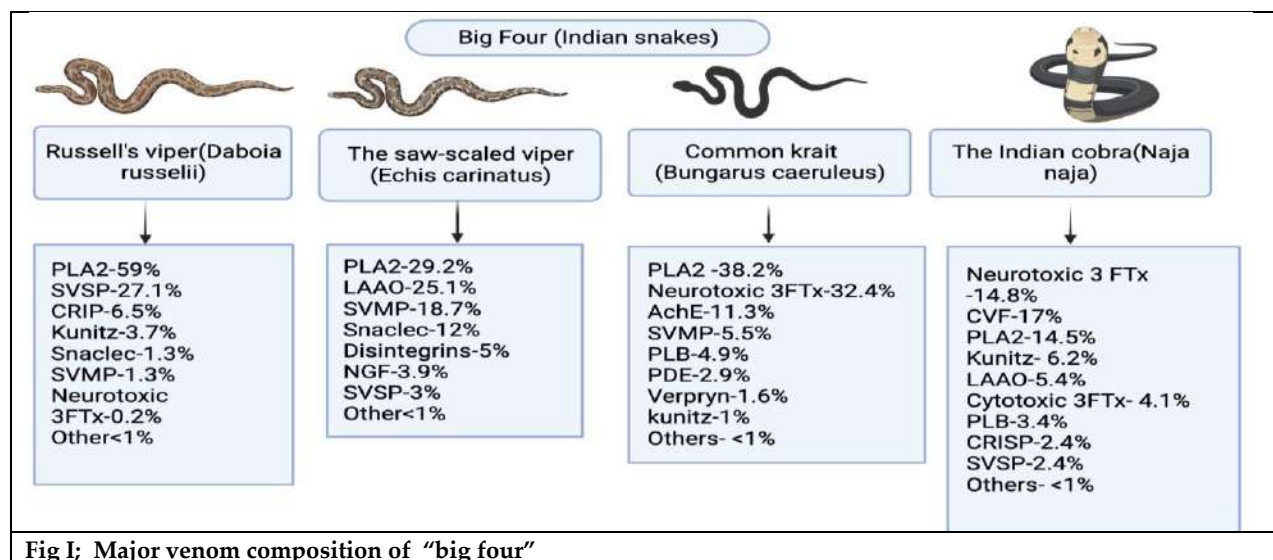
Fig I; Major venom composition of "big four"

Amrita Babu *et al.,*

Table I: Commonly Used Plants Which Have Antivenin Property

Sl no	Name of the plant	Parts used	Inhibited activities	Sl no	Name of the plant	Parts used	Inhibited activities
	Anacardium occidentale	Bark	PLA_2, proteolytic, SVH		*Andrographis paniculata*	Whole plant, Stem and leaf extract	
	Tylophoraindica	Leaf, root	PLA_2		*Andrographis serpyllifolia*	Whole plant	
	Vitis vinifera.	Seed	Proteolytic, SVH		*Carmona retusa*	Whole plant	
	Ophiorrhizamungos	Root	Hemorrhage		*Desmodiummotorium*	whole plant	
	Morus alba	Leaf	Proteolytic, SVH		*Ehretiacanarensis*	root bark	
	Acalypha indica	Leaf	Hemorrhage		*Lantana indica*	Leaf	
	Leucas aspera	Leaf, root	PLA_2		*Polyalthiakorinti*	Root	
	Aristolochiaindica	Root	LAAO, proteolytic		*Polygala arvensis*	whole plant	
	Aristolochiabracteolata	Leaf, root, Aqueous leaf and root extract.	PLA_2		*Aristolochia indica*	Plant extract	
	Tylophoraindica	Leaf, root	PLA_2		*Wattakakavolubilis*	Leaf and root	-
	Hemidesmusindicus	Root	Hemorrhage		*Abutilon indicum*	Leaf extract	-
	Crinum jagus	Bulb	Hemorrhage		*Acorus calamus*	Root extract	-
	Senna auriculata	Leaf	PLA_2, proteolytic, SVH		*Ecliptaprostrata*	Aerial parts	-

RESEARCH ARTICLE

Regulatory Requirements for Combination Products in the US, China, and Japan

Harshitha P[1]*, Shivanand Mutta[2] and C. S. Lakshmeesha[3]

[1]M. Pharm Student, Dept. of Pharmaceutical Regulatory Affairs, Acharya and BM Reddy College of Pharmacy, Bengaluru- 560107, Karnataka, India
[2]Professor and Head, Dept, of Pharmaceutical Regulatory Affairs, Acharya and BM Reddy College of Pharmacy, Bengaluru- 560107, Karnataka, India
[3]Professor Dept. of Pharmaceutical Regulatory Affairs, Acharya and BM Reddy College of Pharmacy, Bengaluru- 560107,Karnataka, India

*Address for Correspondence
Harshitha P
M. Pharm Student,
Dept. of Pharmaceutical Regulatory Affairs,
Acharya and BM Reddy College of Pharmacy,
Bengaluru- 560107, Karnataka, India
E.Mail: harshithap.21.draf@acharya.ac.in

ABSTRACT

The regulatory environment is one of the most crucial factors in bringing a cutting-edge medical product to market, such as a drug-device combination product. Drug-device combinations have developed a method for product development, regulatory approval, and business interactions that has provided crucial information for the creation of subsequent generations of combination goods. Drugs, equipment, and/or biological products may be combined to create therapeutic and diagnostic medical products known as combination products. The medical device markets, which are often viewed as having high growth potential and offering higher profit margins and better patient outcomes, now include devices that can deliver medications and biologics to particular sites. Combination product development, clinical translation, and regulatory review are intricate and difficult processes. The main ideas for comprehending the USFDA, Japan, and China's thoughts on combination goods are outlined in this article. The combination of product provisions and the approval process are discussed in this article.

Keywords: Drug-device combinations, USFDA, China, Japan, Medical device, Clinical translation, Regulatory review.

INTRODUCTION

Since ancient times, the traditional medical system has been practised, however, treating new ailments with traditional medicine is becoming an increasingly challenging process. Currently, the unique technology makes use of combination products (1). In the early 2000s, the medical device, pharmaceutical, and biological industries started to understand that the future of therapeutic interventions did not lie just in specialized subsets of those products. A transdisciplinary approach results in true innovation, which can lead to considerably increased therapeutic value. For instance, the growing development of complex combination products is a result of ongoing technological developments in drug and biological research as well as those in engineering and producing medications, biologics, and devices (2). Because medical devices, biologics, and drugs alone may not be sufficient to treat disease or harm. In reality, every field of medicine will gain from this since disease or physical harm may eventually be reversed rather than just stopped.

Regulatory requirements for Combination products in US
As two or three products combining medical equipment, medicines, and biological products, combination products first appeared in 1970 and gained distinctive efficacy (4). The Federal Food, Drug, and Cosmetic Act (FFD&C) was revised in 1990 by the Safe Medical Device Act (SMDA), which marked the start of the development of regulations for combination items in the US. Prior to these things being managed on an as-needed basis, there was no formal regulatory system in existence (5). Combination goods are expanding in scope and complexity as manufacturing technology advances. The first definition of combination goods appeared in Title 21 of CFR 3.21 in 1991 (6).

Combination products are defined in 21 CFR 3.2(e). The term combination product includes:
1. A product consisting of two or more regulated components, such as a drug and a device, a biologic and a device, a drug and a biologic, or a drug and a device and a biological, and produced as a single entity by physical, chemical, or other processes.
2. Examples of two or more different products that are packaged together in a single container or as a single unit are drug and device goods, device and biological products, or biological and drug products.
3. A drug, device, or biological product packaged separately that, according to its investigational plan or proposed labelling, is intended for use only with an approved individually specified drug, device, or biological product when both are required to achieve the intended use, indication, or effect and when, after the proposed product's approval, the labelling of the approved product would need to be changed.
4. Any experimental drug, apparatus, or biological product that is packaged separately and, in accordance with its planned labelling, is only to be used in conjunction with another such product, when both are required to achieve the intended use, indication, or effect (7).

Combination Product Types (8)
Table 1-Types of combination products

Office of Combination products
The requirements of the Medical Device User Fee and Modernization Act (MDUFMA) in 2002 led to the establishment of the Office of Combination Products. The primary agency responsible for regulating and grading combination products is chosen by OCP (9).

- It acts as the primary point of contact for staff and the industry with regards to inquiries concerning combination items. The creation of guidelines, rules, and standard operating procedures to make the laws governing combination goods clearer.
- Facilitate the settlement of disagreements about the premarket examination of timetables for combination products.
- Modernization of contracts, policies, or procedures pertaining to the assignment of combination goods (10).

PMOA.
Combination products will have more than one mode of action since they are composed of more than one regulated product category (such as a biological product, device, or medication), and each component contributes its own mode of action. Therefore, the FDA defines the primary mode of action (PMOA) as "the single mode of action of a combination product that produces the most important therapeutic action of the combination product." The most crucial therapeutic effect is the one that is anticipated to have the greatest influence on all of the intended therapeutic advantages of the product (11).

Pre-Request for Designation process
The sponsor provided the details in written form to the OCP to identify combination products. The feedback period has a 60-day calendar constraint. During the review, the sponsor is always able to connect to OCP and ask any questions they may have. OCP informed the sponsor of a longer review period if it was unable to provide comments within 60 days. Any substantial changes to the product made by the sponsor, such as changes to the indication or a component, must be communicated to OCP. It is necessary to file a separate pre-Request for Designation for each product if it has various configurations, ingredients, applications, or indications (13).

Request for Designation
21 CFR 3.2, (j), states a request letter from an applicant is another name for an RFD, It is an OCP written contribution. RFDs ask for an assessment of
(1) The product's categorization or regulatory designation as a drug, device, biological product, or combination product, and/or
(2) Which FDA division will oversee a non-combination product if one exists? Which agency center will be in charge of premarket regulation and inspection if it's a combined one?

The designation letter is FDA's official response to an RFD and constitutes a legally-binding determination of the center's classification and/or assignment. However, as per 21 CFR 3.2(i) of the regulations, this determination may be modified in accordance with the criteria set forth in 563 of the FD&C Act and 21 CFR 3.9 rules (14).

Product approval procedure
After the lead center has been designated the product developer can submit the required market application to the lead center in order to approach it for market authorization. The product should be submitted as an NDA if the lead center is CDER; if it is allocated to CBER, the application is a BLA; similarly, if the lead center is CDRH, the application is either a 510k or a PMA, depending on the device's classification. CDRH, CBER, and CDER collect the device user fee and the registration charge in order to approve and review a combination product (15).
Application for combination products in accordance with the PMOA and the evaluation period (16).

Regulatory requirements for Combination products in China

The primary Chinese regulatory authority is the CFDA/NMPA (China Food and Drug Administration/National Medical Product Administration) (17). The NMPA has regulated combination goods since 2002(18). The regulatory requirements for drug-device combination products were first made clear in the NMPA's Notice on Matters Concerning the Registration of Drug-Device Combination Products, which was published in November 2009. The Announcement on the Registration of Drug-Device Combination Products was published in 2021 by the NMPA(19). According to the statement, a medication-device combination product's primary mode of action (PMOA) must be considered when determining whether to regulate it as a medicine or a device. When the PMOA is a device and vice versa, the product must adhere to the regulatory process for devices (20). The PMOA for combined items is validated by the Centre for Medical Device Standard Administration. The development of China's regulatory science for medical devices is covered in this portion of the Regulatory Science Action Plan (RSAP), which was introduced by the NMPA in 2019.

Harshitha *et al.,*

In China, a Combination product is defined as "a single, manufactured item that consists of both pharmaceuticals and medical equipment" (21).

Registration of Drug-Device Combination Products

- Products that combine medications and devices must be declared and registered in accordance with the applicable drug regulations.
- Products combining medicines and devices that principally depend on medical devices' functionality must be declared and registered in line with the relevant medical device standards.
- The accompanying marketing certification documents for any medications or medical devices included in a combination of drugs and devices that have been given the go-ahead for marketing in China or the country (area) of manufacture must be included with the registration application.
- The applicant must thoroughly evaluate all of the characteristics of the stated medicine and device combination product. In order to define the management qualities of the medication and device combination product, the applicant must first submit an application to the State Medical Products Administration's Medical Device Standards Management Centre.
- The standard management canter shall review the accepted application materials for the definition of the attributes of drug-device combination products, solicit input on that definition in accordance with the procedures, notify the applicant in the information system for that purpose, and promptly post the outcomes of that definition on its website.
- The applicant must identify a "drug-device combination product" on the application form and submit an application to the State Medical Products Administration for registration of medications or medical devices based on the outcomes of defining the product's qualities (22).

Regulatory Requirements of Combination Products in Japan

The regulating body in Japan is the PMDA (Pharmaceuticals Medicine and Device Agency). It is a department of the Ministry of Health, Labour, and Welfare (MHLW). A "combination product" in Japan is a product that is advertised as a single drug, medical device, or cellular and tissue-based product but actually combines two or more different types of drugs, devices, processed cells, etc. that ordinarily fall into the drug, medical device, or cellular and tissue-based product categories if marketed separately (24).

Examples of Combination Products

These comparable drug-combination products are only a few examples. Prefilled syringes and asthma medicine are delivered through inhalers with a programmable respiratory intake mechanism. Heparin-coated catheters, antimicrobial bone cement, and drug-eluting stents are a few examples of combination items that correlate to medical devices. Cell suspensions in prefilled syringes and a pair of cell suspension and scaffold goods used for impregnation in clinical settings are two examples of cellular and tissue-based combination products.

The following goods are permitted in combination products:

a) A collection of products (integrated goods where each component can be sold as a distinct medication, medical device, or cell and tissue product since the pharmaceuticals, etc., are not indivisible).
b) Kit products ("In Handling Kit and Other goods That Combine Solutions, etc. with Injections, it says "kit products.") (PAB/ELD Notice No. 2-98 by the Directors of the Office of Pharmaceutical Affairs, Ministry of Health and Welfare's First Division of Evaluation and Registration, Second Division of Evaluation and Registration, and Division of Biological Products, dated 12 March 1986)
c) Products, such as medical equipment, etc., that cannot be utilized independently from pharmaceuticals and in which the constituent drugs, etc., cannot be marketed individually. (Excluding kit products).

Handling of Marketing Application

- Cellular and tissue-based products, medical devices, and medication combinations must be submitted as a single product.
- It is not necessary for pharmaceuticals, medical devices, or cellular and tissue-based products that are part of a combination product to have individual marketing permission, certification, or notice, even if they are manufactured at a different manufacturing facility than the final combination product.
- The marketing authorization holder will require a separate license and marketing clearance if the medication, device, or another component of the combination product is offered as a finished good.
- When filing your marketing approval application, be sure to specify whether your product has a clinical necessity since set products—with the exception of those with a need—are often not accepted.
- Specify in the comments area of the application which "Combination Products" match to which medications. If the combination products match the "Kit products" specified in the "Combination Products" section of the Handling of Kit and Other Goods that Combined Solutions, etc. to Injections, then they are "Kit products".
- Be sure to put "combination products" in the section of the application form designated for comments, and request the chance to submit either the application for a partial modification or the minor change notice for combination items (25).

Decision-Making Procedures

In Japan, combination products are evaluated on a case-by-case basis. The primary mode of action is the primary criterion for classifying a substance as a drug or a device. The Ministry of Health, Labour, and Social Services will examine the matter. The Office of New Drugs of the PMDA will oversee the review if the product is classified as a pharmaceutical. The PMDA's Office of Medical Devices will take the lead if the item is a medical device (26).

License, Manufacture, and Quality Management

The company must get the license to develop any combination of drugs, medical devices, or products made from cellular tissues. Combination products need to follow GMP for medications and quasi-drugs, QMS for medical devices, in vitro diagnostics, and cellular and tissue-based products.

CONCLUSION

Combination products are the new approach that has been used in a vast range because in some scenarios it may be difficult to treat the diseases with the drug, biologics, and medical device alone. The regulations of Combination products in the US, China, and Japan are discussed in this article. The primary mode of action is the primary factor in determining whether a combination product should be classified as a medicine, biologic, or medical device in each of the three counties, and the regulatory pathway that results from that classification. The field of Combination products in the US is very well developed with transparency when compared to China and Japan.

ACKNOWLEDGEMENT

REFERENCES

1. Bayarri L. Drug-device combination products: regulatory landscape and market growth. Drugs of Today (Barcelona, Spain: 1998). 2015 Aug 1;51(8):505-13.
2. Privitera MB, editor. Applied human factors in Medical Device design. Academic Press; 2019 Jun 15.

3. Tian J, Song X, Wang Y, Cheng M, Lu S, Xu W, Gao G, Sun L, Tang Z, Wang M, Zhang X. Regulatory perspectives of combination products. Bioactive Materials. 2022 Apr 1;10:492-503

4. Elson RA, Jephcott AE, McGechie DA, Verettas D. Antibiotic-loaded acrylic cement. The Journal of bone and joint surgery. British volume. 1977 May;59(2):200-5.

5. Commissioner Oof the. Classification of produc ts as drugs and devices and additional issues [Internet]. U.S. Food and Drug Administration. FDA; [cited 2023Jan6]. Available from: https://www.fda.gov/regulatory-information/search-fda-guidance-documents/classification-products-drugs-and-devices-and-additional-product-classification-issues

6. Sanduria S, Tripathy S, Murthy PN, Patra BP, Dureja H. Voicing regulatory perspectives of the combination products. Journal of Generic Medicines. 2020 Sep;16(3):101-11.

7. Code of Federal Regulations Title 21 3.2(e). https://ecfr.federalregister.gov/curr ent/title-21/chapter-I/subchapter-A/part-3, 1991

8. Commissioner Oof the. Combination product definition combination product types [Internet]. U.S. Food and Drug Administration. FDA; [cited 2023Jan7]. Available from: https://www.fda.gov/combination-products/about-combination-products/combination-product-definition-combination-product-types

9. Commissioner Oof the. Acts, rules and regulations [Internet]. U.S. Food and Drug Administration. F.DA; [cited 2023Jan7]. Available from: https://www.fda.gov/combination-products/guidance-regulatory-information/acts-rules-and-regulations

10. Commissioner Oof the. Office of Combination Products [Internet]. U.S. Food and Drug Administration. [cited 2023Jan7]. Available from: https://www.fda.gov/about-fda/office-clinical-policy-and-programs/office-combination-products

11. Commissioner Oof the. Frequently asked questions about combination products [Internet]. U.S. Food and Drug Administration. FDA; [cited 2023Jan8]. Available from: https://cacmap.fda.gov/combination-products/about-combination-products/frequently-asked-questions-about-combination-products

12. Kapoor V, Kaushik D. A comparative study of regulatory prospects for drug-device combination products in major pharmaceutical jurisdictions. Journal of Generic Medicines. 2013 Jun;10(2):86-96.

13. Commissioner Oof the. How to prepare a pre-request for designation (Pre-RFD) [Internet]. U.S. Food and Drug Administration. FDA; [cited 2023Jan27]. Available from: https://www.fda.gov/regulatory-information/search-fda-guidance-documents/how-prepare-pre-request-designation-pre-rfd

14. Commissioner Oof the. How to write a request for designation (RFD) [Internet]. U.S. Food and Drug Administration. FDA; [cited 2023Jan9]. Available from: https://www.fda.gov/regulatory-information/search-fda-guidance-documents/how-write-request-designation-rfd

15. Commissioner Oof the. Combination products guidance documents [Internet]. U.S. Food and Drug Administration. FDA; [cited 2023Jan10]. Available from: https://www.fda.gov/regulatory-information/search-fda-guidance-documents/combination-products-guidance-documents

16. Kapoor A, Aggarwal G. Pre-filled syringes in the developed and developing region: An insight into Regulatory considerations. International Journal of Drug Regulatory Affairs (IJDRA). 2019;7(2):42-50.

17. Information of NMPA, www.emergobyul.com/resour ces/china/china-food-drug-administration (Accessed on 2023 Jan 10)

18. Nmpa.gov.cn.Available at: https://www.nmpa.gov.cn/xxgk/fgwj/gzwj/gzwjylqx/20020816010101116.html (Accessed: January 11, 2023).

19. Tian J, Song X, Wang Y, Cheng M, Lu S, Xu W, Gao G, Sun L, Tang Z, Wang M, Zhang X. Regulatory perspectives of combination products. Bioactive Materials. 2022 Apr 1;10:492-503.

20. Cheng WX, Liu YZ, Meng XB, Zheng ZT, Li LL, Ke LQ, Li L, Huang CS, Zhu GY, Pan HD, Qin L. PLGA/β-TCP composite scaffold incorporating cucurbitacin B promotes bone regeneration by inducing angiogenesis. Journal of orthopaedic translation. 2021 Nov 1;31:41-51

21. Available from : Circular of the State Food and Drug Administration on Matters Related to the Registration of Drug-Device Combination Products (No. 2021 of 52) (nmpa.gov.cn) (Accessed: January 13, 2023)

22. Sanduria S, Tripathy S, Murthy PN, Patra BP, Dureja H. Voicing regulatory perspectives of the combination products. Journal of Generic Medicines. 2020 Sep;16(3):101-11.

23. Nmpa.gov.cn.[cited2023Jan20].Availablefrom:https://www.nmpa.gov.cn/xxgk/ggtg/qtggtg/20210727154135199.html?type=pc&m= Accessed: January 18, 2023)

24. Pharmaceuticals and Medical Devices Agency Handling of a marketing application for combination products https://www.pmda.go.jp/files/000153158.pdf (2014), Accessed on 2023 Jan21

25. Available from:NOTifIcation-PMDA(no date). Available at: https://www.pmda.go.jp/files/000153158.pdf (Accessed: January 22, 2023)

26. Cartwright, A.C., and Matthews, B.R. (2016) International Pharmaceutical Product Registration, Second edition. CRC Press.

Table 1-Types of combination products

Type	Description	Common Example(s)
1	Convenience Kit or Co-Package *Drug and device are provided as individual constituent parts within the same package*	Drug or biological product vials packaged with device(s) or accessory kits (empty syringes, auto-injectors, transfer sets), first aid or surgical kits containing devices and drugs
2	Prefilled Drug Delivery Device/ System *Drug is filled into or otherwise combined with the device AND the sole purpose of the device is to deliver drug*	Prefilled drug syringe, auto-injectors, metered-dose inhalers, dry powder inhalers, nasal-spray, pumps, transdermal systems, prefilled iontophoresis system or microneedle "patch"
3	Prefilled Biologic Delivery Device/ System *Biological product is filled into or otherwise combined with the device AND the sole purpose of the device is to deliver biological product*	Vaccine or other biological product in a prefilled syringe, autoinjector, nasal spray, transdermal systems or microneedle patch pre-loaded with biological product
4	Device Coated/ Impregnated/ Otherwise Combined with Drug *Device has an additional function in addition to delivering the drug*	Drug pills embedded with sensors, contact lens coated with a drug, drug-eluting stents, drug-eluting leads, condoms with spermicide, dental floss with fluoride, antimicrobial coated catheters/sutures, bone cements with antibiotics
5	Device Coated or Otherwise Combined with Biologic *Device has an additional function in addition to delivering the drug*	Live cells seeded on or in a device scaffold, extracorporeal column with column-bound protein
6	Drug/Biologic Combination	Antibody-drug conjugates, progenitor cells combined with a drug to promote homing
7	Separate Products Requiring Cross Labeling	Light-activated drugs or biological products not co-packaged but labeled for use with a specific light source device
8	Possible Combination Based on Cross Labeling of Separate Products	Drug/biological product under development utilizes a device, but unclear whether the final product will require that the two be cross-labeled
9	Other Type of Part 3 Combination Product (e.g., Drug/Device/ Biological Product) Combination product not otherwise described	All 3 articles are combined in a single product (e.g., a prefilled syringe containing an antibody-drug conjugate), device to manufacture a biologic also includes a drug or biologic in the kit, or the product contains two different combination product types (e.g., Type 1 and Type 2 are provided together).

Harshitha *et al.,*

Table 2-US regulatory agencies application type and review period

Lead Centre	Application type	Review clock
Centre for Drug Evaluation and Research or Centre for Biologics Evaluation and Research	New Drug Application / Biologic License Application	6 Months (Priority Review) or 10 Months (Standard Review)
Centre for Devices and Centre Radiological Health	Humanitarian Device Exemption	75 days
	510k (Premarket notification)	90 days
	Pre-market approval (PMA)	180 days

Fig. 1. Representative diagrams of combination products. A. drug-eluting stents. B. catheters with antibacterial coatings. C. antibiotic-loaded bone cements for total knee replacement. D. stitches containing antibacterial ingredients and their inhibition halo. E. Intracranial drug-eluting stent system. Images were provided by the manufacturers.

Fig 1: Examples of Combination Products (3)

Fig 2: Algorithm of PMOA in US (12)

Fig 3: Drug/device combination product attributes-definition application procedure in China (21)

Harshitha *et al.,*

Fig 4: Combination products Approval Process in China (23)
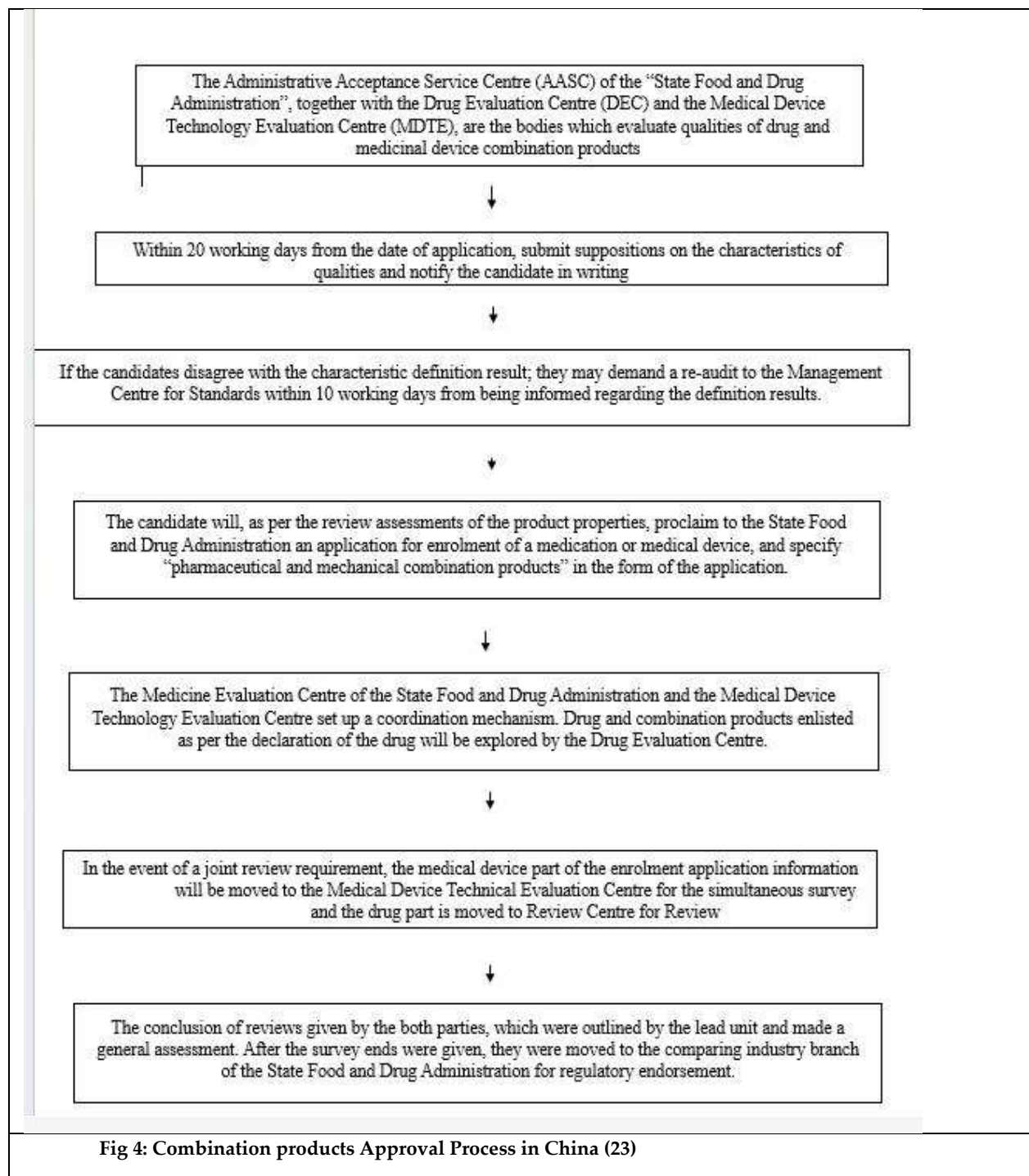
RESEARCH ARTICLE

Studies on the Exploitation of ITK Practices Adopted by the Farmers of the Cauvery Delta Region for the Control of Brown Leaf Spot and Blast Disease in Rice

R.Livitha[1]*, D. John Christopher[2] and V. Jai Ganesh[3]

[1]Ph.D (Scholar), Department of Plant Pathology, Faculty of Agriculture, Annnamalai University, Annamalai Nagar – 608002, Tamil Nadu, India
[2]Professor, Department of Plant Pathology, Faculty of Agriculture, Annnamalai University, Annamalai Nagar – 608002, Tamil Nadu, India.
[3]Assistant Professor, Department of Plant Pathology, Faculty of Agriculture, Annnamalai University, Annamalai Nagar – 608002,Tamil Nadu, India.

*Address for Correspondence
R.Livitha
Ph.D (Scholar),
Department of Plant Pathology,
Faculty of Agriculture,
Annnamalai University,
Annamalai Nagar – 608002,
Tamil Nadu, India.
E.Mail: livitharajendiran@gmail.com

ABSTRACT

Rice (*Oryzae sativa* L.) is the most important food for over two billion people in Asia. Which is mainly infested by Brownspot and blast diseases and cause maximum yield loss.The present study was undertaken to find out the efficacy of different Indigenous Technical Knowledge (ITK) practices (Panchagavya, Mint leaf extract, Five leaf extract and Fish amino acid) alone and in combination against the diseases and also characterization of antimicrobial compound against disease causing pathogens. The rice plant are treated with combined application of Panchagavya, Five leaf extract, Mint leaf extract and cd with seed treatment @20ml/ kg of seeds and foliar spray @10 % conc. on 20 and 40 Days after transplanting (T7) recorded minimum disease incidence and significantly enhanced the yield parameters. Several antimicrobial compounds were identified from the ITK components which were found to possess antimicrobial compounds against fungal and bacterial pathogens causing diseases in crop plants. These compounds could be the reason for inducing resistant in the plant against the pathogen causing major disease in rice.

Keywords: Rice, ITK, Panchagavya, Fish amino acid.

INTRODUCTION

Rice (*Oryza sativa* L.) is the most important and extensively grown crop in tropical and subtropical regions of the world and consuming as a staple food for more than 70 percent of the world's population. It is grown in almost all the states of India. In Tamil Nadu rice crop (paddy) is predominantly grown in the Cauvery delta region which is also known as the rice bowl of Tamil Nadu. Rice crop is affected by serious biotic factors like diseases caused by fungi, bacteria and viruses leads to the economic loss and non-availability of food to the population. Among the diseases, Brown leaf spot disease caused by *Bipolaris oryzae* and blast incited by *Pyricularia oryzae* are considered to be major constrain is rice cultivation due to extensive distribution of numerous physiological races (Arshad et al., 2008) and resulting in yield loss of about 27–35 percent (Deepak CA et al., 2021).

Diseases of Rice is managed by seed treatment with fungicides and spraying of fungicides in the field that break down the natural ecological balance. The use of Indigenous Technical knowledge (ITK) practices may help in avoiding environmental pollution as well as increase the production of pesticide-free produce. The ITK components *Viz,*. Panchagavya, Fish amino acid, Five leaf extract, 3G solution, Mooligai viratti, Tulsi leaf extract, Mint leaf extract and Ten leaf extract, etc., generally refers to knowledge systems embedded in the cultural traditions of regional or local communities (Talukdar et al. 2012).The information on traditional agriculture pertinent on efficacy of ITK components against rice diseases and characterization of antimicrobial compounds available in ITK components have never been recorded or documented. With the background, the present investigation was done to study the efficacy and characterization of antimicrobial compounds of ITK components against the diseases incited by *Bipolaris oryzae* and *Pyricularia oryzae*.

MATERIALS AND METHODS

Isolation of *B. oryzae*
Ten Strains of *B. oryzae* was obtained from foliar lesions of the rice variety ADT-36 by pure culture technique and was grown on a rice flour medium (rice flour, 14g; yeast extract, 4g; agar-agar, 15g; distilled water, 1000ml) the culture was maintained at 28Â°C under continuous fluorescent lighting (Michelena and Castilo, 1984). The pathogenic isolates of *B. oryzae* were designated as (AUBO-1 to AUBO-10).

Isolation of *P. oryzae*
Ten isolates of *P. oryzae* was isolated from the seeds of ADT-36 by pure culture technique and was grown on prune-agar medium (prune,40g; agar-agar,20g; distilled water, 1000ml) (Ram B. Khadka et al. 2012). Petri plates inoculated with *P. oryzae* was incubated at 28Â°C for 7 days in the dark, and for further 3 days at the same temperature under continuous fluorescent lighting. The pathogenic isolates of *P.oryzae* were designated as (AUPO-1 to AUPO-10).

Pathogenicity proving of the fungal pathogen
The efficacy of ten isolates of pathogenic fungi such as and *Bipolaris oryzae* and *Pyricularia oryzae* were tested by pathogenicity proving study and the isolates Bo$_8$ & Po$_7$ were found to be effective in cause the disease symptom in pot cultural condition. Hence *Bipolaris oryzae* Bo$_8$ and *Pyricularia oryzae* Po$_7$ were used for further studies. From the result of the pathogenicity test the virulent isolates of each pathogen Bo$_8$ and Po$_7$ were subjected to molecular confirmation through ITS region sequencing. the sequence thus obtained was analyzed by using the BLAST analysis tool of the NCBI database. Based on the BLAST search, isolate Bo$_8$ is confirmed as *B. oryzae* and Po$_7$ as *P. oryzae*. The sequences analysed were deposited in the Gen Bank database and the accession number is obtained. The pathogen isolates with accession numbers were given below:

Isolate	Organism	Accesion number
Bo$_8$	*Bipolaris oryzae*	OQ349750
Po$_7$	*Pyricularia oryzae*	OQ359421

Preparation of ITK components.
Panchagavya

The Panchagavya was prepared by using cow dung (5 parts), cow urine (3 parts), milk (2 parts), curd (2 parts), and ghee (1 part). The fresh cow dung was thoroughly mixed with ghee in a wide-mouth mud pot and kept for three days. The above mixture was thoroughly mixed once daily. On the fourth day, other ITK were added to the mud pot, mixed properly, and covered with a nylon net to prevent flies into the pot. The pot was placed in a shed and mixed thoroughly twice for thirty days. (Krishna kumar et al., 2020)

Five leaf extract

Collect leaves of the Neem, Pungam, Calotrophis, Adathoda and, Vitex at the rate of each 1 Kg and clean well with water, grind into paste form with water, soak in an equal amount of water or cow urine and keep it undisturbed overnight. In the morning for better effect, boil the extract for 1/2 -1 hour at 70-80°C in a closed container. After boiling, leave it for another 12 hours to cool, the cooled suspension must be filtered with Kada cloth and the filtrate is stored in a clean glass bottle and can be stored upto 15 days. Mix the extract with the recommended quantity of water for the crop.

Mint leaf extract

Mint leaves are purchased from the local market. The fresh leaves are washed in sterilized distilled water. The aqueous extract was then prepared by macerating 10 g of leaves in 100 ml of sterilized distilled water. Subsequently, the extract was filtered twice with Whatmann filter paper 1. This extract was used for investigations.

Fish amino acid

The fish amino acid was prepared from fish waste obtained from the local fish market. An equal amount of fish waste and jaggery was taken (1 kg of each fish waste and jaggery). The fish waste was taken in an air-tight plastic jar/bottle and jaggery was added. The materials were mixed well and stored in a cool dry place. It was kept away from direct sunlight. After 10 days, the liquid portion was filtered and used for spraying (Maghirang, 2011). The final product was viscous fluid and smelled of panchamirtham.

Gas chromatography–mass spectrometry (GC-MS):

The compounds present in the ITK components *Viz* Panchagavya, five leaf extract, mint leaf extract and fish amino acid were characterized through GC-MS analysis at Bio Focus Research Centre, Thanjavur using Thermo Scientific Trace GC Ultra chromatograph system (Thermo Fischer Scientific, Austria) coupled to Thermo Scientific DSQ II quadruple mass spectrometer. Methanolic extracts of Panchagavya, five leaf extract and mint leaf extract were separated using a TG-SQC capillary column (15 m in length, 0.25mm I.D. and 0.25 μm film thicknesses). Helium gas was used as a carrier gas with a flow rate of 1.0 mL/min and split mode was used with the split flow of 10 mL. The injector temperature was set at 207°C. The column temperature programs consisted of the following: initial temperature of 50°C (held 1 min), increased to 150°C at a rate of 25°C/min. After each injection, the column temperature was increased to 250°C and then held for 7.0 min to remove the residues that were potentially retained in the column. The transfer line temperature and MS source temperature were 265 and 200°C, respectively. Ions with masses of 44 and 56 were selected for the quantification of compounds. The sample extraction and introduction were fully automated using a Triplus RSH Head Space Autosampler. The volume of syringe used was 2.5mL and needle length was 65mm. The 20mL headspace vials were incubated for 1 min in the agitator with temperature 300°C. Filling and injection speed was maintained at 20mL/min. Pre-injection and post-injection flush were given using nitrogen gas to avoid contamination. The time for pre-injection and post-injection flushing was 5 s and 30 s respectively. Raw hexanal (99 per cent purity) purchased from Sigma Aldrich is used as the standard check.

Pot culture experiment

A pot culture study was conducted with sterilized garden land soil in completely randomized block design with ten treatments and three replications each at Department of Plant Pathology, Annamalai University, Annamalai nagar from September 2021 to January 2022. Rectangular cement pot of size 18" x 12" x 12" filled with 45 kg of paddy field

soil under puddle condition were used for this study. BPT 5204 rice seeds were used (Figure I). The plants in the `pots were maintained with uniform, regular and judicious watering. The ITK components viz., Panchagavya, Mint leaf extract, Five leaf extract, and Fish amino acid and the chemical Tricyclazole were tested against the *Pyricularia oryzae, Bipolaris oryzae*. Twenty percent concentration of ITK components such as Panchagavya, Fish amino acid, Five leaf extract and Mint leaf extract treated with seed @20 ml/ kg of seeds and foliar spray @10 % conc. on 20 and 40 Days after transplanting. The chemical tricyclazole used as foliar spray at 0.6g/ha first standard chemical check. The spore suspension of *Bipolaris oryzae, Pyricularia oryzae* 20 days culture grown on PDA were inoculated the plants using the sterile pinpricking method 15 days after transplanting rice plants. The inoculated plants were incubated in a humid chamber for 48 h and subsequently moved to the greenhouse and it is maintained at 22-28℃, 70-90% relative humidity. Under a light intensity of 85 μmol m^{-1} S^{-1}, 12 h photoperiod and subsequently transfer to pot culture yard. The treatment schedules were designed on the basis of the above phenomena.

Treatment schedule
T_1- Application of panchagavya with seed treatment @20ml/kg of seeds and foliar spray @10 % conc. on 20 and 40 Days after transplanting, T_2 **-** Application of five leaf extract with seed treatment @20ml/ kg of seeds and foliar spray @10 % conc. on 20 and 40 Days after transplanting T_3 **-** Application of mint leaf extract with seed treatment @20ml/ kg of seeds and foliar spray @10 % conc. on 20 and 40 Days after transplanting T_4**-** Application of fish amino acid with seed treatment @20ml/ kg of seeds and foliar spray @10 % conc. on 25 and 50 Days after transplanting T_5**-**T_1+T_2 T_6 **-** T_5+T_3 T_7 **-** T_6+T_4 T_8 **-** Application of Tricyclazole @ 0.6 % conc. on 20 and 40 Days after transplanting T_9 **-** Healthy Control T_{10} **-** Inoculated Control.

Assessment of the disease severity in the field
Twelve plants from each plot were randomly selected and tagged for grading the severity of diseases. The severity of two diseases *viz.* brown leaf spot and leaf blast were recorded following IRRI scales (Standard Evaluation System for Rice, 1980). The disease severity was recorded at 30,50 and at the time of harvest and per cent diseases index was determined us usual.

Field trial
The field trials were conducted at Nalladai, Mayiladudurai district of Tamilnadu during September 2021 to January 2022, in field with a history of brown leaf spot, blast and sheath blight incidence (Figure II). The trial was laid out in plots (5x4 m) arranged in randomized block design. Rice seeds of cv. BPT 5204 were sown in the plot and transplanted in 30 DAS in row with row/ plant spacing of 12.5 x 10 cm. Three replicate plots were maintained for each treatment. Regular cultivation practices were followed as per the recommendation. Treatment application details and experimental observation were the same as in greenhouse experiment.

Treatment schedule
T_1 - Application of panchagavya with seed treatment @20 ml/ kg of seeds and foliar spray @10 % conc. on 20 and 40 Days after transplanting, T_2 - Application of five leaf extract with seed treatment @20ml/ kg of seeds and foliar spray @10 % conc. on 20 and 40 Days after transplanting, T_3- Application of mint leaf extract with seed treatment @20ml/ kg of seeds and foliar spray @10 % conc. on 20 and 40 Days after transplanting, T_4 -T_1+T_2, T_5 - T_4+T_3, T_6 - Application of Tricyclazole @ 0.6 % conc. on 20 and 40 Days after transplanting, T_7 – Contro

Data analysis
The data obtained from the studies conducted under laboratory and field conditions were subjected to the analysis of variance techniques (ANOVA) and were applied to completely randomized design (CRD) and randomized block design (RBD). The data obtained on per cent inhibition were transformed using angular (arc sine) transformation.

Livitha *et al.,*

RESULTS

Evaluation of combined application of ITK components against blast and brown leaf spot incidence of rice Brown leaf spot disease incidence. The Effect of ITK components were tested against the Brown leaf spot disease of rice under pot culture condition. The result revealed that all the ITK components were found to be effective in inhibiting the progress of disease development than the untreated control. Among the various treatments, the plants are treated with standard chemical check Tricyclazole (T8) @ 0.6 % conc. on 20 and 40 days after transplanting (T8) recorded minimum brown leaf spot disease incidence which recorded 7.82 %, 10.04 % and 11.65 % percent disease incidence on 30, 50 and at the time of harvest 68.83%,71.27% and 70.62% respectively and followed by the plant are treated with combined application of Panchagavya, Five leaf extract, Mint leaf extract and Fish amino acid with seed treatment @20ml/ kg of seeds and foliar spray @10 % conc. on 20 and 40 Days after transplanting (T7) recorded brown leaf spot disease incidence 7.99%, 10.22% and 11.72% percent disease incidence on 30, 50 and at the time of harvest 72.14%,71.77% and 70.44% respectively and combined application Panchagavya, Five leaf extract and Mint leaf extract with seed treatment @20ml/ kg of seeds and foliar spray @10 % conc. on 20 and 40 Days after transplanting (T6) recorded brown leaf spot disease incidence 8.35%, 11.18% and 12.24% percent disease incidence on 30, 50 and at the time of harvest 70.89%, 69.11% and 69.13% respectively and the above three treatments were at par with each other in controlling the disease incidence. The same trend was observed in field trial also. The minimum disease incidence was registered with treatment T6 which recorded the brown leaf spot disease incidence of 7.98 %, 9.87 % and 10.84 % on 30, 50 and at the time of harvest respectively and followed by T5 recording 8.32 %, 10.13 % and 11.12 % percent disease incidence and T4 which recorded 9.40 %, 12.76 % and 13.32 % percent disease incidence on 30, 50 and at the time of harvest respectively. However all the above three treatments were statistically on par with each other in controlling the brown leaf spot disease incidence and significantly superior than all other treatments. Combined applications of ITK components significantly reduce blast disease incidence than the individual application of ITK components (Table III,IV)

Blast disease incidence.
The result of the experiments revealed that all the ITK components were effectively arrested the progress of disease development than the untreated control. The maximum percent disease control was observed with the plants are treated with standard chemical check Tricyclazole (T8) @ 0.6 % conc. on 20 and 40 days after transplanting (T8) recorded minimum blast disease incidence which recorded 8.50 %, 12.76 % and 13.32 % percent disease incidence on 30, 50 and at the time of harvest 74.53%, 66.46% and 66.18% respectively and followed by the plant are treated with combined application of Panchagavya, Five leaf extract, Mint leaf extract and Fish amino acid with seed treatment @20ml/ kg of seeds and foliar spray @10 % conc. on 20 and 40 Days after transplanting (T7) recorded minimum blast disease incidence which recorded 9.09 %, 12.22 % and 13.60 % percent disease incidence on 30, 50 and at the time of harvest 72.76%, 67.88% and 66.49% respectively and combined application Panchagavya, Five leaf extract and Mint leaf extract with seed treatment @20ml/ kg of seeds and foliar spray @10 % conc. on 20 and 40 Days after transplanting (T6) recorded minimum blast disease incidence which recorded 10.12 %, 13.07 % and 14.12 % percent disease incidence on 30, 50 and at the time of harvest 70.03%, 65.64% and 64.15% respectively. The treatments T8,T7andT6 were statistically at par with each other to manage the disease incidence. The same result was observed in field trial also. The maximum percent disease control was observed with treatment T6 ,which recorded 9.85 %, 11.74 % and 12.83 % percent disease incidence on 30, 50 and at the time of harvest respectively and followed by treatment T5 recording 10.16 %, 12.12 % and 13.48 % percent disease incidence and treatment T4 which recorded 11.45 %, 13.23 % and 14.09 %percent disease incidence on 30, 50 and at the time of harvest respectively. The maximum percent disease control was observed with treatment T6, How ever all the above three treatments were statistically on par with each other in controlling the blast disease incidence and significantly superior than all other treatments. Combined applications of ITK components significantly reduce blast disease incidence than the individual application of ITK components (Table III,IV)

Livitha *et al.,*

Evaluation of different ITK components on growth and yield parameters of rice

The results pot culture experiment revealed that among the ten treatments, the plants are treated with combined application of Panchagavya, Five leaf extract, Mint leaf extract and Fish amino acid with seed treatment @20ml/ kg of seeds and foliar spray @10 % conc. on 20 and 40 Days after transplanting (T7) recorded maximum plant height (90.45 cm), grain yield (32 g/plant), straw weight (117.5 g/plant), number of tillers (22/ clump). It was followed by standard chemical check Tricyclazole @ 0.6 % conc. on 20 and 40 days after transplanting (T8) which registered plant height (91.57 cm), grain yield (34 g/plant), straw weight (122.51 g/plant), number of tillers (24/ clump) and combined application of Panchagavya, Five leaf extract and Mint leaf extract with seed treatment @20ml/ kg of seeds and foliar spray @10 % conc. on 20 and 40 Days after transplanting (T6)   recording plant height (92.14 cm), grain yield (33 g/plant), straw weight (116.56 g/plant), number of tillers (21/ clump). In field trial experiments similar observation was recorded. The maximum growth and yield were observed with treatment T5 which recorded maximum plant height (90.56 cm), grain yield (4.36 t/ha) and followed by T6 which recorded plant height (91.67 cm), grain yield (4.50 t/ha) and T4 recording plant height (88.93 cm), grain yield (3.49 t/ha) and the treatment T4 recording plant height (88.93 cm), grain yield (3.49 t/ha). However all the above three treatments were statistically on par in enhancing the growth and yield parameters and significantly superior than all other treatments. (Table I,II)

Gas Chromatography Mass Spectroscopy (GC MS) Analysis:
Characterization of antimicrobial compounds from methanolic solvent of ITK components through GC-MS.
 Panchagavya.

The methanolic extract of Panchagavya was analysed in GC-MS for its antimicrobial properties. The analysis shown that, two antibiotics & antimicrobials such as Squalene &Octadecanoic acid and two antioxidants & pesticide compounds, n-Hexadecanoic acid & Hexadecanoic acid and one induce systemic acquired resistance (ISR) ie 2,3-Butanediol. The retention time, name of the compound, biological activity, molecular weights, molecular formula and structure of the compound are presented in the table V.

Mint leaf extracts

The antimicrobial and antibiotic compounds identified from mint leaf extract by GC-MS. are recorded as, two antimicrobials *Viz* Nitrogen oxide (N2O) (CAS) Nitrous oxide & 1-Octadecyne and Citronellyl acetate. The compounds Cyclohexanol, 2-methyl-5-(1-methylethenyl)-, (1α,2α,5β) having antimicrobial, antibacterial, antifungal and antiviral property also identified. The retention time, name of the compound, biological activity, molecular weights, molecular formula and structure of the compound are presented in the table VI.

Five leaf extract.

The antimicrobial and antibiotic compounds identified from five leaf extract by GC-MS are recorded. Three antimicrobials compounds *Viz* Phenol (CAS) Izal, Benzoic acid (CAS) Retardex and Peracetic acid and one pesticide compound of Carbamic acid Phenyl ester were identified. Peracetic acid also noticed as antifungal activity. The retention time, name of the compound, biological activity, molecular weights, molecular formula and structure of the compound are presented in the table VII.

Fish amino acid (FAA)

The extract of fish amino acid was analysis for its antimicrobial property by GC-MS. The analysis shown that two antioxidants, nematicide & pesticidal activity compounds such as n-Hexadecanoic acid & Hexadecanoic acid and one antimicrobial as octadecanoic acid. The retention time, name of the compound, biological activity, molecular weights, molecular formula and structure of the compound are presented in the table VIII.

DISCUSSION

Efficacy of combined application of ITK components against blast and brown leaf spot

The efficacy of ITK components *viz.,* Panchagavya, Fish amino acid, Five leaf extract and Mint leaf extract were tested at different combinations against brown leaf spot and blast diseases of rice under pot culture and field conditions. Plants treated with combined application of Panchagavya, Fish amino acid, Five leaf extract and Mint leaf extract as seed treatment @ 20ml/kg of seeds and foliar spray @10 % conc. on 20 and 40 DAT was found to significantly manage the brown leaf spot and blast diseases and in influencing yield parameters. Similar findings were made by several workers using ITK components viz., Panchagavya, Fish amino acid, Five leaf extract, Mint leaf extract. Panchagavya has played a significant role in providing resistance to pests and diseases, resulting in increased overall yields (Tharmaraj et al., 2011). Panchagavya possess the properties of fertilizers and bio pesticides and resulted in positive effect on growth and productivity of crops (Somasundaram *et al*. 2003 and Sireesha, 2013). Yadav and Lourduraj (2006) studied that foliar spray of Panchagavya recorded significantly higher physical characteristics like grain size, 1000-grain weight and milling quality as well as cooking quality. Abassi (2011) said that fish emulsions is an excellent model system for development of an organic amendment as fertilizer with disease suppressing effects. Cow dung and Hen litter at 20% conc. was found to inhibit the mycelial growth of *P. oryzae* (Anandeeswari and John Christopher 2020).   Kamalakannan et al. (2001) studied the efficacy of different plant extracts against blast disease under pot culture conditions and reported that, pre and post inoculation spray of *Prosophis julifera*, *Zizyphus jujuba* and *Azadirachta indica* exhibited greater reduction in disease incidence. However, pre-inoculation spray was comparatively more effective than post inoculation spray in reducing disease incidence.

Characterization of antimicrobial compounds from ITK components.

Several antimicrobial compounds were identified from the ITK components through GC-MS. All the components were found to possess antimicrobial compounds against fungal and bacterial pathogens causing diseases in crop plants, (Reference listed in table 5,6,7,8).   similar findings were reported by several workers, Omotoso et al. (2014), Yi Shi et al. (2018), Lozano-Grande et al. (2018) I G Mamedov and Y V Mamedova (2021), Alicja Synowiec et al. (2021), Carlos et al. (2021), Sermakkani and Thangapandian (2012), D Akachukwu and R I. Uchegbu (2016), R.C. Gupta (2014), David et al. (2016), Zhilin Zhang et al. (2018) Vijayakumar and Pannerselvam (2013) and Blechert et al., (1995). The plants are treated with ITK components *viz.,* Panchagavya, Fish amino acid, Five leaf extract and Mint leaf extract, the compounds as listed in the table directly interact with mitochondria of plants and reaches the endoplasmic reticulum hence significantly enhance the structure like cutin, suberin and wax artificially in the plants system thereby the plant will escape from the disease incidence during adverse conditions .These findings are supported by many research workers Zhukov (2015) and Thirukumar et al., (2017). Besides Hexadecaconic acid and octadecanoic acid are the 16 carbon and 18 carbon compounds and their derivatives act as a signalling molecules, modulating diseases related physiologies in plants.

CONCLUSION

The results reported here indicated that Rice crop treated with complained application of Indigenous Technical Knowledges (ITKs) components viz., Panchagavya, Mint leaf extract, Five leaf extract and Fish amino acid were trigging the metabolic pathway of plant system against disease causing pathogens due to antimicrobial compound present in the ITKs components.

REFERENCES

1. Arshad HMI, Khan JA, Jamil FF. Screening of rice germplasm against blast and brown spot diseases. Pak. J. Phytopathol 2008;20: 52–57.
2. Deepak CA, Turaidar, V, Reddy M, Anantapur R, Krupa KN, Dalawai N, Kumar KH. Rice Sheath Blight: Major Disease in Rice. Inter J of Curr Microbiol and Appl sci 2021;7:976-988.

3. Talukdar RK, Barman S, Hussain A. Documentation and perceived rationale of ITK utilized in Boro rice cultivation by farmers of Kamrup district of Assam. J Acad Indus Res 2012;1(7): 412-417.

4. Michelena VV, Castillo FJ. Production of amylase by Aspergillus foetidus on rice flour medium and characterization of the enzyme. Journal of applied bacteriology 1984;56(3):395-407.

5. Ram. BK, Sundar M, Shrestha, Hira KM, Gopal BKC. Study on Differential response of Pyricularia grisea Isolates from Rice, Finger millet and Panicum sp. With Local and Alien Media, and their host range. Nepal Journal of Science and Technology 2012;13(2):225-230.

6. Krishna Kumar, Ghanshyam V, Ram V, Suraj K, Popin K. Exploitation of Panchagavya, benefits and ecofriendly management of plant diseases: A review Journal of Entomology and Zoology Studies 2020;8(4): 2360-2364.

7. Maghirang RG. Organic Fertilizers from Farm Waste Adopted by Farmers in the Philippines 2011.

8. Tharmaraj K, Suresh K, Ganesh R. Biochemical characterization and antibacterial activity of panchagavya. Golden Res. Thoughts 2011;1: 4- 5.

9. Somasundaram E. Evaluation of organic sources of nutrients and panchagavya spray on the growth and productivity of maize - sunflower - greengram system. Ph.D., Thesis, Tamil Nadu Agric. Univ, Coimbatore 2003.

10. Sireesha O.Effect of plant products, panchagavya and biocontrol agents on rice blast disease of paddy and yield parameters. Int J Res Biol Sci 2013;3:48-50.

11. Yadav BK, Christopher Lourduraj A. Effect of organic manures and Panchagavya spray on rice (*Oryza sativa* L.) quality. Cr Res 2006;31(1): 6-10.

12. Abassi PA. Exploiting and Understanding Disease Suppressing Effects of Fish Emulsion for Soil-borne and Foliar Diseases. Ontario Canada Global Sciences Books 2011.

13. Anandeeswari D, John Christopher D. Efficacy of plant products and animal products for management of *Sarocladium oryzae* (Sawada) gams and hawks worth causing sheath rot disease in rice. J Pharmacogn Phytochem 2020;9(5): 96-100.

14. Kamalakannan A, Shanmugam V, Srendran M. Effect of plant extracts on susceptibility of rice seedlings to blast disease and consequent biochemical changes in rice plants 2001;108(5): 536-543.

15. Omotoso A, Ezealisiji K, Mkparu KI. Chemometric profiling of methanolic leaf extract of *Cnidoscolus aconitifolius* (Euphorbiaceae) using UV-VIS, FTIR and GC-MS techniques. Peak J. Medicinal Plant Res 2014;2(1): 6-12.

16. Yi Shi, Xinju L, Yuanyuan F, Qing T, Hanyu J, Huiling M. 2, 3-Butanediol activated disease-resistance of creeping bentgrass by inducing phytohormone and antioxidant responses. Plant Physiology and Biochemistry 2018;129: 244-250.

17. Lozano-Grand AM, Shela G, Eduardo Espitia R, Gloria DO, Alma LMA (). Plant Sources, Extraction Methods, and Uses of Squalene". International Journal of Agronomy 2018;13.

18. Mamedov IG, Mamedova YV. Biological activity of novel pentasubstituted cyclohexanol against some microorganisms. Indian Journal of Chemistry 2021;60: 283-286.

19. Alicja S, Żyła K, Gniewosz M, Kieliszek M. An effect of positional isomerism of benzoic acid derivatives on antibacterial activity against Escherichia coli. Open Life Sciences 2021;16(1):594-601.

20. Carlos TD, Leydiane BB, Mayane MV, Renato AS, Douglas HP, Grasiele SC. Fenton-type process using peracetic acid: Efficiency, reaction elucidations and ecotoxicity. Journal of Hazardous Materials 2021;403.

21. Sermakkani M, Thangapandian V. GC-MS analysis of *Cassia italica* leaf methanol extract. Asian J Pharm Clin Res 2012;5: 90-94.

22. Akachukwu D, Uchegbu RI. GC-MS, antimicrobial and in vitro antioxidant assay of the leaf extract of *Alternanthera dentate*. J Adv Med Pharm Sci 2016;11(2): 1-7.

23. Gupta RC, Miller M, Jitendra KM, Robin BD, Wolf DD, Dejan M. Biomarkers in Toxicology (Second Edition Chapter 26 – Insecticides. Academic Press 2019;455-475.

24. David T, Dormanns K, Brown RG. The role of nitric oxide in neurovascular coupling. Journal of Theoretical Biology 2016;394: 1-17.

25. Zhang   Z. Antifungal activity of monoterpenes against Botryosphaeria dothidea. Natural Product Communications 2018;13-12.

26. Vijayakumar R, Raja S, Durai T, Chinnasamy M, Nooruddin T, Panneerselvam A. Antimicrobial Efficiency of a Marine Streptomyces sp. VPTSA1-4 Isolated from Coromandel Coast of Bay of Bengal, India 2023; 23: 16-25.

27. Blechert S. The octadecanoic pathway: signal molecules for the regulation of secondary pathways. Proceedings of the National Academy of Sciences 1995;92(10): 4099-4105.
28. Zhukov A. Palmitic acid and its role in the structure and functions of plant cell membranes. Russian journal of plant physiology 2015;62 (5): 706-713.
29. Thirukkumar S, Vennila P, Maheshwari TU. Investigation of total antioxidant activity and phenol in India noni fruit (Morinda citrifolia Linn). Juice extraction. Journal of Pharmocognosy and Phytochemistry 2017;6(2):241-243.
30. Thirumurugan, D, Ramasamy V. A potent fish pathogenic bacterial killer Streptomyces sp. isolated from the soils of east coast region, South India. J Coast Life Med 2013;1(3): 175-180.

Table I: Evaluation of combined application of ITK practices on the growth and yield parameters of rice under Pot culture condition

Tr. No	Plant height (Cm)	No. of tillers/ clump	Straw yield g/plant	Grain yield g/plant
T$_1$	84.43	20	106.98	28
T$_2$	83.21	19	104.42	26
T$_3$	80.32	18	103.97	25
T$_4$	72.93	16	100.29	21
T$_5$	88.47	20	118.87	31
T$_6$	92.14	21	116.56	33
T$_7$	91.57	24	122.51	34
T$_8$	90.45	22	117.54	32
T$_9$	80.41	11	98.22	16
T$_{10}$	78.52	9	94.63	13

Table II: Evaluation of combined application of ITK practices on the growth and yield parameters of rice under Field study

Tr. No	Plant height (Cm)	No. of tillers/ clump	Straw yield t/ha	Grain yield t/ha
T$_1$	85.43	20	3.98	3.22
T$_2$	82.21	18	3.42	2.78
T$_3$	79.32	16	2.97	2.33
T$_4$	88.93	22	4.29	3.49
T$_5$	91.67	24	5.14	4.50
T$_6$	90.56	23	4.97	4.36
T$_7$	80.43	13	2.21	1.57

Table III: Evaluation of combined application of ITK practices on the Brown leaf spot and blast incidence of rice (Pot culture)

Tr. No	Brown leaf spot						Blast					
	Disease incidence (%)			Disease over control (%)			Disease incidence (%)			Disease over control (%)		
	30 DAT	50DAT	At Harvest	30 DAT	50 DAT	At Harvest	30 DAT	50 DAT	At Harvest	30 DAT	50 DAT	At Harvest
T$_1$	14.85 (22.66)	18.42 (25.41)	19.94 (26.52)	48.22	49.12	49.71	15.45 (23.15)	17.71 (24.89)	20.45 (26.89)	53.70	53.44	48.08

63213

Livitha *et al.,*

T₂	16.97 (24.33)	20.05 (26.60)	21.55 (27.66)	40.83	44.61	45.65	17.07 (24.40)	18.58 (25.53)	22.56 (28.36)	48.85	51.16	42.73
T₃	17.23 (24.53)	21.55 (27.66)	22.26 (28.15)	39.92	40.47	43.86	18.23 (25.28)	19.73 (26.37)	23.17 (28.77)	45.37	48.13	41.18
T₄	23.40 (28.93)	27.76 (31.79)	29.32 (32.78)	18.41	23.31	26.05	25.63 (30.42)	27.28 (31.49)	31.23 (33.98)	23.19	28.29	20.72
T₅	10.42 (18.83)	13.33 (21.41)	14.12 (22.07)	63.67	63.18	64.39	12.44 (20.65)	15.27 (23.00)	16.87 (24.25)	62.72	59.86	57.17
T₆	8.35 (16.80)	11.18 (19.53)	12.24 (20.47)	70.89	69.11	69.13	10.12 (18.54)	13.07 (21.19)	14.12 (22.07)	70.03	65.64	64.15
T₇	7.99 (16.41)	10.22 (18.64)	11.72 (20.01)	72.14	71.77	70.44	9.09 (17.54)	12.22 (20.46)	13.60 (21.30)	72.76	67.88	66.49
T₈	7.82 (16.24)	10.04 (18.47)	11.65 (19.95)	68.83	71.27	70.62	8.50 (16.95)	12.76 (20.92)	13.32 (21.40)	74.53	66.46	66.18
T₉	8.94 (17.39)	12.76 (20.93)	14.67 (22.52)				10.47 (18.87)	13.63 (21.66)	15.73 (23.36)			
T₁₀	28.68 (32.38)	36.20 (36.98)	39.65 (39.03)				33.77 (35.29)	38.04 (38.08)	39.39 (38.87)			
C.D.	0.88	1.12	1.18				1.02	1.11	1.20			
SE(d)	0.42	0.52	0.56				0.48	0.52	0.57			

Table IV: Evaluation of combined application of ITK practices on the Brown leaf spot and Blast incidence of rice (Field study)

Tr. No	Brown leaf spot						Blast					
	Disease incidence (%)			Disease over control (%)			Disease incidence (%)			Disease over control (%)		
	30 DAT	50 DAT	At Harvest	30 DAT	50 DAT	At Harvest	30 DAT	50 DAT	At Harvest	30 DAT	50 DAT	At Harvest
T₁	10.34 (18.75)	13.42 (21.48)	14.94 (22.73)	56.65	52.45	49.73	12.87 (21.02)	15.67 (23.31)	16.49 (23.95)	58.47	54.51	56.31
T₂	11.97 (20.24)	16.21 (23.74)	15.55 (23.22)	50.10	42.56	47.68	16.97 (24.32)	18.00 (25.10)	19.50 (26.20)	45.24	47.75	48.33
T₃	12.23 (20.47)	20.59 (26.98)	21.26 (27.45)	49.02	27.04	28.47	15.46 (23.15)	17.56 (24.77)	18.24 (25.28)	50.11	49.03	51.66
T₄	9.40 (17.85)	12.76 (20.92)	13.32 (21.41)	60.82	54.78	55.18	11.45 (19.77)	13.23 (21.33)	14.09 (22.04)	63.05	61.59	62.66
T₅	8.32 (16.76)	10.13 (18.74)	11.12 (19.47)	65.32	64.10	62.59	10.16 (18.68)	12.12 (20.37)	13.48 (21.54)	67.22	64.82	64.28
T₆	7.98 (16.41)	9.87 (18.31)	10.84 (19.22)	66.74	65.02	63.53	9.85 (17.29)	11.74 (20.04)	12.83 (20.99)	68.22	65.92	66
T₇	23.99 (29.33)	28.22 (32.08)	29.72 (33.03)				30.99 (33.83)	34.45 (35.94)	37.74 (37.90)			
C.D.	0.80	1.04	1.06				1.01	1.14	1.25			
SE(d)	0.36	0.47	0.48				0.46	0.51	0.57			

Table V: Characterization of antimicrobial compounds from aqueous extract of Panchagavya

S. No	Compound	Biological activity	Molecular Weight (g/mol)	Molecular formula	Retention time	Structure	Reference
1.	n-Hexadecanoic acid	Antioxidant, Nematicide, Pesticide	256.42	$C_{16}H_{32}O_2$	13.903		Omotoso et al. (2014)
2.	Hexadecanoic acid	Antioxidant, Pesticide, Nematicide,	256.42	$C_{16}H_{32}O_2$	11.736		Sermakkani and Thangapandian (2012) and Vijayakumar and Pannerselvam (2013)
3.	Squalene	Antimicrobials, antibiotics, repellents.	410.71	C30H50	19.829		Lozano-Grande et al. 2018
4.	2,3-Butanediol	Initiate induced systemic resistance (ISR)	90.12	C4H10O2	1.668		Yi Shi et al. (2018)
5.	Octadecanoic Acid	Antibiotic and antimicrobials	284.47	C18H36O2	15.969		Blechert et al 1995

Table VI: Characterization of antimicrobial compounds from aqueous extract of Mint leaf extract

S. No	Compound	Biological activity	Molecular Weight	Molecular formula	Retention time	Structure	Reference
1.	Cyclohexanol, 2-methyl-5-(1-methylethenyl)-, (1α,2α,5β)	Antimicrobial, antibacterial, antifungal, antiviral	154.24	$C_{10}H_{18}O$	4.941		I G Mamedov and Y V Mamedova (2021)
2.	Citronellyl acetate	Antifungal Activity	198.30	$C_{12}H_{22}O_2$	12.882		Zhilin Zhang et al. 2018
3.	Nitrogen oxide (N2O) (CAS) Nitrous oxide	Antimicrobial activity	40.14	N_2O	13.029		David et al. 2012
4.	1-Octadecyne	Antimicrobial activity	250	$C_{18}H_{34}$	12.553		D Akachukwu and R I. Uchegbu 2016

Table VII: Characterization of antimicrobial compounds from aqueous extract of Five leaf extract

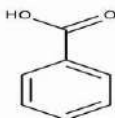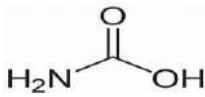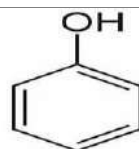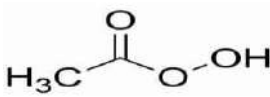| S. No	Compound	Biological activity	Molecular Weight	Molecular formula	Retention time	Structure	Reference
1.	Benzoic acid (CAS) Retardex	Antimicrobial activity	122.12	$C_7H_6O_2$	4.614		Alicja Synowiec et al. 2021
2.	Carbamic acid, Phenyl ester	Pesticide	61.04	CH_3NO_2	4.067		R.C. Gupta 2014
3.	Phenol (CAS) Izal	Antimicrobial activity	94.11	C_6H_6O	2.815		Alicja Synowiec et al. 2021
4.	Peracetic acid	Antifungal and antimicrobial activity	76.05	CH_3CO_3H	1.300		Carlos et al. 2021

Table VIII: Characterization of antimicrobial compounds from aqueous extract of fish amino acid (FAA)

S. No	Compound	Biological activity	Molecular Weight (g/mol)	Molecular formula	Retention time	Structure	Reference
1.	n-Hexadecanoic acid	Antioxidant, Nematicide, Pesticide	256.42	$C_{16}H_{32}O_2$	13.903		Omotoso et al. (2014)
2.	Hexadecanoic acid	Antioxidant, Pesticide, Nematicide,	256.42	$C_{16}H_{32}O_2$	11.736		Sermakkani and Thangapandian (2012) and Vijayakumar and Pannerselvam (2013)
3.	Octadecanoic Acid	Antibiotic and antimicrobials	284.47	$C_{18}H_{36}O_2$	15.969		Blechert et al 1995

Figure I: Pot culture experiment	**Figure II: Field trial**

RESEARCH ARTICLE

Trapezoidal Intuitionistic Fuzzy Sequencing Problem

R. Santhi[1]* and A.Nandhini[2]

[1]Assistant Professor, PG and Research Department of Mathematics, Nallamuthu Gounder Mahalingam College, Pollachi-642001, Tamil Nadu, India.
[2]Research Scholar, PG and Research Department of Mathematics, Nallamuthu Gounder Mahalingam College, Pollachi-642001, Tamil Nadu, India.

*Address for Correspondence
R. Santhi
Assistant Professor,
PG and Research Department of Mathematics,
Nallamuthu Gounder Mahalingam College,
Pollachi-642001, Tamil Nadu, India.
E.Mail: santhifuzzy@yahoo.co.in

ABSTRACT

This study examines various sequencing issues where the processing times are trapezoidal intuitionistic fuzzy numbers. Through the use of Graded Mean Ranking Methodology of Pascal's Triangle and the Zero Identifier method, an algorithm is shown for determining the ideal sequence, the minimum total time spent and the idle time for each machine. To demonstrate the viability of the sequencing problem, numerical examples have been provided.

Keywords: Trapezoidal Intuitionistic Fuzzy Number, Optimal Sequence, Total elapsed time, Idle time, Pascal's Triangle Graded Mean Ranking value.

INTRODUCTION

Operations Research assists us in making wiser judgements in difficult situations. Considered to be one of the most crucial applications of operations research is the Sequencing problem. When we are worried about the situation, where there is an option regarding how a number of activities can be done, job sequencing concerns occurs. Sequencing refers to a set of actions or tasks that must be carried out in a particular order. Johnson's method [1] , which he provided in 1954 for production scheduling and which minimized the overall idle time of machines and the total production times of the jobs, is one of the most well-known works in this field still being used today. Later in 1967, Smith and Dudek created a general method for the flow shop's 'n' task on 'm' machines sequencing problem when the number of passing is permitted. In most cases, Processing times in sequencing problems are accurately

63217

valued. However, in reality, it seems as though the processing time needed to do a task varies and unreliable. So, we employ Fuzzy Numbers to manage these uncertainties. The uncertainty in determining the data can be replaced by the fuzzy notions which was introduced by Zadeh [2] in the year 1965. Later, Intuitionistic Fuzzy Set was created by Atanassov [3] as a generalization of fuzzy sets. With help of Zero Identifier method [4] , we need not to convert the 'n' jobs on three machines or 'n' jobs on 'm' machines problem to 'n' jobs on two machines problem for finding the optimal sequence. Using Graded Mean of Pascal's Triangle [5] and Zero Identifier approach, we use the key concepts and definitions of fuzzy numbers in this work to solve Trapezoidal Intuitionistic Sequencing Problem and obtain the shortest processing times for each machine.

PRELIMINARIES

Definition 2.1[2]:

A Fuzzy Set $\tilde{A}$ in X is a set of ordered pairs defined by
$\tilde{A} = \{(x, \mu_{\tilde{A}}(x)) : x \in X, \mu_{\tilde{A}}(x) \in [0,1]\}$, where $\mu_{\tilde{A}}(x)$ is a membership function.

Definition 2.2[2]:

A fuzzy set $\tilde{A}$ defined on a set of real numbers $\mathbb{R}$ is claimed as a Fuzzy Number, if its membership function $\mu_{\tilde{A}}(x) : \mathbb{R} \to [0,1]$ that satisfies the following properties:

a. $\tilde{A}$ is convex.

b. $\tilde{A}$ is normal.

c. $\mu_{\tilde{A}}(x)$ is piecewise continuous.

Definition 2.3[3]:

Consider X to be a non-empty set. An Intuitionistic Fuzzy Set is defined as
$\widetilde{A^I} = \{(x, \mu_{\widetilde{A^I}}(x), \vartheta_{\widetilde{A^I}}(x)) : x \in X\}$ which assigns to each element x, a membership degree $\mu_{\widetilde{A^I}}(x)$ and a non membership degree $\vartheta_{\widetilde{A^I}}(x)$ under the condition $0 \leq \mu_{\widetilde{A^I}}(x) + \vartheta_{\widetilde{A^I}}(x) \leq 1$, for all $x \in X$.

Definition 2.4[6]:

An Intuitionistic Fuzzy Subset $\widetilde{A^I} = \{(x, \mu_{\widetilde{A^I}}(x), \vartheta_{\widetilde{A^I}}(x)) : x \in \mathbb{R}\}$ of the real line $\mathbb{R}$ is called an Intuitionistic Fuzzy Number (IFN) if the following conditions hold:

i.   There exists $m \in \mathbb{R}$ such that $\mu_{\widetilde{A^I}}(m) = 1$ and $\vartheta_{\widetilde{A^I}}(m) = 0$.

ii. $\mu_{\widetilde{A^I}}$ is a continuous function from $\mathbb{R} \to [0,1]$ such that $0 \leq \mu_{\widetilde{A^I}}(x) + \vartheta_{\widetilde{A^I}}(x) \leq 1$, for all $x \in X$.

iii. The membership and non-membership functions of $\widetilde{A^I}$ are in the following form:

$$\mu_{\widetilde{A^I}}(x) = \begin{cases} 0, & -\infty < x \leq a_1 \\ f(x), & a_1 \leq x \leq a_2 \\ 1, & x = a_2 \\ g(x), & a_2 \leq x \leq a_3 \\ 0, & a_3 \leq x \leq \infty \end{cases}$$

and $$\gamma_{\widetilde{A^I}}(x) = \begin{cases} 1, & -\infty < x \leq a_1^{'} \\ f^{'}(x), & a_1^{'} \leq x \leq a_2 \\ 0, & x = a_2 \\ g^{'}(x), & a_2 \leq x \leq a_3^{'} \\ 1, & a_3^{'} \leq x \leq \infty \end{cases}$$

where $f, f^{'}, g, g^{'}$ are functions from $\mathbb{R} \to [0,1]$, f and $g^{'}$ are strictly increasing functions, and g and $f^{'}$ are strictly decreasing functions with the conditions $0 \leq f(x) + f^{'}(x) \leq 1$ and $0 \leq g(x) + g^{'}(x) \leq 1$.

Santhi and Nandhini

Definition 2.5[7]:

An Intuitionistic fuzzy number $\widetilde{A^I} = \{(a_1, a_2, a_3; a_1', a_2, a_3')\}$ is supposed to be called as a Triangular Intuitionistic Fuzzy Number if its membership and non-membership functions are respectively given by

$$\mu_{\widetilde{A^I}}(x) = \begin{cases} \dfrac{x - a_1}{a_2 - a_1}, & a_1 \le x \le a_2 \\ \dfrac{a_3 - x}{a_3 - a_2}, & a_2 \le x \le a_3 \\ 0, & otherwise \end{cases} \quad \text{and} \quad \vartheta_{\widetilde{A^I}}(x) = \begin{cases} \dfrac{a_2 - x}{a_2 - a_1'}, & a_1' \le x \le a_2 \\ \dfrac{x - a_2}{a_3' - a_2}, & a_2 \le x \le a_3' \\ 1, & otherwise \end{cases}$$

Here $a_1' \le a_1 \le a_2 \le a_3 \le a_3'$ and $\mu_{\tilde{A}}(x) + \vartheta_{\tilde{A}}(x) \le 1$ or $\mu_{\tilde{A}}(x) = \vartheta_{\tilde{A}}(x)$ for all $x \in X$.

Definition 2.6[8]

An Intuitionistic fuzzy number $\widetilde{A^I} = \{(a_1, a_2, a_3, a_4; b_1, b_2, b_3, b_4)\}$ is said to be a Trapezoidal Intuitionistic Fuzzy Number if its membership and non-membership functions are respectively given by

$$\mu_{\widetilde{A^I}}(x) = \begin{cases} \dfrac{x - a_1}{a_2 - a_1}, & a_1 \le x \le a_2 \\ 1, & a_2 \le x \le a_3 \\ \dfrac{a_4 - x}{a_4 - a_3}, & a_3 \le x \le a_4 \\ 0, & otherwise \end{cases} \quad and \quad \vartheta_{\widetilde{A^I}}(x) = \begin{cases} \dfrac{b_2 - x}{b_2 - b_1}, & b_1 \le x \le b_2 \\ 0, & b_2 \le x \le b_3 \\ \dfrac{x - b_3}{b_4 - b_3}, & b_3 \le x \le b_4 \\ 1, & otherwise \end{cases}$$

Here $b_1 \le a_1 \le b_2 \le a_2 \le a_3 \le b_3 \le a_4 \le b_4$ and $\mu_{\widetilde{A^I}}(x) + \vartheta_{\widetilde{A^I}}(x) \le 1$ or $\mu_{\widetilde{A^I}}(x) = \vartheta_{\widetilde{A^I}}(x)$ for all $x \in X$. The membership and non-membership functions of Trapezoidal Intuitionistic Fuzzy Number is given in Fig.1.

ARITHMETIC OPERATIONS ON TRAPEZOIDAL INTUITIONISTIC FUZZY NUMBER

Let $\widetilde{A^I} = \{(a_1, a_2, a_3, a_4; b_1, b_2, b_3, b_4)\}$ and $\widetilde{B^I} = \{(a_1', a_2', a_3', a_4'; b_1', b_2', b_3', b_4')\}$. Then

1. Addition:
$$\widetilde{A^I} + \widetilde{B^I} = \{(a_1 + a_1', a_2 + a_2', a_3 + a_3', a_4 + a_4'; b_1 + b_1', b_2 + b_2', b_3 + b_3', b_4 + b_4')\}$$

2. Subtraction:
$$\widetilde{A^I} - \widetilde{B^I} = \{(a_1 - a_4', a_2 - a_3', a_3 - a_2', a_4 - a_1'; b_1 - b_4', b_2 - b_3', b_3 - b_2', b_4 - b_1')\}$$

3. Scalar Multiplication:

If $k \ge 0$, $k\widetilde{A^I} = (ka_1, ka_2, ka_3, ka_4)$

If $k \le 0$, $k\widetilde{A^I} = (ka_4, ka_3, ka_2, ka_1)$

RANKING USING PASCAL'S TRIANGULAR GRADED MEAN[5]

Let $\widetilde{A^I} = \{(a_1, a_2, a_3, a_4; b_1, b_2, b_3, b_4)\}$ be a trapezoidal intuitionistic fuzzy number.

The ranking function is given by

R(A) = Max[mag($\tilde{A}_\mu^I$), mag($\tilde{A}_\vartheta^I$)]

where mag($\tilde{A}_\mu^I$) $= \dfrac{a_1 + 3a_2 + 3a_3 + a_4}{8}$ and mag($\tilde{A}_\vartheta^I$) $= \dfrac{b_1 + 3b_2 + 3b_3 + b_4}{8}$

ALGORITHM FOR SOLVING INTUITIONISTIC FUZZY SEQUENCING PROBLEM USING ZERO IDENTIFIER METHOD [4]

Processing 'n' jobs on two machines

Let $A_{11}, A_{21}, \ldots A_{n1}$ be the processing times of 'n' jobs on machine I and let

$A_{12}, A_{22}, \ldots A_{n2}$ be the processing times of 'n' jobs on machine II.

Steps involved in the algorithm:

63219

Santhi and Nandhini

1. Identify $\text{Min}(A_{i1}, A_{i2})$, $i = 1, 2, \ldots, n$.
2. (a) If we get minimum on machine I say A_{i1}, then process the ith job first.
   (b) If we get minimum on machine II say A_{m2}, then process the mth job last.
   (c) If there is a tie, that is, $A_{i1} = A_{m2}$, process the ith job first and m^{th} job last.
3. Cancel the jobs already assigned and repeat the procedure till each jobs have been assigned.

Processing 'n' jobs on three machines:
Let A,B,C be three machines and processing each job in the proper sequence A,B,C. Instead of converting this problem into 'n' jobs across two machines, the following steps shows us the way to get the optimal sequence using Zero Identifier method.
1. Convert the Trapezoidal Intuitionistic Fuzzy Number into crisp value using Graded Mean Ranking Function of Pascal's Triangle and identify the minimum processing time.
2. Subtract all components from this minimum processing time.
3. Locate the zeros; they might happen in any of the machines.
4. Give preference to the first machine if zeros are present and the order of sequence is from left to right.
5. If zeros occur in the second machine or third machine, prefer that machine from left to right and the order of sequence is from right to left.
6. Cancel the jobs already assigned and repeat the process until all jobs have been assigned and compute the time in and time out.

Processing 'n' jobs on 'm' machines:
Let $A_1, A_2, \ldots\ldots A_m$ be 'm' machines processed over 'n' jobs and each job be processed in the sequence $A_1, A_2, \ldots\ldots A_m$. Instead of converting this problem into 'n' jobs on two machines, we use Zero Identifier method to obtain the optimal sequence.
1. Convert the Trapezoidal Intuitionistic Fuzzy Number into crisp value using Graded Mean Ranking Function of Pascal's Triangle and identify the minimum processing time'
2. Subtract all components from this minimum processing time.
3. Locate the zeros; they might happen in any of the machines.
4. If zeros occur in the first machine, give priority to machine 1 and the order of sequence is from left to right.
5. If zeros occur in the second, third,…m^{th} machine, give priority to that machine from left to right and the order of sequence is from right to left.
6. Cancel the jobs already assigned and repeat the process until all jobs have been assigned and compute the time in and time out.

NUMERICAL EXAMPLES

Example: 1 ('n' jobs on two machines)
There are 5 jobs, each of which is intended to be completed by two machines M_1, M_2 in the sequence $M_1 M_2$. Processing time (in hours) is given below:

Jobs	Machine (M_1)	Machine (M_2)
A	(2,3,4,5; 1,3,4,6)	(4,5,6,7; 2,5,6,9)
B	(8,9,10,11; 6,9,10,13)	(6,7,8,9; 5,7,8,10)
C	(5,6,7,8; 4,6,7,9)	(11,12,13,14; 9,12,13,16)
D	(4,5,6,7; 2,5,6,9)	(10,11,12,13; 7,11,12,16)
E	(10,11,12,13; 7,11,12,16)	(13,14,15,16; 12,14,15,17)

Obtain the optimal sequence, minimum total elapsed time and idle time for each machine.
Solution:

Using Graded mean ranking function of Pascal's triangle, we convert the Trapezoidal Intuitionistic fuzzy number into crisp one and obtain the optimal sequence as: $A \rightarrow D \rightarrow C \rightarrow E \rightarrow B$.

To find the total elapsed time:

Jobs	Machine(M_1) Time in – Time Out	Machine(M_2) Time in – Time out
A	(0,0,0,0; 0,0,0,0) - (2,3,4,5; 1,3,4,6)	(2,3,4,5; 1,3,4,6) - (6,8,10,12; 3,8,10,15)
D	(2,3,4,5; 1,3,4,6) - (6,8,10,12; 3,8,10,15)	(6,8,10,12; 3,8,10,15) - (16,19,22,25; 11,19,22,30)
C	(6,8,10,12; 3,8,10,15) - (11,14,17,20; 7,14,17,24)	(16,19,22,25; 11,19,22,30) - (27,31,35,39; 20,31,35,46)
E	(11,14,17,20; 7,14,17,24) - (21,25,29,33; 14,25,29,40)	(27,31,35,39; 20,31,35,46) - (40,45,50,54; 32,45,50,63)
B	(21,25,29,33; 14,25,29,40) - (29,34,39,44; 20,34,39,53)	(40,45,50,54; 32,45,50,63) - (46,52,58,63; 37,52,58,73)

Jobs	Idle time(M_1)	Idle time (M_2)
A	-	(2,3,4,5; 1,3,4,6)
D	-	(-6,-2,2,6; -12,-2,2,12)
C	-	(-9,-3,3,9; -19,-3,3,19)
E	-	(-12,-4,4,12; -26,-4,4,26)
B	-	(-14,-5,5,14; -31,-5,5,31)
Total	(2,13,24,34; -16,13,24,53)	(-39,-11,18,46; -87,-11,18,94)

Minimum Total Elapsed Time = (46,52,58,63; 37,52,58,73) hours
Idle time for Machine M_1= (2,13,24,34; -16,13,24,53) hours
Idle time for Machine M_2 = (-39,-11,18,46; -87,-11,18,94) hours

Example:2 ('n' jobs on three machines)

Three machines M_1, M_2 and $M_3$are to process each of the five jobs in the following order M_1, M_2, M_3. Processing time (in hours) is given below:

Jobs	Machine(M_1)	Machine(M_2)	Machine(M_3)
A	(3,5,7,9; 1,5,7,11)	(4,5,6,7; 3,5,6,8)	(5,8,9,10; 3,8,9,12)
B	(7,8,9,10; 6,8,9,11)	(2,4,6,8; 0,4,6,10)	(1,2,3,4; 0,2,3,5)
C	(5,8,9,10; 3,8,9,12)	(2,3,4,5; 1,3,4,6)	(8,9,10,11; 5,9,10,14)
D	(4,5,6,7; 3,5,6,8)	(3,5,7,9; 1,5,7,11)	(1,2,3,6; 0,2,3,7)
E	(8,9,10,11; 5,9,10,14)	(1,2,3,6; 0,2,3,7)	(2,4,6,8; 0,4,6,10)

Obtain the optimal sequence and also determine the minimum total elapsed time and idle time for each of the machine.

Solution

Using New Zero Identifier Method, we get the optimal sequence as follows:

Jobs	M_1	M_2	MM_{3_3}	Jobs	M_1	M_2	M_3
A	6	5.5	8.25	A	3.5	3	5.75
B	5.5	5	2.5	B	6	2.5	0
C	8.25	3.5	11	C	5.75	1	8.5
D	5.5	6	2.75	D	3	3.5	0.25
E	9.5	2.75	5	E	7	0.25	2.5

Santhi and Nandhini

Jobs	M_1	M_2	MM_{33}
A	3.25	2.75	5.5
B	6	2.5	0
C	5.5	0.75	8.25
D	2.75	3.25	0
E	6.75	0	2.25

Jobs	M_1	M_2	MM_{33}
A	2.5	2	4.75
B	6	2.5	0
C	4.75	0	7.5
D	2.75	3.25	0
E	6.75	0	2.25

Jobs	M_1	M_2	MM_{33}
A	0.5	0	2.75
B	6	2.5	0
C	4.75	0	7.5
D	2.75	3.25	0
E	6.75	0	2.25

Therefore, Optimal Sequence: A→C→D→E→B
To find the total elapsed time:

Jobs	Machine (M_1) Time in-Time out	Machine (M_2) Time in-Time out	Machine (M_3) Time in-Time out
A	(0,0,0,0; 0,0,0,0) – (3,5,7,9; 1,5,7,11)	(3,5,7,9; 1,5,7,11) – (7,10,13,16; 3,10,13,20)	(7,10,13,16; 3,10,13,20) – (12,18,22,26; 6,18,22,32)
C	(3,5,7,9; 1,5,7,11) – (8,13,16,19; 4,13,16,23)	(8,13,16,19; 4,13,16,23) – (10,16,20,24; 5,16,20,29)	(12,18,22,26; 6,18,22,32) – (20,28,34,40; 13,28,34,47)
D	(8,13,16,19; 4,13,16,23) – (12,18,22,26; 7,18,22,31)	(12,18,22,26; 7,18,22,31) – (15,23,29,35; 12,23,29,42)	(20,28,34,40; 13,28,34,47) – (21,30,37,46; 13,30,37,54)
E	(12,18,22,26; 7,18,22,31) – (20,27,32,37; 12,27,32,45)	(20,27,32,37; 12,27,32,45) – (21,29,35,43; 12,29,35,52)	(21,30,37,46; 13,30,37,54) – (23,34,43,54; 13,34,43,64)
B	(20,27,32,37; 12,27,32,45) – (27,35,41,47; 18,35,41,56)	(27,35,41,47; 18,35,41,56) – (29,39,47,55; 18,39,47,66)	(23,34,43,54; 13,34,43,64) – (30,41,50,59;18,41,50,71)
Idle time	(-17,6,9,32; -38,6,9,53)	(-73,-5,51,115; -149,-5,51,187)	(-77,-11,43,107; -144,-11,43,

Minimum Total Elapsed Time = (30,41,50,59; 18,41,50,71) hours
Idle time for Machine M_1 = (-17,6,9,32; -38,6,9,53) hours
Idle time for Machine M_2 = (-73,-5,51,115; -149,-5,51,187)hours
Idle time for Machine M_3 = (-77,-11,43,107; -144,-11,43,174) hours

Example 3: ('n' jobs on 'm' machines)
Find the best order for the next sequencing issue with four jobs and four machines when passing is prohibited, of which processing time (in hours) are given below:

Jobs	Machine(M_1)	Machine(M_2)	Machine(M_3)	Machine(M_4)
A	(3,5,7,9; 1,5,7,11)	(1,2,3,4; 0,2,3,5)	(2,3,4,5; 1,3,4,6)	(2,4,6,8; 0,4,6,10)
B	(7,8,9,10; 6,8,9,11)	(4,5,6,7; 2,5,6,9)	(1,3,4,5; 0,3,4,6)	(4,7,8,9; 2,7,8,11)
C	(8,9,10,11; 5,9,10,14)	(2,3,4,5; 1,3,4,6)	(4,5,6,8; 3,5,6,9)	(1,2,3,4; 0,2,3,5)
D	(5,6,7,8; 4,6,7,9)	(3,5,7,9; 1,5,7,11)	(3,5,7,8; 1,5,7,10)	(8,9,10,11; 5,9,10,14)

Solution:

Using Pascal's Triangular graded mean and zero identifier method, we get

Jobs	M_1	M_2	MM_{3_3}	MM_{4_3}
A	6	2.5	3.5	5
B	8.5	5.5	3.375	7.25
C	9.5	3.5	5.625	2.5
D	6.5	6	5.875	9.5

Jobs	M_1	M_2	MM_{3_3}	MM_{4_3}
A	3.5	0	1	2.5
B	6	3	0.875	4.75
C	7	1	3.125	0
D	4	3.5	3.375	7

Jobs	M_1	M_2	MM_{3_3}	MM_{4_3}
A	3.5	0	1	2.5
B	5.125	2.125	0	3.875
C	7	1	3.125	0
D	6.5	2.625	2.5	6.125

Jobs	M_1	M_2	MM_{3_3}	MM_{4_3}
A	3.5	0	1	2.5
B	5.125	2.125	0	3.875
C	7	1	3.125	0
D	4	0.125	0	3.625

Therefore, Optimal Sequence: D→B→C→A

To find total elapsed time:

Jobs	Machine (M_1) Time in-Time out	Machine (M_2) Time in-Time out	Machine (M_3) Time in-Time out	Machine (M_4) Time in-Time out
D	(0,0,0,0;0,0,0,0) - (5,6,7,8;4,6,7,9)	(5,6,7,8;4,6,7,9) – (8,11,14,17;5,11,14,20)	(8,11,14,17;5,11,14,20) – (11,16,21,25;6,16,21,30)	(11,16,21,25;6,16,21,30) – (19,25,31,36;13,25,31,42)
B	(5,6,7,8;4,6,7,9) - (12,14,16,18;10,14,16,20)	(12,14,16,18;10,14,16,20) – (16,19,22,25;12,19,22,29)	(16,19,22,25;12,19,22,29) – (17,22,26,30;12,22,26,35)	(19,25,31,36;13,25,31,42) – (23,32,39,45;15,32,39,53)
C	(12,14,16,18;10,14,16,20) – (20,23,26,29;15,23,26,33)	(20,23,26,29;15,23,26,33) – (22,26,30,34;16,26,30,40)	(22,26,30,34;16,26,30,40) – (26,31,36,42;19,31,36,49)	(23,32,39,45;15,32,39,53) – (24,34,42,49;15,34,42,58)
A	(20,23,26,29;15,23,26,33) – (23,28,33,38;16,28,33,45)	(23,28,33,38;16,28,33,45) – (24,30,36,42;16,30,36,50)	(26,31,36,42;19,31,36,49) – (28,34,40,47;20,34,40,55)	(24,34,42,49;15,34,42,58) – (26,38,48,57;15,38,48,68)
Idle Time	(-12,5,20,34; -30,5,20,52)	(-32,7,44,80; -79,7,44,95)	(-46,2,47,93; -102,2,47,149)	(-53,-5,42,89; -104,-5,42,140)

Finally,

Minimum Total Elapsed Time = (26,38,48,57; 15,38,48,68) hours

Idle time for Machine M_1　　= (-12,5,20,34; -30,5,20,52) hours

Idle time for Machine M_2　　= (-32,7,44,80; -79,7,44,95)hours

Idle time for Machine M_3　　= (-46,2,47,93; -102,2,47,149) hours

Idle time for Machine M_4　　= (-53,-5,42,89; -104,-5,42,140) hours.

CONCLUSION

Using Trapezoidal intuitionistic fuzzy numbers, we have solved several kinds of fuzzy sequencing problems in this study. With the aid of Graded Mean Ranking function of Pascal's Triangle and Zero Identifier approach, we are able to process all jobs through machines in the most efficient order and with the least amount of time spent on each job. The fuzzy sequencing problem notion offers an useful foundation for resolving the practical issue.

REFERENCES

1. Johnson, S. M. Optimal two and three stage production schedules with setup times included, Naval Research Logistics Quarterly,1, (1954) 61-68.
2. Zadeh, L.A. Fuzzy sets, Information and control, John Wiley and Sons, New York,8(1965), 338-353.
3. Atanassov. K.T. Intuitionistic fuzzy sets, Fuzzy sets and systems,(1986) 20: 87-96.
4. V. T. Lakshmi. Finding Minimum total elapsed Time in a Sequencing Problem by a New Zero Identifier Method, International Journal of Novel Research and Development (2022) Volume 7, ISSN: 2456-4184.
5. P. Rajarajeswari and G. Menaka: A New Approach for Ranking of Octagonal Intuitionistic   Fuzzy Numbers, International Journal of Fuzzy Logic systems(IJFLS) Vol.7, No.2, April 2017.
6. K. T. Atanassov, Intuitionistic Fuzzy Sets: Theory and Applications, Physica, Heidelberg, Germany, 1999.
7. Radhakrishnan, S. and Saikeerthana, D. Triangular Intuitionistic Fuzzy Sequencing Problem, Kong. Res. J. (2021),8(2):61-68.
8. L.G.N. Velu, J. Selvaraj, D. Ponnialagan: A New Ranking Principle for ordering Trapezoidal Intuitionistic fuzzy numbers, Complexity, Volume 2017 (2017), Article ID: 3049041, 1-24.
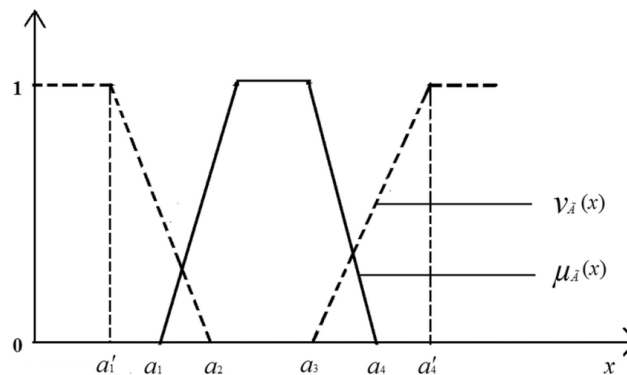
Fig 1: Trapezoidal Intuitionistic Fuzzy Number

RESEARCH ARTICLE

In – vitro Evaluation of Neuroprotective Potential of Siddha Medicine *Sagala Noi Choornam*

Shalini.V[1]*, Sivakkumar.S[2] and Meenakumari. R[3]

[1]PG Scholar, Department of Gunapadam, National Institute of Siddha, Ministry of Ayush, Chennai - 600047, Tamil Nadu, India,

[2]Associate Professor, Department of Gunapadam, National Institute of Siddha, Ministry of Ayush, Chennai 600047, Tamil Nadu, India.

[3]Director, National Institute of Siddha, Ministry of Ayush, Chennai 600047, Tamil Nadu, India

*Address for Correspondence
Shalini.V
PG Scholar,
Department of Gunapadam,
National Institute of Siddha,
Ministry of Ayush, Chennai - 600047,
Tamil Nadu, India,
E.Mail: shalinibsms49@gmail.com

ABSTRACT

Neurocognitive disorders are characterized by impairment in cognitive functions which is present in many neurological and mental disorders such as Alzheimer's disease, traumatic brain injury, fronto-temporal degeneration, infections, schizophrenia, and bipolar disorder etc., Neurocognitive disorders are divided into major and minor neurocognitive disorder. Dementia also known as major neurocognitive disorder is a group of symptoms caused by decreased mental function. A worldwide estimation of people affected by dementia is around 30 million by the year 2008 and it will rise to 59 million by 2030 and 104 million by 2050. In India, 3.01 million people were already affected by dementia. Currently, available treatment modalities, Cholinesterase inhibitors are the only choice of drug for the treatment of neurocognitive disorders, it might be helpful to manage symptomatically. Prolonged administration of Cholinesterase inhibitors may cause adverse side effect which includes dyspepsia, anorexia, asthenia, dizziness, muscle cramps, insomnia, diarrhea, etc., In the Siddha system of medicine various conditions of Neurocognitive disorders are treated through highly effective herbal preparations, *Sagala Noi choornam* (SNC) is one among them. Which is used for treating *Vatha-related* diseases, urolithiasis, insomnia, slurred speech, cervical lymphadenopathy, delirium, ulcers, etc, The study was designed to evaluate the neuroprotective activity of SNC through the AChE enzyme Inhibition assay method. In this study, the trial drug SNC was studied in various concentrations (25, 50, 100,250, 500 µg/ml) by Acetylcholinesterase inhibition assay method, Physostigmine was used as a standard drug. The

Shalini *et al.,*

maximum inhibition of AChE enzyme by SNC and the standard drug was 45.63 4.40% and 93.9 5.36 % respectively. The present study indicates that the test drug SNC was effective in inhibiting the AChE enzyme at a stipulated concentration dose independently. The percentage of inhibition and IC50 value were calculated and compared with standards. This study concluded that the test drug *Sagala Noi choornam* (SNC) has shown proven neuroprotective activity through the acetylcholinesterase enzyme inhibition assay method. Further studies must be conducted in the future to confirm its Neuroprotective activity clinically.

Keywords: Acetylcholinesterase, Neuroprotective activity. *Sagala Noi choornam*, Siddha medicine.

INTRODUCTION

Siddha system of medicine offers a holistic approach to treatment along with a list of nootropic herbs and therapeutic formulations that are a rich source of neuroprotective, anti-oxidant, anti-amyloidogenic, adaptogenic, anti-inflammatory, and immune-modulatory compounds that are found to enhance cognitive functions and improves quality of life. Neurocognitive disorders are characterized by cognitive impairment associated with depression, progressive memory loss, agitation, language deficits, and various neurodegenerative disorders including Alzheimer's disease (AD), Parkinsonism and epilepsy is a major health issues. Neurological disorders ranked as the second most common cause of global mortality in the year 2016 [1].

The estimated number of people in 2010 and 2015 living with major Neurocognitive disorders are 3.7 million and 4.1 million respectively.[2] Owing to various side effects, limited efficacy of neuroprotective drugs, and poor patient compliance for recent rationally designed therapies scientists to searching for new and effective alternative medicines with low adverse effects.[3] The Siddha system of medicine is one of the traditional systems of medicine that gives effective treatment and has minimal side effects after chronic consumption of medicines.[4]

Choornam is one type of internal medicine that is used to regulate the vital humors (*Vaatham*, *Pittham*, *Kabham*).[5] *Sagala Noi choornam* (SNC) is one of the Siddha polyherbal formulations that is therapeutically used for sirasu noigal (Neurological disorders), Vaikonal (Facial palsy), Vaikularal (Slurring of speech) etc. [6] [7] *Sagala Noi Choornam* is composed of multiple herbs as most of the ingredients in *Sagala Noi Choornam* exhibited AChE inhibitory, decreased lipid peroxidation, and anti-oxidant activities.

Acetylcholinesterase inhibitors are the only choice of drug for the treatment of Neurocognitive disorders especially Alzheimer's disease, but it gives only symptomatic relief. Also currently available drugs for AChE inhibitors have shown various illnesses in a person's life including bradycardia, weight loss, miosis, hypotension, urinary incontinence, diaphoresis, emesis, Gastrointestinal upset.etc.,[8] Patients with cardiac conduction diseases, Gastric ulcers, urinary retention, and previous allergic history are contraindicated for AChE inhibitors.[9],[10]. This research study focused on scientifically validating the Neuroprotective potential of *Sagala Noi Choornam* through *in-vitro* acetylcholinesterase inhibition assay method.

MATERIALS AND METHODS

The SNC was procured from GMP-certified IMPCOPS Pharmacy in Thiruvanmiyur, Chennai.

Method of Preparation

Each 35 grams of *Cuminum Cyminum, Glycyrrhiza glabra, Nigella sativa, Anethum graveolens*, *Cycas circinalis, Cinnamomum verum* purified raw drugs, Coriandrum sativum – 210 grams, and *seeni karkandu* 420 g were taken and ground all these ingredients separately. Then mix all the powdered drugs well and store in air tight glass container.

Procurement of test drug for analysis
The test drug Sagala noi choornam (SNC) was prepared in the above manner and procured from GMP-certified IMPCOPS pharmacy in Thiruvanmiyur, Chennai, and then given for analysis.

Drug dosage: *Verukadiyalavu* (2 times a day)
Adjuvant: Hot water

Indication:
➤   Sirasu noigal (Neurological disorders),
➤   Vaikonal (Facial paly),
➤   Vaikularal(Slurring of speech),
➤   Delirium (Unmaatham),
➤   Sleep Disturbances (Insomnia).

In-vitro AChE enzyme Inhibition Assay – Methodology
The test drug *Sagala Noi Choornam* (SNC) was procured from GMP-certified   IMPCOPS pharmacy in Thiruvanmiyur, Chennai, and used for analysis. AChE activity of Siddha poly herbal formulation *Sagala Noi Choornam* (SNC) was measured using a modified 96-well microplate assay based on Ellman's method, enzyme hydrolyses the substrate acetylthiocholine resulting, the experiment, a buffer solution of 50 Mm Tris- HCL at a PH of 8.0 was employed. The reaction involved the conversion of thiocholine into 2-nitrobenzoate-5-mercaptothiocholine and 5-thio-2-nitrobenzoate when it interacted with Ellman's reagent (DTNB), with detection carried out at a wavelength of 412nm.AChE enzyme stock solution (518 U/ml) was kept at -80oC and the enzyme dilution was done in 0.1% BSA in the buffer.

DTNB was dissolved in a buffer solution comprising 0.1 M Nacl and 0.02 M MgCl2, while ATCI was dissolved in deionized water. In each of the 96-well plates, the following components were added: 100µl of 3Mm DTNB, 20 µl of 0.26 U/ml AChE, and 40 µl of buffer with a PH of 8.0 containing 50 Mm Tris. To these wells, 20 µl of the test drug at various concentration (25,50,100,250 and 500 µl/ml) dissolved in a buffer containing no more than 0% methanol were introduced. After thorough mixing, the plate was incubated for 15 minutes. The enzymatic reaction was initiated by the addition of 20 µl of 15 mM acetylthiocholine iodide and the hydrolysis of acetylthiocholine was monitored by reading the absorbance every 5 min for 20 min at 412 nm. Physostigmine (5, 10, 20 and 40 µg/ml) was used as positive control. All the reactions were performed in triplicate.[12],[13]

Statistical analysis
The statistical analysis was done by one-way ANOVA (Graph pad Prism 5 computer program). Numerical data were expressed as the mean value ± standard deviation (SD).

RESULTS

Inhibition of the AChE enzyme by the test drug, expressed as a percentage

Effect of *Sagala Noi Choornam* (SNC) in AChE Enzyme Inhibition Activity
The result obtained from the present study indicates that the test drug SNC was effective in inhibiting the AChE enzyme at the stipulated concentration dose-dependently. Maximum percentage inhibition of about 45.63 ± 4.405 % was observed at 500 µg/ml with the IC 50 value of 519.4 ± 87.56 µg/ml. The results are shown in Fig 1 and Table 2.

Effect of Physostigmine on AChE Enzyme Inhibition Activity

The results obtained from the present study have been compared with the Standard drug Physostigmine (a well-known AChE inhibitor), the results revealed that the maximum inhibition of AChE Enzyme at the concentration of 40 % is 93.9 ± 5.306 % with the IC50 value of 13.47 ± 2.115 μg/ml. Results are expressed in Fig no 2 and Table no 3.

DISCUSSION

5th edition of the Diagnostic and Statistical Manual of Mental Disorders (DSM-IV) provides a framework for diagnosing neurocognitive disorders. That is, explaining the main cognitive syndromes and defining criteria to delineate particular aetiological subtypes of mild and major NCD.[14] According to the DSM-5 dementia was developed step by step decline of memory and cognitive functions. Alzheimer's disease is one of the most common causes of Neurocognitive disorders it develops slowly after the age of 65. Nowadays, Symptomatic management is only provided to NCD patients if these drugs will cause severe side effects in the future.

Herbal drugs possess Neuroprotective activity it have been used in many countries because of their therapeutic potency, safety, and efficacy. *Sagala Noi Choornam* (SNC) has AChE inhibition properties in a stipulant dose-dependent manner. Among the ingredients *Cuminum Cyminum, Glycyrrhiza glabra, Nigella sativa, Anethum graveolens, Coriandrum sativum, Cycas circinalis, Cinnamomum verum* are known for its anti Alzheimer's, nootrophic, and neuroprotective activities. *Cuminum cyminum* seeds have protective effects against Alzheimer's disease, Parkinson's disease, and other Neurodegenerative diseases. Azetidine,2-methyl -1-phenyl isolated from *Cuminum cyminum* seeds was used for preventing or treating Alzheimer's disease, Parkinson's disease.[15] Cuminaldehyde was isolated from *Cuminum Cyminum* seeds' neuroprotective activity was performed using *an in vitro* SH-SY5Y cells model. In the results MTT assay shows that, Cuminaldehyde has a Neuroprotective activity against neuronal damage caused by dexamethasone. [16]

Nigella sativa has been used as a therapeutic agent for various disorders especially Neurodegenerative disorders.[17] The bioactive component present in the herb like Thymoquinone has a significant role in neuroprotection like the improvement of memory & learning, neuroinflammation, and reduction of ROS.[18] Research studies have shown that *Coriandrum sativum* exhibits numerous therapeutic effects including anti-anxiety, anti-convulsant, oxidative stress reduction, and improvement of memory and cognitive functions. [19] Linalool a compound separated from Coriandrum *sativum* has higher retention performance in induced AD in mice. [20]. *Glycyrrhiza glabra* has a protective effect against neurological disorders. Glabridin a compound isolated from the *Glycyrrhiza glabra* which was improved memory and cognitive functions in mice by oral administration (5, 25, and 50 mg/kg, p.o.). [21] *Cinnamomum verum* essential oil shows acetylcholinesterase (AChE) and butyrylcholinesterase (BuChE) inhibitory activities. [22] From the literature evidence Ingredients of *Sagala Noi Choornam* (SNC) have been proven Neuroprotective activity, Anti-oxidant, Anti- Alzheimer's activities in various *in-vitro/in- vivo* activities.This research article revealed that the *Sagala Noi Choornam* (SNC) has a promising Neuroprotective effect and the above-mentioned evidence provides the SNC can be used to manage and prevent Neurocognitive disorders.

CONCLUSION

This study concluded that the Neuroprotective activity of *Sagala Noi Choornam* was studied based on *an in vitro* assay. The results show *Sagala Noi Choornam* has promising Neuroprotective activity. In the future, proper clinical studies to be conducted to confirm its therapeutic effect.

REFERENCES

1. Feigin VL, Nichols E, Alam T, Bannick MS, Beghi E, Blake N, Culpepper WJ, Dorsey ER, Elbaz A, Ellenbogen RG, Fisher JL. Global, regional, and national burden of neurological disorders, 1990–2016: a systematic analysis for the Global Burden of Disease Study 2016. The Lancet Neurology. 2019 May 1;18(5):459-80.

2. Puneeth u malapur , Nripendra kumar, Sudhir K, Khandelwal , Manjari Tripathi , cost of illness of Major neurocognitive disorders in india , Vol.69, No.5, September – October, Doi: 10.413/0028-3886.329606 .

3. Sharma R, Kuca K, Nepovimova E, Kabra A, Rao MM, Prajapati PK. Traditional Ayurvedic and herbal remedies for Alzheimer's disease: from bench to bedside. Expert review of Neurotherapeutics, 2019 May 4;19(5):359-74.

4. Singh A, Agarwal S, Singh S. Age related neurodegenerative Alzheimer's disease: Usage of traditional herbs in therapeutics. Neuroscience letters. 2020 Jan 19;717:134679.

5. Keerthana R, Visweswaran S, Sivakkumar S, Maariappan A, Banumathi V. Evaluation Of Antioxidant Activity Of Seeraga Chooranam In-Vitro Assay (a Siddha Polyherbal Preparation). International Journal of Ayurveda and Pharma Research. 2018 Aug 18.

6. Thiyagarajan R., Naagamunivar thalai noi maruthuvam ,India maruthuvathurai iyakkunaragam, First edition, 1976.

7. Sambasivam pillai T V , Dictionary of Medicine , Chemistry , Botany and Allied sciences, Directorate of Indian medicine and Homeopathy, Madras – 600 106 , 1991.

8. Ohbe H, Jo T, Matsui H, Fushimi K, Yasunaga H. Cholinergic Crisis Caused by Cholinesterase Inhibitors: a Retrospective Nationwide Database Study. J Med Toxicol. 2018 Sep;14(3):237-241.

9. Gill SS, Anderson GM, Fischer HD, Bell CM, Li P, Normand SL, Rochon PA. Syncope and its consequences in patients with dementia receiving cholinesterase inhibitors: a population-based cohort study. Arch Intern Med. 2009 May 11;169(9):867-73.

10. Triantafylidis LK, Clemons JS, Peron EP, Roefaro J, Zimmerman KM. Brain Over Bladder: A Systematic Review of Dual Cholinesterase Inhibitor and Urinary Anticholinergic Use. Drugs Aging. 2018 Jan;35(1):27-41.

11. Murugesa mudhiyar K S., Gunapadam mudhal vaguppu- Mooligai,, Indian medicine and Homeopathy,Chennai -600 106,2013.

12. Ellman GL, Courtney KD, Andres V, Featherstone RM (1961) A new and rapid colorimetric determination of acetylcholinesterase activity. Biochem. Pharmacol 7: 88–95.

13. Sivaraman D. Evaluation of AChE enzyme inhibition potential of Indian Medicinal Herbs Ficus hispida, Morinda tinctoria, Sapindus emarginatus and their Biological significance in Alzheimer's Disease Therapy. Research Journal of Biotechnology. 2018;13 (8):110-115.

14. Sachdev S, Perminder S et al. "Classifying neurocognitive disorders: the DSM-5 approach." *Nature reviews. Neurology* vol. 10,11 (2014): 634-42. doi:10.1038/nrneurol.2014.181

15. Arirudran B, Oswin MA, Balabhaskar R. GC/MS determination of bioactive components from Cuminum Cyminum L. World Journal of Pharmaceutical Research. 2018 Jul 22;212584360.

16. Koppula S, Choi DK. Cuminum cyminum extract attenuates scopolamine-induced memory loss and stress-induced urinary biochemical changes in rats: a noninvasive biochemical approach. Pharmaceutical biology. 2011 Jul 1;49(7):702-8.

17. Kanter ME, Coskun O, Kalayc M, Buyukbas S, Cagavi F. Neuroprotective effects of Nigella sativa on experimental spinal cord injury in rats. Human & experimental toxicology. 2006 Mar;25(3):127-33.

18. Farkhondeh T, Samarghandian S, Shahri AM, Samini F. The neuroprotective effects of thymoquinone: A review. Dose-response. 2018 Apr 11;16(2):1559325818761455.

19. Hosseini M, Boskabady MH, Khazdair MR. Neuroprotective effects of Coriandrum sativum and its constituent, linalool: A review. Avicenna Journal of Phytomedicine. 2021 Sep;11(5):436.

20. Sabogal-Guáqueta AM, Osorio E, Cardona-Gómez GP. Linalool reverses neuropathological and behavioral impairments in old triple transgenic Alzheimer's mice. Neuropharmacology. 2016 Mar 1;102:111-20.

21. Hasanein P. Glabridin as a major active isoflavan from Glycyrrhiza glabra (licorice) reverses learning and memory deficits in diabetic rats. Acta Physiologica Hungarica. 2011 Jun 1;98(2):221-30.

Shalini *et al.,*

22. Saeedi M, Iraji A, Vahedi-Mazdabadi Y, Alizadeh A, Edraki N, Firuzi O, Eftekhari M, Akbarzadeh T. Correction: Cinnamomum verum J. Presl. Bark essential oil: in vitro investigation of anti-cholinesterase, anti-BACE1, and neuroprotective activity. BMC Complementary Medicine and Therapies. 2022 Dec;22(1):

Table:1 Ingredients of *Sagala Noi Choornam* [11]

S.No	Name of the drug	Botanical Name	Common Name	Taste	Quantity
1	*Seeragam*	*Cuminum Cyminum* L.	Cumin	Pungent, Sweet	35 grams
2	*Athimathuram*	*Glycyrrhiza glabra* L.	Liquorice	Sweet, Bitter	35 grams
3	*Karunjeeragam*	*Nigella sativa* L.	Black cumin	Bitter	35 grams
4	*Sathakuppai*	*Anethum graveolens* L.	Dill	Sweet, Pungent	35 grams
5	*Kottha malli*	*Coriandrum sativum* L.	Cilantro seeds	Pungent	210grams
6	*Madhanakama poo*	*Cycas circinalis* L.	Queen sago	Sweet	35 grams
7	*Sanna lavangam*	*Cinnamomum verum* J.S. Presl	Cinnamon	Pungent, Sweet	35 grams

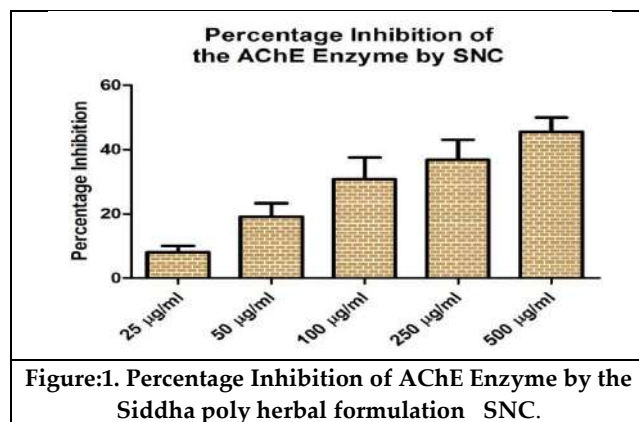**Table 2 : Inhibition of the AChE enzyme by the test drug (SNC), expressed as a percentage.**

Concentration of SNC in µg/ml	Percentage Inhibition of AChE Enzyme by Test Drug
SNC 25	8.133 ± 1.898
SNC 50	19.13 ± 4.207
SNC 100	30.72 ± 6.778
SNC 250	36.79 ± 6.271
SNC 500	45.63 ± 4.405

Each value represents the mean ± SD. N=3

Table 3 : Percentage Inhibition of AChE Enzyme by Standard Drug

Concentration of Physostigmine in µg/ml	Percentage Inhibition of AChE Enzyme by Std Drug
5	21.35 ± 5.205
10	47.44 ± 5.589
20	77.96 ± 2.3427
40	93.9 ± 5.306

Each value represents the mean ± SD. N=3

Figure:1. Percentage Inhibition of AChE Enzyme by the Siddha poly herbal formulation   SNC.

Fig 2: Percentage Inhibition of AChE Enzyme by Physostigmine

RESEARCH ARTICLE
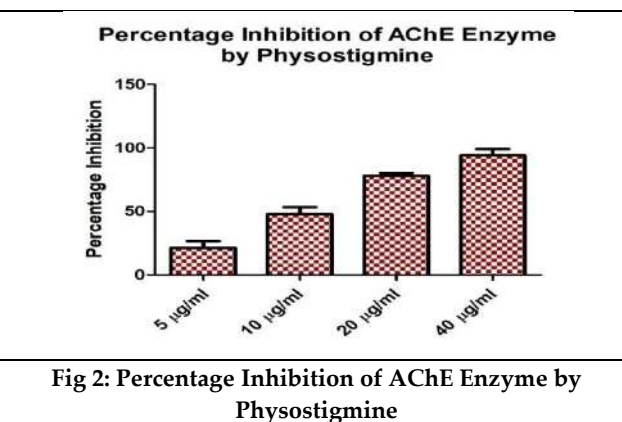
Spatial - Radio Mapping System using Mobile Access Point Model with Mobile Sensor

A.Kavitha[1]* and M.Gobi[2]

[1]Research Scholar, Department of Computer Science, Chikkanna Government Arts College, Tirupur, Tamil Nadu, India
[2]Assistant Professor, Department of Computer Science, Chikkanna Government Arts College, Tirupur, Tamil Nadu, India

*Address for Correspondence
A.Kavitha
Research Scholar,
Department of Computer Science,
Chikkanna Government Arts College,
Tirupur, Tamil Nadu, India.
E.Mail: kavigopi@gmail.com

ABSTRACT

RSS based localization systems are widely applied in indoor positioning for generating and distribution of radio map with co-ordinate system. Even for a large indoor space, system linked with spatial information is vital. In this paper, we propose spatial radio mapping system (SRMS) that effectively combines mobile access point model (MAPM) and mobile phone sensor to perform both spatial and Radio mapping. This SRMS consists of Synchronization, position estimation, mapping and create real time spatial and radio signals. In synchronization process number of different dimensions and time required to receive signals data collected from MAP and Mobile phone signals collected based on sensing time are stored in one node. Localization, a geographic feature is used to identify number of neighbour nodes based on movement direction and axes are measured same co-ordinates to extract spatial and radio map. We estimate the distance between mobile phone and the access points using the mathematical model of RSS from received signal strength. These can be more effective in heterogeneous property and adopted changing environments than RSSI Fingerprints. By this way, we can reduce the effect of the most problems on indoor positioning system. Current models assume that the spatial network of wireless terminal to locate people without requiring them to carry or wear any electronic device. This paper gives an overview of indoor localization technologies, methods and performance metrics, and makes benchmark of existing solutions of Wi-Fi fingerprinting technique with detailed presentation of performances and limitations related to most important recent advances.

Keywords: SRMS, MAPM, RSSI, SPATIAL MAP, RADIO MAP

INTRODUCTION

The Global Positioning System (GPS) is the most widely used localization system for outdoor use. However, GPS doesn't work well indoors because walls block the direct view between the satellites and the passengers. For this reason, researchers are trying to use some of the telecommunicationstools available indoors. Such as Wi-Fi, Bluetooth, inertial sensors (Accelerometer, gyroscope, magnetometer, barome-ter, etc.), RFID, cameras, light, and others. [1]With the development of mobile computing technology, location-based service (LBS) has become more and more requiring in our daily life. [2].This scope is recently been developed to large indoor spaces [3]. In particular, with increasing use of mobile phones and developments in telecommunication devices, indoor localization technology is being closely utilized in the field of life safety, e.g., for emergency calls and emergency exit guidance [4]. received signal strength (RSS) or received signal strength indicator (RSSI) is a measurement of the strength of a received radio signal. In theory, the RSS value decreases as the distance between transmitter and receiver increases [5]. Other methods include measurement of the time difference of arrival [6] and angle of arrival [7]. However, their widespread use in the public domain is limited owing to the high cost of purchasing, installing, managing, and maintaining specially designed devices such as ultra-wideband (UWB) [8,9]. Conversely, the fingerprinting method can implement the RSS of WiFi and Bluetooth devices without the need of additional devices, which are representative pervasive network devices installed for cloud computing. Hence, the RSS-based finger- printing method, which does not require additional costs even in the case of mobile phones, is being developed into a practical indoor localization technology. RSS is an indoor positioning technique that estimates the position coordinates by measuring received signal strength during communication [10]. This method can use the mathematical model (the telecommunication equation) that relates signal strength.

The aims of this paper are to provide the reader with mobile sensor and access point wireless techniques from that generate radio and spatial map. There are following consideration are required to apply the radio RSS-based localization method. First measure received signal strength from different mobile access point .This method can use the mathematical model that relate signal strength to distance.[11].connectivity with spatial map[12].Mobile sensor (geograph)is compatiable with generate spatial data than Lidar.The different calculation methods are used to locate the device.Then solution is generated in which position is estimated by algorithm.The time required to build the radio map is directly releated to cost of implementating localization.[13]As complexity of above mentioned,this study proposes a novel SRMS can simultaneously bulid spatial and Radio map in real time.SRMS collect data from mobile sensor data and mobile access point to estimate the distance range, collected one node position and simultaneously build spatial and radio map.This system combine advanced technology of mobile phone- GPS sensor[14] and mobile access point(MAPM)method to extract spatial data..[11]. Due to improved mapping efficiency, reliable accuracy, and connectivity with the spatial map when building the radio map. Considering that the spatial and radio maps are built using the position estimated through mobile GIS sensor -based localization technology, the location coordinate system of both maps is automatically registered to a common coordinate system. Hence, the RSS Based location of the radio map can ensure reliable accuracy. This study also developed by identifying trends of a mobile phone's motion data and radio signals. Mobile GIS sensor data achieving efficient and real-time mapping, and reduce cost.[14].Visual tracking is kind of indoor positioning that uses mobile sensor to position of user.

RELATED WORKS

Several works have already shown that human presence and motion alters the way radio signals propagate, enabling the localization and tracking of people. Different measurement modalities, models, algorithms and applications have been proposed, having all as objective to locate people with high accuracy. Most approaches achieve sub meter localization accuracy. However, a comparison of the results obtained by these systems is difficult since they differ considerably in nodes number, type of indoor environment, hardware, communication protocols, size The RSS-based fingerprinting localization method contains two stages: the offline and online stage. The basic idea of fingerprinting localization for estimating user's position is matching the online RSS readings with offline prebuilt radio map. Radio

map is composed of extensive location-labeled fingerprints at specific reference points (RPs). Generally, at each RP, several tens of samples are performed and the average RSS vector is stored as fingerprint in the radio map. Sometimes, to avoid the sheltering impact of the human body on RSS, the data collection procedure requires signal sampling in four directions[1,2]. Obviously, as the system coverage expands, the workload and time are greatly increased. Therefore, the radio map construction is time-consuming and labor-sensitive, hindering the wide use of Wi-Fi fingerprinting localization system. Although there are many challenges for constructing radio map, it is inevitable impact of the human body on RSS, the data collection procedure requires signal sampling in four directions [1,2].

Obviously, as the system coverage expands, the workload and time are greatly increased. Therefore, the radio map construction is time-consuming and labor-sensitive, hindering the wide use of Wi-Fi fingerprinting localization system. Although there are many challenges for constructing radio map, it is inevitable for fingerprinting-based approaches. of the monitored area, just to name a few parameters.[15] To implement radio RSS-based indoor localization technology, a radio map whose coordinate system is linked with the spatial map must be provided beforehand. This is typically implemented by designating fingerprint location containing the collected radio received signal information used as the spatial map [16,17]. As a result, the floorplan and actual radio fingerprint location are frequently inconsistent. In some investigations, to address the limitations of PDR, SLAM using a LiDAR and a panoramic camera is employed to construct a spatial map, and then it is manually linked with a radio map [18]. The spatial map is used only for extracting the ground-truth location information of the waypoints for the challenge. The operator constructs a radio map for the location of the waypoints defined on the spatial map with PMC method. LiDAR-based SLAM is applied to the construction of radio maps, but a system that can build both spatial and radio maps concurrently as in the case of SRS is not provided.

A learning-based approach designates some labeled fingerprint locations on the spatial map and adds fingerprint information for unknown areas according to the learning model. The method enables building a radio map of the entire area by specifying a few labeled fingerprints, thus reducing manual calibration cost compared to PMC. However, the method requires efforts to designate the labeled fingerprint locations on the spatial map. Usually, this method can be used only in indoor environments that include a place where the reference location can be known, such as GPS. [17]. Accordingly, to address the limitations of the existing techniques, next study, SRS which combines the data acquired from LiDAR and mobile phone to simultaneously build and distribute the spatial and radio maps. Additionally, to confirm the applicability of SRS as a base technology for indoor LBS, its performance was experimentally verified in terms of securing radio-map fingerprint accuracy, registration of location information using the spatial map, and improvement of mapping efficiency.[19].

To enhance the accuracy of RSS-based DFL. The improvements concern four aspects: exploiting channel diversity, deriving a more accurate spatial model for the human-induced RSS changes, proposing a measurement model that determines the probability of the person being inside the modeled area, and taking into consideration the direction of the RSS changes[15] . Accordingly, to above existing techniques, in this study we propose SRMS, which the data received from mobile sensor and mobile access point to build and distribute spatial and radio map.[14] Additionally this system work to limit the static access point and also undetected access point also determine their positions. This study reveals the technologies and methods to apply to develop indoor localization system to generate spatial and radio Map. The different clustering algorithms can use future research and data extraction from spatial data and different simulation tools to system process and database process also carried out.

SYSTEM OVERVIEW

SPATIAL RADIO MAPPING SYSTEM (SRMS)
SRMS can simultaneously build spatial and radio maps in different axed points and signals measured from mobile sensor and mobile access points. In Synchronous procedure radio signals are received from different dimensions and time acquired from mobile phone sensor and multiple access point (MAP) connected through WLAN and stored in

one node. Localization step estimate the position based on mathematical algorithm and difference directions. In the mapping step, estimated positions are used to construct spatial map .The estimated position and radio signals can be used to build the radio map. Map in real time has been generated by visualization of spatial data.

Synchronization

Mobile phone sensor and mobile access point connected via WLAN,.to synchronize the sensing data different nodes signal and sensing details(s_i) are collected and radio signals (r_i) received combined as one node(n_i).Fig(1.1)

$N_{i=\{S_i,r_i\}}$ ------------------------- (1)

Those are constructed as single node based on time acquired from the mobile access point and mobile sensor. The position origin is calculated from x horizontal direction and y vertical directions .(x,y,distance).

Localization

Multiple access points(MAP) and mobile sensor(GIS) measure the locations of nearby objects at uniform bearing angle arrival. Fig(1.2)shows x,y, and z determination of location. To estimate the location using RSSI Mathematical model ,it require calibration between environmental changes.

Algorithm1.MAPM Localization Algorithm'

Input:
X_i-The horizontal coordinate of node position
Y_i-The verticial coordinate of node position
id-Node number
F_s=Sample frequency
F_0=Signal Frequency
N_s=Number of nodes

Output:
X_o=estimated output
Y_o=estimated output
D_e=estimated distance
P_r=Received Strength

Begin
Algorithm initialization
 For new input data t<-t+1 do
  <Synchronization>
Node generation= $N_{i=\{S_i,r_i\}}$
<localization>
  1.Insert data into database(x_o,yo,id)
2.Insert user random data
3.Measure the received signal strength (p_r)between user.
4.estimate the location.
If sensing data==true then
  Polygon shapes are created
End if
End for

Algorithm2:
Main function(Estimate position)
5.Select Id_{sap}
6.Select the SAPs connected node
7.SAP/LOCATION
if the number of communications is greater than or equal to two
then
 Estimate node position
  end if   =

 Map Generation
After estimate the position MAP algorithm generate map for store into database.
Algorithm 3:
Main function
8.select x and y co-ordinates
9.select the device connected with x
10.if the number of node is great than or equal to two then Estimate the position
11.end if
12.insert map connected to the user into database
13.End

Spatial data is information about shape and location of geographic features. It contains two types of data that's called raster and vector data. We use vector data format is used to represents geographical features by set of co-ordinates. It's represented as two dimensional spaces where features are represented by co-ordinates on two axes. It is formed use of geometry .Fig (1.3) represents 3 dimensional It is combined one or more interconnected vertices. Fig (1.4) A vertex describe position in space using x, y and optionally z axis.

Therefore an intermediate location of neighboring nodes can be selected as the positions.Calculate the global position , by using the Euclidean distance formula.
We give the Euclidean equation for deduce the position co-ordintes

$D_{jk}^2=[(x_{k-xj)]}^2+(y_k-y_j)^2$ ------------------- (2)

Where x_j,y_j is the user co-ordinate position ,x_k,y_k is the access point position coordinates and D_{jk} is the distance between the j and k access point. The system is well adapted to the change of environment.

CONCLUSION

In this study, we proposed an SRMS that can simultaneously generate spatial and radio maps even in large indoor environments. The SRMS effectively fuses the sensing data obtained from, Mobile sensor (GIS) scanner and a mobile access point to generate spatial and radio maps in real time. SRMS achieves high accuracy, real-time performance, efficiency advancement, and localization applicability in both spatial and radio mapping. Furthermore, the applicability of the SRMS to actual LBS was confirmed by utilizing the constructed maps   to well-known RSS mathematical   localization algorithms and heterogeneous Mobile   phones. SRMS requires specialized wireless device mobile sensor, thus it is suitable for   creating an initial radio map in an unknown environment by map building operators instead of public users. Considering the accessibility of SRMS equipment, in the case of a site where the radio maps are provided in advance, the cloud collection method that can update the existing maps with only mobile phones might be more effective than SRS in terms of map management cost.

In the future works, therefore, we will aim to add a function to update the radio map constructed by SRMS using a cloud strategy. Because the cloud method constructs radio maps in various ways, uniform accuracy cannot be ensured.

REFERENCES

1. X. Zhang, X. Liu, H. Samani, and B. Jalaian, ''Cooperative spectrum sensing in cognitive wireless sensor networks,'' Int. J. Distrib. Sensor Netw., vol. 2015, Jan. 2015, Art. no. 1.
2. R. Zhu, M. Ma, Y. Zhang, and J. Hu, ''Collaborative wireless sensor networks and applications,'' Int. J. Distrib. Sensor Netw., vol. 2015, pp. 1–3, Jan. 2015.
3. X. Wang, X. Wei, Y. Liu, S. Gao, Received signal strength–based localization for large space indoor environments, Int. J. Distrib. Sens. Netw. 13 (1) (2017) 1–12.
4. W. Sun, M. Xue, H. Yu, H. Tang, A. Lin, Augmentation of fingerprints for indoor WiFi localization based on Gaussian process regression, IEEE Trans. Veh. Technol. 67 (11) (2018) 10896–10905.
5. Guo, G.; Chen, R.; Ye, F.; Peng, X.; Liu, Z.; Pan, Y. Indoor Smartphone Localization: A Hybrid WiFi RTT-RSS Ranging Approach. IEEE Access 2019, 7, 176767–176781. [CrossRef]
6. M. Kolakowski, V. Djaja-Josko, TDOA-TWR Based positioning algorithm for UWB localization system, in: Proc. of IEEE MIKON, Krakow, Poland, 2016, pp. 1–4.
7. J. Xu, M. Ma, C.L. Law, Cooperative angle-of-arrival position localization, Measurement 59 (2015) 302–313.
8. Z. Xu, Z. Liang, Z. Zhou, Z. Li, G.-M. Du, X. Wang, Y.-K. Song, A precise 3D positioning approach based on UWB with reduced base stations, in: Proc. of IEEE ASID, Xiamen, China, 2021, pp. 145–149.
9. R. Bazo, C.A. da Costa, L.A. Seewald, L.G. da Silveira, R.S. Antunes, R.da Rosa Righi, V.F. Rodrigues, A survey about real-time location systems in healthcare environments, J. Med.Syst. 45 (3) (2021)1–13.
10. S. He and S.-H. G. Chan, ''Wi-Fi fingerprint-based indoor positioning: Recent advances and comparisons,'' *IEEE Commun. Surveys Tuts.*, vol. 18,no. 1, pp. 466–490, 1st Quart., 2015.
11. Youssef ibnatta,Mohammed Khaldoun,and Mohammed Sadik,Indoor localization system Based on Mobile Access point model MAPM Using RSS with UWB-OFDM ,.data of publication April 18,2022,.dtae of current version may 4.,2022
12. H. Zou, M. Jin, H. Jiang, L. Xie, C.J. Spanos, WinIPS: Wifi-based non-intrusive indoor positioning system with online radio map construction and adaptation, IEEE Trans. Wirel. Commun. 16 (12) (2017) 8118–8130.
13. Y. Shu, et al., Gradient-based fingerprinting for indoor localization and tracking, IEEE Trans. Ind. Electron. 63 (4) (2016) 2424–2433.
14. F H Saad1* , O Z Jasim1 and M M A Albayati1Literature review of mobile spatial data collection and related to reality as a basis for the geomatics applications, IOP Conf. Series: Earth and Environmental Science 1129 (2023) 012009 IOP Publishing doi:10.1088/1755-1315/1129/1/012009.
15. Ossi Kaltiokallio, Maurizio Bocca, and Neal Patwari Member, IEEE, A Multi-Scale Spatial Model for RSS-based Device-Free Localization,
16. X. Luo, W.J. O'Brien, C.L. Julien, Comparative evaluation of received signal- strength index (RSSI) based indoor localization techniques for construction jobsites, Adv. Eng. Inf. 25 (2011) 355–363.
17. Z. Yang, C. Wu, Y. Liu, Locating in fingerprint space: wireless indoor localization with little human intervention, in: Proc. of ACM MOBICOM, Istanbul, Turkey, 2012, pp. 269–280.
18. V.Renaudin,etal., Evaluating indoor positioning systems in a shopping mall:The lessons learned from the IPIN 2018 competition, IEEE Access 7 (2019) 148594–148628.
19. Yu-Cheol Lee*,SRS: Spatial-tagged radio-mapping system combining LiDAR and mobile-phone data for indoor location-based services, 1474-0346/© 2022 The Author(s). Published by Elsevier Ltd. This is an open access article under the CC BY-NC-ND license.

20. Dr. M. Gobi, J. John Bosco ., A Secured Service Model of Cloud Computing Environment using ECC Algorithm (IJSTE/ Volume 3 / Issue 02 / 019).
21. Dr. M.Gobi, B Arunapriya., Solitude Adaptable User Profile Matching for Mobile Social Cloud Networks,. International Journal of Computer Networks and Applications IJCNA) DOI: 10.22247/ijcna/2022/214506 Volume 9, Issue 4, July – August (2022).
22. M.Gobi and D.Kannan., A Secured Public Key Cryptosystem for Biometric Encryption.,IJCSNS International Journal of Computer Science and Network Security, VOL.15 No.1, January 2015.
23. G. Kishore Kumar, Dr. M. Gobi ., Role of Cryptography & its Related Techniques in Cloud Computing Security., nternational Journal for Research in Applied Science & Engineering Technology (IJRASET) ISSN: 2321-9653; IC Value: 45.98; SJ Impact Factor:6.887Volume 5 Issue VIII, August 2017.
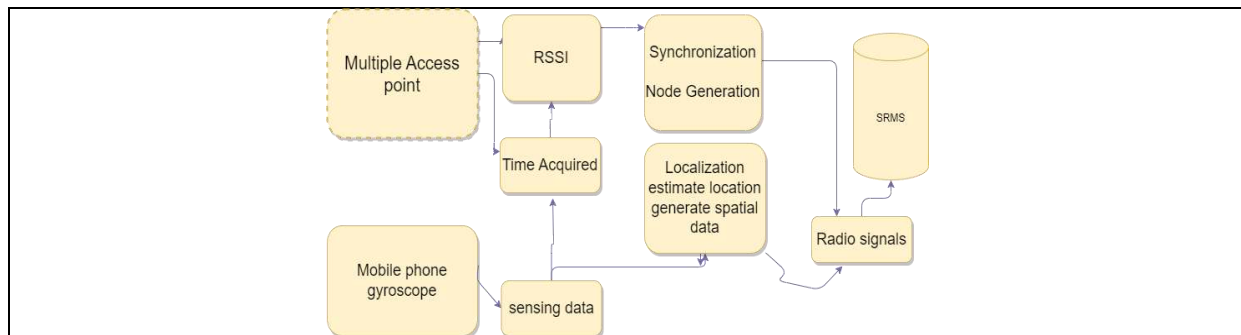
Fig 1..Overview of the proposed spatial radio mapping system
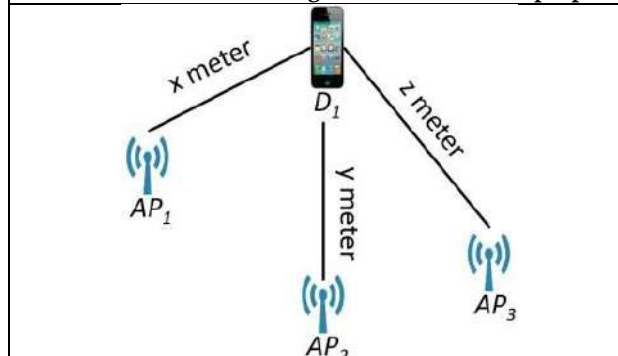
Fig. 2 Location determination
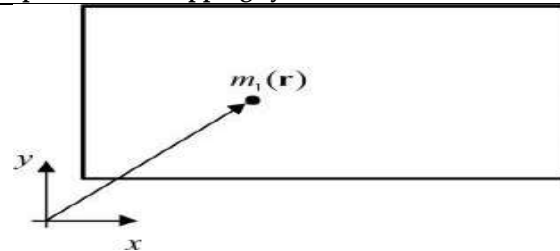
Fig..3.Spatial co-ordinates

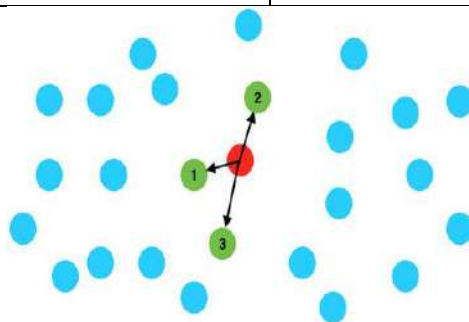**Fig. 4 .vector data represents 3 dimensional**

RESEARCH ARTICLE

IFsgp* Compositional Relation in Pattern Recognition Application

Chandhini. J[1]* and Uma. N[2]

[1]Research Scholar, PG and Research Department of Mathematics, Sri Ramakrishna College of Arts & Science, Coimbatore, Tamil Nadu, India.
[2]Asso. Prof. and Head, PG and Research Department of Mathematics, Sri Ramakrishna College of Arts & Science, Coimbatore, Tamil Nadu, India.

*Address for Correspondence
Chandhini. J
Research Scholar,
PG and Research Department of Mathematics,
Sri Ramakrishna College of Arts & Science,
Coimbatore, Tamil Nadu, India.
E.Mail: chandhujk@gmail.com

ABSTRACT

A new approach of pattern recognition using the IFsgp* Relational Composition is studied in this paper. The Relational Composition of the Intuitionistic Fuzzy Semi Generalized Pre-Star (IFsgp*) in Intuitionistic Fuzzy Topological Spaceis one of the important features.Few numerical examples of pattern recognition are provided for two and three parametric members and it is found that the three parametric methodology is more accurate.

Keywords: Intuitionistic Fuzzy Sets; Intuitionistic Fuzzy Relations; Intuitionistic Fuzzy Sets with parameters, Pattern Recognition

INTRODUCTION

The concept of an Intuitionistic fuzzy semi generalized pre-star set Relational Composition (IFsgp*S) with some preliminary informations are introduced in the first stage of this research. Then the novel method is proposed and analysedfor the pattern recognition process. Several additional concepts of higher-order FSs have been presented since Zadeh [9] established the Fuzzy Sets theory. Among them, Atanassov's [2] Intuitionistic Fuzzy Sets (IFsS) give a flexible mathematical framework for dealing with reluctance caused by defective or imprecise knowledge, in addition to the presence of vagueness. When dealing with incomplete information and ambiguous knowledge, various IFSs features have been exploited for pattern identification. Li Dengfeng and Li Yanhong [7, 8] submitted an application in pattern recognition. As a result, several scholars widely utilized IFS to decision-making analysis and pattern identification.

63238

PRELIMINARIES

In this section, some basic concepts related to *IFS*s were discussed.

Definition 2.1 [2]: An Intuitionistic Fuzzy Set (*IFS*) M in X and *IFS* is an object having the form $M = \{< x, \mu_M(x), \nu_M(x) > x \in X\}$ where the functions $\mu_M(x): X \longrightarrow [0,1]$ and $\nu_M(x): X \longrightarrow [0,1]$ denote the degree of membership (namely $\mu_M(x)$) and the degree of non - membership (namely $\nu_M(x)$) of each element $x \in X$ to a set M and $0 \leq \mu_M(x) + \nu_M(x) \leq 1$ for each $x \in X$.

The value $\pi_A(x) = 1 - (\mu_A(x) + \nu_A(x))$ is called the hesitation part which may cater to either membership value or non-membership value or both.

Definition 2.2 [2]: Let M and N be *IFS*s of the form $M = \{< x, \mu_M(x), \nu_M(x) > x \in X\}$ and $N = \{< x, \mu_N(x), \nu_N(x) > x \in X\}$ Then

a) $M \subset N$ if and only if $\mu_M(x) \leq \nu_N(x)$ and $\nu_M(x) \geq \nu_N(x)$ for all $x \in X$,
b) $M = N$ if and only if $M \subseteq N$ and $N \subseteq M$,
c) $M^C = \{< x, \mu_M(x), \nu_M(x) > x \in X\}$,
d) $M \cap N = \{< x, \mu_M(x) \cap \mu_N(x), \nu_M(x) \cup \nu_N(x) > /x \in X\}$,
e) $M \cup N = \{< x, \mu_M(x) \cup (x), \nu_M(x) \cap \nu_N(x) > /x \in X\}$,

For the sake of simplicity, the notation $M = < x, \mu_M, \nu_M >$ shall be used instead of $M = \{< x, \mu_M(x), \nu_M(x) > x \in X\}$. Also, the notation $M = \{< x, (\mu_M, \mu_N), (\nu_M, \nu_N) >\}$ is used instead of $M = \{< x, (M/\mu_M, N/\mu_N), (M/\nu_M, N/\nu_N) >\}$. The Intuitionistic Fuzzy Sets $0_\sim = \{< x, 0,1 > / x \epsilon X\}$ and $1_\sim = \{< x, 1,0 > / x \epsilon X\}$ are the empty set and the whole set of X, respectively.

RELATION WITH IFsgp* SETS

This section describes the Intuitionistic Fuzzy generalized pre star Relation

Definition 3.1 [6]: An Intuitionistic Fuzzy Set A of an Intuitionistic Fuzzy Topological Sets (*IFTS*) isreferred as **Intuitionistic Fuzzy semi generalized pre star closed** (briefly IFsgp* - closed) if $scl(A) \subseteq U$ whenever $A \subseteq U$ and U is IFgp* - open set in X.

Example 3.2: Let $X = \{a, b\}$ and let $\tau = \{0_\sim, T, 1_\sim\}$ be an IFT on X, where $T = \{x, (0.6, 0.8), (0.4, 0.2)\}$. Then the IFS $A = \{x, (0.1, 0.2), (0.9, 0.8)\}$ is an IFsgp*cs in X.

Example 3.3: Let $X = \{a, b\}$ and let $\tau = \{0_\sim, T, 1_\sim\}$ be an IFT on X, where $T = \{x, (0.4, 0.5), (0.6, 0.5)\}$. Then the IFS $A = \{x, (0.3, 0.4), (0.7, 0.6)\}$ is an IFsgp*cs in X.

Example 3.4: Let $X = \{a, b\}$ and let $\tau = \{0_\sim, T, 1_\sim\}$ be an IFT on X, where $T = \{x, (0.2, 0.3), (0.8, 0.7)\}$. Then the IFS $A = \{x, (0.1, 0.1), (0.9, 0.9)\}$ is an IFsgp*cs in X.

Definition 3.5: The Intuitionistic Fuzzy semi generalized pre star Relation **(IFsgp*Relation)** R on A is defined as $R = \{\langle (x,y), \mu_R(x,y), \nu_R(x,y)\rangle / (x,y) \in A \times A\}$.

Definition 3.6: Let X be a non-empty set and A and B be the IFsgp*Ss in X given by the membership $\mu_A(x)$, $\mu_B(x)$ and the non membership $\nu_A(x)$, $\nu_B(x)$ such that $\mu_A(x)$, $\mu_B(x)$, $\nu_A(x)$ and $\nu_B(x)$ are the IFsgp*S drawn from the unit interval $[0,1]$.

Let $A \times B$ be the IFsgp*S in $X \times X$ defined as
$\mu_{A \times B}(x,y) = \min\{\mu_A(x), \mu_B(x)\}$ and
$\nu_{A \times B}(x,y) = \max\{\nu_A(x), \nu_B(x)\}$ for all $x, y \in X$.

Then the relation R from A and B is said to **be IFsgp*Relation** if $R \subseteq A \times B$ such that $R = \{\langle (x,y), \mu_R(x,y), \nu_R(x,y)\rangle / (x,y) \in A \times B\}$ where $\mu_R(x,y) \leq \mu_{A \times B}(x,y)$ and $\nu_R(x,y) \geq \nu_{A \times B}(x,y)$ with the condition $0 \leq \mu_R(x,y) + \nu_R(x,y) \leq 1$.

Example 3.7: Let X = {a, b, c}, A = {a₁|(0.3, 0.6), a₂|(0.4, 0.4), a₃|(0.7, 0.2)} and
B = {b₁|(0.4, 0.2), b₂|(0.5, 0.5), b₃|(0.3, 0.5)}, then R =

Definition 3.8: Let $R : A \rightarrow B$ and $S : B \rightarrow C$ be two **IFsgp* Relations**. The **Composition** $S \circ R$ is an **IFsgp* Relation** from A to C. For every $(x, z) \in A \times C$ and for every $y \in B$ the membership function is

$$\mu_{S \, o \, R}(x,z) = \bigvee_y \left\{ \mu_R(x,y) \bigwedge \mu_S(y,z) \right\}$$

and the non-membership function is

$$v_{S \, o \, R}(x,z) = \bigwedge_y \left\{ v_R(x,y) \bigvee v_S(y,z) \right\}$$

Example 3.9: We show by means of an example that the **Composition** $S \circ R$ is an **IFsgp* Relation** from X to Z

$$R = \begin{array}{c} \\ x_1 \\ x_2 \end{array} \begin{array}{cc} y_1 & y_2 \\ \left[(0.6, 0.2) \right. & (0.2, 0.4) \\ \left. (0.3, 0.3) \right. & (0.7, 0.3) \end{array} \right], \quad S = \begin{array}{c} \\ y_1 \\ y_2 \end{array} \begin{array}{ccc} Z_1 & Z_2 & Z_3 \\ \left[(0.6, 0.4) \right. & (0.6, 0.4) & (0.4, 0.2) \\ \left. (0.5, 0.5) \right. & (0.4, 0.4) & (0.7, 0.3) \end{array} \right]$$

$$S \circ R = \begin{array}{c} \\ y_1 \\ y_2 \end{array} \begin{array}{ccc} Z_1 & Z_2 & Z_3 \\ \left[(0.6, 0.4) \right. & (0.6, 0.4)(0.4, 0.3) \\ \left. (0.4, 0.4) \right. & (0.5, 0.4)(0.7, 0.3) \end{array} \right]$$

PATTERN RECOGNITION USING IFsgp*R COMPOSITION

In order to recognize instances of these patterns, identify the patterns that exist in various types of data, and reach the appropriate conclusions, pattern recognition is required. The following discussion of the pattern recognition issues serves to illustrate the use of the IFsgp* R composition. The recognition principle specifies considering the highest degree of confidence between the IFsgp* R composition to determine the proper pattern in one of the patterns. The IFsgp*Rs are represented by specific patterns in the examples below in order to choose the most useful approach among the two methods for decision analysis.

Methodology I:

1. Compute $T = R \circ Q$, where the membership function

$$\mu_T = \mu_{RoQ} = \bigvee_s \left\{ \mu_Q(p,s) \bigwedge \mu_T(s,d) \right\}$$

and the non-membership function is

$$v_T = v_{RoQ} = \bigwedge_s \left\{ v_Q(p,s) \bigvee v_R(s,d) \right\}$$

2. Calculate $X = \left(\mu_X(p,d), \, v_X(p,d) \right)$ were

$$\mu_X(p,d) = \bigvee_j \mu_T$$

$$v_X(p,d) = \bigwedge_j v_T$$

3. Consider $Y = \mu_X(p,d)$

4. Find the $Max\{Y\}$.

Methodology II:

1. Compute $T = R \circ Q$, where the membership function

$$\mu_T = \mu_{RoQ} = \bigvee_s \left\{ \mu_Q(p,s) \bigwedge \mu_T(s,d) \right\}$$

and the non-membership function is

$$v_T = v_{RoQ} = \bigwedge_s \left\{ v_Q(p,s) \bigvee v_R(s,d) \right\}$$

2. Calculate $X = \left(\mu_X(p,d), v_X(p,d) \right)$ were

$$\mu_X(p,d) = \bigvee_j \mu_T$$

$$v_X(p,d) = \bigwedge_j v_T$$

$$\pi_X(p,d) = 1 - \mu_X(p,d) - v_X(p,d)$$

3. Consider $Y = \mu_X(p,d) - [v_X(p,d) * \pi_X(p,d)]$

EXAMPLE4.1:

The IFsgp* R composition Pattern I, Pattern II, and Pattern III defined here are Intuitionistic Fuzzy Sets, each consisting of two elements.

Let X = {A₁, A₂, A₃, A₄........ Aₙ} with Pattern I, Pattern II, and Pattern III is the IFsgp*R composition defined on X as

Pattern I = {⟨(0.4,0.3), (0.5, 0.4)⟩}

Pattern II = {⟨(0.6,0.4), (0.8, 0.2)⟩}

If the testing IFsgp* R composition Pattern III is defined as

Pattern III = {⟨(0.7, 0.3), (0.6, 0.2)⟩}

Then the pattern identification using the *IFsgp*R* Composition between

Pattern (I, III)   in Method I = 0.5 and Method II = 0.44and

Pattern (II, III)   in Method I = 0.6 and Method II = 0.54

The desired decision is the maximum value thus the testing Pattern III belongs to the Pattern II type

EXAMPLE 4.2:

The IFsgp*R composition Pattern I, Pattern II, and Pattern III defined here are Intuitionistic Fuzzy Sets, each consisting of three elements.

Let X = {A₁, A₂, A₃, A₄........ Aₙ} with Pattern I, Pattern II,Pattern III, Pattern IV, Pattern V and Pattern VI is the IFsgp* R composition defined on X as

Pattern I = {⟨(0.5,0.3), (0.2, 0.2), (0.2, 0.3) ⟩}

Pattern II = {⟨(0.1,0.9), (0.2, 0.8), (0.3, 0.6) ⟩}

Pattern III = {⟨(0.1,0.9), (0.8, 0.1), (0.1, 0.8) ⟩}

Pattern IV = {⟨(0.2,0.8), (0.1, 0.7), (0.4, 0.5))}

Pattern V = {⟨(0.1,0.8), (0.2, 0.7), (0.2, 0.4))}

If the testing *IFsgp*R* composition Pattern VI is defined as

Pattern VI = {⟨(0.2, 0.8), (0.9, 0.1), (0.4, 0.3))}

Then the pattern identification using the *IFsgp*R* Composition between

Pattern (I, VI)   in Method I = 0.3 and Method II = 0.05and

Pattern (II, VI)   in Method I = 0.6 and Method II = 0.24and

Pattern (III, VI)   in Method I = 0.8 and Method II = 0.79and

Pattern (IV, VI)   in Method I = 0.5 and Method II = 0.35and

Pattern (V, VI)   in Method I = 0.4 and Method II = 0.04

The desired decision is the maximum value thus the testing Pattern VI belongs to the Pattern III type

EXAMPLE 4.3:

The IFsgp* *R* composition X1, X2, X3 and X4 defined here is of Intuitionistic Fuzzy Sets, each consisting of two elements. Let X = {A$_1$, A$_2$, A$_3$, A$_4$........ A$_n$} with X1, X2, X3 and X4 are the *IFsgp*R* composition defined on X as

X1 = {⟨(0.5,0.5), (0.4, 0.4))}

X2 = {⟨(0. 3,0.6), (0.2, 0.4))}

X3 = {⟨(0.1,0.9), (0.2, 0.4))}

And the Pattern X4 of *IFsgp*R* composition is referred as

Pattern X4 = {⟨(0.2,0.5), (0.4, 0.4))}

The proposed *IFsgp*R* Composition measure is used for the pattern identification.

In Method I: Pattern (X1, X4) is 0.4; Pattern (X2, X4) is 0.4&Pattern (X3, X4) is 0.4

In Method II: Pattern (X1, X4) is 0.32;   Pattern (X2, X4) is0.04&Pattern (X3, X4) is 0.04

The desired decision is the maximum value. Hence, the testing Pattern X4 belongs to the Pattern X1 type

EXAMPLE 4.4:

The IFsgp*R composition X1, X2, X3 and X4 defined here is of Intuitionistic Fuzzy Sets, each consisting of four elements. Let X = {A$_1$, A$_2$, A$_3$, A$_4$........ A$_n$} with X1, X2, X3 and X4 are the IFsgp*R composition defined on X as

X1= {⟨(0. 3,0.3), (0.3, 0.5), (0.4, 0.3), (0.8, 0.1))}

X2 = {⟨(0.3,0.6), (0.3, 0.7), (0.3, 0.6), (0.2, 0.6))}

X3 = {⟨(0.1,0.3), (0.1, 0.9), (0.2, 0.1), (0.7, 0.4))}

And the Pattern X4 of *IFsgp* R* compositionis referred as

Pattern X4 = {⟨(0.4,0.2), (0.5, 0.5), (0.2, 0.4), (0.9, 0.1))}

From **Method I**: **Pattern (X1, X4) is 0.8**; Pattern (X2, X4) is 0.6&Pattern (X3, X4) is 0.7

And Method II : Pattern (X1, X4) is 0.79; Pattern (X2, X4) is 0.24&Pattern (X3, X4) is 0.13
The desired decision is the maximum value.Hence, the testing Pattern X4 belongs to the Pattern X1 type

Atabular column for comparative analysis is given below (Table 2)
It is evident from the Pattern Recognition Examples, that Method II can be used to make decisions more effectively than Method I.

Three parametric calculations are more accurate in the *IFsgp*R* COMPOSITION than two parametric calculations.
From the Pattern Recognition Examples, it is clear that a better decision can be made using Method II more efficiently than Method I. In the *IFsgp* R* COMPOSITION, calculation with three parametric is effective than with two parametric.

As in the analysis of the Pattern (X1, X4), Pattern (X2, X4), and Pattern (X3, X4) all the result are found to be identical numerical values of 0.4, the Pattern Recognition **Example 4.3** cannot be decided using Method I. The numerical evaluation between Pattern (X1, X4), Pattern (X2, X4), and Pattern (X3, X4) provided by Method II gives values of 0.32, 0.04, and 0.04; as a result, the high confidence of **0.32** identifies the decision analysis as the testing **Pattern X4 belongs to Pattern X1 type**.
Therefore, it is clear that **Method 2** is comparatively a better method than Method 1

CONCLUSION

This work investigates a novel method of pattern identification utilizing the IFsgp* Relational Composition. One of the key characteristics is the Relational Composition of the Intuitionistic Fuzzy Semi Generalized Pre-Star (IFsgp*) in Intuitionistic Fuzzy Topological Space. For two and three parametric members, a few numerical instances of pattern recognition are shown, and it is discovered that the three parametric methodology is more accurate.This method can be expanded to other problems such as handwritten character identification, fingerprint recognition, human face recognition, and X-ray picture classification.

ACKNOWLEDGEMENT

REFERENCES

1. Atanassov K, On Intuitionistic Fuzzy Sets Theory. Sofia Bulgaria,2012
2. Atanassov K, Intuitionistic Fuzzy Sets, Fuzzy Sets and Systems, 20(1986), 87-96.
3. Atanassov K, New operations defined over Intuitionistic Fuzzy Sets, Fuzzy Sets and Systems,61(1994), 137-142.
4. Biswas R, Intuitionistic Fuzzy Relations, Bull. Sous. Ens. Flous. Appl.(BUSEFAL), 70(1997) 22-29.
5. Biswas R, On Fuzzy Sets and Intuitionistic Fuzzy Sets, NIFS, 3(1997), 3-11.
6. J. Chandhini, N. Uma, IFsgp* - Closed Sets, Open sets in Intuitionistic Fuzzy Topological Spaces, International Journal for Research in Applied Science & Engineering Technology (IJRASET), Vol 10 Issue XII, Dec 2022, DOI – https://doi.org/10.22214/ijraset.2022.48169.
7. Li Dengfeng and Cheng Chuntian, "New similarity measures of intuitionistic fuzzy sets and applications to pattern recognitions," Pattern Recognition Letters, vol. 23, 2002, pp. 221-225.
8. Li Yanhong, David L.Olson, and Qin Zheng, "Similarity measures between intuitionistic fuzzy (vague) sets: A comparative analysis," Pattern Recognition Letters, vol. 28, 2007, pp. 278-285.
9. Zadeh, L. A., "Fuzzy sets", Information and Control, Vol. 8, pp. 338–353, 1965.

Chandhini and Uma

Table 1. IFsgp* Relation

R	b_1	b_2	b_3
a_1	(0.3,0.6)	(0.3,0.6)	(0.3,0.6)
a_2	(0.4,0.4)	(0.4,0.5)	(0.3,0.5)
a_3	(0.4,0.2)	(0.5,0.5)	(0.3,0.5)

Table 2. - Pattern recognition using the *IFsgp*R* Composition

Pattern Recognition using the *IFsgp*R* Composition	Method I	Method II	Result
Example4.1: *IFsgp*R* Composition betweenPattern (I, III) and Pattern (II, III). The Pattern I, II and III are the *IFsgp*R*composition have equalIFSs,each **consisting of two elements**.	Pattern (I, III) =0.5 Pattern (II, III) = **0.6**	Pattern (I, III) =0.44 Pattern (II, III) =**0.54**	The maximum value is the required decision. **The testing Pattern III belongs to Pattern II type**
Example 4.2: *IFsgp*R* Composition betweenPattern (I, III) and Pattern (II, III). The Pattern I, II, III, IV, V and VI are the *IFsgp*R*composition have equal IFSs,each **consisting of three elements**.	Pattern (I, VI) =0.3 Pattern (II, VI) = 0.6 Pattern (III, VI) = **0.8** Pattern (IV, VI) = 0.5 Pattern (V, VI) = 0.4	Pattern (I, VI) =0.05 Pattern (II, VI) =0.24 Pattern (III, VI) = **0.79** Pattern (IV, VI) = 0.35 Pattern (V, VI) = 0.04	The maximum value is the required decision. **The testing Pattern VI belongs to Pattern III type**
Example 4.3: *IFsgp*R* Composition between Pattern (X1, X4), Pattern (X2, X4), and Pattern (X3, X4).The Pattern X1, X2, X3 and X4 are the *IFsgp*R* composition have equal IFSs, each **consisting of two elements.**	Pattern (X1, X4) = **0.4** Pattern (X2, X4) = 0.4 Pattern (X3, X4) = 0.4	Pattern (X1, X4) = **0.32** Pattern (X2, X4) = 0.04 Pattern (X3, X4)= 0.04	The maximum value is the required decision. **Hence, the testingPattern X4 belongs to Pattern X1 type**
Example 4.4: Considering the Numerical Evaluation using *IFsgp*R* Composition between Pattern (X1, X4), Pattern (X2, X4), and Pattern (X3, X4).The Pattern X1, X2, X3 and X4 are the *IFsgp*R* composition defined IFSs, each consisting of **four elements.**	Pattern (X1, X4) = **0.8** Pattern (X2, X4) = 0.6 Pattern (X3, X4) = 0.7	Pattern (X1, X4) = **0.79** Pattern (X2, X4) = 0.24 Pattern (X3, X4)= 0.13	The maximum value is the required decision. **Hence, the testingPattern X4 belongs to Pattern X1 type**

RESEARCH ARTICLE

Algebraic Operations on Quin – Terranean Fuzzy Numbers

P. Rajarajeswari[1]*, T. Thirunamakkani[2], and P. Pooranadevi[3]

[1]Assistant Professor, Department of Mathematics, Chikkanna Government Arts College, Tirupur – 641602, Tamil Nadu, India.
[2]Research Scholar, Department of Mathematics, Chikkanna Government Arts College, Tirupur – 641602, Tamil Nadu, India.
[3]Assistant Professor, Department of Science and Humanities, Info Institute of Engineering, Coimbatore – 641107, Tamil Nadu, India.

*Address for Correspondence**
P. Rajarajeswari
Assistant Professor,
Department of Mathematics,
Chikkanna Government Arts College,
Tirupur – 641602, Tamil Nadu, India.
E.Mail: p.rajarajeswari29@gmail.com.

ABSTRACT

Quin-Terranean Fuzzy Set is a more sophisticated set that produces effective results than Intuitionistic Fuzzy Set, Pythagorean Fuzzy Set, and Fermatean Fuzzy Set. Quin-Terranean fuzzy set is the most effective tool for managing uncertainty. By using Quin-Terranean fuzzy set, we have defined Quin – Terranean Fuzzy Number. In this paper we defined some of the algebraic operations such as addition, multiplication, scalar multiplication and power rule on Quin – Terranean Fuzzy Numbers. Several properties of the algebraic operations on Quin – Terranean Fuzzy Numbers are also studied.

INTRODUCTION

In 1965, Zadeh [12] introduced the concept of fuzzy sets which are sets with varying degrees of membership. Fuzzy sets are extension to the traditional concept of set theory. Zadeh introduced the idea of fuzzy numbers and fuzzy arithmetic. In 1998, Shan – Huo Chen [6] presented the way to treat the operations of fuzzy numbers with step form by using function principle. In 2003, Witold Kosinski et al. [10] have developed the novel idea of an ordered fuzzy number, which is symbolized by an ordered pair of real continuous functions and defined four algebraic operations

Rajarajeswari *et al.,*

on ordered fuzzy numbers. In 2003, Jae Duek Myung [2] introduced the two types of algebraic operations on fuzzy number utilizing piecewise linear function. He also demonstrated that the Zadeh implication is smaller than the Diense - Rescher implication, which is smaller than the Lukasiewicz implication. There are some situations in which fuzzy sets are not sufficient to manage uncertainty. In order to manage such situations, in 1986, Atanassov [1] defined the extended concept of Fuzzy set theory known as Intuitionistic fuzzy set (IFS). He also defined the operations of IFS and analyzed their properties. In 2014, Sankar Prasad Mondal et al. [5] discussed some nonlinear arithmetic operations on generalised triangular Intuitionistic fuzzy numbers. They have also provided examples along with an application.

In 2014 Yager [11] introduced the concept of Pythagorean fuzzy set (PFS) which was a logical extension of this limitation in IFS, where in certain cases, unlike the examples observed in IFSs, the total of the degree of acceptance and the degree of non-acceptance may be higher than one. In Pythagorean fuzzy set, the total of the square of the degree of acceptance and square of the degree of non-acceptance is lesser than one. In 2019, Shu-Ping Wan et al. [7] proposed a new order relation for Pythagorean fuzzy numbers (PFNs). They have applied it in multi-attribute group decision making (MAGDM). They have also demonstrated the effectiveness of the suggested method through a venture capital investment selection example. In some circumstances, unlike the examples observed in PFS, the total of the square of the degree of acceptance and square of the degree of non-acceptance may be more than one. The Fermatean fuzzy sets (FFSs) concept was a logical result of this restriction in PFS. In 2019, Senapathi and Yager [8] introduced Fermatean fuzzy set in which the sum of the cube of the degree of acceptance and cube of the degree of non-acceptance is less than or equal to one. In 2019, Tapan Senapati and Ronald Yager [9] introduced the three new operations namely subtraction, division, and Fermatean arithmetic mean operations over Fermatean fuzzy sets. They have provided great detail on their properties. They developed a Fermatean fuzzy weighted product model to address the multi-criteria decision-making issue. They have also provided a practical example of choosing a suitable bridge construction method to illustrate the approach they developed and to confirm its viability. The Quin-Terranean Fuzzy Set (QTFS), a revolutionary concept that we invented in 2023 [4], is the most significant and practical way to handle uncertainty and contingency when compared to IFS, PFS, and FFS. We defined the basic set theory operations, such as union, intersection and complement for Quin-Terranean Fuzzy sets. Based on these operations, a number of the properties have been investigated. We have seen that the Quin-Terranean Fuzzy set satisfies the De Morgan's rule, associative property, commutative property, and distributive property.

Preliminaries

This section consists of the basic concepts and definitions related to the paper.

Definition 2.1 [8]

The Pythagorean fuzzy sets defined on a non-empty set X as objects having the form $\mathcal{P} = \{\langle \tilde{x}, \alpha_P(\tilde{x}), \beta_P(\tilde{x}) \rangle : \tilde{x} \in X\}$, where the function $\alpha_P(\tilde{x}): X \rightarrow [0,1]$ and $\beta_P(\tilde{x}): X \rightarrow [0,1]$, denote the degree of membership and degree of non-membership of each element $\tilde{x} \in X$ to the set $\mathcal{P}$ respectively, and $0 \leq \left(\alpha_P(\tilde{x})\right)^2 + \left(\beta_P(\tilde{x})\right)^2 \leq 1$ for all $\tilde{x} \in X$. For any Pythagorean fuzzy set $\mathcal{P}$ and $\tilde{x} \in X$, $\pi_P(\tilde{x}) = \sqrt{1 - \left(\alpha_P(\tilde{x})\right)^2 - \left(\beta_P(\tilde{x})\right)^2}$ is called the degree of indeterminacy of $\tilde{x}$ to $\mathcal{P}$.

Definition 2.2 [8]

Let X be a universe of discourse. A Fermatean fuzzy set $\mathcal{F}$ in X is an object having the form
$\mathcal{F} = \{\langle \tilde{x}, \alpha_\mathcal{F}(\tilde{x}), \beta_\mathcal{F}(\tilde{x}) \rangle : \tilde{x} \in X\}$,
where $\alpha_\mathcal{F}(\tilde{x}): X \rightarrow [0,1]$ and $\beta_\mathcal{F}(\tilde{x}): X \rightarrow [0,1]$, including the condition
$0 \leq \left(\alpha_P(\tilde{x})\right)^3 + \left(\beta_P(\tilde{x})\right)^3 \leq 1$,
for all $\tilde{x} \in X$. The $\alpha_\mathcal{F}(\tilde{x})$ and $\beta_\mathcal{F}(\tilde{x})$ denote, respectively, the degree of membership and the degree of non-membership of the element $\tilde{x}$ in the set $\mathcal{F}$.

For any FFS $\mathcal{F}$ and $\tilde{x} \in X$,
$\pi_\mathcal{F}(\tilde{x}) = \sqrt[3]{1 - \left(\alpha_P(\tilde{x})\right)^3 - \left(\beta_P(\tilde{x})\right)^3}$

is identified as the degree of indeterminacy of $\tilde{x}$ to $\mathcal{F}$.

In the interest of simplicity, we shall mention the symbol $\mathcal{F} = (\alpha_{\mathcal{F}}, \beta_{\mathcal{F}})$ for the FFS $\mathcal{F} = \{\langle \tilde{x}, \alpha_{\mathcal{F}}(\tilde{x}), \beta_{\mathcal{F}}(\tilde{x}) \rangle : \tilde{x} \in X\}$.

Definition 2.3 [4]

Let X denotes a universe of discourse. A Quin – Terranean fuzzy set $\widetilde{Q}$ in X is the element possess the configuration $\widetilde{Q} = \{\langle \tilde{x}, \sigma_{\widetilde{Q}}(\tilde{x}), \delta_{\widetilde{Q}}(\tilde{x}) \rangle : \forall \tilde{x} \in X\}$,

where $\sigma_{\widetilde{Q}}(\tilde{x}) : X \longrightarrow [0,1]$ and $\delta_{\widetilde{Q}}(\tilde{x}) : X \longrightarrow [0,1]$ represents the degree of dependence and degree of non – dependence of the element respectively, satisfying the condition $0 \leq \left(\sigma_{\widetilde{Q}}(\tilde{x})\right)^{4^5} + \left(\delta_{\widetilde{Q}}(\tilde{x})\right)^{\frac{5}{4}} \leq 1, \forall \tilde{x} \in X$.

For any Quin – Terranean fuzzy set $\widetilde{Q}$ and $\forall \tilde{x} \in X$, $\varphi_{\widetilde{Q}}(\tilde{x}) = \left\{1 - \left(\sigma_{\widetilde{Q}}(\tilde{x})\right)^{4^5} - \left(\delta_{\widetilde{Q}}(\tilde{x})\right)^{\frac{5}{4}}\right\}^{\frac{4}{5}}$ is the degree of hesitance of $\tilde{x}$ to X.

Definition 2.4 [3]

A Quin – Terranean fuzzy number $\widetilde{Q}$ is defined as,

a Quin – Terranean fuzzy subset of the real line

normal, that is, there exist $\tilde{x}_0 \in R$ such that $\sigma_{\widetilde{Q}}(\tilde{x}_0) = 1$ and $\delta_{\widetilde{Q}}(\tilde{x}_0) = 0$.

a convex set for the acceptance function $\sigma_{\widetilde{Q}}(\tilde{x})$, that is,

$$\sigma_{\widetilde{Q}}(\lambda \tilde{x}_1 + (1 - \lambda)\tilde{x}_2) \geq \boldsymbol{min}\left(\sigma_{\widetilde{Q}}(\tilde{x}_1), \sigma_{\widetilde{Q}}(\tilde{x}_2)\right) \quad \forall \tilde{x}_1, \tilde{x}_2 \in R, \lambda \in [0,1]$$

a concave set for the non-acceptance function $\delta_{\widetilde{Q}}(\tilde{x})$, that is,

$$\delta_{\widetilde{Q}}(\lambda \tilde{x}_1 + (1 - \lambda)\tilde{x}_2) \leq \boldsymbol{max}\left(\delta_{\widetilde{Q}}(\tilde{x}_1), \delta_{\widetilde{Q}}(\tilde{x}_2)\right) \quad \forall \tilde{x}_1, \tilde{x}_2 \in R, \lambda \in [0,1].$$

and satisfies the condition, $0 \leq \left(\sigma_{\widetilde{Q}}(\tilde{x})\right)^{4^5} + \left(\delta_{\widetilde{Q}}(\tilde{x})\right)^{\frac{5}{4}} \leq 1$.

A doublet expressed by $\widetilde{Q} = \langle \sigma_{\widetilde{Q}}(\tilde{x}), \delta_{\widetilde{Q}}(\tilde{x}) \rangle$ is known as Quin – Terranean fuzzy number. The Zero and one Quin – Terranean fuzzy number is denoted by (0,0) and (1,0) respectively.

Definition 2.5 [4]

Let $\widetilde{Q} = \{\langle \tilde{x}, \sigma_{\widetilde{Q}}(\tilde{x}), \delta_{\widetilde{Q}}(\tilde{x}) \rangle : \forall \tilde{x} \in X\}$, $\widetilde{Q}_1 = \{\langle \tilde{x}, \sigma_{\widetilde{Q}_1}(\tilde{x}), \delta_{\widetilde{Q}_1}(\tilde{x}) \rangle : \forall \tilde{x} \in X\}$, $\widetilde{Q}_2 = \{\langle \tilde{x}, \sigma_{\widetilde{Q}_2}(\tilde{x}), \delta_{\widetilde{Q}_2}(\tilde{x}) \rangle : \forall \tilde{x} \in X\}$ be three Quin – Terranean fuzzy set, then their operations are expressed as follows,

$\widetilde{Q}_1 \subset \widetilde{Q}_2$ *iff* $\{\langle \tilde{x}, \sigma_{\widetilde{Q}_1}(\tilde{x}) \leq \sigma_{\widetilde{Q}_2}(\tilde{x})$ *and* $\delta_{\widetilde{Q}_1}(\tilde{x}) \geq \delta_{\widetilde{Q}_2}(\tilde{x}) \rangle : \forall \tilde{x} \in X\}$,

$\widetilde{Q}_1 = \widetilde{Q}_2$ *iff* $\{\langle \tilde{x}, \sigma_{\widetilde{Q}_1}(\tilde{x}) = \sigma_{\widetilde{Q}_2}(\tilde{x})$ *and* $\delta_{\widetilde{Q}_1}(\tilde{x}) = \delta_{\widetilde{Q}_2}(\tilde{x}) \rangle : \forall \tilde{x} \in X\}$,

$\widetilde{Q}_1 \cup \widetilde{Q}_2 = \left\{\langle \tilde{x}, \boldsymbol{max}\left(\sigma_{\widetilde{Q}_1}(\tilde{x}), \sigma_{\widetilde{Q}_2}(\tilde{x})\right), \boldsymbol{min}\left(\delta_{\widetilde{Q}_1}(\tilde{x}), \delta_{\widetilde{Q}_2}(\tilde{x})\right) \rangle : \forall \tilde{x} \in X\right\}$,

$\widetilde{Q}_1 \cap \widetilde{Q}_2 = \left\{\langle \tilde{x}, \boldsymbol{min}\left(\sigma_{\widetilde{Q}_1}(\tilde{x}), \sigma_{\widetilde{Q}_2}(\tilde{x})\right), \boldsymbol{max}\left(\delta_{\widetilde{Q}_1}(\tilde{x}), \delta_{\widetilde{Q}_2}(\tilde{x})\right) \rangle : \forall \tilde{x} \in X\right\}$,

$$\widetilde{Q}^c = \{\langle \tilde{x}, \delta_{\widetilde{Q}}(\tilde{x}), \sigma_{\widetilde{Q}}(\tilde{x}) \rangle : \forall \tilde{x} \in X\}$$

MAIN RESULT

In this section, the definitions of certain algebraic operations on Quin-Terranean Fuzzy numbers including addition, multiplication, scalar multiplication, and exponentiation are given. Some of the features of the model operators ⊞ and ⊠, scalar multiplication and exponentiation of the Quin-Terranean Fuzzy numbers, are also explored based on the algebraic operations that have been specified.

Algebraic Operation on Quin – Terranean Fuzzy Number:

Definition 3.1

Let $\widetilde{\mathbb{Q}} = \langle \sigma_{\widetilde{\mathbb{Q}}}(\tilde{x}), \delta_{\widetilde{\mathbb{Q}}}(x) \rangle$, $\widetilde{\mathbb{Q}}_1 = \langle \sigma_{\widetilde{\mathbb{Q}}}(\tilde{x}), \delta_{\widetilde{\mathbb{Q}}}(x) \rangle$ and $\widetilde{\mathbb{Q}}_2 = \langle \sigma_{\widetilde{\mathbb{Q}}_2}(\tilde{x}), \delta_{\widetilde{\mathbb{Q}}_2}(\tilde{x}) \rangle$ be three Quin – Terranean Fuzzy Numbers and $\lambda > 0$, then their operations are expressed as follows:

Rajarajeswari *et al.,*

$$\widetilde{\mathbb{Q}}_1 \boxplus \widetilde{\mathbb{Q}}_2 = \left\langle \left\{ \left(\sigma_{\widetilde{\mathbb{Q}}_1}(\tilde{x})\right)^{4^5} + \left(\sigma_{\widetilde{\mathbb{Q}}_2}(\tilde{x})\right)^{4^5} - \left(\sigma_{\widetilde{\mathbb{Q}}_1}(\tilde{x})\right)^{4^5}\left(\sigma_{\widetilde{\mathbb{Q}}_2}(\tilde{x})\right)^{4^5} \right\}^{\frac{1}{4^5}}, \delta_{\widetilde{\mathbb{Q}}_1}(\tilde{x})\delta_{\widetilde{\mathbb{Q}}_2}(\tilde{x}) \right\rangle$$

$$\widetilde{\mathbb{Q}}_1 \boxtimes \widetilde{\mathbb{Q}}_2 = \left\langle \sigma_{\widetilde{\mathbb{Q}}_1}(\tilde{x})\sigma_{\widetilde{\mathbb{Q}}_2}(\tilde{x}), \left\{ \left(\delta_{\widetilde{\mathbb{Q}}_1}(\tilde{x})\right)^{\frac{5}{4}} + \left(\delta_{\widetilde{\mathbb{Q}}_2}(\tilde{x})\right)^{\frac{5}{4}} - \left(\delta_{\widetilde{\mathbb{Q}}_1}(\tilde{x})\right)^{\frac{5}{4}}\left(\delta_{\widetilde{\mathbb{Q}}_2}(\tilde{x})\right)^{\frac{5}{4}} \right\}^{\frac{4}{5}} \right\rangle$$

$$\lambda\widetilde{\mathbb{Q}} = \left\langle \left\{ 1 - \left(1 - \left(\sigma_{\widetilde{\mathbb{Q}}}(\tilde{x})\right)^{4^5}\right)^{\lambda} \right\}^{\frac{1}{4^5}}, \delta_{\widetilde{\mathbb{Q}}}(\tilde{x})^{\lambda} \right\rangle$$

$$\widetilde{\mathbb{Q}}^{\lambda} = \left\langle \sigma_{\widetilde{\mathbb{Q}}}(\tilde{x})^{\lambda}, \left\{ 1 - \left(1 - \left(\delta_{\widetilde{\mathbb{Q}}}(\tilde{x})\right)^{\frac{5}{4}}\right)^{\lambda} \right\}^{\frac{4}{5}} \right\rangle$$

Properties of Algebraic Operations on Quin – Terranean Fuzzy Numbers:
Several properties of algebraic operations on Quin – Terranean Fuzzy Numbers are given as follows,

Theorem 3.1:
For three Quin – Terranean Fuzzy numbers $\widetilde{\mathbb{Q}} = \langle \sigma_{\widetilde{\mathbb{Q}}}(\tilde{x}), \delta_{\widetilde{\mathbb{Q}}}(\tilde{x})\rangle$, $\widetilde{\mathbb{Q}}_1 = \langle \sigma_{\widetilde{\mathbb{Q}}_1}(\tilde{x}), \delta_{\widetilde{\mathbb{Q}}_1}(\tilde{x})\rangle$ and $\widetilde{\mathbb{Q}}_2 = \langle \sigma_{\widetilde{\mathbb{Q}}_2}(\tilde{x}), \delta_{\widetilde{\mathbb{Q}}_2}(\tilde{x})\rangle$, the following ones are valid,

$$\widetilde{\mathbb{Q}}_1 \boxplus \widetilde{\mathbb{Q}}_2 = \widetilde{\mathbb{Q}}_2 \boxplus \widetilde{\mathbb{Q}}_1$$
$$\widetilde{\mathbb{Q}}_1 \boxtimes \widetilde{\mathbb{Q}}_2 = \widetilde{\mathbb{Q}}_2 \boxtimes \widetilde{\mathbb{Q}}_1$$
$$\lambda\left(\widetilde{\mathbb{Q}}_1 \boxplus \widetilde{\mathbb{Q}}_2\right) = \lambda\widetilde{\mathbb{Q}}_1 \boxplus \lambda\widetilde{\mathbb{Q}}_2 , \qquad \lambda > 0$$
$$(\lambda_1 + \lambda_2)\widetilde{\mathbb{Q}} = \lambda_1\widetilde{\mathbb{Q}} \boxplus \lambda_2\widetilde{\mathbb{Q}} , \qquad \lambda_1, \lambda_2 > 0$$
$$\left(\widetilde{\mathbb{Q}}_1 \boxtimes \widetilde{\mathbb{Q}}_2\right)^{\lambda} = \widetilde{\mathbb{Q}}_1^{\lambda} \boxtimes \widetilde{\mathbb{Q}}_2^{\lambda} , \qquad \lambda > 0$$
$$\widetilde{\mathbb{Q}}^{(\lambda_1 + \lambda_2)} = \widetilde{\mathbb{Q}}^{\lambda_1} \boxtimes \widetilde{\mathbb{Q}}^{\lambda_2} , \quad \lambda_1, \lambda_2 > 0$$

Proof:
Let us consider $\widetilde{\mathbb{Q}} = \langle \sigma_{\widetilde{\mathbb{Q}}}(\tilde{x}), \delta_{\widetilde{\mathbb{Q}}}(\tilde{x})\rangle$, $\widetilde{\mathbb{Q}}_1 = \langle \sigma_{\widetilde{\mathbb{Q}}_1}(\tilde{x}), \delta_{\widetilde{\mathbb{Q}}_1}(\tilde{x})\rangle$ and $\widetilde{\mathbb{Q}}_2 = \langle \sigma_{\widetilde{\mathbb{Q}}_2}(\tilde{x}), \delta_{\widetilde{\mathbb{Q}}_2}(\tilde{x})\rangle$ be three Quin – Terranean Fuzzy Numbers and $\lambda, \lambda_1, \lambda_2 > 0$, then using definition 3.1, we can acquire,
L.H.S = $\widetilde{\mathbb{Q}}_1 \boxplus \widetilde{\mathbb{Q}}_2$

$$= \left\langle \left\{ \left(\sigma_{\widetilde{\mathbb{Q}}_1}(\tilde{x})\right)^{4^5} + \left(\sigma_{\widetilde{\mathbb{Q}}_2}(\tilde{x})\right)^{4^5} - \left(\sigma_{\widetilde{\mathbb{Q}}_1}(\tilde{x})\right)^{4^5}\left(\sigma_{\widetilde{\mathbb{Q}}_2}(\tilde{x})\right)^{4^5} \right\}^{\frac{1}{4^5}}, \delta_{\widetilde{\mathbb{Q}}_1}(\tilde{x})\delta_{\widetilde{\mathbb{Q}}_2}(\tilde{x}) \right\rangle$$

$$= \left\langle \left\{ \left(\sigma_{\widetilde{\mathbb{Q}}_2}(\tilde{x})\right)^{4^5} + \left(\sigma_{\widetilde{\mathbb{Q}}_1}(\tilde{x})\right)^{4^5} - \left(\sigma_{\widetilde{\mathbb{Q}}_2}(\tilde{x})\right)^{4^5}\left(\sigma_{\widetilde{\mathbb{Q}}_1}(\tilde{x})\right)^{4^5} \right\}^{\frac{1}{4^5}}, \delta_{\widetilde{\mathbb{Q}}_1}(\tilde{x})\delta_{\widetilde{\mathbb{Q}}_2}(\tilde{x}) \right\rangle$$

$= \widetilde{\mathbb{Q}}_2 \boxplus \widetilde{\mathbb{Q}}_1$ = R.H.S

L.H.S = $\widetilde{\mathbb{Q}}_1 \boxtimes \widetilde{\mathbb{Q}}_2 = \left\langle \sigma_{\widetilde{\mathbb{Q}}_1}(\tilde{x})\sigma_{\widetilde{\mathbb{Q}}_2}(\tilde{x}), \left\{ \left(\delta_{\widetilde{\mathbb{Q}}_1}(\tilde{x})\right)^{\frac{5}{4}} + \left(\delta_{\widetilde{\mathbb{Q}}_2}(\tilde{x})\right)^{\frac{5}{4}} - \left(\delta_{\widetilde{\mathbb{Q}}_1}(\tilde{x})\right)^{\frac{5}{4}}\left(\delta_{\widetilde{\mathbb{Q}}_2}(\tilde{x})\right)^{\frac{5}{4}} \right\}^{\frac{4}{5}} \right\rangle$

$$= \left\langle \sigma_{\widetilde{\mathbb{Q}}_1}(\tilde{x})\sigma_{\widetilde{\mathbb{Q}}_2}(\tilde{x}), \left\{ \left(\delta_{\widetilde{\mathbb{Q}}_1}(\tilde{x})\right)^{\frac{5}{4}} + \left(\delta_{\widetilde{\mathbb{Q}}_2}(\tilde{x})\right)^{\frac{5}{4}} - \left(\delta_{\widetilde{\mathbb{Q}}_1}(\tilde{x})\right)^{\frac{5}{4}}\left(\delta_{\widetilde{\mathbb{Q}}_2}(\tilde{x})\right)^{\frac{5}{4}} \right\}^{\frac{4}{5}} \right\rangle$$

$= \widetilde{\mathbb{Q}}_2 \boxtimes \widetilde{\mathbb{Q}}_1$ = R.H.S

L.H.S = $\lambda\left(\widetilde{\mathbb{Q}}_1 \boxplus \widetilde{\mathbb{Q}}_2\right)$

$$= \lambda\left(\left\langle \left\{ \left(\sigma_{\widetilde{\mathbb{Q}}_1}(\tilde{x})\right)^{4^5} + \left(\sigma_{\widetilde{\mathbb{Q}}_2}(\tilde{x})\right)^{4^5} - \left(\sigma_{\widetilde{\mathbb{Q}}_1}(\tilde{x})\right)^{4^5}\left(\sigma_{\widetilde{\mathbb{Q}}_2}(\tilde{x})\right)^{4^5} \right\}^{\frac{1}{4^5}}, \delta_{\widetilde{\mathbb{Q}}_1}(\tilde{x})\delta_{\widetilde{\mathbb{Q}}_2}(\tilde{x}) \right\rangle \right)$$

$$= \left\langle \left\{ 1 - \left(1 - \left(\left\{ \left(\sigma_{\widetilde{\mathbb{Q}}_1}(\tilde{x})\right)^{4^5} + \left(\sigma_{\widetilde{\mathbb{Q}}_2}(\tilde{x})\right)^{4^5} - \left(\sigma_{\widetilde{\mathbb{Q}}_1}(\tilde{x})\right)^{4^5}\left(\sigma_{\widetilde{\mathbb{Q}}_2}(\tilde{x})\right)^{4^5} \right\}^{\frac{1}{4^5}}\right)^{4^5} \right)^{\lambda} \right\}^{\frac{1}{4^5}}, \delta_{\widetilde{\mathbb{Q}}_1}(\tilde{x})^{\lambda}\delta_{\widetilde{\mathbb{Q}}_2}(\tilde{x})^{\lambda} \right\rangle$$

$$= \left\langle \left\{ 1 - \left(\left(1 - \left(\sigma_{\widetilde{\mathbb{Q}}_1}(\tilde{x})\right)^{4^5}\right) - \left(\sigma_{\widetilde{\mathbb{Q}}_2}(\tilde{x})\right)^{4^5}\left(1 - \left(\sigma_{\widetilde{\mathbb{Q}}_1}(\tilde{x})\right)^{4^5}\right) \right)^{\lambda} \right\}^{\frac{1}{4^5}}, \delta_{\widetilde{\mathbb{Q}}_1}(\tilde{x})^{\lambda}\, \delta_{\widetilde{\mathbb{Q}}_2}(\tilde{x})^{\lambda} \right\rangle$$

Rajarajeswari *et al.,*

$$= \langle \left\{ 1 - \left(1 - \left(\sigma_{\widetilde{\mathbb{Q}}_1}(\tilde{x})\right)^{4^5}\right)^\lambda \left(1 - \left(\sigma_{\widetilde{\mathbb{Q}}_2}(\tilde{x})\right)^{4^5}\right)^\lambda \right\}^{\frac{1}{4^5}}, \delta_{\widetilde{\mathbb{Q}}_1}(\tilde{x})^\lambda \, \delta_{\widetilde{\mathbb{Q}}_2}(\tilde{x})^\lambda \rangle$$

$$R.H.S = \langle \left\{ 1 - \left(1 - \left(\sigma_{\widetilde{\mathbb{Q}}_1}(\tilde{x})\right)^{4^5}\right)^\lambda \right\}^{\frac{1}{4^5}}, \delta_{\widetilde{\mathbb{Q}}_1}(\tilde{x})^\lambda \rangle \boxplus$$

$$\langle \left\{ 1 - \left(1 - \left(\sigma_{\widetilde{\mathbb{Q}}_2}(\tilde{x})\right)^{4^5}\right)^\lambda \right\}^{\frac{1}{4^5}}, \delta_{\widetilde{\mathbb{Q}}_2}(\tilde{x})^\lambda \rangle$$

$$= \langle \left\{ \left(\left\{ 1 - \left(1 - \left(\sigma_{\widetilde{\mathbb{Q}}_1}(\tilde{x})\right)^{4^5}\right)^\lambda \right\}^{\frac{1}{4^5}} \right)^{4^5} + \left(\left\{ 1 - \left(1 - \left(\sigma_{\widetilde{\mathbb{Q}}_2}(\tilde{x})\right)^{4^5}\right)^\lambda \right\}^{\frac{1}{4^5}} \right)^{4^5} \right.$$

$$\left. - \left(\left\{ 1 - \left(1 - \left(\sigma_{\widetilde{\mathbb{Q}}_1}(\tilde{x})\right)^{4^5}\right)^\lambda \right\}^{\frac{1}{4^5}} \right)^{4^5} \left(\left\{ 1 - \left(1 - \left(\sigma_{\widetilde{\mathbb{Q}}_2}(\tilde{x})\right)^{4^5}\right)^\lambda \right\}^{\frac{1}{4^5}} \right)^{4^5} \right\}^{\frac{1}{4^5}}, \delta_{\widetilde{\mathbb{Q}}_1}(\tilde{x})^\lambda \delta_{\widetilde{\mathbb{Q}}_2}(\tilde{x})^\lambda \rangle$$

$$= \langle \left\{ 1 - \left(1 - \left(\sigma_{\widetilde{\mathbb{Q}}_1}(\tilde{x})\right)^{4^5}\right)^\lambda \left(1 - \left(\sigma_{\widetilde{\mathbb{Q}}_2}(\tilde{x})\right)^{4^5}\right)^\lambda \right\}^{\frac{1}{4^5}}, \delta_{\widetilde{\mathbb{Q}}_1}(\tilde{x})^\lambda \, \delta_{\widetilde{\mathbb{Q}}_2}(\tilde{x})^\lambda \rangle$$

From (1) and (2), L.H.S = R.H.S implies $\lambda\left(\widetilde{\mathbb{Q}}_1 \boxplus \widetilde{\mathbb{Q}}_2\right) = \lambda\widetilde{\mathbb{Q}}_1 \boxplus \lambda\widetilde{\mathbb{Q}}_2 , \; \lambda > 0.$

L.H.S $= (\lambda_1 \boxplus \lambda_2)\widetilde{\mathbb{Q}} = (\lambda_1 + \lambda_2)\langle \sigma_{\widetilde{\mathbb{Q}}}(\tilde{x}), \delta_{\widetilde{\mathbb{Q}}}(\tilde{x}) \rangle$

$$= \langle \left\{ 1 - \left(1 - \left(\sigma_{\widetilde{\mathbb{Q}}}(\tilde{x})\right)^{4^5}\right)^{\lambda_1 + \lambda_2} \right\}^{\frac{1}{4^5}}, \delta_{\widetilde{\mathbb{Q}}}(\tilde{x})^{\lambda_1 + \lambda_2} \rangle$$

$$= \langle \left\{ 1 - \left(1 - \left(\sigma_{\widetilde{\mathbb{Q}}}(\tilde{x})\right)^{4^5}\right)^{\lambda_1} \left(1 - \left(\sigma_{\widetilde{\mathbb{Q}}}(\tilde{x})\right)^{4^5}\right)^{\lambda_2} \right\}^{\frac{1}{4^5}}, \delta_{\widetilde{\mathbb{Q}}}(\tilde{x})^{\lambda_1 + \lambda_2} \rangle$$

$$= \langle \left\{ 1 - \left(1 - \left(\sigma_{\widetilde{\mathbb{Q}}}(\tilde{x})\right)^{4^5}\right)^{\lambda_1} \right\}^{\frac{1}{4^5}}, \delta_{\widetilde{\mathbb{Q}}}(\tilde{x})^{\lambda_1} \rangle \boxplus \langle \left\{ 1 - \left(1 - \left(\sigma_{\widetilde{\mathbb{Q}}}(\tilde{x})\right)^{4^5}\right)^{\lambda_2} \right\}^{\frac{1}{4^5}}, \delta_{\widetilde{\mathbb{Q}}}(\tilde{x})^{\lambda_2} \rangle$$

$= \lambda_1\widetilde{\mathbb{Q}} \boxplus \lambda_2\widetilde{\mathbb{Q}} = $ R.H.S

$\therefore, (\lambda_1 + \lambda_2)\widetilde{\mathbb{Q}} = \lambda_1\widetilde{\mathbb{Q}} \boxplus \lambda_2\widetilde{\mathbb{Q}} , \; \lambda_1, \lambda_2 > 0.$

Hence, (iv) proved.

L.H.S $= \left(\widetilde{\mathbb{Q}}_1 \boxtimes \widetilde{\mathbb{Q}}_2\right)^\lambda$

$$= \left(\langle \sigma_{\widetilde{\mathbb{Q}}_1}(\tilde{x})\sigma_{\widetilde{\mathbb{Q}}_2}(\tilde{x}), \left\{ \left(\delta_{\widetilde{\mathbb{Q}}_1}(\tilde{x})\right)^{\frac{5}{4}} + \left(\delta_{\widetilde{\mathbb{Q}}_2}(\tilde{x})\right)^{\frac{5}{4}} - \left(\delta_{\widetilde{\mathbb{Q}}_1}(\tilde{x})\right)^{\frac{5}{4}}\left(\delta_{\widetilde{\mathbb{Q}}_2}(\tilde{x})\right)^{\frac{5}{4}} \right\}^{\frac{4}{5}} \rangle \right)^\lambda$$

$$= \langle \sigma_{\widetilde{\mathbb{Q}}_1}(\tilde{x})^\lambda \sigma_{\widetilde{\mathbb{Q}}_2}(\tilde{x})^\lambda, \left\{ 1 - \left(1 - \left(\left\{ \left(\delta_{\widetilde{\mathbb{Q}}_1}(\tilde{x})\right)^{\frac{5}{4}} + \left(\delta_{\widetilde{\mathbb{Q}}_2}(\tilde{x})\right)^{\frac{5}{4}} - \left(\delta_{\widetilde{\mathbb{Q}}_1}(\tilde{x})\right)^{\frac{5}{4}}\left(\delta_{\widetilde{\mathbb{Q}}_2}(\tilde{x})\right)^{\frac{5}{4}} \right\}^{\frac{5}{4}} \right)^{\frac{5}{4}} \right)^\lambda \right\}^{\frac{4}{5}} \rangle$$

$$= \langle \sigma_{\widetilde{\mathbb{Q}}_1}(\tilde{x})^\lambda \sigma_{\widetilde{\mathbb{Q}}_2}(\tilde{x})^\lambda, \left\{ 1 - \left(\left(1 - \left(\delta_{\widetilde{\mathbb{Q}}_1}(\tilde{x})\right)^{\frac{5}{4}}\right) - \left(\delta_{\widetilde{\mathbb{Q}}_2}(\tilde{x})\right)^{\frac{5}{4}}\left(1 - \left(\delta_{\widetilde{\mathbb{Q}}_1}(\tilde{x})\right)^{\frac{5}{4}}\right) \right)^\lambda \right\}^{\frac{4}{5}} \rangle$$

$$= \langle \sigma_{\widetilde{\mathbb{Q}}_1}(\tilde{x})^\lambda \sigma_{\widetilde{\mathbb{Q}}_2}(\tilde{x})^\lambda, \left\{ 1 - \left(\left(1 - \left(\delta_{\widetilde{\mathbb{Q}}_1}(\tilde{x})\right)^{\frac{5}{4}}\right)\left(1 - \left(\delta_{\widetilde{\mathbb{Q}}_2}(\tilde{x})\right)^{\frac{5}{4}}\right) \right)^\lambda \right\}^{\frac{4}{5}} \rangle$$

$$= \langle \sigma_{\widetilde{\mathbb{Q}}_1}(\tilde{x})^\lambda \sigma_{\widetilde{\mathbb{Q}}_2}(\tilde{x})^\lambda, \left\{ 1 - \left(1 - \left(\delta_{\widetilde{\mathbb{Q}}_1}(\tilde{x})\right)^{\frac{5}{4}}\right)^\lambda \left(1 - \left(\delta_{\widetilde{\mathbb{Q}}_2}(\tilde{x})\right)^{\frac{5}{4}}\right)^\lambda \right\}^{\frac{4}{5}} \rangle$$

Rajarajeswari *et al.,*

$$= \left\{ \langle \sigma_{\widetilde{\mathbb{Q}}_1}(\tilde{x})^\lambda, \left\{ 1 - \left(1 - \left(\delta_{\widetilde{\mathbb{Q}}_1}(\tilde{x}) \right)^{\frac{5}{4}} \right)^\lambda \right\}^{\frac{4}{5}} \rangle \boxtimes \langle \sigma_{\widetilde{\mathbb{Q}}_2}(\tilde{x})^\lambda, \left\{ 1 - \left(1 - \left(\delta_{\widetilde{\mathbb{Q}}_2}(\tilde{x}) \right)^{\frac{5}{4}} \right)^\lambda \right\}^{\frac{4}{5}} \rangle \right\}$$

$= \widetilde{\mathbb{Q}}_1^{\ \lambda} \boxtimes \widetilde{\mathbb{Q}}_2^{\ \lambda} =$ R.H.S

R.H.S $= \widetilde{\mathbb{Q}}^{\lambda_1} \boxtimes \widetilde{\mathbb{Q}}^{\lambda_2}$

$$= \left\{ \langle \sigma_{\widetilde{\mathbb{Q}}}(\tilde{x})^{\lambda_1}, \left\{ 1 - \left(1 - \left(\delta_{\widetilde{\mathbb{Q}}}(\tilde{x}) \right)^{\frac{5}{4}} \right)^{\lambda_1} \right\}^{\frac{4}{5}} \rangle \boxtimes \langle \sigma_{\widetilde{\mathbb{Q}}}(\tilde{x})^{\lambda_2}, \left\{ 1 - \left(1 - \left(\delta_{\widetilde{\mathbb{Q}}}(\tilde{x}) \right)^{\frac{5}{4}} \right)^{\lambda_2} \right\}^{\frac{4}{5}} \rangle \right\}$$

$$= \langle \sigma_{\widetilde{\mathbb{Q}}}(\tilde{x})^{\lambda_1} \sigma_{\widetilde{\mathbb{Q}}}(\tilde{x})^{\lambda_2}, \left\{ 1 - \left(1 - \left(\delta_{\widetilde{\mathbb{Q}}}(\tilde{x}) \right)^{\frac{5}{4}} \right)^{\lambda_1} \left(1 - \left(\delta_{\widetilde{\mathbb{Q}}}(\tilde{x}) \right)^{\frac{5}{4}} \right)^{\lambda_2} \right\}^{\frac{4}{5}} \rangle$$

$$= \langle \sigma_{\widetilde{\mathbb{Q}}}(\tilde{x})^{\lambda_1 + \lambda_2}, \left\{ 1 - \left(1 - \left(\delta_{\widetilde{\mathbb{Q}}}(\tilde{x}) \right)^{\frac{5}{4}} \right)^{\lambda_1 + \lambda_2} \right\}^{\frac{4}{5}} \rangle$$

$= \widetilde{\mathbb{Q}}^{(\lambda_1 + \lambda_2)} =$ L.H.S

Theorem 3.2

Let $\widetilde{\mathbb{Q}}_1 = \langle \sigma_{\widetilde{\mathbb{Q}}_1}(\tilde{x}), \delta_{\widetilde{\mathbb{Q}}_1}(\tilde{x}) \rangle$, $\widetilde{\mathbb{Q}}_2 = \langle \sigma_{\widetilde{\mathbb{Q}}_2}(\tilde{x}), \delta_{\widetilde{\mathbb{Q}}_2}(\tilde{x}) \rangle$ and $\widetilde{\mathbb{Q}}_3 = \langle \sigma_{\widetilde{\mathbb{Q}}_3}(\tilde{x}), \delta_{\widetilde{\mathbb{Q}}_3}(\tilde{x}) \rangle$ be three Quin – Terranean Fuzzy Numbers, then,

$$(\widetilde{\mathbb{Q}}_1 \cap \widetilde{\mathbb{Q}}_2) \boxplus \widetilde{\mathbb{Q}}_3 = (\widetilde{\mathbb{Q}}_1 \boxplus \widetilde{\mathbb{Q}}_3) \cap (\widetilde{\mathbb{Q}}_2 \boxplus \widetilde{\mathbb{Q}}_3)$$
$$(\widetilde{\mathbb{Q}}_1 \cup \widetilde{\mathbb{Q}}_2) \boxplus \widetilde{\mathbb{Q}}_3 = (\widetilde{\mathbb{Q}}_1 \boxplus \widetilde{\mathbb{Q}}_3) \cup (\widetilde{\mathbb{Q}}_2 \boxplus \widetilde{\mathbb{Q}}_3)$$
$$(\widetilde{\mathbb{Q}}_1 \cap \widetilde{\mathbb{Q}}_2) \boxtimes \widetilde{\mathbb{Q}}_3 = (\widetilde{\mathbb{Q}}_1 \boxtimes \widetilde{\mathbb{Q}}_3) \cap (\widetilde{\mathbb{Q}}_2 \boxtimes \widetilde{\mathbb{Q}}_3)$$
$$(\widetilde{\mathbb{Q}}_1 \cup \widetilde{\mathbb{Q}}_2) \boxtimes \widetilde{\mathbb{Q}}_3 = (\widetilde{\mathbb{Q}}_1 \boxtimes \widetilde{\mathbb{Q}}_3) \cup (\widetilde{\mathbb{Q}}_2 \boxtimes \widetilde{\mathbb{Q}}_3)$$

Proof:

For the three Quin – Terranean Fuzzy Numbers $\widetilde{\mathbb{Q}}_1 = \langle \sigma_{\widetilde{\mathbb{Q}}_1}(\tilde{x}), \delta_{\widetilde{\mathbb{Q}}_1}(\tilde{x}) \rangle$, $\widetilde{\mathbb{Q}}_2 = \langle \sigma_{\widetilde{\mathbb{Q}}_2}(\tilde{x}), \delta_{\widetilde{\mathbb{Q}}_2}(\tilde{x}) \rangle$ and $\widetilde{\mathbb{Q}}_3 = \langle \sigma_{\widetilde{\mathbb{Q}}_3}(\tilde{x}), \delta_{\widetilde{\mathbb{Q}}_3}(\tilde{x}) \rangle$, we get,

L.H.S $= (\widetilde{\mathbb{Q}}_1 \cap \widetilde{\mathbb{Q}}_2) \boxplus \widetilde{\mathbb{Q}}_3$

$= \langle min\{\sigma_{\widetilde{\mathbb{Q}}_1}(\tilde{x}), \sigma_{\widetilde{\mathbb{Q}}_2}(\tilde{x})\}, max\{\delta_{\widetilde{\mathbb{Q}}_1}(\tilde{x}), \delta_{\widetilde{\mathbb{Q}}_2}(\tilde{x})\} \rangle \boxplus \langle \sigma_{\widetilde{\mathbb{Q}}_3}(\tilde{x}), \delta_{\widetilde{\mathbb{Q}}_3}(\tilde{x}) \rangle = \langle \left\{ min\{\sigma_{\widetilde{\mathbb{Q}}_1}(\tilde{x})^{4^5}, \sigma_{\widetilde{\mathbb{Q}}_2(\tilde{x})}^{4^5}\} + \left(\sigma_{\widetilde{\mathbb{Q}}_3}(\tilde{x}) \right)^{4^5} - min\sigma\mathbb{Q}1(x)45, \sigma\mathbb{Q}2(x)45 \sigma\mathbb{Q}3(x)45145, max\delta\mathbb{Q}1(x), \delta\mathbb{Q}2(x)\delta\mathbb{Q}3(x) \right.$

$= \langle \left\{ \left(1 - (\sigma_{\widetilde{\mathbb{Q}}_3}(\tilde{x}))^{4^5} \right) min\{\sigma_{\widetilde{\mathbb{Q}}_1}(\tilde{x})^{4^5}, \sigma_{\widetilde{\mathbb{Q}}_2}(\tilde{x})^{4^5}\} + (\sigma_{\widetilde{\mathbb{Q}}_3}(\tilde{x}))^{4^5} \right\}^{\frac{1}{4^5}}, max\{\delta_{\widetilde{\mathbb{Q}}_1}(\tilde{x})\delta_{\widetilde{\mathbb{Q}}_3}(\tilde{x}), \delta_{\widetilde{\mathbb{Q}}_2}(\tilde{x})\delta_{\widetilde{\mathbb{Q}}_3}(\tilde{x})\} \rangle$

R.H.S $= (\widetilde{\mathbb{Q}}_1 \boxplus \widetilde{\mathbb{Q}}_3) \cap (\widetilde{\mathbb{Q}}_2 \boxplus \widetilde{\mathbb{Q}}_3)$

$= \langle \left\{ (\sigma_{\widetilde{\mathbb{Q}}_1}(\tilde{x}))^{4^5} + (\sigma_{\widetilde{\mathbb{Q}}_3}(\tilde{x}))^{4^5} - (\sigma_{\widetilde{\mathbb{Q}}_1}(\tilde{x}))^{4^5}(\sigma_{\widetilde{\mathbb{Q}}_3}(\tilde{x}))^{4^5} \right\}^{\frac{1}{4^5}}, \delta_{\widetilde{\mathbb{Q}}_1}(\tilde{x})\delta_{\widetilde{\mathbb{Q}}_3}(\tilde{x}) \rangle \cap$

$$\langle \left\{ (\sigma_{\widetilde{\mathbb{Q}}_2}(\tilde{x}))^{4^5} + (\sigma_{\widetilde{\mathbb{Q}}_3}(\tilde{x}))^{4^5} - (\sigma_{\widetilde{\mathbb{Q}}_2}(\tilde{x}))^{4^5}(\sigma_{\widetilde{\mathbb{Q}}_3}(\tilde{x}))^{4^5} \right\}^{\frac{1}{4^5}}, \delta_{\widetilde{\mathbb{Q}}_2}(\tilde{x})\delta_{\widetilde{\mathbb{Q}}_3}(\tilde{x}) \rangle$$

$$= \langle min \left\{ \left\{ (\sigma_{\widetilde{\mathbb{Q}}_1}(\tilde{x}))^{4^5} + (\sigma_{\widetilde{\mathbb{Q}}_3}(\tilde{x}))^{4^5} - (\sigma_{\widetilde{\mathbb{Q}}_1}(\tilde{x}))^{4^5}(\sigma_{\widetilde{\mathbb{Q}}_3}(\tilde{x}))^{4^5} \right\}^{\frac{1}{4^5}}, \left\{ (\sigma_{\widetilde{\mathbb{Q}}_2}(\tilde{x}))^{4^5} + (\sigma_{\widetilde{\mathbb{Q}}_3}(\tilde{x}))^{4^5} \right. \right.$$

$$\left. \left. - (\sigma_{\widetilde{\mathbb{Q}}_2}(\tilde{x}))^{4^5}(\sigma_{\widetilde{\mathbb{Q}}_3}(\tilde{x}))^{4^5} \right\}^{\frac{1}{4^5}} \right\}, max\{\delta_{\widetilde{\mathbb{Q}}_1}(\tilde{x})\delta_{\widetilde{\mathbb{Q}}_3}(\tilde{x}), \delta_{\widetilde{\mathbb{Q}}_2}(\tilde{x})\delta_{\widetilde{\mathbb{Q}}_3}(\tilde{x})\} \rangle$$

$$= \langle min \left\{ \left\{ \left(1 - (\sigma_{\widetilde{\mathbb{Q}}_3}(\tilde{x}))^{4^5} \right) (\sigma_{\widetilde{\mathbb{Q}}_1}(\tilde{x}))^{4^5} + (\sigma_{\widetilde{\mathbb{Q}}_3}(\tilde{x}))^{4^5} \right\}^{\frac{1}{4^5}}, \left\{ \left(1 - (\sigma_{\widetilde{\mathbb{Q}}_3}(\tilde{x}))^{4^5} \right) (\sigma_{\widetilde{\mathbb{Q}}_2}(\tilde{x}))^{4^5} \right. \right.$$

$$\left. \left. + (\sigma_{\widetilde{\mathbb{Q}}_3}(\tilde{x}))^{4^5} \right\}^{\frac{1}{4^5}} \right\}, max\{\delta_{\widetilde{\mathbb{Q}}_1}(\tilde{x})\delta_{\widetilde{\mathbb{Q}}_3}(\tilde{x}), \delta_{\widetilde{\mathbb{Q}}_2}(\tilde{x})\delta_{\widetilde{\mathbb{Q}}_3}(\tilde{x})\} \rangle$$

$= \langle \left\{ \left(1 - (\sigma_{\widetilde{\mathbb{Q}}_3}(\tilde{x}))^{4^5} \right) min\{\sigma_{\widetilde{\mathbb{Q}}_1}(\tilde{x})^{4^5}, \sigma_{\widetilde{\mathbb{Q}}_2}(\tilde{x})^{4^5}\} + (\sigma_{\widetilde{\mathbb{Q}}_3}(\tilde{x}))^{4^5} \right\}^{\frac{1}{4^5}}, max\{\delta_{\widetilde{\mathbb{Q}}_1}(\tilde{x})\delta_{\widetilde{\mathbb{Q}}_3}(\tilde{x}), \delta_{\widetilde{\mathbb{Q}}_2}(\tilde{x})\delta_{\widetilde{\mathbb{Q}}_3}(\tilde{x})\} \rangle =$ L.H.S.

63250

Rajarajeswari *et al.,*

$\therefore, (\widetilde{\mathbb{Q}}_1 \cap \widetilde{\mathbb{Q}}_2) \boxplus \widetilde{\mathbb{Q}}_3 = (\widetilde{\mathbb{Q}}_1 \boxplus \widetilde{\mathbb{Q}}_3) \cap (\widetilde{\mathbb{Q}}_2 \boxplus \widetilde{\mathbb{Q}}_3).$

Hence, (i) proved.

L.H.S = $(\widetilde{\mathbb{Q}}_1 \cup \widetilde{\mathbb{Q}}_2) \boxplus \widetilde{\mathbb{Q}}_3$

$= \langle max\{\sigma_{\widetilde{\mathbb{Q}}_1}(\tilde{x}), \sigma_{\widetilde{\mathbb{Q}}_2}(\tilde{x})\}, min\{\delta_{\widetilde{\mathbb{Q}}_1}(\tilde{x}), \delta_{\widetilde{\mathbb{Q}}_2}(\tilde{x})\}\rangle \boxplus \langle \sigma_{\widetilde{\mathbb{Q}}_3}(\tilde{x}), \delta_{\widetilde{\mathbb{Q}}_3}(\tilde{x})\rangle$

$= \langle \{max\{\sigma_{\widetilde{\mathbb{Q}}_1}(\tilde{x})^{4^5}, \sigma_{\widetilde{\mathbb{Q}}_2}(\tilde{x})^{4^5}\} + (\sigma_{\widetilde{\mathbb{Q}}_3}(\tilde{x}))^{4^5} - max\{\sigma_{\widetilde{\mathbb{Q}}_1}(\tilde{x})^{4^5}, \sigma_{\widetilde{\mathbb{Q}}_2}(\tilde{x})^{4^5}\}(\sigma_{\widetilde{\mathbb{Q}}_3}(\tilde{x}))^{4^5}\}^{\frac{1}{4^5}}, min\{\delta_{\widetilde{\mathbb{Q}}_1}(\tilde{x}), \delta_{\widetilde{\mathbb{Q}}_2}(\tilde{x})\}\delta_{\widetilde{\mathbb{Q}}_3}(\tilde{x})\rangle$

$= \langle \{\left(1 - (\sigma_{\widetilde{\mathbb{Q}}_3}(\tilde{x}))^{4^5}\right) max\{\sigma_{\widetilde{\mathbb{Q}}_1}(\tilde{x})^{4^5}, \sigma_{\widetilde{\mathbb{Q}}_2}(\tilde{x})^{4^5}\} + (\sigma_{\widetilde{\mathbb{Q}}_3}(\tilde{x}))^{4^5}\}^{\frac{1}{4^5}}, min\{\delta_{\widetilde{\mathbb{Q}}_1}(\tilde{x})\delta_{\widetilde{\mathbb{Q}}_3}(\tilde{x}), \delta_{\widetilde{\mathbb{Q}}_2}(\tilde{x})\delta_{\widetilde{\mathbb{Q}}_3}(\tilde{x})\}\rangle$

R.H.S = $(\widetilde{\mathbb{Q}}_1 \boxplus \widetilde{\mathbb{Q}}_3) \cup (\widetilde{\mathbb{Q}}_2 \boxplus \widetilde{\mathbb{Q}}_3)$

$= \langle \{\left(\sigma_{\widetilde{\mathbb{Q}}_1}(\tilde{x})\right)^{4^5} + \left(\sigma_{\widetilde{\mathbb{Q}}_3}(\tilde{x})\right)^{4^5} - \left(\sigma_{\widetilde{\mathbb{Q}}_1}(\tilde{x})\right)^{4^5}\left(\sigma_{\widetilde{\mathbb{Q}}_3}(\tilde{x})\right)^{4^5}\}^{\frac{1}{4^5}}, \delta_{\widetilde{\mathbb{Q}}_1}(\tilde{x})\delta_{\widetilde{\mathbb{Q}}_3}(\tilde{x})\rangle \cup$

$\langle \{\left(\sigma_{\widetilde{\mathbb{Q}}_1}(\tilde{x})\right)^{4^5} + \left(\sigma_{\widetilde{\mathbb{Q}}_3}(\tilde{x})\right)^{4^5} - \left(\sigma_{\widetilde{\mathbb{Q}}_1}(\tilde{x})\right)^{4^5}\left(\sigma_{\widetilde{\mathbb{Q}}_3}(\tilde{x})\right)^{4^5}\}^{\frac{1}{4^5}}, \delta_{\widetilde{\mathbb{Q}}_1}(\tilde{x})\delta_{\widetilde{\mathbb{Q}}_3}(\tilde{x})\rangle$

$= \langle max\{\{\left(\sigma_{\widetilde{\mathbb{Q}}_1}(\tilde{x})\right)^{4^5} + \left(\sigma_{\widetilde{\mathbb{Q}}_3}(\tilde{x})\right)^{4^5} - \left(\sigma_{\widetilde{\mathbb{Q}}_1}(\tilde{x})\right)^{4^5}\left(\sigma_{\widetilde{\mathbb{Q}}_3}(\tilde{x})\right)^{4^5}\}^{\frac{1}{4^5}}, \{\left(\sigma_{\widetilde{\mathbb{Q}}_2}(\tilde{x})\right)^{4^5} + \left(\sigma_{\widetilde{\mathbb{Q}}_3}(\tilde{x})\right)^{4^5}$

$- \left(\sigma_{\widetilde{\mathbb{Q}}_2}(\tilde{x})\right)^{4^5}\left(\sigma_{\widetilde{\mathbb{Q}}_3}(\tilde{x})\right)^{4^5}\}^{\frac{1}{4^5}}\}, min\{\delta_{\widetilde{\mathbb{Q}}_1}(\tilde{x})\delta_{\widetilde{\mathbb{Q}}_3}(\tilde{x}), \delta_{\widetilde{\mathbb{Q}}_2}(\tilde{x})\delta_{\widetilde{\mathbb{Q}}_3}(\tilde{x})\}\rangle$

$= \langle max\{\{\left(1 - (\sigma_{\widetilde{\mathbb{Q}}_3}(\tilde{x}))^{4^5}\right)\left(\sigma_{\widetilde{\mathbb{Q}}_1}(\tilde{x})\right)^{4^5} + \left(\sigma_{\widetilde{\mathbb{Q}}_3}(\tilde{x})\right)^{4^5}\}^{\frac{1}{4^5}}, \{\left(1 - (\sigma_{\widetilde{\mathbb{Q}}_3}(\tilde{x}))^{4^5}\right)\left(\sigma_{\widetilde{\mathbb{Q}}_2}(\tilde{x})\right)^{4^5}$

$+ \left(\sigma_{\widetilde{\mathbb{Q}}_3}(\tilde{x})\right)^{4^5}\}^{\frac{1}{4^5}}\}, min\{\delta_{\widetilde{\mathbb{Q}}_1}(\tilde{x})\delta_{\widetilde{\mathbb{Q}}_3}(\tilde{x}), \delta_{\widetilde{\mathbb{Q}}_2}(\tilde{x})\delta_{\widetilde{\mathbb{Q}}_3}(\tilde{x})\}\rangle$

$= \langle \{\left(1 - (\sigma_{\widetilde{\mathbb{Q}}_3}(\tilde{x}))^{4^5}\right) max\{\sigma_{\widetilde{\mathbb{Q}}_1}(\tilde{x})^{4^5}, \sigma_{\widetilde{\mathbb{Q}}_2}(\tilde{x})^{4^5}\} + (\sigma_{\widetilde{\mathbb{Q}}_3}(\tilde{x}))^{4^5}\}^{\frac{1}{4^5}}, min\{\delta_{\widetilde{\mathbb{Q}}_1}(\tilde{x})\delta_{\widetilde{\mathbb{Q}}_3}(\tilde{x}), \delta_{\widetilde{\mathbb{Q}}_2}(\tilde{x})\delta_{\widetilde{\mathbb{Q}}_3}(\tilde{x})\}\rangle$ = L.H.S.

$\therefore, (\widetilde{\mathbb{Q}}_1 \cup \widetilde{\mathbb{Q}}_2) \boxplus \widetilde{\mathbb{Q}}_3 = (\widetilde{\mathbb{Q}}_1 \boxplus \widetilde{\mathbb{Q}}_3) \cup (\widetilde{\mathbb{Q}}_2 \boxplus \widetilde{\mathbb{Q}}_3).$

Hence, (ii) proved.

L.H.S = $(\widetilde{\mathbb{Q}}_1 \cap \widetilde{\mathbb{Q}}_2) \boxtimes \widetilde{\mathbb{Q}}_3$

$= \langle min\{\sigma_{\widetilde{\mathbb{Q}}_1}(\tilde{x}), \sigma_{\widetilde{\mathbb{Q}}_2}(\tilde{x})\}, max\{\delta_{\widetilde{\mathbb{Q}}_1}(\tilde{x}), \delta_{\widetilde{\mathbb{Q}}_2}(\tilde{x})\}\rangle \boxplus \langle \sigma_{\widetilde{\mathbb{Q}}_3}(\tilde{x}), \delta_{\widetilde{\mathbb{Q}}_3}(\tilde{x})\rangle$

$= \langle min\{\sigma_{\widetilde{\mathbb{Q}}_1}(\tilde{x}), \sigma_{\widetilde{\mathbb{Q}}_2}(\tilde{x})\}\sigma_{\widetilde{\mathbb{Q}}_3}, \{max\{\delta_{\widetilde{\mathbb{Q}}_1}(\tilde{x})^{\frac{5}{4}}, \delta_{\widetilde{\mathbb{Q}}_2}(\tilde{x})^{\frac{5}{4}}\} + (\delta_{\widetilde{\mathbb{Q}}_3}(\tilde{x}))^{\frac{5}{4}} - max\{\delta_{\widetilde{\mathbb{Q}}_1}(\tilde{x})^{\frac{5}{4}}, \delta_{\widetilde{\mathbb{Q}}_2}(\tilde{x})^{\frac{5}{4}}\}(\delta_{\widetilde{\mathbb{Q}}_3}(\tilde{x}))^{\frac{5}{4}}\}^{\frac{4}{5}}\rangle$

$= \langle min\{\sigma_{\widetilde{\mathbb{Q}}_1}(\tilde{x})\sigma_{\widetilde{\mathbb{Q}}_3}(\tilde{x}), \sigma_{\widetilde{\mathbb{Q}}_2}(\tilde{x})\sigma_{\widetilde{\mathbb{Q}}_3}(\tilde{x})\}, \{\left(1 - (\delta_{\widetilde{\mathbb{Q}}_3}(\tilde{x}))^{\frac{5}{4}}\right) max\{\delta_{\widetilde{\mathbb{Q}}_1}(\tilde{x})^{\frac{5}{4}}, \delta_{\widetilde{\mathbb{Q}}_2}(\tilde{x})^{\frac{5}{4}}\} + (\delta_{\widetilde{\mathbb{Q}}_3}(\tilde{x}))^{\frac{5}{4}}\}^{\frac{4}{5}}\rangle$

R.H.S = $(\widetilde{\mathbb{Q}}_1 \boxtimes \widetilde{\mathbb{Q}}_3) \cap (\widetilde{\mathbb{Q}}_2 \boxtimes \widetilde{\mathbb{Q}}_3)$

$= \langle \sigma_{\widetilde{\mathbb{Q}}_1}(\tilde{x})\sigma_{\widetilde{\mathbb{Q}}_3}(\tilde{x}), \{(\delta_{\widetilde{\mathbb{Q}}_1}(\tilde{x}))^{\frac{5}{4}} + (\delta_{\widetilde{\mathbb{Q}}_3}(\tilde{x}))^{\frac{5}{4}} - (\delta_{\widetilde{\mathbb{Q}}_1}(\tilde{x}))^{\frac{5}{4}}(\delta_{\widetilde{\mathbb{Q}}_3}(\tilde{x}))^{\frac{5}{4}}\}^{\frac{4}{5}}\rangle \cap$

$\langle \sigma_{\widetilde{\mathbb{Q}}_2}(\tilde{x})\sigma_{\widetilde{\mathbb{Q}}_3}(\tilde{x}), \{(\delta_{\widetilde{\mathbb{Q}}_2}(\tilde{x}))^{\frac{5}{4}} + (\delta_{\widetilde{\mathbb{Q}}_3}(\tilde{x}))^{\frac{5}{4}} - (\delta_{\widetilde{\mathbb{Q}}_2}(\tilde{x}))^{\frac{5}{4}}(\delta_{\widetilde{\mathbb{Q}}_3}(\tilde{x}))^{\frac{5}{4}}\}^{\frac{4}{5}}\rangle$

$= \langle min\{\sigma_{\widetilde{\mathbb{Q}}_1}(\tilde{x})\sigma_{\widetilde{\mathbb{Q}}_3}(\tilde{x}), \sigma_{\widetilde{\mathbb{Q}}_2}(\tilde{x})\sigma_{\widetilde{\mathbb{Q}}_3}(\tilde{x})\}, max\{\{(\delta_{\widetilde{\mathbb{Q}}_1}(\tilde{x}))^{\frac{5}{4}} + (\delta_{\widetilde{\mathbb{Q}}_3}(\tilde{x}))^{\frac{5}{4}} - (\delta_{\widetilde{\mathbb{Q}}_1}(\tilde{x}))^{\frac{5}{4}}(\delta_{\widetilde{\mathbb{Q}}_3}(\tilde{x}))^{\frac{5}{4}}\}^{\frac{4}{5}}, \{(\delta_{\widetilde{\mathbb{Q}}_2}(\tilde{x}))^{\frac{5}{4}} + (\delta_{\widetilde{\mathbb{Q}}_3}(\tilde{x}))^{\frac{5}{4}}$

$- (\delta_{\widetilde{\mathbb{Q}}_2}(\tilde{x}))^{\frac{5}{4}}(\delta_{\widetilde{\mathbb{Q}}_3}(\tilde{x}))^{\frac{5}{4}}\}^{\frac{4}{5}}\}\rangle$

$$= \langle min\{\sigma_{\widetilde{\mathbb{Q}}_1}(\tilde{x})\sigma_{\widetilde{\mathbb{Q}}_3}(\tilde{x}), \sigma_{\widetilde{\mathbb{Q}}_2}(\tilde{x})\sigma_{\widetilde{\mathbb{Q}}_3}(\tilde{x})\}, max\left\{\left\{\left(1-(\delta_{\widetilde{\mathbb{Q}}_3}(\tilde{x}))^{\frac{5}{4}}\right)(\delta_{\widetilde{\mathbb{Q}}_1}(\tilde{x}))^{\frac{5}{4}} + (\delta_{\widetilde{\mathbb{Q}}_3}(\tilde{x}))^{\frac{5}{4}}\right\}^{\frac{4}{5}}, \left\{\left(1-(\delta_{\widetilde{\mathbb{Q}}_3}(\tilde{x}))^{\frac{5}{4}}\right)(\delta_{\widetilde{\mathbb{Q}}_2}(\tilde{x}))^{\frac{5}{4}} + \right.\right.$$

$$\left.\left.(\delta_{\widetilde{\mathbb{Q}}_3}(\tilde{x}))^{\frac{5}{4}}\right\}^{\frac{4}{5}}\right\}\rangle$$

$$= \langle min\{\sigma_{\widetilde{\mathbb{Q}}_1}(\tilde{x})\sigma_{\widetilde{\mathbb{Q}}_3}(\tilde{x}), \sigma_{\widetilde{\mathbb{Q}}_2}(\tilde{x})\sigma_{\widetilde{\mathbb{Q}}_3}(\tilde{x})\}, \left\{\left(1-(\delta_{\widetilde{\mathbb{Q}}_3}(\tilde{x}))^{\frac{5}{4}}\right)max\left\{\delta_{\widetilde{\mathbb{Q}}_1}(\tilde{x})^{\frac{5}{4}}, \delta_{\widetilde{\mathbb{Q}}_2}(\tilde{x})^{\frac{5}{4}}\right\} + (\delta_{\widetilde{\mathbb{Q}}_3}(\tilde{x}))^{\frac{5}{4}}\right\}^{\frac{4}{5}}\rangle = \text{L.H.S.}$$

Hence, $(\widetilde{\mathbb{Q}}_1 \cap \widetilde{\mathbb{Q}}_2) \boxtimes \widetilde{\mathbb{Q}}_3 = (\widetilde{\mathbb{Q}}_1 \boxtimes \widetilde{\mathbb{Q}}_3) \cap (\widetilde{\mathbb{Q}}_2 \boxtimes \widetilde{\mathbb{Q}}_3).$

L.H.S $= (\widetilde{\mathbb{Q}}_1 \cup \widetilde{\mathbb{Q}}_2) \boxtimes \widetilde{\mathbb{Q}}_3$
$= \langle max\{\sigma_{\widetilde{\mathbb{Q}}_1}(\tilde{x}), \sigma_{\widetilde{\mathbb{Q}}_2}(\tilde{x})\}, min\{\delta_{\widetilde{\mathbb{Q}}_1}(\tilde{x}), \delta_{\widetilde{\mathbb{Q}}_2}(\tilde{x})\}\rangle \boxplus \langle \sigma_{\widetilde{\mathbb{Q}}_3}(\tilde{x}), \delta_{\widetilde{\mathbb{Q}}_3}(\tilde{x})\rangle$

$$= \langle max\{\sigma_{\widetilde{\mathbb{Q}}_1}(\tilde{x}), \sigma_{\widetilde{\mathbb{Q}}_2}(\tilde{x})\}\sigma_{\widetilde{\mathbb{Q}}_3}(\tilde{x}), \left\{min\left\{\delta_{\widetilde{\mathbb{Q}}_1}(\tilde{x})^{\frac{5}{4}}, \delta_{\widetilde{\mathbb{Q}}_2}(\tilde{x})^{\frac{5}{4}}\right\} + (\delta_{\widetilde{\mathbb{Q}}_3}(\tilde{x}))^{\frac{5}{4}} - min\left\{\delta_{\widetilde{\mathbb{Q}}_1}(\tilde{x})^{\frac{5}{4}}, \delta_{\widetilde{\mathbb{Q}}_2}(\tilde{x})^{\frac{5}{4}}\right\}(\delta_{\widetilde{\mathbb{Q}}_3}(\tilde{x}))^{\frac{5}{4}}\right\}^{\frac{4}{5}}\rangle$$

$$= \langle max\{\sigma_{\widetilde{\mathbb{Q}}_1}(\tilde{x})\sigma_{\widetilde{\mathbb{Q}}_3}(\tilde{x}), \sigma_{\widetilde{\mathbb{Q}}_2}(\tilde{x})\sigma_{\widetilde{\mathbb{Q}}_3}(\tilde{x})\}, \left\{\left(1-(\delta_{\widetilde{\mathbb{Q}}_3}(\tilde{x}))^{\frac{5}{4}}\right)min\left\{\delta_{\widetilde{\mathbb{Q}}_1}(\tilde{x})^{\frac{5}{4}}, \delta_{\widetilde{\mathbb{Q}}_2}(\tilde{x})^{\frac{5}{4}}\right\} + (\delta_{\widetilde{\mathbb{Q}}_3}(\tilde{x}))^{\frac{5}{4}}\right\}^{\frac{4}{5}}\rangle$$

R.H.S $= (\widetilde{\mathbb{Q}}_1 \boxtimes \widetilde{\mathbb{Q}}_3) \cup (\widetilde{\mathbb{Q}}_2 \boxtimes \widetilde{\mathbb{Q}}_3)$

$$= \langle \sigma_{\widetilde{\mathbb{Q}}_1}(\tilde{x})\sigma_{\widetilde{\mathbb{Q}}_3}(\tilde{x}), \left\{(\delta_{\widetilde{\mathbb{Q}}_1}(\tilde{x}))^{\frac{5}{4}} + (\delta_{\widetilde{\mathbb{Q}}_3}(\tilde{x}))^{\frac{5}{4}} - (\delta_{\widetilde{\mathbb{Q}}_1}(\tilde{x}))^{\frac{5}{4}}(\delta_{\widetilde{\mathbb{Q}}_3}(\tilde{x}))^{\frac{5}{4}}\right\}^{\frac{4}{5}}\rangle \cap \langle \sigma_{\widetilde{\mathbb{Q}}_2}(\tilde{x})\sigma_{\widetilde{\mathbb{Q}}_3}(\tilde{x}), \left\{(\delta_{\widetilde{\mathbb{Q}}_2}(\tilde{x}))^{\frac{5}{4}} + (\delta_{\widetilde{\mathbb{Q}}_3}(\tilde{x}))^{\frac{5}{4}} - \right.$$

$\delta\mathbb{Q}2(x)54\delta\mathbb{Q}3(x)5445$

$$= \langle max\{\sigma_{\widetilde{\mathbb{Q}}_1}(\tilde{x})\sigma_{\widetilde{\mathbb{Q}}_3}(\tilde{x}), \sigma_{\widetilde{\mathbb{Q}}_2}(\tilde{x})\sigma_{\widetilde{\mathbb{Q}}_3}(\tilde{x})\}, min\left\{\left\{(\delta_{\widetilde{\mathbb{Q}}_1}(\tilde{x}))^{\frac{5}{4}} + (\delta_{\widetilde{\mathbb{Q}}_3}(\tilde{x}))^{\frac{5}{4}} - (\delta_{\widetilde{\mathbb{Q}}_1}(\tilde{x}))^{\frac{5}{4}}(\delta_{\widetilde{\mathbb{Q}}_3}(\tilde{x}))^{\frac{5}{4}}\right\}^{\frac{4}{5}}, \left\{(\delta_{\widetilde{\mathbb{Q}}_2}(\tilde{x}))^{\frac{5}{4}} + (\delta_{\widetilde{\mathbb{Q}}_3}(\tilde{x}))^{\frac{5}{4}}\right.\right.$$

$$\left.\left. - (\delta_{\widetilde{\mathbb{Q}}_2}(\tilde{x}))^{\frac{5}{4}}(\delta_{\widetilde{\mathbb{Q}}_3}(\tilde{x}))^{\frac{5}{4}}\right\}^{\frac{4}{5}}\right\}\rangle$$

$$= \langle max\{\sigma_{\widetilde{\mathbb{Q}}_1}(\tilde{x})\sigma_{\widetilde{\mathbb{Q}}_3}(\tilde{x}), \sigma_{\widetilde{\mathbb{Q}}_2}(\tilde{x})\sigma_{\widetilde{\mathbb{Q}}_3}(\tilde{x})\}, min\left\{\left\{\left(1-(\delta_{\widetilde{\mathbb{Q}}_3}(\tilde{x}))^{\frac{5}{4}}\right)(\delta_{\widetilde{\mathbb{Q}}_1}(\tilde{x}))^{\frac{5}{4}} + (\delta_{\widetilde{\mathbb{Q}}_3}(\tilde{x}))^{\frac{5}{4}}\right\}^{\frac{4}{5}}, \left\{\left(1-(\delta_{\widetilde{\mathbb{Q}}_3}(\tilde{x}))^{\frac{5}{4}}\right)(\delta_{\widetilde{\mathbb{Q}}_2}(\tilde{x}))^{\frac{5}{4}}\right.\right.$$

$$\left.\left. + (\delta_{\widetilde{\mathbb{Q}}_3}(\tilde{x}))^{\frac{5}{4}}\right\}^{\frac{4}{5}}\right\}\rangle$$

$$= \langle max\{\sigma_{\widetilde{\mathbb{Q}}_1}(\tilde{x})\sigma_{\widetilde{\mathbb{Q}}_3}(\tilde{x}), \sigma_{\widetilde{\mathbb{Q}}_2}(\tilde{x})\sigma_{\widetilde{\mathbb{Q}}_3}(\tilde{x})\}, \left\{\left(1-(\delta_{\widetilde{\mathbb{Q}}_3}(\tilde{x}))^{\frac{5}{4}}\right)min\left\{\delta_{\widetilde{\mathbb{Q}}_1}(\tilde{x})^{\frac{5}{4}}, \delta_{\widetilde{\mathbb{Q}}_2}(\tilde{x})^{\frac{5}{4}}\right\} + (\delta_{\widetilde{\mathbb{Q}}_3}(\tilde{x}))^{\frac{5}{4}}\right\}^{\frac{4}{5}}\rangle = \text{L.H.S.}$$

Hence, $(\widetilde{\mathbb{Q}}_1 \cup \widetilde{\mathbb{Q}}_2) \boxtimes \widetilde{\mathbb{Q}}_3 = (\widetilde{\mathbb{Q}}_1 \boxtimes \widetilde{\mathbb{Q}}_3) \cup (\widetilde{\mathbb{Q}}_2 \boxtimes \widetilde{\mathbb{Q}}_3).$

CONCLUSION

In this paper, we defined the algebraic operations addition, multiplication, scalar multiplication, and exponentiation on Quin-Terranean Fuzzy numbers. We have investigated certain Quin-Terranean Fuzzy number properties based on these operations. We have proven that the model operators satisfy the distributive and commutative properties. We note that the distributive property is also satisfied by these model operators as well as in combination with the basic operations of union and intersection on Quin-Terranean Fuzzy numbers. In future, Quin-Terranean Fuzzy Numbers may be used for other operations and their properties may be researched. Additionally, these algebraic operations on Quin-Terranean Fuzzy Numbers have applications in a various fields including decision-making, agriculture, and healthcare, etc.

Rajarajeswari *et al.,*

REFERENCES

1. Krassimir T. Atanassov. Intuitionistic Fuzzy Sets, Fuzzy Sets and Systems; 1986; 20(1):87-96.
2. Jae Deuk Myung. Algebraic operations on Fuzzy Numbers using of Linear Functions, Kangweon – Kyungki Math. Jour; 2003; 11(1):1-7.
3. Rajarajeswari P, Thirunamakkani T. Application of Quin-Terranean Fuzzy Set in Transportation Problem under Fuzzy Environment, Journal of Asiatic Society of Mumbai; 2023; XCVI(12):171-181.
4. Quin – Terranean Fuzzy set. Bulletin of Calcutta Mathematical Society. *Accepted.*
5. Sankar Prasad Mondal and Tapan Kumar Roy. Non-Linear arithmetic operation on generalized triangular Intuitionistic fuzzy numbers, Notes on Intuitionistic Fuzzy Sets; 2014; 20(1):9-19.
6. Shan – Huo Chen. Operations of fuzzy numbers with step form membership function using function principle, Journal of Information Sciences; 1998; 108:149 – 155.
7. Shu-Ping Wan, Zhen Jin, Jiu-Ying Dong. A new order relation for Pythagorean fuzzy numbers and application to multi-attribute group decision making, Knowledge and Information Systems; 2020; 62:751-785.
8. Tapan Senapati, Ronald R. Yager. Fermatean fuzzy sets, Journal of Ambient Intelligence and Humanized Computing; 2019; 11(2):663-674.
9. Tapan Senapati, Ronald R. Yager. Some New Operations Over Fermatean Fuzzy Numbers and Application of Fermatean fuzzy WPM in Multi Criteria Decision Making, Informatica; 2019; 30(2):391-412.
10. Witold Kosinski, Piotr Prokopowicz and Dominik Slezak. On Algebraic Operations on Fuzzy Numbers, Intelligent Information Processing and Web Mining; 2003; 22:353-362.
11. Yager R R. Pythagorean membership Grades in Multi criteria Decision Making, in IEEE Transaction on Fuzzy Systems; 2014; 22(4):958-965.
12. Zadeh L A. Fuzzy Sets, Information and Control; 1965; 8:338-353.

RESEARCH ARTICLE

Energy Level Connectedness on Fuzzy Graphs

R.Buvaneswari[1] and K.Senbaga Priya[2]*

[1]Assistant Professor, Department of Mathematics, Sri Krishna Arts and Science College, Coimbatore, Tamil Nadu, India-614008.

[2]Research Scholar, Department of Mathematics, Sri Krishna Arts and Science College, Coimbatore, Tamil Nadu, India-641008.

*Address for Correspondence
K. Senbaga Priya,
Research Scholar,
Department of Mathematics,
Sri Krishna Arts and Science College,
Coimbatore, Tamil Nadu, India -641008.
E. Mail: ksenbagapriya@gmail.com

ABSTRACT

The connectedness energy $CL(\hat{G})$ of laplacian matrix H is defined to improve the bounds on connectedness energy on $\hat{G}$ in terms of vertex membership, edge membership and the connectedness strength between v_i and v_j . Also, κ and κ ' on $\hat{G}$ are compared to connectivity spectral bounds enhancing the application in communication networks.

Keywords: Laplacian eigenvalue, Second largest eigenvalue, Algebraic connectivity, Spectral radii, fuzzy connectivity of vertex and edge *(κ, κ ')*, connectivity bounds.

INTRODUCTION

Theory of spectral graphs holds significance among various aspects of algebraic graph theory as it aids in deriving the characteristics that define a graph's structure based on its graph spectrum. The concept of the Spectrum of a graph was originally introduced by Collatz and Sinogowitz in 1957. Fiedler's work demonstrated that 0 serves as the unique eigenvalue of the Laplacian matrix $L(G)$ if and only if graph G is connected. This discovery led to the introduction of the term "algebraic connectivity", denoting the eigenvalue μ_{n-1} of the Laplacian matrix. Lecture on spectral graph theory by Jiaqi Jiang focussed on the connection between the eigen values of the laplacian matrix and graph connectivity. To determine the connectivity of a graph becomes the most difficult task when dealing with applications. The property of eigen vectors of non-negative symmetric matrices by Fiedler (1975) provoked the researchers in analysing the spectral properties and robustness in complex networks. In 2010, S.M.Cioaba gave improvements on the eigenvalues of regular graphs and described their edge-connectivity. The Connectivity determining the spectral bounds of regular graphs with given order is explained briefly in [1]. λ_2 and μ_{n-1} measures

63254

Buvaneswari and Senbaga Priya

the connectivity as defined by Fiedler in [1]. Later in 2019, results involving μ_{n-1} and λ_2 are characterized in [2] defining the vertex connectivity.

Graphs encounter limitations in accurately representing problems involving uncertain measures. The introduction of fuzzy set theory, following Zadeh's pioneering work in 1965, emerged as a means to address uncertainty through the concept of fuzzy subsets. Building upon Zadeh's fuzzy relations applied to fuzzy graphs, Kaufmann and Rosenfeld developed concepts related to bridges, paths, cycles, trees, and connectedness in their work [3]. The groundwork laid by Yeh and Bang in terms of connectivity parameters paved the way for Mathew and Sunitha [4] to categorize edges within various fuzzy graphs. This classification involved identifying α-strong, β-strong and δ-weak edges based on the degree of connectedness, thereby establishing notions of fuzzy connectivity of vertex and edge [5]. In this paper, the connectedness energy $CL(\hat{G})$ of Laplacian matrix H to improve the bounds on connectedness energy on $\hat{G}$ is defined to apply the parameters in network in a 'strong' sense. Also, κ and κ ' on fuzzy graphs $\hat{G}$ are compared to connectivity spectral bounds enhancing the application in communication networks as the connectivity bounds are more stronger.

Preliminaries
Definition 2.1
A graph G = (σ, μ) is categorized as a fuzzy graph with n vertices and m edges, where $\hat{G}$: σ(u, v) ≤ σ(u) ∧ σ(v) for all u, v ∈ J. The adjacency matrix ($\hat{A}$) of any undirected fuzzy graph $\hat{G}$ possesses n real eigenvalues, denoted as $\hat{\lambda}_i$: $\hat{\lambda}_1 \geq \hat{\lambda}_2 \geq ,.., \geq \hat{\lambda}_n$ of $\hat{A}$. These eigenvalues, along with their multiplicities, form the fuzzy spectrum of $\hat{G}$. The laplacian matrix L(G) = D(G)- A(G) has eigen values that are represented by $0 = \hat{\mu}_1 \geq \hat{\mu}_2 \geq \cdots \geq \hat{\mu}_n$. A square matrix of size p × p for $\hat{G}$ constitutes the degree matrix D($\hat{G}$) = [d$_{ij}$], where $d_{ij} = d_{\mathcal{G}(v_i)}$ when $i = j$, and is zero otherwise.

Definition 2.2
A discontinuity in the fuzzy graph refers to the vertex D subtracting them results in an unruncated graph or a one-line graph. The vertex connectivity of a fuzzy graph G, denoted as $\kappa(G)$, is the minimum weight of the disconnection within G. The edge connectivity of G, denoted as κ '(G), is defined as the minimum weight among cut-sets in G. The strong degree of a node $v \in \sigma^*$ is the sum of membership values of all strong arcs incident to v, denoted as d$_s$(v). The minimum and maximum strong degree is denoted as δ$_s$(G) and Δ$_s$(G) respectively.

Definition 2.3
The matrix C representing the connectedness strength of is characterized by C = [c$_{ij}$] where,
$$c_{ij} = \begin{cases} \mu^\infty(\mu_{ij}) & whenever\ i \neq j \\ 0 & when\ i = j \end{cases}$$
The eigenvalues of C are represented as $\hat{\zeta}_1, \hat{\zeta}_2, \ldots, \hat{\zeta}_n$, and the connectedness energy of a fuzzy graph is the total sum of the eigenvalues of C represented as $CE(\hat{G})$.

Properties on Energy Level Connectedness in FG's
Definition 3.1. The spectral radius $\hat{\rho}(A)$ of a graph $\hat{G}$ is characterized as the maximum absolute value present within the graph spectrum ie.., eigenvalues of respective adjacency fuzzy matrix $(\hat{\lambda}_1, \hat{\lambda}_2,.., \hat{\lambda}_n)$.
$$\hat{\rho}(A) = \max_{1 \leq i \leq n} |\hat{\lambda}_i|$$
Theorem 3.2. Consider $\hat{G}$ as a fuzzy graph with μ edges and a spectral radius of $\hat{\rho}$.Then,
i) $\hat{\rho}(\hat{\rho} + 1) \leq 2 \sum_{i \in [1,n]} \mu_i$

ii) If $\hat{G}$ is connected, then $\hat{\rho} \leq \sqrt{2 \sum_i \mu_i - \sum_i \sigma_i + 1}$, with equality only for K_n and $K_{1,n-1}$.

Proof: Since the spectral radius of $\hat{G}$ is the largest eigenvalue of any connected component and $\hat{\rho}$≤ k$_{max}$ ≤ n − 1. This indicates that $\hat{\rho}(\hat{\rho} + 1)$ is bounded by 2 times the sum of terms 1 through n, each denoted by μi which follows from $\hat{\rho} \leq \sqrt{2 \sum_i \mu_i - \sum_i \sigma_i + 1}$. Let Av = $\hat{\rho}$v such that vv^T = 1 where v is normalized. Then for each vertex v$_i$, we have $\sum_{j \sim i} v_j = \hat{\rho} v_i$. Using Cauchy-Schwartz inequality, $\hat{\rho}^2 v_i^2 \leq d_i \sum_{j \sim i} v_j^2$ where d_i represents the degree of each vertex v_i.

63255

Summing over i results in $\hat{\rho}^2 \leq \sum_i d_i(1 - v_i^2 - \sum_{k \neq i} v_k^2) \leq 2\mu_i - \sum_i d_i v_i^2 - \sum_k(\sigma_i - 1 - d_i)v_k^2 = 2\mu - (\sigma_i - 1)$ for all i. Since $d_i \geq 0$, equality holds for K_n and $K_{1,n-1}$.

Definition 3.3. The measure of connectedness strength on H within the context of $\hat{G}$ is established as H = [h$_{ij}$], wherein

$$h_{ij} = \begin{cases} d_i^* & if\ i = j \\ -\mu^\infty(\mu_{ij}) & if\ i \neq j \\ 0 & otherwise \end{cases}$$

The eigen values of H are denoted by $\hat{\varphi}_1, \hat{\varphi}_2, \dots, \hat{\varphi}_n$ and the connectedness energy of $\hat{G}$ corresponds to the summation of distances between Laplacian eigen values within the matrix of connectedness strength H, along with their average degree $d_i^*(\hat{G})$.

$$CL(\hat{G}) = \left| \hat{\varphi}_i - \frac{2\sum_{i,j \in [1,n]} \mu_{ij}}{n} \right|$$

such that $\hat{\varphi}_1 \geq \hat{\varphi}_2 \geq \cdots \geq \hat{\varphi}_n$ are the laplacian eigenvalues of H.

Theorem 3.4. If $\hat{G}$ represents a fuzzy graph with $|\sigma| = n$ and $\mu = m^*$. Then the connectedness energy CL$(\hat{G})$ remains consistently greater than or equal to E$(\hat{G})$.
Proof: Consider E$(\hat{G})$ and CL$(\hat{G})$ as representations of the total sum of eigenvalues within the Laplacian matrix L of $\hat{G}$ and the matrix H denoting the connectedness strength of $\hat{G}$, respectively. The elements of L includes d$_i$ when v$_i$ and v$_j$ are equal. The negation of µ(v$_i$, v$_j$) exists when the vertices are adjacent and expressed as 0 when vertices are not adjacent. The diagonal entries fill the membership degrees of each vertex (v$_i$, v$_j$) and μ^∞(v$_i$, v$_j$) elsewhere. Therefore, the sum of eigen values of H is greater than L. This implies $CL(\hat{G}) \geq E(\hat{G})$. This equality holds only for complete fuzzy graphs with H and L are equal.

Example 3.5. Consider Fig.3.1 representing a simple undirected fuzzy graph $\hat{G}$ as depicted.
The matrix L corresponding to $\hat{G}$ is defined as follows,

$$L = \begin{bmatrix} 0.4 & -0.2 & 0 & 0 & -0.2 \\ -0.2 & 0.8 & -0.3 & 0 & -0.3 \\ 0 & -0.3 & 0.8 & -0.2 & -0.3 \\ 0 & 0 & -0.2 & 0.4 & -0.2 \\ -0.2 & -0.3 & -0.3 & -0.2 & 1 \end{bmatrix}$$

The eigenvalues of L is {0, 0.35, 0.63, 1.15, 1.27}. The energy of $\hat{G}$= 2.72. The strength matrix H of $\hat{G}$ is given by,

$$H = \begin{bmatrix} 0.4 & -0.2 & -0.2 & -0.2 & -0.2 \\ -0.2 & 0.8 & -0.3 & -0.2 & -0.3 \\ -0.2 & -0.3 & 0.8 & -0.2 & -0.3 \\ -0.2 & -0.2 & -0.2 & 0.4 & -0.2 \\ -0.2 & -0.3 & -0.3 & -0.2 & 1.0 \end{bmatrix}$$

The connectedness laplacian eigenvalues of H is {−0.26, 0.6, 0.71, 1.1, 1.24}. The connectedness laplacian energy CL$(\hat{G})$ = 3.23.

Lemma 3.6. For a fuzzy graph $\hat{G}$ with $|\sigma_i| = n*$ and $\hat{\mu}_i$ signifying the Laplacian eigenvalue has the connectedness laplacian energy of the form,

$$2\sqrt{\sum \mu_{ij}^2 + \frac{1}{2}\left(\sum_{i\in[1,n^*]} d_{\hat{G}}(u_i) - \frac{2\sum_{ij\in[1,n^*]}\mu_{ij}}{n^*}\right)^2} \leq CL(\hat{G})\ \ and$$

$$CL(\hat{G}) \leq \sqrt{2\sum \mu_{ij}^2 + \left(\sum_{i\in[1,n^*]} d_{\hat{G}}(u_i) - \frac{2\sum_{ij\in[1,n^*]}\mu_{ij}}{n^*}\right)^2} \cdot n^*.$$

The bounds on the connectedness laplacian energy of $\hat{G}$ in terms of edge membership, vertex membership and the strength of connectedness are described below.

Theorem 3.7. Consider $\hat{G}$ with $|\sigma| = n$ and $\mu = m^*$. Then,
i) $CL(\hat{G}) \leq 2\sum \mu_{ij}$ where $\mu_{ij} \in E$
ii) $(n - 1)\sum_{r=1}^n \sigma(v_r) \geq CL(\hat{G})$ where $v_r \in \sigma$
Proof: Proof of (i) is obvious.

Buvaneswari and Senbaga Priya

$CL(\hat{G}) \leq \sum \mu_{ij} = 2\sum_{r=1}^{n(n-1)/2} \mu_{ij}$ for all $r > m^*, \mu_{ij} = 0$.

From the definition of fuzzy graphs,

$CL(\hat{G}) \leq 2\sum_{r\in[1,m^*]} \mu_{ij}$ where $m^* = \dfrac{n(n-1)}{2}$

$$= \sum_{r=1}^{m^*} \mu_i + \mu_j$$
$$\leq \sum \sigma(v_{r_1}) + \sigma(v_{r_2})$$
$$\leq \sum_{r=[1,n]} \sigma(v_r).$$

Theorem 3.8. Let $\hat{G}$ denote a fuzzy graph with $|\sigma| = $ n and $\mu = $ m*. If $\mu_{ij} = -\mu^\infty(v_i, v_j)$, then the strength of connectedness is given by

$$\frac{2\mu_{ij}}{\sigma_i} + \sqrt{(\sigma_i - 1)\left[2Q - \left(\frac{2\mu_{ij}}{\sigma_i}\right)^2\right]} \leq CL(\hat{G}) \leq \frac{2\mu_{ij}}{\sigma_i} + 1$$

Where, $Q = \sum_{i,j=[1,n]} \mu_{ij}^2 + \frac{1}{2}\left(\sum_{i\in[1,n^*]} d_{\hat{G}}(u_i) - \frac{2\sum_{ij\in[1,n^*]}\mu_{ij}}{n^*}\right)^2$.

Proof: Let $\hat{\varphi}_1, \hat{\varphi}_2, \dots, \hat{\varphi}_n$ be the eigen values of H of $\hat{G}= (\sigma, \mu)$. Applying Cauchy Schwartz inequality to connectedness strength laplacian matrix H and for every i in the range from 1 to n,

$$|\hat{\varphi}_i|^2 \geq \frac{1}{n}\sum_{i=1}^{n} |\hat{\varphi}_i|^2$$

Suppose, $\hat{G}$ contains k components and $\hat{\varphi}_1 \geq \hat{\varphi}_2 \geq \cdots \geq \hat{\varphi}_n$, then $\hat{\varphi}_{n-i} = 0$ for any $i = 0,1,..,k-1$ and $\hat{\varphi}_{n-k} > 0$. This implies that,

$CL(\hat{G}) \geq k.\frac{2\mu_{ij}}{\sigma_i}$ $- - - - - (1)$

If $\hat{G}$ possess atleast one edge, then (1) can be written as,

$\mu_1 \geq \dfrac{2\mu_{ij}}{\sigma_i} + 1$ $- - - - - $ (2)

since, $\hat{\gamma}_{n-i} = \dfrac{-2\mu_{ij}}{\sigma_i}$. Therefore, for any, $\hat{\gamma}_1 \geq 1$ implies, $CL(\hat{G}) \geq k.\frac{2\mu_{ij}}{\sigma_i} + 1$. Setting $k = 1$ results in an upper bound.

$CL(\hat{G}) \geq \dfrac{2\mu_{ij}}{\sigma_i} + 1$ $- - - - - $ (3)

Let $a = \dfrac{2\mu_{ij}}{\sigma_i}$ and consider the function, $f(x) = ax + \sqrt{(\sigma - x)(2Q - a^2x)}; 0 \leq x \leq n$. The function $f'(x) = 0$ iff

$2a\sqrt{(\sigma - x)(2Q - a^2x)} \leq 2Q + a^2n - 2a^2x$

Where, $Q = \sum_{i,j=[1,n]} \mu_{ij}^2 + \frac{1}{2}\left(\sum_{i\in[1,n^*]} d_{\hat{G}}(u_i) - \frac{2\sum_{ij\in[1,n^*]}\mu_{ij}}{n^*}\right)^2$

Since, the upper bound increases with decreasing k, and by setting $k = 1$,

$$CL(\hat{G}) \leq \frac{2\mu_{ij}}{\sigma_i} + \sqrt{(\sigma_i - 1)\left[2Q - \left(\frac{2\mu_{ij}}{\sigma_i}\right)^2\right]}   \quad - - - -(4)$$

From (3) and (4), we get,

$$\frac{2\mu_{ij}}{\sigma_i} + \sqrt{(\sigma_i - 1)\left[2Q - \left(\frac{2\mu_{ij}}{\sigma_i}\right)^2\right]} \leq CL(\hat{G}) \leq \frac{2\mu_{ij}}{\sigma_i} + 1$$

This condition holds for any $\hat{G} = (\sigma, \mu)$ graphs.

Example 3.9. Consider the Fig.3.1 $\hat{G}$ having the laplacian energy E($\hat{G}$) = 2.72 and connectedness energy CL($\hat{G}$) = 3.23. Upper bound=4.66, Lower bound=2.21. This implies, CL($\hat{G}$) ≥ E($\hat{G}$) and 2.21 < 3.23 < 4.66.

Theorem 3.10. If $\hat{G}$ is a non-trivial, non-complete fuzzy graph, then κ ≥ μ2.

Proof: Consider $\hat{G}$ with $|\sigma| = $ n and $\mu = $ m, where V₁ represents the vertex cut such that $V_2 = V - V_1 \neq \phi$ where $V = V_1 \cup V_2$ is a decomposition of V. Any subgraph $\hat{G}_2$ of $\hat{G}$ generated on Vᵢ yields, κ($\hat{G}$) ≤ (κ($\hat{G}_1$) + V₂) ∧ (κ($\hat{G}_2$) + V₁). Since the subgraph $\hat{G}_2$ of $\hat{G}$ generated on V₂ is not connected, it yields κ($\hat{G}$) ≥ μ₂($\hat{G}$).

Remark: For every non-trivial fuzzy graph, $\kappa' \geq \mu_2$ holds, as $\kappa' \geq \kappa$. Consider fig.3.1 to depict the result as follows, $\kappa = 0.4$; $\kappa' = 0.4$; $\mu_2 = 0.35 \implies \kappa \geq \mu_2$ and $\kappa'(\hat{G}) \geq \mu_2(\hat{G})$.

Proposition 3.11. Consider $\hat{G}$ as an n-vertex regular fuzzy graph characterized by the strong degree $\hat{d}_s(v)$, where $|\sigma| = n$. Assuming, $\hat{\lambda}_2(\hat{G}) > \hat{d}_s(v) - 1 - \frac{\hat{d}_s(v)}{|\sigma_i| - \hat{d}_s(v)}$, it can be concluded that $\kappa' \leq \hat{d}_s(v)$.

Proposition 3.12. Consider $\hat{G}$ to be an n-vertex regular fuzzy graph characterized by the strong degree $\hat{d}_s(v)$, where $|\sigma| = n$. Assuming, $\hat{\mu}_{n-1}(\hat{G}) > \hat{d}_s(v) - 1 - \frac{\hat{d}_s(v)}{|\sigma_i| - \hat{d}_s(v)}$, it can be concluded that $\kappa' \leq \hat{d}_s(v)$.

Proposition 3.13. Consider $\hat{G}$ as a regular fuzzy graph possessing a maximum strong degree of $\Delta_s(\hat{G})$. Then,

i) $\hat{\lambda}_2 \geq \Delta_s - 2$ whenever $\hat{\mu}_{n-1} \geq \Delta_s - 2$

ii) $\kappa' \leq \Delta_s$

Proposition 3.14. Consider $\hat{G}$ as a regular fuzzy graph possessing a minimum strong degree of $\delta_s(\hat{G})$. Then,

i) $\hat{\lambda}_2 \geq \delta_s - 2$ whenever $\hat{\mu}_{n-1} \geq \delta_s - 2$

ii) $\kappa' \geq \delta_s$

Example 3.15. Consider $\hat{G}$ as shown in Fig.3.2

From the given example 3.15, we say that the propositions (3.11-3.14) are satisfied.

CONCLUSION

Reformulating the concepts of fuzzy connectivity of vertices and edges in clustering techniques and connectedness energy of fuzzy graph paved the way for new connectivity parameters, Connectedness strength matrix H and Connectedness laplacian energy of fuzzy graphs $CL(\hat{G})$ obtained from the laplacian eigenvalues of $\hat{G}$. This motivated to apply the parameters in network in a stronger sense. The newly defined parameter effectively applies in many areas including network analysis as the connectivity bounds are more stronger.

ACKNOWLEDGEMENTS

REFERENCES

1. Aida Abiad, Boris Brimkov, Xavier Martinez-Rivera, Suil O, Jingmei Zhang: Spectral Bounds for the Connectivity of Regular Graphs with Given Order. Electronic Journal of Linear Algebra, 2006; ISSN-1081-3810, V-34,428-443.
2. Zhen-Mu Hong, Zheng-Jiang Xia, Hong-Jian Lai: Vertex-Connectivity and Eigenvalues of Graphs. Linear Algebra and its Applications,2019; 72-88.
3. K. R. Bhutani and A. Rosenfeld: Strong arcs in fuzzy graphs. Information Sciences,2003;152, 319 - 322.
4. Sunil Mathew, M. S. Sunitha: Types of arcs in a fuzzy graph. Information Sciences,2009; 179 (11), 1760 - 1768.
5. Sunil Mathew, M. S. Sunitha: Menger's theorem for fuzzy graphs. Information Sciences,2013: 222, 717 - 726.
6. P. Bhattacharya: Some Remarks on Fuzzy Graphs. Patteren Recognition Letters,1987; 6 (5), 297 - 302.
7. Sunil Mathew, M.S.Sunitha: Node Connectivity and Arc Connectivity of a Fuzzy Graph. Information Sciences,2010; 519-531.
8. K. Kalpana, S. Lavanya: Connectedness Energy of Fuzzy Graph. Journal of Computer and Mathematical Sciences, 2018; 9(5), 485-492.
9. Jiaqi Jiang, An Introduction to Spectral Graph theory.
10. Zadeh,L.A.: Fuzzy Sets. Information Sciences and Control,1965; 338-353.
11. Sunil Mathew, John N. Mordeson, Davender S.Malik: Fuzzy Graph Theory. Studies in Fuzziness and Soft Computing, 2018; vol 363.
12. A. Kaufmann: Theory of Expertons and Fuzzy Logic. Fuzzy Sets and Systems,1988; 3(28), 295-304.

Buvaneswari and Senbaga Priya
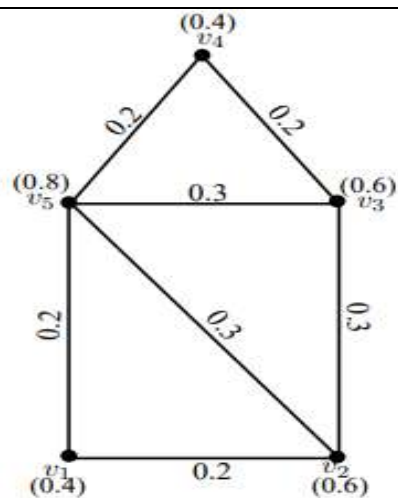
Fig. 3.1 A fuzzy graph $\hat{G}$
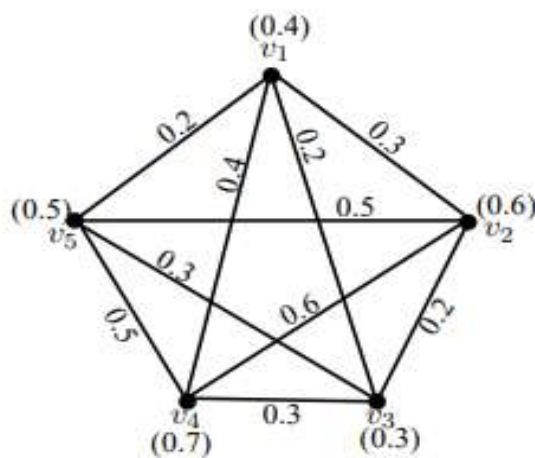
Fig. 3.2 Regular fuzzy graph $\hat{G}$

RESEARCH ARTICLE

Special Restricted Interval Valued Picture Fuzzy Matrix and its Applications in Decision Making

P. Rajarajeswari[1] and D. Nandhini[2]*

[1]Associate Professor, Department of Mathematics, Chikkanna Govt Arts College, Tirupur-02, Tamil Nadu, India.
[2]Research Scholar, Department of Mathematics, Chikkanna Govt Arts College, Tirupur-02, Tamil Nadu, India.

*Address for Correspondence
D. Nandhini
Research Scholar,
Department of Mathematics,
Chikkanna Govt Arts College,
Tirupur-02, Tamil Nadu, India.

ABSTRACT

In this paper, the new concept of interval valued picture fuzzy matrices, restricted interval valued picture fuzzy matrices, and special restricted interval valued picture fuzzy matrices are established. Two different types of $\langle [\alpha_L, \alpha_U], [\beta_L, \beta_U], [\gamma_L, \gamma_U] \rangle$-cut of a specific restricted interval valued square picture fuzzy matrix are presented, and their important properties are investigated. Also, the determinant and adjoint of the square picture fuzzy matrix are established. Here, an interval valued picture fuzzy matrix application to a decision-making problem is described.

Keywords : Picture fuzzy matrix, Interval valued intuitionistic fuzzy matrix, Determinant of interval valued picture fuzzy matrix, Adjoint of square interval valued picture fuzzy matrix.

INTRODUCTION

In the past few years, it has been found that Fuzzy can be utilized to resolve a wide range of challenging issues including uncertainties that come up in the areas of engineering, social science, economics, and other sciences. Every area of life is filled with uncertainty in the real world. This type of issue plays itself well to Zadeh's classical fuzzy set[10] notion. Higher order fuzzy sets have been proposed for various uses in a wide range of disciplines ever since the fuzzy set theory was first proposed. The Atanassov[1] intuitionistic fuzzy set[2] has been shown to be particularly advantageous and flexible among higher fuzzy sets. The intuitionistic fuzzy set was expanded by Attanassov and Gargov[2] to the interval valued intuitionistic fuzzy set, which is distinguished by a membership function with interval values. By Coung[3], the picture fuzzy set was generalized. Used as one of the components of an picture fuzzy set are membership, neutral, and non-membership functions. Hashimoto created the concept of fuzzy matrices. Later, Ragab and Emam investigated the max-min composition of fuzzy matrices as well as the determinant of a square fuzzy matrix. Generalised fuzzy matrices were first

proposed by Kim and Roush. Pal [7]proposed the concept of fuzzy matrices with fuzzy columns and rows. Pal studied fuzzy matrices with interval values and such rows and columns.Triangular fuzzy matrix norm research was conducted by Pradhan and Pal.As a generalization of intuitionistic fuzzy set, picture fuzzy set was invented by Cuong and Kreinovich. Wei looked at multi-attribute decision-making issues in a picture fuzzy environment. In this paper, the new concept special restricted interval valued picture fuzzy matrices, we also introduce the new idea of determinant and adjoint of square interval valued picture fuzzy matrix. we also have been studied their application in Decision making with numerical example.

Preliminaries

Definition 1(1986, Atanassov) An IFS Cover the set of universe X is defind as
C =$\{\langle x, \zeta_C(x), \theta_C(x)\rangle : x \in X\}$ where $\zeta_C(x) \in [0,1]$ is the measure of membership and$\theta_C(x) \in [0,1]$ is the measure of non-membership of x in C with $0 \le \lambda_C(x) + \le 1$ for all$x$ in C.

Definition 2. (Khan et al.2002) An IFM C of order $a \times b$ is defined as C=$\left(\langle C_{ij_\zeta}, C_{ij_\theta}\rangle\right)$, where $C_{ij_\lambda} \in [0,1]$ is the measure of membership of C_{ij} (ij th element of C) and $C_{ij_\zeta} \in [0,1]$ is the measure of non-membershipC_{ij} with the condition$0 \le C_{ij_\zeta} + C_{ij_\theta} \le 1$ for i=1,2,……….,a and j=1,2,……….,b.
An IFM C is said to SIFM if the number of rows is equal to the number of columns.

Definition 3.(Cuong and Kreinovich 2013) A PFS Cover the set of universe X is defined as C=$\{\langle x, \zeta_C(x), \eta_C(x), \theta_C(x)\rangle : x \in X\}$ where $\zeta_C(x) \in [0,1]$,$\eta_C(x) \in [0,1]$,   is the measure of membership, neutral membership and$\theta_C(x) \in [0,1]$ is the measure of non-membership of $x \in X$ with the condition $0 \le \zeta_C(x) + \eta_C(x) + \theta_C(x) \le 1$ for all $x \in X$.

Definition 4.
A IVPFM of size $\boldsymbol{a \times b}$ is defined as $\left(\langle [C_{ij\zeta_L}, C_{ij\zeta_U}], [C_{ij\eta_L}, C_{ij\eta_L}], [C_{ij\theta_L}, C_{ij\theta_U}]\rangle\right)$ $\boldsymbol{where\ C_{ij\zeta_L}, C_{ij\zeta_U} \in [0,1]}$ are the lower and upper

limit of membership degree,$C_{ij\eta_L}, C_{ij\eta_L} \in [0,1]$ are the lower and upper limit of neutral membership degree, and $C_{ij\theta_L}, C_{ij\theta_U} \in [0,1]$ are the lower and upper limit of non-membership *degree of the element*of C_{ij} for i=1,2,……,a and j=1,2,…….,b satisfying

$0 \le C_{ij\zeta_U} + C_{ij\eta_u} + C_{ij\zeta_U} \le 1.$

Definition 5

A special restricted SIVPFM is referred to as an identity special restricted IVPFM if it has nondiagonal values $\langle [\phi_{1L}, \phi_{1U}], [\phi_{2L}, \phi_{2U}], 0\rangle$, as well as diagonal entries of $\langle 0, [\phi_{2L}, \phi_{2U}], [\phi_{3L}, \phi_{3U}]\rangle$

Definition 6

If a special restricted SIVPFM has all entries$\langle 0, [\phi_{2L}, \phi_{2U}], [\phi_{3L}, \phi_{3U}]\rangle$, Then it is called null special restricted IVPFM.

It is clear that when $\phi_2 = 0, \phi_1 = 1, \phi_{3=}1$ Then $0 \le ([C_{ij\zeta_L}, C_{ij\zeta_U}]) \le 1, (\langle [C_{ij\eta_L}, C_{ij\eta_L}]\rangle) = 1, 0 \le ([C_{ij\theta_L}, C_{ij\theta_U}]) \le 1$ with $0 \le (\langle [C_{ij\zeta_L}, C_{ij\zeta_U}], [C_{ij\eta_L}, C_{ij\eta_L}], [C_{ij\theta_L}, C_{ij\theta_U}]\rangle) \le 1$. Now,by replacing the measure membership by the measure of neutral membership and the measure of non-membership IVPFM is obtained. Thus, null IVIFM is obtained with all entries $\langle 0, \phi_3\rangle = \langle 0,1\rangle$ and identity IVIFM is obtained with diagonal entries $\langle \phi_1, 0\rangle = \langle 0,1\rangle$ and non -diagonal entries $\langle 0, \phi_3\rangle = \langle 0,1\rangle$ so identity IVIFM and null IFM, respectively.

Different types of $\langle[\alpha_L, \alpha_U], [\beta_L, \beta_U], [\gamma_L, \gamma_U]\rangle$-cut of SIVPFM

In this section, we define different types of $\langle[\alpha_L, \alpha_U], [\beta_L, \beta_U], [\gamma_L, \gamma_U]\rangle -$ cut of special restricted SIVPFM and study some properties related to these.

Definition 1.

Let $C = (\langle[C_{ij\zeta_L}, C_{ij\zeta_U}], [C_{ij\eta_L}, C_{ij\eta_L}], [C_{ij\theta_L}, C_{ij\theta_U}]\rangle)$ be a special restricted SIVPFM for three real numbers $[\phi_{1L}, \phi_{1U}] \subseteq [0,1], [\phi_{2L}, \phi_{2L}] \subseteq [0,1]$ and $[\phi_{3L}, \phi_{3U}] \subseteq [0,1]$ with $\phi_{1U} + \phi_{2U} = 1$ and $\phi_{2U} + \phi_{3U} = 1$. Then type-I

$\langle[\alpha_L, \alpha_U], [\beta_L, \beta_U], [\gamma_L, \gamma_U]\rangle -$**cut** of C is the special restricted SIVPFM $C^{\langle[\alpha_L,\alpha_U],[\beta_L,\beta_U],[\gamma_L,\gamma_U]\rangle} = (\langle[e_{ij\zeta_L}, e_{ij\zeta_U}], [e_{ij\eta_L}, e_{ij\eta_L}], [e_{ij\theta_L}, e_{ij\theta_U}]\rangle)$ given by $(\langle[e_{ij\lambda_L}, e_{ij\lambda_U}], [e_{ij\eta_L}, e_{ij\eta_L}], [e_{ij\zeta_L}, e_{ij\zeta_U}]\rangle) =$

$$\begin{cases} \langle[\phi_{1L}, \phi_{1U}], [\phi_{2L}, \phi_{2U}], 0\rangle, & when \left((\langle[c_{ij\zeta_L}, c_{ij\zeta_U}], [c_{ij\eta_L}, c_{ij\eta_L}], [c_{ij\theta_L}, c_{ij\theta_U}]\rangle)\right) \geq \langle[\alpha_L, \alpha_U], [\beta_L, \beta_U], [\gamma_L, \gamma_U]\rangle \\ \langle0, [\phi_{2L}, \phi_{2U}], [\phi_{3L}, \phi_{3U}]\rangle, & otherwise \end{cases}$$

where $[\alpha_L, \alpha_U] \subseteq [\phi_{1L}, \phi_{1U}], [\beta_L, \beta_U] = [\phi_{2L}, \phi_{2U}]$ and $[\gamma_L, \gamma_U] \subseteq [\phi_{3L}, \phi_{3U}]$ with

$0 \leq \alpha_U + \beta_U + \gamma_U \leq 1$.

Definition 2.

Let $C = (\langle[C_{ij\zeta_L}, C_{ij\zeta_U}], [C_{ij\eta_L}, C_{ij\eta_L}], [C_{ij\theta_L}, C_{ij\theta_U}]\rangle)$ be a special restricted SIVPFM for three real numbers $[\phi_{1L}, \phi_{1U}] \subseteq [0,1], [\phi_{2L}, \phi_{2U}] \subseteq [0,1]$ and $[\phi_{3L}, \phi_{3U}] \subseteq [0,1]$ with $\phi_{1U} + \phi_{2U} = 1$ and $\phi_{2U} + \phi_{3U} = 1$. Then type-II

$\langle[\alpha_L, \alpha_U], [\beta_L, \beta_U], [\gamma_L, \gamma_U]\rangle$**cut** of C is the special restricted SIVPFM $C_{\langle[\alpha_L,\alpha_U],[\beta_L,\beta_U],[\gamma_L,\gamma_U]\rangle} = (\langle[e_{ij\zeta_L}, e_{ij\zeta_U}], [e_{ij\eta_L}, e_{ij\eta_L}], [e_{ij\theta_L}, e_{ij\theta_U}]\rangle)$ given by $(\langle[e_{ij\zeta_L}, e_{ij\zeta_U}], [e_{ij\eta_L}, e_{ij\eta_L}], [e_{ij\theta_L}, e_{ij\theta_U}]\rangle)$

$$\begin{cases} \left(\langle[C_{ij\zeta_L}, C_{ij\zeta_U}], [C_{ij\eta_L}, C_{ij\eta_L}], [C_{ij\theta_L}, C_{ij\theta_U}]\rangle\right), & when(\langle[C_{ij\zeta_L}, C_{ij\zeta_U}], [C_{ij\eta_L}, C_{ij\eta_L}], [C_{ij\theta_L}, C_{ij\theta_U}]\rangle) \geq \\ & \langle[\alpha_L, \alpha_U], [\beta_L, \beta_U], [\gamma_L, \gamma_U]\rangle \\ \langle[\alpha_L, \alpha_U], [\beta_L, \beta_U], [\gamma_L, \gamma_U]\rangle & otherwise \end{cases}$$

where $[\alpha_L, \alpha_U] \subseteq [\phi_{1L}, \phi_{1U}], [\beta_L, \beta_U] = [\phi_{2L}, \phi_{2U}]$ and $[\gamma_L, \gamma_U] \subseteq [\phi_{3L}, \phi_{3U}]$ with

$0 \leq \alpha_U + \beta_U + \gamma_U \leq 1$.

Proposition 1.

Let C and D be two specials restricted SIVPFMs Then $C \geq D \Rightarrow C^{\langle[\alpha_L,\alpha_U],[\beta_L,\beta_U],[\gamma_L,\gamma_U]\rangle} \geq D^{\langle[\alpha_L,\alpha_U],[\beta_L,\beta_U],[\gamma_L,\gamma_U]\rangle}$

Proof

Let $C = (\langle[C_{ij\zeta_L}, C_{ij\zeta_U}], [C_{ij\eta_L}, C_{ij\eta_L}], [C_{ij\theta_L}, C_{ij\theta_U}]\rangle)$ and $D = (\langle[d_{ij\zeta_L}, d_{ij\zeta_U}], [d_{ij\eta_L}, d_{ij\eta_L}], [d_{ij\theta_L}, d_{ij\theta_U}]\rangle)$ be two special restricted SIVPFM of order a for three real numbers $[\phi_{1L}, \phi_{1U}] \subseteq [0,1], [\phi_{2L}, \phi_{2U}] \subseteq [0,1]$ and $[\phi_{3L}, \phi_{3U}] \subseteq [0,1]$ with $\phi_{1U} + \phi_{2U} = 1$ and $\phi_{2U} + \phi_{3U} = 1$. Then

$(\langle[C_{ij\zeta_L}, C_{ij\zeta_U}], [d_{ij\zeta_L}, d_{ij\zeta_U}] \subseteq [\phi_{1L}, \phi_{1U}][C_{ij\eta_L}, C_{ij\eta_L}] = [d_{ij\eta_L}, d_{ij\eta_L}] = [\phi_{2L}, \phi_{2U}], ([C_{ij\theta_L}, C_{ij\theta_U}], [d_{ij\theta_L}, d_{ij\theta_U}]\rangle) \subseteq [\phi_{3L}, \phi_{3U}]$ for i,j=1,2,3,.........a.

$C \geq D \Rightarrow ([C_{ij\zeta_L}, C_{ij\zeta_U}]) \supseteq ([d_{ij\theta_L}, d_{ij\theta_U}]), ([C_{ij\eta_L}, C_{ij\eta_L}]) \subseteq ([d_{ij\eta_L}, d_{ij\eta_L}])$ and $([C_{ij\theta_L}, C_{ij\theta_U}]) \subseteq ([d_{ij\theta_L}, d_{ij\theta_U}])$

Let $C^{\langle[\alpha_L,\alpha_U],[\beta_L,\beta_U],[\gamma_L,\gamma_U]\rangle} = (\langle[e_{ij\zeta_L}, e_{ij\zeta_U}], [e_{ij\eta_L}, e_{ij\eta_L}], [e_{ij\theta_L}, e_{ij\theta_U}]\rangle)$

$D^{\langle[\alpha_L,\alpha_U],[\beta_L,\beta_U],[\gamma_L,\gamma_U]\rangle} = (\langle[f_{ij\lambda_L}, f_{ij\lambda_U}], [f_{ij\eta_L}, f_{ij\eta_L}], [f_{ij\zeta_L}, f_{ij\zeta_U}]\rangle)$

Where $(\langle[e_{ij\lambda_L}, e_{ij\lambda_U}], [e_{ij\eta_L}, e_{ij\eta_L}], [e_{ij\zeta_L}, e_{ij\zeta_U}]\rangle) =$

$$\begin{cases} \langle[\phi_{1L}, \phi_{1U}], [\phi_{2L}, \phi_{2U}], 0\rangle, & when(\langle[c_{ij\lambda_L}, c_{ij\lambda_U}], [c_{ij\eta_L}, c_{ij\eta_L}], [c_{ij\zeta_L}, c_{ij\zeta_U}]\rangle) \geq \\ & \langle[\alpha_L, \alpha_U], [\beta_L, \beta_U], [\gamma_L, \gamma_U]\rangle \\ \langle0, [\phi_{2L}, \phi_{2U}], [\phi_{3L}, \phi_{3U}]\rangle, & otherwise \end{cases}$$

Rajarajeswari and Nandhini

$$(\langle[f_{ij\lambda_L}, f_{ij\lambda_U}], [f_{ij\eta_L}, f_{ij\eta_L}], [f_{ij\zeta_L}, f_{ij\zeta_U}]\rangle) =$$

And $\begin{cases} \langle[\phi_{1L}, \phi_{1U}], [\phi_{2L}, \phi_{2U}], 0\rangle, & when(\langle[d_{ij\lambda_L}, d_{ij\lambda_U}], [d_{ij\eta_L}, d_{ij\eta_L}], [d_{ij\zeta_L}, d_{ij\zeta_U}]\rangle) \geq \\ & \langle[\alpha_L, \alpha_U], [\beta_L, \beta_U], [\gamma_L, \gamma_U]\rangle \\ \langle0, [\phi_{2L}, \phi_{2U}], [\phi_{3L}, \phi_{3U}]\rangle, & otherwise \end{cases}$

Case 1:

$(\langle[c_{ij\lambda_L}, c_{ij\lambda_U}], [c_{ij\eta_L}, c_{ij\eta_L}], [c_{ij\zeta_L}, c_{ij\zeta_U}]\rangle) \geq \langle[\alpha_L, \alpha_U], [\beta_L, \beta_U], [\gamma_L, \gamma_U]\rangle$ and $(\langle[d_{ij\lambda_L}, d_{ij\lambda_U}], [d_{ij\eta_L}, d_{ij\eta_L}], [d_{ij\zeta_L}, d_{ij\zeta_U}]\rangle) \geq \langle[\alpha_L, \alpha_U], [\beta_L, \beta_U], [\gamma_L, \gamma_U]\rangle$ Then

$C^{\langle[\alpha_L,\alpha_U],[\beta_L,\beta_U],[\gamma_L,\gamma_U]\rangle} = \langle[\phi_{1L}, \phi_{1U}], [\phi_{2L}, \phi_{2U}], 0\rangle$ and $D^{\langle[\alpha_L,\alpha_U],[\beta_L,\beta_U],[\gamma_L,\gamma_U]\rangle} = \langle[\phi_{1L}, \phi_{1U}], [\phi_{2L}, \phi_{2U}], 0\rangle$

$C^{\langle[\alpha_L,\alpha_U],[\beta_L,\beta_U],[\gamma_L,\gamma_U]\rangle} = D^{\langle[\alpha_L,\alpha_U],[\beta_L,\beta_U],[\gamma_L,\gamma_U]\rangle}$

Case 2:

$(\langle[c_{ij\lambda_L}, c_{ij\lambda_U}], [c_{ij\eta_L}, c_{ij\eta_L}], [c_{ij\zeta_L}, c_{ij\zeta_U}]\rangle) \ngeq \langle[\alpha_L, \alpha_U], [\beta_L, \beta_U], [\gamma_L, \gamma_U]\rangle$ and $(\langle[d_{ij\lambda_L}, d_{ij\lambda_U}], [d_{ij\eta_L}, d_{ij\eta_L}], [d_{ij\zeta_L}, d_{ij\zeta_U}]\rangle) \ngeq \langle[\alpha_L, \alpha_U], [\beta_L, \beta_U], [\gamma_L, \gamma_U]\rangle$ Then

$C^{\langle[\alpha_L,\alpha_U],[\beta_L,\beta_U],[\gamma_L,\gamma_U]\rangle} = \langle0, [\phi_{2L}, \phi_{2U}], [\phi_{3L}, \phi_{3U}]\rangle$ and $D^{\langle[\alpha_L,\alpha_U],[\beta_L,\beta_U],[\gamma_L,\gamma_U]\rangle} = \langle0, [\phi_{2L}, \phi_{2U}], [\phi_{3L}, \phi_{3U}]\rangle$

$C^{\langle[\alpha_L,\alpha_U],[\beta_L,\beta_U],[\gamma_L,\gamma_U]\rangle} = D^{\langle[\alpha_L,\alpha_U],[\beta_L,\beta_U],[\gamma_L,\gamma_U]\rangle}$

Case 3

$(\langle[c_{ij\lambda_L}, c_{ij\lambda_U}], [c_{ij\eta_L}, c_{ij\eta_L}], [c_{ij\zeta_L}, c_{ij\zeta_U}]\rangle) \geq \langle[\alpha_L, \alpha_U], [\beta_L, \beta_U], [\gamma_L, \gamma_U]\rangle$ and $(\langle[d_{ij\lambda_L}, d_{ij\lambda_U}], [d_{ij\eta_L}, d_{ij\eta_L}], [d_{ij\zeta_L}, d_{ij\zeta_U}]\rangle) \ngeq \langle[\alpha_L, \alpha_U], [\beta_L, \beta_U], [\gamma_L, \gamma_U]\rangle$ Then

$C^{\langle[\alpha_L,\alpha_U],[\beta_L,\beta_U],[\gamma_L,\gamma_U]\rangle} = \langle[\phi_{1L}, \phi_{1U}], [\phi_{2L}, \phi_{2U}], 0\rangle$ and $D^{\langle[\alpha_L,\alpha_U],[\beta_L,\beta_U],[\gamma_L,\gamma_U]\rangle} = \langle0, [\phi_{2L}, \phi_{2U}], [\phi_{3L}, \phi_{3U}]\rangle$

$C^{\langle[\alpha_L,\alpha_U],[\beta_L,\beta_U],[\gamma_L,\gamma_U]\rangle} \geq D^{\langle[\alpha_L,\alpha_U],[\beta_L,\beta_U],[\gamma_L,\gamma_U]\rangle}$.

Case 4

$(\langle[c_{ij\lambda_L}, c_{ij\lambda_U}], [c_{ij\eta_L}, c_{ij\eta_L}], [c_{ij\zeta_L}, c_{ij\zeta_U}]\rangle) \ngeq \langle[\alpha_L, \alpha_U], [\beta_L, \beta_U], [\gamma_L, \gamma_U]\rangle$ and $(\langle[d_{ij\lambda_L}, d_{ij\lambda_U}], [d_{ij\eta_L}, d_{ij\eta_L}], [d_{ij\zeta_L}, d_{ij\zeta_U}]\rangle) \geq \langle[\alpha_L, \alpha_U], [\beta_L, \beta_U], [\gamma_L, \gamma_U]\rangle$,similarly we have proved the result as in case3.hence in all cases $C^{\langle[\alpha_L,\alpha_U],[\beta_L,\beta_U],[\gamma_L,\gamma_U]\rangle} \geq D^{\langle[\alpha_L,\alpha_U],[\beta_L,\beta_U],[\gamma_L,\gamma_U]\rangle}$

Proposition 2

Let C and D be two special restricted SIVPFMs.
Then$(C \vee D)^{\langle[\alpha_L,\alpha_U],[\beta_L,\beta_U],[\gamma_L,\gamma_U]\rangle} \geq C^{\langle[\alpha_L,\alpha_U],[\beta_L,\beta_U],[\gamma_L,\gamma_U]\rangle} \vee D^{\langle[\alpha_L,\alpha_U],[\beta_L,\beta_U],[\gamma_L,\gamma_U]\rangle}$

Proof

Let C=$(\langle[C_{ij\lambda_L}, C_{ij\lambda_U}], [C_{ij\eta_L}, C_{ij\eta_L}], [C_{ij\zeta_L}, C_{ij\zeta_U}]\rangle)$ and D=$(\langle[d_{ij\lambda_L}, d_{ij\lambda_U}], [d_{ij\eta_L}, d_{ij\eta_L}], [d_{ij\zeta_L}, d_{ij\zeta_U}]\rangle)$be two special restricted SIVPFM of order a for three real numbers $[\phi_{1L}, \phi_{1U}] \subseteq [0,1], [\phi_{2L}, \phi_{2U}] \subseteq [0,1] and [\phi_{3L}, \phi_{3U}] \subseteq [0,1]$with $\phi_{1U} + \phi_{2U} = 1$ and $\phi_{2U} + \phi_{3U} = 1$.Then

$(\langle[C_{ij\lambda_L}, C_{ij\lambda_U}], [d_{ij\lambda_L}, d_{ij\lambda_U}] \subseteq [\phi_{1L}, \phi_{1U}] [C_{ij\eta_L}, C_{ij\eta_L}] = [d_{ij\eta_L}, d_{ij\eta_L}] = [\phi_{2L}, \phi_{2U}], ([C_{ij\zeta_L}, C_{ij\zeta_U}], [d_{ij\zeta_L}, d_{ij\zeta_U}]\rangle) \subseteq [\phi_{3L}, \phi_{3U}]$for i,j=1,2,3,………a

Case 1

$(\langle[c_{ij\lambda_L}, c_{ij\lambda_U}], [c_{ij\eta_L}, c_{ij\eta_L}], [c_{ij\zeta_L}, c_{ij\zeta_U}]\rangle) \geq \langle[\alpha_L, \alpha_U], [\beta_L, \beta_U], [\gamma_L, \gamma_U]\rangle$ and $(\langle[d_{ij\lambda_L}, d_{ij\lambda_U}], [d_{ij\eta_L}, d_{ij\eta_L}], [d_{ij\zeta_L}, d_{ij\zeta_U}]\rangle) \geq \langle[\alpha_L, \alpha_U], [\beta_L, \beta_U], [\gamma_L, \gamma_U]\rangle$ Then $C^{\langle[\alpha_L,\alpha_U],[\beta_L,\beta_U],[\gamma_L,\gamma_U]\rangle} = \langle[\phi_{1L}, \phi_{1U}], [\phi_{2L}, \phi_{2U}], [0,0]\rangle$ and $D^{\langle[\alpha_L,\alpha_U],[\beta_L,\beta_U],[\gamma_L,\gamma_U]\rangle} = \langle[0,0], [\phi_{2L}, \phi_{2U}], [\phi_{3L}, \phi_{3U}]\rangle$ then$C^{\langle[\alpha_L,\alpha_U],[\beta_L,\beta_U],[\gamma_L,\gamma_U]\rangle} \vee D^{\langle[\alpha_L,\alpha_U],[\beta_L,\beta_U],[\gamma_L,\gamma_U]\rangle}$ =$(\langle[\phi_{1L}, \phi_{1U}] \vee [\phi_{1L}, \phi_{1U}], [\phi_{2L}, \phi_{2U}] \wedge [\phi2L,\phi2U],[0,0]\wedge[0,0]=\phi1L,\phi1U,\phi2L,\phi2U,0$ (by proposition 2) it is known that $C\vee D \geq C$.(by proposition 12)$C \vee D^{\langle[\alpha_L,\alpha_U],[\beta_L,\beta_U],[\gamma_L,\gamma_U]\rangle} \geq C^{\langle[\alpha_L,\alpha_U],[\beta_L,\beta_U],[\gamma_L,\gamma_U]\rangle} = \langle[\phi_{1L}, \phi_{1U}], [\phi_{2L}, \phi_{2U}], [0,0]\rangle = C^{\langle[\alpha_L,\alpha_U],[\beta_L,\beta_U],[\gamma_L,\gamma_U]\rangle} \vee D^{\langle[\alpha_L,\alpha_U],[\beta_L,\beta_U],[\gamma_L,\gamma_U]\rangle}$.

Case 2:

Let $\left(\langle\left[c_{ij\lambda_L}, c_{ij\lambda_U}\right], \left[c_{ij\eta_L}, c_{ij\eta_L}\right], \left[c_{ij\zeta_L}, c_{ij\zeta_U}\right]\rangle\right) \geq$
$\langle[\boldsymbol{\alpha_L}, \boldsymbol{\alpha_U}], [\boldsymbol{\beta_L}, \boldsymbol{\beta_U}], [\boldsymbol{\gamma_L}, \boldsymbol{\gamma_U}]\rangle$ and $\left(\langle\left[d_{ij\lambda_L}, d_{ij\lambda_U}\right], \left[d_{ij\eta_L}, d_{ij\eta_L}\right], \left[d_{ij\zeta_L}, d_{ij\zeta_U}\right]\rangle\right) \ngeq \langle[\boldsymbol{\alpha_L}, \boldsymbol{\alpha_U}], [\boldsymbol{\beta_L}, \boldsymbol{\beta_U}], [\boldsymbol{\gamma_L}, \boldsymbol{\gamma_U}]\rangle$ Then
$C^{\langle[\alpha_L,\alpha_U],[\beta_L,\beta_U],[\gamma_L,\gamma_U]\rangle} = \langle[\phi_{1L}, \phi_{1U}], [\phi_{2L}, \phi_{2U}], 0\rangle$ and $D^{\langle[\alpha_L,\alpha_U],[\beta_L,\beta_U],[\gamma_L,\gamma_U]\rangle} = \langle0, [\phi_{2L}, \phi_{2U}], [\phi_{3L}, \phi_{3U}]\rangle$

Thus $C^{\langle[\alpha_L,\alpha_U],[\beta_L,\beta_U],[\gamma_L,\gamma_U]\rangle} \vee D^{\langle[\alpha_L,\alpha_U],[\beta_L,\beta_U],[\gamma_L,\gamma_U]\rangle} = \left(\langle[\phi_{1L}, \phi_{1U}] \vee 0, [\phi_{2L},\phi_{2U}] \wedge [\phi_{2L},\phi_{2U}], [0,0] \wedge [\phi_{3L},\phi_{3U}]\rangle\right) =$
$\langle[\phi_{1L}, \phi_{1U}], [\phi_{2L}, \phi_{2U}], 0\rangle$ by proposition 2,it is known that $C \vee D \geq C$. Then by proposition
12. $C \vee D^{\langle[\alpha_L,\alpha_U],[\beta_L,\beta_U],[\gamma_L,\gamma_U]\rangle} \geq C^{\langle[\alpha_L,\alpha_U],[\beta_L,\beta_U],[\gamma_L,\gamma_U]\rangle} = \langle[\phi_{1L}, \phi_{1U}], [\phi_{2L}, \phi_{2U}], 0\rangle =$
$C^{\langle[\alpha_L,\alpha_U],[\beta_L,\beta_U],[\gamma_L,\gamma_U]\rangle} \vee D^{\langle[\alpha_L,\alpha_U],[\beta_L,\beta_U],[\gamma_L,\gamma_U]\rangle}$.

Case 3

$\left(\langle\left[c_{ij\lambda_L}, c_{ij\lambda_U}\right], \left[c_{ij\eta_L}, c_{ij\eta_L}\right], \left[c_{ij\zeta_L}, c_{ij\zeta_U}\right]\rangle\right) \ngeq \langle[\boldsymbol{\alpha_L}, \boldsymbol{\alpha_U}], [\boldsymbol{\beta_L}, \boldsymbol{\beta_U}], [\boldsymbol{\gamma_L}, \boldsymbol{\gamma_U}]\rangle$ and $\left(\langle\left[d_{ij\lambda_L}, d_{ij\lambda_U}\right], \left[d_{ij\eta_L}, d_{ij\eta_L}\right], \left[d_{ij\zeta_L}, d_{ij\zeta_U}\right]\rangle\right) \geq$
$\langle[\boldsymbol{\alpha_L}, \boldsymbol{\alpha_U}], [\boldsymbol{\beta_L}, \boldsymbol{\beta_U}], [\boldsymbol{\gamma_L}, \boldsymbol{\gamma_U}]\rangle$ Then

$$C^{\langle[\alpha_L,\alpha_U],[\beta_L,\beta_U],[\gamma_L,\gamma_U]\rangle} = \langle[0,0], [\phi_{2L}, \phi_{2U}], [\phi_{3L}, \phi_{3U}]\rangle$$

and $D^{\langle[\alpha_L,\alpha_U],[\beta_L,\beta_U],[\gamma_L,\gamma_U]\rangle} = \langle[\phi_{1L}, \phi_{1U}], [\phi_{2L}, \phi_{2U}], [0,0]\rangle$ it follows that

$C^{\langle[\alpha_L,\alpha_U],[\beta_L,\beta_U],[\gamma_L,\gamma_U]\rangle} \vee D^{\langle[\alpha_L,\alpha_U],[\beta_L,\beta_U],[\gamma_L,\gamma_U]\rangle} = (\langle0 \vee \phi_1, \phi_2 \wedge \phi_2, \phi_3 \wedge 0\rangle) = \langle[\phi_{1L}, \phi_{1U}], [\phi_{2L}, \phi_{2U}], 0\rangle$ by proposition 2,it
is known that $C \vee D \geq C$.

Then by proposition
12. $C \vee D^{\langle[\alpha_L,\alpha_U],[\beta_L,\beta_U],[\gamma_L,\gamma_U]\rangle} \geq D^{\langle[\alpha_L,\alpha_U],[\beta_L,\beta_U],[\gamma_L,\gamma_U]\rangle} = \langle[\phi_{1L}, \phi_{1U}], [\phi_{2L}, \phi_{2U}], 0\rangle =$
$C^{\langle[\alpha_L,\alpha_U],[\beta_L,\beta_U],[\gamma_L,\gamma_U]\rangle} \vee D^{\langle[\alpha_L,\alpha_U],[\beta_L,\beta_U],[\gamma_L,\gamma_U]\rangle}$.

Case 4.

$\left(\langle\left[c_{ij\lambda_L}, c_{ij\lambda_U}\right], \left[c_{ij\eta_L}, c_{ij\eta_L}\right], \left[c_{ij\zeta_L}, c_{ij\zeta_U}\right]\rangle\right) \ngeq \langle[\boldsymbol{\alpha_L}, \boldsymbol{\alpha_U}], [\boldsymbol{\beta_L}, \boldsymbol{\beta_U}], [\boldsymbol{\gamma_L}, \boldsymbol{\gamma_U}]\rangle$ and $\left(\langle\left[d_{ij\lambda_L}, d_{ij\lambda_U}\right], \left[d_{ij\eta_L}, d_{ij\eta_L}\right], \left[d_{ij\zeta_L}, d_{ij\zeta_U}\right]\rangle\right) \ngeq$
$\langle[\boldsymbol{\alpha_L}, \boldsymbol{\alpha_U}], [\boldsymbol{\beta_L}, \boldsymbol{\beta_U}], [\boldsymbol{\gamma_L}, \boldsymbol{\gamma_U}]\rangle$ Then

$C^{\langle[\alpha_L,\alpha_U],[\beta_L,\beta_U],[\gamma_L,\gamma_U]\rangle} = \langle0, [\phi_{2L}, \phi_{2U}], [\phi_{3L}, \phi_{3U}]\rangle$ and $D^{\langle[\alpha_L,\alpha_U],[\beta_L,\beta_U],[\gamma_L,\gamma_U]\rangle} = \langle0, [\phi_{2L}, \phi_{2U}], [\phi_{3L}, \phi_{3U}]\rangle$ and
$D^{\langle[\alpha_L,\alpha_U],[\beta_L,\beta_U],[\gamma_L,\gamma_U]\rangle} = \langle0, [\phi_{2L}, \phi_{2U}], [\phi_{3L}, \phi_{3U}]\rangle$ it follows that

$C^{\langle[\alpha_L,\alpha_U],[\beta_L,\beta_U],[\gamma_L,\gamma_U]\rangle} \vee D^{\langle[\alpha_L,\alpha_U],[\beta_L,\beta_U],[\gamma_L,\gamma_U]\rangle} = (\langle0 \vee 0, \phi_2 \wedge \phi_2, \phi_3 \wedge \phi_3\rangle) = \langle0, [\phi_{2L}, \phi_{2U}], [\phi_{3L}, \phi_{3U}]\rangle$ by proposition 2,it
is known that $C \vee D \geq C$. Then by proposition
12. $C \vee D^{\langle[\alpha_L,\alpha_U],[\beta_L,\beta_U],[\gamma_L,\gamma_U]\rangle} \geq D^{\langle[\alpha_L,\alpha_U],[\beta_L,\beta_U],[\gamma_L,\gamma_U]\rangle} = \langle0, [\phi_{2L}, \phi_{2U}], [\phi_{3L}, \phi_{3U}]\rangle =$
$C^{\langle[\alpha_L,\alpha_U],[\beta_L,\beta_U],[\gamma_L,\gamma_U]\rangle} \vee D^{\langle[\alpha_L,\alpha_U],[\beta_L,\beta_U],[\gamma_L,\gamma_U]\rangle}$.

Proposition 3

Let C be a special restricted SIVPFM. Then$(C^t)^{\langle[\alpha_L,\alpha_U],[\beta_L,\beta_U],[\gamma_L,\gamma_U]\rangle} = (C^{\langle[\alpha_L,\alpha_U],[\beta_L,\beta_U],[\gamma_L,\gamma_U]\rangle})^t$.

Proof

Let C=$(\langle\left[C_{ij\lambda_L}, C_{ij\lambda_U}\right], \left[C_{ij\eta_L}, C_{ij\eta_L}\right], \left[C_{ij\zeta_L}, C_{ij\zeta_U}\right]\rangle)$be a special restricted SIVPFM of order a for three
real numbers $[\phi_{1L}, \phi_{1U}] \subseteq [0,1], [\phi_{2L}, \phi_{2U}] \subseteq [0,1]$ and$[\phi_{3L}, \phi_{3U}] \subseteq [0,1]$with $\phi_{1U} + \phi_{2U} = 1$ and $\phi_{2U} + \phi_{3U} = 1$.Then
$(\langle\left[C_{ij\lambda_L}, C_{ij\lambda_U}\right], \subseteq [\phi_{1L}, \phi_{1U}] \left[C_{ij\eta_L}, C_{ij\eta_L}\right] = [\phi_{2L}, \phi_{2U}], (\left[C_{ij\zeta_L}, C_{ij\zeta_U}\right]) \subseteq [\phi_{3L}, \phi_{3U}]$for i,j=1,2,3,………a
Let $C^{\langle[\alpha_L,\alpha_U],[\beta_L,\beta_U],[\gamma_L,\gamma_U]\rangle} = E = (\langle\left[e_{ij\zeta_L}, e_{ij\zeta_U}\right], \left[e_{ij\eta_L}, e_{ij\eta_L}\right], \left[e_{ij\theta_L}, e_{ij\theta_U}\right]\rangle)$
where$(\langle\left[e_{ij\zeta_L}, e_{ij\zeta_U}\right], \left[e_{ij\eta_L}, e_{ij\eta_L}\right], \left[e_{ij\theta_L}, e_{ij\theta_U}\right]\rangle) =$

$$\begin{cases} \langle[\phi_{1L}, \phi_{1U}], [\phi_{2L}, \phi_{2U}], 0\rangle, & when(\langle\left[c_{ij\lambda_L}, c_{ij\lambda_U}\right], \left[c_{ij\eta_L}, c_{ij\eta_L}\right], \left[c_{ij\zeta_L}, c_{ij\zeta_U}\right]\rangle) \geq \\ & \langle[\boldsymbol{\alpha_L}, \boldsymbol{\alpha_U}], [\boldsymbol{\beta_L}, \boldsymbol{\beta_U}], [\boldsymbol{\gamma_L}, \boldsymbol{\gamma_U}]\rangle \\ \langle0, \phi_2, \phi_3\rangle, & otherwise \end{cases}$$

Now,$(C^{\langle[\alpha_L,\alpha_U],[\beta_L,\beta_U],[\gamma_L,\gamma_U]\rangle})^t = E^t = (\langle\left[c_{ij\lambda_L}, c_{ij\lambda_U}\right], \left[c_{ij\eta_L}, c_{ij\eta_L}\right], \left[c_{ij\zeta_L}, c_{ij\zeta_U}\right]\rangle) =$
$(\langle\left[e_{ij\zeta_L}, e_{ij\zeta_U}\right], \left[e_{ij\eta_L}, e_{ij\eta_L}\right], \left[e_{ij\theta_L}, e_{ij\theta_U}\right]\rangle), where (\langle\left[e_{ij\zeta_L}, e_{ij\zeta_U}\right], \left[e_{ij\eta_L}, e_{ij\eta_L}\right], \left[e_{ij\theta_L}, e_{ij\theta_U}\right]\rangle) =$

Rajarajeswari and Nandhini

$$\begin{cases} \langle[\phi_{1L},\phi_{1U}],[\phi_{2L},\phi_{2U}],0\rangle, & when(\langle[c_{ij\lambda_L},c_{ij\lambda_U}],[c_{ij\eta_L},c_{ij\eta_L}],[c_{ij\zeta_L},c_{ij\zeta_U}]\rangle) \geq \\ & \langle[\alpha_L,\alpha_U],[\beta_L,\beta_U],[\gamma_L,\gamma_U]\rangle \\ \langle 0,\phi_2,\phi_3\rangle, & otherwise \end{cases}$$

$$C^t = \left((\langle[C_{ij\lambda_L},C_{ij\lambda_U}],[C_{ij\eta_L},C_{ij\eta_L}],[C_{ij\zeta_L},C_{ij\zeta_U}]\rangle)\right)^t = (\langle[C_{ji\lambda_L},C_{ji\lambda_U}],[C_{jin_L},C_{jin_L}],[C_{ji\zeta_L},C_{ji\zeta_U}]\rangle)$$

$(C^t)^{\langle[\alpha_L,\alpha_U],[\beta_L,\beta_U],[\gamma_L,\gamma_U]\rangle} = (\langle[f_{ij\zeta_L},f_{ij\zeta_U}],[f_{ij\eta_L},f_{ij\eta_L}],[f_{ij\theta_L},f_{ij\theta_U}]\rangle)$ where$(\langle[f_{ij\zeta_L},f_{ij\zeta_U}],[f_{ij\eta_L},f_{ij\eta_L}],[f_{ij\theta_L},f_{ij\theta_U}]\rangle)$

$$\begin{cases} \langle[\phi_{1L},\phi_{1U}],[\phi_{2L},\phi_{2U}],0\rangle, & when(\langle[c_{ij\lambda_L},c_{ij\lambda_U}],[c_{ij\eta_L},c_{ij\eta_U}],[c_{ij\zeta_L},c_{ij\zeta_U}]\rangle) \\ & \geq \langle[\alpha_L,\alpha_U],[\beta_L,\beta_U],[\gamma_L,\gamma_U]\rangle \\ \langle 0,\phi_2,\phi_3\rangle, & otherwise \end{cases}$$

$(\langle[e_{ij\zeta_L},e_{ij\zeta_U}],[e_{ij\eta_L},e_{ij\eta_L}],[e_{ij\theta_L},e_{ij\theta_U}]\rangle)=(\langle[f_{ij\zeta_L},f_{ij\zeta_U}],[f_{ij\eta_L},f_{ij\eta_L}],[f_{ij\theta_L},f_{ij\theta_U}]\rangle)$for i,j=1,2,3,……a.$(C^t)^{\langle[\alpha_L,\alpha_U],[\beta_L,\beta_U],[\gamma_L,\gamma_U]\rangle}=(C^{\langle[\alpha_L,\alpha_U],[\beta_L,\beta_U],[\gamma_L,\gamma_U]\rangle})^t$.

Proposition 4

For a reflexive Special restricted SIVPFM,$C_{\langle[\alpha_L,\alpha_U],[\beta_L,\beta_U],[\gamma_L,\gamma_U]\rangle}$ *is* reflexive.

Proof

Let C=$(\langle[c_{ij\zeta_L},c_{ij\zeta_U}],[c_{ij\eta_L},c_{ij\eta_L}],[c_{ij\theta_L},c_{ij\theta_U}]\rangle)$ and D=$(\langle[d_{ij\zeta_L},d_{ij\zeta_U}],[d_{ij\eta_L},d_{ij\eta_L}],[d_{ij\theta_L},d_{ij\theta_U}]\rangle)$be two special restricted SIVPFM of order a for three real numbers $[\phi_{1L},\phi_{1U}] \subseteq [0,1], [\phi_{2L},\phi_{2U}] \subseteq [0,1] and [\phi_{3L},\phi_{3U}] \subseteq [0,1]$with $\phi_{1U} + \phi_{2U} = 1 \ and \ \phi_{2U} + \phi_{3U} = 1.$Then

$(\langle[c_{ij\zeta_L},c_{ij\zeta_U}],[d_{ij\zeta_L},d_{ij\zeta_U}] \subseteq [\phi_{1L},\phi_{1U}][C_{ij\eta_L},C_{ij\eta_L}] = [d_{ij\eta_L},d_{ij\eta_L}] = [\phi_{2L},\phi_{2U}],([c_{ij\theta_L},c_{ij\theta_U}],[d_{ij\theta_L},d_{ij\theta_U}]) \subseteq [\phi_{3L},\phi_{3U}]$for i,j=1,2,3,………aSince C is reflexive, C=$(\langle[C_{ij\lambda_L},C_{ij\lambda_U}],[C_{ij\eta_L},C_{ij\eta_L}],[C_{ij\zeta_L},C_{ij\zeta_U}]\rangle) = \langle[\phi_{1L},\phi_{1U}],[\phi_{2L},\phi_{2U}],0\rangle$

i=1,2,3, ……. ,a. Let$C_{\langle[\alpha_L,\alpha_U],[\beta_L,\beta_U],[\gamma_L,\gamma_U]\rangle}=(\langle[e_{ij\zeta_L},e_{ij\zeta_U}],[e_{ij\eta_L},e_{ij\eta_L}],[e_{ij\theta_L},e_{ij\theta_U}]\rangle)$,

Where $(\langle[e_{ij\lambda_L},e_{ij\lambda_U}],[e_{ij\eta_L},e_{ij\eta_L}],[e_{ij\zeta_L},e_{ij\zeta_U}]\rangle) = $

$$\begin{cases} (\langle[c_{ij\zeta_L},c_{ij\zeta_U}],[c_{ij\eta_L},c_{ij\eta_L}],[c_{ij\theta_L},c_{ij\theta_U}]\rangle), & when(\langle[c_{ij\zeta_L},c_{ij\zeta_U}],[c_{ij\eta_L},c_{ij\eta_L}],[c_{ij\theta_L},c_{ij\theta_U}]\rangle) \\ & \geq \langle[\alpha_L,\alpha_U],[\beta_L,\beta_U],[\gamma_L,\gamma_U]\rangle \\ \langle[\alpha_L,\alpha_U],[\beta_L,\beta_U],[\gamma_L,\gamma_U]\rangle & otherwise \end{cases}$$

Then $(\langle[e_{ij\zeta_L},e_{ij\zeta_U}],[e_{ij\eta_L},e_{ij\eta_L}],[e_{ij\theta_L},e_{ij\theta_U}]\rangle) = \langle[\phi_{1L},\phi_{1U}],[\phi_{2L},\phi_{2U}],[0,0]\rangle$

$\langle\phi_1,\phi_2,0\rangle = \langle\langle[\alpha_L,\alpha_U],[\beta_L,\beta_U],[\gamma_L,\gamma_U]\rangle\rangle$ So clearly $C^{\langle[\alpha_L,\alpha_U],[\beta_L,\beta_U],[\gamma_L,\gamma_U]\rangle}$ is reflexive.

Determinant Of SIVPFM.

In this section, we define determinant of SIVPFM and study some corresponding basic results related to it.

Definition 3

Let C=$(\langle[c_{ij\lambda_L},c_{ij\lambda_U}],[c_{ij\eta_L},c_{ij\eta_L}],[c_{ij\zeta_L},c_{ij\zeta_U}]\rangle)$ be a SIVPFM of order a. Then determinant of C is denoted by |C| and is defined by

$$|C|=\langle \bigvee_{\beta\in F_a}(C_{1\beta(1)\zeta_L} \wedge C_{2\beta(2)\zeta_L} \wedge \ldots\ldots \wedge C_{a\beta(a)\zeta_L}), \bigvee_{\beta\in F_a}(C_{1\beta(1)\zeta_U} \wedge C_{2\beta(2)\zeta_U} \wedge \ldots\ldots \wedge C_{a\beta(a)\zeta_U}),$$

$$\bigwedge_{\beta\in F_a}(C_{1\beta(1)\eta_L} \wedge C_{2\beta(2)\eta_L} \wedge \ldots\ldots \wedge C_{a\beta(a)\eta_L}), \bigvee_{\beta\in F_a}(C_{1\beta(1)\eta_U} \wedge C_{2\beta(2)\eta_U} \wedge \ldots\ldots \wedge C_{a\beta(a)\eta_U})\rangle$$

$$\bigwedge_{\beta\in F_a}(C_{1\beta(1)\theta_L} \vee C_{2\beta(2)\theta_L} \vee \ldots\ldots \vee C_{a\beta(a)\theta_L}), \bigvee_{\beta\in F_a}(C_{1\beta(1)\theta_U} \vee C_{2\beta(2)\theta_U} \vee \ldots\ldots \vee C_{a\beta(a)\theta_U}),$$

Where F_a be the set of permutation on the set$\{1,2,3,\ldots\ldots.a\}$.

Example 1

Let us consider a SIVPFMs of order 3 as follows.

Rajarajeswari and Nandhini

$$C=\begin{pmatrix} \langle[0.3,0.5],[0.2,0.3],[0.1,0.2]\rangle & \langle[0.1,0.2],[0.3,0.4],[0.3,0.4]\rangle & \langle[0.2,0.3],[0.4,0.5],[0.1,0.2]\rangle \\ \langle[0.2,0.3],[0.5,0.6],[0.1,0.1]\rangle & \langle[0.1,0.2],[0.5,0.6],[0.1,0.2]\rangle & \langle[0.3,0.4],[0.3,0.4],[0.1,0.2]\rangle \\ \langle[0.5,0.6],[0.1,0.1],[0.2,0.3]\rangle & \langle[0.4,0.5],[0.1,0.2],[0.2,0.3]\rangle & \langle[0.1,0.2],[0.2,0.2],[0.5,0.6]\rangle \end{pmatrix}$$

To find out the determinant of C, it needs to find out all permutations on{1,2,3}. The permutations on {1,2,3} *are*

$$\psi_1 = \begin{pmatrix} 1 & 2 & 3 \\ 1 & 2 & 3 \end{pmatrix} \psi_2 = \begin{pmatrix} 1 & 2 & 3 \\ 1 & 3 & 2 \end{pmatrix} \psi_3 = \begin{pmatrix} 1 & 2 & 3 \\ 2 & 1 & 3 \end{pmatrix}$$
$$\psi_4 = \begin{pmatrix} 1 & 2 & 3 \\ 2 & 3 & 1 \end{pmatrix} \psi_5 = \begin{pmatrix} 1 & 2 & 3 \\ 3 & 1 & 2 \end{pmatrix} \psi_6 = \begin{pmatrix} 1 & 2 & 3 \\ 3 & 2 & 1 \end{pmatrix}$$

The membership of det(C) is

$(C_{1\psi_1(1)\zeta_L} \wedge C_{1\psi_2(1)\zeta_L} \wedge C_{1\psi_1(3)\zeta_L})\,(C_{1\psi_1(1)\zeta_U} \wedge C_{1\psi_1(2)\zeta_U} \wedge C_{1\psi_1(3)\zeta_U})$

$\qquad\qquad \vee (C_{1\psi_2(1)\zeta_L} \wedge C_{2\psi_2(2)\lambda_L} \wedge C_{3\psi_2(3)\zeta_L})\,(C_{1\psi_2(1)\zeta_U} \wedge C_{2\psi_2(2)\zeta_U} \wedge C_{3\psi_2(3)\zeta_U})$

$\qquad\qquad \vee (C_{1\psi_3(1)\zeta_L} \wedge C_{2\psi_3(1)\zeta_L} \wedge C_{3\psi_3(3)\zeta_L})\,(C_{1\psi_3(1)\zeta_U} \wedge C_{2\psi_3(2)\zeta_U} \wedge C_{3\psi_3(3)\zeta_U})$

$\qquad\qquad \vee (C_{1\psi_4(1)\zeta_L} \wedge C_{2\psi_4(1)\zeta_L} \wedge C_{3\psi_4(3)\zeta_L})\,(C_{1\psi_4(1)\zeta_U} \wedge C_{2\psi_4(2)\zeta_U} \wedge C_{3\psi_4(3)\zeta_U})$

$\qquad\qquad \vee (C_{1\psi_5(1)\zeta_L} \wedge C_{\psi_5(1)\zeta_L} \wedge C_{3\psi_5(3)\zeta_L})\,(C_{1\psi_5(1)\zeta_U} \wedge C_{2\psi_5(2)\zeta_U} \wedge C_{3\psi_5(3)\zeta_U})$

$\qquad\qquad \vee (C_{1\psi_6(1)\zeta_L} \wedge C_{2\psi_6(1)\zeta_L} \wedge C_{3\psi_6(3)\zeta_L})\,(C_{1\psi_6(1)\zeta_U} \wedge C_{2\psi_6(2)\zeta_U} \wedge C_{3\psi_6(3)\zeta_U})$

$=(c_{11}\zeta_L \wedge c_{22}\zeta_L \wedge c_{33}\zeta_L)(c_{11}\zeta_U \wedge c_{22}\zeta_U \wedge c_{33}\zeta_U)$

$\qquad\qquad \vee (c_{11}\zeta_L \wedge c_{23}\zeta_L \wedge c_{32}\zeta_L)(c_{11}\zeta_U \wedge c_{23}\zeta_U \wedge c_{32}\zeta_U)$

$\qquad\qquad \vee (c_{12}\zeta_L \wedge c_{21}\zeta_L \wedge c_{33}\zeta_L)(c_{12}\zeta_U \wedge c_{21}\zeta_U \wedge c_{33}\zeta_U)$

$\qquad\qquad \vee (c_{12}\zeta_L \wedge c_{23}\zeta_L \wedge c_{31}\zeta_L)(c_{12}\zeta_U \wedge c_{23}\zeta_U \wedge c_{31}\zeta_U)$

$\qquad\qquad \vee (c_{13}\zeta_L \wedge c_{21}\zeta_L \wedge c_{32}\zeta_L)(c_{13}\zeta_U \wedge c_{21}\zeta_U \wedge c_{32}\zeta_U)$

$\qquad\qquad \vee (c_{13}\zeta_L \wedge c_{22}\zeta_L \wedge c_{31}\zeta_L)(c_{13}\zeta_L \wedge c_{22}\zeta_L \wedge c_{31}\zeta_L)$

$=(0.3 \wedge 0.1 \wedge 0.1)(0.5 \wedge 0.2 \wedge 0.2) \vee (0.3 \wedge 0.3 \wedge 0.4)(0.5 \wedge 0.4 \wedge 0.5) \vee (0.1 \wedge 0.2 \wedge 0.1)(0.2 \wedge 0.3 \wedge 0.2) \vee (0.1 \wedge 0.3 \wedge$
0.50.2∧0.4∧0.6∨0.2∧0.2∧0.40.30.3∧0.5∨0.2∧0.1∧0.50.3∧0.2∧0.6

$=([0.1,0.2] \vee [0.3,0.4] \vee [0.1,0.2] \vee [0.1,0.2] \vee [0.2,0.3] \vee [0.2,0.2])$

$=[0.3,0.4]$

The neutral membership of det(C) is

$= (C_{1\psi_1(1)\eta_L} \wedge C_{2\psi_1(2)\eta_L} \wedge C_{1\psi_1(3)\eta_L})\,(C_{1\psi_1(1)\eta_U} \wedge C_{2\psi_1(2)\eta_U} \wedge C_{1\psi_1(3)\eta_U})$

$\qquad\qquad \vee (C_{1\psi_2(1)\eta_L} \wedge C_{2\psi_2(2)\eta_L} \wedge C_{3\psi_2(3)\eta_L})\,(C_{1\psi_2(1)\eta_U} \wedge C_{2\psi_2(2)\eta_U} \wedge C_{3\psi_2(3)\eta_U})$

$\qquad\qquad \vee (C_{1\psi_3(1)\eta_L} \wedge C_{2\psi_3(2)\eta_L} \wedge C_{3\psi_3(3)\eta_L})\,(C_{1\psi_3(1)\eta_U} \wedge C_{2\psi_3(2)\eta_U} \wedge C_{3\psi_3(3)\eta_U})$

$\qquad\qquad \vee (C_{1\psi_4(1)\eta_L} \wedge C_{2\psi_4(2)\eta_L} \wedge C_{3\psi_4(3)\eta_L})\,(C_{1\psi_4(1)\eta_U} \wedge C_{2\psi_4(2)\eta_U} \wedge C_{3\psi_4(3)\eta_U})$

$\qquad\qquad \vee (C_{1\psi_5(1)\eta_L} \wedge C_{2\psi_5(2)\eta_L} \wedge C_{3\psi_5(3)\eta_L})\,(C_{1\psi_5(1)\eta_U} \wedge C_{2\psi_5(2)\eta_U} \wedge C_{3\psi_5(3)\eta_U})$

$\qquad\qquad \vee (C_{1\psi_6(1)\eta_L} \wedge C_{2\psi_6(2)\eta_L} \wedge C_{3\psi_6(3)\eta_L})\,(C_{1\psi_6(1)\eta_U} \wedge C_{2\psi_6(2)\eta_U} \wedge C_{3\psi_6(3)\eta_U})$

$=(c_{11}\eta_L \wedge c_{22}\eta_L \wedge c_{33}\eta_L)(c_{11}\eta_U \wedge c_{22}\eta_U \wedge c_{33}\eta_U)$

$\qquad\qquad \wedge (c_{11}\eta_L \wedge c_{23}\eta_L \wedge c_{32}\eta_L)(c_{11}\eta_U \wedge c_{23}\eta_U \wedge c_{32}\eta_U)$

$\qquad\qquad \wedge (c_{12}\eta_L \wedge c_{21}\eta_L \wedge c_{33}\eta_L)(c_{12}\eta_U \wedge c_{21}\eta_U \wedge c_{33}\eta_U)$

$\qquad\qquad \wedge (c_{12}\eta_L \wedge c_{23}\eta_L \wedge c_{31}\eta_L)(c_{12}\eta_U \wedge c_{23}\eta_U \wedge c_{31}\eta_U)$

$\qquad\qquad \wedge (c_{13}\eta_L \wedge c_{21}\eta_L \wedge c_{32}\eta_L)(c_{13}\eta_U \wedge c_{21}\eta_U \wedge c_{32}\eta_U)$

$\qquad\qquad \wedge (c_{13}\eta_L \wedge c_{22}\eta_L \wedge c_{31}\eta_L)(c_{13}\eta_U \wedge c_{22}\eta_U \wedge c_{31}\eta_U)$

$=(0.2 \wedge 0.5 \wedge 0.2)(0.3 \wedge 0.6 \wedge 0.2) \wedge (0.2 \wedge 0.3 \wedge 0.1)(0.3 \wedge 0.4 \wedge 0.2) \wedge (0.3 \wedge 0.5 \wedge 0.2)(0.4 \wedge 0.6 \wedge 0.2) \wedge (0.3 \wedge 0.3 \wedge$
0.10.4∧0.4∧0.1∧0.4∧0.5∧0.10.5∧0.6∧0.2∧0.4∧0.5∧0.10.5∧0.6∧0.1

$=([0.2,0.2] \wedge [0.1,0.2] \wedge [0.2,0.2] \wedge [0.1,0.1] \wedge [0.1,0.2] \wedge [0.1,0.1])$

$=[0.1,0.1]$

Rajarajeswari and Nandhini

The non- membership of det(C) is

$$= (C_{1\psi_1(1)\theta_L} \vee C_{2\psi_1(2)\theta_L} \vee C_{1\psi_1(3)\theta_L})(C_{1\psi_1(1)\theta_U} \vee C_{2\psi_1(2)\theta_U} \vee C_{3\psi_1(3)\theta_U})$$

$$\wedge (C_{1\psi_2(1)\theta_L} \vee C_{2\psi_2(2)\theta_L} \vee C_{3\psi_2(3)\theta_L})(C_{1\psi_2(1)\theta_U} \vee C_{2\psi_2(2)\theta_U} \vee C_{3\psi_2(3)\theta_U})$$

$$\wedge (C_{1\psi_3(1)\theta_L} \vee C_{2\psi_3(2)\theta_L} \vee C_{3\psi_3(3)\theta_L})(C_{1\psi_3(1)\theta_U} \vee C_{2\psi_3(2)\theta_U} \vee C_{3\psi_3(3)\theta_U})$$

$$\wedge (C_{1\psi_4(1)\theta_L} \vee C_{2\psi_4(2)\theta_L} \vee C_{3\psi_4(3)\theta_L})(C_{1\psi_4(1)\theta_U} \vee C_{2\psi_4(2)\theta_U} \vee C_{3\psi_4(3)\theta_U})$$

$$\wedge (C_{1\psi_5(1)\theta_L} \vee C_{2\psi_5(2)\theta_L} \vee C_{3\psi_5(3)\theta_L})(C_{1\psi_5(1)\theta_U} \vee C_{2\psi_5(2)\theta_U} \vee C_{3\psi_5(3)\theta_U})$$

$$\wedge (C_{1\psi_6(1)\theta_L} \vee C_{2\psi_6(2)\theta_L} \vee C_{3\psi_6(3)\theta_L})(C_{1\psi_6(1)\theta_U} \vee C_{2\psi_6(2)\theta_U} \vee C_{3\psi_6(3)\theta_U})$$

$$=(c_{11}\theta_L \vee c_{22}\theta_L \vee c_{33}\theta_L)\zeta(c_{11}\theta_U \vee c_{22}\theta_U \vee c_{33}\theta_U)$$

$$\wedge (c_{11}\theta_L \vee c_{23}\theta_L \vee c_{32}\theta_L)(c_{11}\theta_U \vee c_{23}\theta_U \vee c_{32}\theta_U)$$

$$\wedge (c_{12}\theta_L \vee c_{21}\theta_L \vee c_{33}\theta_L)(c_{12}\theta_U \vee c_{21}\theta_U \vee c_{33}\theta_U)$$

$$\wedge (c_{12}\theta_L \vee c_{23}\theta_L \vee c_{31}\theta_L)(c_{12}\theta_U \vee c_{23}\theta_U \vee c_{31}\theta_U)$$

$$\wedge (c_{13}\theta_L \vee c_{21}\theta_L \vee c_{32}\theta_L)(c_{13}\theta_U \vee c_{21}\theta_U \vee c_{32}\theta_U)$$

$$\wedge (c_{13}\theta_L \vee c_{22}\theta_L \vee c_{31}\theta_L)(c_{13}\theta_U \vee c_{22}\theta_U \vee c_{31}\theta_U)$$

$=(0.1 \vee 0.1 \vee 0.5)(0.2 \vee 0.2 \vee 0.6) \wedge (0.1 \vee 0.1 \vee 0.2)(0.2 \vee 0.2 \vee 0.3) \wedge (0.3 \vee 0.1 \vee 0.5)(0.4 \vee 0.1 \vee$ 0.6) $\wedge$ (0.3 $\vee$ 0.1 $\vee$
0.20.4$\vee$0.2$\wedge$0.3$\wedge$0.1$\vee$0.1$\vee$0.20.2$\vee$0.1$\vee$0.3$\wedge$0.1$\vee$0.1$\vee$0.20.2$\vee$ 0.2$\vee$0.3

$=([0.5,0.6] \wedge [0.2,0.3] \wedge [0.5,0.6] \wedge [0.3,0.4] \wedge [0.2,0.3] \wedge [0.2,0.3])$

$=[0.2,0.3]$

So det(C) =$\langle[0.3,0.4], [0.1,0.1], [0.2,0.3]\rangle$

Proposition 5

Let C=$(\langle[C_{ij\zeta_L}, C_{ij\zeta_U}], [C_{ij\eta_L}, C_{ij\eta_L}], [C_{ij\theta_L}, C_{ij\theta_U}]\rangle)$ be a SIVPFM and C^t be the transpose of C. Then det (C^t)=det(C)

Proof

Let C=$(\langle[C_{ij\zeta_L}, C_{ij\zeta_U}], [C_{ij\eta_L}, C_{ij\eta_L}], [C_{ij\theta_L}, C_{ij\theta_U}]\rangle)$ be a SIVPFM of order a Then

$$C^t = (\langle(\langle[C_{ij\zeta_L}, C_{ij\zeta_U}], [C_{ij\eta_L}, C_{ij\eta_L}], [C_{ij\theta_L}, C_{ij\theta_U}]\rangle))^t = ((\langle[C_{ij\zeta_L}, C_{ij\zeta_U}], [C_{ij\eta_L}, C_{ij\eta_L}], [C_{ij\theta_L}, C_{ij\theta_U}]\rangle))$$

Now, det (C)

$$\langle \overset{\vee}{_{\beta\in F_a}}(C_{1\beta(1)\zeta_L} \wedge C_{2\beta(2)\zeta_L} \wedge \ldots\ldots \wedge C_{a\beta(a)\zeta_L}), \overset{\vee}{_{\beta\in F_a}}(C_{1\beta(1)\zeta_U} \wedge C_{2\beta(2)\zeta_U} \wedge \ldots\ldots \wedge C_{a\beta(a)\zeta_U}),$$
$$\overset{\wedge}{_{\beta\in F_a}}(C_{1\beta(1)\eta_L} \wedge C_{2\beta(2)\eta_L} \wedge \ldots\ldots \wedge C_{a\beta(a)\eta_L}), \overset{\vee}{_{\beta\in F_a}}(C_{1\beta(1)\eta_U} \wedge C_{2\beta(2)\eta_U} \wedge \ldots\ldots \wedge C_{a\beta(a)\eta_U})\rangle$$
$$\overset{\wedge}{_{\beta\in F_a}}(C_{1\beta(1)\theta_L} \vee C_{2\beta(2)\theta_L} \vee \ldots\ldots \vee C_{a\beta(a)\theta_L}), \overset{\vee}{_{\beta\in F_a}}(C_{1\beta(1)\theta_U} \vee C_{2\beta(2)\theta_U} \vee \ldots\ldots \vee C_{a\beta(a)\theta_U}),$$

Where F_a be the set of permutation on the set$\{1,2,3, \ldots\ldots., a\}$
det (C^t)=

$$\overset{\vee}{_{\beta\in F_a}}(C_{\beta(1)1_L} \wedge C_{\beta(2)2_L} \wedge \ldots\ldots \wedge C_{\beta(a)a_L}), \overset{\vee}{_{\beta\in F_a}}(C_{\beta(1)1_U} \wedge C_{\beta(2)2_U} \wedge \ldots\ldots \wedge C_{\beta(a)a_U}),$$
$$\langle \overset{\wedge}{_{\beta\in F_a}}(C_{\beta(1)1\eta_L} \wedge C_{\beta(2)2\eta_L} \wedge \ldots\ldots \wedge C_{\beta(a)a\eta_L}), \overset{\vee}{_{\beta\in F_a}}(C_{\beta(1)1\eta_U} \wedge C_{\beta(2)2\eta_U} \wedge \ldots\ldots \wedge C_{\beta(a)a\eta_U})\rangle$$
$$\overset{\wedge}{_{\beta\in F_a}}(C_{\beta(1)1\zeta_L} \vee C_{\beta(2)2\zeta_L} \vee \ldots\ldots \vee C_{\beta(a)a\zeta_L}), \overset{\vee}{_{\beta\in F_a}}(C_{\beta(1)1\zeta_U} \vee C_{\beta(2)2\zeta_U} \vee \ldots\ldots \vee C_{\beta(a)a\zeta_U}),$$

Let ψe the permutation on {1,2,3,……a} such that $\psi\beta\beta$where l_a
 Is the identity permutation {1,2,3,……a} then Let $\psi \neq \beta^1$.Here ψchanges through all permutation because βdoes go.Let
$\beta\zeta = \psi$then i= β^1.(j)=$\psi(j)$. Since i runs from 1 to a, j also runs from 1 to a.so$\beta(j)i = j\psi(j)$.
Thus, it can be written as det(C^t)=det(C).

Proposition 6

The determinant of an identity special restricted IVPFM C of order a is$\langle\phi_{1L},\phi_{1U},\phi_{2L},\phi_{2U}, 0\rangle$

Proof

Let C=$(\langle[C_{ij\zeta_L}, C_{ij\zeta_U}], [C_{ij\eta_L}, C_{ij\eta_L}], [C_{ij\theta_L}, C_{ij\theta_U}]\rangle)$ and be an identity special restricted SIVPFM of order a for three real numbers $\phi_{1L}, \phi_{1U} \in [0,1], \phi_{2L}, \phi_{2U} \in [0,1] and \phi_{3L}, \phi_{3U} \in [0,1]$ with

$\phi_{1U} + \phi_{2U} = 1\ and\ \phi_{2U} + \phi_{3U} = 1$. Then $(\langle[C_{ij\zeta_L}, C_{ij\zeta_U}], [d_{ij\zeta_L}, d_{ij\zeta_U}] \in [\phi_{1L}, \phi_{1U}][C_{ij\eta_L}, C_{ij\eta_L}] = [d_{ij\eta_L}, d_{ij\eta_L}] = [\phi_{2L}, \phi_{2U}], [C_{ij\theta_L}, C_{ij\theta_U}], [d_{ij\theta_L}, d_{ij\theta_U}]\rangle) \in [\phi_{3L}, \phi_{3U}]$ with $0 \le (\langle[C_{ij\zeta_L}, C_{ij\zeta_U}] + [C_{ij\eta_L}, C_{ij\eta_L}] + [C_{ij\theta_L}, C_{ij\theta_U}]\rangle) \le 1$

for i,j=1,2,3,………a. Here the diagonal entries of C are $\langle\phi_{1L}, \phi_{1U}, \phi_{2L}, \phi_{2U}, 0\rangle$ for i=1,2,3,…….a.

Now, det(c)   =

$$\underset{\beta \in F_a}{\vee}(C_{1\beta(1)\lambda_L} \wedge C_{2\beta(2)\lambda_L} \wedge \dots\dots \wedge C_{a\beta(a)\lambda_L}), \underset{\beta \in F_a}{\vee}(C_{1\beta(1)\lambda_U} \wedge C_{2\beta(2)\lambda_U} \wedge \dots\dots \wedge C_{a\beta(a)\lambda_U}),$$

$$\langle\underset{\beta \in F_a}{\wedge}(C_{1\beta(1)\eta_L} \wedge C_{2\beta(2)\eta_L} \wedge \dots\dots \wedge C_{a\beta(a)\eta_L}), \underset{\beta \in F_a}{\vee}(C_{1\beta(1)\eta_U} \wedge C_{2\beta(2)\eta_U} \wedge \dots\dots \wedge C_{a\beta(a)\eta_U})\rangle$$

$$\underset{\beta \in F_a}{\wedge}(C_{1\beta(1)\zeta_L} \vee C_{2\beta(2)\zeta_L} \vee \dots\dots \vee C_{a\beta(a)\zeta_L}), \underset{\beta \in F_a}{\vee}(C_{1\beta(1)\zeta_U} \vee C_{2\beta(2)\zeta_U} \vee \dots\dots \vee C_{a\beta(a)\zeta_U}),$$

Where F_a be the set of permutation on the set {1,2,3,……a}.

Now, for $\beta = I_a$, (*identity permutation*),

$\beta(i) = i$ for i=1,2,3,……a

So, for identity permutation.

$$C_{1\beta(1)\lambda_L} \wedge C_{2\beta(2)\lambda_L} \wedge \dots\dots \wedge C_{a\beta(a)\lambda_L}, C_{1\beta(1)\lambda_U} \wedge C_{2\beta(2)\lambda_U} \wedge \dots\dots \wedge C_{a\beta(a)\lambda_U}$$

$=\phi_{1L} \wedge \phi_{1L} \wedge \phi_{1L} \wedge \dots\dots\wedge \phi_{1L}, \phi_{1U} \wedge \phi_{1U} \wedge \dots\dots\wedge \phi_{1U}$.

$$C_{1\beta(1)\eta_L} \wedge C_{2\beta(2)\eta_L} \wedge \dots\dots \wedge C_{a\beta(a)\eta_L}, C_{1\beta(1)\eta_U} \wedge C_{2\beta(2)\eta_U} \wedge \dots\dots \wedge C_{a\beta(a)\eta_U}.$$

$=\phi_{2L} \wedge \phi_{2L} \wedge \dots\dots\wedge \phi_{2L}, \phi_{2U} \wedge \phi_{2U} \wedge \dots\dots\wedge \phi_{2U}$.

$C_{1\beta(1)\zeta_L} \vee C_{2\beta(2)\zeta_L} \vee \dots\dots \vee C_{a\beta(a)\zeta_L}, C_{1\beta(1)\zeta_U} \vee C_{2\beta(2)\zeta_U} \vee \dots\dots \vee C_{a\beta(a)\zeta_U}$

$=0\vee 0 \vee \dots\dots\dots \vee 0 = 0$.

Thus ,it can be writien as

det(C)=

$$\left(\phi_{1L} \vee \underset{\beta \in F_a}{\vee}(C_{1\beta(1)\zeta_L} \wedge C_{2\beta(2)\zeta_L} \wedge \dots\dots \wedge C_{a\beta(a)\zeta_L})\right), \left(\phi_{1U} \vee \underset{\beta \in F_a}{\vee}(C_{1\beta(1)\zeta_U} \wedge C_{2\beta(2)\zeta_U} \wedge \dots\dots \wedge C_{a\beta(a)\zeta_U})\right)$$

$$\langle\left(\phi_{2L} \wedge \underset{\beta \in F_a}{\wedge}(C_{1\beta(1)\eta_L} \wedge C_{2\beta(2)\eta_L} \wedge \dots\dots \wedge C_{a\beta(a)\eta_L})\right), \left(\phi_{2L} \wedge \underset{\beta \in F_a}{\vee}(C_{1\beta(1)\eta_U} \wedge C_{2\beta(2)\eta_U} \wedge \dots\dots \wedge C_{a\beta(a)\eta_U})\right)\rangle$$

$$\left(0 \wedge \underset{\beta \in F_a}{\wedge}(C_{1\beta(1)\theta_L} \vee C_{2\beta(2)\zeta_L} \vee \dots\dots \vee C_{a\beta(a)\theta_L})\right), \left(0 \wedge \underset{\beta \in F_a}{\vee}(C_{1\beta(1)\theta_U} \vee C_{2\beta(2)\theta_U} \vee \dots\dots \vee C_{a\beta(a)\theta_U})\right)$$

$=\langle\phi_{1L}, \phi_{1U}, \phi_{2L}, \phi_{2U}, 0\rangle$

5.Adjoint of SIVPFM

In this part, we define the adjoint of a SIVPFM and look at some associated fundamental features.

Definition 4

Let C=$(\langle[C_{ij\zeta_L}, C_{ij\zeta_U}], [C_{ij\eta_L}, C_{ij\eta_L}], [C_{ij\theta_L}, C_{ij\theta_U}]\rangle)$ be a SIVPFM of order a. Then adjoint of C is denoted by adj(C) and is defined as the SIVPFM E=$(\langle[e_{ij\zeta_L}, e_{ij\zeta_U}], [e_{ij\eta_L}, e_{ij\eta_L}], [e_{ij\theta_L}, e_{ij\theta_U}]\rangle)$=adj(C),

Where

$$([e_{ij\zeta_L}, e_{ij\zeta_U}]) = \underset{\beta \in F_{a_j n_i}}{\vee}\left(\underset{w \in a_j}{\wedge}C_w\beta(w)\zeta_L, \underset{w \in a_j}{\wedge}C_w\beta(w)\zeta_U\right)$$

$$([e_{ij\eta_L}, e_{ij\eta_L}]) = \underset{\beta \in F_{a_j a_i}}{\wedge}\left(\underset{w \in a_j}{\wedge}C_w\beta(w)\eta_L, \underset{w \in a_j}{\wedge}C_w\beta(w)\eta_U\right)$$

$([e_{ij\theta_L}, e_{ij\theta_U}])= \underset{\beta \in F_{a_j n_i}}{\wedge}\left(\underset{w \in a_j}{\vee}C_w\beta(w)\theta_L, \underset{w \in a_j}{\vee}C_w\beta(w)\theta_U\right)$

Here $a_j = \{1,2,3, \dots\dots a\}$ -$\{a\}$ and $F_{a_j a_i}$ is the set of all permutations on the set a_j over the set a_i.

Proposition 7

Let C be a SIVPFM. Then adj$(C^t) = \left(adj(C)\right)^t$.

Proposition 8

Let C and D be two SIVPFM of same order. Then $C \le D \Rightarrow adj(C) \le adj(D)$.

Proof

Let C=$(\langle[c_{ij\zeta_L}, c_{ij\zeta_U}], [c_{ij\eta_L}, c_{ij\eta_L}], [c_{ij\theta_L}, c_{ij\theta_U}]\rangle)$ and D=$(\langle[d_{ij\zeta_L}, d_{ij\zeta_U}], [d_{ij\eta_L}, d_{ij\eta_L}], [d_{ij\theta_L}, d_{ij\theta_U}]\rangle)$two SIVPFM of order a. Let E= adj(C) and G= adj(D).

$$\text{Then}\left(\left\langle \begin{array}{c} \beta \in F_{a_j n_i}\left(\overset{\vee}{w \in a_j} C_w\beta(w)\zeta_L, \overset{\wedge}{w \in a_j} c_w\beta(w)\zeta_U\right), \beta \in F_{a_j a_i}\left(\overset{\wedge}{w \in a_j} C_w\beta(w)\eta_L, \overset{\wedge}{w \in a_j} C_w\beta(w)\eta_U\right), \\ \beta \in F_{a_j n_i}\left(\overset{\wedge}{w \in a_j} C_w\beta(w)\theta_L, \overset{\vee}{w \in a_j} C_w\beta(w)\theta_U\right) \end{array}\right\rangle\right)$$

$$(\langle[g_{ij\zeta_L}, g_{ij\zeta_U}], [g_{ij\eta_L}, g_{ij\eta_L}], [g_{ij\theta_L}, g_{ij\theta_U}]\rangle)=$$
$$\left(\left\langle \begin{array}{c} \beta \in F_{a_j n_i}\left(\overset{\vee}{w \in a_j} d_w\beta(w)\zeta_L, \overset{\wedge}{w \in a_j} d_w\beta(w)\zeta_U\right), \beta \in F_{a_j a_i}\left(\overset{\wedge}{w \in a_j} d_w\beta(w)\eta_L, \overset{\wedge}{w \in a_j} d_w\beta(w)\eta_U\right), \\ \beta \in F_{a_j n_i}\left(\overset{\wedge}{w \in a_j} d_w\beta(w)\theta_L, \overset{\vee}{w \in a_j} d_w\beta(w)\theta_U\right) \end{array}\right\rangle\right)$$

$(C_w\beta(w)\zeta_L, C_w\beta(w)\zeta_U) \le (d_w\beta(w)\zeta_L, d_w\beta(w)\zeta_U)$
$(C_w\beta(w)\eta_L, C_w\beta(w)\eta_U) \le (d_w\beta(w)\eta_L, d_w\beta(w)\eta_U)$
$(d_w\beta(w)\theta_L, d_w\beta(w)\theta_U) \ge (d_w\beta(w)\theta_L, d_w\beta(w)\theta_U)$ for every w$\neq j, \beta(w) \neq i$, consequently, E$\le F, i.e,$
adj(C)$\le adj(D)$.

Proposition 9.

Let C be a special restricted SIVPFM, then adj (C$\vee D$) $\ge$ adj(C) $\vee adj(D)$.

Proof

Let C=$(\langle[c_{ij\zeta_L}, c_{ij\zeta_U}], [c_{ij\eta_L}, c_{ij\eta_L}], [c_{ij\theta_L}, c_{ij\theta_U}]\rangle)$ and D=$(\langle[d_{ij\zeta_L}, d_{ij\zeta_U}], [d_{ij\eta_L}, d_{ij\eta_L}], [d_{ij\theta_L}, d_{ij\theta_U}]\rangle)$two SIVPFM of order a. Let E= adj(C) and G= adj(D).it is known from proposition 2.that C,D$\le$ C $\vee$ D.it follows that adj(C)$\le$ adj(C $\vee D$) and adj(D)$\le adj$(C $\vee D$). Thus adj(C)$\vee$ adj(D)$\le adj$(C $\vee D$).

Proposition 10.

Let C be any special restricted SIVPFM and I be an identity special restricted IVPFM whose order is equal to the order of C. Then adj (C).C$\ge |C|.I$.

Proof

Let C=$(\langle[c_{ij\zeta_L}, c_{ij\zeta_U}], [c_{ij\eta_L}, c_{ij\eta_L}], [c_{ij\theta_L}, c_{ij\theta_U}]\rangle)$ be a special restricted SIVPFM of order a for three real numbers $\phi_{1L}, \phi_{1U} \in [0,1], \phi_{2L}, \phi_{2U} \in [0,1]$ and $\phi_{3L}, \phi_{3U} \in [0,1]$ with$\phi_{1U} + \phi_{2U} = 1$ and $\phi_{2U} + \phi_{3U} = 1$. $[C_{ij\lambda_L}, C_{ij\lambda_U}] \in [\phi_{1L}, \phi_{1U}]$, $[C_{ij\eta_L}, C_{ij\eta_L}] = [\phi_{2L}, \phi_{2U}]$ and $[C_{ij\zeta_L}, C_{ij\zeta_U}] \in [\phi_{3L}, \phi_{3U}]$ with 0$\le (\langle[c_{ij\zeta_L}, c_{ij\zeta_U}] + [C_{ij\eta_L}, C_{ij\eta_L}] + [c_{ij\theta_L}, c_{ij\theta_U}]\rangle) \le 1$
For i,j=1,2,3,……….a.
It is observed that$\langle C_1, C_2, C_3\rangle = \langle\phi_{1L}, \phi_{1U}, \phi_{2L}, \phi_{2U}, 0\rangle = |C|$ and is $\langle C_1, C_2, C_3\rangle.\langle 0, \phi_{2L}, \phi_{2U}, \phi_{3L}, \phi_{3U}\rangle = \langle 0, \phi_{2L}, \phi_{2U}, \phi_{3L}, \phi_{3U}\rangle$.here ,$i^{th}$ row of adj(C)
is$(\langle[C_{1i\zeta_L}, C_{1i\zeta_U}], [C_{1i\eta_L}, C_{1i\eta_L}], [C_{1i\theta_L}, C_{1i\theta_U}]\rangle), (\langle[C_{2i\zeta_L}, C_{2i\zeta_U}], [C_{2i\eta_L}, C_{2i\eta_L}], [C_{2i\theta_L}, C_{2i\theta_U}]\rangle),\ldots\ldots\ldots\ldots\ldots$
$(\langle[C_{ai\zeta_L}, C_{ai\zeta_U}], [C_{ai\eta_L}, C_{ai\eta_L}], [C_{ai\theta_L}, C_{ai\theta_U}]\rangle)$and j^{th} column of C is

$$\left(\begin{array}{c}(\langle[C_{1i\zeta_L}, C_{1i\zeta_U}], [C_{1i\eta_L}, C_{1i\eta_L}], [C_{1i\theta_L}, C_{1i\theta_U}]\rangle), (\langle[C_{2i\zeta_L}, C_{2i\zeta_U}], [C_{2i\eta_L}, C_{2i\eta_L}], [C_{2i\theta_L}, C_{2i\theta_U}]\rangle), \ldots\ldots\ldots \\ \ldots\ldots\ldots. (\langle[C_{ai\zeta_L}, C_{ai\zeta_U}], [C_{ai\eta_L}, C_{ai\eta_L}], [C_{ai\theta_L}, C_{ai\theta_U}]\rangle)\end{array}\right)^t$$

Let E=adj(C) is C=$(\langle[e_{ij\zeta_L}, e_{ij\zeta_U}], [e_{ij\eta_L}, e_{ij\eta_L}], [e_{ij\theta_L}, e_{ij\theta_U}]\rangle)$
where$\left((\langle[e_{ij\zeta_L}, e_{ij\zeta_U}], [e_{ij\eta_L}, e_{ij\eta_L}], [e_{ij\theta_L}, e_{ij\theta_U}]\rangle)\right) =$
$\langle\overset{V}{_k}(C_{ki\lambda_L}, C_{ki\lambda_U} \wedge C_{ki\lambda_L}, C_{ki\lambda_U}), \overset{\wedge}{_k}(C_{ki\eta_L}, C_{ki\eta_U} \wedge C_{ki\eta_L}, C_{ki\eta_U}), \overset{\wedge}{_k}(C_{ki\zeta_L}, C_{ki\zeta_U} \vee C_{ki\zeta_L}, C_{ki\zeta_U})\rangle$
it　　　　　　　　　　　　　　follows　　　　　　　　　　　　　　that
$\left((\langle[e_{ij\zeta_L}, e_{ij\zeta_U}], [e_{ij\eta_L}, e_{ij\eta_L}], [e_{ij\theta_L}, e_{ij\theta_U}]\rangle)\right) = \langle\overset{V}{_k}(C_{ki\lambda_L}, C_{ki\lambda_U} \wedge C_{ki\lambda_L}, C_{ki\lambda_U}), \overset{\wedge}{_k}(C_{ki\eta_L}, C_{ki\eta_U} \wedge C_{ki\eta_L}, C_{ki\eta_U}), \overset{\wedge}{_k}(C_{ki\zeta_L}, C_{ki\zeta_U} \vee$
$Cki\zeta L, Cki\zeta U = |C|$.　　　　　　Thus,$eij\zeta L, eij\zeta U, eij\eta L, eij\eta L, eij\theta L, eij\theta U = |$　　　　　$C|$　　　　and
$(\langle[e_{ij\zeta_L}, e_{ij\zeta_U}], [e_{ij\eta_L}, e_{ij\eta_L}], [e_{ij\theta_L}, e_{ij\theta_U}]\rangle) \ge \langle 0, \phi_{2L}, \phi_{2U}, \phi_{3L}, \phi_{3U}\rangle$for i$\neq j$.so, adj(C).C $\ge |C|.I$.

Proposition 11

Let C be a symmetric SIVPFM. Then adj(C) is Symmetric.

Rajarajeswari and Nandhini

Proof

Let D=adj(C) then $D=(\langle[d_{ij\zeta_L}, d_{ij\zeta_U}], [d_{ij\eta_L}, d_{ij\eta_L}], [d_{ij\theta_L}, d_{ij\theta_U}]\rangle)$

$$=\left(\left\langle \begin{matrix} \overset{\vee}{\beta \in F_{a_j a_i}}\left(\overset{\wedge}{w \in a_j}c_w\beta(w)\zeta_L, \overset{\wedge}{w \in a_j}c_w\beta(w)\zeta_U\right), \overset{\wedge}{\beta \in F_{a_j a_i}}\left(\overset{\wedge}{w \in a_j}c_w\beta(w)\eta_L, \overset{\wedge}{w \in a_j}c_w\beta(w)\eta_U\right), \\ \overset{\wedge}{\beta \in F_{a_j a_i}}\left(\overset{\vee}{w \in a_j}c_w\beta(w)\theta_L, \overset{\vee}{w \in a_j}c_w\beta(w)\theta_U\right) \end{matrix} \right\rangle\right)$$

Now, $D^t = \left(adj(C)\right)^t$

$$=\left(\left\langle \begin{matrix} \overset{\vee}{\beta \in F_{a_j a_i}}\left(\overset{\wedge}{w \in a_j}c_w\beta(w)w\zeta_L, \overset{\wedge}{w \in a_j}c_w\beta(w)w\zeta_U\right), \overset{\wedge}{\beta \in F_{a_j a_i}}\left(\overset{\wedge}{w \in a_j}c_w\beta(w)w\eta_L, \overset{\wedge}{w \in a_j}c_w\beta(w)w\eta_U\right), \\ \overset{\wedge}{\beta \in F_{a_j a_i}}\left(\overset{\vee}{w \in a_j}c_w\beta(w)w\theta_L, \overset{\vee}{w \in a_j}c_w\beta(w)w\theta_U\right) \end{matrix} \right\rangle\right)$$

$$=\left(\left\langle \begin{matrix} \overset{\vee}{\beta \in F_{a_j a_i}}\left(\overset{\wedge}{w \in a_j}c_w\beta(w)\zeta_L, \overset{\wedge}{w \in a_j}c_w\beta(w)\zeta_U\right), \overset{\wedge}{\beta \in F_{a_j a_i}}\left(\overset{\wedge}{w \in a_j}c_w\beta(w)\eta_L, \overset{\wedge}{w \in a_j}c_w\beta(w)\eta_U\right), \\ \overset{\wedge}{\beta \in F_{a_j a_i}}\left(\overset{\vee}{w \in a_j}c_w\beta(w)\theta_L, \overset{\vee}{w \in a_j}c_w\beta(w)\theta_U\right) \end{matrix} \right\rangle\right)$$ as C is Symmetric.

=D.

Definition 5

Let $C=(\langle[c_{ij\zeta_L}, c_{ij\zeta_U}], [c_{ij\eta_L}, c_{ij\eta_L}], [c_{ij\theta_L}, c_{ij\theta_U}]\rangle)$ be a SIVPFM of order a, Then   it is called constant SIVPFM if $(\langle[C_{ek\zeta_L}, C_{ek\zeta_U}], [C_{ek\eta_L}, C_{ek\eta_L}], [C_{ek\theta_L}, C_{ek\theta_U}]\rangle)=(\langle[C_{fk\zeta_L}, C_{fk\zeta_U}], [C_{fk\eta_L}, C_{fk\eta_L}], [C_{fk\theta_L}, C_{fk\theta_U}]\rangle)$ for k, e, f=1,2,3,…………,a, i.e. rows are equal.

Proposition 12

 Let C be a constant   SIVPFM, then C. adj(C) is constant.

Proof

Let $C(\langle[c_{ij\zeta_L}, c_{ij\zeta_U}], [c_{ij\eta_L}, c_{ij\eta_L}], [c_{ij\theta_L}, c_{ij\theta_U}]\rangle)=$ be a order which is constant, Then

$\langle[e_{jk\zeta_L}, e_{jk\zeta_U}], [e_{jk\eta_L}, e_{jk\eta_L}], [e_{jk\theta_L}, e_{jk\theta_U}]\rangle = \langle[e_{jk\zeta_L}, e_{jk\zeta_U}], [e_{jk\eta_L}, e_{jk\eta_L}], [e_{jk\theta_L}, e_{jk\theta_U}]\rangle$ for i, j, k =1,2,3,……..a ie, row are equal.

Let $(\langle[e_{ij\zeta_L}, e_{ij\zeta_U}], [e_{ij\eta_L}, e_{ij\eta_L}], [e_{ij\theta_L}, e_{ij\theta_U}]\rangle)=$C. adj(C)

Now,i^{th} row of C is $(\langle[C_{1\zeta_L}, C_{1\zeta_U}], [C_{1\eta_L}, C_{1\eta_L}], [C_{1\theta_L}, C_{1\theta_U}]\rangle), (\langle[C_{2\zeta_L}, C_{2\zeta_U}], [C_{2\eta_L}, C_{2\eta_L}], [C_{2\theta_L}, C_{2\theta_U}]\rangle) … … … … ….$
$…….(\langle[C_{ja\zeta_L}, C_{ja\zeta_U}], [C_{ja\eta_L}, C_{ja\eta_L}], [C_{ja\theta_L}, C_{ja\theta_U}]\rangle)$

 And j^{th} column of adj(C) is

$(\langle[C_{j1\zeta_L}, C_{j1\zeta_U}], [C_{j1\eta_L}, C_{j1\eta_L}], [C_{j1\theta_L}, C_{j1\theta_U}]\rangle), (\langle[C_{j2\zeta_L}, C_{j2\zeta_U}], [C_{j2\eta_L}, C_{j2\eta_L}], [C_{j2\theta_L}, C_{j2\theta_U}]\rangle) … … … … ….$
$…….(\langle[C_{ja\zeta_L}, C_{ja\zeta_U}], [C_{ja\eta_L}, C_{ja\eta_L}], [C_{ja\theta_L}, C_{ja\theta_U}]\rangle)$

Then$(\langle[e_{ij\zeta_L}, e_{ij\zeta_U}], [e_{ij\eta_L}, e_{ij\eta_L}], [e_{ij\theta_L}, e_{ij\theta_U}]\rangle)$

$$\left(\left\langle \begin{matrix} \overset{\vee}{\underset{k}{}}\left(C_{ik\zeta_L} \wedge C_{jk\zeta_L}, C_{ik\zeta_U} \wedge C_{jk\zeta_U}\right), \overset{\wedge}{\underset{k}{}}\left(C_{ik\eta_L} \wedge C_{jk\eta_L}, C_{ik\eta_U} \wedge C_{jk\eta_U}\right), \\ \overset{\wedge}{\underset{k}{}}\left(C_{ik\theta_L} \vee C_{jk\theta_L}, C_{ik\theta_U} \vee C_{jk\theta_U}\right) \end{matrix} \right\rangle\right)$$

$$\left(\left\langle \begin{matrix} \overset{\vee}{\underset{k}{}}\left(C_{ik\zeta_L} \wedge C_{jk\zeta_L}, C_{ik\zeta_U} \wedge C_{jk\zeta_U}\right), \overset{\wedge}{\underset{k}{}}\left(C_{jk\eta_L} \wedge C_{jk\eta_L}, C_{jk\eta_U} \wedge C_{jk\eta_U}\right), \\ \overset{\wedge}{\underset{k}{}}\left(C_{ik\theta_L} \vee C_{jk\theta_L}, C_{ik\theta_U} \vee C_{jk\theta_U}\right) \end{matrix} \right\rangle\right)$$

Consequently, C. adj(C) is constant.

Proposition 13

Let C be a special restricted SIVPFM. Then adj(C) is reflexive whenever C is reflexive.

Proof

Let $C=(\langle[c_{ij\zeta_L}, c_{ij\zeta_U}], [c_{ij\eta_L}, c_{ij\eta_L}], [c_{ij\theta_L}, c_{ij\theta_U}]\rangle)$ be a special restricted SIVPFM of order a for three real numbers $\phi_{1L}, \phi_{1U} \in [0,1], \phi_{2L}, \phi_{2U} \in [0,1]$ and $\phi_{3L}, \phi_{3U} \in [0,1]$ with$\phi_{1U} + \phi_{2U} = 1$ and $\phi_{2U} + \phi_{3U} = 1$. $[C_{ij\lambda_L}, C_{ij\lambda_U}] \in [\phi_{1L}, \phi_{1U}]$, $[C_{ij\eta_L}, C_{ij\eta_L}] = [\phi_{2L}, \phi_{2U}]$ and $[C_{ij\zeta_L}, C_{ij\zeta_U}] \in [\phi_{3L}, \phi_{3U}]$ with $0\le (\langle[C_{ij\zeta_L}, C_{ij\zeta_U}] + [C_{ij\eta_L}, C_{ij\eta_L}] + [C_{ij\theta_L}, C_{ij\theta_U}]\rangle) \le 1$ For i,j=1,2,3,……….a. since C is reflexive,

$[C_{ij\lambda_L}, C_{ij\lambda_U}]=\phi_{1L}, \phi_{1U}$,$[C_{ij\eta_L}, C_{ij\eta_L}] = \phi_{2L}, \phi_{2U}$ and $[C_{ij\zeta_L}, C_{ij\zeta_U}] = 0$ for i=1,2,3……..a.

 Let adj (c)=$E=(\langle[e_{ij\zeta_L}, e_{ij\zeta_U}], [e_{ij\eta_L}, e_{ij\eta_L}], [e_{ij\theta_L}, e_{ij\theta_U}]\rangle)$

Then $(\langle[e_{ij\lambda_L}, e_{ij\lambda_U}], [e_{ij\eta_L}, e_{ij\eta_L}], [e_{ij\zeta_L}, e_{ij\zeta_U}]\rangle)$

Rajarajeswari and Nandhini

=

$$\left(\left\langle \beta \in F_{a_j a_i} \left(\underset{w \in a_j}{\overset{\wedge}{}} c_w \beta(w) w\zeta_L, \underset{w \in a_j}{\overset{\wedge}{}} c_w \beta(w) w\zeta_U \right), \beta \in F_{a_j a_i} \left(\underset{w \in a_j}{\overset{\wedge}{}} c_w \beta(w) w\eta_L, \underset{w \in a_j}{\overset{\wedge}{}} c_w \beta(w) w\eta_U \right), \right.\right.$$
$$\left.\left. \beta \in F_{a_j a_i} \left(\underset{w \in a_j}{\overset{\vee}{}} c_w \beta(w) w\theta_L, \underset{w \in a_j}{\overset{\vee}{}} c_w \beta(w) w\theta_U \right) \right\rangle \right)$$

Now, when $\beta = I_x \beta(w) = w$

So,$\left(\langle [e_{ij\zeta_L}, e_{ij\zeta_U}], [e_{ij\eta_L}, e_{ij\eta_L}], [e_{ij\theta_L}, e_{ij\theta_U}] \rangle \right)$

$$\geq \begin{pmatrix} [C_{11\zeta_L} \wedge C_{11\zeta_U}][C_{22\zeta_L} \wedge C_{22\zeta_U}] \wedge \dots \dots \wedge c_i - 1i - 1[\zeta_L, \zeta_U] \wedge c_i + 1i \\ +1[\zeta_L, \zeta_U] \dots \dots \dots c_{aa}[\theta_L, \theta_U], \end{pmatrix}$$
$$\begin{pmatrix} [C_{11\eta_L} \wedge C_{11\eta_U}][C_{22\eta_L} \wedge C_{22\eta_U}] \wedge \dots \dots \wedge c_i - 1i - 1[\eta_L, \eta_U] \wedge c_i + 1i \\ +1[\eta_L, \eta_U] \dots \dots \dots c_{aa}[\eta_L, \eta_U], \end{pmatrix}$$
$$[C_{11\theta_L} \wedge C_{110\theta_U}][C_{220\theta_L} \wedge C_{22\theta_U}] \wedge \dots \dots \wedge c_i - 1i - 1[\theta_L, \theta_U] \wedge c_i + 1i$$
$$+1[\theta_L, \theta_U] \dots \dots \dots c_{aa}[\theta_L, \theta_U].$$
$$= \langle \phi_{1L}, \phi_{1U}, \phi_{2L}, \phi_{2U}, 0 \rangle$$

Consequently $[e_{ij\zeta_L}, e_{ij\zeta_U}] = [\phi_{1L}, \phi_{1L}], [e_{ij\eta_L}, e_{ij\eta_L}] = [\phi_{2L}, \phi_{2U}], [e_{ij\theta_L}, e_{ij\theta_U}] = 0$ for i=1,2,3,……..a. It follows that E is reflexive.

APPLICATION
The IVPFM is a valuable resource that may be utilised to resolve various forms of problem-based decision-making.

Algorithm
We are using an interval-valued picture fuzzy matrix to obtain a chosen list of canditateselected to the government job.

Step 1: All IVPFSs from two IVPFMs over the set of political parties should be obtained.

Step 2: convert the given interval valued picture fuzzy decision matrix into Trapezoidal picture fuzzy decision matrix. C =$\left(\langle [c_{ij\zeta_L}, c_{ij\zeta_U}], [c_{ij\eta_L}, c_{ij\eta_L}], [c_{ij\theta_L}, c_{ij\theta_U}] \rangle \right)$ D=$\left(\langle [d_{ij\zeta_L}, d_{ij\zeta_U}], [d_{ij\eta_L}, d_{ij\eta_L}], [d_{ij\theta_L}, d_{ij\theta_U}] \rangle \right)$ as follows.

$\beta(C, D)=$

$$\sqrt{\frac{1}{3n} \sum_{i,j=1}^{n} \left[(a_{ijL} - a_{ijL}')^2 (a_{ijU} - a_{ijU}')^2 + (b_{ijL} - b_{ijL}')^2 (b_{ijU} - b_{ijU}')^2 + (c_{ijL} - c_{ijL}')^2 (c_{ijU} - c_{ijU}')^2 + (r_{ijL} - r_{ijL}')^2 (r_{ijU} - ri_{jU}')^2 \right]}$$

where $a_i = [c_{ij\zeta_L}, c_{ij\zeta_U}], b_i = [c_{ij\eta_L}, c_{ij\eta_L}] c_i = [c_{ij\theta_L}, c_{ij\theta_U}]$, $d_C(x_i) = 1 - a_i - b_i - c_i$ are respectively, the measure of membership, neutral membership, non- membership and denial membership of x_i in C and $a_{ij}' = [d_{ij\zeta_L}, d_{ij\zeta_U}] b_{ij}' = [d_{ij\eta_L}, d_{ij\eta_L}] c_{ij}' = [d_{ij\theta_L}, d_{ij\theta_U}]$
$a_i' = d_C(x_i) = 1 - a_i' - b_i' - C_i'$ are respectively, the measure of membership, neutral membership, non-membership and denial membership of x_i in D.

Step 3: convert obtain Trapezoidal picture fuzzy decision matrix into picture fuzzy decision matrix.

Step 4: To calculate the distance formula between two picture fuzzy decision matrix.

Step 5: Now, a IVPFM C=$\left(\langle [c_{ij\zeta_L}, c_{ij\zeta_U}], [c_{ij\eta_L}, c_{ij\eta_L}], [c_{ij\theta_L}, c_{ij\theta_U}] \rangle \right)$ of size 5 x 3 is considered in the following which represent AO towards a Govt.

Case study
Consider the five candidate S=s_1, s_2, s_3, s_4, s_5 *as the universal set* to apply the government job J=$j_1, j_2, j_3$where represent the AE post, JA post, JEE post. Let the candidate selected to quota Q =q_1, q_2, q_3 where represent quotas are open competition quota, Ex-serviceman quota, Sports quotaare successful selected to the candidate in quota category to be promoted to the government officer.

IVPFM C =$\left(\langle [c_{ij\zeta_L}, c_{ij\zeta_U}], [c_{ij\eta_L}, c_{ij\eta_L}], [c_{ij\theta_L}, c_{ij\theta_U}] \rangle \right)$ of size 5 x 3 is following represents the Canditate.

$$\begin{array}{c} \begin{matrix} q_1 & q_2 & q_3 \end{matrix} \\ S = \begin{matrix} s_1 \\ s_2 \\ s_3 \\ s_4 \\ s_5 \end{matrix} \begin{pmatrix} ([0.6,0.7][0,0.1][0,0.1][0.1,0.4]) & ([0.1,0.2][0.1,0.2][0.1,0.2][0.4,0.7]) & ([0.1,0.2][0.1,0.2][0.1,0.2][0.4,0.7]) \\ ([0.3,0.4][0.3,0.4][0,0.1][0.1,0.4]) & ([0.5,0.65][0,0.1][0.1,0.2][0.05,0.4]) & ([0.2,0.3][0.2,0.3][0.2,0.3][0.1,0.4]) \\ ([0.6,0.7][0,0.1][0,0.1][0.1,0.4]) & ([0.1,0.2][0.1,0.2][0.1,0.2][0.4,0.7]) & ([0.4,0.5][0.2,0.3][0,0.1][0.1,0.4]) \\ ([0.4,0.5][0.2,0.3][0,0.1][0.1,0.4]) & ([0.5,0.6][0.1,0.2][0,0.1][0.1,0.1]) & ([0.3,0.4][0.2,0.3][0.1,0.2][0.1,0.4]) \\ ([0.6,0.7][0,0.1][0,0.1][0.1,0.4]) & ([0.6,0.7][0,0.1][0,0.1][0.1,0.4]) & ([0.4,0.5][0.2,0.3][0,0.1][0.1,0.4]) \end{pmatrix} \end{array}$$

IVPFM D=$(\langle [d_{ij\zeta_L}, d_{ij\zeta_U}], [d_{ij\eta_L}, d_{ij\eta_L}], [d_{ij\theta_L}, d_{ij\theta_U}] \rangle)$ of size 3 x 3 is following represents the job of government office

$$\begin{array}{c} J = \begin{matrix} q_1 & q_2 & q_3 \end{matrix} \\ \begin{matrix} j_1 \\ j_2 \\ j_3 \end{matrix} \begin{pmatrix} ([0.6,0.7][0,0.1][0,0.1][0.1,0.4]) & ([0.2,0.3][0.2,0.3][0.3,0.4][0,0.3]) & ([0.2,0.3][0.2,0.3][0.3,0.4][0,0.3]) \\ ([0.1,0.2][0.2,0.3][0.3,0.4][0.1,0.4]) & ([0.6,0.75][0,0.15][0,0.1][0.4]) & ([0.4,0.5][0.1,0.2][0.2,0.3][0,0.3]) \\ ([0.2,0.3][0.3,0.4][0.2,0.3][0.0,0.3]) & ([0.3,0.4][0.1,0.2][0.3,0.4][0,0.3]) & ([0.6,0.75][0,0.15][0.0,0.1][0.4]) \end{pmatrix} \end{array}$$

Step 2

Interval valued picture fuzzy matrix into Trapezoidal picture fuzzy decision matrix

$$\begin{array}{c} \begin{matrix} q_1 & q_2 & q_3 \end{matrix} \\ C = \begin{matrix} s_1 \\ s_2 \\ s_3 \\ s_4 \\ s_5 \end{matrix} \begin{pmatrix} (0.65,0.05,0.05,0.25) & (0.15,0.15,0.15,0.55) & (0.15,0.15,0.15,0.55) \\ (0.35,0.35,0.05,0.25) & (0.58,0.05,0.15,0.23) & (0.25,0.25,0.25,0.25) \\ (0.65,0.05,0.05,0.25) & (0.15,0.15,0.15,0.15,0.55) & (0.45,0.25,0.05,0.55) \\ (0.45,0.25,0.05,0.25) & (0.55,0.15,0.05,0.25) & (0.35,0.25,0.15,0.55) \\ (0.65,0.05,0.05,0.25) & (0.65,0.05,0.05,0.25) & (0.45,0.25,0.05,0.55) \end{pmatrix} \end{array}$$

$$\begin{array}{c} \begin{matrix} q_1 & q_2 & q_3 \end{matrix} \\ D = \begin{matrix} j_1 \\ j_2 \\ j_3 \end{matrix} \begin{pmatrix} (0.65,0.05,0.05,0.25) & (0.15,0.25,0.35,0.25) & (0.25,0.35,0.25,0.1) \\ (0.25,0.25,0.35,0.15) & (0.68,0.08,0.05,0.2) & (0.35,0.15,0.35,0.15) \\ (0.25,0.25,0.35,0.15) & (0.45,0.15,0.25,0.15) & (0.68,0.08,0.05,0.20) \end{pmatrix} \end{array}$$

Step 3 & 4

To calculate the distance formula between two PFSs the following matrix Z= (Z_{ij})

Where z_{ij} is the distance between c_i and d_j for i=1,2,3,4,5 and j=1,2,3

$$\begin{array}{c} \begin{matrix} j_1 & j_2 & j_3 \end{matrix} \\ Z = \begin{matrix} s_1 \\ s_2 \\ s_3 \\ s_4 \\ s_5 \end{matrix} \begin{pmatrix} 0.2211 & 0.3429 & 0.3263 \\ 0.2096 & 0.1570 & 0.2175 \\ 0.2380 & 0.3347 & 0.2876 \\ 0.2333 & 0.2093 & 0.2381 \\ 0.2560 & 0.2570 & 0.2797 \end{pmatrix} \end{array}$$

The following is a list of the candidate selected to each government, as calculated $s_1 \rightarrow j_2, s_2 \rightarrow j_3, s_3 \rightarrow j_2, s_4 \rightarrow j_3, s_5 \rightarrow j_3$.

CONCLUSION

We have defined interval valued picture fuzzy matrix, which is the extension of picture fuzzy matrix, and gives excellent accuracy and improves the efficacy in various practical domains. Also we have defined Different types of $\langle [\alpha_L, \alpha_U], [\beta_L, \beta_U], [\gamma_L, \gamma_U] \rangle$-cut of SIVPFM,determinant and adjoint of Square interval valued picture fuzzy matrix have been studied. Here is an application of interval valued picture fuzzy matrix being used in decision-making. We predict that the results of this study will spark a growing interest among researchers in the further development and generalization of current research.

REFERENCES

1. Atannassov.K, Intuitionistic fuzzy sets and systems 20(1)(1986)87-96.
2. Atannassov.K and Gargov.G,Interval value dintuitionistic fuzzy sets,fuzzy setsandsystems3(1)(1989)343-349.

3. Buicongcuong, Picture fuzzy sets, Journal of computer science andcybernetics,V.30,N.4(2014),409-420.
4. Khan SK.Shymal Ak ,Pal M (2002) Intuitionistic fuzzy matrices
5. M.Bora, B.Bora, T.J.Neog and D.K.Sut, Intuitionistic fuzzys of t matrix theory and its application in medical diagnosis, Ann. Fuzzy Math. Inform.7(1) (2014)143–153.
6. P.Rajarajeswari and P.Dhanalakshmi, An application of interval valued intuitionistic fuzzys of t matrix theoryinmedicaldiagnosis,9(3)(2015),pp.463-472.
7. Pal M Intutitionistic fuzzy determinant. V.U.J. phys sci 7:87-93
8. Ragab MG,Emam EG the determinant and adjoint of a square fuzzy matrices. Fuzzt sets syst 61 (3):297-307.
9. Shovan Dogra, Madhumangal pal (2020) Picture fuzzy matrix and its application.
10. Zadeh.L.A, fuzzy set. Information and control,8(1965):338.

RESEARCH ARTICLE

A Study on the Infusion of Genetic Algebra and its Constituents

Karen Felicita C[1]* and   Sahaya Sudha A[2],

[1]Research Scholar, Department of Mathematics, Nirmala College for Women, Coimbatore, Tamil Nadu, India.
[2]Associate Professor, Department of Mathematics, Nirmala College for Women, Coimbatore, Tamil Nadu, India.

*Address for Correspondence
Karen Felicita C
Research Scholar,
Department of Mathematics,
Nirmala College for Women,
Coimbatore, India.

ABSTRACT

Algebras when infused with certain principles with Biological sciences turns out to be one of the significant interdisciplinary approaches in the field of scientific approach. Genetics, being the study of genes and heredity of organisms stands as a branch of biology. Genetics being the important aspect of human heredity can be infused with algebra called Genetic Algebra. The basic preliminaries and terminologies are discussed in terms of both genetics and Mathematical Sciences. A walk back of Genetic Algebra from the past years have been illustrated and viewed. Different Algebraic concepts which constitute Genetic Algebras are showcased in this paper. An attempt has been made to investigate the Algebra of Genetics in the heredity of organisms using different approaches. Certain case studies in Genetic Algebra are interpreted and analysed in this paper. Constituents which constitute Genetic Algebra are studied for further application. Genetic Algebra is further applied in the quality of crops in agriculture which will optimize the productivity of crops. It is noted and emphasised that Genetic Algebra will enhance and maintain the quality with high productivity rate of crops with the association of biological investigation. This paper projects and elevates the infusion of genetic algebra for the improvisation of plant crops.

Keywords: Algebra, Biological Science, Mathematical Sciences, Genetic Algebra, Genetics, Agriculture, Optimize

Karen Felicita and Sahaya Sudha

INTRODUCTION

Mathematics, known as queen of Science has its walk through in many applications. Mathematical Sciences when combined with Biological Sciences serves as a best approach in Interdisciplinary research which has its progress all way forward. Such a combination is Mathematics with Agriculture. Agriculture being the holistic area which holds the entire system together. Many researches have been done in many ideologies and results have been produced so as to increase the productivity of crops, assigning work in the process of agriculture, distribution of yield, etc., In the beginning of Crop breeding, by various techniques has undergone many revolutions in the few decades so as to increase the crop yield. Researches have been done in the genetic diversity (Kotowska-2009) which resulted in higher plant productivity and survival at high genotypic diversity yet did not consider about the phenotypic diversity of the plants[2]. Abishek Kumar suggested the Genetic manipulation of photosynthesis to enhance crop productivity under changing environmental conditions where the plant develops tolerance to cope with changing environmental conditions. Julia Bailey-Serres(2019) explored emerging strategies for enhancing sustainable crop production. Most of the reviews focuses on the external risk factors and in improvisation of tolerance in the plant itself[1].

Suggestions by Euan T Smithers for both biologists and mathematicians illustrated the biological insights afforded by mathematical modelling and demonstrated the breadth of mathematically rich problems available within plant sciences[3]. Recent review of Meselu Tegenie Mellaku and Ashebir Sidelil Sebside exclaims that the promotion of mathematical model-based decision making through accessible mobile application technology integrated with national and regional agronomy, climate and market information systems will be an option to enhance the sustainable performance of agriculture in the face of climate change [4]. Mathematical and theoretical biology are the interdisciplinary scientific research fields with a range of their applications. This combination of Mathematics along with Biology is known as "Mathematical Biology" or "Bio-Mathematics' to stress the side of Mathematics in its diversity. Mathematical Biology synchronizes the Mathematical tools to study or forecast biological systems [5]. It has its wide range of applications using techniques and tools of applied Mathematics by Mathematical representation, treatment and modelling process has both theoretical and practical application in the fields of biology, biomedical science and biotechnology[6].

Many findings reveal and verify the importance of Mathematics behind biology which includes that the population growth would be "geometric" while resources would grow arithmetically[7]. It is foremost important that Mathematics could be neglected in the growth of evolution. It is one of the upcoming fields in the current trend and in research of biodiversity and it is astonishing that Mathematical Sciences play a vital role in the successive progression of the result. Moving on from Bio-Mathematics to one of the specialized concepts called Mathematical genetics which is far now concerned as "genetic algebras'. They are possibly non-associative used to model inheritance in genetics. In the recent years, many authors have tried to investigate the difficult problem of classification of algebra. Lyubich Y illustrates that in an evolution algebra associated to be the free population is introduced and by using the non-associative algebra many valid results are obtained in explicit form [8]. In the year 2008, a new type of algebra was introduced which describes some evolution laws of genetics [9]. The main aim of the study is to infuse and verify the genetic algebra constituents in the improvisation of plant crops.

Preliminaries
Genetic Algebra
Let g be an algebra over the field K. Assume that g admits a basis $\{e_1, e_2, \dots e_n\}$ such that multiplication constants $P_{1ij,k}$ with respect to this basis, are given by
$e_i \cdot e_j = e_i \cdot$
We say that g is a genetic algebra if the multiplication constants. In that case, the basis $\{e_1, e_2, \dots e_n\}$ is called a natural basis.

Walk Back of Genetic Algebra

This section deals with the history of Genetic Algebra along with its different constituents. Genetic Algebra is most profoundly deals with the evolution of organisms. The study of genetic algebras was eventually commenced by Ivor Etherington where it was studied in the non-associative algebras which arise in the symbolism of genetics [11]. In the utilization of genetics, this genetic algebras play a major role which has a basis corresponding to the genetically different gametes. Added to it, the structure constant of the algebra encode the probabilities of producing offspring of various types. Some special cases, different algebras such as classes of algebra called train algebras and that this class includes algebras called special train algebras could be defined [12].

Train Algebra

A branch of genetic algebra in a specialized format is the Train algebra which was introduced by Etherington,1939. A newer specialized algebra is known as special train algebra has its walkway through genetic algebra[13].

Baric Algebra

Another specialized feature of genetic algebra is the baric algebra or known as weighted algebra. The baric algebra over the field K is a possibly non-associative algebra over *K* together with a homomorphism *w,* called the weight, from the algebra to *K*

METHODOLOGY

The principal tool of investigation of the genetic algebra is the transformation algebra [13]. Transformation Algebra helps us to transform the trait we require and enable it so as to verify our assumption.

Step 1: **Converting the phenotypes to algebraic structures**

Plants have the phenotype which exists with the plant which showcases the traits of them. In this case, we consider the phenotypes into algebraic structures and verify the properties.

Step 2: **Explicating the non-associative property of Algebra**

The so formed algebraic structures with phenotypes are therein treated with the property of non-associativity of algebra where non-associative algebra or distributive algebra is an algebra over a field where the binary multiplication operation is not assumed to be associative[AB not equals BA].

Step 3: **Implying the result verified in Plant Productivity**

After changing the phenotypes to non-associative algebraic format, the endured mathematical model will now be transferred in real life world by stimulating it in plant productivity wherein the seeds will be transferred as a seed what we have favored and preferred for.

Step 4: **Optimizing the productivity of the yield plant crop.**

The above such treated seed will be cultivated and the yield will be optimized using Operation Research models and the optimum result will be obtained.

CONCLUSION

This paper enables the bridge between Mathematical Sciences and Biological Sciences which will be a quantitative technique in Agricultural Sciences. Furthermore, research and findings will give a broad spectrum of idealogy in its future trends. Thus, the Genetic Algebra along with its properties when infused with plant technology provides a door for the revolution in plant productivity.

The main objective of the paper is to enhance and improvise the plant production in accordingly to increase the yield and enhance the taste of the food crop.

REFERENCES

1. Kotowska, A.M., Cahill Jr, J.F. and Keddie, B.A. (2010), Plant genetic diversity yields increased plant productivity and herbivore performance. Journal of Ecology, 98: 237-245.
2. Bailey-Serres J, Parker JE, Ainsworth EA, Oldroyd GED, Schroeder JI(2019). Genetic strategies for improving crop yields. Nature. 575(7781):109-118.
3. Euan T Smithers (2019), Mathematical principles and models of plant growth mechanics: from cell wall dynamics to tissue morphogenesis, *Journal of Experimental Botany*, Volume 70, Issue 14, Pages 3587–3600
4. Mellaku MT, Sebsibe AS.(2022) Potential of mathematical model-based decision making to promote sustainable performance of agriculture in developing countries: A review article. Heliyon, 8(2)
5. Longo, Giuseppe; Soto, Ana M. (2016). "Why do we need theories?" (PDF). Progress in Biophysics and Molecular Biology. From the Century of the Genome to the Century of the Organism: New Theoretical Approaches. 122 (1): 4– 10.
6. Vitthalrao B. Khyade & Hanumant V Wanve (2018), Mathematicas for Biological Sciences, Global Journal of Science frontier Research: C Bilogical Science, Volume 18(1),65-70.
7. Mallet, James (2001). "Mimicry: An interface between psychology and evolution". PNAS. 98 (16): 8928–8930
8. Lyubich Y I (1992), Mathematical Structures in Population Genetics, Springer- Verlag, Berlin
9. Tian J P (2008) Evolution algebras and their applications, Lecture Notes in Mathematics ,Springer-Verlag, Berlin.
10. Mallet, James (July 2001). "Mimicry: An interface between psychology and evolution". PNAS. 98 (16): 8928–8930.
11. I. M. H. Etherington, " Genetic algebras," Proceedings of the Royal Society of Edinburgh, Vol. 59 (1939), pp. 242-258.
12. Speciial train algebras," Quarterly Journal of Mathematics (Oxford), vol. 12 (1941), pp. 1-8
13. A. A. Albert, "Non-associative algebras I. Fundamental concepts and isotopy," Annals of Mathematics, vol. 43 (1942), pp. 685-707.

RESEARCH ARTICLE

Interval Valued Picture Fuzzy Matrices and its Application in Medical Diagnosis

P. Rajarajeswari [1*] and D. Nandhini[2]

[1]Associate Professor, Department of Mathematics, Chikkanna Govt Arts College, Tirupur-02, Tamil Nadu, India
[2]Research Scholar, Department of Mathematics, Chikkanna Govt Arts College, Tirupur-02, Tamil Nadu, India.

*Address for Correspondence
P.Rajarajeswari
Associate Professor,
Department of Mathematics,
Chikkanna Govt Arts College,
Tirupur-02, Tamil Nadu, India

ABSTRACT

Picture Fuzzy sets (PFS), which are direct extension of fuzzy sets and intuitionistic fuzzy sets and are more suited to dealing with vague, unreliable and ambiguous data. In some situations, we cannot predict the precises value, in such cases the concept of interval valued picture fuzzy sets are used in which the membership, neutral and non-membership degrees are represented as intervals. The classical matrix cannot solve the problems involving various types of uncertainties. In this paper, by using the concept of interval valued picture fuzzy sets we introduce a new type of matrices namely interval valued picture fuzzy matrices and we defined special restriction on interval valued picture fuzzy matrices. Also we have defined some basic operations namely addition, multiplication, transpose and complement on square interval valued picture fuzzy matrices. Based on these operations some properties of square interval valued picture fuzzy matrices are studied and illustrated with suitable examples. By using the concept of interval valued picture fuzzy matrices, we have studied their application in medical diagnosis with numerical examples.

Keywords: Picture fuzzy matrix, Interval valued picture fuzzy set, Special restricted Square picture fuzzy matrix.

INTRODUCTION

In recent years, it has been found that Fuzzy can be used to solve a variety of complicated problems involving uncertainties that arise in the fields of engineering, social science, economics, and other sciences. In the real world, there are many uncertainties in every aspect of life. When dealing with problems of this kind, Zadeh's conventional fuzzy set[9] concept works well. Since the initial proposal of fuzzy set theory, higher order fuzzy sets have been suggested for various applications in a wide range of domains. Among higher fuzzy sets, the Atanassov intuitionistic fuzzy set[2] has been proven to be especially beneficial and adaptable. Attanassov and Gargov[3] enlarged the intuitionistic fuzzy set to the interval valued intuitionistic fuzzy set, which is distinct by a membership function with interval values. Fuzzy matrices were introduced by Hashimoto. Ragab and Emam later looked into the determinant of a square fuzzy matrix and the max-min composition of fuzzy matrices. By Kim and Roush , the idea of generalised fuzzy matrices was first developed. Pal introduced the idea of fuzzy matrices with fuzzy rows and columns. Pal looked into interval valued fuzzy matrices that have such rows and columns. Pradhan and Pal researched the triangular fuzzy matrix norm.In this paper we introduce the new concept of interval valued picture fuzzy matrix . we also introduce the concept of restricted interval valued picture fuzzy matrix and some basic operations. we have studied their application with numerical example in medical diagnosis.

Preliminaries

Definition 1(1986, Atanassov)An IFS Cover the set of universe X is defind as

C =$\{\langle x, \lambda_C(x), \zeta_C(x)\rangle : x \in X\}$where $\lambda_C(x) \in [0,1]$ is the measure of membership and$\zeta_C(x) \in [0,1]$ is the measure of non-membership of x in C with $0 \leq \lambda_C(x) + \zeta_C(x) \leq 1$ for all$x$ in C.

Definition 2.   Let k_1 and k_2 be two real numbers with $K_1 \in [0,1]$and $K_2 \in [0,1]$,

with $0 \leq K_1 + K_2 \leq 1$.Then k=<k_1, k_2> is called IFV.

Definition 3. (Khan et al.2002) An IFM C of order $a \times b$ is defined as C=$\left(\langle C_{ij_\lambda}, C_{ij_\zeta}\rangle\right)$, where $C_{ij_\lambda} \in [0,1]$ is the measure of membership of C_{ij} (ij th element of C) and $C_{ij_\zeta} \in [0,1]$ is the measure of non-membershipC_{ij} with the condition$0 \leq C_{ij_\lambda} + C_{ij_\zeta} \leq 1$ for i=1,2,………,a and j=1,2,……….,b.

An IFM C is said to SIFM if the number of rows is equal to the number of columns.

Definition 4.(Sriram and Murugadas2010) An identify IFM I of order a is the SIFM of order a with all diagonal entries $\langle 1,0\rangle$ and non-diagonal entries $\langle 0,1\rangle$.

Definition 5.(Sriram and Murugadas2010) A null IFM 0 of order a is the SIFM of order a with all entries$\langle 0,1\rangle$.It is to be noted that $\langle 1,0\rangle$ *is the* greatest IFV and $\langle 0,1\rangle$ is n the least IFV. so, to define identity IFM and null IFM,Least IFV and greatest IFV are needed.

Considering more possible types of uncertainty and including the measure of neutral membership, Cuong introduced PFS in 2013.

Definition 6.(Cuong   and   Kreinovich   2013)   APFS   Cover   the   set   of   universe   X   is   defined   as C=$\{\langle x, \lambda_C(x), \eta_C(x), \zeta_C(x)\rangle : x \in X\}$ where $\lambda_C(x) \in [0,1]$,$\eta_C(x) \in [0,1]$,   is   the   measure   of   membership,   neutral membership   and$\zeta_C(x) \in [0,1]$ is   the   measure   of   non-membership   of $x \in X$ with   the   condition $0 \leq \lambda_C(x) + \eta_C(x) + \zeta_C(x) \leq 1$ for all $x \in X$.

Rajarajeswari and Nandhini

Definition 7. Let k_1, k_2 and k_3 be three real numbers with $K_1 \in [0,1]$ and $K_2 \in [0,1]$, $K_3 \in [0,1]$,

with $0 \leq K_1 + K_2 + K_3 \leq 1$. Then $k = \langle k_1, k_2, K_3 \rangle$ is called PFV.

Based Following our definition of IVPFM based on IVPFS.

Interval valued picture fuzzy matrix.

To generalize the idea ofInterval valued intuitionistic fuzzy matrix(IVIFM), let's defineInterval valued picture fuzzy matrix(IVPFM)as follows

Definition 8.

A IVPFM of size $a \times b$ is defined as $(\langle [C_{ij\lambda_L}, C_{ij\lambda_U}], [C_{ij\eta_L}, C_{ij\eta_L}], [C_{ij\zeta_L}, C_{ij\zeta_U}] \rangle)$ where $C_{ij\lambda_L}, C_{ij\lambda_U} \in [0,1]$ are the lower and upper limit of membership degree, $C_{ij\eta_L}, C_{ij\eta_L} \in [0,1]$ are the lower and upper limit of neutral membership degree, and $C_{ij\zeta_L}, C_{ij\zeta_U} \in [0,1]$ are the lower and upper limit of non-membership *degree of the element* of C_{ij} for i=1,2,……,a and j=1,2,…….,b satisfying $0 \leq C_{ij\lambda_U} + C_{ij\eta_u} + C_{ij\zeta_U} \leq 1$.

Definition 9.

A IVPFM is said to be SIVPFM if the number of rows is equal to the number of columns.

Definition 10.

Let C $= (\langle [C_{ij\lambda_L}, C_{ij\lambda_U}], [C_{ij\eta_L}, C_{ij\eta_L}], [C_{ij\zeta_L}, C_{ij\zeta_U}] \rangle)$ be a IPFM of order a x b. Then β by Scalar multiplication is given by

$\beta.C = ([\beta \wedge C_{ij\lambda_L}, \beta \wedge C_{ij\lambda_U}], [\beta \wedge C_{ij\eta_L}, \beta \wedge C_{ij\eta_L}], [\beta \wedge C_{ij\zeta_L}, \beta \wedge C_{ij\zeta_U}])$.

Definition 10.

LetC$= (\langle [C_{ij\lambda_L}, C_{ij\lambda_U}], [C_{ij\eta_L}, C_{ij\eta_L}], [C_{ij\zeta_L}, C_{ij\zeta_U}] \rangle)$ and D$= (\langle [d_{ij\lambda_L}, d_{ij\lambda_U}], [d_{ij\eta_L}, d_{ij\eta_L}], [d_{ij\zeta_L}, d_{ij\zeta_U}] \rangle)$ be two SIVPFMs of order a. Then the product C.D is defined as E =C.D $= (\langle e_{ij_\lambda}, e_{ij_\eta}, e_{ij_\zeta} \rangle)$ where $e_{ij_\lambda} = [\vee_k (C_{ik\lambda_L} \wedge d_{kj\lambda_L}), \vee_k (C_{ik\lambda_U} \wedge d_{kj\lambda_U}]$

$e_{ij_\eta} = [\wedge_k (C_{ik\eta_L} \wedge d_{kj\eta_L}), \wedge_k (C_{ik\eta_U} \wedge d_{kj\eta_U})]$ and $e_{ij_\zeta} = [\wedge_k (C_{ik\zeta_L} \vee d_{kj\zeta_L}), \wedge_k (C_{ik\zeta_U} \vee d_{kj\zeta_U})]$ for i,j =1,2,………,a .

Definition 11.

Let C$= (\langle [C_{ij\lambda_L}, C_{ij\lambda_U}], [C_{ij\eta_L}, C_{ij\eta_L}], [C_{ij\zeta_L}, C_{ij\zeta_U}] \rangle)$ andD$= (\langle [d_{ij\lambda_L}, d_{ij\lambda_U}], [d_{ij\eta_L}, d_{ij\eta_L}], [d_{ij\zeta_L}, d_{ij\zeta_U}] \rangle)$ be two SIVPFMs of order a. Then $C \leq D$

if $[C_{ij\lambda_L}, C_{ij\lambda_U}] \subseteq [d_{ij\lambda_L}, d_{ij\lambda_U}]$, $[C_{ij\eta_L}, C_{ij\eta_L}] \supseteq [d_{ij\eta_L}, d_{ij\eta_L}]$, $[C_{ij\zeta_L}, C_{ij\zeta_U}] \supseteq [d_{ij\zeta_L}, Cd_{ij\zeta_U}]$ for i,j=1,2,……….,a.

Definition 12.

Let C$= (\langle [C_{ij\lambda_L}, C_{ij\lambda_U}], [C_{ij\eta_L}, C_{ij\eta_L}], [C_{ij\zeta_L}, C_{ij\zeta_U}] \rangle)$ be a SIVPFMs Then multiplication by a IVPFV k $= \langle [k_{1L}, k_{1U}], [k_{2L}, k_{2U}], [k_{3L}, k_{3U}] \rangle$ is defined as

k .C $= (\langle [k_{1L} \wedge C_{ij\lambda_L}, k_{1U} \wedge C_{ij\lambda_U}], [k_{2L} \wedge C_{ij\eta_L}, k_{2U} \wedge C_{ij\eta_L}], [k_{3L} \vee C_{ij\zeta_L}, k_{3U} \vee C_{ij\zeta_U}] \rangle)$.

Definition 13.

Let C$= (\langle [C_{ij\lambda_L}, C_{ij\lambda_U}], [C_{ij\eta_L}, C_{ij\eta_L}], [C_{ij\zeta_L}, C_{ij\zeta_U}] \rangle)$ be a SIVPFM. Also Let $([x_L, x_U], [y_L, y_U], [z_L, z_U])$ be a IVPFV for $(\langle [C_{ij\lambda_L}, C_{ij\lambda_U}], [C_{ij\eta_L}, C_{ij\eta_L}], [C_{ij\zeta_L}, C_{ij\zeta_U}] \rangle) \geq (x, y, z)$ it means

63280

that$[C_{ij\lambda_L}, C_{ij\lambda_U}] \geq [x_L, x_U]$, $[C_{ij\eta_L}, C_{ij\eta_L}] \geq [y_L, y_U]$, $[C_{ij\zeta_L}, C_{ij\zeta_U}] \leq [z_L, z_U]$.$(\langle[C_{ij\lambda_L}, C_{ij\lambda_U}], [C_{ij\eta_L}, C_{ij\eta_L}], [C_{ij\zeta_L}, C_{ij\zeta_U}]\rangle) \geqq$ $([x_L, x_U], [y_L, y_U], [z_L, z_U])$ it means that three inequalities $C_{ij\lambda_L} \geq x_L, C_{ij\lambda_U} \geq x_U$, $C_{ij\eta_L} \geq y_L, C_{ij\eta_U} \geq y_U, C_{ij\zeta_L} \leq z_L, C_{ij\zeta_U} \leq z_U$do not hold at a time. We will now propose restricted interval valued picture fuzzy matrices by limiting the measure of membership, neutral membership and non-membership but keeping their sum in the interval.

Definition 14.

For three chosen interval valued real numbers $[\phi_{1L}, \phi_{1U}] \in [0,1], [\phi_{2L}, \phi_{2U}] \in [0,1]$ $and[\phi_{3L}, \phi_{3U}] \in [0,1]$ with $\phi_{1U} + \phi_{2U} = 1, and \ \phi_{2U} + \phi_{3U} = 1$ a   restricted   IVPFM   namely   C   of   size $a \times b$ is   defined   as C=$(\langle[C_{ij\lambda_L}, C_{ij\lambda_U}], [C_{ij\eta_L}, C_{ij\eta_L}], [C_{ij\zeta_L}, C_{ij\zeta_U}]\rangle)$where$[C_{ij\lambda_L}, C_{ij\lambda_U}]$, $[C_{ij\eta_L}, C_{ij\eta_L}]$ $and[C_{ij\zeta_L}, C_{ij\zeta_U}]$are   respectively,the measure of membership, neutral membership and non-membership of C_{ij} for i=1,2, 3, ……, a; j=1,2, 3, ……, b with $[C_{ij\lambda_L}, C_{ij\lambda_U}] \subseteq [\phi_{1L}, \phi_{1U}], [C_{ij\eta_L}, C_{ij\eta_U}] \subseteq [\phi_{2L}, \phi_{2U}], [C_{ij\zeta_L}, C_{ij\zeta_U}] \subseteq [\phi_{3L}, \phi_{3U}]$ satisfying 0$\leq C_{ij\lambda_U} + C_{ij\eta_u} + C_{ij\zeta_U} \leq 1$.

A special restricted SIVPFM is a restricted SIVPFM if $[C_{ij\eta_L}, C_{ij\eta_L}]=[\phi_{2L}, \phi_{2L}]$ for i,j=1,2,3,……..,a.

Any restricted SIVPFM C = $(\langle x, y, z \rangle)$ of order 2.Let us consider a SIVPFM D of order 2 with all diagonal entries $\langle \phi_{1L}, \phi_2, 0 \rangle$ and non-diagonal entries $\langle 0, \phi_2, \phi_3 \rangle$.Then $x \in [0, \phi_1], y \in [0, \phi_1]$ $and \ z \in [0, \phi_1]$.Let E=C.D=$(\langle[e_{ij\lambda_L}, e_{ij\lambda_U}], [e_{ij\eta_L}, e_{ij\eta_L}], [e_{ij\zeta_L}, e_{ij\zeta_U}]\rangle)$Then $(\langle[e_{ij\lambda_L}, e_{ij\lambda_U}], [e_{ij\eta_L}, e_{ij\eta_L}], [e_{ij\zeta_L}, e_{ij\zeta_U}]\rangle) = \langle (x \wedge \phi_1) \vee$ $(x \wedge \phi_2), (y \wedge \phi_2) \wedge (y \wedge \phi_2), (z \vee 0) \wedge (z \wedge \phi_3) \rangle =(x, y, z).$ $similarly,$ it can be shown that rest entries of R are also (x, y, z). Consequently C.D = C.

For having lowest IVPFV$\langle 0, \phi_2, \phi_3 \rangle \leq (x, y, z), i.e, 0 \leq x, \phi_2 \leq y, \phi_3 \geq z$ which concludes that for existing least IVPFV $y = \phi_2. so$ for defining null and identity IVPFM.it needs special restricted SIVPFM.

Identity special restricted IVPFM and null special restricted IVPFM are described as follows based on the aforementioned idea.

Definition 15

A special restricted SIVPFM is referred to as an identity special restricted IVPFM if it has nondiagonal values $\langle[\phi_{1L}, \phi_{1U}], [\phi_{2L}, \phi_{2U}], 0\rangle$, as well as diagonal entries of $\langle 0, [\phi_{2L}, \phi_{2U}], [\phi_{3L}, \phi_{3U}]\rangle$

Definition 16

If a special restricted SIVPFM has all entries$\langle 0, [\phi_{2L}, \phi_{2U}], [\phi_{3L}, \phi_{3U}]\rangle$, Then it is called null special restricted IVPFM.

It is clear that when$\phi_2 = 0, \phi_1 = 1, \phi_3 = 1$ Then $0 \leq (\langle[C_{ij\lambda_L}, C_{ij\lambda_U}]\rangle) \leq 1, (\langle[C_{ij\eta_L}, C_{ij\eta_L}]\rangle) = 1, 0 \leq (\langle[C_{ij\zeta_L}, C_{ij\zeta_U}]\rangle) \leq 1$ with $0 \leq (\langle[C_{ij\lambda_L}, C_{ij\lambda_U}], [C_{ij\eta_L}, C_{ij\eta_L}], [C_{ij\zeta_L}, C_{ij\zeta_U}]\rangle) \leq 1$. Now ,by replacing the measure membership by the measure of neutral membership and the measure of non-membership IVPFM is obtained. Thus, null IVIFM is obtained with all entries$\langle 0, \phi_3 \rangle = \langle 0,1 \rangle$ and identity IVIFM is obtained with diagonal entries $\langle \phi_1, 0 \rangle = \langle 0,1 \rangle$ and non -diagonal entries $\langle 0, \phi_3 \rangle = \langle 0,1 \rangle$ so identity IVIFM and null IFM, respectively.

Now, Let us define some basic operations on SIVPFMs.

Definition 17

Let C and D be two SIVPFMs of order a then the following operations are defined.

(i)   C ⊙D= $(\langle[C_{ij\lambda_L} . d_{ij\lambda_L}, C_{ij\lambda_U} . d_{ij\lambda_U}], [C_{ij\eta_L} . d_{ij\eta_L}, C_{ij\eta_U} . d_{ij\eta_U}], [C_{ij\zeta_L} . d_{ij\zeta_L}, C_{ij\zeta_U} . d_{ij\zeta_U}]\rangle)$,

(ii)   C ∨D= $(\langle[C_{ij\lambda_L} \vee d_{ij\lambda_L}, C_{ij\lambda_U} \vee d_{ij\lambda_U}], [C_{ij\eta_L} \wedge d_{ij\eta_L}, C_{ij\eta_U} \wedge d_{ij\eta_U}], [C_{ij\zeta_L} \wedge d_{ij\zeta_L}, C_{ij\zeta_U} \wedge d_{ij\zeta_U}]\rangle)$,

(iii)   C ∧D= $(\langle[C_{ij\lambda_L} \wedge d_{ij\lambda_L}, C_{ij\lambda_U} \wedge d_{ij\lambda_U}], [C_{ij\eta_L} \wedge d_{ij\eta_L}, C_{ij\eta_U} \wedge d_{ij\eta_U}], [C_{ij\zeta_L} \vee d_{ij\zeta_L}, C_{ij\zeta_U} \vee d_{ij\zeta_U}]\rangle)$,

(iv) $C^t = (\langle[C_{ji\lambda_L}, C_{ji\lambda_U}], [C_{ji\eta_L}, C_{ji\eta_L}], [C_{ji\zeta_L}, C_{ji\zeta_U}]\rangle)$,

(v) $\overline{C} =(\langle[C_{ij\zeta_L}, C_{ij\zeta_U}], [C_{ij\eta_L}, C_{ij\eta_L}], [C_{ij\lambda_L}, C_{ij\lambda_U}]\rangle)$(complement of SIVPFM P)

A few properties on SPFM

The proposition that follows will be used in this investigation of some ground properties of SIVPFM.

Proposition 1.

Let C and D two SIVPFM of same order. Then

(i) $C \wedge D = D \wedge C$,

(ii) $C \vee D = D \vee C$,

(iii) $(C^t)^t = C$,

(iv) $(\bar{C})^t = (\bar{C^t})$,

(v) $C \wedge (D \vee E) = (C \wedge D) \vee (C \wedge E)$

(vi) $C \vee (D \vee E) = (C \vee D) \wedge (C \vee E)$

(vii) $(K.C)^t = K.C^t$ for a IVPFV $k = \langle [k_{1L}, k_{1U}], [k_{2L}, k_{2U}], [k_{3L}, k_{3U}] \rangle$,

(viii) $\lim\limits_{n \to \infty} C \odot C \odot C \dots \dots \dots \odot C(n \text{ times}) = (\langle (0,0), (0,0), (0,0) \rangle)$

When ever $0 \leq (\langle [C_{ij\lambda_L}, C_{ij\lambda_U}] \rangle) < 1, 0 \leq (\langle [C_{ij\eta_L}, C_{ij\eta_L}] \rangle) < 1, 0 \leq (\langle [C_{ij\zeta_L}, C_{ij\zeta_U}] \rangle) < 1$.

Proof

Let $C = (\langle [C_{ij\lambda_L}, C_{ij\lambda_U}], [C_{ij\eta_L}, C_{ij\eta_L}], [C_{ij\zeta_L}, C_{ij\zeta_U}] \rangle)$ and $D = (\langle [d_{ij\lambda_L}, d_{ij\lambda_U}], [d_{ij\eta_L}, d_{ij\eta_L}], [d_{ij\zeta_L}, d_{ij\zeta_U}] \rangle)$ be two SIVPFM of order a.

(i) We have,

$C \wedge D = (\langle [C_{ij\lambda_L} \wedge d_{ij\lambda_L}, C_{ij\lambda_U} \wedge d_{ij\lambda_U}], [C_{ij\eta_L} \wedge d_{ij\eta_L}, C_{ij\eta_U} \wedge d_{ij\eta_U}], [C_{ij\zeta_L} \vee d_{ij\zeta_L}, C_{ij\zeta_U} \vee d_{ij\zeta_U}] \rangle)$

$= (\langle [d_{ij\lambda_L} \wedge c_{ij\lambda_L}, d_{ij\lambda_U} \wedge c_{ij\lambda_U}], [d_{ij\eta_L} \wedge c_{ij\eta_L}, d_{ij\eta_U} \wedge c_{ij\eta_U}], [d_{ij\zeta_L} \vee c_{ij\zeta_L}, d_{ij\zeta_U} \vee c_{ij\zeta_U}] \rangle)$

$\quad = D \wedge C$,

(ii) We have

$\qquad C \vee D = (\langle [C_{ij\lambda_L} \vee d_{ij\lambda_L}, C_{ij\lambda_U} \vee d_{ij\lambda_U}], [C_{ij\eta_L} \wedge d_{ij\eta_L}, C_{ij\eta_U} \wedge d_{ij\eta_U}], [C_{ij\zeta_L} \wedge d_{ij\zeta_L}, C_{ij\zeta_U} \wedge d_{ij\zeta_U}] \rangle)$

$= (\langle [d_{ij\lambda_L} \vee c_{ij\lambda_L}, d_{ij\lambda_U} \vee c_{ij\lambda_U}], [d_{ij\eta_L} \wedge c_{ij\eta_L}, d_{ij\eta_U} \wedge c_{ij\eta_U}], [d_{ij\zeta_L} \wedge c_{ij\zeta_L}, d_{ij\zeta_U} \wedge c_{ij\zeta_U}] \rangle)$

$\qquad\qquad\qquad = D \vee C$,

(iii) We have

$\qquad C^t = \left((\langle [C_{ij\lambda_L}, C_{ij\lambda_U}], [C_{ij\eta_L}, C_{ij\eta_L}], [C_{ij\zeta_L}, C_{ij\zeta_U}] \rangle) \right)^t$

$= (\langle [C_{ji\lambda_L}, C_{ji\lambda_U}], [C_{ji\eta_L}, C_{ji\eta_L}], [C_{ji\zeta_L}, C_{ji\zeta_U}] \rangle)$

$\qquad (C^t)^t = \left((\langle [C_{ji\lambda_L}, C_{ji\lambda_U}], [C_{ji\eta_L}, C_{ji\eta_L}], [C_{ji\zeta_L}, C_{ji\zeta_U}] \rangle) \right)^t$

$= (\langle [C_{ij\lambda_L}, C_{ij\lambda_U}], [C_{ij\eta_L}, C_{ij\eta_L}], [C_{ij\zeta_L}, C_{ij\zeta_U}] \rangle)$

$\qquad = C$

(iv) Here

$\bar{C} = (\langle [C_{ij\zeta_L}, C_{ij\zeta_U}], [C_{ij\eta_L}, C_{ij\eta_L}], [C_{ij\lambda_L}, C_{ij\lambda_U}] \rangle)$

Therefore

$\qquad (\bar{C})^t = \left((\langle [C_{ij\zeta_L}, C_{ij\zeta_U}], [C_{ij\eta_L}, C_{ij\eta_L}], [C_{ij\lambda_L}, C_{ij\lambda_U}] \rangle) \right)^t$

$\qquad = (\langle [C_{ji\zeta_L}, C_{ji\zeta_U}], [C_{ji\eta_L}, C_{ji\eta_L}], [C_{ji\lambda_L}, C_{ji\lambda_U}] \rangle)$

$\qquad \text{Now}, \left((\langle [C_{ij\lambda_L}, C_{ij\lambda_U}], [C_{ij\eta_L}, C_{ij\eta_L}], [C_{ij\zeta_L}, C_{ij\zeta_U}] \rangle) \right)^t$

$\qquad = (\langle [C_{ji\lambda_L}, C_{ji\lambda_U}], [C_{ji\eta_L}, C_{ji\eta_L}], [C_{ji\zeta_L}, C_{ji\zeta_U}] \rangle)$

Rajarajeswari and Nandhini

Therefore

$$(\bar{C}^t) = (\langle [C_{ji\zeta_L}, C_{ji\zeta_U}], [C_{ji\eta_L}, C_{ji\eta_L}], [C_{ji\lambda_L}, C_{ji\lambda_U}] \rangle)^t \text{ Thus } (\bar{C})^t = (\bar{C^t})$$

(v)$C \wedge (D \vee E) = (\langle [C_{ij\lambda_L}, C_{ij\lambda_U}], [C_{ij\eta_L}, C_{ij\eta_L}], [C_{ij\zeta_L}, C_{ij\zeta_U}] \rangle) \wedge$

$(\langle [C_{ij\lambda_L} \wedge (d_{ij\lambda_L} \vee e_{ij\lambda_L}), C_{ij\lambda_U} \wedge (d_{ij\lambda_U} \vee e_{ij\lambda_U})], [C_{ij\eta_L} \wedge (d_{ij\eta_L} \wedge e_{ij\eta_L}), C_{ij\eta_L} \wedge (d_{ij\eta_U} \wedge e_{ij\eta_U})], [C_{ij\zeta_L} \wedge (d_{ij\zeta_L} \wedge e_{ij\zeta_L}), C_{ij\zeta_L} \wedge (d_{ij\zeta_U} \wedge e_{ij\zeta_U})] \rangle)$

$= ([C_{ij\lambda_L} \wedge d_{ij\lambda_L} \vee C_{ij\lambda_L} \wedge e_{ij\lambda_L}][C_{ij\lambda_U} \wedge d_{ij\lambda_U} \vee C_{ij\lambda_U} \wedge e_{ij\lambda_U}], [C_{ij\eta_L} \wedge d_{ij\eta_L} \vee C_{ij\eta_L} \wedge e_{ij\eta_L}]_{(\langle [C_{ij\lambda_L} \wedge (d_{ij\lambda_L} \vee}$

$e_{ij\lambda_L}), C_{ij\lambda_U} \wedge (d_{ij\lambda_U} \vee e_{ij\lambda_U})], [C_{ij\eta_L} \wedge (d_{ij\eta_L} \wedge e_{ij\eta_L}), C_{ij\eta_L} \wedge (d_{ij\eta_U} \wedge e_{ij\eta_U})], [C_{ij\zeta_L} \wedge (d_{ij\zeta_L} \wedge e_{ij\zeta_L}), C_{ij\zeta_L} \wedge (d_{ij\zeta_U} \wedge e_{ij\zeta_U})] \rangle)$

$=(C \wedge D) \vee (C \wedge E)$

(vi) $C \vee (D \wedge E) = (\langle [C_{ij\lambda_L}, C_{ij\lambda_U}], [C_{ij\eta_L}, C_{ij\eta_L}], [C_{ij\zeta_L}, C_{ij\zeta_U}] \rangle) \vee$

$(\langle [C_{ij\lambda_L} \vee (d_{ij\lambda_L} \wedge e_{ij\lambda_L}), C_{ij\lambda_U} \vee (d_{ij\lambda_U} \wedge e_{ij\lambda_U})], [C_{ij\eta_L} \vee (d_{ij\eta_L} \wedge e_{ij\eta_L}), C_{ij\eta_L} \vee (d_{ij\eta_U} \wedge e_{ij\eta_U})], [C_{ij\zeta_L} \vee (d_{ij\zeta_L} \wedge e_{ij\zeta_L}), C_{ij\zeta_U} \vee (d_{ij\zeta_U} \wedge e_{ij\zeta_U})] \rangle)$

$= ([C_{ij\lambda_L} \wedge d_{ij\lambda_L} \vee C_{ij\lambda_L} \wedge e_{ij\lambda_L}][C_{ij\lambda_U} \wedge d_{ij\lambda_U} \vee C_{ij\lambda_U} \wedge e_{ij\lambda_U}], [C_{ij\eta_L} \wedge d_{ij\eta_L} \vee C_{ij\eta_L} \wedge e_{ij\eta_L}]_{(\langle [C_{ij\lambda_L} \wedge (d_{ij\lambda_L} \vee}$

$e_{ij\lambda_L}), C_{ij\lambda_U} \wedge (d_{ij\lambda_U} \vee e_{ij\lambda_U})], [C_{ij\eta_L} \wedge (d_{ij\eta_L} \wedge e_{ij\eta_L}), C_{ij\eta_L} \wedge (d_{ij\eta_U} \wedge e_{ij\eta_U})], [C_{ij\zeta_L} \wedge (d_{ij\zeta_L} \wedge e_{ij\zeta_L}), C_{ij\zeta_L} \wedge (d_{ij\zeta_U} \wedge e_{ij\zeta_U})] \rangle)$

$=(C \vee D) \wedge (C \vee E)$

 (vii)We have

$$(K.C)^t = (\langle \langle [k_{1L}, k_{1U}], [k_{2L}, k_{2U}], [k_{3L}, k_{2U}] \rangle . (\langle [C_{ij\lambda_L}, C_{ij\lambda_U}], [C_{ij\eta_L}, C_{ij\eta_L}], [C_{ij\zeta_L}, C_{ij\zeta_U}] \rangle) \rangle)^t$$

$$=(\langle [k_{1L} \wedge C_{ij\lambda_L}, k_{1U} \wedge C_{ij\lambda_L}], [k_{2L} \wedge C_{ij\eta_L}, k_{2U} \wedge C_{ij\eta_L}], [k_{3L} \vee C_{ij\zeta_L}, k_{3U} \vee C_{ij\zeta_U}] \rangle)^t$$

$$= \left((\langle [k_{1L}, k_{1U}] \wedge [C_{ij\lambda_L}, C_{ij\lambda_U}], [k_{2L}, k_{2U}] \wedge [C_{ij\eta_L}, C_{ij\eta_L}], [k_{3L}, k_{3U}] \vee [C_{ij\zeta_L}, C_{ij\zeta_U}] \rangle) \right)^t$$

$$=(\langle [k_{1L}, k_{1U}] \wedge [C_{ji\lambda_L}, C_{ji\lambda_U}], [k_{2L}, k_{2U}] \wedge [C_{ji\eta_L}, C_{ji\eta_L}], [k_{3L}, k_{3U}] \vee [C_{ji\zeta_L}, C_{ji\zeta_U}] \rangle)$$

$$(\langle \langle [k_{1L}, k_{1U}], [k_{2L}, k_{2U}], [k_{3L}, k_{2U}] \rangle . (\langle [C_{ji\lambda_L}, C_{ji\lambda_U}], [C_{ji\eta_L}, C_{ji\eta_L}], [C_{ji\zeta_L}, C_{ji\zeta_U}] \rangle) \rangle)$$

$$=k.C^t$$

(viii) $C \odot C = (\langle [C_{ij\lambda_L}, C_{ij\lambda_U}], [C_{ij\eta_L}, C_{ij\eta_L}], [C_{ij\zeta_L}, C_{ij\zeta_U}] \rangle) . (\langle [C_{ij\lambda_L}, C_{ij\lambda_U}], [C_{ij\eta_L}, C_{ij\eta_L}], [C_{ij\zeta_L}, C_{ij\zeta_U}] \rangle)$

$$(\langle [C_{ij\lambda_L} . C_{ij\lambda_L}, C_{ij\lambda_U} . C_{ij\lambda_U}], [C_{ij\eta_L} . C_{ij\eta_L}, C_{ij\eta_U} . C_{ij\eta_U}], [C_{ij\zeta_L} . C_{ij\zeta_U}, C_{ij\zeta_L} . C_{ij\zeta_U}] \rangle)$$

$=(\langle [C_{ij\lambda_L}{}^2, C_{ij\lambda_U}{}^2], [C_{ij\eta_L}{}^2, C_{ij\eta_U}{}^2], [C_{ij\zeta_L}{}^2, C_{ij\zeta_U}{}^2] \rangle) C \odot C \odot C = (\langle [C_{ij\lambda_L}{}^3, C_{ij\lambda_U}{}^3], [C_{ij\eta_L}{}^3, C_{ij\eta_U}{}^3], [C_{ij\zeta_L}{}^3, C_{ij\zeta_U}{}^3] \rangle).$ Proceeding in this way. It is obtained that

$C \odot C \odot \dots \dots \dots \odot C(n \text{ times}) = (\langle [C_{ij\lambda_L}{}^n, C_{ij\lambda_U}{}^n], [C_{ij\eta_L}{}^n, C_{ij\eta_U}{}^n], [C_{ij\zeta_L}{}^n, C_{ij\zeta_U}{}^n] \rangle).$ since $(\langle [C_{ij\lambda_L}, C_{ij\lambda_U}] \rangle) \subseteq [0,1], (\langle [C_{ij\eta_L}, C_{ij\eta_L}] \rangle) \subseteq [0,1], (\langle [C_{ij\zeta_L}, C_{ij\zeta_U}] \rangle) \subseteq [0,1],$

$$\lim_{n\to\infty} [C_{ij\lambda_L}{}^n, C_{ij\lambda_U}{}^n] = [0,0], \lim_{n\to\infty} [C_{ij\eta_L}{}^n, C_{ij\eta_U}{}^n] = [0,0], \lim_{n\to\infty} [C_{ij\zeta_L}{}^n, C_{ij\zeta_U}{}^n]$$
$$= [0,0] \lim_{n\to\infty} C \odot C \odot \dots \dots \dots \odot C(n \text{ times}) = (\langle [0,0], [0,0], [0,0] \rangle).$$

Proposition 2

Let C and D be two Special restricted SIVPFMs of same order a. Then $C \vee D \geq C$ and $C \vee D \geq D$.

Proof

Let C=$(\langle [C_{ij\lambda_L}, C_{ij\lambda_U}], [C_{ij\eta_L}, C_{ij\eta_L}], [C_{ij\zeta_L}, C_{ij\zeta_U}] \rangle)$ and D=$(\langle [d_{ij\lambda_L}, d_{ij\lambda_U}], [d_{ij\eta_L}, d_{ij\eta_L}], [d_{ij\zeta_L}, d_{ij\zeta_U}] \rangle)$be two SIVPFM of order $a$and restricted for three interval valued real numbers $[\phi_{1L}, \phi_{1U}] \subseteq [0,1], [\phi_{2L}, \phi_{2U}] \subseteq [0,1]$ and $[\phi_{3L}, \phi_{3U}] \subseteq$

[0,1]with

$\phi_{1U} + \phi_{2U} = 1 \ and \ \phi_{2U} + \phi_{3U} = 1$.Then$[C_{ij\lambda_L}, C_{ij\lambda_U}] and [d_{ij\lambda_L}, d_{ij\lambda_U}] \subseteq [\phi_{1L}, \phi_{1U}]$, $[C_{ij\eta_L}, C_{ij\eta_L}] and [d_{ij\eta_L}, d_{ij\eta_L}] = [\phi_{2L}, \phi_{2U}]$,$([C_{ij\zeta_L}, C_{ij\zeta_U}] and [d_{ij\zeta_L}, d_{ij\zeta_U}]) \subseteq [\phi_{3L}, \phi_{3U}]$.

Now $C \vee D = (\langle [C_{ij\lambda_L} \vee d_{ij\lambda_L}, C_{ij\lambda_U} \vee d_{ij\lambda_U}], [C_{ij\eta_L} \wedge d_{ij\eta_L}, C_{ij\eta_U} \wedge d_{ij\eta_U}], [C_{ij\zeta_L} \wedge d_{ij\zeta_L}, C_{ij\zeta_U} \wedge d_{ij\zeta_U}])$for i,j=1,2,3,……..a.

It is observed that$[C_{ij\lambda_L} \vee d_{ij\lambda_L}, C_{ij\lambda_U} \vee d_{ij\lambda_U}] \supseteq [C_{ij\lambda_L}, C_{ij\lambda_U}]$

$([C_{ij\eta_L} \wedge d_{ij\eta_L}, C_{ij\eta_U} \wedge d_{ij\eta_U}]) \supseteq [C_{ij\eta_L}, C_{ij\eta_L}]$

$([C_{ij\zeta_L} \wedge d_{ij\zeta_L}] \wedge [[d_{ij\zeta_L} \wedge d_{ij\zeta_U}]]) \subseteq [C_{ij\zeta_L}, C_{ij\zeta_U}]$.

hence by using the Definition 11 we have $C \vee D \geq C$

Similarly we can prove that $C \vee D \geq D$.

Proposition 3

Let C and D be two Special restricted SIVPFMs of same order a. Then $C \vee D \geq C \wedge D$.

Proof

Let C=$(\langle [C_{ij\lambda_L}, C_{ij\lambda_U}], [C_{ij\eta_L}, C_{ij\eta_L}], [C_{ij\zeta_L}, C_{ij\zeta_U}])$ and D=$(\langle [d_{ij\lambda_L}, d_{ij\lambda_U}], [d_{ij\eta_L}, d_{ij\eta_L}], [d_{ij\zeta_L}, d_{ij\zeta_U}])$be two SIVPFM of order a.Then

$$C \vee D = (\langle [C_{ij\lambda_L} \vee d_{ij\lambda_L}, C_{ij\lambda_U} \vee d_{ij\lambda_U}], [C_{ij\eta_L} \wedge d_{ij\eta_L}, C_{ij\eta_U} \wedge d_{ij\eta_U}], [C_{ij\zeta_L} \wedge d_{ij\zeta_L}, C_{ij\zeta_U} \wedge d_{ij\zeta_U}])$$

C $\wedge$D= $(\langle [C_{ij\lambda_L} \wedge d_{ij\lambda_L}, C_{ij\lambda_U} \wedge d_{ij\lambda_U}], [C_{ij\eta_L} \wedge d_{ij\eta_L}, C_{ij\eta_U} \wedge d_{ij\eta_U}], [C_{ij\zeta_L} \vee d_{ij\zeta_L}, C_{ij\zeta_U} \vee d_{ij\zeta_U}])$

It is Clear that$([C_{ij\lambda_L} \vee d_{ij\lambda_L}, C_{ij\lambda_U} \vee d_{ij\lambda_U}]) \supseteq ([C_{ij\lambda_L} \wedge d_{ij\lambda_L}, C_{ij\lambda_U} \wedge d_{ij\lambda_U}])$

$([C_{ij\eta_L} \wedge d_{ij\eta_L}, C_{ij\eta_U} \wedge d_{ij\eta_U}]) \supseteq ([C_{ij\eta_L} \wedge d_{ij\eta_L}, C_{ij\eta_U} \wedge d_{ij\eta_U}])$

$([C_{ij\zeta_L} \wedge d_{ij\zeta_L}, C_{ij\zeta_U} \wedge d_{ij\zeta_U}]) \subseteq ([C_{ij\zeta_L} \vee d_{ij\zeta_L}, C_{ij\zeta_U} \vee d_{ij\zeta_U}])$

So $C \vee D \geq C \wedge D$.

Proposition 4

Let C, D and E be three Special restricted SIVPFMs of same order. Then C$\vee E \geq$ D $\vee E$ whenever $C \geq D$.

Proof

Let C=$(\langle [C_{ij\lambda_L}, C_{ij\lambda_U}], [C_{ij\eta_L}, C_{ij\eta_L}], [C_{ij\zeta_L}, C_{ij\zeta_U}])$ and D=$(\langle [d_{ij\lambda_L}, d_{ij\lambda_U}], [d_{ij\eta_L}, d_{ij\eta_L}], [d_{ij\zeta_L}, d_{ij\zeta_U}])$E= $(\langle [e_{ij\lambda_L}, e_{ij\lambda_U}], [e_{ij\eta_L}, e_{ij\eta_L}], [e_{ij\zeta_L}, e_{ij\zeta_U}])$

be three Special restricted SIVPFM of order a by three interval valued real numbers $[\phi_{1L}, \phi_{1U}] \subseteq [0,1], [\phi_{2L}, \phi_{2U}] \subseteq [0,1] and [\phi_{3L}, \phi_{3U}] \subseteq [0,1]$with $\phi_{1U} + \phi_{2U} = 1 \ and \ \phi_{2U} + \phi_{3U} = 1$.Then$[C_{ij\lambda_L}, C_{ij\lambda_U}], [d_{ij\lambda_L}, d_{ij\lambda_U}] \ and [e_{ij\lambda_L}, e_{ij\lambda_U}] \subseteq [\phi_{1L}, \phi_{1U}]$, $[C_{ij\eta_L}, C_{ij\eta_L}], [d_{ij\eta_L}, d_{ij\eta_L}] and [e_{ij\eta_L}, e_{ij\eta_L}] = [\phi_{2L}, \phi_{2U}]$,$([C_{ij\zeta_L}, C_{ij\zeta_U}], [d_{ij\zeta_L}, d_{ij\zeta_U}]) and [e_{ij\zeta_L}, e_{ij\zeta_U}] \subseteq [\phi_{3L}, \phi_{3U}]$

$C \geq D \Rightarrow ([C_{ij\lambda_L}, C_{ij\lambda_U}]) \supseteq ([d_{ij\lambda_L}, d_{ij\lambda_U}])$,

$([C_{ij\eta_L}, C_{ij\eta_L}]) \supseteq ([d_{ij\eta_L}, d_{ij\eta_L}]), ([[C_{ij\zeta_L}, C_{ij\zeta_U}]]) \subseteq ([[d_{ij\zeta_L}, d_{ij\zeta_U}]])$

$When ([C_{ij\lambda_L}, C_{ij\lambda_U}]) \supseteq ([d_{ij\lambda_L}, d_{ij\lambda_U}]) \supseteq ([e_{ij\lambda_L}, e_{ij\lambda_U}])$,

$([C_{ij\lambda_L}, C_{ij\lambda_U}]) \vee ([e_{ij\lambda_L}, e_{ij\lambda_U}]) = ([[C_{ij\lambda_L}, C_{ij\lambda_U}]]) \ and ([[d_{ij\lambda_L}, d_{ij\lambda_U}]]) \vee ([e_{ij\lambda_L}, e_{ij\lambda_U}]) = ([[d_{ij\lambda_L}, d_{ij\lambda_U}]])$

Rajarajeswari and Nandhini

When $([C_{ij\lambda_L}, C_{ij\lambda_U}]) \supseteq ([e_{ij\lambda_L}, e_{ij\lambda_U}]) \supseteq ([d_{ij\lambda_L}, d_{ij\lambda_U}]), ([[C_{ij\lambda_L}, C_{ij\lambda_U}]]) \vee ([e_{ij\lambda_L}, e_{ij\lambda_U}]) = ([[C_{ij\lambda_L}, C_{ij\lambda_U}]])$

and $([[d_{ij\lambda_L}, d_{ij\lambda_U}]]) \vee ([e_{ij\lambda_L}, e_{ij\lambda_U}]) = ([[e_{ij\lambda_L}, e_{ij\lambda_U}]])$

When

$([e_{ij\lambda_L}, e_{ij\lambda_U}]) \supseteq ([c_{ij\lambda_L}, c_{ij\lambda_U}]) \supseteq ([d_{ij\lambda_L}, d_{ij\lambda_U}]), ([[C_{ij\lambda_L}, C_{ij\lambda_U}]]) \vee ([e_{ij\lambda_L}, e_{ij\lambda_U}]) = ([[e_{ij\lambda_L}, e_{ij\lambda_U}]])$

and $([[d_{ij\lambda_L}, d_{ij\lambda_U}]]) \vee ([e_{ij\lambda_L}, e_{ij\lambda_U}]) = ([[e_{ij\lambda_L}, e_{ij\lambda_U}]])$

Now

when $([C_{ij\eta_L}, C_{ij\eta_U}]) \supseteq ([d_{ij\eta_L}, d_{ij\eta_U}]) \supseteq ([e_{ij\eta_L}, e_{ij\eta_U}]), ([[C_{ij\eta_L}, C_{ij\eta_U}]]) \wedge ([e_{ij\eta_L}, e_{ij\eta_U}]) = ([[e_{ij\eta_L}, e_{ij\eta_U}]])$

and $([[d_{ij\eta_L}, d_{ij\eta_U}]]) \wedge ([e_{ij\eta_L}, e_{ij\eta_U}]) = ([[e_{ij\eta_L}, e_{ij\eta_U}]])$

When

$([C_{ij\eta_L}, C_{ij\eta_U}]) \supseteq ([[e_{ij\eta_L}, e_{ij\eta_U}]]) \supseteq ([d_{ij\lambda_L}, d_{ij\lambda_U}]), ([[C_{ij\eta_L}, C_{ij\eta_U}]]) \wedge ([e_{ij\eta_L}, e_{ij\eta_U}]) = ([e_{ij\eta_L}, e_{ij\eta_U}])$

and $([d_{ij\eta_L}, d_{ij\eta_U}]) \wedge ([[e_{ij\eta_L}, e_{ij\eta_U}]]) = ([[[d_{ij\eta_L}, d_{ij\eta_U}]]])$

When

$([e_{ij\eta_L}, e_{ij\eta_U}]) \supseteq ([C_{ij\eta_L}, C_{ij\eta_U}]) \supseteq ([d_{ij\lambda_L}, d_{ij\lambda_U}]), ([[C_{ij\eta_L}, C_{ij\eta_U}]]) \wedge ([e_{ij\eta_L}, e_{ij\eta_U}]) = ([[[c_{ij\eta_L}, c_{ij\eta_U}]]])$

and $([[d_{ij\lambda_L}, d_{ij\lambda_U}]]) \vee ([e_{ij\eta_L}, e_{ij\eta_U}]) = ([[[d_{ij\eta_L}, d_{ij\eta_U}]]])$

Also

when $([C_{ij\zeta_L}, C_{ij\zeta_U}]) \subseteq ([d_{ij\zeta_L}, d_{ij\zeta_U}]) \subseteq ([e_{ij\zeta_L}, e_{ij\zeta_U}]), ([[C_{ij\zeta_L}, C_{ij\zeta_U}]]) \wedge ([[e_{ij\zeta_L}, e_{ij\zeta_U}]]) = ([[c_{ij\zeta_L}, c_{ij\zeta_U}]])$

and $([[d_{ij\zeta_L}, d_{ij\zeta_U}]]) \wedge ([[e_{ij\zeta_L}, e_{ij\zeta_U}]]) = ([d_{ij\zeta_L}, d_{ij\zeta_U}])$

When

$([C_{ij\zeta_L}, C_{ij\zeta_U}]) \subseteq ([[e_{ij\zeta_L}, e_{ij\zeta_U}]]) \subseteq ([d_{ij\zeta_L}, d_{ij\zeta_U}]), ([[C_{ij\zeta_L}, C_{ij\zeta_U}]]) \wedge ([[e_{ij\zeta_L}, e_{ij\zeta_U}]]) = ([C_{ij\zeta_L}, C_{ij\zeta_U}])$

and $([[d_{ij\lambda_L}, d_{ij\lambda_U}]]) \wedge ([[e_{ij\zeta_L}, e_{ij\zeta_U}]]) = ([[[e_{ij\zeta_L}, e_{ij\zeta_U}]]])$

When

$([e_{ij\zeta_L}, e_{ij\zeta_U}]) \subseteq ([C_{ij\zeta_L}, C_{ij\zeta_U}]) \subseteq ([d_{ij\zeta_L}, d_{ij\zeta_U}]), ([[C_{ij\zeta_L}, C_{ij\zeta_U}]]) \wedge ([[e_{ij\zeta_L}, e_{ij\zeta_U}]]) = ([[e_{ij\zeta_L}, e_{ij\zeta_U}]])$

and $([[d_{ij\lambda_L}, d_{ij\lambda_U}]]) \vee ([[e_{ij\zeta_L}, e_{ij\zeta_U}]]) = ([[[e_{ij\zeta_L}, e_{ij\zeta_U}]]])$

Therefore, it is obtained that $([[C_{ij\lambda_L}, C_{ij\lambda_U}]]) \vee ([e_{ij\lambda_L}, e_{ij\lambda_U}]) \supseteq ([d_{ij\lambda_L}, d_{ij\lambda_U}]) \vee ([e_{ij\lambda_L}, e_{ij\lambda_U}])$

$([[C_{ij\lambda_L}, C_{ij\lambda_U}]]) \wedge ([e_{ij\eta_L}, e_{ij\eta_U}]) \supseteq ([d_{ij\lambda_L}, d_{ij\lambda_U}]) \wedge ([e_{ij\lambda_L}, e_{ij\lambda_U}]) ([[C_{ij\lambda_L}, C_{ij\lambda_U}]]) \wedge ([e_{ij\lambda_L}, e_{ij\lambda_U}]) \subseteq ([d_{ij\lambda_L}, d_{ij\lambda_U}]) \wedge ([e_{ij\lambda_L}, e_{ij\lambda_U}])$ for i,j=1,2,3,………a. consequently,

C$\vee E \geq$ D $\vee E$.

Proposition 5.

Let C,D and E be three Special restricted SIVPFMs of same order. Then C$\wedge E \leq$ D $\wedge E$ *whenever* $C \leq D$.

Proof

Similarly we can prove as in proposition 4.

Proposition 6.

Let C ,D and E be three Special restricted SIVPFMs of same order. Then $C \leq D$ implies $C \wedge E = 0$ whenever $D \wedge E = 0$.

Proof

Let C=$(\langle[C_{ij\lambda_L}, C_{ij\lambda_U}], [C_{ij\eta_L}, C_{ij\eta_L}], [C_{ij\zeta_L}, C_{ij\zeta_U}]\rangle)$ and D=$(\langle[d_{ij\lambda_L}, d_{ij\lambda_U}], [d_{ij\eta_L}, d_{ij\eta_L}], [d_{ij\zeta_L}, d_{ij\zeta_U}]\rangle)$be two SIVPFM of order x for three real numbers $[\phi_{1L}, \phi_{1U}] \in [0,1], [\phi_{2L}, \phi_{2U}] \in [0,1]$ and $[\phi_{3L}, \phi_{3U}] \in [0,1]$ with $\phi_{1U} + \phi_{2U} = 1$ and $\phi_{2U} + \phi_{3U} = 1$.Then $([C_{ij\lambda_L}, C_{ij\lambda_U}], [d_{ij\lambda_L}, d_{ij\lambda_U}]) \in [\phi_{1L}, \phi_{1U}] [C_{ij\eta_L}, C_{ij\eta_L}] = [d_{ij\eta_L}, d_{ij\eta_L}] = [\phi_{2L}, \phi_{2U}]([C_{ij\zeta_L}, C_{ij\zeta_U}], [d_{ij\zeta_L}, d_{ij\zeta_U}]) \in [\phi_{3L}, \phi_{3U}]$ with $0 \leq (\langle[C_{ij\lambda_L}, C_{ij\lambda_U}] + [C_{ij\eta_L}, C_{ij\eta_L}] + [C_{ij\zeta_L}, C_{ij\zeta_U}]\rangle) \leq 1. 0 \leq (\langle[d_{ij\lambda_L}, d_{ij\lambda_U}] + [d_{ij\eta_L}, d_{ij\eta_L}] + [d_{ij\zeta_L}, d_{ij\zeta_U}]\rangle) \leq 1$.for i,j=1,2,3,………a.

Now C≤D $\Rightarrow C \wedge E \leq D \wedge E = (\langle0, [\phi_{2L}, \phi_{2U}], [\phi_{3L}, \phi_{3U}]\rangle)$

(by proposition 5)$C \wedge E = S = (\langle[s_{ij\lambda_L}, s_{ij\lambda_U}], [s_{ij\eta_L}, s_{ij\eta_L}], [s_{ij\zeta_L}, s_{ij\zeta_U}]\rangle)$

$(\langle[s_{ij\lambda_L}, s_{ij\lambda_U}], [s_{ij\eta_L}, s_{ij\eta_L}], [s_{ij\zeta_L}, s_{ij\zeta_U}]\rangle) \leq (\langle0, \phi_{2L}, \phi_{2U}, \phi_{3L}, \phi_{3U}\rangle)([s_{ij\lambda_L}, s_{ij\lambda_U}]) \leq 0, ([s_{ij\eta_L}, s_{ij\eta_L}]) \leq [\phi_{2L}, \phi_{2U}], ([s_{ij\zeta_L}, s_{ij\zeta_U}]) \geq [\phi_{3L,}\phi_{3U}]$ for 1,2,3,………a.

$[s_{ij\lambda_L}, s_{ij\lambda_U}] = 0, [s_{ij\eta_L}, s_{ij\eta_L}] = [\phi_{2L}, \phi_{2U}], [s_{ij\zeta_L}, s_{ij\zeta_U}] = [\phi_{3L,}\phi_{3U}]$ for1,2,3,…….a

Consequently S=$(\langle0, [\phi_{2L}, \phi_{2U}], [\phi_{3L}, \phi_{3U}]\rangle)$=0.

Proposition 7

Let C, D and E be three Special restricted SIVPFMs of same order. Then $C \geq D$ implies $C \vee D = (\langle\phi_1, \phi_2, 0\rangle)$ whenever $D \wedge E = (\langle[\phi_{1L}, \phi_{1U}], [\phi_{2L}, \phi_{2U}], 0\rangle)$.

Proof

Let C=$(\langle[C_{ij\lambda_L}, C_{ij\lambda_U}], [C_{ij\eta_L}, C_{ij\eta_L}], [C_{ij\zeta_L}, C_{ij\zeta_U}]\rangle)$ and D=$(\langle[d_{ij\lambda_L}, d_{ij\lambda_U}], [d_{ij\eta_L}, d_{ij\eta_L}], [d_{ij\zeta_L}, d_{ij\zeta_U}]\rangle)$E= $(\langle[e_{ij\lambda_L}, e_{ij\lambda_U}], [e_{ij\eta_L}, e_{ij\eta_L}], [e_{ij\zeta_L}, e_{ij\zeta_U}]\rangle)$

be three SIVPFM of order x for three real numbers $[\phi_{1L}, \phi_{1U}] \in [0,1], [\phi_{2L}, \phi_{2U}] \in [0,1], [\phi_{3L}, \phi_{3U}] \in [0,1]$ with $\phi_{1U} + \phi_{2U} = 1$ and $\phi_{2U} + \phi_{3U} = 1$.Then

$(\langle[C_{ij\lambda_L}, C_{ij\lambda_U}], [d_{ij\lambda_L}, d_{ij\lambda_U}], [e_{ij\lambda_L}, e_{ij\lambda_U}] \in [\phi_{1L}, \phi_{1U}] [C_{ij\eta_L}, C_{ij\eta_L}] = [d_{ij\eta_L}, d_{ij\eta_L}] = [e_{ij\eta_L}, e_{ij\eta_L}] = \phi_{2L}, \phi_{2U}, [C_{ij\zeta_L}, C_{ij\zeta_U}], [d_{ij\zeta_L}, d_{ij\zeta_U}], [e_{ij\zeta_L}, e_{ij\zeta_U}]\rangle) \in [\phi_{3L}, \phi_{3U}]$ with $0 \leq (\langle[C_{ij\lambda_L}, C_{ij\lambda_U}] + [C_{ij\eta_L}, C_{ij\eta_L}] + [C_{ij\zeta_L}, C_{ij\zeta_U}]\rangle) \leq 1, 0 \leq (\langle[d_{ij\lambda_L}, d_{ij\lambda_U}] + [d_{ij\eta_L}, d_{ij\eta_L}] + [d_{ij\zeta_L}, d_{ij\zeta_U}]\rangle) \leq 1, 0 \leq (\langle[e_{ij\lambda_L}, e_{ij\lambda_U}] + [e_{ij\eta_L}, e_{ij\eta_L}] + [e_{ij\zeta_L}, e_{ij\zeta_U}]\rangle) \leq 1$.for i,j=1,2,3,………a.

Now C≥D $\Rightarrow C \vee E \leq D \vee E = (\langle[\phi_{1L}, \phi_{1U}], [\phi_{2L}, \phi_{2U}], 0\rangle)$ (by proposition 4)

$$C \vee E \geq (\langle[\phi_{1L}, \phi_{1U}], [\phi_{2L}, \phi_{2U}], 0\rangle)$$

Let $C \vee E = S = (\langle[s_{ij\lambda_L}, s_{ij\lambda_U}], [s_{ij\eta_L}, s_{ij\eta_L}], [s_{ij\zeta_L}, s_{ij\zeta_U}]\rangle)$

$(\langle[s_{ij\lambda_L}, s_{ij\lambda_U}], [s_{ij\eta_L}, s_{ij\eta_L}], [s_{ij\zeta_L}, s_{ij\zeta_U}]\rangle) \geq (\langle[\phi_{1L}, \phi_{1U}], [\phi_{2L}, \phi_{2U}], 0\rangle) \leq 0, [s_{ij\lambda_L}, s_{ij\lambda_U}] \geq [\phi_{1L}, \phi_{1U}]([s_{ij\eta_L}, s_{ij\eta_L}]) \geq [\phi_{2L}, \phi_{2U}], ([s_{ij\zeta_L}, s_{ij\zeta_U}]) \leq [\phi_{3L}, \phi_{3U}]$ for 1,2,3,………a.

$$[s_{ij\lambda_L}, s_{ij\lambda_U}] = [\phi_{1L}, \phi_{1U}], [s_{ij\eta_L}, s_{ij\eta_L}] = [\phi_{2L}, \phi_{2U}], [s_{ij\zeta_L}, s_{ij\zeta_U}] = 0 \text{ for1,2,3,…….a}$$

Consequently, S=$(\langle[\phi_{1L}, \phi_{1U}], [\phi_{2L}, \phi_{2U}], 0\rangle)$.

Definition 18

Let $C=(\langle[C_{ij\lambda_L}, C_{ij\lambda_U}], [C_{ij\eta_L}, C_{ij\eta_L}], [C_{ij\zeta_L}, C_{ij\zeta_U}]\rangle)$ and $D=(\langle[d_{ij\lambda_L}, d_{ij\lambda_U}], [d_{ij\eta_L}, d_{ij\eta_L}], [d_{ij\zeta_L}, d_{ij\zeta_U}]\rangle)$ be two special restricted SIVPFM. Then a binary operation $'\ominus'$between them is defined by

$C\ominus D=(\langle[e_{ij\lambda_L}, e_{ij\lambda_U}], [e_{ij\eta_L}, e_{ij\eta_L}], [e_{ij\zeta_L}, e_{ij\zeta_U}]\rangle), where\ (\langle[e_{ij\lambda_L}, e_{ij\lambda_U}], [e_{ij\eta_L}, e_{ij\eta_L}], [e_{ij\zeta_L}, e_{ij\zeta_U}]\rangle)=$

$$\begin{cases} (\langle[C_{ij\lambda_L}, C_{ij\lambda_U}], [C_{ij\eta_L}, C_{ij\eta_L}], [C_{ij\zeta_L}, C_{ij\zeta_U}]\rangle), & when(\langle[C_{ij\lambda_L}, C_{ij\lambda_U}], [C_{ij\eta_L}, C_{ij\eta_L}], [C_{ij\zeta_L}, C_{ij\zeta_U}]\rangle) \\ & \geq (\langle[d_{ij\lambda_L}, d_{ij\lambda_U}], [d_{ij\eta_L}, d_{ij\eta_L}], [d_{ij\zeta_L}, d_{ij\zeta_U}]\rangle) \\ \langle0, [\phi_{2L}, \phi_{2U}], [\phi_{3L}, \phi_{3U}]\rangle & otherwise \end{cases}$$

Definition 19

Let $C=(\langle[C_{ij\lambda_L}, C_{ij\lambda_U}], [C_{ij\eta_L}, C_{ij\eta_L}], [C_{ij\zeta_L}, C_{ij\zeta_U}]\rangle)$ *be special restricted* SIVPFM of order $a.$ Then C is reflexive if$[C_{ii\lambda_L}, C_{ii\lambda_U}] = [\phi_{1L}, \phi_{1U}], [C_{ii\eta_L}, C_{ii\eta_L}] = [\phi_{2L}, \phi_{2U}], [C_{ii\zeta_L}, C_{ii\zeta_U}] = 0$ for i=1,2,3,…..a.

Definition 20

Let $C=(\langle[C_{ij\lambda_L}, C_{ij\lambda_U}], [C_{ij\eta_L}, C_{ij\eta_L}], [C_{ij\zeta_L}, C_{ij\zeta_U}]\rangle)$ *be special restricted* SIVPFM of order $a.$ Then C   irreflexive if $[C_{ii\lambda_L}, C_{ii\lambda_U}] = 0 [C_{ii\eta_L}, C_{ii\eta_L}] = [\phi_{2L}, \phi_{2U}] [C_{ii\zeta_L}, C_{ii\zeta_U}] = [\phi_{3L}, \phi_{3U}]$ for i=1,2,3,…..a.

Definition 21.

Let C and D be two SIVPFMs of order $x.$ Then the convex combination of C and D is denoted by $C* D$ and is defined by $C* D = (\langle[e_{ij\lambda_L}, e_{ij\lambda_U}], [e_{ij\eta_L}, e_{ij\eta_L}], [e_{ij\zeta_L}, e_{ij\zeta_U}]\rangle),$

where
$$[e_{ij\lambda_L}, e_{ij\lambda_U}] = [\beta \wedge C_{ij\lambda_L}, \beta \wedge C_{ij\lambda_U}] \vee [(1-\beta) \wedge d_{ij\lambda_L}, (1-\beta) \wedge d_{ij\lambda_U}].$$
$$[e_{ij\eta_L}, e_{ij\eta_L}] = [\beta \wedge C_{ij\eta_L}, \beta \wedge C_{ij\eta_U}] \vee [(1-\beta) \wedge d_{ij\eta_L}, (1-\beta) \wedge d_{ij\eta_U}].$$
$$[e_{ij\zeta_L}, e_{ij\zeta_U}] = [\beta \wedge C_{ij\zeta_L}, \beta \wedge C_{ij\zeta_U}] \vee [(1-\beta) \wedge d_{ij\zeta_L}, (1-\beta) \wedge d_{ij\zeta_U}].$$

for i,j=1,2,3,…….,a;Where $0\leq \beta \leq 1$.

As a result, it is noted that the convex combination of two SIVPFMs is nothing more than the convex combination of their entries, each of which contains three different sorts of membership values. Convex combination of the entries' respective membership values is used during convex combination of the entries.

Definition 22.

A SIVPFM $C=(\langle[C_{ij\lambda_L}, C_{ij\lambda_U}], [C_{ij\eta_L}, C_{ij\eta_L}], [C_{ij\zeta_L}, C_{ij\zeta_U}]\rangle)$ is said to be idempotent with respect to some operation '∘' if $C∘C =C.$

Proposition 8

Every SIVPFM is idempotent with respect to convex combination '∗'.

Proof

Let $C=(\langle[C_{ij\lambda_L}, C_{ij\lambda_U}], [C_{ij\eta_L}, C_{ij\eta_L}], [C_{ij\zeta_L}, C_{ij\zeta_U}]\rangle)$ be a SIVPFM of order $x.$
$C* C=(\langle[e_{ij\lambda_L}, e_{ij\lambda_U}], [e_{ij\eta_L}, e_{ij\eta_L}], [e_{ij\zeta_L}, e_{ij\zeta_U}]\rangle)$

Rajarajeswari and Nandhini

where

$$[e_{ij\lambda_L}, e_{ij\lambda_U}] = [\beta \wedge C_{ij\lambda_L}, \beta \wedge C_{ij\lambda_U}] \vee [(1-\beta) \wedge c_{ij\lambda_L}, (1-\beta) \wedge c_{ij\lambda_U}].$$

$$[e_{ij\eta_L}, e_{ij\eta_L}] = [\beta \wedge C_{ij\eta_L}, \beta \wedge C_{ij\eta_U}] \vee [(1-\beta) \wedge c_{ij\eta_L}, (1-\beta) \wedge c_{ij\eta_U}].$$

$$[e_{ij\zeta_L}, e_{ij\zeta_U}] = [\beta \wedge C_{ij\zeta_L}, \beta \wedge C_{ij\zeta_U}] \vee [(1-\beta) \wedge c_{ij\zeta_L}, (1-\beta) \wedge c_{ij\zeta_U}] \text{for i,j=1,2,3,}\ldots\ldots\text{,a.}$$

Therefore $C* C$=C.So, C is idempodent SIVPFM with respect to '$*$'.

Proposition 9.

For an irreflexive special restricted SIVPFM C, C$\ominus I$ is irreflexive.

Proof

Let C=$(\langle [C_{ij\lambda_L}, C_{ij\lambda_U}], [C_{ij\eta_L}, C_{ij\eta_L}], [C_{ij\zeta_L}, C_{ij\zeta_U}] \rangle)$ be an irreflexive

special   restricted   of   order a for   three   interval   valued   real   numbers $[\phi_{1L}, \phi_{1U}] \subseteq [0,1], [\phi_{2L}, \phi_{2U}] \subseteq [0,1] and [\phi_{3L}, \phi_{3U}] \subseteq [0,1]$ with $\phi_{1U} + \phi_{2U} = 1$ and $\phi_{2U} + \phi_{3U} = 1$.Then

$[C_{ij\lambda_L}, C_{ij\lambda_U}] \subseteq [\phi_{1L}, \phi_{1L}][C_{ij\eta_L}, C_{ij\eta_L}] = [\phi_{2L}, \phi_{2U}], [C_{ij\zeta_L}, C_{ij\zeta_U}] \subseteq [\phi_{3L}, \phi_{3U}]$ for i,j=1,2,3,$\ldots\ldots$a.Since C is irreflexive $(\langle [C_{ii\lambda_L}, C_{ii\lambda_U}], [C_{ii\eta_L}, C_{ii\eta_L}], [C_{ii\zeta_L}, C_{ii\zeta_U}] \rangle) = \langle 0, [\phi_{2L}, \phi_{2U}], [\phi_{3L}, \phi_{3U}] \rangle$ for i,j =1,2,3,$\ldots\ldots$a. the entries in (i,i) position of C$\ominus I$ are $\langle 0, [\phi_{2L}, \phi_{2U}], [\phi_{3L}, \phi_{3U}] \rangle$for i,j=1,2,3,$\ldots\ldots$a.so C$\ominus I$ is irreflexive.

Proposition 10.

Let C and D be two Special restricted SIVPFMs. Then C$\vee D \geq$ C $\ominus D$.

Proof

Let   C=$(\langle [C_{ij\lambda_L}, C_{ij\lambda_U}], [C_{ij\eta_L}, C_{ij\eta_L}], [C_{ij\zeta_L}, C_{ij\zeta_U}] \rangle)$ and   D=$(\langle [d_{ij\lambda_L}, d_{ij\lambda_U}], [d_{ij\eta_L}, d_{ij\eta_L}], [d_{ij\zeta_L}, d_{ij\zeta_U}] \rangle)$be two special restricted SIVPFM of order a for three real numbers$[\phi_{1L}, \phi_{1U}] \subseteq [0,1], [\phi_{2L}, \phi_{2U}] \subseteq [0,1] and \phi_{3L}, \phi_{3U} \subseteq [0,1]$with $\phi_{1U} + \phi_{2U} = 1$ and $\phi_{2U} + \phi_{3U} = 1$.Then$(\langle [C_{ij\lambda_L}, C_{ij\lambda_U}], [d_{ij\lambda_L}, d_{ij\lambda_U}] \in [\phi_{1L}, \phi_{1U}][C_{ij\eta_L}, C_{ij\eta_L}] = [d_{ij\eta_L}, d_{ij\eta_L}] = [\phi_{2L}, \phi_{2U}], [C_{ij\zeta_L}, C_{ij\zeta_U}], [d_{ij\zeta_L}, d_{ij\zeta_U}] \rangle) \in [\phi_{3L}, \phi_{3U}]$ with$0 \leq (\langle [C_{ij\lambda_L}, C_{ij\lambda_U}] + [C_{ij\eta_L}, C_{ij\eta_L}] + [C_{ij\zeta_L}, C_{ij\zeta_U}] \rangle) \leq 1.0 \leq (\langle [d_{ij\lambda_L}, d_{ij\lambda_U}] + [d_{ij\eta_L}, d_{ij\eta_L}] + [d_{ij\zeta_L}, d_{ij\zeta_U}] \rangle) \leq 1$.for i,j=1,2,3,$\ldots\ldots$a.

Now,$C \vee D = (\langle [C_{ij\lambda_L}, C_{ij\lambda_U}], [C_{ij\eta_L}, C_{ij\eta_L}], [C_{ij\zeta_L}, C_{ij\zeta_U}] \rangle) \vee (\langle [d_{ij\lambda_L}, d_{ij\lambda_U}], [d_{ij\eta_L}, d_{ij\eta_L}], [d_{ij\zeta_L}, d_{ij\zeta_U}] \rangle) =$

$(\langle [C_{ij\lambda_L} \vee d_{ij\lambda_L}, C_{ij\lambda_U} \vee d_{ij\lambda_U}], [C_{ij\eta_L} \vee d_{ij\eta_L}, C_{ij\eta_U} \vee d_{ij\eta_U}], [C_{ij\zeta_L} \vee d_{ij\zeta_L}, C_{ij\zeta_U} \vee d_{ij\zeta_U}] \rangle)$ and

C$\ominus$D=$(\langle [e_{ij\lambda_L}, e_{ij\lambda_U}], [e_{ij\eta_L}, e_{ij\eta_L}], [e_{ij\zeta_L}, e_{ij\zeta_U}] \rangle), where (\langle [e_{ij\lambda_L}, e_{ij\lambda_U}], [e_{ij\eta_L}, e_{ij\eta_L}], [e_{ij\zeta_L}, e_{ij\zeta_U}] \rangle)$

$$\begin{cases} (\langle [C_{ij\lambda_L}, C_{ij\lambda_U}], [C_{ij\eta_L}, C_{ij\eta_L}], [C_{ij\zeta_L}, C_{ij\zeta_U}] \rangle), & when (\langle [C_{ij\lambda_L}, C_{ij\lambda_U}], [C_{ij\eta_L}, C_{ij\eta_L}], [C_{ij\zeta_L}, C_{ij\zeta_U}] \rangle) \\ & \geq (\langle [d_{ij\lambda_L}, d_{ij\lambda_U}], [d_{ij\eta_L}, d_{ij\eta_L}], [d_{ij\zeta_L}, d_{ij\zeta_U}] \rangle) \\ \langle 0, [\phi_{2L}, \phi_{2U}], [\phi_{3L}, \phi_{3U}] \rangle & otherwise \end{cases}$$

It is observed that $([c_{ij\lambda_L}, c_{ij\lambda_U}]) \vee ([d_{ij\lambda_L}, d_{ij\lambda_U}]) \geq ([c_{ij\lambda_L}, c_{ij\lambda_U}]),$

$$([c_{ij\eta_L}, c_{ij\eta_L}]) \wedge ([d_{ij\eta_L}, d_{ij\eta_L}]) \geq ([c_{ij\eta_L}, c_{ij\eta_L}]),$$

$$([c_{ij\zeta_L}, c_{ij\zeta_U}]) \wedge ([d_{ij\zeta_L}, d_{ij\zeta_U}]) \leq ([c_{ij\zeta_L}, c_{ij\zeta_U}]).$$

$$([c_{ij\lambda_L}, c_{ij\lambda_U}]) \vee ([d_{ij\lambda_L}, d_{ij\lambda_U}]) \geq 0,$$

$$([c_{ij\eta_L}, c_{ij\eta_L}]) \wedge ([d_{ij\eta_L}, d_{ij\eta_L}]) \geq [\phi_{2L}, \phi_{2U}]$$

$$([c_{ij\zeta_L}, c_{ij\zeta_U}]) \wedge ([d_{ij\zeta_L}, d_{ij\zeta_U}]) \leq [\phi_{3L}, \phi_{3U}]$$

Consequently, C$\vee D \geq$ C $\ominus D$.

Proposition 11.

Let C and D be two Special restricted SIVPFMs of same order. Then, $(C \vee D) \vee (C \ominus D) = C \vee D$.

Proof

Let $C = (\langle [C_{ij\lambda_L}, C_{ij\lambda_U}], [C_{ij\eta_L}, C_{ij\eta_L}], [C_{ij\zeta_L}, C_{ij\zeta_U}] \rangle)$ and $D = (\langle [d_{ij\lambda_L}, d_{ij\lambda_U}], [d_{ij\eta_L}, d_{ij\eta_L}], [d_{ij\zeta_L}, d_{ij\zeta_U}] \rangle)$ be two special restricted SIVPFM of order a for three real numbers $[\phi_{1L}, \phi_{1U}] \subseteq [0,1], [\phi_{2L}, \phi_{2U}] \subseteq [0,1]$ and $[\phi_{3L}, \phi_{3U}] \subseteq [0,1]$ with $\phi_{1U} + \phi_{2U} = 1$ and $\phi_{2U} + \phi_{3U} = 1$. Then

$(\langle [C_{ij\lambda_L}, C_{ij\lambda_U}], [d_{ij\lambda_L}, d_{ij\lambda_U}] \subseteq [\phi_{1L}, \phi_{1U}] [C_{ij\eta_L}, C_{ij\eta_L}] = [d_{ij\eta_L}, d_{ij\eta_L}] = [\phi_{2L}, \phi_{2U}], ([C_{ij\zeta_L}, C_{ij\zeta_U}], [d_{ij\zeta_L}, d_{ij\zeta_U}] \rangle) \subseteq [\phi_{3L}, \phi_{3U}]$ for i,j=1,2,3,.........a. $C \vee D =$

$(\langle [C_{ij\lambda_L} \vee d_{ij\lambda_L}, C_{ij\lambda_U} \vee d_{ij\lambda_U}], [C_{ij\eta_L} \wedge d_{ij\eta_L}, C_{ij\eta_U} \wedge d_{ij\eta_U}], [C_{ij\zeta_L} \wedge d_{ij\zeta_L}, C_{ij\zeta_U} \wedge d_{ij\zeta_U}] \rangle)$. Also, let

$(C \ominus D) = (\langle [e_{ij\lambda_L}, e_{ij\lambda_U}], [e_{ij\eta_L}, e_{ij\eta_L}], [e_{ij\zeta_L}, e_{ij\zeta_U}] \rangle)$, where $(\langle [e_{ij\lambda_L}, e_{ij\lambda_U}], [e_{ij\eta_L}, e_{ij\eta_L}], [e_{ij\zeta_L}, e_{ij\zeta_U}] \rangle) =$

$$\begin{cases} (\langle [C_{ij\lambda_L}, C_{ij\lambda_U}], [C_{ij\eta_L}, C_{ij\eta_L}], [C_{ij\zeta_L}, C_{ij\zeta_U}] \rangle), & when (\langle [C_{ij\lambda_L}, C_{ij\lambda_U}], [C_{ij\eta_L}, C_{ij\eta_L}], [C_{ij\zeta_L}, C_{ij\zeta_U}] \rangle) \\ & \geq (\langle [d_{ij\lambda_L}, d_{ij\lambda_U}], [d_{ij\eta_L}, d_{ij\eta_L}], [d_{ij\zeta_L}, d_{ij\zeta_U}] \rangle) \\ \langle 0, [\phi_{2L}, \phi_{2U}], [\phi_{3L}, \phi_{3U}] \rangle & otherwise , \end{cases}$$

Now, $[C_{ij\lambda_L}, C_{ij\lambda_L}] \vee , [d_{ij\lambda_L}, d_{ij\lambda_L}] \vee , [C_{ij\lambda_L}, C_{ij\lambda_L}] = ([c_{ij\lambda_L}, c_{ij\lambda_U}]) \vee ([d_{ij\lambda_L}, d_{ij\lambda_U}])$

$([C_{ij\lambda_L} \vee d_{ij\lambda_L}, C_{ij\lambda_U} \vee d_{ij\lambda_U}]) \vee ([C_{ij\lambda_L}, C_{ij\lambda_U}]) = ([C_{ij\lambda_L} \vee d_{ij\lambda_L}, C_{ij\lambda_U} \vee d_{ij\lambda_U}])$

$(([c_{ij\eta_L}, c_{ij\eta_L}]) \wedge ([d_{ij\eta_L}, d_{ij\eta_L}])) \wedge [c_{ij\eta_L}, C_{ij\eta_L}] = ([c_{ij\eta_L}, c_{ij\eta_L}]) \wedge ([d_{ij\eta_L}, d_{ij\eta_L}])$

and $([c_{ij\zeta_L}, c_{ij\zeta_U}]) \wedge ([d_{ij\zeta_L}, d_{ij\zeta_U}]) \wedge ([C_{ij\zeta_L}, C_{ij\zeta_U}]) = ([c_{ij\zeta_L}, c_{ij\zeta_U}]) \wedge ([d_{ij\zeta_L}, d_{ij\zeta_U}])$.

$(([c_{ij\lambda_L}, c_{ij\lambda_U}]) \vee ([d_{ij\lambda_L}, d_{ij\lambda_U}])) \vee 0 = ([c_{ij\lambda_L}, c_{ij\lambda_U}]) \vee ([d_{ij\lambda_L}, d_{ij\lambda_U}])$,

$([c_{ij\eta_L}, c_{ij\eta_L}]) \wedge ([d_{ij\eta_L}, d_{ij\eta_L}]) \wedge \phi_2 = ([c_{ij\eta_L}, c_{ij\eta_L}]) \wedge ([d_{ij\eta_L}, d_{ij\eta_L}])$

$([c_{ij\zeta_L}, c_{ij\zeta_U}]) \wedge ([d_{ij\zeta_L}, d_{ij\zeta_U}]) \wedge \phi_3 = ([c_{ij\zeta_L}, c_{ij\zeta_U}]) \wedge ([d_{ij\zeta_L}, d_{ij\zeta_U}])$.

Thus $(C \vee D) \vee (C \ominus D) = C \vee D$

APPLICATION IN MEDICAL DIAGNOSIS.

The interval valued picture fuzzy matrix is an important tool that can be used in numerous types of medical diagnosis problems. Suppose there is a set of m patients C= {c_1, c_2, c_3, … … .. c_m} with a set of n symptoms T= {t_1, t_2, t_3, … … … t_n}connected to a set of k diseases D= {d_1, d_2, d_3, … … … d_k}. we apply interval valued picture fuzzy matrix to determine which patient is afflicted with which disease. we calculate the two-interval valued picture fuzzy matrix C and D multiply the two matrices. next we compute the interval valued picture fuzzy matrix into picture fuzzy matrix. we conclude that Picture fuzzy matrix into crisp value. Finally find maximum value that the patient is affected from which disease.

Algorithm.

- The two-interval valued picture fuzzy sets from interval valued picture fuzzy matrix
- Compute multiplying the two-interval valued picture fuzzy matrix
- Find the average value of interval valued picture fuzzy matrix lower bound+ upper bound by dividing into two
- Interval valued picture fuzzy matrix can be converted into the picture fuzzy matrix
- Picture matrix into the crisp value using harmonic mean
- find the maximum score value
- we come to the conclusion that the patients C_i has a diseased d_i

Case study: Consider the five patients C= {c_1, c_2, c_3, c_4,c_5}as the universal set in a hospital with symptoms fever, cold, cough, headache. Let the disease related to the above symptoms be High temperature, malaria, corona. C= {c_1, c_2, c_3, c_4,c_5} where c_1, c_2, c_3 and $c_4$represent patients. Let T= {t_1, t_2, t_3}as the set of symptoms where t_1, t_2 and $t_3$represent symptoms respectively. Now, a interval valued picture fuzzy matrix $C = (\langle [C_{ij\lambda_L}, C_{ij\lambda_U}], [C_{ij\eta_L}, C_{ij\eta_U}], [C_{ij\zeta_L}, C_{ij\zeta_U}] \rangle)$ of size 5 x 3 in the following represents the patients.

Rajarajeswari and Nandhini

$$
C=\begin{array}{c}\\ C_1 \\ C_2 \\ C_3 \\ C_4 \\ C_5 \end{array}
\begin{pmatrix}
([0.5,0.6][0,0.1][0,0.1]) & ([0.1,0.2][0.1,0.2][0.1,0.2]) & ([0.1,0.2][0.1,0.2][0.1,0.2]) \\
([0.3,0.4][0.3,0.4][0,0.1]) & ([0.6,0.65][0,0.1][0.1,0.2]) & ([0.2,0.3][0.2,0.3][0.2,0.3]) \\
([0.3,0.4][0.2,0.3][0.1,0.2]) & ([0.2,0.3],[0.2,0.3][0.1,0.2]) & ([0.5,0.55][0,0.1][0,0.1]) \\
([0.4,0.5][0.2,0.3][0,0.1]) & ([0.5,0.6][0.1,0.2][0,0.1]) & ([0.3,0.4][0.2,0.3][0.1,0.2]) \\
([0.6,0.7][0,0.1][0,0.1]) & ([0.3,0.4][0.2,0.3][0.1,0.2]) & ([0.4,0.5][0.2,0.3][0,0.1])
\end{pmatrix}
$$

Next matrix D=$\langle[d_{ij\lambda_L},d_{ij\lambda_U}],[d_{ij\eta_L},d_{ij\eta_L}],[d_{ij\zeta_L},d_{ij\zeta_U}]\rangle$ of size 3x3 in the following represents the disease and their symptoms.

$$
D=\begin{array}{c}\\ t_1 \\ t_2 \\ t_3 \end{array}
\begin{pmatrix}
([0.6,0.7][0,0.1][0.1,0.2]) & ([0.1,0.2][0.2,0.3][0.3,0.4]) & ([0.2,0.3][0.3,0.4][0.2,0.3]) \\
([0.2,0.3][0.2,0.3][0.3,0.4]) & ([0.7,0.75][0.1,0.15][0,0.1]) & ([0.3,0.4][0.1,0.2][0.3,0.4]) \\
([0.2,0.3][0.2,0.3][0.3,0.4]) & ([0.4,0.5][0.1,0.2][0.2,0.3]) & ([0.7,0.75][0.1,0.15][0,0.1])
\end{pmatrix}
$$

STEP 1: Multiplying the two matrices

C ⊙ D =

$$
\begin{array}{c}\\ C_1 \\ C_2 \\ C_3 \\ C_4 \\ C_5 \end{array}
\begin{pmatrix}
([0.11,0.18][0.01,0.04][0.02,0.06]) & ([0.05,0.12][0.01,0.12][0.01,0.04]) & ([0.07,0.14][0.01,0.13][0.01,0.04]) \\
([0.11,0.19][0.01,0.05][0.03,0.07]) & ([0.18,0.24][0.03,0.07][0.01,0.05]) & ([0.13,0.18][0.03,0.075][0.01,0.05]) \\
([0.11,0.18][0.013,0.043][0.013,0.043]) & ([0.12,0.19],[0.02,0.052][0.01,0.04]) & ([0.15,0.21][0.02,0.065][0.02,0.05]) \\
([0.13,0.22][0.013,0.02][0.01,0.04]) & ([0.17,0.25][0.02,0.14][0.01,0.04]) & ([0.15,0.22][0.03,0.07][0,0.03]) \\
([0.16,0.25][0.026,0.06][0.01,0.5]) & ([0.143,0.23][0.013,0.045][0,0.03]) & ([0.16,0.25][0.013,0.048][0.01,0.04])
\end{pmatrix}
$$

$d_1 \quad d_2 \quad d_3$

STEP 2: Interval valued Picture fuzzy matrix into picture fuzzy matrix

$$
S=\begin{array}{c}\\ C_1 \\ C_2 \\ C_3 \\ C_4 \\ C_5 \end{array}
\begin{pmatrix}
(0.15,0.025,0.04) & (0.085,0.065,0.025) & (0.105,0.07,0.025) \\
(0.15,0.03,0.05) & (0.21,0.05,0.03) & (0.16,0.05,0.03) \\
(0.145,0.028,0.028) & (0.16,0.036,0.025) & (0.18,0.0425,0.035) \\
(0.175,0.0165,0.025) & (0.21,0.08,0.025) & (0.185,0.05,0.15) \\
(0.205,0.043,0.03) & (0.19,0.029,0.015) & (0.205,0.030,0.025)
\end{pmatrix}
$$

$d_1 \quad d_2 \quad d_3$

STEP 3 : The above using the hormonic mean picture fuzzy matrix is converted into crisp value as follows

$$
S=\begin{array}{c}\\ C_1 \\ C_2 \\ C_3 \\ C_4 \\ C_5 \end{array}
\begin{pmatrix}
0.0122 & 0.01175 & 0.0135 \\
0.015 & 0.1775 & 0.0155 \\
0.0106 & 0.012 & 0.0164 \\
0.0085 & 0.0204 & 0.0118 \\
0.0163 & 0.0091 & 0.0125
\end{pmatrix}
$$

$d_1 \quad d_2 \quad d_3$

Therefore conclude that all the five patients are maximum score affected by the $c_1 \to d_3, c_2 \to d_2, c_3 \to d_3, c_4 \to d_2, c_5 \to d_1$.

CONCLUSION

In many practical fields, asking questions about matrix theory has made a significant contribution. We have defined interval valued picture fuzzy matrix, which is the extension of picture fuzzy matrix and provides high accuracy and improves the effectiveness. Also we have defined special rrestricted picture fuzzy matrix,some basic operationson these matrices, based on these we have studied some basic properties of these defined matrices. This research can be seen as a generalization of the interval valued picture fuzzy matrix research. An application of interval valued picture fuzzy matrix in medical diagnosis have been provided to solve the medical diagnosis problem which is illustrated with a numerical example. we expect that the current study will start increasing researchers' interest in the further generalization and development of future works.

REFERENCES

1. Buicongcuong, Picture fuzzy sets, Journal of computer science and cybernetics, V.30,N.4(2014),409-420.
2. K. Atannassov, Intuitionistic fuzzy sets and systems 20(1)(1986)87-96.
3. K.Atannassov and G.Gargov, Interval valued intuitionistic fuzzy sets, fuzzy sets and systems 3(1)(1989)343-349.
4. Khan SK.Shymal Ak ,Pal M (2002) Intuitionistic fuzzy matrices
5. M.Bora, B.Bora,T.J.Neog and D.K.Sut, Intuitionistic fuzzy soft matrix theory and its application inmedical diagnosis, Ann.FuzzyMath.Inform.7(1) (2014)143–153.
6. P.Rajarajeswari and P.Dhanalakshmi, An application of interval valued intuitionistic fuzzys of t matrix theoryinmedicaldiagnosis,9(3)(2015),pp.463-472.
7. P.Rajarajeswari and P.Dhanalakshmi, Interval valued intuitionistic fuzzys of t matrix theory, International Journal of Mathematical Archive 5(1)(2014)152–161.
8. Shovan Dogra, Madhumangal pal (2020) Picture fuzzy matrix and its application.
9. Zadeh.L. A, fuzzy set. Information and control,8(1965):338.

RESEARCH ARTICLE

A Study on Multicriteria Decision Making Approach based on Crop Diseases of Crop Amirtha [Co 09004]

Amala Kaavya .C[1] * and A.Sahaya Sudha[2]

[1]Research Scholar, Department of Mathematics, Nirmala College for Women, Coimbatore, Tamil Nadu, India
[2]Assistant Professor, Department of Mathematics, Nirmala College For Women, Coimbatore, Tamil Nadu, India

*Address for Correspondence
Amala Kaavya .C
Research Scholar,
Department of Mathematics,
Nirmala College for Women,
Coimbatore, Tamil Nadu, India
E.Mail: amala2297@gmail.com

ABSTRACT

In India, sugarcane is a major crop used for sugar production which is naturally exposed to various diseases that leads to significant economic loss. In this research paper a study of crop diseases in sugarcane using the Decision-Making Trial and Evaluation Laboratory (DEMATEL) method in accordance of a novel fuzzy set. DEMATEL is a useful tool for understanding the cause-and-effect outcome among different factors in complex manner. The objective of this study is to identify the key factors contributing to the spread of sugarcane diseases in a particular crop variety namely, Co 09004 (Amritha) .The approach in this paper helps for similar studies in other crops and agricultural systems, providing more effective disease management strategies.

Keywords: crop diseases, sugarcane, DEMATEL method, causal relationships, disease management, agriculture.

INTRODUCTION

Sugarcane (*Saccharum officinarum* L.) is a cash crop of utmost importance providing a great economic significance to the agro-industrial sector. In Tamil Nadu, sugarcane occupies an important position in agricultural production, making an economic contribution to the state's economy. The incidence of crop diseases is a major obstacle to the sustainable development of sugarcane. Crop diseases pose a threat to agricultural productivity and food quality, impacting the yield of crops.
Prince Kumaret..al;[4] studied an analytical Research Paper On Sugarcane Disease Detection Model. The main cause of the disease is progressed by factors such aspoor drainage system, weather conditions, and economically

63292

agronomic practiceswhich not only reduces yield but also it affects the quality of the harvested cane. Shukla Adil Zubair et.al [12] elaborated the concept of Sugarcane Varieties Identified By AICPR(S) In India Thus, broad approach for disease management involves traditionally practices, the methods of disease-free planting material are used, and regular check are kept for the evaluation of disease management. The Decision-Making Trial and Evaluation Laboratory (DEMATEL) method emerges as a useful tool, providing an insightful approach to solve these most interdependencies. A. Gabus[4] solved the Framework of DEMATEL.As governments, and individual's faces with multiple challenges, the DEMATEL method offers a structured process to show cause-and-effect relationships enabling informed and effective decision-making.

Thi Hai Ninh Do et.al.[18] demonstrated that the DEMATEL method demands a systematic approach. Accurate data collection analysis are main components of the process. By employing the DEMATEL method, decision-makers can analyze the factors that are more informed and aligned with the complexities of the criteria that are solved. Sheng-Li Si et.al [13] explained about the DEMATEL Technique has a Systematic Review of the State-of-the-Art Literature on Methodologies and its Applications.2015 Sangaiah et.al[15] discussed about that a fuzzy DEMATEL approach based on intuitionistic fuzzy information for evaluating knowledge transfer effectiveness in GSD projects . This study also shows how DEMATEL works well for getting a comprehensive grasp of complicated agricultural systems and the problems they present.RasappaViswanathanet.al[16]demonstrated   the Brown spot of sugarcane: an emerging disease in South Western region in India.Yanli Chen et.al[22] studied a concept to illustrate the Identification of Sugarcane with NDVI Time Series Based on HJ-1 CCD and MODIS Fusion in the year 2020.Liu, Zhong[7]discussed about the extraction of sugarcane in the southern hills using multi-temporal GF-1 WFV data.

In the 1960s,Fuzzy set theory is a groundbreaking concept introduced by Lotfi A. Zadeh, revolutionized how we perceive and handle uncertainty in various domains. Tareq M. Al-shami [17](2,1)-Fuzzy sets with its properties, weighted aggregated operators and their applications to multi-criteria decision-making methods..Anoop Kumar Tiwaria[2] showed an intuitionistic fuzzy-rough set model and its application to feature selection. A classical fuzzy set theory involves with a degree of membership. This is linked relevant in real-world situation with the concepts are vague or subject to interpretation according to the fuzzy set.

Atanassov K.T [1] gives a clear picture and detailed study On Intuitionistic fuzzy sets theory with itsfuture work. The aim of the fuzzy set theory lies the concept of membership functions. Yager.R.R [21] demonstrated Pythagorean Membership Grades in Multi Criteria Decision Making stand as an example for many MCDM methods. An Intuitionistic fuzzy set is a fundamental concept within fuzzy set theory. Muhammad Saeed [11]investigated the Theoretical Development of Cubic Pythagorean Fuzzy Soft Set with Its Application in Multi-Attribute Decision Making .It is characterized by a membership function with two categories. Muhammad Jabir Khan[10] gave a detailed study in the knowledge measure for the q-rung orthopair fuzzy sets.Arshad Ahmad Khan et.al.[3]gave a clear picture on A New Ranking Methodology for Pythagorean Trapezoidal Uncertain Linguistic Fuzzy Sets Based on Einstein Operations. Krishna Prabhaa et.al.[6]Studied a Geometric Mean with Pythagorean Fuzzy Transportation Problem. Vakkas Uluçay et.al.[19] studied about the Intuitionistic trapezoidal fuzzy which are capable of representing gradual changes in membership with more precision than traditional triangular fuzzy sets.In this Paper ,q-Rung orthopedic fuzzy hyper soft ordered aggregation operators by Salma Khan et.al[12].Jianhua Jin et.al.[5] showed a concept ofQuintuple Implication Principle on interval-valued intuitionistic fuzzy sets.

QIFS fuzzy sets are both extensions of theoryand offers an effective representation, while enrich our capacity to model with membership transitions.The defined Quad Intuitionistic Fuzzy set(QIFS) is worked with the DEMATEL method to produce the results for uncertainty. The Quad Intuitionistic Fuzzy set consists to values of Membership Degree (MD) and Non Membership Degree(NMD).The aim is to specify the point that Quad Intuitionistic Fuzzy set is capable to handle the greater levels of vague concepts. In section -2 shows the preliminaries results used for the study. In section-3, the paper focuses on the fundamental ideas of QIFS. In section-4 shows the characteristics of CropAmirtha.In section-5, the proposed methodology of DEMATEL is explained in QIFS. In section-6 the application

of proposed method is discussed.In section-7 presents the conclusions and in section-8 results with the reference following.

Preliminaries

Intuitionistic Fuzzy Set [1]
An Intuitionistic fuzzy set A on a universe X is an object of the form
$A = \{(x, \mu_A(x), \nu_A(x))|x \in X\}$
where$\mu_A(x) \in [0,1]$ is called the degree of membership of x in A, and $\nu_A(x) \in [0,1]$ is called the degree of non-membership of x in A.

Pythagorean Fuzzy Set[6]
A Pythagorean fuzzy set P in a finite universe of discourse X is given as

$P = \{< x, \mu_P(x), \nu_P(x) > x \in X\}$

where$\mu_P(x), \nu_P(x):X \to [0,1]$ be the degree of membership and non membership of the element $x \in X$ to the set P,

respectively, with the condition that

$0 \le \mu_P{}^2(x) + \nu_P{}^2(x) \le 1$.

The degree of indeterminacy(hesitation) between the membership function is given by

$\pi_P(x) = \sqrt{1 - \mu_P{}^2(x) - \nu_P{}^2(x)}$

$(\mu_P(x), \nu_P(x))$ called a Pythagorean fuzzy numbers denoted by$P = (\mu_P, \nu_P)$.

Quad Intuitionistic Fuzzy Set:

Definition
Let A be the Quad Intuitionistic Fuzzy Set(QIFS) in X is defined by
$A = \{x, [a, b, c, d], \mu(x), \nu(x)|x\epsilon X\}$
where $\mu_A(x) \in [0,1]$ is called the degree of membership of x in X, and $\nu_A(x) \in [0,1]$ is called the degree of non-membership of x in X; a,b,c,d$\epsilon X \to [0,1]$ are the finite collections of objects in the universe X,$\pi_A(x) = 1 - \mu_A(x) - \nu_A(x)$ called the degree of indeterminacy of $x\epsilon X$ to QIFS.$\pi_A(x)$ gives the information whether x belongs to A or not.

Algorithms for the DEMATEL method:
DEMATEL involves a series of steps to analyze and visualize the relationships between factors. The overview of the steps involved:

STEP I:
Initiation of Direct relation matrix:The decision maker assesses the correlation between the groups of paired criteria to identify the direct influence of each criteria.

$A = \begin{pmatrix} 0 & a_{12} & a_{1n} \\ a_{21} & 0 & a_{2n} \\ a_{i1} & a_{i2} & a_{in} \end{pmatrix}$

STEP II:
Normalization of Direct Relation matrix
X= k A,where $K = \dfrac{1}{max_{1 \le i \le n} \sum_{j=1}^n a_{ij}} i, j = 1,2,3,..n$

Amala Kaavya and Sahaya Sudha

STEP III:

Estimation of the Total relation matrix

The total relation matrix is estimated with the Identify matrix .

T is the matrix denotes the total relationship within each pair of criteria.

$$T = Y(I - Y)^{-1}$$

STEP IV:

Evaluate the sums of rows and columns in T matrix

$$D = \left[\sum_{j=1}^{n} t_{ij} \right]_{n*1}$$

$$= [t_i]_{n*1}, i = 1,2, \dots n$$

$$R = \left[\sum_{i=1}^{n} t_{ij} \right]_{i*n}$$

$$= \left[t_j \right]_{n*1}, j = 1,2, \dots n$$

STEP V:

Defining the threshold value α.Average of the elements in the Total matrix T

$$\alpha = \frac{\sum_{i=1}^{n} \sum_{j=1}^{n} t_{ij}}{N}$$

STEP VI:

Formation of the casual Diagram

It provides information to identify the most important criteria and their influence levels in order to recognize the driving variables of the considered problem in a complex system and design for reasonable measures to take care of the issues based on the attribute type and influence level.

Application to detect the Cane Crop Diseases Using DEMATEL method:

The number of sugarcane plants that can be grown per acre depends on factors like the spacing of the plants, soil fertility, climate,etc.Usually,Sugarcane is typically planted with 4 to 6 feet of distance between adjacent rows of sugarcane plants(Space between rows) For space within a row the cane should be planted within 2 to 3 feet of distance between sugarcane plants in the same row(Space within rows).

Let us consider the planting cultivation of 5 feet between rows and 3 feet plants within a row, the number of sugarcane plants per acre is given below:

Space between rows

Number of plants to be cultivated = 43560 feet / 5 feet =8712 plants per row

Space within a row

Number of rows to be cultivated = 43560 feet / 3 feet = 14520 rows per acre

Total number of plants per acre

Number of plants per row × Number of rows per acre

= 8712 x14520 ≈ 1,26,498,240 plants per acre

Quad Intuitionistic Fuzzy sets in terms of PDI:

One acre is divided into Quadrant I,II,III,IV

RESULTS AND DISCUSSIONS

The utilization of the DEMATEL method in accordance with Quad Intuitionistic Fuzzy Sets to investigate the relationship among Red Rot, Smut, Grassy Shoot and Ratoon Stunting Diseases in a 1-acre land of cane cultivation area.In conclusion, the application of the DEMATEL method with Quad Intuitionistic Fuzzy Sets gives a detailed framework for understanding the factors of Red Rot, Smut, and Ratoon Stunting Diseases based on the divided quadrants of cane cultivation of 1 acreThe detailed study provides the distribution of these diseases in the four different quadrants, enabling to analyze the potential effects and the percentage of the prevalence among the four quadrants. All the specified each quadrant representing a distinct section of the cultivating Co 09004 Amirtha in the peninsular region. The diseasespresent in each quadrant stands for the identification of patterns andcorrelations. The DEMATEL method with Quad Intuitionistic Fuzzy Sets, shows the uncertainty and imprecision that are intrinsic to real-world agricultural scenarios.

REFERENCES

1. Atanassov K.T (2012),"On Intuitionistic fuzzy sets theory", Studies in Fuzziness and Soft Computing ,Vol.283 ,147-193.
2. Anoop Kumar Tiwaria, ShivamShreevastavab, KarthikeyanSubbiaha and T. Som(2019) ,"An intuitionistic fuzzy-rough set model and its application to feature selection",Journal of Intelligent & Fuzzy Systems,Vol. 36 ,4969–4979 https://doi.org/10.3233/JIFS-179043
3. Arshad Ahmad Khan,Saleem Abdullah, Muhammad Shakeel, Faisal Khan, Noor ul Amin and JianchaoLuo(2019)"A New Ranking Methodology for Pythagorean Trapezoidal Uncertain Linguistic Fuzzy Sets Based on Einstein Operations" ,Symmetry,Vol. 11,1-29. https://doi.org/10.3390/sym11030440
4. A. Gabus and E. Fontela, World Problems, "An Invitation to Further Tought within Te Framework of DEMATEL, Battelle Geneva Research Centre", Geneva, Switzerland, 1972.
5. JianhuaJin,MingfeiYe,WitoldPedrycz(2020),"Quintuple Implication Principle on interval-valued intuitionistic fuzzy sets", Soft Computing ,Vol. 24,12091–12109 . https://doi.org/10.1007/s00500-019-04649-1
6. S.KrishnaPrabhaa , S. Sangeethab , P. Hemac , MuhammedBasheerd , and G. Veeramala(2021) "Geometric Mean with Pythagorean Fuzzy Transportation Problem",Turkish Journal of Computer and Mathematics Education , Vol.12 No.7, 1171-1176 https://doi.org/10.17762/turcomat.v12i7.2727
7. Liu, Zhong, Xu, & Chen (2014)," Sugarcane extraction in the southern hills using multi-temporal GF-1 WFV data", Guangdong Agricultural Sciences, Vol.41(18), 149–154.
8. Muhammad Jabir Khan,PoomKumam,MeshalShutaywi(2021), "Knowledge measure for the q-rung orthopair fuzzy sets" ,International Journal of Intelligent Systems Vol.36,628–655. https://doi.org/10.1002/int.22313
9. Muhammad Saeed,MuhammadHarisSaeed,RimshaShafaqat,Salvatore Sessa, Umar Ishtiaq and Ferdinando di Martino(2022), "A Theoretical Development of Cubic Pythagorean Fuzzy Soft Set with Its Application in Multi-Attribute Decision Making", Symmetry,Vol.14,Issue.12, 2639 https://doi.org/10.3390/sym14122639
10. PerumalGovindaraj,K.Bhagayalakshmi (2017)"Co 09004(AMRITHA) a new early maturing and high sugar variety for cultivation in peninsular zone",ICAR-Sugarcane Breeding Institute,Coimbatore, Vol.37 No.3
11. Prince Kumar, MayankSonker andVikash(2021), "Research Paper On Sugarcane Disease Detection Model", Turkish Journal of Computer and Mathematics Education ,Vol.12 ,No.6 ,5167-5174.
12. Salma Khan, Muhammad Gulistan, NasreenKausar, DraganPamucar , EbruOzbilge and Nasser El-Kanj (2022)"q-Rung orthopair fuzzy hypersoft ordered aggregation operators and their application towards green supplier" Vol.10 , 249–262. https://doi.org/10.3389/fenvs.2022.1048019
13. Sheng-Li Si,Xiao-Yue You, Hu-Chen Liu ,Ping Zhang(2018) "DEMATEL Technique: A Systematic Review of the State-of-the-Art Literature on Methodologies and Applications", Mathematical Problems in Engineering Vol.2018,1-33. https://doi.org/10.1155/2018/3696457
14. Shukla Adil Zubair , Awasthi, Pathak(2018) ,"Sugarcane Varieties Identified By AICPR(S) In India", All India Coordinated Reserch Project On Sugarcane ,ICAR-Indian Institute Of Sugarcane Research,1-111.

15. A. K. Sangaiah, X. Z. Gao, M. Ramachandran, and X. Zheng (2015), "A fuzzy DEMATEL approach based on intuitionistic fuzzy information for evaluating knowledge transfer effectiveness in GSD projects," International Journal of Innovative Computing and Applications, Vol. 6 ,no. 3-4, 203–215. http://dx.doi.org/10.1504/IJICA.2015.073006

16. Rasappa Viswanathan,Ashwin(2020) ,"Brown spot of sugarcane: an emerging disease in South Western region in India",Journal of Sugarcane Research Vol.10(1),87-93.https://doi.org/10.37580/JSR.2020.1.10.87-93

17. Tareq M. Al-shami (2023) ,"(2,1)-Fuzzy sets: properties, weighted aggregated operators and their applications to multi-criteria decision-making methods" , Complex & Intelligent Systems ,Vol. 9,1687–1705.https://doi.org/10.1007/s40747-022-00878-4

18. ThiHaiNinh Do, Wurong Shih (2016), "Destination Decision-Making Process Based on a Hybrid MCDM Model Combining DEMATEL and ANP: The Case of Vietnam as a Destination, College of Business", Southern Taiwan University of Science and Technology,Vol.7 No.9. https://doi.org/10.4236/me.2016.79099

19. VakkasUluçay, IrfanDeli,Mehmet Sahin(2019), "Intuitionistic trapezoidal fuzzy multi-numbers and its application to multi-criteria decision-making problems",Complex& Intelligent Systems ,Vol.5,65–78. https://doi.org/10.1007/s40747-018-0074-z

20. Valmohammadiand Sofyabadi (2015), "Modeling cause and effect relationships of strategy map using fuzzy DEMATEL and fourth generation of balanced scorecard," Benchmarking, Vol. 22, no. 6, 1175–1191.http://dx.doi.org/10.1108/BIJ-09-2014-0086

21. Yager.R.R (2013), "Pythagorean Membership Grades in Multi Criteria Decision Making",IEEE Trans Fuzzy System,Vol.22,958-965

22. YanliChen,LipingFeng, JianfeiMo,Weihua Mo, MeihuaDing,Zhiping Liu(2020), "Identification of Sugarcane with NDVI Time Series Based on HJ-1 CCD and MODIS Fusion",Journal of the Indian Society of Remote Sensing Vol.48(2),249–262 .

Table: 1. Representing the PDI interms of QIFS

Crop Diseases	I $x = 0.1$	II $x = 0.5$	III $x = 0.4$	IV $x = 0.8$
Red Rot	0	$x, [0.7,0.6,0.2,0.1], 0.8,0.1$	$x, [0.4,0.3,0.5,0.7], 0.6,0.9$	$x, [0.3,0.8,0.4,0.6], 0.4,0.8$
Smut	$x, [0.3,0.2,0.1,0.5], 0.2,0.7$	0	$x, [0.5,0.4,0.1,0.3], 0.7,0.8$	$x, [0.8,0.2,0.1,0.3], 0.2,0.9$
Ratoon Stunting Disease	$x, [0.4,0.3,0.2,0.7], 0.3,0.4$	$x, [0.3,0.6,0.8,0.9], 0.1,0.3$	0	$x, [0.8,0.3,0.9,0.4], 0.6,0.5$
Grassy Shoot Disease	$x, [0.9,0.7,0.4,0.2], 0.8,0.5$	$x, [0.2,0.8,0.6,0.4], 0.3,0.5$	$x, [0.1,0.5,0.2,0.5], 0.3,0.6$	0

Table 2. :Forming QIFS in terms of PDI

Crop Diseases	Percentage Disease Incidence(PDI) in reference with two decision makers $[\mu(x), v(x)]$			
Co 09004 Amirtha	Quadrant I	Quadrant II	Quadrant III	Quadrant IV
Red Rot	0	[0.8,0.1]	[0,0]	[0.5,0.2]
Smut	[0.4,0.6]	0	[0.2,0.2]	1
Ratoon Stunting Disease	[0.3,0.4]	[0.06,0.5]	0	[0.8,0.6]
Grassy Shoot Disease	[0.5,1]	[0.15,0.2]	[0.3,0.6]	0

Amala Kaavya and Sahaya Sudha

Table 3. Defining the Direct –Relation Matrix

Crop Diseases	Percentage Disease Incidence(PDI)			
Co 09004 Amirtha	Quadrant I	Quadrant II	Quadrant III	Quadrant IV
Red Rot	0	0.4	0	0.3
Smut	0.5	0	0.2	1
Ratoon Stunting Disease	0.3	0.2	0	0.19
Grassy Shoot Disease	0.7	0.10	0.12	0

Table 4 .Comparison Scale in terms of PDI

Percentage Disease Incidence(PDI)	Grades
0	Free (F)
0.1-0.4	Resistant (R)
0.5-0.9	Moderately Resistant (MR)
0.10-0.14	Moderately Liable (ML)
0.15 and above	Liable (L)

Table 5. Determination of PDI in terms of grades

Crop Diseases	Percentage Disease Incidence(PDI)			
Co 09004 Amirtha	Quadrant I	Quadrant II	Quadrant III	Quadrant IV
Red Rot	F	R	F	R
Smut	MR	F	R	L
Ratoon Stunting Disease	R	R	F	MR
Grassy Shoot Disease	MR	ML	R	F

Table 6. Normalizingthe Matrix

Co 09004 Amirtha	Quadrant I	Quadrant II	Quadrant III	Quadrant IV	sum
Red Rot	0	0.4	0	0.3	0.7
Smut	0.5	0	0.2	1	1.7
Ratoon Stunting Disease	0.3	0.2	0	0.19	0.6
Grassy Shoot Disease	0.7	0.10	0.12	0	0.9

Table 7. Attaining the Total Relation Matrix

Co 09004 Amirtha	Quadrant I	Quadrant II	Quadrant III	Quadrant IV
Red Rot	0.789	0.235	0.912	0.356
Smut	0.678	0.945	1.240	1.256
Ratoon Stunting Disease	0.346	0.268	0.236	0.646
Grassy Shoot Disease	0.853	0.376	1.123	0.432

Amala Kaavya and Sahaya Sudha

Table 8 : Producing a casual diagram

Co 09004 Amirtha	Quadrant I	Quadrant II	Quadrant III	Quadrant IV	D
Red Rot	0.789	0.235	0.912	0.356	2.292
Smut	0.678	0.945	1.240	1.256	4.119
Ratoon Stunting Disease	0.346	0.268	0.236	0.646	1.496
Grassy Shoot Disease	0.853	0.376	1.123	0.432	2.784
R	2.666	1.824	3.511	2.690	

Table 9: Determination of Effect and Cause

Co 09004 Amirtha	D	R	D-R	D+R	Effect/Cause
Red Rot	2.292	2.666	-0.374	4.958	Effect
Smut	4.119	1.824	2.295	5.943	Cause
Ratoon Stunting Disease	1.496	3.511	-2.015	5.007	Effect
Grassy Shoot Disease	2.784	2.690	0.094	5.474	Cause

Table 10 Determining the value of Threshold

Co 09004 Amirtha	Quadrant I	Quadrant II	Quadrant III	Quadrant IV
Red Rot	**0.789**	0.235	**0.912**	0.356
Smut	**0.678**	**0.945**	**1.240**	**1.256**
Ratoon Stunting Disease	0.346	0.268	0.236	0.646
Grassy Shoot Disease	**0.853**	0.376	**1.123**	0.432
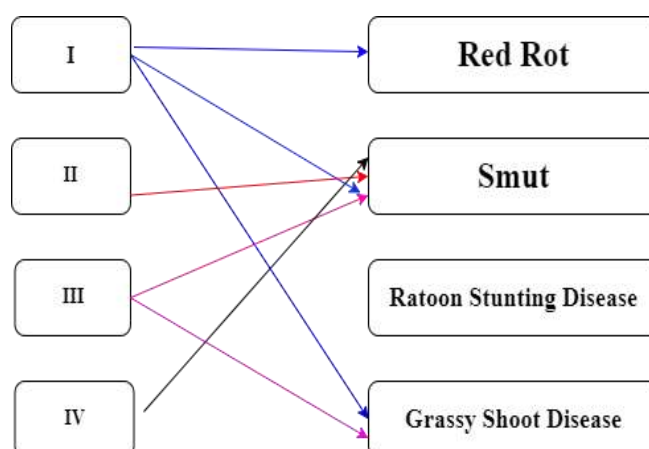
Fig 1. Casual diagram in comparison with the criterion

RESEARCH ARTICLE

A Study on Control of Fuzzy based Compound Fraction Defectives in a Production Process using Control Chart Technique

N. Arunthadhi[1] and S. Devaarul[2]*

[1]Research Scholar, Department of Statistics, Government Arts College, Coimbatore – 641 018, Tamil Nadu, India
[2]Associate Professor and Head, Department of Statistics, Government Arts College, Coimbatore – 641 018, Tamil Nadu, India

*Address for Correspondence
S. Devaarul
Associate Professor and Head,
 Department of Statistics,
Government Arts College,
Coimbatore – 641 018,
Tamil Nadu, India.
E.Mail: deardeva@gmail.com

ABSTRACT

A Shewhart control chart is one of the important tools in Statistical Process Control (SPC) to monitor and analyze a process parameter over time. Process Control Techniques are useful to identify assignable causes of variations. Any significant variations in the production process can be easily detected using Control Charts. In few industries existing control charts may not be suitable since the data could be vague or imprecise. Hence to control the vagueness and process control parameters, a new Fuzzy control chart is developed to handle such quality control environment. In this article a new fuzzy based compound binomial control chart is developed and designed to monitor the fraction defectives and to control the variability in the sample size. A new fuzzy control chart which can handle the uncertainty of sample size and compound fraction defective is developed using α - level midrange. ARL (Average Run Length) is determined and analyzed for newly developed control chart. It is found that the ARL is better over other types of control charts.

Keywords - Process control, Compound Binomial, Fuzzy set, α - level midrange.

INTRODUCTION

In the current scenario of a statistical quality control, the enhancement of process control techniques stands as a crucial quality strategy. Statistical Process Control (SPC) holds a pivotal position inside numerous quality control environments. Control charts were developed with the purpose of overseeing processes and identifying changes in the average and variability of quality characteristics, ensuring the satisfactory performance of these processes. Even though Shewhart initially proposed the concept of control charts in 1920, modern times still see emerging areas of application that deserve further investigation. Uncertainty is a common aspect in many real-world systems, which introduces challenges in applying statistical process control. Consequently, the utilization of fuzzy set theory becomes pertinent for the purpose of elucidating and conceptualizing these problems in quality control techniques.

This paper introduces the new approach of fuzzy control charts for controlling or to monitor compound fraction defectives. The compound fraction defectives control chart is new approach of control chart based on Compound Binomial Distribution. This chart can control both fraction defective and monitor variability of sample size in single chart. The compound fraction defective control chart may not be suitable in some situations such as the data involved could be vague or imprecise. Thus, Fuzzy control charts are used to handle such situations and a fuzzy based compound fraction defectives control chart is developed.

The section of the article is organised as follows. Section 2 shows the review of literature. Section 3 contains the methodology of the work. Section 4 describes the illustration of the proposed work. Section 5 contains results and discussions.

REVIEW OF LITERATURE

Shewhart (1926) introduced a concept of control chart to monitor the quality of process in the industry. Zadeh (1965) proposed a concept of fuzzy based on mathematical method for representing vagueness and uncertainty in decision making. H. Taleb and M. Limam (2002) proposed different procedures for constructing control charts based on fuzzy and probabilistic approach. Gulbay, Kahraman and Ruan (2004) designed a α - cut fuzzy control chart for attribute data for utilize the tightness of the inspection. Further, M. Gulbay and C. Kahraman (2006) also designed fuzzy control charts for linguistic and imprecise data. These fuzzy control charts are applied to p and c charts. To monitor multivariate attribute data Taleb et.al (2006) developed a control chart called fuzzy multinomial control charts. Sevil and Nihal (2009) proposed a fuzzy $\widetilde{\overline{X}}$-$\widetilde{R}$ and $\widetilde{\overline{X}}$-$\widetilde{S}$ control charts with α cuts.

Hung Shu and Chung Wu (2011) developed a fuzzy $\overline{X}$ and R control charts using the fuzzy dominance approach. This approach can compare fuzzy averages and variances to their respective fuzzy control limits. To monitor attribute quality characteristics Sogandi, et.al (2014) developed a fuzzy P chart. Alakoc and Apaydin (2018) designed a fuzzy control chart approach for attribute and variable data based on decision function, α- cut fuzzy numbers, fuzzy 3σ control limits. Prabu and Nanthakumar (2020) designed a fuzzy control chart for number of defects using process capability. Devaarul and Arunthadhi (2023) designed a Truncated Poisson Exponentially Weighted Moving Average (TPEWMA) control chart for an unstabilized production process.

METHODOLOGY

Compound Fraction Defectives Control Chart
Let X be random variable, then the probability density function of binomial distribution is $P(X=r) = \binom{n}{r} p^r q^{n-r}$;   r = 0,1,2……..n   ----------------- (1)
Take n as another random variable which follows the Poisson distribution.

$$P(n=k) = \frac{e^{-\lambda}\lambda^{k}}{k!} \; ; \; k = 0,1,2,3…… \qquad \text{---------------- (2)}$$

The probability density function of compound binomial distribution is derived from the joint probability of X and n.

$$P(X=r) = \frac{e^{-\lambda p}(\lambda p)^{r}}{r!} \; ; \; r = 0,1,2,…… \qquad \text{----------------- (3)}$$

Then, the mean and variance of compound binomial distribution is λp.

The n as a fixed constant in Binomial distribution becomes a random variable in Poisson distribution. Thus, the mean and variance of compound binomial distribution becomes np^{2}.

Then the Control limits for compound fraction defectives are as follows,

$$CL = \overline{np^{2}} \qquad \text{----------------- (4)}$$

$$UCL = \overline{np^{2}} + 3\sqrt{\overline{np^{2}}} \qquad \text{----------------- (5)}$$

$$LCL = \overline{np^{2}} - 3\sqrt{\overline{np^{2}}} \qquad \text{----------------- (6)}$$

The control limit can control both the number of defectives and variability in sample size as compound fraction defectives.

Fuzzy Compound Fraction Defectives Control Chart based on Triangular fuzzy number

Let us consider the compound fraction defectives as triangular fuzzy numbers which are represented as (CF_a, CF_b, CF_c) for each fuzzy sample. Then the control limits for fuzzy compound binomial control chart is determined based on triangular fuzzy number are as follows,

$$CL = (CL_a, CL_b, CL_c) = (\overline{np^2}_a, \overline{np^2}_b, \overline{np^2}_c) \qquad \text{------------ (7)}$$

$$(\overline{np^2}_a, \overline{np^2}_b, \overline{np^2}_c) = (\tfrac{\sum CF_a}{m}, \tfrac{\sum CF_b}{m}, \tfrac{\sum CF_c}{m}) \qquad \text{------------ (8)}$$

$$UCL = (UCL_a, UCL_b, UCL_c) = (\overline{np^2}_a + 3\sqrt{\overline{np^2}_a} \, , \, \overline{np^2}_b + 3\sqrt{\overline{np^2}_b} \, , \, \overline{np^2}_c + 3\sqrt{\overline{np^2}_c}) \qquad \text{------ (9)}$$

$$LCL = (LCL_a, LCL_b, LCL_c) = (\overline{np^2}_a - 3\sqrt{\overline{np^2}_a} \, , \, \overline{np^2}_b - 3\sqrt{\overline{np^2}_b} \, , \, \overline{np^2}_c - 3\sqrt{\overline{np^2}_c}) \qquad \text{------ (10)}$$

where, m = number of subgroups.

Fuzzy Compound Fraction Defectives Control chart based on α - Level Midrange

To enhance the uncertainty of compound binomial control chart the α – level midrange is applied to fuzzy compound binomial control chart. The α – level midrange comes into play when the centre of these fuzzy control limits is determined. Now applying the α – level midrange to fuzzy compound binomial control chart the centre line of the control chart is as follows,

$$CL = (CL_a^{\alpha}, CL_b, CL_b^{\alpha}) = (\overline{np^2}_a^{\alpha}, \overline{np^2}_b, \overline{np^2}_c^{\alpha}) \qquad \text{----------------- (11)}$$

Similarly,

$$(\overline{np^2}_a^{\alpha}, \overline{np^2}_b, \overline{np^2}_c^{\alpha}) = (\tfrac{\sum CF_a^{\alpha}}{m}, \tfrac{\sum CF_b}{m}, \tfrac{\sum CF_c^{\alpha}}{m}) \qquad \text{----------------- (12)}$$

where,

$$\overline{np^2}_a^{\alpha} = \overline{np^2}_a + \alpha \, (\overline{np^2}_b - \overline{np^2}_a) \qquad \text{----------------- (13)}$$

$$\overline{np^2}_c^{\alpha} = \overline{np^2}_c - \alpha \, (\overline{np^2}_c - \overline{np^2}_b) \qquad \text{----------------- (14)}$$

α – Level fuzzy Midrange for Compound Fraction Defectives Control Chart

To design the fuzzy compound binomial control limit the α – level midrange is applied and the control limits are as follows,

$$CL_{mid}^{\alpha} = \tfrac{1}{2}(\overline{np^2}_a^{\alpha} + \overline{np^2}_c^{\alpha}) \qquad \text{----------------- (15)}$$

$$UCL_{mid}^{\alpha} = \tfrac{1}{2}(\overline{np^2}_a^{\alpha} + \overline{np^2}_c^{\alpha}) + 3\sqrt{\tfrac{1}{2}(\overline{np^2}_a^{\alpha} + \overline{np^2}_c^{\alpha})} \qquad \text{----------------- (16)}$$

$$LCL_{mid}^{\alpha} = \tfrac{1}{2}(\overline{np^2}_a^{\alpha} + \overline{np^2}_c^{\alpha}) - 3\sqrt{\tfrac{1}{2}(\overline{np^2}_a^{\alpha} + \overline{np^2}_c^{\alpha})} \qquad \text{----------------- (17)}$$

The α – level fuzzy midrange for sample i for the fuzzy compound binomial control chart is,

$$S^{\alpha}_{mid,i} = \frac{(CF_{a_j} + CF_{c_j}) + \alpha\,[(CF_{b_j} - CF_{a_j}) - (CF_{c_j} - CF_{b_j})]}{2}$$ ----------------- (18)

Then the condition of process control for each sample can be defined as,

Process Control = $\begin{cases} \text{in control} & ; \ LCL^{\alpha}_{mid} \leq S^{\alpha}_{mid,i} \leq UCL^{\alpha}_{mid} \\ \text{out of control} & ; \text{Otherwise} \end{cases}$

ILLUSTRATION

In this section an example is illustrated for the proposed work. The control limits, control chart and ARL are derived in this section. Let us consider the example.

The sample size from the Table 1 can be fuzzifie based on Triangular fuzzy number. Then the control limits for compound fraction defectives based on triangular fuzzy number is as follows,

CL = (1.07, 1.008, 0.97)
UCL = (4.184, 4.019, 3.923)
LCL = (0, 0, 0)

Now apply the α level midrange to the control chart of triangular fuzzy number. Then the control limits for α – level fuzzy midrange for Compound Fraction Defectives chart are as follows,

$CL^{0.5}_{mid}$ = 1.01

$UCL^{0.5}_{mid}$ = 4.04

$LCL^{0.5}_{mid}$ = 0

Calculation for ARL

To comparing the proposed fuzzy based compound defective control chart with normal compound defective control chart ARL is used. ARL is the average number of samples which could occur before the out of control condition.

$$ARL = \frac{1}{P(X > UCL)}$$

Hence the ARL for the proposed control chart is 264.
Based on various values of compound fraction defectives the ARL is shown in following table.

RESULT AND DISCUSSION

In this article, a new control chart is developed to monitor fuzzy based compound fraction defectives. Uncertainty is a common aspect in many real-world systems, which introduces challenges in applying statistical process control. Consequently, the utilization of fuzzy set theory becomes pertinent for the purpose for the purpose of elucidating and conceptualizing these issues. Thus, in this paper a fuzzy based compound fraction defectives control chart is developed with help of α – level fuzzy midrange. The ARL for the newly developed control chart is derived and calculated. For various shifts the ARL for fuzzy based compound fraction defectives is calculated. It gives a better performance than other charts. As, industries continue to evolve and face new challenges, the adoption of fuzzy based approaches holds significant promise for optimising quality control practices and ensuring the delivery of products.

REFERENCES

1. Shewhart WA. Quality Control Charts. Bell System Technical Journal 1926; 5:593-602.
2. Zadeh LA. Fuzzy sets. Information and Control 1965; 8(3):338-353.
3. Taleb H, Limam M. On Fuzzy and Probabilistic Control Charts. International Journal of Production Research 2002; 40(2):2849-2863.
4. Gulbay M, Kahraman C, Ruan D. α-Cut Fuzzy Control Charts for Linguistic Data.International Journal of Intelligent Systems 2004; 19(12):1173-1195.
5. Gulbay M, Kahraman. Design of Fuzzy Process Control Charts for Linguistic and Imprecise Data. Studies in Fuzziness and Soft Computing 2006; l(201):59-88.
6. Taleb H, Limam M, Hirota K. Multivariate Fuzzy Multinomial Control Charts. Quality Technology and Quantitative Management 2006; 3(4):437-453.
7. Sevil Senturk, Nihal Erginel. Development of Fuzzy $\widetilde{\overline{X}}$-$\widetilde{R}$ and $\widetilde{\overline{X}}$-$\widetilde{S}$ Control Charts with α cuts. Information Sciences 2009; 179:1542-1551.
8. Ming-Hung Shu, Hsien-Chung Wu. Fuzzy $\overline{X}$ and R Control Charts: Fuzzy Dominance Approach. Computers and Industrial Engineering 2011; 61:676-685.
9. Sogandi F, Meysam Mousavi S, Ghanaatiyan R. An Extension of Fuzzy P- Control Chart based on α - Level Midrange. Advanced Computational Techniques in Electromagnetics 2014; 2014:1-8.
10. Pekin Alakoc N, Apaydin A. A Fuzzy Control Chart Approach for Attributes and Variables. Engineering, Technology & Applied Science Research 2018; 8(5):3360-3365.
11. Prabu S, Nanthakumar C. Construction of Fuzzy Control Chart for Number of Defects Using Process Capability. International Journal of Creative Research Thoughts (IJCRT) 2020; 8:1340-1348.
12. Devaarul S, Arunthadhi N. Design of Geometric Moving Average Control Chart to Monitor Poisson Mean for an Unstabilized Production Process. International Journal of Statistics and Applied Mathematics 2023; 8(3):26-35.

Table1. Observation data

Sample size (n)	Number of Defects (d)	Sample size (n)	Number of Defects (d)
100	12	120	8
80	8	110	6
80	6	80	8
100	9	80	10
110	10	80	7
110	12	90	5
100	11	100	8
100	16	100	5
90	10	100	8
90	6	100	10
110	21	90	6
120	15	90	9
120	9		

*Source: Montgomery, D. C. (2009), "Introduction to Statistical Quality Control", Sixth Edition, Wiley India, New Delhi.

Table 2. ARL for fuzzy based Compound fraction defectives when α = 0.5

Shifts	ARL
0.75	137
0.99	285
1.008	264
1.250	544
2.140	155
2.500	235
3.150	193
3.500	302
3.880	443
4.002	351
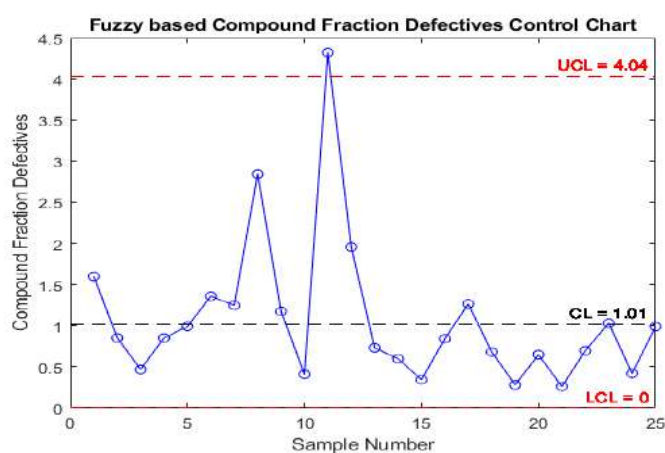
Figure 1. Control chart for fuzzy based compound fraction defectives

RESEARCH ARTICLE

A New Ranking for Solving Trapezoidal and Pentagonal Picture Fuzzy Transportation Problem

T.Narppasalai Arasu[1]* and [2]M.Sivapriya[2]

[1]Associate Professor, Department of Mathematics, Chikkanna Govt. Arts College, Tirupur-02, Tamil Nadu, India

[2]Research Scholar, Department of Mathematics, Chikkanna Govt. Arts College, Tirupur-02, Tamil Nadu, India

*Address for Correspondence
T.Narppasalai Arasu
Associate Professor,
Department of Mathematics,
Chikkanna Govt. Arts College,
Tirupur-02, Tamil Nadu, India
E.Mail: narppasalai@gmail.com

ABSTRACT

In this paper a new ranking formula is used to find an Initial Basic Feasible Solution to a Trapezoidal Picture Fuzzy Transportation Problem and Pentagonal Picture Fuzzy Transportation Problem. Three types of Transportation Problem are considered namely Type 1(supply and demand), Type 2 (cost only) and Type 3 (supply, demand and cost) in which the above parameters are represented as Trapezoidal Picture Fuzzy Numbers and Pentagonal Picture Fuzzy Numbers. Also the results obtained for Type 1,Type 2 and Type 3 for Trapezoidal Picture Fuzzy Transportation Problem and Pentagonal Picture Fuzzy Transportation Problem are compared with each other. It is observed that Pentagonal Picture Fuzzy Transportation Problem gives better approximation for the estimation cost of transportation better than Trapezoidal Picture Fuzzy Transportation Problem.

Keywords: Picture Fuzzy Sets, Trapezoidal Picture Fuzzy Number, Pentagonal Picture Fuzzy number, Picture Fuzzy transportation problem, Ranking formula.

INTRODUCTION

A Trapezoidal Picture Fuzzy Transportation Problem (TPFTP) and Pentagonal Picture Fuzzy Transportation Problem (PPFTP) are transportation problems in which the Transportation Problems (TP) is classified into Type 1, Type 2 and Type 3. An extension of Fuzzy Set by Zadeh [3] and Intuitionistic Fuzzy Set by Atanassov [1] is a Picture Fuzzy Set (PFS). A. Nagoorgani and S. Abbas, [2] find a new method for solving Intuitionistic Fuzzy Transportation Problem. Sathya Geetha et.al [4]. solved TP under Picture Fuzzy environment. Muhammad Athar Mehmood et al.[5]

find Extended TP based on PFS. In this paper a TPFTP and PPFTP was solved by using a new ranking formula for converting Trapezoidal Picture Fuzzy Number (TPFN) and Pentagonal Picture Fuzzy Number (PPFN) into crisps value and VAM technique is used to find an Initial Basic Feasible Solution (IBFS).

Basic definitions

Definition 2.1 [6]: A PFS in U is defined by P $=\{x, (m_p(x), a_p(x), n_p(x))/x \in U\}$ where $(m_p(x), a_p(x), n_p(x)) \in$ [0,1], $0 \leq (m_p(x) + a_p(x) + n_p(x)) \leq 1$. The $(m_p(x), a_p(x), n_p(x)) \in [0,1]$ denote respectively the positive membership degree, neutral, negative membership degree of the element of x in the set P. For each PFS P in U, the refusal membership degree is described as

$r_p(x) = 1 - (m_p(x) + a_p(x) + n_p(x))$.

Definition 2.2 [6]: A Picture Fuzzy Number (PFN) n is defined in a PFS, where $n \in R$, as

n $=\{\xi, (m_n(\xi), a_n(\xi), n_n(\xi))/\xi \in R\}$, where

$$m(\xi) = \begin{cases} f_n^l(\xi), & for \ \ p_1 \leq \xi < q \\ \alpha_n, & for \ q \leq \xi \leq r \\ f_n^u(\xi), & for \ r \leq \xi < \ s_1 \\ 0, & otherwise \end{cases}$$

$$a(\xi) = \begin{cases} g_n^l(\xi), & for \ \ p_2 \leq \xi < q \\ \beta_n, & for \ q \leq \xi \leq r \\ g_n^u(\xi), & for \ r \leq \xi < \ s_2 \\ 0, & otherwise \end{cases}$$

$$n(\xi) = \begin{cases} h_n^l(\xi), & for \ \ p_3 \leq \xi < q \\ \gamma_n, & for \ q \leq \xi \leq r \\ h_n^u(\xi), & for \ r \leq \xi < \ s_3 \\ 0, & otherwise \end{cases}$$

Definition 2.3 [6]: A TPFN 't_n' is defined in a picture fuzzy subset in R with the following membership function $m_n(\xi)$, neutral $a_n(\xi)$ and non-membership function $n_n(\xi)$.

$$m_n(\xi) = \begin{cases} f_n^l(\xi) = \dfrac{\xi - p_1}{q - p_1} \alpha_n^q, & for \ \ p_1 \leq \xi < q \\ \alpha_n, & for \ q \leq \xi \leq r \\ f_n^u(\xi) = \dfrac{s_1 - \xi}{s_1 - r} \alpha_n, & for \ r \leq \xi < \ s_1 \\ 0, & otherwise \end{cases}$$

$$a_n(\xi) = \begin{cases} g_n^l(\xi) = \dfrac{q - \xi + \beta_n(\xi - p_2)}{q - p_2}, & for \ \ p_2 \leq \xi < q \\ \beta_n, & for \ q \leq \xi \leq r \\ g_n^u(\xi) = \dfrac{\xi - r + \beta_n(s_2 - \xi)}{s_2 - r}, & for \ r \leq \xi < \ s_2 \\ 0, & otherwise \end{cases}$$

$$n_n(\xi) = \begin{cases} h_n^l(\xi) = \dfrac{q - \xi + \gamma_n(\xi - p_3)}{q - p_3}, & for \ \ p_3 \leq \xi < q \\ \gamma_n, & for \ q \leq \xi \leq r \\ h_n^u(\xi) = \dfrac{\xi - r + \gamma_n(s_3 - \xi)}{s_3 - r}, & for \ r \leq \xi < \ s_3 \\ 0, & otherwise \end{cases}$$

Where $P_3 \leq P_2 \leq P_1 \leq q \leq r \leq S_1 \leq S_2 \leq S_3$ for all $\xi \epsilon X$ with the constraints $0 \leq \alpha_n, \beta_n, \gamma_n \leq 1$ and $\alpha_n + \beta_n + \gamma_n \leq 1$. TPFN '$t_n'$ is denoted by

$t_n = (P_1, q, r, S_1; P_2, q, r, S_2; P_3, q, r, S_3)$.

Narppasalai Arasu and Sivapriya

Definition 2.4 : A PPFN′P_n′of PFS is defined as P_n ={(a1, b1, c1,d1, e1)(a2 , b2, c2, d2, e2) (a3, b3, c3, d3, e3)} where all $a1, b1, c1 , d1, e1, a2 , b2, c2, d2, e2 ,a3, b3, c3, d3, e3$are real numbers and its membership function $m_n(\xi)$, neutral $a_n(\xi)$ and non-membership function $n_n(\xi)$.

$$m_n(\xi) = \begin{cases} 0, for\ \xi < a_1 \\ (\dfrac{\xi - a_1}{b_1 - a_1})\alpha_n^q, \ for\ \ a_1 \le \xi < b_1 \\ \dfrac{\xi - b_1}{c_1 - b_1}\alpha_n^q, \ for\ \ b_1 \le \xi < c_1 \\ \alpha_n , \qquad\qquad for\ \xi = c_1 \\ \dfrac{d_1 - \xi}{d_1 - c_1}\alpha_n, \ for\ \ c_1 \le \xi < d_1 \\ \dfrac{e_1 - \xi}{e_1 - d_1}\alpha_n, \ for\ \ c_1 \le \xi < d_1 \\ 0, for\ \xi > e_1 \end{cases}$$

$$a_n(\xi) = \begin{cases} 0, for\ \xi < a_2 \\ \dfrac{b_2 - \xi}{b_2 - a_2}\beta_n, \ for\ \ a_2 \le \xi < b_2 \\ \dfrac{c_2 - \xi}{c_2 - b_2}\beta_n, \ for\ \ b_2 \le \xi < c_2 \\ \beta_n , \qquad\qquad for\ \xi = c_1 \\ \dfrac{\xi - c_2}{d_2 - c_2}\beta_n, \ for\ \ c_2 \le \xi < d_2 \\ \dfrac{\xi - d_2}{e_2 - d_2}\beta_n, \ for\ \ d_2 \le \xi < e_2 \\ 1, for\ \xi > e_2 \end{cases}$$

$$n_n(\xi) = \begin{cases} 1, for\ \xi < a_3 \\ \dfrac{b_3 - \xi}{b_3 - a_3}\gamma_n, \ for\ \ a_3 \le \xi < b_3 \\ \dfrac{c_3 - \xi}{c_3 - b_3}\gamma_n, \ for\ \ b_3 \le \xi < c_3 \\ \gamma_n , \qquad\qquad for\ \xi = c_1 \\ \dfrac{\xi - c_3}{d_3 - c_3}\gamma_n, \ for\ \ c_3 \le \xi < d_3 \\ \dfrac{\xi - d_3}{e_3 - d_3}\gamma_n, \ for\ \ d_3 \le \xi < e_3 \\ 1, for\ \xi > e_3 \end{cases}$$

with the constraints $0\le \alpha_n, \beta_n, \gamma_n \le 1 and\ \alpha_n + \ \beta_n + \gamma_n \le 1$.

Definition 2.5:Mathematical Formulation of TPFTP (or PPFTP)

A Picture Fuzzy Transportation Problem (PFTP) is defined as

$$Minimum\ \tilde{z}^P = \sum_{i=1}^{m}\sum_{j=1}^{n} \tilde{c}_{ij}^P \otimes \tilde{x}_{ij}^P$$

Subject to the constraints,

$$\sum_{j=1}^{n} \tilde{x}_{ij}^P = \tilde{a}_i^P, i = 1,2,3 \dots m$$

$$\sum_{i=1}^{m} \tilde{x}_{ij}^P = \tilde{b}_i^P, j = 1,2,3 \dots n$$

$\tilde{x}_{ij}^P \ge 0, i = 1,2, \dots m, j = 1,2, \dots n$

The above PFTP is called TPFTP (or PPFTP).

Narppasalai Arasu and Sivapriya

If $\tilde{c}_{ij}^P$ is the unit Trapezoidal(or Pentagonal) picture fuzzy transporting cost from i^{th} source to j^{th} destination.

$\tilde{a}_i^P$ is the Trapezoidal (or Pentagonal)picture fuzzy availability of the commodity at the ith source to j^{th} destination.

$\tilde{b}_i^P$ is the Trapezoidal (or Pentagonal) picture fuzzy demand of the commodity at the ith source to j^{th} destination.

$\tilde{x}_{ij}^P$ is the number of units of commodity transported from the ith source to j^{th} destination.

Note: The above TPFTP (or PPFTP) represent Type 3 problem. Suppose $\tilde{c}_{ij}^P$ is represented as crisp valuesthen the above TPFTP (or PPFTP) represent Type 1and supply and demand are represented as crisp values then the above TPFTP (or PPFTP) represent Type 2

Definition 2.6: Ranking formula for TPFN

If $t_n = (P_1, q, r, S_1; P_2, q, r, S_2; P_3, q, r, S_3)$.is a TPFN, then the crisp value of t_n,ais given below.

$$a = \frac{p_1 + 2q + 2r + s_1 + p_2 + 2q + 2r + s_2 + p_3 + 2q + 2r + s_3}{18}$$

Definition 2.7: Ranking formula for PPFN

If $P_n = (a_1, b_1, c_1, d_1, e_1; a_2, b_2, c_2, d_2, e_2; a_3, b_3, c_3, d_3, e_3)$.is a PPFN, then the crisp value of P_n,b is given below.

$$b = \frac{a_1 + 2b_1 + 2c_1 + 2d_1 + e_1 + a_2 + 2b_2 + 2c_2 + 2d_2 + e_2 + a_3 + 2b_3 + 2c_3 + 2d_3 + e_3}{24}$$

Algorithm for the TPFTP and PPFTP

Step (1): Check whether the given transportation problem is balanced or not. If not, introduce a dummy row or column for making the transportation problem a balanced one.

Step (2): Each type1,type2 and type3 the TPFN and PPFN are converted into crisp value using respective ranking formula.

Step (3): Existing method namely, VAM technique for the given three types of TPFTP and PPFTP to find the IBFS.

Step (4): Compare the IBFS obtained from the TPFTP and PPFTP.

NUMERICAL EXAMPLES

Example 4.1: Consider TPFTP of Type-1 is shown in TPFTP Table 1 (TPFTPT 1)

TPFTPT 1

	D1	D2	D3	D4	Supply
C1	5	1	3	3	(3,4,5,9; 2.5,4,5,9.5; 2,4,5,10)
C2	3	3	5	4	(7,11,12,13; 6.5,11,12,13.5; 6,11,12,14)
C3	6	4	4	3	(6,10,11,12; 5,10,11,13; 4,10,11,14)
C4	4	1	4	2	(3,7,8,9; 2.5,7,8,9.5; 2,7,8,10)
Demand	(10,14,15,17; 9,14,15,17.5; 7,14,15,18)	(2,7.5,8.1,10.5; 1,7.5,8.1,11; 1,7.5,8.1,12)	- (1,2,3,6; 0.5,2,3,7; 0,2,3,9)	(5,9,10,11; 4.5,9,10,11.5; 4,9,10,12)	

Convert given Trapezoidal supply and demand into crisp value by using ranking formula 2.5 and we get the Crisp Transportation Table 2 (CTT 2)

Narppasalai Arasu and Sivapriya

CTT 2

	D1	D2	D3	D4	Supply
C1	5	1	3	3	5
C2	3	3	5	4	11
C3	6	4	4	3	10
C4	4	1	4	2	7
Demand	14	7	3	9	33

Applying VAM Technique to find IBFS.

IBFS Table 3

	D1	D2	D3	D4	Supply
C1	5	5 | 1	3	3	5
C2	11 | 3	3	5	4	11
C3	3 | 6	4	3 | 4	4 | 3	10
C4	4	2 | 1	4	5 | 2	7
Demand	14	7	3	9	33

Z = 5*1+11*3+3*6+3*4+4*3+2*1+5*2

Z = 92

Example 4.2: Consider TPFTP of Type-2 is shown in TPFTPT 4

TPFTPT 4

	D1	D2	D3	D4	Supply
C1	(0,1,2,3; -4,1,2,4; -8,1,2,5)	(12,16,17,21;11,16,17,22;10,16,17,23)	(12,13,14,18;11.5,13,14,18.5;11,13,14,19)	(7,8,9,10;6,8,9,11;5,8,9,12)	34
C2	(3,4,5,9;2.5,4,5,9.5;2,4,5,10)	(7,11,12,16;6,11,12,17;5,11,12,18)	(6,10,11,12;5,10,11,13;4,10,11,14)	(4,7,8,11;3,7,8,12;2,7,8,13)	15
C3	(12,15,16,17;11,15,16,17.5;9,15,16,18)	(6,8,9,11;5,8,9,12;4,8,9,13)	(1,2,3,6;0.5,2,3,7;0,2,3,9)	(7,9,10,12;6,9,10,13;5,9,10,14)	12
C4	(10,12,13,18;9,12,13,19;8,12,13,20)	(5,6,7,8;4,6,7,9;3,6,7,10)	(3,13,14,15; 2.5,13,14,15.5; 2,13,14,16)	(2,6,7,11; 1,6,7,12; 0,6,7,13)	19
Demand	21	25	17	17	

Convert given Trapezoidal cost into crisp value by using ranking formula 2.5 and we get the CTT 5

CTT 5

	D1	D2	D3	D4	Supply
C1	1	16.5	14	8.5	34
C2	5	11.5	10	7.5	15
C3	15	8.5	3	9.5	12
C4	13	6.5	12	6	19
Demand	21	25	17	17	80

Applying VAM Technique to find IBFS.

IBFS Table 6

	D1	D2	D3	D4	Supply
C1	21 / 1	16.5	14	13 / 8.5	34
C2	5	6 / 11.5	5 / 10	4 / 7.5	15
C3	15	8.5	12 / 3	9.5	12
C4	13	19 / 6.5	12	6	19
Demand	21	25	17	17	

Z = 21*1+13*8.5+6*11.5+5*10+4*7.5+12*3+19*6.5

Z = 440

Example 4.3: Consider TPFTP of Type-3 is shown in TPFTPT 7

TPFTPT 7

	D1	D2	D3	D4	Supply
C1	(0,1,2,3;-4,1,2,4;-8,1,2,5)	(12,16,17,18;11.5,16,17,18.5;11,16,17,19)	(12,13,14,18;11.5,13,14,18.5;11,13,14,19)	(7,8,9,13;6.5,8,9,13.5;6,8,9,14)	(2,3,4,8;1.5,3,4,8.5;1,3,4,9)
C2	(3,4,5,9;2.5,4,5,9.5;2,4,5,10)	(7,11,12,13;6.5,11,12,13.5;6,11,12,14)	(6,10,11,12;5,10,11,13;4,10,11,14)	(3,7,8,9;2.5,7,8,9.5;2,7,8,10)	(5,7,8.2,10;4,7,8.2,11;2,7,8.2,13)
C3	(12,15,16,17;11,15,16,17.5;9,15,16,18)	(4,8,9,10;3.5,8,9,10.5;3,8,9,11)	(1,2,3,6;0.5,2,3,7;0,2,3,9)	(5,9,10,11;4.5,9,10,11.5;4,9,10,12)	(7,8,9,13;6,8,9,14;5,8,9,15)
C4	(10,12,13,18;9,12,13,19;8,12,13,20)	(5,6,7,9;4.5,6,7,12;4,6,7,14)	(3,13,14,15;2.5,13,14,15.5;2,13,14,16)	(2,6,7,8;1.5,6,7,8.5;1,6,7,9)	(6,10,11,12;5.5,10,11,12.5;5,10,11,13)
Demand	(3,5,6,10;2.5,5,6,11;2,5,6,13)	(1,4,5,7;0,4,5,8;-2,4,5,9)	(7,7.5,8.6,12;6,7.5,8.6,13;5,7.5,8.6,14)	(9,12,13,14;7,12,13,15;5,12,13,16)	

Narppasalai Arasu and Sivapriya

Convert given Trapezoidal cost, supply and demand into crisp value by using ranking formula 2.5 and we get the CTT 8

CTT 8

	D1	D2	D3	D4	Supply
C1	1	16	14	9	4
C2	5	11	10	7	7.5
C3	15	8	3	9	9
C4	13	7	12	6	10
Demand	6	4	8.5	12	

Applying VAM Technique to find IBFS.

IBFS Table 9

	D1	D2	D3	D4	Supply
C1	4 / 1	16	14	9	4
C2	2 / 5	11	10	5.5 / 7	7.5
C3	15	0.5 / 8	8.5 / 3	9	9
C4	13	3.5 / 7	12	6.5 / 6	10
Demand	6	4	8.5	12	

Z=4*1+2*5+5.5*7+0.5*8+8.5*3+3.5*7+6.5*6
Z=145.5

Example 4.4: Consider PPFTP of Type-1 is shown in PPFTPTable 10 (PPFTPT 10)

PPFTPT 10

	D1	D2	D3	D4	Supply
C1	5	1	3	3	(3,4.5,6,7.5,9; 2.5,4.25,6,7.75,9.5;2,4, 6,8,10)
C2	3	3	5	4	(7,8.5,10,11.5,13; 6.5,8.25,10,11.75, 13.5; 6,8,10,12,14)
C3	6	4	4	3	(6,7.5,9,10.5,12; 5,7,9,11,13; 4,6.5,9,11.5,14)
C4	4	1	4	2	(3,4.5,6,7.5,9; 2.5,4.25,6,7.75,9.5;2,4, 6,8,10)

Narppasalai Arasu and Sivapriya

| Demand | (10,11.75,13.5, 15.25,17; 9,11.125,13.25, 15.375,17.5;7,9.75,12. 5,15.25,18) | (2,4.125,6.25,8.375,10.5; 1,3.5,6,8.5,11;   - 1,3.5,6,8.5,12) | (1,2.25,3.5,4.75,6; 0.5,2.125,3.75,5.35,7; 0,2.25,4.5,6.75,9) | (5,6.5,8,9.5,11; 4.5,6.25,8,9.75,1 1.5; 4,6,8,10,12) | |

Convert given Pentagonal supply and demand into crisp value by using ranking formula 2.6 and we get the CTT 11

CTT 11

	D1	D2	D3	D4	Supply
C1	5	1	3	3	6
C2	3	3	5	4	10
C3	6	4	4	3	9
C4	4	1	4	2	6
Demand	13	6	4	8	31

Applying VAM technique to find IBFS.
IBFS Table 12

	D1	D2	D3	D4	Supply
C1	5	6 / 1	3	3	6
C2	10 / 3	3	5	4	10
C3	3 / 6	4	4 / 4	2 / 3	9
C4	4	0 / 1	4	6 / 2	6
Demand	13	6	4	8	31

Z = 6*1+10*3+3*6+4*4+2*3+0*1+6*2 =88

Example 4.5: Consider PPFTP of Type-2 is shown in PPFTPT 13
PPFTPT 13

	D1	D2	D3	D4	Supply
C1	(0,0.75,1.5,2.25,3; -4,-2,0,2,4; -8,-4.75,- 1.5,1.75,5)	(12,14.25,16.5,18.75,21;11,1 3.75,16.5,19.25,22;10,13.25, 16.5,19.75,23)	(12,13.5,15,16.5,18;11.5, 13.25, 15, 16.75, 18.5;11,13,15,17,19)	(7,7.75,8.5,9.25,10;6,7. 25,8.5,9.75,11;5,6.75,8. 5,10.25,12)	34
C2	(3,4.5,6,7.5,9;2.5,4.25,6,7.7,9 .5;2,4,6,8,10)	(7,9.25,11.5,13.75,16;6,8.75, 11.5,14.25,17;5,8.25,11.5,14 .75,18)	(6,7.5,9,10.5,12;5,7,9,11, 13;4,6.5,9,11.5,14)	(4,5.75,7.5,9.25,11;3,5. 25,7.5,9.75,12;2,4.75,7. 5,10.25,13)	15

Narppasalai Arasu and Sivapriya

C3	(12,13.25,14.5,15.75,17;11,12.63,14.25,15.88,17.5;9,11.25,13.5,15.75,18)	(6,7.25,8.5,9.75,11;5,6.75,8.5,10.25,12;4,6.25,8.5,10.75,13)	(1,2.25,3.5,4.75,6;0.5,2.125,3.75,5.375,7;0,2.25,4.5,6.75,9)	(7,8.25,9.5,10.75,12;6,7.75,9.5,11.25,13;5,7.25,9.5,11.75,14)	12
C4	(10,12,14,16,18;9,11.5,14,16.5,19;8,11,14,17,20)	(5,5.75,6.5,7.25,8;4,5.25,6.5,7.75,9;3,4.75,6.5,8.25,10)	(3,6,9,12,15; 2.5,5.75,9,12.25,15.5; 2,5.5,9,12.5,16)	(2,4.25,6.5,8.75,11;1,3.75,6.5,9.25,12;0,3.25,6.5,9.75,13)	19
Demand	21	25	17	17	

Convert given Pentagonal cost into crisp value by using ranking formula 2.6 and we get the CTT 14
CTT 14

	D1	D2	D3	D4	Supply
C1	0	16.5	15	8.5	34
C2	6	11.5	9	7.5	15
C3	14	8.5	4	9.5	12
C4	14	6.5	9	6	19
Demand	21	25	17	17	80

Applying VAM Technique to find IBFS.
IBFS Table 15

	D1	D2	D3	D4	Supply
C1	21 — 0	16.5	15	13 — 8.5	34
C2	6	6 — 11.5	5 — 9	4 — 7.5	15
C3	14	8.5	12 — 4	9.5	12
C4	14	19 — 6.5	9	6	19
Demand	21	25	17	17	

Z=21*0+13*8.5+6*11.5+5*9+4*7.5+12*4+19*6.5
Z = 426

Example 4.6: Consider PPFTP of Type-3 is shown in PPFTPT 16
PPFTPT 16

	D1	D2	D3	D4	Supply
C1	(0,0.75,1.5,2.25,3; -4,-2,0,2,4; -8,-4.75,-1.5,1.75,5)	(12,13.5,15,16.5,18;11.5,13.25,15,16.75,18;5,11,13,15,17,19)	(12,13.5,15,16.5,18;11.5,13.25,15,16.7518.5;11,13,15,17,19)	(7,8.5,10,11.5,13;6.5,8.25,10,11.75,13.5;6,8,10,12,14)	(2,3.5,5,6.5,8;1.5,3.25,5,6.75,8.5;1,3,5,7,9)

Narppasalai Arasu and Sivapriya

C2	(3,4.5,6,7.5,9;2.5,4.25,6,7.7,9.5;2,4,6,8,10)	(7,8.5,10,11.5,13;6.5,8.25,10,11.75,13.5;6,8,10,12,14)	(6,7.5,9,10.5,12;5,7,9,11,13;4,6.5,9,11.5,14)	(3,4.5,6,7.5,9;2.5,4.25,6,7.75,9.5;2,4,6,8,10)	(5,6.25,7.5,8.75,10;4,5.75,7.5,9.25,11;2,4.75,7.5,10.25,13)
C3	(12,13.25,14.5,15.75,17;11,12.63,14.25,15.88,17.5;9,11.25,13.5,15.75,18)	(4,5.5,7,8.5,10;3.5,5.25,7,8.75,10.5;3,5,7,9,11)	(1,2.25,3.5,4.75,6;0.5,2.125,3.75,5.375,7;0,2.25,4.5,6.75,9)	(5,6.5,8,9.5,11;4.5,6.25,8,9.75,11.5;4,6,8,10,12)	(7,8.5,10,11.5,13;6,8,10,12,14;5,7.5,10,12.5,15)
C4	(10,12,14,16,18;9,11.5,14,16.5,19;8,11,14,17,20)	(5,6,7,8,9;4.5,6.375,8.25,10.13,12;4,6.5,9,11.5,14)	(3,6,9,12,15;2.5,5.75,9,12.25,15.5;2,5.5,9,12.5,16)	(2,3.5,5,6.5,8;1.5,3.25,5,6.75,8.5;1,3,5,7,9)	(6,7.5,9,10.5,12;5.5,7.25,9,10.75,12.5;5,7,9,11,13)
Demand	(3,4.75,6.5,8.25,10;2.5,4.625,6.75,8.875,11;2,4.75,7.5,10.25,13)	(1,2.5,4,5.5,7;0,2,4,6,8;-2,0.75,3.5,6.25,9)	(7,8.25,9.5,10.75,12;6,7.75,9.5,11.25,13;5,7.25,9.5,11.75,14)	(9,10.25,11.5,12.75,14;7,9,11,13,15;5,7.75,10.5,13.5,16)	

Convert given Pentagonalcost, supply and demand into crisp value by using ranking formula 2.6 and we get the
CTT 17
CTT 17

	D1	D2	D3	D4	Supply
C1	0	15	15	10	5
C2	6	10	9	6	7.5
C3	14	7	4	8	10
C4	14	8	9	5	9
Demand	7	4	9.5	11	31.5

Apply VAM Technique to find IBFS
IBFS Table 18

	D1		D2		D3		D4		Supply
C1	5	0		15		15		10	5
C2	2	6		10		9	5.5	6	7.5
C3		14	0.5	7	9.5	4		8	10
C4		14	3.5	8		9	5.5	5	9
Demand	7		4		9.5		11		

Z = 5*0+2*6+5.5*6+0.5*7+9.5*4+3.5*8+5.5*5
Z = 142

Comparison and Conclusion:
The comparison of IBFS for Type1, 2 and 3 TPFTP and PPFTP can be made and shown in Table 19

Table 19

Types	TPFTP	PPFTP
Type-1	92	88
Type-2	440	426
Type-3	145.5	142

In this paper, a new ranking formula is used to solve TPFTP and PPFTP. Based on the results shown in Table 19 it has been found that PPFTP gives better solution than the TPFTP.

REFERENCES

1. K.Atanassov, Intuitionistic fuzzy sets and systems, 20(1986): 87-96.
2. A.NagoorganiandS.Abbas, A new method for solving Intuitionistic fuzzy Transportation problem. Applied Mathematical Sciences 7(28),(2013): 1357-1365.
3. L.A Zadeh,Fuzzysets.*Information andcontrol,*8(1965):338-353.
4. S.Sathya Geetha and K.Selvakumari, A picture fuzzy approach to solving transportation problem, ISSN 2515-8260, volume 07, issue 02,2020.
5. Muhammad Athar Mehmood and Shahida Bashir, Extended transportation models based on picture fuzzy sets(2022).
6. Muhammad Akram, Amna Habib, Jose Carlos R.Alcantud, An optimization study based on dijikstra algorithm for a network with trapezoidal picture fuzzy numbers(2020).

RESEARCH ARTICLE

Special Algebraic Operations on Quin – Terranean Fuzzy Numbers

P. Rajarajeswari[1] and T. Thirunamakkani[2]*

[1]Assistant Professor, Department of Mathematics, Chikkanna Government Arts College, Tirupur – 641602, Tamil Nadu, India,
[2]Research Scholar, Department of Mathematics, Chikkanna Government Arts College, Tirupur – 641602, Tamil Nadu, India.

*Address for Correspondence
T. Thirunamakkani
Research Scholar,
Department of Mathematics,
Chikkanna Government Arts College,
Tirupur – 641602, Tamil Nadu, India.
E.Mail: thirunamakkani2015@gmail.com.

ABSTRACT

In this paper, we introduce some special model algebraic operations on Quin – Terranean Fuzzy numbers such as $\ominus$ and $\oslash$ on Quin – Terranean fuzzy numbers. Based on the special model algebraic operations defined, we have analyzed several properties of Quin – Terranean Fuzzy numbers.

Mathematics Subject Classification: 03E72

Keywords: Quin – Terranean Fuzzy set, Quin – Terranean Fuzzy Number, special model algebraic operations such as $\ominus$ and $\oslash$ on Quin – Terranean Fuzzy Numbers.

INTRODUCTION

In 1965, Zadeh [17] introduced the concept of Fuzzy set theory which is an extension of classical set theory. In 2011, Taleshian et al. [13] provided a method for multiplying two trapezoidal Fuzzy numbers. The proposed analytical approach is the most accurate, but when the membership function is complex, it is challenging to alpha-cuts interval. They have given examples to explain this approach. They generalized Fuzzy number operations from the operations of a crisp interval. In 2013, Rajarajeswari et al. [9] defined an innovative operation on hexagonal fuzzy numbers such that the methods of addition, subtraction, and multiplication have been adapted with some conditions. They have presented new operations for hexagonal Fuzzy number addition, subtraction, and multiplication on the basis of alpha cut sets of fuzzy numbers. In 2015, Chandrasekaran et al. [3] analyzed the arithmetic operations on Fuzzy numbers such as addition, subtraction, multiplication, division, inverse, exponential, logarithm, square root and n[th]

63317

root of a Fuzzy number using α-cut method. In 2016, Md. Yasin Ali et al. [8] compared the α-cut method and the standard approximation method for multiplying triangular Fuzzy numbers, and provided examples and graphical demonstration for each comparison. In 2018, Jayasri and Elavarasi [6] studied Fuzzy set theory and arithmetic operations such as addition, subtraction, multiplication and division operations on Fuzzy numbers. In order to handle situations in which Fuzzy sets are insufficient, in 1986, Atanassov [1] defined the extended concept of Fuzzy set theory known as Intuitionistic Fuzzy Set (IFS). He defined the operations of IFS and also analyzed their properties.

In 2014 Yager [16] introduced the extended concept of IFS known as Pythagorean Fuzzy set(PFS) in which the total of the square of the degree of acceptance and square of the degree of non-acceptance is lesser than or equal to one. In 2010, Chuan-qiang Fan et al. [5] proposed the new (α,β)-pythagorean Fuzzy descriptor systems using pythagorean Fuzzy sets and T-S Fuzzy descriptor systems. They discussed relationship between (α,β)-Pythagorean Fuzzy descriptor systems and T-S Fuzzy descriptor systems, along with the definition of these systems and a study of their stability. They conducted a thorough study on the stability of (α,β)-Pythagorean Fuzzy descriptor systems which handles the challenges associated with actual non-linear control more effectively and the (α,β)-Pythagorean Fuzzy controller. They have also provided a concrete example to highlight the viability of the suggested approach. In 2019, Senapathi and Yager [14] introduced Fermatean Fuzzy Set (FFS) in which the sum of the cube of the degree of acceptance and cube of the degree of non-acceptance is less than or equal to one. In 2019, Tapan Senapati and Ronald Yager [15] introduced the three new operations namely subtraction, division and Fermatean arithmetic mean operations over Fermatean Fuzzy Numbers. They have provided great detail on their properties. They developed a Fermatean Fuzzy weighted product model to address the multi-criteria decision-making issue. They have also provided a practical example of choosing a suitable bridge construction method to illustrate the approach they developed and to confirm its viability. The Quin-Terranean Fuzzy Set (QTFS) [11], a novel concept we developed in 2023, is the most significant and useful technique to address uncertainty and contingency, when compared to IFS, PFS, and FFS. Quin-Terranean Fuzzy sets fundamental set theory operations, such as complement, intersection, and union, were defined. Several of the properties are investigated in regard to these operations. The Quin-Terranean Fuzzy set has been shown to satisfy the De Morgan's rule, associative property, commutative property, and distributive property.

Preliminaries
This section consists of the basic concepts and definitions related to the paper.

Definition 2.1 [14]
The Pythagorean fuzzy sets defined on a non-empty set X as objects having the form $\mathcal{P} = \{\langle \tilde{x}, \alpha_P(\tilde{x}), \beta_P(\tilde{x})\rangle : \tilde{x} \in X\}$, where the function $\alpha_P(\tilde{x}): X \to [0,1]$ and $\beta_P(\tilde{x}): X \to [0,1]$, denote the degree of membership and degree of non-membership of each element $\tilde{x} \in X$ to the set $\mathcal{P}$ respectively, and $0 \leq \left(\alpha_P(\tilde{x})\right)^2 + \left(\beta_P(\tilde{x})\right)^2 \leq 1$ for all $\tilde{x} \in X$. For any Pythagorean fuzzy set $\mathcal{P}$ and $\tilde{x} \in X$, $\pi_P(\tilde{x}) = \sqrt{1 - \left(\alpha_P(\tilde{x})\right)^2 - \left(\beta_P(\tilde{x})\right)^2}$ is called the degree of indeterminacy of $\tilde{x}$ to $\mathcal{P}$.

Definition 2.2 [14]
Let X be a universe of discourse. A Fermatean fuzzy set $\mathcal{F}$ in X is an object having the form
$\mathcal{F} = \{\langle \tilde{x}, \alpha_{\mathcal{F}}(\tilde{x}), \beta_{\mathcal{F}}(\tilde{x})\rangle : \tilde{x} \in X\}$,
where $\alpha_{\mathcal{F}}(\tilde{x}): X \to [0,1]$ and $\beta_{\mathcal{F}}(\tilde{x}): X \to [0,1]$, including the condition
$0 \leq \left(\alpha_P(\tilde{x})\right)^3 + \left(\beta_P(\tilde{x})\right)^3 \leq 1$,
for all $\tilde{x} \in X$. The $\alpha_{\mathcal{F}}(\tilde{x})$ and $\beta_{\mathcal{F}}(\tilde{x})$ denote, respectively, the degree of membership and the degree of non-membership of the element $\tilde{x}$ in the set $\mathcal{F}$.

For any FFS $\mathcal{F}$ and $\tilde{x} \in X$,

$$\pi_{\mathcal{F}}(\tilde{x}) = \sqrt[3]{1 - (\alpha_P(\tilde{x}))^3 - (\beta_P(\tilde{x}))^3}$$

is identified as the degree of indeterminacy of $\tilde{x}$ to $\mathcal{F}$.

In the interest of simplicity, we shall mention the symbol $\mathcal{F} = (\alpha_{\mathcal{F}}, \beta_{\mathcal{F}})$ for the FFS $\mathcal{F} = \{\langle \tilde{x}, \alpha_{\mathcal{F}}(\tilde{x}), \beta_{\mathcal{F}}(\tilde{x}) \rangle : \tilde{x} \in X\}$.

Definition 2.3 [11]

Let X denotes a universe of discourse. A Quin – Terranean fuzzy set $\tilde{Q}$ in X is the element possess the configuration $\tilde{Q} = \{\langle \tilde{x}, \sigma_{\tilde{Q}}(\tilde{x}), \delta_{\tilde{Q}}(\tilde{x}) \rangle : \forall \tilde{x} \in X\}$,

where $\sigma_{\tilde{Q}}(\tilde{x}): X \longrightarrow [0, 1]$ and $\delta_{\tilde{Q}}(\tilde{x}): X \longrightarrow [0, 1]$ represents the degree of dependence and degree of non-dependence

of the element respectively, satisfying the condition $0 \leq \left(\sigma_{\tilde{Q}}(\tilde{x})\right)^{4^5} + \left(\delta_{\tilde{Q}}(\tilde{x})\right)^{\frac{5}{4}} \leq 1, \forall \tilde{x} \in X$.

For any Quin – Terranean fuzzy set $\tilde{Q}$ and $\forall \tilde{x} \in X$, $\varphi_{\tilde{Q}}(\tilde{x}) = \left\{1 - \left(\sigma_{\tilde{Q}}(\tilde{x})\right)^{4^5} - \left(\delta_{\tilde{Q}}(\tilde{x})\right)^{\frac{5}{4}}\right\}^{\frac{4}{5}}$ is the degree of

hesitance of $\tilde{x}$ to X.

Definition 2.4 [10]

A Quin – Terranean fuzzy number $\tilde{Q}$ is defined as,

a Quin – Terranean fuzzy subset of the real line

normal, that is, there exist $\tilde{x}_0 \in R$ such that $\sigma_{\tilde{Q}}(\tilde{x}_0) = 1$ and $\delta_{\tilde{Q}}(\tilde{x}_0) = 0.$

a convex set for the acceptance function $\sigma_{\tilde{Q}}(\tilde{x})$, that is,

$$\sigma_{\tilde{Q}}(\lambda\tilde{x}_1 + (1-\lambda)\tilde{x}_2) \geq min\left(\sigma_{\tilde{Q}}(\tilde{x}_1), \sigma_{\tilde{Q}}(\tilde{x}_2)\right) \quad \forall \tilde{x}_1, \tilde{x}_2 \in R, \lambda \in [0,1]$$

a concave set for the non-acceptance function $\delta_{\tilde{Q}}(\tilde{x})$, that is,

$$\delta_{\tilde{Q}}(\lambda\tilde{x}_1 + (1-\lambda)\tilde{x}_2) \leq max\left(\delta_{\tilde{Q}}(\tilde{x}_1), \delta_{\tilde{Q}}(\tilde{x}_2)\right) \quad \forall \tilde{x}_1, \tilde{x}_2 \in R, \lambda \in [0,1].$$

and satisfies the condition, $0 \leq \left(\sigma_{\tilde{Q}}(\tilde{x})\right)^{4^5} + \left(\delta_{\tilde{Q}}(\tilde{x})\right)^{\frac{5}{4}} \leq 1$.

A doublet expressed by $\tilde{Q} = \langle \sigma_{\tilde{Q}}(\tilde{x}), \delta_{\tilde{Q}}(\tilde{x}) \rangle$ is known as Quin – Terranean fuzzy number. The Zero and one Quin – Terranean fuzzy number is denoted by (0,0) and (1,0) respectively.

Definition 2.5 [11]

Let $\tilde{Q} = \{\langle \tilde{x}, \sigma_{\tilde{Q}}(\tilde{x}), \delta_{\tilde{Q}}(\tilde{x}) \rangle : \forall \tilde{x} \in X\}$, $\tilde{Q}_1 = \{\langle \tilde{x}, \sigma_{\tilde{Q}_1}(\tilde{x}), \delta_{\tilde{Q}_1}(\tilde{x}) \rangle : \forall \tilde{x} \in X\}$, $\tilde{Q}_2 = \{\langle \tilde{x}, \sigma_{\tilde{Q}_2}(\tilde{x}), \delta_{\tilde{Q}_2}(\tilde{x}) \rangle : \forall \tilde{x} \in X\}$ be three Quin – Terranean fuzzy set, then their operations are expressed as follows,

$\tilde{Q}_1 \subset \tilde{Q}_2 \ iff \ \{\langle \tilde{x}, \sigma_{\tilde{Q}_1}(\tilde{x}) \leq \sigma_{\tilde{Q}_2}(\tilde{x}) \ and \ \delta_{\tilde{Q}_1}(\tilde{x}) \geq \delta_{\tilde{Q}_2}(\tilde{x}) \rangle : \forall \tilde{x} \in X\}$,

$\tilde{Q}_1 = \tilde{Q}_2 \ iff \ \{\langle \tilde{x}, \sigma_{\tilde{Q}_1}(\tilde{x}) = \sigma_{\tilde{Q}_2}(\tilde{x}) \ and \ \delta_{\tilde{Q}_1}(\tilde{x}) = \delta_{\tilde{Q}_2}(\tilde{x}) \rangle : \forall \tilde{x} \in X\}$,

$\tilde{Q}_1 \cup \tilde{Q}_2 = \left\{\langle \tilde{x}, max\left(\sigma_{\tilde{Q}_1}(\tilde{x}), \sigma_{\tilde{Q}_2}(\tilde{x})\right), min\left(\delta_{\tilde{Q}_1}(\tilde{x}), \delta_{\tilde{Q}_2}(\tilde{x})\right)\rangle : \forall \tilde{x} \in X\right\}$,

$\tilde{Q}_1 \cap \tilde{Q}_2 = \left\{\langle \tilde{x}, min\left(\sigma_{\tilde{Q}_1}(\tilde{x}), \sigma_{\tilde{Q}_2}(\tilde{x})\right), max\left(\delta_{\tilde{Q}_1}(\tilde{x}), \delta_{\tilde{Q}_2}(\tilde{x})\right)\rangle : \forall \tilde{x} \in X\right\}$,

$$\tilde{Q}^c = \{\langle \tilde{x}, \delta_{\tilde{Q}}(\tilde{x}), \sigma_{\tilde{Q}}(\tilde{x}) \rangle : \forall \tilde{x} \in X\}.$$

Definition 2.6 [12]

Let $\tilde{\mathbb{Q}} = \{\langle \tilde{x}, \sigma_{\tilde{\mathbb{Q}}}(\tilde{x}), \delta_{\tilde{\mathbb{Q}}}(x) \rangle : \forall \tilde{x} \in X\}$, $\tilde{\mathbb{Q}}_1 = \{\langle \tilde{x}, \sigma_{\tilde{\mathbb{Q}}_1}(\tilde{x}), \delta_{\tilde{\mathbb{Q}}_1}(\tilde{x}) \rangle : \forall \tilde{x} \in X\}$ and $\tilde{\mathbb{Q}}_2 = \{\langle \tilde{x}, \sigma_{\tilde{\mathbb{Q}}_2}(\tilde{x}), \delta_{\tilde{\mathbb{Q}}_2}(\tilde{x}) \rangle : \forall \tilde{x} \in X\}$ be three Quin – Terranean Fuzzy numbers and $\lambda > 0$, then their operations are expressed as follows:

$$\tilde{\mathbb{Q}}_1 \boxplus \tilde{\mathbb{Q}}_2 = \left\{\langle \tilde{x}, \left\{\left(\sigma_{\tilde{\mathbb{Q}}_1}(\tilde{x})\right)^{4^5} + \left(\sigma_{\tilde{\mathbb{Q}}_2}(\tilde{x})\right)^{4^5} - \left(\sigma_{\tilde{\mathbb{Q}}_1}(\tilde{x})\right)^{4^5} \left(\sigma_{\tilde{\mathbb{Q}}_2}(\tilde{x})\right)^{4^5}\right\}^{\frac{1}{4^5}}, \delta_{\tilde{\mathbb{Q}}_1}(\tilde{x})\delta_{\tilde{\mathbb{Q}}_2}(\tilde{x}) \rangle : \forall \tilde{x} \in X\right\}$$

$$\tilde{\mathbb{Q}}_1 \boxtimes \tilde{\mathbb{Q}}_2 =$$

$$\left\{ \langle \tilde{x}, \sigma_{\mathbb{Q}_1}(\tilde{x})\sigma_{\mathbb{Q}_2}(\tilde{x}), \left\{ \left(\delta_{\mathbb{Q}_1}(\tilde{x}) \right)^{\frac{5}{4}} + \left(\delta_{\mathbb{Q}_2}(\tilde{x}) \right)^{\frac{5}{4}} - \left(\delta_{\mathbb{Q}_1}(\tilde{x}) \right)^{\frac{5}{4}} \left(\delta_{\mathbb{Q}_2}(\tilde{x}) \right)^{\frac{5}{4}} \right\}^{\frac{4}{5}} \rangle : \forall \tilde{x} \in X \right\}$$

$$\lambda \widetilde{\mathbb{Q}} = \left\{ \langle \tilde{x}, \left\{ 1 - \left(1 - \left(\sigma_{\widetilde{\mathbb{Q}}}(\tilde{x}) \right)^{4^5} \right)^{\lambda} \right\}^{\frac{1}{4^5}}, \delta_{\widetilde{\mathbb{Q}}}(\tilde{x})^{\lambda} \rangle : \forall \tilde{x} \in X \right\}$$

$$\widetilde{\mathbb{Q}}^{\lambda} = \left\{ \langle \tilde{x}, \sigma_{\widetilde{\mathbb{Q}}}(\tilde{x})^{\lambda}, \left\{ 1 - \left(1 - \left(\delta_{\widetilde{\mathbb{Q}}}(\tilde{x}) \right)^{\frac{5}{4}} \right)^{\lambda} \right\}^{\frac{4}{5}} \rangle : \forall \tilde{x} \in X \right\}.$$

MAIN RESULT

In 2006, Atanassov and Riecan [2] established and discussed on the subtraction and division operations in Intuitionistic Fuzzy sets. In 2007, Chen [4] discussed the Intuitionistic Fuzzy Comparable operations. In 2014, these operations are used on hesitant fuzzy sets by Liao and Xu [7]. In 2019, Senapathi and Yager [15] discussed on subtraction and division operation on Fermatean Fuzzy numbers. Now, we discuss on some special algebraic model operators such as $\ominus$, $\oslash$ on Quin – Terranean fuzzy numbers and Quin-Terranean Arithmetic mean operation. Based on these special algebraic model operations defined, some of the properties of these model operators on Quin – Terranean Fuzzy numbers and Quin-Terranean Arithmetic mean operation are also analyzed.

Special algebraic model operators over Quin-Terranean Fuzzy Numbers

Definition 3.1
Let $T_1 = \langle T_1, T_1 \rangle$ and $T_2 = \langle T_2, T_2 \rangle$ be two Quin-Terranean Fuzzy numbers, then,

$$T_1 \ominus T_2 = \langle \left\{ \frac{\sigma_{T_1}{}^{4^5} - \sigma_{T_2}{}^{4^5}}{1 - \sigma_{T_2}{}^{4^5}} \right\}^{\frac{1}{4^5}}, \frac{\delta_{T_1}}{\delta_{T_2}} \rangle , \text{ if } \sigma_{T_1} \geq \sigma_{T_2}, \ \delta_{T_1} \leq min\left\{ \delta_{T_2}, \frac{\delta_{T_2}\varphi_1}{\varphi_2} \right\} ;$$

$$T_1 \oslash T_2 = \langle \frac{\sigma_{T_1}}{\sigma_{T_2}}, \left\{ \frac{\delta_{T_1}{}^{\frac{5}{4}} - \delta_{T_2}{}^{\frac{5}{4}}}{1 - \delta_{T_2}{}^{\frac{5}{4}}} \right\}^{\frac{4}{5}} \rangle , \text{ if } \sigma_{T_1} \leq min\left\{ \sigma_{T_2}, \frac{\sigma_{T_2}\varphi_1}{\varphi_2} \right\} , \ \delta_{T_1} \geq \delta_{T_2}.$$

Properties of Special algebraic model operators over Quin-Terranean fuzzy Numbers:

Theorem 3.2.1
Let $T = \langle \sigma_T, \delta_T \rangle$, $T_1 = \langle \sigma_{T_1}, \delta_{T_1} \rangle$ and $T_2 = \langle \sigma_{T_2}, \delta_{T_2} \rangle$ represents three Quin-Terranean Fuzzy numbers and $\lambda, \lambda_1, \lambda_2 > 0$, then

$\lambda(T_1 \ominus T_2) = \lambda T_1 \ominus \lambda T_2$, if $\sigma_{T_1} \geq \sigma_{T_2}$, $\delta_{T_1} \leq min\left\{ \delta_{T_2}, \frac{\delta_{T_2}\varphi_1}{\varphi_2} \right\}$;

$(T_1 \ominus T_2)^{\lambda} = T_1{}^{\lambda} \ominus T_2{}^{\lambda}$, if $\sigma_{T_1} \leq min\left\{ \sigma_{T_2}, \frac{\sigma_{T_2}\varphi_1}{\varphi_2} \right\}$, $\delta_{T_1} \geq \delta_{T_2}$;

$\lambda_1 T \ominus \lambda_2 T = (\lambda_1 - \lambda_2)T$, if $\lambda_1 \geq \lambda_2$;

$\widetilde{T}^{\lambda_1} - \widetilde{T}^{\lambda_2} = \widetilde{T}^{(\lambda_1 - \lambda_2)}$, if $\lambda_1 \geq \lambda_2$;

Proof:
Let T, T_1, T_2 be three Quin-Terranean Fuzzy numbers and $\lambda, \lambda_1, \lambda_2 > 0$.
Since, $\sigma_{T_1} \geq \sigma_{T_2}$, $\delta_{T_1} \leq min\left\{ \delta_{T_2}, \frac{\delta_{T_2}\varphi_1}{\varphi_2} \right\}$, we have,

$$\delta_{T_1} \leq \frac{\delta_{T_2}\varphi_1}{\varphi_2} \ \Rightarrow \delta_{T_1}\varphi_2 \leq \delta_{T_2}\varphi_1 \Rightarrow \delta_{T_1}{}^{\frac{5}{4}}\varphi_2{}^{\frac{5}{4}} \leq \delta_{T_2}{}^{\frac{5}{4}}\varphi_1{}^{\frac{5}{4}}$$

$$\Rightarrow \delta_{T_1}{}^{\frac{5}{4}}\delta_{T_2}{}^{\frac{5}{4}} + \delta_{T_1}{}^{\frac{5}{4}}\varphi_2{}^{\frac{5}{4}} \leq \delta_{T_1}{}^{\frac{5}{4}}\delta_{T_2}{}^{\frac{5}{4}} + \delta_{T_2}{}^{\frac{5}{4}}\varphi_1{}^{\frac{5}{4}} \Rightarrow \delta_{T_1}{}^{\frac{5}{4}}\left(\delta_{T_2}{}^{\frac{5}{4}} + \varphi_2{}^{\frac{5}{4}} \right) \leq \delta_{T_2}{}^{\frac{5}{4}}\left(\delta_{T_1}{}^{\frac{5}{4}} + \varphi_1{}^{\frac{5}{4}} \right)$$

Rajarajeswari and Thirunamakkani

$$\Rightarrow \delta_{T_1}^{\frac{5}{4}}\left(1-\sigma_{T_2}{}^{4^5}\right) \le \delta_{T_2}^{\frac{5}{4}}\left(1-\sigma_{T_1}{}^{4^5}\right) \Rightarrow \frac{\delta_{T_1}^{\frac{5}{4}}}{\delta_{T_2}^{\frac{5}{4}}} \le \frac{\left(1-\sigma_{T_1}{}^{4^5}\right)}{\left(1-\sigma_{T_2}{}^{4^5}\right)} \Rightarrow \left[\frac{\delta_{T_1}^{\frac{5}{4}}}{\delta_{T_2}^{\frac{5}{4}}}\right]^{\lambda} \le \left[\frac{\left(1-\sigma_{T_1}{}^{4^5}\right)}{\left(1-\sigma_{T_2}{}^{4^5}\right)}\right]^{\lambda}$$

$$\Rightarrow 1 + \left[\frac{\delta_{T_1}^{\frac{5}{4}}}{\delta_{T_2}^{\frac{5}{4}}}\right]^{\lambda} \le 1 + \left[\frac{\left(1-\sigma_{T_1}{}^{4^5}\right)}{\left(1-\sigma_{T_2}{}^{4^5}\right)}\right]^{\lambda} \Rightarrow 1 - \left[\frac{\left(1-\sigma_{T_1}{}^{4^5}\right)}{\left(1-\sigma_{T_2}{}^{4^5}\right)}\right]^{\lambda} + \left[\frac{\delta_{\widetilde{T}_1}^{\frac{5}{4}}}{\delta_{\widetilde{T}_2}^{\frac{5}{4}}}\right]^{\lambda} \le 1$$

$$\Rightarrow 1 - \left[\frac{\left(1-\sigma_{T_1}{}^{4^5}\right)}{\left(1-\sigma_{T_2}{}^{4^5}\right)}\right]^{\lambda} + \left[\frac{\delta_{T_1}^{\frac{5}{4}}}{\delta_{T_2}^{\frac{5}{4}}}\right]^{\lambda} \le 1 \Rightarrow \left\{\left(1-\left[\frac{\left(1-\sigma_{T_1}{}^{4^5}\right)}{\left(1-\sigma_{T_2}{}^{4^5}\right)}\right]^{\lambda}\right)^{4^5}\right\}^{\frac{1}{4^5}} + \left[\frac{\delta_{T_1}^{\lambda}}{\delta_{T_2}^{\lambda}}\right]^{\frac{5}{4}} \le 1.$$

Then from definition 3.1 and 2.4, we get,

$$\lambda(T_1 \ominus T_2) = \lambda\left(\left\langle \left\{\frac{\sigma_{T_1}{}^{4^5}-\sigma_{T_2}{}^{4^5}}{1-\sigma_{T_2}{}^{4^5}}\right\}^{\frac{1}{4^5}}, \frac{\delta_{T_1}}{\delta_{T_2}}\right\rangle\right) = \left\langle \left\{1-\left(1-\left[\frac{\sigma_{T_1}{}^{4^5}-\sigma_{T_2}{}^{4^5}}{1-\sigma_{T_2}{}^{4^5}}\right]^{4^5}\right)^{\lambda}\right\}^{\frac{1}{4^5}}, \frac{\delta_{T_1}^{\lambda}}{\delta_{T_2}^{\lambda}}\right\rangle$$

$$= \left\langle \left\{1-\left(\frac{1-\sigma_{T_2}{}^{4^5}-\sigma_{T_1}{}^{4^5}+\sigma_{T_2}{}^{4^5}}{1-\sigma_{T_2}{}^{4^5}}\right)^{\lambda}\right\}^{\frac{1}{4^5}}, \frac{\delta_{T_1}^{\lambda}}{\delta_{T_2}^{\lambda}}\right\rangle = \left\langle \left\{1-\left(\frac{1-\sigma_{T_1}{}^{4^5}}{1-\sigma_{T_2}{}^{4^5}}\right)^{\lambda}\right\}^{\frac{1}{4^5}}, \frac{\delta_{T_1}^{\lambda}}{\delta_{T_2}^{\lambda}}\right\rangle$$

and $\lambda T_1 \ominus \lambda T_2 = \left\langle \left\{1-\left(1-\sigma_{\widetilde{T}_1}{}^{4^5}\right)^{\lambda}\right\}^{\frac{1}{4^5}}, \delta_{\widetilde{T}_1}^{\lambda}\right\rangle \ominus \left\langle \left\{1-\left(1-\sigma_{\widetilde{T}_2}{}^{4^5}\right)^{\lambda}\right\}^{\frac{1}{4^5}}, \delta_{\widetilde{T}_2}^{\lambda}\right\rangle$

$$= \left\langle \left\{\frac{\left(\left\{1-\left(1-\sigma_{\widetilde{T}_1}{}^{4^5}\right)^{\lambda}\right\}^{\frac{1}{4^5}}\right)^{4^5} - \left(\left\{1-\left(1-\sigma_{\widetilde{T}_2}{}^{4^5}\right)^{\lambda}\right\}^{\frac{1}{4^5}}\right)^{4^5}}{1-\left(\left\{1-\left(1-\sigma_{\widetilde{T}_2}{}^{4^5}\right)^{\lambda}\right\}^{\frac{1}{4^5}}\right)^{4^5}}\right\}^{\frac{1}{4^5}}, \frac{\delta_{\widetilde{T}_1}^{\lambda}}{\delta_{\widetilde{T}_2}^{\lambda}}\right\rangle$$

$$= \left\langle \left\{\frac{1-\left(1-\sigma_{\widetilde{T}_1}{}^{4^5}\right)^{\lambda} - 1 + \left(1-\sigma_{\widetilde{T}_2}{}^{4^5}\right)^{\lambda}}{1-1+\left(1-\sigma_{\widetilde{T}_2}{}^{4^5}\right)^{\lambda}}\right\}^{\frac{1}{4^5}}, \frac{\delta_{\widetilde{T}_1}^{\lambda}}{\delta_{\widetilde{T}_2}^{\lambda}}\right\rangle$$

$$= \left\langle \left\{\frac{\left(1-\sigma_{\widetilde{T}_2}{}^{4^5}\right)^{\lambda} - \left(1-\sigma_{\widetilde{T}_1}{}^{4^5}\right)^{\lambda}}{\left(1-\sigma_{T_2}{}^{4^5}\right)^{\lambda}}\right\}^{\frac{1}{4^5}}, \frac{\delta_{\widetilde{T}_1}^{\lambda}}{\delta_{\widetilde{T}_2}^{\lambda}}\right\rangle = \left\langle \left\{1-\left[\frac{1-\sigma_{\widetilde{T}_1}{}^{4^5}}{1-\sigma_{T_2}{}^{4^5}}\right]^{\lambda}\right\}^{\frac{1}{4^5}}, \frac{\delta_{\widetilde{T}_1}^{\lambda}}{\delta_{\widetilde{T}_2}^{\lambda}}\right\rangle$$

$$\therefore, (\widetilde{T}_1 \ominus \widetilde{T}_2) = \widetilde{T}_1 \ominus \widetilde{T}_2.$$

Hence, (i) proved.

Similarly, we can prove for $\left(\widetilde{T}_1 \ominus \widetilde{T}_2\right)^{\lambda} = \widetilde{T}_1{}^{\lambda} \ominus \widetilde{T}_2{}^{\lambda}$, if $\sigma_{\widetilde{T}_1} \le min\left\{\sigma_{\widetilde{T}_2}, \frac{\sigma_{\widetilde{T}_2}\varphi_1}{\varphi_2}\right\}$, $\delta_{\widetilde{T}_1} \ge \delta_{\widetilde{T}_2}$.

$$\lambda_1\widetilde{T} \ominus \lambda_2\widetilde{T} = \left\langle \left\{1-\left(1-\sigma_{\widetilde{T}}{}^{4^5}\right)^{\lambda_1}\right\}^{\frac{1}{4^5}}, \delta_{\widetilde{T}}^{\lambda_1}\right\rangle \ominus \left\langle \left\{1-\left(1-\sigma_{\widetilde{T}}{}^{4^5}\right)^{\lambda_2}\right\}^{\frac{1}{4^5}}, \delta_{\widetilde{T}}^{\lambda_2}\right\rangle$$

$$= \left\langle \left\{\frac{\left(\left\{1-\left(1-\sigma_{\widetilde{T}}{}^{4^5}\right)^{\lambda_1}\right\}^{\frac{1}{4^5}}\right)^{4^5} - \left(\left\{1-\left(1-\sigma_{\widetilde{T}}{}^{4^5}\right)^{\lambda_2}\right\}^{\frac{1}{4^5}}\right)^{4^5}}{1-\left(\left\{1-\left(1-\sigma_{\widetilde{T}}{}^{4^5}\right)^{\lambda_2}\right\}^{\frac{1}{4^5}}\right)^{4^5}}\right\}^{\frac{1}{4^5}}, \frac{\delta_{\widetilde{T}}^{\lambda_1}}{\delta_{\widetilde{T}}^{\lambda_2}}\right\rangle$$

$$= \left\langle \left\{\frac{1-\left(1-\sigma_{\widetilde{T}}{}^{4^5}\right)^{\lambda_1} - 1 + \left(1-\sigma_{\widetilde{T}}{}^{4^5}\right)^{\lambda_2}}{1-1+\left(1-\sigma_{\widetilde{T}}{}^{4^5}\right)^{\lambda_2}}\right\}^{\frac{1}{4^5}}, \frac{\delta_{\widetilde{T}}^{\lambda_1}}{\delta_{\widetilde{T}}^{\lambda_2}}\right\rangle$$

Rajarajeswari and Thirunamakkani

$$= \langle \left\{ 1 - \left(1 - \sigma_{\widetilde{T}}^{\,4^5}\right)^{(\lambda_1-\lambda_2)} \right\}^{\frac{1}{4^5}}, \delta_{\widetilde{T}}^{\,(\lambda_1-\lambda_2)} \rangle = (\lambda_1 - \lambda_2)\widetilde{T}.$$

$$\therefore, \lambda_1\widetilde{T} \ominus \lambda_2\widetilde{T} = (\lambda_1 - \lambda_2)\widetilde{T}.$$

Hence, (iii) proved.

Similarly, we can prove, $\widetilde{T}^{\lambda_1} - \widetilde{T}^{\lambda_2} = \widetilde{T}^{(\lambda_1-\lambda_2)}$, if $\lambda_1 \geq \lambda_2$.

Theorem 3.2.2

Let $\widetilde{T}_1 = \langle \sigma_{\widetilde{T}_1}, \delta_{\widetilde{T}_1} \rangle$ and $\widetilde{T}_2 = \langle \sigma_{\widetilde{T}_2}, \delta_{\widetilde{T}_2} \rangle$ represents two Quin-Terranean Fuzzy numbers, then,

$(\widetilde{T}_1 \ominus \widetilde{T}_2) \boxplus \widetilde{T}_2 = \widetilde{T}_1$ if $\sigma_{\widetilde{T}_1} \geq \sigma_{\widetilde{T}_2}$, $\delta_{\widetilde{T}_1} \leq min\left\{\delta_{\widetilde{T}_2}, \frac{\delta_{\widetilde{T}_2}\varphi_1}{\varphi_2}\right\}$.

$(\widetilde{T}_1 \oslash \widetilde{T}_2) \boxtimes \widetilde{T}_2 = \widetilde{T}_1$ if $\sigma_{\widetilde{T}_1} \leq min\left\{\sigma_{\widetilde{T}_2}, \frac{\sigma_{\widetilde{T}_2}\varphi_1}{\varphi_2}\right\}$, $\delta_{\widetilde{T}_1} \geq \delta_{\widetilde{T}_2}$.

Proof:

Consider two Quin-Terranean Fuzzy numbers $\widetilde{T}_1 = \langle \sigma_{\widetilde{T}_1}, \delta_{\widetilde{T}_1} \rangle$ and $\widetilde{T}_2 = \langle \sigma_{\widetilde{T}_2}, \delta_{\widetilde{T}_2} \rangle$.

Since, $\sigma_{\widetilde{T}_1} \geq \sigma_{\widetilde{T}_2}$, $\delta_{\widetilde{T}_1} \leq min\left\{\delta_{\widetilde{T}_2}, \frac{\delta_{\widetilde{T}_2}\varphi_1}{\varphi_2}\right\}$, then

$$L.H.S = (\widetilde{T}_1 \ominus \widetilde{T}_2) \boxplus \widetilde{T}_2 = \langle \left\{\frac{\sigma_{\widetilde{T}_1}^{\,4^5} - \sigma_{\widetilde{T}_2}^{\,4^5}}{1 - \sigma_{\widetilde{T}_2}^{\,4^5}}\right\}^{\frac{1}{4^5}}, \frac{\delta_{\widetilde{T}_1}}{\delta_{\widetilde{T}_2}} \rangle \boxplus \langle \sigma_{\widetilde{T}_2}, \delta_{\widetilde{T}_2} \rangle$$

$$= \langle \left\{\left[\left(\frac{\sigma_{\widetilde{T}_1}^{\,4^5} - \sigma_{\widetilde{T}_2}^{\,4^5}}{1 - \sigma_{\widetilde{T}_2}^{\,4^5}}\right)^{\frac{1}{4^5}}\right]^{4^5} + \sigma_{\widetilde{T}_2}^{\,4^5} - \left[\left(\frac{\sigma_{\widetilde{T}_1}^{\,4^5} - \sigma_{\widetilde{T}_2}^{\,4^5}}{1 - \sigma_{\widetilde{T}_2}^{\,4^5}}\right)^{\frac{1}{4^5}}\right]^{4^5} \sigma_{\widetilde{T}_2}^{\,4^5} \right\}^{\frac{1}{4^5}}, \frac{\delta_{\widetilde{T}_1}\delta_{\widetilde{T}_2}}{\delta_{\widetilde{T}_2}} \rangle$$

$$= \langle \left\{\left(\frac{\sigma_{\widetilde{T}_1}^{\,4^5} - \sigma_{\widetilde{T}_2}^{\,4^5}}{1 - \sigma_{\widetilde{T}_2}^{\,4^5}}\right) + \sigma_{\widetilde{T}_2}^{\,4^5} - \left(\frac{\sigma_{\widetilde{T}_1}^{\,4^5} - \sigma_{\widetilde{T}_2}^{\,4^5}}{1 - \sigma_{\widetilde{T}_2}^{\,4^5}}\right)\sigma_{\widetilde{T}_2}^{\,4^5}\right\}^{\frac{1}{4^5}}, \delta_{\widetilde{T}_1} \rangle$$

$$= \langle \left\{\frac{\sigma_{\widetilde{T}_1}^{\,4^5} - \sigma_{\widetilde{T}_2}^{\,4^5} + \sigma_{\widetilde{T}_2}^{\,4^5} - \sigma_{\widetilde{T}_2}^{\,4^5}\sigma_{\widetilde{T}_2}^{\,4^5} - \sigma_{\widetilde{T}_1}^{\,4^5}\sigma_{\widetilde{T}_2}^{\,4^5} + \sigma_{\widetilde{T}_2}^{\,4^5}\sigma_{\widetilde{T}_2}^{\,4^5}}{1 - \sigma_{\widetilde{T}_2}^{\,4^5}}\right\}^{\frac{1}{4^5}}, \delta_{\widetilde{T}_1} \rangle$$

$$= \langle \left\{\frac{\sigma_{\widetilde{T}_1}^{\,4^5}\left(1 - \sigma_{\widetilde{T}_2}^{\,4^5}\right)}{\left(1 - \sigma_{\widetilde{T}_2}^{\,4^5}\right)}\right\}^{\frac{1}{4^5}}, \delta_{\widetilde{T}_1} \rangle = \langle \left\{\sigma_{\widetilde{T}_1}^{\,4^5}\right\}^{\frac{1}{4^5}}, \delta_{\widetilde{T}_1} \rangle = \langle \sigma_{\widetilde{T}_1}, \delta_{\widetilde{T}_1} \rangle = \widetilde{T}_1 = R.H.S.$$

$$\therefore, (\widetilde{T}_1 \ominus \widetilde{T}_2) \boxplus \widetilde{T}_2 = \widetilde{T}_1.$$

Hence, (i) proved.

Since, $\sigma_{\widetilde{T}_1} \leq min\left\{\sigma_{\widetilde{T}_2}, \frac{\sigma_{\widetilde{T}_2}\varphi_1}{\varphi_2}\right\}$, $\delta_{\widetilde{T}_1} \geq \delta_{\widetilde{T}_2}$, then,

$$L.H.S = (\widetilde{T}_1 \oslash \widetilde{T}_2) \boxtimes \widetilde{T}_2 = \langle \frac{\sigma_{\widetilde{T}_1}}{\sigma_{\widetilde{T}_2}}, \left\{\frac{\delta_{\widetilde{T}_1}^{\frac{5}{4}} - \delta_{\widetilde{T}_2}^{\frac{5}{4}}}{1 - \delta_{\widetilde{T}_2}^{\frac{5}{4}}}\right\}^{\frac{4}{5}} \rangle \boxtimes \langle \sigma_{\widetilde{T}_2}, \delta_{\widetilde{T}_2} \rangle$$

$$= \langle \frac{\sigma_{\widetilde{T}_1}\sigma_{\widetilde{T}_2}}{\sigma_{\widetilde{T}_2}}, \left\{\left[\frac{\delta_{\widetilde{T}_1}^{\frac{5}{4}} - \delta_{\widetilde{T}_2}^{\frac{5}{4}}}{1 - \delta_{\widetilde{T}_2}^{\frac{5}{4}}}\right]^{\frac{4}{5}}\right\}^{\frac{5}{4}} + \delta_{\widetilde{T}_2}^{\frac{5}{4}} - \left\{\left[\frac{\delta_{\widetilde{T}_1}^{\frac{5}{4}} - \delta_{\widetilde{T}_2}^{\frac{5}{4}}}{1 - \delta_{\widetilde{T}_2}^{\frac{5}{4}}}\right]^{\frac{4}{5}}\right\}^{\frac{5}{4}}\delta_{\widetilde{T}_2}^{\frac{5}{4}} \rangle$$

$$= \langle \sigma_{\widetilde{T}_1}, \left[\frac{\delta_{\widetilde{T}_1}^{\frac{5}{4}} - \delta_{\widetilde{T}_2}^{\frac{5}{4}} + \delta_{\widetilde{T}_2}^{\frac{5}{4}} - \delta_{\widetilde{T}_2}^{\frac{5}{4}}\delta_{\widetilde{T}_2}^{\frac{5}{4}} - \delta_{\widetilde{T}_1}^{\frac{5}{4}}\delta_{\widetilde{T}_2}^{\frac{5}{4}} + \delta_{\widetilde{T}_2}^{\frac{5}{4}}\delta_{\widetilde{T}_2}^{\frac{5}{4}}}{1 - \delta_{\widetilde{T}_2}^{\frac{5}{4}}}\right]^{\frac{4}{5}} \rangle$$

$$= \langle \sigma_{\widetilde{T}_1}, \left\{\frac{\delta_{\widetilde{T}_1}^{\frac{5}{4}}\left(1 - \delta_{\widetilde{T}_2}^{\frac{5}{4}}\right)}{\left(1 - \delta_{\widetilde{T}_2}^{\frac{5}{4}}\right)}\right\}^{\frac{4}{5}} \rangle = \langle \sigma_{\widetilde{T}_1}, \left\{\delta_{\widetilde{T}_1}^{\frac{5}{4}}\right\}^{\frac{4}{5}} \rangle = \langle \sigma_{\widetilde{T}_1}, \delta_{\widetilde{T}_1} \rangle = \widetilde{T}_1 = R.H.S.$$

$$\therefore, (\widetilde{T}_1 \ominus \widetilde{T}_2) \boxplus \widetilde{T}_2 = \widetilde{T}_1.$$

Hence, (ii) proved.

Rajarajeswari and Thirunamakkani

Theorem 3.2.3

Let $\widetilde{T}_1 = \langle \sigma_{\widetilde{T}_1}, \delta_{\widetilde{T}_1} \rangle$, $\widetilde{T}_2 = \langle \sigma_{\widetilde{T}_2}, \delta_{\widetilde{T}_2} \rangle$ and $\widetilde{T}_3 = \langle \sigma_{\widetilde{T}_3}, \delta_{\widetilde{T}_3} \rangle$ represents three Quin-Terranean Fuzzy numbers, then,

$(\widetilde{T}_1 \ominus \widetilde{T}_2) \ominus \widetilde{T}_3 = (\widetilde{T}_1 \ominus \widetilde{T}_3) \ominus \widetilde{T}_2$ if $\sigma_{\widetilde{T}_1} \geq max\{\sigma_{\widetilde{T}_2}, \sigma_{\widetilde{T}_3}\}$, $\delta_{\widetilde{T}_1} \leq min\left\{\delta_{\widetilde{T}_2} \delta_{\widetilde{T}_3}, \frac{\delta_{\widetilde{T}_2} \varphi_1}{\varphi_2}, \frac{\delta_{\widetilde{T}_3} \varphi_1}{\varphi_3}\right\}$,

$$\frac{\sigma_{\widetilde{T}_1}{}^{45} - \sigma_{\widetilde{T}_2}{}^{45} - \sigma_{\widetilde{T}_3}{}^{45} + \sigma_{\widetilde{T}_2}{}^{45}\sigma_{\widetilde{T}_3}{}^{45}}{\left(1 - \sigma_{\widetilde{T}_2}{}^{45}\right)\left(1 - \sigma_{\widetilde{T}_3}{}^{45}\right)} + \frac{\delta_{\widetilde{T}_1}{}^{\frac{5}{4}}}{\delta_{\widetilde{T}_2}{}^{\frac{5}{4}}\delta_{\widetilde{T}_3}{}^{\frac{5}{4}}} \leq 1.$$

$(\widetilde{T}_1 \oslash \widetilde{T}_2) \oslash \widetilde{T}_3 = (\widetilde{T}_1 \oslash \widetilde{T}_3) \oslash \widetilde{T}_2$ if $\delta_{\widetilde{T}_1} \geq max\{\delta_{\widetilde{T}_2}, \delta_{\widetilde{T}_3}\}$, $\sigma_{\widetilde{T}_1} \leq min\left\{\sigma_{\widetilde{T}_2} \sigma_{\widetilde{T}_3}, \frac{\sigma_{\widetilde{T}_2} \varphi_1}{\varphi_2}, \frac{\sigma_{\widetilde{T}_3} \varphi_1}{\varphi_3}\right\}$,

$$\frac{\delta_{\widetilde{T}_1}{}^{\frac{5}{4}} - \delta_{\widetilde{T}_2}{}^{\frac{5}{4}} - \delta_{\widetilde{T}_3}{}^{\frac{5}{4}} + \delta_{\widetilde{T}_2}{}^{\frac{5}{4}}\delta_{\widetilde{T}_3}{}^{\frac{5}{4}}}{\left(1 - \delta_{\widetilde{T}_2}{}^{\frac{5}{4}}\right)\left(1 - \delta_{\widetilde{T}_3}{}^{\frac{5}{4}}\right)} + \frac{\sigma_{\widetilde{T}_1}{}^{45}}{\sigma_{\widetilde{T}_2}{}^{45}\sigma_{\widetilde{T}_3}{}^{45}} \leq 1.$$

Proof:

Consider three Quin-Terranean Fuzzy numbers $\widetilde{T}_1 = \langle \sigma_{\widetilde{T}_1}, \delta_{\widetilde{T}_1} \rangle$, $\widetilde{T}_2 = \langle \sigma_{\widetilde{T}_2}, \delta_{\widetilde{T}_2} \rangle$ and $\widetilde{T}_3 = \langle \sigma_{\widetilde{T}_3}, \delta_{\widetilde{T}_3} \rangle$.

Since, $\sigma_{\widetilde{T}_1} \geq max\{\sigma_{\widetilde{T}_2}, \sigma_{\widetilde{T}_3}\}$, $\delta_{\widetilde{T}_1} \leq min\left\{\delta_{\widetilde{T}_2} \delta_{\widetilde{T}_3}, \frac{\delta_{\widetilde{T}_2} \varphi_1}{\varphi_2}, \frac{\delta_{\widetilde{T}_3} \varphi_1}{\varphi_3}\right\}$,

$$\frac{\sigma_{\widetilde{T}_1}{}^{45} - \sigma_{\widetilde{T}_2}{}^{45} - \sigma_{\widetilde{T}_3}{}^{45} + \sigma_{\widetilde{T}_2}{}^{45}\sigma_{\widetilde{T}_3}{}^{45}}{\left(1 - \sigma_{\widetilde{T}_2}{}^{45}\right)\left(1 - \sigma_{\widetilde{T}_3}{}^{45}\right)} + \frac{\delta_{\widetilde{T}_1}{}^{\frac{5}{4}}}{\delta_{\widetilde{T}_2}{}^{\frac{5}{4}}\delta_{\widetilde{T}_3}{}^{\frac{5}{4}}} \leq 1.$$

L.H.S $= (\widetilde{T}_1 \ominus \widetilde{T}_2) \ominus \widetilde{T}_3 = \left\langle \left\{\frac{\sigma_{\widetilde{T}_1}{}^{45} - \sigma_{\widetilde{T}_2}{}^{45}}{1 - \sigma_{\widetilde{T}_2}{}^{45}}\right\}^{\frac{1}{45}}, \frac{\delta_{\widetilde{T}_1}}{\delta_{\widetilde{T}_2}} \right\rangle \ominus \langle \sigma_{\widetilde{T}_3}, \delta_{\widetilde{T}_3} \rangle$

$= \left\langle \left\{\frac{\left[\left(\frac{\sigma_{\widetilde{T}_1}{}^{45} - \sigma_{\widetilde{T}_2}{}^{45}}{1 - \sigma_{\widetilde{T}_2}{}^{45}}\right)^{\frac{1}{45}}\right]^{45} - \sigma_{\widetilde{T}_3}{}^{45}}{\left(1 - \sigma_{\widetilde{T}_3}{}^{45}\right)}\right\}^{\frac{1}{45}}, \frac{\delta_{\widetilde{T}_1}}{\delta_{\widetilde{T}_2}\delta_{\widetilde{T}_3}} \right\rangle$

$= \left\langle \left\{\frac{\sigma_{\widetilde{T}_1}{}^{45} - \sigma_{\widetilde{T}_2}{}^{45} - \sigma_{\widetilde{T}_3}{}^{45} + \sigma_{\widetilde{T}_2}{}^{45}\sigma_{\widetilde{T}_3}{}^{45}}{\left(1 - \sigma_{\widetilde{T}_2}{}^{45}\right)\left(1 - \sigma_{\widetilde{T}_3}{}^{45}\right)}\right\}^{\frac{1}{45}}, \frac{\delta_{\widetilde{T}_1}}{\delta_{\widetilde{T}_2}\delta_{\widetilde{T}_3}} \right\rangle$

and R.H.S $= (\widetilde{T}_1 \ominus \widetilde{T}_3) \ominus \widetilde{T}_2 = \left\langle \left\{\frac{\sigma_{\widetilde{T}_1}{}^{45} - \sigma_{\widetilde{T}_3}{}^{45}}{1 - \sigma_{\widetilde{T}_3}{}^{45}}\right\}^{\frac{1}{45}}, \frac{\delta_{\widetilde{T}_1}}{\delta_{\widetilde{T}_3}} \right\rangle \ominus \langle \sigma_{\widetilde{T}_2}, \delta_{\widetilde{T}_2} \rangle$

$= \left\langle \left\{\frac{\left[\left(\frac{\sigma_{\widetilde{T}_1}{}^{45} - \sigma_{\widetilde{T}_3}{}^{45}}{1 - \sigma_{\widetilde{T}_3}{}^{45}}\right)^{\frac{1}{45}}\right]^{45} - \sigma_{\widetilde{T}_2}{}^{45}}{\left(1 - \sigma_{\widetilde{T}_2}{}^{45}\right)}\right\}^{\frac{1}{45}}, \frac{\delta_{\widetilde{T}_1}}{\delta_{\widetilde{T}_2}\delta_{\widetilde{T}_3}} \right\rangle$

$= \left\langle \left\{\frac{\sigma_{\widetilde{T}_1}{}^{45} - \sigma_{\widetilde{T}_3}{}^{45} - \sigma_{\widetilde{T}_2}{}^{45} + \sigma_{\widetilde{T}_2}{}^{45}\sigma_{\widetilde{T}_3}{}^{45}}{\left(1 - \sigma_{\widetilde{T}_2}{}^{45}\right)\left(1 - \sigma_{\widetilde{T}_3}{}^{45}\right)}\right\}^{\frac{1}{45}}, \frac{\delta_{\widetilde{T}_1}}{\delta_{\widetilde{T}_2}\delta_{\widetilde{T}_3}} \right\rangle$ = L.H.S.

$\therefore (\widetilde{T}_1 \ominus \widetilde{T}_2) \ominus \widetilde{T}_3 = (\widetilde{T}_1 \ominus \widetilde{T}_3) \ominus \widetilde{T}_2$.

Hence, (i) proved.

Since, $\delta_{\widetilde{T}_1} \geq max\{\delta_{\widetilde{T}_2}, \delta_{\widetilde{T}_3}\}$, $\sigma_{\widetilde{T}_1} \leq min\left\{\sigma_{\widetilde{T}_2} \sigma_{\widetilde{T}_3}, \frac{\sigma_{\widetilde{T}_2} \varphi_1}{\varphi_2}, \frac{\sigma_{\widetilde{T}_3} \varphi_1}{\varphi_3}\right\}$,

$$\frac{\delta_{\widetilde{T}_1}{}^{\frac{5}{4}} - \delta_{\widetilde{T}_2}{}^{\frac{5}{4}} - \delta_{\widetilde{T}_3}{}^{\frac{5}{4}} + \delta_{\widetilde{T}_2}{}^{\frac{5}{4}}\delta_{\widetilde{T}_3}{}^{\frac{5}{4}}}{\left(1 - \delta_{\widetilde{T}_2}{}^{\frac{5}{4}}\right)\left(1 - \delta_{\widetilde{T}_3}{}^{\frac{5}{4}}\right)} + \frac{\sigma_{\widetilde{T}_1}{}^{45}}{\sigma_{\widetilde{T}_2}{}^{45}\sigma_{\widetilde{T}_3}{}^{45}} \leq 1.$$

L.H.S $= (\widetilde{T}_1 \oslash \widetilde{T}_2) \oslash \widetilde{T}_3 = \left\langle \frac{\sigma_{\widetilde{T}_1}}{\sigma_{\widetilde{T}_2}}, \left\{\frac{\delta_{\widetilde{T}_1}{}^{\frac{5}{4}} - \delta_{\widetilde{T}_2}{}^{\frac{5}{4}}}{1 - \delta_{\widetilde{T}_2}{}^{\frac{5}{4}}}\right\}^{\frac{4}{5}} \right\rangle \oslash \langle \sigma_{\widetilde{T}_3}, \delta_{\widetilde{T}_3} \rangle$

$$= \langle \frac{\sigma_{\widetilde{T}_1}}{\sigma_{\widetilde{T}_2}\sigma_{\widetilde{T}_3}}, \left\{ \frac{\left[\left(\frac{\delta_{\widetilde{T}_1}^{\frac{5}{4}} - \delta_{\widetilde{T}_2}^{\frac{5}{4}}}{1 - \delta_{\widetilde{T}_2}^{\frac{5}{4}}} \right)^{\frac{4}{5}} \right]^{\frac{5}{4}} - \delta_{\widetilde{T}_3}^{\frac{5}{4}}}{\left(1 - \delta_{\widetilde{T}_3}^{\frac{5}{4}} \right)} \right\}^{\frac{4}{5}} \rangle$$

$$= \langle \frac{\sigma_{\widetilde{T}_1}}{\sigma_{\widetilde{T}_2}\sigma_{\widetilde{T}_3}}, \left\{ \frac{\delta_{\widetilde{T}_1}^{\frac{5}{4}} - \delta_{\widetilde{T}_2}^{\frac{5}{4}} - \delta_{\widetilde{T}_3}^{\frac{5}{4}} + \delta_{\widetilde{T}_2}^{\frac{5}{4}}\delta_{\widetilde{T}_3}^{\frac{5}{4}}}{\left(1 - \delta_{\widetilde{T}_2}^{\frac{5}{4}} \right)\left(1 - \delta_{\widetilde{T}_3}^{\frac{5}{4}} \right)} \right\}^{\frac{4}{5}} \rangle$$

and R.H.S $= \left(\widetilde{T}_1 \oslash \widetilde{T}_3 \right) \oslash \widetilde{T}_2 = \langle \frac{\sigma_{\widetilde{T}_1}}{\sigma_{\widetilde{T}_3}}, \left\{ \frac{\delta_{\widetilde{T}_1}^{\frac{5}{4}} - \delta_{\widetilde{T}_3}^{\frac{5}{4}}}{1 - \delta_{\widetilde{T}_3}^{\frac{5}{4}}} \right\}^{\frac{4}{5}} \rangle \oslash \langle \sigma_{\widetilde{T}_2}, \delta_{\widetilde{T}_2} \rangle$

$$= \langle \frac{\sigma_{\widetilde{T}_1}}{\sigma_{\widetilde{T}_2}\sigma_{\widetilde{T}_3}}, \left\{ \frac{\left[\left(\frac{\delta_{\widetilde{T}_1}^{\frac{5}{4}} - \delta_{\widetilde{T}_3}^{\frac{5}{4}}}{1 - \delta_{\widetilde{T}_3}^{\frac{5}{4}}} \right)^{\frac{4}{5}} \right]^{\frac{5}{4}} - \delta_{\widetilde{T}_2}^{\frac{5}{4}}}{\left(1 - \delta_{\widetilde{T}_2}^{\frac{5}{4}} \right)} \right\}^{\frac{4}{5}} \rangle$$

$$= \langle \frac{\sigma_{\widetilde{T}_1}}{\sigma_{\widetilde{T}_2}\sigma_{\widetilde{T}_3}}, \left\{ \frac{\delta_{\widetilde{T}_1}^{\frac{5}{4}} - \delta_{\widetilde{T}_3}^{\frac{5}{4}} - \delta_{\widetilde{T}_2}^{\frac{5}{4}} + \delta_{\widetilde{T}_2}^{\frac{5}{4}}\delta_{\widetilde{T}_3}^{\frac{5}{4}}}{\left(1 - \delta_{\widetilde{T}_2}^{\frac{5}{4}} \right)\left(1 - \delta_{\widetilde{T}_3}^{\frac{5}{4}} \right)} \right\}^{\frac{4}{5}} \rangle = \text{L.H.S.}$$

$\therefore \left(\widetilde{T}_1 \oslash \widetilde{T}_2 \right) \oslash \widetilde{T}_3 = \left(\widetilde{T}_1 \oslash \widetilde{T}_3 \right) \oslash \widetilde{T}_2$.

Hence, (ii) proved.

CONCLUSION

In this paper, we have defined some algebraic model operators such as $\ominus$ and $\oslash$ on Quin – Terranean Fuzzy numbers and Quin-Terranean Arithmetic mean operation. Based on these operations we have studied some properties of Quin – Terranean Fuzzy numbers. We have proved that the model operators satisfy scalar multiplication and exponentiation property. We observe that these model operators together with the fundamental operations of union, intersection and model operations such as $\boxplus$ and $\boxtimes$ on Quin – Terranean Fuzzy numbers are also satisfies several properties. In future, these special algebraic operations on Quin – Terranean Fuzzy Numbers can be applied in various research areas such as medicine, agriculture, transportation problem and decision making, etc.

REFERENCES

1. Krassimir T. Atanassov. Intuitionistic Fuzzy Sets, Fuzzy Sets and Systems; 1986; 20(1):87-96.
2. Krassimir T. Atanassov, Riecan B. On two operations over Intuitionistic fuzzy set, Journal of Applied Mathematics, Statistics and Informatics; 2006; 2(2):145-148.
3. Chandrasekaran S and Tamilmani E. Arithmetic Operations of Fuzzy Numbers using α-Cut Method, International Journal of Innovative Science, Engineering and Technology; 2015; 2(10): 299-315.
4. Chen T Y. Remarks on the subtraction and division operations over Intuitionistic fuzzy sets and interval – valued fuzzy sets, International Journal of Fuzzy Systems; 2007; 9(3):169-172.
5. Chuan-qiang Fan, Wei-he Xie and Feng Liu. (α,β) Pythagorean Fuzzy Numbers Descriptor Systems, Fuzzy Systems; 2020; 20(1):23-35.

6. Jayasri P and Elavarasi P. Fuzzy Set Theory and Arithmetic operations on Fuzzy Numbers, International Journal of Scientific Research and Management; 2018; 6(2):14-16.
7. Liao H and Xu Z. Subtraction and division operations over hesitant fuzzy sets, Journal of Intelligent and Fuzzy Systems; 2014; 27:65-72.
8. Md. Yasin Ali, Abeda Sultana and Khodadad A F M. Comparison of Fuzzy Multiplication Operation on Triangular Fuzzy Number, IOSR Journal of Mathematics; 2016; 12(4):35-41.
9. Rajarajeswari P, Sahaya Sudha A and Karthika R. A New Operation on Hexagonal Fuzzy Number, International Journal of Fuzzy Logic Systems; 2013; 3(3):15-26.
10. Rajarajeswari P, Thirunamakkani T. Application of Quin-Terranean Fuzzy Set in Transportation Problem under Fuzzy Environment, Journal of Asiatic Society of Mumbai; 2023; XCVI(12):171-181.
11. Quin – Terranean Fuzzy set. Bulletin of Calcutta Mathematical Society. *Accepted.*
12. Algebraic Operations on Quin – Terranean Fuzzy Number. Indian Journal of Natural Sciences. *Communicated.*
13. Taleshian A and Rezvani S. Multiplication Operation on Trapezoidal Fuzzy Numbers, Journal of Physical Sciences; 2011; 15:17-26.
14. Tapan Senapati, Ronald R. Yager. Fermatean fuzzy sets, Journal of Ambient Intelligence and Humanized Computing; 2019; 11(2):663-674.
15. Tapan Senapati, Ronald R. Yager. Some New Operations over Fermatean Fuzzy Numbers and Application of Fermatean fuzzy WPM in Multi Criteria Decision Making, Informatica; 2019; 30(2):391-412.
16. Yager R R. Pythagorean membership Grades in Multi criteria Decision Making, in IEEE Transaction on Fuzzy Systems; 2014; 22(4):958-965.
17. Zadeh L A. Fuzzy Sets, Information and Control; 1965; 8:338-353.

RESEARCH ARTICLE

Dominating Function in Fractional Directed Graph

M. Meenakshi* and V. Pankajam

Department of Mathematics, Sri GVG Visalakshi college for Women, Udumalpet-642128, Tiruppur, Tamil Nadu, India.

*Address for Correspondence
M. Meenakshi
Department of Mathematics,
Sri GVG Visalakshi College for Women,
Udumalpet-642128, Tiruppur,
Tamil Nadu, India.

ABSTRACT

In this paper the concept of a dominating function on a fractional directed graph G has been introduced. The fractional parameters like domination number and upper domination number of a fractional directed graph G are determined. Linear Program solver software is used to find domination number and upper domination number of fractional directed graph with fuzzy & Intuitionistic fuzzy environment.

Keywords: Digraph, domination number, fractional graph and fractional digraph

INTRODUCTION

Let G =(V,E) be a directed graph or digraph, where V is the set of vertices and VxV is a set of edges. A vertex u is said to be dominates vertex v (or vertex v is dominated by vertex u) if edge (u,v) is in G. The edge (u,v) is shown graphically as u→v. Fuzzy digraph dominance is about controlling the vertices of a graph with fuzzy sets rather than binary (0,1) values. A fuzzy digraph is a graph in which the edges are marked with fuzzy values that indicate the degree of connectivity between the vertices.

Let $f:V\to\{0,1\}$ be a function that assigns an element of the set $\{0,1\}$ to each node of the digraph. f is said to be dominant if $f[v]\geq1$ for all $v\in V$. f is called as minimal dominant function if there is no dominant function $g: V\to\{0,1\}$, $f\neq g$ with $g(v) \leq f(v)$ for all $v\in V$. Then the number of dominances and the upper number of dominances of the digraph G can be defined as $\gamma(G)=$ min $\{w(f)/$ f is the dominant function of G$\}$ and $\Gamma(G)=$max$\{w(f)/$ f is the minimal dominant function on G$\}$

63326

Fractional graph theory concerns the generalization of the concept of integer graph theory, a theory that assumes fractional values as weights in the interval [0,1]. The digraph G=(V,E) and f: V→[0,1] is a function whose weights are assigned to each vertex of the digraph in the interval [0,1]. f is said to be a dominant function (DF) if f(N[v])=$\sum_{u \in N[v]} f(u) \geq 1$ for all v∈V. f is a minimal dominant function (MDF) if there is no dominant function f≠g such that g(v) ≤ f(v) for all v∈V. Correspondingly, f is MDF if for every v with f(v) > 0 there exists a vertex w∈N[v] such that f(N[w]) or $\sum_{u \in N[w]} f(u)$ = 1. So one can define the fractional number of dominances and the upper number of dominances G as γf(G)= min{|f| :f is MDF G} and Γf(G)= max {|f| : f is MDF G} in [4].

To determine the number of dominances and the upper number of dominances using the LIPS algorithm[6].This is the concept of a digraph convert it to a fractional version, which is an integer program formula, and then convert it to linear programming as an optimization problem that is Minimization problem or Maximization Problem . We find an effective solution. This solution is the dominance number & higher dominance number. In this article you will find the number of dominance & the largest number of dominances in the situation of an intuitionistic fuzzy digraph [5].

In point 2 the definition of the dominance function ,the number of dominances (γ) and the upper number of dominances (Γ) of the digraph is explained with a suitable example. In Section 3, find the dominance and upper dominance number in the intuitionistic fuzzy digraph.Also, use the LIPS algorithm to calculate the number of dominance & the upper dominance number by the fractional digraph and the intuitionistic fuzzy digraph.

Domination Function on fractional Digraph

Fuzzy digraph:
A fuzzy digraph G$_D$=(V ,σ_D,μ_D) is a pair of function σ_D :V→ [0,1] and μ_D: VxV → [0,1], where u,v ϵ V and μ_D (u,v) ≤ $\sigma_D(u) \wedge \sigma_D(v)$

Fractional Digraph:
A fractional digraph or fuzzy digraph is a graph which means that weights are represented in fractional values.

Domination Function on a fuzzy or Fractional Digraph:
Let G$_D$=(V ,σ_D ,μ_D) be a fuzzy digraph. An edge e=$\overrightarrow{uv}$ of a fuzzy digraph is called an effective arc if $\mu_D(u,v)$=$\sigma_D(u) \wedge \sigma_D(v)$ for all u,v∈ V. Then the vertex $\sigma_D(u)$ dominates $\sigma_D(v)$ in G$_D$. The fuzzy cardinality of a minimum dominating set is called the domination number of G$_D$ and is denoted by $\gamma(G_D)$, that is $\gamma(G_D)$ = min$\sum_{x \in s} \sigma_D(u)$. The open neighborhood N_{G_D}(v) and the closed neighbourhood N[v] of v are defined byN_{G_D}(v)= { u∈V;$\mu_D(u,v)$=$\sigma_D(u) \wedge \sigma_D(v)$ } and N_{G_D}[v] = N_{G_D}(v) ∪ {v}. Sinceσ_D: V→{0,1} be a function which assigns to each vertex of a graph an element of the set {0,1}. For a vertex v∈V, let σ_D(N[V]) equal the sum of values of σ_D (v) for every vertex u∈N_{G_D} [v]. Given a function σ_D is called the minimal dominating function (MDF),if there does not exist a dominating function τ_D: V → {0,1},$\sigma_D \neq \tau_D$, for whichσ_D (v)≤τ_D (v) for every v∈V. Then σ_D is MDF if for every v such that σ_D (v)>0, there exist a vertex u∈$N[V]$ Then the domination numberγ_f, and upper domination numberΓ_f in a fuzzy environment are defined as the following Linear Programming Problem

$\gamma_f(G_D) = min \sum_{i=1}^{n} \sigma_D(v_i)$, subject to N.$X_f \geq \overrightarrow{1_n}$ with $\sigma_D(v_i)$ ϵ{0,1} and

$\Gamma_f(G_D)$=$max \sum_{i=1}^{n} f(v_i)$, subject to N.$X_f \geq \overrightarrow{1_n}$ with $\sigma_D(v_i)$ ϵ{0,1}

where N is the closed neighborhood matrix and X_f= [σ_D (v₁), …σ_D (vₙ)]ᵗ be the column vector.

Example

Let σ_D: V→{0,1} be a function of a graph G_D $=(V, \sigma_D, \mu_D)$ in figure 2.1 with vertex V={$v_1, v_2, v_3, v_4,$ },E={$v_1 v_2, v_2 v_3, v_3 v_4, v_4 v_1$}

Here$N_{G_D}[v_1] = \{v_1, v_2, v_4\}, N_{G_D}[v_2] = \{v_1, v_2 v_3\}, N_{G_D}[v_3] = \{v_2, v_3 v_4\}, N_{G_D}[v_4] = \{v_3, v_{4,} v_1\}$,f is dominating function of G_D.

$\sigma_D(v_1) = 1/2$,$\sigma_D(v_2) = 1/2$, $\sigma_D(v_3) = 1/2$, $\sigma_D(v_4) = 1/2$

$\mu_D(v_1 v_2)$=1/2,$\mu_D(v_2 v_3)$=1/2,$\mu_D(v_3 v_4)$=1/2,$\mu_D(v_4 v_1)$=1/2,

Now $\sigma_D(N_{G_D}[v_1])$= $\sum_{v_{1 \epsilon N_{G_D}}[v_1]} \sigma_D(v_1)$= $\sigma_D(v_1)$+$\sigma_D(v_2)$ + $\sigma_D(v_3)$.

Find the Domination Number $\gamma_f(G_D)$ in fig 2.1 by solving the following linear Programming Problem Which is formulated using G_D.

Minimize z =$\sigma_D(v_1)$ +$\sigma_D(v_2)$ +$\sigma_D(v_3)$ +$\sigma_D(v_4)$

Subject to $\sigma_D(v_1)$+$\sigma_D(v_2)$ + $\sigma_D(4)$ ≥1,$\sigma_D(v_1)$+$\sigma_D(v_2)$ + $\sigma_D(v_3)$ ≥1,$\sigma_D(v_2)$+$\sigma_D(v_3)$ + $\sigma_D(v_4)$ ≥1, $\sigma_D(v_1)$+$\sigma_D(v_3)$ + $\sigma_D(v_4)$ ≥1 and $0 \le \sigma_D(v_i) \le 1$ for all V(G_D)

Solution: Minimize z =$\sigma_D(v_1)$ +$\sigma_D(v_2)$ +$\sigma_D(v_3)$ +$\sigma_D(v_4)$

$$\begin{pmatrix} 1 & 1 & 0 & 1 \\ 1 & 1 & 1 & 0 \\ 0 & 1 & 1 & 1 \\ 1 & 0 & 1 & 1 \end{pmatrix} \begin{pmatrix} \sigma_D(v_1) \\ \sigma_D(v_2) \\ \sigma_D(v_3) \\ \sigma_D(v_4) \end{pmatrix} \ge \begin{pmatrix} 1 \\ 1 \\ 1 \\ 1 \end{pmatrix}$$ and$\sigma_D(v_i) \epsilon$ [0,1] for all $v_i \epsilon$ V(G) where

N=$\begin{pmatrix} 1 & 1 & 0 & 1 \\ 1 & 1 & 1 & 0 \\ 0 & 1 & 1 & 1 \\ 1 & 0 & 1 & 1 \end{pmatrix}$, X_{fD}=$\begin{pmatrix} \sigma_D(v_1) \\ \sigma_D(v_2) \\ \sigma_D(v_3) \\ \sigma_D(v_4) \end{pmatrix}$ $\overrightarrow{1_n}$ = $\begin{pmatrix} 1 \\ 1 \\ 1 \\ 1 \end{pmatrix}$ be the coloumn vector with respect to the constraint part of L.P.P.

Then the optimal solution of the above L.P.P is Minimize Z= 4/3 where $\sigma_D(v_1)$=1/3,$\sigma_D(v_2)$=1/3 $\sigma_D(v_3)$ =1/3 ,$\sigma_D(v_4)$=1/3.

Hence the domination number $\gamma_f(G_D)$= 4/3.

Find the upper Domination Number $\Gamma_f(G_D)$ in fig 2.1 by solving the following linear Programming Problem Which is formulated using G_D.

Maximize z =$\sigma_D(v_1)$ +$\sigma_D(v_2)$ +$\sigma_D(v_3)$ +$\sigma_D(v_4)$

Subject to $\sigma_D(v_1)$+$\sigma_D(v_2)$ + $\sigma_D(4)$ ≤1,$\sigma_D(v_1)$+$\sigma_D(v_2)$ + $\sigma_D(v_3)$ ≤1,$\sigma_D(v_2)$+$\sigma_D(v_3)$ + $\sigma_D(v_4)$ ≤1, $\sigma_D(v_1)$+$\sigma_D(v_3)$ + $\sigma_D(v_4)$ ≤1 and $0 \le \sigma_D(v_i) \le 1$ for all V(G_D)

Solution: Maximize z =$\sigma_D(v_1)$ +$\sigma_D(v_2)$ +$\sigma_D(v_3)$ +$\sigma_D(v_4)$

$$\begin{pmatrix} 1 & 1 & 0 & 1 \\ 1 & 1 & 1 & 0 \\ 0 & 1 & 1 & 1 \\ 1 & 0 & 1 & 1 \end{pmatrix} \begin{pmatrix} \sigma_D(v_1) \\ \sigma_D(v_2) \\ \sigma_D(v_3) \\ \sigma_D(v_4) \end{pmatrix} \le \begin{pmatrix} 1 \\ 1 \\ 1 \\ 1 \end{pmatrix}$$ and$\sigma_D(v_i) \epsilon$ [0,1] for all $v_i \epsilon$ V(G) where

N=$\begin{pmatrix} 1 & 1 & 0 & 1 \\ 1 & 1 & 1 & 0 \\ 0 & 1 & 1 & 1 \\ 1 & 0 & 1 & 1 \end{pmatrix}$, X_{fD}=$\begin{pmatrix} \sigma_D(v_1) \\ \sigma_D(v_2) \\ \sigma_D(v_3) \\ \sigma_D(v_4) \end{pmatrix}$ $\overrightarrow{1_n}$ = $\begin{pmatrix} 1 \\ 1 \\ 1 \\ 1 \end{pmatrix}$ be the coloumn vector with respect to the constraint part of L.P.P.

Then the optimal solution of the above L.P.P is Maximize Z= 4/3 where $\sigma_D(v_1)$=1/3,$\sigma_D(v_2)$=1/3 $\sigma_D(v_3)$ =1/3 ,$\sigma_D(v_4)$=1/3.

Hence the domination number$\Gamma_f(G_D)$= 4/3.

Domination Function on an Intuitionistic fuzzy Digraph

Intuitionistic fuzzy set

The intuitionistic fuzzy set (IFS) in universe X is an object of the form A={ x,μ_A(x), $\gamma_A(x)$/xϵX}, where μ_A(X) ϵ [0,1] is the degree of the membership of X in A, , γ_A (x) ϵ [0,1] is called a degree of Non-membership function of x in A, and μ_A , γ_A satisfy the condition : for all xϵ X, μ_A(X) + γ_A (x) $\leq$ 1.

Intuitionistic Fuzzy-Digraph

Theintuitionisticfuzzy-graph with set V is defined asthepairG_D= (A:B), where the functionμ_A:V$\rightarrow$ [0,1] and γ_A:V$\rightarrow$ [0,1] is the degree of membership and non-membership of the element x ϵ V such that 0 $\leq \mu_A$(X) + γ_A (x) $\leq$1 for each x ϵ V and the functionsμ_B:E$\subseteq$ VXV$\rightarrow$ [0,1] andγ_B: E $\subseteq$VXV$\rightarrow$ [0,1] are givenμ_B(x,y) $\leq$ min(μ_A(X),μ_A(y))and $\gamma_B(x,y) \geq$ max (γ_A(X), γ_A(Y)) such that 0$\leq \mu_B$(x,y) + $\gamma_B(x,y)$ $\leq$ 1for every (x,y) ϵ E. Let A be the intuitionistic fuzzy set of vertices V, let B be the intuitionistic fuzzy set ofedgesG_D.

Dominant function on an intuitionistic fuzzy digraph

 Let G_D=(V_D, E_D,σ,μ) be an intuitionistic fuzzy digraph (IFG_D),where σ=(σ_1, σ_2), μ = (μ_1, μ_2). The neighborhood of any vertex v is defined as N(v)=(N_{σ_1}, N_{σ_2}) where N_{σ_1}(v)={WϵV; μ_1(u,v)=σ_1(u) $\wedge$ σ_1(v)} N_{σ_2}(v)={WϵV:μ_1(u,v)= σ_2(u)$\vee\sigma_2$(v) } and N[v] = N(v)U {v} will bea closed neighborhood v. The degree of neighborhood of a vertex and the degree of neighborhood of a closed vertex are defined as asd_N(v) = ($d_{N_{\sigma_1}}$(v), $d_{N_{\sigma_2}}$(v)) and d_N[v] = ($d_{N_{\sigma_1}}$[v], $d_{N_{\sigma_2}}$[v]) where d_N[v] = ($d_{N_{\sigma_1}}$[v], $d_{N_{\sigma_2}}$[v]) where $d_{N_{\sigma_1}}$(v)= $\sum_{u\epsilon N(v)}\sigma_1$(u) , $d_{N_{\sigma_2}}$(v)= $\sum_{u\epsilon N(v)}\sigma_2$(u) , $d_{N_{\sigma_1}}$[v] = $\sum_{u\epsilon N(v)}\sigma_1$(u) + σ_1(v) and $d_{N_{\sigma_2}}$[v]= $\sum_{u\epsilon N(v)}\sigma_2$(u)+ σ_2(v). Becauseσ_1: V $\rightarrow$ [0,1] is a function assigns the degree of membership of each node of the graph to the element u ϵN_{σ_1}[v]. Then $\sigma_1$is called the dominant function$\sigma_1$if $d_{N_{\sigma_1}}$[v] = $\sum_{u\epsilon N_{\sigma_1}[v]}\sigma_1$(u) $\geq$ 1 for every v ϵ V where $\sum_{u\epsilon N_{\sigma_1}[v]}\sigma_1$(u) = $\sum_{u\epsilon N(v)}\sigma_1$(u) + σ_1(v). Similarly σ_2: V $\rightarrow$ [0,1] is a function assigns the degree to which each node belongs to an element of the set [0,1]. For vertex v ϵ V, let $d_{N_{\sigma_2}}$[v] equal the sum of the values ofσ_2(v) for each vertex uϵN_{σ_2}(v). Then σ_2 is called the σ_2 $-$dominant function if $d_{N_{\sigma_2}}$[v]= $\sum_{u\epsilon N\sigma 2[v]}\sigma_2$(u)<1 for every v ϵ V, where$\sum_{u\epsilon N\sigma 2[v]}\sigma_2$(u) = $\sum_{u\epsilon N(v)}\sigma_2$(u) + σ_2(v). A function: V $\rightarrow$ [0,1] is called dominant function $G_D$if it is a σ_1-dominant and σ_2-dominant function with0 $\leq \sigma_1$(u)+ σ_2(v) $\leq$ 1 for each v ϵ V where σ_1(v) $\geq$ 0 , σ_2(v) < 1. for each v ϵ V where σ_1(v) $\geq$ 0 , σ_2(v) < 1.Lowestdominant function (MDF) if $\sum_{u\epsilon N_{\sigma_1}[v]}\sigma_1$(u) =1, $\sum_{u\epsilon N\sigma 2[v]}\sigma_2$(u)<1 for any u$\epsilon$ N[v] , for every v ϵV , where σ_2(v) $\neq$ 1. Then the dominance number $\gamma_{if}$and the upper dominance number Γ_{if}in the intuitionistic fuzzy environment are defined as

γ_{if}(G_D) = ($\gamma_{if_{\sigma_1}}$(G_D) ,$\gamma_{if_{\sigma_2}}$(G_D)) and Γ_{if}(G_D) = ($\Gamma_{if\sigma_1}$(G_D), $\Gamma_{if\sigma_2}$(G_D)) where

$\gamma_{if_{\sigma_1}}$ = min $\sum_{i=1}^n\sigma_1$(v_i) , subject to N. $X_{if} \geq \vec{1}$ with σ_1(v_i)ϵ [0,1] $\forall v_i\epsilon$ V(G_D)

$\gamma_{if_{\sigma_2}}$ = min$\sum_{i=1}^n\sigma_2$(v_i) , subject to N. $X_{if} \geq \vec{1}$ with σ_2(v_i)ϵ [0,1] $\forall v_i\epsilon$ V(G_D)

$\Gamma_{if\sigma_1}$ = max$\sum_{i=1}^n\sigma_1$(v_i) , subject to N. $X_{if} \leq \vec{1}$ with σ_1(v_i)ϵ [0,1] $\forall v_i\epsilon$ V(G_D)

$\Gamma_{if\sigma_2}$ = max$\sum_{i=1}^n\sigma_2$(v_i) , subject to N. $X_{if} \leq \vec{1}$ with σ_2(v_i)ϵ [0,1] $\forall v_i\epsilon$ V(G_D)

and N is closed neighbourhood of $\sigma_1 -$ dominating and $\sigma_2 -$ dominating function value of the matrix, X_{if} be the $\sigma_1 -$ dominating and $\sigma_2 -$ dominating function value of the coloumn vector $[\sigma_1 (v_1), \sigma_1(v_2), \ldots \ldots \sigma_1(v_n)]^t$ and $[\sigma_2 (v_1), \sigma_2(v_2), \ldots \ldots \sigma_2(v_n)]^t$.

Example

σ_1 : V $\rightarrow$ [0,1] and σ_2 : V $\rightarrow$ [0,1] be a function of a graph G_D = <V,E,σ, μ > in the following figure with σ_1 (v_1) = $\frac{1}{4}$, σ_2 (v_1) =$\frac{1}{3}$, σ_1(v_2)= $\frac{1}{2}$, σ_2 (v_2) = $\frac{2}{5}$, σ_1(v_3)= $\frac{1}{3}$, σ_2 (v_3) = $\frac{1}{5}$, σ_1(v_4) = $\frac{3}{4}$,σ_2(v_3) =$\frac{1}{5}$, μ_1 (v_1) = $\frac{1}{4}$, μ_2 (v_1) = $\frac{1}{3}$, μ_1 (v_2) = $\frac{1}{2}$, μ_2 (v_2) = $\frac{2}{5}$, μ_1 (v_3) = $\frac{1}{3}$, μ_2 (v_3) = $\frac{1}{5}$, μ_1 (v_4) = $\frac{1}{3}$, μ_2 (v_3) =$\frac{1}{5}$,

Here $N[v_1] = \{v_1, v_2, v_4\}$, $N[v_2] = \{v_1, v_2, v_3\}$, $N[v_3] = \{v_3, v_2, v_4\}$, $N[v_4] = \{v_1, v_4, v_3\}$

Now $d_{N_{\sigma_1}}[v_1] = \sum_{u \in N_{\sigma_1}[v1]} \sigma_1(v_1) = 1.5 \geq 1$, $d_{N_{\sigma_2}}[v1] = \sum_{u \in N_{\sigma_2[v1]}} \sigma_2(v_1) = 0.9 < 1$.

with $0 \leq \sigma_1(v_i) + \sigma_2(v_i) \leq 1$, where $\sigma_1(v_i) \geq 0$, $\sigma_2(v_i) < 1$, σ_1 and σ_2 is a σ_1 − dominating and σ_2 − dominating function of G_D. It is also dominating function of σ of G_D and MDF of G_D .

Find the dominating number ($\gamma_{if\sigma_1}$) in above figure , by solving the following Linear Programming Problem which is formulated using G_D.

Minimize Z = $\sigma_1(v_1) + \sigma_1(v_2) + \sigma_1(v_3) + \sigma_1(v_4)$ subject to $\sigma_1(v_1) + \sigma_1(v_2) + \sigma_1(v_4) \geq 1$, $\sigma_1(v_1) + \sigma_1(v_2) + \sigma_1(v_3) \geq 1$, $\sigma_1(v_2) + \sigma_1(v_3) + \sigma_1(v_4) \geq 1$, $\sigma_1(v_1) + \sigma_1(v_3) + \sigma_1(v_4) \geq 1$ and $0 \leq \sigma_1(v_i) \leq 1$ for all $v_i \in V(G_D)$

Solution :

Minimize Z = $\sigma_1(v_1) + \sigma_1(v_2) + \sigma_1(v_3) + \sigma_1(v_4)$, $\begin{pmatrix} 1 & 1 & 0 & 1 \\ 1 & 1 & 1 & 0 \\ 0 & 1 & 1 & 1 \\ 1 & 0 & 1 & 1 \end{pmatrix} \begin{pmatrix} \sigma_1(v_1) \\ \sigma_1(v_2) \\ \sigma_1(v_3) \\ \sigma_1(v_4) \end{pmatrix} \geq \begin{pmatrix} 1 \\ 1 \\ 1 \\ 1 \end{pmatrix}$ and $\sigma_1(v_i) \in [0,1]$ for all $v_i \in$ V(G)

where

N= $\begin{pmatrix} 1 & 10 & 1 \\ 1 & 11 & 0 \\ 0 & 11 & 1 \\ 1 & 01 & 1 \end{pmatrix}$, $X_{if} = \begin{pmatrix} \sigma_1(v_1) \\ \sigma_1(v_2) \\ \sigma_1(v_3) \\ \sigma_1(v_4) \end{pmatrix}$ $\overrightarrow{\mathbf{1_n}} = \begin{pmatrix} 1 \\ 1 \\ 1 \\ 1 \end{pmatrix}$ be the coloumn vector with respect to the constraint part of L.P.P.

 Then the optimal solution of the above L.P.P is Minimize Z= 4/3 where $\sigma_1(v_1)$=1/3,$\sigma_1(v_2)$=1/3

$\sigma_1(v_3)$ =1/3 ,$\sigma_1(v_4)$=1/3

Hence the domination number $\gamma_{if\sigma_1}(G_D)$= 4/3.

Find the dominating number ($\gamma_{if\sigma_2}$) in above figure , by solving the following Linear Programming Problem which is formulated using G_D.

Minimize Z = $\sigma_1(v_1) + \sigma_2(v_2) + \sigma_2(v_3) + \sigma_2(v_4)$ subject to $\sigma_2(v_1) + \sigma_2(v_2) + \sigma_2(v_4) \geq 1$, $\sigma_2(v_1) + \sigma_2(v_2) + \sigma_2(v_3) \geq 1$, $\sigma_2(v_2) + \sigma_2(v_3) + \sigma_2(v_4) \geq 1$, $\sigma_2(v_1) + \sigma_2(v_3) + \sigma_2(v_4) \geq 1$ and $0 \leq \sigma_2(v_i) \leq 1$ for all $v_i \in$ V(G_D)

Solution :

Minimize Z = $\sigma_1(v_1) + \sigma_1(v_2) + \sigma_1(v_3) +$

$\sigma_1(v_4)$, $\begin{pmatrix} 1 & 10 & 1 \\ 1 & 11 & 0 \\ 0 & 11 & 1 \\ 1 & 01 & 1 \end{pmatrix} \begin{pmatrix} \sigma_2(v_1) \\ \sigma_2(v_2) \\ \sigma_2(v_3) \\ \sigma_2(v_4) \end{pmatrix} \geq \begin{pmatrix} 1 \\ 1 \\ 1 \\ 1 \end{pmatrix}$ and $\sigma_2(v_i) \in [0,1]$ for all $v_i \in$ V(G) where

N= $\begin{pmatrix} 1 & 10 & 1 \\ 1 & 11 & 0 \\ 0 & 11 & 1 \\ 1 & 01 & 1 \end{pmatrix}$, $X_{if} = \begin{pmatrix} \sigma_2(v_1) \\ \sigma_2(v_2) \\ \sigma_2(v_3) \\ \sigma_2(v_4) \end{pmatrix}$ $\overrightarrow{\mathbf{1_n}} = \begin{pmatrix} 1 \\ 1 \\ 1 \\ 1 \end{pmatrix}$ be the coloumn vector with respect to the constraint part of L.P.P.

 Then the optimal solution of the above L.P.P is Minimize Z= 0 where $\sigma_2(v_1)$=0,$\sigma_2(v_2)$=0

$\sigma_2(v_3)$ = 0 ,$\sigma_2(v_4)$=1/3

Hence the domination number $\gamma_{if\sigma_2}(G_D)$= 0.

Meenakshi and Pankajam

Find the upper dominating number ($\Gamma_{if\sigma_1}$) in above figure , by solving the following Linear Programming Problem which is formulated using G_D.

Maximize Z = $\sigma_1(v_1)$+ $\sigma_1(v_2)$ + $\sigma_1(v_3)$+ $\sigma_1(v_4)$ subject to $\sigma_1(v_1)$+ $\sigma_1(v_2)$ + $\sigma_1(v_4)$≤ 1, $\sigma_1(v_1)$+ $\sigma_1(v_2)$ + $\sigma_1(v_3)$ ≤ 1, $\sigma_1(v_2)$+ $\sigma_1(v_3)$ + $\sigma_1(v_4)$ ≤ 1, $\sigma_1(v_1)$+ $\sigma_1(v_3)$ + $\sigma_1(v_4)$ ≤ 1 and 0≤ $\sigma_1(v_i)$ ≤ 1 for all $v_i \epsilon$ V(G_D)

Solution :

Maximize Z = $\sigma_1(v_1)$+ $\sigma_1(v_2)$ + $\sigma_1(v_3)$+ $\sigma_1(v_4)$, $\begin{pmatrix} 1 & 10 & 1 \\ 1 & 11 & 0 \\ 0 & 11 & 1 \\ 1 & 01 & 1 \end{pmatrix} \begin{pmatrix} \sigma_1(v_1) \\ \sigma_1(v_2) \\ \sigma_1(v_3) \\ \sigma_1(v_4) \end{pmatrix} \leq \begin{pmatrix} 1 \\ 1 \\ 1 \\ 1 \end{pmatrix}$ and $\sigma_1(v_i)\epsilon$ [0,1] for all $v_i\epsilon$ V(G)

where

N= $\begin{pmatrix} 1 & 10 & 1 \\ 1 & 11 & 0 \\ 0 & 11 & 1 \\ 1 & 01 & 1 \end{pmatrix}$, X_{if}= $\begin{pmatrix} \sigma_1(v_1) \\ \sigma_1(v_2) \\ \sigma_1(v_3) \\ \sigma_1(v_4) \end{pmatrix}$ $\overrightarrow{1_n}$ = $\begin{pmatrix} 1 \\ 1 \\ 1 \\ 1 \end{pmatrix}$ be the coloumn vector with respect to the constraint part of L.P.P.

Then the optimal solution of the above L.P.P is Maximize Z= 4/3 where $\sigma_1(v_1)$=1/3,$\sigma_1(v_2)$=1/3

$\sigma_1(v_3)$ =1/3 ,$\sigma_1(v_4)$=1/3

Hence the domination number $\Gamma_{if\sigma_1}(G_D)$= 4/3.

Find the upper dominating number ($\Gamma_{if\sigma_2}$) in above figure , by solving the following Linear Programming Problem which is formulated using G_D.

Maximize Z = $\sigma_1(v_1)$+ $\sigma_2(v_2)$ + $\sigma_2(v_3)$+ $\sigma_2(v_4)$ subject to $\sigma_2(v_1)$+ $\sigma_2(v_2)$ + $\sigma_2(v_4)$≥ 1, $\sigma_2(v_1)$+ $\sigma_2(v_2)$ + $\sigma_2(v_3)$ ≥ 1, $\sigma_2(v_2)$+ $\sigma_2(v_3)$ + $\sigma_2(v_4)$ ≥ 1, $\sigma_2(v_1)$+ $\sigma_2(v_3)$ + $\sigma_2(v_4)$ ≥ 1 and 0≤ $\sigma_2(v_i)$ ≤ 1 for all $v_i\epsilon$ V(G_D)

Solution :

Minimize Z = $\sigma_1(v_1)$+ $\sigma_1(v_2)$ + $\sigma_1(v_3)$+ $\sigma_1(v_4)$, $\begin{pmatrix} 1 & 10 & 1 \\ 1 & 11 & 0 \\ 0 & 11 & 1 \\ 1 & 01 & 1 \end{pmatrix} \begin{pmatrix} \sigma_2(v_1) \\ \sigma_2(v_2) \\ \sigma_2(v_3) \\ \sigma_2(v_4) \end{pmatrix} \geq \begin{pmatrix} 1 \\ 1 \\ 1 \\ 1 \end{pmatrix}$ and $\sigma_2(v_i)\epsilon$ [0,1] for all $v_i\epsilon$ V(G) where

N= $\begin{pmatrix} 1 & 10 & 1 \\ 1 & 11 & 0 \\ 0 & 11 & 1 \\ 1 & 01 & 1 \end{pmatrix}$, X_{if}= $\begin{pmatrix} \sigma_2(v_1) \\ \sigma_2(v_2) \\ \sigma_2(v_3) \\ \sigma_2(v_4) \end{pmatrix}$ $\overrightarrow{1_n}$ = $\begin{pmatrix} 1 \\ 1 \\ 1 \\ 1 \end{pmatrix}$ be the coloumn vector with respect to the constraint part of L.P.P.

Then the optimal solution of the above L.P.P is Minimize Z= 4/3 where $\sigma_2(v_1)$=1/3,$\sigma_2(v_2)$=1/3

$\sigma_2(v_3)$ = 1/3 ,$\sigma_2(v_4)$=1/3

Hence the domination number $\Gamma_{if\sigma_2}(G_D)$= 4/3.

CONCLUSION

For the dominance function of any fractional digraph G_D, the determination of the lower and upper dominance number bythe linear programming method is discussed. This procedure was applied toan intuitionistic fuzzy graph to find the number ofdominances and the upper dominance number.

REFERENCES

1. Atanassov. K.T., Intuitionistic fuzzy sets: theory of applications, Physica, New Yark,(1999).
2. Karunabigai M.G and Sathiskumar.A, dominating function in intuitionistic fractional graph, Malaya Journal of Matematik 8(4)(2020).
3. Enrico C Enuquez, Grace M Estrade, C.M.Loquias.,Domination in fuzzy Directed graphs, Researchgate(2021)
4. A. Bozhenyuk,S. Belyakov, I. Rozenberg.,On computing Domination set in Intuitionistic fuzzy graph, Russia (2021)
5. Karunabigai M.G and Sathiskumar. .A., Dominating function in fractional graph, Journal of physics (2021).
6. Manickam. R,JulianaGnanaselvi. K, Anitha.G., Minimum Domination set in Intuitionistic fuzzy digraph Protocol for certificate Revocation List Dissemination, Coimbatore.

Figure-2.1
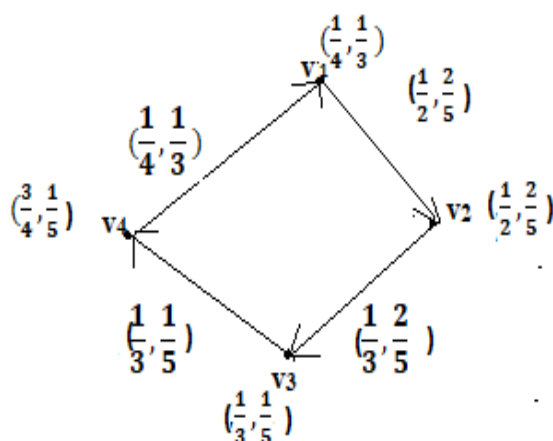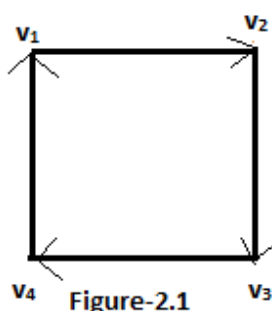
Some Properties of Fuzzy Soft n-Paranormal Operator

A Radharamani[1]* and T Nagajothi[2]

[1]Assistant Professor, Department of Mathematics, Chikkanna Govt.Arts College, Tirupur, Tamil Nadu, India.
[2]Assistant Professor, Department of Mathematics, PSG College of Arts and Science, Coimbatore, , Tamil Nadu, India

*Address for Correspondence
A Radharamani
Assistant Professor,
Department of Mathematics,
Chikkanna Govt.Arts College,
Tirupur, Tamil Nadu, India.

ABSTRACT

The purpose of this search is to introduce some concepts of the fuzzy soft n- paranormal operator defined on fuzzy soft Hilbert space, including some key characteristics of this operator, as well as a discussion of various theorems related to this operator.

Keywords: Fuzzy soft n-power paranormal operator, fuzzy soft Hilbert space, fuzzy soft *-paranormal operator, fuzzy soft paranormal operator, fuzzy soft n- paranormal operator

INTRODUCTION

To solve a number of issues in pure mathematics, the discipline of functional analysis was founded more than a century ago. In addition to regularly presenting us with uncertainty, the phenomena under study's ambiguity also provides us with instruments for assessing faults in solutions to issues with both infinite and limited dimensions. In a variety of fields, including engineering, business, medicine, and economics, this kind of problem might be encountered. Our conventional mathematical methods frequently fall short in addressing such problems.So, in 1965, L. Zadeh offered a generalisation of set theory. The resulting theory was given the name fuzzy set theory. It didn't take long for fuzzy set theory to become a potent tool for handling uncertain situations. In classical set theory, the basis function from a set x to set [0,1] defines the set x.

On the other hand, in fuzzy set theory, a set is defined by its membership function, which spans from x to the closed interval between 0 and 1. Additionally, Molodtsov created a novel generalisation for handling uncertainty in 1999. This study led to the development of soft set theory. Since then, it has been used in a variety of disciplines, including

63333

computer science, engineering, medicine, and others, to address challenging problems. A parametrized collection of a universal set is known as a soft set. Soft set gave rise to the concepts of soft point, soft normed space, soft inner product space, and soft Hilbert space, which were later used in functional analysis to deal with a variety of mathematical subjects.

Maji et al. presented the idea of a fuzzy soft set for the first time in 2001. The concept was developed by combining a fuzzy set and a soft set. It was required to combine the two ideas in order to provide results that were more accurate and comprehensive. Fuzzy soft point and fuzzy soft normed spacewere developed as a result of the addition of these additional ideas to the framework. Fuzzy soft Hilbert spaces were introduced in 2020 by Fariedet al. Also included are the fuzzy soft linear operators. In this article, we provide a novel kind of Fuzzy soft n-power paranormal operator and establish various related theorems.

PRELIMINARIES

The notations, definitions, and introductions for fuzzy set, soft set, and fuzzy soft set that will be used in the discussion that follows are provided in this section.

Definition 2.1: Fuzzy set

If fuzzy set $\check{A}$over $\mathfrak{X}$ is a set characterized by a membership function

$\eta_{\check{A}}: \mathfrak{X} \to \mathfrak{I}$, such as $\mathfrak{I} = [0,1]$and $\check{A} = \left\{ \frac{\eta_{\check{A}}(x)}{x} : x \in \mathfrak{X} \right\}$.

And $\mathfrak{I}^{\mathfrak{X}} = \{\check{A} : \check{A} \ is \ a \ function \ from \ \mathfrak{X} \ into \ \mathfrak{I}\}$

Definition 2.2: Soft set

Let $\mathcal{P}(\mathfrak{X})$ the power set of $\mathfrak{X}$ and E be set of parameters and $A \subseteq E$. The mapping $\mathbb{G}: A \to \mathcal{P}(\mathfrak{X})$, when $(\mathbb{G}, A) = \{\mathbb{G}(l)\epsilon\mathcal{P}(\mathfrak{X}): l \in A\}$. As a result $(\mathbb{G}, A)$ is called the soft set.

Definition 2.3: Fuzzy soft set

The soft set $\mathbb{G}_A$ we say that fuzzy soft set over $\mathfrak{X}$, when $\mathbb{G}: A \to \mathfrak{I}^{\mathfrak{X}}$, and $\{\mathbb{G}(l)\epsilon\mathfrak{I}^{\mathfrak{X}}: l \in A\}$. The collection of all fuzzy soft sets denoted by $FSS(\widetilde{\mathfrak{X}})$.

Definition 2.4: Fuzzy soft point

The fuzzy soft set $(\mathbb{G}, A) \in FSS(\widetilde{\mathfrak{X}})$is called a fuzzy soft point over $\mathfrak{X}$, denoted by $\tilde{l}_{\eta_{\mathbb{G}(e)}}$ if

$e \in A, x \in \mathfrak{X}$

$\eta_{\mathbb{G}(e)}(x) = \begin{cases} \alpha, \ if \ l = l_0 \in \mathfrak{X} \ and \ e = e_0 \in A, \\ 0, \ if \ l \in \mathfrak{X} - \{l_0\} \ or \ e \in A - \{e_0\} \end{cases}$, such that $\alpha \in (0,1]$

Definition 2.5: Fuzzy soft Hilbert space

A fuzzy soft inner product space is defined as $(\widetilde{\mathfrak{X}}, \ \widetilde{\langle.,.\rangle})$. This space, which is fuzzy soft complete in the induced fuzzy soft norm indicated in Theorem (2.10), is thus referred to as a fuzzy soft Hilbert space and denoted by $(\tilde{\hbar}, \ \widetilde{\langle.,.\rangle})$. Every fuzzy soft Hilbert space is obviously a fuzzy soft banach space.

Definition 2.6: Fuzzy soft adjoint operator in $\tilde{\hbar}$

The fuzzy soft adjoint operator $\widetilde{\mathbb{T}}^*$of a fuzzy soft linear operator $\widetilde{\mathbb{T}}$ is defined by

$\langle \widetilde{\mathbb{T}}\tilde{l}^1_{\eta_{1_{\mathbb{G}(e_1)}}}, \tilde{l}^2_{\eta_{2_{\mathbb{G}(2)}}} \rangle \cong \langle \tilde{l}^1_{\eta_{1_{\mathbb{G}(e_1)}}}, \widetilde{\mathbb{T}^*}\tilde{l}^2_{\eta_{2_{\mathbb{G}(2)}}} \rangle$

for all $\tilde{l}^1_{\eta_{1_{\mathbb{G}(e_1)}}}, \tilde{l}^2_{\eta_{2_{\mathbb{G}(e_2)}}} \in \tilde{\hbar}$

Definition 2.7:Fuzzy soft Normal Operator

Let $\tilde{\hbar}$ be an FS Hilbert space and$\widetilde{\mathbb{T}} \in \mathfrak{B}(\tilde{\hbar})$. Then, $\widetilde{\mathbb{T}}$ is said to be an FS normal operator if $\widetilde{\mathbb{T}}\widetilde{\mathbb{T}}^* \cong \widetilde{\mathbb{T}}^*\widetilde{\mathbb{T}}$

Radharamani and Nagajothi

Definition 2.8: Fuzzy soft self adjoint operator
The FS-operator $\tilde{\mathfrak{T}}$ of FSH-space $\tilde{h}$ is called fuzzy soft self adjoint (FS-self adjoint operator)
if $\tilde{\mathfrak{T}} \cong \tilde{\mathfrak{T}}^{*}$

Definition 2.9: Fuzzy soft isometry operator
Let $\tilde{h}$ be an FS Hilbert space and $\tilde{\mathfrak{T}} \in \mathfrak{B}(\tilde{h})$. Then, $\tilde{\mathfrak{T}}$ is said to be an FSisometry
operator if $\langle \tilde{\mathfrak{T}} \widetilde{l^1}_{\eta_{1_{\mathfrak{g}(e_1)}}}, \tilde{\mathfrak{T}} \widetilde{l^2}_{\eta_{2_{\mathfrak{g}(e_2)}}} \rangle \cong \langle \tilde{l}^1_{\eta_{1_{\mathfrak{g}(e_1)}}}, \widetilde{l^2}_{\eta_{2_{\mathfrak{g}(2)}}} \rangle$ for all $\tilde{l}^1_{\eta_{1_{\mathfrak{g}(e_1)}}}, l^2_{\eta_{2_{\mathfrak{g}(e_2)}}} \tilde{\in} \tilde{h}$

Definition 2.10: Fuzzy soft projection operator
Consider $\tilde{h}$ to be a fuzzy soft Hilbert space. A fuzzy soft linear operator $\tilde{\mathfrak{T}}: \tilde{h} \to \tilde{h}$ is called a fuzzy soft projection
operator in $\tilde{h}$ if $\tilde{\mathfrak{T}}^2 \cong \tilde{\mathfrak{T}}$ ie, $\tilde{\mathfrak{T}}$ is an idempotent.

Definition 2.11: Fuzzy soft hyponormaloperator
Consider $\tilde{h}$ to be a fuzzy soft Hilbert space. $\tilde{\mathfrak{T}} \in \mathfrak{B}(\tilde{h})$ is called fuzzy soft hyponormal operator if $\left\| \tilde{\mathfrak{T}}^{*} \tilde{l}_{\eta_{\mathfrak{g}(e)}} \right\| \leq \left\| \tilde{\mathfrak{T}} \tilde{l}_{\eta_{\mathfrak{g}(e)}} \right\|$
for all $\tilde{l}_{\eta_{\mathfrak{g}(e)}} \tilde{\in} \tilde{h}$ or equivalently $\tilde{\mathfrak{T}}^{*}\tilde{\mathfrak{T}} \geq \tilde{\mathfrak{T}}\tilde{\mathfrak{T}}^{*}$

Definition 2.12: M-Fuzzy soft hyponormaloperator
Let $\tilde{h}$ be an FS Hilbert space and let $\tilde{\mathfrak{T}} \in \mathfrak{B}(\tilde{h})$ is called M – fuzzy soft hyponormal operator if there exist a real
number $\mathcal{M}$, such that $\left\| \widetilde{(\tilde{\mathfrak{T}} \tilde{\approx} \tilde{\mathfrak{e}} I)^{*}} \tilde{l}_{\eta_{\mathfrak{g}(e)}} \right\| \tilde{\lesssim} \tilde{\mathcal{M}} \left\| \widetilde{(\tilde{\mathfrak{T}} \tilde{\approx} \tilde{\mathfrak{e}} I)} \tilde{l}_{\eta_{\mathfrak{g}(e)}} \right\|$
for all $\tilde{l}_{\eta_{\mathfrak{g}(e)}} \tilde{\in} \tilde{h}$ and for all $\tilde{\mathfrak{e}} \tilde{\in} \mathbb{C}(\mathbb{A})$

MAIN RESULTS

The definition of the fuzzy soft n-power paranormal operator in fuzzy soft Hilbert space is provided in this section.

Definition 3.1: Fuzzy Soft Paranormal Operator (FSPN)
Let $\tilde{h}$ be an FS Hilbert space and let $\tilde{\mathfrak{T}} \in \mathfrak{B}(\tilde{h})$ then $\tilde{\mathfrak{T}}$ is a FSPN operator if
$\left\| \widetilde{\mathfrak{T}^2 \tilde{l}_{\eta_{\mathfrak{g}(e)}}} \right\| \left\| \widetilde{\tilde{l}_{\eta_{\mathfrak{g}(e)}}} \right\| \tilde{\gtrless} \left\| \widetilde{\mathfrak{T}\tilde{l}_{\eta_{\mathfrak{g}(e)}}} \right\|^2$ for all $\tilde{l}_{\eta_{\mathfrak{g}(e)}} \tilde{\in} \tilde{h}$

Definition 3.2: Fuzzy Soft n-Paranormal Operator (FSn-PN)
Let $\tilde{h}$ be an FS Hilbert space and let $\tilde{\mathfrak{T}} \in \mathfrak{B}(\tilde{h})$ then $\tilde{\mathfrak{T}}$ is a FSPN operator if
$\left\| \widetilde{\mathfrak{T}^{n+1} \tilde{l}_{\eta_{\mathfrak{g}(e)}}} \right\| \tilde{\gtrless} \left\| \widetilde{\mathfrak{T}\tilde{l}_{\eta_{\mathfrak{g}(e)}}} \right\|^{n+1}$ forall $\tilde{l}_{\eta_{\mathfrak{g}(e)}} \tilde{\in} \tilde{h}$

Theorem 3.3:
Let $\tilde{\mathfrak{T}} \in \mathfrak{B}(\tilde{h})$, then $\tilde{\mathfrak{T}}$ is FSPN operator if $\tilde{\mathfrak{T}}$ is an fuzzy soft n-paranormal operator
Proof:
Given $\tilde{\mathfrak{T}}$ is fuzzy soft n-paranormal operator
By the definition, $\left\| \widetilde{\mathfrak{T}^{n+1} \tilde{l}_{\eta_{\mathfrak{g}(e)}}} \right\| \tilde{\gtrless} \left\| \widetilde{\mathfrak{T}\tilde{l}_{\eta_{\mathfrak{g}(e)}}} \right\|^{n+1}$
Put $n = 1$, $\left\| \widetilde{\mathfrak{T}^{1+1} \tilde{l}_{\eta_{\mathfrak{g}(e)}}} \right\| \tilde{\gtrless} \left\| \widetilde{\mathfrak{T}\tilde{l}_{\eta_{\mathfrak{g}(e)}}} \right\|^{1+1}$
$\left\| \widetilde{\mathfrak{T}^2 \tilde{l}_{\eta_{\mathfrak{g}(e)}}} \right\| \tilde{\gtrless} \left\| \widetilde{\mathfrak{T}\tilde{l}_{\eta_{\mathfrak{g}(e)}}} \right\|^2$
Therefore, $\tilde{\mathfrak{T}}$ is FSPN operator

Theorem 3.4:
Let $\tilde{\mathfrak{T}} \in \mathfrak{B}(\tilde{h})$, then $\tilde{\mathfrak{T}}$ is FSn-PN operator if $\tilde{\mathfrak{T}}$ is an fuzzy soft paranormal operator

Proof:

Take $\tilde{l}_{\eta_{\mathfrak{g}(e)}} \tilde{\in} \tilde{\hbar}$

By using the mathematical induction, if $n = 1$

$$\left\| \widetilde{\mathbb{T}^{1+1}\tilde{l}_{\eta_{\mathfrak{g}(e)}}} \right\| \cong \left\| \widetilde{\mathbb{T}^2 \tilde{l}_{\eta_{\mathfrak{g}(e)}}} \right\| \gtrsim \left\| \widetilde{\mathbb{T}\tilde{l}_{\eta_{\mathfrak{g}(e)}}} \right\|^2$$

$$\gtrsim \left\| \widetilde{\mathbb{T}\tilde{l}_{\eta_{\mathfrak{g}(e)}}} \right\|^{1+1}$$

$$\left\| \widetilde{\mathbb{T}^{1+1}\tilde{l}_{\eta_{\mathfrak{g}(e)}}} \right\| \gtrsim \left\| \widetilde{\mathbb{T}\tilde{l}_{\eta_{\mathfrak{g}(e)}}} \right\|^{1+1}$$

If $n = 2$,

$$\left\| \widetilde{\mathbb{T}^{2+1}\tilde{l}_{\eta_{\mathfrak{g}(e)}}} \right\| \cong \left\| \widetilde{\mathbb{T}^3 \tilde{l}_{\eta_{\mathfrak{g}(e)}}} \right\| \gtrsim \left\| \widetilde{\mathbb{T}\tilde{l}_{\eta_{\mathfrak{g}(e)}}} \right\|^3$$

$$\gtrsim \left\| \widetilde{\mathbb{T}\tilde{l}_{\eta_{\mathfrak{g}(e)}}} \right\|^{2+1}$$

$$\left\| \widetilde{\mathbb{T}^{2+1}\tilde{l}_{\eta_{\mathfrak{g}(e)}}} \right\| \gtrsim \left\| \widetilde{\mathbb{T}\tilde{l}_{\eta_{\mathfrak{g}(e)}}} \right\|^{2+1} \text{etc.,}$$

If $n = k$ is true

$$\left\| \widetilde{\mathbb{T}^{k+1}\tilde{l}_{\eta_{\mathfrak{g}(e)}}} \right\| \gtrsim \left\| \widetilde{\mathbb{T}\tilde{l}_{\eta_{\mathfrak{g}(e)}}} \right\|^{k+1}$$

Now we have to prove that it is true for $n = k + 1$

Let $\left\| \widetilde{\mathbb{T}\tilde{l}_{\eta_{\mathfrak{g}(e)}}} \right\|^{k+1+1} \cong \left\| \widetilde{\mathbb{T}\tilde{l}_{\eta_{\mathfrak{g}(e)}}} \right\|^{k+1} \left\| \widetilde{\tilde{l}_{\eta_{\mathfrak{g}(e)}}} \right\|$

$$\lesssim \left\| \widetilde{\mathbb{T}^{k+1}\tilde{l}_{\eta_{\mathfrak{g}(e)}}} \right\| \left\| \widetilde{\tilde{l}_{\eta_{\mathfrak{g}(e)}}} \right\|$$

$$\left\| \widetilde{\mathbb{T}\tilde{l}_{\eta_{\mathfrak{g}(e)}}} \right\|^{k+1+1} \lesssim \left\| \widetilde{\mathbb{T}^{k+1+1}\tilde{l}_{\eta_{\mathfrak{g}(e)}}} \right\|$$

Therefore, $\widetilde{\mathbb{T}}$ is FSn-PN operator

Definition 3.5: Fuzzy Soft n – power Paranormal Operator

Let $\tilde{\hbar}$ be an FS Hilbert space and let $\widetilde{\mathbb{T}} \in \mathfrak{B}(\tilde{\hbar})$ then $\widetilde{\mathbb{T}}$ is a FSn –power paranormal operator if
$\left\| \widetilde{\mathbb{T}^{2n}\tilde{l}_{\eta_{\mathfrak{g}(e)}}} \right\| \left\| \widetilde{\tilde{l}_{\eta_{\mathfrak{g}(e)}}} \right\| \gtrsim \left\| \widetilde{\mathbb{T}^n \tilde{l}_{\eta_{\mathfrak{g}(e)}}} \right\|^2$ for all $\tilde{l}_{\eta_{\mathfrak{g}(e)}} \tilde{\in} \tilde{\hbar}$

Theorem 3.6:

Let $\widetilde{\mathbb{T}}, \tilde{\tilde{e}} \in \mathfrak{B}(\tilde{\hbar})$, if $\widetilde{\mathbb{T}}, \tilde{\tilde{e}}$ are fuzzy soft self adjoint operator then $\widetilde{\mathbb{T}} \tilde{\mp} \tilde{\tilde{e}}$ is fuzzy soft n-power –paranormal operator .

Proof:

Take $\tilde{l}_{\eta_{\mathfrak{g}(e)}} \tilde{\in} \tilde{\hbar}$ with $\left\| \widetilde{\tilde{l}_{\eta_{\mathfrak{g}(e)}}} \right\| \cong 1$

Let $\left\| (\widetilde{\mathbb{T} \tilde{\mp} \tilde{\tilde{e}})^n} \tilde{l}_{\eta_{\mathfrak{g}(e)}} \right\|^2 \cong \langle (\widetilde{\mathbb{T} \tilde{\mp} \tilde{\tilde{e}})^n} \tilde{l}_{\eta_{\mathfrak{g}(e)}}, \widetilde{(\widetilde{\mathbb{T} \tilde{\mp} \tilde{\tilde{e}})^n}} \tilde{l}_{\eta_{\mathfrak{g}(e)}} \rangle$

$$\cong \langle \left(\left(\widetilde{\mathbb{T} \tilde{\mp} \tilde{\tilde{e}}} \right)^n \right)^* \widetilde{(\widetilde{\mathbb{T} \tilde{\mp} \tilde{\tilde{e}}})^n} \tilde{l}_{\eta_{\mathfrak{g}(e)}}, \tilde{l}_{\eta_{\mathfrak{g}(e)}} \rangle$$

$$\cong \langle \left(\left(\widetilde{\mathbb{T}^*} + \tilde{\tilde{e}}^* \right)^n \widetilde{(\widetilde{\mathbb{T} \tilde{\mp} \tilde{\tilde{e}}})^n} \tilde{l}_{\eta_{\mathfrak{g}(e)}}, \tilde{l}_{\eta_{\mathfrak{g}(e)}} \right) \rangle$$

$$\cong \langle \left(\left(\widetilde{\mathbb{T} \tilde{\mp} \tilde{\tilde{e}}} \right)^n \widetilde{(\widetilde{\mathbb{T} \tilde{\mp} \tilde{\tilde{e}}})^n} \tilde{l}_{\eta_{\mathfrak{g}(e)}}, \tilde{l}_{\eta_{\mathfrak{g}(e)}} \right) \rangle$$

$$\cong \langle \left(\left(\widetilde{\mathbb{T} \tilde{\mp} \tilde{\tilde{e}}} \right)^{2n} \tilde{l}_{\eta_{\mathfrak{g}(e)}}, \tilde{l}_{\eta_{\mathfrak{g}(e)}} \right) \rangle$$

$$\left\| (\widetilde{\mathbb{T} \tilde{\mp} \tilde{\tilde{e}})^n} \tilde{l}_{\eta_{\mathfrak{g}(e)}} \right\|^2 \lesssim \langle \left((\widetilde{\mathbb{T} \tilde{\mp} \tilde{\tilde{e}})^{2n}} \tilde{l}_{\eta_{\mathfrak{g}(e)}}, \tilde{l}_{\eta_{\mathfrak{g}(e)}} \right) \rangle$$

$\left\| (\widetilde{\mathbb{T} \tilde{\mp} \tilde{\tilde{e}})^n} \tilde{l}_{\eta_{\mathfrak{g}(e)}} \right\|^2 \lesssim \left\| (\widetilde{\mathbb{T} \tilde{\mp} \tilde{\tilde{e}})^{2n}} \tilde{l}_{\eta_{\mathfrak{g}(e)}} \right\| \left\| \widetilde{\tilde{l}_{\eta_{\mathfrak{g}(e)}}} \right\|$ implies that

$$\left\| (\widetilde{\mathbb{T} \tilde{\mp} \tilde{\tilde{e}})^n} \tilde{l}_{\eta_{\mathfrak{g}(e)}} \right\|^2 \lesssim \left\| (\widetilde{\mathbb{T} \tilde{\mp} \tilde{\tilde{e}})^{2n}} \tilde{l}_{\eta_{\mathfrak{g}(e)}} \right\|$$

Therefore, $\widetilde{\mathbb{T}} \tilde{\mp} \tilde{\tilde{e}}$ is fuzzy soft n-power paranormal operator

Theorem 3.7:

Let $\widetilde{\mathbb{T}},\widetilde{\mathbb{e}} \in \mathfrak{B}(\tilde{\hbar})$, if $\widetilde{\mathbb{T}},\widetilde{\mathbb{e}}$ are fuzzy soft self adjoint operator then $\widetilde{\mathbb{T}}\widetilde{\mathbb{e}}$ is fuzzy soft n-power –paranormal operator.

Proof:

Take $\widetilde{l}_{\eta_{\mathfrak{g}(e)}} \widetilde{\in} \tilde{\hbar}$ with $\left\| \widetilde{\widetilde{l}_{\eta_{\mathfrak{g}(e)}}} \right\| \cong 1$

Let $\left\| \widetilde{(\widetilde{\mathbb{T}}\widetilde{\mathbb{e}})^{n}\widetilde{l}_{\eta_{\mathfrak{g}(e)}}} \right\|^{2} \cong \langle (\widetilde{\mathbb{T}}\widetilde{\mathbb{e}})^{n}\widetilde{l}_{\eta_{\mathfrak{g}(e)}}, (\widetilde{\mathbb{T}}\widetilde{\mathbb{e}})^{n}\widetilde{l}_{\eta_{\mathfrak{g}(e)}} \rangle$

$$\cong \langle \left((\widetilde{\mathbb{T}}\widetilde{\mathbb{e}})^{n} \right)^{*}\widetilde{(\widetilde{\mathbb{T}}\widetilde{\mathbb{e}})}^{n}\widetilde{l}_{\eta_{\mathfrak{g}(e)}}, \widetilde{l}_{\eta_{\mathfrak{g}(e)}} \rangle$$

$$\cong \langle \left((\widetilde{\mathbb{T}}\widetilde{\mathbb{e}})^{*} \right)^{n}\widetilde{(\widetilde{\mathbb{T}}\widetilde{\mathbb{e}})}^{n}\widetilde{l}_{\eta_{\mathfrak{g}(e)}}, \widetilde{l}_{\eta_{\mathfrak{g}(e)}}) \rangle$$

$$\cong \langle \left(\widetilde{\mathbb{e}}^{*}\widetilde{\mathbb{T}}^{*} \right)^{n}\widetilde{(\widetilde{\mathbb{T}}\widetilde{\mathbb{e}})}^{n}\widetilde{l}_{\eta_{\mathfrak{g}(e)}}, \widetilde{l}_{\eta_{\mathfrak{g}(e)}}) \rangle$$

$$\cong \langle \left(\widetilde{\mathbb{e}}\widetilde{\mathbb{T}} \right)^{n}\widetilde{(\widetilde{\mathbb{T}}\widetilde{\mathbb{e}})}^{n}\widetilde{l}_{\eta_{\mathfrak{g}(e)}}, \widetilde{l}_{\eta_{\mathfrak{g}(e)}}) \rangle$$

$$\cong \langle \left(\widetilde{\mathbb{T}}\widetilde{\mathbb{e}} \right)^{n}\widetilde{(\widetilde{\mathbb{T}}\widetilde{\mathbb{e}})}^{n}\widetilde{l}_{\eta_{\mathfrak{g}(e)}}, \widetilde{l}_{\eta_{\mathfrak{g}(e)}}) \rangle$$

$$\cong \langle \left(\widetilde{\mathbb{T}}\widetilde{\mathbb{e}} \right)^{2n}\widetilde{l}_{\eta_{\mathfrak{g}(e)}}, \widetilde{l}_{\eta_{\mathfrak{g}(e)}}) \rangle$$

$$\lesssim \left\| (\widetilde{\mathbb{T}}\widetilde{\mathbb{e}})^{2n}\widetilde{l}_{\eta_{\mathfrak{g}(e)}} \right\| \left\| \widetilde{l}_{\eta_{\mathfrak{g}(e)}} \right\|$$

$$\left\| (\widetilde{\mathbb{T}}\widetilde{\mathbb{e}})^{n}\widetilde{l}_{\eta_{\mathfrak{g}(e)}} \right\|^{2} \lesssim \left\| (\widetilde{\mathbb{T}}\widetilde{\mathbb{e}})^{2n}\widetilde{l}_{\eta_{\mathfrak{g}(e)}} \right\|$$

Therefore, $\widetilde{\mathbb{T}}\widetilde{\mathbb{e}}$ is fuzzy soft n-power paranormal operator

Theorem 3.8:

Let $\widetilde{\mathbb{T}} \in \mathfrak{B}(\tilde{\hbar})$ is a FSHS and fuzzy soft self adjoint operator. If $\widetilde{\mathbb{T}}$ is a fuzzy soft n-power paranormal operator then $\widetilde{\mathbb{T}}^{n}$ is a fuzzy soft n-power paranormal operator.

Proof:

Take $\widetilde{l}_{\eta_{\mathfrak{g}(e)}} \widetilde{\in} \tilde{\hbar}$ with $\left\| \widetilde{\widetilde{l}_{\eta_{\mathfrak{g}(e)}}} \right\| \cong 1$

We know that, $\widetilde{\mathbb{T}}$ is fuzzy soft n-power paranormal operator

ie), $\left\| \widetilde{\mathbb{T}}^{n}\widetilde{l}_{\eta_{\mathfrak{g}(e)}} \right\|^{2} \lesssim \left\| \widetilde{\mathbb{T}}^{2n}\widetilde{l}_{\eta_{\mathfrak{g}(e)}} \right\|$

To show that $\left\| (\widetilde{\mathbb{T}}^{n})^{n}\widetilde{l}_{\eta_{\mathfrak{g}(e)}} \right\|^{2} \lesssim \left\| (\widetilde{\mathbb{T}}^{n})^{2n}\widetilde{l}_{\eta_{\mathfrak{g}(e)}} \right\|$

Let $\left\| (\widetilde{\mathbb{T}}^{n})^{n}\widetilde{l}_{\eta_{\mathfrak{g}(e)}} \right\|^{2} \cong \langle (\widetilde{\mathbb{T}}^{n})^{n}\widetilde{l}_{\eta_{\mathfrak{g}(e)}}, (\widetilde{\mathbb{T}}^{n})^{n}\widetilde{l}_{\eta_{\mathfrak{g}(e)}} \rangle$

$$\cong \langle \left((\widetilde{\mathbb{T}}^{n})^{n} \right)^{*}(\widetilde{\mathbb{T}}^{n})^{n}\widetilde{l}_{\eta_{\mathfrak{g}(e)}}, \widetilde{l}_{\eta_{\mathfrak{g}(e)}} \rangle$$

$$\cong \langle \left((\widetilde{\mathbb{T}}^{*})^{n} \right)^{n}(\widetilde{\mathbb{T}}^{n})^{n}\widetilde{l}_{\eta_{\mathfrak{g}(e)}}, \widetilde{l}_{\eta_{\mathfrak{g}(e)}} \rangle$$

$$\cong \langle (\widetilde{\mathbb{T}}^{n})^{n}(\widetilde{\mathbb{T}}^{n})^{n}\widetilde{l}_{\eta_{\mathfrak{g}(e)}}, \widetilde{l}_{\eta_{\mathfrak{g}(e)}} \rangle$$

$$\cong \langle (\widetilde{\mathbb{T}}^{n})^{2n}\widetilde{l}_{\eta_{\mathfrak{g}(e)}}, \widetilde{l}_{\eta_{\mathfrak{g}(e)}} \rangle$$

$\left\| (\widetilde{\mathbb{T}}^{n})^{n}\widetilde{l}_{\eta_{\mathfrak{g}(e)}} \right\|^{2} \lesssim \left\| (\widetilde{\mathbb{T}}^{n})^{2n}\widetilde{l}_{\eta_{\mathfrak{g}(e)}} \right\| \left\| \widetilde{l}_{\eta_{\mathfrak{g}(e)}} \right\|$ implies that

$$\left\| (\widetilde{\mathbb{T}}^{n})^{n}\widetilde{l}_{\eta_{\mathfrak{g}(e)}} \right\|^{2} \lesssim \left\| (\widetilde{\mathbb{T}}^{n})^{2n}\widetilde{l}_{\eta_{\mathfrak{g}(e)}} \right\|$$

Therefore, $\widetilde{\mathbb{T}}^{n}$ is a fuzzy soft n-power paranormal operator

Theorem 3.9:

Let $\widetilde{\mathbb{T}} \in \mathfrak{B}(\tilde{\hbar})$ is a FSHS. If $\widetilde{\mathbb{T}}$ is a fuzzy soft n-power paranormal operator and fuzzy soft self adjoint operator then $\widetilde{\mathbb{T}}^{*}$ is a fuzzy soft n-power paranormal operator.

Proof:

Take $\widetilde{l}_{\eta_{\mathfrak{g}(e)}} \widetilde{\in} \tilde{\hbar}$ with $\left\| \widetilde{\widetilde{l}_{\eta_{\mathfrak{g}(e)}}} \right\| \cong 1$

since $\widetilde{\mathbb{T}}$ is fuzzy soft n-power paranormal operator

ie), $\left\|\widetilde{\mathbb{T}}^n\widetilde{l_{\eta_{\mathfrak{g}(e)}}}\right\|^2 \lesssim \left\|\widetilde{\mathbb{T}}^{2n}\widetilde{l_{\eta_{\mathfrak{g}(e)}}}\right\|$

To show that $\left\|(\widetilde{\mathbb{T}}^*)^n\widetilde{l_{\eta_{\mathfrak{g}(e)}}}\right\|^2 \lesssim \left\|(\widetilde{\mathbb{T}}^*)^{2n}\widetilde{l_{\eta_{\mathfrak{g}(e)}}}\right\|$

Let $\left\|(\widetilde{\mathbb{T}}^*)^n\widetilde{l_{\eta_{\mathfrak{g}(e)}}}\right\|^2 \cong \langle (\widetilde{\mathbb{T}}^*)^n\widetilde{l_{\eta_{\mathfrak{g}(e)}}}, (\widetilde{\mathbb{T}}^*)^n\widetilde{l_{\eta_{\mathfrak{g}(e)}}}\rangle$

$$\cong \langle \left((\widetilde{\mathbb{T}}^*)^n\right)^*(\widetilde{\mathbb{T}}^*)^n\widetilde{l_{\eta_{\mathfrak{g}(e)}}}, \widetilde{l_{\eta_{\mathfrak{g}(e)}}}\rangle$$
$$\cong \langle \left((\widetilde{\mathbb{T}}^*)^*\right)^n(\widetilde{\mathbb{T}}^n)^n\widetilde{l_{\eta_{\mathfrak{g}(e)}}}, \widetilde{l_{\eta_{\mathfrak{g}(e)}}}\rangle$$
$$\cong \langle (\widetilde{\mathbb{T}}^*)^n(\widetilde{\mathbb{T}}^*)^n\widetilde{l_{\eta_{\mathfrak{g}(e)}}}, \widetilde{l_{\eta_{\mathfrak{g}(e)}}}\rangle$$
$$\cong \langle (\widetilde{\mathbb{T}}^*)^{2n}\widetilde{l_{\eta_{\mathfrak{g}(e)}}}, \widetilde{l_{\eta_{\mathfrak{g}(e)}}}\rangle$$

$\left\|(\widetilde{\mathbb{T}}^*)^n\widetilde{l_{\eta_{\mathfrak{g}(e)}}}\right\|^2 \lesssim \left\|(\widetilde{\mathbb{T}}^*)^{2n}\widetilde{l_{\eta_{\mathfrak{g}(e)}}}\right\| \left\|\widetilde{l_{\eta_{\mathfrak{g}(e)}}}\right\|$ implies that

$$\left\|(\widetilde{\mathbb{T}}^*)^n\widetilde{l_{\eta_{\mathfrak{g}(e)}}}\right\|^2 \lesssim \left\|(\widetilde{\mathbb{T}}^*)^{2n}\widetilde{l_{\eta_{\mathfrak{g}(e)}}}\right\|$$

Therefore, $\widetilde{\mathbb{T}}^*$ is a fuzzy soft n-power paranormal operator

Theorem 3.10:

Let $\widetilde{\mathbb{T}} \in \mathfrak{B}(\tilde{\hbar})$ is a FSHS. If $\widetilde{\mathbb{T}}$ is a fuzzy soft paranormal operator then $\widetilde{\mathbb{T}}$ is a fuzzy soft n-power paranormal operator.

Proof:

Take $\tilde{l}_{\eta_{\mathfrak{g}(e)}} \widetilde{\in} \tilde{\hbar}$ with $\left\|\widetilde{l_{\eta_{\mathfrak{g}(e)}}}\right\| \cong 1$

Since $\widetilde{\mathbb{T}} \in \mathfrak{B}(\tilde{\hbar})$ is a fuzzy soft paranormal operator

$\left\|\widetilde{\mathbb{T}}\widetilde{l_{\eta_{\mathfrak{g}(e)}}}\right\|^2 \lesssim \left\|\widetilde{\mathbb{T}^2}\widetilde{l_{\eta_{\mathfrak{g}(e)}}}\right\|$

By using the mathematical induction,

If $n = 1$, then it is correct because $\widetilde{\mathbb{T}}$ is fuzzy soft paranormal operator

Let $\left\|\widetilde{\mathbb{T}^2}\widetilde{l_{\eta_{\mathfrak{g}(e)}}}\right\| \cong \left\|\widetilde{\mathbb{T}^{2.1}}\widetilde{l_{\eta_{\mathfrak{g}(e)}}}\right\| \gtrsim \left\|\widetilde{\mathbb{T}}\widetilde{l_{\eta_{\mathfrak{g}(e)}}}\right\|^2$

$\gtrsim \left\|\widetilde{\mathbb{T}^1}\widetilde{l_{\eta_{\mathfrak{g}(e)}}}\right\|^2$

i.e) $\left\|\widetilde{\mathbb{T}^2}\widetilde{l_{\eta_{\mathfrak{g}(e)}}}\right\| \gtrsim \left\|\widetilde{\mathbb{T}^1}\widetilde{l_{\eta_{\mathfrak{g}(e)}}}\right\|^2$ etc.,

If $n = k$ is true, then

$\left\|\widetilde{\mathbb{T}^k}\widetilde{l_{\eta_{\mathfrak{g}(e)}}}\right\|^2 \lesssim \left\|\widetilde{\mathbb{T}^{2k}}\widetilde{l_{\eta_{\mathfrak{g}(e)}}}\right\|$

Now we have to prove that it is true for $n = k + 1$

Let $\left\|\widetilde{\mathbb{T}^{k+1}}\widetilde{l_{\eta_{\mathfrak{g}(e)}}}\right\|^2 \cong \langle \widetilde{\mathbb{T}^{k+1}}\widetilde{l_{\eta_{\mathfrak{g}(e)}}}, \widetilde{\mathbb{T}^{k+1}}\widetilde{l_{\eta_{\mathfrak{g}(e)}}}\rangle$

$\cong \langle \widetilde{\mathbb{T}}\widetilde{\mathbb{T}}^k\tilde{l}_{\eta_{\mathfrak{g}(e)}}, \widetilde{\mathbb{T}}\widetilde{\mathbb{T}}^k\tilde{l}_{\eta_{\mathfrak{g}(e)}}\rangle$

$\cong \left\|\widetilde{\mathbb{T}}\widetilde{\mathbb{T}^k}\widetilde{l_{\eta_{\mathfrak{g}(e)}}}\right\|^2$

$\lesssim \left\|\widetilde{\mathbb{T}}\right\|^2 \left\|\widetilde{\mathbb{T}^k}\widetilde{l_{\eta_{\mathfrak{g}(e)}}}\right\|^2$

$\lesssim \left\|\widetilde{\mathbb{T}}\right\|^2 \left\|\widetilde{\mathbb{T}^k}\widetilde{l_{\eta_{\mathfrak{g}(e)}}}\right\|^2 \left\|\widetilde{l_{\eta_{\mathfrak{g}(e)}}}\right\|$

$\lesssim \left\|\widetilde{\mathbb{T}^2}\right\| \left\|\widetilde{\mathbb{T}^{2k}}\widetilde{l_{\eta_{\mathfrak{g}(e)}}}\right\| \left\|\widetilde{l_{\eta_{\mathfrak{g}(e)}}}\right\|$

$\lesssim \left\|\widetilde{\mathbb{T}^2}\widetilde{\mathbb{T}^{2k}}\widetilde{l_{\eta_{\mathfrak{g}(e)}}}\right\| \left\|\widetilde{l_{\eta_{\mathfrak{g}(e)}}}\right\|$

$\lesssim \left\|\widetilde{\mathbb{T}^{2k}}\widetilde{\mathbb{T}^2}\widetilde{l_{\eta_{\mathfrak{g}(e)}}}\right\| \left\|\widetilde{l_{\eta_{\mathfrak{g}(e)}}}\right\|$

$\lesssim \left\|\widetilde{\mathbb{T}^{2k+2}}\widetilde{l_{\eta_{\mathfrak{g}(e)}}}\right\| \left\|\widetilde{l_{\eta_{\mathfrak{g}(e)}}}\right\|$

$\left\|\widetilde{\mathbb{T}^{k+1}}\widetilde{l_{\eta_{\mathfrak{g}(e)}}}\right\|^2 \lesssim \left\|\widetilde{\mathbb{T}^{2(k+1)}}\tilde{l}_{\eta_{\mathfrak{g}(e)}}\right\| \left\|\widetilde{l_{\eta_{\mathfrak{g}(e)}}}\right\|$ implies that

$$\left\| \widetilde{\mathbb{T}^{k+1}\tilde{l}_{\eta_{g(e)}}} \right\|^2 \lesssim \left\| \widetilde{\mathbb{T}^{2(k+1)}\tilde{l}_{\eta_{g(e)}}} \right\|$$

Therefore, $\widetilde{\mathbb{T}}$ is a fuzzy soft n-power paranormal operator

Theorem 3.11:

Let $\widetilde{\mathbb{T}} \in \widetilde{\mathfrak{B}}(\tilde{\hbar})$ is a FSHS. If $\widetilde{\mathbb{T}}$ is a fuzzy soft n - paranormal operator then $\widetilde{\mathbb{T}}$ is a fuzzy soft n-power paranormal operator.

Proof:

By the definition of fuzzy soft n - paranormal operator

$$\left\| \widetilde{\mathbb{T}^{n+1}\tilde{l}_{\eta_{g(e)}}} \right\| \gtrsim \left\| \widetilde{\widetilde{\mathbb{T}}\tilde{l}_{\eta_{g(e)}}} \right\|^{n+1}$$

It will be shown that $\left\| \widetilde{\mathbb{T}^{2n}\tilde{l}_{\eta_{g(e)}}} \right\| \gtrsim \left\| \widetilde{\mathbb{T}^{n}\tilde{l}_{\eta_{g(e)}}} \right\|^2$

Take $\tilde{l}_{\eta_{g(e)}} \widetilde{\in} \tilde{\hbar}$ with $\left\| \widetilde{\tilde{l}_{\eta_{g(e)}}} \right\| \cong 1$

We will prove, by using mathematical induction,

Since $\widetilde{\mathbb{T}} \in \widetilde{\mathfrak{B}}(\tilde{\hbar})$ is a fuzzy soft n - paranormal operator

By using the mathematical induction, if $n = 1$

$$\left\| \widetilde{\mathbb{T}^1\tilde{l}_{\eta_{g(e)}}} \right\|^2 \cong \langle \widetilde{\mathbb{T}^1\tilde{l}_{\eta_{g(e)}}}, \; \widetilde{\mathbb{T}^1\tilde{l}_{\eta_{g(e)}}} \rangle$$

$$\cong \langle \widetilde{\mathbb{T}^*\widetilde{\mathbb{T}}\tilde{l}_{\eta_{g(e)}}}, \; \tilde{l}_{\eta_{g(e)}} \rangle$$

$$\lesssim \left\| \widetilde{\mathbb{T}^*\widetilde{\mathbb{T}}\tilde{l}_{\eta_{g(e)}}} \right\| \left\| \widetilde{\tilde{l}_{\eta_{g(e)}}} \right\|$$

$$\lesssim \left\| \widetilde{\mathbb{T}^2\tilde{l}_{\eta_{g(e)}}} \right\|$$

$$\left\| \widetilde{\mathbb{T}^1\tilde{l}_{\eta_{g(e)}}} \right\| \lesssim \left\| \widetilde{\mathbb{T}^2\tilde{l}_{\eta_{g(e)}}} \right\|$$

If $n = k$, then

$$\left\| \widetilde{\mathbb{T}^k\tilde{l}_{\eta_{g(e)}}} \right\|^2 \cong \langle \widetilde{\mathbb{T}^k\tilde{l}_{\eta_{g(e)}}}, \; \widetilde{\mathbb{T}^k\tilde{l}_{\eta_{g(e)}}} \rangle$$

$$\cong \langle \widetilde{(\widetilde{\mathbb{T}}^k)^* \widetilde{\mathbb{T}}^k\tilde{l}_{\eta_{g(e)}}}, \; \tilde{l}_{\eta_{g(e)}} \rangle$$

$$\cong \langle \widetilde{(\widetilde{\mathbb{T}}^*)^k \widetilde{\mathbb{T}}^k\tilde{l}_{\eta_{g(e)}}}, \; \tilde{l}_{\eta_{g(e)}} \rangle$$

$$\cong \langle \widetilde{\mathbb{T}}^k \widetilde{\mathbb{T}}^k\tilde{l}_{\eta_{g(e)}}, \; \tilde{l}_{\eta_{g(e)}} \rangle$$

$$\cong \langle \widetilde{\mathbb{T}^{2k}\tilde{l}_{\eta_{g(e)}}}, \; \tilde{l}_{\eta_{g(e)}} \rangle$$

$$\left\| \widetilde{\mathbb{T}^k\tilde{l}_{\eta_{g(e)}}} \right\|^2 \lesssim \left\| \widetilde{\mathbb{T}^{2k}\tilde{l}_{\eta_{g(e)}}} \right\| \left\| \widetilde{\tilde{l}_{\eta_{g(e)}}} \right\|$$

$$\left\| \widetilde{\mathbb{T}^k\tilde{l}_{\eta_{g(e)}}} \right\|^2 \lesssim \left\| \widetilde{\mathbb{T}^{2k}\tilde{l}_{\eta_{g(e)}}} \right\|$$

It will be shown that it is true for $n = k + 1$

$$\left\| \widetilde{\mathbb{T}^{k+1}\tilde{l}_{\eta_{g(e)}}} \right\|^2 \cong \langle \widetilde{\mathbb{T}^{k+1}\tilde{l}_{\eta_{g(e)}}}, \; \widetilde{\mathbb{T}^{k+1}\tilde{l}_{\eta_{g(e)}}} \rangle$$

$$\cong \langle \widetilde{(\widetilde{\mathbb{T}}^{k+1})^* \widetilde{\mathbb{T}}^{k+1}\tilde{l}_{\eta_{g(e)}}}, \; \tilde{l}_{\eta_{g(e)}} \rangle$$

$$\cong \langle \widetilde{(\widetilde{\mathbb{T}}^*)^{k+1} \widetilde{\mathbb{T}}^{k+1}\tilde{l}_{\eta_{g(e)}}}, \; \tilde{l}_{\eta_{g(e)}} \rangle$$

$$\cong \langle \widetilde{\mathbb{T}}^{k+1} \widetilde{\mathbb{T}}^{k+1}\tilde{l}_{\eta_{g(e)}}, \; \tilde{l}_{\eta_{g(e)}} \rangle$$

$$\cong \langle \widetilde{\mathcal{T}}^{2(k+1)}\widetilde{\tilde{l}_{\eta_{\mathfrak{g}(e)}}} , \tilde{l}_{\eta_{\mathfrak{g}(e)}} \rangle$$

$$\left\| \widetilde{\mathcal{T}^{k+1}\tilde{l}_{\eta_{\mathfrak{g}(e)}}} \right\|^2 \tilde{\le} \left\| \widetilde{\mathcal{T}^{2(k+1)}\tilde{l}_{\eta_{\mathfrak{g}(e)}}} \right\| \left\| \widetilde{\tilde{l}_{\eta_{\mathfrak{g}(e)}}} \right\|$$

$$\left\| \widetilde{\mathcal{T}^{k+1}\tilde{l}_{\eta_{\mathfrak{g}(e)}}} \right\|^2 \tilde{\le} \left\| \widetilde{\mathcal{T}^{2(k+1)}\tilde{l}_{\eta_{\mathfrak{g}(e)}}} \right\|$$

Hence $\widetilde{\mathcal{T}}$ is a fuzzy soft n-power paranormal operator.

Theorem 3.12:

Let $\widetilde{\mathcal{T}} \in \widetilde{\mathfrak{B}}(\tilde{\hbar})$ is a FSHS. If $\widetilde{\mathcal{T}}$ is a fuzzy soft n - paranormal operator and $\widetilde{\mathcal{T}}^{-1}$ exist then$\widetilde{\mathcal{T}}^{-1}$ is a fuzzy soft n-power paranormal operator.

Proof:

Since $\widetilde{\mathcal{T}}$ is a fuzzy soft n-power paranormal operator

$$\left\| \widetilde{\mathcal{T}^n\tilde{l}_{\eta_{\mathfrak{g}(e)}}} \right\|^2 \tilde{\le} \left\| \widetilde{\mathcal{T}^{2n}\tilde{l}_{\eta_{\mathfrak{g}(e)}}} \right\|$$

Now we replace $\tilde{l}_{\eta_{\mathfrak{g}(e)}}$ by $\left(\widetilde{\mathcal{T}}^{-1}\right)^{2n}\tilde{l}_{\eta_{\mathfrak{g}(e)}}$

$$\left\| \widetilde{\mathcal{T}^n\left(\widetilde{\mathcal{T}}^{-1}\right)^{2n}}\tilde{l}_{\eta_{\mathfrak{g}(e)}} \right\|^2 \tilde{\le} \left\| \widetilde{\mathcal{T}^{2n}\left(\widetilde{\mathcal{T}}^{-1}\right)^{2n}}\tilde{l}_{\eta_{\mathfrak{g}(e)}} \right\| \left\| \widetilde{\left(\widetilde{\mathcal{T}}^{-1}\right)^{2n}}\tilde{l}_{\eta_{\mathfrak{g}(e)}} \right\|$$

$$\left\| \widetilde{\mathcal{T}^n\left(\widetilde{\mathcal{T}^n}\right)^{-2}}\tilde{l}_{\eta_{\mathfrak{g}(e)}} \right\|^2 \tilde{\le} \left\| \widetilde{\tilde{l}_{\eta_{\mathfrak{g}(e)}}} \right\| \left\| \widetilde{\left(\widetilde{\mathcal{T}}^{-1}\right)^{2n}}\tilde{l}_{\eta_{\mathfrak{g}(e)}} \right\|$$

$$\left\| \widetilde{\left(\widetilde{\mathcal{T}}^{-1}\right)^n}\tilde{l}_{\eta_{\mathfrak{g}(e)}} \right\|^2 \tilde{\le} \left\| \widetilde{\tilde{l}_{\eta_{\mathfrak{g}(e)}}} \right\| \left\| \widetilde{\left(\widetilde{\mathcal{T}}^{-1}\right)^{2n}}\tilde{l}_{\eta_{\mathfrak{g}(e)}} \right\|$$

$$\left\| \widetilde{\left(\widetilde{\mathcal{T}}^{-1}\right)^{2n}}\tilde{l}_{\eta_{\mathfrak{g}(e)}} \right\| \left\| \widetilde{\tilde{l}_{\eta_{\mathfrak{g}(e)}}} \right\| \tilde{\ge} \left\| \widetilde{\left(\widetilde{\mathcal{T}}^{-1}\right)^n}\tilde{l}_{\eta_{\mathfrak{g}(e)}} \right\|^2$$

Hence $\widetilde{\mathcal{T}}^{-1}$ is fuzzy soft n-power paranormal operator

Definition 3.13: Fuzzy Soft * -Paranormal Operator (FS*-PN)

Let$\widetilde{\mathcal{T}}$is fuzzy soft self adjoint operatorand let $\tilde{\hbar}$ be an FS Hilbert space

An operator $\widetilde{\mathcal{T}} \in \widetilde{\mathfrak{B}}(\tilde{\hbar})$ is called FS*-PN if $\left\| \widetilde{\mathcal{T}^2\tilde{l}_{\eta_{\mathfrak{g}(e)}}} \right\| \tilde{\ge} \left\| \widetilde{\mathcal{T}^*\tilde{l}_{\eta_{\mathfrak{g}(e)}}} \right\|^2$ for all $\tilde{l}_{\eta_{\mathfrak{g}(e)}} \tilde{\in} \tilde{\hbar}$

Theorem 3.14:

Let $\widetilde{\mathcal{T}}, \tilde{\mathcal{e}} \in \widetilde{\mathfrak{B}}(\tilde{\hbar})$, if $\widetilde{\mathcal{T}}, \tilde{\mathcal{e}}$ are fuzzy soft self adjoint operator then $\widetilde{\mathcal{T}}\tilde{\mp}\tilde{\mathcal{e}}$ is fuzzy soft * –paranormal operator.

Proof:

Take$\tilde{l}_{\eta_{\mathfrak{g}(e)}} \tilde{\in} \tilde{\hbar}$ with $\left\| \widetilde{\tilde{l}_{\eta_{\mathfrak{g}(e)}}} \right\| \cong 1$

Let $\left\| \widetilde{\left(\widetilde{\mathcal{T}}\tilde{\mp}\tilde{\mathcal{e}}\right)^*}\tilde{l}_{\eta_{\mathfrak{g}(e)}} \right\|^2 \cong \langle \widetilde{\left(\widetilde{\mathcal{T}}\tilde{\mp}\tilde{\mathcal{e}}\right)^*\tilde{l}_{\eta_{\mathfrak{g}(e)}}} , \widetilde{\left(\widetilde{\mathcal{T}}\tilde{\mp}\tilde{\mathcal{e}}\right)^*\tilde{l}_{\eta_{\mathfrak{g}(e)}}} \rangle$

$$\cong \langle \left(\widetilde{\left(\widetilde{\mathcal{T}}\tilde{\mp}\tilde{\mathcal{e}}\right)^*}\right)^* \widetilde{\left(\widetilde{\mathcal{T}}\tilde{\mp}\tilde{\mathcal{e}}\right)^*}\tilde{l}_{\eta_{\mathfrak{g}(e)}} , \tilde{l}_{\eta_{\mathfrak{g}(e)}} \rangle$$

$$\cong \langle \left(\left(\widetilde{\mathcal{T}}\tilde{\mp}\tilde{\mathcal{e}}\right)\widetilde{\left(\widetilde{\mathcal{T}}^* + \tilde{\mathcal{e}}^*\right)}\right)\tilde{l}_{\eta_{\mathfrak{g}(e)}} , \tilde{l}_{\eta_{\mathfrak{g}(e)}} \rangle$$

$$\cong \langle \left(\left(\widetilde{\mathcal{T}}\tilde{\mp}\tilde{\mathcal{e}}\right)\widetilde{\left(\widetilde{\mathcal{T}}\tilde{\mp}\tilde{\mathcal{e}}\right)}\right)\tilde{l}_{\eta_{\mathfrak{g}(e)}} , \tilde{l}_{\eta_{\mathfrak{g}(e)}} \rangle$$

$$\cong \langle \left(\left(\widetilde{\mathcal{T}}\tilde{\mp}\tilde{\mathcal{e}}\right)^2\tilde{l}_{\eta_{\mathfrak{g}(e)}}\right) , \tilde{l}_{\eta_{\mathfrak{g}(e)}} \rangle$$

$$\left\| \widetilde{\left(\widetilde{\mathcal{T}}\tilde{\mp}\tilde{\mathcal{e}}\right)^*}\tilde{l}_{\eta_{\mathfrak{g}(e)}} \right\|^2 \tilde{\le} \langle \left(\left(\widetilde{\mathcal{T}}\tilde{\mp}\tilde{\mathcal{e}}\right)^2\tilde{l}_{\eta_{\mathfrak{g}(e)}}\right) , \tilde{l}_{\eta_{\mathfrak{g}(e)}} \rangle$$

$$\left\| \widetilde{\left(\widetilde{\mathcal{T}}\tilde{\mp}\tilde{\mathcal{e}}\right)^*}\tilde{l}_{\eta_{\mathfrak{g}(e)}} \right\|^2 \tilde{\le} \left\| \widetilde{\left(\widetilde{\mathcal{T}}\tilde{\mp}\tilde{\mathcal{e}}\right)^2}\tilde{l}_{\eta_{\mathfrak{g}(e)}} \right\| \left\| \widetilde{\tilde{l}_{\eta_{\mathfrak{g}(e)}}} \right\| \text{implies that}$$

$$\left\| \widetilde{\left(\widetilde{\mathcal{T}}\tilde{\mp}\tilde{\mathcal{e}}\right)^*}\tilde{l}_{\eta_{\mathfrak{g}(e)}} \right\|^2 \tilde{\le} \left\| \widetilde{\left(\widetilde{\mathcal{T}}\tilde{\mp}\tilde{\mathcal{e}}\right)^2}\tilde{l}_{\eta_{\mathfrak{g}(e)}} \right\|$$

Therefore, $\widetilde{\mathcal{T}}\tilde{\mp}\tilde{\mathcal{e}}$ is fuzzy soft *- paranormal operator

Theorem 3.15:

Let $\widetilde{\mathfrak{T}}, \widetilde{\mathfrak{e}} \in \widetilde{\mathfrak{B}}(\check{\hbar})$, if $\widetilde{\mathfrak{T}}, \widetilde{\mathfrak{e}}$ are fuzzy soft self adjoint operator then $\widetilde{\mathfrak{T}}\widetilde{\mathfrak{e}}$ is fuzzy soft *–paranormal operator.

Proof:

Take $\widetilde{\mathfrak{e}}_{\mathfrak{g}0} \in^{\sim}$ with $\left\|\widetilde{\mathfrak{g}0}\right\| \cong 1$

Let $\left\|\widetilde{(\widetilde{\mathfrak{T}}\widetilde{\mathfrak{e}})^{*}}_{\mathfrak{g}0}\right\|^{2} \cong \langle \widetilde{(\widetilde{\mathfrak{T}}\widetilde{\mathfrak{e}})^{*}}_{\mathfrak{g}0}, \widetilde{(\widetilde{\mathfrak{T}}\widetilde{\mathfrak{e}})^{*}}_{\mathfrak{g}0}\rangle$

$\cong \langle \left(\widetilde{((\widetilde{\mathfrak{T}}\widetilde{\mathfrak{e}})^{*})^{*}} \widetilde{(\widetilde{\mathfrak{T}}\widetilde{\mathfrak{e}})^{*}}_{\mathfrak{g}0}, \widetilde{}_{\mathfrak{g}0}\rangle \right.$

$\cong \langle \left(\widetilde{(\widetilde{\mathfrak{e}}^{*}\widetilde{\mathfrak{T}}^{*})^{*}} \widetilde{(\widetilde{\mathfrak{T}}\widetilde{\mathfrak{e}})^{*}}_{\mathfrak{g}0}, \widetilde{}_{\mathfrak{g}0}\right)\rangle$

$\cong \langle \left(\widetilde{(\widetilde{\mathfrak{e}}\widetilde{\mathfrak{T}})^{*}} \widetilde{(\widetilde{\mathfrak{e}}^{*}\widetilde{\mathfrak{T}}^{*})}_{\mathfrak{g}0}, \widetilde{}_{\mathfrak{g}0}\right)\rangle$

$\cong \langle \left(\widetilde{(\widetilde{\mathfrak{e}}^{*}\widetilde{\mathfrak{T}}^{*})} \widetilde{(\widetilde{\mathfrak{e}}^{*}\widetilde{\mathfrak{T}}^{*})}_{\mathfrak{g}0}, \widetilde{}_{\mathfrak{g}0}\right)\rangle$

$\cong \langle \left(\widetilde{(\widetilde{\mathfrak{T}}^{*}\widetilde{\mathfrak{e}}^{*})} \widetilde{(\widetilde{\mathfrak{T}}^{*}\widetilde{\mathfrak{e}}^{*})}_{\mathfrak{g}0}, \widetilde{}_{\mathfrak{g}0}\right)\rangle$

$\cong \langle \left(\widetilde{(\widetilde{\mathfrak{T}}\widetilde{\mathfrak{e}})^{2}}_{\mathfrak{g}0}, \widetilde{}_{\mathfrak{g}0}\right)\rangle$

$\lesssim \left\|\widetilde{(\widetilde{\mathfrak{T}}\widetilde{\mathfrak{e}})^{2}}_{\mathfrak{g}0}\right\| \left\|\widetilde{}_{\mathfrak{g}0}\right\|$

$\left\|\widetilde{(\widetilde{\mathfrak{T}}\widetilde{\mathfrak{e}})^{*}}\widetilde{\iota}_{\eta_{\mathfrak{g}(e)}}\right\|^{2} \lesssim \left\|\widetilde{(\widetilde{\mathfrak{T}}\widetilde{\mathfrak{e}})^{2}}\widetilde{\iota}_{\eta_{\mathfrak{g}(e)}}\right\|$

Therefore, $\widetilde{\mathfrak{T}}\widetilde{\mathfrak{e}}$ is fuzzy soft *- paranormal operator

CONCLUSION

The concepts of normed space, metric space, and Hilbert space have all been given soft and fuzzy updates by numerous academics. The results of merging soft and fuzzy concepts are more widely applicable. In this paper, the Fuzzy soft n-power paranormal operator has been described and defined.

ACKNOWLEDGEMENT

REFERENCES

1. Beaula and M.M. Priyanga, A new notion for fuzzy soft normed linear space, Int. J. Fuzzy Math. Arch. 9(1), 81-90 (2015)
2. N. Faried, M.S.S. Ali and H.H. Sakr, On fuzzy soft linear operators in fuzzy soft Hilbert Spaces, Abst. Appl. Anal.2020
3. N. Faried, M.S.S. Ali and H.H. Sakr. Fuzzy soft inner product spaces, Appl.Math. Inf. Sci. 14(4), 709-720(2020)
4. N. Faried, M.S.S. Ali and H.H. Sakr. Fuzzy soft Hilbert spaces, J. Math. Comp. Sci. 22(2021), 142-157 (2020)
5. N. Faried, M.S.S. Ali and H.H. Sakr. A Note on Fuzzy soft Isometry operators, Math.Sci.Lett.10, No.1, 1-3(2021)
6. P.K. Maji, R. Biswas and A.R. Roy, Fuzzy soft set , J. Fuzzy Math.. 9(3), 677-692 (2001)
7. K. Maji, R. Biswas, and A.R. Roy, "Soft set theory", Computers & Mathematics with Application, vol.45, no. 4-5, pp. 555-562, 2003
8. D. Molodtsov, Soft set theory-First results, Comput. Math.Appl. 37. 19-31 (1999)
9. Dr.SalimDawood, Ali QassimJabur, On fuzzy soft normal operators, Journal of Physics: Conference series 1879(2021) 032002
10. Dr.SalimDawood, Ali QassimJabur, On fuzzy soft projection operators in Hilbert space, Al-Qadisiyah journal of pure science vol.(26) issue (1)(2021)PP math.112-123

11. Radharamani. A etal., Fuzzy partial isometry operator and its characteristics, IOSR Journal of Engineering (IOSRJEN) , VOL.09.NO.08, 2019, PP.54-58

12. Radharamani. A etal., Fuzzy unitary operator in Fuzzy Hilbert space and its properties, International Journal of Research and Analytic Reviews(IJRAR) , 2018, 5(4), 258-261

13. Radharamani.A , T Nagajothi, Fuzzy soft hyponormal operator in Fuzzy soft Hilbert space, Strad Research, Vol.9, issue 3-2022

14. Radharamani. A, T Nagajothi , M-Fuzzy soft hyponormal operator in Fuzzy soft Hilbert space, Journal of Data Acquisition and Processing, Vol.38, issue (1)2023

15. L.A. Zadeh, Fuzzy sets, Inf.Control, vol.8, no.3,pp. 338-353, 1965

RESEARCH ARTICLE

Third Order Semi-Canonical Nonlinear Difference Equations

S. Kaleeswari[1] and S. Rangasri[2]*

[1]Department of Mathematics, Nallamuthu Gounder Mahalingam College, Pollachi, Tamil Nadu, India - 642201.
[2]Research Scholar Department of Mathematics, Nallamuthu Gounder Mahalingam College, Pollachi, Tamil Nadu, India – 642201

*Address for Correspondence
S. Rangasri
Research Scholar Department of Mathematics,
Nallamuthu Gounder Mahalingam College,
Pollachi, Tamil Nadu, India - 642201.
E. Mail: rangasrisuresh97@gmail.com

ABSTRACT

We provide some novel oscillation conditions for semi-canonical difference equations using the canonical transformation method. Our findings reinforce and improve certain earlier ones. Examples have been generated to highlight the relevance of the consequences.

Keywords: Semi-canonical, asymptotic, oscillatory, difference equation, nonlinear.

INTRODUCTION

Consider the third order difference equation in this instance.
$$\Delta(q(\varsigma)\Delta(r(\varsigma)\Delta\Psi(\varsigma))) = s(\varsigma)\Psi^{\kappa}(\varrho(\varsigma)), \varsigma \geq \varsigma_0 \qquad (1.1)$$
where ς_0 is a positive integer. We assume the subsequent hypothesis
H1) $\{q(\varsigma)\}, \{r(\varsigma)\}, \{s(\varsigma)\}$ are positive real sequences;
H2) $\{\varrho(\varsigma)\}$ is an increasing sequence of positive integer with $\varrho(\varsigma) \geq \varsigma + 1$;
H3) κ is a real positive integer with $\kappa > 1$;
H4) the equation (1.1) is in semi canonical form, that is
$\sum_{\varsigma=\varsigma_0}^{\infty} \frac{1}{q(\varsigma)} = \infty$ and $\sum_{\varsigma=\varsigma_0}^{\infty} \frac{1}{r(\varsigma)} < \infty.$ (1.2)
A real sequence $\{\Psi(\varsigma)\}$ that satisfies (1.1) for any $\varsigma \geq \varsigma_0$ is referred to as a solution of (1.1). Nontrivial solutions to (1.1) are either oscillatory or non oscillatory depending on whether the final result is positive or negative.
Finding out the qualitative behavior of various types of second order difference equations has garnered a lot of attention in recent years. Despite the fact that discrete models are used in many other areas of mathematics, including economics, mathematical biology, and [1] and [2], difference equations have a wide range of applications in these fields.

Kaleeswari and Rangasri

A number of publications have concentrated on the oscillatory and asymptotic solutions of (1.1), see [3]-[13] and the cited references throughout. However, the publication devotes the majority of its space to equation of the canonical form, (i.e),

$$\sum_{\varsigma=\varsigma_0}^{\infty} \frac{1}{q(\varsigma)} = \infty \text{ and } \sum_{\varsigma=\varsigma_0}^{\infty} \frac{1}{r(\varsigma)} = \infty.$$

In [14], the authors studied difference equation of the form

$$\Delta\left(q(\varsigma)\Delta\left(r(\varsigma)\Delta\Psi(\varsigma)\right)\right) = s(\varsigma)f\left(\Psi(\varrho(\varsigma))\right), \qquad \varsigma \geq \varsigma_0$$

with semi-canonical condition

$$\sum_{\varsigma=\varsigma_0}^{\infty} \frac{1}{q(\varsigma)} < \infty \text{ and } \sum_{\varsigma=\varsigma_0}^{\infty} \frac{1}{r(\varsigma)} = \infty.$$

In [15], the authors discussed about the difference equation of the form

$$\Delta(q(\varsigma)\Delta(r(\varsigma)\Delta\Psi(\varsigma))) + w(\varsigma)f(\Psi(\sigma(\varsigma))) - s(\varsigma)g(\Psi(\tau(\varsigma))) = 0.$$

with semi-canonical condition

$$\sum_{\varsigma=\varsigma_0}^{\infty} \frac{1}{q(\varsigma)} < \infty \text{ and } \sum_{\varsigma=\varsigma_0}^{\infty} \frac{1}{r(\varsigma)} = \infty.$$

To the greatest extent of our knowledge, the oscillatory features of the relevant equation have not been studied when

$$\sum_{\varsigma=\varsigma_0}^{\infty} \frac{1}{q(\varsigma)} = \infty \text{ and } \sum_{\varsigma=\varsigma_0}^{\infty} \frac{1}{r(\varsigma)} < \infty.$$

Therefore, the aim of this paper is to provide the qualitative behavior of (1.1) if condition (1.2) is satisfied. This is initially established by transforming semi-canonical to canonical, after which we approach to develop some novel criteria for oscillatory solution of (1.1).

MAIN RESULTS

To make it easier to read, the following symbols will be used:

$$Q(\varsigma) = \sum_{t=\varsigma_1}^{\varsigma-1} \frac{1}{\gamma(t)}, \qquad R(\varsigma) = \sum_{t=\varsigma}^{\infty} \frac{1}{r(t)}, \qquad \xi(\varsigma) = r(\varsigma)R(\varsigma)R(\varsigma+1),$$

$$\gamma(\varsigma) = \frac{q(\varsigma)}{R(\varsigma+1)}, \qquad S(\varsigma) = s(\varsigma)R^{\kappa}(\varrho(\varsigma)), \qquad \Xi(\varsigma) = \sum_{t=\varsigma_1}^{\varsigma-1} \frac{1}{\xi(t)},$$

$$F(\varsigma) = \frac{1}{\gamma(t)} \sum_{u=\varsigma}^{\infty} S(u), \qquad T(\varsigma) = \sum_{s=\varsigma_1}^{\varsigma-1} \frac{1}{\xi(s)} \sum_{t=\varsigma_1}^{s-1} \frac{1}{\gamma(t)}.$$

where $\varsigma \geq \varsigma_1 \geq \varsigma_0$ and ς_1 is large enough.

Theorem 2.1. Assume that

$$\sum_{\varsigma=\varsigma_0}^{\infty} \frac{1}{\gamma(\varsigma)} = \infty \qquad\qquad\qquad (2.1)$$

Then (1.1) has the following canonical representation

$$\Delta\left(\frac{q(\varsigma)}{R(\varsigma+1)}\Delta\left(r(\varsigma)R(\varsigma)R(\varsigma+1)\Delta\left(\frac{\Psi(\varsigma)}{R(\varsigma)}\right)\right)\right) = \Delta(q(\varsigma)\Delta(r(\varsigma)\Delta\Psi(\varsigma))). \qquad (2.2)$$

Proof. Direct computation demonstrates that

$$\frac{q(\varsigma)}{R(\varsigma+1)}\Delta\left(r(\varsigma)R(\varsigma)R(\varsigma+1)\Delta\left(\frac{\Psi(\varsigma)}{R(\varsigma)}\right)\right) \quad = \frac{q(\varsigma)}{R(\varsigma+1)}\Delta(r(\varsigma)R(\varsigma)\Delta\Psi(\varsigma) + \Psi(\varsigma))$$

$$= \frac{q(\varsigma)}{R(\varsigma+1)}[R(\varsigma+1)\Delta(r(\varsigma)\Delta\Psi(\varsigma))]$$

$$= q(\varsigma)\Delta(r(\varsigma)\Delta\Psi(\varsigma))$$

Hence

$$\Delta\left(\frac{q(\varsigma)}{R(\varsigma+1)}\Delta\left(r(\varsigma)R(\varsigma)R(\varsigma+1)\Delta\left(\frac{\Psi(\varsigma)}{R(\varsigma)}\right)\right)\right) = \Delta(q(\varsigma)\Delta(r(\varsigma)\Delta\Psi(\varsigma))).$$

As we can see from (2.1),

$$\sum_{\varsigma=\varsigma_0}^{\infty}\frac{R(\varsigma+1)}{q(\varsigma)} = \infty, \quad (2.3)$$

and since

$$\sum_{\varsigma=\varsigma_0}^{\infty}\frac{1}{r(\varsigma)R(\varsigma)R(\varsigma+1)} = \sum_{\varsigma=\varsigma_0}^{\infty}\Delta\left(\frac{1}{R(\varsigma)}\right) = \lim_{\varsigma\to\infty}\frac{1}{R(\varsigma)}-\frac{1}{R(\varsigma_0)} = \infty,$$

we assess that (2.2) is in canonical form

Corollary 2.2. Assume that (2.1) holds. Then the semi-canonical difference equation (1.1) possesses a solution $\Psi(\varsigma)$ if and only if the canonical equation

$$\Delta(\gamma(\varsigma)\Delta(\xi(\varsigma)\Delta\Phi(\varsigma))) = S(\varsigma)\Phi^{\kappa}(\varrho(\varsigma)) \qquad (2.4)$$

has the positive solution $\Phi(\varsigma) = \frac{\Psi(\varsigma)}{R(\varsigma)}$.

In the following section, we provide the structure of a potential non-oscillatory solution to (2.4), which is deduced from an analogy involving the discrete knesers theorem and canonical form of (2.4)

$$\Phi(\varsigma) \in \mathcal{N}_0 : \Phi(\varsigma) > 0, \Delta\Phi(\varsigma) > 0, \Delta(\xi(\varsigma)\Delta(\Phi(\varsigma))) < 0, \Delta(\gamma(\varsigma)\Delta(\xi(\varsigma)\Delta\Phi(\varsigma))) > 0$$

and

$$\Phi(\varsigma) \in \mathcal{N}_3 : \Phi(\varsigma) > 0, \Delta\Phi(\varsigma) > 0, \Delta(\xi(\varsigma)\Delta(\Phi(\varsigma))) > 0, \Delta(\gamma(\varsigma)\Delta(\xi(\varsigma)\Delta\Phi(\varsigma))) > 0.$$

Lemma 2.3. Assuming $\Phi(\varsigma) \in \mathcal{N}_3$ is a positive solution of (2.4) and

$$\sum_{u=\varsigma_1}^{\infty} S(u)T^{\kappa}(\varrho(u)) = \infty. \qquad (2.5)$$

Then $\frac{\Phi(\varsigma)}{T(\varsigma)}$ is eventually increasing $\forall \; \varsigma \geq K$.

The preceding lemma's proof resembles that of in [3].

Theorem 2.4. Assuming that (2.1) is true,

$$\sum_{t=\varsigma_1}^{\varsigma-1}\frac{1}{\xi(t)}\sum_{u=t}^{\infty}F(t) = \infty \qquad (2.6)$$

and

$$\limsup_{\varsigma\to\infty}\left(\frac{1}{\Xi^{\kappa}(\varrho(\varsigma))}\sum_{t=\varsigma_1}^{\varsigma-1}\Xi^{\kappa}(\varrho(t))\Xi(t+1)F(t) + \sum_{t=\varsigma}^{\varrho(t)-1}\Xi(t+1)F(t) + \Xi(\varrho(\varsigma))\sum_{t=\varrho(\varsigma)}^{\infty}F(t)\right) = \infty. \qquad (2.7)$$

Then all non-oscillatory solution of (1.1) meets $\lim_{\varsigma\to\infty}\frac{\Psi(\varsigma)}{R(\varsigma)} = 0$.

Proof. Let $\{\Psi(\varsigma)\}$ be an non-oscillatory solution (1.1). Without losing generality, suppose that $\{\Psi(\varsigma)\}$ is a positive solution of (1.1). Then, from corollary 2.2, relevant sequence $\{\Phi(\varsigma)\}$ is also a positive solution of (2.4) and $\Phi(\varsigma) \in \mathcal{N}_0$ or $\Phi(\varsigma) \in \mathcal{N}_3$ for all $\varsigma \geq \varsigma_1$. Now consider that $\Phi(\varsigma) \in \mathcal{N}_0$ for all $\varsigma \geq \varsigma_1$. From the monotonicity of $\xi(\varsigma)\Delta\Phi(\varsigma)$, we carry

$$\Phi(\varsigma) \geq \Phi(\varsigma)-\Phi(\varsigma_1) = \sum_{t=\varsigma_1}^{\varsigma-1}\frac{\xi(t)\Delta\Phi(t)}{\xi(t)} \geq \xi(\varsigma)\Delta\Phi(\varsigma)\Xi(\varsigma)$$

which suggest that

$$\Delta\left(\frac{\Phi(\varsigma)}{\Xi(\varsigma)}\right) = \left(\frac{\Xi(\varsigma)\Delta\Phi(\varsigma)-\Phi(\varsigma)\frac{1}{\xi(\varsigma)}}{\Xi(\varsigma)\Xi(\varsigma+1)}\right) \leq 0 \qquad (2.8)$$

Hence $\frac{\Phi(\varsigma)}{\Xi(\varsigma)}$ is decreasing.

On the other hand, summing twice (2.4) from ς to ∞ gives

$$\xi(\varsigma)\Delta\Phi(\varsigma) \geq \sum_{t=\varsigma}^{\infty}\frac{\Phi^{\kappa}(\varrho(t))}{\gamma(t)}\sum_{u=t}^{\infty}S(u)$$

$$\geq \sum_{t=\varsigma}^{\infty}\Phi^{\kappa}(\varrho(t))F(t).$$

Again, summing from ς_1 to $\varsigma-1$, we carry

$$\Phi(\varsigma) \geq \sum_{t=\varsigma_1}^{\varsigma-1} \frac{1}{\xi(t)} \sum_{u=\varsigma}^{\infty} \Phi^\kappa(\varrho(u)) F(u)$$

$$= \Xi(\varsigma) \sum_{u=\varsigma}^{\infty} \Phi^\kappa(\varrho(u)) F(u) + \sum_{t=\varsigma_1}^{\varsigma-1} \Xi(t+1) \Phi^\kappa(\varrho(t)) F(t)$$

Hence

$$\Phi(\varrho(\varsigma)) \geq \sum_{t=\varsigma_1}^{\varsigma-1} \Xi(t+1) \Phi^\kappa(\varrho(t)) F(t) + \sum_{t=\varsigma}^{\varrho(\varsigma)-1} \Xi(t+1) \Phi^\kappa(\varrho(t)) F(t) + \Xi(\varrho(\varsigma)) \sum_{t=\varrho(\varsigma)}^{\infty} \Phi^\kappa(\varrho(t)) F(t).$$

Using $\Phi(\varsigma)$ is increasing and $\frac{\Phi(\varsigma)}{\Xi(\varsigma)}$ decreasing, we obtain

$$\Phi(\varrho(\varsigma)) \geq \frac{\Phi^\kappa(\varrho(\varsigma))}{\Xi^\kappa(\varrho(\varsigma))} \sum_{t=\varsigma_1}^{\varsigma-1} \Xi^\kappa(\varrho(t)) \Xi(t+1) F(t) + \Phi^\kappa(\varrho(\varsigma)) \sum_{t=\varsigma}^{\varrho(\varsigma)-1} \Xi(t+1) F(t) + \Phi^\kappa(\varrho(\varsigma)) \Xi(\varrho(\varsigma)) \sum_{t=\varrho(\varsigma)}^{\infty} F(t)$$

or

$$\Phi^{1-\kappa}(\varrho(\varsigma)) \geq \frac{1}{\Xi^\kappa(\varrho(\varsigma))} \sum_{t=\varsigma_1}^{\varsigma-1} \Xi^\kappa(\varrho(t)) \Xi(t+1) F(t) + \sum_{t=\varsigma}^{\varrho(\varsigma)-1} \Xi(t+1) F(t) + \Xi(\varrho(\varsigma)) \sum_{t=\varrho(\varsigma)}^{\infty} F(t).$$

(2.9)

Since $\Phi(\varsigma)$ is positive and increasing, $\exists$ a constant $A > 0 \ni \Phi(\varsigma) \geq A$, and so we carry $\Phi^{1-\kappa}(\varrho(\varsigma)) \leq A^{1-\kappa}$. Using this in (2.9) we obtain

$$A^{1-\kappa} \geq \frac{1}{\Xi^\kappa(\varrho(\varsigma))} \sum_{t=\varsigma_1}^{\varsigma-1} \Xi^\kappa(\varrho(t)) \Xi(t+1) F(t) + \sum_{t=\varsigma}^{\varrho(\varsigma)-1} \Xi(t+1) F(t) + \Xi(\varrho(\varsigma)) \sum_{t=\varrho(\varsigma)}^{\infty} F(t).$$

Taking limsup as $\varsigma \to \infty$ of the aforementioned inequality, which contradicts (2.7)

Next, we assume that $\Phi(\varsigma) \in \mathcal{N}_3$. Since $\Phi(\varsigma)$ is positive and increasing, there exists $\lim_{\varsigma \to \infty} \Phi(\varsigma) = e \geq 0$. Suppose that $e > 0$, then $\Phi(\varsigma) \geq e > 0$. Summing twice (2.4) from ς to ∞ and again summing from ς_1 to $\varsigma - 1$, which gives

$$\Phi(\varsigma) \geq e^\kappa \sum_{t=\varsigma_1}^{\varsigma-1} \frac{1}{\xi(t)} \sum_{u=t}^{\infty} F(t),$$

which contradicts (2.6) and so

$$\lim_{\varsigma \to \infty} \Phi(\varsigma) = \lim_{\varsigma \to \infty} \frac{\Psi(\varsigma)}{R(\varsigma)} = 0.$$

Hence the proof is completed.

Theorem 2.5. Let (2.1) and (2.5) hold, and

$$\lim_{\varsigma \to \infty} w^{\frac{1}{\kappa}-1}(\varsigma) = M_1^{\frac{1}{\kappa}-1} < \infty. \tag{2.10}$$

Suppose

$$\limsup_{\varsigma \to \infty} \left\{ \frac{1}{T(\varrho(\varsigma))} \sum_{t=\varsigma}^{\varrho(\varsigma)-1} \frac{1}{\xi(t)} \sum_{u=\varsigma}^{t-1} \frac{1}{\gamma(u)} \sum_{v=\varsigma}^{u-1} S(v) T^\kappa(\varrho(v)) \right\} > M_1, \tag{2.11}$$

then $\mathcal{N}_3$ is $\emptyset$ for (1.1).

Proof. Let $\{\Psi(\varsigma)\}$ be an positive solution of (1.1). By Corollary 2.2 the corresponding function $\{\Phi(\varsigma)\}$ is a positive solution of (2.4). Let us assume that $\Phi(\varsigma) \in \mathcal{N}_3$ for all $\varsigma \geq \varsigma_1$. Summing (2.4) from ς to $m-1$, we have

$$\Delta(\xi(m)\Delta\Phi(m)) \geq \frac{1}{\gamma(m)} \sum_{t=\varsigma}^{m-1} S(t) \Phi^\kappa(\varrho(t))$$

$$\geq \frac{1}{\gamma(m)} \sum_{t=\varsigma}^{m-1} S(t) \frac{\Phi^\kappa(\varrho(t))}{T^\kappa(\varrho(t))} T^\kappa(\varrho(t))$$

$$\geq \frac{\Phi^\kappa(\varrho(\varsigma))}{T^\kappa(\varrho(\varsigma))} \frac{1}{\gamma(m)} \sum_{t=\varsigma}^{m-1} S(t) T^\kappa(\varrho(t)).$$

Again summing, we get

$$\Delta\Phi(m) \geq \frac{\Phi^\kappa(\varrho(\varsigma))}{T^\kappa(\varrho(\varsigma))} \frac{1}{\xi(m)} \sum_{t=\varsigma}^{m-1} \frac{1}{\gamma(t)} \sum_{u=\varsigma}^{t-1} S(u) T^\kappa(\varrho(u)).$$

Summing once again, we obtain

$\Phi(m) \geq \frac{\Phi^\kappa(\varrho(\varsigma))}{T^\kappa(\varrho(\varsigma))} \sum_{t=\varsigma}^{m-1} \frac{1}{\xi(t)} \sum_{u=\varsigma}^{t-1} \frac{1}{\gamma(u)} \sum_{v=\varsigma}^{u-1} S(v)T^\kappa(\varrho(v)).$

Now, we have to define $m = \varrho(\varsigma)$ and $w(\varsigma) = \frac{\Phi^\kappa(\varrho(\varsigma))}{T^\kappa(\varrho(\varsigma))}.$

$$\Phi(\varrho(\varsigma)) \geq w(\varsigma) \sum_{t=\varsigma}^{\varrho(\varsigma)-1} \frac{1}{\xi(t)} \sum_{u=\varsigma}^{t-1} \frac{1}{\gamma(u)} \sum_{v=\varsigma}^{u-1} S(v)T^\kappa(\varrho(v)),$$

$w^{\frac{1}{\kappa}-1}(\varsigma) \geq \frac{1}{T(\varrho(\varsigma))} \sum_{t=\varsigma}^{\varrho(\varsigma)-1} \frac{1}{\xi(t)} \sum_{u=\varsigma}^{t-1} \frac{1}{\gamma(u)} \sum_{v=\varsigma}^{u-1} S(v)T^\kappa(\varrho(v)).$

Taking limit as $\varsigma \to \infty$ on above inequality, we get

$$\limsup_{\varsigma\to\infty} w^{\frac{1}{\kappa}-1}(\varsigma) \geq \limsup_{\varsigma\to\infty} \frac{1}{T(\varrho(\varsigma))} \sum_{t=\varsigma}^{\varrho(\varsigma)-1} \frac{1}{\xi(t)} \sum_{u=\varsigma}^{t-1} \frac{1}{\gamma(u)} \sum_{v=\varsigma}^{u-1} S(v)T^\kappa(\varrho(v)).$$

Which contradicts (2.11). Thus, $\mathcal{N}_3$ is $\emptyset$ for (1.1). This completes the proof.

Theorem 2.6. If all the conditions of Theorem 2.4 and 2.5 hold, then the solution $\Psi(\varsigma)$ of (1.1) is oscillatory or satisfies $\lim_{\varsigma\to\infty} \frac{\Psi(\varsigma)}{R(\varsigma)} = 0$

3. EXAMPLES

Example 3.1. Take

$\Delta\left(\frac{1}{(2^{\varsigma+1})^2} \Delta\left(\frac{1}{2^{\varsigma+1}} \Delta\Psi(\varsigma)\right)\right) = (2^{\varsigma+2})^2 \Psi^3(\varsigma + 2), \varsigma \geq 1$ (3.1)

Here $q(\varsigma) = \frac{1}{(2^{\varsigma+1})^2}, r(\varsigma) = \frac{1}{2^{\varsigma+1}}, s(\varsigma) = (2^{\varsigma+1})^2, \kappa = 3, \varrho(\varsigma) = \varsigma + 2, R(\varsigma) = \sum_{t=\varsigma}^{\infty} 2^{t+1} = 2^\varsigma, \gamma(\varsigma) = \frac{1}{(2^{\varsigma+1})^3}, \xi(\varsigma) = 2^\varsigma, S(\varsigma) = (2^{\varsigma+2})^5, Q(\varsigma) \approx (2^{\varsigma+2})^3, T(\varsigma) \approx 2^\varsigma(2^{\varsigma+1})^3, \Xi(\varsigma) = \frac{1}{2^\varsigma}, F(\varsigma) = (2^{\varsigma+1})^2.$ Therefore (2.4) becomes

$\Delta\left(\frac{1}{(2^{\varsigma+1} + 1)^3} \Delta(2^\varsigma \Delta\Phi(\varsigma))\right) = (2^{\varsigma+2})^5 \Phi^3(\varsigma + 2).$

is canonical.

Clearly

$$\sum_{\varsigma=\varsigma_0}^{\infty} \frac{1}{\gamma(\varsigma)} = \sum_{\varsigma=1}^{\infty} (2^{\varsigma+1})^2 = \infty$$

and

$$\sum_{t=\varsigma_1}^{\varsigma-1} \frac{1}{2^t} \sum_{u=t}^{\infty} 2^{u+1} = \infty$$

Also (2.7) becomes

$$\limsup_{\varsigma\to\infty} \left(2^{\varsigma+2} \sum_{t=1}^{\varsigma-1} \frac{1}{2^{t+2}} \frac{1}{2^{t+1}} (2^{t+1})^2 + \sum_{t=\varsigma}^{\varsigma+1} (2^{t+1}) + \frac{1}{2^{\varsigma+1}} \sum_{t=\varsigma+2}^{\infty} (2^{t+1})^2\right) = \infty.$$

(i.e), (2.7) is verified. Hence by Theorem 2.4, every non-oscillatory solution $\Psi(t)$ of (3.1) satisfies

$\lim_{\varsigma\to\infty} \frac{1}{2^\varsigma} \Psi(\varsigma) = 0.$

Example 3.2. Take

$\Delta\left(\frac{1}{\varsigma^2} \Delta(\varsigma(\varsigma + 1)\Delta\Psi(\varsigma))\right) = \varsigma(\varsigma + 2)^2 \Psi^2(\varsigma + 1).$ (3.2)

Here $q(\varsigma) = \frac{1}{\varsigma^2}, r(\varsigma) = \varsigma(\varsigma + 1), s(\varsigma) = \varsigma(\varsigma + 2)^2, \kappa = 2, \varrho(\varsigma) = \varsigma + 1, R(\varsigma) = \sum_{t=\varsigma}^{\infty} \frac{1}{t(t+1)} = \frac{1}{\varsigma},$ $\gamma(\varsigma) = \frac{1}{\varsigma}, \xi(\varsigma) = 1, S(\varsigma) = \varsigma(\varsigma + 2)^2 \frac{1}{(\varsigma+1)^2}, Q(\varsigma) \approx \varsigma, T(\varsigma) \approx \varsigma^2, \Xi(\varsigma) \approx \varsigma.$ Take $M = 1$, therefore (2.4) becomes

$\Delta\left(\frac{1}{\varsigma} (\Delta(\Delta\Phi(\varsigma)))\right) = \varsigma(\varsigma + 2)^2 \frac{1}{(\varsigma + 1)^2} \Phi^2(\varsigma + 1),$

is canonical.

Clearly

$\sum_{\varsigma=\varsigma_0}^{\infty} \frac{1}{\gamma(\varsigma)} = \sum_{\varsigma=1}^{\infty} \varsigma = \infty$

and

$$\sum_{u=\varsigma_1}^{\infty} S(u)T^{\kappa}(\varrho(u)) = \sum_{u=\varsigma_1}^{\infty} u(u+2)^2 = \infty$$

and

$$\lim_{\varsigma \to \infty} w^{\frac{1}{\varsigma}-1}(\varsigma) = 1 < \infty$$

is true.

Also (2.11) becomes

$$\limsup_{\varsigma \to \infty} \left\{ \frac{1}{\varsigma+1} \sum_{t=1}^{\varsigma} \sum_{u=1}^{t-1} \frac{1}{\varsigma} \sum_{v=1}^{u-1} v(v+2)^2 \right\} = \infty > M_1.$$

Hence all the conditions of Theorem 2.5 are verified, so every solution $\Psi(\varsigma)$ of (3.2) is oscillatory.

CONCLUSION

This study finds some fresh oscillatory and asymptotic conditions for semi-canonical difference equations. The conclusions reached in this study have a high degree of generality, and they enhance and add to prior conclusions for specific instances of equation (1.1).

REFERENCES

1. Kaleeswari, S., Selvaraj, B., Removing Noise Through a Nonlinear Difference OperatorMT, International Journal of Applied Engineering Research, 9 (21), 5100-5106, 2014.
2. Kaleeswari, S., Selvaraj,B., Thiyagarajan, M., A New Creation of Mask from Difference Operator to Image Analysis, Journal of Theoretical and Applied Information Technology, 69(1), 2014.
3. Agarwal, R.P., Difference Equations and Inqualities, Theory, Methods and Applications, Second Edition, Revised and Expanded, New York, Marcel Dekker, 2000.
4. Ahmed Mohamed Hassan, Higinio Ramos, Osama Moaaz, Second order dynamic equations with noncanonical operator: Oscillatory behavior, Fractal Fract, 7, 2023, 134.
5. Elaydi, S. An Introduction to Difference Equations, Springer-Verlag, New York, 1996.
6. John R. Graef, Canonical, Noncanonical, and semi-canonical Third Order Dynamic Equations on Time Scales, Results in Nonlinear Analysis, 5 N0. 3, (2022) 273-278.
7. Martin Bohner, Srinivasan, R., Thandapani, E., Oscillation of second order damped noncanonical differential equations with superlinear neutral term, Journal of Inequalities And Special Functions, Vol. 2, 3(2021)44-53.
8. Martin Bohner, Kumar, S. Vidhyaa, Thandapani, E.,Oscillation of noncanonical second order advanced differential equations via canonical transformConstructive Mathematical Analysis, 5 No. 1,(2022), pp. 7-13
9. Saker, S.H., Selvarangam, S., Geetha, S., Thandapani, E., Alzabut, J., Asymptotic behavior of third order delay difference equations with a negative middle term, Advance in Difference Equations, (2021), 248 .
10. Selvaraj, B., Kaleeswari, S., Oscillation of solutions of second order nonlinear difference equations, Bulletin of Pure and Applied Sciences-Mathematics and Statistics, 32 (1), 8392(2013).
11. Srinivasan, R., Dharuman, C., John R. Graef, Thandapani, E.,Asymptotic properties of kneser type solutions for third order half linear neutral difference equations, Miskolc Mathematical Notes, Vol. 22 No. 2, (2021), pp. 991-1000.
12. Srinivasan, R., Dharuman, C., Oscillation and property B for third order difference equations with advanced arguments, Int.Journal of Pure and Applied Mathematics, 113(16), 2017, 352360.
13. Walter, G.K., Allan, C.P., Difference Equations Introduction with Applications, Second Edition, Academic Press, 1991.
14. Chatzarakis, G., Srinivasan, R., Thandapani, E., Oscillation and property B for semicanonical third order advanced differene equations, Nonauton.Dyn.Syst., 9, 2022,11-20.

15. Gopal Thangavel, AyyapanGovindasamy, Thandapani, E., Oscillation and asymptotic behavior of third order semi-canonical difference equations with positive and negative terms, Int. J. Nonlinear Anal. Appl. 14, 1, (2023) 2519-2527.

RESEARCH ARTICLE

Triple Connected Certified Domination in Graphs

G. Mahadevan[1*], S. Kaviya[2] and C. Sivagnanam[3]

[1]Associate Professor, Department of Mathematics, The Gandhigram Rural Institute (Deemed to be University), Gandhigram, Dindigul, Tamil Nadu, India.
[2]Full- Time Research Scholar, Department of Mathematics, The Gandhigram Rural Institute (Deemed to be University), Gandhigram, Dindigul, Tamil Nadu, India.
[3]Assistant Professor, Department of General Requirements, University of Technology and Applied Sciences- Sur, Sultanate of Oman.

*Address for Correspondence
G.Mahadevan
Associate Professor,
Department of Mathematics,
The Gandhigram Rural Institute (Deemed to be University),
Gandhigram, Dindigul, Tamil Nadu, India.
E. Mail: drgmaha2014@gmail.com

ABSTRACT

The notion of certified domination was proposed by Magda Dettlaf *et al.*, and the concept of triple connected domination number was introduced by G.Mahadevan *et al*. Motivated by these papers in this article we introduce a new domination parameter called triple connected certified domination number of a graph. A dominating Set S is said to be a triple connected certified dominating set, if every vertex in S has either zero or at least two neighbours in $V - S$ and $< S >$ is triple connected. The minimum cardinality of a triple connected certified dominating set in G is called the triple connected certified domination number of a graph G and is denoted by $\gamma_{Tcc}(G)$. In this paper we initiate a study of this parameter.

Keywords: Domination, triple connected, certified domination, triple connected certified domination.

INTRODUCTION

The triple connected graph was initiated by Paulraj Joseph *et al.*[3], followed by this, triple connected domination number of a graph was introduced by G.Mahadevan *et al.* [4]. The idea of certified domination was initiated by Magda Dettlaff *et al.* [5]. Motivated by these papers, here we initiate a parameter called triple connected certified domination number. The graphs used here are connected and undirected graphs. Following are the definitions of some special type of graphs which are referred from [6]. The Flower graph F_r is a graph obtained from the Helm H_r

of joining each pendent vertex to the center of the helm. The Moser Spindle Graph has 7 points that can be placed so that its 11 edges all have the same length and is a unit-distance graph for any norm in the plane. Subdivide every edge in the graph G, join subdivided vertices that are adjacent to a common vertex, the obtained graph is called middle graph M(G). The shadow graph $S^{'}(G)$ is constructed by adding a new vertex v' for each vertex v of G and joining v' to the neighbours of v in G. Subdivide every edge in the graph G, join the vertices that are adjacent in G, and join the subdivided vertices that are adjacent to a common vertex. The obtained graph is called total graph T(G). The splitting graph S(G) is constructed by taking a copy of G for each vertex v_i in G corresponds to $v_i{'}$ in the copy of G and the joining $v_i^{'}$ to the neighbours of v_i in G. The Mirror graph $M_r(G) = P_2 \times G$. Book graph can be formed by joining r copies of C_3 with a common edge B_r. Crown graph is obtained to the complete bipartite graph by removing the Horizontal edges. The Double Wheel graph $DW_r = 2C_r + K_1$. The power graph G^t of a graph G has $V(G^t) = V(G)$ with u and v are adjacent in G^t whenever deg(u, v) $\leq$ t. G^2, G^3 is square and cube graph respectively.

TCCD- number

Definition 2.1:
A dominating set S is said to be a triple connected certified dominating set (TCCD-set), if $|N(v) \cap (V - S)| = 0$ or k, k $\geq$ 2 and any three vertices of S Lie on a path in $< S >$. The minimum cardinality of (TCCD-set) is called the triple connected certified domination number (TCCD-number) and is denoted by γ_{TCC}.
Example 2.2:
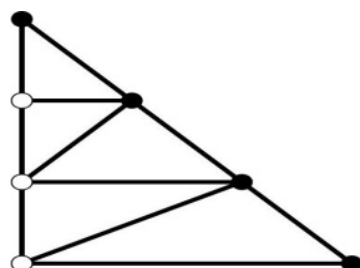
Figure 2.1

The graph given in figure 2.1, lightened vertices forms a TCCD-set of cardinality 3 which is minimum and hence $\gamma_{TCC} = 3$.
Observation 2.3: For a graph G, $\gamma \leq \gamma_{cer} \leq \gamma_{TCC}$.
Example 2.4:
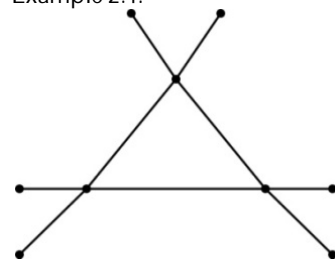
Figure 2.2

Illustration: The graph given in figure 2.2, $\gamma = \gamma_{cer} = \gamma_{TCC} = 3$.
Example 2.5:

Mahadevan *et al.*,
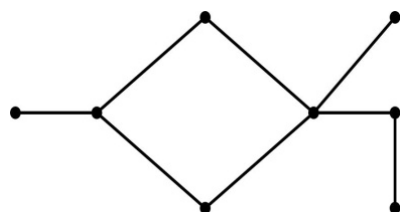
Figure 2.3

Illustration: The graph given in figure 2.3 $\gamma = 3, \gamma_{cer} = 4, \gamma_{TCC} = 5$.

Observation 2.6: For a graph G, $3 \leq \gamma_{TCC}(G) \leq n$.

Observation 2.7: For G, $\gamma_{TCC}(G) \geq \left\lceil \frac{n}{\Delta+1} \right\rceil$ and the bound is sharp.

Since $\left\lceil \frac{n}{\Delta+1} \right\rceil \leq \gamma(G) \leq n - \Delta$ also $\gamma \leq \gamma_{TCC}$, we have $\gamma_{TCC} \geq \left\lceil \frac{n}{\Delta+1} \right\rceil$.

Example 2.8:
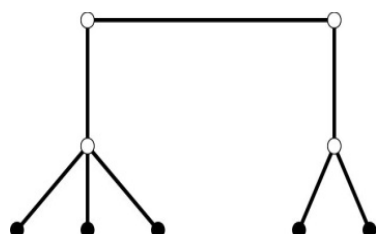
Figure : 2.4

Illustration: In this graph the set of white vertices is a TCCD set whose cardinality is minimum and hence $\gamma_{TCC}(G) = 4$.

Example2.9:
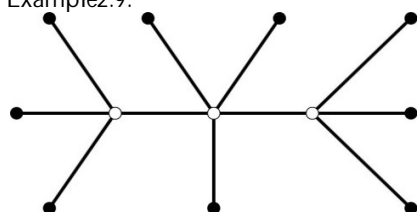
Figure 2.5

Illustration: In this graph the TCCD set is a set of white vertices whose cardinality is minimum and hence $\gamma_{TCC}(G) = 3$.

Exact Value of TCCD Numbers For Some Peculiar Graphs

Observation 3.1

If a graph G is a Wheel graph $(n \geq 5)$ or complete graph $(n \geq 5)$ or star graph$(n \geq 5)$ or Double Wheel graph DW_r $(r \geq 7)$ or Book graph B_r $(r \geq 3)$ or Moser spindle graph or Crown graph $(where\ n \geq 10)$ (or) Flower graph F_r then $\gamma_{TCC}(G) = 3$ and i) $\gamma_{TCC}(\overline{P_n}) = 3$ ii) $\gamma_{TCC}(\overline{C_n}) = 3$ iii) $\gamma_{TCC}(\overline{M_r(P_n)}) = 3$ iv) $\gamma_{TCC}(\overline{M_r(C_n)}) = 3$.

Observation 3.2

$\gamma_{TCC}(M_r\overline{(P_n)}) = \gamma_{TCC}(M_r\overline{(C_n)}) = 4$.

Observation 3.3

For path and cycle $(n \geq 3)$, $\gamma_{TCC}(G) = n$.

Observation 3.4

1. $\gamma_{TCC}(K_{r,s}) = 3$ (if $2 \geq r \geq s, s \leq 3$).

2. $\gamma_{TCC}(Ll_r) = \begin{cases} r - 1 & \text{if } r = 6,8 \\ r & \text{otherwise.} \end{cases}$

3.　　　$\gamma_{TCC}\big(M(P_n)\big) = n - 1$ if $n \geq 3$.

4.　　　$\gamma_{TCC}\big(M(C_n)\big) = \begin{cases} 3 & \text{if } n = 3 \\ n - 1 & \text{if } n \geq 4. \end{cases}$

5.　　　$\gamma_{TCC}\big(T(P_n)\big) = \begin{cases} 3 & \text{if } n = 4 \\ n - 2 & \text{if } n \geq 5. \end{cases}$

6.　　　$\gamma_{TCC}\big(T(C_n)\big) = \begin{cases} 3 & \text{if } n = 3 \\ n - 1 & \text{if } n \geq 4. \end{cases}$

7.　　　$\gamma_{TCC}\big(S'(P_r)\big) = \begin{cases} 3 & \text{if } r = 4 \\ r - 2 & \text{if } r \geq 5. \end{cases}$

8.　　　$\gamma_{TCC}\big(S'(C_r)\big) = \begin{cases} 3 & \text{if } r = 3,4 \\ r - 2 & \text{if } r \geq 5. \end{cases}$

9.　　　$\gamma_{TCC}\big(D(P_r)\big) = \begin{cases} 3 & \text{if } r = 3,4 \\ n - 2 & \text{if } r \geq 5. \end{cases}$

10.　　$\gamma_{TCC}\big(D(C_r)\big) = \begin{cases} 3 & \text{if } r = 3,4 \\ n - 2 & \text{if } r \geq 5. \end{cases}$

TCCD-Number of Some Special Types of Graphs

Theorem 4.1: For a path P_a, $a \geq 7$. $\gamma_{TCC}\big(P_a^2\big) = \begin{cases} 3 & \text{if } a = 7 \\ \left\lfloor \frac{a}{2} \right\rfloor - 1 & \text{if } a \geq 8. \end{cases}$

Proof:　Let　$V(P_a^2) = \{h_1, h_2, h_3, \ldots, h_a\}$　and　$E(P_a^2) = \{h_j h_{j+1}, h_j h_{j+2}, 1 \leq i \leq a - 1, 1 \leq j \leq a - 2\}$.　Take　$S_1 = \{h_i : i \equiv 1 (\bmod\, 2)\} - \{h_1\}$

For $a \geq 8$, take $S = \begin{cases} S_1 & \text{if } a \equiv 0 (\bmod\, 2) \\ S_1 - h_a & \text{if } a \equiv 1 (\bmod\, 2). \end{cases}$

It is clear that if $a = 7$ then, $\gamma_{TCC}\big(P_a^2\big) = 3$. Then S is a TCCD-set of P_a^2 and hence

$\gamma_{TCC}\big(P_a^2\big) \leq |S| = \left\lfloor \frac{a}{2} \right\rfloor - 1$ if $a \geq 8$.

Consider a TCCD-set S' of P_a^2. Since, $D \subseteq V$ of cardinality at most $k = \left\lfloor \frac{a}{2} \right\rfloor - 2$ if $a \geq 8$.

Contains an isolated vertex $< D >$, then D is not a TCCD-set, we have

Thus $|S'| \geq k + 1 = \begin{cases} 3 & \text{if } a = 7 \\ \left\lfloor \frac{a}{2} \right\rfloor - 1 & \text{if } a \geq 8. \end{cases}$

Hence the proof.

Theorem 4.2: For a cycle C_a, $a \geq 5$, $\gamma_{TCC}\big(C_a^2\big) = \begin{cases} 3 & \text{if } a = 5 \text{ or } 6 \text{ or } 7 \\ \left\lfloor \frac{a}{2} \right\rfloor - 1 & \text{if } a \geq 8. \end{cases}$

Proof: Let $V(C_a^2) = \{h_1, h_2, h_3, \ldots, h_a\}$ let $E\big(C_a^2\big) = \{h_j h_{j+1}, h_j h_{j+2}, h_j h_q, h_j h_{q-1}, 1 \leq i \leq a - 1, 1 \leq j \leq a - 2\}$.

Take $S = \{h_i : i \equiv 1 (\bmod\, 2)\} - \{h_a\}$

For $a \geq 8$, take $S = \begin{cases} S_1 & \text{if } a \equiv 1 (\bmod\, 2), \\ S_1 - \{h_{a-1}\} & \text{if } a \equiv 0 (\bmod\, 2). \end{cases}$

It is clear that if $5 \leq a \leq 7$ then, $\gamma_{TCC}\big(C_a^2\big) = 3$.

Then S is a TCCD-set of C_a^2 and hence $\gamma_{TCC}\big(C_a^2\big) \leq |S| = \left\lfloor \frac{a}{2} \right\rfloor - 1$ if $a \geq 8$.

Consider a TCCD-set S' of C_a^2. Since, $D \subseteq V$ of cardinality at most

$k = \left\lfloor \frac{a}{2} \right\rfloor - 2$ if $a \geq 8$

contains an isolated vertex $< D >$, then D is not a TCCD-set, we have

Thus $|S'| \geq k + 1 = \begin{cases} 3 & \text{if } a = 5 \text{ or } 6 \text{ or } 7 \\ \left\lfloor \frac{q}{2} \right\rfloor - 1 & \text{if } a \geq 8. \end{cases}$

Hence the proof.

Theorem 4.3 : For a path P_a $a \geq 5$, $\gamma_{TCC}\big(P_a^3\big) = \begin{cases} 3 & \text{if } 5 \leq a \leq 10 \\ \left\lfloor \frac{a}{3} \right\rfloor & \text{if } a \equiv 2 \,(\bmod\, 3) \\ \left\lfloor \frac{a}{3} \right\rfloor - 1 & \text{if } a \equiv 0 \text{ or } 1 \,(\bmod\, 3). \end{cases}$

Proof: Let $V(P_a^3) = \{h_1, h_2, h_3, \ldots, h_a\}$ and $E(P_a^3) = \{h_i h_{i+1}, h_j h_{j+2}, h_k h_{k+3}, 1 \leq i \leq a - 1, 1 \leq j \leq a - 2, 1 \leq k \leq a - 3\}$.

Mahadevan *et al.*,

Take $S_1 = \{h_i : i \equiv 1 \pmod 3\} - \{h_1\}$

For $a \geq 11$, take $S = \begin{cases} S_1 - \{h_a\} & \text{if } a \equiv 1 \pmod 3 \\ S_1 & \text{if } a \equiv 0, 2 \pmod 3. \end{cases}$

It is clear that if $5 \leq a \leq 10$ then, $\gamma_{TCC}(P_a^3) = 3$. Then S is a TCCD-set of P_a^3 and hence

$$\gamma_{tcc}(P_a^3) \leq |S| = \begin{cases} \left\lfloor \frac{a}{3} \right\rfloor & \text{if } a \equiv 2 \pmod 3 \\ \left\lfloor \frac{a}{3} \right\rfloor - 1 & \text{if } a \equiv 0 \text{ or } 1 \pmod 3. \end{cases}$$

Consider a TCCD-set S' of P_a^3. Since, $D \subseteq V$ of cardinality at most

$$k = \begin{cases} \left\lfloor \frac{a}{3} \right\rfloor - 1 & \text{if } a \equiv 2 \pmod 3, \\ \left\lfloor \frac{a}{3} \right\rfloor - 2 & \text{if } a \equiv 0 \text{ or } 1 \pmod 3. \end{cases}$$

contains an isolated vertex $< D >$, then D is not a TCCD-set, we have

Thus $|S'| \geq k + 1 = \begin{cases} 3 & \text{if } 5 \leq a \leq 10 \\ \left\lfloor \frac{a}{3} \right\rfloor & \text{if } a \equiv 2 \pmod 3 \\ \left\lfloor \frac{a}{3} \right\rfloor - 1 & \text{if } a \equiv 0 \text{ or } 1 \pmod 3. \end{cases}$

Hence the proof.

Theorem 4.4: For a cycle C_a $a \geq 5$, $\gamma_{TCC}(C_a^3) = \begin{cases} 3 & \text{if } 5 \leq a \leq 10 \\ \left\lfloor \frac{a}{3} \right\rfloor & \text{if } a \equiv 2 \pmod 3 \\ \left\lfloor \frac{a}{3} \right\rfloor - 1 & \text{if } a \equiv 0 \text{ or } 1 \pmod 3. \end{cases}$

Proof: Let $V(C_a^3) = \{h_1, h_2, h_3, \ldots, h_a, h_1\}$ and $E(C_a^3) = (h_i h_{i+1}, h_j h_{j+2}, h_k h_{k+3}, h_a h_1, h_a h_2, h_a h_3, h_{a-1}h, h_{a-1}h_2, h_{a-1}h_1, 1 \leq i \leq a-1, 1 \leq j \leq a-2, 1 \leq k \leq a-3\}$.

Take $S_1 = \{h f_i : i \equiv 1 \pmod 3\}$

For $a \geq 11$, take $S = \begin{cases} S_1 - \{h_{a-2}\} & \text{if } a \equiv 0 \pmod 3 \\ S_1 - \{h_{a-3}, h_a\} & \text{if } a \equiv 1 \pmod 3 \\ S_1 - \{h_{a-1}\} & \text{if } a \equiv 2 \pmod 3. \end{cases}$

It is clear that if $5 \leq a \leq 10$ then, $\gamma_{TCC}(C_a^3) = 3$. Then S is a TCCD-set of C_a^3 and hence

$$\gamma_{tcc}(C_a^3) \leq |S| = \begin{cases} \left\lfloor \frac{a}{3} \right\rfloor & \text{if } a \equiv 2 \pmod 3 \\ \left\lfloor \frac{a}{3} \right\rfloor - 1 & \text{if } a \equiv 0 \text{ or } 1 \pmod 3. \end{cases}$$

Consider a TCCD-set S' of C_a^3. Since, $D \subseteq V$ of cardinality at most

$$k = \begin{cases} \left\lfloor \frac{a}{3} \right\rfloor - 1 & \text{if } a \equiv 2 \pmod 3 \\ \left\lfloor \frac{a}{3} \right\rfloor - 2 & \text{if } a \equiv 0, 1 \pmod 3. \end{cases}$$

contains an isolated vertex $< D >$, then D is not a TCCD-set, we have

Thus $|S'| \geq k + 1 = \begin{cases} 3 & \text{if } 5 \leq a \leq 10 \\ \left\lfloor \frac{a}{3} \right\rfloor & \text{if } a \equiv 2 \pmod 3 \\ \left\lfloor \frac{a}{3} \right\rfloor - 1 & \text{if } a \equiv 0 \text{ or } 1 \pmod 3. \end{cases}$

Hence the proof.

CONCLUSION

In this paper we have initiated and analyzed Triple connected certified domination number of a graph. Also we have found its exact values for some special types of graphs. In the succeeding papers we will extend the study for product related graphs.

Mahadevan *et al.*,

ACKNOWLEDGMENT

REFERENCES

1. F.Harary "Graph Theory", Addison Wesley Publishing Company pvt Ltd USA(1969).
2. T.W.Haynes, S.T.Hedetniemi and P.J.Slater, "Fundamentals of Domination in graphs", Marcel Dekker Inc., New York (1998).
3. J. Paulraj Joseph, M. K. Angel Jebitha, P. Chitra Devi, and G. Sudhana, 'Triple Connected Graphs', Indian Journal Mathematics and Mathematical Sciences, Vol 8(1) pp 61-75(2012).
4. G. Mahadevan, A. Selvam and J. Paulraj Joseph, 'Triple connected Domination number of a graph", International Journal of Mathematical Combinatorics, Vol 3 pp 93-104 (2012).
5. M.Dettlaff, M.Lemanska, and J.Topp, "Certified Domination", AKCE International Journal of Graphs and Combinatorics – Vol 17 pg 86-97 June (2020).
6. Chartrand and L.Lesnaik, Graphs and digraphs. CRC, (2005).

RESEARCH ARTICLE

On Neutrosophic Mildly Generalized Star αJ - Closed Sets In Neutrosophic Topological Spaces

R M Samukthaa * and C Suganthi

Department of Mathematics, Excel Engineering College (Autonomous), Komarapalayam, Namakkal – 637303, Tamil Nadu, India

*Address for Correspondence
R M Samukthaa
Department of Mathematics,
Excel Engineering College (Autonomous),
Komarapalayam, Namakkal – 637303.
Tamil Nadu, India.
E. Mail: samukthaatn@gmail.com

ABSTRACT

The Neutrosophic moderately generalised star αJ - closed sets in Neutrosophic topological spaces are a novel class of sets that we present in this study (briefly Neu - mg*αj - closed sets). Here, we study the concepts and discuss the properties of Neu - mg*αj - closed sets.

Keywords: Neutrosophic set, Neutrosophic topological space, Neutrosophic Mildly Generalized Star αJ - closed sets, Neutrosophic mildly generalized star αJ - open sets, Neutrosophic mildly generalized star αJ– Neighbourhoods

INTRODUCTION

Since Zadeh[13] introduced the fuzzy set notation in 1965, it has spread to practically all areas of mathematics. Chang[2] (1968) proposed and developed the idea of fuzzy topological space, and since then, To create fuzzy topological spaces, numerous concepts from classical topology have been used. Initially, the intuitionistic fuzzy set's concept was proposed in 1988 by Atanassov[1]. Thakur and Chaturvedi[12] (2006) established and extended the concept behind the generalized intuitionistic fuzzy closed set. After Smarandache[4] (2000) proposed and expanded the notions of the neutrosophic set along with neutrosophy. This article covers the concepts of generalized mildly Star αJ - closed sets and several interesting properties and some theorems are also discussed.

Preliminaries
Here, we review several essential Neutrosophic set findings as well as their basic operation and Definition.

Definition 2.1[4]
Non-empty fixed set Y must be Y. Neutrosophic sets E is the object in following form:
E = $\{\langle y, \mu_E(y), \sigma_E(y), \gamma_E(y)\rangle; y \in Y\}$
With,
$\mu_E(y)$ is the membership function degree
$\sigma_E(y)$ is the indeterminacy degree
$\gamma_E(y)$ is the non-membership function degree

Remark 2.2:[4]
The Neutrosophic sets E = $\{\langle y, \mu_E(y), \sigma_E(y), \gamma_E(y)\rangle; y \in Y\}$ may be identified as an ordered triple E = $\langle \mu_E, \sigma_E, \gamma_E\rangle$ in] -0, 1+ [on Y.

Remark 2.3:[4]
We can denote, the Neutrosophic sets E = $\{\langle y, \mu_E(y), \sigma_E(y), \gamma_E(y)\rangle; y \in Y\}$ as E = $\langle y, \mu_E(y), \sigma_E(y), \gamma_E(y)\rangle$"

Definition 2.4[5]
Every non-empty Intuitionistic fuzzy set in Y is called the Neutrosophic set. Where the topological space we may define O_N and I_N as follows:
For all $y \in Y$

"$O_1 =$	$\langle y, 1,0,0\rangle$	$N_1 =$	$\langle y, 1,0,0\rangle$
$O_2 =$	$\langle y, 1,0,1\rangle$	$N_2 =$	$\langle y, 1,0,1\rangle$
$O_3 =$	$\langle y, 1,1,0\rangle$	$N_3 =$	$\langle y, 1,1,0\rangle$
$O_4 =$	$\langle y, 1,1,1\rangle$	$N_4 =$	$\langle y, 1,1,1\rangle$"

Definition 2.5[5]
For all $y \in Y$, the complement of Neutrosophic sets E [shortly C - E] is expressed as
C – E = $\{\langle y, \gamma_E(y), 1-\sigma_E(y), \mu_E(y)\rangle\}$

Definition 2.6[6]
For all $y \in Y$,
the two Neutrosophic sets E & F are given by
"E = $\langle y, \mu_E(y), \sigma_E(y), \gamma_E(y)\rangle$"
and
"F = $\langle y, \mu_F(y), \sigma_F(y), \gamma_F(y)\rangle$"
Then, the subset $(E \subseteq F)$ is $E \subseteq F \Longleftrightarrow \mu_E(y) \le \mu_F(y), \sigma_E(y) \le \sigma_F(y), \gamma_E(y) \le \gamma_F(y)$

Proposition 2.7:[3]
Any Neutrosophic set E meets the undergiven requirements
$O_N \subseteq E, O_N \subseteq O_N$
$E \subseteq I_N, I_N \subseteq I_N$

Definition 2.8[3]
For any non-empty set E the intersection and union of any 2 Neutrosophic sets E and F, where
E = $\langle y, \mu_E(y), \sigma_E(y), \gamma_E(y)\rangle$" and F = $\langle y, \mu_F(y), \sigma_F(y), \gamma_F(y)\rangle$ is given by
$E \cup F = \langle y \quad \mu_E(y) \wedge \mu_F(y) \quad \sigma_E(y) \wedge \sigma_F(y)$
$E \cap F = \langle y \quad \mu_E(y) \vee \mu_F(y) \quad \sigma_E(y) \vee \sigma_F(y) \quad$ respectively

Proposition 2.9[4]

The two Neutrosophic sets E and F are subject to the following criteria.

i. $C - (A \cap B) = \quad C - A \cup C - B$

ii. $C - (A \cup B) = \quad C - A \cap C - B$

Definition 2.10[6]

A family τ_N of Neutrosophic subsets in Neutrosophic topological set Y holds the following axioms

$O_N, I_N \in \tau_N$

$for\ any\ M_1, M_2 \in \tau_N, M_1 \cap M_2 \in \tau_N$

$for\ each\ \{M_i; i \in J\} \subseteq \tau_N, \cup M_I \in \tau_N$

The pair (Y, τ_N) is thus referred to as neutrosophic topological space. Neutrosophic open sets are the constituents of Neutrosophic topological space τ_N, while Neutrosophic closed sets works as complements of open sets.

Definition 2.11 [5]

The Neutrosophic closure and interior of a family (Y, τ_N) Neutrosophic topological space for a Neutrosophic set

E = $\{\langle y, \mu_E(y), \sigma_E(y), \gamma_E(y)\rangle; y \in Y\}$ in Y is defined by

Neu – cl (E) = $\cap \{G: G\ is\ a\ Neutrosophic\ closed\ set\ in\ Y\ and\ E \subseteq G\}$

Neu – Int (E) = $\cup \{J: J\ is\ a\ Neutrosophic\ open\ set\ in\ Y\ and\ E \subseteq J\}$ respectively and it holds the following conditions

E is Neutrosophic open set if, E = Neu-Int (E)

E is Neutrosophic closed set if, E = Neu-cl (E)

Proposition 2.12:[4]

For any Neutrosophic set E of a family (Y, τ_N) Neutrosophic topological space, we've

"Neu-cl(C - E) = C – (Neu – Int(E))

Neu-Int(C - E) = C – (Neu – cl(E))"

Proposition 2.12:[7]

Any two E and F Neutrosophic sets have the aforementioned characteristics in Neutrosophic topological space (Y, τ_N)

1. $Neu - Int(E) \subset E$

2. $E \subseteq Neu - cl(E)$

3. $E \subseteq F \Rightarrow Neu - Int(E) \subseteq Neu - Int(F)$

4. $E \subseteq F \Rightarrow Neu - cl(E) \subseteq Neu - cl(F)$

5. $Neu - Int(Neu - Int(E)) = Neu - Int(E)$

6. $Neu - cl(Neu - cl(E)) = Neu - cl(E)$

7. $Neu - Int(E \cap F) = Neu - Int(E) \cap Neu - Int(F)$"

8. $Neu - cl(E \cup F) = Neu - cl(E) \cap Neu - cl(F)$

9. $Neu - Int(O_N) = O_N$

10. $Neu - Int(I_N) = I_N$

11. $Neu - cl(O_N) = O_N$

12. $Neu - cl(I_N) = I_N$

13. $E \subseteq F \Rightarrow C - E \subseteq C - F$

14. $Neu - cl(E \cap F) \subseteq Neu - cl(E) \cap Neu - cl(F)$

15. $Neu - Int(E \cup F) \supseteq Neu - Int(E) \cap Neu - Int(F)$

Definition 2.13[7]

A subset E of a Neutrosophic topological space (Y, τ_N) is known as a generalized Neutrosophic closed if $Neu - cl(E) \subseteq U, whenever E \subseteq U$ and U is Neutrosophic closed set.

Neutrosophic Mildly Generalized Star αJ - closed sets

We present and explore the novel idea of Neutrosophic slightly generalised star αJ - closed sets in Neutrosophic topological spaces in this part.

Definition 3.1:

Neutrosophic slightly generalised star αJ closed sets are a Neutrosophic subset E of a Neutrosophic topological space(Y, τ_N) (shortly Neu – mg$\cdot\alpha J$ - closed) if $Neu - Jcl(E) \subseteq U$ whenever $E \subseteq U$ and U is Neutrosophic mildly generalised open (Neu – mg – open) in Neutrosophic set E.

Theorem 3.2:

Every set that is Neu-closed is Neu - mg*αJ - closed.

Proof:

Now consider any Neutrosophic "closed-set E and $E \subseteq U$,

Where U is" Neutrosophic mildly generalized open (Neu – mg – open)

Since, E is Neutrosophic closed (Neu-closed) $Neu - Jcl(E) \subseteq Neu - cl(E)$

Therefore, $Neu - Jcl(E) \subseteq E \subseteq E \subseteq U$

Hence, E is Neu – mg$\cdot\alpha J$ - closed in Y.

Remark 3.3:

Finite union of Neu – mg*αJ - closed need not be Neu – mg$\cdot\alpha J$ - closed

Finite intersection of Neu – mg$\cdot\alpha J$ - closed need not be Neu – mg$\cdot\alpha J$–closed"

Definition 3.4:

The intersection of all Neu - mg*αJ - closed sets including a given subset E of "Neutrosophic topological space" (Y, τ_N) is referred to as Neu - mg*αJ - closure of E and we can denote it by Neu – mg$\cdot\alpha J$ -cl(E).

Symbolically, $Neu - \text{mg}^* \, \alpha J \text{ - cl}(E) = \cap \{K : E \subset K, K \, is \, Neu - \text{mg}^*\alpha J - \text{closed in } Y\}$

Remark 3.5:

The following conditions hold for a subsets E and F of Neutrosophic topological space

1. $Neu - \text{mg}^* \, \alpha J \text{ - cl}(\varphi) = \varphi \, and \, Neu - \text{mg}^* \, \alpha J \text{ - cl}(X) = X$

2. $E \subset F \Rightarrow Neu - \text{mg}^* \, \alpha J \text{ - cl}(E) \subset Neu - \text{mg}^* \, \alpha J \text{ - cl}(F)$

3. $E \subset F \Rightarrow Neu - \text{mg}^* \, \alpha J \text{ - cl}\left(Neu - \text{mg}^* \, \alpha J \text{ - cl}(E)\right) = Neu - \text{mg}^* \, \alpha J \text{ - cl}(E)$

4. $Neu - \text{mg}^* \, \alpha J \text{ - cl}(E \cup F) \supseteq Neu - \text{mg}^* \, \alpha J \text{ - cl}(F) \cup Neu - \text{mg}^* \, \alpha J \text{ - cl}(F)$

5. $Neu - \text{mg}^* \, \alpha J \text{ - cl}(E \cap F) \subseteq Neu - \text{mg}^* \, \alpha J \text{ - cl}(E) \cap Neu - \text{mg}^* \, \alpha J \text{ - cl}(F)$

Neutrosophic mildly generalized star αJ - open sets and Neutrosophic mildly generalized star αJ– Neighbourhoods

Here we introduced the notion of Neutrosophic mildly generalized star αJ - open sets and by using it we obtain the characterizations of Neutrosophic mildly generalized star neighbourhoods.

Definition 4.1:

The term "Neutrosophic mildly generalized star αJ -open set" refers to a subset E of a Neutrosophic topological space. If C - A is $Neu - \text{mg}^* \, \alpha J$ -closed in Y, then (briefly $Neu - \text{mg}^* \, \alpha J$ -open). All Neutrosophic family mildly generalized star αJ - open sets can be denoted by $Neu - MG * \alpha J(Y, \tau_N)$

Remarks 4.2:

Finite union of Neu – mg*αJ - open sets require not be Neu – mg$\cdot\alpha J$ - open

Finite intersection of Neu – mg$\cdot\alpha J$ - open sets require not be Neu – mg$\cdot\alpha J$–open"

Definition 4.3:

Any point in the Neutrosophic topological space Y will do as y. If and only if a Neu - mg*αJ - open set N exists such that $y \in N \subseteq M$, a subset M of Y is said to be a Neu - mg*αJ - neighbourhood of Y.

Definition 4.4:

A subset M of a topological space with neutrosophic properties Y is referred to as a Neu - mg*αJ - $E \subset Y$ neighbourhood if there exists a Neu – mg*αJ - open set N such that $E \subseteq N \subseteq M$

Remark 4.5:

Each neighbourhood M of $y \in Y$ is a Neu – mg*αJ - neighbourhood of y

Definition 4.6:

The Neu - mg*αJ - neighbourhood system at y for every point y in a Neutrosophic topological space Y is the collection of all Neu - mg*αJ - neighbourhoods, and it is denoted by Neu - mg*αJ - M (y).

Theorem 4.7:

For all $y \in Y$ and Y be a Neutrosophic topological space, let Neu – mg*αJ - M(y) be the collection of all Neu – mg*αJ - neighbourhood of y, then it holds the following conditions

1. $\forall y \in Y$, Neu - mg* - M$(y) \neq \varphi$
2. $M \in$ Neu - mg* - M$(y) \Rightarrow y \in M$
3. $M \cup \in$ Neu - mg* - M$(y), N \supset M \Rightarrow N \in$ Neu - mg* - M(y)
4. $M \in$ Neu - mg* - M$(y) \Rightarrow \exists$ N $\in$ Neu - mg* - M$(y) \ni N \subset M$ and $N \in$ Neu - mg* - M$(z) \forall z \in N$

Definition 4.8:

Suppose E represent a subset of Neutrosophic space Y. If there is a Neu - mg*αJ -open set N such that $y \in N \subseteq E$, a $y \in Y$ point is said to be a Neu - mg*- internal point of E. The term "Neu - mg*αJ - interior of E" refers to the set of all Neu - mg*αJ - interior points of E and we can denote it by Neu – mg*αJ - int(E)

Theorem 4.9:

The following assertions are valid, for subsets E and F of Neutrosophic topological space Y,

1. $Neu - \mathrm{mg}^*\alpha J - int(E)$ is union of all $Neu - \mathrm{mg}^*\alpha J$ −open E subsets.
2. $E = Neu - \mathrm{mg}^*\alpha J - int(E)$ if E is Neu $- \mathrm{mg}^*\alpha J -$ open
3. $Neu - \mathrm{mg}^*\alpha J - int(Neu - \mathrm{mg}^*\alpha J - int(E)) = Neu - \mathrm{mg}^*\alpha J - int(E)$
4. $Neu - \mathrm{mg}^*\alpha J - int(E) = E \backslash Neu - D_{\mathrm{mg}^*\alpha J}(Y \backslash E)$
5. $Y \backslash Neu - \mathrm{mg}^*\alpha J - int(E) = Neu - \mathrm{mg}^*\alpha J - cl(Y \backslash E)$
6. $Y \backslash Neu - \mathrm{mg}^*\alpha J - cl(E) = Neu - \mathrm{mg}^*\alpha J - int(Y \backslash E)$
7. $E \subseteq F \Rightarrow Neu - \mathrm{mg}^*\alpha J - int(E) \subseteq Neu - \mathrm{mg}^*\alpha J - int(F)$
8. $Neu - \mathrm{mg}^*\alpha J - int(E) \cup Neu - \mathrm{mg}^*\alpha J - int(F) \subseteq Neu - \mathrm{mg}^*\alpha J - int(E \cup F)$
9. $Neu - \mathrm{mg}^*\alpha J - int(E \cup F) \subseteq Neu - \mathrm{mg}^*\alpha J - int(E) \cap Neu - \mathrm{mg}^*\alpha J - int(F)$

Definition 4.10:

The $Neu - \mathrm{mg}^*\alpha J$ - border and the $Neu - \mathrm{mg}^*\alpha J$ - frontier of E; E is any subset of the Neutrosophic topological space Y is given by the set $Neu - b_{\mathrm{mg}^*\alpha J}(E) = E \backslash Neu - \mathrm{mg}^*\alpha J - int(E)$ and the set $Neu - \mathrm{Fr}_{\mathrm{mg}^*\alpha J}(E) = Neu - \mathrm{mg}^*\alpha J - cl(E) \backslash Neu - \mathrm{mg}^*\alpha J - int(E)$ respectively.

Remarks 4.11:

$Neu - b_{\mathrm{mg}^*\alpha J}(E) = Neu - \mathrm{Fr}_{\mathrm{mg}^*\alpha J}(E)$ if E is an $Neu - \mathrm{mg}^*\alpha J$ - closed subset of Neutrosophic topological space Y

Theorem 4.12:

Mentioned below are the conditions hold for any subset E of the Neutrosophic topological space Y

1. $E = Neu - \mathrm{mg}^*\alpha J - int(E) \cup Neu - b_{\mathrm{mg}^*\alpha J}(E)$
2. $Neu - \mathrm{mg}^*\alpha J - int(E) \cap Neu - b_{\mathrm{mg}^*\alpha J}(E) = \varphi$
3. $Neu - b_{\mathrm{mg}^*\alpha J}(E) = \varphi$ if E is an Neu $- \mathrm{mg}^*\alpha J - $ open set
4. $Neu - b_{\mathrm{mg}^*\alpha J}(Neu - \mathrm{mg}^*\alpha J - int(E)) = \varphi$
5. $Neu - \mathrm{mg}^*\alpha J - int\left(Neu - b_{\mathrm{mg}^*\alpha J}(E)\right) = \varphi$
6. $Neu - b_{\mathrm{mg}^*\alpha J}\left(Neu - b_{\mathrm{mg}^*\alpha J}(E)\right) = Neu - b_{\mathrm{mg}^*\alpha J}(E)$
7. $Neu - b_{\mathrm{mg}^*\alpha J}(E) = E \cap Neu - \mathrm{mg}^*\alpha J - cl(Y \backslash E)$

8. $Neu - b_{\mathrm{mg}^*\alpha J}(E) = E \cap Neu - D_{\mathrm{mg}^*\alpha J}(Y\backslash E)$

Theorem 4.13:
The following assertions are valid, for subsets E of Neutrosophic topological space Y,

1. $Neu - \mathrm{mg}^*\alpha J - cl(E) = Neu - \mathrm{mg}^*\alpha J - int(E) \cup Neu - \mathrm{Fr}_{\mathrm{mg}^*\alpha J}(E)$
2. $Neu - \mathrm{mg}^*\alpha J - int(E) \cup Neu - \mathrm{Fr}_{\mathrm{mg}^*\alpha J}(E) = \varphi$
3. $Neu - b_{\mathrm{mg}^*\alpha J}(E) \subseteq Neu - \mathrm{Fr}_{\mathrm{mg}^*\alpha J}(E)$
4. $Neu - \mathrm{Fr}_{\mathrm{mg}^*\alpha J}(E) = Neu - b_{\mathrm{mg}^*\alpha J}(E) \cup Neu - D_{\mathrm{mg}^*\alpha J}(E)\backslash Neu - \mathrm{mg}^*\alpha J - int(E)$
5. $Neu - \mathrm{Fr}_{\mathrm{mg}^*\alpha J}(E) = Neu - b_{\mathrm{mg}^*\alpha J}(Y\backslash E) if E is an Neu - \mathrm{mg}^*\alpha J - open set$
6. $Neu - \mathrm{Fr}_{\mathrm{mg}^*\alpha J}(E) = Neu - \mathrm{mg}^*\alpha J - cl(E) \cap Neu - \mathrm{mg}^*\alpha J - cl(Y\backslash E)$
7. $Neu - \mathrm{Fr}_{\mathrm{mg}^*\alpha J}(E) = Neu - \mathrm{Fr}_{\mathrm{mg}^*\alpha J}(Y\backslash E)$
8. $Neu - \mathrm{Fr}_{\mathrm{mg}^*\alpha J}(E) is Neu - \mathrm{mg}^*\alpha J - closed$
9. $Neu - \mathrm{Fr}_{\mathrm{mg}^*\alpha J}\left(Neu - \mathrm{Fr}_{\mathrm{mg}^*\alpha J}(E)\right) \subseteq Neu - \mathrm{Fr}_{\mathrm{mg}^*\alpha J}(E)$
10. $Neu - \mathrm{Fr}_{\mathrm{mg}^*\alpha J}\left(Neu - \mathrm{mg}^*\alpha J - int(E)\right) \subseteq Neu - \mathrm{Fr}_{\mathrm{mg}^*\alpha J}(E)$
11. $Neu - \mathrm{Fr}_{\mathrm{mg}^*\alpha J}\left(Neu - \mathrm{mg}^*\alpha J - cl(E)\right) \subseteq Neu - \mathrm{Fr}_{\mathrm{mg}^*\alpha J}(E)$
12. $Neu - \mathrm{mg}^*\alpha J - int(E) = E\backslash Neu - \mathrm{Fr}_{\mathrm{mg}^*\alpha J}(E)$

Definition 4.14:
The $Neu - \mathrm{mg}^*\alpha J$ –exterior of E; E is any subset of Y given by $Neu - \mathrm{mg}^*\alpha J$ –the interior of Y\E and we can be denoted by $Neu - \mathrm{Ext}_{\mathrm{mg}^*\alpha J}(E)$. That is, $Neu - \mathrm{Ext}_{\mathrm{mg}^*\alpha J}(E) = Neu - \mathrm{mg}^*\alpha J - int(Y\backslash E)$

Theorem 4.15
The following assertions are valid, for subsets E and F of Neutrosophic topological space Y,

1. $Neu - \mathrm{Ext}_{\mathrm{mg}^*\alpha J}(E) = Neu - \mathrm{mg}^*\alpha J - open$
2. $Neu - \mathrm{Ext}_{\mathrm{mg}^*\alpha J}(E) = Y\backslash Neu - \mathrm{mg}^*\alpha J - cl(E)$
3. $Neu - \mathrm{Ext}_{\mathrm{mg}^*\alpha J}\left(Neu - \mathrm{Ext}_{\mathrm{mg}^*\alpha J}(E)\right) = Neu - \mathrm{mg}^*\alpha J - int\left(Neu - \mathrm{mg}^*\alpha J - cl(E)\right) \supseteq Neu - \mathrm{mg}^*\alpha J - int(E)$
4. $Neu - \mathrm{Ext}_{\mathrm{mg}^*\alpha J}(F) \subseteq Neu - \mathrm{Ext}_{\mathrm{mg}^*\alpha J}(E) if E \subseteq F$
5. $Neu - \mathrm{Ext}_{\mathrm{mg}^*\alpha J}(E \cup F) \subseteq Neu - \mathrm{Ext}_{\mathrm{mg}^*\alpha J}(E) \cap Neu - \mathrm{Ext}_{\mathrm{mg}^*\alpha J}(F)$
6. $Neu - \mathrm{Ext}_{\mathrm{mg}^*\alpha J}(E \cap F) \supseteq Neu - \mathrm{Ext}_{\mathrm{mg}^*\alpha J}(E) \cup Neu - \mathrm{Ext}_{\mathrm{mg}^*\alpha J}(F)$
7. $Neu - \mathrm{Ext}_{\mathrm{mg}^*\alpha J}(Y) = \varphi$
8. $Neu - \mathrm{Ext}_{\mathrm{mg}^*\alpha J}(\varphi) = Y$
9. $Neu - \mathrm{Ext}_{\mathrm{mg}^*\alpha J}(E) = Neu - \mathrm{Ext}_{\mathrm{mg}^*\alpha J}\left(Y\backslash Neu - \mathrm{Ext}_{\mathrm{mg}^*\alpha J}(E)\right)$
10. $Y = Neu - \mathrm{mg}^*\alpha J - int(E) \cup Neu - \mathrm{Ext}_{\mathrm{mg}^*\alpha J}(E) \cup Neu - \mathrm{Fr}_{\mathrm{mg}^*\alpha J}(E)$

CONCLUSION

In this paper, we defined some new classes of Neutrosophic Mildly Generalized Star αJ - closed sets and studied some of their basic properties. Finally we have introduced Neutrosophic mildly generalized star αJ - open sets and Neutrosophic mildly generalized star αJ– Neighbourhoods in Neutrosophic topological space and studied some their properties.

REFERENCES

1.   Atanassov. K, Intuitionistic fuzzy sets, Fuzzy Sets and Systems 20(1986),87-94
2.   Chang. C.L., Fuzzy Topological Spaces, J.Math.Anal.Appl.24(1968),182-190

3. Dhavaseelan. Rand Jafari. S, Generalized Neutrosophic closed sets new trends in Neutrosophic theory and applications**II**pp261-273, 2018

4. Florentin Smarandache, Neutrosophic and Neutrosophic Logic First International Conference on Neutrosophy, Neutrosophic Logic, Set, Probability, and Statistics University of New Mexico, Gallup,NM87301,USA, smarand@unm.edu, 2002

5. Floretin Smaradache, Neutrosophic Set A Generalization of Intuitionistic Fuzzyset, Journal of Defense Resources Management.**1** pp107-114,2010

6. Iswarya. P and Bageerathi. K, On Neutrosophic semi-open sets in Neutrosophic topological spaces, International Journal of Mathematics Trends and Technology **37**3 pp24-33, 2016

7. Salama. A.A and Alblowi. S.A., Neutrosophic set and Neutrosophic topological space, ISORJ.mathematics,**3** 4pp31-35, 2012

8. Salama. A.A and Alblowi. S.A, Generalized Neutrosophic set and generalized Neutrosophic topological spaces Journal Computer Sci. Engineering**2**7pp129-132, 2012

9. Shanthi. V.K Chandrasekar. S, Safina Begam. K, Neutrosophic Generalized Semi   Closed   Sets   in Neutrosophic Topological Spaces International Journal of Research in Advent technology **6** 7pp1739-1743, 2018.

10. Sindhu. G, Neutrosophic Regular Generalized star b – closed sets in Neutrosophic topological spaces, the international journal of analytical and experimental modal analysis,Vol.XI, Issue 11, 2019

11. Sudha. R and Meenakshi.PL.,"αJ - closed sets in Topological spaces", Journal of Xi'an University of Architecture & Technology, Vol. XIII, Issue 5, 2021.

12. Thakur. S, Chaturvedi, Generalized closed set in Intuitionistic Fuzzy Topology, The Journal of Fuzzy Mathematics, 16(3),2008,559-572.

13. Zadeh. L.P., FuzzySets, Inform andControl**8** pp 338-353, 1965.

RESEARCH ARTICLE

Contribution to Six Sigma Based Waiting Time Control Chart With (M|M|1) (∞|FCFS) Queuing Model Using Process Capability

Mani N[1] and P. K. Sivakumaran[2]*

[1]Research Scholar of Statistics, Govt. Arts College, Coimbatore and Assistant Professor of Statistics Sri Ramakrishna College of Arts and Science (Autonomous), Coimbatore-641006, Tamil Nadu, India.
[2]Assistant Professor of Statistics, Govt. Arts College, Coimbatore-641018, Tamil Nadu, India.

*Address for Correspondence
P. K. Sivakumaran
Assistant Professor of Statistics,
Govt. Arts College, Coimbatore-641018,
Tamil Nadu, India.
E. Mail: kumaranpks2010@gmail.com

ABSTRACT

Customers feedback and assessments have a huge impact on the long term success of the organisation. The main contribution of This paper is to analyses six sigma based waiting time control chart (M|M|1) (∞|FCFS) Queuing Model using Process Capability to monitor the queue and improve performance of the system explained with numerical examples

Keywords: Six Sigma. Control chart, Queuing Theory, Process Capability, Waiting time.

INTRODUCTION

Today's technological development has contributed with big data .Customers satisfaction is critical to the long term viability of an online and offline firm. This can be accomplished by focussing on the shortest possible response time. When the waiting time is reduced, the tendency is offer a higher rating, if higher rating increases, resulting in higher customer satisfaction. The adoption of six sigma based waiting time control chart and process capability would be extremely beneficial in monitoring queue length and performance of the system.

Control Charts
Control charts are used to monitor and analyse fluctuations in the performance of a process over time. They are commonly used in quality control to set upper and lower limits that demonstrate process stability. Extensive study has been undertaken in this sector, beginning with product faults. Control charts are using currently being used to examine queuing systems, specifically factors such as customer waiting time, no. of customers in the system, and those queue. These elements are critical in ensuring client happiness[12].

REVIEW OF LITERATURE

Haim Shore (2007) proposed an attribute control chart [2]. While M.V.Karparde and S.D Dhabe (2010) developed control chart with random queue length for queuing model (M/M/1): (∞/FCFS) [4]. T, Poongodi and S. Muthulakshmi (2013) investigated system waiting time using control chart for (M/M/1): (∞ /FCFS) Queuing model [7]. A.R Sudamani Ramasamy and Vennila (2012) investigated skewness in control chart for random queue length[1] . N. Pukazhendhi and S. Poornima (2018) created a waiting time control chart for (M/M/S): (∞/FCFS) queueing model using process capability [8]. Mani. N and P.K.Sivakumaran (2023) contributed six sigma based control chart for single server queuing model [5]. Mani N and P.K.Sivakumaran(2023) developed six sigma based control chart for single server , infinite capacity Markovian Queuing model using process capability[6]y.

Six Sigma

Six Sigma is a methodology consisting of techniques designed to eliminate errors, improve quality, and achieve operational excellence. It was first established in 1980 by Motorola. In 2008, the quality levels related to Six Sigma were developed and refined by Radhakrishnan and Sivakumaran (2010) [10,14]. This work paved the way for the subsequent development of control charts based on Six Sigma for defect monitoring by the team of Radhakrishnan and Balamurugan (2010)[11]. The process capability index (PCI) is a metric that evaluates the accuracy and consistency of the performance of a system under assessment.

Mean waiting time of the customers in the Queue [1]

$$E(w_q) = \frac{\rho_q}{\mu(1-\rho_q)} \text{ --------- (1)}$$

$$E(w_q^2) = \frac{2\rho_q}{\mu^2(1-\rho_q)2} \text{ --------- (2)}$$

$$var(w_q) = E(w_q^2) - [E(w_q)]^2 = \frac{\rho_q(2-\rho_q)}{\mu^2(1-\rho_q)^2} \text{ ----- (3)}$$

$$S.D(W_q) = \sqrt{var(w_q)} = \sqrt{\frac{\rho_q(2-\rho_q)}{\mu^2(1-\rho_q)^2}} \text{ ------ (4)}$$

Shewhart Control chart- Performance of the average waiting time of the customers in the queue is given below[5,6]

$$LCL(W_q) = E(W_q) - 3\times \sqrt{var(W_q)}$$

$$= \frac{\rho_q}{\mu(1-\rho_q)} - 3 \times \sqrt{\frac{\rho_q(2-\rho_q)}{\mu^2(1-\rho_q)^2}} \text{ ------- (5)}$$

$$CL(W_q) = E(W_q) = \frac{\rho_q}{\mu(1-\rho_q)} \text{ -------- (6)}$$

$$UCL(W_q) = E(W_q) + 3\times \sqrt{var(W_q)} \text{ ------ (7)}$$

Six Sigma based Control chart performance of the waiting time in the queue by using process capability is given by [5,6]

The process capability index, Cp, is calculated as TL/ 6, where TL represents the tolerance level defined as the range between the highest and lowest values within the expected standard deviation range for the given λ and μ assumptions[7].

$$UCL(6\sigma_{wq}) = E(W_q) + \sqrt{V(W_q)} \times \sigma pc$$

$$= \frac{\rho_q}{\mu(1-\rho_q)} + \sqrt{\frac{\rho_q(2-\rho_q)}{\mu^2(1-\rho_q)^2}} \times 6\sigma_{pc} \text{ ------ (8)}$$

$$LCL(6\sigma_{w_q}) = E(W_q) - \sqrt{V(W_q)} \times \sigma pc$$

$$= \frac{\rho_q}{\mu(1-\rho_q)} - \sqrt{\frac{\rho_q(2-\rho_q)}{\mu^2(1-\rho_q)^2}} \times 6\sigma_{pc} \text{ ------- (9)}$$

CONCLUSION

The use of control charts within queue theory is a growing area within the statistical quality control domain. Customer satisfaction depends on both the waiting time of customers in the queue and the amount of time spent on the service per customer. This is why the focus of this research is on the single server, infinite capacity queue. The main focus is on monitoring customers waiting time in the queue using Six Sigma based control charts. Implementing Six Sigma methodologies reduces variation and keeps the number of customers waiting time in the queue within the optimal range. This increases system efficiency.

REFERENCES

1. Gross D and Harris C.M(1998). "Fundamentals of queueing theory", John Wiley and sons.
2. Haim Shore (2000), "General control charts for attributes", IIE Transactions, 32:12, 1149-1160,DOI: 10.1080/07408170008967469.
3. Kantiswarup, Gupta, P.K. and Man Mohan (2011), "Operations Research", Sultan Chand &Sons, New Delhi.
4. Khaparde M.V and Dhabe S.D 2010. "Control chart for random queue length N for (M/M/1):(∞/FCFS) queueing model",International Journal of Agricultural and Statistical sciences, Vol.1:319-334.
5. Mani N*, Sivakumaran P.K. (2023). Contribution to Six Sigma Based Control Chart with Single Server Queuing Model. *Journal of Optoelectronics Laser, 42*(3), 12–17. Retrieved from http://gdzjg.org/index.php/ JOL/article/view/1478
6. Mani N, Sivakumaran P.K (2023). "Six Sigma Based Control Chart for Single Server, Infinite Capacity Markovian Queueing Model using Process Capability", *Bulletin of Mathematics And Statistics Research,* Vol.11.Issue.2.2023 (April-June), pp 44-48 , ISSN:2348-0580, 2023.
7. Montgomery D.C. (2005). "Introduction to Statistical Quality Control", John Wiley &Sons,Inc.
8. Poongodi T and Muthulakshmi S 2013. "Control chart for waiting time in system of (M/M/S):(∞/FCFS) Queuing model", Journal of Mathematics, Vol. 5(6): 48-53.
9. Pukhazhenthi.N and Poornima.S(2018), "Construction of control chart for waiting time in (M/M/S): (∞/FCFS) Queuing model using process capability", Journal of Emerging Technologiesand Innovative Research (JETIR),Vol-5,Issue-11,PP 490-499, ISSN-2349-5162.
10. Radhakrishnan and Sivakumaran (2008). "Construction and Selection of Six Sigma Sampling Planindexed through Six Sigma Quality Level" International Journal of Statistics and Systems, Vol.3,No.2, pp.153-159.
11. Radhakrishnan R and Balamurugan P (2012)," Construction of control charts based on sixsigma initiatives for fractiondefectives with varying sample size", Journal of Statistics & Management Systems, Vol.15(4-5): 405-413.
12. Shore H (2000). "General control charts for attributes", IIE transactions, 32: 1149-1160.
13. Shewhart W.A (1931). "Economic control of quality of manufactured product", Van Nostrand,New York.
14. Sivakumaran (2009). "Contribution to the Construction of Attribute Sampling Plans indexedthrough Six Sigma Quality Levels". PhD Thesis, Bharathiar University, Coimbatore.
15. SudamaniRamasamy A. R and Vennila.B (2012), "Construction of Control chart for RandomQueue length for (M/M/c) : (∞/FCFS) Queuing using Skewness" International Journal ofScientific and Research Publications,Vol-2,Issue 12,PP 1-18,ISSN:2250-3153.

Table 1: Shewhart control chart and Six Sigma based waiting time control chart using Process capability for fixed μ

λ	μ	ρ	SD(σ)	SCHEWHART			$6\sigma_{pc}$- waiting time in the queue	
				LCL	CL= E(W_q)	UCL	LCL	UCL
2.5	9	0.27778	0.10641	-0.27649	0.04274	0.36196	-0.10126	0.18674
2.75	9	0.30556	0.11513	-0.29649	0.04889	0.39427	-0.09511	0.19289
3	9	0.33333	0.12423	-0.31712	0.05556	0.42823	-0.08844	0.19956
3.25	9	0.36111	0.13379	-0.33857	0.06280	0.46418	-0.08120	0.20680
3.5	9	0.38889	0.14392	-0.36104	0.07071	0.50246	-0.07329	0.21471
3.75	9	0.41667	0.15471	-0.38477	0.07937	0.54350	-0.06463	0.22337
4	9	0.44444	0.16630	-0.41000	0.08889	0.58778	-0.05511	0.23289
4.25	9	0.47222	0.17882	-0.43704	0.09942	0.63587	-0.04458	0.24342
4.5	9	0.50000	0.19245	-0.46624	0.11111	0.68846	-0.03289	0.25511
4.75	9	0.52778	0.20741	-0.49804	0.12418	0.74640	-0.01982	0.26818
5	9	0.55556	0.22395	-0.53297	0.13889	0.81074	-0.00511	0.28289
5.25	9	0.58333	0.24242	-0.57169	0.15556	0.88280	0.01156	0.29956
5.5	9	0.61111	0.26322	-0.61507	0.17460	0.96428	0.03060	0.31860
5.75	9	0.63889	0.28693	-0.66421	0.19658	1.05737	0.05258	0.34058
6	9	0.66667	0.31427	-0.72059	0.22222	1.16503	0.07822	0.36622
6.25	9	0.69444	0.34625	-0.78621	0.25253	1.29126	0.10853	0.39653
6.5	9	0.72222	0.38426	-0.86389	0.28889	1.44166	0.14489	0.43289
6.75	9	0.75000	0.43033	-0.95766	0.33333	1.62433	0.18933	0.47733
7	9	0.77778	0.48750	-1.07361	0.38889	1.85138	0.24489	0.53289

Table 2: Shewhart control chart and Six Sigma based waiting time control chart using Process capability for fixed

λ	μ	ρ	SD(σ)	SCHEWHART			$6\sigma_{pc}$- waiting time in the queue	
				LCL	CL= E(W_q)	UCL	LCL	UCL
4	7	0.57143	0.30117	-0.71303	0.19048	1.09398	0.11398	0.26698
4	7.25	0.55172	0.27504	-0.65537	0.16976	0.99490	0.09326	0.24626
4	7.5	0.53333	0.25270	-0.60570	0.15238	0.91047	0.07588	0.22888
4	7.75	0.51613	0.23337	-0.56248	0.13763	0.83775	0.06113	0.21413
4	8	0.50000	0.21651	-0.52452	0.12500	0.77452	0.04850	0.20150
4	8.25	0.48485	0.20167	-0.49093	0.11408	0.71909	0.03758	0.19058
4	8.5	0.47059	0.18853	-0.46100	0.10458	0.67015	0.02808	0.18108
4	8.75	0.45714	0.17681	-0.43418	0.09624	0.62666	0.01974	0.17274
4	9	0.44444	0.16630	-0.41000	0.08889	0.58778	0.01239	0.16539
4	9.25	0.43243	0.15682	-0.38810	0.08237	0.55284	0.00587	0.15887
4	9.5	0.42105	0.14825	-0.36819	0.07656	0.52130	0.00006	0.15306
4	9.75	0.41026	0.14045	-0.35000	0.07135	0.49270	-0.00515	0.14785
4	10	0.40000	0.13333	-0.33333	0.06667	0.46667	-0.00983	0.14317
4	10.25	0.39024	0.12681	-0.31800	0.06244	0.44288	-0.01406	0.13894
4	10.5	0.38095	0.12082	-0.30386	0.05861	0.42108	-0.01789	0.13511
4	10.75	0.37209	0.11530	-0.29078	0.05512	0.40103	-0.02138	0.13162
4	11	0.36364	0.11020	-0.27865	0.05195	0.38254	-0.02455	0.12845
4	11.25	0.35556	0.10547	-0.26737	0.04904	0.36545	-0.02746	0.12554
4	11.5	0.34783	0.10108	-0.25685	0.04638	0.34960	-0.03012	0.12288

Figure 1.1 six sigma based waiting time control chart using PC for fixed μ

Figure 2.1 six sigma based waiting time control chart using PC for fixed μ

RESEARCH ARTICLE
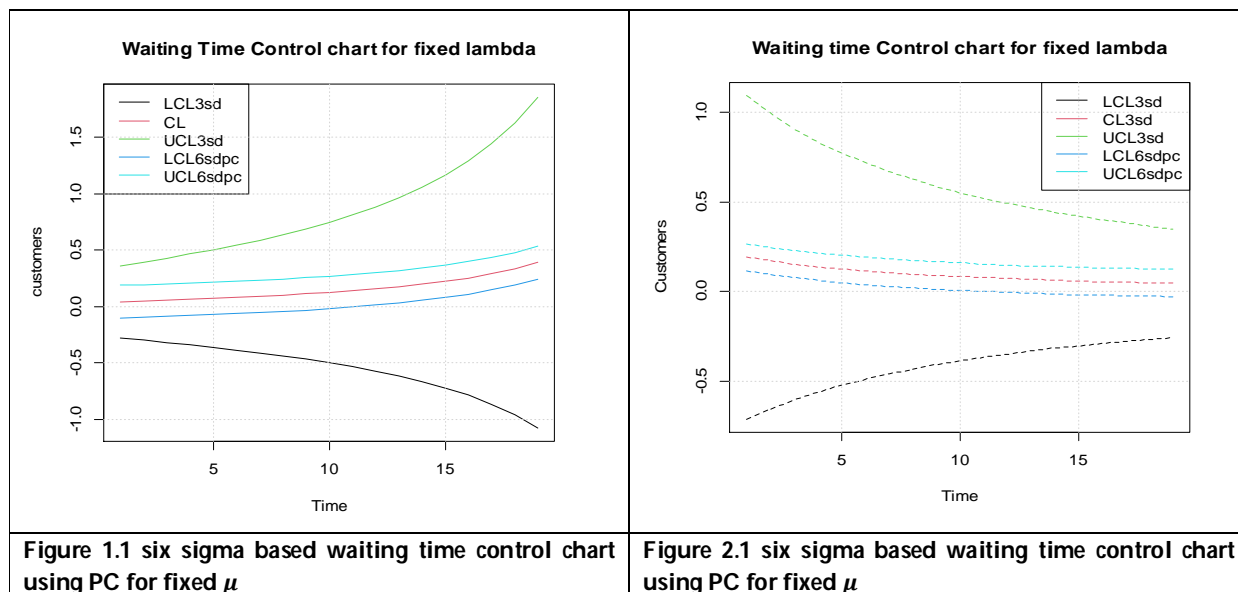
Multi Objective Task Scheduling Optimization in Cloud Computing Environment using Hybrid Firefly and Lion Optimizer (HFLO)

Karunya.N[1*] and D. Gayathri Devi[2]

[1]Research Scholar, Sri Ramakrishna College of Arts and Science for Women, and Assistant Professor of Computer Science, Sri Ramakrishna College of Arts and Science, Coimbatore, Tamil Nadu, India.
[2]Assistant Professor, Department of Computer Science, Sri Ramakrishna College of Arts and Science for Women, Coimbatore, Tamil Nadu, India.

*Address for Correspondence
Karunya.N
Research Scholar,
Sri Ramakrishna College of Arts and Science for Women,
and Assistant Professor of Computer Science,
 Sri Ramakrishna College of Arts and Science,
Coimbatore, Tamil Nadu, India.
E. Mail: karunyakarun95@gmail.com

ABSTRACT

The high performance distributed computing of cloud computing has facilitated its rapid adoption. Via service providers, it provides internet users with services and access to shared resources. One of the most crucial research areas that need to be concentrated on is the effective performance of task scheduling in clouds. Several cloud-based job scheduling algorithms have been evaluated, and they performed well in a timely manner. Examples include in order giving users better services, task scheduling has become crucial. In light of this, the current study intends to offer a task-scheduling method employing the Firefly Algorithm, Lion Optimization Algorithm (LOA), and HFLO (Hybrid Firefly and Lion Optimizer) Algorithm. The HFLO algorithm is superior than the Firefly algorithm, LOA algorithm efficiency and task delay time, energy consumption, resource utilization, and cost, and as a consequence, it can be used to accomplish the best scheduling in cloud computing.

Keywords: Task Scheduling, Job Scheduling, Lion Optimization, Fairfly, HFLO

INTRODUCTION

The utilization of cloud computing allows for pay-as-you-go access to in-demand IT resources from any location at any time. A typical cloud computing datacenter consists of a few computers connected by fast networks. The

63368

calculation of broad and varied groups of jobs is ideally suited to this environment. Different users' tasks are no longer distinguishable from one another. Assigning more jobs to be carried out on the available computing machines is the scheduling difficulty in this situation.

Cloud computing can be characterised by three specific features:

- Unlimited computing resources, such as processing speed, data storage capacity, and application availability on demand as needed to enable high levels of agility and scalability that satisfy business requirements.
- Why there are no long-term commitments; because computing resources are purchased on a month-to-month or even minute-to-minute basis, they are immediately available and may be used for as long as necessary before being decommissioned.
- Pay-as-you-go pricing; as there are no long-term contracts, the price of cloud computing resources is based on how much is used [1].

The flexibility and dependability of cloud-based systems are significantly increased by task scheduling. The primary motivation for allocating tasks to resources in line with time constraints is to determine the optimal order in which to perform various tasks so as to provide the user with the best outcome. In cloud computing, resources are always dynamically assigned in accordance with the order and specifications of the task, subtasks, and resources in any form, such as cups, firewalls, and networks. This causes task scheduling in the cloud to become a dynamic problem because no previously established sequence may be helpful during job processing. Because the flow of tasks is unclear, execution paths are also uncertain, and resources are also uncertain because several tasks are present that are sharing them concurrently at the same time, scheduling is dynamic because of these factors.

The scheduling algorithms used in distributed systems determine the order in which these activities complete by allocating subtasks to resources that improve system performance [2]. In heterogeneous distributed systems, such as the cloud environment, where the allocation of processors and resources to tasks is a complex issue, numerous techniques and algorithms have been developed to lessen the complexity of time and the simultaneous operation of subtasks. Heterogeneous resources, total running time, runtime and productivity convergence speed in meta-heuristic methods, and scheduling method effectiveness are a few of the issues that might be encountered in the field of scheduling activities in heterogeneous distributed systems. This paper presents research on task scheduling for cloud computing jobs in light of the significance of this subject. The task scheduling algorithm is regarded as a complicated procedure since it has to fit a lot of jobs into the resources that are available. On the other hand, when creating a task scheduling algorithm, there are a lot of variables to take into account. From the viewpoint of a Cloud user, several of these factors are significant (i.e., tasks compilation time, cost, and response time). The use of resources, fault tolerance, and power consumption are other factors that are crucial from the standpoint of cloud providers [3].

A problem that is NP-Complete is task scheduling. Hence, by taking into account performance characteristics (such as completion time, cost, resource utilisation, etc.), optimization methodologies could be applied to solve it. The purpose of this research is to create a task scheduling algorithm for the cloud computing environment based on genetic algorithms for allocating and carrying out independent tasks in order to increase task completion times, reduce execution costs, and maximize resource usage. In order to solve NP issues, a number of meta-heuristic-based techniques have been proposed, including the Lion Optimization Algorithm (LOA) [4] and the Firefly Algorithm [5]. These techniques could present several solutions to evaluate the efficient parameters. Some of the proposed firefly-based scheduling algorithms use random approaches in their phases, such as giving the initial population or placing tasks in the workflow at the same level [6][7], while others make use of a straightforward workflow graph. Response time and reliability are taken into account by task scheduling techniques in heterogeneous distributed systems [8]. This paper proposed the HFLO algorithm to identify an appropriate scheduling method for computational applications in accordance with cloud system environments. By creating an optimum initial population, this approach aims to cut down on the number of operations needed to properly distribute workload across available resources.

Proposed Methodology And Suggested Algorithm

One of the most recent technologies today allows customers to send their requests to clouds and pay a set price based on the service received. Yet, cloud environments are actually uniform systems that are suitable for storing huge applications and data for services. Given this, it is crucial that these systems schedule the enormous applications and data they include. Managing tasks within the cloud is largely accomplished through scheduling. The scheduling process establishes which task should be assigned to a specific computer component and estimates the number of resources required to execute the work. It is possible to break up larger subtasks before processing them in parallel. The efficiency of an implementation is improved by breaking a computation into smaller subtasks and executing these subtasks on different processors. Also, the goal of the task scheduling algorithm is not to schedule every work into every available processor in an effort to increase profit (profit here denotes the combination of cheap cost, low memory consumption, and energy conservation) at the expense of the basic needs.

Task scheduling is a challenge. The goal of this work is to introduce a new algorithm for job scheduling in clouds that is based on Firefly and Lion Optimizer. Here is an expression of the suggested combination's specifics. Figure 1 depicts the overall structure of the task scheduling optimization model that has been suggested. As a result of the operation that the virtual machines are supposed to carry out, this process takes place while using a limited task. The scheduler gathers information from the Cloud User, Task Manager, and Resource, computes that information, and then decides which virtual machine should be assigned to each task.

Two algorithms—the Lion optimization method and Firefly—are hybridised in the suggested scheduling. By utilising the benefits of the Firefly and Lion search algorithms, the technique avoids their drawbacks. By combining the two algorithms, their flaws are fixed, and some advantages are quickly acknowledged and focused on, allowing the planning approach to obtain an idea or a shoddy layout in a shorter amount of time. Comparing the novel hybrid algorithm to the Firefly and LOA techniques, it optimises the job and resources more effectively. Experimental comparisons' positive findings supported the effectiveness of the suggested strategy. The execution of each task has to be done in a single VM instance type. If pm = {PM_1, PM_2, … PM_n) is A amalgamation of physical machine (data centers). VM_i = {VM_1, VM_2 … VM_l} which is the sequence followed in A virtual machine VMI types and T = {T_1, T_2 … T_n} is defined as the set of task. Every task considers a set which is derived, T_i = {t_1, t_2, … t_n}. The unique cost of every task be C_1, memory m_i, and energy E_i. Problem factors are defined as a solution to this problem. In this paper, the utmost function depends on three factors such as cost, energy consumption and memory usage. Here each task has individual moving charge. It is possible to define task and resource allocation as the process by which the supplier must identify the best resources to meet incoming customer demands. Although obtaining and releasing resources on demand is one of the major characteristics of cloud computing, ongoing resource monitoring is required. All of the physical servers are housed in data centres, which are components of hardware. Realistic users are not used on physical servers. They are transformed into various virtual machines (VMs) using virtualization, and users' jobs will run on these VMs when scheduling tasks. The VMs are managed by the VM management. A list of suitable candidates is highlighted following the gathering of data on the cloud's resources (VM and HOST). The resource selection algorithm chooses the potential solution that satisfies all criteria and makes the best use of the infrastructure. An optimization algorithm might be used for resource selection. For clouds, some examples are genetic algorithms, ant colonies, and particle swarm optimization.

Problem Statement

In cloud computing systems, the challenge of assigning tasks to virtual machines arises when there are m tasks (V=T1, T2,..., TM) that need to be assigned to different virtual machines. The total number of tasks in this study were randomly chosen from a range of 10 to 80 tasks, and they were then divided into three separate data sets with various numbers of virtual machines. The tasks are created at random. Moreover, VM= "VM1,VM2,...,VMN," where each VM_i is a trinity expressed as VM = (CPU_i, RAM_i- $HOST_i$), 1 I n, where the values of the triplets stand for the corresponding CPU, memory, and bandwidth requirements of VMs. Let PM symbolise a collection of PMs and PM_j denote the jth PM. The values of the triplets indicate the total resource capacity of the jth PM, and PM_j = (CPU_j, RAM_j -$HOST_j$) is used to represent each PM_j. Each VM can only be allocated on one physical machine at a time, which is

one of the absolute restrictions mentioned in the explanation above. The number of resource demands from VMs deployed on the same HOST machines for each type of resource (CPU, memory, and bandwidth) must be less than or equal to the capability/capacity of the PMs hosting them; There are a maximum of m PMs in total that can allocate VMs, where yimi=1 m. Because all systems are same, duties are carried out in a homogeneous manner.

Proposed Task Scheduling Using HFLO
The Firefly and Lion Optimization algorithms were combined to create this hybrid optimization technique. The primary flaw in the Firefly method is the number of iterations required to arrive at an ideal solution, which also adds to its overall time requirement. Lion Optimizer has the drawback that its union speed delays the later investigation step and makes it challenging to reach the local optimum solution. The strategy avoids the drawbacks of the Firefly and Lion Optimizer algorithms by utilising their strengths. By combining the two algorithms, their shortcomings are addressed and certain advantages are realised, allowing the planning methodology to obtain a concept or flawed layout in a shorter computing time.

Proposed Hybrid Algorithm HFLO
Input: m,nMax, i,j,FL,R1,R2
 List of Cloud (Tasks), List of VMs. Initialization parameters
Output: the best solution for minimize the cost, Energy consumption, makespan
1: $n = 1$. Number of iterations
2: **while** n < Max **do** . Executes within the maximum number of iterations
3: Calculate the relative brightness I of fireflies and initialize the lion optimization pheromone matrix
4: **for** i = 1, 2, . . . ,m **do**
5: **for** j = 1, 2, . . . ,m **do**
6: Calculate the probability of selecting the remaining points when the lion optimization departs from point i. Select the departure alternative with the highest probability ki, and update the next city selection for lion i as ki
Step7:Move Towards Safer Place
position for female lion (FL) is expressed as

$$FL = FL + 2D \times random(0,1)\{R1\} + U(-1,1) \times \tan(\theta) \times D \times$$

$$random(0,10\{R2\}$$

$$\{R1\}.\{R2\} = 0, \| R2 \| = 1$$

where FL is the current place of FL, D provides the distance among the FL's position as well as chosen point selected by the tournament chosen in the pride region. {R1} is a vector that indicates the primary point is the earlier place of the FL, and it is focused on the elected position. {R2} is perpendicular to {R1}.
Step 8:For each Nomad lion
Both male and female move randomly in the search space Identify their new position as,
$Lion=\{Lion, if\ rand>pr RAND, otherwise$
$pr=0.1+(0.5 Nomad-BestNomad BestNomad)$
Where, rand is a random number between 0 and 1, pr is a probability, Nomad is the fitness value of the current nomad, and BestNomad is the best fitness value of the nomad lions. %M of females mate with only one male Nomad males attack prides
Step 9: For each pride,
Nomads are %I of the pride that is immigrated.
Do
(i)Every male and female lions under nomad category are sorted according to their fitness score.
(ii) Female lions faring above fitness score are selected and disseminated to prides, filling out the empty positions.
(iii) Lions faring below fitness score are taken out in accordance to maximum permissible count under each gender
Step 10: If (t< Iterations)
Go to step 2

Karunya and Gayathri Devi

Return best solution.

EXPERIMENTAL RESULTS

The suggested scheduling method is based on the fire fly algorithm, which is used to optimise the schedule for handling requests to the cloud network. The proposed method is also concerned with distributing the loads among the cloud system's resources. The processing of the suggested technique is described in the sections above. In this section, using the CloudSim tool and Java programming, we plot the experimental analysis of the suggested scheduling methodology. Java programming is used to create an application based on CloudSim that simulates clouds. The studies are carried out on a computer with a core i5 processor, 4GB of RAM, and a 500GB hard drive.

Execution Time
In this experiment, various quantities of tasks and resources are taken into account when evaluating the suggested mechanism and looking at how it performs over time and from various angles. to determine whether there is a relationship between processing time and repeats. The number of positions was set at 80 for all firefly and LOA population sizes and iterations. The following results are displayed: The following results are based on the subtraction of the various listed algorithms from the suggested algorithm for execution time in order to streamline the comparison. The proposed algorithm has the shortest Execution Time along the amount of tasks, as shown in Figure 2, according to our research.

Evaluation using Makespan:
By giving the last task's completion time, Makespan calculates the maximum completion time. The most common optimization criterion for task scheduling is minimising the makespan. The following equation can be used to compute it:

Makespan=max$_{task\ i}$ (Fn$_{time}$)

A location, Fn Time displays the task's completion time. The HFLO and LOA Firefly methods for computing and minimising make span are compared in this section. The term "make span" refers to the whole amount of time that passed from beginning to end. The phrase is often used in relation to scheduling. There is a huge project that is broken down into numerous smaller assignments. A time comparison of the Firefly, LOA, and HFLO algorithms is shown in Figure 3. The term "make span" refers to the overall amount of time needed for the tasks to finish execution. The task and resource values are changed to assess and analyse Makespan. The lowest span values are produced by the LOA and HFLO algorithms when compared to Firefly. The HFLO approach provides the quickest make span time in Figure 3.

Task Delay Time
The fact that the user d has zero service schedules in the Firefly, LOA, and HFLO scheduling results indicates that the resource management platform has not allocated resources to it, making it impossible for it to schedule urgent tasks in a timely manner. This results in unfair task scheduling and a sharp decline in user satisfaction. The HFLO method developed in this study does not appear to have any scheduling tasks in the scenario described above, and each user has an equitable opportunity to perform tasks. The comparison of the smallest delay across the Firefly, LOA, and HFLO is illustrated in figure 4. The delay time of jobs is slightly less than Firefly, LOA after calculating the three methods of the observed algorithm ms, however HFLO is more efficient while ensuring fairness for the Firefly, LOA algorithm, delay time is improved. When the number of scheduled tasks rises, this paper's task scheduling by HFLO algorithm produces the desired scheduling outcome with a shorter task delay time. The technique can fully utilise cloud computing resources to achieve more efficient job scheduling, more appropriate resource scheduling, and higher resource utilisation. The HFLO algorithm not only ensures the fairness of task assignment, but also outperforms the HFLO,LOA algorithm in terms of efficiency and user satisfaction, further proving that the HFLO

algorithm can successfully resolve the scheduling problem in the cloud environment. This is shown by the aforementioned experimental results.

CONCLUSION

Task scheduling methods for cloud computing have been developed using a variety of metaheuristic optimization algorithms. Throughout this research, a brand-new cloud task-scheduling algorithm that is based on the firefly concept—a freshly developed algorithm based on the behavior of fireflies—was proposed. Comparisons were made between the performance of the proposed algorithm and that of the FF and LOA metaheuristic algorithms. It achieved a remarkable reduction in costs and energy use. Moreover, it resulted in significant resource use. The HFLO algorithm looks into cloud scheduling issues in an effort to cut costs.

REFERENCES

1. M. Hugos, C. Emeritus, S. Advisor, C. T. Officer, T. Weather, C. Interactive, C. I. Officer, C. E. Officer, and E. V. President, Business in the Cloud,book, John Wiley Sons, Inc., Hoboken, New Jersey. USA,)2011
2. M. A. Khan, "Scheduling for heterogeneous systems using constrained critical paths", Parallel Computing, Vol. 38, pp. 175-193, 2012.
3. J. W. Ge and Y. S. Yuan, "Research of cloud computing task scheduling algorithm based on improved genetic algorithm," in Applied Mechanics and Materials, 2013, pp. 2426-2429.
4. S. Periyanatchi and K. Chitra ,"A Lion Optimization Algorithm for an Efficient Cloud Computing With High Security, Volume 64, Issue 1, 2020 **Journal of Scientific Research**
5. Hui Wang,· Zhihua Cui, · Hui Sun,· Shahryar Rahnamayan, · Xin-She Yang,,"Randomly attracted firefly algorithm with neighborhood search and dynamic parameter adjustment mechanism", Soft Computing DOI 10.1007/s00500-016-2116-z
6. Suraj Pandey, (2010), "Scheduling and Management of Data Intensive Application Workflows in Grid and Cloud computing Environments", Doctoral Thesis. Department of Computer Science and Software Engineering, the University of Melbourne, Australia.
7. ADNAN Fida, (2008), "Workflow Scheduling for Service Oriented Cloud Computing"
8. Arash Ghorbannia Delavar & Yalda Aryan, (2012), "A Goal-Oriented Workflow Scheduling in Heterogeneous Distributed Systems", International Journal of Computer Applications, 0975 – 8887.
9. Yang, X.S. (2010). Firefly Algorithm for Multimodal Optimization. In: Stochastic Algorithms: Foundations and Applications, SAGA 2009, Lecture Notes in Computer Science., Vol. 5792, pp. 169-178.
10. Nora Ahmed Almezeini , Alaaeldin Hafez"Task Scheduling in Cloud Computing using Lion Optimization Algorithm", *in* International Journal of Advanced Computer Science and Applications · January 2017
11. Kaveh, S. Mahjoubi,"Lion pride optimization algorithm: A meta-heuristic method for global optimization problems", Sharif University of Technology Scientia Iranica Transactions B: Mechanical Engineering.
12. Karunya N, Dr.T.Deepa," LITERATURE REVIEW ON RESOURCE ALLOCATION IN CLOUD COMPUTING" Shodhasamhita : Journal of Fundamental & Comparative ResearchVol. VIII, No. 1(XXII) : 2022,ISSN: 2277-7067.

| Figure 1: Task Scheduling Model with Optimization Algorithm | Figure 2: Execution Time |

| Figure3: Makespan | Figure4: Task Delay Time |
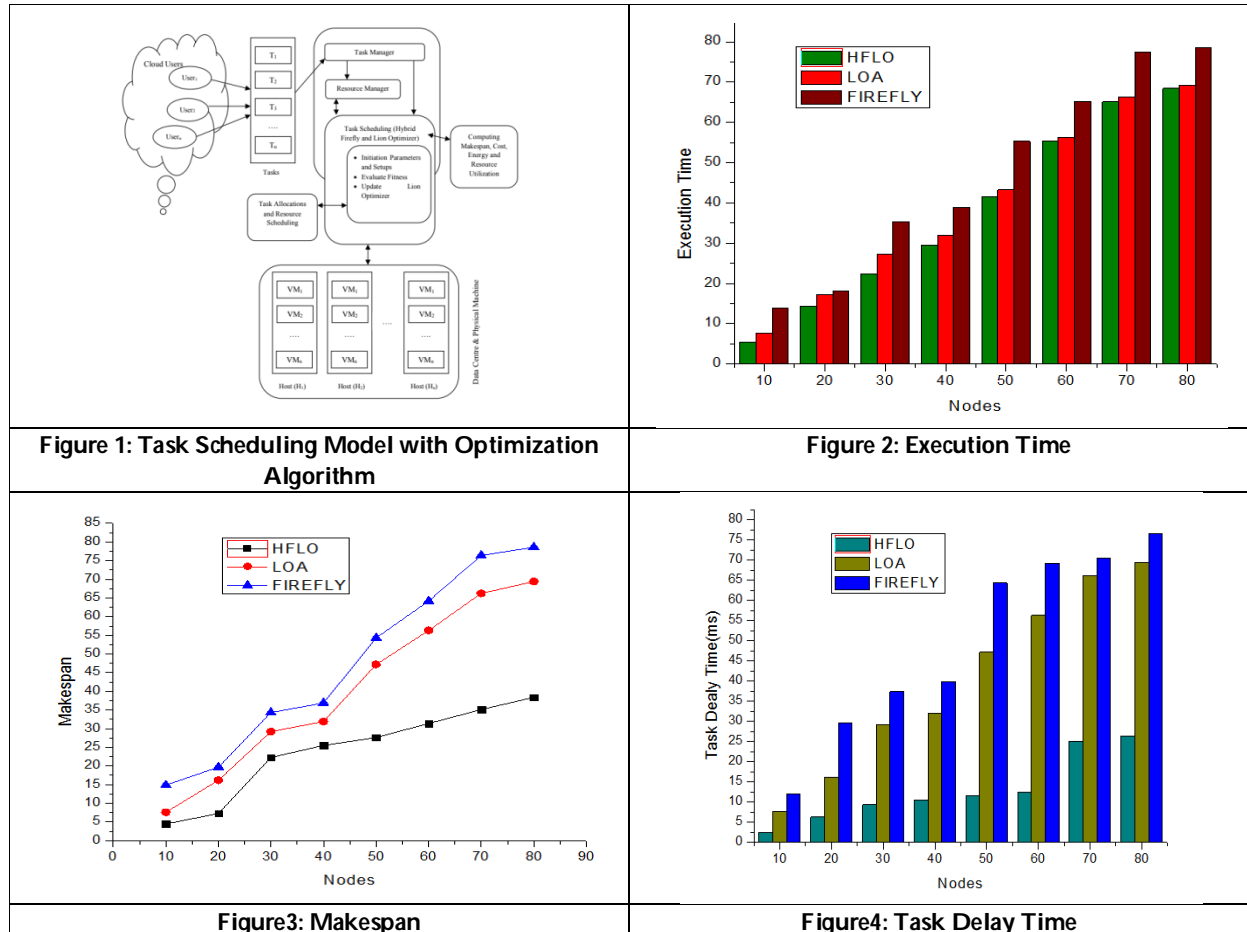
Identifying Locating Sets In Zero Divisor Graph Of A Lattice

S. Nithya[1] and S. Valarmathi[2]*

[1]Assistant Professor, PG and Research Department of Mathematics, St. Xavier's College (Autonomous), Palayamkottai-627002, Affiliated to Manonmaniam Sundaranar University, Abishekapatti, Tirunelveli-627012, Tamil Nadu, India.
[2]Research Scholar, Registration Number: 19221282092011 St. Xavier's College (Autonomous), Palayamkottai-627002, Affiliated to Manonmaniam Sundaranar University, Abishekapatti, Tirunelveli-627012, Tamil Nadu, India

*Address for Correspondence
S.Valarmathi
Research Scholar,
Registration Number: 19221282092011
St. Xavier's College (Autonomous), Palayamkottai-627002,
Affiliated to Manonmaniam Sundaranar University,
Abishekapatti, Tirunelveli-627012, Tamil Nadu, India
E. Mail: valarmathirenisha@gmail.com

ABSTRACT

If A is a lattice with the smallest element being zero, then a zero divisor graph, indicated by the symbol $\alpha(A)$, is an undirected graph whose vertices are nonzero zero divisors of A, with two unique vertices connected by an edge when their meet is zero. In this paper, we investigate the locating number of a graph with zero divisor of the lattice A.

Keywords: Locating set; locating number; lattice; zero divisor; graph with zero divisor

INTRODUCTION

Let A be a lattice with the least element 0. We associate a simple graph $\alpha(A)$ to A with the vertex set $Z(A)^* = Z(A) \setminus \{0\}$, the set of non-zero zero divisors of A and distinct $x, y \in Z(A)^*$ are adjacent if and only if $x \wedge y = 0$. Note that $\operatorname{diam}(\alpha(A)) \leq 3$. There are many papers which interlink graph theory and lattice theory [5, 9, 10, 11, 12]. These papers discussed the properties of graphs derived from partially ordered sets and lattices. S. K. Nimbhokar, M. P. Wasadikar and M. M. Pawar [12] have introduced the notion of coloring in graphs derived from lattices. In [10], E. Estaji and K. Khashyarmanesh associated to any finite lattice A, a simple graph $G(A)$ whose vertex set is $Z(A)^*$ and two vertices x and y are adjacent $\Leftrightarrow x \wedge y = 0$. They studied the structure of $G(A)$ and connections between graph theoretical properties and lattice theoretical properties. The zero divisor graph of various algebraic structures has

Nithya and Valarmathi

been studied by several authors [1, 2, 3, 4, 8]. Let $(A, \vee, \wedge)$ be a lattice with the least element 0. Then $a \in A$ is called an *atom* if there is no $y \in A$ such that $0 < y < a$. The set of all atoms of A is denoted by $\mathcal{T}(A)$. The lattice A is called *atomic* if for any $x \in A$, there exists an element $a \in \mathcal{T}(A)$ such that $a \le x$. A nonempty subset I of A is called an *ideal* if $x, y \in I \implies x \vee y \in I$ and $l \in A, x \in I$ and $l \le x \implies l \in I$. A proper ideal I of A is said to be *prime* if $a, b \in A$ and $a \wedge b \in I \implies a \in I$ or $b \in I$. The undefined terms and notations are from [7].

Let $G = (V, E)$ be a graph. We say that G is *connected* if there is a path between any two vertices of G, otherwise G is called disconnected. The *neighbourhood* of a vertex u is the set $N(u)$ consisting of all vertices v which are adjacent with u. For vertices x and y of G, let $d(x, y)$ be the length of a shortest path from x to y. The diameter of G is $diam(G) = sup\{d(x, y): x, y \in V(G)\}$. The *eccentricity* of a vertex v is defined as $e(v) = max\{d(v, y): y \in V(G)\}$ and the radius of G is given by $rad(G) = min\{e(x): x \in V(G)\}$. Let G be a connected graph with n vertices, where $n \ge 2$. Let $W = \{w_1, w_2, \dots, w_k\}$ be an ordered subset of $V(G)$ and a vertex $\in G$, the *locating code (or code)* of v with respect to W is the k-tuple, $c_W(v) = (d(v, w_1), d(v, w_2), \dots, d(v, w_k))$. The set W is said to be a *locating set* for G if distinct vertices have distinct codes. A locating set of minimum number for a graph G is called a *minimum locating set G*. The locating number denoted by $\iota(G)$ is the number of vertices in the minimum locating set for G. Let G be a connected graph with $|V(G)| \ge 2$. Two distinct vertices u and v of G are *distance similar* if $d(u, x) = d(v, x), \forall x \in V(G) - \{u, v\}$. For basic definitions in graph theory we refer to [6]. Some of the results are well known in the literature, and they are listed for future reference.

Preliminaries

Theorem 2.1.([13, Theorem 2.1]) *Let G be a connected graph. If G is partitioned into r distinct distance similar classes $V_1, V_2, \dots, V_r$ (that is, $x, y \in V_i$ if and only if $d(x, a) = d(y, a)$ for all $a \in V(G) - \{x, y\}$).*
(i) Any locating set W for G contains all but at most one vertex from each V_i.
(ii) Each V_i induces a complete subgraph or a subgraph with no edges.
(iii) $\iota(G) \ge |V(G)| - r$.
(iv) There exists a minimal locating set W for G such that if $|V_i| > 1$, at most $|V_i| - 1$ vertices of V_i are elements of W.
(v) If m is the number of distance similar classes that consist of a single vertex, then $|V(G)| - r \le \iota(G) \le |V(G)| - r + m$.

Theorem 2.2.([13, Theorem 2.2]) *Let G be a connected graph with $diam(G) = m < \infty$. If $\iota(G) = k < \infty$, then $|V(G)| \le (m + 1)^k$.*

Theorem 2.3.([13, Corollary 2.2]) *Let G be a connected graph with finite diameter. Then $|V(G)|$ is finite if and only if $\iota(G)$ is finite.*

Theorem 2.4.([14, Theorem 1.1]) *Let A be a Boolean algebra. Then A is finite if and only if its set of atoms is finite.*

Locating Sets And Numbers Of $\alpha(A)$

Theorem 3.1.*Let A be a Boolean algebra. Then*
(i) $\iota(\alpha(A))$ is finite if and only if A is finite.
(ii) $\iota(\alpha(A))$ is undefined if and only if $A = \{0\}$.

Proof. (i) Let A be finite. Then clearly $\alpha(A)$ is finite and hence $\iota(\alpha(A))$ is finite, by Theorem 2.3. Conversely, assume that $\iota(\alpha(A))$ is finite. Since $diam(\alpha(A)) \le 3$ and by Theorem 2.2, vertex set is finite. Since all the atoms are zerodivisors, atom set is finite. Therefore, by Theorem 2.4., A is finite. (ii) This follows from the fact that the locating number of $\alpha(A)$ is undefined if and only if the vertex set of $\alpha(A)$ is empty.

Theorem 3.2.*Consider A is a lattice. Then*
(i) $\iota(\alpha(A)) = 1 \iff \alpha(A)$ is a path.
(ii) $\iota(\alpha(A)) = |Z(A)^*| - 1 \iff \alpha(A)$ is a complete graph.
(iii) If $\alpha(A)$ is a cycle, then $\iota(\alpha(A)) = 2$.
(iv) If $\alpha(A)$ is a bipartite graph (other than $K_{1,1}$), then $\iota(\alpha(A)) = |Z(A)^*| - 2$.

Proof. This result follows from [13] (Lemma 2.1, Lemma 2.3, and Theorem 2.1).

63376

Notation:D_n = The set of all positive divisors of n, where $n \in \mathbb{N}$. For $a, b \in D_n$, we write $a \leq b$ if and only if $a \mid b$, i.e., $b = ac$ for some $c \in \mathbb{N}$. Then D_n becomes a lattice with the smallest element 1 and $x \wedge y = gcd(x, y)$, $x \vee y = lcm(x, y)$.

Theorem 3.3.￼*Let p and q be two distinct prime numbers.*
(i) If $n = 2p, p \geq 3$, then $\iota(\alpha(A)) = 1$.
(ii) If $n = p^k$ where $k \geq 1$, then $\iota(\alpha(A)) = 0$.
(iii) If $n = p^2 q$, then $\iota(\alpha(A)) = 1$.
(iv) If $n = p^k q, k \geq 3$, then $\iota(\alpha(A)) = |Z(A)^*| - 2$.

Proof.(i) If $n = 2p$ and $p \geq 3$, then $\alpha(D_n)$ contains only two vertices $\{2, p\}$ which are adjacent. Therefore, we get a path and the result follows from Lemma 2.2, [13].
(ii) If $n = p^k$, where $k \geq 1$, then D_n is a chain and so $\alpha(D_n)$ contains only a single vertex $\{p\}$. Since the locating number of a singleton set is zero. Therefore, $\iota(\alpha(A)) = 0$.
(iii) If $n = p^2 q$, When p and q are distinct primes, then $\alpha(D_n)$ is a path of length two. Therefore, $\iota(\alpha(A)) = 1$.
(iv) If $n = p^k q, k \geq 3$, p and q are distinct primes. Thus $\alpha(D_n)$ can be partitioned into two distance similar equivalence classes namely $V_1 = \{q\}$ and $V_2 = \{p^k, k \geq 3\}$. It forms a star graph and so by Theorem 3.2 (iv), $\iota(\alpha(A)) = |Z(A)^*| - 2$.

Theorem 3.4.￼*Let $n = p^{n_1} q^{n_2}$, where p and q are distinct prime numbers and $n_1, n_2 \in \mathbb{N}$. Then there exist prime ideals P_1 and P_2 in $D_n(= A)$ such that $P_1 \cap P_2 = \{1\}$. Moreover $\iota(\alpha(A)) = |Z(A)^*| - 2$.*

Proof. Consider $P_1 = \{1, p, p^2, ..., p^{n_1}\}$ and $P_2 = \{1, q, q^2, ..., q^{n_2}\}$. Clearly $P_1 \cap P_2 = \{1\}$. Let $x_1, x_2 \in P_1$ and then $x_1 \wedge$ (meet)$x_2 = $ gcd (x_1, x_2) and $x_1 \vee$ (join)$x_2 = lcm(x_1, x_2)$. First, we claim that P_1 is an ideal. To prove that $x_1 \vee x_2 \in P_1$.
Case 1. $x_1 = 1$ or $x_2 = 1$. Then $x_1 \vee x_2 = x_1$ or $x_2 \in P_1$.
Case 2. $x_1, x_2 \neq 1$. Assume without sacrificing generality that $x_1 \geq x_2$. Then $x_1 \vee x_2 = $ lcm $(x_1, x_2) = x_1 \in P_1$. If $t \in A - \{1\}, x \in P_1$ and $t \leq x$. Then $t \mid x$ and so x is a multiple of t. Then $t = p^i \in P_1$, for some i and hence P_1 is an ideal. Next, we assert that P_1 is a prime ideal. Let $x, y \in L$ and $x \wedge y \in P_1$. To prove that $x \in P_1$ or $y \in P_1$.
Case 1. $x \wedge y = 1$. Then $x = 1$ and $y = 1, x = 1$ and $y = p^i \in P_1$ for some i.
Case 2. $x \wedge y = p^i, x \leq y$. Then $x = p^i$ and $y = p^j, i < j$. Thus P_1 is prime. Similarly we can demonstrate that P_2 is also a prime ideal.

Theorem 3.5.*If $n = pqr$, where p, q and r are three distinct primes and $A = D_n$ then $\iota(\alpha(A)) = 2$.*

Proof. $A = \{1, p, q, r, pq, qr, pr, pqr\}$ and so $Z(A)^* = \{p, q, r, pq, qr, pr\}$. Let the vertex set of $\alpha(A)$ may be divided into four separate pair wise distance similarity equivalence classes, say $V_1 = \{qr\}, V_2 = \{p\}, V_3 = \{q, r\}, V_4 = \{pr, pq\}$. Then by Theorem 2.1, $\iota(\alpha(A)) \geq 2$. If $W = \{qr, pr\}$, then $c_W(q) = (2,1), c_W(r) = (2,2), c_W(p) = (1,2), c_W(pq) = (3,3)$. Therefore W is a locating set and also it forms a minimum locating set. Hence $\iota(\alpha(A)) \leq 2$.

Theorem 3.6. Let $n = pqrs$, where p, q, r and s are four distinct prime numbers, then $\iota(\alpha(D_n)) = 4$.

Proof. Consider that $\mathcal{K}$ is the locating (discovering) set for $\alpha(D_n)$. Suppose $\mathcal{K} = \{p\}$, then $c_{\mathcal{K}}(pq) = c_{\mathcal{K}}(pr) = c_{\mathcal{K}}(ps) = c_{\mathcal{K}}(pqr) = c_{\mathcal{K}}(prs) = c_{\mathcal{K}}(pqs) = 2$. Using Figure 1, one can check all the possible of singleton set is not a locating set. Suppose $\mathcal{K} = \{p, q\}$. In this case, $c_{\mathcal{K}}(pq) = c_{\mathcal{K}}(pqr) = c_{\mathcal{K}}(pqs) = (2,2)$. Clearly two points set cannot be a locating set. If $\mathcal{K} = \{p, q, r\}$, then $c_{\mathcal{K}}(pq) = c_{\mathcal{K}}(pqs) = (2,2,1)$. Therefore, it is not a locating set. One can examine all the possible of three vertices set is not a locating set. Consider the set $\mathcal{K} = \{p, q, r, s\}, c_{\mathcal{K}}(x)$ not the same as $c_{\mathcal{K}}(y) \forall x, y \in V(\alpha(D_n)) \setminus \mathcal{K}$ and also it forms a minimum locating set.

Theorem 3.7.*If $n = pqrst$ where p, q, r, s and t are five distinct prime numbers, then $\iota(\alpha(D_n)) = 5$.*

Proof. The locating set will be $\mathbb{W}$ for $\alpha(D_n)$. Suppose $\mathbb{W} = \{p\}$. In this case, we can find many vertices such that $c_{\mathbb{W}}(pqrs) = c_{\mathbb{W}}(pqst) = c_{\mathbb{W}}(\text{prst}) = c_{\mathbb{W}}(pqrt) = 2$. Using Figure 2, we can able to see all the possible of singleton set is not a locating set. Suppose $\mathbb{W} = \{p, q\}$. Here also we can find some vertices whose locating code is same (for example, $c_{\mathbb{W}}(pqrs) = c_{\mathbb{W}}(pqst) = c_{\mathbb{W}}(pqrt) = (2,2)$. Clearly two points set cannot be a locating set. Suppose $\mathbb{W} = \{p, q, r\}$, one can investigate two vertices such that $c_{\mathbb{W}}(pq) = c_{\mathbb{W}}(pqs) = (2,2,1)$. Therefore, it is not a locating set. Also a set with three vertices cannot be a locating set. If $\mathbb{W} = \{p, q, r, s\}$, then $c_{\mathbb{W}}(pr) = c_{\mathbb{W}}(prs) = c_{\mathbb{W}}(\text{prst}) = (2,1,2,2)$. Look into all the possible of a set which contains four vertices is not a locating set. Consider the set $\mathbb{W} = \{p, q, r, s, t\}, c_{\mathbb{W}}(x) \neq c_{\mathbb{W}}(y) \forall x, y \in V(\alpha(D_n)) \setminus \mathbb{W}$ and also it forms a minimum locating set.

Theorem 3.8. If $n = (pqr)^k$, where $k \geq 2$ and p, q and r are three distinct primes, then $\iota(\alpha(D_n)) = 3(2^k - 1)$.

Proof. If $n = (pqr)^k$ and $k \geq 2$, then $|Z(D_n)^*| = 3(2^k) + 3$ and $V(\alpha(D_n))$ will be divided into six distinct distance similar equivalence classes namely, $P = \{qr, q^2r, \dots, q^kr, qr^2, \dots, qr^k\}, Q = \{p, p^2, \dots, p^k\}, R = \{q, q^2, \dots, q^k\}, S = \{pr, p^2r, \dots, p^kr, pr^2, \dots pr^k\}, E = \{r, r^2, \dots, r^k\}, T = \{pq, p^2q, \dots, p^kq, pq^2, \dots pq^k\}$. Therefore, by Theorem 2.1. $\iota(\alpha(D_n)) \geq |Z(D_n)^*| - 6 = 3(2^k) + 3 - 6 = 3(2^k) - 3 = 3(2^k - 1)$. Consider $\mathcal{M} = \left\{ \begin{matrix} p^i, q^i, r^i, pq^i, p^iq, (pq)^i, qr^i, \\ q^ir, (qr)^i, pr^i, p^ir, (pr)^i, 2 \leq i \leq k \end{matrix} \right\}$. Refer Figure 3., $c_{\mathcal{M}}(p) \neq c_{\mathcal{M}}(q) \neq c_{\mathcal{M}}(r) \neq c_{\mathcal{M}}(pq) \neq c_{\mathcal{M}}(qr) \neq c_{\mathcal{M}}(pr)$. Hence it forms a locating set with cardinality less than or equal to $|Z(D_n)^*| - 6$.

Remark 3.9. *The locating number of $\alpha(D_n)$, where $n = (pqr)^2$, is $3(2^2 - 1) = 9$.*

Theorem 3.10. *If $n = p^{n_1}qr$, where $n_1 \geq 2 \in \mathbb{N}$ and p, q and r are distinct prime numbers. Then $\iota(\alpha(D_n)) = 3(n_1 - 1)$.*

Proof. Here $|Z(D_n)^*| = 3(n_1 + 1)$. Now, the vertices will be divided into distance-related classes in $\alpha(D_n)$ stated by $V_1 = \{pr, p^2r, \dots, p^{n_1}r\}, V_2 = \{q\}, V_3 = \{p, p^2, \dots p^{n_1}\}, V_4 = \{qr\}, V_5 = \{r\}$ and $V_6 = \{pq, p^2q, \dots, p^{n_1}q\}$. By Theorem 2.1, $\iota(\alpha(D_n)) \geq |Z((D_n)^*)| - 6 = 3(n_1 + 1) - 6 = 3n_1 + 3 - 6 = 3n_1 - 3 = 3(n_1 - 3), n_1 \geq 2$. Consider the set $Q = \{p^i, p^ir, p^iq : 2 \leq i \leq n_1\}$. Refer Figure 4., all the values of $c_Q(p), c_Q(pr), c_Q(pq), c_Q(q)$ and $c_Q(r)$ with respect to Q are distinct. Hence it forms a locating set with cardinality $\leq |Z(D_n)^*| - 6$.

Theorem 3.11. *If $n = pq^2r^3$, where p, q and r are distinct prime numbers. Then $\iota(\alpha(D_n)) = |Z(D_n)^*| - 6$.*
Proof. Here $|Z(D_n)^*| = 17$. $V(\alpha(D_n)^*)$ can be divided into six different distance similar equivalence classes. They are $V_1 = \{qr, q^2r, qr^2, qr^3, q^2r^2, q^2r^3\}, V_2 = \{p\}, V_3 = \{r, r^2, r^3\}, V_4 = \{pq, pq^2\}, V_5 = \{q, q^2\}, V_6 = \{pr, pr^2, pr^3\}$. Hence, by Theorem 2.1, $\iota(\alpha(D_n)) \geq |Z(D_n)^*| - 6$. Consider $\mathcal{S} = \{q^2r, qr^2, qr^3, q^2r^2, q^2r^3, r^2, r^3, pq^2, q^2, pr^2, pr^3\}$. Refer Figure 5, $c_{\mathcal{S}}(p) \neq c_{\mathcal{S}}(q) \neq c_{\mathcal{S}}(r) \neq c_{\mathcal{S}}(pq) \neq c_{\mathcal{S}}(qr) \neq c_{\mathcal{S}}(pr)$. Hence it forms a locating set with cardinality $\leq |Z(D_n)^*| - 6$.

Remark 3.12. *If $n = p^2q^3r, p^2qr^3$, then $\iota(\alpha(D_n)) = |Z(D_n)^*| - 6$.*
Theorem 3.13. *Let $A = M_n$, where $M_n = \{0, a_1, \dots, a_{n-2}, 1\}$ be the lattice in which $a_i \wedge a_j = 0$ and $a_i \vee a_j = 1$ for $i \neq j$ if and only if $\iota(\alpha(M_n)) = n - 3$.*

Proof. Here, the atoms set $\{a_1, a_2, \dots, a_{n-2},\}$ is the vertex set of $\alpha(M_n)$. Also it forms a complete graph with $n - 2$ vertices. Therefore, $\iota(\alpha(M_n)) = n - 3$.

Example 3.14. Consider the lattice $A = M_5$. The zero-divisor graph of the lattice M_5 is a complete graph with 3 vertices. Therefore, $\iota(\alpha(M_n)) = 2$.

Theorem 3.15. *If A is a lattice with finite number of elements. Then*
(i) $\iota(\alpha(D_p \times D_p)) = 1$.
(ii) If $A = D_{2^k} \times D_{2^k}$ and $D_{p^2} \times D_{p^2}$, then $\alpha(A)$ is a complete bipartite graph, where p is prime and $k \geq 1$. Further $\iota(\alpha(A)) = |Z(A)^*| - 2$.

Nithya and Valarmathi

(iii) If $A = D_p \times D_q$, where p and q are prime numbers. Then,$\iota(\alpha(A)) = 1$

Proof.(i) Since the lattices $\alpha(D_p \times D_p)$ contains only two atoms $\{(1,p),(p,1)\}$, then the corresponding zero divisor graph is isomorphic to a path of length 2 . Hence by Lemma 2.1, [13], locating number of this graph is 1 .

(ii) Here $\alpha(D_p \times D_p)$ can be partitioned into two distinct vertex sets, namely $U_1 = \{(1,2),(1,2^2),\dots,(1,2^k)\}$and $U_2 = \{(2,1),(2^2,1),\dots,(2^k,1)\}$. Also $\alpha(D_{p^2} \times D_{p^2})$ can be partitioned into two distinct vertex sets, namely $V_1 = \{(1,p),(1,p^2)\}$and $V_2 = \{(p,1),(p^2,1)\}$. Each graph is isomorphic to a complete bipartite graph$(K_{n,n})$.Thus by Theorem 3.2.,$\iota(\alpha(A)) = |Z(A)^*| - 2$.

(iii) This graph is isomorphic to the path which contains only two vertices$\{(1,p),(q,1)\}$. Therefore, locating number is 1.

REFERENCES

1. D. D. Anderson and M. Naseer, Beck's coloring of a commutative ring, J. Algebra, 159 (1993),$500 - 514$.
2. D. F. Anderson and P. Livingston, The zero divisor graph of a commutative ring, J. Algebra, 217 (1999), 434-447.
3. D. F. Anderson, R. Levy, and J. Shapiro, Zero divisor graphs, von Neumann regular rings and Boolean algebras, J. Pure Appl. Algebra 180 (2003), 221-241.
4. I. Beck, Coloring of Commutative rings, J. Algebra 116 (1988), 208-226.
5. B. Bollobos and I. Rival, The maximal size of the covering graph of a lattice, Algebra Universalis 9 (1979), 371-373.
6. G. Chartrand and P. Zhang, Introduction to Graph theory, Wadsworth and Brooks/Cole, Monterey, CA 1986.
7. B. A. Davey and H. A. Priestley, Introduction to Lattices and Order, Cambridge University Press Cambridge 2002.
8. F. R. Demeyer, T. Mckenzie and K. Schneider, The zero divisor graph of a commutative semigroup, Semigroup Forum 65 (2002), 206-214.
9. D. Duffus and I. Rival, Path length in the covering graph of a lattice, Discrete Math. 19 (1977), 139-158.
10. E. Estaji and K. Khashyarmanesh, The zero divisor graph of a lattice, Results Math. 61 (2012) 1-11.
11. E. Gedeonová, Lattices, whose covering graphs are S-graphs, Colloq Math. Soc. JánosBolyai 33 (1980), 407-435.
12. S. K. Nimbhorkar, M. P. Wasadikar and M. M. Pawar, Coloring of lattices, Math. Slovaca 60 (2010) 419-434.
13. S. Pirzada and R. Raja and S. Redmond Locating sets and numbers of graphs associated to commutative rings, J. Algebra, Vol. 13, No. 7 (2014).
14. T. TamizhChelvam and S. Nithya A note on the zero divisor graph of a lattice, Transactions on Combinatories, Vol. 3 No. 3(2014), pp. 51-59.
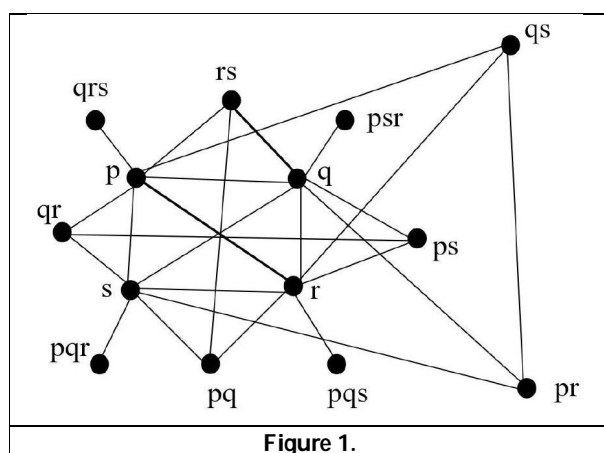
Figure 1.
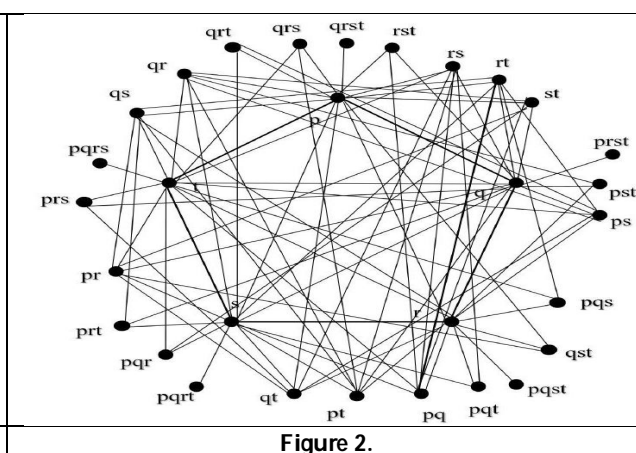
Figure 2.

Nithya and Valarmathi

Figure 3.

Figure 4.

Figure 5.

RESEARCH ARTICLE
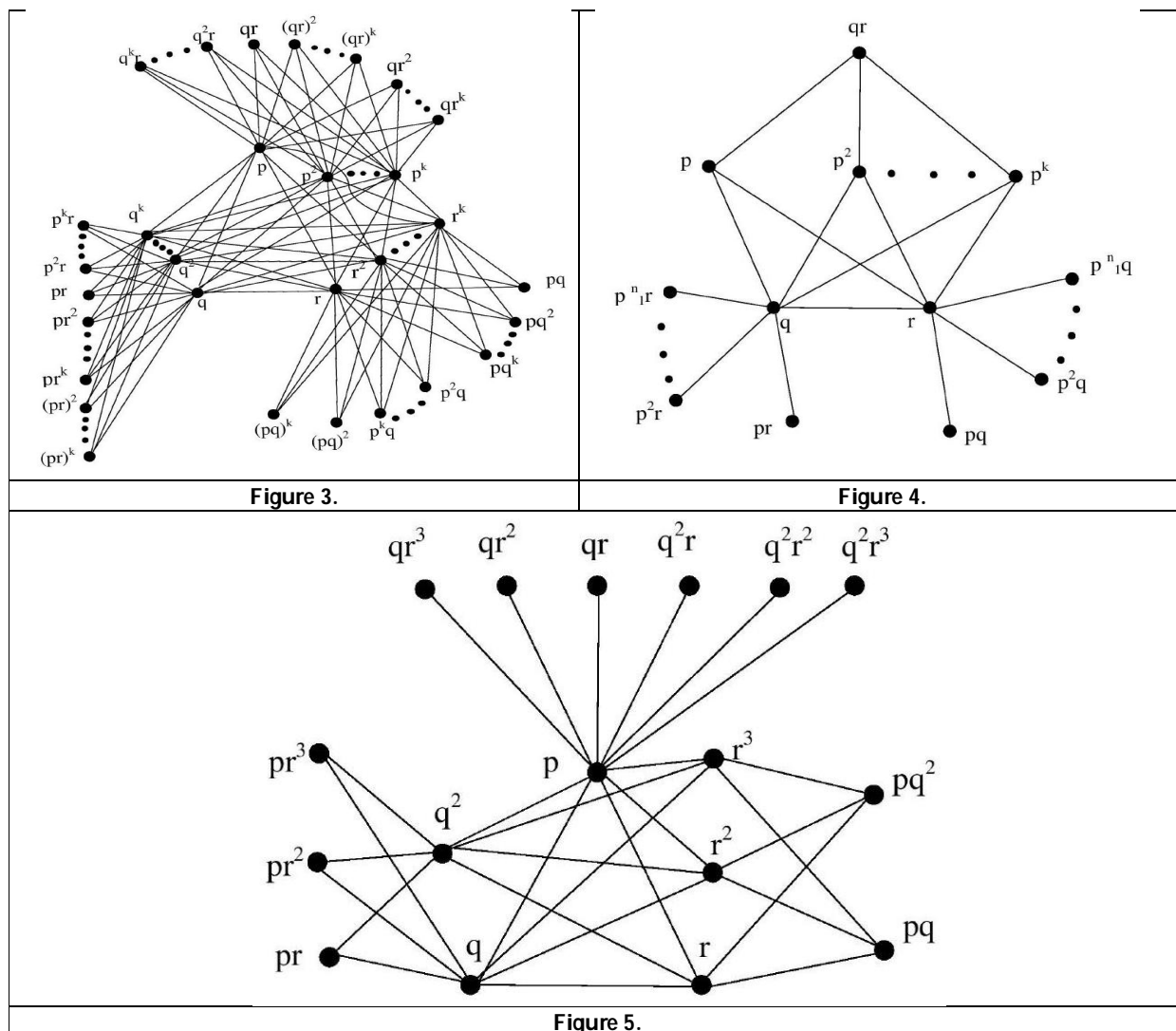
Manufacturing Company Performance Analysis using Time Series

Nanthitha. L[1] and Mani. N[2]*

[1]II M.Sc., Mathematics, Sri Ramakrishna College of Arts and Science, Coimbatore, Tamil Nadu, India.
[2]Assistant Professor of Statistics, Sri Ramakrishna College of Arts and Science, Coimbatore, Tamil Nadu, India

*Address for Correspondence
Mani. N
Assistant Professor of Statistics,
Sri Ramakrishna College of Arts and Science,
Coimbatore, Tamil Nadu, India
E.Mail: mani.n@srcas.ac.in

ABSTRACT

Time series analysis approach provides significant potential to enhance financial planning and performance management in companies. The goal of our research presents an advanced time series analysis approach for predicting a company's performance over the next 6 months and enables decision-makers to make informed strategic decisions with accurate and reliable forecasts and allocate resources effectively.

Keywords: Time Series, Semi Average, Moving Average, Prediction, R Programming,

INTRODUCTION

Time series, is a sequence of numerical data obtained at regular time intervals. Time series analysis is a statistical tool that is useful for a wide range of longitudinal study methods. Such designs involve a single subject or research unit that is measured regularly at regular intervals over a significant number of observations. We can better understand the underlying naturalistic process, the pattern of change through time, or the results of either a planned or unexpected intervention by using time series analysis. Time series analysis is a potent and popular technique in many disciplines, from environmental sciences and engineering to economics, business and finance. It relays on comprehending and identifying significant patterns in data points gathered over time. Time series designs are becoming a more practical way for analyzing significant data for developments in information systems technology. A time series is a collection on observations having a temporal ordering that are recorded at regular intervals. Time series data differ from cross-sectional data, where observations are independent of one another, due to their sequential structure. Time Series Analysis has a variety of goals, it includes predicting future values, spotting anomalies or unusual behavior, figuring out underlying patterns, and making judgements based on such

63381

information. A well-executed Time Series Analysis can produce insightful results that support important decision-making.

Uses of Time Series
- Time series helps to understand the past behavior of the variable under study. Time series is very useful in predicting probable future activities based on the past performance. Time series analysis enables comparison between two or more variables over a period of time.

- Time series helps to determine the type and nature of the changes in the given data. Time series analysis explains why trends appear in historical data and how underlying patterns or processes may be able to account for them. Time series analysis is used to identify the fluctuation in economics and business. Time series helps in evaluating the current achievements. Natural systems cannot be understood without the use of time series analysis, which is a fundamental analytical tool. Examples of natural systems whose behavior can be best investigated using time series analysis include climate cycles, economic swings, volcanic eruptions, and earthquakes.

Major components of Time Series Analysis

Trend component: This aids in predicting future actions. This trend shows whether the data generally tends to rise or fall over a long period of time. A "trend" is a typical, consistent, long-term tendency. Not all increases and decreases must occur simultaneously. As for increasing, declining, or constant patterns, different historical periods show distinct tendencies. A general upward, downward, or constant movement is necessary though.

Seasonal component: The variation in a variable caused by some specified patterns in its behavior is known as the seasonal component of a time series. Any sort of time series, such as individual commodity price quotes, interest rates, exchange rates, stock prices, etc., can be described using this term. These patterns can be daily, weekly, monthly, or occur at regular time intervals. Seasonal components can often be modelled using straightforward regression equations. The term "seasonalized regression" or "bimodal regression" may be used to describe this method.

Cyclical component: The portion of the movement in the variable that can be explained by other cyclical movements in the economy is known as the cyclical component in a time series. In other words, this phrase provides details regarding seasonal patterns.It is also known as the boom-bust process or the long-period (LP) effect. For instance, business cycles typically exhibit slower growth rates during recessions than they did before.

Irregular component: The portion of the movement in the variable that cannot be accounted for by economic cycle is known as the irregular component. Alternatively said, this term provides information on non-seasonal patterns. Changes that are not cyclical are referred to by this phrase. These include boom-bust cycles, long-term trend changes that are permanent, or data that is "not seasonally adjusted" and is typically not included in national income and product accounts such as depreciation, R&D spending and agricultural subsidies.

REVIEW OF LITERATURE

William W. S. Wei (2005) explained the basic concepts and conventional methods,and extended the autoregressive moving average models to represent seasonal series in their book. James D. Hamilton (1994), covers various aspects of time series analysis, including seasonal variation and their detection. It also provides a thorough explanation of seasonal decomposition techniques, which are used to identify and model the seasonal patterns present in time series data. Robert H. Shumway and David S. Stoffer (2017) provided a comprehensive introduction to time series analysis with practical examples using the R programming language. George E. P. Box, Gwilym M. Jenkins, and Gregory C. Reinsel (2015), widely covered the foundational concepts of time series analysis, including ARIMA models and

forecasting. Peter J. Brockwell and Richard A. Davis (2016), gave a solid introduction to time series analysis and forecasting methods, focusing on theoretical aspects and practical applications. Richard G. Graf (2015), geared towards social science researchers, explained time series analysis techniques in a user-friendly manner with examples using R. Rob J. Hyndman and George Athanasopoulos (2021) primarily focused on forecasting methods, and provided excellent coverage of time series analysis concepts and tools. Peter J. Diggle, Patrick J. Heagerty, Kung-Yee Liang, and Scott L. Zeger (2002), covered time series analysis from a statistical perspective, with emphasis on biomedical and public health applications. Pedro Lara-Benitez, Manuel Carranza-Garcia, Jose C Riquelme (2021), experimental review on deep learning architectures for time series forecasting.

RESEARCH METHODOLOGY

Objective
• To find the industry manufacturing process

• To predict expected industry growth for future

Need of the study: There is a need for the research among the industry for predicting the future growth
Data sources: Secondary data is collected from the industry for the analysis

ANALYSIS AND INTERPRETATION
The following statistical methods was used for this study
1. Diagrammatic representation

2. Correlation analysis and

3. Time series analysis

Diagrammatic Representation
From the above diagram (4.1.1), it shows that at the month of March industry ordered and dispatched nearly 71,000 products, followed by the month of June ordered and dispatched nearly 69,000 products, followed by May, the company ordered and dispatched nearly 65,800 products, and on April the industry ordered and dispatched on an average of 65,300, followed by January the company ordered and dispatched nearly 64,000 products, and followed by the month of February the company ordered and dispatched nearly 62,000 products.

Semi Average for total amount for the Material
The above analysis (4.2) shows the semi average of the production of the industry. The semi average of the products ordered and dispatched is maximum during the month of June and minimum during the month of February.

Semi Average for the ordered, dispatched and price of the Material
The above analysis (4.3) shows the semi average of the ordered quantity, dispatched quantity and the price per meter of the material, and the semi average of the ordered and dispatched quantity of the products is equal.

PREDICTION FOR NEXT 6 MONTHS
From the above analysis (4.4), the industry's growth for the next 6 months from the calculated data is predicted.

MONTHLY MOVING AVERAGE
The above analysis (4.5), gives the moving average of the industry's production.

Correlation
From the correlation analysis we observe that ordered quantity and dispatched quantity is strongly correlated, and the ordered quantity and dispatched quantity negatively correlates with the price per meter.

Descriptive Statistics

From the above analysis, it shows that for the six months period, the company ordered and dispatched 1362.73 material on an average with Rs.64.70 per meter. The total number of ordered products is completely dispatched by the company, so that the Mean, Standard Deviation, Median is equal for the ordered and dispatched quantity. The company ordered and dispatched maximum of 2475 products and minimum of 255 products, and the company delivered the product at the maximum price of Rs.70 per meter and minimum price of Rs.60 per meter.

ACKNOWLEDGEMENT

CONCLUSION

In conclusion, the time series analysis presented for the manufacturing company has provided valuable insights into predicting company growth for the next 6 months. Overall, the result of this study serves as a foundation for better preparedness and proactive actions to drive sustainable growth and success for the manufacturing company.

REFERENCES

1. William W. S. Wei, "Time Series Analysis", in Univariate and Multivariate Methods, Second Edition, April 2005.
2. James D. Hamilton, "Time Series Analysis", 1994.
3. Robert H. Shumway and David S. Stoffer, "Time Series Analysis and It's Applications", with R examples, 2017.
4. George E. P. Box, Gwilym M. Jenkins, and Gregory C. Reinsel, "Time Series Analysis: Forecasting and Control", 2015.
5. Peter J. Brockwell and Richard A. Davis, "Introduction to Time Series and Forecasting", 2016.
6. Richard G. Graf, "Applied Time Series Analysis for the Social Sciences", 2015.
7. Rob J. Hyndman and George Athanasopoulos, "Forecasting: Principles and Practice", online textbook, 2021.
8. Peter J. Diggle, Patrick J. Heagerty, Kung-Yee Liang, and Scott L. Zeger, "Time Series: Theory and Methods", 2002.
9. Pedro Lara-Benitez, Manuel Carranza-Garcia, Jose C Riquelme, "An experimental review on deep learning architectures for time series" International journal of neural systems 31 (03), 2130001, 2021.

Table 1. Correlation

	Ordered Quantity	Dispatched Quantity	Price per Mtr
Ordered Quantity	1	1	-0.014211339
Dispatched Quantity	1	1	-0.014211339
Price per Meter	-0.014211339	-0.014211339	1

Table 2. Descriptive Statistics

Month	Mean	Standard Deviation	Median	Maximum	Minimum
Ordered Quantity	1362.726027	649.6863692	1412.5	2475	255
Dispatch Quantity	1362.726027	649.6863692	1412.5	2475	255
Price Per Meter	64.70350736	2.785823437	64.73518421	69.87769977	60.02132815

Fig . 1. Industry Manufacturing process

```
> # Print the result
> print(fab_data)
  Month Ordered_Quantity Despatched_Quantity Price_per_Mtr Total_Amount
1  Jan            64053               64053      3063.740    196241711
2  Feb            62224               62224      3113.193    193715294
3  Mar            71117               71117      3139.113    223244282
4  Apr            65371               65371      3109.057    203242159
5  May            65869               65869      3110.967    204916318
6  Jun            69282               69282      3357.355    232604259
  Semi_Average
1   196241711
2   194978503
3   204400429
4   204110862
5   204271953
6   208994004
> |
```

Fig . 2. Semi Average for total amount for the Material

```
>
> # Print the result
> print(fab_data)
  Month Ordered_Quantity Despatched_Quantity Price_per_Mtr
1   Jan            64053               64053      3063.740
2   Feb            62224               62224      3113.193
3   Mar            71117               71117      3139.113
4   Apr            65371               65371      3109.057
5   May            65869               65869      3110.967
6   Jun            69282               69282      3357.355
  Semi_Avg_Ordered_Quantity Semi_Avg_Despatched_Quantity Semi_Avg_Price_per_Mtr
1                  64053.00                     64053.00               3063.740
2                  63138.50                     63138.50               3088.466
3                  65798.00                     65798.00               3105.348
4                  65691.25                     65691.25               3106.275
5                  65726.80                     65726.80               3107.214
6                  66319.33                     66319.33               3148.904
> |
```

Fig . 3. Semi Average for the ordered, dispatched and price of the Material:

```
>
> # Print the forecasted values
> print(next_6_months)
  Month Semi_Avg_Ordered_Quantity Semi_Avg_Despatched_Quantity Semi_Avg_Price_per_Mtr
1   Jul                  66319.33                     66319.33               3148.904
2   Aug                  66319.33                     66319.33               3148.904
3   Sep                  66319.33                     66319.33               3148.904
4   Oct                  66319.33                     66319.33               3148.904
5   Nov                  66319.33                     66319.33               3148.904
6   Dec                  66319.33                     66319.33               3148.904
> |
```

Fig . 4. Prediction For Next 6 Months

```
>
> # Print the result
> print(fcb_data)
  Month Ordered_Quantity Despatched_Quantity Price_per_Mtr Moving_Avg_Ordered_Quantity Moving_Avg_Despatched_Quantity Moving_Avg_Price_per_Mtr
1   Jan            64053              64053      3063.740                        0.00                           0.00                   0.000
2   Feb            62224              62224      3113.193                        0.00                           0.00                   0.000
3   Mar            71117              71117      3139.113                    65798.00                       65798.00                3105.348
4   Apr            65371              65371      3109.057                    66237.33                       66237.33                3120.454
5   May            65869              65869      3110.967                    67452.33                       67452.33                3119.712
6   Jun            60282              60282      3357.355                    65840.67                       65840.67                3192.160
> |
```

Fig . 5. Monthly Moving Average

RESEARCH ARTICLE

Fuzzy Solution for Fractional Order Tumor System Using Laplace Transform and Stability Analysis

P. Dhanalakshmi[1] and E. Shrilekha[2*]

[1]Associate Professor and Head, Department of Applied Mathematics, Bharathiar University, Coimbatore - 641046, Tamil Nadu, India.
[2]Ph.D Scholar, Department of Applied Mathematics, Bharathiar University, Coimbatore - 641046, Tamil Nadu, India.

*Address for Correspondence
E. Shrilekha
Ph.D Scholar,
Department of Applied Mathematics,
Bharathiar University, Coimbatore - 641046,
Tamil Nadu, India.

ABSTRACT

India's cancer incidence rates have been rising throughout the years. One method of treating cancer is chemotherapy and drugs used for chemotherapy work by preventing or reducing the growth of cancer cells, which can help shrink tumors or prevent them from spreading to other parts of the body. Modelling under a fuzzy environment is essential as it produces more precise, flexible, and easy-to-understand models that can enhance decision-making and performance in a broad range of industries. This paper formulates the fractional tumor model in a fuzzy environment which comprises the parameters involving chemotherapy drug. The existence of the solution is established using the fuzzy Laplace transform. Further, Hyers Ulam Stability is used in illustrating the stability of the fuzzy Caputo fractional order tumor model.

Keywords: Tumor system, Fractional Calculus, Fuzzy Laplace transform, Hyers Ulam Stability.

INTRODUCTION

The term 'cancer' was first coined in ancient Greece by the Greek physician Galen and Hippocrates due to the similarities observed between the swollen vein in some tumors and crabs. In India, there will likely be 14,61,427 tumour cases in 2022. One ninth people of India develop cancer in their lifetime. Among the female and male populations, breast and lung cancer are leading cancers respectively. For children from newborn to 14 years, lymphoid leukaemia is the most widespread form of cancer. Compared to 2020, the incident cases are expected to rise by 12.8% in 2025 [1]-[3]. Analysing a complicated real-world problem in a simple imaginary nature can depict

63387

the precise behavior of the system, which is a remarkable aspect of mathematical modelling. The merits of fractional calculus in the mathematical modelling of various dynamical systems are investigated in [4]-[6]. Cancer cases are continuously rising and the government has taken many initiatives in controlling them. Several researchers have analysed various types of cancers using mathematical modelling which can be referred to in [7]-[8]. Fuzzy solutions allow for a more accurate description of the system by incorporating uncertainty and imprecision. Biological systems are often subject to various sources of uncertainty, such as measurement errors, parameter variations, and inherent variability [9]. The Hyers-Ulam stability theorem extends the concept of stability from differential equations to functional equations. This enables the use of stability analysis techniques in a wide range of mathematical models and systems other than standard differential equations [10] – [12].

The highlights of this work are,

- Incorporating fuzzy concept in terms of initial condition.
- Utilizing fuzzy Laplace transform in solving the system.
- Model's stability is examined by Hyers Ulam concept

Basic Notation

Definition 1: Consider the map μ from $\mathbb{R}$ to [0,1] which stands for fuzzy number when it complies with the criteria:

- μ is normal.
- For $\lambda \in [0, 1]$ and any two arbitrary points u,v there are, $\mu\ (\lambda u + (1-\lambda)\ v) \geq$ min $\{\mu(u, v)\}$ that is, μ is fuzzy convex.
- μ is upper semi-continuous on $\mathbb{R}$.
- Closure of set $Supp(\mu)=\{u\in\mathbb{R}|\mu(u)>0\}$ is compact, where $Supp$ is the support of μ.

Definition 2: Consider ζ which maps from $E \times E$ to $\mathbb{R}$ and let s, r be two fuzzy numbers $s=(\underline{s}(j),\bar{s}(j))\&r=(\underline{r}(j),\bar{r}(j))$. The fuzzy numbers s and r follows Hausdorff distance, if it satisfies

$\zeta(s,r) = \sup_{j \in [0,1]} [\max \{ \mid \underline{s}(j) - \underline{r}(j)\mid , \mid \bar{s}(j) - \bar{r}\ (j)\mid \}]$

The metric ζ in E satisfies the following properties,

- $\zeta(\pi m,\pi n) = \mid \pi \mid \zeta(m,n)$ for all m,$n\in E$, $\pi \in \mathbb{R}$.
- $\zeta(m+s,n+s)=\zeta(m,n)$ for all $m,s,n\in E.$
- $\zeta(m+s,n+t)\leq\zeta(m,s)+\zeta(n,t)$ for all $m,n,s,t\in E.$
- (E,ζ) will denote a complete metric space.

Definition 3: The fractional function g(z) represents derivative under Caputo as

$$^{c}D^{\xi}g(z) = \begin{cases} \dfrac{1}{\Gamma(w-\xi)} \displaystyle\int_{a}^{z}(s-z)^{w-\xi-1}D^{k}g(s)ds, w-1 < \xi < w, z > a, w \in \mathbb{N} \\[2mm] \left(\dfrac{d}{dz}\right)^{w-1}g(z), \qquad \xi = w-1. \end{cases}$$

where the function $g\in F$, where F denotes the collection of fuzzy numbers with respect to $\mathbb{R}$ and $D^{k}g(s)$, for all k, are integrable.

Definition 4: Let s be the positive real parameter. The fuzzy Laplace transform for $\mathcal{G}(z)$, the fractional differential equation is given by,

$$\mathbf{L}\big(\mathcal{G}(z)\big) = \int_{0}^{\infty}e^{-sz}\mathcal{G}(z)dt$$

where $s>0$ and $\mathcal{G}(z) \in$ F.

Property 1: [Convolution Property]

Let $\mathcal{G}(z),\mathcal{H}(z) \in [0,\infty]$ be a continuous function,

$$\mathbf{L}\big((\mathcal{G}.\mathcal{H})(z)\big) = \mathbf{L}\big(\mathcal{G}(z)\big)\mathbf{L}\big(\mathcal{H}(z)\big)$$

Model Formulation

In this study, a tumor-immune system model under chemotherapy treatment is considered. The normal cell population are indicated by $R_{p}(t)$, tumor cell population as $T_{c}(t)$, Effector Immune (EI) cells population as $E_{c}(t)$, the

toxicity of drugs as $T_x(t)$, the concentration of chemotherapeutic agents as $D_c(t)$ based on time t are studied. The tumor system related to chemotherapy is defined with its parameters where $^cD^\xi$ denotes derivative under Caputo sense and ξ represents order $0 < \xi < 1$ as follows,

$$^cD^\xi R_p = m_2 R_p(1 - q_2 R_p) - l_4 R_p T_c,$$
$$^cD^\xi T_c = m_1 T_c(1 - q_1 T_c) - [l_2 E_c + l_3 R_p + p_2 D_c]T_c,$$
$$^cD^\xi E_c = v - d_1 E_c + \left[\sigma \frac{T_c}{l_5 + T_c} - a_2 T_c\right] E_c, \qquad (1)$$
$$^cD^\xi T_x = D_c - \phi T_x,$$
$$^cD^\xi D_c = -\eta_2 D_c + V(t).$$

The parameter descriptions are provided as follows,

Parameters	Description
p_2	Tumor cells killed in chemotherapy under fractional order
q_1	$1/q_1$ is carrying capacity of Tumor cells
q_2	$1/q_2$ is normal cell carrying capacity
l_2	EI cells that destroy cancer cells in a fractional order
l_3	Normal cells that destroy tumor cells in a fractional order
l_4	Tumor cells kill Normal Cells killed by under fractional order
m_1	Cancer cell proliferation pace
m_2	Normal cell proliferation pace
d_1	Mortality rate of EI cells
v	Continuous producion of the EI cells
l_5	The rate of increase in EI cells recruitment determined by slope of the recruitment curve
σ	The highest rate of EI cells recruitment
ϕ	Toxicity of drug elimination rate
η_2	Chemotherapy drug elimination rate
a_2	The degradation rate of chemotherapy and tumor cells-killed effector cells
ξ	Proposed system's order
$V(t)$	External influx of drug depending on time

Table 1: Parameter Description

Now, the system (1) is represented as

$$W_c = \begin{cases} R_p \\ T_c \\ E_c \\ T_x \\ D_c \end{cases},$$

$$X(t, W_c(t)) = \begin{cases} m_2 R_p(1 - q_2 R_p) - l_4 R_p T_c \\ m_1 T_c(1 - q_1 T_c) - [l_2 E_c + l_3 R_p + p_2 D_c]T_c \\ v - d_1 E_c + \left[\sigma \frac{T_c}{l_5 + T_c} - a_2 T_c\right] E_c \\ D_c - \phi T_x \\ -\eta_2 D_c + V(t) \end{cases} \qquad W_c(0, \varrho) = \begin{cases} R_p(0, \varrho) \\ T_c(0, \varrho) \\ E_c(0, \varrho) \\ T_x(0, \varrho) \\ D_c(0, \varrho) \end{cases}$$

$$\qquad (2)$$

Thus, the system (1) is reduced as,
$$^cD^\xi W_c = X(t, W_c(t)) \qquad (3)$$

Existence of Solution

The solution's existence for the above system is derived in this section. The Laplace transform is effective method in solving the differential equation of the dynamical system.

Theorem 1: For $t \geq 0$ and $0 < \xi < 1$, the considered model's solution (1) exists under the initial conditions

$$R_p(0,\varrho) = \left(\underline{R_p}(0,\varrho), \overline{R_p}(0,\varrho)\right),$$

$$T_c(0,\varrho) = \left(\underline{T_c}(0,\varrho), \overline{T_c}(0,\varrho)\right),$$

$$E_c(0,\varrho) = \left(\underline{E_c}(0,\varrho), \overline{E_c}(0,\varrho)\right), \qquad (4)$$

$$T_x(0,\varrho) = \left(\underline{T_x}(0,\varrho), \overline{T_x}(0,\varrho)\right),$$

$$D_c(0,\varrho) = \left(\underline{D_c}(0,\varrho), \overline{D_c}(0,\varrho)\right).$$

where $R_p(0,\varrho), T_c(0,\varrho), E_c(0,\varrho), T_x(0,\varrho)$ and $D_c(0,\varrho) \geq 0$.

Proof

Employing the fuzzy Laplace transform on (1), we obtain,

$$\mathbf{L}[R_p] = \frac{1}{s} R_p(0,\varrho) + \frac{1}{s^{\xi}} \mathbf{L}[m_2 R_p(1 - q_2 R_p) - l_4 R_p T_c],$$

$$\mathbf{L}[T_c] = \frac{1}{s} T_c(0,\varrho) + \frac{1}{s^{\xi}} \mathbf{L}[m_1 T_c(1 - q_1 T_c) - [l_2 E_c + l_3 R_p + p_2 D_c]T_c],$$

$$\mathbf{L}[E_c] = \frac{1}{s} E_c(0,\varrho) + \frac{1}{s^{\xi}} \mathbf{L}\left[v - d_1 E_c + \left[\sigma \frac{T_c}{l_5 + T_c} - a_2 T_c\right] E_c\right], \qquad (5)$$

$$\mathbf{L}[T_x] = \frac{1}{s} T_x(0,\varrho) + \frac{1}{s^{\xi}} \mathbf{L}[D_c - \phi T_x],$$

$$\mathbf{L}[D_c] = \frac{1}{s} D_c(0,\varrho) + \frac{1}{s^{\xi}} \mathbf{L}[-\eta_2 D_c + V(t)].$$

The following equations are obtained by utilizing inverse Laplace transform,

$$R_p = R_p(0,\varrho) + \mathbf{L}^{-1}\left[\frac{1}{s^{\xi}} \mathbf{L}[m_2 R_p(1 - q_2 R_p) - l_4 R_p T_c]\right],$$

$$T_c = T_c(0,\varrho) + \mathbf{L}^{-1}\left[\frac{1}{s^{\xi}} \mathbf{L}[m_1 T_c(1 - q_1 T_c) - [l_2 E_c + l_3 R_p + p_2 D_c]T_c]\right],$$

$$E_c = E_c(0,\varrho) + \mathbf{L}^{-1}\left[\frac{1}{s^{\xi}} \mathbf{L}\left[v - d_1 E_c + \left[\sigma \frac{T_c}{l_5 + T_c} - a_2 T_c\right] E_c\right]\right], \qquad (6)$$

$$T_x = T_x(0,\varrho) + \mathbf{L}^{-1}\left[\frac{1}{s^{\xi}} \mathbf{L}[D_c - \phi T_x]\right],$$

$$D_c = D_c(0,\varrho) + \mathbf{L}^{-1}\left[\frac{1}{s^{\xi}} \mathbf{L}[-\eta_2 D_c + V(t)]\right].$$

which is denoted under fuzzy level set as,

$$\underline{R_p} = \underline{R_p}(0,\varrho) + \mathbf{L}^{-1}\left[\frac{1}{s^{\xi}} \mathbf{L}[m_2 \underline{R_p}\left(1 - q_2 \underline{R_p}\right) - l_4 \underline{R_p T_c}]\right],$$

$$\overline{R_p} = \overline{R_p}(0,\varrho) + \mathbf{L}^{-1}\left[\frac{1}{s^{\xi}} \mathbf{L}[m_2 \overline{R_p}(1 - q_2 \overline{R_p}) - l_4 \overline{R_p T_c}]\right],$$

$$\underline{T_c} = \underline{T_c}(0,\varrho) + \mathbf{L}^{-1}\left[\frac{1}{s^{\xi}} \mathbf{L}[m_1 \underline{T_c}\left(1 - q_1 \underline{T_c}\right) - \left[l_2 \underline{E_c} + l_3 \underline{R_p} + p_2 \underline{D_c}\right]\underline{T_c}]\right],$$

$$\overline{T_c} = \overline{T_c}(0,\varrho) + \mathbf{L}^{-1}\left[\frac{1}{s^{\xi}} \mathbf{L}[m_1 \overline{T_c}(1 - q_1 \overline{T_c}) - [l_2 \overline{E_c} + l_3 \overline{R_p} + p_2 \overline{D_c}]\overline{T_c}]\right],$$

$$\underline{E_c} = \underline{E_c}(0,\varrho) + \mathbf{L}^{-1}\left[\frac{1}{s^{\xi}} \mathbf{L}\left[v - d_1 \underline{E_c} + \left[\sigma \frac{T_c}{l_5 + T_c} - a_2 \underline{T_c}\right]\underline{E_c}\right]\right], \qquad (7)$$

$$\overline{E_c} = \overline{E_c}(0,\varrho) + \mathbf{L}^{-1}\left[\frac{1}{s^{\xi}} \mathbf{L}\left[v - d_1 \overline{E_c} + \left[\sigma \frac{\overline{T_c}}{l_5 + \overline{T_c}} - a_2 \overline{T_c}\right]\overline{E_c}\right]\right],$$

$$\underline{T_x} = \underline{T_x}(0,\varrho) + \mathbf{L}^{-1}\left[\frac{1}{s^{\xi}} \mathbf{L}[\underline{D_c} - \phi \underline{T_x}]\right],$$

$$\overline{T_x} = \overline{T_x}(0,\varrho) + \mathbf{L}^{-1}\left[\frac{1}{s^{\xi}} \mathbf{L}[\overline{D_c} - \phi \overline{T_x}]\right],$$

$$\underline{D_c} = \underline{D_c}(0,\varrho) + \mathbf{L}^{-1}\left[\frac{1}{s^{\xi}} \mathbf{L}[-\eta_2 \underline{D_c} + V(t)]\right],$$

$$\overline{D_c} = \overline{D_c}(0,\varrho) + \mathbf{L}^{-1}\left[\frac{1}{s^{\xi}} \mathbf{L}[-\eta_2 \overline{D_c} + V(t)]\right].$$

Thus, the fuzzy solution of the fractional tumor model (1) is obtained using Laplace transform, proving the existence of solution. Further by utilising the Laplace transform properties, we obtain

Dhanalakshmi and Shrilekha

$$W_c(t) = \int_0^t \frac{(t-s)^{\xi-1}}{\Gamma(\xi)} X(s, W_c(s)) ds + W_c(0).$$

Hyers-Ulam Stability (HUS)

Hyers-Ulam theorem establishes the theoretical basis for stability analysis. It makes a link between functional equation stability and the concept of continuity. This has led to subsequent developments and extensions of the theorem, which has contributed to the understanding of mathematical system stability.

Assumption 1

Let $t \in [0, a]$ and $\epsilon > 0$, ζ $[$ $^C D^{\xi} W_c(t), \ X(t, W_c(t))] \le \epsilon$.

Assumption 2

Consider the continuous function $X: [0,1] \times \mathbb{R} \to \mathbb{R}$.

Lipschitz condition holds for $X(t, W_c(t))$,

$\zeta [X(t, W *_c (t)), X(t, W_c(t))] \le k \zeta [W *_c (t), \ W_c(t)]$, $t \in [0, a]$

where $W *_c (t)$ and $W_c(t)$ are solutions of $^C D^{\xi} W_c = X(t, W *_c (t))$ and (3) respectively.

Theorem: 2

Let the assumptions holds. Consider $1 - C_Q k > 0$, where $C_Q = \frac{a^{\xi}}{\Gamma(\xi+1)}$ then the system (1) under fractional order is stable based on Hyers Ulam Stability theorem.

Proof:

To prove this, the Laplace transform is applied for the solution of (3) and $^C D^{\xi} W_c = X(t, W *_c (t))$, that is, as $W_c(t)$ and $W *_c (t)$, respectively.

$\zeta [W *_c , W_c] =$

$$\zeta \left[W *_c (t), \int_0^t \frac{(t-s)^{\xi-1}}{\Gamma(\xi)} X(s, W_c(s)) ds + W_c(0) \pm \int_0^t \frac{(t-s)^{\xi-1}}{\Gamma(\xi)} X(s, W *_c (s)) ds \right]$$

$$\le C_Q \epsilon + \frac{k}{\Gamma(\xi)} \int_0^t \frac{(t-s)^{\xi-1}}{\Gamma(\xi)} \zeta [W *_c (s), \qquad W_c(s)] ds$$

$$\zeta [W *_c , W_c] \le C_Q \epsilon + C_Q k \zeta [W *_c, W_c]$$

$$\zeta [W *_c , W_c] \le \frac{C_Q}{1 - C_Q k} \epsilon \ \le \ H\epsilon$$

where $H = \frac{C_Q}{1 - C_Q k}$.

CONCLUSION

There are various advantages to mathematically simulating tumor systems that help in comprehending and treating cancer. This study comprises a fuzzy model of the tumor system with drug administration during cancer chemotherapy taken in fractional order. The existence of solution under fuzziness for the tumor model is studied. Finally, the system's stability using HUS concept is verified.

REFERENCES

1. Siegel, R.L., Miller, K.D., Wagle, N.S. and Jemal, A., 2023. Cancer statistics, 2023. CA: a cancer journal for clinicians, 73(1), pp.17-48.
2. Sathishkumar, K., Chaturvedi, M., Das, P., Stephen, S. and Mathur, P., 2023. Cancer incidence estimates for 2022 \& projection for 2025: Result from National Cancer Registry Programme, India. Indian Journal of Medical Research.
3. Financial Aid for Cancer Patients - https://www.worldcancercare.co.in/index-info-gov-fin-sch.html.
4. Palanisami, D. and Elango, S., 2023. Population Dynamics on Fractional Tumor System Using Laplace Transform and Stability Analysis. International Journal of Robotics and Control Systems, 3(3), pp.417-432.
5. Özköse, F., Şenel, M.T. and Habbireeh, R., 2021. Fractional-order mathematical modelling of cancer cells-cancer stem cells-immune system interaction with chemotherapy. Mathematical Modelling and Numerical Simulation with Applications, 1(2), pp.67-83.

6. Dhanalakshmi, P., Senpagam, S. and Mohanapriya, R., 2022. Finite-time fuzzy reliable controller design for fractional-order tumor system under chemotherapy. Fuzzy Sets and Systems, 432, pp.168-181.
7. Subash, A., Bylapudi, B., Thakur, S. and Rao, V.U., 2022. Oral cancer in India, a growing problem: Is limiting the exposure to avoidable risk factors the only way to reduce the disease burden? Oral Oncology, 125, p.105677.
8. Mehrotra, R. and Yadav, K., 2022. Breast cancer in India: Present scenario and the challenges ahead. World Journal of Clinical Oncology, 13(3), p.209.
9. Ahmad, S., Ullah, A., Shah, K., Salahshour, S., Ahmadian, A. and Ciano, T., 2020. Fuzzy fractional-order model of the novel coronavirus. Advances in difference equations, 2020(1), pp.1-17.
10. Wang, S., 2022. The Ulam stability of fractional differential Equation with the Caputo-Fabrizio derivative. Journal of Function Spaces, 2022, pp.1-9.
11. Dai, Q. and Liu, S., 2022. Stability of the mixed Caputo fractional integro-differential equation by means of weighted space method. AIMS Mathematics, 7(2), pp.2498-2511.
12. Wang, X., Luo, D. and Zhu, Q., 2022. Ulam-Hyers stability of caputo type fuzzy fractional differential equations with ti

RESEARCH ARTICLE

Algebraic Operations on Bipolar Pythagorean Fuzzy Matrices

T. Muthuraji[1] and R. Punitha[2]*

[1]Department of Mathematics, Annamalai University, Deputed to Government Arts College, Chidambaram, Tamil Nadu, India.
[2]Research Scholar, Department of Mathematics, Annamalai University, Annamalai Nagar-608002,Chidambaram, Tamil Nadu, India.

*Address for Correspondence
R. Punitha
Department of Mathematics,
Annamalai University,
Chidambaram, Tamilnadu, India.
E. Mail: punitharajney@gmail.com

ABSTRACT

In this paper, we define some basic operations on Bipolar Pythagorean Fuzzy Matrices(BPFMs). Some algebraic properties like commutative, associative, distributive and De Morgan's are discussed for the operations algebraic sum, algebraic product, $\vee$ and $\wedge$. Also we introduce nA and A^n and investigate some results on bipolar pythagorean fuzzy matrices

Keywords: Fuzzy Matrix, Intuitionistic Fuzzy Matrices(IFM), Bipolar Fuzzy Matrices(BFM),Pythagorean Fuzzy Matrix, Bipolar Pythagorean Fuzzy Matrices(BPFM).

INTRODUCTION

Zadeh introduced the concept fuzzy set in 1965, as the generalization of crisp set [14]. Fuzzy matrices are introduced for the first time by Thomason in 1977[11].Some results on fuzzy matrices are discussed by gilchrist [2]. The concept of an intuitionistic fuzzy matrices are introduced by khan[3]. Each element in an intuitionistic fuzzy matrices is expressed by an ordered pair $(a_{ij}a_{ij}^{'})$ of a non negative real numbers $a_{ij}a_{ij}^{'}\in[0,1]$.Monoids on intuitionistic fuzzy matrices are discussed by boobalan[10].Decomposition of Intuitionistic fuzzy matrices are discussed by Muthuraji, Sriram and Murugadas[8]. Some algebraic structures on max-max min-min compositions over intuitionistic fuzzy matrices are studied by Muthuraji and lalitha.[6] The concept of bipolar fuzzy set was first introduced by Zhang[15].The concept of bipolar fuzzy matrices are established by Pal and Mondal [5].Commutative monoids on algebraic sum and algebraic product on bipolar fuzzy sets and bipolar fuzzy matrices are constructed by Muthuraji and Punitha[7]. The concept of bipolar intuitionistic fuzzy matrices are initiated by Lalitha and Dhivya[4]. Pythagorean fuzzy set are established by the extension of the intuitionistic fuzzy sets and characterize the condition that square of sum of its membership and nonmembership is equal to 0 or less than 1. The concept of pythagorean

fuzzy matrices and it's algebraic operations was developed by Silambarasan and Sriram[9].Pythagorean fuzzy subsets and its membership grades in multi criteria decision making are discussed by Yager[12,13].The trace and determinant of bipolar Pythagorean fuzzy square matrices and its novel operations are discussed by Chinnadurai[1].In this paper, Algebraic operations on Pythagorean fuzzy matrices are extended to bipolar Pythagorean fuzzy matrices. We construct $_nA$ and $A^{\bar{n}}$ when n is positive interger for bipolar Pythagorean fuzzy matrices.

Definitions And Preliminaries
In this section, we refer basic definition.
Definition 2.1 (Fuzzy Matrix) [2]
Consider a matrix $A=[(a_{ij})]_{m \times n}$ where $a_{ij} \in [0,1]$ $1 \le i \le m$ and $1 \le i \le n$. Then A is a fuzzy matrix.
Definition 2.2 (Intuitionistic Fuzzy Matrix) [4]
An Intuitionistic fuzzy matrix is a matrix of pairs $A=[(a_{ij}, a'_{ij})]_{m \times n}$ of non negative real numbers $a_{ij}, a'_{ij} \in [0,1]$ satisfying $0 \le a_{ij} + a'_{ij} \le 1$ for all i,j.
Definition 2.3 (Pythagorean Fuzzy Matrix) [9]
A Pythagorean fuzzy matrix is a pair $A=[(a_{ij}, a'_{ij})]$ of non negative real numbers $a_{ij}, a'_{ij} \in [0,1]$ satisfying the condition $a_{ij}^2 + a'^2_{ij} \le 1$ for all i,j.
Definition 2.4 (Bipolar Fuzzy Matrix) [5]
Let $A = (a_{ij})_{l \times m} \in \mathcal{M}_{lm}$, then $a_{ij} = (-a_{ijn}, a_{ijp}) \in \mathcal{B}_F$, where $a_{ijn}, a_{ijp} \in [0,1]$ are the negative and positive membership values of the element a_{ij}, respectively.
Definition 2.5(Bipolar Pythagorean Fuzzy Matrix) [1]
A Bipolar Pythagorean fuzzy matrix of order (m×n) is denoted by M_{mn} and that of order (m×m), that is square BPFM is denoted by M_{mm}. We conclude that the matrix $A = [(-a^n_{ij}, a^p_{ij}, -a^{n'}_{ij}, a^{p'}_{ij})]$, where $-a^n_{ij}, a^p_{ij}, -a^{n'}_{ij}, a^{p'}_{ij} \in [-1,1]$ are the negative and positive membership values of the element a_{ij}, a_{ij}' respectively. Also satisfies $(a^n_{ij})^2 + (a^p_{ij})^2 + (a^{n'}_{ij})^2 + (a^{p'}_{ij})^2 \le 1$ for all i, j and $0 \le (a^p_{ij})^2 + (a^{p'}_{ij})^2 \le 1$, $-1 \le -[(a^n_{ij})^2 + (a^{n'}_{ij})^2] \le 0$.

Operations On Bipolar Pythagorean Fuzzy Matrices
In this section, we discuss some operations on Bipolar Pythagorean Fuzzy Matrices
Let us consider the BPFMs $A = [(-\Phi_{ijn}, \Phi_{ijp}, -\Phi'_{ijn}, \Phi'_{ijp})] \in \mathcal{M}_{mn}$ and $B = [(-\Psi_{ijn}, \Psi_{ijp}, -\Psi'_{ijn}, \Psi'_{ijp})] \in \mathcal{M}_{mn}$. Their operations are defined as follows

$A \vee B = [-max\{\Phi_{ijn}, \Psi_{ijn}\}, max\{\Phi_{ijp}, \Psi_{ijp}\}, -min\{\Phi'_{ijn}, \Psi'_{ijn}\}, min\{\Phi'_{ijp}, \Psi'_{ijp}\}]$

$A \wedge B = [-min\{\Phi_{ijn}, \Psi_{ijn}\}, min\{\Phi_{ijp}, \Psi_{ijp}\}, -max\{\Phi'_{ijn}, \Psi'_{ijn}\}, max\{\Phi'_{ijp}, \Psi'_{ijp}\}]$

$A^c = [(-\Phi'_{ijn}, \Phi'_{ijp}), (-\Phi_{ijn}, \Phi_{ijp})]$

$A \oplus_{BP} B = [-\sqrt{\Phi^2_{ijn} + \Psi^2_{ijn} - \Phi^2_{ijn}\Psi^2_{ijn}}, \sqrt{\Phi^2_{ijp} + \Psi^2_{ijp} - \Phi^2_{ijp}\Psi^2_{ijp}}, -(\Phi'_{ijn}\Psi'_{ijn}), (\Phi'_{ijp}\Psi'_{ijp})]$

$A \odot_{BP} B = [-(\Phi_{ijn}\Psi_{ijn}), (\Phi_{ijp}\Psi_{ijp}), -\sqrt{\Phi'^2_{ijn} + \Psi'^2_{ijn} - \Phi'^2_{ijn}\Psi'^2_{ijn}}, \sqrt{\Phi'^2_{ijp} + \Psi'^2_{ijp} - \Phi'^2_{ijp}\Psi'^2_{ijp}}]$

Following $A \oplus_{BP} B$ and $A \odot_{BP} B$ we get the equations for any integer n>0
$nA = A \oplus_{BP} A \oplus_{BP} \ldots \oplus_{BP} A$

$= [-\sqrt{1 - (1 - \Phi^2_{ijn})^n}, \sqrt{1 - (1 - \Phi^2_{ijp})^n}, -\Phi'^n_{ijn}, \Phi'^n_{ijp}]$

$A^n = A \odot_{BP} A \odot_{BP} \ldots \odot_{BP} A$

$= [-\Phi^n_{ijn}, \Phi^n_{ijp}, -\sqrt{1 - (1 - \Phi'^2_{ijn})^n}, \sqrt{1 - (1 - \Phi'^2_{ijp})^n}]$

Theorem 3.1

www.tnsroindia.org.in ©IJONS

If A and B are BPFMs, n is a positive integer then

(i) $n(A \oplus_{BP} B) = nA \oplus_{BP} nB$

(ii) $(A \odot_{BP} B)^n = A^n \odot_{BP} B^n$

Proof (i) $n(A \oplus_{BP} B)$

$$= \begin{bmatrix} -\sqrt{1-(1-(\Phi_{ij\underline{n}}^2 + \Psi_{ij\underline{n}}^2 - \Phi_{ij\underline{n}}^2\Psi_{ij\underline{n}}^2))^n}, & \sqrt{1-(1-(\Phi_{ij\dot{p}}^2 + \Psi_{ij\dot{p}}^2 - \Phi_{ij\dot{p}}^2\Psi_{ij\dot{p}}^2))^n}, \\ -(\Phi_{ij\underline{n}}'\Psi_{ij\underline{n}}')^n, & (\Phi_{ij\dot{p}}'\Psi_{ij\dot{p}}')^n \end{bmatrix}$$

$$= \begin{bmatrix} -\sqrt{1-(1-\Phi_{ij\underline{n}}^2)^n(1-\Psi_{ij\underline{n}}^2)^n}, & \sqrt{1-(1-\Phi_{ij\dot{p}}^2)^n(1-\Psi_{ij\dot{p}}^2)^n}, \\ -(\Phi_{ij\underline{n}}'\Psi_{ij\underline{n}}')^n, & (\Phi_{ij\dot{p}}'\Psi_{ij\dot{p}}')^n \end{bmatrix} (3.1)$$

$nA \oplus_{BP} nB$

$$= \begin{bmatrix} -\sqrt{1-(1-\Phi_{ij\underline{n}}^2)^n + 1-(1-\Psi_{ij\underline{n}}^2)^n - (1-(1-\Phi_{ij\underline{n}}^2)^n)(1-(1-\Psi_{ij\underline{n}}^2)^n)}, \\ \sqrt{1-(1-\Phi_{ij\dot{p}}^2)^n + 1-(1-\Psi_{ij\dot{p}}^2)^n - (1-(1-\Phi_{ij\dot{p}}^2)^n \, 1-(1-\Psi_{ij\dot{p}}^2)^n)}, \\ -(\Phi_{ij\underline{n}}'^n \Psi_{ij\underline{n}}'^n), \, (\Phi_{ij\dot{p}}'^n \Psi_{ij\dot{p}}'^n) \end{bmatrix}$$

$$= \begin{bmatrix} -\sqrt{1-(1-\Phi_{ij\underline{n}}^2)^n(1-\Psi_{ij\underline{n}}^2)^n}, & \sqrt{1-(1-\Phi_{ij\dot{p}}^2)^n(1-\Psi_{ij\dot{p}}^2)^n}, \\ -(\Phi_{ij\underline{n}}'\Psi_{ij\underline{n}}')^n, & (\Phi_{ij\dot{p}}'\Psi_{ij\dot{p}}')^n \end{bmatrix} (3.2)$$

From equations (3.1) and (3.2), we get the result.

Similarly we can prove $(A \odot_{BP} B)^n = A^n \odot_{BP} B^n$

Theorem 3.2

Let A be a BPFMs, n_1, n_2 are positive integer then

(i) $n_1 A \oplus_{BP} n_2 A = (n_1 + n_2)A$

(ii) $A^{n1} \odot_{BP} A^{n2} = A^{(n1+n2)}$

Proof:(i) $n_1 A \oplus_{BP} n_2 A =$

$$= \begin{bmatrix} -\sqrt{1-(1-\Phi_{ij\underline{n}}^2)^{n1} + 1-(1-\Phi_{ij\underline{n}}^2)^{n2} - (1-(1-\Phi_{ij\underline{n}}^2)^{n1})(1-(1-\Phi_{ij\underline{n}}^2)^{n2})}, \\ \sqrt{1-(1-\Phi_{ij\dot{p}}^2)^{n1} + 1-(1-\Phi_{ij\dot{p}}^2)^{n2} - (1-(1-\Phi_{ij\dot{p}}^2)^{n1} \, 1-(1-\Phi_{ij\dot{p}}^2)^{n2})}, \\ -(\Phi_{ij\underline{n}}^{n1}\Phi_{ij\underline{n}}^{m2}), \, (\Phi_{ij\dot{p}}^{m1}\Phi_{ij\dot{p}}^{m2}) \end{bmatrix}$$

$$= \begin{bmatrix} -\sqrt{1-(1-\Phi_{ij\underline{n}}^2)^{n1+n2}}, & \sqrt{1-(1-\Phi_{ij\dot{p}}^2)^{n1+n2}}, \\ -(\Phi_{ij\underline{n}}')^{n1+n2}, & (\Phi_{ij\dot{p}}')^{n1+n2} \end{bmatrix}$$

$= (n_1 + n_2)A$

Similarly we can prove $A^{n1} \odot_{BP} A^{n2} = A^{(n1+n2)}$

Theorem 3.3

Let A be a BPFMs, n is a positive integer then

(i) $(A^c)^n = (nA)^c$

(ii) $n(A^c) = (A^n)^c$

Proof: (i) $(A^c)^n = \left[\left(-\Phi_{ij\underline{n}}'^n, \ \Phi_{ij\dot{p}}'^n, -\sqrt{1-(1-\Phi_{ij\underline{n}}^2)^n}, \ \sqrt{1-(1-\Phi_{ij\dot{p}}^2)^n}\right)\right]$

$(nA)^c = \left[\left(-\Phi_{ij\underline{n}}'^n, \ \Phi_{ij\dot{p}}'^n, -\sqrt{1-(1-\Phi_{ij\underline{n}}^2)^n}, \ \sqrt{1-(1-\Phi_{ij\dot{p}}^2)^n}\right)\right]$

$\Rightarrow (A^c)^n = (nA)^c$

Similarly we can prove $n(A^c) = (A^n)^c$

Theorem3.4

If A and B are BPFMs, n is a positive integer then

(i)$n(A\vee B) = nA \vee nB$

(ii) $(A\vee B)^n = A^n \vee B^n$

Proof:(i) $(A\vee B) = \left[-max\{\Phi_{ij\underline{n}}, \ \Psi_{ij\underline{n}}\}, \ max\{\Phi_{ij\dot{p}}, \ \Psi_{ij\dot{p}}\}, -min\{\Phi_{ij\underline{n}}', \Psi_{ij\underline{n}}'\}, \ min\{\Phi_{ij\dot{p}}', \Psi_{ij\dot{p}}'\}\right]$

$n(A\vee B) = \begin{bmatrix} -\sqrt{1-(1-\max\{\Phi_{ij\underline{n}}^2\Psi_{ij\underline{n}}^2\})^n}, \sqrt{1-(1-\max\{\Phi_{ij\dot{p}}^2\Psi_{ij\dot{p}}^2\})^n}, \\ -\min\{\Phi_{ij\underline{n}}'^m, \Psi_{ij\underline{n}}'^m\}, \min\{\Phi_{ij\dot{p}}'^m, \Psi_{ij\dot{p}}'^m\} \end{bmatrix}$ (3.3)

$nA\vee nB = \begin{bmatrix} -\sqrt{1-(1-\Phi_{ij\underline{n}}^2)^n}, \sqrt{1-(1-\Phi_{ij\dot{p}}^2)^n}, -\Phi_{ij\underline{n}}'^n, \Phi_{ij\dot{p}}'^n \\ \vee \\ -\sqrt{1-(1-\Psi_{ij\underline{n}}^2)^n}, \sqrt{1-(1-\Psi_{ij\dot{p}}^2)^n}, -\Psi_{ij\underline{n}}'^n, \ \Psi_{ij\dot{p}}'^n \end{bmatrix}$

$= \begin{bmatrix} -max\left\{\sqrt{1-(1-\Phi_{ij\underline{n}}^2)^n}, \ \sqrt{1-(1-\Psi_{ij\underline{n}}^2)^n}\right\}, \\ max\left\{\sqrt{1-(1-\Phi_{ij\dot{p}}^2)^n}, \ \sqrt{1-(1-\Psi_{ij\dot{p}}^2)^n}\right\}, \\ -\min\{\Phi_{ij\underline{n}}'^m, \Psi_{ij\underline{n}}'^m\}, \min\{\Phi_{ij\dot{p}}'^m, \Psi_{ij\dot{p}}'^m\} \end{bmatrix}$

$= \begin{bmatrix} -\sqrt{1-(1-max\{\Phi_{ij\underline{n}}^2\Psi_{ij\underline{n}}^2\}^n)}, \sqrt{1-(1-max\{\Phi_{ij\dot{p}}^2\Psi_{ij\dot{p}}^2\}^n)}, \\ -\min\{\Phi_{ij\underline{n}}'^m, \Psi_{ij\underline{n}}'^m\}, \min\{\Phi_{ij\dot{p}}'^m, \Psi_{ij\dot{p}}'^m\} \end{bmatrix}$ (3.4)

From equation (3.3) and (3.4), we get the result .

Similarly we can prove$(A\vee B)^n = A^n \vee B^n$

Theorem 3.5(Commutative law)

Let A and B are BPFMs, then

(i)$A\oplus_{BP}B = B\oplus_{BP} A$

(ii)$A\odot_{BP}B = B\odot_{BP} A$

The proof (i) and (ii) are trivial.

Theorem 3.6 (Associative law)

Let A and B are two BPFMs,   then

(i)$(A\oplus_{BP}B)\oplus_{BP}C = A\oplus_{BP}(B\oplus_{BP}C)$

(ii)$(A\odot_{BP}B)\odot_{BP}C = A\odot_{BP} (B\odot_{BP}C)$

Proof: (i) $(A\oplus_{BP}B)\oplus_{BP}C$

$$=\begin{bmatrix}-\sqrt{(\Phi_{ij\underline{n}}^2 + \Psi_{ij\underline{n}}^2 - \Phi_{ij\underline{n}}^2\Psi_{ij\underline{n}}^2) + \Upsilon_{ij\underline{n}}^2 - (\Phi_{ij\underline{n}}^2 + \Psi_{ij\underline{n}}^2 - \Phi_{ij\underline{n}}^2\Psi_{ij\underline{n}}^2)(\Upsilon_{ij\underline{n}}^2),} \\ \sqrt{(\Phi_{ij\dot{p}}^2 + \Psi_{ij\dot{p}}^2 - \Phi_{ij\dot{p}}^2\Psi_{ij\dot{p}}^2) + \Upsilon_{ij\dot{p}}^2 - (\Phi_{ij\dot{p}}^2 + \Psi_{ij\dot{p}}^2 - \Phi_{ij\dot{p}}^2\Psi_{ij\dot{p}}^2)(\Upsilon_{ij\dot{p}}^2),} \\ -(\Phi_{ij\underline{n}}'\Psi_{ij\underline{n}}'\Upsilon_{ij\underline{n}}'), \quad (\Phi_{ij\dot{p}}'\Psi_{ij\dot{p}}'\Upsilon_{ij\dot{p}}')\end{bmatrix}$$

$$=\begin{bmatrix}-\sqrt{\Phi_{ij\underline{n}}^2 + \Psi_{ij\underline{n}}^2 + \Upsilon_{ij\underline{n}}^2 - \Phi_{ij\underline{n}}^2\Psi_{ij\underline{n}}^2 - \Phi_{ij\underline{n}}^2\Upsilon_{ij\underline{n}}^2 - \Psi_{ij\underline{n}}^2\Upsilon_{ij\underline{n}}^2 + \Phi_{ij\underline{n}}^2\Psi_{ij\underline{n}}^2\Upsilon_{ij\underline{n}}^2,} \\ \sqrt{\Phi_{ij\dot{p}}^2 + \Psi_{ij\dot{p}}^2 + \Upsilon_{ij\dot{p}}^2 - \Phi_{ij\dot{p}}^2\Psi_{ij\dot{p}}^2 - \Phi_{ij\dot{p}}^2\Upsilon_{ij\dot{p}}^2 - \Psi_{ij\dot{p}}^2\Upsilon_{ij\dot{p}}^2 + \Phi_{ij\dot{p}}^2\Psi_{ij\dot{p}}^2\Upsilon_{ij\dot{p}}^2,} \\ -(\Phi_{ij\underline{n}}'\Psi_{ij\underline{n}}'\Upsilon_{ij\underline{n}}'), \quad (\Phi_{ij\dot{p}}'\Psi_{ij\dot{p}}'\Upsilon_{ij\dot{p}}')\end{bmatrix} \quad (3.5)$$

$A\oplus_{BP}(B\oplus_{BP}C)$

$$=\begin{bmatrix}-\sqrt{\Phi_{ij\underline{n}}^2 + (\Psi_{ij\underline{n}}^2 + \Upsilon_{ij\underline{n}}^2 - \Psi_{ij\underline{n}}^2\Upsilon_{ij\underline{n}}^2) - (\Upsilon_{ij\underline{n}}^2)(\Psi_{ij\underline{n}}^2 + \Upsilon_{ij\underline{n}}^2 - \Psi_{ij\underline{n}}^2\Upsilon_{ij\underline{n}}^2),} \\ \sqrt{\Phi_{ij\dot{p}}^2 + (\Psi_{ij\dot{p}}^2 + \Upsilon_{ij\dot{p}}^2 - \Psi_{ij\dot{p}}^2\Upsilon_{ij\dot{p}}^2) - (\Upsilon_{ij\dot{p}}^2)(\Psi_{ij\dot{p}}^2 + \Upsilon_{ij\dot{p}}^2 - \Psi_{ij\dot{p}}^2\Upsilon_{ij\dot{p}}^2),} \\ -(\Phi_{ij\underline{n}}'\Psi_{ij\underline{n}}'\Upsilon_{ij\underline{n}}'), \quad (\Phi_{ij\dot{p}}'\Psi_{ij\dot{p}}'\Upsilon_{ij\dot{p}}')\end{bmatrix}$$

$$=\begin{bmatrix}-\sqrt{\Phi_{ij\underline{n}}^2 + \Psi_{ij\underline{n}}^2 + \Upsilon_{ij\underline{n}}^2 - \Phi_{ij\underline{n}}^2\Psi_{ij\underline{n}}^2 - \Phi_{ij\underline{n}}^2\Upsilon_{ij\underline{n}}^2 - \Psi_{ij\underline{n}}^2\Upsilon_{ij\underline{n}}^2 + \Phi_{ij\underline{n}}^2\Psi_{ij\underline{n}}^2\Upsilon_{ij\underline{n}}^2,} \\ \sqrt{\Phi_{ij\dot{p}}^2 + \Psi_{ij\dot{p}}^2 + \Upsilon_{ij\dot{p}}^2 - \Phi_{ij\dot{p}}^2\Psi_{ij\dot{p}}^2 - \Phi_{ij\dot{p}}^2\Upsilon_{ij\dot{p}}^2 - \Psi_{ij\dot{p}}^2\Upsilon_{ij\dot{p}}^2 + \Phi_{ij\dot{p}}^2\Psi_{ij\dot{p}}^2\Upsilon_{ij\dot{p}}^2,} \\ -(\Phi_{ij\underline{n}}'\Psi_{ij\underline{n}}'\Upsilon_{ij\underline{n}}'), \quad (\Phi_{ij\dot{p}}'\Psi_{ij\dot{p}}'\Upsilon_{ij\dot{p}}')\end{bmatrix} \quad (3.6)$$

From equation (3.5) and (3.6), we get the result.

Similarly we can prove $(A\odot_{BP}B)\odot_{BP}C=A\odot_{BP}(B\odot_{BP}C)$

Theorem 3.7(De Morgan's law)

Let A and B are BPFMs, then

(i) $A^c \vee B^c=(A\wedge B)^c$

(ii) $A^c \wedge B^c=(A\vee B)^c$

(iii)$A^c\oplus_{BP}B^c=(A\odot_{BP}B)^c$

(iv) $A^c\odot_{BP}B^c=(A\oplus_{BP}B)^c$

Proof: (i) $A^c \vee B^c =\left[-max\{\Phi_{ij\underline{n}}', \Psi_{ij\underline{n}}'\}, max\{\Phi_{ij\dot{p}}', \Psi_{ij\dot{p}}'\}, -min\{\Phi_{ij\underline{n}}, \Psi_{ij\underline{n}}\}, min\{\Phi_{ij\dot{p}}, \Psi_{ij\dot{p}}\}\right]$

$(A\wedge B)^c =\left[-min\{\Phi_{ij\underline{n}}, \Psi_{ij\underline{n}}\}, min\{\Phi_{ij\dot{p}}, \Psi_{ij\dot{p}}\}, -max\{\Phi_{ij\underline{n}}', \Psi_{ij\underline{n}}'\}, max\{\Phi_{ij\dot{p}}', \Psi_{ij\dot{p}}'\}\right]$

$= A^c \vee B^c$

Similarly we can prove (ii)$A^c \wedge B^c= (A\vee B)^c$

(iii)$A^c\oplus_{BP}B^c=\left[-\sqrt{\Phi_{ij\underline{n}}'^2 + \Psi_{ij\underline{n}}'^2 - \Phi_{ij\underline{n}}'^2\Psi_{ij\underline{n}}'^2}, \sqrt{\Phi_{ij\dot{p}}'^2 + \Psi_{ij\dot{p}}'^2 - \Phi_{ij\dot{p}}'^2\Psi_{ij\dot{p}}'^2}, -(\Phi_{ij\underline{n}}\Psi_{ij\underline{n}}), (\Phi_{ij\dot{p}}\Psi_{ij\dot{p}})\right]$

$(A\odot_{BP} B)^c=\left[-\sqrt{\Phi_{ij\underline{n}}'^2 + \Psi_{ij\underline{n}}'^2 - \Phi_{ij\underline{n}}'^2\Psi_{ij\underline{n}}'^2}, \sqrt{\Phi_{ij\dot{p}}'^2 + \Psi_{ij\dot{p}}'^2 - \Phi_{ij\dot{p}}'^2\Psi_{ij\dot{p}}'^2}, -(\Phi_{ij\underline{n}}\Psi_{ij\underline{n}}), (\Phi_{ij\dot{p}}\Psi_{ij\dot{p}})\right]$

$=A^c\oplus_{BP}B^c$

Similarly we can prove (iv) $A^c\odot_{BP}B^c = (A\oplus_{BP} B)^c$

Theorem 3.8

Let A and B are BPFMs, then

(i)$(A\vee B) \oplus_{BP} (A\wedge B)=A\oplus_{BP} B$

(ii)$(A\vee B) \odot_{BP} (A\wedge B)=A\odot_{BP} B$

Proof (i)$(A\vee B) \oplus_{BP}(A\wedge B)$

Muthuraji and Punitha

$$= \begin{bmatrix} -\sqrt{max\{\Phi_{ij\underline{n}}^2, \Psi_{ij\underline{n}}^2\} + min\{\Phi_{ij\underline{n}}^2, \Psi_{ij\underline{n}}^2\} - max\{\Phi_{ij\underline{n}}^2, \Psi_{ij\underline{n}}^2\} min\{\Phi_{ij\underline{n}}^2, \Psi_{ij\underline{n}}^2\}}, \\ \sqrt{max\{\Phi_{ij\underline{p}}^2, \Psi_{ij\underline{p}}^2\} + min\{\Phi_{ij\underline{p}}^2, \Psi_{ij\underline{p}}^2\} - max\{\Phi_{ij\underline{p}}^2, \Psi_{ij\underline{p}}^2\} min\{\Phi_{ij\underline{p}}^2, \Psi_{ij\underline{p}}^2\}}, \\ -\left(min\{\Phi_{ij\underline{n}}', \Psi_{ij\underline{n}}'\} max\{\Phi_{ij\underline{n}}', \Psi_{ij\underline{n}}'\}\right), \left(min\{\Phi_{ij\underline{p}}', \Psi_{ij\underline{p}}'\} max\{\Phi_{ij\underline{p}}', \Psi_{ij\underline{p}}'\}\right), \end{bmatrix}$$

$$= \left[-\sqrt{\Phi_{ij\underline{n}}^2 + \Psi_{ij\underline{n}}^2 - \Phi_{ij\underline{n}}^2 \Psi_{ij\underline{n}}^2}, \sqrt{\Phi_{ij\underline{p}}^2 + \Psi_{ij\underline{p}}^2 - \Phi_{ij\underline{p}}^2 \Psi_{ij\underline{p}}^2}, - (\Phi_{ij\underline{n}}', \Psi_{ij\underline{n}}'), (\Phi_{ij\underline{p}}', \Psi_{ij\underline{p}}') \right]$$

$= A \oplus_{BP} B$

Similarly we can prove (ii) $(A \vee B) \odot_{BP} (A \wedge B) = A \odot_{BP} B$

Theorem 3.9 (Distributive laws)
Let A, B and C are BPFMs, then
(i) $(A \vee B) \wedge C = (A \wedge C) \vee (B \wedge C)$
(ii) $(A \wedge B) \vee C = (A \vee C) \wedge (B \vee C)$
(iii) $(A \vee B) \oplus_{BP} C = (A \oplus_{BP} C) \vee (B \oplus_{BP} C)$
(iv) $(A \wedge B) \oplus_{BP} C = (A \oplus_{BP} C) \wedge (B \oplus_{BP} C)$
(v) $(A \vee B) \odot_{BP} C = (A \odot_{BP} C) \vee (B \odot_{BP} C)$
(vi) $(A \wedge B) \odot_{BP} C = (A \odot_{BP} C) \wedge (B \odot_{BP} C)$
Proof:(i)$(A \vee B) \wedge C$

$$= \begin{bmatrix} -min\{max\{\Phi_{ij\underline{n}}, \Psi_{ij\underline{n}}\}\Upsilon_{ij\underline{n}}\}, min\{max\{\Phi_{ij\underline{p}}, \Psi_{ij\underline{p}}\}\Upsilon_{ij\underline{p}}\}, \\ -max\{min\{\Phi_{ij\underline{n}}', \Psi_{ij\underline{n}}'\}, \Upsilon_{ij\underline{n}}'\}, max\{min\{\Phi_{ij\underline{p}}', \Psi_{ij\underline{p}}'\}, \Upsilon_{ij\underline{p}}'\} \end{bmatrix}$$

$$= \begin{bmatrix} -max\left\{min\{\Phi_{ij\underline{n}}, \Psi_{ij\underline{n}}\}, min\{\Phi_{ij\underline{n}}, \Upsilon_{ij\underline{n}}\}\right\}, max\left\{min\{\Phi_{ij\underline{p}}, \Psi_{ij\underline{p}}\}, min\{\Phi_{ij\underline{p}}, \Upsilon_{ij\underline{p}}\}\right\}, \\ -min\left\{max\{\Phi_{ij\underline{n}}', \Psi_{ij\underline{n}}'\}, max\{\Psi_{ij\underline{n}}', \Upsilon_{ij\underline{n}}'\}\right\}, min\left\{max\{\Phi_{ij\underline{p}}', \Psi_{ij\underline{p}}'\}, max\{\Psi_{ij\underline{p}}', \Upsilon_{ij\underline{p}}'\}\right\} \end{bmatrix}$$

$$= \begin{bmatrix} (-min\{\Phi_{ij\underline{n}}, \Upsilon_{ij\underline{n}}\}, min\{\Phi_{ij\underline{p}}, \Upsilon_{ij\underline{p}}\}), (-max\{\Phi_{ij\underline{n}}', \Upsilon_{ij\underline{n}}'\}, max\{\Phi_{ij\underline{p}}', \Upsilon_{ij\underline{p}}'\}), \\ \vee \\ (-min\{\Psi_{ij\underline{n}}, \Upsilon_{ij\underline{n}}\}, min\{\Psi_{ij\underline{n}}, \Upsilon_{ij\underline{p}}\})(-max\{\Psi_{ij\underline{n}}',, \Upsilon_{ij\underline{n}}'\}, max\{\Psi_{ij\underline{p}}',, \Upsilon_{ij\underline{p}}'\}) \end{bmatrix}$$

$= (A \wedge C) \vee (B \wedge C)$

Similarly we can prove (ii) $(A \wedge B) \vee C = (A \vee C) \wedge (B \vee C)$

(iii)$(A \vee B) \oplus_{BP} C$

$$= \begin{bmatrix} -\left(\sqrt{max\{\Phi_{ij\underline{n}}^2, \Psi_{ij\underline{n}}^2\} + \Upsilon_{ij\underline{n}}^2 - max\{\Phi_{ij\underline{n}}^2, \Psi_{ij\underline{n}}^2\}\Upsilon_{ij\underline{n}}^2}\right), \\ \left(\sqrt{max\{\Phi_{ij\underline{p}}^2, \Psi_{ij\underline{p}}^2\} + \Upsilon_{ij\underline{p}}^2 - max\{\Phi_{ij\underline{p}}^2, \Psi_{ij\underline{p}}^2\}\Upsilon_{ij\underline{p}}^2}\right), \\ -(min\{\Phi_{ij\underline{n}}', \Psi_{ij\underline{n}}'\}\Upsilon_{ij\underline{n}}'), (min\{\Phi_{ij\underline{p}}', \Psi_{ij\underline{p}}'\}\Upsilon_{ij\underline{p}}') \end{bmatrix}$$

$$= \begin{bmatrix} -\left(\sqrt{(1 - \Upsilon_{ij\underline{n}}^2)max\{\Phi_{ij\underline{n}}^2, \Psi_{ij\underline{n}}^2\} + \Upsilon_{ij\underline{n}}^2}\right), \left(\sqrt{(1 - \Upsilon_{ij\underline{p}}^2)max\{\Phi_{ij\underline{p}}^2, \Psi_{ij\underline{p}}^2\} + \Upsilon_{ij\underline{p}}^2}\right), \\ -(min\{\Phi_{ij\underline{n}}'\Upsilon_{ij\underline{n}}', \Psi_{ij\underline{n}}'\Upsilon_{ij\underline{n}}'\}), (min\{\Phi_{ij\underline{p}}'\Upsilon_{ij\underline{p}}', \Psi_{ij\underline{p}}'\Upsilon_{ij\underline{p}}'\}) \end{bmatrix} (3.7)$$

$(A \oplus_{BP} C) \vee (B \oplus_{BP} C)$

$$= \begin{bmatrix} -\left(-max\left\{\sqrt{\Phi_{ij\underline{n}}^2 + \Upsilon_{ij\underline{n}}^2 - \Phi_{ij\underline{n}}^2 \Upsilon_{ij\underline{n}}^2}, \sqrt{\Psi_{ij\underline{n}}^2 + \Upsilon_{ij\underline{n}}^2 - \Psi_{ij\underline{n}}^2 \Upsilon_{ij\underline{n}}^2}\right\}\right), \\ \left(max\left\{\sqrt{\Phi_{ij\underline{p}}^2 + \Upsilon_{ij\underline{p}}^2 - \Phi_{ij\underline{p}}^2 \Upsilon_{ij\underline{p}}^2}, \sqrt{\Psi_{ij\underline{p}}^2 + \Upsilon_{ij\underline{p}}^2 - \Psi_{ij\underline{p}}^2 \Upsilon_{ij\underline{p}}^2}\right\}\right), \\ -(min\{\Phi_{ij\underline{n}}'\Upsilon_{ij\underline{n}}', \Psi_{ij\underline{n}}'\Upsilon_{ij\underline{n}}'\}), (min\{\Phi_{ij\underline{p}}'\Upsilon_{ij\underline{p}}', \Psi_{ij\underline{p}}'\Upsilon_{ij\underline{p}}'\}) \end{bmatrix}$$

Muthuraji and Punitha

$$= \begin{bmatrix} -\left(max\left\{\sqrt{(1-\Upsilon^2_{ij\eta})\Phi^2_{ij\eta}+\Upsilon^2_{ij\eta}} , \sqrt{(1-\Upsilon^2_{ij\eta})\Psi^2_{ij\eta}+\Upsilon^2_{ij\eta}}\right\}\right), \\ \left(max\left\{\sqrt{(1-\Upsilon^2_{ij\dot{p}})\Phi^2_{ij\dot{p}}+\Upsilon^2_{ij\dot{p}}} , \sqrt{(1-\Upsilon^2_{ij\dot{p}})\Psi^2_{ij\dot{p}}+\Upsilon^2_{ij\dot{p}}}\right\}\right), \\ -(min\{\Phi'_{ij\eta}\Upsilon'_{ij\eta}, \Psi'_{ij\eta}\Upsilon'_{ij\eta}\}), (min\{\Phi'_{ij\dot{p}}\Upsilon'_{ij\dot{p}}, \Psi'_{ij\dot{p}}\Upsilon'_{ij\dot{p}}\}) \end{bmatrix}$$

$$= \begin{bmatrix} -\left(\sqrt{(1-\Upsilon^2_{ij\eta})max\{\Phi^2_{ij\eta}, \Psi^2_{ij\eta}\}+\Upsilon^2_{ij\eta}}\right), \left(\sqrt{(1-\Upsilon^2_{ij\dot{p}})max\{\Phi^2_{ij\dot{p}}, \Psi^2_{ij\dot{p}}\}+\Upsilon^2_{ij\dot{p}}}\right), \\ -(min\{\Phi'_{ij\eta}\Upsilon'_{ij\eta}, \Psi'_{ij\eta}\Upsilon'_{ij\eta}\}), (min\{\Phi'_{ij\dot{p}}\Upsilon'_{ij\dot{p}}, \Psi'_{ij\dot{p}}\Upsilon'_{ij\dot{p}}\}) \end{bmatrix} \quad (3.8)$$

From equation (3.7) and (3.8), we get the result.

Similarly we can prove (iv) (A∧B) ⊕BP C = (A⊕BP C)∧(B⊕BP C)

(v)(A∨B) ⊙BP C

$$= \begin{bmatrix} -(max\{\Phi_{ij\eta}, \Psi_{ij\eta}\}\Upsilon_{ij\eta}), (max\{\Phi_{ij\dot{p}}, \Psi_{ij\dot{p}}\}\Upsilon_{ij\dot{p}}), \\ -\left(\sqrt{min\{\Phi^2_{ij\eta}, \Psi'^2_{ij\eta}\}+\Upsilon^2_{ij\eta}-min\{\Phi'^2_{ij\eta}, \Psi^2_{ij\eta}\}\Upsilon^2_{ij\eta}}\right), \\ \left(\sqrt{min\{\Phi^2_{ij\dot{p}}, \Psi'^2_{ij\dot{p}}\}+\Upsilon^2_{ij\dot{p}}-min\{\Phi'^2_{ij\dot{p}}, \Psi^2_{ij\dot{p}}\}\Upsilon'^2_{ij\dot{p}}}\right) \end{bmatrix}$$

$$= \begin{bmatrix} -(max\{\Phi_{ij\eta}, \Psi_{ij\eta}\}\Upsilon_{ij\eta}), (max\{\Phi_{ij\dot{p}}, \Psi_{ij\dot{p}}\}\Upsilon_{ij\dot{p}}), \\ -\left(\sqrt{(1-\Upsilon'^2_{ij\eta})min\{\Phi'^2_{ij\eta}, \Psi'^2_{ij\eta}\}+\Upsilon'^2_{ij\eta}}\right), \left(\sqrt{(1-\Upsilon'^2_{ij\dot{p}})min\{\Phi'^2_{ij\dot{p}}, \Psi'^2_{ij\dot{p}}\}+\Upsilon'^2_{ij\dot{p}}}\right) \end{bmatrix} \quad (3.9)$$

(A⊙BP C)∨(B⊙BP C)

$$= \begin{bmatrix} -(max\{\Phi_{ij\eta}\Upsilon_{ij\eta}, \Psi_{ij\eta}\Upsilon_{ij\eta}\}), (max\{\Phi_{ij\dot{p}}\Upsilon_{ij\dot{p}}, \Psi_{ij\dot{p}}\Upsilon_{ij\dot{p}}\}), \\ -\left(min\left\{\sqrt{\Phi'^2_{ij\eta}+\Upsilon'^2_{ij\eta}-\Phi'^2_{ij\eta}\Upsilon'^2_{ij\eta}} , \sqrt{\Psi'^2_{ij\eta}+\Upsilon'^2_{ij\eta}-\Psi'^2_{ij\eta}\Upsilon'^2_{ij\eta}}\right\}\right), \\ \left(min\left\{\sqrt{\Phi'^2_{ij\dot{p}}+\Upsilon'^2_{ij\dot{p}}-\Phi'^2_{ij\dot{p}}\Upsilon'^2_{ij\dot{p}}} , \sqrt{\Psi'^2_{ij\dot{p}}+\Upsilon'^2_{ij\dot{p}}-\Psi'^2_{ij\dot{p}}\Upsilon'^2_{ij\dot{p}}}\right\}\right) \end{bmatrix}$$

$$= \begin{bmatrix} -(max\{\Phi_{ij\eta}, \Psi_{ij\eta}\}\Upsilon_{ij\eta}), (max\{\Phi_{ij\dot{p}}, \Psi_{ij\dot{p}}\}\Upsilon_{ij\dot{p}}), \\ -\left(\sqrt{(1-\Upsilon^2_{ij\eta})min\{\Phi'^2_{ij\eta}, \Psi'^2_{ij\eta}\}+\Upsilon'^2_{ij\eta}}\right), \left(\sqrt{(1-\Upsilon'^2_{ij\dot{p}})min\{\Phi'^2_{ij\dot{p}}, \Psi'^2_{ij\dot{p}}\}+\Upsilon'^2_{ij\dot{p}}}\right) \end{bmatrix} (3.10)$$

From equation (3.9) and (3.10), we get the result.

Similarly we can prove (vi) (A∧B) ⊙BP C = (A⊙BP C)∧(B⊙BP C

CONCLUSION

In this paper, we discuss the Algebraic operators on Bipolar Pythagorean Fuzzy matrices such as algebraic sum, algebraic product,∨ and ∧. In this operators we discussed about De Morgan's laws and Distributive laws, and also discussed about n integers are greater than zero. In future we discuss about some new operators on Bipolar Pythagorean Fuzzy matrices

REFERENCES

1. Chinnadurai.V, Thirumurugan.G and Umamaheshwari.M, Trace and Determinant of Bipolar Pythagorean Fuzzy Squares matrices,Journal of Shanghai University, ISSn: 1007-1172.
2. Clayton Gilchrist, Some Results on Fuzzy Matrices, Department of Mathematics, Georgia   college, Milledgeville, GA 31061,2019.
3. Khan S.K. and M.Pal, Some operators on Intuitionistic Fuzzy Matrices, ActaCiencia Indica, Vol.32(2006) 515-524.

4. Lalitha K and Dhivya T, Bipolar Intuitionistic fuzzy Matrices, Indian Journal of Natural Sciences, December /2021/Vol.12/Issue 69.

5. Madhumangal pal and SanjibMondal, Bipolar fuzzy matrices, Springer- verlag Gmbh Germany part of Springer (2019).DOI:10.1007/s00500-019-03912-9

6. Muthuraji.T and Lalitha.k (2020), Some algebraic structures on max-max, min-min compositions over intuitionistic fuzzy matrices, Advanced in Mathematics: Scientific Journal,9(8),pp.5683-5691.

7. Muthuraji.TPunitha.R, Commutative monoids on algebraic sum and algebraic product over bipolar fuzzy set and bipolar fuzzy matrices. Paper Presented in third international conference on mathematical techniques and application.(Communicated in AIP).

8. Muthuraji.T, Sriram.S and Murugadas P, (2016), Decomposition of Intuitionistic fuzzy matrices, Fuzzy Information and Engineering, 8(3), pp.345-354.

9. Silambarasan. I and Sriram.S, Algebraic operations on Pythagorean fuzzy matrices, Mathematical Sciences International Research Journal Vol. 7(2)(2018), 406-414.

10. Sriram S and Boobalan J, Monoids of Intuitionistic fuzzy matrices, Annals of fuzzy Mathematics and Informatics, September 2015.

11. Thomason MG, (1977) Convergence of powers of a fuzzy matrix. J Math Anal Appl 57: 476-480.

12. Yager.R.R, Pythagorean fuzzy subsets, In: Proc Joint IFSA Worls Congress and NAFIPS Annual Meeting, Edmonton, Canada, (2013) 57-61.

13. Yager. R.R Pythagorean membership grades in multi-criteria decision making, IEEE Transactions on Fuzzy Systems, Vol.22 (2014) 958-965.

14. Zadeh L.A., Fuzzy Sets, Journal of information and control, 8(1965) 338-353.

15. Zhang W (1994) Bipolar fuzzy sets and relations: a computational frame work for cognitive modeling and multiagent decision analysis In IEEE. PP 305-309.

RESEARCH ARTICLE

Triangular Path Decomposition of Triangular Cyclic Snake Graphs

M.Subbulakshmi[1] and S.Chitra Devi[2]*

[1]Associate Professor, PG and Research Department of Mathematics, G .Venkataswamy Naidu College, Kovilpatti. Affiliated to Manonmaniam Sundaranar University, Tirunelveli, Tamil Nadu, India.
[2]Research Scholar, Reg. No. 19222052092002, PG and Research Department of Mathematics, G.Venkataswamy Naidu College, Kovilpatti. Affiliated to Manonmaniam Sundaranar University, Tirunelveli, Tamil Nadu, India.

*Address for Correspondence
S.Chitra Devi
Research Scholar,
 Reg. No. 19222052092002,
PG and Research Department of Mathematics,
G.Venkataswamy Naidu College, Kovilpatti.
Affiliated to Manonmaniam Sundaranar University,
Tirunelveli, Tamil Nadu, India.

ABSTRACT

Let G = (V, E) be a simple connected graph of order p and size q. If $G_1, G_2, G_3, \ldots, G_n$ are edge disjoint subgraphs of G such that $E(G) = E(G_1) \cup E(G_2) \cup \ldots \ldots \cup E(G_n)$, then $(G_1, G_2, G_3, \ldots, G_n)$ is said to be a Decomposition of a graph G. A graph of size $q = \binom{n+2}{3}$ is said to have a Triangular decomposition (TD) if G can be decomposed into n - subgraphs $G_1, G_2, G_3, \ldots, G_n$ such that each G_i is connected and $|E(G_i)| = \binom{i+1}{2}$ for $1 \le i \le n$. A TD in which each G_i is a path is said to be a Triangular path decomposition (TPD). In this paper, we investigate TPD of Triangular cyclic snake graphs.

Keywords – Decomposition, Triangular decomposition, Triangular path decomposition, Triangular cyclic snake graphs.

INTRODUCTION

 A graph G, referred to here is an undirected connected graph without loops or multiple edges. A path is a type of open walk where neither edges nor vertices are allowed to repeat. There is a possibility that only the starting vertex and ending vertex are same in a path. A path of length n is denoted by P_n. Different types of decomposition of a graph G have been studied in the literature by imposing suitable conditions on the subgraphs G_i. A TD in which each G_i is a path of length $\binom{i+1}{2}$ in G, then we say that G admits Triangular path decomposition (TPD). In this paper we

discuss about the necessary and sufficient conditions for the existence of Triangular path decomposition of Triangular cyclic snake graphs.

Definition 1.1
A decomposition of a graph G is a collection of edge disjoint subgraphs $G_1, G_2, G_3, \ldots, G_n$ of G such that every edge of G belongs to exactly one of the subgraph G_i.

Definition 1.2
A graph G of size $q = \binom{n+2}{3}$ is said to have a Triangular decomposition (TD) if G can be decomposed into n - subgraphs $G_1, G_2, G_3, \ldots, G_n$ such that each G_i is connected and $|E(G_i)| = \binom{i+1}{2}$ for $1 \leq i \leq n$.

Definition 1.3
A Triangular decomposition (TD) in which each G_i is a path is said to be Triangular path decomposition (TPD).

Definition 1.4
A kC_t – snake has been defined as a connected graph in which all the blocks are isomorphic to the cycle C_t and the block – cut point graph is a path P, where P is the path of least length that contains all the cut vertices of a kC_t - snake. A kC_t cyclic snake graph has 2k + 1 vertices and tk edges where k is the number of blocks in the cyclic snake graph. Assuming t is odd, then the cyclic snake graph kC_t is said to be an odd cyclic snake graph.

Note :1.5
Throughout this paper the base path $v_0 v_1 v_2 \ldots v_k$ is a path that contains all the cut vertices of kC_t – cyclic snake graph and here $d(v_i, v_{i+1}) = 1, 0 \leq i \leq k - 1$.

Definition 1.6
A **Triangular snake graph** kC_3 is obtained from a path $v_0 v_1 v_2 \ldots v_k$ by joining v_i and v_{i+1} to a new vertex u_{i+1} for $0 \leq i \leq k - 1$. That is every edge of a path of size k is replaced by a triangle C_3. A Triangular snake graph has 2k + 1 vertices and 3k edges where k is the number of blocks in the Triangular snake graph.

Triangular Decomposition of Triangular cyclic snake graphs
Theorem 2.1
Odd cyclic snake graphs $\frac{(tm-2)(tm-1)m}{6} C_t$ admits TPD $(P_1, P_2, P_3, \ldots, P_n) \Leftrightarrow n = tm-2$ where t is a odd number, $t \geq 3$ and $m \in N$.

Proof:
Assume $\frac{(tm-2)(tm-1)m}{6} C_t$ admits TPD $(P_1, P_2, P_3, \ldots, P_n)$. Then $q\left(\frac{(tm-2)(tm-1)m}{6} C_t\right) = t\left(\frac{(tm-2)(tm-1)m}{6}\right)$. That is $\frac{(tm-2)(tm-1)tm}{6} = \frac{n(n+1)(n+2)}{6}$. Implies n = tm-2 where $m \in N$.

Conversely, to prove $\left(\frac{(tm-2)(tm-1)m}{6}\right) C_t$ admits TPD $(P_1, P_2, P_3, \ldots, P_n)$, where n = tm-2, t is odd, $t \geq 3$ and $m \in N$. We prove the theorem by using mathematical induction on 'm'. When m = 1, $q\left(\frac{(tm-2)(tm-1)m}{6} C_t\right) = \frac{(t-2)(t-1)(t)}{6}$. Clearly $\frac{(t-2)(t-1)(t)}{6}$ admits TPD $(P_1, P_2, P_3, \ldots, P_{t-2})$. Assume that the result is true for m = k. That is $\left(\frac{(tk-2)(tk-1)k}{6}\right) C_t$ admits TPD $(P_1, P_2, P_3, \ldots, P_n)$ where n = tk-2, t is odd, $t \geq 3$ and $m \in N$. We prove the result is true for a positive integer m = k + 1. That is to prove $\left(\frac{(t(k+1)-2)(t(k+1)-1)(k+1)}{6}\right) C_t$ admits TPD $(P_1, P_2, P_3, \ldots, P_{t(k+1)-2})$. Now $q\left(\frac{(t(k+1)-2)(t(k+1)-1)(k+1)}{6} C_t\right) = \frac{(t(k+1)-2)(t(k+1)-1)(k+1)}{6} t = \frac{(t^2 k^3 + 3t^2 k^2 - 3tk^2 + 3t^2 k - 6tk + t^2 - 3t + 2 + 2k)}{6} t = \left(\frac{t^2 k^3 - 3t k^2 + 2k}{6}\right) t + \left(\frac{3t^2 k^2 + 3t^2 k - 6tk + t^2 - 3t + 2}{6}\right) t$ and the sum of edges of $(P_{tk -}$

Subbulakshmi and Chitra Devi

$_1$, P$_{tk}$,............,P$_{(k + 1)t-2}$) equal to ($\frac{3t^2k^2+3t^2k-6tk+t^2-3t+2}{6}$)t and hence ($\frac{(t(k+1)-2)(t(k+1)-1)(k+1)}{6}$)C$_t$ can be decompose into(P$_1$, P$_2$, P$_3$, ..., P$_{t(k + 1)-2}$). We conclude by the induction principle that odd cyclic snake graphs $\frac{(tm-2)(tm-1)m}{6}$C$_t$ admits TPD (P$_1$, P$_2$, P$_3$, ….............,P$_n$)⇔n = tm-2 where t is a odd number, t ≥ 3 and m ∈ N.

Theorem 2.2
Odd cyclic snake graphs $\frac{(tm-1)m(tm+1)}{6}$C$_t$ admits TPD (P$_1$, P$_2$, P$_3$, ….….....,P$_n$)⇔n = tm-1 where t is a odd number, t ≥ 3 and m ∈ N.

Proof :
Assume $\frac{(tm-1)m(tm+1)}{6}$C$_t$ admits TPD (P$_1$, P$_2$, P$_3$, ..., P$_n$). Then q($\frac{(tm-1)m(tm+1)}{6}$C$_t$) = t($\frac{(tm-1)m(tm+1)}{6}$). That is $\frac{(tm-1)tm(tm+1)}{6}$ = $\frac{(n-1)n(n+1)}{6}$. Implies n = tm -1, m ∈ N.

Conversely, to prove ($\frac{(tm-1)m(tm+1)}{6}$)C$_t$ admits TPD (P$_1$, P$_2$, P$_3$, ...,P$_n$), where n = tm - 1, t is a odd number, t ≥ 3 and m∈ N. We prove the theorem by using mathematical induction on 'm'. When m = 1, q($\frac{(tm-1)m(tm+1)}{6}$C$_t$) = $\frac{(t-1)t(t+1)}{6}$. Clearly $\frac{(t-1)t(t+1)}{6}$ admits TPD (P$_1$, P$_2$, P$_3$, ….........,P$_{t-1}$). Assume that the result is true for m = k. T h a t i s ($\frac{(tk-1)k(tk+1)}{6}$)C$_t$ admits TPD (P$_1$, P$_2$, P$_3$, ..., P$_n$) where n = tk – 1, t is odd, t ≥ 3 and m ∈ N. We prove the result is true for a positive integer m = k + 1. That is to prove ($\frac{(t(k+1)-1)(k+1)(t(k+1)+1)}{6}$)C$_t$ admits TPD (P$_1$,P$_2$,P$_3$,....................,P$_{t(k+1)}$ $_{- 1}$)). Now q($\frac{(t(k+1)-1)(k+1)(t(k+1)+1)}{6}C_t$) = $\frac{(t(k+1)-1)(k+1)(t(k+1)+1)}{6}$ t $\frac{(t^2k^3 + 3t^2k^2 + 3t^2k-k+t^2-1)}{6}$t = ($\frac{t^2k^3 - k}{6}$)t + ($\frac{3t^2k^2+3t^2k+t^2-1}{6}$)t and the sum of edges of (P$_{tk}$, P$_{tk + 1}$, P$_{tk + 2}$,...................,P$_{((k + 1)t - 1)}$) equal to ($\frac{3t^2k^2+3t^2k+ t^2-1}{6}$)t and hence ($\frac{(t(k+1)-1)(k+1)(t(k+1)+1)}{6}$)C$_t$ can be decompose into (P$_1$, P$_2$, P$_3$,.............,P$_{((k + 1)t - 1)}$). We conclude by the induction principle that odd cyclic snake graphs $\frac{(tm-1)m(tm+1)}{6}$C$_t$ admits TPD (P$_1$, P$_2$, P$_3$, ….….....…....., P$_n$) ⇔ n = tm-1 where t is a odd number, t ≥ 3 and m ∈ N.

Theorem 2.3
Odd cyclic snake graphs $\frac{m(tm+1)(tm+2)}{6}$ C$_t$ admits TPD (P$_1$, P$_2$, P$_3$, ...,P$_n$)⇔ n = tm where t is a odd number, t ≥ 3 and m ∈ N.

Proof :
Assume $\frac{m(tm+1)(tm+2)}{6}$C$_t$ admits TPD (P$_1$, P$_2$, P$_3$,...........,P$_n$). Then q($\frac{m(tm+1)(tm+2)}{6}$C$_t$) = t($\frac{m(tm+1)(tm+2)}{6}$). That is $\frac{tm(tm+1)(tm+2)}{6}$ = $\frac{n(n+1)(n+2)}{6}$. Implies n = tm, m ∈ N.

Conversely, to prove ($\frac{m(tm+1)(tm+2)}{6}$)C$_t$ admits TPD (P$_1$, P$_2$, P$_3$, ..., P$_n$), where n = tm, t is odd, t ≥ 3 and m∈ N. We prove the theorem by using mathematical induction on 'm'. When m = 1, q($\frac{m(tm+1)(tm+2)}{6}$C$_t$) = $\frac{t(t+1)(t+2)}{6}$. Clearly $\frac{t(t+1)(t+2)}{6}$ admits TPD (P$_1$, P$_2$, P$_3$, ..., P$_t$). Assume that the result is true for m = k. T h a t i s ($\frac{k(tk+1)(tk+2)}{6}$)C$_t$ admits TPD (P$_1$, P$_2$, P$_3$, ..., P$_n$) where n = tk, t is odd, t ≥ 3 and m ∈ N. We prove the result is true for a positive integer m = k + 1. That is to prove ($\frac{(k+1)(t(k+1)+1)(t(k+1)+2)}{6}$)C$_t$ admits TPD (P$_1$,P$_2$,P$_3$,..................,P$_{t(k+1)}$). Now q($\frac{(k+1)(t(k+1)+1)(t(k+1)+2)}{6}$ C$_t$) =$\frac{(k+1)(t(k+1)+1)(t(k+1)+2)}{6}$t $\frac{(t^2k^3 + 3t^2k^2 + 3tk^2+3t^2k+6tk+t^2+3t+2+2k)}{6}$t = ($\frac{t^2k^3+3t k^2+2k}{6}$)t + ($\frac{3t^2k^2+3t^2k+6tk+ t^2+3t+2}{6}$)t and the sum of edges of (P$_{tk + 1}$, P$_{tk + 2}$,..........,P$_{(k + 1)t}$) equal to ($\frac{3t^2k^2+3t^2k+6tk+ t^2+3t+2}{6}$)t and hence ($\frac{(k+1)(t(k+1)+1)(t(k+1)+2)}{6}$)C$_t$ can be decompose into(P$_1$, P$_2$, P$_3$,.............,P$_{(k + 1)t}$). We conclude by the induction principle that odd cyclic snake graphs $\frac{m(tm+1)(tm+2)}{6}$C$_t$ admits TPD   (P$_1$, P$_2$, P$_3$, ..., P$_n$) ⇔ n = tm where t is a odd number, t ≥ 3 and m ∈ N.

Theorem 2.4

Any Triangular cyclic snake graphs $\frac{(3m-2)(3m-1)m}{6}C_3$ admits TPD $(P_1, P_2, P_3, \ldots\ldots,P_n) \Leftrightarrow n = 3m\text{-}2$, $m \in N$.

Proof:

Assume $\frac{(3m-2)(3m-1)m}{6}C_3$ admits TPD $(P_1, P_2, P_3,\ldots,P_n)$. Then $q(\frac{(3m-2)(3m-1)m}{6}C_3) = 3(\frac{(3m-2)(3m-1)m}{6})$. That is $\frac{(3m-2)(3m-1)3m}{6} = \frac{n(n+1)(n+2)}{6}$. Implies $n = 3m\text{-}2$, $m \in N$.

Conversely, suppose $n = 3m\text{-}2$, $m \in N$. Let $V = \{v_0, w_1, v_1, w_2, v_2, \ldots, w_{\frac{9m^3-9m^2+2m}{6}}, v_{\frac{9m^3-9m^2+2m}{6}}\}$ be the set of vertices of the base path of $(\frac{(3m-2)(3m-1)m}{6})C_3$. Let v_0 and $v_{\frac{9m^3-9m^2+2m}{6}}$ are the beginning and end vertices of the base path respectively. Let the base path be $P_{\frac{9m^3-9m^2+2m}{6}}$. Also we consider the path $v_0, u_1, v_1, u_2, v_2, \ldots, u_{\frac{9m^3-9m^2+2m}{6}}, v_{\frac{9m^3-9m^2+2m}{6}}$ of length $2(\frac{9m^3-9m^2+2m}{6})$. To prove $(\frac{(3m-2)(3m-1)m}{6})C_3$ admits TPD $(P_1,P_2,P_3,\ldots,P_n)$ where $n = 3m\text{-}2$ and $m \in N$. We prove the theorem by using mathematical induction on 'm'. When $m = 1$, $q(\frac{(3m-2)(3m-1)m}{6}C_3) = \frac{(3-2)(3-1)(3)}{6}$. Clearly $\frac{(3-2)(3-1)(3)}{6}$ admits TPD P_1. Assume that the result is true for $m = k$. That is $(\frac{(3k-2)(3k-1)k}{6})C_3$ admits TPD $(P_1, P_2, P_3, \ldots, P_n)$ where $n = 3k\text{-}2$. We prove the result is true for a positive integer $m = k + 1$. That is to prove $(\frac{(3(k+1)-2)(3(k+1)-1)(k+1)}{6})C_3$ admits TPD $(P_1, P_2, P_3,\ldots,P_{3k+1})$. Now $q(\frac{(3(k+1)-2)(3(k+1)-1)(k+1)}{6}C_3) = (\frac{9k^3+27k^2-9k^2+27k-18k+9-9+2+2k}{6})3 = (\frac{9k^3-9k^2+2k}{6})3 + \frac{27k^2+9k+2}{2}$ and the sum of edges of $(P_{3k-1}, P_{3k}, P_{3k+1})$ equal to $\frac{27k^2+9k+2}{2}$ and hence $(\frac{(3(k+1)-2)(3(k+1)-1)(k+1)}{6})C_3$ can be decompose into $(P_1, P_2, P_3, \ldots, P_{3k+1})$. We conclude by the induction principle that any Triangular cyclic snake graphs $\frac{(3m-2)(3m-1)m}{6}C_3$ admits TPD $(P_1, P_2, P_3, \ldots, P_n) \Leftrightarrow n = 3m\text{-}2$, $m \in N$.

List of first ten TPD of $(\frac{(3m-2)(3m-1)(m)}{6})C_3$
Illustration 2.5
Figure(1) TPD $(P_1, P_2, \ldots, P_7)$ Of $_{28}C_3$

Theorem 2.6

Any Triangular cyclic snake graphs $\frac{(3m-1)m(3m+1)}{6}C_3$ admits TPD $(P_1, P_2, P_3, \ldots, P_n) \Leftrightarrow n = 3m\text{-}1$, $m \in N$.

Proof :

Assume $(\frac{(3m-1)m(3m+1)}{6})C_3$ admits TPD $(P_1, P_2, P_3,\ldots,P_n)$. Then $q(\frac{(3m-1)m(3m+1)}{6})C_3 = 3(\frac{(3m-1)m(3m+1)}{6})$. That is $3(\frac{(3m-1)m(3m+1)}{6}) = \frac{n(n+1)(n+2)}{6}$. This implies $n = 3m\text{-}1$, $m \in N$.
Conversely, Suppose $n = 3m\text{-}1$, $m \in N$. Let $V = \{v_0, w_1, v_1, w_2, v_2, \ldots, w_{\frac{9m^3-m}{6}}, v_{\frac{9m^3-m}{6}}\}$ be the set of vertices of the base path of $(\frac{(3m-1)m(3m+1)}{6})C_3$. Let v_0 and $v_{\frac{9m^3-m}{6}}$ are the beginning and end vertices of the base path respectively. Let the base path be $P_{\frac{9m^3-m}{6}}$. Also we consider the path $v_0, u_1, v_1, u_2, v_2, \ldots, u_{\frac{9m^3-m}{6}}, v_{\frac{9m^3-m}{6}}$ of length $2(\frac{9m^3-m}{6})$. To prove $(\frac{(3m-1)m(3m+1)}{6})C_3$ admits TPD $(P_1, P_2, P_3, \ldots, P_n)$ where $n = 3m\text{-}1$, $m \in N$. We prove the theorem by using mathematical induction on 'm'. When $m = 1$, $q(\frac{(3m-1)m(3m+1)}{6}C_3) = \frac{(3-1)3(3+1)}{6}$. Clearly $\frac{(3-1)3(3+1)}{6}$ admits TPD (P_1, P_2). Assume that the result is true for $m = k$. That is $(\frac{(3k-1)k(3k+1)}{6})C_3$ admits TPD $(P_1, P_2, P_3, \ldots, P_n)$ where $n = 3k-1$. We prove the result for a positive integer $m = k + 1$. That is to prove $(\frac{(3(k+1)-1)(k+1)(3(k+1)+1)}{6})C_3$ admits TPD $(P_1, P_2, P_3, \ldots, P_{3k+2})$. Now $q(\frac{(3(k+1)-1)(k+1)(3(k+1)+1)}{6}C_3) = (\frac{9k^3+27k^2+27k-k+9-1}{6})3 = (\frac{9k^3-k}{6})3 + \frac{27k^2+27k+8}{2}$ and the sum of edges of $(P_{3k}, P_{3k+1}, P_{3k+2})$ equal to $\frac{27k^2+27k+8}{2}$

Subbulakshmi and Chitra Devi

and hence $(\frac{(3(k+1)-1)(k+1)(3(k+1)+1)}{6})C_3$ can be decompose into $(P_1, P_2, P_3,\ldots\ldots,P_{3k+2})$. We conclude by the induction principle that any Triangular cyclic snake graphs $\frac{(3m-1)m(3m+1)}{6}C_3$ admits TPD $(P_1, P_2, P_3, \ldots\ldots, P_n) \Leftrightarrow n = 3m-1, m \in N$.

Theorem 2.8

Any Triangular cyclic snake graphs $\frac{(m)(3m+1)(3m+2)}{6}C_3$ admits TPD $(P_1, P_2, P_3, \ldots\ldots,P_n)$ $\Leftrightarrow n = 3m, m \in N$.

Proof :

Assume $\frac{(m)(3m+1)(3m+2)}{6}C_3$ admits TPD $(P_1, P_2, P_3,\ldots\ldots,P_n)$. Then $q(\frac{(m)(3m+1)(3m+2)}{6})C_3 = 3(\frac{(m)(3m+1)(3m+2)}{6})$. That is $3(\frac{(m)(3m+1)(3m+2)}{6}) = \frac{n(n+1)(n+2)}{6}$. This implies n = 3m, m ∈ N.

Conversely, suppose n = 3m, m ∈ N. Let $V = \{v_0, w_1, v_1, w_2, v_2, \ldots\ldots, w_{\frac{9m^3+9m^2+2m}{6}}, v_{\frac{9m^3+9m^2+2m}{6}}\}$ be the set of vertices of the base path of $(\frac{m(3m+1)(3m+2)}{6})C_3$. Let v_0 and $v_{\frac{9m^3+9m^2+2m}{6}}$ are the beginning and end vertices of the base path respectively. Let the base path be $P_{\frac{9m^3+9m^2+2m}{6}}$. Also we consider the path $v_0, u_1, v_1, u_2, v_2, \ldots\ldots, u_{\frac{9m^3+9m^2+2m}{6}}, v_{\frac{9m^3+9m^2+2m}{6}}$ of length $2(\frac{9m^3+9m^2+2m}{6})$. To prove $(\frac{m(3m+1)(3m+2)}{6})C_3$ admits TPD

$(P_1, P_2, P_3, \ldots\ldots, P_n)$ where n = 3m, m∈ N. We prove the theorem by using mathematical induction on 'm'. When m = 1, $q(\frac{m(3m+1)(3m+2)}{6}C_3) = \frac{3(3+1)(3+2)}{6}$. Clearly $\frac{3(3+1)(3+2)}{6}$ admits TPD (P_1, P_2, P_3). Assume that the result is true for m = k. That is $(\frac{k(3k+1)(3k+2)}{6})C_3$ admits TPD $(P_1, P_2, P_3, \ldots\ldots, P_n)$ where n = 3k. We prove the result for a positive integer m = k + 1. That is to prove $(\frac{(k+1)(3(k+1)+1)(3(k+1)+2)}{6})C_3$ admits TPD $(P_1, P_2, P_3, \ldots\ldots\ldots, P_{3(k+1)})$. Now $q(\frac{(k+1)(3(k+1)+1)(3(k+1)+2)}{6}C_3) = \frac{(k+1)(3(k+1)+1)(3(k+1)+2)}{6}3 = \frac{(9k^3+27k^2+9k^2+27k+18k+9+9+2+2k)}{6}3 = (\frac{9k^3+9k^2+2k}{6})3 + (\frac{27k^2+45k+20}{2})$ and the sum of edges of $(P_{3k+1}, P_{3k+2}, P_{3(k+1)})$ equal to $(\frac{27k^2+45k+20}{2})$ and hence $(\frac{(k+1)(3(k+1)+1)(3(k+1)+2)}{6})C_3$ can be decompose into $(P_1, P_2, P_3,\ldots\ldots,P_{3(k+1)})$. We conclude by the induction principle that any Triangular cyclic snake graphs $\frac{m(3m+1)(3m+2)}{6}C_3$ admits TPD $(P_1, P_2, P_3, \ldots\ldots, P_n) \Leftrightarrow n = 3m, m \in N$.

CONCLUSION

The Triangular path decomposition of kC_3 has been studied. The study can be extended for any odd cyclic snake graphs.

REFERENCES

1. Suthiesh Goldy J and E.Ebin Raja Merly, "Even Path Decomposition of Even Cyclic Snake Graphs", Journals of Computer and Mathematical Sciences, Vol.9(6), 625-630 June 2018.
2. N.Gnanadhas and J.Paulraj Joseph, "Continuous Monotonic Decomposition Of Cycles", International Journal Of Management and Systems, 19(2003), No.1, Page 65-76.
3. A Nagarajan and S.Navaneetha Krishnan, "Continuous Monotonic Decomposition Of some special Class of Graphs", International Journal Of Management and Systems, 21(2005), No.3, Page 91-106.
4. Frank Harary, Graph theory, Addition- Wesley Publishing Company (1972).
5. N.Gnanadhas and J.Paulraj Joseph, "Continuous Monotonic Decomposition Of Graphs", International Journal Of Management and Systems, 16(2000), No.3, Page 333-334.

Subbulakshmi and Chitra Devi

Table 1. List of first ten TPD of $\left(\frac{(3m-2)(3m-1)(m)}{6}\right)C_3$

m	q	TPD$(P_1, P_2, P_3, \ldots, P_n)$
3	84	(P1, P2, P3, … , P7)
6	816	(P1, P2, P3, … , P16)
9	2925	(P1, P2, P3, … , P25)
12	7140	(P1, P2, P3, … , P34)
15	14190	(P1, P2, P3, … , P43)
18	24804	(P1, P2, P3, … , P52)
21	39711	(P1, P2, P3, … , P61)
24	59640	(P1, P2, P3, … , P70)
27	85320	(P1, P2, P3, … , P79)
30	117480	(P1, P2, P3, … , P88)

Table 2. List of first ten TPD of $\left(\frac{9m^3-m}{6}\right)C_3$

m	q	TPD$(P_1, P_2, P_3, \ldots, P_n)$
3	120	(P1, P2, P3, … , P8)
6	969	(P1, P2, P3, … , P17)
9	3276	(P1, P2, P3, … , P26)
12	7770	(P1, P2, P3, … , P35)
15	15180	(P1, P2, P3, … , P44)
18	26235	(P1, P2, P3, … , P53)
21	41664	(P1, P2, P3, … , P62)
24	62196	(P1, P2, P3, … , P71)
27	88560	(P1, P2, P3, … , P80)
30	121485	(P1, P2, P3, … , P89)

Table 3. List of first ten TPD of $\left(\frac{9m^3+9m^2+2m}{6}\right)C_3$

m	q	TPD$(P_1, P_2, P_3, \ldots, P_n)$
3	165	(P1, P2, P3,……,P9)
6	1140	(P1, P2, P3, … , P18)
9	3654	(P1, P2, P3, … , P27)
12	8436	(P1, P2, P3, … , P36)
15	16215	(P1, P2, P3, … , P45)
18	27720	(P1, P2, P3, … , P54)
21	43680	(P1, P2, P3, … , P63)
24	64824	(P1, P2, P3, … , P72)
27	91881	(P1, P2, P3, … , P81)
30	125580	(P1, P2, P3, … , P90)

Illustration 2.5

$28C_3$

Figure 1. TPD (P1, P2,...., P7) Of 28C₃

$40C_3$

P_1 P_2 P_3

P_4

P_5
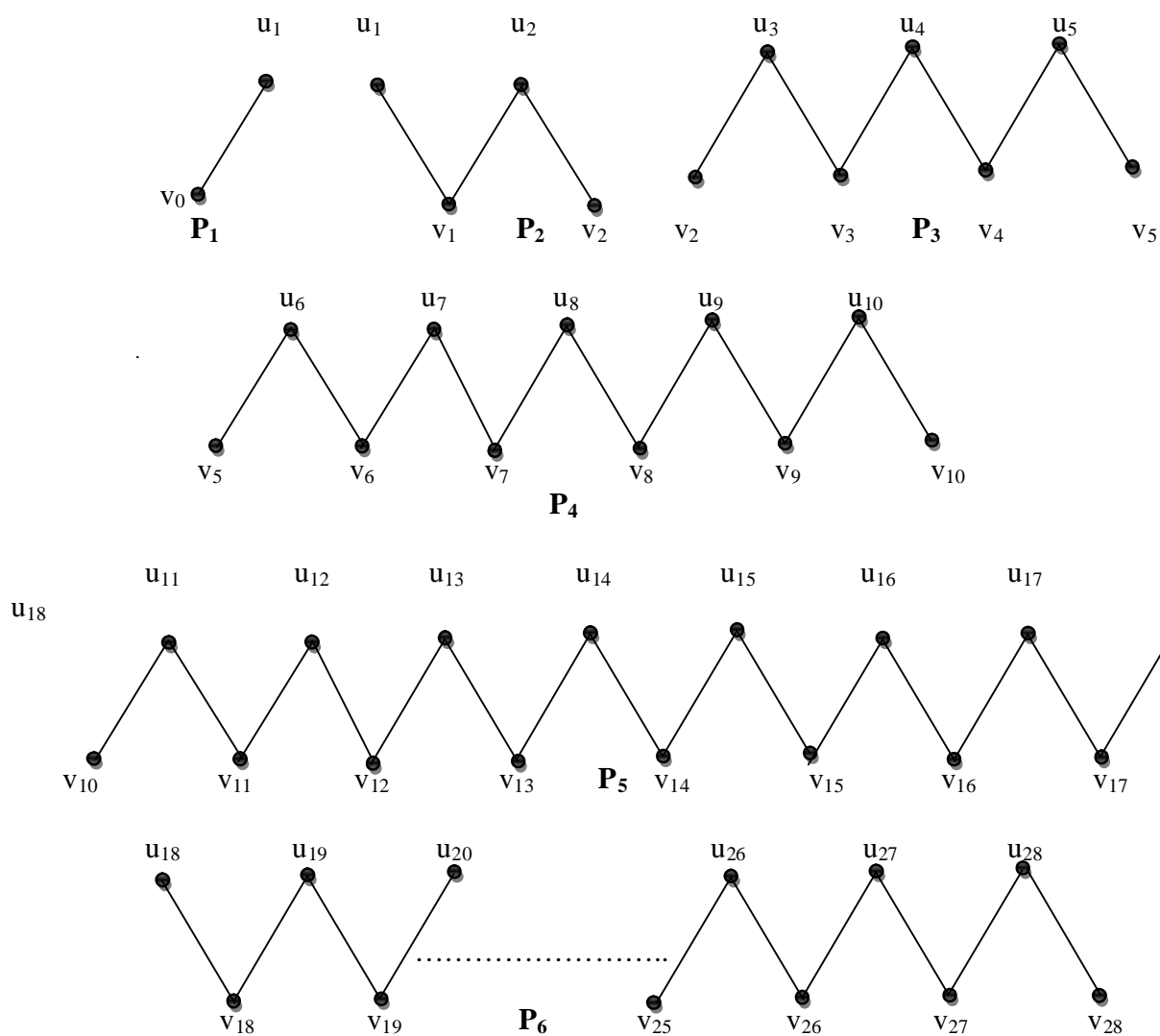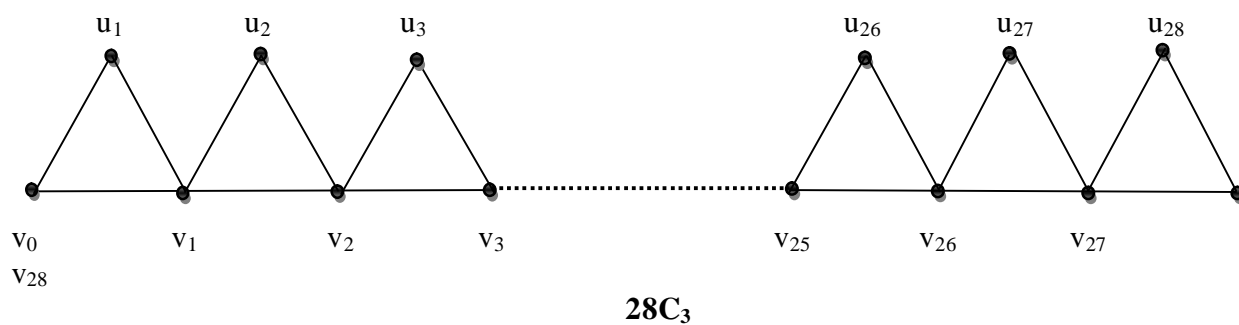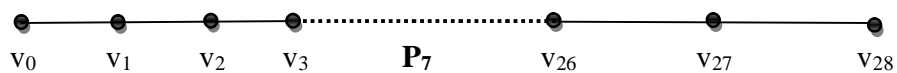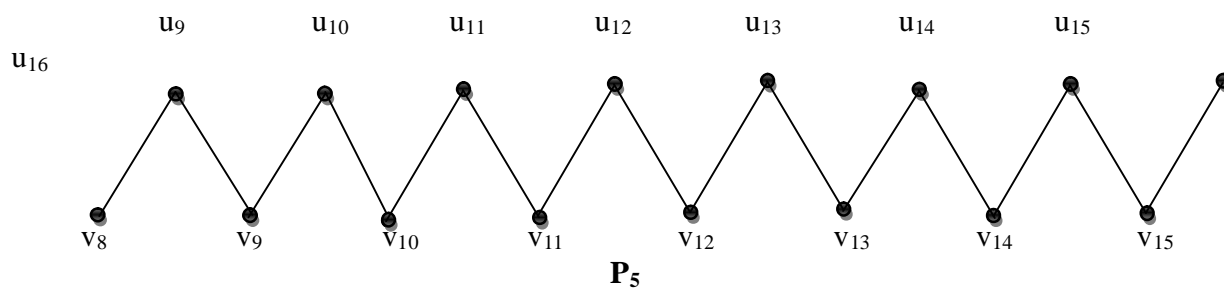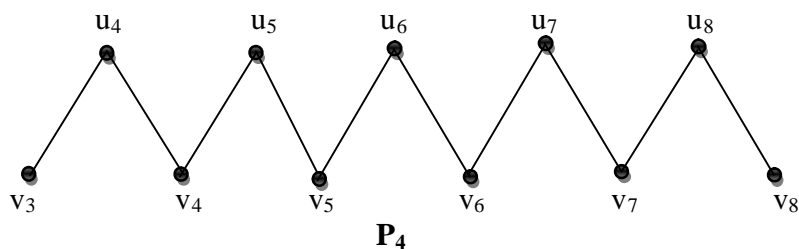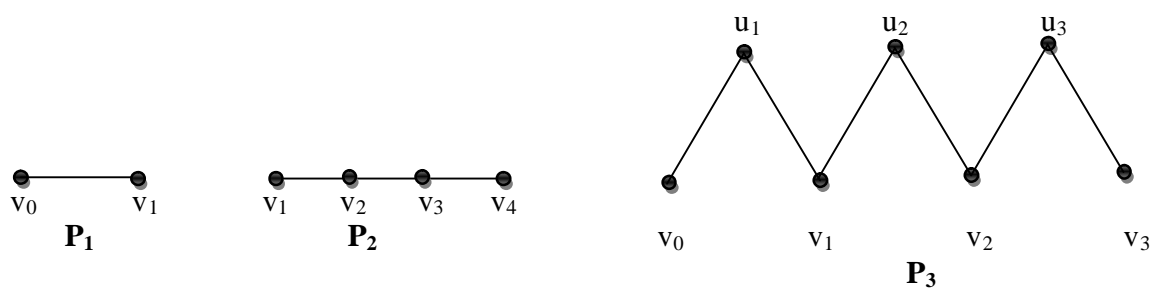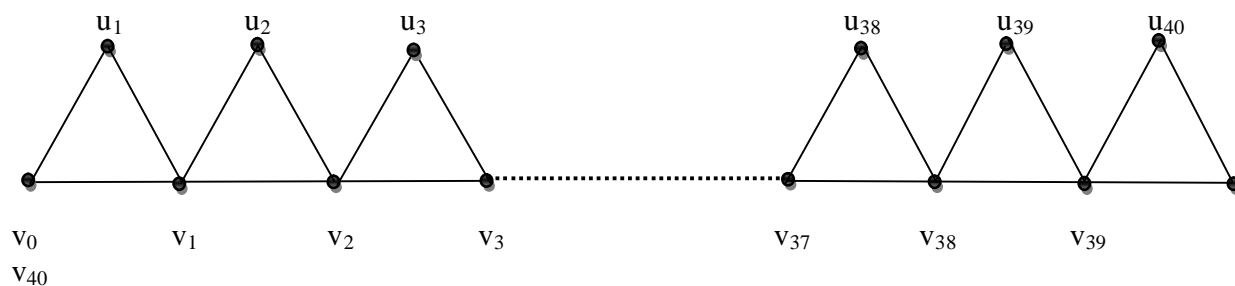
Subbulakshmi and Chitra Devi
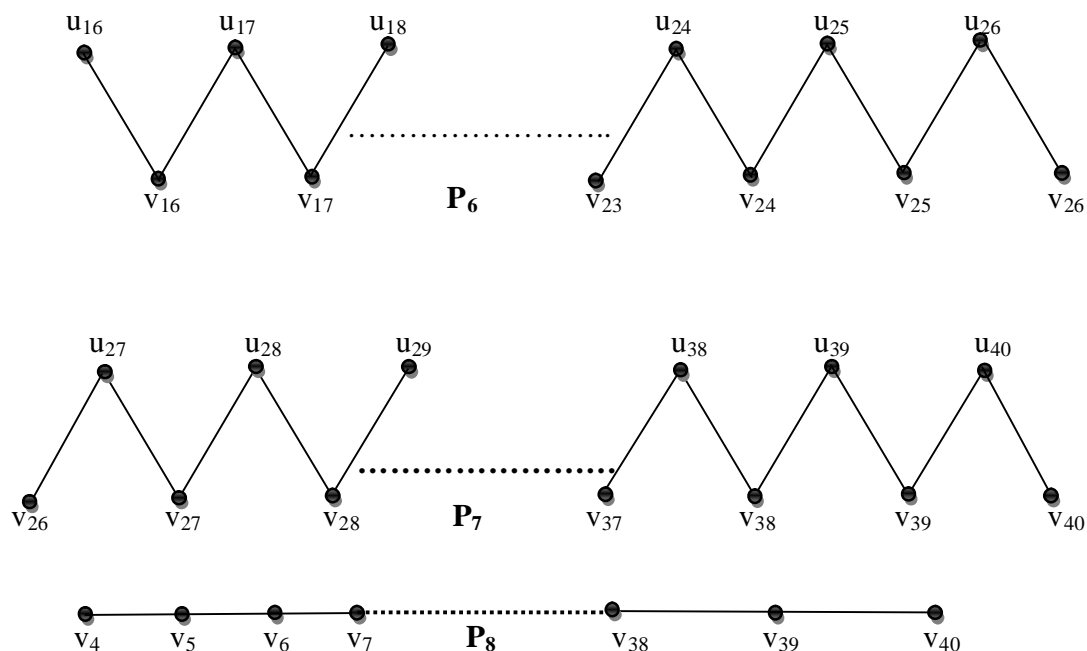
Figure 2. TPD (P1, P2,……… , P8) Of 40C₃
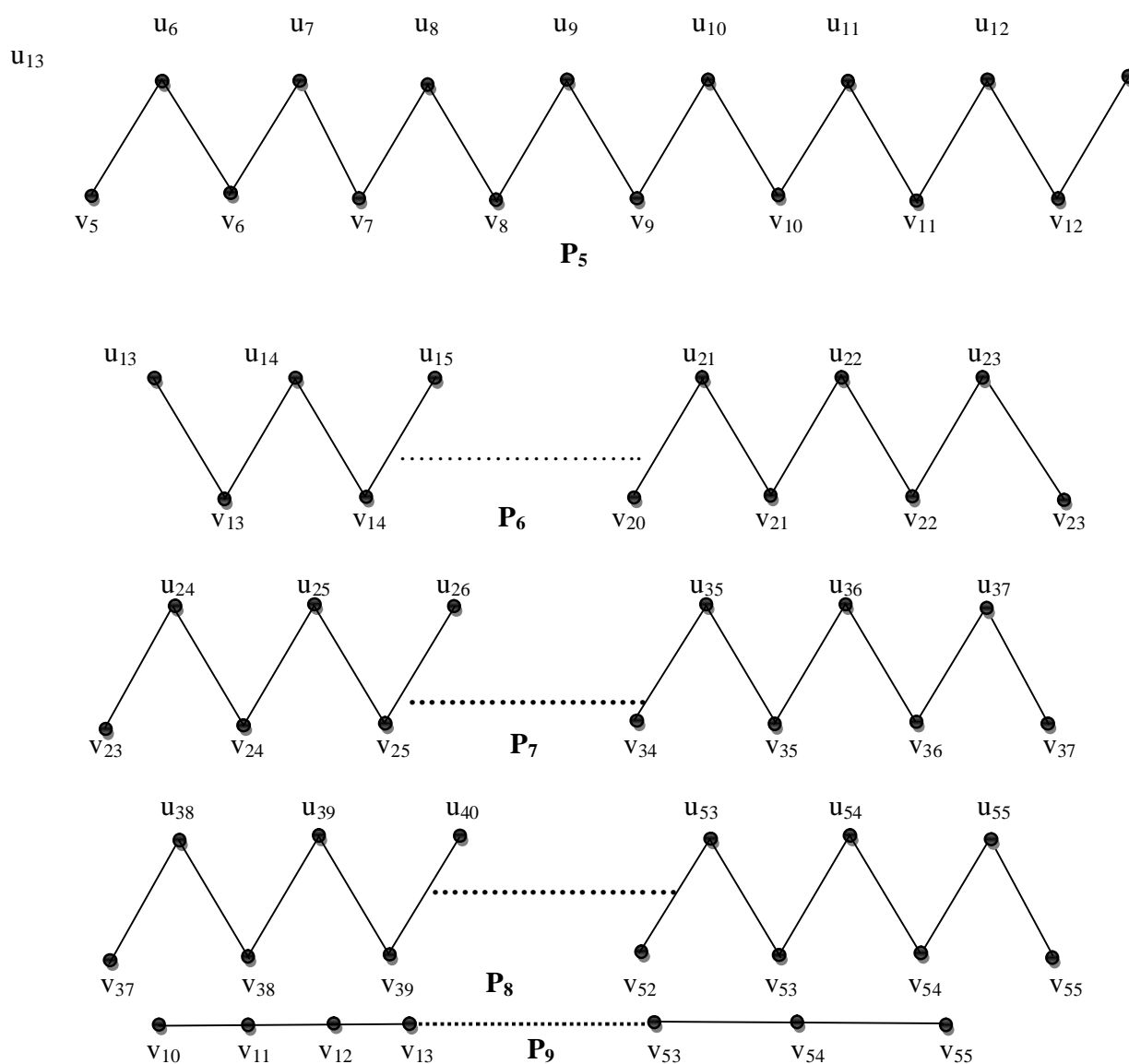
55C₃

Figure 3. TPD (P1, P2,………., P9) Of 55C₃

RESEARCH ARTICLE

Preliminary Phytochemical Studies on Tropical Fruit: *Lansium domesticum* Correa (Meliaceae)

Sruthi Gopan.M[1] and Sudha Bai.R[2]*

[1]Research Scholar,Post Graduate and Research, Department of Botany, University College, Thiruvananthapuram, Kerala– 695 034, India.
[2]Professor and Head, Post Graduate and Research Department of Botany, University College, Thiruvananthapuram, Kerala– 695 034, India.

*Address for Correspondence
Sudha Bai.R
Professor and Head,
Post Graduate and Research Department of Botany,
University College, Thiruvananthapuram,
Kerala– 695 034, India.
E.Mail: sudharvinayan@gmail.com

ABSTRACT

Lansium domesticum bearing clusters of edible fruits is a tree belonging to the family Meliaceae. There are two distinct varieties namely *Lansium domesticum var. pubescens* and *Lansium domesticum var. domesticum* commonly known as Langsat and Duku. It is an exotic species native to Southeast Asian countries like Indonesia, Thailand, Philippines. The present investigation focused on the preliminary phytochemical evaluation of Fruit Peel and Pulp of *Lansium domesticum.* Based on the polarity, seven solvents - Acetone, Methanol, Chloroform, Ethyl acetate, Petroleum ether, Hexane and Distilled water were selected for extraction and analysis of phytochemicals. Yield and colour of the extracts were also determined. On quantitative basis, the methanolic extract of the fruit peel of Langsat and duku showed high yield and the methanolic extract of pulp of langsat and distilled water extract of duku indicated high yield. The positivity of the phytochemical tests showed best results in the acetone, methanol and distilled water extracts and poor results in the non-polar solvents such as hexane and petroleum ether. The preliminary investigations of both the fruit peel concluded the presences of flavonoids, phenols, tannins, terpenoids, carbohydrates, saponins, triterpenoids, fats and fixed oils. Among these, fats and fixed oils showed positive results for fruit peel extract analysis in all solvents. The fruit pulp extract in different solvents also revealed the presence of various phytoconstituents. The more polar solvents like acetone, methanol and distilled water were detected as best for extraction of phytochemicals. The Fruit peel and pulp of Langsat and Duku were selected for quantification of flavonoids, tannins, phenols, terpenoids and saponins. The acetone extract of the Langsat Peel exhibited high (mg/g) tannin (3.94±0.74) and phenolic content (5.06±0.39) compared to Duku Peel extract of other solvents. The distilled water extract of fruit

pulp of both suggested high (mg/g) tannin (2.38±0.59, 1.88±0.07 respectively) and phenolic (2.89±0.58, 2.60±0.33 respectively) content compared to other solvents. The flavonoid content was negligible in ethyl acetate extract of both fruit peel. Terpenoids and saponins were also quantified from both fruit parts.

Keywords: *Lansium domesticum*, Phytochemical analysis, flavonoids, tannins, phenols, terpenoids, saponins

INTRODUCTION

Lansium domesticum Correa is an exotic tree form bearing edible fruits belongs to the family Meliaceae. The family is also known as Mahagony family. There are two distinct varieties: *Lansium domesticum var. pubescens* and *Lansium domesticum var. domesticum* commonly known by langsat and duku. Native to Southeast Asian countries like Malaysia, Thailand, Indonesia, Philippines. The raw fruit is green in colour and on maturity, it turns pale yellow to light brown. The pulp appeared as white translucent part, which is the edible part and the seeds are bitter in taste. The fruit is highly nutritious and rich in many vitamins [1]. Langsat fruits are oblong-ovoid, thin- skinned and possess latex, while Duku fruits are nearly round, thick- skinned and contains mild latex or latex free. The fruit peel is used as insect repellent [2]. The iron and mineral content of both the fruits is higher than apples and oranges[3].Traditionally, the bark is used to treat venomous insects bites, as dysentery medicine and used to eradicate cancer cells [4]. The present investigation focused on the preliminary phytochemical analysis of peel and pulp of *Lansium domesticum* fruits. The presence of phytoconstituents in the samples suggests the scope for studies on bioactivities and identification of compounds responsible for it. It may have several medicinal properties and can be included in the health care system.

AIM OF THE STUDY
Phytochemical analysis to evaluate the fruit samples of *Lansium domesticum* on qualitative and quantitative basis employing solvents with different polarity indices.

MATERIALS AND METHODS

Collection of plant materials
The samples for the study include mature fruit peel and fruit pulp of *Lansium domesticum*. The fruits samples (Figure 1 and Figure 2) were collected from the home garden near Ernakulam and Kottayam district respectively in Kerala. After the shade drying process, they were powdered and stored in labelled bottles.

Preparation of Successive Extracts
Preparation of extract by cold extraction method.

Preliminary Qualitative Phytochemical Analysis
A stock solution (mg/ml) of extract from different solvents (acetone, methanol, chloroform, ethyl acetate, petroleum ether, hexane and distilled water) was prepared. These extracts along with blanks were analyzed qualitatively for the presence of various phytochemicals in the fruit pulp and fruit peel samples. Phytochemical investigations were carried out for all fruit extracts of *Lansium domesticum* as per standard methods [5].

Quantitative Phytochemical Analysis:
Flavonoids, Phenol, Tannin, Terpenoids, Saponins were determined quantitatively [6][7][8][9][10][11].

Statistical analysis

The experimental data were recorded on basis of three independent trials of each parameter. Mean value and standard deviation (SD) were computed and the results are tabulated as Mean $\pm$ SD for each triplicates.

RESULTS AND DISCUSSION

In the present investigation, the study focused on preliminary phytochemical analysis of fruit peel and fruit pulp of *Lansium domesticum var. pubescens* and *Lansium domesticum var. domesticum*. The extract of fruit peel and fruit pulp were taken using seven different solvents - acetone , methanol, chloroform, ethyl acetate, petroleum ether, hexane and distilled water based on their polarity. The present study aimed to detect the presence of flavonoids, phytosterols/ terpenoids, tannins, cardiac glycosides, phenols, triterpenoids, anthraquinone glycosides, carbohydrates, proteins, fats and fixed oils and saponins using the standard protocol. In addition to the phytochemical studies, morphological characteristics of leaf were studied and tabulated in Table 1.

Yield of extracts

The extraction yield of fruits peel and fruits pulp of *Lansium domesticum* in seven solvents were analyzed. The yield of crude extract was determined by measuring its dry weight and the yield per 100g was calculated and tabulated in Table 2 and Table 3.

$$\text{Extraction yield} \ = \ \frac{\text{mass of extract}}{\text{mass of dry matter}}$$

From the present studies of fruits peel, it is noticed that the highest yield of extract is possible in methanol, the polar solvent and the lowest yield were shown in the non-polar solvent. The extraction yield mainly depend on the extraction techniques. In addition to that it also depends on the solvent used for the extraction of the samples [12][13].The yield of extract from methanolic pulp of langsat fruit and distilled water pulp of duku fruit were monitored as relatively higher. Poor yield were detected in the hexane extract of both the fruits pulp samples. The yield of extract of fruits peel and fruits pulp showed variations in different solvents it may be due to the polarity of the solvent as well as the phytochemicals present in the samples.

Phytochemical Investigation

Phytochemical studies on qualitative and quantitative basis were carried out using the standard procedure and the results are explained for the assessment of phytochemical profile of the fruits peel and fruits pulp of *Lansium domesticum* Correa.

Qualitative phytochemical analysis

A preliminary phytochemical investigation of fruits peel and fruits pulp of *Lansium domesticum* Correa was performed using the standard protocol. The results of the qualitative analysis are illustrated in Tables 4 to 7. Based on the intensity of the reaction products from the qualitative tests, the data were graded as very high (**+++**), high (**++**), moderate (**+**) and nil (**-**). In the present study, phytochemicals except alkaloids, cardiac glycosides, anthraquinone glycosides, proteins were not detected in any of the seven solvent extract of peel of both the fruits samples. The polar solvents acetone, methanol and distilled water showed good intensity of results. In the preliminary analysis the pulp of both of the fruits samples showed the presence of various phytoconstituents. The intensities of results were found to be low in the non-polar solvents – petroleum ether and hexane for both the fruit pulp. Alkaloids, cardiac glycosides, anthroquinone glycosides and proteins also showed no positive results in the langsat and duku fruits pulp.

The phytoconstituents present in the fruit peel and fruit pulp of *Lansium domesticum* could be extracted in different solvents. The variation on efficiency in the extraction of phytochemicals in seven solvents employed is based on

differences in their polarity. Acetone, methanol and distilled water showed efficient extraction of phytochemicals in the present investigation. The extraction of the samples is monitored as higher in the polar solvents than the non-polar solvents. The extraction and purification of the plant materials for the antioxidant and the phytochemicals present in it depends upon the temperature, time, concentration of the solvent as well as polarity of the solvent. All the phytochemicals present in the samples will get eluted on different solvents not on a single solvent[14][15]. So the selection of the appropriate solvent for the extraction of the plant samples is very important in phytochemical evaluation.

Quantitative phytochemical analysis
The quantitative phytochemical studies was carried out to estimate the quantity of phytoconstituents present in the fruits peel and fruits pulp of *Lansium domesticum*. The results from seven solvent extracts are illustrated in Table 8 to 12. The quantitative analysis of flavonoids was done in seven solvents. Quercetin was used as the standard (1mg/ml). The ethyl acetate extract of the langsat peel (0.38 ± 0.04 mg/g) and duku peel (0.38 ± 0.10) showed the highest flavonoid contents. The lowest flavonoid contents were detected in chloroform and hexane extracts of both the fruits peel samples. The distilled water extract of the fruits pulp showed the highest (0.50 ± 0.00 mg/g, 0.25 ± 0.06 mg/g) and lowest were observed in the methanol and chloroform extract. Flavonoids have several medicinal properties such as neuro and cardio protective and bioactivities like antioxidant, anti inflammatory, anticancer, antimicrobial, anti-viral properties. These properties of bioactivities depends upon the bioavailability and its mode of action [16]. For the estimation of tannin, tannic acid (1mg/ml) was used as the standard. Tannin is observed to be highest, in the acetone extract of langsat peel (3.94 ± 0.74mg/g) than the duku peel (1.08 ± 0.23 mg/g) extract and lowest in the hexane extract of the both the fruits peel extract. Langsat pulp (2.38 ± 0.59 mg/g) in the distilled water extract showed highest tannin content than the duku pulp (1.88 ± 0.07mg/g). Lowest were observed in the chloroform, petroleum ether and hexane extract of the fruits pulp. Tannins act as defensive agents for plants and protect it from insects, microorganisms and animals [17][18][19][20].

 Gallic acid (1mg/ml) was used as the standard for the estimation of phenol. The phenolic content of both the fruits peel exhibited highest in the acetone extract and fruit pulp in the distilled water extract. And the phenolic content were not observed in the ethyl acetate, petroleum ether, hexane extract of all fruits samples. Duku peel of chloroform extract also don't exhibited the phenolic content. The ability of the donating power of hydrogen atom by phenolic and the flavonoid molecules are responsible for the antioxidant activity. They can inactivate the free radicals their by reducing the damage caused by the free radicals[21]. Synthetic antioxidants have potential toxic effects[22]. To overcome this effects, natural antioxidant like flavonoids and phenolic compounds are used [23].

 For the determination of terpenoid contents in the fruits samples, the method of Indira *et al.*, 2012 was followed. Among the fruits peel and fruits pulp, duku fruit samples exhibited high terpenoids (0.56 ± 0.00 mg/g ,0.53 ± 0.00 mg/g respectively) content. Terpenoids are one of the important secondary metabolites found in plants. It plays an important role in plant development and growth. They possess hypoglycemic, antimalarial, antiviral, antibacterial, antitumour, anti-inflammatory activities [24]. Langsat peel (9.20±0.56 mg/g) and the duku pulp (14.00±0.56 mg/g) were observed to be high in saponin content. Saponin content was found to be higher than other phytochemicals present in the fruits samples. Saponins are amphiphilic molecules used as formulation of several traditional and herbal medicines. They also possess several bioactivities such as antioxidant, anticancerous, anti-inflammatory, antiviral, fungicidal, antimicrobial and immunomodulatory effects[25].

The present study concluded that acetone, methanol and distilled water are the best solvents for the extraction of phytochemicals from the peel and pulp of fruits of *Lansium domesticum*. The quantitative analysis of the fruits samples done spectrophotometrically in seven solvents except for terpenoid and saponins which were evaluated on basis of weighing method. The data illustrated from the preliminary phytochemical analysis supported the results from the quantification of the fruits samples of *Lansium domesticum*. The present investigation is only the preliminary studies about the plant. Further studies are needed, that will result in the use of this tropical fruits in health care. The

Sruthi Gopan and Sudha Bai

phytoconstituents present in the samples maybe responsible for different bioactivities. So identification and characterization of compounds responsible for the bioactivities of the fruit extract is needed for the future studies.

ACKNOWLEDGEMENTS

REFERENCES

1. 1.Venkatachalam K. Bioactive compounds of longkong fruit (*Lansium domesticum* Corr.). Bioactive Compd. Underutilized Fruits Nuts 2020; 107–122.
2. Quisumbing E. Medicinal plants of the Philippines. Dept of Agri and Comm, Philippine Islands Technical Bulletin1951;16.
3. Mabberley D. Jupiter Botanicus: robert brown of the British museum. Braunschweig. 1985.
4. Mitsuoka T. Beneficial microbial aspects (probiotics). Int Dairy Congr Proc 15th 1990;2:1226-37.
5. Sofowora A. Research on Medicinal Plants and Traditional Medicine in Africa. J Altern Complement Med 1996; 2: 365-372.
6. Edeoga HO, Mbaebe BO, Afolayan AJ, Adesuyi AO. Phytochemical analysis and antioxidants activities of aqueous stem bark extract of *Schotia latifolia* Jacq. Asian Pac J Trop Biomed 2012;(2)2:118-124.
7. Lee Wei Har, Intan Safinar Ismail. Antioxidant activity, total phenolics and total flavonoids of *Syzygium polyanthum* (Wight) Walp leaves. J Med Aromat Plants2012; 2(2): 219-228.
8. Kamtekar, Samidha, Vrushali Keer and Vijaya Patil. Estimation of phenolic content, flavonoid content, antioxidant and alpha amylase inhibitory activity of marketed polyherbal formulation. J Appl Pharm Sci2014; 4 (09): 61-65.
9. Indira G, Kavitha Chandran C. Quantitative estimation of total phenolic, flavonoids, tannin and chlorophyll content of leaves of *Strobilanthes kunthiana* (Neelakurinji). J Med Plants Stud2016; 4(4): 282-292.
10. Malik SK, Ahmad M and Khan F. Qualitative and quantitative estimation of terpenoid contents in some important plants of Punjab, Pakistan. Pak J Sci2017; 69(2):150.
11. *11.Ukpabi Chibueze, Akubugwo Emmanuel I, Agbafor Kingsley, Wogu Chidi, Chukwu Henry C. Phytochemical and heavy metal composition of Telfairia occidental and Talinium triangulare grown in Aba Nigeria and environmental health implications. Am J Biochem 2013; 3(3): 67-73.*
12. Ajanal M, Gundkalle M and Nayak S. Estimation of total alkaloid in Chitrakadivati by UV-Spectrophotometer. Anc Sci Life2012; 31(4): 198–201.
13. Mahdi-Pour B, Jothy SL, Latha LY, Chen Y and Sasidharan S. Antioxidant activity of methanol extracts of different parts of *Lantana camara*. Asian Pac J Trop Biomed.2012; 2(12): 960–965.
14. Lapornik B, Prošek M, Wondra AG. Comparison of extracts prepared from plant by-products using different solvents and extraction time. J Food Eng 2005;71(2):214-222.
15. Iloki-Assanga SB, Lewis-Luján LM, Lara-Espinoza CL, GilSalido AA, Fernandez-Angulo D, Rubio-Pino JL, *et al*. Solvent effects on phytochemical constituent profiles and antioxidant activities, using four different extraction formulations for analysis of *Bucida buceras* L. and *Phoradendron californicum*. BMC Res Notes. 2015;8(1):396.
16. Ullah A, Munir S, Badshah SL, Khan N, Ghani L, Poulson BG, Emwas AH, Jaremko M. Important Flavonoids and Their Role as a Therapeutic Agent. Mol2020;11,25(22):5243.
17. De Bruyne T, Pieters L, Deelstra H, Vlietinck A. Condensed vegetable tannins: biodiversity in structure and biological activities. Biochem Syst Ecol 1999; 27 (4) : 445-459.
18. Hagerman AE, Riedl KM, Jones GA, Sovik KN, Ritchard NT, Hartzfeld PW, Riechel TL. High molecular weight plant polyphenolics (tannins) as biological antioxidants. J Agric Food Chem. 1998; 46 (5):1887-1892.
19. 19.Khanbabaee K, Van Ree T. Tannins: classification and definition. Nat Prod Rep 2001;18 (6) : 641-649

Sruthi Gopan and Sudha Bai

20. K.P. Sharma KP.Tannin degradation by phytopathogen's tannase: a Plant's defense perspective. Biocatal Agric Biotechnol 2019; 21.
21. Amarowicz R, Pegg R, Rahimi-Moghaddam P, Barl B, Weil J. Free-radical scavenging capacity and antioxidant activity of selected plant species from the Canadian prairies. Food Chem. 2004;84:551–562
22. Liu J, Jia L, Kan J and Jin CH. In vitro and in vivo antioxidant activity of ethanolic extract of white button mushroom (*Agaricus bisporus*). Food Chem Toxicol 2013; 51: 310–316.
23. Zhong RZ and Zhou DW. Oxidative stress and role of natural plant derived antioxidants in animal reproduction. J Integr Agric2013; 12 (10): 1826–1838.
24. Yang W, Chen X, Li Y, Guo S, Wang Z, Yu X. Advances in Pharmacological Activities of Terpenoids. Nat Prod Commun 2020;15(3).
25. Juang YP, Liang PH. Biological and Pharmacological Effects of Synthetic Saponins. Molecules. 2020; 27, 25(21):4974.

Table 1: MORPHOLOGICAL CHARACTERISTICS OF LEAF
 Morphological characteristics of the leaves are examined and tabulated in Table 1.

SI no	Characteristics	Langsat	Duku
1.	No:of leaflets	9 nos	9 nos
2.	Leaf type	Odd pinnately compound,	Odd pinnately compound,
3.	Leaf arrangement	Alternate leaflets	Alternate leaflets
4.	No: of major veins	9/10 pairs	11/12 pairs
5.	No: of minor veins	18/20 pairs	21/23 pairs
6.	Length of midrib (Length of leaf)	25.5 cm	24.0 cm
7.	Shape of leaf	Elliptical and long	Ovate, larger in size
8.	Nature of leaf	Smooth	Rough and glabrous
9.	Leaf apex	Narrowly acuminate, pointed	Acute
10	Leaf width	10.5 cm	11.5 cm
11	Length of petiole	1.4 cm	1.7 cm
12	Leaf margin	Entire	Entire
13	Leaf lamina	Thin and soft	Slightly rough

Table 2: The Yield And Nature of Extracts of Fruits Peel of *Lansium domesticum* Correa After Extraction (Duration of extraction = 48 hours; Treatment temperature = 40⁰C)

Name of the solvent	Langsat peel			Duku peel		
	Yield of extract(g)	Yield/ 100g	Colour of the extract	Yield of extract (g)	Yield/ 100g	Colour of the extract
Acetone	1.29	25.8	Dark brown	0.78	15.6	Golden yellow
Methanol	2.27	45.5	Greenish yellow	1.96	39.2	Light yellow
Chloroform	1.23	24.6	Brown	1.06	21.2	Dark brown
Ethyl acetate	1.73	34.6	Greenish brown	1.89	37.8	Greenish yellow
Petroleum ether	0.51	10.2	Light brown	0.69	13.8	Light brown
Hexane	0.46	9.2	Light brown	0.41	8.2	Golden yellow
Distilled water	0.94	18.8	Greenish brown	0.84	16.8	Dark brown

Table 3: the yield and nature of extracts of fruits pulp of *lansium domesticum* correa after extraction (Duration of extraction = 48 hours; Treatment temperature = 40⁰C)

Name of the solvent	Langsat pulp			Duku pulp		
	Yield of extract(g)	Yield/ 100g	Colour of the extract	Yield of extract (g)	Yield/ 100g	Colour of the extract
Acetone	0.76	15.2	Dark brown	0.88	17.5	Light brown
Methanol	1.63	32.54	Greenish brown	0.69	13.94	Light brown
Chloroform	0.38	7.52	Dark brown	0.33	6.6	Dark brown
Ethyl acetate	0.34	6.76	Dark brown	0.27	5.42	Light brown
Petroleum ether	0.37	7.36	Dark brown	0.15	3.08	Light brown
Hexane	0.27	5.34	Light brown	0.13	2.52	Light brown
Distilled water	0.99	19.8	Dark brown	1.31	26.2	Brown

Table 4: Qualitative Phytochemical Analysis of Peel (LANGSAT) of *Lansium domesticum* Correa

SI No:	Name of the phytoconstituents	Name of the test	Name of the solvents						
			A	M	C	EA	PE	H	DW
1.	Alkaloids	a) Dragendroff's test	-	-	-	-	-	-	-
		b) Wagner's test	-	-	-	-	-	-	-
2.	Flavonoids	a) Ammonium test	-	-	-	+	-	-	-
		b) Alkaline reagent test	-	-	-	-	-	-	-
		c) Shinoda test	-	-	-	-	-	-	-
3.	Phytosterols/ Terpenoids	Liebermann-Burchard's test	+++	++	+	+++	-	-	+
4.	Tannins	Ferric chloride test	+++	+	-	+	-	-	+
5.	Cardiac glycosides	Keller-Kiliani test	-	-	-	-	-	-	-
6.	Phenols	Ferric chloride test	-	++	-	-	-	-	-
7.	Triterpenoids	Salkowski test	+++	-	-	+++	+	+	-
8.	Anthraquinone glycosides	Hyhydroxyanthraquinone test	-	-	-	-	-	-	-
9.	Carbohydrates	a) Molisch's test	+++	-	+++	++	-	++	+++
		b) Fehling's test	-	-	+++	-	-	-	-
10.	Proteins	Biuret test	-	-	-	-	-	-	-
11.	Fats and fixed oils		+++	+++	++	+++	+++	+++	+++
12.	Saponins	Foam test	-	-	++	-	-	-	+++

(A-Acetone; M-Methanol; C-Chloroform; EA-Ethyl acetate; PE- petroleum ether; H-Hexane; DW-Distilled water)

Table 5: Qualitative Phytochemical Analysis of Peel (DUKU) OF *Lansium domesticum* Correa

SI No:	Name of the phytoconstituents	Name of the test	Name of the solvents						
			A	M	C	EA	PE	H	DW
1.	Alkaloids	a) Dragendroff's test	-	-	-	-	-	-	-
		b) Wagner's test	-	-	-	-	-	-	-
2.	Flavonoids	a) Ammonium test	-	-	-	+	-	-	-
		b) Alkaline reagent test	-	-	-	-	-	-	-
		c) Shinoda test	-	-	-	-	-	-	-
3.	Phytosterols/ Terpenoids	Liebermann-Burchard's test	++	+	+	++	-	-	+
4.	Tannins	Ferric chloride test	++	+	-	+	-	-	+
5.	Cardiac glycosides	Keller-Kiliani test	-	-	-	-	-	-	-
6.	Phenols	Ferric chloride test	-	++	-	-	-	-	++
7.	Triterpenoids	Salkowski test	+	-	-	+++	+	++	-

Sruthi Gopan and Sudha Bai

8.	Anthraquinone glycosides	Hyhydroxyanthraquinone test	-	-	-	-	-	-	-
9.	Carbohydrates	a) Molisch's test	++	-	++	++	-	++	++
		b) Fehling's test	-	-	++	-	-	-	-
10.	Proteins	Biuret test	-	-	-	-	-	-	-
11.	Fats and fixed oils		+++	+++	+++	+++	+++	+++	+++
12.	Saponins	Foam test	-	-	++	-	-	-	+++

(A-Acetone; M-Methanol; C-Chloroform; EA-Ethyl acetate; PE- petroleum ether; H-Hexane; DW-Distilled water)

Table 6: Qualitative Phytochemical Analysis of Pulp (LANGSAT) OF *Lansium domesticum* Correa

SI No:	Name of the phytoconstituents	Name of the test	Name of the solvents						
			A	M	C	EA	PE	H	DW
1.	Alkaloids	a) Dragendroff's test	-	-	-	-	-	-	+
		b) Wagner's test	-	-	-	-	-	-	+
2.	Flavonoids	a) Ammonium test	-	-	-	-	-	-	-
		b) Alkaline reagent test	-	-	-	-	-	-	+
		c) Shinoda test	-	-	-	-	-	-	-
3.	Phytosterols/ Terpenoids	Liebermann-Burchard's test	+	+	-	+	-	-	+
4.	Tannins	Ferric chloride test	+	+	-	-	-	-	+++
5.	Cardiac glycosides	Keller-Kiliani test	-	-	-	-	-	-	-
6.	Phenols	Ferric chloride test	+	-	-	-	-	-	+++
7.	Triterpenoids	Salkowski test	-	-	-	+	-	-	-
8.	Anthraquinone glycosides	Hyhydroxyanthraquinone test	-	-	-	-	-	-	-
9.	Carbohydrates	a) Molisch's test	+++	+	++	-	-	-	+++
		b) Fehling's test	-	-	+++	-	-	-	-
10.	Proteins	Biuret test	-	-	-	-	-	-	-
11.	Fats and fixed oils		+++	+++	+++	+++	+++	-	+++
12.	Saponins	Foam test	-	-	-	-	-	-	+++

(A-Acetone; M-Methanol; C-Chloroform; EA-Ethyl acetate; PE- petroleum ether; H-Hexane; DW-Distilled water)

Table 7: Qualitative Phytochemical Analysis of Pulp (DUKU) OF *Lansium domesticum* Correa

SI No:	Name of the phytoconstituents	Name of the test	Name of the solvents						
			A	M	C	EA	PE	H	DW
1.	Alkaloids	a) Dragendroff's test	-	-	-	-	-	-	+
		b) Wagner's test	-	-	-	-	-	-	+
2.	Flavonoids	a) Ammonium test	-	-	-	-	-	-	+
		b) Alkaline reagent test	-	-	-	-	-	-	-
		c) Shinoda test	-	-	-	-	-	-	-
3.	Phytosterols/ Terpenoids	Liebermann-Burchard's test	++	+	-	+	-	-	+
4.	Tannins	Ferric chloride test	+	-	-	-	-	-	++
5.	Cardiac glycosides	Keller-Kiliani test	-	-	-	-	-	-	-
6.	Phenols	Ferric chloride test	+	+	-	-	-	-	+++
7.	Triterpenoids	Salkowski test	-	-	-	+	-	-	-
8.	Anthraquinone glycosides	Hyhydroxyanthraquinone test	-	-	-	-	-	-	-
9.	Carbohydrates	a) Molisch's test	+++	+	++	-	-	+	+++
		b) Fehling's test	-	-	+++	-	-	-	-
10.	Proteins	Biuret test	-	-	-	-	-	-	-

11.	Fats and fixed oils		+++	+++	+++	+++	+++	+++	+++
12.	Saponins	Foam test	-	-	-	-	-	-	+++

(A-Acetone; M-Methanol; C-Chloroform; EA-Ethyl acetate; PE- petroleum ether; H-Hexane; DW-Distilled water)

Table 8: Estimation Of Flavonoids Present in the Fruits Peel and Fruits Pulp Of *Lansium domesticum* Correa

SI no:	Solvents used	Langast Peel	Duku Peel	Langsat Pulp	Duku Pulp
1.	Acetone	0.06 ± 0.01	0.06 ± 0.01	0.02 ± 0.01	0.02 ± 0.01
2.	Methanol	0.05 ± 0.02	0.05 ± 0.02	0.00 ± 0.00	0.01 ± 0.00
3.	Chloroform	0.00 ± 0.00	0.01 ± 0.00	0.00 ± 0.01	0.00 ± 0.00
4.	Ethyl acetate	0.38 ± 0.04	0.38 ± 0.10	0.03 ± 0.00	0.03 ± 0.00
5.	Petroleum ether	0.02 ± 0.00	0.02 ± 0.02	0.01 ± 0.00	0.00 ± 0.00
6.	Hexane	0.00 ± 0.00	0.01 ± 0.00	0.01 ± 0.00	0.00 ± 0.00
7.	Distilled water	0.04 ± 0.06	0.01 ± 0.00	0.50 ± 0.00	0.25 ± 0.06

[Data shown as mean ± SD (n = 3)]

Table 9: Estimation of Tannins Present in the Fruits Peel and Fruits Pulp of *Lansium domesticum* Correa

SI no:	Solvents used	Langast Peel	Duku Peel	Langsat Pulp	Duku Pulp
1.	Acetone	3.94 ± 0.74	1.08 ± 0.23	0.12 ± 0.01	0.14 ± 0.01
2.	Methanol	0.71 ± 0.04	0.76 ± 0.05	0.18 ± 0.04	0.08 ± 0.01
3.	Chloroform	0.04 ± 0.01	0.01 ± 0.00	0.00 ± 0.00	0.01 ± 0.00
4.	Ethyl acetate	0.17 ± 0.01	0.23 ± 0.25	0.05 ± 0.01	0.02 ± 0.00
5.	Petroleum ether	0.03 ± 0.01	0.06 ± 0.01	0.00 ± 0.00	0.01 ± 0.02
6.	Hexane	0.02 ± 0.01	0.02 ± 0.00	0.00 ± 0.00	0.00 ± 0.00
7.	Distilled water	0.54 ± 0.01	0.62 ± 0.10	2.38 ± 0.59	1.88 ± 0.07

[Data shown as mean ± SD (n = 3)]

Table 10: Estimation of Phenols Present in the Fruits Peel And Fruits Pulp of *Lansium domesticum* Correa

SI no:	Solvents used	Langast Peel	Duku Peel	Langsat Pulp	Duku Pulp
1.	Acetone	5.06 ± 0.39	4.25 ± 1.76	0.18 ± 0.01	0.2 ±0.01
2.	Methanol	2.58 ± 1.55	2.43 ± 0.87	0.08 ± 0.03	0.18± 0.02
3.	Chloroform	0.01± 0.01	-	0.04 ± 0.04	0.06± 0.05
4.	Ethyl acetate	-	-	-	-
5.	Petroleum ether	-	-	-	-
6.	Hexane	-	-	-	-
7.	Distilled water	0.91 ± 0.02	1.73± 0.14	2.89 ± 0.58	2.60 ± 0.33

[Data shown as mean ± SD (n = 3)]

Table 11: Estimation of Terpenoids Present in the Fruits Peel and Fruits Pulp of *Lansium domesticum* Correa

SI no:	Sample	Quantity (mg/g)
1.	Langast Peel	0.29 ± 0.01
2.	Duku Peel	0.56 ± 0.00
3.	Langsat Pulp	0.28 ± 0.01
4.	Duku Pulp	0.53 ± 0.00

[Data shown as mean ± SD (n = 3)]

Sruthi Gopan and Sudha Bai

Table 12: Estimation of Saponins Present in the Fruits Peel and Fruits Pulp of *Lansium domesticum* Correa

SI no:	Sample	Quantity (mg/g)
1.	**Langast Peel**	9.20±0.56
2.	**Duku Peel**	8.26±0.46
3.	**Langsat Pulp**	12.60±0.28
4.	**Duku Pulp**	14.00±0.56

[Data shown as mean ± SD (n = 3)]
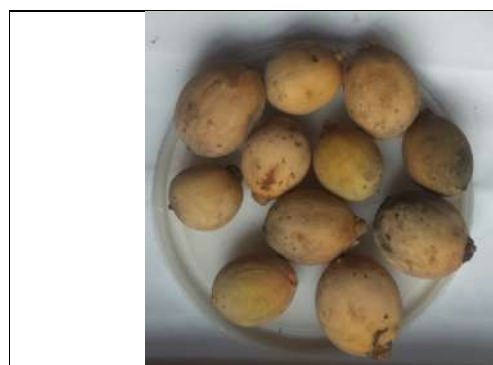
| Figure 1: Langsat Fruit (*Lansium domesticum var pubescens*) | Figure 2: Duku Fruit (*Lansium domesticum var domesticum*) |
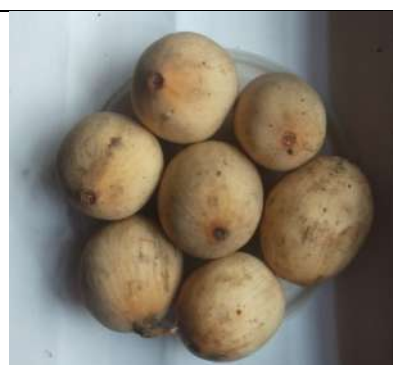
RESEARCH ARTICLE

Silver and Copper Nanoparticles Enhance *In-vitro* Plant Growth and Secondary Metabolites Production: Current Status and Future Perspectives

Chetna* and Simranjeet Kaur

Student, M.Sc. Hons. Biotechnology, School of bioengineering and Biosciences, Lovely Professional University, Phagwara, Punjab, India

*Address for Correspondence
Chetna
Student, M.Sc. Hons. Biotechnology,
School of bioengineering and Biosciences,
Lovely Professional University,
Phagwara, Punjab, India
E.Mail: chetna1536@gmail.com

ABSTRACT

Nanotechnology is one of the most promising fields in science and technology. Nanotechnology is expanding in all the sectors including agriculture, pharmaceuticals, food and medical industries. It plays important role in plant tissue culture and shows various applications in producing disease free plants, conservation of endangered plant species and gene manipulation. The effect of silver and copper Nanoparticles are evaluated on different plant species, whereas it is observed that how nanoparticles influence the growth morphology and secondary metabolites production. Different plant species shows different result, some shows increase in growth of root & shoot structures while other are having negative effect on growth. It has been observed that when high concentration of nanoparticles is used it results in enhancement of secondary metabolites production due to stress induced condition. Silver and copper nanoparticles along and in combination enhances the plant growth and accumulation of secondary metabolites like, flavonoid, proline, antioxidant enzymes glutathione in some plant's species. In this review, it has reported that when exposed to different plant species, silver nanoparticles and copper nanoparticles show positive as well negative effects depending on their size, types, concentration and structure.

Keywords: Silver nanoparticles, Copper nanoparticles, Secondary metabolites, Plant growth regulators.

Chetna and Simranjeet Kaur

INTRODUCTION

Nanoparticles have emerged as promising tools in various fields, including agriculture, due to their unique physicochemical properties and potential applications. Nano is Greek word which means dwarf.[1] Nano-sized particle are frame up in a way so their properties could utilize in various field. Nanomaterial is mainly of two types organic and inorganic. In 2000s Nano era has begun where the applications of nanomaterial have become widely utilized and acceptable for welfare of humans, both positive as well as negative effects of nanoparticles were seen in plant growth,CuNPs and AgNPs are among many nanoparticles that are widely used in many industries. Agriculture-relevant nano fertilizers based on nanotechnology boost agricultural productivity and efficiency while lowering environmental stress.Nanotechnology is used in agricultural field to improve the crop production and also to ensure food security. Use of nanotechnology effectively in agriculture for long-term sustainability.Nanoparticles can be present in any shape spherical, flat, cylindrical, conical, irregular they have large surface to volume area ratio so that property make them highly reactive.[2] The use of nanomaterials for agricultural purposes may offer a powerful solution to current challenges and dangers to food security. To maintain food hygiene and safety, this has transformed the fields of storing food and packaging. The focus of the review is to understand the effect of CuNPs and AgNPson different plant species as growth promoter or growth inhibitor and to know that by varying concentrations of nanoparticles how it could influence production of secondary metabolites polyphenol, flavonoids, and phenols in plants. CuONPs have been applied to agriculture as insecticides, herbicides, fertilizers, soil-remediation additives, and growth regulators. CuNPs have demonstrated diverse effects on plant growth and development. CuNPs have been reported to promote seed germination, root elongation, and shoot biomass in several plant species.[3] Furthermore, CuNPs can influence various physiological processes, including photosynthesis, mineral nutrient uptake, enzyme activities, and oxidative stress responses in plants.[4] Studies have also indicated that CuNPs can modulate the production of secondary metabolites, such as alkaloids, flavonoids, andterpenoids, thereby impacting the nutritional and medicinal value of plants.[5]Since Cu functions as a micronutrient in plants, it was thought that Cu in nano form may have a similar positive effect. CuONPs have become increasingly used over the past few decades, finally becoming a growth stimulant. CuONPs affected growth, physiological effectiveness, biochemical assays, and the antioxidant system.[6]

AgNPs have been widely investigated for their antimicrobial properties, which make them attractive for plant protection against pathogens. Additionally, AgNPs have been reported to enhance seed germination, root elongation, shoot biomass, and overall plant growth.[7]These nanoparticles can also influence physiological and biochemical processes in plants, such as photosynthesis, nutrient uptake, enzyme activities, and antioxidant defence mechanisms.[8]Moreover, AgNPs have been shown to modulate the production of secondary metabolites, including phenolics, flavonoids, and essential oils, which are known to play crucial roles in plant defence mechanisms and human health benefits.[9]AgNPs are currently being produced by plants, which is a sensible method and can prevent and control plant diseases.AgNPs function as growth stimulators and are advantageous for seed germination and growth. Usage of AgNPs, has been beneficial for callus induction, organogenesis, the development of somatic embryos, Soma clonal variation, genetic change, and the creation of secondary metabolites as well as successfully controlling microbial contamination from explants. AgNPs have unique properties that make them useful in a variety of applications, including plant growth and development, their effects on plants can vary depending on the species and the application method used. AgNPs is helpful in developing and growing plants. Additionally, advances in nanoscience have helped us better understand the best way for nanoparticles to work in plants, resulting in improved the development and growth of plants. AgNPs are now being used more frequently to increase crop productivity. Studies have shown that AgNPs can enhance seed germination and plant growth, as well as increase metabolite production in some plant species. However, conflicting outcomes have been observed in different plant species, highlighting the need for more research to better understand the complex mechanisms involved in nanoparticle action and their phytotoxic.The amount produced of total phenol compounds, total flavonoids, and saponins is reduced when some herbal plant is exposed to copper heavy metals, which has been demonstrated to diminish its effectiveness. The review also discusses the mechanisms of action of AgNPs on plants and the limitations faced in applying these nanoparticles on a commercial scale. While the potential of AgNPs in plant tissue

culture is promising, more research is needed to determine the optimal conditions for their use and to ensure that their application does not have adverse effects on the environment and human health.[10]

Role of Nanotechnology in plant tissue culture
Nanotechnology is playing very precious role in plant biotechnology field. Plant biotechnology is important for improving the growth and development of plants. Through the help of nanotechnology, we can understand the important function and mechanism in biological system. Nanotechnology has shown various applications in the field of Plant biotechnology. It has major impact on *in-vitro* plant growth production. Under *in-vitro* conditions, plant is grown with sterile controlled conditions. There are different types of nanoparticles which shows great effect on *in-vitro* plant. Several types of nanoparticles are utilized for proper growth of plant. Nanoparticles shows various advantages in *in-vitro* plant growth and developments. Under different stress conditions, plants are not able to survive, so this nanotechnology is helpful is enhancing the endurance and tolerance level of plant. [11]In plant biotechnology, plant tissue culture is a technique which is helpful in growing disease-free plant. In plant tissue culture, culture medium is provided with various types of nutrients such as vitamins and minerals. Nutrients is essential for the growth & development of the plants. Various types of bio-products which are in great demand can be produced through the help of plant tissue culture. In plant tissue culture, microbial contamination is the main problem which affects the growth and development of the plant[12] but with the combining of the nanotechnology with nanoparticles, it resulted in removal of microbial contamination. It also shows positive effects in production of various bioactive compounds, secondary metabolites, induction of callus, somatic embryogenesis, genetic transformation & organogenesis. It has great applications in producing disease-free plants, conservation of endangered plant species, genetic manipulation (genetical changes) and many others shown in figure A1.The main purpose of genetically change the plant is to get an enhanced variety of plant which gives better yield, highly bioactive compounds and helps in production of secondary metabolites.[13]Contamination causes problem in *in-vitro* plants, explants & consist of various kinds of contamination (contains various harmful pathogens) so, this problem should be solved.[14] In vanilla explant (*Vanilla Planifolia* Jacks ex-Andrews), AgNPs are added in Morishige and Skoog medium with varies concentration and it results in lowering the bacterial contamination.[15]There are several factors which is important for the plant tissue culture. Aseptic technique is one of the most important and basic need for plant tissue culture. There are different stages of culturing the plant but there are many obstacles like bacteria (e.g., *Pseudomonas syringae, Bacillus licheniformis*) and fungi which causes the bacterial and fungal contamination. This is due to improper washing of explants, inadequate tools, and controlled conditions.[16]To reduce the microbial contamination, explant is washed with mercuric chloride, ethanol, sodium hypochlorite. Secondly, different kinds of antibiotics and fungicides added into culture medium. Although these exhibits various phytotoxic, hinders nucleic acid synthesis, protein synthesis and disturbs cell membrane synthesis but the main purpose of adding these is to protect the plant from infection. These nanomaterials can act as decontaminant agent in plant tissue culture.[14]In plant tissue culture, nanomaterials and nanoparticles is playing a major role and developing very rapidly. The properties of nanoparticles are depending on types of nanoparticles utilized in the medium and it has shape, size and distribution.[17] Various researchers have been conducted on the utilization of nanoparticles in seed germination, plant improvement, and genetic manipulation [18]. Nanoparticles such as silica (SiO_2)-AgNPs are utilized for conserving and maintaining the health of plants tissue culture. Nanoparticles can act as surface sterilization. It can sterilize the explants and help in eliminating the contamination such as bacterial and fungal. It is useful in genetic engineering techniques and can enhance the endurance of explant.[19] Metal and non-metal oxides influence the plant growth and development. It acts as decontaminate against contaminated surface [20]. Different nanoparticles play various roles in plant tissue culture. Nanoparticles such as ZnONPs, TiO_2NPs, AgNPs helps in disinfection. To induce the Soma clonal variation AuNPs and AgNPs is utilized. Al_2O_3NPs, TiO_2NPs and AgNPs can enhance the secondary metabolites in various plants. In genetic transformation dendrimers is beneficial for the process [21].

Effects of AgNPs in plant growth and development
From the past few years, nanomaterials play an important role in various research fields like biomedical, chemical sciences and agriculture etc. In the field of agriculture and pharmaceuticals, the utilization of nanoparticles has been increased due to different method of synthesizing the nanoparticles. Specific and unique shapes and size of

Chetna and Simranjeet Kaur

synthesizing the nanoparticles has enhanced the application of nanoparticles. The Chemical and physical properties of AgNPs have been studied in order to boost the application in different fields [22]. Plant are the important elements of biosphere and it is very necessary source for the living things. So, it is very important to known about the effects of AgNPs on the growth and development of plants [23]. Scientists have organised various experiment in which they studied that nanoparticle extend the post- harvest shelf life of cut flowers and also it acts as regulator for various plant species. The very first step to grow a plant is seed germination and it is very important step because it is the initial seedling that is at risk of contamination such as bacterial and fungal. Other environment factors also effect the growth of the plant such as soil, salinity, water etc. For the initial stage, water is the essential components which is required for the growth and after certain period of time, embryonic axis develops from the seed coat.Radicle and plumule formation also occur, which further gives rise to roots and shoots.[24]For the growth of the plant, tissue culture utilized various media which is nutritive in nature. Aseptic conditions also utilized for the growth of the plant to avoid the contamination. To obtain the disease-free plants and transformation of plant genome, *in-vitro*techniques are applied.[25] AgNPs enhances the growth & development of plant.

Nanomaterials can be utilized for the purpose of delivering gene at particular site, which is helpful in the functioning of the plant. Different type of physical and structural changes is observed when plants are exposed to nanomaterials. Plants express various functional changes which is depend on various factors like varying in the size of the nanoparticles, interaction of nanoparticles, surface coating and also changes varies from one plant species to another plant species. The nanoparticles of Ag are ranging in between 1 nm-100 nm. AgNPs can be synthesized by various method such as Chemical and Physical method. Both this method involves high energy and hazardous chemicals. Each method has its own advantages as well as disadvantages. AgNPs can be synthesized by biological method and which is advantageous because biological synthesized AgNPs are eco-friendly, non-toxic and less expensive.[26] Nowadays, AgNPs used widely because it exhibits various unique properties. Through the mechanism of action of AgNPs, the outcomes in growth of the plant can be enhanced.[27] AgNPs are one of the most important nanoparticles to study the effects on plants. AgNPs have the great potential that can acts as antimicrobial agents. Nowadays, AgNPs are taken into consideration due to its specific physicochemical properties and exhibiting the antimicrobial properties. This resulted in broad application in extensive variety of products with promising results.[28] Nano silver enhanced the production & growth of *in-vitro* plant. The effects of AgNPs on different types of plants are discussed in table A1. A study was conducted in order to check the effects of silver nitrate on *in-vitro* plant (date palm) growth. Different concentrations of silver nitrate were added into the culture medium (date palm). The outcome of adding silver nitrate into culture medium enhanced the regeneration stage. It increased the length of the shoots and also enhanced the number of leaves and shoots. The culture medium comprised of MS medium and in that medium plant growth hormone is added. Different types of plant growth hormones are added such as 0.1mg/l NAA, 2.0 mg/l BA& 0.5 mg/l GA3. The main purpose of adding plant growth hormones is to increase the growth of the plant.[39]

AgNPs synthesized by green method, in which the extract is taken from plant *Swertia chirata* (Gentianaceae). To solve the issue related with the conservation of the medicinal plant via, plant tissue culture, leaf extract of *S.chirata* plant was taken into consideration. *S.chirata* plant is an endangered as well as economically crucial plant. Due to over exploration of this plant, this plant become completely extinct from natural habitat. To preserve the plant species, *in-vitro* culture method is utilized. The nanoparticles are prepared which is 20 nm in size and it comprises of various types of phytochemicals. Nanoparticles increased the growth of shoot culture including shoot induction and proliferation. The variety of AgNPs such as AgNO3 and $Ag_2S_2O_3$ enhanced the regeneration of *in-vitro* plant as compare to sample of controls. AgNPs enclosed with phytochemicals has the capacity to change the chemical reactions which is occurring in plant regeneration. These will acknowledge the future utilization of bio-fabricated AgNPs in the field of agriculture and plant sciences.[40] It has a particular size,shape and it exhibits some properties like environment- friendly. Currently, nanoparticles it is widely utilized in horticulture because it provides various advantages and exert different properties. So today, in the field of horticulture, more attention is given on nutrient properties and antimicrobial properties. To improve the growth of the plant, it involves several types of pathways. Pathways involves different types of effects on different enzyme, growth hormones (Ethylene) and metabolism like

63424

Chetna and Simranjeet Kaur

nitrogen metabolism. If the concentration on plant is accurate than it does not show any toxicity on the growth of the plants.[41] AgNPs can also play a role in handling the contaminants which is derived from explants. AgNPs can enhance the growth of callus induction (explant), secondary metabolites production.[42]The explant of *Tecomella undulata (Roxb.)* is cultured on medium and along with the medium PGRs (6 BAP & IAA) is added. AgNPs (5–80 mg L^{-1}) is also added to evaluate the effect.The results indicated that the AgNPs (10 mg L^{-1}) along with the PGRs, BAP (2.5 mg L^{-1}) and IAA (0.1 mg L^{-1}) enhanced the number of shoots of explants and also increased the endurance of the plant due to barrier in ethylene.[43]Ethylene gas is utilized for culturing the *Rosa hybrida L.* under *in-vitro* condition. Leaf abscission of this plant is controlled by adding the nanoparticles such as AgNPs & CuNPs. It was observed that the AgNPs enhanced the height of shoots & improves the shoot multiplication coefficient. Many of the plantlets are not able to survive at the nursery stage. AgNPshelps in increasing the viability rate of young plant, which is at nursery stage. For the propagation of shoot, AgNPs are considered as important factor for growth and development.[44]A study showed that for culturing the *Psidium friedrichsthalianum,* AgNPs play important role in sterilizing the culture media. It acts as sterilizing agent because it has antimicrobial properties and it can fight against multiple pathogens. It increases the leaf area and also helps in growing the mass shoot. It brushes up the genetic transformation, enhance the callus induction (derived from explants) and metabolic production. AgNPs such as Argovit™ is added in *in- vitro* culture of *Vanilla planifolia and* it resulted that it did not show any toxic and genotoxic (harmful to genetic material) effects on plant. Also, it helps in improving the plant growth, yield of the plant, enhances the total phenolic content & rising the shoots growth. Argovit™ AgNPs minimise the contamination such as bacterial contamination in culture medium. AgNPs have been utilized to boost up the physical as well as biochemical properties of the plant which includes photosynthetic growth, improves flavonoid and phenolic content, reduces the toxic metals. To enhance the *in-vitro* culture of plants like medicinal plants, AgNPs is considered as best option for the growth of plant.[45]The explant of the plant can be sterilized with AgNPs as it can remove the microbial contamination and reduces the bacterial contamination in the culture media.

It also plays a role in improving the structure of explant.[46] AgNPs exhibits antifungal as well as antiviral properties. Nanoparticles such as AgNPs help in increasing the growth of plant through improving the germination of seeds. Concentration of AgNPs is considered as important for the growth of plant. Optimum concentration is required by the plant, if the concentration of AgNPs is not specific then it can also show the negative effects. To minimise the pests in the crops, an experiment has been conducted with the use of AgNPs. The purpose of this experiment is to protect the plant from harmful pest and improve the nutritional value. This is helpful in decreasing the use of pesticides in farming. Chemical pesticides helpful in killing the pests. To protect the plant from harmful and pathogenic microorganism, the liquid silver solution is applied on plants. It helps in growth and development of the plants, increase the physiological activity and tolerate the stress in plants. In case of rice and grasserie, AgNPs nanoparticles is applied and it resulted that after 2 months of treatment, the rice does not show any effects, So, it is suggested that AgNPs is considered as best in protecting the seed. AgNPs considered suitable for plant growth stimulator [47].

Effects of AgNPs on secondary metabolite accumulation and production
The Medicinal plants are gaining more interest because they are rich in producing various vital secondary metabolites. There are several factors that influence the growth and development of the plants such as environmental factor (light, temperature, humidity etc). These factors directly influence the pathways in plants such as anabolic pathways. Thus, it has major impact on secondary metabolites. To increase the production from the plant and to improve the quality of the different kinds of medicinal plants, plant industries are using several kinds of unnatural lights.[48] In a study *Caralluma tuberculate* (traditional medicinal plant)cultured under *in-vitro*condition. In the culture media, along with the plant growth regulators different concentration of AgNPs were added. The purpose of adding the AgNPs in *in-vitro* cultures is to enhanced the production of antioxidant and secondary metabolites.[49]*Caralluma tuberculata* (Chung) is very useful plant which is rich in antioxidant potential and bioactive metabolites. This plant has some medicinal properties and it used in treating various diseases like asthma, diabetes & paralysis. The extract of this plant (*in-vitro* assays) is beneficial in carcinoma cell lines.[50] In the callus media, if concentration of AgNPs is boost up, then it enhanced the antioxidant enzyme activity. In a culture medium of *Catharanthus roseus (Apocynaceae)*

AgNPs is added in different concentration. At concentration of 75mg/L it shows higher concentration of alkaloid that is vinsblastine. To analyse the secondary metabolite, dichloromethane is utilized. The size of nanoparticles utilized for this purpose is 40nm.[51]In an experiment, the seeds of *Ricinus communis* (castor oil plant) was treated with AgNPsand it resulted that the seed which are treated with AgNPs enhances the production of antioxidant enzymes as compare to the seeds which are not treated with AgNPs.[52] In case of *Proteus vulgaris*, when AgNPs added in growth media or along with plant growth regulators like NAA (α-naphthalene acetic acid) auxin hormones increases the growth of callus, antioxidant potential and various secondary metabolites.[53]In the field of science especially in plant biotechnology, nanoparticles are usedwidely in this field and it has capacity to initiate the formulation of phytochemicals.[54] In a recent study, it is reported that adding the elicitors in the cell suspension culture can rise the formulation of various phytochemicals.[55]Elicitors have the potential to trigger the biological defence mechanism in plants. Along with the defence mechanism elicitors play important role in initiating the different kinds of pathways such as biosynthetic pathways. Pathways are activated according to the compound used in the treated plants.[56] Elicitors can be of two types biotic as well as abiotic, it has potential to boost up the production of various types of phytochemicals present in cell suspension culture of different plants.[57] The effect of AgNPs on different species is shown in table A2.(Ghanati and Bakhtiaria, 2014) reported that on addition of AgNPs into the media of *Calendula officinalis L (Asteraceae)* results in decrease in anthocyanin, carotenoid & flavonoid.[58]

The size of AgNPs is 40nm.In a case study, it is reported that the effects of nanoparticles on plants is dependent on the types of nanoparticles, size, concentration, structure, and the way how nanoparticles are exposed to plants. A studyshowed that AgNPs can enhanced the secondary metabolites production. This method is helpful in determining the bioactive compounds at mass production via cell suspension culture (liquid medium) and it is beneficial for bioprocessing engineering. AgNPs is prepared by under the presence of *hay bacillus*extracts. It is synthesized by reducing Ag^+ into Ag^0. These AgNPs added into the cell suspension culture. The main aim of the study is to check the effects of AgNPs on phenolic compounds (individual), total phenolic content, total flavonoid content, accumulation of biomass production which can be dry or fresh. Along with this, it is used to check the pharmaceutical activities such as antibacterial, antioxidant, antifungal, and anticancer in bitter gourd *(Momordica charantia L.)*. Addition of AgNPsin cell suspension culture increased the phenolic components of flavanols, such hydroxybenzoic and hydroxycinnamic acids. These acids were in higher amount in cell suspension culture as compare to the culture which does not contain theAgNPs.

AgNPs-elicited showed that there is increase in H_2O_2 contents and Malondialdehyde in cell suspension culture. AgNPs-elicited culture shows that there is enhanced in phenolic compounds as well as in pharmacological activities such as antimicrobial when compare to non-elicited AgNPs.[59] The most important approach for the increase in the outcome of secondary metabolites is elicitation. Elicitation has the potential to regulate the biotic as well as abiotic elicitors. The abiotic component of elicitation includes various kinds of heavy metals like silver, gold etc. and all these metals can boost up the production of secondary metabolites. In case of *S. miltiorrhiza*, silver metal (Ag) is considered as best for the enhancement for secondary metabolites. In root culture of *S. miltiorrhiza*, Ag^+ is added and it shows effect on diterpenoid tanshinone accumulation. The effects are depended on the concentrations of Ag^+ used in the culture. In culture medium, $Ag_2S_2O_3$ is added and it resulted in enhancement in the yields of all three diterpenoid tanshinone i.e., tanshinone I, tanshinone IIA, cryptotanshinone. Sometimes, Ag^+ have shown adverse effect in plant tissue culture like disturbing cell membrane. It is reported that heavy metals ion at low concentration can improve the flexibility of cell membrane. It also led to suppression of the growth but does not cause any cell death.[65] Heavy metals ions such as Ag^+, Cd^{2+}, Cu^{2+} can improve the alkaloids production in *Brugmansia candida*and lead to create membrane disruption in case of *Datura stramonium*.[66]

Effect of CuNPs in Plant Growth and development
Copper is one of essential trace elements which is having great properties even in small concentration. CuNPs has shown the fungicidal properties in plant-based diseases. When the nanoparticles are present in high concentration it effects plant cell wall and plasma membrane nanoparticles can enter through root directly it get translocated in plant through various physiological pathway it firstly enter to plant by crossing cell wall , the limit for crossing cell wall is

Chetna and Simranjeet Kaur

5-20 nm which allow nanoparticles to easily penetrate inside due to their smaller size but large nanoparticles faces difficulty some nanoparticles even creates pore in cell wall which facilitates their entry. Due to high reactivity, small size, distinct morphology nanoparticles have been widely used in plant growth and development. One of the eight crucial micronutrients for plants is copper. Copper is necessary for the formation of chlorophyll, seeds, and numerous enzymatic processes in plants. Copper plays an important role in plant cell functioning.[67] Nanotechnology overall utilized for increasing the crop yield and nutrient absorption capacity of plant through latest applications.[68]Lower concentration of copper sulphate nanoparticles has seen increasing the shoot and root length in case of *Verbena bipinnatifida Nutt.* CuNPs has wide range of properties including antimicrobial, antibacterial and catalytic properties. They have high surface to volume ratio and has large interaction with other particles this property makes it a good drug loading source. Simple, environment friendly, low cost, copper-based nanoparticles can be designed.[69] CuNPs have been investigated for their potential effects on plant growth and development. Several studies have examined the impact of CuNPs on various plant species, and the findings indicate both positive and negative effects depending on the concentration as shown in table A3. One study conducted by Li et al. (2018) investigated the effects of CuNPs on the growth of wheat *(Triticum aestivum)* plants.[85].

The researchers exposed the plants to different concentrations of CuNPs and assessed their impact on plant height, biomass, chlorophyll content, and root development. They found that low concentrations of CuNPs had a stimulatory effect on plant growth, increasing plant height, biomass, and chlorophyll content. However, higher concentrations of CuNPs inhibited plant growth and development, leading to reduced plant height, biomass, and chlorophyll content. The study concluded that CuNPs can have both positive and negative effects on plant growth depending on their concentration. Another study by Sharma et al. (2019) investigated the effects of CuNPs on the growth and development of soybean *(Glycine max)* plants. The researchers exposed the plants to different concentrations of CuNPs and evaluated their impact on plant height, leaf area, root length, and seed yield. The results showed that low concentrations of CuNPs promoted plant growth, increasing plant height, leaf area, and root length. However, higher concentrations of CuNPs negatively affected plant growth, leading to reduced plant height, leaf area, and root length. The study suggested that the concentration of CuNPs plays a crucial role in determining their effects on plant growth and development.[86]. These studies demonstrate that CuNPs can have both positive and negative effects on plant growth and development, depending on their concentration. Low concentrations of CuNPs may have stimulatory effects, while high concentrations can inhibit plant growth and development.

It is important to carefully regulate the application and concentration of CuNPs to minimize any potential negative impacts on plants.Analysis of three species *Cajanus cajon L.*, *Elodeadensa planch* and *Allium cepa* plants is exposedto CuNPs at different concentration. The effect of CuNPs (20 nm) is seen on (*Cajanus cajon L.*) species in the colloidal suspension it enhances the growth and development of pigeon pea plant as shown in figure A2. It also improves the photosynthesis activity and act as a growth nutrient. The biomass of pigeon pea plant having less dry weight and less wet weight when it is not exposed to CuNPs but after exposure of CuNPs it shows high biomass and its root and shoot has been harvested for 4 weeks.[81] Anexperiment was conducted on wheat 'Gazul' seed, weight of twenty seeds has been measured and germinated on Petri dish, suspended in CuNPs in different concentrations of 1,5,10,25,50,100 mg/L after 5 days results were observed and metabolic efficiency of seeds were observed. Analysis of variance has performed for detectingthe presence of CuNPs, where wheat seeds shown increasing tendency, dry weight of shoot does not show much influence while the dry weight of root is lower in presence of CuNPs.[87]

Effect of CuNPs on Secondary Metabolite Accumulation and Production
The effect of CuNPs on secondary metabolite production can vary depending on the specific secondary metabolite and the biological system in which it is produced. Secondary metabolites are organic compounds that are not directly involved in the growth, development, or reproduction of an organism but often play important roles in defence mechanisms and interactions with the environment. CuNPs can have inhibitory effects on secondary metabolite production. They may interfere with the enzymes involved in the biosynthetic pathways of secondary metabolites, leading to reduced production. Additionally, CuNPs can disrupt cellular processes and overall metabolic activity, which can indirectly affect secondary metabolite production. CuNPs can modify the chemical composition of

secondary metabolites. They may induce structural changes or chemical modifications in the metabolites, resulting in altered properties or activities. This alteration can have both positive and negative consequences, depending on the specific metabolite and its biological function. The effect of CuNPs on secondary metabolite production can vary across different species, making it important to consider the specific organism of interest.[88] One study conducted by Parveen et al. (2018) investigated the influence of CuNPs on the production of secondary metabolites in *Catharanthus roseus (Madagascar periwinkle)*. The researchers treated *C. roseus* plants with different concentrations of CuNPs and analysed the levels of secondary metabolites, including alkaloids, phenolics, and flavonoids. The study found that the application of CuNPs led to a significant increase in the accumulation of secondary metabolites in *C. roseus* plants. The enhanced production of secondary metabolites was attributed to the elicitation effect of CuNPs, which stimulated the plants defence mechanisms and secondary metabolite biosynthesis pathways.[89] Another study by Abbas et al. (2020) investigated the impact of CuNPs on the production of secondary metabolites in *Ocimum basilicum* (basil) plants. The researchers treated basil plants with CuNPs and evaluated the levels of essential oil, which is a valuable secondary metabolite in basil.[90] The study demonstrated that the application of CuNPs significantly increased the content of essential oil in basil plants.

The enhanced production of essential oil was associated with the upregulation of key enzymes involved in secondary metabolite biosynthesis pathways, which were triggered by the presence of CuNPs.Some studies have reported that exposure to low concentrations of CuNPs can enhance the accumulation of secondary metabolites in plants. These metabolites may include phenolics, flavonoids, alkaloids, terpenoids, and essential oils. The stimulation of secondary metabolite production is often attributed to the nanoparticles ability to induce oxidative stress and activate defence mechanisms in plants, leading to increased synthesis of protective compounds. CuNPs possess inherent redox properties, and they can act as antioxidants or pro-oxidants depending on their concentration. At low concentrations, CuNPs can scavenge reactive oxygen species (ROS) and mitigate oxidative stress in plants, thereby promoting secondary metabolite synthesis. On the other hand, at higher concentrations, CuNPs may generate excess ROS, leading to oxidative damage and potentially inhibiting secondary metabolite accumulation. Different plant species can exhibit varying responses to CuNPs exposure.

Some plants may show increased secondary metabolite production, while others may experience inhibition or no significant changes. Additionally, variations in the nanoparticle size, shape, surface charge, and coating can influence the interaction between CuNPs and plant cells, leading to different outcomes in secondary metabolite accumulation. The effects of CuNPs on secondary metabolites and production is shown in table A4. The concentration or dose of CuNPs is a crucial factor determining their impact on secondary metabolites. Low concentrations are more likely to induce positive responses, while high concentrations can lead to toxicity and inhibit secondary metabolite synthesis. It is important to note that the optimal concentration range for stimulating secondary metabolites may vary for different plant species. Environmental conditions such as light intensity, temperature, humidity, and nutrient availability can interact with CuNPs and modulate their effects on secondary metabolite accumulation.[96].

Natural polymer chitosan polyvinyl alcohol hydrogels in addition with use of CuNPs has been studied in tomato (*Solanum lycopersicon L*.). It has shown the positive results towards biotic and abiotic stress by increasing the phenol content, lycopene, vitamin C content and also shows enhancement in enzymatic activity. Plants were treated with chitosan PVA hydrogel in concentration of 1gm, 100mM NaCl, 3.75 EDTA and leaves were covered in aluminium bag and frozen at -80°C at 23, 28, 42 delivered at terminal. Copper oxide nanoparticles effect is analysed on activity of antioxidant enzyme present in rice supernatant in different concentration 2,4,8,16 mg/l at 30 and 45 mg/l) sprayed on plant along with the distilled water, the antioxidant level of plant has shown tremendous increase by use of copper oxide nanoparticles. Furthermore, the effect has been seen in activity of soil and enzyme, copper oxide nanoparticles reduce the peroxidase and polyphenol oxidase activity. To know whether the antioxidant activity is relevant of the all given values CuNPs toxicity has been widely documented in a variety of plant species, but there have also been several reports of their beneficial effects. CuONPs impact on the environment must therefore be carefully assessed, and standards for sustainable applications must be established.[97]. In case of *Sesbania virgata*, the effect of copper oxide nanoparticles is seen on its seed, it causes inhibition in growth of root and surface temperature is increased in

seeds so it shows that Copper oxide nanoparticles are having negative effect in growth of *S. virgata* by effecting initial development status. Effect of nanoparticle of copper has detected on tomato plant when it is affected by Fusarium wilt which is caused by fungus named *Fusarium oxysporum*. It effects tomato plants at concentration of 0.5 mg/ml but if the concentration is increased it shows strong inhibitory effect. It promotes tomato plant growth because when the fungicide is used (copper hydroxide) it causes the unwanted uptake of copper ions and thus shows negative effects on plant. This study shows one of application of CuNPs as fungicide.[98] Other effect of copper-based nanoparticles is seen on oomycete *Phytophthora cinnamomic* at 50 mg/l concentration where CuNPs are integrated with copper oxychloride (non-nano) cause growth inhibition while in the case of wheat it shows that combinatory effect of CuNPs with copper oxychloride promotes growth as rate of seed germination increased.[99] Other effect is seen on (*Coriandrum sativum*) where the plant which is treated with CuNPs shows decrease in root length and biomass as compared to plant which is untreated it also result in less level of chlorophyll a and chlorophyll b, increased electrolyte leakage and amount of H_2O_2. Genotypic effect is also seen by using Random amplified DNA technology and it shows that genetic composition has also manipulated by CuNPs.[100]

CONCLUSION AND FUTURE PERSPECTIVE

The importance of nanoparticles has been increased in various sectors of plant biotechnology. Several studies have shown the antimicrobial, antibacterial and catalytic properties of AgNPs and CuNPs. CuNPs have high surface to volume ratio and has large interaction with other particles which makes it a good drug loading source. The effects of AgNPs & CuNPs have been dependent on the size and shape. They show positive as well as negative effects on different plant species. AgNPs are in great demand because its production is very economical. The impact of CuONPs on environment must be carefully assessed, and standards for sustainable applications must be established. In order to create an integrative assessment suitable for regulation, future studies in nanotoxicology, which must systematically incorporate low concentrations and account for soil complexity in biology and physio-chemical variation in their experimental designs. Our findings also point to the significant potential for non-invasive optical techniques to be used as analytical tools for determining the physiological effects of nanoparticles on plants in their early stages of growth .According to different studies it is reported that, using modest doses of CuONPs increased the manufacture of phytochemical components in wheat shoots while also enhancing germination, vigor, plumule, and radicle length.

Due to the build-ups of Cu and toxicity in plant tissue, high concentrations of CuONPs have inhibitory effects. Nanosilver is also utilized at low concentration because it is reported that high amount of nano-silver can produces harmful chemicals which can affect the growth & development of plant. A feasible way to achieve favourable outcomes in germination and development of seedlings as well as increased manufacturing of secondary metabolites is the use of CuONPs in green synthesis. AgNPs & CuNPs influence the production of secondary metabolites such as flavonoid, proline, antioxidant enzymes glutathione which in form of secondary metabolites when they get accumulate by heavy metal use, they were not able to protect the plant from different biotic and abiotic stress conditions. Green synthesis of AgNPs & CuNPs utilizing plant-based product is comparatively nontoxic, cost effective and environmentally friendly. It is previously known that nanoparticles are helpful in activating the various bioactive compounds in roots, shoots which is grown *in-vitro*. It also enhances the secondary metabolites production in plant species. Flavonoid are most important bioactive compound which demonstrate the strong oxidative property to plant. It is important to know about the interaction of nanoparticles with plant cell, to get more theoretical knowledge in order to develop new practical applications.

ABBREVIATION

AgNPs- Silver nanoparticles, CuNPs- Copper nanoparticles, PGRs- Plant growth regulators, SiO_2 – Silicon dioxide, $Ag_2S_2O_3$- Silver thiosulfate, IAA- Indole acetic acid, ZnONPs- Zinc oxide nanoparticles, TiO_2NP- Titanium dioxide,

PVA- Polyvinyl alcohol,EDTA- Ethylenediaminetetraacetic acid, nm- nanometer, ppm- parts per million, NEF- nitrite embedded filtrate.

REFERENCES

1. Pantarotto, D., Briand, J. P., Prato, M., & Bianco, A. (2004). Translocation of bioactive peptides across cell membranes by carbon nanotubes. *Chemical communications*, (1), 16-17.
2. Machado, S., Pacheco, J. G., Nouws, H. P. A., Albergaria, J. T., &Delerue-Matos, C. (2015). Characterization of green zero-valent iron nanoparticles produced with tree leaf extracts. *Science of the total environment*, *533*, 76-81.
3. Ahmad, P., et al. (2018). Copper oxide nanoparticles alleviate the negative effects of NaCl stress on photosynthesis and growth in wheat. Frontiers in Plant Science, 9, 1422.
4. Khan, M. N., et al. (2019). Copper oxide nanoparticles modulate the physiological and molecular responses of Arabidopsis thaliana. Environmental Science and Pollution Research, 26(7), 7154-7163.
5. Azimi, R., et al. (2020). Role of copper nanoparticles in influencing secondary metabolites production in medicinal plants. Industrial Crops and Products, 145, 112104.
6. Rodrigues CT, de Andrade FB, de Vasconcelos LRSM, Midena RZ, Pereira TC, Kuga MC, Duarte MAH, Bernardineli N. Antibacterial properties of silver nanoparticles as a root canal irrigant against Enterococcus faecalis biofilm and infected dentinal tubules. Int Endod J. 2018 Aug;51(8).
7. Rajput, V. D., et al. (2016). Effect of silver nanoparticles on growth and physiological activities of Brassica juncea. Acta Physiologiae Plantarum, 38(1), 1-11.
8. Tripathi, D. K., et al. (2017). Silicon nanoparticles more effectively alleviate arsenate toxicity than silicon in maize cultuvars. Ecotoxicology and Environmental Safety, 144, 131-140.
9. Das, R. K., et al. (2018). Impact of silver nanoparticles on plant growth and associated physiological changes. Journal of Nanoscience and Nanotechnology, 18(3), 1808-1823.
10. Ashrafi, S. J., Rastegar, M. F., Jafarpour, B., & Kumar, S. A. (2010). Possibility use of silver nano particle for controlling Fusarium wilting in plant pathology. In *Symposium of international conference on food and agricultural applications of nanotechnologies, São Pedro SP, Brazil. ISBN* (pp. 978-85).
11. Al-Qudah, Tamara; Mahmood, Sami H.; Abu-Zurayk, Rund; Shibli, Rida; Khalaf, Aya; Lambat, Trimurti L.; Chaudhary, Ratiram G.2022. Nanotechnology Applications in Plant Tissue Culture and Molecular Genetics: A Holistic Approach. Bentham Science Publishers. Current Nanoscience, Volume 18, Number 4, 2022, pp. 442-464(23).
12. Bhandari, S., Sinha, S., Nailwal, T. K., & Thangadurai, D. (2022). Nanotechnology: an approach for enhancement of plant system in terms of tissue culture. In *Biogenic Nanomaterials* (pp. 163-192). Apple Academic Press.
13. Singh, Rachana; Ahamad, Shadab. 2022. Integration of Nanotechnology in Plant Tissue Culture. Current Nanoscience, Volume 18, Number 5, 2022, pp. 604-610(7).
14. Álvarez, S. P., Tapia, M. A. M., Vega, M. E. G., Ardisana, E. F. H., Medina, J. A. C., Zamora, G. L. F., & Bustamante, D. V. (2019). Nanotechnology and plant tissue culture. *Plant Nanobionics: Volume 1, Advances in the Understanding of Nanomaterials Research and Applications*, 333-370.
15. Spinoso-Castillo, J. L., Chavez-Santoscoy, R. A., Bogdanchikova, N., Pérez-Sato, J. A., Morales-Ramos, V., & Bello-Bello, J. J. (2017). Antimicrobial and hormetic effects of silver nanoparticles on in vitro regeneration of vanilla (Vanilla planifolia Jacks. ex-Andrews) using a temporary immersion system. *Plant Cell, Tissue and Organ Culture (PCTOC)*, *129*, 195-207.
16. Omamor, I. B., Asemota, A. O., Eke, C. R., &Eziashi, E. I. (2007). Fungal contaminants of the oil palm tissue culture in Nigerian institute for oil palm research (NIFOR). *African Journal of Agricultural Research*, *2*(10), 534-537.14]
17. Jain, D., Daima, H. K., Kachhwaha, S., & Kothari, S. L. (2009). Synthesis of plant-mediated silver nanoparticles using papaya fruit extract and evaluation of their anti-microbial activities. *Digest journal of nanomaterials and biostructures*, *4*(3), 557-563.

18. Ong, G. H., Wong, L. S., Tan, A. L., & Yap, C. K. (2016). Effects of metal-contaminated soils on the accumulation of heavy metals in gotu kola (Centella asiatica) and the potential health risks: a study in Peninsular Malaysia. *Environmental monitoring and assessment*, *188*, 1-10.

19. Hwan KD, Gopal J, Sivanesan I (2017) Nanomaterials in plant tissue culture: the disclosed and undisclosed. RSC Adv 7:36492–36505

20. Prasad, G. K., Mahato, T. H., Singh, B., Ganesan, K., Srivastava, A. R., Kaushik, M. P., &Vijayraghavan, R. (2008). Decontamination of sulfur mustard and sarin on titania nanotubes. *AIChE journal*, *54*(11), 2957-2963.

21. Kim, D. H., Gopal, J., & Sivanesan, I. (2017). Nanomaterials in plant tissue culture: the disclosed and undisclosed. *RSC advances*, *7*(58), 36492-36505.

22. Dawadi, S., Katuwal, S., Gupta, A., Lamichhane, U., Thapa, R., Jaisi, S., ... & Parajuli, N. (2021). Current research on silver nanoparticles: Synthesis, characterization, and applications. *Journal of nanomaterials*, *2021*, 1-23.

23. Yan, A., & Chen, Z. (2019). Impacts of silver nanoparticles on plants: a focus on the phytotoxicity and underlying mechanism. *International Journal of Molecular Sciences*, *20*(5), 1003.

24. Srivastava M. L., 2022. Plant growth and development. Academic press. 757-772.

25. Espinosa-Leal, C. A., Puente-Garza, C. A., & García-Lara, S. (2018). In vitro plant tissue culture: means for production of biological active compounds. *Planta*, *248*, 1-18.

26. Chaudhuri, S. K., &Malodia, L. (2017). Biosynthesis of zinc oxide nanoparticles using leaf extract of Calotropis gigantea: characterization and its evaluation on tree seedling growth in nursery stage. *Applied Nanoscience*, *7*(8), 501-512.

27. Mahajan, S., Kadam, J., Dhawal, P., Barve, S., &Kakodkar, S. (2022). Application of silver nanoparticles in in-vitro plant growth and metabolite production: revisiting its scope and feasibility. *Plant Cell, Tissue and Organ Culture (PCTOC)*, *150*(1), 15-39.

28. Tortella, G. R., Rubilar, O., Durán, N., Diez, M. C., Martínez, M., Parada, J., & Seabra, A. B. (2020). Silver nanoparticles: Toxicity in model organisms as an overview of its hazard for human health and the environment. *Journal of hazardous materials*, *390*, 121974.

29. Sadak, M. S. (2019). Impact of silver nanoparticles on plant growth, some biochemical aspects, and yield of fenugreek plant (Trigonella foenum-graecum). *Bulletin of the National Research Centre*, *43*(1), 1-6.

30. Rai, P. K., Kumar, V., Lee, S., Raza, N., Kim, K. H., Ok, Y. S., & Tsang, D. C. 2018. Nanoparticle-plant interaction: Implications in energy, environment, and agriculture. *Environment international*, *119*, 1-19.

31. Kumar, P., Pahal, V., Gupta, A., Vadhan, R., Chandra, H., & Dubey, R. C. (2020). Effect of silver nanoparticles and Bacillus cereus LPR2 on the growth of Zea mays. *Scientific reports*, *10*(1), 1-10.

32. Vishwakarma, K., Upadhyay, N., Singh, J., Liu, S., Singh, V. P., Prasad, S. M. & Sharma, S. (2017). Differential phytotoxic impact of plant mediated silver nanoparticles (AgNPs) and silver nitrate (AgNO3) on Brassica sp. *Frontiers in Plant Science*, *8*, 1501.

33. Rastogi, A., Zivcak, M., Tripathi, D. K., Yadav, S., Kalaji, H. M., &Brestic, M. (2019). Phytotoxic effect of silver nanoparticles in Triticum aestivum: Improper regulation of photosystem I activity as the reason for oxidative damage in the chloroplast. *Photosynthetica*, *57*(1), 209-216.

34. Feregrino-Perez, A. A., Magaña-López, E., Guzmán, C., & Esquivel, K. (2018). A general overview of the benefits and possible negative effects of the nanotechnology in horticulture. *Scientia Horticulturae*, *238*, 126-137.

35. Tomaszewska-Sowa, M., Siwik-Ziomek, A., Figas, A., & Bocian, K. (2018). Assessment of metal nanoparticle-induced morphological and physiological changes in in vitro cultures of rapeseed (Brassica napus L.). *Electronic Journal of Polish Agricultural Universities*, *21*(4).

36. Dimkpa, C. O., McLean, J. E., Martineau, N., Britt, D. W., Haverkamp, R., & Anderson, A. J. (2013). Silver nanoparticles disrupt wheat (Triticum aestivum L.) growth in a sand matrix. *Environmental science & technology*, *47*(2), 1082-1090.

37. Liu, X. M., Zhang, F. D., Zhang, S. Q., He, X. S., Fang, R., Feng, Z., & Wang, Y. J. (2005). Effects of nano-ferric oxide on the growth and nutrients absorption of peanut. *Plant Nutr. Fert. Sci*, *11*, 14-18.

38. Khan, M., Khan, A. U., Moon, I. S., Felimban, R., Alserihi, R., Alsanie, W. F., & Alam, M. (2021). Synthesis of biogenic silver nanoparticles from the seed coat waste of pistachio (Pistacia vera) and their effect on the growth of eggplant. *Nanotechnology Reviews*, *10*(1), 1789-1800.

39. Elsayh, S. A., Arafa, R. N., Ali, G. A., Abdelaal, W. B., Sidky, R. A., & Ragab, T. I. (2022). Impact of silver nanoparticles on multiplication, rooting of shoots and biochemical analyses of date palm Hayani cv. by in vitro. *Biocatalysis and Agricultural Biotechnology*, *43*, 102400.

40. Saha, N., & Dutta Gupta, S. (2018). Promotion of shoot regeneration of Swertia chirata by biosynthesized silver nanoparticles and their involvement in ethylene interceptions and activation of antioxidant activity. *Plant Cell, Tissue and Organ Culture (PCTOC)*, *134*, 289-300.

41. Sarmast, M. K., & Salehi, H. (2016). Silver nanoparticles: an influential element in plant nanobiotechnology. *Molecular Biotechnology*, *58*, 441-449.

42. Mahendran, D., Geetha, N., & Venkatachalam, P. (2019). Role of silver nitrate and silver nanoparticles on tissue culture medium and enhanced the plant growth and development. *In vitro Plant Breeding towards Novel Agronomic Traits: Biotic and Abiotic Stress Tolerance*, 59-74.

43. Aghdaei, M., Sarmast, M. K., & Salehi, H. (2012). Effects of silver nanoparticles on Tecomellaundulata (Roxb.) Seem. micropropagation. *Effects of Silver Nanoparticles on Tecomellaundulata (Roxb.) Seem. Micropropagation*, 21-24.

44. Ha, N. T. M., Manh Do, C., Hoang, T. T., Ngo, N. D., Van Bui, L., & Nhut, D. T. (2020). The effect of cobalt and silver nanoparticles on overcoming leaf abscission and enhanced growth of rose (Rosa hybridaL.'Baby Love') plantlets cultured in vitro. *Plant Cell, Tissue and Organ Culture (PCTOC)*, *141*, 393-405.

45. Andújar, I., González, N., García-Ramos, J. C., Bogdanchikova, N., Pestryakov, A., Escalona, M., & Concepción, O. (2020). Argovit™ silver nanoparticles reduce contamination levels and improve morphological growth in the in vitro culture of Psidium friedrichsthalianum (O. Berg) Nied. *SN Applied Sciences*, *2*, 1-9.

46. Kim, D. H., Gopal, J., & Sivanesan, I. (2017). Nanomaterials in plant tissue culture: the disclosed and undisclosed. *RSC advances*, *7*(58), 36492-36505.

47. Kale, S. K., Parishwad, G. V., & Patil, A. S. H. A. S. (2021). Emerging agriculture applications of silver nanoparticles. *ES Food & Agroforestry*, *3*, 17-22.

48. Lu, N., Bernardo, E. L., Tippayadarapanich, C., Takagaki, M., Kagawa, N., &Yamori, W. (2017). Growth and accumulation of secondary metabolites in perilla as affected by photosynthetic photon flux density and electrical conductivity of the nutrient solution. *Frontiers in Plant Science*, *8*, 708.

49. Ali, A., Mohammad, S., Khan, M. A., Raja, N. I., Arif, M., Kamil, A., & Mashwani, Z. U. R. (2019). Silver nanoparticles elicited in vitro callus cultures for accumulation of biomass and secondary metabolites in Caralluma tuberculata. *Artificial cells, nanomedicine, and biotechnology*, *47*(1), 715-724.

50. Ansari, N. M., Houlihan, L., Hussain, B., & Pieroni, A. (2005). Antioxidant activity of five vegetables traditionally consumed by south-Asian migrants in Bradford, Yorkshire, UK. *Phytotherapy Research: An International Journal Devoted to Pharmacological and Toxicological Evaluation of Natural Product Derivatives*, *19*(10), 907-911.

51. Shahin, H. (2018). Enhanced production of secondary metabolites by methyl jasmonate and silver nanoparticles elicitation in tissue culture of Catharanthus roseus (Apocynaceae). *Al-Azhar Journal of Pharmaceutical Sciences*, *57*(1), 62-69.

52. Yasur, J., & Rani, P. U. (2013). Environmental effects of nanosilver: impact on castor seed germination, seedling growth, and plant physiology. *Environmental Science and Pollution Research*, *20*, 8636-8648.

53. Fazal, H., Abbasi, B. H., Ahmad, N., & Ali, M. (2016). Elicitation of medicinally important antioxidant secondary metabolites with silver and gold nanoparticles in callus cultures of Prunella vulgaris L. *Applied biochemistry and biotechnology*, *180*, 1076-1092.

54. Sharafi, E., KhayamNekoei, S. M., Fotokian, M. H., Davoodi, D., Mirzaei, H. H., &Hasanloo, T. (2013). Improvement of Hypericin and Hyperforin Production Using Zinc and Iron Nano-oxides as Elicitors in Cell Suspension Culture of St John's wort (Hypericum perforatum L.). *Journal of Medicinal plants and By-product*, *2*(2), 177-184.

55. Cai, Z., Knorr, D., &Smetanska, I. (2012). Enhanced anthocyanins and resveratrol production in Vitis vinifera cell suspension culture by indanoyl-isoleucine, N-linolenoyl-l-glutamine and insect saliva. *Enzyme and Microbial Technology*, *50*(1), 29-34.

56. Thakur, M., & Sohal, B. S. (2013). Role of elicitors in inducing resistance in plants against pathogen infection: a review. *International Scholarly Research Notices*, *2013*.

57. Zhao, D. X., Fu, C. X., Han, Y. S., & Lu, D. P. (2005). Effects of elicitation on jaceosidin and hispidulin production in cell suspension cultures of Saussurea medusa. *Process biochemistry*, *40*(2), 739-745.

58. Ghanati, F., &Bakhtiarian, S. (2014). Effect of methyl jasmonate and silver nanoparticles on production of secondary metabolites by Calendula officinalis L (Asteraceae). *Tropical Journal of Pharmaceutical Research*, *13*(11), 1783-1789.

59. Chung, I. M., Rekha, K., Rajakumar, G., & Thiruvengadam, M. (2018). Elicitation of silver nanoparticles enhanced the secondary metabolites and pharmacological activities in cell suspension cultures of bitter gourd. *3 Biotech*, *8*, 1-12.

60. Solanki, S., Lakshmi, G. B. V. S., Dhiman, T., Gupta, S., Solanki, P. R., Kapoor, R., & Varma, A. (2023). Co-Application of Silver Nanoparticles and Symbiotic Fungus Piriformospora indica Improves Secondary Metabolite Production in Black Rice. *Journal of Fungi*, *9*(2), 260.

61. Bhat, P., & Bhat, A. (2016). Silver nanoparticles for enhancement of accumulation of capsaicin in suspension culture of Capsicum sp. *Journal of Experimental Sciences*, *7*, 1-6.

62. Khan, I., Raza, M. A., Awan, S. A., Shah, G. A., Rizwan, M., Ali, B., ... & Huang, L. (2020). Amelioration of salt induced toxicity in pearl millet by seed priming with silver nanoparticles (AgNPs): The oxidative damage, antioxidant enzymes and ions uptake are major determinants of salt tolerant capacity. *Plant Physiology and Biochemistry*, *156*, 221-232.

63. Hayat, K., Ali, S., Ullah, S., Fu, Y., & Hussain, M. (2021). Green synthesized silver and copper nanoparticles induced changes in biomass parameters, secondary metabolites production, and antioxidant activity in callus cultures of Artemisia absinthium L. *Green Processing and Synthesis*, *10*(1), 61-72.

64. Begum, Shabana; Zahid, Ayesha; Khan, Tariq; Khan, Nadir Zaman; Ali, Waqar (2020). Comparative analysis of the effects of chemically and biologically synthesized silver nanoparticles on biomass accumulation and secondary metabolism in callus cultures of Fagonia indica. Physiology and Molecular Biology of Plants.

65. Zhang, C., Yan, Q., Cheuk, W. K., & Wu, J. (2004). Enhancement of tanshinone production in Salvia miltiorrhiza hairy root culture by Ag+ elicitation and nutrient feeding. *Planta medica*, *70*(02), 147-151.

66. Pitta–Alvarez, S. I., Spollansky, T. C., & Giulietti, A. M. (2000). The influence of different biotic and abiotic elicitors on the production and profile of tropane alkaloids in hairy root cultures of Brugmansia candida. *Enzyme and Microbial Technology*, *26*(2-4), 252-258.

67. V.patil. N.P2 and S.S Extracellular synthesis of copper nanoparticles using different plant extracts, international journal of applied science volume 5 issue 4 ,Issn no. 2319-4014

68. Siddiqui, Manzer & Al-whaibi, Mohamed & Mohammad, Firoz & Al-Khaishany, Mutahhar. (2015). Role of Nanoparticles in Plants.

69. Sriram. (2021). Impacts on Foliar Application of Copper Nanoparticles for the Growth in Zea mays. Bioscience Biotechnology Research Communications. 14. 1248-1255.

70. Sui, H. J., Zhang, J. Z., & Wang, Z. Y. (2014). Toxicity of copper oxide engineered nanoparticles to maize (Zea Mays L.) at different aging times. In *Advanced Materials Research* (Vol. 881, pp. 972-975). Trans Tech Publications Ltd.

71. Nhan Le Van, Chuanxin Ma, Jianying Shang, Yukui Rui, Shutong Liu, Baoshan Xing, Effects of CuO nanoparticles on insecticidal activity.Volume 144, 2016, Pages 661-670, ISSN 0045-6535,

72. Ochoa, L., Medina-Velo, I. A., Barrios, A. C., Bonilla-Bird, N. J., Hernandez-Viezcas, J. A., Peralta-Videa, J. R., & Gardea-Torresdey, J. L. (2017). Modulation of CuO nanoparticles toxicity to green pea (Pisum sativum Fabaceae) by the phytohormone indole-3-acetic acid. *Science of the Total Environment*, *598*, 513-524.

73. Chong yang and Cheng yang, 2018. ZExcellent degradation performance of 3D hierarchical nanoporous structures of copper towards organic pollutants, journal of material chemistry, issue 42

74. Thiruvengadam, S., Ganesan, M., &Vanniappan, P. (2021). Green Synthesis of Silver nanoparticles and its effect on the growth of Zea mays L. *Current Trends in Biotechnology and Pharmacy*, *15*(5), 480-488.

75. Junfei Gu, Zhenxiang Zhou, Zhikang Li, Ying Chen, Zhiqin Wang, Hao Zhang, Rice (Oryza sativa L.) with reduced chlorophyll content exhibit higher photosynthetic rate and efficiency, improved canopy light distribution, and greater yields than normally pigmented plants, Field Crops Research, Volume 200, 2017, Pages 58-70, ISSN 0378-4290,

76. Ortega-Ortiz, H., Gaucin-Delgado, J. M., Preciado-Rangel, P., Fortis-Hernandez, M., Hernandez-Montiel, L. G., La CRUZ-LAZARO, E. D., & Liliana, L. C. (2022). Copper oxide nanoparticles biosynthetized improve germination and bioactive compounds in wheat sprouts. *NotulaeBotanicae Horti Agrobotanici Cluj-Napoca*, *50*(1), 12657-12657.

77. Liu, J., Simms, M., Song, S., King, R. S., & Cobb, G. P. (2018). Physiological effects of copper oxide nanoparticles and arsenic on the growth and life cycle of rice (Oryza sativa japonica 'Koshihikari'). *Environmental science & technology*, *52*(23), 13728-13737.

78. Margenot, Andrew &Rippner, Devin & Dumlao, Matt & Nezami, Sareh & Green, Peter & Parikh, Sanjai & Mcelrone, Andrew. (2018). Copper oxide nanoparticle effects on root growth and hydraulic conductivity of two vegetable crops. Plant and Soil. 431.

79. Mahadimane P, Vishwaprakash& Ananda, S. & KS, Shashidhara &Govindaiah, Shobha. (2019). In Vitro Cytotoxicity Study of Green Synthesized Copper Nanoparticles. Research journal of biotechnology. 14. 105-111.

80. Zakharova, O., Kolesnikov, E., Shatrova, N., & Gusev, A. (2019). The effects of CuO nanoparticles on wheat seeds and seedlings and Alternaria solani fungi: in vitro study. In *IOP conference series: earth and environmental science* Vol. 226, No. 1, p. 012036.

81. Shende, S., Rathod, D., Gade, A., & Rai, M. (2017). Biogenic copper nanoparticles promote the growth of pigeon pea (Cajanus cajan L.). *IET Nanobiotechnology*, *11*(7), 773-781.

82. Khan, A. R., Fan, X., Salam, A., Azhar, W., Ulhassan, Z., Qi, J., ... & Gan, Y. (2023). Melatonin-mediated resistance to copper oxide nanoparticles-induced toxicity by regulating the photosynthetic apparatus, cellular damages and antioxidant defense system in maize seedlings. *Environmental Pollution*, *316*, 120639.

83. Ezzat A. Genady, 2016, International Journal of Pharmaceutical Research&Allied Sciences, 2016, 5(1):196-202

84. AlQuraidi, A. O., Mosa, K. A., & Ramamoorthy, K. (2019). Phytotoxic and genotoxic effects of copper nanoparticles in coriander (Coriandrum sativum—Apiaceae). *Plants*, *8*(1), 19.

85. Li, H., Ma, C., Wang, H., Wei, L., & Zhu, X. (2018). Copper nanoparticles stimulate wheat yield by interacting with soil nutrients. Journal of Plant Nutrition and Soil Science, 181(1), 61-69.

86. Sharma, P., Bhatt, D., Zaidi, M. G. H., Saradhi, P. P., Khanna, P. K., & Arora, S. (2019). Impact of copper nanoparticles exposure on growth, metabolic profile and toxicity symptoms of soybean (Glycine max L.) plants. Ecotoxicology and Environmental Safety, 169, 17-25.

87. Chaudhuri, A., Paul, A., Sikder, A., & Singh, N. P. (2021). Single component photoresponsive fluorescent organic nanoparticles: a smart platform for improved biomedical and agrochemical applications. *Chemical Communications*, *57*(14), 1715-1733.

88. Velmurugan, P., Cho, M., Lim, S., Seo, S. K., Oh, B. T., & Kamala-Kannan, S. (2019). Engineered Copper-Based Nanomaterials: Mechanistic Understanding of Their Antimicrobial Activity. Chemical Research in Toxicology, 32(9), 868–877.

89. Parveen, A., Mazumder, P. M., Ansari, M. M., & Adil, M. (2018). Influence of copper nanoparticles on secondary metabolites production and antioxidant capacity in Catharanthus roseus. Biocatalysis and Agricultural Biotechnology, 14, 258-263.

90. Abbas, Z., Hussain, M., Ahmad, M. S. A., Mehmood, S., Rizwan, M., Iqbal, M. M., & Javed, M. R. (2020). Copper oxide nanoparticles enhance essential oil production in Ocimumbasilicum through up-regulation of genes involved in secondary metabolite biosynthesis pathways. Environmental Science and Pollution Research, 27(6), 6022-6031.

91. Ibrahim, M. H., Chee Kong, Y., & Mohd Zain, N. A. (2017). Effect of cadmium and copper exposure on growth, secondary metabolites and antioxidant activity in the medicinal plant Sambung Nyawa (Gynura procumbens (Lour.) Merr). *Molecules*, *22*(10), 1623.

92. Ghazal, B., Saif, S., Farid, K., Khan, A., Rehman, S., Reshma, A., ... & Ahmad, N. (2018). Stimulation of secondary metabolites by copper and gold nanoparticles in submerge adventitious root cultures of Stevia rebaudiana (Bert.). *IET nanobiotechnology*, *12*(5), 569-573.

93. Janova, A., Kolackova, M., Bytesnikova, Z., Capal, P., Chaloupsky, P., Svec, P. & Huska, D. (2021). New insights into mechanisms of copper nanoparticle toxicity in freshwater algae Chlamydomonas reinhardtii: Effects on the pathways of secondary metabolites. *Algal Research*, *60*, 102476.

Chetna and Simranjeet Kaur

94. Ahmad Faraz and Mohammad Faizan,2022 Foliar Application of Copper Oxide Nanoparticles Increases the Photosynthetic Efficiency and Antioxidant Activity in Brassica juncea", Journal of Food Quality, vol. 2022, Article ID 5535100, 2022.

95. Javed, R., Yucesan, B., Zia, M., & Gurel, E. (2018). Elicitation of secondary metabolites in callus cultures of Stevia rebaudiana Bertoni grown under ZnO and CuO nanoparticles stress. *Sugar Tech*, *20*, 194-201.

96. J. L Smith and N.tran , 2022. Robust bulk micro-nano hierarchical copper structures possessing exceptional bactericidal efficacy, Biomaterials,Volume 280.

97. Rajput, V. D., Minkina, T., Suskova, S., Mandzhieva, S., Tsitsuashvili, V., Chapligin, V., & Fedorenko, A. (2018). Effects of copper nanoparticles (CuO NPs) on crop plants: a mini review. *BioNanoScience*, *8*, 36-42.

98. Lopez-Lima, D., Mtz-Enriquez, A. I., Carrión, G., Basurto-Cereceda, S., & Pariona, N. (2021). The bifunctional role of copper nanoparticles in tomato: Effective treatment for Fusarium wilt and plant growth promoter. *Scientia Horticulturae*, *277*, 109810.

99. Banik, S., & Pérez-de-Luque, A. (2017). In vitro effects of copper nanoparticles on plant pathogens, beneficial microbes and crop plants. *Spanish Journal of Agricultural Research*, *15*(2), e1005-e1005.

100. Zhu, Y., Xu, J., Lu, T., Zhang, M., Ke, M., Fu, Z. & Qian, H. (2017). A comparison of the effects of copper nanoparticles and copper sulfate on Phaeodactylumtricornutum physiology and transcription. *Environmental Toxicology and Pharmacology*, *56*, 43.

Table 1: Effects of AgNPs on plant growth & development

Nanoparticles	Particle size	Concentration	Plant growth hormones	Plant species	Effect on plant growth & development	References
AgNPs	<1000nm	40mg/l	IAA	*Trigonella foenum-graecum*	Increase shoot length, no. of leaves, shoot dry weight	[29]
AgNPs	100nm	1000ppm	-	*Oriental lilies*	Enhance flowering, biomass of bulb and leave	[30]
AgNPs	60nm	-	IAA	*Zea mays*	Increase in germination rate	[31]
AgNO₃NPs	47nm	3mM	-	Brassica	Root and shoot length revealed	[32]
AgNO₃NPs	-	-	-	*Acalypha indica Linn.*	Plant germination is more effective	[30]
AgNPs	20nm	5mM	-	*Triticum aestivum*	Increase root shoot length	[33]
AgNPs	-	50ppm	-	*Pennisetum glaucum*	Germination rate of seed increased	[34]
AgNPs	-	30g/ml	-	*Oryza sativa*	Increase root development	[35]
AgNPs	-	100mg/l	-	*Lupinus seedlings*	Increase root branching	[36]
AgNPs	-	15ml	-	*Phaseolus vulgaris L.*	Increase root and shoot length	[37]
AgNPs	20nm	75mg/l	-	*Pistacia vera*	Increase in plant growth	[38]

Chetna and Simranjeet Kaur

Table 2: Effects of silver nanoparticles on secondary metabolite production of different plant species

Name of the nanoparticles	Particle size	concentration	Name of the solvent	Concentration of solvent	Plant species	Effect on secondary metabolites	References
AgNPs	-	30 µg l–1	Methanol	1ml	*Prunella vulgaris L.*	Enhanced total phenolic content	[53]
AgNPs	40nm	0.4 mM	Acidic methanol& deionised water aqueous acetone Ethyl acetate	99:1(v/v) & 1.25mL 80 % -	*Calendula officinalis L (Asteraceae)*	Decrease in anthocyanin & flavonoid Decreased carotenoid content in the plant by 30 - 50 % Increase in saponin content (177 % of the control)	[58]
AgNPs	8nm	5 mg/L	Methanol	10ml (80%)	*Momordica charantia L.*	Showed a higher amount of flavanol's (1822.37 µg/g), hydroxybenzoic (1713.40 µg/g) and hydroxycinnamic (1080.10 µg/g) acids	[59]
AgNPs	40nm	75 mg/L	dichloromethane	5ml	*Catharanthus roseus (Apocynaceae)*	High concentration of alkaloid i.e., vinblastine observed	[51]
AgNPs	80-120 nm	300 ppm	Methanol	10ml	*Black rice*	Flavonoids such as quercetin, apigenin, myricetin, catechin, kaempferol, isorhamnetin, luteolin, and tricine were increased significantly except luteolin glucosides and isorhamnetin glucosides. Terpenoids such as beta cymene,	[60]

Chetna and Simranjeet Kaur

			MilliQ water	10ml		gamma terpinene, terpinene-4-ol, alpha element, linalool, caryophyllene, beta ocimene, trans linalool, and myrcene were significantly increased Saffrole, a toxic benzodioxole element, was not detected in any of the treatments.	
AgNPs	-	1.0 mg/L	Distilled water & acetonitrile	-	*Cucumis anguria*	Enhanced total phenolic and flavonoid contents	[59]
AgNO3	-	3mg/L	Methanol	5ml	*Capsicum sp.*	Increases only total phenolic content	[61]
AgNPs	100nm	80ppm	Distilled water	3.5 ml	*Pennisetum Glaucum L.*	High concentration of AgNPs produces more TFC High dosage of AgNPs inhibited the accrual of TPC	[62]
Ag& CuNPs	-	3:1 1:3	Ethanol Methanol	1.5ml 2ml (80%)	*Artemisia absinthium L.*	Increase TFC content Maximum TPC was recorded	[63]
Bio-AgNPs	15nm	250 µg/mL 31.25 µg/mL	Methanol Methanol	- -	*Fagonia indica*	TPC increases as the concentration of AgNPs increased TFC decreased with increasing concentrations of BioAgNPs	[64]

Chetna and Simranjeet Kaur

Table 3: Effect of CuNPs on different species of plant

Nanoparticles	Particle size	Concentration	Plant growth regulators	Plant species	Effect on plant growth & development	References
CuONPs	-	500mg/l	-	*Zea mays*	Inhibit maize growth	[70]
CuONPs	-	10mg/l	ABA, IAA	*Bt transgenic cotton*	Inhibit growth development and nutrient content	[71]
CuONPs	100nm	50mg/kg	IAA	*Pisum sativum*	Improve the nutritional quality of plant	[72]
CuONPs		1000mg/l	Proline	*Oryza sativa*	Photosynthetic rate, transpiration rate, stomatal conductance, maximal quantum yield of PSII declined	[73]
CuNPs	-	20ppm	-	*Zea mays* L.	Optimum growth character observed	[74]
CuONPs	-	100-200mg/l	-	*S. virgata*	Decrease in length, reduction in root length and plant growth	[75]
CuONPs	-	(0.5 mg/l)	-	*Citrus X sinensis*	Improved germination, vigor, plumule and radicle length, in addition to increasing the biosynthesis of phytochemical compounds.	[76]
CuO+AsNPs	-	1.4-7 mg/l	-	*Oryza sativa japonica*	Decrease rice and seed germination	[77]
CuONPs	16nm	(798.9 mg/ l	-	*Lettuce*	Increase in root diameter	[78]
Cu2ONPs	-	20ppm	-	*Lycoperesculentum*	When enzymes are highly antioxidant, lipid peroxidation increases and DPPH's ability to scavenge free radicals declines.	[79]
CuONPs	-	0.01-1 mg/l	-	*Alternaria solani*	Inhibit mycelium development and spore germination	[80]
CuONPs	-	20ppm	-	*Cajanus cajan L.*	increase in height, root length, fresh and dry weights	[81]
CuONPs	-	300mg/l	-	*Maize seedling*	reduction in all plant growth traits and induced toxicity in maize.	[82]
CuSO4-NPs	-	-	-	*Verbena bipinnatifida Nutt*	Enhance phenolic content	[83]

CuNPs	20nm	-	-	*Coriandrum sativum*	Root length and biomass decreased also effect genetic composition	[84]

Table 4: Effect of CuNPs on secondary metabolites production

Nanoparticles	Particle size	Concentration	Name of solvent	Concentration of solvent	Plant species	Effect on secondary metabolites	References
CuNPs	-	4mg/l	Hoagland sol.	50%	*G. procumbens.*	Reduce the production of total flavonoid, phenol, saponins	[91]
CuNPs	760 nm	30µg l^{-1}	Aluminium chloride sodium hydroxide	-	*Stevia rebaudiana*	Enhance production of phenol and flavonoids	[92]
CuNPs	2.1 nm	-	Copper sulphate, demineralized water	10ml	*Chlamydomonas Reinhardtian*	Enhance phenolic production	[93]
CuO NPs	-	8mg/l	-	-	*Mustard*	Increase sec. metabolite production	[94]
CuO NPs	-	6mg/ ml	-	-	*Citrus X sinensis*	Enhance production of secondary metabolites	[76]
CuNPs	-	5ml	Copper sulphate solution	0.001M	*Zea mays* L.	Enhance sec. metabolite production	**[74]**
CuO NPs	-	100mg/l	-	-	*Stevia rebaudiana*	High flavonoid and phenolic content	[95]

Figure 1: Role of nanotechnology in plant tissue culture [14].

Figure 2: *Biomass analysis of Cajanus cajon*

RESEARCH ARTICLE
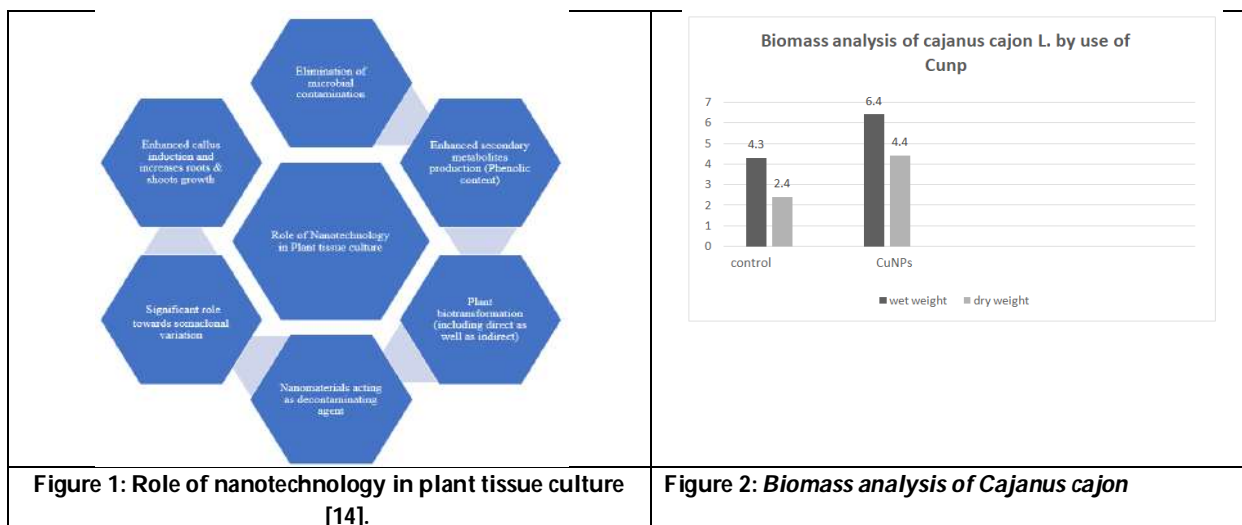
A New Algorithm for Trapezoidal Picture Fuzzy Linear Programming Problem

B.Thenmozhi[1]* and M.Haripriya[2]

[1]Associate Professor, Department of Mathematics, Chikkanna Govt. Arts College, Tirupur-02, Tamil Nadu, India.
[2]Research Scholar, Department of Mathematics, Chikkanna Govt. Arts College, Tirupur-02, Tamil Nadu, India.

*Address for Correspondence
B.Thenmozhi
Associate Professor,
Department of Mathematics,
Chikkanna Govt. Arts College,
Tirupur-02, Tamil Nadu, India.

ABSTRACT

A powerful tool to handle situation involving uncertainty and ambiguity, the Picture Fuzzy Set (PFS) is an extension of the Intuitionistic Fuzzy Set (IFS).Each element in the PFS is represented by three parameters: membership, neutrality and non-membership degrees. By utilizing the picture fuzzy numbers in which the membership, neutral, and non-membership degrees are represented as four and five tuples, respectively were introduced. Trapezoidal picture fuzzy numbers can be used to solve the picture fuzzy linear programming problem. In this research, we propose a new ranking algorithm to defuzzify the Trapezoidal picture fuzzy number. By considering two types, Type 1 (constraints) and Type 2 (cost) , in which the mentioned parameters are represent as Trapezoidal picture fuzzy numbers, we can use this ranking formula to find an initial basic feasible solution (IBFS) to a Trapezoidal picture fuzzy linear programming problem. We also compared and examined from the given data and Trapezoidal picture fuzzy linear programming problem.

Keywords: Trapezoidal Picture Fuzzy number, Linear Programming Problem, Trapezoidal Picture Fuzzy Linear Programming problem, Ranking formula.

INTRODUCTION

Zadeh [1] introduced the fuzzy sets. In the field of Intuitionistic Fuzzy Numbers (IFNs), Grzegorzewski [2] constructed two families of metrices and suggested a ranking mechanism for Intuitionistic Fuzzy Numbers (IFNs) based on these metrices. By adopting a statistical perspective and understanding each Trapezoidal Intuitionistic

63441

Fuzzy Number (TIFN)as an ensemble of regular fuzzy numbers, Mitchell [3] extended the natural ordering of real numbers to these numbers. Li [4] suggested a Trapezoidal Intuitionistic Fuzzy Numbers (TIFN) Ranking Order Relation utilizing Lexicographic Technique. Ranking Fuzzy Numbers with an area between the centroid point and Original point was introduced by T.C.Chu and C.T. Tsao [5]. Linear programming method for multi attribute decision making using if sets was introduced by D.F.Li,G.H.Chen and Z.G.Huang [6]. In this paper, a Trapezoidal Intuitionistic Fuzzy Numbers (TIFNs) was first defined. Our main goal has been to investigate a useful method for dealing with linear programming issues when the data are presented as intuitive fuzzy integers. A way to resolve linear programming issues involving Trapezoidal Intuitionistic Fuzzy Numbers is suggested using the new ranking function.

Basic Definitions

Definition 2.1 : A PFS in V is defined by B $=\{t, (p_s(t), b_s(t), q_s(t))/t \in V\}$ where $(p_s(t), b_s(t), q_s(t)) \in [0,1], 0 \leq (p_s(t) + b_s(t) + q_s(t)) \leq 1$. The$(p_s(t), b_s(t), q_s(t)) \in [0,1]$ signify respectively, the element of t's degree of positive, neutral and negative membership in the collection B . For each PFS B in V, the refusal membership degree is described as

$u_S(t) = 1 - (p_s(t) + b_s(t) + q_s(t))$.

Definition 2.2 : A Picture Fuzzy Number (PFN) q is defined in a PFS, where q $\in S$, as

$=\left\{\sigma, \left(p_q(\sigma), b_q(\sigma), q_q(\sigma)\right)/\sigma \in S\right\}$, where

$$p(\sigma) = \begin{cases} v_q^k(\sigma), \; for \; m_1 \leq \sigma < n \\ \beta_q, \; for \, n \leq \sigma \leq o \\ v_q^e(\sigma), for \, o \leq \sigma < \; g_1 \\ 0, otherwise \end{cases}$$

$$b(\sigma) = \begin{cases} w_q^k(\sigma), \; for \; m_2 \leq \sigma < n \\ \gamma_q, \; for \, n \leq \sigma \leq o \\ w_q^e(\sigma), for \, o \leq \sigma < \; g_2 \\ 0, otherwise \end{cases}$$

$$q(\sigma) = \begin{cases} x_q^k(\sigma), \; for \; m_3 \leq \sigma < n \\ \delta_q, \; for \, n \leq \sigma \leq o \\ x_q^e(\sigma), for \, o \leq \sigma < \; g_3 \\ 0, otherwise \end{cases}$$

Definition 2.3 : A TPFN 'z_q' is defined in a picture fuzzy subset in S with the following positive $m_q(\sigma)$, neutral $b_q(\sigma)$ and negative-membership function $q_q(\sigma)$.

$$p_q(\sigma) = \begin{cases} v_q^k(\sigma) = \dfrac{\sigma - m_1}{n - m_1} \beta_q^n, \; for \; m_1 \leq \sigma < n \\ \beta_q, \; \qquad\qquad for \, n \leq \sigma \leq o \\ v_q^e(\sigma) = \dfrac{g_1 - \sigma}{g_1 - o} \beta_q, for \, o \leq \sigma < \; g_1 \\ 0, otherwise \end{cases}$$

$$b_q(\sigma) = \begin{cases} w_q^k(\sigma) = \dfrac{n - \sigma + \gamma_q(\sigma - m_2)}{n - m_2}, \; for \; m_2 \leq \sigma < n \\ \gamma_q, \qquad\qquad\qquad for \, n \leq \sigma \leq o \\ w_q^e(\sigma) = \dfrac{\sigma - o + \gamma_q(g_2 - \sigma)}{g_2 - o}, for \, o \leq \sigma < \; g_2 \\ 0, otherwise \end{cases}$$

63442

Thenmozhi and Haripriya

$$n_n(\xi) = \begin{cases} x_q^k(\sigma) = \frac{n-\sigma+\delta_q(\sigma-m_3)}{n-m_3}, & for\ m_3 \leq \sigma < n \\ \delta_q\ , & for\ n \leq \sigma \leq o \\ x_q^e(\sigma) = \frac{\sigma-o+\delta_q(g_3-\sigma)}{g_3-o}, & for\ o \leq \sigma < g_3 \\ 0\ , & otherwise \end{cases}$$

Where $m_3 \leq m_2 \leq m_1 \leq n \leq o \leq g_1 \leq g_2 \leq g_3$ for all $\sigma\ \epsilon\ Y$ with the constraints
$0\leq\ \beta_q, \gamma_{q,\delta_q} \leq 1\ and\ \beta_q\ +\gamma_q + \delta_q \leq 1.$
TPFN $'z_q'$ is denoted by
$z_q = (m_1, n, o, g_1; m_2, n, o, g_2; m_3, n, o, g_3).$

Definition 2.4 : TPFN of Ranking formula
If $z_q = (m_1, n, o, g_1; m_2, n, o, g_2; m_3, n, o, g_3)$ is a TPFN, then the crisp value of z_q, is given below.
$$f = \frac{m_1 + 2n + 2o + g_1 + m_2 + 2n + 2o + g_2 + m_3 + 2n + 2o + g_3}{18}$$

Algorithm
Step (1) : Consider the Trapezoidal Picture Fuzzy Linear Programming Problem.
Step (2) : Convert the considered Trapezoidal Picture Fuzzy Linear Programming Problem into Crisp Linear Programming Problem using ranking function
Step (3) : Identify whether the provided LPP's objective function can be maximized or minimized, and then use the conclusion to transform the problem into one of maximization.
Minimum z = -Maximum (-z).
Step (4) : By including slack and surplus variables in the constraints, all of the inequalities of the constraints can be transformed into equations. Set the costs of these factors to zero.
Step (5) : Obtain the initial basic feasible solution to the problem in the form $x_B = B^{-1}$ b and put it in the first column of the simple table
Step (6) : Compute the net evaluation $z_j\text{-}c_j$ (i=1,2,3,….n) by using the relation $z_j\text{-}c_j = c_{ij}y_j - c_j$ where $y_j = B^{-1}a$
Examine the sign $z_j\text{-}c_j$
if all $(z_j\text{-}c_j) \geq 0$ then the initial basic feasible solution x_B is an optimum basic feasible solution.
If atleast one $(z_r\text{-}c_r) < 0$
If there are more than one negative $z_j\text{-}c_j$ then choose the most negative of them. Let it be $z_r\text{-}c_r$ for some j = r.

Numerical Examples
Example 4.1:
$$\widetilde{max}\ \tilde{5}x_1 + \tilde{3}x_2$$
Subject to:
$$\tilde{4}x_1 + \tilde{3}x_2 \leq \widetilde{12}$$
$$\tilde{1}x_1 + \tilde{3}x_2 \leq \tilde{6}$$
$$x_1, x_2 \geq 0.$$

Trapezoidal
$c_1 = \tilde{5} = \{(4,4.68,5.36,6.04),(4,4.68,5.36,6.04),(4,\ 4.68,5.36,6.1)\}$
$c_2 = \tilde{3} = \{(2.5,2.62,2.97,3.2),(2.3,2.62,2.97,3.29),(2.2,2.62,2.97,3.5)\}$
$a_{11} = \tilde{4} = \{(3.5,3.68,4.12,4.1),(3.2,\ 3.68,4.12,4.61),(3,\ 3.68,4.12,5.01)\}$
$a_{12} = \tilde{3} = \{(2.5,2.78,3.16,3.49),(2.3,\ 2.78,3.16,3.53),(2.4,\ 2.78,3.16,3.6)\}$
$a_{21} = \tilde{1} = \{(0,0.67,1.34,2.01),(0,0.67,1.34,2.01),(0,0.67,1.34,2.01)\}$
$a_{22} = \tilde{3} = \{(2.8,2.82,3,3.19),(2.6,2.82,3,3.2),(2.5,2.82,3,3.19)\}$
$b_1 = \widetilde{12} = \{(11,11.83,12.66,13.01),(11,11.83,12.66,13.49),(11,11.83,12.66,14)\}$
$b_2 = \tilde{6} = \{(5.5,6.1,6.93,7.5),(5.3,6.1,6.93,7.1),(5,6.1,6.93,8.09)\}$

Thenmozhi and Haripriya

CRISP

$c_1 = \tilde{5} = 5.02$
$c_2 = \tilde{3} = 2.796$
$a_{11} = \tilde{4} = 3.9011$
$a_{12} = \tilde{3} = 2.97$
$a_{21} = \tilde{1} = 0.938$
$a_{22} = \tilde{3} = 2.911$
$b_1 = \widetilde{12} = 12.246$
$b_2 = \tilde{6} = 6.515$

Max Z $= 5.02x_1 + 2.796x_2$
Subject to
$3.9011x_1 + 2.97x_2 \le 12.246$
$0.938x_1 + 2.911x_2 \le 6.515$
$x_1, x_2 \ge 0.$

After introducing slack variables:

Max Z $= 5.02x_1 + 2.796x_2 + 0S_1 + 0S_2$
Subject to
$3.9011x_1 + 2.97x_2 + S_1 + 0 = 12.246$
$0.938x_1 + 2.911x_2 + 0 + S_2 = 6.515$
 and $x_1, x_2, S_1, S_2 \ge 0.$

Iteration-1		C_j	5.02	2.796	0	0	
B	C_B	X_B	X_1	X_2	S_1	S_2	Min ratio $\frac{X_B}{X_1}$
S_1	0	12.246	(3.9011)	2.97	1	0	3.1391→
S_2	0	6.515	0.938	2.911	0	1	6.9456
Z=0		Z_j	0	0	0	0	
		$Z_j - C_j$	-5.02↑	-2.796	0	0	

Table (a)

Negative minimum $Z_j - C_j$ is -5.02 and its column index is 1.So,the entering variable is X_1. Minimum ratio is 3.139 and its row index is 1.So,the leaving basis variable is S_1.
∴ The pivot element is 3.9011.

Iteration-2		C_j	5.02	2.796	0	0	
B	C_B	X_B	X_1	X_2	S_1	S_2	Min ratio $\frac{X_B}{X_1}$
X_1	5.02	3.1391	1	0.7613	0.2563	0	
S_2	0	3.5705	0	2.1969	-0.2404	1	
Z=15.7584		Z_j	5.02	3.8218	1.2868	0	
		$Z_j - C_j$	0	1.0258	1.2868	0	

Table (b)

Hence, optimal solution is arrived with value of variables as:
$X_1 = 5.02, X_2 = 1.0258,$ Max Z $= 15.7584$

Thenmozhi and Haripriya

Example 4.2:

$$\widetilde{max}\ \widetilde{25}x_1 + \widetilde{48}x_2$$

Subject to:

$$15x_1 + 30x_2 \leq 45000$$
$$24x_1 + 6x_2 \leq 24000$$
$$21x_1 + 14x_2 \leq 28000$$
$$x_1, x_2 \geq 0.$$

TRAPEZOIDAL

$c_1 = \widetilde{25} = \{(19,23.5,28.5,33.01),(18.5,23.5,28.5,33.5),(18,23.5,28.5,33.5)\}$
$c_2 = \widetilde{48} = \{(44,47.33,51.16,53.99),(43.5,47.33,51.16,54.99),(43,47.33,51.16,55.99)\}$

CRISP

$c_1 = \widetilde{25} = 26$
$c_2 = \widetilde{48} = 49.24$

Max $26x_1 + 49.24x_2$

Subject to:

$$15x_1 + 30x_2 \leq 45000$$
$$24x_1 + 6x_2 \leq 24000$$
$$21x_1 + 14x_2 \leq 28000$$
$$x_1, x_2 \geq 0.$$

After introducing slack variables:

Max Z $= 26x_1 + 49.245x_2 + 0S_1 + 0S_2 + 0S_3$

Subject to

$$15x_1 + 30x_2 + S_1 + 0S_2 + 0S_3 = 45000$$
$$24x_1 + 6x_2 + 0S_1 + S_2 + 0S_3 = 24000$$
$$21x_1 + 14x_2 + 0S_1 + 0S_2 + S_3 = 28000$$

and $x_1, x_2, S_1, S_2, S_3 \geq 0.$

Iteration-1		C_j	26	49.245	0	0	0	
B	C_B	X_B	X_1	X_2	S_1	S_2	S_3	Min ratio $\frac{X_B}{X_1}$
S_1	0	45000	15	(30)	1	0	0	1500→
S_2	0	24000	24	6	0	1	0	4000
S_3	0	28000	21	14	0	0	1	2000
Z=0		Z_j	0	0	0	0	0	
		$Z_j - C_j$	-26	-49.245	0	0	0	

Table (c)

Negative minimum $Z_j - C_j$ is -49.245 and its column index is 2.So,the entering variable is X_2. Minimum ratio is 1500 and its row index is 1.So,the leaving basis variable is S_1.

∴ The pivot element is 3

Iteration-2		C_j	26	49.245	0	0	0	
B	C_B	X_B	X_1	X_2	S_1	S_2	S_3	Min ratio $\frac{X_B}{X_1}$
X_2	49.245	1500	0.5	1	0.0333	0	0	3000
S_2	0	15000	21	0	-0.2	1	0	714.2857

Thenmozhi and Haripriya

S_3	0	7000	(14)	0	-0.4667	0	1	500→
Z=73867.5		Z_j	24.6225	49.245	1.6415	0	0	
		$Z_j - C_j$	-1.3775 ↑	0	1.6415	0	0	

Table (d)

Hence, optimal solution is arrived with value of variables as:

X_1 = 5.02, X_2= 1.0258, Max Z = 15.7584

Iteration-3		C_j	26	49.245	0	0	0	
B	C_B	X_B	X_1	X_2	S_1	S_2	S_3	Min ratio $\dfrac{X_B}{X_1}$
X_2	49.245	1250	0	1	0.05	0	-0.0357	
S_2	0	4500	0	0	0.5	1	-1.5	
X_1	26	500	1	0	-0.0333	0	0.0714	
Z=74556.25		Z_j	26	49.245	1.5956	0	0.0984	
		$Z_j - C_j$	0	0	1.5956	0	0.0984	

Table (e)

Hence, optimal solution is arrived with value of variables as:

X_1 = 26, X_2= 49.245, Max Z = 74556.25

COMPARISON AND CONCLUSION

The Comparison of Optimum solution of given data and TPFLPP can be made and shown in the table

GIVEN DATA	TPFLPP
11.6872	15.7584
70500	74556.25

Table (f)

In this paper, we conclude that given data and TPFLPP gives better solution, then the existing method.

REFERENCES

1. Lofi A. Zadeh. Fuzzy sets. Information and Control, 8:338-353,1965.
2. P.Grzegorzewski. Distances and orderings in a family of Intuitionistic Fuzzy Numbers. In Proceedings of the Third Conference on Fuzzy logic and Technology (Eusflat03), pages 223-227,2003.
3. H.B. Mitchell. Ranking Intuitionistic Fuzzy Numbers. International Journal of Uncertainity, Fuzziness and Knowledge-Based Systems, 12:377-386,2004.
4. J.X. Nan and D-F.Li. A lexicographic method for matrix games with payoffs of Triangular Intuitionistic Fuzzy Numbers (TIFN). Inernational Jornal of Computational Inelligence Systems,3:280-289,2010.
5. T.C.Chu and C.T. Tsao. Ranking Fuzzy Numbers with an area between the centroid point and Original point. Computers Mathematics and Applications, 43:111-117,2002.
6. D.F.Li,G.H.Chen and Z.G.Huang. Linear programming method for multiattribute decision making using if sets. Information Sciences, 180:1591-1609,2010.

RESEARCH ARTICLE

A New Generalization of Power Rama Distribution with Characterizations and Applications in Medical Sciences

Soumya V. P[1]*, V. Rajagopalan[2] and V Sreejith[3]

[1]Research Scholar Annamalai University, Annamalai Nagar, Tamil Nadu and Research Coordinator, Dr.Vithalrao Vicky Patil Medical College and Hospital, Ahmed Nagar, Maharashtra, India.
[2]Professor, Annamalai University, Annamalai Nagar, Tamil Nadu, India,
[3]Assistant Professor , Government Arts College, Thiruvananthapuram, Kerala,India

*Address for Correspondence
Soumya V. P
Research Scholar,
Annamalai University,
Annamalai Nagar, Tamil Nadu and
Research Coordinator,
Dr.Vithalrao Vicky Patil Medical College and Hospital,
Ahmed Nagar, Maharashtra, India.
        E.Mail: soumyaponnan@gmail.com

ABSTRACT

In this paper, a new study of power Rama distribution called as weighted power Rama distribution has been proposed. Its different statistical properties have been investigated and the model parameters of the proposed new distribution are estimated by using the method of maximum likelihood estimation. Finally, a new distribution has been examined and analysed with real lifetime data set from medical sciences to discuss its superiority and flexibility.

Keywords: Power Rama distribution, Weighted distribution, Order statistics, Survival analysis, Maximum likelihood estimation.

INTRODUCTION

In recent times, researchers have applied various probability models for modeling lifetime data occurring from diversified fields like engineering, medical sciences, finance, insurance etc. There are various cases were classical distributions may not provide best fit to lifetime data. In such a situation an attempt has been made to generalize the classical probability distributions by adding an extra parameter to the existing classical distribution. This extra parameter can be added through various techniques. One such technique is of weighted technique. The concept of

63447

Soumya *et al.*,

weighted distribution is useful in distribution theory because it provides a new outlook to the existing classical distributions. Fisher (1934) studies the concept of weighted distribution to model the ascertainment bias, which was later formalized by Rao (1965) in a unified manner while modeling the statistical data when the standard distributions were not appropriate to record the observations with equal probabilities. The weighted distribution provides a collective approach to deal with model specification and data interpretation problems. The weighted distributions are remarkable for efficient modeling of statistical data and prediction, obviously when standard distributions are not appropriate.

The weighted distributions arise when the observations are recorded by an investigator in nature according to certain stochastic model, the distribution of recorded observation will not have the original distribution unless each and every observation is given an equal chance of being recorded. The weighted distributions are applied to modify the probabilities of events as observed and transcribed. The weighted distributions play a dominant role to attract large number of researchers to contemplate on and to carry out research on this topic. The weighted distributions are applied in various research areas related to reliability, ecology, biomedicine, Meta analysis, analysis of family data, analysis of intervention data and other areas for the improvement of proper statistical models. The weighted distribution reduces to length biased distribution when the weight function considers only the length of units of interest. The concept of length biased sampling was introduced by Cox (1969) and Zelen (1974).

Many authors have studied the various weighted probability models along with their illustrations and applications in different fields. Kersey (2010) constructed the weighted inverse Weibull distribution (WIWD) and beta-inverse Weibull distribution (BIWD). Ye et al. (2012) developed a weighted generalized beta distribution (WGBD) of second kind. Bashir and Rasul (2015) discussed the weighted Lindley distribution. Das and kundu (2016) developed the weighted exponential distribution and its length biased version. Saghir et al. (2017) studies weighted distribution with a brief review, perspective and characterizations. Shanker, Shukla and Leonida (2019) introduced weighted quasi Lindley distribution with properties and application. Kilany (2016) developed the weighted Lomax distribution and discuss its properties and application.Mahdi (2020) executed weighted exponential Lomax distribution with applications. Bashir and Rasul (2018) constructed new weighted Rayleigh distribution with properties and applications on lifetime data. Rather and Subramanian (2019) presented weighted Sushila distribution with properties and applications. Dar, Ahmed and Reshi (2020) constructed the weighted gamma-Pareto distribution and its application. Recently Rajagopalan, Ganaie and Nair (2023) presented the weighted three parameter Pranav distribution with applications in industrial and medical sciences.

Power Rama distribution is a two parametric lifetime model proposed by Abebe, Tesfay, Eyob and Shanker (2019) of which one parameter Rama distribution is a particular case of power Rama distribution. Its various statistical and reliability properties which include moments, survival function, hazard rate function, mean residual life function, shapes of density for varying values of parameters, the mean and variance have been discussed. The method of maximum likelihood estimation has been discussed for estimating the parameters of proposed distribution. Shanker (2017) studied one parameter Rama distribution and obtained its various mathematical and statistical properties. The parameters have also been estimated through the method of moments and maximum likelihood estimation. Edith, Ebele and Henrietta (2019) developed two parameter Rama distribution, obtained its various mathematical and statistical properties and estimate its parameters through method of moments and maximum likelihood estimation.

Weighted Power Rama (WPR) Distribution

The probability density function of power Rama distribution is given by

$$f(x;\theta,\alpha) = \frac{\alpha\,\theta^4}{\theta^3+6}\left(1+x^{3\alpha}\right)x^{\alpha-1}e^{-\theta x^{\alpha}}\;;\; x>0, \theta>0,\ \alpha>0 \qquad (1)$$

and the cumulative distribution function of power Rama distribution is given by

Soumya *et al*.,

$$F(x;\theta,\alpha) = 1 - \frac{\theta^3 e^{-\theta x^\alpha} + \Gamma(4,\theta x^\alpha)}{\theta^3 + 6}; \ x > 0, \theta > 0, \alpha > 0 \tag{2}$$

Let X be the random variable following non negative condition having probability density function $f(x)$. Let its non-negative weight function be $w(x)$, then the probability density function of weighted random variable X_w is given by

$$f_W(x) = \frac{w(x)f(x)}{E(w(x))}, \ x > 0.$$

Where the non-negative weight function be $w(x)$ and $E(w(x)) = \int w(x)f(x)dx < \infty.$

In this paper, we have to obtain the weighted version of power Rama distribution, particularly when $w(x) = x^c$, resulting distribution is called weighted distribution. We have considered the weight function as $w(x) = x^c$ to obtain the weighted power Rama distribution and its probability density function is given by

$$f_w(x) = \frac{x^c f(x)}{E(x^c)} \tag{3}$$

Where $\ E(x^c) = \int\limits_0^\infty x^c f(x)dx$

$$E(x^c) = \frac{\alpha\theta^3 \Gamma\dfrac{(\alpha+c)}{\alpha} + \Gamma\dfrac{(4\alpha+c)}{\alpha}}{\alpha\theta^{\frac{c}{\alpha}}\left(\theta^3 + 6\right)} \tag{4}$$

By using the equations (1) and (4) in equation (3), we will obtain the probability density function of weighted power Rama distribution as

$$f_w(x) = \frac{\alpha\theta^{\frac{4\alpha+c}{\alpha}}}{\alpha\theta^3 \Gamma\dfrac{(\alpha+c)}{\alpha} + \Gamma\dfrac{(4\alpha+c)}{\alpha}} x^{\alpha+c-1}\left(1 + x^{3\alpha}\right)e^{-\theta x^\alpha} \tag{5}$$

and cumulative distribution function of weighted power Rama distribution can be obtained as

$$F_w(x) = \int\limits_0^x f_w(x)dx$$

$$F_w(x) = \int\limits_0^x \frac{\alpha\theta^{\frac{4\alpha+c}{\alpha}}}{\alpha\theta^3 \Gamma\dfrac{(\alpha+c)}{\alpha} + \Gamma\dfrac{(4\alpha+c)}{\alpha}} x^{\alpha+c-1}\left(1 + x^{3\alpha}\right)e^{-\theta x^\alpha}dx$$

$$F_w(x) = \frac{1}{\alpha\theta^3 \Gamma\dfrac{(\alpha+c)}{\alpha} + \Gamma\dfrac{(4\alpha+c)}{\alpha}} \int\limits_0^x \alpha\theta^{\frac{4\alpha+c}{\alpha}} x^{\alpha+c-1}\left(1 + x^{3\alpha}\right)e^{-\theta x^\alpha}dx$$

$$F_w(x) = \frac{1}{\alpha\theta^3\Gamma\frac{(\alpha+c)}{\alpha}+\Gamma\frac{(4\alpha+c)}{\alpha}}\left(\alpha\theta^{\frac{4\alpha+c}{\alpha}}\int_0^x x^{\alpha+c-1}e^{-\theta x^\alpha}dx + \alpha\theta^{\frac{4\alpha+c}{\alpha}}\int_0^x x^{4\alpha+c-1}e^{-\theta x^\alpha}dx\right)$$

(6)

Put $\theta x^\alpha = t \Rightarrow x^\alpha = \frac{t}{\theta} \Rightarrow x = \left(\frac{t}{\theta}\right)^{\frac{1}{\alpha}}$

Also $\alpha\theta x^{\alpha-1}dx = dt \Rightarrow dx = \frac{dt}{\alpha\theta x^{\alpha-1}} \Rightarrow dx = \frac{dt}{\alpha\theta\left(\frac{t}{\theta}\right)^{\frac{\alpha-1}{\alpha}}}$

After the simplification of equation (6), we will obtain the cumulative distribution function of weighted power Rama distribution as

$$F_w(x) = \frac{1}{\alpha\theta^3\Gamma\frac{(\alpha+c)}{\alpha}+\Gamma\frac{(4\alpha+c)}{\alpha}}\left(\alpha\theta^3\gamma\left(\frac{(\alpha+c)}{\alpha},\theta x^\alpha\right) + \alpha\gamma\left(\frac{(4\alpha+c)}{\alpha},\theta x^\alpha\right)\right)$$

(7)

Survival Analysis
In this section, we have obtained the survival function, hazard rate function, reverse hazard rate function and Mills ratio of the weighted power Rama distribution.

Survival function
The survival function or reliability function of weighted power Rama distribution can be obtained as
$S(x) = 1 - F_w(x)$

$$S(x) = 1 - \frac{1}{\alpha\theta^3\Gamma\frac{(\alpha+c)}{\alpha}+\Gamma\frac{(4\alpha+c)}{\alpha}}\left(\alpha\theta^3\gamma\left(\frac{(\alpha+c)}{\alpha},\theta x^\alpha\right) + \alpha\gamma\left(\frac{(4\alpha+c)}{\alpha},\theta x^\alpha\right)\right)$$

Hazard function
The hazard function is also known as hazard rate or failure rate or force of mortality and is given by

$$h(x) = \frac{f_w(x)}{1-F_w(x)}$$

$$h(x) = \frac{\alpha\theta^{\frac{4\alpha+c}{\alpha}}x^{\alpha+c-1}\left(1+x^{3\alpha}\right)e^{-\theta x^\alpha}}{\left(\alpha\theta^3\Gamma\frac{(\alpha+c)}{\alpha}+\Gamma\frac{(4\alpha+c)}{\alpha}\right)-\left(\alpha\theta^3\gamma\left(\frac{(\alpha+c)}{\alpha},\theta x^\alpha\right)+\alpha\gamma\left(\frac{(4\alpha+c)}{\alpha},\theta x^\alpha\right)\right)}$$

Soumya *et al.,*

Reverse hazard function

The reverse hazard rate function is given by

$$h_r(x) = \frac{f_w(x)}{F_w(x)}$$

$$h_r(x) = \frac{\alpha\theta^{\frac{4\alpha+c}{\alpha}} x^{\alpha+c-1}\left(1+x^{3\alpha}\right)e^{-\theta x^{\alpha}}}{\left(\alpha\theta^3\gamma\left(\frac{(\alpha+c)}{\alpha},\theta x^{\alpha}\right) + \alpha\gamma\left(\frac{(4\alpha+c)}{\alpha},\theta x^{\alpha}\right)\right)}$$

Mills Ratio

$$M.R = \frac{1}{h_r(x)} = \frac{\left(\alpha\theta^3\gamma\left(\frac{(\alpha+c)}{\alpha},\theta x^{\alpha}\right) + \alpha\gamma\left(\frac{(4\alpha+c)}{\alpha},\theta x^{\alpha}\right)\right)}{\alpha\theta^{\frac{4\alpha+c}{\alpha}} x^{\alpha+c-1}\left(1+x^{3\alpha}\right)e^{-\theta x^{\alpha}}}$$

Structural Properties

In this section, we have obtained the various statistical properties of weighted power Rama distribution these include moments, harmonic mean, MGF and characteristic function.

Moments

Let X denotes the random variable following weighted power Rama distribution with parameters θ, α and c, then the rth order moment $E(X^r)$ of proposed distribution can be obtained as

$$E(X^r) = \mu_r' = \int_0^{\infty} x^r f_w(x)dx$$

$$E(X^r) = \int_0^{\infty} x^r \frac{\alpha\theta^{\frac{4\alpha+c}{\alpha}}}{\alpha\theta^3\Gamma\frac{(\alpha+c)}{\alpha} + \Gamma\frac{(4\alpha+c)}{\alpha}} x^{\alpha+c-1}\left(1+x^{3\alpha}\right)e^{-\theta x^{\alpha}} dx$$

$$E(X^r) = \int_0^{\infty} \frac{\alpha\theta^{\frac{4\alpha+c}{\alpha}}}{\alpha\theta^3\Gamma\frac{(\alpha+c)}{\alpha} + \Gamma\frac{(4\alpha+c)}{\alpha}} x^{\alpha+c+r-1}\left(1+x^{3\alpha}\right)e^{-\theta x^{\alpha}} dx$$

$$E(X^r) = \frac{\alpha\theta^{\frac{4\alpha+c}{\alpha}}}{\alpha\theta^3\Gamma\frac{(\alpha+c)}{\alpha} + \Gamma\frac{(4\alpha+c)}{\alpha}} \int_0^{\infty} x^{\alpha+c+r-1}\left(1+x^{3\alpha}\right)e^{-\theta x^{\alpha}} dx$$

$$E(X^r) = \frac{\alpha\,\theta^{\frac{4\alpha+c}{\alpha}}}{\alpha\,\theta^3 \Gamma\frac{(\alpha+c)}{\alpha}+\Gamma\frac{(4\alpha+c)}{\alpha}}\left(\int_0^{\infty} x^{\alpha+c+r-1}\,e^{-\theta x^{\alpha}}\,dx \;+\; \int_0^{\infty} x^{4\alpha+c+r-1}\,e^{-\theta x^{\alpha}}\,dx \right) \tag{8}$$

Put $x^{\alpha}=t \;\Rightarrow x=t^{\frac{1}{\alpha}}$

Also $\alpha\,x^{\alpha-1}dx=dt \;\Rightarrow dx=\dfrac{dt}{\alpha x^{\alpha-1}} \;=\dfrac{dt}{\alpha\,t^{\frac{\alpha-1}{\alpha}}}$

After simplification, equation (8) becomes

$$E(X^r)=\mu_r{}' \;\;=\; \frac{\alpha\,\theta^3\Gamma\dfrac{(\alpha+c+r)}{\alpha}+\Gamma\dfrac{(4\alpha+c+r)}{\alpha}}{\alpha\theta^{\frac{r}{\alpha}}\left(\alpha\theta^3\Gamma\dfrac{(\alpha+c)}{\alpha}+\Gamma\dfrac{(4\alpha+c)}{\alpha}\right)} \tag{9}$$

By putting *r*= 1, 2, 3 and 4 in equation (9), we will obtain the first four moments of weighted power Rama distribution as

$$E(X)=\mu_1{}'= \frac{\alpha\,\theta^3\Gamma\dfrac{(\alpha+c+1)}{\alpha}+\Gamma\dfrac{(4\alpha+c+1)}{\alpha}}{\alpha\theta^{\frac{1}{\alpha}}\left(\alpha\,\theta^3\Gamma\dfrac{(\alpha+c)}{\alpha}+\Gamma\dfrac{(4\alpha+c)}{\alpha}\right)}$$

$$E(X^2)=\mu_2{}'= \frac{\alpha\theta^3\Gamma\dfrac{(\alpha+c+2)}{\alpha}+\Gamma\dfrac{(4\alpha+c+2)}{\alpha}}{\alpha\theta^{\frac{2}{\alpha}}\left(\alpha\theta^3\Gamma\dfrac{(\alpha+c)}{\alpha}+\Gamma\dfrac{(4\alpha+c)}{\alpha}\right)}$$

$$E(X^3)=\mu_3{}'= \frac{\alpha\,\theta^3\Gamma\dfrac{(\alpha+c+3)}{\alpha}+\Gamma\dfrac{(4\alpha+c+3)}{\alpha}}{\alpha\theta^{\frac{3}{\alpha}}\left(\alpha\theta^3\Gamma\dfrac{(\alpha+c)}{\alpha}+\Gamma\dfrac{(4\alpha+c)}{\alpha}\right)}$$

$$E(X^4)=\mu_4{}'= \frac{\alpha\,\theta^3\Gamma\dfrac{(\alpha+c+4)}{\alpha}+\Gamma\dfrac{(4\alpha+c+4)}{\alpha}}{\alpha\theta^{\frac{4}{\alpha}}\left(\alpha\theta^3\Gamma\dfrac{(\alpha+c)}{\alpha}+\Gamma\dfrac{(4\alpha+c)}{\alpha}\right)}$$

$$\text{Variance} = \frac{\alpha\,\theta^3\Gamma\dfrac{(\alpha+c+2)}{\alpha}+\Gamma\dfrac{(4\alpha+c+2)}{\alpha}}{\alpha\theta^{\frac{2}{\alpha}}\left(\alpha\,\theta^3\Gamma\dfrac{(\alpha+c)}{\alpha}+\Gamma\dfrac{(4\alpha+c)}{\alpha}\right)} - \left(\frac{\alpha\theta^3\Gamma\dfrac{(\alpha+c+1)}{\alpha}+\Gamma\dfrac{(4\alpha+c+1)}{\alpha}}{\alpha\theta^{\frac{1}{\alpha}}\left(\alpha\,\theta^3\Gamma\dfrac{(\alpha+c)}{\alpha}+\Gamma\dfrac{(4\alpha+c)}{\alpha}\right)}\right)^2$$

$$S.D(\sigma) = \sqrt{\left(\frac{\alpha\,\theta^3\Gamma\dfrac{(\alpha+c+2)}{\alpha}+\Gamma\dfrac{(4\alpha+c+2)}{\alpha}}{\alpha\theta^{\frac{2}{\alpha}}\left(\alpha\,\theta^3\Gamma\dfrac{(\alpha+c)}{\alpha}+\Gamma\dfrac{(4\alpha+c)}{\alpha}\right)} - \left(\frac{\alpha\,\theta^3\Gamma\dfrac{(\alpha+c+1)}{\alpha}+\Gamma\dfrac{(4\alpha+c+1)}{\alpha}}{\alpha\theta^{\frac{1}{\alpha}}\left(\alpha\,\theta^3\Gamma\dfrac{(\alpha+c)}{\alpha}+\Gamma\dfrac{(4\alpha+c)}{\alpha}\right)}\right)^2\right)}$$

Harmonic mean

The harmonic mean for the proposed weighted power Rama distribution can be obtained as

$$H.M = E\left(\frac{1}{x}\right) = \int_0^\infty \frac{1}{x} f_w(x)dx$$

$$H.M = \int_0^\infty \frac{\alpha\theta^{\frac{4\alpha+c}{\alpha}}}{\alpha\,\theta^3\Gamma\dfrac{(\alpha+c)}{\alpha}+\Gamma\dfrac{(4\alpha+c)}{\alpha}} x^{\alpha+c-2}\left(1+x^{3\alpha}\right)e^{-\theta x^\alpha}dx$$

$$H.M = \frac{\alpha\theta^{\frac{4\alpha+c}{\alpha}}}{\alpha\theta^3\Gamma\dfrac{(\alpha+c)}{\alpha}+\Gamma\dfrac{(4\alpha+c)}{\alpha}} \int_0^\infty x^{\alpha+c-2}\left(1+x^{3\alpha}\right)e^{-\theta x^\alpha}dx$$

$$H.M = \frac{\alpha\theta^{\frac{4\alpha+c}{\alpha}}}{\alpha\,\theta^3\Gamma\dfrac{(\alpha+c)}{\alpha}+\Gamma\dfrac{(4\alpha+c)}{\alpha}} \left(\int_0^\infty x^{\alpha+c-2}\,e^{-\theta x^\alpha}dx + \int_0^\infty x^{4\alpha+c-2}\,e^{-\theta x^\alpha}dx\right) \qquad (10)$$

Put $x^\alpha = t \implies x = t^{\frac{1}{\alpha}}$

Also $\alpha\,x^{\alpha-1}dx = dt \Rightarrow dx = \dfrac{dt}{\alpha\,x^{\alpha-1}} \implies dx = \dfrac{dt}{\alpha\,t^{\frac{\alpha-1}{\alpha}}}$

After the simplification of equation (10), we obtain

$$H.M = \frac{\alpha\,\theta^3\Gamma\dfrac{(\alpha+c-1)}{\alpha}+\Gamma\dfrac{(4\alpha+c-1)}{\alpha}}{\alpha\theta^{\alpha}\left(\alpha\,\theta^3\Gamma\dfrac{(\alpha+c)}{\alpha}+\Gamma\dfrac{(4\alpha+c)}{\alpha}\right)}$$

Moment generating function and characteristic function

Let X denotes the random variable following weighted power Rama distribution with parameters θ, α and c, then the moment generating function of proposed distribution can be obtained as

$$M_X(t) = E\left(e^{tx}\right) = \int_0^\infty e^{tx} f_w(x) dx$$

Using Taylor series, we obtain

$$= \int_0^\infty \left(1 + tx + \frac{(tx)^2}{2!} + \dots\right) f_w(x) dx$$

$$= \int_0^\infty \sum_{j=0}^\infty \frac{t^j}{j!} x^j f_w(x) dx$$

$$= \sum_{j=0}^\infty \frac{t^j}{j!} \mu_j{'}$$

$$= \sum_{j=0}^\infty \frac{t^j}{j!} \left(\frac{\alpha\theta^3 \Gamma \frac{(\alpha+c+j)}{\alpha} + \Gamma \frac{(4\alpha+c+j)}{\alpha}}{\alpha\theta^{\frac{j}{\alpha}} \left(\alpha\theta^3 \Gamma \frac{(\alpha+c)}{\alpha} + \Gamma \frac{(4\alpha+c)}{\alpha}\right)} \right)$$

$$M_X(t) = \frac{1}{\alpha\left(\alpha\theta^3\Gamma\frac{(\alpha+c)}{\alpha} + \Gamma\frac{(4\alpha+c)}{\alpha}\right)} \sum_{j=0}^\infty \frac{t^j}{j!\,\theta^{\frac{j}{\alpha}}} \left(\alpha\theta^3\Gamma\frac{(\alpha+c+j)}{\alpha} + \Gamma\frac{(4\alpha+c+j)}{\alpha}\right)$$

Similarly, the characteristic function of weighted power Rama distribution can be determined as

$$\varphi_X(t) = M_X(it)$$

$$M_X(it) = \frac{1}{\alpha\left(\alpha\theta^3\Gamma\frac{(\alpha+c)}{\alpha} + \Gamma\frac{(4\alpha+c)}{\alpha}\right)} \sum_{j=0}^\infty \frac{it^j}{j!\,\theta^{\frac{j}{\alpha}}} \left(\alpha\theta^3\Gamma\frac{(\alpha+c+j)}{\alpha} + \Gamma\frac{(4\alpha+c+j)}{\alpha}\right)$$

Order Statistics

Order statistics is a useful in statistical sciences and have wide range of applicability in reliability and life testing. Let $X_{(1)}$, $X_{(2)}$,..., $X_{(n)}$ denotes the order statistics of a random sample X_1, X_2,..., X_n from a continuous population with

probability density function $f_x(x)$ and cumulative distribution function $F_X(x)$, then the probability density function of rth order statistics $X_{(r)}$is given by

$$f_{x(r)}(x) = \frac{n!}{(r-1)!(n-r)!} \, f_X(x) \, (F_X(x))^{r-1} (1-F_X(x))^{n-r} \tag{11}$$

By using the equations (5) and (7) in equation (11), we will have obtained the probability density function of rth order statistics of weighted power Rama distribution as

$$f_{x(r)}(x) = \frac{n!}{(r-1)!(n-r)!} \left(\frac{\alpha\theta^{\frac{4\alpha+c}{\alpha}}}{\alpha\theta^3\Gamma\frac{(\alpha+c)}{\alpha} + \Gamma\frac{(4\alpha+c)}{\alpha}} x^{\alpha+c-1}\left(1+x^{3\alpha}\right)e^{-\theta x^{\alpha}} \right)$$

$$\times \left(\frac{1}{\alpha\theta^3\Gamma\frac{(\alpha+c)}{\alpha} + \Gamma\frac{(4\alpha+c)}{\alpha}} \left(\alpha\theta^3\gamma\left(\frac{(\alpha+c)}{\alpha},\theta x^{\alpha}\right) + \alpha\gamma\left(\frac{(4\alpha+c)}{\alpha},\theta x^{\alpha}\right) \right) \right)^{r-1}$$

$$\times \left(1 - \frac{1}{\alpha\theta^3\Gamma\frac{(\alpha+c)}{\alpha} + \Gamma\frac{(4\alpha+c)}{\alpha}} \left(\alpha\theta^3\gamma\left(\frac{(\alpha+c)}{\alpha},\theta x^{\alpha}\right) + \alpha\gamma\left(\frac{(4\alpha+c)}{\alpha},\theta x^{\alpha}\right) \right) \right)^{n-r}$$

Therefore, the probability density function of higher orderstatistic $X_{(n)}$ of weighted power Rama distribution can be obtained as

$$f_{x(n)}(x) = \frac{n\alpha\theta^{\frac{4\alpha+c}{\alpha}}}{\alpha\theta^3\Gamma\frac{(\alpha+c)}{\alpha} + \Gamma\frac{(4\alpha+c)}{\alpha}} x^{\alpha+c-1}\left(1+x^{3\alpha}\right)e^{-\theta x^{\alpha}}$$

$$\times \left(\frac{1}{\alpha\theta^3\Gamma\frac{(\alpha+c)}{\alpha} + \Gamma\frac{(4\alpha+c)}{\alpha}} \left(\alpha\theta^3\gamma\left(\frac{(\alpha+c)}{\alpha},\theta x^{\alpha}\right) + \alpha\gamma\left(\frac{(4\alpha+c)}{\alpha},\theta x^{\alpha}\right) \right) \right)^{n-1}$$

and the probability density function of first order statistic $X_{(1)}$ of weighted power Rama distribution can be obtained as

Soumya *et al.*,

$$f_{x(1)}(x) = \frac{n\alpha\theta^{\frac{4\alpha+c}{\alpha}}}{\alpha\,\theta^3\Gamma\frac{(\alpha+c)}{\alpha} + \Gamma\frac{(4\alpha+c)}{\alpha}} x^{\alpha+c-1}\left(1+x^{3\alpha}\right)e^{-\theta x^{\alpha}}$$

$$\times\left(1 - \frac{1}{\alpha\,\theta^3\Gamma\frac{(\alpha+c)}{\alpha} + \Gamma\frac{(4\alpha+c)}{\alpha}}\left(\alpha\,\theta^3\gamma\left(\frac{(\alpha+c)}{\alpha},\theta x^{\alpha}\right) + \alpha\gamma\left(\frac{(4\alpha+c)}{\alpha},\theta x^{\alpha}\right)\right)\right)^{n-1}$$

Likelihood Ratio Test

Let the random sample $X_1, X_2,….X_n$ of size n from the power Rama or weighted power Rama distribution. To test we use the hypothesis

$$H_O : f(x) = f(x;\theta,\alpha) \qquad \text{against} \quad H_1 : f(x) = f_w(x;\theta,\alpha,c)$$

In order to determine whether the random sample of size n comes from the power Ramadistribution or weighted power Rama distribution, the following test procedure is used

$$\Delta = \frac{L_1}{L_o} = \prod_{i=1}^{n}\frac{f_w(x;\theta,\alpha,c)}{f(x;\theta,\alpha)}$$

$$\Delta = \frac{L_1}{L_o} = \prod_{i=1}^{n}\left(\frac{\alpha\theta^{\frac{c}{\alpha}}x_i^{c}\left(\theta^3+6\right)}{\alpha\,\theta^3\Gamma\frac{(\alpha+c)}{\alpha} + \Gamma\frac{(4\alpha+c)}{\alpha}}\right)$$

$$\Delta = \frac{L_1}{L_o} = \left(\frac{\alpha\theta^{\frac{c}{\alpha}}\left(\theta^3+6\right)}{\alpha\,\theta^3\Gamma\frac{(\alpha+c)}{\alpha} + \Gamma\frac{(4\alpha+c)}{\alpha}}\right)^{n}\prod_{i=1}^{n}x_i^{c}$$

We should refuse to accept the null hypothesis if

$$\Delta = \left(\frac{\alpha\theta^{\frac{c}{\alpha}}\left(\theta^3+6\right)}{\alpha\,\theta^3\Gamma\frac{(\alpha+c)}{\alpha} + \Gamma\frac{(4\alpha+c)}{\alpha}}\right)^{n}\prod_{i=1}^{n}x_i^{c} > k$$

Equivalently, we should also refuse to retain the null hypothesis where

$$\Delta^{*} = \prod_{i=1}^{n}x_i^{c} > k\left(\frac{\alpha\,\theta^3\Gamma\frac{(\alpha+c)}{\alpha} + \Gamma\frac{(4\alpha+c)}{\alpha}}{\alpha\theta^{\frac{c}{\alpha}}\left(\theta^3+6\right)}\right)^{n}$$

Soumya *et al.*,

$$\Delta^* = \prod_{i=1}^{n} x_i^{\,c} > k^*, \text{Where } k^* = k \left(\frac{\alpha\theta^3\Gamma\dfrac{(\alpha+c)}{\alpha} + \Gamma\dfrac{(4\alpha+c)}{\alpha}}{\alpha\theta^{\frac{c}{\alpha}}\left(\theta^3 + 6\right)} \right)^n$$

Whether for the large sample of size *n, 2log Δ* is distributed as chi-square distribution with one degree of freedom and also chi-square distribution is employed for determining *p* value. Thus, we reject to retain the null hypothesis if the probability value is given by

$$p\left(\Delta^* > \beta^*\right), \text{Where } \beta^* = \prod_{i=1}^{n} x_i^{\,c} \text{ is lower than a specified level of significance and } \prod_{i=1}^{n} x_i^{\,c}$$

is the detected value of the statistic Δ^*.

Bonferroni and Lorenz Curves

The bonferroni and Lorenz curves also termed as classical curves are used to measure the distribution of inequality in income or poverty. The bonferroni and Lorenz curves are given by

$$B(p) = \frac{1}{p\mu_1'} \int_0^q x f_w(x)dx$$

and $\quad L(p) = pB(p) = \dfrac{1}{\mu_1'} \displaystyle\int_0^q x f_w(x)dx$

Where $\mu_1' = \dfrac{\alpha\theta^3\Gamma\dfrac{(\alpha+c+1)}{\alpha} + \Gamma\dfrac{(4\alpha+c+1)}{\alpha}}{\alpha\theta^{\frac{1}{\alpha}}\left(\alpha\theta^3\Gamma\dfrac{(\alpha+c)}{\alpha} + \Gamma\dfrac{(4\alpha+c)}{\alpha}\right)}$ $\quad$ and $\quad q = F^{-1}(p)$

$$B(p) = \frac{\alpha\theta^{\frac{1}{\alpha}}\left(\alpha\theta^3\Gamma\dfrac{(\alpha+c)}{\alpha} + \Gamma\dfrac{(4\alpha+c)}{\alpha}\right)}{p\left(\alpha\theta^3\Gamma\dfrac{(\alpha+c+1)}{\alpha} + \Gamma\dfrac{(4\alpha+c+1)}{\alpha}\right)} \int_0^q \frac{\alpha\theta^{\frac{4\alpha+c}{\alpha}}}{\alpha\theta^3\Gamma\dfrac{(\alpha+c)}{\alpha} + \Gamma\dfrac{(4\alpha+c)}{\alpha}} x^{\alpha+c}\left(1 + x^{3\alpha}\right)e^{-\theta x^{\alpha}}dx$$

$$B(p) = \frac{\alpha\theta^{\frac{4\alpha+c+1}{\alpha}}}{p\left(\alpha\theta^3\Gamma\dfrac{(\alpha+c+1)}{\alpha} + \Gamma\dfrac{(4\alpha+c+1)}{\alpha}\right)} \int_0^q x^{\alpha+c}\left(1 + x^{3\alpha}\right)e^{-\theta x^{\alpha}}dx$$

$$B(p) = \frac{\alpha\theta^{\frac{4\alpha+c+1}{\alpha}}}{p\left(\alpha\theta^3\Gamma\dfrac{(\alpha+c+1)}{\alpha} + \Gamma\dfrac{(4\alpha+c+1)}{\alpha}\right)} \left(\int_0^q x^{\alpha+c}e^{-\theta x^{\alpha}}dx + \int_0^q x^{4\alpha+c}e^{-\theta x^{\alpha}}dx\right) \tag{12}$$

Put $x^{\alpha} = t \Rightarrow x = t^{\frac{1}{\alpha}}$

Also $\alpha x^{\alpha-1} dx = dt \Rightarrow dx = \dfrac{dt}{\alpha x^{\alpha-1}} \Rightarrow dx = \dfrac{dt}{\alpha t^{\frac{\alpha-1}{\alpha}}}$

After simplification equation (12) becomes

$$B(p) = \frac{\theta^{\frac{4\alpha+c+1}{\alpha}}}{p\left(\alpha\theta^3\Gamma\frac{(\alpha+c+1)}{\alpha} + \Gamma\frac{(4\alpha+c+1)}{\alpha}\right)}\left(\gamma\left(\frac{(\alpha+c+1)}{\alpha},\theta q\right) + \gamma\left(\frac{(4\alpha+c+1)}{\alpha},\theta q\right)\right)$$

$$L(p) = \frac{\theta^{\frac{4\alpha+c+1}{\alpha}}}{\left(\alpha\theta^3\Gamma\frac{(\alpha+c+1)}{\alpha} + \Gamma\frac{(4\alpha+c+1)}{\alpha}\right)}\left(\gamma\left(\frac{(\alpha+c+1)}{\alpha},\theta q\right) + \gamma\left(\frac{(4\alpha+c+1)}{\alpha},\theta q\right)\right)$$

Maximum Likelihood Estimation and Fisher's Information Matrix

In this section, we will discuss the parameter estimation of weighted power Rama distribution by using the method of maximum likelihood estimation. Let $X_1, X_2…,X_n$ be a random sample of size *n* from the weighted power Rama distribution, then the likelihood function can be written as

$$L(x) = \prod_{i=1}^{n} f_w(x)$$

$$L(x) = \prod_{i=1}^{n}\left(\frac{\alpha\theta^{\frac{4\alpha+c}{\alpha}}}{\alpha\theta^3\Gamma\frac{(\alpha+c)}{\alpha} + \Gamma\frac{(4\alpha+c)}{\alpha}} x_i^{\alpha+c-1}\left(1+x_i^{3\alpha}\right)e^{-\theta x_i^{\alpha}}\right)$$

$$L(x) = \left(\frac{\alpha\theta^{\frac{4\alpha+c}{\alpha}}}{\alpha\theta^3\Gamma\frac{(\alpha+c)}{\alpha} + \Gamma\frac{(4\alpha+c)}{\alpha}}\right)^n \prod_{i=1}^{n}\left(x_i^{\alpha+c-1}\left(1+x_i^{3\alpha}\right)e^{-\theta x_i^{\alpha}}\right)$$

$$L(x) = \frac{\alpha\theta^{n\left(\frac{4\alpha+c}{\alpha}\right)}}{\left(\alpha\theta^3\Gamma\frac{(\alpha+c)}{\alpha} + \Gamma\frac{(4\alpha+c)}{\alpha}\right)^n} \prod_{i=1}^{n}\left(x_i^{\alpha+c-1}\left(1+x_i^{3\alpha}\right)e^{-\theta x_i^{\alpha}}\right)$$

The log likelihood function is given by

Soumya *et al*.,

$$\log L = n\left(\frac{4\alpha + c}{\alpha}\right)\log \alpha\theta - n\log\left(\alpha\,\theta^3\Gamma\frac{(\alpha+c)}{\alpha} + \Gamma\frac{(4\alpha+c)}{\alpha}\right)$$

$$+(\alpha+c-1)\sum_{i=1}^{n}\log x_i + \sum_{i=1}^{n}\log\left(1+x_i^{\,3\alpha}\right) - \theta\sum_{i=1}^{n}x_i^{\,\alpha} \qquad (13)$$

By differentiating the log likelihood equation (13) with respect to θ, α and c and must satisfy the following normal

equations

$$\frac{\partial \log L}{\partial \theta} = \frac{n\alpha}{\alpha\theta}\left(\frac{4\alpha+c}{\alpha}\right) - n\left(\frac{3\alpha\,\theta^2\Gamma\frac{(\alpha+c)}{\alpha}}{\alpha\,\theta^3\Gamma\frac{(\alpha+c)}{\alpha} + \Gamma\frac{(4\alpha+c)}{\alpha}}\right) - \sum_{i=1}^{n}x_i^{\,\alpha} = 0$$

$$\frac{\partial \log L}{\partial \alpha} = -\frac{n\theta\,c}{\alpha^3\theta} - n\left(\frac{\theta^3\Gamma\frac{(\alpha+c)}{\alpha}}{\alpha\theta^3\Gamma\frac{(\alpha+c)}{\alpha} + \Gamma\frac{(4\alpha+c)}{\alpha}}\right) + \sum_{i=1}^{n}\log x_i + \sum_{i=1}^{n}\frac{x_i^{\,3\alpha}\log x_i}{\left(1+x_i^{\,3\alpha}\right)} - \theta\sum_{i=1}^{n}x_i^{\,\alpha}\log x_i = 0$$

$$\frac{\partial \log L}{\partial c} = \frac{n}{\alpha}\log\alpha\theta - n\psi\left(\alpha\theta^3\Gamma\frac{(\alpha+c)}{\alpha} + \Gamma\frac{(4\alpha+c)}{\alpha}\right) + \sum_{i=1}^{n}\log x_i = 0$$

Where ψ (.)is the digamma function.

The above system of non linear equations are too complicated to solve it algebraically. Therefore we use R and wolfram mathematics for estimating the required parameters of the proposed distribution.

In order to use the asymptotic normality results for obtaining the confidence interval. We have that if $\hat{\lambda} = \left(\hat{\theta},\hat{\alpha},\hat{c}\right)$ denotes the MLE of $\lambda = (\theta,\alpha,c)$, we can state the result as

$$\sqrt{n}(\hat{\lambda} - \lambda) \to N_3\left(0, I^{-1}(\lambda)\right)$$

Where $I(\lambda)$ is Fisher's Information matrix.i.e .

$$I(\lambda) = -\frac{1}{n}\begin{pmatrix} E\left(\dfrac{\partial^2 \log L}{\partial \theta^2}\right) & E\left(\dfrac{\partial^2 \log L}{\partial \theta\,\partial \alpha}\right) & E\left(\dfrac{\partial^2 \log L}{\partial \theta\,\partial c}\right) \\[2mm] E\left(\dfrac{\partial^2 \log L}{\partial \alpha\,\partial \theta}\right) & E\left(\dfrac{\partial^2 \log L}{\partial \alpha^2}\right) & E\left(\dfrac{\partial^2 \log L}{\partial \alpha\,\partial c}\right) \\[2mm] E\left(\dfrac{\partial^2 \log L}{\partial c\,\partial \theta}\right) & E\left(\dfrac{\partial^2 \log L}{\partial c\,\partial \alpha}\right) & E\left(\dfrac{\partial^2 \log L}{\partial c^2}\right) \end{pmatrix}$$

Here, we show that

63459

Soumya *et al.*,

$$E\left(\frac{\partial^2 \log L}{\partial \theta^2}\right) = -\frac{n\alpha^2}{(\alpha\theta)^2}\left(\frac{4\alpha+c}{\alpha}\right) - n\left(\frac{\left(\alpha\theta^3\Gamma\frac{(\alpha+c)}{\alpha} + \Gamma\frac{(4\alpha+c)}{\alpha}\right)\left(6\alpha\theta\,\Gamma\frac{(\alpha+c)}{\alpha}\right) - \left(3\alpha\,\theta^2\Gamma\frac{(\alpha+c)}{\alpha}\right)\left(3\alpha\,\theta^2\Gamma\frac{(\alpha+c)}{\alpha}\right)}{\left(\alpha\theta^3\Gamma\frac{(\alpha+c)}{\alpha} + \Gamma\frac{(4\alpha+c)}{\alpha}\right)^2}\right)$$

$$E\left(\frac{\partial^2 \log L}{\partial \alpha^2}\right) = \frac{3n\alpha^2\theta^2 c}{\left(\alpha^3\theta\right)^2} + n\left(\frac{\left(\theta^3\Gamma\frac{(\alpha+c)}{\alpha}\right)\left(\theta^3\Gamma\frac{(\alpha+c)}{\alpha}\right)}{\left(\alpha\theta^3\Gamma\frac{(\alpha+c)}{\alpha} + \Gamma\frac{(4\alpha+c)}{\alpha}\right)^2}\right) + \sum_{i=1}^n \frac{\left(1 + x_i^{3\alpha}\right)x_i^{3\alpha}\left(\log x_i\right)^2 - \left(x_i^{3\alpha}\log x_i\right)^2}{\left(1 + x_i^{3\alpha}\right)^2}$$

$$-\theta\sum_{i=1}^n\left(x_i^{\alpha}\log x_i\right)^2$$

$$E\left(\frac{\partial^2 \log L}{\partial c^2}\right) = -n\psi'\left(\alpha\theta^3\Gamma\frac{(\alpha+c)}{\alpha} + \Gamma\frac{(4\alpha+c)}{\alpha}\right)$$

$$E\left(\frac{\partial^2 \log L}{\partial \theta\,\partial \alpha}\right) = -n\left(\frac{\left(\alpha\,\theta^3\Gamma\frac{(\alpha+c)}{\alpha} + \Gamma\frac{(4\alpha+c)}{\alpha}\right)\left(3\theta^2\Gamma\frac{(\alpha+c)}{\alpha}\right) - \left(\theta^3\Gamma\frac{(\alpha+c)}{\alpha}\right)\left(3\alpha\theta^2\Gamma\frac{(\alpha+c)}{\alpha}\right)}{\left(\alpha\theta^3\Gamma\frac{(\alpha+c)}{\alpha} + \Gamma\frac{(4\alpha+c)}{\alpha}\right)^2}\right) - \sum_{i=1}^n x_i^{\alpha}\log x_i$$

$$E\left(\frac{\partial^2 \log L}{\partial \theta\,\partial c}\right) = \frac{n\alpha}{\alpha^2\theta} - n\psi\left(\frac{3\alpha\,\theta^2\Gamma\frac{(\alpha+c)}{\alpha}}{\alpha\theta^3\Gamma\frac{(\alpha+c)}{\alpha} + \Gamma\frac{(4\alpha+c)}{\alpha}}\right)$$

$$E\left(\frac{\partial^2 \log L}{\partial \alpha\,\partial c}\right) = -\frac{n\theta}{\alpha^3\theta} - n\psi\left(\frac{\theta^3\Gamma\frac{(\alpha+c)}{\alpha}}{\alpha\theta^3\Gamma\frac{(\alpha+c)}{\alpha} + \Gamma\frac{(4\alpha+c)}{\alpha}}\right)$$

Where $\psi(.)'$ is the first order derivative of digamma function. Since λ being unknown, we estimate $I^{-1}(\lambda)$ by $I^{-1}(\hat{\lambda})$ and this can be used to obtain asymptotic confidence intervals for θ, α and c.

Soumya *et al.*,

Application

In this section, we have fitted a real lifetime data set in weighted power Rama distribution to discuss its goodness of fit and the fit has been compared over power Rama, two parameter Rama and one parameter Rama distributions. The real lifetime data set is given below as The following real lifetime data set consists of 100 samples represents the birth weight of babies collected by the researcher from a private hospital in Kerala India during the year 2021. The real life time data set is given below in table 1 as

In order to determine the model comparison criterion values, the unknown parameters are also computed through the technique of R software. In order to compare the performance of weighted power Rama distribution with power Rama, two parameter Rama and one parameter Rama distributions, we use the criterions like Bayesian Information criterion (*BIC*), Akaike Information Criterion (*AIC*), Akaike Information Criterion Corrected (*AICC*) and *-2logL*. The better distribution is which corresponds to the lesser values of *AIC,BIC, AICC* and *-2logL*. For computing the criterions like *AIC, BIC, AICC* and *-2logL* following formulas are used

$$AIC = 2k - 2\log L, \qquad BIC = k \log n - 2 \log L \qquad \text{and} \qquad AICC = AIC + \frac{2k(k+1)}{n-k-1}$$

Where *k* is the number of parameters in the statistical model, *n* is the sample size and *–2logL* is the maximized value of log-likelihood function under the considered model.

From table 2 given above, it has been clearly seen from the results that the weighted power Rama distribution has the lesser *AIC,BIC, AICC* and *-2logL* values as compared to the power Rama, two parameter Rama and one parameter Rama distributions. Hence, it can be concluded that the weighted power Rama distribution provides a better fit over power Rama, two parameter Rama and one parameter Rama distributions.

CONCLUSION

The present paper established a new model of power Rama distribution termed as weighted power Rama distribution has been executed. The new distribution is generated by using the weighted technique to the classical distribution. Its various statistical properties which include moments, survival function, hazard rate function, moment generating function, harmonic mean, shape of the pdf and cdf, order statistics, bonferroni and lorenz curves have been studied. The parameters of new distribution have also been estimated by using the method of maximum likelihood estimation. Finally, a new distribution has been demonstrated with real lifetime data set to discuss its supremacy and it is observed from the result that the weighted power Rama distribution fits quite satisfactory over power Rama, two parameter Rama and one parameter Rama distributions.

REFERENCES

1. Abebe, B., Tesfay, M., Eyob, T. and Shanker, R. (2019). A two-parameter power Rama distribution with properties and applications. *Biometrics & Biostatistics International Journal*, 8(1), 6-11.
2. Bashir, S. and Rasul, M. (2015). Some properties of the weighted Lindley distribution. *International Journal of Economics and Business Review*, 3, 11-17.
3. Bashir, S. and Rasul, M. (2018). A new weighted Rayleigh distribution: Properties and Applications on lifetime data. *Open Journal of Statistics*, 8, 640-650.
4. Cox, D. R. (1969). Some sampling problems in technology, In New Development in Survey Sampling, Johnson, N. L. and Smith, H., Jr .(eds.) New York Wiley- *Interscience*, 506-527.
5. Dar, A. A., Ahmed, A. and Reshi, J. A. (2020). Weighted Gamma-Pareto distribution and its application. *Pak.J.Statist.*, 36(4), 287-304.

Soumya *et al.,*

6. Das, S. and Kundu, D. (2016). On weighted exponential distribution and its length biased version. *Journal of the Indian Society for Probability and Statistics*, 17, 57-77.

7. Edith, U. U., Ebele, T. U. and Henrietta, A. I. (2019). A two-parameter Rama distribution. *EarthlineJournal of Mathematical Sciences*, Vol. 2, No. 2, 365-382.

8. Fisher, R. A. (1934). The effects of methods of ascertainment upon the estimation of frequencies. *Annals of Eugenics*, 6(1), 13-25.

9. Kersey, J. X. (2010). Weighted inverse Weibull and Beta-inverse Weibull distribution. *M.SC. Thesis, University of Georgia Southern.*

10. Kilany, N. M. (2016). Weighted Lomax distribution. *SpringerPlus*, 5(1), doi: 10.1186/s40064-016-3489-2.

11. Mahdi, A. A. (2020). Weighted exponential Lomax distribution. *AI-Bahir Quarterly Adjudicated Journal for Natural and Engineering Research and Studies*, Vol. 12, No. 23 and 24, 27-36.

12. Rajagopalan, V., Ganaie, R. A. and Nair, S. R. (2023). A new extension of two parameter Pranav distribution with applications in Industrial and Medical Sciences. *Journal of Statistics Applications & Probability*, 12(1), 231-246.

13. Rao, C. R. (1965). On discrete distributions arising out of method of ascertainment, in classical and Contagious Discrete, G.P. Patiled; Pergamum Press and Statistical publishing Society,Calcutta. 320-332.

14. Rather, A. A. and Subramanian, C. (2019). On weighted Sushila distribution with properties and its applications. *International Journal of Scientific Research in Mathematical and Statistical Sciences*, Vol. 6, Issue 1, 105-117.

15. R core team (2019). R version 3.5.3: A language and environment for statistical computing. R Foundation for statistical computing, Vienna, Austria.URL https:// www.R-project .org/.

16. Saghir, A., Hamedani, G. G., Tazeem, S. and Khadim, A. (2017). Weighted distributions: A brief Review, Perspective and Characterizations. *International Journal of Statistics and Probability*, 6(3), 109-131.

17. Shanker, R. (2017). Rama distribution and its application. *International Journal of Statistics and Applications*, 7(1), 26-35.

18. Shanker, R., Shukla, K. K. and Leonida, T. A. (2019). Weighted quasi Lindley distribution with properties and applications. *International Journal of Statistics and Applications*, 9(1), 8-20.

19. Ye, Y., Oluyede, B. O. and Pararai, M. (2012). Weighted generalized beta distribution of the second kind and related distributions. *Journal of Statistical and Econometric Methods*, 1, 13-31.

20. Zelen, M. (1974), Problems in cell kinetic and the early detection of disease, in Reliability and Biometry, F. Proschan & R. J. Sering, eds, *SIAM, Philadelphia*, 701-706.

Table 1: Data regarding the birth weight of babies in Kerala during the year 2021

3.005	3.35	2.805	2.92	3.065	3.55	2.77	2.715	2.885	3.145
2.76	3.865	2.8	3.34	3.78	3.135	3.14	3.6	2.95	3.295
3.105	2.91	3.435	1.66	2.38	2.8	2.625	3.05	2.695	2.15
3.11	1.08	3.975	2.71	3.19	0.985	3.125	3.22	2.875	2.94
3.035	3.43	3.06	2.67	2.915	2.77	2.95	2.7	2.67	2.68
3.43	1.635	2.6	3.07	2.32	3.025	2.98	3.09	2.8	2.865
3.965	2.35	2.805	2.625	3.02	3.06	2.71	3.07	2.035	3.41
2.63	2.88	3.135	3.57	2.55	3.745	3.36	2.995	3.58	2.25
2.98	2.96	2.77	3.33	3.78	3.3	2.795	3.045	1.96	3.11
3.265	2.72	2.98	2.095	2.495	4.035	3.725	3.09	3.61	3.2

Table 2: Comparison and Performance of Fitted Distributions

Distributions	MLE	S.E	- 2logL	AIC	BIC	AICC
Weighted Power Rama	$\hat{\alpha} = 0.86969944$ $\hat{\theta} = 8.08415153$ $\hat{c} = 15.36203894$	$\hat{\alpha} = 0.02100096$ $\hat{\theta} = 1.40328122$ $\hat{c} = 3.34534534$	139.6608	145.6608	153.4763	145.9108

Power Rama	$\hat{\alpha} = 0.80922370$ $\hat{\theta} = 1.32358451$	$\hat{\alpha} = 0.04788841$ $\hat{\theta} = 0.07390590$	307.9417	311.9417	317.152	312.0654
Two Parameter Rama	$\hat{\alpha} = 0.00100000$ $\hat{\theta} = 1.35744128$	$\hat{\alpha} = 0.01003002$ $\hat{\theta} = 0.03604148$	277.9187	281.9187	287.129	282.0424
Rama	$\hat{\theta} = 1.15134710$	$\hat{\theta} = 0.05229817$	322.2909	324.2909	326.896	324.3317
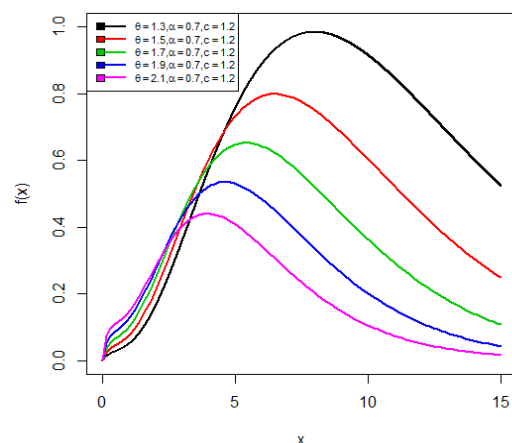
Fig.1:Pdf plot of Weighted Power Rama Distribution
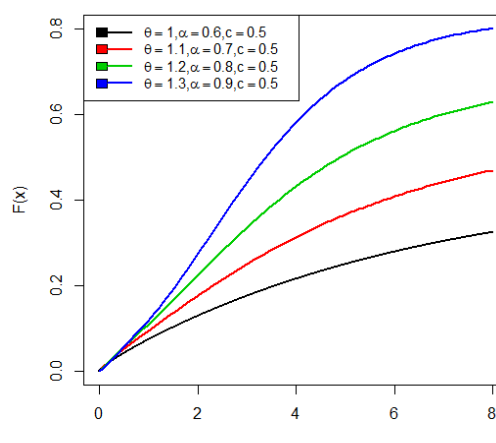
Fig.2:Cdf plot of Weighted Power Rama Distribution
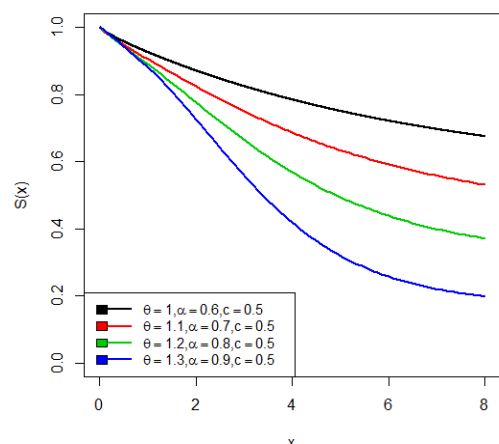
Fig.3:Survival plot of Weighted Power Rama Distribution
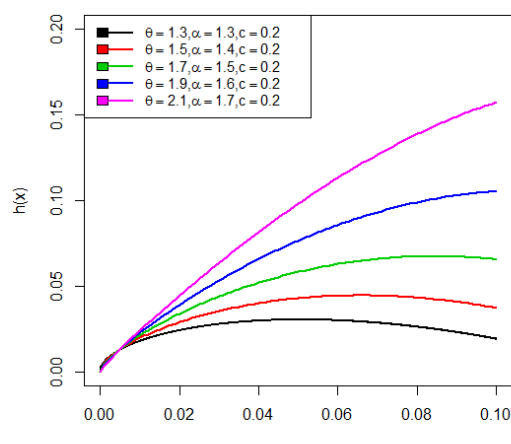
Fig.4:Hazard Plot of Weighted Power Rama Distribution

RESEARCH ARTICLE

Johan Coloring of Network Graphs

S.Florence Poornima[1]* and A.Arokia Lancy[2]

[1]Research Scholar, PG and Research Department of Mathematics, Nirmala College for Women, Coimbatore - 641018,Tamil Nadu, India.
[2]Assistant Professor, PG and Research Department of Mathematics, Nirmala College for Women, Coimbatore - 641018, Tamil Nadu, India

*Address for Correspondence
S.Florence Poornima
Research Scholar,
PG and Research Department of Mathematics,
Nirmala College for Women.
Coimbatore-641018, Tamil Nadu, India.
E. Mail: florence.poornima25@gmail.com

ABSTRACT

A type of graph labelling is graph colouring. It is the process of assigning the vertices of a graph with colors so that no two neighbouring vertices have the same colour. Assume G is a graph with the chromatic coloring C specified. The rainbow neighbourhood in G is the closed neighbourhood of a vertex v belonging to V(G) and containing at least one coloured vertex of each colour in G's chromatic colouring C. Johan colouring or J-coloring is possible if every vertex of G belongs to a rainbow neighbourhood of Graph G. We investigate Johan Coloring of several network types Graph in this paper.

Keywords: Rainbow neighbourhood, Johan Coloring, Johan Coloring Number, Honeycomb Network, Seirpinski Triangle, Triangular Grid Graph, Hexagonal Mesh, Butterfly Network, Benes Netwok.

INTRODUCTION

The challenge of how to colour the countries on a map so that no two countries sharing a border have the same colour is where the concept of graph colouring first arose. A planar graph can be created by representing the countries as points on a plane and connecting each pair of points that represent countries that share a border. A network is a collection of nodes that are linked together by edges or connections that link them with one another. In mathematics, networks are frequently referred to as graphs. The role of networks plays an essential part in electrical, electronic, and computer engineering. The graph theory principle is applied in the network to establish the relationship between the networked computers. There is an important application of graph theory in network research

63464

Florence Poornima and Arokia Lancy

Network theory is utilized in many fields, such as statistical physics, biology, public health, and sociology. The Internet, logistical networks, social networks, and other networks are examples of applications of network theory. Vertex colouring, commonly referred to as graph colouring, is the process of giving labels or colours to the vertices of a graph under particular conditions. Proper colouring of a graph occurs when its vertices are coloured so that no two adjacent vertices share the same colour. The minimal number of distinct colours required for a graph G to be properly coloured is known as its chromatic number.

Preliminaries
For fundamental terms and definitions related to graphs we refer [1][2].
Definition:2.1 [3]
Let G be a graph with a chromatic colouring C defined on it. The rainbow neighbourhood in G is the closed neighbourhood N[v] of a vertex $v \in V$ (G) which contains at least one coloured vertex of each colour in the chromatic colouring C of G.

Definition:2.2 [3]
Let G be a graph with a chromatic colouring C defined on it. The number of vertices in G yielding rainbow neighbourhoods is called the rainbow neighbourhood number of the graph G, denoted by $r_x(G)$.

Definition:2.3 [4]
A proper k-coloring C of a graph G is called the Johan coloring or the J-Coloring of G if C is the maximal coloring such that every vertex of G belongs to a rainbow neighbourhood of G. A graph G is J-Colorable if it admits J-Coloring.

Definition:2.4[4]
The J-colouring number of a graph G, denoted by J (G) is the maximum number of colours in A J-colouring of G.
Definition:2.5[6]
The Sierpinski Triangle is a fractal and geomentric figure in which similar pattern recur progressively in smaller scales. In 1915, it was named after the polish mathematician Walcaw Sierpinski who described it. The Sierpinski triangle can be created from an equilateral triangle by continually dividing it into 4 small congruent equilateral triangles while eliminating the middle triangle. Sierpinski Gasket is another name for it.

Definition:2.6[7]
A triangular grid T_n is the graph created from interpreting the order (n+1) triangular grid as a graph, with grid line intersections serving as the vertices and line segments between vertices as the edges.

Definition:2.7[8]
HX_n is a hexagonal mesh of dimension n with $3n^2-3n+1$ nodes and $9n^2-15n+6$ lines. The corner nodes of HX_n has degree 3 and there are 6 corner nodes.
There are 2n-1 vertical lines for every n dimensions of the hexagonal mesh HX_n. Vertical lines are denoted by the letter X .
The central nodes of the hexagonal mesh are denoted as X_0 and are referred to as the hexagonal mesh's spine.
$X_1, X_2, ...X_{n+1}$ are the numbers to the left of X_0 while the right side are denoted as $X_{-1}, X_{-2}, ...X_{-n+1}$.

Definition:2.8[9]
The k-dimensional butterfly network, denoted by BF(k), has a node set V = {(m, i): m $\in$ V (Q_k), $0 \le i \le k$}. Two nodes (m, i) and (n, j) are linked by a line in BF(k) iff j = i + 1 and either (i) m = n, or (ii) m differs from n in precisely the j th bit. For m=y, the line is said to be a straight line. Otherwise, the line is a cross line. For fixed i, the node (m, i) is a node on level i. The BF(k) has $(k+1)2^k$ nodes because BF(k) has k + 1 stages and there are 2^k nodes in every stage. Each node on stage 0 and k is of degree 2, otherwise, every node is of degree 4.

Definition:2.9[9]
The back-to-back butterfly network which forms the m-dimensional benes network BB(m) has 2m+1 levels and $(2m+1)2^m$ nodes and $m2^{m+2}$ lines.[7]

Definition:3.0[10]
A unit honeycomb network is represented by the hexagon denoted by HC(1). Six hexagons were added around the HC(1) network's boundary edges to create the honeycomb network of size 2, or HC(2). By surrounding the boundary edges of HC(n - 1) with a layer of hexagons, the honeycomb network HC(n) can be inductively constructed from HC(n - 1).

HC(n) has $6n^2$ nodes and $9n^2-3n$ lines.

In HC(n), each node is denoted by a pair (a, b), where a is the line number in which the node exists and b is the node's position in the line. The first node on line number one has the address 1,1. Node 1,2 denotes the second node on line 1, and so on.[11]

Johan Coloring of Network Graphs
Theorem:3.1
Honeycomb Network admits Johan Coloring.
Proof:
Let us consider a honeycomb network HC(n).
Each node in a honeycomb network is denoted as (a,b).
Let us color the nodes of the HC(n) with colors c_1, c_2,.. respectively.
When a=1,2,3.. and when b is even the nodes are colored with color c_1 and when b is odd the nodes are colored with colors c_2.
Thus by definition of Johan coloring every vertices of HC(n) has rainbow neighbourhood .
Thus the honeycomb network HC(n) admits Johan coloring The Johan coloring number of HC(n) is 2.

Theorem:3.2
Seirpinski Triangle admits Johan Coloring.
Proof:
Let us consider an Sierpinski Triangle S(n).Let us color the vertices of S(n) with colors c_1, c_2, c_3,… respectively. Since Sierpinski Triangle is constructed by subdividing the larger equilateral triangles into four smaller triangles. And each triangles in S(n) are colored with three colors .
By the definition of Johan Coloring, every vertices of Sierpinski triangle has a rainbow neighbourhood. Thus S(n) admits Johan Coloring.
The Johan Coloring Number of sierpinski Triangle is 3.

Theorem:3.3
Triangular Grid Graph admits Johan Coloring.
Proof:
Let us consider a Triangular Grid Graph T_n
Let the vertices of T_n be v_1 ,v_2 ,v_3 ,.. respectively.
The Triangular Grid Graph T_n has n triangles and (n+1) vertices on each side. Let us color the vertices of T_n with c_1,c_2,.. respectively.
By the definition of Johan Coloring,every vertices of T_n has a rainbow neighbourhood.
Thus the Triangular Grid Graph admits Johan Coloring.
The Johan Coloring Number of T_n is 3.

Theorem:3.4
Hexagonal Mesh admits Johan Coloring.

Florence Poornima and Arokia Lancy

Proof:

Let us consider a n-dimensional Hexagonal Mesh HX_n .

HX_nconsists of $3n^2 -3n+1$ nodes and $9n^2-15n+6$ lines.It has totally $2n-1$ vertical lines. The nodes of HX_n are colored with colors c_1, c_2, …respectively. By the definition of Johan coloring, we color the nodes of HX_n with 4 colors alternatively.

Thus every vertices of HX_n has rainbow neighbourhood.

The Johan coloring number of Hexagonal Mesh is 4 .

Theorem:3.5

Butterfly Network admits Johan Coloring.

Proof:

Let us consider a Butterfly Network BF(k).The butterfly network has (k+1) stages and there are 2^k nodes in every stage of BF(k). The nodes of BF(k) are colored with colors c_1,c_2 ,…respectively.

Let us color every nodes of stage 0 with color c_1 since every nodes in stage 0 are not adjacent to each other .

Similarly every nodes in stage 1 are also not adjacent to each other so the nodes of stage 1 are colored with color c_2.

Thus, the remaining stages in BF(k) are colored with colors c_1 and c_2 alternatively.

By the definition of Johan Coloring, every nodes in BF(k) has rainbow neighbourhood. Thus butterfly network admits Johan Coloring.

The Johan coloring Number of BF(k) is 2.

Theorem:3.6

Benes Network admits Johan Coloring.

Proof: Let us Consider a benes network of m-dimension. The benes network has 2m+1 levels and $(2m+1)2^m$ nodes and $m2^{m+2}$ lines. The nodes of BB(m) are colored with $c_1,c_2,…$ respectively. Since no nodes at level 0 are adjacent to each other, so each node in the benes network in this level is coloured c_1. Similarly, every node in level1, level 2,… are colored with colors c_1 and c_2 alternatively. By the definition of Johan Coloring, every nodes in BB(m) has rainbow neighbourhood. Thus the Benes Network admits Johan Coloring. The Johan coloring Number of BB(m) is 2.

CONCLUSION

In this paper, we discussed Johan coloring of Honeycomb network, Sierpinski Triangle, Triangular Grid Graph, Hexagonal Mesh, Butterfly Network and Benes Network and we have also determined the Johan Coloring Number for these Graphs.

REFERENCES

1. J. A. Bondy and U. S. R. Murty, Graph theory with application, North Holland, New York, 1982.
2. Harary.F ,Graph Theory , Addison-Wesley,Reading,Mass,1972.
3. J. Kok, N. K. Sudev and M. K. Jamil, Rainbow neighbourhood number of graphs, arXiv:1703.01089v1 (2019).
4. Johan Kok,Sudev Naduvath,Johan Coloring of Graph Operations, arXiv:1704.02869v1, April(2017).
5. N.K.Sudev, On Certain J-Coloring Parameters of a Graph, arXiv:1612.04194v2(2017).
6. Alberto M. Teguia, Anant P. Godbole, Sierpinski Gasket Graphs and their Properties, arXiv: math/0509259v1, sep(2005).
7. Valery S. Gordon, Yury L. Orlovich, Frank Werner, Hamiltonian properties of triangular grid graphs, Discrete Mathematics, 308(24) (2008), 6166-6188.
8. D.Antony Xavier, R.C.Thivyarathi, Proper Lucky Number of Hexagonal Mesh and Honeycomb Network, International Journal Of Mathematical Trends and Technology, Vol:48, Number:4,August 2017.
9. D.Florence Isido V.M.Chitra, On Difference Cordial Labeling Of Networks,International Journal of Innovative Technology and Exploring Engineering,Vol:8,Issue:7 May(2019).

Florence Poornima and Arokia Lancy

10. Bharathi Rajan, Indra Rajasingh and Francis Xavier.D, Harmonious Coloring of Honeycomb Network,Journal of Computer and Mathematical Sciences, Volume 2, Issue 6,(2011).
11. Sharieh A, Qatawneh M, Almobaideen W, Sleit A, "HexCell: Modeling, Topological Properties and Routing Algorithm", European Journal of Scientific Research, Vol. 22 No.2 , 457-468, (2008).
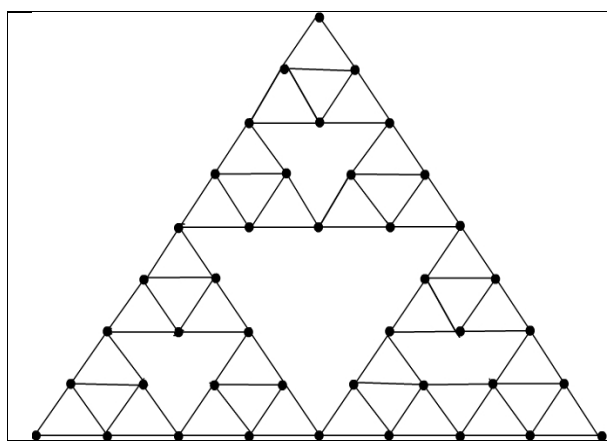
Fig. 1.Seirpinski Triangle
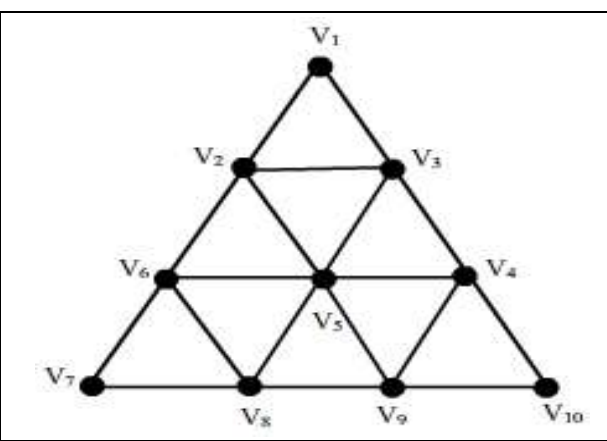
Fig. 2.Triangular Grid Graph
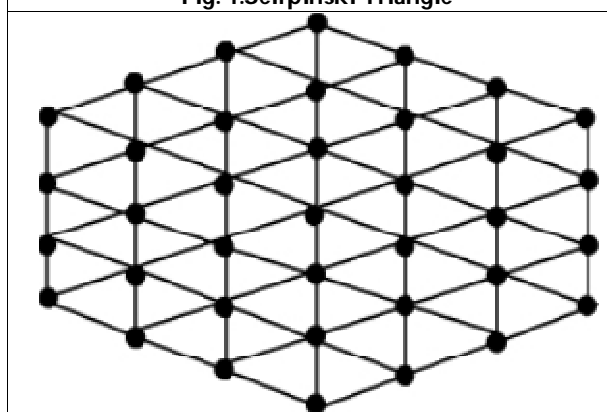
Fig. 3.Hexagonal Mesh
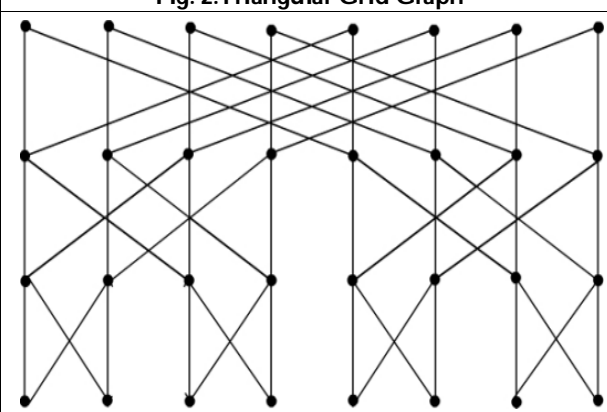
Fig. 4.Butterfly Network
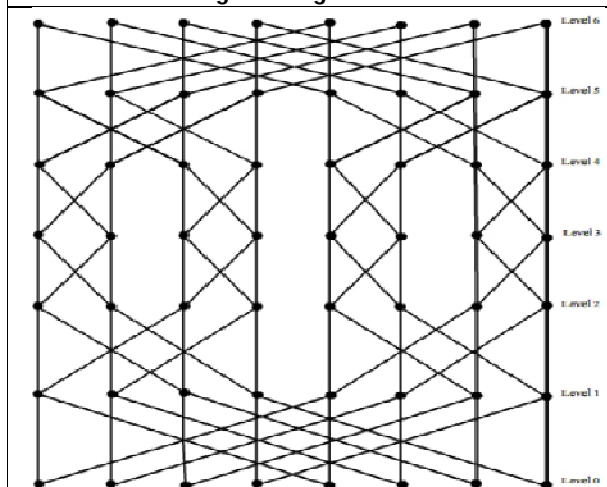
Fig. 5.Benes Network

Fig. 6.Honeycomb Network

63468

Florence Poornima and Arokia Lancy

Fig. 7.Addressing in HC(3)

Fig. 8. Johan Coloring of Honeycomb Network HC(2)

Fig. 9.Johan Coloring of S(3).

Fig. 10. Johan Coloring of Triangular Grid Graph

Fig. 11.Johan Coloring of HX₃

Fig. 12.Johan Coloring of BF(3)

Fig. 13.Johan Coloring of BB(2)

RESEARCH ARTICLE
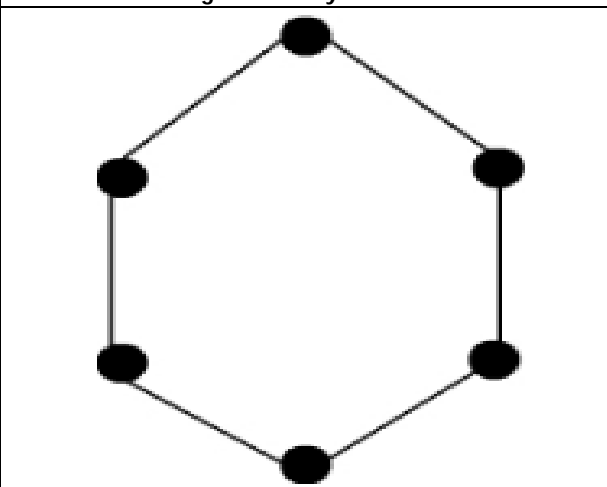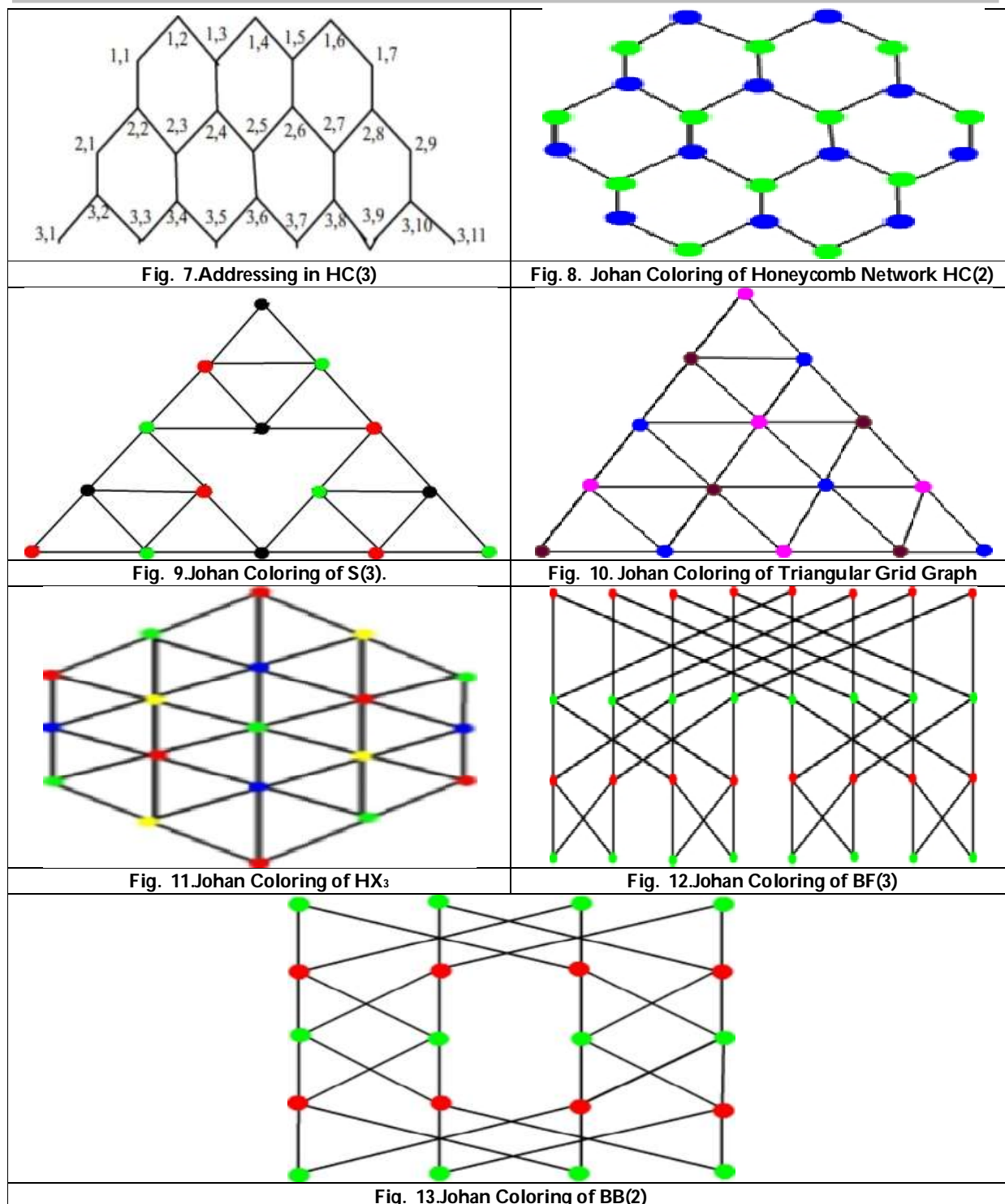
Optimizing Transportation Problem with Pentagonal Fuzzy Numbers

Madhav R Fegade[1] and Aniket A. Muley[2]*

[1]Department of Statistics, Digambarrao Bindu Arts, Commerce and Science College, Bhokar-431801 (M. S.), India

[2]School of Mathematical Sciences, Swami Ramanand Teerth Marathwada University, Nanded-431606 (M. S.), India

*Address for Correspondence
Aniket Muley
School of Mathematical Sciences,
Swami Ramanand Teerth Marathwada University,
Nanded-431606 (M. S.), India
E. Mail: aniket.muley@gmail.com

ABSTRACT

In this paper, we have proposed a new algorithm to find optimal solutions to fuzzy transportation problems. Here, defuzzified the pentagonal numbers by implementing the ranking methodology. This article gives methodology that brings down the optimal solution. The numerical example illustrates the validity of our proposed method.

Keywords: Transportation, fuzzy, optimality, ranking, pentagonal fuzzy numbers.

INTRODUCTION

Operations Research is a state of art approach used for problem-solving and decision making. It helps any organization to achieve their best performance under the given constraints or situations. The transportation problem (TP) is one of the special areas found worldwide which is helpful to solve real life problems. It is important to deal with production, distribution etc. purposes in minimizing the cost function. There are numerous things that make an impact on the transportation cost viz., distance, path, mode, number of units, speed, etc. In this paper, it is observed that there are several research studies to bring the best optimal solution to the transportation problems. The problem that needs to be resolved is to reach cost effective production in various production companies. Our main focus is to transport the optimal number of commodities with minimum transportation cost that will be fruitful to design optimal location decisions. Maheswari and Ganesan [6] dealt with TP with a fuzzy environment where the availability and requirements at sources and destinations were denoted by pentagonal fuzzy numbers. Further, it is being dealt with robust ranking technique and a new fuzzy arithmetic on pentagonal fuzzy numbers. Geetha and Selvakumari [4] proposed a new move towards the key of the TP under a fuzzy environment with transportation

63470

costs are taken as fuzzy pentagonal numbers. The fuzzy numbers and fuzzy values are predominantly used in various fields such as experimental sciences, artificial intelligence, etc. because of their uncertainty. They have converted fuzzy pentagonal numbers into crisp values by using range technique and then solved by the max-min approach. Mitlif *et al.* [9] dealt with optimizing TP with fuzzy pentagonal numbers for the cost, supply, and demand. Further, it has been transformed into crisp values by new ranking methodology. George *et al.* [3] optimize a fuzzy TP algorithm which gives initial solution is closer to optimal solution having trapezoidal fuzzy numbers. It is observed that, the optimal solution is verified by using the fuzzy Modified Distribution method without transforming into its correspondent classical form.

Christi and Kasthuri [2] developed a method that can be dealt with pentagonal intuitionistic fuzzy numbers. TP is a generalization of linear programming problems on distribution and transport of goods from one place to a different with least cost objective. They have used ranking methodology for pentagonal fuzzy number and Russell's technique. Nasir and Beenu [11] proposed a ranking method depends on value and vagueness index of pentagonal intuitionistic fuzzy number is used to answer the unbalanced TP. Menaka [8] proposed for finding optimal TP cost values are pentagonal intuitionistic fuzzy numbers. Mondal and Mandal [10] introduces Pentagonal fuzzy number and some basic arithmetic operations. Das [5] discussed a TP with pentagonal neutrosophic numbers where the supply, demand and transportation cost is uncertain. Maheswari and Vijaya [7] developed a method for obtaining the initial basic feasible solution of fuzzy TP based on the proposed ranking method of trapezoidal fuzzy number using centroid of in centers. They are focused on interval based transportation problems. Further, it is converted to fuzzy TP and then a proposed ranking based on centroid of in centres is applied for the adaptation of crisp numbers to find its initial basic feasible solution. Sengupta *et al.* [12] proposed a reduction method for the pentagonal fuzzy number using the expected value criterion. They proposed reduction method, a single objective carbon cost integrated solid transportation problem minimizing the transportation cost along with the emission cost is solved with the parameters as the pentagonal fuzzy number and it is validated the proposed reduction method and with the existing expected value reduction methods. Chakraborty *et al.* [1] envisaged the hexagonal number from various distinct rational perspectives and viewpoints to give it a look of a conundrum. Hexagonal fuzzy number is used as a trustworthy to ease understanding of vague information. They have proposed a new ranking method.

Preliminaries

Definitions
Fuzzy set: $\tilde{A}$ is fuzzy set on R is defined as a set ordered pairs $\tilde{A} = \{X_0, \mu_A(X_0) \mid X_0 \in \tilde{A}, \mu_A(X_0) \rightarrow$
[0,1]\}, where $\mu_A(X_0)$ is said to be the membership function.
Fuzzy Number $\tilde{A}$ is fuzzy set on R, likely bounded to the stated conditions given beneath
i. $\mu_A(X_0)$ is part by continuous
ii. There exist at one $X_0 \in R$ with $_A(X_0) = 1$
iii. $\tilde{A}$ is a regular and convex
Pentagonal Fuzzy Number A fuzzy number $\tilde{A}$ on R is said to be the pentagonal fuzzy number or linear number which is names as $(\tilde{a}_1 \tilde{a}_2, \tilde{a}_3, \tilde{a}_4, \tilde{a}_5)$ if it membership function $\mu_A(X_0)$ has the following characteristic

Madhav Fegade and Aniket Muley

$$\mu_A(X) = \begin{cases} 0, & X < \tilde{a}_1 \\ \tilde{u}_1 \dfrac{X - \tilde{a}_2}{\tilde{a}_3 - \tilde{a}_2}, & \tilde{a}_2 \leq X \leq \tilde{a}_3 \\ ((1 - (1 - \tilde{u}_1))\dfrac{X - \tilde{a}_2}{\tilde{a}_3 - \tilde{a}_2}, & \tilde{a}_2 \leq X \leq \tilde{a}_3 \\ 1, & X = \tilde{a}_3 \\ ((1 - (1 - \tilde{u}_2))\dfrac{\tilde{a}_4 - X}{\tilde{a}_4 - \tilde{a}_3}, & \tilde{a}_3 \leq X \leq \tilde{a}_4 \\ \tilde{u}_2 \dfrac{\tilde{a}_5 - X}{\tilde{a}_5 - \tilde{a}_4}, & \tilde{a}_4 \leq X \leq \tilde{a}_5 \\ 0, & X > \tilde{a}_5 \end{cases}$$

Here, the midpoint $\tilde{a}_3$ has the grade of membership 1 and $\tilde{a}_2$, $\tilde{a}_4$ has grades $\tilde{u}_1$, $\tilde{u}_2$ respectively. Note that, every pentagonal fuzzy number is connected with two weights $\tilde{u}_1$, $\tilde{u}_2$.

Arithmetic operations

Let, $\tilde{a}_A = (\tilde{a}_1, \tilde{a}_2, \tilde{a}_3, \tilde{a}_4, \tilde{a}_5)$ and $\tilde{b}_B = (\tilde{b}_1 \tilde{b}_2, \tilde{b}_3, \tilde{b}_4, \tilde{b}_5)$ are two fuzzy numbers where $\tilde{a}_1 \leq \tilde{a}_2 \leq \tilde{a}_3 \leq$

$\tilde{a}_4 \leq \tilde{a}_5$ and $\tilde{b}_1 \leq \tilde{b}_2 \leq \tilde{b}_3 \leq \tilde{b}_4 \leq \tilde{b}_5$, then the arithmetic operations are defined are as follows: Addition: $\tilde{a}_A + \tilde{b}_B = (\tilde{a}_1 + \tilde{b}_1, \tilde{a}_2 + \tilde{b}_2, \tilde{a}_3 + \tilde{b}_3, \tilde{a}_4 + \tilde{b}_4, \tilde{a}_5 + \tilde{b}_5)$

Subtraction: $\tilde{a}_A - \tilde{b}_B = (\tilde{a}_1 - \tilde{b}_1, \tilde{a}_2 - \tilde{b}_2, \tilde{a}_3 - \tilde{b}_3, \tilde{a}_4 - \tilde{b}_4, \tilde{a}_5 - \tilde{b}_5)$

Multiplication: $\tilde{a}_A * \tilde{b}_B = \left(\dfrac{\tilde{a}_1}{5}\tilde{Y}_B, \dfrac{\tilde{a}_2}{5}\tilde{Y}_B, \dfrac{\tilde{a}_3}{5}\tilde{Y}_B, \dfrac{\tilde{a}_4}{5}\tilde{Y}_B, \dfrac{\tilde{a}_5}{5}\tilde{Y}_B\right)$ if $\tilde{Y}_B \neq 0$

$Where, \tilde{Y}_B = (\tilde{b}_1 + \tilde{b}_2 + \tilde{b}_3 + \tilde{b}_4 + \tilde{b}_5)$

Division: $\tilde{a}_A * \tilde{b}_B = \left(\dfrac{5\tilde{a}_1}{\tilde{Y}_B}, \dfrac{5\tilde{a}_2}{\tilde{Y}_B}, \dfrac{5\tilde{a}_3}{\tilde{Y}_B}, \dfrac{5\tilde{a}_4}{\tilde{Y}_B}, \dfrac{5\tilde{a}_5}{\tilde{Y}_B}\right)$ $Where, \tilde{Y}_B = (\tilde{b}_1 + \tilde{b}_2 + \tilde{b}_3 + \tilde{b}_4 + \tilde{b}_5)$

F_B F_B F_B F_B F_B

Scalar Multiplication: $k\tilde{a}_A = \{k\tilde{a}_1, k\tilde{a}_2, k\tilde{a}_3, k\tilde{a}_4, k\tilde{a}_5 \text{ if } k > 0 \ k\tilde{a}_5, k\tilde{a}_4, k\tilde{a}_3, k\tilde{a}_2, k\tilde{a}_1 \text{ if } k < 0$

METHODOLOGY

Algorithm

Step 1: To ensure whether the given TP is fair or unequal.1.1: If it is balanced, then go to step 2. : If it is unbalanced, then add a dummy row or dummy column to fulfil the requirement.

Step2: Convert the given pentagonal fuzzy numbers to crisp number using following ranking function:

$$R(\hat{a}_A) = \frac{a_1 + 2a_2 + 3a_3 + 2a_4 + a_5}{9}$$

Step 3: Discover, First smallest amount and second minimum of each row and make the difference between them. i.e. (2nd Minimum-1st Minimum) and the difference is separated by the digit of row in the given table in each iteration.

Step 4: Find the First minimum and second minimum of each column and make the difference between them. i.e. (2nd Minimum-1st Minimum) and the difference is separated by the digit of column in the given table in respective iteration.

Step 5: After simplifying step 3 and 4, select the largest difference and allocate as much as possible to the smallest element in the respective row (Column).

Madhav Fegade and Aniket Muley

Step 6: If maximum difference ratio value may occur more than once in the rows or columns thenarbitrarily select any one row or column but not both.

Step 7: Locate the smallest value obtained from the certain row or column then allot the quantitymaximum possible quantity to fulfil the demand or to exhaust the availability.

Step 8: Repeat the step 3 to 7, until all the availability and demand will get exhausted or fulfilled.

Step 9: To check the allocations are equal to m+n-1 or not. If it is less than m+n-1, then apply theMODI method to check the optimality of the given problem.

RESULT AND DISCUSSION

A motion that established fuzzy TP which includes: transportation cost, customer desires and demands and existence of commodities with pentagonal fuzzy numbers. Examined the following TPas stated in Table 1[13]:

Total Minimum cost=38 × 4.4444 + 2 × 3 + 50 × 4.4444 + 18 × 4.3333 + 30 × 4.8888 + 4 × 5.3333+ 5× 6.4444 = 676.3266

The comparison of the proposed method with NCWM, LCM, Russell's Approximation method, Rowminima method, column minima method and VAM is tabulated below (Table 9):

CONCLUSION

In this study, the proposed algorithm gives us better solution for the TP with pentagonal fuzzy numbers. In general, this algorithm can be useful for all types of fuzzy TP and can be generalized for similar kinds of studies. The proposed method will be helpful in decision making process for selection of new location having more than two destinations. It is observed that, cost of TP is minimized after implementing the proposed methodology. Hence, the good results achieved with theproposed perspective.

REFERENCES

1. Chakraborty, A., Maity, S., Jain, S., Mondal, S. P., Alam, S. (2021). Hexagonal fuzzy number and its distinctive representation, ranking, defuzzification technique and application in production inventory management problem. Granular Computing, 6(3), 507-521.
2. Christi,M. A., Kasthuri, B. (2016). Transportation Problem with Pentagonal Intuitionistic Fuzzy Numbers Solved Using Ranking Technique and Russell's Method; Int. Journal of Engineering Research and Applications, 6(2), 82-86.
3. George, G., Maheswari, P. U., Ganesan, K. (2020). A modified method to solve fuzzy transportation problem involving trapezoidal fuzzy numbers. In AIP Conference Proceedings. AIP Publishing LLC. 2277(1), p. 090005.
4. Geetha, S. S., Selvakumari, K. (2020). A new method for solving fuzzy transportation problem using pentagonal fuzzy numbers. Journal of Critical Reviews, 7(9), 171-174.
5. Kumar Das, S. (2020). Application of transportation problem under pentagonal Neutrosophic environment. Journal of fuzzy extension and applications, 1(1), 27-41.
6. Maheswari, P. U., Ganesan, K. (2018). Solving fully fuzzy transportation problem using pentagonal fuzzy numbers. In Journal of physics: conference series, 1000 (1), p. 012014. IOP Publishing.
7. Maheswari, P., Vijaya, M. (2019). On initial basic feasible solution (IBFS) of fuzzy transportation problem based on ranking of fuzzy numbers using centroid of incenters. Int. J. Appl. Eng. Res, 14(4), 155-164.
8. Menaka, G. (2017). Ranking of octagonal intuitionistic fuzzy numbers. IOSR Journal of Mathematics, 13(3), 63-71.
9. Mitlif, R. J., Rasheed, M., Shihab, S. (2020). An Optimal Algorithm for a Fuzzy Transportation Problem. Journal of Southwest Jiaotong University, 55(3).
10. Mondal, S. P., Mandal, M. (2017). Pentagonal fuzzy number, its properties and application in fuzzy equation. Future Computing and Informatics Journal, 2(2), 110-117.

Madhav Fegade and Aniket Muley

11. Nasir,V. K., Beenu, V. P. (2021). Unbalanced transportation problem with pentagonal intuitionistic fuzzy number solved using ambiguity index. Malaya Journal of Matematik, 9(1), 720-724.

12. Sengupta, D., Datta, A., Das, A., Bera, U. K. (2018). The Expected Value Defuzzification Method for Pentagonal Fuzzy Number to Solve a Carbon Cost Integrated Solid Transportation Problem. In 2018 3rd International Conference for Convergence in Technology. IEEE 1-6.

13. Srinivasan, R., Karthikeyan, N., & Jayaraja, A. (2021). A Proposed Ranking Method to Solve Transportation Problem by Pentagonal Fuzzy Numbers. Turkish Online Journal of Qualitative Inquiry (TOJQI). 12(3), 277-286

Table 1: Given dataset

	D_1	D_2	D_3	D_4	Availability
O_1	(2,4,6,8,9)	(3,5,7,8,9)	(2,4,5,6,7)	(3,4,6,7,12)	30
O_2	(0,2,5,6,8)	(4,5,6,8,11)	(2,3,5,7,11)	(1,5,6,9,11)	27
O_3	(1,2,3,4,5)	(2,3,4,6,8)	(4,5,6,8,9)	(6,7,8,9,13)	40
O_4	(3,5,6,7,8)	(1,5,6,7,8)	(2,7,8,9,10)	(3,3,4,5,9)	50
Demand	20	38	34	55	147

By using ranking technique (Step 2) we have defuzzified the given transportation problem and represented Table 2.

Table 2: Defuzzified Transportation problem

	D_1	D_2	D_3	D_4	Availability
O_1	5.8888	6.5555	4.8888	6.1111	30
O_2	4.3333	6.5555	5.3333	6.4444	27
O_3	3	4.4444	6.3333	8.3333	40
O_4	5.8888	6.6666	7.5555	4.4444	50

Table 3: First Iteration

	D_1	D_2	D_3	D_4	Availability	$\dfrac{2nd\ Min - 1st\ Min}{4}$
O_1	5.8888	6.5555	4.8888	6.1111	30	0.25
O_2	4.3333	6.5555	5.3333	6.4444	27	0.25
O_3	3	**38** 4.4444	6.3333	8.3333	40	03611
O_4	5.8888	6.6666	7.5555	4.4444	50	03611
Demand	20	38	34	55		
$-\dfrac{2nd\ Min - 1st\ Min}{4}$	0.3332	0.5277 t	0.1111	0.4166		

Madhav Fegade and Aniket Muley

Table 4: Second Iteration

	D_1	D_3	D_4	Availability	$2nd\ Min - 1st\ Min$ —————— 3
O_1	5.8888	4.8888	6.1111	30	0.3333
O_2	4.3333	5.3333	6.4444	27	0.3333
O_3	2 3	6.3333	8.3333	2	1.1111 ←
O_4	5.8888	7.5555	4.4444	50	0.4814
Demand	20	34	55		
$2nd\ Min - 1st\ Min$ —————— 4	0.3332	0.1111	0.4166		

Table 5: Third Iteration

	D_1	D_3	D_4	Availability	$2nd\ Min - 1st\ Min$ —————— 3
O_1	5.8888	4.8888	6.1111	30	0.3333
O_2	4.3333	5.3333	6.4444	27	0.3333
O_4	5.8888	7.5555	**50** 4.4444	50	0.4814
Demand	18	34	55		
$2nd\ Min - 1st\ Min$ —————— 3	0.5185	0.1481	0.5555 t		

Table 6: Fourth Iteration

	D_1	D_3	D_4	Availability	$2nd\ Min - 1st\ Min$ 2
O_1	5.8888	4.8888	6.1111	30	0.5
O_2	**18** 4.3333	5.3333	6.4444	27	0.5
Demand	18	34	5		
$2nd\ Min - 1st\ Min$ 3	0.5185 t	0.1481	0.1111		

Table 7: Fifth Iteration

	D_3	D_4	Availability	$2nd\ Min - 1st\ Min$ 2
O_1	**30** 4.8888	6.1111	30	0.6111 ←
O_2	5.3333	6.4444	9	0.5555
Demand	34	5		
$2nd\ Min - 1st\ Min$ 2	0.2222	0.1665		

Madhav Fegade and Aniket Muley

Table 8: Final Iteration

		D_3	D_4	Availability	$2nd\ Min - 1st\ Min$
O_2		**4** 5.3333	**5** 6.4444	9	0.5555
Demand		4	5		
$2nd\ Min - 1st\ Min$ ——————— 2		0.2222	0.1665		

Table 9: Comparative Results

Methods	Optimal Solutions
NCWM [13]	896.12
LCM [13]	727.19
Russell's Approximation Method [13]	727.19
Row Minima Method [13]	721.19
Column Minima Method [13]	727.19
VAM Method [13]	717.86
Ranking method [13]	714.47
Proposed method	676.3266

RESEARCH ARTICLE

A New Algorithm for Solving Interval Valued Picture Fuzzy Transportation Problems

P.Rajarajeswari[1] and K.Vanithamani[2]*

[1]Associate Professor, Department of Mathematics, Chikkanna Govt. Arts College, Tirupur-02, Tamil Nadu, India.
[2]Research Scholar, Department of Mathematics, Chikkanna Govt. Arts College, Tirupur-02, Tamil Nadu, India.

*Address for Correspondence
K.Vanithamani
Research Scholar,
Department of Mathematics,
Chikkanna Govt. Arts College,
Tirupur-02, Tamil Nadu, India.
E.Mail: vanitha200985@gmail.com

ABSTRACT

Researchers and entrepreneurs are growing more interested in Picture Fuzzy Sets (PFS) to resolve uncertainty and hesitance in real world problems. Interval Valued Picture Fuzzy Sets (IVPFN) is a more useful method for handling ambiguity and impressions. In this paper, three types of Interval Valued Picture Fuzzy Transportation problem(IVPFTP) that are taken into consideration are Type 1(demand and supply), Type 2(cost only) and Type 3(demand, supply and cost) with the above parameters represented as IVPFS. Additionally the three different types of formulae namely WIDTH, HM and PERT were developed and they are used to covert the IVPFS into crisp values in the three different types of IVPFTP. After that the Initial Basic Feasible Solution(IBFS) was found using the RANGE method. Finally a comparison of the Type 1, Type 2 and Type 3 IVPFTP results are produced.

Keywords: Picture Fuzzy Sets, Interval Valued Picture Fuzzy Sets, RANGE method

INTRODUCTION

In 1965, Zadeh[10] introduced Fuzzy Set (FS) and Interval Valued Fuzzy Set (IVFS), both of which are effective in handling uncertainty. The membership degree in FS and IVFS is essentially a sub interval of [0,1].Atanassov[3] introduced Intuitionistic Fuzzy Sets, a distinct extension of Fuzzy Sets. The membership and non-membership functions are two functions found in IFSs, each requiring a sum within a closed unit interval. Atanassov and Gargov[3] introduced the Interval Valued Intuitionistic Fuzzy Set (IVIFS).IVIFS stipulates that the total supremum of

these intervals must belong to the intervals [0,1]. Coung[6] introduced the concept of PFS, which comprises membership, neutral, and non-membership functions, ensuring their sum must fit within a closed unit interval. Coung introduces Interval Valued Picture Fuzzy Sets, specifying membership, neutral, and non-membership degrees within a closed subinterval of [0,1], with the supremum of all three subintervals within a closed unit interval. IVPFSs are superior in describing fuzzy information compared to other types of FSs, IVFSs, IFSs, IVIFS, and PFSs. The Transportation Problem (TP) aims to find the best solution for minimizing transportation costs, considering supply and demand limitations, from origin to destination. The optimal TP solution can be determined through two stages: identifying an Initial Basic Feasible Solution (IBFS) and determining the optimal solution from an IBFS. Scholars have conducted three well-known IBFS studies: Northwest Corner Method (NCM), Least Cost Method (LCM), and Vogel's Approximation Method (VAM)[9]. Juman and Hoque proposed the Juman Hoque Method (JHM) for obtaining IBFS, while Ahmed et al. presented the Incessant Allocation Method (IAM) for transportation problem. In order to deliver items to clients in amore proper way, the transportation problem provides feasible solutions. Real world problems, unpredictable occurrences, such as traffic restrictions and weather conditions frequently occur. In this situation, Sathya Geetha and Selvanayaki[8] given the A Picture Fuzzy Approach to Solving Transportation Problem. From The IVPFS is a highly effective method for addressing ambiguity and impressions. We introduce and generalize IVPFTP, an efficient alternative to PFTP, and develop a new algorithm for finding IBFS, comparing it with existing methods.

Preliminaries

In this section we define a few fundamental terms to make the following sections easier to understand for readers. The universal set is called X.

Definition 2.1. A FS on X is defined as:

$T = \{x, \Omega(x) \mid x \in X\}$,   (1)

where the term $\Omega(x)$ refers tomembership function,$\Omega: X \rightarrow [0, 1]$ that expresses the degree to which an object is a member of a non-empty set.Each $\Omega(x)$ is known as a fuzzy number.

Definition 2.2. An IVFS on X is defined as:

$T = \{x, \Omega_T(x) \mid x \in X\}$,   (2)

where $\Omega_T = [\Omega_{TL}, \Omega_{TU}]$ is subinterval of [0, 1] and it expresses the degree of membership by sub-interval and each $\Omega(x)$ is called IVFN.

Definition 2.3. An IFS on X is defined as:

$T = \{x, \Omega(x), \delta(x) \mid x \in X\}$,   (3)

where $\Omega, \delta: X \rightarrow [0,1]$ are called membership and non-membership functions. An IFS has a condition that the sum of both functions must lie in unit interval and the degree of refusal is defined as $r(x) = 1 - (\Omega(x) + \delta(x))$. A duplet $(\Omega(x), \delta(x))$ is called an intuitionistic fuzzy number (IFN).

Definition 2.4. An IVIFS on a universal set X is defined as:

$T = \{x, \Omega_T(x), \delta_T(x) \mid x \in X\}$,   (4)

where $\Omega_T = [\Omega_{TL}, \Omega_{TU}]$, $\delta_T = [\delta_{TL}, \delta_{TU}]$ and $\Omega_T, \delta_T: X \rightarrow [0,1]$. An IVIFS has a condition that the sum of supremum of membership and non-membership functions must lie in unit interval. A duplet $(\Omega(x), \delta(x))$ is called interval-valued intuitionistic fuzzy number (IVIFN).

Definition 2.5. A PFS on X is defined as:

$T = \{x, \Omega(x), \Lambda(x), \delta(x) \mid x \in X\}$,   (5)

where $\Omega, \Lambda, \delta: X \rightarrow [0,1]$ are called membership, abstinence, and non-membership functions. A PFS has a condition that the sum of all three functions must lie in unit interval and the degree of refusal is defined as $(x) = 1 - (\Omega(x) + \Lambda(x) + \delta(x))$. A triplet $(\Omega(x), \Lambda(x), \delta(x))$ is called a PFN.

Definition 2.6. An IVPFS on a universal set X is defined as:

$T = \{x, \Omega_T(x), \Lambda(x), \delta(x) \mid x \in X\}$,   (6)

where $\Omega_T = [\Omega_{TL}, \Omega_{TU}]$, $\Lambda_T = [\Lambda_{TL}, \Lambda_{TU}]$, $\delta_T = [\delta_{TL}, \delta_{TU}]$ and $\Omega_T, \Lambda_T, \delta_T: X \rightarrow [0,1]$. An IVPFS has a condition that the sum of supremum of all three functions must lie in unit interval. A triplet $(\Omega(x), \Lambda(x), \delta(x))$ is called interval-valued picture fuzzy number (IVPFN).

Definition 2.7 : Type 1 IVPFTP

In this type of interval valued picture fuzzy transportation problem, the transportation costs are crisp values and the supply, demand are interval valued picture fuzzy numbers.

IVPFTP Table 1

S_1	C_{11}	C_{12}	C_{13}	...	C_{1n}	$([a_{s\Omega_1},b_{s\Omega_1}],$ $[a_{s\Lambda_1},b_{s\Lambda_1}],[a_{s\delta_1},b_{s\delta_1}]),$
S_2	C_{21}	C_{22}	C_{23}	...	C_{2n}	$([a_{s\Omega_2},b_{s\Omega_2}],$ $[a_{s\Lambda_2},b_{s\Lambda_2}],[a_{s\delta_2},b_{s\delta_2}]),$
S_3	C_{31}	C_{32}	C_{33}	...	C_{3n}	$([a_{s\Omega_3},b_{s\Omega_3}],$ $[a_{s\Lambda_3},b_{s\Lambda_3}],[a_{s\delta_3},b_{s\delta_3}]),$
⋮	⋮	⋮	⋮	...	⋮	
S_m	C_{m1}	C_{m2}	C_{m3}	...	C_{mn}	$([a_{s\Omega_m},b_{s\Omega_m}],$ $[a_{s\Lambda_m},b_{s\Lambda_m}],[a_{s\delta_m},b_{s\delta_m}]),$
Demand	$([a_{d\Omega_1},b_{d\Omega_1}],$ $[a_{d\Lambda_1},b_{d\Lambda_1}],$ $[a_{d\delta_1},b_{d\delta_1}]),$	$([a_{d\Omega_2},b_{d\Omega_2}],$ $[a_{d\Lambda_2},b_{d\Lambda_2}],$ $[a_{d\delta_2},b_{d\delta_2}]),$	$([a_{d\Omega_3},b_{d\Omega_3}],$ $[a_{d\Lambda_3},b_{d\Lambda_3}],$ $[a_{d\delta_3},b_{d\delta_3}]),$	...	$([a_{d\Omega_n},b_{d\Omega_n}],$ $[a_{d\Lambda_n},b_{d\Lambda_n}],$ $[a_{d\delta_n},b_{d\delta_n}]),$	

In the above IVPFTP table1 where

C_{ij} – be the costs,

$[a_{d\Omega_j},b_{d\Omega_j}], [a_{d\Lambda_j},b_{d\Lambda_j}], [a_{d\delta_j},b_{d\delta_j}])$- be the demands,

$[a_{s\Omega_i},b_{s\Omega_i}], [a_{s\Lambda_i},b_{s\Lambda_i}], [a_{s\delta_i},b_{s\delta_i}])$-be the supply.

Definition 2.7. Type 2 IVPFTP

IVPFTP Table 2

	D_1	D_2	D_3	...	D_n	Supply
S_1	$([a_{\Omega_{11}},b_{\Omega_{11}}],$ $[a_{\Lambda_{11}},b_{\Lambda_{11}}],$ $[a_{\delta_{11}},b_{\delta_{11}}])$	$([a_{\Omega_{12}},b_{\Omega_{12}}],$ $[a_{\Lambda_{12}},b_{\xi_{12}}],$ $[a_{\delta_{12}},b_{\delta_{12}}]),$	$([a_{\Omega_{13}},b_{\Omega_{13}}],$ $[a_{\Lambda_{13}},b_{\xi_{13}}],$ $[a_{\delta_{13}},b_{\delta_{13}}]),$	...	$([a_{\Omega_{1n}},b_{\Omega_{1n}}],$ $[a_{\Lambda_{1n}},b_{\xi_{1n}}],$ $[a_{\delta_{1n}},b_{\delta_{1n}}]),$	C_{s1}
S_2	$([a_{\Omega_{21}},b_{\Omega_{21}}],$ $[a_{\Lambda_{21}},b_{\xi_{21}}],$ $[a_{\delta_{21}},b_{\delta_{21}}])$	$([a_{\Omega_{22}},b_{\Omega_{22}}],$ $[a_{\Lambda_{22}},b_{\xi_{22}}],$ $[a_{\delta_{22}},b_{\delta_{22}}]),$	$([a_{\Omega_{23}},b_{\Omega_{23}}],$ $[a_{\Lambda_{23}},b_{\xi_{23}}],$ $[a_{\delta_{23}},b_{\delta_{23}}]),$	...	$([a_{\Omega_{2n}},b_{\Omega_{2n}}],$ $[a_{\Lambda_{2n}},b_{\xi_{2n}}],$ $[a_{\delta_{2n}},b_{\delta_{2n}}]),$	C_{s2}
S_3	$([a_{\Omega_{31}},b_{\Omega_{31}}],$ $[a_{\Lambda_{31}},b_{\Lambda_{31}}],$ $[a_{\delta_{31}},b_{\delta_{31}}]),$	$[a_{\Omega_{32}},b_{\Omega_{32}}],$ $[a_{\Lambda_{32}},b_{\Lambda_{32}}],$ $[a_{\delta_{32}},b_{\delta_{32}}]),$	$[a_{\Omega_{33}},b_{\Omega_{33}}],$ $[a_{\Lambda_{33}},b_{\Lambda_{33}}],$ $[a_{\delta_{33}},b_{\delta_{33}}]),$	...	$([a_{\Omega_{3n}},b_{\Omega_{3n}}],$ $[a_{\Lambda_{3n}},b_{\Lambda_{3n}}],$ $[a_{\delta_{3n}},b_{\delta_{3n}}]),$	C_{s3}
⋮	⋮	⋮	⋮	⋮		⋮
S_m	$([a_{\Omega_{m1}},b_{\Omega_{m1}}],$ $[a_{\Lambda_{m1}},b_{\xi_{m1}}],$ $[a_{\delta_{m1}},b_{\delta_{m1}}]),$	$([a_{\Omega_{m2}},b_{\Omega_{m2}}],$ $[a_{\Lambda_{m2}},b_{\Lambda_{m2}}],$ $[a_{\delta_{m2}},b_{\delta_{m2}}]),$	$([a_{\Omega_{m3}},b_{\Omega_{m3}}],$ $[a_{\Lambda_{m3}},b_{\Lambda_{m3}}],$ $[a_{\delta_{m3}},b_{\delta_{m3}}]),$	...	$([a_{\Omega_{mn}},b_{\Omega_{mn}}],$ $[a_{\Lambda_{mn}},b_{\Lambda_{mn}}],$ $[a_{\delta_{mn}},b_{\delta_{mn}}]),$	C_{sm}
Demand	C_{d1}	C_{d2}	C_{d3}	...	C_{dn}	

In the IVPFTP type 2,the transportation costs are interval valued picture fuzzy numbers and the supply, demands are crisp values. The Type 2 IVPFTP from the above IVPFTP Table 2, where

$[a_{\Omega_{ij}},b_{\Omega_{ij}},a_{\Lambda_{ij}},b_{\xi_{ij}},a_{\delta_{ij}},b_{\delta_{ij}}]$ are costs,

C_{dj} be the demand,

C_{si} be the supply.

Type 3 IVPFTP

This type of IVPFTP have transportation costs, supply and demands are interval valued picture fuzzysets. The following table represents IVPFTP Type 3.

IVPFTP Table 3

	D_1	D_2	D_3	...	D_n	Supply
S_1	$([a_{\Omega_{11}},b_{\Omega_{11}}],$ $[a_{\Lambda_{11}},b_{\xi_{11}}],$ $[a_{\delta_{11}},b_{\delta_{11}}])$	$([a_{\Omega_{12}},b_{\Omega_{12}}],$ $[a_{\Lambda_{12}},b_{\xi_{12}}], [a_{\delta_{12}},b_{\delta_{12}}])$	$([a_{\Omega_{13}},b_{\Omega_{13}}],$ $[a_{\Lambda_{13}},b_{\xi_{13}}],$ $[a_{\delta_{13}},b_{\delta_{13}}])$	...	$([a_{\Omega_{1n}},b_{\Omega_{1n}}],$ $[a_{\Lambda_{1n}},b_{\xi_{1n}}],$ $[a_{\delta_{1n}},b_{\delta_{1n}}]),$	$([a_{s\Omega_1},b_{s\Omega_1}],$ $[a_{s\Lambda_1},b_{s\Lambda_1}],$ $[a_{s\delta_1},b_{s\delta_1}])$
S_2	$([a_{\Omega_{21}},b_{\Omega_{21}}],$ $[a_{\Lambda_{21}},b_{\xi_{21}}],$ $[a_{\delta_{21}},b_{\delta_{21}}])$	$([a_{\Omega_{22}},b_{\Omega_{22}}],$ $[a_{\Lambda_{22}},b_{\xi_{22}}], [a_{\delta_{22}},b_{\delta_{22}}])$	$([a_{\Omega_{23}},b_{\Omega_{23}}],$ $[a_{\Lambda_{23}},b_{\xi_{23}}],$ $[a_{\delta_{23}},b_{\delta_{23}}])$	...	$([a_{\Omega_{2n}},b_{\Omega_{2n}}],$ $[a_{\Lambda_{2n}},b_{\xi_{2n}}],$ $[a_{\delta_{2n}},b_{\delta_{2n}}]),$	$([a_{s\Omega_2},b_{s\Omega_2}],$ $[a_{s\Lambda_2},b_{s\Lambda_2}],$ $[a_{s\delta_2},b_{s\delta_2}])$
S_3	$([a_{\Omega_{31}},b_{\Omega_{31}}],$ $[a_{\Lambda_{31}},b_{\Lambda_{31}}],$ $[a_{\delta_{31}},b_{\delta_{31}}])$	$([a_{\Omega_{32}},b_{\Omega_{32}}],$ $[a_{\Lambda_{32}},b_{\Lambda_{32}}],$ $[a_{\delta_{32}},b_{\delta_{32}}])$	$([a_{\Omega_{33}},b_{\Omega_{33}}],$ $[a_{\Lambda_{33}},b_{\Lambda_{33}}],$ $[a_{\delta_{33}},b_{\delta_{33}}])$	...	$([a_{\Omega_{3n}},b_{\Omega_{3n}}],$ $[a_{\Lambda_{3n}},b_{\Lambda_{3n}}],$ $[a_{\delta_{3n}},b_{\delta_{3n}}])$	$([a_{s\Omega_3},b_{s\Omega_3}],$ $[a_{s\Lambda_3},b_{s\Lambda_3}],$ $[a_{s\delta_3},b_{s\delta_3}])$
⋮	⋮	⋮	⋮	⋮	⋮	⋮
S_m	$([a_{\Omega_{m1}},b_{\Omega_{m1}}],$ $[a_{\Lambda_{m1}},b_{\xi_{m1}}],$ $[a_{\delta_{m1}},b_{\delta_{m1}}])$	$([a_{\Omega_{m2}},b_{\Omega_{m2}}],$ $[a_{\Lambda_{m2}},b_{\Lambda_{m2}}],$ $[a_{\delta_{m2}},b_{\delta_{m2}}])$	$([a_{\Omega_{m3}},b_{\Omega_{m3}}],$ $[a_{\Lambda_{m3}},b_{\Lambda_{m3}}],$ $[a_{\delta_{m3}},b_{\delta_{m3}}])$	...	$([a_{\Omega_{mn}},b_{\Omega_{mn}}],$ $[a_{\Lambda_{mn}},b_{\Lambda_{mn}}],$ $[a_{\delta_{mn}},b_{\delta_{mn}}])$	$([a_{s\Omega_m},b_{s\Omega_m}],$ $[a_{s\Lambda_m},b_{s\Lambda_m}],$ $[a_{s\delta_m},b_{s\delta_m}])$
Demand	$([a_{d\Omega_1},b_{d\Omega_1}],$ $[a_{d\Lambda_1},b_{d\Lambda_1}],$ $[a_{d\delta_1},b_{d\delta_1}])$	$([a_{d\Omega_2},b_{d\Omega_2}],$ $[a_{d\Lambda_2},b_{d\Lambda_2}],$ $[a_{d\delta_2},b_{d\delta_2}])$	$([a_{d\Omega_3},b_{d\Omega_3}],$ $[a_{d\Lambda_3},b_{d\Lambda_3}],$ $[a_{d\delta_3},b_{d\delta_3}])$	...	$([a_{d\Omega_n},b_{d\Omega_n}],$ $[a_{d\Lambda_n},b_{d\Lambda_n}],$ $[a_{d\delta_n},b_{d\delta_n}])$	

In Type 3, IVPFTP Table 3

$C_{ij} = ([a_{\Omega_{ij}},b_{\Omega_{ij}}], [a_{\Lambda_{ij}},b_{\Lambda_{ij}}], [a_{\delta_{ij}},b_{\delta_{ij}}])$ for i =1,2,3…m and j =1,2,3…n represents the transportation cost for transporting one unit from the ith origin to j^{th} destination ,where $[a_{\Omega_{ij}},b_{\Omega_{ij}}]$ represents the membership,$[a_{\Lambda_{ij}},b_{\Lambda_{ij}}]$ represents abstinence and $[a_{\delta_{ij}},b_{\delta_{ij}}]$ represents non-membership values which are Interval Valued Picture Fuzzy Sets

Algorithm to IBFS for IVPFTP

RANGE method for IBFS of IVPFTP. The following algorithm is used to find IBFS for IVPTP.

Step 1: Find width by using the following formulae

$d_{\Omega_{ij}}=(b_{\Omega_{ij}}- a_{\Omega_{ij}})/2,$ $d_{\Lambda_{ij}}=(b_{\Lambda_{ij}}- a_{\Lambda_{ij}})/2$ and
$d_{\delta_{ij}}=(b_{\delta_{ij}}- a_{\delta_{ij}})/2$ and we get the values of $d_{\Omega_{ij}}, d_{\vartheta_{ij}}, d_{\varpi_{ij}},$
where i =1,2,3…m and j =1,2,3…n

Step 2: Find the number between the interval $([a_{\Omega_{ij}},b_{\Omega_{ij}}], [a_{\vartheta_{ij}},b_{\vartheta_{ij}}], [a_{\delta_{ij}},b_{\delta_{ij}}])$ by using following.

$e_{\Omega_{ij}}= a_{\Omega_{ij}}+ d_{\Omega_{ij}}$; $e_{\Lambda_{ij}} = a_{\Lambda_{ij}}+ d_{\Lambda_{ij}}$ and $e_{\delta_{ij}} = a_{\delta_{ij}}+ d_{\delta_{ij}},$
where i =1,2,3…m and j =1,2,3…n

Form,
$T_{\Omega_{ij}}= (a_{\Omega_{ij}}, e_{\Omega_{ij}}, b_{\Omega_{ij}});$ $T_{\vartheta_{ij}}= (a_{\Lambda_{ij}}, e_{\Lambda_{ij}}, b_{\Lambda_{ij}}),$ and $T_{\delta_{ij}}= (a_{\delta_{ij}}, e_{\delta_{ij}}, b_{\delta_{ij}}),$
where i =1,2,3…m and j =1,2,3…n

Step 3: Use the HM formula and find the value of triangular values. After that, get PFSare following.

$$C_{\Omega_{ij}}=\frac{3}{\left(\frac{1}{a_{\Omega_{ij}}}\right)+\left(\frac{1}{e_{\Omega_{ij}}}\right)+\left(\frac{1}{b_{\Omega_{ij}}}\right)}$$

$$C_{\Lambda_{ij}}=\frac{3}{\left(\frac{1}{a_{\Lambda_{ij}}}\right)+\left(\frac{1}{e_{\Lambda_{ij}}}\right)+\left(\frac{1}{b_{\Lambda_{ij}}}\right)}$$

$$C_{\delta_{ij}}=\frac{3}{\left(\frac{1}{a_{\delta_{ij}}}\right)+\left(\frac{1}{e_{\delta_{ij}}}\right)+\left(\frac{1}{b_{\delta_{ij}}}\right)}, \text{ where } i \text{ =1,2,3…m and } j \text{ =1,2,3…n}$$

Step 4: Use the ranking formula namely PERT formula and change the PFS into crisp values in the IVPFTP.
$C_{ij}= (C_{\Omega_{ij}}+(4xC_{\vartheta_{ij}})+ C_{\delta_{ij}})/6$, where i =1,2,3…m and j =1,2,3…n

Step 5. Find the range for each row and each column, where range = largest cost- smallest cost.

Step 6. Find the row or column with the largest range. For the minimum cost in the selected row or column assign the corresponding demand or supply, whichever is minimum. Supply and demand in related to the value that was assigned to the cell. Once you have crossed the fully satisfied row or column, continue.

Step 7. Steps 5 and 6 should be repeated until all conditions are fulfilled.

Step 8. Calculate the Transportation Cost.

Example1 represent the Type 1 IVPFTP.

IVPFTP Table 4

	D_1	D_2	D_3	D_4	Supply
S_1	0.7	0.2	0.6	0.1	([0.7,0.8], [0,0.1], [0.05,0.1])
S_2	0.3	0.1	0.9	0.2	([0.3,0.4], [0.1,0.3], [0.2,0.3])
S_3	0.4	0.2	0.7	0.1	([0.5,0.6], [0.2,0.3], [0,0.1])
S_4	0.3	0.3	0.1	0.3	([0.3,0.4], [0.1,0.3], [0.2,0.3])
Demand	([0.5,0.6], [0.2,0.3], [0,0.1])	([0.7,0.8], [0,0.1],[0.05,0.1])	([0.3,0.4], [0.1,0.3],[0.2,0.3])	([0.1,0.2],[0.5,0.6], [0,0.1])	

Use the steps 1-5 from the algorithm and get the following table values.

	D_1	D_2	D_3	D_4	Supply
S_1	0.7	0.2	0.6	0.1	0.13
S_2	0.3	0.1	0.9	0.2	0.38
S_3	0.4	0.2	0.7	0.1	0.25
S_4	0.3	0.3	0.1	0.3	0.19
Demand	0.25	0.13	0.19	0.38	

IVPFTP Table 5

The IBFS table is given below by the steps 6-8 from the proposed algorithm.

IVPFTP Table 6

	D_1	D_2	D_3	D_4	Supply
S_1	0.7	0.2	0.6	0.13 0.1	0.13
S_2	0.25 0.3	0.13 0.1	0.9	0.2	0.38
S_3	0.4	0.2	0.7	0.25 0.1	0.25
S_4	0 0.3	0.3	0.19 0.1	0.3	0.19
Demand	0.25	0.13	0.19	0.38	

Z=(0.25*0.3)+(0.13*0.1)+(0*0.3)+(0.19*0.1)+(0.25*0.1)+(0.13*0.1)

=0.145

Example2

This example represented the Type 2 model and it has the costs are IVPFS and the supply, demands are crisp values.

IVPFTP Table 7

	D$_1$	D$_2$	D$_3$	D$_4$	Supply
S$_1$	([0.6,0.7], [0,0.1],[0.05,0.1])	([0.4,0.5],[0.2,0.3],[0.1, 0.2])	([0.3,0.4],[0.2,0.3],[0.1, 0.2])	([0.7,0.8], [0,0.1],[0.05,0.1])	0.4
S$_2$	([0.1,0.2],[0.5,0.6],[0,0.1])	([0.4,0.5],[0.2,0.3],[0,0.1])	([0.7,0.8],[0,0.1],[0,0])	([0.3,0.4],[0.4,0.5],[0,0.1])	0.1
S$_3$	([0.2,0.3],[0.3,0.4],[0,0.1])	([0.6,0.7],[0.2,0.3],[0,0])	([0.5,0.6],[0.2,0.3],[0,0.1])	([0.5,0.6],[0.1,0.2],[0,0.2])	0.1
S$_4$	([0.3,0.4],[0.2,0.4],[0.1, 0.2])	([0.7,0.8],[0.1,0.2],[0,0])	([0.3,0.4],[0.5,0.6],[0,0])	([0.6,0.7],[0,0.1],[0.05, 0.1])	0.7
Demand	0.4	0.1	0.6	0.2	

Used the steps 1-5 from the algorithm we get the below table values.

IVPFTP Table 8

	D$_1$	D$_2$	D$_3$	D$_4$	Supply
S$_1$	0.11	0.26	0.19	0.13	0.4
S$_2$	0.39	0.24	0.12	0.36	0.1
S$_3$	0.42	0.22	0.27	0.12	0.1
S$_4$	0.25	0.27	0.27	0.18	0.7
Demand	0.4	0.1	0.6	0.2	

The IBFS table is given below by the steps 6-8 from the proposed algorithm.

	D$_1$	D$_2$	D$_3$	D$_4$	Supply
S$_1$	0.4 0.11	0.26	0.19	0 0.13	0.4
S$_2$	0.39	0.24	0.1 0.12	0.36	0.1
S$_3$	0.42	0.22	0.27	0.12	0.1
S$_4$	0.25	0.1 0.27	0.5 0.27	0.1 0.18	0.7
Demand	0.4	0.1	0.6	0.2	

IVPFTP Table 9

Z=(0.4*0.1)+(0*0.13)+(0.1*0.12)+(0.1*0.12)+(0.1*0.27)+(0.5*0.27)+(0.1*0.18)

=0.236

Example 3.

In this example all costs, supply and demands are IVPFS.

Rajarajeswari and Vanithamani

IVPFTP Table 10

	D₁	D₂	D₃	D₄	Supply
S₁	([0.7,0.8], [0,0.1],[0.05,0.1])	([0.3,0.4],[0.1,0.3],[0.2,0.3])	([0.4,0.5],[0.2,0.3],[0.1,0.2])	([0.6,0.7],[0,0.1],[0.05,0.1])	([0.5,0.6],[0.2,0.3],[0,0.1])
S₂	([0.1,0.2],[0.5,0.6],[0,0.1])	([0.4,0.5],[0.2,0.3],[0,0.1])	([0.7,0.8],[0,0.1],[0,0])	([0.3,0.4],[0.4,0.5],[0,0.1])	([0.7,0.8],[0,0.1],[0,0.1])
S₃	([0.5,0.6],[0.2,0.3],[0,0.1])	([0.6,0.7],[0.2,0.3],[0,0])	([0.2,0.3],[0.3,0.4],[0,0.1])	([0.5,0.6],[0.1,0.2],[0,0.2])	([0.4,0.5],[0.2,0.3],[0,0.1])
S₄	([0.3,0.4],[0.2,0.4],[0.1,0.2])	([0.7,0.8],[0.1,0.2],[0,0])	([0.3,0.4],[0.5,0.6],[0,0])	([0.6,0.7],[0,0.1],[0.05,0.1])	([0.3,0.4],[0.2,0.4],[0,0.1])
Demand	([0.4,0.5],[0.2,0.3],[0,0.1])	([0.3,0.4],[0.2,0.4],[0,0.1])	([0.5,0.6],[0.2,0.3],[0,0.1])	([0.7,0.8],[0,0.1],[0,0.1])	

Using the steps 1 to 5 we get the following table values.

IVPFTP Table 11

	D₁	D₂	D₃	D₄	Supply
S₁	0.14	0.19	0.26	0.12	0.25
S₂	0.39	0.24	0.12	0.36	0.12
S₃	0.27	0.22	0.42	0.12	0.24
S₄	0.25	0.27	0.27	0.18	0.24
Demand	0.24	0.24	0.25	0.12	

By the step 4 to 8 for calculate the IBFS for the IVPFTP.

	D₁	D₂	D₃	D₄	Supply
S₁	0.24 0.14	0.01 0.19	0.26	0.12	0.25
S₂	0.39	0.24	0.12 0.12	0.36	0.12
S₃	0.27	0.12 0.22	0.42	0.12 0.12	0.24
S₄	0.25	0.11 0.27	0.13 0.27	0.18	0.24
Demand	0.24	0.24	0.25	0.12	

Z=(0.24*0.14)+(0.01*.019)+(0.12*.22)+(.012*0.12)+(0.11*0.27)+(0.12*0.12)+(0.13*0.27)=0.155

Comparing the results with the Type 1,Type 2 and Type 3 of IVPFN by using proposed algorithm.

IVPFTP Table 13

IVPFTP	Type 1	Type 2	Type 3
	0.145	0.236	0.155

From the above IVPFTP Table 13, Type 1 IVPFTP given the better result.

CONCLUSION

The Transportation Problem is generalized into IVPFTP using IVPFN, and a new algorithm, Range Method, is developed to find the Interval Valued Picture Fuzzy (IBFS) for given IVPFTP. Comparing the method with each other, the proposed method is found to be an alternating method.

REFERENCES

1. Ahmed MM, Khan AR, Ahmed F, Uddin S. Incessant allocation method for solving transportation problems. Am JOper Res 2016;6(May):236–44.
2. Ahmed MM, Khan AR, Uddin S, Ahmed F. A new approach to solve transportation problems. Open J Optim 2016;5(March):22–30.
3. Atanassov, K.; Gargov, G. Interval valued intuitionistic fuzzy sets. Fuzzy Sets Syst. 1989, 31, 343–349. Atanassov, K.T. Intuitionistic fuzzy sets. Fuzzy Sets Syst. 1986, 20, 87–96.
4. Coung, B.C. Picture fuzzy sets. J. Comput. Sci. Cybern. 2014, 30, 409–420. 8. Dengfeng L.; Chuntian, C. New similarity measures of intuitionistic fuzzy sets and application to pattern recognitions. Pattern Recognit. Lett. 2002, 23, 221–225.
5. Cuong, B.C. Picture Fuzzy Sets-First Results. Part 1, Seminar Neuro-Fuzzy Systems with Applications; Instiute of Mathematics: Hanoi, Vietnam, 2013.
6. Cuong, B.C. Picture Fuzzy Sets-First Results. Part 2, Seminar Neuro-Fuzzy Systems with Applications; Instiute of Mathematics: Hanoi, Vietnam, 2013
7. Hitchcock FL. The distribution of a product from several sources to numerous localities. J Math Phys 1941;20:224– 30.
8. Sathya Geetha S, Seelvakumari K A Picture Fuzzy Approach to Solving Transportation Problem. European Journal of Molecular & Clinical Medicine. ISSN: 2515-8260 Volume 07, Issue 02,2020.
9. Vogel and N.V., W.R. Mathematical Programming Englewood Cliffs. NJ: Prentice -Hall (1958)
10. Zadeh, L.A. Fuzzy Sets. Inf. control 1965, 8, 338–353.
11. Zadeh, L.A. The concept of a linguistic variable and its application to approximate reasoning. Inf. Sci. 1975, 8, 199– 249

RESEARCH ARTICLE

A Study on School Education System, in East Godavari District of Andhra Pradesh

M. Anuradha[1] and Kannuru Hari Krishna[2]*

[1]Asst. Professor and Head, Department of Social Work, Dr.B.R.Ambedkar University, Srikakulam, Andhra Pradesh, India
[2]Research Scholar, Dept of Social Work, Dr.BR Ambedkar University, Srikakulam, Andhra Pradesh, India.

*Address for Correspondence
Kannuru Hari Krishna
Research Scholar,
Dept of Social Work,
Dr. BR Ambedkar University,
Srikakulam, Andhra Pradesh, India
E. Mail: kannuruhari2021@gmail.com

ABSTRACT

Education is the basic requirement, and fundamental right of every citizen. It is a human right, which also enables people to access other types of rights. Ancient philosopher and historian Plato describes that, education helps to the comprehensive development of every individual. It gives knowledge to take the decisions for the fulfilment of their responsibilities. However; Education as a means for knowledge and cultural transmission is very essential for humankind's sustainable development. Besides that; school education is helps to inclusive development of the children. It is the basement to the higher education of the every child. But; the Low Enrolment and Retention Rates are caused to the inadequate education, which has a detrimental effect on family future growth and development. Another side the family socio-economic perceptions are shows negative impact of further investments in education. The East Godavari District is, one of the state's most populous and densely inhabited districts, in the state of Andhra Pradesh. According to the 2011 Census; the East Godavari total population are 52.86 lakhs, with a geographical area of 12805 square kilometres. The population density is 413 people per square kilometre, and only 24.86 percent of the population resides in urban regions, leaving 75.14 percent in rural areas. The literacy rate in the District is 70.50 percent. In the District, agriculture provides a living for a big portion of the working population. According to the 2011 Census; the population of scheduled castes in the District is 18.10 percent, it means 9.57 lakhs. While; the number of scheduled tribes is 2.97 lakhs, it accounting for 5.62 percent of the total population of the district. The methodology of the present paper is, mainly used the secondary data sources and its analysis; the secondary data was collected from various Governments, International Organizations, and from eminent scholar's articles. The main aim of

63485

Anuradha and Kannuru Hari Krishna

the present study is, to understand the contemporary school education system of East Godavari Dist, Andhra Pradesh. Another aim of the paper is, to discuss about the, socio-economic conditions of East Godavari District.

Keywords: School-Education, East Godavari, Community Participation, Andhra Pradesh, Sustainable Development Goals

INTRODUCTION

Education is the basic requirement and fundamental right of every citizen. Education is a human right, which also enables people to access other types of rights. It is helps to build a character and personality of every Individual. Education as a means for knowledge and cultural transmission is very essential for mankind's sustainable development. According to Plato; "Education is helps to the comprehensive development of every individual. It is gives a knowledge to take the decisions for the fulfilment of their responsibilities". According to Radden; education is the process through which a more experienced individual has a positive, long-lasting impact on less experience individuals.

United Nations Organisation-(UNO's) said that; the goal number four, in the Sustainable Development Goal-(SDGs), are clarifies about, the "quality education" to every individual on earth. However; this objective can only be attained if other socioeconomic objectives, like SDGs 1 to 6 and 17, are also met (UNDP, 2022). Whereas; the "Universal elementary education-(UEE)" is not a new concept, it is a one of the component of the Millennium Development Goal-(MDGs) established by the United Nations in late 1990's. Here we need to understand that, the education is assist to the accomplishment of a range of individual and social objectives, if it is of a desirable standard. The United Nations Education and Socio-Cultural Organisation-(UNESCO's), and its allied institute, the Institute of Education (UIE) 2004) said that; Education consists of qualitatively defined processes and outcomes. The emphasis on education quality at the international level can be traced back to the 1990s, when the 'World Declaration on Education for All' suggested that education should become worldwide affordable and strengthened significantly.

The Planning Commission of India stated; in its annual report for 2011, India has noticed that the Net Enrolment Ratio-(NER) at the primary level has improved significantly and was on the same level with other developed nations in 2007, , (NITI Aayog, Planning Commission, Annual Report 2011).   As per Bangay, Latham, Govinda, and Bandyopadhya, the same "Net Enrolment Ratio-(NER)", Quality The year 2007 witnessed progressive school exclusion as a consequence of low learning levels, considerable repetition rates, and the inability to speak. Complex interdependencies exist between enrolment, retention, and educational quality, (Govinda and Bandopadhyay, 2010).

Low enrolment and retention rates are caused by inadequate education, which has a detrimental effect on family perceptions of the value of further investments in education. The educational process is slowed down by poor enrolment and retention rates. Policymakers, educators, and others involved in education have become increasingly aware of the significant role communities can play in the administration, management, and oversight of educational institutions. There is accumulating evidence; that community involvement in education can have a profound effect on educational access, retention, and quality. According to a 2014 study from UNESCO, "quality education" has become a multifaceted notion that takes into account things like students' individual traits and the context in which they are learning. Teachers, textbooks, computers, and other resources all play a role in a student's capacity to learn, as does the quality of the school itself.

Anuradha and Kannuru Hari Krishna

The Kothari Commission (1964–1986) emphasised; the importance of decentralising school education, involving parents and community organisations in the enhancement of schools, (Kothari Commission, 1966). National Policy on Education (NPE) of 1986 emphasised that; the decentralised planning, and the administration of primary education above all else. Moreover, it emphasises the elimination of inequalities in the educational system and seeks to equalise school education opportunities. Through the Programme of Action-(POA) in 1992, the village committees are became a stronger, (National Policy on Education, 1986). In addition, the Sarva Siksha Abhiyan-(SSA) is a one Inclusive Educational Development Programme, which is implementing by the Govt of India, from the year of 2001. The main goal of the programme is; to achieve a, "Universal Elementary Education-(UEE)", through the support of the community. The community support and its participation is in different forms like, "Gram Panchayats-(GP's), Parent-Teacher Associations-(PTA), Mother-Teacher Associations-(MTA), Village Education Committees-(VEC)" etc., (SSA, 2001).

In addition, the Right to Education-(RTE) Act of 2009 is the most significant declaration, of the commitment and obligation made by the government towards education. The Act makes it crystal clear, that the state is responsible for providing eight years of free, compulsory schooling to all children ages 6 to 14. Besides that; the Act establishes minimum requirements for infrastructure necessities, educational amenities, and curriculum that all categories of institutions must meet.

Furthermore; the RTE Act clearly specified that, the teacher-students ratio is must be 1:30 ratio in every school. Moreover; it is mentioned the Educational Qualifications of the teachers, and their roles and responsibilities. The RTE Act-2009; gives a more importance to the Community Participation in the school administration, through GP's, SMC's, PTA's and other forms in School Education System. The act noted that; community role in the School Education is, supports to not only improve the Quality and Equity of the School Education, and it helps to comprehensive development of the society, (RTE Act 2009). According to Anderson; encouraging students to participate in hands-on learning can ensure quality education in the contemporary period. The dedicated teachers are utilising their skills and knowledge to the development of the students. Through a curriculum based on evidence and an activity-based teaching-learning process, the quality of education is enhanced in order to increase and produce men with greater knowledge, self-assurance, creativity, potential, and competencies. There are numerous ways to improve the quality of education, including by educating parents, enhancing instructor resources, creating new educational models, and so on. Moreover; the Qualitative Education is always helps to the development of the students, in the way of acquiring skills, rational thinking, development of communication skills, self discipline, communal and environmental harmony, and so forth, (Anderson, 2013).

The RTE Act of 2009 mandates the age-appropriate enrolment and special training, for out-of-school children, in order to bring them up to par with other children. Section 4 of the Act states that; Where a child above the age of six has not been admitted to any school or, though admitted, could not complete his or her elementary education, he or she shall be admitted in a class appropriate to his or her age; provided that where a child is directly admitted to a class appropriate to his or her age, he or she shall, in order to be at par with others, have the right to receive special training in such a manner and within such a time period as the State. In addition; Sarva Siksha Abhiyan-(SSA) seeks to "Universalize Elementary Education (UEE)" through the involvement and participation of the general public. SSA places a premium on the methodical involvement of communities and the establishment of a decentralised decision-making system. Through decentralisation, when it comes to interventions in schools, SSA advocates for community involvement. Under SSA, there have been concerted attempts to include the local community in advancing education, building schools, and monitoring their daily operations.

It supports a community-based monitoring system that is open and honest. Every institution must make grant information available to the public as just one more piece of data. However; the 2001 SSA study suggests that schools, families, and the Panchayati Raj might work together, (SSA, 2001).

METHODOLOGY

The methodology of the present paper mainly based on the secondary data sources and it analysis.. The secondary data was collected from various Governments, International Organizations, and from eminent scholar's articles. The main aim of the present study is, to understand the contemporary school education system of East Godavari Dist, Andhra Pradesh. Another aim of the paper is, to discuss about the, socio-economic conditions of East Godavari District.

DISCUSSION

The ASER reports indicate that; the majority of primary-aged students in villages, across India are lack of the necessary reading and math skills for daily life. Worryingly, between the years 2005 and 2011, elementary school performance declined in most of the states, (ASER, 2012). Using ASER data, the organisation calculated a Learning Achievement Index-(LAI) is, set for the most populous states in India. It has been shown that, the Indian states of, West Bengal, Andhra Pradesh, Haryana, Kerala, Maharashtra, and Punjab. Have all shown and maintained strong performance on the basis of LAI between the period of 2008 and 2012. In the meantime, the states of, Tamil Nadu, Gujarat, Uttar Pradesh, Assam and, Rajasthan have shown persistently low performance. Surprisingly; Tamil Nadu is recognised for achieving development through social means. Nonetheless, persistently subpar learning outcomes cast doubt on the state's actual social infrastructure quality. Another problem is that; it needs the further investigation, it is alarming drop in education standards in Madhya Pradesh.

However, the problem of low academic achievement is not unique to India. It affects the majority of the world's impoverished nations (ASER, 2012). The National University of Educational Planning and Administration (NUEPA) conducted a study on secondary education in 2016, finding that the average ratio of high schools to elementary schools was 0.77 percent. Data from NUEPA shows that middle and high schools take up the same amount of land as elementary and middle schools combined.

The National Sample Survey of Educational Attainment (NUEPA) found that in 2016–17, there were 6.13 crores students enrolled in India, with 3.98 crores located in rural regions and 2.15 crores in urban areas. The aforementioned study found that as of April 2017, India had a total of 36 lakh teachers, with 22.13 lakh residing in rural areas and 13.86 lakh in urban areas. About half (48.86%) of all employees are educators. In the United States as a whole, female students make up an average of 47.50 percent of the student body. The average ratio of students to teachers is 17 to 1, and on average, the student-to-classroom proportion is 43 to 1. The national average number of professors per school is 14, (NUEPA 2016-17).

Brief Information Regarding erstwhile East Godavari District of Andhra Pradesh
East Godavari District is located in the north eastern part of Andhra Pradesh, between 160°30′N and 180°20′N in latitude and 810°30′E and 836°30′E in longitude, as stated by the state government. The district comprises a sizeable portion of the Godavari River delta, and has a total area of 12805 square kilometres. This district is located, on the northeast coastal region of the Andhra Pradesh. The Visakhapatnam District and the state of Orissa are to the north, the Bay of Bengal is to the east, the Godavari and Khammam Districts are to the south, and the Godavari and Khammam Districts are to the west of the area. The district may be roughly broken into delta, upland, and agency natural zones. It is 12,805 square kilometres in size. East Godavari's district headquarters, Kakinada, is conveniently accessible by train, road, and the 144-kilometre-long Kakinada Natural Port. According to the chief planning officer of the East Godavari district; the environmental conditions are fairly consistent, and while it is quite warm in May with a high of 37.70 °C and quite cold in January with a low of 28.50 °C, the actual rainfall from June 2018 to May 2019 was 987.70 mm compared to the average rainfall of 1217.80 mm. Less than -18.90 percentages of the variance

from the mean is observed. The preponderance of the remainder, 132.1 mm, fell during the North-East monsoon period from October to December 2018, (East Godavari Hand Book, 2019).

According to the chief planning officer for the East Godavari district, there are seven revenue divisions with headquarters in Kakinada, Peddapuram, Rajamahendravaram, Rampachodavaram, Ramachandrapuram, Amalapuram, and Yetiapaka. In addition, the district consists of 64 Revenue Mandals and 62 Mandal Parishad. There are 1069 Grama Panchayats in the region. The district consists of two municipal corporations, such as Kakinada and Rajamahendravaram. Moreover; it has seven municipalities, those are Samalkot, Pithapuram, Peddapuram, Tuni, Ramachandrapuram, Mandapeta, and Amalapuram. Besides that; it has a three Nagar Panchayats, namely Yeleswaram, Mummadi Varam, and Gollaprolu. This district contains 1595 inhabited villages, 89 uninhabited villages, and 25 municipalities, (District Hand Book, 2019). According to the 2011 Census; the population is 51.54 million, and the land area is 1,280.05 square kilometres. The district of East Godavari is one of the most populous and densely populated districts in the state. The population density is 413 inhabitants per square kilometre. In the District; in this district, the majority (74.5%) of people still live in rural regions, while the minority (25.5%) live in urban regions. The literacy rate in this area is 70.99 percent. A significant proportion of the working population earns a livelihood through agriculture. According to the 2011 Census, scheduled castes make up 18.10 percentage of the district's total population, while scheduled tribes account for 5.62 percentages, (District Census Hand Book 2011).

Present School Education Status in the state of Andhra Pradesh and East Godavari Dist
Enrolments are the process of making arrangements to attend a school, and enrol in specific courses. This term may also refer, to the number of students enrolled in a school or course at the present time. Enrolment refers to the act of registering for school and/or specific classes or other extracurricular activities at a particular institution. After a pupil is admitted to a particular institution, the enrolment procedure is complete. Students can then choose courses, through their school's online student information system. Andhra Pradesh Gross Enrolment Ratio-(GER) in institutions is, significantly lower than the national average, as reported by the Hindu newspaper on June 25, 2018. In primary institutions, the national GER is 99.21 percentages, but in A.P., it is only 84.48 percentages. In addition; nearly one lakh children have dropped out of the school, it is indicating a Herculean task for the officials as schools reopen soon. In comparison to the national average of 92.84 percentages, of the GER in upper primary institutions, is 83.96 percent in Andhra Pradesh.

However; in secondary institutions, it is 79.15percentages, which is near the national average of 80 percentages. The GER in elementary schools decreased from 91 percentages in 2010–2011 to 83 percentages in 2016–2017. During the same time period, the rate increased from 77 percentages to 81 percentages in upper-level primary institutions. Programmes such as 'Badi Bata,' 'Badi Pilustundi,' and 'Manna Vooru-Manna Badi', have reportedly failed to produce the desired outcome. In 2017-18; 99,833 children were not in school. According to a study conducted using the mobile app AP-GER. Compared with other states like Kerala, the attrition rate is high. Nevertheless, it is lower than the national average of 5.13 percentages for primary education. In 2015-16, which the government considers a benchmark year, the attrition rate was 6.27 percentages. According to Ravi Kumar and Venugopal; there was a downward trend in enrolment growth at government elementary institutions. As a result of the availability of the "Mid-Day Meal Scheme-(MDMS)" in government schools, private schools have improved their educational amenities to attract students and keep them enrolled. The amount spent on the Mid Day Meal Scheme (MDMS) has no impact on enrolment in elementary government institutions in erstwhile Andhra Pradesh, (Ravi Kumar, J & Venugopala Rao, K P, 2017).

The NUEPA secondary education report for 2016–17 states that; the ratio of upper primary to secondary institutions in Andhra Pradesh is 1percentages. 33.70 percent of secondary institutions in Andhra Pradesh are higher secondary schools. In 2016–17, the enrolment ratio of females to boys at the secondary and higher secondary levels was 0.90 percent, according to the report cited above. In 2016–17, the enrolment ratio of females to boys at the secondary level in the Indian state of Andhra Pradesh was 0.93 percent and 0.0 percent at the higher secondary school level,

according to the report cited above. Nonetheless, 97.81 percent of students in the state transition from elementary to secondary education, (NUEPA, 2016).

According to the NUPEA-2017; dropout rate is very high within in the country and state, moreover dropout rate between classes of IX to X class is 50 percentages, and it is more than 200 percentages, when compared with national average. NUPEA Report-2017 that, the academic year of 2016-17 promotion rates of the India and the state of Andhra Pradesh. According to the report eighth class promotion rate in India is 99.89 percent, and in Andhra Pradesh it is 97.81 percent. In ninth class promotion rate are 82.93 percent in India, 98.6 percent in Andhra Pradesh. The tenth class promotion rate in India is 94.1; the data is not available for Andhra Pradesh. Whereas, eleventh class promotion rate in India is 76.05 percent, the data is not available for Andhra Pradesh. The IX to X class promotion rate in Andhra Pradesh is 49.85 percent, it is in national wide 88.1 percent. But, the classes of XI to XII, the promotion rate data was not available for both country and the state, (NUEPA, 2017). According to the UDISE Report-2019; the total Enrolments in the academic year 2018-19 of Andhra Pradesh state is 70.4 lakhs, out of this 36.8 lakhs are boys and 33.6 lakhs are girls.

The UDISE report (2018–19) found that 37.93% of schools in Andhra Pradesh had School Building Committees (SBCs) and that 24.71% of primary (including upper primary, intermediate, and higher secondary) schools had School Monitoring and Development Committees (SMDCs). In addition to universities and colleges, 19.89% of elementary and secondary schools at the upper-primary level also have SMDCs. School building committees (SBCs) are in place in just 35.91 percent of schools. The School Monitoring and Development Committees (SMDCs) are present in 3.55 percent of primary schools, and School Building Committees (SBCs) are present in 13.91 percent of primary schools. 11.82 percent of upper primary schools (in addition to secondary schools) possess School Monitoring and Development Committees (SMDCs), and 30.63 percent of primary schools (in addition to upper primary and secondary schools) have School Building Committees (SBCs). School building committees are present in 9.09 percent of secondary institutions. School Monitoring and Development Committees (SMDCs) are present in 33.33 percent of secondary and senior secondary institutions. School monitoring and development committees were present in 10.93 percent of schools, while school building committees were present in 28.37 percent of schools, (Unified District Information System for Education plus Report-(UDISE+), 2019).

As per District Educational Officer (D.E.O) of the East Godavari district; explains about the management wise (Govt. and Private), and total availability of schools in East Godavari district as on December/2021, is as follows. The total primary schools in the district are 3833, upper primary schools are 955. Whereas; secondary schools in the district are 1216, higher secondary schools are 286 and finally total schools in the district are 6290 schools. The D.E.O of East Godavari said that; in the District the overall enrolments in the govt schools, during the academic year 2021-22 are nearly 47.2 lakhs, (Management Information System 2020).

As per the table no.1; the East Godavari District totals boys Gross Enrolment Ratio (GER) is 91.17 percent and girls Gross Enrolment Ratio (GER) is 90.3 percent. Whereas; the boys Net Enrolment Ratio (NER) are 70.26 percent and girls Net Enrolment Ratio (NER) are 70.62 percent. The boys Transition rate from class VIIITO IX is 97.64 percent, girls Transition rate from class VIII TO IX is 98.87 percent and total Transition rate from class VIII TO IX are 98.25 percent. The total Retention Rate-(RR) is 94.19 percent, the Dropout Ratio - (DR) is 4.1 percent, and it is 5.16 percent in boys and 3.02 percent in girls. The Promotion Rate-(PR) is 100 percent, Gender Parity Index-(GPI) is 1 percent and finally the Gender Gap Rate- (GGR) is .049 percent in the district. Meanwhile; Andhra Pradesh total literacy rate is 67.35 percentages, in that female literacy is 59.96 percentages, and male literacy is 74.77 percentages.

Table no.2 reveals that; the East Godavari District has a 70.50 percentage of literacy rate, out of that, the rural literacy rate is 67.08 percent, and the urban literacy rate is 80.78 percent. Out of the 67.08 percent of rural literacy, 70.65 percent is rural male literacy, and 63.53 percent is rural female literacy. In the district, the urban literacy rate is 80.78

percent. According to the 2011 Andhra Pradesh Census Handbook, 84.62 percent of urban men and 77.07 percent of urban women are literate.

When compared the National, State, and District level literacy rates, the literacy rates are has so much variations, especially in rural women and girl child education. Delliswararao said that; Illiteracy or Lack of Education to the women and the girl child is increases the gender disparities in the developing countries like India, (Delliswararao, 2021). According to the Delliswararao K; education is a one of the key factor to the women empowerment, at least up to secondary school education is assures the girls, to acquires a self confidence, knowledge about the society, and how to protect their selves in the worst situations. It is reducing the stress on the parents and their kins, (Delliswararao, 2018). Rao and Vasanta Srinivas (2009) observed that community participation, is enhancing education is minimal, in the East Godavari district of Andhra Pradesh. Besides that; the authors are said that, the members of School Management Committee-(SMCs) have a limited knowledge on the Sarva Siksha Abhiyan-(SSA). The vast majority of school instructors (87.2 percentages) were aware of the Sarva Siksha Abhiyan, compared to 61 percentages of PRI members and 52 percentages of parents of school-aged children. The tribal community members took part in some or all of the school-related activities. The school education management committees in this district of Andhra Pradesh played a crucial role in micro-planning, particularly in the development of a village education plan and school enhancement plans, (Rao, Vasanta Srinivasa. 2009).

Suggestions
- Development of school infrastructures at village level is very important to development of district literacy rates.
- School Monitoring Committees are needed to play an active role, in enrolment and retention of the students in the schools.
- District and state officials need to focus the fulfilment of the teacher's vacancies, it is helps to the development of education standards and literacy rates within the district.
- Community and parental active participation; are given an assurance the quality of education, to children and society. Hence; the district administration responsibility is, to focus and stress the active participation of the parents and community in the school education.
- Skill based training, communication skills development programmes must be included in the student's curriculum, and it helps to enhance the employment opportunities in the students.

CONCLUSION

East Godavari District and the state of Andhra Pradesh; have made great strides in primary school enrolment, but they are still facing a significant challenges. Like; significant number of dropouts in the schools, the shortage of skilled teachers, and insufficient school facilities. Moreover; extremely low teacher and student participation, and poor educational outcomes. In the states with higher enrolment rates, there is a greater likelihood that a school will be available, but the state's physical and human infrastructure is frequently worse. For obvious reasons, this means more children will register for school, but that doesn't mean they'll perform well academically.

The Department of Education must provide support by issuing a regulation that allows the school committee to actively participate and maximise its role, particularly in the fields of supporting agency and mediating agency; principals should make efforts to include the school committee in the control and evaluation of a policy, educational programme being implemented, or output of education. With an increase in student attendance, a high-quality educational environment will be fostered in and around schools. The appropriate maintenance of school facilities will increase the school attendance of children. Moreover, community involvement is required to enhance and maintain the equilibrium of enrolment, the retention of students, and school education quality. Common development issues, along with the inclusion of the community in school education, necessitate resolving these issues and it helps to improving school education outcomes. Researchers, policymakers, instructors, officials, and the

community are required to provide necessary suggestions for appropriate community participation and quality education in the school education system for children.

Conflict of Interest
None

REFERENCES

1. Anderson V (2013); impure community: a framework for contact in inter nationalised higher education journal of intercultural studies, 34(1), 34-54, 2013.
2. Delliswararao, K. (2018). A Brief Study of Women Empowerment Index in India. International Journal of Scientific Research and Reviews, 7 (4), 720-736.
3. Delliswararao, K. (2021). Anthropological Perspective on Gender Disparities in India. International Journal of Social Science and Management, 8 (3), 416-425.
4. Delliswararao, K. (2023). Climate Change and its Impacts on Bay of Bengal Region. Indian Journal of Natural Science, 13 (76), 0976-0997.
5. District Hand Book (2011); District Census Hand Book-2011, Directorate of Census Operations, Andhra Pradesh, Govt of India, 2011.
6. Govinda and Bandopadhyay (2010); Changing framework of local governance and community participation in elementary education in India, Consortium for Research on Educational Access, T. a. E., & National University of Educational Planning and Administration (India), 2010.
7. Hand Book (2019); East Godavari-2019 Directorate of Economics& Statistics, Vijayawada, Andhra Pradesh, 2019.
8. Hindu (2018); Cover Story on School Education of Andhra Pradesh school education, dated on 25 June 2018.
9. Kothari Commission (1966); Kothari Commission Report on Education System in India (1964-66), Publication Unit, NCERT, New Delhi, 1-138.
10. MIS (2019-20); Management Information System - 2020, District Project Office, A.P., Samagra Shiksha, Kakinada, East Godavari District, 2020.
11. National Education Policy (2020); National Educational Policy - 2020, Ministry Human Resource Development, New Delhi, India, 2020
12. NPE (1986); National Policy on Education1986, Ministry of Human Resource Development, Department of Education, Govt. of India, New Delhi, 23.
13. NUEPA (2016); Annual Report- 2015-16, National Institute of Educational Planning and Administration (NIEPA), 17-B, New Delhi, 2016.
14. NUEPA (2017); Annual Report-2016-17, National Institute of Educational Planning and Administration (NIEPA), 17-B, New Delhi, 2016.
15. Rao, Vasanta Srinivasa (2009); Lack of Community Participation in the Sarva Shiksha Abhiyan: A Case Study. Economic and Political Weekly. Vol. XLIV (8). February 21.
16. Ravi Kumar, J. & Venugopala Rao, K.P (2017); Universalization of Elementary Education: A Study of Elementary Schools Enrolments of Undivided Andhra Pradesh, International Journal of Research in Economics

and Social Sciences (IJRESS), pp.393-409,ISSN(o) :2249-7382, Impact Factor: 6.939. https://www.researchgate.net/publication/331036711.

17. Retrieved from URL: https://www.asercentre.org/education/India/status/p/html
18. /2012/pdf/Accessedon05Aug 2022
19. Retrieved from, URL: https://www.education.gov.in/SarvaSikshaAbhiyan/annual report/2001/Accessed on 05 June /2022.
20. Retrieved from, URL: https: //www.education.gov.in/sites/upload-files/MHRD/files
21. /NEP-1986/_Final_English_0.pdf/Accessedon21thAugust/2022.
22. Retrieved from, URL: https: //www.digitallibrary.un.org/UNCIEF/annual report/1992/ Accessed on 1st August /2022.
23. Retrieved fromURL: https://www.legislative.gov.in/files/RTE/ACT/2009/pdf/Accessed on9 July / 2022.
24. Retrieved from, URL: https: //www.niti.gov.in/planning/commission/annual report/2011/Accessed on 30st June /2022.
25. Retrieved from, URL: https://www.undp.org/sdgs/Accessedon15thJune/2022.
26. State Hand Book (2011); Andhra Pradesh Census Hand Book-2011, Directorate of Census Operations, Andhra Pradesh, Govt of India, 2011.
27. UDISE (2019); Unified District Information System for Education plus Report-2019 (UDISE-2018-19), Ministry of Education, Govt of India, 2019.
28. UDISE (2020); Unified District Information System for Education plus Report-2020 (UDISE-2019-20), Ministry of Education, Govt of India, 2020.
29. UIE Report (2004); UNESCO Institute For Education (UIE) Annual Report-2004, United Nations Educational, Scientific and Cultural Organisation (UNESCO), Paris, France, 2004
30. UNESCO (2014); Achieving transparency in pro-poor education incentives. International Institute for Educational Planning, Paris. http://etico.iiep.unesco.org/fileadmin/user_upload/ETICO/Publications/PDF/Pro-poor_incentives.pdf.

Table no.1: Distribution of Educational Growth Rate			
Particulars	**Boys**	**Girls**	**Total**
Gross Enrolment (GER)	91.17 percentages	90.03percentages	90.73percentages
Net Enrolment Rate (NER)	70.26 percentages	70.62percentages	70.44percentages
Transition Ratio (TR) VIII to IX	97.64 percentages	98.87percentages	98.25percentages
Retention Rate	92.45percentages	96.01percentages	94.19percentages
Dropout Rate (DPR)	5.16percentages	3.02percentages	4.1percentages
The Promotion Rate (PR)	100percentages	100percentages	100percentages
Source: U-DISE*			

* **Note**: **U-DISE:** (Unified District Information System for Education); is an online database containing information regarding colleges in India. The database was developed by the joint group organisation. The organisation is form with the Ministry of Education, and National Informatics Centre-(NIC), of Govt of India.

Table No.2: Distribution of Literacy Rate of East Godavari District, Andhra Pradesh			
Literacy Rate (As per Census 2011)	**Male (In Percentages)**	**Female (In Percentages)**	**Total (In Percentages)**
Rural	71.0	64.17	67.62
Urban	84.62	77.07	80.78
Total	74.51	67.52	70.99

RESEARCH ARTICLE

Antiviral Prophylaxis: Impending Cradles in Covid -19 Outburst

Kavya Nainita Manchikanti[1], K Vinod Kumar[2], Nawaz Mahammed[3] , P. Chiranjeevi[4] ,G.Kranthi Kumar[4] * and T.Reshma

[1]Student, Department of Pharmaceutical Quality Assurance, Raghavendra Institute of Pharmaceutical Education and Research, Anantapur, Andhra Pradesh, India.
[2]Professor, Department of Pharmaceutical Analysis, Raghavendra Institute of Pharmaceutical Education and Research, Anantapur, Andhra Pradesh, India
[3]Associate Professor, Department of Pharmaceutics, Raghavendra Institute of Pharmaceutical Education and Research, Anantapur, Andhra Pradesh, India.
[4]Assistant Professor, Raghavendra Institute of Pharmaceutical Education and Research, Department of Pharmaceutical Analysis, Krishnam Reddy Palli Cross, Anantapur, Chiyyedu, Andhra Pradesh-515721, India

*Address for Correspondence
G Kranthi Kumar
Assistant Professor ,
Raghavendra Institute of Pharmaceutical Education and Research,
Department of Pharmaceutical Analysis,
Krishnam Reddy Palli Cross, Anantapur,
Chiyyedu, Andhra Pradesh-515721, India
E. Mail: ok.kranthikumar23@gmail.com

ABSTRACT

A report of pneumonia was identified with a unique form of the pathogen in Wuhan city of China. It was titled "Novel corona virus" by WHO. The revelation on November 24, 2021 in South Africa of the severely altered Omicron of the severe acute respiratory syndrome corona virus 2 (SARS-CoV-2) aroused numerous worries. According to a peer-reviewed study backed by the French government, the novel B.1.640.2 strain from the lineage has infected 12 persons in the nation. Until December 2021, more than half a million genome sequences from all six continents have been reported to the Global Initiative on Sharing Avian Influenza Data (GISAID) to detect variations. The worldwide healthcare system is dealing with several issues as a result of the COVID - 19 pandemic. While news of the vaccine roll-out lifted many people's optimism, the mutant virus threatened that hope and sparked another wave of fear and uncertainty. The imaginable uses of Ayurveda which is the Indian herbal treatment system publicized an immune system enhancer. It helps COVID-19 patients with increased average cure efficiency, and many natural products possess antiviral characteristics where they can be used for future perspectives. Prescription prophylaxis is one approach where prophylactic antiviral drug therapy is emerging the world over. There is an immediate need for both prevention and therapeutic interventions for this

63494

Kavya Nainita Manchikanti *et al.,*

condition, and more than 500 clinical trials are underway. Here, in this review, we studied several articles, newsletters and had provided the latest evidence on immune boosters, prophylactic antiviral therapy, approved vaccines and currently ongoing clinical trials to treat corona virus.

Keywords: Antiviral treatment, COVID-19,Probiotics, variants, Clinical trials.

INTRODUCTION

The rapid evolution of corona virus disease 2019 (COVID-19) is becoming a concerning issue that has jolted the entire world. Since December 2019, a new virulent strain of corona virus has attacked millions of individuals globally, resulting in enormous mortality. There have been at least eleven documented versions. SARS-CoV-2 variations were identified (Alpha, Beta, Gamma, Delta, Delta Plus, Epsilon, Eta, Theta, Iota, Kappa, and Lambda), and the number is expected to increase as different strains appear.[1] A pathogen that causes COVID-19 is nCoV, it was identified firstly in January 2020 and the international committee on taxonomy titled it SARS-CoV-2 on February 11, 2020. It is a big group of single-stranded RNA viruses. French researchers have discovered a novel Covid variation, most likely of Cameroonian origin, and have given it the tentative name 'IHU.' Our human body has some immune systems in which it protects from disease. As a result, understanding the underlying mechanism of immunological deficiencies in COVID-19 patients might help with illness management. At present, several clinical trials where antiviral therapy are testing like inhibiting the enzymes that are responsible for replication. Currently, some of the drugs for managing COVID-19 and repurpose drugs are given to infected patients like anti-HIV to manage *influenza*. Remdesivir, chloroquine, favipiravir, ivermectin, nitazoxanide and ritonavir are also used as antiviral against corona virus. [1] Some researchers are looking into using a combination of medications to treat COVID-19.[2] We can boost up our immunity with some of the natural spices like vitamin supplements, some other changes in our lifestyle like sleep, physical exercise and water supplements. Few studies suggest that immune boosters tend to control the corona virus, where doctors recommend as many antiviral medications as possible to prevent or treat it. To combat corona virus infection, the population is puzzled by immune boosters and antiviral therapy. Unfortunately, to treat the novel COVID-19, there is no such proper drug or therapy known yet. It can even take months or years to develop antiviral medications or vaccines if urgent action is appropriate to avoid this extraordinarily infectious disease, but the Indian government appreciates the use of conventional herbal or natural remedies to heal contaminated patients. Several research on the efficacy of both prevention and therapy are shortly proceeding. Antivirals are not just therapeutic, but also prophylactic against many viruses. In light of current knowledge, combinational antiviral drugs are to be considered as shown in table 1.

2. BUDDING IMMUNOTHERAPEUTIC TACTICS FOR COVID-19

There is a strong indication of SARS-CoV-2 induced immunopathology. But regrettably, many glucocorticoids, antivirals haven't shown any durable improvement in the survival of patients. Where targeting the immune profiles of COVID-19 in specific can lead to treatment for severe cases. Enhancement of lymphocytes, immune modulators, Janus kinase inhibitors, plasma therapy.[5] Raise the amount of turmeric, cumin, coriander, and garlic. As our health care professionals fight the war against the Covid-19 pandemic, our responsibility is to prevent exposure to viruses by staying home, maintaining social distance, consuming balanced foods and following the simple hygiene protocol. The human body is designed to defend the body from illness and disease with a complex and effective immune response as presented in Figure 1. The priority of this current research is to highlight the human body's immune system to tackle this pandemic phase of COVID-19. Ayurveda, which is commonly used in ancient times around the world, is the various kinds of principles to improve immunity combined with the resistance function of the body to combat many diseases. The imbalance of these three induces many diseases and limits the strength of our immunity. It is understood that some compounds derived from plants have an antiviral function as shown in Figure 2.

Kavya Nainita Manchikanti *et al.*,

Role of Immunity After Vaccination

There were 91 COVID-19 vaccines in clinical development and 184 in preclinical development (Malayala, Mohan, Vasireddy, &Atluri, 2021). The mRNA vaccines appear to give adequate protection against the B.1.1.7 COVID-19 mutation, according to the data. Before the South African variation (B.1.351 or 20H/501Y.V2) strain was identified, the Pfizer and Moderna messenger RNA (mRNA) vaccines were approved in the US (Vasireddy, Vanaparthy, Mohan, Malayala, &Atluri, 2021). Vaccines are critical in educating our immune systems on how to detect and fight the COVID-19 virus. The neutralizing antibodies take around two weeks to form following the second dosage of mRNA vaccinations. However, further research is needed to determine how well the vaccinations prevent the virus from spreading but for how long they give protection. Sinovac Biotech has begun clinical studies, which have shown that the CoronoVac vaccine is 50% successful in preventing P.1 variant infection in Brazil. Bharat Biotech's COVAXIN vaccine has been shown to neutralize well and is 78 percent effective over the double mutant strain, B.1.617, as per the Indian Council of Medical Research Virology lab. Although SARS-CoV-2 reinfection has been documented, scientific knowledge of natural infection-derived immunity is still developing (Y. Sui, Bekele, &Berzofsky, 2021). When compared to the original Wuhan-Hu-1 strain, sera obtained from earlier infected people before they were vaccinated provided a considerably lower, and in some cases missing, neutralizing response to the B.1.351 (Beta) variation (Stamatatos *et al.*, 2021). Looking throughout the region, we observe the same broad patterns, with India by far the most concerning in levels of infections per million, but Nepal fast narrows the gap due to its considerably higher infection rate as shown in figure 3.

Vitamins

This is an important supplement, fat-soluble, and holds a significant involvement in the regulation of vision, development, and maturity, and defence of the human body's mucosal and epithelial integrity. [6] Since the removal of the SARS-CoV-2 virus involves antibodies, especially T-cells, thiamine deficiency can lead to insufficient antibody responses and consequently serious symptoms (Sufficient amounts of thiamine are also liable to help in effective immune responses in infection with SARS-CoV-2). Thiamine also acts as an inhibitor of carbonic anhydrase isoenzyme.[7] Since the removal of the SARS-CoV-2 virus involves antibodies, especially T-cells, thiamine deficiency can lead to insufficient antibody responses and consequently serious symptoms. (Sufficient amounts of thiamine are also liable to help in effective immune responses in infection with SARS-CoV-2.) Thiamine also acts as an inhibitor of carbonic anhydrase isoenzyme.[7] It has been shown that riboflavin and UV light are beneficial against the MERS-CoV virus, indicating that they may be effective against SARS-CoV-2.[8] Riboflavin-UV reduced the amount of the SARS-CoV-2 infectious titer which is below the concentration level in the blood, plasma as well as platelet products.[9] It has been shown that vitamin C intake reduces the period and incidence of infections at the upper respiratory tract that is mostly believed to be related to viral infections, like cold infections.[10][11] It scavenges ROS as an antioxidant, inhibits the peroxidation of lipids and alkylation of proteins, and thereby defends cells from cellular damage triggered by oxidative stress. [12] C-vitamin supplementation and quercetin supplementation have also been found to have a mutually beneficial antiviral, antioxidant, and immunomodulatory effect in studies.[13] In a case study where a patient was cured with high-dose of vitamin C after the ARDS development, she was detached from the ventilator after 5 days, as she was also medicated with some antiviral as well. [14] Fat-soluble vitamin- D has a huge advantages for good health and immunity improvement. It governs the development of a protein that destroys infectious agents selectively and bacteria and viruses included. Vitamin D increases monocytes and macrophages pathogen-fighting effects-white blood cells (WBC) that are essential parts of immune defence and reduce inflammation, which helps stimulate an immune response. Vitamin D changes the action and amount of WBC, referred to as T2 Killer lymphocytes, which can decrease the transmission of viruses and bacteria. Vitamin D3 and vitamin D2 are agreed for the stoppage and management of vitamin D deficiency but are not expressly approved license to prevent or treat any infection caused by COVID-19, including the novel corona virus. A modern study showed that the administration of vitamin D could decrease admittance to thorough care in adults with COVID-19 who got hospitalized.[15]

Kavya Nainita Manchikanti *et al.*,

Trace Elements
Copper
A trace element that shows a crucial part in the enactment of components in the immune system, like natural killer cells, neutrophils, macrophages, and monocytes. [18] Copper deficiency is linked to weakened immune responses to virulence and infections. [19] Based on the evidence, it was presumed that the copper levels of plasma will increase adaptive and innate immunity, it shows preventive and therapeutic effects against corona virus. [20] A recent review has shown that copper shows its activity in combination with N– acetyl cysteine, colchicine, or Remdesivir as COVID -19 treatment. [21] Corona virus, which is antagonistic to the copper surface, in the case of cell-based study Cu2+ is liable for papain-like protease – 2 blockage which is a protein prerequisite for the replication of SARS-COV-1. [22] Nanoparticles (CuONPs) of oxidized Cu oxide (CuO) are commonly used as catalysts so, CuONPs can limit the application of viruses is improved. [23]

Zinc
A mineral that has a role in immunity, particularly in innate and acquired immunological responses to viral infections. It is alleged that zinc is an important mineral in COVID-19 infection due to its dual properties of immune-modulatory and antiviral. Zinc shows inhibition of the synthesis, transcription complex, and replication of corona viruses.[24] [25] Especially, Zn2+ with zinc ionophore pyrithione are revealed the SARS- corona virus RNA polymerase inhibition by its decrease in replication. [24]

Selenium
Due to its action on the immune system in antibody production, deficient levels of Se are responsible for a decrease in cytotoxicity of natural killer cells, cellular immunity impairment and low vaccination response. Sodium selenite, a selenium salt that has been proposed for therapy in decreasing the blood clot formation risk.[26] which is mostly seen in SARS-COV- 2, which is the surety death cause of COVID-19. [27] [28]Selenium has certain beneficial benefits when combined with vitamins D and E. [29]

Probiotics
The concept of probiotics is live micro-organisms that carry the host's nutritional benefits, including the gastrointestinal tract, insufficient proportions as treated.[30][31] Multistrain probiotics are also additional powerful than mono-strain probiotics.[32] as showed in table 3 . Recently, it was shown in a computerized docking analysis of metabolites Plantaricin JLA-9, Plantaricin W and Plantaricin D greatly inhibited the ACE2 receptors binding to SARS-CoV-2 blocking the entrance of the virus into the cells and indicated the anti-viral properties of Lactobacillus Plantarum to SARS-CoV-2. [33] Therefore, by meddling with the viruses entry into cells or inhibiting the repetition of the virus, probiotics may serve as antivirals. The path of COVID-19 can also be altered by the regeneration of the intestine, immune system, respiratory microbiota and gut-lung axis. [34] In comparison, in contrast to antiviral medications, immunomodulators, or new methods studied in COVID-19, probiotics are available readily, oral administration comparatively safe, and cost-effective. [35] In animal models, much of the information available today on the enhancement of immune health by probiotics has been illustrated. Intranasal inoculation of L. Plantarum and L. reuteri has been ensured to safeguard alongside fatal infection by the pneumonia virus in mice. [36] Probiotics are very safe even in weak populations. Oral probiotics have ability to reduce the severity and incidence of viral respiratory tract infections.

Antiviral Prophylaxis Of Corona Virus
Repurposed drugs were FDA approved for any indications to treat patients of COVID-19 as presented in Figure 4 and shown in Table 3. The drugs should be adequate, treatment should be highly sage, low costs. It has become a challenge due to the unavailability of approved drugs from the FDA which are specific to COVID-19. Currently, the emergency of COVID-19 warrants the fast development of effective strategies for people protection who are at high risk of infection, especially in health care workers, close contacts.

Hydroxychloroquine and Chloroquine
It should be noted that the USFDA has issued an emergency use authorization for the use of HCHL in the treatment of COVID-19. These have shown to come up with antiviral effects where some of the studies reported to have inhibition of human CoV-229E replication, HCoV OC43 and SARS-CoV. [37] [38] [39] This results in insufficient hemoglobin used to transport O2 and Co2 (respiratory insufficiency). Chloroquine was discovered to block glycoproteins viral surface from heme attacking for the formation of porphyrin and binding of glycoproteins inhibition to porphyrins, relieves the respiratory distress symptoms effectively. [40]

Remdesevir
In this period, to fight back with COVID-19 is with remdesivir which was derived from the final stages of many effective vaccines. It's the most promising medication for fighting RNA viruses since it offers a wide range of antiviral properties. It was initially established by Gilead Sciences to defeat the Ebola virus, and undergone clinical trials in the Ebola outbreak. Even though it was effective against Ebola, it was proved for human's safety, where it was allowed to conduct clinical trials in COVID-19 emergency. [41]

Bamlanivimab
This was issued by the FDA as an emergency use authorization, which is a monoclonal antibody directed against the SARS-CoV-2 spike protein on 9 Nov 2020. The EUA licenses bamlanivimab to administer in treating mild to moderate COVID-19 in adults and pediatrics aged 12 years and high risk for progressing to severe COVID-19.

Casirivimab and Imdevimab
On 21 Nov 2020, USFDA issued EUA for Casirivimab and imdevimab to administer combined for the mild to the moderated cure of COVID-19 in both pediatrics and adults, who are aged 65 years old and who have conditions of chronic. These both are not approved for patients who need oxygen therapy because of COVID-19. Both monoclonal antibodies may associate with some worse clinical outcomes when they are given to COVID-19 hospitalized patients who require mechanical ventilation.

Baricitinib
EUA has been issued by USFDA for emergency use of Baricitinib in combination with remdesivir, to treat laboratory-confirmed hospitalized COVID-19 adults and 2 years of pediatrics. It's not FDA approved for mentioned uses. The dosage of Baricitinib recommended under EUA is 4 mg daily once for adults and 9 years of pediatrics and 2 mg daily once for 2 years to < 9 years of pediatrics. The optimal duration for treatment is not known. The suggested treatment duration is 2 weeks or else until hospital discharge.

CONCLUSION

Universal spread of the corona virus has arisen to be a big challenge to reduce. Desperately, many scientists are looking for a vaccine. Few drugs are effectively potentially and in case of efficacy is still in progress where they need more experimental work. Many natural sources are in connection with us by minimizing the usage of medications. And may repurposed drugs are existing by few studies and FDA approval to treat the mild to moderate cases of COVID-19. Immune boosters and antiviral prophylaxis are the only sources right now which can save us from the severity of corona virus. Compiling the information available on COVID-19 the immune boosters and antiviral prophylaxis are in widespread use and promising way to cure.

Conflict of Interest
The authors declare no conflict of interest, financial or otherwise.

Kavya Nainita Manchikanti *et al.*,

REFERENCES

1. Dhama K, Sharun K, Tiwari R, Dadar M, Malik YS, Singh KP, *et al.* COVID-19, an emerging corona virus infection: advances and prospects in designing and developing vaccines, immunotherapeutics, and therapeutics. Human vaccines & immunotherapeutics. 2020;16(6):1232-8.
2. Velavan TP, Meyer CG. The COVID-19 epidemic. Tropical medicine & international health. 2020;25(3):278.
3. Liu Y, Sun W, Li J, Chen L, Wang Y, Zhang L, *et al.* Clinical features and progression of acute respiratory distress syndrome in corona virus disease 2019. MedRxiv. 2020.
4. Malayala SV, Mohan G, Vasireddy D, Atluri P. Purpuric Rash and Thrombocytopenia After the mRNA-1273 (Moderna) COVID-19 Vaccine. Cureus. 2021;13(3).
5. Vasireddy D, Vanaparthy R, Mohan G, Malayala SV, Atluri P. Review of COVID-19 Variants and COVID-19 Vaccine Efficacy: What the Clinician Should Know? Journal of Clinical Medicine Research. 2021;13(6):317.
6. Sui Y, Bekele Y, Berzofsky JA. Potential SARS-CoV-2 immune correlates of protection in infection and vaccine immunization. Pathogens. 2021;10(2):138.
7. Stamatatos L, Czartoski J, Wan Y-H, Homad LJ, Rubin V, Glantz H, *et al.* mRNA vaccination boosts cross-variant neutralizing antibodies elicited by SARS-CoV-2 infection. American Association for the Advancement of Science; 2021.
8. AHuang Z, Liu Y, Qi G, Brand D, Zheng SGJJocm. Role of vitamin A in the immune system. 2018;7(9):258[ ]Bde Andrade MIS, de Macêdo PFC, de Oliveira TLPS, da Silva Lima NM, da Costa Ribeiro I, Santos TM. Vitamin A and D deficiencies in the prognosis of respiratory tract infections: A systematic review with perspectives for COVID-19 and a critical analysis on supplementation.
9. Özdemir ZÖ, Şentürk M, Ekinci DJJoei, chemistry m. Inhibition of mammalian carbonic anhydrase isoforms I, II and VI with thiamine and thiamine-like molecules. 2013;28(2):316-9.
10. Ragan I, Hartson L, Pidcoke H, Bowen R, Goodrich RJPo. Pathogen reduction of SARS-CoV-2 virus in plasma and whole blood using riboflavin and UV light. 2020;15(5):e0233947.
11. Keil SD, Ragan I, Yonemura S, Hartson L, Dart NK, Bowen RJVS. Inactivation of severe acute respiratory syndrome corona virus 2 in plasma and platelet products using a riboflavin and ultraviolet light-based photochemical treatment. 2020.
12. Van Driel ML, Beller EM, Thielemans E, Deckx L, Price-Haywood E, Clark J, *et al.* Oral vitamin C supplements to prevent and treat acute upper respiratory tract infections. 2019;2019(3).
13. Carr AC, Maggini SJN. Vitamin C and immune function. 2017;9(11):1211.
14. Traber MG, Stevens JFJFRB, Medicine. Vitamins C and E: beneficial effects from a mechanistic perspective. 2011;51(5):1000-13.
15. Colunga Biancatelli RML, Berrill M, Catravas JD, Marik PEJFii. Quercetin and vitamin C: an experimental, synergistic therapy for the prevention and treatment of SARS-CoV-2 related disease (COVID-19). 2020;11:1451.
16. Khan HMW, Parikh N, Megala SM, Predeteanu GSJTAjocr. Unusual early recovery of a critical COVID-19 patient after administration of intravenous vitamin C. 2020;21:e925521-1.
17. Castillo ME, Costa LME, Barrios JMV, Díaz JFA, Miranda JL, Bouillon R, *et al.* Effect of calcifediol treatment and best available therapy versus best available therapy on intensive care unit admission and mortality among patients hospitalized for COVID-19: A pilot randomized clinical study. 2020;203:105751.
18. Besold AN, Culbertson EM, Culotta VCJJJoBIC. The Yin and Yang of copper during infection. 2016;21(2):137-44.
19. AMaggini S, Beveridge S, Sorbara P, Senatore GJCRPiA, Veterinary Science, Nutrition, Resources N. Feeding the immune system: the role of micronutrients in restoring resistance to infections. 2008;3(098):1-21[ ]BVan Doremalen N, Bushmaker T, Morris DH, Holbrook MG, Gamble A, Williamson BN, *et al.* Aerosol and surface stability of SARS-CoV-2 as compared with SARS-CoV-1. 2020;382(16):1564-7.

20. Raha S, Mallick R, Basak S, Duttaroy AKJMH. Is copper beneficial for COVID-19 patients? 2020:109814.
21. ANDREOU A, TRANTZA S, FILIPPOU D, SIPSAS N, TSIODRAS SJiv. COVID-19: The Potential Role of Copper and N-acetylcysteine (NAC) in a Combination of Candidate Antiviral Treatments Against SARS-CoV-2. 2020;34(3 suppl):1567-88.
22. Báez-Santos YM, John SES, Mesecar ADJAr. The SARS-corona virus papain-like protease: structure, function and inhibition by designed antiviral compounds. 2015;115:21-38.
23. Ishida TJWSN. Antiviral Activities of Cu2+ Ions in Viral Prevention, Replication, RNA Degradation, and for Antiviral Efficacies of Lytic Virus, ROS-Mediated Virus, Copper Chelation. 2018;99:148-68.
24. Te Velthuis AJ, van den Worm SH, Sims AC, Baric RS, Snijder EJ, van Hemert MJJPp. Zn2+ inhibits corona virus and arterivirus RNA polymerase activity in vitro and zinc ionophores block the replication of these viruses in cell culture. 2010;6(11):e1001176.
25. Finzi EJIJoID. Treatment of SARS-CoV-2 with high dose oral zinc salts: A report on four patients. 2020.
26. Kieliszek M, Lipinski BJMH. Selenium supplementation in the prevention of corona virus infections (COVID-19). 2020;143:109878.
27. Fogarty H, Townsend L, Ni Cheallaigh C, Bergin C, Martin-Loeches I, Browne P, *et al.* COVID19 coagulopathy in Caucasian patients. 2020.
28. Lipinski BJJoAiM, Research M. Can selenite be an ultimate inhibitor of EBOLA and other viral infections? 2015:319-24.
29. Delesderrier E, Cople-Rodrigues CS, Omena J, Kneip Fleury M, Barbosa Brito F, Costa Bacelo A, *et al.* Selenium Status and Hemolysis in Sickle Cell Disease Patients. 2019;11(9):2211.
30. Sanders MEJCid. Probiotics: definition, sources, selection, and uses. 2008;46(Supplement_2):S58-S61.
31. Kumar S, Singhi SJM. Role of probiotics in prevention of Candida infection in critically ill children. 2013;56(3):204-11.
32. Timmerman H, Koning C, Mulder L, Rombouts F, Beynen AJIjofm. Monostrain, multistrain and multispecies probiotics—a comparison of functionality and efficacy. 2004;96(3):219-33.
33. Anwar F, Altayb HN, Al-Abbasi FA, Al-Malki AL, Kamal MA, Kumar VJJoBS, *et al.* Antiviral Effects of Probiotic metabolites on COVID-19. 2020(just-accepted):1-11.
34. Baud D, Agri VD, Gibson GR, Reid G, Giannoni EJFiPH. Using Probiotics to Flatten the Curve of Corona virus Disease COVID-2019 Pandemic. 2020;8.
35. Infusino F, Marazzato M, Mancone M, Fedele F, Mastroianni CM, Severino P, *et al.* Diet Supplementation, Probiotics, and Nutraceuticals in SARS-CoV-2 Infection: A Scoping Review. 2020;12(6):1718.
36. Gabryszewski SJ, Bachar O, Dyer KD, Percopo CM, Killoran KE, Domachowske JB, *et al.* Lactobacillus-mediated priming of the respiratory mucosa protects against lethal pneumovirus infection. 2011;186(2):1151-61.
37. Keyaerts E, Vijgen L, Maes P, Neyts J, Van Ranst MJB, communications br. In vitro inhibition of severe acute respiratory syndrome corona virus by chloroquine. 2004;323(1):264-8.
38. Keyaerts E, Li S, Vijgen L, Rysman E, Verbeeck J, Van Ranst M, *et al.* Antiviral activity of chloroquine against human corona virus OC43 infection in newborn mice. 2009;53(8):3416-21.
39. Jang C-H, Choi J-H, Byun M-S, Jue D-MJR. Chloroquine inhibits production of TNF-α, IL-1β and IL-6 from lipopolysaccharide-stimulated human monocytes/macrophages by different modes. 2006;45(6):703-10.
40. ALiu W, Li HJPro. COVID-19: attacks the 1-beta chain of hemoglobin and captures the porphyrin to inhibit human heme metabolism. 2020;10(04)[ ]BGautret P, Lagier J-C, Parola P, Meddeb L, Mailhe M, Doudier B, *et al.* Hydroxychloroquine and azithromycin as a treatment of COVID-19: results of an open-label non-randomized clinical trial. 2020:105949.
41. Mulangu S, Dodd LE, Davey Jr RT, Tshiani Mbaya O, Proschan M, Mukadi D, *et al.* A randomized, controlled trial of Ebola virus disease therapeutics. 2019;381(24):2293-303.
42. Liu J, Cao R, Xu M, Wang X, Zhang H, Hu H, *et al.* Hydroxychloroquine, a less toxic derivative of chloroquine, is effective in inhibiting SARS-CoV-2 infection in vitro. Cell discovery. 2020;6(1):1-4.
43. Ohashi H, Watashi K, Saso W, Shionoya K, Iwanami S, Hirokawa T, *et al.* Multidrug treatment with nelfinavir and cepharanthine against COVID-19. BioRxiv. 2020.

44. de Steenhuijsen Piters WA, Heinonen S, Hasrat R, Bunsow E, Smith B, Suarez-Arrabal M-C, *et al*. Nasopharyngeal microbiota, host transcriptome, and disease severity in children with respiratory syncytial virus infection. American journal of respiratory and critical care medicine. 2016;194(9):1104-15.

45. ALuoto R, Ruuskanen O, Waris M, Kalliomäki M, Salminen S, Isolauri E. Prebiotic and probiotic supplementation prevents rhinovirus infections in preterm infants: a randomized, placebo-controlled trial. Journal of Allergy and Clinical Immunology. 2014;133(2):405-13[ ]

46. BKawase M, He F, Kubota A, Harata G, Hiramatsu M. Oral administration of lactobacilli from human intestinal tract protects mice against influenza virus infection. Letters in applied microbiology. 2010;51(1):6-10.

47. Olivares M, Díaz-Ropero MP, Sierra S, Lara-Villoslada F, Fonollá J, Navas M, *et al*. Oral intake of Lactobacillus fermentum CECT5716 enhances the effects of influenza vaccination. Nutrition. 2007;23(3):254-60.

48. Makino S, Ikegami S, Kume A, Horiuchi H, Sasaki H, Orii N. Reducing the risk of infection in the elderly by dietary intake of yoghurt fermented with Lactobacillus delbrueckii ssp. bulgaricus OLL1073R-1. British Journal of Nutrition. 2010;104(7):998-1006.

49. Taipale T, Pienihäkkinen K, Isolauri E, Larsen C, Brockmann E, Alanen P, *et al*. Bifidobacterium animalis subsp. lactis BB-12 in reducing the risk of infections in infancy. British Journal of Nutrition. 2011;105(3):409-16.

50. Park M-K, Ngo V, Kwon Y-M, Lee Y-T, Yoo S, Cho Y-H, *et al*. Lactobacillus plantarum DK119 as a probiotic confers protection against influenza virus by modulating innate immunity. PloS one. 2013;8(10):e75368.

51. Berggren A, Ahrén IL, Larsson N, Önning G. Randomised, double-blind and placebo-controlled study using new probiotic lactobacilli for strengthening the body immune defence against viral infections. European journal of nutrition. 2011;50(3):203-10.

52. AWang M, Cao R, Zhang L, Yang X, Liu J, Xu M, *et al*. Remdesivir and chloroquine effectively inhibit the recently emerged novel corona virus (2019-nCoV) in vitro. Cell research. 2020;30(3):269-71[ ]BSavarino A, Di Trani L, Donatelli I, Cauda R, Cassone A. New insights into the antiviral effects of chloroquine. The Lancet infectious diseases. 2006;6(2):67-9[ ]

53. CVincent MJ, Bergeron E, Benjannet S, Erickson BR, Rollin PE, Ksiazek TG, *et al*. Chloroquine is a potent inhibitor of SARS corona virus infection and spread. Virology journal. 2005;2(1):1-10[ ]DSui J, Li W, Murakami A, Tamin A, Matthews LJ, Wong SK, *et al*. Potent neutralization of severe acute respiratory syndrome (SARS) corona virus by a human mAb to S1 protein that blocks receptor association. Proceedings of the National Academy of Sciences. 2004;101(8):2536-41.

54. Sangawa H, Komeno T, Nishikawa H, Yoshida A, Takahashi K, Nomura N, *et al*. Mechanism of action of T-705 ribosyl triphosphate against influenza virus RNA polymerase. Antimicrobial agents and chemotherapy. 2013;57(11):5202-8.

55. Nukoolkarn V, Lee VS, Malaisree M, Aruksakulwong O, Hannongbua S. Molecular dynamic simulations analysis of ritronavir and lopinavir as SARS-CoV 3CLpro inhibitors. Journal of theoretical biology. 2008;254(4):861-7.

56. Mulangu S, Dodd LE, Davey Jr RT, Tshiani Mbaya O, Proschan M, Mukadi D, *et al*. A randomized, controlled trial of Ebola virus disease therapeutics. New England Journal of Medicine. 2019;381(24):2293-303.

57. ASaraya MA, Amal AE-AI. Dexamethasone as adjunctive therapy for treatment of varicella pneumonia. Egyptian Journal of Chest Diseases and Tuberculosis. 2012;61(3):9-13[ ]BLecoq L, Vincent P, Lavoie-Lamoureux A, Lavoie J-P. Genomic and non-genomic effects of dexamethasone on equine peripheral blood neutrophils. Veterinary immunology and immunopathology. 2009;128(1-3):126-31.

58. Walls AC, Park Y-J, Tortorici MA, Wall A, McGuire AT, Veesler D. Structure, function, and antigenicity of the SARS-CoV-2 spike glycoprotein. Cell. 2020;181(2):281-92. e6.

59. Somvanshi VS, Ellis BL, Hu Y, Aroian RV. Nitazoxanide: nematicidal mode of action and drug combination studies. Molecular and biochemical parasitology. 2014;193(1):1-8.

60. Dowty ME, Lin TH, Jesson MI, Hegen M, Martin DA, Katkade V, *et al*. Janus kinase inhibitors for the treatment of rheumatoid arthritis demonstrate similar profiles of in vitro cytokine receptor inhibition. Pharmacology research & perspectives. 2019;7(6):e00537.

61. Spagnuolo V, Castagna A, Lazzarin AJEoop. Darunavir for the treatment of HIV infection. 2018;19(10):1149-63.

Kavya Nainita Manchikanti *et al.*,

Table 1: Combinational medication in the treatment of corona virus

Combination of drugs	Category	Advantages	References
Chloroquine + hydroxyl chloroquine	Anti-malarial	Because of its anti-inflammatory effect, it is used as a repurposed drug to treat SARS-CoV-2.	[3]
Nelfinavir + Cepharanthine	Protease inhibitor + alkaloid	Inhibition of viral proliferation and minimizes virus transmission.	[4]

Table 2: Probiotics-targeted viral infections

Probiotic bacterial strain	Viral respiratory infection	Consequence	Reference
Streptococcus, Moraxella	Respiratory syncytial virus	The researchers wanted to see if distinct nasopharyngeal microbiota are linked to different host transcriptome profiles and infection severity in RSV-infected kids. The findings revealed that the interaction between RSV and the nasopharyngeal microbiota may moderate host immune responses, thereby changing the disease's clinical severity.	[16]
Lactobacillus Rhamnosus	Respiratory tract infections, influenza virus	In a cohort analysis of preterm babies, the researchers predicted that early prebiotic or probiotic supplementation might reduce the incidence of virus-associated RTIs throughout the first year of life. The findings showed that changing the gut microbiota with specific prebiotics and probiotics might be a unique and cost-effective way to reduce the risk of rhinovirus infections.	[17]
Lactobacillus Fermentum	Influenza	The ability of the breast-milk-isolated strain Lactobacillus fermentum to serve as a co-adjuvant with an anti-influenza vaccination was tested. This study found that taking L. fermentum orally boosts the T-helper type 1 response and elicits virus-neutralizing antibodies, which may improve protection by increasing the T-helper type 1 response and evoking virus-neutralizing antibodies.	[18]
Lactobacillus Bulgaricus	Respiratory tract infections	This study looked at whether eating yoghurt fermented with Lactobacillus delbrueckii ssp. bulgaricus may keep you from catching a cold. Intake of yoghurt fermented with L. bulgaricus enhanced natural killer cell activity and decreased the chance of developing a cold in the elderly, according to the findings.	[19]
BifdobacteriumAnimalis	Respiratory tract infections	viral titer reduced	[20]
Lactobacillus Plantarum	H1N1 and H3N2 influenza viruses	It enhances the innate immunity of antiviral cytokines and macrophage cells.	[21]
Lactobacillus Paracasei	Common cold virus	Oral ingestion of this probiotics minimizes the symptoms of cold infections.	[22]

Kavya Nainita Manchikanti *et al.*,

Table 3: Mechanism, Targets and side effects of anti-SARS-CoV-2 prophylactic drugs

Drugs	Category	Mechanism of action	Side effects
Chloroquine (Aralen) / hydroxychloroquine (Plaquenil) [23]	Anti-malarial	Cytotoxicity inhibition; immunosuppression; ACE2 receptor and spike protein glycosylation changes.	Nausea, vomiting, hair loss, the sensitivity of light is increased.
Remdesivir, favipiravir (Avigan) [23D, 24]	Anti-viral	Inhibition of viral RNA polymerase through chain termination inhibits viral replication and transcription.	Production of erythrocytes is reduced and liver function parameters will be increased in influenza conditions. In COVID-19 the symptoms are reduced.
Lopinavir (Kaletra), Rotinavir (norvir) [25]	Antiretroviral	SARS-CoV 3 CL proenzyme inhibition, inhibits SARS-CoV-2 replication of Vero E6 cells, protease, CYP4503A.	Headache, chest pain, dizziness and stomach pain.
Oseltamavir (Tamiflu) [23D, 26]	Anti-viral	Neuraminidase inhibitor. The mechanism is still not yet known on SARS-CoV-2.	Hypersensitivity.
Dexamethasone (Decadron) [27]	corticosteroid	Genomic and non-genomic mechanisms	Agitation, headache, changes in mood, high appetite.
Umefenovir (Arbidol) [28]	Anti-viral	Blocks the trimerization of SARS-CoV-2 spike glycoprotein that leads to form of immature virus which is infection less.	Sensitivity is increased to medication in below 2 years.
Nitazoxanide [29]	Antiviral and anti-parasitic	Reduces the inhibitory effect of interferon which is triggered by SARS-CoV-2.	Discolored urine, stomach pain, and headache.
Darunavir (Prezista) [30][31]	Anti-viral	A non-peptidyl HIV-1 protease inhibitor inhibits HIV protease dimerization, inhibits cleave of Gag-Pol polyprotein.	Rashes, stomach pain, vomiting, nausea, diarrhea.
Ivermectin (Stromectol)	Anthelmintic	Inhibits the nuclear import of viral and host proteins by inhibition of importin 1 heterodimer. It inhibits IMP $\alpha/\beta1$- mediated nuclear import.	Muscle aches, mild skin rash, discolored urine, nausea.

Kavya Nainita Manchikanti *et al*.,
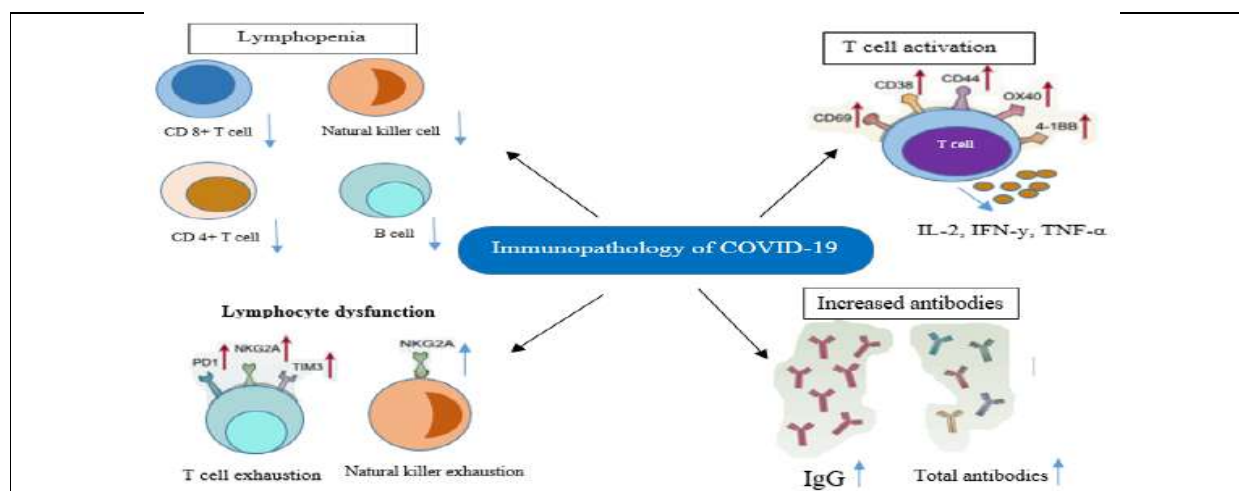
Figure 1: Immune configurations of COVID-19
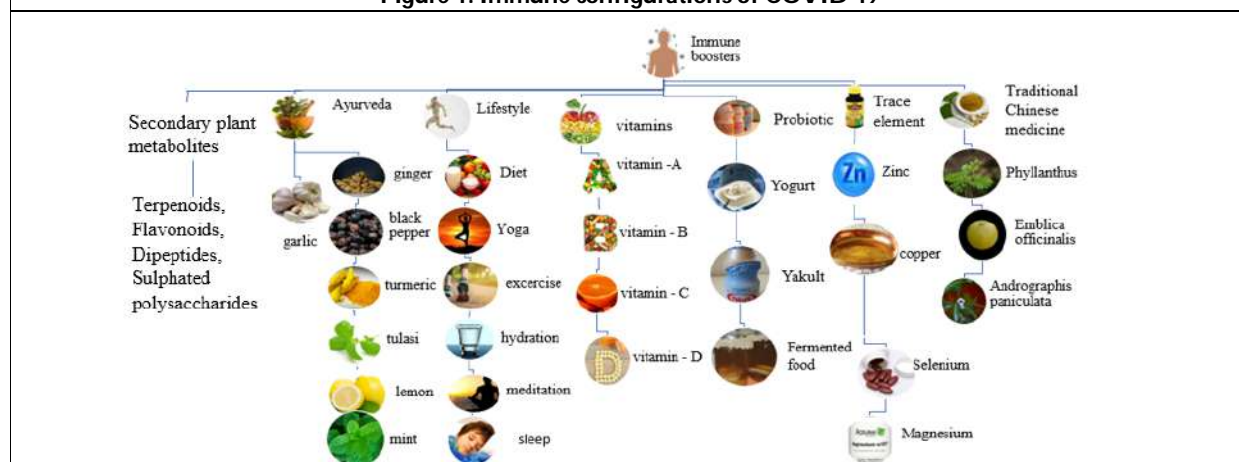
Figure 2: Immune boosters fight against COVID -19
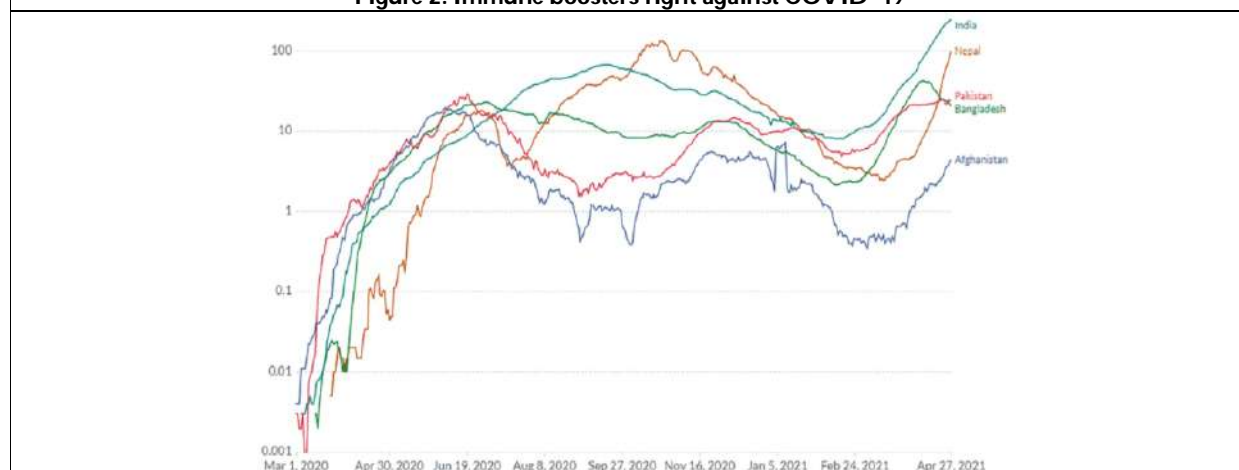
Figure 3: Data Analysis on India's Covid-19 Epidemic

Kavya Nainita Manchikanti *et al.,*
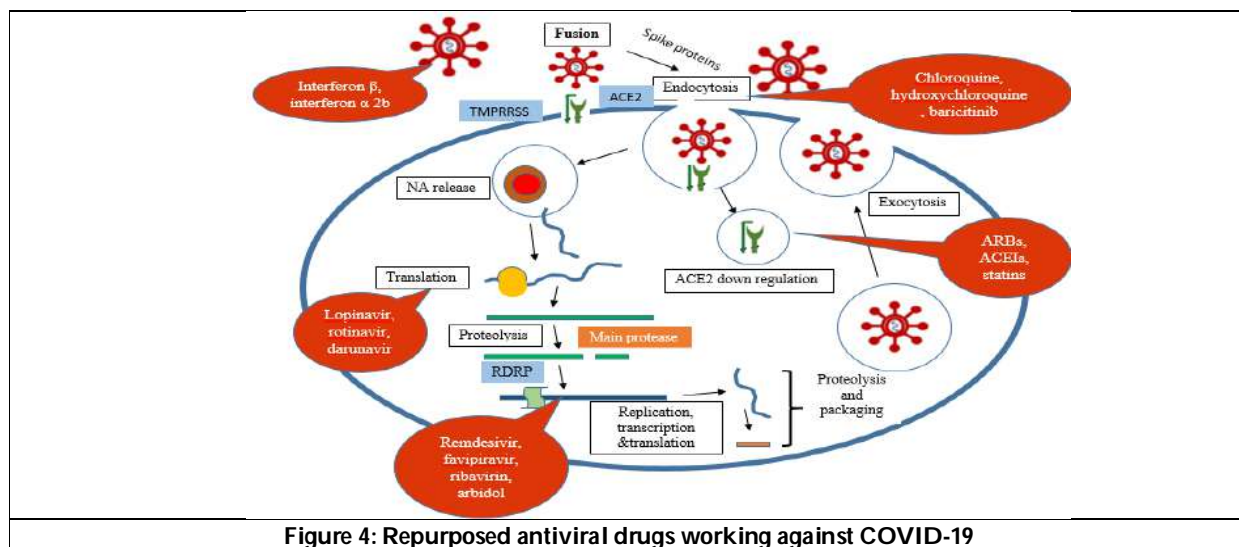
Figure 4: Repurposed antiviral drugs working against COVID-19

RESEARCH ARTICLE

Phytochemical Constituency Profiling and Antimicrobial Activity of *Haloplegma duperreyi* From The Mandapam, Rameshwaram Coast, Tamil Nadu.

M. Shantha[1] and A. Arockia Jenecius Alphonse[2]*

[1]Research Scholar, Department of Botany, St. Mary's College (Autonomous), (Affiliated to Manonmaniam Sundaranar University, Tirunelveli), Thoothukudi-628001,Tamil Nadu, India.
[2]Assistant Professor, Department of Botany, St. Mary's College (Autonomous), (Affiliated to Manonmaniam Sundaranar University, Tirunelveli), Thoothukudi-628001, Tamil Nadu, India

*Address for Correspondence
Arockia Jenecius Alphonse,
Assistant Professor,
Department of Botany, St. Mary's College (Autonomous),
(Affiliated to Manonmaniam Sundaranar University, Tirunelveli),
Thoothukudi-628001, Tamil Nadu, India.
E. Mail: researchscholarsmc21@gmail.com

ABSTRACT

This work aims to evaluate the antimicrobial potential of methanolic extracts of *Haloplegma duperreyi* . Agar well diffusion method has been used to determine the antimicrobial activities of *Haloplegma duperreyi* against gram- positive bacteria (*Salmonella para typhi, Staphylococcus aureus), gram – Negative bacteria (Escherichia coli ,Klebsiella neminiae and fungus(Candida albicans, Aspergillus fumicates).* The extracts exhibited both antifungal and antibacterial activities against tested microorganisms. Thus, the result shows that red algae *Haloplegma Duperreyi* has good biological activity, and further it can be carried out in pharmaceutical, food preservatives, and cosmetic purpose.

Keywords: *Aspergillus fumigates, Klebsiella neminiae, Haloplegma Duperreyi, Salmonella para typhi Staphylococcus aureus*, Antibacterial*.

INTRODUCTION

Antimicrobial agents play a crucial role in lowering the burden of infectious diseases worldwide [1]. However, because there are fewer or often no effective antimicrobial medicines available to treat infections brought on by pathogenic bacteria, the rise and spread of multidrug resistant (MDR) strains of pathogenic bacteria have become a significant public health problem [2, 3].Seaweeds are considered as a variety of sources for secondary metabolites

63506

with a wide range of biological [1] activities Seaweeds are photosynthetic microalgae and are categorised as red [2], brown [3], and green [4] algae based on the components of their pigments. *Haloplegma Duperreyi* is Rhodophyta (red seaweeds). Additionally, it has been demonstrated by results from earlier studies that seaweeds contain bioactive components that can help humanity by preventing the growth of bacteria (5,6). Examples of substances found in seaweeds that exhibit antimicrobial and antibacterial properties include phenols, terpenes, acetogenins, indoles, fatty acids, and volatile halogenated hydrocarbons (7); Some of the most well-known species of seaweed, include *Porphyra sp.*. and *Chondrus crispus*, are found in Rhodophyta and are extremely popular in Asia [8,9,10] and Ireland [11], respectively, particularly as a component in their culinary traditions. Several investigations have focused on specific species, including *Osmundea pinnatifida* (e.g., [11,12]), *Sphaerococcus coronopifolius* (e.g., [13,14,11]), and *Plocamium cartilagineum* (e.g., [15,16,17,18]), In Asia, crude extracts of the Asian plant *Calotropis gigantean* exhibit encouraging antifungal efficacy against the pathogenic fungus *Candida albicans*, *Aspergillus niger*, *Aspergillus ochraceus*, *Aspergillus ustus*, and *Rizopus oryzae*. [19]. In Another study found that an ethanolic extract of *Plumbago zeylanica* root has effective antibacterial properties against *Curvularia lunata, Colletotrichum corchori, P. aeruginosa, V. cholerae*, and *E. coli*. [20,21,22]. So, the objective of the present study is to investigate different compounds such as phenols, flavonoids, terpenoids, and steroids as well as their antiomicrobial properties in *Haloplegma Duperreyi* . The studied marine algae showed antibacterial activities. They could be potentially used for applications in medicine, food production and the cosmetic industry [23].

MATERIALS AND METHODS

Sample Preparation
Haloplegma duperreyi was collected Rameshwaram coast, Ramanathapuram, Tamil Nadu. The collected sample was authenticated by Botanical Survey of India (BSI), Coimbatore, Tamil Nadu, India.

Processing Of Collected Sample
The collected seaweeds were initially rinsed with seawater to eliminate dirt and debris along with epiphytes, sand particles and shells. Later, they were washed with running tap water followed by distilled water and dried in dark conditions. The resulting dried material was coarsely powdered (passing through a 40-size sieve) and utilized for further pharmacognostic and phytochemical studies.

Preparation Of Seaweed Extracts Using The Different Solvent Method
The shade-dried *Haploplegma duperreyi* were powdered using a milling machine and further subjected to Soxhlet extraction (Borosil, Mumbai, India) using five different solvents namely Methanol, Ethylacetate, Aqueous, Chloroform, and Hexane. The powdered samples were subjected to 20gm thimble using handmade filter paper. Later, *Haploplegma duperreyi* the filled thimble was carefully placed within the extractor chamber and poured with chosen five dissimilar solvents as a 1:10 ratio. The reservoir round bottom flask was excited to 60°C in a heating mantle. Each sample was run at least 15 refluxes to get good quality seaweed solvent extracts and the resultant solvent extracts were condensed using a rotary evaporator (Buchi, Bangalore, India) within condensed temperature under vacuum conditions. Finally, the precipitant was collected in a glass container and stored under -20°C for further analysis.

Qualitative Analysis of Phytochemical Screening of *Haploplegma duperreyi*
The phytochemical screening aqueous, ethanol, methanol, ethyl acetate and chloroform extracts of plant sample was subjected to different chemical tests for the detection of different phyto constituents using standard procedures. To identify the presence of alkaloids, flavonoids,tannins, saponins, steroids, terpenoids, glycosides, phenols, carbohydrates and proteins. [24] [25]. (Peach and Tracey, 1995; Raaman, 2006)

Shantha and Arockia Jenecius Alphonse

Alkaloids
Meyar's reagent (potassium iodide)
1.3 g of mercuric chloride was dissolved in 60 ml distilled water and 5.0 g of potassium iodide in 10 ml of water. The two solutions were mixed and diluted to 100 ml with distilledwater. A few drops of reagent were applied to 1.0 ml of leaf extract. Alkaloids were detected by the formation of white or pale yellow precipitate.

Phenols
Ferric chloride test
To 1.0 ml of leaf extract 2.0 ml of distilled water, followed by a few drops of 10 % aqueous $FeCl_3$ solution was added. Appearance of blue or green colour indicates the presence of phenols.

Flavanoids
In the test tubes containing 0.5 ml of leaf extract, 5-10 drops of dilute HCl and small piece of zinc or magnesium were added and the solution was boiled for a few minutes. Reddish pink or dirty brown colour was produced it showed the presence of flavonoids.

Tannins
Ferric chloride test
To 1- 2 ml of leaf extract, few drops of 5 % aqueous $FeCl_3$ solution was added.A bluish black colour, which disappears on the addition of a few ml of dilute H_2SO_4 was followed by the formation of a yellowish brown precipitate.

Saponins
In a test tube containing about 5.0 ml of leaf extract, a drop of sodium bicarbonatesolution was added. The mixture was vigorously shaken and keft for three minutes.. A honey comb like froth was developed and it showed the presence of saponins.

Terpenoids
Salkwski reaction
5.0 ml of leaf extract was mixed in 2.0 ml of chloroform and concentrated H_2SO_4 (3.0 ml) was carefully added to form a layer. A reddish brown coloration in the inter phase formed to show positive results for the presence of terpenoids.

Steroids
Libermann-Burchard's test
To 1.0 ml of leaf extract, 1.0 ml of conc. H_2SO_4 was added, followed by the addition of 2.0 ml of acetic anhydride solution. A greenish colour developed and turned blue indicates the presence of steroids.

Carbohydrates
Benedict's test
173 g of sodium citrate and 100 mg of sodium carbonate was dissolved in 500 ml of water. To this solution 17.3 g of copper sulphate dissolved in 100 ml of water was added. To 0.5ml of the leaf extract, 5.0 ml of Benedict's reagent was added and boiled for 5 minutes.Formation of a bluish green colour showed the presence of carbohydrates.

Glycosides
A small amount of leaf extract was dissolved in 1.0 ml of water and then an aqueous sodium hydroxide solution was added. Formation of a yellow colour indicates the presence of glycosides.

Aminoacids And Proteins
Biuret's test
To 1.0 ml of leaf extract, 5-8 drops of 5 % sodium hydroxide solution were added, followed by one or two drops of 1 % copper sulphate. Formation of pink or purple colour confirmed the presence of proteins and amino acids.

Antimicrobial Activity
Test Microorganisms
The test organisms used were clinical isolates *viz., Staphylococcus aureus, Escherichia coli Salmonella paratyphi and Klebsiellanemoniae.* The human fungal pathogens like *Aspergillus fumigates* and *Candida albicans,*which were obtained from Department of Microbiology, Coimbatore medical college and hospital (CMHC), Coimbatore. The bacterial and the fungal cultures were maintained on nutrient agar medium and potato dextrose agar (PDA) medium respectively.

Growth and Maintenance of Test Microorganism for Antimicrobial Studies
The bacterial and fungal cultures were maintained on nutrient broth (NB) at37°C and fungus was maintained on Potato dextrose agar (PDA) at 28°C.

Preparation of Inoculum
The gram positive bacteria *Escherichia coli, Staphylococcus aureus* and gram negative bacteria *Salmonella paratyphi and Klebsiella nemoniae* were pre-cultured in nutrient broth overnight in a rotary shaker at 37°C, centrifuged at 10,000 rpm for 5 min, pellet was suspended in double distilled water and the cell density was standardized spectro photometrically (A_{610} nm). The fungal inoculums *Aspergillus fumigatus* and *Candida albicans,* were prepared from 5 to 10 day old culture grown on Potato dextrose agar medium. The Petri dishes were flooded with8 to 10 ml of distilled water and the conidia were scraped using sterile spatula. The spore density of each fungus was adjusted with spectrophotometer (A_{595}nm) to obtain a final concentration of approximately 10^5 spores/ml.

Anti-bacterial Activity (Anonymous, 1996)
The samples were tested by the well diffusion method. Different concentration of the samples (10,20,30 μg/ml) was prepared. The test microorganisms were seeded into respective medium by spread plate method 10 μl (10 cells/ml) with the 24h cultures of bacteria growth in nutrient broth. After solidification the filter paper wells (5 mm in diameter) impregnated with the extracts were placed on test organism-seeded plates. Amoxicillin (10 μg) used as standard for antibacterial test. The antibacterial assay plates were incubated at 37°C for 24 hrs. The diameters of the inhibition zones were measured in mm.

Antifungal Activity (Taylor *et al.*, 1995)
The antifungal activity was tested by well diffusion method. The potato dextrose agar plates were inoculated with each fungal culture (10 days old) by point inoculation. The filter paper wells (5 mm in diameter) impregnated with 100 μg concentrations of the synthesized silver nanoparticles were placed on test organism-seeded plates. Amoxicillin (10 μgwell 1) used as positive control. The activity was determined after 72 hrs of incubation at 28°C. The diameters of the inhibition zones were measured in mm.

RESULT AND DISCUSSION

Qualitative analysis of *Haloplegma duperreyi*
The present study revealed that the polar to non polar extracts of *Haloplegma duperreyi* contained alkaloids, flavonoids, glycosides, phenols, resins, saponins, steroids, tannins, terpenoids , carbohydrates and proteins (Table .1). However, phenols, terpenoids, steroids, proteins and carbohydrates were moderately presented in four solvents such as aqueous chloroform, ethyl acetate and methanol. Next to methanol extract, ethyl acetate extracts of both parts showed the presence of rich variety of secondary metabolites. Ethyl acetate and chloroform extracts showed the less variety of these secondary metabolites. Compared to all other solvent extracts, ethanolic extracts had higher

Shantha and Arockia Jenecius Alphonse

number of secondary metabolites with high degree of precipitation (+++). Saponin and tannin were determined to be present with lesser amount (+) only in all extracts.

Quantitative analysis of *Haloplegma duperreyi*

The quantitative phytochemical analysis of *Haloplegma duperreyi* revealed the highest phenolics content of the *Haloplegma duperreyi* was found to be 4.72±0.35 mg GAE/g in Methanol extract . While the lowest amount of phenolic content was found in the chloroform extract (2.90±0.55 mg GAE/g). The alkaloid content was found to be the highest in methanol extract. However highest steroid, flavanoids and terpenoids content observed in methanol extract (Table 2). In previous studies alkaloids were found to be present in aq. extracts of the Punica granatum while terpenoids were not detected (Wadood *et al.*, 2013).Similarly, in current study terpenoids and tannins were detected in Ficus microcarpa while in previous studies alkaloids and steroids have also been reported (Shripad *et al.*, 2012).(27-28)

Antimicrobial Activity

These results indicate significant capacity of *Haloplegma duperreyi* as new bioactive compounds as antimicrobial agent in the treatment of pathogenic organisms. The antibacterial and anti fungal activity of *Haloplegma duperreyi* were determined in both gram positive and gram negative bacteria and fungus. In the preliminary phytochemical assay of five different organic solvents like Ethanol, methanol,aqueous, ethyl acetate and choloroform. Only methanol extracts showing antimicobial activity were considered for further study. The zone of inhibition produced by these extracts against pathogenic microorganisms is summarized in Figure 1-6. Different species showed sensitivity for methanol extract. The extract of *Haloplegma duperreyi* showed activity against S.aureus. Some studies reported the antimicrobial property of A. vulgaris against S. aureus and E. coli similarly to our fnding [29]

CONCLUSION

Phytochemical analysis of . *Haloplegma duperreyi* shown the presence of various metabolites such as flavonoids, alkaloids, phytosterols and steroids are present and antibacterial potential of seaweed extract for the synthesis novel antibiotics.. Future studies (in vitro and in vivo) are required to prove the potential medicinal properties of the *Haloplegma duperreyi* (red algae).

REFERENCES

1. Cox S, Abu-Ghannam N, Gupta S. An assessment of the antioxidant and antimicrobial activity of six species of edible Irish seaweeds. Int. Food Res. J. 2010: 17: 205-220.
2. Richard JP, Cannell RJP, Owsianka AM, Walker JM. Result of a large scale screening programmes to detect antibacterial activity from fresh water algae. Br. Phycol. J. 1988: 23: 41-44.
3. Smit AJ. Medicinal and pharmaceutical uses of seaweed natural products: Areview. J. Appl. Phycol. 2004: 16: 245-262.
4. AL-Haj NA, Mashan NI, Mariana N, Shamsudin MN, Mohamad H, Vairappan CS, Sekawi Z. Antibacterial Activity of Marine Source Extracts Against Multidrug Resistance Organisms. Am. J. Pharmacol. Toxicol. 2010: 5(2): 95-10
5. Souza, Bartolomeu WS, *et al.* "Antioxidant potential of two red seaweeds from the Brazilian coasts." *Journal of Agricultural and Food Chemistry* 59.10 (2011): 5589-5594.
6. Kanatt, Sweetie R., *et al.* "Kappaphycus alvarezii: Its antioxidant potential and use in bioactive packaging films." *Journal of Microbiology, Biotechnology and Food Sciences* 2021 (2021): 1-6.
7. El Shafay, Shimaa M., Samh S. Ali, and Mostafa M. El-Sheekh. "Antimicrobial activity of some seaweeds species from Red sea, against multidrug resistant bacteria." *The Egyptian Journal of Aquatic Research* 42.1 (2016): 65-74.
8. Soares-Filho, Britaldo, *et al.* "Cracking Brazil's forest code." *Science* 344.6182 (2014): 363-364.

Shantha and Arockia Jenecius Alphonse

9. Seenivasan, R., *et al.* "Antibacterial Activity and Phytochemical Analysis of Selected Seaweeds from Mandapam Coast, India." (2012).

10. Isaka, S.; Cho, K.; Nakazono, S.; Abu, R.; Ueno, M.; Kim, D.; Oda, T. Antioxidant and Anti-Inflammatory Activities of Porphyran Isolated from Discolored Nori (Porphyra yezoensis). Int. J. Biol. Macromol. 2015, 74, 68–75. https://doi.org/10.1016/j.ijbi- omac.2014.11.043.

11. Patarra, R.F.; Paiva, L.; Neto, A.I.; Lima, E.; Baptista, J. Nutritional Value of Selected Macroalgae. J. Appl. Phycol. 2011, 23, 205– 208. https://doi.org/10.1007/s10811-010-9556-0.

12. Campos, A.M.; Matos, J.; Afonso, C.; Gomes, R.; Bandarra, N.M.; Cardoso, C. Azorean Macroalgae (Petalonia binghamiae, Halop- teris scoparia and Osmundea pinnatifida) Bioprospection: A Study of Fatty Acid Profiles and Bioactivity. Int J. Food Sci. Technol. 2019, 54, 880–890. https://doi.org/10.1111/ijfs.14010.

13. Pinteus, S.; Alves, C.; Rodrigues, A.; Mouga, T.; Pedrosa, R. Algae from the Peniche Coast (Portugal) Exhibit New Promising Antibacterial Activities against Fish Pathogenic Bacteria. Curr. Opin. Biotechnol. 2011, 22, 33–34. https://doi.org/10.1016/j.cop- bio.2011.05.074.

14. .Alves, C.; Serrano, E.; Silva, J.; Rodrigues, C.; Pinteus, S.; Gaspar, H.; Botana, L.M.; Alpoim, M.C.; Pedrosa, R. Sphaerococcus coronopifolius Bromoterpenes as Potential Cancer Stem Cell-Targeting Agents. Biomed. Pharmacother. 2020, 128, 110275. https://doi.org/10.1016/j.biopha.2020.110275

15. Valentão, P.; Trindade, P.; Gomes, D.; Guedes de Pinho, P.; Mouga, T.; Andrade, P.B. Codium tomentosum and Plocamium cartilagineum: Chemistry and Antioxidant Potential. Food Chem. 2010, 119, 1359–1368. https://doi.org/10.1016/j.food- chem.2009.09.015.

16. Alves, C.; Pinteus, S.; Rodrigues, A.; Horta, A.; Pedrosa, R. Algae from Portuguese Coast Presented High Cytotoxicity and Antiproliferative Effects on an in Vitro Model of Human Colorectal Cancer. Pharmacogn. Res. 2018, 10, 24–30. https://doi.org/10.4103/pr.pr_151_16

17. Young, R.M.; von Salm, J.L.; Amsler, M.O.; Lopez-Bautista, J.; Amsler, C.D.; McClintock, J.B.; Baker, B.J. Site-Specific Variability in the Chemical Diversity of the Antarctic Red Alga Plocamium cartilagineum. Mar. Drugs 2013, 11, 2126–2139. https://doi.org/10.3390/md11062126.

18. Santos, M.A.Z.; Colepicolo, P.; Pupo, D.; Fujii, M.T.; de Pereira, C.M.P.; Mesko, M.F. Antarctic Red Macroalgae: A Source of Polyunsaturated Fatty Acids. J. Appl. Phycol. 2017, 29, 759–767. https://doi.org/10.1007/s10811-016-1034-x.

19. Parvin S, Abdul Kader M, Uzzaman Chouduri A, Abu Shuaib Rafshanjani M, Ekramul Haque M, Md Abdul Kader C. Antibacterial, antifungal, and insecticidal activities of the n-hexane and ethyl-acetate fractions of methanolic extract of the leaves of Calotropis gigantea Linn. J Pharmacogn Phytochem. 2014; 2(5):47–51. 22.

20. Chuah E, Zakaria Z, Suhaili Z, Abu Bakar Jamaludin S, Mohd Desa M. Antimicrobial activities of plant extracts against methicillin-susceptible and methicillin-resistant Staphylococcus aureus. J Microbiol Res. 2014; 4(1):6–13.

21. Kebede, Taye, Eshetu Gadisa, and Abreham Tufa. "Antimicrobial activities evaluation and phytochemical screening of some selected medicinal plants: A possible alternative in the treatment of multidrug-resistant microbes." *PLoS One* 16.3 (2021): e0249253.

22. Kumaresan, M., *et al.* "Seaweed Sargassum wightii mediated preparation of zirconia (ZrO2) nanoparticles and their antibacterial activity against gram positive and gram negative bacteria." *Microbial pathogenesis* 124 (2018): 311-315.

23. Saidani, Karima, *et al.* "Bioactive Compounds Identification, Antioxidant and Antibacterial Activities of Algerian Marine Algae Extracts." *Current Bioactive Compounds* 18.8 (2022): 81-93.

24. Raaman, N. (2006). Phytochemicals techniques. New India publishing agency, New Delhi., 19-

25. 25.Peach, D and Tracey, M.V. (1955). Modern methods of plant analysis. 4 th edn., Springer Berlin,Verlag., 373 - 374. Mishra, V. K., *et al.* "Lipids of the red alga, Palmaria palmata." (1993): 169-174.

26. Taylor, R.S.L., N.P. Manandhar, J.B. Hudson and G.H.N. Towers, (1995). Screening of selected medicinal plants of Nepal for antimicrobial activities. J. Ethnopharmacol., 546: 153-159.

27. Anonymous,(1996). Pharmacopiea of India (The Indian Pharmacopiea), 3rdEdn., Govt. of India, rd New Delhi, Ministry of Health and Family Welfare.

28. Harborne, J.B. (1973). Phytochemical methods, Chapman and Hall, New York, 1-226.

Shantha and Arockia Jenecius Alphonse

29. A. Changhiz, M. Alireza, R. Ali, P. Mehrdad, and J. Behbood, "Antibacterial activity of methanolic extract and essence of Sagebrush (Artemisia vulgaris) against pathogenic bacteria," Bulletin of Environment, Pharmacology and Life Sciences, vol. 3, no. 2, pp. 121–125, 2014

30. M. P. Raghavendra, S. Satish, and K. A. Raveesha, "Phytochemical analysis and antibacterial activity of Oxalis corniculata; a known medicinal plant," myScience, vol. 1, no. 1, pp. 72–78, 2006

Table 1. Composition of Nutrient agar medium

Peptone	5.0 g
Beef extract	3.0 g
Agar	15.0 g
Distilled water	1000 ml
pH	7.0

Table 2. Composition of PDA medium

Potato	200.0 g
Dextrose	20.0 g
Agar	15.0 g
Distilled water	1000 ml
pH	6.2

Table : 1 3.1. Qualitative analysis of phytochemicals in different solvent extracts from *Haloplegma Duperreyi*

Phytochemicals	Aqueous	Ethanol	Methanol	Ethyl acetate	Chloroform
Alkaloids	++	+++	+++	++	+
Phenols	++	++	++	++	+
Flavonoids	++	+++	++	++	+
Tannins	-	+	-	-	-
Saponins	+	++	+	-	-
Terpenoids	+	+++	++	+	++
Steroids	+	++	++	++	++
Carbohydrates	++	++	++	-	+
Glycosides	++	+	++	-	+
Amino acids	+	++	+	+	+
Proteins	++	++	+	++	+

+ → present in small concentration; ++ → present in moderately high concentration;
+++ → present in very high concentration;--→ absent.

Table 2. Quantitative Analysis of Phytochemicals in different solvent extracts from *Haloplegma duperreyi*

Secondary metabolites	Ethanol extract	Methanol extract	Aqueous extract	Ethyl acetate extract	Chloroform extract
Alkaloids (mg/g sample)	4.72±0.42	5.08±0.23	3.40 ±0.66	5.93±0.20	3.49±0.50
phenols (mg/g sample)	3.30 ±0.09	3.27±0.30	2.80 ±0.20	4.72±0.35	2.90±0.55
Flavonoids (mg/g sample)	1.73±0.19	1.62±0.23	1.50 ±0.10	3.55±0.85	-
Terpenoids (mg/g sample)	2.63±0.35	3.09±0.22	2.30 ±0.80	4.20±0.10	3.50±0.50
Steroids (mg/g sample)	2.45±0.13	2.85±0.35	2.86±0.20	5.30±0.10	--

Values are expressed as mean±SD (n=3).

Shantha and Arockia Jenecius Alphonse

Table :3 Growth inhibition of methanol extracts of *H. duperreyi* against Gram negative and gram positive bacteria

S.No	Pathogenic bacteria	Zone of inhibition (mm)			Standard (Amoxicillin)
		10 µl	20 µl	30 µl	
1.	*Escherichia coli*	07	07	14	22
2.	*Staphylococcus aureus*	07	07	14	22
3.	*Salmonella paratyphi*	07	07	14	24
4.	*Klebsiellanemoniae*	07	07	12	22

Table :4 Growth inhibition of methanol extracts of *H. duperreyi* against fungus

S.No	Pathogenic fungus	Zone of inhibition (mm)			Standard (Amoxicillin)
		10 µl	20 µl	30 µl	
1.	*Candida albicans*	07	07	12	18
2.	*Aspergillusfumigatus*	07	07	14	18

Eshcheria coli   *Klebsiella nemoniae*

Staphylococcus aureus   *Salmonella paratyphi*

Shantha and Arockia Jenecius Alphonse

Aspergillus fumigatus   *Candida albicans*

Figure 1-6. **Growth inhibition zone of methanol extracts of** *H. duperreyi* **against Gram negative and gram positive bacteria and fungus**
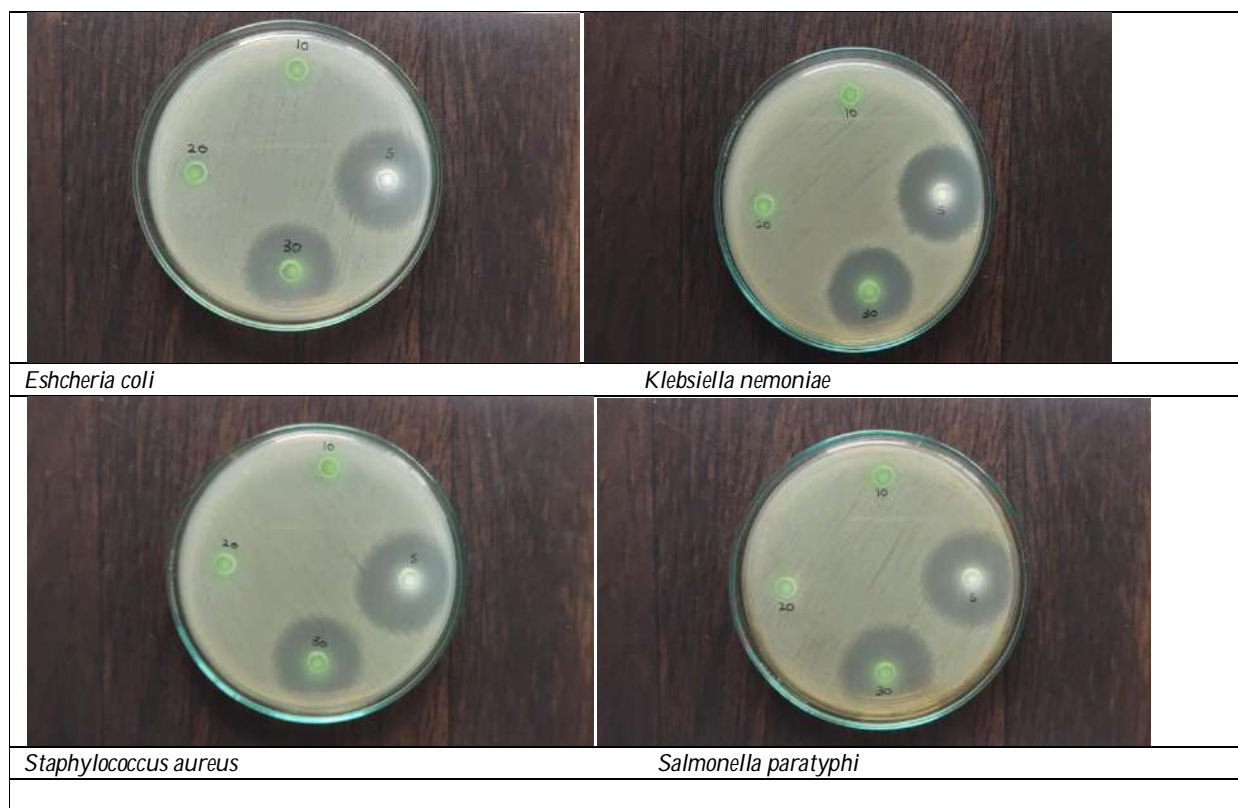
RESEARCH ARTICLE
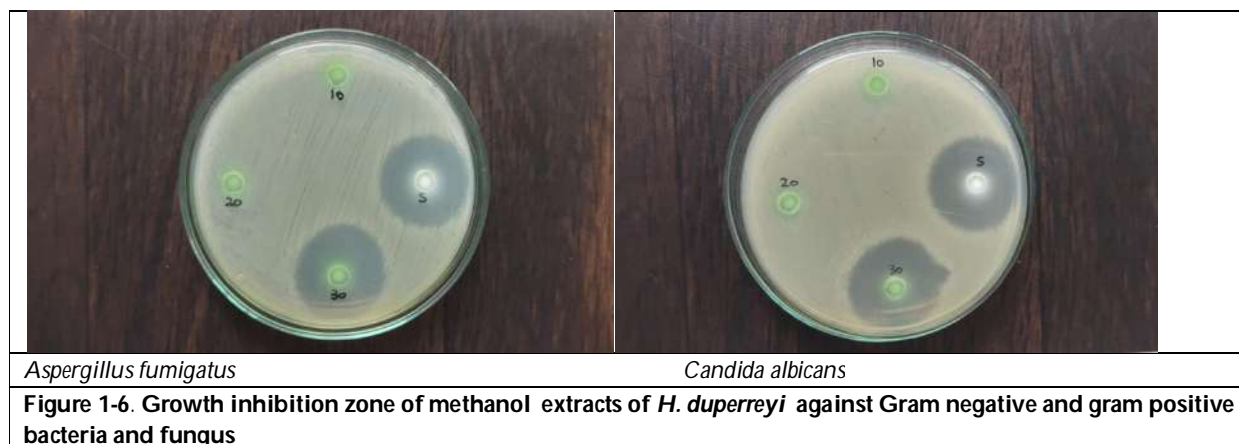
Fuzzy Logic Control based Solar Fed Microgrid and Damping Method of Droop Control

M.Kondalu[1]* , P. Mallikarjun[2] and P.Satyaendra Kumar[2]

[1]Professor, Malla Reddy Engineering College, Secunderabad-500100, Hyderabad, Telangana, India.
[2]Assistant Professor, Malla Reddy Engineering College, Secunderabad-500100, Hyderabad, Telangana, India

*Address for Correspondence
M.Kondalu
Professor,
Malla Reddy Engineering College,
Secunderabad-500100,
Hyderabad, Telangana, India.

ABSTRACT

In this paper propose FLC based solar fed Microgrid to establish synchronization. Due to in stable of Power electronic converters, solar power generation plays a of the essence role and it does not have normal inertia and damping characteristics. This paper makes employ of the grid-linked photovoltaic muscle era gadget base on DC voltage instinct control because the research item, and establishes the static synchronous generator (SSG) representation of the gadget among a analysis to make the capacitance of the middle time scale take part in the grid frequency response without including additional device. The model is used to study the amount of one factor that has an impact on the system's inertia, damping and synchronization characteristics as well as the legal plan of that govern their affect. The findings screen that the capacitor's electricity garage contact on a medium time scale might purpose the system to exhibit inertia traits. In terms of manage parameters, the inertia characteristic proven via the device turns into more potent because the droop coefficient Dp lowers. The damping produce of the device is bigger the bigger the DC voltage outer loop proportional coefficient Kp is. The stronger the synchronization functionality of the device, the bigger the DC voltage outer loop integral coefficient Ki. in addition, the Simulink/ MATLAB , simulation platform is used to make certain that the theoretical approximation.

Keywords: Hybrid energy system; Model predictive control, fuzzy logic controller.

INTRODUCTION

With the worldwide electricity emergency and ecological contamination transforming into gradually more now not energetically, kidding developing smooth energy has become the improvement conformity of all countries on earth. The electric powered motors, FACTS hardware and the environmentally pleasant power generation be roughly highly developed [1][2]. Lattice coupled photovoltaic electricity age, as a delegate of environmentally friendly power generation improvement, has shown hazardous development by prudence of its bountiful belongings and infectivity unfastened benefits [3][4]. In the established power framework, the essential collection of force ages is the rotating coordinated generator (RSG), and RSG itself has the massive dormancy and stable damping potential. In the network tied photovoltaic energy era framework, the actual characteristics of the network related inverter are really now not moderately similar to RSG. As a power digital machine, the lattice tied inverter itself does not have actual state of being inactive. It is related to the framework for a massive scope with the qualities of low employment and feeble damping, bringing in the order of a diminution in the dormancy of the power agenda and exhausting extreme difficulties to the protected and stable hobby of the strength lattice [5][6]. Separately, photovoltaic power generation has excessive, regions of power for instability, and clean irregular, with a purpose to critically have an effect on the steady motion of the power lattice[7].

Hence, while photovoltaic electricity is integrated into the power matrix, they by using and massive must be equipped with a selected degree of strength stockpiling to give latency [7]. In [8] the mixture of the daylight based totally age and power stockpiling framework has been taken because the exploration object, and the plan and manipulate system studies are directed to further expand the frame work dependability of the photovoltaic strength era coordinated into the lattice. Be that as it is able to, attributable to little aggravations, the power stockpiling framework is much less efficient, and the essential electricity and its converter's sizeable probable in latency and it are not completely used to sodden characteristics reenactment.In [9], it's far delivered up that the DC aspect capacitor of the network tied inverter has comparative powerful behavior traits to the RSG rotor, and the capacitor voltage at the DC aspect of the matrix tied inverter can vacillate inside a selected reach, giving a selected latency guide, but it didn't dissect the dormancy, damping and synchronization characteristics of the whole framework together with the capacitor dynamic. In [10], it's far proven that the framework tied new strength technology framework has correspondence with the standard strength era framework, and in keeping with the viewpoint of electromechanical brief cycle displaying, it demonstrates the matrix tied inverter inside the new electricity lattice tied power technology framework and the RSG within the traditional energy technology framework has a comparative actual factor and equal unique version.

A SSG model this is suitable for the research of the DC voltage time scale dynamic attributes of the matrix tied converter framework is proposed, and the idleness, damping and synchronization qualities of the lattice tied converter framework underneath voltage and contemporary twofold close circle control is examined. In [11], by using laying out the SSG version, the aspect of a static coordinated compensator for smothering the energy swaying of force framework is dissected. In [10], the short energy remuneration (RPC) based totally recurrence manipulate method is created to upgrade the converter capability to repay the framework awkwardness strength, through completely taking advantage of the converter inactive limit. The numerical verification confirmed the advanced exhibition of the RPC method as far as recurrence deviation concealment versus grasp manage, and as some distance as RoCoF concealment as opposed to idleness manipulate, with indistinguishable converter restriction. In [12] the SSG version-based exam strategy is used to dissect the idleness and damping features of the matrix tied electricity stockpiling framework underneath two different manage techniques.

ROCOF DROOP CONTROL OF PMSG-BASED WIND TURBINES FOR SYSTEM

This proposes a RoCoF hang manipulate, which eases the brief recurrence trade process by using controlling the energy of the DC side capacitor. Right off the bat, take a look at and represent the control time size of the breeze power framework (WPS). Under the electromagnetic time scale, consolidate the low-bypass channel (LPF) and the

Kondalu *et al.*,

differential connect with get the control connection of the framework. Consequently, the brief course of RoCoF is really moved along. Besides, primarily based on the dormancy examination of the first simultaneous generator, additional inference and research of the RoCoF hold manage inactivity attributes. Contrasted and ordinary hang manipulate, RoCoF grasp have power over empowers the inverter to can equally expand recurrence deviation [8]. Then, the element research of the transport capacitance voltage to the framework latency guide is given, the relationship between capacitor keep restriction and RoCoF is inferred, which confirms the practicability of capacitor-helped recurrence adjustment. At long last, the trial examination with the hang manage method is completed in view of the RT-LAB stage [9].

This study facilities round the quick power response of community side inverters under RoCoF hang manage exclusively while the framework recurrence drops under DVT high-recurrence unsettling have an effect on. Thusly, the control method for turbine-aspect rectifier may not be in calculation pointed out on this paper. At the point while the framework is disillusioned by using power awkwardness, the WPS can be separated into electromechanical time scale (second-stage response) and electromagnetic time scale (millisecond-level response) as per the particular reaction season of various designs [10].

As located in Figure1, Due to the sizeable distinction eventually scale, the AC contemporary manage circle and mechanical power rotor velocity and can be disregarded all through the recurrence drop transient cycle. All matters considered the capacitor voltage dynamic interaction is breaking down underneath DVT, and the issue of unreasonable RoCoF is concentrated on underneath high-recurrence unsettling influences. The RoCoF grasp manage is displayed in Figure three, wherein Udc addresses the deliberate voltage, and Udcref addresses the given voltage. The reference really worth of dynamic modern can be acquired with the aid of taking the charging direction of the capacitor modern-day because the reference heading and alluding to the DC voltage manipulate target

$$I_{d\,ref} = -\left(K_p + \frac{K_i}{s}\right)(U_{dcref} + U_{dc0} - U_{dc}) \qquad (2)$$

The RoCoF grasp manage circle is embedded in the DC voltage manipulate circle. The power recurrence ω0 short the lattice recurrence ωg is recurrence deviation 1ω. Since the lattice recurrence is in a rather regular nation, 1ω is beaten via low-recurrence elements. By changing low-bypass channel cutoff recurrence ωc, the high-recurrence commotion contained in this is wiped out, so the inverter solutions principally to low recurrence signal. The RoCoF of the framework is gotten via the differential connection, and in a while grasp coefficient Kh is applied to change the sign to get the helper voltage order Udc0.

Because of high-recurrence unsettling affects, this has a look at proposes a RoCoF cling control methodology mild the problems of recurrence variation and severe RoCoF. The aftereffects of the correlation among the impacts of ordinary hold and RoCoF dangle manage procedure on WPS, the primary factors and pastime thing display that: shown in the figure2

RESULTS AND DISCUSSION

In the figure2 of without droop control ,DC-to-DC converter do not react to the frequency variations of the grid, so the DC voltage and Output Power remain constant as depicted in fig 3 and fig 4.

With Voltage Droop Control
With droop control when the frequency of the grid decreases, the capacitor reacts to the frequency changes and the dc voltage decreases to release the energy and the output Power rises as depicted in fig5 and fig 6

Kondalu *et al.,*

Effect of Droop Coefficient D$_p$ on DC Voltage

Fig 2 a grid-tied PV system by keeping the Proportional coefficient Kp and Integral coefficient K$_i$ constant and by increasing the droop coefficient D$_P$, DC voltage drops as presented in fig 7fig 8 and fig 9. In fig 2 a grid integrated PV system which is controlled by the DC voltage droop control, when simulated in MATLAB using Simulink using Fuzzy Logic Controller the results are observed. Smaller the Dp value, the system will show strong inertia characteristics shown in fig 10,11 and 12.

Influence Of Dp On Output Power

Fromfig 2, the waveforms of fig 13,14 and 15 it is observed that the output power is stable with fewer oscillations. In summary, the smaller Droop coefficient value output power is stable.

CONCLUSION

In this paper we propose FLC based solar fed Microgrid to found synchronization. Due to in constant of s Power electronic converters, solar power generation plays a vital role and it does not have natural inertia and damping characteristics. The latency, damping and synchronization of the network tied photovoltaic power period structure in view of DC voltage droop not entirely set in stone by the fundamental boundaries, control boundaries and consistent state working marks of the framework. From the point of view of control boundaries, the more modest the hang coefficient Dp, the further grounded the inactivity normal for the framework; the bigger the DC voltage external circle corresponding coefficient Kp, the more grounded the damping impact of the framework; the more noteworthy the DC voltage external circle essential coefficient Ki Larger, the more grounded the synchronization ability of the framework. The examination finish of this paper have particular significance for more developing the repetition security of framework allied photovoltaic power age framework under little upsetting influence, and establish a hypothetical starting point for the well-disposed mix of photovoltaic power age into the power network.

REFERENCES

1. Z. Zhou, Y. Cai, S. Su, X. Tang and Y. Cao, "Electric Vehicles Scale Evolution Model Considering Social Attributes," in IEEE Access, vol. 8, pp. 168784-168792, 2020, doi: 10.1109/ACCESS.2020.3022780.
2. W. Binbing, X. Abuduwayiti, C. Yuxi and T. Yizhi, "RoCoF Droop Control of PMSG-Based Wind Turbines for System Inertia Response Rapidly," in IEEE Access, vol. 8, pp. 181154-181162, 2020, doi: 10.1109/ACCESS.2020.3027740.
3. H. Wang, Y. Liu, and B. Zhou, ``Taxonomy research of articial intelli- gence for deterministic solar power forecasting,'' Energy Convers. Man- age., vol. 214, Jun. 2020, Art. no. 112909.
4. D. Xu, Q. Wu, B. Zhou, C. Li, L. Bai and S. Huang, "Distributed Multi-Energy Operation of Coupled Electricity, Heating, and Natural Gas Networks," in IEEE Transactions on Sustainable Energy, vol. 11, no. 4, pp. 2457-2469, Oct. 2020, doi: 10.1109/TSTE.2019.2961432.
5. T. Shintai, Y. Miura and T. Ise, "Oscillation Damping of a Distributed Generator Using a Virtual Synchronous Generator," in IEEE Transactions on Power Delivery, vol. 29, no. 2, pp. 668-676, April 2014, doi: 10.1109/TPWRD.2013.2281359.
6. L. Xiong, X. Liu, C. Zhao and F. Zhuo, "A Fast and Robust Real-Time Detection Algorithm of Decaying DC Transient and Harmonic Components in Three-Phase Systems," in IEEE Transactions on Power Electronics, vol. 35, no. 4, pp. 3332-3336, April 2020, doi: 10.1109/TPEL.2019. 2940891.
7. J. Alipoor, Y. Miura and T. Ise, "Power System Stabilization Using Virtual Synchronous Generator with Alternating Moment of Inertia," in IEEE Journal of Emerging and Selected Topics in Power Electronics, vol. 3, no. 2, pp. 451-458, June 2015, doi: 10.1109/JESTPE.2014.2362530.
8. J. Liu, Y. Miura and T. Ise, "Comparison of Dynamic Characteristics Between Virtual Synchronous Generator and Droop Control in Inverter-Based Distributed Generators," in IEEE Transactions on Power Electronics, vol. 31, no. 5, pp. 3600-3611, May 2016, doi: 10.1109/TPEL.2015.2465852.

Kondalu *et al.*,

9. L. Xiong, X. Liu, Y. Liu and F. Zhuo, "Modeling and stability issues of voltage-source converter dominated power systems: A review," in CSEE Journal of Power and Energy Systems, doi: 10.17775/CSEEJPES.2020.03590.

10. N. Soni, S. Doolla and M. C. Chandorkar, "Improvement of Transient Response in Microgrids Using Virtual Inertia," in IEEE Transactions on Power Delivery, vol. 28, no. 3, pp. 1830-1838, July 2013, doi: 10.1109/TPWRD.2013.2264738.

11. M. S. Pilehvar and B. Mirafzal, "PV-Fed Smart Inverters for Mitigation of Voltage and Frequency Fluctuations in Islanded Microgrids," 2020 International Conference on Smart Grids and Energy Systems (SGES), 2020, pp. 807-812, doi: 10.1109/SGES51519.2020.00149.

12. Ahmadi, Saleh & Shokoohi, Shoresh & Bevrani, H. (2015). A fuzzy logic-based droop control for simultaneous voltage and frequency regulation in an AC microgrid. International Journal of Electrical Power & Energy Systems. 64. 148–155. 10.1016/j.ijepes.2014.07.024.
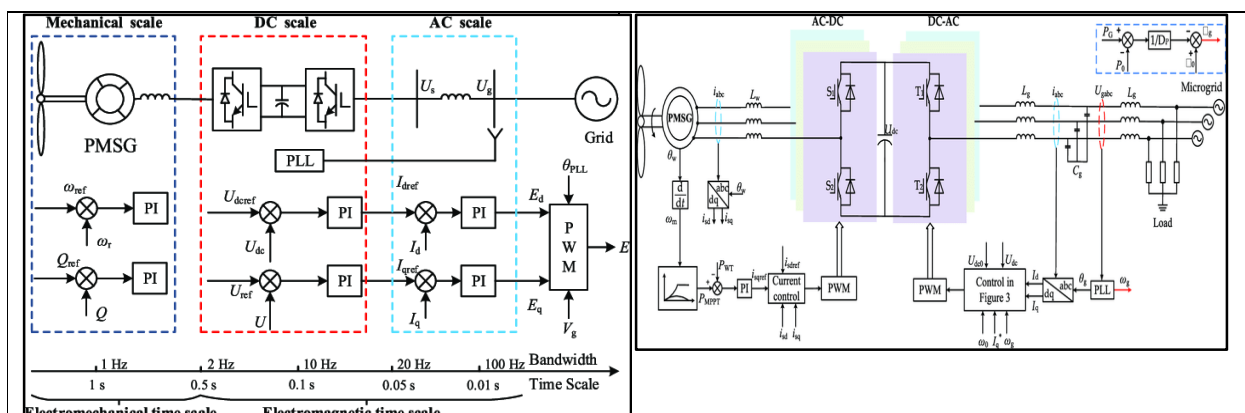
Fig. 1. Circuit diagram of power timescale for wind power structure
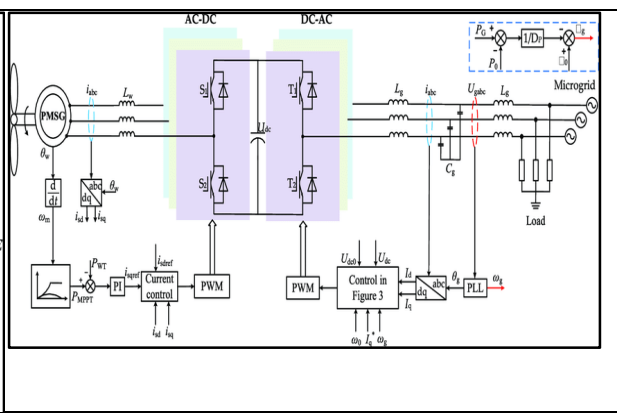
Fig. 2. The structure diagram of the wps
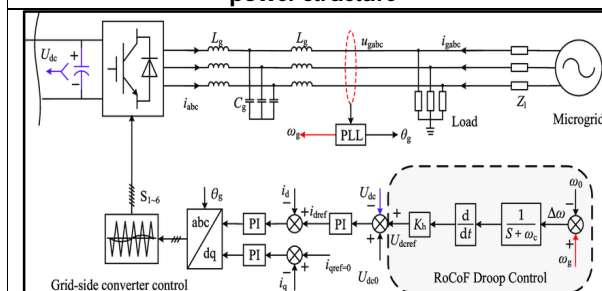
Fig. 3. Circuit diagram of Grid side inverter control block
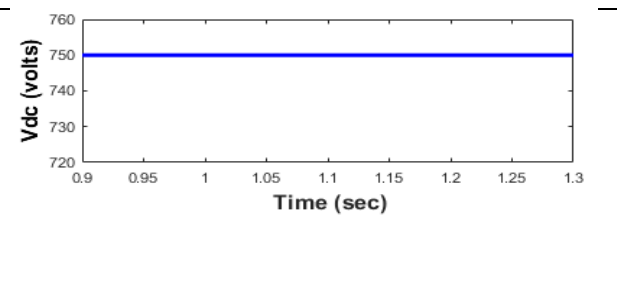
Fig.4. DC voltage waveform of without droop control
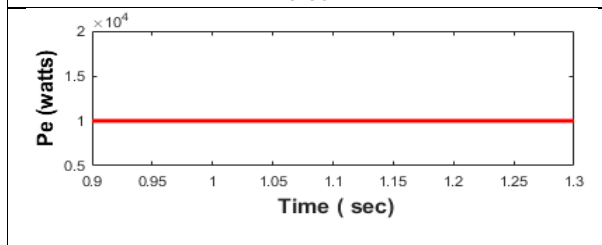
Fig. 5. Output waveform of Power without volatge droop

Fig. 6. DC voltage waveform of with droop control

Fig. 7. Output Power waveform of with droop control

Fig. 8 . DC volatge waveform at Dp 60

Fig.9 . DC voltage waveform at Dp 80

Fig. 10. DC voltage waveform Dp 100

Fig .11. DC voltage waveform at Dp 60

Fig.12. DC voltage waveform of Dp 80

Fig 13. DC voltage waveform of Dp 100

Fig 14. Output Power waveform of Dp 60

Fig 15. Output Power waveform of Dp 80

Fig 16. Output Power waveform of Dp 100

RESEARCH ARTICLE
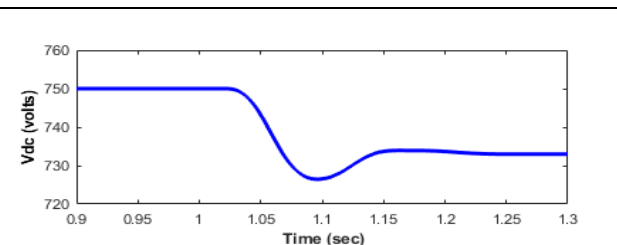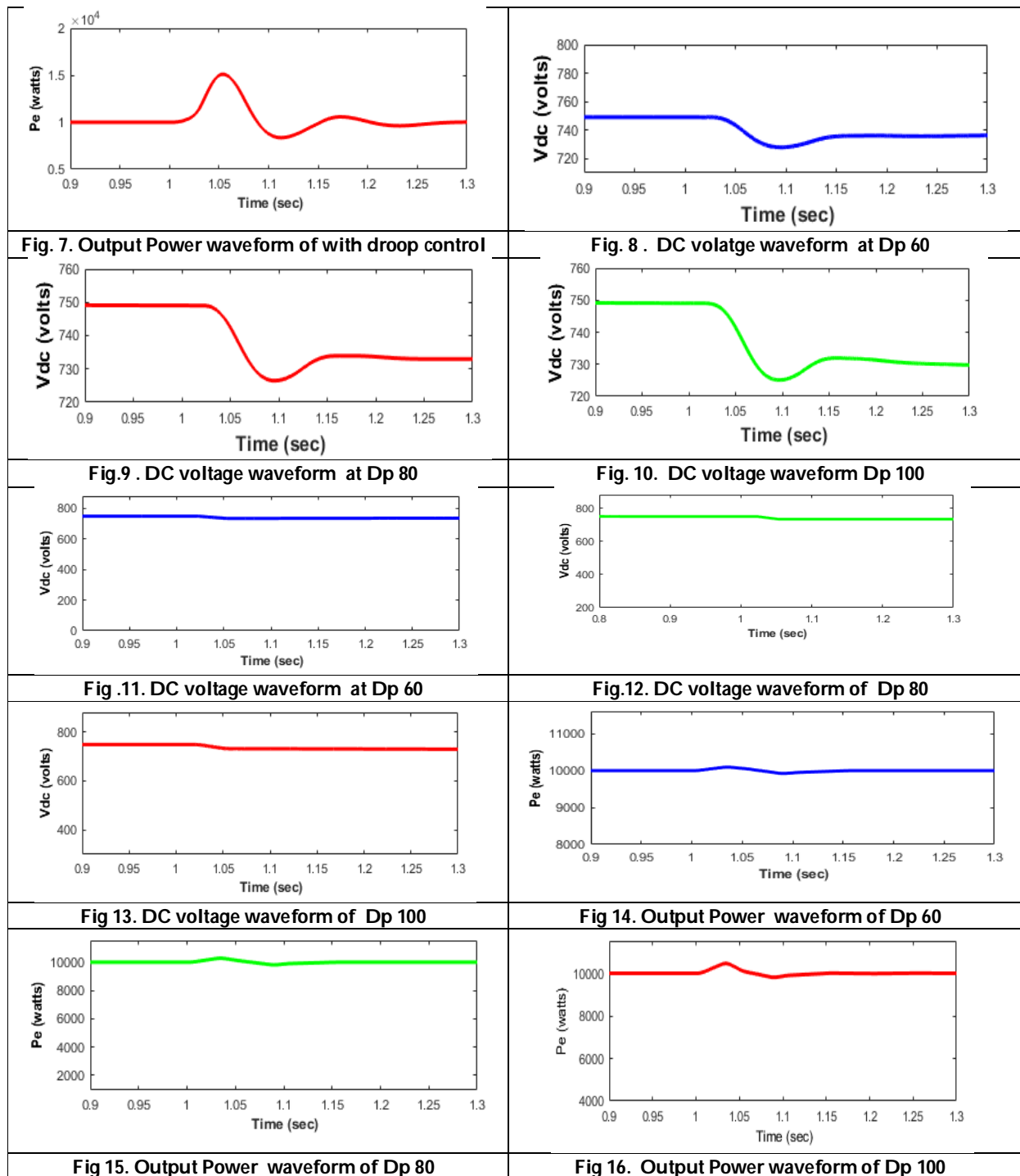
Ethnobotanical Studies of Wild Edible Plants used by the Indigenous Tribe of Chakhesang, Phek District, Nagaland

Vepu[1]* and T.Lirola Sangtam[2]

[1]Research Scholar, Department of Botany, St. Joseph University, Virgin Town, Ikishe Model Village, Dimapur, Nagaland-797115, India .
[2]Assistant Professor, Department of Botany, St. Joseph University, Virgin Town, Ikishe Model Village, Dimapur, Nagaland-797115,India.

*Address for Correspondence
Vepu[1]*
Research Scholar, Department of Botany,
St. Joseph University,
Virgin Town, Ikishe Model Village,
Dimapur, Nagaland-797115, India .
Email: vepupfuno@gmail.com

ABSTRACT

The present studies deals with the preliminary survey of the wild edible plants used by the indigenous Chakhesang Tribe of Phek District. The district holds a vast area of thickly dense forest which comprises of highly diversified flora. The study was carried out in between January 2021 to August 2022. Ethnobotanical data were collected by interviewing the villagers especially the elders and herbalists who has well acquainted with the forest. The data were collected through semi structure questioners by interacting with the informants face to face. Altogether 74 wild edible plant species were recorded from 64 genera and 39 families. The present studies indicates that the tribal people depends on the forest for their food and for commercial purpose for their livelihood and regularly collect and consume leafy vegetables, ferns, fruits, tubers, mushrooms etc. from the mountainous forest and have acquired a vast knowledge of wild edible plants. The present study aims to identified, document, and explore of wild edible plants used by the indigenous tribe of Chakhesang of Phek District.

Keywords: Chakhesang, Ethnobotanical, wild edible plants, Identified, Document, Explore.

INTRODUCTION

Nagaland one of the eight sister of North East India is located in the northern and eastern hemisphere at Latitudinal expanse of 25°6′ N to 27°4 N and Longitudinal expanse of 93°2′E to 95°15′E. The total area of Nagaland is 16,579 sq km (6401 sq miles). Nagaland is bounded in the east by the country Myanmar, the west by the state Assam, in the

63521

North partly by the sate Arunachal Pradesh and Assam and in the south by Manipur. It has a population of about 1,980,602 as per the 2011 census of India. Nagaland consist of 18 tribes namely Angami, Ao, Chakhesang, Chang, Dimasa Kachari, Khiamniugan, Konyak, Kuki, Lotha, Phom, Pochury, Rengma, Sangtam, Sumi, Tikhir, Yimkhiung and Zeliang. It has 16th district Chumoukedima, Dimapur, Kiphiri, Kohima, Longleng, Mokokchung, Mon, Niuland, Noklak, Peren, Phek, Shamator, Tseminyu, Tuensang, Wokha and Zunheboto.

Phek district of Nagaland is mainly inhabited by Chakhesang and Pochury tribe. The district hold a very large covered of wild forest and many villagers depends on the abundance of nature for their survivals like cultivated and wild eatable plants and fruits which provide a good scope for the Ethnobotanical studies. Since ages Chakhesang people live a very close relationship with nature and are well acquainted with their surrounding plants and their beneficial utilities for various purposes like medicine, food, animal fodders, agriculture, basketry works, furniture, house building, musical instruments, tools, utensils, dyes, cloths, hunting and defence equipments etc. for their self sustenance and daily needs. Many plants are used by the indigenous Chakhesang tribe for their medicinal purposes which are available in their locality. The plants in and around the villages plays an integral role in their culture and the information about the significance of plants are pass down orally from generation to generation without any written record. If those useful information about the knowledge of plants are not documented or tapped at the earliest, it may be lost forever with the generation gap. Besides, the vast beautiful forest which are fast disappearing due to shifting cultivation, unwanted fires due to hunting, making of concrete road, timber business, firewood and other socio-economic activities in the region.

In the past years, many researchers have contributed on ethnobotany in the North-East region of India: Jamir,N. S & Rao R.R. 1982a; Jamir N. S & Rao R.R 1982b; Kar, A. 2004, Lokho A, Moa, A.A & Odyuo, N. 2007. Lokho, A. 2012; Takatemje et al. 2010; Takatemje et al. 2010; Salam. S. Et al 2010. Some of the recent contribution from the state of Nagaland: Mozhui, R, ET al. 2011; Pfozo, N. L. Et al. 2012 Medhi, P, Kar, A. & Borthakur, S.K 2013; Singh et al. 2015; Limasenla & Lea Nelia 2020; Konyak Zenwang & Konyak Phongle 2020. According to the survey, there is, still lots of works to be done in the field of ethnobotany. More field research is needed to tap the vast scientific resources before it gets diminishes with the rapid development of human activities.

STUDY AREA

Phek district lies between 25°37′N-25°39′N latitude and 94°35′E-94°38′E longitude. Altitude varies from 520m to 2900m above the sea level with a total area of 2026 km2. The district is bounded by Manipur state on the south, Kiphiri and Zunheboto on the North, Kohima in the west and Myanmar country in the south-east. The district consists of rich evergreen sub-tropical and temperate coniferous forest supporting vast amount of flora and fauna. Agriculture is the main occupation of the indigenous tribe with Rice as their stable diet. The Chakhesang practices terrace cultivation in the hilly terrains and sub-terrain areas where they mostly cultivate Rice and others minor crops alongside the paddy field. Jhum (slash and burn) cultivation is also practice by the tribe but with the passage of time it has decrease drastically with villagers knowing the importance of biodiversity and its conservation.

METHODOLOGY

Frequent field trips were conducted in between January 2021 to August 2022 to different villages of the Chakhesang tribe of Phek district, Nagaland. Data collections were done through group discussions, personal interview to local healers/Kobiraj, elders of the village and even youngsters who have certain knowledge about the wild edible plants in their locality. Questionnaires based surveys were carried out from the participants for further analysis. The diversity and the economy of the wild edible plants were documented by frequent visit to villages in different seasons with the availability of the plant species. Most of the plant species were collected from the wild habitats with the help of the informants but a few of them were collected from their market places which were sold near the village

road and gate. The plants were identified with the help of expert consultants, locally available literatures of different authors and Botanical Survey of India, Shillong, Meghalaya.

RESULT AND DISCUSSION

During the study period, a total of 74 wild edibles plants belonging to 64 genera and 39 families used by the Chakhesang tribe of Phek district are documented. Wild edible plants family and its number of species occurrence were arranged alphabetically in the *Table 1*. Poaceae and Rosaceae family with highest number of 6 plant species each, followed by solanaceae of 5 plant species, Amaranthecea of 4 plant species and Apiaceae, Cucurbitaceae, Lamiaceae & Araceae with 3 each species and Athyriaceae, Asteraceae, Brassicaceae, Dioscoreaceae, Fabaceae, Leguminoceae, Moraceae, Polygonaceae & Urticaceae with two each plant species and the rest of the 22 families consist of only one species each. Wild eatable plant part uses and its occurrence were given in *Table 2*, out of which 51 number of plants species have only one part eatable i.e either shoots, leaves, flowers or seeds or fruits while 17 plant species are found to have two eatable parts and 3 plants are taken as a whole plant. 47 plant species are found to have only one uses whereas 24 plant species are found to have an additional uses like animal feeds and medicinal values. Altogether 4 bamboo species and 2 fern species are recorded. 33 fruits/seeds wild eatable plants, 32 leafy vegetables, 12 shoots, 6 tuber, 8 Flowers/inflorescence and 3 whole wild edible plants are recorded.

The edible parts of the wild plant is found as fruits with the highest number of consumption followed by leaves, shoots flowers and tubers. Habit wise of plants are found are trees, herbs, shrubs and climbers. 3 numbers of plants have found to use as whole plants like *Colocassia esculenta* Linn. (tuber petiole leaves), *Houttuynia cordata* Thunb. (shoot, roots, leaves) and *Centella asiatica* Linn. (leaves, shots and roots). In the enumeration of *table 3*, plant species name are arrange alphabetically with family, vernacular name, part used, preparation and any medicinal or other uses were indicated. Some prominent plants like *Centella asiatica* Linn., *Diplazium esculenta* Retzius Swartz , *Oenanthe javanica* Blume Candolle and *Rhus chinensis* Miller have high medicinal value and also use frequently and become household medicine among the Chakhesang tribe.

The present study approach shows the tribal people involved closely with the nature of wild edible plants for their food and commercial purpose for their livelihood. Wild edible plants were collected and consumed regularly from the nearby forest. The tribe also have acquired a vast knowledge of wild edible plants for various uses since generation. Many valuable plants are threatened due to rampant deforestation for agriculture purpose and various developmental activities. With the fast declining of deep forest, there is urgent need to educate the tribal to conserve, protect and to manage forest resources for the sustainability of mankind and nature.

ACKNOWLEDGEMENT

REFERENCES

1. Jamir, N.S. & Rao, R.R. 1982a. Ethnobotanical study of Nagalnad – 1. Medicinal plants. *Econ. Bot* 36(2): 176 – 181.
2. Jamir, N.S & Rao R.R 1982b. Ethnobotanical study of Nagaland +. Fifty four medicinal plants used by Nagas. *J. Econ. Taxon.* Bot. 3: 11 – 17
3. Kar, A. 2004. Common wild vegetables of Aka tribe of Arunachal Pradesh. *Indian J. Trad. Knowl.* 3(3): 305 – 313

Vepu and Lirola Sangtam

4. Deorani, S.C and Sharma, G.D. 2007. *Medicinal plants of Nagaland.* Bishen Singh Mahendra Pal Singh, Dehra Dun, India.

5. Lokho, A. 2012. The folk medicinal plants of the Moa Naga in Manipur, North east India. *Intn. J. Sci. Res.* Publ. 2(6): 1 – 8

6. Moa, A.A. & Odyuo, N. 2007. Traditional fermented foods of the Naga tribes of Northeastern India. *Indian J. Trad. Knowl.* 6(1): 37 – 41

7. Moa, A.A., Hynniewta, T.M & Sanjappa, M. Plant wealth of northeast India with reference to ethnobotany. Indian Journal of Traditional Knowledge. 8(1): 96 – 103, 2008.

8. Takatemjen; Jamir, N.S & Deb, M.S. 2009. Wild edible fruits of Wokha district of Nagaland, India. *Pleione* 3(1): 59 – 62

9. Plant Resource of Nagaland. Nagaland Bio Resource Mission Publication, Government of Nagaland, Kohima, Nagaland. 2009, ISBN: 978 – 93 – 80500 – 02 – 7.

10. Salam, S.; Kumar. P.K & Jamir, N.S. 2010. Wild edible plants used by the Tangkhul Naga tribe of Ukhrul district of Manipur, India. *Pleione* 4(2): 284 – 287

11. Medhi, P, Kar, A. & Borthakur, S.K. 2013. Medicinal uses of wild edible plants among the Ao Nagas of Mokukchung and its vincinity of Nagaland, India. *Asian Reson.* 2(4):64 – 67.

12. Mozhui, R,: Rongsensashi; Limasenla & Changkija, S. 2011. Wild edible fruits used by the tribals of dimapur district of Nagaland, India. *Pleione* (5): 56 – 64.

13. Pfozo, N.L.; Kumar, Y; Sheik, N. & Myrboh, B. 2012. Assesement of local dependency on selected wild edible plants and fruits from Senapati District, Manipur, Northeast India. *Ethno. Res. Applic.* 10: 357 – 367.

14. Flora of Nagaland Vol-I & Vol-II by Sapu Changkija & P.B. Gurung. 2017.

15. Sapu Changkija, Biodiversity of Nagaland published by Department of Forest, Ecology, Environment and Wild life, Government of Nagaland.

16. Singh, A.K.; & Teron R. 2015. Diversity of wild edible plants used by the Angami-Nagas in Kohima District of Nagaland, India. *Pleione* 9(2): 311 – 324.

17. Lea, Nelia. & Limasenla. 2020. Traditional Knowledge of medicinal plants used by the Chakhesang Naga tribe in Phek District of Nagaland, India. *Pleione* 14(2): 237 - 247

18. Konyak, Zenwang & Konyak Phongle. E. 2020. Documentation of wild edible fruits (WEFs) from mon District of Nagaland, India. *Journal of medicinal plants Studies* 202; 8(5): 101-106

Table 1: Edible wild plants family and its number of species occurrence

Family Name	Number of plant species occurrence
Amarantheceae	4
Anacardiaceae	1
Apiaceae	3
Araceae	3
Asteraceae	2
Brassicaceae	2
Campanulaceae	1
Convolvulaceae	1
Crassulaceae	1
Cucurbitaceae	3
Dioscoreaceae	2
Ebenaceae	1
Elaegnaceae	1
Euphorbiaceae	1
Fabaceae	2
Fagaceae	1

Vepu and Lirola Sangtam

Juglandaceae	1
Lamiaceae	3
Leguminoceae	2
Malvaceae	1
Melastomotaceae	1
Moraceae	2
Musaceae	1
Myricaceae	1
Passifloraceae	1
Phyllantheceae	1
Plantaginaceae	1
Poaceae	6
Polygonaceae	2
Rhamaceae	1
Rosaceae	6
Rutaceae	1
Sapindaceae	1
Saururaceae	1
Solanaceae	5
Urticaceae	2
Viburnaceae	1
Zingiberaceae	1

Table 2: Wild plant edible parts and it's number of occurrences

Edible leaf	Edible Shoot	Edible Tuber	Edible Fruit/seed	Edible Flower/ Inflorescence	Edible whole plant	Edible 2 parts of plant	Edible one part of plant
33 plant species	12 plant species	6 plant species	32 plant species	8 plant species	3 plant species	17 plant species	51 plant species

Table 3: Wild edible plants of Chakhesang tribe of Phek District, Nagaland.

Botanical name	Family	Vernacular name	Part used	Preparation	Medicinal/ Other uses
Alocasia machrorrhizos (Linnaeus) G Don.	Araceae	Bü	Leaves and Tuber	Boiled curry and chutney	
Alternanthera philoxeroides (Martius) Grisebach	Amarantheceae	Menhyipa	Young shoot and leaves	Cook as vegetable curry	Pig feed
Amaranthus spinosus (Linnaeus)	Amaranthaceae	Kadzünhü	Leaves	Boiled with potato	Controlled high Bp/animal feed
Amaranthus viridis (Linnaeus)	Amaranthceae	Kadzünhü	Leaves and shoots	Cook with potato/ meat/ boiled/Fried	Animal feed/reduce diabetes

63525

Vepu and Lirola Sangtam

Bambusa tulda Roxb.	Poaceae	Kavü	Tender Shoots	Fresh/fermented cooked with meat	
Bauhinia variegate Linnaeus	Leguminoceae	Mewupa	Leaves and flowers	Boiled with tomato, green chillies and potato	Cattle feed
Brassica oleraceae (Linnaeus)	Brassicaceae	Münayie	Leaves	Boiled/cooked with meat/potato/tomato	Lower Bp
Bryophyllum pinnatum (Lam.) Oken	Crassulaceae	Tsonyü	Leaves	Crush and drink	Kidney stone removal
Cardamine hirsute Linnaeus	Brassicaceae	Thüvüga	Shoots	Cooked with garlic, ginger and chillies	
Centella asiatica (Linnaeus) Urban	Apiaceae	Gapre	Whole plant	Boiled/cook with rice	Purify blood
Chimonobambusa collosa (Mitford) makino	Poaceae	Kavü	Tender shoots	Fresh and fermented shoot is cook with meat	
Chinopodium album Linnaues	Amaranthaceae	Chüzhünhü	Leaves	Cooked with meat	
Clerodendrum colebrookianum Walp.	Lamiaceae	Gatherü	Young leaves	Boiled//cook with potato and tomato	Lower Bp
Coix lacryma-jobi Linnaeus	Poaceae	Tuchiebe	Seeds	Roasted seed is crush and cook	Kidney problem
Colocassia esculanta (Linnaeus) Schott	Araceae	Büküto	Whole plant	Cooked with pork or dry fish	
Curcuma angustifolia Roxb.	Zingiberaceae	Ketupa	Inflorescence	Cooked with meat or other vegetables	
Debregeasia longifolia (Burm.f.)Wedd	Urticaceae	Ziche	Fruits	Ripe fruit are eaten	
Dendrocalamus hamiltonii Gamble	Poaceae	Kavü	Tender shoots	Fresh/ fermented cooked with meat	
Dendrocalamus giganteus Munro	Poaceae	Kavü küdeo	Tender shoots	Fermented shoots	
Diplazium esculentum (Retzius) Swartz	Athyriaceae	Kütsaga	Tender leaves	Boiled/Cooked with Crab	Anti Gastric
Dilplazium maximum (D. Don) C. Chr.	Athyraceae	Mrüshünhü	Leaves	Cooked with potato/dry fish/tomato	
Diascorea bulbifera Linnaeus	Dioscoreaceae	Rupfu	Tubers	Boiled/cook with dry meat	
Dioscorea deltoidea Wall. Ex Griseb	Dioscoreaceae	Muthu	Tuber	Cooked and eat as vegetables	
Diospyros kaki Thunb.	Ebenaceae	Zhiedeshe	Fruit	Ripe fruit eaten raw	

Vepu and Lirola Sangtam

Docynia indica (wallich) Decaisne	Rosaceae	Ciephose	Fruits	Ripe fruit fresh or dried eaten	Diarrhoea
Elaeagnus conferta Roxb	Elaeagnaceae	Tsütucie	Fruits	Ripe fruit eaten raw	
Elatostema lineolatum Wight	Urticaceae	Tsüyie	Leaves and tender shoots	Boiled or cook with rice called Galho	
Elsholtzia griffithi Hook.f	Lamiaceae	Sawhe	Leaves and inflorescence	Use as spices in curry	Stomach upset and headache
Eryngium foetidum Linnaeus	Apiaceae	Burma dunyia	Leaves	Used in chutney or fish curry as spices	Asthma
Fagopyrum sp.	Polygonaceae	Gare	Leaves	Boiled or cooked with meat	
Ficus auriculata Lour.	Moraceae	Kabuse	Fruit	Ripe fruit eaten raw	Use for cattle and pig feed
Gynura nepalensis De Candolle	Asteraceae	Letsüyie	Leaves	Boiled/ cook with rice as Galho	Antidiabetic
Hibiscus sabdariffa Linnaeus	Malvaceae	Kükhropa/ Kekhropa	Leave and seeds cover	Cook with meat or potato.	Anti fever
Houttuynia cordata Thunb.	Saururaceae	Posükuma/Wesenyü	Whole plant	Taken raw or make into a chutney/salad	
Ipomea batatus (Linnaeus) Lamarck	Convolvulaceae	Dzümucie	Leaves and tuber	Boiled	Animal feed
Juglans regia Linnaeus	Juglandaceae	Lepfüchie	Seeds	Ripe seeds crack open and eat	
Lasia spinosa (Linnaeus)	Araceae	Dzüye	Leaves	Boiled/cook with potato or meat	
Leucaena leucocephala (Lam.) de Wit	Fabaceae	Prücie	Fruits/seeds	Eat when tender/chutney	
Litchi chinensis Sonn.	Sapindaceae	Litchibo	Fruits	Ripe fruit eaten raw	
Luffa cylindrica (Linnaeus) Roemer	Cucurbitaceae	Kashüchie	Fruits	Tender fruits boiled/ fried with potato or meat	
Lycopersicum esculentum Miller	Solanaceae	Dongachie	Fruits	Used in almost all the curry	
Melocana baccifera (Roxb.) Kurz	Poaceae	Kavü	Tender shoots	Fresh tender shoots with chutney	
Manihot esculenta Crantz	Euphorbiaceae	Chi-alu	Leaves and tuber	Boiled	Animals feed
Melostoma malabathricum Linnaeus	Melastomataceae	Seprüpra	Fruits	Ripe fruit eaten raw	Animal fooder
Momordica balsamina	Cucurbitaceae	Keriela	Fruits	Boiled or fried	Blood pressure

Linnaeus					controlled
Momordica foetida Schumacher	Cucurbitaceae	Bhat keriela	Fruits	Boiled or fried	Blood pressure controlled
Morus alba Linnaeus	Moraceae	Zucie	Fruits and leaves	Ripe fruit taken raw, tender leaves boiled.	Animal feed
Musa paradisiaca (Linnaeus)	Musaceae	Nganchie	Fruits and inner stem	Ripe fruit raw eat. Stem cook with potato or meat.	
Myrica esculenta Buch.-Ham. Ex D.Don	Myricaceae	Nhuche	Fruits	Ripe fruit eaten raw	
Ocimum tenuiflorum Linnaeus	Lamiaceae	Nhetsu	Leaves and inflorescence	Used as spices in chutney and curry	Fever
Oenanthe javanica (Blume) de Candolle	Apiaceae	Lekroyie	Leaves and tender shoots	Boiled	Lower Blood pressure
Parkia roxburghii G. Don	Fabaceae	Yonjak	Fruit/seeds	Chutney	
Passiflora edulis John Sims	Passifloraceae	Bel	Tender leaves and fruits	Boiled or taken raw	Lower Blood pressure
Phyllanthus emblica Linnaeus	Phyllantheceae	Tsühose	Fruits	Raw taken or pickle	Washing face
Physallis sp.	Solanaceae		Fruits	Mature fruit taken raw	
Plantago major Linnaeus	Plantaginaceae	Gapa	Leaves	Boiled or cook with other vegetables	
Polygonum molle D. Don	Polygonaceae	Ghazie	Leaves	Boiled	
Pratia begonifolia (Wall.) Lidl.	Campanulaceae	Letuche	Leaves and young shoot	Cooked and eaten as a vegetables	
Prunus nepalensis (Ser.) Steud.	Rosaceae	Mutroho	Fruit	Ripe fruit eaten raw	
Pyrus pashia Buchanan-hamilton ex D. Don	Rosaceae	Kazhuche	Fruits	Ripe fruit eaten raw	
Prunus persica (Linnaeus) Batsch	Rosaceae	Mekrocie/Mekricie	Fruits	Ripe fruit eaten raw	
Quercus serrata Murray	Fagaceae	Pfücie	Fruits	Roasted seed eaten/ is a coffee substitute	
Rhus chinensis Miller	Anacardiaceae	Mvü	Fruits	Used as spices in many curry	Food poison, allergy, indigestion, dysentery
Rubus ellipticus Sm	Rosaceae	Tsamhise	Fruits	Ripe fruit eaten raw	

Vepu and Lirola Sangtam

Rubus idaeus Linnaeus	Rosaceae	Lemucie	Fruits	Ripe fruit can be eaten raw	
Solanum anguivi Lamarck	Solanaceae	Küpfüchie	Fruits	Boiled/in chutney	
Solanum betaceum Cav.	Solanaceae	Chi dongachie	Fruits	Used in many curry	
Solanum torvum Sw.	Solanaceae	Küpfüchie	Fruits	Cook/fresh/burn	
Spillanthes acmella (Linnaeus)	Asteraceae	Kiti küvü prü	Leaves and flowers	Boiled	
Tamarindus indica Linnaeus	Leguminoceae	Khromvütsü chie	Fruits	Ripe fruit eaten raw	
Viburnum foetidum Linnaeus	Viburnaceae	Tsakhrose	Fruits	Ripe fruit eaten raw	
Zanthoxylum acanthopodium DC.	Rutaceae	Mothise	Fruits and leaves	Boiled or chutney	
Zanthoxylum oxyphyllum Edgeworth	Rutaceae	Mijinga patta	Leaves and fruits	Used as spices in curry	
Ziziphus mauritiana Lam.	Rhamnaceae	Buguri	Fruits	Eaten fresh or make into pickle	

REVIEW ARTICLE

Animal Models for Preclinical Drug Research on Ulcerative Colitis: A Review

Shamal R. Borude[1]* and Devendra S. Shirode[2]

[1]Ph.D Scholar, Dr. D. Y. Patil College of Pharmacy, Akurdi, Pune -411044, Maharashtra, India.
[2]Associate Professor, Dr. D. Y. Patil College of Pharmacy, Akurdi, Pune -411044, Maharashtra, India.

*Address for Correspondence
Shamal R. Borude
Ph.D Scholar,
Dr. D. Y. Patil College of Pharmacy,
Akurdi, Pune -411044, Maharashtra, India.
E. Mail: shamalrb2016@gmail.com

ABSTRACT

Inflammatory bowel disease has two major forms, one of them is Ulcerative colitis. Ulcerative colitis is characterized by mucosal inflammation beginning in the rectum and extending proximally in the colon in a continuous fashion. The inflammation in Ulcerative colitis is particularly limited to the mucosal layer, causing superficial damage of the bowel wall. At present time, the corticosteroids, aminosalicylic acid preparations, immunomodulators, and other drugs, use as a clinical treatment of this disease, but the disease has the characteristics of high recurrence rate, and due to long-term medication adverse reactions can easily occurs. Hence, there is a need in investigating new drugs to manage Ulcerative colitis in a less harmful and more efficient way. There are various animal models which have been used globally by researchers to assess new lead compounds prior they can be tested in humans. There are various types of animal models for assessment named as immunity transfer models, chemical models, composite Models, bacterial models and genetic models. In this review article, we try to give an overview on animal models which can be used in drug research globally to manage Ulcerative colitis.

Keywords: Inflammatory bowel disease, ulcerative colitis, drug research, screening models, India.

INTRODUCTION

UC is an uncontrollable, cancerous, refractory gastrointestinal disease, the pathology of diseases such as colitis or idiopathic colitis as first described by Stephen *et al*[1]. In current years, the incidence of the disease has been increasing, and it has been classified as one of the uncontrolable diseases by the World Health Organization (WHO) [2]. Inflammatory Bowel Disease (IBD) is a globally health problem in that two specific and more prevalent pathologies are: Crohn's disease and Ulcerative colitis. In 1859 Ulcerative colitis (UC) firstly described, and it is one of two major forms of inflammatory bowel disease (IBD). Opposite, the other type of IBD, inflammation in Crohn's disease (CD), reveal patchy lesions that are possibly scattered anywhere in the gastrointestinal tract. The

63530

inflammation in UC is specifically limited to the mucosal layer, causes superficial damage of the bowel wall, although CD is characterized by transmural inflammation (all layers of the bowel wall involved) that leads to fibrosis, stricture and fistula(Fig no. I). It is characterized by painful episodes in the abdominal region, bloody diarrhea and episodes of tenesmus. In addition, some extra intestinal conditions can also occur with primary manifestations in the skin, eyes, liver and joints. whereas diagnosis is made from a combination of symptoms, endoscopy and histology. Currently, there is no effective treatment for UC, and the current main treatment is also based on controlling the inflammatory response of the intestine and controlling complications. Currently, the clinical treatment for this disease mainly uses corticosteroids, immunomodulators, aminosalicylic acid preparations, and other drugs, but the disease has the characteristics of high recurrence rate, and due to long-term medication adverse reactions can easily occurrs. Amid, glucocorticoids and aminosalicylic acid preparations are first-line drugs for the treatment of UC, but due to the complexity of the disease, the cause has not been fully defined, and the clinical efficacy cannot fully meet the needs of patients. With the development of molecular biology, some advancement of treating UC has been made, but how to completely cure this disease is still challenging[3].

Pre-clinical methods may be option to address the issue towards understanding of drug mechanism and body's physiology response. To study the mechanisms of UC development Experimental animal models have many advantages: it can simulate the whole process of UC occurrence and development. Hence, it became critical to build a laboratory animal model of UC disease that is highly similar to the human gut environment. While, prior building an animal model of UC, the most important and basic thing is the selection of laboratory animals. In the selection of experimental animals, consider following four principles: the use of experimental animals alike to human function, structure, metabolism, and disease; the use of systemized experimental animals; the use of experimental animals with some specific reactions, sensitive to stimuli; the use of easily available and economical experimental animals and the use of zoonotic experimental animals[4].

According to the above principles, we should first choose animals that are fit for UC disease modeling, most reflective of clinical drug efficacy and nearest to the human internal environment. In current years, rats and mice have been preferably used in various animal experiments: they are genetically adjacent to humans, domestic and easy to handle, they also have good intraperitoneal injection effect, their white body hair is uncomplicated to observe, and they are low-cost and easy to keep. However, to select an animal that best fits the human intestinal environment and is most worthy for investigating UC disease, it is also important to determine the differences between rats and mice. On the one hand, mice have a tiny intestine and rats have a longer intestine, which is about 114 cm (102-126), and the classification of the rat intestine is identical to that of humans, so rats are more advanced to mice in this respect; and on the other hand, rats are omnivorous, anatomically and physiologically relevant to humans, and have a fast growth and metabolism, rats can be used for pharmacological and nutritional studies. Rats are also the main experimental animals for drug evaluation and It can be made into animal models of experimentally induced genetic defects diseases which is similar to those of humans. These advantages are very helpful for modeling UC diseases, whereas mice do not have a notable advantage in modeling UC, so rats are most preferred for animal modeling. If an animal model of UC that relatable to the human intestinal tract can be strongly established, different experiments can be carried out based on this model to test the therapeutic effects of different clinical drugs on UC as well as further determine the pathogenesis of UC. Finally, we may be able to come up with a set of treatment plan to cure UC via the in-depth study of this model[3].

Animal Screening Models
There are various animal models (Table No. I) which have been used globally by different researchers to assess new lead compounds prior they can be tested in humans. In this review article, we are highlighting the various advantages and disadvantages of animal model, try to give an overview of the important animal models which can be used, Many chemicals, immunity transfer, bacterial, and genetic models have been used in research to induce Ulcerative Colitis in animals.

Shamal R. Borude and Devendra S. Shirode

Chemical Models (Table No.I)

Dextran sulfate sodiumInduced Colitis [3,6,7,8,9].

Dextran sulfate sodium (DSS) is a polyanionic derivative of dextran with a chemical formula of (C6H7Na3O14S3)n. This compound have various applications which include probe hybridization to membrane-immobilized DNA, lipoproteins precipitation, and the release of DNA from DNA-histone complexes. It has been used on a large scale in research to induce intestinal colitis and colorectal cancer in mice and rats[6]. DSS is generally administered in the drinking water per oral treatment of the animals with the compound. 3% concentration of the compound is frequently used[7]. By DSS in wild-type animals an inflammatory response is begin which starts distally after around 5 days and is restricted to the colonic mucosa. How DSS starts the inflammation in the colon it is still not well understood. Although, a recent work investigating DSS both in vitro and in vivo disclosed that on the inner mucus layer DSS has a direct effect, leading to bacterial penetration of this layer prior any inflammatory signs could be seen. Thus, it can be concluded that the development of an inflammatory response start by loss of the inner colon mucus layer is the initial episode which leads to bacterial penetration and ultimately,[8]. DSS-induced colitis has also been used for investigating the effects of the gut microbiota on the development of colitis. This is exemplified by studies demonstrating that the nucleotide binding ligomerization domain containing 2(NOD2) abnormalities give rise to mice that develop changes in susceptibility to DSS colitis and the latter is associated with (or perhaps caused by) changes in the gut microbiome[6].

Mechanism[10].

Dysbiosis of intestinal flora by increasing the permeability of intestinal mucosal cells, Elevated mRNA levels of IL-1, IL-6, TNF-α, and secreted levels in serum.

DSS-induced colitis is a commonly used experimental model for many reasons which are:[9].

• The administration process is simple which is usually done in the drinking water
• Simplicity of dosage control which helps in determining colitis severity
• To study the process of inflammation or recovery process duration control is possible
• Microbial interventions, Multiple chemical compounds, and gene or cell therapy have been found to be effective therapeutically in DSS-induced colitis.

Advantages

high success rate, Easy to perform, lesion symptoms are very similar to human UC good reproducibility.

Disadvantages

Unstable experimental data, difficult to make a successful and stable model influence long modeling period. [3].

2,4,6–trinitrobenzene sulfonic acid Induced Colitis [3,9,18].

An oxidizing Nitroaryl compound Trinitrobenzene sulfonic acid (TNBS) which is administered intrarectally in animals to induce inflammatory bowel disease. This induction causes colonic damage which leads to necrotic regions associated with inflammatory areas. Damage mainly characterized by neutrophilic infiltration into the colonic tissue which is caused by High myeloperoxidase activity. Damage to the colonic epithelium and interstitium results in increase in the mucosal permeability. TNBS may cause a decrease in the mucosal hydrophobicity by interacting with the phospholipids present on the surface of the colonic mucosa. Due to this hydrophobicity is decreased and it is believed to contribute to TNBS-induced inflammation of the colon. Due to TNBS necrosis and deep tissue damage occurs which mimics the transmural involvement of CD; hence, rather than UC it may be preferred to be a better experimental model of CD. TNBS-induced colitis models have helped to be an important source for generating vital information about the cytokines involved in the human IBD. It has also helped in shaping the therapy regimens of the human disease[9]. Colitis induction done by Intra-rectal administration of TNBS dissolved in ethanol (50%) 120mg/ml, continuously for 7 days, causes mucosal barrier destruction. In this UC model, the sulfasalazine is used as a standard drug[18].

Mechanism [3].

Elevated IL-6 and TNF-α, disrupts the structure and composition of the intestinal flora, causing disruption of the flora.

Shamal R. Borude and Devendra S. Shirode

Advantages
Shorter time to induce ulceration, good reproducibility, Simple operation, longer duration of lesions.
Disadvantages
Easy mucosal ulceration perforation, and death, TNBS stimulation is too severe. [3].

Oxazolone Induced colitis [11,17].
Intrarectal administration of the hapten oxazolone(OXA) with ethanol into murine animals results in acute colitis. The condition is characterized by a T helper (Th)2-type immune response with a marked increase in interleukin (IL)-4 and IL-5 production, accompanied by body weight loss, diarrhea, ulcers, and loss of epithelial cells in the large intestine. Thus, it favors UC than the other IBD subtypes, differentiating it from trinitrobenzene sulfonic acid (TNBS)-induced colitis (Th1-mediated immune responses), which copy CD more closely. In oxazolone-induced colitis induction natural killer T cells and their associated cytokine, mainly IL-13, are also intimately involved. To test disease pathology and therapeutic interventions for UC many studies have utilized oxazolone-induced colitis. Nicotine upregulates the nicotine acetylcholine receptors on CD4+ T cells and increases regulatory T cell (Treg) numbers, it was recently shown in oxazolone-treated mice that, accompanied by a decrease in the number of Th17 cells, which develop amelioration of the inflammatory phenotype. Opposite to this, nicotine treatment in TNBS-induced mice, that have CD-like Th1-associated inflammation, upregulates Th17 cell numbers associated with an exacerbation of the inflammatory response. In a different study, suppression of the Th1 response and attenuation of intestinal inflammation in TNBS-induced colitis after mice treated with 3-hydroxy-3-methylglutaryl coenzyme A reductase inhibitor, but not oxazolone-induced colitis. This examples helps to illustrate the importance of choosing an appropriate model to answer a specific question when exploring a therapeutic potential of a drug/compound for a particular disease. In BALB/C strain which is known to favor Th-2 immune responses colitis induction done by OXA solution (7.5 mg/ml in 40% ethanol) through intra-rectal administration. The 5- amino salicylic acid is used as a standard and administered through intra- rectal administration[17].

Mechanism [3].
Increased release of TNF-α and IL-6, Leading to an imbalance in the ratio of Th1/Th2 helper cells, production of antibodies, active secretion of B lymphocytes, and hyperactive humoral immune response, causes an inflammatory response in the intestinal mucosa by activating the complement system.
Advantages
Rapid model establishment, very similar to UC in humans, good reproducibility, Simple operation.
Disadvantages
The exact mechanism is not fully understood and duration of disease is maintained for a relatively short period of time.

Acetic acid-induced colitis [3,11,12,13].
To create chemical injury to the mucosal epithelium that induces a transient phenotype mimicking UC intrarectal administration of diluted acetic acid provides an alternative method. The first result of this animal model was illustrated by MacPherson and Pfeiffer[12]. where for 10 seconds they instilled 10%–50% acetic acid into the rat rectum, followed by flushing the lumen with saline three times. In an acetic acid dose-dependent manner a diffuse colitis was observed in these rats, with histopathological features including ulceration of the distal colon and crypt abnormalities[12]. The injured and ulcerated mucosa, with destruction occasionally extending to the LP, starts to heal within days in mice and a few weeks after in rats[13]. Subsequent modifications and optimization several years focused on altering the concentration of acetic acid and the contact time. Concentrated acetic acid enemas into the lumen usually cause perforations; the recent protocol is carried out using 4% acetic acid with 15–30 seconds of exposure. There are a several reports that shows compounds that can ameliorate acetic acid-induced colitis. Compounds aiming to target reactive oxidative species such as N-acetyl cysteine, trimetazidine, vitamin E, and melatonin included, indicating that acetic acid-induced colitis may be a good model to study the efficacy of drugs that intended to interfere with reactive oxidative species pathogenesis[3,11]. Of note, within the first 24 hours the

epithelial injury observed after acetic acid induction is not immunologic in nature. Drug should be tested at a time point after 24 hours postinduction, that target immune responses

Advantages
Low cost and the ease of administration

DNCB Induced Colitis [14,16].
Chemical hapten 2,4-dinitro-1-chlorobenzene(DNCB), which binds to tissue protein and is responsible for induction of delayed-type hypersensitivity when applied to the skin or the intestinal lesion. In the skin the pathological lesion a small vessel vasclitis occurs involving the dermis and the subcutaneous tissue. Around the venules a mononuclear cellular infiltration occurs, along with endothelial proliferation. There is a necrosis or little fibrosis. In DNCB – induced colitis, some of the histological features associated with idiopathic human colitis occurs in the large bowel. By a mononuclear cell infiltration, vascular congestion and perivascular cuffing, the lesion is characterized. Additionally, there is epithelial erosion, frank ulceration and mucosal haemorrhage. By intra-colonic instillation of 25 mg of DNBS per rat dissolved in 50% alcohol, colitis induction done. After 4 days, the colonic mucosal damage was analyzed along with body weight, food intake, spleen weight, colon weight, myeloperoxidase activity, histological damage, malondialdehyde levels, reduced nitric oxide and glutathione levels in colonic tissue homogenate[16].

Mechanism [3].
Significant increase in NO and TNF-α activity by activation induced by T cells.

Advantages
High similarity in pathology to human UC, simple operation.

Disadvantages
Requires prior sensitization, More tedious operation, inflammation is self-healing.

Immunostimulation Models (Table No. II)
Colonic mucosal tissue sensitization method [3].
Injection of antigen containing Fuchs antigen emulsion+enema with ethanol solution used for the colonic mucosal tissue sensitization method. Rats are commonly used for this model.

Advantages
Identical to human UC immunopathogenesis; Longer duration of lesions; fit for screening of new drugs.

Disadvantages
More cumbersome operation; prolonged modeling time; multiple injections of antigen required to maintain sensitization.

Rat colonic bacterial strain method [3].
Bacterial suspensions were made from E. coli in the colon contents of healthy rats, suspensions were injected in rats.

Advantages
Longer maintenance of inflammation; mostly chronic inflammation.

Disadvantages
Requires certain conditions and techniques to prepare E.coli suspension, Longer time required to prepare E. coli suspensions

Fetal rat colonic embedding method [3].
The fetal rat colonic was removed 3-4 cm long and it is surgically planted aseptically under the right kidney pericardium in adult rats.

Advantages
The disease model is alike to the clinical symptoms of UC.

Disadvantages
Low success rate, long experimental period; High technical requirements.

Spontaneous animal models [3].
Abnormalities developing under natural conditions or genetic mutations; obtained by depend on selective breeding and hybridization methods.

Advantages
Deliberate well on the development of UC and the effect of drug treatment.; The adjacent model to the occurrence of UC.

Disadvantages
Onerous to standardize control; and animals are scarce and costly, making it difficult to tough to large-scale experiments or more in-depth studies.

Bacterial Model [11,15].(Table No. III)
Salmonella-induced colitis[11,15].
Gram-negative Salmonella typhimurium and Salmonella Dublin are the Food-borne enteric bacterial pathogens that can cause the intestinal diseases. Direct oral infection of S. typhimurium results in the systemic infection in mice that may hide the phenotype of intestinal inflammation. Although, this problem can be overcome by pretreating mice to upset commensal microbial flora and allow better colonization of S. typhimurium with an oral antibiotic cocktail, resulting in high-density growth of the bacterium within a day. By such colonization the initial inflammation caused which has similar histo¬pathological characteristics to human UC, involving epithelial crypt loss, erosion, and neutrophilic infiltration. Of note, within 5 to 7 days of infection this mode of colitis induction usually results in the systemic infection. Therefore, it is perceived that to study the acute phase S. typhimurium infection is a valuable model, but not next stages, of colitis. Salmonella has been shown to function as a good vector which is used to introduce certain gene components into the mucosa, to determine immune response for vaccines against colitis. Into the intestinal epithelium and Peyer's patches (PP) it can efficiently invade. Therefore, careful and full characterization of its virulence factors is diffficult to efficiently make a safe attenuated strain for such gene therapy vaccination. Vaccinating mice with an attenuated mutant S. typhimurium strain contains deletion of the znuABC operon, that encodes a zinc importer which is responsible for metal recruitment in the infected host, that evokes effective immune responses and protects mice from the subsequent Salmonella infection. In addition, illuminating how S. typhimurium interacts with host epithelial cells facilitates advance understanding of ways to potentially prevent UC onset. For example, the host inflammatory-induced proteins (eg, chitinase 3-like 1 [CHI3L1, also known as YKL-40].) blocks the colon using fit antibodies (Abs) or inhibitors that can stop colonization of S. typhimurium on the intestinal epithelium, thus preventing more invasion.

Adherent–invasive E. coli [11,15].
From the ileum of CD patients the commensal adherent invasive Escherichia coli (AIEC) strain was originally isolated and was exhibit to exacerbate intestinal inflammation in an opportunistic manner. Although, AIEC can stick to both small and large intestinal epithelial cells (IECs) with similar affinity. Induction of colonic inflammation animal models using AIEC infection needs mild epithelial damage, such as low dose DSS treatment, during the course of the infection. The phenotype of the colonic inflammation acts as a UC, including the presence of blood in stool, body weight loss, and colonic neutrophilic infiltrations. A latest study showed that the AIEC encodes a pathogenic form of the chitinase, chiA, that is differentiable from other nonpathogenic E. coli, which is utilized to stick to host epithelial cells by binding with the colonic inducible protein CHI3L1. In mice administration of chitin microparticles (1–10 μm in size) ameliorates colonic intestinal inflammation, probably interaction of bacterial-derived factors (such as AIEC chiA) with host CHI3L1 blocks. Likewise, ameliorative effect also result of anti-CHI3L1 Abs.

Colonization of and Effective invasion into, AIEC in the mucosal epithelium is regularly hindered by the mucosal biofilm formation of probiotic bacteria, such as Lactobacillus casei. Particular antibiotics result in the disruption of the intestinal microflora, as well as the probiotic biofilm, creating an ideal environment for opportunistic AIEC to stick to and invade IECs and macrophages. It has been shown that in non-antibiotic-treated mice AIEC does not adhere efficiently, but colonizes well in the antibiotic-treated animals. This result suggests that the restoration of a

Shamal R. Borude and Devendra S. Shirode

beneficial microbiota, either through the probiotic intake or other methods like fecal microbial transplantation, they can theoretically prevent further exacerbation of the intestinal inflammation by commensal pathogenic bacteria.

Transgenic and gene knockout animal models of ulcerative colitis[11].(Table No. IV)
IL-7 Tg mice
IL-7 is a pleiotropic cytokine, candidate risk gene associated with UC. IECs demonstrate IL-7, which serves as a regulatory factor for the development and homeostasis of lymphocytes that express IL-7 receptor (IL-7R). IL-7 protein expression is notably upregulated and generate its optimal effects in controlling long-lived memory of CD4+ T cells in the colonic mucosa, in UC patients. IL-7 seems to mediate the persistence of chronic colitis via IL-7Rα chain expressed especially on CD4+ T cells, but not on the other cell types. Consequently, blocking IL-7R functions has shown to be fruitful in suppressing adoptive transfer-induced intestinal inflammation in an mice. Administration of fixed anti-IL-7R Ab into the murine colitis models (eg, Helicobacter bilis-infected Mdr1 KO mice) as well controls dendritic cell (DC) and macrophage expansion.

IL-7 Tg mice express the murine IL-7 complementary DNA mechanically develop acute colitis at or near 1–3 weeks of age, which is characterized by a mixed cellular infiltration that involves neutrophils and lymphocytes. At 8–12 weeks of age, the Tg mice exhibit rectal prolapse and remittent intestinal bleeding, with goblet cell loss, rectal erosion, and occasional crypt abscesses. Upregulation of IL-7R on the mucosal lymphocytes is also associated with disease progression. Thus, an IL-7 Tg mouse model is fruitfull to understand the T-cell-mediated pathogenesis of colitis for the therapeutic treatment targeting T-cell functions.

TCRα KO mice
Mombaerts *et al* in 1993, showed that the T-cell receptor α chain (TCRα) KO mice instinctively developed chronic colitis, which was mediated by a Th2-type of immune response which is similar to human UC with an inflammatory pattern restricted primarily to colonic mucosa. At 4–6 months of age, nearly 60% of TCRα KO mice formed soft stools, which is associated with loss of goblet cells, and a mixed cellular infiltration mostly consisting of the lymphocytes and neutrophils in the affected LP. Spontaneous colitis starts in TCRα KO animals when raised in a helicobacter-free/SPF facility, but not in the conventional (CV) environments. When SPF-born TCRα KO mice were later transferred into the CV environment, the mice started attenuated mild colitis. This supports the concept that early life exposure to an environmental microbes which may be protective against colitis risk later in life. Various therapeutic treatment have been tested in TCRα KO mice with effectiveness. Oral administration of dexamethasone 3 mg/kg(Daily) an member of the glucocorticoid class of steroid drugs, into an TCRα KO mice was effectual to prevent the goblet cell loss and leukocyte infiltration. An Immunotherapy innervations by using anti-IL-4 Abs has also been exhibited to defeat the clinical and histological symptoms of colitis by regulating the Th2-type cytokine productions. Purified immunoglobulin G, Administration with a mixture of monoclonal auto-Abs reactive against colonic epithelial cells, can weaken colitis in B-cell-deficient TCRα KO mice. Carbon monoxide, a well known component in cigarette smoking, which exerts anti-inflammatory effects in an TCRα KO mice via suppression of IL-1β, tumor necrosis factor-α (TNFα) and the IL-4, also through induction of IL-10 production, giving molecular insights into how smoking has an protections against UC. In addition, chitin microparticles oral administration into TCRα KO colitic mice also displayed suppression of IL-4 and TNFα production and increased interferon-γ (IFNγ) production in mesenteric lymph nodes (MLNs). It was found that in TCRα control groups chitin treatment exhibit expansion of a certain genre of commensals microbes.

Wiskott–Aldrich syndrome protein KO mice
Patients with Wiskott–Aldrich syndrome have not only immunodeficiency but also frequently autoimmune manifestations, with 5% to 10% of patients growing colonic inflammation. They either lack or express a defective form of Wiskott–Aldrich syndrome protein (WASP), an intracellular molecule particular to hematopoietic cells. In actin polymerization WASP has major biological role, and it is critical for multiple cellular functions like cell motility, activation, and signaling. Such as, their human counterpart, an WASP KO mice on 129 SvEv mouse background also spread spontaneous colitis from the 4 months of age. At 6 months of age full penetrance was observed. The pancolitic

marking of the inflammation together with increase in Th2 cytokines in the colonic LP which is associated with this model which has similar features of UC. At first, it was hypothesized that abnormally activated effector T cells also deficient and dysfunctional Tregs similar with WASP deficiency bore the only responsibility for colitis development, but latest studies have disclosed a role of the WASP KO innate immune cells in disrupting mucosal regulation. The advantages of using this model for study of ulcerative colitis pathogenesis Th2-skewed cytokine profile similar as a human disease, aberrant natural Treg and, the innate immune cell function, and a human correlate where a subset of patients with same genetic defect also suffer from the colitis.

Different types of the therapeutic strategies have been investigated by using WASP KO animals. In WASP-deficient hematopoietic stem cells the WASP-expressing retrovirus was transduced prior transfer into an lethally irradiated recipient mice, results the weakening of colitis together with normalized populations of the mature B and T cells compared chimeric mice with the control retrovirus-transduced WASP-deficient bone marrow cells which then developed disease. Additionally, given that UC patients were found to produce lower levels of the intestinal alkaline phosphatase, the WASP KO mice were treated with oral intestinal alkaline phosphatase and were found to productively weaken colitis with less cellular infiltration and the reduced production of IL-4 and IFNγ. In addition, direct neutralization of IL-4, but not IFNγ, with injection of anti-IL-4 antibody weekly for 8 weeks ameliorated disease. At the end, administration of a freshly formulated IL-10-immunoglobulin fusion protein completely revoked colitis development in the chimeric mice with WASP-deficient innate immune cells.

Mdr1a KO mice

The multiple drug resistance 1a (mdr1a) gene lack in Mdr1a KO mice, that is encoding for the cell surface P-glycoprotein (P-gp) transporter which pumps small amphiphilic/hydrophobic molecules around the cell membrane. Around 25% of these mice develop the colitis between 8 and 36 weeks of age when increased in an SPF facility, but not in a GF facility. The mucosal thickening and loss of goblet cells that is also accompanied by crypt abscesses and ulceration in the colon are the histological findings in this model. Tto dispose of bacterial breakdown products in the epithelial cells the Mdr1a KO mice has lack of the proper potentiality. The bacterial products accumulation increases excess/abnormal antigen presentation to the neighboring T cells, generate a marked T-cell activation, state that initiate the colitis. Lately, T-cell participation in the growth of colitis in the Mdr1a KO model has been majorly characterized. The lack of Mdr1a (P-gp) limit the growth of inducible Treg cells, consequently producing fewer functional forkhead box P3 (Foxp3)-positive Treg cells and hence small IL-10 production to control and regulate the intestinal inflammation. More serious colitis is an result of Hematopoietic-specific Mdr1a deficiency than the mice that have Mdr1a deficiency only in the IECs, suggesting colitis development immune cell-derived P-glycoprotein has a critical role.

Mdr1a KO mice in a GF facility do not develop colitis, regular finding explains, prophylactic treatment using the broad-spectrum oral antibiotics majorly reduces the incidence of colitis development. Diet containing a polyphenol compound called curcumin (commonly found in spices used in Asian food) fed in Mdr1a KO mice which demonstrated upregulation of the xenobiotic metabolism and also suppression of pro-inflammatory pathways and correlated to the depletion of histological signs of the colitis. Meta-analysis has recognized some polymorphisms in the Mdr1a locus in the human UC, but not in CD, patients that influence its gene expression and regulation. Loss of Mdr1a expression was incriminated in UC development, but not in Crohn's Disease patients. P-glycoprotein expression upregulates after administration of the probiotics Lactobacilli under both normal and the inflammatory conditions, that reduces the myeloperoxidase activity and histological signs of the injury in DSS-treated mice. These results recommend that the Mdr1a KO mice can be utilized in the design of therapeutic drug that target the intestinal epithelial barrier dysfunction and in the determining the mechanisms underlying the benefits of a probiotic treatment.

IL-2 KO mice

IL-2 is an effective regulatory cytokine produced by CD4+ T cells and amplifies stimulatory responses by promoting T lymphocyte expansion. IL-2 KO mice are develop normally before 4 weeks of age they are viable, after that displaying 50 percentage of mortality. The rest of mice when they are in a CV environment, develop colon-limited

inflammation with 100 percentage of the penetrance by a 6 weeks of age, but not in the GF conditions. The histological and clinical characteristic of this inflammation hold up striking resemblance to the human UC, also crypt ulcerations, abscess, and loss of goblet cells. Usually, GF-reared IL-2 KO mice showed the signs of different non-UC phenotypes like disruption in bone marrow hematopoietic cells, hemolytic anemia, generalized autoimmunity, and lymphocytic hyperplasia, but not the colitis. Signs of colonic inflammation shows only at 17–20 weeks of age in SPF-maintained mice , and majorly T-cell and B-cell activation were found to mediate the colitis. These T cells are appearently activated through the altered antigen presentation by the Dendritic cells (DCs). In IL-2 KO mice, colonic Dendritic Cells increase 4 to 5 fold in the inflammatory conditions and localize into the T- and B-cell aggregates, indicating excessive levels of major histocompatibility complex class II, CD80, CD205, CD86, CD40, and C-C chemokine receptor type 5 molecules. These changes in Dendritic cells phenotype may be produced by a certain colitogenic bacteria or antigens. It was manifest that the, colitis do not clear by bacteroides vulgatus mpk monocolonized IL-2 KO mice but it exert the protective effect, opposite to this, disease develop in the E. coli mpk monocolonized IL-2 KO mice, IL-6 expression and semi maturation of LP DCs raise by bacteroides vulgatus mpk-infected IL-2 KO mice a. It was reported that, the intestinal bacterial flora and the endogenous antigens are the chief contributors affecting SPF-associated colitis phenotype but not the environmental antigens, in this murine model. In IL-2 KO mice, particular targets have been recognized to control the severity of colitis. It was pinpoint that 2,4,6-trinitrophenol–ovalbumin-immunized IL-2 KO mice showed notably severe intestinal inflammation as compared with the untreated mice. Opposite to this, against the αEβ7 integrin mice administrated monoclonal Abs together with 2,4,6-trinitrophenol–ovalbumin immunization revealed attenuated disease associated with a reduction in CD4+ cells and IFNγ production in the LP. Additionally, green tea polyphenol extract in drinking water treatment to 8-week-old IL-2 KO mice, which decreased IFNγ and TNFα production later one week of treatment and it showed more clarification in the general histological scores of the spontaneous colitis later 6 weeks.

αi2 KO mice

Within 5–7 weeks of age Guanine nucleotide-binding protein G(i) subunit α-2 (Gαi2) KO mice exhibit marked lethal diffuse colitis phenotype, which associated with histopathological and clinical features same as UC. That include thickening of colon, neutrophilic and lymphocyte infiltrations, goblet and crypt loss, and crypt abscesses. Marked increase in memory CD45RBlow, CD62Llow, and CD44high, CD4+ T cells in LP showed in Cell analysis. Transfer of Gαi2 KO splenic CD3+ T cells, but not MLN CD3+ T cells, into immunodeficient mice causes severe colitis. Hematopoietic compartment B cells in the Gαi2 KO mice appear to be an chief regulatory factor to manage the colitis phenotype, as showed by the decrease in LPS-induced proliferation and IL-10 production. In fact, from wild-type MLNs isolated B cells, that cell transfer can protect Gαi2 KO mice from the colitis. In Gαi2 KO mice, Testing of therapeutic agents has shown the productive results in ameliorating colitis. Into the Gαi2 KO mice, Intraperitoneal injection of the cellular Bordetella pertussis vaccine indicated an increase in regulatory IL-10 production in the intestine, along with a significant reduction in the colitis. Excessive proliferation of CD4+ T cells was controlled upon treatment, along with an increase in apoptosis of activated Th1-type CD4+ T cells. Ex vivo cultures of colons from Gαi2 KO mice, obtained which respond to the methyl-prednisolone an anti-inflammatory drug which is similar as colons from the mice that had been orally treated with same drug, as evaluated by inflammatory-associated gene expression. Therefore, rather than in vivo testing colonic culture systems can be utilized to validate future IBD therapies.

Composite Method [3].(Table No. V)
TNBS +ethanol
Mice are used in this model, TNBS ethanol solution administered by enema, and 7 d later by TNBS ethanol solution by enema.
Advantages
High modeling efficiency; Modeling method is simple and economical; good reproducibility; good model stability; similar to human UC.
Disadvantages
The inflammatory Manifestations are more similar to Crohn's disease.

Shamal R. Borude and Devendra S. Shirode

DNCB +acetic acid
For 14 day DNCB acetone solution drip back once and DNCB ethanol solution for 15 d in rats by enema.
Advantages
High success rate, Consistent with UC characteristics; reproducible and simple, long duration.
Disadvantages
Modeling is Cumbersome

DNCB +ethanol
DNCB ethanol solution for 2 d continuously in rats.
For 4 days DNCB solution applied to abdomen of mice followed by enema of DNCB ethanol solution for 5d.
Advantages
Lack of self-healing of DNCB; overcome the short duration and similar to human UC.
Disadvantages
Long time required for modeling

DSS +acetic acid
DSS solution Free drinking for 7 day, fasting without water for 1 day and enema with acetic acid solution in rats.
Advantages
Short modeling time; good reproducibility; Simple and easy to perform; high success rate; long self-healing time.
Disadvantages
Death caused by Acetic acid enema in rats.

DNCB +acetic acid +ethanol
For 14 day DNCB acetone solution dribbled back, and DNCB ethanol solution for 15 d by enema, aceticacid solution injected at same site for 16 d in rats.
Advantages
Similar to human colorectal UC disease.
Disadvantages
Animal death occurs due to Acetic acid enema.

DMH +DSS
Free drinking of DSS and Intraperitoneal injection of DMH, with 18 weeks in mice.
Advantages
Good reproducibility; Simple and easy; similar to human UC disease.
Disadvantages
Prolonged use of DMH or Large doses can induce intestinal cancer.

CONCLUSION

There are various ways in which potential drugs for UC can be studied in laboratory animals before they are tested in humans. It is hard to find which animal model is the finest, as different factors such as availability of bacterial isolates or chemicals as well as the financial support with the research institute decide the choice of the models also. By the by thorough comparative analysis of different animal models of UC conditions, this paper outline the model progression, animal selection, and UC animal models pathogenic mechanisms and gives a more targeted choice of animal models for upcoming related experiments. We surveyed the research papers published in PubMed, Google Scholar, and Web of Science and discussed the experimental animals, modeling methods. In summary, there are different methods for drawing experimental models of UC animals for the scientific experiments, throughout this the immunostimulation method was the first to use, after the chemical stimulation method and the composite modeling method. In the choice of experimental animals, we compared the advantages and the disadvantages of different

Shamal R. Borude and Devendra S. Shirode

experimental animals for the animal model of Ulcerative colitis and ultimately selected rats as the best experimental animals after combining it with the human intestinal physiological environment.

REFERENCES

1. O. Stephen, M. Sain, U. J. Maduh, and D. U. Jeong, "An efficient deep learning approach to pneumonia classification in healthcare,"Journal of healthcare engineering, vol. 2019, 7 pages, 2019.

2. P. G. Kotze, F. Steinwurz, C. Francisconi *et al.*, "Review of the epidemiology and burden of ulcerative colitis in Latin America," Therapeutic Advances in Gastroenterology, vol. 13, 2020.

3. Xin Gao, Jia Li , Xueping Pang, Kaiyuan Cong, *et al.*, "Research ArticleAnimal Models and Pathogenesis of Ulcerative Colitis", Computational and Mathematical Methods in Medicine, pp- 1-15, 2022

4. E. C. Jung and H. I. Maibach, "Animal models for percutaneous absorption," Journal of Applied Toxicology, vol. 35, no. 1, pp. 1–10, 2015.

5. Kritarth NamanM Singh,Paresh G Koli, "Animal Models for Preclinical Drug Research on Ulcerative Colitis: A Review", Journal of the Scientific Society, Volume 45, Issue 2, May-August 2018.page no-1-4.

6. Barnett M, Fraser A. Animal Models of Colitis: Lessons Learned, and their Relevance to the Clinic. Ulcerative Colitis-Treatments, Special Populations and the Future. IntechOpen; 2011. p. 1-19.

7. Johansson ME, Gustafsson JK, Sjöberg KE, Petersson J, Holm L, Sjövall H, *et al.* Bacteria penetrate the inner mucus layer before inflammation in the dextran sulfate colitis model. PLoS One 2010;5:e12238.

8. Kiesler P, Fuss IJ, Strober W. Experimental models of inflammatory bowel diseases. Cell Mol Gastroenterol Hepatol 2015;1:154-70.

9. Low D, Nguyen DD, Mizoguchi E. Animal models of ulcerative colitis and their application in drug research. Drug Des Devel Ther 2013;7:1341-57.

10. X. Tian, Z. Peng, S. Luo *et al.*, "Aesculin protects against DSSinduced colitis though activating PPARγ and inhibiting NF-κB pathway," European Journal of Pharmacology, vol. 857, p. 172453, 2019.

11. Daren Low, Deanna D Nguyen & Emiko Mizoguchi (2013),"Animal models of ulcerative colitis and their application in drug research, Drug Design, Development and Therapy, 1341-1357, 2013.

12. MacPherson BR, Pfeiffer CJ. Experimental production of diffuse colitis in rats. Digestion. 1978;17(2):135–150.

13. Elson CO, Sartor RB, Tennyson GS, Riddell RH. Experimental models of inflammatory bowel disease. Gastroenterology. 1995;109(4): 1344–1367.

14. M E Glick, Z M Falchuk, "Dintroclorobenzene- induced colitis in the guinea –pig: studies of colonic lamina prpria lymphocytes", Gut, 1981, 22, 120-125.

15. Mizoguchi E. Chitinase 3-like-1 exacerbates intestinal inflammation by enhancing bacterial adhesion and invasion in colonic epithelial cells. Gastroenterology. 2006;130(2):398–411.

16. Shrikant V Joshi, Bhavin A Vyas, Payal D Shah, *et al.*, "Protective effect of aqueous extract of *oroxylum indicum Linn* (Root Bark) against DNBS- induced colitis in rats", Indian journal of Pharmacology 43(6), 656, 2011.

17. Ryotaro Kojima, Satoko Kuroda, Tomiko Ohkishi, et.al., "Oxazolone- induced colitis in BALB/C mice: a new method to evaluate the efficacy of therapeutic agents for ulcerative colitis", Journal of pharmacological sciences 96(3), 307-313, 2004.

18. A V Kulkarni, N S Vyawahare, " Effect of hydro alcoholic extract of *Sida Spinasa L.* 2,4,6- trinitro benzene sulphonic acid induced ulcerative colitis in rats", International journal of pharmaceutical sciences and research, vol.12(1); 1000-09. 2021.

Table No. I: Chemical Models

Name of Model	Evaluation Parameter
1) Dextran sulfate sodium Induced Colitis	mRNA levels of IL-1, IL-6, TNF-α levels, permeability of intestinal mucosal cells, histopathology, MPO activity, MDA level
2) 2,4,6–trinitrobenzene sulfonic acid Induced Colitis	IL-6 and TNF-α,structure and composition of the intestinal flora, MPO activity, MDA level

Shamal R. Borude and Devendra S. Shirode

3)	Oxazolone Induced colitis	TNF-α and IL-6,ratio of Th1/Th2 helper cells, antibodies, B lymphocytes, humoral immune response, MPO activity, MDA level
4)	Acetic acid-induced colitis	Histopathology, oxidative species, MPO activity, MDA level
5)	2,4-dinitro-1-chlorobenzene Induced Colitis	Body weight, food intake, spleen weight, colon weight, myeloperoxidase activity,TNF-α histological damage, malondialdehyde levels, reduced nitric oxide and glutathione levels in colonic tissue homogenate.

Table No. II: Immunostimulation Models

Name of Model	Evaluation Parameter
1) Colonic mucosal tissue sensitization method	Histopathological analysis, pro inflammatory factors, Anti- inflammatory factors imbalance, body weight loss, platelet activity, regulatory T- cell dysregulation.
2) Rat colonic bacterial strain method	
3) Fetal rat colonic embedding method	
4) Spontaneous animal models	

Table No. III: Bacterial Model

Name of Model	Evaluation Parameter
1) Salmonella-induced colitis	Histopathological analysis, pro inflammatory factors, body weight loss
2) Adherent–invasive E. coli	Blood in stool, body weight loss, and colonic neutrophilic infiltrations.

Table No. IV: Transgenic and gene knockout animal models of ulcerative colitis

Name of Model	Evaluation Parameter
1) IL-7 Tg mice	Intestinal bleeding, goblet cell loss, rectal erosion, and crypt abscesses
2) TCRα KO mice	IL-1β, tumor necrosis factor-α (TNFα) and the IL-4
3) Wiskott–Aldrich syndrome protein KO mice	IL-4 and IFNγ
4) Mdr1a KO mice	Histology, myeloperoxidase activity
5) IL-2 KO mice	Colonic Dendritic Cells, histocompatibility complex class II
6) Gαi2 KO mice	thickening of colon, neutrophilic and lymphocyte infiltrations, goblet and crypt loss, and crypt abscesses, Cell analysis, IL-10 production

Table No. IV: Composite Method

Name of Model	Evaluation Parameter
1) TNBS +ethanol	IL-6 and TNF-α, structure and composition of the intestinal flora
2) DNCB +acetic acid	Body weight, food intake, spleen weight, colon weight, myeloperoxidase activity, TNF-α histological damage, malondialdehyde levels, reduced nitric oxide and glutathione levels in colonic tissue homogenate.
3) DNCB +ethanol	Body weight, food intake, spleen weight, colon weight, myeloperoxidase activity, TNF-α histological damage, malondialdehyde levels, reduced nitric oxide and glutathione levels in colonic tissue homogenate.
4) DSS +acetic acid	mRNA levels of IL-1, IL-6, TNF-α levels, permeability of intestinal mucosal cells, histopathology, MPO activity, MDA level
5) DNCB+acetic acid +ethanol	Body weight, food intake, spleen weight, colon weight, myeloperoxidase activity, TNF-α histological damage, malondialdehyde levels, reduced nitric oxide and glutathione levels in colonic tissue homogenate.

Shamal R. Borude and Devendra S. Shirode

6)	DMH +DSS	mRNA levels of IL-1, IL-6, TNF-α levels, permeability of intestinal mucosal cells, histopathology, MPO activity, MDA level

Fig. No. I : Flow chart for Pathophysiology of Ulcerative Colitis

RESEARCH ARTICLE
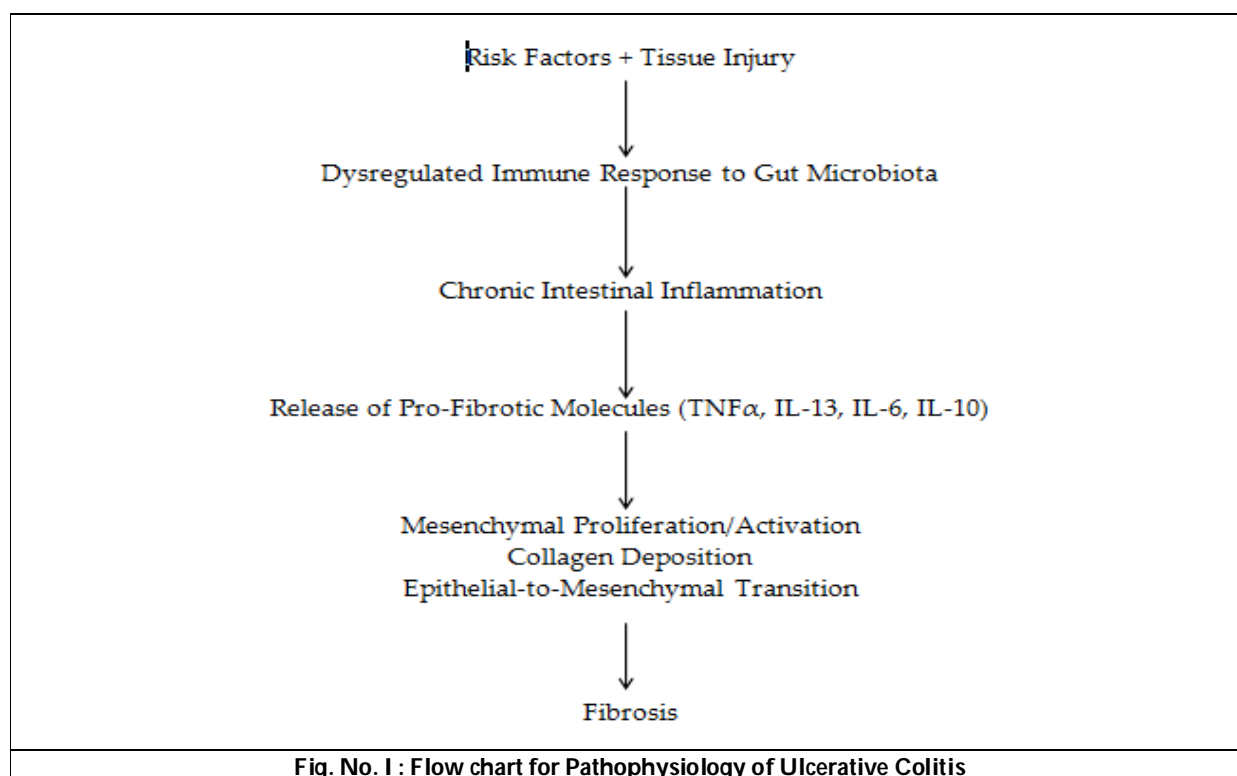
The Significance of Soil Enzymes in Carbon Sequestration

Dhruv Y Haldaria[1] and Hiren K.Patel[2]*

[1]M.Sc Microbiology, P.P.Savani University, Surat-394125, Gujarat, India.
[2]Associate Professor, School of Science and School of Agriculture, P.P.Savani University, Surat- 394125, Gujarat, India.

*Address for Correspondence
Hiren K.Patel
Associate Professor,
School of Science and School of Agriculture,
P.P.Savani University, Surat- 394125, Gujarat, India.
E.Mail: drhkpatel1@gmail.com

ABSTRACT

The increase in atmospheric carbon dioxide (CO_2) due to human activity since the industrial revolution is widely recognized. However, the crucial role that natural and managed soils play in the global carbon cycle is often overlooked. Soil microorganisms are responsible for a large respiratory flux of CO_2 to the atmosphere, which is ten times greater than the annual CO_2 emissions from fossil fuels. Consequently, even small changes in the soil carbon cycle could have a significant impact on atmospheric CO_2 levels. This article focuses on the contribution of soil microbes to the global carbon cycle and the methods used to identify the microorganisms responsible for processing plant carbon inputs to soil. The article also discusses whether current techniques can provide the necessary information to manage agro-ecosystems for carbon sequestration and increased agricultural sustainability. While these techniques are useful in identifying plant-derived carbon-utilizing microbes, they lack the ability to accurately measure carbon use efficiency and destination within the microbial metabolome, which is necessary for rational manipulation of the plant-soil system to promote soil carbon storage.

Keywords: carbon cycling, rhizosphere carbon flow, decomposition, soil microbialrespiration, climate Change, methods, carbon tracking, agroecosystem management.

INTRODUCTION

Soil enzymes play a crucial role in the carbon cycle and can have a significant impact on carbon sequestration in soils. Enzymes are organic molecules that accelerate biochemical reactions, and they are essential for the decomposition of organic matter in soils. As organic matter decomposes, it releases carbon dioxide into the atmosphere. However, if the decomposition rate is slower than the carbon uptake rate by plants, then carbon can be

Dhruv Y Haldaria and Hiren K.Patel

stored in soils for an extended period, leading to carbon sequestration.Soil enzymes can affect carbon sequestration by influencing the rate of decomposition of soil organic matter. For instance, enzymes such as cellulases, ligninases, and proteases break down complex organic molecules, making them available for microbial consumption. The availability of organic matter for microbial consumption, in turn, affects the rate of decomposition and carbon sequestration.Additionally, the activity of soil enzymes can be influenced by environmental factors such as temperature, moisture, and pH, which affect microbial communities' composition and function. Therefore, understanding the relationship between soil enzymes and carbon sequestration can help identify the key factors that influence soil carbon dynamics, which can be useful in developing strategies for mitigating climate change through soil carbon sequestration.

THE SOIL CARBON CYCLE AND MICROBIAL DECOMPOSERS:FUNDAMENTAL PRINCIPLES:
All living organisms depend on the supply of necessary elements from the Earth. Since the Earth is a closed system with a finite supply of essential elements such as hydrogen (H), oxygen (O), carbon (C), nitrogen (N), sulfur (S), and phosphorus (P), recycling of these elements is fundamental to avoid exhaustion. Microbes are critical in the process of breaking down and transforming dead organic material into forms that can be reused by other organisms. This is why the microbial enzyme systems involved are viewed as key 'engines' that drive the Earth's biogeochemical cycles.

The terrestrial carbon cycle is dominated by the balance between photosynthesis and respiration. Carbon is transferred from the atmosphere to soil via 'carbon-fixing' autotrophic organisms, mainly photosynthesizing plants and also photo- and chemoautotrophic microbes, that synthesize atmospheric carbon dioxide (CO_2) into organic material. Fixed carbon is then returned to the atmosphere by a variety of different pathways that account for the respiration of both autotrophic and heterotrophic organisms. The reverse route includes the decomposition of organic material by 'organic carbon-consuming' heterotrophic microorganisms that utilize the carbon of either plant, animal or microbial origin as a substrate for metabolism, retaining some carbon in their biomass and releasing the rest as metabolites or as CO_2 back to the atmosphere [1]. Globally, most soils are unsaturated and oxic, so CO_2 is the main respiration flux. In waterlogged anoxic soils such as rice paddies and peatlands, CO_2 is reduced by hydrogenotrophic archaea in methanogenesis, with the net flux of the methane produced dependent on the relative activity of methanogens (including that of fermenting acetate) versus the activity of aerobic methane-oxidizing bacteria (methanotrophs) residing in the surface, oxic layers of soil of such wetland systems and also probably the microbial anaerobic oxidation of methane in anoxic layers [1].

According to[6] , soil microbes play a crucial role in transferring carbon between environmental compartments to ensure their survival through reproduction. Microbes use different organic and inorganic forms of carbon as carbon and energy sources. However, the carbon cycle is closely linked with other essential elements for microbial metabolism, including nitrogen (ranging from the most reduced to the most oxidized) and phosphorus. The availability of these key elements, as well as other environmental factors such as pH, soil texture, mineralogy, temperature, and soil water content, control the rate at which microbes consume and respire carbon. These interactions between environmental conditions and biological processes are essential in controlling the uneven distribution of organic matter across the world's soils, including the largest global concentration of carbon in wet and cool areas in the northern hemisphere, dominated by deep accumulations of peat and permafrost soils. [6] review aims to outline the significance of soil microbial communities to global environmental issues of soil organic matter persistence and climate change through carbon cycle feedbacks. It also discusses the main techniques that can be used to apportion below-ground utilization of plant-derived carbon to specific microbial groups and whether these techniques can provide the information required to underpin the management of agro-ecosystems for carbon sequestration and increased agricultural sustainability.

Dhruv Y Haldaria and Hiren K.Patel

THE SOIL CARBON CYCLE AND MICROBIAL DECOMPOSERS: SIGNIFICANCE AND ENVIRONMENTAL IMPLICATION

The relationship between soil and atmospheric carbon pools is critical to understanding global carbon cycling and climate change. It is estimated that global soil organic carbon stocks are at least three times greater than atmospheric carbon stores[7] Terrestrial ecosystems exchange around 8% of the total atmospheric carbon pool annually via net primary production and terrestrial heterotrophic respiration, predominantly microbial[8]. However, if soil microbial respiration ceased, it would only take about 12 years of primary production at current rates to exhaust atmospheric CO_2 stocks [9]. Net carbon sequestration varies between locations and is significantly affected by land management [10]. Human activity has caused the loss, degradation, and agricultural soil depletion of 42–78 Gt of carbon[3] . Land remediation to restore some of this lost carbon could help offset fossil fuel emissions. Soils play a crucial role in the global carbon cycle, affecting not only the supply of essential plant nutrients but also the climate system. The functioning of microbiological communities within soils influences these processes.

The decomposition of plant-derived carbon and the persistence of soil organic matter are essential components of the global carbon cycle. Above-ground plant litter and below-ground root litter and exudation are the two main inputs for plant organic carbon into the soil system. The relative contribution of each input depends on plant species and crop management. Root exudates consist of a continuous flow of carbon-containing compounds from roots to soil. These exudates are composed of simple molecules such as sugars, amino acids, sugar alcohols, organic acids, and structurally complex secondary metabolites. However, polymers such as lignin, cellulose, and hemicellulose require depolymerisation by extracellular enzymes before they can be metabolised by microbial cells [11].

The mycorrhizal fungi play a significant role in the carbon cycling of soil, particularly in the transfer of carbon between plants and fungi. The arbuscular mycorrhizal fungi (AMF) are obligate symbionts that rely solely on their host plant for carbon, whereas ectomycorrhizal fungi (ECM) are facultative symbionts that can mineralize organic carbon. The AMF symbiosis is found in about 85% of plant families and experimental evidence suggests that up to 20% to 30% of total carbon assimilated by plants may be transferred to the fungal partner. The mycelia quickly respire a proportion of the plant carbon, resulting in a short-circuit of the soil carbon cycle. Soil organic matter (SOM) is composed of fresh to decomposing plant, microbial, and faunal-derived debris and exudates, including the microbial biomass responsible for primary decomposition. The traditional view of SOM has been divided into active and passive pools with varying decomposition kinetics, but recent evidence suggests that environmental and biological factors may play a more significant role in the long-term persistence of SOM. Direct observations have not confirmed the existence of humic macromolecules in soil, and it is suggested that SOM consists of partially decomposed litter and microbial necromass. Soil microbes contribute to the formation of persistent SOM via their necromass and may promote the formation of microaggregates that physically protect SOM from decomposition. Glomalin, a glycoprotein produced by the hyphae of AMF, has been linked to the stabilisation of microaggregates, as well as other hydrophobic proteins produced by mycorrhizal fungi and filamentous bacteria, such as hydrophobins and chaplins ([9, 12]

The carbon cycle has been heavily disturbed by human activities during the industrial period, primarily through the burning of fossil fuels and conversion of natural ecosystems into agricultural land, resulting in increased carbon dioxide (CO_2) emissions to the atmosphere [13]. However, the consequences of these human actions for the global climate are still uncertain, particularly due to limited understanding of soil respiration and its representation in Earth system models. Microbial decomposers play a critical role in the carbon cycle and contribute to climate change through carbon cycle feedbacks, which are complicated by direct and indirect effects and interactions with other factors [14]. For instance, microbial activity and organic carbon decomposition can be accelerated by an increase in temperature, leading to more CO_2 released by respiration, and increased root deposition of easily available exudates can "prime" the turnover of less available soil organic matter constituents [13]; [15]. However, the balance between terrestrial ecosystem sinks (photosynthesis) and sources (respiration) of atmospheric CO_2 under elevated CO_2 remains uncertain, particularly when soil nitrogen availability and its effect on plant growth are considered [14]. Moreover, the actual temperature sensitivity of soil respiration and how this sensitivity is modified by other

Dhruv Y Haldaria and Hiren K.Patel

environmental factors, such as changes in soil moisture during droughts and nutrient limitations, is still unclear. The diversity of soil ecosystems across the world, which vary in their function owing to differences in their forming factors, further complicates the issue[13]. Research in this area is an urgent priority to predict impacts and feedbacks between climate change and the global carbon cycle, particularly in vulnerable ecosystems such as peatlands and permafrost soils [13]; [14].

METHODOLOGIES FOR TRACKING CARBON FLOW BELOW GROUND MICROBIAL GROUPS
The majority of carbon cycle models treat soil microbial biomass as a "black box" despite their crucial role in the carbon cycle and implications for climate change feedbacks [16]. These models typically calculate soil respiration using first-order kinetics based on the size of the carbon pool and an empirically derived decomposition rate constant, which captures the net effect of microbial activity[17, 18]. However, recent studies have suggested that these models need to be modified to include more explicit representations of microbial community and functions that control decomposition [16]. Fortunately, empirical microbial ecology methods, such as stable (SIP) or radioactive (RIP) isotope probing and molecular ecology techniques, can now be used to identify microbial groups responsible for the turnover of plant-derived inputs to soil[19]. These methods involve the use of either stable or radioactive isotopes to track the microbial fate of a labelled carbon source, and they allow for allocation of carbon utilization to specific microbial ribotypes[19]. While these techniques are still in development, they have the potential to shed light on the "black box" of soil microbial biomass and improve our understanding of the carbon cycle.

The use of nucleic acid stable isotope probing (SIP) has been applied for over a decade to study microbial carbon utilization and cycling in various ecosystems [20]. While early studies focused on non-planted systems, recent research has utilized DNA-SIP to examine the cycling of methane [20] and degradation of organic pollutants in soil[21], and rRNA-SIP to track carbon utilization in phenol-utilizing microorganisms in wastewater treatment plants[19] and specific microbial groups in diverse ecosystems (e.g., rivers, tidal flats, aquifers, groundwater) with respect to carbon biogeochemical processes such as methanotrophy[20], degradation of xenobiotics[19, 20], and other ecosystem functions.

The application of nucleic acid-SIP to study the microbial fate of rhizodeposit carbon in soil involves the growth of plants in a $13C-CO_2$ atmosphere to promote 13C labelling of photosynthate and rhizodeposition. However, this approach faces sensitivity issues due to dilution with plant 12C and native 12C SOM [19], making rRNA-SIP a more sensitive and successful approach[22][22]. As rRNA is turned over independently of cell replication with a high copy number within the microbial cell, rRNA-SIP has a greater sensitivity than DNA-SIP[22] and has therefore been used more successfully to directly track plant-derived carbon to microorganisms in the rhizosphere[19, 20]. The promise of mRNA-SIP has also been recently explored for understanding the links between root exudation and bacterial gene expression in the rhizosphere[23] . The SIP approach has been complemented and extended to track plant-derived carbon into biochemical markers other than nucleic acids, such as proteins [24] and phospholipid fatty acids (PLFA-SIP) [25]. Recent studies have combined RNA-SIP, neutral lipid fatty acid (NLFA)-SIP with neutral (NLFA) and phospholipid (PLFA) lipid fatty acids biomarker analyses and/or PLFA-SIP with real-time polymerase chain reaction (PCR) and community fingerprinting techniques to examine how elevated CO_2 or plant genetic modification alters the destination of photosynthetically fixed carbon with respect to its utilization by AMF and mycorrhizosphere bacterial and fungal species[26].

In 1999, FISH-MAR was first demonstrated by two research groups who visualized the incorporation of 14C-labelled substrates in probe-detected bacteria under the microscope. Since then, it has been primarily used to study the in situ physiology of bacteria in biofilms and activated sewage sludge with enhanced biological phosphorus removal. Although FISH-MAR has greater sensitivity than DNA- or RNA-SIP, its application is restricted to either single or small clusters of cells, and the microbial groups to be targeted need to be known in advance. Additionally, the number of different fluorophores that can be detected simultaneously is limited, which restricts the number of microbial groups that can be targeted. However, isotope arrays have been developed to study multiple microbial populations' ability to consume a radioactive substrate in activated sludge samples, and they have given promising

results. Furthermore, FISH-MAR has been used in combination with other methodologies, such as catalyzed reporter deposition and quantitative FISH-MAR, to improve signal detection and quantify cell-specific carbon uptake in probe-targeted bacterial groups. FISH-SIMS and FISH-RAMAN, which combine FISH with secondary ion mass spectrometry and Raman microspectroscopy, respectively, have considerable promise for use in rhizosphere carbon flow tracking experiments.[27]

POTENTIAL FOR MANIPULATING CARBON DYNAMICS IN AGRICULTURAL SYSTEMS

The loss of soil carbon due to intensive agricultural practices is caused by the acceleration of decomposition and reduction of primary production inputs to soil. As a result of tillage and drainage, physically protected organic matter is exposed, and improved aeration leads to the acceleration of decomposition. It is estimated that intensive cultivation has resulted in the loss of 42–78 Gt of carbon historically stored in the soil system. One potential solution to this problem is to increase the capacity of agricultural soils to regain lost carbon, which is currently being discussed as a means of atmospheric carbon remediation and mitigating climate change[28].

Strategies for managing soil for carbon sequestration involve increasing the quantity and quality of primary production inputs and manipulating the fate of these inputs in the soil. Crop plants with extensive root systems, altered physiological traits, cover and inter-cropping, returning crop residues to soil, and adding amendments such as compost or biochar are some ways to increase primary production. However, the addition of crop residues and amendments may not qualify as "soil C sequestration" under the strictest definition of the term since it does not necessarily transfer additional carbon fixed from the atmosphere to land. A second strategy is to encourage the processing of plant-derived carbon to biomass and metabolite precursors of soil organic matter or to secretions that promote the physical protection of carbon substrates against decomposition, rather than to CO_2. The identity of soil microorganisms, especially fungi and bacteria, significantly influences the fate of carbon inputs to soil. The relative abundance of fungi and bacteria may play a critical role in the formation of more stable carbon in soils with high fungal/bacterial biomass ratios. The relationship between soil biodiversity and carbon cycling processes such as respiration requires further study [29].

The influence of microbial diversity and identity on the fate of plant-derived carbon (C) in the rhizosphere remains unclear, as does the extent to which these microbes can be manipulated to promote C sequestration. If the community structure of plant C-utilising microbes is important for C fate, then the next step is to understand which are the most important groups that control soil storage with respect to expression of specific functions (e.g. metabolite production) and the proportion of the plant C inputs they are responsible for processing[30]. However, current methodologies for identifying plant-derived carbon-utilising microbes lack high-throughput abilities to study carbon partitioning at the whole cell level, and there is a need for new methodologies to enable a step-change in understanding [31]. Soil enzymes, produced by microorganisms such as bacteria, fungi, and actinomycetes, play a crucial role in breaking down organic matter into simple compounds that plants can use as nutrients[31] . Research has shown that adding soil enzymes can significantly enhance a soil's ability to capture carbon, increasing organic matter and carbon by up to 10 times[31]. Understanding and manipulating soil enzymes can therefore be an effective strategy for promoting soil carbon storage in diverse agricultural conditions.

The comparison of soil to a kitchen can help in understanding the concept that adding extra ingredients to soil can significantly change it. In the same way that tomato sauce or peanut butter alters food in a pan, organic matter in soil goes into solution while minerals stay on the surface, making soil the "earth's pharmacy." A soil's ability to provide nutrients to plants depends on its health and the presence of soil enzymes responsible for breaking down organic matter into soluble nutrients. The lack of these enzymes or insufficient organic matter can result in poor plant growth rates and yields. There are four basic enzyme types, and to enhance soil health or carbon sequestration, they can be added as liquid or powder. Microbial enzymes are widely available in liquid or powder form and can be mixed with water and organic matter before application. Adding oxygen to liquid enzymes can help them break down organic matter, although they may not be 100% effective. For a soil that is high in organic matter but low in nutrients, a microbial product is recommended, while for a soil that is low in organic matter but rich in nutrients, an animal or

Dhruv Y Haldaria and Hiren K.Patel

human enzyme is preferred [32].Various estimates have been published regarding the potential for global biophysical soil carbon sequestration assuming the widespread adoption of carbon-sequestering practices. These estimates differ in terms of the types of land use and the practices included. Earlier estimates, which were made before 2000, focused on cropland and set-aside to grassland of marginal crop land. Later estimates included a fuller range of options on all agricultural lands. Some estimates provide a range of per annum rates, while others provide a point estimate. Two estimates are shown, one denoting with and one without frontier technologies. The biophysical potential for CO_2 removal and sequestration in soils is dependent on a variety of management practices that can be adopted on agricultural lands to convert CO_2 into soil organic matter. Various estimates have been made over the past 20 years of the soil C sequestration potential globally and for the US. These estimates represent upper-bound estimates of the C sequestration potential assuming widespread adoption of the sequestering practices. Economic or policy-related constraints are generally not considered in these estimates. Most estimates are based on highly aggregated data on total area by land-use type, stratified into broadly defined climate types, and then applying estimates of representative per ha soil C sequestration rates for different management practices or suites of practices, based on measurements from long-term field experiments[32].

The global estimates indicate a potential for technical soil carbon (C) sequestration of 2-5 Gt CO_2 per year, based on existing best conservation management practices, with estimates towards the lower end considering less land area and/or a more restricted set of practices. These estimates align closely due to the two main determining factors, land area by land use type and observed rates of soil C sequestration from long-term field trials, being tightly constrained. Widespread adoption of a broad suite of best management practices (BMPs) for soil C sequestration on global grassland and cropland could potentially result in C storage rates of 4-5 Gt CO_2 per year, sustained for a limited time period of 2-3 decades. The estimate by[28] goes as high as 8 Gt CO_2 per year, including frontier technologies such as biochar amendments and high root C input crop phenotypes, which have much more uncertain technical potentials due to the lack of empirical data on their performance in the field.

The French government announced an initiative called "4 per mille" during the Paris climate accords, advocating for a massive effort to increase global soil C stocks as a core greenhouse gas mitigation strategy. If global soil C stocks in the top 40 cm could be increased on average by 0.4% per year (i.e., 4 per mille), that would be equivalent to about 3.4 GtC/y or 12.6 Gt CO_2/y. This level of net CO_2 uptake could offset most of the current annual increase in atmospheric CO2, assuming that the current ocean and terrestrial C sinks remained intact. However, there is considerable debate about whether this level of soil C sequestration is achievable and whether all soils or mainly agricultural soils should be targeted. Nonetheless, the 4 per mille concept has spurred debate and "raised the profile" of soils as a potentially key mitigation strategy. For comparison, current global greenhouse gas (GHG) emissions are around 40 GtCO2e/year, with approximately 83% of that from fossil fuel combustion, and the goals of the Paris agreement may require negative emissions of about 15 Gt CO_2/year by the end of the century[33].

The use of non-conventional management practices shows potential for sequestering soil carbon (SOC) and producing negative emissions. However, further research is needed to develop necessary technologies and better estimate costs and life-cycle emissions under large-scale deployment[28] . Three promising technologies are the application of biochar to cropland soils, deployment of perennial grain crops, and adoption of annual crops with deeper and larger root systems for enhanced C inputs[3] . Biochar is a carbon-rich solid produced from biomass using a thermochemical conversion process known as pyrolysis[34] . Biochar can increase SOC stocks and improve soil fertility and crop yields [35]. Moreover, biochar is a natural constituent of many soils and does not impair soil function, making it an attractive option for sequestering SOC[36] . However, the efficacy of biochar application depends on factors such as feedstock selection, pyrolysis conditions, and soil type[34]. Perennial grain crops, such as Kernza, have deep root systems that can sequester more carbon in the soil compared to annual crops . These crops can also reduce soil erosion, enhance water quality, and provide other ecosystem services[37] . However, the widespread adoption of perennial grain crops requires overcoming technical, economic, and policy barriers [38]. Finally, annual crops bred to produce deeper and larger root systems also have the potential to sequester more SOC [38]. However, their effectiveness in sequestering SOC under different soil and climate conditions needs further

Dhruv Y Haldaria and Hiren K.Patel

investigation [38]. The use of biochar, perennial grain crops, and enhanced root annual crops offer potential for sequestering SOC and producing negative emissions. However, further research is needed to optimize these practices and overcome technical, economic, and policy barriers to large-scale deployment. According to [39] and [40], biochar amendments can impact soil C storage and net CO_2 removals from the atmosphere in three different ways. First, biochars produced as a coproduct of biofuel pyrolysis processes are highly resistant to microbial decay, resulting in a long mean residence time of 100s of years or more. As a result, the biochar itself represents a carbon stock that persists for a long time when added to soil. Secondly, biochar additions can interact with the native organic matter already present in soils, either stimulating or reducing the rate of decomposition of the native soil organic matter. These interactions can involve several factors, including impacts on soil water holding capacity, soil moisture, changes in pH or nutrient availability, and direct impacts on microbial community activity and composition. Although both positive and negative effects on native SOM decomposition have been found[40] (e.g., [41], in most cases, these effects on the long-term soil C balance are small[40] . Finally, biochar additions can influence plant productivity and hence C inputs to the soil in the form of plant residues.[42] found that biochar additions generally have neutral or positive effects on plant growth, with small increases on average (typically <10%) in temperate cropping systems and larger increases (e.g., 10–25%) in tropical systems, particularly on acid, nutrient-poor soils. Apart from impacts on soil C storage,[43]reported that biochar amendments may decrease soil N_2O emissions, contributing to greenhouse gas mitigation. The meta-analysis reported average reductions of N_2O emissions of 9–12%. However, the study by[44] suggested greater average reductions of almost 50% compared to non-biochar amended soils. The differences in these meta-analyses are due to different selection criteria for the studies included and the weighting factors used. Nevertheless, there is an emerging consensus that biochar applications help to reduce N_2O emissions. The exact mechanisms involved are uncertain since the presence of biochar can impact the controls on nitrification and denitrification processes, such as pH, mineral N concentrations, soil moisture, and O_2 concentrations.

DEPLOYMENT OF PERENNIAL GRAIN CROPS

Over the last 30 years, there has been a focus on developing perennial cereal grains and other annual crops with a perennial growth habit to improve soil health and reduce environmental impacts. Perennial grasses, such as intermediate wheatgrass, have been selected for breeding due to their deep and extensive root systems, which allocate a higher proportion of dry matter belowground compared to conventional annual crops. This leads to increased carbon inputs to the soil, supporting greater soil organic carbon (SOC) stocks and reducing the negative effects of tillage and erosion. Moreover, the deeper and larger root systems can decrease nitrate leaching losses and possibly reduce N_2O emissions.[37, 45] While there are few long-term experiments to document the impact of perennial grain crops on SOC, results from long-term studies and chronosequences of perennial grass systems provide a reasonable proxy. Culman*et al.* (2013) found that intermediate wheatgrass increased labile soil C after four years, but there was no significant increase in total SOC compared to annual winter wheat. In contrast, various managed perennial grassland systems have shown significant rates of SOC change following conversion from annual cropland .Terrestrial soils have three times the stock of carbon in the atmosphere, so small changes in SOC can have a significant impact on climate change. Microorganisms play an essential role in SOC turnover, promoting the formation of macro-aggregates to physically protect carbon and contributing to a stable source of carbon. Simultaneously, microbe-driven soil C decomposition plays a critical role in C cycling, with over half of the cumulative CO_2-C emitted from soil induced by microbial community[46, 47].

Soil organic matter (SOM) is synthesized or degraded by soil enzyme activity, which is closely linked to CO_2 production [48]. Therefore, it is of utmost importance to understand the contribution of microorganisms and enzymes to the accumulation or consumption of SOM in soil for regulating soil carbon (C) and reducing the impact of CO_2 on the climate system[49]. Despite the direct role of microbe-driven decomposition in soil C cycling, the contribution of microorganisms to C turnover is often overlooked in C cycle prediction . Maintaining high richness and diversity of soil microorganisms is critical to mediate C cycling. However, there is less consistency in the research regarding soil microbiological properties, such as soil microbial diversity, microbial community, and enzyme activity[50] .Microorganisms, such as bacteria and fungi, are the most abundant in soil systems and have

Dhruv Y Haldaria and Hiren K.Patel

been reported to facilitate C cycling through increasing metabolic actions and bonding organic particles together or stimulating root secretion of SOM[51, 52]. Some studies found that bacteria contribute to SOM storage more greatly than fungi in the rice and wheat system (Chen *et al.*, 2018). In contrast, arbuscular mycorrhizal (AM) fungi have been thought not to be very important in C decomposition[53] . Both microbial biomass C and diversity are suspected to play a crucial role in influencing the SOM pool [53]. Another study found that microbial biomass had a significant influence on soil C cycling rather than its community composition under manure application . Additionally, soil enzymes, produced by soil microorganisms, are reported to regulate the overall processing of SOM through degrading different molecules or depolymerizing macromolecular substrates. Some enzymes (e.g., β-Glucosidase and β-Xylosidase activities) show a strong relationship with SOM content and are generally reported to be good indicators of soil biological change[5]. Despite the complexity of SOM-related mechanisms, most studies have focused on a single factor, with fewer focused on multiple factors regulating SOM[46]. Moreover, the potential mechanisms by which microbiological properties are linked to C regulation are often ignored [54].

ANALYSIS OF ENZYME ACTIVITY

The present study estimated the activities of four soil enzymes: β-Glucosidase (BG), β-Xylosidase (BXYL), N-acetyl-glucosaminidase (NAG), and leucine aminopeptidase (LAP) following the methods of previous studies[5]. To determine the activities of all enzymes, 4-Methyllumbelliferyl (MUB) and 7-amino-4-methylcoumarin (AMC) were used as substrates for BG, BXYL, NAG (MUB), and LAP (AMC). The study involved mixing 1 g of fresh soil with NaHCO3 buffer (pH = 8) and stirring at 800 rpm for 2.5 min, transferring the slurry into 96-well microplates, adding substrates, and incubating in the dark for 3 h at 25 ∘C. Fluorescence was detected using a multilabel fluorescence reader (Tecan Infinite F200/M200). Phospholipid fatty acids (PLFA) were measured to calculate the soil microbial biomass and diversity following the method described in previous research [55]. Fatty acid methyl esters (FAME) were identified by Gas Chromatograph Agilent Series and calculated by MIDI microbial identification system. Our findings suggest that alterations in microorganism community (i.e., fungal and AM biomass and F/B ratio) and enzyme activities (BXYL and LAP) contribute greatly to C storage in macro-aggregates (>0.25 mm), rather than microbial diversity[5][55].

Moreover, our study indicates that the contribution of microbial processes to C accumulation depends not only on the aggregate size but also on the variety of microbial properties and their interrelationships under different fertilization regimes. The combined application of organic and inorganic fertilizer increased the microbial contribution to C storage compared to inorganic fertilization. Therefore, it is important to use organic matter application to reduce the negative impact of inorganic fertilizers on soil flora while maximizing soil C accumulation in agroecosystems[55].

Future Perspectives on the Significance of Soil Enzymes in Carbon Sequestration

The role of soil enzymes in carbon sequestration has gained significant attention in recent years due to their potential as a sustainable strategy for mitigating climate change. Soil enzymes play a crucial role in the decomposition and transformation of organic matter, affecting soil carbon dynamics and influencing the long-term storage of carbon in terrestrial ecosystems. This review explores the future prospects and research directions regarding the significance of soil enzymes in carbon sequestration, highlighting the potential implications for climate change mitigation.

Advanced Enzyme Characterization Techniques

Future research should focus on the development and application of advanced enzyme characterization techniques to gain a comprehensive understanding of the functional diversity and activity of soil enzymes involved in carbon sequestration. Techniques such as metagenomics, metatranscriptomics, and proteomics can provide insights into the composition and functioning of soil enzyme communities, enabling researchers to identify key enzymes and their roles in carbon cycling processes. References[56].

Dhruv Y Haldaria and Hiren K.Patel

Enzyme Engineering for Enhanced Carbon Storage

Exploring the potential of enzyme engineering offers promising avenues for enhancing carbon storage in soils. By manipulating enzyme properties, such as substrate specificity, activity, and stability, it is possible to optimize enzymatic processes involved in carbon sequestration. This approach can lead to the development of novel enzymes or enzyme variants with improved performance in degrading recalcitrant carbon compounds, accelerating organic matter decomposition, and facilitating carbon stabilization in soils. References [57][58].

Microbial Interactions and Enzyme Synergies

Future research should focus on unraveling the complex interactions between soil enzymes and microbial communities involved in carbon sequestration processes. Understanding the synergistic effects and feedback mechanisms between enzymes and microorganisms can provide insights into how microbial communities modulate enzyme activity, nutrient availability, and carbon dynamics. This knowledge can guide the development of targeted management strategies to enhance soil enzyme activity and promote carbon sequestration. References[59].

Climate Change Feedbacks and Soil Enzyme Function

Investigating the impact of climate change on soil enzyme activity and function is essential for predicting future carbon sequestration potentials. Elevated temperatures, changing precipitation patterns, and altered microbial community dynamics can influence the activity and stability of soil enzymes, potentially affecting carbon turnover rates and the overall capacity of soils to sequester carbon. Integrating climate change scenarios into experimental studies and modeling approaches can help elucidate these complex feedbacks and improve predictions of carbon sequestration potential under future climate conditions. References [60].

CONCLUSION

The significance of soil enzymes in carbon sequestration holds immense potential for climate change mitigation. Advancements in enzyme characterization techniques, enzyme engineering, understanding microbial interactions, and accounting for climate change feedback are critical for harnessing the full capacity of soil enzymes in carbon storage. By integrating these research avenues, we can develop innovative strategies to enhance soil enzyme activity, promote carbon sequestration, and contribute to sustainable land management practices in the face of climate change.

REFERENCES

1. Han, L., *et al.*, *Mobilization of ferrihydrite-associated organic carbon during Fe reduction: adsorption versus coprecipitation.* Chemical Geology, 2019. 503: p. 61-68.
2. Lal, R., *Soil carbon management and climate change.* Carbon Management, 2013. 4(4): p. 439-462.
3. Lal, R., *Soil carbon sequestration to mitigate climate change.* Geoderma, 2004. 123(1-2): p. 1-22.
4. Baldrian, P., *Fungal laccases–occurrence and properties.* FEMS microbiology reviews, 2006. 30(2): p. 215-242.
5. Sinsabaugh, R.L., B.H. Hill, and J.J. Follstad Shah, *Ecoenzymatic stoichiometry of microbial organic nutrient acquisition in soil and sediment.* Nature, 2009. 462(7274): p. 795-798.
6. Hayasaka, Y., *et al.*, *Assessing the impact of smoke exposure in grapes: Development and validation of a HPLC-MS/MS method for the quantitative analysis of smoke-derived phenolic glycosides in grapes and wine.* Journal of Agricultural and Food Chemistry, 2013. 61(1): p. 25-33.
7. Batjes, N.H., *Total carbon and nitrogen in the soils of the world.* European journal of soil science, 2014. 65(1): p. 10-21.
8. Falkowski, P., *et al.*, *The global carbon cycle: a test of our knowledge of earth as a system.* science, 2000. 290(5490): p. 291-296.
9. Schlesinger, W.H. and J.A. Andrews, *Soil respiration and the global carbon cycle.* Biogeochemistry, 2000. 48: p. 7-20.

10. Smith, P., *et al.*, *Global change pressures on soils from land use and management.* Global change biology, 2016. 22(3): p. 1008-1028.

11. Sokol, N.W. and M.A. Bradford, *Microbial formation of stable soil carbon is more efficient from belowground than aboveground input.* Nature Geoscience, 2019. 12(1): p. 46-53.

12. Rousk, J., P.C. Brookes, and E. Bååth, *The microbial PLFA composition as affected by pH in an arable soil.* Soil Biology and Biochemistry, 2010. 42(3): p. 516-520.

13. Crowther, T.W., *et al.*, *Quantifying global soil carbon losses in response to warming.* Nature, 2016. 540(7631): p. 104-108.

14. Bardgett, R.D. and T. Caruso, *Soil microbial community responses to climate extremes: resistance, resilience and transitions to alternative states.* Philosophical Transactions of the Royal Society B, 2020. 375(1794): p. 20190112.

15. Delgado-Baquerizo, M., *et al.*, *Soil microbial communities drive the resistance of ecosystem multifunctionality to global change in drylands across the globe.* Ecology letters, 2017. 20(10): p. 1295-1305.

16. Cotrufo, M.F., *et al.*, *The M icrobial E fficiency-M atrix S tabilization (MEMS) framework integrates plant litter decomposition with soil organic matter stabilization: do labile plant inputs form stable soil organic matter?* Global change biology, 2013. 19(4): p. 988-995.

17. Hagerty, S.B., *et al.*, *Accelerated microbial turnover but constant growth efficiency with warming in soil.* Nature Climate Change, 2014. 4(10): p. 903-906.

18. Davidson, E.A., I.A. Janssens, and Y. Luo, *On the variability of respiration in terrestrial ecosystems: moving beyond Q10.* Global change biology, 2006. 12(2): p. 154-164.

19. Ho, D., *et al.*, *High-rate, high temperature acetotrophic methanogenesis governed by a three population consortium in anaerobic bioreactors.* PloS one, 2016. 11(8): p. e0159760.

20. Neufeld, J.D., *et al.*, *Methodological considerations for the use of stable isotope probing in microbial ecology.* Microbial Ecology, 2007. 53: p. 435-442.

21. Bragina, A., *et al.*, *Sphagnum mosses harbour highly specific bacterial diversity during their whole lifecycle.* The ISME journal, 2012. 6(4): p. 802-813.

22. Whiteley, A.S., *et al.*, *RNA stable-isotope probing.* Nature Protocols, 2007. 2(4): p. 838-844.

23. DeAngelis, K.M., *et al.*, *Microbial communities acclimate to recurring changes in soil redox potential status.* Environmental microbiology, 2010. 12(12): p. 3137-3149.

24. Seifert, K.A., *Progress towards DNA barcoding of fungi.* Molecular ecology resources, 2009. 9: p. 83-89.

25. DeRito, C.M., G.M. Pumphrey, and E.L. Madsen, *Use of field-based stable isotope probing to identify adapted populations and track carbon flow through a phenol-degrading soil microbial community.* Applied and Environmental Microbiology, 2005. 71(12): p. 7858-7865.

26. Drigo, B., *et al.*, *Shifting carbon flow from roots into associated microbial communities in response to elevated atmospheric CO2.* Proceedings of the National Academy of Sciences, 2010. 107(24): p. 10938-10942.

27. Wagner, M., *et al.*, *Microbial community composition and function in wastewater treatment plants.* Antonie Van Leeuwenhoek, 2002. 81: p. 665-680.

28. Keith, P., *et al.*, *Climate-smart soils.* Nature, 2016. 532(7597): p. 49-57.

29. Ogilvie, J.E. and J.D. Thomson, *Site fidelity by bees drives pollination facilitation in sequentially blooming plant species.* Ecology, 2016. 97(6): p. 1442-1451.

30. Bartlett, K.H., *Appendix A Contributed Manuscripts.*

31. Hill, P.W., *et al.*, *Angiosperm symbioses with non-mycorrhizal fungal partners enhance N acquisition from ancient organic matter in a warming maritime Antarctic.* Ecology Letters, 2019. 22(12): p. 2111-2119.

32. Turland, N.J., *et al.*, *International Code of Nomenclature for algae, fungi, and plants (Shenzhen Code) adopted by the Nineteenth International Botanical Congress Shenzhen, China, July 2017.* 2018: Koeltz botanical books.

33. National Academies of Sciences, E. and Medicine, *sequestration of supercritical CO2 in deep sedimentary geological formations.* Negative Emissions Technologies and Reliable Sequestration: A Research Agenda, 2019: p. 273-281.

34. Lehmann, J. and S. Joseph, *Biochar for environmental management: science, technology and implementation.* 2015: Routledge.

35. Jeffery, S., *et al.*, *Biochar boosts tropical but not temperate crop yields.* Environmental Research Letters, 2017. 12(5): p. 053001.

63552

36. Glaser, B., *et al. Potential of pyrolyzed organic matter in soil amelioration.* in *12th ISCO conference'. Beijing.* 2002.

37. Glover, J.D., *et al., Increased food and ecosystem security via perennial grains.* Science, 2010. 328(5986): p. 1638-1639.

38. DeHaan, L., D. Van Tassel, and T. Cox, *Perennial grain crops: A synthesis of ecology and plant breeding.* Renewable Agriculture and Food Systems, 2005. 20(1): p. 5-14.

39. Valeur, B. and M.N. Berberan-Santos, *Molecular fluorescence: principles and applications.* 2012: John Wiley & Sons.

40. Wang, J., Z. Xiong, and Y. Kuzyakov, *Biochar stability in soil: meta-analysis of decomposition and priming effects. GCB Bioenergy 8: 512–523.* 2016.

41. Jonsson, U., *et al., Psychological treatment of depression in people aged 65 years and over: A systematic review of efficacy, safety, and cost-effectiveness.* PloS one, 2016. 11(8): p. e0160859.

42. Verdejo, J., *et al., Thresholds of copper toxicity to lettuce in field-collected agricultural soils exposed to copper mining activities in Chile.* Journal of soil science and plant nutrition, 2016. 16(1): p. 154-158.

43. Topal, A., *et al., Neurotoxic responses in brain tissues of rainbow trout exposed to imidacloprid pesticide: Assessment of 8-hydroxy-2-deoxyguanosine activity, oxidative stress and acetylcholinesterase activity.* Chemosphere, 2017. 175: p. 186-191.

44. Kaiser, S., *et al., Optical properties of a vibrationally modulated solid state Mott insulator.* Scientific reports, 2014. 4(1): p. 3823.

45. Lyu, X., *et al., Enhanced efficiency nitrogen fertilizers maintain yields and mitigate global warming potential in an intensified spring wheat system.* Field Crops Research, 2019. 244: p. 107624.

46. Six, J., *et al., Stabilization mechanisms of soil organic matter: implications for C-saturation of soils.* Plant and soil, 2002. 241: p. 155-176.

47. Liu, M., *et al., Microbial community structure and the relationship with soil carbon and nitrogen in an original Korean pine forest of Changbai Mountain, China.* BMC microbiology, 2019. 19: p. 1-14.

48. Lehmann, J. and M. Kleber, *The contentious nature of soil organic matter.* Nature, 2015. 528(7580): p. 60-68.

49. Evans, S.E. and M.D. Wallenstein, *Soil microbial community response to drying and rewetting stress: does historical precipitation regime matter?* Biogeochemistry, 2012. 109: p. 101-116.

50. Bastida, F., *et al., Differential sensitivity of total and active soil microbial communities to drought and forest management.* Global Change Biology, 2017. 23(10): p. 4185-4203.

51. Lange, M., *et al., Plant diversity increases soil microbial activity and soil carbon storage.* Nature communications, 2015. 6(1): p. 6707.

52. Waring, B.G., *et al., Pervasive and strong effects of plants on soil chemistry: a meta-analysis of individual plant 'Zinke'effects.* Proceedings of the Royal Society B: Biological Sciences, 2015. 282(1812): p. 20151001.

53. Bhattacharyya, S.S., *et al., Soil carbon sequestration–An interplay between soil microbial community and soil organic matter dynamics.* Science of The Total Environment, 2022: p. 152928.

54. Fierer, N., *et al., Comparative metagenomic, phylogenetic and physiological analyses of soil microbial communities across nitrogen gradients.* The ISME journal, 2012. 6(5): p. 1007-1017.

55. Frostegård, A. and E. Bååth, *The use of phospholipid fatty acid analysis to estimate bacterial and fungal biomass in soil.* Biology and Fertility of soils, 1996. 22: p. 59-65.

56. Thapa, S., *et al., Microbial cellulolytic enzymes: diversity and biotechnology with reference to lignocellulosic biomass degradation.* Reviews in Environmental Science and Bio/Technology, 2020. 19: p. 621-648.

57. Gargallo-Garriga, A., *et al., Root exudate metabolomes change under drought and show limited capacity for recovery.* Scientific reports, 2018. 8(1): p. 1-15.

58. Singh, M. and J. Pandey, *Alkaline phosphatase as a bio-indicator of phosphorus-eutrophy in freshwater ecosystems: A review.* International Journal of Sediment Research, 2022.

59. Houfani, A.A., *et al., Insights from enzymatic degradation of cellulose and hemicellulose to fermentable sugars–a review.* Biomass and Bioenergy, 2020. 134: p. 105481.

60. Soong, J.L., *et al., Five years of whole-soil warming led to loss of subsoil carbon stocks and increased CO2 efflux.* Science advances, 2021. 7(21): p. eabd1343.

Dhruv Y Haldaria and Hiren K.Patel

Table 1. microbial decomposers

Soil Enzyme	Significance in Carbon Sequestration	References
Cellulase	Breaks down cellulose in plant material, increasing soil organic matter and carbon sequestration	[2]
Protease	Breaks down proteins in plant and animal residues, increasing soil organic matter and carbon sequestration	*[3]*
Urease	Converts urea to ammonium, increasing plant growth and therefore carbon sequestration through increased photosynthesis	[3]
Laccase	Oxidizes lignin in plant material, increasing soil organic matter and carbon sequestration	[4]
Amylase	Breaks down starch in plant material, increasing soil organic matter and carbon sequestration	[5]

RESEARCH ARTICLE

Real Time Emotion Recognition Using Convolutional Neural Networks

G.S.K.Gayatri Devi[1]*, L.Sailaja[2], P.Kiran[3], B.Priya[3] and G.Govardhan Raju[3]

[1]Professor, ECE Department, Malla Reddy Engineering College, Secunderabad-500100, Hyderabad, India
[2]Assistant Professor, ECE Department, Malla Reddy Engineering College, Secunderabad-500100, Hyderabad, India
[3]B.Tech, Malla Reddy Engineering College, Secunderabad-500100, Hyderabad, India

*Address for Correspondence
G.S.K.Gayatri Devi
Professor, ECE Department,
Malla Reddy Engineering College,
Secunderabad-500100, Hyderabad, India

ABSTRACT

Human emotion detection plays very important role in like Artificial Intelligence particularly in the field of image processing, machine learning etc. The human voice presents vaarious emotions which is an indication of what is going on in mind. Real time emotion recognition is to train the machine to identify and process human emotions. The different modulations which occur in our voice reflects various states of the person. In this paper, a voice input is used to identify the state of person into one of seven predefined emotions by building a multi class classifier. Convolutional neural networks (CNNs) are used for training over voice inputs. Various experiments are conducted with different depths and layers to improve accuracy. The authors present the real-time implementation of emotion recognition which provides accurate results for multiple voice inputs. The results obtained from the research are rather appealing.

Keywords: CNN, Deep learning, Human Emotions, Neural network

INTRODUCTION

Emotion detection from speech [1] or audio is a challenging problem in audio signal processing. A person's characteristics like age, gender, his mental state can be found out from his voice. Recognition of a person's emotion is one among the above. It is completely known fact that the human's speech encloses linguistic content, identity as well as the emotion of speaker. Human emotion plays a major role in daily human interactions. It helps in understanding the feelings of others and also helps others in understanding our feelings. Speech is one such important human emotion. Human- Technology interface is significant in both the quantitative and qualitative

63555

terms. The emotional state and body language of a person can be obtained from Speech communication. Although an enormous effort is invested in recognizing the emotions of a person from speech but still much research is needed. Emotions are universal but their understanding, interpretation and sections are particular and partly culturally specific. Based on the art survey of results in emotion detection, we decided to implement the emotion detection from voice, as most appropriate in the context of application intended. There are many applications to detect the emotion of the persons like in audio surveillance, web-based E learning, and commercial applications, clinical studies, and entertainment etc. Emotion identification can be used as a voice tag in different database access systems. This voice tag is used in telephony shopping, and ATM machine as a password for accessing that particular account. Human emotion recognition is widely gaining more popularity as a research topic. Emotion recognition systems have numerous potential applications, including mental health diagnosis, human- robot interaction, and marketing research. One popular approach to emotion recognition is to use facial expression analysis, where CNNs are trained to detect and classify facial expressions associated with different emotions. Researchers have explored different CNN architectures and training strategies to optimize the performance of these systems.

Zadeh, Milad *et. al.*[2] presented a deep learning based framework for human emotion detection. The framework proposed makes use of the Gabor filters for feature extraction and then the deep CNN. The results depict that the speed and accuracy of training the neural network cabn be increased by the proposed features. Rashid, Munaf *et. al.* [3] presented the design of human emotion recognition system based on sound and spatio-temporal characteristics. The system proposed conducted tests for both genders on audio visual emotion data set.The simulations and results showed that only 74.15 % accuracy can be obtained from visual features alone. An accuracy of 67.39% can be obtained from audio features alone. A significant accuracy of 80.27% can be obtained by mixing both audio and video features. Katsigiannis *et. al.* [4] presented a multimodal database containing EEG and ECG signals which are recorded during affect elicitation using audio-visual stimuli. Anurag Jain *et al.* [5] introduced an algorithm for conversion of emotions. This algorithm needs a database of neural utterances while these can be used for deriving other expressive style utterances. The algorithm proposed relies on linear modification model. Kumar et. al. [6] presented a new approach to envisage human emotions using CNN and to indicate the emotion intensity on a human face.

Salunkeet *et.al.* [7] proposed an artificially intelligent system which can use facial expressions to recognize human emotions. The proposed network has three Convolutional layers which is followed by max pooling and ReLU. Ruiz-Garcia *et. al* [8] provided a deeply-trained model which uses facial expression images for human emotion recognition. Investigational results were presented. Kartali *et. al.*[9] gave an evaluation of five different approaches for four basic human emotion recognition. A comparison of three deep-learning approaches based on CNN and two conventional approaches were given. In [10], Verma *et. al.* proposed a new architecture named Venturi Architecture and evaluated its performance in terms of training accuracy, testing accuracy, training loss and testing loss. Subramanian *et.al* in [11] discussed about the application of emotion recognition where seven different emotions such as happy, sad, neutral, angry, surprise, fear and disgust are obtained. A new hybrid based method was introduced by Rahul *et. al* [12] based on RNN and CNN. These achieved good results by retrieving some parts of the database. The available literature shows that very few works on human emotion recognition based on voice input have been reported earlier. The present work aims to develop a real-time emotion recognition system based on convolution neural networks (CNN's).

MATERIALS AND METHODS

The system is divided broadly into data set formation; pre-processing, feature extraction and classification. MatLab R2014a version is used for programming the system. The Roberson Audio-Visual Database of Emotional Speech and Song (RAVDESS) [1], which consisted of both male and female speech audio samples was used to test for 3 emotions-angry, happy and sad. As a first step, the audio database is divided into two sets namely training and testing sets. Each signal from both the sets is pre processed to make it suitable for data gathering and analysis. In succession, the

features are extracted from the preprocessed signal. The feature vectors are the input to the multi class support vector machine (SVM) classifier which forms a model corresponding to every emotion. Then the test signal is subjected to testing with every model so as to categorize and find out its emotion. Figure 1 shows the recognition model.

Proposed System

Implementation of the DWT

There are several ways to implement DWT. The most straightforward approach is to implement the filters in a Laguerre network (considering first order all-pass filters, A(z),which are reset every N samples). In the second approach, we can implement the filtering by a matrix-vector multiplication in two steps: first we divide the all-pass IIR transfer functions into N terms, and then sample the frequency responses of the warped filter bank to obtain the DWT matrix through an inverse discrete Fourier transform (IDFT).

The second approach is used here which acts as filter bank for an N-tap Finite impulse response filter. Here the inner multiplication of input vector and filter coefficient vector represents the filtering and decimation by N. From Parseval's relation, this is again equal to the inner product of the conjugate DFT of the input and the DFT of the filter coefficients, which is equal to the sampled value of Fk(ejw) for w = (2pk=N) where k = 0;1; :::;N -1: Similarly, we can approximate the result of the filtering with Fk(A(ejw)) as the inner product of the input vector and the IDFT of the sampled sequence of More detailed description about the DWT and its implementations can be found below.

Applying for Speech enhancement:

$$Y_k(t) = X_k(t) + N_k(t), \qquad k = 0, 1, \cdots, M-1$$

A noise signal is assumed to be added to speech signal x. The resulting signal is represented with y. Taking the DWT gives us,

where k denotes the kth the frequency bin, M is the total number of frequency components, and t is the frame index in the time domain, respectively. Given a frame of noisy speech signal, the basic assumption adopted in a speech enhancement approach could be described by the following hypotheses:

The frequencies of these formants are controlled by modifying the shape of the tract. This, for example, could be done by changing the tongue position. An important part of many speech coders and decoders, is the modeling of the vocal tract as a short term filter. The transfer function of vocal tract modeling filter requires to be updated only if it's shape changes. The excitation to the vocal tract filter can be given by forcing air through the vocal cords. Based on their excitation mode, speech sounds can be divided into three types. Sounds are produced when flow of air from lungs to vocal tract is interrupted and this produces air pulses as input. Pitch of the sound can be given as the rate at which opening and closing takes place. By varying the shape of cords, tension in the cords and air pressure behind the cords, pitch can be varied. A high amount of periodicity can be observed which varies between 2ms and 20ms.

This section describes the methodology proposed in this study. This study starts with inputting the real-time voice, followed by the implementation of Convolutional Neural Network (CNN) for recognizing the emotion. Succeeding, the recognized emotion will be displayed. The proposed flowchart in this study is as shown in fig.2. CNN is deep learning based approach which can get high accuracy in recognition. Table 1 show the analysis conducted during training process. The purpose of this analysis is to find the best ratio for dividing the images. The images used for testing the accuracy of application are 80 audio signals. A total number of 80 audio signals have been used during the accuracy testing conducted. From Table 2, there exists a FALSE result to indicate the application is wrongly recognize the emotion. The reason of obtain false result is because the application failed to recognize the correct emotion based on the input voice. For example, the expected result should be sad, but the application recognizes it as happy. Hence, the similarities of the voice cause the application a false result. To conclude overall accuracy performance, the average accuracy is calculated. Equation 1 shows the formula for accuracy calculation.

A=(N/T)*100%   (1)

Where A= Accuracy

N=Number of correct predictions

T=Total number of all cases

Gayatri Devi *et al.*,

Here, the numerator indicates prediction predicted by the application, the denominator indicates number of images that were tested. The quotient is multiplied with 100% to get the percentage of accuracy. In this work, the total accuracy is reported to be 85%.

RESULTS AND DISCUSSION

The results are simulated using Matlab software. Figure 3 shows the GUI window displayed showing options for inputting voice signal. To use the program, the user would select the "Browse" option to select an input voice file. This is depicted in figure 4. Once the file is selected, the program displays it in signal form, which may be a graphical representation of the sound wave. The "preprocess" allows many preprocessing functions like filtering, noise reduction etc. to be performed to improve the accuracy of the voice recognition. The "DWT Features" option likely extracts features from the signal using Discrete Wavelet Transform (DWT), which can be used as inputs for the neural network. The "Database" option likely allows the user to access a database of previously trained data to compare against the input signal. The "NN Training" option likely allows the user to train the neural network on a dataset. Finally, the "Classifier" option likely applies the trained neural network to classify the input signal and provide a voice recognition output.

"Preprocess" option in the user interface window allows applying a filtering algorithm to the input signal. This filtering step likely helped to remove unwanted noise or interference from the signal, making it easier to extract useful features for voice recognition. The step "filtering" is important because it helps in improving accuracy and reliability of further stages. By eliminating noise and other unwanted signals, the filtering step can help to reveal the underlying patterns and features in the input signal that are relevant for the task at hand. Figure 5 shows about DWT. It is a powerful signal processing tool that can be used to analyze and extract features from signals. DWT decomposes a signal into a series of wavelet coefficients at different scales and positions, which can be used to identify important features or patterns in the signal. After applying the DWT to the preprocessed signal, the program likely displayed a wavelet transform signal, which is a graphical representation of the wavelet coefficients at different scales and positions. This signal can provide valuable information about the underlying features and patterns in the signal that are relevant for voice recognition.

Features
Input Voice Signal Features:3.3711e+06
Input Signal Features:
DWT:
Maximum Signal Level:0.6744
Minimum Signal Level: -1.0471
Avg Signal Level: 3.6577e-04
Peak Level:0.6744
Median Filter Signal Level:0.0209
Standard Deviation: 0.0687
Histogram : -3.3712e+06
Entropy Level:3.4420
Zero Crossing Rate: 0.0151
Fundamental Energy Level:19.3565
Loading option allows signal to be loaded into database. This helps in storing and organizing data for speech recognition applications. The screenshot is shown in figure 6.The database can be used to store information about the signal, such as its features, labels, or other metadata, which can be used to train and test voice recognition models.

Figure 7 shows NN training. NN training is a critical step in building an effective voice recognition system. During training, the NN algorithm learns to recognize patterns and features in the input signal that are associated with specific words or phrases. The weights and biases of the network can be adjusted to minimize errors between actual predicted values. The training process is time consuming mainly depending on qmount of data and complexity of architecture employed. NN-based systems can achieve high accuracy. The classifier is also a trained ML algorithm which predicts the emotion based on given voice input. The classifier uses the features extracted from the DWT transform and the preprocessed signal to make its prediction. The classifier program runs and displays the predicted emotions like **"happy", "sad", "angry", or "neutral"**. The screenshot is shown in figure 8.

CONCLUSION

A human emotion recognition system based on voice input using CNN is presented. The application is able to recognize four types of emotions which are happy, sad, normal, and disgusting. The Convolutional Neural Network (CNN) used the Mobile Net algorithm with a custom dataset and evaluated using a confusion expression is a valuable expression that portrays human. The developed application achieved an average accuracy of 92.50% in term of the sensitivity and specificity, it able to achieve 85.00% and 95.00% respectively. Hence, the implementation of CNN in recognizing emotion successfully achieved promising results and could be able to contribute to the succession work in CNN. In future the addition of CNN with any Artificial Intelligence method can be carried for further improvement in performance.

REFERENCES

1. Koolagudi, Shashidhar G., and K. SreenivasaRao. "Emotion recognition from speech: a review." *International journal of speech technology, vol.* 15, pp. 99-117,2012.
2. Zadeh, Milad Mohammad Taghi, Maryam Imani, and BabakMajidi. "Fast facial emotion recognition using convolutional neural networks and Gabor filters." *2019 5th Conference on Knowledge Based Engineering and Innovation (KBEI)*. IEEE, 2019.
3. Rashid, Munaf, S. A. R. Abu-Bakar, and Musa Mokji. "Human emotion recognition from videos using spatio-temporal and audio features." *The Visual Computer,* vol.29,pp. 1269-1275,2013.
4. Katsigiannis, Stamos, and NaeemRamzan. "DREAMER: A database for emotion recognition through EEG and ECG signals from wireless low-cost off-the-shelf devices." *IEEE journal of biomedical and health informatics,* vol.22, No.1,pp. 98-107,2017.
5. Jain, Anurag, S. S. Agrawal, and NupurPrakash. "Transformation of emotion based on acoustic features of intonation patterns for Hindi speech and their perception." *IETE Journal of Research,* vol. 57, No.4, pp. 318-324,2011.
6. G. A. R. Kumar, R. K. Kumar and G. Sanyal, "Facial emotion analysis using deep convolution neural network," 2017 International Conference on Signal Processing and Communication (ICSPC), Coimbatore, India, 2017, pp. 369-374, doi: 10.1109/CSPC.2017.8305872.
7. Salunke, Vibha V., and C. G. Patil. "A new approach for automatic face emotion recognition and classification based on deep networks." *2017 International Conference on Computing, Communication, Control and Automation (ICCUBEA)*. IEEE, 2017.
8. Ruiz-Garcia, Ariel, *et al.* "Deep learning for emotion recognition in faces." *Artificial Neural Networks and Machine Learning–ICANN 2016: 25th International Conference on Artificial Neural Networks, Barcelona, Spain, September 6-9, 2016, Proceedings, Part II 25*. Springer International Publishing, 2016.
9. Kartali, Aneta, *et al.* "Real-time algorithms for facial emotion recognition: A comparison of different approaches." *2018 14th Symposium on Neural Networks and Applications (NEUREL)*. IEEE, 2018.
10. Verma, Abhishek, Piyush Singh, and John Sahaya Rani Alex. "Modified convolutional neural network architecture analysis for facial emotion recognition." *2019 international conference on systems, signals and image processing (IWSSIP)*. IEEE, 2019.

11. Subramanian, R. Raja, *et al.* "Design and evaluation of a deep learning algorithm for emotion recognition." *2021 5th International Conference on Intelligent Computing and Control Systems (ICICCS).* IEEE, 2021.
12. Rahul, Mayur, *et al.* "A New Hybrid Approach for Efficient Emotion Recognition using Deep Learning", *IJEER* ,vol.10, No.1, pp. 18-22,2022.

Training the CNN model:
Table 1:Analysis of Training Process

	Splitting images (%)	Accuracy (%)	Loss (%)	Error Rate	Error Rate (%)
Train	**90**	**94**	**53**		
Test	**5**	**80**	**94**	**9/46**	**19.56**
Validation	**5**	**84**	**66**		
Train	80	94	54		
Test	10	78	79	19/91	20.87
Validation	10	89	66		
Train	70	93	53		
Test	15	78	79	28/100	28
Validation	15	79	79		
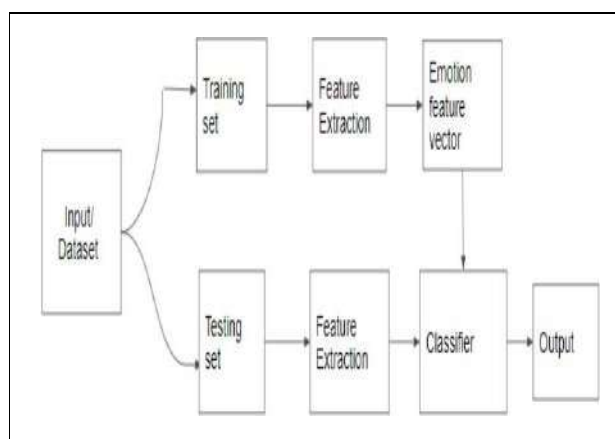
Figure 1: Recognition Model	**Figure 2.Proposed flow chart**
Figure 3:GUI Window	**Figure 4:Browse the Input signal**
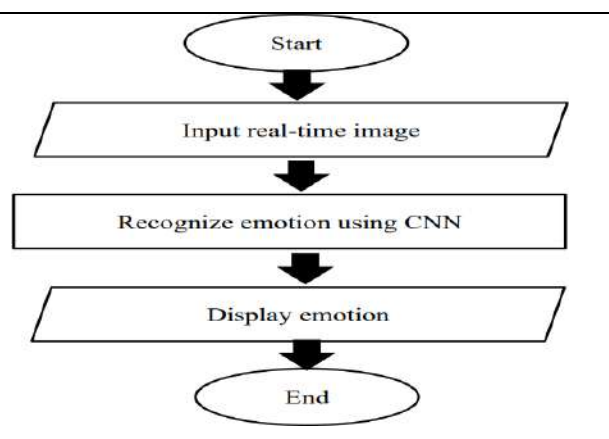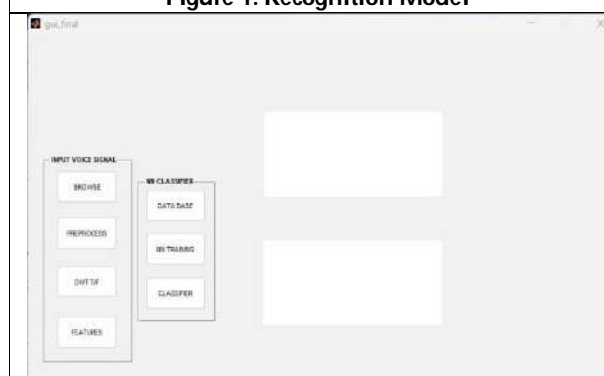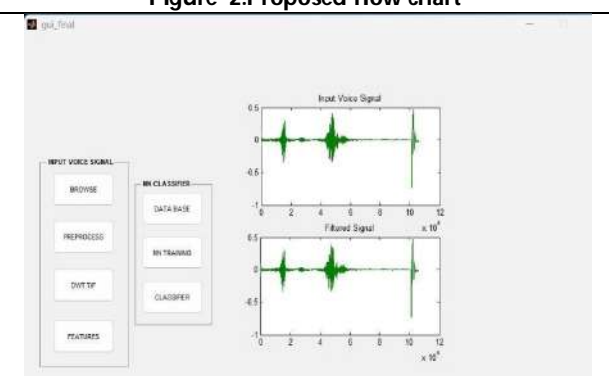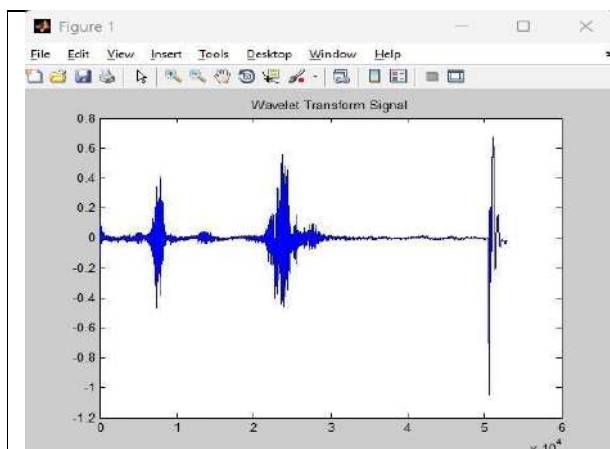
Figure 5: Wavelet Transform Signal
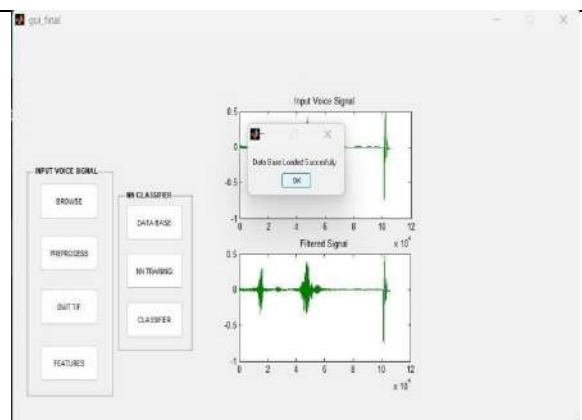
Figure 6: Database
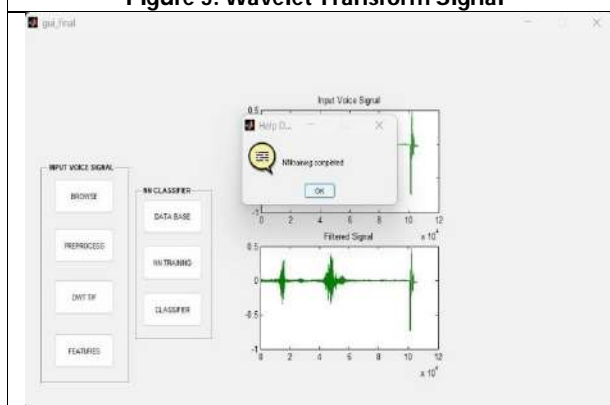
Figure 7: NN Training
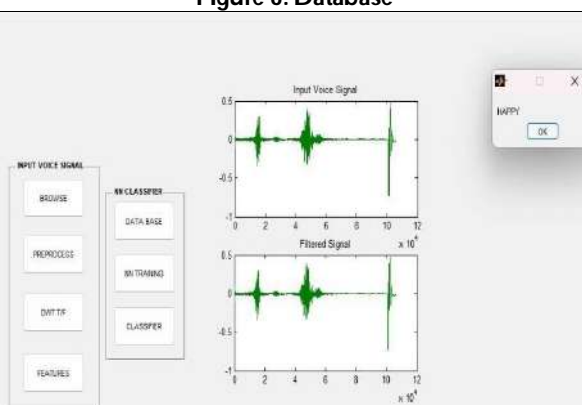
Figure 8: Classifier gives result

RESEARCH ARTICLE

A Novel Mathematical Approach for an Automated Estimation Strategy in Obstetrics using Image Processing Techniques

P.Sheeba Ranjini[1]* and T.Hemamalini [2]

[1]Department of Science and Humanities, Sri Krishna College of Technology, Coimbatore, Tamil Nadu, India
[2]Department of Mathematics, Government Arts College (Autonomous), Coimbatore, Tamil Nadu, India

*Address for Correspondence
P.Sheeba Ranjini
Department of Science and Humanities,
Sri Krishna College of Technology,
Coimbatore, Tamil Nadu, India.

ABSTRACT

Image processing is the projection of object within the human body. The advancement in computing methodologies has led to development of efficient image processing techniques, which are useful in medical diagnosis, treatment planning and research. In clinical diagnosis, segmentation of objects in medical images is a critical task due to noise and varying resolution of objects. A better segmentation can be achieved by integration of useful data from separate images. In this study, an involuntary technique to identify accessible segments through the biparietal plane of the fetal head and the fetal femur in ultrasound images is developed. Once the accurate anatomical segment for measurement is identified by the machine, the placement of the measurement calipers is automatically determined by fitting an active contour model to the structure of interest. The fetal femur length (FL) and biparietal diameter (BPD) are then calculated automatically. The validation data set contained 167 BPD and 197 FL B-mode images extracted using four ultrasound scanners, resulting in varied image quality and gain settings. The mean gestational age (GA) of the fetuses was 20 weeks, ranging from 16 to 41 weeks. A dimension success rate of 90% was achieved for both BPD and FL. The correlation coefficients between the manual and automated measurements were 0.995 (BPD) and 0.967 (FL);mean errors were -1.7 mm (FL) and 0.5 mm (BPD); and error range with 95% confidence interval (CI) was -3.8 to 4.8 mm (BPD) and -11.4 to 8.1 mm (FL). Furthermore, the routine dimension results were consistent in both high- and low-gain settings. The intraclass correlation coefficients between manual and routine measurements were 0.995 (95% CI: 0.981–0.999) for BPD in high-gain, 1.0(95%CI: 0.998–1.0)for BPD in low-gain, 0.998 (95% CI: 0.991–0.999) for FL in high-gain, and 0.999 (95% CI: 0.996–1.0) for FL in low-gain settings. The method was implemented on a portable ultrasound machine designed to be used in low- and middle-income countries. The overall performance of the method supported our hypothesis that automated methods can be used, and are beneficial, within clinical settings.

Keywords : Image Processing, Biparietal Diameter, Femur Length, Portable Ultrasound Machine, Automatic Measurement

INTRODUCTION

An ultrasonography scanning in pregnancy has become common practice in rich countries (RC). It begins from 12th to 18th week, or both. The primary aim of the ultrasonography investigation is to identify the position of the placenta and embryo, number of fetuses, gestational age (GA), evaluated day of delivery (EDD), and anomalies that act as a foundation for further medical administration of fetal. The benefits of using ultrasonography in pregnancy care are crucial in poor countries (PC) as in the RC In PC, inaccurate dating, high rate of fetal growth restriction, and limited detection of twins before delivery are common factors. Although, the use of ultrasonography in PC may be not as extensive as in RC due to many reasons. A significant number f ultrasonography machines enhanced for use in RC may be too sensitive to harsh conditions present in PC. Because of changes in the sources of power and voltage fluctuations, huge shifts in transportation conditions, humidity and temperature, dusty environments, vibration and shock, critical parts break down and cannot be repaired. Another significant challenge is the high cost of ultrasonography machinery. In addition, in the rural regions of PC, there is a lack of technical awareness required for operating ultrasonography machines. Our research team is presently working on developing a prototype of a portable, affordable, and user-friendly ultrasonography machine based on a tablet (Figure 1).

To lesser level the usability device threshold, we are in the process of automating as many portions of the manual estimation methods as possible and implementing them on the proposed machine. We hypothesize that automated estimation processes, combined with a minimalistic user interface (UI), will facilitate the adoption of ultrasonography in PC (Figure 1(b)). With this UI, the functionalities found in conventional ultrasonography machinery are carried out by simple touch interactions. For example, the examine depth will be adjusted by a pinch-zoom gesture on the screen. The cine loop playback is performed by sliding a finger from left to right on the screen. The estimation position calipers can be effortlessly adjusted by drag gestures and additional functions are accessed via side buttons. The anticipated outcome is a robust and inexpensive ultrasonography machine with a satisfactory picture quality, which will be used in PC by personnel with limited technical knowledge. The assessment of GA is vital but frequently absent in PC. It is used to predict the EDD, monitor fetal development, and refine clinical management association with premature delivery and full-term pregnancies. To ascertain GA and EDD, biparietal diameter (BPD) and fetal femur length (FL) are regularly used and well-documented parameters. Usually, these are measured manually by ultrasonography-trained midwives, sonographers, radiographers, or doctors. The fetal dating methodology requires precise positioning of the ultrasonography machine to capture anatomic landmarks and alignment of measurement markers. The estimations are prone to both intra-and inter observer variability. To minimize errors, the measurement procedure is repeated multiple times (typically three) and the mean or maximum value is recorded. Proper adjustment of the picture acquisition setting is vital to acquiring consistent results. Improper setting, whether too high or too low can significantly influence the FL and BPD estimation, consequently affecting the calculated GA. Various methods, ranging from semi-automatic to fully automatic, have been proposed to enhance the accuracy of BPD and FL estimations and stream line the fetal dating procedure. However, none of these methods have been tailored for use with portable ultrasonography machines. The aim of this study was to develop and implement an automated method to identify specific plane across the fetal head and femur, and subsequently measure FL and BPD. The method was designed to run on an off-the-rack tablet with limited computational power. Hence, it could be effortlessly integrated to a compact ultrasonography machine. Another aim was to simplify the technical adjustments in image acquisition settings.

MOTIVATION

The project's motivation arises from the most recent advancements in clinical operations, medical industries, and small-sensor technology, which have provided base frameworks for enhancing efficient and flexible systems. They provide potential for flexible use and scalability of framework. The raspberry Pi has emerged as a perfect essential for such a framework. There are numerous realistic uses for fetal monitoring, for example, monitoring fetal electrocardiogram and electrocardiogram in a fetal externally. Despite designed for passive screening, it can be used for actively updating individuals about BPD and fetal progress.

Sheeba Ranjini and Hemamalini

CHALLANGE

The challenge is to build an automated system to segment anatomical structures within 2D fetal ultrasound images, taken at different GAs (21, 28, and 33 weeks). The challenge is to obtain good-quality image segmentation and to measure BPD and FL. Each measurement obtained from the fetal ultrasound device is then connected with a database, where results are stored. Although the results are sent to individuals through message. To send fetal information to a patient's mobile phone, we have developed a mobile application for 24×7monitoring.

RESEARCH METHODS

The field of obstetrics and gynecology relies on medical uses of ultrasonography devices to estimate GA, delivery date and visualization of maternal–fetal development. This is because this device is easy to use and minimally invasive to mother and fetus. However, ultrasonography examination requires special skills from users, because the accuracy of the ultrasound results depends on the skill of the user. In addition, the resulting image quality also affects the diagnosis. Currently, ultrasonography machines have three- and four-dimensional configurations. However, in developing countries such as Indonesia, the availability of such machines is still limited to big cities. In addition, the equipment is quite expensive, leading to increased expenses for the patient. Hence, many regions of Indonesia still use 2-dimensional ultrasonography machines. It is noteworthy that the ultrasonography machines in the rural area have a low resolution and some essential functions must be executed manually. Also, in some areas, ultrasonography is not at all available. As described in the previous sub segment, in this article, we discuss about the use of image processing techniques in estimating both GA and uterine diameter.

IMPLEMENTATION

Gestational age is different from fetal age. Fetal age is determined based on the normal ovulation cycle occurring about 14 days after menstruation. . If a woman has a 28-day and regular menstrual cycle, the fetus age would be a 2 weeks less than the GA. In other words, if a woman is 8 weeks pregnant, then the age of the fetus will be6 weeks. Meanwhile, the determination of GA through ultrasonography examination can be done in two ways:

Calculation of the diameter of fetal sac (mean sac diameter) is described in Equation1.

$$MSD = \frac{p+l+t}{3} \quad (1)$$

Where p is the length (mm),l is the width (mm), and t is the height(mm).
GA could be estimated using the formula described in Equation 2.

$$\Delta t = MSD + 40 days \quad (2)$$

Where Δt is the gestational age (days) and MSD is the mean sac diameter (1day/1mm after 40 days).
By measuring distance between head and butt fetal (crown length or CL), we can estimate GA using the formula described in Equation3.

$$\Delta t = CL + 60 weeks \quad (3)$$

Where Δt is the gestational age (weeks) and CL is the crown rump length (mm).

IMAGE PROCESSING PROCESS

This interface is divided into three panels, namely the image template panel, the fetal detection panel, and the image processing operation panel. Here's an explanation of each panel:
(i) Image template panel: It has a function to call predefined templates. The template command is as follows:

Sheeba Ranjini and Hemamalini

[Filename pathname]= ui get file({'*.jpg';'*.bmp';}, 'Select an Image'); img name=[pathname filename]; axes(handles. Gambar template); im show (img name);

The UI allows the user to browse and search an image file. Then, it will be saved in the form of filename and pathname matrix. Then, this matrix is displayed on a designated using "axes" command (handles. Gambar template). Then, the image will be displayed on the "Gambar template" axes. The matrix will be displayed on the image template using the "im show" command (img name). After the template selection process is complete, the fetal detection phase can start.

(ii) Fetal detection panel: In this panel, the fetal image detection program has a feature for cropping images, to facilitate the search of fetal image diameter. This detection stage uses the template matching method, which is an image-matching method that involves finding the smallest parts and matching the image template. Template image testing results are presented in the Results and Discussions section.

(iii) Image processing operation panel: It is divided into three parts, namely the binary converter panel, the morphology operation panel, and the edge detection panel. Here's an explanation from each panel:

(a) Binary converter: It has a function to convert grayscale images to binary images. The source code of the binary conversion function is given below:

c=get image (handles.citra_hasil_deteksi);
d=im2bw(c);
axes (handles. operasimorfologi);
im show (d);

The image generated from the "Ubah Biner" button is then displayed using the "in show (d);" function. The image that appears within the "operandi morphology" axes will be recalled to continue with the adaptive thresholding process. This process is crucial to obtain a clearer picture and get an optimal value because each image has a different color intensity. The results of adaptive threshold experiments are presented in the Results and Discussions section.

(b)Morphology operation panel: The morphological operation is a step to clean up the image after it is change to binary. There are several push buttons on the morphology operation panel such as push button dilation, erosion, opening, and closing.

(c) Edge detection: It has a function to clarify the borders within the ultrasonograph image. Edge detection is used only when the borders of the image are not clearly visible. However, if the peripheral borders are clearly visible, no edge detection is performed.

The pregnancy age within the image can be determined by incorporating the MSD formula (Equation 2) into the source code. This is done by combining the MSD formula to the diameter source code, as given below.

usia = MSD+30; set(handles. hasilusia, 'string', usia); axes(handles.axes6);

Source code formula for calculating age is age = MSD + 30,where the MSD is obtained from the diameter result. The sum of MSD and the variable 30 means that the GA is calculated from 30 days. The fetal sac will expand by 1mm/day. Table2 shows some examples of pregnancy age based on diameter measurements and vice versa.

Some of the parameters that affect the results include threshold value, number of morphological operations and edge detection, and errors from GA. According to the threshold, each image gets different threshold treatment. The threshold value determines the quality of the image to be processed further, so that the accurate diameter and GA are obtained. The threshold value has a range between 0 and1. For comparison, we also calculated GA manually. The original USG image was manually measured using Paint software. The first step was inputting the original image to Paint and then measuring it by marking out a straight line. The straight line's measurements were compared with the results of image calculation done using MATLAB. Once the coordinates for each point (in units of pixels) were determined, they were converted into units (mm), where1 pixel corresponded to0.26458 mm. The diameter of the image was measured using the Pythagoras formula. The value of GA obtained via the MSD formula was tested for success rate by comparing it with to the manually calculated pregnancy age. Figure9 shows comparison of GA calculated by MSD and manually.

Sheeba Ranjini and Hemamalini

Some factors that have potential for introducing an error include (i) obtaining original USG images with low resolution and limited contrast. (ii) Resizing the original ultrasound image without considering scaling. (iii) Not using all morphological operations. The operations used are only related to image cleanup. The mean age of MSD calculation results for the entire image dataset was 75.67 days and the data distribution for the calculated MSD age score had a standard deviation of 8.43. The mean age of manual calculations for the overall image was 76.67 days and the data distribution for the age value of the manual calculation had a standard deviation of 7.23.

COMMUNICATION

The dissemination of information including patient data such as MSD, BPD, fetal diameter and fetus age is done by transmitting it to the patient mobile number via SMS or through email. Also, the option of using free services such asthinkspeak.com is available. A majority of upscale hospitals in India all use this kind of services. However, we our purpose is to make it usable primarily to government hospitals and remaining hospitals that are economical.

CONCLUSION

An automated estimation method for obstetrics has been executed and refined on an off-the-shelf tablet. The mechanically measured values of FL and BPD were similar to manual estimations. The accuracy and execution of outcomes were comparable to those of other state-of-the-art automatic models that run only on high-end ultrasonography machines. Through its incorporation in a moderate and simple ultrasonography machine, such as the UF scanner, the technique has potential for clinical usability in PC. Moreover, the automated estimation strategy is adaptable to various image gain settings. This is a feature that will ensure consistent measurement results between clients in PC.As a result, this feature will enhance ease of use and overall quality of measurements. Subsequently, results could be sent to the patient through email or text messages. This feature is very useful for the patients, enabling them to monitor the fetal progress and to become healthy.

REFERENCES

1. Salomon, L. J., et al. "ISUOG practice guidelines: performance of first-trimester fetal ultrasound scan." Ultrasound in obstetrics & gynecology: the official journal of the International Society of Ultrasound in Obstetrics and Gynecology 41.1 (2013): 102.
2. Khan, Naiad Hossain, et al. "Automatic measurement of biparietal diameter with a portable ultrasound device." 2014 IEEE International Ultrasonics Symposium. IEEE, 2014.
3. Khan, Naiad Hossain, et al. "Automatic Detection and Measurement of Fetal Biparietal Diameter and Femur Length—Feasibility on a Portable Ultrasound Device." Open Journal of Obstetrics and Gynecology 7.03 (2017): 334.
4. Campbell, S., and Alison Thoms. "Ultrasound measurement of the fetal head to abdomen circumference ratio in the assessment of growth retardation." BJOG: An International Journal of Obstetrics & Gynaecology 84.3 (1977): 165-174.
5. Queenan, John T., Gregory D. O'Brien, and Stuart Campbell. "Ultrasound measurement of fetal limb bones." American journal of obstetrics and gynecology 138.3 (1980): 297-302.
6. Perni, S. C., et al. "Intra observer and inter observer reproducibility of fetal biometry." Ultrasound in obstetrics & gynecology 24.6 (2004): 654-658.
7. Hanna, Christine W., and Abou Bakr M. Youssef. "Automated measurements in obstetric ultrasound images." Proceedings of International Conference on Image Processing. Vol. 3. IEEE, 1997.
8. Thomas, Judith G., Richard Alan Peters, and Philippe Jeanty. "Automatic segmentation of ultrasound images using morphological operators." IEEE Transactions on Medical Imaging 10.2 (1991): 180-186.
9. Wang, Ching-Wei. "Automatic entropy-based femur segmentation and fast length measurement for fetal

Sheeba Ranjini and Hemamalini

ultrasound images." 2014 International Conference on Advanced Robotics and Intelligent Systems (ARIS). IEEE, 2014.

10. Altman, D. G., and L. S. Chitty. "New charts for ultrasound dating of pregnancy." Ultrasound in Obstetrics and Gynecology 10.3 (1997): 174-191.

11. Bradski, Gary, and Adrian Kaehler. Learning Open CV: Computer vision with the Open CV library. "O'Reilly Media, Inc.", 2008.

12. Gjessing, H. K., et al. "Fetal size monitoring and birth-weight prediction: a new population-based approach." Ultrasound in Obstetrics & Gynecology 49.4 (2017): 500-507.

13. Alexander Muacevic and John R Adler. Artificial intelligence: a new paradigm in obstetrics and gynecology research and clinical practice.

Table1. Examples of pregnancy age based on diameter

Diameter(mm)	Pregnancy age(days)
47	77
33	73
41	71
58	88
50	80
45	75

Figure 1.(a) Measurement of the Biparietal Diameter (BPD). (b) Screen Capture of the user Interface for BPD Measurement
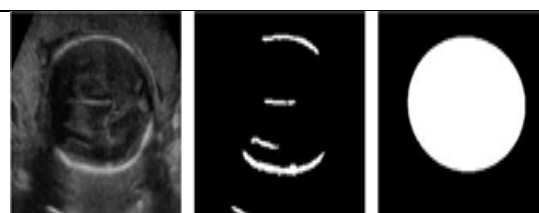
Figure 2. (a)Original Image. (b) Preliminary Segmented Objects. (c) Inscribed Head Ellipse
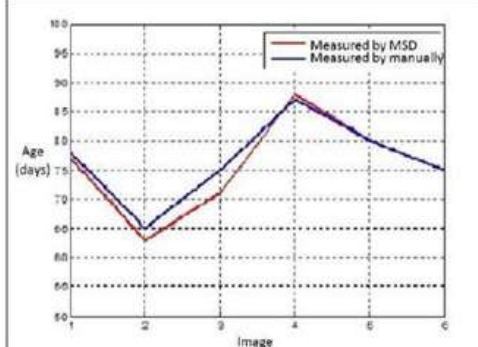
Figure 3. Comparison Graph of Gestational Age Calculated by MSD and Manually

RESEARCH ARTICLE

Identification of Changes in Brain Activity for Alzheimer Disease using Voxel-based Neuroimaging Analysis

Kalpana R[1]*, Swarna Kedia[2] and T.N. Vishalakshi[3]

[1]Associate Professor, Department of Medical Electronics, B.M.S College of Engineering, Bangalore -19 , Karnataka, India
[2]Student, Department of Medical Electronics, B.M.S College of Engineering, Bangalore -19 , Karnataka, India
[3]Professor, Department of Mathematics, B.M.S College of Engineering, Bangalore -19 , Karnataka,India

*Address for Correspondence
Kalpana R
Associate Professor,
Department of Medical Electronics,
B.M.S College of Engineering,
Bangalore -19 , Karnataka, India
E.Mail: rk.ml@bmsce.ac.in

ABSTRACT

Voxel-based morphometric (VBM) is a method for measuring differences in native concentrations of brain tissue through the voxel-wise comparison of various medical imaging of the brain. VBM is one of the most important neuroimaging methods for assessing macroscopical asymmetries in grey matter with high regional specificity. A structural magnetic resonance imaging (sMRI) analytical technique called VBM enables voxel-wise comparisons of native grey material concentrations between two groups of subjects or between each participant's two cerebral hemispheres. It is employed for the examination of several topic teams, which has numerous therapeutic applications. For example, VBM is frequently used to examine aberrant structures in Alzheimer's disease (AD). High-resolution structural magnetic resonance imaging (sMRI) provides the basis for this method. The main sMRI preprocessing steps for cross-sectional VBM analysis are often introduced first. Next, the statistical analysis for the examination of grey matter images from two distinct teams. The expanded VBM (eVBM) technique for sMRI information analysis is next examined. By applying contrast technique eVBM with conventional VBM using a sizable cohort AD dataset.

Keywords : Alzheimer's, MRI, Voxel-Based Morphometry

Kalpana *et al.*,

INTRODUCTION

The human brain is constantly changing and adapting. This could be caused by aging processes, common biological processes, the outcomes of learning and training, or new phenomena that have appeared in the world. In addition to the alterations, the shape of the brain is impacted by a number of systematic factors like gender, illness, and heredity. Because changes and variations in the brain may be evaluated noninvasively and in vivo using magnetic resonance imaging, this method is extremely intriguing for both basic research and clinical testing. Analyzing whole-brain volume is the simplest way to evaluate brain changes (or cluster differences). Yet, evaluating at the level of the entire brain is quite vast. Specific region-of-interest (ROI) analyses have considerably more restrictions than whole-brain assessments, but they measure native changes with a lot more sensitivity. For instance, if only one specific area of the brain is evaluated, other brain structures go unreported, and potential impacts are not observed in the brain. Moreover, ROIs measurements occasionally produce supported individual protocols and are more accurate than the particular "judgement calls," necessitating a distinct, determinable, and unambiguous structure. However it will be challenging to precisely define (or discover) clear boundaries for large portions of the brain. inally, the sensitivity will decrease if an ROI slightly differs. The use of voxel-based morphometry (VBM), which allows for the examination of brain changes and/or cluster variations across the entire brain with high regional specificity (i.e., voxel by voxel), becomes necessary as a result of this. VBM does not necessitate the prior definition of particular ROIs. A wide range of impartial, objective techniques have been developed in recent years to describe anatomical changes in vivo MRI medical image datasets. These methods can be broadly divided into those that alter gross variances in brain structure and those that look at the native make-up of brain tissue after gross variations are taken into account. The former, which represent deformation-based morphometry (DBM), describe the fundamental structure of every person's brain in terms of deformation fields that relate every brain to a standard reference.

It is clear why innovations are being developed to help the fight against Alzheimer's disease; this motivation stems not only from moral considerations but also from the fact that Alzheimer's cases are constantly increasing in our society. A common percentage of the fifty million people who live insanity today have Alzheimer's disease. With a new case of Alzheimer's being reported every three seconds worldwide, the disease has surpassed cancer cases as our most feared ailment. Oasis provided the dataset that was used for the analysis.

LITERATURE REVIEW

A thorough literature survey was allotted on Alzheimer's illness, imaging systems, applied mathematics parameter mapping, and also the nervous tissue volumes. Alzheimer's (AD) poses a significant threat to the ageing health of our nation because citizens are living longer thanks to medical advancements. It is estimated that about two-hundredths of US citizens would be older than 65 by 2030 [3]. Advancing age is said to associate the hyperbolic risk of dementedness. According to calculations, AD accounts for up to 80% of cases of dementedness [1]. Most often, ageing increases the risk of developing Alzheimer's disease and presenile dementia. The Alzheimer's Association estimates that eighty-one percent of patients who have AD are older than seventy-five years of age [1]. The impact of AD on the population is considerable. According to official figures, the number of AD-related deaths increased by 71% between 2000 and 2013 [1]. This is comparable to a reduction in cardiovascular disease on Bastille Day throughout the same time period. In a 10-year period, AD went from being the 25th most taxing sickness in all of us to the 12th, and from the 32nd to the 9th in terms of being worse in terms of years of life lost. This was the most tragic increase in any sickness throughout that time period [1]. Regarding the diagnosis and treatment of AD, the region specifically identifies a number of obstacles. According to studies, several medications and smart treatment options for AD are ineffective when utilised on patients who also have subtle psychosocial impairments. Generally speaking, a diagnosis is clinical and involves the doctor treating the patient. It's crucial to have a thorough medical, familial, and medical specialty history. Routine labs to rule out different causes of dementedness (complete blood count, comprehensive metabolic panel, thyroid-stimulating internal secretion, B-complex vitamin, and folic acid) and further neuroimaging with resonance imaging (MRI) conjointly are ought to be thought as a part of the routine

Kalpana *et al.*,

workup. Serologies for biomarkers and psychological science testing may be used to support the identification as needed. The fluid or cerebrospinal fluid can be used to get the biomarkers that are now being investigated (CSF). Key CSF biomarkers have good specificity and sensitivity for diagnosis, ranging from 85 to 90 percent [4]. Gray brain material volume (GMV) abnormalities in the brain as determined by MRI and using statistical SPM software systems can be automatically investigated using the picture processing and applied mathematics technique known as voxel-based morphometry (VBM). The capacity of VBM to do applied mathematics cluster comparisons of brain volume fluctuations across the entire brain[5] as opposed to just on certain regions of interest is one of its salient features. Through connections to the amygdaloid nucleus and other physical structures, the cortical region is also thought to play a significant role in the regulation of anxiety, aggression, conjugation behaviour, and other aspects of the emotional process. More specifically, the orbital ventromedial greenhouse emission is thought to mediate appropriate behaviour in nerve-wracking situations and sound judgement in situations where showing emotion is intense. [6] This supports the idea that lobe injury has significance to the pathophysiology of AD. Impairments in these skills are either directly apparent in AD patients or lay at the root of the appearance of medical specialty symptoms (such as apathy or agitation). Moreover, a larger understanding concerning lobe abnormalities in AD has relevance given the requirement to differentiate this type of dementedness from different neurodegenerative disorders that conjointly have an effect on the lobe, like frontotemporal dementedness,[6] dementedness with Lewy bodies, and vascular dementedness.[7]

PROPOSED SYSTEM
The proposed method for detecting disorders on magnetic resonance imaging (MRI) consists of four primary steps: I identifying regions of interest, (ii) extracting features, (iii) selecting features, (iv) classifying, and (v) evaluating performance. For the purpose of extracting features from the grey matter, regions of interest must be identified. Areas of interest are those places where a known reduction in grey matter volume has been seen. By comparing two templates that represent two teams, VBM is used to identify these zones of interest. The proposed methodology is divided into two primary sections: I regions of interest are identified by VBM, and (ii) those regions are examined for detection. The pattern recognition pipeline follows VBM and includes First- and second-order statistics were provided by feature extraction, and multiple procedure analyses were supported by feature selection. High-resolution images of the structural brain are used in the study. The T1 weighted images are first split into several tissue types, such as liquid body substance, substantia alba, and grey matter, and then they are corrected for inhomogeneities. The tissue of interest, or the grey matter phase, is subsequently spatially normalised to fit a predetermined template. Eventually, a related isotropic mathematical kernel is used to smooth down the normalised grey matter phase. Lastly, voxel-wise applied math tests are performed on the smoothened normalised grey matter segments in order to map significant effects.

METHODOLOGY

As shown in figure 3.1. The raw 3DT1-weighted images obtained from the MRI scans from the Oasis Dataset will be our major focus which is in .nii format. The SPM software package, created for the analysis of brain imaging data sequences, will be used to further segment the image into grey matter, white matter, cerebrospinal fluid (CSF), fat, and bone. Interest in grey matter pictures will lead to statistical analysis

ABSTRACT SPECIFICATION OF SUB-SYSTEM
Image Acquisition: 3D T1 raw Images
Image acquisition is the first and most important stage. This step's intended goal is to collect the best data available in order to meet the study's data requirements. The Open Access Series of Imaging Studies (OASIS) Brains project provided the dataset. The scientific community can access macroscopic (whole brain) structural MRI neuroimaging datasets from the OASIS Brains project. These facts come from MRI scans, diagnostic exams, and demographic information gathered from test subjects during the diagnosis of Alzheimer's disease. Used was the Oasis 3 Dataset. NIH P50 AG00561, P30 NS09857781, P01 AG026276, P01 AG003991, R01 AG043434, UL1 TR000448, R01 EB009352;

principal investigators: T. Benzinger, D. Marcus, and J. Morris; OASIS-3. Avid Radiopharmaceuticals, an entirely owned subsidary of Eli Lilly, supplied the AV-45 doses. The benefit of these databases is that they may be used to test how well image processing techniques work with various photos and settings.

Viewing the Raw Image in the SPM: Unsegmented Whole Brain Images
After successfully attaining the dataset. Now, we can have a look at how the raw brain MRI images i.e. the unsegmented whole-brain images look with the help of SPM software. To run SPM software, we need the Matlab Software Installed as SPM is an integrated software that works on the algorithm of MATLAB. Since the obtained images are in Nifti format, the SPM is easily compatible with it. Fig. 4.2 shows examples of how the raw MRI Images look with the help of SPM.

Workflow of VBM
The study is based on high-resolution structural brain images, as illustrated in figure 4.3. Prior to classifying the T1-weighted data into completely different tissue types like substantia grisea, substantia alba, and CSF, they are first adjusted for inhomogeneities. The tissue of interest (the grey matter phase) is then spatially adjusted to fit a standard guide. Subsequently, the substantia grisea phase is smoothed once it has been adjusted. Lastly, voxel-wise applied mathematics tests are performed on the smoothened, normalised substantia nigra segments in order to map significant effects.

Tissue Classification
The brain is effectively phased into the substantia grisea, substantia alba, and CSF by tissue categorization, which uses intensity levels to separate out any non-brain components. The target now could be to mechanically establish totally different tissue varieties inside the pictures, through the New Segment choice within the SPM. Then, the Native Space versions of the tissues during which we tend to have an interest are generated, in conjunction with "DARTEL imported" versions of gray and substantia alba. Because these images may later be warped to MNI housing, the native space photos for VBM are normally the c1*.nii files. The segmentation in SPM will operate with images collected via a form of sequences, but the accuracy of the resulting segmentation can depend on the actual attributes of the images. This is true for both the foreign and native tissue category image sets. Although each patient was offered multiple scans, the dataset that will be used only contains the T1-weighted scans.

Following the completion of the segmentation, a large number of recent image files are generated. Files with the prefix "c1" measure what the algorithmic programmerecognises as nervous tissue. If they have a "c2," they are thought to be substantia alba. CSF is measured by the "c3" images. The tissue category images' DARTEL foreign versions, which can be aligned next, have file names that start with "r" (as in "rc1"). Pictures of substantia grisea are shown in Figure 4.4. (ROI).

Run Dartel
The goal of DARTEL is to increase the accuracy of inter-subject alignment by modelling each brain victimisation score's shape (three parameters for every voxel). DARTEL positions substantia alba while simultaneously placing neural tissue in the images. This can be done by creating its own, increasingly precise average guiding knowledge, which will align the information iteratively. This creates "u rc1" files as well as a set of guide photographs by using the foreign "rc1" and "rc2" images. The Dartel guidance produced after 18 iterations is displayed in Fig. 4.5.

Normalize to MNI Space with Smoothening
The individual brains or the native grey substance segments should be spatially normalised in addition to tissue categorization to ensure voxel-wise equivalence. Even if native grey matter volumes in each brain are commonly measured in natives, voxel-wise comparison is difficult to do. After being spatially normalised, every brain has the same size, shape, and overall pattern of major sulci and gyri. The native quantity of the grey material is typically directly compared in voxel-wise applied math evaluations. The Jacobian determinants derived from the deformation fields utilised for spatial control also show that the patterns of volume amendment for each individual are

completely different. The final "u rc1" files are smoothed, spatially normalised, and Jacobian transformed in this step (which cypher the shapes). In this stage, grey substance images for the MNI are smoothed, spatially normalised, and Jacobian scaled using the resulting "u rc1" files (which cypher the forms). Fig. 4.6 displays the images after SPM's spatial social control was depleted.

Statistical Analysis
Although non-parametric tests are also frequently used, statistical models can examine the smoothed normalised tissue segments using parametric tests. Generally, a mass-univariate technique is used to execute these tests, running the same test simultaneously for each voxel. This involves a serious multiple comparison problem, similar to those found in the majority of previous neuroimaging analyses, and must be corrected appropriately. Now that the pre-processed data have been fitted to a GLM, we may deduce the locations of systematic differences between the pre-processed data.

i. Using Basic Models, develop a design matrix that details how the pre-processed data is produced in SPM.
ii. Play about, use Review models, examine the design matrix, etc.
iii. To fit the GLM to the data and determine how smooth the residuals will be for further GRF corrections, use Estimate.
iv. Use the findings to identify any noteworthy differences.

Global Calculation
"Global normalization" for VBM refers to working with different sized brains. Since VBM analyses volumetric differences voxel-by-voxel, it is important to think about how regional volumes can change depending on the size of the entire brain. Bigger brain structures are more likely in larger brains. If we use some sort of "global" brain volume correction, we might obtain more targeted outcomes. The computation of global can be done in a number of ways. For instance, add the values in a "c1" or "mwc1" image and multiply by the volume of each voxel to determine the overall volume of grey matter. Comparably, the sum of the volumes of the grey and white matter can represent the overall volume of the brain. Addition of the CSF, white matter, and grey matter yields the total intracranial volume. This can be estimated using SPM's tissue volumes feature, which returns the grey matter, white matter, and cerebrospinal fluid volume from the original data. The text file containing the estimated brain volumes is shown in Fig.5.1.

Global Normalization
The proper use of "globals" is outlined in this section. Grand mean scaling should be turned off globally. This completely useless option is still included in the SPM programme. Next select Normalization to provide possibilities for using our "globals". In this instance, proportional scaling was applied.

Masking
There are numerous ways to use masking to choose which voxels go into the analysis. The multiple comparison adjustments are supposed to make analyses more sensitive when fewer voxels are included. When the backdrop is evaluated in VBM investigations, instability occurs. The computed variance is extremely near to zero because the background signal is quite weak. The t statistics are proportional to the magnitudes of the differences, squared as the residual variance. It is difficult to divide by zero or by numbers near to zero. Blobs could also penetrate the background deeply, but masking prevents this from happening. Absolute masking was applied in this case.

Design
In this part, the actual design matrix and data are described. If the analysis for the present data can be specified as a Multiple Regression, choose this Design option. Scans, Covariates, and Intercept are the following three fields that must be specified. The "smwc1" files can be selected by clicking Scans -. Including Intercept for Intercept when specifying a menu item. It will serve as a constant term in the design matrix. Double-click Covariates and select New "Covariate" after each click. We'll model gender and age as covariates. Input the following covariates:

63572

1. Type "info(:,1)" as the Vector, "Gender" as the Name, and "No centering" as the Centering options. Values of 0 denote a female subject, while 1 denotes a male subject. 2. Type "Age" as the Name, "info(:,2)" as the Vector, and "No centering" as the Centering options. Now that everything has been spoken, the statistical analysis data should be filled out. Now that we've saved the work, SPM will collect the data required to carry out the statistical analysis when we click the Run button. 'SPM.mat' file, where.

Estimate
The analysis is carried out through the Estimate button. After selecting the freshly formed "SPM.mat" file, click Estimate and wait a while. The design matrix's columns are first linearly combined to fit the data at each voxel. This results in the creation of a sequence of "beta" images, the first of which represents the contribution of the first column, the second representing the contribution of the second column, and so on. Moreover, an image called "ResMS" is created, containing the standard deviations needed to calculate the t statistics. The computation of residual images—used to determine the smoothness of the data—comes next. When they are no longer needed, these photos are automatically erased because they are only transitory.

RESULT

After the GLM has been fitted, images of t statistics can be created using the data from the resulting "beta" and "ResMS" images, along with the "SPM.mat" file. Contrast vectors, which show the linear combination of "beta" images to be tested, are defined. The objective is to locate any regions that significantly deviate from zero in these linear combinations, which are recorded as "con" images. The actual t statistics are stored in "spmT" pictures. It is necessary to make certain adjustments for the number of tests when several voxels are checked. In order to account for numerous dependent comparisons, Gaussian random field theory is applied because the voxels are associated and the pre-processed data are spatially smooth. Select the "SPM.mat" file by clicking the Results button. This activates the SPM contrast manager. Then, click the t-contrasts button, and define the required new contrasts. When the SPM contrast manager says name, enter "-Age" (or another name of your choice). The agenda is to look for regions of the brain with proportionally less gray matter in elderly Alzheimer's patients. This has a t contrast of 0,-1,0. This would be entered into the contrast field.

The fig. 7.1.1,7.1.2,7.1.3 here shows the motor response in the subjects with p<0.05. The motor response was varied according to age and Volume of the brain. The fig. 7.2.1,7.2.2,7.2.3 here shows the common areas of the activation in the subjects with p<0.05. The response was varied according to age and gender. Till now, all the results were according to the t-statistical test. SPM also has a F-statistical test. The difference between the f-test and t-test is that f-test is used to compare the standard deviations of the two samples and understand their variability. However,aT-test is used to test the hypothesis whether the given mean is significantly different from the sample mean or not.
The fig. 7.3.1,7.3.2 here shows the SPM-F image that corresponds to basically the difference (positive or negative) from the left and right responses.

DISCUSSION

fMRI results showed reduced functional activation in the motor areas of the brain (contralateral precentral and post central gyrus), also reduced gray matter in prefrontal cortex and hippocampus region of the brain. It is also observed that the data significantly varies and differs according to age but is less dependent on the overall size and volume of the brain. Research studies have found that a correlation exists between people who have dementia and reduced gray matter volume in the brain. Patients with Alzheimer's disease are observed to experience atrophy in the hippocampus area. Also, the prefrontal cortex in patients reduces

CONCLUSION

Our results show that VBM is generally more sensitive at identifying focal cortical gray matter differences, in the area of voxel signal-to-noise and spatial extent commonly studied. Also, VBM appears to be similar in sensitivity to global gray matter differences as ALV. This suggests that VBM is a better technique for evaluating structural brain differences when compared to the many large scale automated ROI methods. In recent years, VBM studies have been successful in differentiating structural brain differences in many diseases.

FUTURE WORK

Some future aspects of the work that will be improved bythe further the neural quantification can be applied to the data generated from this analysis which will yield a faster result and the whole process can be automated.

REFERENCES

1. Alzheimer's Association. 2015 Alzheimer's disease facts and figures. *Alzheimers Dement.*2015; 11:332–84.
2. Yang J, Pan P, Song W. Voxelwise Meta-analysis of Gray Matter Anomalies in Alzheimer's Disease and Mild Cognitive Impairment Using Anatomic Likelihood Estimation. *J Neurol Sci.* 2012;316:21–29.
3. Velkoff V. The next four decades: The older population in the United States: 2010-2050. *Curr. Popul. Rep.* 2010:1–14.
4. Scheltens P, Blennow K, Breteler MM, et al. Alzheimer's disease. *Lancet.* 2016; 388:505–17.
5. Ashburner J, Friston KJ. Voxel-Based Morphometry-The Methods. *NeuroImage.* 2000;11(6):805–821.
6. Bang J, Spina S, Miller BL. Frontotemporal dementia. *Lancet.* 2015;386(10004):1672–1682.
7. Kalaria RN. Neuropathological diagnosis of vascular cognitive impairment and vascular dementia with implications for Alzheimer's disease. *Acta Neuropathol.* 2016;131(5):659–685.
8. Sarraf S, Anderson J, Tofighi G (2016) Deepad: Alzheimer's disease classification via deep convolutional neural networks using MRI and fMRI. bioRxiv p 070441
9. Frisoni GB, Fox NC, Jack CR, Jr, Scheltens P, Thompson PM. The clinical use of structural MRI in Alzheimer disease. *Nat Rev Neurol.* 2010;6:67–77.
10. Good CD, Johnsrude IS, Ashburner J, Henson RN, Friston KJ, Frackowiak RS. A voxel-based morphometric study of ageing in 465 normal adult human brains. *Neuroimage.* 2001;14:21–36.
11. Busatto GF, Diniz BS, Zanetti MV. Voxel-based morphometry in Alzheimer's disease. *Expert Rev Neurother.* 2008;8(11):1691–702.
12. Raji CA, Lopez OL, Kuller LH, Carmichael OT, Becker JT. Age, Alzheimer disease, and brain structure. *Neurology.* 2009;73(22):1899–905.
13. Guo Y, Zhang Z, Zhou B, Wang P, Yao H, Yuan M, et al. Grey-matter volume as a potential feature for the classification of Alzheimer's disease and mild cognitive impairment: an exploratory study. *Neurosci Bull.* 2014;30(3):477–89.
14. Seeley WW, Crawford RK, Zhou J, Miller BL, Greicius MD. Neurodegenerative diseases target large-scale human brain networks. *Neuron.* 2009;62(1):42–52.

Kalpana *et al.*,

Fig. 1	**Fig. 2.**
Fig. 3	**Fig 4.**
Fig 5.	**Fig 6.**
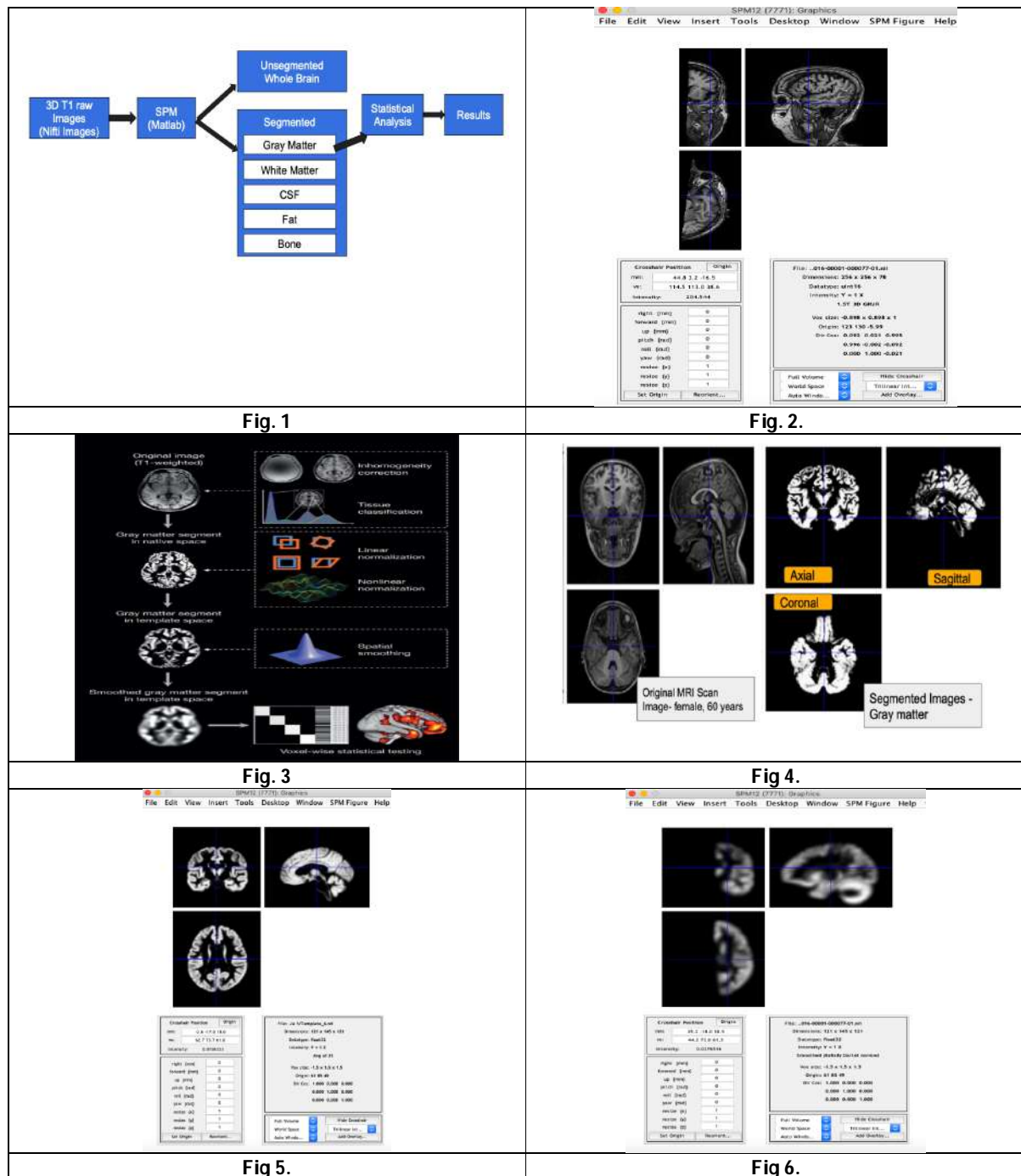
Kalpana *et al.,*

0	60	0.2166	0.1804	0.1319
0	31	0.3005	0.1441	0.0331
1	23	0.5784	0.3365	0.3676
0	50	0.4014	0.3261	0.3510
1	51	0.6251	0.4229	0.2590
0	08	0.5006	0.2094	0.4068
1	88	0.7130	0.4864	0.2238
1	38	0.5961	0.2702	0.1875
1	78	0.6790	0.4466	0.2728
0	75	0.6285	0.2953	0.2099
1	42	0.5014	0.3844	0.3279
0	52	0.6778	0.4831	0.3149
0	55	0.5842	0.3288	0.1436
1	56	0.6451	0.3322	0.2066
1	46	0.4799	0.4152	0.3488
1	45	0.5528	0.3556	0.1799
0	65	0.5629	0.3842	0.2274
0	67	0.5564	0.3812	0.2327
0	72	0.5369	0.3666	0.2755
0	74	0.5364	0.3656	0.2724
1	67	0.6534	0.4854	0.5191

Fig 7.

Fig. 8.

Fig. 9.

Fig. 10

Fig. 11	Fig. 12.

Fig. 13	Fig. 14

Kalpana *et al*.,

Fig.7.3.2

RESEARCH ARTICLE
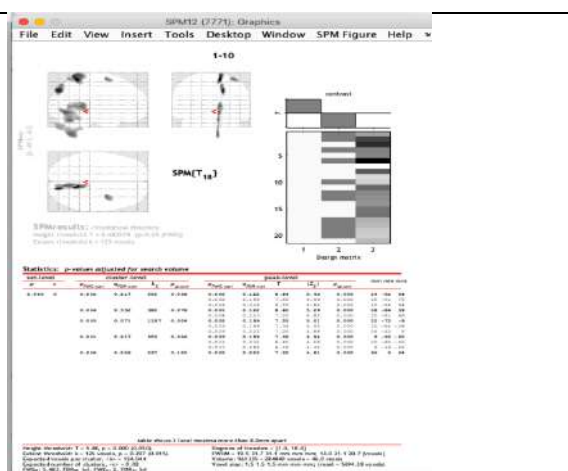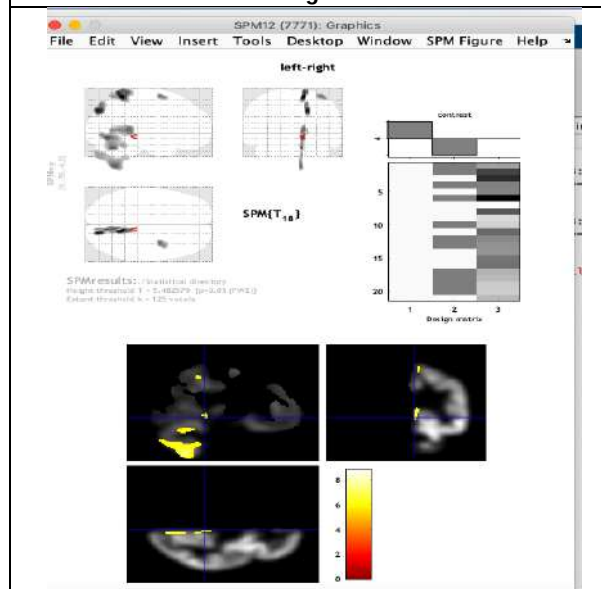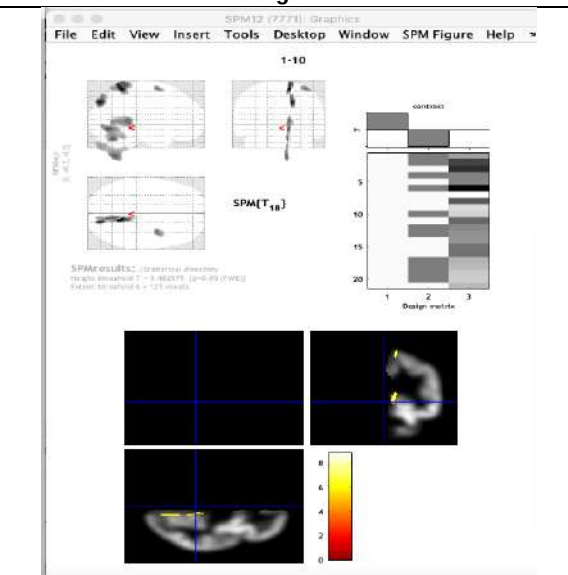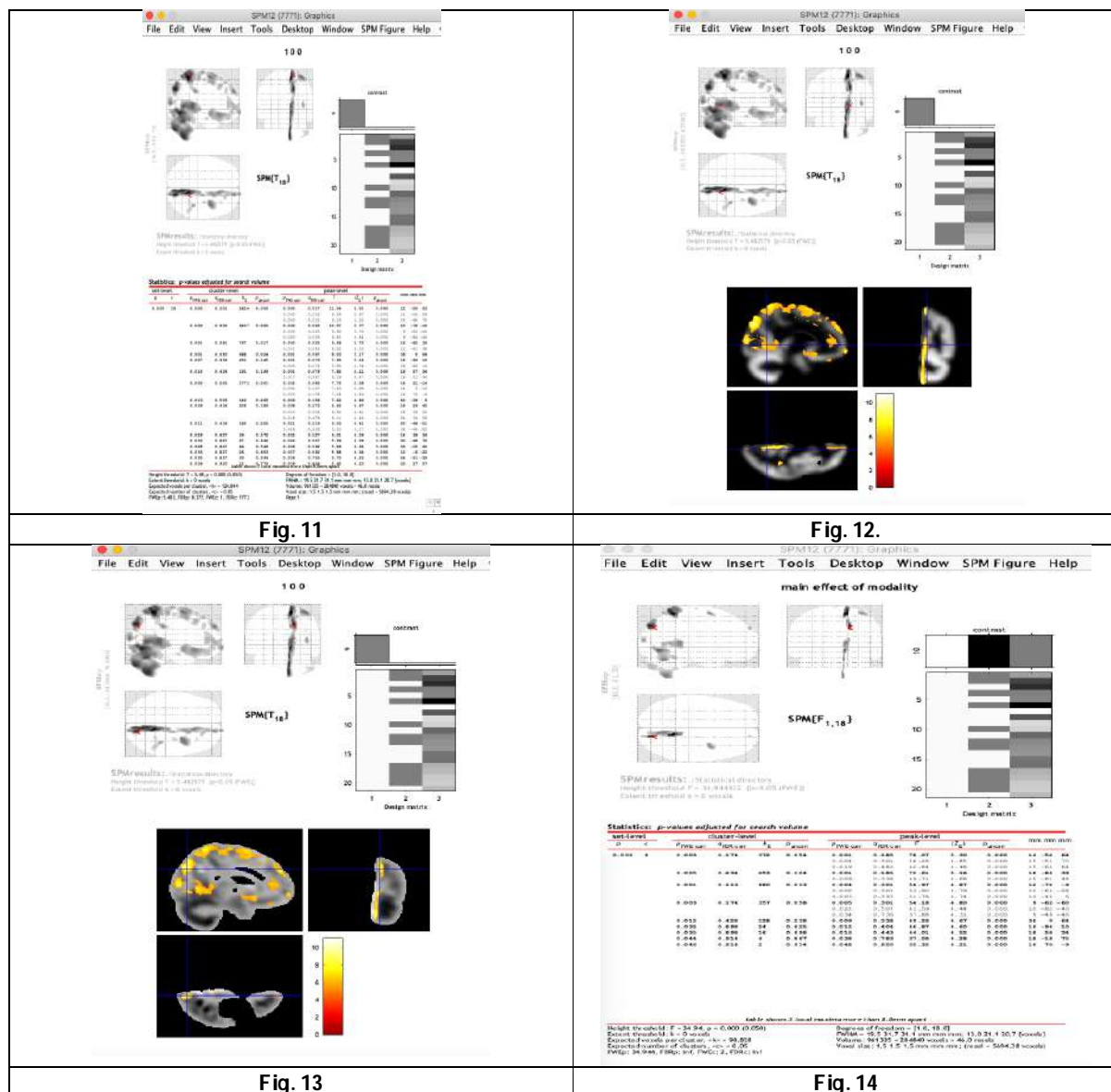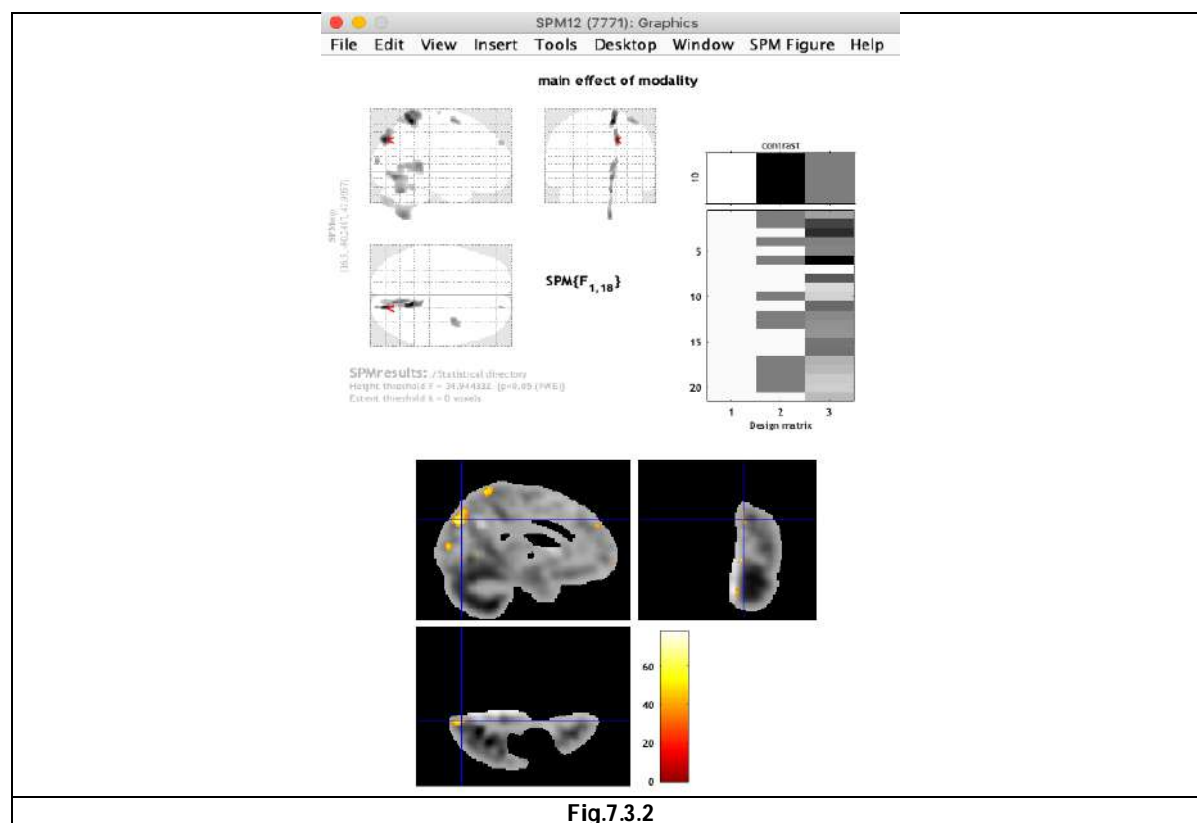
Vertical Electrical Soundings (VES) Exploration Analysis of Vythiri Taluk, Wayanad District, Kerala, India using IPI2WIN

Insaf. M[1]* and D .Nagaraju[2]

[1]Research Scholar, Department of Studies in Earth Science, University of Mysore, Manasagangotri, Mysuru, Karnataka, India.
[2]Professor, Department of Studies in Earth Science, University of Mysore, Manasagangotri, Mysuru, Karnataka, India

*Address for Correspondence
Insaf. M
Research Scholar,
Department of Studies in Earth Science,
University of Mysore, Manasagangotri,
Mysuru, Karnataka, India.
E.Mail: insafwayanad@gmail.com

ABSTRACT

The Resistivity method is aimed at measuring the potential differences on the surface due to the current flow within the ground. Since the mechanisms that control the fluid flow and electric current and conduction are generally governed by the same physical parameters and lithological attributes, the hydraulic and electrical conductivities are dependent on each other (George et al., 2015). Groundwater is the major source that meets the drinking and domestic needs of any area of the world. Thus, its exploration and accessibility assumes a great significance to the scientists and society. In the crystalline hard rock groundwater generally occurs in the weathered basement, or regolith, and the fractured rock (Verma et al., 1980).in many parts of the world groundwater is a primary source of fresh water. Some regions are becoming overly dependent on it, water tables to declining because of consuming groundwater causing unremittingly (Gleick, 1993). Groundwater rights have not changed accordingly by population growth and economic development, the laws governing, even in developed nations. (Livingston, & Garrido, 2004). Groundwater is the subject of growing social concern around the globe. The ownership and control of underground aquifers, the intensive use of groundwater resources, potential changes in both groundwater quality and quantity and the related impacts on natural systems command the attention of scholars and policy makers in many countries. India, with 70–80% of its food production based on groundwater resources, is perhaps the sharpest world example of the challenges involved in managing this resource (Deb Roy and Shah, 2002).

Keywords: Vertical Electrical Sounding (VES), IPI2win Program, Vythiri taluk, Schlumberger array, Groundwater, wells, Aquifer, Vythiri, Kerala

INTRODUCTION

Geophysical survey is necessary to ascertain subsurface geological and hydrogeological conditions and helps to delineate regional hydrogeological features, even pinpoint locations for drilling of boreholes. Geophysical data provides information on local geological environment such as type and extent of surface material, extent and degree of weathered mantle, the nature and extent of underlying bedrock, the structural elements etc. That influence groundwater occurrence and movement. The important geophysical method involved in ground water explorations is Geo Electrical prospecting and several scientists like Bhimasankaram et al.(1975,1976); Benergy (1969); Bindumadhavan (1975); Zambre (1980): Bagdhan(1976); and Mani (1989) have applied the geoelectrical methods to solve various groundwater problems. Patangay (1977) is of the opinion that the electrical methods have greater advantage over the other methods. The proper use of geoelectrical techniques reduces the risk of drilling poor yield wells and can also supplement the geological evaluation of proposed well locations. In an area of salt water intrusion that arises due to over exploitation of groundwater can be studied using electrical resistivity techniques which provide additional data to improve the accuracy of groundwater models, which in turn can be used to determine the extent of the non saline ground water resource (Singh and Mesh, 1982; Sathyamoorthy and Banerjee 1985; Basak and Nazimuddin, 1987). Electrical resistivity methods are widely used for both regional and detailed survey for ground water exploration because of their great resolving powers, low expense compared drilling and wide range of field applicability (keller and frischnecht 1996, balakrishna et al 1978,Chandra and athavale 1979: Chandrasekharan, 1988). Hence in the present study electrical resistivity in particular Vertical Electrical Sounding (VES) is followed.

STUDY AREA
Administratively, Vythiri taluk is located within Kalpetta, the district headquarters of Wayanad district, within the state of Kerala, India.The area of the Vythiri taluk covers 637 square kilometers. This area is covered in the Survey of India topographic sheet (no. 49 M/14, 58A/21, 58A/31, 58A/61) with geographic co-ordinates N 11° 33' 5.97384" and E 76° 2' 24.94356". Vythiri taluk is a famous tourist destination in the Wayanad district. The study area is well connected by road. (Fig.1). National Highway 212, connecting Kozhikode (Calicut) with Mysore and the Calicut–Vythiri–Gudallur (CVG) road passes close to the study area.

Geologically, the Wayanad area is an extension of Dharwar Craton which is perhaps one of the important crustal blocks among the collage of terrains in the Southern Granulite Terrain (SGT) and is occupied by the rocks of the Wayanad Group, Charnockite Group, Peninsular Gneissic Complex (PGC) and Migmatitic Complex. Wayanad Group of rocks are supracrustal and include garnet, sillimanite, biotite gneiss, graphite, kyanite, fuchsite, muscovite, quartz, schist, hornblende, biotite schist and gneiss garnet, amphibolites, quartz sericite schist or quartz mica schist, banded magnetite quartzites (BMQ) and meta ultramafites.   These rocks are found as linear bodies within the PGC. The PGC, represented by hornblende-biotite gneiss and pink granite gneiss, occupies a major part. The Charnockite Group comprises the hilly terrain made up of charnockites. Pyroxene granulite and banded magnetite quartzites occur as narrow bands within the charnockite. Migmatite Complex is represented by biotite hornblende gneiss. (Fig.2)

METHODOLOGY

The most widely used geophysical method for groundwater exploration is electrical resistivity method as it is efficient in detecting water-bearing layers, besides being simple and inexpensive to carry out field investigations (Zohdy, 1974). The method involves measurement of applied current (I) through two electrodes and potential (V) across two other electrodes. Apparent resistivity is derived from these measurements for various electrode separations. There are different electrode arrangements such as Schlumberger, Wenner, Dipole–Dipole, Two-Electrode Array, etc. Geophysical Investigation The geophysical investigation involved the electrical resistivity method. The Vertical Electrical Sounding (VES) technique adopting a Schlumberger array was used. The half current electrode spacing (AB/2) was varied from 1 m to a maximum of 100 m .The choice of the VES stations was

63580

constrained by the geology, structure (lineament) map, terrain, accessibility and representativeness of the spread of the stations. Every VES station was appropriately geo-referenced. Secondary information on existing VES data and borehole records (logs, yield etc.) were assessed re-processed and incorporated. Thirty Vertical Electrical Sounding (VES) data. Lineament analysis followed by resistivity survey is cost effective while studying geomorphologic data. In order to assess the groundwater conditions in the area, electrical resistivity surveys were carried out with Schlumberger electrode configuration to pinpoint the most favorable locations in the area. Integrating hydrogeomorphological data with geophysical investigations, Teeuw (1999), Shahid and Nath (2002) South-East dry agroclimatic zones of Karnataka using Arc GIS 10.2 Version generated different types of thematic maps like top soil map, weathered map, highly weathered map, Apparent resistivity 25mtr, 50mtr, 75mtr, 100mtr and 200mtr. Through these spatial maps we can easily understood about of the surrounding forest area. The typical-hydrogeological section of a hard rock terrain consists of a soil zone followed by a weathered zone are overlying bedrock. A total 30 VES conducted in Vythiri taluk, Wayanad district for deep drilling. The area is underlain by the granites, schists and peninsular gneissic complex of Precambrian to Achaean age. The interpreted results at the recommended sites indicated 4 layered geo electric sections in which the last layer is massive formation. (Table.1)

RESULT AND DISCUSSION

The Field data were interpreted and processed qualitatively and quantitatively of using partial curve matching techniques and computed to obtain the resistivity values of different subsurface layers and their corresponding thickness in the Table.1.several result of VES data interpretations with identification of groundwater types. Location of Mandad, the first layer is weathered soil loam with 2082Ωm resistivity with a thickness of 3m; the second layer is a granitic rock with 10889Ωm resistivity with thickness of 1.92m and third layer Gneissic rock with 175Ωm resistivity with a thickness of 5.97m.Location 6 Moopainad the first layer is silt loam with a resistivity with a thickness of 400Ωm resistivity with a thickness of 5.92m and the second layer loam soil resistivity 20195Ωm and the thickness is 2.55m.

CONCLUSION

Hydrogeophysical studies were carried out ot understand subsurface geology based on resistivity survey in the study area. Thirty Vertical electrical soundings(VES)were conducted in the study area, using schlumberger configuration with a maximum half distance of current electrode separation(AB/2) equal to 100 m until the sounding curve was attained, which is an indication of the establishment of contact of the volcanic rock with the granite basement. Initialy VES data has been interpreted with master curves and later the interpretation was redefined by using IP12Win softwares. The layer curves of different parameters such as resistiivities (P1, P2,P3 and P4) and the thickness(h1,h2 and h3) of various layers indicating top soil, weathered, fractured and basement respectively have been prepared software. The study area suggests that it is hard and compact though with a relatively high weathered zone and minor fractures. Major curves are A and H types which have been plotted in the terrain respectively.

ACKNOWLEDGEMENT

REFERENCES

1. Balasubramanian, A., 1986. Hydrogeological investigations in the Tambrapami River Basin, Tamil Nadu, Unpub. Ph.D. thesis, Univ. of Mysore, 349 p.
2. Balasubramaniam, A. and Sastri, J.C.V. 1985., "Studies on the quality of groundwater of Tambaraparani River basin, Tamil Nadu", Nat,emi,GroundwaterMang, Tamil Nadu, Agricultural University, Coimbatore, pp. 124-128

3. Balasubramanian, A., Subramanian, S. and Sastri, J.C.V. 1991"HYCH -Basic computer program for Hydrochemical studies", Proc. VolNat.Sem. On water. Govtof Kerala, Trivandrum,

4. Agrwal.C.S.(1998) Study of drainage pattern through aerial data in naugarh area of Varanasi district, U.P.Jour.India Soc. Remote Sensing,26(4):169-185.

5. Albert Range, Arlen Feldman, Thomas, S.S., George III and Robert, M., Ragan, 1983. Effective use of Landsat data in hydrologic model. Water Resource Bulletin, AmWater Resources Ass. Vol. 19, No. 2, pp 165-174.

6. A.Ghulam, Q.Qin, L.ZHU. Satellite remote sensing of ground water quantitative modeling and uncertainty reduction using 6S atmospheric simulations. Jour, remote sensing, 10 dec. 2004. vol.25, no.23, pp.5509-5524.

7. A.S.Patel. water resource management and people participation. Journal of applied hydrology. Vol.17, no.4, pp. 1-7.

8. Adedeji, K.J.,(2001) Application of integrated Geophysical methods in groundwater exploration and protection: Ijapo housing estate, Akuve,Ondo state as a case study. M.Sc Thesis, University of Lagos, Nigeria,140 P.

9. garwal C.S (1998), Study of Drainage pattern through aerial data in Naugarh area of Varanasi District. U.P.J Indian Soc. Remote Sensing 26 (4):169-175.

10. Akos Gyulai and Tamas Ormos (1990). A new procedure for the interpretation of VES data: 1.5-D simultaneous inversion method, our. Appl. Geophys., v. 41, pp. 1 -17.

11. Amit Kumar Ray, 1997, Remote Sensing Studies in the Narmada- Tapti Linear zone in Gujarat and part of Madhya Pradesh. Abstract volume, National Symposium on GIS and Geological Remote Sensing, (NAGRES-97), Bharathidasan University, Trichy, pp 24.

12. Anderson, James R., et al. 1976. A Land Use And Land Cover Classification System For Use with Remote Sensor Data: Geological Survey Professional Paper 964. Edited by NJDEP, OIRM, BGIA, 1998, 2000, 2001, 2002, 2005.

13. Anderson, James R., Hardy, Ernest E., and Roach, John T., 1972, A land-use classification system for use with remote-sensor data: U.S. Geol. Survey Cire. 671, 16 p., refs.

14. Anon., (1990) Use of remote sensing for hydrogeological studies in humid tropical areas. A pilot study in West Java, Indonesia. IWACO/TNO/ÎTC. Min. Public Works, Indonesia.

15. Aravindan, S. (1999). Integrated hydrogeological studies in hard rocks aquifer system of Gadilam river basin, Tamil Nadu, India, unpublished Ph.D thesis, Bharathidasan University.

16. Asadi, E., Isazadeh, M.Samadianfard, S., Ramli, M.F., Mosavi, A., Nabipour, N., Shamshirband, S., Hajnal, E., and Chau, K.W., (2020). Groundwater quality assessment for sustainable drinking and irrigation. Sustainability v.12, 177p.http://doi. org/ 10.3390 /su12010177.

17. Ayenew, T., Demlie, M., & Wohnlich, S. (2008). Hydrogeological framework and occurrence of groundwater in the Ethiopian aquifers. *Journal of African Earth Sciences, 52*(3), 97-113.

18. Baali, F., Rouabhia, A., Kherici, N., Djabri, L., Bouchaou, L., & Hani, A. (2007). Underground water quality and contamination risk. The case of the basin of Chéria (NE algeria).

19. Balasubramanian, A. and Nagaraju, D.(2019). Water Chemistry Interpretation Techniques (WATCHIT-Software & its Application Manual) Version – 1 open File Report 01, Centre for advanced Studies, Dept of Studies in Earth Science, University of Mysore.

20. BIS (2003). Indian standard drinking water specifications. IS:10500. Edition 2.2 (2003-2009). Bureau of Indian Standards, New Delhi.

21. Bouma, Johannes, Varallyay, G. and Batjes, N.H (1998). Principal land use changes anticipated in Europe. Agricult. Ecosyst. Environ., v.67 (2-3), pp. 103-119.

22. C.G.W.B. (2017-18). Central Ground Water Board, Ministry of Water Resources, River Development and Ganga Rejuvenation, Govt. of India. Annual Report.

23. Carpenter, S. R., Caraco, N. F., Correll, D. L., Howarth, R. W., Sharpley, A. N., & Smith, V. H. (1998). Nonpoint pollution of surface waters with phosphorus and nitrogen. *Ecological applications, 8*(3), 559-568.

24. Carpenter, S. R., Caraco, N. F., Correll, D. L., Howarth, R. W., Sharpley, A. N., & Smith, V. H. (1998). Nonpoint pollution of surface waters with phosphorus and nitrogen. *Ecological applications, 8*(3), 559-568.

25. Coleman, W.D., Wyn, G. and Timothy, E.J. (2004). Agriculture in the new global economy. Cheltenham, U.K.: Edward Elgar Pub. Pp.147-153.

26. Davis, S.N., and De Weist, R.J.M. (1966). Hydrogeology, KrinegarPulication Co., 476p.

27. Domenico PA, Schwartz FW (1990) Physical and chemical hydrology. Wiley, New York.

28. Eaton, Frank M. (1950). Significance of carbonates in irrigation waters Soil Sci., v.69 (2), pp.123-134.

29. Foster, S. S., Garduno, H., Tuinhof, A., Kemper, K., & Nanni, M. (2011). Urban wastewater as groundwater recharge: Evaluating and managing the risks and benefits. *GW-MATE Briefing Note Series*, (12).

30. Garduño, H., Romani, S., Sengupta, B., Tuinhof, A., & Davis, R. (2011). India groundwater governance case study.

31. Giridharan, L., Venugopal, T., & Jayaprakash, M. (2008). Evaluation of the seasonal variation on the geochemical parameters and quality assessment of the groundwater in the proximity of River Cooum, Chennai, India. *Environmental monitoring and assessment*, *143*(1), 161-178.

32. Gupta, Suresh Kumar and Gupta, I.C.(1987). Management of saline soils and waters. Oxford and I.B.H. Publishing Company, 339p.

33. Jalali, M. (2007). Salinization of groundwater in arid and semi-arid zones: an example from Tajarak, western Iran. *Environmental Geology*, *52*(6), 1133-1149.

34. Jarvie, H. P., Whitton, B. A., & Neal, C. (1998). Nitrogen and phosphorus in east coast British rivers: speciation, sources and biological significance. *Science of the Total environment*, *210*, 79-109.

35. Jassal, R. S., Black, T. A., Novak, M. D., GAUMONT-GUAY, D. A. V. I. D., & Nesic, Z. (2008). Effect of soil water stress on soil respiration and its temperature sensitivity in an 18-year-old temperate Douglas-fir stand. *Global Change Biology*, *14*(6), 1305-1318.

36. Kass, A., Gavrieli, I., Yechieli, Y., Vengosh, A., & Starinsky, A. (2005). The impact of freshwater and wastewater irrigation on the chemistry of shallow groundwater: a case study from the Israeli Coastal Aquifer. *Journal of Hydrology*, *300*(1-4), 314-331.

37. Khazaei, E., Stednick, J. D., Sanford, W. E., & Warner, J. W. (2006). Hydrochemical changes over time in the Zahedan aquifer, Iran. *Environmental monitoring and assessment*, *114*(1), 123-143.

38. Kolahchi Z, Jalali M (2006) Effect of water quality on the leaching of potassium from sandy soil. J Arid Environ 68:624–639

39. Malpe, D.B., Yenkie, R. And Hazarika, B. (2021). Assessment of Irrigation Water Quality of Ghatanji Area, Yavatmal District, Maharashtra. Jour: Geosci. Resi., v.6(1),pp.121-128.

40. MetrohmTitrandi (2020). Manual, Metrohm AG Ch-900 Herisan, Switzerland, pp. 1-15.

41. Murkute, Y. A. (2023). Groundwater quality and suitability of PG2 Watershed, Chandrapur District, Maharashtra; An appraisal of hydrogeochemical behavior. Journal of Geosciences Research Vol.8, No.1, January, 2023, pp.70-78.

42. Oladeji, J.T. (2012). Comparative study of briquetting of few selected agroresidues commonly found in Nigeria. Pacific Jour. Sci. Technol., v.13(2), pp.80-86.

43. Paliwal, K. V., & Gandhi, A. P. (1976). Effect of salinity, SAR, Ca: Mg ratio in irrigation water, and soil texture on the predictability of exchangeable sodium percentage. *Soil Science*, *122*(2), 85-90.

44. Pophare, D. A. (2019). Groundwater Quality in Vicinity of Umrer Coal Mines Area, Nagpur District, Maharashtra. *Groundwater Quality, July*.

45. Pramoda, G., Balasubramnaian, A., Nagaraju, D., & Vybhav, K. (2022). Groundwater Suitability for Irrigation in Chickmagaluru District, Southern Karnataka, India using WATCHIT.

46. Richards, L., A. (1954). Diagnosis and Improvement of Saline and Gupta S, Nayek S, Saha RN (2012) Major ion chemistry and metal distribution in coal mine pit lake contaminated with industrial effluents: constraints of weathering and anthropogenic inputs. Environ Earth Sci 67(7):2053–2061Alkaline Soils. Soil Science Society of America Journal, 18(3), 348. https://doi.org/10.2136/sssaj1954.03615995001800030032x

47. Rouabhia, A., Fehdi, C., Baali, F., Djabri, L., & Rouabhi, R. (2009). Impact of human activities on quality and geochemistry of groundwater in the Merdja area, Tebessa, Algeria. *Environmental geology*, *56*(7), 1259-1268.

48. Simeonov, V., Stratis, J. A., Samara, C., Zachariadis, G., Voutsa, D., Anthemidis, A., ... & Kouimtzis, T. (2003). Assessment of the surface water quality in Northern Greece. *Water research*, *37*(17), 4119-4124.

49. Tayfur, G., Kirer, T., & Baba, A. (2008). Groundwater quality and hydrogeochemical properties of Torbalı Region, Izmir, Turkey. *Environmental Monitoring and Assessment*, *146*(1), 157-169.

50. Todd DK (1980) Groundwater Hydrology, 2nd edn. Wiley, New York, p 535.

51. U.S.S.L.S. (1954). United States Salinity Laboratory Staff, Diagonistic and improvement of saline and alkali soils. U.S. Dept. Agri. Handbook No.60, 160p.

52. WHO (2011). Guidelines for drinking-water quality 2016. World Health Organization, pp. 303-304.

Table .1. layer

SL NO	NAME OF LOCATION	LAYER THICKNESS			RESISTIVITY			
		h1	h2	h3	ϱ1	ϱ2	ϱ3	Curve T
1	MANDAD	3.07	1.92	5.97	2082	10889	175	A
2	KUTTAMANGALAM	1.09	1.33	2.73	2542	16082	70.7	K
3	VADUVANCHAL	0.623	6.45	1	716	1281	2557	A
4	NEDUMBALA	0.5	1.37	1	1181	9166	54.2	H
5	VAKERIKUNNU	5.29	6.76	1	183	194	7536	K
6	MUPPAINAD	1.98	2.54	1	400	20195	764	H
7	MEPPADI TOWN	2	1.15	2.76	875	182	6597	Q
8	KALPETTA BYPASS	0.943	35.3	1	349	9.75	1.12	A
9	KAINATTY	2.89	6.943	5.05	1100	6756	102	K
10	KANIYAMBATTA	0.943	2.89	1	556	16226	45.5	A
11	CHUNDA	1.47	1.25	3.45	590	3547	2041	H
12	SETUKUNNU	8.15	2.46	1	36965	2932	30062	H
13	KAVUMANDAM	0.767	3.3	1	8671	28719	2541	Q
14	POZHUTHANA	4.16	0	1	683	1502	1	K
15	THEKKUMTHARA	9.86	17.9	1	557	1602	1.45	Q
16	KUPPADITHARA	0.761	1.28	7.36	851	18838	57.5	A
17	KOTTAVAYAL	0.5	8.43	13	85.3	2970	138	K
18	VYTHIRI TOWN	3.9	3.29	1	1439	47.1	10837	H
19	THRIKYPATTA	1.17	1.38	1	1456	17605	2246	H
20	MUTTIL	0.5	0.037	3.73	101	5.7	156	K
21	THARIYODE	0.861	0.861	1	91.4	57	6031	K
22	CHOORALMALA	0.88	1.34	8.33	89.4	10140	35.3	K
23	KAMBALAKKAD	0.5	0.691	6.18	237	29407	267	K
24	PADINJARATHARA	1.68	1.14	4.5	366	4421	96.6	K
25	MANDAD KUNNU	0.5	7.5	3.08	634	2677	115	H
26	VENGAPALLY	1.98	1.93	5.54	297	2407	72.3	K
27	PARIYARAM	0.846	3.28	29.9	819	4160	364	K
28	VYTHIRI RESORT	2.2	1.83	4.24	1037	6139	57.6	K
29	RIPPON	1.46	1.24	3.82	549	3183	39.8	A
30	PINANGODE	1.82	1.94	7.48	972	11535	200	H

Insaf and Nagaraju
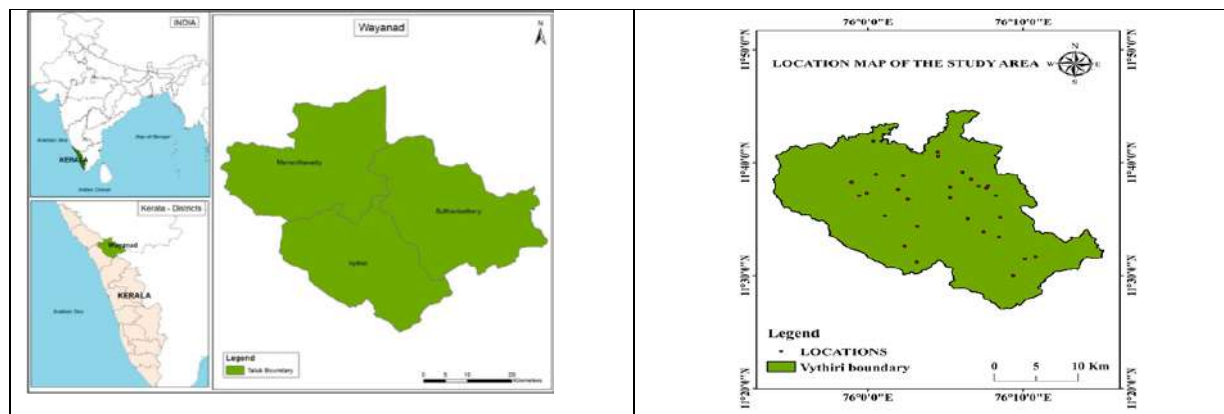
Fig.1 Location Map of the Study Area
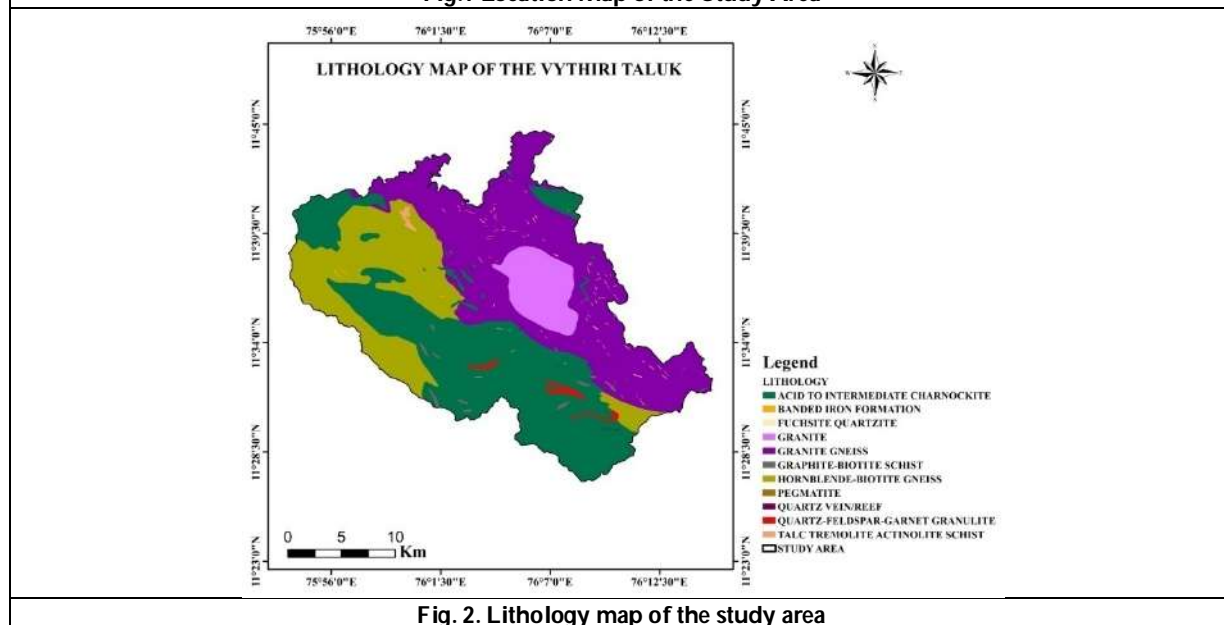
Fig. 2. Lithology map of the study area

RESEARCH ARTICLE

Development and Evaluation of Ezetimibe Oral Fast Dissolving Films

Nandini Jampana[1] and Jyosna Doniparthi[2]*

[1]Department of Pharmaceutics, SKU College of Pharmaceutical Sciences, Sri Krishnadevaraya University, Ananthapuramu, Andra Pradesh, India.
[2]HoD, Department of Pharmaceutics, SKU College of Pharmaceutical Sciences, Sri Krishnadevaraya University, Ananthapuramu, Andra Pradesh, India

*Address for Correspondence
Jyosna Doniparthi
HoD, Department of Pharmaceutics,
SKU College of Pharmaceutical Sciences,
Sri Krishnadevaraya University,
Ananthapuramu, Andra Pradesh, India
E. Mail: jyosna.gms@gmail.com

ABSTRACT

The goal of this investigation was to develop and evaluate Ezetimibe oral fast-dissolving films, which are used to treat hyperlipidemia and prevent cholesterol absorption. The fast-dissolving ezetimibe films were developed using the solvent casting method and included the following ingredients: xanthum gum, dammar gum, gum karaya, which act as film-forming agents; polyethylene glyol 400 (PEG 400), which serves as a plasticizer; croscarmellose sodium, which acts as a super disintegrant, citric acid and stevia powder, which serves as a saliva stimulant and sweetener. The formulated ezetimibe fast-dissolving films were evaluated for film thickness, folding resistance, drug content, air bubble entrapment, and film curling produced findings that fell within the predetermined ranges. In order to determine the drug release from each formulation, the *invitro* diffusion investigations were carried out using the Franz diffusion cell apparatus. The fast dissolving film formulations of E7-E9 prepared by using the gum karaya which showed the drug release upto 97.85 – 99.76% within 15 min. For the optimized E9 formulation, drug releases about 99.76%. The spectra of the E9 formulation showed the principle peaks present in the ezetimibe pure drug, it found that no interaction between the drug and the polymers used. Scanning electron microscopy analysis was carried out for optimized E9 formulation exhibited the smooth even surface.

Keywords: Ezetimibe, solvent casting, fast-disintegrating films, plasticizers, and superdisintegrants.

Nandini Jampana and Jyosna Doniparthi

INTRODUCTION

The oral route of drug administration is the most popular among the different drug delivery methods. For the treatment of a variety of disorders and diseases, about 90% of medications are given to the body orally because this is thought to be the safest, most practical, and most affordable drug delivery technique with the highest patient compliance. (Hema Chaudhary *et al.* 2013,Bhowmik D *et al.* 2009,Aju S *et al.*2011&Verma P *et al.*2010)The medicine is either taken whole or dissolved, and after it enters the systemic circulation, it has the intended effect.(SetouhyDA *et al.* 2010 &Puttalingaiah L *et al.* 2011) Due to self-medication, convenience of administration, and lack of discomfort compared to parenteral route, oral route of drug administration is regarded as the most significant mode of administration of a medicine for systemic impact despite substantial progress in drug delivery. (Siddiqui N *et al.*, Saurabh R *et al.*, Prabhu P *et al.*, 2011 & Bhalla N *et al.* 2012)

Fast-dissolving oral films are a novel class of drug delivery technologies that attempt to improve the safety and effectiveness of a therapeutic molecule in order to increase patient compliance. It is a reliable method of drug delivery in which a film is put on the surface or the bottom of the tongue. When placed on the tongue, this film instantly melts, releasing the medication, which dissolves in the saliva. As saliva descends into the stomach, some medications are absorbed from the mouth, pharynx, and oesophagus. In this situation, improving tongue feel, eliminating choking danger, and increasing drug absorption are important. To get around this issue of swallowing difficulty, fast dissolving drug delivery systems are being developed.(Flesch G *et al.*, 1997&Rajesh K *et al.* 2013)This fast dissolving process is principally driven by the film's enormous surface area, which quickly becomes wet when exposed to a moist environment. The hydrophilic polymer used it to produce FDF quickly dissolves on the tongue or in the buccal cavity, allowing the drug to reach the bloodstream through the buccal mucosa. In order to increase bioavailability of medications with low doses and substantial first pass metabolism, quick dissolving drug delivery systems were developed. (Vidyadhara S *et al.* 2015 &Balakrishna T *et al.* 2018)

Ezetimibe is a cholesterol absorption inhibitor which is used to treat familial and primary hyperlipidemia by lowering total cholesterol, LDL cholesterol, Apoprotein B (Apo-B) cholesterol, and non-HDL cholesterol. Additionally, people with homozygous sitosterolemia may use ezetimibe to lower excessive sitosterol and campesterol levels (phytosterolemia). It can be administered alone or taken in combination with statins (HMG-CoA reductase inhibitor). In this current research Ezetimibe drug was formulated as oral fast dissolving film, by using different film forming agents, plasticizers and superdisintegrants which showed better solubilty, dissolution rate and enhanced therapeutic efficacy.

MATERIALS AND METHODS

Ezetimibe a gift sample from Alkem Laboratories Bangalore, Xanthum gum, Dammar gum, Gum karaya(film forming agents), polyethylene Glycol 4000(PEG 4000), (pasticizer) and croscarmellose sodium, the superdisintegrant were obtained from Yarrow chem, Ltd., Mumbai, stevia powder which is natural disintegrant obtained from High-pure fine Chem., Chennai.

Preparation Of Ezetimibe Fast Disintegrating Films
Solvent casting was used to produce the buccal films for Ezetimibe Fast Dissolving. Individual 100ml beakers of aqueous solutions of the plasticizers xanthum gum, gum karaya, and dammar gum were prepared to obtain clear solutions. After thoroughly combining the xanthum gum solution with the aqueous gum karaya solution, a homogeneous solution known as solution A was obtained. A drug and plasticizer solution known as solution B was prepared by weighing and dissolving specified amounts of ezetimibe and saccharin sodium in the appropriate amount of PEG 400. The homogeneous aqueous solution A was added to the solution B, and they were thoroughly mixed.

Nandini Jampana and Jyosna Doniparthi

The resulting solution was cast onto a non adhesive base plate and allowed to dry for 24 hours under an infrared lamp. The films were sliced into the necessary sizes after they had fully dried. To optimize the method of preparation of ezetimibe buccal films, numerous studies were carried out. The following is a list of the ingredients in ezetimibe buccal films seen in Table 1.

Evaluation of Physical Parameters For Ezetimibe Fast Disintegrating Films
The ezetimibe oral fast dissolving films were evaluated for physical parameters such as Thickness uniformity, folding endurance, drug content uniformity. The results were given in Table 2.

Thickness Uniformity
At different places on the film, the thickness was measured using screw gauze with a minimum count of 0.01 mm. On the film, the thickness was measured at 3 distinct places, and the average was calculated. Results given in Table 2.

Folding Endurance
In terms of what is referred to as folding endurance, the film's flexibility is measured. The film's folding resistance was tested by repeatedly folding a small strip of it until it broke. The value of folding endurance is determined by how many folds of the film can be made without breaking. Results given in Table 2.

Drug Content Uniformity
The films underwent UV-visible spectrophotometric testing to determine the uniformity of their drug content. From the cast film, films of the necessary sizes were sliced three times. Each cut film was put into a 100 ml volumetric flask and dissolved with a buffer with a pH of 6.8. From this, 1 ml was pipetted into a 10 ml volumetric flask, where it was added to the required volume to reach a pH of 6.8. Using a UV visible spectrophotometer, the absorbance of the resultant solution was determined at 296 nm against a blank. Using the standard graph, the percentage of drug content was determined. Results obtained in Table 2. It is challenging to mimic these natural conditions and measure using an appropriate approach when it comes to oral films since the disintegration and dissolution are difficult to determine if the oral films concurrently dissolve in a little volume of saliva. The media used in previous tests for dissolution and disintegration were in significant quantities and weren't physiologically present in the oral cavity. Independent approaches were provided for the assessment of disintegration and dissolution behaviour. Only a minimal amount of media was required for this procedure.

Dissolution test by Franz Diffusion Cell
The volume of the Franz Diffusion Cell is approximately 15 ml. A strip of film containing 10 mg of ezetimibe is placed in the Franz Diffusion Cell, along with 10 ml of pH 6.8 phosphate buffer (pH of saliva). Place the cell on a magnetic stirrer, keep the medium at a temperature of about $400°C$ and the speed of the bead in the cell at 50 RPM. Then, take out 1 ml of samples at intervals of 1, 2.5, 5, 10, and 15, make up to 5 ml with pH 6.8 phosphate buffer, and measure the absorbance in UV at 296 nm using pH 6.8 phosphate buffer as a blank. The drug release profiles for all the film formulations were shown in Figures 1,2,&3 and values obtained in Table 3.

Dispersion Test
A 200 ml of 6.8 pH buffer and a strip of film containing 20 mg of ezetimibe are combined, stirred for three minutes with a glass rod, and then the mixture is run through a 22-mesh screen to determine whether the film passed the dispersion test.

In vitro Diffusion Studies
All of the Ezetimibe fast-dissolving films were subjected to in vitro diffusion tests utilizing Franz diffusion cell apparatuses with pH 6.8 phosphate buffer as the dissolution medium. For each formulation, the dissolving studies took place over a 15-minute timeframe. Studies on dissolution were conducted in triplicate while maintaining sink conditions for all formulations. At regular intervals, a 5 ml aliquot of samples was taken, filtered, and measured spectrophotometrically at 295 nm. For each of the film formulations, the drug release profiles were displayed.

Nandini Jampana and Jyosna Doniparthi

Evaluation of various *in vitro* Dissolution Parameters
The dissolution parameters such as T_{50}, T_{90}, $DE_{5\%}$ and the first order rate constant were calculated from the dissolution data and the results can be obtained in Table 4.

Characterization
Depending on the results obtained by diffusion studies, some of the formulations were optimized and carried out for characterization.

I.R. Spectral studies
BRUKER FT I.R was used to conduct I.R Spectral analyses on a few chosen films. Before they were put through dissolution tests, these studies on films were done to see whether there were any structural differences between the drug and the excipients used in the film formulation. The drug and E5 formulation seen in Figures 1,2&3 respectively.

Scanning Electron Microscopy (SEM)
A thin layer of gold was applied to the samples using a sputter coater unit (SPI, Sputter, USA). Then, using a scanning electron microscope (model JSM-6390, Japan) operating at an accelerated voltage of 10kV, SEM photographs were taken. Photographs observed in Figures 11-12.

RESULTS AND DISCUSSION

Preparation Of Ezetimibe Oral Fast Dissolving Films.
 The solvent casting method was used to produce ezetimibe fast-dissolving films utilising a variety of film-forming ingredients, including xanthum gum, dammar gum, and gum karaya. The film-forming agents xanthum gum were used to prepare the film formulations E1–E3. The films failed the folding endurance test and were found to be brittle. All of the film formulations passed the tests and shown strong film forming characteristics, but formulation E9 was determined to be the best choice and exhibits excellent flexibility. The formulation shown in Table 1.

Evaluation of Physical Parameters For Ezetimibe Fast Disintegrating Films
The formulation of ezetimibe fast-dissolving films was found to be acceptable for the solvent casting method. To eliminate processing variables, all of the film formulations were created under the same set of circumstances. The following physical characteristics were then used to further assess the film formulations. Table provided the physical parameters for various ezetimibe oral quick dissolving films. A screw gauge was used to measure the film's thickness. All film formulations had thicknesses around 0.030 and 0.034 mm. A small strip of film was folded repeatedly at the location to test the film's folding endurance. In comparison to other formulations, it is noted that formulation E9 has good flexibility. Virtually all of the formulations underwent drug content testing. The range of 9.89 to 0.5 mg was the average drug content across all formulations, which was extremely uniform. Entrapment of air bubbles occurs often in all liquid formulations. The presence of air bubbles causes inconsistent and inappropriate drug content. All formulations are fully free of air bubble entrapment both before and after casting the film. In order to reduce the curling of the film, starch (1.6%) is employed as an anti-curling ingredient in film formulations prepared using the solvent casting method.

***In vitro* Drug Release**
Ezetimibe film formulations were developed with the objective of delivering the drug instantly, improving patient compliance and bioavailability. As a result, materials such as xanthum gum, dammar gum, and gum karaya that are water soluble were employed. For the purpose of producing film, polyethylene glycol 400 and croscarmellose sodium were selected as the superdisintegrant and plasticizer, respectively. All of the film formulations were the subject of dissolution tests utilising Franz diffusion cell equipment. For all film formulations, the release values and drug release profiles were provided in Tables 16 and displayed in figures 6 and 7.The drug released on average

Nandini Jampana and Jyosna Doniparthi

between 90 and 96.4% within 15 minutes in the film formulations E1 to E3, which were developed by increasing the xanthum gum concentration. The film formulations E4–E6 were made with dammar gum and had an average 15-minute drug release of 91–97.88%. The film formulations E7–E9, which were prepared utilising gum karaya, had a 15-minute average drug release range of 97.85–99.76%.

Evaluation of Various *in vitro* Dissolution Parameters
From the dissolution data, dissolution parameters such T50, T90, DE5%, and first order rate constant were computed, and the results are shown in the table 4. Gum Karaya's film formulations were found to have T50, T90, and DE 5% values of 2.5, 9.85, and 22.8%, respectively. All of the film formulations' first order plots were linear. All of the film formulations were found to have first order release rates that were linear, with R2 values ranging 0.946 to 0.994. As a result, the rates of drug release from all film formulations were dependent on concentration and linear with the first order release rate constant (K1). Drug dissolution parameters were given in Table 4.

Fourier-Transform Infra Red (FT-IR) Spectroscopic Analysis
The spectra of ezetimibe showed 3 primary peaks at wave numbers of 1115 cm-1(C-N stretching), 1731 cm-1, (C=C stretching) and 3171 cm-1 (N-H Stretching). All of the major peaks found in ezetimibe in its purest form could be seen in the spectra of the Optimized E9 film formulation. Consequently, there is no interaction between the drug and the formulation's polymers. FTIR spectrum of pure drug, karaya gum and optimized formulations were shown in Figures 7 to 10.

Scanning Electron Microscopy Analysis
SEM photographs were taken for the E9 optimized film and the pure Ezetimibe drug. The SEM photographs were shown in Figures 11&12. The E9 demonstrated an even, smooth surface and uniform without any cracks.

CONCLUSION

Ezetimibe oral fast dissolving films prepared by solvent casting method showed good flexibility and film characteristic properties with good bioavailability. The optimized formulation E9 prepared by utilizing gum karaya showed the average drug release of 99.76% within 15min, which was desirable for faster dissolution and absorption. The drug content on average was found to be 8.71± 0.5, and showed good folding endurance and found that no interactions between the drug and the polymers in FT-IR studies whereas exhibited the smooth surface in SEM analysis. Ezetimibe oral fast dissolving films prepared by solvent casting technique were found to be suitable for the treatment of hyperlipidem.

Conflict Of Interest
The authors declare no conflict of interest.

REFERENCES

1. Hema Chaudhary., Samita Gauri., PermenderRathee., Vikash Kumar. Bulletin ofFaculty of Pharmacy, Development and optimization of fast dissolving oro-dispersible films of granisetron HCl using Box–Behnken statistical design Cairo University Cairo University. 51, 193–201(2013).
2. Bhowmik, D., Chiranjib, B., Krishnakanth, Pankaj., Chandra, R. M. Fast dissolving tablet: an overview. J Chem Pharm Res. 1, 163–77(2009).
3. aju, S., Reddy, P.S., Kumar, V.A., Deepthi, A., Reddy, K.S., Reddy, P.V.M. Flash release oral films of metoclopramide hydrochloride for pediatric use: Formulation and *in-vitro* evaluation. J Chem Pharm Res.3(4), 636–46(2011).
4. Verma, P., Thakur, AS., Deshmukh, K., Jha, A.K., Verma, S. Routes of drug administration. Int J Pharm Studies Res. 1(1), 54–9(2010).

Nandini Jampana and Jyosna Doniparthi

5. Setouhy, D.A., Malak, N.S.A.A.P.S. Formulation of a novel Tianeptine sodium orodispersible film. Pharm Sci Tech. 11(3), 1018–25(2010).
6. Puttalingaiah, L., Kunchu, K., Tamizh, M. Fast disintegrating tablets: an overview of formulation, technology, and evaluation. Res J Pharm Biol Chem Sci. 2(2), 589–601(2011).
7. Siddiqui, N.,Garg, G., Sharma, P.K. A short review of a novel approach in oral fast dissolving drug delivery system and their patents. Adv Biol Res. 5(6), 291–303(2011).
8. Saurabh, R., Malviya, R., Sharma, P.K. Trends in a buccal film: Formulation characterization, recent studies and patents. Eur J Appl Sci. 3(3), 93–101(2011).
9. Prabhu, P., Malli, R., Koland, M., Vijaynarayana, K., Dsouza, U., Shastry, C.S., Charyulu, R.N. Formulation and evaluation of fast dissolving films of levocetirizine dihydrochloride. Int J Pharm Invest. 1(2), 99–104(2011).
10. Bhalla, N., Deep, A., Goswami, M. An overview of a various approaches oral controlled drug delivery system via gastro retention drug delivery system. Int Res J Pharm. 3(4), 128–33(2012).
11. Flesch, G., Lloyd, P., Muller, P.H. Absolute bioavailability and pharmacokinetics of valsartan, an angiotensin II receptor antagonist, in man. Eur J Clin Pharmacol. 52, 115-20(1997).
12. Rajesh, K., Prasanna Raju Y., Nagaraju, R. Dissolution enhancement of valsartan using natural polymers by solid dispersion technique. Der Pharmacia Lettre. 5, 126-34(2013).
13. Vidyadhara, S., Sasidhar, RLC., Balakrishna, T., Santhavardhan, M. Formulation of rizatriptan benzoate fast dissolving buccal films by emulsion evaporation technique. Int. J. Pharm. Investing. 5, 101-06(2015).
14. Balakrishna, T., Vidyadhara, S., Murthy, TEGK., Sasidhar, RLC. Formulation and evaluation of lansoprazole fast dissolving buccal films. Asian J. Pharm. 12, 101-35(2018).
15. Balakrishna, T., Vidyadhara, S., Murthy, TEGK., Ramu, A., Sasidhar, RLC. Formulation and   evaluation of esomeprazole fast dissolving buccal films. Asian J Pharm Clin Res.11, 193-99(2018).
16. Balakrishna, T., Vidyadhara, S., Murthy, TEGK., Sasidhar, RLC., Venkateswarao, J. Formulation and evaluation of lansoprazole fast dissolving buccal films. Asian J. Pharm. 10, 313-19(2016).

Table1. Composition of Ezetimibe Fast Dissolving Films

Ingredients for 10 doses (w/w)	E1	E2	E3	E4	E5	E6	E7	E8	E9
Ezetimibe	100	100	100	100	100	100	100	100	100
Xanthum gum	100	200	300	-	-	-	-	-	-
Dammar gum	-	-	-	100	200	300	-	-	-
Karaya gum	-	-	-	-	-	-	100	200	300
Croscarmellose sodium	5	5	5	5	5	5	5	5	5
Polyethylene Glycol 400	15	15	15	15	15	15	15	15	15
Stevia powder	10	10	10	10	10	10	10	10	10
Methanol (ml)	10	10	10	10	10	10	10	10	10

Table 2. Evaluation of Physical Parameters for Ezetimibe Fast Dissolving Films

Formulation	Weight uniformity (mg)	Drug content (mg/film)	Film thickness (mm)	Folding endurance (no)	Dispersion test	Curling
E1	49	8.77	0.032	90	Passed	Absent
E2	60	8.87	0.034	96	Passed	Absent
E3	69	8.55	0.034	92	Passed	Absent
E4	48	8.44	0.033	97	Passed	Absent
E5	59	8.74	0.033	98	Passed	Absent
E6	60	8.11	0.031	99	Passed	Absent

Nandini Jampana and Jyosna Doniparthi

E7	58	8.86	0.030	96	Passed	Absent
E8	56	8.99	0.033	95	Passed	Absent
E9	70	9.23	0.034	101	Passed	Absent

Table 3. *In vitro* Dissolution Studies of Ezetimibe Fast Dissolving Film Formulations

Time (Mins)	Cumulative % Drug Released								
	E1	E2	E3	E4	E5	E6	E7	E8	E9
1	22.99	31.96	38.96	26.66	34.56	39.16	39.98	41.69	42.88
2.5	38.66	47.33	51.33	39.74	51.66	54.06	57.77	63.99	64.66
5	56.66	71.39	77.39	67.51	61.89	67.49	74.69	77.25	79.45
10	79.22	82.44	89.44	82.37	69.12	72.12	86.32	88.14	90.66
15	90.0	94.41	96.41	91.78	96.88	97.88	97.85	98.63	99.76

Table 4. Evaluation of *Invitro* Dissolution Parameters for Ezetimibe Fast Dissolving Films

S.No	Formulation	T_{50} (min)	T_{90} (min)	DE $_{5\%}$	First order	
					K (min^{-1})	R^2
1.	E1	3.5	14.5	17.4	0.163	0.953
2.	E2	3.0	14.50	19.5	0.181	0.966
3.	E3	3.4	14.65	20.8	0.156	0.946
4.	E4	3.2	12.25	18.6	0.234	0.954
5.	E5	3.0	14.5	19.4	0.226	0.962
6.	E6	3.1	12.6	21.3	0.219	0.967
7.	E7	3.3	13.5	17.85	0.221	0.971
8.	E8	3.2	13.2	19.63	0.246	0.989
9.	E9	2.5	9.85	22.8	0.216	0.994
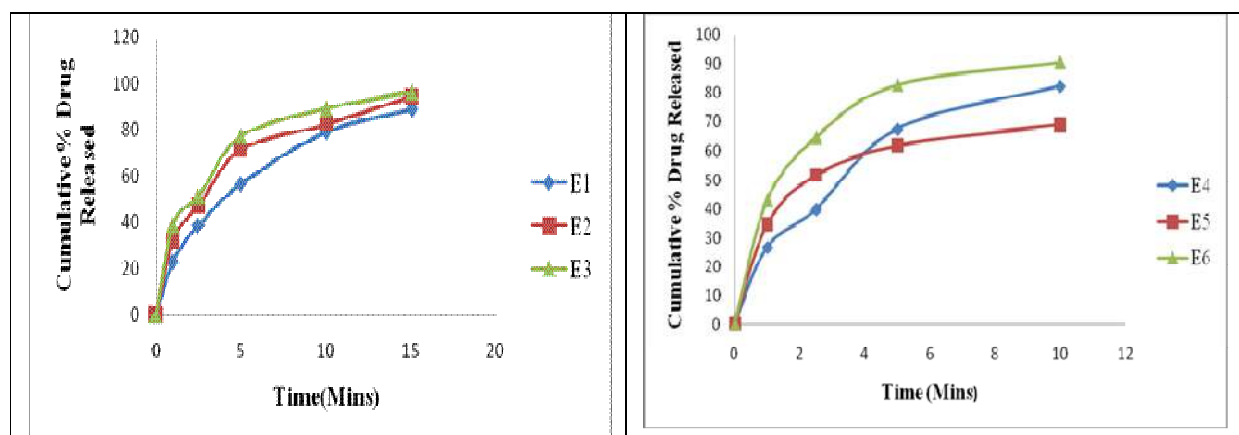
Figure 1. Drug Release Profiles for Ezetimibe Fast Dissolving Films from E1 to E3	**Figure2. Drug Release Profiles for Ezetimibe Oral Fast Dissolving Films from E4 to E6**

Nandini Jampana and Jyosna Doniparthi
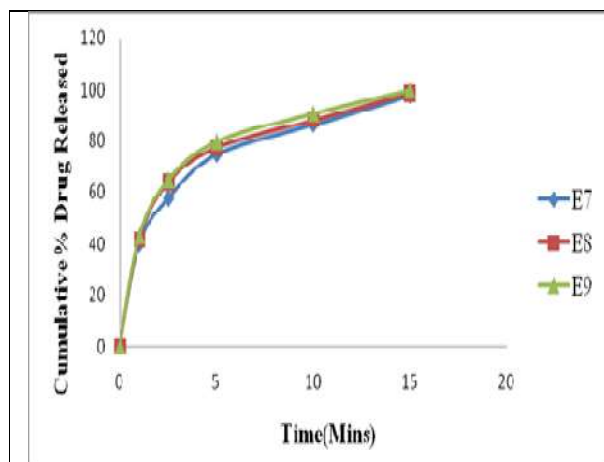
Figure 3. Drug Release Profiles for Ezetimibe Oral Fast Dissolving Films from E7 to E9
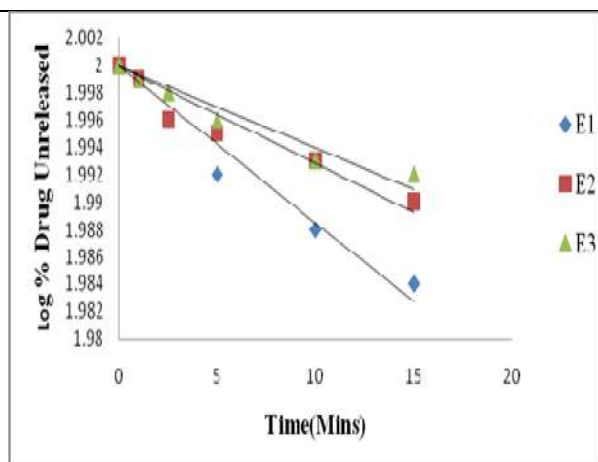
Figure 4. First Order of Ezetimibe Oral Fast Dissolving Films from E1 to E3
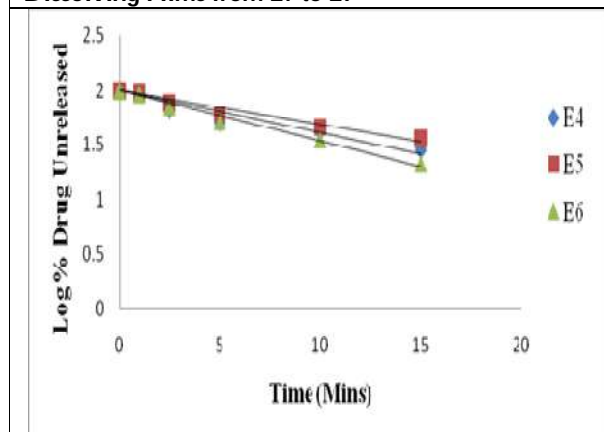
Figure5. First Order of Ezetimibe Oral Fast Dissolving Films from E4 to E6
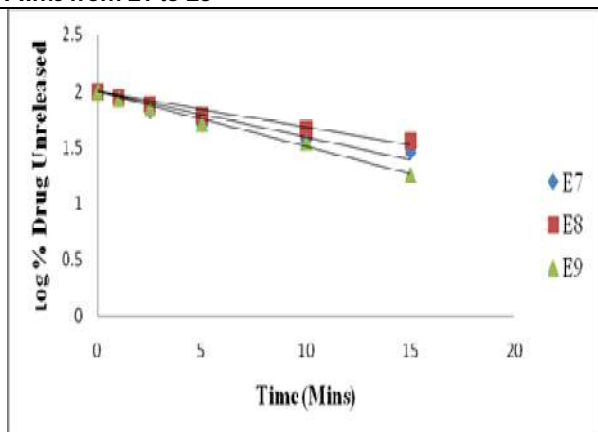
Figure 6. First Order of EzetimibeOral Fast Dissolving Films from E7 to E9
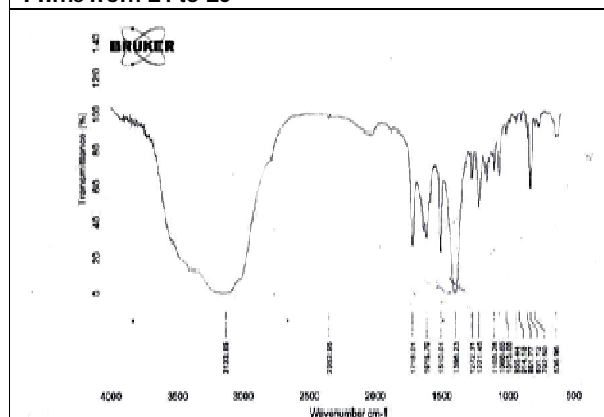
Figure 7. FTIR Spectrum of Ezetimibe Pure Drug
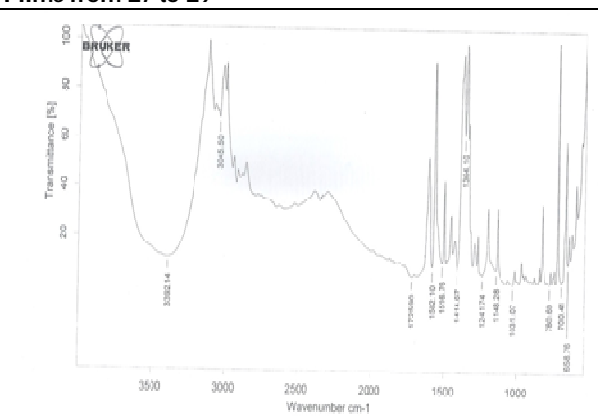
Figure 8. FTIR Spectrum of Gum Karaya

Nandini Jampana and Jyosna Doniparthi
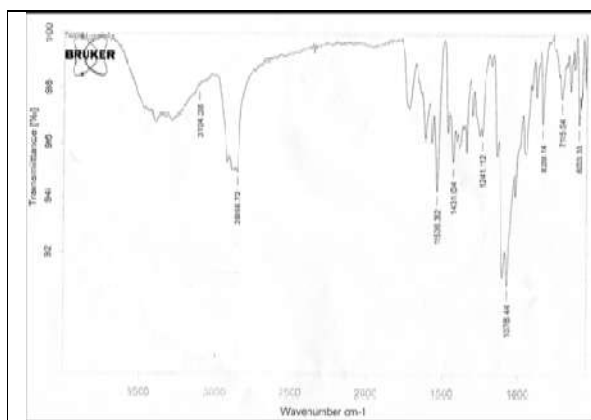
Figure 9. FTIR Spectrum of Xanthum gum
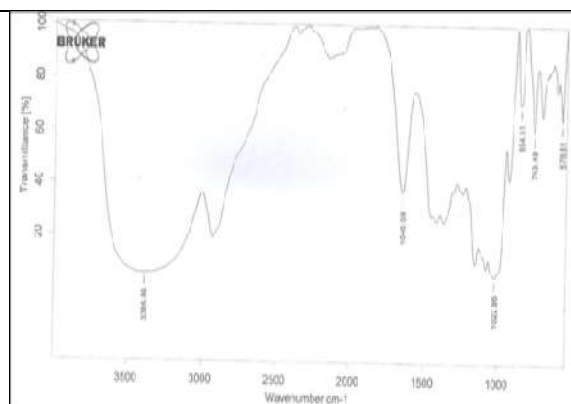
Figure 10. FTIR Spectrum of Optimized Formulation (E9)
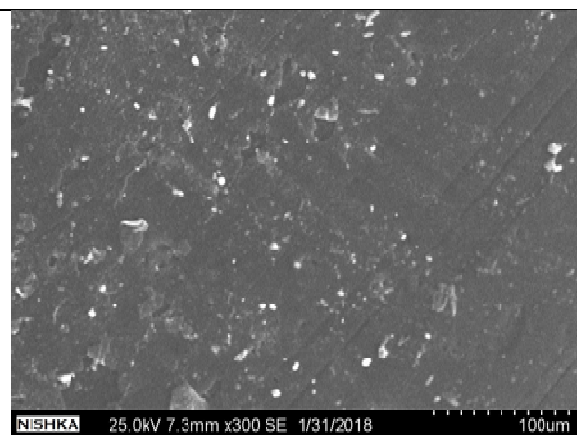
Figure 11. SEM Photograph of Ezetimibe Pure Drug
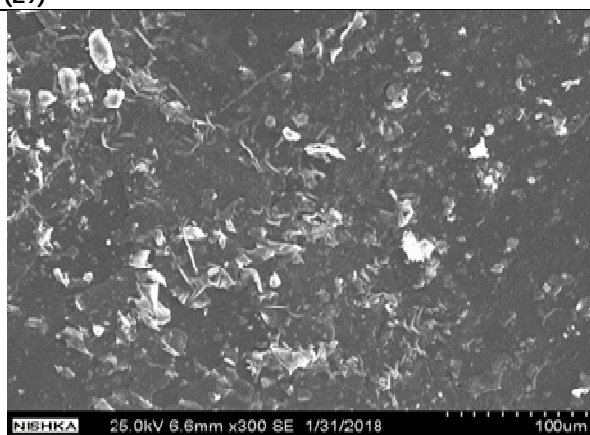
Figure 12. SEM Photograph of Optimized Formulation (E9)

RESEARCH ARTICLE

An Analytical Method for the Determination of Benzodiazepine Drugs from Forensic Biological Matrices

Ravshish Kaur Kohli* and Mridu Sharma

Research Scholar, Amity Institute of Forensic Sciences, Amity University, Sector – 125, Noida, Uttar Pradesh – 201301, India.

****Address for Correspondence**
Ravshish Kaur Kohli
Research Scholar,
Amity Institute of Forensic Sciences,
Amity University,
Sector – 125, Noida,
Uttar Pradesh – 201301, India.

ABSTRACT

Benzodiazepine drug (BZD) is majorly used for the treatment of neuro-psychological ailments. Despite its therapeutic usage, these drugs are misused by drug addicts. These drugs arealso used as sedatives and antidepressants. Hence, the detection and quantification of these drugs are important in forensic toxicology and clinical chemistry. The determination of BZD drugs acts as crucial evidence from forensic biological matrices. In the present study, human blood and viscera were used as forensic biological matrices to detect BZDs, including bromazepam, clonazepam, lorazepam, nordiazepam, and diazepam. A column named AT1000 was used to detect the standard BZDs in forensic biological samples. The isocratic mobile elution was performed using 20mol/Lphosphate buffer (pH 7.0) and methanol (50:50, v/v). 1.0 mL per minute at 214 nm wavelength with a temperature of 40 °C. The linearity graph was made having concentration ranges of 5-500 ng mL^{-1} for alprazolam and oxazepam, 3-500 ng mL^{-1} for diazepam and clonazepam, and 1-500 ng mL^{-1} for lorazepam with a determination coefficient (R^2) greater than 0.9992.This study includes the extraction of drugs from biological matrices followed by the detection using GC-MS instrumentation for the purpose of quantification.

Keywords: Benzodiazepine, Blood, Clinical toxicology, Forensic Science, Gas chromatography

INTRODUCTION

Benzodiazepine misuse is more normal than you might suspect. Left untreated, manhandling these medications can adversely affect your connections, vocation, and your physical and passionate well-being[1]. Benzodiazepine is a kind of drug known as a sedative. Recognizable names incorporate Valium and Xanax. Benzodiazepines are usually mishandled[2]. The misuse is somewhat connected with the harmful impacts that they produce and furthermore to

Ravshish Kaur Kohli and Mridu Sharma

their inescapable accessibility[3]. They can be constantly manhandled or, as seen generally in medical clinic crisis divisions, purposefully or coincidentally taken in glut. Benzodiazepines have likewise been utilized as a "date assault" drug since they can particularly weaken and even annul capacities that typically permit an individual to oppose or even need to oppose sexual hostility or attack. As of late, the location and conviction of individuals engaged with this have expanded emphatically. The medication is typically added to liquor-containing drinks or even soda pops in powder or fluid structures and can be difficult to taste[4].LC combined with API mass spectrometry has now turned into the most amazing asset for the fast location, primary explanation, and evaluation of drug-derived material inside different natural liquids[5]. Programming interface procedures (ESI, APCI) give proficient ionization for different benzodiazepine-related particles, including metabolites. The fundamental benefits of MS/MS are simple test readiness, no expected derivation, and excellent quantitative abilities in the MRM mode. These days, LC-MS is of the highest quality level, especially for identifying extremely low focuses for evaluation in clinical and measurable toxicology[6].Butt-centricstudy a fast elite execution fluid chromatography (HPLC) strategy, involving a solid section in HPLC combined with a diode-exhibit identifier, was produced for the quantitative analysis of benzodiazepines in entire blood. The strategy has been applied to the examiner of eight benzodiazepines among the most often experienced in scientific toxicology- Clonazepam, desalkylflurazepam, diazepam, flunitrazepam, lorazepam, midazolam, nordizepam and oxazepam[7]. Various screening tests are currently accessible to give an underlying test to the presence of benzodiazepines in examples. Their applicability will rely upon the tissue being inspected (Blood/Plasma/Serum or Urine) and the kind of benzodiazepines prone to be available in the example. Earlier enzymatic hydrolysis to change over glucuronide metabolites to immunoreactive species is generally preferred to work on the perceptibility[8]. The Benzodiazepines measure uses gas chromatography-mass spectrometry (GC-MS) for the examination of diazepam, nordiazepam, oxazepam, temazepam, and lorazepam in Blood and Urine.

MATERIALS AND METHODOLOGY

Extraction from Blood
Pre-treatment/Blood deproteinization
Take the sample of blood in a conical flask approximately 20-50 ml.Add a solution of Sodium tungstate with distilled water.Add conc. Sulfuric acid dropwise.Heat the sample on a hot plate for 2-3 minutes at 94°C. Filter the sample using filter paper and collect the filtrate for further basic extraction of the drug.

Extraction from Viscera
Pre-treatment of viscera sample
Take 50gm tissue cut into small pieces in a beaker.Add 20gm of ammonium sulfate and 15 ml of glacial acetic acid into it.Cover the sample with foil.Keep the sample in water for 2 days until the tissue is completely homogenized.Filter the sample using cotton and collect the filtrate for further basic extraction of the drug.

Extraction of the basic layer of drug
Take the filtrate from blood and viscera respectively in the separating funnel. Add ammonia, diethyl ether, and chloroform into it.Shake it for 15 min and keep releasing the gas while opening the knob every 2 min. Keep it undisturbed for 5 min on a separating stand and remove the sample in a conical flask.Collect the organic basic layer by transferring it through sodium sulfate and collect it in an evaporating bowl.Again, do the same process for the second organic basic layer. Collect the layer in the same evaporating bowl.Keep the bowl uncovered overnight and let the organic layer evaporate completely.This bowl can be used for TLC and for the making of GC-MS vials.

Ravshish Kaur Kohli and Mridu Sharma

APPLYING THIN LAYER CHROMATOGRAPHY

Take a fresh TLC plate and cut it according to the number of samples.Mark 1.5cm from both sides using a pencil.The dried sample in an evaporating bowl, add chloroform, and spot the sample. Apply at least 20-25 spots.Meanwhile prepare the chamber for better separation, the solvent system used are as follows-

Chloroform: Acetone (8:2)

Chloroform: Methanol (9:1)

Methanol: Ammonia (9.5:0.5)

Retain the TLC chamber undisturbed for better saturation.Keep the TLC plates in the chamber.Observe the plates carefully for the prevention ofoverrun of the plates.Dry it and spray the reagent for visualization.

Preparationof spraying reagent

Dragendroff reagent- 1gm of bismuth sub-nitrate is dissolved in 3ml of 10M of HCL. It is diluted at 20ml. 1gm of potassium iodide is dissolved in it. If the black precipitate of bismuth triiodideis separated, it is dissolved in 2M HCL. Idoplatinate- 2ml of 5% solution of platinic chloride in 2N HCL+5gms of potassium iodide to 98ml of water with stirring. Marquis reagent- 4 parts of sulfuric acid+6 parts of formalin. Figure 1: (A) and (B) represent the fumes of Sulfuric acid heating on a plate, Filtration, and Filtrate respectively, (C) represents the Filtration of the Viscera sample, (D) represents the sample of Blood separated with Organic basic layer.

RESULTS AND DISCUSSION

Benzodiazepines are used most frequently in today's scenario. They are considered date assaultdrugs because the person doesn't remember anything after the consumption of these drugs. Most of the drugs are basic in nature. Different manufacturers are various concentrations of benzodiazepines along with different other salts combined to form a tablet[9]. The common concentration of tablet available in the market is 0.25mg, 0.5mg, and 1mg. even a minor dose of these drugs can act tremendously on the body[10]. This dissertation focuses on the analysis of benzodiazepines and their salt. The process was followed by the deproteinization of blood and water bath for viscera and then its extraction[11]. Further TLC was run in different solvent systems and the vials for GC-MS were made along with it. The reagents used for spraying TLC are Dragendroff followed by idoplatinate and marquis reagent[12]. The chromatogram shows the peak of the drug present in the sample along with those various other peaks that can be seen. TLC is one of the most common tests performed, retention faction and halfwerecalculated, and it is widely accepted, to look for further quantification of the drug GC-MS was done[13].

CONCLUSION

From the study, it can be concluded that the dissertation primarily focuses on the extraction of drugs from biological matric followed by the detection using GC-MS instrumentation for the purpose of quantification. As almost all these drugs are basic in nature, the basic layer was extracted using ammonia to balance its pH, diethyl ether, and chloroform. The solvent systems and reagents mentioned were used as per the literature available. We would be covering a more detailed analysis on drugs and will also consider drugs beyond benzodiazepines and in further studies biological matrices such as urine and feces will also be analyzed. The different solvent systems not mentioned in the literature will also be tried using the hit-and-trial process for the development of something new which will help us to analyze the drugs in a more effective manner and will also ease out the possibilities of errors.

Ravshish Kaur Kohli and   Mridu Sharma

REFERENCES

1. Persona K, Madej K, Knihnicki P, Piekoszewski W. Analytical methodologies for the determination of benzodiazepines in biological samples. J Pharm Biomed Anal 2015; 113:239–64.
2. Gallager DW. Functional importance of benzodiazepine binding in brain. Brain Res Bull. 1980; 5:833–38.
3. Deveaux M, Chèze M, Pépin G. The role of liquid chromatography-tandem mass spectrometry (LC-MS/MS) to test blood and urine samples for the toxicological investigation of drug-facilitated crimes. Ther Drug Monit.2008; 30:225–28.
4. Westland JL, Dorman FL. QuEChERS extraction of benzodiazepines in biological matrices. J Pharm Anal.2013; 3:509–17.
5. Mercolini L, Mandrioli R, Amore M, Raggi MA. Separation and HPLC analysis of 15 benzodiazepines in human plasma.J Sep Sci. 2008; 31:2619–626.
6. Uddin MN, SamanidouVF,Papadoyannis IN. Development and validation of an HPLC method for the determination of benzodiazepines and tricyclic antidepressants in biological fluids after sequential SPE. J Sep Sci. 2008; 31:2358–70.
7. Samanidou VF, Uddin MN, Papadoyannis IN. Benzodiazepines: sample preparation and HPLC methods for their determination in biological samples. Bioanalysis.2009; 1:755–84.
8. AI-Hawasli H, AI-KhayatMA,AI-Mardini MA. Development of a validated HPLC method for the separation and analysis of a Bromazepam, Medazepam and Midazolam mixture. J Pharm Anal. 2012; 2:484–91.
9. McIntyre IM, Syrjanen ML, Crump K, Horomidis S, Peace AW, Drummer OH. Simultaneous HPLC gradient analysis of 15 benzodiazepines and selected metabolites in postmortem blood. J Anal Toxicol.1993; 17:202–07.
10. Vidal JL, Frenich AG, Aguilera-Luiz MM, Romero-González R. Development of fast screening methods for the analysis of veterinary drug residues in milk by liquid chromatography-triple quadrupole mass spectrometry. Anal Bioanal Chem. 2010; 7:2777–2790.
11. Ferrara SD,Tedeschi L, Frison G, Castagna F. Solid-phase extraction and HPLC-UV confirmation of drugs of abuse in urine. J Anal Toxicol.1992; 16:217–22.
12. Matuszewski BK, Constanzer ML, Chavez-Eng CM. Strategies for the assessment of matrix effect in quantitative bio analytical methods based on HPLC-MS/MS. Anal Chem. 2003; 75:3019–30.
13. Plössl F, Giera M, Bracher F. Multiresidue analytical method using dispersive solid-phaseextraction and gas chromatography/ion trap mass spectrometry to determine pharmaceuticals in whole blood. J Chromatogr A. 2006; 1135: 19–26.

(A)	(B)	(C)	(D)
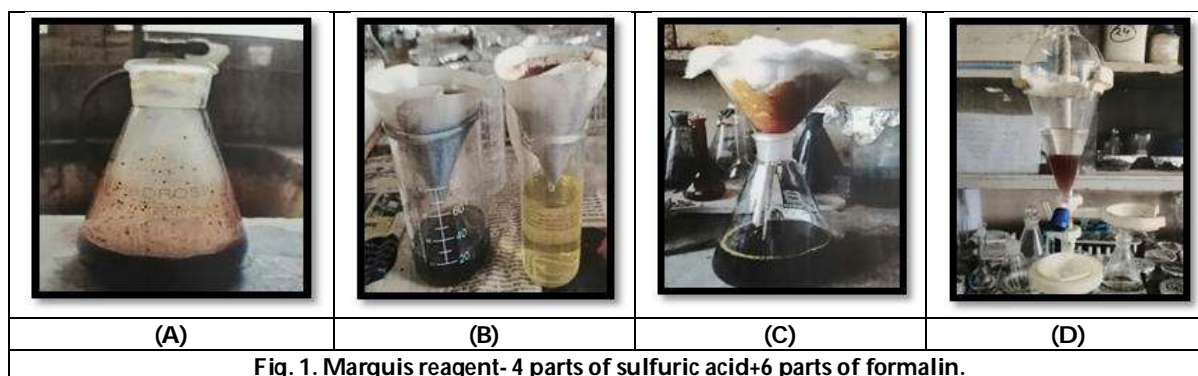
Fig. 1. Marquis reagent- 4 parts of sulfuric acid+6 parts of formalin.

RESEARCH ARTICLE

Implementation of Energy Efficient Hybrid Adder for Approximate Computing Applications

P.Nandha Kumar[1]*, R.V.V.Murali Krishna[2] and B. Narender Reddy[1]

[1]Assistant Professor, Department of ECE, Malla Reddy Engineering College, Secunderabad, Hyderabad, Telangana 500100, India.
[2]Associate Professor, IT Dept., Gayatri Vidya Parishad College of Engineering (Autonomous),Gandhi Nagar, Madhurawada, Visakhapatnam, Andhra Pradesh 530048, India.

*Address for Correspondence**
P.Nandha Kumar
Assistant Professor,
Department of ECE,
Malla Reddy Engineering College,
Secunderabad, Hyderabad,
Telangana 500100, India.
E.Mail: nandha.iarevlsi@gmail.com

ABSTRACT

As the dimensions of transistors have shrunk to sub-micron scales, new challenges, including power efficiency and undetected radiation hazards, have emerged as important areas of concern in the realm of extremely large-scale integration. Because they are key areas of worry, these new problems have recently come to the forefront as important areas of concern. In addition, complementary metal oxide semiconductors, which are more often referred to as CMOS transistors, have a greater consumption of space, power, and delay than the various other kinds of transistors. Because of this, a brand-new 10 Transistor (10T) Multiplexer Logic based Full Adder (MLFA) has been created and is now being simulated. Utilizing both kinds of transistors was necessary in order to achieve this goal, which is considered one of the possible answers to the problems caused by standard CMOS. Additionally, the MLFA that is being presented functions on the basis of a multiplexer selection logic, which has the capability of effectively reducing the route delays as well as the number of transistors. In addition, employing suggested MLFAs allowed for the development of a 4-bit ripple carry adder (RCA). In the end, the simulations are performed with the help of the Tanner-EDA simulation programme. The results of the simulation indicated that the recommended approach resulted in superior performance when compared to other approaches that are presently regarded to be state of the art in the field.
Keywords: Full adder, Multiplexer, hybrid adder, FinFET.

INTRODUCTION

Conventionally, computing systems are built to function with the highest feasible degree of accuracy. However, this tendency is met with significant obstacles in terms of technology, such as high performance and power consumption, as well as dependability of circuits. Computer systems have been gradually improving in both their performance and their power consumption for well over half a century, with scaling technologies being the primary factor in this improvement [1]. It is anticipated that this pattern will maintain its prevalence far into the foreseeable future. In accordance with Dennard's scaling, the size of a transistor has been noticeably smaller during the course of its development, and the supply voltage has likewise become lower. As a direct consequence of this development, electronic circuits can now function at higher frequencies while nearly preserving the same amount of power dissipation. However, because Dennard's scaling is drawing ever-nearer to its end, it is becoming increasingly difficult to achieve additional performance improvements while adhering to the same 10.1109/JPROC.2020.2975695 power limits. This is because Dennard's scaling is getting closer and closer to its conclusion. Consumption of electricity has been a major source of concern for a very long time, and in recent years, it has developed into a problem that impacts the whole industry as a whole and is of critical importance. [2] This is because it is difficult to monitor and avoid parameter fluctuations and defects at advanced nanoscales, which is the reason why this is the case. [3] As a consequence of this, there will be a significant increase in the costs associated with the manufacturing and verification processes in order to ensure the success of the complete accuracy of the signals, logic values, devices, and interconnects.

[4] When it comes to the creation of digital processing devices, with an emphasis on portable systems, the key goals are to lower the amount of power that is needed while concurrently improving the processing speed. In most cases, increasing the speed of the precise processing units results in an increase in the amount of power that is required to run them. [5] The accuracy of the calculation is compromised as one of the strategies for increasing processing power without sacrificing speed. It is possible to utilise this method, which is known as approximative computing, for the applications in which it is acceptable to have some inaccuracies. [6] Among these are the applications in which digital signal processing, often known as DSP, is carried out on the signals connected to human senses. The capabilities of human perception are restricted, thus most of the time, approximation computing is used for processing these signals in bespoke DSP blocks. This is done since it is more accurate than human perception. [7] The realisation of this component utilising the technique of approximation computing was motivated by these facts, which can be found in the previous sentence. Previous studies on approximation adders have focused on either reducing the error weight or the error probability, both of which are considered to be more broad techniques. This is because, in most cases, the majority of the operations take place in the LSB section. The second method makes use of structures that are pure approximation adders. The primary design goals for these adders are to cut down on the amount of power they use and the amount of delay they incur, as well as the error probability associated with the summing. They could also be accompanied with an error correcting unit, which incurs overhead costs in terms of both time and power consumption. [8].

The ECG signals coming from a patient's body are continually monitored by a device based on WBSN. Continuous monitoring results in the production of an excessive amount of data, which, in turn, calls for a greater quantity of storage space, results in higher expenses associated with transmission, and raises the required amount of power consumption. In addition, in order for the Processing Subsystem of the WBSN device to be able to deal with this enormous volume of data, it needs additional processing time to be carried out, which results in an extraordinarily high level of power consumption. As a result, data compression methods are routinely applied in order to accomplish sparse encoding of this data. [9] Sparse encoding has the effect of lowering the needs for processing, which in turn leads to a reduction in the amount of power that is lost by the Processing subsystem. It is possible to reduce the amount of data being transferred by cutting down on the number of bits being sent (which are what make up the packets) [10]. This is due to the fact that the reconstructed signals are not exactly the same as the original signals.

LITERATURE SURVEY

Betzel et al. [11] highlighted the potential advantages of approximation computing for the reduction of communication by conducting a review of three possible strategies for approximate communication. These techniques were compression, relaxed synchronisation, and value prediction. A comparison of the methods is made using an assessment methodology that takes into consideration factors such as the reduction of communication costs, performance, energy reduction, applicability, overheads, and output deterioration. In conclusion, this essay offers a number of recommendations for further research on approximation communication methods. In their paper [12], Mahmud and colleagues presented a thorough assessment with connection to the processing and analysis of large data, of the procedures and techniques of data partitioning and sampling. The first thing that students do when they begin this course is get an overview of the most widely used big data frameworks that can be operated on Hadoop clusters. Following that, we will go through the fundamental approaches to data partitioning, which will include a discussion of the three most frequent horizontal partitioning schemes: range, hash, and random partitioning. Following that, we shall go to the subsequent part of this discussion. The topic of data partitioning on Hadoop clusters is also discussed, along with an overview of novel methodologies for the partitioning of large amounts of data, such as the recently developed Random Sample Partition (RSP) distributed model. In addition, the topic of data partitioning on Hadoop clusters is also discussed. In addition, the topic of data partitioning on Hadoop clusters is covered.

Wei et al. [13] suggested a novel method of using static analysis for the purpose of performing security checks on Android applications, as well as a generic framework known as Amandroid. In an Android app component, Amandroid will do data flow and data dependency analysis on the component in addition to determining points-to information for every objects inside the component in a flow- and context-sensitive manner (which is configured by the user). Additionally, Amandroid monitors the activities of inter-component communication. In order to undertake intra-app or inter-app analysis, it is able to stitch together information at the component level and information at the app level. Stanley-Marbell et al. [14] made the observation that it could be useful to provide an overview of the research results on computer systems that only produce as many mistakes as their end-to-end applications can tolerate. This action was taken as a direct reaction to a suggestion made by the previously stated organisation. [There must be other citations for this] The results include a broad spectrum of academic disciplines, such as information theory, computer-aided circuit design, digital system design, computer architecture, programming languages, and operating systems, to mention just a few of them. Instead of over-provisioning the resources that are controlled by each of these layers of abstraction to prevent errors, it is more efficient to take advantage of the masking of errors that are occurring at one layer in order to stop those errors from propagating to a higher layer. This is because errors that occur at one layer can be masked by errors that occur at higher layers. This is due to the fact that faults that take place at one layer might be concealed by errors that take place at a higher layer. This is because errors that occur at one layer can be masked by errors that occur at higher layers. This is achieved by eliminating the possibility of mistakes arising at a more fundamental level in the first place.

An edge-computing-based lightweight blockchain framework (ECLB) was suggested for mobile devices by Liu et al. [15]. In order to achieve greater performance, this work presents a unique set of ledger structures and implements a transaction consensus procedure. In addition, taking into consideration the permissioned blockchain environment, we make explicit use of various cryptographic approaches in order to create a pluggable transaction regulation module. In conclusion, the results of our security analysis and performance evaluation demonstrate that ECLB is capable of maintaining the same level of security as blockchains similar to Bitcoin while achieving superior performance in terms of the cost of ledger storage in mobile devices, the cost of computing blocks, the throughput of transactions, the confirmation latency of transactions, and the transaction regulation cost.

zhou, et al. [16] created a Java annotation-based offloading framework for android mobile devices and gave it the name MCAF. This framework was created with the intention of easing the process of developing android apps that have the potential to offload their processing to a remote server. The only thing that the developers need to do is import the SDK library of our MCAF, and then they need to annotate the methods that need a lot of calculation.

Nandha Kumar *et al.*,

MCAF has the capability to automatically build the code that will be executed in the cloud as well as extract the annotated source code. In addition, the programmes that make the judgements about offloading are automatically integrated into the code that was originally written. Additionally, they carried out the actual trials in order to demonstrate that our MCAF is applicable. The Wireless Body Sensor Nodes was a concept that was suggested by Gosh et al. [17]. (WBSN). These wireless body sensor networks (WBSNs) initially comprise of bio-sensors that collect signals from a patient's body and wireless transmitters that transfer the acquired data to a server that is located in either a private or public cloud. The collected data may then be analysed. These WBSNs are equipped with the appropriate hardware to process signals before sending them to the cloud in order to be stored there. In energy-constrained WBSNs, the simultaneous occurrence of all of these actions results in a large level of power consumption, which, in turn, shortens the operational lifetime of these networks. The vast majority of these data that are being sent to the servers are, by their very nature, duplicated; as a consequence, the therapeutic value that they have is negligible. This is because error-resilience is an inherent property of signal processing algorithms. In conclusion, the findings of the experiments reveal a 96% increase in system-level energy efficiency with just a 2% reduction in the effect on signal quality.

Liu, et al. [18] suggested An examination of approximation computing from both its past and its potential future. The size of a transistor has been greatly reduced from the beginning in line with Dennard's scaling, and the supply voltage has been decreased during the course of the years. As a direct consequence of this development, electronic circuits can now function at higher frequencies while nearly preserving the same amount of power dissipation. Not only does an increase in power consumption occur when the feature size of complementary metal-oxide-semiconductor (CMOS) technology is reduced to 7 nanometers, but an improvement in reliability also occurs at this point. This is due to the fact that it is more difficult to regulate and steer clear of parameter changes and flaws at advanced nanoscales. It was thought that a reverse carry propagate adder should be used, as stated by Pashaeifar et al. [19]. (RCPA). Even if there is variations in the latency, the overall system will be more stable if you use this sort of carry propagation at the beginning of the process. We describe three distinct implementations of the reverse carry propagate full-adder (RCPFA) cell; each of these implementations differs from the others in terms of the amount of delay, power, and energy it consumes, as well as the accuracy it provides. It is possible to produce hybrid adders with varied degrees of accuracy by combining the structure that has been described with an accurate carry adder that works in reverse. Using a variety of different permutations of these structures allowed for the generation of these adders. The discrete cosine transforms (DCT) block of the JPEG compression and the finite-impulse response (FIR) filter applications are analysed in order to determine whether or not the recommended RCPAs are successful. This is the last but not the least of the topics covered.

Marchisio et al. [20] presented their idea of using deep learning for edge computing. In the beginning, as DNNs increase in complexity, the linked issue of their high energy consumption becomes a difficult one to deal with. This task is made much more difficult by edge computing, in which the computing devices have restricted access to resources and must function within a limited energy budget. As a direct result of this, it is necessary to carry out specific optimizations for deep learning on both the software and the hardware levels. In this work, we undertake a complete analysis of the current trends of such optimizations, and we address key outstanding research concerns both in the medium term and in the long term.

Proposed Method

Because full adders are the fundamental components of any integrated circuit, their design and development must be approached with extreme caution in order to get optimal results. Conventional CMOS full adders have much greater power, delay, and energy consumption figures than their digital counterparts. As a result, the alternative technologies of FinFET and GnrFET are the technologies that may give reduced resource utilisation in lieu of the fundamental CMOS technology. In this part, an in-depth discussion of the creation of a full adder via the use of FinFET and GnrFET technology, together with 10T modelling, is presented. The MLFA is shown in the block diagram seen in figure 1. It demonstrates the operation of adding one bit by making use of a number of different components, such as XOR gates, NOT gates, and a Multiplexer 2 to 1 (MUX21), in that order.The functions of the

MLFA are mostly focused on the switching operations for MUX21. Because of its performance, which is characterised by the rapid triggering of data in comparison to that of other building blocks, the computational complexity of the MUX21 is very low in this instance. In addition to that, the logic of FA is satisfied by this activating procedure. In this setup, each individual component is crafted by the use of the FinFET and GnrFET technologies, in that order. In addition, both the process of sum generation and the process of carry out generation are shown in Table 1. The fact that the lines in Figures 1 as well as Table 1 all have different colours indicates that they represent the same procedure.

In the beginning, inputs A and B are placed into the XOR gate, which ultimately produces the half adder sum output. This is the outcome of the first step. The output of this generation is sent as the data input to the MUX21 once it has been processed (input 0). Additionally, the XOR gate is used on the NOT gate, which leads in the output being referred to as XNOR. This is because of the way in which the XOR gate is utilised on the NOT gate. In addition to this, the result of the XNOR operation is fed into the MUX21 as the data input (input 1), and the MUX21 utilises C in as its selection input in the appropriate manner. In addition, depending on the value of C in, MUX21 will choose the data inputs using either the XOR or XNOR outputs. This is shown by the equations (2) and (3) that are presented below, in that order. The total adder sum, which is represented by the symbol S, is found in equation (1), which can be found below.

$$S = A \oplus B \oplus C_{in} \qquad (1)$$
$$C_{in} = 0 \rightarrow S = A \oplus B \oplus 0 \rightarrow A \oplus B \qquad (2)$$
$$C_{in} = 1 \rightarrow S = A \oplus B \oplus 1 \rightarrow A \odot B \qquad (3)$$

In a similar fashion, the result of the XNOR operation is fed into the second MUX21 as the selection input, with C in serving as "data input 0" and B being the "data input 1." This, in turn, produces the carry out (C out).In addition, Equation 4 demonstrates the fundamental process of MLFA carry out, and it is altered in accordance with the XOR-XNOR logic for implementations that are based on multiplexers.

$$C_{out} = AB + C_{in}(A \oplus B) = C_{in}(A \oplus B) + \bar{B}(A \odot B) \qquad (4)$$

Additionally, equations (5) and (6) illustrate the method of carry out generation in the following manner:

$$A \odot B = 0 \rightarrow C_{out} = C_{in} \qquad (5)$$
$$A \odot B = 1 \rightarrow C_{out} = B \qquad (6)$$

The varied colours in Figure 2 and Table 1, respectively, reflect how these equations are used in practise. This can be seen in both of these figures.

Figure 2 illustrates the FinFET modelling of the proposed MLFA that has been developed. The proposed MLFA is constructed from 5 numbers of FinFET PMOS transistors and 5 numbers of FinFET NMOS transistors, each in their own separate 5 number configuration. Due to the fact that the NMOS and PMOS transistors used in this particular implementation are carbon copies of one another, it is essential to include an equilibrium state into the MLFA. This is done in order to ensure that the unbiased electron-hole pair is both regulated and synchronised. In addition to this, the condition of balance also helps to maintain the appropriate level of power consumption while simultaneously improving energy efficiency. The combination of P1 and N1 FinFET transistors performs the function of an inverter, and it gives the value B minus as the output for any value of B that is input. Therefore, the combination of P2 and N2 FinFET transistors functions as an XOR gate, taking the values B and A as its inputs and producing the values A and B as its outputs.

In addition, as an inverter, the combination of P3 and N3 FinFET transistors causes them to produce the XNOR result AB in response to the XOR input AB. AB is the output of the XNOR operation. This is because the result of performing the XOR operation on AB is AB. In addition, the functionality of a MUX21 is accomplished by combining P4 and N4 FinFET transistors in a single device. The letter C in represents the selection input, data input-0 represents AB, data input-1 also represents AB, and the letter S represents the sum output. This specific arrangement of transistors is referred to as a MUX21 and has been given that name. The MUX21 that is generated by the combination of P5 and N5 FinFET transistors operates in the following manner: A and B are used as the selection input, data

Nandha Kumar *et al.*,

input-0 is used as C in, data input-1 is used as B, and the carry output is created as C out, respectively. This brings us to our final point, which is that the combination of these transistors creates a carry output. The implementation of a MLFA using GnrFETs makes use of the same transistor level circuit as before, and the operation remains the same.

RESULTS AND DISCUSSIONS

For the creation of each and every MLFA design, The Xilinx ISE software was the one that was used. This piece of software has the capacity to generate two separate kinds of outputs, namely simulation and synthesis. These outputs are both possible. The results of the simulation make it possible to conduct an in-depth analysis of the MLFA architecture with relation to the many permutations of input and output byte levels. A simple decoding technique may be approximated by applying a large number of different combinations of inputs and watching a wide variety of outputs while doing a simulation study of accurate encoding. As a consequence of the conclusions of the synthesis, the use of space in proportion to the number of transistors will be carried out. In addition, a time summary will be obtained with reference to the various route delays, and a power summary will be prepared making use of the static and dynamic power consumption. Both of these summaries will be gathered. Both of these summaries will be done.The results of the simulation of the existingMLFA are shown in Figure 3. Here, the outputs are wrong. Further, the results of the simulation of the proposed MLFA are shown in Figure 4.

Table 2 presents a comparison and contrast of the results of performance assessments conducted on a number of different MLFA controllers. In this instance, the proposed MLFA resulted in superior (reduced) performance in terms of transistors, time-delay, and power consumption when compared to conventional approaches such EFA [9], 16T-FA [17], 12T -FA [16], and 11T-FA [13]. This was the case because the MLFA used fewer transistors than the conventional approaches. This was the case because the MLFA was able to reduce the time-delay without sacrificing the number oftransistors.

CONCLUSION

This academic article focuses mostly on the design and manufacturing of a MLFA as well as a 4-bit RCA by making use of FinFET and GnrFET technologies. This is the primary topic of the study. It is engaged between the XOR results and the XNOR outcomes so that the entire output is created. In addition, a second multiplexer enabled the data inputs and produced the carry output, both of which contributed to the successful reduction of the route delays. The suggested MLFA is constructed on the basis of the logic used by the multiplexer selection, and as a result, it is activated between those two possibilities in order to provide the sum output. In addition to this, the technique that was proposed was able to reduce the amount of power that was used by activities that were quickly activated. These libraries were used to create the final product. The results of the simulation make it possible to reach the conclusion that the design that was supplied is an excellent choice for a broad variety of addition-based applications. This conclusion can be reached because the findings of the simulation enable it. In addition to this, this strategy is extensible, meaning that it is used to build the complete subtractor, the subtractor, and the multiplication operations in the order given.

REFERENCES

1. Chiluveru, Samba Raju, et al. "Memory efficient architecture for lifting-based discrete wavelet packet transform." IEEE Transactions on Circuits and Systems II: Express Briefs 68.4 (2020): 1373-1377.
2. Hasan, Md Mehedi, and Khan A. Wahid. "Low-cost lifting architecture and lossless implementation of Daubechies-8 wavelets." IEEE Transactions on Circuits and Systems I: Regular Papers 65.8 (2018): 2515-2523.
3. Basiri, M. Mohamed Asan. "Efficient VLSI architectures of lifting based 3D discrete wavelet transform." IET Computers & Digital Techniques 14.6 (2020): 247-255.

Nandha Kumar *et al.*,

4. Lone, Rafi, and Najeeb-ud-Din Hakim. "Multiplier-less architecture for 4-tap Daubechies wavelet filters using algebraic integers." International Conference on Intelligent Computing and Smart Communication 2019. Springer, Singapore, 2020.

5. Singh, Gyanendra, et al. "Novel Architecture for Lifting Discrete Wavelet Packet Transform With Arbitrary Tree Structure." IEEE Transactions on Very Large Scale Integration (VLSI) Systems 29.7 (2021): 1490-1494.

6. M. T. Khan and R. A. Shaik, "Optimal Complexity Architectures for Pipelined Distributed Arithmetic-Based LMS Adaptive Filter," in IEEE Transactions on Circuits and Systems I: Regular Papers, vol. 66, no. 2, pp. 630-642, Feb. 2019, doi: 10.1109/TCSI.2018.2867291.

7. M. T. Khan, J. Kumar, S. R. Ahamed and J. Faridi, "Partial-LUT Designs for Low-Complexity Realization of DA-Based BLMS Adaptive Filter," in IEEE Transactions on Circuits and Systems II: Express Briefs, vol. 68, no. 4, pp. 1188-1192, April 2021, doi: 10.1109/TCSII.2020.3035693.

8. Di Meo, Gennaro, et al. "A Novel Low-Power High-Precision Implementation for Sign–Magnitude DLMS Adaptive Filters." Electronics 11.7 (2022): 1007.

9. Mula, Subrahmanyam, Vinay ChakravarthiGogineni, and AnindyaSundar Dhar. "Algorithm and VLSI architecture design of proportionate-type LMS adaptive filters for sparse system identification." IEEE Transactions on Very Large Scale Integration (VLSI) Systems 26.9 (2018): 1750-1762.

10. Narendran, S., and B. T. Geetha. "Performance Analysis of Parallel FIR Digital Filter Based on Even Symmetric Fast FIR Algorithm using Different Adders." 2021 5th International Conference on Electronics, Communication and Aerospace Technology (ICECA). IEEE, 2021.

11. Betzel, Filipe, et al. "Approximate communication: Techniques for reducing communication bottlenecks in large-scale parallel systems." ACM Computing Surveys (CSUR) 51.1 (2018): 1-32.

12. Mahmud, Mohammad Sultan, et al. "A survey of data partitioning and sampling methods to support big data analysis." Big Data Mining and Analytics 3.2 (2020): 85-101.

13. Wei, Fengguo, Sankardas Roy, and XinmingOu. "Amandroid: A precise and general inter-component data flow analysis framework for security vetting of android apps." ACM Transactions on Privacy and Security (TOPS) 21.3 (2018): 1-32.

14. Stanley-Marbell, Phillip, et al. "Exploiting errors for efficiency: A survey from circuits to applications." ACM Computing Surveys (CSUR) 53.3 (2020): 1-39.

15. M. Liu, F. R. Yu, Y. Teng, V. C. M. Leung, and M. Song, "Computation offloading and content caching in wireless blockchain networks with mobile edge computing," IEEE Transactions on Vehicular Technology, vol. 67, no. 11, pp. 11008–11021, 2018.

16. Zhou, Yilian, et al. "MCAF: Developing an Annotation-Based Offloading Framework for Mobile Cloud Computing." Scientific Programming 2020 (2020).

17. Ghosh, Avrajit, Arnab Raha, and Amitava Mukherjee. "Energy-efficient IoT-health monitoring system using approximate computing." Internet of Things 9 (2020): 100166.

18. Liu, Weiqiang, Fabrizio Lombardi, and Michael Shulte. "A retrospective and prospective view of approximate computing [point of view." Proceedings of the IEEE 108.3 (2020): 394-399.

19. Pashaeifar, Masoud, et al. "Approximate reverse carry propagate adder for energy-efficient DSP applications." IEEE Transactions on Very Large Scale Integration (VLSI) Systems 26.11 (2018): 2530-2541.

20. Marchisio et al., "Deep Learning for Edge Computing: Current Trends, Cross-Layer Optimizations, and Open Research Challenges," 2019 IEEE Computer Society Annual Symposium on VLSI (ISVLSI), 2019, pp. 553-559, doi: 10.1109/ISVLSI.2019.00105

Nandha Kumar *et al*.,

Table 1: Entire Adder Operating Table Proposed.

Inputs			Sum Output	Comments for sum	Temporary outcome	Carry out outcome	Comments for carry out
C_{in}	A	B	S		XNOR (A, B)	C_{out}	
0	0	0	0	Eq. (3) is indicated by blue color	1	0	Eq. (6) is indicated by red color
0	0	1	1		0	0	
0	1	0	1		0	0	
0	1	1	0		1	1	
1	0	0	1	Eq. (4) is indicated by green color	1	0	Eq. (7) is indicated by violet color
1	0	1	0		0	1	
1	1	0	0		0	1	
1	1	1	1		1	1	

Table 2. Comparison Table

METHOD	Transistor count	Average power	Max power	Delay
EFA [9]	16	15.2uw	1.11mw	20.05ns
16T-FA [17]	15	13.8uw	1.17mw	60.16ns
12T -FA [16]	12	5.477uw	0.963mw	20.21ns
11T-FA [13]	11	4.90uw	0.510mw	40.28ns
proposed MLFA	10	2.90uw	0.421mw	12.34ns

Figure 1: Proposed MLFA block diagram.

Figure 2: FinFET simulation of the suggested MLFA.

Figure 3. Simulation output of existing

Figure 4. Simulation output of proposed MLFA

RESEARCH ARTICLE

Social Media Infodemic during Covid -19 Second Wave in India

Garima Gunawat[1]   and Vaishali Kapoor[2*]

[1]Research Scholar, Department of Journalism and Mass Communication, Manipal   University Jaipur, Jaipur, Rajasthan, India.
[2]Associate Professor, Department of Journalism and Mass Communication, Manipal University Jaipur, Jaipur, Rajasthan, India.

*Address for Correspondence
Vaishali Kapoor
Associate Professor,
Department of Journalism and Mass Communication,
Manipal University Jaipur,
Jaipur, Rajasthan, India.
E.Mail: vaishali.kapoor@jaipur.manipal.edu

ABSTRACT

Authenticity of the information has become the prominent issue which is affecting the society along with the media organizations. Widespread influence has a significant impact on the rapid spread of news on social media, simplifying information that is false, inaccurate, or distorted. The public sphere and possible integrity have been disrupted by the current propagation of fake news. are examined in this paper. This paper also discusses the connection between the problem of fake news and the main activities in India during second Covid-19 wave. Indian authorities and mishandling of entire Covid-19 second wave were criticized by international newspapers and nations. This paper also looks for the Indian authorities, who used a lot of propaganda to try to control the people. Any information aims to unite people on a common ground that makes up the public sphere. Throughout the entire Covid-19 second wave in India, from April 2021 to June 2021, where Indian government must be held liable, concerns have been raised.

Keywords: Mishandling, misinformation, Covid-19, Social media, second wave.

INTRODUCTION

People can quickly share information through the internet and amount of shared information is identified as fake.It has made it extremely difficult to create and fabricate accurate news. Because of the abundance of information available through digital media, people can easily access news from a variety of sources. When multiple media

63607

Garima Gunawat   and Vaishali Kapoor

outlets are reporting the same story, however, discerning the real from the fake becomes more difficult. It becomes simpler and more volatile (Sundaram, Nundy& Mallick, 2020). From various platforms,circulation of fake content quickly as well as easily, suggesting that people are susceptible fake news, low reliability and content that is biased. The fact that people are affected by fake news and global sites is the primary cause of concern.People share incomplete or partially misleading information as a result. During the Covid-19 outbreak, all of this false information had a negative impact and led to the improper use of drugs and treatments for these diseases. People asked a lot of questions about the disease's origin, treatment, home remedies, prevention, and transmission by pets and fly to stay up to date. The bogus reports during the Pandemic were spreading quickly in the beginning phases. Authorities coined the term "Infodemic" to describe the widespread dissemination of false information.

In India, during the second wave of the Coronavirus, numerous lives have been lost, according to BBC news. The country was experiencing an increase in the number of Corona cases. People scrambled for hospital beds, oxygen cylinders, and crucial medications because the nation's health infrastructure was unable to handle the situation(Pathak, Salemi,Sobers, and et.al., 2020).Despite numerous warnings and recommendations from medical professionals, the Indian government didn't adequately formulate for second wave. During second wave, the failures and risks were not effectively communicated to the public by any segment of the public health communication. Instead, the government focused on well-known "babas" who held unscientific beliefs and ignored doctors. (Jafri, 2020).

Fake news propagation during the second covid-19 wave
The World Health Organization said that it's important to figure out how fake information gets out of control. In various domains, there were a lot of false information and myths. The followings are some of the most prevalent myths and false information (Reddy, Suryakumari,Yadav, and et.al. 2020):

- Chloroquine and hydroxychloroquine are used to treat malaria, but they can be combined with Covid-19 medications.
- Coronavirus is additionally started by microscopic organisms.
- Covid-19 can be prevented by sun exposure or drinking alcohol.
- Flies are another vector that can spread Covid-19.
- The effect of 5G networks on how the corona is spread out

According to Erku's (2020) discussion, a pandemic has three parallel tendencies: - False prescriptions, fake drugs, and false news. His research shows that fake news depends on its problem and vice versa during the Covid-19 event. This is due to a correlation between the capacity to identify fake news and news consumption online. Volumes vary across all platforms for social media online (Erku, Belachew, Abrhaand et.al, 2020).

Our health infrastructure and lack of medical preparations were highlighted by the sudden rise in Covid cases. As a result, assistance for the intensive care unit, oxygen cylinders, medications, and vaccines were smuggled over via social media. At first, political leaders also spread false information about vaccination. In a video that was published by The Economic Times, the leader of the Uttar Pradesh Samajwadi Party, Ashutosh Sinha, made the incorrect statement that vaccination might make one infertile. In a similar vein, a claim was made in India Today that Muslims should avoid vaccinations because they contain pork. Furthermore, an unfounded claim suggested that the vaccine contained a microchip, purportedly a means for government surveillance. As a result, all of these claims were untrue and eventually proved false. In addition, Uttar Pradesh's former chief minister Akhilesh Yadav uploaded a video that included caption, "Do we laugh or cry over this?". A group of men in that video covered themselves with cow urine cow dung. They believe it will eradicate the Covid-19 disease and prevent it. (Ramesh, 2021).

Infodemic contribution in misinformation
An information epidemic, also known as an infodemic, has emerged as a result of the proliferation of social media and mobile phones with Internet access across the globe as well as the exponential production of information (Here's

Garima Gunawat   and Vaishali Kapoor

How social media Can Combat the Coronavirus "Infodemic," n.d.).Breaking this dangerous cycle is essential: Misinformation spreads at the same rate as new routes for content production and distribution. As a result, the same infodemic propagates and accelerates false information. How accurate is this information? Just a few. Infodemic makes the pandemic worst: -

- Makes it difficult for individuals, decision-makers, and health professionals to locate reliable guidance and sources when they need them. Apps, scientific organizations, websites, blogs, "influencers," and other sources may be used as sources.
- People may experience feelings of anxiety, depression, overwhelm, emotional exhaustion, and inability to meet important obligations.
- When immediate responses are anticipated and not enough time is allotted to thoroughly analyze the evidence, it can affect decision-making processes.
- There is a lack of quality control over what is published and, occasionally, used to take action and make decisions.
- Anything can be written or published online, including podcasts, articles, and so on. primarily through social media channels (individual and corporate accounts).

EPI-WIN held a two-day global online consultation on managing COVID-19 participants in early April. In addition, over 500 ideas were submitted in an interactive online forum.By developing global resources for fact-checking and misinformation management, infodemic measurement and analysis, evidence synthesis, knowledge translation, risk communication, community engagement, and amplification of messages, the WHO is supporting the response to the infodemic.The World Health Organization (WHO) is also working with search, social, and digital companies like Facebook, Google, Tencent, Baidu, Twitter, TikTok, Weibo, and Pinterest to stop fake news and spread accurate information from reliable sources like the Centers for Disease Control and Prevention(Department of Evidence and Intelligence for Action in Health, N.D.).

RESEARCH METHODOLOGY

During the second wave of Corona, fake news items are gathered from fact-checking and news website websites. Qualitative research will be used in this study. This study uses content analysis as its method. The nature of social media, its sources, motivations, and themes of fake news were discovered through content analysis. Fake information is disseminated through the platforms of social media. During entire India's second Covid-19 wave, from April to July 2021, concerns were raised. In this study, the method of purposive sampling is used. A lot of the collected data and information can be squeezed out with the help of purposeful sampling. In addition to this, it makes it possible for the researchers to talk about their findings' main effects. It includes forty news articles, four WHO documents, and ten research papers. Twelve stories from Indian News's six websites: -The Times of India, Economic Times, NDTV, Indian Express, Hindustan Times and India Today. Six fact-checking websites published ten news articles: - News laundry, Scroll, The Quint, The Print, and Alt News in. The Deutsche Well, BBC, The Guardian , The New York Times , Time, The New Yorker , USA Today, Global Times, Reuters, Lancet, and The Washington Post are just eighteen of the international news articles.

The number of people who receive, share, and post information on social media is the mass media's audience. By disseminating social, entertainment, and political information via social media social media sets agenda. Information purification allows agenda of the mass media to reach the audience. Through accidental exposure, Information that is shared online can be shared with more people. McCombs and Shaw carried out a meticulously organized study of the agenda-setting theory in 1972. The agenda-setting theory, according to Gokce (1993), is based on the strategy of using mass communication tools for presentation. It draws attention to subjects that matter to the audience and influence public opinion. According to McQuail (1994), "society will also consider them more important than other issues and subjects" for subjects and concerns that are marked as important by the media (Demirsoy&Karakoç, 2016).

Garima Gunawat   and Vaishali Kapoor

India's epidemic of false Covid-19 information

World Health Organization (WHO) has completely reversed course and now asserts that Corona patients do not require isolation, quarantine, social isolation, or even transmission from one patient to another. The World Health Organization (WHO) asserts that in the digital age, infodemics spread quickly by fostering uncertainty. It is based on mistrust, anxiety, stigma, and other forms of violent aggression that are evidence of the implementation of public health measures, which frequently result in the loss of many lives.

The social media platform was full of conspiracy theories, unverified news, and fake news. That was making things unclear and making it harder to respond effectively to pandemic crises. The social media platform was full of conspiracy theories, unverified news, and fake news. That was making things unclear and making it harder to respond effectively to pandemic crises. Experts estimate that the actual number of corona cases maybe between five and ten times the official count. during the subsequent wave religious misinformation comes in second, with health-related misinformation coming in third (Krishnan, 2021).

The Times of India reports that the government requested that 100 URLs and posts be removed from popular social media platforms like Instagram, Facebook, Twitter and YouTube. those URLs and posts that were accused of spreading false information and inciting panic about the country's Covid-19 situation. The IT ministry was advised by the home ministry that certain users Inappropriately use social media platforms (Doval, 2021). According to the Times of India, Twitter had already established that it had removed four dozen tweets that appear to criticized how the central government dealt with the corona pandemic. Mallick, The Quint's assistant editor in 2021, stated that he revealed that the Telegram,messaging app was major hothouse for fake news and that he had joined several anti-vaxxer groups on social media platforms. Unlike other social media platforms, there is no limit on the number of people who can connect to a group or channel. In addition, there is no evidence that the message has been multiple times forwarded. As a result, passing off the news was simple.

In India, the WHO issued a medical product alert for counterfeit Covishield vaccine. The Indian legitimate manufacturer of the Covidshield was also confirmed by the Serum Institute of India (SII). World Health Organization (WHO) requested that supply chains in regions and nations that are likely to be affected by fake vaccine products be monitored more closely.Covishield, a product developed by Oxford University and AstraZeneca.Covaxin, product that was developed Bharat Biotech, an Indian startup.According to the USA Today there is no correlation between these two vaccines. There is no connection between these two vaccines. India placed an overall order for approximately 167 million doses, and Only 34 million people got the two doses, according to government data. It represented slightly more than 2% of India's 1.3 billion inhabitants (Sadeghi, 2021).

The Middle gave rules to assist individuals with distinguishing between phony and credible antibodies against the crown (Beam, 2021). West Bengal and Maharashtra are two of the states where the bogus vaccination was administered. On the antibiotic injection that is used to treat bacterial vaccines, the con artists applied fictitious labels for Covishield or Covaxine. The thought process behind counterfeit antibodies is to bring in cash through unlawful strategies other than hurting individuals (Choudhary and et. al., 2021).

Mass gathering during second wave of COVID-19

Tirath Singh Rawat, the Boss Priest of Uttrakhand, said concerning the Kumbh Mela in its crowd that stream contains the gifts of Maa Ganga. when Covid was at its peak. There shouldn't be a corona (Bhatia, 2021). Faith should be respected, but faith is for humans and not vice versa, the unabashed Hindu nationalist CM tweeted prior to the Kumbh Mela. Further added, we should put our faith aside to save humanity during this pandemic and contribute to the nation's fight against the coronavirus. India's ruling Bhartiya Janta Party had never made a statement before that defied logic for the crowd. From April 9 to May 8, Uttarakhand's Haridwar hosted the Kumbh Mela. On April 12,

roughly, At Kumbh, three million individuals swam in the Ganges; however,number of corona cases surpassed all previous records. In Haridwar, approximately 2000 people tested positive.

As indicated by The Indian Express, in the midst of overall worry about the crown and public worry over the mass get-together during the Kumbh Mela. Mela should be "Symbolic," according to PM Modi because it will strengthen the nation's fight against the coronavirus pandemic. I pleaded that "shahi snan" would occur and that the Kumbh would now serve as a symbol, Prime Minister Modi wrote in a tweet. The country's pandemic almost did not affect CM Rawat's front. No one will be halted for the sake of Covid as we are certain the confidence in God will defeat the anxiety toward the infection, CM Rawat stated, as reported by Hindustan Times. No one will be halted for the sake of Covid as we are certain the confidence in God will defeat the anxiety toward the infection. CM Rawat issued a statement in which he insisted that the risk and danger of the Tablighi Jamaat event at Nizamuddin Markaz in Delhi outweighed those of the Maha Kumbh Mela, despite the obvious fact that the Kumbh Mela was clearly increasing the number of cases in Uttarakhand (The Wire).

After the Kumbh Mela, a lot of people criticized the government for letting the festival go on while the entire country was fighting a pandemic. The holy river was used by 900000 people, according to officials. Hindus have faith that bathing in the Ganga River will cleanse them of their sins and bring them back to God. Police officers at the Kumbh Mela have stated that it is difficult for them to impose standards on masses. BBC News reports that on a single day, more than 20,000 samples were collected in that region. 2812 active cases were counted by Haridwar at Kumbh. Some devotees tested positive, some chose to remain alone, and some moved to the city of Haridwar's hospital. Each day, it recorded over a thousand new cases. 14 Hindu groups were found to be positive, and the former Chief Minister of Uttar Pradesh was also found to be positive after visiting the Kumbh Mela. The current Uttar Pradesh chief minister was also positive.

Corona cases increased, and political parties turned their focus on election-related activities like voting and attending rallies in some states. The BJP, India's ruling party, denied that mass gatherings during the Kumbh Mela and election rallies were linked to an increase in cases.BJP pioneer BBC News was informed by Dr. Vijay Chaythaiwale that the high cases have nothing to do with political and religious gatherings.In a few states, including West Bengal, Assam, Tamil Nadu, and Kerala, political parties in India began their election series campaigning.The virus could easily be passed from one person to another People who attended election rallies in a crowded location where they were in proximity to other people for an extended period of time and were not properly communally isolated may have spread the virus.(Goodman, 2021).

In the states where West Bengal's elections were headed, Modi and ministers from his party were doing a lot of campaigning. Akhilesh Jha, deputy director of the Federal Department of Science and Technology, says, as people head to the funerals, you have rallied. Additionally, he asserts People will hold you responsible if you continue to hold rallies.The government spokesperson did not respond to any of the questions regarding the criticism of the government. According to Piyush Goyal, minister of railways, commerce, and industry, Prime Minister Modi works long hours every day to deal with the country's crises. Congress, the national opposition party, organized election rallies in West Bengal during the elections. Before the elections, the BJP insisted that candidates exercise their right under the constitution to campaign for at least 14 days. Nirupama Menon Rao, a former foreign secretary, asks, what number of passings does it take until he realizes that an excessive number of individuals have passed on? (Das and Ahmed, 2021).

Political parties started breaking the rules of the Corona campaign gatherings for assembly elections without the election commission's intervention. The Madras High Court said that constitutional bodies could face murder charges because they were "the only institutions responsible for the situation that we are in right now." The election commission was also criticized by the Calcutta High Court for failing to ensure that political parties would adhere to the Covid protocols following the surge of the second corona. In accordance with Corona protocol, rallies and campaigns were attended by a large number of people. Numerous large rallies were staged by PM Modi and Union

Garima Gunawat   and Vaishali Kapoor

Home Minister Amit Shah, drawing criticism from all over the country. However, West Bengal Chief Minister Mamta Banerjee attributed the state's second Corona outbreak and rise in cases to BJP rallies.Mamta Banerjee, on the other hand, was just as guilty of the high-profile rallies and campaigning that were a serious violation of the Corona Protocol.

The government views the second wave
During the second corona wave, India experienced a rise and fall in corona cases before experiencing a sudden increase. By the middle of April, there were already 1.93 million active corona cases in India. In contrast, the corona cases were treated with flippancy and indifference by government officials. During the pandemic, leaders of the nation's ruling party, the Bhartiya Janta Party, made extremely insensitive remarks We are in the final stages of the India coronavirus pandemic, and in order to win at this point, we really want to go through the following three stages: Keep politics out of the COVID-19 vaccination campaign and put your faith in the science behind it: Trust the science behind COVID-19 vaccines, keep politics

The various regions of the nation were in acute need of oxygen supply during the second wave of the corona. However, According to Union Minister Piyush Goyal, the demand for oxygen cylinders is not controlled by state governments. Medical oxygen demand should be controlled by state governments, Piyush Goyal stated to ANI. Management on the demand side is just as important as supply-side management. State governments are responsible for preventing the spread of Covid-19, and they ought to fulfill this responsibility The statement continued, the country's healthcare system will face a significant challenge if cases continue to rise indefinitely. We support state governments, However, in order to prevent the COVID-19 virus from spreading, they must control demand and take action. On social media, individuals voiced their disapproval of each of these comments. On Twitter, the trending hashtag #toomuchoxygen started.

PM Narendra Modi said, never witnessed a crowd as large. a huge crowd to thousands of people at a rally while campaigning for the elections in West Bengal (NDTV). Despite the leader's lack of concern for Corona protocols portrayed this crowd as the worst-case scenario during the pandemic. I only see people everywhere, he continued. According to The Wire, he should have noticed that people didn't follow corona protocol or wear masks, and were very concerned about social distancing(Sen, 2021).

Condemnation of the Indian Council
Reuters says that the government set up a forum of scientists to warn Indian authorities that the new virus variant is more contagious at the beginning of March. In spite of the early advance notice, the public authority forced no significant limitations to visit the circulation of infection. On the other hand, approximately Ten thousand farmers remained in New Delhi to camp out in opposition to Modi's changes to agriculture policy. The populous nation was experiencing difficulties due to the second corona wave (Ghoshal, 2021). Numerous Indians were disheartened by PM Modi over his terrifying reactions to the Covid flood by tending to in excess of 10,000 individuals at political revitalizes and allowing Hindu adherents to go to the celebration. Some hashtags, like #ResignModi and #SuperspreaderModi, gained popularity and became popular on Twitter. There were heaps of dead bodies that were heaped in the morgues and crematories, need for medical clinic beds and blood, oxygen chambers, and crown tests overwhelmed online entertainment. On the talk show "Mann ki Baat," PM Modi spoke to the nation about his immense popularity and dedication, focusing on the "Mask Zaroori." However, in contrast, the PM spoke to thousands of people at the rally, maintaining the social distance and uttering the phrase "Amazing atmosphere" without mentioning corona-safe behaviors (Narendra Modi, 2021).

Criticism from authorities of foreign media
The Second Wave of Coronavirus is spreading throughout India, according to the New York Times, and there is a shortage of oxygen and supplements that can save lives. While the government of India directed to remove a dozen posts that criticized the government's handling of the pandemic on social media, that order primarily targeted opposition-related posts calling for Modi's resignation. India's public health problems became the political agenda.

Garima Gunawat   and Vaishali Kapoor

Pictures of people desperately seeking hospital beds and oxygen and requesting assistance from the government went viral on the internet, which horrified people all over the world. The ruling party in India became aggressive, arresting a number of journalists and activists, and putting pressure on media organizations to change their stance. In troubled areas, they also block mobile internet access. As a result, they began spreading propaganda against China and blocked advertisements owned by Chinese organizations. Twitter blocked approx. 500 accounts after government suspects them, and government also threatened to arrest their employees.

Prof. Sumit Ganguly writes in a Washington Post column that the Modi government is alert but has made irrational decisions, because of this the second floor of the crown squashed the country. This clearly conveys the following: Policy objectives, political dramaturgy, and electoral prospects are more important than the population's well-being (Times of India, 2021). PM Narendra Modi was criticized by the well-known medical journal The Lancet for saying that removing tweets of criticism rather than attempting to contain the pandemic. Additionally, their lack of Covid-19 mitigation measures was noted as noticeable in the editorial. The Lancet additionally requested that the public authority broadcast exact data quickly. Mr. Modi's ruling Bharatiya Janata Party and other parties have continued to hold massive rallies where thousands of people have been unmasked, even as the number of cases has increased, in their article, the New York Times mentioned. The government has also allowed a massive Hindu festival to attract millions of pilgrims, despite signs that it has accelerated the spread of the virus (Schmall, 2021

According to BBC reports, India's healthcare system is buckling as a record number of Covid-19 cases put pressure on hospital beds and drain oxygen supplies. Some patients are left untreated for hours, leaving families pleading for their critically ill relatives. The sycophantic cabinet ministers who praised Modi for successfully dealing with Covid-19 in India despite testing slowing down and allowing people to become more complacent about the virus bear responsibility. The strongman regime has ignored all warnings (Ayyub, 2021). This was also stated in an article that was published in Times magazine. Global Time in China also said that India had let its guard down. Now According to Oxford Economics, the upward trend will continue for a few weeks, if not months, when tens of thousands of people return to a poor and densely populated nation like India (Sheng, 2021). Further, they added, when thousands of people return to a poor and densely populated nation like India, the upward trend will continue for several weeks, if not months. By allowing state elections, political rallies, and religious festivals to take place and declaring victory over the pandemic, the Prime Minister is also accused of ignoring the warning signs of the second wave, disregarding the advice of scientists, and encouraging a culture of complacency at the highest levels of government.

CONCLUSION

Majority of the world was affected by the corona's second wave. India's situation was grim. The second wave of the virus spread at a much quicker and at a rate that is more complicated than the first wave. During the subsequent wave, Indians knew nothing about crown conventions like veiling, keeping proper social separation, staying away from huge get-togethers, etc. This study aims to spread false information during the second corona wave. It is concluded that a lot of false information and news was spread during the second corona wave. On social media platforms like Facebook, Whatsapp, and YouTube, messages, images, and videos were used to spread a lot of false information. India was marked by a variety of political content and false information regarding cases, deaths, treatment options, and prevention strategies. The lack of medical oxygen, hospital beds, vaccines, and antiviral medications strained the Indian health sector. In the absence of facilities or ambulances, individuals were dying in homes and the parking lots of hospitals. They refused to stop large crowds. Thousands of the coronavirus was found in these pilgrims. The Indian government and its actions were criticized by numerous international media outlets. It is concluded that there was insufficient flexibility and planning. In numerous urban areas in India, the well-being framework fell the government rushed to prepare for the sudden announcement of oxygen plants and other health facilities during the second crisis wave.

REFERENCES

1. Aggarwal, A. (2020, December 28). *Faith or safety? Covid vaccines spark religious concerns over pork gelatin, cow blood*. India Today. https://www.indiatoday.in/coronavirus-outbreak/vaccine-updates/story/religious-hurdle-for-covid-19-vaccines-religious-leaders-raise-concern-over-pork-gelatin-cow-blood-in-vaccines-1753992-2020-12-28)

2. Ayyub, R. (2021, April 23). *"This Is Hell." Prime Minister Modi's Failure to Lead Is Deepening India's COVID-19 Crisis*. Time. https://time.com/5957118/india-covid-19-modi/.

3. BBC News. (2021, April 14). *Haridwar: Hundreds test positive for Covid at Kumbh Mela*. https://www.bbc.com/news/world-asia-india-56742231.

4. Bhatia, R. (2021, May 10). *India's Epidemic of False COVID-19 Information*. The New Yorker. https://www.newyorker.com/news/dispatch/indias-epidemic-of-false-covid-19-information.

5. *BJP's Himanta Sarma's "No Need To Wear Mask" Comment Draws Criticism*. (n.d.). NDTV.com. https://www.ndtv.com/india-news/no-covid-in-assam-no-need-for-face-mask-bjps-himanta-biswa-sarma-2405878.

6. Correspondent, F. (2021, May 8). *Foreign media on India's Covid crisis*. Times of India Blog. https://timesofindia.indiatimes.com/blogs/foreign-media/foreign-media-on-indias-covid-crisis/

7. Correspondent, H. (2021, March 20). *'Devotees' faith will overcome fear of Covid-19 in Mahakumbh': CM Rawat*. Hindustan Times. https://www.hindustantimes.com/cities/others/devotees-faith-will-overcome-fear-of-covid-19-in-mahakumbh-cm-rawat-101616253395877.html.

8. *COVID-19 Mythbusters – World Health Organization*. (n.d.). https://www.who.int/emergencies/diseases/novel-coronavirus-2019/advice-for-public/myth-busters.

9. *COVID-19: As Thousands Gasp for Oxygen, Government Tardiness in Spotlight*. (n.d.). The Wire. https://thewire.in/health/covid-19-as-thousands-gasp-for-oxygen-government-tardiness-in-spotlight.

10. Das, K. N. (2021, April 20). *India's Modi scorned over reckless rallies, religious gathering amid virus mayhem*. Reuters. https://www.reuters.com/world/india/indias-modi-scorned-over-reckless-rallies-religious-gathering-amid-virus-mayhem-2021-04-19/.

11. Demirsoy, A. and Karakoç, E. 2016. "Contribution of Social Media to Agenda Setting Approach". *Atatürk İletişimDergisi*, (10), pp.137-147.

12. *DEPARTMENT OF EVIDENCE AND INTELLIGENCE FOR ACTION IN HEALTH*. (n.d.).https://iris.paho.org/bitstream/handle/10665.2/52052/Factsheetinfodemic_eng.pdf.

13. Doval, P. (2021, April 26). *Ordered only 'fake' Covid posts blocked, not critical ones: IT ministry*. The Times of India. https://timesofindia.indiatimes.com/india/ordered-only-fake-covid-posts-blocked-not-critical-ones-it-ministry/articleshow/82249535.cms.

14. Erku, D. A., Belachew, S. A., Abrha, S., Sinnollareddy, M., Thomas, J., Steadman, K. J., & Tesfaye, W. H. (2020). When fear and misinformation go viral: Pharmacists' role in deterring medication misinformation during the "infodemic" surrounding COVID-19. *Research in Social and Administrative Pharmacy*, *17*(1). https://doi.org/10.1016/j.sapharm.2020.04.032.

15. Express Web Desk. (2021, April 17). *Kumbh should now be symbolic, says PM Narendra Modi amid surge in Covid-19 cases*. The Indian Express. https://indianexpress.com/article/india/narendra-modi-kumbh-mela-coronavirus-surge-7277381/.

16. Ganguly, S. (2021, April 28). *Modi's pandemic choice: Protect his image or protect India. He chose himself.* Washington Post. https://www.washingtonpost.com/outlook/modis-pandemic-choice-protect-his-image-or-protect-india-he-chose-himself/2021/04/28/44cc0d22-a79e-11eb-bca5-048b2759a489_story.html.

17. Ghoshal, D. (2021, May 3). *EXCLUSIVE Scientists say India government ignored warnings amid coronavirus surge*. Reuters. https://www.reuters.com/world/asia-pacific/exclusive-scientists-say-india-government-ignored-warnings-amid-coronavirus-2021-05-01/.

18. Goodman, B. S. M. a. J. (2021, April 29). *India Covid crisis: Did election rallies help spread virus?* BBC News. https://www.bbc.com/news/56858980.

19. *Here's how social media can combat the coronavirus "infodemic."* (n.d.). MIT Technology Review. https://www.technologyreview.com/2020/03/17/905279/facebook-twitter-social-media-infodemic-misinformation/.

20. Hindustan Times (2021b, December 28). *Chandigarh: Former chief justice NK Sodhi succumbs to Covid*. Hindustan Times. https://www.hindustantimes.com/cities/chandigarh-news/chandigarh-former-chief-justice-nk-sodhi-succumbs-to-covid-101640727182668.html.

21. India Today. (2021, April 29). *Is the Election Commission responsible for the second wave of Covid cases?* https://www.indiatoday.in/india-today-insight/story/is-the-election-commission-responsible-for-the-second-wave-of-covid-cases-1796437-2021-04-29.

22. India Today. (2021a, March 7). *We are in the endgame of Covid-19 pandemic in India: Health Minister Harsh Vardhan*. https://www.indiatoday.in/coronavirus-outbreak/story/we-are-in-the-endgame-of-covid-19-pandemic-in-india-vardhan-1776697-2021-03-07.

23. Jafri, A. 2020. *Fake News, Quackery Mar India's COVID Fight but Government is Doing Nothing About Infodemic*. (n.d.). The Wire. https://thewire.in/media/fake-news-quackery-mar-indias-covid-fight-but-government-is-doing-nothing-about-infodemic.

24. Krishnan, M. (2021, May 3). *COVID: Misinformation complicates India's pandemic fight*. dw.com. https://www.dw.com/en/india-covid-misinformation/a-57414876.

25. L. (2021). India's COVID-19 emergency. *The Lancet, 397*(10286), 1683. https://doi.org/10.1016/s0140-6736(21)01052-7 .

26. Mallick, A. (2021, April 12). *Inside India's Anti-Vaxx Telegram Groups, COVID-19 is a Conspiracy*. TheQuint. https://www.thequint.com/news/webqoof/telegram-anti-vaccine-covid-19-misinformation

27. Mashal, M., & Kumar, H. (2021, May 25). *India Covid-19 Crisis Deepened by Missteps and Complacency*. The New York Times. https://www.nytimes.com/2021/04/09/world/asia/india-covid-vaccine-variant.html.

28. Moole, B. J. (2021, April 23). *A nightmare on repeat - India is running out of oxygen again*. BBC News. https://www.bbc.com/news/uk-56841381.

29. Narendra Modi. (2021, April 27). *PM Modi's Mann Ki Baat with the Nation, April 2021* [Video]. YouTube. https://www.youtube.com/watch?v=K8zeo3ID6OY.

30. NDTV. 2021. "Have never ever seen such huge crowds at a rally: PM Modi in Asansol". *NDTV*. Retrieved on 31 March 2022(https://twitter.com/ndtv/status/1383419909128933377?ref_src=twsrc%5Etfw%7Ctwcamp%5Etweetembed%7Ctwterm%5E1383419909128933377%7Ctwgr%5E%7Ctwcon%5Es1_&ref_url=https%3A%2F%2Fthewire.in%2Fpolitics%2Fbjp-leaders-covid-19-pandemic-remarks).

31. NDTV.2021.*"States Must Keep Oxygen Demand Under Control": Union Minister Piyush Goyal*. (n.d.). NDTV.com. https://www.ndtv.com/india-news/covid-oxygen-shortage-piyush-goyal-says-states-must-keep-oxygen-demand-under-control-2416616.

32. Pathak, E. B., Salemi, J. L., Sobers, N., Menard, J., & Hambleton, I. (2020). COVID-19 in Children in the United States: Intensive Care Admissions, Estimated Total Infected, and Projected Numbers of Severe Pediatric Cases in 2020. *Journal of Public Health Management and Practice, 26*(4), 325–333. https://doi.org/10.1097/phh.0000000000001190.

33. Pathak, K. (2020). COVID-19 Infodemic and Indian Media: An Evaluative Study. *IntechOpenEBooks*. https://doi.org/10.5772/intechopen.94230

34. Ramesh, M. (2021, May 12). *What Can Prevent COVID? Repeat After Us – Not Cow Dung or Urine!* TheQuint. https://www.thequint.com/news/india/cow-dung-urine-to-prevent-coronavirus-unscientific#read-more

35. Rand, D. G., McPhetres, J., Zhang, Y., Lu, J. G., & Rand, D. G. (2020). Fighting COVID-19 Misinformation on Social Media: Experimental Evidence for a Scalable Accuracy-Nudge Intervention. *Psychological Science, 31*(7), 770–780. https://doi.org/10.1177/0956797620939054.

36. Ray, M. 2021. *How to identify fake Covid-19 vaccines? Centre issues guidelines.* (2021, September 5). Hindustan Times. https://www.hindustantimes.com/india-news/how-to-identify-fake-covid-19-vaccines-centre-issues-guidelines-101630831462696.html

37. Recchia, F., & Vijayan, S. (2021, May 6). *In India, social media is a lifeline. It's being silenced.* Washington Post. https://www.washingtonpost.com/opinions/2021/05/06/india-social-media-covid-19/.

38. Reddy, P., Suryakumari, V. B. P., Yadav, S. S., Doshi, D., Palle, A. R., &Gopikrishna, M. (2020). Myths regarding COVID-19 among Indian population – An online survey. *Journal of Global Oral Health*, *3*, 94–100. https://doi.org/10.25259/jgoh_29_2020 .

39. Rodríguez, C., Carballido, B. V., Redondo-Sama, G., Guo, M., Ramis-Salas, M., &Flecha, R. (2020). False news around COVID-19 circulated less on Sina Weibo than on Twitter. How to overcome false information? *RIMCIS : International and Multidisciplinary Journal of Social Sciences*. https://doi.org/10.17583/rimcis.2020.5386.

40. Sadeghi, M. K. (2021, May 12). Today, M. S. U. *Fact check: India's COVID-19 surge not connected to vaccinations.* USA TODAY. https://www.usatoday.com/story/news/factcheck/2021/05/11/fact-check-indias-covid-19-surge-not-connected-vaccinations/4988690001/

41. Schmall, E. (2021, May 5). *India Scrambles to Supply Oxygen as Covid-19 Patients Gasp for Breath.* The New York Times. https://www.nytimes.com/2021/04/23/world/asia/india-covid-oxygen-hospitals.html.

42. Sen, J. 2021. *Nine Things BJP Leaders Said Recently About the Pandemic – But Shouldn't Have.* (n.d.). The Wire. https://thewire.in/politics/bjp-leaders-covid-19-pandemic-remarks.

43. Sheng, W. 2021. Times, G. (n.d.). *Surging coronavirus variants continue to shadow economies.* Copyright 2021 by the Global Times. https://www.globaltimes.cn/page/202104/1220720.shtml.

44. Sundaram, S., Nundy, S., & Mallick, T. K. (2020). How India is dealing with COVID-19 pandemic. *Sensors International*, *1*, 100021. https://doi.org/10.1016/j.sintl.2020.100021 .

45. Sundaram, S., Nundy, S., & Mallick, T. K. (2020b). How India is dealing with COVID-19 pandemic. *Sensors International*, *1*, 100021. https://doi.org/10.1016/j.sintl.2020.100021.

46. T. S. ., & T. S. . (2021b, December 28). *Misinformation on vaccines, farmers and minorities: India's fact-checkers had a busy 2021.* Newslaundry. https://www.newslaundry.com/2021/12/28/misinformation-on-vaccines-farmers-and-minorities-indias-fact-checkers-had-a-busy-2021.

47. Tewari, R. (2021, April 14). *Poll rallies to Kumbh Mela — Modi-Shah's conscience must take a look at latest Covid surge.* ThePrint. https://theprint.in/opinion/politricks/poll-rallies-to-kumbh-mela-modi-shahs-conscience-must-take-a-look-at-latest-covid-surge/639526/.

48. The Economic Times. (2021a, January 3). *COVID-19 vaccine might make a person impotent, claims SP leader.* The Economic Times. https://economictimes.indiatimes.com/news/politics-and-nation/covid-19-vaccine-might-make-a-person-impotent-sp-leader/videoshow/80079030.cms?from=mdr.

49. The Guardian.2021. *"Everybody is angry": Modi under fire over India's Covid second wave.* (2021, May 17). The Guardian. https://www.theguardian.com/world/2021/may/17/everybody-is-angry-modi-under-fire-over-indias-covid-second-wave

50. The Guardian.2021. *"The system has collapsed": India's descent into Covid hell.* (2021, April 21). The Guardian. https://www.theguardian.com/world/2021/apr/21/system-has-collapsed-india-descent-into-covid-hell

51. Timesofindia.Com. (2021, April 25). *"Need to stop panic & misinformation": Govt clarifies on Twitter move.* The Times of India. https://timesofindia.indiatimes.com/india/need-to-stop-panic-misinformation-govt-clarifies-on-social-media-move/articleshow/82241793.cms.

52. World Health Organization: WHO. (2020, September 23). *Managing the COVID-19 infodemic: Promoting healthy behaviours and mitigating the harm from misinformation and disinformation.* https://www.who.int/news/item/23-09-2020-managing-the-covid-19-infodemic-promoting-healthy-behaviours-and-mitigating-the-harm-from-misinformation-and-disinformation.

53. World Health Organization: WHO. (2021, April 27). *Fighting misinformation in the time of COVID-19, one click at a time.* https://www.who.int/news-room/feature-stories/detail/fighting-misinformation-in-the-time-of-covid-19-one-click-at-a-time.

54. World Health Organization: WHO. (2021b, August 31). *Medical Product Alert N°5/2021: Falsified COVISHIELD vaccine (Update)*. https://www.who.int/news/item/31-08-2021-medical-product-alert-n-5-2021-falsified-covishield-vaccine.

55. Zarocostas, J. (2020). How to fight an infodemic. *The Lancet, 395*(10225), 676. https://doi.org/10.1016/S0140-6736(20)30461-X

RESEARCH ARTICLE

Rapid Stability Indicating HPLC Method for the Estimation of Teriflunamide in Teriflunomide Pharmaceutical Dosage Forms

Suresh Kumar Raju.V[1]*, P. Sanjeeva[2] and P. Venkata Ramana[3]

[1]Research Scholar, Department of Chemistry, Sri Krishnadevaraya University, Ananthapuramu, Andhra Pradesh, India.
[2]Lecturer, Department of Chemistry, Sri Krishnadevaraya University, Ananthapuramu, Andhra Pradesh, India.
[3]Professor, Department of Chemistry, Sri Krishnadevaraya University, Ananthapuramu, Andhra Pradesh, India.

*Address for Correspondence
Suresh Kumar Raju.V
Research Scholar,
Department of Chemistry,
Sri Krishnadevaraya University,
Ananthapuramu, Andhra Pradesh, India.
E.Mail: sureshkumarraju03@gmail.com

ABSTRACT

A simple, accurate, precise method was developed for the estimation of the Teriflunomide in a tablet dosage form and optimized separation was achieved on a Inertsil C8 column (250 mm×4.6 mm; 5 μm) using mobile phase composition of buffer pH 6.0 and acetonitrile in the ratio of 45:55 (v/v), at a flow rate of 1.5 mL/min in isocratic elution. UV detection was carried out at a wavelength of 250 nm. The temperature was maintained at Ambient. Well-resolved peak were observed with high numbers of theoretical plates, lower tailing factor and reproducible relative retention time. The method was validated and all the validation parameters were found to be within the acceptance limits.

Keywords: Teriflunomide, Phenyl isoxazole, 4-(trifluoromethyl) aniline, RP-HPLC method development, Validation.

INTRODUCTION

Teriflunomide (trade name Aubagio, marketed by Sanofi) is an Immunosuppressive Agent. Teriflunomide was investigated as a medication for multiple sclerosis (MS) and act by inhibiting pyrimidinede novo synthesis by blocking the enzyme dihydroorotate dehydrogenasee [1,3,4,5].

63618

Suresh Kumar Raju *et al.,*

A literature search confirms that there is no method reported for the simultaneous estimation of Teriflunomide quantitatively in pharmaceutical dosage forms of Tablets. Hence the present work aimed to develop a simple stability indicating RP-HPLC method for the separation and quantification of Teriflunomide. Considering the BCS classification, solubility, and the influence of gastrointestinal pH on solubility of drug substances, in vitro dissolution studies of formulations containing both drugs are very important to check the release and solubilization of the active drug substance from the drug product and to predict the in vivo performance of different formulations. The main aim of this method was to determine and validate the Teriflunomide based on International Conference on Harmonization guidelines [2]. This method was made use of a reproducible procedure for the quantitative analysis of drug samples in tablet dosage forms. The designed method was considered as an advisable to develop precise, accurate, simple RP-HPLC method.

MATERIAL AND METHODS

Chemicals, reagents and instruments
Teriflunomide, Ortho phosphoric acid (H_3PO_4), potassium dihydrogen phosphate (KH_2PO_4), Potassium hydroxide (KOH), Acetonitrile and Milli-Q water. Inertsil C8 250 x 4.6mm, 5μm column, HPLC instrument equipped with UV-VIS spectrophotometer.

Mobile phase and solutions preparation
Preparation of buffer
Pipette 0.5 mL of Orthophosphoric acid in 500 mL of water, adjusted pH of the solution is 6.0 with diluted potassium hydroxide solution.

Preparation of Mobile phase:
Mix 45 mL of buffer, 55 mL of acetonitrile and sonicate to degas.

Preparation of Dissolution media
Weigh and dissolve 6.8 g of potassium dihydrogen phosphate in 1000 mL of water, add 0.8 g of sodium hydroxide pellets, adjust the pH of the solution to 6.8 with diluted sodium hydroxide solution.

Standard Preparation
Accurately Weighed and transferred 18mg of Teriflunamide standard into a 50 ml clean dry volumetric flask, add acetonitrile to dissolve the material by sonication and make up to the final volume with acetonitrile.
For 7 mg: Further pipette 1 mL stock solution into 50 mL of volumetric flask and diluent to volume with dissolution media.
For 14 mg: Further pipette 2 mL stock solution into 50 mL of volumetric flask and diluent to volume with dissolution media.

Sample Preparation
Dissolution parameters, i.e., USP dissolution apparatus type II (paddle type), at 50 rpm and 1000 mL dissolution medium containing 0.05M phosphate buffer pH 6.8 were selected as per FDA guidelines [6] for in vitro dissolution. The medium was equilibrated at 37.0 ± 0.5 °C, and tablet samples were added to each dissolution bowl. Sample collection as per the prescribed schedule at 30 min. At specified time intervals10 mL of sample was collected using a bent cannula from half way between the top of the medium and the top of the paddle, not less than 1 cm away from the wall of the bowl and each sample aliquot from bowl was filtered through a 0.45-μm nylon filter (Millipore). With the progress of International Conference on Harmonization (ICH) guidelines, the method has developed into more clearly and obligatory. Hence the necessity of separation of several components through the study of stability samples, HPLC has gained reputation in stability studies due to its specificity, sensitivity and high-resolution capacity. The work planned in this research was subjected towards the study of the chromatographic actions of the

samples of stress degradation of teriflunamide and its impurities in the tablet dosage formulation. The stability indicating study of present drug has not reported so far in the literature as per our knowledge and motivated us to develop an RP-HPLC- PDA stability indicating test where the degradation products were resolved from the integral drugs.

Method development

The standard drug solution containing 7.2 µg/mL concentrations of Teriflunomide was initially used for method development studies, the blank chromatogram in the Figure 1,placebo chromatogram in the Figure 2, standard chromatogram in Figure 3 and Sample chromatogram in Figure 4.

Method validation

The method was validated as per ICH guidelines. The different validation parameters which were performed asfollowing: linearity, precision, accuracy, specificity, limit of detection, limit of quantification and robustness.

System suitability test

System suitability was evaluated with freshly prepared standard solutions. Five replicate standard solution injections were performed and calculated the % RSD for retention time and peak area. Other parameters theoretical plates and tailing factor were measured. System suitability results were tabulated in table 1. % RSD values were within the limit 2%.

Specificity and Placebo Interference

Specificity of the method is important to check interference of excipients and dissolution medium on the response of the drug substance. A composite solution of placebo was prepared from all excipients of tablets, i.e., except the active ingredient, in the same medium. This solution was analyzed using the same chromatographic conditions, and baseline was evaluated for peak response. Placebo interference was also ensured by spiking the reference solution with appropriate levels of excipients and evaluating for any interference or additional peak other than known peaks of Teriflunomide. No inference was observed from placebo at retention time of Teriflunomide. Placebo, standard and sample chromatograms in figure-5 to 7.

Linearity

Linearity parameter was evaluated with standard solutions by preparing six different concentrations. Linearity levels are 20%, 50%, 75%, 100%, 125%, 150% concentrations. All six linearity solutions were injected into the HPLC system and calculated the correlation coefficient values. Correlation coefficient was calculated for concentration versus peak area. Results were obtained in table 2 &3. Results were satisfactory, correlation coefficient values were above 0.99.

Precision

Precision was performed by injecting the six dissolution bowl solutions and all solutions were carried out as per the test procedure mentioned in the materials and method section. Method precision % of RSD results were calculated and tabulated in table 3. Precision results were found satisfactory and % RSD values were below 5 %.

Acceptance Criteria

The % RSD should not be more than 5%.

Accuracy

Accuracy of the method was determined on three concentration levels by recovery experiments. The recovery studies were carried out by different concentration of organic impurities added to the sample 20%, 50 %, 100 % and 150 % were evaluated. Accuracy recovery and % RSD were calculated and tabulated in table 4. % of recovery results were between 95 % to 105 % and % RSD values were below 5.0 %.

Limit of detection and limit of quantification

Limit of detection (LOD) is the least concentration of analyte in a sample that can be identified but not quantified. Limit of quantification (LOQ) is defined as least concentration of analyte in a sample that can be estimated with tolerable precision, accuracy and reliability by a specified method under affirmed experimental conditions. Teriflunomide LOD & LOQ were found to be 0.6 µg/mL& 2.1 µg/mL respectively.

Robustness

Robustness of the method was performed with flow rate, mobile phase pH, temperature variations evaluated. System suitability was conducted to check the variation changes and results were found satisfactory.

RESULTS AND DISCUSSIONS

The current study describes new and simple, reliable, economic elution RP-HPLC method for the estimation of Teriflunomide in the tablet dosage form. To our present knowledge, no such detailed method has been presented as of now for this drug. The developed method finished use of UV as a tool confirmation. *In vitro* dissolution studies of pharmaceutical dosage form are very important and a vital criterion for the product quality control. In vitro dissolution is used to evaluate the release and solubilization of the active drug substance from the drug product and to predict correctly the delivery of the required drug substance to the patients. In this context, it is important to have an accurate and precise RP-HPLC analytical method to quantify the amount of drug substance in dissolution medium simultaneously. The proposed RP-HPLC analytical method was successfully validated according to the requirements of USP and ICH guidelines for validation of analytical procedure. All the results of the complete agreement with the required limits and criteria. The validated method was successfully applied to determination of dissolution profiles of the tablet dosage form, using USP apparatus II. It is concluded that the method is accurate, precise, linear, and specific for the simultaneous determination of Teriflunomide and can be applied to routine quality control analysis of tablet dosage form in vitro dissolution studies.

ACKNOWLEDGEMENT

REFERENCES

1. Bruneau JM, Yea CM, Spinella-Jaegle S, Fudali C, Woodward K, Robson PA, Sautès C, Westwood R, Kuo EA, Williamson RA, Ruuth E. Purification of human dihydro-orotate dehydrogenase and its inhibition by A77 1726, the active metabolite of leflunomide. The Bioch J., 1998; 336(2): 299–03.
2. *International Conference on Harmonization (ICH); Validation of analytical procedures: Methodology, Q2B (CPMP/ICH/281/95), 1995. Available at:* http://www.ich.org.
3. Marriott J, O'Connor P. emerging therapies in relapsing-remitting multiple sclerosis. Rev Recent Clin Trials, 2010; 5(3): 179–88.
4. O'Connor PW, Li D, Freedman MS, Bar-Or A, Rice GP, Confavreux C, etal.A Phase II study of the safety and efficacy of Teriflunomide in multiple sclerosis with relapses. Neurology, 2006; 66(6): 894–900.
5. Osiri M, Shea B, Robinson V, Suarez-Almazor M, Strand V, Tugwell P, Wells G. Leflunomide for treating rheumatoid arthritis. Cochrane database of syst rev (Online), 2003; (1): CD002047.
6. US FDA, Center for Drug Evaluation and Research (CDER), Generic drugs division of bioequivalence: FDA-recommended dissolution method. https://www.accessdata.fda.gov/scripts/cder/dissolution/dsp_ Search Results. cfm.

Suresh Kumar Raju *et al.*,

Table 1(a): System suitability results for 7 mg strength

Teriflunomide				
Injections	Retention Time(min)	Area	USP Plate Count	USP Tailing factor
1	4.02	593584	8542	1.21
2	4.03	593458	8558	1.22
3	4.05	593845	8525	1.21
4	4.02	593545	8534	1.23
5	4.03	593615	8562	1.21
Mean	4.03	593609	8544	1.21
Std. Dev.		144.26		
% RSD		0.0		

Table 1 (b): System suitability results for 14 mg strength

Teriflunomide				
Injections	Retention Time(min)	Area	USP Plate Count	USP Tailing factor
1	4.10	1195142	7584	1.14
2	4.12	1196458	7548	1.16
3	4.10	1194258	7514	1.12
4	4.11	1196158	7558	1.14
5	4.10	1194251	7565	1.13
Mean	4.11	1195253	7554	1.13
Std. Dev.		1034.09		
% RSD		0.1		

Table 2: Linearity concentration table

Linearity level	Teriflunomide	
	Concentration (µg/mL)	Peak area
20%	1.4432	116058
50 %	3.6079	295456
75 %	5.4119	438900
100 %	7.2158	585252
125 %	9.0198	735974
150 %	10.8237	878475
Correlation coefficient	0.999	

Table 3: Method precision results

S. No	%drug dissolved of Teriflunomide	
	7 mg strength	14 mg strength
1.	95	96
2.	96	98
3.	98	95
4.	96	96

Suresh Kumar Raju *et al.*,

5.	97	97
6.	96	98
Mean	96	97
S.D	1.03	1.21
%RSD	1.1	1.2

Table 4: Accuracy results

Accuracy (%Recovery)		
S. No	Recovery level	Teriflunomide
1.	20%-1	97.1
2.	20%-2	97.5
3.	20%-3	96.3
4.	50%-1	98.0
5.	50%-2	98.5
6.	50%-3	98.1
7	100%-1	98.9
8	100%-2	98.4
9	100%-3	98.2
10	150%-1	101.5
11	150%-2	100.1
12	150%-3	99.2
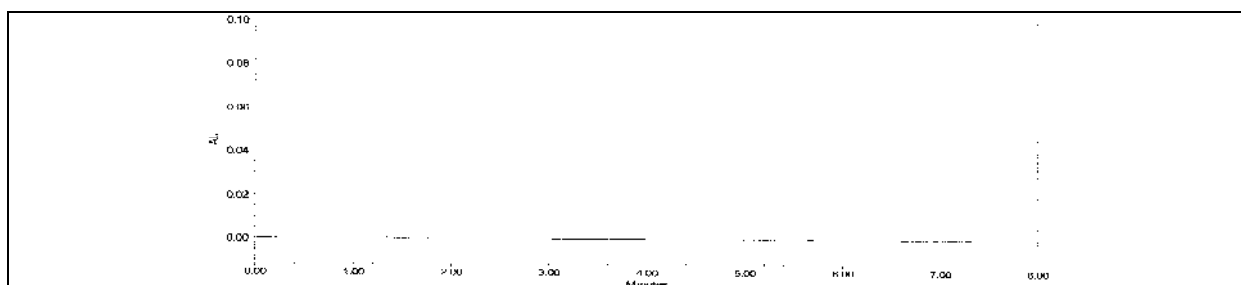
Figure 1: Blank chromatogram
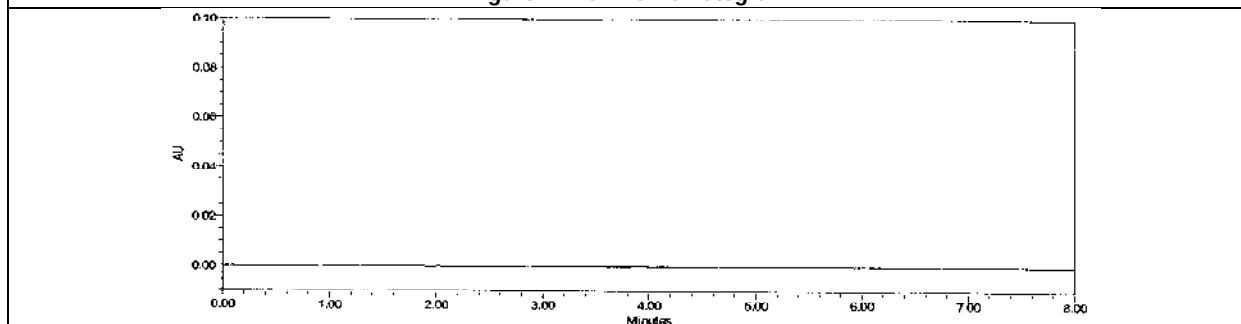
Figure 2: Placebo chromatogram

63623

Suresh Kumar Raju *et al.*,
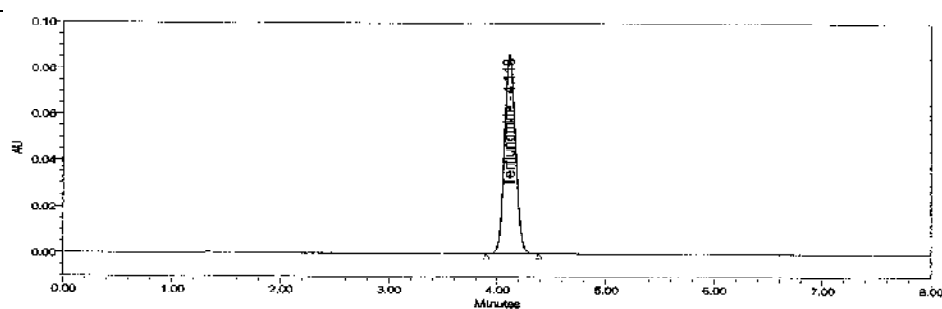
Figure 3: Standard chromatogram
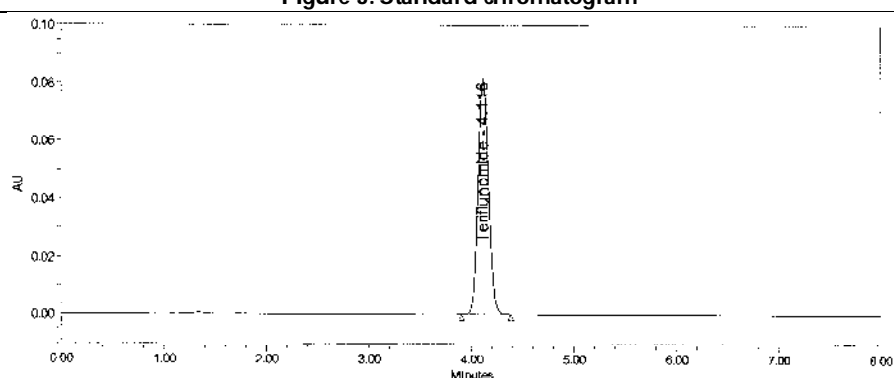
Figure 4: Sample chromatogram
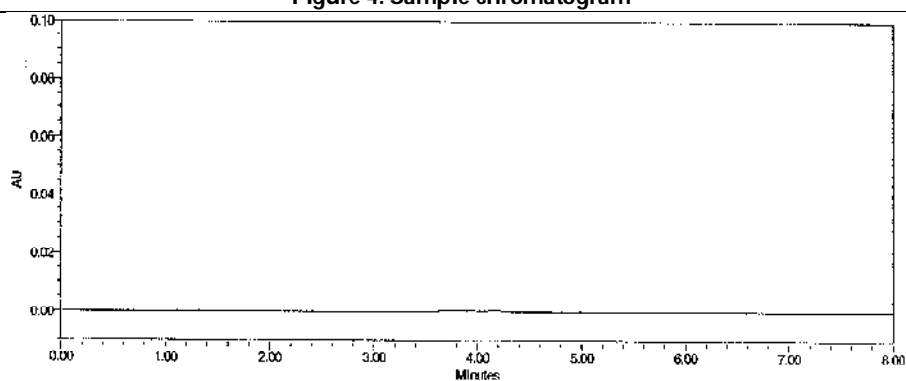
Figure 5: Placebo chromatogram
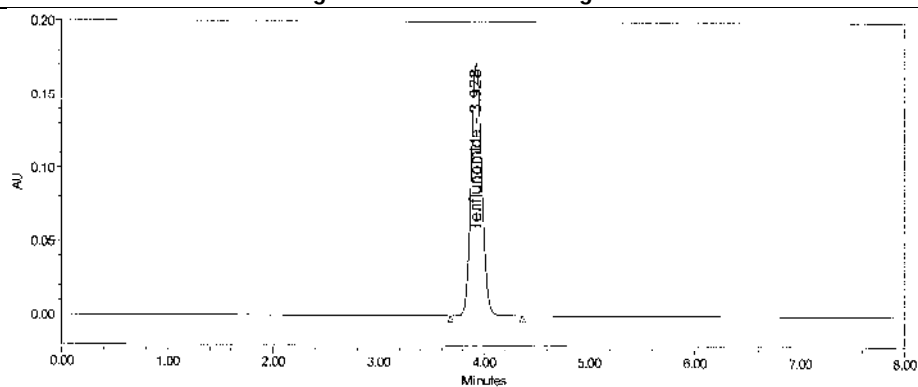
Figure 6: Standard chromatogram
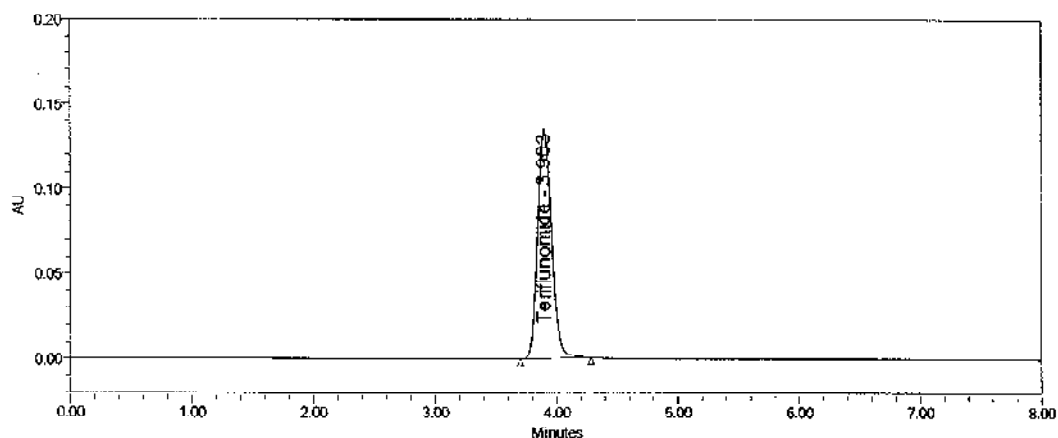
Figure 7: Sample chromatogram
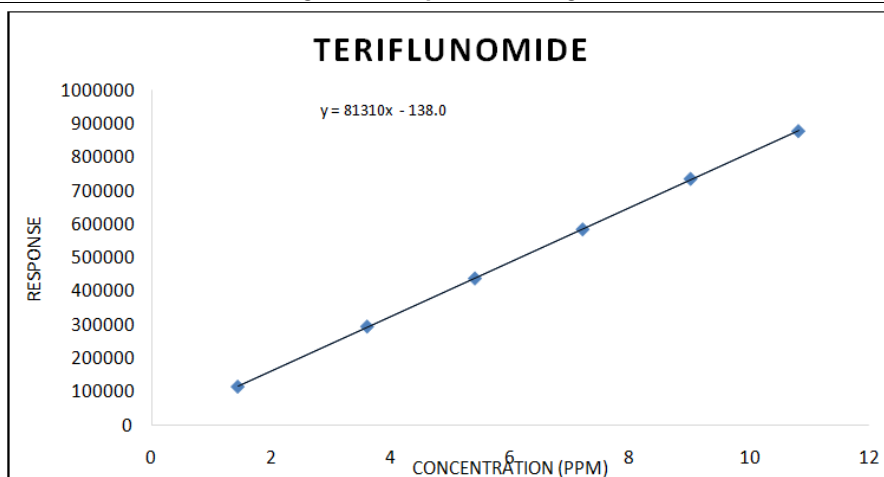
Figure 8: Linearity graph for Teriflunomide

RESEARCH ARTICLE

Intelligent Cruising and Road Quality Mapping

K.Kabilan[1]* and K.Madheswari[2]

[1]Assistant Professor (Sr), School of Computer Science and Engineering, VIT, Chennai - 600127, Tamil Nadu, India.
[2]Associate Professor, School of Computer Science and Engineering, VIT, Chennai - 600127, Tamil Nadu, India.

*Address for Correspondence
K.Kabilan
Assistant Professor (Sr),
School of Computer Science and Engineering,
VIT, Chennai - 600127,
Tamil Nadu, India.
E.Mail: @gmail.com

ABSTRACT

This paper presents Intelligent Cruising and Road Quality Mapping which monitors the road conditions and detects the bumps and potholes in the road and alerts regarding the same. Over the decades of evolution, there are promising develop- ments across the world yet with its own significant demerits. One such arena is road transportation. Transportation to varsities, colleges, business parks, and other occupational grounds is majorly covered by terrain commutations. The standard of roads plays a significant role in shaping the journey of each citizen. Bad roads cause disruptions within the routine. Bumps and potholes within the roads cause wear and tear of the vehicle and discomfort to the passengers. Hence, it's desirable to own a mechanism for detecting the condition of roads and to induce them repaired as soon as possible. An android application that involves Google Maps API, firebase as database and a Machine learning model that uses linear acceleration data to assess road quality, is developed that non-intrusively detects road conditions that are updated on a real-time basis and alerts drivers for future endeavors. Alerts are issued regarding potholes, speed breakers, and bumpy roads so as to boost passenger experience and absolve the proposed demerits. The dataset for the model is collected manually by driving through the roads of Chennai city. Upon training the single layer perceptron, a significant accuracy of 80.75% has been achieved.

Index Terms—Road Quality Mapping, Intelligent Cruising, machine learning, neural networks, tensorflow.

INTRODUCTION

With the development of technology in road transportation, there have been promising developments across the globe yet with its own significant demerits. Transportation to schools, colleges, business parks, and other occupational grounds is majorly covered by terrain commutations. The quality of roads often shape the journey of every individual. Bumps and potholes in the roads cause wear and tear of the vehicle and discomfort to the passengers. Although comfort in road navigation has been a prevalent topic of importance over the decade, it is, however, difficult to train an application that can detect the presence of hurdles such as potholes and speed breakers which often are impediments to commuting. Hence, it is desirable to have a mechanism for detecting the condition of roads and to get them repaired as soon as possible, thereby reducing government investment in the production of new roads and casualty relief funds. As a result, working on monitoring road conditions has gained significant attention in recent times. Smartphones in the current day come with inbuilt sensors that range from gyroscope to her monitoring. Owing to the availability of low-cost sensors in smartphones and the rapid increase in the rate of smartphone users, it has never been more salient to develop one such monitoring application. In this project we have developed an android application that uses Google Maps API to map potholes, firebase as database and developed a machine learning model that uses linear acceleration data from sensors to assess road quality and non-intrusively detect road conditions that are updated on a real-time basis. Alerts are issued regarding potholes, speed breakers, and bumpy roads in order to enhance passenger experience and absolve the proposed demerits. Section II deals with related works on this forum highlight- ing the use of different technologies, Section III discusses the methodology proposed for the project we developed with its architecture, Section IV has the experimental observations and conclusions derived from processing the data set.

RELATED WORKS

Road Quality Mapping attempts to classify accelerometer data into categories such as pothole, speed breaker and normal road. Different systems have been designed that can identify different characteristics of given accelerometer data. Some of the existing works:

Real Time Pothole Detection using Android Smartphones with Accelerometers

Mednis et al, describe a mobile sensing system for road irregularity detection using Android OS based smartphones. Selected data processing algorithms are discussed and their evaluation presented with true positive rate as high as 90% us- ing real world data. The optimal parameters for the algorithms are determined and the recommendations for their application are described [1].

Pothole Patrol

Eriksson et al, describe an application of mobile sensing: detecting and reporting the surface conditions of roads. It describes a system and associated algorithms to monitor this important civil infrastructure using a collection of sensor- equipped vehicles. This system, which is called as the Pothole Patrol (P2), uses the inherent mobility of the participating vehicles, opportunistically gathering data from vibration and GPS sensors, and processing the data to assess road surface conditions [3].

Pothole Detection and Warning System using Wireless Sensor Networks

This paper aims at proposing a novel pothole detection system which assists the driver in avoiding potholes on the roads, by giving prior warnings. Interest in Intelligent Vehicle Systems comes from the problems caused by traffic congestion worldwide and a synergy of new information technologies for simulation, real-time control and communications networks. The architectural design further proposes a low response time, low maintenance and deployment cost solution to this problem [8].

Pothole Detection System using Machine Learning on Android

Aniket Kulkarni et al. has proposed a paper called Pothole detection system using machine learning on android in

which the pothole sensor plug-in monitors the changes in the accel- eration in order to detect potholes. For this, the user needs to have an Android Smartphone. The device's built-in accelerom- eter is used to collect the x, y and z axis accelerations. The pothole detection algorithm is good, in terms of speed and accuracy. This algorithm accepts the training set and displays the pothole scenario in the particular area [2].

Pothole Detection System using Wi-Fi Access Point
Sudam Pawar et al has proposed a system where the system is divided into three subsystems. First, a sensing subsystem which is used to sense the potholes encountered by it. Second is communication subsystem which handles the information transfer between Wi-Fi Access Point and Mobile Node. Third subsystem is the localization subsystem which analyses the data received from Access Points and warns the driver regarding the occurrence of potholes[10].

Traffic Sense
Traffic Sense is a system for rich monitoring of road and traffic conditions using mobile smartphones equipped with an array of sensors (GPS, accelerometer, microphone) and communication radios. In this system, they have focused on the sensing component of Traffic Sense, specifically on how these sensors and radios are used to detect bumps and potholes, braking, and honking, and to localize the phone in an energy efficient manner [7].

A Pothole Detection System using Z-Thresh
Kruthik M S et al. has proposed a system which uses accelerometer data and GPS data. They have assumed some threshold values on Z-axis. The threshold values are set by trail and error method. [9].

SYSTEM DESIGN
Upon driving a vehicle, the linear acceleration data collected using the sensor present in the smartphone is aggregated over an interval of 3 seconds periodically. Mean and median for the data acquired is calculated and fed as input to the TfLite model. The TfLite model upon classification decides if the processed data is a pothole or a speed breaker or a normal road. If the result is pothole or a speed breaker, the location is geo- hashed into an alphanumeric string containing 0-9 characters and is uploaded to the firebase database. The Navigation App, used by the drivers, scans the database for potholes within a specified radius of 700 metres from the current location regularly. Based on the proximity of the vehicle to the pothole an alert is issued to the driver when he is under a 100 metre distance so that he can maneuver accordingly to either safely avoid or slow down the vehicle to minimize the effect of impact. The driver can also enter the destination and get optimal routes with less number of potholes. Figure 1. Briefly illustrates the workflow and the system design.

EXPERIMENTATION

Dataset
The dataset used in this assignment was created by collect- ing, real time acceleration data using a smart phone on a road surface with the help of custom developed android application. Driving through the roads of the city in a four wheeled vehicle, we collected the linear acceleration data of the three axes, with an aggregation, over an interval of 5 seconds. The interval split was done using timestamp to segment the continuous data. The live data collected was labelled and uploaded into a firebase database. The data collected manually is bound to contain human errors such as incorrectly classifying a normal road as pothole. These outliers collectively decrease the efficiency of the TfLite Model which takes the aggregation of the collected data as input.

To remove such outliers, Interquartile ranges (IQR) are found and values within 25th and 75th percentile are consistent and clean with no outliers. Figure 2. portrays the data collection app screen. The data collection button is used to collect normal road data. While this button is active, pothole or speed breaker button can be clicked to record 5 seconds of linear acceleration data. For this recorded data, mean and median for all 3 axes is calculated, labelled

and uploaded to the firebase database. From Figure 3, it can be seen that pothole graph contains a single crest while the speed breaker graph contains 2 crests. This is due to the movement of two wheels both front and back over the speed breaker consecutively. There is no significant change in the normal road graph due to the flat surface of the road.

Training
Instead of using popular scikit package for creating machine learning model we are using tensorflow lite model which is the only model that can run on smartphones. In order to simulate the model, a single layer single node model is considered to replicate a machine learning model that has a softmax activation function. The input shape is 6 (mean x, mean y, mean z, median x, median y, median z) and the output shape is 3 (pothole, speed breaker, normal). Softmax was used to give the probability of occurrence of each class out of 3. The input data is trained for 1000 epochs. For gradient optimization, the adam optimizer is used and loss is calculated using sparse categorical cross entropy.

Figure 4. portrays the accuracy of the model as 82.75% and the validation accuracy being 80.43% and also displays the loss and validation loss of the model as 0.5799% and 0.6599% respectively.

Navigation App
The Navigation App, used by the drivers, scans the database for potholes within a specified radius of 700 metres from the current location regularly. Based on the proximity of the vehicle to the pothole an alert is issued to the driver when he is under a 100 metre distance so that he can maneuver accordingly to either safely avoid or slow down the vehicle to minimize the effect of impact. GeoFire library is used to fetch potholes within a specific radius. This is an open-source library for Java that allows to store and query a set of keys based on their geographic location. It uses Geo Hashing method which is an encoding technique used to encode geographic coordinates (latitude, longitude) into an alphanumeric string delineating an area on map, which is called a cell, with varying resolutions. The precision of the location is proportional to the number of characters in the string.

PERFORMANCE ANALYSIS
In this section, we evaluate the results of the proposed architecture. There are 700 samples each for pothole, speed breaker and normal road in the data set. From this, using softmax, probability distribution values for potholes, speed breakers and normal roads are generated. The performance metric used is accuracy. Accuracy in classification task is the number of correct predictions made by the model over all other predictions made.

CONCLUSION

In this paper, we illustrated the task of Intelligent Cruising and Road Quality Mapping with a tensorflow lite model having single layer single node, suitable to run on smartphones. The data set for this task is collected using sensors built in smartphones, consisting of linear acceleration data from various kinds of roads. The data set was recorded in and around Chennai city. The samples are pre-processed to remove outliers. They are then trained using machine learning. This system achieved an overall accuracy of 82.75% . Future work of this project focuses on enhancing the accuracy, which can be done by altering the architecture. Further, the overall accuracy of this task can be improved by using Long Short Term Memory (LSTM) and considering data as time series and not as aggregation.

REFERENCES

1. A. Mednis, G. Strazdins, R. Zviedris, G. Kanonirs and L. Selavo, "Real time pothole detection using Android smartphones with accelerometers," 2011 International Conference on Distributed Computing in Sensor Systems and Workshops (DCOSS), Barcelona, 2011, pp. 1-6.
2. Aniket Kulkarni , Nitish Mhalgi , Sagar Gurnani , Dr. Nupur Giri. "Pothole Detection System using Machine

Kabilan and Madheswari

Learning on Android". International Journal of Emerging Technology and Advanced Engineering, Volume 4, Issue 7, July 2014.

3. Eriksson, J., Girod, L., Hull, B., Newton, R., Madden, S., and Balakrishnan H. "The pothole patrol: Using a mobile sensor network for road surface monitoring". In: Sixth Annual International conference on Mobile Systems, Applications and Services (MobiSys 2008). IEEE, Breckenridge, U.S.A. (June 2008).

4. Gunjan Chugh, Divya Bansal and Sanjeev Sofat. "Road Condition Detection Using Smartphone Sensors". International Journal of Electronic and Electrical Engineering. ISSN 09742174, Volume 7, Number 6 (2014), pp. 595-602.

5. H. Hautakangas and J. Nieminen, "Data mining for pothole detection." Presented at the Pro gradu seminar, University of Jyvaskyla, February 2011.

6. K. De Zoysa, C. Keppitiyagama, G. Seneviratne, and W. Shihan. "A public transport system based sensor network for road surface condition monitoring". In Proc. NSDR'07, pp. 9–14 (2007).

7. P. Mohan, V. N. Padmanabhan, and R. Ramjee, "Nericell using mobile smartphones for rich monitoring of road and traffic conditions," in Proceedings of the 6th ACM conference on Embedded network sensor systems, ser. SenSys '08. New York, NY, USA ACM, 2008, pp. 357–358.

8. Rode, Sudarshan & Vijay, Shonil & Goyal, Piyush & Kulkarni, Purushottam & Arya, Kavi. (2009). "Pothole Detection and Warning System: Infrastructure Support and System Design". Electronic Computer Technology, International Conference on. 286-290. 10.1109/ICECT.2009.152.

9. S, Kruthik & Vali, D. (2018). "Pothole Detection System". 398-400. 10.21467/proceedings.1.62.

10. Sudam Pawar, Shubham Admuthe, Mugdha Shah, Sachita Kulkarni, Rahul Thengadi."Pothole Detection and Warning System using IBM Bluemix Platform" Volume: 03 Issue:11 — Nov-2016.

11. "Realtime maps, traffic information and directions from Google Maps" [Online] https://developers.google.com/maps/documentation/an droid- sdk/intro

12. "GeoFire library for android to query keys with geographic location" [Online] https://github.com/firebase/geofire-android

13. "Android SDK for developing android apps that runs on smartphones" [Online] https://developer.android.com/

Table I:Details of the road samples

Data set-road segments		
Class label	**No. of training samples**	**No.of testing samples**
Normal Road	462	281
Pothole	462	238
Speed Breaker	462	238
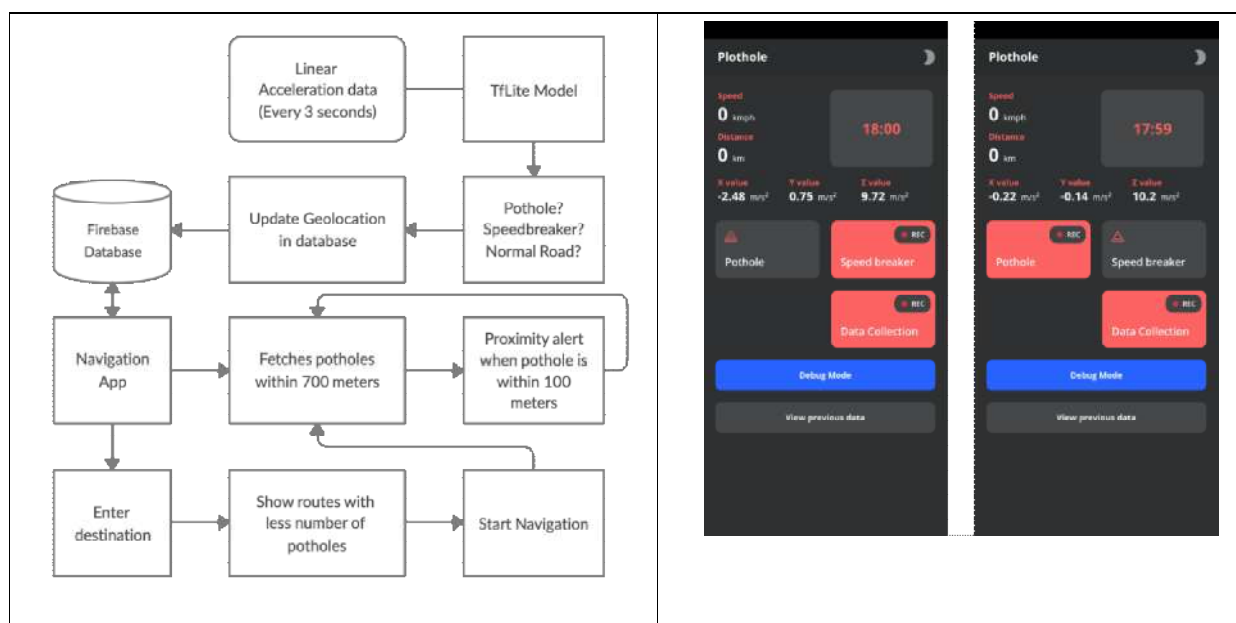
Fig. 1: System Design

Fig. 2: Data Collection App
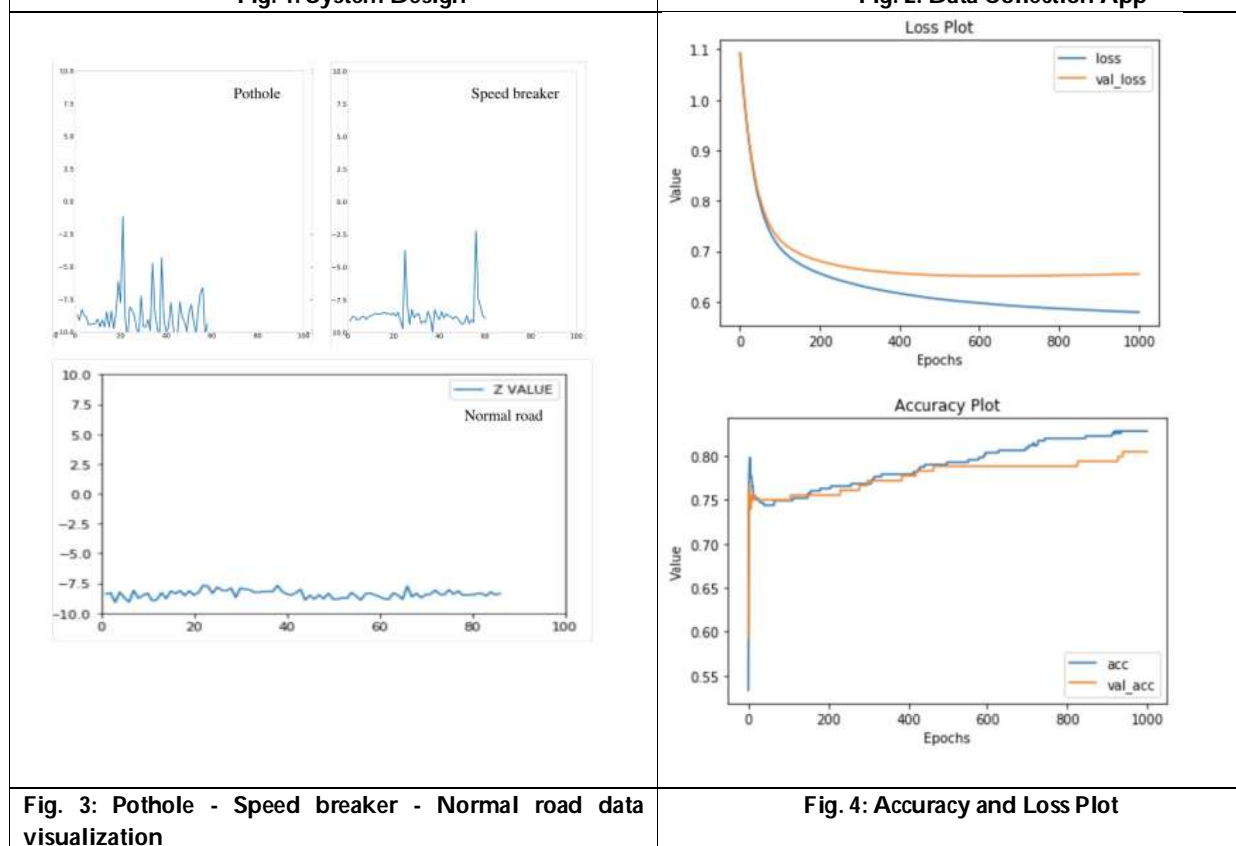
Fig. 3: Pothole - Speed breaker - Normal road data visualization

Fig. 4: Accuracy and Loss Plot
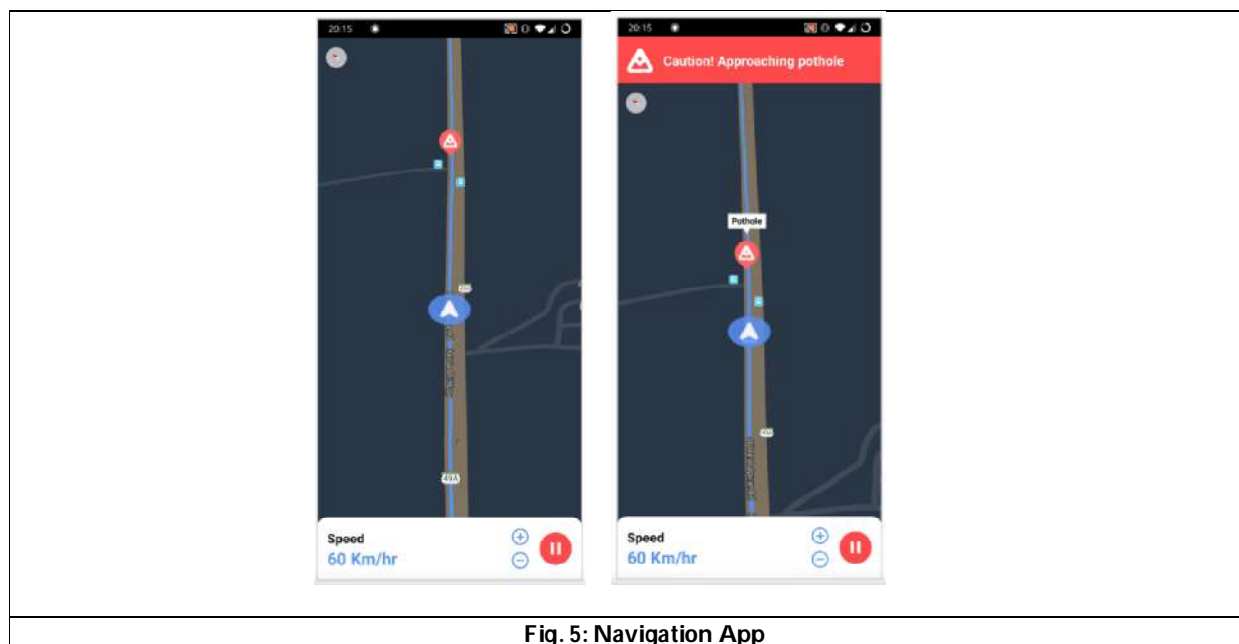
Fig. 5: Navigation App

RESEARCH ARTICLE

Musculoskeletal Pain in Patients with Paraplegic Spinal Cord Injury: Prevalence and Severity

Jenny D. Chaudhari[1], Vivek H. Ramanandi[2]*, Mahima Y. Tailor[1] and Priyanshi R. Patel[1]

[1]Consultant Physiotherapist, Surat, Gujarat, India.
[2]Associate Professor, SPB Physiotherapy College, Surat, Gujarat, India

*Address for Correspondence
Vivek H. Ramanandi
Associate Professor,
SPB Physiotherapy College,
Surat, Gujarat, India
E.Mail: vivekramanandi@gmail.com

ABSTRACT

Traumatic spinal cord injury (SCI) patients can be affected by numerous immediate or long-term complications. Musculoskeletal (MSK) pain is among the most typical consequences. Primary objective of the study was to find prevalence of MSK pain & its severity in paraplegic SCI patients in Gujarat, India. Secondary objective was to find areas commonly affected & factors associated with MSK pain. An observational study was conducted including 142 patients with paraplegic SCI. MSK pain & area of body was assessed through Nordic Musculoskeletal Questionnaire (NMQ), severity of pain was assessed through Numeric pain rating scale (NPRS). Majority participants were male (n=142) and were from younger age group having their mean age 34.73 ± 6.72 years. MSK pain prevalence was 57% and reported moderate to severe intensity pain reflected as mean NPRS value (4-10 integers). Shoulder was most commonly (52.8%) affected followed by lower back (33.1%) and then upper back pain (21.8%). The findings of this study suggest that the majority of SCI patients experience moderate to severe MSK pain and the areas of the shoulder and back are most affected areas.

Keywords: Musculoskeletal, pain, paraplegia, prevalence, spinal cord injury.

INTRODUCTION

Spinal cord injury (SCI) is defined as damage to the spinal cord that results in loss of motor, sensory &/or autonomic function and affects young adults predominantly [1,2]. Therefore, SCI usually leads to a long-lasting serious disability, which requires rehabilitation. The prevalence of SCI is 365/million population in America and around 12,500 new cases of SCI are reported in North America, according to the National Spinal Cord Injury Statistical

63633

Center [3,4]. In India, the incidence & prevalence of SCI are 15/million and 236/million respectively [3]. The SCI affects not only one person but also the whole family as they may require help for assistance with basic day to day activities like dressing, feeding, bladder & bowel and also includes managing household chores, finance, shopping etc. [5,6]. The SCI patients suffer from several types of pain such as musculoskeletal (MSK) pain, visceral pain and neuropathic pain [8]. MSK pain is a common problem for many people with SCI which generally arises from bones, ligaments and muscles either in acute post injury phase or chronic overuse of muscles [8, 9].MSK pain is found to interfere with everyday life causing stress, anxiety &also negatively affects mood, interfere with sleep, quality of life (QOL). The mechanisms of MSK pain in SCI patients are somewhat similar to the general population. For example, MSK pain involving the neck, shoulders, and upper limbs may be related to overuse, extreme joint postures, high mechanical stresses, and repetitive movements associated with transfers and use of wheelchairs [7,10].

The study of pain prevalence can indicate the MSK issues of patient with SCI, although its prevalence varies in different studies, thus study of general prevalence of pain is of great importance. In this study we want to know if the factors like age, types of injury, and level of injury have a significant role in MSK pain or not because these factors are directly related to changes in the mechanical efficiency of joints. Besides significant impairments, patient with SCI also face with significant acute & chronic complication which have negative impact on survival, functional independence and QOL. Understanding the factors and pain is of critical importance not only for patient but also for family and caregivers. The aim of the present study is to find MSK pain prevalence and severity in SCI patients in Gujarat.

METHODS

An observational study using survey form for SCI patients was conducted after receiving ethical approval certificate from Institutional ethics committee of SPB Physiotherapy College, Surat. Various physiotherapy and rehabilitation centers were approached and permission to undertake data collection from paraplegic SCI patients attending their setups was received. The subjects were invited for participation and after screening for inclusion and exclusion criteria eligible candidates were included for study. Traumatic SCI paraplegic patients, between 18-50 years, and had injury before 12 months were included. Patients with acute SCI (within 12 months), clinically unstable patients, quadriplegic patients, or other spinal cord pathology were excluded. As shown in fig.1, based upon criteria 142 participated had been selected. After receiving informed consent, the participants had filled the assessment and data collection form. The assessment and data collection sheet consist of demographics data, screening form, Nordic Musculoskeletal Questionnaire (NMQ) and Numeric pain rating scale (NPRS). The data was tabulated, sorted and stored using Microsoft Office Excel and analyzed using descriptive statistics. SPSS (Statistical Package of Social Science) software version 20.0 and Microsoft Office Excel were used for analyses and plotting graphs.

RESULTS AND DISCUSSION

A spinal cord injury causes a person to have a serious injury to their spinal cord. The severity of the impairment it produces can lessen a person's activity and participation restrictions. Table 1 shows demographic characteristics of 142 paraplegic patients. It was seen that most of the participants were male (n=117, 82.4%) and majority belonged to younger age groups of 18-30 years and 41-50 years, 78% approximately. Approximately 52% participants had history of road accidents and 54% had complete SCI. Most of the patients (n=113, 79.60%) had thoracic and thoraco-lumbar spinal injury. In this study the participant mean age is 34.72 ± 6.72 years. This study shows that 29% (n=41) of participants were between the age group of 18-30 years. In a previous study, it was found that the majority of the spinal cord injury patients mean age was 45.91 ± 6.69 years (20-66 years) [11]. Also, it was reported in one study that the most common SCI patient's affected average age group who had pain in their upper limb was 42.2 ±12 years[12]. The reason for spinal cord damage differs from one person to the next and from one region to another. In this study it was found that 31.7% (n=45) were injured by fall from height, 52.1% (n=74) were by motor vehicle or road traffic accident, 6.3 % (n=9) from diving, 4.1% (n=7) sports related and 4.1% (n=7) from violence. In this study it was also

Jenny D. Chaudhari *et al.*,

found that road traffic accident is the highest cause of injury, secondly fall from height and the third highest rate is due diving. Mehta et. al. (2014) in Turkey found that 51% of SCI patients were injured due to this cause followed by 24% from fall, 11% from Gunshot [13].

The aim of the study was to find MSK pain prevalence in the paraplegic spinal cord injury patients in Gujarat. MSK pain can interfere with daily activities and affects the muscles, bones, ligaments, tendons, nerves, and joints. MSK pain may be acute (with a sudden onset strong symptoms) and chronic (long lasting). [14] We found that about 57% of SCI patients complains of MSK pain while rest 43% of patients reported no complains of MSK pain. Gupta N, Solomon J and Raja K (2011) surveyed that among 600 individuals were taken to study survey for pain & they found that 57% of SCI patients complained of pain [15]. Few other studiessuggested that SCI induced MSK pain hasvaryingprevalence ranging from 33-92%, one third of patients with spinal cord injuries who experience pain after their injury endure severe pain. [16-19]. Graph 1 shows that from 142 paraplegic SCI patients about 57% of SCI patients reported MSK pain.

Graph 2 shows anatomical areas of body reported to be affected by SCI patients. It was reported that among 81 patients who had complains of pain, 75 had shoulder pain; 47 had lower back pain, 31 had upper back pain, 18 had neck pain, 13 had elbow pain and 4 of them complained of wrist pain. Graph 3 shows the distribution of pain intensity for paraplegic SCI patients on the basis of NPRS scores. It shows that 42.96% of SCI paraplegic patients felt moderate type of pain, 11.27% of them felt severe pain in their body and 2.82% of them felt mild pain

MSK pain can be localized in one area, or widespread. Discomfort, minor aches, and sprains are some of more thoughtful health problems of MSK symptoms which require medical treatment. Anyone can experience MSK pain. It is most often caused by injury to the bone, joint, muscle, tendon, ligaments or nerves. In our study among all about 57% (n=81) of patients complains of pain, 52.8% (n=75) of them complains of shoulder pain, 33.1% (n=47) had lower back pain, 21.8% (n=31) had upper back pain, 11% (n=18) neck pain, 7% (n=13) elbow pain and 2% (n=4) of them complains of wrist pain. According to an epidemiological study conducted in India, about 20,000 new instances of SCI are reported annually, with shoulder pain being the most common symptom (60-70 %). One study shows that 74.2% (n=89) women were having pain compared to 60.1% of the men [20]. With using NPRS in this study we found that among 142 patients of paraplegic spinal cord injury 44% complains of moderate type of pain, 10% of severe pain, 3% of them complains of mild pain. So, we can say that SCI patients are having moderate-severe type of pain. 43% patients complains that they are not having any type of MSK pain. In the study of Hassan M &Kamrujjaman M (2019) with using NPRS it was found that MSK pain in SCI patients is 92% which termed as high prevalence rate & in many studies in most of SCI patients' pain was found to be moderate to high prevalence rate. [17].

The questions were focused on asking the patients if they had any difficulties related to or complaints such as tightness, transferring, lifting & moving wheelchair in surrounding area. Table 2 shows that 25.4% (n=36) of patients fells tightness/contracture in any joint of their body and 74.6% (n=106) did not fell contracture or tightness in their body. 38.7% (n=55) paraplegic patients of SCI felt pain while moving wheelchair by their own and 61.3% (n=87) paraplegic patients of SCI did not felt pain while moving wheelchair by their own. 37.3% (n=53) patients fell pain while transferring activity or self-transfer and 62.7% (n=89) patients did not felt any pain while transferring activity. Only 16.2% (n=23) patients felt pain by lifting objects from surroundings and 83.8% (n=119) patients did not feel any pain while lifting. Limitations of this study was convenience sampling was used that was not reflecting the wider population under the study and the prevalence of the MSK pain was only for traumatic and paraplegic SCI patients. Future studies may include larger sample size with stratified sampling across the state and long-term studies including various intervention strategies for such pain can be conducted.

Jenny D. Chaudhari *et al.,*

CONCLUSION

This study came to the conclusion that 57 percent of SCI paraplegic patients report experiencing MSK pain. MSK discomfort ranges from moderate to severe in intensity. Lower back and upper back pain come in second and shoulder joint pain is more common than in other joints.

ACKNOWLEDGEMENT

REFERENCES

1. Khazaeipour Z, Rezaei-Motlagh F, Ahmadipour E, Azarnia-Ghavam M, Mirzababaei A, Salimi N, Salehi-Nejad A. Burden of care in primary caregivers of individuals with spinal cord injury in Iran: its association with sociodemographic factors. Spinal Cord. 2017 Jun;55(6):595-600.
2. Backx AP, Spooren AI, Bongers-Janssen HM, Bouwsema H. Quality of life, burden and satisfaction with care in caregivers of patients with a spinal cord injury during and after rehabilitation. Spinal cord. 2018 Sep;56(9):890-9.
3. Gopal VV, Baburaj PT, Balakrishnan PK. Caregiver's burden in rehabilitation of patients with neurological deficits following traumatic spinal cord injury. Journal of Spinal Surgery. 2017 Jan 1;4(1):9.
4. Alizadeh A, Dyck SM, Karimi-Abdolrezaee S. Traumatic spinal cord injury: an overview of pathophysiology, models and acute injury mechanisms. Frontiers in neurology. 2019 Mar 22;10:282.
5. O'Sullivan, S.B., Schmitz T.J, and Fulk GU, Physical Rehabilitation, 6th Edition. 2019: F.A. Davis Company.
6. Umphred, Darcy A. Umphreds Neurological Rehabilitation. St. Louis, 6th Edition. Mo: Elsevier/Mosby, 2013.
7. Anjum A, Yazid MD, Fauzi Daud M, Idris J, Ng AM, Selvi Naicker A, Ismail OH,Athi Kumar RK, Lokanathan Y. Spinal cord injury: pathophysiology, multimolecular interactions, and underlying recovery mechanisms. International journal of molecular sciences. 2020 Oct 13;21(20):7533.
8. Rupp R, Biering-Sørensen F, Burns SP, Graves DE, Guest J, Jones L, Read MS, Rodriguez GM, Schuld C, Tansey-Md KE, Walden K. International standards for neurological classification of spinal cord injury: revised 2019. Topics in spinal cord injury rehabilitation. 2021;27(2):1-22.
9. Mahnig S, Landmann G, Stockinger L, Opsommer E. Pain assessment according to the International Spinal Cord Injury Pain classification in patients with spinal cord injury referred to a multidisciplinary pain center. Spinal cord. 2016 Oct;54(10):809-15.
10. Das A, Equebal A, Kumar S. Incidence of musculoskeletal pain and its impact on daily & functional activities among Indian spinal cord injury patients. Int J Physioth Res. 2013; (3): 99-106.
11. Hassanijirdehi M, Khak M, Afshari-Mirak S, Holakouie-Naieni K, Saadat S, Taheri T, Rahimi-Movaghar V. Evaluation of pain and its effect on quality of life and functioning in men with spinal cord injury. The Korean journal of pain. 2015 Apr 1;28(2):129-36.
12. Dalyan M, Cardenas DD, Gerard B. Upper extremity pain after spinal cord injury. Spinal cord. 1999 Mar;37(3):191-5.
13. Mehta S, Teasell RW, Loh E, Short C, Wolfe DL, Hsieh JT. Pain following spinal cord injury. Spinal Cord injury rehabilitation evidence. Version. 2014;5:1-79.
14. Kalirathinam D, Manoharlal M, Chidambaram R, Mokashi BS. Prevalence of chronic pain and its effect on functional independence in spinal cord injury patients. IOSR J Nurs Health Sci. 2015;4:61-.
15. Gupta N, Solomon J, Raja K. Employment after paraplegia in India: a postal survey. Spinal cord. 2011 Jul;49(7):806-11.
16. NorrbrinkBudh C, Lund I, Hultling C, Levi R, Werhagen L, Ertzgaard P, Lundeberg T. Gender related differences in pain in spinal cord injured individuals. Spinal cord. 2003 Feb;41(2):122-8.

17. Hassan MR, Kamrujjaman M. A Cross Sectional Study of Spinal Cord Injury-Induced Musculoskeletal Pain. Journal of Current Medical Research and Opinion. 2019 Dec 9;2(12):367-71.
18. Kalirathinam D, Manoharlal M, Chidambaram R, Mokashi BS. Prevalence of chronic pain and its effect on functional independence in spinal cord injury patients. IOSR J Nurs Health Sci. 2015;4:61-64.
19. Barbetta DC, Lopes AC, Chagas FN, Soares PT, Casaro FM, Poletto MF, de Carvalho Paiva Ribeiro YH, Ogashawara TO. Predictors of musculoskeletal pain in the upper extremities of individuals with spinal cord injury. Spinal Cord. 2016 Feb;54(2):145-9.
20. NorrbrinkBudh C, Lund I, Hultling C, Levi R, Werhagen L, Ertzgaard P,Lundeberg T. Gender related differences in pain in spinal cord injured individuals. Spinal cord. 2003 Feb;41(2):122-8.

Table 1: Demographic Characteristics of Participants (n=142)

Characteristics		Frequency (n)	Percentage (%)
Gender	Female	25	17.60%
	Male	117	82.40%
Age (years)	18-30	41	29%
	31-40	69	49%
	41-50	32	22%
Cause of injury	Accident	75	52.10%
	Diving	9	6.30%
	Falls	45	31.70%
	Sports	7	4.90%
	Violence	7	4.90%
Type of injury	Complete	77	54%
	Incomplete	65	46%
Level of injury	Thoracic	73	51.40%
	Thoraco-lumbar	40	28.20%
	Lumbar	26	18.30%
	Sacral	3	2.10%

Table 2: Complaints related to MSK problems in SCI patients (n=142)

Questions	Yes/No	Frequency (n)	Percentage (%)
Have you felt tightness or contracture in any joint of your body?	Yes	36	25.40%
	No	106	74.60%
Have you felt pain while moving wheelchair by your own?	Yes	55	38.70%
	No	87	61.30%
Have you felt pain while transferring activity or self?	Yes	53	37.30%
	No	89	62.70%
Have you felt pain by lifting objects from your surrounding?	Yes	23	16.20%
	No	119	83.80%

Jenny D. Chaudhari *et al.,*

Figure 1: Participant Flow

Graph 1: Prevalence of Musculoskeletal Pain in SCI patients (n=142)

Graph 2: Frequency of Anatomical Areas Involved (n=142)

Graph 3: The Distribution of Pain Severity (n=142)

RESEARCH ARTICLE
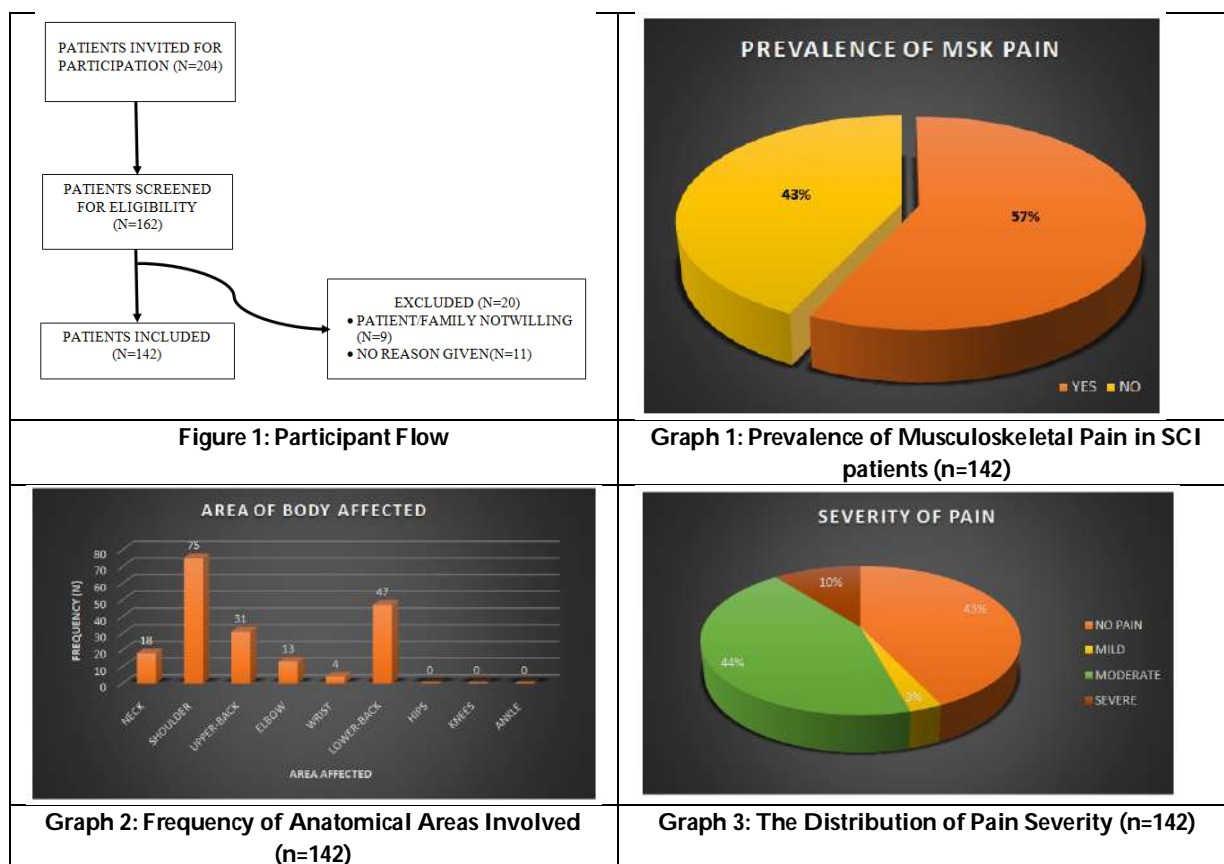
A Study to Analyze the Prescribing Pattern and the Role of Diuretics in Systolic Heart Failure Patients

Angel Mariam Titus[1], Neenu Mathew[1], Neethu.J[1], Parvathi Baiju[1], Sujith Kumar.S [2], Jeny Samuel[3]* and Boby Johns G[4]

[1]Pharm D Internship , Department of Pharmacy Practice, St Joseph's College of Pharmacy, Cherthala, Kerala, India

[2]Head of Department and Senior Consultant, Department of Cardiology, Lourdes Hospital, Ernakulum, Kerala, India.

[3]Associate Professor, Department of Pharmacy Practice, St Joseph's College of Pharmacy ,Cherthala, Kerala, India

[4]Professor, Department of Pharmaceutics, St Joseph's College of Pharmacy , Cherthala, Kerala, India.

*Address for Correspondence
Jeny Samuel
Associate Professor,
Department of Pharmacy Practice,
St Joseph's College of Pharmacy,
Cherthala, Kerala, India
E.Mail: jenysam14@gmail.com

ABSTRACT

The primary objective of the study is to identify the diuretic prescribing pattern including prevalence of monotherapy and combination therapy, role and adverse effects of diuretics in patients with HFrEF or left ventricular systolic dysfunction and evaluation of diuretic tolerance. Diuretics are considered as a corner stone in reducing the symptoms of congestion in heart failure patients with reduced ejection fraction although the quality of evidence regarding this is poor and their effect on morbidity and mortality is not clearly understood. This was a 6-month prospective study of 98 left ventricular systolic heart failure patients who received diuretics for symptomatic treatment (Inclusion: minimum samplesize: 93). Torsemide (10mg) was the drug most prescribed both at admission and during hospital stay. Combinations of furosemide + spironolactone (20/50mgPO) and torsemide +spironolactone (10/50mg PO) were found more prevalent (21.4%) on discharge. Of the total population, 90.80% of patients got symptomatically improved on diuretics and there is a significant difference existing between urine output before and after administration. ADRs were seen in 27 patients, of which diuretic induced renal failure was more frequently observed. Based on the causality assessment of adverse drug reactions using Naranjo Scale, 10 ADR's were found to be probable and 17ADR's were possible.12patients among the total population developed diuretic tolerance.

Angel Mariam Titus *et al.,*

Diuretics play a central role in patients with heart failure to relieve the symptoms of congestion. However, electrolyte imbalances and worsening of renal function may arise from the administration of diuretics. Thus, the use of diuretics in patients should be continuously monitored for the development of these adverse effects.

Keywords: Heart Failure, Diuretics, Adverse effects, Symptomatic improvement, Urine output, Tolerance

INTRODUCTION

Heart failure is defined as a structural or a functional abnormality of the heart that leads to elevated intracardiac pressure and inadequate cardiac output (at rest or during exercise[1]. Diuretics are commonly prescribed to people with heart failure to alleviate the congestive symptoms of the disease [2].Side effects of diuretic therapy are mainly due to the fluid and electrolyte imbalance induced by all diuretics [3]. Diuretic resistance is the failure to achieve effective relief from congestion despite appropriate doses of diuretic[4]

MATERIALS AND METHOD. STUDY DESIGN

It is a prospective analysis during a period of six months (October 2021- April 2022)conducted in cardiology department of a multi- specialty tertiary care hospital.

METHOD OF SLECTION
Inclusion criteria: Patients diagnosed with moderate or severe LV systolic dysfunction on diuretics and Symptomatic LV dysfunction patients on diuretics.

Exclusion criteria: Cases in which adequate data were not available, patients diagnosed with renal or hepatic impairment, and special population including pregnant and lactating women were excluded.

SAMPLE SIZE: A total of 98 patients who met the inclusion and exclusion criteria were selected in the study. (Minimum sample size required was found tobe93).

STATISTICAL ANALYSIS: The collected data were analyzed and interpreted using Microsoft excel and SPSS..

RESULTANDDISCUSSION

Ninety eight cases of systolic heart failure patients on diuretics managed in a tertiary care hospital during a period of six months (1-10-2021to30-4-2022) prospectively were randomly studied and evaluated for diuretic prescribing pattern, prevalence of monotherapy and combination therapy, role in symptomatic relief, ADR using Naranjo scale, tolerance and its management.

DIURETIC PRESCRIBING PATTERN
The study evaluated the prescribing pattern of diuretics according to WHO prescribing indicators. The rational use of diuretics were analyzed based on average number of drugs per encounter and percentage of drugs prescribed from essential drug list or hospital formulary.

Angel Mariam Titus *et al.,*

PREVALENCE OF MONOTHERAPY AND COMBINATION THERAPY
Monotherapy showed higher prevalence at admission (61.2%) and during hospital stay(60.2%)while combination therapy showed higher prevalence at discharge (54.1%).

DIURETIC PRESCRIBINGPATTERN BASED ONDRUG
Considering patients on monotherapy, 60 patients were treated with diuretics at admission ,59 during hospital stay and 44 on discharge. Out of 60 patients, 32(32.7%) were treated ontorsemide,21 (21.4%)onfurosemideand7(7.1%)on spironolactone. Out of 59 patients,33(33.7%) were on torsemide,22(22.4%) on furosemide and 4(4.1%)on spironolactone.Outof44 patients, 25 (25.5%) were on torsemide, 15(15.3%) on furosemide and4(4.1%)on spironolactone. Considering patients on combination therapy, 29 patients were treated with diuretics at admission, 40 during hospital stay and 53 on discharge. Out of 29 patients 16(16.3%) were on furosemide+ spironolactone ,7(7.1%)ontorsemide+spironolactoneand6(6.1%) on furosemide+ amiloride. Out of 40patients, 17(17.3%) were on furosemide + spironolactone, 16(16.3%) on torsemide + spironolactone and 7 (7.1%) on furosemide + amiloride. Out of 53 patients,21(21.4%)were on furosemide+ spironolactone,21(21.4%) on torsemide + spironolactone and 11 (11.2%) on furosemide+ amiloride.

ROLE OF DIURETICS IN SYMPTOMATIC TREATMENT
On monotherapy during hospital stay, 32 patients (32.7%) got symptomatically improved out of 33on torsemide,17 (17.3%)out of 22 on furosemide and 3(3.1%) out of 4 on spironolactone. And in combination therapy during hospital stay, 16(16.3%) patients got symptomatically improved on the combination of furosemide+ spironolactone out of 17, 15 (15.3%) out of 16 on combination of torsemide + spironolactone and7 (7.1%)out of 7 on combination of furosemide+ amiloride.

COMPARISON OF URINE OUTPUT BEFORE AND AFTER DRUG ADMINISTRATION USING WILCOXON SIGNED RANKTEST

Out of 98 patients ,67 achieved negative balance within first 24hrs.Among the remaining31, again 21 achieved negative balance on the subsequent days, only 5 patients showed a negative response. Positive changes are the number of patients with negative urine output after drug administration, negative changes are the number of patients with positive urine output after the drug administration. Z value is 2.942 (p < 0.01). Hence there is a significant difference existing between urine output before and after drug administration.

ADVERSE EFFECTS OF DIURECTICS DIURETICTOLERANCE
Resistance or tolerance to diuretic therapy can occur overtime, making volume management more difficult. Among the 12 patients who developed diuretic tolerance,6(6.12%) patients were tolerant to furosemide,4(4.4%) tolerant to torsemide and2(2.0%)tolerant to spironolactone.

CONCLUSION

Our study analyzed prescribing pattern of diuretics including the prevalence of monotherapy and combination therapy, role in symptomatic treatment, adverse effects and tolerance to diuretics in patients with systolic heart failure admitted to a tertiary care hospital during six months period. We came to understand that torsemide was found to be more prevalent at admission and during hospital stay while the combination therapy of furosemide+ spironolactone and torsemide + spironolactone found to be prevalent on discharge. The prescribing pattern of the total population concluded rational use of diuretics as per WHO core indicators. Majority of the patients got symptomatically improved on diuretics and there is a significant difference existing between urine output before and after administration. Symptomatic improvements in patients on monotherapy relating to combination therapy were found out using Odds Ratio. Diuretic induced renal failure was shown to be the most frequently occurred ADR. Based on the causality assessment of adverse drug reactions using Naranjo Causality Assessment Scale, probable and

Angel Mariam Titus *et al.,*

possible were the occurred ADR. Only the patients who had positive urine output and not symptomatically improved even after the drug administration got tolerant to diuretics. LV dysfunction has no significant association with the diuretic tolerance. Some of the limitations of our study was acknowledged. Majority of the patients were bedridden and their weight was unable to assess, so we evaluated role of diuretics only through symptomatic improvement and urine output although weight change was also having beneficial effect on the same .Since one of the patients from our study sample was expired during the study period we were not able to obtain the complete data. The study can be extended to a multi-center study with a large sample size so that more clearer results can be obtained. Understanding prescribing pattern of diuretics will help in better management of tolerance.

REFERENCES

1. McDonaghTA,MetraM,AdamoM,Gardner RS, Baumbach A, Böhm M, Burri H,Butler J, Čelutkienė J, ChioncelO, ClelandJG. 2021 ESC Guidelines for the diagnosis and treatment of acute and chronic heart failure: Developed by the Task Force for thediagnosis and treatment of acute and chronic heart failure of the European Society of Cardiology (ESC) With the special contribution of the Heart Failure Association(HFA) of the ESC.European heart journal.2021Sep 21;42(36):3599-726.
2. Casu G, Merella P. Diuretic therapy in heart failure - current approaches. Eur Cardiol [Internet].2015;10(1):42–7.Availablefrom:http://dx.doi.org/10.15420/ecr.2015.10.01.42
3. Prichard BN, Owens CW, Woolf AS. Adverse reactions to diuretics. Eur Heart J [Internet].1992;13SupplG:96–103.Availablefrom:http://dx.doi.org/10.1093/eurheartj/13.suppl_g
4. Shams E, Bonnice S, Mayrovitz HN. Diuretic Resistance Associated With Heart Failure.Cureus. 2022 Jan18;14(1).

Table .1 : odds ratio for symptomatic improvement in patients on mono therapy relating to combination therapy.

	No symptomatic improvement	Symptomatic improvement	Odds ratio	Confidence interval
Mono therapy	7 (11.9%)	52 (88.1%)	2.5 5	0.503-13.004
Combination therapy	2 (5%)	38 (95%)		

Table .2 : comparison of urine output before and after drug administration using Wilcoxon signed rank test

Test	n	+ve change	-ve change	No change	z-value	p-value
Initial- Final urine output difference	98	21	5	72	2.942	*p <0.01*

Table 3.1: Naranjo's causality Assessment of ADRs4.

		Naranjo score	
		Probable	possible
ADR	Hyponatremia	2	1
	Hyponatremia, Hypokalemia	0	1
	Hypokalemia	0	2
	Diuretic induced renal failure	7	11
	Hyponatremia+ renal failure	1	2
	Total	10	17

Angel Mariam Titus *et al.,*
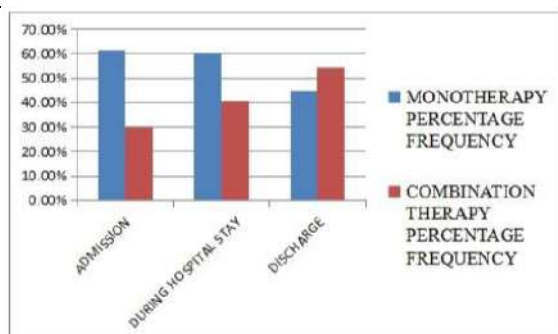
Fig. 1: prevalence of mono therapy and combination
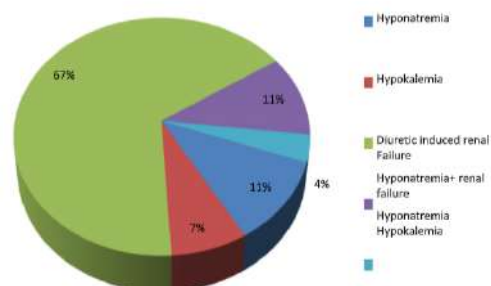
Fig 2. Observed ADRs

REVIEW ARTICLE

A Review on Syntheisis of DHA (Dehydroacetic Acid) based Hetrocyclic Schiff's base and their Metal Complexes Having Different Applications in Various Fields

Satvinder Khatkar[1], Sushil Kumar[2], Vivek Sharma[1], Vikash Singh[1], Dhruvin Pareek[1] and Bhawna Pareek[3]*

[1]Ph.D Scholar, Department of Chemistry, Maharishi Markandeshwar (Deemed to be University), Mullana, Ambala, India.
[2]Senior Scientist, Research and Development Centre at "Biozenta Life Science Pvt. Ltd." Una (Himachal Pradesh), India.
[3]Professor and Head, Department of Chemistry, Maharishi Markandeshwar (Deemed to be University), Mullana, Ambala, Haryana, India.

*Address for Correspondence
Bhawna Pareek
Professor and Head,
Department of Chemistry,
Maharishi Markandeshwar (Deemed to be University),
Mullana, Ambala, Haryana, India.
E.Mail: dr.pareekbhawna@gmail.com

ABSTRACT

Primary amines and carbonyl compounds condense to form Schiff bases [1]. There are numerous reported synthetic methods in the literature, but the non-standard method using microwave-assisted reactions has attracted significant attention since it takes less time and produces acceptable yields. Microwave synthesis increases repeatability and facilitates handling. The flexible methods for synthesising Schiff bases and its coordination chemistry are described in the current paper. Supra molecular chemistry, biological applications, catalysts, material science, and chemical separation have all claimed relevance to this [2]. They also have a wide range of uses, including analgesic drugs [7], ant tubercular [3], antimalarial [4], verso-relaxing [5], and anticancer [6].

Keywords : Antimicrobial, unconventional, microwave-assisted reactions, Schiff Base, DHA, Heterocyclic.

Satvinder Khatkar *et al.*,

INTRODUCTION

Schiff base name derived from "Hugo Schiff's [8] a Germen Chemist who synthesize first schiff base through condensation reaction of primary amines [9] and aldehydes or ketones. Schiff base prepared from aliphatic carbonyls compounds are less stable in comparison of schiff base derived from aromatic carbonyls[10] compounds due to the presence of aromatic phenyl moiety which is responsible for separation of electron density on a large surface area which provide extra stability to the schiff bases because electron density per unit area [11]goes on decreasing. During condensation reaction Schiff base functional group obtained which contain a double bond between carbon and nitrogen(-C=N-).[12] Schiff base also known with different names like imine or azomethine on the basis of structural features that is presence of double bond between carbon and nitrogen.[13] Rate of formation of schiff bases explain on the basis of type of reaction occurs during schiff base formation, which is nucleophillic[14] addition and elimination reaction[15] in which primary amines[16] act as a nucleophile and carbonyl compounds[17] act as an electrophile if carbonyl compound[18] is aldehydes, [19]then it reacts faster because they have high electrophilicity[20] and less sterically hindered[21] in comparison of ketones which are less electrophilic[22] and more sterically hindered. Mechanism of formation [23] of schiff bases are nucleophillic addition and elimination reaction in first step primary amines act as a nucleophile and attacks on carbonyls compounds which act as an electrophile and formed a tetrahedral intermediate similar to hemi acetal [24]and hemi-ketal [25]and in second step elimination reaction occurs in which water molecule eliminate [26] and a double bond is formed between carbon and nitrogen. Due to their availability and diversity, schiff-base complexes are regarded as the most significant stereo chemical models [27] in main group and transition metal coordination chemistry. Environmentally friendly synthetic technologies have gained relevance recently. Because chlorinated hydrocarbons are poisonous and flammable by nature, organic synthesis processes that utilise them as solvents have wreaked havoc on the biosphere [28]. Thus, safer chemicals and solvents must be used in order to reduce such mishaps. As most solvents are poisonous or flammable today and raise the cost of synthesis overall, a solvent-free approach has shown to be appealing. However, compared to conventional approaches, the solvent-free approach enhances selectivity, shortens reaction times, and makes product separation and purification simpler [29-33]. A significant obstacle in green chemistry is the creation of cleaner processes. The elimination of volatile organic solvents from the reaction medium is one of the many components of green chemistry and is crucial [34-35]. It is increasingly vital for chemists to explore for ecologically friendly methods due to the growing economic concerns. Due to the diversity of their steric and electronic properties, Schiff bases generated from aromatic carbonyl compounds have been extensively explored using metalloproteinase models and asymmetric catalysis. While there are no harsh reaction conditions, using water as a solvent [36-38] is one of the better alternatives. The challenge of eliminating solvents from the reaction mixture or liquid is frequently encountered in the traditional synthesis of Schiff bases. As a result, microwave-assisted reactions have undergone extensive research [39-41] and are frequently employed in chemical synthesis.

SYNTHESIS ROUTES

In claimed eggshells, Suresh Patil et al. [42] produced Schiff Bases using 4-methoxyaniline and 4- hydroxy benzaldehyde (Scheme-1). This innovative environmentally friendly grinding technique produced a moderate to good yield when used to synthesise Schiff bases using CES (heterogeneous catalyst).
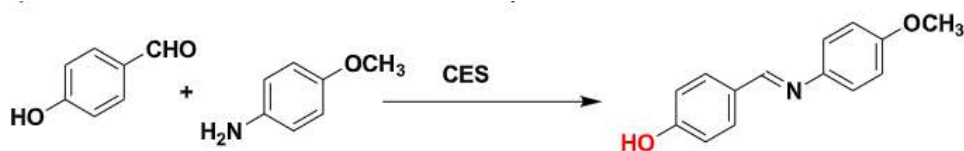
Scheme 1

Using microwave irradiation, J. Panda et al. [43] refluxed Schiff Base of Isatin utilising substituted aniline (Scheme-2) to generate 85% product.

Satvinder Khatkar *et al.*,
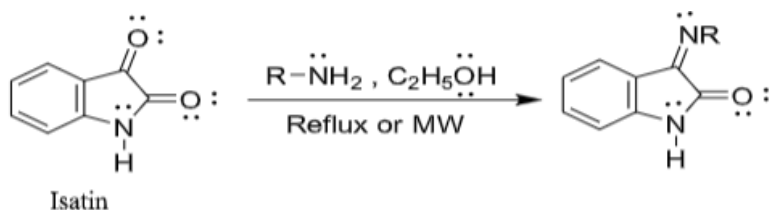
Scheme 2

For the preparation of Schiff bases, Arshi Nakvi et al. [44] investigated three alternative green techniques. 10-ml of water was mixed into a combination of 3-chloro-4-fluoro aniline and substituted benzaldehyde (Scheme-3), and crystallised product was produced. The use of " ;microwave jump- start "synthesis," ;grindstone friction activated "; synthesis, and water-based reactions in greener methodologies has many advantages because water is a less expensive reaction medium, is safe for the environment, is simple to handle, and has no corrosive or carcinogenic effects.
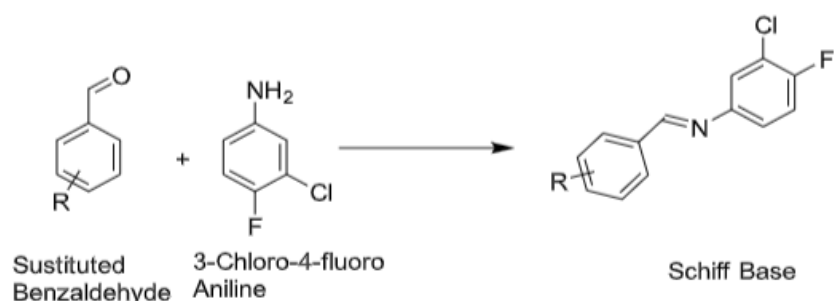
Scheme 3

By reacting p-toluidine and 3,4,5-trimethoxybenzaldehyde with neutral alumina and dichloromethane while it was being microwaved for four minutes, Zhaoqi Yang et al. [45] created the Schiff Bases (Scheme-4). With a good yield, microwave irradiation synthesis uses the least amount of time.

Scheme 4

Schiff bases made from carboxy ethyl thiophenes were created by B. Sindhu Kumari [46]. (Scheme- 5). The addition of ethanolic Lanthanide (III) chloride solution to the Schiff Base and subsequent 15- minute irradiation of the combination resulted in the further production of the metal complex.
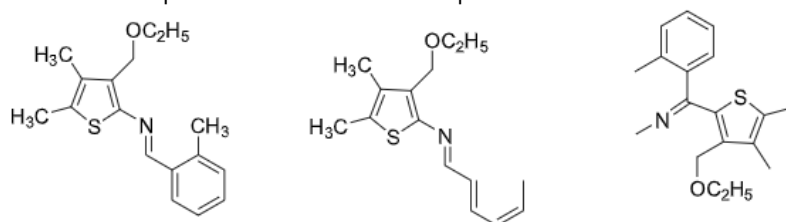
Scheme 5

With the aid of natural acid catalysts like grape juice, lemon juice (Scheme 6), and mango juice, Garima Yadav et al. [47] created the Schiff Base. Fruit juice's increasing popularity can be attributed in large part to its enzymatic activity, acidic qualities, environmentally friendly nature, and commercial availability. The chemistry of natural catalysts will spur a lot of research in the near future.

Satvinder Khatkar *et al.*,

Scheme 6
Dehydroacetic acid (DHA)
DHA, a biologically active compound, has shown to have good antibiotic and antifungal effects. It was isolated from natural sources and is now available in the industrial sector thanks to a variety of synthetic techniques. DHA and its derivatives have been demonstrated to have a wide range of applications in chemical synthesis. The research has been evaluated, as well as investigations on related pyrone derivatives. The carbonyl of the acetyl group, the carbon atom terminating the conjugated carbon at position-6, the lactone carbonyl, and the carbonyl carbon at position-4 are all vulnerable to attack by nucleophillic reagents since it has numerous reactive sites. An electrophile, on the other hand, can attack at C (3) or C (5). position all these position shown below with numbering.
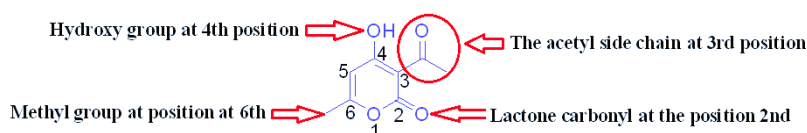
According to a review of the literature, reacting DHA and its derivatives with various reagents provides a flexible pathway to the synthesis of a wide range of heterocyclic compounds.. Since the studies embodied in this review are aimed at further exploring the potentiality of this aspect, it will be worthwhile to review the literature work concerning the synthesis of 'Nitrogen' and 'Oxygen' containing heterocyclic compounds from the reactions of DHA and its derivatives[48].

THE HETEROCYCLIC COMPOUNDS SYNTHESIZED FROM DHA AND ITS DERIVATIVES ARE CATEGORIZED AS:

PYRIDINES
S Garratt et al, synthesize pyridines (18) by treating DHA with NH 3 & amines. During the transformation of DHA into pyridines two intermediate [(16), (17)] are isolated and identified.[49].

"PYRIDONES"
M Iqbal *et al*, synthesize substituted-4-pyridones [(22), R=H, CH3] by treating 3-Cinnamoyl-4-hydroxy-6-methyl-2H-pyran-2-ones (11) with primary amines. During the reaction intermediate (21) that is Schiff's base formed [50].

N, N'-LINKED BI(HETEROARYLS)
"M P Sammesh and coworkers" also prepared " N, N'-linked bi(heteroaryl) compounds" by treating amino triazolewith Dehydroacetic acid. Alarge number of variations are observed of this reactionwhen DHA, (1) reacts with hydrazine, N-aminoheterocycles(24)&N-amino pyridiniumsalts(27).After completion of the reaction,we obtained different products of N,N'-linkedbi(heteroaryl)compounds [51-52] that is (25), (26) & (28).

N, N'-LINKED BI(HETEROARYLS)
M P Sammesh and coworkers also synthesized N, N'-linked bi(heteroaryl) compounds by the reaction of DHA with aminotriazole. Many interesting versions of this reaction When hydrazine reacts with N- amino heterocycles, it

produces. As a result of the reactions of DHA with aminotriazole24, hydrazine, and N-aminopyridinium salts 27, N, N'-linked bi(heteroaryl) compounds 25, 26, and 28 are formed[52].

PYRAZOLYLPYRIMIDINES

H Batra et al, synthesised Condensation of 4-acetoacetyl-5-hydroxy-3-methyl-1H-substituted pyrazoles 3 and guanidine carbonate in ethanolic NaOH yields 2-amino-6-methyl-4-(5-hydroxy-3- methyl-1-substitutedpyrazol-4-yl0pyrimidines 23. (40 percent). Some of these chemicals have been discovered to have mild antifungal activity[53].

"PYRIDONES"

M Iqbal et al, synthesize substituted-4-pyridones [(22), R=H, CH3] by treating 3-Cinnamoyl-4- hydroxy-6-methyl-2H-pyran-2-ones (11) with primary amines. During the reaction intermediate (21) that is Schiff's base formed [50].

"N, N'-LINKED BI(HETEROARYLS)"

"M P Sammesh and coworkers" also prepared " N, N'-linked bi(heteroaryl) compounds" by treating amino triazole with Dehydroacetic acid. A large number of variations are observed of this reaction when DHA, (1) reacts with hydrazine, N- amino heterocycles (24) & N-amino pyridinium salts (27). After completion of the reaction, we obtained different products of N, N;-linked bi(heteroaryl) compounds [51-52] that is (25), (26) & (28).

Satvinder Khatkar *et al.*,
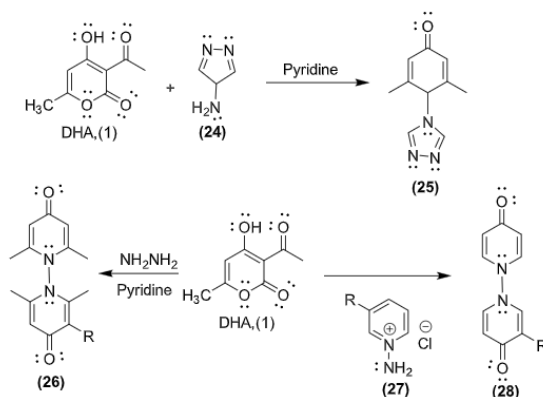
"PYRAZOLYLPYRIMIDINES"

"H Batra et al", prepared 2-amino-6-methyl-4-(5-hydroxy-3- methyl-1-substitutedpyrazol-4- ylopyrimidines (23) with yield (40 percent) by treating pyrazoles (3), guanidine carbonate and 4- acetoacetyl-5-hydroxy-3-methyl-1H-substituted (22) by using $C_2H_5OH/NaOH$ via condensation process. Among these chemicals some them shows mild antifungal activity [53].
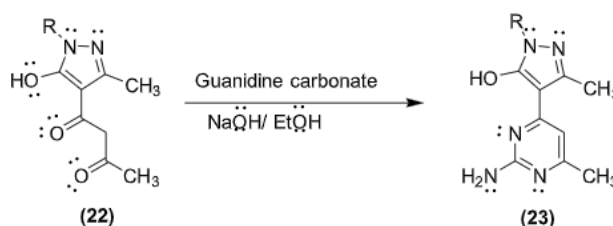
"BENZIMIDAZOLES"

"M A Qayyoom et al", synthesized 2- methyl-5-substituted benzimidazoles (31) by treating DHA (1) with substituted o-phenylenediamines (29), via intermediate formation i.e. 3-[N- (substituted-amino phenyl) acetimidoyl]-4-hydroxy-6-methyl-2h-pyrones (30), which further converted into (31) by pyrolysis [54].
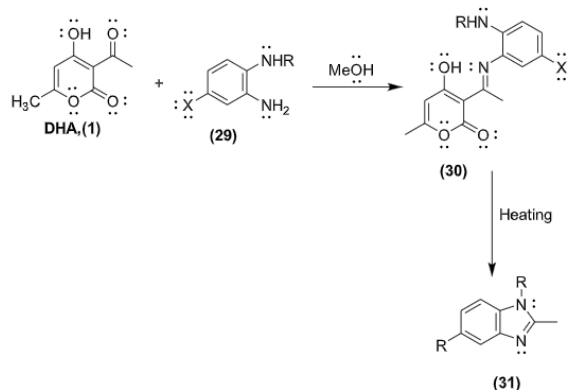
"PYRAZOLOPYRIDONES"

"K Ogawa et al", synthesize 3,6-dimethyl-1-phenyl-1H-pyrazolo[4,3-c] by using pyridine-4-thiones, pyridine- 4-ones

Satvinder Khatkar *et al.*,

and DHA as a starting material & tested in vitro for activity. The activity of the synthesized substances activities was compared with mirlinone, which was used as a control. Most of the substances have greater potential of activity in comparison of than milrinone [55].
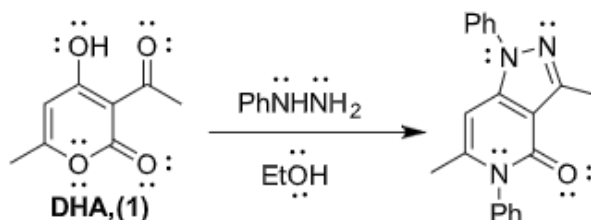
"PYRANOPYRANS"

"V Y Sosnovskikh & coworkers", developed another method for the preparation of pyranopyrans i.e., 2-Substituted-7-methylpyrano[4,3-b]-4H,5H-diones (47). In this method they treated DHA, (1) with esters RCO2 Et in the presence of LiH/THF & formation of intermediate, [diketones of the type (3- acetoacetyl- 4-hydroxy-6-methyl-2H-pyran-2-ones)] (46) is formed which further converted into final product (47) in
the presence of conc. H_2SO_4 via cyclization process[56].
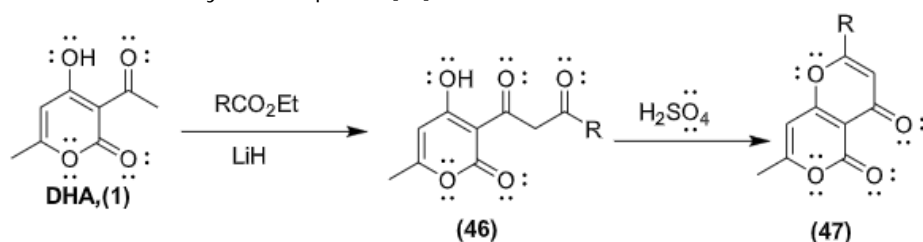
"PYRANOPYRANS (1)"

"V K Mahesh et al", synthesized 3-acetyl-4,7-dimethylpyrano[4,3-b] pyran-2H,5H- dione 47(a) by treating DHA, (1) with ethyl 3-oxobutyrate under mild alkaline condition via formation of intermediate 46(a) by condensation mechanism. This intermediate 46(a) further cyclized and gives desired product [57].
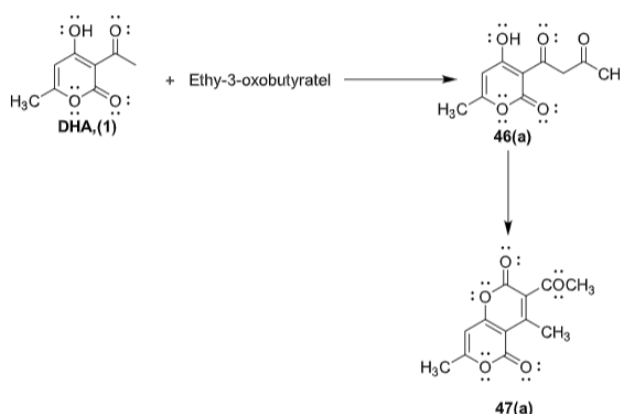
"PYRANOPYRANS (2)"

M Siddiq et al, by removing an acetyl group from 3-acetyl-4,7-dimethylpyrano[4,3-b] pyran-2H,5H- dione (48), a dipyrone derivative, "4,7-dimethylpyrano[4,3-b] pyran-2H,5H-dione" (49) was produced [58].
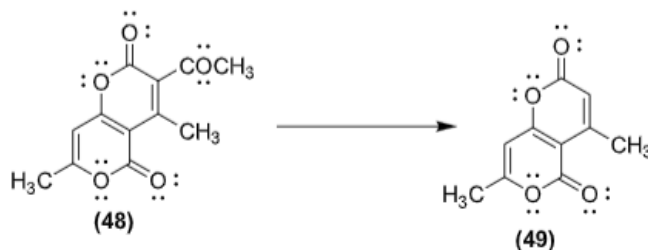
"Important Biological perspective of Schiff bases":
"Antimalarial activity":

More than 100 nations are affected from "Malaria disease" & has resulted in significant health issues all over the world. Almost 3 million of the 550 million people who are affected by this disease each year die from it; 90% of these deaths occur in Africa, mostly in children [48]. "*P. falsiparum*", "*P. vivax*", "*P. ovale*" & "*P. malariae*" are the major causes of human malaria. The vector of Plasmodium is a female mosquito belonging to the species Anopheles [59].

Antibacterial activity
The interest in Schiff base complexes has grown as bio-inorganic chemistry has advanced, as many Schiff base complexes function as promising antibacterial compounds. Bacteria are directly responsible for the rising infectious disease death rate. The creation of novel antibacterial substances with improved modes of action is unquestionably necessary nowadays. The potential of schiff bases as antibacterial agents has been acknowledged [60].

Anticancer activities
Schiff's base "3-methylbenzyl-2-(6-methylpyridin-2-ylmethylene) hydrazine carbodithioate" produced by treating S-3- methylbenzyldithiocarbazate with 6-methylpyridine-2-aldehyde via condensation mechanism. This Schiff's base act as a tridentate ligand in which donner atoms are "N" & "S" through which it form octahedral complexes with di-positive metal ions [Cu (II), Ni (II), Zn (II) & Cd (II)]. These metal complexes show excellent activity against breast cancer cell lines [61]. Ligand show high activity against both cancer cell lines and its complexes are highly selective with metal ion [Cu(II), Ni(II) & Zn(II)] these complexes active only against one cancer cell lines. On the other hand, its complex with Cd (II) ion active against all other cancer cell line [62].
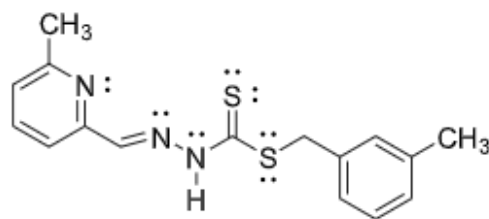
Structure of ligand having anti-cancer activity
The "Schiff's base 2- [(2,3-dihydro-1H-inden-4- ylimino) methyl]-5-nitrophenol" & its complexes with metal ions [Cu (II), Mn (II), Pd (II) & Zn (II)] shows good anticancer activity in "MCF-7 (human breast adenocarcinoma)" & "HT- 29 (colon carcinoma)" cells in vitro. According to the findings, greatest cytotoxic action of the complex of di-positive metal ion palladium observed against "MCF-7 cells", with an IC_{50} of 5.94 M, which is on par with "cisplatin". The ligand & its combination with dipositive zinc metal ion shows "broad spectrum activity" against two-three gram-"negative & gram-positive bacteria" [63].

Satvinder Khatkar *et al.,*
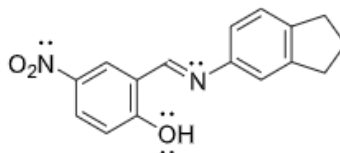
Structure of metal complexes having anti-cancer activity

Schiff's base ligand synthesize from condensation mechanism by treating benzaldehyde, 2-amino-3- methyl-butanoic acid & 4-amino-antipyrine. This ligand formed complexes with di-positive metal ion [Cu (II) & Zn (II)] which shows excellent biological activities. Cytotoxic activity of the synthesized complex test in vitro by using "trypan blue dye exclusion assay" against an Ehrlich ascites carcinoma (EAC) tumor model. The complexes show highest degree of cytotoxicity [64].
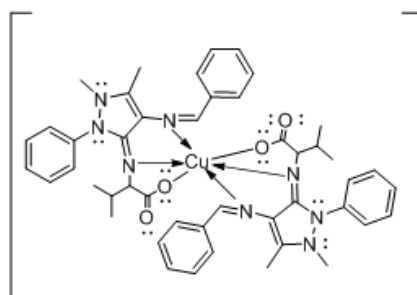
Copper (II) Complex
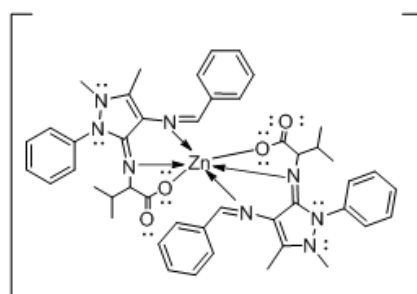
Zinc (II) complex

Structure of synthesized "metal complexes"
"Catalytic activities of Schiff's base metal complexes"

There are various parameters such as the ligand's composition, the availability of a coordination site & the character of the metal ion with which it forms are used to determine the catalytic activity of the synthesized Schiff's base metal complexes. The base metal complexes of Schiff can be used as catalysts in both homogeneous and heterogeneous catalysis [65]. Due to the possibility of varied oxidation states, metal complexes, particularly those with a vacant coordination site, can operate as a suitable catalyst and provide a location for reaction to occur. "Schiff's base metal complexes" have been utilized as a "catalyst" in "polymerization" [66], "hydrogenation" [67], "epoxidation" [68], "oxidation" [69] & "ring opening" [70], among other applications. In asymmetric transformations, the chirality of the Schiff's base ligand is crucial. A chiral salen [72] type ligand is used as Jacobsen's catalyst in the enantioselective transformation of prochiral alkenes into matching epoxides. Ryoji Noyori created a copper-base Schiff's complex for metal-carbenoid cyclopropanation of styrene in 1968, which contains chiral ligand coupled with copper metal ion for metal-carbenoid cyclopropanation of styrene [73].

Satvinder Khatkar *et al.*,

Noyon's Catalyst   **Jacobsen's catalyst**
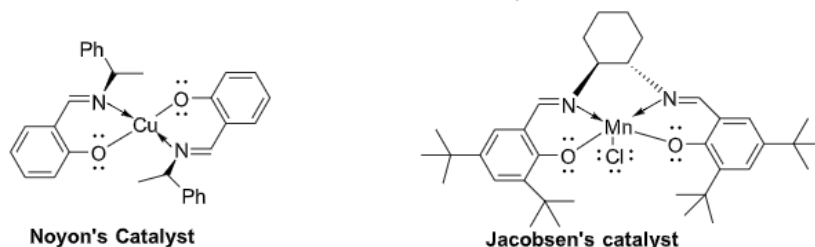
Structure of Noyon's (Left) and Jacobsen's catalyst (Right)

Oxidation reactions

The enantioselective epoxidation of "Cis -1,2-Diphenylethylene", "(E)-non-3-ene" & "(E)-4-Octene" using "iodoso- Benzene" as an oxidizing agent carried out in presence of dissymmetric chiral Schiff's base of tri positive metal ion manganese & ruthenium complexes. On the behalf of olefins studied, overall chemical yields for corresponding epoxides achieved with Mn (II) catalysts were superior than those obtained with Ru (III) catalysts [74]. The conversion of trans-3-nonane to its epoxides rises linearly as more electron withdrawing groups are present on ligands. Other substrates under investigation did not show similar tendencies, although ligands containing nitro groups always provide greater translation and a higher cis/trans ratio. The ligand with the MeOH substituent in the fifth position yields the least. These findings underlined the importance of the ligand substituent at the 5th position in the conversion of substrates to their epoxides. The catalytic potential of "zeolites encapsulating Schiff's base complexes" of tri-positive chromium ion & di-positive metal ion of copper, iron, nickel, cobalt, manganese was investigated during oxidation reaction of C_6H_6 to $C_6H_{12}O$ & $C_6H_{10}O$. Among all these "zeolites encapsulating Schiff's base complexes", highest catalytic potential was obtained for Schiff base complexes of di-positive manganese ion. Oxidation of Ethenylbenzene to Benzenecarbaldehyde in presence of oxygen aerobic oxidation was carried out by using zeolites-Y which contain tri-positive complexes of manganese ion with "N, N-ethylene bis-(salicylideneaminato) salen", "N, N-ethylene bis-(5-chlorosalicylideneaminato)CI salen" & "N, N- ethylene bis-(5-bromosalicylideneamina) Most effective oxidation of reactive substrates like "carbolic acids & aldehydes" were observed in case of Schiff's base complexes of dipositive cobalt ion[75].

M= Mn(II), Ru(III) & Co(II)
Structure of metal complex
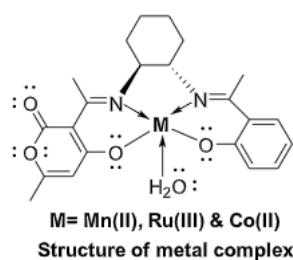
Hydrogenation reactions

The catalytic effectiveness of di-positive palladium ion complex with "poly(3,6-dibenzaldimino-N- vinylcarbazole)" has been studied in hydrogenation processes. Excellent heterogeneous catalytic activity showed by the polymer complex during the hydrogenation processes. In these processes normal reaction conditions were required like 1 atm pressure of H_2 gas along with ambient temperature for the reduction of alkenes, benzaldehyde, Schiff's bases, aromatic nitro compounds & alkynes [76].

Satvinder Khatkar *et al.*,
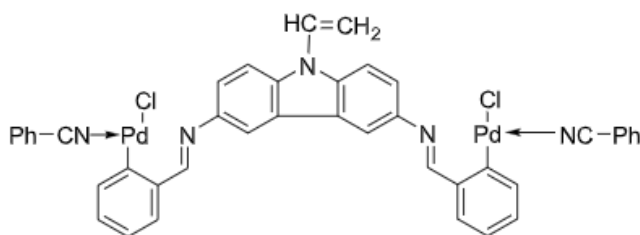
Structure of Pd complex having catalytic activity towards hydrogenation rteaction

Asymmetric reduction of di-alkyl ketones to alcohols are carried out by using transition metal Schiff's base complexes as catalysts during the reaction, in the absence of catalysts i.e., transition metal Schiff's base complexes these conversions are not possible. It was also possible to reduce ketones using ruthenium and iridium analogues. The reduction rate was discovered to be controlled by the type of the central metals, with Rhir Ru as the observed order. In addition, instead of bipyridine complexes, chiral compounds were used to reduce ketones [77]. The reduction of ketones effectively carried out by using Schiff's bases which have chirality with 51 percent ee and a 99 percent yield. In the case of aryl ketones, the position and electrical characteristics of ring substituents influence the enantioselectivity of reduction, as evidenced by results acquired from catalyti c reduction of a range of ketones. In comparison to ortho substituted acetophenones, meta and para substituted ketones were less enantioselective [78]. The hydrogenation of acetophenone to 1-phenylethanol was particularly active in zeolites supported cobalt (II) complexes of salicylidenediaminocyclohexane [79]. These catalysts had a selectivity of 99 percent and a conversion of 98 percent, which was comparable to homogeneous catalysts. The optimum temperature for best ee with homogeneous catalysts was -10 °C, whereas the Schiff's base catalyst showed best activity at 25 °C, which is a major advantage over the conventional one [80].
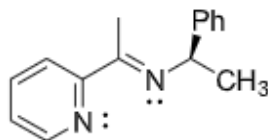
Structure of chiral Schiff's base

ACKNOWLEDGMENT

CONCLUSION

We have reviewed the most recent developments in the study of Schiff bases, as well as their structure, characterization, and biological uses, in this review paper. Both the industrial and medical areas heavily dependent on "ligands & their metal complexes". A number of reports of Schiff bases in antibiotic and antiviral of therapeutic interest have lately been reported in several journals, despite the fact that research on the Schiff bases is growing every day. However, further study is still required before these metal complex medicines may be developed. Finally, Novel Schiff's bases prepared via chemically described methods by treating cobalt dicyanamide compounds with N 2 –containing heterocyclic compounds. We prepared a new class of "chalcones" which further tested for "antibacterial activity". As a result of the findings, all chemicals were shown excellent activities against to all microorganisms during testing. In addition, the conjugated carbonyl region was changed to cyanopyridine,

pyrimidines, pyrazoles & isooxazoline. On the basis of these changed components nitro containing pyrazoles are most effective as an antibacterial inhibitor. Observed results indicated that moderate to exceptional bioactivities in vitro shown by the several examined substances.

REFERENCES

1. Abu-Hussen, J. Coorcl. Chem. 2006, 59,157.
2. S Karthikeyan, M.,' Jagadesh Prasad, D.,' Poojary, B., S. Bhat, Bioorg. Med. Chem. 2006, 14, 7482.
3. 5. Singh, K., Barwa, M. S.,' Tyagi, P. Eur. J. Med. Chem. 2006, 41, 1.
4. Pannerselvarn, P., Nair, R.R., Viyayalakshmi, G.; Suhranianian, E.H.,' Sridhar, S.. Eur. J. Med. Chem. 2005, 40, 225.
5. Sridliar, S. K.; Caravan, M., Ramesh, A. Eur. J. Med. Chem. 2001, 36, 615.
6. Pandeya, S. N., Sriram, D., Nath, G.; Declercq, E. Eur. J. Pharmacol. 1999, 9, 25.
7. Mladetiova, R., M., Manolova, N.; Pet+-o va, T., Rashkov, I. Eur. Poly+n. J. 2002, 38, 989
8. Liu X, Hamon JR. Recent developments in penta-, hexa-and heptadentate Schiff base ligands and their metal complexes. Coordination Chemistry Reviews. 2019 Jun 15;389:94-118.
9. Sun Y, Lu Y, Bian M, Yang Z, Ma X, Liu W. Pt (II) and Au (III) complexes containing Schiff-base ligands: A promising source for antitumor treatment. European Journal of Medicinal Chemistry. 2021 Feb 5;211:113098.
10. Tsantis ST, Tzimopoulos DI, Holynska M, Perlepes SP. Oligonuclear actinoid complexes with Schiff bases as ligands—older achievements and recent progress. International Journal of Molecular Sciences. 2020 Jan 15;21(2):555.
11. Banerjee A, Chattopadhyay S. Synthesis and characterization of mixed valence cobalt (III)/cobalt (II) complexes with N, O-donor Schiff base ligands. Polyhedron. 2019 Feb 1;159:1-1.
12. Tüzün B. Investigation of pyrazoly derivatives schiff base ligands and their metal complexes used as anti-cancer drug. Spectrochimica Acta Part A: Molecular and Biomolecular Spectroscopy. 2020 Feb 15;227:117663.
13. El-Sonbati AZ, Mahmoud WH, Mohamed GG, Diab MA, Morgan SM, Abbas SY. Synthesis, characterization of Schiff base metal complexes and their biological investigation. Applied Organometallic Chemistry. 2019 Sep;33(9):e5048.
14. Kargar H, Ardakani AA, Tahir MN, Ashfaq M, Munawar KS. Synthesis, spectral characterization, crystalstructure and antibacterial activity of nickel (II), copper (II) and zinc (II) complexes containing ONNO donor Schiff base ligands. Journal of Molecular Structure. 2021 Jun 5;1233:130112.
15. El-Gammal OA, Mohamed FS, Rezk GN, El-Bindary AA. Synthesis, characterization, catalytic, DNA binding and antibacterial activities of Co (II), Ni (II) and Cu (II) complexes with new Schiff base ligand. Journal of Molecular Liquids. 2021 Mar 15;326:115223.
16. Fekri R, Salehi M, Asadi A, Kubicki M. Synthesis, characterization, anticancer and antibacterial evaluation of Schiff base ligands derived from hydrazone and their transition metal complexes. Inorganica Chimica Acta. 2019Jan 1;484:245-54.
17. Kargar H, Ardakani AA, Tahir MN, Ashfaq M, Munawar KS. Synthesis, spectral characterization, crystal structure determination and antimicrobial activity of Ni (II), Cu (II) and Zn (II) complexes with the Schiff base ligand derived from 3, 5-dibromosalicylaldehyde. Journal of Molecular Structure. 2021 Apr 5;1229:129842.
18. Gao B, Zhang D, Li Y. Synthesis and photoluminescence properties of novel Schiff base type polymer-rare earth complexes containing furfural-based bidentate Schiff base ligands. Optical Materials. 2018 Mar 1;77:77-86.
19. Andiappan K, Sanmugam A, Deivanayagam E, Karuppasamy K, Kim HS, Vikraman D. In vitro cytotoxicity activity of novel Schiff base ligand–lanthanide complexes. Scientific reports. 2018 Feb 14;8(1):1-2.
20. Vinusha HM, Kollur SP, Revanasiddappa HD, Ramu R, Shirahatti PS, Prasad MN, Chandrashekar S, Begum M. Preparation, spectral characterization and biological applications of Schiff base ligand and its transition metal complexes. Results in Chemistry. 2019 Jan 1;1:100012.
21. Shaygan S, Pasdar H, Foroughifar N, Davallo M, Motiee F. Cobalt (II) complexes with Schiff base ligands derived from terephthalaldehyde and ortho-substituted anilines: Synthesis, characterization and antibacterial

activity. Applied Sciences. 2018 Mar 6;8(3):385.

22. Wang HL, Peng JM, Zhu ZH, Mo KQ, Ma XF, Li B, Zou HH, Liang FP. Step-by-step and competitive assembly of two Dy (III) single-molecule magnets with their performance tuned by Schiff base ligands. Crystal Growth & Design. 2019 Jul 26;19(9):5369-75.

23. Abd El-Halim HF, Mohamed GG, Anwar MN. Antimicrobial and anticancer activities of Schiff base ligand and its transition metal mixed ligand complexes with heterocyclic base. Applied Organometallic Chemistry. 2018 Jan;32(1):e3899.

24. Yaşar Ü, Gönül İ, Türkeş C, Demir Y, Beydemir Ş. Transition-metal complexes of bidentate Schiff-Base ligands: In vitro and in silico evaluation as non-classical carbonic anhydrase and potential acetylcholinesterase inhibitors. ChemistrySelect. 2021 Aug 6;6(29):7278-84.

25. Jamshidvand A, Sahihi M, Mirkhani V, Moghadam M, Mohammadpoor-Baltork I, Tangestaninejad S, Rudbari HA, Kargar H, Keshavarzi R, Gharaghani S. Studies on DNA binding properties of new Schiff base ligands using spectroscopic, electrochemical and computational methods: influence of substitutions on DNA-binding. Journal of Molecular Liquids. 2018 Mar 1;253:61-71.

26. Kargar H, Aghaei-Meybodi F, Behjatmanesh-Ardakani R, Elahifard MR, Torabi V, Fallah-Mehrjardi M, Tahir MN, Ashfaq M, Munawar KS. Synthesis, crystal structure, theoretical calculation, spectroscopic and antibacterial activity studies of copper (II) complexes bearing bidentate Schiff base ligands derived from 4-aminoantipyrine: influence of substitutions on antibacterial activity. Journal of Molecular Structure. 2021 Apr 15;1230:129908.

27. Mohapatra RK, Sarangi AK, Azam M, El-ajaily MM, Kudrat-E-Zahan M, Patjoshi SB, Dash DC. Synthesis, structural investigations, DFT, molecular docking and antifungal studies of transition metal complexes with benzothiazole based Schiff base ligands. Journal of Molecular Structure. 2019 Mar 5;1179:65-75.

28. J. M. DeSimone, "Practical approaches to green solvents," Science, vol. 297, no. 5582, 2002, pp. 799—803.

29. 22 I. G. W. V. Cave, C. L. Raston, and J. L. Scott, "Recent advances in solventless organic reactions.' towards benign synthesis with remarkable versatility, " Chemical Communications, no. 21, 2001 pp. 2159—2169.

30. 12 C. Imrie, P. Kleyi, V. O. Nyamori, T. I. A. Gerber, D. C. Levendis, rind J. Look, "Further solvent-free reactions of ferrocenylaldehyde.s.' synthesis o] 1, I -ferrocenyldiimine.s ‹mid ferrocenylac rylonitriles, " Journ‹il oJ Organometallic Chemistry, vol. 692, no. 16, 2007, pp. 3443—3453.

31. J.Metzger, "Solvent-j!ree organic syntheses, " Angewandte Chemie—International Edition, vol. 37, no. 21, , 1998, pp. 2975—2978.

32. C. J. Li cmd T. H. Chan, "Organic syntheses using indium mediated and catalyzed reactions in aqueous media," Tetrahedron, vol. 55, no. 37, 1999, pp. 11149—111 76.

33. T. P. Loh, J. M. Huang, S. H. Goh, and J. J. Vittal, "Aldol reaction under solvent-j!rec conditions. Highly stereo selective synthc•sis of 1,3-amino alcohols," Organic Letters, vol. 2, no. 9, 2000, pp. 1291—1294.

34. R. S. Varma and V. V. Namboodiri, "Solvent-free preparation of ionic liquids using a household microwave oven," Pure and Applied Chemistry, vol. 73, no. 8, 2001, pp. 1309—1313.

35. K. Tanaka and F. Toda, "Solvent-free organic synthesis," Chemical Reviews, 100, (3),2000, 1025—1074.

36. S. S. Pawar, M. S. Shingare, and S. N. Thore, "A novel approach for ligand promoted palladium (II)- catalyzed suzuki coupling in aqueous media," Lett in Organic Chemistry, vol. 4, no. 7, 2007,48d—490.

37. Y. Ren and C. Cai, "Iodine catalysis in aqueous medium: an improved reaction system for knoevenagel and nitroaldol condensation," Catalysis Letters, vol. 118, no. 1-2, 2007, 134—138.

38. V. K. Rao, S. S. Reddy, B. S. Krishna, K. R. M. Naidu, C. N. Raju,and S. K. Ghosh, "Synthesis of schiff bases in aqueous medium: a green alternative approach with effective mass yield and high reaction rates," Green Chemistry Letters and Reviews, vol. 3, no. 3, 2010, 217—223.

39. Somani R., et al. Optimization of Microwave Assisted Synthesis of some Schiff Bases. International Journal of ChemTech Research 2, 2010, 172-179

40. Kulshrestha A. and Baluja S., Microwave Promoted Synthesis of Some Schiff Bases, Scholars Research Library 2, 2010, 221-224

41. Yang Z. and Sun P., Compare of three ways ofsynthesis ofsimple Schiff base. Molbank, 2006, 12-14

42. Suresh Patil, S. D. Jadhav, S. K. Shinde, Organic Chemistry International Volume, 2012, 153159, 1-5

43.   Jnyanaranjan Panda, V. Jagannath Patro, Biswa Mohan Sahoo, and Jitendriya Mishra, Journal of Nanoparticles, 2013, Article ID 549502, 1-5

44.   Arshi Naqvi, Mohd.. Shahnawaaz, Arikatla V. Rao, Daya S. Seth and Nawal K Sharma, E-Journal of Chemistry, 2009, 6(SI), 575-578

45.   Zhaoqi Yang, Pinhua Sun, Molbank 2006, M514 1-3

46.   B. Sindhu Kumari, G. Rijulal & K. Mohanan, Synthesis and reactivity in inorganic metal-organic and Nano- metal chemistry, 2011, Page 24-31.

47.   Garima Yadav, Jyoti V. Mani, International Journal of Science and Research (IJSR), 2015, Volume 4 Issue 2, 121-127

48.   S.F. Vasilevsky, E.V. Tretyakov, and J. Elguero. Adv. Heterocycl. Chem. 82, 1 (2002).

49.   R.M. Moriarty, R.K. Vaid, V.T. RaviKumar, T.E. Hopkins, and P. Farid. Tetrahedron, 45, 1605 (1989).

50.   J.S. Yadav, V.B. Reddy, and V. Geetha. Synlett, 3, 513 (2002).

51.   O. Prakash, A. Kumar, A. Sadana, and S.P. Singh. Synth. Commun. 32, 2663, (2002).

52.   O. Prakash, A. Kumar, and S.P. Singh. J. Indian Chem. Soc. 80, 1035, (2003).

53.   O. Prakash, A. Kumar, and S.P. Singh. Heterocycles, 63, 1193, (2004).

54.   S.P. Singh, O. Prakash, and R.K. Vaid. Indian J. Chem. 23B, 191 (1984).

55.   G. Jones and S.P. Stanforth. Organic reactions. Vol. 56. Edited by L.A. Paquette. John Wiley and Sons, New York. 2000. p. 355.

56.   M.A. Kira, M.N. Aboul-Enein, and M.I. Korkor. J. Heterocycl. Chem. 7, 25 (1970).

57.   M.A. Kira, Z. Nofal, and K.Z. Gadella. Tetrahedron Lett. 42 15 (1970).

58.   M.A. Kira, M.C.A. Rahman, and K.Z. Gadella. Tetrahedron Lett. 10, 9 (1969).

59.   Bohach GA, Fast DJ, Nelson RD, Schlievert PM. Malaria. In. Rodes J, Benhamou JP, Blei A, Reichen J, Rizzetto M, editors. The textbook of hepatology, Oxford (UK): Wiley Blackwell,' 2007. p. I029—34.

60.   Kayser 0, Kiderlen AF, Croft SL. Natural products as potential antiparasitic drugs. Parasitol Res 2003,-90 (Suppl 2):555—62.

61.   de Souza AO, Galetti FCS, Silva CL, Bicalho B, Parma MM, Fonseca SF, et al. Antimycobacterial and cytotoxicity activity ofsynthetic and natural compounds. Quim Nova, 2007;30(7):1563—6.

62.   Koser, G. F. [Hydroxy(tosyloxy)iodobenzene] and closely related iodanes: The second stage of development. Aldrichimica Acta 2001, 34, 89–101.

63.   Schardt, B. C.; Hill, C. L. Inorg. Chem. 1983 , 22, 1563.

64.   Ochiai, M.; Ukita, S.; Lawki, S.; Nagao, Y.; Fujita, E. Oxidative grob fragmentation of g-tributyl-stannyl alcohols with a combination of iodosobenzene dicyclohexyl carbodimide and boron trifluoride. J. Org. Chem. 1989, 54, 4832–4840.

65.   Moriarty, R. M.; John, L. S.; Du, P. C. J. Chem. Soc., Chem. Commun. 1981, 641–642.

66.   Prakash, O.; Kaur, H.; Pundeer, R.; Dhillon, R. S.; Singh, S. P. An improved iodine(III)-mediated method for thiocyanation of 2-arylindan-1,3-diones, phenols, and anilines. Synth. Comm. 2003, 33, 4037–4042.

67.   Jones, G. The Vilsmeier reaction of fully conjugated carbocycles and heterocycles. Org. React. 1997, 49, 1–327.

68.   Hlasta, D. J.; Ackerman, J. H.; Court, J. J.; Farrell, R. P.; Johnson, J. A.; Kofron, J. L.; Robinson, D. T.; Talomie, T. G. A novel class of cyclic b-dicarbonyl leaving groups and their use in the design of benzisothiazolone human leukocyte elastase inhibitors. J. Med. Chem. 1995, 38, 4687–4692.

69.   Cantos, A.; March, P.; Manas, M. M.; Pla, A.; Ferrnado, F. S.; Virgili, A. Synthesis of pyrano[4,3-c]pyrazol-4(1H)-ones and -4(2H)-ones from dehydroacetic acid. Homo and heteronuclear selective NOE measurements for unambiguious structure assignment. Bull. Chem. Soc. Jpn. 1987, 60, 4425–4431.

70.   Furniss, B. S.; Hannaford, A. J.; Smith, P. W.G.; Tatchell, A. R. Vogel's Text Book of Practical Organic Chemistry, 5th ed.; Longman Group: England, 1991, pp. 869–870.

71.   Banerjee, K. S.; Deshpande, S. S. Synthesis of 2-methyl-6-ethyl and 2-methyl-6-npropyl-g-pyrones. J. Indian. Chem. Soc. 1975, LII, 41–44.

72.   Hershberg E B, J Org Chem, 13, 1948, 542.

73.   Hagiwara H & Uda H, J Org Chem, 53, 1988, 2308.

74.   Varvoglis A in Hypervalent Iiodine in Organic Synthesis edited by Katritzky A R, Meth-Cohn O and Rees C W

Satvinder Khatkar *et al.*,

(Academic Press, London), 1997.

75. Zhdankin V V & Stang P J, Chem Rev, 102, 2002, 2523.
76. Hypervalent Iodine Chemistry, Modern Developments in Organic Synthesis edited by Wirth T (Springer, Berlin) 224, 2003.
77. Moriarty R M, J Org Chem, 70, 2005, 2893.
78. Moriarty R M, Chany II C J & Kosmeder II J W, in Enclopedia of Reagents in Organic Synthesis edited by Paquette L A (John Wiley & Sons Ltd., Chichester), 2, 1995, 1479.
79. Prakash O & Singh S P, Aldrichimica Acta, 27, 1994, 15.
80. Somogyi L, Liebigs Ann Chem, 1999.

RESEARCH ARTICLE

A Note on Fuzzy Soft Unitary Operator in Fuzzy Soft Hilbert space

A Radharamani[1]* and T Nagajothi[2]

[1]Assistant Professor, Department of Mathematics, Chikkanna Govt.Arts College, Tirupur, Tamil Nadu, India
[2]Assistant Professor, Department of Mathematics, PSG College of Arts and Science, Coimbatore, , Tamil Nadu, India

*Address for Correspondence
A Radharamani
Assistant Professor,
Department of Mathematics,
Chikkanna Govt.Arts College,
Tirupur, Tamil Nadu, India.

ABSTRACT

The purpose of this search is to introduce some concepts of the fuzzy soft unitary operator defined on fuzzy soft Hilbert space, including some key characteristics of this operator, as well as a discussion of various theorems related to this operator. The aim of this search is to explain some basic ideas about the fuzzy soft unitary operator defined on fuzzy soft Hilbert space, along with a discussion of some of the operator's essential properties and related theorems.

Keywords: Fuzzy soft normal operator, fuzzy soft Hilbert space, fuzzy soft hyponormal operator, fuzzy soft unitary operator, fuzzy soft isometric isomorphism

INTRODUCTION

To solve a number of issues in pure mathematics, the discipline of functional analysis was founded more than a century ago. In addition to regularly presenting us with uncertainty, the phenomena under study's ambiguity also provides us with instruments for assessing faults in solutions to issues with both infinite and limited dimensions. In a variety of fields, including engineering, business, medicine, and economics, this kind of problem might be encountered. Our conventional mathematical methods frequently fall short in addressing such problems. So, in 1965, L. Zadeh offered a generalisation of set theory. The resulting theory was given the name fuzzy set theory. It didn't take long for fuzzy set theory to become a potent tool for handling uncertain situations. In classical set theory, the basis function from a set x to set [0,1] defines the set x.

On the other hand, in fuzzy set theory, a set is defined by its membership function, which spans from x to the closed interval between 0 and 1. Additionally, Molodtsovcreated a novel generalisation for handling uncertainty in 1999. This study led to the development of soft set theory. Since then, it has been used in a variety of disciplines, including computer science, engineering, medicine, and others, to address challenging problems. A parametrized collection of a universal set is known as a soft set. Soft set gave rise to the concepts of soft point, soft normed space, soft inner product space, and soft Hilbert space, which were later used in functional analysis to deal with a variety of mathematical subjects.

Maji et al. presented the idea of a fuzzy soft set for the first time in 2001. The concept was developed by combining a fuzzy set and a soft set. It was required to combine the two ideas in order to provide results that were more accurate and comprehensive. Fuzzy soft point and fuzzy soft normed space were developed as a result of the addition of these additional ideas to the framework. Fuzzy soft Hilbert spaces were introduced in 2020 by Fariedet al. Also included are the fuzzy soft linear operators. In this article, we provide a novel kind of Fuzzy soft unitary operator and establish various related theorems.

PRELIMINARIES
The notations, definitions, and introductions for fuzzy set, soft set, and fuzzy soft set that will be used in the discussion that follows are provided in this section.

Definition 2.1: Fuzzy set
If fuzzy set $\check{A}$over $\mathfrak{X}$ is a set characterized by a membership function
$\eta_{\check{A}}: \mathfrak{X} \rightarrow \mathfrak{I}$, such as $\mathfrak{I} = [0,1]$and $\check{A} = \left\{ \frac{\eta_{\check{A}}(x)}{x} : x \in \mathfrak{X} \right\}$.
And $\mathfrak{I}^{\mathfrak{X}} = \{\check{A} : \check{A} \; is \; a \; function \; from \; \mathfrak{X} \; into \; \mathfrak{I}\}$

Definition 2.2: Soft set
Let $\mathcal{P}(\mathfrak{X})$ the power set of $\mathfrak{X}$ and E be set of parameters and $A \subseteq E$. The mapping $\mathbb{G}: A \rightarrow \mathcal{P}(\mathfrak{X})$, when $(\mathbb{G}, A) = \{\mathbb{G}(l)\epsilon\mathcal{P}(\mathfrak{X}): l \in A\}$. As a result $(\mathbb{G}, A)$ is called the soft set.

Definition 2.3: Fuzzy soft set
The soft set $\mathbb{G}_A$ we say that fuzzy soft set over $\mathfrak{X}$, when $\mathbb{G}: A \rightarrow \mathfrak{I}^{\mathfrak{X}}$, and $\{\mathbb{G}(l)\epsilon\mathfrak{I}^{\mathfrak{X}}: l \in A\}$. The collection of all fuzzy soft sets denoted by $FSS(\widetilde{\mathfrak{X}})$.

Definition 2.4: Fuzzy soft point
The fuzzy soft set $(\mathbb{G}, A) \in FSS(\widetilde{\mathfrak{X}})$is called a fuzzy soft point over $\mathfrak{X}$, denoted by $\tilde{l}_{\eta_{\mathbb{G}(e)}}$ if
$e \in A, x \in \mathfrak{X}$
$\eta_{\mathbb{G}(e)}(x) = \begin{cases} \alpha, & if \; l = l_0 \in \mathfrak{X} \; and \; e = e_0 \in A, \\ 0, & if \; l \in \mathfrak{X} - \{l_0\} \; or \; e \in A - \{e_0\} \end{cases}$, such that $\alpha \in (0,1]$

Definition 2.5: Fuzzy soft Hilbert space
A fuzzy soft inner product space is defined as $(\widetilde{\mathfrak{X}}, \widetilde{\langle.,.\rangle})$. This space, which is fuzzy soft complete in the induced fuzzy soft norm indicated in Theorem (2.10), is thus referred to as a fuzzy soft Hilbert space and denoted by $(\tilde{\hbar}, \widetilde{\langle.,.\rangle})$. Every fuzzy soft Hilbert space is obviously a fuzzy soft banach space.

Definition 2.6: Fuzzy soft linear operator in $\tilde{\hbar}$
Consider $\tilde{\hbar}$ to be a fuzzy soft Hilbert space. A fuzzy soft linear operator $\widetilde{\mathcal{T}}: \tilde{\hbar} \rightarrow \tilde{\hbar}$is called a fuzzy soft linear operator in $\tilde{\hbar}$, then $\widetilde{\mathcal{T}}$ is a fuzzy soft linear operator on $\tilde{\hbar}$ which is denoted as$\widetilde{\mathcal{T}} \widetilde{\in} \widetilde{\mathbb{L}}(\tilde{\hbar})$. $\widetilde{\mathcal{T}}$ is fuzzy soft bounded if there exists $\tilde{\kappa} \widetilde{\in} \Re(\mathbb{A})$: $\left\| \widetilde{\mathcal{T}}\left(\widetilde{\tilde{l}_{\eta_{\mathfrak{g}(e)}}}\right) \right\| \widetilde{\leqq} \tilde{\kappa} \left\| \tilde{l}_{\eta_{\mathfrak{g}(e)}} \right\|$ $\forall \tilde{l}_{\eta_{\mathfrak{g}(e)}} \widetilde{\in} \tilde{\hbar}$, then $\widetilde{\mathcal{T}} \widetilde{\in} \mathfrak{B}(\tilde{\hbar})$

Definition 2.7: Fuzzy soft adjoint operator in $\tilde{h}$

The fuzzy soft adjoint operator $\mathbb{T}^*$ of a fuzzy soft linear operator $\mathbb{T}$ is defined by
$\langle \widetilde{\mathbb{T}\tilde{l}^1}_{\eta_{1_{\mathbb{G}(e_1)}}}, \tilde{l}^2_{\eta_{2_{\mathbb{G}(2)}}} \rangle \cong \langle \tilde{l}^1_{\eta_{1_{\mathbb{G}(e_1)}}}, \widetilde{\mathbb{T}^*\tilde{l}^2}_{\eta_{2_{\mathbb{G}(2)}}} \rangle$
for all $\tilde{l}^1_{\eta_{1_{\mathbb{G}(e_1)}}}, \tilde{l}^2_{\eta_{2_{\mathbb{G}(e_2)}}} \; \widetilde{\in} \; \tilde{h}$

Definition 2.8: Fuzzy soft Normal Operator

Let $\tilde{h}$ be an FS Hilbert space and $\tilde{\mathbb{T}} \in \mathfrak{B}(\tilde{h})$. Then, $\tilde{\mathbb{T}}$ is said to be an FS normal
operator if $\tilde{\mathbb{T}}\tilde{\mathbb{T}}^* \cong \tilde{\mathbb{T}}^*\tilde{\mathbb{T}}$

Definition 2.9: Fuzzy soft self adjoint operator

The FS-operator $\tilde{\mathbb{T}}$ of FSH-space $\tilde{h}$ is called fuzzy soft self adjoint (FS-self adjoint operator)
if $\tilde{\mathbb{T}} \cong \tilde{\mathbb{T}}^*$

Definition 2.10: Fuzzy soft isometry operator

Let $\tilde{h}$ be an FS Hilbert space and $\tilde{\mathbb{T}} \in \mathfrak{B}(\tilde{h})$. Then, $\tilde{\mathbb{T}}$ is said to be an FSisometry
operator if $\langle \widetilde{\tilde{\mathbb{T}}\tilde{l}^1}_{\eta_{1_{g(e_1)}}}, \tilde{\mathbb{T}}\tilde{l}^2_{\eta_{2_{g(e_2)}}} \rangle \cong \langle \tilde{l}^1_{\eta_{1_{g(e_1)}}}, \tilde{l}^2_{\eta_{2_{g(2)}}} \rangle$ for all $\tilde{l}^1_{\eta_{1_{g(e_1)}}}, \tilde{l}^2_{\eta_{2_{g(2)}}} \; \widetilde{\in} \; \tilde{h}$

Definition 2.11: Fuzzy soft projection operator

Consider $\tilde{h}$ to be a fuzzy soft Hilbert space. A fuzzy soft linear operator $\tilde{\mathbb{T}}: \tilde{h} \rightarrow \tilde{h}$ is called a fuzzy soft projection
operator in $\tilde{h}$ if $\tilde{\mathbb{T}}^2 \cong \tilde{\mathbb{T}}$ ie, $\tilde{\mathbb{T}}$ is an idempotent.

Definition 2.12: Fuzzy soft hyponormaloperator

Consider $\tilde{h}$ to be a fuzzy soft Hilbert space. $\tilde{\mathbb{T}} \in \mathfrak{B}(\tilde{h})$ is called fuzzy soft hyponormal operator if $\left\| \tilde{\mathbb{T}}^* \tilde{l}_{\eta_{g(e)}} \right\| \leq \left\| \tilde{\mathbb{T}}\tilde{l}_{\eta_{g(e)}} \right\|$
for all $\tilde{l}_{\eta_{g(e)}} \; \widetilde{\in} \; \tilde{h}$ or equivalently $\tilde{\mathbb{T}}^*\tilde{\mathbb{T}} \geq \tilde{\mathbb{T}}\tilde{\mathbb{T}}^*$

Definition 2.13: M-Fuzzy soft hyponormaloperator

Let $\tilde{h}$ be an FS Hilbert space and let $\tilde{\mathbb{T}} \in \mathfrak{B}(\tilde{h})$ is called M – fuzzy soft hyponormal operator if there exist a real
number $\mathcal{M}$, such that $\left\| \left(\widetilde{\tilde{\mathbb{T}} \tilde{\approx} \tilde{e}\tilde{I}}\right)^* \tilde{l}_{\eta_{g(e)}} \right\| \widetilde{\leq} \widetilde{\mathcal{M}} \left\| \widetilde{\left(\tilde{\mathbb{T}} \tilde{\approx} \tilde{e}\tilde{I}\right)\tilde{l}}_{\eta_{g(e)}} \right\|$
for all $\tilde{l}_{\eta_{g(e)}} \; \widetilde{\in} \; \tilde{h}$ and for all $\tilde{e} \; \widetilde{\in} \; \mathbb{C}(\mathbb{A})$

Remark 2.14:

Any fuzzy soft Hilbert space $\tilde{h}$ has the same fuzzy soft conjugate space $\tilde{h}^*$,
ie) $\tilde{h}^* \cong \tilde{h}$ ($\tilde{h}$ and $\tilde{h}^*$ are fuzzy soft isomorphic).

MAIN RESULTS

The definition of the fuzzy soft unitary operator in fuzzy soft Hilbert space is provided in this section.

Definition 3.1: [9]

Suppose that $\tilde{h}$ is an FS Hilbert space. If $\tilde{\mathbb{6}}^*\tilde{\mathbb{6}} \cong \tilde{I} \cong \tilde{\mathbb{6}}\tilde{\mathbb{6}}^*$, then $\tilde{\mathbb{6}} \in \mathfrak{B}(\tilde{h})$ is known as a fuzzy soft unitary operator.

Note 3.2:

Every FSU operator also acts as an FSN operator

Theorem 3.3:

Let $\tilde{\mathbb{6}} \in \mathfrak{B}(\tilde{h})$, then the following are all equivalent:
i) $\tilde{\mathbb{6}}^*\tilde{\mathbb{6}} \cong \tilde{I}$

  ii) $\langle \widetilde{\tilde{\mathbb{6}}\tilde{l}^1}_{\eta_{1_{g(e_1)}}}, \tilde{\mathbb{6}}\tilde{l}^2_{\eta_{2_{g(e_2)}}} \rangle \cong \langle \tilde{l}^1_{\eta_{1_{g(e_1)}}}, \tilde{l}^2_{\eta_{2_{g(e_2)}}} \rangle$ for all $\tilde{l}^1_{\eta_{1_{g(e_1)}}}, \tilde{l}^2_{\eta_{2_{g(e_2)}}} \; \widetilde{\in} \; \tilde{h}$

iii) $\left\|\widetilde{\mathfrak{b}}\widetilde{l_{\eta_{\mathfrak{g}(e)}}}\right\| \cong \left\|\widetilde{l_{\eta_{\mathfrak{g}(e)}}}\right\|$ for all $\tilde{l}_{\eta_{\mathfrak{g}(e)}} \tilde{\in} \tilde{\hbar}$

Theorem 3.4:

Assume that $\tilde{\mathfrak{b}} \in \tilde{\mathfrak{B}}(\tilde{\hbar})$. If $\widetilde{\mathbb{U}}$ is fuzzy soft unitary operator iff $\left\|\widetilde{\mathfrak{b}}\widetilde{l_{\eta_{\mathfrak{g}(e)}}}\right\| \cong \left\|\widetilde{l_{\eta_{\mathfrak{g}(e)}}}\right\|$
for all $\tilde{l}_{\eta_{\mathfrak{g}(e)}} \tilde{\in} \tilde{\hbar}$ and $\tilde{\mathfrak{b}}$ is surjective in that case $\left\|\widetilde{\mathfrak{b}^{-1}\widetilde{l_{\eta_{\mathfrak{g}(e)}}}}\right\| \cong \left\|\widetilde{l_{\eta_{\mathfrak{g}(e)}}}\right\|$
for all $\tilde{l}_{\eta_{\mathfrak{g}(e)}} \tilde{\in} \tilde{\hbar}$ and $\|\tilde{\mathfrak{b}}\| \cong \tilde{1} \cong \|\tilde{\mathfrak{b}}^{-1}\|$

Proof:

For $\tilde{l}^1{}_{\eta_{1_{\mathfrak{g}(e_1)}}} \tilde{\in} \tilde{\hbar}$ we have

$\left\|\widetilde{\mathfrak{b}}\widetilde{l_{\eta_{\mathfrak{g}(e)}}}\right\|^2 - \left\|\widetilde{l_{\eta_{\mathfrak{g}(e)}}}\right\|^2 \cong \langle \widetilde{\mathfrak{b}}l_{\eta_{\mathfrak{g}(e)}}, \widetilde{\mathfrak{b}}l_{\eta_{\mathfrak{g}(e)}}\rangle - \langle \tilde{l}_{\eta_{\mathfrak{g}(e)}}, \tilde{l}_{\eta_{\mathfrak{g}(e)}}\rangle$

$\cong \langle \widetilde{\mathfrak{b}^*\mathfrak{b}}l_{\eta_{\mathfrak{g}(e)}}, \tilde{l}_{\eta_{\mathfrak{g}(e)}}\rangle - \langle \tilde{l}_{\eta_{\mathfrak{g}(e)}}, \tilde{l}_{\eta_{\mathfrak{g}(e)}}\rangle$

$\cong \langle (\widetilde{\mathfrak{b}^*\mathfrak{b} - \tilde{I}})l_{\eta_{\mathfrak{g}(e)}}, \quad \tilde{l}_{\eta_{\mathfrak{g}(e)}}\rangle$

Since $\tilde{\mathfrak{b}}^*\tilde{\mathfrak{b}} - \tilde{I}$ is self adjoint fuzzy soft operator it follows from that $\tilde{\mathfrak{b}}^*\tilde{\mathfrak{b}} \cong \tilde{I}$ iff
$\left\|\widetilde{\mathfrak{b}}\widetilde{l_{\eta_{\mathfrak{g}(e)}}}\right\| \cong \left\|\widetilde{l_{\eta_{\mathfrak{g}(e)}}}\right\|$ for all $\tilde{l}_{\eta_{\mathfrak{g}(e)}} \tilde{\in} \tilde{\hbar}$ and $\tilde{\mathfrak{b}}$ is surjective, then $\tilde{\mathfrak{b}}^*\tilde{\mathfrak{b}} \cong \tilde{I}$ and $\tilde{\mathfrak{b}}$ is bijective,
Therefore, $\tilde{\mathfrak{b}}\tilde{\mathfrak{b}}^* \cong (\tilde{\mathfrak{b}}\tilde{\mathfrak{b}}^*)\tilde{I}$
$\cong (\tilde{\mathfrak{b}}\tilde{\mathfrak{b}}^*) . (\tilde{\mathfrak{b}}\tilde{\mathfrak{b}}^{-1})$
$\cong \tilde{\mathfrak{b}}(\tilde{\mathfrak{b}}^*\tilde{\mathfrak{b}})\tilde{\mathfrak{b}}^{-1}$
$\cong \tilde{\mathfrak{b}}\tilde{\mathfrak{b}}^{-1}$
[since $\tilde{\mathfrak{b}}$ is fuzzy soft unitary, $\tilde{\mathfrak{b}}\tilde{\mathfrak{b}}^* \cong \tilde{I} \cong \tilde{\mathfrak{b}}^*\tilde{\mathfrak{b}}$]
ie) $\tilde{\mathfrak{b}}\tilde{\mathfrak{b}}^* \cong \tilde{I}$, therefore $\tilde{\mathfrak{b}}$ is fuzzy soft unitary
Conversely, if $\tilde{\mathfrak{b}}$ is fuzzy soft unitary then $\tilde{\mathfrak{b}}\tilde{\mathfrak{b}}^* \cong \tilde{I}$ and $\tilde{\mathfrak{b}}^{-1} \cong \tilde{\mathfrak{b}}^*$ in that
$\left\|\widetilde{\mathfrak{b}}\widetilde{l_{\eta_{\mathfrak{g}(e)}}}\right\| \cong \left\|\widetilde{l_{\eta_{\mathfrak{g}(e)}}}\right\|$ for all $\tilde{l}_{\eta_{\mathfrak{g}(e)}} \tilde{\in} \tilde{\hbar}$ and $\widetilde{\mathbb{U}}$ is surjective in that case it follows that
$\left\|\widetilde{\mathfrak{b}^{-1}\widetilde{l_{\eta_{\mathfrak{g}(e)}}}}\right\| \cong \left\|\widetilde{l_{\eta_{\mathfrak{g}(e)}}}\right\|$ for all $\tilde{l}_{\eta_{\mathfrak{g}(e)}} \tilde{\in} \tilde{\hbar}$
taking the supremum over all $\tilde{l}_{\eta_{\mathfrak{g}(e)}} \tilde{\in} \tilde{\hbar}$ with $\left\|\widetilde{l_{\eta_{\mathfrak{g}(e)}}}\right\| \tilde{\leq} \tilde{1}$
then we get, $\|\tilde{\mathfrak{b}}\| \cong \tilde{1} \cong \|\tilde{\mathfrak{b}}^{-1}\|$

Theorem 3.5:
Consider $\tilde{\mathfrak{b}}_1, \tilde{\mathfrak{b}}_2 \in \tilde{\mathfrak{B}}(\tilde{\hbar})$, if $\tilde{\mathfrak{b}}_1$ and $\tilde{\mathfrak{b}}_2$ are FSU operator, then $\tilde{\mathfrak{b}}_1\tilde{\mathfrak{b}}_2$ is also FSU.
Let $\tilde{\mathfrak{b}}_1 \tilde{\mp} \tilde{\mathfrak{b}}_2$ is FSU iff it is surjective and $\left(\widetilde{\tilde{\mathfrak{b}}_1\tilde{l}_{\eta_{\mathfrak{g}(e)}}, \tilde{\mathfrak{b}}_2\tilde{l}_{\eta_{\mathfrak{g}(e)}}}\right) \cong -\frac{1}{2}$,
$\tilde{l}_{\eta_{\mathfrak{g}(e)}} \tilde{\in} \tilde{\hbar}$ with $\|\tilde{\mathfrak{b}}\| \cong \tilde{1}$
Proof:
Given $\tilde{\mathfrak{b}}_1$ and $\tilde{\mathfrak{b}}_2$ are FSU operator on $\tilde{\hbar}$
To prove that $\tilde{\mathfrak{b}}_1\tilde{\mathfrak{b}}_2$ is FSU
Let $(\tilde{\mathfrak{b}}_1\tilde{\mathfrak{b}}_2)^*\tilde{\mathfrak{b}}_1\tilde{\mathfrak{b}}_2 \cong \tilde{\mathfrak{b}}_2{}^*(\tilde{\mathfrak{b}}_1{}^*\tilde{\mathfrak{b}}_1)\tilde{\mathfrak{b}}_2$
$\cong \tilde{\mathfrak{b}}_2{}^*\tilde{\mathfrak{b}}_2$
$(\tilde{\mathfrak{b}}_1\tilde{\mathfrak{b}}_2)^*\tilde{\mathfrak{b}}_1\tilde{\mathfrak{b}}_2 \cong \tilde{I}$
Therefore, $\tilde{\mathfrak{b}}_1\tilde{\mathfrak{b}}_2$ is FSU
Consider $\tilde{\mathfrak{b}}_1 \tilde{\mp} \tilde{\mathfrak{b}}_2$ is surjective and
$Re\left(\widetilde{\tilde{\mathfrak{b}}_1\tilde{l}_{\eta_{\mathfrak{g}(e)}}, \tilde{\mathfrak{b}}_2\tilde{l}_{\eta_{\mathfrak{g}(e)}}}\right) \cong -\frac{1}{2}, \tilde{l}_{\eta_{\mathfrak{g}(e)}} \tilde{\in} \tilde{\hbar}$ with $\|\tilde{\mathfrak{b}}\| \cong \tilde{1}$
From above theorem $\tilde{\mathfrak{b}}_1 \tilde{\mp} \tilde{\mathfrak{b}}_2$ is FSU
Conversely,
To prove that it is surjective and $Re\left(\widetilde{\tilde{\mathfrak{b}}_1\tilde{l}_{\eta_{\mathfrak{g}(e)}}, \tilde{\mathfrak{b}}_2\tilde{l}_{\eta_{\mathfrak{g}(e)}}}\right) \cong -\frac{1}{2}, \tilde{l}_{\eta_{\mathfrak{g}(e)}} \tilde{\in} \tilde{\hbar}$ with $\|\tilde{\mathfrak{b}}\| \cong \tilde{1}$

$\left\|(\tilde{\mathfrak{b}}_1 \tilde{\mp} \tilde{\mathfrak{b}}_2)\tilde{l}_{\eta_{\mathfrak{g}(e)}}\right\|^2 \cong \langle (\tilde{\mathfrak{b}}_1 \tilde{\mp} \tilde{\mathfrak{b}}_2)\tilde{l}_{\eta_{\mathfrak{g}(e)}}, (\tilde{\mathfrak{b}}_1 \tilde{\mp} \tilde{\mathfrak{b}}_2)\tilde{l}_{\eta_{\mathfrak{g}(e)}}\rangle$

$$\left\|\tilde{l}_{\eta_{\mathfrak{g}(e)}}\right\|^2 \cong \langle \widetilde{\mathfrak{b}_1\tilde{l}_{\eta_{\mathfrak{g}(e)}}, \widetilde{\mathfrak{b}_1}\tilde{l}_{\eta_{\mathfrak{g}(e)}}\rangle \widetilde{+} \langle \widetilde{\mathfrak{b}_1\tilde{l}_{\eta_{\mathfrak{g}(e)}}, \widetilde{\mathfrak{b}_2}\tilde{l}_{\eta_{\mathfrak{g}(e)}}\rangle \widetilde{+} \langle \widetilde{\mathfrak{b}_2\tilde{l}_{\eta_{\mathfrak{g}(e)}}, \widetilde{\mathfrak{b}_1}\tilde{l}_{\eta_{\mathfrak{g}(e)}}\rangle \widetilde{+} \langle \widetilde{\mathfrak{b}_2\tilde{l}_{\eta_{\mathfrak{g}(e)}}, \widetilde{\mathfrak{b}_2}\tilde{l}_{\eta_{\mathfrak{g}(e)}}\rangle$$

$$\langle \tilde{l}_{\eta_{\mathfrak{g}(e)}}, \tilde{l}_{\eta_{\mathfrak{g}(e)}}\rangle \cong \langle \widetilde{\tilde{l}_{\eta_{\mathfrak{g}(e)}}, \tilde{l}_{\eta_{\mathfrak{g}(e)}}\rangle \widetilde{+} \langle \widetilde{\mathfrak{b}_1\tilde{l}_{\eta_{\mathfrak{g}(e)}}, \widetilde{\mathfrak{b}_2}\tilde{l}_{\eta_{\mathfrak{g}(e)}}\rangle \widetilde{+} \langle \widetilde{\mathfrak{b}_2\tilde{l}_{\eta_{\mathfrak{g}(e)}}, \widetilde{\mathfrak{b}_1}\tilde{l}_{\eta_{\mathfrak{g}(e)}}\rangle \widetilde{+} \langle \widetilde{\tilde{l}_{\eta_{\mathfrak{g}(e)}}, \tilde{l}_{\eta_{\mathfrak{g}(e)}}\rangle$$

$$\langle \tilde{l}_{\eta_{\mathfrak{g}(e)}}, \tilde{l}_{\eta_{\mathfrak{g}(e)}}\rangle \cong 2\langle \widetilde{\tilde{l}_{\eta_{\mathfrak{g}(e)}}, \tilde{l}_{\eta_{\mathfrak{g}(e)}}\rangle \widetilde{+} 2\, Re\, \langle \widetilde{\mathfrak{b}_1\tilde{l}_{\eta_{\mathfrak{g}(e)}}, \widetilde{\mathfrak{b}_2}\tilde{l}_{\eta_{\mathfrak{g}(e)}}\rangle$$

Hence by the Theorem 3.4,

$\mathfrak{b}_1 \widetilde{+} \mathfrak{b}_2$ is FSU, iff it is surjective and

$$\langle \widetilde{\tilde{l}_{\eta_{\mathfrak{g}(e)}}, \tilde{l}_{\eta_{\mathfrak{g}(e)}}\rangle \widetilde{+} 2\, Re\, \langle \widetilde{\mathfrak{b}_1\tilde{l}_{\eta_{\mathfrak{g}(e)}}, \widetilde{\mathfrak{b}_2}\tilde{l}_{\eta_{\mathfrak{g}(e)}}\rangle \cong \tilde{0} \Rightarrow 2\, Re\, \langle \widetilde{\mathfrak{b}_1\tilde{l}_{\eta_{\mathfrak{g}(e)}}, \widetilde{\mathfrak{b}_2}\tilde{l}_{\eta_{\mathfrak{g}(e)}}\rangle \cong -\frac{1}{2},$$

for all $\tilde{l}_{\eta_{\mathfrak{g}(e)}} \widetilde{\in} \tilde{\hbar}$

Definition 3.6:Fuzzy soft isometric isomorphism:

Consider the fuzzy soft normed linear spaces $\tilde{\mathfrak{m}}$ *and* $\tilde{\mathfrak{n}}$. A fuzzy soft isometric isomorphism of $\tilde{\mathfrak{m}}$ *and* $\tilde{\mathfrak{n}}$ and $\tilde{\mathfrak{n}}$ is a one-to-one linear transformation $\mathfrak{b}$ of $\tilde{\mathfrak{m}}$ *into* $\tilde{\mathfrak{n}}$ such that $\left\|\widetilde{\mathfrak{b}\tilde{l}_{\eta_{\mathfrak{g}(e)}}}\right\| \cong \left\|\widetilde{\tilde{l}_{\eta_{\mathfrak{g}(e)}}}\right\|$ for every $\tilde{l}_{\eta_{\mathfrak{g}(e)}} \widetilde{\in} \tilde{\hbar}$.

Theorem 3.7:

Assume that $\tilde{\hbar}$ is an FSH space and that $\mathfrak{b} \in \mathfrak{B}(\tilde{\hbar})$. If $\mathfrak{b}$ is an isometric isomorphism of $\tilde{\hbar}$ onto itself, then it is an FSU operator.

Proof:

If $\mathfrak{b}$ is an FSU operator, it is onto by definition.

It is an isometric isomorphism of $\tilde{\hbar}$ onto itself, and it preserves fuzzy soft norm by the definition.

Conversely, if $\mathfrak{b}$ is an isometric isomorphism of $\tilde{\hbar}$ onto itself, then $\mathfrak{b}^{-1}$ exists.

By the definition, we have $\mathfrak{b}^*\mathfrak{b} \cong \tilde{I}$, multiplying on both sides by $\mathfrak{b}^{-1}$

$(\mathfrak{b}^*\mathfrak{b})\mathfrak{b}^{-1} \cong \tilde{I}\mathfrak{b}^{-1}$

$\Rightarrow \mathfrak{b}^* \cong \mathfrak{b}^{-1}$

$\Rightarrow \mathfrak{b}\mathfrak{b}^* \cong \tilde{I} \cong \mathfrak{b}^*\mathfrak{b}$

Hence $\mathfrak{b}$ is a FSU operator.

Note:

Let $\mathfrak{b} \in \mathfrak{B}(\tilde{\hbar})$. since $\langle \widetilde{\mathfrak{b}\tilde{l}^1_{\eta_{1_{\mathfrak{g}(e_1)}}}, \tilde{l}^2_{\eta_{2_{\mathfrak{g}(e_2)}}}\rangle \cong \langle \tilde{l}^1_{\eta_{1_{\mathfrak{g}(e_1)}}}, \widetilde{\mathfrak{b}^*\tilde{l}^2_{\eta_{2_{\mathfrak{g}(e_2)}}}}\rangle$

for all $\tilde{l}^1_{\eta_{1_{\mathfrak{g}(e_1)}}}, \tilde{l}^2_{\eta_{2_{\mathfrak{g}(e_2)}}} \widetilde{\in} \tilde{\hbar}$

Then i) $\mathfrak{b}$ isfuzzy soft normal iff $\langle \widetilde{\mathfrak{b}\tilde{l}^1_{\eta_{1_{\mathfrak{g}(e_1)}}}, \widetilde{\mathfrak{b}\tilde{l}^2_{\eta_{2_{\mathfrak{g}(e_2)}}}}\rangle \cong \langle \widetilde{\mathfrak{b}^*\tilde{l}^1_{\eta_{1_{\mathfrak{g}(e_1)}}}, \widetilde{\mathfrak{b}^*\tilde{l}^2_{\eta_{2_{\mathfrak{g}(e_2)}}}}\rangle$

ii) Fuzzy soft unitary iff $\langle \widetilde{\mathfrak{b}\tilde{l}^1_{\eta_{1_{\mathfrak{g}(e_1)}}}, \widetilde{\mathfrak{b}\tilde{l}^2_{\eta_{2_{\mathfrak{g}(e_2)}}}}\rangle \cong \langle \widetilde{\tilde{l}^1_{\eta_{1_{\mathfrak{g}(e_1)}}}, \tilde{l}^2_{\eta_{2_{\mathfrak{g}(e_2)}}}}\rangle \cong \langle \widetilde{\mathfrak{b}^*\tilde{l}^1_{\eta_{1_{\mathfrak{g}(e_1)}}}, \widetilde{\mathfrak{b}^*\tilde{l}^2_{\eta_{2_{\mathfrak{g}(e_2)}}}}\rangle$

iii) Self-adjoint fuzzy soft operator iff $\langle \widetilde{\mathfrak{b}\tilde{l}^1_{\eta_{1_{\mathfrak{g}(e_1)}}}, \tilde{l}^2_{\eta_{2_{\mathfrak{g}(e_2)}}}}\rangle \cong \langle \tilde{l}^1_{\eta_{1_{\mathfrak{g}(e_1)}}}, \widetilde{\mathfrak{b}\tilde{l}^2_{\eta_{2_{\mathfrak{g}(e_2)}}}}\rangle$

We also know that the geometry of $\tilde{\hbar}$ can be described by a fuzzy soft inner product on $\tilde{\hbar}$.

Therefore, an operator $\mathfrak{b}$ is fuzzy soft unitary if neither $\mathfrak{b}$ nor $\mathfrak{b}^*$ modify the geometry of $\tilde{\hbar}$, and an operator $\mathfrak{b}$ is fuzzy soft normal if $\mathfrak{b}$ and $\mathfrak{b}^*$ modification the geometry of $\tilde{\hbar}$ in the same way.In addition to this, a fuzzy soft unitary operator is also referred to as a fuzzy soft isomorphism of Hilbert space.

Theorem 3.8:

Consider $\mathfrak{b} \in \mathfrak{B}(\tilde{\hbar})$ and $K \cong \tilde{\varphi}$. Then there are a unique self adjoint fuzzy soft operators $\tilde{P}$ and $\tilde{\varphi}$ on $\tilde{\hbar}$ such that $\mathfrak{b} \cong \tilde{P} \widetilde{+} i\tilde{\varphi}$.Moreover, $\mathfrak{b}$ is fuzzy soft normal iff $\tilde{P}\tilde{\varphi} \cong \tilde{\varphi}\tilde{P}$, fuzzy soft unitary iff $\tilde{P}\tilde{\varphi} \cong \tilde{\varphi}\tilde{P}$ and $\tilde{P}^2 \widetilde{+} \tilde{\varphi}^2 \cong \tilde{I}$ and $\mathfrak{b}$ is self adjoint fuzzy soft operator iff $\tilde{\varphi} \cong \tilde{0}$

Proof:

Let $\tilde{P} \cong \frac{\mathfrak{b} \widetilde{+} \mathfrak{b}^*}{2}$ and $\tilde{\varphi} \cong \frac{\mathfrak{b} \cong \mathfrak{b}^*}{2i}$

Then $\tilde{P}$ and $\tilde{\varphi}$ are self adjoint fuzzy soft operator and $\mathfrak{b} \cong \tilde{P} \widetilde{+} i\tilde{\varphi}$

If we also have $\mathfrak{b} \cong \tilde{P}_1 \widetilde{+} i\tilde{\varphi}_1$

Where $\tilde{P}_1$ *and* $\tilde{\varphi}_1$ self adjoint fuzzy soft operator then, $\mathfrak{b}^* \cong \tilde{P}_1 \cong i\tilde{\varphi}_1$

Radharamani and Nagajothi

So that $\tilde{\mathbb{P}}_1 \cong \frac{\tilde{\mathbb{t}} \tilde{+} \tilde{\mathbb{t}}^*}{2} \cong \tilde{\mathbb{P}}$ and $\tilde{\mathbb{q}}_1 \cong \frac{\tilde{\mathbb{t}} \tilde{-} \tilde{\mathbb{t}}^*}{2i} \cong \tilde{\mathbb{q}}$

Thus, $\tilde{\mathbb{P}}$and $\tilde{\mathbb{q}}$ are unique.

Now $\tilde{\mathbb{t}}$ is fuzzy soft normal iff $(\tilde{\mathbb{P}} \tilde{-} i\tilde{\mathbb{q}})(\tilde{\mathbb{P}} \tilde{+} i\tilde{\mathbb{q}}) \cong \tilde{\mathbb{t}}^* \tilde{\mathbb{t}} \cong \tilde{\mathbb{t}} \tilde{\mathbb{t}}^* \cong (\tilde{\mathbb{P}} \tilde{+} i\tilde{\mathbb{q}})(\tilde{\mathbb{P}} \tilde{-} i\tilde{\mathbb{q}})$

ie) $\tilde{\mathbb{P}}\tilde{\mathbb{q}} \cong \tilde{\mathbb{q}}\tilde{\mathbb{P}}$

Similarly, $\tilde{\mathbb{t}}$ is fuzzy soft unitaryiff$\tilde{\mathbb{t}}\tilde{\mathbb{t}}^* \cong \tilde{I} \cong \tilde{\mathbb{t}}^* \tilde{\mathbb{t}}$

$$(\tilde{\mathbb{P}} \tilde{+} \tilde{\mathbb{q}})(\tilde{\mathbb{P}} \tilde{-} \tilde{\mathbb{q}}) \cong \tilde{\ } \cong (\tilde{\mathbb{P}} \tilde{-} \tilde{\mathbb{q}})(\tilde{\mathbb{P}} \tilde{+} \tilde{\mathbb{q}})$$

ie) $(\tilde{\mathbb{P}}^2 \tilde{+} \tilde{\mathbb{q}}^2) + (\tilde{\mathbb{q}}\tilde{\mathbb{P}} \tilde{-} \tilde{\mathbb{P}}\tilde{\mathbb{q}}) \cong \tilde{\ } \cong (\tilde{\mathbb{P}}^2 \tilde{+} \tilde{\mathbb{q}}^2) + (\tilde{\mathbb{q}}\tilde{\mathbb{P}} \tilde{-} \tilde{\mathbb{P}}\tilde{\mathbb{q}})$

It can be easily seen that this is equivalent to

$\tilde{\mathbb{P}}^2 \tilde{+} \tilde{\mathbb{q}}^2 \cong \tilde{\ }and\tilde{\mathbb{q}}\tilde{\mathbb{P}} \tilde{-} \tilde{\mathbb{P}}\tilde{\mathbb{q}} \cong \tilde{0}$

Finally, $\tilde{\mathbb{t}}$ is self adjoint fuzzy soft operator iff$\tilde{\mathbb{P}} + \tilde{\mathbb{q}} \cong \tilde{\mathbb{P}} \tilde{-} i\tilde{\mathbb{q}}; ie)$ $\tilde{\mathbb{P}}\tilde{\mathbb{q}} \cong \tilde{0}$

CONCLUSION

Numerous scholars have updated the ideas of normed space, metric space, and Hilbert space in soft and fuzzy ways. The outcomes of the fusion of fuzzy and soft notions are more broadly applicable. The Fuzzy Soft Unitary Operator has been defined and explained in this study.

ACKNOWLEDGEMENT

ABBREVIATION

FSU – fuzzy soft unitary operator, FSN – fuzzy soft normal operator,
FSHS – fuzzy soft Hilbert space

REFERENCES

1. Beaula and M.M. Priyanga, A new notion for fuzzy soft normed linear space, Int. J. Fuzzy Math. Arch. 9(1), 81-90 (2015)
2. N. Faried, M.S.S. Ali and H.H. Sakr, On fuzzy soft linear operators in fuzzy soft Hilbert Spaces, Abst. Appl. Anal.2020
3. N. Faried, M.S.S. Ali and H.H. Sakr. Fuzzy soft inner product spaces, Appl.Math. Inf. Sci. 14(4), 709-720(2020)
4. N. Faried, M.S.S. Ali and H.H. Sakr. Fuzzy soft Hilbert spaces, J. Math. Comp. Sci. 22(2021), 142-157 (2020)
5. N. Faried, M.S.S. Ali and H.H. Sakr. A Note on Fuzzy soft Isometry operators, Math.Sci.Lett.10, No.1, 1-3(2021)
6. P.K. Maji, R. Biswas and A.R. Roy, Fuzzy soft set , J. Fuzzy Math.. 9(3), 677-692 (2001)
7. K. Maji, R. Biswas, and A.R. Roy, "Soft set theory", Computers & Mathematics with Application, vol.45, no. 4-5, pp. 555-562, 2003
8. D. Molodtsov, Soft set theory-First results, Comput. Math.Appl. 37. 19-31 (1999)
9. Dr.SalimDawood, Ali QassimJabur, On fuzzy soft normal operators, Journal of Physics: Conference series 1879(2021) 032002
10. Dr.SalimDawood, Ali QassimJabur, On fuzzy soft projection operators in Hilbert space, Al-Qadisiyah journal of pure science vol.(26) issue (1)(2021)PP math.112-123
11. Radharamani. A etal., Fuzzy partial isometry operator and its characteristics, IOSR Journal of Engineering (IOSRJEN) , VOL.09.NO.08, 2019, PP.54-58

12. Radharamani. A etal., Fuzzy unitary operator in Fuzzy Hilbert space and its properties,   International Journal of Research and Analytic Reviews(IJRAR) , 2018, 5(4), 258-261

13. Radharamani.A , T Nagajothi, Fuzzy soft hyponormal operator in Fuzzy soft Hilbert space, Strad Research, Vol.9, issue 3-2022

14. Radharamani. A, T Nagajothi , M-Fuzzy soft hyponormal operator in Fuzzy soft Hilbert space, Journal of Data Acquisition and Processing, Vol.38, issue (1)2023

15. LA. Zadeh, Fuzzy sets, Inf.Control, vol.8, no.3,pp. 338-353, 1965

Spherical Picture Fuzzy Sets

Rajarajeswari Palanisamy[1*] and Reshma Ranganathan[2]

[1]Associate Professor, Department of Mathematics, Chikkanna Govt Arts College, Tirupur-02, Tamil Nadu, India.
[2]Research Scholar, Department of Mathematics, Chikkanna Govt Arts College, Tirupur-02, Tamil Nadu, India.

*Address for Correspondence
Rajarajeswari Palanisamy
Associate Professor,
Department of Mathematics,
Chikkanna Govt Arts College,
Tirupur-02, Tamil Nadu, India.
E.Mail: p.rajarajeswari29@gmail.com

ABSTRACT

In this paper, we introduce the concept of Spherical Picture Fuzzy Sets and we have analyzed the geometrical interpretation of Picture Fuzzy Sets and Spherical Picture Fuzzy Sets for the first time in literature. Spherical Picture Fuzzy sets are extensions of the standard Intuitionistic Fuzzy Sets, Circular Intuitionistic Fuzzy Sets, Picture Fuzzy Sets and hence of the Zadeh'sFuzzy Sets(FS). Here, some of the operations and relations over Spherical Picture Fuzzy Sets are defined and based on these operations some of its properties are studied.

Keywords : Fuzzy set, Circular-Intuitionistic Fuzzy Sets, Picture fuzzy set, Spherical picture fuzzy set.

INTRODUCTION

In daily life, we deal problems with uncertainty in some way in kind of situation, as new mathematical tools are required since the standard mathematical tools(crisp sets) are insufficient to deal with overcome uncertainities. The concept of Fuzzy Set theory established by Zadeh [18] in 1965 in which the element has membership degree, the degree of belongingness is used to deal the problem under uncertain environment. In 1981, Masaharu Mizumoto and Kokichi Tanaka [15] discussed about the algebraic properties of fuzzy sets under these new bounded-sum and bounded-difference operations as well as the properties of fuzzy sets when these new operations are combined with the well-known union, intersection, algebraic product, and algebraic sum operations. In 1983, Atanassov [1] introduced the concept of Intuitionistic Fuzzy Sets (IFSs) which is the prime extension of Zadeh's Fuzzy Set. It describing an element with membership and non-membership values such that sum of these two values less than or

63666

equal to one. The two best examples of an orthopair fuzzy set are Atanassov's [1, 2] classical intuitionistic fuzzy set and second type of intuitionistic fuzzy set in which the total of the acceptance degree and non-acceptance degree has one as a boundary in a classical intuitionistic fuzzy set. In 1994, Atanassov [4] was defined some other operations over the Intuitionistic Fuzzy Sets. In [12] Atanassov defined the relations on IFSs and [13] have studied various properties of Intuitionistic Fuzzy Relations. In 2001, Atanassov [6] examined the Sanchez's approach for medical diagnosis and it's application is expanded using the idea of IFS theory which is a generalization of fuzzy set theory. Later, the important aspect of neutrality degree isseen as lacking in Intuitionistic Fuzzy Set theory. In 2014, Coung [10] introduced the conceptof the Picture Fuzzy Sets which is the prime extension of Fuzzy Sets and Intuitionistic Fuzzy Sets by including the neutrality degree for each element along with membership and non-membership degrees in such that sum of these three degrees must not exceed one. Coung and Kreinovich [11] has analyzed new operations and properties over Picture Fuzzy Sets. In 2018, Nguyen Van Dinh and Nguyen XuanThao [16] analyzed the concepts of difference between PFS-sets, distance measure, and dissimilarity measure between picture fuzzy sets are introduced and along with the formulas for determining these values. They also illustrate how it can be used in Multi Attribute Decision Making. In 2017, Chunyong Wang and et.al., [14] established the a few geometric operators of Picture Fuzzy Sets and discussed some of its properties and also they have applied these operators to resolve involving Multiple Attribute Decision Making in a Picture Fuzzy environment. The concept of Circular Intuitionistic Fuzzy Sets (CIFSs) introduced by Atanassov [8] in 2020 which is the expansion of Intuitionistic Fuzzy Sets.Circular Intuitionistic Fuzzy Sets is characterized by describing a circle with radius r amongeach point of the IFS set. In [9], Atanassov defined the range of the radius of C-IFSs lies in $[0,\sqrt{2}]$ since the points with center⟨0, 1⟩and ⟨1, 0⟩are necessary to cover the entire Intuitionistic Fuzzy Sets triangle, which can be valid only when r≥$\sqrt{2}$. Picture Fuzzy Set(PFS) is animportant and interesting concept in Fuzzy mathematics as they provide wide applications inhuman opinions such as decision making, pattern recognition and data processing, etc. In thispaper, we have introduced the Spherical Picture Fuzzy Set which is the extension of PFSs andis characterized by describing a sphere with radius r among each elements of the Picture Fuzzy Sets. As said above here also the range of the radius lies in $[0,\sqrt{2}]$ since the points with center⟨0, 1, 0⟩, ⟨0, 0, 1⟩and ⟨1, 0, 0⟩are necessary to cover the entire Picture Fuzzy Set triangular pyramid. By using the proposed definition of Spherical Picture Fuzzy Sets (SPFSs) we have defined some operations on SPFSs and studied their properties based on this operations.

Preliminaries
In this section, few pre-requisites that are needed for this study overviewed.

Definition 2.1. [18] Fuzzy Set
Let X be a non-empty universal set. Each set is mapped to [0,1] by membership function is defined as
$E = \{⟨x, \tau_E(x)⟩/x \in X\}$
where $\tau_E: X \to [0, 1]$ is the degree of membership function of the fuzzy set E and $\tau_E(x) \in [0, 1]$ is the membership value of the element x ∈X in the fuzzy set E.

Definition 2.2. [1] IFS:
Let X be a non-empty universal set. An intuitionistic fuzzy set (IFS) E in X is defined as
$E = \{⟨x, \tau_E(x), \upsilon_E(x)⟩/x \in X\}$
where $\tau_E: X \to [0, 1]$ and $\upsilon_E: X \to [0, 1]$ with $0 \le \tau_E(x) + \upsilon_E(x) \le 1$ for all x ∈X represents the degrees of membership and non-membership of the element x to the IFS E. For each IFS, the intuitionistic index or hesitancy degree of the element x in X to the IFS E is$\pi_E(x) = 1 - \tau_E(x) - \upsilon_E(x)$.

Definition 2.3. [8] C-IFS:
Let X be the universe and E be its subset then, the set C-IFS is defined as,
$E_r^* = \{⟨x, \tau_E(x), \upsilon_E(x); r⟩/x \in X\}$
where $\tau_E: X \to [0, 1]$ and $\vartheta_E: X \to [0, 1]$ with $0 \le \tau_E(x) + \upsilon_E(x) \le 1$ and r ∈$[0,\sqrt{2}]$ is the radius of the circle around each element x ∈E, and functions $\tau_E: X \to [0, 1]$ and $\upsilon_E: X \to [0,1]$ represent membership degree and non-membership degree of element x ∈X to a fixed set E ⊆X. We also define the hesitancy margin $\pi_E: X \to [0, 1]$ by $\pi_E(x) =$

63667

$1-\tau_E(x)-\upsilon_E(x)$ which corresponds to the degree of indeterminacy. The radius r defined in C-IFS takes on values from the interval [0,1].

Definition 2.4. [10] PFS:

A Picture Fuzzy Set(PFS) E on a universe X is an object in the form of

P = {⟨x, $\tau_E(x)$, $\omega_E(x)$, $\upsilon_E(x)$⟩/x ∈X}

where $\tau_E(x)$ ∈[0, 1] is called the degree of positive membership of x in E, $\omega_E(x)$ ∈[0, 1] is called the degree of neutral membership of x in E and $\upsilon_E(x)$ ∈[0, 1] is called the degree of negative membership of x in E. where $\tau_E(x)$, $\omega_E(x)$ and $\upsilon_E(x)$ satisfy the following condition

(x∈X) $0 \le \tau_E(x)+\omega_E(x)+\upsilon_E(x) \le 1$ Now, $\sigma_E(x) = (1-(\tau_E(x)+\omega_E(x)+\upsilon_E(x)))$ could be called the degree of refusal membership of x in E.

Operations over Spherical Picture Fuzzy Sets

In this section, we have defined the concept of Spherical Picture Fuzzy Sets and some fundamentalOperations for Spherical Picture Fuzzy Sets are defined and based on the operations some of their properties are discussed. In addition, we have drawn the geometrical interpretation of the Picture Fuzzy Set, geometrical interpretation of the Spherical Picture Fuzzy Set.

Geometrical interpretation of PFS

The following Figure 1 represents the Geometrical interpretation of the PFS.

The Picture Fuzzy Interpretation Triangular Pyramid (PFITP) is used to represent the elements of a fixed universe as points. Every element x is evaluated with three parameters namely degree of membership ($\tau_E(x)$) and degree of non-membership ($\omega_E(x)$) and also degree of neutrality ($\upsilon_E(x)$) to a fixed subset E of the universe, is represented as a point having coordinates ($\tau_E(x)$, $\omega_E(x)$, $\upsilon_E(x)$), where $\tau_E(x)$, $\omega_E(x)$, $\upsilon_E(x)$ ∈[0, 1] such that $0 \le \tau_E(x)+\omega_E(x)+\upsilon_E(x) \le 1$.

Definition 3.1. Spherical Picture Fuzzy Sets(SPFSs)

Let us have a fixed universe X and E be its subset then, the set SPFSs is defined as,

$P_r^* = $ {⟨x, $\tau_E(x)$, $\omega_E(x)$, $\upsilon_E(x)$; r⟩/x ∈X}

where functions τ_E: X → [0, 1], ω_E: X → [0, 1] and υ_E: X → [0, 1] with $0 \le \tau_E(x)+\omega_E(x)+\upsilon_E(x) \le 1$ and r ∈[0,√2] is the radius of the sphere around each element x ∈E, represent membership degree, neutral degree and non-membership degree of element x ∈Xto a fixed set E ⊆X. We also define the hesitancy marginπ_E: X → [0, 1] by $\pi_E(x) = 1 - \tau_E(x) - \omega_E(x) - \upsilon_E(x)$ which corresponds to the degree of indeterminacy.

Geometrical interpretation of SPFS

In SPFS, each element is represented by a sphere with centre ($\tau_E(x)$, $\omega_E(x)$, $\upsilon_E(x)$) and radius r, compared to the normal PFSs, where each element is represented by a point in the picture fuzzy interpretation triangular pyramid.

Let L^*={⟨a, b, c⟩ suchthata,b,c∈[0,1] and a + b + c ≤ 1}.

Therefore P_r^*can be rewritten in the form as

$P_r^* = $ {⟨x,$O_r(\tau_E(x)$, $\omega_E(x)$, $\upsilon_E(x))$; r⟩/x ∈X}

Where,

$O_r(\tau_E(x)$, $\omega_E(x)$, $\upsilon_E(x))$={⟨a, b, c⟩such that a,b,c∈[0,1]

And$\sqrt{(\tau_E(x) - a)^2 + (\omega_E(x) - b)^2 + (\upsilon_E(x) - c)^2} \le$ r}∩ L^*

= {⟨a, b, c⟩such that a,b,c∈[0,1]

and$\sqrt{(\tau_E(x) - a)^2 + (\omega_E(x) - b)^2 + (\upsilon_E(x) - c)^2} \le$ r

and a + b + c ≤ 1}

Definitions 3.2. Relations over SPFSs

Let us have two Spherical Picture Fuzzy SetsE_r and $F_s$are given by

63668

E_r = {⟨x, τ_E (x), ω_E (x), υ_E (x); r)/x ∈X}and F_s = {⟨x, τ_F (x), ω_F (x), υ_F (x); s)/x ∈X} then the following relations are,

E_r⊆F_s⟺⇒(x ∈X)(r ≤ s&τ_E(x) ≤ τ_F(x)ω_E(x) ≤ω_F(x)&υ_E(x) ≥ υ_F(x))
E_r= F_s= (x ∈X)(r = s&τ_E(x) = τ_F(x)ω_E(x) = ω_F(x)&υ_E (x) =υ_F (x))

Definition 3.3.
Let us have two Spherical Picture Fuzzy Sets E_r and $F_s$are given by
E_r= {⟨x, τ_E (x), ω_E (x), υ_E (x); r)/x ∈X}and F_s= {⟨x, τ_F (x), ω_F (x), υ_F (x); s)/x ∈X} then
the following operations are defined,
(a) $E_r \cup_{max} F_s$=
{⟨x, max(τ_E(x), τ_F(x)), min(ω_E(x), ω_F(x)), min(υ_E(x), υ_F(x)), max(r, s)⟩/x ∈X}
(b)$E_r \cup_{min} F_s$=
{⟨x, max(τ_E (x), τ_F(x)), min(ω_E (x), ω_F(x)), min(υ_E (x), υ_F (x)), min(r, s)⟩/x ∈X}
(c)$E_r \cap_{max} F_s$=
{⟨x, min(τ_E (x), τ_F (x)), min(ω_E (x), ω_F(x)), max(υ_E (x), υ_F (x)), max(r, s)⟩/x ∈X}
(d)$E_r \cap_{min} F_s$=
{⟨x, min(τ_E (x), τ_F (x)), min(ω_E (x), ω_F(x)), max(υ_E (x), υ_F (x)), min(r, s)⟩/x ∈X}
(e) $E_r +_{min} F_s$=
{⟨x, (τ_E (x) +τ_F(x)−τ_E (x).τ_F(x)), (ω_E (x).ω_F(x)), (υ_E (x).υ_F (x)), min(r, s)⟩/x ∈X}
(f)$E_r +_{max} F_s$=
{⟨x, (τ_E (x) + τ_F(x)−τ_E (x).τ_F(x)), (ω_E (x).ω_F(x)), (υ_E (x).υ_F (x)), max(r, s)⟩/x ∈X}
(g) $E_{r \cdot min} F_s$=
{⟨x, (τ_E (x).τ_F(x)), (ω_E (x)+ω_F(x) -ω_E (x).ω_F(x)), (υ_E (x)+ υ_F (x)−υ_E (x).υ_F (x)), min(r, s)⟩/x ∈X}

(h) $E_{r.max} F_s$= {⟨x, (τ_E(x).τ_F(x)), (ω_E(x) + ω_F(x) − ω_E(x).ω_F(x)), (υ_E(x) + υ_F(x) − υ_E(x).υ_F(x)), max(r, s))/x ∈X}
(i) $E_r@_{min}F_s$={⟨x, $\frac{\tau_E(x)+\tau_F(x)}{2}$,$\frac{\omega_E(x)+\omega_F(x)}{2}$,$\frac{\upsilon_E(x)+\upsilon_F(x)}{2}$,min(r, s))/x ∈X}
(j)$E_r@_{max}F_s$={⟨x, $\frac{\tau_E(x)+\tau_F(x)}{2}$,$\frac{\omega_E(x)+\omega_F(x)}{2}$,$\frac{\upsilon_E(x)+\upsilon_F(x)}{2}$,max(r, s))/x ∈X}

Remark 3.4.
Let us have one complement of Spherical Picture Fuzzy Sets →$E_r$are given by, when r=0
→ E =→ E0 = {⟨x, υ_E(x), ω_E(x), τ_E(x); 0)/x ∈X}

Proposition 3.5.
The following commutative properties for union and intersection are valid for any two
SPFSs $E_r$and $F_s$are given by E_r= {⟨x, τ_E(x), ω_E(x), υ_E(x); r)/x ∈X} and
F_s= {⟨x, τ_F(x), ω_F(x), υ_F(x); s)/x ∈X},
(i) $E_r \cup_{max} F_s$=$F_s \cup_{max} E_r$(Proof follows from the Definition 3.3 (a)
(ii) $E_r \cup_{min} F_s$= $F_s \cup_{min} E_r$(Proof follows from the Definition 3.3 (b)
(iii) $E_r \cap_{max} F_s$= $F_s \cap_{max} E_r$(Proof follows from the Definition 3.3 (c)
(iv) $E_r \cap_{min} F_s$= $F_s \cap_{min} E_r$(Proof follows from the Definition 3.3 (d)

Proposition 3.6.
The following commutative properties for addition operator are valid for any two SPFSs
$E_r$and $F_s$are given by E_r = {⟨x, τ_E(x), ω_E(x), υ_E (x); r)/x ∈X} and
F_s= {⟨x, τ_F(x), ω_F(x), υ_F(x); s)/x ∈X},
(i)$E_r+_{max}F_s$=$F_s+_{max}E_r$(Proof follows from the Definition 3.3 (f)
(ii) $E_r+_{min}F_s$=$F_s+_{min}E_r$(Proof follows from the Definition 3.3 (e)

Proposition 3.7.

The following commutative properties for multiplication operator are valid for any two SPFSs E_r and F_s are given by $E_r = \{\langle x, \tau_E(x), \omega_E(x), \upsilon_E(x); r\rangle/x \in X\}$ and $F_s = \{\langle x, \tau_F(x), \omega_F(x), \upsilon_F(x); s\rangle/x \in X\}$,

(i) $E_r._{max}F_s = F_s._{max}E_r$ (Proof follows from the Definition 3.3 (h)

(ii $E_r._{min}F_s = F_s._{min}E_r$ (Proof follows from the Definition 3.3 (g)

Proposition 3.8.

The following commutative properties for average sum operator are valid for any two SPFSs E_r and F_s are given by $E_r = \{\langle x, \tau_E(x), \omega_E(x), \upsilon_E(x); r\rangle/x \in X\}$ and $F_s = \{\langle x, \tau_F(x), \omega_F(x), \upsilon_F(x); s\rangle/x \in X\}$,

(i) $E_r@_{max}F_s = F_s@_{max}E_r$ (Proof follows from the Definition 3.3 (j)

(ii) $E_r@_{min}F_s = F_s@_{min}E_r$ (Proof follows from the Definition 3.3 (i)

Proposition 3.9. (Associative property)

Let us have three Spherical Picture Fuzzy Sets E_r, F_s and G_t given by,

$E_r = \{\langle x, \tau_E(x), \omega_E(x), \upsilon_E(x); r\rangle/x \in X\}, F_s = \{\langle x, \tau_F(x), \omega_F(x), \upsilon_F(x); s\rangle/x \in X\}$

And $G_t = \{\langle x, \tau_G(x), \omega_G(x), \upsilon_G(x); t\rangle/x \in X\}$ then the following associative properties for union and intersection are hold,

(i) $E_r \cup_{max}(F_s \cup_{max} G_t) = (E_r \cup_{max} F_s) \cup_{max} G_t$

(ii) $(E_r \cup_{min} F_s) \cup_{min} G_t = E_r \cup_{min}(F_s \cup_{min} G_t)$

(iii) $(E_r \cap_{max} F_s) \cap_{max} G_t = E_r \cap_{max}(F_s \cap_{max} G_t)$

(iv) $(E_r \cap_{min} F_s) \cap_{min} G_t = E_r \cap_{min}(F_s \cap_{min} G_t)$

Proof (i).LHS:

$E_r \cup_{max}(F_s \cup_{max} G_t)$

$= \{\langle x, _{max}(\tau_E(x), \tau_G(x)), _{min}(\omega_E(x), \omega_G(x)), _{min}(\upsilon_E(x), \upsilon_G(x)), _{max}(s, t)\rangle/x \in X\}$

$= \{\langle x, _{max}(\tau_E(x), _{max}(\tau_E(x), \tau_G(x)), _{min}(\omega_E(x), _{min}(\omega_E(x), \omega_G(x)), _{min}(\upsilon E(x), _{min}(\upsilon_E(x), \upsilon_G(x)), _{max}(r, s, t)\rangle/x \in X\}$

$= \{\langle x, max(max(\tau_E(x), \tau_F(x)), \tau_G(x)), min(min(\omega_E(x), \omega_F(x)), \omega_G(x)), min(min(\upsilon_E(x), \upsilon_F(x)), \upsilon_G(x)), max(r, s, t)\rangle/x \in X\}$

$= (E_r \cup_{max} F_s) \cup_{max} G_t = RHS$

Thus, $(E_r \cup_{max} F_s) \cup_{max} G_t = E_r \cup_{max}(F_s \cup_{max} G_t)$.

Similarly, we can prove the result (ii), (iii) and (iv).

Proposition 3.10.

Let us have three Spherical Picture Fuzzy Sets E_r, F_s and G_t given by,

$E_r = \{\langle x, \tau_E(x), \omega_E(x), \upsilon_E(x); r\rangle/x \in X\}, F_s = \{\langle x, \tau_F(x), \omega_F(x), \upsilon_F(x); s\rangle/x \in X\}$

And $G_t = \{\langle x, \tau_G(x), \omega_G(x), \upsilon_G(x); t\rangle/x \in X\}$

Then the following additive properties hold,

(i) $(E_r +_{max} F_s) +_{max} G_t = E_r +_{max}(F_s +_{max} G_t)$

(ii) $(E_r +_{min} F_s) +_{min} G_t = E_r +_{min}(F_s +_{min} G_t)$

Proof (i).LHS: $(E_r +_{max} F_s) +_{max} G_t$

$= \{\langle x, (\tau_E(x) + \tau_F(x) - \tau_E(x).\tau_F(x)), (\omega_E(x).\omega_F(x)), (\upsilon_E(x).\upsilon_F(x)), max(r, s)\rangle/x \in X\}$

$= \{\langle x, (\tau_E(x) + \tau_F(x) + \tau_G(x) - \tau_E(x).\tau_F(x) + \tau_G(x) - \tau_E(x) + \tau_F(x).\tau_G(x) + \tau_E(x).\tau_F(x).\tau_G(x)), (\omega_E(x).\omega_F(x).\omega_G(x)), (\upsilon_E(x).\upsilon_F(x).\upsilon_G(x)), max(r, s, t)\rangle/x \in X\}$

$= \{\langle x, (\tau_E(x) + \tau_F(x) + \tau_G(x) - \tau_E(x) + \tau_F(x).\tau_G(x) - \tau_E(x).\tau_F(x) + \tau_G(x) + \tau_E(x).\tau_F(x).\tau_G(x)), (\omega_E(x).\omega_F(x).\omega_G(x)), (\upsilon_E(x).\upsilon_F(x).\upsilon_G(x)), max(r, s, t)\rangle/x \in X\}$

$= \{\langle x, (\tau_E(x) + (\tau_F(x) + \tau_G(x) - \tau_F(x).\tau_G(x)) - \tau_E(x).(\tau_F(x) + \tau_G(x) - \tau_F(x).\tau_G(x)), (\omega_E(x).\omega_F(x).\omega_G(x)), (\upsilon_E(x).\upsilon_F(x).\upsilon_G(x)), max(r, s, t)\rangle/x \in X\}$

Rajarajeswari Palanisamy and Reshma Ranganathan

$=E_{r+max}(F_s+{}_{max}G_t) = RHS$

Thus, $(E_{r+max}F_s) +_{max} G_t=E_{r+max}(F_s+{}_{max}G_t)$.

Similarly, we can prove the result (ii).

Proposition 3.11.

Let us have three Spherical Picture Fuzzy Sets E_r, F_s and G_t given by,

E_r = {⟨x, τ_E(x), ω_E(x), υ_E (x); r⟩/x ∈X}, F_s= {⟨x, τ_F(x), ω_F(x), υ_F(x); s⟩/x ∈X}

And G_t= {⟨x, τ_G(x), ω_G(x), υ_G(x); t⟩/x ∈X}

Then the following multiplicative properties hold,

(i).$(E_{r.min}F_s) ._{min}G_t =E_{r.min}(F_{s.min}G_t)$

(ii).$(E_{r.max}F_s) ._{max}G_t =E_{r.max}(F_{s.max}G_t)$

Proof(i).LHS:

$(E_{r.min}F_s) ._{min}G_t$= {⟨x, ($\tau_E$(x).$\tau_F$(x)), ($\omega_E$(x) + ω_F(x) − ω_E(x).ω_F(x)), (υ_E(x) + υ_F(x) − υ_E(x).υ_F(x)), min(r, s)⟩/x ∈X}

= {⟨x, (τ_E (x).τ_F(x)).τ_G(x), (ω_E(x) + ω_F(x) − ω_E(x).ω_F(x)) + ω_G(x) − (ω_E(x) + ω_F(x)− ω_E(x).ω_F(x)).ω_G(x), (υ_E(x)+υ_F(x)−υ_E(x).υ_F(x))+υ_G(x)−(υ_E(x)+υ_F(x)−υ_E(x).υ_F(x)).υ_G(x), min(r, s, t)⟩/x ∈X}

= {⟨x, (τ_E(x).τ_F(x)).τ_G(x), (ω_E(x) + ω_F(x) + ω_G(x) − ω_E(x).ω_F(x) + ω_G(x) − ω_E(x) + ω_F(x).ω_G(x)+ ω_E(x).ω_F(x).ω_G(x)), (υ_E(x) + υ_F(x) + υ_G(x) − υ_E(x).υ_F(x) + υ_G(x) − υ_E(x) + υ_F(x).υ_G(x) + υ_E(x). υ_F(x).υ_G(x)), min(r, s, t)⟩/x ∈X}

={⟨x, τ_E(x).τ_F(x).τ_G(x), (ω_E(x)+ω_F(x)+ω_G(x)−ω_E(x)+ω_F(x).ω_G(x)−ω_E(x).ω_F(x)+ω_G(x)+ ω_E(x).ω_F(x).ω_G(x)), (υ_E(x)+υ_F(x)+υ_G(x)−υ_E(x)+υ_F(x).υ_G(x)−υ_E(x).υ_F(x)+υ_G(x)+ υ_E(x).υ_F(x).υ_G(x)), min(r, s, t)⟩/x ∈X}

= {⟨x, τ_E(x).τ_F(x).τ_G(x), ω_E(x) + (ω_F(x) + ω_G(x) − ω_F(x).ω_G(x)) − ω_E(x).(ω_F(x) + ω_G(x)+ ω_F(x).ω_G(x)), υ_E(x)+(υ_F(x)+υ_G(x)−υ_F(x).υ_G(x))−υ_E(x).(υ_F(x)+υ_G(x)+υ_F(x).υ_G(x)), min(r, s, t)⟩/x ∈X}

= $E_{r.min}(F_{s.min}G_t)$ = RHS

Thus, $(E_{r.min}F_s) ._{min}G_t =E_{r.min}(F_{s.min}G_t)$.

Similarly, we can prove the result (ii).

Proposition 3.12. De Morgan's Law

Let us have two Spherical Picture Fuzzy Sets E_r and F_s are given by,

E_r= {⟨x, υ_E (x), ω_E (x), τ_E (x); r⟩/x ∈X} and

F_s= {⟨x, υ_F (x), ω_F (x), τ_F(x); s⟩/x ∈X}

Then the following De Morgan's law for union, intersection laws hold,

(i). $\to(E_r \cap_{max} F_s) = \to E_r \cup_{max} \to F_s$

(ii). $\to(E_r \cup_{max} F_s) = \to E_r \cap_{max} \to F_s$

Proof (i).LHS:

$E_r \cap_{max} F_s$)

= {⟨x, min(τ_E (x), τ_F (x)), min(ω_E (x), ω_F (x)), max(υ_E (x), υ_F (x)), max(r, s)⟩/x ∈X}

$\to(E_r \cap_{max} F$s)

= {⟨x, max(υ_E (x), υ_F (x)), min(ω_E (x), ω_F (x)), min(τ_E (x), τ_F (x)), max(r, s)⟩/x ∈X}

RHS:

$\to E_r \cup_{max} \to F$s

$\to E_r$= {⟨x, υ_E (x), ω_E (x), τ_E (x); r⟩/x ∈X}

$\to F$s = {⟨x, υ_F (x), ω_F (x), τ_F (x); s⟩/x ∈X}

= {⟨x, max(υ_E (x), υ_F (x)), min(ω_E (x), ω_F (x)), min(τ_E (x), τ_F (x)), max(r, s)⟩/x ∈X}

=⇒$\to(E \cap_{max}F) = \to E\cup_{max}\to F$

63671

Similarly, we can prove the result (ii).

Remark 3.13.

Spherical picture fuzzy sets does not satisfies the following De Morgan laws under the '+'
and '.'operation which is illustrated with suitable example in the given below.

(i). $\rightarrow(E_r + \max F_s) = \rightarrow E_{r.\max} \rightarrow F_s$

(ii). $\rightarrow(E_{r.\max} F_s) = \rightarrow E_r + \max \rightarrow F_s$

Example 3.14. Let us have two Spherical Picture Fuzzy Sets E_r and F_s are given by,

$E_r = \{\langle x, \upsilon_E(x), \omega_E(x), \tau_E(x); r\rangle/x \in X\}$ and

$F_s = \{\langle x, \upsilon_F(x), \omega_F(x), \tau_F(x); s\rangle/x \in X\}$

Then the following De Morgan's law does not satisfy under the addition and multiplication
operations $E_r = \{(u, 0, 0.8, 0.2; 0.5), (v, 0.6, 0.2, 0.2; 0.5), (w, 0.3, 0.7, 0; 0.5)\}$

$F_s = \{(u, 0, 0.5, 0.5; 0.6), (v, 0.4, 0.2, 0, 4; 0.6), (w, 0.4, 0.5, 0.1; 0.6)\}$

$\rightarrow E_r = \{(u, 0.2, 0.8, 0; 0.5), (v, 0.2, 0.2, 0.6; 0.5), (w, 0, 0.7, 0.3; 0.5)\}$

$\rightarrow F_s = \{(u, 0.5, 0.5, 0; 0.6), (v, 0.4, 0.2, 0, 4; 0.6), (w, 0.1, 0.5, 0.4; 0.6)\}$

LHS:

$\rightarrow(E_r + \max F_s) = \{(u, 0.1, 0.4, 0.8; 0.5), (v, 0.8, 0.4, 0.76; 0.5), (w, 0, 0.35, 0.58; 0.5)\}$

RHS:

$\rightarrow E_{r.\max} \rightarrow F_s = \{(u, 0.1, 0.6, 0.8; 0.6), (v, 0.8, 0.36, 0.76; 0.6), (w, 0, 0.85, 0.58; 0.6)\}$

=⇒LHS ≠RHS

=⇒$\rightarrow(E_r + \max Fs) \neq \rightarrow E_{r.\max} \rightarrow F_s$

Example 3.15. Let X={u,v,w} be the universal set.

E = $\{(u, 0, 0.8, 0.2; 0.5), (v, 0.6, 0.2, 0.2; 0.5), (w, 0.3, 0.7, 0; 0.5)\}$

F = $\{(u, 0, 0.5, 0.5; 0.6), (v, 0.4, 0.2, 0, 4; 0.6), (w, 0.4, 0.5, 0.1; 0.6)\}$

$\rightarrow E_r = \{(u, 0.2, 0.8, 0; 0.5), (v, 0.2, 0.2, 0.6; 0.5), (w, 0, 0.7, 0.3; 0.5)\}$

$\rightarrow F_s = \{(u, 0.5, 0.5, 0; 0.6), (v, 0.4, 0.2, 0, 4; 0.6), (w, 0.1, 0.5, 0.4; 0.6)\}$

LHS:

$\rightarrow(E_r.\max F_s) = \{(u, 0.6, 0.9, 0.9; 0.6), (v, 0.52, 0.36, 0.24; 0.6), (w, 0.1, 0.85, 0.12; 0.6)\}$

RHS:

$\rightarrow E_r + \max \rightarrow F_s = \{(u, 0.6, 0.4, 0; 0.6), (v, 0.52, 0.4, 0.24; 0.6), (w, 0.1, 0.35, 0.12; 0.6)\}$

⇒LHS ≠RHS

⇒$\rightarrow(E_r.\max F_s) \neq \rightarrow E_r + \max \rightarrow F_s$

Proposition 3.16: (Distributive property)

Let us have three Spherical Picture Fuzzy Sets E_r, F_s and G_t given by,

$E_r = \{\langle x, \tau_E(x), \omega_E(x), \upsilon_E(x); r\rangle/x \in X\}$, $F_s = \{\langle x, \tau_F(x), \omega_F(x), \upsilon_F(x); s\rangle/x \in X\}$ and

$G_t = \{\langle x, \tau_G(x), \omega_G(x), \upsilon_G(x); t\rangle/x \in X\}$

Then the following distributive properties hold,

(i) $(E_r \cap_{max} F_s) \cup_{max} G_t = (E_r \cup_{max} G_t) \cap_{max} (F_s \cup_{max} G_t)$

(ii)$(E_r \cap_{min} F_s) \cup_{min} G_t = (E_r \cup_{min} G_t) \cap_{min} (F_s \cup_{min} G_t)$.

Proof (i).LHS:

$(E_r \cap_{max} F_s) \cup G_t$

$= \{\langle x, \min(\tau_E(x), \tau_F(x)), \min(\omega_E(x), \omega_F(x)), \max(\upsilon_E(x), \upsilon_F(x)), \max(r, s)\rangle/x \in X\}$

$= \{\langle x, \max(\min(\tau_E(x), \tau_F(x)) + \tau_G(x)), \min(\min(\omega_E(x), \omega_F(x)) + \omega_G(x)), \min(\max(\upsilon_E(x),$
$\upsilon_F(x) + \upsilon_G(x))), \max(r, s, t)\rangle/x \in X\}$

$= \{\langle x, \max(\min(\tau_E(x) + \tau_G(x), \tau_F(x) + \tau_G(x)), \min(\min(\omega_E(x) + \omega_G(x), \omega_F(x) + \omega_G(x)),$
$\min(\max(\upsilon_E(x) + \upsilon_G(x), \upsilon_F(x) + \upsilon_G(x))), \max(r, s, t)\rangle/x \in X\}$

$= \{\langle x, \min(\max(\tau_E(x) + \tau_G(x)), \max(\tau_F(x) + \tau_G(x)), \min(\min(\omega_E(x) + \omega_G(x), \min(\omega_F(x)+$

Rajarajeswari Palanisamy and Reshma Ranganathan

ω_G (x)), max(min(υ_E (x) + υ_G (x)), min(υ_F (x) + υ_G (x)), max(r, s, t))/x ∈X}

=$(E_r \cup_{max} G_t) \cap (F_s \cup_{max} G_t)$ = RHS

Hence, $(E_r \cap_{max} F_s) \cup_{max} G_t$= (Er $\cup_{max} G_t) \cap (F_s \cup_{max} G_t)$.

Similarly, we can prove the result (ii).

Proposition 3.17.

Let us have three Spherical Picture Fuzzy Sets E_r,$F_s$and $G_t$given by,

E_r= {⟨x, τ_E (x), ω_E (x), υ_E (x); r)/x ∈X}, F_s= {⟨x, τ_F (x), ω_F (x), υ_F (x); s)/x ∈X} and

G_t= {⟨x, τ_G (x), ω_G (x), υ_G (x); t)/x ∈X}

Then the following properties hold,

(i) E_r+min $(F_s \cup_{min} G_t)$ = $(E_r$+min $F_s) \cup_{min} (E_r$+min $G_t)$.

(ii) E_r+min $(F_s \cap_{min} G_t)$ = $(E_r$+min $F_s) \cap_{min}(E_r$+min $G_t)$.

Proof (i). LHS:

E_r+min $(F_s \cup_{min} G_t)$

= {⟨x, max(τ_F (x), τ_G (x)), min(ω_F (x), ω_G (x)), min(υ_F (x), υ_G (x)), min(s, t))/x ∈X}

= {⟨x, (τ_E (x) + max(τ_F (x), τ_G (x)) −

(τ_E (x).max(τ_F (x), τ_G (x))), (ω_E (x).min(ω_F (x).ω_G (x))), υ_E (x).

min(υ_F (x).υ_G (x)), min(r, s, t))/x ∈X}

= {⟨x, max(τ_E (x) + τ_F (x), τ_E (x) + τ_G (x)) −

max(τ_E (x).τ_F (x), τ_E (x).τ_G (x)), min(ω_E (x).ω_F (x), ω_E (x).

ω_G (x)), min(υ_E (x).υ_F (x), υ_E (x).υ_G (x)), min(r, s, t))/x ∈X}

=

{⟨x, max(τ_E (x)+τ_F (x)−τ_E (x).τ_F (x), τ_E (x)+τ_G (x))−τ_E(x).τ_G(x)), min(ω_E (x).ω_F (x), ω_E (x).

ω_G (x)), min(υ_E (x).υ_F (x), υ_E (x).υ_G (x)), min(r, s, t))/x ∈X}

= $(E_r$+min $F_s) \cup_{min}(E_r$+min $G_t)$ = RHS

Hence, E_r+min $(F_s \cup_{min} G_t)$ = $(E_r$+min $F_s) \cup_{min} (E_r$+min $G_t)$.

Similarly, we can prove the result (ii).

Proposition 3.18.

Let us have three Spherical Picture Fuzzy Sets E_r,$F_s$and $G_t$given by,

E_r= {⟨x, τ_E (x), ω_E (x), υ_E (x); r)/x ∈X}, F_s= {⟨x, τ_F (x), ω_F (x), υ_F (x); s)/x ∈X} and

G_t= {⟨x, τ_G (x), ω_G (x), υ_G (x); t)/x ∈X} Then the following additive properties hold,

(i) $E_{r.min}$ $(F_s \cup_{min} G_t)$ = $(E_{r.min}F_s) \cup_{min} (E_{r.min}G_t)$

(ii) $E_{r.min}$ $(F_s \cap_{min} G_t)$ = $(E_{r.min}F_s) \cap_{min}(E_{r.min}G_t)$.

Proof. (i).LHS:

$E_{r.min}(F_s \cup_{min} G_t)$

= {⟨x, max(τ_F (x), τ_G (x)), min(ω_F (x), ω_G (x)), min(υ_F (x), υ_G (x)), max(s, t))/x ∈X}

= {⟨x, (τ_E (x).max(τ_F (x), τ_G (x))), (ω_E (x)+min(ω_F (x), ω_G (x))−(ω_E (x).min(ω_F (x), ω_G (x))),

(υ_E (x) + min(υ_F (x), υ_G (x))) − (υ_E (x).min(υ_F (x), υ_G (x))), min(r, s, t))/x ∈X}

= {⟨x, (max(τ_E (x).τ_F (x), τ_E (x).τ_G (x))), (min(ω_E (x) + ω_F (x), ω_E (x) + ω_G (x)) − min(ω_E (x).

ω_F (x), ω_E (x).ω_G (x))), min(υ_E (x) + υ_F (x), υ_E (x) + υ_G (x)) − min(υ_E (x).υ_F (x), υ_E (x).υ_G (x)),

min(r, s, t))/x ∈X}

= {⟨x, (max(τ_E (x).τ_F (x), τ_E (x).τ_G (x))), min(ω_E (x) + ω_F (x) − ω_E (x).ω_F (x), ω_E (x) + ω_G (x)-

ω_E (x).ω_G (x)), min(υ_E (x) + υ_F (x) − υ_E (x).υ_F (x), υ_E (x) + υ_G (x) − υ_E (x).υ_G (x)), min(r, s, t))

/x ∈X}

=$(E_{r.min}F_s) \cup_{min} (E_{r.min}G_t)$ = RHS

Hence, $E_{r.min}$ $(F_s \cup_{min} G_t)$ = $(E_{r.min}F_s) \cup_{min} (E_{r.min}G_t)$.

Similarly, we can prove the result (ii).

CONCLUSION

In this paper, a new concept of Spherical Picture fuzzy set was introduced which is an expansion of Circular-Intuitionistic fuzzy sets and in addition we have presented the geometrical interpretation of PFSs and SPFSs. The basic operations like union, intersection, complement, addition and multiplication are defined on SPFSs and based on the operations some of their properties over Spherical picture fuzzy sets are discussed. We observe that, Spherical Picture Fuzzy Sets satisfies commutative, associative, complementary and distributive properties under the union, intersection, addition and multiplication. In addition, it satisfies De Morgan 'slaws for the operations union and intersection and it does not satisfy the De Morgan's laws for the operations addition and multiplication which is illustrated with suitable example. As a future work some more properties and distance measures over Spherical Picture Fuzzy sets will be studied, which will be more useful to study their applications in the field of medical diagnosis, pattern recognition and decision making.

Conflicts of Interest
The authors declare that they have no conflicts of interest.

Funding
Not applicable.

Authors Contributions
All authors contributed equally to this work and read and approved the final version of the manuscript.

Ethical Conduct
Not applicable

Data Availability
No data were used to support the findings of this study.

REFERENCES

1. Atanassov, K T. A second type of Intuitionistic Fuzzy Sets, Fuzzy sets and systems, 56, 1983, 66-70.
2. Atanassov, K T. Intuitionistic Fuzzy Sets, Fuzzy sets and systems, 20, 1986, 87-96.
3. Atanassov, K T. More on Intuitionistic Fuzzy Sets, Fuzzy sets and systems, 33, 1989, 37-46.
4. Atanassov, K T. New operations defined over the intuitionistic fuzzy sets, Fuzzy Sets and Systems 61, 1994,137-142.
5. Atanassov, K T. Intuitionistic fuzzy sets, Springer, Heidelberg, Germany, 1999, 1-137.
6. Atanassov, K T. An application of Intuitionistic fuzzy sets in medical diagnosis, Fuzzy sets and systems,117, 2001, 209-213.
7. Atanassov, K T. On Intuitionistic fuzzy sets Theory; Springer:Berlin, Germany, 2012.
8. Atanassov, K T. Circular Intuitionistic fuzzy sets.J.Intell. Fuzzy Syst, 39, 2020, 5981-5986.
9. Atanassov, K T and Evgeniy Marinov. Four Distances for Circular Intuitionistic fuzzy sets, Mathematics,9, 2021, 1121.
10. Bui Cong Cuong, Picture Fuzzy Sets, Journal of computer science and cybernetics, 30(4), 2014, 409-420.
11. Bui Cong Cuong and Kreinovich, Picture fuzzy sets-a new concept for computational intelligence problems, Proceedings of the Third World Congress on Information and Communication Technologies WICT'2013,Hanoi, Vietnam, 2013, 1–6.
12. Burillo.P, and Bustince.H, Intuitionistic fuzzy relations. (parti), Mathware and Soft Computing, 2, 2008,5–38.

Rajarajeswari Palanisamy and Reshma Ranganathan

13. Bustince.H, Construction of intuitionistic fuzzy relations with predetermined properties, Fuzzy Sets andSystems, 109, 2000, 379–403.
14. Chunyong Wang, et.al., Some geometric aggregation operators based on picture fuzzy sets and their applicationin multiple attribute decision making , Italian journal of pure and applied mathematics, 37, 2017,477-492.
15. Masaharu Mizumoto and Kokichi Tanaka, Fuzzy Sets and Their Operations, Information and Control, 48,1981, 30-48.
16. Nguyen Van Dinh and Nguyen Xuan Thao, Some Measures of Picture Fuzzy Sets and Their Application inMulti-attribute Decision Making , I.J. Mathematical Sciences and Computing, 3, 2018, 23-41.
17. Silambarasan.L, Some algebraic properties of picture fuzzy sets, Bull. Int Math. Virtual Inst., 11(3), 2021,429-442.
18. Zadeh.L. A, Fuzzy Sets, Information and Control, 8, 1965, 338-353.
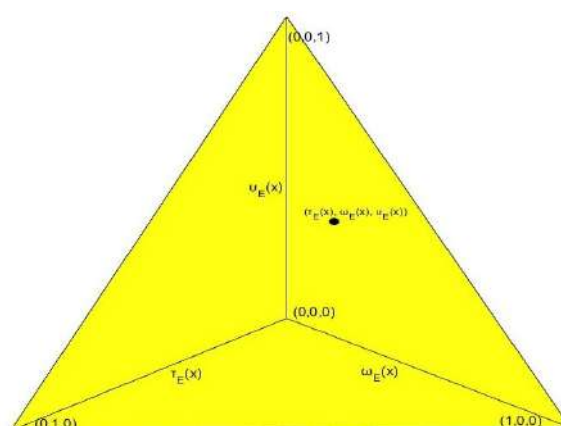
Figure 1. Geometrical interpretation of PFS
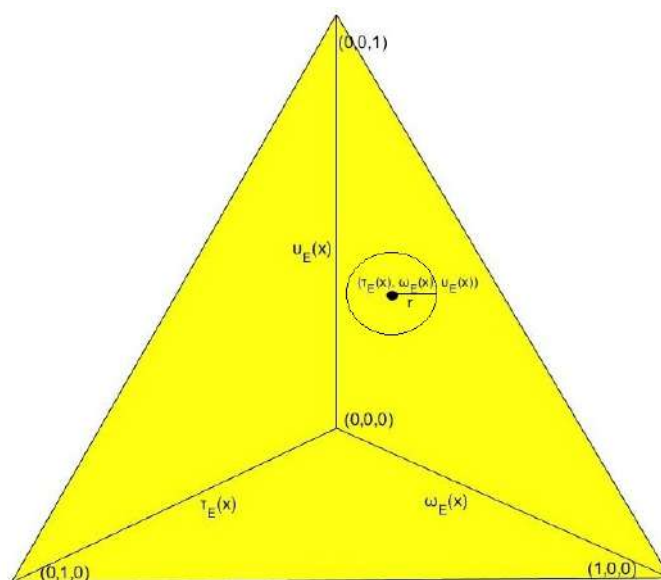
Figure 2. Geometrical interpretation of SPFSs

RESEARCH ARTICLE

Solving Matrix Games with Trapezoidal Intuitionistic Fuzzy Payoff using Score Function

G.Sasikala[1]* and S. A.Sahathana Thasneem[2]

[1]Associate Professor, Department of Mathematics, Chikkanna Government Arts College, Tirupur, Tamil Nadu, India.
[2]Research Scholar, Department of Mathematics, Chikkanna Government Arts College,Tirupur, Tamilnadu, India.

*Address for Correspondence
G.Sasikala
Associate Professor,
Department of Mathematics,
Chikkanna Government Arts College,
Tirupur, Tamil Nadu, India.
E.Mail: sasiganesh2306@gmail.com

ABSTRACT

In this paper the score function is used to solve Matrix game with Trapezoidal Intuitionistic Fuzzy(TrIF) payoff. The proposed method is applied to defuzzify the payoff matrix and the matrix is solved by mixed strategy method. The technique is illustrated by a numerical example.

Keywords: Matrix game, Intuitionistic fuzzy set, Trapezoidal Intuitionistic fuzzy number, (α, β) −cut sets, score function.
MSC: 91-05

INTRODUCTION

Game theory is the study of handling the situations where two conflicting interests exist. In general the matrix games with $m \times n$ payoffs are reduced to 2×2 matrix to find the optimal strategies and value of the game [3]. The payoff matrix may or may not have saddle points. The matrix without saddle points are reduced to 2×2 matrix by the most popular dominance principle [7].In real life situations there are lot of problems arises which cannot be explained in simple crisp sense. Zadeh [5] introduced the concept of fuzzy sets used in game theory to deal with that. The concept of Intuitionistic fuzzy sets developed by Atnassov [4] provides membership as well as non-membership functions which are found more useful in game theory to represents the players acceptance level and the hesitance level regarding a decision making situation [8]. In the multi criteria decision making the method of solving the vague set

Sasikala and Sahathana Thasneem

by using the score function is established by S.M.Chen[13] and Q.Zhang [12]. Then the method is applied on Intuitionistic fuzzy sets [9]. The average index and deviation index are used to denote the level of belongingness and non-belongingness of the payoff . The method is designed to overcome the drawbacks of the existing method and gives more accuracy level in finding the optimal solution for the decision maker[6]. In this paper Trapezoidal Intuitionistic fuzzy payoff matrix is considered then reduced into the crisp payoff matrix using the score function.

This paper is organized as follows. In section 2 basic definitions of Intuitionistic fuzzy and Trapezoidal Intuitionistic fuzzy number are given with their cut sets and arithmetic operations. The score function for TrIFN is defined in section 3 and in section 4 a numerical example of voting share problem between two political parties is solved which is to help the voting agent to find the possible number of votes will be registered in the area before the poling day. The conclusion has been drawn in section 5.

Preliminaries
Definition 2.1:
Let $X = \{x_1, x_2, \ldots, x_n\}$ be a finite universal set. An intuitionistic fuzzy set $\tilde{l}$ in a given universal set □ is of the form
$$\tilde{l} = \{\langle x_i, \mu_{\tilde{l}}(x_i), v_{\tilde{l}}(x_i)\rangle : x_i \in X\},$$
where the functions $\mu_{\tilde{l}}(x_i), v_{\tilde{l}}(x_i)$ are the degree of membership and degree of non - membership of an element $x_i \in X$, and they satisfy the condition $0 \leq \mu_{\tilde{l}}(x_i) + v_{\tilde{l}}(x_i) \leq 1, \forall\, x_i \in X,$
$i = 1,2,3,\ldots$

Definition 2.2:
A Trapezoidal Intuitionistic Fuzzy Number (TrIFN) is an Intuitionistic fuzzy number denoted as
$\tilde{l} = \langle(\underline{l}, \underline{h}, \overline{l}, \overline{h}); \chi_{\tilde{l}}, \eta_{\tilde{l}}\rangle$ in $\mathbb{R}$ with membership function and non-membership function are defined as

$$\mu_{\tilde{l}}(x) = \begin{cases} \dfrac{x - \underline{l}}{\underline{h} - \underline{l}}\chi_{\tilde{l}} & , \quad \underline{l} \leq x \leq \underline{h} \\ \chi_{\tilde{l}} & , \quad \underline{h} \leq x \leq \overline{l} \\ \dfrac{\overline{h} - x}{\overline{h} - \overline{l}}\chi_{\tilde{l}} & , \quad \overline{l} \leq x \leq \overline{h} \\ 0, & otherwise \end{cases}$$

And

$$v_{\tilde{l}}(x) = \begin{cases} \dfrac{(\underline{h} - x) + \eta_{\tilde{l}}(x - \underline{l})}{(\underline{h} - \underline{l})} & , \quad \underline{l} \leq x \leq \underline{h} \\ \eta_{\tilde{l}} & , \quad \underline{h} \leq x \leq \overline{l} \\ \dfrac{(x - \overline{l}) + \eta_{\tilde{l}}(\overline{h} - x)}{(\overline{h} - \overline{l})} & , \quad \overline{l} \leq x \leq \overline{h} \\ 1, & otherwise \end{cases}$$

Arithmetic operations on TrIFN:
Let $\tilde{l} = \langle(\underline{l}, \underline{h}, \overline{l}, \overline{h}); \chi_{\tilde{l}}, \eta_{\tilde{l}}\rangle$ and $\tilde{f} = \langle(\underline{f}, \underline{g}, \overline{f}, \overline{g}); \chi_{\tilde{f}}, \eta_{\tilde{f}}\rangle$ be two TrIF numbers. The arithmetic operations between the two numbers are of the form

$\tilde{l} + \tilde{f} = \langle(\underline{l} + \underline{f}, \underline{h} + \underline{g}, \overline{l} + \overline{f}, \overline{h} + \overline{g}); \chi_{\tilde{l}} \wedge \chi_{\tilde{f}}, \eta_{\tilde{l}} \vee \eta_{\tilde{f}}\rangle$

$\tilde{l} - \tilde{f} = \langle(\underline{l} - \overline{□}, \underline{h} - \overline{□}, \overline{l} - \underline{□}, \overline{h} - \underline{□}); \chi_{\tilde{l}} \wedge \chi_{\tilde{f}}, \eta_{\tilde{l}} \vee \eta_{\tilde{f}}\rangle$

$$\tilde{l} \times \tilde{f} = \begin{cases} \left(\underline{l}\underline{f}, \underline{h}\underline{g}, \overline{l}\overline{f}, \overline{h}\overline{g}\right); \chi_{\tilde{l}} \wedge \chi_{\tilde{f}}, \eta_{\tilde{l}} \vee \eta_{\tilde{f}}, & if\ \tilde{l} > 0\ and\ \tilde{f} > 0 \\ \left(\underline{l}\overline{g}, \underline{h}\overline{f}, \overline{l}\underline{g}, \overline{h}\underline{f}\right); \chi_{\tilde{l}} \wedge \chi_{\tilde{f}}, \eta_{\tilde{l}} \vee \eta_{\tilde{f}}, & if\ \tilde{l} < 0\ and\ \tilde{f} > 0 \\ \left(\overline{h}\underline{f}, \overline{l}\underline{g}, \underline{h}\overline{f}, \underline{l}\overline{g}\right); \chi_{\tilde{l}} \wedge \chi_{\tilde{f}}, \eta_{\tilde{l}} \vee \eta_{\tilde{f}}, & if\ \tilde{l} > 0\ and\ \tilde{f} < 0 \\ \left(\overline{h}\overline{g}, \overline{l}\overline{f}, \underline{h}\underline{g}, \underline{l}\underline{f}\right); \chi_{\tilde{l}} \wedge \chi_{\tilde{f}}, \eta_{\tilde{l}} \vee \eta_{\tilde{f}}, & if\ \tilde{l} < 0\ and\ \tilde{f} < 0 \end{cases}$$

$$\frac{\tilde{l}}{\tilde{f}} = \begin{cases} \left(\underline{l}/\overline{g}, \underline{h}/\overline{f}, \overline{l}/\underline{g}, \overline{h}/\underline{f}\right); \chi_{\tilde{l}} \wedge \chi_{\tilde{f}}, \eta_{\tilde{l}} \vee \eta_{\tilde{f}}, \text{if } \tilde{l} > 0 \text{ and } \tilde{f} > 0 \\ \left(\overline{h}/\overline{g}, \overline{l}/\overline{f}, \underline{h}/\underline{g}, \underline{l}/\underline{f}\right); \chi_{\tilde{l}} \wedge \chi_{\tilde{f}}, \eta_{\tilde{l}} \vee \eta_{\tilde{f}}, \text{ if } \tilde{l} < 0 \text{ and } \tilde{f} > 0 \\ \left(\overline{l}/\underline{f}, \underline{h}/\underline{g}, \underline{l}/\overline{f}, \overline{h}/\overline{g}\right); \chi_{\tilde{l}} \wedge \chi_{\tilde{f}}, \eta_{\tilde{l}} \vee \eta_{\tilde{f}}, \text{if } \tilde{l} > 0 \text{ and } \tilde{f} < 0 \\ \left(\overline{h}/\underline{f}, \overline{l}/\underline{g}, \underline{h}/\overline{f}, \underline{l}/\overline{g}\right); \chi_{\tilde{l}} \wedge \chi_{\tilde{f}}, \eta_{\tilde{l}} \vee \eta_{\tilde{f}}, \text{if } \tilde{l} < 0 \text{ and } \tilde{f} < 0 \end{cases}$$

For any real number λ,

$$\lambda \tilde{l} = \begin{cases} \langle(\lambda \underline{l}, \lambda \underline{h}, \lambda \overline{l}, \lambda \overline{h}); \chi_{\tilde{l}}, \eta_{\tilde{l}}\rangle, \text{if } \lambda > 0 \\ \langle(\lambda \overline{h}, \lambda \overline{l}, \lambda \underline{h}, \lambda \underline{l}); \chi_{\tilde{l}}, \eta_{\tilde{l}}\rangle, \text{if } \lambda < 0 \end{cases}$$

$$\tilde{l}^{-1} = \langle(1/\overline{h}, 1/\overline{l}, 1/\underline{h}, 1/\underline{l}); \chi_{\tilde{l}}, \eta_{\tilde{l}}\rangle$$

Cut sets of TrIF Numbers:

For $\tilde{l} = \langle(\underline{l}, \underline{h}, \overline{l}, \overline{h}); \chi_{\tilde{l}}, \eta_{\tilde{l}}\rangle$ the (α, β) cut sets of $\tilde{l}$ is a subset of $\mathbb{R}$ defined as $\tilde{l}_{\alpha,\beta} = \{x : \mu_{\tilde{l}}(x) \geq \alpha, v_{\tilde{l}}(x) \leq \beta\}$. α −cut of $\tilde{l}$ is

$$\tilde{l}_\alpha = \left[\underline{l} + \frac{\alpha(\underline{h} - \underline{l})}{\chi_{\tilde{l}}}, \overline{h} - \frac{\alpha(\overline{h} - \overline{l})}{\chi_{\tilde{l}}}\right]$$

β −cut of $\tilde{l}$ is

$$\tilde{l}_\beta = \left[\frac{(1 - \beta)\underline{h} + (\beta - \eta_{\tilde{l}})\underline{l}}{1 - \eta_{\tilde{l}}}, \frac{(1 - \beta)\overline{l} + (\beta - \eta_{\tilde{l}})\overline{h}}{1 - \eta_{\tilde{l}}}\right]$$

Definition 2.3:

The mean values of the (α, β) cut sets of $\tilde{l}$ are denoted as $P(\tilde{l}_\alpha)$ and $P(\tilde{l}_\beta)$ written as

$$P(\tilde{l}_\alpha) = \frac{\chi_{\tilde{l}}(\underline{l} + \overline{h}) + \alpha(\underline{h} - \underline{l}) - \alpha(\overline{h} - \overline{l})}{2\chi_{\tilde{l}}}$$

And

$$P(\tilde{l}_\beta) = \frac{(1 - \beta)(\underline{h} + \overline{l}) + (\underline{l} + \overline{h})(\beta - \eta_{\tilde{l}})}{2(1 - \eta_{\tilde{l}})}$$

Definition 2.4:

The average index of membership and non-membership functions is denoted as $T_\mu(\tilde{l})$ and $T_v(\tilde{l})$ for the TrIFN $\tilde{l}$ which are defined as

$$T_\mu(\tilde{l}) = \int_0^{\chi_{\tilde{l}}} P(\tilde{l}_\alpha) d\alpha$$

$$= \int_0^{\chi_{\tilde{l}}} \frac{\chi_{\tilde{l}}(\underline{l} + \overline{h}) + \alpha(\underline{h} - \underline{l}) - \alpha(\overline{h} - \overline{l})}{2\chi_{\tilde{l}}} d\alpha$$

$$= \frac{\chi_{\tilde{l}}}{4}\left[\underline{l} + \overline{h} + \underline{h} + \overline{l}\right]$$

$$T_v(\tilde{l}) = \int_{\eta_{\tilde{l}}}^1 P(\tilde{l}_\beta) d\beta$$

$$= \int_{\eta_{\tilde{l}}}^1 \frac{(1 - \beta)(\underline{h} + \overline{l}) + (\underline{l} + \overline{h})(\beta - \eta_{\tilde{l}})}{2(1 - \eta_{\tilde{l}})} d\beta$$

$$= \frac{1}{4(1 - \eta_{\tilde{l}})}\left[(\underline{l} + \overline{h} + \underline{h} + \overline{l})(1 + \eta_{\tilde{l}}^2) + 2\eta_{\tilde{l}}(\underline{h} + \overline{l} - \underline{l} - \overline{h})\right]$$

Definition 2.5:

The deviation index of the membership function is denoted as $\rho_\mu(\tilde{l})$ and non-membership function is denoted as $\rho_v(\tilde{l})$ defined by using the mean values $\rho(\tilde{l}_\alpha)$ and $\rho(\tilde{l}_\beta)$ where

$$\rho(\tilde{l}_\alpha) = \frac{[(\chi_{\tilde{l}} - \alpha)(\overline{h} - \underline{l})]}{2\chi_{\tilde{l}}}$$

$$\rho(\tilde{l}_\beta) = \frac{[(\beta - \eta_{\tilde{l}})(\overline{h} - \underline{l})]}{2(1 - \eta_{\tilde{l}})}$$

The deviation index is calculated as

$$\rho_\mu(\tilde{l}) = \int_0^{\chi_l} \rho(\tilde{l}_\alpha)\, d\alpha$$
$$= \int_0^{\chi_l} \frac{[(\chi_l - \alpha)(\overline{h} - \underline{l})]}{2\chi_l}\, d\alpha$$
$$= \frac{1}{4}\chi_l(\overline{h} - \underline{l})$$

And

$$\rho_v(\tilde{l}) = \int_{\eta_l}^1 \rho(\tilde{l}_\beta)\, d\beta$$
$$= \int_{\eta_l}^1 \frac{[(\beta - \eta_l)(\overline{h} - \underline{l})]}{2(1 - \eta_l)}\, d\beta$$
$$= \frac{1}{4}(1 - \eta_l)(\overline{h} - \underline{l})$$

Comparer Index

For two TrIFNs $\tilde{l}$ and $\tilde{f}$ the average index of the membership functions are $T_\mu(\tilde{l})$ and $T_\mu(\tilde{f})$ for non-membership functions $T_v(\tilde{l})$ and $T_v(\tilde{f})$. The deviation index for the membership and non-membership functions of two TrIFNs are $\rho_\mu(\tilde{l}), \rho_\mu(\tilde{f})$ and $\rho_v(\tilde{l}), \rho_v(\tilde{f})$ then the comparer index between the two numbers is defined as

$$\mathcal{C}_{\tilde{l},\tilde{f}} = \frac{\pi(\tilde{f})\{T_v(\tilde{l}) - T_\mu(\tilde{l})\} - \pi(\tilde{l})\{T_v(\tilde{f}) - T_\mu(\tilde{f})\}}{\pi(\tilde{l})\pi(\tilde{f}) \max_{\tilde{l}=\tilde{l},f}\left(\rho_v(\tilde{l}) - \rho_\mu(\tilde{l})\right)}$$

Which leads to the following results

i. If $\mathcal{C}_{\tilde{l},\tilde{f}} < 0$ then $\tilde{f}$ is greater than $\tilde{l}$, denoted as $\tilde{f} \widetilde{>} \tilde{l}$
ii. If $\mathcal{C}_{\tilde{l},\tilde{f}} > 0$, then $\tilde{f} \widetilde{<} \tilde{l}$
iii. If $\mathcal{C}_{\tilde{l},\tilde{f}} = 0$, then $\tilde{f} \cong \tilde{l}$ where $\widetilde{>}, \widetilde{<}$ and $\cong$ are the Intuitionistic equal symbols of $>, <$ and $=$.

Example 2.1:

The comparer Index of TrIF numbers is illustrated with a numerical example. Let
$\tilde{l} = \langle(10,12.5,14,17); 0.5,0.3\rangle$ and $\tilde{f} = \langle(11,13,14.5,16); 0.6,0.2\rangle$ be two TrIFN. The average index values of $\tilde{l}, \tilde{f}$ are $T_\mu(\tilde{l}) = 6.69$, $T_\mu(\tilde{f}) = 8.18$, $T_v(\tilde{l}) = 20.72$ and $T_v(\tilde{f}) = 17.76$. The deviation index values of $\tilde{l}, \tilde{f}$ are $\rho_\mu(\tilde{l}) = 0.875, \rho_\mu(\tilde{f}) = 0.75$, $\rho_v(\tilde{l}) = 1.225$ and $\rho_v(\tilde{f}) = 1$

$$\mathcal{C}_{\tilde{l},\tilde{f}} = \frac{(0.2)(20.72 - 6.69) - (0.2)(17.76 - 8.18)}{(0.2)(0.2)(1.225 - 0.875)} = 63.57 > 0$$

Which implies $\tilde{f} \widetilde{<} \tilde{l}$.

Score Function

The score function for Trapezoidal Intuitionistic Fuzzy Numbers is defined as

$$E(\tilde{l}) = \frac{T_v(\tilde{l}) - T_\mu(\tilde{l})}{\pi(\tilde{l})}$$

And it has the following two properties
i. $E(\tilde{l} + \tilde{f}) = E(\tilde{l}) + E(\tilde{f})$
ii. $E(\lambda\tilde{l}) = \lambda E(\tilde{l})$

TrIFN In Matrix Form :

For players C and D, player C has m number of strategies and player D has n number of strategies . The players choose their own strategy and attains an outcome depend upon their choice. At the end of the game the outcome is known as the payoff matrix. The $m \times n$ payoff matrix of the TrIFN
$\tilde{l} = \langle(\underline{l}, \underline{h}, \overline{l}, \overline{h}); \chi_l, \eta_l\rangle$ is of the form

$$D_1 \quad D_2 \quad \dots \quad \quad D_n$$

$$\begin{array}{c} C_1 \\ C_2 \\ \vdots \\ C_m \end{array} \begin{bmatrix} \tilde{l}_{11} & \tilde{l}_{12} & \dots & \tilde{l}_{1n} \\ \tilde{l}_{21} & \tilde{l}_{22} & \dots & \tilde{l}_{2n} \\ \vdots & \dots & \ddots & \vdots \\ \tilde{l}_{m1} & \tilde{l}_{m2} & \dots & \tilde{l}_{mn} \end{bmatrix}$$

If player C chooses strategy i and D chooses strategy j then the payoff is $\tilde{l}_{ij}$. For the TrIF game the minmax and maximin strategies are to maximize the minimum gain and minimize the maximum loss. For $\tilde{l}$ the strategy is defined as

$Max\text{-}min = \vee_i \left\{ \wedge_j \left\{ \langle (\underline{l}_{ij}, \underline{h}_{ij}, \overline{l}_{ij}, \overline{h}_{ij}); \chi_{\tilde{l}_{ij}}, \eta_{\tilde{l}_{ij}} \rangle \right\} \right\}$

$Min\text{-}max = \wedge_j \left\{ \vee_i \left\{ \langle (\underline{l}_{ij}, \underline{h}_{ij}, \overline{l}_{ij}, \overline{h}_{ij}); \chi_{\tilde{l}_{ij}}, \eta_{\tilde{l}_{ij}} \rangle \right\} \right\}$

The saddle point of the TrIF game is the $(k,r)^{th}$ position of the payoff matrix satisfy the condition

$\langle (\underline{l}_{kr}, \underline{h}_{kr}, \overline{l}_{kr}, \overline{h}_{kr}); \chi_{\tilde{l}_{kr}}, \eta_{\tilde{l}_{kr}} \rangle$

$$= \bigvee_i \left\{ \bigwedge_j \left\{ \langle (\underline{l}_{ij}, \underline{h}_{ij}, \overline{l}_{ij}, \overline{h}_{ij}); \chi_{\tilde{l}_{ij}}, \eta_{\tilde{l}_{ij}} \rangle \right\} \right\}$$

$$= \bigwedge_j \left\{ \bigvee_i \left\{ \langle (\underline{l}_{ij}, \underline{h}_{ij}, \overline{l}_{ij}, \overline{h}_{ij}); \chi_{\tilde{l}_{ij}}, \eta_{\tilde{l}_{ij}} \rangle \right\} \right\}$$

Simply written as

$$\tilde{} = \bigvee \left\{ \bigwedge \tilde{} \right\} = \bigwedge \left\{ \bigvee \{\} \right\}$$

The saddle point $\tilde{}$ is called the value of the TrIF game and denoted as . The strategies are the optimal strategies of the game.

Definition 3.1:
The expected payoff for the strategies $y = (y_1, y_2, \dots \dots, y_m)$ and $z = (z_1, z_2, \dots \dots, z_n)$ for the TrIFN $\tilde{l}$ is defined as

$$\tilde{E}(y,z) = \sum_{j=1}^{n} \sum_{i=1}^{m} \langle (\underline{l}_{ij}, \underline{h}_{ij}, \overline{l}_{ij}, \overline{h}_{ij}); \chi_{\tilde{l}_{ij}}, \eta_{\tilde{l}_{ij}} \rangle y_i z_j$$

For players C and D, player C choose strategy y to maximize his expectation and D chooses z to minimize the maximum expectation of C.

$$\min_z \max_y \tilde{E}(y,z) = \tilde{E}(y^*, z^*) = \max_y \min_z \tilde{E}(y,z)$$

$\tilde{E}(y^*, z^*)$ is the strategic saddle point of the game and $V = \tilde{E}(y^*, z^*)$ is the value of the game.

Voting share Problem
The voting share problem is defined in a situation where an election is going to be conducted in a city and there are two major political parties competing with each other to gain more votes and win the election. The number of voters in the city is constant. So ,it is same for both the parties. Each parties have their own set of strategies to increase their possibility of winning the election. Let C and D be the two political parties.

Party C's strategies are as follows,

C_1: Increasing door to door campaigning

C_2: Making alliances with small political parties in the area

C_3: Doing campaigning and rallies by celebrities.

Party D's strategies are,

D_1: Making lot of promises to people and pledges to execute them

D_2: Addressing the current problems of the voters and promises to rectify them

D_3: Capturing the mistakes of the previous ruling party and giving assurance to solve them.

Now the voting agents of the Election commission can not say the exact voting percentage of the area before the voting day. But they have certain level of confidence and also hesitance due to bad weather forecast ,or previous

Sasikala and Sahathana Thasneem

election results or the opinion poll. In this situation we consider the payoff matrix as Trapezoidal Intuitionistic fuzzy number.

$$
\begin{array}{c}
\ \ \ \ D_1 \ \ \ \ \ \ \ \ \ \ \ \ \ \ \ \ D_2 \ \ \ \ \ \ D_3 \\
\begin{array}{c} C_1 \\ C_2 \\ C_3 \end{array}
\begin{bmatrix}
\langle(5,6,7,8);0.6,0.2\rangle & \langle(5,7,8,9);0.5,0.3\rangle & \langle(4,6,7,9);0.4,0.2\rangle \\
\langle(4,6,7,9);0.5,0.2\rangle & \langle(4,5,6,7);0.4,0.3\rangle & \langle(5,7,9,10);0.5,0.1\rangle \\
\langle(6,7,8,9);0.4,0.2\rangle & \langle(3,5,6,7);0.6,0.2\rangle & \langle(3,5,7,8);0.5,0.3\rangle
\end{bmatrix}
\end{array}
$$

Here the payoff $\langle(5,6,7,8);0.6,0.2\rangle$ denotes the player C chooses strategy C_1 and player D chooses strategy D_1. The expected votes in favour of C is between 6 and 7 lakhs with lower bound of 5 lakhs and upper bound of 8 lakhs. The confidence level is 0.6 and the hesitance level is 0.2 .

Using the ranking method mentioned above we get table 1

By using the score function the crisp payoff matrix is

$$
\begin{array}{c}
\ \ \ \ D_1 \ \ \ \ \ \ \ D_2 \ \ \ \ \ \ D_3 \\
\begin{array}{c} C_1 \\ C_2 \\ C_3 \end{array}
\begin{bmatrix}
22.75 & 39.375 & 14.625 \\
17.33 & 21.2 & 12.19 \\
16.875 & 19 & 31.475
\end{bmatrix}
\end{array}
$$

Here $\vee_i\{\wedge_j \tilde{l}_{ij}\} = (3,1) \neq (1,1) = \wedge_j\{\vee_i \tilde{l}_{ij}\}$. So the game does not have saddle point. Using the method of dominance the payoff matrix is reduced into 2×2 payoff matrix of the form

$$
\begin{array}{c}
\ \ \ \ D_1 \ \ \ \ \ \ \ D_3 \\
\begin{array}{c} C_1 \\ C_3 \end{array}
\begin{bmatrix}
22.75 & 14.625 \\
16.875 & 31.475
\end{bmatrix}
\end{array}
$$

By using mixed strategies method the probabilities for player C plays strategies C_1 and C_3 are $p_1^* = \frac{37}{50}$ and $p_2^* = \frac{13}{50}$. Similarly $q_1^* = \frac{16}{25}$ and $q_2^* = \frac{9}{25}$ are the probabilities for player D chooses strategies D_1 and D_3 . And value of the game is 20.65 .The optimal score is in favour of player C. The value of the game in form of TrIFN is written as

$$\frac{16}{25}\langle(5,6,7,8);0.6,0.2\rangle + \frac{9}{25}\langle(6,7,8,9);0.4,0.2\rangle = \langle(5.36,6.36,7.36,8.36);0.4,0.2\rangle$$

For player C the expected optimal votes are between 6.36 and 7.36 lakhs. Which could be as low as 5.36 lakhs and as high as 8.36 lakhs. The maximum confidence level and minimum hesitance level are 0.4 and 0.2 .

CONCLUSION

In this paper payoff matrix with TrIF values is solved. The TrIF payoff matrix is converted into crisp payoff matrix using the score function. The method is applied on voting share problem between two political parties. The merit of this method is it can be used to find the optimal solution as nearly as possible.

Statements and Declaration

The authors declare that they have no known competing financial interests or personal relationships that could have appeared to influence the work reported in this paper.

REFERENCES

1. H.J.Zimmermann, "Fuzzy set theory and it's Applications", *Norwell,M.A.Kluwer*(1985).
2. J.F.Nash, "Non Cooperative Games", *Annals of Mathematics*, 286-295 (1951).
3. J.Von Neumann, D.Morgenstern, "The Theory of Games in Economics Behaviour", *New York , Wiley*(1944).
4. K.Atanassov, "Intuitionistic Fuzzy sets", *Fuzzy sets and systems,* 87-96(1986).
5. L.A.Zadeh, "Fuzzy Sets" , *Inform.contr.*vol-8.338-353(1965).

63681

6. M.R.Seikh, P.K.Nayak, M.Pal, "Generalized Triangular Fuzzy Numbers in Intuitionistic Fuzzy Environment", *International Journal of Engineering and Research and Development*, vol 5,Issue 1,08-13,(2012).

7. Kanti Swarup, P.K.Gupta, Manmohan, "An Introduction to management science",

8. *Operations Research, Sultan&sons,newdelhi.,*(2010).

9. K.Atanassov,C.Georgiev, "Intuitionistic fuzzy prolog", *Fuzzy sets syst,*vol-53,pp 121-128,(1993).

10. I.Nihizaki, M.Sakawa, "Max-min solution for fuzzy Multi objective Matrix Games", *Fuzzy sets and systems*, vol-61,pp 265-275,(1994).

11. P.K.Nayak, M.Pal, "Linear Programming Technique to solve Two person Matrix games with Interval Payoffs",*Asia-Pacific Journal of Operational Research*, vol-26,pp 285-305,(2009).

12. Q.Zhang ,Y.Meng, "A Note on handling multicriteria fuzzy decision making problem based on vague set theory", *IEEE International Conference on Systems*, Man and cybernetics,(2006).

13. S.M.Chen ,J.M.Tan, "Handling Multicriteria Fuzzy decision making problems based on vague set theory",*Fuzzy sets and systems,*vol-144,pp 103-113,(2000).

Table 1: The average and deviation index values of the payoff matrix

i,j	$T_\mu(\tilde{l}_{ij})$	$T_v(\tilde{l}_{ij})$	$\rho_\mu(\tilde{l}_{ij})$	$\rho_v(\tilde{l}_{ij})$
$i = 1, j = 1$	3.9	8.45	0.45	0.6
$i = 1, j = 2$	3.625	11.5	0.5	0.7
$i = 1, j = 3$	2.6	8.45	0.5	1
$i = 2, j = 1$	3.25	8.45	0.625	1
$i = 2, j = 2$	2.2	8.56	0.3	0.525
$i = 2, j = 3$	3.875	8.75	0.625	1.125
$i = 3, j = 1$	3	9.75	0.3	0.6
$i = 3, j = 2$	3.15	6.95	0.6	0.8
$i = 3, j = 3$	2.875	9.17	0.625	0.875

RESEARCH ARTICLE

(α,β) Quasi Class (Q) and (α, β) Quasi Normal Composition and Weighted Composition Operators

Radharamani[1*] and N. Sathyavathi[2]

[1]Assistant Professor, Department of Mathematics, Chikkanna Govt. Arts College, Tirupur, Tamil Nadu, India
[2]Research Scholar, Department of Mathematics, Chikkanna Govt. Arts College, Tirupur, Tamil Nadu, India

*Address for Correspondence
Radharamani
Assistant Professor,
Department of Mathematics,
Chikkanna Govt. Arts College,
Tirupur, Tamil Nadu, India
E.Mail: radhabtk@gmail.com

ABSTRACT

In this paper Composition and Weighted Composition of (α, β) Quasi normal and (α, β) Quasi class Q operators on L^2- Spaces are characterized and including some key characteristics of this operator, as well as a discussion of various theorems related to this operator.

Mathematics Subject Classification: 47B20, 47B37 , 47B38.
Keywords: Operator, Hilbert space, (α, β) Quasi normal operator, (α, β) Quasi class Q operator, Joint (α, β)-quasi normal operator.

INTRODUCTION

Let H be a complex Hilbert space, an operator T is normal if T T*= T*T . In this paper, we will study some properties of (α,β) Quasi-Class (Q) operators. This has been done by relaxing some conditions of normality and introducing classes such as (α,β)-Quasi Normal as covered in [4] and [9] . E-Rasoul, M.Farzollah and Ali Morassaei [5] presented the concept of (α,β) – Normal operators in Hilbert spaces. Throughout the paper, H denotes the usual Hilbert space over the complex field and the separable, infinite-dimensional B (H) Banach algebra of all bounded linear algebra in Hilbert space H.

Preliminaries
Let B(H) stand for the complex Hilbert space H's Banach algebra of all bounded linear operators.

Definition 2.1
It is referred to as an operator T ∈ B(H) is said to be Class (Q) if $T^{*2}T^2 = (T^*T)^2$

Definition 2.2
It is referred to as an operator T ∈ B(H) is said to be Quasi-Class (Q) if $T(T^{*2}T^2)=(T^*T)^2T$

Definition 2.3
It is referred to as an operator T ∈ B(H) is said to be (α,β) Class (Q) if
$[\alpha^2 T^{*2}T^2] \leq (T^*T)^2 \leq [\beta^2 T^{*2}T^2]$

Definition 2.4
It is referred to as an operator T ∈ B(H) is said to be Normal if $T^*T = TT^*$

Definition 2.5 [2]
It is referred to as an operator T ∈ B(H) is said to be (α,β)- Normal if
$\beta^2 T^*T \geq TT^* \geq \alpha^2 T^*T$

MAIN RESULTS
When an operator T∈B(H) is said to be (α,β) Quasi-class (Q) if $T[\alpha^2 T^{*2}T^2] \leq (T^*T)^2 T \leq T[\beta^2 T^{*2}T^2]$ and (α,β)-quasi normal operator $T[\alpha^2 T^*T] \leq [TT^*]T \leq T[\beta^2 T^*T]$ for $0 \leq \alpha \leq 1 \leq \beta$ where T^* is the ad joint of the operator T. Assume (A, Σ, μ) be a $'\sigma'$ finite measure space. A Σ-measurable mapping from X onto itself is a transformation T on (A, Σ) such that $C_Tf = f \circ T$ for f in $L^2(\mu)$. It is known that T induces a bounded linear operator CT on L^2 if and only if the measure $\mu_0 T^{-1}$ is absolutely continuous in relation to the measure μ and h = $d\mu_0 T^{-1}/d\mu$ is the Radon . Nikodyn derivative of measure μT^{-1} with respect to the μ. A weighted composition operator is linear transformation acting on a set of complex valued Σ-measurable function f of the form $Wf = wf \circ T$ where w is complex valued, Σ-measurable function.

(α,β) Quasi Class (Q) and (α,β) Quasi Normal Composition Operators
Theorem 3.1.1
If T∈B(H), $C_T \in B(L^2(\mu))$ then C_T is (α, β) normal iff
$\alpha^2(C_T^*C_T) \leq C_T C_T^* \leq \beta^2(C_T^*C_T)$.

Proof
C_T is (α,β) normal $\alpha^2(C_T^*C_T) \leq C_T C_T^* \leq \beta^2(C_T^*C_T)$
$\alpha^2(C_T^*C_T) \leq C_T C_T^*$
$\Leftrightarrow (\alpha^2 C_T^*C_T - C_T C_T^*)f, f) \leq 0$
$\Leftrightarrow \langle \alpha^2 hf|f \rangle - \langle h \circ TPf|f \rangle \leq 0$
$\Leftrightarrow \|(h.T)^{1/2}Pf\|^2 \geq |\alpha^2|\|h^{1/2}f\|^2$ --------------(1)

Consider
$C_T C_T^* \leq \beta^2(C_T^*C_T)$
$\Leftrightarrow (C_T C_T^* - \beta^2(C_T^*C_T))f, f) \leq 0$
$\Leftrightarrow \langle h \circ TPf|f \rangle - \langle \beta^2 hf|f \rangle \leq 0$
$\Leftrightarrow |\beta^2|\|h^{1/2}f\|^2 \geq \|(h.T)^{1/2}Pf\|^2$ --------------(2)

From (1) and (2)
$|\alpha^2|\|h^{1/2}f\|^2 \leq \|(h.T)^{1/2}Pf\|^2 \leq |\beta^2|\|h^{1/2}f\|^2$

Theorem 3.1.2

If T∈B(H), C_T is (α, β) class (Q) iff $|\alpha^2|h_0 \leq f_0^2 \leq |\beta^2|h_0$

Proof

If C_T is (α,β) class (Q) then

$\alpha^2 C_T^{*2} C_T^2 \leq (C_T^* C_T)^2 \leq \beta^2 C_T^{*2} C_T^2$

Consider

$\alpha^2 C_T^{*2} C_T^2 \leq (C_T^* C_T)^2$

$(\alpha^2 C_T^{*2} C_T^2 - (C_T^* C_T)^2 f, f) \leq 0$

$|\alpha^2|h_0 \leq f_0^2$ ------------(3)

Consider

$(C_T^* C_T)^2 \leq \beta^2 C_T^{*2} C_T^2$

$(C_T^* C_T)^2 - (\beta^2 C_T^{*2} C_T^2 f, f) \leq 0$

$f_0^2 \leq |\beta^2|h_0$ -------------(4)

From (3) and (4)

$|\alpha^2|h_0 \leq f_0^2 \leq |\beta^2|h_0$

Theorem 3.1.3

If T∈B(H), $C_T \in B(L^2(\mu))$ then C_T is (α, β) Quasi normal iff

$\alpha^2 T(C_T^* C_T) \leq (C_T C_T^*) T \leq \beta^2 T(C_T^* C_T)$.

Proof

C_T is (α,β) normal $\alpha^2 T(C_T^* C_T) \leq (C_T C_T^*) T \leq \beta^2 T(C_T^* C_T)$

$\alpha^2 T(C_T^* C_T) \leq (C_T C_T^*) T$

$\Leftrightarrow \quad (\alpha^2 T(C_T^* C_T) - C_T C_T^* T) f, f) \leq 0$

$\Leftrightarrow \quad \langle \alpha^2 Thf|f \rangle - \langle h° TPTf|f \rangle \leq 0$

$\Leftrightarrow \| (h.T)^{1/2} PfT \|^2 \geq |\alpha^2| \| Th^{1/2} f \|^2$ --------------(5)

Consider

$(C_T C_T^*) T \leq \beta^2 T(C_T^* C_T)$

$\Leftrightarrow \quad (C_T C_T^* T - \beta^2 T(C_T^* C_T)) f, f) \leq 0$

$\Leftrightarrow \quad \langle h° TPTf|f \rangle - \langle \beta^2 Thf|f \rangle - \leq 0$

$\Leftrightarrow \quad |\beta^2| \| Th^{1/2} f \|^2 \geq \| (h.T)^{1/2} PfT \|^2$ --------------(6)

From (5) and (6)

$|\alpha^2| \| Th^{1/2} f \|^2 \leq \| (h.T)^{1/2} PfT \|^2 \leq |\beta^2| \| Th^{1/2} f \|^2$

Theorem 3.1.4

If T∈B(H), C_T is Quasi class (Q) if $Th_0 = f_0^2 T$ a.e.

Proof

C_T is Quasi class(Q)

$T(C_T^{*2} C_T^2) = (C_T^* C_T)^2 T$

$\Leftrightarrow \langle T(C_T^{*2} C_T^2) - (C_T^* C_T)^2 Tf|f \rangle = 0$

$\Leftrightarrow \langle T(C_T^{*2} C_T^2) f|f \rangle - \langle (C_T^* C_T)^2 Tf|f \rangle = 0$

$\Leftrightarrow Th_0 = f_0^2 T$ a.e.

Theorem 3.1.5

If T∈B(H), C_T is (α, β) Quasi class (Q) iff $T|\alpha^2|h_0 \leq f_0^2 T \leq T|\beta^2|h_0$

Radharamani and Sathyavathi

Proof

If C_T is (α,β) Quasi class (Q) then

$$T\alpha^2(C_T^{*2}C_T^2) \leq (C_T^*C_T)^2 T \leq T\beta^2(C_T^{*2}C_T^2)$$

Consider

$$T\alpha^2(C_T^{*2}C_T^2) \leq (C_T^*C_T)^2 T$$

$$(T\alpha^2(C_T^{*2}C_T^2) - (C_T^*C_T)^2 Tf, f) \leq 0$$

$$T|\alpha^2|h_0 \leq f_0^2 T \qquad\qquad\qquad\text{------------------(7)}$$

Consider

$$(C_T^*C_T)^2 T \leq T\beta^2(C_T^{*2}C_T^2)$$

$$((C_T^*C_T)^2 T - T\beta^2(C_T^{*2}C_T^2)f, f) \leq 0$$

$$f_0^2 T \leq T|\beta^2|h_0 \qquad\qquad\qquad\text{--------------------(8)}$$

From (7) and (8)

$$T|\alpha^2|h_0 \leq f_0^2 T \leq T|\beta^2|h_0$$

(α,β) Quasi Class (Q) and (α,β) Quasi Normal Weighted Composition Operators
Theorem 3.2.1

If $T \in B(H)$, Suppose $T^{-1}\sum = \sum$ Then W is (α, β) normal iff

$$\alpha^2(WW^*) \leq (W^*W) \leq \beta^2(WW^*)$$

Proof

Consider $\alpha^2(WW^*) \leq (W^*W)$

$$\Leftrightarrow \langle\alpha^2(WW^*) - (W^*W)f|f\rangle \leq 0 \quad \forall f \in L^2$$

$$\Leftrightarrow \alpha^2 w^2(h \circ T) \leq hw^2 \circ T^{-1} \qquad\qquad\text{----------------------------(9)}$$

Consider $(W^*W) \leq \beta^2(WW^*)$

$$\Leftrightarrow \langle(W^*W) - \beta^2(WW^*)f|f\rangle \leq 0 \qquad \forall f \in L^2$$

$$\Leftrightarrow hw^2 \circ T^{-1} \leq \beta^2 w^2(h \circ T) \qquad\qquad\text{----------------------------(10)}$$

From (9) and (10)

$$\alpha^2 w^2(h \circ T) \leq hw^2 \circ T^{-1} \leq \beta^2 w^2(h \circ T)$$

Theorem 3.2.2

If $T \in B(H)$, W is (α, β) Class (Q) iff $\alpha^2[hE(w^2 \circ T^{-1})]^2 \leq h_2 E(W_2^2) \circ T^{-1} \leq \beta^2[hE(w^2 \circ T^{-1})]^2$

Proof

Let $Wf = w(f \circ T)$ and $W^*f = hE(wf) \circ T^{-1}$

W is (α,β) Class (Q)

$$\alpha^2(WW^*)^2 \leq (WW^*)^2 \leq \beta^2(WW^*)^2$$

Consider

$$\Leftrightarrow \alpha^2(WW^*)^2 \leq (WW^*)^2$$

$$\Leftrightarrow \langle\alpha^2(W^*W)^2 - (W^*W)^2 f|f\rangle \leq 0 \ \forall f \in L^2$$

$$\Leftrightarrow \alpha^2[hE(w^2 \circ T^{-1}]^2 \leq h_2 E(W_2^2) \circ T^{-1} \qquad\qquad\text{--------------------(11)}$$

Consider

$$\Leftrightarrow (WW^*)^2 \leq \beta^2(WW^*)^2$$

$$\Leftrightarrow \langle(W^*W)^2 f - \beta^2(W^*W)^2 f|f\rangle \leq 0 \qquad \forall f \in L^2$$

$$\Leftrightarrow h_2 E(W_2^2) \circ T^{-1} \leq \beta^2[hE(w^2 \circ T^{-1}]^2 \qquad\qquad\text{--------------------(12)}$$

From (11) and (12)

$$\alpha^2[hE(w^2 \circ T^{-1}]^2 \leq h_2 E(W_2^2) \circ T^{-1} \leq \beta^2[hE(w^2 \circ T^{-1}]^2$$

Theorem 3.2.3

If T∈B(H), Suppose $T^{-1}\sum = \sum$ Then W is (α, β) Quasi normal iff
$$T[\alpha^2(WW^*)] \leq [(W^*W)]T \leq T[\beta^2(WW^*)]$$

Proof

Consider $T[\alpha^2(WW^*)] \leq [(W^*W)]T$
$\Leftrightarrow \langle T\alpha^2(WW^*) - (W^*W)Yf|f \rangle \leq 0 \quad \forall f \in L^2$
$\Leftrightarrow T\alpha^2 w^2(h^\circ T) \leq hw^2 {}^\circ T^{-1}T$ --------------------(13)

Consider $(W^*W)T \leq T[\beta^2(WW^*)]$
$\Leftrightarrow \langle (W^*W)T - T\beta^2(WW^*)f|f \rangle \leq 0 \quad \forall f \in L^2$
$\Leftrightarrow hw^2 {}^\circ T^{-1}T \leq T\beta^2 w^2(h^\circ T)$ ----------------------------(14)
From (13) and (14)
$$T\alpha^2 w^2(h^\circ T) \leq hw^2 {}^\circ T^{-1}T \leq T\beta^2 w^2(h^\circ T)$$

Theorem 3.2.4

If T∈B(H), W is (α, β) Quasi Class (Q) iff
$$T\alpha^2[hE(w^2 {}^\circ T^{-1}]^2 \leq h_2 E(W_2^2) {}^\circ T^{-1}T \leq T\beta^2[hE(w^2 {}^\circ T^{-1}]^2$$
Proof
Let $Wf = w(f^\circ T)$ and $W^*f = hE(wf) {}^\circ T^{-1}$
W is (α, β) Quasi Class (Q)
$T[\alpha^2(WW^*)^2] \leq [(WW^*)^2]T \leq T[\beta^2(WW^*)^2]$
Consider
$\Leftrightarrow T[\alpha^2(WW^*)^2] \leq [(WW^*)^2]T$
$\Leftrightarrow \langle T\alpha^2(W^*W)^2 - (W^*W)^2 Tf|f \rangle \leq 0 \quad \forall f \in L^2$
$\Leftrightarrow T\alpha^2[hE(w^2 {}^\circ T^{-1}]^2 \leq h_2 E(W_2^2) {}^\circ T^{-1}T$ --------------------(15)
Consider
$\Leftrightarrow [(WW^*)^2]T \leq T[\beta^2(WW^*)^2]$
$\Leftrightarrow \langle (W^*W)^2 fT - T\beta^2(W^*W)^2 f|f \rangle \leq 0 \forall f \in L^2$
$\Leftrightarrow h_2 E(W_2^2) {}^\circ T^{-1}T \leq T\beta^2[hE(w^2 {}^\circ T^{-1}]^2$ --------------------(16)
From (15) and (16)
$$T\alpha^2[hE(w^2 {}^\circ T^{-1}]^2 \leq h_2 E(W_2^2) {}^\circ T^{-1}T \leq T\beta^2[hE(w^2 {}^\circ T^{-1}]^2$$

CONCLUSION

We defined as the idea on (α, β)- Quasi Class (Q) and (α, β)-Quasi normal Composition and Weighted Composition Operators is relatively new. We attempted to prove some properties on (α, β) - Quasi Class (Q) and (α, β)-Quasi normal Composition and Weighted Composition Operators in complex Hilbert space. The results of this paper will be accessible for further research to develop application side of Functional Analysis.

REFERENCES

1. M. Berkani. 1999." On a class of quasi Fredholm operators, Integral Equations Operator Theory" .34 : 244-249.
2. David J. Harrington , Robert Whitely., "Seminormal Composition Operators"., *Journal of Operator theory* 11(1984)., 125-135
3. S.S Dragomir.,M.S Moslehian, 2008.,"Some inequalities for (α, β) Normal operators in Hilbert spaces"., *Series Math and Informatics.*, pp. 39-47
4. M.S Moslehian., 2007. "On (α, β) Normal operators in Hilbert spaces"., Pbm IMAGE: pp. 39-47
5. E. Rasoul, M. Farzollah and Ali Morassaei," More on (α, β)-Normal operators in Hilbert spaces", *Abstract and Applied Analysis*, 2012(2012).

Radharamani and Sathyavathi

6. D. Senthilkumar, P. Maheswan Naik and D. Kiruthika "Quasi class Q composition operators" , *International Journal of Math Science and Eng. Appls (IJMSEA).,* ISSN 0973-9424. Volume. 5., No IV, July 2011., pp., 01-09.

7. C.R Putnam, 1951., "On the Normal operators on Hilbert spaces"., *Am.J.Math.,*73: 357-362.

8. S. Panayappan ," Non Hyponormal Weighted Composition Operators"., Indian J. Pure appl. Mathematics and Computing., Vol(19)(2005),(573-578)

9. K. Vidhyapraba , A. Sivasathya and V. Vimala.," Some Properties of Quasi Normal Operators"., *International Journal of Sci Research and Management.,* 02(12)(2014)., 1811-1814.

RESEARCH ARTICLE

Solving Fuzzy Game of Order 3x3 using Nonagonal Fuzzy Numbers

G.Sasikala[1*] and R.Umamaheswari[2]

[1]Associate Professor, Department of Mathematics, Chikkanna Government Arts College, Tirupur Tamil Nadu, India.
[2]Research Scholar, Department of Mathematics, Chikkanna Government Arts College, Tirupur Tamil Nadu, India.

*Address for Correspondence
G.Sasikala
Associate Professor,
Department of Mathematics,
Chikkanna Government Arts College,
Tirupur Tamil Nadu, India.
E.Mail: mahiramasamyuma@gmail.com

ABSTRACT

In this article, we think about a two persons zero sum game of order 3 x 3 with estimated values in payoff matrix. All the estimated values are pretended to be Nonagonal fuzzy numbers. The solution of this kind of fuzzy games with pure strategies by maximin-minimax principles are argued.

Keywords: Fuzzy numbers, Nonagonal, Ranking of fuzzy numbers.

INTRODUCTION

Game theory is a decision theory applicable to competitive situations. It is normally used during two or more individuals or organisations with inconsistent purpose try to make outcomes. In such position , outcome made by one outcome maker affects the outcome made by one or more of the remaining outcome makers. Game theory is based on the minimax principle which chances that every competitor will perform so as to minimize his maximum loss. (or maximise his minimum gain).Game theory is relevant to position such as two players harrowing to winatchess, contestant dispute an election, hard harrowing to continue their market stake, etc..

Fuzzyset[27]
Let X be a non-empty set. A fuzzy set A in X is characterized by its membership function A→[0,1] and A(x) is interpreted as the degree of membership of element x in fuzzy A for each x ∈ X.

63689

The value zero is to represent complete non-membership the value one is used to represent complete membership and values in between are used to represent intermediate degrees of membership. The mapping A is also called the membership function of fuzzy set A.

Crispset[26]

Acrispset is a special case of a fuzzy set, in which the membership function only takes two values, commonly defined as 0 and 1.

Fuzzy number[27]

A fuzzy number $\tilde{A}$ is a fuzzy set on the real line R, must satisfy the following conditions.

(i)   There exist at least one x $R0 \in$RR with $\mu_{\tilde{A}}(x_0)$=1.

(ii)   µ $R\bar{A}R$(x)is piecewise continuous.

(iii) $\bar{A}$ must be normal and convex.

Nonagonal fuzzy numbers:

Definition 2.1.

An Nonagonal fuzzy number denoted by $\tilde{A}R_WR$ is defined to be the ordered quadruple
$\tilde{A}R_WR$= (fR_1R(r), hR_1R(t),gR(s),fR_2R(r),hR_2R(t)) for r$\in[0,k_1]$, s$\in[k_1,k_2]$and t$\in[k_2,1]$ where

1. fR_1R(r)is abounded left continuous non-decreasing function over $[0,k_1]$, $[0 \le r \le k_1]$
2. hR_1R(t) is abounded left continuous non-decreasing function over $[k_2,1]$, $[k_2 \le r \le 1]$
3. gR(s) is a bounded continuous function over $[k_1,k_2]$,$[k_1 \le s \le k_2]$.
4. fR_2R(r) is abounded right continuous non-increasing function over $[0,k_1]$, $[0 \le r \le k_1]$

hR_2R(t)is abounded right continuous non-increasing function over $[k_2,1]$, $[k_2 \le r \le 1]$

Definition 2.2[28]

A Nonagonal fuzzy number $\bar{A}$=(a_1, a_2, a_3, a_4, a_5, a_6, a_7, a_8, a_9) is a normal fuzzy number where a_1, a_2, a_3, a_4, a_5, a_6, a_7, a_8, a_9 are real number sand its membership function is given by

$$\mu_{\bar{A}}(x)=\begin{cases} \frac{1}{4}\left(\frac{x-a_1}{a_2-a_1}\right) & for a_1 \le x \le a_2 \\ \frac{1}{4}+\frac{1}{4}\left(\frac{x-a_2}{a_3-a_2}\right) & for a_2 \le x \le a_3 \\ \frac{1}{2}+\frac{1}{4}\left(\frac{x-a_3}{a_4-a_3}\right) & for a_3 \le x \le a_4 \\ \frac{3}{4}+\frac{1}{4}\left(\frac{x-a_4}{a_5-a_4}\right) & for a_4 \le x \le a_5 \\ 1-\frac{1}{4}\left(\frac{x-a_5}{a_6-a_5}\right) & for a_5 \le x \le a_6 \\ \frac{3}{4}-\frac{1}{4}\left(\frac{x-a_6}{a_7-a_6}\right) & for a_5 \le x \le a_6 \\ \frac{1}{2}-\frac{1}{4}\left(\frac{x-a_7}{a_8-a_7}\right) & for a_7 \le x \le a_8 \\ \frac{1}{4}\left(\frac{a_9-x}{a_9-a_8}\right) & for a_8 \le x \le a_9 \\ o & otherwise \end{cases}$$

α-cutofan Nonagonal fuzzy number

The α-cut of an nonagonal fuzzy number $\bar{A}$=(a_1, a_2, a_3, a_4, a_5, a_6, a_7, a_8, a_9) is

$$[\bar{A}]_\alpha = \begin{cases} (f_1(r), f_2(r)) & r \in [0, k_1] \\ g(s) & s \in [k_1, k_2] \\ (h_1(t), h_2(t)) & t \in [k_2, 1] \end{cases}$$

Sasikala and Umamaheswari

$$[\bar{A}]_\alpha = \begin{cases} \left(a_1 + \frac{r}{k_1}(a_2 - a_1) + a_9 - \frac{r}{k_1}(a_9 - a_8)\right) & r \in [0, k_1] \\ a_3 + \frac{s-k_1}{k_2-k_1}(a_4 - a_3) & s \in [k_1, k_2] \\ a_5 + \frac{t-k_2}{1-k_2}(a_6 - a_5) + a_7 - \frac{t-k_2}{1-k_2}(a_7 - a_6) & t \in [k_2, 1] \end{cases}$$

Where $f_1(r) = a_1 + \frac{r}{k_1}(a_2 - a_1)$

$g(s) = a_3 + \frac{s-k_1}{k_2-k_1}(a_4 - a_3)$

$h_1(t) = a_5 + \frac{t-k_2}{1-k_2}(a_6 - a_5)$

$f_2(r) = a_9 - \frac{r}{k_1}(a_9 - a_8)$

$h_2(t) = a_7 - \frac{t-k_2}{1-k_2}(a_7 - a_6)$

Ranking of Nonagonal fuzzy numbers

A measure of a number $\bar{A}_w$ is a function $R_\alpha : R_\omega(I) \to R^+$ which assign a non- negative real number R_{Non} that expresses the measure of $\bar{A}_w$.

$R_{Non} = \frac{1}{2}\int_0^{k_1}(f_1(r) + f_2(r))dr + \int_{k_1}^{k_2} g(s)\,ds + \frac{1}{2}\int_{k_2}^1(h_1(t) + h_2(t))dt$.

Where $r \in [0, k_1]$, $s \in [k_1, k_2]$, $t \in [k_2, 1]$.

Definition3.1.

The measure of an Nonagonal fuzzy number is obtained by the average of

The two fuzzy side areas, left side are a and right side area, and the center part of the area from membership function to α-axis.

Definition3.2.

Let$\bar{A}$ be a normal octagonal fuzzy number. The value R_{Non} called the measure of calculated as follows:

$R_{Non} = \frac{1}{2}\int_0^{k_1}(f_1(r) + f_2(r))dr + \int_{k_1}^{k_2} g(s)\,ds + \frac{1}{2}\int_{k_2}^1(h_1(t) + h_2(t))dt$

$= \frac{1}{4}\{(a_5 + 2a_6 + a_7) + (a_1 + a_2 - 2a_3 - 2a_4 + a_8 + a_9)k_1 + (2a_3 + 2a_4 - a_5 + 2a_6 - a_7)k_2\}$

Where $0 \leq k_1 \leq k_2 \leq 1$.

Solution of all 3x3 matrix game[26]

Consider the general 3×3 game matrix A=$\begin{pmatrix} a_{11} & a_{12} & a_{13} \\ a_{21} & a_{22} & a_{23} \\ a_{31} & a_{32} & a_{33} \end{pmatrix}$

To solve this game we proceed as follows:

(i)   Test for as addle point.

(ii)   If there is no saddle point, solve by finding equalizing strategies.

The Optimal mixed strategies for player A= (pR_1R,pR_2R) and for playerB = (qR_1R,qR_2R)

$P_1 = \frac{a_{22}-a_{21}}{\lambda}$,P_2 =1-P_1 .$q_1 = \frac{a_{22}-a_{12}}{\lambda}$,q_2=1-q_1

$\lambda = (a_{11} + a_{22}) - (a_{12} + a_{21})$

Value of the game V=$\frac{a_{11}a_{22}-a_{12}a_{21}}{(a_{11}+a_{22})-(a_{12}+a_{21})}$

Ranking of Nonagonal

$R_{Non} = \frac{1}{2}\int_0^{k_1}(f_1(r) + f_2(r))dr + \int_{k_1}^{k_2} g(s)\,ds + \frac{1}{2}\int_{k_2}^1(h_1(t) + h_2(t))dt$

$= \frac{1}{2}\int_0^{k_1}\left(a_1 + \frac{r}{k_1}(a_2 - a_1) + a_9 - \frac{r}{k_1}(a_9 - a_8)\right)dr + \int_{k_1}^{k_2} a_3 + \frac{s-k_1}{k_2-k_1}(a_4 - a_3))ds +$

$$\frac{1}{2}\int_{k_2}^1\left(a_5 + \frac{t-k_2}{1-k_2}(a_6 - a_5) + a_7 - \frac{t-k_2}{1-k_2}(a_7 - a_6)\right)dr$$

$\frac{1}{2}\int_0^{k_1}\left(a_1 + \frac{r}{k_1}(a_2 - a_1) + a_9 - \frac{r}{k_1}(a_9 - a_8)\right)dr = \frac{1}{2}\left\{ \begin{array}{c} (a_1 + a_9)(r)_0^{k_1}) + \\ (\frac{r^2}{2k_1})_0^{k_1}(a_2 - a_1 - a_9 + a_8) \end{array} \right\}$

$= \frac{1}{4}(a_1 + a_9 + a_2 + a_8)k_1$

$\int_{k_1}^{k_2} a_3 + \frac{s-k_1}{k_2-k_1}(a_4 - a_3))\,ds = a_3(s)_{k_1}^{k_2} + \int_{k_1}^{k_2}\frac{s}{k_2-k_1}(a_4 - a_3)\,ds - \int_{k_1}^{k_2}\frac{k_1}{k_2-k_1}(a_4 - a_3)ds$

Sasikala and Umamaheswari

$=\frac{1}{4}\{2a_3k_2 - 2a_4k_1 - 2a_3k_1 + 2a_4k_2\}$

$\frac{1}{2}\int_{k_2}^{1}(a_5 + (\frac{t-k_2}{1-k_2})(a_6 - a_5) + a_7 - (\frac{t-k_2}{1-k_2})(a_7 - a_6))\mathrm{dt} = \frac{1}{4}\{(a_5 + 2a_6 + a_7) - a_5k_2 + 2a_6k_2 - a_7k_2\}.$

$\frac{1}{2}\int_{0}^{k_1}\left(a_1 + \frac{r}{k_1}(a_2 - a_1) + a_9 - \frac{r}{k_1}(a_9 - a_8)\right)dr + \int_{k_1}^{k_2} a_3 + \frac{s-k_1}{k_2-k_1}(a_4 - a_3))\mathrm{ds} +$

$\frac{1}{2}\int_{k_2}^{1}\left(a_5 + \frac{t-k_2}{1-k_2}(a_6 - a_5) + a_7 - \frac{t-k_2}{1-k_2}(a_7 - a_6)\right)dr$ =

$\frac{1}{4}(a_1 + a_9 + a_2 + a_8)k_1 + \frac{1}{4}\{2a_3k_2 - 2a_4k_1 - 2a_3k_1 + 2a_4k_2\} + \frac{1}{4}\{(a_5 + 2a_6 + a_7) - a_5k_2 + 2a_6k_2 - a_7k_2\}$

$=\frac{1}{4}\{(a_5 + 2a_6 + a_7) + (a_1 + a_2 - 2a_3 - 2a_4 + a_8 + a_9)k_1 + (2a_3 + 2a_4 - a_5 + 2a_6 - a_7)k_2\}$

Where $0 \le k_1 \le k_2 \le 1$.

Numerical Example

Consider the following   Nonagonal fuzzy game problem.

Player B

Player A $\begin{pmatrix} (-3,-1,0,1,2,3,4,5,6) & (1,3,4,5,7,8,9,10,11) & (2,3,4,5,6,7,8,9,10) \\ (-3,-1,3,6,8,9,10,12,13) & (1,2,3,5,6,10,12,13,14) & (-3,-2,-1,1,3,6,8,10,13) \\ (-5,-4,-3,-2,1,2,3,4,5) & (-1,0,1,2,3,4,5,8,12) & (-5,-4,-3,-2,5,6,7,8,9) \end{pmatrix}$

Solution:

$R_{Non} = \frac{1}{2}\int_{0}^{k_1}(f_1(r) + f_2(r))dr + \int_{k_1}^{k_2} g(s)\, ds + \frac{1}{2}\int_{k_2}^{1}(h_1(t) + h_2(t))dt$

$=\frac{1}{2}\int_{0}^{k_1}\left(a_1 + \frac{r}{k_1}(a_2 - a_1) + a_9 - \frac{r}{k_1}(a_9 - a_8)\right)dr + \int_{k_1}^{k_2} a_3 + \frac{s-k_1}{k_2-k_1}(a_4 - a_3))\mathrm{ds} +$

$$\frac{1}{2}\int_{k_2}^{1}\left(a_5 + \frac{t-k_2}{1-k_2}(a_6 - a_5) + a_7 - \frac{t-k_2}{1-k_2}(a_7 - a_6)\right)dr$$

$R_{Non} = \frac{1}{4}\{(a_5 + 2a_6 + a_7) + (a_1 + a_2 - 2a_3 - 2a_4 + a_8 + a_9)k_1 + (2a_3 + 2a_4 - a_5 + 2a_6 - a_7)k_2\}$, Where $0 \le k_1 \le k_2 \le 1$.

Taking k_1=0.4 and k_2=0.6

$a_{11}= (-3,-1,0,1,2,3,4,5,6)$

$R_{Non}(a_{11}) = \frac{1}{4}\{(2 + 2(3) + 4) + (-3 - 1 - 2(0) - 2(1) + 5 + 6)(0.4) + (2(0) + 2(1) - 2 + 2(3) - 4)(0.6)\}$

$\qquad = \frac{1}{4}\{12 + 2 + 1.2\}$

$R_{Non}(a_{11})$=3.8

$a_{12}= (1,3,4,5,7,8,9,10,11) \Rightarrow R_{Non}(a_{12})$=11.4, $a_{13}= (2,3,4,5,6,7,8,9,10) \Rightarrow R_{Non}(a_{13})$=10.3

$a_{21}= (-3,-1,3,6,8,9,10,12,13) \Rightarrow R_{Non}(a_{21})$=12,

$a_{22}= (1,2,3,5,6,10,12,13,14) \Rightarrow R_{Non}(a_{22})$=13.6,

$a_{23}= (-3,-2,-1,1,3,6,8,10,13) \Rightarrow R_{Non}(a_{23})$=7.7

$a_{31}= (-5,-4,-3,-2,1,2,3,4,5) \Rightarrow R_{Non}(a_{31})$=1.2

$a_{32}= (-1,0,1,2,3,4,5,8,12) \Rightarrow R_{Non}(a_{32})$=6.2

$a_{33}= (-5,-4,-3,-2,5,6,7,8,9) \Rightarrow R_{Non}(a_{33})$=4.3

Pay off matrix

$$\begin{pmatrix} 3.8 & 11.4 & 10.3 \\ 12 & 13.6 & 7.7 \\ 1.2 & 6.2 & 4.3 \end{pmatrix}$$

Minimax = 10.3, Maximin = 7.7, Minimax $\ne$ Maximin

It does not exist a saddle point.

Row 3 is dominated by Row 1, So we delete Row 3.

$$\begin{pmatrix} 3.8 & 11.4 & 10.3 \\ 12 & 13.6 & 7.7 \end{pmatrix}$$

Column 2 is dominated by Column 3, So we delete Column 2.

$$\begin{pmatrix} 3.8 & 10.3 \\ 12 & 7.7 \end{pmatrix}$$

a_{11}=3.8, a_{12}=10.3, a_{21}=12, a_{22}=7.7.

$\lambda = (a_{11} + a_{22}) - (a_{12} + a_{21}) = (3.8+7.7) - (10.3+12), \lambda$= -10.8

Sasikala and Umamaheswari

$P_1 = \frac{a_{22} - a_{21}}{\lambda} = \frac{7.7 - 10.3}{-10.8} = 0.24$, $P_2 = 1 - P_1 = 1 - 0.24 = 0.76$

$q_1 = \frac{a_{22} - a_{12}}{\lambda} = \frac{7.7 - 12}{-10.8} = 0.398$

$q_2 = 1 - q_1 = 1 - 0.398 = 0.602$

Value of the game $V = \frac{a_{11}a_{22} - a_{12}a_{21}}{(a_{11} + a_{22}) - (a_{12} + a_{21})} = \frac{(3.8*7.7) - (10.3*12)}{-10.8}$

$V = 8.7$.

Doing in this way we can solve nonagonal & decogonal problems for the type of $4 \times 3, 5 \times 3, 3 \times 5$ etc.

CONCLUSION

In this article, a method deal with 3 x 3 fuzzy game problem applying ranking of fuzzy numbers has been advised. The parameter k can be changed by the outcome maker to obtain the applicable decision. We may get various types of fuzzy game value for various values of k for the same fuzzy competitor.

REFERENCES

1. A.J.Kamble and T.Venkatesh, Some results on fuzzy numbers, Annals of Pure and Applied Mathematics,7(2)(2004).
2. H.Basirzadeh and R.Abbasi,A new approach for ranking fuzzy numbers based on α cuts, journal of applied MathematicsandInformatics,26(2008).
3. G.BortolanandR.Degani,Areviewofsomemethodforrankingfuzzysets,Fuzzysetsand systems,15 (1985)..
4. M.Delgado,J.L.VerdegayandM.A.Vila,Aprocedureforrankingfuzzynumbers,Fuzzysets and systems,26(1988).
5. K.H.Lee, FirstCourseonFuzzyTheoryandApplication,Springer,2005.
6. V.K.KapoorandS.Kapoor,OperationResearch-techniquesforManagement,Edition-7.S.Chand,2001.
7. T.S.LiouandM.J.Wang,Rankingfuzzynumberswithintegralvalue,FuzzySetssystems 50(3) (1992).
8. I.Nishizaki and M.Sakawa, Equilibrium solution for multiobjectivebimatrix games incorporatin fuzzy goals, Journal of Optimization Theory and Application,86(1995).
9. Y.X.Yuan, Criteria for evaluating fuzzy ranking method, Fuzzy Sets and Systems,44(1991).
10. Bellman, R.E. and Zadeh, L.A (1970). Decision making in fuzzy environment. Management Science, 17, 141-164
11. Bhaumik ,A., Roy S.K. and Li, D.F.,(2017). Analysis of triangular intuitionistic fuzzy matrix games using robust ranking. Journal of intelligent & fuzzy systems,33, 327-336.
12. Cevikel, A.C. & Ahlatcioglu, M. (2010). Solution for fuzzy matrix games. Computer and mathematics with application,60, 399-410.
13. Dhanalakshmi, V and Kennedy, F.C (2014). Some ranking methods for octagonal fuzzy numbers. International Journal of Mathematical Archive, 5(6), 177-188.
14. Hussain, R.J and Priya, A (2016). Solving fuzzy game problem using hexagonal fuzzy number. Journal of Computer, 1(2), 53-59
15. Jain, R (1976). Decision making in the presence of fuzzy variables.IEEE Transactions on Systems, Man and Cybernetics, 6, 698-703.
16. S.,Chopra, R and Saxena, R.R (2013). Method to solve fuzzy game matrix. International Journal of Pure and Applied Mathematics, 89(5), 679-687.
17. Kumar, R.S and Kumaraghuru, S(2015). Solution of fuzzy game problem using triangular fuzzy number.International Journal of Innovative Science, Engineering & Technology, 2, 497-502.
18. Kumar,A., Singh,P., Kaur, P., Kaur, A(2010). A new approach for ranking of generalized trapezoidal fuzzy numbers. International Journal of computer and information engineering, 4(8), 1217-1220.
19. Li Deng- Feng (2012). A fast approach to compute fuzzy values of matrix games with payoffs of triangular fuzzy numbers. European journal of operational research, 223, 421-429.

20. Li and Hong (2012). Solving constrained matrix games with payoffs of triangular fuzzy numbers. Computers and Mathematics with applications, 64, 432-446.

21. Namarta, Thakur, N. I, & Gupta, U.C. (2017). Ranking of heptagonal fuzzy numbers using incentre of centroids. International journal of advanced technology in engineering and science. 5(7),248-255.

22. Nan, J. X., Zhang, M.U., and Li, D.F., (2014). A methodology for matrix games with payoffs of triangular intuitionistic fuzzy number. Journal of intelligent & fuzzy systems, 26, 2899-2912.

23. Selvakumari, K. and Lavanya, S. (2014). On solving fuzzy game problem using octagonal fuzzy numbers. Annals of Pure and Applied Mathematics, 8(2), 211-217.

24. Selvakumari, K. and Lavanya, S.(2015). An approach for solving fuzzy game problem. Journal of Science and Technology, 8(15),1-6.

25. Swarup, K., Gupta, P.K., Mohan,M., (2010). Operation Research. Sultanchand and sons.

26. B.Krishnapriya and Dr.K.Senbagam ,Solving Fuzzy Game Problem Using Pentagonal and hexagonal fuzzy Numbers, International Journal of Scientific Reasearch and Review ISSN NO:2279-543X

27. R.Senthilkumar and K.Gnanaprakah, "Solving fuzzy game of order 3×3 using octagonal fuzzy numbers. IJISET-vol. 3 Issue 8, Agust 2016-ISSN(ONLINE) 2348-7968. Impact factor (2015)-4.332.

28. V.R.Bindu Kumari and Dr. R.Govindarajan, "EPRA International journal off multidisciplinary Research(IJMR)"-ISSN(online):2455-3662.Vol 5,Issue 9-september 2019.SJIF Impact Factor :5.614-ISI I.F Value : 1.188

RESEARCH ARTICLE

Distance Measures for Spherical Picture Fuzzy Sets and its Application in Multi Criteria Decision Making

Rajarajeswari Palanisamy[1] and Reshma Ranganathan[2] *

[1]Associate Professor, Department of Mathematics, Chikkanna Govt Arts College, Tirupur, Tamil Nadu, India.
[2] Research Scholar, Department of Mathematics, Chikkanna Govt Arts College, Tirupur, Tamil Nadu, India.

***Address for Correspondence**
Reshma Ranganathan
Research Scholar,
Department of Mathematics,
Chikkanna Govt Arts College,
Tirupur, Tamil Nadu, India.
E.Mail: reshmaranganathan1608@gmail.com

ABSTRACT

In this paper, we have introduced Euclidean and Hamming distance measures for Spherical Picture Fuzzy Sets (SPFS) for the first time in literature. Spherical Picture Fuzzy sets are extensions of the standard Intuitionistic Fuzzy Sets, Circular Intuitionistic Fuzzy Sets, Picture Fuzzy sets, and hence of Zadeh's Fuzzy Sets (FS). It is a new generalized representation of distance metrics applied to Spherical Picture Fuzzy Sets and Spherical Picture Fuzzy Values. Spherical Picture Fuzzy Sets used to identify the assessment data with uncertainty in complicated realistic decision making situations when Picture Fuzzy sets are insufficient. Multiple criteria decision-making MCDM research has grown rapidly and is still a notable area of study for tackling complex decision problems. We have applied the proposed distances for finding radius to deal with MCDM under picture Fuzzy environment. The proposed approach helps decision analysts truly understand the entire evaluation process and can provide a more precise and efficient decision support tool compared to Picture Fuzzy sets. The effectiveness of Spherical Picture Fuzzy approach is illustrated with suitable example.

Keywords: Picture fuzzy set, Picture fuzzy number, Spherical Picture Fuzzy Sets and Multiple attribute decision making.

Rajarajeswari Palanisamy and Reshma Ranganathan

INTRODUCTION

In daily life, we deal problems with uncertainty in some way in kind of situation, as new mathematical tools are required since the standard mathematical tools(crisp sets) are insufficient to deal with overcome uncertainties. The concept of Fuzzy Set theory established by Zadeh [15] in 1965 in which the element has membership degree, the degree of belongingness is used to deal the problem under uncertain environment. In 1983, Atanassov [1] introduced the concept of Intuitionistic Fuzzy Sets (IFSs) which is the prime extension of Zadeh's Fuzzy Set. It describing an element with membership and non-membership values such that sum of these two values less than or equal toone. In 1994, Atanassov [4] was defined some other operations over the Intuitionistic Fuzzy Sets. In 2001, Atanassov [6] examined the Sanchez's approach for medical diagnosis andit's application is expanded using the idea of IFS theory which is a generalization of fuzzy set theory. Later, the important aspect of neutrality degree is seen as lacking in Intuitionistic Fuzzy Set theory. In 2014, Coung [10] introduced the concept of the Picture Fuzzy Sets which is the prime extension of Fuzzy Sets and Intuitionistic Fuzzy Sets by including the neutrality degree for each element along with membership and non-membership degrees in such that sum of these three degrees must not exceed one. Coung and Kreinovich [10] has analyzed new operations and properties over Picture Fuzzy Sets. In 2018, Nguyen Van Dinh and Nguyen Xuan Thao [13] analyzed the concepts of difference between PFS-sets, distance measure, and dissimilarity measure between picture fuzzy sets are introduced and along with the formulas for determining these values. They also illustrate how it can be used in Multi Attribute Decision Making. In 2017, Chunyong Wang and et.al., [12] established the a few geometric operators of Picture Fuzzy Sets and discussed some of its properties and also they have applied these operators to resolve involving Multiple Attribute Decision Making in a Picture Fuzzy environment. The concept of Circular Intuitionistic Fuzzy Sets (CIFSs) introduced by Atanassov [8] in 2020 which is the expansion of Intuitionistic Fuzzy Sets.Circular Intuitionistic Fuzzy Sets is characterized by describing a circle with radius r among each point of the IFS set. In [9], Atanassov defined the range of the radius of C-IFSs lies in [0,√2] since the points with center⟨0, 1⟩and ⟨1, 0⟩are necessary to cover the entire Intuitionistic Fuzzy Sets triangle, which can be valid only when r≥√2. In this paper, we have introduced the distance measures for Spherical Picture Fuzzy Sets. Distance measures over Spherical Picture fuzzy sets applied to Multi criteria Decision Making for finding a radius which is used to overcome the insufficient situation in Picture fuzzy sets.

Preliminaries
In this section, few pre-requisites that are needed for this study overviewed.

Definition 2.1. [15] Fuzzy Set
Let X be a non-empty universal set. Each set is mapped to [0,1] by membership function is defined as
$E = \{⟨x, \tau_E(x)⟩/x \in X\}$
where $\tau_E: X \to [0, 1]$ is the degree of membership function of the fuzzy set E and $\tau_E(x) \in [0, 1]$ is the membership value of the element x $\in$X in the fuzzy set E.

Definition 2.2. [1]IFS
Let X be a non-empty universal set. An intuitionistic fuzzy set (IFS) E in X is defined as
$E = \{⟨x, \tau_E(x), \upsilon_E(x)⟩/x \in X\}$
where $\tau_E: X \to [0, 1]$ and $\upsilon_E: X \to [0, 1]$ with $0 \leq \tau_E(x) + \upsilon_E(x) \leq 1$ for all x $\in$X represents the degrees of membership and non-membership of the element x to the IFS E. For each IFS, the intuitionistic index or hesitancy degree of the element x in X to the IFS E is $\pi_E(x) = 1 - \tau_E(x) - \upsilon_E(x)$.

Definition 2.3. [8] C-IFS
Let X be the universe and E be its subset then, the set C-IFS is defined as,
$E_r^* = \{⟨x, \tau_E(x), \upsilon_E(x); r⟩/x \in X\}$
where $\tau_E: X \to [0, 1]$ and $\upsilon_E: X \to [0, 1]$ with $0 \leq \tau_E(x) + \upsilon_E(x) \leq 1$ and r $\in$[0,√2] is the radius of the circle around each element x $\in$E, and functions $\tau_E: X \to [0, 1]$ and $\upsilon_E: X \to$[0,1] represent membership degree and non-membership

Rajarajeswari Palanisamy and Reshma Ranganathan

degree of element x $\in$X to a fixed set E $\subseteq$X. We also define the hesitancy margin π_E: X → [0, 1] by π_E(x) = 1−τ_E(x)−υ_E(x) which corresponds to the degree of indeterminacy. The radius r defined in C-IFS takes on values from the interval [0,1].

Definition 2.4. [10] PFS

A Picture Fuzzy Set(PFS) E on a universe X is an object in the form of

P = {⟨x, τ_E(x), ω_E(x), υ_E(x)⟩/x $\in$X}

where τ_E(x) $\in$[0, 1] is called the degree of positive membership of x in E, ω_E(x) $\in$[0, 1] is called the degree of neutral membership of x in E and υ_E(x) $\in$[0, 1] is called the degree of negative membership of x in E. where τ_E(x), ω_E(x) and υ_E(x) satisfy the following condition

(x$\in$X) $0 \le \tau_E$(x)+ω_E(x)+υ_E(x) ≤ 1 Now, σ_E(x) = (1−(τ_E(x)+ω_E(x)+υ_E(x)) could be called the degree of refusal membership of x in E.

Definition 2.5.(Spherical Picture Fuzzy Sets (SPFSs))

Let us have a fixed universe X and E be its subset then, the set SPFSs is defined as,

P_r^*= {⟨x, τ_E(x), ω_E(x), υ_E(x); r⟩/x $\in$X}

where functions τ_E: X → [0, 1], ω_E: X → [0, 1] and υ_E: X → [0, 1] with $0 \le \tau_E$(x) +ω_E(x) + υ_E(x) ≤ 1 and r $\in$[0,√2] is the radius of the sphere around each element x $\in$E,represent membership degree, neutral degree and non-membership degree of element x $\in$Xto a fixed set E $\subseteq$X. We also define the hesitancy margin π_E: X → [0, 1] by π_E(x) =$1 - \tau_E$(x) − ω_E(x) − υ_E(x) which corresponds to the degree of indeterminacy.

Definition 2.6. (Distance Properties)

AmetriconasetXisafunction$d$: $X \times X \to R$whichsatisfythefollowingthreeconditions:

1. $d(x,y) \ge 0$forall$x,y \in X$andequalityholdsiff$x=y$.
2. $d(x,y)=d(y,x)$forall$x,y \in X$(similarity)
3. $d(x,z) \le d(x,y)+d(y,z)$forall$x,y,z \in X$(Thetriangleinequality)Here,$d(x,y)$representsthedistancebetweentheobjectsxandy.

Definition 2.7.

Consider two points x=$(x_1,x_2,....x_n)$ and y=$(y_1,y_2,....y_n)$ $\in R^n$. Following are the two most popular distance metrics available in literature.

1. $d_2\left(x, y\right) = \sqrt{\sum_{i=1}^{n}(x_i - y_i)^2}$
2. $d_1\left(x, y\right) = \sum_{i=1}|x_i - y_i|$

Definition 2.8.

Let α = (τ_α, ω_α, υ_α) and β = (τ_β, ω_β, υ_β) be two picture fuzzy numbers, then

(1) $\alpha \cdot \beta$ = ((τ_α + ω_α)(τ_β + ω_β) − $\omega_\alpha\omega_\beta$, $\omega_\alpha\omega_\beta$, 1 − (1 −$\upsilon_\alpha$)(1 − υ_β));

(2) α^λ = ((τ_α +ω_α)$^\lambda$ −ω_α^λ, $\omega_{\alpha'}^\lambda$, 1 − (1 − υ_α)$^\lambda$), $\lambda > 0$.

Definition 2.9.[14]

If we consider α = (τ_α, ω_α, υ_α, ϱ_α) be a picture fuzzy numbers, we can define a score function S as S(α) = $\frac{\tau_\alpha - \upsilon_\alpha + \sqrt{2}r(2\rho-1)}{3}$ and the accuracy function H as H(α) = τ_α + ω_α + υ_α, where S(α) $\in$ [−1, 1] and H(α) $\in$ [0, 1] respectively. We can take two picture fuzzy numbers α and β

   (i) if S(α) > S(β), then α is superior to β, denoted by $\alpha > \beta$;

   (ii) if S(α) = S(β), then

(1) H(α) = H(β), implies that α is equivalent to β, represented by $\alpha \sim \beta$;

(2) H(α) > H(β), implies that α is superior to β, represented by $\alpha \succ \beta$.

Rajarajeswari Palanisamy and Reshma Ranganathan

Definition 2.10.
Let us assume that p_j (j = 1, 2, ..., n) is a set of PFNs, then the picture fuzzy weighted geometric (PFWG) operator is defined as follow:

$PFWG_w(p_1, p_2, ..., p_n) = \prod_{j=1}^{n} p_j^{w_j}$, where w = $(w_1, w_2, w_3, \ldots w_n)$, and $w_j > 0$

Definition 2.11. (Distance Measures for C-IFSs)

The radius of the $(\tau(x), v(x))$ is the maximum of the Euclidean distance

$$r_i = \max \sqrt{\left[\left(\tau(x) - m_{i,j}\right)^2 + \left(v(x) - n_{i,j}\right)^2\right]}$$

Euclidean Distance

$$E_2(E, F) = \frac{1}{2}\left(\frac{|r_E - r_F|}{\sqrt{2}} + \sqrt{\frac{1}{2}\sum_{X \in E}[(\tau_E(x) - \tau_F(x))^2 + (v_E(x) - v_F(x))^2]}\right)$$

$$E_3(E, F) = \frac{1}{2}\left(\frac{|r_E - r_F|}{\sqrt{2}} \sqrt{\frac{1}{2}\sum_{X \in E}[(\tau_E(x) - \tau_F(x))^2 + (v_E(x) - v_F(x))^2 + (\pi_E(x) - \pi_F(x))^2]}\right)$$

Hamming Distance

$$H_2(E, F) = \frac{1}{2}\left(\frac{|r_E - r_F|}{\sqrt{2}} + \frac{1}{2}\sum_{X \in E}[|\tau_E(x) - \tau_F(x)| + |v_E(x) - v_F(x)|]\right)$$

$$H_3(E, F) = \frac{1}{2}\left(\frac{|r_E - r_F|}{\sqrt{2}} + \frac{1}{2}\sum_{X \in E}[|\tau_E(x) - \tau_F(x)| + |v_E(x) - v_F(x)| + |\pi_E(x) - \pi_F|]\right)$$

Hausdorff Distance

$$HD_2(E, F) = \frac{1}{2}\left(\frac{|r_E - r_F|}{\sqrt{2}} + \frac{1}{n}\sum_{X \in E} max[|\tau_E(x) - \tau_F(x)|, |v_E(x) - v_F(x)|]\right)$$

$$HD_3(E, F) = \frac{1}{2}\left(\frac{|r_E - r_F|}{\sqrt{2}} + \frac{1}{n}\sum_{X \in E} max[|\tau_E(x) - \tau_F(x)|, |v_E(x) - v_F(x)|, |\pi_E(x) - \pi_F(x)|]\right)$$

Definition 2.12. (Distance Measures for PFSs)

Euclidean Distance

$$E_3(E, F) \sqrt{\frac{1}{2}\sum_{X \in E}[(\tau_E(x) - \tau_F(x))^2 + (\omega_E(x) - \omega_F(x))^2 + (v_E(x) - v_F(x))^2]}$$

$$E_4(E, F) \sqrt{\frac{1}{2}\sum_{X \in E}[(\tau_E(x) - \tau_F(x))^2 + (\omega_E(x) - \omega_F(x))^2 + (v_E(x) - v_F(x))^2 + (\pi_E(x) - \pi_F(x))^2]}$$

Hamming Distance

$$H_3(E, F) = \frac{1}{2}\sum_{X \in E}[|\tau_E(x) - \tau_F(x)| + |\omega_E(x) - \omega_F(x)| + |\upsilon_E(x) - \upsilon_F(x)|]$$

$$H_4(E, F) = \frac{1}{2}\sum_{X \in E}[|\tau_E(x) - \tau_F(x)| + |\omega_E(x) - \omega_F(x)| + |\upsilon_E(x) - \upsilon_F(x)| + |\pi_E(x) - \pi_F)|]$$

Hausdorff Distance

$$HD_3(E, F) = \frac{1}{n}\sum_{X \in E} max[|\tau_E(x) - \tau_F(x)|, |\omega_E(x) - \omega_F(x)|, |\upsilon_E(x) - \upsilon_F(x)|]$$

$$HD_4(E, F) = \frac{1}{n}\sum_{X \in E} max[|\tau_E(x) - \tau_F(x)|, |\upsilon_E(x) - \upsilon_F(x)|, |\omega_E(x) - \omega_F(x)|, |\pi_E(x) - \pi_F(x)|]]$$

Distance measures for Spherical Picture Fuzzy Sets
In this section, we have defined the distance measures for Spherical Picture Fuzzy Sets which is an extension of Circular Intuitionistic Fuzzy Sets is given as follows.

Euclidean Distance

$$E_3(E, F) = \frac{1}{2}(\frac{|r_E - r_F|}{\sqrt{2}} + \sqrt{\frac{1}{2}\sum_{X \in E}[(\tau_E(x) - \tau_F(x))^2 + (\omega_E(x) - \omega_F(x))^2 + (\upsilon_E(x) - \upsilon_F(x))^2]}$$

$$E_4(E, F) = \frac{1}{2}(\frac{|r_E - r_F|}{\sqrt{2}} \sqrt{\frac{1}{2}\sum_{X \in E}[(\tau_E(x) - \tau_F(x))^2 + (\omega_E(x) - \omega_F(x))^2 + (\upsilon_E(x) - \upsilon_F(x))^2 + (\pi_E(x) - \pi_F(x))^2]}$$

Hamming Distance

$$H_3(E, F) = \frac{1}{2}(\frac{|r_E - r_F|}{\sqrt{2}} + \frac{1}{2}\sum_{X \in E}[|\tau_E(x) - \tau_F(x)| + |\omega_E(x) - \omega_F(x)| + |\upsilon_E(x) - \upsilon_F(x)|]$$

$$H_4(E, F) = \frac{1}{2}(\frac{|r_E - r_F|}{\sqrt{2}} + \frac{1}{2}\sum_{X \in E}[|\tau_E(x) - \tau_F(x)| + |\omega_E(x) - \omega_F(x)| + |\upsilon_E(x) - \upsilon_F(x)| + |\pi_E(x) - \pi_F)|]$$

Hausdorff Distance

$$HD_3(E, F) = \frac{1}{2}(\frac{|r_E - r_F|}{\sqrt{2}} + \frac{1}{n}\sum_{X \in E} max[|\tau_E(x) - \tau_F(x)|, |\upsilon_E(x) - \upsilon_F(x)|]$$

$$HD_4(E, F) = \frac{1}{2}(\frac{|r_E - r_F|}{\sqrt{2}} + \frac{1}{n}\sum_{X \in E} max[|\tau_E(x) - \tau_F(x)|, |\upsilon_E(x) - \upsilon_F(x)|, |\omega_E(x) - \omega_F(x)|, |\pi_E(x) - \pi_F(x)|]]$$

The radius of the $(\mu(x), \omega(x), \upsilon(x))$ is the maximum of the Euclidean distance

$$r_i = max\sqrt{[(\tau(x) - m_{i,j})^2 + (\omega(x) - m_{i,j})^2 + (\upsilon(x) - n_{i,j})^2}$$

Theorem 3.1.
For any two E_{rE}, $F_{rF} \in$ SPFSs(X) that is E,F∈ PFS where r_E, $r_F \in [0, \sqrt{2}]$ the distance measures over SPFSs are well defined distance measures.

Rajarajeswari Palanisamy and Reshma Ranganathan

Proof:

We have to demonstrate that the proposed measures H3(E_{r_E}, F_{r_F}), H4(E_{r_E}, F_{r_F}),E3(E_{r_E}, F_{r_F}) and H4(E_{r_E}, F_{r_F}) given in definition satisfies the three axioms of distance measures over SPFSs.

We know that distance measures for C-IFS formulas are well defined in Circular Intuitionistic Fuzzy Sets(X).

Similar manner, we can prove for SPFS formulas.

Case(i): we show that the distance property

D(E_{r_E}, F_{r_F})≥0 holds

$$D(E_{r_E}, F_{r_F}) = \frac{1}{2}\left(\frac{|r_E - r_F|}{\sqrt{2}} + \sqrt{\frac{1}{2}\sum_{X\in E}[(\tau_E(x) - \tau_F(x))^2 + \left(\omega_E(x) - \omega_F(x)\right)^2 + (\upsilon_E(x) - \upsilon_F(x))^2]}\right.$$

We know that,

D(E,F) ≥ 0 holds for the C-IFSs E and F

From the distance property, d(x,y) ≥ 0

For all x,y ∈X and equality holds iff x=y.

|x-y| ≥ 0

|r_E-r_F| ≥ 0

Hence, D(E_{r_E}, F_{r_F}) ≥ 0 and when E_{r_E}=F_{r_F}in C-IFS (E) and r_A-r_B=0 iff E=F in IFS(E)Thereforethe validity of the first axioms for a distance is proved.

Case(ii):

Let us take D(E,F)=$\frac{1}{2}\left(\frac{|r_E - r_F|}{\sqrt{2}} + \sqrt{\frac{1}{2}\sum_{X\in E}[(\tau_E(x) - \tau_F(x))^2 + \left(\omega_E(x) - \omega_F(x)\right)^2 + (\upsilon_E(x) - \upsilon_F(x))^2]}\right.$

D(F,E)=$\frac{1}{2}\left(\frac{|r_F - r_E|}{\sqrt{2}} + \sqrt{\frac{1}{2}\sum_{X\in E}[(\tau_F(x) - \tau_E(x))^2 + \left(\omega_F(x) - \omega_E(x)\right)^2 + (\upsilon_F(x) - \upsilon_E(x))^2]}\right.$

Which satisfies the symmetric condition

Therefore, second axiom can be proved since D is symmetric.

Case(iii):

We consider a third SPFS G_t we have to satisfy that the triangle property

$$D(E_{r_E}, G_{r_G}) = \frac{1}{2}\left(\frac{|r_E - r_C|}{\sqrt{2}} + \sqrt{\frac{1}{2}\sum_{X\in E}[(\tau_E(x) - \tau_G(x))^2 + \left(\omega_E(x) - \omega_G(x)\right)^2 + (\upsilon_E(x) - \upsilon_G(x))^2]}\right.$$

$$D(E_{r_E}, G_{r_G}) = \frac{1}{2}\left(\frac{|r_E - r_F + r_F + r_G|}{\sqrt{2}}\right.$$

$$+ \sqrt{\frac{1}{2}\sum_{X\in E}[(\tau_E(x) - \tau_F(x) + \tau_F(x) + \tau_G(x))^2 + (\omega_E(x) - \omega_F(x) + \omega_F(x) + \omega_G(x))^2 + (\upsilon_E(x) - \upsilon_F(x) + \upsilon_F(x) + \upsilon_G(x))^2]}$$

D(E_{r_E}, G_{r_G}) ≤ D(E_{r_E}, F_{r_F}) + D(F_{r_F}, G_{r_G}) holds.

We know that,

D(E,G) ≤ D(E,F)+D(F,G)

According to a wellknown inequality |x|+|y|≥|x+y| for three real numbers,

|r_E,r_G|≤|r_E,r_F|+|r_F,r_G|

for all possible combinations of r_E, $r_F$and r_G∈ [0, √2].

As a result, when both sides of the last two inequality formulas, 2 and 3 are applied together,

the validity of 1, i.e) the axioms for distance is held.

A Method for Multiple Attribute Decision making with spherical picture fuzzy information

In this section, we will use the existing operators to handle various attributes in a spherical picture fuzzy information. The MADM issues for alternative assessment with spherical picture fuzzy information are represented by the following presumptions or notations. Let R= {R_1, R_2, ..., R_m} be a set of m alternatives and S = {S_1, S_2, ..., S_n} be a set of n attributes. Let P be the picture fuzzy decision matrix. Assume that the picture fuzzy decision matrix P = (p_{ij})$_{mn}$, where p_{ij} (i = 1,2,..., m), (j = 1, 2,..., n) are in the form of PFNs, is the picture fuzzy decision matrix. The PFWG operator is used in the following to evaluate alternatives in MADM issues using spherical picture fuzzy information.

Step 1.

Rajarajeswari Palanisamy and Reshma Ranganathan

We calculate the overall preference values (i = 1, 2,..., m) of the alternative Ai using the decision data given in the matrix P and the PFWG operator.

Step 2. Evaluate the scores S($\tilde{p}$i) (i = 1, 2, ..., m) of the overall picture fuzzy values $\tilde{p}$ by

Definition 2.9.

Step 3. Rank all the alternatives Ri (i = 1, 2, ..., m) according to the values of S ($\tilde{p}$i) (i = 1, 2, ..., m) and choose the best alternative.

Numerical example

Let there be five project Ri (i=1,2,3,4,5) and we have to choose best one. External choose five criteria to evaluate the project: (1) R1 is the relevance; (2) R2 is the effectiveness; (3) R3 is the creativity; (4) R4 is the impact. The experts must evaluate five projects under the aforementioned four criteria in anonymity in order to prevent them from influencing one another.The Decision matrix P=p_{ij} giveninTable1.

MCDM Algorithm

Now, we use the proposed strategy to evaluate a project with spherical picture fuzzy information.

Step 1: utilize the decision information given in matrix P_i and

$\tilde{p}_l$ =PFWG$_w$(P_{i1},P_{i2},P_{i3}, …,P_{in})

We have,

$\tilde{p}_1$=(0.439853,0.133514,0.198915)

$\tilde{p}_2$=(0.302763,0.252098,0.272259)

$\tilde{p}_3$=(0.520169,0.137973,0.175133)

$\tilde{p}_4$=(0.632456,0,0.175133)

$\tilde{p}_5$=(0.437,0.115,0.20)

Step 2: Calculate the scoresS($\tilde{p}$i) (i=1,2,3,4) of the overall picture fuzzy preference values $\tilde{p}_l$ by Definition 2.9.

$$S(\tilde{p}_1)=0.402,$$
$$S(\tilde{p}_2)=0.052,$$
$$S(\tilde{p}_3)=0.262,$$
$$S(\tilde{p}_4)=0.761,$$
$$S(\tilde{p}_5)=0.374.$$

Step 3: Rank all the alternatives Ri (i=1,2,3,4) in accordance with the values of S($\tilde{p}$i): R4>R1>R5>R3>R2.

Comparison Analysis.

First, when the input arguments are Picture Fuzzy Numbers, our method can be applied as already stated, Spherical Picture Fuzzy Sets are extensions of the standard Intuitionistic Fuzzy Sets, Circular Intuitionistic Fuzzy Sets and hence of Zadeh's Fuzzy Sets. This method can be plays predominant role in decision making situations. Next, our approach can be examined with PFWG.

Finally we conclude that, in picture fuzzy sets scores deviation between candidates H1and H5 is very very less which is difficult for us to rank. By using Spherical Picture Fuzzy Sets scores, it improves the accuracy and enhance the deviation between H1 and H5. Hence it is easy to us to rank.

CONCLUSION

In this paper, a new distance measures of the Spherical Picture fuzzy set was introduced which is an expansion of Circular-Intuitionistic fuzzy sets and picture fuzzy sets. In addition, we have presented a new approach for the Spherical picture fuzzy environment. We have used SPFS distance measures to solve multiple attribute decision-

making issues where the attribute values are represented by picture fuzzy information. Finally, an accurate instance of project evaluation has been provided to illustrate how feasible and useful the new approach. Asa future work some more applications will be studied.

REFERENCES

1. Atanassov, K T. A second type of Intuitionistic Fuzzy Sets, Fuzzy sets and systems, 56, 1983, 66- 70.
2. Atanassov, K T. Intuitionistic Fuzzy Sets, Fuzzy sets and systems, 20, 1986, 87-96.
3. Atanassov, K T. More on Intuitionistic Fuzzy Sets, Fuzzy sets and systems, 33, 1989, 37-46.
4. Atanassov, K T. New operations defined over the intuitionistic fuzzy sets, Fuzzy Sets and Systems 61, 1994,137-142.
5. Atanassov, K T. Intuitionistic fuzzy sets, Springer, Heidelberg, Germany, 1999, 1-137.
6. Atanassov, K T. An application of Intuitionistic fuzzy sets in medical diagnosis, Fuzzy sets and systems,117, 2001, 209-213.
7. Atanassov, K T. On Intuitionistic fuzzy sets Theory; Springer:Berlin, Germany, 2012.
8. Atanassov, K T. Circular Intuitionistic fuzzy sets.J.Intell. Fuzzy Syst, 39, 2020, 5981-5986.
9. Atanassov, K T and Evgeniy Marinov. Four Distances for Circular Intuitionistic fuzzy sets, Mathematics,9, 2021, 1121.
10. Bui Cong Cuong, Picture Fuzzy Sets, Journal of computer science and cybernetics, 30(4), 2014, 409-420.
11. Bui Cong Cuong and Kreinovich, Picture fuzzy sets-a new concept for computational intelligence problems, Proceedings of the Third World Congress on Information and Communication echnologies WICT'2013,Hanoi, Vietnam, 2013, 1–6.
12. Chunyong Wang, et.al., Some geometric aggregation operators based on picture fuzzy sets and their applicationin multiple attribute decision making , Italian journal of pure and applied mathematics, 37, 2017,477-492.
13. Nguyen Van Dinh and Nguyen Xuan Thao, Some Measures of Picture Fuzzy Sets and Their Application inMulti-attribute Decision Making, I.J. Mathematical Sciences and Computing, 3, 2018, 23-41.
14. Imanov G and Aliyev A, Circular Intuitionistic Fuzzy Sets in evaluation of human capital, Revista científica del instituto iberoamericano de desarrollo empresarial, 1, 2021.
15. .Zadeh.L. A, Fuzzy Sets, Information and Control, 8, 1965, 338-353.

Table1: Picture fuzzy decision matrix P

	S1	S2	S3	S4
R1	(0.2,0.3,0.1,0.4)	(0.7,0.1,0.1,0.1)	(0.1,0.2,0.6.0.1)	(0.4,0.1,0.2,0.3)
R2	(0.4,0.2,0.3,0.1)	(0.1,0.6,0.1,0.2)	(0.3,0.2,0.4,0.1)	(0.3,0.1,0.4,0.2)
R3	(0.2,0.5,0.1,0.2)	(0.6,0.1,0.1,0.2)	(0.5,0.1,0.2,0.2)	(0.5,0.1,0.3,0.1)
R4	(0.2,0.3,0.1,0.4)	(0.6,0.2,0.1,0.1)	(0.5,0.3.0.2,0)	(0.5,0,0.3,0.2)
R5	(0.7,0.2,0.2,0.1)	(0.4,0.1,0.2,0.1)	(0.7,0.1,0.2,0.1)	(0.3,0.1,0.2,0.1)

The information of the attribute weights are referred to as: w=(0.2,0.4,0.1,0.3)

Table 2. Comparison Analysis.

	Picture fuzzy values	Scores (PFS)	Scores (SPFS)
H1	(0.4398,0.1335,0.1989)	0.239	0.402
H2	(0.3027,0.2520,0.2722)	0.030	0.052
H3	(0.5201,0.1379,0.1751)	0.345	0.262
H4	(0.6324,0,0.1751)	0.457	0.761
H5	(0.437,0.115,0.20)	0.237	0.374

RESEARCH ARTICLE

Joint (α, β) – Quasi Normal Operators in Several Variables

Radharamani[1]* and N. Sathyavathi[2]

[1]Assistant Professor, Department of Mathematics, Chikkanna Govt. Arts College, Tirupur, Tamil Nadu, India
[2]Research Scholar, Department of Mathematics, Chikkanna Govt. Arts College, Tirupur, Tamil Nadu, India

*Address for Correspondence
Radharamani
Assistant Professor,
Department of Mathematics,
Chikkanna Govt. Arts College,
Tirupur, Tamil Nadu, India
E.Mail: radhabtk@gmail.com

ABSTRACT

In this work we focus our study on (α, β)-quasi normal operators by acting on a complex Hilbertspace H. When an operator $T \in B(H)$ is said to be (α, β)-quasi normal operator then $T[\alpha^2 T^*T] \leq [TT^*]T \leq T[\beta^2 T^*T]$ where $0 \leq \alpha \leq 1 \leq \beta$. We demonstrate that a joint (α, β) –quasi normal tuple is produced when an m-tuple of operators satisfying appropriate requirements is multiplied by a joint (α, β) - quasi normal tuple.

Mathematics Subject Classification: 47B20, 47B37 , 47B38.

Keywords: Operator, Hilbert space, Normal, (α, β) - quasi normal operator, joint (α, β)-quasi normal operator.

INTRODUCTION

In this paper, we will study some properties of joint (α, β) - quasi normal operators in several variables. Let H be a complex Hilbert space, an operator T is normal if TT*= T*T . This has been done by relaxing some conditions of normality and introducing classes such as (α,β) quasi normal operators. E - Rasoul, M . Farzollah and Ali Morassaei [9] presented the concept of(α,β) – Normal operators in Hilbert spaces. Throughout the paper, H denotes the usual Hilbert space over the complex field and the separable, infinite-dimensional B (H) Banach algebra of all bounded linear algebra in Hilbert space H. T is a normal operator for α=1=β and for α=1 we perceive from the left inequality

that T˙ is hyponormal and for β=1, from the right inequality we say that T is hyponormal. Moslehian has declared this class of operators as covered in [7].

Preliminaries

Let B(H) denote the Banach algebra of all bounded linear operators on a Complex Hilbert space H.

Definition 2.1
It is referred to as an operator T ∈ B(H) is said to be Normal if T˙T = TT˙

Definition 2.2
It is referred to as an operator T ∈ B(H) is said to be (α,β)- Normal if $\beta^2 T^* T \geq T\, T^* \geq \alpha^2 T^* T$

Joint (α, β) Quasi Normal Operators
Proposition 3.1
Let $T \in B(H)$ be (α, β) quasi normal. Then, $T = (T, \ldots\ldots, T) \in B(H)^m$ is joint (α, β) quasinormal. In point of fact, since T is (α, β) - quasi normal, it follows that
$T[\alpha^2 \langle Tx \,|\, Tx\rangle] \leq [\langle T^*x \,|\, T^*x\rangle]T \leq T[\beta^2 \langle Tx \,|\, Tx\rangle], \forall\ x \in H.$

Proof
Let $x_1, x_2, \ldots\ldots\ldots\ldots x_n \in$ H and for $x = \sum_{1 \leq i \leq m} x_i$, then we can write
$T[\beta^2 \langle T(\sum_{1 \leq i \leq m} x_i) \,|\, T(\sum_{1 \leq i \leq m} x_i)\rangle] - [\langle T^*(\sum_{1 \leq i \leq m} x_i) \,|\, T^*(\sum_{1 \leq i \leq m} x_i)\rangle]T \geq 0$ ----------(1)
$[\langle T^*(\sum_{1 \leq i \leq m} x_i) \,|\, T^*(\sum_{1 \leq i \leq m} x_i)\rangle]T - T[\alpha^2 \langle T(\sum_{1 \leq i \leq m} x_i) \,|\, T(\sum_{1 \leq i \leq m} x_i)\rangle] \geq 0$ ----------(2)
Then
$T[\beta^2 (\sum_{1 \leq i,j \leq m} \langle Tx_i \,|\, Tx_j\rangle)] - (\sum_{1 \leq i,j \leq m} \langle T^*x_i \,|\, T^*x_j\rangle)T \geq 0$ ----------(3)

$(\sum_{1 \leq i,j \leq m} \langle T^*x_i \,|\, T^*x_j\rangle)T - T[\alpha^2 (\sum_{1 \leq i,j \leq m} \langle Tx_i \,|\, Tx_j\rangle)] \geq 0$ ----------(4)
for $x_1, x_2 \ldots\ldots x_m \in H.$
Therefore, T is joint (α, β) – quasi normal.

Proposition 3.2
Let $T \in B(H)$ and consider $T = (T, \ldots\ldots, T) \in B(H)^m$. Then, T is joint (α, β) – quasinormal if and only if T is (α, β) - quasi normal.
Proof
Let T is (α, β) quasi normal and by proposition (2.1) we say that joint (α, β) – quasi normal.Conversely, assume that T is (α, β) – quasi normal. By known definition, it becomes

$T[\beta^2 (\sum_{1 \leq i,j \leq m} \langle Tx_i \,|\, Tx_j\rangle)] - (\sum_{1 \leq i,j \leq m} \langle T^*x_i \,|\, T^*x_j\rangle)T \geq 0$ -------------(5)

$(\sum_{1 \leq i,j \leq m} \langle T^*x_i \,|\, T^*x_j\rangle)T - T[\alpha^2 (\sum_{1 \leq i,j \leq m} \langle Tx_i \,|\, Tx_j\rangle)] \geq 0$ -------------(6)

for each $x_1, x_2 \ldots\ldots x_m \in H.$ In general, we get

$T[\beta^2 \langle Tx \,|\, Tx\rangle] - \langle T^*x \,|\, T^*x\rangle T \geq 0$ -------------(7)

and

$\langle T^*x \,|\, T^*x\rangle T - T[\alpha^2 \langle Tx \,|\, Tx\rangle] \geq 0$ -------------(8)

or equivalently

$T[\alpha^2 \langle Tx \,|\, Tx\rangle] \leq \langle T^*x \,|\, T^*x\rangle T \leq T[\beta^2 \langle Tx \,|\, Tx\rangle]$ -------------(9)

Therefore, T is (α, β) - quasi normal.

Theorem 3.3

Let T = (T$_1$,..........................,T$_m$) be m-tuple of operators on H and let $0 \leq \alpha \leq 1 \leq \beta$ and assume that

$$T[\beta^2 T_i^* T_j] - [T_j T_i^*]T = 0 \; for \; i \neq j$$

$$[T_j T_i^*]T - T[\alpha^2 T_i^* T_j] = 0 \; for \; i \neq j$$

Then, T=(T$_1$,.......,T$_m$) is joint (α, β) - quasi normal tuple iff each T_i is (α, β) - quasi normal for i=1,2,   m.

Proof
Let T = (T$_1$, ...,T$_m$) is joint (α, β) - quasi normal tuple iff

$$\begin{cases} T[\beta^2(T)] - [T^*]T \geq 0 \\ T[T^*] - T[\alpha^2[T] \geq 0 \end{cases} \qquad\qquad \text{------------(10)}$$

By applying (8),we get,

$$\Leftrightarrow \begin{cases} T[\beta^2 \left(\sum_{1 \leq k \leq m} \|T_k x\|^2 \right)] - \left(\sum_{1 \leq k \leq m} \|T_k^* x\|^2 \right)T] \\ \left(\sum_{1 \leq k \leq m} \|T_k^* x\|^2 \right)T - T[\alpha^2 \left(\sum_{1 \leq k \leq m} \|T_k x\|^2 \right)] \end{cases} \geq 0, \forall \; x \in H$$

$$\begin{cases} T[\beta^2(T)] - [T^*]T \geq 0 \\ T[T^*] - T[\alpha^2[T] \geq 0 \end{cases} \Leftrightarrow \begin{cases} [(\sum_{1 \leq k \leq m} T(\beta^2 \|T_k x\|^2) - \|T_k^* x\|^2 T)] \\ [\sum_{1 \leq k \leq m} (\|T_k^* x\|^2 T - T(\alpha^2 \|T_k x\|^2)] \end{cases} \geq 0, \forall \; x \in H$$

$$\Leftrightarrow \begin{cases} [(T(\beta^2 \|T_k x\|^2 - \|T_k^* x\|^2 T)] \\ [\|T_k^* x\|^2 T - T(\alpha^2 \|T_k x\|^2] \end{cases} \geq 0, \forall \; x \in H$$

Therefore, T_k is (α, β) - quasi normal for k = 1,2,...............................m.

Theorem 3.4

Let T = (T$_1$,.......,T$_m$) $\in B(H)^m$ and let $(\alpha, \beta) \in R^2$ such that $0 \leq \alpha \leq 1 \leq \beta$. If

$T_i T_j^* = 0$ for all i≠ j , then T is joint (α, β)- quasi normal if and only if $T^* = (T_1^*,............T_m^*)$ is joint $(1/\beta , 1/\alpha)$ quasi normal.

Proof

Assume that T is joint (α, β) quasi normal and we have to prove that T^* is joint

$(1/\beta , 1/\alpha)$ quasi normal

Radharamani and Sathyavathi

Consider

$$T[\alpha^2(\sum_{1\leq k\leq m}\|T_k x\|^2)] \leq (\sum_{1\leq k\leq m}\|T_k^* x\|^2)T \leq T[\beta^2(\sum_{1\leq k\leq m}\|T_k x\|^2)]\forall\ x \in H \text{ ------(10)}$$

Then (10) becomes

$$T[\frac{1}{\beta^2}(\sum_{1\leq k\leq m}\|T_k x\|^2)] \leq (\sum_{1\leq k\leq m}\|T_k^* x\|^2)T \leq T[\frac{1}{\alpha^2}(\sum_{1\leq k\leq m}\|T_k x\|^2)]\forall\ x \in H \text{ ------(11)}$$

Hence, T^* is joint $(1/\beta,\ 1/\alpha)$ quasi normal tuble and conversely let T^* is joint $(1/\beta,\ 1/\alpha)$ quasi normal tuble, we have

$$T[\frac{1}{\beta^2}(\sum_{1\leq k\leq m}\|T_k x\|^2)] \leq (\sum_{1\leq k\leq m}\|T_k^* x\|^2)T \leq T[\frac{1}{\alpha^2}(\sum_{1\leq k\leq m}\|T_k x\|^2)]\forall\ x \in H \text{ ------(12)}$$

which means that

$$T[\alpha^2(\sum_{1\leq k\leq m}\|T_k x\|^2)] \leq (\sum_{1\leq k\leq m}\|T_k^* x\|^2)T \leq T[\beta^2(\sum_{1\leq k\leq m}\|T_k x\|^2)]\forall\ x \in H \text{ ------(13)}$$

Therefore, T is joint (α,β) quasi normal tuble.

Example 3.5

Let $A=\begin{pmatrix}0 & 1 \\ 1 & 1\end{pmatrix}$, $B=\begin{pmatrix}0 & -1 \\ -1 & 0\end{pmatrix}$ which are $(\alpha,\ \beta)$-quasi normal operators and their product

$\begin{pmatrix}-1 & 0 \\ -1 & -1\end{pmatrix}$ is not $(\alpha,\ \beta)$-quasi normal operator.

The above example proves that, by proposition 3.2 even if A and B are joint (α,β)- quasi normal operators, their product AB is not joint (α,β)-quasi normal operator.

CONCLUSION

We defined as the idea on joint (α,β)-Quasi normal operators in several variables are relatively new. We attempted to prove some properties of joint (α,β)-Quasi normal operators in several variables in complex Hilbert space. The results of this paper will be accessible for further research to develop application side of Functional Analysis.

REFERENCES

1. A.Athavale 1988. "On joint hyponormality of operators, Proceedings of the American Mathematical Society". vol.103 :no.2 pp.417-423.
2. Bakiouti H, Feki K, and O.A.M Sid Ahmed Mahmoud, "Joint normality of operators in semi – Hildertian spaces"., *Linear and Multilinear Algebra.*, Vol .,68., No.4.,pp.,845- 866,2020.
3. Bachir A , Prasad T., Fuglede Putnam theorem forgeries., "(α,β)-normal operators"., *Rendiconti del Circolo Mathematico di Palermo* S Vol.,69.,No.3.,pp.,1243-1249.,2020
4. Dragomir, S.S. Moslehian, M.S. 2008. "Some inequalities for (α,β)-normal operators in Hilbert spaces". *Series Mathematics and Informatics*": pp. 39-47
5. Douglas, R.G. 1966. "On majorization, factorization and range inclusion of operators on Hilbert spaces". *Proc.Am.Math.*Soc.17: 413-415.
6. Gupta A , Sharma P., (α,β) Normal composition operators., *Thai Journal of Mathematics.*, vol.,14.,no.1.,pp.,83-92.,2016
7. Moslehian. M.S. 2007. "On (α,β)-normal operators in Hilbert spaces". *Problem IMAGE*: pp. 39-47

8. Senthilkumar D,S. M. Sherin Joy. 2012. "On totally (α, β)-normal operators" *Far East Journal of Mathematical Sciences*(1) "

9. E. Rasoul, M. Farzollah and Ali Morassaei, "More on (α,β)-Normal operators in Hilbert spaces, Abstract and Applied Analysis", 2012(2012).

10. Stamofli J.G., "Hyponormal operators Pac"., *Journal of Mathematics.*, Vol.,12.,No . 4., pp., 1453 – 1458.,1962.

11. Sid Ahmed Ould Ahmed Mahmoud, Ahmed Himadan Ahmed and Ahmad Sarosh., "(α, β)-normal operators in several variables"., Volume 2022,Article ID 3020449.

12. E. Rasoul, M. Farzollah and Ali Morassaei,"More on (α,β)-Normal operators in Hilbert spaces", *Abstract and Applied Analysis*, 2012(2012).

13. K. Vidhyapraba , A. Sivasathya and V. Vimala.,"Some Properties of Quasi Normal Operators"., *International Journal of Sci Research and Management.*, 02(12)(2014)., 1811-1814.

RESEARCH ARTICLE

A Novel Simplex Technique to Solve the Linear Fractional Programming Problem using the Trapezoidal Fuzzy Neutrosophic Number

P.Rajarajeswari [1*] and M.Shyamala[2]

[1]Department of Mathematics, Chikkanna Government Arts College, Tirupur- 641602, Tamil Nadu, India
[2]Department of Mathematics, VLB Janakiammal College of Arts and Science,Coimbatore-641042, Tamil Nadu, India

*Address for Correspondence
P.Rajarajeswari
Department of Mathematics,
Chikkanna Government Arts College,
Tirupur- 641602, Tamil Nadu, India
E.Mail: p.rajarajeswari29@gmail.com

ABSTRACT

In many real time applications such as planning, production, inventory and in other domains, the decision makers plays an important role. Trapezoidal Fuzzy Neutrosophic Number (TFNN) has an major role to measure the vagueness and uncertainty data of real life. In this research work, we presented a new method for solving Linear fractional programming problem (LFPP) using simplex method technique and a ranking function of TFNN. In LFPP, the coefficients of the objective function and constraints were represented as TFNN .Further, numerical examples were illustrated to make   a comparative study with the existing methods. Finally, we observe that our proposed methodology gives the most optimized solution than the existing methods.

Keywords - Fuzzy numbers, Neutrosophic Number, Trapezoidal Fuzzy Neutrosophic Number and Linear Programming Problem.

INTRODUCTION

Linear fractional programming problem (LFPP) is represented as the ratio of two linear functions namely real cost/standard cost, inventory/sale and other ratios which measure the efficiency of the LFPP. In real time applications, the decision makers may find it difficult to make decisions due to incomplete and obscure information. In such cases, LFPP is a major focus of several researchers due to its application in various fields namely traffic planning, production planning, financial planning, game theory , hospital and health care planning .Isbell and Marlow [5]   introduced a methodology for solving a LFPP by using a sequence of linear programming

problem[LPP].Charnes and Cooper [3] have proposed a variable transformation method for solving LFPP. Later on,Swarup[11] solved the LFPP using different types of solution procedures based on the simplex method developed by Danzig where as Bitran and Novas [2] have solved the LFPP by computing the generalization of the derivative to multivariate functions of objective functions.Fuzzy linear fractional programming problem is generalization of the LFPP with fuzzy number. Neutrosophic number is the major focus of several researchers due to its scope in various research domains. Hence, researchers have developed many novel methods to solve LFPP using neutrosophic and different types of fuzzy concepts. Smarandache[10] introduced the neutrosophic set to handle incomplete, uncertainty and indeterminacy. Later on,Abdel-Basset[1] have introduced a method for solving the fully neutrosophic linear programming problems. Sapan Kumar Das et.al.,[9] have developed an intelligent dual simplex technique to solve LFPP by considering all the coefficients of the objective function and constraints as triangular neutrosophic number except the decision variables. Rasha Jalal Mitlif [8] developed an efficient method for solving fuzzy linear fractional programming problem through ranking function with triangular fuzzy number in their work and included few examples to prove the advantage of their method. Elhadidi et.al.,[4] introduced a ranking function for solving LFPP with trapezoidal neutrosophic number.In this paper, we have introduced a new method by combining TFNN and simplex method technique for solving LFPP.

PRELIMINARIES
The basic terminologies involving Trapezoidal Fuzzy Neutrosophic Number and Score Function are outlined in this section.

Definition 2.1: Trapezoidal Fuzzy Neutrosophic Number [6]
If $T_{\tilde{a}}, I_{\tilde{a}}, F_{\tilde{a}} \in [0,1]$ and $e_1, e_2, e_3, e_4 \in$ R   such that $e_1 \leq e_2 \leq e_3 \leq e_4$ then   we define Trapezoidal Fuzzy Neutrosophic   Number by $\tilde{a} = \langle (e_1, e_2, e_3, e_4) ; T_{\tilde{a}}, I_{\tilde{a}}, F_{\tilde{a}} \rangle$ whose truth-membership ($T_{\tilde{a}}$) , indeterminacy-membership ($I_{\tilde{a}}$) and falsity-membership($F_{\tilde{a}}$) functions are given as follows.

$$\mu(x) = \begin{cases} \frac{(x-e_1)\,T_{\tilde{a}}}{e_2-e_1}, & e_1 \leq x \leq e_2 \\ T_{\tilde{a}} & , \; e_2 \leq x \leq e_3 \\ \frac{(e_4-x)T_{\tilde{a}}}{e_4-e_3} & , e_3 \leq x \leq e_4 \\ 0, & Otherwise \end{cases}$$

$$\Theta(x) = \begin{cases} \frac{e_2-x+(x-e_1)I_{\tilde{a}}}{e_2-e_1}, & e_1 \leq x \leq e_2 \\ I_{\tilde{a}} & , \; e_2 \leq x \leq e_3 \\ \frac{x-e_3+(e_4-x)I_{\tilde{a}}}{e_4-e_3}, & e_3 \leq x \leq e_4 \\ 1 & otherwise \end{cases}$$

$$\lambda(x) = \begin{cases} \frac{(e_2-x)+(x-e_1)\,F_{\tilde{a}}}{e_2-e_1}, & e_1 \leq x \leq e_2 \\ F_{\tilde{a}} & , \; e_2 \leq x \leq e_3 \\ \frac{x-e_3+(e_4-x)\,F_{\tilde{a}}}{e_4-e_3}, & e_3 \leq x \leq e_4 \\ 1 & otherwise \end{cases}$$

Definition 2.2 : Score Function [6]
Let $\tilde{a} = \langle (e_1, e_2, e_3, e_4) ; T_{\tilde{a}}, I_{\tilde{a}}, F_{\tilde{a}} \rangle$ be the Trapezoidal Fuzzy Neutrosophic Number then the special ranking of TFNN   named Score Function is given by
S ($\tilde{a}$) = $\frac{1}{16}$ $(e_1 + e_2 + e_3 + e_4)\left(T_{\tilde{a}} + (1 - I_{\tilde{a}}) + (1 - F_{\tilde{a}})\right)$

Proposed method for solving LFPP
In this paper ,we introduce an intelligent method for solving the LFPP in which the coefficients of the objective function and the constraints are TFNN except the decision variables.

Let us consider the LFPP as follows.

Max (or)Min $z(x) = \frac{z_1(x)}{z_2(x)}$ s.t $x \, \varepsilon T$ (1)

where the objective functions $z_1(x)$ and $z_2(x)$ are the two linear functions and the set T is defined as T = $\{x/Ax \le B, x > 0\}$. Here A is a fuzzy matrix.

Step 1: We consider the general form of LFPP with m constraints and n variables which is represented as

$$\text{Max(or)Min} z(x) = \frac{\sum_{j=1}^{n} c_j \, x_j + \alpha}{\sum_{j=1}^{n} d_j \, x_j + \beta}$$

$$\text{s.t} \quad \sum_{i=1}^{m} a_{ij} \, x_j \le b_i$$

$$x_j \ge 0 \quad where \quad j = 1,2,\ldots,n. \tag{2}$$

Step 2: In the above LFPP, we represent all the coefficients in the objective function and the constraints as TFNN like below

$$\text{Max(or)Min } z(x) = \frac{\sum_{j=1}^{n}(b_j, d_j, e_j, f_j; T_{c_j}, I_{c_j}, F_{c_j}) \, x_j + (\alpha_1, \alpha_2, \alpha_3, \alpha_4; \; T_\alpha, I_\alpha, F_\alpha)}{\sum_{j=1}^{n}(c_j, e_j, f_j, g_j; T_{d_j}, I_{d_j}, F_{d_j}) \, x_j + (\beta_1, \beta_2, \beta_3, \beta_4; \; T_\beta, I_\beta, F_\beta)}$$

Subject to

$$\sum_{i=1}^{m}\left(b_{ij}, c_{ij}, d_{ij}, e_{ij}; \; T_{a_{ij}}, I_{a_{ij}}, F_{a_{ij}}\right) x_j \le \left(p_i, q_i, r_i, s_i; T_{b_i}, I_{b_i}, F_{b_i}\right).$$

$$x_j \ge 0 , \; j = 1,2,\ldots,n.$$

We proposed a novel methodology for solving LFPP by using TFNN with a idea of Simplex Method.The following algorithm explains the proposed methodology.

Step 3: In the above LFPP, we decompose the objective function into two LPPs as below.

(P-1)

Max (or)Min $z_1(x) = \sum_{j=1}^{n}(b_j, d_j, e_j, f_j; T_{c_j}, I_{c_j}, F_{c_j}) \, x_j + (\alpha_1, \alpha_2, \alpha_3, \alpha_4; \; T_\alpha, I_\alpha, F_\alpha)$

s.t $\sum_{i=1}^{m}\left(b_{ij}, c_{ij}, d_{ij}, e_{ij}; \; T_{a_{ij}}, I_{a_{ij}}, F_{a_{ij}}\right) x_j \le \left(p_i, q_i, r_i, s_i; T_{b_i}, I_{b_i}, F_{b_i}\right).$

$$x_j \ge 0 \quad where \quad j = 1,2,\ldots,n.$$

(P-2)

Max (or)Min $z_2(x) = \sum_{j=1}^{n}(c_j, e_j, f_j, g_j; T_{d_j}, I_{d_j}, F_{d_j}) \, x_j + (\beta_1, \beta_2, \beta_3, \beta_4; \; T_\beta, I_\beta, F_\beta)$

s.t $\sum_{i=1}^{m}\left(b_{ij}, c_{ij}, d_{ij}, e_{ij}; \; T_{a_{ij}}, I_{a_{ij}}, F_{a_{ij}}\right) x_j \le \left(p_i, q_i, r_i, s_i; T_{b_i}, I_{b_i}, F_{b_i}\right).$

$$x_j \ge 0 \quad where \quad j = 1,2,\ldots,n.$$

Step 4: Using the definition 2.2 in above LPP given in (P-1) and (P-2) ,we get the modified LPPs as below

(P-3)

Max (or)Min $z_1(x) = \sum_{j=1}^{n} S\left(b_j, d_j, e_j, f_j; T_{c_j}, I_{c_j}, F_{c_j}\right) x_j + S(\alpha_1, \alpha_2, \alpha_3, \alpha_4; \; T_\alpha, I_\alpha, F_\alpha)$

s.t $\sum_{i=1}^{m} S\left(b_{ij}, c_{ij}, d_{ij}, e_{ij}; \; T_{a_{ij}}, I_{a_{ij}}, F_{a_{ij}}\right) x_j + S(p_i, q_i, r_i, s_i; T_{b_i}, I_{b_i}, F_{b_i})$

$$x_j \ge 0 \quad where \quad j = 1,2,\ldots,n.$$

(P-4)

Max (or) Min $z_2(x) = \sum_{j=1}^{n} S\left(c_j, e_j, f_j, g_j; T_{d_j}, I_{d_j}, F_{d_j}\right) x_j + S(\beta_1, \beta_2, \beta_3, \beta_4; \; T_\beta, I_\beta, F_\beta)$

s.t $\sum_{i=1}^{m} S\left(b_{ij}, c_{ij}, d_{ij}, e_{ij}; \; T_{a_{ij}}, I_{a_{ij}}, F_{a_{ij}}\right) x_j + S(p_i, q_i, r_i, s_i; T_{b_i}, I_{b_i}, F_{b_i})$

$$x_j \ge 0 \quad where \quad j = 1,2,\ldots,n.$$

Step 5: By solving the above LPP given in (P-3) and (P-4) by Simplex Method to get the optimal solutions namely $z_1(x)$ and $z_2(x)$.

Step 6: The optimal solution of the given LFPP is got by using the formula below

Max Z(x) $= \frac{z_2(x)}{z_1(x)}$ and Min Z(x) $= \frac{z_1(x)}{z_2(x)}$

If the objective function is of minimization type then convert it into maximization type by using the formula Max Z(x)= - Min Z(x)

Application of proposed method
Numerical Example 3.1:

Here we illustrate a numerical example in the field of Production of Casting Company

A casting company in coimbatore produces two kinds of products namely Grey Iron and S.G .Iron with profits around 8 rupees   and 18 rupees per product respectively. However, the cost of the 100 grams of Grey Iron is around Rs.16 and cost of 100 grams of S.G .Iron is around Rs.18 .It is assumed that a fixed cost of Rs.12 is added to the cost function for the process of production. Suppose the raw materials needed for manufacturing the products Grey Iron and S.G.Iron are about Rs.64 per Kg and Rs.82 per Kg respectively, then the supply for the raw material is restricted to Rs.95. Product Grey Iron requires 8 hours per Kg of processing time and Product S.G.Iron requires 10 hour per kg of processing time ,but total time available is about 22 hours daily. Determine , how many Kg's of Grey Iron and S.G. Iron should be manufactured in order to maximize the total profit.

Solution: Let X_1 and X_2 denote the number of units of two kinds of products produced namely Grey Iron and S.G .Iron.

Step 1: Formulating the above as the LFPP ,we get

Max Z(x) = $\frac{8 X_1 + 18 X_2}{16 X_1 + 18 X_2 + 12}$ (3)

Subject to

$64 X_1 + 82 X_2 \le 95$, $8 X_1 + 10 X_2 \le 22$, $X_1, X_2 \ge 0$

Step 2: We have represented all the coefficients used in objective function and the constraints as TFNN like below

Max Z(x) = $\frac{(1,6,10,13;0.9,0.1,0.3)X_1 + (11,16,20,23;0.9,0.1,0.3)X_2}{(5,15,25,30;0.7,0.5,0.6)X_1 + (11,16,20,23;0.9,0.1,0.3)X_2 + (4,8,17,25;0.3,0.6,0.4)}$

s.t.

$(60,62,64,66;0.2,0.5,0.6)X_1 + (80,82,85,86;0.3,0.6,0.4) X_2 \le (92,94,97,100;0.8,0.2,0.4)$

$(1,6,10,13;0.9,0.1,0.3)X_1 + (1,6,11,15;0.7,0.6,0.3) X_2 \le (16,18,22,23;0.3,0.6,0.4)$ and $X_1, X_2 \ge 0$

Step 3: In the above LFPP, we decompose the objective function into two LPPs as follows.

(P-1)

Max $z_1(x)$ = $(1,6,10,13;0.9,0.1,0.3)X_1 + (11,16,20,23;0.9,0.1,0.3)X_2$

s.t.

$(60,62,64,66;0.2,0.5,0.6) X_1 + (80,82,85,86;0.3,0.6,0.4) X_2 \le (92,94,97,100;0.8,0.2,0.4)$

$(1,6,10,13;0.9,0.1,0.3) X_1 + (1,6,11,15;0.7,0.6,0.3) X_2 \le (16,18,22,23;0.3,0.6,0.4)$

 and $X_1, X_2 \ge 0$

(P-2)

                Max $z_2(x)$ = $(5,15,25,30;0.7,0.5,0.6)X_1 + (11,16,20,23;0.9,0.1,0.3)X_2 + (4,8,17,25;0.3,0.6,0.4)$

s.t.

$(60,62,64,66;0.2,0.5,0.6) X_1 + (80,82,85,86;0.3,0.6,0.4) X_2 \le (92,94,97,100;0.8,0.2,0.4)$

$(1,6,10,13;0.9,0.1,0.3) X_1 + (1,6,11,15;0.7,0.6,0.3) X_2 \le (16,18,22,23;0.3,0.6,0.4)$ and $X_1, X_2 \ge 0$

Step 4: The crisp value of each TFNN is calculated using definition 2.2

$S(\widetilde{8})$ = 4.68, $S(\widetilde{10})$ =3.71, $S(\widetilde{12})$ = 4.39 , $S(\widetilde{16})$=7.5 , $S(\widetilde{18})$ = 10.94,

$S(\widetilde{22})$ = 6.42, $S(\widetilde{64})$ =17.33 , $S(\widetilde{82})$ =18.73 , $S(\widetilde{95})$ =52.66

By substituting the crisp values in (P- 1) and (P- 2), we get the modified LPPs as follows

(P- 3)

Max $z_1(x)$ = (4.68) X_1 + (10.94) X_2

s.t $17.33 X_1 + 18.73 X_2 \le 52.66$, $4.68 X_1 + 3.71 X_2 \le 6.42$ and $X_1, X_2 \ge 0$

(P-4)

Max $z_2(x)$ = $7.5 X_1 + 10.94 X_2 + 4.39$

s.t $17.33X_1 + 18.35 X_2 \leq 52.66$, $4.68X_1 + 3.71X_2 \leq 6.42$ and $X_1, X_2 \geq 0$

Step 5: Solving (P-3) and (P-4) by using simplex method, we get Max $z_1(x) = 18.93$ where $X_1 = 0, X_2 = 1.73$ and Max $z_2(x)$ = 23.32 where $X_1 = 0$, $X_2 = 1.73$.

Step 6: The optimum solution of the LFPP is got by applying the below formula

Max $Z = \frac{z_2}{z_1} = \frac{23.32}{18.93}$ $= 1.23$

Numerical Example3.2 [12]:

Let us consider the problem solved by Sumon Kumar Saha et.al.,[12] in Section 4, Example 1

Step 1 : Consider the LFPP

Min $Z(x) = \frac{-2X_1 + X_2 + 2}{X_1 + 3X_2 + 4}$ (4)

   s.t $-X_1 + X_2 \leq 4$, $2 X_1 + X_2 \leq 14$, $X_2 \leq 6$ and $X_1, X_2 \geq 0$

Step 2: We represent the coefficients used in the objective function and the constraint's as   TFNN like below

$$\text{Min } Z(x) = \frac{-(1,3,5,6; 0.2,0.3,0.5)x_1 + (0,2,4,5; 0.8,0.6,0.4)x_2 + (1,3,5,6; 0.2,0.3,0.5)}{(0,2,4,5; 0.8,0.6,0.4)x_1 + (1,2,5,6; 0.2,0.5,0.6)x_2 + (1,2,5,7; 0.5,0.4,0.9)}$$

s.t.

$-(0,2,4,5; 0.8,0.6,0.4) X_1 + (0,2,4,5; 0.8, 0.6, 0.4) X_2 \leq (1,2,5,7; 0.5,0.4,0.9)$

$(1,3,5,6; 0.2,0.3,0.5) X_1 + (0,2,4,5; 0.8, 0.6, 0.4) X_2 \leq (7,10,19,30; 0.8,0.4,0.7)$

$(0,2,4,5; 0.8, 0.6, 0.4) X_2 \leq (3,7,9,12; 0.7,0.2,0.5)$ and $X_1, X_2 \geq 0$

Step 3: In the above LFPP, we decompose the objective function into two LPPs as follows.

(P-1)

Min $z_1(x) = -(1,3,5,6; 0.2,0.3,0.5)x_1 + (0,2,4,5; 0.8,0.6,0.4)x_2 + (1,3,5,6; 0.2,0.3,0.5)$

   s.t.

$-(0,2,4,5; 0.8,0.6,0.4) X_1 + (0,2,4,5; 0.8, 0.6, 0.4) X_2 \leq (1,2,5,7; 0.5,0.4,0.9)$

$(1,3,5,6; 0.2,0.3,0.5) X_1 + (0,2,4,5; 0.8, 0.6, 0.4) X_2 \leq (7,10,19,30; 0.8,0.4,0.7)$

$(0,2,4,5; 0.8, 0.6, 0.4) X_2 \leq (3,7,9,12; 0.7,0.2,0.5)$ and $X_1, X_2 \geq 0$

(P-2)

Min $z_2(x) = (0,2,4,5; 0.8,0.6, 0.4)x_1 + (1,2,5,6; 0.2,0.5,0.6)x_2 + (1,2,5,7; 0.5,0.4,0.9)$

   s.t.

$-(0,2,4,5; 0.8,0.6,0.4) X_1 + (0,2,4,5; 0.8, 0.6, 0.4) X_2 \leq (1,2,5,7; 0.5,0.4,0.9)$

$(1,3,5,6; 0.2,0.3,0.5) X_1 + (0,2,4,5; 0.8, 0.6, 0.4) X_2 \leq (7,10,19,30; 0.8,0.4,0.7)$

$(0,2,4,5; 0.8, 0.6, 0.4) X_2 \leq (3,7,9,12; 0.7,0.2,0.5)$ and $X_1, X_2 \geq 0$

Step 4: The crisp value of each TFNN is calculated using definition 2.2

$S(\tilde{1}) = 1.24$, $S(\tilde{2}) = 1.31$, $S(\tilde{3}) = 0.96$, $S(\tilde{4}) = 1.12$, $S(\tilde{6}) = 3.87$, $S(\widetilde{14}) = 7.01$

By substituting the crisp values in (P- 1) and (P- 2), we get the modified LPPs as follows

 (P-3)

Min $z_1(x) = -(1.31) X_1 + (1.24) X_2 + 1.31$

s.t $-(1.24) X_1 + (1.24) X_2 \leq 1.12$, $(1.31) X_1 + (1.24) X_2 \leq 7.01$, $(1.24) X_2 \leq 3.87$ and $X_1, X_2 \geq 0$

(P-4)

Min $z_2(x) = (1.24) X_1 + 0.96 X_2 + 1.12$

s.t $-(1.24) X_1 + (1.24) X_2 \leq 1.12$, $(1.31) X_1 + (1.24) X_2 \leq 7.01$, $(1.24) X_2 \leq 3.87$ and $X_1, X_2 \geq 0$.

Step 5: Solving (P-3) and (P-4) by simplex method ,we get Min $z_1(x)$ = -5.70 where X_1=5.35, X_2=0 and Min $z_2(x)$ =1.12 where X_1=0, X_2=0.

Step 6: The optimum solution of the LFPP is got by applying the below formula

Min Z(x) = $\frac{Z_1(x)}{Z_2(x)}$ = $\frac{-5.70}{1.12}$ =-5.09 and   Max Z(x) = - Min [Z(x)]=-[-5.09]=5.09

We observe that the same problem given in Numerical Example 3.2 was solved by Sumon Kumar Saha et.al.,[12] in the Section 4 ,Example 1 and they got the solution as Min Z(x)=-1.09 but the same problem solved by proposed method and gives the solution as Min Z(x)=-5.09.This shows that our proposed method gives the most optimal solution.

Numerical Example 3.3[9]:
Let us consider the problem solved by Sapan kumar Das et.al.,[9] in Section 4.

Step 1: Consider the LFPP

Max Z(x) = $\frac{8X_1+7X_2+9X_3}{8X_1+9X_2+6X_3+1.5}$ (5)

S.t $4X_1 + 3X_2+5X_3 \leq 28$, $5X_1 + 3X_2+3X_3 \leq 20$ and $X_1,X_2,X_3 \geq 0$

Step 2: We represent the coefficients used in the objective function and the constraint's as   TFNN like below

Max Z= $\frac{(1,6,10,13;0.9,0.1,0.3)\,X_1+\,(5,8,9,13;0.4,0.6,0.8)X_2+\,(6,8,10,15;0.6,0.4,0.7)X_3}{(1,6,10,13;0.9,0.1,0.3)X_1+\,(6,8,10,15;0.6,0.4,0.7)X_2+(3,7,9,12;0.7,0.2,0.5)X_3+(0.5,1,1.5,2;0.75,0.5,0.25)}$

s.t.

$(1,2,5,7; 0.5, 0.4, 0.9)\,X_1 + (1,2,5,6; 0.2, 0.5, 0.6)\,X_2+ (2,4,7,10; 0.8, 0.2, 0.4)\,X_3 \leq (24,26,28,30; 0.4, 0.25, 0.5)$

$(2,4,7,10; 0.8, 0.2, 0.4)\,X_1 + (1,2,5,6; 0.2, 0.5, 0.6)\,X_2+(1,2,5,6; 0.2, 0.5, 0.6)\,X_3 \leq (10,12,27,30; 0.2, 0.3, 0.5)$

$X_1, X_2, X_3 \geq 0$

Step 3: In the above LFPP,we decompose the objective function into two LPP as follows.

(P-1)

Max $z_1(x)$ = $(1,6,10,13;0.9,0.1,0.3)X_1 + (5,8,9,13;0.4,0.6,0.8)X_2 + (6,8,10,15,0.6,0.4,0.7)X_3$

s.t.

$(1,2,5,7; 0.5, 0.4, 0.9)\,X_1 + (1,2,5,6; 0.2, 0.5, 0.6) +X_2\ (2,4,7,10; 0.8, 0.2, 0.4)\,X_3 \leq (24,26,28,30; 0.4, 0.25, 0.5)$

$(2,4,7,10; 0.8, 0.2, 0.4)\,X_1 + (1,2,5,6; 0.2, 0.5, 0.6)\,X_2+(1,2,5,6; 0.2, 0.5, 0.6)\,X_3 \leq (10,12,27,30; 0.2, 0.3, 0.5)$

$X_1, X_2, X_3 \geq 0$

(P-2)

Max $z_2(x)$ = $(1,6,10,13;0.9,0.1,0.3)X_1 + (6,8,10,15;0.6,0.4,0.7)X_2 + (3,7,9,12;0.7,0.2,0.5)X_3$
     $+ (0.5,1,1.5,2;0.75,0.5,0.25)$

s.t $(1,2,5,7; 0.5, 0.4, 0.9)\,X_1 + (1,2,5,6; 0.2, 0.5, 0.6)\,X_2+ (2,4,7,10; 0.8, 0.2, 0.4)\,X_3 \leq (24,26,28,30; 0.4, 0.25, 0.5)$

     $(2,4,7,10; 0.8, 0.2, 0.4)\,X_1 + (1,2,5,6; 0.2, 0.5, 0.6)\,X_2+(1,2,5,6; 0.2, 0.5, 0.6)X_3 \leq (10,12,27,30; 0.2, 0.3, 0.5)$

     $X_1, X_2, X_3 \geq 0$

Step 4: The crisp value of each TFNN is calculated using definition 2.2

 S($\tilde{3}$) = 0.96 , S ($\tilde{4}$) =1.13 , S ($\tilde{5}$) = 3.16, S ($\tilde{6}$) = 3.88, S ($\tilde{7}$) = = 2.19, S ($\tilde{8}$) = 4.69, S ($\widetilde{1.5}$) = 0.63,   S($\widetilde{20}$) = 6.91 ,S ($\widetilde{28}$) = 11.14

By substituting the crisp values in (P- 1) and (P- 2), we get the modified LPPs as follows

(P-3)

Max $z_1(x)$ = $4.69X_1$ + $2.19 X_2$ + $3.66 X_3$

s.t $1.13X_1 + 0.96 X_2 + 3.16 X_3 \leq 11.14$, $3.16X_1 + 0.96X_2 + 0.96 X_3 \leq 6.91$ and $X_1, X_2, X_3 \geq 0$

(P- 4)

Max $z_2(x)$ = $4.69 X_1$ + $3.66 X_2$ + $3.88X_3$ + 0.63

s.t $1.13 X_1 + 0.96X_2 + 3.16X_3 \leq 11.14$, $3.16 X_1 + 0.96X_2 + 0.96X_3 \leq 6.91$

   and $X_1, X_2, X_3 \geq 0$

Step 5 : Solving (P-3) and (P-4) by simplex method ,we get Max $z_1(x)$=18.59 where X_1 =0, X_2 =5.28, X_3 = 1.92 and Max Z_2(x) =27.4 where X_1 =0, X_2=5.28, X_3 = 1.92.

Step 6: The optimum solution of the LFPP is got by applying the below formula

Max Z = $\frac{z_2(x)}{z_1(x)}$ = $\frac{27.4}{18.59}$ = 1.47

We observe that the same problem given in Numerical Example 3.3 was solved by Sapan kumar Das et.al.,[9] using Triangular Neutrosophic Number and they got the solution as Max Z=1.16 but the same problem solved by our proposed method gives the solution as Max Z=1.47.We observe that the proposed method gives the best optimal solution.

RESULTS AND DISCUSSION

We have developed a new method for solving LFPP using TFNN and made its intensive studies. The various optimal solutions obtained for the LFPP by using Triangular Neutrosophic Number and TFNN are shown in the comparison table and a multiple bar diagram is shown to prove the stability of the proposed method.We conclude that the optimal solution obtained by the proposed method using TFNN gives the most optimized value than the existing one.

A Multiple Bar Diagram is shown below to visualize the optimal solutions obtained by the proposed methods with some of the existing methods.

CONCLUSION

 In this paper, a new ranking method for solving LFPP by combining TFNN with simplex method was introduced. A real time application of proposed method   has been taken to prove the advantage ,stability and accuracy of proposed method.By comparing and analyzing the optimal solutions arrived ,we conclude that   our proposed method gives the most higher optimal solution and it is better than the existing techniques. In future, researchers can extend this technique with some different score function and ranking function to convert TFNN into a crisp value which will be helpful in the field of science and technology.

Conflicts of Interest:

The authors declare that they have no conflicts of interest.

Authors Contribution

All authors contributed equally to this work and read and approved the final version of the manual script.

REFERENCES

1. M.Abdel-Bas set,M.Gunasekaran, M.Mohamed & F.Smarandache ,A novel method forsolving the fully neutrosophic linear programming problems,Neural Computing and Applications ,2019,31,1595-1605.
2. Bitran G.R.andNovaes A.G., Linear programming with a fractional objective function,   Journal of operation research,vol.21, p.22-29, (1973).
3. A.Charnes and W.W.Cooper, An explicit general solution in linear fractional programming, Naval Research Logistics, vol.20, no. 3, pp. 449–467, 1973.
4. A.M.Elhadidi,O.E.Emam ,A.M.Abdelfadel and Mansour Lotayij,. Linear Fractional Programming based on Trapezoidal Neutrosophic Numbers.
5. J. Isbell and W. Marlow, Attrition games. Naval Research Logistics Quarterly, 3 (1956) 71–94
6. Mai Mohamed,Mohamed Abdel-Basset,Abdel-Nasser Hussien,Florentin Smarandache, Using Neutrosophic Sets to obtain PERT Three –Times Estimates in Project Management, June 2016
7. Palash Dutta and Gourangajit Borah ,Multicriteria group decision making via generalized trapezoidal intuitionistic fuzzy number-based novel similarity measure and its application to diverse COVID- 19 scenarios, Springer Nature B.V. 2022 ,7 September 2022.
8. Rasha Jalal Mitlif ,An Efficient Algorithm for Fuzzy Linear Fractional Programming Problems via Ranking Function,Baghdad Science Journal 2022,19(1):71-76,Feb 2022.
9. Sapan Kumar Das, S.A.Edalatpanah, J.K.Dash, Paper's title ,An intelligent Dual Simplex Method to solve Triangular Neutrosophic Linear Fractional Programming Problem ,University of Mexico,2020.
10. F.Smarandache, *AUnifying Field in Logics: Neutrosophic Logic. Neutrosophy, Neutrosophic Set, Neutrosophic Probability and Statistics*, InfoLearnQuest. Philadelphia, PA, USA, 6th edition, 2007. Smarandach.
11. Swarup, K. (1964) Linear Fractional Functional Programming. Operations Research, 13,   1029-1036.http://dx.doi.org/10.1287/opre.13.6.1029
12. Sumon Kumar Saha,Md.Rezwan Hossain ,Md.Kutub Uddin ,Rabindra Nath Mondal,A New Approach of Solving Linear Fractional Programming problem (LFP) by using Computer Algorithm.

Table 1. Optimal Value

Particulars	Optimal Value for Numerical Example 3.1	Optimal Value for Numerical Example3. 2	Optimal Value for Numerical Example 3.3
Linear fractional programming problem[LFPP]	Max Z=0.63	Min Z=(-12/11)=-1.09 Base Paper[12]	Max Z=1
Triangular Neutrosophic Number[TNN]	Max Z=1.17	Min Z=-3.02	Max Z=1.16 Base Paper[9]
Proposed Method	Max Z=1.23	Min Z=-5.09	Max Z=1.47
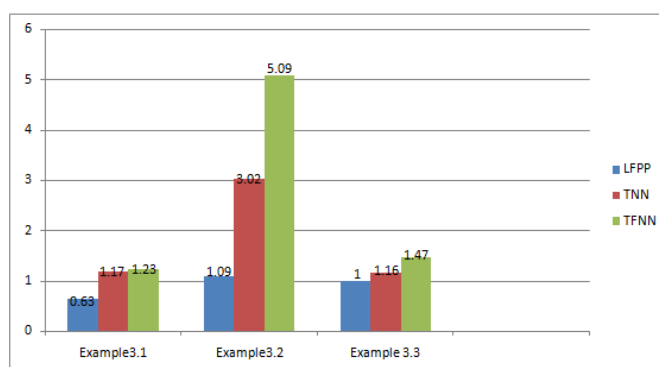
Fig.1. Optimal Value

RESEARCH ARTICLE

Fuzzy Multi Number's Ranking Measure in Transportation Problem

E.Vivek[1]*, N. Uma[2] and M. Kanishkar[3]

[1]Assistant Professor, Department of Mathematics, Sri Ramakrishna College of Arts and Science, Coimbatore, Tamil Nadu, India
[2]Associate Professor, Department of Mathematics, Sri Ramakrishna College of Arts and Science, Coimbatore, Tamil Nadu, India.
[3]Student of M.Sc. Mathematics, Sri Ramakrishna College of Arts and Science, Coimbatore, Tamil Nadu, India.

*Address for Correspondence
E.Vivek
Assistant Professor,
Department of Mathematics,
Sri Ramakrishna College of Arts and Science,
Coimbatore, Tamil Nadu, India
E.Mail: vivek@srcas.ac.in

ABSTRACT

The Fuzzy Multi Transportation Problem (FMTP) is solved in this paper by considering the ranking technique of the Fuzzy Multi Numbers. Here, we consider the Triangular Fuzzy Multi Number of the FMTP. The Fuzzy Multi Numbers (FMN) are transformed to crisp data by the ranking technique and based on this ranking crisp data, the initial and the optimal solution of the Fuzzy Multi Transportation Problem are obtained. The numerical examples of balanced and unbalanced Triangular Fuzzy Multi Number with its membership functions of the FMTP shows the efficiency of the procedure explained.

Keywords: Fuzzy Set, Fuzzy Multi Set, Fuzzy Number, Triangular Fuzzy Multi Number, Fuzzy Transportation Problem, Ranking Technique.

INTRODUCTION

Hitchcock in 1941 introduced the basic transportation model with the transportation constraints on crisp values. Transportation problem is a particular class of linear programming, which is associated with day-to-day activities in our real life. It helps in solving problem on distribution and transportation of resources from one place toanother.Themainobjectiveistominimizethetransportationcostpossiblebysatisfyingthedemandatdestinationfromsupplyconstraint. But in present situation, due to several uncontrolled reasons, the transportation parameters like demand, supply and unit transportation costar uncertain. Hence, the fuzzy transportation problems were formulated

63716

and solved by many researchers. **O'heigeartaigh [7]** was who proposed a method to solve the fuzzy transportation problem with fuzzy demand and supply.

Lotfi A. Zadeh[9] in 1965 introduced the Fuzzy set theory, Since then fuzzy mathematics has been applied in various fields like decision making, pattern recognition, information processing and various analysis methodologies. The Fuzzy set theory is a class of objects with a membership between 0 and 1.Zimmermann [10] proposed the basic definitions of fuzzy sets and algebraic operations. Alsoin1975, Lotfi A. Zadeh proposed the Fuzzy numbers, most used fuzzy tools in fuzzy applications. The Fuzzy Number was defined by Dijkmanet.all[4], are basically fuzzy sets satisfying the properties of normality, convexity and piece-wise continuity.Buckley [1] use fuzzy numbers to express their preferences and Li & Lee [5] proposed the order of fuzzy numbers based on the concept of probability measure of fuzzy events. Triangular fuzzy numbers, Trapezoidal fuzzy numbers and Pentagonal fuzzy numbers are most popular forms of fuzzy numbers used in various applications. Later, a new method to find the fuzzy optimal solution of fully fuzzy linear programming problems with triangular fuzzy number was proposed by Nagoor Gani & Mohamed Assarudeen [6].Ranking the fuzzy numbers is an important aspect of decision making in a fuzzy environment for practical applications, and Chen [2] the ordering value of each fuzzy number and uses these values to determine the order of the *n* fuzzy numbers.Yager [8] first discussed fuzzy multisets, he uses the term of fuzzy bag; an element of X may occur more than once with possibly of the same or different membership values.

In this paper, we have applied the fuzzy multi ranking technique of triangular fuzzy multi numbers with its membership function in the transportation problem of uncertainty. As the efficiency of the defined fuzzy multi ranking techniques is analyzed using the numerical examples. The numerical examples were of balanced, unbalanced transportation problems whose supply, demand and costswere in the form of triangular fuzzy multi numbers. Hence, it is recommended to use this ranking measure for any multi decision making situations.

PRELIMINARIES
In this section, the basis notions, concepts and definitions are reviewed.

Definition: 2.1
Let X be a nonempty set. A **fuzzy set** $\overline{A}$ of X is defined as $\overline{A}$ = { < x, $\mu_{\overline{A}}(x)$> / x$\in X$ }, where $\mu_{\overline{A}}(x)$ is called membership function and it maps each element of X to a value between 0 and 1.

Definition: 2.2
A **multi set(MS)**is an unordered collection of objects in which, unlike an ordinary set, objects are allowed to repeat. Each individual occurrence of an object is a **multi-set** which is called its element.

Definition: 2.3
Let X be a nonempty set. A **fuzzy multi set (FMS)** A in X is characterized by the count membership function Mc such that Mc : $X \rightarrow Q$ where Q is the set of all crisp multi sets in [0,1]. Hence, for any $x \in X$, Mc(x) is the crisp multi set from [0, 1]. The membership sequence is defined as $(\mu_A^1(x), \mu_A^2(x), \ldots\ldots\mu_A^p(x))$ where $\mu_A^1(x) \geq \mu_A^2(x) \geq \cdots \geq \mu_A^p(x)$ Therefore, **FMS A**is given by $A = \{\langle x, (\mu_A^1(x), \mu_A^2(x), \ldots\ldots\mu_A^p(x)) \rangle / x \in X \}$

Definition: 2.4
A **fuzzy number** is a generalization of a regular real number. It does not refer to a single value but rather to a connected set of possible values, where each possible value has its weight between 0 and 1. The weight is called the membership function.

A fuzzy number $\overline{A}$ is a convex normalized fuzzy set on the real line R such that there exist at least one x ∈ R with $\mu_{\overline{A}}(x)$= 1 and $\mu_{\overline{A}}(x)$is piecewise continuous.

Definition: 2.5

A **triangular fuzzy number**A is denoted by 3 – tuples (a, b, c), where $a, b \ and \ c$ are real numbers and $a \leq b \leq c$ with membership function defined as

$$\mu_A(x) = \begin{cases} 0 & for \quad x \leq a \\ \dfrac{x-a}{b-a} & for \ a \leq x \leq b \\ \dfrac{c-x}{c-b} & for \ b \leq x \leq c \\ 0 & for \quad x \geq c \end{cases}$$

Definition: 2.6

The **ranking** function is approach of ordering fuzzy numbers which is an efficient. The ranking function is denoted by F $(\mathbb{R})$, where $\mathbb{R}$: F$(\mathbb{R}) \rightarrow \mathbb{R}$, and F $(\mathbb{R})$ is the set of fuzzy numbers defined on a real line, where a natural order exist.

Let $a, b \in \mathbb{R}$, then **ranking function** for real numbers a, b is defined as

(i) $D(a,b) > 0 \Leftrightarrow D(a,0) > D(b,0) \Leftrightarrow a > b$
(ii) $D(a,b) < 0 \Leftrightarrow D(a,0) < D(b,0) \Leftrightarrow b < a$
(iii) $D(a,b) = 0 \Leftrightarrow D(a,0) = D(b,0) \Leftrightarrow b = a$

RANKING MEASURES OF FUZZY MULTI NUMBERS

Definition: 3.1

A **fuzzy multi number** is a generalization of a regular real number. It does not refer to a single value but rather to a connected set of possible values, where each possible value has its weight between 0 and 1. The weight is called the membership function. The membership sequence is in the form $(\mu_A^1(x), \mu_A^2(x), \dots\dots \mu_A^p(x))$ where $\mu_A^1(x) \geq \mu_A^2(x) \geq \cdots \geq \mu_A^p(x)$.

Definition: 3.2

The **cardinality** of the membership function Mc(x) is the length of an element x in the Fuzzy Multi Set *A* denoted as η, defined as η = Mc(x)

If A, B, C are the *FMS* defined on *X*, then their cardinality η = Max { η(A), η(B), η(C) }.

Definition: 3.3

A **triangular fuzzy multi number**A_i is denoted by 3 – tuples (a_i, b_i, c_i), where $a_i, b_i \ and \ c_i$ are real numbers and $a_i \leq b_i \leq c_i$ with membership function defined as

$$\mu_{A_i}(x) = \begin{cases} 0 & for \quad x \leq a_i \\ \dfrac{x-a_i}{b_i-a_i} & for \ a_i \leq x \leq b_i \\ \dfrac{c_i-x}{c_i-b_i} & for \ b_i \leq x \leq c_i \\ 0 & for \quad x \geq c_i \end{cases}$$

Definition: 3.4

In general, a fuzzy number A is described as any fuzzy subset of real line R, whose membership function μ_A satisfies the condition that$\mu_A$is a continuous mapping from R to the closed interval [0,1]. Then the **Ranking Measure of Graded Mean Integration Representation** proposed by **Chen and Hsieh [3]**is as follows for the membership sequence is in the form $(\mu_A^1(x), \mu_A^2(x), \dots\dots \mu_A^p(x))$ where $\mu_A^1(x) \geq \mu_A^2(x) \geq \cdots \geq \mu_A^p(x)$with the Cardinality, the length of an element x in the Fuzzy Multi Set *A* denoted as η. We have used the introduced ranking measures of the

Vivek *et al.*,

triangular fuzzy multi number A_i, extended from the of Graded Mean Representation Method by Chen & Hsieh for the fuzzy numbers.

The defined Ranking Measure the Graded Mean Integration Representation of the triangularfuzzy multi number A_i of (a_i, b_i, c_i) is $R(A_i) = \frac{1}{\eta} \sum_{i=1}^{\eta} \frac{(a_i + 4b_i + c_i)}{6}$

Clearly it satisfies the properties of the ranking measure

(i) $R(A_i)$ *is always* > 0
(ii) $R(A_i, b_i) > 0 \Leftrightarrow R(A_i) > R(B_i) \Leftrightarrow A_i > B_i$
(iii) $R(A_i, b_i) < 0 \Leftrightarrow R(A_i) < R(B_i) \Leftrightarrow A_i < B_i$
(iv) $R(A_i, b_i) = 0 \Leftrightarrow R(A_i) = R(B_i) \Leftrightarrow A_i = B_i$

IV MATHEMATICAL MODEL & COMPUTATIONAL ALGORITHM OF FUZZY MULTI TRANSPORTATION PROBLEM

Mathematical model for Fuzzy Multi Transportation Problem with Triangular Fuzzy Number
The transportation problem with m origins (rows) and n destinations (columns) is considered with C_{ij}, the cost of transporting one unit of the product from i^{th} FM (Fuzzy Multi) origin to j^{th} FM (Fuzzy Multi) destination.

$\overline{a} = \left(a_i^1, a_i^2, a_i^3\right)$ be the quantity of commodity available at origin i.
$\overline{b} = \left(b_j^1, b_j^2, b_j^3\right)$ the quantity of commodity needed at FM (Fuzzy Multi) destination j.
$\overline{x} = \left(x_{ij}^1, x_{ij}^2, x_{ij}^3\right)$ is the quantity transported from i^{th} origin to j^{th} destination, so as to minimize the FM (Fuzzy Multi) transportation cost.

$$Minimum\ \overline{Z}^I = \sum_{i=1}^{m} \sum_{j=1}^{n} C_{ij} \otimes \left(x_{ij}^1, x_{ij}^2, x_{ij}^3\right)$$

Subject to, $\sum_{j=1}^{n} \left(x_{ij}^1, x_{ij}^2, x_{ij}^3\right) = \left(a_i^1, a_i^2, a_i^3\right)\ for\ i = 1,2,\dots,m$

$\sum_{j=1}^{n} \left(x_{ij}^1, x_{ij}^2, x_{ij}^3\right) = \left(b_j^1, b_j^2, b_j^3\right)\ for\ j = 1,2,\dots,n$
$\left(x_{ij}^1, x_{ij}^2, x_{ij}^3\right) \geq 0\ \ for\ i = 1,2,\dots,m\ and\ for\ j = 1,2,\dots,n$
Where m is the number of supply points and n is the number of demand points.

Computational Algorithm

First, in this triangular fuzzy multi transportation problem; the quantities are reduced into an integer using the ranking measure of triangular fuzzy multi number. Then to find the basic feasible solution, VAM method is used as the advantage of this method is that it gives an initial solution which is nearer to an optimal solution. Also, in this paper MODI method is used to find the optimal solution.

NUMERICAL EXAMPLES
The triangular fuzzy multi numbers can be used to represent uncertain and incomplete information in decision-making, risk evaluation, and expert systems. Measurement of similarity should keep some parameters of triangular fuzzy numbers. Shape and midpoint are important metrics of a triangular fuzzy number. Therefore, they should be taken into consideration when measuring the similarity of triangular fuzzy multi numbers.

Vivek *et al*.,

EXAMPLE: 4.1
An FMTP of 3x4with cost as the Triangular Fuzzy Multi Number is considered below

First, we reduce triangular fuzzy multi number to a crisp data:
The above 3×4 matrix is of balanced transportation problem with the triangular fuzzy multi numbers, which has four repeated fuzzy triangular numbers in each cell. These measures are considered for four different times in day (morning, afternoon, evening and night).We have to convert the fuzzy multi number to a corresponding crisp number and for this we use the concept of ranking measure. By using the formula of the Ranking Measure of theTriangular fuzzy multi numbers of Chen & Hsieh

A_i (a_i, b_i, c_i) as $\frac{1}{\eta} \sum_{i=1}^{\eta} \frac{(a_i + 4b_i + c_i)}{6}$, wecan get the crisp data. Here, the cardinality $\eta = 4$,

Using the VAM method, the initial solution obtained is represented in the following table

Using the MODI method of the fuzzy multi transportation table and checking the optimality for all dij > 0, the solution is found to be optimum and unique as$32 + 2\epsilon_1 + 4\epsilon_2$.

EXAMPLE: 4.2
A **Balanced FMTP of 3x3with** supply and demand as the triangular fuzzy multi numbers is considered below

And here, we reduce triangular fuzzy multi number to a crisp data by Graded Mean Integration Representation by Chen & HsiehA_i (a_i, b_i, c_i) as $\frac{1}{\eta} \sum_{i=1}^{\eta} \frac{(a_i + 4b_i + c_i)}{6}$, wecan get the crisp data. Here, the cardinality $\eta = 3$, The above 3×3 matrix is of balanced transportation problem with measures of three different times in day (morning, afternoon and night).

Using the VAM method, the initial solution obtained is represented in the following table and whose Initial Cost of this IFTP is 820 + 30∈

Using the MODI method of the fuzzy multi transportation table and checking the optimality for all dij > 0, the solution is found to be optimum and unique as 820 + 5∈

EXAMPLE: 4.3
This is an unbalanced FMTP of 3x3 with supply and demand as the triangular fuzzy multi numbers

Once again to reduce the triangular fuzzy multi numbers to a crisp data, we use the same ranking measurer of Graded Mean Integration Representation. The cardinality $\eta = 3$,
as the 3×3 unbalanced transportation problem is of three different times in day (morning, afternoon and night).

Using the VAM method, the initial solution obtained is represented in the following table

Using the MODI method of the fuzzy multi transportation table and checking the optimality for all dij > 0, the solution is found to be optimum and unique as 31.

CONCLUSION

In this paper, a method of finding the initial and the optimal solution for fuzzy multi transportation problem with the triangular fuzzy multi number has been proposed. We have used the ranking technique of graded mean integration representation by Chen & Hsieh of triangular fuzzy multi number. The numerical examples 4.1, 4.2 and

Vivek *et al.*,

4.3 illustrate the efficiency of the proposed technique for both balanced and unbalanced FMTP. In Future,this approach of solving the FMTP may also be utilized for trapezoidal, pentagonal, hexagonal and octagonal fuzzy multi transportation problems.

REFERENCES

1. Buckley . J.J, A fuzzy ranking of fuzzy numbers, Fuzzy Sets and Systems 33, 119—121 (1989).
2. Chen . S. H, Ranking fuzzy numbers with maximizing set and minimizing set, Fuzzy Sets and Systems 17, 113-129 (1985).
3. Chen, S. H. and Hsieh, C. H. , "Graded Mean Integration Representation of Generalized Fuzzy Number", Journal of the Chinese Fuzzy System Association, Vol. 5, No. 2, pp. 1-7, 1999.
4. Dijkman . J. G, Van Haeringen . H and De Lange . S.J, Fuzzy numbers, Journal of mathematical analysis and applications 92, 301-341 (1983).
5. Lee .E.S and Li. R.J., "Comparison of fuzzy numbers based on the probability measure of fuzzy events ", Computational Mathematical Application, Volume 15, No. 10, pp. 887-896, (1988).
6. Nagoor Gani A and Mohamed Assarudeen S N 2012 A new operation on triangular fuzzy number for solving fuzzy linear programming problem *Applied Mathematical Sciences* 6(11)   pp525 -532
7. O'heigeartaigh O, A fuzzy transportation algorithm, *Fuzzy Sets and Systems (1982), 235-243.*
8. Yager . R. R, On the theory of bags, Int. J. General Systems, Vol. 13, pp. 23–37, 1986.
9. Zadeh, L.A. Fuzzy sets. Information and Control, 8(3), 338-356,1965.
10. Zimmermann . H. J, Fuzzy Set Theory and Its Applications, Kluwer Academic Publishers, Boston, Mass, USA, Second edition, 1996.

Table 1. An FMTP of 3x4with cost as the Triangular Fuzzy Multi Number is considered below

	D1	D2	D3	D4	**Supply**
S1	{(1,1,1) (1,2,3) (2,3,4) (4,6,8)}	{(4,5,6) (3,6,9) (5,7,9) (9,10,11)}	{(3,4,5) (4,5,6) (3,6,9) (8,9,10)}	{(1,1,1) (2,4,6) (4,5,6) (4,6,8)}	**5**
S2	{(1,1,1) (1,2,3) (1,2,3) (2,3,4)}	{(1,1,1) (1,2,3) (2,4,6) (8,9,10)}	{(1,1,1) (1,2,3) (2,4,6) (4,5,6)}	{(1,1,1) (1,1,1) (1,2,3) (2,4,6)}	**2**
S3	{(1,1,1) (2,3,4) (2,4,6) (7,8,9)}	{(1,1,1) (2,3,4) (2,3,4) (4,5,6)}	{(4,5,6) (7,8,9) (8,9,10) (9,10,11)}	{(4,5,6) (3,6,9) (1,2,3) (5,7,9)}	**3**
Demand	**3**	**3**	**2**	**2**	

Table 2. Crisp Data

	D1	D2	D3	D4	**Supply**
S1	3	7	6	**4**	**5**
S2	2	4	3	**2**	**2**
S3	4	3	8	**5**	**3**
Demand	**3**	**3**	**2**	**2**	

63721

Vivek *et al.*,

Table 3. VAM method,

	D1		D2	D3		D4		Supply
S1	3	**3**	7	6		4	2	**5**
S2	2		4	3	**2**	2	$\in_1$	**2 + $\in_1$**
S3	4	$\in_2$	3	3	8		5		**3 + $\in_2$**
Demand	**3 +$\in_2$**		**3**	**2**		**2 +$\in_1$**		

Table 4. Initial Cost of this IFTP is 32 + 2$\in_1$ + 4$\in_2$.

	D1		D2	D3		D4		Supply
S1	3	**3**	7	6		4	2	**5**
S2	2		4	3	**2**	2	$\in_1$	**2 + $\in_1$**
S3	4	$\in_2$	3	3	8		5		**3 + $\in_2$**
Demand	**3 +$\in_2$**		**3**	**2**		**2 +$\in_1$**		

Table 5. Balanced FMTP of 3x3with supply and demand as the triangular fuzzy multi numbers

	D1	D2	D3	Supply
S1	50	30	220	{(1,1,1) (1,1,1) (1,1,1)}
S2	90	45	170	{(1,2,3) (2,3,4) (2,4,6)}
S3	250	200	50	{(2,3,4) (2,4,6) (4,5,6)}
Demand	{(2,4,6) (1,2,3) (4,6,8)}	{(1,1,1) (1,2,3) (2,3,4)}	{(1,1,1) (1,1,1) (2,4,6)}	

Table 6. Graded Mean Integration Representation

	D1	D2	D3	Supply
S1	50	30	220	**1**
S2	90	45	170	**3**
S3	250	200	50	**4**
Demand	**4**	**2**	**2**	

Table 7. VAM method,

	D1		D2		D3		Supply
S1	50	**1**	30	∈	220		**1+∈**
S2	90	3	45		170		**3**
S3	250		200	2	50	2	**4**
Demand	**4**		**2+∈**		**2**		

Table 8.MODI method

	D1		D2		D3		Supply
S1	50	**1** +∈	30		220		**1+∈**
S2	90	3 - ∈	45	∈	170		**3**
S3	250		200	2	50	2	**4**
Demand	**4**		**2+∈**		**2**		

Table 9. Unbalanced FMTP of 3x3

	D1	D2	D3	Supply
S1	4	3	2	{(4,5,6) (5,10,15) (10,15,20)}
S2	2	5	0	{(10,11,12) (12,13,14) (10,15,20)}
S3	3	8	6	{(10,11,12) (11,12,13) (12,13,14)}
Demand	{(6,7,8) (7,8,9) (8,9,10)}	{(2,4,6) (4,5,6) (4,6,8)}	{(1,1,1) (4,5,6) (4,6,8)}	

Table 10. Graded Mean Integration Representation

	D1	D2	D3	Supply
S1	4	3	2	**10**
S2	2	5	0	**13**
S3	3	8	6	**12**
Demand	**8**	**5**	**4**	

Vivek *et al.*,

Table 11. VAM method,

	D1		D2		D3		D4		Supply
S1	4		3	4	2		0	6	**10**
S2	2	8	5	1	0	4	0		**13**
S3	3		8		6		0	12	**12**
Demand	**8**		**5**		**4**		18		

Table 12. Initial Cost of this IFTP

	D1		D2		D3		D4		Supply
S1	4		3	5	2		0	5	**10**
S2	2	8	5		0	4	0	1	**13**
S3	3		8		6		0	12	**12**
Demand	**8**		**5**		**4**		18		

An Efficient Numerical Approach Based on Wavelets Operational Matrices for Multi Term Fractional Differential Equations

R. Aruldoss[1] and K. Balaji[2]*

[1]Assistant Professor, Department of Mathematics, Government Arts College (Autonomous),(Affiliated to Bharathidasan University,Tiruchirappalli), Kumbakonam- 612 002, Tamil Nadu, India.
[2]Research Scholar, Department of Mathematics, Government Arts College (Autonomous),(Affiliated to BharathidasanUniversity,Tiruchirappalli), Kumbakonam- 612 002, Tamil Nadu, India.

*Address for Correspondence
K. Balaji
Research Scholar,
Department of Mathematics, Government Arts College (Autonomous),
(Affiliated to BharathidasanUniversity,Tiruchirappalli),
Kumbakonam- 612 002, Tamil Nadu, India.
E. Mail: krvarul@gmail.com

ABSTRACT

In this article, an efficient numerical algorithm based on Legendre wavelets operational matrix is proposed for solving multi term fractional differential equations with variable coefficients. Legendre wavelets operational matrix for fractional integration is derived and it is employed to reduce fractional differential equations into a system of algebraic equations. Some numerical examples are included to elucidate the simplicity and the efficiency of the proposed method. The absolute errors are also compared with some existing numerical techniques.

Keywords: Caputo fractional derivative, Legendre wavelets, Operational matrix, Multi term Fractional differential equations with variable coefficients.

INTRODUCTION

The origin of fractional calculus is traced back to the end of seventeenth century. Fractional calculus, as a generalization of ordinary calculus, deals with an arbitrary order integration and differentiation. Nowadays many fractional models have a great attention in various disciplines, such as Medicine, Economics, Dynamical problems, Mathematical physics, Traffic model, Fluid flow, Bio Sciences, Bio Engineering, Electro chemistry, Electromagnetism, Viscoelasticy and so on. Moreover, most fractional order differential equations have no exact solution. Owing this fact, many researchers have engaged in developing the numerical techniques for fractional order differential equations. Some of these numerical approaches include Finite element method, Finite difference method, Adomian decomposition method, Homotopy perturbation method, Homotopy analysis method, Variational iteration method, Spectral tau method and Spline collocation method. Some polynomials namely, Laguerre polynomials[6], Bernoulli

Aruldoss and Balaji

polynomials[19], Chelyshkov polynomials[20], fractional-order Lagrange polynomials[18], Bernstein Polynomials[7], Shifted Chebyshev polynomials[1] are also employed to solve fractional order integral and differential equations numerically. Recently, orthogonal wavelets have become more popular numerical techniques for solving differential and integral equations due to their excellent properties. Many researchers have employed the operational matrices of fractional integrations of Legendre wavelets[16, 17, 22], Taylor wavelets[21], Müntz-Legendre wavelets[15], Haar wavelets[11], Chebyshev wavelets[5], Second kind Chebyshev wavelets[23], Euler wavelets[24] and Bernoulli wavelets[14] to find the approximate solutions of arbitrary order differential and integral equations. The main objective of this paper is to find the numerical solutions of multi term fractional order differential equations having variable coefficients based on Legendre wavelet operational matrix. The proposed method converts the fractional order differential equations into simultaneous algebraic equations by Legendre wavelet operational matrix. The large system of algebraic equations may some times lead to a greater computational complexity and a large amount of storage requirements, but the Legendre wavelets operational matrix is a structurally sparse matrix, which decreases the computational complexity of the resultant algebraic equations. This article is classified as follows. In section 2, we briefly describe some basic definitions and properties of fractional calculus. A brief overview of Legendre wavelets, function approximation and operational matrix for fractional integration of Legendre wavelets is presented in section 3. In section 4, the applicability and the efficiency of the proposed approach are elucidated on some numerical examples and error estimations are also presented. Finally we conclude our work in section 5.

Preliminaries

We discuss here fractional order integral and differential operators with the preliminary mathematical facts of fractional calculus.

Definition 2.1 [4,10,12,13] *The fractional integral with order $\mu \geq 0$, of the function $h(x) \in L^1([0, \infty))$, in Riemann-Liouville sense, is given by*

$$J^\mu h(x) = \begin{cases} \dfrac{1}{\Gamma(\mu)} \displaystyle\int_0^x (x - v)^{\mu-1} h(v) dv, & \mu > 0. \\[4mm] h(x), & \mu = 0. \end{cases}$$

Let $h(x), g(x) \in L^1([0, \infty))$, $\lambda, \gamma \in \mathbb{R}$, $v > -1$, $\mu \geq 0$.
Then
(i) $J^\mu(\lambda h(x) + \gamma g(x)) = \lambda J^\mu h(x) + \gamma J^\mu g(x)$.
(ii) $J^\mu x^v = \dfrac{\Gamma(v + 1)}{\Gamma(v + \mu + 1)} x^{\mu+v}$.

Definition 2.2 [4,10,12,13] *The fractional derivative with order $\mu \geq 0$, of the function $h(x) \in L^1([0, \infty))$, in Caputo sense, is given by*

$$D^\mu h(x) = J^{m-\mu}(D^m h(x)) = \begin{cases} \dfrac{1}{\Gamma(m - \mu)} \displaystyle\int_0^x \dfrac{h^{(m)}(v)}{(x - v)^{\mu-m+1}} dv, & m - 1 < \mu < m, m \in \mathbb{N}. \\[4mm] \dfrac{d^m}{dx^m} h(x), & \mu = m \in \mathbb{N}. \end{cases}$$

Let $h(x), g(x) \in L^1([0, \infty))$, $\lambda, \gamma \in \mathbb{R}$, $\mu \geq 0$.
Then
(i) $D^\mu k = 0$, *where k is a constant.*
(ii) $D^\mu(\lambda h(x) + \gamma g(x)) = \lambda(D^\mu h(x)) + \gamma(D^\mu g(x))$.
(iii) $D^\mu(J^\mu h(x)) = h(x)$.
(iv) $J^\mu(D^\mu h(x)) = h(x) - \displaystyle\sum_{k=0}^{m-1} h^{(k)}(0^+) \dfrac{x^k}{k!}$, $m - 1 < \mu \leq m$,

where $m \in \mathbb{N}$, $x > 0$ and $h^{(k)}(0^+) := \lim_{x \to 0^+} D^{(k)} h(x)$, $k = 0,1,2,\dots,m - 1$.

Legendre wavelets approximations of functions

We now discuss the Legendre wavelet and its operational matrix for fractional order integration.

Legendre Wavelets

Wavelets represent a family of functions generated from dilations and translations of a mother wavelet function $\psi(t)$ over $\mathbb{R}$. Varying the dilation parameter b and the translation parameter c continuously, we obtain the following family of continuous wavelets,

$$\psi_{bc}(t) = |b|^{-\frac{1}{2}}\psi\left(\frac{t-c}{b}\right), b \neq 0, c \in \mathbb{R}.$$

Restricting the parameters b and c to discrete values as $b = b_0^{-u}$, $c = vc_0 b_0^{-u}$, $b_0 > 1$, $c_0 > 0$, $u, v \in \mathbb{N}$, we arrive the family of discrete wavelets,

$$\psi_{uv}(t) = |b_0|^{-\frac{u}{2}}\psi(b_0^u t - vc_0),$$

where $\{\psi_{uv}(t)\}$ forms a basis for $L^2(\mathbb{R})$. Particularly, when $b_0 = 2$ and $c_0 = 1$, $\{\psi_{uv}(t)\}$ forms an orthonormal basis for $L^2(\mathbb{R})$. The Legendre wavelets are defined over the interval [0,1) as

$$\psi_{pq}(t) = \begin{cases} \left(q+\frac{1}{2}\right)^{\frac{1}{2}} 2^{\frac{k}{2}} L_q(2^k t - \hat{n}), & t \in [\frac{\hat{n}-1}{2^k}, \frac{\hat{n}+1}{2^k}). \\ 0, & otherwise, \end{cases} \quad (1)$$

where $\hat{n} = 2p - 1$, $p = 1,2,3,\ldots,2^{k-1}$, $q = 0,1,2,\ldots,M-1$ and $M, k \in \mathbb{N}$. In (1), 2^{-k} is the dilation parameter, $\hat{n}2^{-k}$ is the translation parameter and the coefficient $\left(q+\frac{1}{2}\right)^{\frac{1}{2}}$ is used for orthonormality. Moreover, $L_q(t)$, $q = 0,1,2,\ldots,M-1$, are mutually orthogonal Legendre polynomials of order q with regard to the weight function $\omega(t) = 1$ over the interval $[-1,1]$ and satisfy the following recurrence formulae,

$$L_0(t) = 1, L_1(t) = t, L_{q+1}(t) = \left(\frac{2q+1}{q+1}\right)tL_q(t) - \left(\frac{q}{q+1}\right)L_{q-1}(t), \quad q = 1,2,3,\ldots$$

Approximation of Square Integrable Functions

An arbitrary function $h(t)$ from $L^2([0,1))$ can be written in terms of Legendre wavelets as

$$h(t) = \sum_{p=1}^{\infty}\sum_{q=0}^{\infty} c_{pq}\psi_{pq}(t), \quad (2)$$

where the coefficients c_{pq} are resolved by the inner product

$$\langle h(t), \psi_{pq}(t)\rangle = \int_0^1 h(t)\psi_{pq}(t)dt.$$

If we truncate the series in (2), then $h(t)$ can be approximated as

$$\tilde{h}(t) = \sum_{p=1}^{2^{k-1}}\sum_{q=0}^{M-1} c_{pq}\psi_{pq}(t). \quad (3)$$

For simplicity, (3) can be written as

$$\tilde{h}(t) = \sum_{i=1}^{N} c_i\psi_i(t) = C^T\Psi(t), \quad (4)$$

where $N = 2^{k-1}M$, $c_i = c_{pq}$, $\psi_i(t) = \psi_{pq}(t)$, $C = [c_1, c_2, \ldots, c_N]^T$ is the coefficient vector, $\Psi(t) = [\psi_1(t), \psi_2(t), \ldots, \psi_N(t)]^T$ and the index i is determined by the relation $i = (p-1)M + q + 1$.

Discretizing (4) at the collocation points $t_i = \frac{2i-1}{2N}$, $i = 1,2,3,\ldots,N$, we attain

$$H \simeq C^T\Phi_{N\times N}, \quad (5)$$

where $H = [h(t_1), h(t_2), \ldots, h(t_N)]_{1\times N}$ is the vector of the function $h(t)$ at the collocation points and $\Phi_{N\times N} = [\Psi(t_1), \Psi(t_2), \ldots, \Psi(t_N)]$ is a Legendre wavelet coefficient matrix of order N. Specifically, the Legendre wavelet coefficient matrix for $k = 2$ and $M = 3$ becomes

$$\Phi_{6\times 6} = \begin{pmatrix} 1.4142 & 1.4142 & 1.4142 & 0 & 0 & 0 \\ -1.6330 & 0 & 1.6330 & 0 & 0 & 0 \\ 0.5270 & -1.5811 & 0.5270 & 0 & 0 & 0 \\ 0 & 0 & 0 & 1.4142 & 1.4142 & 1.4142 \\ 0 & 0 & 0 & -1.6330 & 0 & 1.6330 \\ 0 & 0 & 0 & 0.5270 & -1.5811 & 0.5270 \end{pmatrix}$$

Aruldoss and Balaji

Lemma 3.1 *Suppose $\tilde{h}(t)$ is the truncated Legendre wavelets expansion of a continuous function h(t) defined on $[0,1)$. If $h(t)$ is bounded by a positive constant η, that is, $|h(t)| < \eta$, then the Legendre wavelet coefficients of h(t) are bounded as*

$$|c_{pq}| \leq \frac{\eta\left(q+\frac{1}{2}\right)^{\frac{1}{2}}}{2^{\frac{k-2}{2}}} \qquad (6)$$

Proof. Suppose $\tilde{h}(t)$ is the truncated Legendre wavelets expansion of $h(t)$. Then

$$\tilde{h}(t) = \sum_{p=1}^{2^{k-1}} \sum_{q=0}^{M-1} c_{pq}\psi_{pq}(t), \qquad (7)$$

where the coefficients c_{pq} can be determined by

$$
\begin{aligned}
c_{pq} = \langle h(t), \psi_{pq}(t)\rangle \quad &= \int_0^1 h(t)\psi_{pq}(t)dt \\
&= \int_{\frac{\hat{n}+1}{2^k}}^{\frac{\hat{n}-1}{2^k}} h(t)\psi_{pq}(t)dt \\
&= 2^{\frac{k}{2}}\left(q+\frac{1}{2}\right)^{\frac{1}{2}} \int_{\frac{\hat{n}+1}{2^k}}^{\frac{\hat{n}-1}{2^k}} h(t)L_q(2^k t - \hat{n})dt
\end{aligned}
$$

Changing the variable $2^k t - \hat{n}$ by y, we have

$$c_{pq} = \frac{\left(q+\frac{1}{2}\right)^{\frac{1}{2}}}{2^{\frac{k}{2}}} \int_{-1}^1 h\left(\frac{y+\hat{n}}{2^k}\right) L_q(y)dy \qquad (8)$$

Since $|h(t)| < \eta$, we have

$$
\begin{aligned}
|c_{pq}| \quad &= \frac{\left(q+\frac{1}{2}\right)^{\frac{1}{2}}}{2^{\frac{k}{2}}} \left|\int_{-1}^1 h\left(\frac{y+\hat{n}}{2^k}\right) L_q(y)dy\right| \\
&\leq \frac{\left(q+\frac{1}{2}\right)^{\frac{1}{2}}}{2^{\frac{k}{2}}} \int_{-1}^1 \left|h\left(\frac{y+\hat{n}}{2^k}\right)\right| |L_q(y)|dy
\end{aligned}
$$

$$|c_{pq}| \leq \frac{\eta\left(q+\frac{1}{2}\right)^{\frac{1}{2}}}{2^{\frac{k}{2}}} \int_{-1}^1 |L_q(y)|dy \qquad (9)$$

Since $|L_q(y)| \leq 1, \forall y \in [-1,1]$, we have

$$\int_{-1}^1 |L_q(y)|dy \leq 2 \qquad (10)$$

Thus

$$|c_{pq}| \leq \frac{\eta\left(q+\frac{1}{2}\right)^{\frac{1}{2}}}{2^{\frac{k-2}{2}}} \qquad (11)$$

Theorem 3.2 *If $h(t)$ is a continuous function defined on $[0,1)$ and $\tilde{h}(t)$ is the approximation of $h(t)$ by using Legendre wavelets, then we have the upper bound error*

$$\| h(t) - \tilde{h}(t) \|_2 \leq \left(\sum_{p=2^{k-1}+1}^{\infty} \sum_{q=0}^{M-1} (\alpha(q))^2\right)^{\frac{1}{2}} + \left(\sum_{p=1}^{\infty} \sum_{q=M}^{\infty} (\alpha(q))^2\right)^{\frac{1}{2}}, (12)$$

where $\alpha(q) = \frac{\eta\left(q+\frac{1}{2}\right)^{\frac{1}{2}}}{2^{\frac{k-2}{2}}}$.

Proof. Suppose $\tilde{h}(t)$ is the truncated Legendre wavelets expansion of $h(t)$.

The truncated error term can then be calculated as

$$h(t) - \tilde{h}(t) = \sum_{p=2^{k-1}+1}^{\infty} \sum_{q=0}^{M-1} c_{pq}\psi_{pq}(t) + \sum_{p=1}^{\infty} \sum_{q=M}^{\infty} c_{pq}\psi_{pq}(t) (13)$$

Thus

Aruldoss and Balaji

$$\left|\left|h(t) - \tilde{h}(t)\right|\right|_2 \leq \left|\left|\sum_{p=2^{k-1}+1}^{\infty}\sum_{q=0}^{M-1} c_{pq}\psi_{pq}(t)\right|\right|_2 + \left|\left|\sum_{p=1}^{\infty}\sum_{q=M}^{\infty} c_{pq}\psi_{pq}(t)\right|\right|_2$$

$$= \left(\int_0^1 \left|\sum_{p=2^{k-1}+1}^{\infty}\sum_{q=0}^{M-1} c_{pq}\psi_{pq}(t)\right|^2 dt\right)^{\frac{1}{2}} + \left(\int_0^1 \left|\sum_{p=1}^{\infty}\sum_{q=M}^{\infty} c_{pq}\psi_{pq}(t)\right|^2 dt\right)^{\frac{1}{2}}$$

$$\leq \left(\sum_{p=2^{k-1}+1}^{\infty}\sum_{q=0}^{M-1} |c_{pq}|^2\right)^{\frac{1}{2}} + \left(\sum_{p=1}^{\infty}\sum_{q=M}^{\infty} |c_{pq}|^2\right)^{\frac{1}{2}}$$

Using Lemma 3.1, *we have*

$$\left|\left|h(t) - \tilde{h}(t)\right|\right|_2 \leq \left(\sum_{p=2^{k-1}+1}^{\infty}\sum_{q=0}^{M-1} \left(\alpha(q)\right)^2\right)^{\frac{1}{2}} + \left(\sum_{p=1}^{\infty}\sum_{q=M}^{\infty} \left(\alpha(q)\right)^2\right)^{\frac{1}{2}}.$$

Legendre wavelets operational matrix of fractional integration

An N-set of Block pulse functions(BPFs) over [0,1) is defined as,

$$b_m(t) = \begin{cases} 1, & [\frac{m-1}{N},\frac{m}{N}), \\ 0, & otherwise, \end{cases}$$

where $m = 1,2,3,\ldots,N$, $N \in \mathbb{N}$.

For $t \in [0,1)$, $b_m(t)b_n(t) = \begin{cases} b_m(t), & m = n. \\ 0, & m \neq n. \end{cases}$

And

$$\int_0^1 b_m(t)b_n(t)dt = \begin{cases} \frac{1}{N}, & m = n. \\ 0, & m \neq n. \end{cases}$$

Any square integrable function $h(t)$ can be expressed in terms of BPFs as

$$h(t) \simeq \sum_{m=1}^{N} h_m b_m(t) = h^T B_N(t),$$

where $h = [h_1, h_2, \ldots, h_N]^T$, $h_m = N\int_{\frac{m-1}{N}}^{\frac{m}{N}} h(t)b_m(t)dt$ and $B_N(t) = [b_1(t), b_2(t), \ldots, b_N(t)]^T$.

The BPFs and Legendre wavelets are connected by the relation
$$\Psi(t) = \Phi_{N\times N}B_N(t). \tag{14}$$

The fractional integration J^{μ}, $\mu \geq 0$ of the vector function $B_N(t)$ is defined as in [9], that is,
$$J^{\mu}(B_N(t)) \simeq F_{N\times N}^{\mu}B_N(t), \tag{15}$$
where $F_{N\times N}^{\mu}$ is the Block pulse operational matrix of $J^{\mu}(B_N(t))$,

$$F_{N\times N}^{\mu} = \frac{1}{N^{\mu}}\frac{1}{\Gamma(\mu+2)}\begin{pmatrix} 1 & \xi_1 & \xi_2 & \xi_3 & \cdots & \xi_{N-1} \\ 0 & 1 & \xi_1 & \xi_2 & \cdots & \xi_{N-2} \\ 0 & 0 & 1 & \xi_1 & \cdots & \xi_{N-3} \\ 0 & 0 & 0 & 1 & \cdots & \xi_{N-4} \\ \vdots & \vdots & \vdots & \vdots & \ddots & \vdots \\ 0 & 0 & 0 & 0 & \cdots & \xi_1 \\ 0 & 0 & 0 & 0 & \cdots & 1 \end{pmatrix}$$

With $\xi_r = (r+1)^{\mu+1} - 2r^{\mu+1} + (r-1)^{\mu+1}$

The fractional order integration J^{μ} of the vector function $\Psi(t)$ can be approximated as,
$$J^{\mu}(\Psi(t)) \simeq P_{N\times N}^{\mu}\Psi(t), \tag{16}$$
where $P_{N\times N}^{\mu}$ is known as operational matrix of Legendre wavelets with order $\mu \geq 0$. By (14) and (17), we obtain
$$J^{\mu}(\Psi(t)) = J^{\mu}(\Phi_{N\times N}B_N(t)) = \Phi_{N\times N}J^{\mu}(B_N(t)) \simeq \Phi_{N\times N}F_{N\times N}^{\mu}B_N(t). \tag{17}$$
Thus, combining (16) and (17), we attain
$$P_{N\times N}^{\mu}\Psi(t) \simeq J^{\mu}(\Psi(t)) \simeq \Phi_{N\times N}F_{N\times N}^{\mu}B_N(t) = \Phi_{N\times N}F_{N\times N}^{\mu}(\Phi_{N\times N})^{-1}\Psi(t)$$
and so
$$P_{N\times N}^{\mu} \simeq \Phi_{N\times N}F_{N\times N}^{\mu}(\Phi_{N\times N})^{-1}. \tag{18}$$

Aruldoss and Balaji

For instance, the operational matrix for fractional integration of Legendre wavelets for $M = 3$, $k = 2$ and $\mu = 0.5$

yields, $P_{6\times6}^{0.5} = \begin{pmatrix} 0.5282 & 0.1819 & -0.0298 & 0.4438 & -0.0871 & 0.0256 \\ -0.1452 & 0.2243 & 0.1329 & 0.0799 & -0.0449 & 0.0198 \\ -0.0598 & -0.0964 & 0.1688 & -0.0417 & -0.0002 & 0.0029 \\ 0 & 0 & 0 & 0.5282 & 0.1819 & -0.0298 \\ 0 & 0 & 0 & -0.1452 & 0.2243 & 0.1329 \\ 0 & 0 & 0 & -0.0598 & -0.0964 & 0.1688 \end{pmatrix}$

Illustrative Examples

The applicability and the efficiency of the proposed strategy are elucidated by the following numerical examples.

Example 4.1 *Let us examine the fractional order differential equation having variable coefficients*

$$D^2h(t) + sin(t)D^{\frac{1}{2}}h(t) + th(t) = f(t), \tag{19}$$

where $f(t) = t^9 - t^8 + 56t^6 - 42x^5 + sin(t)\left\{\frac{32768}{6435}t^{\frac{15}{2}} - \frac{2048}{429}t^{\frac{13}{2}}\right\}$, $t \geq 0$, with regard to the conditions

$$h(0) = 0, \quad h'(0) = 0. \tag{20}$$

The classical solution of (19) is $t^8 - t^7$.

Suppose

$$D^2h(t) \simeq C^T\Psi(t) \text{ and } f(t) \simeq F^T\Psi(t), \text{ where } F^T = [f_1, f_2, \dots, f_N]. \tag{21}$$

Then

$$D^{\frac{1}{2}}h(t) = J^{\frac{3}{2}}\left(D^2(h(t))\right) = C^T P_{N\times N}^{\frac{3}{2}}\Psi(t) \tag{22}$$

and

$$h(t) = C^T P_{N\times N}^2\Psi(t) + h(0) + th'(0) \tag{23}$$

Using (21), (22), (23) in (19), we have

$$C^T\Psi(t) + sin(t)C^T P_{N\times N}^{\frac{3}{2}}\Psi(t) + tC^T P_{N\times N}^2\Psi(t) = F^T\Psi(t) \tag{24}$$

We can attain the coefficient vector C^T by solving the equation (24) at the collocation points. Using the coefficient vector C^T in (23), we get the numerical solutions of (19). Table 1 exhibits that the absolute errors become smaller when the values of k are increased. Table 1 also shows that the numerical solutions rapidly converge to the classical solution. Table 2 exhibits the absolute errors of the shifted Chebyshev polynomial method (SCPM)[1] and the proposed strategy. Table 2 clearly shows that the proposed strategy is superior to SCPM.

Example 4.2 Let us examine the multi term fractional order differential equation

$$D^2h(t) + D^{\frac{1}{2}}h(t) + g(t)Dh(t) + h(t) = f(t), \tag{25}$$

where $g(t) = -2$, $f(t) = t^7 + \frac{2048}{429\sqrt{\pi}} + t^{6.5} - 14t^6 + 42t^5 - t^2 - \frac{8}{3\sqrt{\pi}}t^{1.5} + 4t - 2$, $t \geq 0$, with regard to the conditions

$$h(0) = h'(0) = 0. \tag{26}$$

The classical solution of (25) is $t^7 - t^2$.

Suppose

$$D^2h(t) \simeq C^T\Psi(t) \text{ and } f(t) \simeq F^T\Psi(t), \text{ where } F^T = [f_1, f_2, \dots, f_N]. \tag{27}$$

Then

$$D^{\frac{1}{2}}h(t) = C^T P_{N\times N}^{\frac{3}{2}}\Psi(t) \tag{28}$$

$$Dh(t) = C^T P_{N\times N}\Psi(t) \tag{29}$$

and

$$h(t) = C^T P_{N\times N}^2\Psi(t) + h(0) + th'(0) \tag{30}$$

Using (27), (28), (29), (30) in (25), we have

$$C^T\Psi(t) + C^T P_{N\times N}^{\frac{3}{2}}\Psi(t) - 2C^T P_{N\times N}\Psi(t) + C^T P_{N\times N}^2\Psi(t) = F^T\Psi(t) \tag{31}$$

Aruldoss and Balaji

Solving the equation (31) at the collocation points, we attain unknown coefficient vector C^T. Using the coefficient vector C^T in (30), we get the numerical solutions of (25). Table 3 exhibits that the absolute errors become smaller when the values of k are increased. Table 3 also shows that the numerical solutions rapidly converge to the classical solution. Table 4 exhibits the absolute errors of the Triangular function method(TF)[3], Block pulse function method(BPF)[3] and the proposed method. Table 4 clearly shows that the proposed strategy reaches a higher precision than TF and BPF.

Example 4.3 Let us examine the multi term nonlinear fractional order differential equation having variable coefficients

$$D^2 h(t) + t^{\frac{7}{2}} D^{\frac{3}{2}} h(t) + h^2(t) + h(t) = f(t), \tag{32}$$

where $f(t) = \left(1 + \frac{4}{\sqrt{\pi}}\right) t^4 + 2, \ t \geq 0,$

with regard to the initial conditions

$$h(0) = h'(0) = 0. \tag{33}$$

The classical solution of (32) is t^2.

Suppose

$$D^2 h(t) \simeq C^T \Psi(t) \text{and} f(t) \simeq F^T \Psi(t), \text{where } F^T = [f_1, f_2, \dots, f_N]. \tag{34}$$

Then

$$D^{\frac{3}{2}} h(t) = C^T P^{\frac{1}{2}}_{N \times N} \Psi(t) \tag{35}$$

and

$$h(t) = C^T P^2_{N \times N} \Psi(t) + h(0) + t h'(0) \tag{36}$$

Using (34), (35), (36) in (32), we have

$$C^T \Psi(t) + t^{\frac{7}{2}} \left(C^T P^{\frac{1}{2}}_{N \times N} \Psi(t) \right) + (C^T P^2_{N \times N} \Psi(t))^2 = F^T \Psi(t) \tag{37}$$

Solving the equation (37) at the collocation points, we attain unknown coefficient vector C^T. Using the coefficient vector C^T in (36), we get the numerical solutions of (32). Table 5 exhibits the absolute errors of Chebyshev operational matrix method (COM)[2]. Clearly Table 5 shows the proposed strategy is superior to Legendre wavelet method.

Example 4.4 *Let us examine the multi term fractional order differential equation having variable coefficients*

$$D^{\frac{3}{2}} h(t) + 2Dh(t) + 3\sqrt{t} D^{\frac{1}{2}} h(t) + (1-t)h(t) = f(t), \tag{38}$$

where $f(t) = \frac{2}{\Gamma(1.5)} x^{0.5} + 4x + \frac{4}{\Gamma(1.5)} x^2 + (1-t)t^2, \ t \geq 0,$

with regard to the conditions

$$h(0) = h'(0) = 0. \tag{39}$$

The classical solution of (38) is t^2.

Suppose

$$D^{\frac{3}{2}} h(t) \simeq C^T \Psi(t) \text{and} f(t) \simeq F^T \Psi(t), \text{where } F^T = [f_1, f_2, \dots, f_N]. \tag{40}$$

Then

$$D^{\frac{1}{2}} h(t) = C^T P_{N \times N} \Psi(t) \tag{41}$$

$$Dh(t) = C^T P^{\frac{1}{2}}_{N \times N} \Psi(t) \tag{42}$$

and

$$h(t) = C^T P^{\frac{3}{2}}_{N \times N} \Psi(t) + h(0) + t h'(0) \tag{43}$$

Using (40), (41), (42), (43) in (38), we have

$$C^T \Psi(t) + 2C^T P^{\frac{1}{2}}_{N \times N} \Psi(t) + 3\sqrt{t} C^T P_{N \times N} \Psi(t) + (1-t) C^T P^{\frac{3}{2}}_{N \times N} \Psi(t) = F^T \Psi(t) \tag{44}$$

Solving the equation (44) at the collocation points, we attain unknown coefficient vector C^T. Using the coefficient vector C^T in (43), we get the numerical solutions of (38). Table 6 exhibits that the absolute errors become smaller

when the values of k are increased. Table 6 shows that the numerical solutions rapidly converge to the classical solution.

CONCLUSION

In this article, an efficient numerical algorithm based on Legendre wavelets operational matrix was derived and successfully employed to solve multi term fractional differential equations having variable coefficients. The Legendre wavelet operational matrix is structurally a sparse matrix, which reduces the computational complexity in solving the system of algebraic equations. Moreover, the proposed numerical technique gives solutions with high precision of accuracy. Error tables and graphical demonstrations of numerical examples reveal that the proposed strategy is superior to Shifted Chebyshev polynomial method, Triangular function method, Block pulse function method and Chebyshev operational matrix method in solving multi term fractional differential equations with variable coefficients.

REFERENCES

1. Ali, A., & Ali, N. H. M., On numerical solution of multi-terms fractional differential equations using shifted chebyshev polynomials, International Journal of Pure and Applied Mathematics, 120(1) (2018), 111-125.
2. Atabakzadeh, M. H., Akrami, M. H., & Erjaee, G. H., Chebyshev operational matrix method for solving multi-order fractional ordinary differential equations, Applied Mathematical Modelling 37(20-21) (2013), 8903-8911.
3. Damarla, S. K., & Kundu, M., Numerical solution of multi-order fractional differential equations using generalized triangular function operational matrices, Applied Mathematics and Computation, 263 (2015), 189-203.
4. Diethelm, K., The analysis of fractional differential equations: an application-oriented exposition using operators of caputo type, Springer (2004).
5. Farooq, U., Khan, H., Baleanu, D., & Arif, M., Numerical solutions of fractional delay differential equations using Chebyshev wavelet method, Computational and Applied Mathematics, 38(4) (2019), 1-13.
6. Ji, T., & Hou, J., Numerical solution of the Bagley-Torvik equation using Laguerre polynomials. SeMA Journal, 77(1) (2020), 97-106.
7. Kadkhoda, N., A numerical approach for solving variable order differential equations using Bernstein polynomials, Alexandria Engineering Journal, 59(5) (2020), 3041-3047.
8. Khader, M. M., EL Danaf, T. S., & Hendy, A. S., Efficient spectral collocation method for solving multi-term fractional differential equations based on the generalized Laguerre polynomials, J. Fractional Calc. Appl, 3 (2012), 1-14.
9. Kilicman, A., & Al Zhour, Z. A. A., Kronecker operational matrices for fractional calculus and some applications, Applied Mathematics and Computation, 187(1) (2007), 250-265.
10. Miller, K. S., & Ross, B., An introduction to the fractional calculus and fractional differential equations, Wiley (1993).
11. Mohammadi, A., Aghazadeh, N., & Rezapour, S., Haar wavelet collocation method for solving singular and nonlinear fractional time-dependent Emden-Fowler equations with initial and boundary conditions, Mathematical Sciences, 13(3) (2019), 255-265.
12. Oldham, K. B., & Spanier, J., The Fractional Calculus, Academic Press, New York (1974).
13. Podlubny, I., Fractional differential equations: an introduction to fractional derivatives, fractional differential equations, to methods of their solution and some of their applications, (Vol. 198). Elsevier (1999).
14. Rahimkhani, P., & Moeti, R., Numerical Solution of the Fractional Order Duffing–van der Pol Oscillator Equation by Using Bernoulli Wavelets Collocation Method, International Journal of Applied and Computational Mathematics, 4(2) (2018), 1-18.
15. Rahimkhani, P., Ordokhani, Y., & Babolian, E., Müntz-Legendre wavelet operational matrix of fractional-order integration and its applications for solving the fractional pantograph differential equations, Numerical

Algorithms, 77(4) (2018), 1283-1305.

16. Razzaghi, M., & Yousefi, S., Legendre wavelets direct method for variational problems, Mathematics and computers in simulation, 53(3) (2000), 185-192.

17. Razzaghi, M., & Yousefi, S., The Legendre wavelets operational matrix of integration, International Journal of Systems Science, 32(4) (2001), 495-502.

18. Sabermahani, S., Ordokhani, Y., & Yousefi, S. A., Numerical approach based on fractional-order Lagrange polynomials for solving a class of fractional differential equations, Computational and Applied Mathematics, 37(3) (2018), 3846-3868.

19. Sahu, P. K., & Mallick, B., Approximate solution of fractional order Lane-Emden type differential equation by orthonormal bernoulli's polynomials, International Journal of Applied and Computational Mathematics, 5(3) (2019), 1-9.

20. Talaei, Y., & Asgari, M., An operational matrix based on Chelyshkov polynomials for solving multi-order fractional differential equations, Neural Computing and Applications, 30(5) (2018), 1369-1376.

21. Toan, P. T., Vo, T. N., & Razzaghi, M., Taylor wavelet method for fractional delay differential equations, Engineering with Computers,(2019), 1-10.

22. ur Rehman, M., & Khan, R. A., The Legendre wavelet method for solving fractional differential equations, Communications in Nonlinear Science and Numerical Simulation, 16(11) (2011), 4163-4173.

23. Wang, Y., & Fan, Q., The second kind Chebyshev wavelet method for solving fractional differential equations, Applied Mathematics and Computation, 218(17) (2012), 8592-8601.

24. Wang, Y., Zhu, L., & Wang, Z., Solving the nonlinear variable order fractional differential equations by using Euler wavelets, Computer Modeling in Engineering & Sciences, 118(2) (2019), 339-350.

Table 1: Absolute errors of Example 4.1 obtained by the proposed strategy for $M = 3$ and different values of k.

t	$k = 4$	$k = 5$	$k = 6$	$k = 7$	$k = 8$
0.0625	1.2784e-08	3.5312e-08	2.7676e-09	3.4999e-10	6.0736e-11
0.1875	2.1658e-06	1.3301e-06	2.1540e-07	4.4809e-08	1.2051e-08
0.3125	2.1718e-05	9.1652e-06	2.0342e-06	6.8218e-07	3.8829e-07
0.4375	8.9130e-05	3.4167e-05	1.2310e-05	7.5941e-06	6.4770e-06
0.5625	2.3500e-04	1.0550e-04	6.7192e-05	5.7522e-05	5.4926e-05
0.6875	4.7475e-04	3.1623e-04	2.9617e-04	2.8621e-04	2.8238e-04
0.8125	7.3332e-04	8.4457e-04	9.7158e-04	9.8441e-04	9.8299e-04
0.9375	4.0433e-04	1.6523e-03	2.2491e-03	2.3496e-03	2.3635e-03

Table 2: Absolute errors of Example 4.1 attained by the proposed strategy and SCPM.

t	SCPM	The proposed strategy $(M = 2, k = 4)$
0.1	2.521476e-04	2.0114e-07
0.2	5.142769e-04	1.1124e-05
0.3	8.289741e-04	7.2013e-05
0.4	9.248573e-04	7.8780e-05
0.5	3.452169e-04	4.8732e-04
0.6	5.485201e-04	3.9816e-04
0.7	6.129357e-04	8.5205e-04
0.8	2.968571e-04	1.7584e-04
0.9	5.685742e-04	3.1318e-04

Table 3: Absolute errors of Example 4.2 obtained by the proposed strategy for $M = 3$ and different values of k.

t	$k = 5$	$k = 6$	$k = 7$	$k = 8$	$k = 9$
0.0625	1.0745e-04	2.6864e-05	6.7151e-06	1.6786e-06	4.1960e-07

0.1875	9.9732e-05	2.5095e-05	6.2858e-06	1.5724e-06	3.9315e-07
0.3125	7.3914e-05	1.9530e-05	4.9849e-06	1.2571e-06	3.1549e-07
0.4375	3.4211e-06	2.8077e-06	1.0885e-06	3.1598e-07	8.4134e-08
0.5625	2.0063e-04	4.0729e-05	9.1468e-06	2.1662e-06	5.2711e-07
0.6875	6.3477e-04	1.3848e-04	3.2347e-05	7.8180e-06	1.9220e-06
0.8125	1.4859e-03	3.3318e-04	7.8913e-05	1.9205e-05	4.7377e-06
0.9375	3.0117e-03	6.8648e-04	1.6393e-04	4.0058e-05	9.9015e-06

Table 4: Maximum absolute errors of Example 4.2 obtained by the proposed strategy, TF and BPF method for $h = 0.01$.

TF	BPF	The proposed strategy $M = 3, k = 8$
3.96626e-04	0.01261473	3.1693e-05

Table 5: Absolute errors of Example 4.3 obtained by COM and the proposed method.

t	COM	The proposed strategy $(M = 3, k = 4)$	The proposed strategy $(M = 3, k = 5)$
0.2	8.8×10^{-4}	4.3390e-04	1.0848e-04
0.4	7.8×10^{-3}	4.3213e-04	1.0804e-04
0.6	3.8×10^{-2}	4.2473e-04	1.0620e-04
0.8	2.8×10^{-2}	4.0609e-04	1.0155e-04

Table 6: Absolute errors of Example 4.4 attained by the proposed method for $M = 2$ and different values of k.

t	$k = 5$	$k = 6$	$k = 7$	$k = 8$	$k = 9$
0.0625	3.3867e-04	6.8162e-05	1.0863e-05	3.7567e-07	8.0652e-07
0.1875	2.0627e-04	8.6279e-06	1.6765e-05	1.2699e-05	7.0835e-06
0.3125	4.2434e-06	9.1757e-05	6.6746e-05	3.7604e-05	1.9501e-05
0.4375	2.7972e-04	2.3475e-04	1.3856e-04	7.3607e-05	3.7531e-05
0.5625	6.3156e-04	4.1213e-04	2.2772e-04	1.1834e-04	5.9946e-05
0.6875	1.0324e-03	6.1403e-04	3.2914e-04	1.6920e-04	8.5433e-05
0.8125	1.4638e-03	8.3094e-04	4.3802e-04	2.2379e-04	1.1277e-04
0.9375	1.9087e-03	1.0544e-03	5.5007e-04	2.7994e-04	1.4089e-04
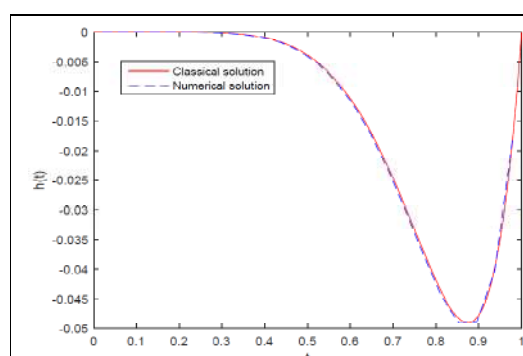
Figure 1: Comparison of the attained numerical solutions for $M = 3, k = 4$ with the classical solution of Example 4.1.	**Figure 2: Comparison of the attained numerical solutions for $M = 3, k = 4$ with the classical solution of Example 4.2.**
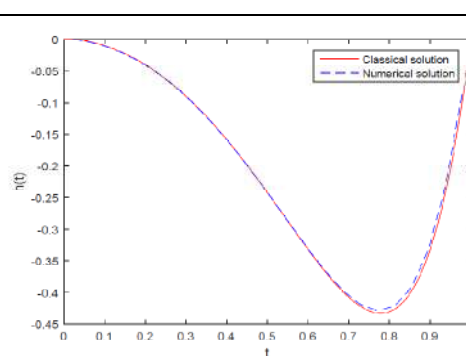
Aruldoss and Balaji

Figure 3: Comparison of the attained numerical solutions for $M = 3$, $k = 4$ with the classical solution of Example 4.3.

Figure 4: Comparison of the attained numerical solutions for $M = 3$, $k = 4$ with the classical solution of Example 4.4.

RESEARCH ARTICLE
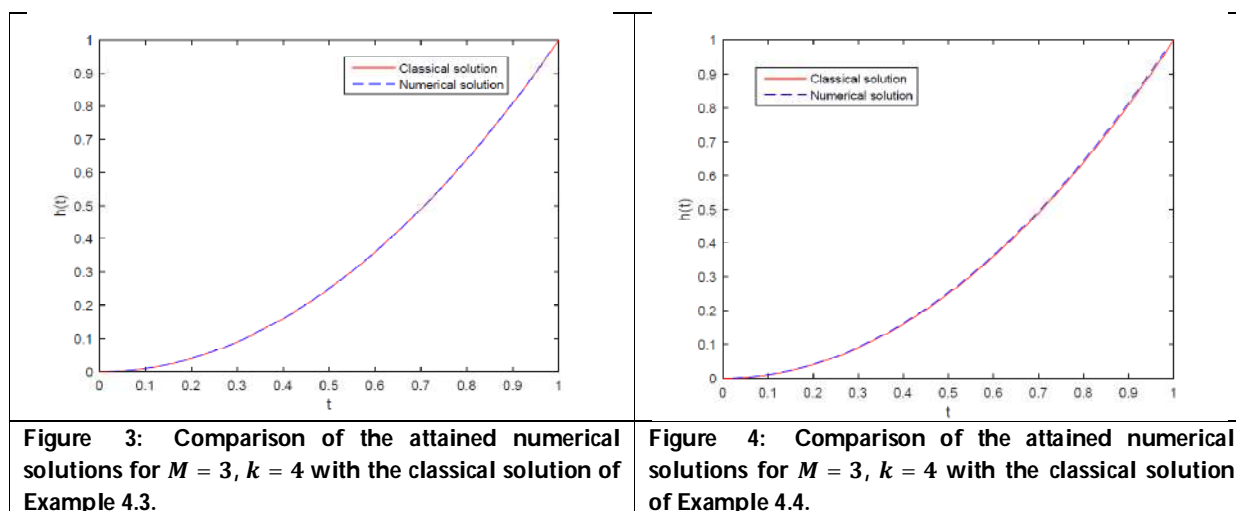
Titanium Dioxide Nanoparticles as a Highly Efficient Reusable Catalyst for the Synthesis of 2-Amino-4H-Pyran

Abdulfatah Abdullah Abdu Saifan[1], Amat Alrahman Othman[2], Priyanka Sunil Pinate[1], Nabeel M. S. Kaawash[3] and Sangita Sanjay Makone[4]*

[1]Research Scholar, School of Chemical Sciences, Swami Ramanand Teerth Marathwada University, Nanded, 431606, Maharashtra, India.
[2]Research Scholar, Department of Chemistry, University of Delhi 110007, India.
[3]Research Scholar, School of Physical Sciences, Swami Ramanand Teerth Marathwada University, Nanded, 431606, Maharashtra, India.
[4]Professor, School of Chemical Sciences, Swami Ramanand Teerth Marathwada University, Nanded, 431606, Maharashtra, India.

*Address for Correspondence
Sangita Sanjay Makone
Professor,
School of Chemical Sciences,
Swami Ramanand Teerth Marathwada University,
Nanded, 431606, Maharashtra, India.
E.Mail: ss_makone@rediffmail.com

ABSTRACT

Titanium dioxide nanoparticles were developed as a new and efficient heterogeneous catalyst for the synthesis of 2-amino-4H-pyran annulated heterocyclic systems by reacting ethyl/methyl acetoacetate with aldehyde and malononitrile. At 80^0C for half an hour, a reaction between different aldehydes, methyl acetoacetate, and malononitrile was carried out in EtOH as a green solvent. In good yields, this process produced 2-amino-4H-pyran-containing heterocyclic compounds, including thirteen derivatives.Titanium dioxide nanoparticles were recycled and reused five times with no reduction in catalyst quantity or efficiency. Because titanium dioxide is a cheap, readily accessible, non-toxic, and recyclable catalyst, this method is exceedingly efficient, economical, and environmentally friendly.

Keywords: Titaniumdioxide, Aldehyde , Ethyl/Methyl Acetoacetate, Malononitrile, 2-amino-4H-pyran.

Abdulfatah Abdullah Abdu Saifan *et al.,*
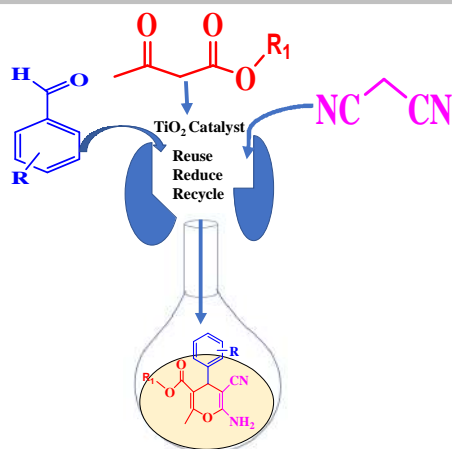
R= OH, CH₃, OCH₃. CI, Br, NO₂, H,
R¹= Ethyl (a1, a9), Methyl (a10, a14)

INTRODUCTION

With growing concern about environmental pollution, the development of innovative green approaches in chemical synthesis has received a lot of attention. Heterogeneous catalysis and green solvents are critical to the successful development of green chemistry, and promising techniques have been reported[1]. The dangers of organic solvents drew researchers' attention to the development of new methods for using EtOH as a solvent[2,3]. Recently, several papers have proven the relevance of ethanol in chemical processes [4]. Catalytic processes generated by heterogeneous catalysts provide advantages such as ease of handling, easy work up, and catalyst renew-ability. TiO₂ is a low-cost and widely available heterogeneous acidic catalyst with numerous commercial uses, including selective NOx reduction in stationary sources, photocatalysis for pollutant elimination or organic synthesis, sensors, photovoltaic devices, and paints [5]. Metal oxides with nanoscale dimensions exhibit remarkable magnetic, physical, surface chemical, and catalytic characteristics [6,7]. TiO₂ nanoparticles have been used as a catalyst in organic syntheses such as the Friedel Crafts alkylation of indoles with epoxides [8]. amino-4H-pyrans are important biological compounds that have spasmolytic, analgesic, anticonvulsant, antibacterial, anticancer, anti-tubercular, anthelmintic, antioxidant, antiglycation, and antidepressant properties [9-11].

2-amino-4H-pyrans, which are annulated heterocyclic structures, exhibit anti-bacterial, anti-tumor, anti-hypertensive, and vasodilator properties. As a result, the development of new greener techniques for their synthesis remains of interest [12-15]. Following our attempts to explore new approaches for the synthesis of heterocyclic molecules[16,17]. Within some of the min, a green approach for the synthesis of 2-amino-4H-pyrans in ethanol with TiO2 NPs as the heterogeneous reusable catalyst was devised. (Scheme 1). In this work, we have synthesized 2-amino-4H-pyrans derivatives efficiently in a one-pot synthesis employing nano-sized titanium dioxide as a heterogeneous catalyst. The current approach has various advantages, including excellent yields, short reaction durations (20-60 min), and ecologically friendly and mild reaction conditions. The catalyst is easily isolated from the reaction products and can be recovered in high purity for direct reuse. Because they may be easily recovered from the reaction mixture by simple filtration and reused after activation, heterogeneous catalysts have an economic advantage over traditional homogeneous catalysts.

Abdulfatah Abdullah Abdu Saifan *et al.,*

Experimental

Materials were purchased from chemist supply companies like Merck, Fluka, and Aldrich. The melting points (in degrees Celsius) were measured with an open-glass capillary on an Electrothermal MK_3 equipment. TLC was used to track reaction completion on silica gel plates using a chloroform solvent solution ($CHCl_3$). The functional groups were examined using FTIR. All of the substances' IR spectra were measured using a Perkin Elmer FT-IR 550 spectrophotometer. Bruker DRX-400 spectrometer was used to measure 1H and ^{13}C NMR spectra. The X-ray diffraction investigation was performed using the Philips Xpert X-ray diffraction system (XRD). The KYKY EM-3200 scanning electron microscope was used to get the SEM pictures.

Synthesis of Titanium dioxide (TiO_2) nanoparticles.

In a typical experiment, synthesize titanium dioxide by dissolving 5 ml of $TiCl_4$ solutions into 45 ml of distilling water under vigorous stirring at room temperature for 25 min. then o.1 mole of urea was added to the reaction and heated in Water Bath at 60oC for 15 to 40 min. then got the precipitates and then filtration and dried(white powders) and characterized by (SEM, EDX, Mapping, IR, and XRD).

Characterization

Using a Bruker (D5005) X-ray diffractometer with graphite monochromatized CuK radiation (=1.54056), the crystalline properties of the synthesized TiO_2 -NPs were investigated. It was decided to use a 40 kV accelerating voltage and a 30 mA emission current for the tests. The structure of the TiO_2 -NPs was verified with both XRD and FTIR spectroscopy measurements. SEM was utilized to investigate the TiO2 -NPs' chemical makeup. The Hitachi S-4800 high-resolution (HR) field emission scanning electron microscope was used for the SEM observations. Elements were analyzed with the help of an EDAX spectrometer, which was included with the FE-SEM instruments. Using a spectrophotometer (Jasco V 670), we obtained absorption spectra of the samples in the 200-1000 nm range while recording them in the diffused reflectance spectrum (DRS) mode.Adsorption edge values were extrapolated to obtain band gap values.

General procedure for the synthesis of 2-amino-4H-pyrans.

In this method, in a two-neck round bottom flask, a combination of aromatic aldehyde, malononitrile, and ethyl/methyl acetoacetate (1:1:1 mol ratio) with the titanium dioxide catalyst (10 mg) was added. Then, the ethanol as solvent was added to the reaction vessel and refluxed at 80^0C under continuous stirring. TLC plates were used to monitor the reaction's progress, while a TLC tank was filled with a 7:3 mixture of ethyl acetate and n-hexane. After the reaction was finished, the mixture was filtered to remove the solvent, and the result was mixed with a little amount of hot alcohol. The catalyst was separated by filtration after the product had been stirred and dissolved in alcohol. Finally, the catalyst was rinsed multiple times with hot alcohol to thoroughly collect all products. After evaporating the ethanol, place the filtrate at room temperature to collect the 2-amino-4H-pyran derivatives as showing in Fig. 1.

Synthesis of ethyl 6-amino-5-cyano-2-methyl-4-(4-chlorophenyl)-4H-pyran-3-carboxylate(1a)

M.p.; $175-177^0C$; Yield: 92%; IR (ATR, CM^{-1}): 3365, 3404 (-NH primary amine), 1675 (-C=O), 2191 (-CN), 834 (-C-Cl); Anal. Calcd. For $C_{16}H_{15}ClN_2O_3$: N-8.74, H-4.72, C-60.20; Found: N-8.79, Cl-11.12, H-4.47, H-4.47; ^1H NMR: 4.03 (m,2H,-CH2), 1.29 (t,3H,-CH₃ ester), 6.80 (s,2H,NH₂), 2.2 (s,3H,CH₃), 6.4-4.7 (m,4H,Ar-H); ^{13}C NMR (100 MHz, DMSO-d6,ppm): 156.15 (C-12), 158,39 (C-10), 156.92 (C-9), 143.84 (C-6), 131.42 (C-3), 128.97 (C-1,C-5), 128,25 (C-2,C-4), 119,47 (CN), 106.74 (C-8), 60.09 (C-13), 56.90 (C-11), 39.09 (C-7), 18.18 (CH₃), 13.67 (C-14). m/z: 319.7

Synthesis of ethyl 6-amino-5-cyano-2-methyl-4-(3-hydroxyphenyl)-4H-pyran-3-carboxylate (2a).

M.p.; $163-164^0C$; Yield: 93%; IR (ATR, CM^{-1}): 3365, 3404 (-NH primary amine), 1675 (-C=O), 2191 (-CN), 3580 (-OH); Anal. Calcd. For $C_{16}H_{16}N_2O_4$: N-5.72, C-63.78, H-5.27; Found: N-9.33%, H-5.37, C-63,99; ^1H NMR: 4.03 (m,2H,-CH2), 1.29 (t,3H,-CH₃ ester), 6.80 (s,2H,NH₂), 2.2 (s,3H,CH₃), 6.4-6.7 (m,4H,Ar-H), 4.41 (s,iH,OH); ^{13}C NMR (100 MHz, DMSO-d6,ppm): 165.30 (C-12), 158,46 (C-10), 156.93 (C-9), 144.10 (C-6), 130.42 (C-4), 134.10 (C-2), 128.10 (C-1), 126.35

Abdulfatah Abdullah Abdu Saifan *et al.,*

(C-5), 126,22 (C-3), 119,42 (CN), 106.81 (C-8), 60.11 (C-13), 56.96 (C-11), 39.09 (C-7), 18.20 (CH$_3$), 13.69 (C-14). m/z: 301.1

Synthesis of ethyl 6-amino-5-cyano-2-methyl-4-(4-nitrophenyl)-4H-pyran-3-carboxylate(3a).
M.p.; 176-177^{0}C; Yield: 96%; IR (ATR, CM^{-1}): 3365, 3404 (-NH primary amine), 1680(-C=O), 2198 (-CN), 1516 (-N=O); Anal. Calcd. For C$_{16}$H$_{15}$N$_3$O$_5$: N-12.07, C-58.00, H-4.34; Found: N-12.76%, H-4.59, C-58.36; ^{1}H NMR: 4.03 (m,2H,-CH$_2$), 1.29 (t,3H,-CH$_3$ ester), 6.80 (s,2H,NH$_2$), 2.2 (s,3H,CH$_3$), 7.4-8.1 (m,4H,Ar-H); ^{13}C NMR (100 MHz, DMSO-d6,ppm): 164.90 (C-12), 158,49 (C-10), 157.93 (C-9), 152.40 (C-6), 146.42 (C-3), 128.10 (C-2.C-4), 123.10 (C-1.C-5), 119,19 (CN), 105.95 (C-8), 60.17 (C-13), 56.21 (C-11), 39.08 (C-7), 18.28 (CH$_3$), 13.62 (C-14). m/z: 330.1

Synthesis of ethyl 6-amino-5-cyano-2-methyl-4-(2-hydroxyphenyl)-4H-pyran- 3-carboxylate(4a).
M.p.; 165-167^{0}C; Yield: 90%; IR (ATR, CM^{-1}): 3365, 3404 (-NH primary amine), 1675(-C=O), 2191 (-CN), 3580 (-OH); Anal. Calcd. For C$_{16}$H$_{16}$N$_2$O$_4$: N-9.07, C-63.42, H-5.30; Found: N-9.33%, H-5.37, C-63.99; ^{1}H NMR: 4.03 (m,2H,-CH$_2$), 1.29 (t,3H,-CH$_3$ ester), 6.80 (s,2H,NH$_2$), 2.2 (s,3H,CH$_3$), 6.86-7.27 (m,4H,Ar-H), 9.68(s,1H,OH); ^{13}C NMR (100 MHz, DMSO-d6,ppm): 165.25 (C-12), 158,29 (C-10), 156.89 (C-9), 143.90 (C-6), 131.4 (C-1), 128.77 (C-2), 127.10 (C-3),126.90 (C-4), 126.57 (C-5), 119,39 (CN), 106.78 (C-8), 60.20 (C-13), 56.92 (C-11), 39.08 (C-7), 18.24 (CH$_3$), 13.64 (C-14). m/z: 301.1

Synthesis of ethyl 6-amino-5-cyano-2-methyl-4-phenyl-4H-pyran-3-carboxylate(5a).
M.p.; 189-190^{0}C; Yield: 91%; IR (ATR, CM^{-1}): 3365, 3397 (-NH primary amine), 1692(-C=O), 2168 (-CN); Anal. Calcd. For C$_{16}$H$_{16}$N$_2$O$_3$: N-9.80, C-67.42, H-5.43; Found: N-9.85%, H-5.67, C-67.59; ^{1}H NMR: 4.03 (m,2H,-CH$_2$), 1.29 (t,3H,-CH$_3$ ester), 6.80 (s,2H,NH$_2$), 2.2 (s,3H,CH$_3$), 6.86-7.27 (m,5H,Ar-H); ^{13}C NMR (100 MHz, DMSO-d6,ppm): 164.95 (C-12), 158,32 (C-10), 157.12 (C-9), 145.1 (C-6), 126.8 (C-1,C-5), 128.9 (C-2,C-4), 127.10 (C-3), 126.90 (C-4), 126.57 (C-5), 119,39 (CN), 285.11

Synthesis of methyl 6-amino-4-(4-chlorophenyl)-5-cyano-2-methyl-4H-pyran-3-carboxylate(9a).
M.p.; 192-194^{0}C; Yield: 97%; IR (ATR, CM^{-1}): 3365, 3404 (-NH primary amine), 1675(-C=O), 2191 (-CN), 834 (-C-Cl); Anal. Calcd. For C$_{15}$H$_{13}$N$_2$O$_3$: N-9.07, C-59.00, H-4.15; Found: N-9.19%, H-4.30, C-59.11; ^{1}H NMR: 6.80 (s,2H,NH$_2$), 2.31 (s,3H,CH$_3$), 3.61 (s,3H,CH$_3$), 7.15-721 (m,4H,Ar-H); ^{13}C NMR (100 MHz, DMSO-d6,ppm): 165.16 (C-12), 158,39 (C-10), 156.93 (C-9), 142.80 (C-6),131.42(C-3), 128.97 (C-1.C-5),128.24 (C-2.C-4), 119,49 (CN), 106.95 (C-8), 60.07 (C-13), 56.91 (C-11), 39.08 (C-7), 18.18 (CH$_3$), 13.66 (C-14). m/z: 305.0

Synthesis of methyl 6-amino-5-cyano-4-(3-hydroxyphenyl)-2-methyl-4H-pyran-3-carboxylate(10a).
M.p.; 163-165^{0}C; Yield: 90%; IR (ATR, CM^{-1}): 3365, 3404 (-NH primary amine), 1675(-C=O), 2191 (-CN), 3580 (-OH); Anal. Calcd. For C$_{15}$H$_{14}$N$_2$O$_4$: N-9.65, C-62.42, H-4.73; Found: N-9.79%, H-4.93, C-62.93; ^{1}H NMR: 6.80 (s,2H,NH$_2$), 2.31 (s,3H,CH$_3$), 3.61 (s,3H,CH$_3$), 6.7-7.0 (m,4H,Ar-H); ^{13}C NMR (100 MHz, DMSO-d6, ppm): 165.31 (C-12), 158,47 (C-10), 156.93 (C-9), 144.80 (C-6),134.11 (C-2), 130,41 (C-4), 128.97 (C-1), 126.35(C-5),126.22(C-3),119,41 (CN), 106.81 (C-8), 60.11 (C-13), 56.95 (C-11), 39.08 (C-7), 18.19 (CH$_3$), 13.68 (C-14). m/z: 287.09

Synthesis of methyl 6-amino-5-cyano-2-methyl-4-(4-nitrophenyl)-4H-pyran-3-carboxylate(11a).
M. p.; 175-177^{0}C; Yield: 94%; IR (ATR, CM^{-1}): 3370, 3440 (-NH primary amine), 1680(-C=O), 2198 (-CN), 1516 (-N=O); Anal. Calcd. For C$_{15}$H$_{13}$N$_3$O$_5$: N-13.13, C-57.09, H-4.10; Found: N-13.33%, H-4.16, C-67.14; ^{1}H NMR: 6.80 (s,2H,NH$_2$), 2.31 (s,3H,CH$_3$), 3.61 (s,3H,CH$_3$), 7.0-8.0 (m,4H,Ar-H); ^{13}C NMR (100 MHz, DMSO-d6, ppm): 164.90 (C-12), 158,49 (C-10), 157.87 (C-9), 152.41 (C-6),146.3 (C-3), 138,3 (-C2,C-4), 123.6 (C-1,-C5), 119,91 (CN), 105.97 (C-8), 60.18 (C-13), 56.21 (C-11), 39.08 (C-7), 18.29 (CH$_3$), 13.62 (C-14). m/z: 316.09 (C-3), 126.90 (C-4), 126.57 (C-5), 119,39 (-CN), 106.79 (C-8), 60.18 (C-13), 56.93 (C-11), 39.08 (C-7), 18.25 (CH$_3$), 13.64 (C-14). m/z: 287.09

Synthesis of methyl 6-amino-5-cyano-2-methyl-4-phenyl-4H-pyran-3-carboxylate(12a).
M.p.; 194-195^{0}C; Yield: 96%; IR (ATR, CM^{-1}): 3340, 3397 (-NH primary amine), 1692(-C=O), 2186 (-CN); Anal. Calcd. For C$_{15}$H$_{14}$N$_2$O$_3$: N-10.27, C-66.42, H-5.13; Found: N-10.36%, H-5.22, C-66.66; ^{1}H NMR: 6.80 (s,2H,NH$_2$), 2.31

Abdulfatah Abdullah Abdu Saifan *et al.,*

(s,3H,CH$_3$), 3.61 (s,3H,CH$_3$), 6.5-7,5 (m,5H,Ar-H); ^{13}C NMR (100 MHz, DMSO-d6, ppm): 164.98 (C-12), 158,32 (C-10), 157.12 (C-9), 145.01 (C-6),128.9 (C-2,-C4), 126,08 (-C1,-C5), 127.16 (C-3). m/z: 271.1

RESULTS AND DISCUSSION

The sol-gel technique was used to create nano-sized titanium dioxide from titanium tetrachloride and ethanol, as described in the literature [18]. According to the data, the prepared titanium dioxide has a surface area of 51.859 m^2/g. Based on a calculation assuming a spherical shape for the catalyst particles, this corresponds to a size of 18.94 nm. An XRD pattern revealed a distinctive peak at 25.34^0. Fig.2. shows the XRD peaks for anatase associated with the (101), (004), (200), (105), and (204) reflections, which correspond with the reported findings [19]. For this sample, the crystallite diameters are determined to be 10 nm from the half-height width of 2^0 of the peak at 25.34^0 for anatase associated with The (101) TiO$_2$, using the Scherrer formula. The disparity in particle size between the specific surface area measurement and the XRD diffraction pattern is owing to the difference in particle shape assumption, i.e. the BET analysis assumes a spherical shape whereas the XRD analysis is based on the anatase phase. The morphological SEM picture indicates that the particles are roughly 29 nm in size and agglomerate showing in Fig. 3. The study of TiO$_2$ nanoparticles (anatase and rutile) using energy-dispersive X-ray spectroscopy (EDX) reveals peaks for Titanium and oxygen. There is no trace of any other contaminants in the EDX study, as shown in Fig. 4. TiO$_2$ energy-dispersive x-ray diffraction (EDX) spectrum (anatase and rutile). Fig. 5. shows the (FT-IR) spectra of titanium dioxide nanoparticles. The FT-IR spectra were captured between 4,000 and 400 cm^{-1}. Bands with frequencies of 3,445 cm^{-1} for OH, 1,640 cm^{-1} for C=O stretching, and bending of nitro N-O (1,395 cm^{-1}). The creation of titanium dioxide nanoparticles was approved by the peak at 650 cm^{-1} that were absorbed.

To begin, we investigated the treatment of aldehyde and amine as a model reaction in H$_2$O using various catalysts to assess the effectiveness of titanium dioxide nanoparticles in this process. The reaction conditions for the production of 2-amino-4H-pyran derivatives were optimized. Optimization of catalyst quantity (Table 3, entries 1-4), temperature (Table 3, entries 5-11), and solvent (Table 3, entries 12-15) were studied, as in the preceding section. As a result, the reaction of benzaldehyde, malononitrile, and ethyl acetoacetate was chosen as the model reaction Table. 4. The ideal condition for the model reaction, according to these investigations, is shown in entry 10. Table.2. displays some of the findings from tests conducted on different types of catalysts. TiO$_2$ nanoparticles outperformed both TiO$_2$at room temperature and the other catalysts indicated in Table 2 in terms of yield and reaction rate. Ce-ZSM-11, Fe$_3$O$_4$@g-C$_3$N$_4$, MNP@PEG-ImOH, HPNb, and Zn^{+2}/4A, were initially tested as catalysts, However, even at large catalyst loadings, the yields achieved were only modest (Table 2, entries 1–6). Titanium dioxide nanoparticles in ethanol had a 96% isolated yield, which was the best result (Table 2, entry 7). TiO$_2$ nanoparticles may be more effective than other catalysts because they have a larger surface area.

An increase in catalyst loading from 10% to 20% did not improve the yield significantly while lowering the catalyst loading from 10% to 8% and decreasing the temperature from 80 to 45 ^{0}C lowered the yield and increased the reaction time. To illustrate the catalyst's efficiency, a blank reaction was performed in the absence of the catalyst in the presence of refluxing EtOH. Only 30% of the product was separated after 6 h of stirring, classical work-up, and recrystallization from ethanol (Table 3, entry 9). We then continued to optimize the above-mentioned model reaction by measuring the efficiency of numerous classical solvents used as comparison medium (Table 3). In each case, the substrates were combined with 10% titanium dioxide nanoparticles and agitated with 2 ml solvent. It was discovered that CH$_2$Cl$_2$, toluene, CH$_3$CN, H$_2$O, and the solventless system were unfavorable for the synthesis of the product (Table 3, entries 1- 6). The effect of temperature was also studied by carrying out the influence of temperature was further investigated by running the model response at various temperatures (Table 3, entries 8-10). When the reaction was carried out in EtOH at 80 ^{0}C, the product produced an excellent yield (Table 3, entry 8). Using a variety of structurally different aldehydes, we assessed the efficacy and applicability of our methodology for component condensation. Table 4 shows the results of smooth cyclo condensation of several aliphatic, aromatic, and aldehydes in good to outstanding yields. As indicated in this Table, aromatic aldehydes with electron-deficient or electron-rich

Abdulfatah Abdullah Abdu Saifan *et al.,*

substituents on the aromatic ring, as well as aliphatic aldehydes, gave excellent yields of the required 2-amino-4H-pyran(Table 4, entry 1-13). In terms of ecologically friendly techniques, the benefits of the utilized catalyst are considerably greater if it can be recovered and reused. To investigate the recyclability of the catalyst, titanium dioxide nanoparticles were recovered from the reaction mixture in the model reaction using a simple workup and employed in five consecutive runs without substantial loss of catalytic activity (Table 5). Reaction conditions: benzaldehyde (1mol), malononitrile (1mol), ethyl acetoacetate (1mol), 10 gm of TiO_2NPs in ETOH at 80^0C

CONCLUSIONS

We discovered a simple and effective approach for synthesizing 2-amino-4H-pyran in EtOH utilizing titanium dioxide nanoparticles as catalysts. This approach has various advantages, including a high yield, a quick reaction time, a simple work-up procedure that avoids the discharge of toxic organic solvents, ease of separation, and the catalyst's recyclability.

ACKNOWLEDGMENTS

DECLARATION OF COMPETING INTEREST

The authors declare that they have no known conflicting financial or personal interests that may have seemed to affect the work presented in this study.

REFERENCES

1.   S. M. George,Introduction: heterogeneous catalysis. Chemical Reviews. 1995. 95, 475.
2.   G. Nagendrappa,Organic synthesis under solvent-free condition:An environmentally benign procedure—I. Resonance. 2002. 7, 59-68.
3.   M. O. Simon, C. J. Li, Green chemistry oriented organic synthesis in water. Chemical Society Reviews. 2012. 41(4), 1415-1427.
4.   P. A. Grieco,Transition metal based ionic liquid (bulk and nanofiber composites) used as catalyst for reduction of aromatic nitro compounds under mild conditions. RSC advances 3.10 (2013): 3399-3406.
5.   A. Maldotti, A. Molinari, R. Amadelli, Photocatalysis with organized systems for the oxofunctionalization of hydrocarbons by O_2. Chemical Reviews.2002. 102(10), 3811-3836.
6.   R. Richards, W. Li, S. Decker, C. Davidson, O. Koper, V. Zaikovski, K. J. Klabunde, Consolidation of metal oxide nanocrystals. Reactive pellets with controllable pore structure that represent a new family of porous, inorganic materials.Journal of the American Chemical Society. 2000. 122(20), 4921-4925.
7.   B. M. Choudary, M. L. Kantam, K. V. Ranganath, K. Mahendar, B. Sreedhar, Bifunctional nanocrystalline MgO for chiral epoxy ketones via Claisen– Schmidt condensation– asymmetric epoxidation reactions. Journal of the American Chemical Society. 2004. 126(11), 3396-3397.
8.   M. L. Kantam, S. Laha, J. Yadav, B. Sreedhar, Friedel–Crafts alkylation of indoles with epoxides catalyzed by nanocrystalline titanium (IV) oxide.Tetrahedron letters. 2006. 47(35), 6213-6216.
9.   E. C. Witte, P. Neubert, A. Roesch, 7-(Piperazinylpropoxy)-2H-1-benzopyran-2-ones. Ger Offen DE. 1986. 3427985.
10. T. Siddiqui, M. G. Alam, N. Islam, A two step facile synthesis of new steroidal linear and angular pyranones having anti-mycobacterial activity.Chinese Chemical Letters. 2009. 20(2), 153-157.

11. L. Bonsignore, G. Loy, D. Secci, A. Calignano, Synthesis and pharmacological activity of 2-oxo-(2H) 1-benzopyran-3-carboxamide derivatives.European Journal of Medicinal Chemistry. 1993. 28(6), 517-520.

12. Y. Sarrafi, E. Mehrasbi, A. Vahid, M. Tajbakhsh, Well-ordered mesoporous silica nanoparticles as a recoverable catalyst for one-pot multicomponent synthesis of 4H-chromene derivatives. Chinese Journal of Catalysis. 2012. 33(9-10), 1486-1494.

13. S. M. Baghbanian, N. Rezaei, H. Tashakkorian, Nanozeolite clinoptilolite as a highly efficient heterogeneous catalyst for the synthesis of various 2-amino-4 H-chromene derivatives in aqueous media.Green Chemistry. 2013. 15(12), 3446-3458.

14. V. M. Joshi, R. L. Magar, P. B. Throat, S. U. Tekale, B. R. Patil, M. P. Kale, R. P. Pawar, Novel one-pot synthesis of 4H-chromene derivatives using amino functionalized silica gel catalyst. Chinese Chemical Letters. 2014. 25(3), 455-458.

15. S. Nemouchi, R. Boulcina, B. Carboni, A. Debache, Phenylboronic acid as an efficient and convenient catalyst for a three-component synthesis of tetrahydrobenzo [b] pyrans. Comptes Rendus Chimie. 2012. 15(5), 394-397.

16. L. Edjlali, The Regiospecific Synthesis of Some New 3, 5-Disubstituted Isoxazoles. Journal of the Chinese Chemical Society. 2008. 55(6), 1322-1325.

17. Y. R. Mirzaei, L. Edjlali,Synthesis and characterization of 2-alkyl-5-{4-[(3-nitrophenyl-5-isoxazolyl) methoxy] phenyl}-2 H-tetrazoles. Journal of the Iranian Chemical Society. 2010. 7, 685-694.

18. G. Li, L. Li, J. Boerio-Goates, B. F. Woodfield, Synthesis and characterization of 2-alkyl-5-{4-[(3-nitrophenyl-5-isoxazolyl) methoxy] phenyl}-2 H-tetrazoles.Journal of the American Chemical Society. 2005. 127(24), 8659-8666.

19. T. Tong, J. Zhang, B. Tian, F. Chen, D. He, Preparation and characterization of anatase TiO2 microspheres with porous frameworks via controlled hydrolysis of titanium alkoxide followed by hydrothermal treatment.Materials Letters. 2008. 62(17-18), 2970-2972.

20. S. Balaji, R. Guda, B.K. Mandal, M. Kasula, E. Ubba, F.-R.N. Khan, Green synthesis of nano-titania (TiO 2 NPs) utilizing aqueous Eucalyptus globulus leaf extract: applications in the synthesis of 4 H-pyran derivatives.Research on Chemical Intermediates. 2021. 47, 3919-3931.

21. R. R. Magar, G. T. Pawar, S. P. Gadekar, M. K. Lande, Ce-ZSM-11 Zeolite: An Efficient Heterogeneous Catalyst for One-Pot Synthesis of 4H-Pyran Derivatives. Iranian Journal of Chemistry and Chemical Engineering. 2020. 39(1), 91-104.

22. N. Azizi, T. S. Ahooie, M. M. Hashemi, I. Yavari. Magnetic graphitic carbon nitride-catalyzed highly efficient construction of functionalized 4H-pyrans. Synlett, 2018. 29(05), 645-649.

23. M. Fallah-Mehrjardi, M. Shirzadi, S.H. Banitaba, A New Basic Ionic Liquid Supported on Magnetite Nanoparticles: An Efficient Phase-Transfer Catalyst for the Green Synthesis of 2-Amino-3-Cyano-4 H-Pyrans. Polycyclic Aromatic Compounds. 2020. 1–12.

24. L. F. Gutierrez, E. Nope, H. A. Rojas, J. A. Cubillos, Á. G. Sathicq, G. P. Romanelli, J. J. Martínez, New application of decaniobate salt as basic solid in the synthesis of 4 H-pyrans by microwave assisted multicomponent reactions.Research on Chemical Intermediates. 2018. 44, 5559-5568.

25. Á. Magyar, Z. Hell, One-pot, three-component, selective synthesis of the polyfunctionalized 4H-pyran and 4H-benzo [b] pyran derivatives in the presence of a highly efficient molecular sieve-supported zinc catalyst.Green Processing and Synthesis. 2018. 7(4), 316-322.

26. A. Martínez-Grau, J. Marc, Friedländer reaction on 2-amino-3-cyano-4H-pyrans: Synthesis of derivatives of 4H-pyran [2, 3-b] quinoline, new tacrine analogues. Bioorganic & Medicinal Chemistry Letters. 1997. 7(24), 3165-3170.

27. J. Quintela, C. Peinador, M. J. Moreira, A novel synthesis of pyrano [2, 3-d] pyrimidine derivatives.Tetrahedron. 1995. 51(20), 5901-5912.

28. S. Banerjee, A. Horn, H. Khatri, G. Sereda, A green one-pot multicomponent synthesis of 4H-pyrans and polysubstituted aniline derivatives of biological, pharmacological, and optical applications using silica nanoparticles as reusable catalyst.Tetrahedron Letters. 2011. 52,1878-1881.

29. S. S. Mansoor, K. Logaiya, K. Aswin, P. N. Sudhan, An appropriate one-pot synthesis of 3, 4-dihydropyrano [c] chromenes and 6-amino-5-cyano-4-aryl-2-methyl-4H-pyrans with thiourea dioxide as an efficient, reusable organic catalyst in aqueous medium.Journal of Taibah University for Science. 2015. 9(2), 213-226.

Abdulfatah Abdullah Abdu Saifan *et al.,*

30. M. Amirnejad, M. R. Naimi-Jamal, H. Tourani, H. Ghafuri, A facile solvent-free one-pot three-component method for the synthesis of 2-amino-4 H-pyrans and tetrahydro-4 H-chromenes at ambient temperature.Monatshefte für Chemie-Chemical Monthly. 2013. 144, 1219-1225.

31. S. Banerjee, A. Horn, H. Khatri, G. Sereda, A green one-pot multicomponent synthesis of 4H-pyrans and polysubstituted aniline derivatives of biological, pharmacological, and optical applications using silica nanoparticles as reusable catalyst.Tetrahedron Letters. 2011. 52,1878-1881.

32. G. P. Lu, C. Cai, A facile, one-pot, green synthesis of polysubstituted 4H-pyrans via piperidine-catalyzed three-component condensation in aqueous medium.Journal of Heterocyclic Chemistry. 2011. 48(1), 124-128.

33. M. Amirnejad, M. R. Naimi-Jamal, H. Tourani, H. Ghafuri, A facile solvent-free one-pot three-component method for the synthesis of 2-amino-4 H-pyrans and tetrahydro-4 H-chromenes at ambient temperature.Monatshefte für Chemie-Chemical Monthly. 2013. 144, 1219-1225.

34. X. S. Wang, Z. S. Zeng, M. M. Zhang, Y. L. Li, D. Q. Shi, S. J. Tu, Z. M. Zong, A convenient and clean procedure for the synthesis of pyran derivatives in aqueous media catalysed by TEBAC. Journal of Chemical Research. 2006. 2006(4), 228-230.

35. D. Kumar, V. B. Reddy, S. Sharad, U. Dube, S. Kapur, A facile one-pot green synthesis and antibacterial activity of 2-amino-4H-pyrans and 2-amino-5-oxo-5, 6, 7, 8-tetrahydro-4H-chromenes.European journal of medicinal chemistry. 2009. 44(9), 3805-3809.

36. S. Banerjee, A. Horn, H. Khatri, G. Sereda, A green one-pot multicomponent synthesis of 4H-pyrans and polysubstituted aniline derivatives of biological, pharmacological, and optical applications using silica nanoparticles as reusable catalyst.Tetrahedron Letters. 2011. 52,1878-1881.

37. X. S. Wang, Z. S. Zeng, M. M. Zhang, Y. L. Li, D. Q. Shi, S. J. Tu, Z. M. Zong, A convenient and clean procedure for the synthesis of pyran derivatives in aqueous media catalysed by TEBAC. Journal of Chemical Research. 2006. 2006(4), 228-230.

38. M.G. Dekamin, M. Eslami, Highly efficient organocatalytic synthesis of diverse and densely functionalized 2-amino-3-cyano-4 H-pyrans under mechanochemical ball milling.Green Chemistry. 2014. 16 (12) 4914-4921.

Table.1.Optimization of substituted 2-amino-4H-pyran derivatives synthesis conditions.

Entry	Amount of Catalyst(mg)	Solvent	Conditions	Time(h:min)	Yield(%)
1	7	EtOH/H2O(1:1)	80 ℃	2:20	80
2	20	EtOH	80 ℃	1:30	95
3	10	EtOH	80 ℃	3:00	60
4	10	EtOH	70 ℃	2:45	74
5	20	EtOH/H2O(1:1)	Reflux	2:50	89
6	15	EtOH	80 ℃	1:40	82
7	10	EtOH	25 ℃	2:20	43
8	10	EtOH/H2O(1:1)	80 ℃	2:20	72
9	10	EtOH	Reflux	3:40	88
10	10	EtOH	80 ℃	1:20	96
11	10	H2O	80 ℃	2:00	85
12	10	EtOH	60 ℃	2:20	80
13	10	EtOH/H2O(1:1)	90 ℃	1:50	90
14	10	EtOH	100 ℃	1:30	83
15	10	Solvent free	100 ℃	1:00	85

Abdulfatah Abdullah Abdu Saifan *et al.,*

Table.2. Comparison of catalytic activity of titanium dioxide nanoparticles with some other catalysts.

Entry	Catalyst	Condition	Time(h:min)	Yield(%)	Ref.
1	TiO$_2$ NPs (15 mol%)	H$_2$O, R.T.	04:00	77	20
2	Ce-ZSM-11 (100 mg)	EtOH, Reflflux	01:30	85	21
3	Fe$_3$O$_4$@g-C3N4 (20 mg)	EtOH, 60 C	00.30	80	22
4	MNP@PEG-ImOH (200 mg)	H$_2$O, R.T.	00.25	89	23
5	HPNb (100 mg)	Solvent-free,MW, 80 C	02:00	91	24
6	Zn^{2+}/4A (100 mg)	EtOH, Reflflux	04:00	95	25
7	TiO$_2$ NPs (10 mg)	EtOH 80 C	00.40	96	This work

Reaction conditions: benzaldehyde: malononitrile: ethyl acetoacetate (1:1:1).

Table. 3. The efficiency of several classical solvents

Entry	Solvent	Temperature 0C	Time (h)	Yield(%)
1	-	25	6	60
2	-	80	6	68
3	CH$_3$CN	Reflux	6	35
4	CH$_3$CN	Reflux	6	45
5	Toluene	Reflux	6	50
6	H$_2$O	Reflux	6	30
7	H$_2$O+ETOH	Reflux	6	42
8	ETOH	80	00.40	96
9	ETOH	40	6	78
10	ETOH	25	4	45

Abdulfatah Abdullah Abdu Saifan *et al.,*

Table.4.Synthesizing substituted 2-amino-4H-pyran derivatives catalyzed by Titanium dioxide

Entry	Aldehyde	Prodect	Time(min)	Yield(%)	M.P(Obsd)^{0}C	M.P(Lit)^{0}C
1	4-Chlorobenzaldehyde	1a	15	92	175-177	127-174[26]
2	3-Hydroxybenzaldehyde	2a	18	93	163-164	164-165[27]
3	4-Nitrobenzaldehyde	3a	15	96	176-177	176-179[28]
4	2-Hydroxybenzaldehyde	4a	35	90	165-167	163-165[29]
5	Benzaldehyde	5a	21	91	189-190	191-192[30]
6	4-Methoxybenzaldehyde	6a	20	95	135-137	136-138[31]
7	4- Bromobenzaldehyde	7a	40	93	170-172	172-174[32]
8	2-Nitrobenzaldehyde	8a	40	89	181-182	180-181[33]
9	4-Chlorobenzaldehyde	9a	35	97	192-194	190-192[34]
10	3-Hydroxybenzaldehyde	10a	25	90	163-165	164-165[35]
11	4-Nitrobenzaldehyde	11a	40	94	175-177	176-178[36]
12	Benzaldehyde	12a	20	96	194-195	195-196[37]
13	4-Methoxybenzaldehyde	13a	35	84	134-136	136-137[38]

Reaction conditions: aromatic aldehyde: malononitrile: ethyl/methyl acetoacetate (1:1:1),Titanium dioxide (10 mg), EtOH 80 ^{0}C.

Table. 5.Recyclability of the catalyst in the model reaction

Entry	Cycle	Yielda(%)
1	1	91
2	2	90
3	3	88
4	4	87
5	5	85

Abdulfatah Abdullah Abdu Saifan *et al.,*
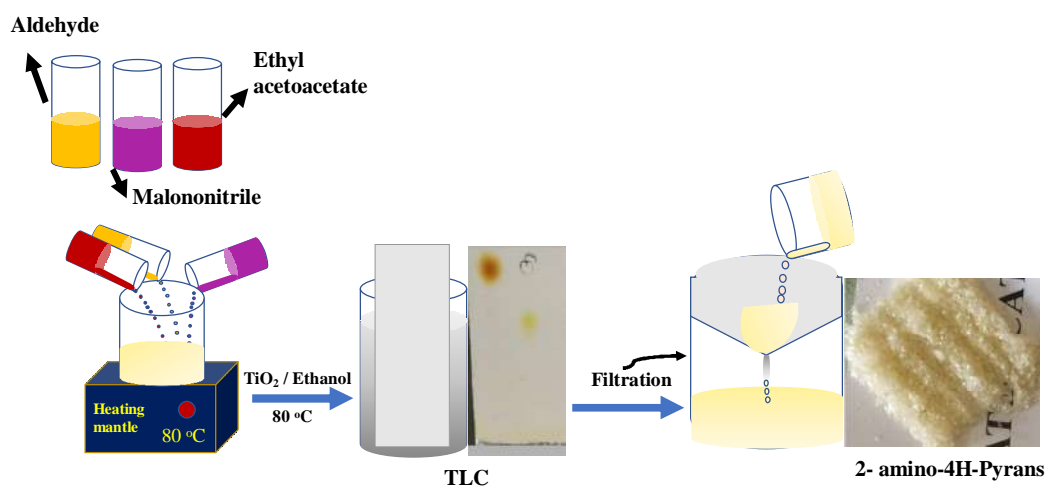
Fig. 1. Preparation of 2-amino-4h-pyrans by using titanium dioxide as catalyst.
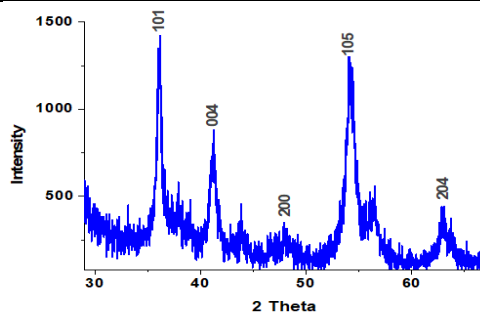
Fig.2. XRD pattern of TiO₂ nanoparticles
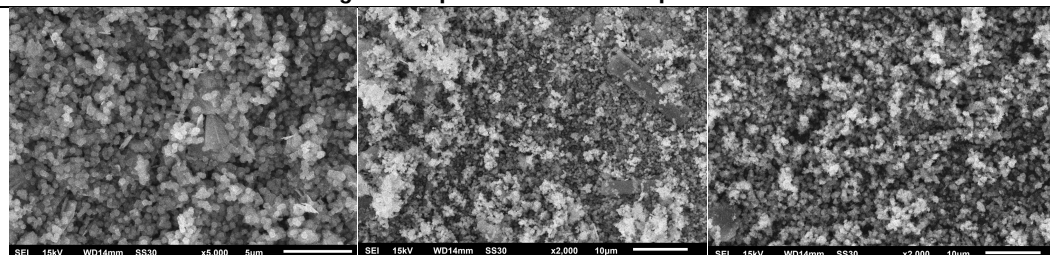
Fig. 3. SEM image of the synthesised TiO₂.
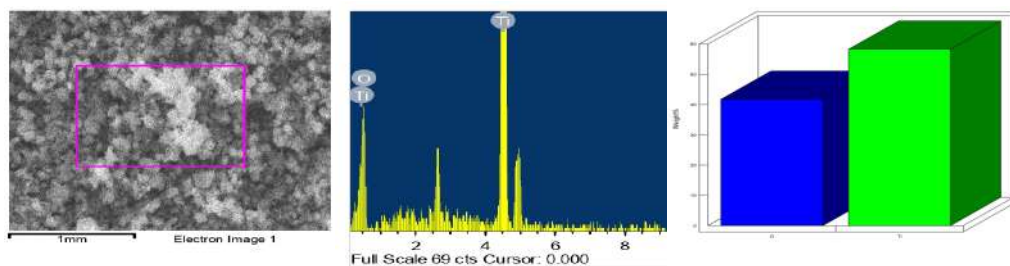
Fig. 4. EDX AND Mapping of TiO₂ nanoparticles.

Abdulfatah Abdullah Abdu Saifan *et al.*,
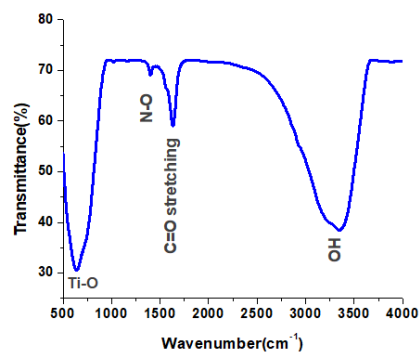
Fig. 5. FT-IR pattern of titanium dioxide nanoparticles.
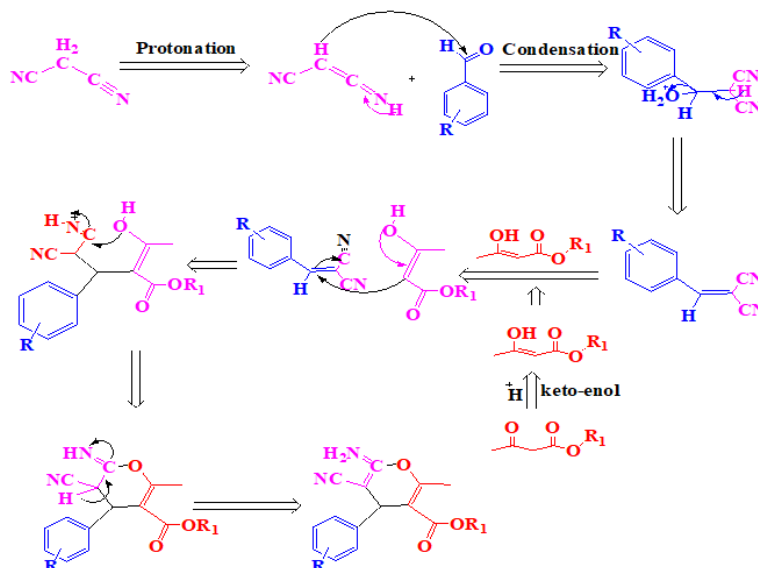
Scheme 1.A plausible mechanism for the synthesis of 2-amino-4H-pyrans.
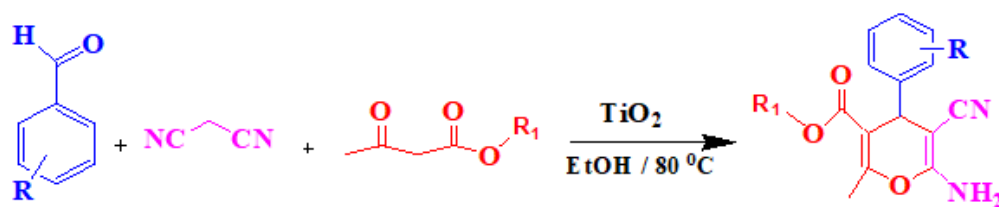
R= OH, CH₃, OCH₃. Cl, Br, NO₂, H,
R¹= Ethyl (a1, a9), Methyl (a10, a14)

Scheme 2.

RESEARCH ARTICLE

Prim's Algorithm based on New Ranking Method for Minimum Spanning Tree Problem in a Z-Graph

P. Vijayalakshmi*

Research Scholar (Part time), Reg.No: P 5291, Madurai Kamaraj University, Madurai and Lecturer in Mathematics, Government Polytechnic College, Checkanurani, Madurai- 625514, Tamil Nadu, India

*Address for Correspondence
P. Vijayalakshmi
Research Scholar (Part time), Reg.No: P 5291,
Madurai Kamaraj University,
Madurai and Lecturer in Mathematics,
Government Polytechnic College,
Checkanurani, Madurai- 625514, Tamil Nadu, India
E.Mail: shreevijiharish@gmail.com

ABSTRACT

In graph theory, the minimum spanning tree (MST) problem is an important problem with many practical applications. The MST problem in fuzzy graphs has been already studied. In this paper, we discuss the MST problem in graph with Z- number weighted edges(Z-graph). Anew ranking function for Z-numbers (the ratio ranking function) is introduced. Prim's algorithm based on new ranking procedure is then used to find the MST in Z-graph.

Keywords: Minimum Spanning tree, Z-number, Prim's Algorithm, Graph with Z-number weighted edges, Ratio ranking function.

INTRODUCTION

A variety of algorithms such as the Prim's algorithm, the Kruskal algorithm are available to find minimum spanning tree (MST) in classic graph theory. Chang and Lee [1],De Almeida [2], Archana A.Deshpande, and Onkar K-Chaudhari [3], Anita Pal and Arindam Dev [4] have studied the MST problem in a fuzzy environment.
In this paper, we present a novel approach to the problem of an MST in a graph with Z-number weighted edges. The solution involves a new type of ranking function for the Z-numbers called the ratio ranking function.

Vijayalakshmi

PRELIMINARIES
Definition: Minimum Spanning tree
A Minimum Spanning Tree (MST) is a subset of edges of a connected weighted undirected graph that connects all the vertices with the minimum possible total edge weight.

Definition: Z- number
A Z–number Z= (A, B) is an ordered pair of fuzzy numbers. The first component A is a restriction of real-valued uncertain variable X. The second component B is a measure of the reliability of the first component.

Definition: Z-Graph
A Z-graph is a simple connected graph with Z-number weighted edges.

Definition: Momentum ranking function of Z-number [5]
Let R_1 and R_2 be any two ranking functions for fuzzy numbers. Then for the Z-number A and B define the momentum ranking function [MRF] by M (A,B)=R_1(A) *R_2(B).

Definition: min R Operation [6]
Let * be any one of the basic arithmetic operations addition, subtraction, multiplication or division. Let R_k be any suitably chosen ranking function. Then the min R Operation[14] is defined by (A, B)(*,min)(C, D)=(A*C, min(B, D)), where A*C is calculated by using the extension principle, min(B, D) = B if $R_k(B) \leq R_k(D)$ and D if $R_k(D) < R_k(B)$

Example: Sum of two triangular Z-numbers by min R
Take Z_1=(A_1, B_1)=$\left((a_{11}, a_{12}, a_{13}), (b_{11}, b_{12}, b_{13})\right)$,and Z_2 = (A_2, B_2) = $\left((a_{21}, a_{22}, a_{23}), (b_{21}, b_{22}, b_{23})\right)$ are any two Z-numbers. The sum of two triangular Z-numbers Z_1 and Z_2 is defined by $Z_1(+,min)Z_2 = \left((a_{11} + a_{21}, a_{12} + a_{22}, a_{13} + a_{23}), min(B_1, B_2)\right)$.

NOVEL ALGORITHM FOR FINDING ZMST IN A GRAPH
A novel ranking function for Z- number is given below:

Ratio ranking function
Let us consider a minimization problem for Z-valued cost function. So, when we are interested in minimizing the cost given by Z-number (A,B) we need to minimize the first component A which represents the cost but maximize the second component B which refers to the reliability. Since the second component is non negative it is enough to minimize the reciprocal of the second component.

Hence, we define the ratio ranking function $RA\left((A,B)\right) = \frac{R_1(A)}{R_2(B)}$, Where R_1, R_2 are ranking functions on set of fuzzy numbers.

Example: Consider the two edges E and F respectively with weights([6,7,8],[.8,.9,1]) and ([8,9,10],[.4,.5,.6]).
Common sense suggests that the edge E should be preferred since the fuzzy cost associated with it is lesser than the fuzzy cost associated with the edge F, while the reliability of information regarding edge E is higher than the reliability of information regarding edge F.

Take $R_1 = R_2 = R$ where $R([x,y,z]) = \frac{x+y+z}{3}$.

Then $RA([6,7,8],[.8,.9,1]) = \frac{7}{.9} = 7.78$ and $RA([8,9,10],[.4,.5,.6]) = \frac{9}{.5} = 18$
So, the ratio ranking function leads to the correct conclusion, that the edge E is associated with the minimum cost.

63749

Vijayalakshmi

Some researchers had applied momentum ranking function for solving minimization problem. For example, refer to [7] ,the momentum ranking function was applied by the researcher to handle the shortest path problem in this article.

Suppose herewe apply momentum ranking function for the above-mentioned edges E and F.

Here also consider $R_1 = R_2 = R$ where $R([x, y, z]) = \frac{x+y+z}{3}$.

Then MRF$[([6,7,8], [.8, .9, 1])] = R_1[6,7,8] * R_2[.8, .9, 1] = 7 * .9 = 6.3$
MRF $[([8,9,10], [.4, .5, .6])] = R_1[8,9,10] * R_2[.4, .5, .6] = 9 * .5 = 4.5$
This leads to the conclusion that the edge F has minimum cost, which is obviously wrong.
Because of this, it is preferable to use the ratio ranking function rather than momentum ranking function, to solve minimization problem such as shortest path problems and MST problems.

Problem formulation for ZMST
Consider a simple connected graph G consisting of 'n' number of vertices $V = \{v_1, v_2, \cdots, v_n\}$ and 'm' number of edges E ⊆V X V.
The ZMST Problem is formulated as follows:$Y = min \sum C_e X_e$,where the minimum is taken over the spanning tree of subgraph of G, Subject to$\sum X_e = n - 1$
Here, C_e-represents the weight of an edge e, which is a Z-number.
$\sum X_e$ - represents the number of edges in ZMST is n-1, where$X_e = \begin{cases} 1, if\ e\ is\ in\ ZMST \\ 0, if\ e\ is\ not\ in\ ZMST \end{cases}$

Y-Total cost of ZMST

Prim's algorithmis generally used to find the MST in a graph.
While adapting algorithms which work with crisp numbers so that they can deal with Z-numbers two issues need to be tackled:(i) Formal arithmetic operations as outlined by Zadeh are too complicated. So suitable simplified operations proposed by Stephenare used. (ii) Comparison of two Z-numbers by a suitable ranking procedure. Here we are interested in a minimization problem, so we can utilize the ratio ranking function.

Modified Prim's Algorithm
Input:
Let G= (V, E) be a simple connected graph with Z-number weighted edges.
Let $V = \{v_1, v_2, \cdots, v_n\}$ and $E = \{e_1, e_2, \cdots, e_m\}$, n(V)=n, n(E)=m
cost (e_i) – weight ofe_i, i=1 to m.

Aim: To find ZMST T(W, B) of G
Process
Initialization
Let W= $\{v_1\}$\\v_1 is a starting vertex of T
B= { }   \\ B is the edge set of T
Cost= 0   \\ corresponding Z-number is ((0,0), (1, 1))

Procedure
Start from v_1
While V\W≠Φ, Do
Among all the edges with one end in W and another end in V\W,
We find an edge (v_1, v_i) with minimum cost;
Cost=cost $(+, min)$ cost (v_1, v_i);
B=BU (v_1, v_i);

W= (W U $\{v_1, v_i\}$)\W;
end while

Output

T= (W, B) is the minimum spanning tree of G,n (W)= n,n (B) = n-1
Start from the vertex v_1. Among all the edges with one end in W and another end in V\W, we find an edge with a minimum weight. The edge with the minimum weight is chosen by a suitable ranking method. Suppose v_2 in V\W is adjacent to v_1 with a minimum weight.

Now W= $\{v_1,v_2\}$, and among all the edges which have one end in W and another end in V\W, find the edges which are adjacent to v_1,v_2 with a minimum weight. Continuing like this, we find a tree that includes all the vertices of G and the edgeswith minimum weight. Hence, we get a spanning tree with n vertices and n-1 edges.

Example

Consider graph G given in the figure 1. The edge weights are given in the table 1. The problem is to find the minimum spanning tree of G.

Here, V= {a, b, c, d, e,f}

To find the minimum spanning tree T of a graph with Z-number weighted edge and its cost.
Using the modified Prim's algorithm, the output isW= {a, b, c, f, e, d}, B= {ab, bc, bf, fe, fd}
The Spanning tree is and the corresponding cost is ((150,180,210),(.6,.65,.7))

CONCLUSION

In this paper, a new ranking method for Z-numbers has been introduced to deal with optimization problems where the objective function has to be minimized .The modified form of Prim's algorithm for finding MST in a simple graph with Z-number weighted edges has been presented.We have demonstrated the proposed algorithm using numerical example. This algorithm finds the ZMST and its corresponding cost.

REFERENCES

1. A. N. C. Kang, R. C. Lee, C. L. Chang, and S. K. Chang, Storage reduction through minimal spanning trees and spanning forests,
2. T. A. De Almeida, A. Yamakami and M. T. Takahashi, An evolutionary approach to solve minimum spanning tree problem with fuzzy parameters, in null. IEEE (2005) 203-208.
3. Archana A.Deshpande and Onkar K.Chaudhari, Fuzzy approach to compare an MST problem by using various algorithms, Advances in Fuzzy Mathematics,Vol.15, 1(2020) pp.47-58.
4. Anita Pal and Arindam Dey, Prim's algorithm for solving minimum spanning tree problem in fuzzy environment, vol.12, 3(2016) pp 419-430.
5. Parameswari.K, Momentum Ranking of Z- numbers and its applications to game theory, Baghdad scienceJournal, vol, 20 No .1(SI)(2023):1(Special Issue) ICAAM.
6. Stephen. S, Novel Binary Operations on Z-numbers and their application in Fuzzy Critical Path Method, Advances in Mathematics: Scientific Journal 9 (2020), no 5, 3111-3120.
7. Veerammal P ,"Fuzzy Z- Number Shortest Path Problem using Dijkstra Algorithm" Periodico di Mineralogia, Volume 91, No. 5, 2022.
8. A. Dey, L. Son, A. Pal, Fuzzy Minimum Spanning Tree with Interval Type 2 Fuzzy Arc Length: Formulation and A New Genetic Algorithm, Soft computing, (2019), 1-12.

Vijayalakshmi

9. A. Janiak and A. Kasperski, The minimum spanning tree problem with fuzzy costs, Fuzzy Optimization and Decision Making, 7(2) (2008) 105–118.

10. J. A. Bondy and U. S. R. Murty, Graph theory with applications,Macmillan London 290 1973

11. Dubois.D and H.Prade, Operations on fuzzy numbers, International Journal of systems science, 9(6) (1978) 613–626.

12. J. B. Kruskal, on the shortest spanning subtree of a graph and the traveling salesman problem, Proceedings of the American Mathematical Society 7(1) (1956) 48–50.

13. J. C. Gower and G. Ross, Minimum spanning trees and single linkage cluster analysis, Applied statistics, (1969) 54–64.

14. J. Gao and M. Lu, Fuzzy quadratic minimum spanning tree problem, Applied Mathematics and Computation, 164(3) (2005) 773–788.

15. Kartick Mohanta, Arindam Dey, Narayan C. Debnath, and Anita pal, an algorithmic approach for finding MST in an intuitionistic fuzzy graph, Epic Series in Computing, Vol. 63, (2019), 140-149.

16. R. L. Graham and P. Hell, on the history of the minimum spanning tree problem, Annals of the History of Computing, 7 (1) (1985) 43–57.

17. T. Itoh and H. Ishi, An approach based on necessity measure to the fuzzy spanning tree problems, Journal of the Operations Research Society of Japan 39 (2) (1996) 247-257.

18. Zadeh L. A. (1965): Fuzzy Sets Information and Control, 8, (1965), 338- 353.

Table 1 The edge weights

Edges	Weight
ab	((30,35,40),(.6,.65,.7))
af	((50,60,70),(.8,.85,.9))
ae	((60,65,70).(.9,.95,1))
bc	(10,15,20),(.6,.65,.7))
bf	((40,45,50),(.7,.75,.8))
cd	((60,65,70).(.8,.85,.9))
cf	((40,45,50),(.75,.8,.9))
fe	((20,30,40),(.6,.65,.7))
fd	((50,55,60),(.8,.85,.9))
ed	((80,85,90),(.9,.95,1))
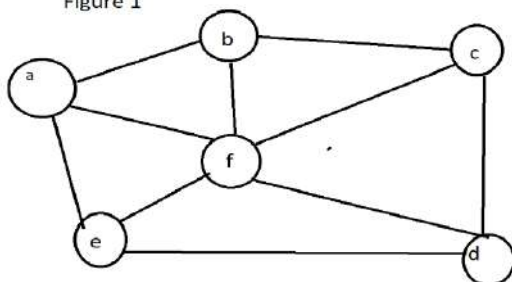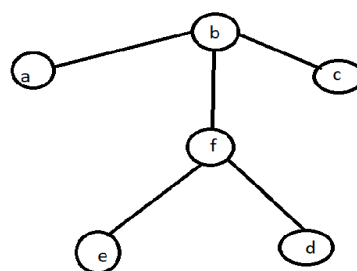
Fig 1. Graph G	Figure 2. The spanning tree

RESEARCH ARTICLE

Analysis of a Morkovian Retrial Queue with Feedback, Recurrent Customers and Server Vacation

S.Pazhani Bala Murugan[1]* and P.Madhangi[2]

[1]Assistant Professor, Department of Mathematics, Annamalai University, Annamalai Nagar-608002, Chidambaram, Tamil Nadu, India.
[2]Guest Lecturer, Department of Mathematics, Government Arts and Science College, Manalmedu, Mayiladuthurai-609202,Tamil Nadu, India.

*Address for Correspondence
S.Pazhani Bala Murugan
Assistant Professor,
Department of Mathematics,
Annamalai University, Annamalai Nagar-608002,
Chidambaram, Tamil Nadu, India.
E.Mail: spbm1966@gmail.com

ABSTRACT

In this article, we examine Analysis of a Markovian retrial queue with Feedback, Recurrent customers and server vacation. In this model, all service times, retrial times and vacation times are assumed to have an exponential distribution. We obtain the probability generating function for the number of customers in the system. We also compute the average number of customers and waiting time in the system. Some of the special cases are discussed. To calibrate the model's stability some numerical examples are illustrated.

Keywords: Retrial Queue, Feedback, Recurrent customers, Server vacation, Steady-state equations.
MSC 2010 No.: 60K25, 68M20, 90B22

INTRODUCTION

The queueing systems, which include the possibility of a customer after receiving one service, returning to the server for additional service, are called queue with feedback. Formation of queues with feedback mechanism was first introduced by Takecs(1963) discipline In this paper, an M/M/1 Retrial queueing model with Recurrent Customers and Server Vacation is taken. Retrial queues are characterized by the phenomenon that arriving customers who find the server busy join the retrial group (called orbit) to repeat their request for service after some random time. Retrial queuing systems have been widely used to model many practical problems in telephone switching systems, telecommunication networks, and computers competing to gain service from a central processing unit. For recent

bibliographies on retrial queues, see [2,3,8,9,14]. Boxma and Cohen[4] studied a M/G/1 queue in which there is a fixed number of permanent customers present who rejoin the queue on their completion of service. This sys tem with permanent customers in the retrial context was analzed by Farahmand[11]. Queues with vacations have been studied extensively in the past: a comprehensive survey can be found in Teghem[14] and Doshi[7]. The Organization of the paper is as follows: The model under consideration is described in section 2. In section 3, we analyze the model by deriving the system steady state equations. Using the equations, the probability generating function of queue length are obtained in section 4.

MODEL DESCRIPTION

We consider an M/M/1 Feedback-retrial queue with transit (also called ordinary) customers and a fixed number K (K ≥ 1) of recurrent (also called permanent) customers. After service completion, recurrent customers always return to the retrial group and transit customers leave the system forever.

Transit customers arrive according to a Poisson process with rate λ. If a transit customer finds the server free on his arrival, he occupies the server, otherwise, he enters the re-trail group in accordance with an FCFS discipline. We will assume that only the transit customers at the head of the orbit is allowed for access to the server. Successive inter retrial times of any transit customer follow an exponential distribution with rate α. The service times for the transit customers are exponentially distributed with rate μ_1. There is a fixed number K of permanent customers in the system. After having received service, recurrent customers immediately return to the retrial group in accordance with an FCFS discipline. We will assume that only the recurrent customer at the head of orbit is allowed for access to the server. Successive inter-retrial times of any recurrent customer follow an exponential distribution with rate . The service times for the recurrent customers are exponentially distributed with rate μ_2. After each service, the next customers to be served is determined by a competition between the retrial time of transit customers, recurrent customers. After completion of service there is no transit customers in the orbit the server takes the vacation of random length. At the end of vacation, if the server finds no transit customer in the orbit, he immediately takes another vacation and continuous in this manner until he finds atleast one transit customer upon return from vacation. The vacation times are the exponentially distributed with parameter . The inter arrival times, retrial times, service times and vacation times are mutually independent. Let O(t) be the number customers in the orbit at time t and C(t) denotes the server state at time t.
We observe that (O(t), C(t)): t ≥ 0 is a continuous Markov chain.

MODEL ANALYSIS EQUATIONS

We define the following limiting probabilities for our subsequent analysis of the queueing

$$P_{0,n} \lim_{t\to\infty}\{C(t) = 0, \quad O(t) = n, \qquad n \geq k + 1$$

$$P_{1,n} \lim_{t\to\infty}\{C(t) = 1, \quad O(t) = n, \qquad n \geq k + 1$$

$$P_{2,n} \lim_{t\to\infty}\{C(t) = 2, \quad O(t) = n, \qquad n \geq k + 1$$

$$P_{3,n} \lim_{t\to\infty}\{C(t) = 3, \quad O(t) = n, \qquad n \geq k + 1$$

The system has the following set of steady state equations:

Pazhani Bala Murugan and Madhangi

$$(\lambda + \alpha + \beta)P_{0,n} = q\mu_1 P_{1,n} + \mu_2 P_{2,n-1} + \mu_1 P_{1,n-1} + \theta P_{3,n} \; ; \; n \ge k+1 \qquad (1)$$

$$(\lambda + \mu_1)P_{1,k} = \alpha P_{0,k+1} \qquad (2)$$

$$(\lambda + \mu_1)P_{1,n} = \lambda P_{0,n} + \lambda P_{1,n-1} + \alpha P_{0,n+1} ; \qquad n \ge k+1 \qquad (3)$$

$$(\lambda + \mu_2)P_{2,k} = \beta P_{0,k+1}; \qquad (4)$$

$$(\lambda + \mu_2)P_{2,n} = \beta P_{0,n+1}; \; \lambda P_{2,n-1}; \qquad n \ge k+1 \qquad (5)$$

$$\lambda P_{3,k} = q\mu_1 P_{1,k} \qquad (6)$$

$$(\lambda + \theta)P_{3,n} = \lambda P_{3,n-1} \qquad n \ge k+1 \qquad (7)$$

PROBABILITY GENERATING FUNCTIONS OF QUEUE LENGTH

We define the following probability generating functions:

$$P_0(z) = \sum_{n=k+1}^{\infty} P_{0,n}z^n \quad P_1(z) = \sum_{n=k}^{\infty} P_{1,n}z^n$$

$$P_2(z) = \sum_{n=k}^{\infty} P_{2,n}z^n \qquad P_3(z) = \sum_{n=k-1}^{\infty} P_{3,n}z^n \qquad (8)$$

applying (8) into equations (1)-(7), we get

$$(\lambda + \alpha + \beta)P_0(z) = \mu_1(q+pz)P_1(z) + \mu_2 z P_2(z) + \theta P_3(z) - (\lambda + \theta)P_{3,k}z^k \qquad (9)$$

$$(\lambda - \lambda z + \mu_1)P_1(z) = \left(\lambda + \frac{\alpha}{z}\right)P_0(z) \qquad (10)$$

$$(\lambda - \lambda z + \mu_2)P_2(z) = \left(\frac{\beta}{z}\right)P_0(z) \qquad (11)$$

$$(\lambda - \lambda z + \theta)P_3(z) = (\lambda + \theta)P_{3,k}z^k \qquad (12)$$

substituting equations (10), (11) and (12) in (9), we get

$$P_0(z) = \frac{-(\lambda+\theta)P_{3,k}z^k(\lambda-\lambda z+\mu_1)(\lambda-\lambda z+\mu_2)[\lambda-\lambda z]}{(\lambda-\lambda z+\theta)\left[\begin{array}{c}(\lambda+\alpha+\beta)(\lambda-\lambda z+\mu_1)(\lambda-\lambda z+\mu_2)\\-\mu_1(q+pz)(\lambda+\alpha z^{-1})(\lambda-\lambda z+\mu_2)-\mu_2\beta(\lambda-\lambda z+\mu_1)\end{array}\right]} \qquad (13)$$

Substituting (13) in (10), we get

$$P_1(z) = \frac{-(\lambda+\theta)P_{3,k}z^k(\lambda+\alpha z^{-1})(\lambda-\lambda z+\mu_2)[\lambda-\lambda z]}{(\lambda-\lambda z+\theta)\left[\begin{array}{c}(\lambda+\alpha+\beta)(\lambda-\lambda z+\mu_1)(\lambda-\lambda z+\mu_2)\\-\mu_1(q+pz)(\lambda+\alpha z^{-1})(\lambda-\lambda z+\mu_2)-\mu_2\beta(\lambda-\lambda z+\mu_1)\end{array}\right]} \qquad (14)$$

Substituting (15) in (11), we get

$$P_2(z) = \frac{-(\lambda+\theta)P_{3,k}z^k\beta z^{-1}(\lambda-\lambda z+\mu_2)[\lambda-\lambda z]}{(\lambda-\lambda z+\theta)\left[\begin{array}{c}(\lambda+\alpha+\beta)(\lambda-\lambda z+\mu_1)(\lambda-\lambda z+\mu_2)\\-\mu_1(q+pz)(\lambda+\alpha z^{-1})(\lambda-\lambda z+\mu_2)-\mu_2\beta(\lambda-\lambda z+\mu_1)\end{array}\right]} \qquad (15)$$

From (12), we get

$$P_3(z) = \frac{-(\lambda+\theta)P_{3,k}z^k}{(\lambda-\lambda z+\theta)} \qquad (16)$$

Let us define P (z) = P 0 (z) + z(P 1 (z) + P 2 (z)) + P 3 (z) the pgf for number of customers in the system.

$$P(z) = \frac{-(\lambda-\lambda z+\mu_2)(\lambda z+\alpha)\mu_1[1-p]z}{\left[\begin{array}{c}(\lambda-\lambda z+\theta)[(\lambda+\alpha+\beta)\lambda z(\lambda-\lambda z+\mu_1+\mu_2)\\-(\lambda z+\alpha)\lambda\mu_1-\beta z\,\lambda\mu_2-\alpha\mu_1\mu_2+p\mu_1(\lambda z+\alpha)(\lambda-\lambda z+\mu_2)]\end{array}\right]}(\lambda+\theta)P_{3,k} \qquad (17)$$

Applying the normalizing condition P(1) =1, in equation (18), we get

63755

Pazhani Bala Murugan and Madhangi

$$P_{3,k} = \frac{1}{1-p}\left[\frac{1}{1+\frac{\lambda}{\theta}}\right]\left[\frac{1}{1+\frac{\lambda}{\alpha}} - \frac{\lambda}{\mu_1}\left(1 + \frac{\beta\mu_1}{(\lambda+\alpha)\mu_2}\right) - p\right] \qquad (18)$$

Which implies that the utilization factor is $\varrho = \dfrac{\frac{\lambda}{\mu_1}\left(1+\frac{\beta\mu_1}{(\lambda+\alpha)\mu_2}\right) - p}{\frac{1}{1+\frac{\lambda}{\alpha}}}$ and the steady state

condition is therefore

$$\frac{\frac{\lambda}{\mu_1}\left(1+\frac{\beta\mu_1}{(\lambda+\alpha)\mu_2}\right)}{\frac{1}{1+\frac{\lambda}{\alpha}}} \leq 1 \qquad (19)$$

Particular cases

i)   If $\theta\to\infty$ p=0 and q=1, then the present model will be remodeled as an M/M/1 retrial queue with recurrent customers.

ii)   If $\alpha\to\infty$ and $\theta\to\infty$, p=0 and q=1, then the present model will be remodeled as an M/M/1 queue with recurrent customers.

iii) If $\alpha\to\infty$, $\theta\to\infty$, p=0,q=1 and k=0 then the present model will be remodeled as an M/M/1 queue.

iv)   If k=0, p=0andq=1, then the present model will be remodeled as an M/M/1 retrial queue with server vacation.

v)   If k=0,p=0,q=1 and $\theta\to\infty$, then the present model will be remodeled as an M/M/1 retrial queue.

OPERATING CHARACTERTISTICS

Let E(L) denote the mean number of customers in the system. The Probability generating function for the number of customers in the system is

$$P(z) = \frac{N(z)}{D(z)}P_{3,k}$$

$$N(z)$$
$$= -(\lambda+\theta)(\lambda - \lambda z + \mu_2)(\lambda z + \alpha)\mu_1[q + pz - z]z^k$$

$$D(z) = \left[\begin{array}{l}(\lambda - \lambda z + \theta)[(\lambda + \alpha + \beta)\lambda z(\lambda - \lambda z + \mu_1 + \mu_2) \\ -(\lambda z + \alpha)\lambda\mu_1 - \beta z\lambda\mu_2 - \alpha\mu_1\mu_2 + p\mu_1(\lambda z + \alpha)(\lambda - \lambda z + \mu_2)]\end{array}\right]$$

$$P_{3,k} = \frac{1}{1-p}\left[\frac{1}{1+\frac{\lambda}{\theta}}\right]\left[\frac{1}{1+\frac{\lambda}{\alpha}} - \frac{\lambda}{\mu_1}\left(1 + \frac{\beta\mu_1}{(\lambda+\alpha)\mu_2}\right) - p\right]$$

Differentiating with respect to z

$$P(z) = \frac{D(z)N'(z) - D'(z)N(z)}{[D(z)]^2}P_{3,k}$$

$$N(z) = -(\lambda+\theta)(\lambda z + \alpha)(\lambda - \lambda z + \mu_2)z^k$$
$$N'(z) = -(\lambda + \theta)\mu_1[\lambda(\lambda - \lambda z + \mu_2)z^k + (\lambda z + \alpha)(-\lambda)z^k + (\lambda z + \alpha)(\lambda - \lambda z + \mu_2)kz^{k-1}]$$

$$D(z) = \left[\begin{array}{l}(\lambda - \lambda z + \theta)(\lambda + \alpha + \beta)\lambda z(\lambda - \lambda z + \mu_1 + \mu_2) \\ -(\lambda z + \alpha)\lambda\mu_1 - \beta z\lambda\mu_2 - \alpha\mu_1\mu_2\end{array}\right]$$

$$D'(z) = \left[\begin{array}{l}(-\lambda)[(\lambda + \alpha + \beta)\lambda z(\lambda - \lambda z + \mu_1 + \mu_2) \\ -(\lambda z + \alpha)\lambda\mu_1 - \beta z\lambda\mu_2 - \alpha\mu_1\mu_2] \\ +(\lambda - \lambda z + \theta)[(\lambda + \alpha + \beta)\lambda(\lambda - \lambda z + \mu_1 + \mu_2) + \\ (\lambda + \alpha + \beta)\lambda z(-\lambda) - \lambda^2\mu_1 - \beta\lambda\mu_2]\end{array}\right]$$

NUMERICAL RESULTS

The curved graph constructed in Figure 1 and the values tabulated in the Table 1 are obtained by setting the fixed values $\nu=2, \alpha=1, \beta=2.5, k=1, \theta=1, p=0.4, q=0.6$, t = 0.3 and varying the values of λ from 1 to 2 incremented with 0.2 and extending the values of μ from 1 to 2 in steps of 0.5. We observed that as λ rises L_s also rises which shows the stability of the model.

The curved graph constructed in Figure 2 and the values tabulated in the Table 2 are obtained by setting the fixed values μ=1.5, $\alpha=1, \beta=2.5, k=1$, $\theta=1, p=0.4$ q=0.6, t = 0.3 and varying the values of λ from 1 to 2 incremented with 0.2 and extending the values of μ_2 from 3 to 7 in steps of 2. We observed that as λ rises L_s also rises which shows the stability of the model.

The curved graph constructed in Figure 3 and the values tabulated in the Table 3 are obtained by setting the fixed values μ=1, $\alpha=1.5, \nu=3, k=1, \theta=1, p=0.4$, q=0.6, t = 0.3 and varying the values of λ from 1 to 2 incremented with 0.2 and extending the values of β from 3 to 4.2 insteps of 0.6. We observed that as λ rises L_s also rises which shows the stability of the model.

The curved graph constructed in Figure 4 and the values tabulated in the Table 4 are obtained by setting the fixed values μ = 2, β = 2.5, ν = 4, θ = 1, k = 1, p = 0.4 q = 0.6, t = 0.3 and varying the values of λ from 1 to 2 incremented with 0.2 and extending the values of α from 0.5 to 1.5 in steps of 0.5. We observed that as λ rises L_s also rises which shows the stability of the model.

CONCLUSION

In this paper, analysis of a Markovian retrial queue with recurrentcustomers, feedback and server vacation is evaluated. We obtain the PGF for the number of customers and the mean number of customers in the orbit. We workout the waiting time distribution. We also derive the performance measures. We perform some particular cases. We illustrate some numerical results.

REFERENCES

1. J.R.Artalijo, "Analysis of an M/G/1 queue with constant repeated attempts and server vacation", Computers and Operations Research 24(6)(1997) 493-504.
2. J.R.Artalijo, "Accessible bibliography on retrial queues", Mathematical and computer Modelling 30(1999) 1-6.
3. O.J Boxma, J.W.Cohen, "The M/G/1 queue with permanent customers" IEEE Journal on selected Areas in communication 9(2)(1991) 179-184.
4. O.J.Boxma, S.Schlegel and U.Yechiali, ``M/G/1 queue with waiting server timer and vacations", American Mathematical Society Translations, 2(207), pp.25-35(2002).
5. V.M.Chandrasekaran, K.Indhira, M.C.Saravanarajan and P.Rajadurai, ``A survey on working vacation queueing models", International Journal of Pure and Applied Mathematics, 106(6), pp.33-41 (2016).
6. B.W.Conolley, "A difference equation technique applied to the simple queue", j.Roy.Statist. Soc.Ser.B, 20(1958 a) 165-167.
7. G.I.Falin, J.G.C.Templeton, "Retrial Queues", Chapman and Hall, London, 1997.
8. K.Farahmand, "Single line queue with repeated demands" Queueing Systems 6(1990) 223-228.
9. K.Farahmand, "Single line queue with recurrent demands", Queueing Systems 22(1996) 425-435.

10. R.Kalyanaraman and S.Pazhani Bala Murugan.S, "A single server queue with addi tional optional service in batches and server vacation", Vol.2 56(2008), 2765- 2776.

11. R.Kalyanaraman and S.Pazhani Bala Murugan.S.(2008), ``A single server retrial queue with vacation", J.Appl.Math.and Informatics, 26(3-4), pp.721-732.

12. J.D.C.Little, "A proof of the queueing formula: L = λW ", Operations Res., Vol.9, No. 3(1961), 773-781.

13. J.Teghem, "Control of the service process in queueing system". Eur.J.Oper. Res., Vol.23(1986), 141-158.

14. Takacs.L., A single server queue with feedback, Bell system Technical Journal, Vol.42(1963)509-519.

15. Takine.T. Takagi. H., and Hasegawa.T., Sojourn times in vacation and polling system with Bernoulli feedback, J.Appl.Prbo.,28(1991)422-432.

Table1: L_s with turnover of λ

λ	$\mu =1$	$\mu=1.5$	$\mu=12$
1.0	1.37705	1.6783	1.0122
1.2	1.75706	1.56923	1.42941
1.4	2.08181	1.90298	1.76926
1.6	2.37506	2.19946	2.06733
1.8	2.64836	2.47301	2.34015
2.0	2.90805	2.73134	2.59649

Table 2: L_s with turnover of λ

Λ	$\mu_2=3$	$\mu_2=5$	$\mu_2=7$
1.0	1.13277	1.03061	0.954587
1.2	1.57374	1.5145	1.46316
1.4	1.92949	1.89079	1.85035
1.6	2.23977	2.21188	2.17666
1.8	2.52273	2.5008	2.46806
2.0	2.78788	2.76923	2.73754

Table 3: L_s with turnover of λ

Λ	$\beta=3$	$\beta=3.6$	$\beta=4.2$
1.0	1.12222	1.18125	1.23333
1.2	1.55489	1.60501	1.64978
1.4	1.90973	1.95673	1.99909
1.6	2.22274	2.26915	2.31128
1.8	2.51036	2.55741	2.60037
2.0	2.78788	2.76923	2.73754

Table 4: L_s with turnover of λ

λ	$\alpha=0.5$	$\alpha=1$	$\alpha=1.5$
1.0	1.43362	0.907895	0.422727
1.2	1.82298	1.42323	1.08291
1.4	2.14633	1.81655	1.54657
1.6	2.4331	2.14808	1.91892
1.8	2.69745	2.44393	2.24147
2.0	2.94706	2.71723	2.53379
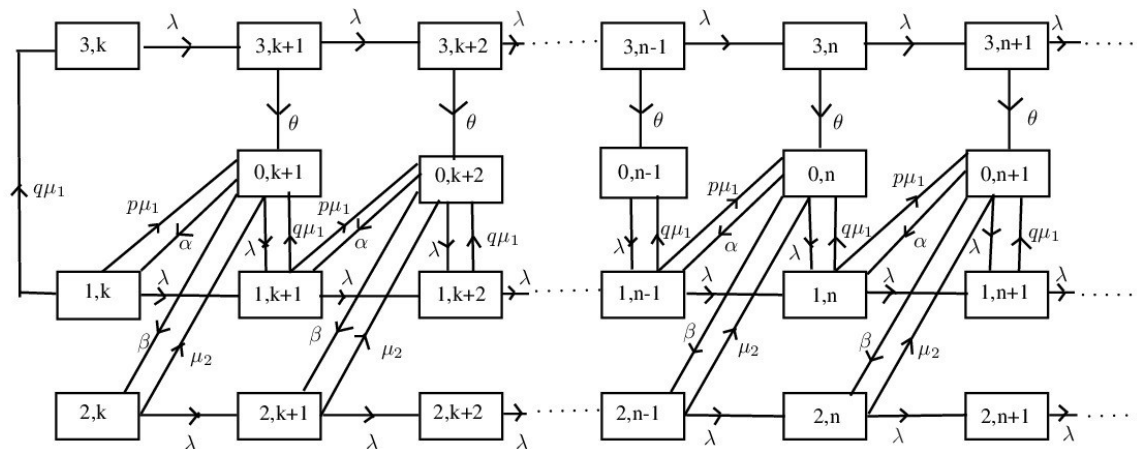
Figure 1: Transition state diagram of the system model.

Table1: Lₛ with turnover of λ

Figure 3: Lₛ with turnover of λ

Figure 4: Lₛ with turnover of λ

Figure 5: Lₛ with turnover of λ

RESEARCH ARTICLE
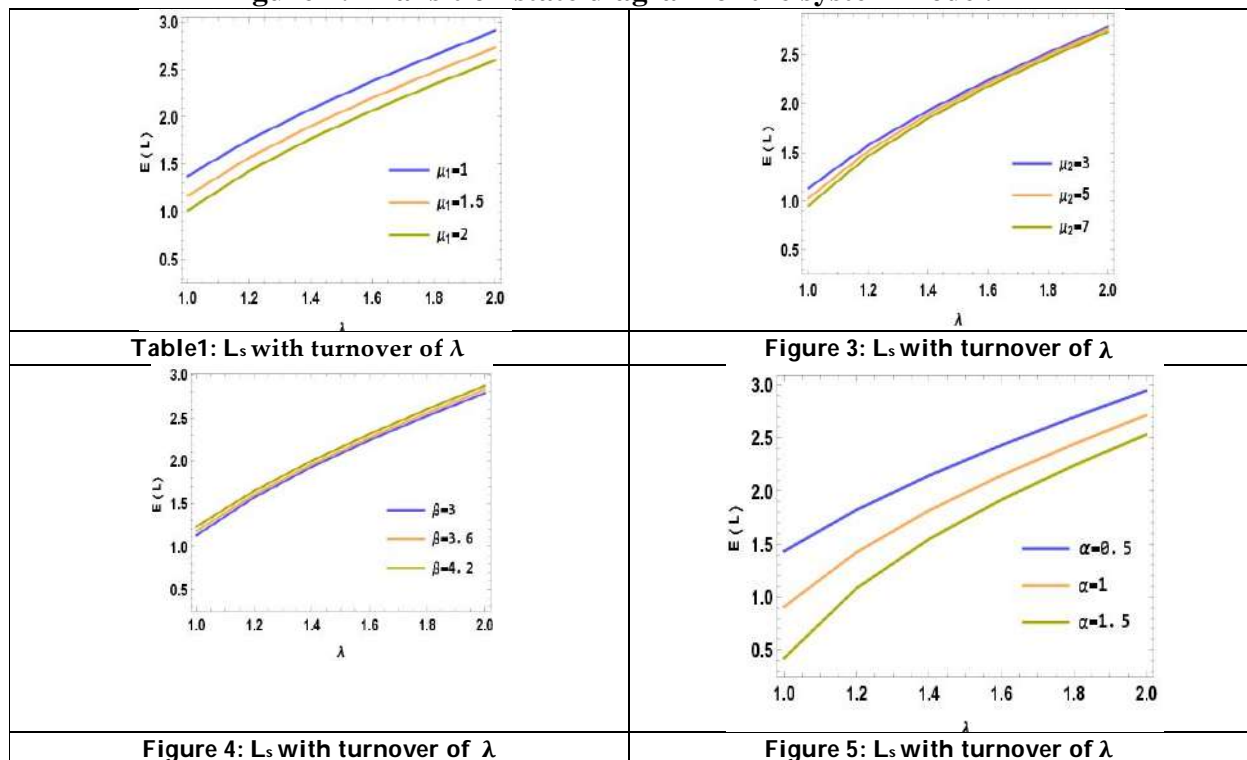
Periodontal Risk Assessment and Oral Microbiome Profile : A Comprehensive Two-Way Diagnosis for Enhanced Understanding and Clinical Significance

J.Bhuvaneswarri[1*], Julius Amaldas[2], Ramya.V[1] and Snophia Rani Rajamani[3]

[1]Professor, Department of Periodontology, Sree Balaji Dental College, Chennai, Tamil Nadu, India.
[2]Professor and Head of the Department, Department of Biochemistry, Sree Balaji Dental College, Chennai, Tamil Nadu, India
[3]Professor, Department of Periodontology, Thai Moogambigai Dental College, Chennai, Tamil Nadu, India.

*Address for Correspondence
J.Bhuvaneswarri
Professor,
Department of Periodontology,
Sree Balaji Dental College,
Chennai, Tamil Nadu, India.
E.Mail: drbhuvana22@gmail.com

ABSTRACT

Periodontal diseases are complex inflammatory conditions affecting the supporting structures of the teeth, with a significant impact on oral health. Traditional diagnostic approaches for periodontal diseases have relied on clinical parameters and subjective assessments, often leading to limited predictive capabilities and suboptimal treatment outcomes. In recent years, there has been a growing recognition of the crucial role played by the oral microbiome in periodontal health and disease. This article highlights the significance of integrating periodontal risk assessment and oral microbiome profiling as a comprehensive two-way diagnostic approach to enhance our understanding of the disease and improve clinical outcomes. By considering both host-related factors and the composition of the oral microbiome, this approach offers a more accurate assessment of disease susceptibility, severity, and treatment response. The integration of periodontal risk assessment and oral microbiome profiling holds great promise in guiding personalized treatment strategies and improving overall patient care.

Keywords: periodontal diseases, periodontal risk assessment, oral microbiome, diagnostic approach, clinical significance

Bhuvaneswarri *et al.*,

INTRODUCTION

Periodontal diseases, including gingivitis and periodontitis, are prevalent inflammatory conditions that affect the supporting tissues surrounding the teeth. These diseases can result in tissue destruction, tooth loss, and have implications for systemic health. Traditional diagnostic approaches for periodontal diseases have primarily relied on clinical parameters, such as probing depth and bleeding on probing, along with subjective assessments. However, these methods often provide limited predictive capabilities and fail to consider the complex interplay between the host immune response and the oral microbiome. In recent years, there has been a remarkable advancement in our understanding of the oral microbiome and its role in periodontal health and disease. The oral cavity harbors a diverse microbial ecosystem consisting of bacteria, viruses, fungi, and other microorganisms. The composition, diversity, and functional potential of this oral microbiome have been recognized as key factors influencing the development and progression of periodontal diseases [1]. With the advent of molecular techniques and high-throughput sequencing, researchers have gained unprecedented insights into the oral microbiome's intricate relationship with periodontal health and disease. The use of methods such as 16S rRNA gene sequencing and metagenomics has allowed for a comprehensive characterization of the oral microbiome, enabling the identification of microbial signatures associated with health and disease states. This deeper understanding of the oral microbiome has paved the way for a paradigm shift in periodontal disease diagnosis and management.

Recognizing the limitations of traditional diagnostic approaches, there is a growing recognition of the importance of integrating periodontal risk assessment and oral microbiome profiling as a comprehensive two-way diagnostic approach. By considering both host-related factors and the composition of the oral microbiome, this integrated approach provides a more accurate assessment of disease susceptibility, severity, and treatment response. The aim of this article is to highlight the significance of this comprehensive two-way diagnostic approach in enhancing our understanding of periodontal diseases and improving clinical outcomes. By combining periodontal risk assessment with oral microbiome profiling, clinicians can tailor treatment plans more effectively, identify high-risk individuals, predict disease progression, and develop personalized therapeutic interventions. In this article, we will explore the current knowledge surrounding periodontal risk assessment and oral microbiome profiling. We will examine the clinical significance of this integrated approach, its implications for treatment planning, and its potential to guide personalized interventions. Furthermore, we will discuss the future directions and challenges in the field, emphasizing the need for standardized protocols, validated diagnostic thresholds, and novel therapeutic strategies based on the comprehensive two-way diagnosis.

Overall, the integration of periodontal risk assessment and oral microbiome profiling holds great promise in improving our understanding of periodontal diseases and revolutionizing their diagnosis and management. By harnessing the power of both host-related factors and microbial analysis, we can enhance clinical decision-making, optimize treatment outcomes, and ultimately improve the oral health and well-being of individuals affected by periodontal diseases.

Periodontal Disease: A Multifactorial Condition
Periodontal disease is a chronic inflammatory condition affecting the supporting structures of the teeth, including the gums, periodontal ligament, and alveolar bone. It is one of the most prevalent oral diseases worldwide, with varying degrees of severity ranging from gingivitis (inflammation of the gums) to periodontitis (destruction of the supporting tissues) [1]. Etiology and Pathogenesis The development and progression of periodontal disease are influenced by a combination of factors, making it a multifactorial condition. While bacterial plaque accumulation is recognized as the primary etiological factor, numerous host-related factors contribute to disease susceptibility and severity. These factors include genetic predisposition, systemic conditions, lifestyle habits, and oral hygiene practices [2]. Genetic Predisposition Growing evidence suggests that genetic variations can modulate an individual's susceptibility to periodontal disease. Several genes involved in immune response, extracellular matrix remodeling, and inflammatory pathways have been implicated in disease susceptibility. For example, polymorphisms in genes

encoding interleukins (IL-1), tumor necrosis factor-alpha (TNF-α), and matrix metalloproteinases (MMPs) have been associated with increased risk of periodontitis [3]. Systemic Factors Systemic conditions, such as diabetes mellitus, cardiovascular disease, and immunodeficiencies, can influence the onset, progression, and severity of periodontal disease. Bidirectional relationships exist between periodontal disease and systemic health, with inflammatory processes in the oral cavity potentially exacerbating systemic conditions and vice versa. Moreover, systemic conditions may compromise the host's immune response, impairing the ability to control the oral microbiota and promoting periodontal disease progression [4]. Lifestyle Habits and Oral Health Certain lifestyle habits, such as smoking, poor nutrition, and alcohol consumption, have been associated with an increased risk and severity of periodontal disease. Smoking has a significant impact on the initiation and progression of periodontitis, as it alters the host's immune response and compromises tissue healing [5].

Traditional Diagnostic Methods and Limitations

Traditionally, the diagnosis of periodontal disease has relied on clinical parameters, including probing depth, clinical attachment level, bleeding on probing, and radiographic assessment. While these methods provide valuable information about the current state of periodontal health, they have certain limitations that hinder a comprehensive understanding of the disease.

Limitations of Traditional Diagnostic Methods

Subjectivity and Intra-observer Variability Clinical parameters such as probing depth and attachment level measurements are subjective and prone to intra-observer variability. Variations in probing force and angulation can lead to inconsistent measurements, affecting the accuracy and reliability of the diagnosis. Lack of Predictive Value Traditional diagnostic methods primarily assess the current disease status but may not provide predictive information about future disease progression. Identifying individuals at risk of developing periodontal disease or experiencing disease progression is crucial for early intervention and preventive strategies [6]. Inability to Assess Disease Activity Traditional methods often fail to capture the dynamic nature of periodontal disease and assess disease activity accurately. They do not provide information about the ongoing tissue destruction and inflammatory processes within the periodontal tissues. Limited Understanding of Disease Mechanisms Clinical parameters alone do not provide insights into the underlying pathogenic mechanisms involved in periodontal disease. Understanding the complex interplay between the host immune response, the oral microbiome, and other contributing factors is essential for effective management and personalized treatment approaches [7]. Advanced Diagnostic Approaches To overcome the limitations of traditional diagnostic methods, advanced diagnostic approaches have emerged, focusing on a more comprehensive assessment of periodontal disease. These approaches include periodontal risk assessment and oral microbiome profiling, which provide valuable insights into disease susceptibility, severity, and microbial dysbiosis.

Periodontal Risk Assessment Periodontal risk assessment involves evaluating various patient-specific factors, such as genetic predisposition, systemic conditions, lifestyle habits, and oral hygiene practices, to determine an individual's risk of developing or experiencing progression of periodontal disease. By considering these factors, clinicians can identify high-risk individuals who may benefit from tailored treatment strategies and preventive measures [8]. Oral Microbiome Profiling The oral microbiome plays a crucial role in periodontal health and disease. Advanced sequencing technologies allow for the identification and quantification of microbial species or groups within the oral cavity. Oral microbiome profiling provides valuable information about the composition, diversity, and dysbiosis associated with periodontal disease. This knowledge can aid in understanding disease mechanisms, predicting disease progression, and developing targeted therapeutic interventions [9].

Advancements in Periodontal Risk Assessment

Genetic Predisposition and Periodontal Risk Genetic factors play a significant role in periodontal disease susceptibility and severity. Advances in genetic research have identified specific genetic variations associated with increased risk of developing periodontal disease. Polymorphisms in genes involved in the immune response, extracellular matrix remodeling, and inflammatory pathways have been investigated in relation to periodontal risk [10]. For example, studies have shown that variations in the interleukin-1 (IL-1) gene cluster, specifically the IL-1α and IL-1β genes, are associated with increased susceptibility to periodontitis. These genetic variations are linked to an exaggerated inflammatory response and impaired tissue repair mechanisms. Additionally, genetic variations in genes encoding matrix metalloproteinases (MMPs), which are involved in extracellular matrix degradation, have been associated with increased periodontal risk [11. Systemic Factors and Periodontal Disease Systemic conditions can influence the development and progression of periodontal disease. Advances in periodontal risk assessment have focused on understanding the bidirectional relationships between periodontal disease and systemic health [11]. For example, individuals with diabetes mellitus have an increased risk of periodontitis, and poor glycemic control can worsen periodontal disease outcomes. The interaction between periodontal pathogens and the host immune response in diabetes contributes to the chronic inflammation seen in both conditions. Similarly, systemic conditions such as cardiovascular disease, rheumatoid arthritis, and immunodeficiencies can impact the severity and progression of periodontal disease [12,13]. Lifestyle Habits and Oral Health Lifestyle habits, including smoking, nutrition, and alcohol consumption, can influence periodontal health. Advances in periodontal risk assessment have considered the impact of these habits on disease susceptibility and severity [14].

Cigarette smoking is a well-established risk factor for periodontal disease. Smoking affects the host immune response, impairs tissue healing, and alters the composition of the oral microbiota, leading to an increased risk of periodontitis. Additionally, poor nutrition, specifically a dietlacking in essential nutrients such as vitamins C and D, can compromise periodontal health and contribute to disease progression [15]. Oral Hygiene Practices and Periodontal Health Oral hygiene practices are critical for maintaining periodontal health. Advancements in periodontal risk assessment have explored the influence of oral hygiene habits on disease progression [16]. Effective oral hygiene practices, including regular toothbrushing, flossing, and interdental cleaning, help remove bacterial plaque and prevent its accumulation. Inadequate oral hygiene practices can lead to plaque buildup, gingival inflammation, and subsequent periodontal disease. Additionally, the use of adjunctive tools such as antimicrobial mouthwashes and interdental brushes can contribute to improved periodontal health [17]. These advancements in periodontal risk assessment provide clinicians with a more comprehensive understanding of individual susceptibility to periodontal disease and facilitate personalized treatment planning for improved clinical outcomes.

Oral Microbiome: The Key Player in Periodontal Disease

The oral microbiome refers to the diverse community of microorganisms that inhabit the oral cavity, including bacteria, fungi, viruses, and archaea. It plays a crucial role in maintaining oral health and has a significant impact on the development and progression of periodontal disease. Composition of the Oral Microbiome The oral cavity provides a unique environment for microbial colonization, with different ecological niches such as the teeth, gingival sulcus, tongue, and saliva. The oral microbiome is highly diverse, consisting of hundreds of different species. While some species are considered beneficial and contribute to oral health, others can be pathogenic and lead to the development of periodontal disease [18]. Dysbiosis and Periodontal Disease Periodontal disease is associated with a shift in the composition and diversity of the oral microbiome, a condition known as dysbiosis. Dysbiosis in the oral microbiome refers to an imbalance in the microbial community, characterized by an increase in the proportion of pathogenic species and a decrease in beneficial species [19]. Pathogenic bacteria, such as *Porphyromonas gingivalis*, *Treponema denticola*, and *Tannerella forsythia*, have been strongly associated with the development and progression of periodontal disease. These bacteria possess virulence factors that enable them to evade the host immune response, adhere to tooth surfaces, invade periodontal tissues, and initiate destructive inflammatory processes. Moreover, the presence of specific microbial complexes, such as the red complex (*P. gingivalis, T. denticola, and T. forsythia)*, has been linked to increased disease severity [20].

The dysbiotic oral microbiome generates a host immune response, leading to chronic inflammation within the periodontal tissues. This sustained inflammatory state contributes to the destruction of the periodontium, including the loss of periodontal ligament attachment and alveolar bone resorption, characteristic of periodontal disease. Role of the Oral Microbiome in Disease Progression The oral microbiome not only initiates periodontal disease but also plays a crucial role in its progression. As the disease advances, the dysbiotic oral microbiome can form biofilms, also known as dental plaque, on tooth surfaces and below the gum line. These biofilms provide a protected environment for bacterial colonization, making them more resistant to host immune responses and antimicrobial therapies [21]. Additionally, the dysbiotic oral microbiome can induce shifts in the local microenvironment, promoting a pro-inflammatory state and further exacerbating tissue destruction. The interaction between microbial virulence factors, host immune responses, and the local environment contributes to the chronic nature of periodontal disease [21]. Understanding the composition and dynamics of the oral microbiome has important clinical implications for the diagnosis, treatment, and prevention of periodontal disease. Advances in high-throughput sequencing technologies, such as next-generation sequencing, have allowed for a more comprehensive analysis of the oral microbiome and its association with periodontal health and disease.

Integrating Periodontal Risk Assessment and Oral Microbiome Profiling
Personalized Approach to Periodontal Diagnosis Integrating periodontal risk assessment and oral microbiome profiling allows for a more personalized approach to periodontal diagnosis. By assessing individual risk factors and analyzing the composition of the oral microbiome, clinicians can gain a deeper understanding of a patient's susceptibility to periodontal disease and tailor their diagnosis accordingly. Periodontal risk assessment considers factors such as genetic predisposition, systemic conditions, lifestyle habits, and oral hygiene practices to determine an individual's risk of developing or experiencing progression of periodontal disease. Oral microbiome profiling provides insights into the composition, diversity, and dysbiosis of the oral microbiome, which can help identify specific bacterial species or complexes associated with periodontal disease [22]. By integrating these two approaches, clinicians can better evaluate a patient's overall periodontal health status and make more accurate and informed diagnoses. This personalized approach enhances the understanding of the underlying causes of periodontal disease and helps guide treatment decisions.

Targeted Treatment Strategies for High-Risk Individuals Integrating periodontal risk assessment and oral microbiome profiling enables the development of targeted treatment strategies for high-risk individuals. High-risk patients, identified through the assessment of risk factors and oral microbiome analysis, may require more aggressive and personalized interventions to achieve optimal periodontal health outcomes [23]. For example, individuals with a genetic predisposition to periodontal disease or those harboring specific pathogenic bacterial species can benefit from targeted antimicrobial therapy. By identifying the presence of specific pathogens through oral microbiome profiling, clinicians can select antimicrobial agents that specifically target those bacteria, improving treatment efficacy. Additionally, high-risk individuals may require more frequent periodontal maintenance visits and supportive periodontal therapy to manage disease progression effectively. Interventions can also be tailored to address lifestyle factors such as smoking cessation counseling, nutritional guidance, and oral hygiene education, further enhancing treatment outcomes.[24]Monitoring Treatment Outcomes and Adjustments Integrating periodontal risk assessment and oral microbiome profiling facilitates the monitoring of treatment outcomes and the necessary adjustments in the management plan. By regularly assessing the oral microbiome and periodontal risk factors during and after treatment, clinicians can track changes in microbial composition and disease progression. Oral microbiome profiling can provide valuable information on the success of treatment interventions by assessing shifts in microbial diversity, the presence or absence of specific pathogenic species, and the establishment of a more balanced microbial community. Periodontal risk assessment allows for the evaluation of improvements in systemic conditions, lifestyle habits, and oral hygiene practices, which may impact periodontal health [25]. Monitoring treatment outcomes and making adjustments to the management plan based on changes in the oral microbiome and risk factors can optimize treatment success and long-term periodontal stability. Regular re-evaluation of the personalized treatment approach ensures that interventions remain tailored to the patient's specific needs and enhances the effectiveness of periodontal therapy.

Clinical Significance and Implications

Integrating periodontal risk assessment and oral microbiome profiling holds significant clinical significance and implications for periodontal diagnosis, treatment, and prevention. This comprehensive approach provides clinicians with a deeper understanding of individual susceptibility to periodontal disease and allows for personalized treatment planning, resulting in improved clinical outcomes. By considering various risk factors, such as genetic predisposition, systemic conditions, lifestyle habits, and oral hygiene practices, clinicians can identify high-risk individuals who may require more intensive interventions and tailored treatment strategies. This personalized approach optimizes treatment outcomes by addressing specific risk factors and targeting pathogenic bacteria identified through oral microbiome profiling.[26]Furthermore, the integration of periodontal risk assessment and oral microbiome profiling enhances the monitoring of treatment outcomes and facilitates necessary adjustments to the management plan. Regular evaluation of the oral microbiome and risk factors allows for the tracking of changes in microbial composition and disease progression. This iterative process ensures that treatment interventions remain tailored to the patient's evolving needs, leading to long-term periodontal stability.

Future Perspectives and Research Directions

The integration of periodontal risk assessment and oral microbiome profiling opens up promising avenues for future research and clinical applications. Some potential future directions include: Development of personalized treatment algorithms: Further research can focus on developing algorithms that integrate periodontal risk factors, oral microbiome data, and clinical parameters to guide personalized treatment decisions and improve treatment outcomes [27]. Targeted antimicrobial therapy: Future studies can explore the efficacy and safety of antimicrobial agents specifically targeted at pathogenic bacteria identified through oral microbiome profiling, leading to more precise and effective treatment interventions [28,29]. Long-term monitoring and prediction of disease progression: Continued monitoring of the oral microbiome and risk factors can help predict the risk of disease progression and guide preventive interventions to maintain long-term periodontal health.Therapeutic modulation of the oral microbiome: Investigating interventions aimed at modulating the oral microbiome, such as probiotics, prebiotics, and microbial therapies, may offer new avenues for preventing and managing periodontal disease. Integration with emerging technologies: Integration with emerging technologies, such as artificial intelligence and machine learning, can enhance the interpretation and analysis of complex oral microbiome data, leading to improved risk assessment and treatment planning.

CONCLUSION

The integration of periodontal risk assessment and oral microbiome profiling represents a significant advancement in periodontal diagnosis, treatment, and prevention. This comprehensive approach allows for a personalized understanding of individual susceptibility to periodontal disease, guiding targeted interventions and enhancing treatment outcomes. By considering various risk factors and analyzing the composition and dynamics of the oral microbiome, clinicians can tailor their approach to each patient, ensuring optimal periodontal health. Future research in this field holds promise for the development of personalized treatment algorithms, targeted antimicrobial therapies, and the exploration of emerging technologies to further enhance periodontal care.

REFERENCES

1. Offenbacher S, Barros SP, Singer RE, Moss K, Williams RC, Beck JD. Periodontal disease at the biofilm-gingival interface. J Periodontol. 2007;78(10):1911-1925.
2. Papapanou PN, Neiderud AM, Papadimitriou A, et al. Dissecting the role of genetic and environmental factors in human periodontitis. Periodontol 2000. 2020;83(1):165-178.
3. Sanz M, Ceriello A, Buysschaert M, et al. Scientific evidence on the links between periodontal diseases and diabetes: Consensus report and guidelines of the joint workshop on periodontal diseases and diabetes by the

63765

International Diabetes Federation and the European Federation of Periodontology. J Clin Periodontol. 2018;45(2):138-149.

4. Tonetti MS, Van Dyke TE; Working Group 1 of the Joint EFP/AAP Workshop. Periodontitis and atherosclerotic cardiovascular disease: Consensus report of the Joint EFP/AAP Workshop on Periodontitis and Systemic Diseases. J Periodontol. 2013;84(4 Suppl):S24-S29.

5. Chapple IL, Bouchard P, Cagetti MG, et al. Interaction of lifestyle, behaviour or systemic diseases with dental caries and periodontal diseases: Consensus report of group 2 of the joint EFP/ORCA workshop on the boundaries between car

6. Lang NP, Bartold PM. Periodontal health. J Periodontol. 2018;89 Suppl 1:S9-S16.

7. Sanz M, Ceriello A, Buysschaert M, et al. Scientific evidence on the links between periodontal diseases and diabetes: Consensus report and guidelines of the joint workshop on periodontal diseases and diabetes by the International Diabetes Federation and the European Federation of Periodontology. J Clin Periodontol. 2018;45(2):138-149.

8. Belstrøm D, Holmstrup P, Bardow A, et al. Temporal stability of the salivary microbiota in oral health. PLoS One. 2016;11(1):e0147472.

9. Meuric V, Le Gall-David S, Boyer E, et al. Signature of microbial dysbiosis in periodontitis. Appl Environ Microbiol. 2017;83(17):e00462-17.

10. Offenbacher S, Divaris K, Barros SP, et al. Genome-wide association study of biologically informed periodontal complex traits offers novel insights into the genetic basis of periodontal disease. Hum Mol Genet. 2016;25(10):2113-2129.

11. Shusterman A, Salzberg S, Golubchik P, et al. Interleukin-1 polymorphisms in periodontal disease: A meta-analysis. J Dent Res. 2016;95(3):278-286.

12. Lalla E, Lamster IB, Drury S, et al. Diabetes mellitus promotes periodontal destruction in children. J Clin Periodontol. 2007;34(4):294-298.

13. D'Aiuto F, Orlandi M, Gunsolley JC. Evidence that periodontal treatment improves biomarkers and CVD outcomes. J Clin Periodontol. 2013;40 Suppl 14:S85-S105.

14. Bergström J. Tobacco smoking and chronic destructive periodontal disease. Odontology. 2004;92(1):1-8.

15. Chapple ILC, Bouchard P, Cagetti MG, et al. Interaction of lifestyle, behaviour or systemic diseases with dental caries and periodontal diseases: Consensus report of group 2 of the joint EFP/ORCA workshop on the boundaries between caries and periodontal diseases. J Clin Periodontol. 2017;44 Suppl 18:S39-S51.

16. Van der Weijden GA, Slot DE. Oral hygiene in the prevention of periodontal diseases: The evidence. Periodontol 2000. 2011;55(1):104-123.

17. Hajishengallis G, Darveau RP, Curtis MA. The keystone-pathogen hypothesis. Nat Rev Microbiol. 2012;10(10):717-725.

18. Lamont RJ, Hajishengallis G. Polymicrobial synergy and dysbiosis in inflammatory disease. Trends Mol Med. 2015;21(3):172-183.

19. Kumar PS. From focal sepsis to periodontal medicine: A century of exploring the role of the oral microbiome in systemic disease. J Physiol. 2017;595(2):465-476.

20. Socransky SS, Haffajee AD. Periodontal microbial ecology. Periodontol 2000. 2005;38:135-187.

21. Paraskevas S, Timmerman MF, van der Velden U, van der Weijden GA. The effect of mechanical plaque control on gingival bleeding. J Clin Periodontol. 2004;31(5):394-397.

22. Armitage GC. Development of a classification system for periodontal diseases and conditions. Ann Periodontol. 1999;4(1):1-6.

23. Kinane DF, Stathopoulou PG, Papapanou PN. Periodontal diseases. Nat Rev Dis Primers. 2017;3:17038.

24. Griffen AL, Beall CJ, Campbell JH, et al. Distinct and complex bacterial profiles in human periodontitis and health revealed by 16S pyrosequencing. ISME J. 2012;6(6):1176-1185.

25. Mombelli A, Casagni F, Madianos PN, Canullo L. Biofilm formation, gingival inflammation, and susceptibility to periodontitis in systemic diseases. J Dent Res. 2018;97(10):1122-1130.

26. Huang S, Yang F, Zeng X, et al. Preliminary characterization of the oral microbiota of Chinese adults with and without gingivitis. BMC Oral Health. 2011;11:33.

27. Han YW, Wang X. Mobile microbiome: Oral bacteria in extra-oral infections and inflammation. J Dent Res. 2013;92(6):485-491.

28. Sanz M, Beighton D, Curtis MA, et al. Role of microbial biofilms in the maintenance of oral health and in the development of dental caries and periodontal diseases. Consensus report of group 1 of the joint EFP/ORCA workshop on the boundaries between caries and periodontal diseases. J Clin Periodontol. 2017;44 Suppl 18:S5-S11.

29. Tonetti MS, Chapple IL, Jepsen S, et al. Primary and secondary prevention of periodontal and peri-implant diseases: Introduction to, and objectives of the 11th European Workshop on Periodontology consensus conference. J Clin Periodontol. 2015;42 Suppl 16:S1-S4.

RESEARCH ARTICLE

Antimicrobial Activity of Biosynthesized Silver Nanoparticles

Chitra Rathod[1],Vijay Jagdish Upadhye[2] and Anupama Shrivastav[3]*

[1]Research Scholar, Department of Microbiology, Parul University, Vadodara, Gujarat, India.
[2]Center of Research for Development (CR4D), Parul Institute of Applied Sciences (PIAS), Parul University, (DSIR-SIRO Recognized), PO Limda, Tal Waghodia 391760, Vadodara ,Gujarat, India
[3]Associate Professor, Microbiology Department, ITM vocational University, Vadodara, Gujarat, India.

*Address for Correspondence
Anupama Shrivastav
Associate Professor,
Microbiology Department,
ITM vocational University,
Vadodara, Gujarat, India.
E. Mail: anupamam@itmvu.in

ABSTRACT

Biosynthesized nanoparticles are used in the study to detect their antimicrobial activity against *E.coli, B.subtilis, P.aeruginosa, S.aureus, A.niger* and *C.albicans.* The nanoparticles were produced from *S.aureus* cell free broth. The antimicrobial activity was determined using two methods: minimum inhibitory concentration and zone of inhibition using the Kirby-Bauer method. Positive controls were included using antibiotics. The results of both tests showed that the biosynthesized nanoparticles exhibited antimicrobial activity, which could have potential applications in the future.

Keywords: *E.coli, B.subtilis, P.aeruginosa, S.aureus, A.niger* and *C.albicans.*

INTRODUCTION

Nanoparticles have emerged as a promising substance in the medical field, particularly for combating multidrug resistant bacteria. However, chemically synthesized metallic nanoparticles are known to be environmentally hazardous. In contrast, biosynthesized nanoparticles are considered eco-friendly. Biosynthesized silver nanoparticles have been shown to possess antimicrobial properties and can be used as an antimicrobial agent. This study investigated the effect of biosynthesized silver nanoparticles on different microorganisms using two common methods: minimum inhibitory concentration and zone of inhibition. The minimum inhibitory concentration is the lowest concentration of a medicinal material that can prevent visible growth of microorganisms and can be expressed as mg/L or µg/ml. The IC50 value is the concentration at which a substance expresses half of its maximum inhibitory effect. The zone of inhibition refers to the area in media where microorganisms cannot grow due to the activity of a

63768

drug substance present in that area and can be observed with the naked eye. The zone size is typically measured in mm.

METHODOLOGY

Minimum Inhibitory Concentration Method

0.5 McFarland Standard dilution of microbes to be used for the study. 500 µl diluted log cultures of bacteria were added to the micro centrifuge tube, along with 10 µl of prepared treatment dilutions of different concentrations, and incubated for 24 hours. After incubation, all content was transferred to the 96 well plate, and readings were taken by the Elisa Plate Reader (iMark Biorad) at 490 nm and 595 nm. Different antibiotics were used as positive controls.

Positive control used in the MIC assay

Name of organism	Name of antibiotic
B.subtilis	Ciprofloxacin (100µg)
E.coli	Ciprofloxacin (100µg)
P.aeruginosa	Ciprofloxacin (100µg)
S.aureus	Ciprofloxacin (100µg)
C.albicans	Amphotericin B (25µg/ml)

Zone of Inhibition Method

The antibacterial activity was checked by following the Zone Inhibition Method (Kirby-Bauer method). The MHA plates were inoculated by spreading 100 µl of different bacterial cultures (adjusted to 0.5 McFarland units) and followed by placing the discs containing 10 µl of different concentrations (0 to 100 mg/ml). One disc in each plate was loaded with solvent alone, which served as vehicle control, and Ciprofloxacin discs (10µg) were taken as positive controls. The plates of bacterial cultures were incubated at 37 °C for 24 hours. Clear zones observed around the disc were measured and recorded. The antifungal activity was checked by following the Zone Inhibition Method (Kirby-Bauer method) for two fungal cultures. The PDA plates were inoculated by spreading 100 µl of fungal culture, *A.niger*. The SDA plates were inoculated by spreading 100 µl of fungal culture, *C.albicans* (adjusted to 0.5 McFarland Unit), followed by placing the discs containing 10 µl of different concentrations (0 to 50 mg/ml). One disc in each plate was loaded with solvent alone, which served as vehicle control, and a fluconazole disc (750µg) was taken as positive control against *A.niger*. Amphotericin B discs (25 µg) were taken as positive controls against *C.albicans*. The plates were then incubated for 48 hours. A clear zone created around the disc was measured and recorded.

RESULTS

Minimum Inhibitory Concentration

Name of microorganism	IC50 value µg/ml
E.coli	1.512
B.subtilis	6.816
P.aeruginosa	2.129
S.aureus	18.99
A.niger	3.125

Chitra Rathod *et al.,*

Zone of inhibition

Name of microorganisms: *Ecoli*	
Amount µg/disk	**Zone size in mm**
0	0
62.5	0
125	6.5
250	8
500	10
1000	11

Name of microorganisms: *B.subtilis*	
Amount µg/disk	**Zone size in mm**
0	0
62.5	7
125	9.5
250	10
500	13.5
1000	15

Name of microorganisms: *C.albicans*	
Amount µg/disk	**Zone size in mm**
0	0
31.25	7
62.5	8
125	7.5
250	10
500	10

Name of microorganisms: *A.niger*	
Amount µg/disk	**Zone size in mm**
0	0
31.25	8
62.5	9
125	9
250	10
500	11

Name of microorganisms: *P.aeruginosa*	
Amount µg/disk	**Zone size in mm**
0	0
62.5	10
125	10
250	10
500	11
1000	11

DISCUSSION

As chemical antimicrobial materials become increasingly resistant to antibiotics, there is a growing need to find more effective agents to combat microorganisms. While silver salts have been used as antimicrobial materials, their effect can be limited by interference with the effect of salts. However, using silver in nano form can overcome this limitation. Silver nanoparticles have a positive charge and can continuously release silver ions, which increases the surface area between the silver ion and microorganisms, resulting in a more powerful effect. In this study, biosynthesized silver nanoparticles made from the cell-free supernatant of S.aureus were used for their antimicrobial activity against different microorganisms. The tested microorganisms included *E.coli, B.subtilis, P.aeruginosa, S.aureus, A.niger* and *C.albicans.* The results showed that the biosynthesized nanoparticles had effective antimicrobial activity. The highest minimum inhibitory concentration (IC50) was found in *B.subtilis* at 6.816 µg/ml. During the zone of inhibition test, a clear zone was observed surrounding wells in different microorganisms. While only six strains were used in this study due to time constraints, these nanoparticles may be effective against a broad range of microorganisms, including resistant and genetically mutated strains. Additionally, these biosynthesized nanoparticles are free from any redox reactions, which makes them a promising candidate for future use as an antimicrobial agent.

CONCLUSION

The biosynthesis of silver nanoparticles using *S.aureus* cell-free broth is a useful, eco-friendly, and cost-effective method. These biosynthesized nanoparticles have potential applications in the medicinal field and have been proven to be an effective antimicrobial agent. This study demonstrates that the use of biological methods to synthesize nanoparticles is effective and useful against a broad range of microorganisms, making them a promising candidate for future medicinal purposes. One of the advantages of using biosynthesized nanoparticles is their eco-friendliness and non-hazardous nature to the environment. In contrast, chemically synthesized nanoparticles via redox reactions can be environmentally hazardous. Therefore, the use of biosynthesized nanoparticles can help reduce environmental impact while still providing an effective solution for antimicrobial applications. Overall, the biosynthesis of silver nanoparticles using S.aureus cell-free broth is a promising approach that can offer numerous benefits in the field of medicine.

REFERENCES

1. Antibacterial activity and characteristics of silver nanoparticles biosynthesized from *Carduus crispus* Enerelt Urnukhsaikhan, Bum-Erdene Bold, Aminaa Gunbileg, Nominchimeg Sukhbaatar & Tsogbadrakh Mishig-Ochi
2. Antimicrobial effect of silver nanoparticles (AgNPs) and their mechanism – a mini review Kaleemullah Kalwar, Dan Shan
3. Antimicrobial activities of silver nanoparticles synthesized from *Lycopersicon esculentum* extract Swarnali Maiti, Deepak Krishnan, Gadadhar Barman, Sudip Kumar Ghosh & Jayasree Konar Laha
4. Antimicrobial activity of biosynthesized silver nanoparticles, amoxicillin, and glassionomer cement against *Streptococcus mutans* and *Staphylococcus aureus* Enas Tawfik Enan8,1,2, Amal A Ashour3, Sakeenabi Basha 4, Nayef H Felemban5 and Sanaa M F Gad El-Rab 8,6,7
5. The antimicrobial activity of biogenic silver nanoparticles synthesized from extracts of Red and Green European pear cultivars Sohail Simon Nicole Remaliah Samantha Sibuyi Adewale Oluwaseun Fadaka, Mervin Meyer, Abram Madimabe Madiehe Marlen Geraldine du Preez

63771

Enhancing the Biotic Stress Resistance in Horticultural Crops using Recombinant DNA Technology

Niyati[1], Kuenga Penjor Gyeltshen[1], Tshering Tobgay Dorji[1], Muskan[1] and Suruchi Jindal[2]*

[1]Undergraduate Student (Biotechnology), Department of Biotechnology, School of Bioengineering and Biosciences, Lovely Professional University, Phagwara, Punjab-144411, India.
[2]Assistant Professor, Division of Molecular Biology and Genetic Engineering, School of Bioengineering and Biosciences, Lovely Professional University, Phagwara, Punjab-144411, India.

*Address for Correspondence
Suruchi Jindal
Assistant Professor,
Division of Molecular Biology and Genetic Engineering,
School of Bioengineering and Biosciences,
Lovely Professional University,
Phagwara, Punjab-144411, India.
E. Mail: suruchi.28640@lpu.co.in

ABSTRACT

Horticultural crops are prone to a wide variety of biotic stresses, like nematodes, bacteria, viruses, fungus, and oomycetes owing to occurrence of changing climatic conditions. The infections caused by the pathogens restrict horticulture crops' resilience and geographic range and affect their rate of development, production, and value. Continuous cropping approach employed in horticultural establishments significantly lowers productivity and quality while exacerbating soil-borne illnesses. Recombinant DNA technology using state of the art biotechnological tools such as RNA interference and genome editing tools based upon the CRISPR-Cas9 system are the powerful aids that can be utilized for the production of resistant varieties. RNAi exploits the gene silencing mechanism in which the genes of the pathogenic species are knocked out or knocked down by designing the hairpin constructs. The most recent CRISPR based genome/gene editing is being widely exploited in developing disease resistant horticultural crops because of its number of advantages. The most common application of CRISPR is to edit the susceptibility genes in the host so that they can be resilient to many diseases. Various case studies of developing resistance horticultural crops using the recombinant DNA technology is discussed in this review.

Keywords: biotic stress, resistant, recombinant DNA technology, RNAi, CRISPR genome editing

INTRODUCTION

Horticulture is an ancient agricultural strategy that has gained worldwide prominence [1]. Fruits, vegetables, and medicinal, fragrant, and visually pleasing plants are examples of horticultural crops. These plants supply essential dietary nutritional components, pharmaceuticals, and fragrances, as well as significant aesthetic value to humans [2]. The Indian economy has a significant impact on the horticultural sector which accounts for around 33% of agricultural GDA. Aside from ensuring the nutritional security of the country, it also provides alternative rural employment opportunities, diversification of farm activities, and handsome income to farmers. Improved demand for horticultural produce due to increased health awareness, rising income, export demands, and population growth offers a challenge for expanding horticultural crop production and productivity. Change in climate has raised the chances of uncertainties and dangers, also putting extra stress on industrial systems. In agriculture, plant diseases inflict significant economic, quality, and quantity losses. Plant diseases must be controlled because agricultural yield accounts for 70% of the Indian economy [3]. Pathogens and pests impair agricultural yield numerically and qualitatively, causing economic losses and jeopardizing food security with the largest impact proved in resource-poor areas with fleetly rising populations. Plants face a wide range of biotic stressors generated from numerous inhabiting creatures such as viruses, fungus, insects/pest, bacteria's, nematodes and other organism. These biotic stressors induces a number of illnesses, outbreaks and harms the crop, eventually leading to decreased crop output [4].The protection of crop cultivars against pests and diseases and the enhancement of crop cultivars for improved yield are critical concerns. The scarcity of disease-resistant crop varieties is causing significant losses in agricultural production for farmers.Plant breeding is essential for developing agricultural cultivars that are resistant to pests and diseases, and that have enhanced productivity, which in turn provides food and nutrition security. Resistance breeding is a technique that combines genetic modifications and advanced molecular techniques with transgenic plants to create superior crop cultivars with increased resistance to pests and diseases. By using transgenic technologies, plant breeders can use cross species and integrate genes from unrelated plants and other organisms into crop plants, further enhancing their resistance to pests and diseases [5]. Numerous biotechnological methods as well as methodologies are being explored not only to increase the diversity and value of horticultural crops but also making the crops more resilient to combat the climatic challenges particularly biotic stresses.Various state of the art biotechnological tools, techniques and strategies that are imparting the viral, bacterial, fungal, insect resistances are discussed in this review.

Viral Resistance
In modern agriculture, plant viruses pose substantial risks to a wide range of crops, and the financial losses brought on by viral infections are second only to those brought on by other pathogens [6].Depending upon the type, some viruses have an extremely large number of hosts. Tomato spotted wilt virus(TSWV) has been linked to more than a thousand crops across 85 families including several veggies, tobacco and peanuts and cucumber mosaic virus are recognized for infecting over 1200 plant species across hundred families consisting the utmost of vegetables and decorative flowers [7].Multiple efforts have been put forward in order to create resistance to viral agents in plants by expressing the virus's proteins from transgenes via pathogen-derived resistance or small RNA-based RNA silencing mechanism[8]. RNA interference (RNAi) acts as a typical genome modification procedure providing widely adopted as a strategy for gene manipulation to improve immunity to viruses in crops used in agriculture. Small interfering RNAs (siRNAs) have been employed to identify and destroy RNA from viruses, thereby decreasing viral reproduction and spread. An apparent method for inhibiting a desired gene while without significantly impairing the activity of any other genes in the plant is provided by the RNAi process[9].Various strategies were employed for activating antiviral suppression, which fall under four subcategories: sense gene-induced post-transcriptional gene silencing, hairpin RNA-induced post-transcriptional gene silencing (hp-PTGS), trans-acting siRNA generated PTGS (TAS), and artificial miRNA induced PTGS (AMIR) [10].S-PTGS were utilized at the very early stages of advancement of growth for viral suppression. s-ptgs is a genetic modification method designed in order to enhance the susceptibility to viruses in horticulture crops. The procedure includes inserting a virus sense gene set inside the host plant's genome, resulting in RNA-mediated suppression of genes and providing virus resistance [11].(Hp-PTGS)

Niyati *et al*.,

"Hairpin RNA-induced post-transcriptional gene silencing" is another genome editing technique used to improve viral resistivity in horticultural crops [12].This approach entails the inserting of a reversed repeat sequence that forms a hairpin design, which produces double-stranded RNA that triggers RNA-mediated gene suppression and imparts viral sensitivity [13].AMIR is a third-generation technology in which the complete miRNA sequences in the natural miRNA initial transcripts are substituted by particular RNA sequences that have properties comparable to targeted virus strains as well as favorable RISC (RNA Induced Silencing Complex) loading capabilities, resulting in the production of a novel synthetic miRNA gene. The AMIR genes went through transcription and is translated into developed miRNA via the appropriate motifs by the cellular miRNA biosynthesis pathway that imparts unique viral resistance once plants were modified [14]. The RNAi methodology is believed to be utilized consistently to yield Papaya ringspot virus (PRSV)-resistant papaya species.The modified papaya crops synthesize short hairpin RNA (shRNA) that addresses the PRSV coat protein molecule, forming siRNAs that break down viral RNA and offer resistance to PRSV infection.

The RNAi-mediated degradation of PRSV RNA was identified utilizing reverse transcription-via quantitative polymerase chain reaction (RT-qPCR), which exhibited a strong correlation with the traditional RT-qPCR approach for PRSV detection. While comparison with non-recombinant plants, recombinant papaya crops illustrated a substantial amount of immunity to PRSV infection[15].The researchers created shRNA (short hairpin RNAs) complexes that targeted the TYLCV (Tomato yellow leaf curl virus) coat protein gene and introduced them into tomato plants. Transgenic tomato plants had lessened TYLCV invasion as well signs than non-transgenic plants, demonstrating successful RNAi-mediated viral resistance [16].The researchers designed a construct encoding a hairpin RNA targeting the *CMV 2b*gene and introduced it into cucumber plants using Agrobacterium-mediated transformation. The shRNA strands are assigned to a carrier virus, which infects plant tissue and causes the shRNA to be expressed. After that, the shRNA can direct the RISC to locate and deteriorate the supplementary CMV RNA molecules. In transgenic cucumber crops, researchers observed decreased CMV transmission rates and expression rates as compared to non-transgenic plants [17].CRISPR/Cas9 technology enables the creation of a wide variety of CRISPR deviations that can be utilized for a wide range of functions which was previously effectively used to build virus-resistant plant cultivars. Moreover, gene interruption is among the most prevalent practice or approaches for the CRISPR/Cas9 technique, which assists in addressing the error-prone nature of cellular NHEJ (DNA-repair machinery) [18]. Nucleotide insertion/deletion (InDel) at sgRNA-targeted locations causes a frameshift transformation and it affects genes activity [19].

This method was previously utilized within the domain of virus resistance construction to create tolerance through modifying the expression of the susceptible (S) gene(s), disrupting crop-virus contact, and ultimately leading to decreased viral efficiency in the host plant. Another technique is to insert InDels into a gene's promoter instead of the coding region [18]. CRISPR-mediated promoter rupture inhibits the whole DNA transcription as well as their effector-binding region in highly susceptible crops through blocking a virus activator from attaching along the promoters [20]. This strategy also has the potential to design virus resistance in plants due to the gene clusters. In many hosts, removing chromosomal regions adjacent to S gene clusters would result in long-term viral resistance. Aside from virus silencing, CRISPR-mediated DNA substitution enables researchers towards exploring vital S domains[21]. An operational evaluation on vulnerability genes gives us a better understanding of how genes are regulated. Most guest proteins serve a critical purpose for the genome's pathogenesis, manifesting in the activation and positioning during viral infection. A number of resistance (R) gene(s) have been found among native varieties, while effective resistance transmission into cultivated horticultural crops has been established [19]. Utilizing combinatorial homology-directed repair (HDR) procedures, such an approach might substitute erroneous as well as inadequately operating R genes against domesticated varieties of crops with a working R gene generated by a virus-immune cultivar. CRISPR-mediated alteration generated by the bio-mimicry method alters the intended region back into sequences of a virus-immune variety [20]. This approach is useful as this permit the insertion of just particular alterations linked to virus-silencing feature instead of modifying each and every gene. As a result, changes within the nucleotide chains of particular genes between farmed and natural varieties are not adequate enough to impart long-term resistance to many viruses that affect plants. In this case, the Cas9 tool may be employed to tweak a specific

gene to provide long-term resistance in plants [22]. Figure 1 illustrates the mechanism of CRISPR/Cas9 system in diagrammatic representation. CRISPR-Cas9 is being utilized in targeting a Citrus tristeza virus (CTV) along with the Citrus psorosis virus (CPsV) in citrus.The researchers targeted the *CTV p23* gene as well as CPsV coat protein gene utilizing CRISPR-Cas9 system.When analyzed alongside the unmodified plants, the altered plants had fewer virus indications and smaller viral loads [23].In pepper crops, CRISPR-Cas9 has been implemented for gaining tolerance to the Banana bunchy top virus (BBTV). Using the CRISPR-Cas9 technology, scientists have addressed the BBTV *Rep* gene [24].

Fungal Resistance

Although fungicides are frequently employed to treat a large spectrum of microbial infections, they are typically vague and eliminate both productive bacteria and infectious agents. Furthermore, the majority of fungicides are detrimental to the well-being of people as well as the natural ecosystem. Therefore, repeated exposure to these chemicals can result in fungicide resistance [25].As a result, generating fungal disease-resistant strains could be a viable optional strategy for efficient aesthetic productivity while minimizing fungal pathogen losses. Conventional rearing for fungal disease resistance is hampered by a number of constraints, including a lack of genetic sources for numerous illnesses, the transmission of unwanted characteristics through genes that are resistant, with the quick development of infections' ability to circumvent plant-silencing techniques [26].Genetic engineering, on the other hand, has the capacity to surpass the limits of traditional breeding procedures by manipulating the plant's capability to identify and fight fungal diseases. Researchers have been able to better comprehend the molecular basis of plant defensive responses because of the advancements in genetic engineering, which has resulted in the development of novel disease-fighting strategies. Unlike traditional cultivation, genetic manipulation enables the simultaneous rise of pathogenic tolerance against various diseases, along with the desired gene that can be put into the intended target host regardless of whether it isn't present in the natural gene reservoir [25]. According to a recent study, establishing suppression within crops for cultivation using controlling mechanisms is feasible and efficient. *B.cinerea*, a necrotrophic fungus generates the short RNAs (sRNAs) that act as crucial trigger in inducing host defense [27]. Host plants can in turn, transfer sRNAs into *B. cinerea* via extracellular vesicles, which reduces the production of pathogenicity-related genes. Host resistance is enhanced or inhibited by over expression or reduction of transmitted host sRNAs. The results of this study imply that transmitted host sRNAs help to protect the host by suppressing fungal DNA [28].

Also, the long non-coding RNAs (lncRNAs) serve substantial roles in a wide range of biochemical actions involving crop defense response pathways [29].Within tomatoes, lncRNA16397 stimulates SlGRX articulation and later it initiates ROS buildup as well as structure damage, while lncRNA33732 induces RBOH activity for boosting H_2O_2 formation and so improves tomato immunity towards *Phytophthora infestans* [30].Grapes have 71 and 83 lncRNAs that respond to or are resistant against powdery mildewing transmission, correspondingly. According to new investigations, they promote a variety of reactions, including ROS, $Ca^{2+,}$ membrane strengthening, PR generation of protein, phytohormones, and secondary metabolic processes [31].The result of these increases the knowledge towards the comprehension of lncRNA modulation in the resistivity of horticultural plants. Another effective approach to generating resistance in cultivated crops may be translational surveillance of mRNA by regulatory element modification. In eukaryotes, upstream open reading frames (uORFs) are key regulators in mRNA translation [32].In one of the intriguing works, altering the uORF of *LsGGP2*, resulting in the generation of a critical chemical ascorbic acid production in lettuce, that enhances oxidative damage sensitivity as well as ascorbate concentration. Additionally, CRISPR/Cas9 enables the creation of transgene-free crop variants having enhanced characteristics which has major substantial implications for agricultural development [33].Correspondingly, constitutive *AtNPR1* expression in 35S: uorfs TBF1-AtNPR1 plants results in evident broad-spectrum resistance to disease with little growth implications. Since uORFs are persistent in eukaryotic mRNAs, which can be anticipated as controlling components that are going be tweaked for promoting wide-ranging tolerance while not having any effect upon typical development along with considerably aiding genetic potential among horticulture plants. TALEs (transcription activator-like effectors) serve as an emerging priority in the execution of gene discoveries that have the potential towards influencing resistance. TALEs possess the ability to adhere to effector binding elements (EBEs)

within the host plant inducer along with they can stimulate the expression of resistance (R) genes and host susceptibility(S) in *Xanthomonas* [34].Tomato *Bs4* (bacterial spot resistance locus no. 4) is a TALE-sensing NLR polypeptide which recognizes *AvrBs4* and stimulates disease resistance in the hosts. TALE-based approaches are ought to be utilized for finding effector R genes among different horticultural crops. Throughout the recent decade, many valuable technologies, like TALE nuclease (TALEN) machinery including the split-TALE (sTALE) framework, which were recently created enable genetic engineering, transcriptome controlling, as well as proteomics research [30].The advancement of all these approaches will contribute towards the acceleration of wide-spectrum fungal disease tolerance throughout horticultural development programs. One of the most severe diseases, *Fusarium oxysporum* f. sp. niveum (FON) causes watermelon (*Citrullus lanatus*) wilt, which has an impact on watermelon quality and yields globally [35].The phytosulfokine (PSK) precursor is encoded by the *Clpsk1* gene, which is knocked out using the CRISPR/Cas9 system to greatly increase watermelon's resistance to FON [36].

Insect/Pest Resistance

The *Bacillus thuringiensis* soil bacterium's *Bt* (*cry*) gene has proven to be particularly successful in controlling a wide range of lepidopteran insects in numerous crops. The *Bt* gene in tomatoes was initially associated with insect resistance in 1987. In transgenic *Bt* tomato plants, resistance to *Spodoptera lituria* and *Heliothis virescens* was seen [37]. *Agrobacterium tumefaciens* was used to alter the brinjal (*Solanum melongena* cv. Pusa Purple Long) utilising the synthesised *cry1Ab* gene that codes for an insecticidal crystal protein [38]. The synthesised *cryIA(b)*gene was developed for transforming the cauliflower cultivar Pusa Snowball K-1, and the transgenic plants indicated the transgene's productiveness in suppressing diamond back moth (*Plutella xylostella*) larval invasion through insect bioassays. Researchers created the transgenic cabbage (*Brassica oleracea* var. capitata) line DTC 507 to control resistance to the diamondback moth by encoding a translated integration result of cry1B and cry1Ab endotoxins from *B. thuringiensis* [39].Okra (*Abelmoschus esculentus*) was effectively transformed and expressed with the *Bt* gene (*Cry1Ac*) [40].During insect bio assay, fruits from transgenic lines exhibited a 100 percent rate of death for larvae. A variety of horticulture crops were given resistance by the insertion of both synthetic and natural insect resistance genes. Vine weevil resistance (*Otiorhynchus sulcatus*) has been demonstrated using transgenic strawberries via a continuous promoter producing a (*Vigna unguiculata*) cowpea proteolytic inhibitor oftrypsin gene (*CpTi*). Through the use of insect bioassays, the CpTi transgenic strains decreased the rate of weevil larval and pupal mortality. In resistance to the codling insect pest, produced transgenic apple varities that had a trypsin inhibitor conveying the *CpTI* gene through the cow peas with a*cry-1-A(c)* gene via *Bacillus thuringiensis* [41].

RNA interference technology has allowed the development of insect resistance in horticultural crops. RNAi-based insect resistance had been developed in citrus against Asian citrus psyllid [42], for making transgenic potato resistant against Colorado potato beetle and the potato tuber moth [43]. RNAi technology is also being utilized to develop tomato plants having resistance against tomato fruitworm and pinworm [44]. Strawberries are a widely cultivated horticultural crop that is susceptible to several insect pests, including the two-spotted spider mite and the strawberry bud weevil. RNAi technology has been used to develop strawberry plants that are resistant to these pests by targeting genes involved in their feeding and development. A study conducted in Japan showed that RNAi-based insect resistance in strawberries can significantly reduce pest damage and increase yield [45].Another approach to creating insect and pest resistance in horticultural plants is through CRISPR mediated genome editing tool.Diamondback moth (*Plutella xylostella*) is a major pest in cabbage production worldwide. The CRISPR-mediated genome editing was used to create diamondback moth-resistant cabbage plants by targeting and disabling a gene involved in the production of glucosinolates, which are toxic compounds that cabbage plants produce in response to diamondback moth feeding. The gene-edited cabbage plants were shown to be highly resistant to diamondback moth without compromising plant growth and yield [46]. The CRISPR-mediated genome editing was used to create tomato plants that are resistant to tomato fruit borer by targeting and disabling a gene involved in the production of jasmonic acid, a hormone that is released in response to insect feeding. The gene-edited tomato plants were shown to be highly resistant to tomato fruit borer without compromising plant growth and yield [47].

Niyati *et al.*,

Bacterial Resistance

Bacteria resistance is one of the major concerns in the world of horticulture, as it can help in the reduction of crop yield and quality. Plant pathogens or disease-causing bacteria pose a significant threat to horticultural crops, reducing their productivity and marketability. Some of the major bacterial diseases in horticulture crops include bacterial wilt, bacterial leaf spot, bacterial blight, and fire blight. Many bacterial pathogens develop resistance to one or more antibiotics that are commonly used to control bacterial infection. Such defense mechanisms can arise due to genetic mutations or transfer of resistance genes between different bacteria. Once the resistance gene is present, it can spread rapidly throughout bacterial populations and lead to the emergence of one or more virulent strains that can cause serious agricultural problems. The management of bacterial diseases in horticulture crops requires the careful use of antibiotics and other chemicals that are proven to be effective against bacterial pathogens. However, this approach leads to the development of antibiotic-resistant strains of bacteria, which eventually renders the chemicals useless. Therefore, new strategies are required to manage bacterial diseases in horticultural crops that do not rely on antibiotics or other chemical treatments [48]. The resistance to bacterial diseases like *Xanthomonas campestris* and *Pseudomonas syringae* had been acquired via RNAi using the hairpin construct [49]. The hypersensitive response-assisting protein (HrpZ) which contributes to the release of virulent markers is encoded due to *HrpZ* gene, which is present in various plant pathogenic bacteria. It was showed that the *HrpZ* gene, which was placed into tomato and tobacco varieties, confers defense against pathogenic bacteria such *Pseudomonas syringae* [50].

The*Rpm1* gene encodes a protein that is recognized for influencing bacteria's activity and initiating a defensive mechanism in *Arabidopsis thaliana*. Tomato plants were genetically engineered using the *Rpm1 gene*which provideddefense against *Pseudomonas syringae* [51].The *Xa21* from rice had been used to genetically engineer the tomato which was capable of providing defense against bacterial diseases like *Xanthomonas campestris* [52]. *X. campestris* is an essential pathogen affecting cruciferous plants, notably broccoli and cabbage.It has been revealed that the toxicity of *X. campestris* in cabbage as well as broccoli can be decreased by utilizing RNAi to silence the *hrpX* gene, which is implicated in the release of virulence proteins [53].A prominent agent of citrus crops is *X. axonopodis*. It has been revealed that the virulence of *X. axonopodis* in citrus can be artificially decreased by utilizing RNA interference to knock down the *gumB* gene, which participates in the generation of extrinsic polysaccharides [54].Pear and apple trees are seriously harmed by *E. amylovora*. It was successfully demonstrated the virulence of *E. amylovora* in pear and apple trees can be decreased by employing RNA interference to silence the *pelL* gene, which participates in the breakdown of pectin [55].A significant pathogen of several horticultural crops, such as tomato, pepper, and cucumber, is *P. syringae*. It has been discovered that *P. syringae* virulence in these crops can be decreased by utilizing RNA interference to silence genes involved in type III secretory structure, which are in charge of delivering effector molecules into the cells of plants [56].

CONCLUSION

In the present review article, the potential applications of recombinant-DNA technology or genetic engineering for developing disease resistant horticultural crops have been discussed in detail. The state of the art biotechnological tools implementing the recombinant DNA technology has multiple applications in the farming industry as a result of the growing world population and demand for effective intensification, which is causing food insecurity. Biotechnology has had limited success in business to date in horticultural crops, such as fruits, vegetables, flowers, and landscape plants, compared to the increasing global adoption of biotech field crops. We can't ignore the potential of this technology at this moment in time to modify our horticultural crops to overcome various production limits like biotic or abiotic stressors and increased quality of fruit. Resolving many regulatory obstacles will make it possible for commercial distribution of an array of transgenic crops, enabling consumers and different beneficiaries to get the most from this remarkable technology.

Niyati *et al.*,

REFERENCES

1. He M, Kong X, Jiang Y, Qu H, Zhu H. MicroRNAs: emerging regulators in horticultural crops. Trends Plant Sci. 2022;27(9):936-951.
2. Mall M, Kumar R, Akhtar MQ. Horticultural crops and abiotic stress challenges. InStress Tolerance in Horticultural Crops. Woodhead Publishing.2021. p. 1-19
3. Sandhu GK, Kaur R. Plant disease detection techniques: a review. In2019 international conference on automation, computational and technology management (ICACTM) 2019 (p. 34-38). IEEE.
4. Jeger M, Beresford R, Bock C, Brown N, Fox A, Newton A, Vicent A, Xu X, Yuen J. Global challenges facing plant pathology: multidisciplinary approaches to meet the food security and environmental challenges in the mid-twenty-first century. CABI Agriculture and Bioscience. 2021;2(1):1-8.
5. Yin Y, Wang C, Xiao D, Liang Y, Wang Y. Advances and Perspectives of Transgenic Technology and Biotechnological Application in Forest Trees. Front Plant Sci. 2021; 12:786328.
6. Simón-Mateo C, García JA. Antiviral strategies in plants based on RNA silencing. Biochim Biophys Acta. 2011;1809(11-12):722-31.
7. Zitter TA, Murphy JF. Cucumber mosaic. The Plant Health Instructor. 2009;10(1094):2009-051801
8. Palukaitis P. The road to RNA silencing is paved with plant-virus interactions. Plant Patho Journal. 2011;27(3):197-206.
9. Gautam P, Kumar R, Feroz Z, Vijayaraghavalu S, Kumar M. RNA Interference Technology in Plants: Mechanisms and Applications in Crop Improvement. InPlant Genomics for Sustainable Agriculture. Singapore: Springer Nature Singapore.2022. p. 265-290.
10. Khalid A, Zhang Q, Yasir M, Li F. Small RNA Based Genetic Engineering for Plant Viral Resistance: Application in Crop Protection. Front Microbiol. 2017;8:43.
11. Harries PA, Palanichelvam K, Yu W, Schoelz JE, Nelson RS. The cauliflower mosaic virus protein P6 forms motile inclusions that traffic along actin microfilaments and stabilize microtubules. Plant Physiol. 2009;149(2):1005-16.
12. Pumplin N, Voinnet O. RNA silencing suppression by plant pathogens: defence, counter-defence and counter-counter-defence. Nat Rev Microbiol. 2013 (11):745-60.
13. Mitter N, Worrall EA, Robinson KE, Li P, Jain RG, Taochy C, Fletcher SJ, Carroll BJ, Lu GQ, Xu ZP. Clay nanosheets for topical delivery of RNAi for sustained protection against plant viruses. Nat Plants. 2017;3:16207.
14. Vu TV, Choudhury NR, Mukherjee SK. Transgenic tomato plants expressing artificial microRNAs for silencing the pre-coat and coat proteins of a begomovirus, Tomato leaf curl New Delhi virus, show tolerance to virus infection. Virus Res. 2013;172(1-2):35-45.
15. Hamim I, Borth WB, Marquez J, Green JC, Melzer MJ, Hu JS. Transgene-mediated resistance to Papaya ringspot virus: challenges and solutions. Phytoparasitica. 2018;46:1-8.
16. Pooggin MM. RNAi-mediated resistance to viruses: a critical assessment of methodologies. Curr Opin Virol. 2017 ;26:28-35.
17. Holeva MC, Sklavounos A, Rajeswaran R, Pooggin MM, Voloudakis AE. Topical Application of Double-Stranded RNA Targeting 2b and CP Genes of *Cucumber mosaic virus* Protects Plants against Local and Systemic Viral Infection. Plants (Basel). 2021; 10(5):963.
18. Zaidi SS, Mahas A, Vanderschuren H, Mahfouz MM. Engineering crops of the future: CRISPR approaches to develop climate-resilient and disease-resistant plants. Genome Biol. 2020;21(1):289.
19. Mushtaq M, Mukhtar S, Sakina A, Dar AA, Bhat R, Deshmukh R, Molla K, Kundoo AA, Dar MS. Tweaking genome-editing approaches for virus interference in crop plants. Plant Physiol Biochem. 2020;147:242-250.
20. Cao Y, Zhou H, Zhou X, Li F. Control of Plant Viruses by CRISPR/Cas System-Mediated Adaptive Immunity. Front Microbiol. 2020;11:593700.
21. Pramanik D, Shelake RM, Park J, Kim MJ, Hwang I, Park Y, Kim JY. CRISPR/Cas9-Mediated Generation of Pathogen-Resistant Tomato against *Tomato Yellow Leaf Curl Virus* and Powdery Mildew. Int J Mol Sci. 2021;22(4):1878.

22. Shahriar SA, Islam MN, Chun CNW, Rahim MA, Paul NC, Uddain J, Siddiquee S. Control of Plant Viral Diseases by CRISPR/Cas9: Resistance Mechanisms, Strategies and Challenges in Food Crops. Plants (Basel). 2021;10(7):1264.

23. Dutt M, El-Mohtar CA, Wang N. Biotechnological approaches for the resistance to citrus diseases. The Citrus Genome. 2020:245-57.

24. Tripathi L, Ntui VO, Tripathi JN, Kumar PL. Application of CRISPR/Cas for Diagnosis and Management of Viral Diseases of Banana. Front Microbiol. 2021;11:609784.

25. Mekapogu M, Jung JA, Kwon OK, Ahn MS, Song HY, Jang S. Recent Progress in Enhancing Fungal Disease Resistance in Ornamental Plants. Int J Mol Sci. 2021;22(15):7956.

26. Wani SH. Inducing fungus-resistance into plants through biotechnology. Notulae Scientia Biologicae. 2010;2(2):14-21.

27. Weiberg A, Wang M, Lin FM, Zhao H, Zhang Z, Kaloshian I, Huang HD, Jin H. Fungal small RNAs suppress plant immunity by hijacking host RNA interference pathways. Science. 2013;342(6154):118-23.

28. Cai Q, Qiao L, Wang M, He B, Lin FM, Palmquist J, Huang SD, Jin H. Plants send small RNAs in extracellular vesicles to fungal pathogen to silence virulence genes. Science. 2018;360(6393):1126-1129.

29. Zaynab M, Fatima M, Abbas S, Umair M, Sharif Y, Raza MA. Long non-coding RNAs as molecular players in plant defense against pathogens. Microb Pathog. 2018 ;121:277-282.

30. Xu X, Chen Y, Li B, Zhang Z, Qin G, Chen T, Tian S. Molecular mechanisms underlying multi-level defense responses of horticultural crops to fungal pathogens. Hortic Res. 2022;9:uhac066.

31. Bhatia G, Upadhyay SK, Upadhyay A, Singh K. Investigation of long non-coding RNAs as regulatory players of grapevine response to powdery and downy mildew infection. BMC Plant Biol. 2021;21(1):265.

32. Zhang H, Wang Y, Wu X, Tang X, Wu C, Lu J. Determinants of genome-wide distribution and evolution of uORFs in eukaryotes. Nat Commun. 2021;12(1):1076.

33. Zhang H, Si X, Ji X, Fan R, Liu J, Chen K, Wang D, Gao C. Genome editing of upstream open reading frames enables translational control in plants. Nat Biotechnol. 2018;36(9):894-898.

34. Nowack MK, Holmes DR, Lahaye T. TALE-induced cell death executors: an origin outside immunity? Trends Plant Sci. 2022;27(6):536-548.

35. Rahman MZ, Ahmad K, Bashir Kutawa A, Siddiqui Y, Saad N, Geok Hun T, Hata EM, Hossain MI. Biology, Diversity, Detection and Management of Fusarium oxysporum f. sp. niveum Causing Vascular Wilt Disease of Watermelon (Citrullus lanatus): A Review. Agronomy. 2021;11(7):1310.

36. Zhang M, Liu Q, Yang X, Xu J, Liu G, Yao X, Ren R, Xu J, Lou L. CRISPR/Cas9-mediated mutagenesis of Clpsk1 in watermelon to confer resistance to Fusarium oxysporum f.sp. niveum. Plant Cell Rep. 2020;39(5):589-595.

37. Perlak FJ, Deaton RW, Armstrong TA, Fuchs RL, Sims SR, Greenplate JT, Fischhoff DA. Insect resistant cotton plants. Biotechnology (N Y). 1990;8(10):939-43.

38. Clark D, Klee H, Dandekar A. Despite benefits, commercialization of transgenic horticultural crops lags. California agriculture. 2004;58(2).

39. Chakrabarty R, Viswakarma N, Bhat SR, Kirti PB, Singh BD, Chopra VL. Agrobacterium-mediated transformation of cauliflower: optimization of protocol and development of Bt-transgenic cauliflower. J Biosci. 2002;27(5):495-502.

40. Mishra GP, Seth T, Karmakar P, Sanwal SK, Sagar V, Singh PM, Singh B. Breeding strategies for yield gains in Okra (Abelmoschus esculentus L.). InAdvances in Plant Breeding Strategies: Vegetable Crops: Volume 9: Fruits and Young Shoots 2021 Aug 26 (pp. 205-233). Cham: Springer International Publishing.

41. Parmar N, Singh KH, Sharma D, Singh L, Kumar P, Nanjundan J, Khan YJ, Chauhan DK, Thakur AK. Genetic engineering strategies for biotic and abiotic stress tolerance and quality enhancement in horticultural crops: a comprehensive review. 3 Biotech. 2017;7(4):239.

42. Taning CN, Andrade EC, Hunter WB, Christiaens O, Smagghe G. Asian Citrus Psyllid RNAi Pathway - RNAi evidence. Sci Rep. 2016;6:38082.

43. Zhang J, Khan SA, Heckel DG, Bock R. Next-Generation Insect-Resistant Plants: RNAi-Mediated Crop Protection. Trends Biotechnol. 2017;35(9):871-882.

44. Kanakala S, Ghanim M. RNA Interference in Insect Vectors for Plant Viruses. Viruses. 2016;8(12):329.

45. Schwab W, Hoffmann T, Kalinowski G, Preuß A. Functional genomics in strawberry fruit through RNAi-mediated silencing. Genes Genomes Genomics. 2011;5(1):91-101.

46. Huang Y, Chen Y, Zeng B, Wang Y, James AA, Gurr GM, Yang G, Lin X, Huang Y, You M. CRISPR/Cas9 mediated knockout of the abdominal-A homeotic gene in the global pest, diamondback moth (Plutella xylostella). Insect Biochem Mol Biol. 2016;75:98-106.

47. Ma Q, Hu Z, Mao Z, Mei Y, Feng S, Shi K. A novel leucine-rich repeat receptor-like kinase MRK1 regulates resistance to multiple stresses in tomato. Hortic Res. 2022 ;9:uhab088.

48. Chen Z, Hartmann HA, Wu MJ, Friedman EJ, Chen JG, Pulley M, Schulze-Lefert P, Panstruga R, Jones AM. Expression analysis of the AtMLO gene family encoding plant-specific seven-transmembrane domain proteins. Plant Mol Biol. 2006;60(4):583-97.

49. Liu T, Chen Y, Tian S, Li B. Crucial Roles of Effectors in Interactions between Horticultural Crops and Pathogens. Horticulturae. 2023;9(2):250.

50. Kloek AP, Verbsky ML, Sharma SB, Schoelz JE, Vogel J, Klessig DF, Kunkel BN. Resistance to Pseudomonas syringae conferred by an Arabidopsis thaliana coronatine-insensitive (coi1) mutation occurs through two distinct mechanisms. Plant J. 2001 ;26(5):509-22.

51. Russell AR, Ashfield T, Innes RW. Pseudomonas syringae Effector AvrPphB Suppresses AvrB-Induced Activation of RPM1 but Not AvrRpm1-Induced Activation. Mol Plant Microbe Interact. 2015;28(6):727-35.

52. Ercoli MF, Luu DD, Rim EY, Shigenaga A, Teixeira de Araujo A Jr, Chern M, Jain R, Ruan R, Joe A, Stewart V, Ronald P. Plant immunity: Rice XA21-mediated resistance to bacterial infection. Proc Natl Acad Sci U S A. 2022;119(8):e2121568119.

53. Rubel MH, Robin AHK, Natarajan S, Vicente JG, Kim HT, Park JI, Nou IS. Whole-Genome Re-Alignment Facilitates Development of Specific Molecular Markers for Races 1 and 4 of Xanthomonas campestris pv. campestris, the Cause of Black Rot Disease in Brassica oleracea. Int J Mol Sci. 2017;18(12):2523.

54. Scortichini M. Sustainable management of diseases in horticulture: Conventional and new options. Horticulturae. 2022;8(6):517.

55. Meena M, Swapnil P, Zehra A, Aamir M, Dubey MK, Patel CB, Upadhyay RS. Virulence factors and their associated genes in microbes. InNew and future developments in microbial biotechnology and bioengineering 2019 Jan 1 (pp. 181-208). Elsevier.

56. Majumdar R, Rajasekaran K, Cary JW. RNA Interference (RNAi) as a Potential Tool for Control of Mycotoxin Contamination in Crop Plants: Concepts and Considerations. Front Plant Sci. 2017;8:200.
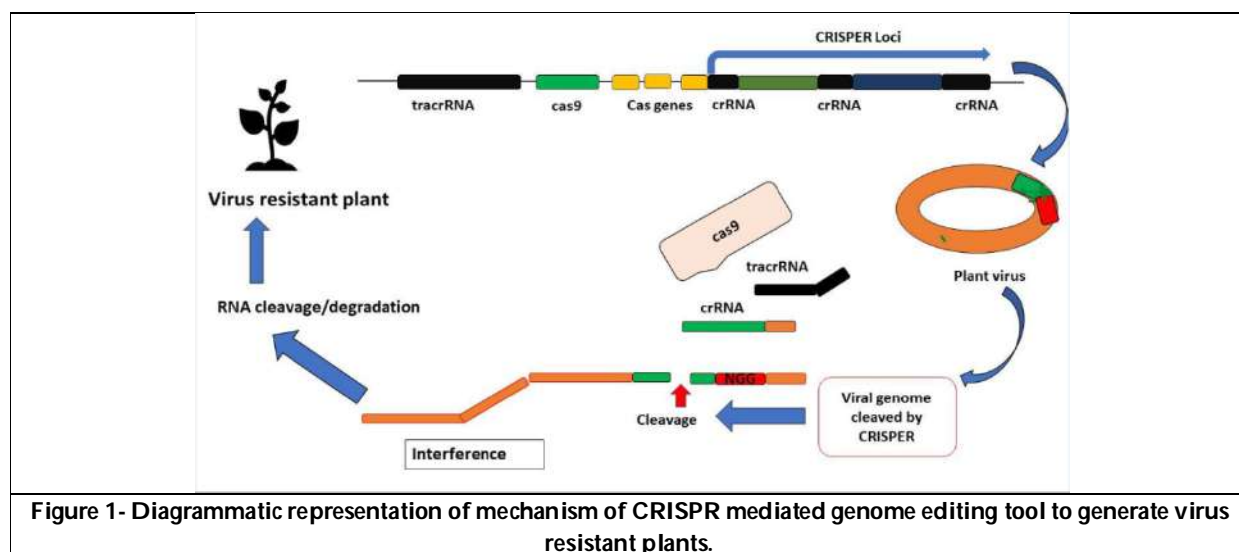
Figure 1- Diagrammatic representation of mechanism of CRISPR mediated genome editing tool to generate virus resistant plants.

RESEARCH ARTICLE

Utilization of Diets Amended Probiotics for the Growth Performances and Immune Responses to Infection with *Vibrio harveyi* in *Litopenaeus vannamei*

Venkatesan.M[1*] , Sudhakar.S [2] and Jayaprakash. R[1]

[1]Research scholar, Centre of Advanced Study in Marine Biology, Faculty of Marine Sciences, Annamalai University, Parangipettai- 608502, Tamil Nadu, India.
[2]Research Guide, Centre of Advanced Study in Marine Biology, Faculty of Marine Sciences, Annamalai University, Parangipettai-608502, Tamil Nadu, India.

*Address for Correspondence
Venkatesan, M
Research scholar,
Centre of Advanced Study in Marine Biology,
Faculty of Marine Sciences,
Annamalai University,
Parangipettai- 608502, Tamil Nadu, India.

ABSTRACT

The experiment was conducted to examine the effects of dietary administration of commercially available probiotic, Zymetin (ZY) on growth performance and immune responses of white shrimp (*Litopenaeus vannamei*). Shrimp (0.31±0.04 g) was fed with basal diet (control without challenge test (-) and control with challenge test (+)), supplemented with 2.5%, 5.0%, 7.5%, and 10.0% Zymetin was encapsulated with commercial feed (CP Aqua) for 30 days. Five shrimp were sampled from each tank after the feeding experiment to determine bacterial levels and immunity. Finally all the shrimp were challenged by *V. harveyi* infection for 7 days. Shrimp week growth rates and food conversion ratios were significantly better in the ZY treatment after 30 days than in the control group. A higher Total Haemocyte Count (THC) and phenoloxidase activity were also measured in all ZY treatments than in the control group. Following a co-infection challenge test, probiotic treatments had higher PO, THC, and Respiratory Burst (RB) activity than the control (+). Then, the lowest survival rate of shrimp was observed in the control (+), whereas higher survivability was observed in Zymetin treated groups

Keywords: Shrimp culture; *Litopenaeus vannamei*, Probiotics, Zymetin, *Vibrio harveyi.*

INTRODUCTION

Aquaculture production has increased dramatically in recent years, with Penaeid shrimps being one of the most significant cultivated species worldwide, particularly in Asia, due to their high economic worth and exportability [1]. More than 5 million metric tonnes of prawns are produced each year, but the current global demand for both wild and farmed prawns is more than 6.5 million metric tonnes per year [2]. Nowadays, despite high levels of shrimp production by culture, shrimp farmers have suffered significant economic losses due to disease problems that have plagued the industry. The continuous outbreak of the White Spot Syndrome Virus (WSSV) disease in *Penaeus monodon* culture has led to a loss of shrimp culture in India. As a result, farmers are actively seeking alternative shrimp species for culture. In 2008, the Coastal Aquaculture Authority (CAA) of India introduced *Litopenaeus vannamei*, a new shrimp species, as an alternative Penaeid species for culture and export. *Litopenaeus vannamei* exhibits a fast growth rate, and its culture period is significantly reduced compared to *Penaeus monodon*. Therefore, *Litopenaeus vannamei* has been established as an alternative to *Penaeus monodon* for shrimp farming in several countries, including East, Southeast, and South Asia [3].

The spread of infectious disorders, especially those brought on by viruses and bacteria, is one of the issues with white prawn intensive farming. *Vibrio harveyi*, a bacterium, was the source of the bacterial sickness that affected the white prawns [4]. Around the world, *Vibrio harveyi* has been identified as a dangerous infection for a variety of aquaculture organisms [5]).The condition has been managed using a variety of strategies. The use of antibiotics or other chemicals in aquaculture may increase the danger of infections that are resistant to antibiotics [6]. In order to prepare prawns for innate immunity by boosting their resistance to infections, probiotics were administered as a disease-controlling alternative. Probiotics are seen of as a live microbial food supplement that enhances the host's and their culture environments' microbial balance and wellness [7]. Probiotics significantly enhance disease resistance and modulate gastrointestinal microbiota in shrimp [8], lobster [9], and sea cucumber [10], parrot fish [11] and koi [12]. The present study aimed to determine the most optimum concentration of probiotic, Zymetin on the growth performance, immune response and disease resistance to infection with *V. harveyi* of shrimp (*L. vannamei*).

MATERIALS AND METHODS

Probiotic and Diet Preparation
Commercially available probiotic, Zymetin (ZY) was used in this study. Two hundred milliliter of the ZY with rice bran, tapioca flour, sugar and yeast were added to 200 L of freshwater and left overnight with vigorous aeration. After fermentation, the slurry was applied evenly in the ponds. The dosage of the probiotic was increased as the culture days increased. four experimental diets were prepared with different concentration of probiotics supplemented with 2.5%, 5.0%, 7.5%, and 10.0% was encapsulated with commercial feed for 30 days. Diets were then stored in clean plastic bags at 4°C until use.

Culture Condition
A commercial hatchery in Sirkazhi, Tamil Nadu, India provided the experimental post-larval vannamei (PL) prawn, which was reared there for 21 days before testing. Shrimp with a mean initial body weight of 0.33 g and a density of 15 per tank were randomly placed in triplicate tanks (30 35 40 cm; volume 0.3 m³ The shrimp were fed four times a day until they reached their target weight, with 10% of the total biomass in each feeding. Water temperature was maintained at 27-29°C; salinity ranged from 29–32‰; pH 7.4–7.5 and dissolved oxygen (DO) between 4.5-6.5 mg/L as well as ammonia nitrogen levels less than 0.016 mg L-1 inside culture vessels

Growth and Feed Conversion Ratio
After 1 month, the total number of prawns was counted and the mean body weight was calculated. Based on this weight of shrimp and the quantity of shrimp counted, the Daily Growth Rate (DGR) and Feed Conversion Ratio (FCR) were determined using the following equations:

$$DGR\,(\%) = \left(\sqrt[t]{W_t / W_o} - 1\right) \times 100 \qquad FCR = \frac{F}{Bt + Bm - Bo}$$

where,

DGR is the specific growth rate in weight (% g),

W_t and W_o are shrimp weight at current time (t) and at the beginning of the experiment (o), respectively,

t is the number of rearing days (day).

FCR is food conversion ratio,

F is the total dry food consumed (g) and

Bt, Bm and Bo is the total biomass of the shrimp (g) at current time (t), due to mortality of shrimp (m) and at the beginning of the experiment (o), respectively, whereas t is the number of rearing days (day).

Challenged Test

The bacteria *Vibrio harveyi* was procured in CAS in Marine biology, Parangipettai, Tamilnadu, India. For the challenge test; ten shrimp were injected with a dose of live *V. harveyi* bacteria equal to 10^3 CFU per tank from a 24 h culture grown in ZMA medium at 29°C. The shrimp mortality rate was observed for 7 days following injection

Immune Parameter Assay

Using a syringe filled with anticoagulant solution, hemolymph was drawn from the ventral sinus. The identical samples obtained from the five prawns kept in the same tank were combined and utilized as a single batch. The anticoagulant solution for haemolymph (10 mM EDTA, 340 mM NaCl, 30 mM trisodium citrate, and pH 7.0). A 1:2 (v/v) anticoagulant solution was extensively incorporated into the haemolymph. Shrimp haemolymph samples were taken twice, once after 30 days of feeding (before the challenge test) and once after the challenge test with *V. harveyi* was completed (7 days later). The THCs were determined using a haemocytometer at 100 times magnification. Cells were counted on both sides of the grids. THCs were calculated using the following equation:

THC = Cells counted × dilution factor × 1000 = Volume of grid ($0.1\ mm^3$)

According to Liu and Chen [13], phenoloxidase activity was measured. Briefly, 50 L of haemolymph were combined with 50 L of 0.1% trypsin in CAC buffer, which was incubated at 25°C for 10 min. After that, 50 L of L-DOPA (0.3% in CAC buffer) were added, mixed, and the ideal density was assessed at 490 nm. An increase of 0.001 min/mg protein in absorbance was used to measure one unit of enzyme activity.

The method of Song and Hsieh [14] was used to evaluate the Respiratory Burst (RB) activity of haemoglobin by reducing NBT (nitrobluetetrazolium) as a gauge of superoxide anion (O_2^-). After being incubated for 30 minutes at room temperature, a total of 300 mL of the haemolymph-anticoagulant combination was centrifuged for 20 minutes at 3000 rpm, with the supernatant being discarded. After that, 100 mL of NBT (HBSS solution containing 0.3% NBT) was added, and stand for 2 hours at room temperature. The mixture was centrifuged at 3000 rpm for 10 min, the supernatant was collected, and 100 mL of 100% methanol was added. This was followed by another 10 min at 3000 rpm centrifugation, with the supernatant being discarded. Then, two times, 70% methanol was used to rinse the formed pellets. The next 120 mL KOH (2 M) and 140 mL of dimethyl sulfoxide (DMSO) was added to dissolve the pellet. Insoluble pellet was then inserted into the microplate to measure Optical Density (OD) using a microplate reader at a wave length of 630 nm. Respiratory burst expressed as NBT reduction per 10 μL haemolymph.

Statistical Analyses

Results are presented as Mean ±SD (standard deviation of means). Data analysis was done with statistical analysis methods at a 95% confidence interval (α = 0.05). Statistical analyses were performed using a statistic program SPSS (version, 17.0). One-way analysis of variance (One-way ANOVA) was used to determine significant differences between the treatments followed by Duncan's Multiple Range Test (DMRT).

RESULTS AND DISCUSSION

Growth and Feed Conversion Ratio

Supplementation of ZY appears to increase the WGR and decrease the FCR as compared to the controls. The highest DGR (9.94±0.18%) and the lowest FCR (1.42±0.05), respectively observed in 7.5% ZY treatment and was significantly different than control groups (p<0.05; Fig. 1). The 2.5% ZY treatment has no significant difference in growth performances compared with the control groups (p>0.05). Similar findings were made for the European lobster (*Homarus gammarus* L.), which when fed a probiotic diet comprising a combination of *Bacillus* spp. and MOS showed considerably higher weight gain, SGR, and FCR [9]. *Bacillus subtilis* and fructo oligosaccharide (FOS) were shown to improve growth performance in juvenile large yellow croaker (*Larimichthy scrocea*) by Ai et al. [15].

Immune Response

Total Haemocyte Count (THC) of shrimp fed on different doses of probiotic is shown in Fig. 2. After 30 days of culture, THC increased significantly in the group treated with probiotic 7.5% (C) compared with control groups. THC of shrimp from the groups fed ZY supplemented with 2.5%, 5.0%, 7.5% and10.0% were higher (p<0.05) compared control (+). Shrimp fed with the control positive diet produced the lowest THC. According to Rodriguez and Le Moullac [16], Smith et al. [17], and Hauton [18], the haemocyte produces inflammatory-type reactions such as phagocytosis, haemocyte clumping, generation of reactive oxygen metabolites, and release of microbial proteins. After the challenge test, THC levels in all prawn treatments decreased. The body's defence mechanisms, including phagocytosis activity, encapsulation, nodule formation, and the degranulation process for system prophenoloxidase activation (ProPO), had an impact on the reduction of cells' hemocytes following the challenge test [17].

Phenoloxidase (PO) activities in haemolymph showed increasing tendency with the increasing doses of ZY in diets (Fig. 3). The shrimp in treatment 7.5% ZY and 10% ZY produced the highest PO activities with, followed by shrimp fed with treatment 5.0% ZY and they were significantly higher than the control groups (Fig. 3; p<0.05). After being given the challenge test with *V. harveyi*, PO activities in control (-), control (+) and all treatments showed an increase. According to data, PO activity of shrimp before challenge test known to be positively correlated with the value of THC. Hemocytes of shrimp function within the production and release of PO into hemolin in the form of inactive pro-enzyme called ProPO [17]. After being given a challenge test all treatments showed an increase. Increased activity of PO indicates a high immune response of shrimp. Lesmanawati [19], stated that an increase in PO activity occurs on the fifth day post-infection IMNV and shrimp on synbiotic treatment resulted in an increase in PO was higher than the control.

In this study, respiratory burst activities (RB) for all treatments were presented in Fig. 4. After feeding trial for 30 days, RB activity in Haemolymph was not significantly different between probiotic treatments and controls (Fig. 4; p>0.05). In contrast, RB activity after challenged with *V. harveyi* significantly increased and was significantly different with controls (Fig. 4; p>0.05). According to Rodriguez and Le Moullac [16], respiratory burst (RB) is an oxygen-dependent killing mechanism used by phagocytic cells to rid themselves of foreign particles. According to the findings, probiotic therapy does not boost RB activity; rather, *V. harveyi* infection is to blame for the rise. Numerous investigations [11, 20] revealed that the treatment of probiotics had no discernible effect on RB activity.

Survival

Shrimp survival after the 30 days of experimental period was similar in all experimental groups. Shrimp survivals after challenged with *V. harveyi* significantly increase as the dose of dietary probiotic in diet increased (Fig. 5; p<0.05). Shrimp fed with the control positive diet produced the lowest survival and were significantly different (p<0.05) from the groups fed synbiotic supplemented with ZY 2.5%, 5.0%, 7.5% and 10.%. This probiotic had significantly reduced mortality of the shrimp challenged by infection with *V. harveyi* and also stimulate immunity of the shrimp. In the previous study, probiotic SKT-b had been reported that probiotic may enhance resistance of shrimp (*L. vannamei*) to *V. harveyi* [21]. Similarly, the result has been reported that SKT-b is known to inhibit the growth

Venkatesan *et al.*,

of *V. harveyi* pathogens effectively both *in vitro* and *in vivo* on tiger shrimp (*Penaeus monodon*) larva [22]. The high resistance of survival shrimp might be caused by enhanced of innate immunity. Results of this study showed that probiotic, Zymetin (ZY) in shrimp diets can significantly improve growth and disease resistance by enhancing immunity, as well as presumably modulating microflora in the shrimp's gut. The results showed that the most optimum dose of dietary probiotic in this study was shrimp 7.5% ZY.

REFERENCES

1. Sekhar M, Alam A, Easwaran S, Srinivasa P, Kathirvelpandian A, Aparna C, Gopal K. Genetic diversity among three Indian populations of black tiger shrimp (*Penaeus monodon* Fabricious, 1798) using microsatellite DNA markers. Indian Journal of Fisheries 2014;61(3):45-51.
2. Karthik R, Hussain AA, Muthezhilan R. Effectiveness of *Lactobacillus* sp (AMET1506) as Probiotic against Vibriosis in *Penaeus monodon* and *Litopenaeus vannamei* Shrimp Aquaculture. Biosciences, Biotechnology Research Asia 2014;11: 297-305.
3. Karuppasamy A, Mathivanan V, Selvisabhanayakam. Comparative growth analysis of *Litopenaeus vannamei* in different stocking density at different farms of the Kottakudi Estuary, South East Coast of India. International journal of fisheries and aquatic studies 2013;1(2):40-44.
4. Austin B, Zhang XH. *Vibrio harveyi*: A significant pathogen of marine vertebrates and invertebrates. Lett Applied Microbiol 2006;43:119-124.
5. Soto-Rodriguez SA, Gomez-Gil B, Lozano R. del Rio-Rodriguez R, Dieguez AL, Romalde JL. Virulence of *Vibrio harveyi* responsible for the Bright-red syndrome in the pacific white shrimp *Litopenaeus vannamei*. J Invertebr Pathol 2012;109:307-317.
6. Balcazar JL, de Blas I, Ruiz-Zarzuela I, Cunningham D, Vendrell D, Muzquiz JL. The role of probiotics in aquaculture. Vet Microbiol, 2006;114:173-186.
7. Verschuere L, Rombaut G, Sorgeloos P, Verstraete, W. Probiotic bacteria as biological control agents in aquaculture. Microbiol Mol Biol Rev 2000;64: 655-671.
8. Li J, Tan B, Mai K. Dietary probiotic *Bacillus* OJ and iso malto oligosaccharides influence the intestine microbial populations, immune responses and resistance to white spot syndrome virus in shrimp (*Litopenaeus vannamei*). Aquaculture 2009;291:35-40.
9. Daniels CL, Merrifield DL, Boothroyd DP, Davies SJ, Factor JR, Arnold KE. Effect of dietary *Bacillus* spp. and mannan oligosaccharides (MOS) on European lobster (*Homarus gammarus* L.) larvae growth performance, gut morphology and gut microbiota. Aquaculture 2010;304:49-57.
10. Zhang Q, Ma H, Mai K, Zhang W, Liufu Z, Xu W. Interaction of dietary *Bacillus subtilis* and fructooligosaccharide on the growth performance, non-specific immunity of seacucumber, *Apostichopusjaponicus*. Fish Shellfish Immunol 2010;29:204-211.
11. Yogananth N, Akila M, Syed Ali M, Jayaprakashvel M, Muthezhilan R. Determination of probiotic bacteria from intestine of *Sparisoma viride* and bioencapsulation of *Artemia salina* with probionts. Research journal of microbiology 2020;15: 1-8.
12. Lin S, Mao S, Guan Y, Luo L, Luo L, Pan Y. Effects of dietary chitosan oligosaccharides and *Bacillus coagulans* on the growth, innate immunity and resistance of koi (*Cyprinuscarpio koi*). Aquaculture 2012;342-343:36-41.
13. Liu CH, Chen JC. Effect of ammonia on the immune response of white shrimp *Litopenaeus vannamei* and its susceptibility to *Vibrio alginolyticus*. Fish Shellfish Immunol 2004;16:321-334.
14. Song YL, Hsieh YT. Immunostimulation of tiger shrimp (*Penaeus monodon*) hemocytes for generation of microbicidal substances: Analysis of reactive oxygen species. Dev Comp Immunol 1994;18:201-209.
15. Ai Q, Xu H, Mai K, Xu W, Wang J, Zhang W, Effects of dietary supplementation of *Bacillus subtilis* and fructo oligosaccharide on growth performance, survival, non-specific immune response and disease resistance of juvenile large yellow croaker, *Larimichthy scrocea*. Aquaculture 2011;317:155-161.
16. Rodriguez J, Le Moullac G. State of the art of immunological tools and health control of penaeid shrimp. Aquaculture 2000;191:109-119.

Venkatesan *et al.*,

17. Smith VJ, Brown JH, Hauton C. Immunostimulation in crustaceans: Does it really protect against infection? Fish Shellfish Immunol 2003;15:71-90.
18. Hauton C. 2012. The scope of the crustacean immune system for disease control. J Invertebr Pathol 110:251-260.
19. Lesmanawati W. Applications of synbiotic on shrimp *Litopenaeus vannamei*: Resistance against infectious virus myonecrosis and growth performance. Master Thesis, Bogor Agricultural University, Indonesia. 2013.
20. Cerezuela R, Guardiola FA, Meseguer J, Esteban MA. Increases in immune parameters by inulin and *Bacillus subtilis* dietary administration to gilthead seabream (*Sparus aurata* L.) did not correlate with disease resistance to *Photobacterium damselae.* Fish Shellfish Immunol 2012;32:1032-1040
21. Arisa II. Application of probiotic, prebiotic and synbiotic to enhance the immune response of shrimp *Litopenaeus vannamei* against *Vibrio harveyi* infection. Master Thesis, Bogor Agricultural University, Indonesia. 2011.
22. Widanarni W, Suwanto A, Sukenda S, Lay BW. Potency of *Vibrio* isolates for biocontrol of vibriosis in tiger shrimp (*Penaeus monodon*) larvae. J Biotropia 2003;20:11-23.
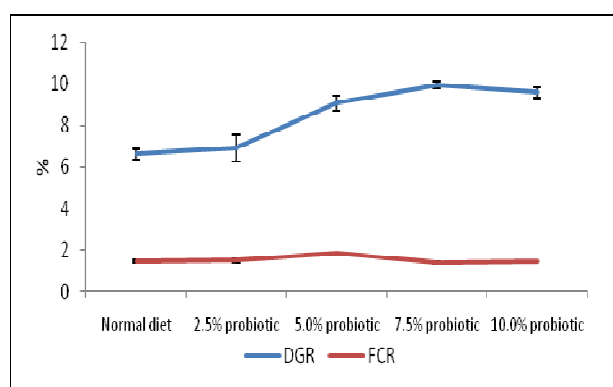
Fig 1: Daily growth rateand feed conversion ratio of *L. vannamei*
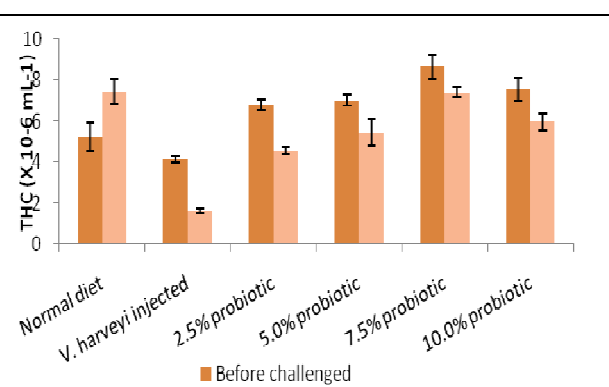
Fig 2: Total Haemocyte Count of *L. vannamei*
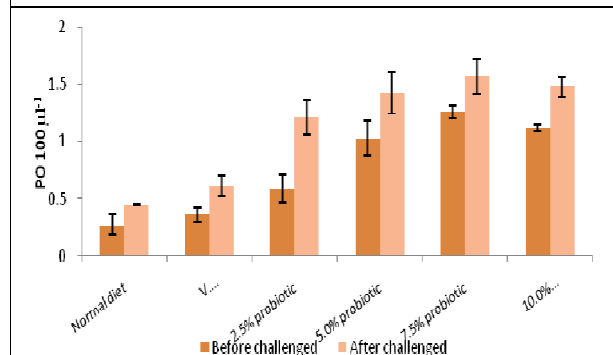
Fig 3: Phenoloxidase activities in haemolymph of *L. vannamei*
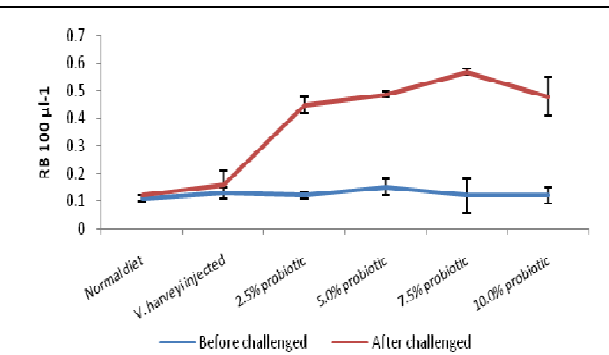
Fig 4: Respiratory burst activities of *L. vannamei*
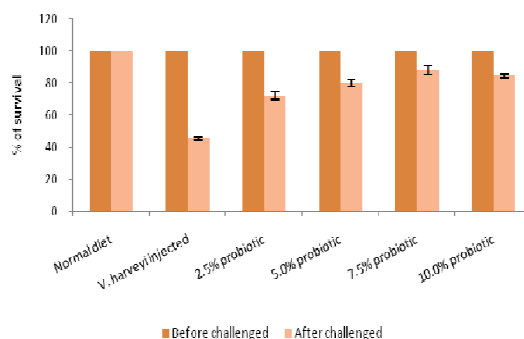
Fig 5: Survival rate of *L. vannamei*

RESEARCH ARTICLE

Text Mining and Health Care

Jayasudha.J* and Manju.V

Assistant Professor, Department of Computer Science, Sri Ramakrishna College of Arts and Science for Women, Coimbatore -641044, Tamil Nadu, India

*Address for Correspondence
Jayasudha.J
Assistant Professor,
Department of Computer Science,
Sri Ramakrishna College of Arts and Science for Women,
Coimbatore -641044, Tamil Nadu, India
E.Mail: jayasudhayuvaraaj@gmail.com

ABSTRACT

Text mining is the process of extracting hidden information from unstructured to semi-structured material. Text mining is the process of discovering new information by mechanically extracting it from various written resources. As vast amount of data is generated every minute some meaningful information should be extracted from the available resource and these data provide information and knowledge which will be very helpful for analysis. This paper focuses a main area based on health care records and also illustrates the methods and techniques in text mining .As health care databases are growing drastically we need to extract knowledge from the available sources.

Keywords : Machine Learning, Text Mining, Health Care, Medical Records, Text Analytics**.**

INTRODUCTION

Text mining also called as Text Data Mining or Text Analytics is the process of drawing out content based on meaning and context from vast amount of text. It transforms the unstructured text into structured data for easy analysis and it used Natural Language Processing (NLP) to understand the human language for natural processing. Text mining extracts valuable insights from unstructured text. By analyzing vast amount of data generated, text mining analyzes complex and large dataset in a simple and effective way. In businesses large amount of data are generated every day as an opportunity and challenge. This data helps the companies to get smarter insights about people's, opinions about a product or service which may be e-mail, product reviews, social media posts, customer feedback etc. So to process these kinds of data text mining uses simple methods and techniques, makes us understand about the working of text mining.[1] In the recent years Text Mining gained the attention of the users due to massive amount of data and it automates the process of classifying texts by sentiment, topic, and intent. Not

63788

only businesses, as healthcare databases are growing exponentially, it collects text and numerical information about patient's visits, prescriptions, and physician notes and so on. The medical service combined with e-clinical records could lead to improve the quality of healthcare and research initiatives, fewer medical errors, and lower costs.

TEXT MINING BACKGROUND

Data mining is a statistical technique for processing raw, structured data. Usually this is done with preexisting databases and spreadsheets to gather information. Here statistical tools are used for analyzing data. It is a combination of Artificial Intelligence, Machine Learning and Statistics mainly used in areas like marketing and health care. Considering healthcare, text mining improves the quality of treatments, increasing revenues or lower costs of healthcare organization such as a hospital. Data mining is widely used area in computer science, economics, communication and marketing, allowing finding important patterns on information that are, otherwise, difficult to analyze. As text mining is closely related to Data Mining, it is used to process collection of unstructured text files such as Word documents, PDF files, text excerpts, and XML files. These textual data are used in academic research literature, health care, biology and marketing.

Text mining is a variation of data mining from text data collections. The main aim of text mining is to find the knowledge from text data, which are unstructured or semi-structured. Text mining is a branch of Data Mining (DM) using KDD to discover knowledge from various data sources, which includes text data, relational databases, Web data, user log data, etc. Text Mining is related to other research areas like Machine Learning (ML), Information Retrieval (IR), Natural Language Processing (NLP), [9] Information Extraction (IE), Statistics, Pattern Recognition (PR), Artificial Intelligence (AI), etc. As all the data generated today are in the form of e-mails, text messages, documents and files and to know the best insights of data and its patterns text mining came into existence. Text mining is considered as a semi-automated process of extraction patterns and discovering knowledge from unstructured data.

Until the introduction of Text mining, data mining was the dominant approach as they had to control only structured data. As Data volumes are exploding and most of this is unstructured and text mining is necessary to deal with unstructured data. so to handle both structured and unstructured data to provide greater insights in the business operations and decision making, we are in need of text mining.[2]Most businesses will collect huge amount of data through customer feedback, product reviews and social media posts. So to analyze this kind of vast amount of data text mining is necessary to find the valuable opinion and feedback of the customers clearly. Without text mining above mentioned task is a challenge to categorize the opinion and automation helps the companies to overcome their drawbacks by going through more feedbacks using opinion mining.

TEXT MINING TECHNIQUES

The process of Text mining involves various activities to gather structured information from the unstructured text by parsing, adding linguistic features and removing unnecessary patterns from database .[3]By structured data final evaluation will be done and the output will be interpreted. So this is an automatic process that extracts the valuable insights from data collected. These techniques deploy various text mining tools and applications for their execution. To make the data structured the steps to be followed are

Information Extraction- A most famous text mining process used to extract meaningful and valuable information from unprocessed or unstructured massive amounts of data. This is the initial step for identifying key phrases and relationships ,tokenization, focuses on identifying the extraction of attributes, entities, relationship from semi-structured or unstructured text. Extracted information is stored in the associated database or some separate storage for additional processing with precision and recall processes.

Informational Retrieval- By using this process relevant and associated pattern are extracted based on specific set of words. With the help of algorithms,

different behavior of users is identified and discovers the relevant data and information. Search engines uses query based algorithms for Information retrieval to derive relevant documents according to the keywords used in search

Natural Language Processing (NLP): Text mining uses various methodologies for text processing, includes **natural language processing (NLP)**. NLP is a subfield of computer science, linguistics, data science, and artificial intelligence deals with the interaction between humans and machines. It allows computers to understand both speech and text forms. Text analytics usually breaks down the sentences into words or phrases before analyzing. So unstructured text contents are separated apart to know the details in it. Using NLP, Text mining exact theme of the contents specified will be extracted. Text mining includes seven steps as shown in Fig.1 like Language identification, Tokenization, Sentence Breaking, Part of Speech Tagging (POS), Chunking, Syntax Parsing and Sentence Chaining. Each step is very ihortant to handle unstructured data in text mining

* ❖ **Language Identification**: The first step in text analytics is language identification that identifies in what language the text is written in. It may be Spanish, Singlish, Arabic, English and so on. Lexanalytics is a text mining technology and NLP feature, processes each text document that goes through to transform data into structured data and also supports nearly 25 languages with more alphabets.
* ❖ **Tokenization**: The second step is to break the sentence into pieces called tokens. Tokens are individual units like words, Punctuations, Hyperlinks or phonemes. Tokens are used in the process of text mining. The process of breaking the sentences into words is called Tokenization and it is language specific as every language follows different tokenization requirements. For Example English language uses punctuation methods and spaces to separate tokens .But logographic languages like Chinese have no space to break between words, so it differs based on the language. So algorithms can also be used to tokenize the sentences in various languages.
* ❖ **Sentence Breaking**: After token identification, next step is to identify the end of the sentences. To separate the sentences also we need some spaces and punctuation symbols to identify the end of the sentence. Some deeper text analytics should be used to identify the sentences using boundary recognition.
* ❖ **Part of Speech Tagging and chunking**: After language identification and tokenization, broken words should be tagged. After token identification and sentence breaking we should tag the words.Part of Speech tagging used to identify things like whether a given token represents a proper noun or a common noun, or if it's a verb, an adjective, or something else entirely. This step is an important step in text analytics.
* ❖ **Chunking**: Chunking is a process of extracting phrases from unstructured text, by analyzing a sentence to identify the constituents. So chunking refers to breaking sentences into component phrases.PoS tagging means assigning parts of speech to tokens whereas Assigning PoS-tagged tokens to phrases is called chunking.
* ❖ **Syntax Parsing:** The syntax parsing is a way to determine the structure of a sentence. Syntax parsing is one of the most computationally-intensive steps in text analytics. Unsupervised machine learning models are used in Lexanalytics, works on more input words and complex matrix factorization, which helps to understand syntax just like a human.
* ❖ **Sentence Chaining**: The final step in preparing unstructured text for deeper analysis is **sentence chaining**, also known as sentence relation that uses Lexalytics which utilizes a technique called "lexical chaining" to relate sentences. Even if paragraphs apart in a document, the lexical chain will flow through the document and help a machine detect overarching topics and quantify the overall "feel.

* • **Clustering-** Most crucial text mining technique that identifies intrinsic structures in text and organize into different subgroups called clusters. So a meaningful cluster should be formed from the unlabelled data without prior information. Tools like Cluster analysis helps in data distribution .Clustering is one of the most crucial text mining techniques. It tries to identify in-depth structures in textual information and organize them into relevant subgroups or 'clusters' for analysis. A challenge in the clustering process is to form clusters from the unlabeled textual data without having any prior knowledge on them. Different clustering techniques are hierarchical, distribution, density centroid, and k-means clustering, used for analyzing unstructured text documents.

* • **Categorization** :Texts are categorized and assigned to predefined set of topics based on their content.The main task of text classification/text categorization is to increase the detection of information that can lead to a better decision. Using Natural Language Processing (NLP) it gathers text documents for processing and analyzing to uncover the

right topics or indexes for each document. So co-referencing method is used to extract relevant synonyms and abbreviations from textual data. This methodology is used in healthcare systems to identify disease categories, operation procedures, and insurance reimbursement codes. Some useful analytical classification models, used to categorize text, are naive Bayesian classifier, nearest neighbor classifier, decision trees, and support vector machines. Applications included in categorization are document organization, spam filtering, SMS categorization, and hierarchical categorization of web pages.

- **Text visualization –**This technique is used to represent textual information into a visual map which produces large textual information into visual layout. It enhances browsing capabilities and also improves the discovery of relevant information**.** Text flags are used to show the document category to represent individual or group of documents with the help of colors to show the density. It also helps us to know the hierarchy levels visually. The process of visualization involves Data preparation, Data analysis and extraction and visualization mapping.

- **Summarization–** Generating compressed text automatically, from multiple text sources to analyze and summarize the text contained in these multiple text sources. So, summarization collects various parts of the textual data to make a meaningful text. Lexicon lists are generated in this stage on the basis of phrase or words in the document. Length of the Sentence, fixed phrase, paragraph, thematic words and upper case word identification features can be analyzed for text summarization. This technique can be applied on multiple documents at the same time. Quality and type of classifiers depend on nature and theme of the text documents. So text summarization is used to create a summary according to the meaning of the text. Text summarization involves text pre processing, it is performed to clean the data to remove the spelling errors, avoid duplication and replacing acronyms.

There are other approaches used in text mining for interpreting and exporting keywords. *Keyword based association* is based on association analysis that reduces the incorrect retrieval using some stop words, keywords or idiomatic expressions. *Document classification* method is used in libraries to assign tags to document, classifying genre and type of writing for tagging. *Trend Analysis* finds patterns on information for future event prediction and also estimates the events of past. *Vector space model* is a technique which is representing documents or searches by vectors to find similarities between them. *Indexing Techniques* uses tables and id of all documents for making related searches faster. *Inverse document frequency* finds out the words based on the importance of words and to search with more precision to extract keywords. Text mining techniques and methods are available to derive valuable insights from text data. Most commonly used text mining techniques are Word frequency ,The concept of finding out the recurrent terms from the data set and most mentioned words in unstructured text is very useful in analyzing customer reviews, social media conversations or in feedbacks. So here the terms that are frequently used are analyzed in word frequency. Then Collocation which refers to combination of words which appear together most of the times. Some words usually come together, it may be bigrams(two words) like "get started "or trigrams (three words) like "keep in touch ".So identifying collocation and using word improves the granularity of the text, for better understanding of its semantic structure and more accurate text mining results. Finally Concordance used to recognize the particular context or a word or set of words appears. As human language can be ambiguous and the same word can be used in different contexts.

METHODS USED IN TEXT MINING
There are various techniques being developed to solve the text mining problems, they are basically the relevant information retrieval according to the requirement of users. Counting on the information retrieval techniques, [1] some common methods are shown in Fig.2.

Term Based Method: Term is defined as a word which has a well-explained meaning in a document. Every term in a document is having a specific meaning and documents are analyzed on the basis of term weight age. Even this method is facing problems like polysemy and synonymy. A word has multiple meanings is called polysemy and

multiple words having the same meaning is called synonymy. So by finding out the semantic meaning of many terms is not sure for answering what exactly users want.

Phrase Based Method: When compared to term this provides semantic information and is less confusing as Phrase carries more semantics like information and is less ambiguous. In phrase based method document is analyzed on phrase basis and more distinct when compared with terms. The reason to choose phrase based methods include Phrases have inferior is statistical properties to terms, and low frequency of occurrence, Extensive replication and noisy phrases are present among them.

Concept Based Method: Here analysis done on sentence and document level. Two terms can have same frequency in same document, but the meaning is that one term contributes more appropriately than the other term. The terms that capture the semantics of the text should be given more importance. This model included three components. The first component analyzes the semantic arrangement of sentences. The second component designs a conceptual ontological graph (COG) to explain the semantic structures and the last component extract top concepts based on the first two components to build feature vectors using the standard vector space model. Concept-based model can easily differentiate between non important terms and meaningful terms which describe a meaning in the sentence .It uses natural language processing techniques and Feature selection is used in query concepts to optimize the representation and remove noise and ambiguity.

Pattern Taxonomy Method: Here documents are analyzed on pattern basis. And Patterns can be structured into taxonomy by applying a relation. Association rule mining, frequent item set mining, sequential pattern mining and closed pattern mining are used in Data Mining to discover Patterns .Use of discovered knowledge (patterns) in the field of text mining is difficult and ineffective, because some useful long patterns with high specificity lack in support. Frequent short patterns lead to misinterpretation and results in ineffective performance. This method uses two processes pattern deploying and pattern evolving to refine the discovered patterns in text documents.

TEXT MINING AND HEALTH CARE

One of the most noticeable areas of text mining is medical record processing and health care. There are different types of medical information sources like which maintains data such as symptoms, patient history, treatments, and medications should be considered for perfect output. So with the help of data mining, text mining it is possible to process the unstructured medical records, as it generates vast amount of online medical records. Due to the increase of electronic medical records, there is an opportunity to classify correct diagnosis for a particular patient, with the help of symptoms, diseases, disorders etc. Different types of medical information sources like Hospital Information System(HIS) can manage medical, administrative, financial and legal aspects of a hospital, Electronic Health Records (EHR) are a collection of medical records of individual patient to keep track of patients status and offer [8]decision support mechanisms .and Electronic Medical Records (EMR) allows to store all relevant patient information in electronic format, but all these facilities doesn't provide the exact information for diagnosing the disease. Text contains more valuable quantitative information that is difficult to use in statistical modeling. So by converting text data into numeric form which can be used in analysis in areas like sociology and communication to extract the hidden words. So by implementing text mining in health care it is possible for early detection of diseases, symptoms, notes, remarks made by one or more physicians ,diet and fitness suggestions and adverse reaction etc. These documents may be structured or unstructured and can contain some errors in grammatical ,abbreviations ,vocabulary which is very difficult to analyze and categorize.

Data mining is considered as an artifact to leverage health data. So by using ML techniques it is has been widely used to summarize, explain and to find the relationships between completed data. It includes various aspects like medical and operational aspects including diagnosis, health monitoring, health care planning, and management of hospitals and health services. Text analytics is also used to derive quality insights using Natural Language Processing (NLP) automatically. So, some text mining methodologies like disease surveillance is used to identify influenza in as it affects millions of people a year. So monitoring these type of diseases will be very helpful in

identifying at an early stage. Next behavioral medicine which helps us to understand the behavior of a person using nicotine and tobacco products using online surveillance by NLP. Clinical records are more complex to analyze and extract using text mining because of abbreviations of medical terms, acronyms and local dialectal terms. Spelling mistakes, punctuations, and hyphens may lead to change the meaning of text which is difficult to analyze in case of tokenization. More medical records are considered to analyze and extract information like patient review, medical notes, images, and observations. So some preprocessing should be done to create datasets and some machine learning models are constructed to interpret and classify the previously acquired data. More legal and ethical aspects are considered to manage patient privacy and security. So confidential data should be removed in Electronic Medical Records and some identification keys are included. Finally with the help of pattern matching it is possible to identify patterns with sentences, words, and expressions. But it is difficult to identify if the content is of different languages. Ontology based extraction [8] enables the classification to find the relation between words and it achieves a higher accuracy in medical term extraction when compared to other approaches.

Another approach is relation extraction that finds pairs of terms that are syntactically or semantically related .So associated information and its values are considered like weight, age, blood pressure, pulse etc. It helps the clinicians to know about the relativity of diseases, symptoms, parts infected and history of related .so here it plays an important role to extract terms like diseases, symptoms. Human body parts with semantic analysis and it is defined in the ontology. But syntactic relation is difficult in major cases as a sentence may contain more than two terms. In some cases we can use decision tree based classification to obtain information theory, information gain of the predictor and dependent variable.

Text mining applied to medical records
This section discusses the application of text mining in Electronic Medical Records (EMR), main challenges and most used techniques. Clinical records can be very complex to analyze and extract using text mining. [6] These documents mostly are presented in a free text format or pre-formatted formularies, and can hold intricate vocabulary with medical terms, abbreviations, acronyms, and local dialectal terms. Additionally, there are a few concerns to take into account: texts may have countless mistakes and misspellings, especially on medical notes, and some values or terms are difficult to interpret, punctuations such as periods or hyphens. Another challenge is the many different types of source data to analyze and extract, namely, patient interviews, laboratory analysis, medical notes, images, and observations. Within this data it is possible to find several relevant features and abnormal values, making this a challenging task for performance and classification processes. These data sources are pre-processed to generate the datasets for text mining. These datasets are, most of the times, unbalanced, making them very difficult to analyze. After applying pre-processing techniques, it then follows a machine learning approach. Using available data, Machine learning "learns" and constructs models to classify data, considering legal, ethical and social aspects, to manage privacy and security of patient personal information, reducing possible breaches in confidentiality. Therefore, it may be necessary to remove or replace the identification of a certain patient. It is, however, possible to use some of this personal information for diagnose classification, such as age, gender or social aspects. Anonymized data and de-identified data are the ways to conceal the private patient information. Anonymous data consists in removing all private information and replacing patient identification with keys only known by authorized persons. Other private information is removed. De-identified data encrypts all patient information to be analysed. Finally, identified data is used when patient information is collected with their consent. Many approaches can be used in information extraction in medical records. Pattern-matching can be useful to discovery patterns within sentences, expressions, words, etc. Other approaches that can be applied are shallow and full syntactic parsing for non-robust texts. Ontology based extraction methodology helps us to classify and the find relations between words. There are several algorithms that can be used in machine learning, although white box algorithms should be adopted, considering that physicians are still apprehensive with this kind of technology and its low level accuracy. White box methodology recognizes the features of an algorithm but it is not possible with a black box approach even with more powerful algorithms to deduce relevant information.

Information Extraction of EMR Based on Text Mining

Text Mining is also used to acquire knowledge and wealth of valuable [7]information from biomedical text for identifying drug reaction, early detection of symptoms etc. Usually text mining process consists of steps like Information Retreival(IE),Information Extraction(IE),Knowledge Discovery and Knowledge Application. Information Retreival is used to collect the data ,Information Extraction is to extract the predefined information from the collected data. The Third process of Knowledge Discovery is acquiring knowledge from the collected data, Knowledge Application applies the unknown facts inferred from text to practice. Usually the data collected from the medical records are unstructured or semi structured , so here regular method of pre-processing cannot be used. So convert any type of text into structured format NLP is used. In this process, the key technologies involved include named-entity recognition (NER) and relation extraction (RE).

i) Named-Entity Recognition Technology: This technology is used to identify particular names or symbols in documents.[5] NER method identifies medical entities related to treatment such as disease names, symptoms and drug names. As the doctors writing of medical terms are not clear and ambiguity in terms of abbreviations, some medical terms are composed of phrases or compounds modified that is particularly prominent. All the mentioned issues reduces the effect of identifying entities. So to overcome these issues NER uses two processes namely ,entity boundary identification and entity class determination. Three important indexes that serve NER are, precision rate (P), recall rate (R), and F-score, F-score, the harmonic average of the precision and recall rate, is a comprehensive evaluation of the test results. When the F-score is higher, the experimental results are better. P = the number of entities identified correctly the number of entities identified, R = the number of entities identified correctly the number of entities present in the test set, F-score = $P * R * 2 P + R$. To identify clinical events and associated temporal expressions NER methods are divided into three types namely the rule-based approach, the dictionary-based approach, and the machine learning approach.

A. *Rule Based NER Approach*: This approach identifies the rules and validate only the named entity from medical text follows the rule, otherwise it is not considered. So for constructing these rule templates and dictionaries for rule-based approach and dictionary based approach we need the assistance of some medical expert.
B. *Dictionary-Based NER Approach*: This is the widely used methodology for clinical text annotation and indexing. But due to existence of more medical terms unable to cover all the things in the single library. So dictionary based approaches provides the corresponding ID after recognizing the target term in the dictionary. Bio-entity name recognition is another key step for information extraction from biomedical literature which consist of three steps namely construction and expansion of the bio entity name dictionary, the approximate string matching, and the post processing.
C. *Machine Learning NER Approach*: Here algorithms and features are two important factors that largely affect the performance of ML-based NER systems. So an appropriate Machine Learning algorithm is used to establish an entity recognition model using statistical characteristics. Machine learning model requires training set as it is data-driven and application-oriented. Various ML models Hidden Markov models (HMM), support vector machines (SVM), conditional random field (CRF) and maximum entropy (ME) are available, but CRF and SVM is considered as more popular and SVM produces more accurate result when compared to CRF.

Relation Extraction (RE)

Once the entity is identified, next task is to extract the relation between entities. The entity relations in EMR can be divided into three categories, including the relation between diseases, the relation between diseases and medical examinations, and the relation between diseases and treatment. Three common methods used to extract entity relation are co occurrence-based extraction, pattern-based extraction, and machine learning approaches. When two entities appear in the same sentence, it shows the correlation between two named entities in that sentence, so higher frequency of correlation strengthens the relation. Sometimes hybrid approach, combination of two approaches also used for better results. Convolutional Neural Networks are also used to extract relations between scientific concepts such as synonyms and hyponyms, through pre-processing, CNN and rule-based post processing.

Text mining applied to Social Media Health Care Documents

Social media makes people to share and discuss their views and opinions about health-related information and general-purpose social media. Advancements in automated data processing, Machine learning and Natural Language Processing uses huge data for public health monitoring and surveillance has been especially popular and fruitful.[4] Numerous studies have been published recently in this realm on pharmacovigilance, identifying smoking cessation patterns, identifying user social circles with common experiences, monitoring malpractice and tracking infectious disease spread. So social media serves as a unique platform to discuss approaches of text and data mining methods which responds to specific requirements in health surveillance such as early detection of diseases, Medication safety, including drug interactions and dietary supplement, Health behaviors and smoking. Social network analysis is a field of research open and adaptable to the medical and health. More recently, web-based disease surveillance research has moved in new directions with potentially higher impact: Other infectious diseases More recent social media research has given more importance on disease surveillance, Forecasting and higher impact locations etc. some key areas of public health for which social media mining has been especially popular and fruitful, with an emphasis on how these focus areas are evolving to increase public health impact.

Pharmacovigilance : It involves monitoring adverse actions caused by medications. This is a notable use case where discussion about the drugs prescribed, reaction and side effects on treatments will be shared. This makes social media unique and robust sources of information regarding treatments. By utilizing data from specialized forums and communities online review of drugs and medications for adverse reaction detection. By analyzing the datasets using supervised classification and association to identify the adverse reaction between drugs and specific reactions.

Behavioral Medicine: Smoking, Drug abuse and Diet fitness: Another important area of social media surveillance is about understanding behaviours that affects health such as smoking and diet. Here behavioural medicine plays a prominent role in the digital revolution. Social media can be used to understand the interest in various nicotine and tobacco products much faster than traditional sources. It helps in understanding and analyzing smoking cessation. Other issues like trends in alcohol use and problems in drug abuse. Specialized social networks have been used for analyzing the effects of drug reformulation. Based on the food consumption patterns mentioned in social media and physical activities measuring the outcomes of the fitness goals.

Disease Surveillance: One of the most important and longest running cases for social media is disease surveillance. Influenza has been by far the most commonly surveilled disease, in part due to its widespread prevalence it reacts millions of people each year, So Google's Flu trends services continue to share their data with academic research labs and search queries for web-based disease surveillance. Main aim of using social media mining is influenza can be prevailed and estimated in real-time when compared to traditional government methods of taking survey by Centers for Disease Control and Prevention as it may be out dated. So when compared to traditional methods web-based surveillance research moved research in new directions with greater impact. Apart from influenza social media research helps us to find other diseases like *Cholera, Ebola*, and *E.Coli.* So mining data in social media helps us to track more diseases.

Infectious Diseases Propagation: It analyzes the transmission of infectious diseases in hospitals using a network centric perspective. Here spread of disease may occur through Patients, nurses, doctors or workers who are closely connected to each other and those connections form a network through which transmission can occur. The density of this network should be strong and spread of diseases may occur fastly.

Predicting Pandemic Increase investigation: By using twitter as a reporting tool using filtering and normalization, it indicates the increased infection spread. So tweets help us to identify the infection earlier. Regression frameworks can be used to extract simple features and reduce error associated with modeling which helps us to identify diseases like influenza by correlating the tweets and search terms used. With this type of online clinical data physicians are able to make forecast of influenza 2 weeks before. So by early work, able to forecast and control the spread of diseases through planning and preparedness.

Modeling the Hospital Structure Network : To know the relationship between social entities Social Network nalysis(SNA) method is used which helps us in identifying structural relationships in hospital administration. SNA for Health Social Network With the continued advances of different Social Networks, the health's Social Networks became very popular. Despite the success of social media for better connecting and changing information, these Medias can also change the users' health behaviors,to become more healthy.

APPLICATIONS OF TEXT MINING

Analyzing survey responses: Open Survey Questions will help respondents to expose the view or opinion of the respondents. It helps to know more about customer's opinion and expectations, which seems better when compared to traditional questionnaires. Now a days social media is a place where a person can express their opinions clearly, So by using Text mining it analyzes the information in the form of text.

Fraud Detection: Technology advancement allow us to [3] easily identify any fraud texts. Text mining has helped achieve that. Text mining plays a vital role in classifying and filtering text .So it is used to classify and filter unnecessary e-mails by analyzing certain words and phrases in the e-mail. Such e-mails are automatically discarded and marked as spam. By using this text mining system it also alerts the mail to remove those mails with offending words or content.

Analyzing Health Care Records: Mostly in business organizations information maintenance is in the form of text. Health care collects huge amounts of textual and numeric information about patients, visits, prescriptions etc. The information collected using EMR improves healthcare quality, promotion of clinical and research initiatives, fewer medical errors and lower costs. So by collecting these contents electronically and using some text mining algorithms, helps the practitioner to diagnose the actual situation.

Crawling web sites: Another area of text mining is web content mining, contents of web page is analyzed to find the list of terms frequently used on the site. So by using this, it is easy to find the important terms in the website. With this, competitor's ability can be known to deliver efficient business.

Risk Management and Decision making: By analyzing the flow of the business, one should be able to avoid risk while doing business. So risk management is one of the important activity which allows the business people to make correct decisions using text mining .Fails to take correct decision will leads to risk and loss in business. So text mining helps the person to know the flow of work and supports about pros, cons in making clear decisions for betterment.

Business Intelligence: For Businesses' data is their backbone, which can be used for or against the company. by analyzing and using the data properly, it supports the business people for efficient running of business .It also finds the feedback from the customers to know the actual requirement .

Challenges in Social Media Mining

Main challenge with automated data mining social media is with the help of standard Natural Language processing (NLP) tools. So these tools support only formal or regular languages and doesn't support informal or non-standard text online. Some tools like POS taggers and Named entity recognizers are used in twitter to analyze the tweets, but this doesn't provide a general-purpose solution. Because a tool designed for a specific social media will not work perfectly for others due to medical terminology.[9] So by finding the text which specifies common symptoms rather than specific illness, language normalizations should be done for social media text to identify the terms.

Next, Sentimental Analysis classifies the opinions as positive, Negative and neutral in understanding important health issues, in case of smoking and drug abuse, diet and fitness, vaccination opinions etc.. Sentiment has also been analyzed in the context of drug abuse, in order to understand public interest in drugs. By analyzing the online reviews about doctors and health care providers helps us to identify patient perceptions of care quality. However,

sentiment analysis does not work as well for short text, such as tweets. Sentiment classification is an active area of NLP research, and improvements in this technology will lead to improvements in understanding public opinion and awareness.

Most research on social media mining for health monitoring has used relatively simple methods of text analysis, such as dictionary associations. Simple approaches can work reasonably well and future improvements will require NLP tools that can extract richer meaning from text .As a word having multiple meanings it is difficult to understand in what aspect they tweet. Richer NLP techniques can be used to extract the detail. Lexicon based approaches are the older methods to identify the content in social media and some health related lexicon resources also have been developed ,but the usage of colloquial language limits the performance these approaches. Some supervised algorithms may be used to improve the promising performance in quantitative evaluations. Another hurdle gaining trust from practitioners and public. Due to significant failings reported by practitioners web-based disease surveillance system lost its attention. So more work should be carried out to validate the social media models carefully to ensure progress is being made. Considering data being accessed, in social media data is publicly available and sometimes it need to be private. For that machine learning algorithms can make inference about private attributes ,even if not explicitly stated in public data.

REFERENCES

1. Gaikwad, S. V., Chaugule, A., &Patil, P. (2014). Text mining methods and techniques. International Journal of Computer Applications, 85(17).
2. Adeva, J. G., Atxa, J. P., Carrillo, M. U., &Zengotitabengoa, E. A. (2014). Automatic text classification to support systematic reviews in medicine. Expert Systems with Applications, 41(4), 1498-1508.
3. Talib, R., Hanif, M. K., Ayesha, S., & Fatima, F. (2016). Text mining: techniques, applications and issues. International Journal of Advanced Computer Science and Applications, 7(11).
4. Paul, M. J., Sarker, A., Brownstein, J. S., Nikfarjam, A., Scotch, M., Smith, K. L., & Gonzalez, G. (2016). Social media mining for public health monitoring and surveillance. In Biocomputing 2016: Proceedings of the Pacific symposium (pp. 468-479).
5. Wegrzyn-Wolska, K., Bougueroua, L., &Dziczkowski, G. (2011, October). Social media analysis for e-health and medical purposes. In 2011 International Conference on Computational Aspects of Social Networks (CASoN) (pp. 278-283). IEEE.
6. Zhou, X., Han, H., Chankai, I., Prestrud, A., & Brooks, A. (2006, April). Approaches to text mining for clinical medical records. In Proceedings of the 2006 ACM symposium on Applied computing (pp. 235-239).
7. Sun, W., Cai, Z., Li, Y., Liu, F., Fang, S., & Wang, G. (2018). Data processing and text mining technologies on electronic medical records: a review. Journal of healthcare engineering, 2018.
8. Luque, C., Luna, J. M., Luque, M., & Ventura, S. (2019). An advanced review on text mining in medicine. Wiley Interdisciplinary Reviews: Data Mining and Knowledge Discovery, 9(3), e1302.
9. Gaikwad,S.V.,Chaugule,A.,&Patil, P. (2014). Text mining methods and techniques. International Journal of Computer Applications, 85(17).

Jayasudha and Manju

INFORMATION EXTRACTION

INFORMATIONAL RETRIEVAL

NATURAL LANGUAGE PROCESSING

CLUSTERING

CATEGORIZATION

TEXT VISUALIZATION

SUMMARIZATION

Fig.1. Informational Retrieval

LANGUAGE IDENTIFICATION — TOKENIZATION — PART OF SPEECH TAGGING — CHUNKING — SYNTAX PARSING — SENTENCE CHAINING

Fig.2. Text Mining steps

TERM BASED METHODS | CONCEPT BASED METHODS
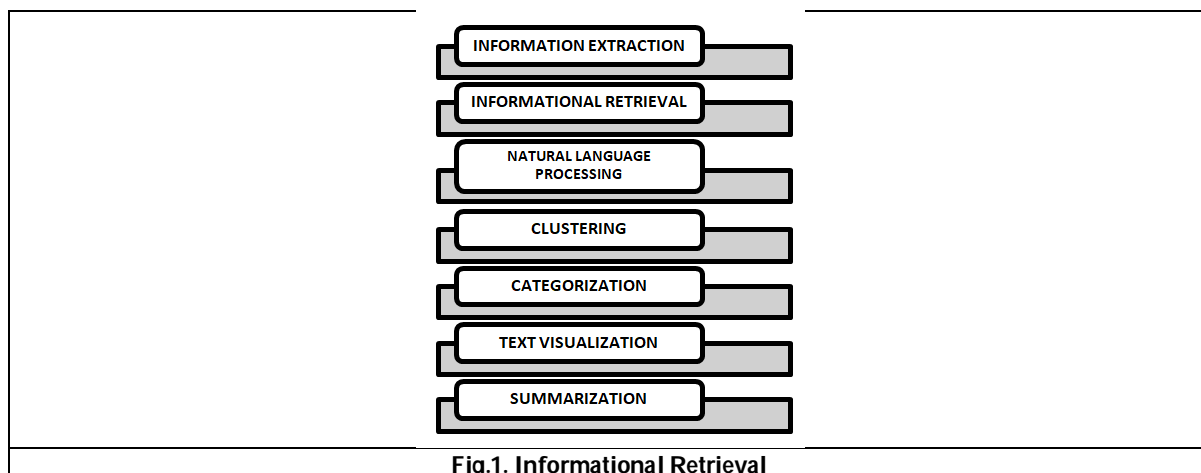
TEXT MINING METHODS

PHRASE BASED METHODS | PATTERN BASED METHODS
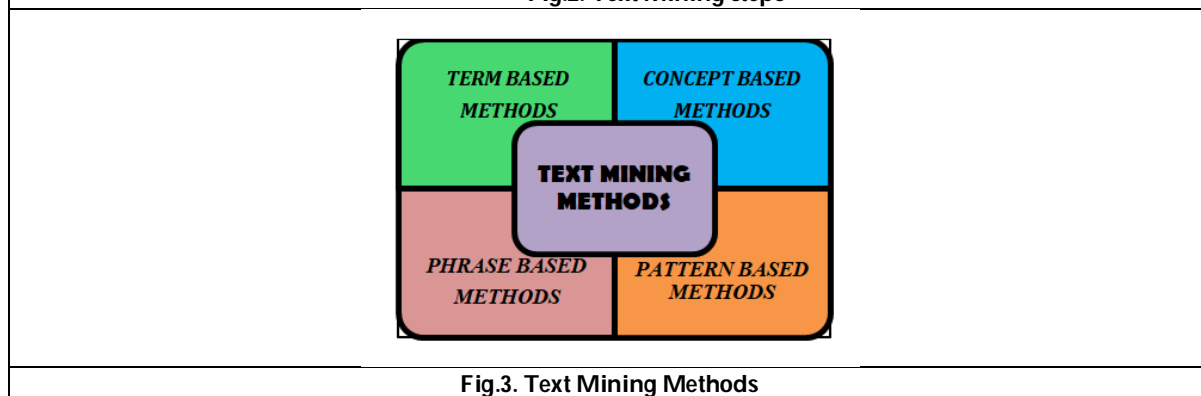
Fig.3. Text Mining Methods

REVIEW ARTICLE

A Review on Various Analytical Methods for Analysis of Ramipril

Rama Rao Tadikonda[1]* and Ramya Alwala [2]

[1]Professor and Principal, CMR College of Pharmacy, Hyderabad, Telangana, India.
[2]M. Pharmacy Student, Department of Pharmaceutical Analysis, CMR College of   Pharmacy, Hyderabad, Telangana, India.

*Address for Correspondence
Rama Rao Tadikonda
Professor and Principal,
CMR College of Pharmacy,
Hyderabad, Telangana, India.
E.Mail: tadikondarao7@gmail.com

ABSTRACT

Hypertension is a serious medical condition that significantly increases the risk of heart, Brain, kidneys and other diseases. Blood pressure is a force exerted by circulating body against the walls of the body's arteries, the major blood vessels in the body. It is the elevation of systolic blood pressure, Diastolic blood pressure or both above the normal levels. It effects above 1-Billion people worldwide and it is estimated that by 2025 up to 1.58 billion adults worldwide will suffer from complications of hypertension. It is the major public health problem in India. It accounts for 57% of all stroke deaths and 24% of all coronary heart diseases, deaths in India. Adequate management of hypertension can eventually reduce the risk of stroke, myocardial infection, chronic kidney disease and heart failure. The initial antihypertensive agent should be generally selected from one of the drug classes like Thiazide diuretics, Angiotensin converting enzyme(ACE) Inhibitors, Angiotensin receptor blockers(ARB'S) & Calcium channel blockers shown to reduce cardiovascular events. One of the angiotensin-converting enzyme (ACE) inhibitor class of medication is Ramipril. It is used to treat high blood pressure and lowering of high bold pressure which in turn helps to prevent strokes, heart attacks, & kidney problems. Ramipril is also used to improve survival after heart attacks and also used to treat heart failure in patents who have had a recent heart attack. Various analytical methods such as UV-Spectroscopy, High performance thin layer chromatography (HPTLC), High performance liquid chromatography (HPLC), Ultra-performance liquid chromatography (UPLC), Mass spectroscopy, Liquid chromatography-Mass spectroscopy (LC-MS), and UV-Spectrophotometric methods for the determination of Ramipril as single and in combination with other drugs have been reported. The present review covers the analytical methods which have been used for analysis of Ramipril.

Keywords: Ramipril, UV-spectrophotometric methods, HPLC, HPTLC, UPLC.

Rama Rao Tadikonda and Ramya Alwala

INTRODUCTION

converting Ramipril to ramiprilat and in a less extent converted in kidneys. Ramipril is mostly used in treatment of congestive heart failure and nephropathy and in hypotension. Angiotensin converting enzyme (ACE) involves in conversion of angiotensin-I to angiotensin-II, this ACE-II is the key constituent of RAAS system (Renin angiotensin-aldosterone system) and regulates blood pressure. Ramipril is a potent inhibitor of ACE and prevents the conversion of angiotensin-I to angiotensin-II [1]. Ramipril is a long acting angiotensin converting enzyme inhibitor and it exhibits similar actions as that of captopril and enalapril [2]. The active metabolite of ramipril called ramiprilat has the long elimination half-life, permitting once in a day administration. The daily dose of ramipril in a hypertensive patient is 2.5 to 20mg and it is usually effective in reducing high blood pressure and maintaining satisfactory control during long-term treatment. People who do not respond to ramipril monotherapy, usually respond with the addition of diuretics [3]. The anti-hypertensive efficacy of ramipril is maintained in patients with diabetes mellitus and the primary data indicate that the drug has the beneficial effects of decreasing urinary albumin excretion in diabetic patients with nephropathy. Ramipril also have a beneficial effect in the treatment of patients with more established heart failures [4].

Chemical structure
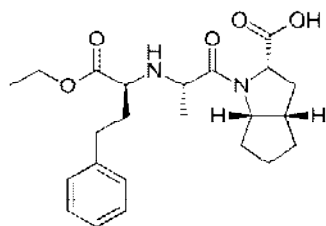
IUPAC Name:
(2S,3aS,6aS)-1-[(2S)-2-[[(2S)-1-Ethoxy-1-oxo-4-phenylbutan-2-yl]amino]propanoyl]-3,3a,4,5,6,6a-hexahydro-2H-cyclopenta[b]pyrrole-2-carboxylic acid.

Melting point: 109 $^{\circ}$C
Molecular weight: 416.518 g. mol^{-1}:
Trade Name: Altace
Dose: 1.25 mg, 2.5 mg, 5 mg, and 10 mg

Ramipril Indications:
1. Hypertension
2. Prevention of heart failure progression after myocardial infarction.
3. Heart Failure with a reduced ejection fraction
4. Risk reduction of MI and stroke.

Pharmacokinetic Data of Ramipril:
Ramipril is a prodrug that is converted in to an active metabolite called ramiprilat. The bioavailability of ramipril is 28% and *it rapidly distributes to all tissues*, with the liver, kidneys and lungs showing higher concentrations of the drug than the blood. The protein binding capacity of ramipril is 73% and the active metabolite ramiprilat is 56% and metabolized through the liver and eliminated via kidneys (60%) and feces (40%). The elimination half-life of the drug is 13-17 hours.

Rama Rao Tadikonda and Ramya Alwala

Side effects of Ramipril:
1. Dry cough
2. Postural hypotension.
3. Elevated serum creatinine
4. Hyperkalemia
5. Angioedema
6. Fatigue and mouth dryness in early stages [5,6].

Previous studies to estimate Ramipril:

There are different methods used to estimate ramipril in pharmaceutical preparations and human serum samples in addition to multiple environmental models. Several analytical methods such as UV, HPLC, HPTLC, UPLC, LC/MS, methods have been reported. The current review is an attempt made to compile all the analytical methods which have been used for the analysis of ramipril.

UV-SPECTROSCOPIC METHODS:

Various UV spectroscopic methods have been reported for the determination of Ramipril in single and combined with other drugs. OE Afieroho1, O. Okorie, and TJN Okonkwo (2012) developed a simple and cost-effective spectrophotometer method for the determination of ACE inhibitor ramipril in dosage forms. UV spectrophotometry was used to develop and validate a simple method for the assay of ramipril in solid dosage form at λmax of 210 nm, as per International Conference on Harmonization (ICH) guidelines. Aqueous methanol (5 %) was used as the blank solvent. The method was validated for linearity, recovery, accuracy, precision, and specificity in the presence of excipients, and also for inter-day stability under laboratory conditions. The Validation results showed linearity in the range 1 – 38 µg/ml; recovery accuracy of 101.55%; regression equation Y = 0.0256X + 0.0697, R² of 0.9942; precision RSD < 2.00 %; and negligible interference from common excipients and colorants. The method was accurate (95 % confidence limit) compared to the standard liquid chromatography (LC) method, with comparable reproducibility when used to assay a commercial product (Ramitace®, 2 and 5 mg tablets). The validated data were within allowable limits and therefore, the proposed method is recommended for routine quality control (QC) analysis [7].

Syed Iftequar,, Lahoti Swaroop, Zahid Zaheer, Mirza Shahid, Sayad Imran,M H Dehghan (2012) reported on a new, simple, rapid and novel spectrophotometric method for estimation of Ramipril (RAM). For this absorption maximum Method (method A) and Area under Curve Method (Method B) is used. The method involved measurement of absorbance at wavelengths 210 nm for method A and method B involved measurement of area under curve in the wavelength range 202 to 237.5 nm for RAM. Beer's law obeyed in the concentration range of 0.1 to 3.5 µg/ mL by both methods. The proposed methods are recommended for routine analysis since they are rapid, simple, accurate and also sensitive and specific. The results obtained are reproducible with a coefficient of variation less than 2%. These methods were validated for precision, reproducibility, linearity and accuracy as per ICH guidelines [8].

Lakshmana Rao A, Prasanthi T, Anusha, Prasanna MR, Jyothi P (2016) discussed a simple, validated, accurate, and precise simultaneous UV Spectrophotometric method for the simultaneous estimation of Telmisartan (TEM) and Ramipril (RAM) in the pharmaceutical dosage form. Telmisartan exhibits absorption maximum at 254.4 nm and Ramipril shows an absorption maximum at 209 nm in methanol. The Beer's law obeyed the concentration range of 2-12µg/ml for both TEM and RAM. Mean recovery of 99.14% for TEM and 99.05% for RAM respectively signifies the accuracy of the method. The method was validated as per ICH guidelines. The method shows good linearity, accuracy, precision, limit of detection and limit of quantification. This method can be successfully employed for the routine simultaneous estimation of TEM and RAM in pharmaceutical dosage forms [9].

Gadireddy Sujana, G. Aruna, G. Sivagangaram (2014 developed a simple, rapid and accurate UV Spectroscopic (Simultaneous Equation method and First order derivative method) and an isocratic RP – HPLC methods showed excellent sensitivity, reproducibility, accuracy, and repeatability. In simultaneous UV method, the overlaid spectra of mixture of Ramipril HCl and Metoprolol Tartrate were recorded. From the spectra, 206 nm for Ramipril HCl and 222

nm for Metoprolol Tartrate was selected as wavelength to construct simultaneous equation. The percentage label claim present in tablet formulation was found to be 101% and 103% for Ramipril HCl and Metoprolol Tartrate respectively. In second method, the same spectrums were derivatized and 205 nm selected for detection of Ramipril HCl where Metoprolol Tartrate shows zero crossing and also 210 nm selected for detection of Metoprolol Tartrate where Ramipril HCl shows zero crossing. The percentage label claim present in formulation was found to be 98.5% and 101% for Ramipril HCl and Metoprolol Tartrate respectively. In RP-HPLC method, mobile phase used is acetonitrile: methanol: acetate buffer pH 5.0 (30:50:20 V/V) with flow rate of 0.9 ml per min, the retention time of Metoprolol Tartrate and were found to be 2.84 and, 3.55 respectively. The percentage purity was found to be 99.76% and 99.82% for Metoprolol Tartrate and Ramipril HCl, respectively. The low % RSD values for recovery indicated that the method was found to be accurate [10].

N. Vanaja, Ch. Preethi, Dr. S.Y. Manjunath, Krishanu Pal (2015) studied a method development and validation for simultaneous estimation of Telmisartan and Ramipril by UV-Spectrophotometric method using 0.1N NAOH as solvent and λmax of Telmisartan and Ramipril were found to be 232 nm and 222 nm respectively. Concentration ranges were found to be 4-20µg/mL for both drugs. The R^2 values were found to be 0.996 and 0.999 for Telmisartan and Ramipril respectively. The method was validated statistically and by recovery studies, percentage assay and recovery were found to be 95-105% for Telmisartan and Ramipril. LOD and LOQ ranges were found to be 0.177 and 0.539µg/mL and 0.298 and 0.903 µg/mL for Telmisartan and Ramipril respectively. This method was validated using ICH guidelines [11].

Sathishkumar, S (2012) developed simple, precise and accurate methods for the estimation of Atorvastatin Calcium, Aspirin, Ramipril and Metoprolol Tartrate in bulk and in combined pharmaceutical dosage form and to validate the developed methods by UV-spectroscopy and HPTLC. The solubility of individual drugs was checked and from the list of solvents the common and stable solvent for the four drugs was selected. The solvent selected for both UV spectroscopy and HPTLC must be cheap and readily available. The various steps involved in the method development as follows, UV Spectroscopy Selection of appropriate analytical wavelength and selection of suitable method determination of working concentration range, Analysis of synthetic mixture, Simultaneous analysis of the formulation by using the developed method HPTLC Method Determination of suitable detection wavelength, Optimization of chromatographic conditions, Analysis of formulation, System suitability testing.

The two methods were found to be accurate, precise and rapid for the simultaneous estimation of these drugs. This was confirmed by low percentage RSD values. The spectrophotometric method is found to be economical when compared to the HPTLC method. But HPTLC is more sensitive than UV spectrophotometric method. The low percentage RSD value in the recovery studies suggests that the excipients do not interfere in the analysis of formulation and hence all the methods are accurate. HPTLC is found to be more sensitive than other method. Because the linearity range, LOD, LOQ were less in HPTLC method than UV spectroscopic method. Hence it is suggested that these two methods can be applied successfully for the routine quality control analysis for the simultaneous estimation of Atorvastatin Calcium, Aspirin, Ramipril and Metoprolol Tartrate in bulk and in pharmaceutical dosage form and the obtained results will be presented elsewhere [12].

Khairunnisa Tasneem, Sonia K, & Lakshmi K S (2020) developed method development and analytical validation of an original, accurate and correct UV-Visible Spectrophotometric methods for the fixed dose assessment of Ramipril and Amlodipine besylate. The working solutions of Telmisartan and Ramipril were scanned at 240 nanometer and 210 nanometer respectively. The regression strength of Amlodipine besylate and Ramipril over its absorbances takes place as y=0.4291x+0.0084 and y=0.0399x+0.310 respectively with a correlation coefficient (r^2) of 0.9998 for Amlodipine besylate and 0.9993 for Ramipril. The intra-day precision in addition inter-day precision for Amlodipine besylate and its % RSD were obtained as 0.08% and 0.25% respectively. The intra-day precision in addition interday precision for Ramipril and% RSD were obtained as 0.16% and 0.24% respectively. The precise amount of tablet formulation were added which holds Alkaline (0.1 N Sodium hydroxide), Acidic (0.1 N Hydrochloric acid) reflux for 3 hours, 3% Oxydol at 50ºC, heat (60ºC), humidity (75 percentage Relative humidity) for 24 hr. and after the

particular time diluted to distilled water, separated using Filter paper. From this stock solution, 5 mL section of the filtrate was pipetted out and further thinned with distilled water in a 100 mL standard flask (10 μg/mL). The standard stock solution of two drugs were prepared and compared against a label claim [13].

Vaishali Pawar, Archana Tiwari, Dr. P.K. Dubey (2022) developed a rapid, specific and economic UV spectrophotometric method has been developed using Methanol as a solvent for simultaneous determination of Atorvastatin Calcium (ATR) and Ramipril (RMP) content in bulk and pharmaceutical tablet dosage formulations. The absorbance values at 246 nm and 226 nm were used for the estimation of Atorvastatin Calcium (ATR) and Ramipril (RMP). The absorption maxima of Atorvastatin Calcium (ATR) and Ramipril (RMP) shown at 246 nm and 226 nm and methanol was used as solvent. This method obeyed Beer's law in the concentration range of 2–20 μg /ml for atorvastatin calcium and 1-6 μg /ml for ramipril. The Simultaneous Estimation method was developed and validated according to ICH guidelines for linearity, precision, accuracy, LOD and LOQ. Atorvastatin calcium found to be linear within concentration range of 2-20 µg/ml with regression coefficient of 0.998 and ramipril found to be linear within concentration range of 1-6 µg/ml with regression coefficient of 0.999. The accuracy was assessed by the standard addition method of three replicate determinations of three different solutions containing 8, 10 and 12 µg/ml of RMP and ATR. The average % recoveries for three different concentrations were found to be 90.14 % for ATR and RMP 99.05 % using proposed UV spectrophotometric method. The limit of detection and limit of quantification were found to be 0.31µg/ml and 0.1023µg/ml for Atorvastatin Calcium and 0.2805µg/ml and 0.85µg/ml for Ramipril respectively by proposed UV spectrophotometric method. The results of validation parameters indicates that the developed method was also found to be accurate, precise and sensitive and such simple & economic method can be used for the simultaneous estimation of atorvastatin calcium and ramipril. The obtained results proved that the method can be employed for the routine analysis of simvastatin and Ezetimibe in bulks as well as in the commercial formulation [14].

Manish Kumar , Mohit Jindal , Shailendra Bhatt , A. Pandurangan1 , Anuj Malik , Vichitra Kaushik, Prabhat Kumar Upadhaya and G.Arunachalam (2019) discussed that Amlodipine Besylate is used to treat hypertension and Coronary Artery Disease. It is a calcium channel blocker. Amlodipine Besylate blocks calcium movement into certain tissues and arteries which leads to the relaxation of arteries so that blood can flow more easily into our heart. Ramipril is also used to treat hypertension, prevent strokes, heart attacks and kidney problems. It is an angiotensin converting enzyme (ACE) inhibitors. ACE is an enzyme which produces the chemical angiotensin II. Only a few spectrophotometric methods have been reported for simultaneous estimation of Amlodipine Besylate and Ramipril in tablet dosage forms. Hence an attempt has been made to develop and validate in accordance with ICH guidelines [15].

HPLC METHODS

Kurade VP, Pai MG, Gude (2009) Preformed A rapid high performance liquid chromatographic method has been developed and validated for the estimation of ramipril and telmisartan simultaneously in combined dosage form. A Genesis C18 column having dimensions of 4.6×250 mm and particle size of 5 μm in isocratic mode, with mobile phase containing a mixture of 0.01 M potassium dihydrogen phosphate buffer (adjusted to pH 3.4 using orthophosphoric acid): methanol: acetonitrile (15:15:70 v/v/v) was used. The mobile phase was pumped at a flow rate of 1.0 ml/min and the eluents were monitored at 210 nm. The selected chromatographic conditions were found to effectively separate ramipril (R_t: 3.68 min) and telmisartan (R_t: 4.98 min) having a resolution of 3.84. The method was validated in terms of linearity, accuracy, precision, specificity, limit of detection and limit of quantitation. Linearity for ramipril and telmisartan were found in the range of 3.5-6.5 μg/ml and 28.0-52.0 μg/ml, respectively. The percentage recoveries for ramipril and telmisartan ranged from 99.09-101.64% and 99.45-100.99%, respectively. The limit of detection and the limit of quantitation for ramipril was found to be 0.5 μg/ml and 1.5 μg/ml respectively and for telmisartan was found to be 1.5 μg/ml and 3.0 μg/ml, respectively. The method was found to be robust and can be successfully used to determine the drug content of marketed formulations [16].

Rama Rao Tadikonda and Ramya Alwala

Shi-Ying Dai, Shi-Ting Qiu, Wei Wu, Chun-Mei Fu (2013) developed an RP-HPLC method for the simultaneous determination of Ramipril (RP) and Amlodipine (AL) in tablets was developed and validated by Chinese Pharmacopoeia 2010. The linearity of the proposed method was investigated in the range of 0.01–0.25 mg/mL (r^2=0.9998) for RP and 0.014–0.36 mg/mL (r^2=0.9997) for AL. The limits of detection (LOD) were 0.06 μg/mL and 0.02 μg/mL for RP and AL, and the limits of quantitation (LOQ) were 0.2 μg/mL and 0.07 μg/mL, respectively. Some major impurities and degradation products did not disturb the detection of RP and AL and the assay can thus be considered stability-indicating [17].

Jinesh Bahubali Nagavi, Preethi Gotadake Anantharaju (2014) reported an HPLC method for the simultaneous estimation of Ramipril and Hydrochlorothiazide in tablets. The developed method involves Purosphere   Star Rp18e, 5 μm, 150×4.6 mm column with mobile phase composition of acetonitrile and sodium perchlorate (pH 2.5) buffer in the ratio of 3:2, at a flow rate of 1.0 ml/min and UV detection at 316 nm for first five minutes for Hydrochlorothiazide and 210 nm for Ramipril. The method was validated as per ICH guidelines, Linearity was observed over concentration range of 17.5 to 32.5 μg/ml for Ramipril and   87.5   to 162.5   μg/ml for Hydrochlorothiazide. The Accuracy of the proposed method was determined by recovery studies and found to be 97.95-102.3% and 97.98-102.66% for Ramipril and Hydrochlorothiazide respectively. The proposed method was extended for estimation of Ramipril and Hydrochlorothiazide in marketed tablet formulation (Ramace-H) and it was found to be well within the acceptance limit. The developed and validated HPLC method for simultaneous estimation of Ramipril and Hydrochlorothiazide was found to be linear, accurate, precise, robust and rugged. Hence it can be used for routine analysis of Ramipril and Hydrochlorothiazide in tablets [18].

Vaibhav Rajoriya, Amrita Soni, Varsha Kashaw developed a stable, linear, rapid, accurate and selective HPLC method for the quantification of Ramipril in FDT using buffer and acetonitrile: methanol (60:40 v/v) ratio in combination as mobile phase and at the flow rate of 1 ml/minute at λmax 210 nm. Chromatographic separation was performed on Shimadzu SPD-20A, SD-M10 AVP-Shimadzu, an ODS C-18 Kromacil (250 mm × 4.60 mm) column used as stationary phase. The quantitation of Ramipril done by HPLC, parameters studied were retention time, linearity, accuracy, precision, detection between response and concentration in the range of 5-30 μg/ml; detection carried out at λmax 2.910 min. Percent recoveries obtained for Ramipril was 99.58-100.15%. LOD and LOQ value was 0.802 μg/ml and 1.4 μg/ml for Ramipril respectively. The result suggested that proposed method gives good peak resolution of Ramipril within short analysis time (<10 min) and high percentages of the recovery shown that method is free from interference of excipient present in the formulation. The % RSD of each parameter lies below the limit of 2%, proven the suitability. The statistical analysis proved that the proposed method is precise, accurate, selective and rapid for the HPLC estimation of Ramipril [19].

Mousumi Kar, Sujit Pillai, Gaurav Sharma, Nitin Deshmukh, Kunwar Nagendra Krishna Singh (2019) reported on the estimation of Atorvastatin and Ramipril in pharmaceutical dosage forms by developing fast and precise RP-HPLC method. Chromatographic separations on C18 column (4.6mm×250mm, 5μm) were achieved using mixture of 0.1% OPA buffer (pH-3.0): Acetonitrile: Methanol, (45:50:05 v/v). pH adjustment of aqueous phase was done by using 0.5% Triethylamine. The peak response was monitored at 227 nm after injecting the sample into HPLC system at a flow rate of 1.0 ml/min. The calibration curve was linear over the range of Ramipril 10-30 μg / ml and Atorvastatin 20-60 μg / ml. Atorvastatin's average RT was 9.2826 ± 0.0107 and Ramipril was 4.548±0.0366. Atorvastatin's percentage recovery value is 99.47% and Ramipril's 98.50% which confirms the excipients do not interfere in the formulation. Thus, the suggested HPLC technique can therefore be used for the simultaneous determination of these two drugs in pharmaceutical dosage forms due to speed, simplicity and high accuracy [20].

Thotakati, Muralikrishna (2012) developed a sensitive, simple, rapid and accurate analytical method for the simultaneous estimation of Ramipril and Telmisartan in formulations and validation of developed method by using RP-HPLC technique. In simultaneous RP-HPLC method development, Waters 2695 Separations Module with PDA Detector and column used is C8 SB ZORBAX (150 X 4.6mm) column with3.5-micron particle size. Injection volume of 10 μL is injected and eluted with the mobile phase selected after optimization was Phosphate buffer and Acetonitrile

63804

in the ratio of 70:30 was found to be ideal. The flow rate was found to be optimized at 1.0 mL/min. Detection was carried out at 230 nm. This system produced symmetric peak shape, good resolution and reasonable retention times of Ramipril and Telmisartan were found to be 2.275 and 4.261 minutes respectively. The Ramipril and Telmisartan showed linearity in the range of 20-60 μg/mL and 160-480 μg/mL respectively. Precision of the developed method was studied under system precision and method precision. The %RSD values for precision was found to be within the acceptable limit, which revealed that the developed method was precise. The developed method was found to be robust. The %RSD value for percentage recovery of Ramipril and Telmisartan was found to be within the acceptance criteria. The results indicate satisfactory accuracy of method for simultaneous estimation of the Ramipril and Telmisartan [21].

Elham Anwar Taha , Manal Mohammed Fouad , Ali Kamal Attia and Zainab Mahmoud Yousef (2019) developed a rapid and sensitive High Performance Liquid Chromatography (HPLC) method and validated as per ICH guidelines for simultaneous determination of ramipril and felodipine binary mixture. Chromatographic separation was achieved on a Hyperchom C18 column (250 × 4.6 mm id., 5 μm) using an isocratic mobile phase of potassium di-hydrogen phosphate (pH = 3.4): methanol: acetonitrile in the ratio 15:15:70 (*v:v:v*). The flow rate was 1.5 mL/min, temperature of the column was maintained at 30 °C and detection was made at 210 nm. Linearity studies indicated that the drugs obey Beer's law over the range of 10-80 μg/mL for ramipril and 5-80 μg/mL for felodipine. The proposed method is precise, accurate, linear and robust. The short retention time allows the analysis of a large number of samples in a short period of time and, therefore, considered to be cost-effective that can be used for routine analysis of both drugs in the pharmaceutical industry [22].

Vassa, S., Vairagar, P., Mulgund, S., & Korhale, R. (2013) reported on development and validation of a simple and rapid isocratic reversed-phase high-performance liquid chromatographic method (RP-HPLC) for the simultaneous estimation of S (-) Amlodipine besylate and Ramipril in combined dosage form. The HPLC system was operated isocratically at flow rate of 1ml/min at 40°C ± 0.5° C for 15 min. The mobile phase found to be most suitable for analysis was Acetonitrile: 0.02M Potassium dihydrogen ortho phosphate buffer (0.1 % of triethylamine, 0.1 % of 6-heptane sulphonic acid salt): 35:65% v/v, pH adjusted to 2.5 with O-phosphoric acid, detection was carried out at 210 nm using Hypersil BDS C-18 (150*4.6mm) 5μ column with injection volume 20 μl. The retention time of Ramipril and S (-) Amlodipine Besylate were 5.61±0.3 and 7.41±0.3 respectively. The proposed method was validated according to International Conference on Harmonization [ICH Q2 (R1)] and was found to be precise, accurate, selective and rapid for the simultaneous determination of Ramipril and S (-) Amlodipine Besylate in bulk and tablet dosage forms. The linearity for Ramipril (r^2=0.9914) and S (-) Amlodipine besylate (r^2=0.9930) was established in the range of 25.14 - 75.41 and 25.46 - 76.38μg/mL respectively. This new developed method was found to be precise with satisfactory %RSD values for inter and intraday precision [23].

Raut, P. V., Padwal, S. L., Bachute, M. T. and Polshettiwar, S. A. (2021) developed a simple, rapid, selective, reproducible and isocratic reversed-phase high performance liquid chromatographic (RP-HPLC) method and validated as per ICH guidelines. Analysis was performed on a Thermo, Sunniest C8 (150 mm x 4.6 mm, 5 μm) with the mobile phase consisting of mixing 500 mL of buffer solution and 500 mL of acetonitrile at a flow rate of 1.0 mL/min. UV detection was performed at 210 nm and the Run time for Ramipril and Hydrochlorothiazide were 10 minutes. The calibration curve was linear (correlation coefficient = 1.000) in the selected range for both analytes. The optimized dissolution conditions include the USP Type 1 (Basket) rotation rate of 100 rpm and 750 mL of 0.1 N Hydrochloric acid as dissolution medium, at 37.0 ± 0.5°C. The method was validated for precision, linearity, specificity, accuracy, limit of quantitation and ruggedness. The system suitability parameters, such as theoretical plate, tailing factor and relative standard deviation (RSD) between six standard replicates were well within the limits. The stability result shows that the drug is stable in the prescribed dissolution medium [24].

Hari Krishna developed a new method was established for simultaneous estimation of Atorvastatin calcium and Ramipril by RP-HPLC method. Chromatographic separations were carried using Phenomenex Luna C18 (250 × 4.6 mm, 5 μm) column with a mobile phase composition of methanol in addition to phosphate cradle (0.1% v/v

triethylamine pH 4.5 well balanced with 0.1% v/v orthophosphoric harsh) have been delivered at a flow rate of 1 ml/min and the detection was carried out using waters HPLC auto sampler, separation module 2695 HPLC system with PDA detector at wavelength 254 nm. The running time 12 min. The retention time for Atorvastatin and Ramipril were 3.02 and 6.10 minute respectively. The correlation coefficient values in linearity were found to be 0.999 and concentration range 20-70 μg/ml for Atorvastatin and 20-70 µg/ml for Ramipril respectively. For accuracy the total recovery was found to be 99.8% and 99.8% for Atorvastatin and Ramipril. LOD and LOQ for Atorvastatin 2.95 and 9.96. LOD and LOQ for Ramipril 3.34 and 10. respectively [25].

Rajesh Sharma, Sunil Khanna, And Ganesh P. Mishra (2012) reported on a simple, sensitive, accurate and rapid reverse phase high performance liquid chromatographic method for the simultaneous estimation of ramipril, aspirin and atorvastatin in pharmaceutical preparations. Chromatography was performed on a 25cm×4.6 mm i.d, 5μm particle, C18 column with Mixture of (A) acetonitrile methanol (65:35) and (B) 10 mM sodium dihydrogen phosphate monohydrate (NaH2PO4 .H2O) buffer and mixture of A:B (60:40 v/v) adjusted to pH 3.0 with o-phosphoric acid (5%v/v) was used as a mobile phase at a flow rate of 1.5 ml min–1. UV detection was performed at 230 nm. Total run time was less than 12 min; retention time for Ramipril, aspirin and Atorvastatin were 3.620, 4.920 min and 11.710 min respectively. The method was validated for accuracy, precision, linearity, specificity and sensitivity in accordance with ICH guidelines. Validation revealed that the method is specific, rapid, accurate, precise, reliable, and reproducible. Calibration plots were linear over the concentration ranges 05-50 μg mL−1 for Ramipril, 05-100 μg/mL−1 for aspirin and 02-20 μg mL−1 for atorvastatin. Limits of detection were 0.014, 0.10 and 0.0095 ng mL−1 limits of quantification were 0.043, 0.329 and 0.029 ng mL−1 for ramipril aspirin and atorvastatin respectively. The high recovery and low coefficients of variation confirm the suitability of the method for simultaneous analysis of the all three drugs in the dosage forms. The validated method was successfully used for quantitative analysis of marketed pharmaceutical preparations [26].

Bilal Yilmaz (2010) developed a procedure based on high-performance liquid chromatography (HPLC) for determination of ramipril in pharmaceutical preparations. Separation of ramipril was achieved on a Ace C18 column (5 μm, 250×4.6 mm i.d.) using UV detection with λ=208 nm. The mobile phase consisted of 20 mM phosphate buffer (pH 2.5) containing 0.1% trifluoroacetic acid (TFA) - acetonitrile (50:50, v/v). The analysis was performed in less than 5 min with a flow rate of 1.0 mL min-1. Calibration curve was linear over the concentration range of 0.25-7.5 μg mL-1. Intra- and inter-day precision values for ramipril were less than 4.95, and accuracy (relative error) was better than 4.00%. The mean recovery of ramipril were 99.7% for pharmaceutical preparations. The limits of detection (LOD) and quantification (LOQ) were 0.10 and 0.25 μg mL-1 , respectively. Also, the method was successfully applied for the quality control of commercial ramipril dosage forms to quantify the drug and to check the formulation content uniformity [27].

P. P. Vairagar, S. MulgundS. P. Vassa, R. Korhale (2013) reported on development and validation of a simple and rapid isocratic reversed-phase high-performance liquid chromatographic method (RP-HPLC) for the simultaneous estimation of S (-) Amlodipine besylate and Ramipril in combined dosage form. The HPLC system was operated isocratically at flow rate of 1ml/min at 40°C ± 0.5° C for 15 min. The mobile phase found to be most suitable for analysis was Acetonitrile: 0.02M Potassium dihydrogen ortho phosphate buffer (0.1 % of triethylamine, 0.1 % of 6-heptane sulphonic acid salt): 35:65% v/v, pH adjusted to 2.5 with O-phosphoric acid, detection was carried out at 210nm using Hypersil BDS C-18 (150*4.6mm) 5μ column with injection volume 20μl. The retention time of Ramipril and S (-) Amlodipine Besylate were 5.61±0.3 and 7.41±0.3 respectively. The proposed method was validated according to International Conference on Harmonization [ICH Q2 (R 1)] and was found to be precise, accurate, selective and rapid for the simultaneous determination of Ramipril and S (-) Amlodipine Besylate in bulk and tablet dosage forms. The linearity for Ramipril (r 2 =0.9914) and S (-) Amlodipine besylate (r 2 =0.9930) was established in the range of 25.14 - 75.41 and 25.46-76.38μg/mL respectively. This new developed method was found to be precise with satisfactory %RSD values for inter and intraday precision [28].

K. Pallavi, Pranitha, Sampath Kumar (2015) developed and validated a simple reversed-phase high performance chromatography (RP-HPLC) method for simultaneous estimation of ramipril and losartan in pharmaceutical dosage form. Chromatographic analysis was performed on a Inertsil ODS (250 4.6 x 5µ) column at ambient temperature with a mixture of 10 mm KH2PO4: ACN (3:70) v/v (1.36gm of potassium di hydrogen phosphate was weighed and dissolved in 1000ml of water and adjust the pH to 3.0 using ortho phosphoric acid. The buffer was filtered through 0.45 µ filters to remove all fine particles and gases) as mobile phase, at a flow rate of 1.0 ml/min-1. UV detection was performed at 211 nm. The method was validated for accuracy, precision, specificity, linearity and sensitivity. The limit of detection was 0.24 and 1.09 µg ml-1 and quantification limit was 0.72 µg ml-1 and 3.30 µg ml-1 for ramipril and losartan. The retention times of Ramipril and losartan were 2.667 and 3.887 min, respectively. The accuracy of proposed method was determined by recovery studies and found to be 100.12% to 100.43%. Commercial tablet formulation was successfully analyzed using the developed method and the proposed method was applicable to outline analysis of determination of ramipril and losartan in pharmaceutical tablet dosage form [29].

K. Rao, K. Srinivas (2010) studied on a simple, specific and accurate reverse phase liquid chromatographic method for the simultaneous determination of losartan potassium and ramipril in table dosage forms. A hypersil ODS C18, 4.6×250 mm, 5 µm column in isocratic mode, with mobile phase acetonitrile:methanol:10 mM tetra butyl ammonium hydrogen sulphate in water in the ratio of 30:30:40% v/v/v was used. The flow rate was 1.0 ml/min and effluent was monitored at 210 nm. The retention times of losartan potassium and ramipril were 4.7 and 3.3 min, respectively. The linearity range for losartan potassium and ramipril were in the range of 0.04-100 µg/ml and 0.2-300 µg/ml, respectively. The proposed method was also validated and successfully applied to the estimation of losartan potassium and ramipril in combined tablet formulations [30].

Vatchavai Bhaskara Raju, Bonthu Mohan Gandhi, Kamatham Srinivas Sumanth, Kolli Srinivas, Tupakula N Venkata Lakshmi Neeraja (2017) developed a new, precise, accurate, rapid and simple reverse-phase high-performance liquid chromatographic (RP-HPLC) method for the simultaneous estimation of Telmisartan (TEL) and Ramipril (RAM) in pharmaceutical formulation and in bulk. The drugs were estimated using Shiseido C18 (250 x 4.6 mm, 5µm) column. The mobile phase is 0.5% ortho phosphoric acid (A), combination of acetonitrile: methanol (70:30, v/v) (B). A: B in the ratio of (50:50, v/v) at a flow rate of 1 ml/min was used for the separation. Detection was carried out at 210 nm .Linearity was obtained in the concentration range of 40-120 µg/ml for TEL, 5-15 µg/ml for RAM with retention times of 3.218 minutes and 4.803 minutes respectively. The correlation coefficient values were found to be greater than 0.99. Precision studies showed % RSD values less than 2% for both the drugs in all the selected concentrations. The percentage recoveries of TEL and RAM are in the range of 99.91-99.97% and 99.76-99.86% respectively. The assay results of TEL and RAM are 99.91% and 99.82% respectively. The limit of detection (LOD) and limit of quantification (LOQ) were 0.01 µg /ml, 0.8 µg /ml for TEL and 0.1µg /ml, 3µg /ml for RAM respectively. The method was validated as per ICH guidelines. The proposed validated method can be successfully used for the quantitative analysis of Telmisartan (TEL) and Ramipril (RAM) in bulk and commercially available dosage form [31].

G. Nagarajan, B. Govardhan1 , B. V. Ramana, K. Sujatha, S. Rubina, T. Arundathi and R. Soumya (2013) reported a simple reversed-phase high-performance liquid chromatographic (RP-HPLC) method and validated for simultaneous determination of Enalapril maleate and Ramipril in bulk and tablet dosage form. Chromatographic analysis was performed on a Oyster BDS C18 column (250x 4.6 mm, 5µm) column temperature 65°C with a mixture of buffer A and buffer B in the ratio 50:50 [Buffer A preparation: 2 gm of sodium per chloride in 800 ml water and add 0.5 ml tri ethyl amine, adjust the pH to 3.6 ± 0.1 with phosphoric acid and add 200 ml of acetonitrile. Buffer B preparation: 2 gm of sodium per chloride in 300 ml water and add 0.5 ml tri ethyl amine, adjust the pH to 2.6 ± 0.1 with phosphoric acid and add 700 ml of acetonitrile] as mobile phase, at a flow rate of 1.0 mL min-1. UV detection was performed at 208 nm. The method was validated for accuracy, precision, specificity, linearity and sensitivity. The retention times of Enalapril maleate and Ramipril were 4.197 and 5.819 min, respectively. Calibration plots were linear over the concentration ranges 5–30 µg mL-1 and 5–30 µg mL-1 for Enalapril maleate and Ramipril, respectively. The Limit of detection was 0.571 and 1.090 µg mL-1 and the quantification limit was 1.733 µg mL-1 and 3.303 µg mL-1 for Enalapril maleate and Ramipril, respectively. The accuracy of the proposed method was

Rama Rao Tadikonda and Ramya Alwala

determined by recovery studies and found to be 98.06% to 100.47%. Commercial tablet formulation was successfully analyzed using the developed method and the proposed method is applicable to routine analysis of determination of Enalapril maleate and Ramipril in bulk and tablet dosage form [32].

Praveen S. Rajput, Amanjot Kaur, Navdeep Kaur Gill, Karan Mittal and Ganti Subrahmanya Sarma (2012) worked on a Simple and precise HPLC method for the simultaneous estimation of Ramipril and Amlodipine in pure drug and pharmaceutical dosage forms. The separation was carried out using C18 Column (250 × 4.6 mm i.d. 5 μm particle size), with mobile phase compressing of Acetonitrile, Sodium phosphate buffer and Methanol in the ratio of 50: 20:25 v/v/v, pH= 6.8 (pH adjusted with OPA). The flow rate was 0.8 ml/min and the detection was carried out using PDA detector at 210 nm. The retention times were 2.64 and 7.45 mins for Ramipril and Amlodipine respectively. Calibration curves were linear with correlation coefficient 0.998 and 0.996 over concentration range of 1 - 16 μg/ml for Ramipril and 0.2 – 3.2 μg/ml for Amlodipine respectively. Recovery was found in between 100.21% and 100.82% for Ramipril and Amlodipine respectively. Method was found to be reproducible with relative standard deviation (R.S.D) for intra and inter day precision less than 2%. The method was validated by evaluation of different parameters such as accuracy, linearity, precision, LOD and LOQ [33].

N.Sriram developed a simple reversed-phase high-performance liquid chromatographic (RP-HPLC) method and validated for simultaneous determination of Ramipril and Losartan in pharmaceutical tablet dosage form. Chromatographic analysis was performed on a Inertsil ODS (250Ã—4.6Ã— 5Âµ) column at ambient temperature with a mixture of 10M KH2PO4:ACN (30:70) v/v as mobile phase, at a flow rate of 1.0 ml/min-1. UV detection was performed at 211 nm. The method was validated for accuracy, precision, specificity, linearity and sensitivity. The retention times of Ramipril and Losartan were 2.667 and 3.887 min, respectively. Calibration plots were linear over the concentration ranges 3-7 μg mL-1 and 60-140 μg mL-1 for Ramipril and Losartan, respectively. The Limit of detection was 0.24 and 1.09 Âµg mL-1 and the quantification limit was 0.72 Âµg mL-1 and 3.30 Âµg mL-1 for Ramipril and Losartan, respectively. The accuracy of the proposed method was determined by recovery studies and found to be 100.12% to 100.43%. Commercial tablet formulation was successfully analyzed using the developed method and the proposed method is applicable to routine analysis of determination of Ramipril and Losartan in pharmaceutical tablet dosage form [34].

S. Ashutosh Kumar, Manidipa Debnath, J.V.L.N.Seshagiri Rao, D. Gowri Sankar performed a precise and reproducible stability indicating RP-HPLC method for the simultaneous estimation of hydrochlorothiazide, ramipril and losartan potassium in plasma by using Symmetry C18 column (4.6 x 150mm, 5Pm, Make: Hypersil) in an isocratic mode. The drug was spiked in the plasma and extracted with mobile phase by precipitation method. The mobile phase was consisted of potassium dihydrogen phosphate (KH2PO4) and acetonitrile [HPLC Grade] in the ratio of 68:32 (% v/v). The detection was carried out at 210 nm. The percentage mean recoveries of hydrochlorothiazide, ramipril and losartan potassium were found to be 98.21-101.13, 98.82-100.93 and 99.69-100.98 percentage respectively. This reveals that the method is quite accurate. The method was linear over the concentration range for hydrochlorothiazide 12.5-32.5, ramipril 1.25-3.25 and losartan 50.0 -130.0 Pg/mL. The percentage relative standard deviation for inter-day and intra-day precision was found to be within limits. The lower limit of quantification was found to be 0.647, 1.283 and 2.647 μg/mL for hydrochlorothiazide, ramipril and losartan respectively. The percentage relative standard deviation obtained for the drugs spiked in plasma for stability studies were less than 2 %. The validation of method was carried out utilizing ICH-guidelines [35].

Jinesh Bahubali Nagavi, Preethi Gotadake Anantharaju (2014) developed and validated a HPLC method for simultaneous estimation of Ramipril and Hydrochlorothiazide in tablets. The developed method involves Purosphere, Star Rp18e, 5μm,150×4.6mm column with mobile phase composition of acetonitrile and sodium perchlorate (pH2.5) buffer in the ratio of 3:2, at a flow rate of 1.0 ml/min and UV detection at 316nm for first five minutes for Hydrochlorothiazide and 210nm for Ramipril. The method was validated as per ICH guidelines, Linearity was observed over concentration range of 17.5 to 32.5 μg/ml for Ramipril and 87.5 to 162.5 μg/ml for Hydrochlorothiazide. The Accuracy of the proposed method was determined by recovery studies and found to be

Rama Rao Tadikonda and Ramya Alwala

97.95-102.3% and 97.98-102.66% for Ramipril and Hydrochlorothiazide respectively. The proposed method was extended for estimation of Ramipril and Hydrochlorothiazide in marketed tablet formulation (Ramace-TM) and it was found to be well within the acceptance limit. The developed and validated HPLC method for simultaneous estimation of Ramipril and Hydrochlorothiazide was found to be linear, accurate, precise, robust and rugged. Hence it can be used for routine analysis of Ramipril and Hydrochlorothiazide in tablets [36].

B. Raj Kumar, G. Nagarajan, D. Prashanthi Reddy, E.V.S.Naveen Chowdary, G. Kamalesh, P. Anil Kumar Yadav, developed a simple, precise, rapid and accurate reverse phase HPLC method for the determination of Telmisartan and Ramipril in combined tablet dosage form. A reverse phase C18 column was used as stationary phase of 250x4.6 mm i.d and 5mm partial size, with mobile phase consisting of phosphate buffer of pH 3.0 and acetonitrile in the proportion of 60:40 v/v respectively was used. The flow rate was 1.0 ml/min and the effluents were monitored at 245nm. The retention time was 5.35 and 10.3 minutes. The detector response was linear in the concentration of 16 to 24 µg/ml for Telmisartan with 0.9998 as the value of correlation coefficient and for Ramipril the linearity in the range of 2 to 3 µg/ml with 0.9998 as the value of correlation coefficient. The Limit of measurements such as limit of detection and limit of quantification were found to be 9.47 µg and 31.57 µg for Telmisartan and for Ramipril 1.16µg and 3.88 µg, respectively. The percentage relative standard deviations for the assay values were found to be 1.11 and 0.518 for Telmisartan and Ramipril. The method was validated by determining its accuracy, precision and system suitability. The results of the study showed that the proposed RP-HPLC method is simple, rapid, precise and accurate. Hence, this method can be easily and conveniently adopted for routine analysis of Telmisartan and Ramipril in combined tablet dosage form [37].

N. Sanni Babu , S. Mutta Reddy (2015) reported a simple, rapid, precise, and reliable reverse phase HPLC method was developed for the separation and estimation of four drugs Aspirin, Ramipril, Atenolol and Atorvastatin in cardiovascular polypill based synthetic mixture. The estimation was carried out using Inertsil ODS-3V (250 mm × 4.6 mm, 5 μm) column; mobile phase consisting of acetonitrile, methanol and buffer (pH=2.5); flow rate of 0.8 mL/min and ultraviolet detection at 225 nm. All the drugs were properly eluted within run time of 10 min with retention times about 4.1 min for Aspirin; 5.9 min for Atorvastatin; 7.2 min for Atenolol; and 8.3 min for Ramipril 8.333 min, respectively. The method was validated as a final verification of method development with respect to precision, linearity, accuracy, ruggedness, and robustness. This validated method was successfully applied to the commercially available pharmaceutical dosage form, yielding very good and reproducible result [38].

Manzoor Ahmed, Manohara Y.N, Rachana R. Yeligar developed a simple, accurate, precise and rapid RP-HPLC method with subsequently validated as per ICH guidelines for the determination of Ramipril (RAM) and Metolazone (MET) using mobile phase [mixture of water and acetonitrile in the ratio of 70:30 and potassium dihydrogen ortho phosphate buffer of pH-3 (using OPA)] as the solvent. The proposed method involves the measurement of Retention time at selected analytical wavelength. 220.0 nm was selected as the analytical wavelength. The retention time of MET and RAM was found to be 4.245 and 6.567 respectively. The linearity of the proposed method was investigated in the range of 10-50 µg/ml (r = 0.9999) for MET and 20-100 µg/ml (r = 0.9998) for RAM respectively. The method was statistically validated for its linearity, accuracy and precision. Both inter-day and intra-day variation was found to be showing less % RSD (Relative Standard Deviation) value indicating high grade of precision of the method [39].

Andal Naga Jyothi Kapuganti, Bonthu Mohan Gandhi, Vasthavai Bhaskara Raju, Kamatham Srinivas Sumanth, Venkata Koteswaramma Kagitapurapu , Kolli Srinivas, Parimi Harika (2016) developed and validated a simple, fast, precise, selective and accurate RP-HPLC method for the simultaneous determination Ramipril(RAM), Aspirin (ASP) and Simvastatin (SIM) in a Pharmaceutical dosage form. The separation of these three drugs was achieved on a SHISHEDO C18, 250×4.6mm, 5 micron size column with a mobile phase consisting of 0.5% Ortho phosphoric acid ACN:Methanol (20:10:70 v/v) at a flow rate of 1ml/min and UV detection at 226nm.The retention times were observed to be 2.1, 2.7 and 9.6 minutes for Ramipril (RAM), Aspirin (ASP) and Simvastatin (SIM) respectively. Linearity was found to be 5-15 µg/ml, 50-150 µg/ml, 20-60 µg/ml for Ramipril(RAM), Aspirin(ASP) and Simvastatin(SIM) respectively. The method was statistically validated for linearity, recovery, limit of detection, limit

Rama Rao Tadikonda and Ramya Alwala

of quantification, accuracy and precision. The stress testing of the drugs individually and their mixture was carried out under acidic, alkaline, oxidation, photo-stability and thermal degradation conditions and its degradation products were well resolved from the analyte peaks. This method was successfully validated for accuracy, precision, and linearity, limit of detection and limit of quantification [40].

Makwana, C. J., Patel, P. D., Thummar, J. M., Dey, S., Upadhyay, U. M Studied about Ramipril is angiotensin-converting enzyme inhibitor. Chlorthalidone is one of the oldest and widely used thiazide diuretics. Simple, accurate and economic RP-HPLC method have been described for the simultaneous estimation of Ramipril and Chlorthalidone in bulk and combined dosage form. Reverse Phase high-performance liquid chromatographic method was developed for the determination of Ramipril and Chlorthalidone using Acetonitrile: Water (40:60 v/v) of as the mobile phase and measuring the response at λmax 215 nm. The analysis was performed on a C18 (250X4.6 mm ID), 5.0 µ column. The calibration curve was obtained for Ramipril and Chlorthalidone at 2-12 µg/ml and 5-30 µg/ml respectively. The mean recovery was found to be 98.21% and 98.46% for Ramipril and Chlorthalidone respectively. The LOD and LOQ value for ramipril was found to be 0.069 and 0.218 respectively. The LOD and LOQ value for Chlorthalidone was found to be 0.0076 and 0.025 respectively. The method was validated according to the ICH guidelines [41].

Saida Naik, Dheeravath, Kasani. Ramadevi, Zilla. Saraswthi, Dheeravath. Maniklal, Bhagawan. D (2013) reported a new, simple, rapid, specific and sensitive reverse phage high performance liquid chromatographic method for estimation of Ramipril and Amlodipine. For this validation following parameters like precision, accuracy, linearity, limit of detection, limit of quantification, robustness have been studied. The developed method is recommended for routine analysis since it is rapid, simple, precious and robust quantitative analytical method for simultaneous estimation of Ramipril and Amlodipine. Validation has done according to international conference for harmonization (ICH) [42].

Dipak.A.Patil, Shyam.S.Rangari, Prashant.P.Nikumbh, Sandip.S.Chaudhari and Mayur.R. Bhurat (2022) studied about the present work that explains the development and validation of a simple and reliable RP-HPLC method for the quantitative determination of Ramipril (RMP). Chromatography was carried out by reversed-phase technique on a Fortis C18 (100 mm × 4.6 mm; 2.5 µm particle size). The optimized mobile phase was consisted of Methanol and citric acid sodium citrate buffer solution (50:50 v/v) having pH 3.0. The retention times were 3.645 min for RMP. The detection was carried out at 270 nm and a column temperature of 25 °C. The method was evaluated for the various validation parameters, such as linearity, accuracy, precision, LOD, LOQ, specificity, selectivity, and sample stability. The proposed method was validated and successfully applied for the analysis of pharmaceutical formulations and laboratory-prepared mixture containing Ramipril respectively [43].

Chandrabatla Varaprasad and K. Ramakrishna (2015) performed a cost-effective RP-HPLC method using a PDA detector at 210nm wavelength for simultaneous estimation of Metoprolol, Ramipril and Atorvastatin in pharmaceutical dosage forms. The method was validated as per ICH guidelines over a range of 62.5-625 µg/mL, 6.25-62.5 µg/mL and 12.5-125µg/mL for Metoprolol, Ramipril and Atorvastatin respectively. Analytical column X-bridge C18, 4.6 x 150mm, 5µ was used at a temperature of 30°C ± 0.5°C. OPA Buffer and Acetonitrile composition were used as mobile phase in a gradient flow at a flow rate of 1.0 mL/min. Retention times of 2.4 ± 0.5, 6.1 ± 0.5 min and 7.8 ± 0.5 min were obtained for Metoprolol, Ramipril and Atorvastatin respectively. The percentage recoveries of Metoprolol, Ramipril and Atorvastatin, are 100.82%, 100.05% and 100.7% respectively [44].

Koduru Swathi , Mitta chaitanya, Kalepu swathi (2015) developed and validated a selective and sensitive stability-indicating high-performance liquid chromatographic method was for the determination of Ramipril & Clopidogrel. The λmax of the two ingredients i.e. Ramipril & Clopidogrel , were found to be 210 nm and 225 nm respectively in methanol as solvent system. Accurately weighed 100 mg of Ramipril and 100 mg of Clopidogrel were transferred to 100 ml volumetric flask. About 40 ml of HPLC grade methanol was added and sonicated to dissolve. The volume was made up to mark with same solvent. Then 10 ml of the above solution was diluted to 100 ml with the solvent

system. Mobile phase was prepared by taking Potassium dihydrogen phosphate buffer + Dipotassium hydrogrn phosphate (0.01 M, pH 3.0): acetonitrile (30:70). Mobile phase was filtered through 0.45 µm membrane filter and degassed under ultrasonic bath prior to use. The mobile phase was pumped through the column at a flow rate of 1.0 ml/min. The HPLC system was set with the optimized chromatographic conditions to run the standard solution of Clopidogrel and Ramipril for 15 min. The retention time were found to be 2.03 min and 9.93 min respectively [45].

Abdullah A. Elshanawane, Lobna M. Abdelaziz, Magda M. Kamal (2014) studied about Telmisartan angiotensin-II-receptor antagonist (ARA II), which is used in treatment of hypertension alone or in combination with other antihypertensive drugs such as Ramipril and Amlodipine besylate or in combination with antihyperlipidemic agent such as Atorvastatin calcium. The RP- HPLC method was developed for the assay of Telmisartan, Ramipril, Amlodipine besylate, and Atorvastatin calcium. The method was performed by reversed phase high performance liquid chromatography using a mobile phase consisting of 0.025 M potassium dihydrogen phosphate (pH 6.0):acetonitrile = 60:40, v/v, with detection at 205 nm on a BDS Hypersil C18 (250 × 4.6 mm, 5 µm i.d) at a flow rate of 1.5 mL/min in an isocratic manner. Analytical run time was 8 min. Method exhibited good linear relationship in concentration ranges (10–60, 16–96, 10–60, 10–60 µg/mL); recovery percentages (100.06, 100.85, 99.54, 100.8%); LOD (0.58, 0.16, 0.72, 0.3 µg/mL); and LOQ (1.92 0.55, 2.4, 0.98 µg/mL) for Ramipril, Telmisartan, Amlodipine besylate, and Atorvastatin calcium, respectively. Method validation was developed following the recommendations for analytical method validation of International Conference on Harmonization (ICH) and Food and Drug Administration (FDA) organizations [46].

Raju Chandra , Manisha Pant , Harchan Singh , Deepak Kumar , Ashwani Sanghi (2016) discussed about a reliable and reproducible reversed-phase high performance liquid chromatography (RP-HPLC) for the quantitative determination of Ramipril drug content from marketed bulk tablets. The active ingredient of Ramipril separation achieved with C18 column using the methanol water mobile phase in the ratio of 40:60 (v/v). The active ingredient of the drug content quantify with UV detector at 215 nm. The retention time of Ramipril is 5.63 min. A good linearity relation (R^2=0.999) was obtained between drug concentration and average peak areas. The limit of detection and limit of quantification of the instrument were 0.03 and 0.09 µg/mL, respectively. The accuracy of the method validation was 102.72% by recoveries method [47].

Maste M.M, Kalekar M.C., Kadian N. and Bhat A.R (2011) described a precise, accurate and reproducible Reverse phase High Performance Liquid Chromatographic (RP-HPLC) method for simultaneous estimation of Ramipril and Amlodipine in tablet dosage form on Phenomenex C18 column (245 mm × 4.5 mm, 5 µm, particle size) using acetonitrile: phosphate buffer, (60:40 v/v) as mobile phase at flow rate of 1.0 ml/min and the detection wavelength was 222 nm. The retention time for Ramipril and Amlodipine was found to be 3.41 and 6.10 min respectively. Proposed method was validated for precision, accuracy, linearity range, robustness and ruggedness [48].

Akhil Nagar , Sumit Deore, Atul Bendale, Rajanikant Kakade , Chetankumar Sonawane (2020) developed a rapid, accurate, and precise ratio spectra derivative spectroscopic high-performance liquid chromatography method and validated for the estimation of Ramipril (RAM) and Candesartan cilexetil (CAN) in synthetic mixture. The estimation of RAM, CAN (6 µg/ml) was used as a devisor and for the estimation of CAN, RAM (5 µg/ml) used as a devisor. The wavelengths selected for quantitative estimation were 331 nm for RAM and 231 nm for CAN. The result for validation shows that linearity of the developed method was 0.9976 and 0.9994 in the range of 5–10 µg/ml and 6–16 µg/ml for RAM and CAN, respectively. Phenomenex C18 column (250 mm×4.6 mm, 5 µm particle size) column was used. Acetonitrile:water (0.5% TEA, pH 4.5 adjusted with 10% orthophosphoric acid) (85:15 v/v) as a mobile phase, flow rate 1 ml/min and detection carried out at 220 nm. The retention time of RAM and CAN was 3.607 and 5.613 min, respectively. Linearity of the developed method was found to be 0.9956 and 0.9974 in the range of 0.5–0.9 µg/ml and 1.60–2.88 µg/ml for RAM and CAN, respectively. From the mentioned results, we can conclude that the developed methods were validated successfully as per the ICH guideline and are accurate, robust, and precise [49].

Rama Rao Tadikonda and Ramya Alwala

Anuruddha Rajaram Chabukswar, Pramod Hindurao Sakpal (2021) developed a Cost effective, Accurate, Precise Accelerated degradation method for determination of Atorvastatin and Amlodipine in combination dosage form of tablet and validated as directed by ICH guidelines. The 0.02 M potassium dihydrogen phosphate: acetonitrile: methanol (30:10:60 v/v/v) was used as mobile phase and pH 4 adjusted using ortho phosphoric acid at flow rate 1.0 ml/min. The column used for method development was Octadecylsilane-C18 (5 μm, 25 cm × 4.6mm, i. d.). The peaks obtained in the chromatogram were well resoluted. The scanning wavelength used was 244 nm with PDA detector.The linearity for both the drugs was found between 05 - 30 μg/ml for both drugs with regression coefficient equation 0.995 and 0.999 at retention time 8.32 min and 11.09 min for Amlodipine and Atorvastatin respectively. The results obtained were statistically validated as directed by ICH guidelines and was found satisfactory. The developed and validated method was found to be very specific, accurate and precise. It can be utilized for routine analysis of combined dosage form of Amlodipine and Atorvastatin in the laboratory [50].

M. Vishnu Priya, Dr.P.Madhavan, Dr.Pramod Kumar, Dr.Raj Kumar (2016) reported a simple, accurate, precise assay and rapid stability-indicating reversed phase high performance liquid chromatography (RP-HPLC) method with an effective resolution and subsequently validated for the simultaneous estimation of Metformin HCl, Ramipril and Glimiperide from their combination drug product. The method was developed using Hypersil BDS C18, 250 x 4.6 mm, 5μm , L1 packing, maintained at an ambient temperature. The optimum mobile phase used in this method was a mixture of Methanol and 0.02M KH2PO4 buffer in the ratio of 850:150 v/v, flow rate of mobile phase was set 0.8mL min -1 at 210 nm compounds was eluted and monitored. Metformin HCl, Ramipril and Glimepiride are subjected to stress conditions of acid, base, oxidative, thermal and photolytic degradation. The degradation products were well separated from the main peak proving the stability-indicating ability of the method. The developed method was validated as per International Conference on Harmonization (ICH) guidelines [51].

K. S. Lakshmi And Lakshmi Sivasubramanian developed a simple, sensitive and validated HPLC method to determine Valsartan And Ramipril simultaneously in synthetic mixture. Chromatographic separation was achieved on A C-18 Column using a mixture of acetonitrile and water in the ratio 55:45 (V/V), pH adjusted to 3.6 with 88% orthophosphoric acid at a wavelength of 215 nm. Linearity Of The method was found to be in the concentration range of 50-250 μg/ml for valsartan and I00-500 μg/ml for Ramipril with correlation coefficient greater than 0.999. the total eluting time for the two Components Is less than five minutes. The method can be used for simultaneous determination of valsartan and Ramipril [52].

N. Sanni Babu, S. Mtta Reddy (2015) studied a simple, rapid, precise, and reliable reverse phase HPLC method was developed for the separation and estimation of four drugs Aspirin, Ramipril, Atenolol and Atorvastatin in cardiovascular polypill based synthetic mixture. The estimation was carried out using Inertsil ODS-3V (250 mm × 4.6 mm, 5 μm) column; mobile phase consisting of acetonitrile, methanol and buffer (pH=2.5); flow rate of 0.8 mL/min and ultraviolet detection at 225 nm. All the drugs were properly eluted within run time of 10 min with retention times about 4.1 min for Aspirin; 5.9 min for Atorvastatin; 7.2 min for Atenolol; and 8.3 min for Ramipril 8.333 min, respectively. The method was validated as a final verification of method development with respect to precision, linearity, accuracy, ruggedness, and robustness. This validated method was successfully applied to the commercially available pharmaceutical dosage form, yielding very good and reproducible result [53].

HPTLC METHODS
Darshana A. Parmar, Dinesh V. Thakkar, Rashmin B. Patel, Mrunali R. Patel (2015) Studied about validated high-performance thin-layer chromatography (HPTLC) methods for simultaneous estimation of ramipril (RAM) and losartan potassium (LOS) in pure powder and formulation. The HPTLC separation was achieved on an aluminum-backed layer of silica gel 60F254 using methanol: ethyl acetate: toluene: glacial acetic acid (1:9:1:0.2 v/v/v/v) as mobile phase. Quantification in HPTLC method was achieved with UV detection at 210 nm over the concentration range of 300 – 1300 ng/spot for RAM and 3000 – 13000 for LOS, respectively, with recovery of 98.93 - 99.73 and 98.96 - 100.11 % for RAM and LOS, respectively. These methods are simple, specific, precise, sensitive and robust; they are applicable for the simultaneous determination of RAM and LOS in pure powder and formulation [54].

Devanshi A. Desai, & Renu S. Chauhan & Ragini D. Kushwaha,(2018) developed and validated a simple, accurate and precise high performance thin layer chromatographic method for simultaneous estimation of hydrochlorothiazide and ramipril (RAM) in tablets and a stability indicating HPTLC method for estimation of hydrochlorothiazide (HCTZ) in tablets. The method employed TLC aluminium plates precoated with silica gel 60F254 as the stationary phase. Mobile phase toluene: methanol: ethyl acetate: TEA (6: 3: 1: 0.2 v/v/v) gave compact, dense and well separated bands for hydrochlorothiazide and ramipril at R_f values 0.32 and 0.55 respectively. The linear regression analysis data for the calibration plots showed a linear relationship in the concentration range 750–3750 ng/band with R^2= 0.9947 for hydrochlorothiazide and 300 – 1500 ng/band with R^2= 0.9935 for ramipril. Mobile phase toluene: ethyl acetate: methanol: glacial acetic acid (5: 4: 1: 0.2 v/v/v) gave compact and dense bands for hydrochlorothiazide at R_f 0.43 and well separated degradation products produced under acidic, alkaline, neutral hydrolysis, and oxidation. The methods were found to be suitable for simultaneous estimation of hydrochlorothiazide and ramipril in their combined tablets and for estimation of hydrochlorothiazide in its tablets [55].

Bokka Ramesh, Kothapalli Hari babu, Vanka Uma Maheswara Sarma, Potturi Sita Devi (2011) developed a new high-throughput HPTLC/ ESI-MS method to separate and quantify ramipril, hydrochlorothiazide and telmisartan in solid pharmaceutical formulations. Separation was performed on silica gel 60F plates using a saturated mixture of toluene: chloroform: methanol: acetonitrile(3:3:2:2 v/v) as mobile phase. After chromatography, multi-wavelength densitometric detection was carried out by measuring the UV-absorbance at 210 nm for ramipril, 273 nm for hydrochlorothiazide and 300 nm for telmisartan. The R_f values were 0.51, 0.61 and 0.69 for ramipril, hydrochlorothiazide and telmisartan respectively. The method exhibited good linearity over a dynamic range of 50-400 ng per band for ramipril, 250-1000 ng per band and 800-3200 ng per band for hydrochlorothiazide, telmisartan respectively. Recoveries were between 99.55% and 99.97%.The validated lowest limit of detection was 9.38ng/band, 2.76ng/b and 7.31ng/band whereas lowest limit of quantification was 31.29ng/band, 9.22ng/band and 24.31ng/band for ramipril, hydrochlorothiazide and telmisartan respectively. Mass confirmation was accomplished in positive electrospray ionization full scan mode for ramipril and telmisartan and in negative mode for hydrochlorothiazide. This simple yet a reliable HPTLC/ESI-MS facilitated the separation and determination of the compounds understudy in one analytical run with reduced analysis cost, good chromatographic selectivity and a reliable alternative for routine analysis of pharmaceutical formulations [56].

V. A. Patel, P. G. Patel, B. G. Chaudary, N. B. Rajgor, S. G. Rathi developed and validated thin layer liquid chromatography (TLC) method for the simultaneous estimation of telmisartan and ramipril in a combined dosage form. Procedure does not require prior separation of components from the sample. Telmisartan and Ramipril were determined by High Performance Thin Layer chromatography method (HPTLC) in tablet dosage form. The method was carried out in TLC Precoated silica gel on aluminum plate 60 F 254, (10 cm ×10 cm, prewashed by methanol and activated at 60° C for 5 min prior to chromatography). The solvent system was Acetone: enzene: Ethyl acetate: Glacial acetic acid in the proportion of 5:3:2:0.03, (v/v/v/v) with R_f Value for telmisartan and ramipril was 0.673 and 0.353 respectively. The linearity regression analysis for calibration showed 0.996 and 0.998 for telmisartan and ramipril with respect to peak area and height in the concentration range of 100- 1800 ng/spot and 300-1800 ng/spot respectively. The method developed can be used for routine analysis of drugs content in tablet dosage form [57].

Kamini Sethy , Janhavi R Rao , K Raja Rajeswari and KEV Nagoji (2019) developed a new, simple, precise, and accurate HPTLC method for simultaneous estimation of Metoprolol succinate and Ramipril as the bulk drug and in tablet dosage forms. Chromatographic separation of the drugs was performed on aluminum plates precoated with silica gel 60 F254 as the stationary phase and the solvent system consisted of Methanol: Toluene: Ethyl Acetate: Ammonia (2.5:3:5:0.7v/v/v/v). Densitometric evaluation of the separated zones was performed at 209 nm. The two drugs were satisfactorily resolved with RF values 0.67, and 0.37 for Metoprolol Succinate and Ramipril, respectively. The accuracy and reliability of the method was assessed by evaluation of linearity (2000-12000 ng/spot for Metoprolol succinate and 200–1200 ng/spot for Ramipril), precision (intra-day RSD 0.471–1.036% and inter-day RSD 1.085–1.580% for Metoprolol Succinate and intra-day RSD 1.057–1.63% and inter-day RSD 1.024–1.746% for

63813

Ramipril,), accuracy (98.95 ± 0.16 % for Metoprolol and 98.98 ± 0.41 % for Ramipril), and specificity, in accordance with ICH guidelines [58].

Shirish P. Lokhande, Surya Prakash Gupta, K.Sureshkumar, J. Dharuman, Gopal Garg, Neeraj Upmanyu (2012) reported a simple, precise, accurate and rapid high-performance thin-layer chromatographic method for the estimation of ramipril and valsartan simultaneously in combined dosage form. The stationary phase used was precoated silica gel 60F254. The mobile phase used was a mixture of chloroform: ethyl acetate: methanol: glacial acetic acid (5.0:5.0:1.0:02 v/v/v/v). The detection of spots was carried out at 210 nm. The method was validated in terms of linearity, accuracy, and precision. The calibration curve was found to be linear between 0.4 to 2.0 µg/spot for Ramipril and 0.2 to 1.0 µg/spot for valsartan. The limit of detection and the limit of quantification for ramipril were found to be 200 ng/spot and 640 ng/spot for ramipril and 100 ng/spot and 330 ng/spot respectively. The proposed method can successfully be used to determine the drug content of marketed formulations [59].

Laxman V. Potale , Mrinalini C. Damle , Amol S. Khodke and K. G. Bothara,(2010) studied about Telmisartan, an angiotensin II antagonist and Ramipril, a long acting ACE inhibitor in combination in tablet dosage form used for the treatment of high blood pressure. The present study deals with development of validated stability indicating method for simultaneous estimation of Telmisartan and Ramipril using TLC plate precoated with Silica gel 60 F254 and the mobile phase consisting of Methanol: Chloroform in the ratio of 1:6v/v. Telmisartan and Ramipril were well resolved with R_f 0.68 ± 0.03 and 0.38 ± 0.03 respectively. Wavelength selected for quantization was 210 nm. At this wavelength, Telmisartan and Ramipril show high absorbance. Inherent stability of these drugs was studied by exposing both drugs to various stress conditions as per ICH guidelines viz. Dry heat, oxidative, photolysis (UV and cool white fluorescent light), and hydrolytic conditions under different pH values. Both drugs were not degraded under acidic condition. Both drugs show degradation under alkaline, dry heat, oxidative condition and photolytic condition. The developed method is found to be simple, specific, precise and stability indicating. The specificity of the method was confirmed by peak purity profile of the resolved peaks [60].

Sunil Singh (2012) developed and validated thin layer liquid chromatography (TLC) method for the simultaneous estimation of telmisartan and Ramipril in a combined dosage form. Telmisartan and Ramipril were determined by High Performance Thin Layer chromatography method (HPTLC) in tablet dosage form. The method was carried out in TLC Precoated silica gel on aluminum plate 60 F 254, (10 cm ×10 cm, prewashed by methanol and activated at 60° C for 5 min prior to chromatography). The solvent system was Acetone: Benzene: Ethyl acetate: Glacial acetic acid in the proportion of 6:4:1:0.05, (v/v/v/v) with Rf Value for telmisartan and ramipril was 0.673 and 0.353 respectively. The linearity regression analysis for calibration showed 0.999 and 0.998 for telmisartan and Ramipril with respect to peak area and height in the concentration range of 150- 1700 ng/spot and 300-1900 ng/spot respectively. The method developed can be used for routine analysis of drugs content in tablet dosage form [61].

Jitendra A. Wayadande, Ramkumar Dubey, Vidhya K. Bhusari and Sunil R. Dhaneshwar (2011) developed a new, simple, precise, and accurate HPTLC method for simultaneous estimation of Ramipril and Metolazone as the bulk drug and in tablet dosage forms. Chromatographic separation of the drugs was performed on aluminum plates precoated with silica gel 60 F254 as the stationary phase and the solvent system consisted of toluene : ethyl acetate : methanol : glacial acetic acid (4 : 4 : 1 : 0.2 v/v/v/v). Densitometric evaluation of the separated zones was performed at 223 nm. The two drugs were satisfactorily resolved with RF values 0.33 ± 0.02 and 0.59 ±0.02 for Ramipril and Metolazone respectively. The accuracy and reliability of the method was assessed by evaluation of linearity (600-2100 ng/spot for Ramipril and 100-350 ng/spot for Metolazone) precision (intra-day % RSD was 1.28 – 1.58 and inter-day % RSD was 1.14 – 1.83 for Ramipril and intra-day % RSD was 0.67 – 1.03 and inter-day % RSD was 0.49 – 1.18 for Metolazone), accuracy (99.44 ± 0.15 for Ramipril and 99.85 ± 0.39 for Metolazone), and specificity in accordance with ICH guidelines [62].

Alagar Raja. M, Sunitha, David Banji1 , Rao. K. N. V , Selva Kuamar. D (2015) reported a simple, Accurate, precise method for the simultaneous determination and validation of the telmisartan and ramipril in Tablet dosage form.

Rama Rao Tadikonda and Ramya Alwala

Chromatogram was run through thermo BDS (250mm 4.6mm, 5µ). mobile phase containing Buffer and Acetonitrile in the ratio of 60:40A was pumped through column at a flow rate of 1ml/min. Buffer used in this method was 0.02N KH2PO4 buffer at PH 3.0 temperature was maintained at 30ºC. Optimized wavelength for telmistran and ramipril was 245nm. Retention time of telmistran and ramipril were found to be 5.35 min and 10.3 min. % RSD of the telmistran and ramipril were found to be 1.11 and 0.518 respectively. %Recover was Obtained as 99.12 and 99.22 for telmistran and ramipril respectively. LOD, LOQ values are obtained from regression equation telmistran and ramipril 9.47 and 1.16 and 31.57 and 3.88 respectively. The HPTLC method % RSD 0.37 and 0.53 % Recover was obtained 99.85 and 99.73 respectively. The LOD LOQ was found to be 6.23 and 103 respectively [63].

OTHER ANALYTICAL METHODS:

Raja Kumar Seshadri , Makarand Madhukar Desai , Thummala Veera Raghavaraju , Deepa Krishnan , Dama Venugopala Rao , Ivon Elisha Chakravarthy (2010) developed a simple ultra-performance liquid chromatographic (UPLC) method has been developed for the simultaneous estimation of Metoprolol (MT), Atorvastatin (AT) and Ramipril (RM) from capsule dosage form. The method was developed using Zorbax XDB-C18 (4.6 mm x 50 mm, 1.8 µm) column with a mobile phase consisting of 0.06% ortho phosphoric acid in Milli Q water having an ion pair reagent, 0.0045 M Sodium lauryl sulphate as buffer, at ratio of buffer: Acetonitrile (50:50 v/v), at 55°C column temperature with a flow rate of 1.0 ml/min. Detection was carried out with ultra-violet detection at 210 nm for RM, MT and AT respectively. The retention times were about 1.3, 2.1 and 2.6 min for MT, AT and RM respectively, the method was validated for linearity, accuracy, precision, specificity, robustness and ruggedness. The % mean recoveries are 101.9, 102.1 and 101.4 for MT, AT and RM respectively. The method was found to be rugged and robust and can be successfully used to determine the three drugs and its combinations [64].

Pudage A, Kamat S (2010) discussed about a validated UPLC-MS/MS assay for determination of ramipril and ramiprilat from human plasma samples. The assay is capable of isolating phase II metabolites of ramipril from in vivo study samples which is otherwise not possible using conventional HPLC conditions. Both analytes were extracted from human plasma using solid-phase extraction technique. Chromatographic separation of analytes and their respective internal standards was carried out using an Acquity UPLC BEH C_{18} (2.1×100 mm), 1.7 µm column followed by mass spectrometric detection using an Waters Quattro Premier XE. The method was validated over the range 0.35–70.0 ng/mL for ramipril and 1.0–40.0 ng/mL for ramiprilat [65].

Sherif A Abdel-Gawad1,, Safar M Alqahtani (2020) developed a sensitive and accurate ultra-performance liquid chromatography–tandem mass spectrometric (UPLC-MS) method for quantification of ramipril in human plasma. Ramipril was extracted from biological fluid using equal volumes of n-hexane and propanol (1:1, v/v), and then chromatographed in a suitable C18 column with methanol: 0.1 % HCOOH (4: 1, v/v) as mobile phase. Atorvastatin was used as an internal standard for the chromatographic separation and quantification. The method was validated according to the United States Food and Drug Administration guidelines for standard indices. Ramipril was determined in the concentration range 0.05 and 1000 ng/mL the validation procedure exhibited a correlation coefficient of 0.9979 + 0.002 (p = 0.05). The studied drug was quantified with lower ceiling of 0.05 ng/mL, and showed an accuracy of 105.00 %. A sensitive UPLC-MS analytical method has been successfully developed for the quantification of ramipril in human plasma. This method can be applied efficiently for the quantification of ramipril in bioavailability and pharmacokinetic studies [66].

Eman S. Elzanfaly1 , Sherif A. Abdel-Gawad (2017) studied about formulation containing Ramipril (RAM), glimepiride (GLM) and metformin (MET) for the treatment of diabetes and cardiovascular disorders. This work introduces a liquid chromatography–tandem mass spectrometric (LC-MS/MS) method for the simultaneous determination of the three drugs in human plasma after liquid-liquid extraction. This method made use of atorvastatin as internal standard (IS). Analytes were recovered from plasma by n-hexane: butanol (50:50%, v/v) and subsequently separated on Waters Acquity TM UPLC BEH shield RP-C18 column using methanol: water containing 0.1% formic acid (90:10%, v/v) as a developing system. The calibration curves were linear (r2 > 0.99) over a range of 0.1 - 1000 ng/mL for RAM & GLM and 250 - 2000 ng/mL for MET. The intra-day and inter-day precisions were below

Rama Rao Tadikonda and Ramya Alwala

14.32% and the accuracy was all within ±15%. Moreover, other validation parameters for the proposed method like matrix effect, selectivity, recovery and stability were adopted. The proposed method can be applied for the sensitive and selective quantification of the analytes in bioavailability and pharmacokinetics studies [67].

CONCLUSION

Presented systematic review covers the current analytical methods for the determination of Ramipril and it's combinations in pharmaceutical and biological samples like serum and plasma. HPLC methods were found to be most widely used for Ramipril. The other analytical methods like UV, HPTLC, UPLC, LC/MS are also used for the determination of Ramipril in blood, serum & pharmaceutical dosage forms. The presented information is useful for the future study for researcher involved in formulation development and quality control of Ramipril.

ACKNOWLEDGEMENT

REFERENCES

1. A. Scidkumar I, Verma S, Chaudhary A. Formulation of Ramipril Tablets Containing Solid Dispersion Employing Selective Polymers to Enhance Dissolution Rate. Journal of Drug Delivery and Therapeutics. 2020; 10(3-s):142-149.
2. Mills TP. Ramipril: a review of the new ACE inhibitor. J Ark Med Soc. 1992 Feb;88(9):437-40. PMID: 1532570.
3. Odd PA, Benfield P. Ramipril. A review of its pharmacological properties and therapeutic efficacy in cardiovascular disorders. Drugs. 1990 Jan;39(1):110-35. doi: 10.2165/00003495-199039010-00009. PMID: 2138076.
4. Frampton JE, Peters DH. Ramipril. An updated review of its therapeutic use in essential hypertension and heart failure. Drugs. 1995 Mar;49(3):440-66. doi: 10.2165/00003495-199549030-00008. PMID: 7774515.
5. Available at https://en.wikipedia.org/wiki/Ramipril.
6. Chauhan M, Patel JB, Ahmad F. Ramipril. [Updated 2022 Jul 4]. In: StatPearls [Internet]. Treasure Island (FL): StatPearls Publishing; 2022 Jan.
7. OE Afieroho , O Okorie And TJN Okonkwo. A Spectrophotometric Method For The Determination Of Ramipril In Solid Dosage Forms.Tropical Journal Of Pharmaceutical Research April 2012; 11 (2): 275-279. Available Online At Http://Www.Tjpr.Org Http://Dx.Doi.Org/10.4314/Tjpr.V11i2.15.
8. Syed Iftequar,,Lahoti Swaroop,Zahid Zaheer, Mirza Shahid, Sayad Imran,M H Dehghan. UV Spectrophotometric Methods For Estimation Of Ramipril In Pharmaceutical Dosage Form By Absorption Maxima Method And Area Under Curve, International Journal Of Drug Development & Research | January-March 2012 | Vol. 4 | Issue 1 | ISSN 0975-9344 | Available Online Http://Www.Ijddr.In.
9. Lakshmana Rao A, Prasanthi T, Anusha ,Prasanna MR, Jyothi P. Method Development And Validation For Simultaneous Determination Of Telmisartanand Ramipril By UV Spectrophotometry. Indian Journal Of Pharmacy And Pharmacology. DOI:10.18231/2393-9087.2016.0018,221-224.
10. Gadireddy Sujana , G. Aruna, G. Sivagangaram. Analytical Method Development And Validation Of Ramipril Hcl And Metoprolal Tartrate In Pure And In Combinations By Uv Spectrophotometry And RP-HPLC. International Journal Of Pharmaceutical Development & Technology E ISSN - 2248 - 910X , ISSN - 2248 – 9096, IJPDT / 4(4), 2014, 214-224.
11. N. Vanaja, Ch. Preethi, S.Y. Manjunath, Krishanu Pal. Method Development and Validation for Simultaneous Estimation of Telmisartan and Ramipril by UV-Spectrophotometric Method in Pharmaceutical Dosage Form. Asian J. Pharm. Ana. 5(4): October- December, 2015; Page 187-194. doi: 10.5958/2231-5675.2015.00030.7.

12. Sathishkumar, S ,*Development and Validation of Analytical Methods for the Simultaneous Estimation of Atorvastatin Calcium, Aspirin, Ramipril and Metoprolol Tartrate in Bulk and in Pharmaceutical Dosage form by UV Spectroscopy and Hptlc,* The Tamil Nadu Dr. M.G.R. Medical University, Chennai – 600 032.

13. Khairunnisa Tasneem, Sonia K, & Lakshmi K S. (2020). Method Development and Validation of simultaneous estimation for Ramipril and Amlodipine besylate by UV- VISIBLE Spectrophotometric method. International Journal of Research in Pharmaceutical Sciences, 11(3), 3828–3832. Retrieved from https://ijrps.com/index.php/home/article/view/893.

14. Vaishali Pawar , Archana Tiwari, Dr. P.K. Dubey. Development and Validation of Spectrophotometric Method for Simultaneous Estimation of Atorvastatin Calcium and Ramipril from Tablet Dosage Form. International Journal of Research Publication and Reviews, Vol 3, no 2, pp 206-212, February 2022.

15. Manish Kumar, Mohit Jindal1 , Shailendra Bhatt1 , A. Pandurangan1 , Anuj Malik1 , Vichitra Kaushik1, Prabhat Kumar Upadhaya and G.Arunachalam. Simultaneous Estimation of Amlodipine Besylate and Ramipril in Tablets Dosage Form by UV Spectrophotometric Method, J. Pharm. Sci. & Res. Vol. 11(2), 2019, 667-670.

16. Kurade VP, Pai MG, Gude R. RP-HPLC Estimation of Ramipril and Telmisartan in Tablets. Indian Journal of Pharmaceutical Science. 2009 Mar;71(2):148-51. doi: 10.4103/0250-474X.54283. PMID: 20336215; PMCID: PMC2839403.

17. Shi-Ying DaiShi-Ting QiuWei WuChun-Mei Fu. Development and validation of an RP-HPLC method for simultaneous determination of Ramipril and Amlodipine in tablet. Journal of Pharmaceutical Analysis,2095-1779 & 2013 ,http://dx.doi.org/10.1016/j.jpha.2013.09.002.

18. Jinesh Bahubali Nagavi, Preethi Gotadake Anantharaju. Analytical RP-HPLC Method Development and Validation for the Simultaneous Estimation of Ramipril and Hydrochlorothiazide in Tablet Dosage Form, American journal of pharmatech research.2014;4(4),IISN:22493387.https://www.researchgate.net/publication/277713717_Analytical_RPHPLC_Method_Development_and_Validation_for_the_Simultaneous_Estimation_of_Ramipril_and_Hydrochlorothiazide_in_Tablet_Dosage_Form.

19. **Vaibhav Rajoriya, Amrita Soni, Varsha Kashaw. Method Development And Validation Of Fast Dissolving Tablet Of Ramipril By Hplc Method. International journal of pharmacy and pharmaceutical science. ISSN:0975-1491.**

20. Mousumi Kar, Sujit Pillai, Gaurav Sharma, Nitin Deshmukh, Kunwar Nagendra Krishna Singh. Method Development and Validation for the Estimation of Ramipril and Atorvastatin in Pharmaceutical Formulation by RP-HPLC. Manipal Journal of Pharmaceutical Sciences, September 2019 , Volume 5 , Issue 2,pg.no:47-49.

21. Thotakati, Muralikrishna (2012). *Method Development and Method Validation for Ramipril and Telmisartan by RP-HPLC in Pharmacentical Dosage form.* Masters thesis, JKKMMRF college of pharmacy.

22. Elham Anwar Taha , Manal Mohammed Fouad , Ali Kamal Attia and Zainab Mahmoud Yousef. RP-HPLC method development and validation for simultaneous estimation of ramipril and felodipine. European Journal of Chemistry 10 (2) (2019) 113-117.

23. Vassa, S., Vairagar, P., Mulgund, S., & Korhale, R. (2013). RP-HPLC Method Development And Validation For Simultaneous Estimation Of Ramipril And S (-) Amlodipine In Tablet Dosage Form. Asian Journal of Pharmaceutical Research and Development, 1(4), 81-87. Retrieved from https://ajprd.com/index.php/journal/article/view/94.

24. Raut, P. V., Padwal, S. L., Bachute, M. T. and Polshettiwar, S. A. (2021) "Development and Validation of RP-HPLC Chromatographic Dissolution Method for the Simultaneous Estimation of Ramipril and Hydrochlorothiazide from Solid Dosage Formulation", Journal of Pharmaceutical Research International, 33(42B), pp. 203-217. doi: 10.9734/jpri/2021/v33i42B32440.

25. Hari Krishna. Development and Validation of RP-HPLC Method for Simultaneous Estimation of Atorvastatin Calcium and Ramipril in Tablet Dosage Forms. Journal of Pharmaceutical Analysis, e-ISSN: 2320-0812.

26. Rajesh Sharma, Sunil Khanna, And Ganesh P. Mishra. Development and Validation of RP-HPLC Method for Simultaneous Estimation of Ramipril, Aspirin and Atorvastatin in Pharmaceutical Preparations, ISSN: 0973-4945; CODEN ECJHAO E-Journal of Chemistry http://www.ejchem.net 2012, 9(4), 2177-2184.

Rama Rao Tadikonda and Ramya Alwala

27. Bilal Yilmaz. Determination Of Ramipril In Pharmaceutical Preparations By High-Performance Liquid Chromatography,.International Journal Of Pharmaceutical Sciences Review And Research,Volume 1, Issue 1, March – April 2010; Article 008, Available Online At Www.Globalresearchonline.Net.

28. Vairagar, P. P. Et Al. "Rp-Hplc Method Development And Validation For Simultaneous Estimation Of Ramipril And S (-) Amlodipine In Tablet Dosage Form." (2013).

29. Pallavi, K. et al. "RP-HPLC method development and validation for the simultaneous estimation of ramipril and losartan in tablet and pharmaceutical dosage form." (2015).

30. **K. Srinivasa Rao and K. Srinivas. RP-HPLC Method fo determination of losartan-potassium and ramipril in combined dosage form.** Indian Jornal of Pharmaceutical Science 2010, 72 (1): 108-111,Aavilale at https://www.ijpsonline.com/articles/rphplc-method-for-the-determination-of-losartan-potassium-and-ramipril-in-combined-dosage-form.html**.**

31. Vatchavai Bhaskara Raju, Bonthu Mohan Gandhi, Kamatham Srinivas Sumanth, Kolli Srinivas, Tupakula N Venkata Lakshmi Neeraja. RP-HPLC Method Development and Validation for Simultaneous Estimation of Telmisartan and Ramipril in pure and Pharmaceutical Dosage forms. Asian J. Research Chem. 2017; 10(2):179-185. doi: 10.5958/0974-4150.2017.00030.X.

32. G. Nagarajan, B. Govardhan1 , B. V. Ramana, K. Sujatha, S. Rubina, T. Arundathi and R. Soumya. Development and validation of a RP- HPLC method for simultaneous estimation of enalapril maleate and ramipril in bulk and tablet dosage form. Scholars Research Library Der Pharmacia Lettre, 2013, 5 (1):69-76 ISSN 0975-5071 Usa CODEN: DPLEB4 (http://scholarsresearchlibrary.com/archive.html).

33. Praveen S. Rajput, Amanjot Kaur, Navdeep Kaur Gill, Karan Mittal and Ganti Subrahmanya Sarma, Simultaneous Estimation of Ramipril and Amlodipine in Bulk and tablet Dosage form by RP-HPLC Method Journal of Applied Pharmaceutical Science 02 (07); 2012: 160-165, ISSN: 2231-3354, DOI: 10.7324/JAPS.2012.2724.

34. Prof. N. Sriram. RP-HPLC Method Development And Validation For The Simultaneous Estimation Of Ramipril And Losartan In Tablet And Pharmaceutical Dosage Form. International Journal Of Pharmacy And Analytical Research, Volme-3,Issue-4**,**Online-Issn No :2320-2831.

35. Dr. S. Ashutosh Kumar, Manidipa Debnath, Dr. J.V.L.N.Seshagiri Rao, Dr. D. Gowri Sankar. New Validated Stablity Indicating Rp-Hplc Bioanalytical Method Development And Validation For Simultaneous Estimation Of Hydrochlorothiazide, Ramipril And Losartan In Human Plasma By Using PDA Detector,https://papers.ssrn.com/sol3/papers.cfm?abstract_id=2791168.

36. Jinesh Bahubali Nagavi, Preethi Gotadake Anantharaju. Analytical RP-HPLC Method Development and Validation for the Simultaneous Estimation of Ramipril and Hydrochlorothiazide in Tablet Dosage Form. American journal of pharma tech reseach 2014,4(4),ISSN:2249-3387.

37. Raj Kumar , G. Nagarajan, D. Prashanthi Reddy, E.V.S.Naveen Chowdary, G. Kamalesh, P. Anil Kumar Yadav. A New Method Development And Validation For The Simultaneous Estimation Of Telmisartan And Ramipril By Rp-HPLC. World Journal Of Pharmacy And Pharmaceutical Science, Https://Www.Wjpps.Com/Assets/Images/Isnno.Png.

38. N. Sanni Babu , S. Mutta Reddy, Development of RP-HPLC method for simultaneous estimation of Aspirin, Ramipril, Atenolol and Atorvastatin, International Journal Of Bioassays,4.12 (2015): 4596-4600, ISSN: 2278-778X.

39. Manzoor Ahmed, Manohara Y.N, Rachana R. Yeligar. RP-HPLC Method Development And Validation For Simultaneous Estimation Of Ramipril And Metolazone In Combined Tablet Dosage Form. World Journal Of Pharmacy And Pharmaceutical Sciences, Impact Factor 2.786 Volume 3, Issue 7, 487-497,ISSN 2278 – 4357

40. Andal Naga Jyothi Kapuganti, Bonthu Mohan Gandhi, Vasthavai Bhaskara Raju, Kamatham Srinivas Sumanth, Venkata Koteswaramma Kagitapurapu , Kolli Srinivas, Parimi Harika. Development and Validation of Stability Indicating RP-HPLC Method for Simultaneous Estimation of Ramipril, Aspirin and Simvastatin in Bulk and Pharmaceutical Dosage Form. Asian Journal of Biomedical and Pharmaceutical Sciences, doi: 10.15272/ajbps.v6i53.771 ,2016,14-20.

41. Makwana, C. J., Patel, P. D., Thummar, J. M., Dey, S., Upadhyay, U. M., Development and Validation of RP-HPLC Method for Simultaneous Estimation of Ramipril and Chlorthalidone in Bulk and Combined Dosage Form. International Journal for Pharmaceutical Research Scholars,volume-3,Issue-2,Pg.no-28-38.

Rama Rao Tadikonda and Ramya Alwala

42. Saida Naik, Dheeravath, Kasani. Ramadevi, Zilla. Saraswthi, Dheeravath. Maniklal, Bhagawan. D Reproted Rp-Hplc Method Development For Simultaneous Determination Of The Drugs Ramipril And Amlodipine, -International Journal Of Scientific Research ,Volume-2, Issue:2,Issn:2277-8179, February-2013.

43. Dipak.A.Patil, Shyam.S.Rangari, Prashant.P.Nikumbh, Sandip.S.Chaudhari And Mayur.R. Bhurat. Analytical Method Development For The Determination And Quantification Of Ramipril In Pharmaceutical Formulation By HPLC. International Journal For Research Trends And Innovation 2022 Ijrti ,Volume 7, Issue 9 , Issn: 2456-3315,Pg.No:910-915 (www.Ijrti.Org).

44. Chandrabatla Varaprasad and K. Ramakrishna. Gradient Rp-HPLC Method For Simultaneous Estimation Of Metoprolol, Ramipril And Atorvastatin In Tablet Dosage Form. Rasayan journal of chemistry, Vol. 8, No.4, 404 – 410, October - December | 2015 ISSN: 0974-1496 | e-ISSN: 0976-0083.

45. Koduru Swathi , Mitta chaitanya, Kalepu swathi. Method Development and Its Validation for Simultaneous Estimation of Ramipril & Clopidogrel by RP-HPLC in Combination Tablet Dosage Form, International Journal of Pharma Research and Health Sciences, Volume 3 (3), 2015, Page-737-741.

46. Abdullah A. Elshanawane, Lobna M. Abdelaziz, Magda M. Kamal. Quantitative Determination Of Telmisartan, Ramipril, Amlodipine Besylate, And Atorvastatin Calcium By HPLC. Journal of liiquid chromatography and Related Technologies,Volume-37, Issue-2,2014.

47. Raju Chandra , Manisha Pant , Harchan Singh , Deepak Kumar , Ashwani Sanghi. Development and Validation of A Reversed Phase-High Performance Liquid Chromatography Method for the Quantitative Estimation of Ramipril Drug Content from Formulated Dosage Form. International Journal of Drug Delivery Technology 2016; 6(3); 64-67 ISSN: 0975 4415.

48. Maste M.M., Kalekar M.C., Kadian N. and Bhat A.R. Development of RP- HPLC Method for Simultaneous Estimation of Amlodipine and Ramipril in Tablet Dosage form. Asian J. Research Chem. 4(8): August, 2011 1210 ISSN 0974-4169.

49. Akhil Nagar , Sumit Deore , Atul Bendale , Rajanikant Kakade , Chetankumar Sonawane. Analytical method development and validation of Ramipril and Candesartan Cilexetil in synthetic mixture. Journal Innovations in Pharmaceuticals and Pharmacotherapy, Apr-Jun 2020 , Vol 8 , Issue 2, Doi: 10.31690/ipp.2020,pg.no:14-20.

50. Anuruddha Rajaram Chabukswar1 , Pramod Hindurao Sakpal. RP-HPLC Accelerated Degradation Method Development and Validation for Determination of Amlodipine and Atorvastatin in Combination Dosage Form of Tablet. Indian Journal of Pharmaceutical Education and Research , Vol 55 , Issue 2 , Apr-Jun, 2021.

51. M. Vishnu Priya , Dr.P.Madhavan , Dr.Pramod Kumar , Dr.Raj Kumar. RP-HPLC Method for Simultaneous Estimation of Metformin HCL, Ramipril and Glimepiride in Bulk and Their Combination Tablet Dosage Form. Journal of Pharmacy and Biological Sciences (IOSR-JPBS) e-ISSN:2278-3008, p-ISSN:2319-7676. Volume 11, Issue 3 Ver. IV (May - Jun.2016), PP 16-23 www.iosrjournals.org.

52. K. S. Lakshmi And Lakshmi Sivasubramanian. A Stability Indicating Hplc Method For The Simultaneous Determination Of Valsartan And Ramipril In Binary Combination. Journal of the Chilean Chemical Society, ISSN 0717-9707.

53. N. Sunni Babu, S. Mutta Reddy, Development of RP-HPLC method for simultaneous estimation of Aspirin, Ramipril, Atenolol and Atorvastatin. International journal of Bioassays, Dec 1, 2015. https://doi.org/10.21746/ijbio.2015.12.004.

54. Darshana A. Parmar, Dinesh V. Thakkar, Rashmin B. Patel, Mrunali R. Patel. HPTLC method for simultaneous estimation of Ramipril and Losartan potassium in pharmaceutical dosage form: Development and Validation consideration. Thai journal of pharmaceutical Sciences. 39 (3), July-September 2015: 83-88.

55. Devanshi A. Desai, & Renu S. Chauhan & Ragini D. Kushwaha. Development And Validation Of HPTLC Method For Simultaneous Estimation Of Hydrochlorothiazide And Ramipril In Their Combined Tablet Dosage Form & Stability Indicating HPTLC Method For Estimation Of Hydrochlorothiazide. International Journal of Research and Analytical Reviews, [Volume 5 I Issue 3 I July – Sept 2018] issn 2348 –1269, Print Issn 2349-5138.

56. Bokka Ramesh, Kothapalli Hari babu, Vanka Uma Maheswara Sarma, Potturi Sita Devi. Development and validation of a HPTLC-ESI/MS Method for the Simultaneous, Determination of Ramipril, Hydrochlorothiazide and Telmisartan in Tablet Dosage Form. Journal of Pharmacy Research 2011,4(12),4541-4545.

Rama Rao Tadikonda and Ramya Alwala

57. V. A. Patel, P. G. Patel, B. G. Chaudary, N. B. Rajgor, S. G. Rathi. Development and Validation of HPTLC Method for the Simultaneous Estimation of Telmisartan and Ramipril in Combined Dosage Form. International journal of biological and pharmaceutical research. January 2010. https://www.researchgate.net/publication/50590006_Development_and_Validation_of_HPTLC_Method_for_the_ Simultaneous_Estimation_of_Telmisartan_and_Ramipril_in_Combined_Dosage_Form.

58. Kamini Sethy , Janhavi R Rao , K Raja Rajeswari and KEV Nagoji. Validated HPTLC method for simultaneous estimation of metoprolol succinate and ramipril in bulk drug and marketed formulation, Clinical and Medical Reports, ISSN: 2516-5283 2019 doi: 10.15761/CMR.1000152 Volume 2: 1-4.

59. Shirish P. Lokhande, Surya Prakash Gupta, K.Sureshkumar, J. Dharuman, Gopal Garg, Neeraj Upmanyu. Development and Validation of a HPTLC Method for the Simultaneous Estimation of Ramipril and Valsartan. International Journal of Pharmacy Teaching & Practices, ISSN - 1986-8111,, 2012, Vol.3, Issue 1, 225-227.

60. Laxman V. Potale , Mrinalini C. Damle , Amol S. Khodke And K. G. Bothara. A Validated Stability Indicating HPTLC Method For Simultaneous Estimation Of Ramipril And Telmisartan. International Journal Of Pharmaceutical Sciences Review And Research, Volume 2, Issue 2, 2010; Article 007, Issn 0976 – 044x,Pg.No:35-39.

61. Sunil Singh. Simultaneous Estimation Of Telmisartan And Ramipril In Combined Dosage Form By Using HPTLC. Scholars Research Library , Der Pharmacia Lettre, 2012, 4 (2):509-514.

62. Jitendra A. Wayadande, Ramkumar Dubey, Vidhya K. Bhusari and Sunil R. Dhaneshwar. Validated HPTLC Method for Simultaneous Estimation of Ramipril and Metolazone in Bulk Drug and Formulation. Pelagia Research Library Der Pharmacia Sinica, 2011, 2 (4): 286-294.

63. Alagar Raja. M, Sunitha, David Banji , Rao. K. N. V , Selva Kuamar. D, HPTLC Estimation Of Telmisartan And Ramipril In Pharmaceutical Dosage Form And Its Method Validation. International Journal of Research in Pharmaceutical and Nano Sciences. 4(4), 2015, 180 - 187.

64. Raja Kumar Seshadri , Makarand Madhukar Desai , Thummala Veera Raghavaraju , Deepa Krishnan , Dama Venugopala Rao , Ivon Elisha Chakravarthy. Simultaneous Quantitative Determination of Metoprolol, Atorvastatin and Ramipril in Capsules by a Validated Stability-Indicating RP-UPLC Method. Scientia Pharmacetica. 2010; 78: 821–834.

65. Pudage A, Kamat S. Development and validation of UPLC tandem mass spectrometry assay for separation of a phase II metabolite of ramipril using actual study samples and its application to a bioequivalence study. Biomed Chromatography. 2011 Jun;25(6):664-73. doi: 10.1002/bmc.1500. Epub 2010 Aug 31. PMID: 20812207.

66. Sherif A Abdel-Gawad, Safar M Alqahtani. Ultra-performance liquid chromatography–tandem mass spectrometric determination of ramipril in human plasma. Tropical Journal of Pharmaceutical Research April 2020; 19 (4): 851-857 ISSN: 1596-5996 (print); 1596-9827.

67. Eman S. Elzanfaly1 , Sherif A. Abdel-Gawad. Simultaneous quantification of ramipril, glimepiride and metformin in human plasma by ultra-performance liquid chromatography – tandem mass spectrometry. Journal of Applied Pharmaceutical Science Vol. 7 (07), pp. 062-069, July, 2017, Available online at http://www.japsonline.com DOI: 10.7324/JAPS.2017.70711 ISSN 2231-3354.

REVIEW ARTICLE

A Review on Herbal Transdermal Drug Delivery System: Pulmonary Disorder

Komala M* and Logesh V

Department of Pharmaceutics, School of Pharmaceutical Sciences, Vel's Institute of Science, Technology and Advanced Studies, Pallavaram, Chennai – 600 117, Tamil Nadu, India.

*Address for Correspondence**
Komala M
Department of Pharmaceutics,
School of Pharmaceutical Sciences,
Vel's Institute of Science,
Technology and Advanced Studies,
Pallavaram, Chennai – 600 117,
Tamil Nadu, India.
E.Mail: komala.sps@velsuniv.ac.in

ABSTRACT

In this review, herbs are delivered using transdermal drug delivery systems (TDDS) for targeted delivery of respiratory medications. As an alternative to conventional treatments, herbal TDDS has several advantages, including non-invasiveness, controlled release, reduced side effects, and improved patient compliance. It is possible to deliver herbal compounds to the respiratory system effectively with herbal TDDS. As a result, systemic side effects can be reduced and healing can be improved. In the future, formulation design should be optimized, herbal products should be standardized, and safety and efficacy research should be conducted. It is likely that herbal TDDS will prove to be a highly effective and tailored treatment option for respiratory ailments.

Keywords: Transdermal drug delivery system, herbal treatments, patient compliance, pulmonary disorder

INTRODUCTION

The complexity of the respiratory system creates significant challenges when treating pulmonary disorders, as well as the need to deliver drugs precisely to the affected areas. There are limitations to conventional treatments, such as inhalations and oral medications, in terms of efficacy, patient compliance, and systemic side effects. Transdermal

drug delivery systems (TDDS) are among the novel drug delivery approaches that have gained popularity in recent years [1]. Herbal TDDS is a method of delivering targeted drugs to the body by applying herbs to the skin to facilitate systemic absorption and targeted drug delivery. Compared to conventional routes of drug delivery, transdermal drugs are less invasive, have a longer time period of release, have a higher bioavailability, and are more likely to be tolerated by patients [2]. There are a number of advantages to using this technique for pulmonary disorders where localized treatment is desirable in order to minimize the impact on the systemic system. By targeting directly, the affected respiratory tissues, TDDS is an important treatment for pulmonary disorders [3]. In order to achieve optimal therapeutic outcomes, medications must reach the site of action efficiently. There is a risk of causing irritation or systemic side effects when traditional treatment approaches, such as inhalation therapy, are used. With herbal TDDS, therapeutic agents are delivered directly into the bloodstream without having to travel through the lung [4].

A review of herbal TDDS is presented here to assess its potential as a drug of choice for pulmonary disorders [5]. This study aims to provide a comprehensive analysis of the advantages, challenges, and future prospects of herbal TDDS in the treatment of respiratory conditions based on an analysis of the available literature and research studies. In addition, we will highlight the potential benefits and limitations of herbal TDDS in comparison with conventional treatments [6]. Various strategies for formulating herbal transdermal patches or gels will be examined to facilitate a deeper understanding of herbal TDDS, including the selection of appropriate herbal extracts and formulation techniques. As well as discussing the potential adverse effects associated with herbal TDDS, we will also discuss the importance of preclinical and clinical studies to evaluate efficacy and safety [7]. In addition to highlighting the unique advantages and limitations of herbal TDDS, this review will also compare it with conventional treatment methods, such as inhalation therapy and oral medications [8]. Furthermore, regulatory considerations and standardization of herbal products will be discussed, as well as future perspectives and challenges. An overview of herbal TDDS will be presented in this review in order to provide an overview of its significance in the treatment of pulmonary disorders in addition to analyzing its potential as a drug of choice for the treatment of such disorders.

Pulmonary Disorders and Current treatment approaches
There are two common pulmonary disorders that have a significant impact on respiratory function and quality of life: asthma and chronic obstructive pulmonary disease (COPD).

Asthma
It is characterized by breathing difficulties, wheezing, coughing, and tightness of the chest. There is no age limit to its prevalence, but it is most common in childhood. Occupational exposures and allergens, air pollution, and respiratory infections are among the environmental factors contributing to asthma. The symptoms of asthma are caused by inflamed, narrowed airways and excessive mucus. It is important to note that asthma attacks are triggered by a variety of factors, including allergens (e.g., pollen, dust mites, pet dander), exercise, cold air, respiratory infections, and irritants (e.g., smoke, strong smells). Symptoms of asthma must be relieved temporarily while long-term control must be maintained to prevent exacerbations. It is common to use inhaled corticosteroids for long-term control as well as bronchodilators for acute symptom relief (for instance, short-acting beta-agonists). It may be necessary to prescribe oral corticosteroids in severe cases. The development of an asthma action plan and identifying asthma triggers are essential for asthmatic individual**s [9].**

Chronic Obstructive Pulmonary Disease (COPD)
Chronic obstructive pulmonary disease causes persistent airflow limitation and inflammation in the lungs. Inhaling harmful inhalants, such as cigarette smoke, is the primary cause of COPD. There are also genetic factors, such as an alpha-1 antitrypsin deficiency, and occupational exposure to dust and chemicals. A person with COPD is typically suffering from chronic bronchitis and emphysema at the same time. The presence of chronic bronchitis is characterized by inflammation and narrowing of the bronchial tubes, resulting in recurrent respiratory infections, excessive mucus production, and chronic coughing. A lung disease called emphysema, on the other hand, causes the air sacs in the lung to become damaged, which results in a reduced ability to exchange oxygen and the inability to

breathe. Shortness of breath, chest tightness, coughing, wheezing, and fatigue are symptoms of COPD. In addition to affecting quality of life and daily activities, the disease is a progressive and irreversible illness. As part of the treatment plan, symptoms will be relieved, disease progression will be slowed, and exacerbations will be prevented. Inhaled treatments, brochodilators, and corticosteroids are common. Patients with advanced lung disease may also benefit from pulmonary rehabilitation programs and oxygen therapy [10]. The treatment of asthma and COPD requires long-term management and an individualized treatment plan. Managing these pulmonary disorders effectively and improving quality of life for affected individuals requires proper diagnosis, medication adherence, lifestyle modifications, and ongoing monitoring.

Limitations and challenges
There are certain limitations and challenges with current treatment methods for pulmonary disorders, such as inhalation therapy and oral medications.

Inhalation therapy
Technique and Device Dependence: The delivery of drugs to the lungs requires proper technique and coordination. Suboptimal therapeutic outcomes can be caused by incorrect inhaler technique.

Patient Compliance: Patients with cognitive or physical impairments may have difficulty adhering to prescribed inhalation therapy regimens. Symptoms of asthma can be exacerbated by inconsistent or improper use of inhalers.

Device Availability and Cost: Depending on their design, availability, and cost, inhalers and other inhalation devices can vary greatly. There are disparities in treatment options due to the cost or accessibility of certain inhaler devices.

Oral medications
Systemic Side Effects: The large distribution of oral medications used to treat pulmonary disorders frequently results in systemic effects. Other organs or systems may be adversely affected, unrelated to the intended target, as a result of this.

Variable Bioavailability: Food intake and gastric pH may affect the bioavailability of orally administered drugs, as they pass through the digestion system. This variability can affect their consistency and efficacy.

First-Pass Metabolism: The liver performs first-pass metabolism of drugs taken orally before they enter the circulation system. To achieve therapeutic effects, higher doses or more frequent administration are required due to the reduced concentration and bioavailability of the drug as a result of this metabolism. It is often the case that both inhalation therapy and oral medications lead to systemic drug distribution, reaching tissues and organs that are not targeted by the drug. Optimal therapeutic outcomes and a minimal impact on other body parts are achieved by delivering drugs locally to the lungs for pulmonary disorders. Factors such as genetic variation, coexisting medical conditions, and drug interactions can affect the response to inhalation therapy and oral medications. In order to tailor treatments to individual needs and to optimize drug selection [11], a multitude of factors need to be taken into account. It is crucial for successful management of pulmonary disorders that patients are educated about treatment techniques, medication schedules, and the importance of adhering to them. Patients with chronic illnesses may find it difficult to understand and adhere to their treatment plans for long periods of time.

Transdermal Drug delivery system
It is a form of administering medications through the skin so they can be absorbed into the bloodstream systemically. Compared to orally administered orally or via injection, it offers several advantages.

Mechanism

It is possible to facilitate drug absorption through transdermal drug delivery because of the skin's unique properties. There are several layers in the skin, including a protective layer called stratum corneum, which is located at the outermost layer. However, the stratum corneum also serves as the primary site of drug permeation in transdermal delivery[12]. As transdermal systems penetrate the stratum corneum, drugs are infused into the deep layers of the stratum corneum from which they are absorbed into the bloodstream. Many strategies are used to enhance drug permeation, such as permeation enhancers, drug carriers, or specialized drug delivery systems such as patches, gels, and creams.

Advantages

Controlled and Sustained Drug Release: In transdermal drug delivery systems, medications are released slowly and continuously over a prolonged period of time. This reduces the need for frequent dosing and maintains therapeutic levels over a longer period of time due to the steady concentration of the drug in the bloodstream.

Non-Invasive Administration: Injections and surgical procedures are not necessary for transdermal drug delivery. Especially for those with aversions to needles or difficulties with oral administration, this is a much more convenient and comfortable method.

Improved Patient Compliance: The ease and convenience of transdermal drug delivery systems contribute to better compliance among patients. Healthcare professionals can lessen the need for patient assistance by administering transdermal patches or topical formulations themselves.

Avoidance of First-Pass Metabolism: Prior to reaching the systemic circulation, orally administered drugs undergo first-pass metabolism in the liver. A drug's bioavailability can be reduced by this metabolic process. Since transdermal delivery bypasses the digestive tract and liver, drugs are directly absorbed into the bloodstream without first-pass metabolic degradation.

Reduced Systemic Side Effects: It is possible to deliver drugs locally and specifically through transdermal delivery. A skin delivery system reduces systemic exposure to medication, reducing systemic side effects and improving the drug's safety profile by delivering it directly into the bloodstream.

Flexibility in Drug Formulations: Small molecules, macromolecules, and even nanoparticles are capable of being delivered through transdermal drug delivery systems. There are many different formulations of patches, gels, and creams that can be tailored to meet the specific needs of patients and the properties of specific drugs.

Potential for Drug Withdrawal: In the event of adverse effects or when the treatment is no longer needed, transdermal drug delivery systems can be easily removed or discontinued.

Importance over management of pulmonary disorder

Pneumonia can be effectively managed with transdermal delivery of drugs, which offers specific advantages making it a valuable technique.

Targeted Drug Delivery to the Lungs: Airways and lung tissues are affected primarily by pulmonary disorders. By delivering targeted drugs directly to the lungs, transdermal drug delivery provides a unique advantage. A drug can be delivered through the skin to reach the pulmonary tissues, bypassing the digestive tract. By targeting drug delivery, systemic side effects are minimized and the local therapeutic effect is maximized.

Localized Treatment of Respiratory Inflammation: Lung tissue and airways are frequently inflamed in many pulmonary diseases. Anti-inflammatory medications can be formulated into transdermal drug delivery systems to

address and reduce inflammation in the lungs. Inflammatory processes associated with pulmonary disorders are managed by this localized treatment approach [13].

Sustained and Controlled Drug Release: Medications can be delivered transdermally in a controlled and sustained manner. The benefit of this is particularly apparent when treating pulmonary diseases, where maintaining consistent drug levels over time is essential for a successful outcome. In addition to reducing dosage frequency and enhancing patient convenience, transdermal drug delivery ensures a continuous therapeutic effect by maintaining a steady concentration of medication in the bloodstream.

Improved Patient Compliance: Managing pulmonary disorders requires patient compliance with treatment regimens. It is possible to improve patient compliance by using transdermal drug delivery systems. Compared to transdermal patches or topical formulations, transdermal patches are more user-friendly, non-invasive, and do not require frequent dosing. Treatment outcomes and disease management can be improved by improving patient compliance [14].

Minimization of Systemic Side Effects: Medication used to treat pulmonary disorders can sometimes have systemic side effects. Transdermal drug delivery bypasses the gastrointestinal tract and delivers drugs directly to the bloodstream. By delivering the drug locally, the potential for systemic side effects are minimized. As a result, medications can be delivered effectively to the target site while minimizing the impact on other organs or systems.

Alternative Route of Administration: In addition to oral medications and inhalation therapies, transdermal drug delivery may be an alternative route of administration for those who have difficulty with other methods. Those with compromised lung function, children, and the elderly who may have trouble swallowing oral medications or using inhalers will particularly benefit from this.

Potential for Combination Therapy: In addition to delivering multiple medications simultaneously or sequentially, transdermal drug delivery systems provide the possibility of combination therapy. Using different drugs that have complementary actions can provide optimal therapeutic effects in the treatment of complex pulmonary disorders.

Herbal medicines for pulmonary disorders
An herbal medicine is a medicinal preparation derived from plants, also known as a botanical medicine or phytomedicine. The therapeutic properties of these preparations can be harnessed from leaves, roots, stems, flowers, and seeds of plants. In ancient civilizations such as Egypt, China, Greece, and India, herbal medicines were used for thousands of years. There have been numerous traditional medical systems which utilize herbal remedies for promoting health and treating illnesses, including Traditional Chinese Medicine (TCM) [15], Ayurveda, and Indigenous Medicine. The medicinal properties of plants are attributed to numerous bioactive compounds, such as alkaloids, flavonoids, terpenoids, phenolic compounds, and essential oils. Therapeutic effects are determined by the combination of constituents in each species of plant.

There are a variety of health conditions that can be treated with herbal medicines. The herbal remedies used by different cultures treat digestive disorders, respiratory conditions, skin conditions, musculoskeletal issues, hormonal imbalances, and more. Generations of people have passed down the knowledge of traditional uses. Physiological processes and bioactive compounds in herbal medicines interact to produce therapeutic effects. Medicinal effects can be exerted by these compounds by activating receptors, enzymes, ion channels, and signaling pathways. A variety of herbal medicines have different patterns of action, with some acting broadly and others acting specifically. If herbal medicines are used properly, they are generally considered safe; however, they may have side effects and interact with other medicines. In addition, certain plants can cause allergic reactions in some people. In order to ensure safe and effective use, it is recommended that you consult a qualified healthcare professional or herbalist. Recent scientific research has concentrated on the therapeutic potential of herbal medicines, analyzing their pharmacological activities, mechanisms of action, safety profiles, and clinical efficacy. Several herbal medicines are being used in

modern healthcare based on this growing body of evidence. Herbal medicines are popular for their anti-inflammatory properties, antibacterial properties, and nutrition benefits. *Echinacea* and *Ginkgo biloba* are popular for their immune system boosting properties, while peppermint and garlic are popular for their antacid and cardiovascular properties. With progress in research, scientists are examining new applications, standardization methods [16], and integrating herbal medicine with conventional medicine. The field of herbal medicine is evolving and presents opportunities for further exploration and understanding.

Review of specific herbs traditionally used for respiratory conditions
Eucalyptus (*Eucalyptus globulus*)
The herb eucalyptus is known to have beneficial effects on respiratory health. Among the compounds found in its composition are cineole, which has antimicrobial and expectorant properties. Oils and leaves of eucalyptus are commonly used for respiratory problems such as congestion, coughs, and bronchial inflammation through steam inhalation or cough syrups.

Liquorice (*Glycyrrhiza glabra*)
There have been a number of uses for liquorice root in traditional medicine over the centuries, including its soothing and anti-inflammatory properties. The herb contains glycyrrhizin, which is used to alleviate respiratory symptoms including coughs and throat irritations. Traditionally, liquorice root is used in teas and herbal formulations to relieve respiratory conditions such as bronchitis and sore throats.

Thyme (*Thymus vulgaris*)
The expectorant and antimicrobial properties of thyme have long been recognized. As well as enhancing mucus expulsion, it contains volatile oils, including thymol, which can soothe bronchial spasms. The herb thyme is commonly used to alleviate coughs, congestion, and respiratory infections through teas, inhalation blends, and herbal preparations.

Mullein (*Verbascum thapsus*)
Traditional herbal medicine has used mullein leaves and flowers to treat respiratory conditions for centuries. As an anti-inflammatory and soothing herb, it has a number of benefits. Coughs, bronchitis, and congestion are often treated with mullein herbal formulations. Inhalation of steam is possible with this tea[17].

Marshmallow Root (*Althaea officinalis*)
For respiratory conditions, marshmallow root is beneficial due to its demulcent and soothing properties. Coughs are relieved and irritation is soothed by its protective coating. Dry coughs, sore throats, and bronchial irritation can be relieved with marshmallow root in herbal cough syrups and teas.

Coltsfoot (*Tussilago farfara*)
Traditional medicine has used coltsfoot for respiratory conditions for centuries. A mucilage compound in it soothes the respiratory tract and relieves coughing. To relieve bronchial congestion and cough caused by respiratory infections, coltsfoot is commonly used in herbal cough remedies and expectorant formulations.

Osha Root (*Ligusticum porteri*)
Native American herbs such as osha root are known for their respiratory benefits. Antimicrobial and expectorant compounds are found in it. As a cough syrup and respiratory formula ingredient, osha root is often used to relieve cough, congestion, and inflammation in the lungs. Cold and flu season is a time when it is particularly beneficial for respiratory health.

Ginger (*Zingiber officinale*)
The benefits of ginger go beyond digestive health. Ginger also plays a role in respiratory health. Respiratory symptoms can be alleviated by its anti-inflammatory and antimicrobial properties. Coughs, congestion, and sore throats are often relieved by ginger tea, syrups, and formulations.

Advantages of herbal transdermal drug delivery system
Non-Invasive Administration: It offers the advantage of being non-invasive, which is a key benefit of herbal transdermal drug delivery. Transdermal delivery involves applying the medication topically to the skin, as opposed to oral medications or injections, which require ingestion or injection. Patients can avoid needles and swallowing pills using this method, making it convenient and comfortable.

Controlled and Prolonged Release
Over an extended period of time, transdermal drug delivery systems release the medication controlled and sustained. Herbal compounds are absorbed steadily into the bloodstream, minimizing fluctuations and maintaining therapeutic levels. A reduction in the frequency of dosing can improve treatment efficacy [18].

Avoidance of First-Pass Metabolism: A medication taken orally passes through the digestive system and the liver before it reaches the circulatory system. During this process, called first-pass metabolism, active compounds in the drug can be broken down or altered. The herbal compounds are delivered transdermally without passing through the liver, resulting in greater bioavailability.

Reduced Systemic Side Effects: By delivering herbal compounds transdermally, side effects can be reduced by targeting local delivery rather than systemic distribution. In this way, medication can be directly applied to the affected area to optimize its concentration, while minimizing its exposure to other tissues. The application of this technique can be particularly useful when treating localized conditions, such as skin disorders or pain.

Improved Patient Compliance: Transdermal drug delivery improves patient compliance with medication regimens because it is convenient and easy to use. With the patches or gels, patients are less likely to forget to take their medication or skip doses because they can be applied once or a few times a day. As a result of transdermal delivery, medication schedules are simplified since there is no need for multiple daily administrations.

Enhanced Stability of Herbal Compounds: In the GI tract and in the stomach, some herbal compounds are susceptible to degradation. Unlike oral drugs, transdermal drugs bypass the digestive system, helping to preserve their stability. In this way, active ingredients remain intact in the bloodstream, maintaining their therapeutic properties.

Flexibility and Ease of Dose Adjustment: It is possible to adjust the dosage based on the individual needs of patients with transdermal drug delivery systems. The dosage can easily be customized by healthcare professionals by modifying its size or frequency. When treating patients with varying needs, this adaptability can be especially useful.

Improved Absorption for Poorly Absorbed Compounds: Because they are poorly absorbed or rapidly metabolized, some herbal compounds are not as bioavailable as others. This limitation is overcome by transdermal drug delivery, which delivers active ingredients directly into the bloodstream. By doing so, poorly absorbed compounds can be better absorbed, resulting in improved therapeutic outcomes.

Strategies for herbal transdermal drug delivery system
Selection of Appropriate Herbal Compounds: A transdermal drug delivery system using herbal compounds begins with the selection of suitable herbal compounds. The best compounds are those that can penetrate the skin barrier

effectively and have the desired therapeutic effects. A variety of factors should be considered during the selection of a compound, including its molecular weight, lipophilicity, and solubility in skin-compatible vehicles.

Enhancement of Skin Permeation:
Drugs are not absorbed through the stratum corneum, the outermost layer of the skin. Permeation of the skin can be enhanced by the following strategies:

Use of Penetration Enhancers: It is possible for herbal compounds to penetrate the stratum corneum by disrupting it with penetration enhancers, like fatty acids, surfactants, and chemical permeation enhancers, such as surfactants.

Physical Enhancement Techniques: Herbal compounds can be better absorbed through the skin by physical methods like microneedling, ultrasound, and iontophoresis.

Nanoparticles and Liposomes: Due to their small size and ability to bind with skin lipids, nanoparticles and liposomes are effective at enhancing the penetration of herbal compounds through the skin.

Formulation Design:
To ensure optimal drug delivery and skin penetration, the formulation of a transdermal drug delivery system is crucial. The following considerations should be taken into account when designing formulations:

Selection of Suitable Vehicles: A vehicle for solubilizing herbal compounds and controlling their release, such as gels, creams, ointments, patches, is critical.

Optimization of Drug Concentration: The formulation must contain the optimal concentration of herbal compounds so that therapeutic efficacy can be achieved while minimizing local irritations or systemic side effects.

Use of Skin Penetration Enhancers: Permeation enhancers are incorporated in the formulation to ensure herbs penetrate the skin barrier more effectively.

Delivery System Design: Transdermal drug delivery systems must be designed in a way that ensures proper release and adhesion to the skin. For the design of delivery systems, the following considerations need to be taken into account:

Patch or Patchless Systems: There are old-fashioned adhesive patches available as well as newer technologies such as microemulsions or hydrogels that don't require a patch to apply.

Control of Drug Release: Controlled-release mechanisms, such as reservoirs, matrix systems, or nanoparticles loaded with drugs, are employed to guarantee sustained and controlled release of herbal compounds.

Skin Adhesion and Comfort: Achieving effective skin retention and comfort, as well as preventing irritations and allergic reactions.

Safety and Stability Considerations: Transdermal drug delivery systems based on herbal materials should be thoroughly tested for safety and stability. The following factors should be considered

Skin Irritation and Sensitization: In order to ensure that the delivery system does not cause adverse skin reactions, skin irritation and sensitization studies are conducted.

Stability of Herbal Compounds: The formulation and shelf life of the product should maintain the stability of the herbal compounds.

63828

Preservative Systems: Maintaining formulation integrity by incorporating appropriate preservatives.

Preclinical and Clinical Evaluation: An assessment of the efficacy and safety of the herbal transdermal drug delivery system requires preclinical and clinical trials. To assess drug release, skin permeation, therapeutic efficacy, and potential side effects, we conduct *in vitro* and animal studies as well as clinical trials.

Comparison with conventional treatment methods
Herbal transdermal drug delivery versus conventional treatments both have their own strengths and limitations, and it is important to note that both have some similarities but also some differences. As a patient, you may have a wide range of preferences when it comes to the type of treatment method you choose [19]. This is due to multiple factors, including the specific condition being treated, the properties of the herbal compound, your preferences, and the advice of your healthcare provider. There are a number of factors that need to be considered when choosing the most suitable treatment approach for an individual patient, including consulting with healthcare professionals.

Future perspectives and challenges
Potential Future Developments and Advancements
Nano-based Delivery Systems: The skin can deliver and target herbal compounds more effectively when compounds are delivered through nanoparticles, liposomes, and other nanotechnology-based approaches. A controlled release system can improve the bioavailability, stability, and bioavailability of herbal active ingredients. Microneedle Technology: Herbal compounds penetrate better through micropores created by microneedles. In the future, microneedle delivery systems may provide a painless, efficient, and convenient method of delivering medication to the skin.

Hybrid Systems: Combined transdermal delivery with oral or inhalation delivery can improve therapeutic outcomes and synergistic effects. Personalized treatments could be provided by these hybrid systems according to a patient's needs and conditions.

Regulatory Considerations and Standardization of Herbal Products
Safety and Efficacy Assessment: It is imperative that herbal transdermal drug delivery systems be evaluated using standardized methods. As herbal products have unique characteristics and potential interactions, regulatory authorities need to develop specific guidelines. Quality Control and Standardization: Integrating herbal compounds into transdermal formulations requires ensuring consistency in quality and potency. Keeping product consistency and patient safety can be achieved by implementing rigorous quality control measures and standardization processes. Registration and Certification: It will be easier to incorporate herb transdermal drug delivery systems into mainstream health care practices if clear regulations and procedures are developed for their registration and certification. In addition, criteria for safety, efficacy, and quality assurance need to be established.

Research on Herb-Drug Interactions and Safety
Herb-Drug Interactions: Herbal compounds delivered via transdermal systems may interact with conventional medications, but further research is needed to clarify these interactions. As a result, healthcare professionals and patients will be able to make informed decisions regarding concurrent use in order to prevent adverse effects and reduced efficacy. Long-term Safety Assessment: Studying the risks and benefits of herbal transdermal drug delivery systems for long periods of time will provide comprehensive data. Identifying rare or delayed adverse effects can be accomplished by monitoring patients over an extended period.

Education and Awareness
Healthcare Provider Training: In order for herbal transdermal drug delivery systems to become more widely used in clinical practices, healthcare providers must be educated and aware of their benefits and limitations. Curriculums in medicine and pharmacy must incorporate herbal medicine education.

Patient Education: The more information patients have about herbal transdermal drug delivery systems, their benefits, and the proper way to use them, the more likely they are to accept them. Making sure that patients are informed about indications, dosing, application methods, and possible side effects will enable them to make informed choices.

Sustainability and Ethical Considerations

Sustainable Sourcing: It is important to prioritize sustainable sourcing of herbal ingredients, cultivate and conserve herbs, and ensure fair trade in order to support ethical production and environmental preservation. Cultural Preservation: It is important to respect and protect traditional herbal medicine knowledge and practices. It is possible to bridge the gap between traditional wisdom and modern science by collaborating between traditional healers, scientists, and regulatory bodies.

CONCLUSION

A key finding of this review of herbal transdermal drug delivery systems (TDDS) is that they are effective at delivering targeted medications. TDDS herbals are advantageous because they are non-invasive, controlled, prolonged release, resistant to first-pass metabolism, have a reduced systemic side effect profile, can be tailored to patients' needs, and can enhance patient compliance. As a result of these advantages, herbal TDDS offers a promising alternative to conventional methods of treating respiratory conditions. In the treatment of pulmonary disorders, herbal TDDS can be an effective alternative. Herbal compounds can be delivered directly to the respiratory system to create targeted therapeutic effects, thereby reducing systemic side effects and improving treatment results. Herbal compounds release controlled and sustained amounts of compounds, which can increase their efficacy when treating respiratory symptoms like coughs, congestion, and bronchitis. Chronic respiratory conditions can benefit greatly from herbal TDDS, especially if long-term treatment is necessary. There are several areas in which herbal TDDS can be applied in the future for research and clinical applications. A further study is needed to optimize formulation design, increase skin permeation, and increase the efficiency in which herbal compounds are delivered to the skin. Nanoparticles, microneedles, and hybrid systems are just a few of the technologies that can be explored. Secondly, herbal products must be regulated and standardized in order to ensure their quality, safety, and efficacy. As part of this process, guidelines and safety assessments will be developed, and registration and certification procedures will be established that are specific to herbal TDDS. Additionally, further research is needed to determine the long-term safety, efficacy, and interaction between herbal TDDS and other drugs.

REFERENCES

1. Huarong S., Xinli G., Ruiqing L. Research progress of transdermal absorption of traditional Chinese medicine. Chin. Anim. Husb. Vet. Med. 2009;2018
2. Feng N. Chinese Medicine Transdermal Administration and Functional Cosmetics. China Medicel Technology; Beijing, China: 2019.
3. Huang S.-H., Lee C.-H., Wang H.-M., Chang Y.-W., Lin C.-Y., Chen C.-Y., Chen Y.-H. 6-Dehydrogingerdione Restrains Lipopolysaccharide-Induced Inflammatory Responses in RAW 264.7 Macrophages. J. Agric. Food Chem. 2014;62:9171–9179.
4. Zhang C., Zhang J., Wu Q., Xu B., Jin G., Qiao Y., Zhao S., Yang Y., Shang J., Li X., et al. Sulforaphene induces apoptosis and inhibits the invasion of esophageal cancer cells through MSK2/CREB/Bcl-2 and cadherin pathway in vivo and in vitro. Cancer Cell Int. 2019;19:1–10.
5. Chang Y.W., Wu Y.C., Huang S.H., Wang H.D., Kuo Y.R., Lee S.S. Autologous and not allogeneic adipose-derived stem cells improve acute burn wound healing. PLoS ONE. 2018;13:e0197744.

6. Kim C.-S., Kawada T., Kim B.-S., Han I.-S., Choe S.-Y., Kurata T., Yu R. Capsaicin exhibits anti-inflammatory property by inhibiting IkB-a degradation in LPS-stimulated peritoneal macrophages. Cell. Signal. 2003;15:299–306.

7. Chan T., Tomlinson B., Tse L., Chan J., Chan W., Critchley J. Aconitine poisoning due to Chinese herbal medicines: A review. Vet. Hum. Toxicol. 1994;36:452–455.

8. Gülçin İ., Büyükokuroğlu M.E., Oktay M., Küfrevioğlu Ö.İ. Antioxidant and analgesic activities of turpentine of PinusnigraArn. subsp. pallsiana (Lamb.) Holmboe. J. Ethnopharmacol. 2003;86:51–58.

9. Mayes S, Ferrone M. Fentanyl HCI patient-controlled iontophoretic transdermal system for the management of acute postoperative pain. Ann Pharmacother. 2006;40:2178–2186.

10. Sieg A, Guy RH, Delgado-Charro MB. Noninvasive and minimally invasive methods for transdermal glucose monitoring. Diabetes TechnolTher. 2005;7:174–197.

11. Morgan TM, Reed BL, Finnin BC. Enhanced skin permeation of sex hormones with novel topical spray vehicles. J Pharm Sci. 1998;87:1213–1218.

12. Williams AC, Barry BW. Penetration enhancers. Adv Drug Deliv Rev. 2004;56:603–618.

13. Smith EW, Maibach HI, editors. Boca Raton, FL: Taylor and Francis Group; 2006. Percutaneous Penetration Enhancers.

14. Bozdaganyan, M.E.; Orekhov, P.S. Synergistic Effect of Chemical Penetration Enhancers on Lidocaine Permeability Revealed by Coarse-Grained Molecular Dynamics Simulations. Membranes 2021, 11, 410.

15. Cho, C.W.; Shin, S.C. Enhanced transdermal delivery of atenolol from the ethylene-vinyl acetate matrix. Int. J. Pharm. 2004, 287, 67–71.

16. Dragicevic, N.; Maibach, H.I. Percutaneous Penetration Enhancers Physical Methods in Penetration Enhancement; Springer: Berlin/Heidelberg, Germany, 2017.

17. Kanikkannan, N.; Singh, M. Skin permeation enhancement effect and skin irritation of saturated fatty alcohols. Int. J. Pharm. 2002, 248, 219–228.

18. Ogiso, T.; Hata, T.; Iwaki, M.; TANINO, T. Transdermal absorption of bupranolol in rabbit skin in vitro and in vivo. Biol. Pharm. Bull. 2001, 24, 588–591.

19. Van Zyl, L.; Du Preez, J.; Gerber, M.; Du Plessis, J.; Viljoen, J. Essential fatty acids as transdermal penetration enhancers. J. Pharm. Sci. 2016, 105, 188–193.

RESEARCH ARTICLE

Investigation on Photodegradation Efficacy of Malachite Green Dye by Nickel Sulfide with Graphene Oxide (NiS/GO) Nanocomposite

G.Priyadharshini[1], D.Geetha[2]* and P.S.Ramesh[3]

[1]Research Scholar, Department of Physics, Annamalai University, Annamalai Nagar - 608 002, Chidambaram, Tamil Nadu ,India
[2]Associate Professor, Department of Physics, Annamalai University, Annamalai Nagar -608 002,Chidambaram, Tamil Nadu , India
[3]Associate Professor, Thiru Kolanjiappar Govt. Arts and Science College, Virudhachalam, Tamil Nadu, India.

*Address for Correspondence
D.Geetha
Associate Professor,
Department of Physics,
Annamalai University,
Annamalai Nagar -608 002,
Chidambaram, Tamil Nadu , India
E.Mail: geeramphyau@gmail.com

ABSTRACT

The nickel sulphide (NiS), graphene oxide (GO) and nickel sulphide with grapheme oxide (NiS/GO) have been synthesized. The graphene oxide (GO) was synthesized by modified Hummer's method and pure NiS, NiS/GO nanocomposite have been prepared by simple hydrothermal method. The nature of nanocomposite (NiS/GO) Viz., structural, morphological and physical properties were analyzed by TG-DTA, XRD, UV-DRS, FE- SEM/EDX, FT- RAMAN, PL and XPS analysis. FE-SEM measurements showed the presence of surface attachment of the NiS nanoparticles onto the graphene oxide. The NiS/GO nanocomposite integrates the high conductivity of GO and electrocatalytic activity of NiS in a single material. The effect of GO with NiS on degradation performance has been investigated. The effective photocatalytic degradation (86%) of organic dye malachite green (MG) was examined and reported. The degradation of MG with nanocomposite was found to be happening within 110 min.

Keywords: Nickel sulfide/ Graphene oxide, nanocomposite, photodegradation.

Priyadharshini *et al.,*

INTRODUCTION

Water pollution is the major environmental problem because it seriously endangers human health. In the recent years, emerging organic contaminants (EOC) will pollute the water resources that involve medicinal drugs, industrial wastes, personal care products and so on [1]. There are many kind of process that is available to purify the contaminated water bodies. The main process viz., physical process and chemical process which includes ultrafiltration, reverse osmosis, flocculation, ion- exchange and adsorption process, etc., Photocatalysis is one of the easier and low expense methods for purifying contaminated water bodies. Advanced Oxidation Process (AOP) will produce functional hydroxyl radicals which will be rapidly oxidizing carbon included dyes. On considering the metal sulphide nanocomposite in recent years; it has unique optical, magnetic, electronic and catalytic properties , hence researchers are performing their best in many tasks to enrich the photocatalytic behaviour of various semiconductors and metal oxides/ sulfides like ZnS, CdS, FeS, CuS, CoS, MnS, ZnO, SnO 2 , CrS, MgS and so on[2] . Among them, nickel sulfide catalyst is a well-known industrial application in hydrogenation reactions. It has efficient ionic conductivity due to oxygen vacancies . Nickel sulfide has wide bandgap (3.12 eV) which is lowering its catalytic process in the presence of natural sunlight irradiation; this is the most significant disadvantage for its photosensitivity . To overcome this issue the hybrid nanostructures of metal sulphide with conductive GO is chosen to enrich the degradation process .

Graphene oxide exhibits both P-type and n-type conductivity, in P- type it has oxygen high electro negativity compared to carbon, in n-type, the graphene covalent bond to electron donating nitrogen containing functional groups . GO that contains highest oxidation degree level has increased the energy of band gap and limiting the absorption level of the light and lowest photocatalytic activity with lower oxidation degree [3]. The photo degradation is attractive as it has a highest active radicals which is unsystematically and quickly decompose organic pollutants that will resulting in the production of hazardless products such as carbon dioxide and water molecules. On the surface of photocatalysts dye compounds will first adsorbed in which common reaction like oxidation and reduction will occur . This redox reaction happens due to the forced vibration activity of photogenerated holes in the valence band (VB) and electrons in the conduction band (CB) . Since, grapheme is an electron acceptor and transporter which can reduce the recombination rate of light that excite the electrons and donors in NiS . NiS/GO nanocomposite contains high activity and stability, graphene based metals have theoretical and experimental guidance. Also sulfide- graphene based materials are more potential than the oxide-graphene based transition metals [4]. In this paper, GO, NiS and NiS/GO nanocomposites were prepared and their photo degradation on organic dye malachite green (MG) under natural sunlight was investigated and the results were reported.

EXPERIMENTAL DETAILS
MATERIALS AND METHODS

The chemicals purchased from Sigma Aldrich Scientific company and are utilized without any further purification process. The chemicals purchased are graphite powder, nickel nitrate hexahydrate, thiourea, hydrogen peroxide, hydrochloric acid, potassium permanganate and so on.

Synthesis of NiS Nanoparticles
In a typical procedure, 1 mol of nickel nitrate hexahydrate and 3 mmol of sulfur were dissolved into 50 ml deionized water. The reaction mixture was stirred for about 2 hours to form an aqueous solution. Then the homogeneous mixture was kept in an autoclave at 180°C for about 12 hours to obtain a precipitate. Further, the above solution was cleaned with deionized water and ethanol to separate impurities. Then the above filtered sample was dried in a vacuum hot air oven at 45°C about 1 hour to obtain NiS nanoparticles. The concentration ratio is 1:1, 1:2 and 1:3 of nickel and sulfur source. When concentration of sulfur increases, new phase of nickel sulfide (Ni_7S_3) was occurred ue to more number of sulfur ions.

Priyadharshini *et al.,*

Synthesis of graphene oxide

Graphene oxide was prepared by modified Hummers method. First 10 ml of sulfuric acid (H_2SO_4) and 2ml of phosphoric acid (H_3PO_4) in the volume ratio of 7:1 was mixed and stirred for an hours, while stirring 0.1g of graphite powder was added and then 1.2g of potassium permanganate ($KMnO_4$) was included pinch by pinch into the solution while stirring. After the solution became dark green, to eliminate excess $KMnO_4$, hydrogen peroxide (H_2O_2) was added dropwise, exothermic reaction occurs and the solution is said to cool down. Then 5ml of hydrochloric acid and 10 ml of deionized water was added for 8 hours the solution is centrifuged and kept in oven for dry(2 hours) at 80 and the powder sample is obtained.

Synthesis of NiS/GO nanocomposites

Nickel nitrate hexahydrate of 1 mol was mixed with 2 mol of sulfur source of thiourea in 50 ml of deionized water. After the GO was sonicated by distilled water, 60mg of GO was included into the above suspension. The above homogeneous mixture was allowed to stir for about 2 hours. After stirring, the above suspension was kept in an autoclave heated at 130 o C for about 18 hours. The obtained black precipitate was centrifuged and filtered. Finally, the composite NiS/GO was allowed to dry in a hot air oven at 60 o C for about 2 hours.

Characterization

The thermal analysis of the sample was studied by TG-DTA using thermal analyser NETZSCH-STA 449F3 Jupiter. The crystal structure was made by Xpert pro-PAnalytic instrument. The morphology of the sample was observed by FESEM/EDAX (model CARL ZEISS-SIGMA 300). The optical nature of the samples were analysed by UV-DRS and PL. FT-Raman was taken by imaging spectrograph STR 500mm Focal length laser Raman spectrometer to find the Raman spectra of the sample. The chemical composition of the sample was characterised using Thermo fisher instrument for XPS analysis.

Photocatalytic measurement

The photocatalytic degradation examination of NiS/GO nanocomposites was determined on malachite green . The concentration was fixed to be 10 -4 M, which is mixed in 400ml distilled water for the process of degradation [5]. In a 100ml beaker of a dye solution, 50ml of dye solution was taken and about 2 mg of catalyst was added into it to make a photocatalytic process . The dye solution made are stirred continuously for about 60 minutes and the collected test solutions of malachite green dye was analyzed by the UV- Visible.

RESULT AND DISCUSSION

Thermogravimetric study (TG-DTA)

To know the phase transformation/weight loss of the nanoparticles, thermogravimetric differential thermal analysis (TG-DTA) was performed. First weight loss of about 5.6% was observed below 120o C represents the evaporation of water in the prepared sample and endothermic reaction exhibits the dehydration of the sample. The second weight loss of about 5.6% between 120o C and 300o C indicates the excess sulfur, combustion of carbon, and other impurity elements that are excluded from the precursor. The third weight loss about 5.5% in the TGA curve at 300 o C to 420oC resulting the removal of sulfur. From the TG-DTA curve, the weight loss of 2.2 % including the range of temperature about 400oC to 500oC is recognized. A weight loss of about 1.1% is concluded from a TG-DTA curve at a temperature range below 420 o C [6]. The NiS is converted to NiO at a temperature weight loss of above 500 o C at 15.3% which is an oxidation state of NiS. The molecular weight for NiS is 90.75 g mol -1 and for NiO is 74.69 g mol -1 . This shows that at certain temperature (& 500oC) sulfur is converted to oxide form. The change in mass of a sample in a fractional second converts the NiS to NiO around 17.8%. The mass change from the figure strongly denotes the change of nickel sulfide to nickel oxide.

Structural analysis (XRD)

To analyse the phase structure of the prepared pure nickel sulfide (NiS),grapheme oxide(GO) and nickel sulfide/graphene oxide (NiS/GO) nanocomposite, the X-ray diffraction analysis technique was adopted and presented in Fig 3.(a to c) . Fig. 3(a) confirms the graphene oxide,3(b) confirms the nickel sulfide nanostructures and 3(c) shows that the nanostructures of composite nickel sulfide/graphene oxide(NiS/GO)[7]. A strong diffraction peak at (001) corresponds to GO which is located at 11.5 o shows the formation of GO [8]. The diffraction peaks at 2 values 29 o , 34 o , 45 o , 53 o are assigned to the plane values (015), (303), (306), (330) (JCPDS Card no:76-2306) for pure NiS and composite NiS/GO respectively. Cornflake like structure (NiS and NiS/GO) of nanoparticles were observed. The crystallite size of the sample is calculated by Debye Scherrer formula. The average crystallite size was 30nm.Due to the low crystallinity and low content of GO, there are no obvious diffraction peaks corresponding to GO observed in the XRD spectra of the NiS/GO nanocomposite.

Thus, the Raman spectra of the NiS/GO nanocomposite were collected because Raman spectroscopy is vital technique for investigating carbon-based materials. The Raman spectra of the NiS/GO nanocomposites and pure GO were collected, shown in Fig.3. Two characteristic peaks corresponding to the carbon based material can be observed in all of the Raman spectra, which are designated as the D (1357 cm -1) and G (1589 cm -1) peaks. The D peak originates from the degree of defects and disorder in the carbon based materials, while the G peak is mainly related to the internal vibrations of the carbon atom.

Morphological analysis (FE-SEM)

The surface morphology of NiS/GO nanocomposite was evaluated through FESEM. Fig. 4(a) shows the cornflake like structure of NiS nanoparticles, the grain size was about 80 nm[9]. Fig 4(b) shows the FESEM image of cornflake like shape with 60 nm size for NiS/GO nanocomposite FESEM image shows a thick and rough structure indicating the high degradable activity. The powder sample were adhered on carbon tape and a stub was exposed to plasma coating inside a sputter chamber for coating. The coating material contains gold and palladium in 80:20 ratios. After coating, a 20kV potential was used to excite electrons from the surface of samples. An average 45mm area was used to get FE-SEM image of materials. NiS/GO illustrate bit intensified patches which could have been localized because of Ni 3d 8 of NiS/GO as there is no proper split of 3d 3/2 and 3d 5/2 electrons. Hence these electronic energies might have induced the localized activities which are expressed in the FESEM images. The cloudy flasky surfaces with a larger magnification infer anchoring of NiS/GO nanocomposites with grain size of 60nm.

Elemental analysis (EDX)

The electron dispersive X-ray spectroscopy (EDX) for NiS and NiS/GO are given in Fig. 4(a) and (b). An elemental composition of (Ni=64.70%) and (S=35.30%) peaks and (Ni=36.46%), (S=23.26%), (C=21.49%) and (O=18.79%) peaks reveals the presence of pure NiS and NiS/GO nanocomposite respectively [10].

Absorption studies (UV-Vis DRS)

Fig. 5(a to d) shows UV-DRS absorption spectra of NiS/GO. The samples were dispersed in water by sonication @ 3 KHz. Fig. 5(b) depicts a higher absorption for NiS/GO due to stronger interactions of unengaged electrons of groups of GO with UV-Vis light. The interaction of sp 2 and lone pair electrons of groups and of GO both accommodate the NiS nanoparticles within the GO exfoliated sheets. Excess lone pair electrons of –OH, -O, -C, =O and –COOH are comparatively engaged and interact with photons at a lower energy. The h from UV strikes sp 2 electrons to excite them to a high energy state causing positive holes (oxidation state) with h + (positive hole) charge at it's native orbital and negative charge (reduced state) or negative holes (e -) at excited states, which may reduces dye molecule. The catalysis by creating positive hole by exciting electron e - , to negative holes a conduction band attains a higher energy level compared to valance band with lower energy level [11]. The main principle of UV-DRS is that some of the light will undergoes specular reflections at the powder surface of the sample [12]. The sample has a strong absorption of light that has visible ranges from 390 and 700 nm for pure NiS and for NiS/GO composite same 390 and 700 nm have a strong absorption of light that is showed in the figure [13]. The band gap energy for UV-DRS can be

Priyadharshini *et al.*,

calculated by a kubelka-munk model. The band gap energy for pure Nis is about 2.3eV and for composite NiS/GO is about 2.9eV. The below figures shows the UV-DRS spectrum and energy band gap for pure nickel sulfide (NiS) and nickel sulfide/graphene oxide (NiS/GO) nanocomposite.

Emission studies (PL)

The photoluminescence study room temperature shows the excitation wavelength at 362 nm. The broad peak appeared at 351 to 372 nm which indicates that the recombination of photogenerated electron-hole pairs[14]. For NiS/GO nanocomposite the excitation wavelength is at 360 nm and the broad peak appeared at 350 to 380 nm[15]. Interestingly, the emission intensity was gradually decreases after adding graphene oxide(GO) denoting the recombination of photogenerated electron-hole pairs are covered by GO. This may enhance the catalytic performance. The low brightness of the peaks are occurred in the infrared region that are due to the gap present in between the localized states of impurities and the imperfections. It is one of the non-contact and non-destructive methods for the probing materials .

FT-RAMAN analysis

Raman spectroscopy is one of the main characterization technique used to determine the organic based compounds like carbon, graphene and its hybrid. Figure 7(a) represents the presence of nickel, sulfide peaks and Figure7(b) denotes the presence of nickel, sulfide, carbon and oxygen peaks [16]. But the peak at 1400 cm -1 to 1581 cm -1 will represent the charge transfer between carbon and nickel sulfide [17]. FT-RAMAN analysis shows the D and G bands of characteristic peaks appears at 1105.2 and 1418.3 cm -1 [18]. The I D /I G value is 1.02 for NiS/GO nanocomposite which is greater than pure NiS.

X-ray photoelectron spectroscopy

XPS spectra determine chemical composition and oxidation states of NiS/GO nanocomposite having Ni, S, C and O infer an authenticity of NiS/GO synthesis.

XPS for NiS

The doublet peaks of two spin orbits of nickel (Ni_2p_3) has a binding energy of 854.19ev were obtained for Ni2p spectrum. For sulfur (S_2p) the peak is obtained at 163.2ev for pure NiS. This shows that XPS analyses denote the NiS formation for photocatalytic property [19]. The below figures for XPS denotes that for pure NiS, elements like Nickel and sulfur are present.

XPS for NiS/GO

The peaks for NiS/GO XPS spectrum includes some elements such as nickel (Ni_2p), sulfur (S_2p), carbon (C_1s) and oxygen (O1s). The binding energy for NiS/GO nanocomposite corresponds to 854.10 eV for nickel (Ni2p), 532.31 eV for sulfur (S2p), 284.92 eV for carbon (C1s) and 162.27 eV for oxygen (O1s). While NiS on GO, changes in D, G bands and 2D intensity infer variable exfoliations of nanomaterials. Also the (-COOH, -OH, -O, and =CO) could be replaced with other groups to dope GO to study pattern of binding energies. Binding energy and electron spin of 3p of Ni is at 75 eV. The Ni2p binding energy is at 854.10eV. A lowering intensity of C1s for C and O1s for O atoms was observed.

Photocatalytic studies

To evaluate the degradation efficiency time of malachite green dye, 5mg of catalyst sample was added into the 0.1g solution of MG dye, the setup was kept under natural sunlight and was stirred continuously . The degradation time for MG dye was fixed for about 2 hours. The UV-VIS absorbance peaks for malachite green dye in the absence of catalyst was 320,427 nm. For UV analysis, 10 ml of dye sample with catalyst was collected for every 15 minutes. The absorption and absorbance plots peaks from 625 to 695 nm shows the 86% degradation of dye solution by lowering the concentration (Fig. 9(a) and (b))[20]. The π-π electrostatic interactions affect reduction by GO and NiS/GO as GO has several hydrophilic groups that faster MG reduction. The –COOH groups exist at edges of GO layers and –O and –OH groups are incorporated in layer, which results in a slightly acidic or negatively charged surfaces to faster reduction rate of positively charged MG molecule. The interaction of MG and GO occurs due to stronger electrostatic

Priyadharshini *et al.*,

forces which are neutralized by h + and e - holes. The main components of NiS-GO are C-C and C=C bonds which contribute to abundant π electron clouds to NiS-GO, considering O-C=O and –OH. A double bond of NiS (Ni=S) interacts with C-C and C=C bonds of GO to conjugate and stabilize a resultant structure for MG reduction. MG and NiS-GO both adjoin together due to their π-π interactions. Thus a consumption of energy of a molecules induces stronger reduction activities which could be extended to their π conjugated rings.

Photocatalyst (NiS/GO) + hγ →h$^+$ VB +e$^-$ CB
h$^+$ VB + e$^-$ CB → energy (heat)
H_2O + h$^+$ VB → OH (hydroxyl radical + H$^+$
O_2 +e$^-$ CB → O_2/ Super oxide radical
OH + pollutant → intermediate → H_2O +CO_2
O_2 + pollutant → intermediate →H_2O + CO_2

CONCLUSION

Ecofriendly stoichiometry of oxidizing mixture using simple methodology to prepare GO and NiS/GO were adopted. NiS/GO nanocomposite were synthesized by hydrothermal route successfully and the corresponding structural behaviour are confirmed from TG-DTA, XRD, UV-Vis, FESEM/EDX and XPS techniques. The XRD and FESEM studies revealed that well crystalline cornlike shape of NiS/GO with average size of about 30 nm by XRD and 60nm from FE-SEM, which is uniformly distributed over the surface of GO. The synthesized highly active sites structures of NiS and incorporating with excellent electrical conductivity (graphene oxide) can provide the fast electron transport matrix. The photodegradation result of NiS/GO on organic dye malachite green (MG) in the uniform reaction condition was observed 86% with 110 minutes. Based on the observed results it may be concluded that the prepared NiS/GO nanocomposite have large amount of charge separation and high surface area. Further more, the proposed method could be a favourable approach to the synthesis of other metal sulfides with graphene oxide.

Conflict of interest
The author mentions there is no conflict of interest in this research paper and agreed to publish this manuscript in this journal.

ACKNOWLEDGEMENT

REFERRENCES

1. Manikandan, V., Elancheran, R., Revathi, P., Suganya, P., & Krishnasamy, K. (2020). Efficient photocatalytic degradation of crystal violet by using graphene oxide/nickel sulphide nanocomposites. Bulletin of Materials Science, 43(1), 1-10.
2. Irshad, M. A., Nawaz, R., ur Rehman, M. Z., Adrees, M., Rizwan, M., Ali, S., ... & Tasleem, S. (2021). Synthesis, characterization and advanced sustainable applications of titanium dioxide nanoparticles: A review. Ecotoxicology and environmental safety, 212, 111978.
3. Zhang, S., Ueno, K., Dokko, K., & Watanabe, M. (2015). Advanced Energy Materials. Go to reference in article.
4. Dai, H., Yuan, X., Jiang, L., Wang, H., Zhang, J., Zhang, J., & Xiong, T. (2021). Recent advances on ZIF-8 composites for adsorption and photocatalytic wastewater pollutant removal: Fabrication, applications and perspective. Coordination Chemistry Reviews, 441, 213985.
5. Wang, Z., Fan, J., Cheng, B., Yu, J., & Xu, J. (2020). Nickel-based cocatalysts for photocatalysis: Hydrogen evolution, overall water splitting and CO_2 reduction. Materials Today Physics, 15, 100279.

6. Olivas, A., Cruz-Reyes, J., Petranovskii, V., Avalos, M., & Fuentes, S. (1998). Synthesis and characterization of nickel sulfide catalysts. Journal of Vacuum Science & Technology A: Vacuum, Surfaces, and Films, 16(6), 3515-3520.

7. Huang, L., Hou, H., Liu, B., Zeinu, K., Yuan, X., Zhu, X., ... & Yang, J. (2017). Phase- controlled solvothermal synthesis and morphology evolution of nickel sulfide and its pseudocapacitance performance. Ceramics International, 43(3), 3080-3088.

8. Anwer, H., Mahmood, A., Lee, J., Kim, K. H., Park, J. W., & Yip, A. C. (2019). Photocatalysts for degradation of dyes in industrial effluents: Opportunities and challenges. Nano Research, 12(5), 955-972.

9. Alagiri, M., Ponnusamy, S., & Muthamizhchelvan, C. (2012). Synthesis and characterization of NiO nanoparticles by sol–gel method. Journal of Materials Science: Materials in Electronics, 23(3), 728-732.

10. Mei, X., Meng, X., & Wu, F. (2015). Hydrothermal method for the production of reduced graphene oxide. Physica E: Low-dimensional Systems and Nanostructures, 68, 81-86.

11. Harish, S., Naveen, A. N., Abinaya, R., Archana, J., Ramesh, R., Navaneethan, M., ... & Hayakawa, Y. (2018). Enhanced performance on capacity retention of hierarchical NiS hexagonal nanoplate for highly stable asymmetric supercapacitor. Electrochimica Acta, 283, 1053-1062.

12. Ghosh, S., Kumar, J. S., Murmu, N. C., Ganesh, R. S., Inokawa, H., & Kuila, T. (2019). Development of carbon coated NiS2 as positive electrode material for high performance asymmetric supercapacitor. Composites Part B: Engineering, 177, 107373.

13. Karthikeyan, R., Navaneethan, M., Archana, J., Thangaraju, D., Arivanandhan, M., & Hayakawa, Y. (2014). Shape controlled synthesis of hierarchical nickel sulfide by the hydrothermal method. Dalton Transactions, 43(46), 17445-17452.

14. Huang, Z., Wang, L., Wu, H., Hu, H., Lin, H., Qin, L., & Li, Q. (2022). Shape-controlled synthesis of CuS as a Fenton-like photocatalyst with high catalytic performance and stability. Journal of Alloys and Compounds, 896, 163045.

15. Luo, X., Hu, H., Pan, Z., Pei, F., Qian, H., Miao, K., ... & Feng, G. (2020). Efficient and stable catalysis of hollow Cu9S5 nanospheres in the Fenton-like degradation of organic dyes. Journal of hazardous materials, 396, 122735.

16. Bibi, S., Ahmad, A., Anjum, M. A. R., Haleem, A., Siddiq, M., Shah, S. S., & Al Kahtani, A. (2021). Photocatalytic degradation of malachite green and methylene blue over reduced graphene oxide (rGO) based metal oxides (rGO-Fe$_3$O$_4$/TiO$_2$) nanocomposite under UV-visible light irradiation. Journal of Environmental Chemical Engineering, 9(4), 105580.

17. Wang, Y., Zhang, W., Guo, X., Liu, Y., Zheng, Y., Zhang, M., ... & Zhang, T. (2020). One-step microwave-hydrothermal preparation of NiS/rGO hybrid for high-performance symmetric solid-state supercapacitor. Applied Surface Science, 514, 146080.

18. Khan, M. A., Hussain, W., Tufail, K., Sulaman, M., Ayub, A. R., Khan, W. A., & Li, H. (2021). Relative study of Ni sulfides synthesized from single and multisource precursors for photocatalytic and battery applications. Energy Reports, 7, 7615-7627.

19. Patil, A. M., Lokhande, A. C., Shinde, P. A., Kim, J. H., & Lokhande, C. D. (2018). Vertically aligned NiS nano-flakes derived from hydrothermally prepared Ni (OH) 2 for high performance supercapacitor. Journal of energy chemistry, 27(3), 791-800.

20. Wang, Y., Zhang, W., Guo, X., Liu, Y., Zheng, Y., Zhang, M., ... & Zhang, T. (2020). One-step microwave-hydrothermal preparation of NiS/rGO hybrid for high-performance symmetric solid-state supercapacitor. Applied Surface Science, 514, 146080.

Priyadharshini *et al.,*
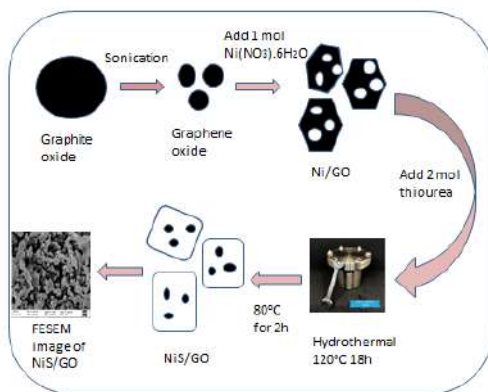
Fig.1. Graphical Representation of NiS/GO Nanocomposite
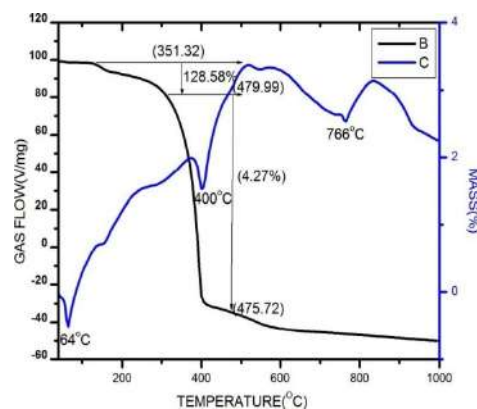
Fig.2. TG-DTA curve of NiS/GO nanocomposite from 50 °C to 1000 °C
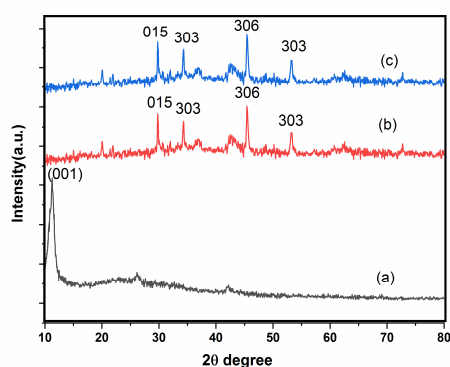
Fig.3. X- ray diffraction analysis of (a) GO, (b) pure NiS and (c) NiS/GO nanocomposite
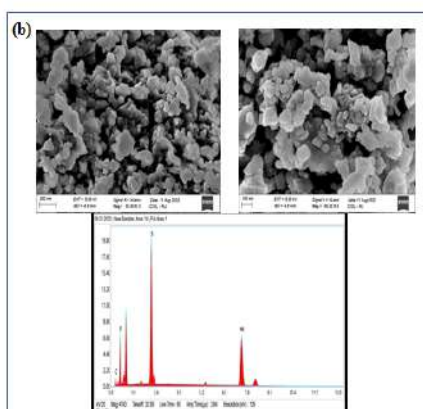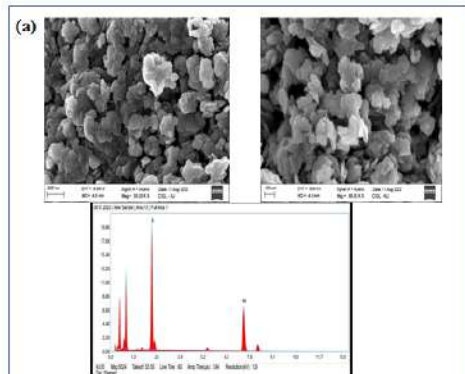
Fig.4. (a) FE-SEM/EDX image of NiS nanostructure
(b) FE-SEM/EDX image of NiS/GO Nanocomposite

Priyadharshini *et al.,*
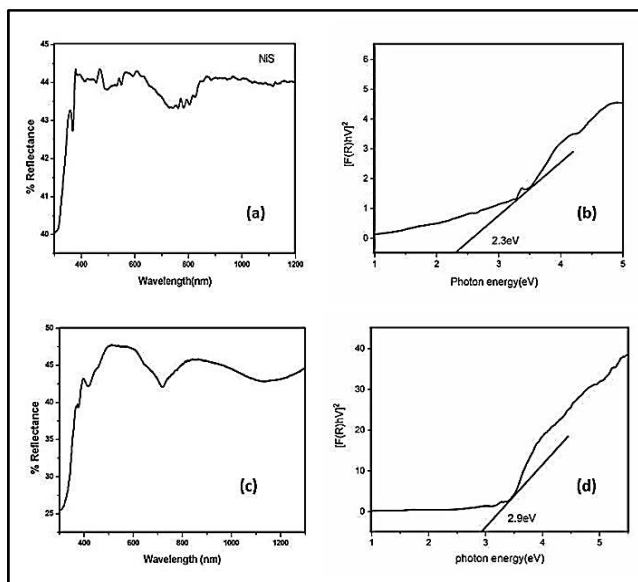
Fig.5. (a) UV-Vis DRS spectra of NiS (b) Kubela-munk model of NiS (c) UV-Vis DRS spectra of NiS/GO (d) Kubelka munk model of NiS/GO
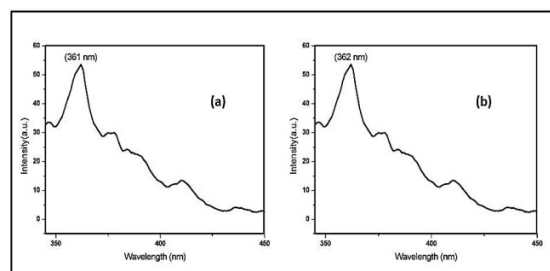
Fig.6. Photoluminescence spectra of (a) pure NiS (b) NiS/GO nanocomposite
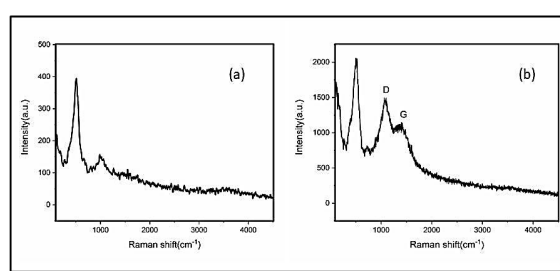
Fig.7. FT-Raman spectra of (a) pure NiS (b) NiS/GO nanocomposite
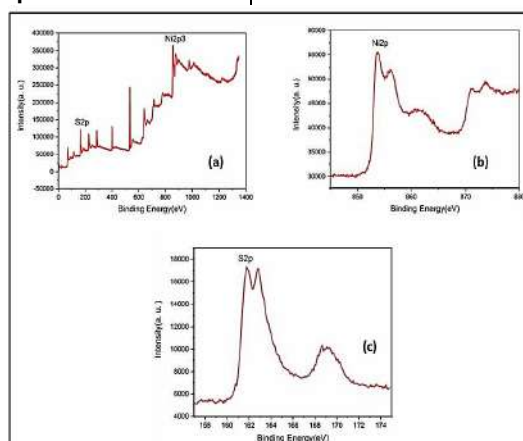
XPS for Fig.8. (a) XPS survey spectra of NiS (b) Ni2p spectra (c) S2p spectra

Priyadharshini *et al.,*
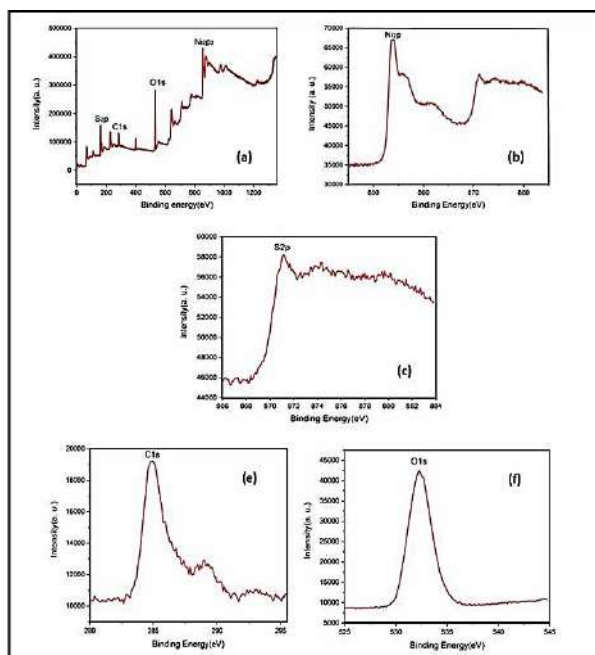
Fig.9. (a) XPS survey spectra of NiS/GO (b) Ni2p spectra (c) S2p spectra (d) C1s

spectra (e) O1s spectra
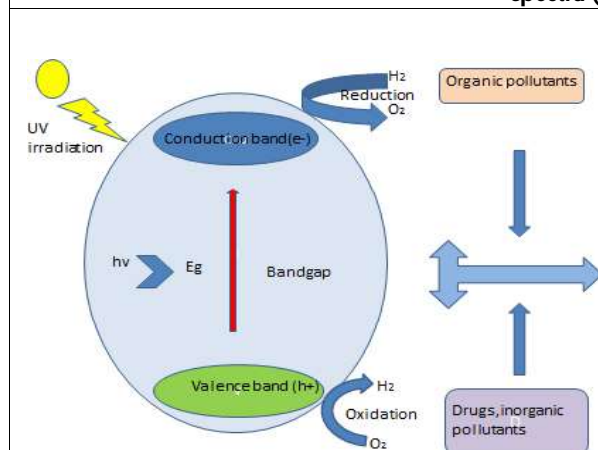
Fig. 10. Photodegradation mechanism
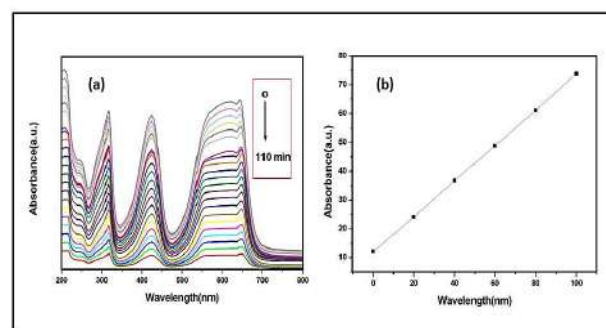
Fig.11 (a) Absorption spectra of malachite green degraded by NiS/GO Nanocomposite
with time hydrothermal method under natural sunlight tradiation
(b)Kinetic analysis of photodegradation of malachite green dye catalyzed by NiS/GO

Nanocomposites

RESEARCH ARTICLE

Impact of Religious Teachings in Causing Transition among Older Adults

Dakshita Pandey[1]* and Rajat Kanti Mitra[2]

[1]Student, M.A Clinical Psychology 2021-2023, Amity University, Noida, Uttar Pradesh, India
[2]Amity University, Noida, Uttar Pradesh, India

*Address for Correspondence
Dakshita Pandey
Student,
M.A Clinical Psychology 2021-2023,
Amity University, Noida,
Uttar Pradesh, India
E.Mail: dakshitapande@gmail.com

ABSTRACT

This qualitative study explored the impact of Hindu religious teachings on older adults' well-being and transitions. In-depth interviews were conducted with 20 religiously practicing participants aged 60 and above. Thematic analysis identified key themes, revealing that religious teachings provided guidance and support during life transitions. Participants found solace and purpose in teachings emphasizing acceptance, resilience, and finding meaning in changes. Religious practices positively impacted their spiritual well-being, overall health, and mental well-being. Personal religious experiences deepened faith and fostered compassion and empathy. Participants anticipated continued guidance from their religious beliefs in future challenges. The findings highlight the transformative power of religious teachings, contributing to understanding the role of Hinduism in older adults' well-being and transitions.

Keywords: Hinduism, religious teachings, older adults, life transitions, well-being, coping strategies, thematic analysis.

INTRODUCTION

Aging is a transformative phase of life that presents individuals with unique challenges and opportunities. As people grow older, they experience physical, cognitive, social, and emotional changes that require adaptation and resilience. In the face of these transitions, many individuals turn to religious teachings for guidance, support, and a sense of purpose. This study aims to explore the impact of religious teachings on the transition experiences and well-being of older adults. Religion has long been recognized as a fundamental aspect of human existence, providing individuals

with spiritual beliefs, practices, and values that shape their worldview. Religious teachings encompass a wide range of subjects, including the nature of the divine, the meaning and purpose of life, moral values, and rituals that express and strengthen religious beliefs. These teachings often serve as a compass, guiding individuals through life's challenges and helping them find direction, meaning, and a sense of community. Scholars and psychologists have approached religion from various perspectives, offering insights into its significance in the lives of individuals. Some view religion as a source of solace and comfort, providing a framework for coping with existential fears and uncertainties. Others see it as a way to explore one's psyche and spiritual nature, offering a path to self-realization and transcendence. Religion is also regarded as fulfilling basic human needs for belonging, purpose, and connection with something greater than oneself.

In the context of aging, religious teachings can play a crucial role in helping older adults navigate the transitions and challenges they encounter. The process of aging often involves physical health changes, cognitive decline, social isolation, financial constraints, and care giving responsibilities. Older adults may grapple with questions of purpose, existential concerns, and the search for meaning as they face their own mortality. Religious teachings have the potential to address these issues by providing guidance on health and wellness, offering a sense of belonging and community, fostering spiritual growth and self-realization, and instilling values of service and care giving. Within the realm of religious teachings, Hinduism stands as one of the world's oldest and most diverse religions. Hinduism encompasses a broad spectrum of beliefs, practices, and rituals that embrace various aspects of an individual's social and personal existence. Central to Hinduism is the quest for spiritual freedom, achieved through the practice of righteousness (dharma), the pursuit of prosperity (artha), the fulfillment of desires (kama), and ultimately, liberation (moksha). Hinduism acknowledges the existence of multiple deities as representations of the supreme reality known as Brahman. The religion encompasses rituals, ceremonies, and practices such as yoga, meditation, and acts of worship and sacrifice.

Given the multifaceted nature of Hindu religious teachings and their potential relevance to aging and transition, it is essential to explore their impact on the well-being of older adults. This study aims to investigate how Hindu religious teachings influence the transition experiences and well-being of older adults. We will examine the ways in which religious teachings are incorporated into the lives of older Hindus, their effects on physical and mental well-being, the role of religious communities and support networks, and the ways in which religious teachings provide guidance and meaning during the aging process. By shedding light on the impact of religious teachings on transition and well-being among older adults, this study aims to contribute to a deeper understanding of the role of religion in the lives of individuals as they age. The findings may have implications for healthcare providers, policymakers, and religious communities in supporting older adults through the challenges and opportunities of aging. Ultimately, this research endeavors to enhance our knowledge of the complex interplay between religion, aging, and well-being, and pave the way for more holistic and culturally sensitive approaches to supporting older adults in their transitions.

Several studies have examined various aspects of the relationship between religion, spirituality, and the well-being of older adults. For instance, Zheng, Chan, & Zhang (2023) investigated the influence of personal value, motivation, transformation, and behavioral intention on spiritual tourism, finding positive associations with spiritual tourism in their study on Tibet. Similarly, Kenkmann & Burkard (2022) explored the experiences of older individuals during the Covid-19 pandemic, highlighting how alternative formats, such as the cemetery as a meeting point, provided solace for churchgoers. Kim, Ng, & Kim (2021) found that religious activities promoted social integration and emotional well-being among older Korean immigrants in the United States. Additionally, Eschler, Edwards & Gruenewald (2021) conducted a systematic review, underscoring the role of religion and spirituality in successful aging by providing purpose, social connectedness, and coping mechanisms during life transitions. Ano &Vasconcelles (2021) conducted a meta-analysis, revealing that positive religious coping strategies were associated with better mental health outcomes for older adults. Furthermore, studies by Kim, Pargament& Chen (2021), Jadhav& Mali (2021), Bhattacharya & Kar (2021), DeKoekkoek, Lindholm, Jansen, &Postmus (2021), and Holley, Frye, Wilson, & Vail (2021) demonstrated the positive effects of religious involvement and practices on well-being, social support, resilience, mental health, loneliness reduction, and physical function among older adults. These studies collectively

Dakshita Pandey and Rajat Kanti Mitra

contribute to our understanding of how religion and spirituality play a significant role in the lives of older individuals, fostering well-being and enhancing various aspects of their lives. Overall, the review of literature on the impact of religious experiences in causing transitions among older adults suggests that religious involvement can have positive effects on well-being outcomes, such as social support, health, life satisfaction, and resilience to stress. The exact mechanisms by which religious involvement promotes these outcomes may differ by cultural context, race, and individual differences in religious expression. Moreover, the literature highlights the importance of considering spirituality more broadly, beyond traditional religious practices, in understanding its impact on well-being in older adults. Further research is needed to better understand the complex relationship between religious experiences and transitions in later life.

During 2022 and 2023researches on religion were impacted by onset of covid-19. Pre-COVID religious-based research studies primarily focused on the impact of religious beliefs, practices, and participation on various aspects of well-being, including mental health, physical health, social support, and coping mechanisms. These studies aimed to understand the role of religion in promoting positive outcomes among older adults. With the onset of the COVID-19 pandemic, religious communities around the world faced significant disruptions. Places of worship were temporarily closed, religious gatherings and events were cancelled or moved online, and religious practices were modified to adhere to social distancing guidelines. The impact of the pandemic on religious practices and the well-being of older adults has likely influenced the direction of religious-based research. Post-COVID studies may have started exploring topics such as the effects of religious coping strategies during the pandemic, the role of online religious communities in promoting social connectedness, the challenges faced by older adults in maintaining religious practices during lockdowns, and the psychological and social implications of the temporary suspension of religious services.

METHODOLOGY

AIM
The aim of the study was to explore the impact ofHindu religious teachings on older adults.

OBJECTIVE
1. To identify the themes that explains the impact of religious teachings on the well-being of older adults.
2. To develop a framework that captures the complex and nuanced ways in which older adults use religious teachings to cope with transitions.

RATIONALEOF STUDY
This study highlights the potential benefits of religion teachings for older individuals, including improved health, coping skills, social support, and societal engagement. However, there are limitations in the existing literature that call for further research. The current literature predominantly relies on quantitative analysis, while a qualitative approach could provide deeper insights into religion, spirituality, belief, and positive aging. Additionally, there is a lack of studies focusing on Hinduism, despite its prevalence in India. Furthermore, the link between religion teachings and transitions in aging has not been extensively explored. Given the aging population and healthcare challenges, understanding the role of religion, spirituality, and belief in healthy aging becomes increasingly important. This research aims to qualitatively investigate this topic in the lives of older individuals in India and provide recommendations for future action and research based on the findings.

LOCALE OF THE STUDY
The study took place in Delhi's parks and a yoga and meditation center, focusing on older adults practicing Hinduism. Interviews were conducted in a private room at the center, ensuring confidentiality. Participants were selected through personal outreach to eligible community members.

Dakshita Pandey and Rajat Kanti Mitra

DESIGN

The study employed a qualitative research design with open-ended questions to explore the impact of Hindu religious teachings on transitions among older adults. Data was collected through semi-structured interviews with participants, using open-ended questions that allow for in-depth exploration of their experiences, perceptions, and attitudes towards religious teachings and transitions. The interviews was conducted face-to-face or via telephone, and was audio-recorded with participants' consent. The study would recruit a purposive sample of older adults (aged 60 and above) who self-identify as practicing members of a religious community. The analysis of the study involved qualitative content analysis. The analysis was divided into three parts- organization of data, analysis of data and interpretation of data.

SAMPLE

The study aimed to recruit 20 older adults aged 60 and above who self-identified as practicing members of a religious community. Inclusion criteria required participants to have experienced a significant life transition in the past ten years, be willing to participate in a semi-structured interview in English or Hindi, and able to provide informed consent. Exclusion criteria included the inability to provide informed consent, communicate effectively in English or Hindi, or currently experiencing a mental or physical health condition that could hinder participation. Participants were recruited through outreach to religious organizations, community centres, advertising, and referrals. Confidentiality was maintained by assigning case numbers. The study included 8 females and 12 males, with ages ranging from 60 to 75.

TOOL USED

The data collected from the interviews with older adults were transcribed verbatim and subjected to thematic analysis. This involved identifying and coding themes and sub-themes that emerged from the data, and developing a coding framework to capture the key dimensions of the participants' experiences. The analysis was carried out by the researcher and a second coder to ensure credibility. Ethical guidelines were followed, including obtaining informed consent, maintaining confidentiality and anonymity, and obtaining ethical approval from the institutional review board.

An interview schedule was constructed to gather qualitative data, consisting of 10 open-ended questions divided into two sections, the first section being "Introduction and their changes in religious beliefs/ practices during transition" and the second section focused on "Transition experiences and coping up with challenges of old age". The questions aimed to explore participants' experiences and perceptions of how religious teachings influenced their transitions and coping with challenges in old age. The interview schedule underwent expert review (expert rating was done under 4 experts) and feedback from professionals in gerontology and religious studies, resulting in modifications to improve clarity and relevance. Thematic analysis was used to analyze the interview transcripts, identifying patterns, themes, and categories in the data, enhancing the credibility of the findings.

PROCEDURE

The research began with determining the aim, objectives of the study. Immediately after that it was determined what the target population would be for the study. Potential participants were identified through purposive sampling techniques, such as contacting religious organizations or community centres that serve older adults. Participants who express interest in the study were screened for eligibility criteria, such as age and self-identification as a practicing member of a religious community. Prior to data collection, participants were provided with an informed consent form that outlines the purpose of the study, the procedures involved, and their rights as research participants. Participants had the opportunity to ask questions and to withdraw their consent at any time. Semi-structured interviews were conducted with participants, either in person or via telephone, depending on their preference and accessibility. The interviews were audio-recorded with participants' consent and will last from 6 minutes to 30 minutes. The interviews followed a flexible, conversational format that allows participants to share their experiences and perceptions of religious teachings and transitions. The audio recordings will be transcribed verbatim, and the data will be analyzed using thematic analysis. The analysis will involve identifying and coding themes and sub-

63845

themes that emerge from the data, using both inductive and deductive approaches. The analysis will be conducted by the researcher and a second coder to ensure credibility.

QUALITATIVE ANALYSIS METHODS

Thematic analysis is a qualitative research method used to identify and analyze patterns or themes in interview data. The process involves transcribing the interviews, familiarizing oneself with the data, assigning codes to capture key ideas, collating codes into broader themes, reviewing and refining the themes, and finally writing up the results. It is a subjective approach that relies on the researcher's interpretation of the data to uncover meaningful insights.

ANALYSIS OF RESULTS

This study explored the impact of Hindu religious teachings on the transition process of older adults. Thematic analysis of interviews with 20 religious participants aged 60 and above identified ten key themes.

TABLE 2 indicates all the themes along with the sub- themes and the frequency that particular sub theme was stated amongst all the individuals.

Themes & Sub-themes extracted from the interview responses

RELIGIOUS PRACTICES

The significance of religious practices in the transition process of older adults was emphasized by participants in this study. Practices such as chanting mantras, practicing yoga, engaging in meditation, worshiping, and fasting were seen as providing structure, guidance, and a connection to faith. Participants assigned scores to each practice, indicating their frequency or importance. Yoga and meditation received high scores, highlighting their role in physical and mental well-being and spiritual connection. Worshipping/praying received the highest score, underlining its significance in religious practices. Other practices mentioned included fasting, attending spiritual discourses, celebrating festivals, and undertaking pilgrimages. These scores provide an overview of the prominence of each practice in the participants' lives, demonstrating their role in navigating life transitions.

RELIGIOUS BELIEF

The religious beliefs of the participants played a significant role in shaping their transition experiences. Beliefs related to the Bhagavad Gita, Sanatan Dharma, karma, Kabir teachings, Arya Samaj, devotion towards Hindu gods, Parmanand teachings, the cycle of life/reincarnation, belief in impermanence, Vedanta, and Ayurveda were identified as influential in participants' religious worldviews. Participants assigned frequencies to each belief, indicating how frequently they mentioned or emphasized them. The beliefs in Sanatan Dharma and karma received high frequencies, highlighting their prominence in participants' religious beliefs. The Bhagavad Gita and devotion towards Hindu gods were also mentioned frequently. Some participants mentioned being influenced by teachings of Kabir, the principles of Arya Samaj, Parmanand, and Vedanta philosophy. Beliefs in the cycle of life/reincarnation, belief in impermanence, and Ayurveda were also acknowledged by participants. These beliefs provided a framework for understanding the purpose of life, the consequences of actions, and the importance of moral conduct, ultimately shaping the participants' perspectives on transitions and providing guidance in navigating them.

EMOTIONAL WELL-BEING

The impact of religious teachings on emotional well-being was evident among participants. Their faith provided solace, hope, and a sense of peace during emotional distress. Themes related to emotional well-being were identified, with varying frequencies indicating the prominence of each theme. Participants often reported feeling calm, composed, and centered, while also experiencing happiness, positive thinking, and mental resilience. Their religious teachings instilled mental strength, focus, and willpower, reducing stress and anger levels. Participants felt motivated and energized, experiencing satisfaction and contentment in life. The teachings brought comfort, relaxation, and a profound sense of inner peace. Overall, religious teachings played a significant role in shaping participants' emotional well-being, providing them with emotional stability and a positive outlook on life.

Dakshita Pandey and Rajat Kanti Mitra

PHYSICAL WELL BEIN

Participants highlighted the impact of religious teachings on their physical well-being. They reported a reduction in physical limitations and improved capabilities, along with feelings of relaxation and tranquility. Participants attributed their religious teachings to being physically active, engaging in regular exercise or yoga. They also perceived a decrease in illness occurrence and severity, as well as a reduced dependency on medication. Overall, religious teachings played a role in enhancing participants' physical health and well-being, empowering them to lead more active and fulfilling lives.

LIFESTYLE CHANGES

Participants reported that their religious teachings influenced positive lifestyle changes, promoting physical well-being. These changes included adopting early rising routines, maintaining a healthy diet aligned with religious beliefs, prioritizing adequate sleep, and cultivating a disciplined and consistent lifestyle. The integration of religious teachings into their daily lives encouraged participants to lead healthier lifestyles, emphasizing self-discipline, productivity, and adherence to moral and ethical guidelines. These lifestyle changes fostered physical well-being, enabling participants to experience the benefits of improved routines and habits influenced by their religious teachings.

WISDOM

Participants acknowledged the profound impact of religious teachings in imparting wisdom and guidance. They drew upon religious texts, teachings, and spiritual leaders' wisdom to navigate life transitions, gain insights into aging, and make decisions. The themes of wisdom that emerged highlighted the transformative influence of religious teachings on participants' perspectives and attitudes. Participants emphasized the importance of acceptance, groundedness, open-mindedness, and seeking new knowledge. They found meaning and purpose in life through their religious teachings, embraced positivity amidst challenges, and held onto hope for the future. Additionally, their religious teachings encouraged them to appreciate the beauty in the world, fostering a sense of awe and gratitude. Overall, religious teachings provided participants with profound wisdom and shaped their outlook on life.

SOCIAL SUPPORT

Religious communities played a vital role as sources of social support during life transitions. Participants highlighted the importance of their religious community in providing emotional support, practical assistance, and a sense of belonging. Within the theme of social support, several subthemes emerged, reflecting the impact of religious teachings on participants' interactions and community engagement. They engaged in acts of charity and selfless service, embodying the teachings of their faith. Their religious teachings encouraged helpful behavior and fostered strong bonds and increased social connections. Participants developed understanding, empathy, and a culture of compassion and kindness. They also emphasized respect, equality, and being role models to positively influence others. Ultimately, their religious teachings promoted a sense of community and active participation in society.

SPIRITUAL GROWTH AND ENLIGHTENMENT

Religious teachings had a profound impact on participants' spiritual growth and enlightenment during life transitions. Within the theme of spiritual growth and enlightenment, several subthemes emerged. Participants embraced mindfulness, being fully present in the moment, and deepening their connection to the divine. They engaged in self-discovery and self-reflection, exploring their inner selves and spiritual paths. Participants developed a strong connection with a higher power or divine authority, finding guidance, purpose, and meaning in their lives. They practiced gratitude, pursued a quality life, and cultivated a sense of detachment from worldly attachments. Their religious teachings also emphasized the interconnectedness of all beings and facilitated a higher level of consciousness, expanding their understanding of reality.

PERSONAL IDENTITY

Participants reported that their religious teachings had a profound impact on their personal spiritual growth and enlightenment during life transitions. They experienced deepened spirituality, increased self-awareness, and a sense

63847

of connection to the divine. Several subthemes emerged within the theme of spiritual growth and enlightenment. Participants practiced mindfulness, engaged in spiritual exploration, and embarked on a journey of self-discovery. They emphasized living in the present moment, engaging in introspection, and developing a strong connection with a higher power or divine authority. Their religious teachings helped them find meaning in life, cultivate gratitude, and strive for a quality life. Participants also embraced a sense of detachment, recognized the interconnectedness of all beings, and attained a higher level of consciousness.

CHALLENGES FACED WHILE APPLYING RELIGIOUS TEACHING
Participants encountered various challenges when applying their religious practices and beliefs in their daily lives. These challenges included difficulties in remaining consistent and motivated, understanding and fully applying certain teachings, physical limitations, memorization without printed books, sacrificing family time, and for some, no significant challenges. These challenges highlight the complexities individuals face in integrating religious practices, and further exploration can provide insights into strategies for overcoming them. It's important to consider individual circumstances and interpretations when understanding the presence or absence of challenges in incorporating religious practices into one's lifestyle.

DISSCUSION AND ANALYSIS

The study aimed to explore the impact of Hindu religious teachings on older adults and had two objectives. The first objective was to identify the theme explaining the influence of religious teachings on the well-being of older adults. The second objective was to develop a framework capturing how older adults utilize religious teachings to cope with transitions. The qualitative research design employed open-ended questions in semi-structured interviews with older adults in parks and spiritual centers in Delhi. Interviews were audio-recorded, transcribed, and thematically analyzed. Ten key themes emerged, including religious practices, beliefs, well-being, lifestyle changes, wisdom, social support, spiritual growth, personal identity, and challenges faced in applying religion.

Research Question 1.
How has your religious faith affected the way you look at life's changes and transitions? What religious practices or beliefs did you have?
The participants in the study expressed a deep connection to their Hindu faith and practices, which have influenced their perspectives on life's changes and transitions. They find guidance, strength, and purpose in their religious beliefs, relying on practices like worship, fasting, yoga, and meditation. Hindu teachings on impermanence, karma, and dharma help them navigate life's ups and downs. They feel supported by a higher power, believe in the importance of virtuous living, and cherish the sense of community and cultural traditions associated with their religion. Sharing their faith with others and conducting devotional gatherings are important to them. Their religious beliefs have brought personal growth, self-awareness, and gratitude, enabling them to face challenges with resilience and acceptance. Overall, their faith has had a profound impact on their well-being and outlook on life's transitions.

Research Question 2. What specific religious teachings or beliefs have helped guide you through life transitions? If so, how can you describe them?
The participants in the study expressed how Hindu religious teachings and beliefs have profoundly impacted their lives during life transitions. Concepts such as karma, dharma, interconnectedness, and self-discovery have guided them in making mindful choices, finding purpose, and staying grounded. Meditation and yoga have provided them with inner peace and well-being. They value the wisdom of saints and spiritual figures and find solace in practices like satsangs and devotional rituals. The understanding of cyclical time and impermanence has helped them cope with challenges and maintain a positive outlook. Overall, Hindu religious teachings have brought them focus, direction, resilience, and a sense of compassion and acceptance in navigating life transitions.

Research Question 3. How have your religious practices/actions changed since old age? Has being involved in religious practices impacted your health and beliefs?

Participants in the discussion shared their experiences of how religious beliefs and practices have positively impacted their health and overall well-being in old age. Yoga and meditation were highlighted as transformative practices that improved vitality, reduced symptoms, and cultivated inner peace and patience. Religious festivals, rituals, and pilgrimages deepened their understanding of interconnectedness and inspired gratitude and service. Religious practices provided structure, meaning, and a sense of community, fostering resilience and equanimity. Aging reinforced the concept of karma and motivated individuals to follow righteous paths. Improved physical health, mental sharpness, humor, and a deeper sense of purpose were common outcomes. Overall, religious practices played a vital role in promoting physical health, inner peace, positive beliefs, and finding meaning in life during old age.

Research Question 4. Can you describe any of your religious experiences? How have they affected your daily lifestyle?

The participants in the discussion shared their experiences of how religious practices have influenced their daily lifestyles. Yoga and meditation were highlighted as practices that positively impacted physical and mental well-being. Belief in the divine presence in food led to a sense of reverence and gratitude, shaping their dietary choices. Discipline, routine, and daily practices such as prayer and meditation were valued for maintaining spirituality and inner peace. Religious festivals and pilgrimages deepened their connection to the divine, while the belief in interconnectedness and the power of actions fostered compassion and kindness. Maintaining a simple and saattvik lifestyle, prioritizing sleep, and a sense of purpose were also emphasized. Overall, religious experiences profoundly influenced participants' daily lives, shaping their health, routines, choices, and values.

Research Question 5.

Do you think that your religious practices/actions will affect your future life as well? Do you see them playing an important role in your future?

In the discussion, participants shared their perspectives on the role of religious practices in shaping their future lives. Many believed that their practices would continue to impact their well-being and evolution. They saw their religious practices as lifelong commitments and sources of guidance, comfort, and strength. The participants emphasized the importance of passing down their faith and values to future generations. Some mentioned evolving their understanding of religious practices over time, seeking deeper spiritual teachings. The significance of these practices in maintaining physical and mental well-being was highlighted, along with their positive impact on relationships and a sense of universal brotherhood. Overall, the participants had deep faith in their religious practices, considering them essential for their future lives.

Research Question 6. Do you feel that your religious beliefs or practices have helped you maintain a sense of purpose or meaning during life transitions?

The participants in the discussion expressed their belief in the ongoing impact of religious practices on their future lives. They emphasized the importance of practices such as yoga, meditation, and spiritual teachings in shaping their well-being, personal growth, and connection to the divine. The participants viewed their religious practices as lifelong commitments and intended to deepen their spiritual journey as they aged. They also recognized the role of religious practices in passing down values to future generations and fostering community bonds. The participants highlighted the physical and mental benefits of their practices and the evolution of their understanding of spirituality over time. Overall, they strongly believed that their religious practices would continue to guide and shape their future lives.

Research Question 7. Have your religious beliefs helped you cope with the challenges of old age? Can you give any example?

The participants overwhelmingly agreed that their religious beliefs have been vital in navigating the challenges of old age. They emphasized the role of practices like meditation, yoga, prayer, and selfless service in maintaining a positive mindset and finding purpose. Mindfulness and acceptance were highlighted as important in managing physical discomfort, and meditation was particularly valued for cultivating inner peace. Rituals and daily spiritual practices provided solace and support, helping individuals stay connected to their spiritual paths. The belief in a higher power and acceptance of a divine plan brought gratitude, contentment, and optimism, enabling them to face difficulties with hope and peace. Overall, religious beliefs have served as sources of strength, comfort, and resilience in old age.

Research Question 8.

Have you noticed any difference in the way you think or feel since incorporating religious practices into your life? If yes, can you tell about those differences?

The incorporation of religious practices has had a profound impact on individuals' thoughts and emotions. They feel more grounded, centered, and connected to their spiritual path, experiencing inner peace, mindfulness, and tranquility. This has helped them effectively manage stress and negative emotions while cultivating patience, compassion, and understanding towards others. Some have shifted towards a more spiritual outlook, fostering self-awareness and the ability to observe thoughts and emotions without attachment. The practices have deepened their sense of connection, purpose, and gratitude while inspiring a mindful and conscious lifestyle. Positive thinking, self-control, and charitable actions have also been fostered, leading to transformative changes in their lives.

Research Question 9.

What do other people and household members have to say about these religious practices? Have you noticed any change in your social relationships? And what is its effect. (What are your views on working for the welfare of others in your society?)

Participants' responses regarding the impact of religious practices on social relationships highlight the overall positive effects. Many note the support and participation of family and friends in their religious activities, strengthening bonds and fostering unity. The practices have cultivated compassion, patience, and empathy, transforming their demeanor and attitude towards others. These qualities have deepened connections within religious communities and expanded social networks. Engaging in selfless service has been emphasized, leading to positive impacts on relationships and increased involvement in the community. Overall, religious practices have brought personal growth, stronger relationships, and a sense of purpose and fulfillment in social interactions.

Research Question 10.

Have you faced any challenges or struggles while trying to apply religious teachings on life transitions/aging?

Participants' experiences with applying religious teachings to life transitions and aging vary. Some found seamless integration of beliefs and practices, receiving support from family, community, and religious texts. However, others faced challenges in maintaining consistency and adapting teachings to changing circumstances. Time management, discipline, and motivation were common obstacles, but perseverance and seeking guidance helped overcome them. Balancing religious practices with other responsibilities posed additional challenges, requiring careful adjustment. Despite the struggles, respondents acknowledged the transformative power of their practice and the importance of adaptability and staying connected to their spiritual goals. Overall, they found meaning and support in their journeys.

This study identified ten major themes related to the influence of religious teachings on older adults' transitions. The themes include religious practices, beliefs, emotional well-being, physical well-being, lifestyle changes, wisdom, social support, spiritual growth and enlightenment, personal identity, and challenges faced in applying religious teachings. These themes demonstrate the holistic impact of religious teachings on various aspects of older adults' lives, such as their well-being, social connections, personal identity, and spiritual development. The findings confirm

Dakshita Pandey and Rajat Kanti Mitra

the positive effects of religious teachings on older adults' well-being and align with previous research in the field. This study provides valuable insights into the specific mechanisms through which religious teachings shape older adults' experiences during transitional periods.

CONCLUSION

This study aimed to explore the impact of Hindu religious teachings on older adults' transitions. Thematic analysis was conducted on data from in-depth interviews with 20 religious older adults, and ten key themes emerged from the analysis. These themes included religious practices, beliefs, emotional well-being, physical well-being, lifestyle changes, wisdom, social support, spiritual growth and enlightenment, personal identity, and challenges faced in applying religious teachings. The findings highlighted the profound impact of religious faith on the lives of older adults. Religious teachings provided guidance, support, and a sense of purpose during life transitions and aging. Participants found solace in teachings that emphasized acceptance, resilience, and finding meaning in life's changes. Their commitment to religious practices remained strong, positively impacting their spiritual and overall well-being. Religious beliefs played a role in coping with the challenges of old age, providing comfort, peace, and trust in a divine plan. Incorporating religious practices led to changes in thoughts and emotions, fostering mindfulness, gratitude, and a deeper sense of connection with the divine. Participants acknowledged the impact of their religious practices on social relationships, inspiring positive changes in their interactions with others. Despite challenges such as time management and balancing responsibilities, participants displayed resilience and adaptability. They emphasized the importance of seeking guidance, staying connected to spiritual goals, and remaining open-minded. The study's findings contribute to existing literature by providing insights into the role of religious teachings in promoting well-being, personal growth, and a sense of purpose among older adults. The identified themes have implications for interventions, support programs, and healthcare initiatives targeting older adults within a religious context. However, the study has limitations such as a small sample size, potential biases, and limited generalizability, suggesting the need for future research with more diverse populations and contexts.

REFERENCES

1. Ano, G. G., &Vasconcelles, E. B. (2021). Religious coping and mental health outcomes among older adults: A meta-analysis. *Journal of Religion, Spirituality & Aging, 33(2), 161-177.*
2. DeKoekkoek, T., Lindholm, J., Jansen, H., &Postmus, J. (2021). A faith-based intervention to reduce loneliness and improve social support among older adults. *The Gerontologist, 61(4), 573-581.*
3. Eschler, S., Edwards, T., &Gruenewald, T. (2021). The role of religion and spirituality in promoting successful aging among older adults: A systematic review. *Gerontologist, 61(4), e305-e315.*
4. Frankl, V. E. (1959). Man's search for meaning. *Beacon Press.*
5. Freud, S. (1927). The future of an illusion. *Hogarth Press.*
6. Fromm, E. (1950). Psychoanalysis and religion. Yale University Press.
7. Fromm, E. (1956). The art of loving. *New York: Harper & Row.*
8. James, W. (1902). The varieties of religious experience: A study in human nature. *Longmans, Green and Company.*
9. James, W. (1902). The varieties of religious experience: A study in human nature. *New York: Longmans, Green & Co.*
10. Jung, C. G. (1964). Man and his symbols. *Garden City, NY: Doubleday.*
11. Jung, C. G. (1969). The archetypes and the collective unconscious. *Princeton University Press.*
12. Kim, B., Ng, S. H., & Kim, J. (2021). Participation in religious activities and social integration of older Korean immigrants in the United States. *Journal of Gerontological Social Work, 64(3), 261-277.*
13. Kim, J., Pargament, K. I., & Chen, Y. J. (2021). Religious involvement, religious identity, and well-being among older adults: A longitudinal study. *The Journals of Gerontology: Series B, 76(6), e290-e299.*
14. Maslow, A. H. (1970). Motivation and personality. *Harper & Row.*
15. Maslow, A. H. (1971). The farther reaches of human nature. *New York: Viking Press.*

Dakshita Pandey and Rajat Kanti Mitra

Table 1. About the sample

SR NO	CASE NUMBER	AGE	GENDER
1	CASE- 1	66	FEMALE
2	CASE-2	70	FEMALE
3	CASE-3	72	MALE
4	CASE-4	68	FEMALE
5	CASE-5	75	MALE
6	CASE-6	74	MALE
7	CASE-7	71	FEMALE
8	CASE-8	62	FEMALE
9	CASE-9	65	FEMALE
10	CASE-10	66	MALE
11	CASE-11	65	MALE
12	CASE-12	63	FEMALE
13	CASE-13	71	MALE
14	CASE-14	74	MALE
15	CASE-15	67	MALE
16	CASE-16	65	FEMALE
17	CASE-17	68	MALE
18	CASE-18	72	MALE
19	CASE-19	62	MALE
20	CASE-20	67	MALE

Table 2. Result table

SR. NO	THEMES	SUB THEMES	FREQUENCY
1.	RELIGIOUS PRACTICES	CHANTING MANTRA/ CHANTING OM	4
		YOGA	7
		MEDITATION	10
		WORSHIPPING / PRAYING	13
		FASTING	4
		SATSANG / PRAVACHANG	5
		BHAJHANS	1
		CELEBRATION OF FESTIVALS	4
		PILGRIMINAGE	4
2.	RELIGIOUS BELIEF	BHAGVAD GITA	4
		SANATAN DHARMA / DHARMA	12
		KARMA	12
		KABIR TEACHINGS	1
		ARYA SAMAJH	1
		DEVOTION TOWARDS HINDU GODS	8
		PARMANAND TEACHINGS	1
		CYCLE OF LIFE/ REINCARNATION	3
		BELIEF IN IMPERMANENCE	4
		VEDANTA	2
		AYURVEDA	1
3.	EMOTIONAL WELL BEING	CALM/ COMPOSED	9
		FEELING GOOD / HAPPY	8

Dakshita Pandey and Rajat Kanti Mitra

		POSITIVE THINKING	10
		MENTAL STRENGTH / RESILIENCE	15
		FOCUSED/CENTRED	14
		WILL POWER	4
		ENERGY / MOTIVATED	7
		LOW STRESS	11
		LOW ANGER	10
		SATISFIED / CONTENTMENT	8
		COMFORT/ RELAXATON	11
		PEACE	13
4.	PHYSICAL WELLBEING	REDUCED PHYSICAL LIMITATION	4
		RELAXED/ TRANQUIL	5
		PHYSICALLY ACTIVE	8
		REDUCTION IN ILLNESS	8
		REDUCED DEPENDENCY ON MEDICATION	3
5.	LIFE STYLE CHANGES	EARLY RISE	6
		HEALTHY DIET	9
		HEALTHY SLEEP PATTERN	5
		DISCIPLINED / CONSISTENT LIFESTYLE	13
6.	WISDOM	ACCEPTANCE	10
		GROUNDED	10
		OPEN MINDEDNESS & SEEKING NEW KNOWLEDGE	3
		MEANING AND PURPOSE IN LIFE	19
		EMBRACE POSITIVITY/ UPS DOWN	8
		HOPE	7
		APPRECIATE BEAUTY	7
7.	SOCIAL SUPPORT	CHARTIY / SEVA - SELFLESS SERVICE	9
		HELPFUL BEHAVIOUR	9
		INCREASED SOCIAL CONNECTIONS/ STRONG BONDING	11
		INCREASED UNDERSTANDING / EMPATHY	11
		COMPASSION / KINDNESS	17
		CARE FOR ANIMALS AND NATURE	2
		NO DISCRIMNATION	3
		RESPECT FOR ALL	4
		ROLE MODEL FOR INFLUENCING OTHERS	7
		SENSE OF COMMUNITY / ACTIVE MEMBER OF SOCIETY	9
8.	SPIRITUAL GROWTH/ ENLIGHTENMENT	MINDFULNESS	11
		ADHYATMIK / SPIRITUALITY	10
		SELF DISCOVERY	6

Dakshita Pandey and Rajat Kanti Mitra

		LIVING IN THE PRESENT	8
		INTROSPECTIVE/ SELF REFLECTIVE	8
		CONNECTION WITH AUTHORITY	18
		FINDING MEANING	11
		GRATITUDE	5
		QUALITY LIFE	6
		SENSE OF DETACHMENT	7
		INTERCONNECTEDNESS OF ALL BEINGS	6
		HIGHER LEVEL OF CONSCIOUSNESS	5
9.	PERSONAL IDENTITY	ETHICS/ RIGHTEOUSNESS	8
		BELIEF/ VALUES	9
		DECISION & LIFE CHOICES	5
		INCREASED CONFIDENCE	3
		NEW DIRECTION - POSITIVE DIRECTION	18
		FORGIVENESS	1
		PATIENCE	8
		OPTIMISM	5
10.	CHALLENGES FACED WHILE APPLYING	REMAINING CONSISTENT & MOTIVATED	5
		UNDERSTAND FULLY SOME RELIGIOUS TEACHINGS AND APPLYING	4
		DIFFICULTY IN TERMS OF PHYSICAL LIMITATION	1
		MEMORIZING SHOLKAS WITHOUT PRINTED BOOK	1
		NO CHALLENGES	8
		SACRIFICE OF FAMILY TIME	1

RESEARCH ARTICLE

A Study on Search Engine Optimization Vs Social Media Marketing Affecting Consumer Behaviour towards Web Stores

Ramasubramaniam P[1]* and Darthy Agnell Mary[2]

[1]Assistant Professor, Department of Textile, Sardar Vallabhbhai Patel International School of Textiles and Management, Coimbatore, Tamil Nadu, India.
[2]Department of Textile, Sardar Vallabhbhai Patel International School of Textiles and Management, Coimbatore, Tamil Nadu, India.

*Address for Correspondence
Ramasubramaniam P
Assistant Professor,
Department of Textile,
Sardar Vallabhbhai Patel International School of Textiles and Management,
Coimbatore, Tamil Nadu, India.
E.Mail: mytextileclassroom@gmail.com

ABSTRACT

This study aims to explore the impact of search engine optimization (SEO) and social media marketing (SMM) on consumer behaviour towards web stores. This study compared the impact of search engine optimization (SEO) and social media marketing (SMM) on consumer behavior towards web stores. It analyzes the effectiveness of these two digital marketing tools in driving the traffic to the web stores and how they influence consumers' purchasing decisions. The study found that search engine optimization has a greater influence on consumer behavior towards web stores than social media marketing. Online shopping, search engines, and social media platforms play a vital role in shaping consumer behavior and perception. The study also found that search engine optimization had a more significant impact on repeat purchases than social media marketing. Businesses should consider using both SEO and SMM as part of their digital marketing strategy for maximum impact.

Keywords-Search Engine Optimization, Social Media Marketing, Consumer Behaviour, Digital Marketing, Web Store

INTRODUCTION

Digital marketing encompasses all online marketing efforts conducted through various digital channels such as social media, email marketing, search engines, SEO, and other websites. Inbound marketing and digital marketing are closely related, but there are minor differences that experienced marketers have learned through conversations with business owners and marketers from different regions. The best digital marketers understand how each digital

63855

marketing campaign contributes to the overall campaign goals and can utilize both free and paid channels depending on their marketing strategy. Digital marketing channels include websites, pay-per-click advertising on platforms like Google and Facebook, email marketing, video marketing on platforms like YouTube and Instagram, SMS or text message campaigns, and e-commerce through online stores. Online shopping, or e-commerce, allows customers to purchase goods and services conveniently from their homes, leading to significant annual sales and effects on businesses and supply chains. Search engine optimization (SEO) improves a website's visibility and relevance in search engine results, making it easier for users to find and driving organic traffic. Web stores often employ a combination of SEO and SMM to increase traffic and enhance their online presence, with SEO attracting active product searchers and SMM focusing on brand awareness and engagement. Both SEO and SMM have the potential to influence consumer behaviour toward web stores, and a strategic combination of both can be the most effective approach. By optimizing their website for search engines and establishing a strong social media presence, web stores can increase visibility, credibility, consumer trust, and ultimately drive more traffic and sales.

Objectives of the Study
- To understand about Search Engine Optimization and Social Media Marketing.
- To gain knowledge on SMM and SEO that affect young adult's buying behaviour towards Web stores.
- To find out the digital marketing tool that affects the consumer behaviour.

Scope of the Study
- To analyze and compare the impact of Search Engine Optimization (SEO) and Social Media Marketing (SMM) on consumer behaviour towards web stores.
- The study aims to explore how these two digital marketing techniques can influence consumers decision making process.
- The study target consumers who frequently shop online and have experienced SEO or SMM activities by web stores.

Hypothesis of the Study
CRITERIA 1: Search engine optimization has a great impact on consumer behaviour towards web stores.
H0: There is no significant difference in the impact on consumer behaviour towards web stores.
H1: Search engine optimization has a greater impact on consumer behaviour towards webStores.
CRITERIA 2: Social media marketing (SMM) has a greater impact on consumer behavior towards web stores.
H0: There is no significant difference in the impact on consumer behavior towards web stores by social media marketing (SMM).
H1: Social media marketing (SMM) has a greater impact on consumer behavior towards web stores.
CRITERIA 3: Consumer behavior towards web stores is not significantly affected by either.
H0: Consumer behavior towards web stores is not significantly affected by either.
H1: Consumer behavior towards web stores is significantly affected by either.

LITERATURE REVIEW

- Online marketing's importance is evident, yet evaluating its impact poses challenges. Swift user behavior insights are crucial for successful SEO and SMM, while experienced marketers support these strategies. Further research is required to validate these findings for entrepreneurs. The growth of social media marketing is attributed to its cost-effectiveness and wide reach. The marketer decision model improves decision-making, emphasizing the significance of considering consumer behavior when designing SEO and SMM strategies. (Ravneet Singh Bhandari, 2019)
- Search engines are crucial for finding information, and website visibility is key. On-page SEO involves quality content and keyword optimization, while off-page SEO includes link building. Google is the dominant search

engine, requiring optimization techniques for better web results, with White Hat SEO being the most effective. (Ankalkoti, 2017)

- Social media's integration with traditional marketing functions is driven by its popularity, extensive user base, and reliance on internet and mobile-based tools, necessitating an evaluation of its impact through comparing pre- and post-social media marketing practices and technologies, emphasizing the crucial role of user engagement, efficient platform creation, and digital integration in effective digital marketing, as exemplified by the case of Interest and the shift from print to online mediums. (Shamsudeen Ibrahim, 2018)

- The evolving world of marketing has undergone remarkable transformations, with significant changes in practices, tools, and strategies, expanding the market's reach from physical limitations to a global scale through the power of social media, necessitating businesses to stay updated and leverage the collective power of online communities for effective brand positioning, customer engagement, and cost-effective marketing campaigns, ultimately enhancing brand awareness, loyalty, and communication with customers. (Ravi. B, 2021)

- In the digital age, the existence and success of a luxury brand heavily rely on its strong online presence, effective SEO, and strategic social media marketing to attract potential high-class customers, highlighting the importance of exclusivity, limited stock, and status-focused portrayal to create demand and appeal among target audiences. (Ms. Mansi Kumari, 2022)

- Online retailing, known as online shopping, enables consumers to purchase goods or services directly from sellers through a web browser, offering convenience, a wide range of products, and competitive pricing, though concerns exist regarding product verification as a challenge for customers. (AkhilKurup, April 2021)

- With the increasing preference for mobile devices, major e-commerce players like Amazon, Flipkart, Myntra, Snapdeal, and Paytm have embraced mobile applications to cater to the evolving consumer trends, while Myntra, in particular, focuses on mobility, versatility, reachability, and keeping up with the latest fashion trends to effectively market and sell its products. (Sravani, November 2020)

- E-business websites like Myntra and Ajio offer a wide range of products, with Myntra excelling in user interface and usability, as it scored higher in Nielsen's usability criteria compared to Ajio, providing user control, consistency, error prevention, flexibility, efficiency, design aesthetics, system status visibility, and assistance. (Peddinti, October 2022)

METHODOLOGY

Research Design

Descriptive research design is the research method used. Descriptive research design is a scientific method which includes noticing and portraying the way of behaving of a subject without impacting it in at any rate. This kind of design is used for more precise investigation and is preplanned and a structured design. Although qualitative research can also be used for descriptive purposes, descriptive research is typically defined as a type of quantitative research. In order to guarantee the validity and dependability of the outcomes, the research design needs to be carefully developed.

Sampling Method

The method known as snowball sampling is used to select participants from the intended group of young adults who shop online. A non-probability sampling method known as snowball sampling or chain-referral sampling uses samples with uncommon characteristics. This is a method of sampling in which existing subjects serve as referrals to recruit the necessary research sample. This method of sampling can go on and on, like a snowball growing until a researcher has enough data to analyze to draw conclusive conclusions that can assist an organization in making informed decisions.

Sample Size
The sample size taken was 153 responses

Ramasubramaniam and Darthy Agnell Mary

Data Collection
Primary Sources
The primary data is collected by approaching the individuals with a Questionnaire and was filled by the respective respondents. The data that came from the first source is called primary data.

Secondary Sources
The data that have already been gathered for another purpose but are still relevant to research requirements are referred to as secondary data and the researcher is not the only one who gathers the data. It is therefore referred to as secondary.

Analysis method
Percentage analysis
Percentage analysis method involves calculating the percentage of respondents who selected each answer option for a particular question on a survey. Overall, percentage analysis is a useful tool for researchers to make sense of survey data and draw meaningful conclusions from it.

Chi Square Test
The chi-square test is a statistical method used to determine if there is a significant association or relationship between two categorical variables. It evaluates whether the observed frequencies in each category significantly differ from the expected frequencies under a specific hypothesis of no association. The null hypothesis assumes that there is no relationship between the variables, while the alternative hypothesis suggests that there is a relationship. The chi-square test calculates a test statistic known as the chi-square statistic (χ^2) by comparing the observed frequencies with the expected frequencies. It measures the deviation between the observed and expected frequencies and determines whether this deviation is greater than what would be expected by chance.

Data analysis and interpretation
Percentage Analysis

Figure 1 Age group of the respondents (Source: Primary Data)
Interpretation: From the report, 30.1% of respondents are from the age group 16-20 years. The majority of respondents is 51.6% from the age group of 21-25 years and 18.3% of respondents are from 25-28 years age group.

Figure 2 Gender of the Respondents (Source: Primary Data)
Interpretation: From the report, the majority of the respondents are female which is 50.3% and the rest 49.7% is of the male respondents.

Figure 3 How often do you shop online? (Source: Primary Data)
Interpretation: From the report,the majority of the respondents shop online occasionally, followed by monthly, rarely, weekly online shoppers and the daily users are of 2%. This shows that occasional users are the major users.

Figure 4. When you search for a product or services online, which one do you use more? (Source: Primary Data
Interpretation: From the report, 47.7% of respondents are using search engines and 13.1% of respondents are using social media to search for a product or service online. 39.2% of respondents are using both the digital marketing tools equally. This shows that the respondents use search engines more to search for a product or service online.

Figure 5. The amount of times do you seek for goods or services online? (Source: Primary Data)
Interpretation: From the report, majority of the respondents seek few times a week, few times a month and rarely. It is followed by the respondents who seek multiple times a day, once a day, once a week and never for goods or services online. This shows that people browse online in their free time like once a week or month and so it's rare.

Figure 6. How important is it to you that a search engine gets what you're looking for quickly? (Source: Primary Data)

Interpretation: From the report, majority of the respondents are very important, extremely important and moderately important. It is followed by 5.9% of slightly important and 3.3% of not important at all respondents towards the importance of search engine in what you are looking for. This shows that people give very much importance to product or service they search in search engines.

Figure 7. What number of times do you click on the top few search engine results? (Source: Primary Data)

Interpretation: From the report, the respondents of most of the times, sometimes and always are majority, where 7.2% of rarely, 1.4% of neutral and 0.3% of never are the people who click on the top few search engine results. This shows that people mostly click on the top few search engine results.

Figure 8 Do you trust the product or services that appear on the first page of search results more than those that appear on the subsequent pages? (Source: Primary Data)

Interpretation: From the report, majority of the respondents trust them somewhat more, doesn't trust them more or less and much more which is followed by 7.8% and 4.6% of them trust it somewhat less and much less. This shows that people somewhat more trust the search engine result's first page.

Figure 9. How often do you seek for products or services online using social media? (Source: Primary Data)

Interpretation: From the report, a greater number of respondents fall rarely, few times a week, few times a month and once a day, multiple times a day category for seeking goods or services using social media. Then the once a week and never category with 6.5% and 5.9% of respondents are categorized. This shows that people use social media few times a week or month in their free time and so it's rare.

Figure 10. What's the possibility that you will click on a social media advertisement or sponsored post? (Source: Primary Data)

Interpretation: From the report, somewhat likely, neutral, somewhat likely and very unlikely are the most category in which people possibly click on social media advertisements and 6.5% of very likely is followed by those. This shows that people somewhat likely click on the social media ads.

Figure 11 How important is it for you to engage with a company on social media before making a purchase? (Source: Primary Data).

Interpretation: From the report, it is 13.1% extremely important, 29.4% Very important, 33.3% Moderately important, 11.8% Slightly important and 12.4% Not important at all. This shows that people moderately consider to engage with a company's social media page.

Figure 12. Are you a person who has purchased something from a company on social media that you follow? (Source: Primary Data)

Interpretation: From the report, the majority of the respondents have shopped once, have considered it and they don't follow the company on social media. This shows that the respondents are not much engaged and interested in social media engagements.

Figure 13. How inclined are you to use a web store that tops the search engine results page to make a purchase? (Source: Primary Data)

Interpretation: From the report, 47% of the respondents are somewhat inclined, 32.7% are neutral and 12.4% are very inclined. This shows that the respondents are more inclined with search engine results.

Figure 14. Do you intend to buy something from a company that you follow in social media? (Source: Primary data)
Interpretation: From the report, 45.8% responded probably yes, 24.2% are neutral, 13.7% responded as probably not and 13.1% responded as definitely yes. This shows that respondents also show interest towards product or services through social medias.

Figure.15 Would you believe companies with a remarkable social media presence are more trustable? (Source: Primary Data)
Interpretation: From the report, 12.4% strongly believe, 37.9% somewhat believe, 35.9% are neutral, 11.8% somewhat don't believe and 2% strongly don't believe social media presence of a company. This shows that people are somewhat positive and neutral to trust towards a company presence on social media.

Figure 16 How important is it for you to read reviews before making a purchase from webstore? (Source: Primary Data)
Interpretation: From the report, 41.2% respondents say extremely important, 35.3% says very important, 14.4% moderately important, 4.6% slightly important and 4.6% not important at all. This shows that the respondents consider the reviews extremely and very important before making a purchase decision from the webstore.

Figure 17 Which do you believe is more effective in influencing your purchase decisions – search engine optimization or social media marketing? (Source: Primary Data)
Interpretation: From the report, 21.6% responded SEO, 24.2% SMM, 43.8% responded equally effective and 10.5% responded neither. This shows that consumers are getting influenced by both search engines and social media effectively.

Figure 18 From the below stated webstores, which is frequently used by you to shop products and services? (Source: Primary D
Interpretation: From the report, 41.2% respondents say extremely important, 35.3% says very important, 14.4% moderately important, 4.6% slightly important and 4.6% not important at all. This shows that the respondents consider the reviews extremely and very important before making a purchase decision from the webstore.

Figure 19 Which do you believe is more effective in influencing your purchase decisions – search engine optimization or social media marketing? (Source: Primary Data)
Interpretation: From the report, 14.4% people use myntra, 9.2% people use ajio and 76.5% people use amazon webstores. This shows that consumers use amazon online store more.

Figure 20 What factors do you consider when making a purchase from a Webstore? (Source: Primary Data)
Interpretation: From the reports, price, quality of the product or service, return policy, reviews, shipping and delivery options are the major factors that consumers consider when making a purchase from a web store.

Figure 21. Would you be more likely to purchase from a webstore that is easy to find through search engines or that has a strong social media presence? (Source: Primary Data)
Interpretation: From the report, 69.9% of the respondents use search engines and 30.1% of the respondents use social media as they were influenced by one of those to shop in webstores. Hence, search engines dominate the social media in terms of influencing consumers to shop in webstores.

CHI SQUARE TEST

CRITERIA 1: Search engine optimization has a great impact on consumer behaviour towards web stores.
H0: There is no significant difference in the impact on consumer behaviour towards web stores.
H1: Search engine optimization has a greater impact on consumer behaviour towards web stores.

63860

Interpretation: From the analysis, according to chi-square table, X2 value is 40.038a , degree of freedom is 16 and P value is 0.001. Here the P value is lesser than the significant value (0.001<0.05). So, the H1 is accepted and H0 is rejected.

CRITERIA 2: Social media marketing (SMM) has a greater impact on consumer behavior towards web stores.
H0: There is no significant difference in the impact on consumer behavior towards web stores by social media marketing (SMM).
H1: Social media marketing (SMM) has a greater impact on consumer behavior towards web stores.
Interpretation: From the analysis, according to chi-square table, X2 value is 26.897a , degree of freedom is 12 and P value is 0.008. Here the P value is lesser than the significant value (0.008<0.05). So, the H1 is accepted and H0 is rejected.

CRITERIA 3: Consumer behavior towards web stores is not significantly affected by either.
H0: Consumer behavior towards web stores is not significantly affected by either.
H1: Consumer behavior towards web stores is significantly affected by either.

Interpretation: From the analysis, according to chi-square table, X2 value is 99.148a, degree of freedom is 9 and P value is 0.005. Here the P value is lesser than the significant value (0.005<0.05). So, the H1 is accepted and H0 is rejected.

FINDINGS AND CONCLUSIONS

This study aimed to compare the effects of search engine optimization (SEO) and social media marketing (SMM) on consumer behavior towards web stores. The findings of the study suggest that search engine optimization influences consumer behavior more than social media marketing. This conclusion is based on the analysis of data collected from a sample of online shoppers who had experience with both SEO and SMM. Based on the responses provided above, it can be concluded that a significant portion of the population (about 92%) frequently shops online, with the majority doing so on a monthly or occasional basis. When searching for products or services, most people use search engines like Google, Bing, or Yahoo, and consider it important to get relevant results quickly. They also tend to trust the products or services that appear on the first page of search results more than those on subsequent pages. Social media platforms like Instagram, Facebook, and Twitter are also popular sources for seeking products or services, with a significant percentage of people doing so a few times a week or less. However, the likelihood of clicking on social media advertisements or sponsored posts is relatively low, with only about one-third of the respondents saying they are somewhat or very likely to do so. Engagement with companies on social media is moderately important to most people when making a purchase, with about two-thirds saying it is either extremely or very important. Additionally, a significant percentage of people have purchased something from a company on social media that they follow or have considered doing so. Overall, most people are inclined to use a webstore that tops the search engine results page to make a purchase, with about two-thirds of the respondents being somewhat or very inclined to do so. Finally, the data suggests that online shopping, search engines, and social media platforms play a vital role in shaping consumer behavior and perception.

The study found that consumers who accessed web stores through search engines tended to spend more time browsing the website, had higher click-through rates, and were more likely to make a purchase. On the other hand, consumers who accessed web stores through social media platforms tended to spend less time browsing the website, had lower click-through rates, and were less likely to make a purchase. These findings suggest that search engine optimization is a more effective method for driving traffic to web stores and converting visitors into customers. The study also found that consumers who accessed web stores through search engines had a higher level of trust in the website compared to those who accessed web stores through social media platforms. This finding is significant as it suggests that SEO can contribute to building brand credibility and trust, which is an essential factor in influencing

Ramasubramaniam and Darthy Agnell Mary

consumer behavior. Another significant finding of the study was that search engine optimization had a more significant impact on repeat purchases than social media marketing. Consumers who accessed web stores through search engines were more likely to return to the website and make additional purchases compared to those who accessed web stores through social media platforms. This finding highlights the importance of search engine optimization as a long-term strategy for building customer loyalty and repeat business. By using Chi Square Test for the Hypothesis Testing, it was found that Search engine optimization has a greater impact on consumer behaviour towards Web Stores. By using Chi Square Test for the Hypothesis Testing, it was found that social media marketing (SMM) has a greater impact on consumer behavior towards web stores. By using Chi Square Test for the Hypothesis Testing, it was found that Consumer behavior towards web stores is significantly affected by either.

Overall, this study provides valuable insights into the effects of search engine optimization and social media marketing on consumer behavior towards web stores. The findings suggest that search engine optimization is a more effective method for driving traffic to web stores, building brand credibility and trust, and generating repeat business. However, it is essential to note that social media marketing can still be an effective tool for reaching a broader audience and building brand awareness. Therefore, businesses should consider using both SEO and SMM as part of their digital marketing strategy for maximum impact. In conclusion, this study provides a strong foundation for future research in the field of digital marketing and consumer behavior. It demonstrates the importance of search engine optimization in influencing consumer behavior towards web stores and provides insights into the factors that contribute to its effectiveness. The findings of this study can be used by businesses to improve their digital marketing strategies and increase their online presence.

REFERENCES

1. Adel m. Torieh, n. H. (feb 2021). The effect of search engine optimization on egyptian consumer response. International journal of economics, commerce and management, vol. Ix, issue 2.
2. Afrina yasmin, s. T. (april 2015). Effectiveness of digital marketing in the challenging age: an empirical study. International journal of management science and business administration, volume 1, issue 5, pages 69-80.
3. Akhil kurup, n. S. (april 2021). Consumer perception towards amazon in vadodara city. International journal of creative research thoughts (ijcrt), volume 9, issue 4, 4456-4464.
4. Ambuli velayudham, s. R. (2019). Impact of search engine marketing towards customer purchase behavior. International journal of research and innovation in applied science (ijrias), volume iv, issue xii.
5. Ankalkoti, p. (2017). Survey on search engine optimization tools & techniques . Imperial journal of interdisciplinary research (ijir), vol-3, issue-5.
6. Desai, d. M. (march 2019). Digital marketing: a review. International journal of trend in scientific research and development (ijtsrd), pp.196-200.

7. Dr. S. Chandrasekar, d. C. (february 2020). A study on digital marketing- a case study with special reference to amazon.com. Studies in indian place names (sipn), vol-40 issue-12, 594-606.
8. Firas almukhtar, n. M. (2021). Search engine optimization: a review. Applied computer science, vol. 17, no. 1, pp. 69–79.
9. Gaurav gawade, m. A. (july 2020). Literature review on customer perception about online shopping with reference to amazon in india. Juni khyat, vol-10 issue-7 no. 2, 372-384.
10. Hemalatha, g. A. (february 2019). A study on consumer attitude towards digital marketing in myntra online shopping. Journal of management (jom), volume 6, issue 1, pp. 202–206.
11. Mr. Jaysing bhosale, d. R. (march 2020). Usage of social media marketing for small business: a comparative analysis of various actions on social media. Annual research journal of scms, pune, vol. 8, 63-73.

12. Mr. R. Mayilsamy, m. (november 2020). A study on customers' awareness, preferences and satisfaction towards ajio online shopping app in coimbatore city. Epra international journal of research and development (ijrd), volume: 5 issue: 11, 509-512.

13. Ms. Mansi kumari, m. A. (2022). Search engine optimization (seo) and social media marketing techniques and its impact as a marketing tool with special reference to luxury brands. International journal of research publication and reviews, vol 3, issue 7, pp 3913-3920.

14. Peddinti, z. P. (october 2022). A comparative study of analysis of the myntra & ajio e-businesses websites using usability method to evaluate.

15. Ravi. B, s. K. (2021). Social media marketing: a conceptual study. International journal of research and analytical reviews (ijrar), volume 8, issue 1.

16. Ravneet singh bhandari, s. B. (2019). An analysis between search engine optimization versus social media marketingaffecting individual marketer's decision-making behavior. Jindal journal of business research, 8(1) 78–91.

17. Rupesh washisht, m. C. (2020). A comparative study of customer satisfaction of myntra and ajio. European journal of molecular & clinical medicine, volume 7, issue 8, 5820-5828.

18. Shamsudeen ibrahim, s. A. (2018). A study on the impact of social media marketing trends on digital marketing. Shanlax international journal of management, vol. 6, no. S1,pp. 120–125.

19. Sravani, a. (november 2020). M-commerce platform and fashion: myntra.com. Phronimos the kiams journal, vol. No.01, issue no.01, 29-34.

20. Venkatraman, s. (2017). Social media marketing. Global journal of business disciplines, volume 1, number 2, 89-101.

21. Zgódka, m. (2011). Influence of search engines on customer decision process. Proceedings of the federated conference on computer science and information systems, pp. 341–344.

22. Ziaul maula, e. S. (2017). The influence of search engine optimization, social media, and internet-based advertising against online purchase decision in students of faculty of economics of samudra university. International journal of business and information, pp.146-152.

23. Zilincan, j. (march 2015). Search engine optimization. Cbu international conference on innovation, technology transfer and education, pp. 506-510

S.No.	AGE	FREQUENCY	PERCENTAGE
1	16-20	46	30.1%
2	21-25	79	51.6%
3	25-28	28	18.3%
	TOTAL	153	100%

[1]   [2]

[3]   **Figure 1. Age group of the respondents (Source: Primary Data)**

S.No.	GENDER	FREQUENCY	PERCENTAGE
1	Male	76	49.7%
2	Female	77	50.3%
3	Prefer not to say	0	0%
	TOTAL	153	100%

[4]   [5]

[6]   **Figure 2. Gender of the Respondents (Source: Primary Data)**
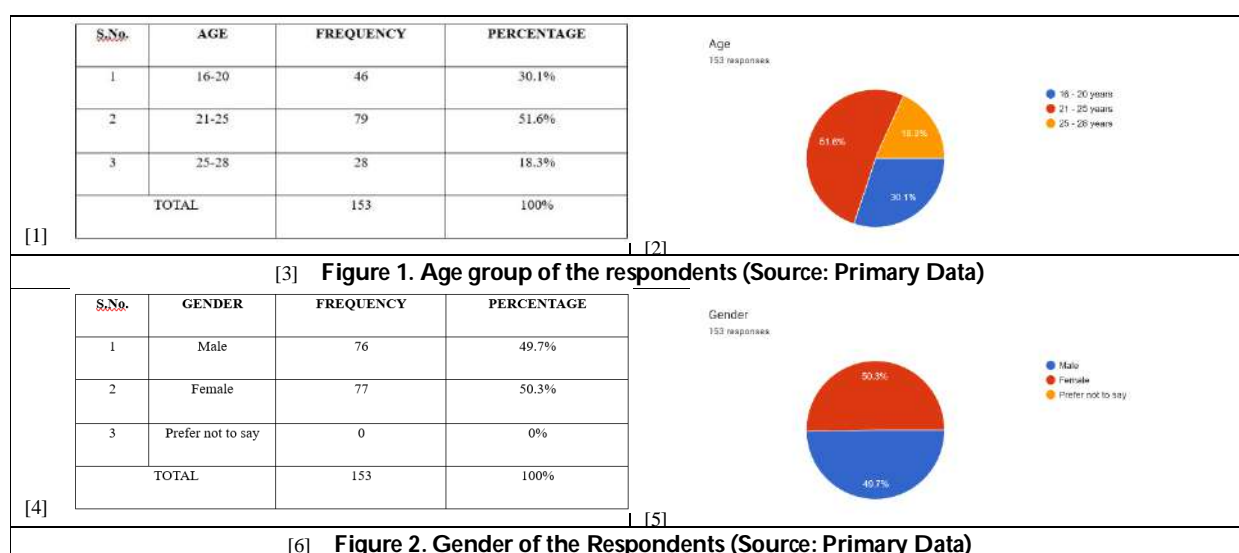
[7]

S.No.	ONLINE SHOPPING	FREQUENCY	PERCENTAGE
1	Daily	3	2%
2	Weekly	16	10.5%
3	Monthly	39	25.5%
4	Occasionally	71	46.4%
5	Rarely	24	15.7%
	TOTAL	153	100%

[8]

[9] **Figure 3. How often do you shop online? (Source: Primary Data)**

[10]

S.No.	ONLINE SERVICE	FREQUENCY	PERCENTAGE
1	Search Engines	73	47.7%
2	Social Media Platforms	20	13.1%
3	Both Equally	60	39.2%
	TOTAL	153	100%

[11]

[12] **Figure.4 When you search for a product or services online, which one do you use more? (Source: Primary Data**

S.No.	SEEKING ONLINE	FREQUENCY	PERCENTAGE
1	Multiple times a day	15	9.8%
2	Once a day	9	5.9%
3	Few times a week	42	27.5%
4	Once a week	9	5.9%
5	Few times a month	41	26.8%
6	Rarely	36	23.5%
7	Never	1	0.7%
	TOTAL	153	100%

[13]

[14]

[15] **Figure 5. The amount of times do you seek for goods or services online? (Source: Primary Data)**

S.No.	SEARCH ENGINE	FREQUENCY	PERCENTAGE
1	Extremely important	34	22.2%
2	Very important	73	47.7%
3	Moderately important	32	20.9%
4	Slightly important	9	5.9%
5	Not important at all	5	3.3%
	TOTAL	153	100%

[16]

[17]

[18] **Figure.6 How important is it to you that a search engine gets what you're looking for quickly? (Source: Primary Data)**

S.No.	SEARCH ENGINE	FREQUENCY	PERCENTAGE
1	Always	25	16.3%
2	Most of the times	65	42.5%
3	Sometimes	49	32%
4	Rarely	11	7.2%
5	Never	1	0.7%
6	Neutral	2	1.3%
	TOTAL	153	100%

[19]

[20]

[21] **Figure 7. What number of times do you click on the top few search engine results? (Source: Primary Data)**

Ramasubramaniam and Darthy Agnell Mary

S.No.	SEARCH ENGINE	FREQUENCY	PERCENTAGE
1	Yes, I trust them much more	30	19.6%
2	Yes, I trust them somewhat more	73	47.7%
3	No, I don't trust them more or less	31	20.3%
4	No, I trust them somewhat less	12	7.8%
5	No, I trust them much less	7	4.6%
	TOTAL	153	100%

Figure 8. Do you trust the product or services that appear on the first page of search results more than those that appear on the subsequent pages? (Source: Primary Data)

S.No.	SOCIAL MEDIA	FREQUENCY	PERCENTAGE
1	Multiple times a day	11	7.2%
2	Once a day	13	8.5%
3	Few times a week	42	27.5%
4	Once a week	10	6.5%
5	Few times a month	29	19%
6	Rarely	39	25.5%
7	Never	9	5.9%
	TOTAL	153	100%

Figure 9 How often do you seek for products or services online using social media? (Source: Primary Data

S.No.	SOCIAL MEDIA	FREQUENCY	PERCENTAGE
1	Very likely	10	6.5%
2	Somewhat likely	51	33.3%
3	Neutral	44	28.8%
4	Somewhat unlikely	22	14.4%
5	Very unlikely	26	17%
	TOTAL	153	100%

Figure 10 What's the possibility that you will click on a social media advertisement or sponsored post? (Source: Primary Data)

S.No.	SOCIAL MEDIA	FREQUENCY	PERCENTAGE
1	Extremely important	20	13.1%
2	Very important	45	29.4%
3	Moderately important	51	33.3%
4	Slightly important	18	11.8%
5	Not important at all	19	12.4%
	TOTAL	153	100%

Figure 11 How important is it for you to engage with a company on social media before making a purchase? (Source: Primary Data)

S.No.	SOCIAL MEDIA	FREQUENCY	PERCENTAGE
1	Yes, multiple times	26	17%
2	Yes, once	45	29.4%
3	No, but I have considered it	42	27.5%
4	No, I haven't considered it	16	10.5%
5	No, I don't follow any companies on social media	24	15.7%
	TOTAL	153	100%

Figure 12 Are you a person who has purchased something from a company on social media that you follow? (Source: Primary Data)

Ramasubramaniam and Darthy Agnell Mary

S.No.	CONSUMER PERCEPTION	FREQUENCY	PERCENTAGE
1	Very inclined	19	12.4%
2	Somewhat inclined	72	47.1%
3	Neutral	50	32.7%
4	Somewhat disinclined	6	3.9%
5	Very disinclined	5	3.3%
6	Very likely	1	0.7 %
	TOTAL	153	100%

[37] [38]

[39] **Figure 13. How inclined are you to use a webstore that tops the search engine results page to make a purchase? (Source: Primary Data)**

S.No.	CONSUMER PERCEPTION	FREQUENCY	PERCENTAGE
1	Yes, definitely	20	13.1%
2	Yes, probably	70	45.8%
3	Neutral	37	24.2%
4	No, probably not	21	13.7%
5	No, definitely not	3	2%
6	Somewhat likely	1	0.7%
7	Very unlikely	1	0.7%
	TOTAL	153	100%

[40] [41]

[42] **Figure 14. Do you intend to buy something from a company that you follow in social media? (Source: Primary Data)**

S.No.	CONSUMER PERCEPTION	FREQUENCY	PERCENTAGE
1	Yes, I strongly believe it	19	12.4%
2	Yes, I somewhat believe it	58	37.9%
3	I'm neutral	55	35.9%
4	No, I somewhat don't believe it	18	11.8%
5	No, I strongly don't believe it	3	2%
	TOTAL	153	100%

[43] [44]

[45] **Figure 15. Would you believe companies with a remarkable social media presence are more trustable? (Source: Primary Data)**

S.No.	CONSUMER PERCEPTION	FREQUENCY	PERCENTAGE
1	Extremely important	63	41.2%
2	Very important	54	35.3%
3	Moderately important	22	14.4%
4	Slightly important	7	4.6%
5	Not important at all	7	4.6%
	TOTAL	153	100%

[46] [47]

[48] **Figure 16. How important is it for you to read reviews before making a purchase from webstore? (Source: Primary Data)**

S.No.	CONSUMER PERCEPTION	FREQUENCY	PERCENTAGE
1	SEO	33	21.6%
2	SMM	37	24.2%
3	Both are equally effective	67	43.8%
4	Neither	16	10.5%
	TOTAL	153	100%

[49] [50]

[51] **Figure 17. Which do you believe is more effective in influencing your purchase decisions – search engine optimization or social media marketing? (Source: Primary Data)**

63866

Ramasubramaniam and Darthy Agnell Mary

S.No.	CONSUMER PERCEPTION	FREQUENCY	PERCENTAGE
1	Myntra	22	14.4%
2	Ajio	14	9.2%
3	Amazon	117	76.5%
	TOTAL	153	100%

[52]

[53]

[54] **Figure 18. From the below stated webstores, which is frequently used by you to shop products and services? (Source: Primary D**

[55]

S.No.	FACTORS	FREQUENCY	PERCENTAGE
1	Price	99	67.7%
2	Quality	122	79.7%
3	Reviews	93	60.8%
4	Trustworthiness	58	37.9%
5	Shipping and delivery options	65	42.5%
6	Return policy	80	52.3%
7	Payment options	57	37.3%
8	Brand reputation	57	37.3%
9	User friendliness of the website	43	28.1%
10	Customer support	44	28.8%
11	Product availability	52	34%
12	Others	3	2%

[56]

[57] **Figure 4.19 What factors do you consider when making a purchase from a Webstore? (Source: Primary Data)**

S.No.	CONSUMER PERCEPTION	FREQUENCY	PERCENTAGE
1	Search engines	107	69.9%
2	Social media	46	30.1%
	TOTAL	153	100%

[58]

[59]

[60] **Figure 20. Would you be more likely to purchase from a webstore that is easy to find through search engines or that has a strong social media presence? (Source: Primary Data)**

	Value	df	Asymp. Sig. (2 sided)
Pearson Chi Square	40.038ᵃ	16	0.001
Likelihood Ratio	35.394	16	0.004
Linear-by-linear association	2.437	1	0.119
No. of Valid Cases	153		

[61]   FIGURE 4.21

	Value	df	Asymp. Sig. (2 sided)
Pearson Chi Square	26.897ᵃ	12	0.008
Likelihood Ratio	29.292	12	0.004
Linear-by-linear association	0.080	1	0.777
No. of Valid Cases	153		

[62]   FIGURE 4.22

[63] **Figure 21. Search engine optimization has a great impact on consumer behaviour towards web stores.**

[64] **Figure 22. Social media marketing (SMM) has a greater impact on consumer behavior towards web stores.**

	Value	df	Asymp. Sig. (2 sided)
Pearson Chi Square	99.148ᵃ	9	0.005
Likelihood Ratio	83.889	9	0.002
Linear-by-linear association	54.961	1	0.110
No. of Valid Cases	153		

[65]   FIGURE 4.23

[66] **Figure 22.CRITERIA 3:Consumer behavior towards web stores is not significantly affected by either.**

RESEARCH ARTICLE

Effect of Hydrologic Variation on Community Structure and Habitat Selection of Stream Fishes in the Western Ghats of Southern Kerala

Ruby Thomas[1]* and K. Raju Thomas[2]

[1]Research Scholar, Department of Zoology, Mar Thoma College, Tiruvalla, Kerala, India.
[2]Assistant Professor, Department of Zoology, Mar Thoma College,Tiruvalla, Kerala, India.

*Address for Correspondence
Ruby Thomas
Research Scholar,
Department of Zoology,
Mar Thoma College,
Tiruvalla, Kerala, India.
E.Mail: rubythomas92@gmail.com

ABSTRACT

Hydrologic variation can have a significant impact on stream fish community structure and habitat choices. This study investigates the impact of hydrologic variation on the community structure and habitat selection of stream fishes in the Western Ghats of southern Kerala. Assessments of fish community structure and stream habitat characteristics were conducted monthly from January 2019 to December 2020. The present study revealed that variation in hydrologic and ecological metrics influences the ichthyofaunal assemblage. Current velocity peaked during the monsoon season and the resident fishes preferred areas with moderate velocity to avoid the shear stress.Pools, riffles, runs, cascades, rapids, falls, glides, and sheets formed the principal habitat/channel units that have been observed. The high summer temperature and hydrologic variations in habitat volume severely reduced the quantity, size, and quality of habitat units in the Western Ghats streams, andimpacted fish assemblage dynamics. Drying and reduced habitat volume may result in a concentration effect, resulting in high fish densities in the pools.

Keywords: Hydrologic variation, Ichthyofauna, Diversity, Habitat, Substrate composition, water depth

Ruby Thomas and Raju Thomas

INTRODUCTION

Hydrologic regimes, also known as flow regimes, play a crucial role in the survival of stream fishes. Fishes have evolved to thrive in specific flow conditions, including water temperature, velocity, and depth. Changes in these flow regimes can have significant impacts on the stream ecosystems and the fish populations that depend on them (Poff and Allan, 1995;Grossman *et al.* 1998; Naiman *et al.* 2008). For example, high flow rates can displace fish from their preferred habitats, while low flow rates can reduce the amount of available habitat and limit feeding opportunities. Yang *et al.* (2020) revealed that the changes in the hydrological regime affect the community structure and habitat selection of fishes. Additionally, changes in water temperature can affect the metabolic rates of fish, potentially leading to changes in growth rates, reproductive success, and overall survival. According to Keller *et al.* (2019), hydrological and water quality variations might alter the availability of habitat for fish to utilise. Therefore, understanding and managing hydrologic regimes is critical to maintaining healthy stream fish populations. Hydrologic variation can be either natural or created by humans. Natural hydrologic fluctuation in streams within an area is often primarily connected to climate, geology, watershed size, and groundwater inputs. Changes in water flow due to climate change or human activities can have significant impacts on fish populations (Yang *et al.* 2008; Junker*et al.* 2015), and understanding how fish respond to these changes can help us to develop better conservation strategies. So, the current study intends to explain the impact of seasonal hydrologic variations on habitat selection and availability to fish assemblages, as well as changes in population structure in response to hydrologic changes in streams.

MATERIALS AND METHODS

Study Area

The study was conducted in five stream systems (S1, S2, S3, S4, and S5)located in the Western Ghats of southern Kerala. The area lies between76° 55' and 77° 17' E longitude and between 9° 10' and 9° 30' N latitude, at an altitudinal range of 100 to 1400 m. Stream substrate in this region ranges from bedrock to silt, with primarily riffle-pool geomorphology.

Assessment of Fish Assemblage Structure and Habitat Selection

We sampled each of the five streams monthly from January 2019 to December 2020. The streams were divided into reaches of 200 m long, and ichthyofaunal sampling and habitat monitoring were carried out. The ichthyofaunal abundance was determined using the number of different species detected throughout the sampling process. Ichthyofaunal specimens were collected simultaneously with habitat assessment, using cast nets and scoop nets. The collected specimens from the streams were preserved in vials, fixed with 10% formalin solution and labelled with the site and habitat identification. Species-level identification was done using the standard keys developed by Talwar and Jhingran (1991), Jayaram (1999), and Froese and Pauly (2021).PAST 4.03 was used to determine diversity for each site in order to examine the community structure of ichthyofauna in the streams. The indices were used to compare the season-wise distribution, abundance, and diversity of species across stream environments.

The substrate composition (Bedrock, Boulder, Cobble and Rubble, Gravel, Sand, and Silt) and stream geomorphic channel units (such as riffle, run, glide, pool, fall, and cascade) were described through visual inspection. Habitat volume is an important component that impacts the assemblage pattern of ichthyofauna in an aquatic environment and is computed from three variables: depth, width, and length of stream stretch (Bastos *et al.* 2010).

abitat volume= Depth×Width×Length (in m³)

The habitat volume is assessed on a seasonal basis (Summer, Monsoon, and Winter) to identify its impact on the ichthyofauna. The qualitative assessment ofhabitat units was further verified by analysing the stream's depth and

63869

Ruby Thomas and Raju Thomas

flow rate. A pigmy-type water current meter, measuring tape, and meter scale were employed for calculating the flow rate, stream width, and depth, respectively.Water temperature was measured in situ by using HM Digital Water Tester (AP-1).

RESULTS AND DISCUSSION

During the study, selected hydrologic and habitat factors (Table 1) across the streams exhibited seasonal fluctuations. The variances in depth, velocity, and bed roughness (substrate size)generate the heterogeneous habitat units (Schneider *et al.* 2015). The current velocity was highest during the monsoon season in all of the analysed stream segments. Summer and winter seasons, on the other hand, were typically distinguished by baseline streamflow. In parts of stream channels with moderate current velocity, resident fishes were over-represented. The ichthyofaunal community prefers the over flooded marginal herbaceous vegetation during monsoon rain days to shield themselves from the shear stress generated by the strong streamflow. Water temperature showed a fall from summer to winter. Fig. 1 depicts a comparison of substrate types from the streams. The most common substrate type in S1 was bedrock (61%), followed by boulder (20%), cobble and rubble (11%), gravel (5%), sand (2%), and silt (1%). The most common stream substrates in S2 were boulders, cobble and rubble. S5 was an ordinary bedrock stream. In S3, sand was the most common substrate, accounting for 62% of the total. Bedrock (42%) and boulder (35%), were the most common substrate types in S4. Mueller and Pyron (2010) point out that substrate composition and fluctuation in water depth are important environmental determinants of fish assemblage composition in an aquatic environment. Pools, riffles, runs, cascades, rapids, falls, glides, and sheets are the principal habitat/channel units recorded in the streams. The number of habitat units per stream reach ranged from 4 to 6. Pools were the most common habitat unit in all stream settings, followed by riffles and runs. Cascades, glides, rapids, and sheets were less common in the selected Western Ghats stream segments. S4 was distinguishable from the other streams by the occurrence of various tiny and large fall patterns. During the summer season in Kerala, the number, extent, and quality of habitat units appear to be considerably diminished. As a result of the drought, the ichthyofauna is forced to use accessible pool units in the vicinity.

The greater depths, slower currents, and structurally complex nature of the pool units allow it to incorporate maximum diversity when compared to others (Thompson and Larsen, 2004; Negi and Negi, 2010).Jeffrey*et al.* (2011) and Perkin *et al.* (2017)reported that drying and habitat volume reduction might subsequently cause a concentration effect, resulting in high fish densities. This can also result in episodic isolation and habitat fragmentation, both of which can impede dispersal and rescue effects. Habitat volume is regarded as a significant determinant of biotic composition and habitat integrity. The habitat volume (m^3) available to resident fishes in the studied stream segments differed with the seasons: summer, monsoon, and winter. The seasonal investigation revealed that the habitat volume peaked during the monsoon season (June-September) because of high rains in the area. Summer temperatures (February-May) resulted in a drop in habitat volume and quality in each stream. S1 had the greatest habitat volume during the 2019-2020 monsoon season, at 1107.9594.11 m^3. Summer emergence in 2019-2020 was observed with the largest habitat volume in S3 (393.9551.63 m^3). In the summer and monsoon seasons of 2019-2020, S2 had the least habitat volume, showing that its narrower stream width had a bigger impact on defining its habitat volume. During the winter, the North-East monsoon provided a modest habitat volume to the Western Ghats streams of southern Kerala.

The composition of ichthyofaunal assemblage varied across the streams in association with different seasons (Fig. 2). This might be due to the changes in the hydrologic regime. Magoulick *et al.* (2021) revealed that spatial and temporal variation in hydrology had a strong influence onfish assemblage dynamics. A similar observation was also made by Tesfay *et al.* (2019). Cyprinidae formed the most abundant family in all streams across all seasons. In S4, Nemacheilidae formed the second abundant ichthyofaunal family, and it showed a significant increasing pattern associated with winter.Belonidae exhibited a slight increase in its abundance during the monsoon season in S1.Variables that modify stream hydrology are expected to influence the fish assemblage dynamics observed (Table

Ruby Thomas and Raju Thomas

2). The diversity indices differed among the investigated streams season-wise. The Shannon and Simpson indices were noted as highest in S4during summer and winter, while S1 scored the highest value in monsoon. S4 exhibited lowest diversity, but maximum evenness in all seasons. Bhat (2004) demonstrated a clear segregation of species in rivers of the central western ghats based on their relationships with environmental and stream features. Arunachalam (2000) revealed that habitat volume was a major determinant of species diversity and abundance in Western Ghats streams; cyprinids were the dominant group in the assemblage, with nearly all cyprinids confined to pools with diverse habitat diversity.

CONCLUSION

The hydrologic variability had a significant impact on the fish community and their habitat preferences. Among the factors, substrate composition, velocity, and water depth changes are critical environmental determinants of fish assemblage composition by regulating channel morphology. Summer temperatures lower habitat units in Kerala, forcing ichthyofauna to rely on available pool units. Drying and habitat volume loss, on the other hand, might result in high fish densities, isolation and fragmentation, and hampered dispersal and rescue operations. The study provides valuable insights into the complex relationships between aquatic ecosystems, hydrology, and biodiversity, which can help us to better understand and manage these delicate ecosystems in the face of climate change and human activities. Further, these findings can help to inform the establishment of effective conservation strategies by providing significant insights into the ecological needs of stream fishes in the Western Ghats.

ACKNOWLEDGEMENTS

REFERENCES

1. Arunachalam M. Assemblage structure of stream fishes in the Western Ghats (India).Hydrobiologia2000; 430: 1-31.
2. Bastos MC, Lilian C, Denise CRF.Meso and Microhabitat analysis and feeding habits of small nektonic characins (Teleostei: Characiformes) in Neotropical streams. Zoologia2010; 27(2): 191-200.
3. Bhat, Anuradha. (2004). Patterns in the distribution of freshwater fishes in rivers of Central Western Ghats, India and their associations with environmental gradients. Hydrobiologia. 529. 83-97. 10.1007/s10750-004-4949-1.
4. Froese R, Pauly D. FishBase. World Wide Web electronic publication; 2021.
5. Grossman GD, RatajczakREJr, Crawford M, Freeman MC. Assemblage organization in stream fishes: Effects of environmental variation and interspecific interactions. EcolMonogr 1998; 68: 395–420.
6. Jayaram KC.The freshwater fishes of the Indian region. Delhi: Narendra Publishing House, 1999.
7. Jeffrey AF, Kurt DF, Robin M, Angela A, Deanna SD, Linda KR, Ramchand O. The role of groundwater pumping and drought in shaping ecological futures for stream fishes in a dryland river basin of the western Great Plains, USA. Ecohydrology 2011; 4: 682–697.
8. Junker J, Heimann FUM, Hauer C, Turowski JM, Rickenmann D,Zappa M,Peter A.Assessing the impact of climate change on brown trout (Salmo trutta fario) recruitment. Hydrobiologia 2015; 751(1): 1-21.
9. Keller K, Allsop Q, Box BJ, Buckle D, Crook DA, Douglas MM, Jackson S, Kennard MJ, Luiz OJ, Pusey BJ, Townsend SA, King AJ. Dry season habitat use of fishes in an Australian tropical river.Scientific Reports 2019; 9 Article No. 5677.
10. Magoulick D,Dekar M, Hodges S, Scott M,Rabalais M, Bare C. Hydrologic variation influences stream fish assemblage dynamics through flow regime and drought. Scientific Reports 2021; 11(1) Article No. 10704.

11. Mueller R, Pyron M. Fish Assemblages and Substrates in the Middle Wabash River, USA. Copeia2010; 1: 47-53.

12. Naiman RJ, Latterell JJ, Pettit NE, Olden JD. Flow variability and the biophysical vitality of river systems. CR Geosci 2008; 340: 629–643.

13. Negi RK, Negi T. Assemblage structure of stream fishes in the Kumaon Himalaya of Uttarakhand State, India. Life Sci J 2010;7(1):9–14.

14. Perkin JS, Gido KB, FalkeJA, FauschKD, Crockett H, Johnson ER, Sanderson J. Groundwater declines are linked to changes in Great Plains stream fish assemblages. Proc Natl Acad Sci USA 2017; 114: 7373–7378.

15. Poff NL, AllanJD. Functional organization of stream fish assemblages in relation to hydrological variability. Ecology 1995; 76:606–627.

16. Schneider JM, Rickenmann D, Turowski JM, Kirchner JW. Self-adjustment of stream bed roughness and flow velocity in a steep mountain channel. Water Resour Res2015; 51: 7838– 7859.

17. Talwar PK,Jhingran AG. Inland Fishes of India and Adjacent Countries.Vol. I and II.New Delhi: Oxford and IBH Co. Pvt. Ltd;1991.

18. Tesfay S, Teferi M, Tsegazeabe HH. Habitat selectivity of fresh water fishes of two second-order tropical streams in Tigray, Northern Ethiopia. Journal of Ecology and Environment 2019; 43. Article No. 9.

19. Thompson LC, Larsen R. Fish habitat in fresh water stream. FWQP Refe Sheet. 2004;10(3):8112.

20. Yang T, Zhang Q, Chen YD, Tao X, Xu C, Chen X.A spatial assessment of hydrologic alteration caused by dam construction in the middle and lower Yellow River, China. Hydrological Processes 2008; 22(18): 3829-3843.

21. Yang B, Ming D, Rui X, Yi-Ming K, Guiqiu L, Lisha S.Effects ofhydrological alteration on fish population structure and habitat in river system: A casestudy in the mid-downstream of the Hanjiang River in China. Global Ecology and Conservation 2020; 23,e01090.

Table 1: Major Hydrologic and Habitat factors recorded from investigated streams of the Western Ghats in southern Kerala

STUDY STREAMS	HYDROLOGIC AND HABITAT FACTORS	SEASONS		
		SUMMER	MONSOON	WINTER
S1	Stream Width (m)	8.36±2.15	19.25±1.38	16.35±4.68
	Stream Depth (cm)	29.7±9.45	44.01±9.25	27.57±7.97
	Average Current Velocity (m/s)	0.658±0.13	5.05±0.23	1.05±0.9
	Water Temperature (°C)	26.52±2.6	25.42±0.65	24.42±1.19
	Habitat Volume (m³)	264.92±94.05	908.27±223.07	355.31±121
	Channel/Habitat Units	Riffle, Pool	Run, Pool, Glide	Pool, Riffle
S2	Stream Width (m)	3.61±0.59	4.96±0.58	4.75±0.65
	Stream Depth (cm)	58.5±4.82	98.56±19.19	45.42±6.84
	Average Current Velocity (m/s)	0.8±0.69	1.09±0.94	0.46±0.1
	Water Temperature (°C)	25.9±1.66	25.9±0.54	25.25±0.56
	Habitat Volume (m³)	217.95±35.85	556.9±362.65	129.5±49.8
	Channel/Habitat Units	Pool	Pool, Riffle, Cascade	Pool
S3	Stream Width (m)	12.55±0.47	12.66±0.4	12.87±0.12
	Stream Depth (cm)	31.5±4.23	58.49±12.3	54.85±37.7
	Average Current Velocity (m/s)	0	0.56±0.1	0.06±0.01
	Water Temperature (°C)	28.87±1.55	26.4±1.1	25.9±1

Ruby Thomas and Raju Thomas

	Habitat Volume (m³)	393.95±44.71	710.64±168.73	702.14±476
	Channel/Habitat Units	Pool	Run, Sheet, Glide	Pool, Riffle
S4	Stream Width (m)	4.56±2.14	7.26±1	6.7±0.41
	Stream Depth (cm)	42.64±42.53	65.25±7.22	56.95±23.9
	Average Current Velocity (m/s)	0.31±0.09	2.08±0.19	1.38±0.9
	Water Temperature (℃)	27.35±0.86	25.37±0.87	24.6±0.33
	Habitat Volume (m³)	441.47±314.46	838.45±263.07	378.75±165
	Channel/Habitat Units	Pool	Pool, Riffle, Run, Cascade, Fall	Pool, Riffle, Cascade
S5	Stream Width (m)	6.76±1.72	13.27±1.56	9.3±2.65
	Stream Depth (cm)	35.04±10.01	48.09±9.37	28.575±2.9
	Average Current Velocity (m/s)	0.54±0.21	9.86±5.8	2.55±0.94
	Water Temperature (℃)	28.35±1.38	26.77±0.83	25.72±1.17
	Habitat Volume (m³)	276.51±167.07	730.38±159.8	311.9±128.2
	Channel/Habitat Units	Pool, Cascade, Riffle	Run, Riffle	Pool, Cascade, Riffle

Table 2: Season-wise fish diversity indices at different study streams

SEASON	DIVERSITY INDICES	S1	S2	S3	S4	S5
SUMMER	No. of ichthyofaunal family	6	4	4	6	4
	Individuals	355	190	360	205	289
	Simpson_1-D	0.1695	0.1492	0.05972	0.4361	0.1592
	Shannon_H	0.4186	0.3559	0.1629	0.8196	0.3233
	Evenness_e^H/S	0.2533	0.3569	0.2942	0.3783	0.3454
	Berger-Parker	0.9099	0.9211	0.9694	0.7171	0.9135
MONSOON	No. of ichthyofaunal family	4	3	3	3	3
	Individuals	258	139	239	143	158
	Simpson_1-D	0.2846	0.1219	0.04926	0.2624	0.1193
	Shannon_H	0.5666	0.2624	0.1347	0.4578	0.2565
	Evenness_e^H/S	0.4406	0.4334	0.3814	0.5268	0.4308
	Berger-Parker	0.8372	0.9353	0.9749	0.8462	0.9367
WINTER	No. of ichthyofaunal family	5	3	2	3	2
	Individuals	455	182	267	109	165
	Simpson_1-D	0.3331	0.03254	0.02951	0.5237	0.1653
	Shannon_H	0.6726	0.09451	0.0778	0.7973	0.3046
	Evenness_e^H/S	0.3919	0.3664	0.5405	0.7399	0.6781
	Berger-Parker	0.8066	0.9835	0.985	0.5229	0.9091

Ruby Thomas and Raju Thomas
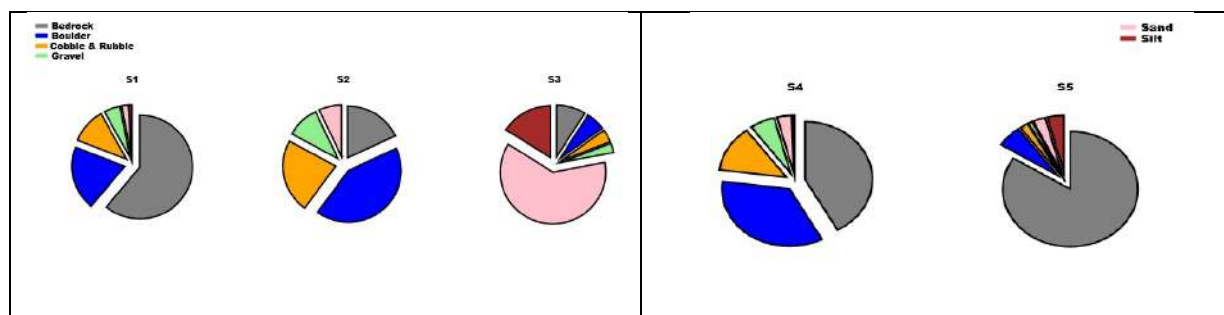
Fig. 1: Substrate composition recorded from study streams
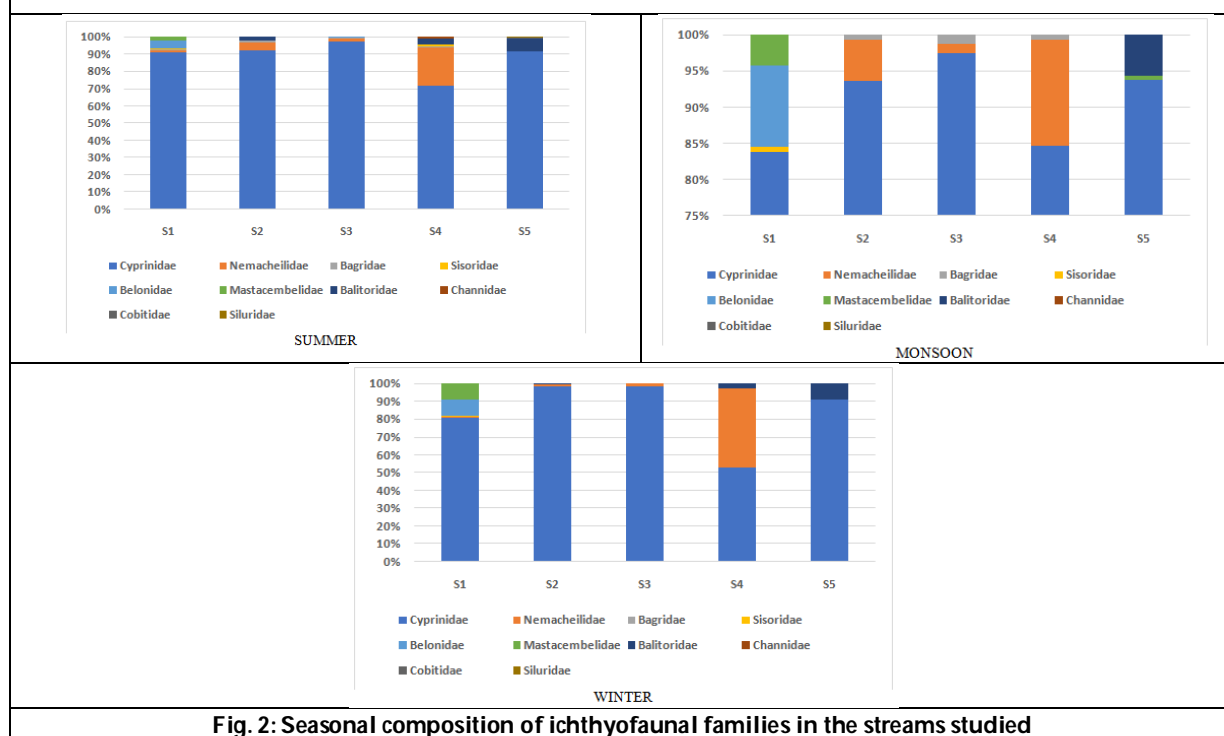
Fig. 2: Seasonal composition of ichthyofaunal families in the streams studied

RESEARCH ARTICLE

Study to Assess the Effectiveness of an Information Booklet on Knowledge Regarding Planned Parenthood among Eligible Couples at Selected Areas of Surat District, Gujarat

Ashwini Patil[1]* and M Jayalakshmi[2]

[1]Research Scholar, P P Savani School of Nursing, P P Savani University, Surat, Gujarat, India
[2]Professor, P P Savani School of Nursing, P P Savani University, Surat, Gujarat, India

*Address for Correspondence
Ashwini Patil
Research Scholar,
P P Savani School of Nursing,
P P Savani University, Surat, Gujarat, India
E. Mail: ashwini.patil@ppsu.ac.in

ABSTRACT

Womanhood is the period in a female's life after she had transitioned through childhood and adolescence and woman refers to adult human beings who are biologically female, that is capable of bearing off springs [1]. Planning about parenthood is considered as a vital step in economic and social planning [2] The aim of this study was to assess the effectiveness of the information booklet on knowledge regarding Planned Parenthood among eligible couples. Quantitative research approach in was used in this study. The study was conducted in selected areas of Surat district Gujarat. The convenience non-probability sampling technique was used to select 30 mothers in selected areas of Surat. A structured knowledge questionnaires were used. Data were analyzed using descriptive and inferential statistics. The data reveals the respondent's knowledge score was high in the post-test (M = 17.16) than that in the pre-test (M = 5.93). The obtained mean difference was 11.23. The obtained 'T Value, t = 2.98 (P = 2.05) was highly significant. Therefore, the research hypothesis (H_1) was accepted at 0.05 level of significance. The above findings supported that information booklet was effective to gain insight and increase knowledge regarding planned parenthood among eligible couples.

Keywords: knowledge, planned parenthood, information booklet, eligible couples.

Ashwini Patil and Jayalakshmi

INTRODUCTION

woman refers to adult human beings who are biologically female, that is capable of bearing offsprings[1]. Pregnancy is a common event that occurs in woman's life. Becoming a parent is considered as one of the maturational milestones of adult life that can be stressful but also rewarding as the woman prepares for a new level of caring and responsibility[2] Planned Parenthood, is a non profit organization that provides reproductive health care in the United States and globally. It is a tax-exempt corporation under Internal Revenue Code section 501(c)(3)[7] and a member association of the International Planned Parenthood Federation (IPPF). Planned Parenthood provided care and education to millions, and fought for the rights of all people.

Statement of the Problem
A study to assess the effectiveness of an information booklet on knowledge regarding Planned Parenthood among eligible couples at selected areas of Surat district, Gujarat.

Objectives of the Study
1. To assess the demographic variable of eligible couples.
2. To assess the pre test knowledge regarding planned parenthood among eligible couples.
3. To evaluate the effectiveness of information booklet on knowledge regarding planned parenthood among eligible couples.
4. To find out the association between pre test knowledge score and selected socio demographic variable

Hypothesis
H1 - There will be significant difference in pre-test and post-test knowledge levels of eligible couples regarding Planned Parenthood
H2 - There will be a significant association between the pre-test knowledge scores of eligible couples with their selected socio-demographic variable

Delimitation
This study is delimited to eligible couples of selected areas of Surat district.

RESEARCH METHODOLOGY

Research Design and Approach
Pre-experimental approach with one group pre test post test design.

Research Setting
The setting of the study was the selected area of Surat district

Sampling Technique
A convenient sampling technique was used to select the samples.

Sample Size
30 samples are selected.

Development of the Tool
Based on the goals and literature review, the researcher created the instrument for the current study. The subject experts and guide improved and validated the tool that was developed.

Description of the Tool

Section A demographic characteristics

The first part of the tool consists of 10 items for obtaining information about the selected background factor such as age (in a year), husband age (in a year), education, occupation, income, married life, area of living, type of family, religion, previous knowledge about Planned Parenthood

Section B knowledge questionnaire

Questionnaire is to assess the knowledge of eligible couples regarding Planned Parenthood. It consist of 30 items of multiple choice question total score is 30.

For right score – 1

For the wrong score – 0

The knowledge level has been arbitrarily divided into three categories based

Adequate knowledge: - above 19

Moderate knowledge:- 09-18

Poor knowledge:- 0-8

RESULT

Analysis and Interpretation of data are based on the objectives and Hypothesis. Analysis of the data collected using a Structured Questionnaire was based on the following heading:

Section – I frequency and percentage distribution of the socio demographic variables

- Majority of the respondents 12(12%)were in the age of 21-25 years,9(9%)respondents were between the age of 26-30 years, 6(6%) respondents were between the age of 18-20 years, and remaining respondents 3 (3%) were between the age of 30-35 years.

- Majorityoftherespondents21(21%)wereintheageof20-25years,9(9%)respondents were between the age of 25-30 years.

- Majority 14(14%) of the respondents were primary school , 15(15%) respondents were secondary school,1(1%)respondents were higher secondary school.

- Majority 15(15%) of the respondents were labour working ,14(14%) respondents were housewife and remaining 1(1%)respondents were job.

- Majority 15(15%)of respondents were of income between 5000-10,000, 14(14%)respondents were of income less than 5000 , remaining 1(1%) respondents were income between 10,000-20,000 and 0(0%) respondents were income is more than 20,000.

- Majority 18(18%) of respondents were of married life between 2-5 year 6(6%) of respondents were of married life between 6 month-1 year, 4(4%) of respondents were on married life between 6-9 year and remaining 2(2%) of respondents of married life is more than 10 year.

- Among the respondents 30(30%)were coming from rural area and0(0%)were coming from urban.

- Distribution of eligible couples according to their family type shows that nuclear24(24%)and 6(6%).

- Majority of respondents 30(30%) were Hindu and remaining all Muslim , Christian ,Otherare0(0%).

- Majority of respondents18(18%) were not having previous information regarding planned parenthood , 6(6%)get information through the mass media , newspaper ,4(4%) get information through the family, friends, relatives and remaining 2(2%) get information through the neighbors.

Section – II

In the pre-test prior to the administration of information booklet data reflects that out of 30 respondents,25(90%)had inadequate knowledge,05(10%)had moderately adequate knowledge and no one had adequate knowledge on

63877

Ashwini Patil and Jayalakshmi

Planned Parenthood. But in the post test was observed that 05(10%) respondents had adequate knowledge, 25(90%) had moderately adequate knowledge and no one had in adequate knowledge Planned Parenthood.

The data reveal the respondent's knowledge score was high in the post-test (M = 17.16) than that in the pre-test (M = 5.93). The obtained mean difference was 11.23. The obtained 'T Value, t = 2.98 (P = 2.05) was highly significant. Therefore, the research hypothesis (H$_1$) was accepted at 0.05 level of significance.

Recommendations

1. On a large sample, a comparative study can be conducted.
2. Different settings might be used for the same investigation.
3. By utilizing various instruments and methods, a comparative study can be conducted.

REFERENCES

1. Women.[online].Available from: URL: http://en.wikipedia.org
2. Pilliteri A. Maternal and child health nursing. Philadelphia: LippincottCompany;1992.
3. Bennet RV, Brown LK. Textbook for midwives. 13th ed. New York: Churchill Livingstone; 2001.
4. Cook AL. Assessment of prenatal experiences by primigravida. 1985 Mar.[online]. Available from: URL:http://docs.google.com.
5. Jacob A. A comprehensive text book of Midwifery. 2nd ed. New Delhi: JaypeeBrothers;2007.
6. Evans A.Antenatal Preparation For Parenthood Classes.2001 Feb.[online].Available From: URL:http://www.dataprevproject.net
7. PlannedParenthoodAnnualReport2012–2013,p.18.
8. Wayne, T. (2011). Planned parenthood. In M. Z. Stange C. K. Oyster & J. E.Sloan(Eds.),Encyclopedia Of Women In Today's World(Vol.4,pp.1107–1108)

Section II

Table 1:Range, mean, and standard deviation of pre-test and post-test awareness score of eligible couples.

Test	Mean	s.d.	T VALUE
Pre test	5.93	172.09	2.98
Post test	17.16	395.83	

Table 2: Table 2 shows that all socio-demographic variables and their the calculated chi-square value were Age(x_2=2.09),Husbandage(x_2=2.16),Education(x_2=6.51),Occupation(x_2=1.52),Income(x_2=4.22), Married Life(x_2=2.49), Area of living(x_2=0),Type of family(x_2=39.72),Religion(x_2=0), previous knowledge(x_2=2.92), is more than the table value P>0.05. Hence there is a significant association between pre-test knowledge scores and selected socio-demographic variables.

SR. NO.	CHARACTERISTICS	CATEGORIES	FREQUENCY	%	level of knowledge			df	chi square	table value	signifi cant
					0-8		>19				
1	AGE (IN YEAR)	18-20	6	20%	2	4	0	6	2.09	12.95	NS
		21-25	12	40%	5	7	0				
		26-30	9	30%	4	5	0				
		30-35	3	10%	0	3	0				
2	HUSBANDAGE(IN YEAR)	20-25	21	60%	10	5	5	6	2.16	12.95	NS
		25-30	9	30%	2	5	3				
		31-34	0	10%	0	0	0				

Ashwini Patil and Jayalakshmi

		ABOVE35	0	0%	0	0	0				
3	EDUCATION	PRIMARY	14	47%	10	2	2				
		SECONDARY	15	50%	12	3	0				
		HIGHER SECONDARY	1	3%	0	1	0				
		GRADUATION AND POST GRADUATION	0	0%	0	0	0	6	6.51	12.95	NS
4	OCCUPATION	OWN BUSINESS	0	0%	0	0	0				
		LABOUR WORK	15	50%	10	5	0				
		JOB	1	3%	0	1	0	6	1.52	12.95	NS
		HOUSEWIFE	14	47%	10	4	0				
5	INCOME	<5000RS.	14	47%	12	2	0				
		5000-10,000RS.	15	50%	10	5	0				
		10,000-20,000RS.	1	3%	0	1	0	6	4.22	12.95	NS
		>20,000RS.	0	0%	0	0	0				
6	MARRIED LIFE	6 MONTH-	6	20%	5	1	0				
		2-5YEAR	18	60%	10	7	1				
		6-9YEAR	4	13%	2	2	0	6	2.49	12.95	NS
		>10YEAR	2	7%	1	1	0				
7	AREA OF LIVING	RURAL	30	100%	20	8	2	2	0	2.75	NS
		URBAN	0	0%	0	0	0				
8	TYPEOF FAMILY	NUCLEAR	24	80%	10	10	4	2	39.72	2.75	S
		JOINT	6	20%	3	3	0				
9	RELIGION	HINDU	30	100%	17	12	1				
		MUSLIM	0	0%	0	0	0				
		CHRISTIAN	0	0%	0	0	0	6	0	12.95	NS
		OTHER	0	0%	0	0	0				
10	PREVIOUS KNOWLEDGE	MASS MEDIA, NEWSPAPER	6	20%	5	1	0				
		FAMILY,FRIENDS, RELATIVES	4	13%	2	2	0				
		NEIGHBOURS	2	7%	2	0	0	6	2.92	12.95	NS
		NO INFORMATION	18	60%	10	8	0				

RESEARCH ARTICLE

Fixed Point of Kannan Type and Asymptotic Set-Valued Maps Defined on Sets in Complete Metric Spaces

Murchana Neog*

Assistant Professor, Department of Mathematics, Assam down town University, Panikhaiti, Guwahati, Asssam-781026, India

*Address for Correspondence
Murchana Neog
Assistant Professor,
Department of Mathematics,
Assam down town University,
Panikhaiti, Guwahati, Asssam-781026, India
E.Mail: murchananeog@gmail.com

ABSTRACT

In this paper, by introducing the notion of a contraction for for Kannan type set-valued mappings with set-valued domain in a metric space we examine the existence as well as uniqueness of fixed points of that map on a complete metric space. Some results are proved using the concept of asymptotic regularity. Also, we provide an elementary proof of Kannan's result for set-valued mapping defined on a complete metric space. Some examples have also been given to demonstrate the non-triviality of our results.

Keywords: Fixed point; Complete metric space, set-valued mapping; set-valued domain; Kannan type set-valued mapping, asymptotic regular map.

INTRODUCTION

In 1968, Kannan [10] established one of the beautiful extension of 'Banach Contraction Principle' . The most important fact of Kannan's result was that the self mapping on a complete metric space need not be continuous. After that Subrahmanyam [18] showed that Kannan's result characterizes the metric completeness concept. Also, it is shown in [17] that Kannan's theorem is independent of the famous Banach Contraction Principle. Due to such ulities, Kannan's theorem has been extensively studied and generalized on many settings, see   ([6], [11], [12]). Very recently, J.Gornicki [9] has proved some fixed point theorems for Kannan type mappings. Fixed point results for set-valued maps play an important role in non-linear analysis. Fixed point theory for multi valued operators is also an important topic for set-valued analysis. Application of set-valued mappings are found in control theory, convex optimization, differential inclusions and economics. Markin [13] and Nadler [14] introduced the fixed point results

63880

Murchana Neog

for set-valued mappings. There have been enormous developments in the area of existence and uniqueness of fixed point for multi valued and set-valued mappings in various directions, see ([1], [2], [3], [5], [7],[8], [15]). In this paper, we prove some fixed point theorems for Kannan type set-valued maps defined on set in the settings of a complete metric space. Our results generalize and extend many existing results in literature, especially those of Gornicki [9].

Preliminaries: Now some important definitions and results are listed below that are necessary in our main results. By $\Box$ and $\Box_+$ we mean the set of natural numbers and non- negative real numbers respectively.

Definition 2.1 [10] Suppose (X, d) is a metric space. The self map R on X is called a Kannan map if there exists some $0 \le \lambda < 1$ such that

$$d(\mathrm{R(x)}, \mathrm{R(y)}) \le \frac{\lambda}{2}[\mathrm{d(x, R(x))} + \mathrm{d(y, R(y))}] , \quad \text{for each } x, y \in X .$$

In 1968, Kannan proved the following theorem.

Theorem 2.2 [10] Suppose R is a Kannan map on a complete metric space (X, d). Then R has a unique fixed point $x \in X$.

By WB(X) we mean the collection of all non-empty closed and bounded subsets of X. If

$$H(\mathrm{E}, \mathrm{F}) = \max_{v_0 \in F}\{\sup \mathrm{D}(v_0, \mathrm{E}), \sup_{u_0 \in E} \mathrm{D}(u_0, \mathrm{F})\}, \quad E, F \in WB(\mathrm{X})$$

where $D(\mathrm{u}_0, \mathrm{F}) = \inf_{v_0 \in F} d(\mathrm{u}_0, \mathrm{v}_0)$. Then $(WB(\mathrm{X}), \mathrm{H})$ forms a metric space and H is said to be Hausdorff metric generated by d.

Definition 2.3 Suppose $\{\mathrm{A}_k\}$ is a sequence of closed subsets of a metric space X and $A_0 \subset X$ is also closed. We say that $A_k \to A_0$ with respect to the Hausdorff metric if and only if $\lim_{k \to \infty} H(\mathrm{A}_k, A_0) = 0$.

Definition 2.4 The set $\mathrm{A}_0 \in WB(\mathrm{X})$ is called a fixed point of $R : WB(\mathrm{X}) \to \mathrm{WB(X)}$ if $A_0 = R(\mathrm{A}_0)$.

In the year of 1969, using the notion of Hausdorff distance between any two sets, Nadler proved the following fixed point results, which generalize the Banach Contraction Principle in set-valued directions.

Theorem 2.5. [14] Suppose (X, d) is a complete metric space and the map $R : \mathrm{X} \to \mathrm{WB(X)}$ satisfies

$$H(\mathrm{R(x}_0), \mathrm{R(y}_0)) \le \beta d(\mathrm{x}_0, \mathrm{y}_0); \quad \text{for each } \mathrm{x}_0, \mathrm{y}_0 \in X$$

where $0 \le \beta < 1$. Then R has a unique fixed point.

In the present paper, we consider the map $R : WB(\mathrm{X}) \to \mathrm{WB(X)}$ instead of $R : \mathrm{X} \to \mathrm{X}$ or $R : \mathrm{X} \to WB(\mathrm{X})$ to investigate the necessary changes that have to be made in the definition of a contraction map in this new setting in order to obtain similar results. Also, we investigate how the proofs of our results are influenced due to these changes.

Kannan Type Set-Valued Mapping With Set-Valued Domain
In this section, we discuss our main results.

Definition 3.1. The function $R : WB(\mathrm{X}) \to \Box_+$ is called lower semi continuous at $A_0 \in WB(\mathrm{X})$ if for any sequence $\{A_n\} \in WB(\mathrm{X})$ such that $A_n \to A_0$ implies $R(A_0) \le \liminf_{n \to \infty} R(A_n)$.

Definition 3.2. The map $R : WB(\mathrm{X}) \to WB(\mathrm{X})$ is called continuous at $\mathrm{A}_0 \in WB(\mathrm{X})$ if $\mathrm{A}_n \to A_0$ implies $\mathrm{R(A}_n) \to R(A_0)$.

Theorem 3.3. Let $(WB(\mathrm{X}), \mathrm{H})$ be a complete metric space and $\mathrm{R : WB(X)} \to WB(\mathrm{X})$ a set-valued map such that there exists $\beta < \frac{1}{2}$ satisfying

Murchana Neog

$$H(R(E_0), R(F_0)) \leq \beta[H(E_0, R(E_0)) + H(F_0, R(F_0))], \quad \text{for each } E_0, F_0 \in WB(X). \qquad (3.1)$$

Then R has a unique fixed point $P_0 \in WB(X)$ and for any $A_0 \in WB(X)$, the sequence of iterates $\{R^n(A_0)\}$

converges to P_0 and $H(R^{n+1}(A_0), P_0) \leq \beta.\left(\dfrac{\beta}{1-\beta}\right)^n H(A_0, R(A_0)), n = 0, 1, 2...$

Before proving the theorem, we prove the following Lemma.

Lemma 3.4. Suppose $(WB(X), H)$ is a complete metric space and $R : WB(X) \to WB(X)$ a set-valued map

such that there exists $\beta < \dfrac{1}{2}$ satisfying 3.1. If for any $E_0 \in WB(X)$, there exists $U_0 \in WB(X)$ such that

$H(U_0, R(U_0)) \leq a.H(E_0, R(E_0))$ and $H(E_0, U_0) \leq b.H(E_0, R(E_0))$, where

$a, b \in \square$ and $a \in [0,1), b > 0$. Then R has at least one fixed point.

Proof: Suppose $A_0 \in WB(X)$. Consider a sequence $\{A_n\} \in WB(X)$ satisfies

$$H(R(A_{n+1}), A_{n+1}) \leq a.H(R(A_n), A_n),$$

and $H(A_{n+1}, A_n) \leq b.H(A_n, R(A_n)), n = 0, 1, 2...$

Now $\quad H(A_{n+1}, A_n) \leq b.H(A_n, R(A_n))$

$\leq b.a.H(A_{n-1}, R(A_{n-1}))$

$\dots$

$\leq b.a^n.H(A_0, R(A_0))$.

Thus for any positive integer m, we get

$$H(A_n, A_{n+m}) \leq H(A_n, A_{n+1}) + H(A_{n+1}, A_{n+2}) + ... + H(A_{n+m-1}, A_{n+m})$$

$$\leq b.a^n H(A_0, R(A_0)) + b.a^{n+1} H(A_0, R(A_0)) + ... + b.a^{n+m-1} H(A_0, R(A_0))$$

$$= a^n(1 + a + a^2 + ... + a^{m-1}).b.H(A_0, R(A_0))$$

$$\leq \frac{a^n(1-a^m)}{1-a}.b.H(A_0, R(A_0)).$$

Since $a \in [0,1)$, we have $a^n \to 0$ as $n \to \infty$. Thus $\{A_n\}$ is a Cauchy sequence in WB(X). As (WB(X), H) is

complete, we get $\lim_{n \to \infty} A_n = P_0$, for some $P_0 \in WB(X)$.

Now, $\quad H(R(P_0), P_0) \leq H(R(P_0), R(A_n)) + H(R(A_n), A_n) + H(A_n, P_0)$

$$\leq \beta[H(P_0, R(P_0)) + H(A_n, R(A_n))] + H(R(A_n), A_n) + H(A_n, P_0)$$

$$\Rightarrow H(R(P_0), P_0) \leq \frac{\beta+1}{1-\beta} H(R(A_n), A_n) + \frac{1}{1-\beta} H(A_n, P_0)$$

$$\leq \frac{\beta+1}{1-\beta} a^n.H(R(A_0), A_0) + \frac{1}{1-\beta} H(A_n, P_0) \quad .$$

Taking $n \to \infty$, we get $H(R(P_0), P_0) = 0$; i.e., $P_0 = R(P_0)$.

Now we proof the **Theorem 3.3.**

Proof. For any $E_0 \in WB(X)$, let $U_0 = R(E_0)$. Then,

$H(U_0, R(U_0)) = H(R(E_0), R(U_0))$

63882

$$\leq \beta[H(E_0, R(E_0)) + H(U_0, R(U_0))]$$

$$\Rightarrow H(U_0, R(U_0)) \leq \frac{\beta}{1-\beta} H(E_0, R(E_0)),$$

By assumption $\frac{\beta}{1-\beta} < 1$ and $H(E_0, U_0) = H(E_0, R(E_0))$. Now for any $A_0 \in WB(X)$, define a sequence

$\{A_n\}$ where $A_{n+1} = R(A_n)$, for $n = 0, 1, 2, \ldots$ Then we have $A_n = R^n(A_0)$. Therefore by **Lemma 3.4.** we have

$\{A_n\}$ converges to $P_0 \in WB(X)$ and $P_0 = R(P_0)$.

Suppose Q_0 is another fixed point of R. Then

$$H(P_0, Q_0) = H(R(P_0), R(Q_0))$$
$$\leq \beta[H(P_0, R(P_0)) + H(Q_0, R(Q_0))]$$
$$= 0.$$

Therefore $P_0 = Q_0$. Hence R has a unique fixed point P_0. Since $A_0 \in WB(X)$ was arbitrary, this gives that for

each $A_0 \in WB(X)$, the sequence $\{R^n A_0\}$ converges to the unique fixed point P_0.

Again for each $A_0 \in WB(X)$,

$$H(R^{n+1}(A_0), R^n(A_0)) \leq \beta[H(R^n(A_0), R^{n+1}(A_0)) + H(R^{n-1}(A_0), R^n(A_0))]$$

$$\Rightarrow H(R^{n+1}(A_0), R^n(A_0)) \leq \frac{\beta}{1-\beta} H(R^{n-1}(A_0), R^n(A_0)).$$

Now, $H(R^{n+1}(A_0), P_0) = H(R^{n+1}(A_0), R(P_0))$

$$\leq \beta[H(R^n(A_0), R^{n+1}(A_0)) + H(P_0, R(P_0))]$$

$$= \beta[H(R^n(A_0), R^{n+1}(A_0))]$$

$$\leq \beta \left(\frac{\beta}{1-\beta}\right)^n H(A_0, R(A_0)), \quad n = 0, 1, 2, \ldots$$

Asymptotic Regularity

In this section, we use the concept of asymptotic regularity and establish its connection with fixed points.

Definition 4.1. Suppose (WB(X), H) is a metric space. A function $R : WB(X) \to WB(X)$ is called asymptotic

regular if $\lim_{n \to \infty} H\left(R^{n+1}(B), R^n(B)\right) = 0$, for all $B \in WB(X)$.

Theorem 4.2. Suppose (WB(X), H) is a complete metric space and $R : WB(X) \to WB(X)$ is an asymptotically

regular mapping such that there exists $\beta < 1$ satisfying equation 3.1. Then R has a unique fixed point.

Proof: Let $B_0 \in WB(X)$. Define a sequence $\{B_n\}$ such that $B_{n+1} = R(B_n)$, for $n = 0, 1, 2, \ldots$ Then we have

$B_n = R^n(B_0)$, for all $n \in \square$. As R is asymptotic regular, for $m, n \in \square$ such that $m > n$ we get,

$$H(B_n, B_m) = H(R^n(B_0), R^m(B_0))$$

$$\leq \beta[H(R^{n-1}(B_0), R^n(B_0)) + H(R^{m-1}(B_0), R^m(B_0))]$$

Which converges to zero if $m, n \to \infty$. This gives that $\{B_n\}$ is a Cauchy sequence. As $(\mathrm{WB(X)}, \mathrm{H})$ is complete, we get $\lim\limits_{n\to\infty} B_n = S_0$, for some $S_0 \in \mathrm{WB(X)}$.

Now, $H(S_0, \mathrm{R}(S_0)) \le H(S_0, \mathrm{R}^n(B_0)) + H(\mathrm{R}^n(B_0), \mathrm{R}(S_0))$

$\le H(S_0, \mathrm{R}^n(B_0)) + \beta[H(\mathrm{R}^{n-1}(B_0), \mathrm{R}^n(B_0)) + H(S_0, \mathrm{R}(S_0))]$

$\Rightarrow (1-\beta)H(S_0, \mathrm{R}(S_0)) \le H(S_0, \mathrm{R}^n(B_0)) + \beta\, \mathrm{H}(\mathrm{R}^{n-1}(B_0), \mathrm{R}^n(B_0))$

$\Rightarrow H(S_0, \mathrm{R}(S_0)) \quad \le \dfrac{1}{1-\beta} H(S_0, \mathrm{R}^n(B_0)) + \dfrac{\beta}{1-\beta} H(\mathrm{R}^{n-1}(B_0), \mathrm{R}^n(B_0))$

which is converge to zero if $n \to \infty$. Hence $S_0 = R(S_0)$. It is obvious that S_0 is unique. Since $B_0 \in WB(X)$ was arbitrary, this gives that for each $B_0 \in WB(X)$, the sequence $\{R^n(B_0)\}$ converges to the unique fixed point S_0.

Remark 4.3. A Kannan type mapping $\mathrm{R} : WB(\mathrm{X}) \to \mathrm{WB(X)}$ satisfies the following property

$\mathrm{H}(\mathrm{R}(E_0), \mathrm{R}(F_0)) < \mathrm{H}(E_0, R(E_0)) + \mathrm{H}(F_0, R(F_0))$, for all $E_0, F_0 \in WB(X)$ with $E_0 \ne F_0$. (4.1)

If R is asymptotically regular then it's not necessary that R contain a fixed point This can be demonstrated with the help of following example.

Example 4.4. Suppose $\mathrm{X} = [0,1], \mathrm{k} \ge 2$. The metric $d : \mathrm{X} \times \mathrm{X} \to \Box_+$ is defined by

$$d(\mathrm{p},\mathrm{q}) = \begin{cases} 0, & if \ \mathrm{p} = \mathrm{q} \\[2mm] \dfrac{1}{k^3}, & if \ p,q \in [0, \frac{1}{2}], \ \text{either } \mathrm{p},\mathrm{q} \in \Box \text{ or } \mathrm{p},\mathrm{q} \in \Box' \\[2mm] \dfrac{1}{k}, & if \ p,q \in [0, \frac{1}{2}], \ \mathrm{p} \in \Box, \mathrm{q} \in \Box' \\[2mm] \dfrac{1}{k^2}, & otherwise \end{cases}$$

Moreover, the Hausdroff metric $H : WB(\mathrm{X}) \to \Box_+$ is defined as

$$\mathrm{H(P,Q)} = \begin{cases} \dfrac{1}{k^3}, & if \ P,Q \subseteq [0, \frac{1}{2}] \\[2mm] \dfrac{1}{k^2}, & if \ P \ or \ Q \ (or\ both) \not\subseteq [0, \frac{1}{2}] \\[2mm] 0, & if \ P = Q \end{cases}$$

The set-valued mapping $\mathrm{R} : WB(\mathrm{X}) \to WB(\mathrm{X})$ is defined as

$$\mathrm{R(P)} = \begin{cases} [0, \frac{2}{3}], & if \ P \subseteq [0, \frac{1}{2}] \\[2mm] [0, \frac{1}{3}], & if \ P \not\subseteq [0, \frac{1}{2}] \end{cases}$$

Now for all $P, Q \in WB(\mathrm{X})$, consider the cases given below:

(i)   If $P, Q \subseteq [0, \frac{1}{2}]$, then we have $\mathrm{H(R(P), R(Q))} = 0$.

Murchana Neog

(ii)   If $P \subseteq [0, \frac{1}{2}]$ and $Q \nsubseteq [0, \frac{1}{2}]$, we have

$$\mathrm{H(R(P), R(Q))} = \frac{1}{k}$$

$$< \frac{2}{k}$$

$$= \frac{1}{k} + \frac{1}{k}$$

$$= H(\mathrm{P, R(P)}) + H(\mathrm{Q, R(Q)}).$$

(iii)   If $P, Q \nsubseteq [0, \frac{1}{2}]$, we have $\mathrm{H(R(P), R(Q))} = 0$.

Hence R satisfies the equation 4.1 for all $P \in WB(\mathrm{X})$. Also R is asymptotically regular, but no fixed point is contain in R.

CONCLUSION

In this paper, using the concept of asymptotic regularity, we have proved some fixed point results for Kannan type set-valued mappings with set-valued domain. Our results unify and extend some existing results in literature. The proofs also give us schemes how to find the desired fixed point of such maps. Similar generalization of well known fixed point results for the map of the type $R : WB(\mathrm{X}) \rightarrow \mathrm{WB(X)}$ would be an interesting topic for the future study.

REFERENCES

1. Abbas, M., Alfuraidan, M. R., Khan, A. R. and Nazir, T. Fixed point results for set contractions on metric spaces with a directed graph. Fixed point Theory Appl., 2015:14:doi: 10.1186/s13663-015-0263-z, 2015.
2. Abbas, M., Nazir, T., Lampert, T. A. and Radenovic, S. Common fixed points of set-valued F-contraction mappings on domain of sets endowed with directed graph. Comp. Appl. Math., doi: 10.1007/s40314-016-0314-z, 2016.
3. Abbas, M., Nazir, T., Propovic, B. Z. and Radenovic, S. On weakly commuting set-valued mappings on domain of sets endowed with directed graph. Results in Mathematics., 71(3-4):1277-1295, 2017.
4. N. A. Assad and W. A. Kirk. Fixed point theorems for set-valued mappings of contractive type. Pac. J. Math., 43(3):553-561, 1972.
5. M. Berinde and V. Berinde. On a general class of multi-valued weakly picard mappings. J. Math. Anal. Appl.,326:772-782, 2007.
6. S. K. Chatterjea. Fixed point theorems. C. R. Acad. Bulgare Sci., 25(6):727-730, 1972.
7. P. Debnath, B. S. Choudhury, and M. Neog. Fixed set of set valued mappings with set valued domain in terms of start set on a metric space with a graph. Fixed Point Theory Appl., 2017:5, DOI: 10.1186/s13663-017-0598-8.
8. D. Eshi, P. K. Das, and P. Debnath. Coupled coincidence and coupled common fixed point theorems on a metric space with a graph. Fixed Point Theory Appl., 37:doi: 10.1186/s13663-016-0530-7, 2016.
9. J. Gornicki. Fixed point theorems for Kannan type mappings. J. Fixed Point Theory Appl., 19 (3):2145-2152, 2017.
10. R. Kannan. Some results on fixed points. Bull. Calc. Math. Soc., 60(1):71-77, 1968.
11. E. Karapinar and H. K. Nashine. Fixed point theorems for Kannan type cyclic weakly contractions. J. Nonlinear Anal. Optim., 4(1):29-35, 2013.
12. Malceski, S. Malceski, K. Anevska, and R. Malceski. New extension of kannan and chatterjea fixed point theorems on complete metric spaces. British J. Math. and Computer Sci., 17(1):1-10, 2016.

Murchana Neog

13. J. T. Markin. A fixed point theorem for set- valued mappings. Bull. Amer. Math. Soc., 74:639-640, 1968.

14. S. B. Nadler. Multi-valued contraction mappings. Pac. J. Math., 30(2):475-488, 1969.

15. M. Neog and P. Debnath. Fixed points of set valued mappings in terms of start point on a metric space endowed with a directed graph. Mathematics, 2017:5 (2):24, DOI: 10.3390/math5020024.

16. B. E. Rhoades. A comparison of various defnitions of contractive mappings. Trans. Amer. Math. Soc., 226:257-290, 1977.

17. P. V. Subrahmanyam. Completeness and fixed points. Monatsh. Math., 80:325-330, 1975.

RESEARCH ARTICLE

Resolvable Odd Cycle Factorization of Tensor Product of Complete Graphs

S. Sampath Kumar[1*] and K.Sankar[2]

[1]Assistant Professor, Department of Mathematics, Sri Sivasubramaniya Nadar College of Engineering, Kalavakkam, Tamil Nadu, India
[2]Assistant Professor, Department of Mathematics, Sri Sai Ram Engineering College, Chennai, Tamil Nadu, India.

*Address for Correspondence
S. Sampath Kumar
Assistant Professor,
Department of Mathematics,
Sri Sivasubramaniya Nadar College of Engineering,
Kalavakkam, Tamil Nadu, India.

ABSTRACT

In this paper it is proved that for odd $k \geq 3, C_k || K_m \times K_n,$ whenever the obvious necessary conditions are satisfied except few values of m and n.

Keywords: Factorization, Tensor Product, Odd cycles, Decomposition, Wreath product.

INTRODUCTION

All graphs considered here are simple and finite. Let C_k (resp.P_{k+1}), denote the cycle (resp. path) of length k. If the edge set of G can be partitioned into edge disjoint cycles of length k, then we write $C_k | G$, and consequently we say that G admits a C_k-decomposition. If each 2-factor of a 2-factorization of G contain only cycles of length k, then we say that G has a $C_k - factorization$ and in notation, we write $C_k || G$. We write $G = H_1 \oplus H_2 \oplus \cdots \oplus H_k$ if $H_1, H_2, \ldots, H_k$ are edge-disjoint subgraphs of G and $E(G) = E(H_1) \cup E(H_2) \cup \ldots \cup E(H_k)$.

For two graphs G and H their *wreath product* $G * H$ has vertex set $V(G) \times V(H)$ in which (g_1, h_1) and (g_2, h_2) are adjacent whenever $g_1 g_2 \in E(G)$ or $g_1 = g_2$ and $h_1 h_2 \in E(H)$. Similarly, $G \times H$, the *tensor product* of the graph G and H has vertex set $V(G) \times V(H)$ in which two vertices (g_1, h_1) and (g_2, h_2) are adjacent whenever $g_1 g_2 \in E(G)$ and $h_1 h_2 \in E(H)$, see Figure 1. It is clear that $(K_m * \overline{K}_n) - nK_m \cong K_m \times K_n$. Clearly, the tensor product is commutative and distributive over edge-disjoint union of graphs, that is, if $G = H_1 \oplus H_2 \oplus \cdots \oplus H_k,$ then $G \times H = (H_1 \times H) \oplus (H_2 \times H) \oplus \cdots \oplus (H_k \times H)$.

63887

Sampath Kumar *et al.*,

Let G and H be simple graphswith vertex sets $V(G) = \{x_0, x_1, \ldots, x_{m-1}\}$ and $V(H) = \{y_0, y_1, \ldots, y_{n-1}\}$. Then $V(G \times H) = V(G) \times V(H)$ and for our convenience, we write $V(G) \times V(H) = \cup_{i=0}^{m-1} X_i$, where X_i stands for $\{x_i\} \times V(H)$. Further, we shall denote the vertices of $X_i, 0 \le i \le m-1$, by $\{x_i^j \mid 0 \le j \le n-1\}$, where x_i^j stands for the vertex (x_i, y_j). We shall call X_i, the ith layer of $G \times H$. As the tensor product is commutative throughout of this paper we assume that m is odd.

Let k be a positive integer and let L be a subset of $\left\{1, 2, \ldots, \left\lfloor \frac{k}{2} \right\rfloor\right\}$. A $circulant X = X(k; L)$ is a graph with vertex set $V(X) = \{u_0, u_1, \ldots, u_{k-1}\}$ and edge set $E(X) = \{u_i u_{i+l} \mid i \in \mathbb{Z}_k, l \in L\}$. The edge $u_i u_{i+l}$, where $l \in L$, is said to be of distance l, and L is called the edge length set of the circulant X.

A $k-$regular graph G is called *Hamilton cycle decomposable* if G is decomposable into $\frac{k}{2}$ Hamilton cycles when k is even and into $\frac{k-1}{2}$ Hamilton cycles together with a perfect matching when k is odd. The problem of finding a C_k-decomposition of K_{2n+1} or $K_{2n} - I$, where I is a one factor of K_{2n} is completely settled by Alspach, Gavlas and Sajna in two different papers, see [2,19]. The *Oberwolfach problem* is equivalent to find a 2-factorization of K_{2n+1} by a given 2-factor F and K_{2n+1}. The *Oberwolfach problem* is still open.

A generalization to the above decomposition problem is to find a C_k-decomposition of $K_m * \overline{K_n}$. As the graph $K_m \times K_n (\cong (K_m * \overline{K_n}) - nK_m)$ is a proper regular spanning subgraph of $K_m * \overline{K_n}$, it is natural to think about the C_k-factorizationproblem of it. The cycle decomposition/factorization problem in product graphs are dealt in [7,9,10,13-16,18,20,21]. For even $k \ge 4$, $C_k \| (K_m \times K_n)$ is considered in [16]. In this paper we have proved that, for any odd integer $k \ge 3$, the necessary conditions for the existence of a C_k-factorization of $K_m \times K_n$ are sufficient with some exceptions on k and n.We list below some of the known results for our future reference.

Theorem 1.1 [3] For odd m, K_m has a 2-factorization F$= \left\{F_1, F_2, \ldots, F_{\frac{m-1}{2}}\right\}$ such that each $F_i, 1 \le i \le \frac{m-1}{2}$, consists of cycles of length 3 or 5 if and only if $m \ne 7 \ or \ 11$.   □

Theorem 1.2 [3] For any odd integer $t \ge 3$, if $m \equiv t(mod \ 2t)$, then $C_t \| K_m$.   □

Theorem 1.3 [14] For $m \ne 2$ and $k \ge 2$, $C_{2k+1} \| C_{2k+1} \times K_m$.   □

Theorem 1.4 [14] For any odd integer $k \ge 3$, $C_k \| C_m \times K_k$.   □

Theorem 1.5 [14] If n is a positive integer, $n \ne 2,6$, then the graph $C_3 * \overline{K_n}$ with partite sets $U = \{u_1, u_2, \ldots, u_n\}, V = \{v_1, v_2, \ldots, v_n\}$, and $W = \{w_1, w_2, \ldots, w_n\}$ has a C_3-factorization in which $\{(u_i, v_i, w_i) \mid 1 \le i \le n\}$ is a C_3-factor.   □

Theorem 1.6 [13] For $k \ge 3$ and $m \ge 3$, $K_m * \overline{K_n}$ has a C_k-factorization if and only if k divides mn and $(m-1)n$ is even, k is even if $m = 2$, $(m,n,k) \ne (3,2,3), (3,6,3), (6,2,3), (2,6,6)$. □

Theorem 1.7 [17] Let $k \ge 1$, and $m \ge 3$. If $a_1, a_2, \ldots, a_k$ are positive integers which are divisible by m and $mn = \sum_i a_i$, then $F \| C_m * \overline{K_n}$, where F consists of k cycles, namely, $C_{a_1}, C_{a_2}, \ldots, C_{a_k}$, except in the cases: (1) $n = 2$ and m odd, (2) $n = 6, m = 3$ and $(a_1, a_2, \ldots, a_k) = (3,3,3,3,3,3)$, in which case the contrary is true.   □

Theorem 1.8 [11] The graph $C_m * \overline{K_n}$ has a Hamilton cycle decomposition.   □

Theorem 1.9 [18] If $C_k \| G$ and $n \mid m$, then $C_{kn} \| G \times K_m$, where $m \ne 2 (mod \ 4)$ when k is odd.

Theorem 1.10 [8] There exists a C_3-factorization of $K_m \times K_n$ if and only if $m, n \ge 3, mn \equiv 0 (mod \ 3)$, and either $m \ or \ n$ is odd except when $(m,n) = (3,6) \ or \ (6,3)$.   □

Theorem 1.11 [16] For $m, n \ge 3$ and even integer $k \ge 4$, $C_k \| K_n \times K_m$ if and only if (1) either $m \ or \ n$ is odd, (2) $k \mid mn$ and (3) $k \le mn$ except possibly $(m,k) = (3,4)$.   □

Odd Cycle Factorization of $K_m \times K_n$

In this section we discuss about the C_k-factorization of $K_m \times K_n$, when k is odd.

Theorem 2.1 For $n \ge 3$ and odd integer $k \ge 3$, $C_k \| (C_3 \times K_n)$ if and only if $k \mid 3n$, except possibly $n \in \{2k, 6k\}$, or if $3 \mid k$ and $n = \frac{2k}{3}$.

Sampath Kumar *et al.*,

Proof. The case $k = 3$ follows from Theorem 1.10. Hence, we assume that $k \geq 5$. The proof of the necessity is obvious. We prove the sufficiency in two cases.

Case 1: $n \neq 0 (mod\, k)$

As $n \neq 0(mod\, k)$ and $k|3n$ implies $3|k$; let $k = 3t$. By the necessary condition, we have $3t|3n$ and hence $t|n$. Let $n = st$. Since $k \geq 5$, we have $t > 1$. From the graph $C_3 \times K_n$ we obtain a new graph $C_3 * \overline{K}_s$ as follows: let the partite sets of the tripartite graph $C_3 \times K_n$ be $X_i = \bigcup_{j=1}^{s} X_{ij}, 1 \leq i \leq 3$, where $X_{ij} = \left\{ x_i^{(j-1)t+2}, x_i^{(j-1)t+2}, \dots, x_i^{jt} \right\}$, we obtain the graph $C_3 * \overline{K}_s$ by identifying the set of vertices X_{ij} of the graph $C_3 \times K_n$ with a vertex v_i^j and joining two vertices by an edge if and only if the corresponding sets of vertices in $C_3 \times K_n$ induce a complete bipartite subgraph $K_{t,t}$ or $K_{t,t} - F$, where F is a 1-factor of $K_{t,t}$. The partite sets of the graph $C_3 * \overline{K}_s$ are $\{v_1^1, v_1^2, \dots, v_1^s\}$, $\{v_2^1, v_2^2, \dots, v_2^s\}$ and $\{v_3^1, v_3^2, \dots, v_3^s\}$. If $3|k$, then by our assumption $n \neq \frac{2k}{3}$, and so $s \neq 2$ (if $s = 2$, then $n = \frac{2k}{3}$). Now for $s \neq 2,6$, the graph $C_3 * \overline{K}_s$ admits a C_3-factorization F   in which $F' = \left\{ (v_1^j, v_2^j, v_3^j)|1 \leq j \leq s \right\}$ is a C_3-factor, by Theorem 1.5. The subgraph of $C_3 \times K_n$ corresponding to the C_3-factor F' of $C_3 * \overline{K}_s$ is the union of s vertex disjoint copies of the graph $C_3 \times K_t$ and $C_{3t}||C_3 \times K_t$, by Theorem 1.9 (while applying Theorem 1.9, we consider $G = C_3, n = m = t$ and further t is odd as k is odd). Similarly, consider the subgraphs of $C_3 \times K_n$ corresponding to each of the C_3-factors in F - F'; each of these subgraphs of $C_3 \times K_n$ is isomorphic to the union of s vertex disjoint copies of the graph $C_3 * \overline{K}_t$. Now $C_{3t}||C_3 * \overline{K}_t$, by Theorem 1.8.

Case 2: $n \equiv 0(mod\, k)$.

Let $n = lk$ for some $l \in \mathbb{N}$. If $l = 1$, then $n = k$ and $n = k$ and $K_n = K_t = C_k \oplus C_k \oplus \dots \oplus C_k$. Now $K_n \times K_m = K_k \times K_m = (C_k \times K_m) \oplus (C_k \times K_m) \oplus \dots \oplus (C_k \times K_m)$. By theorem 1.3, $C_k||C_k \times K_m$ and hence $C_k||K_m \times K_n$. Hence we assume that $l > 1$. As in the previous case, let the partite sets of the tripartite graph $C_3 \times K_n$ be $X_i = \bigcup_{j=1}^{l} \left\{ x_i^{(j-1)k+1}, x_i^{(j-1)k+2}, \dots, x_i^{jk} \right\}, 1 \leq i \leq 3$; from the graph $C_3 \times K_n$ we get a new graph isomorphic to $C_3 * \overline{K}_l$ with partite sets $\{v_1^1, v_1^2, \dots, v_1^l\}, \{v_2^1, v_2^2, \dots, v_2^l\}$ and $\{v_3^1, v_3^2, \dots, v_3^l\}$. For $l \neq 2,6$, the graph $C_3 * \overline{K}_l$ has a C_3-factorization F in which $F' = \left\{ (v_1^j, v_2^j, v_3^j)|1 \leq j \leq l \right\}$ is a C_3-factor, by Theorem 1.5. The subgraph of $C_3 \times K_n$ corresponding to the C_3-factor F' of $C_3 * \overline{K}_l$ is the union of l vertex disjoint copies of the graph $C_3 \times K_k$ and $C_k||C_3 \times K_k$, by Theorem 1.4. Similarly, consider the subgraphs of $C_3 \times K_n$ corresponding to each of the C_3-factors of the graph F$-F'$; each of these subgraphs of $C_3 \times K_n$ is isomorphic to the union of l vertex disjoint copies of the graph $C_3 * \overline{K}_k$ and $C_k||C_3 * \overline{K}_k$, by

Theorem 1.6.

This completes the proof of the theorem.   □

In [3], it is proved that for an odd prime p and an odd integer s with $3 \leq s \leq p, C_p||C_s * \overline{K}_p$. Here, we prove that for odd integer s,k with $3 \leq s \leq k, C_k||C_s * \overline{K}_k$.

We need the following theorem in the proof of Lemma 2.1.

Theorem 2.2 [5] Any connected circulant of degree 4 can be decomposed into Hamilton cycles.

Lemma 2.1 For any odd integer $k \geq 7$, the circulant graph $X \left(k; \left\{ 3,4,\dots,\frac{k-1}{2} \right\} \right)$ has a Hamilton cycle decomposition.

Proof. If $k \equiv 1(mod\, 4)$, the set $S = \left\{ 3,4,\dots,\frac{k-1}{2} \right\}$ contains an even number of elements. We pair the elements of S as $\{3,4\}, \{5,6\}, \dots, \left\{ \frac{k-1}{2} - 1, \frac{k-1}{2} \right\}$. For any such pair $\{l_1, l_2\}$, the graph $H = X(k; \{l_1, l_2\})$ is connected and therefore by Theorem 2.2, H is Hamilton cycle decomposable. Similarly, if $k \equiv 3(mod\, 4)$, the set $S = \left\{ 3,4,\dots,\frac{k-1}{2} \right\}$ contains an odd number of elements; now we pair the elements of $S \backslash \left\{ \frac{k-1}{2} \right\}$ as $\{3,4\}, \{5,6\}, \dots, \left\{ \frac{k-1}{2} - 2, \frac{k-1}{2} - 1 \right\}$. For each of these pairs $\{l_1, l_2\}$ the graph $H = X(k; \{l_1, l_2\})$ is connected and therefore by Theorem 2.2, H is Hamilton cycle decomposable. It is easy to check that the graph $X \left(k; \left\{ \frac{k-1}{2} \right\} \right)$ is a Hamilton cycle of the circulant graph $X \left(k; \left\{ 3,4,\dots,\frac{k-1}{2} \right\} \right)$.

This completes the proof of the lemma.   □

In the following Lemma 2.2, $\overrightarrow{K}_k$ denotes a tournament on k vertices.

63889

Definition. [3] Consider the graph $C_3 * \overline{K}_k$, where $k \geq s \geq 3$, and both s and k are odd. Let $H = u_{j_1} u_{j_2} \ldots u_{j_k} u_{j_1}$ be a directed Hamilton cycle of $\vec{K}_k$. The i-projection of H onto $C_s * \vec{K}_k$ is the k-cycle $u_i^{j_1} u_{i+1}^{j_2} u_{i+2}^{j_3} \ldots u_{i+s-1}^{j_s} u_i^{j_{s+1}} u_{i+1}^{j_{s+2}} u_i^{j_{s+3}} \ldots u_{i+1}^{j_k} u_i^{j_1}$, where the subscript is reduced modulo s.

We use the following two lemmas in the proof of Theorem 2.3.

Lemma 2.2 [3] If $H = u_{j_1} u_{j_2} \ldots u_{j_k} u_{j_1}$ is a directed Hamilton cycle of $\vec{K}_k$, then the $i - projections$ of H onto $C_3 * \overline{K}_k, i = 1,2, \ldots, s$, yield a C_k-factor of $C_s * \overline{K}_k$. Furthermore, if the edge $u_i^j u_{i+1}^l$ appears in one of the k-cycles in the 2-factor, then the edge $u_t^j u_{t+1}^l$ for $t = 1,2, \ldots, s$ appears in the 2-factor.

□

Lemma 2.3 [3] Let s and k be odd integers with $k \geq 5$ and $s \geq 3$. Then $C_s * \overline{K}_k = \left(C_s \times X \left(k; \left\{ 3,4, \ldots, \frac{k-1}{2} \right\} \right) \right) \oplus \left(C_s \times X\{k; \{1,2\}\} \right) \oplus \{ u_i^j u_{i+1}^j : i = 1,2, \ldots, s \text{ and } 1 \leq j \leq k \}$. □

The following Theorem 2.3 is proved in [3] when k is a prime. Also, it is stated in [3] without proof that the theorem is true even if we assume k is odd. However, with the help of Lemma 2.1, it is possible to validate the statement made in [3]. Hence for sake of completion we supply the proof of the following theorem.

Theorem 2.3 If both s and k are odd integers such that $k \geq s \geq 3$, then $C_k || C_s * \overline{K}_k$.

Proof. As in the statement of Lemma 2.3, $C_s * \overline{K}_k$ is the edge disjoint union of two graphs, one of which is $C_5 \times X \left(k; \left\{ 3,4, \ldots, \frac{k-1}{2} \right\} \right)$; this graph has a Hamilton cycle decomposition for $K \geq 7$. For $k = 5$, there is only one graph in the edge disjoint union of Lemma 2.3, namely, $\left(C_s \times X(k; \{1,2\}) \right) \oplus \{ u_i^j u_{i+1}^j : 1 \leq i \leq s \text{ and } 1 \leq j \leq 5 \}$ which will be treated shortly. When $k = 3, s = 3$ must hold and the result is true in this case by simply considering a Kirkman triple system on nine elements, see [12].

For $k \geq 7$ consider a Hamilton cycle decomposition of $X \left(k; \left\{ 3,4, \ldots, \frac{k-1}{2} \right\} \right)$, see Lemma 2.1. The rest of the proof is as in [3]. For a given Hamilton cycle H, assign an arbitrary orientation producing a directed Hamilton cycle H_1. The i-projection of H_1 onto $C_s * \overline{K}_k$ for $i = 1,2, \ldots, s$ yields a 2-factor of $C_s * \overline{K}_k$ of the desired kind, by Lemma 2.2. Reversing the orientation of H_1 yields another directed Hamilton cycle H_2. Again, the i-projections of H_2 onto $C_s * \overline{K}_k$ produces an appropriate 2-factor. Doing this for each Hamilton cycle in the Hamilton cycle decomposition of $C_5 \times X \left(k; \left\{ 3,4, \ldots, \frac{k-1}{2} \right\} \right)$.

Let G denote the graph $(C_s \times X(k; \{1,2\})) \oplus \{ u_i^j u_{i+1}^j : i = 1,2, \ldots, s \text{ and } 1 \leq j \leq k \}$, where $k \geq 5$. It remains to find a C_k-factorization of G. As in the notation of [3], let the vertices of G have the coordinates $(i, j), 0 \leq i \leq s - 1$ and $0 \leq j \leq k - 1$. Define the following sets of edges for each $i, 0 \leq i < s$:

$$A_i = \begin{cases} (i,j)(i+1,j-1) & \text{if } 0 \leq j < s \text{ or } s \leq j \leq k-1 \text{ and } j \text{ is odd} \\ (i,j)(i+1,j+1) & \text{if } s \leq j \leq k-1 \text{ and } j \text{ is odd}, \end{cases}$$

$$B_i = \begin{cases} (i,j-1)(i+1,j) & \text{if } 0 \leq j < s \text{ or } s \leq j \leq k-1 \text{ and } j \text{ is odd} \\ (i,j+1)(i+1,j) & \text{if } s \leq j \leq k-1 \text{ and } j \text{ is odd} \end{cases}$$

$$D_i = \begin{cases} (i,j)(i+1,j) & \text{if } 0 \leq j < s \text{ or } s \leq j \leq k-1 \text{ and } j \text{ is odd} \\ (i,j)(i+1,j+2) & \text{if } s \leq j \leq k-1 \text{ and } j \text{ is odd} \end{cases}$$

$$E_i = \begin{cases} (i,j+1)(i+1,j-1) & \text{if } 0 \leq j < s \text{ or } s \leq j \leq k-1 \text{ and } j \text{ is odd} \\ (i,j+1)(i+1,j+1) & \text{if } s \leq j \leq k-1 \text{ and } j \text{ is odd}, \end{cases}$$

$$F_i = \begin{cases} (i,j-1)(i+1,j+1) & \text{if } 0 \leq j < s \text{ or } s \leq j \leq k-1 \text{ and } j \text{ is odd} \\ (i,j+2)(i+1,j) & \text{if } s \leq j \leq k-1 \text{ and } j \text{ is odd} \end{cases}$$

The sets of edges A_i, B_i, D_i, E_i and F_i for $i = 0,1, \ldots, s-1$ are pairwise disjoint and partition the edges of G. Now let

$$R_1 = A_0 \cup D_1 \cup E_2 \cup D_3 \cup E_4 \cup \ldots \cup D_{s-2} \cup E_{s-1},$$
$$R_2 = D_0 \cup E_1 \cup D_2 \cup E_3 \cup D_4 \cup \ldots \cup D_{s-3} \cup E_{s-2} \cup A_{s-1},$$
$$R_3 = E_0 \cup A_1 \cup A_2 \cup \ldots \cup A_{s-3} \cup A_{s-2} \cup D_{s-1},$$
$$R_4 = B_0 \cup B_1 \cup \ldots \cup B_{s-1},$$
$$R_5 = F_0 \cup F_1 \cup \ldots \cup F_{s-1}.$$

Each of the sub graphs R_1, R_2, R_3, R_4 and R_5 is a C_k-factor.

This completes the proof of the theorem.   □

Sampath Kumar *et al.,*

Remark 2.1 [14] For $k \geq 2$ consider the graph C_{2k+1} with $V(C_{2k+1}) = \{u_1, u_2, \ldots, u_{2k+1}\}$ and $K_m, m \geq 3$ with $V(K_m) = \{v_1, v_2, \ldots, v_m\}$. Let $V(C_{2k+1} * \overline{K}_m) = \bigcup_{i=1}^{2k+1} \mathfrak{U}_i$, where $\mathfrak{U}_i = \{u_i^1, u_i^2, \ldots, u_i^m\}, 1 \leq i \leq 2k+1$. We know that $C_{2k+1}||(C_{2k+1} * \overline{K}_m)$, by Theorem 1.7. By suitably relabelling the vertices, if necessary, we get another C_{2k+1}-factorization of $C_{2k+1} * \overline{K}_m$ in which $F' = \{(u_1^j, u_2^j, \ldots, u_{2k+1}^j)|1 \leq j \leq m\}$ is a C_{2k+1}-factor.

Theorem 2.4 For odd integer $n \geq 3$ and odd prime p with $k \geq p, C_k||C_p \times K_n$ if and only if $k|np$ except possibly (i) $n = 2k$, or (ii) $n = \frac{2k}{p}$ whenever $n \not\equiv 0 (mod\ k)$.

Proof. The proof of the necessity is obvious. We prove the sufficiency in two cases.

Case 1: $n \not\equiv 0 (mod\ k)$.
As $n \not\equiv 0 (mod\ k)$ and $k|pn$ implies $p|k$; let $k = tp$ for some positive integer t. As $k|pn, t|n$. Let $n = st$. If $t = 1$, then $k = p$ and in this case the result follows by Theorem 1.3 and hence we assume that $t > 1$. From the graph $C_p \times K_n$ we obtain a new graph isomorphic to $C_p * \overline{K}_s$ as follows: Let $V(C_p) = \{x_1, x_2, x_3, \ldots, x_p\}$ and let the partite sets of the graph $C_p \times K_n$ be $X_i = \bigcup_{j=1}^{s} X_{ij}, 1 \leq i \leq p$, where $X_{ij} = \{x_{i,(j-1)t+1}, x_{i,(j-1)t+2}, \ldots, x_{i,jt}\}$. For each $i, 1 \leq i \leq p$ and $j, 1 \leq j \leq s$, identify the set of vertices X_{ij} in $C_p \times K_n$ with a vertex $v_{i,j}$ and joining two vertices $v_{i,j}$ and $v_{k,l}$ by an edge if and only if $\langle X_{ij} \cup X_{kl} \rangle$ in $C_p \times K_n$ induce a complete bipartite subgraph $K_{t,t}$ or $K_{t,t} - F$, where F is a 1-factor of $K_{t,t}$. The partite sets of thegraph $C_p * \overline{K}_s$ are $\{v_{1,1}, v_{1,2}, \ldots, v_{1,s}\}, \{v_{2,1}, v_{2,2}, \ldots, v_{2,s}\}, \{v_{3,1}, v_{3,2}, \ldots, v_{3,s}\}, \ldots, \{v_{p,1}, v_{p,2}, \ldots, v_{p,s}\}$. As $p|k$ by hypothesis $n \neq \frac{2k}{p}$, and so $s \neq 2$ (if $s = 2$, then $n = \frac{2k}{p}$). For $s \neq 2$, the graph $C_p * \overline{k}_s$ has a C_p-factorization Fin which $F' = \{(v_{1,j}, v_{2,j}, v_{3,j}, \ldots, v_{p,j})|1 \leq j \leq s\}$, is a C_p-factor, by Remark 2.1. The subgraph of $C_p \times K_n$ corresponding to the C_p-factor F' of $C_p * \overline{K}_s$ is the union of s vertex disjoint copies of $C_p * K_t$. Now $C_{pt}||C_p \times K_t$, by Theorem 1.9 (while we apply Theorem 1.9, consider $G = C_p, n = m = t$ and further t is odd as k is odd). Similarly, consider the subgraphs of $C_p \times K_n$ corresponding to each of the C_p-factors, in F$-F'$, of the graph $C_p * \overline{K}_s$; each of these subgraphs of the graph $C_p \times K_n$ is isomorphic to the union of s vertex disjoint copies of the graph $C_p * \overline{K}_t$ and $C_{pt}||C_p * \overline{K}_t$, by Theorem 1.8.

Case 2: $n \equiv 0 (mod\ k)$.
Let $n = lk$ for some $l \in \mathbb{N}$. If $l = 1$, then $n = k$ and $C_k||(C_p \times K_k)$, by Theorem 1.4. Therefore we assume that $l > 1$. As in the previous case, let the partite sets of the graph $C_p \times K_n$ be $X_i = \bigcup_{j=1}^{l} X_{ij}, 1 \leq i \leq p$,where $X_{ij} = \{x_{i,(j-1)k+1}, x_{i,(j-1)k+2}, \ldots, x_{i,jk}\}$; we get the graph isomorphicto $C_p * \overline{K}_l$ with partitesets $\{v_{1,1}, v_{1,2}, \ldots, v_{1,l}\}, \{v_{2,1}, v_{2,2}, \ldots, v_{2,l}\}, \{v_{3,1}, v_{3,2}, \ldots, v_{3,l}\}, \ldots, \{v_{p,1}, v_{p,2}, \ldots, v_{p,l}\}$. For $l \neq 2$, the graph $C_p * \overline{K}_l$ has a C_p-factorization Fin which$F' = \{(v_{1,j}, v_{2,j}, v_{3,j}, \ldots, v_{p,j})|1 \leq j \leq l\}$, is a C_p-factor, by Remark 2.1. The subgraph of $C_p \times K_n$ corresponding to the C_p-factor F' of $C_p * \overline{K}_l$ is the union of l vertex disjoint copies of $C_p * K_k$. Now $C_{pt}||C_p \times K_t$, by Theorem 1.4. Similarly, consider the subgraphs of $C_p \times K_n$ corresponding to each of the C_p-factors, in F$-F'$, of the graph $C_p * \overline{K}_l$; each of these subgraphs of the graph $C_p \times K_n$ is isomorphic to the union of l vertex disjoint copies of the graph $C_p * \overline{K}_k$ and $C_{pt}||C_p * \overline{K}_k$, by Theorem 2.3. □

Lemma 2.4 [16] If $n \geq 3$ is any integer and $k \geq 3, m \geq 3$ are odd integers such that $k|m$, then $C_k||K_m \times K_n$ except when $(k, m, n) = (3,3,6)$.

Theorem 2.5 Let $m \geq 3$ and $k \geq 5$ be odd integers, then $C_k||K_m \times K_n$, if (1) either m or n is odd, (2) $k|mn$ and $k \leq mn$ except possibly for the following cases:

(i) $(m, n, k) = (m, 2k, k), (m, 6k, k)$.

(ii) $(m, n, k) = \left(m, \frac{2k}{p}, k\right)$, if $p|k$, where $p \in \{3,5,7,11\}$.

(iii) $mn \equiv 2 (mod\ 4)$ when both m and n are not a multiple of k.

Proof. We may assume that m is odd as the tensor product is commutative.
Case 1: $m \equiv 0 (mod\ k)$.
        Proof of this case follows from Lemma 2.4.
Case 2: $n \equiv 0 (mod\ k)$.

Sampath Kumar *et al.,*

First assume that $m \notin \{7,11\}$. Since m is odd, by Theorem 1.1, $K_m = F_1 \oplus F_2 \oplus \dots \oplus F_{\frac{m-1}{2}}$, where each F_i is a 2-factor composed of 3 or 5-cycles. Hence $K_m \times K_n = (F_1 \times K_n) \oplus (F_2 \times K_n) \oplus \dots \oplus \left(F_{\frac{m-1}{2}} \times K_n\right)$; further, as each F_i contains only cycles of length 3 or 5, $F_i \times K_n = (C_3 \times K_n) \oplus (C_3 \times K_n) \oplus \dots \oplus (C_3 \times K_n) \oplus (C_5 \times K_n) \oplus (C_5 \times K_n) \oplus \dots \oplus (C_5 \times K_n)$. Now, $C_k || (C_3 \times K_n)$ and $C_k || (C_5 \times K_n)$ by Theorems 2.1 and 2.4, respectively. Hence, $C_k || (F_i \times K_n), 1 \leq i \leq \frac{m-1}{2}$. This completes the proof of this subcase. If $m = 7 \ or \ 11$, then we decompose K_m into m- cyclesand then consider$K_m \times K_n = (C_m \times K_n) \oplus (C_m \times K_n) \oplus \dots \oplus (C_m \times K_n)$ then by Theorem 2.4, we have a C_k-factorization as required.

Case 3: $m \not\equiv 0 (mod \ k)$ and $n \not\equiv 0 (mod \ k)$.
Let $k = p_1^{\alpha_1} p_2^{\alpha_2} \dots p_l^{\alpha_l}$ be the prime factorization of k. Since k does not divide both m and n and $k | mn$, some prime factors of k divide m and some prime factors of k divide n. Without loss of generality we may assume that $\beta_1 = p_1^{a_1} p_2^{a_2} \dots p_l^{a_l}$ divides m and $\beta_2 = p_1^{\alpha_1 - a_1} p_2^{\alpha_2 - a_2} \dots P_l^{\alpha_l - a_l}$ divides n; let $m = \beta_1 r$ and $n = \beta_2 s$ for some positive integers r and s, where some $\alpha_i's$ and $(\alpha_i - a_i)'s$ may be equal to zero. Since k is odd, both β_1 and β_2 are odd.

Let $V(K_m) = \{x_1, x_2, \dots, x_m\}$ and let $X_i = x_i \times K_n$, then $V(K_m \times K_n) = V(K_m) \times V(K_n) = \cup_{i=1}^{m} X_i$.We partition each X_i into s subsets,each having β_2 vertices, namely, $X_{ij} = \left\{x_i^{(j-1)\beta_2 + 1}, x_i^{((j-1)\beta_2 + 2)}, \dots, x_i^{j\beta_2}\right\}, 1 \leq j \leq s$. As in the proof of Theorem 1.11, Case 2, we obtain a new graph isomorphic to $K_m * \overline{K}_s$ from the graph $K_m \times K_n$ as follows: for each $j, 1 \leq j \leq s$, we identify the set of vertices X_{ij} of the graph $K_m \times K_n$ as vertex $v_i^j, 1 \leq i \leq m$ and joining two vertices by an edge if and only if the corresponding sets of vertices in $K_m \times K_n$ induce a complete bipartite graph K_{β_2, β_2} or $K_{\beta_2, \beta_2} - F$, where F is a 1-factor of the graph $K_{\beta_2 \beta_2}$. The ith partite set of the graph $K_m * \overline{K}_s$ is $\{v_i^1, v_i^2, \dots, v_i^s\}, 1 \leq i \leq m$. The set of vertices in each of the columns of this graph $K_m * \overline{K}_s$ induces a subgraph isomorphic to the complete subgraph K_m; let F' be the s vertex disjoint copies of the graph K_m induced by the s columns of the graph $K_m * \overline{K}_s$. The subgraph of $K_m \times K_n$ corresponding to F' of $K_m * \overline{K}_s$ is the union of s vertex disjoint copies of $K_m \times K_{\beta_2}$. Since, β_1 is odd and $\beta_1 | m, C_{\beta_1} || K_m$, by Theorem 1.2. Hence, by Theorem 1.9, $C_{\beta_1 \beta_2} || K_m \times K_{\beta_2}$. The graph $(K_m * \overline{K}_s) - E(F')$ is isomorphic to $K_m \times K_s$. Since m is odd and $\beta_1 | m$, we have $C_{\beta_1} || K_m \times K_s$, by Lemma 2.4. When we lift back C_{β_1}-factor of $K_m \times K_s$ to the graph $K_m \times K_n$, we get the union of $\frac{ms}{\beta_1}$ vertex disjoint graphs isomorphic to $C_{\beta_1} * \overline{K}_{\beta_2}$, in $K_m \times K_n$. Now $C_{\beta_1 \beta_2} || C_{\beta_1} * \overline{K}_{\beta_2}$, by Theorem 1.8.
This completes the proof of the theorem.

ACKNOWLEDGEMENT

REFERENCES

1. B. Alspach, J.C. Bermond, D.Sotteau, Decomposition into cycles I: Hamilton decompositions, in: Cycles and Rays (eds. G. Hahn et. Al). Kluwer Academic Publishers (1990) 9-18.
2. B. Alspach and H. Gavlas, Cycle decompositions of K_n and $K_n - I$, J. Combinational Theory (Ser. B) 81 (2001) 77-99.
3. B. Alspach, P.J. Schellenberg, D. R. Stinson, and D. Wagner, The Oberwolfach problem and factors of uniform odd length cycles, J. Combinatorial Theory (Ser. A) 52 (1989) 20-43.
4. R. Balakrishnan and K. Ranganathan, A Textbook of Graph Theory, Springer Verlag, New York, 2000.
5. J.-C. Bermond, O. Favaron and M. MAheo, Hamiltonian decomposition of Cayley graphs of degree 4, J. Combinational Theory (Ser. B) 46 (1989) 142-153.
6. J. A. Bondy and U. S. R. Murty, Graph Theory with Applications, The MacMillan Press Ltd., London, 1976.
7. M. Buratti, H. Cao, D. Dai and T. Traetta, A complete solution to the existence of (k,)-cycle frames of type gu, J. Combin. Des. 25 (2017), 197230.

Sampath Kumar *et al.,*

8. Chengmin Wang, Yu Tang, Peter Danziger, Resolvable modified group divisible designs with block size three, J. Combinational Designs 15(2007) 2-14.

9. S. Ganesamurthy and P. Paulraja, 2p-cycle decompositions of some regular graphs and digraphs, Discrete Math. 341 (2018), 21972210.

10. D. G. Hoffman, C. C. Lindner, C. A. Rodger, On the construction of odd cycle systems, J. Graph Theory, 13, 417-426.

11. R. Laskar, Decomposition of some composite graphs into Hamiltonian cycles. Proc. 5th Hungarian Coll. Keszthely, 1976, North Holland, (1978) 705-716.

12. C.C. Lindner, C. A. Rodger, Design Theory, CRC Press, Boca Raton, New York.

13. J. Liu, The equipartiteOberwolfach problem with uniform tables, J. Combinational Theory (Ser. A) 101 (2003) 20-34.

14. R.S. Manikandan and P. Paulraja, C_p-decompositions of some regular graphs, Discrete Math. 306 (2006) 429-451.

15. Muthusamy and A. ShanmugaVadivu, Cycle frames of complete multipartite multigraphs-III, J. Combin. Des. 22 (2014), 473487.

16. P. Paulraja and S. Sampath Kumar, Resolvable even cycle decomposition of the tensor product of complete graphs, Discrete Math. 311 (2011) 1841-1850.

17. W.L. Piotrowski, The solution of the bipartite analogue of the Oberwolfach problem, Discrete Math. 97 (1991) 339-356.

18. Muthusamy and P. Paulraja, Factorizations of product graphs into cycles of uniform length, Graphs and Combin. 11 (1995) 69-90.

19. M. Sajna, Cycle decompositions III. Complete graphs and fixed length cycles, J. Combinatorial designs 10 (2002) 27-78.

20. R. Smith, Decomposing complete equipartite graphs into cycles of length $2p$, J. Combinatorial designs 16 (2006) 244-252.

21. R. Smith, Complete equipartite$3p$-cycle systems, Australasian J. of combinatorics 45 (2009) 125-138.
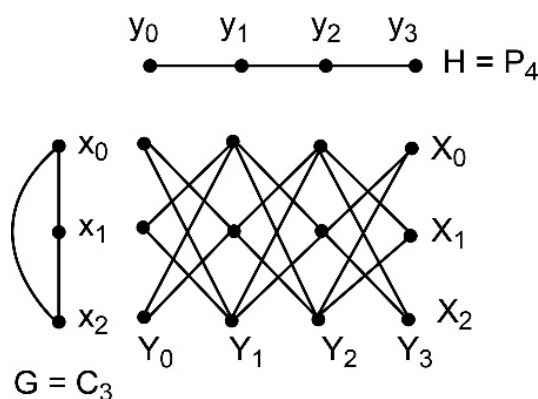
Figure 1 : Graph C_3 x P_4

RESEARCH ARTICLE

Breakthrough Therapy Designation: Examining the Qualification Requirements

Thejesh K S[1]*, Vedamurthy Joshi[2], Prakash Goudanvar[3], Sharath H D[1] and Varshith Kumar[1]

[1]M.Pharm Student, Dept. of Pharmaceutics and Regulatory Affairs, Sri Adichunchanagiri College of Pharmacy, Mandya, Karnataka, India
[2]Associate Professor, Dept. of Pharmaceutics and Regulatory Affairs, CORMIL and CMPAT, Sri Adichunchanagiri College of Pharmacy Mandya, Karnataka, India
[3]Professor and Head, Dept. of Pharmaceutics and Regulatory Affairs, Sri Adichunchanagiri College of Pharmacy, Mandya, Karnataka, India.

*Address for Correspondence
Thejesh K S
M.Pharm Student,
Dept. of Pharmaceutics and Regulatory Affairs,
Sri Adichunchanagiri College of Pharmacy,
Mandya, Karnataka, India
E.Mail: thejasks700@gmail.com

ABSTRACT

The Food and Drug Administration of the United States has established approval paths and designations to facilitate access to medications recommended for serious or life-threatening illnesses for which there are few other effective treatments. The latest, breakthrough therapy designation (BTD), went into effect in 2012. We discovered that the BTD programme had the largest impact on less experienced enterprises and was linked to lower BTD clinical trial design complexity. This essay sought to examine how the US Food and Drug Administration (FDA) positioned the construction of an accelerated drug development pathway for extraordinary new treatments as a high priority and Breakthrough Designation Requirements for approval. Important questions that must be addressed in the development of such a pathway include how to identify a potential breakthrough therapy and how to request for designation may be submitted at the time of IND filing and balance the need to provide sick patients with quick access to breakthroughs against the need to safeguard patients from potentially harmful or ineffective medications through rigorous trials.

Keywords: programme, Designation, Requirements, Administration.

INTRODUCTION

Since 1962, the Food and Drug Administration (FDA) of the United States has required manufacturers to produce proof of the effectiveness and safety of their goods before exposing patients to them.[1] The length of time it takes to introduce novel medicines on the market, especially for circumstances for which there aren't many treatment options, has been widely criticised. This is true even though the FDA review and approval process is designed must ensure that there is sufficient data to demonstrate that the benefits outweigh the hazards. The mystery has drawn a lot of interest.[2] To expedite the process of developing new drugs and to make it easier for drugs used to treat serious or life-threatening conditions to be approved, The FDA Safety and Innovation Act of 2012 was enacted in 2012. [3]The FDA created expedited approval designations and pathways. The most recent inclusion is the breakthrough therapy designation (BTD).[4] A drug may be eligible for a BTD if it treats a serious or life-threatening disease or condition and a surrogate endpoint (such as a test result, radiographic image, or physical sign) demonstrates improvement over current treatment.[5]Present-day therapies (also known as available therapies) are medications that have gained full FDA approval, whereas available therapies are medications that have not yet gotten full FDA approval or are still in the exploratory stages. A drug that helps with BTD qualifies for the fast-track classification as well.[6]

Breakthrough Therapy
The designation of "breakthrough therapy" is granted to drugs that are designed to treat critical illnesses and preliminary clinical evidence indicates that the medication may significantly outperform the standard of care on a clinically meaningful endpoint. The magnitude of the therapy effect, which may include the duration of the effect and the significance of the clinical result observed, is what determines whether the improvement above the current therapy is substantial. Preliminary clinical data should typically show a discernible gain over the norm of treatment.A clinically meaningful endpoint is one that examines the influence on irreversible morbidity or mortality (IMM) or symptoms that signal serious repercussions of the disease for the purposes of identifying "breakthrough therapy."[7]

The creation of the BT designation got the FDA's encouragement. Clearly, the environment for drug development had changed due to changes in the reimbursement landscape and developments in biomedical science. The creation of high-value therapies appeared to be a reinvigorated focus for the pharmaceutical sector as a whole. Particularly targeted medicines were showing notable improvements in selected subpopulations. It was apparent that the development of potentially significant therapeutic advances should not be "business as usual"; in fact, patients with numerous life-threatening illnesses had repeatedly expressed the expectation that the FDA should devote the same attention and focus to accelerating treatments of the regulatory expectations and development pathways for extremely promising investigational pharmaceuticals were not formalised outside of immediate approval (Subpart H). Their conditions as it had to HIV therapies during the AIDS epidemic. In fact, the Centre for Drug Evaluation and Research's (CDER) focus on policy over the past decade has mostly been on the proper assessment of the safety of incremental medicines for the treatment of chronic diseases, at least for new drugs.[8]

Both the FDA's expedited and expanded access programmes have identified breakthrough medications. Exceptions have occurred more frequently than usual in recent years. 22 (or 56%) of the 39 new drugs

licenced in 2012 were accepted under at least one of the fast-track, priority review, or accelerated approval procedures, with 23% eligible for more than one.[9]Although the FDASIA's benefits are primarily already provided by existing laws, rules, or approved FDA procedures, the breakthrough-therapy designation was recognised as having a significant impact on regulatory effectiveness.[10] For instance, the FDASIA mandates that it collaborate closely with the businesses providing funding for novel medications. Subpart E (1988), on the other hand, the conduct and evaluation of clinical trials would be strongly encouraged by top FDA employees, offer "early consultation between FDA and drug sponsors," emphasise the significance of meetings ensure effective phase 2 trial design in collaboration with the FDA, and make it clear that the FDA will actively support these initiatives. [11] It is not obvious how FDASIA will improve the current coordination of staff efforts, although it claims that the appointment of a "cross-disciplinary project lead" may be helpful to support the successful review of breakthrough therapies.The practise of employing fewer evidentiary requirements to determine eligibility for programmes with faster development and approval was continued by the breakthrough-therapy designation.

Some drugs have had their approval based on long-standing surrogate end objectives. Beginning in 1992, the accelerated approval process allowed approval based on "less than well-established surrogate endpoints."[12]The new breakthrough-therapy designation (2012) requires that, one must show "an effect on a pharmacodynamic biomarker(s) that does not meet criteria for an acceptable surrogate endpoint but strongly suggests the potential for a clinically meaningful effect on the underlying disease."[13]This broader threshold would apply to a broader spectrum of potentially novel medications. Such documentation may not be necessary for many years, similar to the bedaquiline approval for MDR tuberculosis. However, under the normal FDA clearance requirements, breakthrough medications must eventually be accepted or denied according to the law.[14]Once breakthrough-therapy designation has been granted based on preliminary evidence, it may be challenging to control demand (whether early access or post-approval), even if the medication turns out to be less effective or more hazardous than previously believed. According to decision theory, decisions should be made with greater care when they are less subject to change.[15] The most recent instance of this issue was the drug bevacizumab, which was recently given fast approval for the treatment of metastatic breast cancer using surrogate end goals.. It took almost a year and substantial pushback to withdraw the indication when follow-up studies showed no benefit in patient survival.[16] Some insurance providers still cover this off-label, non-evidence-based use of the medication. Delaying full research until after a drug has been approved may hinder and prolong the analysis of a medicine's benefit-risk profile.It is now more difficult to enrol patients in clinical trials to evaluate the efficacy of a drug because they can choose to participate in the treatment as part of their regular therapy or sign up for a trial where they could be randomly assigned to receive normal care. This worry is made more pressing by the combination of delayed research and prior designations that might be seen as official endorsements.[17]

Goal of breakthrough therapy designation
Regulatory goal: Drugs that exhibit early clinical evidence of significant improvement for critical illnesses relative to current medications should have the drug development process accelerated.
Public benefit: Because of the coordination between sponsors and FDA reviewers, new treatments can be approved more quickly. This can therefore result in patients with critical diseases receiving new and effective medicines more quickly. [18]

Thejesh *et al.*,

BREAKTHROUGH DESIGNATION REQUIREMENTS

According to Sharma and Schilsky, a significant therapeutic advance "fundamentally changes the way oncologists think about a disease in terms of the prognosis, treatment options, and quality of life of our patients." Future discoveries might not be as obvious to people outside that field as they might be to people who are familiar with an illness they aim to address. It is important to note that not all cancer medications will act on this pathway by default. To provide the process some consistency and predictability, it is vital to define the minimum level of evidence that must be presented in order to receive the Breakthrough designation. Because defining a breakthrough merely in terms of quantitative results based on early outcomes like response rates in comparison to currently available medications may be unrealistic and constricting, for breakthrough designation, we have established qualitative standards that must be met. The qualitative criteria listed below are hypothetical; in the end, it is up to people with the necessary knowledge to decide if a novel medicine satisfies the criteria for a potential breakthrough therapy. Either there is no known SoC for the diseases under study or the acknowledged SoC currently in use yields subpar Clinical results (such as inadequate symptom control, inadequate symptom persistence, inadequate survival, substantial acute or chronic side effects, and inadequate quality of life).

1. Strong preliminary data showing a considerable clinically significant enhancement compared to current treatments in the context of a particular condition should be used to support the designation of a breakthrough.
    a) The possible breakthrough therapy could be given the following moniker based on early indications of strong clinical efficacy:
        i.   The results of early clinical research must significantly outperform comparable recent or historical comparisons in terms of clinical significance.
        ii. acceptable safety in a manageable patient population (patient count matched to illness incidence and prevalence, depending on the mechanism of action and predicted toxicity).
    b) Based on preliminary findings showing a greater clinical therapeutic index compared to SoC in a population with similar criteria, a possible breakthrough therapy may be discovered.
        i.   Must be superior to or obviously maintain equivalent efficacy
        ii. The main factor to be taken into account is superior safety or tolerability.
2. The potential ground-breaking medicine under consideration frequently has a solid scientific foundation and an intriguing method such as focusing on the molecular cause of a physiologically recognised disease (for example, the lung cancer subset that expresses the ALK gene).[19]

Breakthrough Therapies– Categories

We outline various classifications for Breakthrough Therapies as well as the kinds of information that may be needed when a request for Breakthrough designation is made. Remember that a breakthrough designation may also be given to combinations of new agents. Some of these categories in Table 1 are evaluated using the qualitative criteria outlined in the preceding section. In order to focus on a subset of disorders that can be recognised molecularly, a breakthrough therapy for each of these categories will likely co-Dx, short for companion diagnosis. As a result, flexibility in the review of the coDx will be necessary. It is critical to remember that designation as a breakthrough could happen in this scenario

before the diagnostic (Dx) hypothesis has received complete clinical validation or before classification thresholds for the population that is positive for the marker have been established.

Categories

1. Drugs for diseases with a bad prognosis, which can be categorised by their biochemical or clinical subgroups of disease and for which there is neither a demonstrated SoC nor a readily available contemporaneous control.
   a) Drugs that treat conditions that were earlier thought to be incurable, such as ivacaftor for G551D cystic fibrosis and vismodegib for advanced basal cell carcinoma.
   b) Medicines that work well in groups of people who are resistant to treatment, such as brentuximab vedotin in Hodgkin's disease after at least two prior therapies if the patient is not a transplant candidate or when an autologous stem cell transplant fails.
2. for diseases with poor prognoses, which might be identified by a biologic or clinical subset of disease and which provide a significant therapy advance over the already recognised SoC.
   a) New medications that perform differently from the SoC that is currently in use, such as crizotinib for NSCLC with ALK positivity and vemurafenib for metastatic melanoma with a BRAF mutation.
      i. Historical controls should be matched for clinical disease or subtype, context (stage or severity, previously treated), pertinent demographics, and prognostic variables if they are to be used as comparisons. Along with giving out the investigational chemical, any discrepancies in management between the experimental group and controls should be taken into account.
      ii. Retrospective study of clinically extensive annotated biomarkers from tumour banks (such as cooperative group tissue banks). may be used to identify historical controls for new biological subgroups in situations where a molecularly defined population is the focus of the therapy.
   b) Targeted drugs of the second generation that meet unmet needs left unsatisfied by first-generation compounds (e.g., slow reaction time, poor tolerability).
      i. A second-generation therapy may be considered a breakthrough if preliminary clinical evidence suggests that it is significantly superior to its predecessor(s) and has a solid scientific basis supported by preclinical or clinical proof.
      ii. Biopsies of diseases that have progressed after being exposed to first-generation medications and which Clinical proof could be the ability to show the presence of an acquired mutation or alteration that is treated by second-generation therapy.
3. Drugs that, as members of a clearly defined class, provide a SoC with a significant therapeutic index advantage and well-characterized effectiveness and safety (such as non-cardiotoxic anthracyclines and antibody-drug conjugates).
4. Drugs (such as the Hepatitis C treatments boceprevir and teleprevir) that considerably increase the efficiency or toleration of a prescribed regimen
5. In a separate tumour type with the same mutation or modification, medication that has previously demonstrated efficacy in a cancer type caused by a specific mutation or pathway modification may be eligible for breakthrough designation.(for example, crizotinib for the treatment of ALK+ paediatric ALCL). This is based on significant clinical efficacy for the additional tumour type.[20]

63898

Designation Process –Content of request and Timing

The request for designation may be submitted at the time of IND filing or at any time afterward, according to the language of breakthrough therapies. However, it also stipulates that in order to be designated, there must be preliminary clinical proof. We advise that, prior to obtaining marketing authorisation for either its biologics licence application (BLA) or new drug application (NDA), the sponsor initiate negotiations for consideration of a potential breakthrough designation at the time the IND is submitted or at any stage thereafter. Participants would be able to discuss and agree on the preliminary clinical evidence required, the details of the IND, the content of a designation request, the evidence required to meet Breakthrough Therapy criteria, and the potential timetable for a request based on this agreement at the pre-IND meetingA formal request for and decision on Breakthrough designation would still demand and entail the examination of early clinical experience, even though the IND and potential for Breakthrough designation may be reviewed prior to an IND filing in a pre-IND meeting. By outlining the investigational agent's scientific background, method of action, preliminary clinical studies, and outcomes, it should also explain how it meets the requirements for breakthrough designation. Along with prospective clinical development plans for confirming the early-phase studies, the request should also include forward-thinking techniques for streamlining production and developing a companion diagnostic (if required).

Process of Designation - FDA Response

A request for Breakthrough designation must receive a response from the FDA within 60 days. Senior staff members in the office of the Centre Directors will evaluate requests for Breakthrough designation. We recommend providing the FDA the rights to seek advice from outside experts. If necessary, these specialists could also be called for discussions in the future regarding the best layout for clinical research. If the FDA rejects the application, they should explain why in a letter outlining the criteria that must be completed before the product may be given the Breakthrough Designation. [21]

Interactions between FDA and Sponsors: Proposed Timeline

Throughout the development process, we see the FDA providing more general guidelines and the sponsor and the FDA working more closely together. While we recommend hosting a range of meetings, we recommend holding type A meetings as soon as a product is accepted as a breakthrough.We also recommend that the sponsor have access to a completely different style of meeting. These would be established between the FDA's and the sponsor's single points of contact, thus creating a "hotline" to enable real-time communication of study results. Because of this design field, the FDA would be able to actively engage in the decision-making process. Furthermore, Regular evaluation of the approval status based on changing data would be possible. (non-clinical, CMC, etc.).

Phase I :

- When a breakthrough therapy designation is given, the sponsor has access to an FDA Breakthrough Therapy team, a single point of contact, and a communication strategy.
- Conference call or meeting in phase I's middle:
  - ➢ Examine recent interim clinical data.
  - ➢ Agree on the phase II/III protocol description or decide that the phase I extension is adequate given the Breakthrough designation.

> ➢ Simplify the manufacturing qualification/validation plan by using a single lot (for both market and development).
> ➢ Examine the stability and quality control plan.
> ➢ Concur on streamlined companion diagnostic development, including, if necessary, a statistical analysis technique (SAP) for phase I data processing, either prospectively or retroactively.

Conclusion of Phase I - Extension Meeting :

Data from Phase I have been submitted in raw but audited form. deciding whether or not to move on to phase II depending on if phase I extension was adequate. Phase II/III immediately begins after receiving the proper randomised phase II protocol, and a date for the conference for mid-phase II&III is recommended.

Meeting – Mid-phase II/III :

The sponsor team and the FDA look into, debate, and make a conclusion regarding:
- Analysis of study results
- Any modifications to the production plans, data, controls, and related diagnostics
- Create the label's indication, precautions, and administration sections.
- SAP for phase I data prospective or retroactive analysis, as needed for the Dx hypothesis.

Pre-BLA/NDA meeting between mid-phase II/III and the conclusion of phase II&III

- If required, a pre-BLA/NDA meeting would be planned to go through the application's table of contents and plan the further steps. Through email, the FDA and sponsor teams discuss specifics and adjustments based on talks held during mid-phase II and III. The FDA sets the dates for the inspections.
- Discussions with CDRH and CDER about a shortened companion diagnostics process, possibly include a plan to make the IVD available for investigational use before the regulated device is approved.

NDA/BLA submission

All agreed-upon data sets and analyses, complete bioanalytical reports (perhaps without audit), audited non-clinical data, audited manufacturing and controls data, stability and controls plans, module 2 summaries, and labelling must be included in BLA/NDA applications. However, only summaries of clinical, clinical pharmacology, and non-clinical trial results, as well as integrated safety and efficacy when justified (in most cases, this is irrelevant), are allowed. The sponsor simultaneously but separately sends inspection data to the inspection office and/or the field office(s).

NDA/BLA cycle of review

FDA and sponsor teams hold weekly teleconferences to discuss each application component, create the phase IV study and phase IV production commitments, get ready for the advisory committee (if required), choose the final label, and, if necessary, conduct additional research to enable companion diagnostics The recommended evaluation period is three months.

Phase IV – Approval:

- Acceptance of the application (which includes a phase IV plan that has been agreed upon), the start of phase IV (clinical and manufacturing).

Thejesh *et al.*,

- FDA review and approval of promotional materials, and sponsor and FDA review and agreement on revised label elements following phase IV.

Phase IV – Final data:

➢ Data from Phase IV submitted
➢ label updated.[20]

CONCLUSION

Patients can use the BTD to get access to drugs for critical illnesses more quicklyEven if certain drugs authorised with a BTD indicate significant progress in the treatment of an illness, health care practitioners should be aware of the variability in the quality of the evidence supporting these approvals. Providers should be able to adequately inform patients and other healthcare professionals on the safety and efficacy of these medications because there is still much to learn about them. BTT designation in no way implies that the medication is going to be approved, according to the BTT guidance. When preliminary data suggests that a medicine may significantly improve a condition, the BTT programme is intended to encourage sponsorship and FDA collaboration. The drug in question won't be approved if the benefits are ultimately proven to outweigh the dangers (based on the complete amount of evidence acquired both before and after the BTT designation).

REFERENCES

1. Katz R. FDA: evidentiary standards for drug development and approval. NeuroRx : the journal of the American Society for Experimental NeuroTherapeutics. 2004;1(3):307 -316.
2. Light DW, Lexchin JR. Pharmaceutical research and development: what do we get for all that money? BMJ (Clinical research ed). 2012;345:e4348.
3. Kesselheim AS, Wang B, Franklin JM, Darrow JJ. Trends in utilization of FDA expedited drug development and approval programs, 1987 -2014: cohort study. BMJ (Clinical research ed). 2015;351:h4633.
4. Kramer DB, Kesselheim AS. User fees and beyond--the FDA Safety and Innovation Act of 2012. The New England journal of medicine. 2012;367(14):1277 -1279.
5. U.S. Food and Drug Administration. Center for Drug Evaluation and Research (CDER). Center for Biologics Evaluation and Researc (CBER). Guidance for Industry: Expedited Programs for serious Conditions - Drugs and Biologics. May 2014. Available at: https://www.fda.gov/downloads/Drugs/Guidances/UCM358301.pdf.
6. Kwok M, Foster T, Steinberg M. Expedited Programs for Serious Conditions: An Update on Breakthrough Therapy Designation. Clinical therapeutics. 2015;37(9):2104 -2120.
7. Breakthrough therapy [Internet]. U.S. Food and Drug Administration. FDA; [cited 2023 May 22]. Available from: https://www.fda.gov/patients/fast-track-breakthrough-therapy-accelerated-approval-priority-review/breakthrough-therapy
8. US Food and Drug Administration. Code of Federal Regulations, Title 21, Vol. 5 (rev. 1 April 2013). Accelerated approval of new drugs for serious or life-threatening illnesses. 21 CFR 314.500, Subpart H.
9. Fischer S. BIO hails house passage of reconciled user fee package (press release). Washington, DC: Biotechnology Industry Organization, June 21, 2012.

10. Sherman RE, Li J, Shapley S, Robb M, Woodcock J. Expediting drug development — the FDA's new "breakthrough therapy" designation. N Engl J Med 2013;369:1877-80.
11. Investigational new drug, antibiotic, and biological drug product regulations: procedures for drugs intended to treat lifethreatening and severely debilitating illnesses. Fed Regist 1988; 53:41517.
12. Food and Drug Administration. Guidance for industry: fasttrack drug development programs: designation, development and application review. January 2006 (http://www.fda.gov/downloads/ Drugs/Guidances/ucm079736.pdf).
13. Food and Drug Administration. Fast track, breakthrough therapy, accelerated approval and priority review. June 26, 2013 (http://www.fda.gov/ForConsumers/ByAudience/ForPatient Advocates Speeding AccessImportantNewTherapies/ucm128291 .htm).
14. Avorn J. Approval of a tuberculosis drug based on a paradoxical surrogate measure. JAMA 2013;309:1349-50.
15. Etzioni A. The active society: a theory of societal and political processes. London: Collier–Macmillan, 1968.
16. Department of Health and Human Services, Food and Drug Administration. Proposal to withdraw approval for the breast cancer indication for Avastin (bevacizumab): decision of the Commissioner. November 18, 2011 (http://www.fda.gov/downloads/ NewsEvents/Newsroom/UCM280546.pdf).
17. Moore TJ, Furberg CD. Development times, clinical testing, post-market follow-up, and safety risks for the new drugs approved by the US Food and Drug Administration: the class of 2008. JAMA Intern Med 2014;174:90-5
18. Shah A. Breakthrough Therapy Designation: Bringing innovation swiftly to patients.
19. Sharma MR, Schilsky RL. Role of randomized phase III trials in an era of effective targeted therapies. Nature reviews Clinical oncology. 2012;9(4):208-14. Epub 2011/12/07. doi: 10.1038/nrclinonc.2011.190. PubMed PMID: 22143142.
20. Sawyers CL, Haber DA, Horning SJ, Ivy SP, Selig WK. Developing standards for breakthrough therapy designation. Cancer Research. 2012 Nov.
21. US Food and Drug Administration. Draft Guidance for Industry and Food and Drug Administration Staff - In Vitro Companion Diagnostic Devices. In: CDRH, CBER, CDER, editors. 2011.

Table 1: Developmental Paths, Categories, and Potential Breakthrough Criteria

Category	Qualitative Standards	Development Path - Potential
There is no SoC+ and the drug is used to treat serious illnesses.	Early unusual Phase I activity: CRR*, ORR*, or CBR* with acceptable safety	In single-arm research, complete or expedited approval may result from a phase I-B expansion or single-arm pivotal trial.
For a critical illness with poor results, the drug significantly exceeds a well-characterized SoC in terms of effectiveness.	Outstanding early activity in Phase I based on disease management with acceptable safety, response rates (CRR, ORR), and length of response	Full approval could be supported by a randomised phase IIB trial with a moderate sample size and statistical significance. A trial like that might enable crossover. If the efficacy gain is not deemed extraordinary, randomised phase IIB may be used as a phase III screening tool. In extreme circumstances, full or, more

		likely, hastened clearance could occur from Phase IB expansion or a single-arm study.
Compared to a well-characterized SoC, a drug has a significant therapeutic index advantage for a critical illness with poor results.	coupled with higher safety/tolerability and superior or obviously sustained efficacy	Randomised phase IIB study was most frequently employed as a phase III trial screening tool. In a small-scale trial, full approval of a randomised phase IIB trial might be justified if the treatment index shows a striking improvement.

Table 2: Summary of FDA's Programmes for Rapid Development and Review

	Fast Track Designation	Breakthrough Therapy Designation	Accelerated Approval	Priority Review Designation
Year Established	1997	2012	1992	1992
Qualifying Criteria	• A drug used to treat a severe illness; AND • Clinical or nonclinical evidence show potential to treat a medical need that has not yet been satisfied.	• A drug used to treat a severe illness; AND • According to preliminary clinical data, the drug may significantly outperform competing treatments on one or more clinically relevant endpoints.	• A drug used to treat a severe illness; AND • Typically offers real advantages over current treatments, AND • Correlates with a surrogate endpoint that can be reasonably expected to predict patient benefit.	• A prescription for a medication that cures a severe ailment (original or efficacy supplement), AND • Would significantly increase safety and/or effectiveness if approved.
Timeline For FDA Response	Within 60 days of receiving the request	Within 60 days of receiving the request	No specified timeline.	Within 60 days of receiving the request of original BLA, NDA or efficacy supplement

Thejesh *et al.*,

Program Features	• Steps that speed up development and review, like chances for regular communication with the review team • Rolling Review	• Thorough advice on effective medication development • FDA's organisational commitment, which includes senior managers • Rolling Review • Additional steps to quicken the review	• A drug's clinical benefit may be predicted relatively well by its impact on a surrogate endpoint or an intermediate clinical endpoint used in the approval process. • To verify clinical benefit, the drug sponsor must perform post-approval studies.	• Reduces FDA review period from 10 months to 6

REVIEW ARTICLE

A Literature Review on Cloud Computing in Major Sectors

K.Porkodi[1*] and D. Raj Balaji[2]

[1]Ph.D Research Scholar, Department of Computer Science, Rathinam College of Arts and Science, Coimbatore – 641021, Tamil Nadu, India.
[2]Assistant Professor, Department of Computer Science Rathinam college of Arts and Science, Coimbatore – 641021, Tamil Nadu, India.

*Address for Correspondence
K.Porkodi
Ph.D Research Scholar,
Department of Computer Science,
Rathinam College of Arts and Science,
Coimbatore – 641021, Tamil Nadu, India.
E.Mail: rheyakodi@gmail.com

ABSTRACT

In a rapid technology world, Cloud computing is most important role in all the sectors because of any time any where we can access the data easily via internet in all over the world. Cloud Computing is the availability of a vast array of computing services such as data storage, analytics, and networking that are driven automatically with less manual support. It is commonly used for the efficient and smooth functioning of businesses and also providing infrastructure and software support to computing systems. In this study and review paper, it based on how various sectors connected to cloud meanwhile what are the security issues have using cloud computing in all sectors and what are the Cloud Computing techniques used to overcome from that issues.

Keywords: Cloud Computing, Technologies, Data Security, Models

INTRODUCTION

In Modern Technology, all sectors rely on cloud computing for the effective and seamless operation of organizations as well as for the provision of hardware and software to support computer systems. The healthcare industry has historically underutilized technology, especially when it comes to enhancing patient care. Even though the fact that healthcare has been around for sixteen years already, a large number of systems still use paper medical records or other manual processes to notify and make choices in the majority of conditions [1]. Malicious program detection is a challenging task. Network operators and IT managers are faced with a formidable task by the enormous, ever-growing ecosystem of malicious software and tools [2]. One of the newest technological

advancements, cloud computing, together with virtualization, fast connections, and broadband internet, will probably have a big impact on the teaching and learning environment [3].

CLOUD COMPUTING

Instead of using local servers or personal devices to manage applications, cloud computing makes use of pooled computing resources. The simplest definition of cloud computing is relocating services (also known as "cloud services") outside of an organization's firewall. The Web is used to access services like storage and other applications. The cloud customer pays for the services on an as-needed or pay-per-use basis, and they are supplied and used over the Internet.

Cloud Computing Models-

Cloud computing is categorized under a number of categories. It is grouped under the following heading based on the type, location, and usage:
- Public Cloud
- Private Cloud
- Community Cloud
- Hybrid Cloud

Public Cloud

Information can be stored and accessed online utilizing a pay-per-usage model by anyone. Computing resources are managed and run by cloud service providers in public clouds. Amazon EC2, the Windows Azure service platform, and IBM's Blue cloud are a few examples of public clouds. From the figure1, IT services and resources are made available to anybody who subscribes and pays for them by public cloud vendors. It is a kind of external cloud that is offered for public use and is primarily owned and supplied by external organizations.

Private Cloud

It is often referred to as a corporate cloud or an internal cloud. Organizations use it to construct and operate their own data centers, either internally or through a third party. Private cloud refers to commercial organizations' internal data centers that are not accessible to the general public. The private cloud is devoted to the customer directly, as the name implies. Compared to public clouds, these are safer. It makes advantage of virtualization technology. The company's own servers act as the private cloud's host. Eucalyptus, VMware, and OpenStack serve as examples of private cloud technology.

From figure2, an infrastructure or service may be located on-site or off-site and is run purely for the benefit of the one organization that would be the cloud's provider. The administrator has a direct influence on every cloud setup. It may be handled internally by the organization or externally by any reputable third party.

Community Cloud

It enables a collection of diverse groups to access systems and services and share information with the community.

Hybrid Cloud

The cloud is a hybrid of the public and private varieties. It is only partially secure because services running on public clouds can be accessed by anybody, but those running on private clouds can only be accessed by authorized users of the company.

From the figure3, the combining on-premises, public cloud, and private cloud technologies in a hybrid environment are a practical way to begin adopting cloud environments. While still having the flexibility to build new tools at scale and with controlled costs, organizations can retain and use systems that they have historically relied on. Cloud computing is the delivery of computing services over the internet, such as servers, storage databases, networking, and software analytics.

Porkodi and Raj Balaji

SaaS - A service provider that offers software and apps via the internet in cloud computing. Through vendor APIs or the web, users who have subscribed to the software can access it.

PaaS - An entry point to a cloud-based environment where users can create and distribute applications is provided by a service provider (PaaS). The underlying infrastructure is provided by the provider.

IaaS - Storage, networking, servers, and other cloud computing resources are made available to customers on a pay-as-you-go basis by an IaaS vendor.

CLOUD COMPUTING TECHNOLOGIES

The following is a list of cloud computing technologies -

o   Virtualization
o   Service-Oriented Architecture (SOA)
o   Grid Computing
o   Utility Computing

Virtualization

The practice of establishing a virtual environment to run several operating systems and applications on the same server is known as virtualization. The virtual environment can be any combination of different operating systems, storage systems, network application servers, and other environments, including a single instance or a single combination of them. Increased utilization of virtual computers is the idea behind virtualization in cloud computing. A virtual machine is a software computer or software program that can conduct functions like launching apps or programs on demand for the user and can also operate as a physical machine.

Types of Virtualization

*   Hardware virtualization
*   Server virtualization
*   Storage virtualization
*   Operating system virtualization
*   Data Virtualization

Service-Oriented Architecture (SOA)

According to changing business needs, Service-Oriented Architecture (SOA) enables enterprises to use cloud-based computing solutions on demand. It can function both with and without cloud computing. The benefits of SOA include ease of maintenance, platform independence, and great scalability. The two key roles in SOA are service consumer and service provider.

Applications of Service-Oriented Architecture

There are the following applications of Service-Oriented Architecture -

*   It is used in the healthcare industry.
*   It is used to create many mobile applications and games.
*   In the air force, SOA infrastructure is used to deploy situational awareness systems.

The service-oriented architecture is shown below:

From the figure4, a service-oriented architecture, many services interact with one another by exchanging data or coordinating an action between two other services.

Grid Computing

Distributed computing is another name for grid computing. It is a processor architecture that pools numerous computing resources from several places in order to accomplish a single objective. Grid computing creates a computer cluster by connecting the grid through parallel nodes. There are several sizes and operating systems available for these computer clusters.

The following three types of machines are used in grid computing -

• Control Node: This is a collection of servers that manages the entire network.
• Provider: A computer that contributes resources to the network resource pool is known as a provider.
• User: A computer that utilizes network resources is referred to as a user.
Grid computing is mostly employed in back-end infrastructures, marketing research, and ATMs.
From the figure5, Grid computing is a kind of processor architecture that integrates computer resources from many domains to accomplish a shared purpose. The network's computers will collaborate on a project using grid computing, emulating a supercomputer.
Utility Computing

The most popular approach for IT service delivery is utility computing. It offers infrastructure based on the pay-per-use model and on-demand computing resources (computation, storage, and programming services through API). It maximizes resource efficiency while minimizing associated expenditures. Utility computing has the advantages of lower IT costs, more flexibility, and ease of management. Major organizations like Google and Amazon built their computing storage and application utility services.

LITERATURE REVIEW

In 4, the author describes that, the amount of data being stored in data centers is growing daily, which causes a vast amount of data to be stored on the cloud and causes problems like data loss, data breaches, etc. If data is accidentally lost or erased, an effective method must be used to retrieve it from any backup server. Antivirus software is used to identify, stop, and correct any dangerous activity occurring within a computer system. For the effective removal of threats in our computing environment, many malware detection approaches are implemented. Antivirus software is used to identify, stop, and correct any dangerous activity occurring within a computer system. For the purpose of effectively removing threats from our computing environment, many malware detection techniques are implemented [5]. Big data offers insights and information, while cloud computing lets users work whenever and wherever they want. Big Data in the cloud refers to a dataset that is so large that working with it in a conventional local computer-based Database Management System becomes extremely challenging. This dataset may be several dozen terabytes or gigabytes in size. The ability to extend storage, visualize data, manage, and collect becomes extremely time-consuming and expensive, thus using the cloud is the appropriate answer [6].

 Purchasing and selling goods and services online is known as e-commerce. It is made up of two layers from a system approach. A technical architecture made up of hardware and software is the first layer. Other Layers are technologically-based business transactions. Renting hardware and software using cloud computing enables e-commerce businesses to avoid making capital expenditures. Costs associated with system development are reduced [7]. In [8], the author states that to realize the sharing of medical data and health information, coordination of healthcare systems, and effective and cost-containment clinical information system infrastructure through the implementation of a distributed and highly integrated platform, the medical and health information system is based on cloud computing. A service known as cloud storage keeps data up to date, manages and backs it up remotely, and makes data accessible to users over a network (via the internet). Numerous companies offer cloud storage. Most companies offer free storage up to a specific gigabyte limit. When a client can store and manage the data at a reasonable cost as opposed to using the cloud, the concept of cloud storage is not worthwhile. So, the cloud should be created in a way that makes it affordable, autonomously computable, multi-tenant, scalable, accessible, controllable, and efficient [9].

The testing environment, evaluation technology, and evaluation service are the three components that make up the test and evaluation system for cloud computing information security solutions. For cloud computing information security products, the test environment primarily consists of a test platform. Evaluation technology primarily consists of testing tools, testing methods, a basic database, and related standards and specifications. Evaluation services offer the ability to evaluate cloud computing information security products. According to the security

technological requirements, the security testing technique for cloud computing systems may be separated into four categories: security function, security guarantee, environmental adaptability, and performance requirements [10].

MAJOR SECTORS ADOPT CLOUD COMPUTING
A few examples of the many uses for cloud technology include business, data storage, entertainment, business management, social networking, education, medicine, art, and GPS.

E-Governance
In many countries around the world, the use of cloud computing for e-government is growing, and governments have started to benefit from the cloud [11]. The cloud computing industry is a thriving application development that offers an inexpensive and efficient option for any E-Government infrastructure development [12].

Business Trading Sector
Cloud-based e-commerce software enables users and e-businesses to adapt rapidly to growth opportunities. Instead of developing massive static environments scaled for peaks, the cloud is a perfect fit for e-commerce since it allows providing and paying for resources as need them. The objective is automatic provisioning. Environments are static and scalable for peak load without the cloud [13].

From the Figure 8, the Cloud Computing offers some benefits to E-Commerce industries. To combine the processing power of numerous devices, the majority of E-Commerce enterprises employ a hosting server. Online stores operate differently from other websites. To update databases, protect personal information, handle payments, and monitor sales, they require more assistance and flexibility. E-commerce companies can rent hardware and software due to cloud computing rather than purchasing it. It helps in reducing system building costs. E-commerce companies usually purchase all required hardware and software, which leads to significant investment costs, especially for small and medium-sized organizations. Virtualization of cloud computing Depending on their needs, e-commerce companies can select and rent IT services and goods. A technical architecture must be developed. Particularly flexible is the "pay as a service" billing model. This allows growth resource payment for e-commerce companies [14].

Educational Sector
One of the most significant changes brought about by the use of cloud computing in the education sector is the rise of e-learning, online distance learning courses, and student information portals. In this case, cloud computing may prove to be beneficial. The usage of cloud computing is to access any file, document, or even video from anywhere in the world. So it's beneficial to provide fundamental classes to students who can't otherwise afford them. Cloud computing is a new technology that is currently being employed all over the world since it allows us to provide individuals with simple and innovative learning opportunities while also raising the educational level of the nation [15]. Students, professors, and researchers are offered a comfortable environment for learning, teaching, and experimenting in this new learning environment so they can connect to their organization's cloud and access data and information.

Healthcare Sector
Historically, the healthcare industry has underutilized technology, particularly when it comes to enhancing patient care. Even though the fact that healthcare has been around for sixteen years now, there are still a lot of manual or paper-based methods that are used to alert and make choices in most situations, such as patient history [16]. In 17, the author proposed, the adoption of telemedicine technologies like teleradiology, telesurgery, and audio/video conferencing introduces a new way for different healthcare providers to collaborate and communicate. Telehealthcare services enable patients to get clinical care without having to travel and also assist medical specialists in sharing their expertise to handle challenging medical issues.

From the Figure 9, the Cloud Computing offers some benefits to Healthcare industries. Doctor-patient and doctor-doctor communication, as well as the transmission and preservation of medical pictures, may all be made possible

via cloud-based software. Data sharing is made simple by cloud computing, which also effectively streamlines provider communications. It enables experts to conduct virtual consultations to share their knowledge on a case or provide a second opinion for more accurate disease diagnosis and treatment. For healthcare organizations, reliable disaster recovery procedures are ensured by cloud technology, such as patient management software.

Banking and Finance Sector

There are no longer any restrictions associated with this technology since anybody, everywhere can have access to banking systems without the expense and other barriers that are associated with traditional on-premises banking systems. Instead, cloud computing can make enterprise-level banking systems and related technologies available in the cloud on a pay-per-use basis [18]. Cloud computing seems to have the ability to speed up innovation and corporate transformation across industries, including banking. The advantages of this cloud-based technology (instead of its physical servers) for banks are its low prices, speed, adaptability, and security.

The usage of cloud computing can benefit banks in several numbers of ways, including

 • Increasing operational process efficiency;

 •Building secure applications that adhere to regulatory frameworks.

 • Improving products and customer services.

 • Eliminating entry barriers into new business models by being more adaptable. To lead to rising, it is no longer essential to own several of machines; instead, hiring a Cloud provider will be sufficient

A REVIEW – HEALTHCARE SECTOR

The Literature review on Healthcare sector is in a comparative format is given in table1. In 19, the author implemented MES, for utilizes to secure Healthcare sharing and storage mechanisms. And also that compare the various algorithm to analyze some parameters in Healthcare environment. In 20, the author compared to various Algorithms and analyzed to chosen, CBM is most efficiency to secure the data in cloud. In 21, the author proposed, that Lightweight Cryptography is used to secure the EHR in Cloud. The sensitive information is protected by Lightweight protocols. In 22, the author demonstrates the utility of the combination of machine learning and segmentation in order to improve data security. Processing RGB colorful images using cloud resources in a securely. More importantly, in proposed it apply two methods for image enhancement, i.e. Gaussian filtering and pixel intensity.

In 23, the author proposed that, to generate two photo galleries .The OMBD is hold on to secretly in the cloud and the DMBD is used as a honeypot and is remain in the fog. As a result, the user accesses the DMBD by default instead of only doing so when unauthorized access is discovered. Only after confirming the user's legitimacy may they access the OMBD. In 24, the image will be split using a sequence key after being encrypted into ciphertext using the AES technique. The ciphertext is first decrypted after being combined using the same sequence key. In 25, the author is to increase the number of robots in the system from 10 to 100, the time consumption for generating keys differed 0.002–0.003 s. The author framed the methods based on the proposed method's key generation time in comparison to other approaches. When compared to previous

ways, the suggested method reduces the time needed for key generation. The key generation time differs from others by 10 to 15 microseconds. In 26, the author discussed how encryption and anonymization methods have been used for health care data protection as well as presented their limitations.

SECURITY CHALLENGES IN ALL SECTORS

Cloud computing has a lot of security risks. Customers use the cloud because of its on-demand services, cost-effective resource pool, and ability to conduct computer operations from any location at any time. However, the security concerns they endure are causing both clients and cloud service providers to despair. With cloud computing, anyone may instantly host a cloud using a shared pool of resources. The security of data is severely threatened by these interconnected networks. Cloud computing presents several security hurdles and problems [27]. Both external hackers and unauthorized inside personnel can easily access data in cloud models. Internal staff

members have easy access to data, whether on purpose or by accident. Using hacking techniques like session hijacking and network channel eavesdropping, outside hackers may be able to access databases in these environments [28]. All organizations, whether for-profit or nonprofit, have started using the cloud to store data, which raises concerns about the security and privacy of that data. Additionally, the cloud presents several challenges for service providers in terms of data transfer and service utilization. The majority of security threats in cloud computing are associated with cloud data security. Most issues come from the data that consumers upload to the cloud, whether it is a lack of visibility into data, an inability to control data, or data theft in the cloud.

In [29] the author surveys that both internal and external source can provide security risks to businesses. The 2011 Cyber Security Watch Survey found that insiders were responsible for 21% of cyber attacks. According to 33% of respondents, insider attacks are more expensive and devastating to enterprises. The majority of insider threats (63%) and intellectual property theft (32%) involved unauthorized access to and use of corporate information. Certain sensitive data can be accessed by malicious users, which can result in data breaches. As per the study is carried out by the author [30], Access control is a key security tool for cloud computing that enables data protection. It ensures that the requested data, which is kept in the cloud, is only accessible to authorized users. Proper access control is made possible by several security methods in cloud computing. On various network and cloud layers, intrusion detection systems, firewalls, and responsibility separation could be installed. Through the cloud network, a firewall only allows content that has been passed through. Typically, users specify security policies for a firewall and then implement those policies. Demilitarized zones (DMZ), which offer additional data protection, are typically associated with firewalls. In [31], the author illustrated that the subject of account hijacking is one of the most frequently discussed in society. There may be a variety of reasons for hijacking, including providing our credentials to others and offering our data to third parties via online transactions. The hackers who would take over our account might even alter transaction information, falsify data, and utilize other cloud services linked to the account to execute additional attacks

In the healthcare sector, data can be stolen easily because it is stored in plain text, making it simple for anybody to read, write, or modify the data. Because it involves the patient's confidential health information, security in e-healthcare is even more crucial. Attackers can use the open wireless channels' weaknesses to their advantage. The E-healthcare framework can incur a variety of damages as a result of these attacks [32]. For secure the purpose of ensuring online access to banking accounts, the majority of banks offer a user-id, password, as well as a one-time password. The premise that dictionary attacks can ability to get passwords deems this form of authentication procedure entirely unsecure.

Password Hacking Tools used by Hackers:
o   John the ripper
o   THC Hydra
o   Pwdump
o   Rainbow Crack
o   Brutus
o   Cain and Abel

DATA SECURITY IN CLOUD
Typically, data encryption is a key area of concern for cloud security. In [33], the author states that by transforming the data from its readable and intelligible form to a form that is not understandable to unwanted persons, the science of cryptography prevents data from being stolen and interpreted by unauthorized individuals. By using encryption, the scrambled data which makes it virtually impossible for anyone to use it without encryption keys. While attempting to improve the security of cloud data, users should focus on a few key areas.
Be sure to look at the following while trying to secure SMB or industrial systems:
• Encrypting data before it is stored in the cloud: Users can have greater control over how the company manages its encryption methods if it secures individual local data storage devices and operating systems.

63911

Porkodi and Raj Balaji

- End-to-end encryption: To protect the data while it is transmitted to and from the cloud service, be sure the provider provides end-to-end encryption. Sensitive information should always be shielded from interception, such as financial or private data.
- Keep track the Encryption keys: Different keys are required to decrypt data, so it's crucial to handle and protect these keys carefully. Decide whether the cloud provider will manage the keys internally or if users will take charge of that.
- Use a cloud security solution: It is a challenging undertaking that requires assistance to maintain its data encryption efforts. While protecting against existing threats, security technologies like Kaspersky Hybrid Cloud Security can help to decide how to improve local and cloud security efforts.

In [34], the Author analyse that the New Lightweight Cryptography Algorithm, which combines high flexibility and security. The NLCA algorithm reduces processing power and reduces computational complexity. In [35], the most effective functionality of a cloud is directly provided by IaaS, which is present on the sub layer. IaaS also enables hackers to carry out high-resource assaults like brute-force cracking. IaaS offers the perfect platform for hackers to launch assaults that need a lot of attacking instances because it supports multiple virtual machines. Another security concern with cloud models is data loss.

In [36], a security method to thwart this kind of attack is the secure Socket Layer (SSL). Therefore, authentication of the client and the server may not function as it should protect users of cloud technology from a man in the middle of this security technique that is not configured properly. In [37], to provide data confidentiality and information integrity of users' data in the cloud computing environment, the author implemented AES Algorithm and proposed an effective security framework that provides a mechanism through which communication is protected and unauthorized access is restricted.

CONCLUSION AND FUTURE WORK

Cloud computing is an emerging force that has aided numerous sectors over the past few decades as the increasing digitalization has changed over time. The main purpose of this study and review paper, we discussed about basic concept of Cloud computing and Data Security. We review the security challenges in all sectors from various research papers, then how that Data Security challenges are rectified using cloud computing technology. From this paper, the future research process is done from Healthcare Sector. Healthcare is one industry that has greatly benefited from cloud computing in terms of infrastructure. With the introduction of cloud computing, things have drastically changed in the healthcare industry, where a rapid gain is already taking place. This has not only benefited in the growth of the infrastructure and facilities, but it has also created new opportunities for multidisciplinary medical research, which is beneficial for all of humanity. In the table1, we review the various security issues in Healthcare sector and its methods. In future work, we compare and analysis the various algorithms to secure the data efficiently, to implement in Healthcare sectors using cloud technology.

REFERENCES

1. Omkar Warghade et. AI,(2020). "Cloud based Secure Multi Owner Hospital Management System", IJERT, ISSN: 2278-0181, Vol. 9 Issue 01, January-2020.
2. Safaa Salam Hatem (2014). "Malware Detection in Cloud Computing", (IJACSA), Vol. 5, No. 4, 2014.
3. Tuncay Ercan (2010). "Effective use of cloud computing in educational institutions", ELSEVIER, No:35-37, 2010.
4. Manasjyoti Saharia et. AI,(2021)." An Analysis on Data Recovery and Backup Technologies in Cloud Computing", IRJET, Volume: 08 Issue: 06, June 2021.
5. Vasileios A. Memos and Kostas E. Psannis, Member, IEEE (2020). "A New Methodology Based on Cloud Computing for Efficient Virus Detection", IEEE, November 2020.

6. Manoj Muniswamaiah et. Al, (2019). "BIG DATA IN CLOUD COMPUTING REVIEW AND OPPORTUNITIES", IJCSIT, Vol 11, No 4, August 2019.
7. Tamara Almarabeh & Yousef Kh. Majdalawi, (2019). "Cloud Computing of E-commerce", Modern Applied Science; Vol. 13, No. 1; 2019.
8. Yunyong Guo et. Al,(2012). "Cloud Computing for Healthcare Research Information Sharing", IEEE, 2012.
9. Kun Liu, 2012. "Research on Cloud Data Storage Technology and Its Architecture Implementation", ELSEVIER, 2012.
10. Hao Hao Song, (2019). "Testing and Evaluation System for Cloud Computing Information Security Products", ELSEVIER, 2019.
11. Kondra Mounika et. Al,(2017). "A Study on Cloud Computing in E-Governance", IJCSE, Volume-5, Issue-12, IJCSE, 2017.
12. Manoj Kumar et. Al,(2013). "An E Governance model using cloud computing technology for Developing Countries", ResearchGate, 2013.
13. Amir Mohamed Talib, "Cloud Computing Based E-Commerce as a Service Model: Impacts and Recommendations", Kingdom of Saudi Arabia (KSA).
14. Vaibhav P Mujmule,2021. "A Relationship of Cloud Computing With E-Commerce", ResearchGate, August 2021.
15. E.S. Margianti and A.B. Mutiara, 2016. "APPLICATION OF CLOUD COMPUTING IN EDUCATION", ResearchGate, February 2016.
16. Lingkiswaran Devadass et. Al,(2017). "CLOUD COMPUTING IN HEALTHCARE", International Journal of Students' Research In Technology & Management Vol 5, No 1, April 2017.
17. Vaibhav Kamal Nigam and Shubham Bhatia, 2016. "Impact of Cloud Computing on Health Care", IRJET, Volume: 03 Issue: 05, May 2016.
18. Nancy Awadallah, 2016. "Usage of Cloud Computing in Banking System", IJCSI, Volume 13, Issue 1, January 2016.
19. HADEAL ABDULAZIZ AL HAMID et. Al,(2017). "A Security Model for Preserving the Privacy of Medical Big Data in a Healthcare Cloud Using a Fog Computing Facility With Pairing-Based Cryptography", IEEE, VOLUME 5, 2017.
20. R. Priyadarshini et. Al,(2022). "An enhanced encryption-based security framework in the CPS Cloud", Journal of Cloud Computing, Journal of Cloud Computing, Volume 11:64, 2022.
21. Abouelmehdi et al, (2018). "Big healthcare data: preserving security and privacy", Journal of Big Data, Volume 5:1, (2018).
22. V. Vijayakumar et. Al,(2018). "E-Health Cloud Security Using Timing Enabled Proxy Re-Encryption", Mobile Networks and Applications, 2018.
23. R.Josephius Arunkumar, 2017. "ENHANCEMENT OF CLOUD COMPUTING SECURITY IN HEALTH CARE SECTOR", IJCSMC, Vol. 6, Issue. 8, August 2017.
24. MARYAM SHABBIR et. Al,(2021). "Enhancing Security of Health Information Using Modular Encryption Standard in Mobile Cloud Computing", IEEE, 2021.
25. Mbarek Marwan et. Al,(2018). "Security Enhancement in Healthcare Cloud using Machine Learning", The First International Conference On Intelligent Computing in Data Sciences, 2018.
26. Saurabh Jain, 2022. "Security framework to healthcare robots for secure sharing of healthcare data from cloud", Int. j. inf. tecnol. (August 2022).
27. Rohan Jathanna, 2017. "Cloud Computing and Security Issues", Int. Journal of Engineering Research and Application, Vol. 7, Issue 6, June 2017.
28. G . Monika, 2016. "Data Security is the Major Issue in Cloud Computing - A Review", Indian Journal of Science and Technology, Vol 9(43), November 2016.
29. Thilina Dinendra Dharmakeerthi, 2020. "A Study on Secure File Storage in Cloud Computing using Cryptography", ResearchGate, May 2020.
30. Kire Jakimoski, (2016). "Security Techniques for Data Protection in Cloud Computing", International Journal of Grid and Distributed Computing, Vol. 9, No. 1 (2016).

31. Jyoti Gangesh Tiwari, (2020). "Literature Survey on Cloud Cryptography for Data Security", IJARCCE, Vol. 9, Issue 9, September 2020.
32. A. Jsv Sai Bhargav, (2020). "A Review on Cryptography in Cloud Computing", IJSRCSEIT, Volume 6, Issue 6, December 2020.
33. Ali Kadhim Bermani et. Al, (2021). "A hybrid cryptography technique for data storage on cloud computing", Journal of Discrete Mathematical Sciences and Cryptography, ISSN 0972-0529 (Print), ISSN 2169-0065 (Online), March 2021.
34. Fursan Thabit et. Al,(2021). "A new lightweight cryptographic algorithm for enhancing data security in cloud computing", Global Transitions Proceedings, 2021.
35. Sameer A. Nooh, (2020). "Cloud Cryptography: User End Encryption", International Conference on Computing and Information Technology, Volume: 01, Issue: ICCIT- 1441, September 2020.
36. Felix Bentil and Isaac Lartey, 2021. "Cloud Cryptography - A Security Aspect", IJERT, Vol. 10 Issue 05, May-2021.
37. Ansar I. Sheikh et. Al, 2020. "Data Security using Hybrid Cryptography in Cloud", JETIR, Volume 7, Issue 5, May 2020.

Table1: A Comparative Literature Review of Work Done by Various Authors in Healthcare Sector

Refer.No	Problem Identification	Methodology	Pros	Cons	Authors
19	Prevention of security breaches and vulnerabilities in MCC environment	MES Algorithm	Using MES, Health Information system has secure environment to storing and share the data in Mobile Cloud Computing. MES has better performance than other commonly used algorithm in terms of processor utilization rate, less memory utilization, the highest degree of key variances, and highest data colligation rate.	Image-oriented data-set not to be considered. System efficiency is low in Layered model.	Hadeal Abdulaziz Al Hamid et. Al, (2017)

Porkodi and Raj Balaji

20	Due to physical connectivity restrictions, networks are more susceptible to security threats. So the data will be stored in cloud and cyber-security vulnerabilities have been identified in cloud-based healthcare systems	RSA, TWOFISH Algorithm, ICC, FHE Algorithm, BAO(Butter-Ant Optimization Algorithm) CBM(Cross Breed Blowfish & MD5 Algorithm) FET-RT(Fuzzified Effective Trust-based Routing Protocol)	CBM is used to increase the Secure health data in CPS Cloud. MD5 hash generator is useful for encoding the password and encrpyt the data.	Energy consumption is not measured in CBM method	R. Priyadarshini et. Al, (2022)
21	In Electronic Health Record, the data sharing over the unsecured wireless medium brings many security challenges	Hash Function Algorithm	Using Lightweight Cryptography, secure the EHR in Cloud. Using KDF,to ensure end-to-end ciphering of information for preventing misuse. lightweight security protocols with extreme robustness to protect sensitive networks should be developed	Proposed scheme is not cost-effective for Low Power Wide Area Networks (LPWAN) using a local database. Simplicity and robustness	Abouelmehdi et al, (2018)
22	To prevent unauthorized access to medical records and personal health information. Security issues concern in Medical image analysis	Machine Learning Techniques, Support Vector Machines (SVM) and Fuzzy C-means Clustering (FCM) Algorithm, CloudSec	Support Vector Machines (SVM) and Fuzzy C-means Clustering (FCM) to classify image pixels more efficiently. Using CloudSec module, to	Using FCM & SVM, unsuitable to large Datasets.	V. Vijayakumar et. Al, (2018)

			reduce the risk of the potential disclosure of medical information.		
23	Privacy of Medical Big Data in Healthcare Sector	Pairing-based Cryptography and Decoy Techniques Blow-Fish Algorithm	An efficient tri-party authenticated key agreement protocol has been proposed among the user, the DPG, and the OPG based on paring cryptography. Using decoy technique the private healthcare data are accessed and stored securely.	Using FOG, the power consumption is high	R.Josephius Arunkumar, (2017)
24	Secure Patient Related images in Healthcare System	AES	Encrypt and Decrypt the data storage in cloud securely.	In AES the counter mode is complex to implement in software taking both performance and security.	Maryam Shabbir et. AI, (2021)
25	Secure sensitive Healthcare Data in Cloud	Elliptic Curve Cryptography (ECC), Hash-based Message Authentication Code-SHA 1,	The robotics healthcare data is encrypted using an Elliptic Curve Cryptography (ECC)-based mechanism for secure sharing, and Hash-based Message Authentication Code-SHA 1	Internal Threats in System	Mbarek Marwan et. AI, (2018)

				(HMAC-SHA1) is used for maintaining the integrity of the sensitive data.		
26	To prevent security breaches in Big Healthcare data	De-identifcation Methodology Hybrid Execution Model Identity based anonymization	Fraud and Anomaly Detection	Poor usability, Heightened Security risks and Anonymized data set	Saurabh Jain, (2022)	

Fig 1: Public Cloud Computing
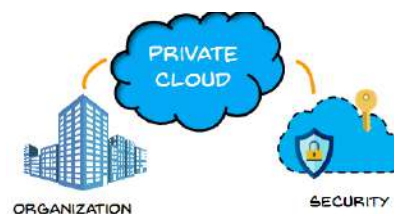
Fig 2: Private Cloud

Fig 3: Hybrid Cloud

Fig 4: Service-Oriented Architecture
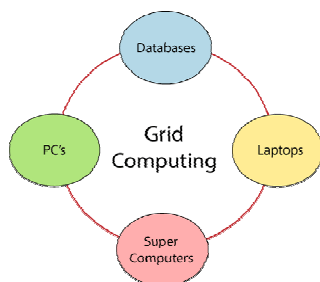
Fig 5: Grid Computing
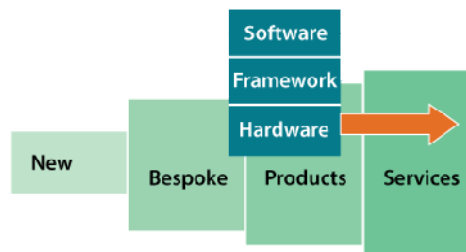
Fig 6: Utility Computing
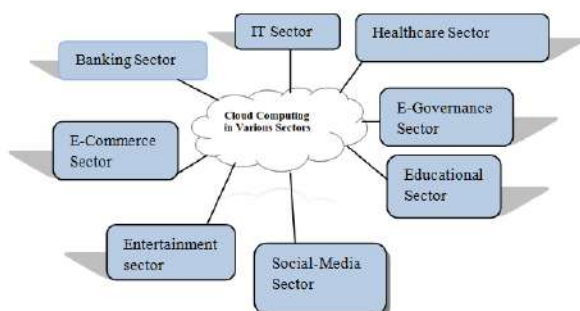
Fig 7: Cloud computing in major Sectors

Fig 8: Benefit of E-Commerce Sector using Cloud computing
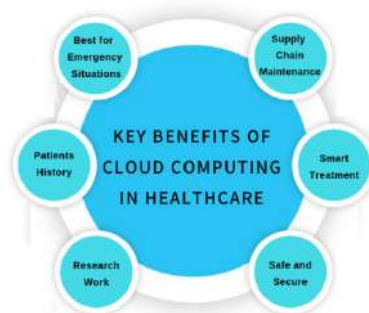
Fig 9: Benefits of Cloud Computing in Healthcare Sector

RESEARCH ARTICLE

Correlation between Level of Stress and Severity of Primary Dysmenorrhea in College Going Girls : A Survey Study

Dolly Shah[1] , Nilesh Parmar[2]* and Bhavana Gadhavi[3]

[1]MPT Scholar, Parul Institute of Physiotherapy, Vadodara, Gujarat, India.
[2]Assistant Professor, Parul Institute of Physiotherapy, Vadodara, Gujarat, India
[3]Dean, Parul Institute of Physiotherapy, Vadodara, Gujarat, India

*Address for Correspondence
Nilesh Parmar
Assistant Professor,
Parul Institute of Physiotherapy,
Vadodara, Gujarat, India
E.Mail: nilesh.parmar281822@paruluniversity.ac.in

ABSTRACT

Dysmenorrhea is one of the most common gynecological health conditions. It is cramping pelvic pain started before or at the onset of menses and lasting 1-3 days. It is also known as painful menstruation. The prevalence of Dysmenorrhea is highest in the 16-25 year age group. Dysmenorrhoea may also affect the stress level among the girls. Dysmenorrhea can limit daily social, recreational, and educational activities, including affects the quality of life of person. To evaluate the prevalence of severity of dysmenorrhea and its correlation with level of stress among college going girls. An online cross-sectional survey was carried out using Google form with sample of 150 students (age group 18-25 years). Outcome measures used are WALIDD and PSS-10to determine the severity of Dysmenorrhea and level of stress respectively. Pain start within 6-12 hours before menses and lasting for one or two days after menses, Lower abdominal, pelvic and body pain lasting 8-12 hours were included in this study. Girls taking oral contraceptive pills due to any hormonal problem, any pelvic surgery, abnormal bleeding was excluded. In this study for analysis of data used the SPSS-20 and Microsoft Excel for descriptive analysis. In which the mean age was 20.82. Then mean and SD of WAILDD score was 5.46 and 2.28984 and PSS-10 score was 20.68and 6.33000 obtained. There is very weak correlation between severity of dysmenorrhea and level of stress. This study concluded that there was prevalence of severity of

Dolly Shah *et al.,*

dysmenorrhea 4.67%(no dysmenorrhea),30.66%(mild),42%(moderate), 22.66%(severe) and level of stress was 11.33%(low),68.66%(moderate), 20%(severe) among girls there was a not statistically significant correlation between the severity of dysmenorrhea and level of stress in girls.

INTRODUCTION

Menstruation known as a monthly period is the regular release of mucosal tissue and blood from the inner lining of uterus (Endometrium) through the vagina. The 1st period generally starts between 12-15 years old; this time is known as menarche.(1)Worldwide, girls experience menstruation every month which is natural physiological process that might be negative effects on girls.(2) Menstruation related health problems like physical & psychological that suffering with abdominal, back pain, blotting, emotional irritability & fatigue.(3) Menstruation period generally getting start during adolescence & mostly 75% of girls have problems associated with menstruation.(4) Dysmenorrhea is a painful gynecological problem derives from the Greek word which means "difficult monthly flow"(5). Dysmenorrhea classified by two types: (1) Primary Dysmenorrhea: It is painful menses with normal pelvic anatomy. It is start within first six months after menarche. Affected girls having sharp, intermittent pain in the suprapubic area. Pain radiating to the back of legs or lower back. (2) Secondary Dysmenorrhea: It is resulting underlying pathology such as pelvic inflammatory diseases, irregular cycles or infertility problems, endometriosis, intra-uterine devices, ovarian cysts, cervical stenos is. In these primary dysmenorrhea is more common.(6,7) Estimates of prevalence amount adolescents range from 25 to 90%. According to Indian studies, the prevalence ranges from 50 to 87.8 % (8). Pain is reported by 5 to 20% of girls who have severe dysmenorrhea that prohibits them from doing their normal activities.(9)PD is neither life threatening nor disabling, but it does cause absenteeism & has a substantial impact on individual's mental stress. The main cause of PD is increased level of prostaglandins. Prostaglandins especially PGF2 which stimulate myometrial contractions, (10)

Psychological problems such as sadness, stress, anxiety, depression, social factors and lifestyle factors include irregular diet, poor sleep all are related to dysmenorrhea & in this mental stress is one of the important cause of the PD among adolescents girls. (11, 12) Minor changes in daily activities like study related stress, family problem and financial trouble which lead to stress and emotional disturbance has a role in the pathogenesis of pain including PD.(13) Dysmenorrhea can limit daily social, recreational, and educational activities, including affects the quality of life of person.(14) In this study, for level of stress measure using the perceived stress scale (PSS). It is 10 item scales. Complete to 5-10 minutes. the reliability of PSS is 0.80.(15)For severity and screening tool using a WaLIDD Score. This tool is very reliable and valid for measuring the severity of dysmenorrhea. (16) However, the relationship between the severity of dysmenorrhea and level of stress among girls has been less studied. So need of this study to evaluate the correlation between level of stress and severity of dysmenorrhea.

AIMS AND OBJECTIVES

AIM: The aim of study is to evaluate the correlation between level of stress and severity of primary dysmenorrhea in college going girls.

OBJECTIVES

➢   To evaluate prevalence of level of stress and severity of dysmenorrhea.
➢   To find the correlation between age and severity of dysmenorrhea.
➢   To find the correlation between age and level of stress.
➢   To find the correlation between severity of dysmenorrhea and level of stress.

METHODOLOGY

- **Source of data:** Parul University.
- **Study design:** A cross sectional study
- **Sampling method:** Convenient sampling
- **Sample size:** 150
- **Study population:** Girls with primary dysmenorrhea.
- **Inclusion criteria:** Age group 18-25 years, Pain start within 6-12 hours before menses, Lower abdominal, pelvic pain, lower back pain, cramps, medial & anterior thigh pain lasting 8-12 hrs. Regular menstrual cycle.
- **Exclusion criteria:** Having secondary dysmenorrhea, Any Urogynecologic diseases, metabolic diseases, neuropsychiatric condition, pelvic surgery, Girls taking oral contraceptive pills due to any hormonal problem.
- **Ethical clearance:** As the study includes human subjects ethical clearance was obtained from Parul university institutional ethical committee for human research. (PU-IECHR).

PROCEDURE

Total 150 subjects were taken who fulfilling the inclusion and exclusion criteria. All the participants were informed about the study and consent was taken from each participants in the signature on the consent form. Privacy and confidentiality of the subjects should be maintained. Personal information such as name, age, address. age of menarche, cycle of days, days of pain during menses etc. After those subjects were asses with WaLIDD and PSS Questionnaires were formulated and organized with the: Google Forms.

OUTCOME MEASURES

1.The WaLIDD Sore is taking for features of dysmenorrhea such as: 1) Number of anatomical pain locations (No part of the body, Lower abdomen, Lumbar region, Lower limbs, Inguinal region) 2) Wong- Beker pain range (Does not hurt, hurts a little, a hurts little more, hurts even more, hurts a lot) 3) Number of days of pain during menstruation (0, 1-2,3-4,>5)4) Frequency of disabling pain to perform their activities (Never, Almost never, Almost always, Always) Each tool's variable provides specific score between 0 and 3 and final score ranged from 0-12 point.

2. Perceived stress scale-10 was taken for evaluate the level of stress about her menstruation moods, anxiety and emotional disturbances. It is a 10 item questionnaire.

Girls were asked to answer the questions about stress, feelings and thoughts during her menstruation period.

STATSTICAL ANALYSIS

Descriptive analysis of age, WALIDD and PSS interpreted by using statistical software IBM SPSS- 20.The descriptive statistics including means and standard deviations were obtained. For the nonparametric correlation between variables spearman's test was applied. A p- value less than 0.05 were considered to be significant.

RESULTS

In this study 150 participants were selected. The IBM SPSS-20 was used for analysis of data and Microsoft Excel was used for descriptive analysis. In which the mean and SD of age, WALIDD and PSS-10 was 20.82 and 1.89, 5.46 and 2.28 and 20.68and 6.33 obtained respectively.

Dolly Shah *et al.,*

Interpretation: Table - 4 shows,

1. Correlation between AGE & WALIDD the p-value is 0.301 which suggest that there is very weak significant correlation; the value of correlation coefficient r is 0.085 which suggest very weak positive correlation.
2. Correlation between AGE & PSS the p-value is 0.267 which suggest that there is very weak significant correlation; the value of correlation coefficient r is 0.091which suggest very weak positive correlation.
3. Correlation between WALIDD & PSS the p-value is 0.968 which suggest that there is very weak significant correlation; the value of correlation coefficient r is 0.003 which suggest very weak positive correlation.

DISCUSSION

The purpose of present study was to find the prevalence of primary dysmenorrhea among girls and its correlation with severity of dysmenorrhea and level of stress. Total 150 girls falling in age group of 18-25 years were selected according inclusion criteria, WALIDD score measure the severity of dysmenorrhea similar screening tool was used by Rabia Butt, Urfah etal Working ability, location, intensity, days of pain dysmenorrhea (WaLIDD)score was used to assess the severity of dysmenorrhea.(17) and PSS was used to assess level of stress. Primary dysmenorrhea may be a common disorder among young women, and uterine ischemia plays a crucial role in pelvic pain. Asymmetric dimethylarginine (ADMA) is accepted as a stronger marker of endothelial dysfunction. Prostaglandins can also cause headache, nausea, vomiting and diarrhea. Hormonal and endocrine imbalance, uterine contractions, uterine bleeding, cervical obstruction and psychological factors are also involved in the pathophysiology of primary dysmenorrhea. Menstrual pain may result from the increased contractions of the uterine muscle which is innervated by the sympathetic nervous system. Stress is supposed to increase the sympathetic activity which may lead to the increase in menstrual pain by enhancing the intensity of the uterine contractions.

The findings of the present study showed a high prevalence of dysmenorrhea in which 4.67% (no dysmenorrhea), 30.66%(mild),42%(moderate), 22.66%(severe) and level of stress was 11.33%(low),68.66%(moderate), 20%(severe) among adolescents girls of Parul university, Farooq Islam, Asim Raza et al. determined that Out of 161 subjects, 12 were having mild dysmenorrhea, 98 were moderate and 51 were severe dysmenorrhea.(17)similar findings were reported by Suresh K. Kumbhar, Mrudula Reddy etal 119 (65%) are dysmenorrheic, 68.4% and 61.2% are from the urban and rural areas respectively.(18)Dysmenorrhea is one of the most frequent discomforting gynecological conditions influencing the quality of lifeand social activities among girls.. Similar study was done by Amir, Farideh etal several factors can affect primary dysmenorrhea and its incidence and severity including mental health. (19)

In this study our results found that very weak positive correlation between age and severity of dysmenorrhea(r= 0.085), age and level of stress.(r= 0.091) and severity of dysmenorrhea with level of stress(r= 0.03) and also no significant level found in college going girls. Similar findings was determined by Karki, Rai Chandra etal. No association was found between incidence of dysmenorrhea and severity of stress.(20)However , wang L etal(21) and Masoumeh Kordi(22) etal found association between high stress level and incidence of dysmenorrhea. The quality of life during dysmenorrhea is comparatively poor among dysmenorrheic girls, loss of physical activity and work satisfaction, personal relationships, confidence& concentration.

CONCLUSION

A total 150 participants were selected for the study from Parul university girls. By this study we concluded that severity of dysmenorrhea and level of stress very weak correlation was obtained, and found that there was a not statistically significant relationship between the severity of dysmenorrhea and level of stress in girls.

Limitations of study
1) Sample size was small.
2) The data was collected from only one university.

Further Recommendations

1) A study can be done with different universities and schools.

2) A study can be done on different age group.

3) A study can be done with large sample size.

4) Other factors can be taken.

REFERENCES

1. Hassan HE. Correlation between quality of life and dysmenorrhea among nursing schools students. International Journal of Nursing. 2017;7(6):123-32.

2. Alshdaifat E, Absy N, Sindiani A, AlOsta N, Hijazi H, Amarin Z, Alnazly E. Premenstrual Syndrome and Its Association with Perceived Stress: The Experience of Medical Students in Jordan. International Journal of Women's Health. 2022 Jun 14:777-85.

3. Priyangani PV, Priyankara EA, Wimalarathna KB. Prevalence and associated factors of menstrual irregularities among student nurses in selected Nursing training schools.

4. Perundurai E, Panneerselvam P. Association of dysmenorrhea and level of perceived stress score with premenstrual and menstrual symptoms in medical and non-medical students. European Journal of Molecular & Clinical Medicine (EJMCM). 2020;7(11):8490-8.

5. Gujral T. Association of Primary Dysmenorrhea with Stress and BMI among Undergraduate Female Students-A Cross Sectional Study. Turkish Journal of Physiotherapy and Rehabilitation. 2022 Jun 16;32(3)

6. Pramanik T, Shrestha R, Sherpa MT, Adhikari P. Incidence of dysmenorrhoea associated with high stress scores among the undergraduate Nepalese medical students. Journal of Institute of Medicine Nepal. 2010;32(3):2-4.

7. Singh A, Kiran D, Singh H, Nel B, Singh P, Tiwari P. Prevalence and severity of dysmenorrhea: a problem related to menstruation, among first and second year female medical students. Indian J Physiol Pharmacol. 2008 Oct 1;52(4):389-97.

8. Zukri SM, Naing L, Hamzah TN. Primary Dysmenorrhea among Medical and Dental University Students in Kelantan: Prevalence and. International Medical Journal. 2009 Jun;16(2):93-9.

9. Diaz AM, Laufer MR, Breech LL. Menstruation in girls and adolescents: using the menstrual cycle as a vital sign. Pediatrics. 2006 Nov 1;118(5):2245-50.

10. Yilmaz FA, Dilek AV. Effect of dysmenorrhea on quality of life in university students: A case-control study. Cukurova Medical Journal. 2020;45(2):648-55.

11. Unsal A, Ayranci U, Tozun M, Arslan G, Calik E. Prevalence of dysmenorrhea and its effect on quality of life among a group of female university students. Upsala journal of medical sciences. 2010 May 1;115(2):138-45.

12. Shehzadi T, Rida M, Imtiaz R. Association of Insomnia and Academic Stress with the onset of Dysmenorrhea among females of Lahore, Pakistan. ScienceOpen Preprints. 2022 Jun 1.

13. Azim R, Paul A, Ghosh B. Evaluating The Effect Of Physical Exercise Therapy On The Mental Stress Of Dysmenorrhea Patients. Webology (ISSN: 1735-188X). 2022;19(3).

14. Atta K, Jawed S, Zia S. Correlating primary dysmenorrhea with its stressors: a cross sectional study investigating the most likely factors of primary dysmenorrhea and its effects on quality of life and general well being. Journal of University Medical & Dental College. 2016;7(4).

15. Baik SH, Fox RS, Mills SD, Roesch SC, Sadler GR, Klonoff EA, Malcarne VL. Reliability and validity of the Perceived Stress Scale-10 in Hispanic Americans with English or Spanish language preference. Journal of health psychology. 2019 Apr;24(5):628-39.

Dolly Shah *et al.*,

16. Teherán AA, Piñeros LG, Pulido F, Mejía Guatibonza MC. WalIDD score, a new tool to diagnose dysmenorrhea and predict medical leave in university students. International journal of women's health. 2018 Jan 17:35-45.

17. Butt RA, Zaigham U, Islam F, Raza A. Effect of dysmenorrhea on instrumental activities of daily living. Rawal Medical Journal. 2021 Jun 8;46(3):628-.

18. Kumbhar SK, Reddy M, Sujana B, Reddy R, Balkrishna C. Prevalence of dysmenorrhea among adolescent girls (14-19 yrs) of Kadapa district and its impact on quality of life: A cross sectional study. National Journal of Community Medicine. 2011 Sep 30;2(02):265-8.

19. Pakpour AH, Kazemi F, Alimoradi Z, Griffiths MD. Depression, anxiety, stress, and dysmenorrhea: a protocol for a systematic review. Systematic reviews. 2020 Dec;9(1):1-6

20. Kumar KP, Kala RC, Sushil K, Gita K. Dysmenorrhea and its association with stress among female students of Kathmandu Medical College. Indian Journal of Basic and Applied Medical Research. 2017 Jun;6(3):554-8.

21. .Wang L, Wang X, Wang W, Chen C, Ronnennberg AG, Guang W, Huang A, Fang Z, Zang T, Xu X. Stress and dysmenorrhoea: a population based prospective study. Occupational and Environmental Medicine. 2004 Dec 1;61(12):1021-6.

22. Kordi M, Mohamadirizi S, Shakeri MT. The relationship between occupational stress and dysmenorrhea in midwives employed at public and private hospitals and health care centers in Iran (Mashhad) in the years 2010 and 2011. Iranian journal of nursing and midwifery research. 2013 Jul;18(4):316.

Table:- 1 Description of Age

	MEAN	SD
AGE	20.82	1.89
WALIDD	5.46	2.28
PSS	20.68	6.33

Table:-2 Distribution of the participants according to Age

AGE	TOTAL	percentage
18-20	74	49.33%
21-23	58	38.66%
24-25	18	12%
	150	

Table:-3 Distribution of participants according WALIDD AND PSS

WALIDD SCORE	TOTAL	percentage	interpretation
0	7	4.67%	No dysmennorhea
1 to 4	46	30.66%	mild
5 to 7	63	42%	moderate
8 to 12	34	22.66%	severe
PSS	**TOTAL**	**percentage**	**interpretation**
0-13	17	11.33%	Low stress
14-26	103	68.66%	moderate
27-40	30	20%	Severe

Table: 4 Correlation between AGE, WaLIDD AND PSS

1.Correlation between AGE and WAILDD				
	Mean	Std-deviation	r-value	p-value
Age	20.826	1.892	0.085	0.301
WaLIDD	5.460	2.289		

Dolly Shah *et al.,*

2.Correlation between AGE and PSSS				
Age	20.826	1.892	0.091	0.267
PSS	20.686	6.330		
3.Correlation between WALIDD and PSS				
WALIDD	5.460	2.289	0.003	0.968
PSS	20.686	6.330		
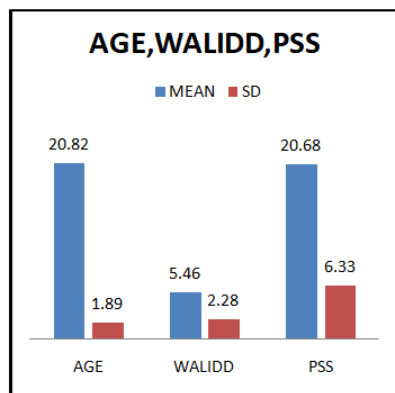
Graph 1: Mean and SD of AGE, WALIDD and PSS.
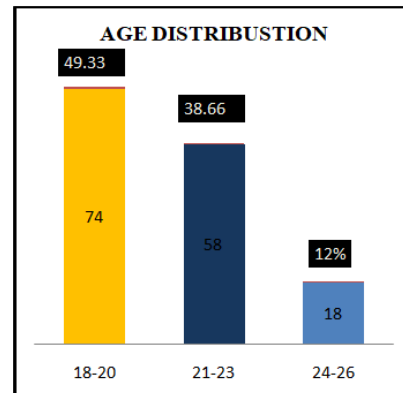
Graph 2: shows a age group distribution.
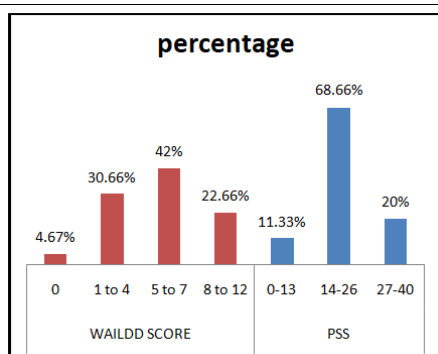
Graph: 3 shows participants' distribution according WALIDD and PSS.
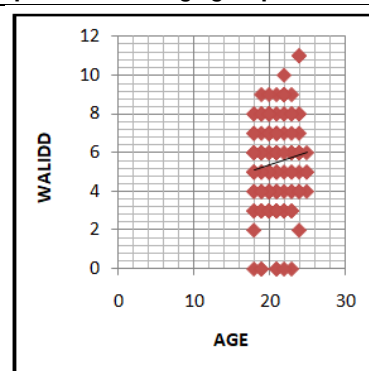
Graph: 4.1 shows correlation between Age and WaLIDD (r= 0.085)
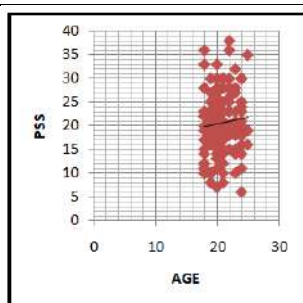
Graph: 4.2 shows correlation between Age and PSS (r= 0.091)
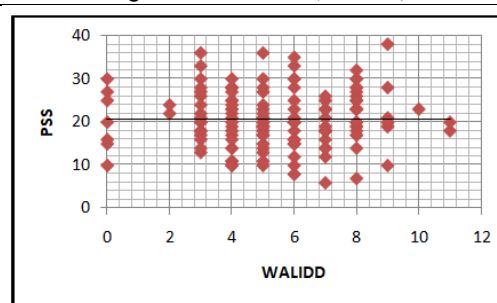
Graph: 4.3 correlation between WALIDD and PSS (r=0.003)

63925

RESEARCH ARTICLE

Independent Semitotal Domination in Product Graphs

J.Sabari Manju[1]* and S.V.Padmavathi[2]

[1]Research Scholar, Department of Mathematics, Saraswathi Narayanan College, (Affiliated to Madurai Kamaraj University), Madurai, Tamil Nadu, India.
[2]Associate Professor, Department of Mathematics, Saraswathi Narayanan College, (Affiliated to Madurai Kamaraj University), Madurai, Tamil Nadu, India.

***Address for Correspondence**
J.Sabari Manju
Research Scholar,
Department of Mathematics,
Saraswathi Narayanan College,
(Affiliated to Madurai Kamaraj University),
Madurai, Tamil Nadu, India.
E.Mail:sabarimanju2009@gmail.com

ABSTRACT

A dominating set S of vertices of a graph G without isolated vertices is an independent semitotal dominating set if it is an independent dominating set and to each u in S there is a v in S at a distance exactly two. The independent semitotal domination number of a graph is the minimum size of an independent semitotal dominating set of vertices in G. In this paper, we have obtained the bounds for independent semitotal domination number in the Cartesian product of paths, path with a cycle and cycles.

AMS Subject Classification: 05C69

Keywords: Cartesian Product of graphs, Total Domination, Semitotal Domination, Independent Semitotal Domination,

INTRODUCTION

Let $G = (V, E)$ be a graph. A set S of vertices of G is a dominating set if for each v in $V - S$ there is a u in S such that uv is an edge. The minimum and maximum cardinality of a minimal dominating set of G are the domination number $\gamma(G)$ and upper domination number $\Gamma(G)$ respectively.

Sabari Manju and Padmavathi

A dominating set S of G is an independent dominating set if < S > consists of isolate vertices. i(G), the independent domination number of G is the minimum cardinality of a minimal independent dominating set.

The maximum cardinality of a maximal independent set of vertices of G is the independence number of G, denoted by β_0(G).

The concept of semitotal domination was introduced in[1]

A set S of vertices of a graph G without isolated vertices is a semitotal dominating set of G if it is a dominating set of G and every vertex in S is within distance 2 of another vertex of S. The semitotal domination number denoted by γ_{t2}(G) is the minimum cardinality of a minimal semitotal dominating set.

An inequality domination chain of a graph connects various parameters was established in [2] as follows ir(G) ≤ γ(G) ≤ i(G) ≤ β_0(G) ≤ Γ(G) ≤ IR(G) .

From the motivation of semitotal domination we introduced a parameter, independent semitotal domination number that lies between independentdomination number, i(G) and independence number β_0(*G*) [3].

A set S of vertices of G is an independent semitotal dominating set if S is an independent dominating set and for each *u* in S there is a *v* in S at a distance exactly two. The minimum and maximum cardinality of a minimal independent semitotal dominating set are called the independent semitotal domination number γ_{it2}(G) and upper independent semitotal domination number Γ_{it2}(G) of G respectively.

This parameter lies between independent domination number i(G) and independence number β_0(G) of a graph. The parameter γ_{it2}(G) extends the chain as

ir(G) ≤ γ(G) ≤ γ_0(G) ≤ i(G) ≤ γ_{it2}(G) ≤ Γ_{it2}(G) ≤ β_0(G) ≤ Γ_0(G) ≤ Γ(G) ≤ IR(G)

Every graph has a β_0 set which is also an independent semitotal dominating set, hence its existence is guaranteed for all non-complete graph. For complete graph β_0(K_n) = 1 and hence γ_{it2}(K_n) is set as 1.

Example 1.1
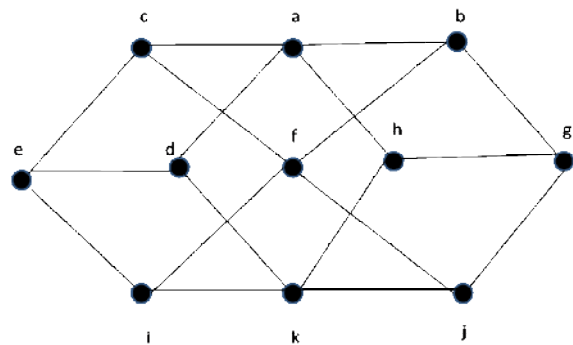
i(G) = |{f, d, h}| = 3.
γ_{it2}(G) = |{f, a, k, e, g}| = 5.
β_0(G) = |{b, c, i, j, d, h}| = 6
i(G) < γ_{it2}(G) < β_0(G)

The Cartesian graph product G□ H called graph product of graphs is a graph with V(G□H) = V(G)xV(H) and (g_1,h_1) (g_2,h_2) ∈E(G□ H) iff either g_1 = g_2 and h_1h_2 ∈E(H) or g_1g_2 ∈ E(G) and h_1=h_2.

In this paper we have obtained the bounds for the Cartesian product of paths, path with a cycle and cycles.

Sabari Manju and Padmavathi

CARTESIAN PRODUCT OF PATHS

Theorem 2.1

(i) $\gamma_{it2}(P_2 \square P_n) = \dfrac{2n}{3} + 1$ for n = 3k , k = 1,2,3…

(ii) $\gamma_{it2}(P_2 \square P_n) = \left\lceil \dfrac{2(n+1)}{3} \right\rceil$ for n ≠ 3k

Proof

Let $V(P_2 \square P_n) = \{(c_1, d_i), (c_2, d_j)\}$ where i, j = 1,2,…..n be the vertex set of $P_2 \square P_n$.

When n = 2 ≠ 3k, the set $S = \{(c_1, d_1), (c_2, d_2)\}$ forms a γ_{it2}- set.

$\gamma_{it2}(P_2 \square P_2) = 2 = \left\lceil \dfrac{2(n+1)}{3} \right\rceil$

When n = 3 = 3k, the set $S = \{(c_1, d_1), (c_2, d_2), (c_1, d_3)\}$ forms a γ_{it2}- set.

$\gamma_{it2}(P_2 \square P_3) = 3 = \dfrac{2n}{3} + 1$.

When n = 4 ≠ 3k, the set $S = \{(c_1, d_i), (c_2, d_j)\}$ where i = 1, 3 and j = 2, 4 forms a γ_{it2}- set.

$\gamma_{it2}(P_2 \square P_4) = 4 = \left\lceil \dfrac{2(n+1)}{3} \right\rceil$

When n = 5 ≠ 3k, the set $S = \{(c_1, d_i), (c_2, d_j)\}$ i = 1,4 and j = 2,5 forms a γ_{it2}- set.

$\gamma_{it2}(P_2 \square P_5) = 4 = \left\lceil \dfrac{2(n+1)}{3} \right\rceil$

In general n = 3k, the set $S = \{(c_1, d_i), (c_2, d_j)\}$ where i = 1,4,….n and j = 2,5,…n-1 forms a γ_{it2}- set.

(c_1, d_i) has $\dfrac{n}{3}$ +1 terms and (c_2, d_j) has $\dfrac{n}{3}$ terms.   Therefore $\gamma_{it2}(P_2 \square P_n) = \dfrac{2n}{3} + 1$.

When n ≠ 3k, the set $S = \{(c_1, d_i), (c_2, d_j)\}$ where i = 1,4,….n-1 and j = 2,5,…n forms a γ_{it2}- set.

(c_1, d_i) has $\left\lceil \dfrac{n+1}{3} \right\rceil$ terms and (c_2, d_j) has $\left\lceil \dfrac{n+1}{3} \right\rceil$ terms.   Therefore $\gamma_{it2}(P_2 \square P_n) = \left\lceil \dfrac{2(n+1)}{3} \right\rceil$

Theorem 2.2

(i) $\gamma_{it2}(P_3 \square P_2) = 3$

(ii) $\gamma_{it2}(P_3 \square P_3) = 4$

(iii) $\gamma_{it2}(P_3 \square P_n) = n$ for n ≥ 4

Proof

(i)   For $P_3 \square P_2$, let $V(P_3 \square P_2) = \{(c_1, d_i), (c_2, d_j), (c_3, d_k)\}$ where i,j,k = 1,2 be the vertex set of $P_3 \square P_2$. The set $S = \{(c_1, d_1), (c_2, d_2), (c_3, d_1)\}$ forms a γ_{it2}- set. Therefore $\gamma_{it2}(P_3 \square P_2) = 3$.

(ii)   For $P_3 \square P_3$, let $V(P_3 \square P_3) = \{(c_1, d_i), (c_2, d_j), (c_3, d_k)\}$ where i,j,k = 1,2,3 be the vertex set of $P_3 \square P_3$. The set $S = \{(c_1, d_2), (c_2, d_1), (c_2, d_3), (c_3, d_2)\}$ forms a γ_{it2}- set. Therefore $\gamma_{it2}(P_3 \square P_3) = 4$.

(iii)   For $P_3 \square P_n$, let $V(P_3 \square P_n) = \{(c_1, d_i), (c_2, d_j), (c_3, d_k)\}$ where i,j,k = 1,2,…n

 When n is even, the set $S = \{(c_1, d_i), (c_3, d_k)\}$ where i = 1,3,5,….n-1 and k = 2,4,…..n forms a γ_{it2}- set.

 (c_1, d_i) has $\dfrac{n}{2}$ terms and (c_3, d_k) has $\dfrac{n}{2}$ terms. Therefore $\gamma_{it2}(P_3 \square P_n) = n$ for n ≥ 4.

Sabari Manju and Padmavathi

When n is odd, the set S = {(c_1, d_i), (c_3, d_k)} where i = 1,3,5,….n and k = 2,4,…..n-1 forms a γ_{it2}- set.

(c_1, d_i) has $\dfrac{n}{2}$ terms and (c_3, d_k) has $\dfrac{n}{2}$ terms. Therefore $\gamma_{it2}(P_3 \Box P_n)$ = n for n ≥ 4.

Theorem 2.3

(i) $\gamma_{it2}(P_4 \Box P_n)$ = n+2 when n is even

(ii) $\gamma_{it2}(P_4 \Box P_n)$ = n+1 when n is odd

Proof

(i)   When n is even

$V(P_4 \Box P_n)$ = {(c_1, d_i), (c_2, d_j), (c_3, d_k) (c_4, d_l)} where i,j,k,l = 1,2,…n

Choose (c_1, d_1), (c_3, d_1) in the 1ˢᵗ column and $(c_2, d_3)(c_4, d_3)$ in the 3ʳᵈ column. Proceeding like this choose upto $(c_2, d_{n-1})(c_4, d_{n-1})$ in the (n-1)ᵗʰ column. Since n is even, $P_4 \Box P_n$ has even number of columns. And two vertices are chosen in each column alternatively. Therefore total number of columns with chosen vertices is n/2. For domination, we have to choose $(c_1, d_n)(c_3, d_n)$ in the nᵗʰ column additionally. Total number of vertices to form a γ_{it2}- set is n+2.

Therefore $\gamma_{it2}(P_4 \Box P_n)$ = n+2.

(ii)   When n is odd

Choose (c_1, d_1), (c_3, d_1) in the 1ˢᵗ column and $(c_2, d_3)(c_4, d_3)$ in the 3ʳᵈ column. Proceeding like this choose upto $(c_1, d_n)(c_3, d_n)$ in the nᵗʰ column. Since n is odd, $P_4 \Box P_n$ has odd number of columns. Therefore total number of columns having the chosen vertices is $\dfrac{n+1}{2}$. Since two vertices are chosen in each column alternatively to form a γ_{it2}- set.   Therefore $\gamma_{it2}(P_4 \Box P_n)$ = n+1.

CARTESIAN PRODUCT OF PATH WITH CYCLE
Theorem 3.1

(i) $\gamma_{it2}(P_2 \Box C_n)$ = $\dfrac{2n}{3}$ n ≡ 0 (mod 3)

(ii) $\gamma_{it2}(P_2 \Box C_n)$ = $\left\lceil \dfrac{2n+3}{3} \right\rceil$ n ≡ 1 (mod 3)

(iii) $\gamma_{it2}(P_2 \Box C_n)$ = $\left\lfloor \dfrac{2n+3}{3} \right\rfloor$ n ≡ 2 (mod 3)

Proof

(i)   When n ≡ 0 (mod 3)

Let n = 3, $V(P_2 \Box C_3)$ = {(c_1, d_i), (c_2, d_j)} where i,j = 1,2,3 be the vertex set.

The set S = {(c_1, d_1), (c_2, d_2)} forms a γ_{it2}- set. Therefore $\gamma_{it2}(P_2 \Box C_3)$ = 2 = $\dfrac{2n}{3}$

Let n = 6, $V(P_2 \Box C_6)$ = {(c_1, d_i), (c_2, d_j)} where i,j = 1,2,3,4,5,6 be the vertex set.

The set S = {(c_1, d_i), (c_2, d_j)}where i = 1,4 and j = 2,5 form a γ_{it2}- set.

Therefore $\gamma_{it2}(P_2 \Box C_6)$ = 4 = $\dfrac{2n}{3}$

In general for n, the set S = {(c_1, d_i), (c_2, d_j)} where i = 1,4,…n-2 and j = 2,5,….n-1 forms a γ_{it2}- set. (c_1, d_i) has $\dfrac{n-2}{3}+1$ terms and (c_2, d_j) has $\dfrac{n-1}{3}$ terms.

Therefore $\gamma_{it2}(P_2 \Box C_n)$ = $\dfrac{2n}{3}$

(ii)   When n ≡ 1 (mod 3)

Sabari Manju and Padmavathi

Let n = 4, $V(P_2 \square C_4) = \{(c_1, d_i), (c_2, d_j)\}$ where i,j = 1,2,3,4 be the vertex set.

The set S = $\{(c_1, d_i), (c_2, d_j)\}$ where i = 1,3 and j = 2,4 forms a γ_{it2}-set.

Therefore $\gamma_{it2}(P_2 \square C_4) = 4 = \left\lceil \dfrac{2n+3}{3} \right\rceil$

In general for $P_2 \square C_n$, the set S = $\{(c_1, d_i), (c_2, d_j)\}$ where i = 1,4,…n-1 and j = 2,5,…n forms a γ_{it2}-set.

(c_1, d_i) has $\dfrac{n-1}{3} + 1$ terms and (c_2, d_j) has $\left\lceil \dfrac{n+1}{3} \right\rceil$ terms.

Therefore $\gamma_{it2}(P_2 \square C_n) = \left\lceil \dfrac{2n+3}{3} \right\rceil$

(iii)   When n ≡ 2 (mod 3)

Let n = 5, $V(P_2 \square C_5) = \{(c_1, d_i), (c_2, d_j)\}$ where i,j = 1,2,3,4,5 be the vertex set.

The set S = $\{(c_1, d_i), (c_2, d_j)\}$ where i = 1,3 and j = 2,4 forms a γ_{it2}- set.

$\gamma_{it2}(P_2 \square C_5) = 4 = \left\lfloor \dfrac{2n+3}{3} \right\rfloor$

In general S = $\{(c_1, d_i), (c_2, d_j)\}$ where i = 1,4,…n-1 and j = 2,5,…n forms a γ_{it2}- set.

(c_1, d_i) has $\left\lfloor \dfrac{n-1}{3} \right\rfloor + 1$ terms and (c_2, d_j) has $\dfrac{n+1}{3}$ terms

Therefore $\gamma_{it2}(P_2 \square C_n) = \left\lfloor \dfrac{2n+3}{3} \right\rfloor$

Theorem 3.2

(i) $\gamma_{it2}(P_3 \square C_n) = n$ n ≡ 0 (mod 3)

(ii) $\gamma_{it2}(P_3 \square C_n) = n+2$ n ≡ 1 (mod 3)

(iii) $\gamma_{it2}(P_3 \square C_n) = n+1$ n ≡ 2 (mod 3)

Proof

(i)   When n ≡ 0 (mod 3)

Let n = 3, $V(P_3 \square C_3) = \{(c_1, d_i), (c_2, d_j), (c_3, d_k)\}$ where i,j,k = 1,2,3 be the vertex set.

The set S = $\{(c_1, d_1), (c_2, d_2), (c_3, d_1)\}$ forms a γ_{it2}- set. Therefore $\gamma_{it2}(P_3 \square C_3) = 3 = n$.

Let n = 6, $V(P_3 \square C_6) = \{(c_1, d_i), (c_2, d_j), (c_3, d_k)\}$ where i,j,k = 1,2,3,4,5,6 be the vertex set.

The set S = $\{(c_1, d_i), (c_2, d_j), (c_3, d_k)\}$ where i = 1,4 j = 3,5 k = 1,4 forms a γ_{it2}-set.

Therefore $\gamma_{it2}(P_3 \square C_6) = 6 = n$.

For the first three columns, two vertices (c_1, d_1), (c_3, d_1) are chosen in 1st column and one vertex is chosen in 3rd column to form Independent semitotal domination.

Similarly for the next three columns, we need three vertices to form independent

semitotal domination. Hence for n columns, we need $3\left(\dfrac{n}{3}\right)$ vertices to form independent semitotal domination.

(ie) $\gamma_{it2}(P_3 \square C_n) = n$.

(ii)   When n ≡ 1 (mod 3)

Therefore n-1 is a multiple of 3. As in case (i) we need $3\left(\dfrac{n-1}{3}\right)$ vertices upto n-1 column. Additionally we need one

vertex in the nth column and two vertices in the (n-1)th column to form independent semitotal domination.

Therefore for $P_3 \square C_n$, we need $3\left(\dfrac{n-1}{3}\right)+3$ vertices to form a γ_{it2}- set.

Therefore $\gamma_{it2}(P_3 \square C_n) = n+2$

(iii)   When $n \equiv 2 \pmod 3$

Therefore $n-2$ is a multiple of 3. As in case (i) we need $3\left(\dfrac{n-2}{3}\right)$ vertices to form independent semitotal domination upto $(n-2)^{th}$ column. Additionally we need one vertex in the nth column and two vertices in the $(n-1)^{th}$ column.

Therefore for $P_3 \square C_n$, we need $3\left(\dfrac{n-2}{3}\right)+3$ vertices to form a γ_{it2}- set.

Therefore $\gamma_{it2}(P_3 \square C_n) = n+1$.

Theorem 3.3
(i) $\gamma_{it2}(P_4 \square C_n) = n$ $n \equiv 0 \pmod 4$
(ii) $\gamma_{it2}(P_4 \square C_n) = n+3$ $n \equiv 1 \pmod 4$
(iii) $\gamma_{it2}(P_4 \square C_n) = n+2$ $n \equiv 2 \pmod 4$
(iv) $\gamma_{it2}(P_4 \square C_n) = n+1$ $n \equiv 3 \pmod 4$

Proof
Let $V(P_4 \square C_n) = \{(c_1, d_i), (c_2, d_j), (c_3, d_k), (c_4, d_l)\}$ where i, j, k, l = 1,2,….n be the vertex set.
Let n= 3, the set S = $\{(c_1, d_1), (c_2, d_3), (c_3, d_1), (c_4, d_3)\}$ form a γ_{it2}- set.
$\gamma_{it2}(P_4 \square C_3) = 4 = n+1$.
(i)   When $n \equiv 0 \pmod 4$
Let n = 4. The set S = $\{(c_1, d_1), (c_2, d_3), (c_3, d_1), (c_4, d_3)\}$ forms a γ_{it2}- set.
(ie) two vertices are chosen in the nth column.   Thus $\gamma_{it2}(P_4 \square C_4) = 4 = n$.
Let n = 8. The set S = $\{(c_1,d_i), (c_2,d_j), (c_3,d_k), (c_4,d_l)\}$ where i=1,5 j=3,7 k=1,5 and l=3,7 forms a γ_{it2}-set. (ie) Two vertices are chosen in 1st, 3rd,5th, and 7th column.
Thus $\gamma_{it2}(P_4 \square C_8) = 8 = n$.
In general for $P_4 \square C_n$, two vertices should be chosen in n/2 columns.

Therefore $\gamma_{it2}(P_4 \square C_n) = 2\left(\dfrac{n}{2}\right) = n$.

(ii)   When $n \equiv 1 \pmod 4$
 Let n = 5. The set S = $\{(c_1,d_i), (c_2,d_j), (c_3,d_k), (c_4,d_l)\}$ where i=1,4 j=3,5 k=1,4 and l=3,5 forms a γ_{it2}-set. Therefore $\gamma_{it2}(P_4 \square C_5) = 8 = n+3$
Here two vertices are choosen upto 3rd column (ie) upto $(n-2)^{th}$ column alternatively. Then again two vertices are chosen in 4th and 5th column (ie) $(n-1)^{th}$ and n^{th} column.

This pattern is carried over for all $n \equiv 1 \pmod 4$. So in general, we need $2\left(\dfrac{n-2+1}{2}\right)+4$

vertices to form a γ_{it2}-set.

        Therefore $\gamma_{it2}(P_4 \square C_n) = n+3$

(iii)   When $n \equiv 2 \pmod 4$
Let n = 6. The set S = $\{(c_1,d_i), (c_2,d_j), (c_3,d_k), (c_4,d_l)\}$ where i=1,5 j=3,6 k=1,5 and l=3,6 forms a γ_{it2}- set. Therefore $\gamma_{it2}(P_4 \square C_6) = 8 = n+2$
Here two vertices are chosen in each alternatively (ie) from 1st, 3rd,5th column and two vertices are chosen in last column (ie) 6th column.

Sabari Manju and Padmavathi

In general, two vertices are chosen upto n-1 column alternatively and two vertices are

Chosen in the nth column. Therefore $\gamma_{it2}(P_4 \Box C_n)$ = $2\dfrac{(n-1)+1}{2}+2$ = n+2

(iv)   When n ≡ 3 (mod 4)

Let n = 7. The set S = {(c_1,d_i), (c_2,d_j), (c_3,d_k), (c_4,d_l)} where i=1,5 j=3,6 k=1,5 l=3,6 forms a γ_{it2}- set. Therefore $\gamma_{it2}(P_4 \Box C_7)$ = 8 = n+1

Here two vertices are chosen in each alternatively (ie) from 1st, 3rd,5th column and two vertices are chosen in 6th column.

In general, two vertices are chosen upto n-2 column alternatively and two vertices are

Chosen in the $(n-1)^{th}$ column. Therefore $\gamma_{it2}(P_4 \Box C_n)$ = $2\dfrac{(n-2)+1}{2}+2$ = n+1

CARTESIAN PRODUCT OF CYCLES

Theorem 4.1

For n ≥ 3, $\gamma_{it2}(C_3 \Box C_n)$ = n.

Proof

Let $V(C_3 \Box C_n)$ = {(c_1, d_i), (c_2, d_j), (c_3, d_k)} where i,j,k = 1,2,3….n be the vertex set of $C_3 \Box C_n$.

Choose one vertex in each column such that all are independent and for every chosen vertex there should be another chosen vertex at distance two. These vertices forms independent semitotal domination. Since there are 'n' number of columns, 'n' number of vertices are chosen to form γ_{it2}- set. Therefore $\gamma_{it2}(C_3 \Box C_n)$ = n.

Theorem 4.2

(i) $\gamma_{it2}(C_4 \Box C_3)$ = 4.

(ii) $\gamma_{it2}(C_4 \Box C_4)$ = 4.

(iii) $\gamma_{it2}(C_4 \Box C_5)$ = 6.

(iv) $\gamma_{it2}(C_4 \Box C_n)$ = n. for n ≥ 6

Proof

(i) Let $V(C_4 \Box C_3)$ = { (c_1, d_i), (c_2, d_j), (c_3, d_k), (c_4, d_l)} where i,j,k,l = 1,2,3 be the vertex set of $C_4 \Box C_3$.

The set S = {(c_1, d_1), (c_2, d_3) , (c_3, d_2), (c_4, d_3)} forms a γ_{it2}- set.

Therefore $\gamma_{it2}(C_4 \Box C_3)$ = 4.

(ii) Let $V(C_4 \Box C_4)$ = { (c_1, d_i), (c_2,d_j), (c_3,d_k), (c_4,d_l)} where i,j,k,l = 1,2,3,4 be the vertex set of $C_4 \Box C_4$.

The set S = {(c_1, d_1), (c_2, d_3) , (c_3, d_1), (c_4, d_3)} forms a γ_{it2}- set.

Therefore $\gamma_{it2}(C_4 \Box C_4)$ = 4.

(iii)Let $V(C_4 \Box C_5)$ = {(c_1, d_i), (c_2,d_j), (c_3,d_k), (c_4,d_l)} where i,j,k,l = 1,2,3,4,5 be the vertex set of $C_4 \Box C_5$.

The set S = {(c_1d_i), (c_2,d_5), (c_3,d_k), (c_4,d_5)}where i=1,3 and k=2,4 forms a γ_{it2}- set.

Therefore $\gamma_{it2}(C_4 \Box C_4)$ = 6.

(iv)Let $V(C_4 \Box C_n)$ = {(c_1, d_i), (c_2, d_j), (c_3, d_k), (c_4,d_l)} where i,j,k,l = 1,2,3….n be the vertex set of $C_4 \Box C_n$.

Choose one vertex in each column such that each should be independent and at a distance two with another vertex.

Therefore $\gamma_{it2}(C_4 \Box C_n)$ = n.

REFERENCES

1. W. Goddard., M.A. Henning and C.A. McPillan., Semitotal domination in graphs,Util.Math.,94(2014), 67-81.

2. E.J. Cockayne., S.T.Hedetniemi., K.J.Miller, Properties of hereditary hypergraphs and middle graphs, Canad.Math.Bull.21(1978), 461-468.

3. S.V. Padmavathi. and J.Sabari Manju., Independent Semitotal Domination in Graphs, (Communicated)

4. J.A. Bondy. and U.S.R. Murthy., Graph theory with applications, Macmillan press,1976.

5. V.R.Girish and P.Usha, Split Domination of Cartesian product graphs, Palestine Journal of Mathematics. Vol. 8(2)(2019), 348-354.

6. T.W. Haynes., S.T. Hedetniemi. and P.J. Slater., Domination in Graphs: Advanced Topics, MarcelDekker, New york,1998.

7. T.W. Haynes., S.T.Hedetniemi and P.J. Slater., Fundamentals of domination in graphs, MarcelDekker, New york,1998.

8. M.S. Jacobson and L.F.Kinch, On the Domination Number of Products of Graphs:I, Ars Combinatoria, Vol. 18(1983), 33-44.

9. Polana Palvic, Janez Zerovnik, A Note on the Domination Number of the Cartesian Product of Paths and Cycles, Krangujevac Journal of Mathematics., 37(2) (2013), 275-285.

10. I. Sahul Hamid. and S.Balamurugan., Isolate domination in graphs, Arab J Math Sci 22(2016), 232-241.

11. Sandi Klavzer, Norbert Seifter, Dominating Cartesian product of cycles, Discrete Applied Mathematics. 59, (1995), 129-136.

RESEARCH ARTICLE

Water Quality Prediction using Machine Learning

Gideon Asante[1] and Kaushal Singh[2]*

[1]M.Sc Data Science, School of Engineering, P.P. Savani University, Surat, Gujarat, India
[2]Assistant Professor, Department of Computer Engineering and IT, P.P. Savani University, Surat, Gujarat, India

*Address for Correspondence
Kaushal Singh
Assistant Professor,
Department of Computer Engineering and IT,
P.P. Savani University,
Surat, Gujarat, India.
E.Mail: Kaushal.singh@ppsu.ac.in

ABSTRACT

Predicting water quality is essential for assuring the availability of clean, safe drinking water, safeguarding aquatic ecosystems, and efficiently managing water resources. The ability of machine learning algorithms to model complicated interactions and produce precise forecasts has made them viable tools for predicting water quality in recent years. Support Vector Machine (SVM) is well known among machine learning techniques and has been extensively used in many disciplines, including water quality prediction. This research thoroughly analyzes current studies on SVM-based water quality prediction. The drawbacks of conventional approaches for predicting water quality are explored, emphasizing the demand for cutting-edge machine learning technologies. The study then thoroughly analyzes several SVM-based methods for forecasting water quality, including various kernel functions, feature selection techniques, and model evaluation procedures, before providing a general review of SVM and outlining its guiding principles, benefits, and drawbacks. The SVM model can manage high-dimensional data, cope with non-linear relationships, and make accurate predictions. The need for large datasets, the selection of the appropriate kernel functions, and issues with uneven data are all noted as challenges and restrictions of SVM-based water quality prediction. Also, possible directions for further research, such as combining SVM with other machine learning algorithms, incorporating domain expertise, and creating ensemble approaches for predicting water quality are considered and discussed. Finally, by improving water management practices, SVM can assist people all around the world to have access to safe and clean drinking water. SVM has demonstrated good results when used to predict water quality.

Keywords: Support Vector Machine (SVM), Machine Learning (ML), Water Quality Prediction

Gideon Asante and Kaushal Singh

INTRODUCTION

No one can live without water, thereby making water a crucial environmental factor. Water quality directly impacts human health, ecosystem sustainability, and economic growth. Monitoring and predicting water quality is essential for ensuring the availability of clean-safe drinking water, protecting aquatic habitats, and managing water resources effectively. The traditional approach used in predicting water quality, such as laboratory analysis and manual monitoring, are frequently labor-intensive, expensive, and time-consuming, making them unsuitable for real-time monitoring and decision-making. [1, 2]

Due to the capacity of SVM to analyze enormous datasets, model intricate relationships, and

produce precise forecasts, machine learning techniques have recently come to the limelight as a promising tool for predicting water quality. Support Vector Machine (SVM), one of the many machine learning algorithms, has drawn a lot of interest in predicting water quality due to its demonstrated and proven performance in managing high-dimensional data, addressing non-linear relationships, and producing reliable forecasts. SVM is a supervised learning technique that is adaptable for various water quality prediction issues because it can be utilized for both classification and regression tasks. [3, 5, 7]

This research work aims to present a thorough overview of SVM-based water quality prediction. The evaluation of the literature on

SVM-based methods for predicting water quality will emphasize the methods' benefits, drawbacks, and potential future directions. The difficulties and factors to be taken into account while using SVM to forecast water quality, including the choice of the best kernel functions, feature selection strategies, model evaluation procedures, and treatment of unbalanced data, will also be covered in this work. [4, 6, 8]

Related Works

A review of machine learning techniques for forecasting water quality, including SVM, artificial neural networks, and decision tree- based algorithms, was done by Muthukumaravel et al. in 2021. In addition to highlighting the significance of data preparation, feature selection, and model validation in machine learning-based water quality prediction, they also

Material and Method

This study's objective is to predict the elements of water quality using machine learning (ML) technology known as Support Vector Machines

(SVM). An overview of the used ML model is given.

Support Vector Machine (SVM)

Support Vector Machine is a supervised learning machine learning algorithm that is greatly used for pattern recognition, classification, and regressions. Function fitting is one of the most popular applications of SVM, so the component of SVM that uses it is known as support vector regression (SVR). Minimizing the error that is different between the model output and observed data is the aim of function fitting using SVM. This can be viewed as an optimization problem, and the following is its mathematical formulation:

Minimize:

Gideon Asante and Kaushal Singh

$$R_{svm}(\omega, \xi^*) = \frac{1}{2} \|\omega\|^2 + C \sum_{i=1}^{l} (\xi_i + \xi_i^*)$$

explored the benefits and drawbacks of these methods. The review provides insights into the difficulties and prospective directions in this area while highlighting the promise of machine learning in forecasting water quality metrics like dissolved oxygen, pH, and nutrient levels [5]. Also, in 2020, Khan and Muhammad conducted an analysis of SVM-based water quality prediction models with an emphasis on the difficulties, uses, and potential future developments in this area. They examined the limits of SVM, including its sensitivity to hyperparameter tuning, choice of kernel functions, and management of unbalanced data, and they reviewed numerous research that used SVM for water quality prediction in various locales and water bodies. The analysis also highlighted the possibility of adopting other machine learning strategies to boost the precision of water quality predictions, including ensemble methods and deep learning [4].

Subject:

$$d_i - \omega\varphi(x_i) + bi \leq \varepsilon + \xi_i$$

$$\omega\varphi(x_i) + bi - d_i \leq \varepsilon + \xi_i$$

$$\xi_i, \xi_i^* \geq 0, 1, \ldots\ldots l,$$

where the normal vector is ω, with a regularization factor of $\frac{1}{2}\|\omega\|^2$, C is also the penalty of error factor, b as the bias, ε as the error function, x_i input factor, d_i is the target value, l is the number of elements in the training dataset, $\varphi(x_i)$ is feature space, and ξ_i and ξ^*_i as the upper and lower excess deviation respectively. [1, 8, 10]

The kernel functions are given as:

i. Linear kernel: $K(x_i, x_j) = x_i^T x_j$

ii. Polynomial kernel: $K(x_i, x_j) = (x_i^T x_j + \gamma)^d,$ $\gamma > 0$

iii. RBF kernel: $K(x_i, x_j) = exp(-\gamma \| x_i - x_j \|)^2, \gamma > 0$

iv. Sigmoid kernel: $k(x_i, x_j) = tanh(\gamma x_i^T x_j + r), \gamma > 0$

the variables x_i, x_j are inputs, and γ – regularization parameter, $\alpha_i = \alpha_i - \alpha_i$ is the Lagrange multiplier. The prediction accuracy is based on three parameters, γ, ε and C, whose values are determined with the firefly algorithm.

Data Collection (Water Dataset)

Water quality measures for 3276 distinct water bodies are included in the water quality dataset that was taken from Kaggle. Ph, hardness, solids, chloramines, sulphate, conductivity, organic carb on, trihalomethanes, turbidity, and potability were a few of the metrics in the dataset.

pH value: When assessing the acid-base balance of water, PH is a crucial metric. It also serves as a gauge for the

water's acidic or alkaline quality. The pH range between 6.5 and 8.5 has been suggested by WHO. The range of the present investigation was 6.52 to 6.83, which is within the range of WHO criteria.

Hardness: Salts of calcium and magnesium are the major contributors to hardness. These salts are released by the geologic formations that water passes through. The ability of water to form soap due to calcium and magnesium precipitation was the original definition of hardness.

Solids (Total dissolved solids, or TDS): Numerous inorganic and organic minerals or salts, such as bicarbonates, chlorides, magnesium, sulphates, potassium, calcium, and sodium, can be dissolved by water. These minerals gave the water an undesirable taste and diminished color. This is a crucial variable while using water. Water with a high TDS rating is one that has a high mineral content. The recommended TDS level for drinking purposes is 500 mg/l, with a maximum limit of 1000 mg/l.

Chloramines: In public water systems, chlorine and chloramine are the main disinfectants utilized. The process of treating drinking water with chlorine and ammonia most frequently results in chloramine formation. The safest level of chlorine in drinking water is 4 mg/L, or 4ppm.

Sulphate: Sulphates are organic compounds that are naturally present in rocks, soil, and minerals. They can be found in the surrounding air, groundwater, vegetation, and food. Sulphate is mostly used in the chemical industry for commercial purposes. The amount of sulphate in saltwater is around 2,700 mg/L. The majority of freshwater sources have values between 3 and 30 mg/L, while certain regions have substantially higher levels (1000 mg/L).

Conductivity: Pure water is an excellent insulator of electrical current rather than a good conductor of current. Increased ion concentration improves water's ability to carry electricity. Electrical conductivity is often based on the quantity of dissolved particles in water. A solution's ionic process, which makes it possible for it to transfer electricity, is really measured by electrical conductivity (EC). The EC value should not be more than 400 S/cm, as per WHO guidelines.

Organic Carbon: Both synthetic and naturally occurring organic matter (NOM) contribute to the total organic carbon (TOC) in source waters. The total amount of carbon (TOC) in organic compounds in pure water is a measurement of this. US EPA estimates that treated drinking water has 2 mg/L of TOC and that source water, which is used for treatment, contains 4 mg/Lit.

Trihalomethanes (THMs): These are substances that can be detected in water that has been chlorinated. The amount of organic matter present, the quantity of chlorine required to treat the water, and the temperature of the treated water all affect the THM levels in drinking water. THM levels up to 80 ppm in drinking water are regarded as safe.

Turbidity: Water turbidity is influenced by how much solid matter is present in a suspended condition. It measures the water's ability to produce light, and the test is used to determine how well waste is discharged in terms of colloidal particles. The mean turbidity value achieved (0.98 NTU) is lower than the WHO's recommended limit of 5.00 NTU.

Potability: Determines if water is fit for human consumption, with 1 denoting drinkable and 0 denoting unfit for potable.

Data Preprocessing

Pre-processing procedures were used to clean up the gathered data, find outliers, and impute missing values. Suitable methods, such as mean, median, or interpolation, were used to impute missing or null data.

Gideon Asante and Kaushal Singh

Feature Selection

The right factors for predicting water quality metrics were chosen using feature selection approaches including correlation analysis, feature importance, and domain knowledge. The machine learning model's input variables were the characteristics that were chosen.

Model Evaluation

Several measures, including accuracy, precision, recall, F1-score, and R-squared, were used to assess how well the machine learning models performed. Different algorithms' performances were examined, and the one that performed the best in terms of accuracy and robustness was chosen.

Statistical Analysis

For the water quality metrics, descriptive statistics including mean, median, standard deviation, and range were determined. The correlations between various factors were found using correlation analysis. Data preparation, model creation, and model assessment were done using statistical tools like Python.

RESULTS AND DISCUSSION

The SVM model was trained using the preprocessed water quality dataset from Kaggle

(water quality dataset), and evaluated using various performance metrics. The following results were obtained:

Precision: For class 0, which denotes water not potable, the precision of the SVM model was determined to be 0.69, meaning that the model accurately predicted 69% of the instances. With a precision of 0.68 for class 1 (good water quality or potable water), the model successfully predicted 68% of the instances of good water quality.

Recall: The SVM model's recall for class 0 was determined to be 0.92, meaning that 92% of the examples with poor water quality were correctly detected by the model. The recall for class 1 was 0.30, meaning that 30% of the instances with good water quality were accurately detected by the model.

F1-score: The SVM model for class 0's F1-score, which balances accuracy and recall, was determined to be 0.79. The model performed worse in predicting good water quality than poor water quality, as evidenced by the F1-score for class 1 of 0.42.

Support: In the test dataset, the SVM model had a total of 680 samples for class 0 (poor water quality) and 402 samples for class 1 (good water quality).

Accuracy and Macro/Micro Average: The SVM model's accuracy was determined to be 0.69, meaning that it accurately predicted the water quality parameters in 69% of the test dataset cases.
Precision, recall, and F1-score were estimated to have macro averages of 0.69, 0.61, and 0.60, respectively. The micro average and accuracy were both 0.69. In contrast to the micro average, which treats all classes equally, the macro average averages performance measures across all classes.

The SVM model's findings show that it performs considerably better in terms of accuracy, recall, and F1-score for class 0 (Non- Potable Water) than for class 1 (Potable Water). This indicates that the model performs worse at recognizing instances with good water quality but performs better at predicting cases with poor water quality. The model may have more false negatives, or instances of good water quality that are not accurately detected by the model, given the lower recall and F1-score for class 1. The imbalanced dataset's greater sample count for class 0 than for class 1 might be one factor contributing to the performance gap between the two classes. The lower recall for class 1 may also have an impact on decision-making regarding water quality or potability, since false negatives may lead to insufficient responses to poor water quality.

Gideon Asante and Kaushal Singh

The performance of the SVM model can be improved by more research and adjustments, such as balancing the dataset using oversampling or under sampling strategies or investigating alternative machine learning algorithms that may be better able to handle unbalanced datasets. The performance of the SVM model may also be enhanced by using cross-validation methods, feature engineering, and model hyper parameter adjustment.

CONCLUSION

With considerably greater accuracy, precision, recall, and F1-score for class 0 (poor water quality) compared to class 1 (good water quality), the SVM model demonstrated reasonable performance in predicting water quality characteristics from the provided dataset. The findings emphasize the significance of resolving unbalanced datasets and further developing the model to increase its accuracy in predicting instances of low water quality and enhance reasoned decision-making in attempts to regulate water quality.

REFERENCES

1. Abobakr Y A S, Ahmed A N, Binti O F, Ibrahim R K, Afan H A, El-Shafie A, Fai CM, Hossain M S, Ehteram M & Elshafie A, Water Quality Prediction Model Based Support Vector Machine Model for Ungauged River Catchment under Dual Scenarios. Water 2019, 11, 1231.https://doi.org/10.3390/w11061231
2. Singh K & Singh A, Water quality prediction using support vector machine: A comprehensive review. Environmental Monitoring and Assessment, 191(3) (2019),154. doi:10.1007/s10661-019-7259-6
3. ,Asadi S & Nasrabadi T, Water quality prediction using a hybrid support vectormachine and gravitational search algorithmapproach. Water, 9(9) (2017) 652. doi:10.3390/w9090652
4. Khan A & Muhammad S, An overview ofsupport vector machine-based water qualityprediction   models: Challenges, applications, and future directions. Science of the Total Environment, 705 (2020) 135825. doi:10.1016/j.scitotenv.2019.135825
5. Muthukumaravel T, Prasanna V K & Venkatramanan S, Water quality prediction using machine learning approaches: Areview. Science of the Total Environment, 799 (2021) 149296.doi:10.1016/j.scitotenv.2021.149296
6. Sahoo S & Sahoo S K, Water quality prediction using support vector machine: A case study in Mahanadi river, Odisha, India.Ecological Engineering, 123 (2018) 86-97.doi:10.1016/j.ecoleng.2018.09.013
7. Kavzoglu T & Sahin A, Water quality prediction in reservoirs using support vector machines. Journal of Hydrology, 568 (2019) 405-415. doi:10.1016/j.jhydrol.2018.11.038
8. Amir H H, Ali H N & Abbas P, Water quality prediction using machine learning methods. Water Quality Research Journal 1February   2018;   53   (1):   3–13. doi: https://doi.org/10.2166/wqrj.2018.025
9. River Water Quality (RWQ) | Malaysia Environmental Performance Index. Available online: http://www.epi.utm.my/v4/?page_id=102 (accessed on 5April 2019).
10. Yan J, Xu Z, Yu Y, Xu H, Gao K, Application of a Hybrid Optimized BP Network Model to Estimate Water Quality Parameters of Beihai Lake in Beijing. Appl.Sci. 2019, 9, 1863.
11. Abd EL-kawyor, Ismail H A, Yehia H M &Allam M A, Egypt J Remote Sens Sp Sci, 22(2019) 237.
12. Bakr N & Afifi A A, Remote Sens Appl SocEnviron, 13 (2019)348.
13. Kussul N, Lavreniuk M, Skakun S & Shelestov A, IEEE Geosci Remote SensLett, 14 (2017) 778.
14. Simonetti D, Simonetti E, Szantoi Z, Lupi A & Eva H D, IEEE Geosci Remote Sens Lett, 12 (2015) 1496.
15. Wang L, Dong Q, Yang L, Gao J & Liu J, Remote Sens, 11(2019) 4.
16. Huang J, Wang H, Dai Q & Han D, IEEE JSel Top Appl Earth Obs Remote Sens, 7(2014) 4374.
17. Avola G, Di Gennaro S F, Cantini C, RiggiE, Muratore F, Tornambe C & Matese A, Remote Sens, 11 (2019) 10.
18. Shih H C, Stow D A, Weeks J R & CoulterL L, IEEE J Sel Top Appl Earth Obs RemoteSens, 9 (2016) 2064.
19. Mostajer Kheirkhah F & Asghari H, IET Comput Vis, 13(2019) 395.
20. JiS, Zhang C, Xu A, Shi Y & Duan Y,Remote Sens, 10 (2018) 1. Peña J M, Gutiérrez P A, Hervás-Martínez C, Six J, Plant R E & López-GranadosF, Remote Sens, 6 (2014) 5019.

21. Viña A, Gitelson A A, Nguy-Robertson A L & Peng Y, Remote Sens Environ, 115 (2011) 3468.Archibald R & Fann G, IEEE GeosciRemote Sens Lett, 4(2007) 674.

22. BerniJ A J, Zarco-Tejada P J, Suárez L & Fereres E, IEEE Trans Geosci Remote Sens,47 (2009) 722.

23. Strohmann, T. R. and Grudic, G. Z.,A Formulation for minimax probability machine regression, In T. G. Editor, S. Editor, & Z. Editor (Eds.), Advances inNeural Information Processing Systems (NIPS) 14, MA. Cambridge: MIT Press,2002.

24. Serre, D. T. Matrices Theory and Applications. Berlin: Springer. 2002.

25. Gandomi, A. H., and Roke, D. A., Intelligent formulation of structural engineering systems. In Seventh M.I.T. Conference on Computational Fluid and Solid Mechanics Focus: Multiphysics & Multiscale, Massachusetts Institute of Technology, Cambridge, MA, 2013.

26. Chandwani, V, Agrawal, V & Nagar, R 2014. Modeling Slump of Ready Mix Concrete Using Genetic Algorithms. Assisted Training of Artificial Neural Networks Expert Systems with Applications, 42(2):885-93

Table 1: Classification report of SVM model

	Precision	Recall	F1-Score	Support
Class 0	0.69	0.92	0.79	680
Class 1	0.68	0.30	0.42	402
accuracy			0.69	1082
Macro avg	0.69	0.61	0.60	1082
Weighted avg	0.69	0.69	0.65	1082

REVIEW ARTICLE

Quantitative Data of Transfer of Drinking Water Fluoride from Pregnant Women to Cord Blood – A Systematic Review

Thippeswamy H.M[1], Nanditha Kumar.M[2]* and Prashanth S.N[3]

[1]Reader, Department of Public Health Dentistry, JSS Dental College and Hospital, JSS Academy of Higher Education and Research, Mysuru, Karnataka, India.
[2]Reader, Department of Prosthodontics, JSS Dental College and Hospital, JSS Academy of Higher Education and Research, Mysuru, Karnataka, India.
[3]Professor and Head, Department of Pediatrics, JSS Medical College and Hospital, JSS Academy of Higher Education and Research, Mysore - 570015, Karnataka, India.

*Address for Correspondence
Nanditha Kumar.M
Reader, Department of Prosthodontics,
JSS Dental College and Hospital,
JSS Academy of Higher Education and Research,
Mysuru, Karnataka, India.
E.Mail: nanditha10@gmail.com

ABSTRACT

Fluoride is one of the most common chemical in water capable of causing adverse health effects, such as dental and skeletal fluorosis, reproductive and neurological effects, and endocrine disorder.This review investigates the amount of fluoride in drinking water is transmitted to the maternal serum and cord blood. A comprehensive literature search was done in five electronic databases of Medline, Scopus, Web of science, Cochrane library and Embase using variant Medical Subject Headings(MeSH) and free terms from 1950 to September 2022. Nine articles were finalized based on the inclusion and exclusion criteria. The minimum fluoride level in drinking water recorded was 0.06 ppm and maximum was 10 ppm in the included studies. In the maternal serum the fluoride levels ranged from 0.014 to 14.1 ppm whereas in cord blood 0.011 to 13.6 ppm Within the limitations of this review it can be concluded that as the fluoride concentration in drinking water increases, the fluoride levels in maternal and cord blood also increases.

Keywords :- Drinking water fluoride, pregnancy, maternal fluoride, cord blood fluoride .

INTRODUCTION

Excessive fluoride intake over a long period of time may result in a serious public health problem called fluorosis, which is characterized by dental mottling and skeletal manifestations such as crippling deformities, osteoporosis, and osteosclerosis. Endemic fluorosis is now known to be global in scope, occurring on all continents and affecting many millions of people(1). Fluoride is one of the most common chemical in water capable of causing adverse health effects, such as dental and skeletal fluorosis, reproductive and neurological effects, and endocrine disorders(2). Exposure to fluoride is common among people around the world. Water and water based beverages are the main sources of systemic ingestion, accounting for approximately 75% of dietary intake. The national toxicology program (NTP) at the national institute of health concluded that prenatal exposure to high levels of fluoride can alter neurodevelopment. Fluoride readily crosses the placenta. Animal studies have proved that fluoride accumulates in critical brain regions involved in learning and memory in foetuses. Biomarkers of fluoride (eg. Urinary fluoride, serum fluoride) directly correlate with fluoride exposure levels (water fluoride concentration, fluoride supplement exposure) in children and pregnant women(3).

99% of the fluoride in humans is found in the hard tissues like bones and teeth, and the rest 1% in soft tissues. The transfer of fluoride from mother through the placenta to the foetus is not very clear as put forth by previous research(4). Although the mechanisms of maternal-foetal transmission of fluoride are poorly understood, many studies have proven that fluoride can readily pass across the placenta and ultimately increase fluoride levels in foetal tissue. Many articles pertaining to the advantages and adverse effects of fluoride on pregnant women and foetuses have also been published(5). Presently many studies have proved that fluoride affects the calcium and vitamin D levels and has neurological effects in foetuses and children. Literature search related to the correlation of fluoride levels in drinking water with fluoride levels in maternal serum and cord blood yielded no reviews. Hence this review was done to check the amount of fluoride transferred from drinking water to maternal serum and then cord blood.

METHODOLOGY

The protocol for this systematic review was in accordance with the Preferred reporting Items for Systematic Review and Meta Analysis (PRISMA) guidelines.

Data source and search strategy

A comprehensive literature search was conducted by two investigators from June 2020 to December 2022. All comprehensive searches related to placental passage of fluoride was carried out with computerized search of five electronic databases of Medline, Scopus, Web of science, Cochrane library and Embase using Medical Subject Headings(MeSH) and free terms from 1950 to December 2022.

Search strategy

Based on the review question keywords were identified and used for the searches. . The search was done using key words in different combinations like fluoride OR Water fluoride OR drinking water fluoride AND maternal fluoride OR pregnant women serum fluoride AND placental barrier OR cord blood OR placental passage OR cord blood fluoride OR placental fluoride. The search was supplemented by hand searching of journals and scanning of references.

Inclusion and exclusion criteria

The present review was undertaken with the following inclusion criteria (i) Studies involving subjects with full term pregnancies (ii) Studies clearly mentioning or assessing drinking water fluoride, maternal serum/plasma fluoride and cord blood fluoride levels (iii) Studies with drinking water fluoride as the only parameter.

The studies were excluded based on the following criteria (i) Studies not mentioning the level of fluoride in drinking water, maternal plasma and cord blood (ii) Conference abstracts , articles for which full texts were not available. (iii) Animal studies

Data extraction
Based on the inclusion and exclusion criteria, nine studies were finalized for the present systematic review(5-13)(Figure 1). Data from eligible studies were extracted into a pre-defined data extraction excel file using a pre-defined list of variables. Our outcome of interest was to correlate the amount/level of fluoride in drinking water to maternal serum/plasma fluoride levels. Data was extracted and segregated under - name of the author, year, location, number of subjects, drinking water fluoride levels, maternal fluoride levels and cord blood fluoride levels. The study selection, data extraction and risk of bias assessment were performed by at least two independent reviewers and consensus was reached in the case of disagreement.

Quality of evidence of the included studies
The quality of the included studies was evaluated using Joanna Briggs Institute(JBI) [14] critical appraisal tool for systematic reviews of analytical cross sectional studies. For each included study, two authors evaluated seven item checklist and scored the JBI questions as :"yes", "no", "unclear" and "not applicable". The final score was determined by the number of "yes" answers.   Based on the number of "yes" answer each article was categorized as "low" risk of bias(ROB)(scores more than 70%), "moderate" ROB(scores from 50 to 69%) and finally "high" ROB if article scores equal or lower than 49%. If there was any confusion between two authors for scoring, third author resolved it. The agreement between the two authors for evaluating was 84%.

RESULTS

The key features of the eligible studies are presented in table 1. Few studies were excluded though they assessed maternal fluoride and cord blood fluoride as they did not mention about drinking water fluoride(details mentioned in figure 1). Majority of the studies showed placental transfer of fluoride increased as the fluoride levels in drinking water also increased. Few studies mentioned drinking water fluoride without categorizing as low and high fluoride levels (9-11,13) while some studies categorized water fluoride level(5-8,12). World health organization recommends 0.7 to 1.2 ppm fluoride level in drinking water. Majority of the eligible studies were at par or below the WHO recommended levels.   The minimum fluoride level in drinking water recorded was 0.06 ppm and maximum was 10 ppm in the included studies. In the maternal serum the fluoride levels ranged from 0.014 to 14.1 ppm whereas in cord blood 0.011 to 13.6 ppm. Among the included studies, fluoride levels were lower in maternal serum and cord blood than in drinking water except in studies by Gardner DW[6] et al and Teotia M(8) et al. Gardner DW(6) et al reported fluoride levels in maternal serum to be higher than in drinking water. But, in a study by Teotia M(8) et al fluoride levels were higher in both maternal and cord blood.(table 1) Out of nine studies only two studies(5,8) reported the placental transfer of fluoride when fluoride in drinking water was above WHO recommended levels. Both the studies observed the results eight to ten times more maternal and cord blood fluoride levels as compared to at or below the 1 ppm of fluoride in drinking water. Most of the studies used ion specific fluoride electrode method for assessment of fluoride. Except for studies by Thippeswamy et al (5) (2020) and Moshe Ron(9) (1985), all other studies used small sample size to assess maternal and cord blood fluoride levels.

Risk of bias of the included studies
 The overview of the ROB of the included studies were presented in Table 2. Out of nine studies seven studies were belong to low risk category. Gardner Dw et al and I. Gedalia et al were scored under moderate category. Both these studies were assessed fluoride levels using Smith and Gardner method and colorimetric methods. All other seven studies fluoride was assessed using Orion ion specific fluoride electrode method which is considered to be most valid and reliable method.

DISCUSSION

Fluoride (F) is an essential trace element, but chronic exposure beyond the permissible limit (1.5 ppm) effectuates dental and skeletal fluorosis(15).The present review tried to find the relationship between fluoride present in drinking water and maternal serum/plasma fluoride and cord blood fluoride. Placenta and umbilical cord are two components of the fetal life support system of a developing fetus inside the uterus. Placenta absorbs nutrients and oxygen from mother's bloodstream and transfers to the fetus via the umbilical cord. The main difference between placenta and umbilical cord is that placenta is a temporary organ which joins mother and the fetus whereas umbilical cord is the connecting link between developing fetus and the placenta of the mother. Placenta is divided into maternal part and fetal part. Maternal placenta bears the maternal origin whereas fetal placenta and the umbilical cord bear fetal origin. In the present review fluoride levels were assessed in cord blood as the umbilical cord blood is considered as purely belonging to fetal origin(16).

The role of the placenta in the movement of fluoride from the mother to the fetus is unclear because of conflicting evidence as to whether fluoride intake or maternal blood fluoride affects the concentration found in the fetus(17). Many aspects of a newborn's health and wellbeing seem to be affected by the mother's nutritional status before and during pregnancy. Fluoride is an important element for the development of foetus and hence needs to be evaluated(18). The present review found nine studies reporting the levels of fluoride present in drinking water of the pregnant women and amount of fluoride transferred through placenta. The results showed direct relationship between drinking water fluoride of the pregnant women, maternal fluoride and placental transfer of fluoride. The results observed from the previous studies show that irrespective of fluoride levels present in drinking water, placenta acts as a partial barrier.

The US Public Health Service set the optimal fluoride concentrations in water from 0.7 to 1.2mg/L to achieve the maximum reduction in tooth decay and minimize the risk of enamel fluorosis Fluorosis, or mottling, of the tooth enamel is due to excess fluoride intake from any source occurring during the period of tooth development. However, the beneficial effects of fluoride predominantly occur at the tooth surface after the teeth have erupted. Therefore, there is no benefit of systemic exposure to fluoride during pregnancy. The evidence showing an association between fluoride exposure and lower IQ scores raises a possible new concern about cumulative exposures to fluoride during pregnancy, even among pregnant women exposed to optimally fluoridated water for the prevention of caries in offspring [25] It is very difficult to draw conclusion from the previous studies because none of the studies have considered dietary history related to fluoride and all the included studies were from different parts of the world with different food habits and practices. I Gedalia et al[7](1964) conducted a study in three different drinking water fluoride levels but did not include samples (more than 1 ppm) from high fluoride areas. Two groups 0.5 to 0.6 ppm and 0.6 to 0.9 ppm samples obtained the same results. Gardner DW et al[6] (1952) conducted study using very low fluoride levels(0.06ppm) in one group and optimum level in another group(1.0 to 1.2 ppm). The result showed that both the groups had higher fluoride levels in maternal serum than in drinking water. Though the fluoride levels in both the groups varied drastically, the fluoride levels in cord blood varied marginally.

CONCLUSION

Within the limitations of this review it can be concluded that as the fluoride concentration in drinking water increases, the fluoride levels in maternal serum/plasma and in cord blood also increases. Though enormous research has been conducted related to effects of fluoride on human health, research related to the exact amount of fluoride transferred from mother to fetus are sparse. Further, well planned research related to the transfer of fluoride from drinking water of mother to foetus needs to be carried out using large sample size to add more information regarding this subject.

Thippeswamy *et al.,*

ACKNOWLEDGEMENT

REFERENCES

1. Barbier O, Arreola-Mendoza L, Razo LMD. Molecular mechanism fluoride toxicity. Chem Biol Interact. 2010;188:319–33 https://doi.org/10.1016/j.cbi.2010.07.011.
2. Jarquín-Yañez L, de Jesús Mejía-Saavedra J, Molina-Frechero N, Gaona E, Rocha-Amador DO, López-Guzmán OD, Bologna-Molina R. Association between urine fluoride and dental fluorosis as a toxicity factor in a rural community in the state of San Luis Potosi. ScientificWorldJournal. 2015;2015:647184. doi: 10.1155/2015/647184. Epub 2015 Feb 19. PMID: 25789336; PMCID: PMC4350618.
3. Till C, Green R, Grundy JG, Hornung R, Neufeld R, Martinez-Mier EA, Ayotte P, Muckle G, Lanphear B. Community Water Fluoridation and Urinary Fluoride Concentrations in a National Sample of Pregnant Women in Canada. Environ Health Perspect. 2018 Oct;126(10):107001. doi: 10.1289/EHP3546. PMID: 30392399; PMCID: PMC6371693.
4. Bashash M, Thomas D, Hu H, Martinez-Mier EA, Sanchez BN, Basu N, et al. Prenatal fluoride exposure and cognitive outcomes in children at 4 and 6–12 years of age in Mexico. Environ Health Perspect. 2017;125:097017.
5. Thippeswamy HM, Devananda D, Nanditha Kumar M, Wormald MM, Prashanth SN. The association of fluoride in drinking water with serum calcium, vitamin D and parathyroid hormone in pregnant women and newborn infants. Eur J Clin Nutr. 2021 Jan;75(1):151-159. doi: 10.1038/s41430-020-00707-2. Epub 2020 Aug 19. PMID: 32814853.
6. Gardner DW, Smith FA, Hodge HC, Overton DE. The fluoride content of placental tissue as related to the fluoride content of drinking water. Science. 1952 Feb 22;115(2982):208-9. doi: 10.1126/science.115.2982.208.
7. Gedalia I, Brzezinski A, Zukerman H, Mayersdorf A. Placental transfer of fluoride in the human fetus at low and high f-intake. J Dent Res. 1964 Sep-Oct;43:669-71. doi: 10.1177/00220345640430050801
8. M Teotia, S.P.S Teotia, RK Singh. Metabolism of fluoride in pregnant women residing in endemic fluorosis areas. Fluoride Journal vol 12(2):, 58-64
9. Ron M, Singer L, Menczel J, Kidroni G. Fluoride concentration in amniotic fluid and fetal cord and maternal plasma. Eur J Obstet Gynecol Reprod Biol. 1986 Apr;21(4):213-8. doi: 10.1016/0028-2243(86)90018-3.
10. Malhotra A, Tewari A, Chawla HS, Gauba K, Dhall K. Placental transfer of fluoride in pregnant women consuming optimum fluoride in drinking water. J Indian Soc Pedod Prev Dent. 1993 Mar;11(1):1-3.
11. Shimonovitz S, Patz D, Ever-Hadani P, Singer L, Zacut D, Kidroni G, Ron M. Umbilical cord fluoride serum levels may not reflect fetal fluoride status. J Perinat Med. 1995;23(4):279-82. doi: 10.1515/jpme.1995.23.4.279.
12. Montherrat-Carret L, Perrat-Mabilon B, Barbey E, Bouloc R, Boivin G, Michelet A, Magloire H. Chemical and X-ray analysis of fluoride, phosphorus, and calcium in human foetal blood and hard tissues. Arch Oral Biol. 1996 Dec;41(12):1169-78. doi: 10.1016/s0003-9969(96)00033-7.
13. Opydo-Szymaczek J, Borysewicz-Lewickaa M. Urinary fluoride levels for assessment of fluoride exposure of pregnant women in Poznan, Poland. Fluoride. 2005;38:312–7.
14. Checklist for Analytical Cross Sectional Studies http://joannabriggs.org/research/critical-appraisal-tools.html accessed on 14 Jan 2021.
15. Dey Bhowmik, A., Shaw, P., Mondal, P. *et al.* Calcium and Vitamin D Supplementation Effectively Alleviates Dental and Skeletal Fluorosis and Retain Elemental Homeostasis in Mice. *Biol Trace Elem Res* (2020). https://doi.org/10.1007/s12011-020-02435-x

16. Panawala, Lakna. (2017). Difference Between Placenta and Umbilical Cord. http://pediaa.com/differencebetween-placentaandumbilicalcord/

17. Shen YW, Taves DR. Fluoride concentrations in the human placenta and maternal and cord blood. Am J Obstet Gynecol. 1974 May 15;119(2):205-7. doi: 10.1016/0002-9378(74)90035-0. PMID: 4823388.

18. Peas DM, Bianchi LP, Gil BA, O.Dopas, Jr., Coronato RG, Aires B. Biochemistry of fluororsis- Methods for evaluating fluoride in blood serum. A critical and comparative study. Fluoride 1980; 13(2): 65-70

19. Armstrong WD, Singer L, Makowski EL. Placental transfer of fluoride and calcium. Am J Obstet Gynecol. 1970 Jun 1;107(3):432-4. doi: 10.1016/0002-9378(70)90571-5. PMID: 5445015.

20. Shen YW, Taves DR. Fluoride concentrations in the human placenta and maternal and cord blood. Am J Obstet Gynecol. 1974 May 15;119(2):205-7. doi: 10.1016/0002-9378(74)90035-0.

21. Motoo Niwa, Jun Takimoto, Tatsuhiko Tsuji, Fluoride and Calcium Interrelationship in Maternal and Cord Blood Sera Studies in Environmental Science, 1986 Volume 27, **pp.** 225-229

22. Gupta S, Seth AK, Gupta A, Gavane AG. Transplacental passage of fluorides. J Pediatr. 1993 Jul;123(1):139-41. doi: 10.1016/s0022-3476(05)81558-6.

23. Goyal LD, Bakshi DK, Arora JK, Manchanda A, Singh P. Assessment of fluoride levels during pregnancy and its association with early adverse pregnancy outcomes. *J Family Med Prim Care.* 2020;9(6):2693-2698.

24. Dariusz Chlubek, Ryszard Poreba and Boguslaw Machalinski. Fluoride and calcium distribution in human placenta Fluoride Vol. 31.(3) 1998. Research Report 131-136

25. Green R, Lanphear B, Hornung R, Flora D, Martinez-Mier EA, Neufeld R, Ayotte P, Muckle G, Till C. Association Between Maternal Fluoride Exposure During Pregnancy and IQ Scores in Offspring in Canada. JAMA Pediatr. 2019 Oct 1;173(10):940-948

26. Abduweli Uyghurturk, D., Goin, D.E., Martinez-Mier, E.A. *et al.* Maternal and fetal exposures to fluoride during mid-gestation among pregnant women in northern California. *Environ Health* **19,** 38 (2020). https://doi.org/10.1186/s12940-020-00581-2

27. Caldera R, Chavinie J, Fermanian J, Tortrat D, Laurent AM. Maternal-fetal transfer of fluoride in pregnant women. Biol Neonate. 1988;54(5):263-9

Table 1:- Salient features of the included studies

Authors	Year	Place and country	Number of subjects	Drinking water fluoride	Maternal fluoride	Cord blood fluoride	Method of assessment
Gardner Dw et al [6]	1952	Rochester Newburg	12 12	0.06 1.0-1.2	0.74 2.09	0.014 0.04	smith and Gardner method
I. Gedalia et al[7]	1964	Jerusalem, Israel	39 12 18	0.06-0.15 ppm F 0.6-0.9 ppm 0.5-0.6 ppm	0.15 0.234 0.234	0.165 0.175 0.175	Colorimetric method
M Teotia, S.P.S Teotia, RK Singh[8]	1979	Meerut,India	15 10	10 01	14.1 1.7	13.6 1.45	Fluoride electrode
Moshe Ron et al[9]	1985	Israel	50 44 29	<0.5ppm	0.033	0.028	Orion ion specific electrode

Thippeswamy *et al.,*

Malhotra A et al[10]	1993	India	25	1.2ppm	25.06 ug/100 ml	22.96ug/100 ml	Orion ion specific electrode
Shlomo Shimonovitz et al[11]	1995	Jerusalem, Israel	22	0.22—0.49 µg/l.	0.0303 µg/ml	0.0183 µg/ml	TISAB buffer
L. Montherrat-carret et al[12]	1996	France	10 03	≤0.1 parts/10^6 ≥ 0.7 parts/10^6	0.034	0.031	TISAB buffer
J Opydo-Szymaczek & M Borysewicz-Lewickaa[13]	2007	Pozan, poland	30	0.4 to 0.8 mg/L.	3.54 µmol/L	2.89 µmol/L	Orion Model 96-09 F ion selective electrode
Thippeswamy HM et al[5]	2020	India	90 90	<1 ppm ≥1ppm	0.014 0.153	0.011 0.11	Fluoride electrode

Table 2:- Joanna Briggs Institute(JBI) Appraisal for analytical cross sectional studies

Studies	Items									
	1	2	3	4	5	6	7	8	Percentage of "yes" answers	Overall classification
Gardner Dw et al 1952	Yes	yes	No	Yes	Not applicable	Not applicable	No	yes	50	Moderate
I. Gedalia et al 1964	yes	yes	No	Yes	Not applicable	Not applicable	No	yes	50	Moderate
M Teotia, S.P.S Teotia, RK Singh 1979	Yes	yes	No	yes	Not applicable	Not applicable	yes	yes	62.5	Moderate
Moshe Ron et al 1985	yes	yes	No	Yes	Not applicable	Not applicable	yes	yes	62.5	Moderate
Malhotra A et al 1993	yes	Yes	No	yes	Not applicable	Not applicable	yes	Yes	62.5	Moderate
Shlomo Shimonovitz et al 1995	yes	Yes	No	yes	Not applicable	Not applicable	yes	Yes	62.5	Moderate
L. Montherrat-carret et al 1996	Yes	Yes	No	Yes	Not applicable	Not applicable	yes	yes	62.5	Moderate
J Opydo-Szymaczek &	yes	yes	No	Yes	Not applicable	Not applicable	yes	yes	62.5	Moderate

M Borysewicz-Lewickaa 2007									
Thippeswamy HM et al 2020	Yes	Yes	Unclear	yes	Yes	yes	yes	Yes	87.5	Low

Were the criteria for inclusion in the sample clearly defined?
Were the study subjects and the setting described in detail?
Was the exposure measured in a valid and reliable way?
Were objective, standard criteria used for measurement of the condition?
Were confounding factors identified?
Were strategies to deal with confounding factors stated?
Were the outcomes measured in a valid and reliable way?
Was appropriate statistical analysis used?
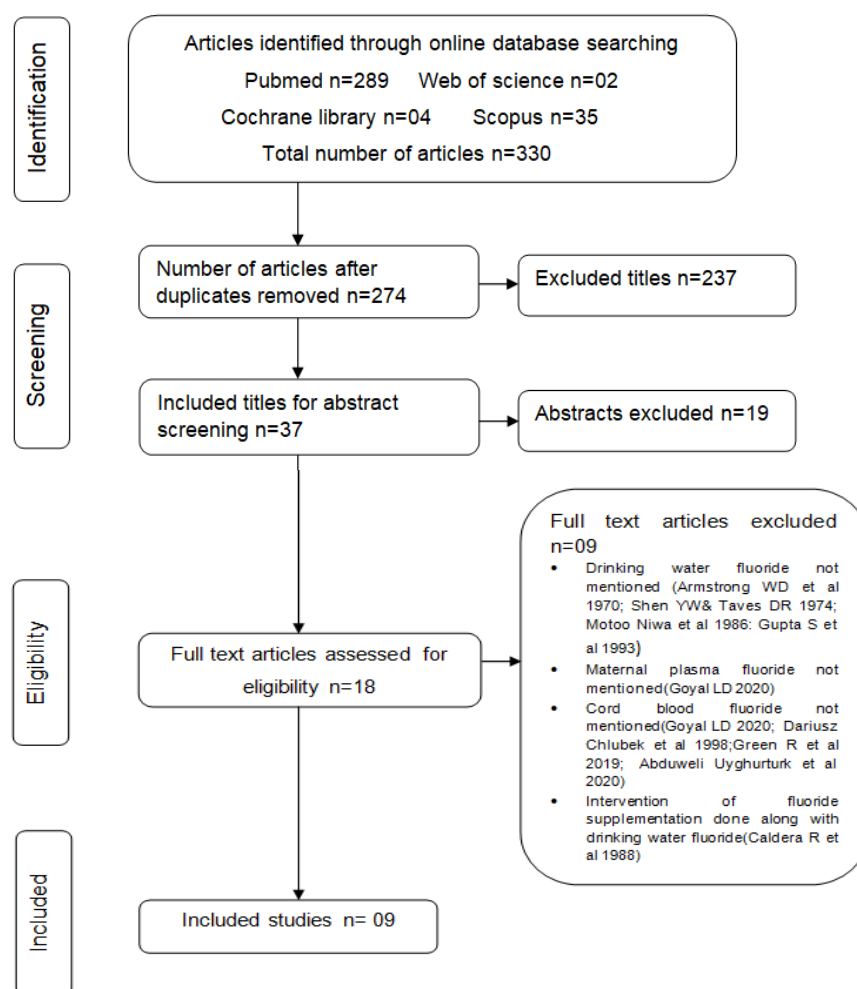
Figure 1: Flow chart for the assessment of articles to be included/ excluded in the systematic review

RESEARCH ARTICLE

Chemical Reaction and Joule heating Effects on MHD Nanofluid Flow Past a Permeable Wedge and a Permeable Cone

Sharad Sinha[1]*, Prachi Gupta[2] and Pankaj Mathur[3]

[1]Assistant Professor, Department of Mathematics, University of Rajasthan, Jaipur, India
[2]Research Scholar, Department of Mathematics, University of Rajasthan, Jaipur, India.
[3]Professor, Department of Mathematics, Government College, Tonk, Rajasthan, India

*Address for Correspondence
Sharad Sinha
Assistant Professor,
Department of Mathematics,
University of Rajasthan, Jaipur, India
E.Mail: sharadsinha89@gmail.com

ABSTRACT

Aim of the present paper is to study the heat and mass transfer in MHD fluid flow past two different geometries, a wedge and a cone, in the presence of chemical reaction and joule heating. It is assumed that the wedge and cone are saturated in porous medium. The Brownian motion and thermophoresis effects are taken into account with non-isothermal and non-isosolutal conditions. The coupled non-linear partial differential equations governing the system are reduced into nonlinear ordinary differential equations by considering similarity transformation. Bvp5c solver of MATLAB is used to find numerical solutions. The influence of various parameters on velocity, temperature, concentration profiles are shown through graphs and skin friction coefficient, Nusselt number, Sherwood number are discussed numerically. A comparative analysis of above mentioned profiles and quantities of physical interest for both the geometries have also been done.
Keywords: MHD, thermophoresis, Brownian motion, chemical reaction, Joule heating **.**

INTRODUCTION

There are many applications such as condensers, power plants, engine cooling, thermal energy storage devices, groundwater systems, paper industry, polymer industry, and high-temperature nanomaterial technology where a high rate of heat transfer is required. To enhance the rate of heat transfer, a variety of methods have been discussed by scientists and engineers. Among them, one method is there, in which nanometre-sized particles are added to some base fluid. The nanometre sized particles are called nanoparticles and have a great capacity to enhance the heat transfer rate when mixed in various base fluids like water, ethylene glycol, oil etc. These nanoparticles can be carbon nanotubes, metal oxides, carbides and metals. The principle of enhancing thermal conductivity by dispersing nano particles in base fluid was given by Choi [1]. Later, Sun et al. [2] used SiC-nanoparticles of sizes 10-20-40-60 nm with

63949

Sharad Sinha *et al.,*

base fluid water and showed that thermal conductivity increases with the increasing size of nanoparticles. Upreti et al. [3] considered a stretching flat plate in a porous medium and investigated the MHD flow of Ag-water nanofluid with Ohmic-viscous dissipation effects, heat generation/absorption, and suction/injection.Sinha et al. [4] investigated heat source/sink and chemical reaction effects on MHD stagnation point nano fluid flow. They used vertical stretching sheet saturated in porous media. Boundary layer flow over a wedge has thermal engineering applications such as the extraction of crude oil, thermal insulation of heat exchangers, groundwater pollution, and the storage of nuclear waste, etc.To analyze this,Uddin et al. [5] considered tangent hyperbolic nanofluid and Carreaunanofluid across a wedge and studied heat as well as flow properties.Heat and mass transfer of hybrid nanofluid flow over curved bodies like cones, ellipses, wavy channels, torus geometries, spherical geometries, cylinders, etc. have a wide range of applications in industry, engineering, and biological science. Fluid flow through a cone has many applications in designing solar energy collectors, steam generators, spacecraft, and nuclear reactors, etc.An analysis of free convection over cone and wedge was done by Ramanaiah and Malarvizhi [6]. They considered mixed thermal boundary conditions and found dual solutions to the problem for flow of $CoFe_2O_4$ with water at 100^0C and 500^0C.

All the models mentioned above are based on single-phase flow. In a single-phase flow, it is assumed that the nanoparticles are fixed with the particles of the base fluid i.e. there is no relative motion between nanoparticles and base fluid. But the assumption is not always true as the nanoparticles move randomly in the base fluid.Buongiorno [7] considered this effect in his model and presented a detailed study on it.Mishra and Upreti [8]analysed Fe_3O_4– $CoFe_2O_4$/EG–water and Ag–MgO/water hybrid nanofluid flow along a curved body and concluded that the mass transfer rate is proportional to Brownian motion and curvature parameters while the other parameters show an opposite trend.Reddy et al. [9] considered MHD nanofluid flow over a vertical cone with convective boundary conditions and explained Brownian motion and thermophoresis effects. Dawar et al. [10] extended the above study for Williamson nanofluid flow through wedge and cone with suction/injection. Jile et al. [11]analyzed the MHD radiated flow with ferrous nanoparticles over a cone numerically. Vajravelu and Nayfeh [12] discussed heat transfer and convection flow in a viscous electrically conducting fluid over a cone and wedge.Butt et al. [13] studied the heat transfer in viscous fluid flow along a horizontal stretching cylinder and analyzed the effect of magnetic field on entropy generation.

The present paper aimed to investigate the thermophoresis and Brownian motion effects on a mixed convective magnetohydrodynamic nanofluid flow over a vertical cone and wedge with joule heating and chemical reaction. The study has many applications in the field of manufacturing and industries. This includes power plants, thermal energy storage devices, crude oil extraction, groundwater pollution, nuclear reactors, solar power collectors, textile coatings and biomedicine, etc.It is also planned in the study to perform a comparative analysis of various effects on flow along both geometries.

MATHEMATICAL FORMULATION

Steady 2-dimensional mixed convective laminar flow of viscous incompressible nanofluid over two different geometries (cone and wedge) is taken into account. The geometries are saturated in porous medium. The x-axis is along the wall of the geometry and y-axis is taken normal to it. The flow is induced by the stretching velocity $u_w \left(= xv/L^2 \right)$ of the surface in the direction of x-axis. The wall of the geometry is assumed to be permeable, so that the fluid can flow through it with suction/injection velocity v_w. To control the flow, an external magnetic field B is applied parallel to the y -axis. Along with this, Brownian motion, thermophoresis, joule heating and chemical reaction effects are considered in the problem. If the half angle of cone and wedge is taken as γ, then conditions for cone and wedge are as follows:

(i) Cone:$\gamma \neq 0$ and $m = 1$

(ii)Wedge:$\gamma \neq 0$ and $m = 0$

The governing equations of flow (see ref. [9], [10], [11]) are given by:

$$\frac{\partial\left(r^m u\right)}{\partial x} + \frac{\partial\left(r^m v\right)}{\partial y} = 0 \qquad (1)$$

$$u\frac{\partial u}{\partial x} + v\frac{\partial u}{\partial y} = \upsilon\frac{\partial^2 u}{\partial y^2} + g\,\beta_T\left(T - T_\infty\right)\cos\gamma - \frac{\sigma B^2}{\rho}u - \frac{\upsilon}{K_1}u \qquad (2)$$

$$u\frac{\partial T}{\partial x} + v\frac{\partial T}{\partial y} = \frac{\kappa}{\rho C_p}\frac{\partial^2 T}{\partial y^2} + \tau\left(D_B\frac{\partial C}{\partial y}\frac{\partial T}{\partial y} + \frac{D_T}{T_\infty}\left(\frac{\partial T}{\partial y}\right)^2\right) + \frac{\sigma B^2}{\rho C_p}u^2 \qquad (3)$$

$$u\frac{\partial C}{\partial x} + v\frac{\partial C}{\partial y} = D_B\frac{\partial^2 C}{\partial y^2} + \frac{D_T}{T_\infty}\frac{\partial^2 T}{\partial y^2} - K_r\left(C - C_\infty\right) \qquad (4)$$

Here, u and v denote component of velocity in x and y -directions, respectively. r is the radius of the cone. T and C are fluid temperature and concentration, D_B and D_T are the coefficient of Brownian motion and thermophoresis, K_1 is the coefficient of permeability of the porous medium, K_r is the coefficient of chemical reaction, υ and κ are kinematic viscosity and thermal conductivity of fluid.

The temperature and concentration conditions at the wall are considered as non-isothermal and non-isosolutal. Under these assumption the boundary conditions can be represented as (see ref. [10])

$$\left.\begin{array}{l} u = u_w = \dfrac{x\upsilon}{L^2},\ v = -v_w,\ T = T_w = T_\infty + ax^{r_1},\ C = C_w = C_\infty + bx^{r_2}\ \text{ at }\ y = 0 \\[2mm] u = 0,\ T = T_\infty,\ C = C_\infty \hspace{4.5cm} \text{ as }\ y \to \infty \end{array}\right\} \qquad (5)$$

In the boundary conditions $a\,\&\,b$ are constants and $r_1\,\&\,r_2$ denote wall temperature &concentration parameter, respectively.

METHOD OF SOLUTION

In the present time, many methods are available to handle nonlinear coupled partial differential equations with boundary conditions. Here, the method of similarity transformation has been used to convert the problem into a system of ordinary differential equations, and for this, the following similarity variable, transformation & dimensionless quantities are introduced:

$$\eta = \frac{y}{L},\ u = \frac{x\upsilon}{L^2}f'(\eta),\ v = -\frac{\upsilon(1+m)}{L}f(\eta),\ \theta(\eta) = \frac{T - T_\infty}{T_w - T_\infty},\ \phi(\eta) = \frac{C - C_\infty}{C_w - C_\infty} \qquad (6)$$

Upon using (6) in equations (1)-(4) it has been observed that the equation of continuity is automatically satisfied, while the remaining equations take the following non dimensional form:

$$f''' + ff'' - f'^2 + \lambda\cos\gamma\,\theta - \left(M + \frac{1}{K}\right)f' = 0 \qquad (7)$$

$$\theta'' + \left(-r_1\,f'\theta + (1+m)f\,\theta' + \theta'\left(N_b\,\phi' + N_t\,\theta'\right) + M\,Ec\,f'^2\right)Pr = 0 \qquad (8)$$

$$\phi'' + \left((1+m)f\,\phi' - r_2\,f'\theta - K_r^{*}\phi\right)Sc + \frac{N_t}{N_b}\theta'' = 0 \qquad (9)$$

Sharad Sinha *et al.*,

where prime denotes differentiation with respect to η and the dimensionless parameters are symbolised as:

$\lambda\left(=\dfrac{Gr}{Re_x}\right)$ mixed convection parameter, $Gr\left(=\dfrac{g\,\beta_T\,(T_w-T_\infty)}{\upsilon^2}L^3\right)$ Grashof number, $Re_x\left(=\dfrac{u_w x}{\upsilon}\right)$

Reynolds number, $M\left(=\dfrac{\sigma B^2}{\rho}\dfrac{L^2}{\upsilon}\right)$ magnetic parameter, $K\left(=\dfrac{K_1}{L^2}\right)$ permeability parameter, $Pr\left(=\dfrac{\upsilon}{\alpha}\right)$ Prandtl

number, $\alpha\left(=\dfrac{\kappa}{\rho C_p}\right)$ thermal diffusivity, $N_b\left(=\dfrac{\tau D_B\,(C_w-C_\infty)}{\upsilon}\right)$ Brownian motion parameter,

$N_t\left(=\dfrac{\tau D_T\,(T_w-T_\infty)}{\upsilon T_\infty}\right)$ thermophoresis parameter, $Ec\left(=\dfrac{u_w^{\,2}}{C_p\,(T_w-T_\infty)}\right)$ Eckert number, $Sc\left(=\dfrac{\upsilon}{D_B}\right)$

Schmidt number and $K_r^{\,*}\left(=\dfrac{K_r L^2}{\upsilon}\right)$ chemical reaction parameter.

The boundary conditions given in (5) take the form

$$\left.\begin{array}{l} f=S,\ f'=1,\ \theta=1,\ \phi=1 \ \ \text{at}\ \eta=0 \\ f'=0,\ \theta=0,\ \phi=0 \qquad\quad \text{as}\ \eta\to\infty \end{array}\right\} \tag{10}$$

where $S\left(=\dfrac{v_w L}{\upsilon(1+m)}\right)$ is the section/injection parameter.

In the study, physical quantities of interest are nondimensional shear stress and rate of heat &mass transfer at the surface. These are given by

$$\left.\begin{array}{l} C_f=\dfrac{2\tau_w}{\rho u_w^2}=2\,\mathrm{Re}_x^{-1/2}\,f''(0) \\[2mm] Nu_x=\dfrac{xq_w}{\kappa\,(T_w-T_\infty)}=-\mathrm{Re}_x^{1/2}\,\theta'(0) \\[2mm] Sh_x=\dfrac{xJ_w}{D_B\,(C_w-C_\infty)}=-\mathrm{Re}_x^{1/2}\,\phi'(0) \end{array}\right\} \tag{11}$$

where the dimensional shear stress, heat &mass flux are given by

$$\tau_w=\mu\left.\dfrac{\partial u}{\partial y}\right|_{y=0},\ q_w=-\kappa\left.\dfrac{\partial T}{\partial y}\right|_{y=0}\ \text{and}\ J_w=-D_B\left.\dfrac{\partial C}{\partial y}\right|_{y=0}.$$

Equations (7)-(9) describe a system of nonlinear coupled ordinary differential equations with boundary conditions (10).To solve these equations numerically along with boundary conditions, bvp5c technique (an inbuilt MATLAB program) has been used. This technique is based on finite difference method implementing four stage Lobatto IIIa formula [14].

The above said technique works on system of first order differential equations and to obtain the system from equations (7)-(9) the following expressions are used:

$$f=f_1,\ f'=f_2,\ f''=f_3,\ f'''=f_3',\ \theta=f_4,\ \theta'=f_5,\ \theta''=f_5',\ \phi=f_6,\ \phi'=f_7,\ \phi''=f_7'$$

Sharad Sinha *et al.*,

The reduced system of first order differential equations is given as:

$$
\left.
\begin{aligned}
f_1' &= f_2 \\
f_2' &= f_3 \\
f_3' &= f_2^2 - f_1 f_3 + \left(M + \frac{1}{K} \right) f_2 + \lambda \cos\gamma\, f_4 \\
f_4' &= f_5 \\
f_5' &= \left(r_1 f_2 f_4 - (1+m) f_1 f_5 - f_5 \left(N_b f_7 + N_t f_5 \right) - M\,Ec\, f_2^2 \right) Pr \\
f_6' &= f_7 \\
f_7' &= \left(r_2 f_2 f_6 + K_r^* f_6 - (1+m) f_1 f_7 \right) Sc - \frac{N_t}{N_b} f_5'
\end{aligned}
\right\}
\tag{12}
$$

and respective boundary conditions are

$$
\left.
\begin{aligned}
f_1(0) &= S,\ f_2(0) = 1,\ f_4(0) = 1,\ f_6(0) = 1 \\
f_2(\infty) &= 0,\ f_4(\infty) = 0,\ f_6(\infty) = 0
\end{aligned}
\right\}
\tag{13}
$$

To achieve high accuracy in numerical computations, the stepsize is taken of order 10^{-4}. A comparative study has been performed in the next section to validate the solution procedure.

RESULTS AND DISCUSSION

In this section, the outcomes of the study are discussed through graphs and tables. Also, a comparative study has been performed between the present and previous studies in Table 1 to verify the correctness of the method.

It is found from the Table 1 than, under limiting cases the present results are in great agreement with previously published results. While plotting graphs and preparing tables, the value of parameter to be analysed is varied and the rest of the parameters are kept as $M = 1,\ K = 100,\ \lambda = 0.2,\ Pr = 5,\ N_b = 0.3,$

$N_t = 0.1,\ Ec = 0.1,\ r_1 = 0.1,\ r_2 = 0.1,\ S = 0.1,\ \gamma = \pi/4,\ Sc = 1$ and $K_r^* = 0.2$

Figure 2(a)-(c) presents the effect of magnetic parameter on various fluid profiles. It is observed that increasing magnetic parameter produces a hike in retarding force called Lorentz force due to which velocity decreases. This retardation converts the kinetic energy into thermal energy and uplifts the temperature. Also, the increased magnetic parameter generates a high capacity in the magnetic field to hold fluid particles, which enhances the concentration profile. The porous media with larger permeability assists the fluid to flow through the porous media with more ease. This assistance enhances the fluid velocity and diminishes the temperature as observed in Figure 3(a)-(b). The consequences of increasing suction parameter are depicted in Figure 4 (a)-(c). When the suction parameter is large, more amount of fluid will be sucked by the surface and causes a drop in fluid velocity. Also, the temperature and concentration at the surface have been taken higher that the free stream, so, increasing suction parameter results in diminishing fluid temperature and concentration. Effects of thermophoresis and Brownian motion parameters on fluid temperature and concentration are shown in Figure 5(a)-(b)&Figure 6(a)-(b). Increasing thermophoresis parameter creates more temperature difference between the surface and free stream, due to which hot fluid particles move from surface to fluid and uplift the fluid temperature and concentration. Also, increasing Brownian motion parameter strengthens the colliding nature of particles. Due to this nature, the nanoparticles get scattered and their concentration decreases and more heat generates which results in enhanced temperature. Figure 7&Figure 8 exhibit the effects of surface temperature and surface concentration on fluid temperature and concentration respectively. As the surface temperature or concentration increases, the difference between the surface temperature/concentration

and free stream temperature/concentration will increase and that causes a drop in fluid temperature or concentration profile. The consequences of increasing Schmidt number or chemical reaction parameter on fluid concentration are presented through Figure 9&Figure 10. For increased Schmidt number or chemical reaction parameter, the concentration profile diminishes. This is because large Schmidt number or chemical reaction parameter corresponds to lesser mass diffusivity and provides more assistance to molecular deterioration. The effects of above discussed dimensionless numbers and parameters on physical quantities of interest i.e. shear stress, rate of heat & mass transfer at the surface are presented in Table 2, Table 3, and Table 4. It is well known that in fluid flow, shear stress is proportional to velocity. Thus upliftment in shear stress can be noticed as the fluid velocity enhances. From Table 2, it is clear that the skin friction coefficient uplifts for larger permeability parameter, while the opposite impact is observed for magnetic parameter and suction parameter. Also, the rate of heat/mass transfer at the surface corresponds to the temperature/concentration difference between the surface and ambient fluid, so, as the difference increases there will be high rate of heat/mass transfer. It is observed from Table 3 that there is upliftment in the Nusselt number at the surface for larger permeability parameter, suction parameter, and surface temperature, while it goes down for magnetic parameter, thermophoresis, or Brownian motion parameter. Table 4 summarizes that increasing the surface concentration, Schmidt number, chemical reactivity parameter or Brownian motion parameter leads to an increase in the Sherwood number while the opposite effect is observed for the magnetic parameter, suction parameter or thermophoresis parameter.

In this work two types of geometries are considered. First is cone (for which $m = 1$) and second is wedge (for which $m = 0$). A comparative study of effects of various parameters on these two geometries is presented here. From Figures 2(a), 3(a) & 4(a) it can be seen that fluid velocity is high for cone than wedge. This is because there is lesser contact between fluid particles and the surface of the cone, rather than the wedge. Similarly, from temperature and concentration profiles for various parameters, it is observed that both temperature and concentration boundary layer thickness are lesser for the cone compared to the wedge. Also, from Tables 2, 3&4 it is noted that skin friction, rate of heat & mass transfer are higher for the cone rather than the wedge.

CONCLUSION

The Brownian motion and thermophoresis effects on a mixed convective MHD flow of nanofluid over a vertical permeable cone & wedge with chemical reaction and joule heating have been explored. Some important results are summarized as follows:
1. Fluid temperature enhances with uplifting values of thermophoresis and Brownian motion parameters.
2. Surface temperature has a proportionality relation with the rate of heat transfer.
3. Fluid concentration can be decreased by uplifting the suction parameter or chemical reaction parameter.
4. For a high rate of heat & mass transfer cone should be used rather than wedge.
5. Skin friction is high for cone and can be diminished by enhancing the suction parameter.

REFERENCES

1. S.Choi, "Enhancing thermal conductivity of fluids with nanoparticles", *The Proceedings of the 1995 ASME International Mechanical Engineering Congress and Exposition*, vol. 66, 1995, pp. 99-105.
2. C.Sun, B.Bai, W.Q. Lu and J.Liu, "Shear-rate dependent effective thermal conductivity of H_2O+SiO_2nano-fluids", *Physics of fluids*, vol. 25, 2013, article 052002.
3. H.Upreti, A.K. Pandey and M. Kumar, "MHD flow of Ag-water nanofluid over a flat porous plate with viscous-Ohmic dissipation, suction/ injection and heat generation/absorption", *Alexandria Engineering Journal*, vol. 57, 2018, pp. 1839–1847.
4. S.Sinha, P.Gupta and A.N.Filippov,"Buoyancy assisting and opposing mixed convective MHD flow of nanofluid along a vertical stretching sheet", *Colloid Journal*, vol. 85(1), 2023, pp. 128-139.

Sharad Sinha *et al.*,

5. I.S.Uddin, I.Siddique, R. Ali, F.Jarad,S. Abdal and S.Hussain, "On heat and flow characteristics of Carreaunanofluid and tangent hyperbolic nanofluid across a wedge with slip effects and bioconvection", *Case Studies in Thermal Engineering*, vol. 39, 2022, article 102390.

6. G.Ramanaiah and G.Malarvizhi, "Free convection about a wedge and a cone subjected to mixed thermal boundary conditions", *ActaMechanica*, vol. 93, 1992, pp. 119-123.

7. J.Buongiorno, "Convective Transport in Nanofluids", *Journal of Heat Transfer*, vol. 128(3), 2006, pp. 240-250.

8. A.Mishra and H.Upreti, "A comparative study of Ag–MgO/water and Fe_3O_4 $CoFe_2O_4$/ EG–water hybrid nanofluid flow over a curved surface with chemical reaction using Buongiorno model", *Partial Differential Equations in Applied Mathematics*, vol. 5, 2022, article 100322.

9. P.S.Reddy,P. Sreedevi and A.J.Chamkha, "Magnetohydrodynamic (MHD) boundary layer heat and mass transfer characteristics of nanofluid over a vertical cone under convective boundary condition", *Propulsion and Power Research*, vol. 7(4), 2018, pp. 308–319.

10. A.Dawar, Z.Shah, A.Tassaddiq, P.Kumam, S.Islam and W.Khan, "A convective flow of Williamson nanofluid through cone and wedge with non-isothermal and non-isosolutal conditions: A revised Buongiorno model", *Case Studies in Thermal Engineering*, vol. 24, 2021, article 100869.

11. H.G.JiLe, N.A.Shah, Y.M.Mahrous, P.Sharma, C.S.K.Rajuand S.M.Upddhya, "Radiated magnetic flow in a suspension of ferrous nanoparticles over a cone with brownian motion and thermophoresis", *Case Studies in Thermal Engineering*, vol. 25, 2021, article 100915.

12. K.Vajravelu and J.Nayfeh, "Hydromagnetic convection at a cone and a wedge", *International Communications in Heat and Mass Transfer*, vol. 19, 1992, pp. 701-710.

13. A.S.Butt, A.Ali and A.Mehmood, "Numerical investigation of magnetic field effects on entropy generation in viscous flow over a stretching cylinder embedded in a porous medium", *Energy*, vol. 99, 2016, pp. 237-249.

14. B.Welfert, "A note on classical Gauss-Radau and Gauss-Lobattoquadratures", *Applied Numerical Mathematics*, vol. 60, 2010, pp. 637-644.

Table 1: Comparison of numerical values of $-\theta'(0)$ for various values of Pr when

$$S = 0, \, M = 0, \, K = 0, \, Ec = 0, \, \lambda = 0, \, m = 0, \, r_1 = 0, \, r_2 = 0 \, \, and \, \, N_b = N_t = 10^{-8}$$

Pr	Upreti et al. [3]	Butt et al. [13]	Present
1	0.5820	0.5820	0.5820
10	2.3080	2.3080	2.3080

Table 2: Numerical results of skin friction coefficient $-f''(0)$ for distinct values of various parameters

m	M	K	S	$-f''(0)$
1	**1**	100	0.1	1.502442
1	**5**	100	0.1	2.532907
0	**1**	100	0.1	1.515441
0	**5**	100	0.1	2.542582
1	1	**1**	0.1	1.815366
1	1	**100**	0.1	1.502442
0	1	**1**	0.1	1.827208
0	1	**100**	0.1	1.515441
1	1	100	**0.1**	1.502442
1	1	100	**0.5**	1.711896
0	1	100	**0.1**	1.515441
0	1	100	**0.5**	1.724683

Sharad Sinha *et al.*,

Table 3:Numerical results of wall temperature gradient $-\theta'(0)$ **for distinct values of various parameters**

m	M	K	S	N_b	N_t	r_1	$-\theta'(0)$
1	**1**	100	0.1	0.3	0.1	0.1	1.744644
1	**5**	100	0.1	0.3	0.1	0.1	1.403196
0	**1**	100	0.1	0.3	0.1	0.1	1.053743
0	**5**	100	0.1	0.3	0.1	0.1	0.642489
1	1	**1**	0.1	0.3	0.1	0.1	1.735710
1	1	**100**	0.1	0.3	0.1	0.1	1.744644
0	1	**1**	0.1	0.3	0.1	0.1	1.028840
0	1	**100**	0.1	0.3	0.1	0.1	1.053743
1	1	100	**0.1**	0.3	0.1	0.1	1.744644
1	1	100	**0.5**	0.3	0.1	0.1	4.023074
0	1	100	**0.1**	0.3	0.1	0.1	1.053743
0	1	100	**0.5**	0.3	0.1	0.1	2.142611
1	1	100	0.1	**0.2**	0.1	0.1	2.017258
1	1	100	0.1	**0.7**	0.1	0.1	0.891600
0	1	100	0.1	**0.2**	0.1	0.1	1.231153
0	1	100	0.1	**0.7**	0.1	0.1	0.515574
1	1	100	0.1	0.3	**0.05**	0.1	1.831520
1	1	100	0.1	0.3	**0.25**	0.1	1.507433
0	1	100	0.1	0.3	**0.05**	0.1	1.110398
0	1	100	0.1	0.3	**0.25**	0.1	0.900482
1	1	100	0.1	0.3	0.1	**0.1**	1.744644
1	1	100	0.1	0.3	0.1	**1.5**	2.750867
0	1	100	0.1	0.3	0.1	**0.1**	1.053743
0	1	100	0.1	0.3	0.1	**1.5**	2.316074

Table 4: Numerical results of mass transfer rate $-\phi'(0)$ for distinct values of various parameters

m	M	S	r_2	Sc	K_r^*	N_b	N_t	$-\phi'(0)$
1	**1**	0.1	0.1	1	0.2	0.3	0.1	0.692099
1	**5**	0.1	0.1	1	0.2	0.3	0.1	0.628261
0	**1**	0.1	0.1	1	0.2	0.3	0.1	0.558438
0	**5**	0.1	0.1	1	0.2	0.3	0.1	0.526706
1	1	**0.1**	0.1	1	0.2	0.3	0.1	0.692099
1	1	**0.5**	0.1	1	0.2	0.3	0.1	0.512422
0	1	**0.1**	0.1	1	0.2	0.3	0.1	0.558438
0	1	**0.5**	0.1	1	0.2	0.3	0.1	0.463967
1	1	0.1	**0.1**	1	0.2	0.3	0.1	0.692099
1	1	0.1	**4**	1	0.2	0.3	0.1	1.864199
0	1	0.1	**0.1**	1	0.2	0.3	0.1	0.558438
0	1	0.1	**4**	1	0.2	0.3	0.1	1.799873
1	1	0.1	0.1	**0.5**	0.2	0.3	0.1	0.125094
1	1	0.1	0.1	**1.5**	0.2	0.3	0.1	1.126220
0	1	0.1	0.1	**0.5**	0.2	0.3	0.1	0.181729
0	1	0.1	0.1	**1.5**	0.2	0.3	0.1	0.849983

Sharad Sinha *et al.,*

1	1	0.1	0.1	1	**0.2**	0.3	0.1	0.692099
1	1	0.1	0.1	1	**1**	0.3	0.1	1.180837
0	1	0.1	0.1	1	**0.2**	0.3	0.1	0.558438
0	1	0.1	0.1	1	**1**	0.3	0.1	1.141085
1	1	0.1	0.1	1	0.2	**0.2**	0.1	0.359145
1	1	0.1	0.1	1	0.2	**0.7**	0.1	1.037283
0	1	0.1	0.1	1	0.2	**0.2**	0.1	0.362250
0	1	0.1	0.1	1	0.2	**0.7**	0.1	0.756728
1	1	0.1	0.1	1	0.2	0.3	**0.05**	0.885050
1	1	0.1	0.1	1	0.2	0.3	**0.25**	0.252848
0	1	0.1	0.1	1	0.2	0.3	**0.05**	0.665184
0	1	0.1	0.1	1	0.2	0.3	**0.25**	0.326185

Figure 1: Physical configuration of the flow problem.

Figure 2(a): Velocity profiles for distinct values of M .

Figure 2(b):Temperature profiles for distinct values of M .

Figure 2(c):Concentration profiles for distinct values of M .

Figure 3(a): Velocity profiles for distinct values of K .

63957
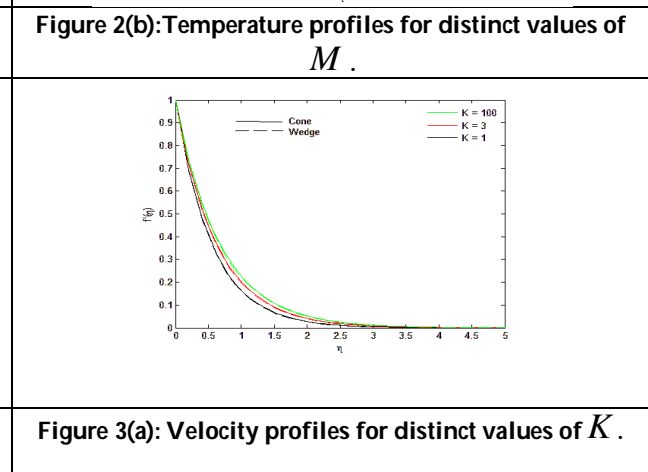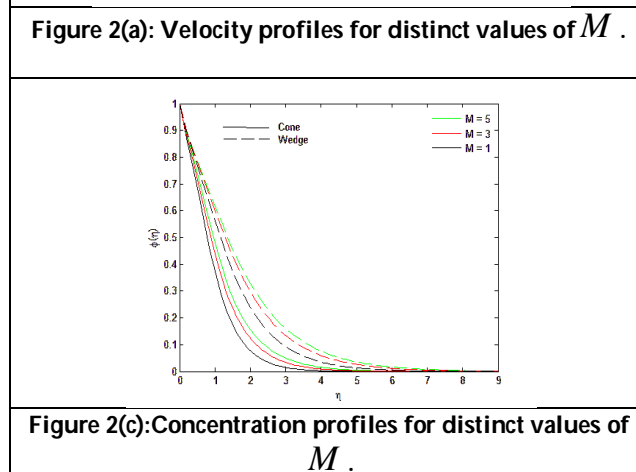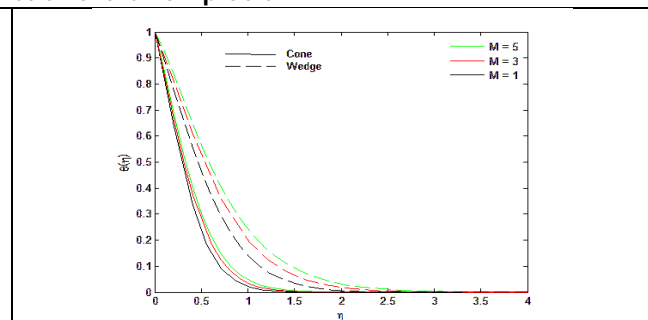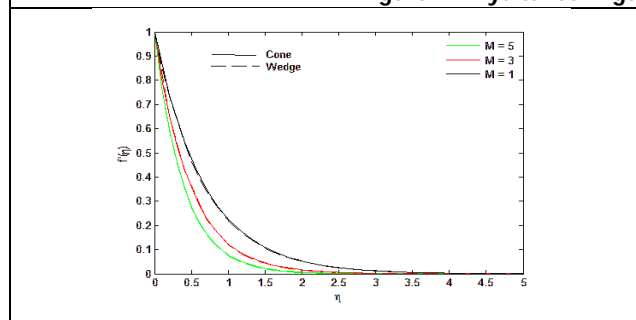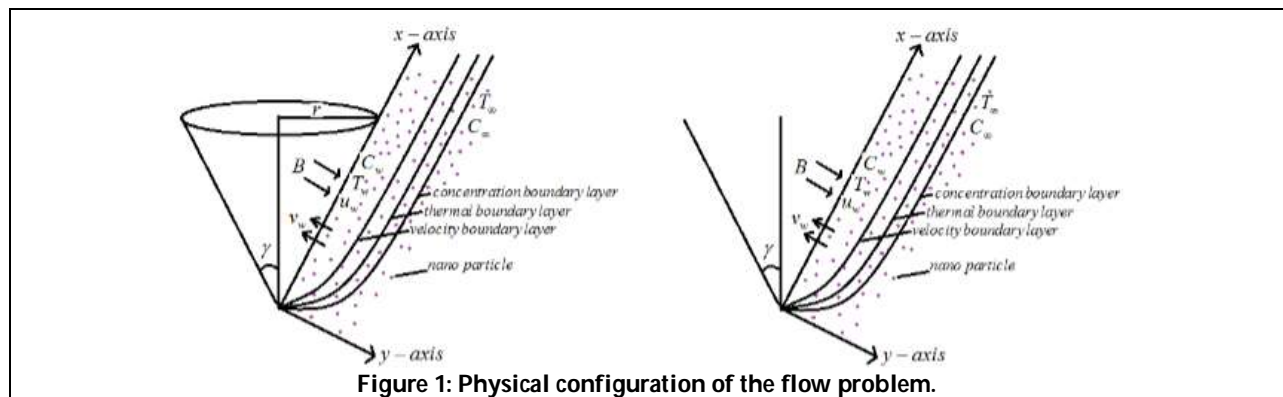
Sharad Sinha *et al.*,
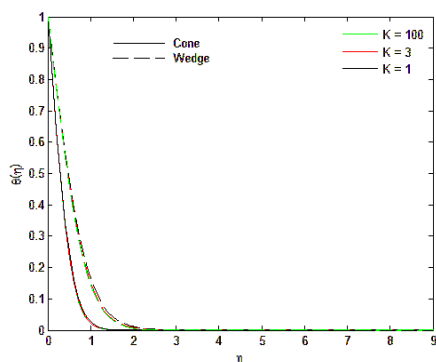
Figure 3(b):Temperature profiles for distinct values of K.
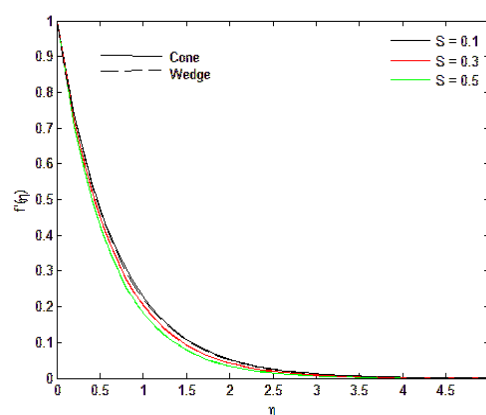
Figure 4(a): Velocity profiles for distinct values of S.
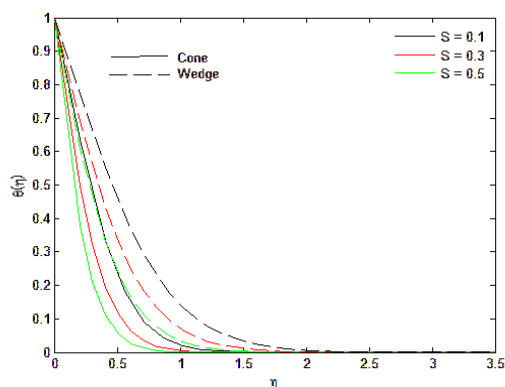
Figure 4(b):Temperature profiles for distinct values of S.
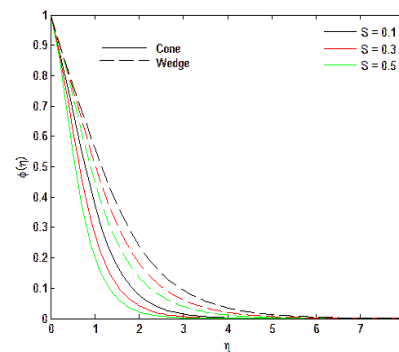
Figure 4(c): Concentration profiles for distinct values of S.
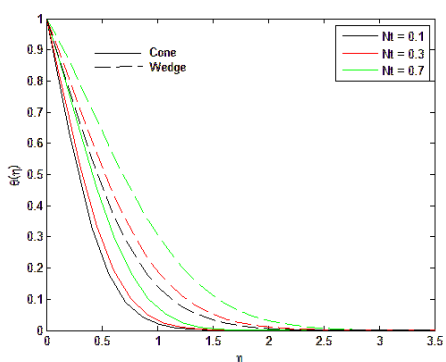
Figure 5(a): Temperature profiles for distinct values of N_t.
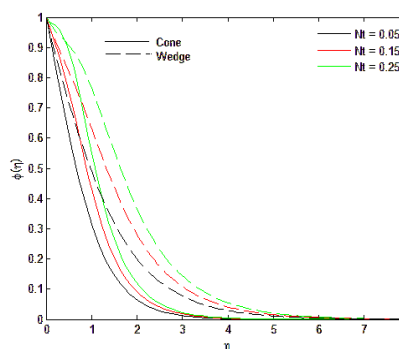
Figure 5(b): Concentration profiles for distinct values of N_t.

Sharad Sinha *et al*.,
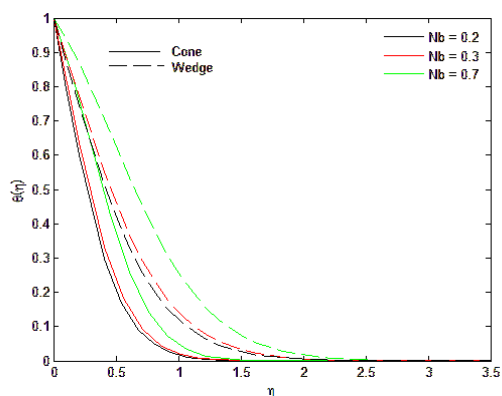
Figure 6(a):Temperature profiles for distinct values of N_b.
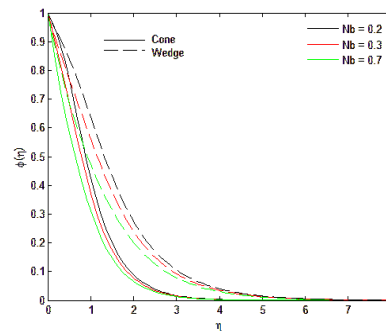
Figure 6(b): Concentration profiles for distinct values of N_b.
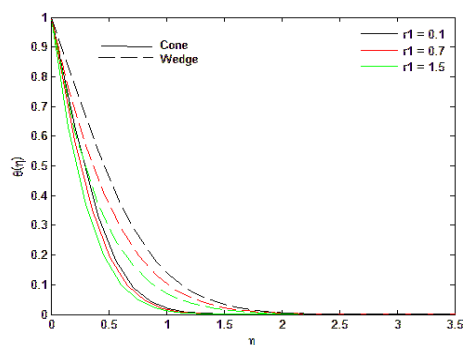
Figure 7: Temperature profiles for distinct values of r_1.
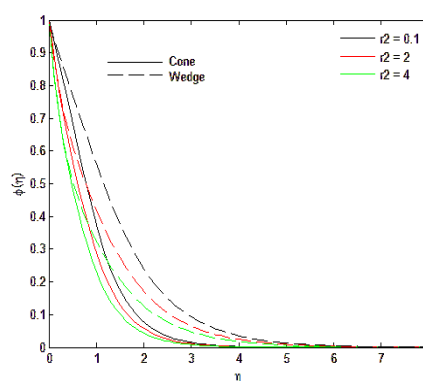
Figure 8: Concentration profiles for distinct values of r_2.
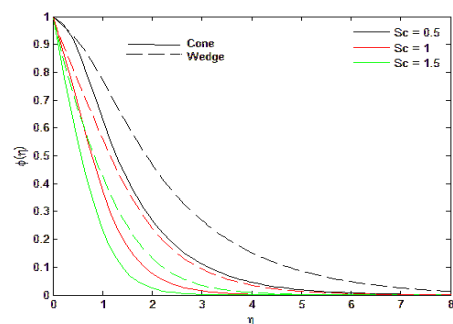
Figure 9: Concentration profiles for distinct values of Sc.
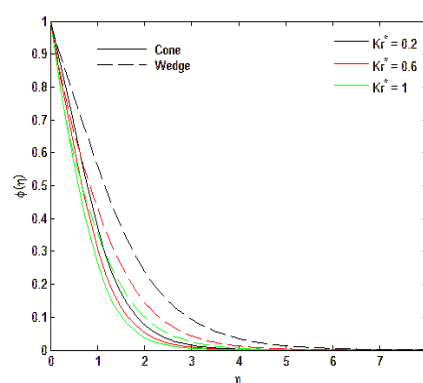
Figure 10: Concentration profiles for distinct values of K_r^*.

RESEARCH ARTICLE

Prevalence of Physical Fitness in Community Dwelling Middle - Aged Women – a Cross Sectional Study

Madhavi Sontakkey[1] and Nidhi Vasava [2*]

[1]Assistant Professor, Parul Institute of Physiotherapy, Parul University, Vadodara , Gujarat, India
[2]MPT Scholar, Parul Institute of Physiotherapy, Parul University, Vadodara, Gujarat, India.

*Address for Correspondence**
Nidhi Vasava
MPT Scholar,
Parul Institute of Physiotherapy,
Parul University, Vadodara,
Gujarat, India.
E.Mail: nidhi.vasava8399@gmail.com

ABSTRACT

when age progress the physical fitness reduces. Less Physical Fitness leads to major disorders affects both Physical and Psychological health conditions. To measure the prevalence of Hamstring flexibility, Aerobic capacity and Balance with sit and reach test, Step test and One leg stand test in villages of Waghodia Taluka, Vadodara. Total 370 Community dwelling middle age women Age raging from 40 – 60 years were included in the study to measure prevalence of Hamstring Flexibility, Aerobic capacity and Balance with sit and reach test, Step test and One leg stand test. All subjects collected from villages of Waghodia Taluka, Vadodara. This study is concluded that 45.94% Participants have less flexibility assess with using sit and reach test, 44.59% Participants have Below average heart rate assess with using Step Test and 61.62% Participants have less balance assess with One leg stand test.

Keywords: Community dwelling middle age women, sit and reach test, Step test, One leg stand test, Hamstring Flexibility, Aerobic Capacity and Balance.

INTRODUCTION

When aging process with time, lesser the physical activity leads mainly to disorders and condition which both affects physical and psychological health condition.[1] Considering women's physical activities are lower than men.[2] Lower activities and movements which are major causes of the lesser functional ability.[3,4] Which is significantly related to higher risk of mortality.[5] Noted down frequently age related changes in women's health around the

Madhavi Sontakkey and Nidhi Vasava

menopause and further beyond.. Regular physical activity has been widely shown to be well-established protective factor which is related to the prevention and the management of a vast number of severe pathological conditions.[6] The Physical fitness can be defined as "the ability to carry out the daily tasks with alertness and vigor, without undue fatigue and with ample energy to enjoy leisure - time pursuits and to meet unforeseen emergencies."[7] Both Exercise and Physical activities are directly relating to high levels of functional fitness, and the smallest change which may be extremely important to the maintenance of functionality in the daily tasks, as well as for the prevention of falls.[8] Physical activities are primary cause of the most pathologies. Physical activity (PA) plays an important role in prevention and treatment of many disease, such as hypertension, diabetes mellitus, heart disease, stroke, colon, breast, endometrium and pulmonary cancer, osteoporosis, obesity and depression.[9] Significant Increasing evidences suggests that being physically inactive with lowering levels of cardiorespiratory fitness are causing the worse cognitive functions in multiple populations of adults.[10] The components of physical finesses which are related to health, include strength, flexibility , endurance of muscles, body composition and cardiovascular & pulmonary endurance.[11]

The Physical fitness is very related to functional limitations.[12] There are some hosts of changes which are associated with a new hormonal environment around the menopausal transition period, such increase in the bodyweight and waist circumferences. In women, Middle Ages are characterized by the biological transformations determined by menopause, which can have the adverse consequences on body weight and metabolic, cardiovascular and bone health. Therefore, to maintain theAdequate level of physical functions, there is a must need to participate in appropriate physical fitness activities.[13] Ability to adapt and perform activities of daily living as well as on personal, social and professional function in the general population are greatly affected by the regular PA.[14]
Regular physical activity practicing promotes an enhancement on the physical fitness parameters, F supported by evidences and which contributes directly to the functional capacity and life quality, of the operating individuals.[15] Women who has been transitioned through perimenopause to post menopause has a declination in muscle strength and muscle power on average of 2-3%, which may suggests that the decline in the physical functioning accelerates already during midlife.[16] Further more to that, little is currently known about the importance of Physical Activity(PA) performed during the different time periods (e.g. 35 – 50 Vs. 50 – 65 years) for maintenance of the muscle mass at old age. Interestingly noted that, we and others have previously showed that PA performed earlier in the life has potential of influencing the physical functions at old age era.[17] So the Need arises Less physical activity leads to a major disorder in middle aged women. Due to increased exposure to risk factors such as Sedentary lifestyle, obesity, lack of physical activity and sometimes malnutrition. The disorders can cause long periods of work disability and treatment is often necessary. This study is helpful to find Physical fitness level with flexibility, aerobic capacity and balance in community dwelling middle age women. Aimed of the study is to evaluate the prevalence of flexibility, aerobic capacity and balance among community dwelling middle age women.

MATERIAL AND METHODOLOGY

- STUDY DESIGN: A Cross sectional study
- STUDY POPULATION: Middle age women from villages of Waghodia taluka
- SOURCE OF DATA: Villages of Waghodia taluka
- SAMPLE METHOD:
- SAMPLE SIZE: These study 370 samples were collected from middle age women.
- SAMPLING: Online calculator
- SELECTION OF SAMPLE: Random sampling (chit method).

INCLUSION CRITERIA
- Age: 40 – 60 years old women
- Only housewives who are functionally independent are included

Madhavi Sontakkey and Nidhi Vasava

EXCLUSION CRITERIA

- Subject who has any prior musculoskeletal conditions, neurological conditions, or vestibular disorders that limits their exercise ability
- Conditions in which the exercises are contraindicated severe aortic stenosis, uncontrolled arrhythmia & acute coronary syndrome 0
- Cancer
- Amputation
- Subjects who are physically disable
- Systemic diseases

MATERIAL USED:

- Paper
- Pen
- Pencil
- Stopwatch
- Metronome
- Measure tape
- Stepstool(12inch)

OUTCOME MEASURES:

- Sit and reach test
- Step test
- One leg stand test

Procedure

A total 370 samples were collected who are fulfilling the inclusion criteria and exclusion criteria. Different villages of waghodiya taluka were selected where the study was conductedin this study, data was collected by using sit and reach test, step test and one leg stand test. A series of different villages were visited and each village women was given a brief introduction and also explained the purpose and procedure of the study. The subject once understands and is willing to participate in the study, a consent form was handed over to each subject in which she fills the basic details and must sign the form. With the use of sit and reach test three readings each for the hamstring flexibility, step test for the aerobic capacity and one leg stand test for the balance.

STATISTICAL ANALYSIS

STATISTICAL SOFTWARE

- For the analysis of the data IBM SPSS version 20 was used.
- Graphs and tables were also generated by Microsoft Excel and Microsoft Word.

STATISTICAL METHOD

- Descriptive analysis was done which include Age, inch measurement for v sit and reach test, heart rate for step test and seconds for one leg stand test.

RESULT

Graph 1 shows the age distribution
Graph 2 Shows the distribution of sit and reach test
Graph 3 shows the distribution of step test
Graph 4 shows the One leg stand test

DISCUSSION

This study aimed to measure the physical fitness in community dwelling middle age women with sit and reach test, Step test and one leg stand test in villages around Parul University. This study has shown, the physical fitness in community dwelling middle aged women. This shows a need for improving physical fitness in community dwelling middle age women. This results are consist with literature on prevalence of hamstring flexibility, aerobic capacity and balance among community dwelling middle age women but unfortunately, no studies specifically looking at community dwelling middle age women. In this study, Graph 1 shows the Age group distribution of 370 middle age women which ranges between 40 - 60 years of age. All these middle age women were divided into 7 age groups. Those 7 age groups are: 40 - 44 years of age (15.4%), 45 - 49 years of age (24.48%), 50 - 54 years of age (22.97%), 55 – 59 years of age (28.1%), 60 - 64years of age (8.64%). Graph 2 shows the categorization of hamstring flexibility of 370 middle age women. All the participants were categorized into 3 different categories according to sit and reach test. The hamstring flexibility of our participants varied from -6 to +4 inch. Their hamstring flexibility distribution are - (45.94%), 0(18.91%) and + (35.13%). Graph 3 shows the categorization of step test of 370 community dwelling middle age women. All the participants were categorized into 5 different categories according to their aerobic capacity in HR. The HR of our participants varied from 93 -140 HR. Their HR distribution are <93 (0), 94 - 106 (18.91%), 107 - 117 (26.48%), 118 - 130 (44.59%), >131 (10%). Graph 4 shows the categorization of one leg stand test of 370 community dwelling middle age women. All the participants were categorized into 5 different categories according to their balance in Secs. The balance in secs of our participants varied from 3.1 – 15.6 Secs. Their balances in Sec distribution are 61.62% in less than 10 sec and 38.87% more than 10 sec.

CONCLUSION

From this study is concluded that 45.94% Participants have less flexibility assess with using sit and reach test, 44.59% Participants have Below average heart rate assess with using Step Test and % Participants have less balance assess with One leg stand test.

ETHICAL APPROVAL
Ethical approval was obtained from the institutional review board from Parul institute of Physiotherapy, waghodia, Vadodara.

CONFLICT OF INTEREST
None

CONSENT FOR PUBLICATION
All individuals participating in this research signed a informed consent form prior to their inclusion in the study.

LIMITATION
Physical Fitness was assessed with Limited outcomes.

FURTHER RECOMMENDATIONS
Physical fitness will be assessed with more outcomes. Physical fitness will also checked in other population.

REFERNCES

1. NURIA CODINA, JOSE V. PESTANTA AND IMMACULADA ARMADANS: PhysicalActivity (PA) among Middle – Aged Women: Initial and Current Influences and Patterns ofParticipation.JournalofWomen&Aging,2013,25:260–272
2. MoniqueL.Schaal, M.s., Woonghee Lee,B.S.,MarleneJ.Egger, Ph.D:PHYSICALACTIVITY PATTERNS IN HEALTHY MIDDLE-AGED WOMEN. Journal of Women &aging,2016;28(6):469-476
3. Miller ME, Rejeski WJ, Reboussin BA, et al.: Physical activity, functional limitations &disabilityinorderadults.JAmGeriatersoc,2000,48:1264-1272s
4. Nakano MM, OtonariTS, Takara KS, et al.: Physical performance,balance,mobilityandmusclestrengthdeclineatdifferentratesinelderlypeople.JPhysTherSci,2014,26:583-586
5. RakoswskiW,MorV: The association of physical activity with mortality among older adults in the Longitud in al Study of Aging(1984-1988).JGerontol,1992,47:M122-M129
6. Brawner, C. A., Churilla, J. R. &Keteyian, S. J. Prevalence of physical activity is loweramongindividualswithchronicdisease. *Med. Sci. Sports Exerc.* **48**, 1062–1067 (2016).
7. Clarke HH: Basic understanding of physical fitness Washington, DC: President's Councilon Physical fitness and Sports,1971.
8. Freiberger E, Häberle L, Spirduso WW, RixtZijlstra GA. Long-term effects of three multicomponent exercise interventions on physical performance and fall-related psychological outcomes in community-dwelling older adults: a randomized controlled trial. Journal of the American GeriatricsSociety.2012 Mar;60(3):437-46.
9. Marcos Ausenka Ribeiro, Milton Arruda Martins, Celso R.F.Carvalho : Intervention toincrease physical activity in middle ag ewomenattheworkplace:ARandomizedControlledTrial.MedSciSportsExerc.2014May1;46(5):1008-5.
10. Bender CM, Sereika SM, Gentry AL, Duquette JE, Casillo FE, Marsland A, Brufsky AM, Evans S,Gorantla VC, Grahovac TL, McAuliffe PF. Physical activity, cardiorespiratory fitness,and cognitive function in post menopausal women with breast cancer. Supportive Carein Cancer. 20 21Jul;29(7): 3743-52.
11. Caspersen CJ, Powell KE, Christenson GM: Physical activity, exercise and physical fitness:definitionanddistinctionsforhealth-relatedresearch,PublicHealthRep,1985,100:126-131
12. MoreyMC,PiperCF,Cornoni-HuntleyJ:Physicalfitnessandfunctionallimitationsincommunity-dwellingolderadults.MedSciSports Exerc,1998,30:715-723
13. Soonee Kang, Sujin Hwang, Aimee B. Klein: Multicomponent exercise for physical fitnessofcommunity–dwellingelderlywomen.J.Phys.Ther.Sci.,2015,25:911-915
14. Hsu PJ, Chou HS, Pan YH, Ju YY, Tsai CL, Pan CY. Sedentary time, physical activity levels andphysical fitness in adults with intellectual disabilities. International journal of environmental researchandpublichealth.2021 May10;18(9):5033.
15. HuckCJ.Effects of Supervised Resistance Training on Fitness and Functional Strength in Patients Succeeding Bariatric Surgery.JStrengthCondRes.2015;29(3):589–95.
16. BondarevD,SipiläS,FinniT,KujalaUM,AukeeP,KovanenV,LaakkonenEK,KokkoK.Associations of physical performance and physical activity with mental well-being in middle-agedwomen.BMCPublicHealth.2021Dec;21(1):1-1.
17. Edholm P, Veen J, Kadi F, Nilsson A. Muscle mass and aerobic capacity in older women Impact of regular exercise at middleage. ExperimentalGerontology.2021May1;147:111259.

Madhavi Sontakkey and Nidhi Vasava
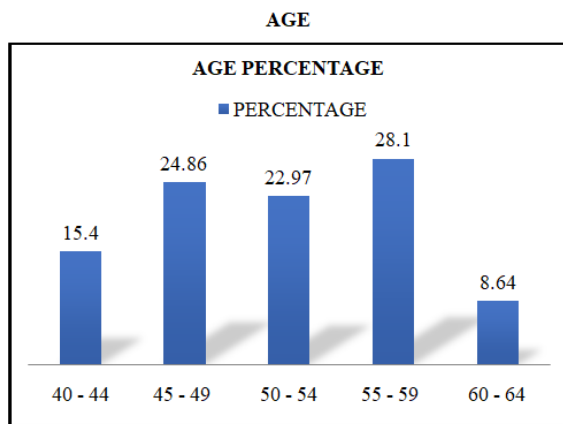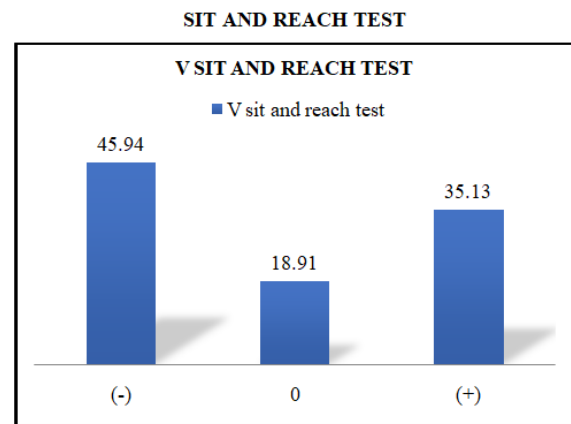
AGE

AGE PERCENTAGE

■ PERCENTAGE

- 15.4 (40 - 44)
- 24.86 (45 - 49)
- 22.97 (50 - 54)
- 28.1 (55 - 59)
- 8.64 (60 - 64)

Graph 1 shows the age distribution

SIT AND REACH TEST

V SIT AND REACH TEST

■ V sit and reach test

- 45.94 (-)
- 18.91 (0)
- 35.13 (+)

Graph 2 Shows the distribution of sit and reach test

STEP TEST

STEP TEST

■ Step Test

- 0 (< 93)
- 18.91 (94 - 106)
- 26.48 (107 - 117)
- 44.59 (118 - 130)
- 10 (> 131)

Graph 3 shows the distribution of step test

ONE LEG STAND TEST

One Leg Stand Test

■ one leg stand test Percentage

- 61.62 (< 10)
- 38.37 (> 10)

Graph 4 shows the One leg stand test

RESEARCH ARTICLE
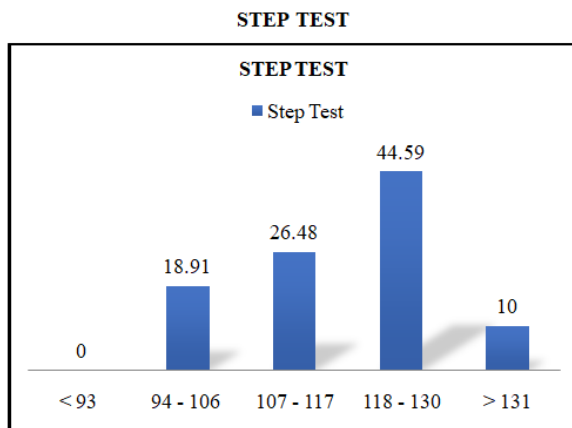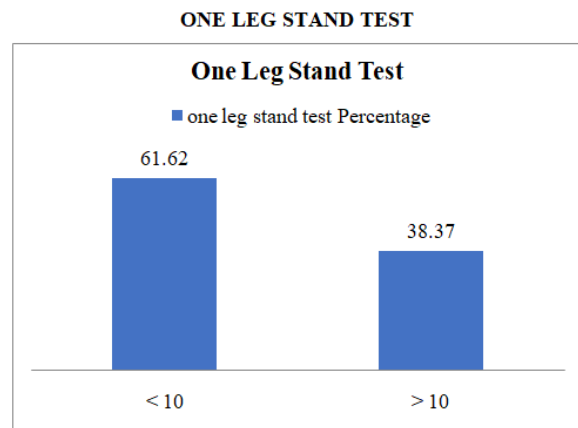
Juvenile Myasthenia Gravis: A Concise Review Case Report

Karra. Geetha[1]*, T. Chandana[2], R. Sakshi[2], Ch. Sai Chandu[2] and T. Rama Rao[3]

[1]Professor, Department of Pharmaceutics, CMR College of Pharmacy, Hyderabad, Telangana, India
[2]Student , Pharm D, CMR College of Pharmacy, Hyderabad, Telangana, India
[3]Principal, Department of Pharma Chemistry, CMR College of Pharmacy, Hyderabad, Telangana, India.

*Address for Correspondence
Karra. Geetha
Professor,
Department of Pharmaceutics,
CMR College of Pharmacy,
Hyderabad, Telangana, India

ABSTRACT

Juvenile myasthenia gravis is a rare childhood disorder that accounts for 10% to 15% of all cases of myasthenia gravis. It is characterized, like the adult form, by an autoimmune attack on acetylcholine receptors at the neuromuscular junction. The majority of patients have ptosis, diplopia, and fatigue. More advanced cases may also have bulbar problems and limb weakness, and may progress to respiratory muscle paralysis. A 12-year-old male patient was admitted to Gandhi hospital, Telangana, that came with complaints of being unable to roll his eyes, watering from the eyes, difficulty in swallowing, throat pain, cough, and fever. It is a known case of myastheniagravis. A neostigmine atropine test was performed, and the result was found to be positive. Ice pack test results were also positive, and intravenous immunoglobulin transfusions were previously administered. As a result, the patient was prescribed pyridostigmine and prednisolone. Based on the clinical presentation and the laboratory results, the patient was diagnosed with Juvenile Myasthenia Gravis with upper respiratory tract infection.

Keywords: Autoimmune, acetylcholine receptors antibodies, ophthalmoplegia, ptosis

INTRODUCTION

The failure of neuromuscular transmission that usually result from the binding of autoantibodies to proteins that are involved in signalling at the neuromuscular junction is the cause of the autoimmune syndrome known as myasthenia gravis (MG) [1].A rare paediatric disease called juvenile myasthenia gravis has numerous clinical characteristics that set it apart from adult myasthenia gravis. Particularly in prepubertal children, isolated ocular symptoms are more common, acetylcholine receptors are less common and remission is likely. Anticholinesterase,

corticosteroids with or without steroid-sparing medications, and more recent immune modifying drugs are frequently used as treatments. Thymectomy raises the likelihood of remission. The child's developmental needs and other factors should be considered in diagnosis and treatment [2].

MYASTHENIA GRAVIS WITH UPPER RESPIRATORY TRACT INFECTION

Myasthenia gravis, is an autoimmune illness that causes muscle weakness, may be worse by upper respiratory tract infection (URTI), including influenza. There is also worry that receiving the influenza vaccine could aggravate existing autoimmune conditions [3].

ETIOLOGY

Myasthenia gravis has an unknown underlying aetiology, while there is strong evidence that it is connected in some way to thymus gland anomalies and that the condition has a genetic component. However, the disease progression is very well understood, despite the lack of a precise cause. The neuromuscular junction or the region where the skeletal muscle and nerve terminals connect is impacted by myasthenia gravis. Nerve terminals at the neuromuscular junction provide impulses to the muscle through a synapse, which causes the muscle to contract. Acetylcholine, a neurotransmitter, is released from vesicles in the nerve ending into the synapse and acetylcholine receptors situated on the muscle side of the synapse when a nerve impulse passes along the neuron.

The reaction lasts just a short while because an enzyme called acetylcholine quickly breaks down the acetylcholine in the receptor into its component molecules, acetate, and choline. Acetylcholine that is still present diffuses away from the receptors. In persons with myasthenia gravis, T-mediated autoantibodies that target and inhibit the body's own acetylcholine receptors interfere with this typical impulse transmission. The main symptom of myasthenia gravis is caused by weak muscular contractions, which occur when enough receptors are blocked by autoantibodies [4].

CLASSIFICATION OF JUVENILE MYASTHENIA GRAVIS

Ocular

Ocular myasthenia gravis comprises up to 10 – 35 % of paediatric instances of myasthenia gravis. 10 to 35 % of paediatric instances of MG are caused by ocular myasthenia gravis. Asian populations have a higher prevalence of OMG in children. The only muscles engaged in OMG are the elevator palpebral and extraocular muscles. Ptosis, diplopia, or strabismus may be the first symptoms or observations that a person presents [5].

Generalized

Extraocular muscles and levatorpalpebrae are impacted in up to 90% of MG patients. The involvement of any other non-ophthalmic skeletal muscle, however, separates ocular from generalized MG. Patients who run or stroll may experience early weariness. A change in voice and other aspects of talking could be affected. There can be facial numbness and swallowing issues. The most concerning symptom is breathing trouble when the diaphragm is affected. Patients may experience respiratory failure and need intubation;therefore, this is an emergency [6].

SUBTYPES OF MYASTHENIA GRAVIS IN CHILDHOOD

Neonatal myasthenia gravis

Unlike juvenile myasthenia gravis and congenital myasthenic syndromes, neonatal myasthenia gravis (NMG) is an immune-mediated that appears after birth in a mother who has autoimmune MG. Transfer of maternal autoantibodies to the foetus through the placenta is the disease's pathophysiological mechanism in these patients. Neostigmine and plasma exchange are two possible treatments, and they could be required to provide respiratory assistance [7].

Juvenile myasthenia gravis

The autoimmune condition known as Juvenile Myasthenia gravis (JMG) affects children and young adults under the age of 19. It differs from adult onset NMG in that it does not result from a structural problem that causes congenital myasthenic syndrome. Patients with MG that are exclusively ocular are less likely to develop serum autoantibodies

that are positive for Acetylcholine receptor (AchR) and muscle specific tyrosine kinase (MuSK). Some patientsare classified as double seronegative MG because they do not have detectable auto antibodies to AchR or MUSK. These kids may, however, have antibodies to other substrates found in the neuromuscular junction, such as agrin, cortactin, or low-density lipoprotein receptor related protein 4 (LRP4). Other autoimmune conditions including Hashimoto's and autoimmune polymyositis may share a link with JMG [8].

Congenital myasthenia syndromes
Congenital myasthenic syndromes (CMS) are a group of disorders that are separate from autoimmunemyasthenia gravis (MG). Typically, onset occurs between childbirth and early infancy. Additionally, these individuals also experience weakness and fatigable ptosis. To separate these illnesses from myopathies or other neurogenic disorders, a strong index of suspicion may be required. These patients' symptoms are not immune-mediated, and instead, a structural change at the NMJ itself causes fatigability, such as modifications to the cholinergic receptor or to the formation and maintenance of endplates. Because the specific treatment for one mutation may be harmful for another mutation, treatment must be tailored to the specific mutation, genetic screening of patients with CMS is important to determine the pathogenic mutation [9].

EPIDEMIOLOGY
JMG is a rare paediatric illness, however, regional differences in incidence and prevalence exist. There are no exact incidence and prevalence statistics available. Asian communities exhibit MG in children more frequently than Caucasian populations do. In Chinese communities, up to 50 % of all cases of MG present in childhood, with a peak age of presentation of 5 to 10 years and a predominance of ocular symptoms Contrarily, Caucasian individuals tend to present as adults, with prepubertal onset occurring in less than 10 % of instances.
Childhood myasthenia gravis is relatively uncommon in western communities, it is common in Asian nations, affecting over 50 % of children under 15 years. They typically exhibit signs of weak extraocular muscles when they first appear [10].

SIGNS AND SYMPTOMS:
● The most common signs and symptoms of myasthenia gravis are as follows:
● Visual issues such as double vision and ptosis of the eyelids (diplopia).
● As muscles are used, muscle weakness and tiredness can increase and fluctuate dramatically in intensity over days or even hours (early fatigue).
● Facial muscle involvement gives the illusion of a mask; a grin may come off as more of a snarl.
● Myasthenia gravis symptoms can mimic those of other diseases. For a diagnosis, visit the doctor.
● Throughout the course of MG, there may be occasional flare-ups and remissions (symptomatic relief). Remissions, however, are not always total or permanent [11].
● Children are at increased risk of chest infection and at risk of choking or aspiration. Impairment of the respiratory muscles needs ventilatory support, this is known as   myasthenic crisis [12].

PATHOPHYSIOLOGY
IgG1 and IgG3 subtype antibodies are present in n- AchR myasthenia gravis. In the postsynaptic membrane of skeletal muscles, they bind to the n-Ach receptor and activate the complement system, causing the membrane assault complex to form Membrane attack complex (MAC). The receptor's final breakdown is caused by MAC. They could potentially work by boosting the endocytosis of the n- Ach receptor that is attached to an antibody or by functionally inhibiting the binding of Ach to its receptor. The antibodies in the myasthenia gravis and low-density lipoprotein receptor related protein 4(LPR4) MG are of the Immunoglobulin G4 (IgG4) subtype and lack the complement activating function. The NMJ's Argin – LPR4 MusK protein complex, whose major job is to maintain the joint, is where they bind. The complex is inhibited, which results in fewer n – Ach receptors. Due to a deficiency in n – Ach receptors, the Ach produced at the nerve terminal cannot produce the postsynaptic potential necessary to trigger an action potential in muscle, which results in symptoms of muscular weakness. Because frequent usage of a muscle group depletes the Ach stored in the NMJ, weakening is more common [13].

DIAGNOSIS
Anyone with myasthenia gravis distinctive weakness may be suspected by a doctor. To confirm the diagnosis of myasthenia gravis, the doctor may prescribe the following types of tests.

ICE test
This is a simple test that may be done in the doctor's office without any extra tools. The doctor will check to see if the patient's eyelid drooping improves after placing an ice packover the patient's eye for a few minutes. Any improvement would suggest a diagnosis of myasthenia gravis [14].

Acetylcholinestarase inhibition
Drugs that increase the amount of acetylcholine can be used to test for myasthenia gravis since acetylcholine receptors are blocked in this condition. Fast-acting acetylcholinesterase inhibitors called edrophonium will temporarily and immediately reduce muscle weakness in people with myasthenia gravis by sparing the body's already existing acetylcholine. Edrophonium starts working within 30 seconds and wears off after only five minutes [15]

Immunohistochemistry of blood
About 85% of persons with myasthenia gravis have anti-acetylcholine receptor antibodies in their serum. However, they are only present in roughly 50% of individuals with symptoms limited to the eye muscles. In roughly 70% of individuals who test negative for anti-acetylcholine receptor antibodies but have the characteristic symptoms of myasthenia gravis, antibodies to muscle-specific kinase (MuSK) have recently been found. TheMuSK protein aids in the organization of acetylcholine receptors on the surface of muscle cells, and this test is emerging as a useful diagnostic tool when the disease's symptoms are present, but no autoantibodies are found [15].

Electrical physiological research
Muscle reactions to light stimulation may be discovered through nerve conduction tests. Myasthenia gravis patients will exhibit progressively smaller or weaker reactions. Although this is the most accurate nerve test for myasthenia gravis, it cannot be used on all muscles and is not always predictive [16].

Thymic imaging and thyroid testing
To evaluate the thyroid and thymus glands' health, many tests may be performed. These include thyroid function tests to identify hyperthyroidism and computed tomography chest scans to reveal a thymoma or enlarged thymus gland [17].

TREATMENT
Traditional therapies for myasthenia gravis come in five different forms:

Inhibitors of acetylcholinesterase:
In order to give the acetylcholine already present in the synapse more time to interact with the accessible receptors, these medications block the enzyme that usually breaks it down in the synapse. Pyridostigmine and neostigmine are the acetylcholinesterase inhibitor most frequently prescribed for myasthenia gravis [18].

Thymectomy
Numerous studies back the surgical removal of the thymus gland, or thymectomy, as a treatment option for people with myasthenia gravis, but these are controversial.

Immunosuppressants:
In myasthenia gravis, immunosuppressants are frequently employed to tame the excessive immunological response. Glucocorticoids like prednisone, azathioprine, cyclosporine, and others may be among these medications. Despite the fact that they are beneficial in many patients, careful monitoringof patients receiving long-term glucocorticoid

therapy is essential due to the serious side effects these medications are known to cause. Long-term usage of glucocorticoids is linked to serious metabolic adverse effects, such as central obesity, decreased insulin sensitivity, and bone loss [20].

Plasmapheresis

Plasmapheresis is particularly helpful before thymus removal surgery. Studies have shown that plasmapheresis is often well tolerated by patients. Reversible hypotension (low blood pressure) and moderate tremor are the most frequent side effects.Plasmapheresis had a low impact on infection and mortality rates, and all patients immediately benefited from the therapy.

Intravenous immunoglobulin

IVIg proved successful in treating chronic inflammatory demyelinating polyneuropathy in controlled clinical studies. Additionally, IVIg has helped certain myasthenia gravis patients. IVIg therapy produces transient alleviation that lasts for a few weeks to months. Although both plasmapheresis and IVIg therapies showed a clinically significant effect in individuals with persistent myasthenia gravis, studies contrasting plasmapheresis and IVIg discovered that the improvement began more quickly with plasmapheresis than with IVIg [19].

CASE REPORT

A 12 years boy born out of non-consanguineous marriage first in birth order was admitted to the PICU (paediatric intensive care unit) with the chief complaints of being unable to scroll his eyes for last 1 week and experiencing watering from the eyes, difficulty in swallowing, cough for last 3 days and the patient had difficulty with throat pain, productive cough that is white and large in quantity, drooping of eyes along with fever for last one day. On examination, the child is active and afebrile. PICCKEL (pallor, icterus, cyanosis, clubbing, koilonychia, lymphadenopathy, oedema) was observed as negative, heart rate is 90 bpm, respiratory rate is 28/minute and P/A (par abdomen) is soft, CNS is NAD (no abnormality detected). The patient had bilateral ptosis. The patient was increased white blood cells, decreased haemoglobin, and more platelets. The clinical serological report is negative for enteric fever and CRP (c-reactive protein). In the urine examination urine was found to be acidic and pale yellow in colour and trace amounts of albumin is found along with pus cells and no RBCs were found in the urine.

The patient had a history of decreased for 3 days and no history of drooling of saliva and blurring of vision. The patient had no history of seizures, loss of consciousness, and altered sensorium. At the initial stage, the child had no chest pain, headache, vomiting, burning micturition, and abdominal pain. It is a known case of seizure disorder at seven years of age;thus, medication is used for 3 years, and history of the same complaints in the past 5 months. And the patient was admitted to Gandhi hospital for 17 days. It is a known case of myasthenia gravis. MRI D.L. spine with screening of whole spine showed evidence of T1 hypointense, T2/STR hypointensejse signal lesion oted in the body, left pedicle and lamina of D5 vertebra with associated wedging of D5 vertebra. Lesion shows intense enhancement on post contract with anterior epidural extension causing canal stenosis and compressing spinal cord. Similar lesion noted in L1, L3 vertebral bodies. Similar soft tissue intensity lesion noted in right iliacwing and body of left iliac bone. Multiple round T2 hyperintense lesion noted in liver. Evidence of peripherally enhancinh central soft tissue lesion measuring 35*35mm noted in superior segment of left lower lobe likely neoplastic etiology. Myasthenia gravis is diagnosed by increased ACH (acetylcholine) receptor antibodies. A neostigmine atropine test has been done, and the result was observed as positive. Ice pack test results also got positive and Iv Ig (intravenous immunoglobulin) transfusions were given in the past. Thus, the patient was started on pyridostigmine and prednisolone medication. The standard treatment for myasthenia gravis is corticosteroids, cholinesterase inhibitors and immune suppressants.

● IV piperacillin 300 mg/kg/day 2.6gm in 20 NS/IV/TID to treat any bacterial infections,
● INJ PCM 20 ml /IV/O is to reduce the fever.
● corticosteroid medication like tab prednisolone @0.5 mg/kg/day to help in limiting antibody production.
● tab azathioprine 25 mg/PO/OD, which is an immune suppressant to alter the patient immune system.

● Tab pyridostigmine @60 mg/PO/QID, which is a choline esterase inhibitor that enhances communication between nerves and muscles.

● tab pantoprazole 20 mg/PO/day, which is a proton pump inhibitor is given to reduce excess acid in the stomach.

● INJ amoxiclav 10MG/kg/day to fight infections.

● INJ.PCM 26ml/iv/QID to reduce the high-grade fever.

● INJ amikacin, is a short-term antibiotic used to treat serious bacterialinfections.

DISCUSSION

Juvenile myasthenia gravis is a rare paediatric disorder that has numerous clinical characteristics that set it apart from adult myasthenia gravis. JMG is an autoimmune disease that develops before the age of 16. It is a rare childhood disorder that affects less than 10-15% of children and has an annual incidence of 1-5 per million [21].The neuromuscular junction or the region where the skeletal muscle and nerve terminals connect is impacted by myasthenia gravis. The main symptom of myasthenia gravis is caused by weak muscular contractions, which occur when enough receptors are blocked by autoantibodies. The diagnosis is made using clinical signs and symptoms, with laboratory and electrophysiological studies used for confirmation. Although thymoma in children is uncommon, the thymus must be imaged (usually by CT) once JMG is diagnosed [22]. Corticosteroids, cholinesterase inhibitors, and immunosuppressants are the choice of drugs for myasthenia gravis. The illness's progression is highly variable. Children with myasthenia have a better long-term outlook than adults.

REFERENCES

1. Conti-Fine BM, Milani M, Kaminski HJ. Myasthenia gravis: *past, present, and future. Journal of Clinical Investigation.* 2006;116(11):2843–2854.

2. P. I. Andrews, J. M. Massey, J. F. Howard, and D. B. Sanders. Race, sex, and puberty influence onset, severity, and outcome in juvenile myasthenia gravis, *Neurology*, vol. 44, no. 7, pp. 1208–1214, 1994.

3. Seok HY, Shin HY, Kim JK, Kim BJ, Oh J, Suh BC, Kim SY, Kang SY, Ahn SW, Bae JS, Kim BJ. The Impacts of Influenza Infection and Vaccination on Exacerbation of Myasthenia Gravis. *J Clin Neurol.* 2017 Oct;13(4):325-330. doi: 10.3988/jcn.2017.13.4.325. PMID: 29057629; PMCID: PMC5653619.

4. Lil XiongWC, MeiL. Nueromuscular junction formation, Aging and disorders. *Annu Rev Physiol.*2018 Feb 10;80: 159- 188.

5. Castro D, Derisavifard S, Anderson M, Greene M, Iannaccone S. Juvenile myasthenia gravis: A twenty-year experience. *J ClinNeuromusc Dis.* 2013; 14:95-102.

6. Nemet AY, Segal O, Mimouni M, Vinker S. Associated morbidity of pediatric ptosis - a large, community based case-control study. *Graefes Arch ClinExpOphthalmol.* 2014; 252:1509-1514.

7. Vanikieti K, Lowwongngam K, Padungkiatsagul T, Visudtibhan A, Poonyathalang A. Juvenile ocular myasthenia gravis: Presentation and outcome of a large cohort. *Pediatr Neurol.* 2018; 87:36-41.

8. Téllez-Zenteno JF, Hernández-Ronquillo L, Salinas V, Estanol B, da Silva O. Myasthenia gravis and pregnancy: clinical implications and neonatal outcome. *BMC MusculoskeletDisord.* 2004; 5:42.

9. Namba T, Brown SB, Grob D. Neonatal myasthenia gravis: Report of two cases and review of the literature. *Pediatrics.* 1970; 45:488-504.

10. JayamThrouth ,Dabi A ,Soliemean N, krurkukumbi M,kalyanam J.Myasthenia gravis a review autoimmune disease. *Autoimmune Dis.* 2012;874680

11. JuelVC, Massey JM. Myasthenia gravis. *Orphanet J rare Dis.* 2007 Nov 06 ;2: 44.

12. Suzuki, NishimotoT, kohnoM, kuwanaM, clinical and immunological predictors of prognosis forjapanese patients with thymoma associated myastgeniagravis. *Jnueroimmunal .*2013 may 15; 258 (1 – 2) 61 – 6.

13. Verchuuren J J, HuijbersMG, PlompJJ,Niks E H ,Molennar PC ,Martinez P ,Gomez AM . Pathophysiology of myasthenia gravis with Antibodies to acetylcholine receptor, Muscle specific kinase.*Autoimmune rev* 2013 july ; 12 (9) : 918 – 23 .

14. I. A. M. Hennessey, A. M. Long, I. Hughes, and G. Humphrey, Thymectomy for inducing remission in juvenile myasthenia gravis.*Pediatric Surgery International.* 2011. vol. 27, no. 6, pp. 591–594.

15. M. Rodriguez, M. R. Gomez, F. M. Howard Jr., and W. F. Taylor, Myasthenia gravis in children: long-term follow-up.*Annals of Neurology.* 1983. vol. 13, no. 5, pp. 504–510.

16. M. M. Tracy, W. McRae, and G. J. Millichap, Graded response to thymectomy in children with myasthenia gravis. *Journal of Child Neurology.* 2009. vol. 24, no. 4, pp. 454–459.

17. C. Schneider-Gold, P. Gajdos, K. V. Toyka, and R. R. Hohlfeld, Corticosteroids for myasthenia gravis.*Cochrane Database of Systematic Reviews.* 2005. vol. 18, no. 2, p. CD002828.

18. H. G. Mertens, G. Hertel, P. Reuther, and K. Ricker, Effect of immunosuppressive drugs (azathioprine). *Annals of the New York Academy of Sciences.* 1981. vol. 377, pp. 691–699.

19. R. Gold, R. Hohlfeld, and K. V. Toyka, Progress in the treatment of myasthenia gravis.*Therapeutic Advances in Neurological Disorders.*2008. vol. 1, no. 2, pp. 36–51.

20. J. Palace, J. Newsom-Davis, and B. Lecky, A randomized double-blind trial of prednisolone alone or with azathioprine in myasthenia gravis, *Neurology.* 1998. vol. 50, no. 6, pp. 1778–1783.

21. Evoli A. Acquired myasthenia gravisin childhood. *CurrOpin Neurol.*2010; 23:536-40.

22. Jaretzki A 3rd, Barohn RJ, Ernstoff RM, Kaminski HJ, Keesey JC, Penn AS, et al. Myasthenia gravis: Recommendations for clinical research standards. *Ann Thoracic Surg*2000; 70:327-34.

Figure I: Anterior posterior view of chest radiograph showing curved spine.

Figure II: Posterior anterior view of chest radiograph showing upper respiratory tract infection.

RESEARCH ARTICLE

A Study to Evaluate the Effectiveness of Sartorius Mobilization with Stretching on Pain among Female Couturiers

S. Senthil Kumar[1] and Natasha Verma[2]*

[1]Professor and Research Supervisor, School of Health Sciences, Department of   Physiotherapy, Garden City University, Bengaluru, Karnataka India.
[2]Assistant Professor, School of Health Sciences, Department of Physiotherapy, Garden City University, Bengaluru, Karnataka, India.

***Address for Correspondence**
Natasha Verma[2]*
Assistant Professor,
School of Health Sciences,
Department of Physiotherapy,
Garden City University,
Bengaluru, Karnataka, India.
E.Mail: vnatasha345@gmail.com

ABSTRACT

The majority of tailors experience pain in the upper arms and lower arms pain as they were exposed to high levels of repetitive tasks and stitching. Prolong sitting and repeated pedaling movements results in pain and discomfort in the lower limb leading to muscular strain. One such muscle involved in repetitive strain due to the pedaling activity is the Sartorius muscle, also known as the tailor's muscle. To assess the effectiveness of Sartorius mobilization with stretching on pain among Female Couturiers. A convenient sample of 30 subjects was solicited. Participants were n=30 and the age range = was 25 - 40 years. Subjects were allocated in two groups. Group A (experimental group) Sartorius Mobilization and Kneeling Stretch along with Hip and knee exercises and Group B (control group) was given hip exercises given for 10 times continuously for 2 weeks. and advice to take hot packs. Each group had a physiotherapist who carried out the interventions. Randomized clinical trial. Numerical pain rating scale. Statistical analysis was done to identify the difference between pre and post-test measurements. The two-tailed p-value is less than 0.0001 by conventional criteria, this difference is considered to be extremely statistically significant. A tailoring occupation makes, repairs, or alters clothing. Due to their prolonged work nature, they tend to have musculoskeletal problems such as joint pain, muscular strain, ligament sprain, and postural deviations. The study concludes that patients with adaptive Sartorius shortening with pain can be reduced by Sartorius mobilization and stretching exercise.

Keywords: Randomized, tailors, Subjects, measurements.

Senthil Kumar and Natasha Verma

INTRODUCTION

According to the Handloom Census 2019-20, about 35,22,512 Handloom workers were employed across the country, out of which 25,46,285 were Women workers with a share of 72.29% of the total handloom workers. In addition, there are around 16,87,534 Women Handicraft artisans registered with the Office of Development Commissioner (Handicrafts)[1]. A preliminary study among the Indian tailor's population found that 79.2% reported musculoskeletal symptoms related to work[2].

Tailoring is an age-old craft that has played a crucial role in the textile industry, providing custom-fit garments to individuals across various cultures and societies. While the profession of tailoring is diverse and encompasses both male and female practitioners, this research focuses specifically on female tailors and the challenges they encounter related to lower extremity problems[3,4]. The main activities performed by the tailors are taking measurements of the customer, cutting the fabric, stitching the fabric, and finishing the stitched garment[4].Female tailors dedicate long hours to their craft, involving activities such as measuring, cutting, and sewing fabric. However, the nature of their work often requires them to assume static, prolonged postures while sitting or standing, which can have adverse effects on their lower extremities. The lower extremities, which include the hips, thighs, knees, and feet, are vital for the mobility and physical well-being of individuals[4]. Given the repetitive and physically demanding nature of tailoring, female practitioners in this field are susceptible to a range of lower extremity problems, which can adversely impact their overall health and quality of life.[5]

One significant lower extremity issue faced by female tailors is musculoskeletal discomfort or pain. The prolonged periods of sitting or standing while working on garments can lead to poor posture and strain on the lower back, hips, and knees. These sustained postures can cause muscle imbalances, joint stiffness, and overall musculoskeletal fatigue, potentially resulting in chronic pain and reduced work productivity[2,5]. Furthermore, female tailors often face challenges associated with foot health. When sitting with their legs crossed to sew, tailors would experience agony along the Sartorius muscle's course. The Sartorius is carried through all of its actions by the motion of crossing its legs, and it is still engaged and active in that position. The Latin word sartor, which means tailor, is where the name of Sartorius's muscle comes from[6]. It was common for tailors to work while sitting cross-legged on the floor, mimicking the shape of the muscle and utilizing one of its functions. The Sartorius's muscle has become adaptively shortened as a result of the prolonged crossing of the legs and continuous, repetitive pedaling actions, which causes pain to radiate from the hip to the leg. This research aims to delve deeper into the challenges faced by female tailors related to lower extremity problems. By shedding light on these aspects, we hope to contribute to the development of targeted strategies and interventions that can alleviate the physical burden experienced by female tailors and enhance their working conditions. [7]

OBJECTIVE OF THE STUDY:

To assess the effectiveness of Sartorius mobilization with stretching on pain among Female Couturiers.

SUBJECTS AND METHODS:

Thirty female tailors who are self-employed were taken up for the studydepending upon the inclusion and exclusion criteria. The inclusion criteria are Female tailors within the age group of20-45 years and pain present along the course of the Sartorius's muscle for at least 3 weeks. NPRS scale of 7 and above were included in the study. The exclusion criteria are Infections, tumors, crush injuries, malunited fractures, muscular insufficiency, deformities, and surgery with metal implantation. Pain intensity was measured by means of the NPRS scale. All the patients were screened and randomized after finding their suitability as per inclusion and exclusion criteria. The numerical Pain Rating Scale (NPRS) where 0 corresponded to "no pain" and 10 corresponded to "worst imaginable pain," was used to measure pain. A randomized trial was designed which included an experimental group and a control group. Group A (experimental group) Sartorius mobilisation and kneeling stretches were given 10 times continuously for 2 weeks. Group B (the control group) in this group was given hip exercises and advice to take hot packs.

PROCEDURE:

The subjects in the experimental group were given sartorius mobilization and active kneeling stretches for the Sartorius musclealong with resisted isometric exercise for the quadriceps muscle and the subjects in the control group were given hip and knee exercises along with hot packs.Pre-test values for NPRS will be recorded. The

intervention will be given for a period of 2 weeks later on which post-test values for pain are recorded. The pre and post-values are recorded for statistical analysis.

PROTOCOL

Group A (Experimental Group)

Sartorius Mobilizations-With the hands, gently press the sartorius muscle in the vicinity of the knot. Begin with light pressure and raise it gradually in accordance with the patient's tolerance. Use a gliding motion to the muscle, moving from knee to hip in a distal-to-proximal path along the length of the sartorius. Make sure the gliding action is pain-free and within the patient's comfort zone as you repeat it multiple times. Kneeling Stretch along with Hip and knee exercises-Kneel with the one-foot level on the floor and the other knee at a 90-degree angle in front. To maintain the balance, lean on a wall for support.Keep the spine upright and the pelvis in a neutral position. While keeping the spine fully erect, lean forward. Keep the pelvis level while pushing it forward. While doing this, clenching the buttock muscles could help to develop a feel for the proper motion.Hold the stretch for 10 to 30 seconds while breathing normally. Then, slowly release the stretch and repeat on the opposite side. Stretch- 3 sets, hold time- 10 to 30 secs. Resisted isometrics of quadriceps- 3 sets, 10 repetitions

Group B (Control)

General hip and knee exercises with hot packs were taken for twoweeks.

RESULTS

The data obtained were tabulated and statistically analyzed. The pre and post-test values for the outcome measures of Pain were calculated and compared. Parametric statistical tests, dependent t-sampletests, and unpaired t-tests were used.

DISCUSSION

Work-related MSDs (WRMSDs) typically arise when there is a mismatch between the physical demands of the job and the human body's physical capabilities, depending on the mechanics, ergonomics, and physical movement characteristics of work tasks[3]. In this study, more emphasis is on the Sartorius muscle as it is the major muscle involved in this profession. Due to its importance, it is known as a tailor's muscle. This Sartorius's muscle tends to go for repeated adaptive shorting due to continuous strain put by repeated pedaling movement and prolonged crossed-leg sitting posture[2,3]. Corrective measures are a must for this rampant problem among thetailors[4]. The study aims in finding the effectiveness of Sartorius muscle mobilization and stretching in reducing pain. The study compared the results of commonly used treatment strategies for patients with adaptive shortness of the Sartorius's muscle. The Numerical pain rating scale was commonly used as an outcome measure in the treatment of Sartorius pain which indicates that the outcome measures are able to detect the changes produced by the treatment[8]. The findings obtained in this randomized controlled study imply that standing Sartorius mobilization and stretch are effective in reducing pain caused by adaptive Sartorius muscle. The results of the present study showed that there was a significant improvement in the experimental group. For the outcome measures NPRS paired t-test analysis showed a significant statistical difference ($p<0.05$) between pre and post-test measurements.The results show that the post-intervention phase NPRS scale 95% confidential interval and a t value is 20.44, standard error of the difference of 0.313.The two-tailed p-value is less than 0.0001 by conventional criteria this difference is considered to be extremely statistically significant. This study concludes to prove the effectiveness of Sartoriusmobilization and stretch for female tailors in reducing pain.

CONCLUSION

Muscle, tendon, and ligament-related physical health issues are referred to as musculoskeletal discomfort. Numerous studies have found that musculoskeletal pain is relatively common among designers. According to the study's findings, tailors have severe musculoskeletal pain at work, particularly in the thigh Sartorius. Repetitive pedaling may cause adaptive shortening. Many of the standard physical therapy procedures work less well here. This study's findings support the use of the Sartorius stretch to relieve pain among female courtiers.

REFERENCES

1. Ministry of Textiles, Govt of India,2022
2. Smrithi A, Pruthviraj R. Prevalence of Musculoskeletal Disorders among Self-Employed Female Tailors in Selected Places of Bengaluru. Indian Journal of Physiotherapy & Occupational Therapy. 2023 Apr 1;17(2).
3. Hagberg C, Silverstein B, Wells R, Smith MJ, Hendrick H, CarayonP, Perusse M. Work related Musculoskeletal Disorders (WRMSDs): a reference book for prevention. London: Taylor&Francis.1
4. Chyuan J-YA, Du C-L, Yeh W-Y, Li C-Y, Musculoskeletaldisorders in hotel restraint workers. Occup Med Oxf Engl. 2004 Jan;54(1):55-7.
5. Jahan N, Das M, Mondal R, Paul S, Saha T, Akhtar R. Prevalence of Musculoskeletal Disorders among the Bangladeshi Garment Workers. SMU Medical Journal. 2015;2(1):102-13.
6. Moore, Keith L.; Dalley, Arthur F.; Agur, A. M. R. (2013). Clinically Oriented Anatomy. Lippincott Williams & Wilkins. pp. 545–546. ISBN 9781451119459.
7. Bulduk S, Bulduk EÖ, Süren T. Reduction of work-related musculoskeletal risk factors following ergonomics education of sewing machine operators. International journal of occupational safety and ergonomics. 2017 Jul 3;23(3):347-52.
8. Dworkin RH, Turk DC, Farrar JT, Haythornthwaite JA, Jensen MP, Katz NP, et al. Core outcome measures for chronic pain clinical trials: IMMPACT recommendations. Pain 2005;113:9–19.

Table.1 Pre-Intervention

SI.No	STATISTICAL MEASUREMENT	GROUP A	GROUP B
1.	MEAN	8.13	8.2
2.	STANDARD DEVIATION	0.74	0.67

Table.2   POST INTERVENTION

SL. No	STATISTICAL MEASUREMENT	GROUP A	GROUP B
1.	MEAN	0.93	5.2
2.	STANDARD DEVIATION	0.45	1.62

Senthil Kumar and Natasha Verma
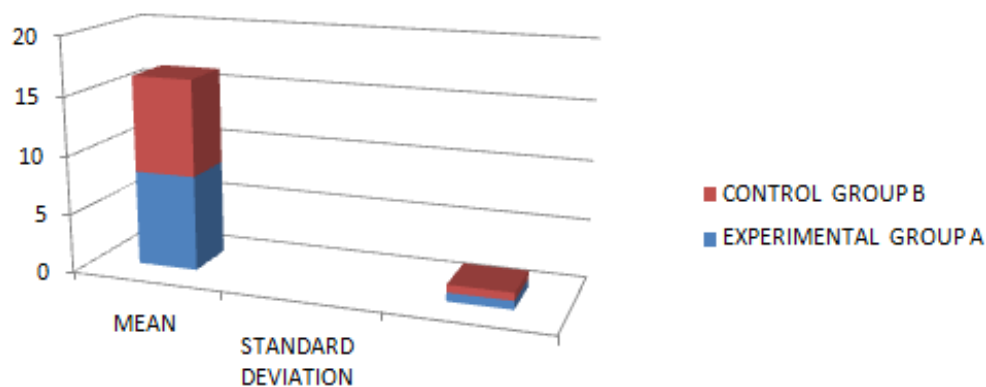
Fig.1 Pre-Intervention Graphical Presentation
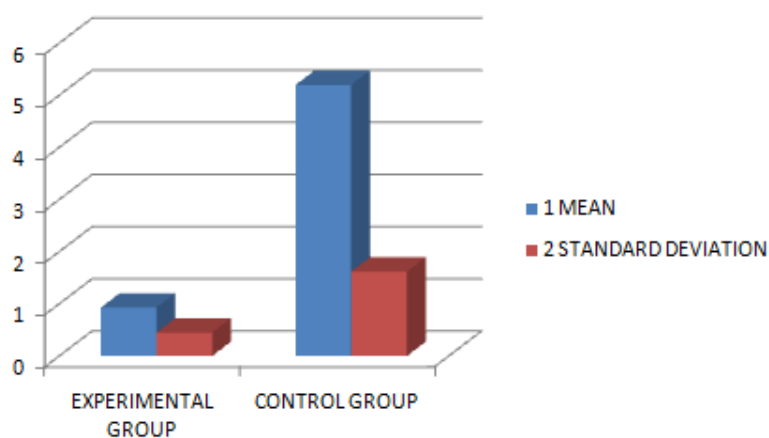
Fig.2 Post-Intervention Graphical Presentation

RESEARCH ARTICLE

The Role of Performance in a Teen's Failure to Excel in Math

R. Prema[1], P. Rajeswari[2], R.S. Sripoorni[3], A. Shanthi[1] and R. Radha[4]*

[1]Associate Professor, Department of Commerce, KPR College of Arts Science and Research, Coimbatore , Tamil Nadu, India.
[2]Assistant Professor, Department of Mathematics, KPR College of Arts Science and Research, Coimbatore, Tamil Nadu, India.
[3] Assistant Professor, Department of Commerce, KPR College of Arts Science and Research, Coimbatore , Tamil Nadu, India
[4]Assistant Professor, Department of Science and Humanities, Karpagam College of Engineering, Coimbatore, Tamil Nadu, India.

*Address for Correspondence
R.Radha
Assistant Professor,
Department of Science and Humanities,
Karpagam College of Engineering,
Coimbatore, Tamil Nadu, India.
E.Mail: radharmat2020@gmail.com&r.radha@kce.ac.in

ABSTRACT

Students can improve their problem-solving skills by strengthening their fundamental knowledge and comprehension of the issue. The purpose of the Mathematical Fineness Camp was to review the fundamental concepts and introduce the approach to problem-based learning with the pupils. The study concentrated on how well fineness camp helped students grasp mathematics. The focus of the study was on how effectively fineness camp assisted kids in understanding mathematics. The Fineness Camp was intended for students who had already taken placement exams. The pre-test and post-test were given to the students every day, before and after the lecture, respectively. To determine the effectiveness of the programme, the research is statistically done in an indirect method. A paired sample t-test was used to check the validity of the hypothesis in light of the different mean values for the pre-test and post-test. The mean value of the study's findings is anticipated to be higher for the post-test than the pre-test.

Keywords: Mathematics Fineness Camp, Paired Sample, Problem Solving, Pre-test and post-test

INTRODUCTION

Surprisingly, this is also apparent in a sense of students enrolled in degree programmes and so therefore students who are perceived to be "talented" in the mathematics domain. From an affective perspective, this issue appears especially intriguing because the students involved frequently experience mathematical failure as a tragedy and, more importantly, struggle to make sense of it at first. For these reasons, it seems essential to look at how emotions are involved in the emergence and management of this crisis, as well as how students' perceptions of mathematics and their own natures change during the tertiary crisis period. The part that emotion plays in pupils' failures in math. Investigating the role emotions play in the emergence and handling of this crisis, as well as how high achiever students' perceptions of mathematics and their own selves change during this crisis time, becomes interesting.

In Arts and Science Institutions offers two programmes namely Department of Commerce (ASCO114) and Department of Computer Science (ASCS110).In addition, a total of seven math chapters were offered to ASCO11 and ASCS110 students. The percentage of failure in math courses in the previous semesters was alarming. Math classes seem to consistently account for the highest number of failures compared to other courses. Figure 1 shows the failure rate for the six mathematics chapters of each program for the semester of June-October 2021. Compared to other courses, mathematics courses appear to be the main reason for consistently high failure rates.

There are three common chapters for both the programmes which are CHAP1, CHAP3 and CHAP5 among sixchapters. Two of these chapters CHAP1 and CHAP3 are prerequisites to others, meaning that students must pass them before enrolling in more advanced courses. Figure 2 compares the failure rates for common subjects in the two programmes. Additionally, it shows that ASCO114 students fail at a higher rate than ASCO110 students. The professors came up with the idea to conduct a "Fineness Camp" mathematical classes to address the high failure rate. We consider that student's weak mathematical foundations are the root cause of the high failure rate.ASCO114students, who are mainly responsible for the high failure rate, were selected for the workshop. These students must repeat CHAP1.Since the programme is a requirement for other advanced mathematics courses like CHAPT3 and serves as the foundation for all other mathematics courses, it was declared mandatory for all repeaters of this subject.

The Fineness Camp took place on January 6 and 7, 2022. The curriculum will be led by experiencedprofessors with more than four years of teaching experience.The Fineness Camp addressed a total of sixchapters. The students took two sets of pre-tests and post-tests to gauge the program's success. On the first day, the first set of pre and post tests, which included three themes, was administered. On the second day, the students received the second set, which had three themes. Table 1 lists the chapters that were tested on both days.

In this work, the paired sample t-test was employed for hypothesis testing. The outcomes are expected to get greater mean vale for post-test than pre-test.

Research Purpose
The goal of this study is to examine the mean value for pre-test and post-test

Hypotheses
H0: Pre and post-mark mean values are equal.
H1: Pre and post-mark mean values are not equal.

Statement of the Problem
This study tries to answer the following research question:
Is there any difference in terms of marks on pre-test and post-test?

Prema *et al.*,

Importance of the study

The "Fineness Camp" was held with the intention of giving the children a foundational understanding of mathematics. In order for the students to improve their foundation at the beginning of the semester, this programme was held during the first week. As a result, they will have a better knowledge of their mathematics classes throughout the semester. Because of this endeavor to lower the failure rate, it is anticipated that the post-test results will have a greater mean than the pre-test.

LITERATURE REVIEW

The ability to solve the problem algebraically is the elementary for all students entering the sciences or social sciences. In order to Fineness Camp and avoid misconceptions in solving mathematical problems, students need to develop their analytical skills during the process of learning (Yin, L. Y, 2005) [1].There are still a few common mistakes in solving mathematical problems. Many researchers are interested in finding out the difficulties that a most students face in solving problem. Gunawardena (2011) [2] found that some students tend to make mistakes in the final step of the equation solving process. According to Nguyen, P. L. and Tran, C. T. H. (2014) [3], types of errors can include faulty calculations, misleading mathematical concepts or theorems, misinterpreted and reckless memory. In the section of the linear equation, research has shown that students tend to use various approaches in problem solving. Lagasse, A (2012) [4] conducted a descriptive study of the various approaches used by college students in solving systems of linear equations problems. There are three types of methods that include substitute method, elimination method and graphing. The results show that most of the students are inclined to use the substitution method, which is easier than other two methods.

In the chapter of indices, there are a few rules and particular cases of indices that students should be aware of. According to Foo, F. Y. et al. (2013) [5], there are five rules and four specific cases in the indices, as can be seen in Tables 2 and 3. The students' common mistakes in fundamental mathematics There are six topics chosen to be used in the "Fitness Camp" as shown in Table 1. For students who take advanced mathematics courses like calculus, the themes cover fundamental concepts in elementary mathematics. These topics are extremely crucial since any false assumptions made in them will result in incorrect interpretation of algebraic problems. Majid,.H (2012) [6] had examined the relationship among different kinds of students mistakes and the knowledge required to solve problems algebraically. His research showed that the inaccuracy was

the primary cause of the majority of student faults. Swedosh,P(1996) [7] stated that the major problematic comes from fallacy. For example, he found that there were students were tested in factorize some mathematics equation such as$(5x + y)^2$- y^2. Around 32% of students were found expanding the equation incorrectly $5x^2$+10xy rather than$(5x + y)^2$- y^2= (5x+y) +y) (5x+y) –y). He also discussed on the common mistakes done by students while simplifying the polynomial. As an instance, the students were asked to shorten$\frac{x^2-4x+4}{x^2-5x-6}$. Those who are weak in mathematics can override identical terms in the numerator and denominator without ending factorization. They found it hard to understand that factorization should be given priority over omission.

In the quadratic chapter, quadratic equations can be solved using either the quadratic formula or factorization, x $=\frac{-b\pm\sqrt{b^2-4ac}}{2a}$. However, a lot of students had gotten the quadratic equation erroneous. The example in thispaper shown that for quadratic equation y^2=1, students gave the incorrect answer y=1 instead of y=±1. Another example is problem solving in the equation of $(y)^2$- y - 2 =0 given one of the   solutions is y =1. Not surprisingly, there are students who still solved it with the wrong approach in which the equation was incorrectly rearranged as $(y)^2$- y = 2 before finding the values of y. Pongchawee, V and Clements, M.A. (2006) [8] has studied on the effects of classroom instruction on students' understanding of quadratic equations.

Prema *et al.,*

Before and after lessons, the same quadratic equations question is presented. The results show that the students who have some concept ideas about quadratic equations prior to the lesson have greatly improved after the lesson.In the chapter of indices, there are some rules and special cases of indices that students should be aware of that, there are five rules and four special cases in indices as shown in Table 2 and Table 3. In Swedosh, P (1996) [9] paper, He identifies some of the common errors with examples like simplifying $3^x \times 3^x$. The correct answershould be 3^{x+x} (or) 3^{2x} but students will give $3^x + 3^x = 6^x$. This completely misunderstands the idea of indices. The same situation happens in the logarithm Table 4 and Table 5.

Many students mistakenly believe that logarithms are objects rather than operations when they use the notation "log". Yen's (1999) [10] report had shown the type of errors made by Australian students in 1998 High school Certificate. Mathematics examination. For instance, some students divided both sides of the equation. In(9x-15) =4 In x by "In" as if it was a variable to obtain 9x-15 = 4x when solving the equation. A study conducted by kaurand Boey (1994) [11] in a junior College in Singapore found that not all students realized that the simplification of log 24-log 4+ log9 = log(24- 4 +9) was incorrect. This error is actually quite common and often called as the linear extrapolation error (Matz, 1980) [12]. For example , when a student asked to solve the equation In(9x-15) =4 In x, the students may solution that In (9x-15) = In 9x -In 15x, Clearly treating "In" as a variable and

distributing it over 9x and 15 (Yen, 1999) [13]. As Harel and Dubinsky (1992) [14],states, work with graphical representations of functions will be affected if students do not understand the language of, domains, images ranges, preimages, and ranges,one-to-one and onto relationships.According to Markovitsal.(1988) [15], Most of students experience very hard with functions because of the symbols. For example, Herscovics (1989) [16] reported that 95% of the students evaluate the expression x+9 when x=3 whereas only 60% of this same group could evaluate g(3) when f(x) = x+7.

METHODOLOGY

The experiment study is to test the effectiveness of "Fineness Camp" inreducing the failure rate for precalculus subject in Arts and Science College. A two-day workshop was conducted due to more failure rate for the subject of precalculus. It includes pre and post-test with six chapters that have been prepared by Mathematics department lectures. The study involved 60 students who are repeating pre-calculus. The test papers were evaluated by the lectures and the marks were classified into grade according to Arts and Science college endexamination standard. Then, the descriptive analysis was used to elaborate the mean and the standard deviation of the marks. The paired t-test was employed to determine whether there was a significant difference between the % marks for the pre- and post-test because it was the same students who provided the percentage marks. For all chapters, the paired t-test was used to evaluate the hypothesis. The alternative hypothesis for the study are:

H1: There is no difference in pre and post-mark in chapter 1
H2: There is no difference in pre and post-mark in chapter 2
H3: There is no difference in pre and post-mark in chapter 3
H4: There is no difference in pre and post-mark in chapter 4
H5: There is no difference in pre and post-mark in chapter 5
H6: There is no difference in pre and post-mark in chapter 6

FINDINGS

The Data collected before and after the test were compiled, which was beneficial for the fineness camp efficacy analysis. Table 6 shows the overall score for both tests in which student scores were categorized into four categories: mediocre, moderate, good and excellent. Table 6 shows that student scores improve after participating in fineness camp. There are 38.33% of students have reached the standard of excellence in post-test compared to the pre-test. It is

followed by good mark of the student, the rate has increased enormously, and there are 46.66% of good students in post-test compared with 21.67% in pre-test. In contrast, there are almost 94% of students fail in the bad and moderate category at the beginning, and the frequency dropped to 6% respectively in the post test.

The table shows the paired sample statistics for the pre-test and post-test marks in six chapters. The lowest average with the average value of 20.00 is found in chapter 3 pre-test implies that students have a very low basic concept of Surds and indices. On the other hand, pre-test of chapter 5 with mean value 50.00 and chapter 2 with the mean value of 42.00 indicated that students have better understanding in solving the equation in one variable and two variable. The chapter of logarithm is still reported having the lowest mean with mean value of 72. 00 in post-test yet the result shows that there is about 52% of improvement after the camp. The greatest mean value is found in chapter 5 post-test with the mean 90.00 and increase 40 % makes it become the highest percentage of increase among six chapters. The figure revealed that the program had strengthened the student's ability to solve one variable and two variables. In the pre-test, the standard deviations are widely scattered compared to the post-test. In general, overall dispersion decreased significantly after the test, with SD values reduced to 20% below.

CONCLUSION

The study strongly indicates that one's success hypotheses and outcome expectations, and in particular the ability to adapt them and acknowledge aspects, are what distinguishes the few who drop out from some who succeed in overcoming the challenges. The result of study viewed that Mathematics camp has positive effect in build-up fundamental Mathematics knowledge. In the pre-test was found that nearly 60% of students were ranked in poor gradeTable 6). Although, the scoreshad highly improved after the camp and the post-test viewed that 41.66% of students were in excellence grade 47% were in good grade and only 6.67% were moderate and only 5% failed.Refer to Table 7, the further analysis on comparison by chapter showed that students were very weak in chapter 3 (Surds and Indices) with the mean value of 20.00. Moreoverpost-test of chapter 3 showed an improvement with the average value of 72.00 increased by 52.00. The average value of six chapters were increased, from 36.66 to75.55.The increasing in the mean valued showed that the students have a better understanding after they attended the camp.The paired t-test result in Table 9 further concluded that there is a significant difference between mean marks of the pre and post-tests for each chapter since all null hypothesis are rejected at 5% significance level. As a result, the statistical analysis may show that educational camps are more successful at enhancing students' comprehension of mathematics. Thus, it would seem that a comprehensive analysis should be conducted into the processes that led to changes in the students' success theories and causal attributions, which highlight the components of one's issues that are within one's control.

REFERENCES

1. Yin, L. Y. Understanding Student's Quadratic Inequality Misconception through an In-Depth Interview. https://paperzz.com/doc/8309931/1-understanding-student-s-quadratic.
2. Gunawardena, E. Secondary School Students' Misconception in Algebra. PhD Theses, University of Toronto, 2011 https://www.semanticscholar.org/paper/Secondary-School-Students.
3. Nguyen, P. L., Tran, C. T. H. 2014. A Survey of 12th Grade Students' Errors in Solving calculus Problems. International Journal of Scientific and Technology Research, 3 (6).
4. Lagasse A, An Analysis of Differences in Approaches to Systems of Linear Equations Problems Given Multiple Choice Answers. Honors Theses, University of New Hampshire, 2012.
5. Foo, F. Y., Azlina, J., Shafaruniza, M., Norzarina, J., Mohammad, N. A. 2013.Intensive Mathematics for Pre-Diploma. ISBN: 978-967-0479-09- 5.
6. Majid, H. et al. 2012. The Relationship between Different Kinds of Students' Errors and the Knowledge Required to Solve Mathematics Word Problems. Bolema, Rio Claro (SP), 26 (42B), 649-665.
7. Swedosh, P. 1996. Mathematical Misconceptions Commonly Exhibited by Entering Tertiary Mathematics

Prema *et al.*,

Students. Technology in Mathematics Education: Proceedings of the 19th annual conference of the Mathematics Education Research Group of Australasia (MERGA).

8. Pongchawee V, Clements, M. A. Mathematical Thinking & Learning: An International Journal , v8 n2 p113-147 2006 https://eric.ed.gov/?id=EJ733810

9. Swedosh, P. 1996. Mathematical Misconceptions Commonly Exhibited by Entering Tertiary Mathematics Students. Technology in Mathematics Education: Proceedings of the 19th annual conference of the Mathematics Education Research Group of Australasia (MERGA). https://www.researchgate.net/publication/4014104_Are_schools_of...

10. Yen, R. 1999. Reflections on Higher School Certificate Examinations: Learning from Their Mistakes, High School Certificate 1998. Reflections, 24(3), 3-8.

11. Kaur, B., Boey, H. P. S. 1994. Algebraic Misconceptions of First Year College Students. Focus on Learning Problems in Mathematics, 16(4), 43 - 58.

12. Matz, M. 1980. Towards a Computational Theory of Algebraic Competence. Journal of Mathematical Behaviour, 3(1), 93 - 166.

13. Yen, R. 1999. Reflections on Higher School Certificate Examinations: Learning from Their Mistakes, High School Certificate 1998. Reflections, 24(3), 3-8.

14. Harel, G., Dubinsky, E. (eds.) Forward to the Concept of Function: Aspects of Epistemology and Pedagogy. MAA Notes 25. Washington (DC): MAA, 1992.https://eric.ed.gov/?id=ED412111.

15. Markovits, Z., Eylon, B., Bruckheimer, M. Difficulties Students have with the Function Concept. In A. Coxford and A. Shulte (eds.) The Ideas of Algebra, K–12.Reston (VA): NCTM, 1988.

16. Herscovics, N. "Cognitive Obstacles Encountered in the Learning of Algebra" In S.Wagner, C. Kieran (eds.) Research Issues in the Learning and Teaching of Algebra. Reston (VA): NCTM, 1989.

17. Baroody, A., Ginsburg, H. 1983. The Effects of Instruction on Children's Understanding of the "Equals" Sign. Elementary School Journal, 84, 199–212.

18. Foo, F. Y., Azlina, J., Shafaruniza, M., Norzarina, J., Mohammad, N. A. 2013.Intensive Mathematics for Pre-Diploma. ISBN: 978-967-0479-09- 5.

19. Gunawardena, E. Secondary School Students' Misconception in Algebra. PhD Theses, University of Toronto, 2011.

20. Harel, G., Dubinsky, E. (eds.) Forward to the Concept of Function: Aspects of Epistemology and Pedagogy. MAA Notes 25. Washington (DC): MAA, 1992.

21. Herscovics, N. "Cognitive Obstacles Encountered in the Learning of Algebra." In S.Wagner, C. Kieran (eds.) Research Issues in the Learning and Teaching of Algebra. Reston (VA): NCTM, 1989.

22. Holly Gritsch de Cordova et al., "Increasing Students' Mathematical Competence by Developing an Interactive Instructional Context for Math 2 and Math 3", FINAL REPORT, June 2005

23. Kaur, B., Boey, H. P. S. 1994. Algebraic Misconceptions of First Year College Students. Focus on Learning Problems in Mathematics, 16(4), 43 - 58.

24. Khairuzaman, K., Suhaila, Z., Khazri, O., Ummu, H. H., Nur Syazwina, M. 2012. Keberkesanan Kem Bahasa Arab dalam Meningkatkan Tahap Motivasidan Keyakinan Pelajar. Persidangan Kebangsaan Pengajaran Dan Pembelajaran Bahasa Arab 2012.

25. Knuth, E. J., Stephens, A. C., McNeil, N. M., Alibali, M.W. 2006. Does Understanding the Equal Sign Matter? Evidence from Solving Equations. Journal for Research in Mathematics Education, 37, 297-312.

26. Lagasse A, An Analysis of Differences in Approaches to Systems of Linear Equations Problems Given Multiple Choice Answers. Honors Theses, University of New Hampshire,2012.

27. Linchevski, L., Williams, J. 1999. Using Intuition from Everyday Life in 'Filling' the Gap in Children's Extension of Their Number Concept to Include the Negative Numbers. Educational Studies in Mathematics, 39, 131 – 147. Ling, S. E., Lai, K. L., Ling, S. C. 2010.

28. Mathematics Camp Model for Primary School. International Conference on Mathematics Education Research 2010 (ICMER 2010), Procedia Social and Behavioral Sciences 8(C) , 248-255.

29. Lorenzo, J. B., Manual, G. 2007. Difficulties in Learning Inequalities in Students of the First Year of Pre-University Education in Spain. Eurasia Journal of Mathematics, Science & Technology Education, 3 (3), 221-229.

30. Majid, H. et al. 2012. The Relationship between Different Kinds of Students' Errors and the Knowledge Required to Solve Mathematics Word Problems. Bolema, Rio Claro (SP), 26 (42B), 649-665.

31. Markovits, Z., Eylon, B., Bruckheimer, M. Difficulties Students have with the Function Concept. In A. Coxford and A. Shulte (eds.) The Ideas of Algebra, K–12.Reston (VA): NCTM, 1988.

32. Matz, M. 1980. Towards a Computational Theory of Algebraic Competence. Journal of Mathematical Behaviour, 3(1), 93 - 166.

33. Mohd Salmi Md Noorani, et al. 2010. Exposing the Fun Side of Mathematics via Mathematics Camp. International Conference on Mathematics Education Research 2010 (ICMER 2010), Procedia Social and Behavioral Sciences, 8, 338-343.

34. Moses, R., Kamii, M., Swap, S.M., Howard, J. 1989. The Algebra Project: Organizing in the Spirit of Ella. Harvard Educational Review 59(4), 423-443.

35. Nguyen, P. L., Tran, C. T. H. 2014. A Survey of 12th Grade Students' Errors in Solving calculus Problems.International Journal of Scientific and Technology Research, 3 (6). Pongchawee Clements, M.A. Mathematical Thinking & Learning: An International Journal . v8 n2 p113-147 2006

36. Soo K. Y., Nor Haniza H. 2004.Analogy as a Tool for the Acquisition of English Verb Tenses among Low Proficiency L2 Learners.English Language Teaching, 7(4).

37. Swedosh, P. 1996. Mathematical Misconceptions Commonly Exhibited by Entering Tertiary Mathematics Students. Technology in Mathematics Education: Proceedings of the 19th annual conference of the Mathematics Education Research Group of Australasia (MERGA).

38. Yen, R. 1999. Reflections on Higher School Certificate Examinations: Learning from Their Mistakes, High School Certificate 1998. Reflections, 24(3), 3-8.

39. Yin, L. Y. Understanding Student's Quadratic Inequality Misconception through an In-Depth Interview. Haselenda Yusop, FooFong Yeng, Azlina Jumadi, Shafaruniza Mahadi, MohanmmaNazir Ali and Norzarina

40. Baroody,A.,Ginsburg,H.1983.TheEffectsofInstructiononChildren'sUnderstandingofthe"Equals"Sign.ElementarySchoolJournal,84,199–212.

41. Foo,F.Y.,Azlina,J.,Shafaruniza,M.,Norzarina,J.,Mohammad,N.A.2013.IntensiveMathematicsforPre-Diploma.ISBN:978-967-0479-09-5.

42. Gunawardena,E.SecondarySchoolStudents'MisconceptioninAlgebra.PhDTheses,UniversityofToronto,2011.

43. Harel,G.,Dubinsky,E.(eds.)ForwardtotheConceptofFunction:AspectsofEpistemologyandPedagogy.MAANotes25.Washington(DC):MAA,1992.

44. Herscovics,N."CognitiveObstacles   EncounteredintheLearningofAlgebra."InS.Wagner,C.Kieran(eds.)ResearchIssuesintheLearningandTeaching of Algebra.Reston(VA): NCTM,1989.

45. HollyGritschdeCordovaetal.,"IncreasingStudents'MathematicalCompetencebyDevelopinganInteractiveInstructionalContextforMath2

46. andMath3",FINALREPORT,June2005

47. Kaur,B.,Boey,H.P.S.1994.AlgebraicMisconceptionsofFirstYearCollegeStudents.FocusonLearningProblemsinMathematics,16(4),43 -58.

48. Khairuzaman, K.,Suhaila, Z., Khazri, O., Ummu, H. H.,NurSyazwina, M. 2012. KeberkesananKemBahasa ArabdalamMeningkatkanTahapMotivasidanKeyakinanPelajar.PersidanganKebangsaanPengajaranDanPembelajaranBahasa Arab 2012.

49. Knuth,E.J.,Stephens,A.C.,McNeil,N.M.,Alibali,M.W.2006.DoesUnderstandingtheEqualSignMatter?EvidencefromSolving Equations.

50. JournalforResearchinMathematicsEducation,37,297-312.

51. Lagasse A, AnAnalysisofDifferencesinApproachestoSystemsofLinearEquationsProblemsGivenMultiple Choice Answers. Honors Theses, University of New Hampshire, 2012.

52. Linchevski,L.,Williams,J.1999.UsingIntuitionfromEverydayLifein'Filling'theGapinChildren'sExtensionofTheirNumberConceptto IncludetheNegativeNumbers.EducationalStudiesinMathematics,39,131–147.

53. Ling,S.E.,Lai,K.L.,Ling,S. C. 2010. Mathematics Camp Model for Primary School. International Conference on Mathematics Education Research 2010(ICMER2010),ProcediaSocialandBehavioral Sciences8(C) ,248-255.

54. Lorenzo,J.B.,Manual,G.2007.DifficultiesinLearningInequalitiesinStudentsoftheFirstYearofPre-UniversityEducationinSpain.EurasiaJournalofMathematics,Science &TechnologyEducation,3(3),221-229.

55. Majid,H.etal.2012.TheRelationshipbetweenDifferentKindsofStudents'ErrorsandtheKnowledgeRequiredtoSolveMathematicsWordProblems.Bolema,RioClaro (SP),26 (42B),649-665.

56. Markovits,Z.,Eylon,B.,Bruckheimer,M.DifficultiesStudentshavewiththeFunctionConcept.InA.CoxfordandA.Shulte(eds.)TheIdeasofAlgebra,K–12.Reston(VA):NCTM,1988.

57. Matz,M. 1980.Towardsa Computational TheoryofAlgebraicCompetence.Journal ofMathematicalBehaviour,3(1), 93-166.

58. MohdSalmiMdNoorani,etal.2010.ExposingtheFunSideofMathematicsviaMathematicsCamp.InternationalConferenceonMathematicsEducationResearch2010(ICMER2010),ProcediaSocialandBehavioralSciences,8,338-343.

59. Moses,R.,Kamii,M.,Swap,S.M.,Howard,J.1989.TheAlgebraProject:OrganizingintheSpiritofElla.HarvardEducationalReview59(4),423-443.

60. Nguyen,P.L.,Tran,C.T.H.2014.ASurveyof12thGradeStudents'ErrorsinSolvingcalculusProblems.InternationalJournalofScientificand TechnologyResearch,3(6).

61. Pongchawee Clements, M.A. Mathematical Thinking & Learning: An International Journal . v8 n2 p113-147 2006

62. SooK.Y.,NorHanizaH.2004.AnalogyasaToolfortheAcquisitionofEnglishVerbTensesamongLowProficiencyL2Learners.EnglishLanguageTeaching,7(4).

63. Swedosh,P.1996.MathematicalMisconceptionsCommonlyExhibitedbyEnteringTertiaryMathematicsStudents.TechnologyinMathematicsEducation: Proceedingsofthe 19th annual conference oftheMathematicsEducationResearchGroupofAustralasia(MERGA).

64. Yen,R.1999.ReflectionsonHigherSchoolCertificateExaminations:LearningfromTheirMistakes,HighSchoolCertificate1998.Reflections,24(3),3-8.

65. Yin, L.Y.UnderstandingStudent'sQuadraticInequalityMisconceptionthrough anIn-DepthInterview.

66. HaselendaYusop, FooFongYeng, AzlinaJumadi, ShafarunizaMahadi, MohanmmaNazir Ali and Norzarina

Table 1: The Fineness Camp contains

TEST	CHAPTER	TITLE	DESCRIPTIONS
Pre and Post Test 1	Chapter 1	Equation, Solving Simultaneous Linear Equation in One variable and two variable	This chapter covered the equation in one variable in finding by using simultaneous method.
	Chapter 2		This chapter covered the equation in two variablein by using Factorization method and quadratic formula
	Chapter 3	Surds and Indices	This chapter covered the rules of indices and solving the surds
	Chapter 4	Probability	This chapter is covered the coin , rolling dice and cards problem
Pre and Post Test 2	Chapter 5	Log	This chapter covered the rules of logarithms question by using the rules and special case of logarithms
	Chapter 6	Simplification	This chapter is covered operations on numerals and the problem by "BODMAS" and Virnaculum rule

Table 2 and Table 3: Rules and Special Cases

Table 2		Table 3	
RULE 1	$b^m \times b^n = b^{(m+n)}$	Special case -1	$b^{-n} = \frac{1}{b^n}$
RULE 2	$b^m \times b^{-n} = b^{(m-n)}$	Special case -2	$b^{\frac{1}{n}} = \sqrt[n]{b}$
RULE 3	$(b^m)^n = b^{(mn)}$	Special case -3	$b^{\frac{m}{n}} = \sqrt[n]{b^m}$
RULE 4	$b^n \times c^n = (bc)^n$	Special case 4	$b^0 = 1$
RULE 5	$b^n \div c^n = (b/c)^n$		

Table 4 & Table 5: Logarithm

	Table 4	Table 5	
RULE 1	$log_a MN = log_a M + log_a N$	Special case -1	$log_a 1 = 0$
RULE 2	$log_a \frac{M}{N} = log_a M - log_a N$	Special case -2	$log_a a = 1$
RULE 3	$log_a M^n = n log_a M$	Special case -3	$log_a M$ is not defined if $M < 0$
		Special case -4	$log_a 0$ is not defined

Table -6: Frequency distribution of before test and after test results

		Before Test		After Test	
Grade	Mark	Frequency	Percentage	Frequency	Percentage
Poor	0-49	35	58.33	3	5.00
Moderate	50-59	11	18.66	4	6.67
Good	60-69	13	21.67	28	46.66
Excellent	80-100	01	3.33	25	41.66
Total		60	100	60	100

Table -7: The paired Samples Statistics of six Chapters

	Pre-test Mark		Post-test Mark	
Chapter	Mean	Standard Deviation	Mean	Standard Deviation
Chapter 1	41.00	20.34	68.3	16.13
Chapter 2	42.00	21.79	73.00	10.87
Chapter 3	20.00	18.37	72.00	12.04
Chapter 4	33.00	22.93	69.00	19.01
Chapter 5	50.33	23.34	90.00	13.88
Chapter 6	34.00	18.07	81.00	13.61
Overall	36.66	2.06	75.55	4.14

Table 9: Paired Sample't' Test

Paired Sample (After-Before) Chapter	Paired Differences (%)		Significance (Two-tailed)
	Mean	Standard Deviation	
Chapter 1	27.3	9.75	.000
Chapter 2	30.8	12.08	.000
Chapter 3	53.4	11.31	.000
Chapter 4	36.4	10.37	.000
Chapter 5	39.4	20.31	.000
Chapter 6	46.8	9.41	.000
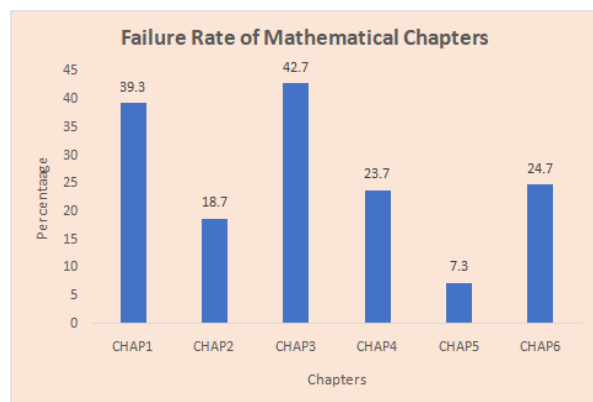
Figure 1: Failure Rate of Mathematic Course
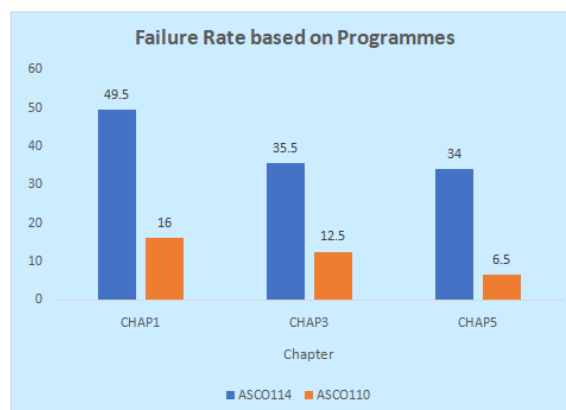
Figure 2: Comparative Failure rate based on Programme

RESEARCH ARTICLE

Losartan Potassium Sustained and Hydrochlorothiazide Immediate Release Formulation Development and Assessment for the Treatment of Hypertension

Bimal Debbarma[1]* and Chandra Kishore Tyagi[2]

[1]Research Scholar, College of Pharmacy, Sri Satya Sai University of Technology and Medical Sciences, Sehore - 466002, Madhya Pradesh, India.
[2]Principal, College of Pharmacy, Sri Satya Sai University of Technology and Medical Sciences, Sehore - 466002, Madhya Pradesh, India.

*Address for Correspondence
Bimal Debbarma[1]*
Research Scholar,
College of Pharmacy,
Sri Satya Sai University of Technology and Medical Sciences,
Sehore - 466002, Madhya Pradesh, India.
E.Mail: bimald32@gmail.com

ABSTRACT

The development of sustained release and immediate release formulations for a single medicine or drug combination uses the technique of region selective dual components. The preparation of dual components of hydrochlorothiazide and losartan potassium in distinct layers for desired release patterns was the major goal of the current study activity. Preformulation studies were performed before compression. The microbeads underwent tests for in-vitro drug release, swelling index, and drug entrapment effectiveness. Using ATR and DSC, tests on the compatibility of drug excipients were conducted. Spectra showed that no interactions between the formulation's excipients and the medications were discovered. According to all pre-compression studies, the outcomes were found to be within the established limitations. According to in-vitro release experiments, the losartan potassium sustained release layer reached 99.14% after 12 hours and the hydrochlorothiazide quick release layer reached 98.41% within 120 minutes. After being exposed to accelerated conditions for a month, stability analyses for both physical properties and in-vitro drug release experiments revealed no alterations despite the release kinetics showing strong linearity and best fitting into the Higuchi model. According to the aforementioned study, the region-selective dual component capsule created met the goal of the research work in treating hypertension.

Keywords: Hydrochlorothiazide, Losartan potassium, Sodium alginate Crospovidone, Ionotropicgelation, Dry granulation, Simultaneous Estimation, UV spectrophotometry.

Bimal Debbarma and Chandra Kishore Tyagi

INTRODUCTION

Hypertension is one of the most common disorders affecting humans throughout the world. It is a chronic medical disorder in which the blood pressure in the arteries is chronically increased. It is also referred to as high blood pressure or arterial hypertension. Systolic and diastolic pressures, which correspond to the arterial system's maximum and minimum pressures, are the two measurements used to express blood pressure. The left ventricle is most contracted during the systole; the left ventricle is most relaxed before the next contraction during the diastole. The term "abnormally high blood pressure" is exceedingly arbitrary and difficult to define. Because the risk to a specific patient may correlate with the degree of hypertension, a threshold for high blood pressure must be agreed upon in clinical practice for screening individuals, implementing diagnostic evaluations, and starting therapy. Thus, there is a need to create practical plans to enhance management.[1,2]

Signs and Symptoms of Hypertension
A severe headache, exhaustion or confusion, visual issues, breathing difficulties, chest discomfort, an irregular heartbeat, blood in the urine, and a pounding in the chest, neck, or ears are some more symptoms that may occur.

Hypertension risk factors
There are a number of illnesses and circumstances that may raise the risk, despite the fact that the precise aetiology of hypertension (high blood pressure) is unknown. They include being overweight and obese, smoking, doing little to no exercise, eating too much salt, drinking too much alcohol, being stressed, having a black ancestry (of African, Caribbean, or South Asian descent), and having a family history of high blood pressure.

Management of Hypertension
Monotherapy
The usual approach for controlling hypertension for many years has been mono medication treatment. Yet, 50 to 60 percent of people who utilize a single medication to regulate their blood pressure are effective in doing so. The routine rise in the dosage of the only medication provided, which results in protracted therapy with high doses and, consequently, an increase in adverse effects, is one factor contributing to the low success rate. In result, patients stop complying. One medicine only tackles one of the various physiological pathways that contribute to hypertension, which is another factor in the inability to manage blood pressure. The pathophysiology of hypertension involves a number of processes. In general, monotherapy will only disrupt one of these pathways, perhaps allowing the other mechanisms to make up for it. Hence, combined therapy is more effective because hypertension is a multifactorial illness. [3]

Combination Therapy
The fundamental effects of pharmaceuticals working through several mechanisms are brought into play by combining two medications from the right classes of drugs, which also work to counter the homeostatic compensations that prevent a blood pressure drop. Combination therapy may be advantageous since it interferes with pathogenetic pathways synergistically. As a result, the issue of dose-dependent side effects is reduced and lower doses can be used. Combination therapy is further justified by the fact that chronic high blood pressure frequently results in heart, renal, and brain problems. Angiotensin-converting enzyme inhibitors (ACE inhibitors), for example, have an effect on target organ illness independently of their antihypertensive effects. Due to the potential stimulation of compensatory mechanisms working to return blood pressure to its predetermined values, the antihypertensive efficacy of a single medication is frequently decreased. Combination therapy enables the administration of lower doses of each antihypertensive drug; as a result, compensatory stimulation may be reduced. The second antihypertensive drug in the combination may, theoretically, counteract this stimulation.

Drugs used for the marketed product

Diuretics, also known as "water pills," caused the kidneys to expel more sodium and water through the urine. They are believed to reduce blood pressure mostly by decreasing the amount of fluid in blood vessels.[3,4]

SIMULTANEOUS ESTIMATION

Pharmaceutical dose forms that combine two or more medications are extremely helpful for a variety of therapy. To maintain the safety and effectiveness of pharmaceutical products throughout their shelf life, including during storage, distribution, and usage, analytical monitoring of the products' individual constituents is required. [5]Because of its patient acceptance, convenience of administration, correct dosing, cost-effective production processes, and stability when compared to other dosage forms, the oral route of drug administration may be the most alluring option for the delivery of pharmaceuticals. Over monotherapy, combination therapy has a number of benefits. The danger associated with dosage was lowered by combining two separate drugs at a low dose; this also minimizes the clinical and metabolic side effects that result from using individual components at their maximum dosage.

SUSTAINED RELEASE DRUG DELIVERY SYSTEM

Because of its unit dosage form, low cost, and straightforward packing, oral drug delivery offers the greatest active surface area of any drug delivery system for the administration of a variety of medications, making it the most popular and practical route. By localizing the drug to the site of action, lowering the dosage needed, and ensuring uniform drug distribution, sustained or controlled delivery systems are intended to decrease the frequency of dosing or increase the effectiveness of the treatment. A modified drug delivery system called a sustained release system can be utilized as an alternative to a traditional medication delivery system. These systems continue the drug release, keep the plasma drug concentration within the therapeutic window, barring any fluctuations, and improve the drug's therapeutic effectiveness. Patient compliance, eliminating numerous doses, raising plasma drug concentration, preventing side effects, and resolving issues with the conventional method are only a few advantages of a sustained release system.[6]

Controlled drug delivery dose systems.

The main goal of therapy is to achieve a steady state blood level that is therapeutically effective and nontoxic for an extended duration. Creating effective dose regimens is a crucial step in achieving this objective. Due to increased design freedom for dosage forms, the oral route of administration for sustained release systems has drawn considerable attention. Several linked and significant factors, including the type of delivery system, the disease being treated, the patient, the length of therapy, and the characteristics of the drug, affect how oral sustained release delivery systems are designed.**[7]**

Limitations

- An active chemical can be maintained on its own if its half-life is long (over six hours).
- Slow release serves no purpose if the pharmacological activity of the active ingredient is unrelated to its blood levels.
- The creation of a time-release product may be difficult if the active compound's absorption includes active transport.
- Lastly, if the active ingredient has a short half-life, a considerable quantity would be needed to maintain a sustained effective dose. To prevent toxicity in this situation, a wide therapeutic window is required; otherwise, the risk is unnecessary, and a different form of administration would be advised.
- Lower small intestine cannot adequately absorb it.[8]

Why Sustain Release Matrix Drug Delivery Systems Were Created?

- To prolong the time the medicine will be effective.
- To reduce variations in plasma level.
- Increased drug usage.
- To provide consistent drug delivery while reducing the frequency of dose.

Bimal Debbarma and Chandra Kishore Tyagi

● To use an unique drug delivery mechanism to change the pharmacokinetics and pharmacodynamic characteristics of pharmacologically active components. [9]

Factors Affecting Oral Sustained Release Dosage Form Design
Biological half-life
Because to the potential reduction in dose frequency, medications with a biological half-life of 2 to 8 hours are thought to be excellent candidates for sustained release dosage forms.

Absorption
Drugs that are absorbed by active transport are only absorbed in the intestine, and the rate of absorption of a sustained dose is dependent on the drug's release rate constant from the dosage form.

Distribution
It lowers the level of medication in the blood, but it also has the potential to be rate-limiting in its equilibrium with blood and extravascular tissue. As a result, the apparent volume of distribution takes on varying values depending on how the drug is degraded over time.

Metabolism
Prior to converting into another form, the metabolic conversion to a medication must be taken into account. A successful sustain release product can be created as long as the location, rate, and extent of metabolism are known.

Drug Properties Relevant to Sustain Release Formulation
Dose size
The maximum dose for a typical dosage form is 500–1000 mg. Due to the narrow therapeutic range associated with the administration of large doses, dose size consideration serves as a criteria for the safety involved.

Ionization, pKa, and aqueous solubility
Most medications are weak acids or bases that must dissolve in the aqueous phase surrounding the delivery site before partitioning into the absorbing membrane in order to be absorbed.

Partition coefficient
Because the biological membrane is lipophilic and the transport of pharmaceuticals over the membrane depends heavily on the partition coefficient of the drug, the partition coefficient has a significant impact on a drug's bioavailability. Since they will be localised in the aqueous phase, drugs with lower partition coefficients are thought to be poor candidates for the sustain release formulation.

Drug stability
Enzymatic degradation and acid-base hydrolysis occur with medicines taken orally. A drug release mechanism that delivers medication over an extended period of time is desirable if the substance is unstable in the stomach. [10]

Methods to achieve oral sustained drug Delivery
They include soft gelatin depot capsules, drug complexes, repeat action, ion exchange resin, fat embedment, plastic matrix, barrier resin beads, and hydrophilic matrix. [11]

IMMEDIATE RELEASE DOSAGE FORM
Any pharmaceutical formulation that does not purposefully or noticeably use galenic adjustments to slow down the rate of drug release from the formulation or absorption is considered to be a "immediate release" formulation. In this instance, the quick release may be achieved using suitable diluents or carriers that are pharmaceutically acceptable and do not appreciably slow down the rate of drug release and/or absorption. Hence, the phrase does not include drug formulations that have been adjusted, controlled, sustained, prolonged, extended, or postponed.[12]

Bimal Debbarma and Chandra Kishore Tyagi

Immediate Release Medication Delivery System Benefits
- Increased convenience and improved compliance.
- Increased steadiness.
- Appropriate for actives with regulated or sustained release.
- Permits heavy drug loading.
- The capacity to deliver liquid therapeutic benefits in the form of a solid formulation.
- Adaptable and compatible with current packaging and processing equipment.
- Economical.

Desired Criteria for Immediate Release Drug Delivery System
- If the dosage is solid, it should quickly dissolve or disintegrate in the stomach.
- It should be suitable with flavour masking in the case of liquid dose form.
- Be transportable without posing a fragility risk.
- Feel good in the mouth.
- It shouldn't leave any or very little tongue residue after being taken orally.
- Be inexpensively produced utilising standard processing and packaging machinery.
- Quick medication breakdown and absorption, which could result in a quick start to action.
- Display little sensitivity to changes in temperature and humidity. [13]

Conventional Technique used in the Preparation of Immediate Release Tablets:
Techniques for making tablets include tablet Moulding, direct compression, wet granulation, bulk extrusion, and solid dispersions. [14]

MICROBEADS
Microbeads are small, solid, free-flowing particulate carriers that contain dispersed drug particles in crystalline or solution form and provide multiple release profiles or sustained release for the safe administration of a range of active pharmaceutical ingredients. Compared to monolithic formulations, microbeads offer superior control over the release of the active components. Because it takes time for food to travel through the intestinal tract when taken orally, the release of microbeads is less impacted by the presence of food.Microbeads are homogeneous polymer particles that range in size from 0.5 to 1000 m. biological components like cells, proteins, or nucleic acids can be separated using bio-reactive chemicals that have been adsorbed or linked to their surface. These are small, solid, free-flowing particulate carriers that contain dispersed drug particles in crystalline or solution form and enable multiple release profiles or prolonged release of treatment with different active agents without experiencing severe side effects.[15]When compared to non-disintegrating single-unit dosage forms, multiple-unit dosage forms, such as microspheres or microbeads, have gained popularity as oral drug delivery systems due to more uniform drug distribution and absorption, decreased local irritation, and elimination of unintended intestinal retention of polymeric material.

The microbeads disperse the active substance via two different mechanisms: diffusion and/or polymer biodegradation. In place of traditional injectable formulations, microbeads can be applied topically, parenterally, or orally. The effectiveness of these Innovative DDS is constrained by their brief stay at the site of absorption, though. Hence, it would be useful to have methods for enabling close contact between the DDS and absorbent membranes. It can be done by creating new delivery methods known as "microbeads" and combining mucoadhesion features to mucoadhesive microbeads.[16]The most popular and quickly evolving technology for controlled medication delivery systems right now is microbeads. Because of the convenience of administration and high levels of patient compliance, it is one of the handy dosages that is more beneficial. It is more cost-effective and uses different polymers to construct medications for sustained release or activity, which increases some drugs' bioavailability. [17]Moreover, they can combine medications to deliver locally at high concentrations, ensuring that therapeutic amounts are achieved at the target site while minimizing side effects by maintaining low systemic concentration. They also sustain functionality under physiological settings. The microbeads are made of a variety of polymers,

Bimal Debbarma and Chandra Kishore Tyagi

including binding substances like gelatin, chondroitin sulphate, and avidin in a specified ratio, cationic polymers like chitosan, anionic polymers like sodium alginate, and cationic polymers like chondroitin sulphate. [18]

Hydrogel beads or Hydrocolloids
A controlled release drug delivery system's primary goal is to maximise a medication's biopharmaceutical, pharmacokinetic, and pharmacodynamic qualities so that it can be used as effectively as possible to regulate conditions quickly and with the least amount of the drug. Moreover, it offers stable drug levels in the blood with less frequent dosage and less side effects, improving patient compliance and reducing negative drug effects. These systems divide the drug dosage into a number of subunits, which are typically made up of thousands of spherical particles with a specific diameter range. These subunits are combined or compressed into a tablet, sachet, or capsule to produce the recommended total dose.[19]When water is added to hydrophilic polymers derived from plant, animal, microbial, or synthetic sources, hydrocolloids are created, which equally spread as minute particles. The polymers entangle with one another at sufficiently high concentrations, generating loose networks that alter the rheological characteristics of solutions. By forming hydrogen bonds within and between polymers, several hydrocolloids, including pectin and gelatin, can also gel. In comparison to other sustained release formulations, formulations based on hydrocolloids may have various advantages. Additionally, because different hydrocolloids behave differently in different areas of the gastrointestinal tract due to factors including swelling in water, pH level, and enzyme activity, their stability and physical qualities (dimensions, strength, etc.) might vary. Modifications in the formulations' physical characteristics may also result in distinct drug-release patterns in various regions of the gastrointestinal tract, offering a variety of potential drug carriers. [20] Additionally, the processes involved in creating hydrocolloid formulations are typically fairly straightforward, and the components themselves are inexpensive. Hydrogel beads are hydrocolloid polymer-based beads that range in size from 0.2 to 3 mm and are primarily spherical to provide the appropriate eye appeal, release qualities, or technical requirements in general.
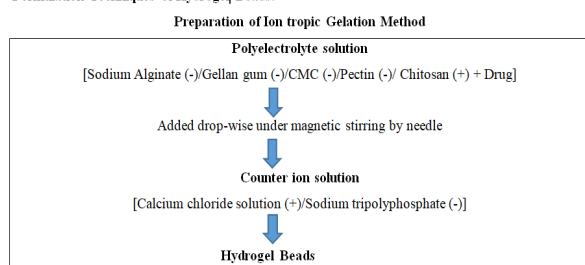
Formulation Techniques of Hydrogel Beads:
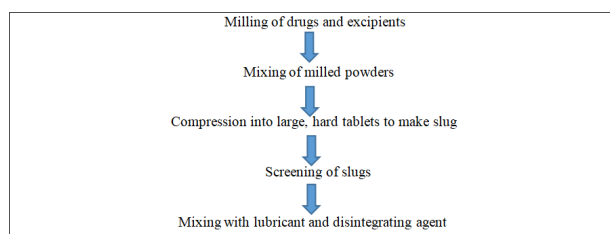Figure 3: Schematic representation of the preparation of hydrogel beads by Ionotropic gelation method. Figure 4: Schematic representation and diagram of the preparation of hydrogel beads by Ionotropic gelation and polyelectrolyte complexation.

Polyelectrolyte complexation
By using the polyelectrolyte complexation method, the quality of hydrogel beads produced by the ionotropic gelation method can be significantly enhanced. The addition of polyelectrolytes with opposing charges to the ionotropically gelated hydrogel beads can increase the mechanical strength and permeability barrier of hydrogels. For example, the presence of polycations enables the formation of a membrane of polyelectrolyte complex on the surface of alginate beads.

Syringe dropping /extruding method
By adding an aqueous solution of poly anion solution into a solution of cation, often calcium chloride, the hydrogel beads can be made in large quantities. While getting particulate drug carriers in this fashion is quick and easy, there is a significant risk of drug loss during formation. In the core of soluble pharmaceuticals, the matrix created is typically relatively porous and the ability to control drug release is minimal at best. As a result, it has been suggested that these hydrogel beads be used preferentially in the administration of medications with limited solubility or small molecular size.

Air atomization method
Furthermore, beads can be made using an air atomization system or a vibration system. A vibration system or an air atomization technique can be used to extrude the poly anion solution, resulting in the formation of relatively smaller droplets. In the latter, compressed air is supplied into a "Turbotak air-atomizer" to mix with the poly anion solution and force tiny liquid droplets out through the nozzle opening. On contact, the cations create micro gel droplets by

Bimal Debbarma and Chandra Kishore Tyagi

cross-linking the droplets of poly anions, which are then further cross-linked by poly electrolytes, such as poly-L-lysine, to form a membrane.[15]

Factors Affecting Ionotropic Gelation Method
Polymer and cross linking electrolyte concentration
The concentration of the polymer and electrolyte plays a significant role in the ionotropic gelation method's formulation of beads. Both should be concentrated in a ratio determined by the quantity of cross-linking units. The type and concentration of electrolytes have an impact on the percentage of entrapment efficiency.

Temperature
The curing period, or the amount of time needed for cross-linking, as well as the size of the beads produced by the ionotropic gelation process, are both significantly influenced by temperature.

pH of cross linking solution
The pH of the cross-linking solution must be taken into account during formulation because it has an impact on the reaction's pace as well as the size, shape, and shape of the beads.

Drug concentration
Since the drug concentration significantly affects the efficiency of the entrapment, the drug to polymer ratio in the beads needs to be accurate. The gel spheres may burst if the ratio is too high, increasing both their density and size and form.

Gas-forming agent concentration
The formulation is modified to create porous gel spheres, which have a significant impact on the size and shape of the gel sphere. Gas-forming substances like calcium carbonate and sodium bicarbonate are added to the formulation.[21]

GRANULES
Excipients and other drug ingredients are among the many components of solid dosage forms that go through various production procedures before becoming the finished product. The pharmaceutical industry utilises granulation techniques to enlarge and densify small powder particles into bigger ones that increase powder flow without segregation so that the material can be processed effectively and efficiently into solid dosage forms. Wet granulation and dry granulation are the two granulation techniques used in pharmaceutical production. In the dry granulation process, a pressure-induced agglomeration technique, granules are prepared with acceptable flowability, compaction properties, compositional uniformity, and chemical stability, particularly for moisture and heat-sensitive drug formulations. Roller compaction is one of the unit operations in this process. The dry powders of the active ingredient and excipients, such as dry binders, disintegrants, diluents, and lubricants, are combined in a blender during the dry granulation process. The powder combinations are then decreased in size and roller compressed to create granules.

Ideal characteristics of granules
The optimal granule properties include being typically spherical in shape, having a smaller particle size distribution with enough fines to fill the spaces between the granules, having acceptable moisture (between 1-3%), having good flow, having good compressibility, and having enough hardness. The size of the drug and excipient particles, the kind of binder (strong or weak), the volume of the binder (less or more), the length of the wet massing time (less or more), the amount of shear used, and the rate of drying all affect how well a substance is granulated (Hydrate formation and polymorphism). [22]

Granulation method
Wet granulation
Just wet massing the powder mixture with a granulating liquid, wet sizing, and drying constitute the wet granulation process.

Disadvantages:
- Labor, space, time, specialized equipment, and energy requirements all add to the cost of the process.
- The process becomes more complex as a result of the numerous processing steps.
- Material loss at different processing phases.
- Drugs that are thermolabile and moisture-sensitive are not good candidates.
- Any compatibility issues among the formulation's ingredients are made worse during processing.

Dry granulation
The powder combination is crushed without the use of heat or a solvent during the dry granulation process. It is the least preferable granulation technique. Compressing a material to create a compact, and then milling that compact to create granules, are the two fundamental processes. There are two approaches to dry granulation. Slugging, in which the powder is precompressed and the resulting tablet or slug is ground to produce the granules, is the more popular technique. The alternative method involves utilising a device like a Chilosonator to precompress the powder using pressure rolls.

Disadvantages:
- To create a slug, a heavy-duty tablet press is needed.
- It is not capable of achieving the same level of colour distribution as wet granulation, where the dye can be mixed with the binder liquid.
- The method often produces more dust than wet granulation, which raises the risk of contamination.[23,24]

SUPERDISINTEGRANTS
Mechanism of Action of Super disintegrants
Super-absorbing materials with specially designed swelling qualities are what superdisintegrants are. They are not intended to absorb a lot of water or other aqueous fluids, but rather to swell quickly. Superdisintegrants are typically used to make disintegrable solid dose forms less structurally rigid. They are physically scattered throughout the dosage form's matrix and will enlarge when it is exposed to a moist environment. These more recent compounds have increased mechanical strength and disintegration efficiency, making them more efficient at lower concentrations. Five major mechanisms for tablet disintegration are as follows-

Swelling
Certain disintegration substances, like starch, are thought to transmit the dissolving action by swelling. The adhesiveness of other substances in a tablet is defeated by swelling when in contact with water, causing the tablet to crumble.

Porosity and Capillary Action (Wicking)
Efficient disintegrants that transmit their disintegration effect by capillary and porosity action cannot swell. Tablet porosity creates passageways for liquid to enter tablets. The low cohesion and compressibility of the disintegrant particles themselves act to increase porosity and provide these entryways into the tablet. By capillary action, the liquid is drawn up or "wicked" into these routes, where it breaks the bonds between the tablet's particles and disintegrates them. For instance, crospovidone and croscarmellose sodium.

Deformation
The prevailing consensus is that starch grains have a "elastic" character, meaning that when pressure is applied, the grains will distort but will immediately return to their former shape. Yet, these grains are reported to be "energy

Bimal Debbarma and Chandra Kishore Tyagi

rich" and to be permanently distorted as a result of the compression forces used in tableting. This energy is said to be released upon contact with water. As comparison to starch grains that have not been distorted by pressure, "energy rich" starch grains have a larger capacity to swell.

Repulsive forces
This disintegration mechanism explains why a tablet manufactured with "non swellable" disintegrants swells. Based on the finding that non-swelling particles also contribute to the disintegration of tablets, Guyot Hermann proposed the particle repulsion theory. The mechanism of disintegration is the electric repulsive interactions between particles, and water is necessary for it.

Enzymatic Reaction
The body's natural enzymes also function as disintegrants. These enzymes aid in disintegration and eliminate the binding action of the binder. The swelling causes pressure to be applied in the tablet's outer direction, which causes it to rupture, or the water's rapid absorption generates a huge rise in the amount of granules, which encourages disintegration.[25,26]

MATERIAL AND METHODS

Drugs and chemicals
Losartan Potassium was procured from Embiotic Laboratories Ltd., Bengaluru and Hydrochlorothiazide was procured from Centurion Laboratories, Gujarat. Polymers and other excipientssuch asSodium Alginate, Chitosan, Cross Povidone, Starch, Acetic Acid, Calcium Chloride, Lactose Monohydrate, Magnesium Stearate, Talc, Sodium Hydroxide,Potassium Dihydrogen Orthophosphate, Potassium Chloride, Hydrochloric Acid are purchased from S.D. Fine Chem. Ltd., Mumbai.

METHODS

PREFORMULATION STUDIES
Determination of Melting Point
A small amount of the drug sample was placed into a capillary tube that had been previously sealed at one end, kept in the digital melting point apparatus, and the temperature range where the drug melted was noted. This method was used to determine the melting points of losartan potassium and hydrochlorothiazide. Three readings were taken, and the mean was noted.

Drug excipients compatibility studies
ATR and DSC tests were utilised to choose appropriate chemically compatible excipients since they can be used to study any physicochemical interaction between components in a formulation. [27]

Attenuated Total Reflectance (ATR)
With the use of the sampling method known as attenuated total reflection (ATR), materials can be studied immediately in their solid or liquid states without the need for any additional preparation.Total internal reflection, which produces an evanescent wave, is a quality used by ATR. An infrared laser beam is directed through the ATR crystal so that it bounces off the interior surface in contact with the sample at least once. The evanescent wave that penetrates the sample is created by this reflection.

Procedure
An IR spectrum was taken to verify the consistency of the pure drug and the physical combination of the pure drug and excipient. An ATR spectrophotometer made by Shimadzu was used to obtain the spectra.A peak was seen after a small amount of pure medicines, polymers, and physical mixes were inserted in the testing chamber.[28]

Differential Scanning Calorimetry:

An IR spectrum was taken to verify the consistency of the pure drug and the physical combination of the pure drug and excipient. An ATR spectrophotometer made by Shimadzu was used to obtain the spectra.A peak was seen after a small amount of pure medicines, polymers, and physical mixes were inserted in the testing chamber.[29]

ANALYTICAL METHODS

Preparation of Standard Solution
Losartan Potassium
Hydrochlorothiazide

Determination of analytical wavelength of Drugs
CX = [(QM – QY) / (QX -QY)] × A1/aX1 (1) CY = [(Qx-Qm)/(Qx-Qy) × A1/ay1 (2)

Losartan potassium and Hydrochlorothiazide
Due to their common aromatic or double-beam composition, the majority of medicines absorb light in the UV area (200 nm–400 nm). Using a Double-beam beam UV spectrophotometer, a solution containing 20 g/ml of losartan potassium and hydrochlorothiazide in buffers with pHs of 1.2 and 7.4 was prepared. The solution was then scanned across the range of 200 nm to 400 nm against the buffers with pHs of 1.2 and 7.4 as a blank. The highest peak that could be measured was designated as λ max.

Simultaneous Estimation of LP and HCTZ in Acidic & Phosphate Buffers
On a UV spectrophotometer, known quantities of solutions containing hydrochlorothiazide and losartan potassium were scanned.Quantitative estimation of LP and HCTZ was carried out by solving the following simultaneous equations:

$$Cx = \frac{Qm - Qy}{Qx - Qy} \times \frac{A1}{ax1} \quad X \quad Cy = \frac{Qm - Qx}{Qy - Qx} \times \frac{A1}{ay1}$$

$$\text{Where,} \quad Qm = \frac{A2}{A1}, \quad Qx = \frac{ax2}{ax1}, \quad Qy = \frac{ay2}{ay1}$$

Where, A1 and A2 were the absorbances of the sample at 257 nm and 272 nm respectively, ax1 and ax2 were the absorptivities of sample 1 at 257 nm and 272 nm respectively and ay1 and ay2 were the absorptivities of sample 2 at 257 nm and 272 nm respectively.[31]

Method of Preparation of Microbeads
Figure11: Flow diagram for the preparation of hydrogel microbeads containing losartan potassium.

PREPARATION OF IMMEDIATE RELEASE GRANULES
In this work hydrochlorothiazide containing an immediate release, granules were prepared by dry granulation technique using crospovidone as super disintegrants

EVALUATION PARAMETERS OF FORMULATED MICROBEADS

Determination of Yield Value

It can be calculated by using the following formula:

$$\text{Percentage Yield} = \frac{\text{Weight of microbeads}}{\text{Weight of drug} + \text{Weight of polymer}} \times 100\,\%$$

Determination of Particle Size

The size of each division of the eyepiece micrometer was determined by using the following formula:

$$\text{Size of each division} = \frac{\text{Number of the division of stage micrometer}}{\text{Number of the division of eyepiece micrometer}} \times 100$$

Surface Morphology

Scanning electron microscopy was used to examine the microspheres' exterior and internal features (SEM). The powder was sparingly sprinkled on a double adhesive tape that was fastened to an aluminum stub to create the samples for SEM. Then, using a gold sputter module in a high-vacuum evaporator, the stubs were coated with gold to a thickness of around 300 while being exposed to an argon environment. A scanning electron microscope was used to acquire photomicrographs of the coated samples after they had been randomly scanned (Jeol JSM-1600, Tokyo, Japan).

Estimation of Drug Content

Losartan potassium-loaded microbeads that were precisely weighed at 50 mg equivalent weights were left in a 7.4 buffer solution overnight. A magnetic stirrer was used to combine the solution. Using a double-beam UV spectrophotometer, the drug content was evaluated following the appropriate dilution (Shimadzu, UV-1700) .[35]

In-vitro Swelling study

Because swelling in the case of hydrogels is directly proportionate to the release of the drug, the behavbehavioriour of the hydrogels affects how the drug is released from its entrapment. The network's pores open when the hydrogel swells, allowing the trapped solute to escape. The produced beads were therefore studied for dynamic swelling. Mass measurement can be used to examine the prepared bead's swelling behavior.

Procedure

Figure 13. Procedure of swelling study

'The swelling index was calculated using the following equation:

$$Q = [(W2-W1)/W1] \times 100$$

Where, Q = percentage of swelling

W1 = mass of the dry beads

W2 = the mass of swollen beads.

In-vitro Dissolution Studies

Using the dissolving apparatus USP XXII, dissolution studies were conducted (Electrolab). Drug-loaded microbeads equivalent to 50 mg of the drug were introduced into the 900 ml of acidic buffer pH 1.2±0.1 for initial 2 hours and in phosphate buffer pH 7.4±0.1 up to 12 hours. The medium was maintained at 37±2ºC at 50 rpm. At regular intervals up to 12 hours, 5ml aliquots were taken out and spectrophotometrically measured at 257nm using a UV 1700, made by Shimadzu in Japan. For each formulation, three trials were run. In order to keep the sink condition throughout the experiment, an equivalent volume of new dissolving media was substituted. Simultaneous equations can be used to compute the dissolution studies profile.[36]

Bimal Debbarma and Chandra Kishore Tyagi

Release Kinetics of Microbeads

The results of in-vitro release data were plotted in different kinetic models, such as zero order, first order, Higuchi model, Korsmeyer-Peppas equation, and Hixson-Crowell model, to examine the process of drug release from the microbeads. [37]

Zero-order kinetics

Cumulative percent drug released versus time. It can be predicted by the following equation.

$$At = A_0 – K_0 t$$

Where, At = drug release at time 't'

A_0 = initial drug concentration.

K_0 = Zero-order rate constant (hr-1)

First order kinetics

Log cumulative percent drug remaining versus time. A first-order would be predicted by the following equation.

$$Log\ C = Log\ C_0 – 303.2Kt$$

Where, C = amount of drug remained at time 't'

C_0 = initial amount of drug.

K = first-order rate constant (hr-1)

Higuchi model

Cumulative percent drug released versus square root of time. Drug released from the matrix devices by diffusion has been described by following Higuchi's classical diffusion equation.

$$Q = \left(\frac{D\varepsilon}{\tau}(2A - \varepsilon C_s)C_s t\right)^{1/2}$$

Where, Q = amount of drug released at the time, "t"

D = diffusion coefficient of the drug in the matrix.

A = total amount of drug in a unit volume of the matrix.

C_S = the solubility of the drug in thediffusion medium.

ε = porosity of the matrix.

τ = tortuosity.

t = time (hrs.) at which 'Q' amount of drug is released.

The equation may be simplified by assuming that, D, CS, and A are constant. Then the equation becomes:

$$Q = Kt^{1/2}$$

Korsmeyer and Peppas release model

The release rates from controlled release polymeric matrices can be described by the equation proposed by Korsmeyer et al.

$$Q = K_1 t^n$$

Where, Q = Percentage of drug released at the time 't'

K = Kinetic constant incorporating structural and geometric characteristics ofthe tablets and

'n'=Diffusional exponent indicative of the release mechanism.

Hixson and Crowell

To account for the particle size decrease and change in surface area accompanying dissolution, Hixson and Crowell's cubic root law of dissolution is used.[38]

$W_0^{1/3} – W^{1/3} = Kt$

EVALUATION PARAMETERS OF IMMEDIATE RELEASE GRANULES

Bulk Density
Bulk density can be determined by using the following formula:

$$\textbf{Bulk Density} = \frac{\text{Mass of Powder}}{\text{Bulk volume of powder}}$$

Tapped Density
The tapped density can be determined by using the following formula:

$$\textbf{Tapped Density} = \frac{\text{Mass of Powder}}{\text{Tapped volume of powder}}$$

Carr's consolidation index
Carr's index can be calculated using the following formula:

$$\textbf{Carr's Index} = \frac{\text{Tapped Density – Bulk Density}}{\text{Tapped Density}} \times 100$$

Hausner's Ratio
It can be calculated by using the formula:

$$\textbf{Hausner's Ratio} = \frac{\text{Tapped Density}}{\text{Bulk Density}}$$

Angle of Repose
The angle of repose is defined as a possible maximum angle (θ) formed between the surface of a pile of powder and the horizontal plane.

Angle of Repose (θ) = $\tan^{-1}(h/r)$

Where, h = height of the pile from the horizontal powder surface.
r = radius of the powder surface.

Estimation of Drug Content
Granules containing hydrochlorothiazide that were precisely weighed at 10 mg equivalent weight were added to a buffer solution with a pH of 1.2. With a magnetic stirrer, the solution was blended. A double beam UV spectrophotometer was used to measure the medication content after the appropriate dilution (Shimadzu, UV-1700).

***In-vitro* dissolution studies**
Using the dissolving apparatus USP XXII, dissolution studies were conducted (Electrolab). Drug-loaded microbeads equivalent to 12.5 mg of the drug were introduced into the 900 ml of acidic buffer pH 1.2±0.1 for up to 2 hours, then in phosphate buffer of 7.4 pH for up to 12 hours. The medium was maintained at 37±2ºC at 50 rpm. For up to two hours, 5 ml aliquots were taken out at regular intervals and examined spectrophotometrically at 272 nm using a UV 1700, made by Shimadzu in Japan. For each formulation, three trials were run. In order to maintain the sink condition throughout the investigation, an equivalent volume of fresh dissolving media was replaced. [39]

Bimal Debbarma and Chandra Kishore Tyagi

RESULTS AND DISCUSSION

Melting point
Losartan potassium's melting point was discovered to be 2650°C, which is within the stated range of 2590–2660°C, while hydrochlorothiazide's melting point wasdiscovered to be 2680°C, which is also within the reported range of 2650–2680°C. That complies with the accepted norm. Thus showing the sample's purity.

Drug excipients compatibility studies
Attenuated Total Reflectance (ATR)
According to the technique, an ATR spectrophotometer was used to carry out compatibility studies. Researchers looked at the IR spectrum of pure drugs, polymers, and physically mixed drugs and polymers. The peaks of the drug spectrum and the peaks found in the spectra of the improved formulation were correlated. This shows that the medicine and the formulation's ingredients got along well.

Differential Scanning Calorimetry (DSC) Analysis
The peaks of the drug spectrum and the peaks found in the spectra of the improved formulation were correlated. This shows that the medicine and the formulation's ingredients got along well.

CHARACTERISATION OF MICROBEADS AND GRANULES
Particle size
According to some reports, gelation happens right away when a drop of alginate solution interacts with Ca2+. Water is pushed out of inner droplets as alginate Ca2+ penetrates them, resulting in a concentration of beads. Consequently, an increase in sodium alginate solution concentration will have a major impact on the beads and cause them to grow in diameter.

Surface Morphology
The sodium alginate-made microbeads in the SEM were spherical, homogeneous, and surfaced with rough wrinkles. Collagens and fusing to the colloidal aqueous polymer dispersion in the alginate matrix may be to blame for this. It is clear from the photomicrographic observation that the formulations' bridging and thick characteristics contributed to the extended drug release.

Swelling Studies
The findings demonstrated a correlation between swelling and polymer concentration, with swelling being more significant for beads with higher polymer contents.

In-vitro drug release:
A pH 1.2 buffer was used for the first two hours of the microbead dissolving investigations, and a pH 7.4 buffer for the remaining studies, lasting up to 12 hours. Due to the limited solubility of the medication in an acidic media, the losartan potassium microbeads' drug release behaviour in an acidic (pH 1.2) buffer was generally very slow. The microbeads' tendency to inflate has an impact on the drug's release rate as well. Due to an increase in the polymer's swelling tendency, the drug release behaviour in pH 7.4 buffer increased in nearly all batches. To calculate the sustained release property of the produced formulations, the *in-vitro* drug release observation was conducted for a further 12 hours. Based on the findings, hydrochlorothiazide was shown to release quickly from immediate-release granules, which may be related to the presence of crospovidone as the super disintegrating agent.

Drug Release Kinetics Losartan Potassium Containing Microbeads
All microbeads displayed nearly zero-order kinetics, according to an analysis of the regression coefficient values of all batches. Since the plots had the maximum linearity ($r2 = 0.902$ to 0.937), Higuchi's equation can best describe the in-vitro release profiles of medicines from all of these formulations. The data were fitted into the Korsmeyer-Peppas

Bimal Debbarma and Chandra Kishore Tyagi

equation to validate the diffusion mechanism. The formulations demonstrated strong linearity (r2 = 0.849 to 0.863) and a slope (n) between 0.845 and 0.905, which seems to point to a non-fiction diffusion process.

STABILITY STUDIES

Accelerated stability tests were performed on the formulation of an improved capsule that contained losartan potassium and hydrochlorothiazide in the form of immediate-release granules and sustained-release microbeads. The improved capsule was inserted in an aluminium pouch and kept in an accelerated stability chamber for one month at 400C and 75% RH. The consistency of the medication content and the appearance of a capsule did not significantly change in samples that were withdrawn after one month.

CONCLUSION

The formulation and assessment of a regioselective dual component capsule were successfully demonstrated in the current work. A layer of hydrochlorothiazide for immediate release was created in the dual component capsule using the dry granulation method with crospovidone as super disintegrants, and a layer of losartan potassium microbeads for sustained release was created using sodium alginate using the ionotropic gelation method with calcium chloride and a blend of chitosan using the ionic and covalent crosslinking method. Using ATR and DSC, tests on the compatibility of drug excipients were conducted. Spectra showed that no interactions between the formulation's excipients and the medications were discovered. According to all pre-compression studies, the outcomes were found to be within the established limitations. According to in-vitro release experiments, the losartan potassium sustained release layer reached 99.14% after 12 hours and the hydrochlorothiazide quick release layer reached 98.41% within 120 minutes. With regard to physical properties and in-vitro drug release investigations, stability testing after exposure to accelerated circumstances for a month revealed no alterations despite the release kinetics showing strong linearity and best fitting into Higuchi's model. With the sequential release of two medications, the manufactured regioselective dual component capsule met the goal of the research study in treating hypertension. These capsules can be the greatest replacement for traditional dose forms with higher frequency of administration because they minimise the frequency of dosage administration and are inexpensive.

ACKNOWLEDGEMENT

REFERENCES

1. www.wikipedia.com.
2. ObinecheEN. Management of hypertension: update and review. Bull The Kuwait Ins Med Spe. 2003;2:73-82.
3. www.webMD.com.
4. Ron G. Hypertension: the use of combination therapy. 1999;86-90.
5. PatilP, ChavankeD,WaghM. A review on ionotropic gelationmethod: A novel approach for controlled gastroretentive gelispheres.
6. Kube RS, Kadam VS, Shendarkar GR, Jadhav SB, Bharkad VB. Sustained release drug delivery system: Areview. Int J Res Ph Biotech. 2015;3(3):246-51.
7. GuptaMM , BrijeshR. A review onsustained release technology. Int J Thera App.2012;8:18-23.
8. PatnaikNA, NagarjunaT, ThulasiramarajuTV. Sustained release drug delivery system: a modern formulation approach. Int J Res Pharm Nano Sci. 2013;2(5): 586-601.
9. MaliAD, BatheRS . A review on sustained release drug delivery system. GCC J Sci Tech. 2015;1(4):107-23.
10. Pharma tutor.

Bimal Debbarma and Chandra Kishore Tyagi

11. KumarKPS, BhowmikD , SrivastavaS, PaswanS, DuttaAS. Sustained release drug delivery system potential. The Pharm Inno. 2012;1(2):46-56.

12. RathodVG, KadamV,Jadhav SB, ZamiruddinM, BharkadVB, BiradarSP, *et al*. Immediate release drug delivery system: areview. World J Ph   PharmSci. 2014;3(6):545-58.

13. Bhandari N, Kumar A, Choudhary A, Choudhary R, Bala R. A review on immediate release drug delivery system. Int Res J Pharm App Sci. 2014;4(1):78-87.

14. SandeepN, GuptaMM. Immediate release dosage form: A review. J Drug Deli Thera. 2013;3(2):155-61.

15. JaiswalAR,VyasMR,Behera1AK,MesharamD. Colon targeted multiparticulate system: hydrogel beads. World J Ph Pharm Sci. 2014;3(4):507-25.

16. ManuboluK, SujathaB, SreenivasuluM,KumarSR, KumarSN,RaoKB, *et al*. Formulation and in-vitroevaluation of gliclazide microbeads. World J Pharm Res. 2015;4(5):1970-82.

17. YS Pathare, HSeema, Fayeza AH. Formulation and characterization of micro particulate carriers for diclofenac sodium. The Pharm Inno J. 2013;2(4):92-6.

18. Avinash GK, ParthibanS , KumarSKS. Formulation and evaluation of ramipril beads for gastro-mucoadhesive drug delivery. Int J Curr Pharm Clini Res. 2013;3(2):55-63.

19. GirhepunjeKM, PillaiK, PalRS, GevariyaHB, ThiumoorthyN. Celecoxib loaded microbeads: a targeted drug delivery for colorectal cancer. Int J Curr Pharm Res. 2010;2(1):46-55.

20. Bhatt MB, Panchal BP, Patel NN, Bhimani BV, Patel GV,Patel UL, *et al*.Formulation and evaluation of ionotropically gelled novel hydrogel beads of valsartan. Int J Pharm Res Bio Sci. 2014;3(2): 845-59.

21. ZamW, BashourG, AbdelwahedW, KhayataW. Formulation and in-vitro release ofpomegranate peels polyphenols microbeads. Int J Pharm Sci Res.2013;4(9):3536-40.

22. SolankiHK, BasuriT, ThakkarJH, PatelCA. Recent advances in granulation technology. Int J Pharm Sci Rev Res. 2010;5(3):48-54.

23. Sheth VP, Ranpura LD, Patel VP, Atara SA, Desai TR.Steamgranulation: novel aspects in granulation techniques.Int J Pharm Sci. 2012;3(3):2170-84.

24. ThejaswiniP, SugunaB, Sumalatha1N, UmasankarK,ReddyPJ. Advanced granulation techniques for pharmaceutical formulations. Int J Res Pharm Nano Sci. 2013;2(6):723-32.

25. Patil R, JagtapVA,PatilA, SarodeS. A review on role of novel superdisintegrants in pharmacy. Euro J Pharm Med Res. 2015; 2(3):390-400.

26. www.Pharmatutor.org

27. Organic laboratory techniques.

28. BuenoJ, LednevIK. Attenuated total reflectance FTIR imaging for rapid andautomated detection of gunshot residue. Anal Chem. 2014;86(7):3389-96.

29. Chandra SBP,SrikanthRP , Valluru R. Formulation and evaluation ofsustained release floating tablets of diltiazem HCl using xanthan gum. Res J Pharm Biological Chem Sci. 2011; 2(2):319-28.

30. Indian pharmacopoeia 2007;(1):245-6.

31. Jani BR, Shah KV. Development and validation of analytical method forsimultaneous estimation of valsartan and pioglitazone hydrochloride by simultaneous equation method. Int J Pharm Res Scholars. 2014;3(3):186-96.

32. PatilJS, MandaveSV,JadhavSM. Ionotropicaly crosslinked and chitosanreinforced losartan potassium loaded complex alginate beads: design, characterization and evaluation.Malaya J Bio Sci. 2014;1(3):126-33.

33. Bhatt MB, Panchal BP, Patel NN, Bhimani BV, Patel GV,Patel UL. Formulation and evaluation of ionotropically gelled novel hydrogel beads of valsartan. Int J Pharm Res Bio Sci. 2014;3(2):845-59.

34. KunduA. Preparation and evaluation of sustained release microbeads of norfloxacin using sodium alginate. 2012;2(3):647-51.

35. MenonTV, SajeethCI. Formulation and evaluation of sustained releasesodium alginate microbeads of carvedilol. Int J Pharm Tech Res. 2013; (2):746-53.

36. Patil JS, MandaveSV,JadhavSM. Ionotropicaly crosslinked and chitosan reinforcedlosartanpotassium loaded complex alginate beads: design,characterization and evaluation. 2014;1(3):126-33.

37. RamanaBV, ParameswariCS,TriveniC, ArundathiT, ReddyV, NagarajanG, *et al*. Formulation and evaluation of sodium alginate microbeads ofsimvastatin. Int J Ph Pharm Sci. 2013;5(3):410-6.

38. RathodVG , KadamVai, JadhavSB,Zamiruddin M,BharkadVB, BiradarSP, *et al*. Immediate release drug delivery system.World J Ph Pharm Sci. 2014;3(6): 545-58.

Table 1: Classification of Hypertension

Classification	Systolic Pressure(mmHg)	Dyastolic Pressure(mmHg)
Normal	90-119	60-79
Pre-hypertension (High Normal)	120-139	80-89
Stage 1 Mild-hypertension	140-159	90-99
Stage 2 Moderate-hypertension	160-179	100-109
Stage 3 Severe-hypertension	180-209	110-119
Stage 4 Very-severe hypertension	>210	>120
Malignant hypertension	>200	>140

Table 2: Composition of hydrochlorothiazide containing granules.

INGREDIENTS	QUANTITY (mg)
Hydrochlorothiazide	12.5
Lactose monohydrate	13
Crospovidone	2.5
Starch mucilage	8
Magnesium stearate	1
Talc	1
Total Weight	**38**

Table No. 3: Flow properties and corresponding angle of repose.

FLOW PROPERTIES	ANGLE OF REPOSE
Excellent	< 25
Good	26 - 30
Moderate	31 - 40
Poor	> 40

Bimal Debbarma and Chandra Kishore Tyagi
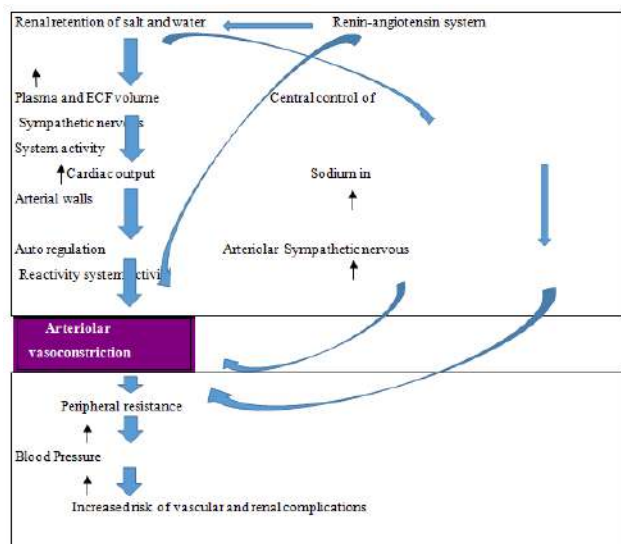
Figure 1: Pathophysiology of Hypertension

Figure 2: Drug levels in the blood with (a) Conventional drug delivery systems.
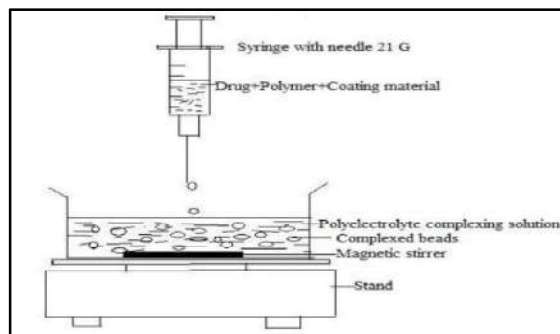
Figure 3: Schematic representation of the preparation of hydrogel beads by Ionotropic gelation method.

Figure 4: Schematic representation and diagram of the preparation of hydrogel beads by Ionotropic gelation and polyelectrolyte complexation.

Figure 5: Steps involved in the dry granulation
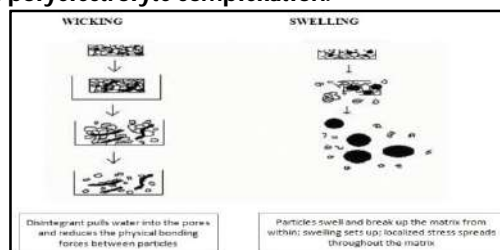
Figure 6: Wicking property of granules and swelling of granules.
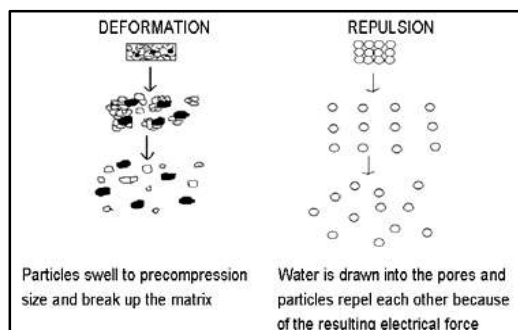
Figure 7: Repulsion of granules and deformation of granules.

Figure 8: Enzymatic reaction of granules.

An accurately weighed quantity of 100 mg of the drug transferred into a 100 ml volumetric flask and dissolved in a small quantity of 1.2 & 7.4 pH buffer solutions separately.

↓

The required volume was made with the respective buffers to get the concentration of 1000 µg/ml. i.e. Stock solution-1.

↓

Pipette out 2 ml exactly from the stock solution-1 into another 100 ml volumetric flasks separately and made the volume with respective buffers to get concentration of 20 µg/ml. i.e. stock solution-2. [30]

Figure 9:Preparation of Standard Solution of Losartan Potassium

Weigh accurately 100 mg of hydrochlorothiazide transferred into two different 100 ml volumetric flask and dissolved in a small quantity of 1.2 & 7.4 pH buffer solutions separately.

↓

The required volume was made with the respective buffers to get the concentration of 1000 µg/ml. i.e. Stock solution-1.

↓

Pipette out 2 ml exactly from the stock solution-1 into another 100 ml volumetric flasks separately & make the volume with respective buffers to get the concentration of 20 µg/ml. i.e. stock solution-2.

Figure 10:Preparation of Standard Solution of Losartan Potassium

Step-I:
Sodium Alginate
(This was previously soaked in the required quantity of distilled water.)

↓

Viscous solution of sodium alginate Stirred until formed homogenous mixture

↓

Drug
Bubbles free solution was filled in syringe with having 21G size needle.

Step-II:

0.5% Chitosan + 1% v/v acetic acid solution

Keep aside for24 hours.   Stirred for 15 minutes.

Viscous solution of chitosan
Filtered

Cleared chitosan solution + 4% w/v 100 ml of CaCl₂ solution
Stirred until formed

homogenous mixture
Chitosan-calcium chloride solution
Add **step-I** product drop-wise with

The help of a syringe containing Stirred for 1 hour
21G size needle.
Filtered with the help of a vacuum

Dried at 50°C ↓

Hydrogel Microbeads

Figure11: Flow diagram for the preparation of hydrogel microbeads containing losartan potassium.

All the ingredients were accurately weighed and passed through sieve no. 80.

↓

Accurately weighed quantity of lactose monohydrate was transferred into a cleaned mortar followed by hydrochlorothiazide and mixed thoroughly with the help of a pestle.

↓

Added crospovidone into the above mixture and mixed it well.

↓

The remaining excipients were added in geometrical proportions and mixed till a homogenous mixture was formed.[32,33]

Figure 12: Preparation of immediate release granules

The 50 mg of beads were incubated into the glass vials, initially with 10 ml of 1.2 pH buffer and then 7.4 pH phosphate buffer solutions.

↓

The beads were taken out at different time intervals and blotted carefully without pressing hard to remove the excess surface liquid.

↓

The swollen beads were weighed using the electronic microbalance.

↓

The weights determined were used for plotting the swelling profile.

Figure 13. Procedure of swelling study

Bimal Debbarma and Chandra Kishore Tyagi

Figure 14: ATR spectra of Losartan Potassium

Figure 15: ATR spectra of Hydrochlorothiazide

Figure16: ATR spectra of Microbeads (LP+Sodium alginate+Chitosan)
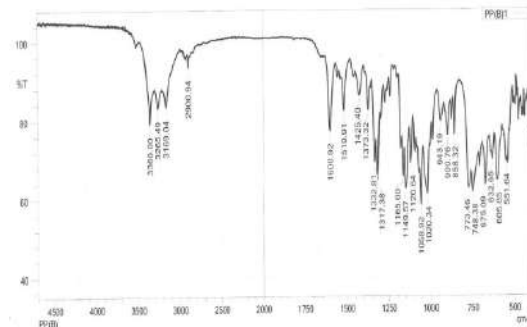
Figure17: ATR spectra of granules (HCTZ+Crospovidone+Lactose+Starch)
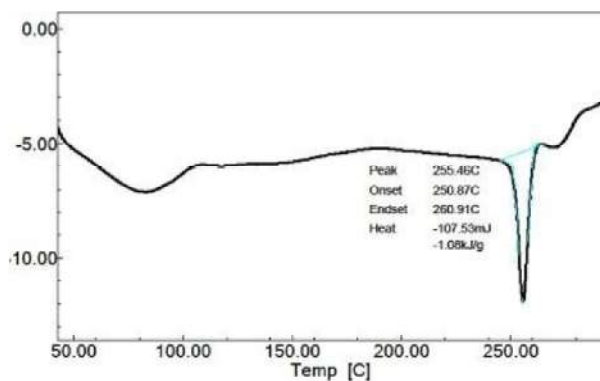
Figure 18: DSC thermogram of Losartan potassium
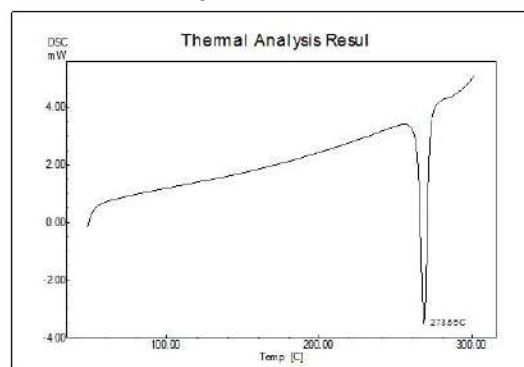
Figure 19: DSC thermogram of Hydrochlorothiazide

Bimal Debbarma and Chandra Kishore Tyagi
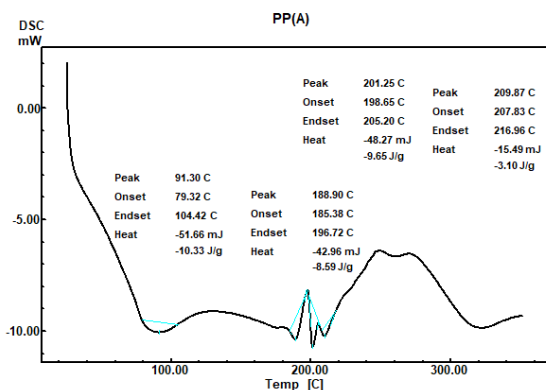
Figure 20: DSC thermogram of Losartanpotassium-containing microbeads.
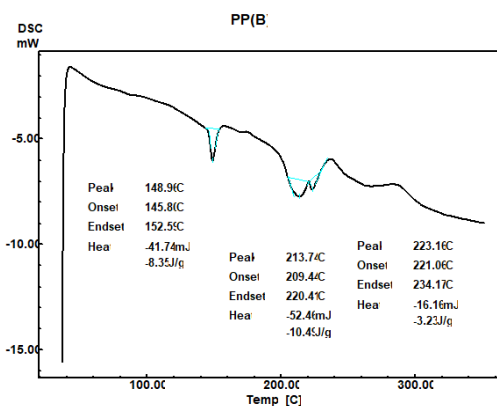
Figure 21: DSC thermogram of Hydrochlorothiazide containing granules.
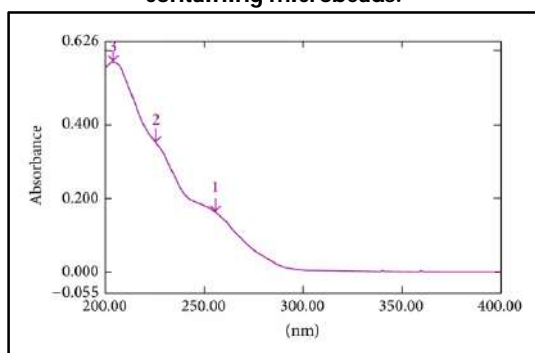
Figure22: Analytical wavelength of Losartan potassium
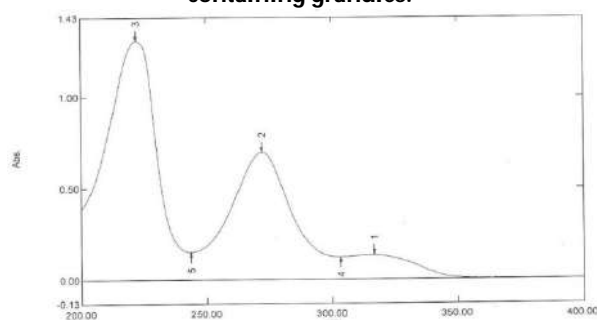
Figure23: Analytical Wavelength of Hydrochlorothiazide.

Figure 24: Microbeads prepared using different concentrations of drug and polymer ratio.

Bimal Debbarma and Chandra Kishore Tyagi
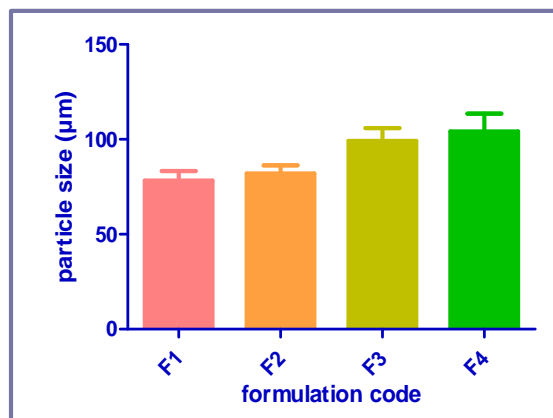
Figure 25: Average particle size of losartan potassium-loaded microbeads.
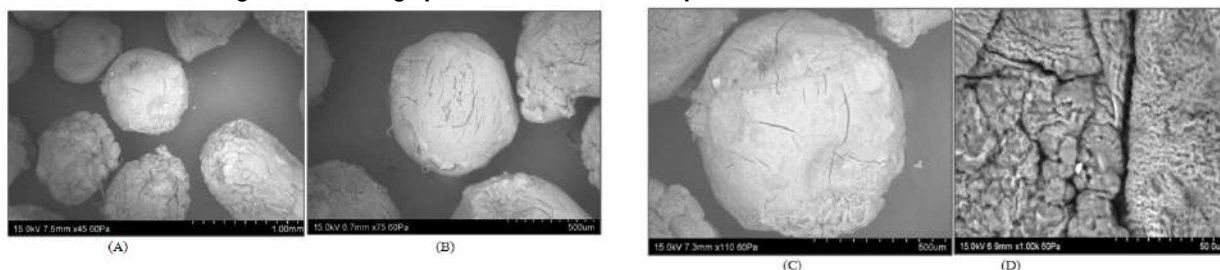
Figure 26: SEM photographic image of microbeads
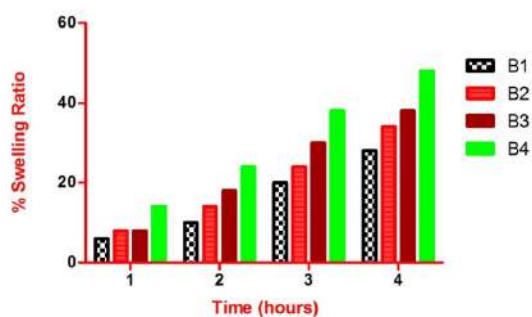
Figure 27: *In-vitro* **swelling index profile of microbeads.**
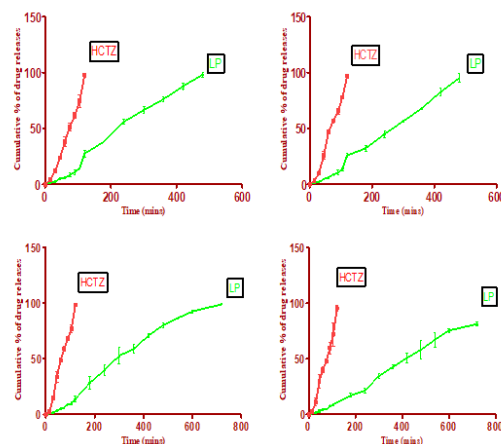
Figure 28: *In-vitro* **drug release profile of B1,B2,B3, and B4**

RESEARCH ARTICLE

Phytochemical Screening and Assessment of Bioactive Constituents Present in *Ganoderma lucidum* using GC-MS Analysis

Manisha Devi[1], Anbu Jayaraman[2]*, Parasuraman Pavadai [3] and Damodar Nayak Ammunje[3]

[1]Research Scholar, Department of Pharmacology, Faculty of Pharmacy, RUAS, Bengaluru, Karnataka, India.
[2]Professor and HoD, Department of Pharmacology, Faculty of Pharmacy, RUAS, Bengaluru, Karnataka, India.
[3]Assistant Professor, Department of Pharmaceutical Chemistry, Faculty of Pharmacy, RUAS, Bengaluru, Karnataka, India.

*Address for Correspondence
Anbu Jayaraman
Professor and HoD,
Department of Pharmacology,
Faculty of Pharmacy, RUAS,
Bengaluru, Karnataka, India.
E-mail: anbu.pg.ph@msruas.ac.in, manisha1996.mc1@gmail.com

ABSTRACT

Medicinal plants have been used as a resource for healing all over the world for many decades. The present study focused on the preliminary phytochemical and phytoconstituents analysis of *Ganoderma lucidum* ethanolic extract. GC-MS analysis method was used for the detection of various bioactive constituents present in *Ganoderma lucidum*. GC-MS analysis results showed the presence of 137 phytoconstituents among which few of them are reported for various biological activities and disease treatments. Hence, the presence of these constituents reveals the application of Ganoderma lucidum for the treatment of various diseases traditionally over the years.

Keywords: *Ganoderma lucidum*, phytochemical, phytoconstituents, GC-MS analysis, biological activities

INTRODUCTION

Since early history, people have been using plants for a wide range of uses. In-depth scientific investigations were previously carried out to ascertain the chemical components of plants and create techniques for the assessment of biological activity [1]. The therapeutic properties of herbs are based on the chemical properties of plants. The medicinal value of the medicinal plant is better understood with a good understanding of the chemical composition

64010

of the plants. Numerous chemical substances synthesized by the plant cell throughout metabolic pathways generated using the basic metabolic pathways are known as secondary metabolites of the plans [2]. Secondary plant metabolites include carbohydrates, alkaloids, glycosides, proteins, steroids, phenols, and related components with have been extensively used in the process of drug discovery [3].

Ganoderma lucidum is an oriental mushroom, belonging to the family Ganodermataceae, possesses extensive medicinal properties. It has a huge, redish brown, glossy, and woody surface mushroom. It has been used for more than 2000 years in TMC and is referred to as "herb of spiritual potency". They are a rich source of polysaccharides, triterpenoids, sterols, proteins and peptides. The active constituents present in *Ganoderma lucidum* acquires many biological activities like anti-oxidant, anti-inflammatory, anti-tumour, anti-diabetic, antiviral, hypoglycaemic, hypolipidemic, anti-hypertensive, cytotoxic and immunomodulatory activity [4-6]. For many years, the analysis of biological samples has been largely carried out using gas chromatography-mass spectroscopy (GC-MS), which has a wide range of uses in the qualitative and quantitative measurement of presented bioactive compounds in drug extracts, mainly for the partition of volatile and thermally stable components. In order to investigate metabolites, this methodology combined the separation properties of gas chromatography with the detection capabilities of mass spectroscopy [7]. This study aimed to assess the phytochemical and phytoconstituents present in ethanolic extract of *Ganoderma lucidum* using phytochemical screening and GC-MS analysis.

MATERIALS AND METHODS

Collection of the Plant Material
Ganoderma lucidum was selected for this study by conducting a systematic literature review and analysing all the proven pharmacological properties including antioxidant, anti diabetic, anti hyperlipidemic, anti tumor, anti androgenic and estrogenic activities. The sun dried *Ganoderma lucidum* fruiting bodies were procured along with botanical authentication from Biobritte Agro Solutions private limited, Jaysingpur, Maharashtra 416101. The obtained mushrooms were pulverized into fine powder using a stainless steel blender for further analysis.

Preparation of Extract
The plant material of *Ganoderma lucidum* was finely powdered and subjected to extraction using soxhlet extraction method. The conditions maintained for soxhlet extraction process were 90% ethanol as extraction solvent, 35ml/g liquid-material ratio, 80°C temperature and 2 hours extraction time respectively in order to obtain a triterpenoid rich fraction. The percentage yield of extract produced by Ganoderma lucidum was 18.533% using ethanol as a solvent.

Preliminary Phytochemical Screening
The presence of various phytoconstituents like carbohydrates, alkaloids, glycosides, proteins, flavonoids, phenolic compounds, tannins, saponins, steroids, terpenoids and triterpenoids in the ethanol extracts of the plants understudy were tested as per the available standard pharmacopoeial procedures.

GC-MS Analysis
The GC-MS analysis of ethanolic extract of *Ganoderma lucidum* was performed using agilent model: CH-GCMSMSO2, 8890 GC System, 7000 GC/TQ. Experimental settings of GC-MS system were as follows: column dimensions 30 m×250 µ×0.25 µ; carrier gas: Helium;, collision gas: Nitrogen; solvent system: diluent- methanol; temperature program: 50°C raised to 280°C at 10°C/min; total run time: 38 min; scan range: 30-900 m/z.

RESULTS AND DISCUSSION

Preliminary Phytochemical Screening
The phytochemical analysis of *Ganoderma lucidum* ethanolic extract revealed the presence of carbohydrates, glycosides, saponins and triterpenoids as detailed in table 1.

GC-MS Analysis

GC-MS analysis of the *Ganoderma lucidum* ethanolic extract fraction revealed the presence of number of phytoconstituents. The mass spectrum produced by GC helped in the identification of the various phytoconstituents as depicted in figure 1. Phytoconstituents recognised in the ethanolic extract of *Ganoderma lucidum* using GC-MS analysis are listed in table 2 along with the reported activity of the individual phytoconstituent. The results revealed the presence of 137 different phytoconstituents, among which few of the components have been isolated and reported for various biological activities and their uses. Hence, isolation and research of individual phytoconstituents of *Ganoderma lucidum* may lead to the identification of novel components for further research.

CONCLUSION

The present study concluded the presence of carbohydrates, glycosides, saponins and triterpenoids in the ethanolic extract of *Ganoderma lucidum*. Further GC-MS analysis helped recognise various phytoconstituents with different chemical structures and biological activities. The bioactive compounds present in Ganoderma lucidum can help in the treatment of various diseases and disorders.

CONFLICT OF INTREST STATEMENT

The authors declare no conflict of interest.

ACKNOWLEDGMENT

REFERENCES

1. Süntar I. Importance of ethnopharmacological studies in drug discovery: role of medicinal plants. Phytochemistry reviews. 2020:19(5):1199-1209.
2. Hussein R A and El-Anssary A A. Plants secondary metabolites: the key drivers of the pharmacological actions of medicinal plants. Herbal medicine. 2019:1(3).
3. Jain C, Khatana S and Vijayvergia R. Bioactivity of secondary metabolites of various plants: a review. International journal of pharmaceutical sciences and research. 2019:10(2):494-504.
4. Cho J Y, Sadiq N B, Kim J C, Lee B, Hamayun M, Lee T S, Kim H S, Park S H, Nho C W, and Kim H Y. Optimization of antioxidant, anti-diabetic, and anti-inflammatory activities and ganoderic acid content of differentially dried Ganoderma lucidum using response surface methodology. Food chemistry. 2021:335:127645.
5. Ahmad M F, Ahmad F A, Khan M I, Alsayegh A A, Wahab S, Alam M I and Ahmed F. Ganoderma lucidum: A potential source to surmount viral infections through β-glucans immunomodulatory and triterpenoids antiviral properties. International journal of biological macromolecules. 2021:187:769-779.
6. Meng J, Wang S Z, He J Z, Zhu S, Huang B Y, Wang S Y, Li M, Zhou H, Lin S Q, and Yang B X. Ganoderic acid A is the effective ingredient of Ganoderma triterpenes in retarding renal cyst development in polycystic kidney disease. Acta pharmacologica sinica. 2020:41(6):782-790.
7. Dat T D, Viet N D, My P L T, Linh N T, Thanh V H, Linh N T T, Ngan N T K, Linh N T T, Nam H M, Phong M T, and Hieu N H. The application of ethanolic ultrasonication to ameliorate the triterpenoid content extracted from Vietnamese Ganoderma lucidum with the examination by gas chromatography. Chemistry select. 2021:6(10):2590-2606.

Manisha Devi *et al.*,

Table 1: Preliminary phytochemical screening of *Ganoderma lucidum*

Sl. No	Tests	Results
1.	Test for alkaloids	-
2.	Test for carbohydrates	+
3.	Test for glycoside	+
4.	Test for amino acids	-
5.	Test for flavonoids	-
6.	Test for phenols	-
7.	Test for tannins	-
8.	Test for saponins	+
9.	Test for phytosterols	-
10.	Test for terpinoids	-
11.	Test for triterpenoids	+

Table 2: Phytoconstituents present in *Ganoderma lucidum* ethanolic extract using GC-MS

Sl. No.	Component Retention Time	Compound Name	Formula	Component Area	Match Factor	Uses
1.	21.3184	2(4H)-Benzofuranone, 5,6,7,7a-tetrahydro-4,4,7a-	$C_{11}H_{16}O_2$	12024918.4	95.3	Flavouring agent
2.	22.1489	1-Hexadecanol	$C_{16}H_{34}O$	9212109.2	95.3	Antioxidant
3.	28.6212	Methyl elaidate or 9-Octadecenoic acid, methyl ester, (E)-	$C_{19}H_{36}O_2$	62954610.8	94.5	No activity reported
4.	14.7784	Glycerol 1,2-diacetate	$C_7H_{12}O_5$	11282483.6	94.0	Fragrance and solvent
5.	16.7313	2-Methoxy-4-vinylphenol	$C_9H_{10}O_2$	31712548.6	93.2	CYP2C9 antagonist
6.	28.5547	9,12-Octadecadienoic acid (Z,Z)-, methyl ester	$C_{19}H_{34}O_2$	31110611.1	92.9	Glucocorticoid receptor signalling pathway antagonist
7.	29.9023	2-Hexadecen-1-ol, 3,7,11,15-tetramethyl-, acetate,	$C_{22}H_{42}O_2$	21064994.2	92.6	Flavouring agent
8.	24.7801	1-Tricosene	$C_{23}H_{46}$	5721119.3	92.4	No activity reported
9.	26.7866	Benzenepropanoic acid, 3,5-bis(1,1-dimethylethyl)-	$C_{18}H_{28}O_3$	22452139.9	92.2	No activity reported
10.	25.1058	Pentadecanal-	$C_{15}H_{30}O$	4761439.3	92.0	No activity reported
11.	21.8247	Phenol, 4-ethenyl-2,6-dimethoxy-	$C_{10}H_{12}O_3$	4068462.9	91.6	Oxidative stress reduction, anticancer
12.	14.6810	1,2,3-Propanetriol, 1-acetate	$C_5H_{10}O_4$	53811850.9	91.5	Anticancer activity
13.	26.9206	n-Hexadecanoic acid	$C_{16}H_{32}O_2$	56618517.6	91.3	Fatty acid binding protein inhibition
14.	28.7673	Phytol	$C_{20}H_{40}O$	46110159.3	90.8	Anti-inflammatory activity
15.	28.7160	2(3H)-Furanone, 5-dodecyldihydro-	$C_{16}H_{30}O_2$	104559086.7	90.6	Flavouring agent
16.	8.8722	Benzeneacetaldehyde	C_8H_8O	3413245.6	90.0	Thyroid stimulating hormone agonist
17.	23.9642	Methyl tetradecanoate	$C_{15}H_{30}O_2$	22597699.5	89.8	Emollient, flavouring agent
18.	25.1844	Pentadecanoic acid, methyl ester	$C_{16}H_{32}O_2$	15209454.5	89.5	No activity reported

64013

Manisha Devi *et al.*,

Sl. No.	Component Retention Time	Compound Name	Formula	Component Area	Match Factor	Uses
19.	26.4768	Hexadecanoic acid, methyl ester	$C_{17}H_{34}O_2$	49134844.0	89.3	Emollient, flavouring agent
20.	30.6725	(Z)-9-octadecen-4-olide	$C_{18}H_{32}O_2$	43377716.2	89.2	No activity reported
21.	21.7407	Dodecanoic acid	$C_{12}H_{24}O_2$	4006491.3	89.1	Androgen receptor signalling pathway antagonist
22.	28.9901	9,12-Octadecadienoic acid (Z,Z)-	$C_{18}H_{32}O_2$	27818860.2	88.6	Antibacterial, antiviral
23.	24.4195	Tetradecanoic acid	$C_{14}H_{28}O_2$	16731351.3	88.5	Estrogen receptor β agonist
24.	18.6088	1-Undecanol	$C_{11}H_{24}O$	5910062.6	88.3	Antioxidant activity
25.	20.9368	2,4-Di-tert-butylphenol	$C_{14}H_{22}O$	132147943.6	87.8	Thyroid receptor pathway inhibitor, aromatase inhibitor
26.	29.0373	9-Octadecenoic acid, (E)-	$C_{18}H_{34}O_2$	25949212.9	87.6	No activity reported
27.	25.8035	1,2-Benzenedicarboxylic acid, bis(2-methylpropyl)	$C_{16}H_{22}O_4$	21480518.2	86.4	No activity reported
28.	17.7355	Phenol, 2,6-dimethoxy-	$C_8H_{10}O_3$	37964270.1	86.2	Cytochrome P450 antagonist
29.	21.8409	Phenol, 4-ethenyl-2,6-dimethoxy-	$C_{10}H_{12}O_3$	5473659.3	85.9	Flavouring agent
30.	30.9484	2(3H)-Furanone, dihydro-5-tetradecyl-	$C_{18}H_{34}O_2$	40935234.1	85.9	Flavouring agent
31.	32.5644	Heneicosane	$C_{21}H_{44}$	8280480.4	85.8	Fragrance component
32.	17.7355	2,3-Dimethoxyphenol	$C_8H_{10}O_3$	35302477.8	85.5	No activity reported
33.	25.8842	1-Hexadecanol	$C_{16}H_{34}O$	6205235.6	85.2	Antioxidant activity
34.	20.7706	2,6-Difluorobenzoic acid, 4-nitrophenyl ester	$C_{13}H_7F_2NO_4$	4025161.3	84.8	No activity reported
35.	26.2912	2-Nonylmalonic acid, dimethyl ester	$C_{14}H_{26}O_4$	25450755.0	84.7	No activity reported
36.	34.3791	Pentacosane	$C_{25}H_{52}$	18891915.6	84.5	No activity reported
37.	23.3564	E-14-Hexadecenal	$C_{16}H_{30}O$	7217866.0	83.5	No activity reported
38.	22.9545	Benzene, (1-propyloctyl)-	$C_{17}H_{28}$	3588576.2	82.8	No activity reported
39.	28.8982	Methyl stearate	$C_{19}H_{38}O_2$	6450470.3	82.6	Emollient, flavouring and fragrance
40.	21.1142	5-Hydroxy-3-methyl-1-indanone	$C_{10}H_{10}O_2$	31982582.1	82.1	Antifungal activity
41.	19.8719	5,9-Undecadien-2-one, 6,10-dimethyl-, (E)-	$C_{13}H_{22}O$	3934407.3	82.0	Flavouring and fragrance
42.	22.2672	Phthalic acid, 4-bromophenyl ethyl ester	$C_{16}H_{13}BrO_4$	2089160.6	82.0	No activity reported
43.	21.1126	Dodecanoic acid, methyl ester	$C_{13}H_{26}O_2$	28658350.8	81.8	Antioxidant activity
44.	26.1757	2-Heptadecanone	$C_{17}H_{34}O$	3986362.7	80.8	Flavouring agent
45.	27.0314	Dibutyl phthalate	$C_{16}H_{22}O_4$	4164839.2	79.8	Estrogen receptor agonist
46.	23.5782	3-Buten-2-one, 4-(4-hydroxy-2,2,6-	$C_{13}H_{20}O_3$	5101258.2	79.4	No activity reported

Manisha Devi *et al.,*

SI. No.	Component Retention Time	Compound Name	Formula	Component Area	Match Factor	Uses
		trimethyl-7-				
47.	30.8060	2-Nonylmalonic acid, dimethyl ester	$C_{14}H_{26}O_4$	19424597.9	79.1	No activity reported
48.	24.6654	6-Hydroxy-4,4,7a-trimethyl-5,6,7,7a-	$C_{11}H_{16}O_3$	4136585.4	79.0	No activity reported
49.	36.1076	9,12-Octadecadienoic acid (Z,Z)-, 2-hydroxy-1-(hydroxymethyl)ethyl ester	$C_{21}H_{38}O_4$	98441154.3	79.0	No activity reported
50.	10.4062	Ketone, methyl 2-methyl-1,3-oxothiolan-2-yl	$C_6H_{10}O_2S$	9889138.5	78.6	No activity reported
51.	22.6252	Tridecanoic acid, methyl ester	$C_{14}H_{28}O_2$	10658221.4	78.3	Solvent, emollient
52.	23.5782	4-Fluorobenzoic acid, tridec-2-ynyl ester	$C_{20}H_{27}FO_2$	4870225.5	78.3	No activity reported
53.	11.7596	I-Norvaline, N-ethoxycarbonyl-, isohexyl ester	$C_{14}H_{27}NO_4$	196742804.5	77.0	No activity reported
54.	29.6648	trans-Geranylgeraniol	$C_{20}H_{34}O$	4688646.2	76.0	Myotoxicity suppression
55.	33.9212	2,3-Dimethylhydroquinone, diacetate	$C_{12}H_{14}O_4$	231066378.4	75.5	No activity reported
56.	36.2297	3,5-Dihydroxybenzaldehyde	$C_7H_6O_3$	9126209.5	75.3	No activity reported
57.	14.3683	1H-Pyrazole, 4,5-dihydro-3-methyl-1-propyl-	$C_7H_{14}N_2$	3513504.6	75.2	No activity reported
58.	30.6145	1,8,11-Heptadecatriene, (Z,Z)-	$C_{17}H_{30}$	4442485.3	75.1	No activity reported
59.	33.066	Phthalic acid, di(2-propylpentyl) ester	$C_{24}H_{38}O_4$	4048518.4	75.1	No activity reported
60.	13.6575	2-Butanone	C_4H_8O	5212492.7	74.8	Adhesive, flavouring agent
61.	11.7668	2-Oxopentanedioic acid	$C_5H_6O_5$	118815678.1	72.8	Human PHD2-Mn(II) binding affinity
62.	25.4556	2-Undecanone, 6,10-dimethyl-	$C_{13}H_{26}O$	4875133.5	72.3	Flavouring agent
63.	24.0964	1-Acetyl-4,6,8-trimethylazulene	$C_{15}H_{16}O$	3869493.1	71.9	No activity reported
64.	10.0526	Thymine	$C_5H_6N_2O_2$	5939868.7	71.7	Anticancer activity
65.	29.0700	Bicyclo[4.1.0]heptane, 7-methylene-	C_8H_{12}	2812105.7	71.6	No activity reported
66.	30.7546	Squalene	$C_{30}H_{50}$	3489191.4	71.4	Antioxidant activity
67.	27.5386	2-Nonylmalonic acid, dimethyl ester	$C_{14}H_{26}O_4$	4485575.3	70.9	No activity reported
68.	30.9536	9-Octadecenoic acid, (E)-	$C_{18}H_{34}O_2$	7958520.8	70.5	No activity reported
69.	22.2069	2-Methoxyformanilide	$C_8H_9NO_2$	11763968.1	70.1	No activity reported
70.	25.3506	1-Octadecyne	$C_{18}H_{34}$	4958789.3	69.4	No activity reported
71.	26.4622	5,9,13-Pentadecatrien-2-one, 6,10,14-trimethyl-,	$C_{18}H_{30}O$	5530487.7	69.1	Flavouring, perfuming
72.	36.365	.alpha.-Tocospiro B	$C_{29}H_{50}O_4$	6977329.3	69.0	Antibacterial activity
73.	32.7082	Hexadecanoic acid, 2-hydroxy-1-(hydroxymethyl)ethyl ester	$C_{19}H_{38}O_4$	7095824.8	68.8	No activity reported

Manisha Devi *et al.*,

SI. No.	Component Retention Time	Compound Name	Formula	Component Area	Match Factor	Uses
74.	35.5727	Phosphvorus P4	P_4	7020583.5	68.8	No activity reported
75.	36.2372	Sesamol, 2-methylpropionate	$C_{11}H_{12}O_4$	14587017.9	68.6	No activity reported
76.	33.4339	5-Tridecylbenzene-1,3-diol	$C_{19}H_{32}O_2$	6799240.0	68.3	COX-2 inhibition activity
77.	11.7593	2-Tetrazene, 1,1-diethyl-4,4-dimethyl-	$C_6H_{16}N_4$	194503458.0	68.2	No activity reported
78.	14.3683	5-Hydroxymethylfurfural	$C_6H_6O_3$	4350202.5	68.2	Mutagenic activity
79.	19.7979	4-Fluorobenzoic acid, tridec-2-ynyl ester	$C_{20}H_{27}FO_2$	4357241.9	68.0	No activity reported
80.	10.3481	Propanoic acid, anhydride	$C_6H_{10}O_3$	9410698.1	67.6	Progesterone and androgen receptor agonist
81.	10.4549	Bis(N-methoxy-N-methylamino)methane	$C_5H_{14}N_2O_2$	9151415.0	67.6	No activity reported
82.	36.241	2,3-Dimethylhydroquinone, diacetate	$C_{12}H_{14}O_4$	50450764.6	67.6	No activity reported
83.	23.9975	2,3-Dihydro-1H-2-isopropylcyclopenta[b]quinoxaline	$C_{14}H_{16}N_2$	2364545.5	67.5	No activity reported
84.	28.7643	1H-1,2,4-Triazole, 3-propyl-	$C_5H_9N_3$	8433493.5	67.4	Antitumor activity
85.	29.0566	2(1H)-Naphthalenone, octahydro-4a-methyl-7-(1-	$C_{14}H_{24}O$	20577299.3	67.2	No activity related
86.	28.6340	1,8,11,14-Heptadecatetraene, (Z,Z,Z)-	$C_{17}H_{28}$	6676394.7	66.9	Antioxidant activity
87.	22.7533	4-Benzyl-4,5-dihydroisoxazole	$C_{10}H_{11}NO$	2402511.9	66.7	No activity reported
88.	7.7142	Glycerin	$C_3H_8O_3$	4062840.3	65.8	Adhesion, binder, plasticizer, flavouring and lubricating activity
89.	18.7750	Cyclopentanol O-tert-butyldimethylsilyl ether	$C_{11}H_{24}OSi$	10820173.5	65.4	No activity reported
90.	25.3523	3,7,11,15-Tetramethyl-2-hexadecen-1-ol	$C_{20}H_{40}O$	5376615.2	64.8	Flavouring agent
91.	35.4626	9-Octadecenoic acid (Z)-, oxiranylmethyl ester	$C_{21}H_{38}O_3$	24442286.6	64.4	No activity reported
92.	10.3887	2-Butanamine, 3,3-dimethyl-	$C_6H_{15}N$	4755974.8	64.3	No activity reported
93.	28.7059	2-Nonylmalonic acid, dimethyl ester	$C_{14}H_{26}O_4$	64433781.2	64.3	No activity reported
94.	20.4722	Benzenepropanal, 4-(1,1-dimethylethyl)-	$C_{13}H_{18}O$	2456818.5	64.2	Estrogen receptor antagonist
95.	31.6055	Supraene	$C_{30}H_{50}$	4860810.5	63.9	Antistatic, emollient, hair conditioning and refatting activity
96.	28.6392	2-Indanone, 4,5,6,7-tetrahydro-	$C_9H_{12}O$	7371616.1	63.4	No activity reported
97.	23.7778	Hexanoic acid, anhydride	$C_{12}H_{22}O_3$	6389735.1	63.3	No activity reported

Manisha Devi *et al.,*

SI. No.	Component Retention Time	Compound Name	Formula	Component Area	Match Factor	Uses
98.	8.8890	5-(2,2,2-Tri(2-cyanoethyl)acetyl)-2-methylpyridine	$C_{17}H_{18}N_4O$	10539484.5	62.9	No activity reported
99.	23.6346	2'-Hydroxyacetophenone, TMS derivative	$C_{11}H_{16}O_2Si$	3648436.1	62.9	No activity reported
100.	14.0433	Benzenemethanol, .alpha.-(1-phenylaminoethyl)-	$C_{15}H_{17}NO$	8595606.8	62.8	No activity reported
101.	32.04	3,5-Dihydroxybenzaldehyde	$C_7H_6O_3$	8216930.9	62.2	Antioxidant activity
102.	27.7189	Pentadecanoic acid, methyl ester	$C_{16}H_{32}O_2$	3431765.3	62.0	Fuel agents
103.	35.45	Z,Z-4,6-Nonadecadien-1-ol acetate	$C_{21}H_{38}O_2$	13382179.5	61.5	No activity reported
104.	18.7722	Silane, [(1,1-dimethyl-2-propenyl)oxy]dimethyl-	$C_7H_{16}OSi$	36647925.2	61.0	No activity reported
105.	29.0433	Eicosen-1-ol, cis-9-	$C_{20}H_{40}O$	60343693.2	61.0	No activity reported
106.	20.5238	1-([4-(Butane-1-sulfonyl)butane]sulfonyl)butane	$C_{12}H_{26}O_4S_2$	8582012.8	60.9	No activity reported
107.	29.2936	Octadecanoic acid	$C_{18}H_{36}O_2$	4448032.0	60.9	Food additives
108.	23.7778	Sarin	$C_4H_{10}FO_2P$	7687686.9	60.4	AChE binding affinity
109.	20.5316	.beta.-D-Glucopyranose, 1,6-anhydro-	$C_6H_{10}O_5$	4874798.1	60.2	No activity reported
110.	3.1267	Propane, 2-fluoro-2-methyl-	C_4H_9F	6245038.8	59.9	No activity reported
111.	27.0359	Phthalic acid, butyl 2-pentyl ester	$C_{17}H_{24}O_4$	5554596.7	59.5	No activity reported
112.	20.0489	Trimethylaluminum	C_3H_9Al	11755733.6	58.2	Catalyst activity
113.	25.3287	Aspidinol	$C_{12}H_{16}O_4$	5316188.0	58.2	Antibacterial activity
114.	28.7682	2,2'-Bifuran, 2,2',5,5'-tetrahydro-	$C_8H_{10}O_2$	14702502.2	58.1	No activity reported
115.	22.6298	Adipic acid, isobutyl pent-4-en-2-yl ester	$C_{15}H_{26}O_4$	2446253.4	57.4	No activity reported
116.	14.6775	Alanylglycine, TMS derivative	$C_8H_{18}N_2O_3Si$	4414120.3	56.4	No activity reported
117.	32.0412	(Z)-9-((5R,8R,8aS)-8-Methyloctahydroindolizin-5-yl)non-5-en-2-ol	$C_{18}H_{33}NO$	3410093.6	56.1	No activity reported
118.	22.3866	Benzoic acid, 4-(trimethylsilyl)-	$C_{10}H_{14}O_2Si$	4180050.3	55.8	No activity reported
119.	10.0475	Methyl vinyl ketone	C_4H_6O	8282211.3	55.3	Mutagenic activity
120.	21.1212	Benzoic acid, 2,4,6-trimethyl-, 2,4,6-trimethylphenyl	$C_{19}H_{22}O_2$	14973246.6	55.2	No activity reported
121.	21.1210	1-Butanone, 2-chloro-3-methyl-1-[4-(1-	$C_{14}H_{19}ClO$	14284947.0	54.9	No activity reported
122.	36.109	1,4-Naphthalenedione, 2-amino-3-chloro-	$C_{10}H_6ClNO_2$	12914432.5	53.8	Anticancer activity
123.	36.0997	Naphtho[1,2-b]furan-6,9-dione, 4,5,7,8-tetrahydroxy-	$C_{12}H_6O_7$	35606478.4	53.7	No activity reported
124.	24.6604	Methyl 3-(4-hydroxy-3-methoxyphenyl)propanoate	$C_{11}H_{14}O_4$	8341698.0	53.6	Antifungal activity
125.	23.9613	2,4-Dimethyl-3-pentanol acetate	$C_9H_{18}O_2$	3012496.0	53.4	No activity reported
126.	24.9076	2-Fluoroaniline, N-pentyl-	$C_{11}H_{16}FN$	2801980.9	53.2	No activity reported
127.	36.1207	9-Octadecenoic acid (Z)-, 2,3-	$C_{21}H_{40}O_4$	66710535.7	52.9	Flavouring, emollient

Manisha Devi *et al.*,

Sl. No.	Component Retention Time	Compound Name	Formula	Component Area	Match Factor	Uses
		dihydroxypropyl ester				and lubricant activity
128.	16.7270	1-Adamantanecarboxylic acid, 2-propenyl ester	$C_{14}H_{20}O_2$	11235672.7	52.8	No activity reported
129.	14.8458	Silane, methoxytripropyl-	$C_{10}H_{24}OSi$	8860227.0	52.5	No activity reported
130.	22.8016	Diazene, 1-naphthalenylphenyl-	$C_{16}H_{12}N_2$	4889503.4	52.5	No activity reported
131.	18.7755	L-Tryptophan, N,N-dimethyl-, methyl ester	$C_{14}H_{18}N_2O_2$	10823227.4	52.2	No activity reported
132.	36.1012	Phthalic acid, ethyl 2-isopropoxyphenyl ester	$C_{19}H_{20}O_5$	18835909.5	52.1	No activity reported
133.	21.8273	Carbamic acid, butyl-, 3-iodo-2-propynyl ester	$C_8H_{12}INO_2$	10029917.6	52.0	P53 signalling pathway agonist
134.	24.4200	L-Norvaline, N-octyloxycarbonyl-, undecyl ester	$C_{25}H_{49}NO_4$	5130181.8	51.8	No activity reported
135.	24.6581	Ethyl homovanillate	$C_{11}H_{14}O_4$	3448945.8	50.8	Anti-inflammatory activity
136.	26.4735	Adipic acid, di(3-chlorophenyl) ester	$C_{18}H_{16}Cl_2O_4$	13713422.4	50.3	No activity reported
137.	30.9524	Phenylacetamide, 3-fluoro-N-methyl-N-[2-[1-azacyclopentyl]ethyl]-	$C_{15}H_{21}FN_2O$	4545031.8	50.3	No activity reported

RESEARCH ARTICLE

Fecundity Study on Selected Ornamental Fishes using Natrum Muriaticum 30c Potency

Sudha.C*

Assistant Professor, PG and Research Department of Zoology, National College, Tiruchirapalli-620001, Tamil Nadu, India

*Address for Correspondence
 Sudha.C*
Assistant Professor,
PG and Research Department of Zoology,
National College, Tiruchirapalli-620001,
Tamil Nadu, India
E.Mail: sudhagoutham@gmail.com.

ABSTRACT

Fish are well known for their high potential fecundity. Spawning in fish was controlled by various environmental factors. So far, in the regulation of reproduction and induced breeding, many products are utilized. The present study assesses the fecundity on exposure to the homeopathic preparation natrummuriaticum 30 c potency in fish viz goldfish, rosy barb, white molly and guppy. It also traces the time taken to spawning in viviparous fish. The experimental goldfish laid 850 ± 104 eggs; the control fish laid 383 ± 75 eggs in 4 days, whereas in rosy barb experimental fish laid 110± 15 eggs and the control fish laid 56 ± 11 eggs in 4 days. The treated white molly released 39±5young ones in19.5±3hours, while the control fish released 20±2 young ones in 72±6 hours, whereas in guppy the control fish released 8±1 young ones in 79±9 hours and the treated released 15±2 young ones 36±9 hours. Present findings demonstrated that homeopathic preparation natrummuriaticum is a highly effective stimulus for breeding of the above mentioned fish. It enhanced the production of matured eggs in oviparous and highly motile young ones in viviparous fish.

Key words: Fecundity, Natrummuriaticum 30c,Oviparous and Viviparous ornamental fish.

INTRODUCTION

Reproduction is an essential component of life and there are a diverse number of reproductive strategies in fish throughout the world. Fish are well known for their high potential fecundity, with most species releasing thousand to millions of egg annually [17]. Fecundity is the general term used to describe the number of eggs produced[17]or the

64019

egg-laying capacity of the fish [20]. The number of eggs ripened by female fish during a spawning season varies from a few dozen to millions [11]. In general, fecundity varies among species, viviparous fish have lower fecundity than ovoviviparous fish, which in turn have lower fecundity than oviparous fish and nest builders have lower fecundity than pelagic spawners. Fecundity can be expressed as the number of mature ova in the ovary, the number of ovulated eggs or the number of eggs deposited during spawning [23]. Breeding is possible for fish in warm water by appropriate control of their environment[5]. Breeding of ornamental fish can be a profitable proposition if it is done in a well monitoredenvironment [20].

Reproductive development and spawning in fish were controlled by various environmental factors such as temperature, nutrition, water quality etc. In aquaculture, embracing fancy fish culture, many species are grown which are far from their original agro-climatic condition. During recent years, intensive aquaculture practices have been emerged, due to this farmer's requirement for fish seed is increasing every year. Inadequacy of quality fish seed supply has been a major constraint in the development and progress of aquaculture. Market demand for fancy fish usually not synchronized with its breeding season. So far, in the regulation of reproduction and induced breeding, many products areutilized [2]. Presently three types of hormones are used for induced breeding purpose, (1) Fish pituitary gonodotropins, (2) HCG (Human Chorionic Gonadotropin,(3) GnRha (Gonadotropin releasing hormone analogue) with or without a dopamineanagonist. Ovaprim is a drug used as a substitute for pituitary extract in induced breeding. Ovaprim gained popularity among the fish farmers who involved in fish seed trade. Trials with ovaprim on Indian major carps administered with single dose on either sex showed excellent results i.e. induced complete spawning [14 &16]. Ovatide is a newly launched ovulating agent developed by an Indian Company Hemma Pharma, Mumbai). It is a synthetic preparation containing salmon GnRH analogue and dopamine antagonist. It has been successfully tested by [15] in *Catlacatla* [13] in *Ompokpabo* [10] in *Channastriatus*. The present study assesses the fecundity on exposure to the homeopathic preparation natrummuriaticum 30 c potency in fish viz goldfish, rosy barb, white molly and guppy. It also traces the time taken to spawning in viviparous fish.

MATERIAL AND METHODS

Animals
Two types of fish (egg layer and live bearer) were selected for this induced breeding study. Sexually mature, healthy and female of gold fish, rosy barb, guppy and white molly were procured from Aqua pet shop in the polythene bags and transferred to big plastic tubes. They were acclimated to the laboratory condition for 10 days. During the period of acclimation, fish were fed with Day Today's complete nutritional food. The water was changed daily. The uneaten feed and faecal pellet were removed daily. Uniform sized fish with identical maturity condition were used for the experiments. The fish were divided into two groups i.e egg layer and live bearer. In each group two types of fish are used i.e., gold fish, rosy barb and guppy and molly respectively. In each type totally 12 fish were taken. Among this, six were used as experimental and six were used as control. Experimental fish were introduced into the medium. On 4th day of the experiment fish were autopsied, eggs were collected and counted in control and experimental group of egg layers. Spawning was observed in the form of young ones number in control and treated group of livebearers.

Homeopathic preparation
The homeopathic preparation, Natrummuriatium of 30c potency was brought from a local homeopathy medial shop. It is kept in a normal room temperature and light. The preparation was diluted by 0.1ml in 400ml of ground water. The medium was prepared in plastic troughs of 2 litre capacity.

Method of treatment
The homeopathic preparation medium was prepared in six plastic troughs considered as experimental ones and six troughs containing only ground water as control. The fish were introduced into medium one in each. The experiment was carried out for three days i.e., the medium was changed morning at 8 am and evening at 4 pm. Evening only ground water was used, at the same time feeding was done. On the day before medication (0 day) and after three

days the oviparous fish were dissected and eggs were pooled out and counted. But for the viviparous the set up was carried out to find the latency period without adding natrummuriaticum after 3 days.

RESULTS

In order to ascertain the effect of natrummuriaticum for the induction of breeding an experiment was conducted in gold fish, rosy barb, guppy and white molly. Each value represented the mean value of six samples for each species. The experimental animal goldfish laid 850 ± 104 eggs in 4 days, the control animal laid 383 ± 75 eggs in 4 days (Table 1, Figure 1, 2A and 2B) whereas in rosy barb experimental animals laid 110 ± 15 eggs in 4 days and the control animal laid 56 ± 11 eggs in 4 days (Table 1, Figure 1, 2C and 2D). Number of eggs level altered significantly between control and experimental animals. The effect of Natrummuriaticum on induced breeding of white molly and guppy are presented in the Table 2 and Figure 3. The natrummuriaticum treated animal laid 39 ± 5 young ones in 19.5 ± 3 hours, while the control animal laid 20 ± 2 young ones in 72 ± 6 hours in white molly (Figure 4A and 4B), whereas in guppy the control animal laid 8 ± 1 young ones in 79 ± 9 hrs and the treated laid 15 ± 2 young ones 36 ± 9 hours (Figure4C and 4D). In viviparous fish also there was a significant changes observed between control and experimental animals.

DISCUSSION

The results suggested the role of natrummuriaticum (homeopathic preparation)in the regulation of breeding in oviparous (goldfish and rosy barb) and viviparous fish(white molly and guppy). Present findings demonstrated that homeopathic preparation natrummuriaticum is a highly effective stimulus for breeding of the above mentioned fish. The experimental preparation natrummuriaticum is also a natural material preparation. There appears to be no experimental information regarding the role of natrummuriaticum in ovulation of teleosts[19]. Only [12] used this homeopathy preparation on major carps for breeding purpose and obtained a positive result. According to [18]*Ompokbimaculatus*an endangered fish, was induced to spawn by a single intramuscular injection of ovaprim (0.5ml/kg).He observed spawning of fish after 5-6hours injection. Each female spawned an average of 4012 eggs. Successful spawning of *C.punctatus*at0.3and 0.5ml/kg and 3000IU/kg body mass of HCG. He also observed successful spawning in *H.fossilis* at 0.3, 0.5 and 0.7ml/kg body mass for ovaprim and1000, 2000and 3000 IU/kg body mass for HCG [7,21]. stated that the single dose administration(30μl/ fish) of pedalium murex, a whole plant extract, induced laying at about 42 hr inblack molly and 20 hr in rosy barb. Similarly single dose administration of (30μl/ fish) *mucunapruriens* seed extract induced spawning at 48hrs in the case of black molly and24 hrs in rosy barb.[22] conducted experiments using natrummuriaticum of 1000cpotency in gold fish induced the spawning within 12 hours against 5 days in the control. He noted that treated animals laid 2856 eggs whereas the control laid 209 eggs.

The endangered riverine catfish, pang as *Pangasius pangasius*, was examined by [8] with 10mg/kg of pituitary gland extracts. He observed that the hatching of fertilized eggs occurred between 28 and 32 hours.[3] reported using five doses of PG extract (1.00, 2.00, 3.00,4.00 and 5.00 ml /kg) in Rajputi *Puntius gonionotus* (Bleeker) affected 100% egg release through induced spawning. Induced breeding of Koi carp and Goldfish by the use of synthetic hormone Synchromate B was highlighted by [9]. He reported that induction at the rate of 0.1ml per gold fish of 25g and 0.25ml per koi carp of 250g yielded potential fry stock of 1600 ± 604 and 30880 ± 7127 respectively. Spawning response of goldfish with ovaprim 0.5μl in female released 1000 ± 115 eggs after 10-12 hr of injection was observed by[6].

The use of ovaprim resulted maximum fecundity in angel fish *Pterophhyllum scalare* suggested by [4]. Maximum fecundity (665.66) was obtained at the optimum dose of ovaprim (0.35ml/kg of body weight). The highest percentage of fertilization in goldfish and koi carp through induced breeding of intraperitonial injection by ovaprim is reported by [1].So when the effectiveness was compared with other hormones, this preparationis found highly effective, cost effective and suitable for farmers. Natrummuriaticumbeing a Swadeshi product, it is easily available, simple to prepare and natural in origin. Further studies on natrummuriaticum will improve our country's economic status, through which more foreign investment may be earned by this Swadeshi product.

From the available references along with the present investigation on the induced breeding in ornamental fish, it was observed that higher levels of fecundity were achieved from a comparatively lower dosage of natrummuriaticum. It enhanced the production of matured eggs in oviparous and highly motile young ones in viviparous within shortperiod by using simple method of breeding. If this technique is employed to increase the production rate, it is possible to meet the domestic demand as well as to enter the international market in turn will fetch foreign exchange to our country.

REFERENCES

1. Ananth Kumar Y, Mohamed Abdul KadherHaniffa, (2014). Interspecific hybridization between cyprinids *Carassiusauratus* goldfish and *Cyprinuscarpio*koicarp; *Asian J.Biol.LifeSci*, 2, (1): 64-67.
2. Anon, (1995). Report on endocrine techniques in aquaculture, Argent Laboratories Press Washington, USA, 30-33.
3. Bhuiyan A.B, Khairul I.M and Zaman T, (2006). Induced spawning of *puntiusgonius* (Bleeker), *J.bio-sci*, 14: 121-125.
4. Chatterjee N.R, Samiran P and Talwar N.A, (2013). Induced Breeding of Fresh Water Angelfish (*PterophyllumScalare*) Using Ova prim: *IOSR* Journal of Agriculture and Veterinary Science, 3(3): 24-28.
5. ChristophMeske, (1985). FISH AQUACULTURE, Pergamon Press, Germany: 1-150.
6. Jagtap H.S, (2011). Comparative study on induction of spawning in goldfish (*Carassiusauratus*) by prostaglandins & other inducing agents, *Indian J. Sci. Technol*, 9 Vol. 4(8), 9-14.
7. KatharHaniffa M.A and Sridhar.S (2002).Induced spawning of spotted murrel(*Channapunctatus*) and catfish (*Heteropneustes fossils*) using human chorionic gonadotropin and synthetic hormone (ovaprim) Veterinarshic arhiv,72(1),51-56.
8. Khan M.H.K and Mollah M.F.A, (2004). Further trials on induced breeding of *Pangasiuspangasius* in Bangladesh, *Asian Fisheries Science*, 17:135-146.
9. Manikandavelu D, Raveneswaran K and Sivakumar T, (2009). Breeding of Koi carp (*Cyprinuscarpio*) and goldfish (*Carassius auratus*) using Synchromate B.(GnRh regulator), *TamilnaduJ.Veterinary& Animal Sciences*, 5 (6):225-227.
10. Marimuthu K, Kumar D and Haniffa M.A. (2007). Induced spawning of striped snakehead, *Channastriatus*, using ovatide. *Journal of Applied Aquaculture*, 19(4): 95-103.
11. Miller B.S and Kendall,A.W(2009).Early life history of marine fishes9Vol,36,No.4) Berkeley,University of California Press, pp 1-240.
12. Mitra S.D and Raizada S, (1986). Gonadal development of major carps through homeopathy, Fishing Chimes, May: 17-18.
13. Mukherjee M and Das S, (2001). Artificial propogation of a fish pabda *Ompokpabo*, *Fishing chimes*,21: 75-79.
14. Pandey A.C and Singh R.N,(1997). Breeding of *Catlacatla, Labeorohita* and *Cirrhinusmrigala* by ovaprim injection for quality seed production, *J. Adv. Zool*, 18: 38-41.
15. Pandey A.K, Baruah A and Biswas S.P, (1998). On the ornamental fish fauna in Brahmaputra drainage system, Inland J Fish, 45: 95–97.
16. Pandey A.X, Koteswaran R and Singh B.N, (2002). Breeding of fishes with synthetic honnone drug ovatide for mass scale seed production. Aquaculture ,3:137-142.
17. Roy P.K, (1996).Observations on the use of ovaprim for induced spawning of Indian Major Carps, ADVANCES IN FISH AND WILDLIFE ECOLOGY AND BIOLOGY, Daya Publishing House,Delhi, pp 1-67.
18. Sridhar S, Vijayakumar C and Haniffa M.A, (1998). Induced spawning and establishment of a captive population for an endangered fish *Ompokbimaculatus* in India, Curr. Sci., 75: 1066-1068.
19. Stacey N.E, (1979). Spontaneous and gonadotropin-induced ovulation in the goldfish *Carassiusauratus*, Journal of Fish Biology,15: 349-361.
20. Swain S.K, Sarangi N, Ayyappan S, (2010). ORNAMENTAL FISH FARMING, ICAR, New Delhi: pp 1-128.
21. Thamilmani K and Subramaian P. (2002). Effect of alcoholic extract of certain aphrodisiac plants on the reproductive ability of ornamental fishes, proc XX SympReprodBiol comp Endocrinol, Jan 7-9:163-164.
22. Vishakan R, (2002). Induced breeding in chosen ornamental fishes using Homeopathy preparation, Ph.D thesis, Bharathidasan University, Tiruchirappalli, Tamilnadu,29-36.

Sudha

23. Webster C.D and Lim,C.(2006)Tilapia:biology,culture and nutrition.CRCPress,New York, pp 1-202.

Table-1.Evaluation of number of eggs in oviparous fish

Animal		Body Length(cm) (Mean±SD)	Body weight(g) (Mean±SD)	Latency period (Hours) (Mean±SD)	Number of eggs (Mean±SD)	't' values
Gold fish	Control	7.2±0.50	8.58±1.02	72	383±75	8.85438 at P<.05 level
	Experimental	7.4±0.58	9.67±0.81	72	850±104	
Rosy barb	Control	5.18±0.19	2.03±0.17	72	56±11	5.23197 at P<.05 level
	Experimental	5.35±0.22	2.38±0.42	72	110±15	

Table-2.Evaluation of number of young ones in viviparous fish

Animal		Body Length(cm) (Mean±SD)	Body weight(g) (Mean±SD)	Latency period (Hours) (Mean±SD)	Number of Young ones (Mean±SD)	't' values
Molly	Control	5.01±0.27	2.84±0.36	72±6	20±2	11.5594 at P<.05 level
	Experimental	5.2±0.31	3.08±0.32	19.5±3	39±5	
Guppy	Control	4.55±0.32	1.24±0.18	79±9	8±1	7.82624 at P<.05 level
	Experimental	4.8±0.36	1.62±0.19	36±9	15±2	
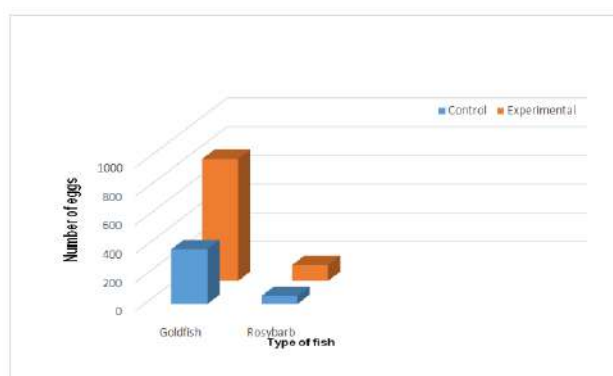
Figure-1-Evaluation of number of eggs in oviparous fish

64023

Figure-2A-Eggs of goldfish (control)

Fig-2B-Eggs of goldfish Experimental

Fig-2C-Eggs of rosy barb (Control)

Fig-2D- Eggs of rosy barbExperimental

Table-2.Evaluation of number of young ones in viviparous fish
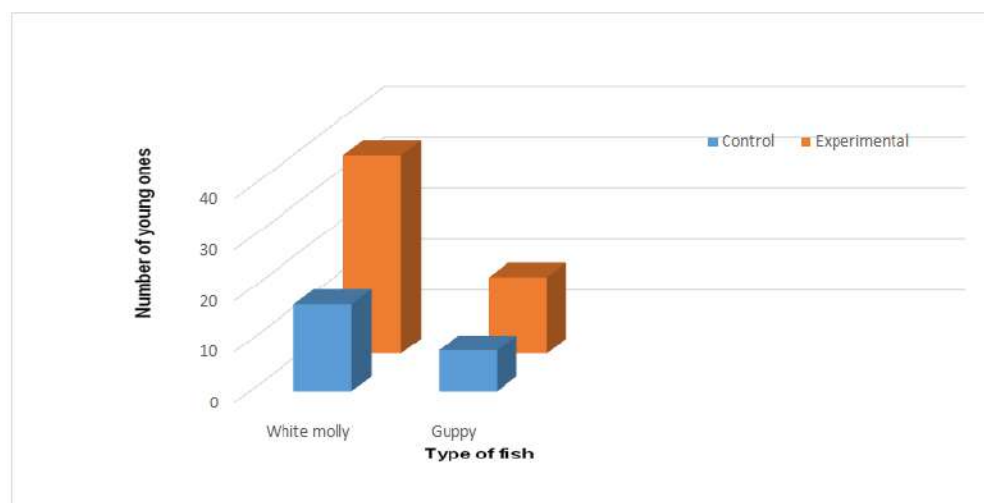
Fig-3-Evaluation of number of youngones in viviparous fish

Fig-4A-Youngones of white molly-(C)

Fig-4B-Youngones of white molly (E)

Fig-4C-Youngones of guppy (C)

Fig-4D Youngones of guppy (E)

RESEARCH ARTICLE

Toxicological Effects of the Organophosphate Pesticide – Quinalphos on the Haematological, Histopathological and Marker Enzyme Level of the Freshwater Fish *Oreochromis mossambicus*

Arshitha A[1] and Pawlin Vasanthi Joseph[2]*

[1]PG Student, PG and Research Department of Zoology, Nirmala College for Women (Autonomous), Red Fields, Coimbatore-641 018, Tamil Nadu, India.
[2]Associate Professor and Head, PG and Research Department of Zoology, Nirmala College for Women (Autonomous), Red Fields, Coimbatore-641 018, Tamil Nadu, India.

*Address for Correspondence
Pawlin Vasanthi Joseph
Associate Professor and Head,
PG and Research Department of Zoology,
Nirmala College for Women (Autonomous),
Red Fields, Coimbatore-641 018,
Tamil Nadu, India.
E.Mail: pawl_06@rediffmail.com

ABSTRACT

The present study investigates the effects of Quinalphos on the haematological, histopathological and marker enzyme level of the freshwater fish *Oreochromis mossambicus*. Fishes were exposed to sublethal concentration (0.009 ml/l) of Quinalphos for 30 days. The WBC indices were significantly increased during the experiment and all other indices like RBC, Hb, PCV, MCV, MCHC, MCH and platelet count decreased during the experiment. The control fishes showed normal histoarchitecture of muscle, gills and liver. Severe degeneration in the muscle fibers, degeneration and necrosis of the respirating epithelium and lamella of gills and hepatic parenchyma with features of severe fatty degeneration and congestion was shown in fishes exposed to Quinalphos. The level of liver marker enzymes such as AST, ALT and ALP showed a significant increase in the Quinalphos-treated fishes than that of the control group. The results of the present study clearly indicated that pesticides have direct impact on the biochemical, physiological and structural alteration in *Oreochromis mossambicus.*

Keywords : Quinalphos, *Oreochromis mossambicus*, Haematology, Histopathology, Liver marker enzyme, Gills, Liver, Muscle, Alkaline phosphatase, Aspartate aminotransferase, Alanine transaminase.

Arshitha and Pawlin Vasanthi Joseph

INTRODUCTION

Environmental pollution is one of the major issues that world is facing. The rate of pollution is increasing every year, causing severe irreparable environmental damage. Water pollution is the most dangerous type of pollution, and it is the biggest threat posed by urbanization, industrialization, and modern agricultural practices. It causes variations in the physical, chemical, and biochemical properties of water bodies[1]. One of the most common categories of toxic substances used in India to manage pests in agricultural lands and control vectors of human disease are insecticides. Rivers and agricultural ponds that receive water from rivers are both impacted by runoff from treated areas [2]. Less than 0.1% of the pesticide used in the fields actually contacts the intended target organism; the other 99% enters the environment. Quinalphos (O,O-diethyl O-quinoxalin-2-yl phosphorothioate), an organophosphorus insecticide, is used worldwide to control agricultural pests. Organophosphorus insecticides are the most widely used synthetic chemicals for controlling agricultural pests. Quinalphos act as a cholinesterase inhibitor and may cause disorders in physiological state of nervous system. It disrupts the passage of impulses across the neuromuscular junction by inhibiting acetylcholinesterase [3].

One of the most frequently usedmethod to evaluate fish physiological status and health is haematological examination. Haematological parameters are crucial in determining the structural and functional rank of a toxicant-treated animal because, blood is the pathophysiological indicator of the entire body. The ability to compare the tissue structures or morphology of healthy and diseased fish allows for the use of histology as a diagnostic tool for fish diseases; however accurate diagnosis and confirmation of disease-related changes require proper specimen processing and a high level of histopathology expertise [4]. It has been suggested that, in general, stress induces elevation of the transamination pathway and the activities of alanine aminotransferase (ALT), aspartate aminotransferase (AST) and alkaline phosphatase (ALP)have been used as relevant stress indicators [5].

The present study aimed to evaluate the insecticide Quinalphos toxicity at the tissue level after its intoxication at sublethal dose in fresh water fish *Oreochromis mossambicus*. The current study's specific objectives were to determine the lethal concentrationLC$_{50}$, to investigate the haematological parameters (RBC, WBC, Hb, PCV, MCH, MCV, MCHC and platelet count), histology of vital tissues such as gills, muscle and liver and to estimate the level pf marker enzymes of *Oreochromis mossambicus* treated with Quinalphos.

MATERIALS AND METHODS

Test animal: The Tilapia fish, *Oreochromis mossambicus* of 10-12 cm was collected from a local fish farm in Thrissur, Kerala. These fishes were transported to the laboratory in oxygenated tubs. The fishes were acclimatized for 15 days in the fish tank containing plain tap water in laboratory and was fed with commercial fish pellets.

Test chemical: In this study, Quinalphos was purchased from commercial store and used for the exposure to the fish. The major use of Quinalphos in farming is to protect corn, cotton and fruit trees against insects. This pesticide is commonly used in Kerala, which act as a cholinesterase inhibitor and may cause disorder in the physiological state of the nervous system in the insects.

Experimental design and treatment: The fishes were acclimatized for 10-15 days in a fish storage tank in the laboratory. They were fed with commercial artificial feed (pellets) twice day. After acclimatization, the *Oreochromis mossambicus* having the size of 10-12cm were randomly distributed in plastic tubs of 10 liters capacity. One tub was maintained as control and other tubs are treated with different concentration of quinalphos as 0.003 ml/l, 0.005 ml/l, 0.007 ml/l, 0.009 ml/l and 0.011 ml/l.Six fishes were used for each concentration of quinalphos placed in each tub and the mortality rate was noted after 24 hrs., 48 hrs., 72 hrs. and 96 hrs.

Then experiment was designed to expose the fish to separate tubs with different sublethal doses of quinalphos. The doses were 0.009 µl/l, 0.007 µl/l, 0.005 µl/l. Each tub was provided with 6 fishes The period of the experiment was 30 days. The fishes were fed with artificial feed twice a day during experimental period. Each day the tubs were refilled with fresh water and the appropriate concentration of quinalphos was induced in the tubs. Fishes were starved for 24 hours. After which the blood specimen was collected. Each fish was caught by a dip net and blood was collected from common cardinal vein using sterilized small insulin needles. To avoid clotting of the blood during collection, sterile evacuate tubes containing EDTA was used. Blood samples were immediately used to determine the hematological parameters such as total erythrocyte, leucocyte count, haemoglobin (Schaperculaus, 1991), red blood cell indices and platelet count (Dacie and Lewis, 2006). And also blood was collected in tubes for estimating the level of liver marker enzymes such as *Aspartate aminotransferase* and *Alanine aminotransferase* (Reitmann and Frankel, 1957) and Alkaline phosphatase (Garen and Levinthal).

After collection of blood samples, Histopathology of vital tissues such as gills, liver and muscles were also assessed after 30 days of treatment and was preserved in 10% buffered formalin for histological studies.

Statistical analysis: The dose responses of mortality was studied using a computer-based probit analysis method. Results were expressed as mean ± standard error of mean of 4 observations. Statistical analyses of data was performed using 't' test, P values of less than 0.05 were considered as significant. Analysis of variance (ANOVA) was employed followed by Duncan's new multirange test to calculate the significance difference between control and experimental means (SPSS Version, 21).

RESULTS AND DISCUSSION

Acute toxicity: The results of Probit analysis is shown in the Table 1 and Fig 1. In the present study, 50% mortality was observed at a concentration of 0.009 ml/l of quinalphos. The log concentration using Probit analysis (Finney, 1953) is 0.905. The corrected mortality data were analyzed by the following method of Finney (1957) to determine the LC_{50} values. Figure X represents the plot of probability (of mortality) is estimated concentration of Quinalphos, which indicates the LC_{50} of 8.035 µl/l of Quinalphos for *Oreochromis mossambicus.*

Effect of Quinalphos on haematological parameters: The results of haematological examination of blood samples from acute toxicity are given in Table 2. The mean control value of the RBC after 30 days of treatment was 4.9±0.2. A statistically significant decrease in RBC content was seen in the entire experimental group of fishes treated with quinalphos concentrations of 5µl/l, 7µl/l and 9µl/l. Its values are as follows ; 4.6±0.436, 4.4±0.361 and 4.2±0.265. After 30 days of exposure in both the control and the experiment, the ANOVA for RBC is statistically insignificant. Blood is a pathophysiological reflector of the body because it is highly susceptible to internal and external environmental fluctuations. Blood parameters are contemplated as a sensitive measure of stress in fish exposed to different water pollutants and toxicants like industrial effluents, metals, pesticides, chemicals, biocides etc. [6].A significant reduction in red blood cell count was observed in this study compared with the control group. Similar observations were already report. This anemic response could result from inhibition of RBCs and haemosynthesis, osmoregulatory dysfunction, and destruction of RBC in hematopoietic organs [7][8].

The mean control value of WBC after 30 days of treatment is 1800±4.359. There is a significant increase in WBC content observed in all experimental groups. The highest WBC content level of 2400±4.583 was observed in the fish group treated with 9 µl/l of the pesticide. The observed WBC level for 5µl/l and 7µl/l is 1700±2.646 and 2000±1.732 respectively. After 30 days of exposure in both the control and the experiment. the one-way ANOVA for WBC is statistically significant at the 99% significance level (p < 0.01).The increase in WBC count in the study indicates the stress condition of the fish caused by Atrazine which might have produced hypoxia and gill damage [9].WBC count was increased significantly when compared to the control animals and this could be due to hemodilution, a mechanism that reduces the concentration of the pollutants in the circulatory system[10].

Arshitha and Pawlin Vasanthi Joseph

The mean control value of haemoglobin after 30 days of treatment is 14.9±0.208. Similar to RBC, a significant decrease in haemoglobin content has been observed in all the experimental groups. The lowest haemoglobin level of 12.7±0.557 was observed in the fish group treated with 9µl/l of the toxic compound. The observed haemoglobin levels for the concentration 5µl/l and 7µl/l of quinalphos were 14.6±0.3 and13.5±0.4 respectively. The one-way ANOVA findings revealed a statistically significant difference(at the 0.01 level) in haemoglobin levels after 30 days of exposure in the control and experimental groups.In such a case, because of decrease in oxygen consumption also reported to cause pronounced haematological changes [11]. Haemoglobin levels significantly decreased after 24 hours may be due to the disruption of iron synthesizing machinery [12]. It may impair oxygen supply to various tissues, thus resulting in a slow metabolic rate and low energy production [13].

PCV level in the control fish population is 45.1±0.132 after 30 days of treatment with no exposure to a toxicant. It was discovered that the amount of PCV in the blood was directly proportional to the amount of exposure. The greatest reduction was observed in the experimental group exposed to 9 µL/l of toxicant, followed by groups exposed to 5 and 7 µl/l of the toxicant. Among the 5- 7µl/l exposure fish groups, the PCV values are 44±0.755, 40±0.1, 38.7±0.458. The one-way ANOVA for PCV between the control and the experiment is statistically significant at the 0.01 level of significance.The PCV values always decrease when a fish loses appetite or becomes diseased or stressed [14]. In the present study, the distinct decrease in the level of Haemoglobin and PCV after exposure to malathion suggests a hemodilution mechanism possibly due to gill damage or impaired osmoregulation.The decrease in the PCV indicates the worsening of the condition of the organism and developing of anemia[15].

After 30 days of treatment, the control value of MCV is 91.9±0.058. A statistically significant drop in MCV content was detected in the entire experimental group, including fish treated with 5 µl/l, 7 µl/l and 9 µl/l of the toxicant. The values are 91.7±0.153, 91.3±0.321, 90.6±0.306. One way ANOVA for MCV after 30 days of exposure in the control and experimental groups is significant at the 0.01 level. The control value of MCH after 30 days of treatment is 32.3±0.252. A significant decrease in MCV content has been observed in the entire experimental group of 5µl/l,7µl/l and 9µl/l treated fishes. The values are 31.2±0.832, 31.1±0.351 and 30.6±0.115 respectively. The ANOVA for MCV after 30 days of exposure in control and experimental are significant at 5% level. The alterations in MCV and MCH were ascribed to hemolysis and impairment in hemoglobin synthesis [16].

The control value of MCHC after 30 days of treatment is 33.73±0.153. A significant decrease in MCV content has been observed in the entire experimental group of 5 µl/l, 7 µl/l and 9 µl/l treated fishes. The values are33.67±0.321, 33.37±0.551 and 33.1±0.346 respectively. The one-way ANOVA for MCV after 30 days of exposure in control and experimental is insignificant.Further, changes in blood cell indices like MCH, MCH, MCHC and MCV were also observed in the study. This may be due to the fact that these are very sensitive and can cause reversible changes in the homeostatic system of fish. Fluctuations in these indices directly correspond with the values of RBC count, Haemoglobin concentration and packed cell volume. The present findings are similar to the earlier reports [17]. The control value of platelet count after 30 days of treatment is 21000±31.048. A significant decrease in platelet content has been observed in the entire experimental group 5 µl/l, 7 µl/l and 9 µl/l of treated fishes. The values are 20000±28.583, 19700±28.054 and 18000±18.33 respectively. The one-way ANOVA for MCV after 30 days of exposure in control and experimental is significant at 1% level.Platelets are nucleated cells responsible for blood clotting in fish; a slight decrease in values observed in this study may signify the effect on platelet (thrombocyte) production [8].

Effects of Quinalphos on vital organs (histopathology):
The muscle in the control section examined was found to be having normal appearing muscle fiber bundles. Degeneration of muscle fibers was noticed in the section which was obtained from the concentration of 5 µl/l of Quinalphos. According to the examination, severe degeneration of muscle fibers were shown by the sections taken from the concentration 7 µl/l and 9 µl/l (Figs. 2,3,4,5).Das and Mukherjee (2000) have studied the effect of different pollutants on fish muscles.The fish showed marked thickening of muscle bundles with severe intracellular edema [18].

The gills in the control section examined was to be normal in appearance, with intact gill filament epithelium and lamella. Degeneration and necrosis of the respirating epithelium and lamella were noticed in sections analyzed from the received biopsy at a concentration of 5 µL/l and 7 µl/l. Segments investigated from the attained biopsy elucidated Severe degeneration and necrosis of the respiratory epithelium and lamella in the fish category exposed to 9 µl/l, confirmed by microscopy (Figs. 6,7,8,9). Since, gills are the respiratory and osmoregulatory organ of fish, the histopathologic changes of the gills might impair the respiratory function of the gills by reducing respiratory surface area resulting in hypoxia, respiratory failure problems [19].

In the control segment, the liver parenchyma is normal-appearing, yet it has a characteristic of congestion. At 5 µL/l, the liver parenchyma in the sections examined appears normal, although there are signs of congestion and fatty degeneration. However, hepatic parenchyma with features of severe fatty degeneration and congestion was noticed in the fish group treated with a concentration of 7 and 9 µl/l of Quinalphos (Fig. 10,11,12,13).Hepatocytes are the most abundant cell types within the liver and perform most of the liver's essential functions, such as converting glucose to glycogen, regulating lipids, and deamination of amino acids [20].

Liver marker enzyme studies: The results of level of liver marker enzymes of blood samples from acute toxicity are given in Table 3.The mean control value of hemoglobin after 30 days of treatment is100.4±0.557. Similar to ALT, a significant increase in AST content has been observed in all the experimental groups. The lowest hemoglobin level of 137.2±0.458 was observed in the fish group treated with 5 µl/l of the toxic compound. The observed AST levels for the concentration 7µl/l and 9 µl/l of quinalphos were 256.8±0.794 and 476.8±0.608 respectively. The one-way ANOVA findings revealed a statistically significant difference(at the 0.01 level) in AST levels after 30 days of exposure in the control and experimental groups.Serum glutamic oxaloacetic transaminase (SGOT) is maximally present in heart followed by liver, skeletal muscles, and kidney. Any damage to these organs raises the SGOT level as in myocardial infarction, Liver diseases such as Liver cirrhosis, Viral Hepatitis, Liver necrosis and skeletal muscle diseases [21].

The mean control value of ALT after 30 days of treatment is 33.03±0.153. There is a significant increase in ALT content observed in all experimental groups. The highest ALT content level of 94.6±0.625 was observed in the fish group treated with 9 µl/l of the pesticide. The observed ALT level for 5µl/l and 7µl/l is43±0.436 and 77.2±0.529 respectively. After 30 days of exposure in both the control and the experiment. the one-way ANOVA for ALT is statistically significant at the 99% significance level ($p < 0.01$).SGPT is in highest concentration in the liver followed by the kidney. Under pesticidal stress, these organs get damaged and the enzyme level elevates in the serum. The SGPT level is found to be raised in liver diseases such as infective hepatitis, liver cirrhosis, cholestatic jaundice and skeletal muscle damage [22].

Under exposure to sublethal concentrations of Quinalphos, the amount of Alkaline Phosphatase (ALP) was found to increase in all the test tissues of Oreochromis mossambicus. In this experiment control shown least ALP content 11.93±0.252. A statistically significant increase in ALP content was seen in the entire experimental group of fishes treated with quinalphos concentrations of 5µl/l, 7µl/l and 9µl/l. Its values are as follows ; 14±0.361, 18.2±0.173 and 66.8±0.458 respectively.Decreased phosphate activity may be due to alteration in membrane permeability, distribution of normal functioning of cell organelles like lysosomes and mitochondria and different suppressor mechanisms associated with toxicity together resulted in significant changes in the level of enzymes in the tissues examined. The decreased activity of ALP in fish is linked to the increased catabolic breakdown in melanomacrophage centers [23].

CONCLUSION

The use of pesticides in the field of agriculture cause disruption in the balance of the ecosystem. O,O-diethyl O-quinoxalin-2-yl phosphorothioate is commonly called as quinalphos which is a organophosphorus insecticide used to control aphids, thrips and mites on paddy, cotton, sugarcane and potato.

Arshitha and Pawlin Vasanthi Joseph

The results of the present study clearly indicated that pesticides have direct impact on the biochemical, physiological and structural alteration in Oreochromis mossambicus. The exposure of fish to this insecticide resulted in reduction in the haematological parameters, degeneration in the vital tissues and a significant increase in the levels of marker enzymes. This negatively affect the growth, reproduction, immunity and even the survival of the fish in the natural environment. This should be also considered by farmers, when they are using quinalphos for pest control in their fields. So awareness should be created among the people to use biocides instead of pesticides and insecticides.

REFERENCES

1. Aswin .B, Binu Kumari .S, Ravisankar .S, Mohan Kumar .M, Ambikadevi .A.P, and Drishya .M.K, "The effect of quinalphos on histopathological changes in the gills of freshwater fish *Anabas testudineus*", *IOSR Journal of Environmental Science, Food and toxicology*, 10(4):12-16, 2016.
2. Begum,G, Carbofuran insecticide induced biochemical alterations in liver and muscle tissues of the fish *Clarias batrachus* and Recovery response. *Aquatic Toxicology*. 66: 83-92, 2004.
3. K.P Greeshma, K.H Mariyam, Laya Paul and E. Pushpalatha, "Biochemical effects of organophosphorus pesticide, Quinalphos on freshwater fish *Oreochromis niloticus* (L.)", *Journal of Advanced Laboratory Research in Biology*, 10(3), pp 95-99, 2019.
4. Abhirami Santhosh, Mubashira P.K and Pawlin Vasanthi Joseph, "Effect of 2,4 Dichlorophenoxy Acetic Acid (Herbicide) on the haematological and histopathological parameters of Freshwater fish *Oreochromis mossambicus*, *International Journal of Zoological Investigations*, 8(2), 06-14, 2022.
5. Ishikawa T.O, Griffin K.J, Banerjee U and Herschman H.R, "The zebrafish genome contains two inducible, functional cyclooxygenase-2 genes", *Biochemical and Biophysical Research communication*, 352(1), 181-187, 2007.
6. Prince Sharma and Pooja Chadha, "Bisphenol A induced toxicity in blood cells of *Channa punctatus* after acute exposure", *Saudi Journal of Biological Sciences,* 28(8), 4738-4750, 2021.
7. Vani T, Saharan N, Mukherjee S, Ranjan R, Kumar R and Brahmchari R, "Deltamethrin induced alterations of haematological and biochemical parameters in fingerlings of *Catla catla* (Ham.) and their amelioration by dietary supplement of vitamin C", *Pestic. Biochem, Physiol*, 101, 16-20, 2011.
8. Soni R, Gaherwal S and Shiv G, "Effect of herbicide 2,4-D on haematological parameters of *Clarias batrachus*", *International Journal of Current Research in Life Sciences,* 7(07), 2441-2444, 2018.
9. Ramesh M, Srinivasan R and Saravana M, "Effect of atrazine (Herbicide) on blood parameters of common carp *Cyprinus carpio*", *African Journal of Environamental Science and Technology*, 3(12), 453-458, 2009.
10. Smit G.L, Hatting J, and Burger A.P, "Haematological assessment of the effects of the anesthetic MS222 in natural and neutralized form in three freshwater fish species: Interspecies differences", *Journal of Fish Biology*, 15, 633-643, 1979.
11. Tilak, K.S and Satyavardhan, K, "Effect of fenvalerate on oxygen consumption and haematological parameters in the fish *Channa punctatus* (Bloch)". *J. Aqua Biol.*, 17: 81-86, 2002.
12. Beena, S and Viswarajan, S., "Effect of Cadmium and Mercury on the haematological parameters of the fish *Cyprinus carpio*",*Environmental Ecology* 5: 726-732,1987.
13. Ahammed, F., Ali, S.S and Shakoori, A.R, "Sublethal effects of Danitol (Fenpropathrin), synthetic pyrethroid on freshwater *Ctenopharyngodon idella.*" *Folia Biologica* 43: 151-159, 1999.
14. Annune P.A and Ahuma F.T.A, "Haematological changes in mudfish *Clarias gariepinus* (Bruchell) exposed to sublethal concentration of copper and lead," *J. Aquati. Sci*, 13, 33-36, 1998.
15. Akinrotimi, O.A., Abu, O.M.G., Ansa, E.J., Edun, O.M. and George, O.S, "Haematological responses of *Tilapia guineensis* to acute stress." *International J National and Applied Sci.*, 5. 338-343, 2009.

Arshitha and Pawlin Vasanthi Joseph

16. Shah A.W, Parveen M, Mir S.H, Sorwar S.G and Yousaf A.R, "Impact of helminth parasitism on fish haematology of Anchar lake, Kashmir", *Pakistan Journal of Nutrition*, 8(1), 42-45, 2009.

17. Balini, T., Szegletes, T., Szegletes, Z, Halasy, K. and Nemcsok, J. "Biochemical and subcellularchanges in carp exposed to the organophosphorus methidathion and the pyrethroid deltamethrin." *Aquatic Toxicology*, 33: 279-295, 1995.

18. Das, B.K. and Mukerjee, S.C, "Toxicity of cypermethrin in *Labeo rohita* fingerlings biochemical, enzymatic and haematological consequences."*Comparative Biochemistry and Physiology* C., 134: 109- 121, 2003.

19. Alazemi, B.M., Lewis J.W. and Andrews, E.B, "Gill damage in the fresh water fish *Gnathonemusptersii*(Family: Mormyridae) exposed to selected pollutants: an ultrastructural study,"*Environmental Technology*, 17, 225-238.1996.

20. Wright, M.C., Mann, D.A., Orrl, J.G., Hawksworthl, G.M., Marek1, C.J., Leel, V., Haughton, E.L., Koruth, M., Murray, G.I., Trim, J.E. and Elrick, L.J. "Intercellular signaling by cytokines and the fibrogenic response of the liver to chronic liver damage." *Toxicology*, 202, 33-127, 2004.

21. Mathur D.S, "Histopathological changes in liver of certain fishes induced by dieldrin. *Sc. and cult*, 31, 1965.

22. Deepak Rawat, Vandana Mishra and Radhey Shyam Sharma," Detoxification of azo dyes in theContext of environmental processes", *Chemosphere*, 155,591-605, 2016.

23. S. Binukumari and M. Manimegala, Impact of Quinalphos on Acid Phosphatase and Alkaline Phosphatase Activity in the Tissues of Freshwater Fish, *Labeo rohita*, Nature Environment and Pollution Technology, 11 (2), 199-201,2012.

Table 1 : LC$_{50}$ value of quinalphos and the 95% confidence limit in *Oreochromis mossambicus*

LC$_{50}$ log concentration	95% confidence		Probit equation	Chi-square
	Lower limit	Upper limit		
0.905	0.807	1.023	y = -6.693 + 7.401x	3.428

Table 2 : Analysis of Hematological parameters in *Oreochromis mossambicus* induced with quinalphos for 30 days

Concentration	RBC in million/ cu mm	WBC in no. of cell/cu mm	Hb in gm%	PCV in gm%	MCV in microns	MCH	MCHC	Platelet count in no. of cell/cu mm
Control	4.9±0.2	1800±4.359	14.9±0.208	45.1±0.132	91.9±0.058	32.3±0.252	33.73±0.153	21000±31.048
5 µl/l	4.6±0.436	1700±2.646	14.6±0.3	44±0.755	91.7±0.153	31.2±0.832	33.67±0.321	20000±28.583
7 µl/l	4.4±0.361	2000±1.732	13.5±0.4	40±0.1	91.3±0.321	31.1±0.351	33.37±0.551	19700±28.054
9 µl/l	4.2±0.265	2400±4.583	12.7±0.557	38.7±0.458	90.6±0.306	30.6±0.115	33.1±0.346	18000±18.33

Values are expressed as mean ± standard error, significant at 1% level

Arshitha and Pawlin Vasanthi Joseph

Table 3 : Analysis of Liver marker enzymes in *Oreochromis mossambicus* induced with quinalphos for 30 days

Concentration	ALP (u/l)	AST (u/l)	ALT (u/l)
Control	11.93±0.252	100.4±0.557	33.03±0.153
5µl	14±0.361	137.2±0.458	43±0.436
7µl	18.2±0.173	256.8±0.794	77.2±0.529
9µl	66.8±0.458	476.8±0.608	94.6±0.625

Values are expressed as mean ± standard error, significant at 1% level
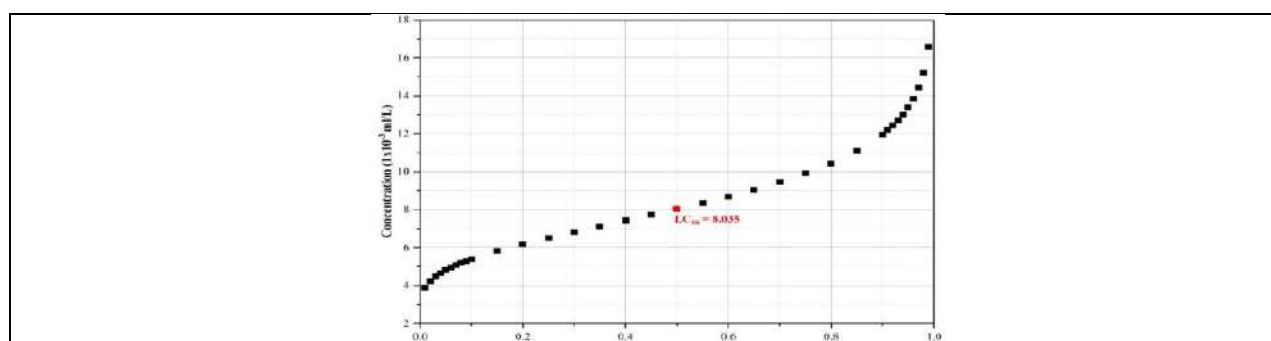
Fig. 1: Mortality rate of *Oreochromis mossambicus* at different concentration of toxicant quinalphos
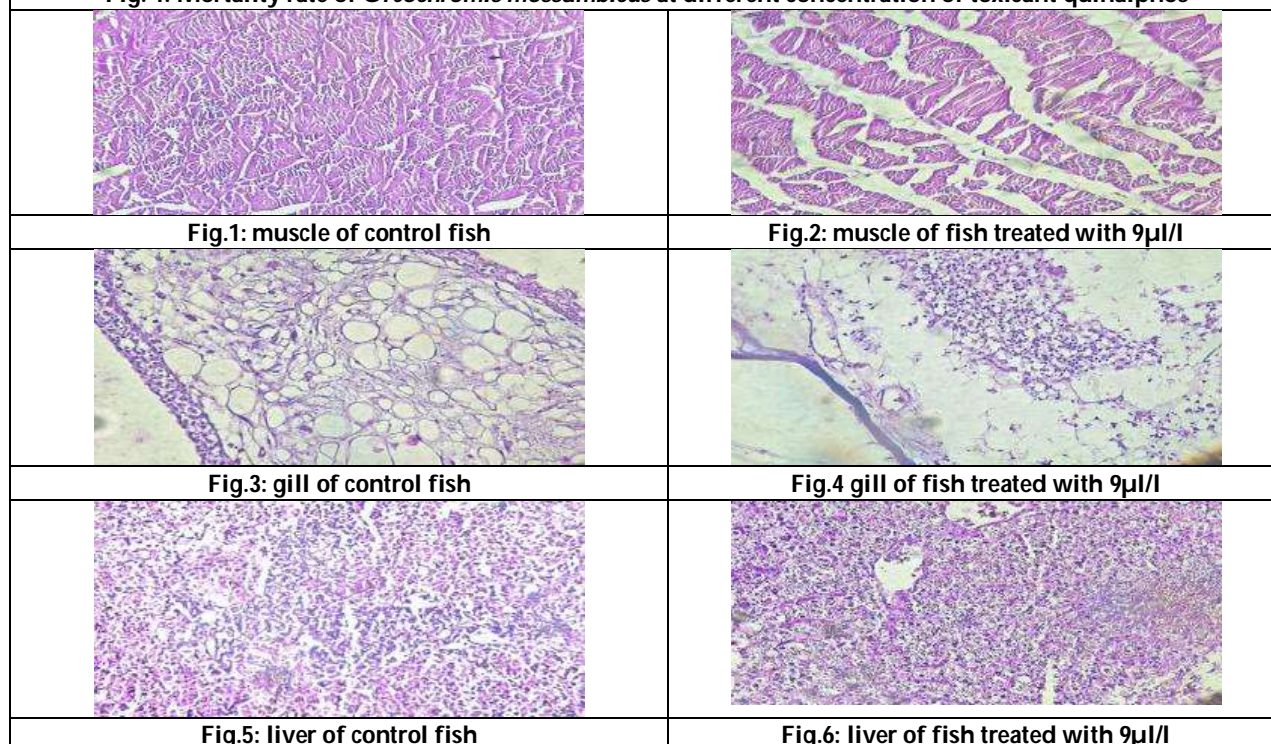
Fig.1: muscle of control fish

Fig.2: muscle of fish treated with 9µl/l

Fig.3: gill of control fish

Fig.4 gill of fish treated with 9µl/l

Fig.5: liver of control fish

Fig.6: liver of fish treated with 9µl/l

RESEARCH ARTICLE

Comparative Study on Efficacy of Instrument Assisted Soft Tissue Mobilization and Strain Counter strain on Pressure Pain Threshold, Muscle Hardness and Neck Functions In Upper Trapezitis Patients

Prachi Patel[1] and Neeti Mishra[2]*

[1]MPT Student , SPB Physiotherapy College, Surat, Gujarat, India.
[2]Professor, SPB Physiotherapy College, Surat, Gujarat, India.

*Address for Correspondence
Neeti Mishra
Professor,
SPB Physiotherapy College,
Surat, Gujarat, India.

ABSTRACT

Trapezitis is defined as inflammation of trapezius muscle. In the upper trapezius muscle area neck pain is very common. At some point in their lives around two thirds of people experience neck pain. Prevalence is highest in middle age and women are more affected than men. Rate of prevalence in male and female in India is 1:10. 3-5% of population is affected worldwide. IASTM techniques use special stainless steel instruments that enable clinicians to locate efficiently and treat soft tissue dysfunctions, such as fibrosis adhesions, chronic inflammation, or degeneration. IASTM technique results in clinical benefits such as improvements in range of motion, strength and pain perception. Strain Counterstrain (SCS) is a gentle manual treatment for muscle pain and spasm which involve resetting muscle tone and enhancing circulation that restores a muscle to its normal resting tone. To compare the effect of Instrument Assisted Soft Tissue Mobilization and Strain Counterstrain on Pressure Pain Threshold, Muscle Hardness and Neck functions in patients with upper Trapezitis. In the present comparative study, total fifty two (52) patients with upper trapezitis with age between 18-40 years were included. They were randomly divided into two groups: Group-A (n=26) and Group-B (n=26). Both group received conventional treatment, in addition Group-A received Instrument Assisted Soft Tissue Mobilization technique and Group-B received Strain Counterstrain technique. Patients were evaluated pre-intervention (0 week) and post-intervention (3 week) for pressure pain threshold (by means of algometer), for muscle hardness (by means of durometer) and for neck function (by means of NPAD). Statistical analysis was done by using SPSS 20 version. Significance level was set at $p<0.05$. Paired 't' test as a parametric and Wilcoxon signed rank test as a non-parametric test was applied for intra-group comparison and results showed that there were statistically significant difference in mean of PPT,MH and NPAD in both the groups during three week intervention period ($p<0.05$). Independent 't' test as a

64033

Prachi Patel and Neeti Mishra

parametric and Mann Whitney U test as anon-parametric test was applied between group comparison and result showed that there were statistically significant difference between IASTM group and SCS group in mean difference of PPT, MH and NPAD during 3 week intervention period (p<0.05). Instrument Assisted Soft Tissue Mobilization Technique along with conventional   treatment is more effective for improving pressure pain threshold, reducing muscle hardness and improving the neck function than Strain Counterstrain technique along with conventional treatment in patient with upper trapezitis.

Keywords: Instrument Assisted Soft Tissue Mobilization Technique (IASTM), Strain Counterstrain (SCS), Positional release technique (PRT), Trapezitis, Trigger points, Pressure Pain Threshold (PPT), Algometer, Durometer, Muscle Hardness (MH), Neck pain and disability scale (NPAD).

INTRODUCTION

Trapezitis is defined as inflammation of trapezius muscle. The upper trapezius muscle is known as the postural muscle and is highly susceptible to overuse.[1] Even during rest the pain is present and exacerbated by activity; from the site of primary inflammation it may be referred to other region.[2] Trapezitis is an inflammatory pain arising from the trapezius muscle causing a severe neck spasm.[3] Trapezitis is an inflammation of trapezius muscle which involve myofascial pain syndrome, that can be commonly encountered in clinical practice.[4] he prevalence of neck pain varies widely in different studies, with a mean point prevalence of 13% (range 5.9%– 38.7%) and a mean prevalence of 50% (range 14.2%–71.0%)[5] .Rate of prevalence in male and female in India is 1:10. 3-5% of population is affected worldwide[6, 7] . Trapezitis is mainly caused due to stress and tension, repetitive movements, forwarded head posture, sitting without back support, working without arm support, prolonged head bending activities, using thick pillow, tight pectoralis major muscle, severe neck spasm [8].

Active trigger points are cause of clinical symptoms and their evoked referred pain is responsible for the patient's pain. Latent trigger points may not be an immediate source of pain, but might produce other muscle dysfunction; i.e. fatigue, restricted range of motion and referred pain with muscle contraction or compression.[9] This clinical distinction has been strongly substantiated by histochemical findings at the trigger points, since higher level of concentration of protons, bradykinin, calcitonin gene-related peptide, substance P, tumor necrosis factor-α , Interleukin-1β, serotonin, and norepinephrine have been recently found in active trigger points.[10] Trigger points develop in the myofascia, mainly in the center of a muscle belly where the motor endplate enters (primary or central TrPs). Those are palpable nodules within the tight muscle at the size of 2-10 mm and can demonstrate at different places in any skeletal muscles of the body. When it happens, TrPs are directly associated with 4 myofascial pain syndrome, somatic dysfunction, psychological disturbance and restricted daily functioning [11].

Conventional treatment include Neck isometric exercises whch cause contraction and relaxation of the neck muscles thus massaging all the toxins, which are responsible for causing inflammation and strengthen the muscle fibers and improve stability of the neck muscles[12, 13] . Various physiotherapy protocols have been advocated in the past like rest, heat, ultrasound therapy (UST), microwave diathermy (MWD), transcutaneous electrical nerve stimulation (TENS), spray and stretch and post–isometric relaxation in treatment of trapezius spasm. IASTM is a skilled myofascial intervention thought to be based upon the rationale by James Cyriax.[14, 15] Unlike the Cyriax approach utilizing digital cross friction, IASTM is applied using specially designed instruments to provide a softtissue massage or mobilization.[15] The use of the instrument is thought to provide a mechanical advantage for the clinician by allowing deeper tissue penetration, vibration feedback sense, and more specific treatment, while also reducing imposed stress on the hands.[16Strain Counterstrain (SCS) is the fourth most commonly used osteopathic

manipulative technique following soft tissue techniques, high velocity low amplitude thrust, and muscle energy technique. [19] It is also known as positional release, SCS is a passive positional technique aimed at relieving musculoskeletal pain and dysfunction through indirect manual manipulation. SCS treatment begins by identifying diagnosticTPs related to musculoskeletal dysfunction.

Studies have found that trapezius stretching combined with positional release technique (PRT) have been found effective in trapezitis, but studies are limited to find which technique is more effective over the other ,due to lack of control group. Hence, this study with Research Question whether positional release technique(Strain Counterstrain)or IASTM ,have more effect in improving pressure pain threshold and reducing muscle hardness and functional disability in subjects with sub-acute trapezitis? Hence, the need of the study is to compare the effect of positional release therapy(Strain Counterstrain) and IASTM in the treatment of subacutetrapezitis on pressure pain threshold, muscle hardness, and functional disability.

IASTM and Strain counter strain have been effectively used as a treatment protocol in trapezitis patients, but till date less comparative studies have been done between IASTM and Strain Counter strain technique. Also there is not availability of a standard protocol for patients of upper trapezitis. Hence this study will significantly contribute for an effective intervention to reduce muscle hardness and improve pain pressure threshold & neck functions in patients with upper trapezitis along with conventional therapy.

AIMS AND OBJECTIVES

• To determine the effect of Instrument Assisted Soft Tissue Manipulation on Pressure Pain Threshold, Muscle Hardness and Neck functions in patients with upper Trapezitis.
• To determine the effect of Strain Counter Strain on Pressure Pain Threshold, Muscle Hardness and Neck functions in patients with upper trapezitis.
• To compare the effect of Instrument Assisted Soft Tissue Mobilization and Strain Counter Strain on Pressure Pain Threshold, Muscle Hardness and Neck functions in patients with upper Trapezitis.

METHODOLOGY

Study design is Pre-post Experimental Study. Study population consists of Patients of upper Trapezitis with 18-40 years of age group. Sampling technique is Purposive sampling . study duration was of 1 Year. For sample size calculation in this study, the effect size was calculated from the result of the pilot study. The sample size was estimated in G Power 3.1.9.2 version with effect size 0.84 and α = 0.05 at 80% power. Sample size calculated was 48, with a drop out chances of 10% the total sample size was 52, 26 samples in IASTM group and 26 samples in SCS group. 6.6 Study setting included SPB Physiotherapy College OPD and other clinical OPDs of Surat

INCLUSION CRITERIA
• Both male and female with age group 18 to 40 years.[25]
• Subjects with acute(7-14 days) and sub-acute(14 days to 3 months) trapezitis.[35]
• Subjects with unilateral trapezitis.[26]
• Subjects with <= grade 3 of trapezius muscle tenderness based on "tenderness grading scale".[26]
• Presence of active MTrPs identifiable by spot tenderness in a taut, muscular band.[25]
• Pressure Pain Threshold value should be ≤3 kg/cm2 . [25]

EXCLUSION CRITERIA
• Malignancy around neck region[27]
• A history of neck surgery during the previous 12 months[27]

Prachi Patel and Neeti Mishra

• If subject had received trigger point injections in the upper trapezius muscle within the past 6 months and taking NSAIDs for trapezitis[27]
• Open wounds around neck region[25]
• Subjects with the traumatic conditions to shoulder region within 6 months[25]
• Subjects with neurological conditions[25]
• Skin lesions around neck region[24]
• Infection or inflammatory edema at MTrPs site[24]
• Subjects with Cervical Spondylosis

PROCEDURE
The patient were screened on the basis of inclusion and exclusion criteria and their demographic data will be taken by an Assessment Performa. Prior to the commencement of the study, detailed procedure of the study was explained to the patients and a signed informed consent form was taken from them. Then the subjects were allocated to any of the two groups by random allocation using lottery method. Description of the groups are given as follows: GROUP-A : Conventional treatment + IASTM GROUP-B : Conventional treatment + Strain CounterStrain technique On the first day of the first week, baseline measurements of Pressure Pain Threshold, Muscle hardness and Neck Pain and Disability Scale (NPAD-G) was taken. 17

OUTCOME MEASURES
1. Pain Pressure Threshold(PPT) was measured using the Algometer[28]. Once an MTP was located, the algometer was used to measure the PPT. Progressive pressure at a rate of 1 kg/s was applied. Study subjects were asked to indicate when pain was elicited. The mean values from three measurements was recorded.
 2. Muscle Hardness was measured using the Durometer[22] : The principle used to measure hardness is based on measuring the resistance force of the penetration of a pin into the test material under a known spring load. The amount of penetration is converted to hardness reading on a scale with 100 units.
 3. Neck function measured using the Neck Pain and Disability Scale (NPAD-G) Gujarati version[23] : The subjects were given a detailed explanation about the Neck Pain and Disability Scale questionnaire.

INTERVENTION : Same Conventional treatment was given to both the groups. Conventional treatment(21) included : - Hot-pack [5 min.] was given prior to starting IASTM or SCS technique. - Trapezius muscle stretching [3 Repetitions with 30 seconds hold] was given after IASTM or SCS technique. - Cryotherapy [10 min. was given in the end of the session.

GROUP-A : [IASTM[54] + Conventional treatment[21]] The patient was in sitting position and the therapist was standing behind the patient. The instrument used was of stainless steel device machined into various shapes. Emollient was applied to the treatment area to prevent skin irritation. Each session included 1 minute of sweeping (longitudinal stroke performed parallel to the muscle fibers similar to an efflurage stroke) with single bevel edge of the IASTM tool at 30o - 60o tilt, 1 minute of swivel (pivoting/rotating back & forth similar to manual compression with oscillations) with the knob of IASTM tool directly over the MTrP, 2 minute of fanning (one end of instrument is held in place & the other end was moved through a semi-circular pattern similar to petrissage) with the convex single bevel edge of the IASTM tool and will be conclude with 1 minute of sweeping with IASTM tool. So, the total duration of IASTM treatment was of 5 minutes in a session and 2 sessions per week for 3 weeks was given

GROUP-B : [SCS[2] + Conventional Treatment[21]] The patient lyed in supine position with therapist standing on the affected side; trigger points was located along the upper fibers of the trapezius muscle. Pressure was applied by pinching the muscle between the thumb and fingers. The patient's head was laterally flexed towards the side of trigger point and rotated opposite to the side of trigger point, then therapist grasped the patient's forearm and abducts shoulder to approximately 90o a slight flexion or extension of shoulder was added to obtain finetune. The ideal position of comfort achieved was held for a period of 90 seconds and followed by a passive return of the body

Prachi Patel and Neeti Mishra

part to an anatomically neutral position continued for 5 minutes in a treatment session and 2 sessions per week for 3 weeks was given. Post treatment measurement was taken after last session of 3rd week

STATISTICAL ANALYSIS: The Statistical software named statistical package of social sciences (SPSS) version 20 (SPSS 20.0) was used for the analysis of the data and Microsoft word 2007 and Excel 2007 was used to generate graphs and tables. Descriptive statistical analysis was carried out at 95% confidence interval. Outcome measurements analyzed were presented as mean ± SD. Significance was assessed at 5 % level of significance with p value set at 0.05; less than this was considered as statistically significant difference. For checking the homogeneity of the data, the Levene's test for equality of variance was done. The data were ensured for their normal distribution using numerical (ShapiroWilk Test) and graphical methods (Normal Q-Q Plots). From that some variables followed the normal distribution and some followed the non-normal distribution. To convert the non-normal distribution to normal distribution, the log transformation was carried out. Then also some variables followed the non-normal distribution. So, both the parametric tests and non-parametric tests were performed. Paired't' test as a parametric and Wilcoxon signed rank test as a non-parametric test have been used to analysis the variables preintervention to post-intervention with calculation of change. Independent't' test as a parametric and Mann Whitney U test as a non-parametric test have been used to compare the means of variables between two groups with calculation of difference between the means.

RESULT

in IASTM group there were 26 subjects with mean age 25.69 years and in SCS group there were 26 subjects with mean age 26 years. In table-1, it shows the results of Levene's test to check the homogeneity of data. It shows homogenous distribution of data in both the groups. In table-2, it shows the results of Shapiro-wilk test which is used to check normality of data. Table-3,demonstrates pre-post mean values of all outcome measures for both group. Table 4 shows within group comparision of muscle hardness and neck function in both IASTM and SCS group (Paired t test was used) and Table 5 shows within group comparision of Pain Pressure Threshold in both IASTM and SCS group (Wilcoxon Signed Ranks Test was used)

DISCUSSION

This study was conducted to compare the effects of Instrument assisted soft tissue mobilization technique and strain counter strain technique on upper Trapezitis. In present study pressure pain threshold, muscle hardness and neck function were taken as the outcome measures and they were scored by using the algometer, durometer and neck pain and disability index, respectively. This study was conducted on 52 subjects with the age group of 18-40 years. The mean age of subjects in IASTM group(Group-A) is 25.69 years with 46% male subjects and 54% female subjects and the mean age of SCS group(Group-B) is 26 years with 38% male subjects and 62% female subjects. Based on the statistical analysis, both group A and B showed a drastic improvement in PPT, MH and NPAD and it has also shown significant improvement clinically in pressure pain threshold, muscle hardness and neck function. The refinement that occurred in IASTM group may come from its ability to induce tissue micro-trauma. Thus, resulting in the regional inflammatory process and increases the release of fibroblast. The fibroblast migration increases collagen synthesis and tissues regeneration that speeds up the healing process. In addition, increasing tissue temperature and blood flow due to friction between tool and tissue may contribute to improve tissue oxygenation and removal of local waste metabolites.18,27]Zeynab et al reported a case study to find out the effects of IASTM technique on upper trapezius trigger points. He reported increase in the pain pressure threshold and decrease in disability (NDI) in his case study.[34] The results of present study were in line with Motimath et al.,[28] who concluded that IASTM technique by using M2T blade is a useful tool which can decrease pain immediately in subjects with upper trapezius spasm. Bulbuli et al.,[29] tested the effect of M2T blade on subjects with heel pain and they found reduction in pain level and increased activity level.

Prachi Patel and Neeti Mishra

In conventional therapy, we used cryotherapy at the end of the treatment session just to overcome the side effects that may appear from IASTM include bruising and soreness. In particular, bruising is a response that appears together with bleeding and occurs more readily in soft tissues that have been injured for a longer period of time. Bruising and soreness can be controlled with cryotherapy, following IASTM. In addition, there are relative and absolute contradictions to IASTM.[30]

In Strain counterstrain technique, the muscles are placed in the greatest comfort position. This causes the relaxation of tissue that improves the vascular circulation and removes the inflammatory chemical mediators, thus leads in enhancing the symptoms.31] By means of an automatic resetting of muscle spindles, this helps to dictate tone and length of the affected tissues by Strain counterstrain technique in pain relief and increasing pain pressure threshold. The descending inhibitory pathways are activated with the application of manual intervention techniques.[32]A reduction of pain and an increase in neck function of 50%-100% occurred in 19 of 20 patients immediately after SCS therapy. The partial improvement was maintained for six months in 11 of 20 patients, and four were still pain-free. This technique has been recommended for physical therapy for treatment of pain in tender points of musculature [33]. Comparing the mean difference of post PPT value, post MH value and post NPAD value of both the groups, then the subjects in group-A who received IASTM and Conventional treatment showed better improvement than the subjects in group-B who received SCS and Conventional treatment when both the groups were compared at the end of three weeks.

The IASTM technique used in this study was proved superior in improving pressure pain threshold, reducing muscle hardness and improving neck function in patients with upper trapezitis comparatively with Strain counterstrain technique. The patients reported better results even after the first application of IASTM technique in comparison with the SCS technique and this gain in pain sensitivity and PPT was reinforced after the next two applications. Disabling myofascial pain after IASTM application can be theoretically attributed to three main mechanisms that have been reported in the literature: a) local temperature and blood flow increase, b) localized tissue manipulation and stretch and c) reduction of fascial adhesions and restrictions

CONCLUSION

Statistically IASTM and SCS were equally effective, but when we compared the mean difference values of PPT, MH and NPAD then IASTM was proved to be more effective than SCS. Hence, we concluded that the Instrument Assisted Soft Tissue Mobilization Technique along with conventional treatment is more effective for improving pressure pain threshold, reducing muscle hardness and improving the neck function than Strain Counterstrain technique along with conventional treatment in patient with upper trapezitis. Limitation & future scope-the evaluation of the effect of therapeutic techniques in the treatment of MTrPs was based only on the assessment pressure pain threshold, muscle hardness and neck function. Moreover, the evaluation of the impact of therapeutic applications had short-term character and was limited to three weeks that lasted the research. Another significant methodological issue that has been recognized as a possible source of measurement errors is the amount of pressure exerted through algometer as maintaining a constant pressure rate reported as the most challenging aspect of algometer. An ideal study evaluating the effect of various techniques on the reduction of adverse effects of MTrPs should assess the therapeutic effect of applied techniques in all the aspects of the functional capacity of the patients and must have long-term evaluation and re-evaluation planning

REFERENCES

1. Kumaresan, A., et al., Effectiveness Of Positional Release Therapy In Treatment Of Trapezitis. 2012. 2.
2. Alagesan, J. and U. Shah, Effect of Positional Release Therapy and Taping On Unilateral Upper Trapezius Tender Points - Randomized Controlled Trial. International Journal of Health and Pharmaceutical Sciences, 2012. 1: p. 13-17.

Prachi Patel and Neeti Mishra

3. Shah, J.P., et al., Myofascial Trigger Points Then and Now: A Historical and Scientific Perspective. PM & R : the journal of injury, function, and rehabilitation, 2015. 7(7): p. 746-761.

4. Fejer, R., K.O. Kyvik, and J. Hartvigsen, The prevalence of neck pain in the world population: a systematic critical review of the literature. Eur Spine J, 2006. 15(6): p. 834-48.

5. Schochat, T. and H. Raspe, Elements of fibromyalgia in an open population. Rheumatology (Oxford), 2003. 42(7): p. 829-35.

6. Draper, D.O., et al., Thermal ultrasound decreases tissue stiffness of trigger points in upper trapezius muscles. Physiother Theory Pract, 2010. 26(3): p. 167-72.

7. Andersen, L.L., et al., Effect of two contrasting types of physical exercise on chronic neck muscle pain. Arthritis Rheum, 2008. 59(1): p. 84-91.

8. Mane, P.A., A. Pawar, and T. Warude. Effect of Myofascial Release and Deep Transverse Friction Massage as an Adjunct to Conventional Physiotherapy in Case Unilateral Upper Trapezitis -Comparative Study. 2017.

9. Simons DG, T.J., Simons LS ; 1999, Myofascial pain and dysfunction: The trigger point manual. 2nd ed. ed. Vol. Volume 1. Baltimore: Williams and Wilkins.

10. Shah, J.P., et al., An in vivo microanalytical technique for measuring the local biochemical milieu of human skeletal muscle. J Appl Physiol (1985), 2005. 99(5): p. 1977-84.

11. Borg-Stein, J. and D.G. Simons, Myofascial pain. Archives of Physical Medicine and Rehabilitation, 2002. 83: p. S40-S47.

12. Falla, D., et al., Effect of neck exercise on sitting posture in patients with chronic neck pain. Phys Ther, 2007. 87(4): p. 408-17.

13. Laudner, K., et al., Acute effects of instrument assisted soft tissue mobilization for improving posterior shoulder range of motion in collegiate baseball players. Int J Sports Phys Ther, 2014. 9(1): p. 1-7.

14. Looney, B., et al., Graston instrument soft tissue mobilization and home stretching for the management of plantar heel pain: a case series. J Manipulative Physiol Ther, 2011. 34(2): p. 138-42.

15. White, K.E., High hamstring tendinopathy in 3 female long distance runners. Journal of chiropractic medicine, 2011. 10(2): p. 93-99.

16. Papa, J.A., Two cases of work-related lateral epicondylopathy treated with Graston Technique® and conservative rehabilitation. The Journal of the Canadian Chiropractic Association, 2012. 56(3): p. 192-200.

17. Cheatham, S.W., et al., The efficacy of instrument assisted soft tissue mobilization: a systematic review. J Can Chiropr Assoc, 2016. 60(3): p. 200-211.

18. Gehlsen, G.M., L.R. Ganion, and R. Helfst, Fibroblast responses to variation in soft tissue mobilization pressure. Med Sci Sports Exerc, 1999. 31(4): p. 531-5.

19. Johnson, S.M. and M.E. Kurtz, Osteopathic manipulative treatment techniques preferred by contemporary osteopathic physicians. J Am Osteopath Assoc, 2003. 103(5): p. 219-24.

20. Hogeweg, J.A., et al., Algometry. Measuring pain threshold, method and characteristics in healthy subjects. Scand J Rehabil Med, 1992. 24(2): p. 99-103.

21. Kim, J., D.J. Sung, and J. Lee, Therapeutic effectiveness of instrument-assisted soft tissue mobilization for soft tissue injury: mechanisms and practical application. J Exerc Rehabil, 2017. 13(1): p. 12-22.

22. Chung-Yoo Kim, J.-H.K., Tae-Sung Park, Intra-Rater Reliability of the Shore Durometer in the Assessment of Upper Trapezius Muscle Hardness. Research J. Pharm. and Tech., 2019. 12(5).

23. Silbaugh, K., Validity of Instrument Assisted Soft Tissue Mobilization for Detecting Myofascial Adhesions through Secondary Diagnostic Ultrasound Analysis. 2013.

24. A.Kumaresan **et.**al., Effectiveness of positional release therapy in treatment of trapezius. 2012.

25. Kaitlyn, S., Validity of Instrument Assisted Soft Tissue Mobilization for Detecting Myofascial Adhesions through Secondary Diagnostic Ultrasound Analysis. 2013.

26. N, R., S. Shridhar, and S. Helen, To compare the effectiveness of myofascial release technique versus positional release technique with laser in patients with unilateral trapezitis. Journal of Evolution of Medical and Dental Sciences, 2014. 3: p. 2161-2166.

27. Russell T. Baker, A.N., Jeff G. Seegmiller, Instrument-Assisted Soft Tissue Mobilization Treatment for Tissue Extensibility Dysfunction. international journal of Athletic Therapy & training, 2013. 18(5): p. 16-21.

28. Dr. Basavaraj Motimath, N.A., Dr. Dhaval Chivate., Immediate effect of instrument assisted soft tissue mobilization (Iastm) With M2T blade technique in trapezitis: An experimental study. International Journal of Applied Research, 2017. 3(5): p. 527-529.
29. Dr Ashwini Bulbuli, N.M., Munpreet Singh, Effect of IASTM Using M2T Blade on Acute Heel Pain: A Pilot Study. Journal of medical science and clinical research, April 2017. 5(4).
30. Hammer, W.I., The effect of mechanical load on degenerated soft tissue. J Bodyw Mov Ther, 2008. 12(3): p. 246-56.
31. Fereira OA, S.A., Effectiveness of strain counterstrain technique and neural tissue mobilisation on cervicogenic headache. Indian Journal of Physiotherapy and Occupational Therapy. 11(3): p. 57-61.
32. Khan, S., Efficacy of ischaemic compression technique in combination with strain countersrain technique in managing upper trapezius myofascial trigger point pain. Indian Journal of Physiotherapy & Occupational Therapy, 2010. 4.
33. Dardzinski, J.A., B.E. Ostrov, and L.S. Hamann, Myofascial pain unresponsive to standard treatment: successful use of a strain and counterstrain technique with physical therapy. J Clin Rheumatol, 2000. 6(4): p. 169-74.
34. Ahmadpour Emshi, Z., et al., The Effects of Instrument-Assisted Soft Tissue Mobilization on Active Myofascial Trigger Points of Upper Trapezius Muscle. Journal of Clinical Physiotherapy Research, 2018. 3(3): p. 133-138.
35. D., B.D., Validation of Gujarati Version of the Neck Pain and Disability Scale in Patients with Chronic Neck Pain. Indian Journal of Physiotherapy and Occupational Therapy, 2017.

Table 1. showstest for homogeneity of data

Independent Samples Test		
Levene's Test for Equality of Variances		
	F	P value
GENDER	.298	.588
AGE	1.050	.310
SIDE	1.406	.241
PREPPT	.335	.565
PREMH	.577	.451
PRENPAD	.810	.372

Table 2. shows tests for normality of data

Tests of Normality			
	Shapiro-Wilk test		
	Statistic	df	Sig.
PREPPT	.592	52	.000
POSTPPT	.805	52	.000
PREMH	.964	52	.120
POSTMH	.963	52	.109
PRENPAD	.981	52	.582
POSTNPAD	.952	52	.036

Table 3. demonstrates pre-post mean values of all outcome measures for both group

	IASTM group	SCS group
PREPPT	1.307692	1.346154
POSTPPT	4.269231	3.615385
PREMH	21.03846	20.15385
POSTMH	8.076923	8.807692
PRENPAD	35.42308	31.26923
POSTNPAD	8.615385	9.615385

Table 4. shows within group comparision of muscle hardness and neck function in both IASTM and SCS group (Paired t test was used)

OUTCOME MEASURES	t value	P VALUE
IASTMPREMH-POSTMH	29.099	.000
IASTMPRENPAD-POSTNPAD	24.824	.000
SCSPREMH-POSTMH	18.835	.000
SCSPRENPAD-POSTNPAD	17.087	.000

Table 5. shows within group comparision of Pain Pressure Threshold in both IASTM and SCS group (Wilcoxon Signed Ranks Test was used)

OUTCOME MEASURES	Z value	P VALUE
IASTMPREPPT-POSTPPT	-4.572[b]	.000
SCSPREPPT-POSTPPT	-4.722[b]	.000

FIG.1Sweeping technique of IASTM

FIG.2Swiveling technique of IASTM

FIG.3Fanning technique of IASTM

FIG. 4.Strain Counter strain technique

Prachi Patel and Neeti Mishra

	CHART TITLE	MEAN DIFFERENCE

GRAPH-1.demonstrates   pre-post mean values of all outcome measures for both group

GRAPH 2.Between Group Comparison of mean Diff of Ppt, Mh And Npad

	MDPPT	MDMH	MDNPAD
IASTM	2.961538	12.961538	26.807692
SCS	2.26923	11.346153	21.653846

REVIEW ARTICLE
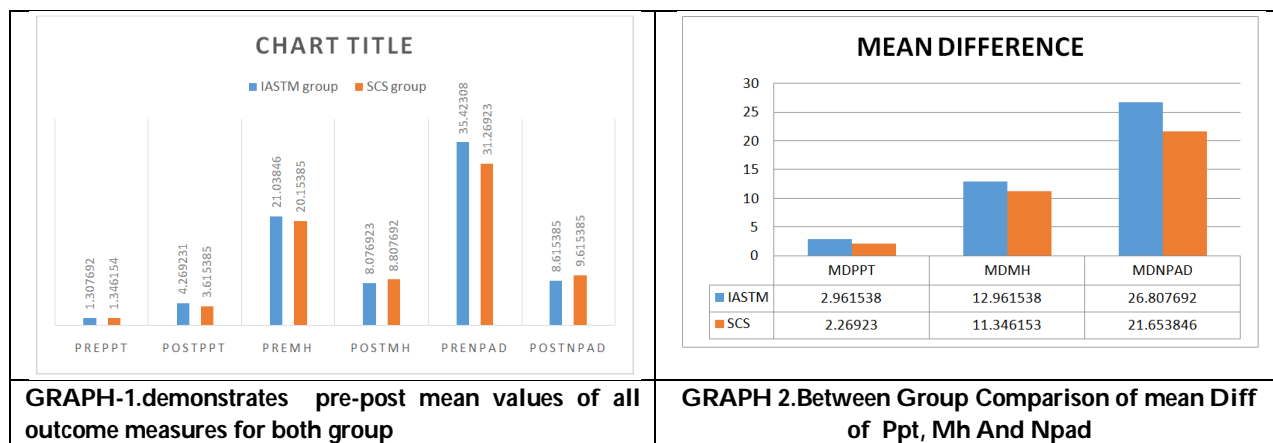
A Comprehensive Review on Medicinal Plant Species of Genus *Ocimum* and *Mentha*: A Promising Hand to treat Urolithiasis

C.S. Tailor[1] and J. Syan[2]*

[1]Assistant Professor, Shri Guru Ram Rai University, Patel Nagar, Dehradun-248001, Uttarakhand, India.
[2]Associate Professor, Shri Guru Ram Rai University, Patel Nagar, Dehradun-248001, Uttarakhand, India

*Address for Correspondence
J. Syan
Associate Professor,
Shri Guru Ram Rai University,
Patel Nagar, Dehradun-248001,
Uttarakhand, India.
E.Mail: jasminsyan1@gmail.com

ABSTRACT

Urolithiasis or kidney stones is defined as the urinary stone originating anywhere in the urinary tract. Urolithiasis plays a significant economic burden in the healthcare system, especially in developing countries owing to changes in food habits and lifestyle due to which there has been significantly increase in the disease over the last few decades. Medicinal plants are established as renewable sources with antiurolitiatic activity. There are many Marketed formulations which are having Antiurolithiatic activity as well as many traditional medicinal plants which is primarily used to dissolve urinary stones in the kidney or urinary bladder. So, the Present Review article represents the potential of Some Traditional Medicinal plants in the treatment of urinary stones. More Research is needed to develop new Plant derived products to treat the formation of kidney stones.

Keywords: Urolithiasis; Medicinal Plants; Anti Urolithiatic activity, Kidney Stones

INTRODUCTION

In order to treat infectious and non-infectious, the modern health care system offers a wide range of possibilities. However, due to cost and accessibility concerns, a number of these medications have their own drawbacks and are not available to the majority of the world's population. As a result, more than 75% of people, particularly in lower income nations, still rely on herbal treatments to address their basic medical needs [1]. Medicinal plants play a significant role in the health care of ancient and modern cultures. Ayurveda, the Indian system of medicine mainly uses plant-based formulations to treat various human diseases because they contain the components of therapeutic

64043

potential. Plant based drugs are an important source of therapeutic agents because of their abundant availability, relatively cheaper cost and non-toxic nature when compared to modern medicine [2]. It is important to consider traditional remedies for non-life-threatening conditions including haemorrhoids and urinary stones. Urolithiasis is a disorder in which a stoneforms or occurs anywhere in the urinary tract. Urinary stones (calculi) are solid crystalline masses that can form anywhere in the renal tract [3].

Stone formation is one of the painful urologic diseases that occur in around 12% of the global population and its occurrence rate in males is 70-81% and 47-60% in female. It is assessed that at least 10% of the population in industrialized part of the world are suffer with the problem of urinary stone formation. The occurrence of the renal calculi is less in the southern part when compared with other parts. Stone formation usually occur due to insufficient urinary discharge, microbial infection in urinary tract, diet with excess oxalates and calcium, vitamin abnormalities like vitamin A deficiencies, excess vitamin D, and metabolic diseases like hyperthyroidism, cystinuria, gout, intestinal dysfunction etc. Kidney stone formation or urolithiasis is a complex procedure that occurs due to imbalance between promoters and inhibitors in the kidneys [4].

Many medications and remedies have been used during the past many years to treat urinary stones. Generally, in the traditional systems of medicine, the majority of the remedies are based on plants and they were proved to be useful though the rationale behind their use is not well established through systematic pharmacological and clinical studies except for some composite herbal drugs and plants. Pharmacotherapy can reduce the recurrence rate. The use of plant products with claimed uses in the traditional systems of medicine assumes importance. In the Ayurvedic system of medicine in India, plants which belongs to 'Pashanabheda' group are claimed to be useful in the treatment of urinary stones. 'Pashanabheda' is the Sanskrit term used for a group of plants with diuretic and antiurolithiatic activities [5].

The mechanism of stone formation is a complex process which results from several physicochemical properties including supersaturation, crystal nucleation, precipitation, crystal growth, aggregation of crystals and retention of urinary stone constituents within tubular cells. There are various types of kidney stones which include cystine stones, calcium oxalate stones, calcium phosphate stones, struvite stones and uric acid stones. However, it is evident that crystal retention, cell apoptosis, renal cell injury, and associated stone promoters or inhibitors play important roles for kidney stone formation [6].

TYPES OF KIDNEY STONES [7,8,9]
Calcareous Stones (Calcium containing stones)
Calcium Oxalate Stones: The most common type of kidney stone which is created when calcium combines with oxalate in the urine. Inadequate calcium and fluid intake, as well as other conditions may contribute to their formulations. Calcium oxalate stones occur as a result of
A. Hypercalciuria –This is idiopathic or results from any disorder that induces even mild hypercalcemia.
B. Hypocitraturia – It is associated with renal lithogenesis. Citrate is an inhibitor of calcium salt formation by forming a soluble complex with calcium. It results from causes of intracellular acidosis such as renal failure, potassium deficiency, distal renal tubular acidosis, chronic diarrhoeal state and drugs such as acetazolamide.
C. Hyperuricosuria – It occurs at high purine intake or chronic diarrhoeal disease.
D. Hyperoxaluria – Oxalate forms an insoluble complex with calcium, resulting in crystal formation.

Calcium Phosphate Stones: It occurs when the kidney loses their ability to lower urinary pH causing calcium phosphate super saturation.

Non-Calcareous Stones

Uric Acid Stones: This is another common type of kidney stones. High purine intake leads to a higher production of monosodium urate may form kidney stones.Uric acid composition seems to be the second most common stone. Urinary uric acid exists in an insoluble form at pH < 5.05 and forms crystals.

Struvite Stones: Struvite is a crystalline substance composed of magnesium ammonium phosphate. These stones are less common and are caused by infections in the upper urinary tract.

Cystine Stones: When kidney do not reabsorb the cystine properly leads to kidney stones.The stones are greenish yellow, flecked with shiny crystallites and are moderately opaque with a rounded appearance.

MECHANISM OF UROLITHIASIS
The diseased state of urolithiasis becomes apparent only when small stones are retained within the urinary system and grow into relevant stones[10].

Crystallization
It represents the first phase of urinary stone formation and includes three steps:
1. Crystal Nucleation
2. Crystal Growth
3. Crystal Aggregation

Crystal Nucleation
The nucleation is a process of formation of a solid crystal in solution. Generation of a crystal can occur by homogenous nucleation when supersaturation allows organization of the atoms into the appropriate lattice. However, heterogenous nucleation occurs within complex mixtures in which proteins provide patterns on their surface to organic molecules for the formation of the crystal lattice11.Nucleation may occur in renal tubules, bladder walls, normal or damaged cells or at interstitial cells[12,13].

Crystal Growth
After nucleation, crystal growth is the next major step of stone formation. In this process, several atoms or molecules in supersaturated liquid starts to form crystals[14].

Crystal Aggregation
Aggregation is an important step of stone development and is commonly defined as a process in which crystals agglomerate and form a larger multicomponent particle in free solution. Aggregation of particles in solution is determined by a balance of forces including both aggregating and disaggregating effects[15].

Stone Retention
After the crystallization process is complete, the retention of urinary stones within the urinary stones within the urinary system is an important step in the development of the diseases[16]. Four different possible modes of stone retention have been identified in the fixed particle hypothesis:
1. Growth over white interstitial plaque
2. Growth over Bellini duct plugs
3. Formation of microliths within collecting ducts
4. Formation in free solution within renal collecting system.

MARKETED HERBAL FORMULATIONS USED IN THE TREATMENT OF UROLITHIASIS
There are many Marketed formulations which are having Anti urolithiatic activity, some of them are:
1. Cystone (Himalaya Drug Company, India)
2. Calcuri (Charak Pharmaceuticals, Bombay, India)
3. Chandraprabhabati (Baidyanath, India)

4. Kidney Detox (Foresta Organics, India)
5. Gokhru Tablets
6. Chywanprash (Organic India)
7. Nerunjil Powder
8. Neeri Syrup

These formulations have been widely used to dissolve urinary calculi in the kidney and urinary bladder. Trinapanchamool consisting of five herbal drugs was found to be effective in preventing the formation and dissolving the pre formed stones[17].

PROMINENT MEDICINAL PLANT SPECIES OF FAMILY LAMIACEAE HAVING ANTI UROLITHIATIC ACTIVITY
Mentha Piperita

Part used: Stem, leaves, flowers
Mentha species are used for their flavouring and medicinal properties widely throughout different countries of the world. It is one of the most economically important aromatic and medicinal crops. It is commonly known as Peppermint, Brandy mint, Candy mint, Lamb mint, Balm mint, pudina.
The plant is a strongly scented, perennial, glabrous, herb 30-90cm in height. The square stems are usually reddish-purple and smooth. The leaves are short 2.5-5cm long, oblong-ovate and serrate. The flowers are purple-pinkish and appear in the summer months. The plant has runners above and below ground. It is native of Europe, Canada and US and have been naturalized in many parts of India[18].

Chemical Composition: The major constituent reported is volatile oil of which the principal component is usually menthol, together with neomenthal and isomenthal. Other monoterpenes include menthone, menthyl acetate, menthofuran, cineol, limonene. Monoterpenes like pinene, terpinene, myrcene, caryophylldene, piperitone, piperitinone, pulegone, eugenol, menthone, isomenthone, carvone, cadinene, dipentene, linalool, ocimene, sabinene, terpinolene, fenchrome[19].

Anti Urolithiatic activity: The present study aims to establish the scientific rationality of anti-urolithiatic activity by in vitro Calcium oxalate crystallization studies; that is, nucleation, aggregation and oxalate depletion assays and in vivo ethylene glycol–induced urolithiasis model in the male albino rats. Peppermint contains rich source of bioactive compounds and has traditionally been used in the treatment of lithiasis[20].

In vitro Crystallization Assay
Nucleation assay: The effects of Calcium oxalate crystallization were studied by nucleation assay. The solutions of calcium chloride and sodium oxalate were prepared in Tris-HCL and NaCl buffer at pH 6.5. Different dilutions of cystone and extract were prepared in distilled water. One milliliter of each dilution (100- 1000 µg/mL) of extract and cystone was mixed with calcium chloride and then sodium oxalate solution was added in each dilution. These dilutions were incubated in oven at 37°C for half an hour then cooled down to room temperature. Optical density was measured using spectrophotometer.

Aggregation assay: The effects of extract on the aggregation of Calcium oxalate crystals were studied. Calcium chloride and sodium oxalate solutions were prepared separately and then mixed together. This mixture was heated in water bath at 60°C, for an hour and then incubated overnight in oven at 37°C. After drying this mixture, Calcium oxalate crystal solution (80 mg/100 mL) was prepared in 0.05 M TrisHCl and 0.05 M NaCl buffer at pH 6.5. One millimeter of each of the dilution of extract and cystone was mixed and vortexed with 3 ml of Calcium oxalate solution. The mixture was incubated in oven at 37°C for half an hour. Optical density was recorded on spectrophotometer at 620 nm[21].

Animal Model of Urolithiasis: Experiments are performed with Wistar albino rats under 100,300,500 mg/kg doses along with lithogenic regimen.

Urine Analysis: At the end of 21st day animals are placed in metabolic cages for the collection of urine samples. 24h urine samples are collected for biochemical analysis, such as urine volume, urine pH, and the levels of uric acid, magnesium, calcium, phosphate, and total protein levels are determined.

Kidney Homogenate Analysis: Kidney homogenate analysis is performed by the end of prophylactic model, whole kidney is separated and washed. Kidney homogenate is prepared by dissolution of 1gm of kidney tissue in 10ml of 0.1M chilled phosphate buffer saline at pH of 7.4 followed by homogenization. The tissue homogenate was then centrifuged at 10000 rpm at 4 degree for 10-15 minutes and the supernatant is separated and stored at -20degree for analysing the levels of protocols.

Serum Analysis: The rats are anesthetized by using combination of ketamine and blood is collected through retro-orbital method and through cardiac puncture. Serum is separated and analysed for blood urea nitrogen and creatinine levels [22].

Ocimum Sanctum
Part used: Stem, Leaves, Seeds

Tulsi (holy basil in English) is an exceptionally adored culinary and restorative fragrant herb that is indigenous to the Indian subcontinent and been utilized inside Ayurvedic medication over 3000 years. In the Ayurveda framework tulsi is frequently alluded to as a "Solution of Life" for its mending powers and has been known to treat a wide range of basic wellbeing conditions. It is an erect, much stretched sub bush 30-60cm tall with furry stems and basic inverse green leaves that are unequivocally scented. Tulsi assumes a crucial job in our regular daily existence and is supposed to be the sovereign of natural plants. Tulsi is an erect pleasant-smelling bush which develops up to a stature of 3 - 5 feet[23].

Chemical Constituents: The leaf volatile oil containseugenol (also called eugenic acid), urosolic acid carvacrol, linalool, limatrol, caryophyllene, methyl carvicol while the seed volatile oil have fatty acids and sitosterol; in addition, the seed mucilage contains some levels of sugars and the anthocyans are present in green leaves. The sugars are composed of xylose and polysaccharides. Although Tulsi is known as a general vitalizer and increases physical endurance, it contains no caffeine or other stimulants. The stem and leaves of holy basil contain a variety of constituents that may have biological activity, including saponins, flavonoids, triterpenoids, and tannins, Rosmarinic acid, apigenin, *cirsimaritin isothymusin* and isothymonin. Two water-soluble flavonoids:Orientin and Vicenin have shown to provide protection against radiation-induced chromosomal damage in human blood lymphocytes [24].

Medicinal Properties: Tulsi is antispasmodic, appetizer, carminative, galactagogue, and stomachic. It is used for stomach cramps, gastric catarrh, vomiting, intestinal catarrh, constipation, and enteritis. It had been sometimes used for whooping cough as an antispasmodic. Tulsi has antioxidant properties and reduces blood glucose levels. Thus, it is useful for diabetics. Tulsi reduces total cholesterol levels. Thus, it is useful for heart disease patients.Tulsi reduces blood pressure. Tulsi plant has many medicinal properties. The leaves are nerve tonic and also sharpen memory. They promote the removal of the catarrhal matter and phlegm from the bronchial tube. The leaves strengthen the stomach and induce copious perspiration. The seed of the plant are mucilaginous. Fever and Common Cold: The leaves of basil are specific for many fevers. During the rainy season, when malaria and dengue fever are widely prevalent, tender leaves, boiled with tea, act as preventive against these diseases.

Nutrition Value : Contain vitamin C, A and minerals like calcium, zinc and iron, as well as chlorophyll and many other phytonutrients. Also enhances the efficient digestion, absorption and use of nutrients from food and other herbs. Protein: 30 Kcal, 4.2 g; Fat: 0.5 g; Carbohydrate 2.3 g; Calcium: 25 mg; Phosphorus 287 mg; Iron: 15.1 mg and Edible portion 25 mg vitamin C per 100 g.

Anti Urolithiatic Activity: *Ocimum sanctum* is effective against the kidney stone. Juice of Tulsi and honey is most effective against kidney stones and if it taken regularly 6 months once a day it will expel them via the urinary tract[25].*Ocimum sanctum* hydroalcoholic extract can effectively inhibitthe nucleation, growthas well as aggregation of Calcium oxalate crystallization process. Hence, it can be used as a phototherapeutic agent to manage urolithiasis at its early stage and can be effective to reduce the chancesof its reoccurrence[26].

CONCLUSION

For Optimum patient treatment and protection, scientific research to explore possibly potential benefits of herbal plants is extremely important. The present review article demonstrated the curative potential of urolithiasis or kidney stones using traditional medicinal plants and herbal marketed formulations. The aim of this study is to Review the Mechanism of kidney stones and represent the medicinal plants belonging to the family Lamiaceae used in Anti urolithiatic activity. More Research is needed to develop New plant derived products to treat the formation of kidney stones.

REFERENCES

1. Nimavat A, Trivedi A, Yadav A, Patel P. A Review on Kidney Stone and Its Herbal Treatment. Journal of Pharmacy and Pharmacology. 2022; 10:195-209.
2. Agbor AG, Ngogang YJ. Toxicity of herbal preparations. Cam. J.Ethnobot. 2005; 1: 23-28.
3. Pareek, S. K."Medicinal Plants in India: Present Status and Future Prospects" In: Prospects of Medicinal Plants, 1996, pp. 14.
4. Shukla AK, Shukla S, Garg A, Garg S. "A Review on anti-urolithiatic activity of herbal folk plants" Asian Journal of Biomaterial Research. 2017;3(2):1-1.
5. Nagal A, Singla RK. "Herbal resources with antiurolithiatic effects: a Review" Indo Glob J Pharm Sci. 2013;3(1):6-14.
6. Butterweck V, Khan SR. Herbal medicines in the management of urolithiasis: alternative or complementary? Planta Med. 2009; 75(10):1095-1103.
7. Fontenelle LF, Sarti TD. Kidney stones: treatment and prevention. American family physician. 2019 Apr 15;99(8):490-6.
8. Frassetto L, Kohlstadt I. Treatment and prevention of kidney stones: an update. American family physician. 2011 Dec 1;84(11):1234-42.
9. Knoll T. Epidemiology, Pathogenesis and Pathophysiology of urolithiasis. Europe Urol Supplements. 2010; 9(12): 802 – 806.
10. Williams JC Jr, McAteer JA. Retention and growth of urinary stones: insights from imaging. J Nephrol 2013; 26: 25-31.
11. Cerini C, Geider S, Dussol B, et al., Nucleation of calcium oxalate crystals by albumin: involvement in the prevention of stone formation. Kidney Int 1999; 55: 1776-1786.
12. Ratkalkar VN, Kleinma JG. Mechanisms of Stone Formation. Clin Rev Bone Miner Metab 2011; 9:187-197.
13. Grases F, Sohnel O. Mechanism of oxalocalcic renal calculi generation. Int. Urol. Nephrol. 1993; 25: 209-214.
14. Basavaraj DR, Biyani CS, Anthony J, Browning A, Cartledge JJ. The role of urinary kidney stone inhibitors and promoters in the pathogenesis of calcium containing renal stones. EAU-EBU Update Series 2007; 5: 126-136.
15. ScottR, East BW, Janczyszyn J, Boddy K, Yates AJ. Concentration of some minor and trace elements in urinary tract stones: a preliminary study. Urol Res 1980; 8: 167-169.
16. Evan AP, Worcester EM, Coe FL, Williams JJr, Lingeman JE, Mechanisms of human kidney stone formation. Urolithiasis 2015;43; 19-32.
17. Singh CM and Sachan SS. Management of urolithiasis by herbal drugs. J. Nepal. Pharm. Assoc. 1989; 7: 81-85.
18. Shah PP, Mello PM. A review of medicinal uses and Pharmacological effects of *Mentha piperita.*

19. Baslas RK and Saxena S, Chromatographic analysis of dementholised essential oil of *Mentha piperita, Indian J Physnat Sci*, 1984, 4A, 32.
20. Jamshed A, Jabeen Q. Pharmacological evaluation of *Mentha piperita* against urolithiasis: An in vitro and in vivo study. Dose-Response. 2022 Jan 10;20(1):15593258211073087.
21. Ahmed S, Khatri MS, Hasan MM. Plants of family lamiaceae: A promising hand for new antiurolithiatic drug development. World J Pharm Pharmaceutical Sci. 2017; 6:90-96.
22. Das M, Malipeddi H. Antiurolithiatic activity of ethanol leaf extract of *Ipomoeaeriocarpa* against ethylene glycol-induced urolithiasis in male Wistar rats. Indian J Pharmacology. 2016; 48:270-274
23. Bhadra P, Sethi L. A Review paper on the Tulsi plant (*Ocimum sanctum*). Indian Journal of Natural Sciences.;10(60):20854-60.
24. Claus, Peter J.; Sarah Diamond, Margaret Ann Mills (2003). South Asian Folklore: An Encyclopedia. Taylor and Francis. p. 619. ISBN 9780415939195.
25. Gulhane NS, Ghode CD, Jadhao AG, Patil PA. Study of medicinal uses of *Ocimumsanctum* (Tulsi). Journal of Pharmacognosy and Phytochemistry. 2021;10(2):1427-31.
26. Faujdar C. Investigating the Effect of Hydroalcoholic Extract of *Ocimum sanctum* on In-vitro Calcium Oxalate Crystallization. Current Trends in Biotechnology and Pharmacy. 2021;15(6):47-52.

Figure 1. *Mentha* Plant Species

Figure 2. *Ocimum* Plant Species

RESEARCH ARTICLE

Effect of Gross Myofascial Release Combined with Focused Myofascial Release Versus Capsular Stretching on Pain and Range of Motion in Individuals with Adhesive Capsulitis: A Comparative Study

Megha Suthar[1], Sonal Thakkar[2] and Gaurav Patel[3]*

[1]MPT Student, Ahmedabad Physiotherapy College, Parul University, Gujarat, India
[2]Assistant Professor, Ahmedabad Physiotherapy College, Parul University, Gujarat, India.
[3]Principal and Professor, Ahmedabad Physiotherapy College, Parul University, Gujarat, India

***Address for Correspondence**
Gaurav Patel
Principal and Professor,
Ahmedabad Physiotherapy College,
Parul University, Gujarat, India
E.Mail: dr.gauravpatel24@gmail.com

ABSTRACT

Adhesive capsulitis is a condition marked by persistent pain, active and passive inability leading to functional inadequacy at shoulder. It results from contraction of the glenohumeral capsule which adheres to the head of the humerus. External rotation of the shoulder is the most restricted movement followed by abduction and internal rotation. Combination release is a Myofascial Release technique in which Gross Myofascial Release and Focused Myofascial Release techniques are combined. Stretching interventions can be used less frequently at high intensity levels to enable time for tissue recovery. In this study there were total of 30 individuals with adhesive capsulitis who had age between 40-65 years was randomly divided 15 into group A with Gross MFR combined with Focused MFR and 15 into group B with Capsular stretching. Intervention was given for 5 days per week for 3 weeks. Outcome measures were NPRS,SPADI and Goniometry. Statistically within Group both groups had a significant difference in outcomes (p<0.05) but no significant difference between groups in outcomes. Gross Myofascial Release combined with Focused Myofascial Release versus capsular Stretch were found to be beneficial in decreasing pain, improving functional activities, and increasing range of motion in people with adhesive capsulitis shoulder.

Keywords: - capsular stretching, gross Myofascial release combined with focused Myofascial release, range of motion, adhesive capsulitis, SPADI, NPRS.

Megha Suthar *et al.,*

INTRODUCTION

Adhesive capsulitis is a condition marked by persistent pain, Active and passive inability leading to functional inadequacy at the Shoulder. Because of thickening decreased volume of the glenoid capsule and contractures in the glenohumeral joint capsule [1]. It results from the contraction of the glenohumeral capsule which adheres to the head of the humerus [2]. Patients usually have a history of debilitating pain and progressive limitation of glenohumeral movements. External rotation of the shoulder is the most restricted movement followed by abduction and internal rotation [3,4]. although a multitude of factors may contribute to the development of a frozen shoulder, the actual cause is unknown. Studies have revealed clinical manifestations, duration, and diagnosis. Although it affects 2-5 per cent of the general population, it affects females in the age group of 40 and 70 more than males. Primary and secondary are the two types. Idiopathic frozen shoulder is a condition in which the cause is unknown. Trauma, inactivity, rotator cuff injuries, hyperglycaemia, biceps inflammation, heart attack, neurological event, mental illnesses, and post-surgical considerations are some of the most common causes of shoulder pain. The pain is usually constant, worst at night. The glenohumeral capsule, which is irritated and inflexible, restricts motion and can cause persistent pain [1].

Though the exact cause remains unknown, Adhesive capsulitis is associated with various precipitating factors. Studies have shown that people who are elderly, females, with diabetes mellitus and abnormal lipid profiles have an increased risk of developing Adhesive capsulitis. There are trigger points surrounding the shoulder joint in adhesive capsulitis. Trigger points in the Myofascial system tender patches can be found in taut bands of stiffened muscle that are always tender and prevents the muscle from fully extending, resulting in muscle weakening [5]. Trigger spots in the internal rotator, shoulder abductor, and scapula protector musculature are common in adhesive capsulitis [6].

Muscle release or Myofascial trigger point release is a technique for treating chronic uncomfortable muscle spasms and increasing range of motion. It involves applying deep pressure to areas of local soreness [7,8]. Myofascial release (MFR) is a technique that focuses on releasing mobility constraints that arise in the body's soft tissues. It's a type of soft tissue therapy that aims to diminish pain and increase movement in people who have been experiencing severe long-lasting pain [9]. MFR is a form of physical therapy that involves applying a low-load, long-duration stretch to the Myofascial system to restore appropriate length, reduce discomfort, and improve function. Myofascial release is used as a treatment in many conditions [10]. Combination release is a Myofascial Release technique in which Gross Myofascial Release and Focused Myofascial Release techniques are combined. Gross Myofascial release uses the first stretch to the muscle is provided via an arm or leg pull approach, whereas guided Myofascial release concentrates on a particular muscle. The Subtle mal alignments that cause the patient's difficulties are recognized and released by focusing on lesser constraints within the Myofascial unit [9]. Patients with adhesive capsulitis benefit from capsular stretching because it reduces pain and improves function [10]. Stretching is a therapeutic procedure that aims to promote soft tissue mobility and, as a result, improve range of motion by stretching components that have become shortened and hypo mobile over time. Manual stretching and self-stretching have been demonstrated to be beneficial in people with hypomobility. Stretching increases the range of motion by extending soft tissue structures beyond their natural length. The result of direct intervention by the therapist is not the same as the result of self-stretching by the patient [11].

METHODOLOGY

The type of study conducted was an experimental study. This study was approved by The Institutional Ethics Committee for Human Research- Sainath Hospital, Ahmedabad (Reg. No: -EC/NEW/INST/2021/1983). Written informed consent was obtained and acknowledged from all the participants and was ensured that their identity was not revealed. The study was carried out in Sainath hospital, bopal, Ahmedabad, and rotary physiotherapy club, JK Orthopedic Hospital, Himmatnagar.

Megha Suthar *et al.*,

Subjects were selected based on inclusion criteria. In this study, 40 to 65 years individuals with adhesive capsulitis were included. There were 17 males and 13 females. Then all subjects were randomly divided into two groups. Group A had 15 subjects were treated with Gross MFR combined with Focused MFR and the rest 15 subjects included in Group B were treated with the capsular stretching technique.

INCLUSION CRITERIA:-
- 40-65 years old both male and female [12]
- Difficulty in reaching behind back [13]
- Clinically diagnosed Adhesive capsulitis [12]
- Restriction of shoulder movement (above 60 degrees of flexion and Abduction, 30 degrees of internal rotation, and 20 degrees of external rotation) [13]
- Adhesive capsulitis stage 2 and stage 3 [14]
- Tenderness over Deltoid, Trapezius, Pectoralis major and minor [12]
- Unilateral adhesive capsulitis [12]

EXCLUSION CRITERIA
- If they mentioned a dislocation, recent trauma, or a fracture at the cervical and shoulder
- Any other shoulder pathologies like soft tissue lesions [12]

INTERVENTION
Eligibility was confirmed and then the baseline measures were taken. The outcome measures reported in this study were the Numerical pain rating scale, range of motion by a universal goniometer, and Shoulder pain and disability index scale. All the individuals were treated 5 days per week for 3 weeks. Baseline values for all the outcome measures were taken and post-intervention after 3 weeks. In the initial evaluation session, the adhesive capsulitis individuals were interviewed and the baseline outcomes of GH joint external rotation and abduction were obtained.

GROUP A:- Gross Myofascial release combined with Focused Myofascial release with Conventional therapy
The patient was in a supine posture, and the first stretch was performed using an arm pull technique based on feedback from the patient's tissue. The arm was abducted to its maximum extent, and the pull was applied by the therapist gripping the patient's wrist with one hand. The stretch was held for 90 seconds each. After that Focused MFR on small restrictions within the Myofascial unit. It was provided for the Pectoralis major and minor muscles, as well as the deltoid and trapezius muscles.5 repetitions were held for 90second. The total duration was 10 to 15 minutes.

GROUP B:- Capsular Stretch with Conventional therapy
15 subjects was treated with capsular stretching
1. ANTERIOR CAPSULAR STRETCHING:-
The patient was standing with his elbow in 90 degrees of flexion and 0 degrees of abduction. A door frame was pressed on the anterior forearm. The patient then progressively rotates their body away from the door frame, creating an external rotation force, which was held for 10 seconds.
2. POSTERIOR CAPSULAR STRETCHING:-
The therapist stretches the back of the problematic shoulder by grabbing the elbow of the concerned arm across the chest and holding it for 10 seconds.
3. INFERIOR CAPSULAR STRETCHING:-
The therapist extends the affected arm above head with the elbow bent and the arm straight forward, stretching it higher overhead and holding the stretch for 10 seconds.

DURATION: - The patient was advised to sustain the stretch for 10 seconds and then repeat the process five times over the course of three weeks.

Megha Suthar *et al*.,

CONVENTIONAL THERAPY:-
· Anterior and posterior glide for shoulder joint 3 sets of 10 repetitions each side
· Interferential current therapy frequency 4100Hz for 10 minute
· Wand exercise
· Pendulum exercise
· Finger ladder exercise
· Towel exercise
Each exercise should be repeated 10 times. For three weeks, and worked five days a week.

OUTCOME MEASURES:-
The shoulder RANGE OF MOTION was measured for shoulder flexion, abduction, and internal and external rotation with a universal goniometer. Shoulder flexion and abduction were measured in the supine position while shoulder internal and external rotations were measured with the shoulder at 90 degrees of abduction [15].

THE SHOULDER PAIN AND DISABILITY QUESTIONNAIRE is a self-administered questionnaire. Five questions about the severity of an individual's pain are included in the pain component. The functional activities component consists of eight questions meant to assess how difficult it is for an individual to perform various daily activities that require the use of the upper extremities. The SPADI is the only reliable and valid shoulder measurement[16].
NPRS(numerical pain rating scale between 1 to 10 where 1 is minimal pain and 10 is maximum pain), In this the patient is asked to make pain ratings, relating to current good and worst pain experienced over the past 24 hours. These ratings represent the patient's level of pain over the previous 24 hours [17].

STATISTICAL ANALYSIS:-To check the improvements of these two treatments statistical analysis were done with statistically package of social science (SPSS 26). Statistically significant was set at p<0.05.

RESULTS

The NPRS, ROM, and SPADI Percentage across baseline and 3rd week follow up showed a significant improvement statistically in their mean score within group A and group B. Statistically Gross Myofascial release combined with focused Myofascial with conventional therapy and capsular stretching with conventional therapy groups are equal in comparison. The Abduction mean value of Group A was 130.53 17.029 and of Group B was 123.13 17.972 with a p-value was o.257.The external rotation means the value of Group A was 60.87 10.836 and of Group B was 55.20 12.667 with a p-value was 0.199. In SPADI the disability components having a mean value of Group A was 30.00 12.950 and Group B have 37.40 16.677 with a p-value was 0.186. The NPRS mean value of Group A was 4.00 1.195 and of Group B was 4.27 0.961 with a p-value was 0.506. There is no significant difference between Group A and Group B. They are significantly equal.

DISCUSSION

The purpose of this study was to see how gross Myofascial release combined with focused Myofascial release affect people with adhesive capsulitis in compare to capsular stretch. Gross Myofascial release combined with focused Myofascial release and capsular stretch had a considerable effect in adhesive capsulitis, according to the findings of this study. The result show there was significant difference in improvement of pain and ROM in both Gross Myofascial release combined with focused Myofascial release and capsular stretching. Relaxation in pain due to MFR technique can be assigned by one of the concept of MFR is that loose the tightness which is leading to weakness. Both Biomechanical and neural reflexive element are responsible for this concept. The hands-on method in this provides afferent stimulation via receptors. This strategy of gross Myofascial release coupled with focused Myofascial release leads to rigid connective tissue loosening when sensory excitation by extension is applied and the operator allows for efferent suppression to happen [18].

Megha Suthar *et al.*,

In a previous study on frozen shoulder patients, author used gross Myofascial release, focused Myofascial release, Maitland mobility, and conventional therapy. They found that combining MFR treatment with traditional treatment will provide additional benefits and a speedier recovery in adhesive capsulitis subjects. This had comparable effects to the current study, where treating trigger points reduced discomfort and increased range of motion [12]. High-grade mobilization was found to be more helpful than capsular stretching in the study. This is in line with the findings of a study by H.B.Sivkumar, who found that high-grade mobilization combined with active exercise is more beneficial than capsular stretching combined with active exercise [19].

Another author studied observed posterior capsular stretch on adhesive capsulitis patients with traditional manual therapy and electrotherapy. They discovered that posterior capsular stretch coupled with mobilization is more beneficial in enhancing ROM and lowering functional disability. This had similar effects to the current trial, in which ROM therapy increased ROM and decreased discomfort [14].

Dr. SwagataPatangarkar et al. conducted a study on the comparison of sustained inferior capsular stretching and passive joint mobilization in Adhesive capsulitis patients, in which sustained inferior capsular stretching with heat and cryotherapy and passive mobilization with heat and cryotherapy were given to two separate groups. They conclude that continuous inferior capsular stretching is superior to passive mobilization in terms of improving ROM and pain reduction [20]. One study of frozen shoulder patients, author compared the efficiency of scapular mobilization, manually posterior capsule stretching, and a relationship between two variable techniques. In one group, they received scapular mobilization, while in the other; they received manual posterior capsule stretching. The results demonstrated that both scapular mobilization and manual posterior capsule stretching were important in enhancing acute joint range of motion [21]

CONCLUSION
Gross Myofascial Release combined with Focused Myofascial Release versus capsular Stretch was found to be beneficial in decreasing pain, improving functional activities, and increasing range of motion in people with adhesive capsulitis shoulder in a three-week therapy program. Statistically, within Group comparison there was a significant difference in outcome measures but there was no significant difference between group comparisons.

LIMITATION
This study was included Short term treatment duration.

FURTHERRECOMMENDATION
It can be compared with other techniques like IASTM or Dry needling, Friction Massage, Ischemic compression. Strength of muscles can be assessed.

REFERENCES

1. LeylaAtasBalcI.Effect of Myofascial Relaxation on individual with Adhesive capsulitis.US national Library of Medicine. May 7,2021
2. Ewald A. Adhesive capsulitis: A review. Am Fam Physician. 2011; 83(4):417-22. Available from: http://www.ncbi.nlm.nih.gov/pubmed/21322517.
3. Calis M, Demir H, Ulker S, Kirnap M, Duygulu F, Calis HT. Is intraarticular sodium hyaluronate injection an alternative treatment in patients with adhesive capsulitis? Rheumatol Int. 2006; 26(6):536-40. Available from: http://www.ncbi.nlm.nih.gov/ pubmed/16091920.
4. Reeves B. The natural history of the frozen shoulder syndrome. Scand J Rheumatol. 1975;4(4):193-96. Available from: http://www.tandfonline.com. ezproxy.med.nyu.edu/doi/pdf/10.3109/03009747509165255.
5. Bron C, De Gast A, Dommerholt J, Stegenga B, Wensing M, Oostendorp RA. Treatment of myofascial trigger points in patients with chronic shoulder pain: a randomized, controlled trial. BMC medicine. 2011 Dec;9(1):8.

6. Simons DG. Understanding effective treatments of myofascial trigger points. Journal of Bodywork and movement therapies. 2002 Apr 1; 6(2):81-8.

7. Gordon CM, Andrasik F, Schleip R, Birbaumer N, Rea M. Myofascial triggerpoint release (MTR) for treating chronic shoulder pain: a novel approach. J BodywMovTher. 2016; 20: 614–22.

8. Bialosky JE, Bishop MD, Price DD, Robinson ME, George SZ. The mechanisms of manual therapy in the treatment of musculoskeletal pain: a comprehensive model. Man Ther.2009;14:531-8

9. Carol J. Manheim. The Myofascial Release Manual, Slack incorporated. 3rd edition, 2003: 40-50pp, 98-100

10. Pravin P Gawali, Ujwalyeol, Biplapnandi. Effect of capsular stretching and maitland mobilization in adhesive capsulitis – a comparative study. Indian Journal of Physical Therapy. Volume 4 Issue 1.January-June 2016.page no 66-69

11. M S Ajimsha, Noora R AI-Mudahka, J A AI Madzhar.Effectivness of Myofascial release: Systmatic review of randomized controlled trials. Journal of body work and movment therapies.Volume 19, issue1,Jan 15,page 102-112

12. PeeyooshaGurudut, Aarti welling, GayatriKudchadkar. Combind effect of gross and focused Myofascial release technique on Trigger points and Mobility in subject with frozen shoulder-A Pi3ot Study. International Journal of Health Science and research vol.9;Issue:4;April 2019

13. Antony Paul, Joshua Samuel Rajkumar,Smita Peter, and Litson Lambert. Effectiveness of Sustained Stretching of the Inferior Capsule in the Management of a Frozen Shoulder. Clinical Orthopedics and Releted Research. 2014 Jul; 472(7): 2262–2268.

14. MadihaMaryam,Muhmmadkashif, Abdul Gafoorsajjat. Effects of Posterior capsule stretch on Adhesive Capsulitis. The Professional Medical Journal 26(08):1272-1277

15. Cynthia C. Norkin, D. Joyce White. Measurment of Joint Motion: A Guide to Goniometry. 3rd Edition.Jaypee Brothers. 2004; Page no 70-72, 78-80, 82-84, 86-88

16. Joy C MacDermid, Patty Solomon,Kennethprkachin.the shoulder pain and disability index demonstrates factor,construct and longitudinal validity. BMC musculoskeletal disorder. 2006; 7: 12.

17. Mawdsley, Roberta H.; Moran, Kelley A.; Conniff, Lisa A.**Reliability of Two Commonly Used Pain Scales With Elderly Patients.** Journal of Geriatric Physical Therapy: Volume 25 Issue 3 p 16-20

18. Shah S, Bhalara A. Myofascial release. International Journal of Health Sciences and Research. 2012 May;2(2):69-77.

19. H.B shivakumar,Chanappa T. S.,R.Balasaravanan and Swathi k. R. A comparative study between the efficacy of high grade mobilization with active exercises versus capsular starching with active exercises on patients with adhesive capsulitis. Journal of evaluation of medical and dental sciencesvol 3,issue 14 April 07,2014 page 3833.

20. Dr. Swagata A. Patangankar and Dr. Amol A. Pandav. A Comparative study of Sustained inferior capsular stretching versus passive joint mobilization in treatment of Adhesive Capsulitis.World Journal of Pharmaceutical and Medical research. 2019, 5(12),90-95

21. IremDuzgun, Elis Turget,NihanKapa.The effect of manual posted stretching and scapular mobilization on range of motion and function in frozen shoulder. Annals of the rheumatic diseases .jan 2014 72(suppl 3):A 573- A57

Given below are the tables for within the group and between the group comparison in Group A which is Gross Myofascial release and Group B which is capsular stretch.

Table: 1. Comparisons within Group A and Group B

Paired t test				
OUTCOME	GROUP	PRE MEAN±SD	POST ±MEAN SD	P value
ABDUCTION	GROUP A	97.53±7.818	130.53±17.029	<0.05
	GROUP B	95.53±15.195	123.13±17.972	
EXTERNAL ROTATION	GROUP A	44.80±15.474	60.87±10.836	
	GROUP B	40.47±13.212	55.20±12.667	
NPRS	GROUP A	7.20±1.521	4.00±1.195	
	GROUP B	7.20±1.207	4.27±.961	

SPADI	GROUP A	76.80±12.417	30.00±12.950	
	GROUP B	75.60±15.380	37.40±16.677	

Table: 2. Comparisons between Group A and Group B

INDEPENDENT t test			
MEASURES	**GROUP**	**MEAN±SD**	**P value**
ABDUCTION	GROUP A	130.5333±17.02883	.257
	GROUPB	123.1333±17.97167	.257
EXTERNAL ROTATION	GROUP A	60.8667±10.83557	.199
	GROUP B	55.2000±12.66717	.199
NPRS	GROUP A	4.0000±1.19523	.506
	GROUP B	4.2667± 96115	.506
SPADI	GROUP A	30.0000±12.95046	.186
	GROUP B	37.4000±16.67676	.186
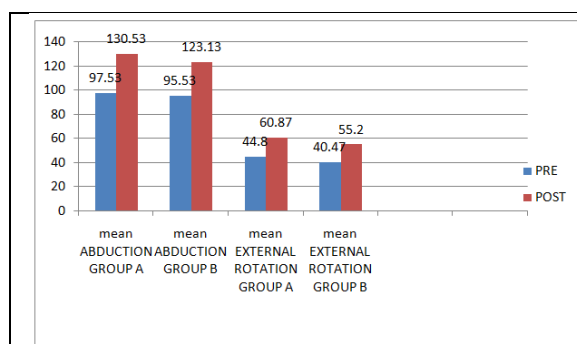
Fig.1. Abduction and External Rotation of Group A and Group B pre post mean	**Fig.2. NPRS and SPADI Group A and Group B pre post mean**
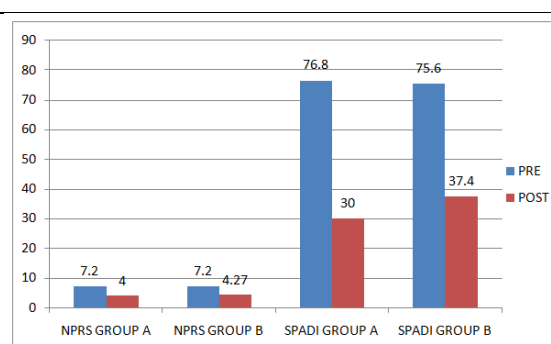
RESEARCH ARTICLE

A Novel Simplex Technique to Solve Linear Fractional Programming Problem using the Pentagonal Neutrosophic Fuzzy Number

P.Rajarajeswari [1*] and M.Shyamala[2]

[1]Department of Mathematics, Chikkanna Government Arts College, Tirupur- 641602, Tamil Nadu, India
[2]Department of Mathematics, VLB Janakiammal College of Arts and Science,Coimbatore-641042, Tamil Nadu, India

*Address for Correspondence
P.Rajarajeswari
Department of Mathematics,
Chikkanna Government Arts College,
Tirupur- 641602, Tamil Nadu, India
E.Mail: p.rajarajeswari29@gmail.com

ABSTRACT

In real world situations, Linear Fractional Programming Problem[LFPP] has inspired several researchers due to its application in engineering, business, production planning, marketing, finance, economics , health care, hospital planning and in various research domains. Pentagonal Neutrosophic Fuzzy Number (PNFN) plays an important role to measure the vagueness ,hesitation and uncertain information . In this , we have provided an efficient ranking method for solving LFPP by using Simplex technique and a ranking method. Here, we represent the coefficients of both the constraints and the objective function alone as PNFN.Further, an illustrative numerical examples were shown to enumerate our proposed method. Further, comparison table and multiple bar diagram was performed with some of the available methods to prove that our proposed method is higher optimized.

Keywords - Fuzzy numbers, Neutrosophic Fuzzy numbers, Pentagonal Neutrosophic Fuzzy Numbers[PNFN], Linear Fractional Programming.

INTRODUCTION

In real life world situations, several methods exist for solving LFPP . Zadeh(1965) [11] introduced fuzzy set theory .Dubois and Prade [5] introduced many types of operations on fuzzy numbers .Several researchers so far introduced different types of fuzzy numbers to measure the vagueness of the existing problems using triangular fuzzy number [6],trapezoidal fuzzy number[4] and pentagonal fuzzy number [2,7] with its membership functions as they have got more applications[10] in risk analysis and reliability. Later Sapan Kumar Das et.al.,[8] introduced a

Rajarajeswari and Shyamala

dual simplex method to solve LFPP using Triangular Neutrosophic Number. Further ,Abdel-Basset et.al.,[1] proposed a new technique with trapezoidal neutrosophic number for solving Linear programming problem[LPP].In this paper ,we solve LFPP by using PNFN to get a better result using the proposed new ranking method. Here, ranking of PNFN plays an important role in solving LFPP and gives the best solution. Further, an efficient ranking method to convert into a crisp number was presented and also explained through numerical examples.In addition, we made a comparison between the proposed method optimal solution with other existing method solutions. Here, we consider LFPP in which coefficients of both the constraints and the objective functions except the decision variables are considered as Pentagonal Neutrosophic Fuzzy Number[PNFN].First LFPP was decomposed into two Linear programming problems[LPPs] and then the decomposed LFPP is converted into crisp LPPs using the ranking method. To get the optimal solution, we put the resultant function in the standard form of LPP and finally ,the problem is solved by our proposed method.

PRELIMINARIES

 Some basic definitions involving Pentagonal Fuzzy Number, Pentagonal Neutrosophic Fuzzy Number, its Score Function and Arithmetic Operations on Pentagonal Neutrosophic Fuzzy Number are outlined in this section.

Definition 2.1 - Pentagonal   Fuzzy Number [2]:

A fuzzy number A=(p_1, q_1, r_1, s_1, t_1) is called pentagonal fuzzy number ,if its membership function is given by

$$\mu_A(x) = \begin{cases} 0 & , p_1 \leq x, t_1 \leq x \\ \frac{x-p_1}{q_1-p_1}, & p_1 \leq x \leq q_1 \\ \frac{x-q_1}{r_1-q_1}, & q_1 \leq x \leq r_1 \\ 1, & x = r_1 \\ \frac{s_1-x}{s_1-r_1}, & r_1 \leq x \leq s_1 \\ \frac{t_1-x}{t_1-s_1}, & s_1 \leq x \leq t_1 \end{cases}$$

Definition 2.2 - Pentagonal Neutrosophic Fuzzy Number [3]:

Pentagonal Neutrosophic Fuzzy Number denoted by $\tilde{a}$ is a subset of a neutrosophic number in R with the   following truth membership function, indeterminacy membership function and falsity membership function given by $\tilde{a}$ = < (p_1, q_1, r_1, s_1, t_1); $\alpha_{\tilde{a}}, \Theta_{\tilde{a}}, \beta_{\tilde{a}}$ > where $\alpha_{\tilde{a}}, \Theta_{\tilde{a}}, \beta_{\tilde{a}} \in$ [0,1]. The truth membership function   T: R $\rightarrow$ [0, $\alpha_{\tilde{a}}$], the indeterminacy membership function I: R$\rightarrow$ [$\Theta_{\tilde{a}}$, 1] and the falsity membership function   F : R $\rightarrow$ [$\beta_{\tilde{a}}$, 1] are defined as follows

$$T(x) = \begin{cases} 0, & p_1 \leq x, t_1 \leq x \\ \frac{\alpha_{\tilde{a}}(x - p_1)}{(q_1 - p_1)}, & p_1 \leq x \leq q_1 \\ \frac{\alpha_{\tilde{a}}(x - q_1)}{(r_1 - q_1)}, & q_1 \leq x \leq r_1 \\ \alpha_{\tilde{a}}, & x = r_1 \\ \frac{\alpha_{\tilde{a}}(s_1 - x)}{(s_1 - r_1)}, & r_1 \leq x \leq s_1 \\ \frac{\alpha_{\tilde{a}}(t_1 - x)}{(t_1 - s_1)}, & s_1 \leq x \leq t_1 \end{cases}$$

$$I(x) = \begin{cases} 0, & p_1 \le x, t_1 \le x \\ \dfrac{\Theta_{\tilde{a}}(x-p_1)}{(q_1-p_1)}, & p_1 \le x \le q_1 \\ \dfrac{\Theta_{\tilde{a}}(x-q_1)}{(r_1-q_1)}, & q_1 \le x \le r_1 \\ \Theta_{\tilde{a}}, & x = r_1 \\ \dfrac{\Theta_{\tilde{a}}(s_1-x)}{(s_1-r_1)}, & r_1 \le x \le s_1 \\ \dfrac{\Theta_{\tilde{a}}(t_1-x)}{(t_1-s_1)}, & s_1 \le x \le t_1 \end{cases}$$

and

$$F(x) = \begin{cases} 0, & p_1 \le x, t_1 \le x \\ \dfrac{\beta_{\tilde{a}}(x-p_1)}{(q_1-p_1)}, & p_1 \le x \le q_1 \\ \dfrac{\beta_{\tilde{a}}(x-q_1)}{(r_1-q_1)}, & q_1 \le x \le r_1 \\ \beta_{\tilde{a}}, & x = r_1 \\ \dfrac{\beta_{\tilde{a}}(s_1-x)}{(s_1-r_1)}, & r_1 \le x \le s_1 \\ \dfrac{\beta_{\tilde{a}}(t_1-x)}{(t_1-s_1)}, & s_1 \le x \le t_1 \end{cases}$$

Definition 2.3 - Score function [2]:

Let $\tilde{a} = <(p_1, q_1, r_1, s_1, t_1); \alpha_{\tilde{a}}, \Theta_{\tilde{a}}, \beta_{\tilde{a}}>$ be the Pentagonal Neutrosophic Fuzzy Number, then the special ranking of Pentagonal Fuzzy Neutrosophic Number called Score function is defined as follows

$$S(\tilde{a}) = \frac{1}{15}(p_1 + q_1 + r_1 + s_1 + t_1)(\alpha_{\tilde{a}} + (1 - \Theta_{\tilde{a}}) + (1 - \beta_{\tilde{a}}))$$

Definition 2.4 - Arithmetic Operations on Pentagonal Neutrosophic Fuzzy Numbers [PNFNs] [3]:

Addition of   two PNFNs:

Let　$\tilde{A} = <(p_1, q_1, r_1, s_1, t_1); \alpha_{\tilde{A}}, \Theta_{\tilde{A}}, \beta_{\tilde{A}}>$

$\tilde{B} = <(p_2, q_2, r_2, s_2, t_2); \alpha_{\tilde{B}}, \Theta_{\tilde{B}}, \beta_{\tilde{B}}>$

then the addition of   two PNFN**s** is given by,

$$\tilde{A} + \tilde{B} = <(p_1 + p_2, q_1 + q_2, r_1 + r_2, s_1 + s_2, t_1 + t_2); \alpha_{\tilde{A}} + \alpha_{\tilde{B}} - \alpha_{\tilde{A}}\alpha_{\tilde{B}}, \Theta_{\tilde{A}}\Theta_{\tilde{B}}, \beta_{\tilde{A}}\beta_{\tilde{B}}>$$

Subtraction of two PNFNs

Let $\tilde{A} = <(p_1, q_1, r_1, s_1, t_1); \alpha_{\tilde{A}}, \Theta_{\tilde{A}}, \beta_{\tilde{A}}>$

$\tilde{B} = <(p_2, q_2, r_2, s_2, t_2); \alpha_{\tilde{B}}, \Theta_{\tilde{B}}, \beta_{\tilde{B}}>$

then the subtraction of   two PNFN**s** is given by,

$$\tilde{A} - \tilde{B} = <(p_1 - p_2, q_1 - q_2, r_1 - r_2, s_1 - s_2, t_1 - t_2); \alpha_{\tilde{A}} + \alpha_{\tilde{B}} - \alpha_{\tilde{A}}\alpha_{\tilde{B}}, \Theta_{\tilde{A}}\Theta_{\tilde{B}}, \beta_{\tilde{A}}\beta_{\tilde{B}}>$$

Multiplication of two PNFNs

Rajarajeswari and Shyamala

Let　$\tilde{A} =< (p_1, q_1, r_1, s_1, t_1); \alpha_{\tilde{A}}, \Theta_{\tilde{A}}, \beta_{\tilde{A}} >$

$\tilde{B} =< (p_2, q_2, r_2, s_2, t_2); \alpha_{\tilde{B}}, \Theta_{\tilde{B}}, \beta_{\tilde{B}} >$

then the multiplication two PNFNs is given by

$\tilde{A}\tilde{B} =< (p_1p_2, q_1q_2, r_1r_2, s_1s_2, t_1t_2); \alpha_{\tilde{A}}\alpha_{\tilde{B}}, \beta_{\tilde{A}} + \beta_{\tilde{B}} - \beta_{\tilde{A}}\beta_{\tilde{B}}, \Theta_{\tilde{A}} + \Theta_{\tilde{B}} - \Theta_{\tilde{A}}\Theta_{\tilde{B}} >$

PROPOSED METHOD

In this proposed method, first we have formulated a LFPP based on real world situations and the essential factors are used in the descriptions of the objective function and constraints. We introduced a new method for solving LFPP where all the coefficients in the objective function and constraints are PNFN except the decision variables and also to find the most optimal value of the objective function.

Consider LFPP as below

Max (or)Min $z(x) = \dfrac{z_1(x)}{z_2(x)}$

Subject to　$x \, \varepsilon \, T$ 　　　　　　　　　　　　　　　　　　　　(1)

where the objective functions $z_1(x)$ and $z_2(x)$ are linear functions and the set T is defined as $T = \{ x / Ax \le B, x > 0\}$ .Here A is fuzzy matrix.

Step-1: We consider the LFPP with m constraints and n variables as below

Max (or)Min $z(x) = \dfrac{\sum_{j=1}^{n} c_j x_j + \alpha}{\sum_{j=1}^{n} d_j x_j + \beta}$ 　　　　　　　　　　　　　(2)

Subject to　$\sum_{i=1}^{m} a_{ij} x_j \le b_i$

$x_j \ge 0$ where $j = 1,2,\dots,n.$

Step-2: In the above , we represented all the coefficients in objective function and constraints as PNFN like below

Max (or)Min $z(x) = \dfrac{\sum_{j=1}^{n}(b_j, d_j, e_j, f_j, g_j; T_{c_j}, I_{c_j}, F_{c_j}) x_j + (\alpha_1, \alpha_2, \alpha_3, \alpha_4, \alpha_5 \,; T_\alpha, I_\alpha, F_\alpha)}{\sum_{j=1}^{n}(c_j, e_j, f_j, g_j, h_j; T_{d_j}, I_{d_j}, F_{d_j}) x_j + (\beta_1, \beta_2, \beta_3, \beta_4, \beta_5, ; T_\beta, I_\beta, F_\beta)}$

Subject to

$\sum_{i=1}^{m}\left(b_{ij}, c_{ij}, d_{ij}, e_{ij}, f_{ij}; T_{a_{ij}}, I_{a_{ij}}, F_{a_{ij}}\right) x_j \le \left(p_i, q_i, r_i, s_i, t_i; T_{b_i}, I_{b_i}, F_{b_i}\right).$

$x_j \ge 0$ where $j = 1,2,\dots,n.$

Step-3: In the above LFPP,we decompose the objective function into two LPPs as follows

(P-1)

Max (or) Min $z_1(x) = \sum_{j=1}^{n}(b_j, d_j, e_j, f_j, g_j; T_{c_j}, I_{c_j}, F_{c_j}) x_j + (\alpha_1, \alpha_2, \alpha_3, \alpha_4, \alpha_5 \,; T_\alpha, I_\alpha, F_\alpha)$

s.t　$\sum_{i=1}^{m}\left(b_{ij}, c_{ij}, d_{ij}, e_{ij}, f_{ij}; T_{a_{ij}}, I_{a_{ij}}, F_{a_{ij}}\right) x_j \le \left(p_i, q_i, r_i, s_i, t_i; T_{b_i}, I_{b_i}, F_{b_i}\right)$

$x_j \ge 0$ where $j = 1,2,\dots,n.$

(P-2)

Max (or)Min $z_2(x) = \sum_{j=1}^{n}(c_j, e_j, f_j, g_j, h_j; T_{d_j}, I_{d_j}, F_{d_j}) x_j + (\beta_1, \beta_2, \beta_3, \beta_4, \beta_5 \,; T_\beta, I_\beta, F_\beta)$

s.t　$\sum_{i=1}^{m}\left(b_{ij}, c_{ij}, d_{ij}, e_{ij}, f_{ij}; T_{a_{ij}}, I_{a_{ij}}, F_{a_{ij}}\right) x_j \le \left(p_i, q_i, r_i, s_i, t_i; T_{b_i}, I_{b_i}, F_{b_i}\right)$

$x_j \ge 0$ where $j = 1,2,\dots,n.$

Step-4: Using the definition 2.2 in the above LPP given in (P-1) and (P-2) ,we get the modified LPPs as below

(P-3)

Max (or) Min $z_1(x) = \sum_{j=1}^{n} S\left(b_j, d_j, e_j, f_j, g_j; T_{c_j}, I_{c_j}, F_{c_j}\right) x_j + S(\alpha_1, \alpha_2, \alpha_3, \alpha_4, \alpha_5; T_\alpha, I_\alpha, F_\alpha)$

Rajarajeswari and Shyamala

s.t $\quad \sum_{i=1}^{m} S\left(b_{ij}, c_{ij}, d_{ij}, e_{ij}, f_{ij}; T_{a_{ij}}, I_{a_{ij}}, F_{a_{ij}}\right) x_j \le S(p_i, q_i, r_i, s_i, t_i; T_{b_i}, I_{b_i}, F_{b_i})$

$\quad x_j \ge 0$ where $j = 1,2,\dots,n$.

(P-4)

Max (or) Min$z_2(x) = \sum_{j=1}^{n} S\left(c_j, e_j, f_j, g_j, h_j; T_{d_j}, I_{d_j}, F_{d_j}\right) x_j + S(\beta_1, \beta_2, \beta_3, \beta_4, \beta_5; T_\beta, I_\beta, F_\beta)$

s.t $\quad \sum_{i=1}^{m} S\left(b_{ij}, c_{ij}, d_{ij}, e_{ij}, f_{ij}; T_{a_{ij}}, I_{a_{ij}}, F_{a_{ij}}\right) x_j \le S(p_i, q_i, r_i, s_i, t_i; T_{b_i}, I_{b_i}, F_{b_i})$

$\quad x_j \ge 0$ where $j = 1,2,\dots,n$.

Step-5: By solving the above LPP given in (P-3) and (P-4) by Simplex Method ,we get the optimal solutions namely $Z_1(x)$ and $Z_2(x)$.

Step-6: The optimal solution of the LFPP is obtained by using the formula

Max (or) Min $Z = \frac{z_2(x)}{z_1(x)}$.

If the objective function is of minimization type then convert it into Min Z(x) by using the formula　Min Z(x)=- Max Z(x)

Application of Proposed Method:

Numerical Example 3.1:

Step 1: Consider the following LFPP

Max Z(x) $= \frac{8 X_1 + 18 X_2}{16X_1 + 18X_2 + 12}$　　　　　　　　　　　　　　　　　(3)

$64 X_1 + 82X_2 \le 95$, $8 X_1 + 10X_2 \le 22$, $X_1, X_2 \ge 0$

Step 2: We have represented the coefficients used in the objective function and the constraints as PNFN as follows

Max Z(x) $= \frac{(1,6,10,13,14;0.9,0.1,0.3)X_1 + (11,16,20,23,24;0.9,0.1,0.3)X_2}{(5,15,25,30,31; 0.7,0.5,0.6)X_1 + (11,16,20,23,24;0.9,0.1,0.3)X_2 + (4,8,17,25,26; 0.3,0.6,0.4)}$

s.t $(60,62,64,66,67;0.2,0.5,0.6) X_1 + (80,82,85,86,88;0.3,0.6,0.4) X_2 \le (92,94,97,100,101;0.8,0.2,0.4)$

$(1,6,10,13,14; 0.9,0.1,0.3) X_1 + (1,6,11,15,16; 0.7,0.6,0.3) X_2 \le (16,18,22,23,24;0.3,0.6,0.4)$　　$X_1, X_2 \ge 0$

Step 3: In the above LFPP,we decompose the objective function into two LPPs namely (P-1) and (P-2) as follows

(P-1)

Max $z_1(x) = (1,6,10,13,14; 0.9,0.1,0.3)X_1 + (11,16,20,23,24; 0.9,0.1,0.3)X_2$

s.t $(60,62,64,66,67;0.2,0.5,0.6) X_1 + (80,82,85,86,88;0.3,0.6,0.4) X_2 \le (92,94,97,100,101;0.8,0.2,0.4)$

$\quad (1,6,10,13,14; 0.9,0.1,0.3) X_1 + (1,6,11,15,16; 0.7,0.6,0.3) X_2 \le (16,18,22,23,24;0.3,0.6,0.4)$

$\quad X_1, X_2 \ge 0$

(P-2) Max$z_2(x) = (5,15,25,30,31; 0.7,0.5,0.6)X_1 + (11,16,20,23,24; 0.9,0.1,0.3)X_2 + (4,8,17,25,26; 0.3,0.6,0.4)$

s.t $(60,62,64,66,67;0.2,0.5,0.6) X_1 + (80,82,85,86,88;0.3,0.6,0.4) X_2 \le (92,94,97,100,101;0.8,0.2,0.4)$

$(1,6,10,13,14;0.9,0.1,0.3) X_1 + (1,6,11,15,16;0.7,0.6,0.3)X_2 \le (16,18,22,23,24;0.3,0.6,0.4)$, $X_1, X_2 \ge 0$

Step 4: To find the crisp value of each PNFN, we use definition 2.2 as follows

S $(\tilde{8}) = 7.33$, S $(\widetilde{10}) = 5.88$, S $(\widetilde{12}) = 6.93$, S$(\widetilde{16}) = 11.31$, S $(\widetilde{18}) = 15.67$, S $(\widetilde{22}) = 8.93$,

S $(\widetilde{64}) = 23.39$, S $(\widetilde{82}) = 36.49$, S $(\widetilde{95}) = 70.99$

By substituting these crisp values in (P- 1) and (P- 2) ,we get the modified LPPs as folows

(P- 3)

Max $z_1(x) = (7.33) X_1 + (15.67) X_2$

s.t $\quad 23.39 X_1 + 36.49X_2 \le 70.99$, $7.33 X_1 + 5.88 X_2 \le 8.93$ and $X_1, X_2 \ge 0$

(P-4)

Max $z_2(x) = 11.31X_1 + 15.67X_2 + 6.93$

s.t $23.39 X_1 + 36.49X_2 \le 70.99$, $7.33X_1 + 5.88 X_2 \le 8.93$ and $X_1, X_2 \ge 0$

Rajarajeswari and Shyamala

Step 5: Solving (P-3) and (P-4) by simplex method ,we get Max $z_1(x)$ =23.80 where X_1=0, X_2=1.52 and Max $z_2(x)$ = 30.73 where X_1=0, X_2=1.52

Step 6: The optimum solution of the crisp LFPP is obtained as follows.
Max Z = $\frac{z_2(x)}{z_1(x)}$ = $\frac{30.73}{23.80}$ = 1.29
Next ,we have illustrated few numerical examples to demonstrate our proposed method

Numerical Example 3.2 [9]:

Step 1: Consider the LFPP
Min Z $(x) = \frac{-2X_1+X_2+2}{X_1+3X_2+4}$ (4)
        s.t $-X_1 + X_2 \leq 4$, $2X_1 + X_2 \leq 14$, $X_2 \leq 6$ and $X_1, X_2 \geq 0$
Step 2: We represent the coefficients used in the objective function and the constraints into   PNFN as follows
Min Z$(x) = \frac{-(1,3,5,6,7;0.2,0.3,0.5)X_1+ (0,2,4,5,7;0.8,0.6,0.4)X_2+(1,3,5,6,7;0.2,0.3,0.5)}{(0,2,4,5,7; 0.8,0.6,0.4)X_1+ (1,2,5,6,7; 0.2,0.5,0.6)X_2+(1,2,5,7,8;0.5,0.4,0.9)}$
s.t $-(0,2,4,5,7; 0.8,0.6,0.4)$ X₁ + (0,2,4,5,7; 0.8, 0.6, 0.4) X₂ ≤(1,2,5,7,8; 0.5,0.4,0.9)
      (1,3,5,6,7; 0.2,0.3,0.5) X₁ + (0,2,4,5,7; 0.8, 0.6, 0.4) X₂ ≤(7,10,19,30,35; 0.8,0.4,0.7)
      (0,2,4,5,7; 0.8, 0.6, 0.4) X₂ ≤(3,7,9,13,16; 0.7,0.2,0.5) and X₁ , X₂≥ 0

Step 3: In the above LFPP,we decompose the objective function into two LPPs as follows
(P-1)
  Min $z_1(x) = -(1,3,5,6,7;0.2,0.3,0.5)X_1 + (0,2,4,5,7;0.8,0.6,0.4)X_2 + (1,3,5,6,7;0.2,0.3,0.5)$
   s.t $-(0,2,4,5,7; 0.8,0.6,0.4)$ X_1 + (0,2,4,5,7; 0.8, 0.6, 0.4) X_2 ≤(1,2,5,7,8; 0.5,0.4,0.9)
      (1,3,5,6,7; 0.2,0.3,0.5) X_1 + (0,2,4,5,7; 0.8, 0.6, 0.4) X_2 ≤(7,10,19,30,35; 0.8,0.4,0.7)
       (0,2,4,5,7; 0.8, 0.6, 0.4) X_2 ≤(3,7,9,13,16; 0.7,0.2,0.5) and $X_{1, 2}$≥ 0
(P-2)
  Min ₂() =(0,2,4,5,7; 0.8,0.6, 0.4)₁ + (1,2,5,6,7; 0.2,0.5,0.6)₂ + (1,2,5,7,8; 0.5,0.4,0.9)
   s.t   -(0,2,4,5,7; 0.8,0.6,0.4)₁ + (0,2,4,5,7; 0.8, 0.6, 0.4)₂ ≤(1,2,5,7,8; 0.5,0.4,0.9)
     (1,3,5,6,7; 0.2,0.3,0.5)₁ + (0,2,4,5,7; 0.8, 0.6, 0.4)₂ ≤(7,10,19,30,35; 0.8,0.4,0.7)
     (0,2,4,5,7; 0.8, 0.6, 0.4)₂ ≤(3,7,9,13,16; 0.7,0.2,0.5) and ₁, ₂≥ 0

Step 4: To find the crisp value of each PNFN, we use definition 2.2 as follows
S $(\tilde{1})$ = 2.16,S $(\tilde{2})$ = 2.05 ,S $(\tilde{3})$ = 1.54 ,S $(\tilde{4})$ = 1.84, S $(\tilde{6})$ = 6.40, S $(\widetilde{14})$ =11.45
 By substituting these crisp values in (P- 1) and (P- 2), we get the modified LPPs as follows
(P-3)
Min ₁() = -(2.05) ₁ + (2.16) ₂+2.05
s.t
-(2.16) ₁ +(2.16) ₂ ≤ 1.84 ,(2.05) ₁ +(2.16) ₂ ≤ 11.45, (2.16) ₂ ≤ 6.40 and ₁, ₂ ≥ 0
(P-4)
Min ₂() = (2.16) ₁ +1.54 ₂ +1.84
s.t
-(2.16) ₁ +(2.16) ₂ ≤ 1.84 ,(2.05) ₁ +(2.16) ₂ ≤ 11.45, (2.16) ₂ ≤ 6.40 and ₁, ₂≥ 0.

Step 5: Solving (P-3) and (P-4) by simplex method ,we get Min ₁() = -9.40 where ₁=5.59, ₂=0 and Min ₂() =1.84 where ₁=0, ₂=0.

Step 6: The optimum solution of the crisp LFPP is obtained as follows.
Max Z = $\frac{₂()}{₁()}$ = $\frac{-9.40}{1.84}$ =-5.11

Rajarajeswari and Shyamala

We observe that the same problem given in example 2 was solved by Sumon Kumar Saha et.al.,[9] in the section 4 ,example 1 using LFPP and they got the solution as Min $Z(x)$=-1.09 but the same problem solved by using Trapezoidal Fuzzy Neutrosophic Number we got the solution as Min $Z(x)$=-5.09.But our proposed method gives the solution as Min $Z(x)$=-5.11.This shows that our proposed method gives the most optimal solution.

Numerical Example 3.3 [8]: Let us consider the problem solved by Sapan kumar Das et.al.,[8] in section 4.

Step 1: Consider the following LFPP

$$\text{Max } Z(x) = \frac{8_1 + 7_2 + 9_3}{8_1 + 9_2 + 6_3 + 1.5} \tag{5}$$

s.t $4_1 + 3_2 + 5_3 \le 28$, $5_1 + 3_2 + 3_3 \le 20$, $_{1,2,3} \ge 0$

Step 2: We represent the coefficients used in the objective function and the constraints as PNFN as follows

$$\text{Max } Z = \frac{(1,6,10,13,14;0.9,0.1,0.3)_1 + (5,8,9,13,14;0.4,0.6,0.8)_2 + (6,8,10,15,16;0.6,0.4,0.7)_3}{(1,6,10,13,14;0.9,0.1,0.3)_1 + (6,8,10,15,16;0.6,0.4,0.7)_2 + (3,7,9,13,16;0.7,0.2,0.5)_3 + (0.5,1,1.5,2,3;0.75,0.5,0.25)}$$

s.t

$(1,2,5,7,8; 0.5, 0.4, 0.9)_1 + (1,2,5,6,7; 0.2, 0.5, 0.6)_2 + (2,4,7,10,11; 0.8, 0.2, 0.4)_3 \le (24,26,28,30,32; 0.4, 0.25, 0.5)$

$(2,4,7,10,11; 0.8, 0.2, 0.4)_1 + (1,2,5,6,7; 0.2, 0.5, 0.6)_2 + (1,2,5,6,7; 0.2, 0.5, 0.6)_3 \le (10,12,27,30,31; 0.2, 0.3, 0.5)$

$_{1,2,3} \ge 0$

Step 3: In the above LFPP,we decompose the objective function into two LPPs namely as follows

(P-1)

$\text{Max }_1() = (1,6,10,13,14; 0.9,0.1,0.3)_1 + (5,8,9,13,14; 0.4,0.6,0.8)_2 + (6,8,10,15,,16; 0.6,0.4,0.7)_3$

s.t.

$(1,2,5,7,8;0.5,0.4,0.9)_1 + (1,2,5,6,7; 0.2, 0.5, 0.6)_2 + (2,4,7,10,11; 0.8, 0.2, 0.4)_3 \le (24,26,28,30,32; 0.4, 0.25, 0.5)$

$(2,4,7,10,11; 0.8, 0.2, 0.4)_1 + (1,2,5,6,7\ 0.2, 0.5, 0.6)_2 + (1,2,5,6,7; 0.2, 0.5, 0.6)_3 \le (10,12,27,30,31; 0.2, 0.3, 0.5)$

$_{1,2,3} \ge 0$

 (P-2)

$\text{Max }_2() = (1,6,10,13,14; 0.9,0.1,0.3)_1 + (6,8,10,15,16,0.6,0.4,0.7)_2 + (3,7,9,13,16; 0.7,0.2,0.5)_3 + (0.5,1,1.5,2,3; 0.75,0.5,0.25)$

s.t.

$(1,2,5,7,8; 0.5, 0.4, 0.9)_1 + (1,2,5,6,7; 0.2, 0.5, 0.6)_2 + (2,4,7,10,11; 0.8, 0.2, 0.4)_3 \le (24,26,28,30,32; 0.4, 0.25, 0.5)$

$(2,4,7,10,11; 0.8, 0.2, 0.4)_1 + (1,2,5,6,7; 0.2, 0.5, 0.6)_2 + (1,2,5,6,7; 0.2, 0.5, 0.6)x_3 \le (10,12,27,30,31; 0.2, 0.3, 0.5)$

$x_1, x_2, x_3 \ge 0$

Step 4: To find the crisp value of each PNFN, we calculate the score function as follows

$S(\tilde{3}) = \frac{1}{15}(1 + 2 + 5 + 6 + 7)(0.2 + (1 - 0.5) + (1 - 0.6)) = 1.54, S(\tilde{4}) = .84, S(\tilde{5}) = 4.99$, $S(\tilde{6}) = 6.40$, $S(\tilde{7}) = 3.27, S(\tilde{8}) = 7.33$, $S(\widetilde{1.5}) = 1.07$, $S(\widetilde{20}) = 10.27, S(\widetilde{28}) = 15.40$

By substituting these score values in (P- 1) and (P- 2), we get the modified LPPs as follows

(P-3)

$\text{Max } z_1(x) = (7.33) x_1 + (3.27) x_2 + (5.50) x_3$

s.t $(1.84) x_1 + (1.54) x_2 + (4.99) x_3 \le 15.40$, $(4.99) x_1 + (1.54) x_2 + (1.54) x_3 \le 10.27$

$x_1, x_2, x_3 \ge 0$

(P-4)

$\text{Max } z_2(x) = (7.33) x_1 + 5.50 x_2 + 6.40 x_3 + 1.07$

s.t $(1.84) x_1 + (1.54)x_2 + (4.99)x_3 \le 15.40$, $(4.99) x_1 + (1.54)x_2 + (1.54)x_3 \le 10.27$

$x_1, x_2, x_3 \ge 0$

Step 5: Solving (P-3) and (P-4) by using simplex method ,we get Max $z_1(x)$= 25.12   where x_1=0, x_2=5.18 , x_3 = 1.49 and Max $z_2(x)$ =39.09   where x_1= 0 , x_2=5.18 , x_3 =   1.49.

Step 6 : The optimum solution of the crisp LFPP is obtained as follows.

Max Z $= \frac{z_2(x)}{z_1(x)}$ $= \frac{39.09}{25.12}$ =1.56

We observe that the same problem given in Numerical Example 3.3 was solved by Sapan kumar Das et.al.,[8] using Triangular Fuzzy Neutrosophic Number ,they got the solution as Max Z=1.16   , using Trapezoidal Fuzzy Neutrosophic Number we got the solution as Max Z=1.47 but the same problem solved by our proposed method gives the solution as Max Z=1.56.We observe that our proposed method gives the most optimal solution.

RESULTS AND DISCUSSION

We have developed a new method for solving LFPP using Pentagonal Neutrosophic Fuzzy Number and made the adequacy of the applied procedure for intensive studies. The various optimal solutions obtained for the LFPP by using Triangular Fuzzy Neutrosophic Number , Trapezoidal Fuzzy Neutrosophic Number and PNFN are shown in the comparison table and a multiple bar diagram was also shown to visualize the optimal results obtained by the proposed methods with some of the existing methods. We conclude that the optimal solution obtained by our proposed method using PNFN gives the most higher optimal value than the existing methods.

We observe that for Numerical Example 3.3

$Max\ Z_{(Proposed\ Method)} = $ 1.56$> Max\ Z_{(TFNN)} = $ 1.47$>Max\ Z_{(Base\ Paper[9])} = $1.16

A Multiple Bar Diagram is shown below to visualize the optimal results obtained by the proposed methods with some of the existing methods.

From the above graph ,we observe that our proposed method is better than the existing methods available to solve LFPP.

CONCLUSION

In this paper ,we introduced a new ranking method with an efficient algorithm to solve a LFPP together with simplex method and PNFN.Here, a unique ranking function has been used to convert PNFN into a crisp value. Assessing the impact of   uncertain information using mathematics is a very challenging process. In this research work ,we have shown the stability and reliability of the proposed method through a novel simplex technique to solve LFPP by using PNFN with the membership functions . In this article ,we focussed on PNFN and its operations due to its application to grab the vagueness and   uncertain information of real life problems .Many researchers   developed various new novel methods   with the de-neutrosophication technique for crisp value. Here, we have generated the idea of crispification of   PNFN.We have also illustrated some numerical examples and made a comparative study of the results derived for the same numerical examples from other research articles with some of the existing methods available to solve LFPP. Finally, by comparing and analyzing the results arrived ,we conclude that our proposed method will give the most optimal solution and it is better than the existing techniques**.** In future, we can extend the concept of PNFN into different types of neutrosophic fuzzy numbers which will be helpful to make mathematical   modelling with uncertainty to solve many real life problems involving LFPPs in cutting stock problem, blending problem, product planning, financial management planning ,health sector development planning and hospital management planning. We can also extend it using Hexagonal Neutrosophic Fuzzy Number, Heptagonal Neutrosophic Fuzzy number , Octagonal Neutrosophic Fuzzy Number   and defuzzication can be made by different techniques which will be helpful in various fields of mobile computing issues ,pattern recognition problem ,image processing, engineering problem and in various research domains.

Conflicts of Interest

The authors declare that they have no conflicts of interest.

Rajarajeswari and Shyamala

Authors Contribution

All authors contributed equally to this work and read and approved the final version of the manual script.

REFERENCES

1. M.Abdel-Basset, M.Gunasekaran, M.Mohamed & F.Smarandache ,A novel method for solving the fully neutrosophic linear programming problems, Neural Computing and Applications ,2019,31,1595-1605.
2. Avinash J. Kamble, Some Notes on Pentagonal Fuzzy Numbers, Intern. J. Fuzzy Mathematical Archive, Vol. 13, No. 2, 2017, 113-121
3. Avishek Chakraborty,Baisakhi Banik,Sankar Prasad Mondal and Shariful Alarm,Arithmetic and Geometric Operators of Pentagonal Neutrosophic Number and its Application in Mobile Communication Service Based MCGDM Problem
4. Bansal.Abhinav.,(2011),Trapezoidal Fuzzy Numbers(a,b,c,d);Arithmetic Behaviour ,International Journal of Physical and Mathematical Sciences,ISSN:2010-1791.
5. D.Dubois and H.Prade, Operations on fuzzy numbers, International Journal of Systems Science, 9(6) (1978) 613-626.
6. Dinnagar.D.Stephen and Latha.K.,(2013),some types of Type 2 –Triangular Fuzzy matrices, International Journal of Pure and Applied Mathematics,vol-82,N0.1,21-32.
7. T.Pathinathan and K.Ponnivalavan, Pentagonal fuzzy numbers, International Journalof Computing Algorithm, 3 (2014) 1003-1005
8. Sapan Kumar Das, S.A.Edalatpanah, J.K.Dash, Paper's title ,An intelligent Dual Simplex Method to solve Triangular Neutrosophic Linear Fractional Programming Problem ,University of Mexico,2020.
9. Sumon Kumar Saha,Md.Rezwan Hossain ,Md.Kutub Uddin ,Rabindra Nath Mondal,A New Approach of Solving Linear Fractional Programming problem (LFP) by using Computer Algorithm.
10. K.H.Lee, First course on Fuzzy Theory and Applications, Springer, 2005
11. L.A.Zadeh, Fuzzy set, *Information and Control*, 8 (1965) 338-353.

Particulars	Optimal Value for Numerical Example 3.1	Optimal Value for Numerical Example3. 2	Optimal Value for Numerical Example 3.3
Linear fractional programming problem[LFPP]	Max Z=0.63	Min Z=(-12/11)=-1.09 Base Paper[9]	Max Z=1
Triangular Neutrosophic Number[TNN]	Max Z=1.17	Min Z=-3.02	Max Z=1.16 Base Paper[8]
Trapezoidal Fuzzy Neutrosophic Number[TFNN]	Max Z=1.23	Min Z=-5.09	Max Z=1.47
Proposed Method using Pentagonal Neutrosophic Fuzzy Number[TNFN]	Max Z=1.29	Min Z=-5.11	Max Z=1.56

Rajarajeswari and Shyamala

RESEARCH ARTICLE
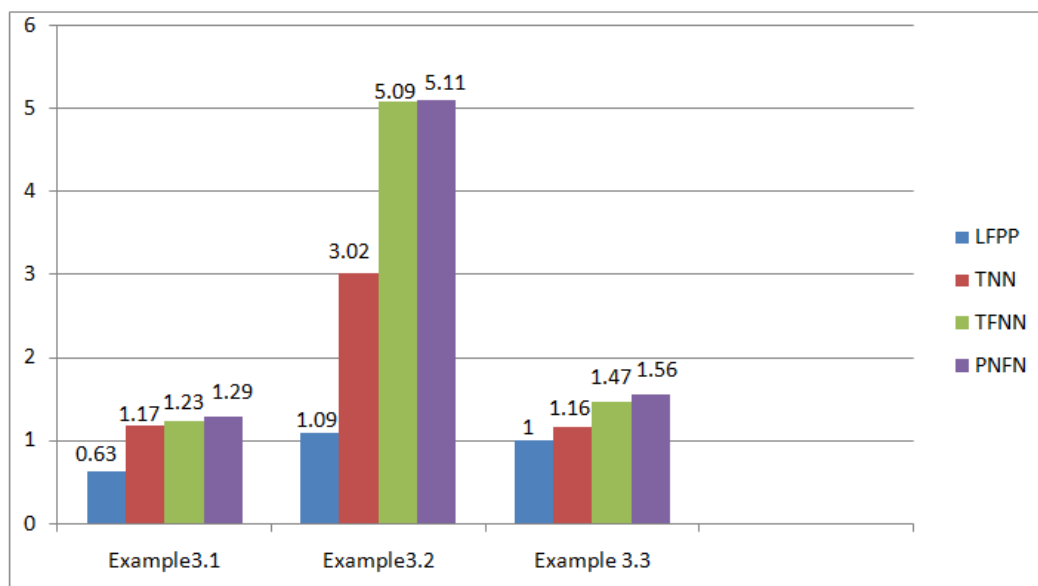
Discovery of Corona Domination Number for Some Notable Graphs

L.Praveenkumar[1], G.Mahadevan[2]* and C.Sivagnanam[3]

[1]Department of Mathematics, The Gandhigram Rural Institute-Deemed to be University, Gandhigram, Tamilnadu-624302, India.
[2]Department of General Requirements, University of Technology and Applied Science-Sur, Sultanate of Oman.

*Address for Correspondence
G. Mahadevan
Department of General Requirements,
University of Technology and Applied Science,
Sur, Sultanate of Oman.
E. Mail: drgmaha2014@gmail.com

ABSTRACT

A dominating set S of a graph H is said to be a corona dominating set ($CD-$ set) if every a vertex in the sub-graph induced by S having a pendant vertex or a support vertex. The minimum cardinality of all corona dominating set is called corona domination number (CD number) and is denoted by $\gamma_{CD}(H)$. In this work we extend the study of CD number for some notable graphs and identify their exact γ_{CD} values.

Keywords: Dominating set, corona dominating set, pendant and support vertex.

INTRODUCTION

Every graph H consider here are finite, undirected without isolated vertex, loops and multiple edges. An *induced subgraph [1]* of a graph H is a graph obtained from the subset of the vertices of the graph and all the edges having both end vertices in it. A *dominating set[2] of H* is a set S of vertices of H with the condition that every $u \in V(H) - S$, $d(u, S) = 1$. The minimum cardinality among all the dominating set is called the domination number of H, denoted by $\gamma(H)$. The theory of *total dominating set* was Proposed by Cockayne *et al.*[3] and defined as the sub-graph induced by the dominating set has no isolated vertices, the total domination number $\gamma_{t(H)}$ denotes the minimum cardinality of a total dominating set. Support vertex is a vertex which adjacent to a pendant vertex. The concept corona domination was introduced by *G*.Mahadevan*etal.* [4] the CD-number of a graph is the minimum cardinality of a dominating set S with the condition that every vertex in the graph induced by S is either a pendent vertex or a support vertices. Let $C_3^1, C_3^2, C_3^3, \ldots, C_3^n$ be the sequence of cycles with 3 vertices *Triangular snake*(T_n)[5] is constructed by pasting any one vertex of C_3^{i+1} to any one vertex of C_3^i $1 \leq i \leq n-1$ and a*lternate triangular snake* $A(T_n)$ [5] is constructed by pasting the

pendant vertices of K_2 in between C_3's, that is pasting one pendant vertex to any one of the vertex in C_3^i and another to any one vertex of $C_3^{i+1} 1 \leq i \leq n-1$.*Double triangular snake and alternative double triangular snake* [5]is constructed by pasting the paths of two triangular snake and alternative triangular snake respectively. Let $C_4^1, C_4^2, C_4^3, \dots, C_4^n$ be the sequence of cycles with 4 vertices *Quadrilateral snake* [6]is constructed by pasting any one vertex of C_4^{i+1} to any one vertex of $C_4^i 1 \leq i \leq n-1$.*Alternate quadrilateral snake* [6]is constructed by pasting the pendant vertices of K_2 in betweenC_4's, that is pasting one pendant vertex to any one of the vertex in C_4^i and another to any one vertex of $C_4^{i+1} 1 \leq i \leq n-1$.*Double quadrilateral snake and alternative double quadrilateral snake* [6] is constructed by pasting paths of two quadrilateral snake and alternative snake respectively. *Friendship graph F_r*is joining any one vertex of r copies of C_3 at a single vertex. The *shadow graph $S'(H)$* of H is obtained by taking two copies of H (say H_1 and H_2) and every vertex $v \in H_1$ is adjacent to $N(v')$ in H_2, where v' is the vertex in H_2 corresponding to v in H_1.A *dumbbell graph*[7]$D_{a,b,c}$is constructed by joining a bridge between two cycles. Let$C_r = (v_1, v_2, v_3, \dots, v_r, v_1)$, $V(K_{1,r}) = \{u_0, u_1, u_2, \dots, u_r\}$ with $\deg(u_0) = \Delta$then the lotus inside circle graph is a graph with $E(LC_r) = \{v_{i-1}u_i, u_iv_i, u_1v_n : 1 \leq i \leq r\}$. A *crown graph*$H_{k,k}$is a graph obtained from the complete bipartite graph $K_{k,k}$ by removing a perfect matching.Consider two even cycles of order r, sharing a common vertex (say v), the butterfly graph $BF_{r,s}$ is obtained by pasting the apex of $K_{1,s}$ to v.Graph domination and associated concepts have been studied for many years; among them many authors investigate the domination number of various graphs, especially for the paths, cycles, complete graph, etc. The authors in [8] have discussed the exact γ_{CD} value for many standard graphs. In continuation of that in this work, we have also determine the exact γ_{CD} for some notable graphs such as Butterfly graph, PVB tree, lotus inside circle graph and some special types of snake graphs. The proof technique used in this work is a well-known number theory concept with some modification, this can also applied to other domination parameter to get the results.

Examining the CD Number for Some Notable Graphs

Observation 2.1.

1.$\gamma_{CD}\left(S'(P_r)\right) = \gamma_{CD}(P_r)$.

2. $\gamma_{CD}\left(S'(C_r)\right) = \gamma_{CD}(C_r)$.

3.$\gamma_{CD}(D_{a,b,c}) = 2\gamma_{CD}(C_r)$.

Theorem 2.2. Let H be a butterfly graph then $\gamma_{CD}(H) = \begin{cases} r & if\ r \equiv 2\ (mod\ 4), \\ r-1 & if\ r \equiv 0\ (mod\ 4). \end{cases}$

Proof: Let $V(H) = \{v_1 = u_1 = v, v_2, v_3, \dots, v_r, u_2, u_3, \dots, u_r, w_1, w_2, w_3, \dots, w_k\}$ and $E(H) = \{v_iv_{i+1}, v_1v_r, u_1u_r, u_iu_{i+1}, vw_j : 1 \leq i \leq r-1, 1 \leq j \leq k\}$.Then $S = \{v_i : i \equiv 1\ or\ 2\ (mod\ 4)\}\cup\{u_j : j \equiv 0\ or\ 1\ (mod\ 4)\}$ is a CD – set of H.

Hence, $\gamma_{CD}(H) \leq |S| = \begin{cases} r & if\ r \equiv 2\ (mod\ 4), \\ r-1 & if\ r \equiv 0\ (mod\ 4). \end{cases}$

Suppose there exist a dominating set D of cardinality at most

$d = \begin{cases} r-1 & if\ r \equiv 2\ (mod\ 4), \\ r-2 & if\ r \equiv o\ (mod\ 4), \end{cases}$then$< D >$ contains an isolated vertex.

Thus $|D| \geq d + 1 = \begin{cases} r & if\ r \equiv 2\ (mod\ 4), \\ r-1 & if\ r \equiv 0\ (mod\ 4). \end{cases}$

Hence, $\gamma_{CD}(H) = \begin{cases} r & if\ r \equiv 2\ (mod\ 4), \\ r-1 & if\ r \equiv 0\ (mod\ 4). \end{cases}$

Theorem 2.3. IfH is PVB tree.Then $\gamma_{CD}(H) = 2p(r-3), p \geq 1, v, b > 1$and $r \geq 6$.

Proof: Consider the main path P_p and p copies of another path P_v with v vertices. Now join the root vertex of the star $K_{1,b}$ to each vertices of p copies of the path P_v. Name the vertices of path P_p are $y_1, y_2, \dots y_p$; vertices of P_v as y_{ij} where $1 \leq i \leq p$ and $1 \leq j \leq v$ and the vertices of the star as y_{ij}^k where $1 \leq i \leq p; 1 \leq j \leq v; 1 \leq k \leq b$. Then join the vertices y_{i1} to y_i where $1 \leq i \leq p$ by using an edge. That is,y_i and y_{i1} are adjacent.

Let S = $\{ v_{ij} : 1 \leq i \leq p, 1 \leq j \leq v\}\cup\{v_{ij}^1 : 1 \leq i \leq p, 3 \leq j \leq v-2\}$ be a CD − set of H and hence $\gamma_{CD}(G) \leq |S| = 2p(r-3)$.

Now let $D \subseteq V$ be any dominating set of cardinality atmost$d = 2p(r-3)-1$, then $< D >$has an isolated vertex.

Thus $|D| \geq d + 1 = 2p\,(r - 3)$. Hence, $\gamma_{CD}\,(H) = 2p\,(r - 3)$.

Example 2.1.

Illustration: For the above graph, the white vertices give us the CD- set and hence the γ_{CD} value is 40.

Theorem 2.4. Let $D(T_r)$be a double triangular snake. Then $\gamma_{CD}\,S((D(T_r))) = 3(r-1) + 2, r \geq 2$.

Proof: Let $V(G)$ ={$_{1,2,3,\cdots,\,,1,2,\cdots-1,1,2,3,\cdots-1,1,2,3,\cdots,\,,}$

$_{11,12,21,22,31,32,\cdots,(-1)1,(-1)2,11,12,21,22,31,32,\cdots,(-1)1,(-1)2}$}an() = { $_{1,\,\,,\,1,(-1)2,(-1)2(-1),\,1,\,2,\,1,\,2}$}.

Let $ = \{: a = 1 \text{ to } r\} \cup \{_{1,\,1}: b = 1 \text{ to } -1\} \cup \{_{(-1)2}\}$. It is clear that is a $-$ set of $\big(\big(()\big)\big)$. Hence, $() \leq || = 3(-1) + 2$.

Now let $\subseteq$ be any dominating set of cardinality atmost $d = 3(r - 1) + 1$ then $<D>$ has isolated vertex.

Thus $|D| \geq d + 1 = 3\,(r - 1) + 2$. Hence, $\gamma_{CD}\,S((D(T_r))) = 3(r - 1) + 2$.

Theorem 2.5. Let $Q_s$be a quadrilateral snake. Then $\gamma_{CD}(Q_s) = 2\left\lfloor\frac{2s}{3}\right\rfloor, r \geq 4$.

Proof: Let$V(G) = \{v_1, v_2, v_3, \dots, v_r, u_{11}, u_{21}, u_{22}, u_{31}, u_{32}, \dots, u_{(s-1)1}, u_{(s-1)2}, u_r\}$ and

$E(G) = \{v_iv_{i+1}, v_1u_1, v_ru_r, v_ju_{j1}, v_ju_{j2} : 1 \leq i \leq s - 1 \text{ and } 2 \leq j \leq s - 1\}$.

Then $S = \{v_i : i \equiv 0 \text{ or } 2\ (mod\ 3)\} \cup \{u_{i\,1}u_{i\,2} : i \equiv 2\ (mod\ 3), j \equiv 0\ (mod\ 3)\}$ is a CD – set of Q_r. Hence $\gamma_{CD}(Q_s) \leq |S| = 2\left\lfloor\frac{2s}{3}\right\rfloor$. Now let $D \subseteq V$ be any dominating set of cardinality atmost $d = 2\left\lfloor\frac{2s}{3}\right\rfloor - 1$ then $< D >$ has an isolated vertex.

Thus $|D| \geq d + 1 = 2\left\lfloor\frac{2s}{3}\right\rfloor$. Hence, $\gamma_{CD}(Q_s) = 2\left\lfloor\frac{2s}{3}\right\rfloor$.

Theorem 2.6. Let $A(Q_r)$ be a alternate quadrilateral snake. Then $\gamma_{CD}A((Q_r)) = 2\left\lfloor\frac{r}{2}\right\rfloor, r \geq 4$.

Proof: Let$V(A(Q_r)) = \{v_1, v_2, v_3, \dots, v_r, v_{i1}, v_{i2}, i = 2k + 1, k = 0,1,2,\dots\}$and

$E(A(Q_r)) = \{v_iv_{i+1}, v_iv_{i\,1}, v_jv_{(j-1)2}, v_{i\,1}v_{i\,2} : 1 \leq i \leq r - 1 \text{ and } 2 \leq j \leq r\}$.

Then S $= \{v_i : i \equiv 0, 2\ (mod\ 3)\} \cup \{v_{i\,2} : i = 2k + 1, k = 0,1,2,3,\dots\}$ is a CD – set of A(Q_r). Hence $\gamma_{CD}(A(Q_r)) \leq |S| = 2\left\lfloor\frac{r}{2}\right\rfloor$.

Now let $D \subseteq V$ be any dominating set of cardinality atmost $d = 2\left\lfloor\frac{r}{2}\right\rfloor - 1$ then$< D >$ has an isolated vertex.

Thus $|D| \geq d + 1 = 2\left\lfloor\frac{r}{2}\right\rfloor$. Hence, $\gamma_{CD}A((Q_r)) = 2\left\lfloor\frac{r}{2}\right\rfloor$.

Theorem 2.7. Let $D(Q_r)$ be the double quadrilateral snake. Then $\gamma_{CD}D((Q_r)) = 3\left\lfloor\frac{r}{2}\right\rfloor, r \geq 4$.

Proof:

Let$V(D(Q_r)) = \{v_1, v_2, v_3, \dots, v_r, v_{11}, v_{12}, v_{21}, v_{22}, v_{31}, v_{32}, \dots, v_{(r-1)1}, v_{(r-1)}, u_{11}, u_{12}, u_{21},$

$u_{22}, u_{31}, u_{32}, \dots, u_{(r-1)1}, u_{(r-1)2}\}$and

$E(D(Q_r)) = \{v_av_{a+1}, v_av_{a\,1}, v_au_{a\,1}, v_bv_{(b-1)2}, v_bv_{(b-2)2}, u_{a\,1}u_{a\,2}, v_{a\,1}v_{a\,2} : 1 \leq a \leq r - 1 \text{ and } 2 \leq b \leq r\}$.Consider

$S = \{v_a : a \equiv 0, 2\ (mod\ 3)\} \cup \{v_{a\,2}, u_{a\,2} : a \equiv 1\ (mod\ 3)\} \cup \{v_{a\,1}, u_{a\,1} : a \equiv 0\ (mod\ 3)\}$,

is a CD – set of$D(Q_r)$. Hence $\gamma_{CD}(D(Q_r)) \leq |S| = 3\left\lfloor\frac{r}{2}\right\rfloor$.

Now let $D \subseteq V$ be any dominating set of cardinality atmost $d = 3\left\lfloor\frac{r}{2}\right\rfloor - 1$ then $< D >$ has an isolated vertex.

Praveenkumar *et al.*,

Thus $|D| \geq d + 1 = 3\left\lfloor\frac{r}{2}\right\rfloor$. Hence, $\gamma_{CD}D((Q_r)) = 3\left\lfloor\frac{r}{2}\right\rfloor$.

Example 2.2.
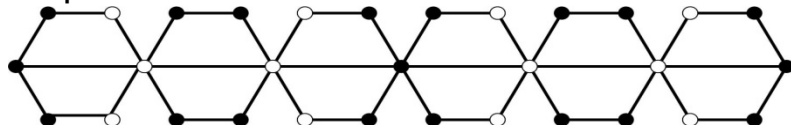
Illustration: Here the white vertices will give us the CD – set of the above graph and hence the γ_{CD} value is 12.

Theorem 2.8. Let H be a lotus inside cycle graph. Then $\gamma_{CD}(H) = \left\lceil\frac{r}{2}\right\rceil + 1$.

Proof: Let $V(H) = \{v, v_1, v_2, v_3, \dots, v_r, u_1, u_2, u_3, \dots, u_r\}$ and $E(H) = \{vv_a, v_b u_{b+1}, v_c u_{c-1} : 1 \leq a \leq r, 1 \leq b \leq r-1, 2 \leq c \leq r\}$

Then $S = \{vv_a : a = 2q + 1, q = 0,1,2,3,\dots\}$ is a CD – set of H.

Hence $\gamma_{CD}(H) \leq |S| = \left\lceil\frac{r}{2}\right\rceil + 1$.

Now let $D \subseteq V$ be any dominating set of cardinality atmost $d = \left\lceil\frac{r}{2}\right\rceil$ then $<D>$ has an isolated vertex.

Thus $|D| \geq d + 1 = \left\lceil\frac{r}{2}\right\rceil + 1$. Hence, $\gamma_{CD}(H) = \left\lceil\frac{r}{2}\right\rceil + 1$.

Example2.3.
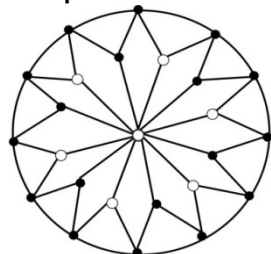
Illustration: Here the white vertices will give us the CD – set of the above mentioned graph and hence the γ_{CD} value is 7.

Observation 2.9.

1. $\gamma_{CD}(F_r) = 2$.

2. $\gamma_{CD}(H_{k,k}) = 4$.

3. $\gamma_{CD}(P_r \odot 1K_1) = $ does not exist , $r \geq 5$.

4. $\gamma_{CD}(P_r \odot 2K_1) = $ does not exist , $r \geq 5$.

5. $\gamma_{CD}(C_r \odot 1K_1) = $ does not exist , $r \geq 5$.

6. $\gamma_{CD}(C_r \odot 2K_1) = $ does not exist , $r \geq 5$.

CONCLUSION

In this work, we have determined the exact γ_{CD} values for some notable graph, instead determine their approximate upper and lower bounds. We will find the results for some general graphs which will be in our successive work.

REFERENCES

1.   Harary F. Graph Theory. Addison Wesley Reading Mass; 1972.
2.   Haynes TW, Hedetniemi S, Slater P. Fundamentals of Domination In Graphs. Marcel Dekker, Inc., New York; 1997.
3.   Cockayne EJ, Dawes RM, Hedetniemi ST. Total Domination in Graphs. Networks 1980; 10(3):211-9.

Praveenkumar *et al.*,

4. Mahadevan G, Vimala SM, Sivagnanam C.Corona Domination of Graphs.Mathematical Modelling and Computational Intelligence Techniques, Spinger proceedings in Mathematics and Statistic2021; 376: 255-265.
5. Sunoj BS, Mathew TK. Square Difference Prime Labeling for Some Snake Graphs. Global Journal of Pure and Applied Mathematics 2017;13(3):1083-1089.
6. Smitha KB, Thirusangu K. Distance Two Labeling of Quadrilateral Snake Families. International Journal of Pure and Applied Mathematical Sciences 2016;9(2):283-298.
7. Wang J, Belardo F, Huang Q, Marzi EM. Spectral Characterizations of Dumbbell Graphs. The Electronic Journal of Combinatorics2010.
8. Praveenkumar, L., Mahadevan, G., & Sivagnanam, C. An Investigation of Corona Domination Number for Some Special Graphs and Jahangir Graph. Baghdad Science Journal, 20(1 (SI)), 0294-0299 (2023).

RESEARCH ARTICLE

Qualitative Behavior of Fourth Order Neutral Difference Equations

S. Kaleeswari and M.Buvanasankari*

Department of Mathematics, Nallamuthu Gounder Mahalingam College, Pollachi, Tamilnadu, India - 642201

***Address for Correspondence**
M.Buvanasankari
Department of Mathematics,
Nallamuthu Gounder Mahalingam College,
Pollachi, Tamilnadu, India – 642201.
E.Mail: buvanasankari@gmail.com

ABSTRACT

"The goal of this paper is to illustrate the qualitative behaviour of a fourth order difference equation with neutral terms of the form

$$\Delta\left(s_1(\vartheta)\left(\Delta^3 q(\vartheta)\right)^{\beta_1}\right) = s_2(\vartheta)y^{\beta_2}(\vartheta - n + 1) + s_3(\vartheta)y^{\beta_3}(\vartheta + n^*)$$

where $q(\vartheta) = y(\vartheta) - s_4(\vartheta)y^{\beta_4}(\vartheta - k)$ Here $\beta_1, \beta_2, \beta_3, \beta_4$ are the ratios of odd positive integers $\beta_1 \geq 1, s_1, s_2, s_3, s_4$ are positive sequences and $n, n^*, k \in N$ are such that $n > 3, n^* > 3, k < n - 2$. With the help of comparison techniques, we are able to acquire some novel oscillations results. Examples are given to illustrate the importance of the discoveries.

Keywords : comparison techniques, fourth order, neutral terms, oscillation.

INTRODUCTION

Due to the fact that neutral difference equations are used in the study of economics, mathematical biology, and many other areas of mathematics, the issue of establishing oscillation phenomena for these equations has drawn a lot of attention in recent years [1],[2],[11],[12],[17]. The sources cited there as well as [4], [21], [22], [23] provide some fascinating new findings on the oscillatory behavior of second-order differential equations. A examination of the literature reveals that every conclusion made for fourth order difference equations with neutral terms ensures that each solution oscillates or monotonically approaches to zero. As far as we are aware, no conclusions have been drawn for fourth order neutral difference equations that suggest that all solutions are just oscillatory. This study's goal is to provide the equation some revised oscillation restrictions as a result.

$$\Delta\left(s_1(\vartheta)\left(\Delta^3 q(\vartheta)\right)^{\beta_1}\right) = s_2(\vartheta)y^{\beta_2}(\vartheta - n + 1) + s_3(\vartheta)y^{\beta_3}(\vartheta + n^*) \qquad (1)$$

where$q(\vartheta) = y(\vartheta) - s_4(\vartheta)y^{\beta_4}(\vartheta - k)$ via comparing first order equations with known oscillatory phenomena, or by comparing second-order difference equations with neutral terms. The reader can refer to [5], [6], [7] for relevant results on oscillation theory of applications.

The following conditions are always considered to hold:

(i) $\beta_1, \beta_2, \beta_3, \beta_4$ are the ratios of odd positive integers with $\beta_1 \geq 1$;

(ii) s_1, s_2, s_3, s_4 are positive sequences;

(iii) $n, n^*, k \in N$ are such that $n > 3, n^* > 3, k < n - 2$.

A solution to (1) is said to be oscillatory if it is neither eventually negative nor finally positive. If not, it is regarded as non-oscillatory. Equation (1) is oscillatory if and only if all of its solutions are oscillatory." The aim of this work is to generate adequate conditions for (1) to oscillate whenever $\beta_4 < 1$ and subject the assumption

$$S_1(\vartheta, \vartheta_1) \rightarrow \infty \text{ as } \vartheta \rightarrow \infty \text{ where} S_1(r, u) = \sum_{\varrho=u}^{r-1} \frac{1}{\frac{1}{s_1^{\beta_1}(\varrho)}} \tag{2}$$

AUXILIARY RESULTS

Lemma 2.1 (see [7], Lemma 1 and 19 , Lemma 2.2).

(I) If the first order delay difference inequality

$\Delta q(\vartheta) - s_2(\vartheta)f(q(\vartheta - n + 1)) \leq 0$

has an eventually positive solution, then so does the corresponding delay difference equation.

(II)If the first order advanced difference inequality

$\Delta q(\vartheta) - s_2(\vartheta)f(q(\vartheta - n^*)) \geq 0$

has an eventually positive solution, then so does the corresponding advanced difference equation.

Lemma 2.2. (see [9])

If $X, Y \geq 0$, then

$$X^\gamma + (\gamma - 1)Y^\gamma - \gamma XY^{\gamma-1} \geq 0 \quad \text{for } \gamma > 1 \tag{3}$$

and

$$X^\gamma + (1 - \gamma)Y^\gamma - \gamma XY^{\gamma-1} \leq 0 \text{ for } 0 < \gamma < 1. \tag{4}$$

Lemma 2.3. Assume (2). Then $\Delta Q(\vartheta) > 0$ eventually, where

$$Q := s_1(\Delta^3 q)^{\beta_1} \tag{5}$$

suggests that one of the below four scenarios occurs:

Case (I). $q(\vartheta) > 0, \quad \Delta q(\vartheta) > 0, \quad \Delta^2 q(\vartheta) > 0 \quad \Delta^3 q(\vartheta) > 0$;

Case (II). $q(\vartheta) > 0, \quad \Delta q(\vartheta) > 0, \quad \Delta^2 q(\vartheta) > 0 \quad \Delta^3 q(\vartheta) < 0$;

Case (III). $q(\vartheta) < 0, \quad \Delta q(\vartheta) < 0, \quad \Delta^2 q(\vartheta) < 0 \quad \Delta^3 q(\vartheta) < 0$;

Case (IV). $q(\vartheta) < 0, \quad \Delta q(\vartheta) > 0, \quad \Delta^2 q(\vartheta) < 0 \quad \Delta^3 q(\vartheta) < 0$.

Proof. From (5), we can find $\vartheta_0 \in N_0$ such that

$$\Delta Q(\vartheta) > 0 \qquad \forall \vartheta \geq \vartheta_0. \tag{6}$$

We suppose that there exists $\vartheta_1 \geq \vartheta_0$ with

$$Q(\vartheta_1) > 0 \tag{7}$$

From (6) and (7), we get, $\forall \vartheta \geq \vartheta_1$.

$$Q(\vartheta) = Q(\vartheta_1) + \sum_{\varrho=\vartheta_1}^{\vartheta-1} \Delta Q(\varrho) \geq Q(\vartheta_1) > 0$$

Thus,

$$\Delta^3 q(\vartheta) > 0 \qquad \forall \vartheta \geq \vartheta_1. \tag{8}$$

From (6) and (7) we obtain, for $\vartheta \geq \vartheta_1$

Kaleeswari and Buvanasankari

$$\Delta^2 q(\vartheta) \quad = \Delta^2 q(\vartheta_1) + \sum_{\varrho=\vartheta_1}^{\vartheta-1} \Delta^3 q(\varrho) = \Delta^2 q(\vartheta_1) + \sum_{\varrho=\vartheta_1}^{\vartheta-1} \frac{Q^{\frac{1}{\beta_1}}(\varrho)}{s_1^{\frac{1}{\beta_1}}(\varrho)}$$

$$\geq \Delta^2 q(\vartheta_1) + \sum_{\varrho=\vartheta_1}^{\vartheta-1} \frac{Q^{\frac{1}{\beta_1}}(\vartheta_1)}{s_1^{\frac{1}{\beta_1}}(\vartheta_1)} \geq \Delta^2 q(\vartheta_1) + Q^{\frac{1}{\beta_1}}(\vartheta_1) S_1(\vartheta, \vartheta_1) \to \infty \quad \text{as } \vartheta \to \infty.$$

because of (2).

Therefore, there exists $\vartheta_2 \geq \vartheta_1$ with

$\Delta^2 q(\vartheta) > 0 \quad \forall \vartheta \geq \vartheta_2.$ (9)

From (8) and (9) we get, $\forall \vartheta \geq \vartheta_2.$

$$\Delta q(\vartheta) \quad = \Delta q(\vartheta_2) + \sum_{\varrho=\vartheta_2}^{\vartheta-1} \Delta^2 q(\varrho) \geq \Delta q(\vartheta_2) + \sum_{\varrho=\vartheta_2}^{\vartheta-1} \Delta^2 q(\vartheta_2)$$

$$= \Delta q(\vartheta_2) + (\vartheta - \vartheta_2)\Delta^2 q(\vartheta_2) \to \infty \quad \text{as } \vartheta \to \infty.$$

Hence, there exists $\vartheta_1 > \vartheta_2$ with $\Delta q(\vartheta) > 0 \quad \forall \vartheta \geq \vartheta_3.$ (10)

From (9) and (10) we obtain for $\vartheta \geq \vartheta_3$,

$$q(\vartheta) \quad = q(\vartheta_3) + \sum_{\varrho=\vartheta_3}^{\vartheta-1} \Delta q(\varrho) \geq q(\vartheta_3) + \sum_{\varrho=\vartheta_3}^{\vartheta-1} \Delta q(\vartheta_3)$$

$$= q(\vartheta_3) + (\vartheta - \vartheta_3)\Delta q(\vartheta_3) \to \infty \quad \text{as } \vartheta \to \infty.$$

Hence, there exists $\vartheta_4 \geq \vartheta_3$ with

$q(\vartheta) > 0 \quad \forall \vartheta \geq \vartheta_4$ (11)

By (8)-(11), we get

$$q(\vartheta) > 0, \Delta q(\vartheta) > 0, \Delta^2 q(\vartheta) > 0, \Delta^3 q(\vartheta) > 0 \forall \vartheta \geq \vartheta_4$$

Thus, Case (I) holds if (7) does not hold, then the only other possibilities is $q(\vartheta) < 0$
for $\vartheta \geq \vartheta_0$ and thus,

$\Delta^3 q(\vartheta) < 0$ for all $\vartheta \geq \vartheta_0$ (12)

we suppose that, there exists $\vartheta_1 \geq \vartheta_0$ with

$\Delta^2 q(\vartheta_1) < 0$ (13)

From (12) and (13) we get, $\forall \vartheta \geq \vartheta_1$

$$\Delta^2 q(\vartheta) = \Delta^2 q(\vartheta_1) + \sum_{\varrho=\vartheta_1}^{\vartheta-1} \Delta^3 q(\varrho) \leq \Delta^2 q(\vartheta_1) < 0$$

Hence

$\Delta^2 q(\vartheta) < 0 \quad \forall \vartheta \geq \vartheta_1$ (14)

Now, from (12) and (13) we obtain for $\vartheta \geq \vartheta_1$

$$\Delta q(\vartheta) \quad = \Delta q(\vartheta_1) + \sum_{\varrho=\vartheta_1}^{\vartheta-1} \Delta^2 q(\varrho) \leq \Delta q(\vartheta_1) + \sum_{\varrho=\vartheta_1}^{\vartheta-1} \Delta^2 q(\vartheta_1)$$

$$\leq \Delta q(\vartheta_1) + (\vartheta - \vartheta_1)\Delta^2 q(\vartheta_1) \to -\infty \quad \text{as } \vartheta \to \infty,$$

Hence there exists $\vartheta_2 \geq \vartheta_1$ with

$\Delta q(\vartheta) < 0 \quad \forall \vartheta \geq \vartheta_2$ (15)

Now, from (14) and (15) we can get, for $\vartheta \geq \vartheta_2$,

$$q(\vartheta) \quad = q(\vartheta_2) + \sum_{\varrho=\vartheta_2}^{\vartheta-1} \Delta q(\varrho) \leq q(\vartheta_2) + \sum_{\varrho=\vartheta_2}^{\vartheta-1} \Delta q(\vartheta_2)$$

$$\leq q(\vartheta_2) + (\vartheta - \vartheta_2)\Delta q(\vartheta_2) \to -\infty \quad \vartheta \to \infty,$$

Thus, there exist $\vartheta_3 \geq \vartheta_2$ with

$q(\vartheta) < 0 \quad \forall \vartheta \geq \vartheta_3$ (16)

By equation (12)-(16), we get $q(\vartheta) < 0, \Delta q(\vartheta) < 0, \Delta^2 q(\vartheta) < 0, \Delta^3 q(\vartheta) < 0.$

Thus, Case III holds. Further, if (13) does not hold, then the only other possibility is

$\Delta^2 q(\vartheta_1) > 0 \quad \forall \vartheta \geq \vartheta_0$ (17)

64074

Suppose that, there exists $\vartheta_1 \geq \vartheta_0$ with

$\Delta q(\vartheta_1) > 0$ (18)

Then, from (17) and (18) we get $\forall \vartheta_1 \geq \vartheta_0$,

$$\Delta q(\vartheta) = \Delta q(\vartheta_1) + \sum_{\varrho=\vartheta_1}^{\vartheta-1} \Delta^2 q(\varrho) \geq \Delta q(\vartheta_1) > 0.$$

Therefore, there exists $\vartheta_2 \geq \vartheta_1$ with

$\Delta q(\vartheta) > 0 \ \forall \vartheta_1 \geq \vartheta_0$ (19)

Now, from (18) and (19)$\forall \vartheta \geq \vartheta_2$,

$$q(\vartheta) = q(\vartheta_2) + \sum_{\varrho=\vartheta_2}^{\vartheta-1} \Delta q(\varrho) \geq q(\vartheta_2) + \sum_{\varrho=\vartheta_2}^{\vartheta-1} \Delta q(\vartheta_2)$$

$$\geq q(\vartheta_2) + (\vartheta - \vartheta_2)\Delta q(\vartheta_2) \to \infty \text{ as } \vartheta \to \infty$$

Hence, there exists $\vartheta_1 \geq \vartheta_2$ with

$q(\vartheta) > 0 \ \forall \vartheta \geq \vartheta_3$.   (20)

By Equations (12),(17),(19),(20) we get, $q(\vartheta) > 0, \Delta q(\vartheta) > 0, \Delta^2 q(\vartheta) > 0, \Delta^3 q(\vartheta) < 0$. Case (II) is so upheld. In the event ϱ (15) does not hold, the sole option is

$\Delta q(\vartheta) > 0 \ \forall \vartheta \geq \vartheta_0$.   (21)

By Equation (12), (14),(16),(21) we get, $q(\vartheta) < 0, \Delta q(\vartheta) > 0, \Delta^2 q(\vartheta) < 0, \Delta^3 q(\vartheta) < 0$, Thus, Case (IV) holds. The rest the article is based on the assumption that

$k_0, k_1, k_2, k_3, k_4 \in \mathbb{N}$ satisfying $3k_0 < n^*, k_1 < n + 2$, and $k_2 < k_3 \leq n + 1 - k$.   (22)

Note 2.4:

1. Consider the constraints $n > 3, n^* > 3$, and $k < n - 2$. For example, one may use $k_0 = k_1 = k_2 = 1, k_3 = 2$ and $k_4 = 4$.

2. Consider that $\vartheta + n^* - 3k_0 > \vartheta$. Since it is always possible $n^* - 3k_0 > 0$. Therefore, equations involving $\vartheta + n^* - 3k_0$ are advanced type. Furthermore

$\vartheta + n^* + k_1 - 2 < \vartheta, \vartheta - n + k - 2 < \vartheta_1, \ \vartheta - n + k - 2 + k_1 < \vartheta$, always since $n + 2 - k_1 > 0, n + 2 - k > 0, n + 2 - k - k_3 > 0$. Therefore, equation containing $\vartheta - n + k_1 - 2 , \vartheta - n + k - 2, \vartheta - n + k - 2 + k_3$ are of delay type.

MAIN RESULTS

We will start looking at the new result.

Theorem 3.1.*Let $\beta_4 < 1$. Assume that*(i)-(iii), (2) and (22) hold. Suppose that there is a sequence $s: Q \to (0, \infty)$. Such that $\lim_{\vartheta \to \infty} (g_1(\vartheta)) = 0$, where

$g_1(\vartheta) := (1 - \beta_4)\beta_4^{\frac{\beta_4}{1-\beta_4}} s^{\frac{\beta_4}{\beta_4-1}}(\vartheta) s_4^{\frac{1}{1-\beta_4}}(\vartheta)$. (23)

Let $\theta_0, \theta_1, \theta_2 \in (0,1)$. If the first-order advanced difference equation

$$\Delta q(\vartheta) = \theta_0 z^{\frac{\beta_3}{\beta_1}}(\vartheta + n^* - 3k_0) \sum_{\varrho=\vartheta-k_0}^{\vartheta-1} \left(\sum_{r=t-k_0}^{\varrho-1} \left(\frac{1}{s_1(\varrho)} \sum_{\gamma=r-k_0}^{r-1} s_3(\gamma) \right)^{\frac{1}{\beta_1}} \right)$$ (24)

and the first order delay difference equation

$\Delta W(\vartheta) + (\theta_1 \theta_2 k)^{\beta_2} s_2(\vartheta)(\vartheta - n + 1)^{\beta_2}(\vartheta - n)^{\beta_2}$

$W^{\frac{\beta_2}{\beta_1}}(\vartheta - n + k_1 - 2)[S_1(\vartheta - n + k_1 - 1, \vartheta - n - 1)]^{\beta_2} = 0$ (25)

$$\Delta W(\vartheta) + \frac{s_2(\vartheta)}{(s_4)^{\frac{\beta_2}{\beta_4}}(\vartheta-n+k+1)} W^{\frac{\beta_2}{\beta_1\beta_4}}(\vartheta - n + k - 2) \left(\sum_{\varrho=\vartheta_1}^{\vartheta-n+k} \left(\sum_{r=t_1}^{t-n+k} S_1(r_1, \vartheta_1) \right) \right) = 0$$

(26)

and

Kaleeswari and Buvanasankari

$$\Delta W(\vartheta) + \frac{s_2(\vartheta)}{s_4^{\frac{\beta_2}{\beta_4}}(\vartheta - n + k + 1)}(k_2 c \theta_0)^{\frac{\beta_2}{\beta_4}}\left[W^{\frac{1}{\beta_1}}(\vartheta - n + k + k_3 - 2)\, S_1(\vartheta - n + k + k_3 - 1,\ \vartheta - n + k + k_3 - 1)\right]^{\frac{\beta_2}{\beta_4}} = 0 \ (27)$$

are oscillatory, then so is (1)

Proof. Suppose thaty is a non oscillatory solution of (1), say $y(\vartheta) > 0, y(\vartheta - k) > 0,\ y(\vartheta - n + k) > 0, y(\vartheta + n^*) > 0$ eventually

$$\Delta\left(s_1(\vartheta)\left(\Delta^3 q(\vartheta)^{\beta_1}\right) = s_2(\vartheta)y^{\beta_2}(\vartheta - n + 1) + s_3(\vartheta)y^{\beta_3}(\vartheta + n^*) > 0 \tag{28}$$

Therefore (5) is fulfilled, and only four cases (I), (II), (III) and (IV) can be done according to Lemma (2.3)

Case (I) and (II):

Using $\gamma = \beta_4 \in (0,1), X = s_4^{\frac{1}{\beta_4}}(\vartheta)y(\vartheta - k), Y = \left(\frac{1}{\beta_4}s(\vartheta)s_4^{\frac{-1}{\beta_4}}(\vartheta)\right)^{\frac{1}{\beta_4 - 1}}$ in (4) we obtain $-(s(\vartheta)y(\vartheta - k) - s_4(\vartheta)y^{\beta_4}(\vartheta - k)) \le g_1(\vartheta)$

$$
\begin{aligned}
y(\vartheta) &= q(\vartheta) + s_4(\vartheta)y^{\beta_4}(\vartheta - k) + s(\vartheta)y(\vartheta - k) - s(\vartheta)y(\vartheta - k)\\
&= q(\vartheta) + s(\vartheta)y(\vartheta - k) - \left(s(\vartheta)y(\vartheta - k) - s_4(\vartheta)y^{\beta_4}(\vartheta - k)\right)\\
&\ge q(\vartheta) + s(\vartheta)y(\vartheta - k) + g_1(\vartheta)\\
&\ge q(\vartheta)\left[1 + \frac{s(\vartheta)y(\vartheta - k) + g_1(\vartheta)}{q(\vartheta)}\right]
\end{aligned}
$$

As q in both cases (I) and (II) is positive and non-decreasing, there exists $L > 0$, fulfilling of $q(\vartheta) > L$, and thus, we obtain

$$y(\vartheta) \ge \left(1 + \frac{s(\vartheta)y(\vartheta - k) + g_1(\vartheta)}{\vartheta}\right)q(\vartheta)$$

Then due to (23), there exists $k \in (0,1)$ such that

$$y(\vartheta) \ge kq(\vartheta) \tag{29}$$

eventually

So, we get

$$\Delta\left(s_1(\vartheta)\left(\Delta^3 q(\vartheta)\right)^{\beta_1}\right) \ge k^{\beta_2}s_2(\vartheta)q^{\beta_2}(\vartheta - n + 1) + k^{\beta_3}s_3(\vartheta)q^{\beta_3}(\vartheta + n^*) \ge 0 \tag{30}$$

Case(I).Using (30), we get

$$\Delta\left(s_1(\vartheta)\left(\Delta^3 q(\vartheta)\right)^{\beta_1}\right) \ge k^{\beta_3}s_3(\vartheta)q^{\beta_3}(\vartheta + n^*) \tag{31}$$

Summing (31) from $\vartheta - k_0$ to $\vartheta - 1$, we have

$$
\begin{aligned}
s_1(\vartheta)\left(\Delta^3 q(\vartheta)\right)^{\beta_1} &= s_1(\vartheta - k_0)\left(\Delta^3 q(\vartheta - k_0)\right)^{\beta_1} + \sum_{\varrho = \vartheta - k_0}^{\vartheta - 1}\Delta\left(s_1(\varrho)\left(\Delta^3 q(\varrho)\right)\right)^{\beta_1}\\
&\ge k^{\beta_3}\sum_{\varrho = \vartheta - k_0}^{\vartheta - 1}s_3(\varrho)q^{\beta_3}(\varrho + n^*)\\
&\ge k^{\beta_3}q^{\beta_3}(\vartheta + n^* - k_0)\sum_{\varrho = \vartheta - k_0}^{\vartheta - 1}s_3(\varrho)
\end{aligned}
$$

So we get,

$$\Delta^3 q(\vartheta) \ge k^{\frac{\beta_3}{\beta_1}}q^{\frac{\beta_3}{\beta_1}}(\vartheta + n^* - k_0)\left(\frac{1}{s_1(\vartheta)}\sum_{\varrho = \vartheta - k_0}^{\vartheta - 1}s_3(\varrho)\right)^{\frac{1}{\beta_1}} \tag{32}$$

Summing (32) again from $\vartheta - k_0$ to $\vartheta - 1$, we get

$$
\begin{aligned}
\Delta^2 q(\vartheta) &= \Delta^2 q(\vartheta - k_0) + \sum_{\varrho = \vartheta - k_0}^{\vartheta - 1}\Delta^3 z(\varrho)\\
&\ge \sum_{\varrho = \vartheta - k_0}^{\vartheta - 1}k^{\frac{\beta_3}{\beta_1}}q^{\frac{\beta_3}{\beta_1}}(\varrho + n^* - k_0)\left(\frac{1}{s_1(\varrho)}\sum_{r = t - k_0}^{\varrho -}s_3(r)\right)^{\frac{1}{\beta_1}}
\end{aligned}
$$

64076

$$\geq k^{\frac{\beta_3}{\beta_1}} q^{\frac{\beta_3}{\beta_1}} (\vartheta + n^* - 2k_0) \sum_{\varrho=\vartheta-k_0}^{\vartheta-1} \left(\frac{1}{s_1(\varrho)} \sum_{r=t-k_0}^{\varrho-} s_3(r) \right)^{\frac{1}{\beta_1}} \tag{33}$$

Summing (33) again from $\vartheta - k_0$ to $\vartheta - 1$, we get

$$\Delta q(\vartheta) = \Delta q(\vartheta - k_0) + \sum_{\varrho=\vartheta-k_0}^{\vartheta-1} \Delta^2 q(\vartheta)$$

$$\geq k^{\frac{\beta_3}{\beta_1}} \sum_{r=\vartheta-k_0}^{\vartheta-1} q^{\frac{\beta_3}{\beta_1}}(\varrho + n^* - 2k_0) \sum_{r=t-k_0}^{\varrho-} \left(\frac{1}{s_1(r)} \sum_{u=r-k_0}^{\vartheta-1} s_3(u) \right)^{\frac{1}{\beta_1}}$$

$$\geq k^{\frac{\beta_3}{\beta_1}} q^{\frac{\beta_3}{\beta_1}}(\vartheta + n^* - 3k_0) \sum_{\varrho=\vartheta-k_0}^{\vartheta-1} \left(\sum_{r=t-k_0}^{\varrho-} \left(\frac{1}{s_1(r)} \sum_{u=r-k_0}^{r-1} s_3(u) \right)^{\frac{1}{\beta_1}} \right)$$

Hence, we conclude that q is a positive and increasing solution of

$$\Delta q(\vartheta) - k^{\frac{\beta_3}{\beta_1}} q^{\frac{\beta_3}{\beta_1}}(\vartheta + n^* - 3k_0) \sum_{\varrho=\vartheta-k_0}^{\vartheta-1} \left(\sum_{r=t-k_0}^{\varrho-} \left(\frac{1}{s_1(r)} \sum_{u=r-k_0}^{r-1} s_3(u) \right)^{\frac{1}{\beta_1}} \right) \geq 0$$

while applying Lemma (2.1)II, (24) also has an eventually positive solution, which is a contradiction.
Case (II). Let

$$W = -s_1 \left(\Delta^3 q \right)^{\beta_1} > 0 \text{ eventually} \tag{34}$$

By (30) we get

$$-\Delta W(\vartheta) \geq k^{\beta_2} s_2(\vartheta) q^{\beta_2}(\vartheta - n + 1) \tag{35}$$

we know that, eventually,

$$q(\vartheta) = q(\vartheta_1) + \sum_{\varrho=\vartheta_1}^{\vartheta-1} \Delta q(\varrho) \geq \sum_{\varrho=\vartheta_1}^{\vartheta-1} \Delta q(\varrho)$$

$$= (\vartheta - \vartheta_1)\Delta q(\vartheta - 1) = l\Delta q(\vartheta - 1)\left(1 - \frac{\vartheta_1}{\vartheta}\right)$$

Since $\frac{\vartheta_1}{\vartheta} \to 0$ as $\vartheta \to \infty$, there exists $\theta_1 \in (0,1)$ such that

$$q(\vartheta) \geq \vartheta \theta_1 \Delta q(\vartheta - 1) \text{ eventually} \tag{36}$$

Next, we have

$$\Delta q(\vartheta) = q(\vartheta_2) + \sum_{\varrho=\vartheta_2}^{\vartheta-1} \Delta^2 q(\varrho) \geq \sum_{\varrho=\vartheta_2}^{\vartheta-1} \Delta^2 q(\vartheta - 1)$$

$$= (\vartheta - \vartheta_2)\Delta^2 q(\vartheta - 1) = \Delta^2 z(\vartheta - 1)\left(1 - \frac{\vartheta_2}{\vartheta}\right)$$

Since $\frac{\vartheta_2}{\vartheta} \to 0$ as $\vartheta \to \infty$ there exists $\theta_2 \in (0,1)$ such that

$$\Delta q(\vartheta) \geq \vartheta \theta_2 \Delta^2 q(\vartheta - 1) \text{ eventually} \tag{37}$$

Now, we get $a = \vartheta - n - 1, b = a + k_1 > a$.
Th
en, f
rom (34) and (28) we geteventually

$$0 \leq \Delta^2 q(b) = \Delta^2 q(a) + \sum_{\varrho=a}^{b-1} \Delta^3 q(\varrho)$$

$$= \Delta^2 q(a) - \sum_{\varrho=a}^{b-1} \frac{W^{\frac{1}{\beta_1}}(\varrho)}{s_1^{\frac{1}{\beta_1}}(\varrho)}$$

$$\leq \Delta^2 q(a) - \sum_{\varrho=a}^{b-1} \frac{W^{\frac{1}{\beta_1}}(b-1)}{s_1^{\frac{1}{\beta_1}}(\varrho)}$$

$$\leq \Delta^2 q(a) - W^{\frac{1}{\beta_1}}(b-1)S_1(b,a)$$

and therefore,

$$\Delta^2 q(a) \geq W^{\frac{1}{\beta_1}}(b-1)S_1(b,a) \tag{38}$$

From (35)-(38), we obtain

$$-\Delta W(\vartheta) \geq k^{\beta_2} s_2(\vartheta) q^{\beta_2}(\vartheta - n + 1)$$

$$\geq (\theta_1 k)^{\beta_2} s_2(\vartheta)(\vartheta - n + 1)^{\beta_2} (\Delta q(\vartheta - n))^{\beta_2}$$

$$\geq (\theta_1 \theta_2 k)^{\beta_2} s_2(\vartheta)(\vartheta - n + 1)^{\beta_2}(\vartheta - n)^{\beta_2} (\Delta^2 q(\vartheta - n - 1))^{\beta_2}$$

$$\geq (\theta_1 \theta_2 k)^{\beta_2} s_2(\vartheta)(\vartheta - n + 1)^{\beta_2}(\vartheta - n)^{\beta_2} W^{\frac{\beta_2}{\beta_1}}(\vartheta - n + k_1 - 2)[S_1(\vartheta - n + k_1 - 1, \vartheta - n - 1)]^{\beta_2}$$

Therefore, W is a positive and decreasing solution of

$$\Delta W(\vartheta) + (\theta_1 \theta_2 k)^{\beta_2} s_2(\vartheta)(\vartheta - n + 1)^{\beta_2}$$

$$(\vartheta - n)^{\beta_2} W^{\frac{\beta_2}{\beta_1}}(\vartheta - n + k_1 - 2)[S_1(\vartheta - n + k_1 - 1, \vartheta - n - 1)]^{\beta_2} \leq 0$$

while applying Lemma 2.1(I), (25) also has an eventually positive solution which contradictory.

Case(III) and (IV):

In the rest of the proof, let W be as in (34). Now,

$$q(\vartheta) = y(\vartheta) - s_4(\vartheta)y^{\beta_4}(\vartheta - k) \geq -s_4(\vartheta)y^{\beta_4}(\vartheta - k) \text{ eventually}$$

Thus,

$$y(\vartheta - k) \geq -\left(\frac{q(\vartheta)}{s_4(\vartheta)}\right)^{\frac{1}{\beta_4}} \tag{39}$$

Here from (1) we get eventually,

$$-\Delta W(\vartheta) = s_2(\vartheta)y^{\beta_2}(\vartheta - n + 1) + s_3(\vartheta)y^{\beta_3}(\vartheta + n^*)$$

$$\geq s_2(\vartheta)y^{\beta_2}(\vartheta - n + 1) \tag{40}$$

$$\geq -\frac{s_2(\vartheta)}{s_4^{\frac{\beta_2}{\beta_4}}(\vartheta - n + k + 1)} q^{\frac{\beta_2}{\beta_4}}(\vartheta - n + k + 1).$$

Case (III).

From (34) and (28) we obtain,

$$\Delta^2 q(\vartheta) = \Delta^2 q(\vartheta_1) + \sum_{\varrho=\vartheta_1}^{\vartheta-1} \Delta^3 q(\varrho)$$

$$= \Delta^2 q(\vartheta_1) - \sum_{\varrho=\vartheta_1}^{\vartheta-1} \frac{W^{\frac{1}{\beta_1}}}{s_1^{\frac{1}{\beta_1}}(\varrho)}$$

$$\leq -\sum_{\varrho=\vartheta_1}^{\vartheta-1} \frac{W^{\frac{1}{\beta_1}}(\vartheta - 1)}{s_1^{\frac{1}{\beta_1}}(\varrho)}$$

$$\leq -W^{\frac{1}{\beta_1}}(\vartheta - 1)S_1(\vartheta, \vartheta_1)$$

eventually, which implies from (28) we get

$$\Delta q(\vartheta) \;\; = \Delta q(\vartheta_1) + \sum_{\varrho=\vartheta_1}^{\vartheta-1} \Delta^2 q(\varrho)$$

$$\leq \sum_{\varrho=\vartheta_1}^{\vartheta-1} \Delta^2 q(\varrho) \leq -\sum_{\varrho=\vartheta_1}^{\vartheta-1} W^{\frac{1}{\beta_1}}(\vartheta-1) S_1(\varrho,\vartheta_1)$$

$$\leq -W^{\frac{1}{\beta_1}}(\vartheta-2) \sum_{\varrho=\vartheta_1}^{\vartheta-1} S_1(\varrho,\vartheta_1) \text{ eventually}$$

Therefore, from (28) we obtain,

$$q(\vartheta) \;\; = q(\vartheta_1) + \sum_{\varrho=\vartheta_1}^{\vartheta-1} \Delta q(\varrho) \leq \sum_{\varrho=\vartheta_1}^{\vartheta-1} \Delta q(\varrho)$$

$$\leq -\sum_{\varrho=\vartheta_1}^{\vartheta-1}\left[W^{\frac{1}{\beta_1}}(\vartheta-2)\left(\sum_{r=\vartheta_1}^{\vartheta-1} S_1(r,\vartheta_1)\right)\right]$$

$$\leq -W^{\frac{1}{\beta_1}}(\vartheta-3)\left[\sum_{\varrho=\vartheta_1}^{\vartheta-1}\left(\sum_{r=\vartheta_1}^{\vartheta-1} S_1(r,\vartheta_1)\right)\right]$$

eventually.

And thus, from (40) we get eventually,

$$-\Delta W(\vartheta) \;\; \geq -\frac{s_2(\vartheta)}{s_4^{\frac{\beta_2}{\beta_4}}(\vartheta-n+k+1)} q^{\frac{\beta_2}{\beta_4}}(\vartheta-n+k+1)$$

$$\geq \frac{s_2(\vartheta)}{s_4^{\frac{\beta_2}{\beta_4}}(\vartheta-n+k+1)}\left[W^{\frac{1}{\beta_1}}(\vartheta-n+k-2)\left[\sum_{\varrho=\vartheta_1}^{\vartheta-n+k}\left(\sum_{r=\vartheta_1}^{\vartheta-n+k} S_1(r,\vartheta_1)\right)\right]\right]^{\frac{\beta_2}{\beta_4}}$$

$$\geq \frac{s_2(\vartheta)}{s_4^{\frac{\beta_2}{\beta_4}}(\vartheta-n+k+1)} W^{\frac{\beta_2}{\beta_1}}(\vartheta-n+k-2)\left[\sum_{\varrho=\vartheta_1}^{\vartheta-n+k}\left(\sum_{r=\vartheta_1}^{\vartheta-n+k} S_1(r,\vartheta_1)\right)\right]^{\frac{\beta_2}{\beta_4}}$$

Hence, W is a positive and decreasing solution of

$$\Delta W(\vartheta) + \frac{s_2(\vartheta)}{s_4^{\frac{\beta_2}{\beta_4}}(\vartheta-n+k+1)} W^{\frac{\beta_2}{\beta_1\beta_4}}(\vartheta-n+k-2)\left[\sum_{\varrho=\vartheta_1}^{\vartheta-n+k}\left(\sum_{r=\vartheta_1}^{\vartheta-n+k} S_1(r,\vartheta_1)\right)\right]^{\frac{\beta_2}{\beta_4}} \leq 0$$

while applying Lemma (2.1) I, we see that (26) also has an eventually positive solution, which contradictory.

Case (IV). Let

$a = m-n+k+1, b = a+k_2 > a, c = a+k_3-1 > b-1, d = a+k_4-1 > c-1,$

First, we get eventually,

$$0 \;\; \geq q(b) = q(a) + \sum_{\varrho=a}^{b-1} \Delta q(\varrho)$$

$$\geq q(a) + \sum_{\varrho=a}^{b-1} \Delta q(b-1)$$

$$\geq q(a) + (b-a)\Delta q(b-1)$$

$$-q(a) \geq (b-a)\Delta q(b-1) \tag{41}$$

Kaleeswari and Buvanasankari

Now, we obtain eventually,

$$0 \leq \Delta q(c) = \Delta q(b-1) + \sum_{\varrho=b-1}^{c-1} \Delta^2 q(\varrho)$$

$$\leq \Delta q(b-1) + (c-b+1)\Delta^2 q(c-1)$$

$$\leq \Delta q(b-1) + c\left(1 - \left(\frac{b-1}{c}\right)\right)\Delta^2 q(c-1)$$

Since $\frac{b-1}{c} \to 0$ as $c \to \infty$, there exists $\theta_0 \in (0,1)$, such that

$$\Delta q(b-1) \geq -c\theta_0 \Delta^2 q(c-1) \text{ eventually.} \tag{42}$$

Then, from (34) and (28) we have

$$\Delta^2 q(d) = \Delta^2 q(c-1) + \sum_{\varrho=c-1}^{d-1} \Delta^3 q(\varrho)$$

$$\leq -\sum_{\varrho=c-1}^{d-1} \frac{W^{\frac{1}{\beta_1}}(\varrho)}{s_1^{\frac{1}{\beta_1}}(\varrho)}$$

$$\leq -W^{\frac{1}{\beta_1}}(d-1)S_1(d, c-1)$$

$$-\Delta^2 q(d) \geq W^{\frac{1}{\beta_1}}(d-1)S_1(d, c-1) \tag{43}$$

Thus, from (40)-(43) we get

$$-\Delta W(\vartheta) \geq \frac{s_2(\vartheta)}{s_4^{\frac{\beta_2}{\beta_4}}(\vartheta - n + k + 1)}[(b-a)\Delta q(b-1)]^{\frac{\beta_2}{\beta_4}}$$

$$\geq \frac{s_2(\vartheta)}{s_4^{\frac{\beta_2}{\beta_4}}(\vartheta - n + k + 1)} k_2^{\frac{\beta_2}{\beta_4}}[-c\theta_0 \Delta^2 q(c-1)]^{\frac{\beta_2}{\beta_4}}$$

$$\geq \frac{s_2(\vartheta)}{s_4^{\frac{\beta_2}{\beta_4}}(\vartheta - n + k + 1)} (k_2 c\theta_0)^{\frac{\beta_2}{\beta_4}}\left[W^{\frac{1}{\beta_1}}(c-2)S_1(c-1, c-1)\right]^{\frac{\beta_2}{\beta_4}}$$

which implies W is a positive and decreasing solution of

$$\Delta W(\vartheta) + \frac{s_2(\vartheta)}{s_4^{\frac{\beta_2}{\beta_4}}(\vartheta - n + k + 1)} (k_2 c\theta_0)^{\frac{\beta_2}{\beta_4}}\left[W^{\frac{1}{\beta_1}}(c-2)S_1(c-1, c-1)\right]^{\frac{\beta_2}{\beta_4}} \leq 0$$

$$\Delta W(\vartheta) + \frac{s_2(\vartheta)}{s_4^{\frac{\beta_2}{\beta_4}}(\vartheta - n + k + 1)} (k_2 c\theta_0)^{\frac{\beta_2}{\beta_4}}\left[W^{\frac{1}{\beta_1}}(\vartheta - n + k + k_3 - 2)S_1(\vartheta - n + k + k_3 - 1, \vartheta - n + k + k_3 - 1)\right]^{\frac{\beta_2}{\beta_4}} \leq 0$$

Using Lemma (2.1) I, (27) also has an eventually positive solution which contradicts.

We provide the next results to demonstrate Theorem 3.1.

Corollary 3.2. Assume that(i)-(iii), (2), (22) and (23) hold. If the first order advanced difference equation (24) and the first oorder delay difference equation (25) and

$$\Delta W(\vartheta) + \min\left\{\frac{s_2(\vartheta)}{s_4^{\frac{\beta_2}{\beta_4}}(\vartheta - n - k + 1)}\left[\sum_{\varrho=\vartheta_1}^{\vartheta - n + k}\left(\sum_{r=t_1}^{t-n+k} S_1(r, \vartheta_1)\right)\right]^{\frac{\beta_2}{\beta_4}},\right.$$

$$\left. \frac{s_2(\vartheta)}{s_4^{\frac{\beta_2}{\beta_4}}(\vartheta - n + k + 1)}(k_2 c\theta_0)^{\frac{\beta_2}{\beta_4}}[S_1(\vartheta - n + k + k_3 - 1, \vartheta - n + k + k_3 - 1)]^{\frac{\beta_2}{\beta_4}}\right\}W^{\frac{\beta_2}{\beta_1\beta_4}}(\vartheta - n + k + k_3 - 2) = 0$$

$$\tag{44}$$

are oscillatory for $1 > \beta_4$ and $\theta_0, \theta_1, \theta_2 \in (0,1)$, then (1) is oscillatory.

Corollary 3.3. Assume $1 > \beta_4$ and $\beta_3 \geq \beta_1 \geq \beta_2$. Let(i)-(iii), (2), (22) and (23) hold. If

$$\limsup_{\vartheta \to \infty} \sum_{\varrho=\vartheta-k_0}^{\vartheta-1} \left(\sum_{r=t-k_0}^{\varrho-} \left(\frac{1}{s_1(\varrho)} \sum_{\xi=r-k_0}^{r-1} s_3(\xi) \right)^{\frac{1}{\beta_1}} \right) = \infty, \tag{45}$$

$$\limsup_{\vartheta \to \infty} s_2(\vartheta)(\vartheta-n+1)^{\beta_2}(\vartheta-n)^{\beta_2} S_1[\vartheta-n+k_1-1, \vartheta-n-1]^{\beta_2} = \infty, \tag{46}$$

$$\limsup_{\vartheta \to \infty} \frac{s_2(\vartheta)}{s_4^{\frac{\beta_2}{\beta_4}}(\vartheta-n+k+1)} \left[\sum_{\varrho=\vartheta_1}^{\vartheta-n+k} \left(\sum_{r=t_1}^{t-n+k} S_1(r, \vartheta_1) \right) \right]^{\frac{\beta_2}{\beta_4}} = \infty, \tag{47}$$

and

$$\limsup_{\vartheta \to \infty} \frac{s_2(\vartheta)}{s_4^{\frac{\beta_2}{\beta_4}}(\vartheta-n+k+1)} (k_2 c \theta_0)^{\frac{\beta_2}{\beta_4}} [S_1(\vartheta-n+k+k_3-1, \vartheta-n+k+k_3-1)]^{\frac{\beta_2}{\beta_4}} = \infty, \tag{48}$$

then (1) is oscillatory.

Corollary 3.4. Let $1 \geq \beta_4$, suppose that(i)-(iii), (12) and (22) hold. Assume $\lim_{\vartheta \to \infty} s(\vartheta) = 0$ where

$$S(\vartheta) = -(\beta_4 s_4(\vartheta))^{\frac{-1}{\beta_4}} \tag{49}$$

Let $\theta_0, \theta_1, \theta_2 \in (0,1)$. If (24)-(27) are oscillatory, then so (1).

Corollary 3.5. Let $1 \geq \beta_4$. Assume that(i)-(iii), (2),(22) and (49) hold. Let $\theta_0, \theta_1, \theta_2 \in (0,1)$. if (24), (25) and (44) are oscillatory then (1) is oscillatory.

Corollary 3.6. Let $1 \geq \beta_4$ and $\beta_3 \geq \beta_1 \geq \frac{\beta_2}{\beta_4}$. Assume that(i)-(iii), (2),(22) and (49) hold. Let $\theta_0, \theta_1, \theta_2 \in (0,1)$. if (45)-(48) hold then (1) is oscillatory.

Examples

Example 4.1. We look at the eqution

$$\Delta \left((\vartheta+2)^3 \left(\Delta^3 \left(y(\vartheta) - \frac{1}{\vartheta} y^{\frac{1}{3}}(\vartheta-1) \right) \right) = \vartheta^2 y(\vartheta-3) + (\vartheta+3)^4 y^3(\vartheta+6) \tag{50}$$

Now (50) is in the form (1) where $\beta_1 = \beta_3 = 3$, $\beta_2 = 1, \beta_4 = \frac{1}{3} k = 1, n = 4$,

$n^* = 6$, $s_1(\vartheta) = (\vartheta+2)^3, s_2(\vartheta) = \vartheta^2, s_3(\vartheta) = (\vartheta+3)^4, s_4(\vartheta) = \frac{1}{\vartheta}$.

Then (i)-(iii) are fulfilled and so is (2), because

$$S_1(b,a) = \sum_{\varrho=a}^{b-1} \left(\frac{1}{s_1(\varrho)} \right)^{\frac{1}{3}} = \sum_{\varrho=a}^{b-1} \frac{1}{t+2} = \sum_{\varrho=a+2}^{b} \frac{1}{t} \to \infty$$

Now, (see Note 2.4) $k_0 = k_1 = k_2 = 1$ and $k_3 = 2$. And thus (22) is fulfilled and we get,

$$\vartheta + n^* - 3k_0 = \vartheta + 3$$
$$\vartheta - n + k_1 - 2 = \vartheta - n + k - 2 = \vartheta - 5$$
$$\vartheta - n + k + k_3 = \vartheta - 3,$$

Furthermore, $\beta_4 < 1$ and $\beta_2 < \beta_1 = \beta_3$. So by corollory 3.3 , we choose $s = s_4$ then

$$\begin{aligned} g_1(\vartheta) &= \frac{2}{3} \left(\frac{1}{3} \right)^{\frac{1}{2}} (s(\vartheta))^{\frac{-1}{2}} (s_4(\vartheta))^{\frac{3}{2}} \\ &= \frac{2}{3} \left(\frac{1}{3} \right)^{\frac{1}{2}} \left(\frac{1}{\vartheta} \right)^{\frac{-1}{2}} \left(\frac{1}{\vartheta} \right)^{\frac{3}{2}} \\ &= \frac{2}{3\sqrt{3}} \left(\frac{1}{\vartheta} \right) \to 0 \text{ as } \vartheta \to \infty. \end{aligned}$$

And so (23) is fulfilled. We also compute

Kaleeswari and Buvanasankari

$$\sum_{\varrho=\vartheta-k_0}^{\vartheta-1} \left(\sum_{r=t-k_0}^{\varrho-1} \left(\frac{1}{s_1(\varrho)} \sum_{\xi=r-k_0}^{r-1} s_3(\xi) \right)^{\frac{1}{\beta_1}} \right) = \left(\frac{s_3(\vartheta-3)}{s_1(\vartheta-1)} \right)^{\frac{1}{3}} = \vartheta^{\frac{1}{3}}$$

$$s_2(\vartheta)(\vartheta-n+1)^{\beta_2}(\vartheta-n)^{\beta_2} S_1[\vartheta-n+k_1-1, \vartheta-n-1]^{\beta_2} = \vartheta^2(\vartheta-4)$$

$$\frac{s_2(\vartheta)}{s_4^{\frac{\beta_2}{\beta_4}}(\vartheta-n+k+1)} \left[\sum_{\varrho=\vartheta_1}^{\vartheta-n+k} \left(\sum_{r=t_1}^{t-n+k} S_1(r, \vartheta_1) \right) \right]^{\frac{\beta_2}{\beta_4}} = \frac{\vartheta^2\left(1-\frac{2}{\vartheta}\right)^3}{\left(1-\frac{4}{\vartheta}\right)^3}$$

and

$$\frac{s_2(\vartheta)}{s_4^{\frac{\beta_2}{\beta_4}}(\vartheta-n+k+1)} (k_2 c\theta_0)^{\frac{\beta_2}{\beta_4}} [S_1(\vartheta-n+k+k_3-1, \vartheta-n+k+k_3-1)]^{\frac{\beta_2}{\beta_4}} = \frac{\vartheta^2\left(1-\frac{2}{\vartheta}\right)^3}{\left(1-\frac{1}{\vartheta}\right)^3}$$

Hence (45)-(48) hold. Now that all of corollary 3.3's criteria have been fulfilled, Equation (50) is oscillatory

Example 4.2.The equations are considered

$$\Delta\left((\vartheta+2)^3\left(\Delta^3\left(y(\vartheta)-\vartheta y^{\frac{1}{3}}(\vartheta-1)\right)\right) = \vartheta^2 y(\vartheta-3) + (\vartheta+3)^4 y^3(\vartheta+6)\right. \tag{51}$$

Now (51) is in the form (1) where $\beta_1 = \beta_3 = 3, \beta_2 = 1, \beta_4 = \frac{1}{3}$

$k = 1, n = 4, n^* = 6, s_1(\vartheta) = (\vartheta+2)^3, s_2(\vartheta) = \vartheta^2, s_3(\vartheta) = (\vartheta+3)^4, s_4(\vartheta) = l$. Furthermore, we have $1 \geq \beta_4$ and $\beta_3 = \beta_1 \geq \frac{\beta_2}{\beta_4}$ from corollary 3.6.

We compute $S(\vartheta) = -(\beta_4 s_4(\vartheta))^{-3} = -\left(\frac{\vartheta}{3}\right)^{-3} = -\left(\frac{3}{\vartheta}\right)^3 \to 0$, as $l \to \infty$ and so (49) is fulfilled because all of the other constraints of corollary 3.6 are satisfied in the same sense as in Example 4.1, (51) is oscillatory

REFERENCES

1. Agarwal, R.P.,Difference Equations and Inequalities: Theory, Methods and Applications, 2nd edition, Monographs and Textbooks in Pure and Applied Mathematics, Dekker, Newyork, 2000, vol 228.
2. Agarwal, R.P., Bohner, M., Grace, S.R., O'Regan, D., Discrete Oscillation Theory, Hindawi Publishing Corporation, Newyork, 2005.
3. Agarwal, R.P., Bohner, M., Li, T., Zhang, C., Hille and Nehari type criteria for third-order delay dynamic equations, J.Differ. Equ. Appl., 2013, 19(10),1563-1579.
4. ElMorshedy, H.A., Grace, S.R., Comparison theorems for second order nonlinear difference equations, J. Math. Anal.Appl., 2005, 306(1), 106-121.
5. Grace, S.R., Oscillatory behavior of third-order nonlinear difference equations with a nonlinear-nonpositive neutral term, Mediterr. J. Math., 2019, 16(5), Article ID 128.
6. Grace, S.R., Agarwal, R.P., Bohner, M., O'Regan, D., Oscillation of second-order strongly superlinear and strongly sublinear dynamic equations, Commun. Nonlinear Sci. Numer.Simul., 2009, 14(8), 3463-3471.
7. Grace, S.R., Alzabut, J., Oscillation results for nonlinear second order difference equations with mixed neutral terms, Adv. Differ. Equ., 2020, 8.
8. Grace, S.R., Bohner, M., Liu, A., On Kneser solutions of third-order delay dynamic equations, Carpath. J. Math., 2010, 26(2),184-192.
9. Hardy, G.H., Littlewood, J.E., Pólya, G., Inequalities, Cambridge Mathematical Library, Cambridge University Press,Cambridge (1988) Reprint of the 1952 edition.
10. Kaleeswari, S., On the oscillation of higher order nonlinear neutral difference equations, Advances in Difference Equations, 2019 (1), 1-10.
11. Kaleeswari. S., Selvaraj, B., Thiyagarajan. M., A New Creation of Mask From Difference Operator To Image Analysis, Journal of Theoretical and Applied Information Technology, 2014, 69 (1).
12. Kaleeswari, S., Selvaraj, B., Thiyagarajan, M., Removing Noise Through a Nonlinear Difference Operator, International Journal of Applied Engineering Research, 2014, 9 (21), 51005106.
13. Kaleeswari, S., Selvaraj, B., On the oscillation of certain odd order nonlinear neutral difference equations, Applied Sciences, 2016, 18, 50-59.

14. Kaleeswari, S., Selvaraj, B., Certain Higher Order Quasilinear Delay Difference Equations International, Journal of Mathematical Analysis, 2015, 9 (18), 907-915.
15. Kaleeswari, S., Oscillatory and asymptotic behavior of third order mixed type neutral difference equations, Journal of Physics: Conference Series, 2020, 1543 (1), 012-005.
16. Kaleeswari, S., Oscillation Criteria For Mixed Neutral Difference Equations, Asian Journal of Mathematics and Computer Research, 2018, 25 (6), 331-339.
17. Kaleeswari, S., Selvaraj, B., An Application of Certain Third Order Difference Equation in Image Enhancement, Asian Journal of Information Technology, 2016, 15 (23), 4945-4954.
18. Kaleeswari S., Selvaraj, B., Oscillation Criteria for Higher Order Nonlinear Functional Difference Equations, British Journal of Mathematics and Computer Science, 2015, 11 (3), 1-8.
19. Li, Q., Wang, C., Li, F., Liang, H., Zhang, Z., Oscillation of sublinear difference equations with positive neutral term, J.Appl. Math.Comput., 2006, 20(1-2), 305-314.
20. Selvaraj, B., Kaleeswari, S., Oscillation theorems for certain fourth order non-linear difference equations, International Journal of Mathematics Research, 2013, 5 (3), 299-312.
21. Selvaraj, B., Kaleeswari, S., Oscillation of solutions of second order nonlinear difference equations, Bulletin of Pure and Applied Sciences-Mathematics and Statistics, 2013, 32 (1), 83-92.
22. Selvaraj, B., Kaleeswari, S., Oscillatory Properties of Solutions For Certain Third Order Non-Linear Difference Equations, Far East Journal of Mathematical Sciences,2015, 98 (8), 963.
23. Selvaraj, B., Kaleeswari, S., Oscillation of Solutions of Certain Nonlinear Difference Equations, Progress in Nonlinear Dynamics and Chaos, 2013, 1, 34-38.
24. Thandapani, E., Selvaraj, B., Oscillatory and Non Oscillatory Behavior of Fourth Order Quasi-linear Difference System, Far East Journal of Mathematical Sciences, 2004, 17(3), 287-307.

RESEARCH ARTICLE

Effectiveness of Back School Protocol Versus Muscle Energy Technique on Pain, Functional Disability, and Range of Motion in Patients with Chronic Mechanical Low Back Pain

Upasti Panchal[1], Dhaval Patel[2] and Gaurav Patel[3]*

[1]MPT Student, Ahmedabad Physiotherapy College, Ahmedabad, Parul University, Gujarat, India.
[2]Professor, Ahmedabad Physiotherapy College, Ahmedabad, Parul University, Gujarat, India.
[3]Principal and Professor, Ahmedabad Physiotherapy College, Ahmedabad, Parul University , Gujarat, India

*Address for Correspondence
Gaurav Patel
Principal and Professor,
Ahmedabad Physiotherapy College,
Ahmedabad, Parul University, Gujarat, India
E.Mail: dr.gauravpatel24@gmail.com

ABSTRACT

Low Back Pain is the most appropriate form of musculoskeletal disorder. It is described as discomfort or pain detected in the area from the 12th rib down to the gluteal area. It acts on annually 5-10% of the adult population. Mechanical low back pain (MLBP) is a major cause of illness and disability, especially in people of working age. Only 39 – 76% of the patients obtain absolute recovery. The study aims to check the effectiveness of back school protocol versus muscle energy technique in patients with chronic mechanical low back pain. 38 patients complaining of chronic mechanical low back pain have participated in the study on the basis of inclusion criteria. Patients were randomly assigned into two equal groups. Group A received Muscle Energy Technique, Group B received Back School Protocol. Both groups underwent a common conventional treatment plan. Treatment was given three times per week for four consecutive weeks. Patients were assessed before and at the end of four weeks by using a numeric pain rating scale (NPRS), Modified Oswestry Disability Low Back Pain Questionnaire (MODQ), Modified - Modified Schober Test (MMST) to assess the intensity of pain, functional disability, and lumbar range of motion. There was a significant decrease in pain, functional disability, and an increase in lumbar range of motion in both groups. Group A showed more improvement post-treatment. The muscle energy technique is more effective compared to the Back School protocol in terms of pain reduction and range of motion whereas Back School is more effective on functional disability in patients with chronic mechanical low back pain (CMLBP).
Keywords : Chronic, Mechanical, Low Back Pain, Muscle Energy Technique, Back School Protocol

Upasti Panchal *et al.,*

INTRODUCTION

Low Back Pain is a very usual condition that occurs due to problems in the muscle and skeletal system [1]. It is described as tenderness and aches detected between the lower ribs and gluteal area. It follows up on every year 5 - 10% of the grown-up populace, with a larger part of 60% to 90% over a long period. By the age of 30, half of the nation will have had a notable episode of Low backache. [2]. only 39 – 76% of the patients obtain   absolute recovery [1]. Chronic low backache is the torment that continues the healing time higher than anticipated, spanning moreover three months. [3]. Frequency of recent and long term LBP in grown-up doubled in the last ten years and continues to increase dramatically in the aging population, influencing men and women overall cultural groups. LBP remarkably affects utilitarian limit, as agony confines word-related exercises and is a significant reason for delinquency. Its financial burden is indicated directly by high healthcare expenses and indirectly by lower productivity. [4]. Mechanical low back pain (MLBP) is still an essential health hazard and a major cause of incapacity in people under the age of 65, so in most cases, there really is no clear underlying pathology. [5]. It comprises unspecific lumbar column damage that could be linked to other causes of lumbar pain. [6]. Mechanical pain results from risky things to do, similar to unfortunate posture, ineffectively planned to seat, and erroneous bowing and lifting movements. There are a few elements incurring mechanical low back torment, as unreasonable masses to typical spinal designs. Posture, body mechanics, trunk strength, and flexibility, as well as the strength of the pelvic arch and lower limbs muscles, all determine the loads conveyed to the spine. [5]. It appears that muscle weakness is associated with MLBP [7]. Mohammad Reza Nourbakhsh et.al, expressed that diminished back extensor muscle endurance is a significant element in ongoing LBP.

The Back School is a conservative form of therapeutic intervention in the management of mechanical low back pain (MLBP) [8]. The Back School method was developed in 1969 in Sweden by Mariane Zachrisson Forssel, with the goal of preventing and avoiding recurrent episodes of low back pain [9]. In later years it became known as the Swedish Back School [10]. The etiological aspects of low back pain, such as biomechanical stress and increased intradiscal pressure, were the basis for the development of the program, which focused primarily on an educational approach to the ergonomic elements related to pain [10]. Modern back schools have advanced into other areas today - of not only managing the pain but also preventing injury to the back that can precipitate back pain [8]. This intervention module was originally developed as an education and training program and involves exercise monitored by a physiotherapist or physician [11]. Common topics of the educational component of the Back School Program include the anatomy of the spine, theories of the etiology of LBP, the function of the backbone, ergonomics, exercise, complications of back pain, and changing unpleasant beliefs about back pain [11]. A practical component that consists of exercise for the maintenance of a healthy back [6].

Muscle Energy Technique is a non-invasive, safe, and inexpensive treatment technique commonly used by physiotherapists, chiropractors, and manual therapists in the treatment of MLBP [12]. This manual therapy technique was founded by Dr. Fred L. Mitchell Sr., who was an osteopathic physician [13]. MET is a versatile technique traditionally used to address different types of muscular strain, pain in different regions, local edema, and joint dysfunction and also improve range of motion (ROM), relieve muscle tension, and increase the strength of the muscle [14]. Muscle energy technique (MET) is a common traditional treatment for spine disease. It is the most popular therapeutic modality aimed at the improvement of elasticity in contractile and non – contractile tissues [1]. This procedure "involves the contraction done by the patient's voluntary group of muscles in a very particular and controlled direction, at varying levels of intensity, against a clearly executed counterforce applied by the therapist [13]. Its plan of action is based on a form for using low amplitude muscular contractions against obstruction in the hopes of affecting both type of static and dynamic posture and vascular dissemination. Isometric constriction principally decreases the tone present in a hypertonic muscle and restores its ordinary resting length by use of reciprocal inhibition. [2]

Upasti Panchal *et al.,*

METHODS AND MATERIALS

A comparative study was carried out at Sainath Hospital. Ethical clearance was taken from ethical committee of Sainath hospital. 38 subjects with chronic mechanical low back pain were taken in the study according to inclusion criteria. They were divided into two groups, 19 in each group. Group A were treated with Muscle Energy Technique along with conventional physiotherapy. Group B were treated with Back School Protocol along with conventional physiotherapy. The inclusion criteria are: (a) Mechanical backache discovered by a registered medical practitioner. (b) At very least 3 months, patient must have chronic mechanical low back pain without peripheral irradiation. (c) Subjects who have pain scores in between 2 to 6 on the NPRS. (d) Age: 18 to 40 years. Exclusion criteria are: (a) Subjects who have gone through past a medical procedure, who had underlying peculiarities, History of spinal fracture, spinal cord pressure, extreme instability, serious osteoporosis. (b) History of any provocative spinal disease (c) Disc prolapsed or Spondylolisthesis (d) Congenital musculoskeletal deformity (e) Any cardiovascular diseases (f) Abnormal neurological signs in the lower extremity and psychosomatic diseases. Outcome measures of present study are The numeric pain rating scale (NPRS), Modified Oswestry Disability Low Back Pain Questionnaire(MODQ), Modified - Modified Schober Test(MMST) .

The numeric pain rating scale (NPRS) is 11 point measure of pain in which patient is asked to rate their pain. It is ranging from 0 indicated as no pain at all to 10 which indicates the worst imaginable pain[15]. Modified Oswestry Disability Low Back Pain Questionnaire(MODQ) is intended to give data about how a patient's low back and leg pain is meaning for his/her regular routine. The questionnaire comprises of 10 things tending to various parts of functions. Each item is scored from 0 to 5, with higher values addressing more noteworthy disabilities. The patient is approached to finish up the questionnaire according to his/her uneasiness in day-by-day exercises[16].
Modified - Modified Schober Test (MMST)

Flexion measurement: - The patients were told to take off their shoes, uncovering their back from gluteal fold to mid-thoracic spine with left and right PSIS completely uncovered. The specialist recognized both the PSIS with her thumb and check a midline point on the sacrum (inferior mark). Then, at that point, the superior mark was set apart on the lumbar spine 15 cm over the sacral mark. The measure tape was kept solidly against the skin and asked to "Bend forward as far as you can while keeping the knee straight". The ROM was the contrast between 15 cm and length estimated toward the end of the movement. Extension measurement: - The patients position and markers were same as flexion. Therapist instruct to "Put the palms of your hands on your butt cheek and bend in reverse to the furthest extent that you would be able". The distance between superior and inferior marks was measured[17].

Group A was treated with Muscle energy technique along with conventional exercises.MET applied for the muscles given below, MET has been used as a post-isometric relaxation treatment. The subjects were instructed to make a contraction of roughly 20 - 30 percent of their most extreme deliberate isometric contraction, hold it around 7-10s, then release around 2-3s after they had sensed the limiting boundary. Proper breathing instructions were given to the patient and afterwards on exhalation the extremity was taken somewhat a long way from the limitation barrier and held on that point around 10-30s, It was completed 3 times per meeting for 12 sessions[18].

Iliopsoas MET: - Patient position - prone lying with a headrest placed under the abdomen area for reduction in lumbar curve. Therapist position - standing on opposite side of the side of muscle which was treated, the table-side hand supporting the thigh. The another one hand was set with the goal that the heel point of the hand was put on the sacrum. Pressure is applied towards the floor, to keep up with pelvic stability. Instructions - The patient was asked to bring his thigh towards table against the therapist's resistance. Patients use 15-25% of him/her maximum voluntary contraction. Hold around 7 to 10s [8].

Hamstring muscles MET: - Patient position- supine lying with treatment leg hanging over the therapist's shoulder.Therapist position- One hand placed on non-treated limb's front distal portion of the thigh, while the other was placed on the treated limb's front distal part of the thigh, simply over the knee, to keep the knee in an

Upasti Panchal *et al.,*

extention.Instructions- patient's hip was passively flexed and the leg extended until tension. The patient was asked to do moderate knee flexion with isometric contraction. Pressing his ankle joint against the therapist's shoulder, followed by relaxation, on and then leg was passively stretched by the therapist up to the tolerance to stretch and hold for 30 seconds[18].

Quadratus lumborum MET: - Patient position- side-lying with the uppermost arm stretched out over the head tightly to hold the edge of the table.Therapist position- Standing behind side-lying patient at the waist level.Instructions- the patient was asked to abduct the uppermost leg around 30° on exhalation. The therapist palpated strong quadratus activity. The patient holds the leg isometrically and gravity gives resistance from the leg. Following 10 second constriction, the patient was approached to hang his leg marginally behind him at the back of the table. The advisor supports the pelvis with two hands with fingers interlocked over the iliac crest moves the pelvis away from the lower ribs on exhalation. The stretch should grasp for 10 to 30 seconds[8].

Erector spine MET: - Patient position- seated on the treatment table his back in the direction of the therapist.Therapist position- Therapist pass his one hand in patent's axilla, across the neck on the side which the patient was rotated. Another hand was placed on the contralateral shoulder.Instructions - Patient was asked to do flexion, side bending, and rotation and that time taken to the comfortable limit of forward bending. patient was asked to hold his breath around 7 to 10s and stare in the direction from whence he rotated before exhaling. On the full exhalation, the patient was again taken to the new restriction[18].

Group-B was treated with Back School Protocol along with conventional therapy. In Back School protocol group patients have given three treatment meetings per week, each lasting 45 minutes to an hour.The program was divided based on educational and practical sessions[6].

THEORY SESSION: General information, history, and methods of back school protocol, Pathology; Anatomy and biomechanical ideas of the spine, The effect of muscle functions on the spine, Etiopathogenesis of the most common conditions that have a detrimental impact on the back, Treatment techniques that are most commonly used, Mechanical forces in varied back movements are inconsistent; relaxation stance, Instructions for sitting and standing positions.

PRACTICAL EXERCISES: Diaphragmatic breathing exercise. (10 reps. In 1set);Stretching of erector spinae muscle, Hamstrings, Calf, and Quadriceps muscles. (30 seconds, repeat 10 times); Pelvic tilting exercise. (10 reps. In 1 set);The abdominal musculature is strengthened. (1 set of 10 repetitions)

CONVENTIONAL PROTOCOL: Infrared radiation, Ultrasonic, Therapeutic exercise program in type of Finger to toes, Bridging exercise, Back expansion from prone, Sit-up work out, Knee to chest work out, Lower back muscle stretching.

RESULT

A comparative study was done on 38 chronic mechanical low back pain patients aged between 18 to 40 years. The subjects were randomly divided into two groups and an Independent t-test was usedto check the pre and post-treatment effects. Graph-1 shows the mean pre-post data of Group-A. Graph-2 shows the mean values of Group-B pre-post data. Table-1 shows Group A and Group B pre and post-mean of Numeric Pain Rating Scale (NPRS), Modified Oswestry Disability Low Back Pain Questionnaire(MODQ), Modified - Modified Schober Test (MMST). The result shows significant improvement in all the outcome measures in both the groups but group-A showed more significant improvement in pain and range of motion whereas Group-B showed more significant improvement in functional disability.

DISCUSSION

The present study compared muscle energy technique and back school protocol. The result of both interventions was investigated and both the groups proved to be effective in the management of chronic mechanical low back pain (CMLBP). The result of this study showed that the two groups were huge in diminishing pain and increasing lumbar flexion and expansion range of motion post-treatment, particularly in group A which is MET. There was a huge improvement in functional ability in both the groups after-treatment, particularly in group B which is back school protocol. Marzouk A. Ellythy[1] et al.; studied and one group got a muscle energy procedure and the other group got Strain Counter Strain treatment for 4weeks. Pain intensity, lumber movements, and functional disability index were taken as outcome measures and In individuals with chronic low back pain, both the MET and SCS approaches were proved to be efficient in lowering pain and functional capability. The diminution in pain caused by the muscular energy approach can be explained by Chaitow'sneurophysiology[19]. He characterized post isometric relaxation (PIR) as the fall in a tone of the agonist's muscle following an isometric contraction. Stretch receptors in the agonist muscle's Golgi tendon cause this to happen. The muscle contraction is inhibited by these receptors which react to overstretching of the muscle. The Golgi tendon organ is triggered by the equal counterforce of a strong agonist muscle contraction. From the Golgi tendon, The afferent nerve impulse travels to the dorsal base of the spinal cord, where it connects to an inhibitory motor neuron. Reestablishing the full stretch length of the muscles reduces the increase in pressure on the afflicted muscles, as well as the pain and dysfunction that follows.

Usman Abba Ahmed et al.; did a scoping review to efficiently assess writing and guide the current The MET technique is a worthwhile and safe intervention that can be beneficial as an independent treatment plan for patients with chronic MLBP, according to a demonstration of its viability and assessment of the retrieved articles. It has the potential to give numerous physical and psychosocial well-being [12]. According to MANIGANDAN S R V (2018), et al., the Muscle energy approach provides an analgesic effect that is understood from both spinal and supraspinal mechanisms. During an isometric contraction, both musculature and joint mechanoreceptors are triggered. This generates sympathoexcitation elicited by somatic efferents, as well as localized initiation of the periaqueductal grey, which helps to minimize pain regulation. Due to mechanoreceptor stimulation, nociceptive inhibition occurs in the dorsal horn of the spinal cord, where synchronized gating of nociceptive impulses occurs [20].

In the present study, a significant reduction in functional disability score was reported after 4 weeks of intervention. Between the two groups, the comparison Back School group showed more reduction in MODQ. This finding supports the finding by Frost [34] et al and Heymans [35] et al that back care education caused improvement in function among patients with nonspecific LBP. According to Snook [36] et al, reduction in pain also led to a reduction in disability status among patients with chronic non-specific LBP.

Bahar SADEGHI-ABDOLLAHI (2012) et al.; studied the efficacy of back school protocol in chronic low back pain in workers. He also stated that BS aims to strengthen the musculature that protects the lumbar spine and discs from excessive stress, as well as to teach the best posture for specific job postures and demonstrate how to lift and push large objects. On top of all, BS is aimed to help people to manage their back pain, by showing them the mechanism of the disease, or whenever they get an inadvertent attack [21]. Andrade et al.; assessed the viability of the Back School Program for a non-specific base. Based on investigation they remark statistically significant differences in functional disability and spinal mobility [22].

CONCLUSION

The muscle energy technique is more effective compared to the Back School protocol in terms of pain reduction and range of motion whereas Back School is more effective on functional disability in patients with chronic mechanical low back pain (CMLBP).

Upasti Panchal *et al.,*

FUTURE RECOMMENDATION OF THE STUDY: A larger sample size should be taken, Follow up should be done for a longer period, Further research should be done with different clinical arms.

CONFLICT OF INTEREST: Nil

REFERENCES

1. Marzouk A. Ellythyet. al.; Efficacy of Muscle Energy Technique Versus Strain Counter Strain on Low Back Dysfunction, Bull. Fac. Ph. Th. Cairo Univ., Vol. 17, No. (2) Jul. 2012
2. Mullai D, Aarti S Tanu A (2011). Comparative Analysis of Muscle Energy Technique and Conventional Physiotherapy in Treatment of Sacroiliac Joint Dysfunction. Indian Journal of Physiotherapy and Occupational Therapy; 5(4): 131-134. 25.
3. Noelle MS, Terry L.G, Kevin MC, Kelli P, Jay H, Susan S (2013). Short-Term Effect of Muscle Energy Technique on Pain in Individuals with Non-Specific Lumbopelvic Pain: A Pilot Study. Journal of Manual and Manipulative Therapy; 17(1):14-18. 26.
4. Deepali S, Siddhartha S (2014). Effects of MET on pain and disability in subjects with SIJ dysfunction. International Journal of Physiotherapy and Research; 2(1):305-11. 27.
5. Ajay K and Deepinder S (2015). Effects of Muscle Energy Technique on pain and disability in patients with non-specific low back pain. Indian Journal of Physiotherapy; 3:128-131. 28. Chaitow L (2001). Muscle Energy Technique. (2nd Edition) London: Churchill Livingston.
6. ShefaliPushp Compare the effect of mckenzie protocol and back school program in mechanical low back pain individual, Physiotherapy and Occupational Therapy Journal Volume 5 Number 2, April - June 2012
7. Mohammad Reza Nourbakhsh, PT, PhD1 Amir Massoud Arab, Relationship Between Mechanical Factors and Incidence of Low Back Pain, Journal of Orthopaedic& Sports Physical Therapy® Downloaded from www.jospt.org at on December 11, 2020
8. Odebiyi DO, MSc (Physiotherapy)1 , Akinpelu AO, PhD2 , Olaogun mob effect of a back school protocol on the referral rate of patients with low back pain to an industrial physiotherapy clinic, sa journal of physiotherapy 2006 vol 62 no 4
9. Alessandra N Garcia1 , Francine LB Gondo2 , Renata A Costa2 , Fábio N Cyrillo2 , Tatiane M Silva1 , Luciola CM Costa1,3 and Leonardo OP Costa1,3* Effectiveness of the back school and mckenzie techniques in patients with chronic non-specific low back pain: a protocol of a randomised controlled trial, BMC Musculoskeletal Disorders 2011, 12:179.
10. L.H. Ribeiro, F. Jennings, A. Jones, R. Furtado, J. Natour Effectiveness of a back school program in low back pain, Clinical and Experimental Rheumatology 2008; 26: 81-88.
11. Mohd Ismail Ibrahim 1 , IzaniUzairZubair 2 , MohdNazriShafei 1 , Interactive Low Back Pain Intervention Module Based on the Back School Program: A Cluster-Randomized Experimental Study Evaluating Its Effectiveness among Nurses in Public Hospitals, International Journal of Environmental Research and Public Health 2020, 17, 5916
12. Usman Abba Ahmeda,b,∗ , ThayanantheeNadasanb , Jessica Van Oosterwijckc,d,e and SonillSooknunanMaharaj The effect of muscles energy technique in the management of chronic mechanical low back pain: A scoping review Journal of Back and Musculoskeletal Rehabilitation 34 (2021) 179–193
13. Krupa D. Tank *1 , PrachiChoksi 2 , Priyanka Makwana to study the effect of muscle energy technique versus mulligan snags on pain, range of motion and functional disability for individuals with mechanical neck pain: a comparative study international journal of physiotherapy and research, int j physiother res 2018, vol 6(1):2582-87. Issn 2321-1822
14. Vivek Dineshbhai Patel1 , Charu Eapen1,*, Zulfeequer Ceepee1 and Ramachandra Kamath2 E®ect of muscle energy technique with and without strain–counterstrain technique in acute low back pain — A randomized clinical trial Hong Kong Physiother. J. 2018.38:41-51

15. Cristiana kahl1 and joshua a. Cleland2,3 visual analogue scale, numeric pain rating scale and the mcgill pain questionnaire: an overview of psychometric properties physical therapy reviews 2005; 10: 123–128 24.

16. Julie M FritzJames J Irrgang A Comparison of a Modified Oswestry Low Back Pain Disability Questionnaire and the Quebec Back Pain Disability Scale Physical Therapy . Volume 81 . Number 2 . February 2001 25.

17. M. Tousignant1, I. Poulin1,4, s. Marchand2, a. Viau2, & c. Place3 The Modified – Modified Schober Test for range of motion assessment of lumbar flexion in patients with low back pain: A study of criterion validity, intra- and inter-rater reliability and minimum metrically detectable change Disability and Rehabilitation, 2005; 27(10): 553 – 559

18. Lone Hansen, PhD,* Mark de Zee, PhD,† John Rasmussen, PhD,† Thomas B. Andersen, PhD,‡ Christian Wong, PhD,§ and Erik B. Simonsen, PhD* Anatomy and Biomechanics of the Back Muscles in the Lumbar Spine With Reference to Biomechanical Modeling, Spine • Volume 31 • Number 17 • 2006

19. Chaitow, L.: Muscle Energy Techniques, 3rd edition, London, Churchill Living stone (1): 152-153, 2006.

20. Manigandan s r v, "impact of mckenzie method enriched by muscle energy technique and strain counter strain technique on pain, range of motion, functional disability and quality of life in patients with chronic non-specific low back pain may 2018

21. Baharsadeghi-abdullahi, anitaeshaghi, siavashnejadhosseini, mojganghahremani, and Fereydoun DAVATCHI The efficacy of Back School on chronic low back pain of workers of a pharmaceutical company in a Tehran Suburb. COPCORD stage II study International Journal of Rheumatic Diseases 2012; 15: 144–153

22. Andrade SC, Araujo AG, Vilor MJ. Back School for the patient with non-specific chronic low back pain. Benefit from the association of an exercise program with patient education. ActaReumatol Port 2008 Oct- Dec; 33(4): 443-50

Table-1: - Comparison of Group-A (MET) and Group-B (Back School)

OUTCOME MEASURES		MEAN	SD	t VALUE	p VALUE
POST NPRS	MET	2.26	0.87	-0.34	0.443
	BACK SCHOOL	2.36	1.01	-0.34	
POST MODQ	MET	17.89	5.03	0.23	0.173
	BACK SCHOOL	17.57	3.07	0.23	
POST MMST FLEXION	MET	7.23	0.97	3.82	0.196
	BACK SCHOOL	5.82	1.27	3.82	
POST MMST EXTENSION	MET	2.63	0.52	2.82	0.911
	BACK SCHOOL	2.15	0.52	2.82	
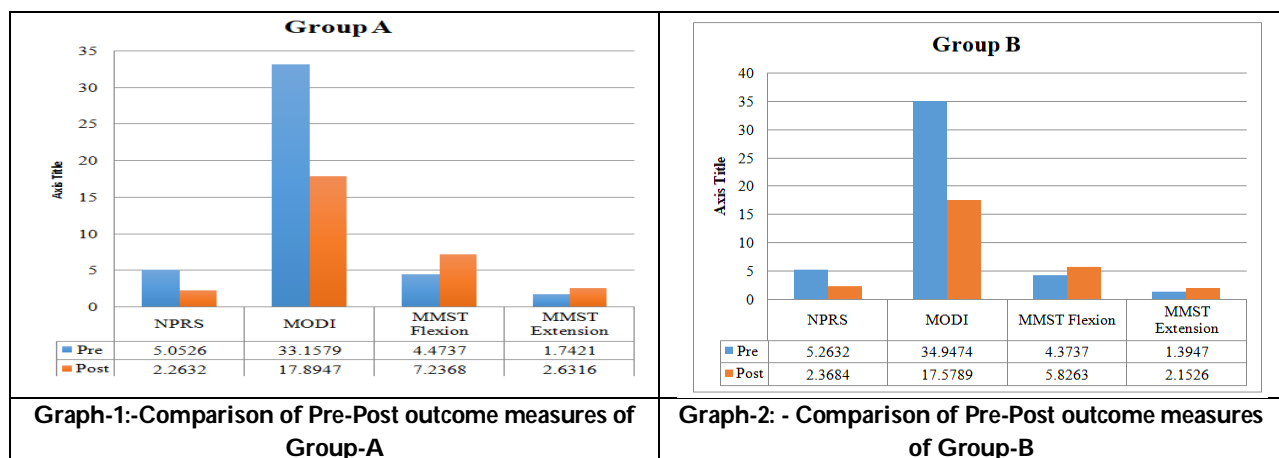
Group A				
	NPRS	MODI	MMST Flexion	MMST Extension
Pre	5.0526	33.1579	4.4737	1.7421
Post	2.2632	17.8947	7.2368	2.6316

Graph-1:-Comparison of Pre-Post outcome measures of Group-A

Group B				
	NPRS	MODI	MMST Flexion	MMST Extension
Pre	5.2632	34.9474	4.3737	1.3947
Post	2.3684	17.5789	5.8263	2.1526

Graph-2: - Comparison of Pre-Post outcome measures of Group-B

RESEARCH ARTICLE

Weakly Coupled Lower and Upper Solutions for anti-Periodic Boundary Value Problem of First Order Delay Differential Equation

Heramb Aiya[1] * and Y. S. Valaulikar[2]

[1]Research Student, School of Physical and Applied Sciences, Goa University, Taleigao Plateau - Goa - India.
[2]Ex-Faculty, Department of Mathematics, Goa University, Taleigao Plateau, Goa, India

*Address for Correspondence
Heramb Aiya
Research Student,
School of Physical and Applied Sciences,
Goa University, Taleigao Plateau - Goa - India.
E.Mail: heramb.aiya@gmail.com

ABSTRACT

We first state lemma concerning bounded linear operator and its inverse and also state Schauder's fixed point theorem. We then define weakly coupled lower and upper solution for anti-periodic boundary value problem of first order delay differential equation of the type, $w'(x) + \theta w(x) = g(x, w(x - k))$. We also provide with the definition of solution for this problem. Then, using stated lemma and Schauder's fixed point theorem we prove that there exists a solution between weakly coupled lower and upper solution. We assume that 'g' to be a non-decreasing function in the second coordinate.

Keywords: lemma, operator, boundary, solution

INTRODUCTION

There are many real world problems in Economics, Biological systems, Physical models and many more involve the study of boundary value problems(BVPs) for differential equations with deviating arguments(DEDA). Thus, it is natural question to ask about existence of solution to such problems. One may refer to ([4], [5])for the existence theory of ordinary differential equations(ODE) as well as delay differential equations(DDE). In proving many existence results in ordinary differential equations, partial differential equations, integral equations and differential equations with deviating arguments, one may seek help of the fixed point theory, which is dealt in [10]. Methods of existence of solutions between lower and upper solutions for BVP of first order ODEs are discussed in ([6], [7], [11], [14]) and for BVP of first order DDEs are discussed in ([1], [2], [3], [8], [9], [12], [13], [15]).

Heramb Aiya and Valaulikar

We seek for a solution to Anti-Periodic Boundary Value Problem (APBVP) of First Order Delay Differential Equation (FODDE) between the weakly coupled lower and upper solution by making use of Schauder's fixed point theorem. Let $\theta > 0$, T > 0, I = [0, T], $0 < k \le T$ and $g : I \times \square \to \square$ be continuous. Then, the APBVP for FODDE, under study, has the form

$$w'(x) + \theta w(x) = g(x, w(x-k)), \ x \in I \ (1.1)$$
$$w(x) = w(0), \ x \in [-k, 0] \ (1.2)$$
$$w(0) = -w(T). \ (1.3)$$

We denote **A** to be the set of all functions defined and continuouson [– k, T] and continuously differentiable on [0, T]. Let $B = \{u \in A : u(x) = u(0), \ \forall \ x \in [-k, 0]\}$ and

$E = \{u \in A : u(x) = 0, \ \forall \ x \in [-k, 0]\}$. The norm on **A** is defined to be,

$$\|u\|_{\infty} = \sup_{x \in [-k, T]} |u(x)| + \sup_{x \in [0, T]} |u'(x)|, \forall u \in A.$$

Then, $\left(A, \|.\|_{\infty}\right), \left(B, \|.\|_{\infty}\right), \left(E, \|.\|_{\infty}\right)$ are Banach spaces.

The norm on $E \times \square$ is given to be, $\left\|(u, \xi)\right\|_{*} = \|u\|_{\infty} + |\xi|, \forall (u, \xi) \in E \times \square$.

So we may say that $\left(E \times \square, \|.\|_{*}\right)$ is also a Banach space. Let $S : B \to E \times \square$ be a linear operator. Then the operator norm of '**S**' is given by,

$$\|S\| = \sup_{\|y\|_{\infty}=1} \|Sy\|_{*}.$$

Below is the Schauder's Fixed point theorem defined without giving the proof.

Schauder's Fixed Point Theorem[10]: Consider a normed linear space '**X**' and $N : X \to X$ be such that '**N**' is continuous and compact map. If '**N(X)**' is bounded, then '**N**' admits a fixed point.

Next, we state the following Lemma's in order to prove existence result for a solution betweenweakly coupled lower and upper solution.

Lemma 1.1. Let $S : B \to E \times \square$ be an operator defined by
S[w(x)] = (u(x), w(0)), where

$$u(x) = \begin{cases} 0; & -k \le x \le 0 \\ w(x) - w(0) + \int_{0}^{x} w(t)dt; & 0 \le x \le T. \end{cases}$$

Then, (1) $S : B \to E \times \square$ is a continuous linear operator.

(2) $S^{-1} : E \times \square \to B$ exists and it is defined by

Heramb Aiya and Valaulikar

$$L^{-1}[u(x)] = \begin{cases} \gamma\,; & -k \le x \le 0 \\ \gamma e^{\theta x} + \int_0^x e^{-\theta(x-t)}u'(t)dt\,; & 0 \le x \le T. \end{cases}$$

(3) $S^{-1}:E\times\square \to B$ is a continuous linear operator.

Lemma 1.2. Let $g,\ p:I\times\square \to \square$ be continuous and $N:B \to E\times\square$ be defined by
N[w(x)] = (v(x), – p(T, w(T))), where

$$v(x) = \begin{cases} 0\,; & -k \le x \le 0 \\ \int_0^x g(t,w(t-r))dt\,; & 0 \le x \le T. \end{cases}$$

Then, $N:B \to E\times\square$ is continuous and compact.

Weakly Coupled Lower and Upper Solutions for Anti-periodic Boundary Value Problem of First Order Delay Differential Equation

We begin first by giving the definition of solution to FODDE (1.1) and (1.2) along with the definition of solution for APBVP (1.1) - (1.3). We move on to define lower and upper solutions for the FODDE (1.1) and (1.2). Then, we define strict lower and upper solution for FODDE (1.1) and (1.2) to prove that under certain conditions on function 'g', the lower solution is less than or equal to the upper solution. We further, define weakly coupled lower and upper solution for the APBVP to obtain existence of solution between weakly coupled lower and upper solution. Also, the definitions of strict weakly coupled lower and upper solution for the APBVP are given to obtain existence of solution strictly between strict weakly coupled lower and upper solution.

Definition 2.1. A function v ∈ A is said to be a solution of APBVP (1.1) - (1.3) if

1. $v'(x) + \theta v(x) = g(x, v(x - k)), x \in I$,

2. $v(x) = v(0), x \in [-k, 0]$,

3. $v(0) = v(T)$.

Definition 2.2. A function v ∈ A is said to be a solution of FODDE (1.1) and (1.3) if

1. $v'(x) + \theta v(x) = g(x, v(x - k)), x \in I$,

2. $v(x) = v(0), x \in [-k, 0]$.

Definition 2.3. A function $\rho \in A$ is said to be a lower solution of FODDE (1.1) and (1.2) if

1. $\rho'(x) + \theta\rho(x) \le g(x, \rho(x - k)), x \in I$,

2. $\rho(x) \le \rho(0), x \in [-k, 0]$.

A function $\sigma \in A$ is said to be an upper solution of FODDE (1.1) and (1.2) if he above inequalities are reversed.

Definition 2.4. A function $\rho \in A$ is called a strict lower solution of FODDE (1.1) and (1.2) if 1.
$$\rho'(x) + \theta\rho(x) < g(x, \rho(x - r)), x \in I,$$
2. $\rho(x) \le \rho(0), x \in [-k, 0]$.

Definition 2.5. A function $\sigma \in A$ is called a strict upper solution of FODDE (1.1) and (1.2) if 1.
$$\sigma'(x) + \theta\sigma(x) > g(x, \sigma(x - k)), x \in I,$$
2. $\sigma(x) \geq \sigma(0), x \in [-k, 0].$

Definition 2.6. A pair of functions $\rho, \sigma \in A$ are called weakly coupled lower and upper solution of APBVP (1.1) - (1.3) if

1. $\rho'(x) + \theta\rho(x) \leq g(x, \rho(x - k)), x \in I,$
2. $\sigma'(x) + \theta\sigma(x) \geq g(x, \sigma(x - k)), x \in I,$
3. $\rho(x) \leq \rho(0), x \in [-k, 0],$
4. $\sigma(x) \geq \sigma(0), x \in [-k, 0],$
5. $\rho(x) \leq \sigma(x), x \in [-k, T],$
6. $\rho(0) \leq -\sigma(T), x \in [-k, 0],$
7. $\sigma(0) \geq -\rho(T), x \in [-k, 0].$

Definition 2.7. A pair of coupled lower and upper solutions $\rho, \sigma \in A$ of APBVP (1.1) - (1.3) are called strict weakly coupled lower and upper solutions of APBVP (1.1) - (1.3) if
1. $\rho'(x) + \theta\rho(x) \leq g(x, \rho(x - k)), x \in I,$
2. $\sigma'(x) + \theta\sigma(x) > g(x, \sigma(x - k)), x \in I.$

Theorem 2.1. Let $g : I \times \square \rightarrow \square$ be continuous and $g(x, u) \leq g(x, v), \forall (x, u), (x, v) \in I \times \square$ such that $u \leq v$. Let $\rho \in B$ be a strict lower solution of FODDE (1.1) and (1.2). Let $\sigma \in B$ be an upper solution of FODDE (1.1) and (1.2). Then, $\rho(0) \leq \sigma(0)$ implies $\rho(x) \leq \sigma(x), \forall x \in [-k, 0]$ and $\rho(x) < \sigma(x), \forall x \in (0, T].$

Proof. It is given that $\rho(0) \leq \sigma(0)$. Therefore, $\rho(x) \leq \sigma(x), \forall x \in [-k, 0].$

Therefore, it is sufficient to prove that $\rho(x) < \sigma(x), \forall x \in (0, T].$

On the contrary, assume that $\exists x_0 \in (0, T]$ such that $\rho(x) < \sigma(x), \forall x \in (0, x_0)$ and $\rho(x_0) = \sigma(x_0).$
Therefore, $\sigma'(x_0) \leq \rho'(x_0).$
This gives, $g(x_0, \sigma(x_0 - k)) < g(x_0, \rho(x_0 - k)).$

CASE-1: Let $0 < x_0 \leq k.$
Therefore, $-k < x_0 - k \leq 0.$
So, we have $\rho(x_0 - k) \leq \sigma(x_0 - k).$
As 'g' is non-decreasing in the second co-ordinate,
we have $g(x_0, \rho(x_0 - k)) \leq g(x_0, \sigma(x_0 - k)),$ which leads to a contradiction.

CASE-2: Let $k < x_0 \leq T.$
Therefore, $0 < x_0 - k < x_0.$

Heramb Aiya and Valaulikar

So, we have $\rho(x_0 - k) \le \sigma(x_0 - k)$.

As 'g' is non-decreasing in the second co-ordinate,

we have $g(x_0, \rho(x_0 - k)) \le g(x_0, \sigma(x_0 - k))$, which leads to a contradiction.

Thus, $\rho(x) < \sigma(x), \ \forall \, x \in (0, T]$.

Hence, $\rho(x) \le \sigma(x), \ \forall \, x \in [-k, 0]$ and $\rho(x) < \sigma(x), \ \forall \, x \in (0, T]$. $\square$

Theorem 2.2. Let $g: I \times \square \to \square$ be continuous and $g(x, u) \le g(x, v), \ \forall (x, u), (x, v) \in I \times \square$ such that $u \le v$. Let $\rho \in B$ be a lower solution of FODDE (1.1) and (1.2). Let $\sigma \in B$ be a strict upper solution of FODDE (1.1) and (1.2). Then, $\rho(0) \le \sigma(0)$ implies $\rho(x) \le \sigma(x), \ \forall \, x \in [-k, 0]$ and $\rho(x) < \sigma(x), \ \forall \, x \in (0, T]$.

Proof. Similar to the proof of theorem 2.1.　　　　　　　　　　　　　$\square$

We are now ready to prove the existence theorem for solution between weakly coupled lower and upper solution for the given APBVP.

Theorem 2.3. Let $g: I \times \square \to \square$ be continuous and $g(x, u) \le g(x, v), \ \forall (x, u), (x, v) \in I \times \square$ such that $u \le v$. Let $\rho, \ \sigma \in B$ be weakly coupled lower and upper solution of APBVP (1.1) - (1.3). Then, the APBVP (1.1) - (1.3) has atleast one solution $w \in B$ such that $\rho(x) \le w(x) \le \sigma(x), \ \forall \, x \in [-k, T]$.

Proof. Let $p: I \times \square \to \square$ be defined by,

$p(x, u) = \max\{ \rho(x), \min\{u, \sigma(x)\} \}, \ \forall \ (x, u) \in I \times \square$.

Then, $\rho(x) \le p(x, u) \le \sigma(x), \ \forall \ (x, u) \in I \times \square$.

Also, $p: I \times \square \to \square$ is continuous and bounded.

Let $G^*: I \times \square \to \square$ be defined by,

$$G^*(x, w) = \begin{cases} g(x, \rho(x-k)); & w \le \rho(x-k), \\ g(x, w); & \rho(x-k) \le w \le \sigma(x-k), \\ g(x, \sigma(x-k)); & \sigma(x-k) \le w. \end{cases}$$

Therefore, $G^*: I \times \square \to \square$ is continuous and bounded.

Let $S: B \to E \times \square$ be defined as in Lemma 1.1.

Therefore, $S: B \to E \times \square$ is linear, continuous and bijective.

Also, $S^{-1}: E \times \square \to B$ exists and is defined as in Lemma 1.1.

Further, $S^{-1}: E \times \square \to B$ is also continuous.

Let $N: B \to E \times \square$ be defined as in Lemma 1.2.

Therefore, $N: B \to E \times \square$ is compact and continuous.

Heramb Aiya and Valaulikar

Let $J=S^{-1} N:B \to B$. Then,

$$J[w(x)] = \begin{cases} -p(T, w(T)); & -k \leq x \leq 0 \\ -p(T, w(T))e^{-\theta x} + \int_0^x e^{-\theta(x-t)}F^*(t, w(t-k)dt; & 0 \leq x \leq T. \end{cases}$$

A fixed point of $J:B \to B$ is a solution of

$$w'(x) + \theta w(x) = F^*(x, w(x-k)), \ x \in I \text{ (2.1)}$$
$$w(x) = w(0), \ x \in [-k, 0]$$
$$w(0) = -p(T, w(T)). \text{ (2.2)}$$

Also, $J:B \to B$ compact and continuous.

Further, 'p' and 'G'' are bounded implies that **J(B)** is a bounded subset of $(B, \|.\|_\infty)$.

So, by applying the Schauder's fixed point theorem, $J:B \to B$ has a fixed point $w \in B.$
Therefore, 'w' is a solution of (2.1), (1.2) and (2.2).

We show that $\rho(x) \leq w(x) \leq \sigma(x), \ \forall\, x \in [-k, T].$
As $-\sigma(0) \leq \rho(T) \leq p(T, w(T)) \leq \sigma(T) \leq -\rho(0)$, we have $\rho(0) \leq -p(T, w(T)) \leq \sigma(0).$
This implies, $\rho(0) \leq w(0) \leq \sigma(0).$
Thus, $\rho(x) \leq w(x) \leq \sigma(x), \ \forall\, x \in [-k, 0].$

Therefore, it is enough to show that $\rho(x) \leq w(x) \leq \sigma(x), \ \forall\, x \in (0, T].$

Let $\varepsilon > 0$ be arbitrary.

Define, $\rho_\varepsilon(x) = \rho(x) - \varepsilon(x + 2k), \ \forall\, x \in [-k, T]$ and $\sigma_\varepsilon(x) = \sigma(x) - \varepsilon(x + 2k), \ \forall\, x \in [-k, T].$
Therefore, $\rho_\varepsilon(0) < w(0) < \sigma_\varepsilon(0).$

So, we prove that $\rho_\varepsilon(x) < w(x) < \sigma_\varepsilon(x) \ \forall\, x \in (0, T].$

On the contrary let us assume that, $\exists\, x_0 \in (0, T]$ such that $\rho_\varepsilon(x) < w(x) < \sigma_\varepsilon(x), \ \forall\, x \in (0, x_0)$ and $w(x_0) = \sigma_\varepsilon(x_0).$

Therefore, $w(x_0) > \sigma(x_0)$ and $\sigma_\varepsilon'(x_0) \leq w'(x_0).$

<u>CASE-1</u>: Let $0 < x_0 \leq k.$
Therefore, $-k < x_0 - k \leq 0.$
So, we have $\rho(x_0 - k) \leq w(x_0 - k) \leq \sigma(x_0 - k).$

Heramb Aiya and Valaulikar

Therefore, $w'(x_0) = G^*(x_0, w(x_0 - k)) - \theta w(x_0)$

$$= g(x_0, w(x_0 - k)) - \theta w(x_0)$$

$$\leq g(x_0, \sigma(x_0 - k)) - \theta \sigma(x_0)$$

$$\leq \sigma'(x_0)$$

$$< \sigma_\varepsilon'(x_0), \text{which leads to a contradiction.}$$

CASE-2: Let $k < x_0 \leq T$.

Therefore, $0 < x_0 - k < x_0$.

So, we have $\rho_\varepsilon(x_0 - k) < w(x_0 - k) < \sigma_\varepsilon(x_0 - k)$.

CASE-2.1: Let $w(x_0 - k) < \rho(x_0 - k)$.

Therefore, $w'(x_0) = G^*(x_0, w(x_0 - k)) - \theta w(x_0)$

$$= g(x_0, \rho(x_0 - k)) - \theta w(x_0)$$

$$\leq g(x_0, \sigma(x_0 - k)) - \theta \sigma(x_0)$$

$$\leq \sigma'(x_0)$$

$$< \sigma_\varepsilon'(x_0), \text{which leads to a contradiction.}$$

CASE-2.2: Let $\rho(x_0 - k) \leq w(x_0 - k) \leq \sigma(x_0 - k)$.

Then by CASE-1 we get $w'(x_0) < \sigma_\varepsilon'(x_0)$, which leads to a contradiction.

CASE-2.3: Let $w(x_0 - k) > \sigma(x_0 - k)$.

Therefore, $w'(x_0) = G^*(x_0, w(x_0 - k)) - \theta w(x_0)$

$$= g(x_0, \sigma(x_0 - k)) - \theta w(x_0)$$

$$< g(x_0, \sigma(x_0 - k)) - \theta \sigma(x_0)$$

$$\leq \sigma'(x_0)$$

$$< \sigma_\varepsilon'(x_0), \text{which leads to a contradiction.}$$

Thus, we conclude that $\rho_\varepsilon(x) < w(x) < \sigma_\varepsilon(x), \forall x \in [0, T]$.

Taking $\varepsilon \to 0$ we get, $\rho(x) \leq w(x) \leq \sigma(x), \forall x \in [0, T]$.

This implies, $\rho(x) \leq w(x) \leq \sigma(x), \forall t \in [-k, T]$.

Therefore, $G^*(x, w(x-k)) = g(x, w(x-k)), \forall x \in I$ and p(T, w(T)) = w(T).

Hence, $w \in B$ is a solution of APBVP (1.1) – (1.3) such that

$\rho(x) \leq w(x) \leq \sigma(x), \forall x \in [-k, T].$ ▢

Consider the following example to illustrate theorem 2.3.

$$w'(x) + w(x) = w(x-1)+1, \ x \in [0, 1],$$

$$w(x) = w(0), \ x \in [-1, 0],$$

$$w(0) = -w(1).$$

Here, k = 1, T = 1, I = [0, 1] and g (x, u) = u + 1, $\forall$ (x, u) $\in$ I × $\square$.

Therefore, g(t, w (x – 1))= w (x – 1) + 1, $\forall$ x $\in$ I.

Also, 'g' is non-decreasing in the second coordinate.

Let $\rho : [-1, 1] \rightarrow \square$ be defined as,

$$\rho(x) = \begin{cases} \dfrac{e^{-1}}{2} - 1; & -1 \leq x \leq 0, \\[4mm] \dfrac{e^{-1}}{2} - e^{-x}; & 0 \leq x \leq 1. \end{cases}$$

Therefore, $\rho(0) = \dfrac{e^{-1}}{2} - 1$ and $\rho(1) = -\dfrac{e^{-1}}{2}.$

Also, $\rho'(x) + \rho(x) = \rho(x-1) + 1, \ \forall x \in [0,1].$

Let $\sigma : [-1, 1] \rightarrow \square$ be defined as,

$$\sigma(x) = \begin{cases} \dfrac{e^{-1}}{2}; & -1 \leq x \leq 0, \\[4mm] \dfrac{e^{-1}}{2} + 1 - e^{-x}; & 0 \leq x \leq 1. \end{cases}$$

Therefore, $\sigma(0) = \dfrac{e^{-1}}{2}$ and $\sigma(1) = \dfrac{e^{-1}}{2} - 1.$

Also, $\sigma'(x) + \sigma(x) = \sigma(x-1) + 1, \ \forall x \in [0,1].$

So, we can say that $\rho \text{ and } \sigma$ are coupled lower and upper solution of the given APBVP.

Now, let $y : [-1, 1] \rightarrow \square$ be defined as,

$$y(x) = \begin{cases} \dfrac{e^{-1}-1}{2}\,; & -1 \le x \le 0, \\[4mm] \dfrac{e^{-1}+1}{2} - e^{-x}\,; & 0 \le x \le 1. \end{cases}$$

Then, 'y' is a solution of given APBVP such that $\rho(x) \le y(x) \le \sigma(x), \ \forall\, x \in [-1,\,1].$

Next we prove the result concerning strict weakly coupled lower and upper solutions
for APBVP (1.1) - (1.3).

Theorem 2.4. Let $g : I \times \Box \rightarrow \Box$ be continuous and $g(x, u) \le g(x, v), \ \forall (x, u), (x, v) \in I \times \Box$ such that $u \le v$.
Let $\rho, \ \sigma \in B$ be strict weakly coupled lower and upper solution of APBVP (1.1) -(1.3). Then, the APBVP (1.1) - (1.3)
has atleast one solution $w \in B$ such that $\rho(x) \le w(x) \le \sigma(x), \ \forall\, x \in [-k,\, 0]$ and
$\rho(x) < w(x) < \sigma(x), \ \forall\, x \in (0,\, T].$

Proof. Let p, G*, S, N and J be as defined in Theorem 2.3.

So, by applying the Schauder's fixed point theorem, $J : B \rightarrow B$ has a fixed point $w \in B.$
Therefore, 'w' is a solution of (2.1), (1.2) and (2.2).

We show that $\rho(x) \le w(x) \le \sigma(x), \ \forall\, x \in [-k,\, T].$
As $-\sigma(0) \le \rho(T) \le p(T, w(T)) \le \sigma(T) \le -\rho(0)$, we have $\rho(0) \le -p(T, w(T)) \le \sigma(0).$
This implies, $\rho(0) \le w(0) \le \sigma(0).$
Thus, $\rho(x) \le w(x) \le \sigma(x), \ \forall\, x \in [-k,\, 0].$

Therefore, it is enough to show that $\rho(x) < w(x) < \sigma(x), \ \forall\, x \in (0,\, T].$

On the contrary let us assume that, $\exists\, x_0 \in (0, T]$ such that $\rho(x) < w(x) < \sigma(x), \ \forall\, x \in (0,\, x_0)$ and
$w(x_0) = \sigma(x_0).$
Therefore, $\sigma'(x_0) \le w'(x_0).$

<u>CASE-1</u>: Let $0 < x_0 \le k.$
This implies, $-k < x_0 - k \le 0.$
So, we have $\rho(x_0 - k) \le w(x_0 - k) \le \sigma(x_0 - k).$
Therefore, $w'(x_0) = G^*(x_0, w(x_0 - k)) - \theta w(x_0)$
$$= g(x_0, w(x_0 - k)) - \theta w(x_0)$$
$$\le g(x_0, \sigma(x_0 - k)) - \theta \sigma(x_0)$$
$$< \sigma'(x_0), \text{ which leads to a contradiction.}$$

Heramb Aiya and Valaulikar

<u>CASE-2</u>: Let $k < x_0 - k \leq T$.

This implies, $0 < x_0 - k < x_0$.

So, we have $\rho(x_0 - k) < w(x_0 - k) < \sigma(x_0 - k)$.

Therefore, $w'(x_0) = G^*(x_0, w(x_0 - k)) - \theta w(x_0)$

$$= g(x_0, w(x_0 - k)) - \theta w(x_0)$$

$$\leq g(x_0, \sigma(x_0 - k)) - \theta \sigma(x_0)$$

$$< \sigma'(x_0), \text{ which leads to a contradiction.}$$

Thus, from CASE-1 and CASE-2 we have $\rho(x) < w(x) < \sigma(x), \forall x \in (0, T]$.

Therefore, $G^*(x, w(x-k)) = g(x, w(x-k)), \forall x \in I$ and $p(T, w(T)) = w(T)$.

Hence, $w \in X$ is a solution of APBVP (1.1) – (1.3) such that

$\rho(x) \leq w(x) \leq \sigma(x), \forall x \in [-k, 0]$ and $\rho(x) < w(x) < \sigma(x), \forall x \in (0, T]$. □

REFERENCES

1. H. Aiya, Y.S.Valaulikar; Some Existence Theorems for Periodic Boundary Value Problem ofFirst Order Delay Differential Equation, Mapana-Journal of Sciences , Vol.22, Special Issue1,(2023), 13-31. ISSN 0975-3303 — https://doi.org/10.12723/mjs.spl.2.
2. M. Bachar, M. A. Khamsi; Delay differential equations: a partially ordered set approach invectorial metric spaces, Fixed point theory and applications: A springer open journal, 193(2014), 1–9.
3. A. Boichuk, J. Diblik, D. Khusainov, M. Ruzickova; Boundary value problems for delay differential systems, Advcs. Difference Eqns., 2010 (2010), Article ID 593834.
4. S. G. Deo, V. Raghavendra, R. Kar, V. Laksmikantham; Textbook of ordinary differentialequations, McGraw Hill, 3 (2015), 1–425.
5. R. D. Driver; Ordinary and delay differential equations, Springer - Verlag, (1977), 225-448.
6. D. Franco, J. Nieto, D. O'Regan; Anti-periodic boundary value problem for nonlinear firstorder ordinary differential equations J. Math. Ineq. Appl., 6 (2003), 477–485.
7. D. Franco, J. Nieto, D. O'Regan; Upper and lower solutions for first order problems withnonlinear boundary conditions. ExtractaMathematicae, 18 (2003), 153–160.
8. L. J. Grimm, K. Schmitt; Boundary value problems for delay differential equations, Bull.Amer. Math. Soc., 5 (1968) 997–1000.
9. T. Jankowski; On delay differential equations with boundary conditions, Dynamic Systemsand applications, 16 (2007), 425–32.
10. M. C. Joshi, R. K. Bose; Some topics in nonlinear functional analysis, Wiley Eastern Ltd., 1(1985), 1–285.
11. V. Lakshmikantham; Periodic boundary value problem for first and second order differentialequations, Jour. of Appl. Math. and Simulation(Vol.2), 3 (1989) 131–138.
12. S. Leela, M. N. Oˇguztoreli; Periodic boundary value problem for differential equations withdelay and monotone iterative method, Journal of Math. Anal. and Appls., 122 (1987) 301–307.
13. S. Ohkohchi; A boundary value problem for delay differential equations, Hiroshima Math. J.,7 (1977), 379–385.
14. C. C. Tisdell; Existence of solutions to first order periodic boundary value problems, J. ofMath. Anl. and Appl., 323 (2006), 1325–1332.
15. G. Zhang, S. S. Cheng; Positive periodic solutions of no autonomous functional differential equations depending on a parameter, Abst. and Appl. Anal., 7 (2002), 279–286.

RESEARCH ARTICLE

Generalized Semi Pre Connected Space in Neutrosophic Topological Spaces

L.Praveenkumar[1], G.Mahadevan [2]* and C.Sivagnanam[3]

[1]Department of Mathematics, The Gandhigram Rural Institute-Deemed to be University, Gandhigram, Tamilnadu-624302, India.
[2]Department of General Requirements, University of Technology and Applied Science-Sur, Sultanate of Oman.

*Address for Correspondence
G.Mahadevan
Department of General Requirements,
University of Technology and Applied Science-Sur,
Sultanate of Oman.
E. Mail: rajeshw851@gmail.com

ABSTRACT

In this manuscript, we inaugurate Neutrosophic generalized semi-pre connected space. We investigate its properties. Also, we add some improvisation of neutrosophic generalized semi pre connected space.

INTRODUCTION

In 2014, the pioneering work of Salama, Smarandache, and Valeri [10] introduced the concept of Neutrosophic closed sets and Neutrosophic continuous functions. Subsequent advancements by Salama and Alblowi [11] led to the development of generalized Neutrosophic sets and generalized Neutrosophic topological spaces. In their publication [25], Rajeshwaran N and Chandramathi N presented the novel idea of Neutrosophic generalized semi pre closed sets within the realm of Neutrosophic topological spaces. Similarly, in another work [26], they introduced the concept of Neutrosophic generalized semi pre Homeomorphisms in the same context. This manuscript seeks to define and investigate the concept of Neutrosophic generalized semi pre-connected space, delving into its inherent properties. The study encompasses an exploration of various related notions and introduces a collection of noteworthy theorems within this domain.

Preliminaries
Definition 2.1: [10] A neutrosophic topology (NT for short) a non-empty set X is a family τ_N of neutrosophic subsets in X adheres the following axioms

(NT1)$0_N, 1_N \in \tau_N$
(NT2)$G_1 \cap G_2 \in \tau_N$
(NT3) $\cup G_i \in \tau_N$, $\forall \{G_i : i \in J\} \subseteq \tau_N$
Here (X_1, τ_N) is called a neutrosophic topological space (NTS for short).

Definition 2.2: [10] Let A_1 *and* A_2 be two Neutrosophic Sets (NS for Short) of the form
$A_1 = \{\langle X, \mu_{A_1}(X), \sigma_{A_1}(X), \gamma_{A_1}(X)\rangle : x \epsilon X\}$, $A_2 = \{\langle X, \mu_{A_2}(X), \sigma_{A_2}(X), \gamma_{A_2}(X)\rangle : x \epsilon X\}$
$A_1 \subseteq A_2$ if and only if
$\mu_{A_1}(X) \leq \mu_{A_2}(X), \sigma_{A_1}(X) \leq \sigma_{A_2}(X)$ and $\gamma_{A_1}(X) \geq \gamma_{A_2}(X)$ for all $x \in X$
(b) $A_1{}^C = \{\langle X, \gamma_{A_1}(X), 1 - \sigma_{A_1}(X), \mu_{A_1}(X)\rangle : x \epsilon X\}$
(c)$A_1 \cap A_2 = \{\langle X, \mu_{A_1}(X) \wedge \mu_{A_2}(X), \sigma_{A_1}(X) \wedge \sigma_{A_2}(X), \gamma_{A_1}(X) \vee \gamma_{A_2}(X)\rangle : x \epsilon X\}$
(d)$A_1 \cup A_2 = \{\langle X, \mu_{A_1}(X) \vee \mu_{A_2}(X), \sigma_{A_1}(X) \vee \sigma_{A_2}(X), \gamma_{A_1}(X) \wedge \gamma_{A_2}(X)\rangle : x \epsilon X\}$

Definition 2.3: [25] Let (X_1, τ_N) be a neutrosophic topological space. A subset A_1 of (X_1, τ_N) is called Neutrosophic generalized semi pre closed set [Neutrosophic gsp-closed] if Nspcl $(A_1) \subseteq W$, whenever $A_1 \subseteq W$ and W is NOS.

Definition 2.4: [25] A NT (X_1, τ_N) is said to be an Neutrosophic C_5-connected (NC$_5$-connected for short) space if the only NS which are both a NOS and a NCS are 0_N and 1_N.

Definition 2.5: [26] A bijection $g: (X_1, \tau_N) \rightarrow (X_2, \sigma_N)$ is denoted NGSP homeomorphism if g is both NGSP continuous and NGSP open map.

Neutrosophic Generalized Semi Pre Connected Space

Definition.3.1: A Neutrosophic topology (X, τ_N) is said to be Neutrosophic generalized semi pre connected space (NGSP connected space for short) if the only NSs which are both a NGSPOS and a NGSPCS are 0_N and 1_N.

Example3.2: Let $X = \{a,b\}$ and $\tau_N = \{0_N, 1_N, K\}$ be a NT on (X, τ_N) where $K = \{x, \langle 0.5, 0.6, 0.5 \rangle, \langle 0.5, 0.4, 0.5 \rangle\}$ .Then (X, τ_N) is a NGSP Connected space.

Theorem: 3.3: Every NGSP connected space is NC$_5$- connected space   but not conversely.

Proof: Let (X, τ_N) be NGSP-connected space. Suppose (X, τ_N) is not an NC$_5$- connected space, then there exists a proper NS D which is both NOS and a NCS in (X, τ_N). That is, D is both NGSPOS and a NGSPCS in (X, τ_N). So, (X, τ_N) is not a NGSP connected space. This is a contradiction. Therefore (X, τ_N) be a NC$_5$- connected space.

Example3.4: Let $X = \{a,b\}$ and $K = \{\langle 0.5, 0.6, 0.5 \rangle, \langle 0.5, 0.4, 0.5 \rangle\}$ .Then $\tau_N = \{0_N, 1_N, K_1\}$ is a NT on (X, τ_N). Then (X, τ_N) is a NC$_5$- connected space but not NGSP connected space, since NS K in (X, τ_N) is both a NGSPCS and NGSPOS in (X, τ_N).

Theorem 3.5: Every NGSP connected space is NGO-connected space but not conversely.

Proof: Let (X, τ_N) is NGSP-connected space. Suppose (X, τ_N) is not a NGO- connected space, then there exists a proper NS D which is both a NGOS and NGCS in (X, τ_N). D is both NGSPOS and NGSPCS in (X, τ_N) . This implies that (X, τ_N) is not a NGSP connected space. This is a contradiction. Therefore (X, τ_N) be a NGO-connected space.

Example 3.6: In Example 3.4, (X, τ_N) is a NGO-connected space but not a NGSP connected space.

Theorem 3.7: The NT (X, τ_N) is a NGSP-connected space if and only if there exists no non-zero NGSPOS A and D in (X, τ_N) such that $A = D^C$.

Proof: Necessity: Assume that (X, τ_N) is an NGSP-connected space. Let A and D be two NGSPOS in (X_1, τ_N) such that $A \neq 0_N \neq D$ and $A = D^C$. Therefore D^C is a NGSPCS. Since $A \neq 0_N$, $D \neq 1_N$. This implies D is a proper NS which is both a NGSPOS and a NGSPCS in (X, τ_N). Hence (X, τ_N) is not a NGSP connected space. But this is a contradiction to our hypothesis. Thus there exists no non-zero NGSPOS A and D in (X, τ_N) such that $A = D^C$.

Sufficiency: Let A both a NGSPOS and NGSPCS in (X, τ_N) such that $1_N \neq A \neq 0_N$. Now let $D = A^C$. Then D is a NGSPOS and $D \neq 1_N$. This implies $D = A^C \neq 0_N$ which is a contradiction to our hypothesis. Therefore (X, τ_N) a NGSP connected space.

Theorem 3.8: A NT (X, τ_N) is an NGSP connected space if and only if there exists no non-zero NGSPOSs A and D in (X, τ_N) such that $A = D^C$, $D = (Nspcl(A))^C$, $A = (Nspcl(D))^C$.

Proof: Necessity: Assume that there exist NSs A and D such that $A \neq 0_N \neq D$, $D = A^C$, $D = (Nspcl(A))^C$, $A = (Nspcl(D))^C$. Since $(Nspcl(A))^C$ and $(Nspcl(D))^C$ are NGSPOSs in (X, τ_N) A and D are NGSPOSs in (X, τ_N). This implies (X, τ_N) is not a NGSP connected space, which is a contradiction. Therefore there exists no non-zero NGSPOSs A and D in (X, τ_N) such that $A = D^C$, $D = (Nspcl(A))^C$, $A = (Nspcl(D))^C$.

Sufficiency: Let A be both a NGSPOS and a NGSPCS in (X, τ_N) such that $1_N \neq A \neq 0_N$. Now by taking $D = A^C$, we obtain a contradiction to our hypothesis. Hence (X, τ_N) is a NGSP connected space.

Remark 3.9: Every Neutrosophic semi-pre $T_{1/2}$ space is an Neutrosophic semi-pre $T_{1/2}$ space but not conversely.

Proof: Let (X, τ_N) be a Neutrosophic semi-pre $T_{1/2}$ space. Let D be an in- Neutrosophic generalized semi-pre closed set in (X, τ_N). By hypothesis D is a Neutrosophic closed set. Since every Neutrosophic closed set is a Neutrosophic semi-preclosed set, D is a Neutrosophic semi-preclosed set in (X, τ_N). Hence (X, τ_N) is a Neutrosophic semi-pre $T_{1/2}$ space.

Example 3.10: In Example 3.4 the NTS (X, τ_N) is a $NT_{1/2}$ space but not a $NSPT_{1/2}$ space, since the NS D is a NGSP closed set in (X, τ_N) but not a NC in (X, τ_N), since $Ncl(D) = D^C \neq D$

Theorem 3.11: If $\varphi_N : (X, \tau_N) \rightarrow (Y, \sigma_N)$ is a NGSP continuous surjection and (X, τ_N) is a NGSP connected space, then (Y, σ_N) is a NC₅-connected space.

Proof: Let (X, τ_N) be a NGSP connected space. Suppose (Y, σ_N) is not an NC₅-connected space, then there exists a proper NS D which is both a NOS and a NCS in (Y, σ_N). Since φ_N is a NGSP continuous mapping, $\varphi_N^{-1}(D)$ is both a NGSPOS and NGSPCS in (X, τ_N). This is a contradiction to our hypothesis. Hence (Y, σ_N) be a NC₅-connected space.

Theorem 3.12: If $\varphi_N : (X, \tau_N) \rightarrow (Y, \sigma_N)$ is a NGSP irresolute surjection and (X, τ_N) is NGSP connected space, then (Y, σ_N) is also NGSP connected space.

Proof: Suppose (Y, σ_N) is not a NGSP connected space, then there exists a proper NS D such that D is both NGSPOS and NGSPCS in (Y, σ_N) Since φ_N is a NGSP irresolute mapping, $\varphi_N^{-1}(D)$ is both NGSPOS and NGSPCS in (X, τ_N). This is a contradiction to our hypothesis. Hence (Y, σ_N) is NGSP connected space.

Theorem 3.13: If a NT (X, τ_N) is NGSP connected between two NS A and B, then it is NC₅-connected between two NSs A and B but the converse may not be true in general.

Proof: Suppose (X, τ_N) is not NC₅-connected between A and B, then there exists a NOS D in (X, τ_N) such that $A \subseteq D$ and $Dq^C B$. Since every NOS is a NGSPOS, there exists a NGSPOS D in (X, τ_N) such that $A \subseteq D$ and $Dq^C B$. This implies (X, τ_N) is not NGSP connected between A and B, a contradiction to our hypothesis. So, (X, τ_N) is NC₅-connected between A and B

Example3.14: Let $X = \{a, b\}$ and $K_1 = \{x, \langle 0.5, 0.4, 0.5 \rangle, \langle 0.5, 0.6, 0.5 \rangle\}$. Then $\tau_N = \{0_N, 1_N, K_1\}$ is a NT on (X, τ_N). Let $A = \{x, \langle 0.4, 0.4, 0.4 \rangle, \langle 0.6, 0.6, 0.6 \rangle\}$ and $B = \{x, \langle 0.3, 0.3, 0.3 \rangle, \langle 0.4, 0.4, 0.4 \rangle\}$ be two NS in (X, τ_N). Then (X, τ_N) is a NC₅-connected between A and B, since there exists no NOS D in (X, τ_N) But it is not NGSP connected between the two NS A and B, since there exists an NGSPOS $D = \{\langle 0.4, 0.4, 0.4 \rangle, \langle 0.5, 0.5, 0.5 \rangle\}$ in (X, τ_N) such that $A \subseteq D$ and $Dq^C B$

Theorem 3.15: A NT (X, τ_N) is NGSP connected between two NS A and B if and only if there is no NGSPOS and NGSPCS D in (X, τ_N) such that $A \subseteq D \subseteq B^C$.

Proof: Necessity: Let (X, τ_N) be NGSP connected between A and B. Suppose that there exists a NGSPOS and NGSPCS D in (X, τ_N) such that $A \subseteq D \subseteq B^C$, then D q B. and $A \subseteq D$. This implies (X, τ_N) is not NGSP connected between A and B, by Definition 3.2 A contradiction to our hypothesis. Therefore there exists no NGSPOS and a NGSPCS D in (X, τ_N) such that $A \subseteq D \subseteq B^C$.

Sufficiency: Suppose that (X, τ_N) is not NGSP connected between A and B. Then there exists a NGSPOS D in (X, τ_N) such that $A \subseteq D$ and D q B. This implies that there exists a NGSPOS D in (X, τ_N) such that $A \subseteq D \subseteq B^C$. This is a contradiction to our hypothesis. Hence (X, τ_N) is NGSP connected.

Theorem 3.16. Let (X, τ_N) be an NTS and A and B be NSs in (X, τ_N). If AqB, then (X, τ_N) is Neutrosophic generalized semi-pre connected between A and B.

Proof: Suppose (X, τ_N) is not Neutrosophic generalized semi-pre connected between A and B. Then there exists a Neutrosophic generalized semi-pre open set $\mathcal{D}$ in (X, τ_N) such that $A \subseteq \mathcal{D}$ and $\mathcal{D} \subseteq B^C$. This implies that $A \subseteq B^C$. That is $Aq^C B$. This is a contradiction to our hypothesis. Therefore (X, τ_N) is Neutrosophic generalized semi-pre connected between A and B.

REFERENCES

1. Atanassov.K. T, Intuitionistic fuzzy sets, Fuzzy Sets and Systems, 20(1986), 87–96.
2. Chang.C. L, Fuzzy topological spaces, Journal of Mathematical Analysis and Application, 24(1968), 183–190.
3. Dhavaseelan.R and Jafari, Generalized Neutrosophic closed sets, new trends in Neutrosophic theory and applications, 2(2018), 261-273.
4. Dogan Coker, An introduction to intuitionstic fuzzy topological spaces, Fuzzy Sets and Systems, 88(1997), 81–89.
5. Floretin Smarandache, Neutrosophy and Neutrosophic Logic, First International Conference on Neutrosophy, Neutrosophic Logic, Set, Probability, and Statistics University of New Mexico, Gallup, NM 87301,USA, 2002.
6. Floretin Smarandache, Neutrosophic Set:- A Generalization of Intuitionistiic Fuzzy set, Journal of Defense Resourses Management, 1(2010),107–116.
7. Floretin Smarandache, A Unifying Field in Logic: Neutrosophic Logic. Neutrosophy, Neutrosophic set, Neutrosophic Probability. Ameican Research Press, Rehoboth, NM, 1999.
8. Ishwarya.P and K. Bageerathi, On Neutrosophicsemi-open sets in Neutrosophic topological spaces, International Jour. of Math. Trends and Tech. 2016, 214-223.
9. Levine N. Generalized closed sets in topology. Rend. Cire. Math. Palermo. 19(2) (1970), 89–96.
10. Salama A.A and Alblowi S.A, Neutrosophic set and Neutrosophic topological space, ISOR J. Mathematics, 3(4)(2012), 31–35.
11. Salama.A.A and Alblowi.S.A, Generalized Neutrosophic Set and Generalized Neutrosophic Topological Spaces, Journal computer Sci. Engineering, 2(7) (2012), 12–23.
12. Shanthi.V.K, Chandrasekar.S and Safina Begam.K, Neutrosophic Generalized Semi Closed sets in Neutrosophic Topological spaces, International Journal of Research in Advent Technology, 6(7)(2018), 2321–9637.
13. SalamaA.A, Florentin Smarandache and Valeri Kroumov, Neutrosophic Closed set and Neutrosophic Continuous Function, Neutrosophic Sets and Systems,4(2014), 4–8.
14. Wadel Faris Al-omeri and Florentin Smarandache, New Neutrosophic Sets via Neutrosophic Topological Spaces, New Trends in Neutrosophic Theory and Applications, Vol(2) June 2016.
15. Zadeh.L.A, Fuzzy set, Inform and Control, 8(1965), 338–353.
16. Al-Omeri, W.F., and Jafari, S., Neutrosophic pre-continuous multifunctions and almost pre-continuous multifunctions, Neutrosophic Sets and Systems, Vol 27, pp 53-69, 2019.
17. Vadivel, M. Seenivasan and C. John Sundar, An introduction to δ-open sets in a neutrosophic topological spaces, Journal of Physics: Conference Series, 1724 (2021), 012011.
18. A. Vadivel and C. John Sundar, Neutrosophic δ-Open Maps and Neutrosophic δ-Closed Maps, International Journal of Neutrosophic Science (IJNS), 13 (2) (2021), 66-74.
19. A. Vadivel, P. Thangaraja and C. John Sundar, Neutrosophic e-continuous maps and neutrosophic e-irresolute maps, Turkish Journal of Computer and Mathematics Education,12 (1S) (2021), 369-375.
20. A. Vadivel, P. Thangaraja and C. John Sundar, Neutrosophic e-Open Maps, Neutrosophic e-Closed Maps and Neutrosophic e-Homeomorphisms in Neutrosophic Topological Spaces, AIP Conference Proceedings, 2364 (2021), 020016.
21. N. Moogambigai, A. Vadivel, and S. Tamilselvan, Neutrosophic Z-continuous maps and Z-irresolute maps, AIP Conference Proceedings, 2364 (2021), 020020.
22. Bhimraj Basumatary, Nijwm Wary,Jeevan Krishna Khaklary and Usha Rani Basumatary, On Some Properties of Neutrosophic Semi Continuous and Almost Continuous Mapping,Computer Modeling in

Engineering & Sciences, cmes.2022.018066

23. Gautam Chandra Ray   and Sudeep Dey, Relation of Quasi-coincidence for Neutrosophic Sets, Neutrosophic Sets and Systems, Vol. 46, 2022.

24. Charanya,Dr.K.Ramasamy, Pre semi Homeomorphisms and Generalized semi pre Homeomorphisms in Topological spaces, International Journal of Mathematics Trends and Technology (IJMTT) – Volume 42 Number 1- February 2017.

25. Rajeshwaran N and Chandramathi N , , Government Arts College, Udumalpet, India GENERALIZED SEMI PRE CLOSED SETS VIA NEUTROSOPHIC TOPOLOGICAL SPACE, pages 174-180, https://doi.org/10.37896/sr8.12/016

26. Rajeshwaran N and Chandramathi N , , Government Arts College, Udumalpet, India. Generalized semi pre-homeomorphisms in neutrosophictopological spaces. http://www.nonlinearstudies.com/index.php /nonlinear /issue/view/205

RESEARCH ARTICLE

An Application of Interval Valued Pythagorean Fuzzy Soft Matrix in Medical Diagnosis

Rajarajeswari. P[1]* and Mathi Sujitha.T[2]

[1] Asst. Prof., Department of Mathematics, Chikkannna Govt. Arts College, Tirupur, Tamil Nadu, India
[2] Asst. Prof., Department of Mathematics, Sree Saraswathi Thyagaraja College, Pollachi, Coimbatore, Tamil Nadu, India

*Address for Correspondence
Rajarajeswari. P
Asst. Prof., Department of Mathematics,
Chikkannna Govt. Arts College,
Tirupur, Tamil Nadu, India

ABSTRACT

In this paper, we have defined different types of reduced Pythagorean fuzzy soft matrices and based on these matrices, a new algorithm is developed for multi - criteria decision making under uncertainty using choice matrix.

Keywords: Soft sets, Fuzzy soft set, Pythagorean fuzzy set, Pythagorean fuzzy soft set, interval-valued Pythagorean fuzzy set, interval valued Pythagorean fuzzy soft set, Pythagorean fuzzy soft matrix.

INTRODUCTION

In today's competitive environment, there are a lot of uncertainties to deal with in a variety of areas, including business, decision-making, and medical science. The George Cantor-introduced classical set theory is insufficient to handle these kinds of circumstances. Zadeh[1] developed the idea of fuzzy set theory, which includes only membership values and somewhat aids us in this purpose. Atanassov[2] proposed the idea of IFS (Intuitionistic Fuzzy Set), an extension of fuzzy set, which is the membership and non-membership degree whose sum is less than or equal to one, in order to advance study in this area. The IVIFS (Interval Valued Intuitionistic Fuzzy Set), created by Atanassov and Gargov [3], is an extension of the IFS and has a membership function and a non-membership function with values that take the form of intervals.

Molodtsov [4] established the soft set theory, which aids in object parameterization. further, the theory of fuzzy soft sets was put forth by Maji P. K., Biswas R., and Roy A. R. [5, 6] and was further extended to include IFSS (Intuitionistic Fuzzy Soft Sets). Following this, Y. Jiang et al. [7] developed the idea of IVIFSS (Interval Valued

Rajarajeswari and Mathi Sujitha

Intuitionistic Fuzzy Soft Set) theory, which is an extension of the IFSS theory, as a result of the increasing convolution of the scientific environment.

In the fields of science and engineering, matrices are significant. The traditional matrix theory is insufficient for dealing with problems containing uncertainties. In order to encode the fuzzy soft set in matrix form and apply it to specific decision-making situations, Yong and Chenli[8] did so. [9] studies a few IFSM (Intuitionistic fuzzy soft matrix) theory outcomes. Interval Valued Intuitionistic Fuzzy Soft Matrix (IVIFSM) and its types were introduced by Rajarajeswari and Dhanalashmi[10], who additionally examined at some operations based on weight. PFS, which is the membership and non-membership degree whose square sum is less than or equal to one was introduced by Yager R. R.[11]because IVIFSM cannot contain more information for decision making. Abhishek Guleria and Rakesh Kumar Bajaj defined the PFSM for a certain set of MCDM issues[12]. Later IVPFSS and IVPFSM were defined by Rajarajeswari and Mathi Sujitha[13, 14] for better decision making. In this research, various reduced Pythagorean fuzzy soft matrix types are established. Based on these matrices, a novel technique for multi-criteria decision making under uncertainty using the choice matrix is devised.

PRELIMINARIES

In this section, we recall some basic definitions such as interval valued Pythagorean fuzzy soft set, interval valued Pythagorean fuzzy soft matrix and choice matrix.

Definition 2.1[13]: Let the parameter set be $\mathbb{E}$. Let $\mathcal{A} \subseteq \mathbb{E}$. A pair $(f, \mathcal{A})$ is called an interval-valued Pythagorean fuzzy soft set (IVPFSS) over $\mathbb{U}$, where $\mathbb{U}$ is the universe and f is a mapping given by $f: \mathcal{A} \to IP^{\mathbb{U}}$, where $IP^{\mathbb{U}}$ denotes the collection of all interval-valued Pythagorean fuzzy subsets of $\mathbb{U}$.

Definition 2.2[14]: Let $\mathcal{A} \subseteq \mathbb{E}$, $\mathbb{E} = \{e_1, e_2, \ldots, e_n\}$ being the parameter set. A pair $(f, \mathcal{A})$ is called an interval-valued Pythagorean fuzzy soft set (IVPFSS) over $\mathbb{U}$, where $\mathbb{U} = \{u_1, u_2, \ldots, u_m\}$ is the universe and f is a mapping given by $f: \mathcal{A} \to IP^{\mathbb{U}}$, where $IP^{\mathbb{U}}$ characterize the collection of all interval-valued Pythagorean fuzzy subsets of $\mathbb{U}$. Then the IVPFSS can be symbolized in the matrix form as $\mathcal{A}^*_{m \times n} = \left[a_{ij}\right]_{m \times n}$ where

$$a_{ij} = \begin{cases} \left(\left[\mu_j^L(u_i), \mu_j^U(u_i)\right]\left[\vartheta_j^L(u_i), \vartheta_j^U(u_i)\right]\right) if\ e_j \in \mathcal{A} \\ ([0,0][1,1]) \qquad\qquad\qquad if\ e_j \notin \mathcal{A} \end{cases}$$

$\left[\mu_j^L(u_i), \mu_j^U(u_i)\right]$ is the membership of u_i in $f(e_j)$, $\left[\vartheta_j^L(u_i), \vartheta_j^U(u_i)\right]$ is the non - membership of u_i in $f(e_j)$ with the condition $\left(\mu_j^U(u_i)\right)^2 + \left(\vartheta_j^U(u_i)\right)^2 \leq 1$.

Definition 2.3: Let η denote the choice matrix which is a square matrix where both m(rows) and n(columns) represent parameters, defined as η_{ij}:

$$\eta_{ij} = \begin{cases} (1,0) when\ i^{th}\ and\ j^{th}\ parameters\ are\ both\ choice\ parameters \\ \qquad\qquad of\ the\ decision\ makers \\ (0,1) otherwise, i.e. when\ at\ least\ one\ of\ the\ i^{th}\ or\ j^{th}\ parameters \\ \qquad\qquad be\ not\ under\ choice \end{cases}$$

INTERVAL VALUED PYTHAGOREAN FUZZY SOFT MATRIX (IVPFSM)

Definition 3.1. Let $\mathbb{U} = \{u_1, u_2, u_3, \ldots, u_m\}$ be the Universal set and $\mathbb{E}$ be the set of parameters given by $\mathbb{E} = \{e_1, e_2, e_3 \ldots, e_n\}$. Let $\mathcal{A} \subseteq \mathbb{E}$ and $(f, \mathcal{A})$ be an interval valued Pythagorean fuzzy soft set in the fuzzy soft class $(\mathbb{U}, \mathbb{E})$ where f is a mapping given by $f: \mathcal{A} \to IP^{\mathbb{U}}$, $IP^{\mathbb{U}}$ characterize the collection of all interval-valued Pythagorean fuzzy subsets of $\mathbb{U}$. Then the interval valued Pythagorean fuzzy soft set is

$$f(e_j) = \{u_i, \left(\left[\mu_j^L(u_i), \mu_j^U(u_i)\right]\left[\vartheta_j^L(u_i), \vartheta_j^U(u_i)\right]\right) \forall e_j \in \mathcal{A}\ and\ \forall u_i \in \mathbb{U}\}$$, $\left[\mu_j^L(u_i), \mu_j^U(u_i)\right]$ represents the membership and $\left[\vartheta_j^L(u_i), \vartheta_j^U(u_i)\right]$ non - membership of u_i in the interval valued Pythagorean fuzzy set $f(e_j)$.

Let w_1, w_2, w_3, w_4 in $[0,1], w_1 + w_2 = 1, w_3 + w_4 = 1$. The Vector $\mathbb{W} = (w_1, w_2, w_3, w_4)$is called weighted vector. The Pythagorean fuzzy soft set $(f_w, \mathcal{A})$over $\mathbb{U}$ such that $(f_w(e_j), \mathcal{A}) = \left\{ u_i, \left(w_1 \mu_j^L(u_i) + w_2 \mu_j^U(u_i), w_3 \vartheta_j^L(u_i) + w_4 \vartheta_j^U(u_i) \right) \forall e_j \in \mathcal{A} \text{ and } \forall u_i \in \mathbb{U} \right\}$is called the Reduced Pythagorean Fuzzy Soft Set(RPFSS) of the interval valued Pythagorean fuzzy soft set with respect to the weighted vector. By adjusting the value of w_1, w_2, w_3, w_4an interval valued Pythagorean fuzzy soft matrix can be converted into reduced Pythagorean fuzzy soft set.

Definition 3.2. Let $\mathbb{U} = \{u_1, u_2, u_3, ..., u_m\}$ be the Universal set and $\mathbb{E}$ be the set of parameters given by $\mathbb{E} = \{e_1, e_2, e_3 ..., e_n\}$. Let $\mathcal{A} \subseteq \mathbb{E}$ and $(f, \mathcal{A})$ be an interval valued Pythagorean fuzzy soft set in the fuzzy soft class $(\mathbb{U}, \mathbb{E})$ where f is a mapping given by $f: \mathcal{A} \to IP^{\mathbb{U}}$, $IP^{\mathbb{U}}$ characterize the collection of all interval-valued Pythagorean fuzzy subsets of $\mathbb{U}$. Let w_1, w_2, w_3, w_4 in $[0,1], w_1 + w_2 = 1, w_3 + w_4 = 1$. Then the reduced Pythagorean fuzzy soft set$(f_w, \mathcal{A})$over $\mathbb{U}$ in a matrix form as $\mathcal{A}^*_{m \times n} = [a_{ij}]_{m \times n}$,i = 1,2,...,m; j = 1,2,3,...,n where

$$a_{ij} = \begin{cases} \left(w\mu_j^L(u_i) + w_2\mu_j^U(u_i), \ w_3\vartheta_j^L(u_i) + w_4\vartheta_j^U(u_i) \right) & if \ e_j \in \mathcal{A} \\ (0,1) & if \ e_j \notin \mathcal{A} \end{cases}$$

so we can find a Reduced Pythagorean fuzzy soft set $(f_w, \mathcal{A})$ in the Pythagorean fuzzy soft class $(\mathbb{U}, \mathbb{E})$ by its Reduced Pythagorean fuzzy soft matrix $\mathcal{A}^*_{m \times n}$.The set of all m × n Reduced Pythagorean Fuzzy Soft Matrices will be denoted by RPFSM$_{m \times n}$.

Definition 3.3. Let $\mathcal{A}^*_{m \times n} = [a_{ij}]_{m \times n} \in$ RPFSM$_{m \times n}$ Then $\mathcal{A}^*_P$ is called Pessimistic Reduced Pythagorean Fuzzy Soft Matrix if $w_1 = 1, w_2 = 0, w_3 = 0, w_4 = 1$, The Pessimistic Reduced Pythagorean Fuzzy Soft set $f_P(e_j) = \left\{ \left(u_i, \left(\mu_j^L(u_i), \vartheta_j^U(u_i) \right) \right) \right\} \forall e_j \in \mathcal{A} \text{ and } \forall u_i \in \mathbb{U}$ over $\mathbb{U}$ in a matrix form as $\mathcal{A}^*_{m \times n} = [a_{ij}]_{m \times n}$, i = 1,2,...,m; j = 1,2,3,...,n   where
$$a_{ij} = \begin{cases} \left(\mu_j^L(u_i), \vartheta_j^U(u_i) \right) & if \ e_j \in \mathcal{A} \\ (0,1) & if \ e_j \notin \mathcal{A} \end{cases}$$
so we can find a Pessimistic Reduced Pythagorean Fuzzy Soft Set$(f_P, \mathcal{A})$ in the Pythagorean fuzzy soft class $(\mathbb{U}, \mathbb{E})$ by its Pessimistic Reduced Pythagorean Fuzzy Soft Matrix $\mathcal{A}^*_P$. The set of all m×n Pessimistic Reduced Pythagorean Fuzzy Soft Matrices will be denoted by PRPFSM$_{m \times n}$.

Definition 3.4. Let $\mathcal{A}^*_{m \times n} = [a_{ij}]_{m \times n} \in$ ROFSM$_{m \times n}$ Then $\mathcal{A}^*_O$ is called optimistic Reduced Pythagorean Fuzzy Soft Matrix if $w_1 = 0, w_2 = 1, w_3 = 1, w_4 = 0$, The Pessimistic Reduced Pythagorean Fuzzy Soft set $f_O(e_j) = \left\{ \left(u_i, \left(\mu_j^L(u_i), \vartheta_j^U(u_i) \right) \right) \right\} \forall e_j \in \mathcal{A} \text{ and } \forall u_i \in \mathbb{U}$ over $\mathbb{U}$ in a matrix form as $\mathcal{A}^*_{m \times n} = [a_{ij}]_{m \times n}$, i = 1,2,...,m; j = 1,2,3,...,n   where
$$a_{ij} = \begin{cases} \left(\mu_j^U(u_i), \vartheta_j^L(u_i) \right) & if \ e_j \in \mathcal{A} \\ (0,1) & if \ e_j \notin \mathcal{A} \end{cases}$$
so we can find a optimistic Reduced Pythagorean Fuzzy Soft Set$(f_o, \mathcal{A})$ in the Pythagorean fuzzy soft class $(\mathbb{U}, \mathbb{E})$ by its Optimistic Reduced Pythagorean Fuzzy Soft Matrix $\mathcal{A}^*_O$. The set of all m×n Optimistic Reduced Pythagorean Fuzzy Soft Matrices will be denoted by ORPFSM$_{m \times n}$.

Definition 3.5. Let $\mathcal{A}^*_{m \times n} = [a_{ij}]_{m \times n} \in$ RNFSM$_{m \times n}$ Then $\mathcal{A}^*_N$ is called Neutral Reduced Pythagorean Fuzzy Soft Matrix if $w_1 = 0.5, w_2 = 0.5, w_3 = 0.5, w_4 = 0.5$, The Neutral Reduced Pythagorean Fuzzy Soft set $f_N(e_j) = \left\{ \left(u_i, \left(\frac{\mu_j^L(u_i) + \mu_j^U(u_i)}{2} \right), \left(\frac{\vartheta_j^L(u_i) + \vartheta_j^U(u_i)}{2} \right) \right) \right\} \forall e_j \in \mathcal{A} \text{ and } \forall u_i \in \mathbb{U}$ over $\mathbb{U}$ in a matrix form as $\mathcal{A}^*_{m \times n} = [a_{ij}]_{m \times n}$, i = 1,2,...,m;   j   =   1,2,3,...,n   where

Rajarajeswari and Mathi Sujitha

$$a_{ij} = \begin{cases} \left(\dfrac{\mu_j^L(u_i) + \mu_j^U(u_i)}{2}, \dfrac{\vartheta_j^L(u_i) + \vartheta_j^U(u_i)}{2} \right) & if \ e_j \in \mathcal{A} \\ (0,1) & if \ e_j \notin \mathcal{A} \end{cases}$$

so we can find a Neutral Reduced Pythagorean Fuzzy Soft Set(f_N, $\mathcal{A}$) in the Pythagorean fuzzy soft class ($\mathbb{U},\mathbb{E}$) by its Neutral Reduced Pythagorean Fuzzy Soft Matrix $\mathcal{A}_N^*$. The set of all m×n Neutral Reduced Pythagorean Fuzzy Soft Matrices will be denoted by NRPFSM$_{m \times n}$.

Application of Interval – Valued Pythagorean Fuzzy Soft Matrix Theory in Decision Making using Choice Matrix
Let us assume that there are 'm' cars $\mathbb{U} = \{u_1, u_2, u_3, ..., u_m\}$ with a set of 'n' alternatives $\mathbb{E} = \{e_1, e_2, e_3, \dots e_n\}$. Now we use interval valued Pythagorean fuzzy soft matrices to find out which of these cars is the optimal decision taken by Mr. X, Y and Z to present it to their friend Mr. D using choice parameters. Construct the interval valued Pythagorean fuzzy soft set $(f, \mathcal{A})$, $(g, \mathcal{B})$, $(h, \mathcal{C})$ over $\mathbb{E}$ where f, g, h is a mapping $f : \mathcal{A} \to IVPF^{\mathbb{E}}$, $g : \mathcal{B} \to IVPF^{\mathbb{E}}$, $h : \mathcal{C} \to IVPF^{\mathbb{E}}$, $IVPF^E$ is the collection of all interval valued Pythagorean fuzzy subsets of $\mathbb{E}$. This gives the interval valued Pythagorean fuzzy soft matrices $\mathcal{A}_{m \times n}^*$, $\mathcal{B}_{m \times n}^*$, $\mathcal{C}_{m \times n}^*$. Convert the interval valued Pythagorean fuzzy soft matrix to a PRPFSM, ORPFSM, NRPFSM by adjusting the weighted vectors. Now we construct the choice matrices according to the choice parameters taken by $\mathcal{A}$, $\mathcal{B}$ and $\mathcal{C}$ respectively. Therefore, here we have developed a new algorithm by using the above data which helps us to find out the optimal choice of the decision makers using the choice parameters.

Algorithm
Step 1: Input the values for interval valued Pythagorean fuzzy soft set $(f, \mathcal{A})$, $(g, \mathcal{B})$, $(h, \mathcal{C})$ and obtain the Pythagorean fuzzy soft matrices $\mathcal{A}_{m \times n}^*$, $\mathcal{B}_{m \times n}^*$, $\mathcal{C}_{m \times n}^*$ corresponding to $(f, \mathcal{A})$, $(g, \mathcal{B})$, $(h, \mathcal{C})$ respectively.
Step 2: Convert the interval valued Pythagorean fuzzy soft matrix to a PRPFSM, ORPFSM, NRPFSM by adjusting the weighted vectors.
Step 3: Construct the combined choice matrix with respect to the choice parameters of the decision makers.
Step 4: Compute the product Pythagorean fuzzy soft matrices by multiplying each converted Pythagorean fuzzy soft matrix with the combined choice matrix
Step 5: Compute the sum of these product Pythagorean fuzzy soft matrices
Step 6: Then compute the maximum weight of each object by adding the membership values, which is the optimal choice. If more than one object has the highest weight then go to the next step.
Step 7: Now compute the minimum weight by adding the non-membership values, which is the optimal choice.

Case Study
Let U be the set of four branded cars given by $\mathbb{U} = \{C_1, C_2, C_3, C_4\}$. Let $\mathbb{E}$ be the set of four alternatives given by, $\mathbb{E}$ = a car {with advanced model, with power steering, with central lock system, comfortable with stereo effect} = {e₁, e₂, e₃, e₄}.

Suppose that the choice parameters of three friends Mr. X, Mr. Y and Mr. Z are $\mathcal{A}$ = {e₁, e₃}, $\mathcal{B}$ = {e₁, e₄}, $\mathcal{C}$ = {e₂, e₄} respectively. Now the interval valued Pythagorean fuzzy soft set $(f, \mathcal{A})$, $(g, \mathcal{B})$, $(h, \mathcal{C})$ according to the choice parameters are

$(f, \mathcal{A})$ = {Advanced model = {C₁ / [0.2,0.8][0.5,0.6] + C₂ / [0.1,0.9][0.2,0.4] + C₃ / [0.3, 0.6][0.6,0.8] + C₄ / [0.4, 0.8][0.1, 0.5]}, Central lock system = {C₁ / [0.2, 0.7][0.3,0.4] + C₂ / [0.2, 0.4][0.7,0.8] + C₃ / [0.3,0.8][0.4,0.6] + C₄ / [0.1,0.4][0.6,0.8]}}

$(g, \mathcal{B})$ = { Advanced model = {C₁ / [0.5,0.7][0.6,0.7] + C₂ / [0.4,0.8][0.5,0.6] + C₃ / [0.2, 0.5][0.7,0.8] + C₄ / [0.3,0.8][0.4,0.5]}, Comfortable with Stereo effect = {C₁ / [0.2, 0.7][0.5,0.7] + C₂ / [0.1, 0.5][0.4,0.7] + C₃ / [0.8,0.9][0.1,0.4] + C₄ / [0.2,0.5][0.6,0.7]}}

Rajarajeswari and Mathi Sujitha

$(h, \mathcal{C})$ = { With power steering = {C_1 / [0.4,0.8][0.3,0.6] + C_2 / [0.7,0.9][0.3,0.4] + C_3 / [0.6, 0.7][0.5,0.6] + C_4 / [0.2,0.5][0.6,0.8]}, Comfortable with Stereo effect = {C_1 / [0.1, 0.3][0.4,0.8] + C_2 / [0.8, 0.9][0.1,0.3] + C_3 / [0.5,0.8][0.4,0.6] + C_4 / [0.5,0.7][0.6,0.7]}}}

The problem is to select one of the branded cars among the four cars to present it for Mr. D which satisfies the choice parameters of Mr. X, Mr. Y and Mr. Z as much as possible.

The values of IVPSS can be represented in IVPFS matrix form as

$$\mathcal{A}^*_{m \times n} = \begin{array}{c} \\ C_1 \\ C_2 \\ C_3 \\ C_4 \end{array} \begin{pmatrix} \overset{e_1}{[0.2,0.8][0.5,0.6]} & \overset{e_2}{[0,1][0,1]} & \overset{e_3}{[0.2,0.7][0.3,0.4]} & \overset{e_4}{[0,1][0,1]} \\ [0.1,0.9][0.2,0.4] & [0,1][0,1] & [0.2,0.4][0.7,0.8] & [0,1][0,1] \\ [0.3,0.6][0.6,0.8] & [0,1][0,1] & [0.3,0.8][0.4,0.6] & [0,1][0,1] \\ [0.4,0.8][0.1,0.5] & [0,1][0,1] & [0.1,0.4][0.6,0.8] & [0,1][0,1] \end{pmatrix}$$

$$\mathcal{B}^*_{m \times n} = \begin{array}{c} \\ C_1 \\ C_2 \\ C_3 \\ C_4 \end{array} \begin{pmatrix} \overset{e_1}{[0.5,0.7][0.6,0.7]} & \overset{e_2}{[0,1][0,1]} & \overset{e_3}{[0,1][0,1]} & \overset{e_4}{[0.2,0.7][0.5,0.7]} \\ [0.4,0.8][0.5,0.6] & [0,1][0,1] & [0,1][0,1] & [0.1,0.5][0.4,0.7] \\ [0.2,0.5][0.7,0.8] & [0,1][0,1] & [0,1][0,1] & [0.8,0.9][0.1,0.4] \\ [0.3,0.8][0.4,0.5] & [0,1][0,1] & [0,1][0,1] & [0.2,0.5][0.6,0.7] \end{pmatrix}$$

$$\mathcal{C}^*_{m \times n} = \begin{array}{c} \\ C_1 \\ C_2 \\ C_3 \\ C_4 \end{array} \begin{pmatrix} \overset{e_1}{[0,1][0,1]} & \overset{e_2}{[0.4,0.8][0.3,0.6]} & \overset{e_3}{[0,1][0,1]} & \overset{e_4}{[0.1,0.3][0.4,0.8]} \\ [0,1][0,1] & [0.7,0.9][0.3,0.4] & [0,1][0,1] & [0.8,0.9][0.1,0.3] \\ [0,1][0,1] & [0.6,0.7][0.5,0.6] & [0,1][0,1] & [0.5,0.8][0.4,0.6] \\ [0,1][0,1] & [0.2,0.5][0.6,0.8] & [0,1][0,1] & [0.5,0.7][0.6,0.7] \end{pmatrix}$$

Optimistic Reduced Pythagorean Fuzzy Soft Matrix

Step 1: By taking the values of weighted vector $w_1 = 0$, $w_2 = 1$, $w_3 = 1$, $w_4 = 0$ we get the Optimistic Reduced Pythagorean Fuzzy Soft Matrices as

$$\mathcal{A}^*_O = \begin{array}{c} \\ C_1 \\ C_2 \\ C_3 \\ C_4 \end{array} \begin{pmatrix} \overset{e_1}{(0.8,0.5)} & \overset{e_2}{(0,1)} & \overset{e_3}{(0.7,0.3)} & \overset{e_4}{(0,1)} \\ (0.9,0.2) & (0.1) & (0.4,0.7) & (0,1) \\ (0.4,0.6) & (0,1) & (0.8,0.4) & (0,1) \\ (0.8,0.1) & (0,1) & (0.4,0.6) & (0,1) \end{pmatrix}$$

$$\mathcal{B}^*_O = \begin{array}{c} \\ C_1 \\ C_2 \\ C_3 \\ C_4 \end{array} \begin{pmatrix} \overset{e_1}{(0.7,0.6)} & \overset{e_2}{(0,1)} & \overset{e_3}{(0,1)} & \overset{e_4}{(0.7,0.5)} \\ (0.8,0.5) & (0.1) & (0,1) & (0.5,0.4) \\ (0.5,0.7) & (0,1) & (0,1) & (0.9,0.1) \\ (0.8,0.4) & (0,1) & (0,1) & (0.5,0.6) \end{pmatrix}$$

$$\mathcal{C}^*_O = \begin{array}{c} \\ C_1 \\ C_2 \\ C_3 \\ C_4 \end{array} \begin{pmatrix} \overset{e_1}{(0,1)} & \overset{e_2}{(0.8,0.3)} & \overset{e_3}{(0,1)} & \overset{e_4}{(0.3,0.4)} \\ (0,1) & (0.9.0.3) & (0,1) & (0.9,0.1) \\ (0,1) & (0.7,0.5) & (0,1) & (0.8,0.4) \\ (0,1) & (0.5,0.6) & (0,1) & (0.7,0.6) \end{pmatrix}$$

Step 2: The combined choice matrix of Mr. X, Mr. Y and Mr. Z are

Rajarajeswari and Mathi Sujitha

$$(\eta_{ij})_{(A,B\wedge C)} = e_A \begin{pmatrix} & e_{(B\wedge C)} & & \\ (0,1) & (0,1) & (0,1) & (1,0) \\ (0,1) & (0,1) & (0,1) & (0,1) \\ (0,1) & (0,1) & (0,1) & (1,0) \\ (0,1) & (0,1) & (0,1) & (0,1) \end{pmatrix} \text{[Since B}\wedge\text{C = \{e}_4\text{\}, A =\{e}_1\text{,e}_3\text{\}]}$$

$$(\eta_{ij})_{(B,C\wedge A)} = e_B \begin{pmatrix} & e_{(C\wedge A)} & & \\ (0,1) & (0,1) & (0,1) & (0,1) \\ (0,1) & (0,1) & (0,1) & (0,1) \\ (0,1) & (0,1) & (0,1) & (0,1) \\ (0,1) & (0,1) & (0,1) & (0,1) \end{pmatrix} \text{[Since C}\wedge\text{A =\{}\phi\text{\}, B = \{e}_1\text{, e}_4\text{\}]}$$

$$(\eta_{ij})_{(C,A\wedge B)} = e_C \begin{pmatrix} & e_{(A\wedge B)} & & \\ (0,1) & (0,1) & (0,1) & (0,1) \\ (1,0) & (0,1) & (0,1) & (0,1) \\ (0,1) & (0,1) & (0,1) & (0,1) \\ (1,0) & (0,1) & (0,1) & (0,1) \end{pmatrix} \text{[Since A}\wedge\text{B = \{e}_1\text{\}, C =\{e}_2\text{,e}_4\text{\}]}$$

Step 3: The product of Pythagorean fuzzy soft matrices and their corresponding choice matrices are,

$$\mathcal{A}_O^* \times (\eta_{ij})_{(A,B\wedge C)} = \begin{matrix} & e_1 & e_2 & e_3 & e_4 \\ C_1 & (0,1) & (0,1) & (0,1) & (0.8,0.3) \\ C_2 & (0,1) & (0,1) & (0,1) & (0.9,0.2) \\ C_3 & (0,1) & (0,1) & (0,1) & (0.8,0.4) \\ C_4 & (0,1) & (0,1) & (0,1) & (0.8,0.1) \end{matrix}$$

$$\mathcal{B}_O^* \times (\eta_{ij})_{(B,C\wedge A)} = \begin{matrix} & e_1 & e_2 & e_3 & e_4 \\ C_1 & (0,1) & (0,1) & (0,1) & (0,1) \\ C_2 & (0,1) & (0,1) & (0,1) & (0,1) \\ C_3 & (0,1) & (0,1) & (0,1) & (0,1) \\ C_4 & (0,1) & (0,1) & (0,1) & (0,1) \end{matrix}$$

$$\mathcal{C}_O^* \times (\eta_{ij})_{(C,A\wedge B)} = \begin{matrix} & e_1 & e_2 & e_3 & e_4 \\ C_1 & (0,1) & (0,1) & (0,1) & (0,1) \\ C_2 & (0,1) & (0,1) & (0,1) & (0,1) \\ C_3 & (0,1) & (0,1) & (0,1) & (0,1) \\ C_4 & (0,1) & (0,1) & (0,1) & (0,1) \end{matrix}$$

Step 4: The sum of these product Pythagorean fuzzy soft matrices is,

$$= \begin{matrix} & e_1 & e_2 & e_3 & e_4 \\ C_1 & (0.8,0.3) & (0,1) & (0,1) & (0.8,0.3) \\ C_2 & (0.9,0.1) & (0,1) & (0,1) & (0.9,0.2) \\ C_3 & (0.8,0.4) & (0,1) & (0,1) & (0.8,0.4) \\ C_4 & (0.7,0.6) & (0,1) & (0,1) & (0.8,0.1) \end{matrix}$$

Step 5: The weights of the cars (sum of the membership values) are,

　　　(i) $w(C_1)$ = 0.8+0+0+0.8 = 1.6

　　　(ii) $w(C_2)$ = 0.9+0+0+0.9 = 1.8

　　　(iii) $w(C_3)$ = 0.8+0+0+0.8 = 1.6

(iv) $w(C_4)$ = 0.7+0+0+0.8 = 1.5

It is clear that the weight of the second row is maximum and hence, C_2 is the optimal choice taken by Mr. X, Mr. Y and Mr. Z to present a car for Mr. D

Pesimistic Reduced Pythagorean Fuzzy Soft Matrix

Step 1: By taking the values of weighted vector w_1 = 1, w_2 = 0, w_3 = 0 , w_4 = 1 we get the Pessimistic Reduced Pythagorean Fuzzy Soft Matrices as

$$\mathcal{A}_P^* = \begin{array}{c} C_1 \\ C_2 \\ C_3 \\ C_4 \end{array} \begin{pmatrix} e_1 & e_2 & e_3 & e_4 \\ (0.8,0.5) & (0,1) & (0.7,0.3) & (0,1) \\ (0.9,0.2) & (0,1) & (0.4,0.7) & (0,1) \\ (0.4,0.6) & (0,1) & (0.8,0.4) & (0,1) \\ (0.8,0.1) & (0,1) & (0.4,0.6) & (0,1) \end{pmatrix}$$

$$\mathcal{B}_P^* = \begin{array}{c} C_1 \\ C_2 \\ C_3 \\ C_4 \end{array} \begin{pmatrix} e_1 & e_2 & e_3 & e_4 \\ (0.7,0.6) & (0,1) & (0,1) & (0.7,0.5) \\ (0.8,0.5) & (0,1) & (0,1) & (0.5,0.4) \\ (0.5,0.7) & (0,1) & (0,1) & (0.9,0.1) \\ (0.8,0.4) & (0,1) & (0,1) & (0.5,0.6) \end{pmatrix}$$

$$\mathcal{C}_P^* = \begin{array}{c} C_1 \\ C_2 \\ C_3 \\ C_4 \end{array} \begin{pmatrix} e_1 & e_2 & e_3 & e_4 \\ (0,1) & (0.8,0.3) & (0,1) & (0.3,0.4) \\ (0,1) & (0.9,0.3) & (0,1) & (0.9,0.1) \\ (0,1) & (0.7,0.5) & (0,1) & (0.8,0.4) \\ (0,1) & (0.5,0.6) & (0,1) & (0.7,0.6) \end{pmatrix}$$

Step 2: Consider the same choice matrix as in Optimistic Reduced Pythagorean Fuzzy Soft Matrix.

Step 3: The product of Pythagorean fuzzy soft matrices and their corresponding choice matrices are,

$$\mathcal{A}_P^* \times \left(\eta_{ij}\right)_{(A,B \wedge C)} = \begin{array}{c} C_1 \\ C_2 \\ C_3 \\ C_4 \end{array} \begin{pmatrix} e_1 & e_2 & e_3 & e_4 \\ (0,1) & (0,1) & (0,1) & (0.2,0.4) \\ (0,1) & (0,1) & (0,1) & (0.2,0.4) \\ (0,1) & (0,1) & (0,1) & (0.3,0.6) \\ (0,1) & (0,1) & (0,1) & (0.4,0.5) \end{pmatrix}$$

$$\mathcal{B}_P^* \times \left(\eta_{ij}\right)_{(B,C \wedge A)} = \begin{array}{c} C_1 \\ C_2 \\ C_3 \\ C_4 \end{array} \begin{pmatrix} e_1 & e_2 & e_3 & e_4 \\ (0,1) & (0,1) & (0,1) & (0,1) \\ (0,1) & (0,1) & (0,1) & (0,1) \\ (0,1) & (0,1) & (0,1) & (0,1) \\ (0,1) & (0,1) & (0,1) & (0,1) \end{pmatrix}$$

$$\mathcal{C}_P^* \times \left(\eta_{ij}\right)_{(C,A \wedge B)} = \begin{array}{c} C_1 \\ C_2 \\ C_3 \\ C_4 \end{array} \begin{pmatrix} e_1 & e_2 & e_3 & e_4 \\ (0.4,0.6) & (0,1) & (0,1) & (0,1) \\ (0.8,0.3) & (0,1) & (0,1) & (0,1) \\ (0.6,0.6) & (0,1) & (0,1) & (0,1) \\ (0.5,0.7) & (0,1) & (0,1) & (0,1) \end{pmatrix}$$

Step 4: The sum of these product Pythagorean fuzzy soft matrices is,

$$= \begin{array}{c} C_1 \\ C_2 \\ C_3 \\ C_4 \end{array} \begin{pmatrix} e_1 & e_2 & e_3 & e_4 \\ (0.4,0.6) & (0,1) & (0,1) & (0.2,0.4) \\ (0.8,0.3) & (0,1) & (0,1) & (0.2,0.4) \\ (0.6,0.6) & (0,1) & (0,1) & (0.3,0.6) \\ (0.5,0.7) & (0,1) & (0,1) & (0.4,0.6) \end{pmatrix}$$

Step 5: The weights of the cars (sum of the membership values) are,

       (i) $w(C_1)$ = 0.4+0+0+0.2 = 0.8

       (ii) $w(C_2)$ = 0.8+0+0+0.2 = 1.0

       (iii) $w(C_3)$ = 0.6+0+0+0.3 = 0.9

Rajarajeswari and Mathi Sujitha

(iv) $w(C_4) = 0.5+0+0+0.4 = 0.9$

It is clear that the weight of the second row is maximum and hence, C_2 is the optimal choice taken by Mr. X, Mr. Y and Mr. Z to present a car for Mr. D

Neutral Reduced Pythagorean Fuzzy Soft Matrix

Step 1: By taking the values of weighted vector $w_1 = 0.5$, $w_2 = 0.5$, $w_3 = 0.5$, $w_4 = 0.5$ we get the Neutral Reduced Pythagorean Fuzzy Soft Matrices as

$$\mathcal{A}_N^* = \begin{array}{c} \\ C_1 \\ C_2 \\ C_3 \\ C_4 \end{array} \begin{pmatrix} e_1 & e_2 & e_3 & e_4 \\ (0.5,0.55) & (0,1) & (0.45,0.35) & (0,1) \\ (0.5,0.3) & (0,1) & (0.3,0.75) & (0,1) \\ (0.45,0.7) & (0,1) & (0.55,0.5) & (0,1) \\ (0.6,0.3) & (0,1) & (0.25,0.7) & (0,1) \end{pmatrix}$$

$$\mathcal{B}_N^* = \begin{array}{c} \\ C_1 \\ C_2 \\ C_3 \\ C_4 \end{array} \begin{pmatrix} e_1 & e_2 & e_3 & e_4 \\ (0.6,0.65) & (0,1) & (0,1) & (0.45,0.6) \\ (0.6,0.55) & (0,1) & (0,1) & (0.3,0.55) \\ (0.35,0.75) & (0,1) & (0,1) & (0.85,0.25) \\ (0.55,0.45) & (0,1) & (0,1) & (0.35,0.65) \end{pmatrix}$$

$$\mathcal{C}_N^* = \begin{array}{c} \\ C_1 \\ C_2 \\ C_3 \\ C_4 \end{array} \begin{pmatrix} e_1 & e_2 & e_3 & e_4 \\ (0,1) & (0.6,0.45) & (0,1) & (0.2,0.6) \\ (0,1) & (0.8.0.35) & (0,1) & (0.85,0.2) \\ (0,1) & (0.65,0.55) & (0,1) & (0.65,0.5) \\ (0,1) & (0.35,0.7) & (0,1) & (0.6,0.65) \end{pmatrix}$$

Step 2: Consider the same choice matrix as in Optimistic Reduced Pythagorean Fuzzy Soft Matrix.

Step 3: The product of Pythagorean fuzzy soft matrices and their corresponding choice matrices are,

$$\mathcal{A}_N^* \times (\eta_{ij})_{(A,B\wedge C)} = \begin{array}{c} \\ C_1 \\ C_2 \\ C_3 \\ C_4 \end{array} \begin{pmatrix} e_1 & e_2 & e_3 & e_4 \\ (0,1) & (0,1) & (0,1) & (0.5,0.35) \\ (0,1) & (0,1) & (0,1) & (0.5,0.3) \\ (0,1) & (0,1) & (0,1) & (0.55,0.5) \\ (0,1) & (0,1) & (0,1) & (0.6,0.3) \end{pmatrix}$$

$$\mathcal{B}_N^* \times (\eta_{ij})_{(B,C\wedge A)} = \begin{array}{c} \\ C_1 \\ C_2 \\ C_3 \\ C_4 \end{array} \begin{pmatrix} e_1 & e_2 & e_3 & e_4 \\ (0,1) & (0,1) & (0,1) & (0,1) \\ (0,1) & (0,1) & (0,1) & (0,1) \\ (0,1) & (0,1) & (0,1) & (0,1) \\ (0,1) & (0,1) & (0,1) & (0,1) \end{pmatrix}$$

$$\mathcal{C}_N^* \times (\eta_{ij})_{(C,A\wedge B)} = \begin{array}{c} \\ C_1 \\ C_2 \\ C_3 \\ C_4 \end{array} \begin{pmatrix} e_1 & e_2 & e_3 & e_4 \\ (0.6,0.45) & (0,1) & (0,1) & (0,1) \\ (0.85,0.2) & (0,1) & (0,1) & (0,1) \\ (0.65,0.5) & (0,1) & (0,1) & (0,1) \\ (0.6,0.65) & (0,1) & (0,1) & (0,1) \end{pmatrix}$$

Step 4: The sum of these product Pythagorean fuzzy soft matrices is,

$$= \begin{array}{c} \\ C_1 \\ C_2 \\ C_3 \\ C_4 \end{array} \begin{pmatrix} e_1 & e_2 & e_3 & e_4 \\ (0.6,0.45) & (0,1) & (0,1) & (0.5,0.35) \\ (0.85,0.2) & (0,1) & (0,1) & (0.5,0.3) \\ (0.65,0.5) & (0,1) & (0,1) & (0.55,0.5) \\ (0.6,0.65) & (0,1) & (0,1) & (0.6,0.3) \end{pmatrix}$$

Step 5: The weights of the cars (sum of the membership values) are,

(i) $w(C_1) = 0.6+0+0+0.5 = 1.1$

(ii) $w(C_2) = 0.85+0+0+0.5 = 1.35$

(iii) $w(C_3) = 0.65+0+0+0.55 = 1.2$

(iv) $w(C_4) = 0.6+0+0+0.6 = 1.2$

Rajarajeswari and Mathi Sujitha

It is clear that the weight of the second row is maximum and hence, C_2 is the optimal choice taken by Mr. X, Mr. Y and Mr. Z to present a car for Mr. D.

CONCLUSION

In the three different reduced interval valued Pythagorean fuzzy matrices, it is found that all the three methods provide C_2 as the optimal choice. But when comparing the weights obtained by the three methods, NRPFSM gives the better result when compared to other methods as shown in the figure 1.

REFERENCES

1.   Zadeh L. A, Fuzzy sets, Information and control, 1985; 8: 338 – 353.
2. K. Atanassov, Intuitionistic fuzzy sets, Fuzzy Sets and Systems 1986; 20: 87–96.
3. K. Atanassov and G. Gargov, Interval valued intuitionistic fuzzy sets, Fuzzy Sets and Systems 1989;3:343–349.
4. D. Molodtsov, Soft set theory-first result, Comput. Math. Appl. 1999;37: 19–31.
5. P. K. Maji, R. Biswas and A. R. Roy, Fuzzy soft set, J. Fuzzy Math. 2001;9: 589–602.
6. P. K. Maji, R. Biswas and A. R. Roy, Intuitionistic fuzzy soft sets, J. Fuzzy Math. 2004;12: 669–683.
7. Y. Jiang, Y. Tang, Q. Chen, H. Liu and J. Tang, Interval valued intuitionistic fuzzy soft sets and their properties, Comput. Math. Appl. 2010;60: 906–918.
8. Yong Yang and Chenli ji., Fuzzy soft matrices and their applications, Lecture notes in computer science, 2011; 7002: 618 – 627.
9. B. Chetia and P. K. Das, Some results of intuitionistic fuzzy soft matrix theory, Advances in Applied Science Research 2012;3: 412–413.
10. P. Rajarajeswari and P. Dhanalakshmi, Interval valued intuitionistic fuzzy soft matrix theory, International Journal of Mathematical Archive 2014;5: 152–161.
11. Yager R.R., Pythagorean fuzzy subsets, In: Proc Joint IFSA World Congress and NAFIPS Annual Meeting, Edmonton, Canada; 2013; 57–61.
12. Abhishek Guleria and Rakesh Kumar Bajaj, On Pythagorean fuzzy soft matrices, operations and their applications in decision making and medical diagnosis 2019;23:7889 - 7900.
13. P. Rajarajeswari and T. Mathi Sujitha, Interval valued Pythagorean fuzzy Soft set and their properties, Journal of the Asiatic Society of Mumbai, 2023;XCVI: 118 - 125
14. P. Rajarajeswari and T. Mathi Sujitha, Interval valued Pythagorean fuzzy soft matrix theory, Journal of Madhya Bharti -Humanities and Social Sciences, 2023;83: 67 – 75.
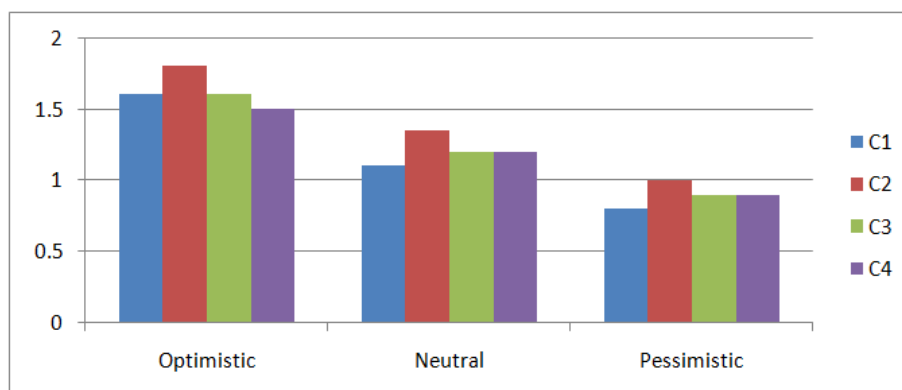
Fig 1: Comparison chart

RESEARCH ARTICLE

A New Form of Separation Axioms in Binary Topological Spaces

Jayalakshmi S[1]* and Manonmani A[2]

[1]Assistant Professor, Department of Mathematics, Government Arts and Science College for Women, Puliyakulam, Coimbatore, Tamil Nadu, India.
[2] Associate Professor, Department of Mathematics, L.R.G. Government Arts College for women, Tirupur, Tamil Nadu, India.

*Address for Correspondence
Jayalakshmi S
Assistant Professor,
Department of Mathematics,
Government Arts and Science College for Women,
Puliyakulam, Coimbatore, Tamil Nadu, India.
E.Mail: iamsjayalakshmi@gmail.com

ABSTRACT

This study aims to present a new type of separation axioms for binary topological spaces utilizing binary $r\beta$-open sets.. Here, a new class of axioms known as Binary $r\beta$ -T_0, Binary $r\beta$ -T_1, Binary $r\beta$ - T_2 spaces, and Binary $r\beta$ - normal space has been described. Their features and linkages have also been examined, along with appropriate examples..

Keywords: Binary $r\beta$- T_0, Binary $r\beta$- T_1, Binary $r\beta$- T_2 spaces, Binary $r\beta$- normal space

INTRODUCTION

In the year 2011, S. Nithyanantha Jothi and P. Thangavelu [1,2] conducted research on binary topological spaces and developed the idea of a binary topology between two non-empty sets that satisfy specific comparable axioms to the axioms of topology. Additionally, in 2012, they [3] developed the idea of binary-T_0, binary-T_1, binary-T_3, and binary-T_4 spaces in binary topological spaces. In 2016, they [4] defined binary semi-open sets in binary topological spaces and examined some of its features. 2019 saw the introduction of $r\beta$-closed sets and $r\beta$ -open sets in topological spaces by A.Manonmani and S.Jayalakshmi [5]. Additionally, in 2020, they [6] introduced and researched the idea of binary $r\beta$ -closed sets and binary $r\beta$ -open sets in binary topological spaces. In this paper we introduce *binary $r\beta$ - T_0, binary $r\beta$ - T_1, binary $r\beta$ - T_2 and binary $r\beta$ - normal spaces* which are respectively $^br\beta$ -T_0, $^br\beta$ -T_1, $^br\beta$ -T_2 and $^br\beta$ - *normal spaces* in

short. In this paper, the symbols $\wp(R)$ and $\wp(S)$ refers to the corresponding power sets of R and S. Also known as *b-cl*(A,B) and *b-int*(A,B) respectively, are *binary closure* of (A,B) and *binary interior* of (A,B).

PRELIMINARIES

Consider any two nonempty sets as R and S. A binary structure $\mathscr{M} \subseteq \wp(R) \times \wp(S)$ that satisfies the axioms namely (i) $(\emptyset,\emptyset)$ and $(R,S) \in \mathscr{M}$ (ii) $(A_1 \cap A_2, B_1 \cap B_2) \in \mathscr{M}$ whenever $(A_1,B_1) \in \mathscr{M}$ and $(A_2,B_2) \in \mathscr{M}$, and (iii) If $\{(A_\alpha,B_\alpha): \alpha \in \Delta\}$ is a family of members of $\mathscr{M}$, then $\left(\bigcup_{\alpha \in \Delta} A_\alpha, \bigcup_{\alpha \in \Delta} B_\alpha\right) \in \mathscr{M}$ is known as a binary topology [3] from R to S and the triplet $(R,S,\mathscr{M})$ is known as a binary topological space. The members of $\mathscr{M}$ are known as the binary open subsets of the binary topological space $(R,S,\mathscr{M})$ and the elements of $R \times S$ are referred to as the binary points of the binary topological space $(R,S,\mathscr{M})$. We refer $(R,\mathscr{M})$ as a binary topological space if $S = R$ in which case $\mathscr{M}$ is referred to as a binary topology on R

Definition 2.1[1]: Let (A,B) and $(C,D) \in \wp(R) \times \wp(S)$ where R and S are any two nonempty sets. If $A \subseteq C$ and $B \subseteq D$ then $(A,B) \subseteq (C,D)$

Definition 2.2 [1]: Let (A,B) and $(C,D) \in \wp(R) \times \wp(S)$ where R and S are any two nonempty sets. If one of the following conditions is true we can state that$(A,B) \not\subseteq (C,D)$
(i) $A \subseteq C$ and $B \not\subseteq D$ (ii) $A \not\subseteq C$ and $B \subseteq D$ (iii) $A \not\subseteq C$ and $B \not\subseteq D$.

Definition 2.3[1]: With $A \subseteq R$, $B \subseteq S$, let $(R,S,\mathscr{M})$ be a binary topological space. If $(R-A,S-B) \in \mathscr{M}$, then (A,B) is known as *binary closed* in $(R,S,\mathscr{M})$

Definition 2.4 [1]: Let $(R,S,\mathscr{M})$ be a binary topological space and assume that $(A,B) \subseteq (R,S)$. Let $(A,B)^{1*} = \cap\{A_\alpha: (A_\alpha, B_\alpha)\}$ is *binary closed* and $(A,B) \subseteq (A_\alpha,B_\alpha)\}$ and $(A,B)^{2*} = \{B_\alpha: (A_\alpha,B_\alpha)$ is *binary closed* and $(A,B) \subseteq (A_\alpha,B_\alpha)\}$. The *binary closure* of (A,B) is then the ordered pair $((A,B)^{1*}, (A,B)^{2*})$ denoted by *b-cl*(A,B) in the binary space $(R,S,\mathscr{M})$ where $(A,B) \subseteq (R,S)$ Here it should be emphasized that $((A,B)^{1*}, (A,B)^{2*})$ is *binary closed* and $(A,B) \subseteq ((A,B)^{1*}, (A,B)^{2*})$.

Definition 2.5 [1]: Assume that $(A,B) \subseteq (R,S)$ where $(R,S,\mathscr{M})$ be a binary topological space. Let us say $(A,B)^{1°} = \cup\{A_\alpha: (A_\alpha, B_\alpha)\}$ is *binary open* and $(A_\alpha, B_\alpha) \subseteq (A,B)\}$ and $(A,B)^{2°} = \cup\{B_\alpha: (A_\alpha, B_\alpha)$ is *binary open* and $(A_\alpha, B_\alpha) \subseteq (A,B)\}$. Then The *binary interior* of (A,B) is then the ordered pair $((A,B)^{1°}, (A,B)^{2°})$ which is represented by *b-int*(A,B). In this case, $((A,B)^{1°}, (A,B)^{2°})$ is *binary open* and $(A,B) \subseteq ((A,B)^{1°}, (A,B)^{2°}) \subseteq (A,B)$.

Definition 2.6 [1]: Consider $(R,S,\mathscr{M})$ be a binary topological space and assume that $(A,B) \subseteq (R,S)$. Define $\mathscr{M}_{(A, B)} = \{(A \cap U, B \cap V) : (U,V) \in \mathscr{M}\}$. Then $\mathscr{M}_{(A, B)}$ is a binary topology from A to B and the binary topological space $(A,B,\mathscr{M}_{(A, B)})$ is called a binary subspace of $(R,S,\mathscr{M})$.

Definition 2.7 [3]: (i)   A binary topological space $(R,S,\mathscr{M})$ is referred to as a *binary-T_0 space* if it contains $(A,B) \in \mathscr{M}$ such that only one of the following conditions applies for any pair of distinct points (a_1,b_1), $(a_2,b_2) \in R \times S$.   (1) $(a_1,b_1) \in (A,B)$, $(a_2,b_2) \in (R-A,S-B)$ (2) $(a_1,b_1) \in (R-A,S-B)$, $(a_2, b_2) \in (A,B)$.
(ii)   If for every pair of distinct points (a_1,b_1), $(a_2,b_2) \in R \times S$, there exists (A,B) and $(C,D) \in \mathscr{M}$, with $(a_1,b_1) \in (A,B)$ and $(a_2, b_2) \in (C, D)$ such that $(a_2, b_2) \in (R-A,S-B)$, $(a_1, b_1) \in (R-C,S-D)$ in a binary topological space $(R,S,\mathscr{M})$, then this is known as a *binary-T_1 space*
(iii)   For each pair of distinct points (a_1,b_1), $(a_2,b_2) \in R \times S$, if there are mutually disjoint *binary open* sets (A,B) and (C,D) such that $(a_1,b_1) \in (A,B)$ and $(a_2,b_2) \in (C,D)$ in a binary topological space $(R,S,\mathscr{M})$, then this is referred to as a *binary-T_2 space*

Definition 2.8 [3]:   If $(R,S,\mathcal{M})$ is a *binary-T_1 space* then a binary topological space $(R,S,\mathcal{M})$ is referred to as a *binary normal* (or) *binary-T_4 space* and for every pair of mutually disjoint *binary closed* sets (A_1,B_1), (A_2,B_2) there exists a pair of mutually disjoint *binary open* sets (U_1,V_1), (U_2,V_2) such that $(A_1,B_1) \subseteq (U_1,V_1)$ and $(A_2, B_2) \subseteq (U_2,V_2)$

Definition 2.9[1]: A pair of *binary open* sets (A,B) and (C,D) are said to be disjoint if $(A \cap C, B \cap D) = (\emptyset,\emptyset)$. This results in $A \cap C = \emptyset$ and $B \cap D = \emptyset$.

Definition 2.10[1]: Let $(R,S,\mathcal{M})$ be a binary topological space and let $(a,b) \in R \times S$. If $a \in A$ and $b \in B$ then the binary open set (A,B) is referred to as a binary neighbourhood of (a,b).

Definition 2.11:   In a binary topological space $(R,S,\mathcal{M})$, a subset (A,B) is referred to as
 (i) a *binary regular open* set [5] (briefly ^{b}*regular open* set) in $(R,S,\mathcal{M})$ if $(A,B) = b\text{-}int(b\text{-}cl(A,B))$ and *binary regular closed* (briefly ^{b}*regular closed* set) if $(A,B)= b\text{-}cl(b\text{-}int(A,B))$.
(ii) a *binary semi open* set [4] (briefly ^{b}*semi open* set) in $(R,S,\mathcal{M})$ if $b\text{-}int(b\text{-}cl(A,B)) \subseteq (A,B)$ and its compliment is called a *binary semi closed* set (briefly ^{b}*semi closed* set) in $(R,S,\mathcal{M})$

Definition 2.12[5]: In a binary topological space $(R,S,\mathcal{M})$ assume $(A,B) \subseteq (R,S)$. If there is a $^b\beta$ - *open* set (U,V) in $(R,S,\mathcal{M})$ such that $b\text{-}rcl(A,B) \subseteq (U,V)$ whenever $(A,B) \subseteq (U,V)$, then (A,B) is is referred to as *a binary $r\beta$ - closed* set (briefly $^br\beta$ - *closed* set) in $(R,S,\mathcal{M})$.
        The compliment of the above *binary $r\beta$ - closed* set is a *binary $r\beta$ - open* set in $(R,S,\mathcal{M})$.

BINARY $r\beta$ - T_0, BINARY $r\beta$ - T_1, BINARY $r\beta$ - T_2 SPACES

We introduce the idea of *binary $r\beta$ - T_0, binary $r\beta$ - T_1, binary $r\beta$ - T_2* and *binary $r\beta$ - normal spaces* (briefly $^br\beta$ -T_0, $^br\beta$ -T_1, $^br\beta$ -T_2 and $^br\beta$ - *normal spaces*) in this chapter and look at some of its characterizations.

Definition 3.1: If for any pair of unique points (a_1,b_1), $(a_2,b_2) \in R \times S$, there exists a $^br\beta$ - *open* set (A, B) such that precisely one of the following holds, the binary topological space $(R,S,\mathcal{M})$ is referred to as a *binary $r\beta$ - T_0 space* (briefly $^br\beta$ -T_0) (i) $(a_1,b_1) \in (A,B)$, $(a_2,b_2) \in (R-A, S-B)$ (ii) $(a_1,b_1) \in (R-A, S-B)$, $(a_2,b_2) \in (A,B)$.

Definition 3.2: A binary topological spaces $(R,S,\mathcal{M})$ is referred to as a *binary $r\beta$ -T_1 space* (briefly $^br\beta$ -T_1) if for any pair of unique points (a_1,b_1), $(a_2,b_2) \in R \times S$, it contains $^br\beta$ - *open* sets (A,B) and (C,D) with $(a_1,b_1) \in (A,B)$ and $(a_2,b_2) \in (C,D)$ such that $(a_2,b_2) \in (R-A, S-B)$, $(a_1,b_1) \in \qquad (R-C, S-D)$.

Definition 3.3: If there are disjoint $^br\beta$ - *open* sets (A,B) and (C,D) such that $(a_1,b_1) \in (A,B)$ and $(a_2,b_2) \in (C,D)$ for any pair of unique points (a_1,b_1), $(a_2,b_2) \in R \times S$ then a binary topological spaces $(R,S,\mathcal{M})$ is said to be a *binary $r\beta$ -T_2 space* (briefly $^br\beta$ -T_2)

Theorem 3.4: Every $^br\beta$ -T_0 space is *binary -T_0 space*, in a binary topological space $(R,S,\mathcal{M})$
Proof: Consider (R,S) be a $^br\beta$ -T_0 space and consider (a_1,b_1) and (a_2,b_2) be a pair of unique points in (R,S). There is a $^br\beta$ - *open* set (A,B) such that $(a_1,b_1) \in (A,B)$ and $(a_2,b_2) \in (R-A, S-B)$ since (R,S) is a *binary-T_0 space*. Due to the fact that any $^br\beta$ -*open* set is *binary open*, (A,B) is also a *binary open* set such that $(a_1,b_1) \in (A,B)$ and $(a_2,b_2) \in (R-A, S-B)$. (R,S) is a *binary -T_0 space* as a result.

Remark 3.5: The following example demonstrates that the converse of the aforementioned theorem is false.
Example 3.6:   Consider $R =\{a,b\}$ and $S =\{1,2,3\}$. Clearly $\mathcal{M} = \{(\emptyset,\emptyset), (\{\emptyset,\{1\}), (\emptyset,\{3\}), (\emptyset, \{1,2\}), (\{\emptyset,\{1, 3\}), (\{\emptyset,S), (\{a\},\{1\}), (\{a\},\{1,2\}) ,(\{a\},\{1,3\}), (\{a\},S) , (\{b\},\emptyset), (\{b\},\{1\}), (\{b\},\{3\}), (\{b\},\{1,2\}), (\{b\}, \{1, 3\}), (\{b\}, S), (R,\{1\}) , (R,\{1,2\}), (R,\{1,3\}), (R,S)\}$ is a binary topology from R to S. Here $^br\beta$ - *open* sets in (R,S) are $\{(\emptyset,\emptyset), (\emptyset,\{1\}), (\emptyset, \{3\}), (\{a\},\{1,2\}) ,(\{a\},S), (\{b\},\emptyset), (\{b\},\{1\}), (\{b\},\{3\}), (\{b\},\{1,3\}), (R,\{1,2\}), (R,\{1,3\}), (R,S)\}$. Let $(a_1,b_1) = (\{a\},\{1\})$ and $(a_2,b_2) = (\{b\},\{3\})$, where (a_1,b_1),

Jayalakshmi and Manonmani

$(a_2,b_2) \in (R,S)$ and $(a_1,b_1) \neq (a_2,b_2)$ there is a *binary open* set $(A,B) = (\{a\},\{1\})$ which is not a $^br\beta$ *-open* set such that $(a_1,b_1) \in (A,B)$ and $(a_2,b_2) \in (R-A, S-B)$. (R,S) is *binary -T_0 space* but not a $^br\beta$ -T_0 space as a result.

Theorem 3.7: Every $^br\beta$ -T_1 space is *binary -T_1 space* in a binary topological space $(R,S,\mathscr{M})$.

Proof: Let (R,S) be a $^br\beta$ -T_1 space and let (a_1,b_1) and (a_2,b_2) be a pair of unique points in (R,S) with $a_1 \neq a_2$, $b_1 \neq b_2$. Then distinct $^br\beta$ - *open* sets (A,B) and (C,D) exist such that $(a_1,b_1) \in (A, B)$, $(a_2,b_2) \in (R-A, S-B)$ and $(a_2,b_2) \in (C,D)$, $(a_1,b_1) \in (R-C, S-D)$. Due to the fact that every $^br\beta$ - *open* set is *binary open*, (A,B) and (C,D) are two different *binary open* sets with (a_1,b_1) and (a_2,b_2) corresponding to (A,B) and (C,D) respectively such that $(a_2,b_2) \in (R-A, S-B)$, $(a_1,b_1) \in (R-C, S-D)$. (R,S) is hence a *binary -T_1 space*.

Remark 3.8: The following example demonstrates that the converse of the aforementioned theorem is false.

Example 3.9: From the Example 3.6, Let $(A,B) = (\{b\}, \{1, 2\})$ and $(C,D) = (\{a\},\{1,3\})$. Let $(a_1,b_1) = (\{a\},\{1\})$ and $(a_2,b_2) = (\{b\},\{1,2\})$ where (a_1,b_1), $(a_2,b_2) \in (R,S)$ and $(a_1,b_1) \neq (a_2,b_2)$ then it is clear that $(a_1,b_1) \in (A,B)$, $(a_2,b_2) \in (R-A, S-B)$ and $(a_2,b_2) \in (C, D)$ and $(a_1,b_1) \in (R-C, S-D)$. Then it is *binary -T_1 space* but not a $^br\beta$ -T_1 *space*.

Theorem 3.10: Every $^br\beta$ -T_2 space is a *binary -T_2 space* in a binary topological space $(R,S,\mathscr{M})$.

Proof: Assume $a_1 \neq a_2$, $b_1 \neq b_2$ in the $^br\beta$ -T_2 space (R,S). If so there are disjoint $^br\beta$ -*open* sets (A,B) and (C,D) that are such that $(a_1,b_1) \in (A,B)$ and $(a_2,b_2) \in (C,D)$. The fact that (A, B) and (C,D) are disjoint *binary open* sets means that $(a_1,b_1) \in (A,B)$ and $(a_2,b_2) \in (C,D)$. This is because every $^br\beta$ -*open* set is *binary open*. (R,S) is a *binary -T_2 space* as a result.

Example 3.11: From the Example 3.6, Let $(a_1,b_1) = (\{b\}, \{3\})$ and $(a_2,b_2) = (\{a\},\{2\})$. Let $(A,B) = (\{a\},\{1,2\})$ and $(C,D) = (\{b\},\{3\})$ where (a_1,b_1), $(a_2,b_2) \in (R,S)$ and $(a_1,b_1) \neq (a_2,b_2)$ then it is clear that $(a_2,b_2) \in (A,B)$, and $(a_1,b_1) \in (C,D)$. Then we can say that it is $^br\beta$ -T_2 *space*. As every $^br\beta$- *open* set is *binary open*, (R,S) is a *binary-T_2 space*.

Theorem 3.12: Every $^br\beta$ -T_1 space is a $^br\beta$ -T_0 space in a binary topological space $(R,S,\mathscr{M})$.

Proof: Let (a_1,b_1) and (a_2,b_2) be two unique points of a $^br\beta$ -T_1 space (R,S). Given that (R,S) is $^br\beta$ -T_1 space there are $^br\beta$ *open* sets (A,B) and (C,D) with $(a_1,b_1) \in (A,B)$ and $(a_2,b_2) \in (C,D)$ such that $(a_2,b_2) \in (R-A, S-B)$, $(a_1,b_1) \in (R-C, S-D)$. As $(a_1,b_1) \in (A,B)$ and $(a_2,b_2) \in (R-A, S-B)$, $^br\beta$ -T_1 space is a $^br\beta$ -T_0 *space*.

Theorem 3.13: Every $^br\beta$ -T_2 space is a $^br\beta$ -T_0 space in a binary topological space $(R,S,\mathscr{M})$.

Proof: Let (R,S) be a $^br\beta$ -T_2 space and let (a_1,b_1) and (a_2,b_2) be two unique points of (R,S). Since (R,S) is $^br\beta$ -T_2 space there exist $^br\beta$- *open* sets (A,B) and (C,D) such that $(a_1,b_1) \in (A,B)$ and $(a_2,b_2) \in (C,D)$. Due to the disjoint nature of (A,B) and (C,D) such that $(a_1,b_1) \in (A,B)$ and $(a_2,b_2) \in (R-A, S-B)$, (R,S) is a $^br\beta$ -T_0 *space* as a result.

Theorem 3.14: Every $^br\beta$ -T_2 space is a $^br\beta$ -T_1 space in a binary topological space $(R,S,\mathscr{M})$.

Proof: Suppose that $(R,S,\mathscr{M})$ is a $^br\beta$ -T_2 space with $(a_1,a_2) \in R$ and $(b_1,b_2) \in S$ with $a_1 \neq a_2$, $b_1 \neq b_2$. Then there are disjoint $^br\beta$ - *open* sets (U_1,V_1), (U_2,V_2) with $(a_1,b_1) \in (U_1,V_1)$, $(a_2,b_2) \in (U_2, V_2)$. We have $(a_1,b_1) \in (R-U_2, S-V_2)$ and $(a_2,b_2) \in (R-U_1, S-V_1)$, since (U_1,V_1) and (U_2,V_2) are disjoint. As can be seen $(R,S,\mathscr{M})$ is a $^br\beta$ -T_1 *space*.

Theorem 3.15: A binary topological space $(R,S,\mathscr{M})$ is a $^br\beta$ -T_0 space if and only if *binary $r\beta$ closure* of unique points is distinct.

Proof: Let (a_1,b_1) and (a_2,b_2) be two unique points of (R,S). There exists a $^br\beta$ - *open* set (U,V), since (R,S) is a $^br\beta$ -T_0 *space* such that $(a_1,b_1) \in (U_1,V_1)$ and $(a_2,b_2) \in (R-U_2, S-V_2)$. In light of this, $((R,S) - (U, V))$ is a $^br\beta$ - *closed* set that includes (a_2,b_2) but excludes (a_1,b_1). But all $^br\beta$ - *closed* set containing (a_2,b_2) are intersected by $^br\beta$-$cl(\{a_2,b_2\})$. Consequently $(a_2,b_2) \in {^br\beta}$-$cl(\{a_2,b_2\})$. On the other hand $(a_1,b_1) \neq {^br\beta}$-$cl(\{a_2,b_2\})$ as $(a_1,b_1) \notin ((R,S)-(U,V))$. Therefore $^br\beta$-$cl(\{a_1,b_1\}) \neq {^br\beta}$-$cl(\{a_2,b_2\})$ and hence *binary $r\beta$ closure* of unique points are distinct.

Conversely, let $^br\beta\text{-}cl(\{a_1,b_1\})$ ⊄ $^br\beta\text{-}cl(\{a_2,b_2\})$ for (a_1,b_1) ≠ (a_2,b_2). Then at least one point $(a_3,b_3)\in(R,S)$ exists such that $(a_3,b_3)\in {}^br\beta\text{-}cl(\{a_1,b_1\})$ but $(a_3,b_3)\notin {}^br\beta\text{-}cl(\{a_2,b_2\})$. We assert that $(a_1,b_1)\notin {}^br\beta\text{-}cl(\{a_2,b_2\})$ because this would implies that $^br\beta\text{-}cl(\{a_1,b_1\})\subseteq {}^br\beta\text{-}cl(\{a_2,b_2\})$ and so $(a_3,b_3)\in {}^br\beta\text{-}cl(\{a_2,b_2\})$, which is a contradiction. Because of this $(a_1,b_1)\notin {}^br\beta cl(\{a_2,b_2\})$, which implies that $(a_1,b_1)\in(R,S)-{}^br\beta\text{-}cl(\{a_2,b_2\})$, which is a $^br\beta$ - *open* set includes (a_1,b_1) but excludes (a_2,b_2). Therefore (R,S) is a $^br\beta$ -T_0 *space*.

Theorem 3.16: A binary topological space $(R,S,\mathcal{M})$ is a $^br\beta$ -T_1 *space* if and only if every binary point is $^br\beta$ - *closed*.
Proof: Consider $(R,S,\mathcal{M})$ to be a $^br\beta$ -T_1 *space*. Let $(r,s)\in R\times S$ and let $(\{r\},\{s\})\in\wp(R)\times\wp(S)$. We must demonstrate that $(\{r\},\{s\})$ is $^br\beta$ - *closed*. For that, it is sufficient to demonstrate that $(R-\{r\},S-\{s\})$ is $^br\beta$ - *open*. Let $(a, b)\in(R-\{r\}, S-\{s\})$. This suggests that $a\in R-\{r\}$ and $b\in R-\{s\}$. Thus a ≠ r and b ≠ s. That is (a,b) and (r,s) are distinct binary points of $R\times S$. Given that $(R,S,\mathcal{M})$ is $^br\beta$ -T_1, there are $^br\beta$ - *open* sets (A,B) and (C,D), $(a, b)\in(A,B)$ and $(r,s)\in(C,D)$ such that $(a,b)\in (R-C,S-D)$ and $(r,s)\in(R-A,S-B)$. Consequently $(A,B)\subseteq(R-\{r\},S-\{s\})$. Therefore the binary neighbourhood of (a,b) is $(R-\{r\},S-\{s\})$. This suggests that $(\{r\},\{s\})$ is $^br\beta$ *closed*.

Conversely, assume that $(\{r\},\{s\})$ is always $^br\beta$ - *closed* for $(r, s)\in R\times S$. With a_1 ≠ a_2, b_1 ≠ b_2, let (a_1,b_1) and $(a_2,b_2)\in R\times S$ .As a result $(a_2,b_2)\in(R-\{a_1\},S-\{b_1\})$ and $(R-a_1),S-\{b_1\})$ is $^br\beta$ - *open*. Also $(a_1,b_1)\in(R-\{a_2\}, S-\{b_2\})$ and $(R-\{a_2\}, S-\{b_2\})$ are $^br\beta$ - *open*. As can be seen $(R,S,\mathcal{M})$ is a $^br\beta$ -T_1 *space*.

Theorem 3.17: If a binary topological space $(R,S,\mathcal{M})$ is a $^br\beta$ -T_0 *space* then $(R,\mathcal{M}_R)$ and $(S,\mathcal{M}_S)$ are $r\beta$-T_0 *spaces*.
Proof: We have $\mathcal{M}_R =\{A\subseteq R :(A,B)\in\mathcal{M}$ for some $B\subseteq S\}$ is a topology on R and $\mathcal{M}_S =\{B\subseteq S : (A,B)\in\mathcal{M}$ for some $A\subseteq R\}$ is a topology on S, because $\mathcal{M}$ is a binary topology from R to S. With a_1 ≠ a_2, b_1 ≠ b_2, let $(a_1,a_2)\in R$ and $(b_1,b_2)\in S$. There exists $r\beta$ - *open* set (A,B) such that either $(a_1,b_1)\in (A,B)$, $(a_2,b_2)\in(R-A,S-B)$ or $(a_1,b_1)\in (R-A,S-B)$, $(a_2,b_2)\in (A,B)$, because $(R,S,\mathcal{M})$ is a $^br\beta$ - T_0 *space*. This suggests that either $a_1\in A$, $a_2\in R-A$, $b_1\in B$, $b_2\in S-B$ or $a_1\in R-A$, $a_2\in A$, $b_1\in S-B$, $b_2\in B$. Therefore $(R,\mathcal{M}_R)$ and $(S,\mathcal{M}_S)$ are $r\beta$-T_0 *spaces*.

Theorem 3.18: If a binary topological space $(R,S, \tau\mathcal{M}(R)\times\sigma\mathcal{M}(S))$ is a $^br\beta$ -T_0 *space*, then the topological spaces (R, τ) and (S, σ) are $r\beta$ -T_0 *spaces*.
Proof: Assume that $(R,S, \tau\mathcal{M}(R)\times\sigma\mathcal{M}(S))$ is a $^br\beta$ -T_0 *space*. With a_1 ≠ a_2, b_1 ≠ b_2, let $(a_1,a_2)\in R$ and $(b_1 b_2)\in S$ .Since $(R,S,\tau\mathcal{M}(R)\times\sigma\mathcal{M}(S))$ is a $^br\beta$ -T_0 *space*, There exists $(A,B)\in\tau\mathcal{M}(R)\times\sigma\mathcal{M}(S)$ such that either $(a_1,b_1)\in(A,B)$, $(a_2,b_2)\in(R-A,S-B)$ or $(a_1,b_1)\in (R-A,S-B)$, $(a_2,b_2)\in(A,B)$, because $(R,S, \tau\mathcal{M}(R)\times\sigma\mathcal{M}(S))$ is a $^br\beta$ -T_0 *space*. This suggests that either $a_1\in A$, $a_2\in R-A$, $b_1\in B$, $b_2\in S-B$ or A, $a\in R-A$, $a_2\in A$, $b_1\in S-B$, $b_2\in B$. and this suggests that either $a_1\in A$, $a_2\in R-A$ or $a_1\in R-A$, $a_2\in A$ and $b_1\in B$, $b_2\in S-B$ or $b_1\in S-B$, $b_2\in B$. Since $(A,B)\in\tau\mathcal{M}(R)\times\sigma\mathcal{M}(S)$, we have $A\in\tau$ and $B\in\sigma$. Hence (R,τ) and (S,σ) are $r\beta$-T_0 *spaces*.

Theorem 3.19: If a binary topological space $(R,S,\mathcal{M})$ is a $^br\beta$ -T_1 *space* then $(R,\mathcal{M}_R)$ and $(S,\mathcal{M}_S)$ are $r\beta$-T_1 *spaces*.
Proof: Since $\mathcal{M}$ is a binary topology from R to S, we have $\mathcal{M}_R =\{A\subseteq R :(A,B)\in\mathcal{M}$ for some $B\subseteq Y\}$ is a topology on R and $\mathcal{M}_S =\{B\subseteq S: (A,B)\in\mathcal{M}$ for some $A\subseteq R\}$ is a topology on S. Let us say $(a_1,a_2)\in R$ and $(b_1,b_2)\in S$ where a_1 ≠ a_2, b_1 ≠ b_2. There are $^br\beta$ - *open* sets (U_1,V_1), (U_2,V_2) with $(a_1,b_1)\in(U_1,V_1)$, $(a_2,b_2)\in(U_2,V_2)$, such that $(a_1,b_1)\in (R-U_2, S-V_2)$, $(a_2,b_2)\in (R-U_1, S-V_1)$, because $(R,S,\mathcal{M})$ is a $^br\beta$ -T_1 *space*. The implication is that $a_1\in U_1$, $a_2\in U_2$ and $b\in V_1$, $b_2\in V_2$ are such that $a_1\in R-U_2$, $a_2\in R-U_1$ and $b_1\in S-V_2$, $b_2\in S-V_1$. As a result, $(R,\mathcal{M}_R)$ and $(S,\mathcal{M}_S)$ are $r\beta$-T_1 *spaces*.

BINARY $r\beta$ – NORMAL SPACE

Using $^br\beta$ - *open* sets we introduce *binary $r\beta$ - normal space* in this section and examine some of its characteristics.

Definition 4.1: A binary topological spaces $(R,S,\mathcal{M})$ is called a *binary $r\beta$ - normal space* (briefly $^br\beta$ – *normal*) if $(R,S,\mathcal{M})$ is $^br\beta$ -T_1 and for every pair of mutually disjoint $^br\beta$ - *closed* sets (A_1,B_1), (A_2,B_2) there exists mutually disjoint $^br\beta$ - *open* sets (U_1,V_1), (U_2,V_2) such that $(A_1,B_1) \subseteq (U_1,V_1)$ and $(A_2,B_2) \subseteq (U_2,V_2)$

Example 4.2:   From the Example 3.6, Let (A_1,B_1) = ({a},{1}) and (A_2,B_2)= ({b},{3}) are mutually disjoint $^br\beta$ - *closed* sets . Let (U_1,V_1) = ({a},{1,2}) and (U_2,V_2) = ({b},{1,3}) Here (a_1,b_1) = ({a}, {1, 2}), (a_2,b_2) = ({b},{1,3})$\in(R,S)$ and (a_1,b_1) ⫫ (a_2,b_2) are mutually disjoint $^br\beta$ – *open* sets. then this shows that $(A_1,B_1)\subseteq(U_1,V_1)\in(A,B)$ and $(A_2,B_2)\subseteq(U_2,V_2)\in(C,D)$ as $(R,S,\mathcal{M})$ is $^br\beta$ -T_1 and so $(R,S,\mathcal{M})$ is a $^br\beta$ – *normal space*.

Theorem 4.3: A $^br\beta$ - *closed* subspace of $^br\beta$ - *normal space* is a $^br\beta$ – *normal space*.

Proof: Let (M,N) be a $^br\beta$ - *closed* subspace of a $^br\beta$ *normal space*. Let (A_1,B_1) and (A_2,B_2) be disjoint $^br\beta$ - *closed* subset of (M,N). Because (M,N) is $^br\beta$ - *closed* in (R,S), the *closed* subsets (A_1,B_1) and (A_2,B_2) are also $^br\beta$ - *closed* in (R,S). The fact rhat (R,S) is $^br\beta$- *normal*, means that there are disjoint $^br\beta$ - *open* sets (U_1,V_1) and (U_2,V_2) in (R,S), such that $(A_1,B_1)\subseteq(U_1,V_1)$ and $(A_2, B_2)\subseteq(U_2,V_2)$. Since both (A_1,B_1) and (A_2,B_2) contained in (M,N), we obtain $(A_1,B_1)\subseteq(M, N)\cap(U_1,V_1)$, $(A_2,B_2)\subseteq(M, N)\cap(U_2,V_2)$ and $((M,N)\cap (U_1,V_1))\cap(M, N)\cap(U_2,V_2)$ = $(\emptyset,\emptyset)$. Due to the fact that (U_1,V_1) and (U_2,V_2) are $^br\beta$ - *open* in (R,S), $(M,N)\cap(U_1,V_1)$ and $(M,N)\cap(U_2,V_2)$ are $^br\beta$ - *open* in (M,N). Thus in the subspace (M,N), we have disjoint $^br\beta$ - *open* sets $((M,N)\cap(U_1,V_1))$ containing (A_1,B_1) and $((M,N)\cap(U_2,V_2))$ containing (A_2,B_2). Consequently the subspace (M,N) is $^br\beta$ - *normal*.

Theorem 4.4:   The topological spaces (R,τ) and (S,σ) are $r\beta$-*normal spaces* if and only if the binary topological space $(R,S, \tau \mathcal{M}(R)\times\sigma \mathcal{M}(S))$ is a $^br\beta$ –*normal space*.

Proof: Assume (R,τ) and (S,σ) are $r\beta$ - *normal spaces* and (A_1,B_1) and (A_2,B_2) be disjoint pair of $^br\beta$ - *closed* sets in $(R,S,\mathcal{M})$. Then A_1,A_2 are disjoint $r\beta$- *closed* sets in (R,τ) and B_1,B_2 are disjoint $r\beta$ - *closed* sets in (S,σ). Since (R,τ) is $r\beta$ - *normal*, there exists disjoint $r\beta$- *open* sets in $U_1,U_2\in\tau$, $A_1\subseteq U_1$ and $A_2\subseteq U_2$. Also, since (S,σ) is $r\beta$-*normal*, there exists disjoint $r\beta$- *open* sets $V_1,V_2\in\sigma$, $B_1\subseteq V_1$ and $B_2\subseteq V_2$. This implies that $(A_1,B_1)\subseteq(U_1,V_1)$ and $(A_2,B_2)\subseteq(U_2,V_2)$. Because U_1 and U_2 are disjoint $r\beta$- *open* sets, we have $U_1\cap U_2$ = $\emptyset$. Also since V_1 and V_2 are disjoint $r\beta$- *open* sets, we have $V_1\cap V_2$ = $\emptyset$. Thus $(U_1\cap U_2,V_1\cap V_2)$ = $(\emptyset, \emptyset)$. Therefore (U_1,V_1) and (U_2,V_2) are disjoint $^br\beta$ -*open* sets. This suggests that $(R,S, \tau \mathcal{M}(R)\times\sigma \mathcal{M}(S))$ is a $^br\beta$ –*normal space*.

Conversely, assume that $(R,S, \tau \mathcal{M}(R)\times\sigma \mathcal{M}(S))$ is $^br\beta$ -*normal*. Let A_1,A_2 be disjoint $r\beta$-*closed* sets in (R,τ) and B_1,B_2 be disjoint $r\beta$-*closed* sets in (S,σ). Then (A_1,B_1), (A_2,B_2) are $^br\beta$ -*closed* in $(R,S, \tau \mathcal{M}(R)\times\sigma \mathcal{M}(S))$. Because of $(R,S, \tau \mathcal{M}(R)\times\sigma \mathcal{M}(S))$ is $^br\beta$ –*normal space*, there are disjoint $^br\beta$ -*open* sets (U_1,V_1) and (U_2,V_2) such that $(A_1, B_1)\subseteq (U_1,V_1)$ and $(A_2, B_2)\subseteq(U_2,V_2)$. That is, $A_1\subseteq U_1$, $A_2\subseteq U_2$ and $B_1\subseteq V_1$, $B_2\subseteq V_2$. Therefore (R,τ) and (S,σ) are $r\beta$-*normal spaces*.

REFERENCES

1. S.Nithyanantha Jothi and P.Thangavelu, Topology between two sets, *Journal of Mathematical Sciences & Computer Applications*, 1(3), (2011), 95-107.
2. S.Nithyanantha Jothi and P.Thangavelu, On binary topological spaces, *Pacific–Asian Journal of Mathematics*, 5(2), (2011), 133-138.
3. S.N. Jothi, P. Thangavelu, On binary continuity and separation axioms, *Ultra Sci.*, 24 (2012), 121-126
4. S.Nithyanantha Jothi, Binary Semi open sets in Binary topological Spaces, *International journal of Mathematical Archieve*, 7(9), (2016), 73-76.
5. A,Manonmani and S,Jayalakshmi, On regular beta closed sets in a Topological spaces, *Int. J. Sci and Research*, Vol 8, (2019), 1756-176
6. S.Jayalakshmi , A.Manonmani , Binary Regular Beta closed sets and Binary Regular Beta open sets in Binary Topological spaces, *The International journal of analytical and   experimental modal analysis*, (ISSN NO:0886-9367) Vol XII, Issue IV, (2020) , 494-497

RESEARCH ARTICLE

2-Antidomatic Number of a Graph

T. Ponnuchamy[1]* G. Mahadevan[1] C. Sivagnanam[2]

[1]Department of Mathematics, The Gandhigram Rural Institute- Deemed to be University, Gandhigram, Dindigul, Tamil Nadu, India.
[2]Department of General Requirements, University of Technology and Applied Sciences-sur, Sultanate of Oman

**Address for Correspondence
T. Ponnuchamy
Department of Mathematics,
The Gandhigram Rural Institute- Deemed to be University,
Gandhigram, Dindigul, Tamil Nadu, India.
E. Mail: tponnuchmay@gmail.com

ABSTRACT

In this paper, we introduce the concept "2-antidomatic number of a graph". A set $S \subseteq V(G)$ is said to be a 2- non dominating set if at least two vertices in $V - S$ are not adjacent to any vertex in S. A partition of the vertices of G into 2- non dominating sets is called 2-antidomatic partition of G. The minimum order of a 2-antidomatic partition is called 2-antidomatic number of G and is denoted by $\overline{d_2}(G)$. Here we discuss many results along with some standard type of graphs of this new parameter.

Keywords: Non dominating set, 2- non dominating set, Antidomatic number, 2- antidomatic number.

INTRODUCTION

Here we have to consider the finite, simple and undirected graph G with maximum degree $\Delta(G) < n - 2$. Let x be any vertex of G. Then the open neighborhood of x is denoted by $N(x)$, defined by $N(x) = \{u \in V(G) : xu \in E(G)\}$. The closed neighborhood of x is denoted by $N[x]$, defined by $N[x] = \{x\} \cup N(x)$.   Let $S \subseteq V(G)$. Then the open neighborhood of S is denoted as $N(S)$, defined as $N(S) = \bigcup_{x \in S} N(x)$. The closed neighborhood of S is denoted as $N[S]$, defined as $N[S] = \bigcup_{x \in S} N[x]$ [1]. A set $S \subseteq V(G)$ is said to be a dominating set if every vertex in $V - S$ are adjacent to some vertex in S [3]. A partition of the vertices of G into dominating sets is called a domatic partition of G. In 4, Zelinka B, introduced the concept of "antidomatic number of a graph". An antidomatic partition of G is a partition of $V(G)$, none of whose classes is a dominating set in G. The minimum number of classes of an antidomatic partition of G is the number $\bar{d}(G)$ of G. Motivated this concept, the authors introduce "2- antidomatic number of a graph". A set $S \subseteq V(G)$ is said to be a 2- non dominating set if at least two vertices in $V - S$ are not adjacent to any vertex in S. A partition of the vertices of G into 2- non dominating sets is called 2-antidomatic partition of G. The

minimum order of a 2-antidomatic partition is called 2-antidomatic number of G and is denoted by $\overline{d_2}(G)$. In this paper, we initiate a study of this parameter.

2- Antidomatic Number

Definition: 2.1

A set $S(\subseteq V(G))$ is said to be a 2-non dominating set if at least two vertices in $V - S$ are not adjacent to any vertex in S. A partition of the vertices of G into 2-non dominating sets is called 2- antidomatic partition of G. The minimum order of a 2- antidomatic partition is called 2- antidomatic number of G and is denoted by $\overline{d_2}(G)$.

Example: 2.2

Consider the graph G,
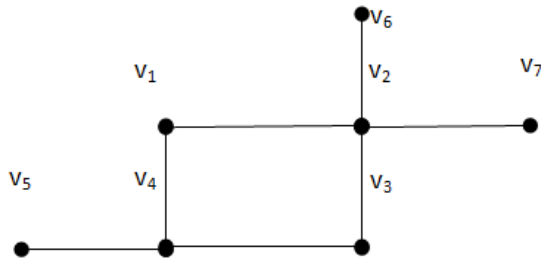
Figure 1 (Graph with 7 vertices and 7 edges)

Here $S_1 = \{v_1, v_3, v_4, v_5\}$ and $S_2 = \{v_2, v_6, v_7\}$ are 2-non dominating sets of G with $S_1 \cup S_2 = V(G)$ and $S_1 \cap S_2 = \emptyset$. Hence $\overline{d_2}(G) = 2$.

Remark: 2.3

If G is a graph with $\Delta(G) < n - 2$ and $n \geq 5$, then $\overline{d_2}(G)$ exists.

Theorem: 2.4

For any graph G, $2 \leq \overline{d_2}(G) \leq n$.

Proof:

Since the vertex set $V(G)$ is a 2-non dominating set of G, $\overline{d_2}(G) \neq 1$ hence $\overline{d_2}(G) \geq 2$ and since $|V(G)| = n$, $\overline{d_2}(G) \leq n$.

Theorem: 2.5

For a path $P_n, n \geq 6, \overline{d_2}(P_n) = 2$.

Proof:

Let $P_n = (v_1, v_2, \ldots, v_n), n \geq 6$ and let $S_1 = \{v_1, v_2, \ldots, v_{n-3}\}$, $S_2 = \{v_{n-2}, v_{n-1}, v_n\}$. It is clear that S_1 and S_2 are 2-non dominating sets of P_n. Also $S_1 \cup S_2 = V(P_n)$ and $S_1 \cap S_2 = \emptyset$. Hence (S_1, S_2) is a 2-antidomatic partition of P_n. Thus $\overline{d_2}(P_n) = 2$.

Remark: 2.6

$\overline{d_2}(P_5) = 3$.

Theorem: 2.7

For a cycle $C_n, n \geq 8, \overline{d_2}(C_n) = 2$.

Proof:

Let $C_n = (v_1, v_2, \ldots, v_n, v_1), n \geq 8$ and let $S_1 = \{v_1, v_2, \ldots, v_{n-4}\}$, $S_2 = \{v_{n-3}, v_{n-2}, v_{n-1}, v_n\}$. It is clear that S_1 and S_2 are 2-non dominating sets of C_n. Also $S_1 \cup S_2 = V(C_n)$ and $S_1 \cap S_2 = \emptyset$. Hence (S_1, S_2) is a 2-antidomatic partition of C_n. Thus $\overline{d_2}(C_n) = 2$.

Remark: 2.8

$\overline{d_2}(C_5) = 5, \overline{d_2}(C_6) = \overline{d_2}(C_7) = 3$.

Theorem: 2.9

If $rad(G) = 1$, then $\overline{d_2}(G)$ does not exist

Ponnuchamy *et al.*,

Proof:

Given $rad(G) = 1$. Then there is a vertex u in G, which is adjacent to every vertex in G. That is $\Delta(G) = n - 1$. By the remark 2.3, $\overline{d_2}(G)$ does not exist.

Theorem: 2.10

For any graph $G\left(\not\cong K_{r,s}; r \neq 3, \ s \neq 3\right), \overline{d_2}(G) = n$ if and only if $rad(G) = diam(G) = 2$.

Proof:

Let $G\left(\not\cong K_{r,s}; r \neq 3, \ s \neq 3\right)$ be a graph of order $n \geq 5$. Assume that $\overline{d_2}(G) = n$. It is clear that $rad(G) \geq 2$. Suppose $rad(G) > 2$, then every vertex in G has at least eccentricity 3. Let u and v be two distinct vertices of G and let $P: u = v_1, v_2, \ldots, v_r = v (r \geq 4)$ be a $u - v$ path in G. If $r \geq 5$, then $\{v_1, v_2\}$ is a 2-non dominating set of G and hence any minimum 2-antidomatic partition contains at most $n - 1$ classes. Hence $r \leq 4$. If $r = 4$, since ≥ 5, there exist a vertex $_1$ is adjacent to either $_2$ or $_3$. Without loss of generality we assume $_{21} \in ()$. If $_{13} \notin ()$, then $\{_1, _1\}$ is a 2- non dominating set of . If $_{13} \in ()$, then there exists a vertex $_2$ is non adjacent to any one of the vertices of $_{1,2}$ and v_3, then either $\{v_1, x_1\}$ or $\{v_1, v_2\}$ is a 2- non dominating set and hence any minimum 2-antidomatic partition contains at most $n - 1$ classes. Thus $\overline{d_2}(G) \leq n - 1$. This is a contradiction. Hence $rad(G) = 2$. Suppose $diam(G) > 2$. Let $P: u_1, u_2, \ldots, u_s = v_1 (s \geq 4)$ be a $u_1 - v_1$ path in G where $d(u_1, v_1) = diam(G)$. If $s \geq 5$, then $\{u_1, u_2\}$ is a 2-non dominating set of G and hence any minimum 2-antidomatic partition contains at most $n - 1$ classes. Hence $s \leq 4$. If $s = 4$, since $n \geq 5$, there exist a vertex x_1 is adjacent to either u_2 or u_3. Without loss of generality we assume $u_2x_1 \in E(G)$. If $x_1u_3 \notin E(G)$, then $\{u_1, x_1\}$ is a 2- non dominating set of G. If $x_1u_3 \in E(G)$, then there exists a vertex x_2 is non adjacent to any one of the vertices of x_1, u_2 and u_3, then either $\{u_1, x_1\}$ or $\{u_1, u_2\}$ is a 2- non dominating set and hence any minimum 2-antidomatic partition contains at most $n - 1$ classes. Thus $\overline{d_2}(G) \leq n - 1$. This is a contradiction. Hence $diam(G) = 2$. Thus $rad(G) = diam(G) = 2$.

Conversely let as assume that $rad(G) = diam(G) = 2$.

Suppose there is a set S with $|S| \geq 2$ is a 2-non dominating set in G. Let $u, v \in S$. Then there exists two vertices $x, y(x \neq y)$ in $V - S$ are non-adjacent to any vertex in S. If $uv \in E(G)$, then $d(u, x) \geq 2$ and $d(v, x) \geq 2$. Suppose $xy \in E(G)$, then either $d(u, y) > 2$ or $d(v, y) > 2$. Hence $diam(G) > 2$. Suppose $xy \notin E(G)$, then either $d(u, y) > 2$ or $d(v, y) > 2$. Hence $diam(G) > 2$. If $uv \notin E(G)$, then any pair of vertices $\{u, v, x, y\}$ have the distance at least 3. Hence $diam(G) > 2$. Thus any set S with $|S| \geq 2$ is not a 2-non dominating set. Hence every singleton set is a 2-non dominating set in G, $\overline{d_2}(G) = n$.

Theorem: 2.11

For a complete bipartite graph $K_{r,s}, r \geq 4 \ and \ s \geq 4, \ \overline{d_2}(K_{r,s}) = 4$.

Proof:

Let $K_{r,s}$ be a complete bipartite graph with bipartition $\{V_1, V_2\}$ where $V_1 = \{u_1, u_2, \ldots, u_r\}$ and $V_2 = \{v_1, v_2, \ldots, v_s\}, r \geq 4, s \geq 4$ and let $S_1 = \{u_1, u_2, \ldots, u_{r-2}\}, S_2 = \{u_{r-1}, u_r\}, S_3 = \{v_1, v_2, \ldots, v_{s-2}\}, S_4 = \{v_{s-1}, v_s\}$. It is clear that S_1, S_2, S_3, S_4 are 2-non dominating set of $K_{r,s}$. Also $S_1 \cup S_2 \cup S_3 \cup S_4 = V(K_{r,s})$and $S_i \cap S_j = \emptyset, i, j = 1,2,3,4 \ and \ i \neq j$. Hence (S_1, S_2, S_3, S_4) is a 2-antidomatic partition of $K_{r,s}$. Thus $\overline{d_2}(K_{r,s}) \leq 4$. Suppose $\overline{d_2}(K_{r,s}) < 4$.

Case:1 If $\overline{d_2}(K_{r,s}) = 3$, then there exists three disjoint set of vertices X_1, X_2 and X_3 are 2- non dominating sets in $K_{r,s}$. Then either any one of $X_i = V_j, i = 1,2,3; j = 1,2$ or there exists one X_i contains some vertices in V_1 and some vertices in V_2. Hence any one X_i is a dominating set. This is a contradiction.

Case: 2 If $\overline{d_2}(K_{r,s}) = 2$, then there exists two disjoint set of vertices X_1 and X_2 are 2- non dominating sets in $K_{r,s}$. Then either any one of $X_i = V_j, i = 1,2; j = 1,2$ or there exists one X_i contains some vertices in V_1 and some vertices in V_2. Hence any one X_i is a dominating set. This is a contradiction. Thus $\overline{d_2}(K_{r,s}) \geq 4$.Hence $\overline{d_2}(K_{r,s}) = 4$.

Theorem: 2.12

For a graph G, if $\overline{d_2}(G) = 2$, then $diam(G) \geq 3$.

Proof:

Assume that $\overline{d_2}(G) = 2$. Let (B_1, B_2) be a 2-antidomatic partition of G. Since B_1 is a 2- non dominating set, there exists two vertices in B_2 has no neighbor in B_1. Let $u_1, u_2 \in B_2$ such that $N(u_i) \cap B_1 = \emptyset, i = 1,2$. Also since B_2 is a 2- non

dominating set, there exists two vertices in B_1 has no neighbor in B_2. Let $v_1, v_2 \in B_1$ such that $N(v_i) \cap B_2 = \emptyset, i = 1,2$. It is clear that u_1 is not adjacent to v_1, $d(u_1, v_1) \neq 1$. Suppose $d(u_1, v_1) = 2$. Then (u_1, u, v_1) is a $u_1 - v_1$ path. Since u_1 has no neighbor in $B_1, u \in B_2$. Also since v_1 has no neighbor in $B_2, u \in B_1$. Then $u \in B_1 \cap B_2$, which is a contradiction. Hence $d(u_1, v_1) \geq 3$. Thus $diam(G) \geq 3$.

Theorem: 2.13
For a graph G, if $diam(G) \geq 5$, then $\overline{d_2}(G) = 2$.
Proof:
Assume that $diam(G) \geq 5$. Let $(u = u_1, u_2, u_3, \ldots, u_t = v); t \geq 6$ be a $u - v$ path in G with $d(u, v) = diam(G)$. Let $A = \{u_{t-1}, u_t\}$, let $X = N[A]$ and let $Y = V - N[A]$. Then (X, Y) is a 2- antidomatic partition of G with minimum order. Hence $\overline{d_2}(G) = 2$.

Theorem: 2.14
Let $G(\neq C_5)$ be a graph on n vertices. Then $\left\lceil \frac{n}{n-1-\delta(G)} \right\rceil \leq \overline{d_2}(G) \leq \Delta(G) + 3$.
Proof:
Let A be a 2-non dominating set of G. Then there exists two vertices $x(\neq)y$ in $V - A$ are not adjacent to any vertex in A. Thus $d(x) \leq n - 1 - |A|$. Also $n - 1 - |A| \geq \delta(G)$. Thus $|A| \leq n - 1 - \delta(G)$. Let $(V_1, V_2, V_3, \ldots, V_k)$ be a 2-antidomatic partition of order k with $\overline{d_2}(G) = k$. Then $n = |V_1| + |V_2| + \ldots + |V_k| \leq k(n - 1 - \delta)$. Thus $\frac{n}{n-1-\delta} \leq k = \overline{d_2}(G)$ and hence $\overline{d_2}(G) \geq \left\lceil \frac{n}{n-1-\delta} \right\rceil$. By the remark 2.3, $\Delta(G) < n - 2$. Let u be the vertex of G such that $d(u) = \Delta(G)$, let $N[u] = \{u, u_1, u_2, u_3, \ldots, u_\Delta\}$. Let $B = V(G) - N[u]$. Since $\Delta < n - 2$, we have $B \neq \emptyset$ and $|B| \geq 2$. Then at least two vertices of B are non-adjacent to u, $\{u\}$ is a 2-non dominating set. Suppose u_i is adjacent to remaining u_j and some vertices in B, then $d(u_i) \geq \Delta + 1$. This is a contradiction. Hence u_i is non-adjacent to some vertices in u_j or all the vertices in A. Suppose u_i is non-adjacent to u_r and u_i is adjacent to u_k, $1 \leq k \leq \Delta$ and $k \neq i, r$. Then u_i is adjacent to at most one vertex in B, $\{u_i\}$ is a 2- non dominating set. If u_i is not adjacent to B, then $\{u_i\}$ is a 2-non dominating set. Hence $\{u_i\}, 1 \leq i \leq \Delta$ is a 2-non dominating set. Suppose $|B| \geq 3$. If there is a vertex $x \in B$ is adjacent to all $u_j's$, then $d(x) = \Delta$. Thus x is non adjacent to every vertex in B. Then $(\{u, x\}, \{u_1\}, \{u_2\}, \ldots, \{u_\Delta\}, B - \{x\})$ is a 2- antidomatic partition of G. Suppose $|B| = 2$. Let $B = \{x, y\}$. If $|N(B) \cap N(u)| \leq \Delta - 1$, then B is a 2- non dominating set. Hence the partition $(\{u\}, \{u_1\}, \{u_2\}, \ldots, \{u_\Delta\}, B)$ is a 2-antidomatic partition of G. If $|N(B) \cap N(u)| = \Delta$.
Case: i
If x is adjacent to every $u_j's$ and y, then $d(x) > \Delta$, which is impossible.
Case: ii
If x is adjacent to every $u_j's$ and non-adjacent to y, then $(\{u\}, \{u_1\}, \{u_2\}, \ldots, \{u_\Delta\}, \{x\}, \{y\})$ is a 2-antidomatic partition of G.
Case: iii
If x and y are non-adjacent to some $u_j's$, then $(\{u\}, \{u_1\}, \{u_2\}, \ldots, \{u_\Delta\}, \{x\}, \{y\})$ is a 2-antidomatic partition of G. Thus $\overline{d_2}(G) \leq \Delta(G) + 3$.

Theorem: 2.15
For any connected graph G on n vertices, $\overline{d_2}(G) = n$ if and only if $\Delta(G) = n - 3$.
Proof:
Given G is a connected graph on n vertices. Assume that $\overline{d_2}(G) = n$, then every singleton set is a 2- non dominating set in G.
Claim: $\Delta = n - 3$.
We know that for any graph G with $\Delta < n - 2$, then $\overline{d_2}(G)$ exists. Hence $\Delta(G) \leq n - 3$.
Suppose assume that $\Delta(G) < n - 3$. Let u be any vertex of G such that $d(u) = \Delta$. Then $N[u] = \{u, u_1, u_2, \ldots, u_\Delta\}$. Since every singleton set is a 2- non dominating set, $\{u\}$ is a 2- non dominating set. Let v_1 and v_2 be any two vertices are not adjacent to u. Let $A = N[v_1] \cap (V - N[u])$ and $B = N[v_2] \cap (V - N[u])$. Since $v_1 \in A$ and $v_2 \in B$. Without loss of generality we may assume that $A \cap B = \emptyset$.

Ponnuchamy *et al.*,

Claim: A is a 2- non dominating set.

Suppose A is not a 2- non dominating set. Then either A is a dominating set or A is a non dominating set.

Case: 1 A is a dominating set.

By the definition of domination, u is adjacent to some vertex in A. This is a contradiction. (since u is adjacent to u_i only).

Case: 2 A is non dominating set.

By the definition non domination, there exists a vertex s in $V - A$ is not adjacent to any vertex in A.

Case: a $s \neq u$. In this case u is adjacent some vertex in A. This is a contradiction to the case:1.

Case: b $s = u$.

Then the vertex v_2 is adjacent to some vertices in A. This implies that $A \cap B \neq \emptyset$. This is the contradiction to our assumption. Suppose there is a vertex $l \neq u$ in $V - A$ is not adjacent to any vertex in A, then A is a 2- non dominating set which is a contradiction. Thus A is a 2- non dominating set. Similarly B is a 2- non dominating set. Therefore the partition $S = (\{u\}, \{u_1\}, \{u_2\}, \ldots , \{u_\Delta\}, A, B)$ is a 2-antidomatic partition of G. Since $d(u) = \Delta$ gives that u is not adjacent to at least 3 vertices. This implies that either $|A| \geq 2$ or $|B| \geq 2$.

Hence $|S| \leq n - 1$. Thus $\overline{d_2}(G) \leq n - 1$, which is a contradiction to our assumption

Hence $\Delta = n - 3$.

Conversely let us assume that $\Delta = n - 3$.

Claim: $\overline{d_2}(G) = n$

Suppose $\overline{d_2}(G) < n$. Then any 2 –antidomatic partition contains at most $n - 1$ classes. Let v be a vertex of G such that $d(v) = \Delta$ and let $N(v) = \{v_1, v_2, v_3, \ldots , v_{n-3}\}$. Also $V - N(v) = \{v, v_{n-2}, v_{n-1}\}$. This implies that $S = (\{v\}, \{v_1\}, \{v_2\}, \{v_3\}, \ldots , \{v_{n-1}\})$ is a 2- antidomatic partition of G and it contains n classes. This is a contradiction to our assumption. Hence $\overline{d_2}(G) \geq n$. Also for any connected graph $G, \overline{d_2}(G) \leq n$. Thus $\overline{d_2}(G) = n$.

Corollary: 2.16

For any connected graph G, $\overline{d_2}(G) = \Delta + 3$ if and only if $rad(G) = diam(G) = 2$.

ACKNOWLEDGMENT

REFERENCES

1. Chartrand G and Lesniak L, Graphs and Digraphs, Chapman and Hall/CRC Press Ltd, New York 1996.
2. Desormeaux W. J, Haynes T. W and Henning M. A, A Note on Non-dominating Partitions in Graphs, Discussiones Mathematicae Graph Theory, 2016; 36, 1043-1050.
3. Haynes T. W, Hedetniemi S. T and Slater P. J, Fundamentals of Domination in Graphs, Marcel Dekker, Inc. New York 1998.
4. Zelinka B, Antidomatic number of a Graph, Archivam Mathematicum, 1997; 33, 3, 191-195.

RESEARCH ARTICLE

Construction of Acceptance Sampling Plans using Stratified Ranked Set Sampling by Logistic Distribution

P. K. Deveka[1] and K.Saranya[2]*

[1]Assistant Professor, Department of Statistics, Government Arts College (Autonomous), Coimbatore – 641 018. (An Autonomous Institution Affiliated to Bharathiar University, Coimbatore), Tamil Nadu, India.
[2]Research Scholar, Department of Statistics, Government Arts College (Autonomous), Coimbatore – 641 018. (An Autonomous Institution Affiliated to Bharathiar University, Coimbatore), Tamil Nadu, India.

*Address for Correspondence
K.Saranya
Assistant Professor,
Department of Statistics,
Government Arts College (Autonomous), Coimbatore – 641 018.
(An Autonomous Institution Affiliated to Bharathiar University, Coimbatore),
Tamil Nadu, India.
E.Mail: saranyagac23@gmail.com

ABSTRACT

The Ranked set sampling is one of the conventional testing techniques utilized for cost decrease and getting more delegated test determination in overviews. At the point when the issue of heterogeneity happens in the population, utilization of delineation is suggested in writing to expand the effectiveness of assessors. Within the sight of heterogeneity and anomalies (outrageous qualities), Stratified Ranked Set Sampling (StRSS) has been proposed. This article proposes another ranked set sampling strategy to appraise the Operating Characteristic Curve, Average Outgoing Quality Curve, and Average Total Inspection using the Stratified Ranked Set Sampling techniques. Reading up the sample portion for corresponding and ideal is two notable strategies in separated examining. It additionally shows the fixed benefit of testing costs in strata. The outcomes for small and medium sample sizes show that StRSS beats its rival methods for both wonderful and defective rankings. A genuine informational index is likewise considered to concentrate on the exact meaning of the recently proposed inspecting system.

Keywords - Ranked Set Sampling, Stratified Ranked Set Sampling (StRSS), Proportional allocation, Optimum allocation, Acceptance Sampling Plans, Logistic Distribution.

INTRODUCTION

In ongoing many years, sampling with ranked sets (RSS) has drawn in a lot of examination interest. McIntyre proposed the idea of RSS in 1952 for assessing the typical rummage and field yields. McIntyre noticed that RSS is considerably more compelling than SRS when it is simpler to rank perceptions. As of late, RSS has been utilized related to other sampling plans, as the last phase of testing in multi-stage plans, or in stratified sampling designs. The accuracy of a simple random sampling gauge relies on the size of the sample and the changeability of the population. The size of the sample can't be unduly expanded: subsequently, the best way to build the accuracy of the gauge is to devise a strategy that will really decrease the sample size. One such strategy is known as the technique of Stratified Random Sampling (StRS). It follows that it will upgrade the accuracy of the gauge since every stratum inside itself will be more homogeneous than the whole population. Samawi (1996) presented the idea of Delineated Positioned Set Examining (StRSS) and Nematollahi et al. (2008) utilized Ranked Set Sampling in the second phase of a two-stage group testing plan to work on the accuracy of the population mean gauge. While separated testing plans are to be utilized, one key inquiry that must be promptly tended to is the number of perceptions that ought to be taken in every stratum. The response to this question is vital in light of the fact that the sample size is a significant component for surmising the population in view of test information.

SAMPLE SIZE ALLOCATIONS

In Stratified Sampling, the distribution of the sample to various strata is the assurance of the size of the sample to be chosen from every stratum, is finished by the thought of these elements viz, i) Stratum size or the total number of units in the Stratum, ii) The variability within the Stratum and iii) The cost of taking observation per sampling unit in the Stratum. A decent portion is where the greatest accuracy is gotten with most extreme assets, That standard of designation is to limit the complete expense for a given difference or limit the fluctuation for a proper expense, In this manner utilizing accessible assets, two strategies for distribution of test size to various Layers are i) Proportional Allocation and ii) Optimum Allocation.

While planning a sample overview of a stratified population, one of the significant contemplations is the manner by which to designate the all-out sample size 'n' among the 'L' recognized strata. On the off chance that unit changes or expenses of inspecting vary among the strata, testing effectiveness can be expanded by over-sampling the variable. Thus, the sample fashioner may choose to limit the fluctuation of assessment for a predetermined expense of taking the sample or to limit the expense for a predefined worth of the difference of the assessment. This allocation technique is depicted as "Optimum allocation". On the off chance that the sampling division is similar in all strata, the delineation is depicted as a definition with relative designation. This portion is utilized to guarantee that the dispersion of the sample in subpopulations (strata) is a "proportional allocation" to their size. With this foundation, corresponding and ideal portions in StRSS for Logistic distribution are described.

Proportional Allocation:
According to the description of proportional sample allocation in StRSS, the number of sample units in the hth stratum (h = 1, 2...., L) is proportional to the stratum size, that is

$$\frac{N_h}{N} \Rightarrow n_h = \frac{n}{N} N_h \qquad (1)$$

Where N_h is the number of sampling units in the hth stratum (h= 1,2, 3,...L), n_h is the number of sampling units selected from the hth stratum,

Optimum Allocation:
Let c_h, h = 1, 2..., L be the cost of sampling for a unit in stratum h. The costs can differ substantially between strata. Assume $n_{0h} = m_h n_h$ be the sample size from h^{th} stratum in StRSS with m_h cycles in h^{th} stratum. The total cost of the survey can be taken as C = $c_0 + \sum_{h=1}^{L} c_h m_h n_h$ (c_0 is the fixed cost, C_h is the cost per unit in the hth stratum). This relation is a linear cost function and c_0 is a fixed cost of sampling. Suppose to minimize the variance of the mean estimator for

Deveka and Saranya

a specified cost C and minimize the cost for a specified variance of the mean estimator, let us consider the two cases, whether an odd or even number of sample units were selected from each stratum in each cycle.

Therefore, $n_h = \frac{N_h S_h}{\sum_{h=1}^{L} N_h S_h} * n$ (2)

Where N_h is the number of sampling units in the hth stratum (h= 1,2, 3,.... L), n_h is the number of sampling units selected from the hth stratum, S_i is the population mean of the h_{th} stratum.

STRATIFIED RANKED SET SAMPLING (StRSS)

In the stratified sampling method, the population of N units is divided into L non-overlapping subpopulations each of N_1, N_2,.... N_L units, respectively, and $N_1+ N_2+....+N_L= N$. These subpopulations are called strata. For full benefit from stratification, the size of the hth subpopulation, denoted by N_h for 1, 2,...,L , must be known. Then the samples are drawn independently from each stratum, producing sample sizes denoted by n_1, n_2,....n_L , such that the total sample size is n $=\sum_{h=1}^{L} n_h \sum_{h=1}^{L} rm_h$. Where 'r' is the number of cycles, m_h is the number of selected units in each stratum and cycle, and m is the number of selected units in each cycle. If the ranked set sample is taken from each stratum, the whole process is described as StRSS.

The following notations were used for the stratified ranked set sample when the ranking is on the variable X. For the hth cycle and the hth stratum, the StRSS is denoted by $(Y_{h[1]i}, X_{h(1)i}),(Y_{h[2]i}, X_{h(2)i}), . . . ,(Y_{h[rh]i}, X_{h(rh)i})$: i= 1, 2, . . . , m; h = 1, 2, . . . , L} , where $Y_{h[i]k}$ is the ith Judgment ordering in the ith set for the study variable and $X_{h(i)k}$ is the ith order statistic in the ith set for the auxiliary variable. The element of the favoured RSS pattern will be inside the shape:

{X [m+1/2, m]ih ; i= 1,2,...m, h=1,2,....,L} m is odd
{X[m/2;m]ih, X[m+2/2;m]kh; i=1,2,...,m/2; k=m+2/2,....m, h= 1,2,...L} m is even

Where $X[m+1/2,m]ih$ is the $(m+1)^{th}$ judgment order statistics of the ith random sample of size m in the h th cycle. It should be noted that all of $X[m+1/2,m]ih$'s are mutually independent and identically distributed. Now, based on the RSS scheme the distribution function, in general, will be:

$$f_{RSS}(x) = \begin{cases} \frac{1}{rm}\sum_{j=1}^{r}\prod_{i=1}^{m} f_{(m+1/2)i}(x) & m \text{ is odd} \\[3mm] \frac{1}{rm}\sum_{j=1}^{r}\prod_{i=1}^{m/2} f_{(m/2)i}(x) + f_{(m+2/2)i}(x) & m \text{ is even} \end{cases}$$

Equivalently to:

$$f_{RSS}(x) = \begin{cases} \frac{1}{rm}\prod_{i=1}^{m} f_{(m+1/2)i}(x) & m \text{ is odd} \\[3mm] \frac{1}{rm}\prod_{i=1}^{m/2} f_{(m/2)i}(x) + f_{(m+2/2)i}(x) & m \text{ is even} \end{cases}$$

The ith order statistic is given by,
$$f_{X(i)}(x) = \frac{n!}{(i-1)!(n-i)} (F(x))^{i-1} (1 - F(x))^{n-i}, -\infty < x < \infty$$

therefore,
$F_{X(i)} = (F(x))^{i-1}(1-F(x))^{n-i}$ $, -\infty < x < \infty$ (3)
Therefore, Stratified Ranked Set Sampling is given by
$F_{StRSS(x)} = (F(x))^{m}(1-F(x))^{m}$ (4)
Most investigations of positioned insights have been ranked data by assessing the population mean. In any case, none of the past research thought about any of the StRSS idea in the acceptance sampling context, this article could be considered as a new contribution in this practical research area.

Deveka and Saranya

CHARACTERIZATION OF THE LOGISTIC DISTRIBUTIONS UNDER StRSS

In this portion, the appropriations could be fundamentally dependent on the StRSS. The effect of the shape parameter on the distribution structure under StRSS using Logistic distribution is obtained as

$$f_{StRSS}(x) = \left[\frac{e^{-(x-\mu/s)}}{[1+e^{-(x-\mu)/s]^2}}\right]^m \left[1 - \frac{e^{-(x-\mu/s)}}{[1+e^{-(x-\mu)/s]^2}}\right]^m \tag{5}$$

OPERATING CHARACTERISTIC (OC) CURVE

Connected with each sampling plan there is an OC curve that portrays the show of the testing plan against perfect and bad quality. The probability that a ton will be recognized under a given sampling plan which is shown by Pa(p) and a plot of Pa(p) against a given worth of part or interaction quality p will yield the OC curve. For one-of-a-kind explanation plans the OC curve, is a curve showing the probability of continuing to permit the communication to happen without change as a component of the interaction quality.

The curve plots the probability of accepting the lot (Pa) versus the lot fraction defective (p)

$$Pa = P\{d \le c\} = \sum_{i=0}^{c} p^i 1 - p^{n-i} \tag{6}$$

Logistic distribution for StRSS will be

$$Pa = \sum_{i=0}^{c} \left[\frac{e^{-(x-\mu/s)}}{s[1+e^{-(x-\mu)/s]^2}}\right]^i \left[1 - \frac{e^{-(x-\mu/s)}}{s[1+e^{-(x-\mu)/s]^2}}\right]^{(n-i)} \tag{7}$$

Table 1: The OC Curve Values for Logistic Distribution using StRSS

The given table shows the OC curve values for StRSS using Logistic distribution for N_1=1200, N_2= 1800, N_3 = 1600, N_4 = 1400, m = 20, s= 4.44, r= 1, 2, 3, 4, 5, 6, n= 50, 100, 150, 200, 250,300 and n_h= 12, 18, 16, 14. The following figure-1and figure-2 shows the OC Curve for Logistic distribution using StRSS (Proportional and Optimum) for the acceptance number c=0, N_1=1200, N_2= 1800, N_3 = 1600, N_4 = 1400, m = 20, s= 4.44, r= 1, 2, 3, 4, 5, 6, n= 50, 100, 150, 200, 250,300 and n_h= 12, 18, 16, 14.

It shows the impact of expanded sample size on the OC curve. We note that each plan utilizes the equivalent percent deficient which can be considered an acknowledgment parcel, the OC curve becomes more extreme and lies nearer to the beginning as the sample size increments.

AVERAGE OUTGOING QUALITY (AOQ) - An ordinary technique, while inspecting and testing is non-unfortunate, is to 100 percent survey excused lots and replaces all defectives with extraordinary units. For this present circumstance, all excused parts are made wonderful and the principal distortions left are those in lots that were acknowledged. AOQs insinuate the excessively long blemish level for this united LASP (Lot Acceptance Sampling Plan) and 100 percent assessment of the excused parts process. In the event that all parts come in with a deformity level of precisely p, and the OC curve for the picked (n, c) LASP demonstrates a probability Pa of tolerating such a lot, for a really long time the AOQ can undoubtedly be demonstrated to be:

$$AOQ = \frac{Pa(p)(N-n)}{N} \tag{8}$$

Where N is the lot size have given expressions for AOQ to different policies adopted for Stratified Ranked Set Sampling (StRSS). In this research, AOQ is approximated as p * Pa(p).

Table 2: The AOQ Values for Logistic Distribution using StRSS

The given table shows the AOQ values for StRSS using Logistic distribution for N_1=1200, N_2= 1800, N_3 = 1600, N_4 = 1400, m = 20, s= 4.44, r= 1, 2, 3, 4, 5, 6, n= 50, 100, 150, 200, 250,300 and n_h= 12, 18, 16, 14.

The following figure-4 and figure-5 shows the AOQ Curve for Logistic distribution using StRSS (Proportional and Optimum) for the acceptance number c=0, N_1=1200, N_2= 1800, N_3 = 1600, N_4 = 1400, m = 20, s= 4.44, r= 1, 2, 3, 4, 5, 6, n=

50, 100, 150, 200, 250,300 and n_h= 12, 18, 16, 14. For the acceptance sampling plan i in which correction isn't finished, the AOQ is equivalent to the approaching quality. Thus, when the lot is either acknowledged or dismissed, the AOQ is equivalent to the nature of the submitted part.

AVERAGE TOTAL INSPECTION (ATI)
Right when excused lots are 100% explored, it is easy to work out the ATI if parts come dependably with a disfigurement level of ' p'. For a Lot Acceptance Sampling Plan (n, c) with a probability Pa of enduring a lot with disfigurement level p, one can have

ATI=n+(1-Pa)(N-n)   (9)

Where N is the lot size, n is the sample size.

Table 3: The ATI Values for Logistic Distribution using StRSS
Table 3 shows the ATI values for StRSS using Logistic distribution for N_1=1200, N_2= 1800, N_3 = 1600, N_4 = 1400, m = 20, s= 4.44, r= 1, 2, 3, 4, 5, 6, n= 50, 100, 150, 200, 250,300 and n_h= 12, 18, 16, 14.

The following figure-6 and figure-7 shows the ATI Curve for Logistic distribution using StRSS (Proportional and Optimum) for the acceptance number c=0, s=4.44, m=20, r= 1, 2, 3, 4, 5, 6 and sample size n=50, 100, 150, 200, 250 and 300. The curve drawn between ATI and the lot quality (p) is known as ATI curve. A typical ATI curve for a single sample plan is shown for n= 50,100, 150, 200, 250 and 300.

PRACTICAL APPLICATION
The plastic chair manufacturing company is working on 4 shift bases, every shift has 6 hours, the first shift has produced 1200 chairs, the second shift produced 1800 chairs, the third shift produced 1600 chairs and the fourth shift produced 1400 chairs per day. End of the day, the manufacturing company produces chairs in lots (N) of 5000 by using Stratified Ranked Set Sampling (StRSS) method, distributed by Logistic distribution. Then, the scale parameter (s) is 4.44, sample set size (m) is 50 and the cycle size (r) is 3. The quality of incoming lot is 0.020 and acceptance numbers are 0 and 1. Find out the sample allocation for Proportional and Optimum.

EXPLANATION
It is given that the plastic chair manufacturing company has produced 1200 Plastic chairs in shift 1 (N_1), 1800 in shift 2 (N_2), 1600 in shift 3 (N_3) and 1400 in shift 4 (N_4). The lot size of the plastic chair company is 5000 (i.e., N = N_1+N_2+N_3+N_4). The sample size of plastic chairs m =50 and sample cycle size r = 3 (specified by the producer). Hence, n= m*r (150 = 50*3).   Using StRSS, the lots (N) is divided by 4 strata. The first stratum (N_1) contains 1200 chairs, the second stratum (N_2) contains 1800 chairs, the third stratum (N_3) contains 1600 chairs and the fourth stratum (N_4) contains 1400 chairs. For a fixed lot quality p = 0.020, the value of the parameter (s) is 4.44. Then $[m,r]_{ij}$ is the $(m,r)^{th}$ order statistics of the ith random sample of size m in the jth cycle. In a sample of n=150 specimens selected from a lot of plastic chairs manufacturing company, using StRSS the allocation of the sample sizes for different strata is done in the following ways: a) Proportional allocation and b) Optimum allocation. If X≤c, the lot is accepted, otherwise reject the lot and inform the management for further action.

In Proportional allocation, If X represents the number of defective plastic chairs in the sample, Then if X=0 the probability of accepting the lot Pa(p) is 0.77, AOQ is 0.76, ATI is 1198. If X=1 the probability of accepting the lot Pa(p) is 0.77, AOQ is 0.77, ATI is 1169.   In Optimum allocation, If X represents the number of defective chairs in the sample, Then if X=0 the probability of accepting the lot Pa(p) is 0.67, AOQ is 0.66, ATI is 1684. If X=1 the probability of accepting the lot Pa(p) is 0.68, AOQ is 0.67, ATI is 1660.

CONCLUSION

In this study, an efficient and easily applicable Stratified Ranked Set Sampling (StRSS) procedure has been proposed for estimating OC Curve, AOQ, and ATI. Real life data set has also been presented to illustrate the relative efficiency of StRSS over its competitor procedures. It concludes that the proposed Stratified Ranked Set Sampling has performed better toward small and persistent shifts detection at small values of smoothing parameters. The StRSS performance by Logistic distributions is far better. It is recommended for future research to propose some ratio, product, regression and exponential type generalized estimators under StRSS for estimating population parameters under heterogeneous environment. This procedure will also be recommended to use in monitoring of location and scale parameters with control chart schemes such as Shewhart, EWMA, CUSUM and also, this study can be extended further for the various parameters such as AQL, LQL, IQL, AOQL, MAPD and MAAOQL. Further it can be extended to Double Sampling Plan, Multi-stage Sampling Plan, other Special Purpose Plans as Chain Sampling, Skip Plot Sampling Plans as well.

REFERENCES

1. Asad Ali, Muhammad Moeen But, Din Azad Zahoor Ahmed and Muhammad Hanif: Stratified Extreme-Cum-Median Ranked Set Sampling. Pak. J. Statist. 2021 Vol. 37(3); 215-235.
2. Mahmoud Ibrahim Syam, Amer Ibrahim AI-Omari: The Efficiency of Stratified Quartile Ranked Set Sampling in Estimating the Population Mean, Tamsui Oxford. Journal of Information and Mathematical Sciences 28(2) (2012);175-190.
3. Muttlak, H. and AI-Sabah: Statistical quality control based on ranked set sampling. Journal of Applied Statistics; 3: 1055- 1078.
4. Shah, I.A., Mir, S.A., Khan : New quartile-based variant of the ranked set sampling scheme. Journal of Indian Society of Agricultural Statistics; 74(3): 255-264.
5. Kaur, A., Patil, G.P. and Taillie, C: Unequal allocation models for ranked set sampling with skew distributions. Technical Report;94-0930.
6. CHEN, Z.: On ranked-set sample quartiles and their applications. Journal of Statistical Planning and Inference; 83:125-135.
7. Amer Ibrahim AI-Omari and Carlos N.Bouza: Review of Ranked Set Sampling: Modification and Applications. Revista Investigaion Operacional; Vol-35: No.3:215-235.
8. Chen, Z., Bai, Z.D. and Sinha, B.K: Ranked set sampling: Theory and applications. Springer; Verlag New York, Inc.
9. Busra Sevinc and ettal: RSSampling: A Pioneering Package for Ranked Set Sampling. The R Journal; Vol. 11/01: June 2019.
10. Rabali Alam and ettal: Estimation of population variance under ranked set sampling method by using the ratio of supplementary information with study variable. Scientific Reports 12; AC 21203(2022).

Deveka and Saranya

Table 1: The OC Curve Values for Logistic Distribution using StRSS

n p	1m		2m		3m		4m C=0		5m		6m	
	Prop	**Opt**	**Prop**	**Opt**	**Prop**	**Opt**	**Prop**	**Opt**	**Prop**	**Opt**	**Prop**	**Opt**
0.010	0.97	0.95	0.93	0.9	0.9	0.86	0.87	0.82	0.84	0.78	0.82	0.74
0.015	0.95	0.92	0.9	0.85	0.85	0.78	0.8	0.72	0.76	0.66	0.72	0.61
0.020	0.91	0.88	0.84	0.77	0.77	0.67	0.7	0.59	0.64	0.51	0.59	0.45
0.025	0.87	0.81	0.75	0.65	0.65	0.53	0.57	0.43	0.49	0.35	0.43	0.28
0.030	0.8	0.72	0.65	0.52	0.52	0.37	0.42	0.27	0.33	0.19	0.27	0.14
0.035	0.72	0.61	0.52	0.37	0.37	0.23	0.27	0.14	0.19	0.09	0.14	0.05
0.040	0.63	0.5	0.39	0.25	0.25	0.12	0.16	0.06	0.1	0.03	0.06	0.02
0.045	0.54	0.4	0.29	0.16	0.16	0.06	0.09	0.03	0.05	0.01	0.03	0.01
0.050	0.48	0.34	0.23	0.11	0.11	0.04	0.05	0.01	0.03	0.01	0.01	0.01
0.055	0.46	0.32	0.22	0.1	0.1	0.03	0.05	0.01	0.02	0.01	0.01	0.01
p							**C=1**					
	Prop	**Opt**	**Prop**	**Opt**	**Prop**	**Opt**	**Prop**	**Opt**	**Prop**	**Opt**	**Prop**	**Opt**
0.010	0.97	0.95	0.94	0.91	0.91	0.86	0.88	0.82	0.85	0.78	0.82	0.74
0.015	0.95	0.92	0.9	0.85	0.85	0.78	0.81	0.72	0.76	0.66	0.72	0.61
0.020	0.92	0.88	0.84	0.77	0.77	0.68	0.71	0.59	0.65	0.52	0.59	0.45
0.025	0.88	0.82	0.76	0.66	0.66	0.54	0.58	0.43	0.5	0.35	0.43	0.28
0.030	0.82	0.73	0.66	0.53	0.53	0.38	0.42	0.27	0.34	0.2	0.27	0.14
0.035	0.74	0.63	0.53	0.38	0.38	0.23	0.28	0.14	0.2	0.09	0.14	0.05
0.040	0.65	0.52	0.41	0.26	0.26	0.13	0.16	0.06	0.1	0.03	0.06	0.02
0.045	0.57	0.42	0.31	0.17	0.17	0.07	0.09	0.03	0.05	0.01	0.03	0.02
0.050	0.51	0.36	0.25	0.12	0.12	0.04	0.06	0.01	0.03	0.01	0.01	0.01
0.055	0.5	0.34	0.23	0.11	0.11	0.03	0.05	0.01	0.02	0.01	0.01	0.01

Table 2: The AOQ Values for Logistic Distribution using StRSS

n p	1m		2m		3m		4m C=0		5m		6m	
	Prop	**Opt**	**Prop**	**Opt**	**Prop**	**Opt**	**Prop**	**Opt**	**Prop**	**Opt**	**Prop**	**Opt**
0.010	0.96	0.95	0.93	0.9	0.9	0.85	0.86	0.8	0.83	0.76	0.8	0.72
0.015	0.94	0.92	0.89	0.84	0.84	0.77	0.79	0.71	0.75	0.65	0.71	0.6
0.020	0.91	0.87	0.83	0.76	0.76	0.66	0.69	0.58	0.63	0.5	0.58	0.44
0.025	0.87	0.81	0.75	0.65	0.65	0.52	0.56	0.42	0.49	0.34	0.42	0.27
0.030	0.8	0.72	0.64	0.51	0.51	0.37	0.41	0.26	0.33	0.19	0.26	0.14
0.035	0.72	0.61	0.52	0.37	0.37	0.23	0.27	0.14	0.19	0.08	0.14	0.05
0.040	0.63	0.5	0.39	0.25	0.25	0.12	0.15	0.06	0.1	0.03	0.06	0.01
0.045	0.54	0.4	0.29	0.16	0.16	0.06	0.09	0.02	0.05	0.01	0.02	0.01
0.050	0.48	0.33	0.23	0.11	0.11	0.04	0.05	0.01	0.03	0.01	0.01	0.01
0.055	0.46	0.32	0.22	0.1	0.1	0.03	0.05	0.01	0.02	0.01	0.01	0.01
p							**C=1**					
	Prop	**Opt**	**Prop**	**Opt**	**Prop**	**Opt**	**Prop**	**Opt**	**Prop**	**Opt**	**Prop**	**Opt**
0.010	0.97	0.95	0.93	0.9	0.9	0.85	0.87	0.81	0.84	0.76	0.81	0.72
0.015	0.95	0.92	0.9	0.85	0.85	0.78	0.8	0.71	0.75	0.65	0.71	0.6
0.020	0.92	0.88	0.84	0.77	0.77	0.67	0.7	0.58	0.64	0.51	0.58	0.44

64132

Deveka and Saranya

0.025	0.88	0.82	0.76	0.66	0.66	0.53	0.57	0.43	0.49	0.34	0.43	0.28
0.030	0.82	0.73	0.65	0.52	0.52	0.38	0.42	0.27	0.34	0.19	0.27	0.14
0.035	0.74	0.63	0.53	0.38	0.38	0.23	0.27	0.14	0.2	0.09	0.14	0.05
0.040	0.65	0.51	0.41	0.26	0.26	0.13	0.16	0.06	0.1	0.03	0.06	0.02
0.045	0.57	0.42	0.31	0.17	0.17	0.07	0.09	0.03	0.05	0.01	0.03	0.02
0.050	0.51	0.36	0.25	0.12	0.12	0.04	0.06	0.01	0.03	0.01	0.01	0.01
0.055	0.49	0.34	0.23	0.11	0.11	0.03	0.05	0.01	0.02	0.01	0.01	0.01

Table 3: The ATI Values for Logistic Distribution using StRSS

n p	1m		2m		3m		4m C=0		5m		6m	
	Prop	Opt	Prop	Opt	Prop	Opt	Prop	Opt	Prop	Opt	Prop	Opt
0.010	178	265	350	516	516	754	676	980	831	1193	980	1395
0.015	280	414	544	793	793	1141	1028	1460	1251	1753	1460	2022
0.020	436	640	834	1198	1198	1684	1529	2109	1832	2479	2109	2801
0.025	669	969	1248	1750	1750	2379	2184	2887	2561	3297	2887	3627
0.030	993	1414	1790	2427	2427	3155	2939	3677	3348	4051	3677	4319
0.035	1408	1955	2419	3146	3146	3871	3668	4312	4043	4581	4312	4745
0.040	1870	2523	3040	3773	3773	4392	4232	4699	4519	4851	4699	4926
0.045	2297	3012	3539	4210	4210	4686	4573	4875	4769	4950	4875	4980
0.050	2591	3328	3839	4441	4441	4813	4731	4937	4870	4979	4937	4993
0.055	2681	3421	3925	4501	4501	4843	4769	4950	4893	4984	4950	4995
p							**C=1**					
	Prop	Opt	Prop	Opt	Prop	Opt	Prop	Opt	Prop	Opt	Prop	Opt
0.010	165	252	337	504	504	742	664	968	819	1182	968	1385
0.015	258	392	523	774	774	1123	1010	1444	1233	1738	1444	2008
0.020	402	607	803	1169	1169	1660	1504	2087	1809	2460	2087	2785
0.025	617	921	1203	1711	1711	2348	2151	2862	2532	3276	2862	3610
0.030	920	1347	1730	2380	2380	3121	2901	3652	3318	4033	3652	4307
0.035	1308	1871	2347	3094	3094	3839	3631	4293	4016	4570	4293	4738
0.040	1746	2425	2963	3725	3725	4368	4202	4687	4500	4845	4687	4923
0.045	2155	2908	3462	4168	4168	4669	4550	4869	4757	4948	4869	4979
0.050	2440	3223	3767	4406	4406	4801	4714	4934	4862	4978	4934	4993
0.055	2529	3317	3854	4469	4469	4832	4754	4947	4886	4983	4947	4995
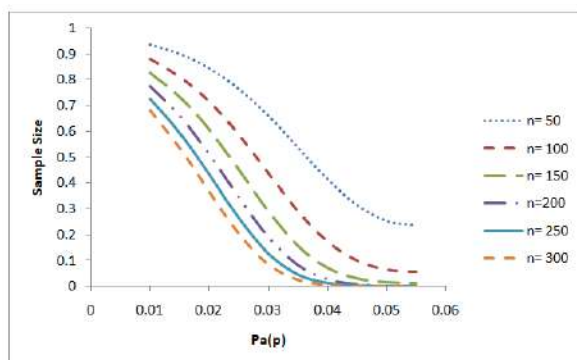
Figure 1: OC Curve for Logistic Distribution using StRSS (Proportional)
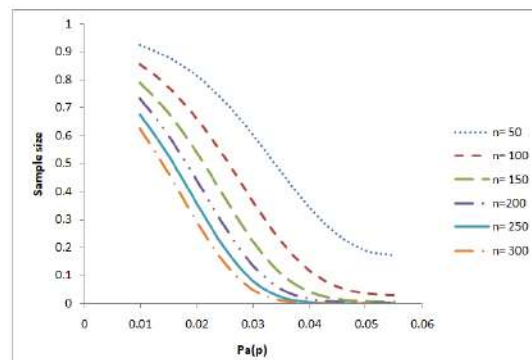
Figure 2: OC Curve for Logistic Distribution using StRSS (Optimum)
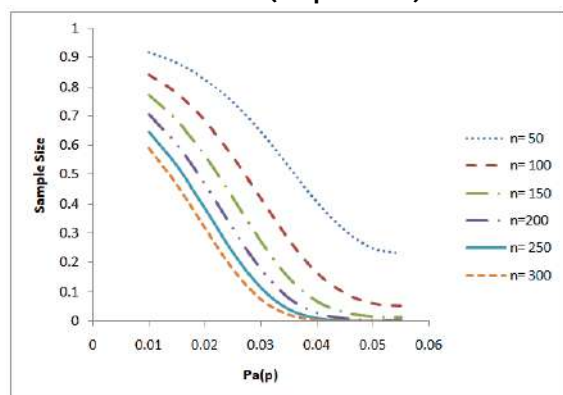
Figure 3: AOQ Curve for Logistic Distribution using StRSS (Proportional)
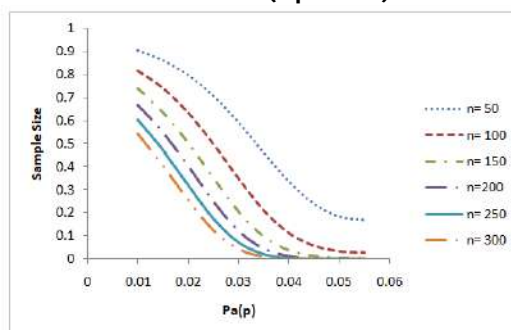
Figure 5: AOQ Curve for Logistic Distribution using StRSS (Optimum)
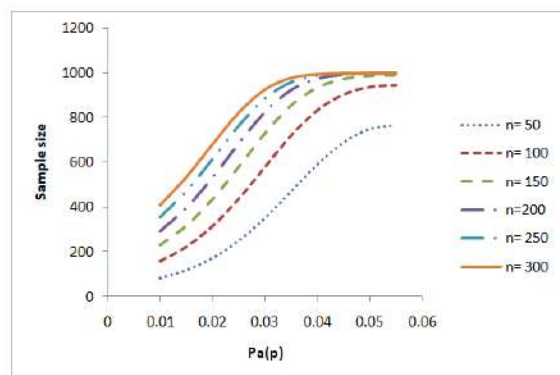
Figure 6: ATI Curve for Logistic Distribution using StRSS (Proportional)
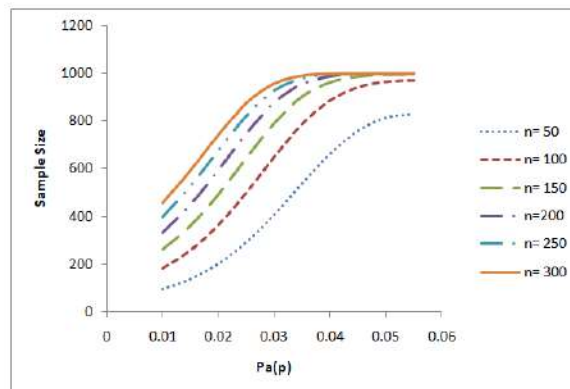
Figure 7: ATI Curve for Logistic Distribution using StRSS (Optimum)

RESEARCH ARTICLE

Some Theorems on Homomorphism of Intuitionistic Multi L –Fuzzy Subgroups

C.Gowrishankar[1]* and M. Akilesh[2]

[1]Research Scholar, SRMV College of Arts and Science, Coimbatore-641 020, Tamil Nadu, India.
[2]Department of Mathematics, SRMV College of Arts and Science, Coimbatore-641 020, Tamil Nadu, India.

*Address for Correspondence
C.Gowrishankar[1]
Research Scholar,
SRMV College of Arts and Science,
Coimbatore-641 020, Tamil Nadu, India.
E.Mail: cgowrishankar88@gmail.com

ABSTRACT

In that paper, the notions of Intuitionistic Multi L–fuzzy subset and Intuitionistic Multi L–fuzzy subgroups are defined and discussed. Intuitionistic Multi L-fuzzy subgroups homeomorphic behavior and inverse homeomorphic images have been discovered. It has been demonstrated some related theorems.

Keywords: Intuitionistic Multi L-Fuzzy Subset (IMLFS), Intuitionistic Multi L–Fuzzy Subgroup (IMLFSG), Homomorphism of Intuitionistic Multi L–Fuzzy Subgroup (HIMLFSG).

INTRODUCTION

The concept of a fuzzy subset A of a set X as a function from X into [0,1] was first developed by L.A. Zadeh [27]. Several studies on the generalization of the idea of fuzzy set were undertaken after L.A. Zadeh introduced the concept of fuzzy set. The terms fuzzy subgroupoid, fuzzy subgroup, fuzzy ideal, and fuzzy homomorphism were initially introduced by Rosenfeld [16]. In addition, he introduced the fuzzy subgroup and fuzzy ideal lattices. As a generalization of the concept of a fuzzy set, Krassimir.T. Attanassov originally proposed the concept of intuitionistic fuzzy sets. Sourier Sebastian and S. Babu Sundar proposed the idea of multi L- fuzzy subgroups [23]. The degree of membership (belongingness) and the degree of non-membership (non-belongingness) of elements of the universe to the intuitionistic fuzzy set are expressed by two functions that make up a fuzzy set. In this article, we define and explain relevant theorems connected to intuitionistic multi-L-fuzzy subgroup under homomorphism and inverse homomorphism.

PRELIMINARIES
The basic definitions that will be used in the sequel are listed in this section.

Definition
Let X be any non-empty set. A fuzzy set μ of X is $\mu: X \to [0,1]$.

Definition
Let $(G, .)$ be a group. A fuzzy subset μ of G is said to be L-fuzzy subgroup (LFSG) of G, if the following conditions are satisfied:

   (i)   μ$(xy) \geq min\{μ(x), μ(y)\}$,
   (ii)   μ$(x^{-1}) = μ(x)$, for all $x, y \in G$.

Definition
Let X be a non-empty set. A Multi L-fuzzy subset (MLFS) μ in X is defined as a set of ordered sequences. $\mu = \{(x, \mu_1(x), \mu_2(x), \ldots, \mu_i(x), \ldots): x \epsilon X\}$, where $\mu_i: X \to [0,1]$, for all i. Also note that, for all $i, \mu_i(x)$ is a decreasingly ordered sequence of elements.
ie., $\mu_1(x) \geq \mu_2(x) \geq \ldots \ldots \geq \mu_i(x) \geq \ldots \ldots$, for all $x \epsilon X$.

Definition
A Multi L-fuzzy subset μ of a group G is called a Multi L-fuzzy subgroup of G (MLFSG), if
   (i) $\mu(xy) \geq min\{\mu(x), \mu(y)\}$,
   (ii) $\mu(x^{-1}) = \mu(x)$, for all $x, y \epsilon G$.

Definition
Let X be a non-empty set. An Intuitionistic L-fuzzy subset (ILFS) μ of X is an object of the form
 $\mu = \{(x, \mu_A(x), \gamma_A(x)): x \epsilon X\}$, where $\mu_A: X \to [0,1]$ and $\gamma_A: X \to [0,1]$.
Define the degree of membership and degree of non-membership of the element $x \epsilon X$ respectively with
$0 \leq \mu_A(x) + \gamma_A(x) \leq 1$, for all $x \epsilon X$.

Remark
   (a)   When $\mu_A(x) + \gamma_A(x) = 1$, ie., when $\gamma_A(x) = 1 - \mu_A(x) = \mu_A^c(x)$. Then μ is called L-fuzzy set.
   (b)   We use the notation $\mu = (\mu_A, \gamma_A)$ to denote the Intuitionistic L-fuzzy subset (ILFS) μ of X.

Definition
Let X be a non-empty set. Let $\mu = \{(x, \mu_A(x), \gamma_A(x)): x \epsilon X\}$ in X is defined as a set of ordered sequences.
ie., $\mu = \left\{ \left(x, \left(\mu_{A_1}(x), \mu_{A_2}(x), \ldots, \mu_{A_i}(x), \ldots \right), \left(\gamma_{A_1}(x), \gamma_{A_2}(x), \ldots, \gamma_{A_i}(x), \ldots \right) \right): x \epsilon X \right\}$.
Where $\mu_{A_i}: X \to [0,1], \gamma_{A_i}: X \to [0,1]$ and $0 \leq \mu_{A_i}(x) + \gamma_{A_i}(x) \leq 1$ for all i.
Here, $\mu_1(x) \geq \mu_2(x) \geq \ldots \geq \mu_i(x) \geq \ldots$, for all $x \epsilon X$ are decreasingly ordered sequence. Then the set μ is said to be an Intuitionistic Multi L-fuzzy subset (IMLFS) of X.

Remark
Since we arrange the membership sequence in decreasing order, the corresponding non-membership sequence may not be in decreasing or increasing order.

Definition
An Intuitionistic Multi L-fuzzy subset is of the form
$\mu = \{(x, (\mu_A(x_1), \mu_A(x_2), \ldots, \mu_A(x_i), \ldots), (\gamma_A(x_1), \gamma_A(x_2), \ldots, \gamma_A(x_i), \ldots)): x \epsilon X\}$ of a group G is said to be Intuitionistic Multi L-fuzzy subgroup of G (IMLFSG) if it satisfies the following: For all $x, y \epsilon G$,

Gowrishankar and Akilesh

(i)　　　$\mu_A(x_1 x_2 x_3 \ldots x_i \ldots) \geq min\{\mu_A(x_1), \mu_A(x_2), \mu_A(x_3), \ldots, \mu_A(x_i), \ldots\}$ and $\gamma_A(x_1 x_2 x_3 \ldots x_i \ldots) \leq max\{\gamma_A(x_1), \gamma_A(x_2), \gamma_A(x_3), \ldots, \gamma_A(x_i), \ldots\}$,

(ii)　　$\mu_A(x_i{}^{-1}) = \mu_A(x_i)$ and $\gamma_A(x_i{}^{-1}) = \gamma_A(x_i)$, *for all i.*

Homomorphism of an Intuitionistic Multi L-Fuzzy Subgroups (HIMLFSG)
In this section we study about Intuitionistic multi L-fuzzy subgroup under homomorphism.

Definition
The function $f: G_1 \rightarrow G_2$ is said to be a homomorphism if $f(xy) = f(x)f(y)$, for all $x, y \in G$.

Definition
The function $f: G_1 \rightarrow G_2$ $(G_1 \text{ and } G_2 \text{ are not necessarily commutative})$ is said to be an anti-homomorphism if $f(xy) = f(y)f(x)$, for all $x, y \in G$.

Definition
Let $G_1 \text{ and } G_2$ be any two groups. The function $f: G_1 \rightarrow G_2$ is said to be an multi homomorphism if $f((x_1 x_2 x_3 \ldots x_i)(y_1 y_2 y_3 \ldots y_i)) = f(x_1 x_2 x_3 \ldots x_i) f(y_1 y_2 y_3 \ldots y_i)$, for all $x_i, y_i \in G_1$.

Definition
Let $G_1 \text{ and } G_2$ be any two groups. Let $f: G_1 \rightarrow G_2$ be a multi homomorphism and onto. Let $\mu: G_1 \rightarrow L$ and $\gamma: G_1 \rightarrow L$ be an Intuitionistic Multi L-fuzzy subgroups of G_1.
(i)　　　Then $f(\mu)$ is an Intuitionistic Multi L-fuzzy subgroup of a group G_2, if μ has a sup property and μ is $f - invariant$.
(ii)　　Then $f(\gamma)$ is an Intuitionistic Multi L-fuzzy subgroup of a group G_2, if γ has a inf property and γ is $f - invariant$.

Theorem
Let $G_1 \text{ and } G_2$ be any two groups. Let $f: G_1 \rightarrow G_2$ be a multi homomorphism and onto. Let $\mu: G_1 \rightarrow L$ and $\gamma: G_1 \rightarrow L$ be an Intuitionistic Multi L-fuzzy subgroups of G_1. Then prove that $f(\mu)$ and $f(\gamma)$ are the Intuitionistic Multi L-fuzzy subgroups of a group G_2, for
(i)　　　if μ has a sup property and μ is $f - invariant$,
(ii)　　if γ has a inf property and γ is $f - invariant$.

Proof
Let $\mu: G_1 \rightarrow L$ and $\gamma: G_1 \rightarrow L$ be an IMLFSG's of G_1.
(a). To prove that $f(\mu)$ be an IMLFSG of G_2.
(i)　　　Let, $f(\mu)((x_1 x_2 x_3 \ldots x_i)(y_1 y_2 y_3 \ldots y_i)) = \max\{\mu((x_1 x_2 x_3 \ldots x_i)(y_1 y_2 y_3 \ldots y_i))/\forall x_i y_i \in G_1,$
$$f((x_1 x_2 x_3 \ldots x_i)(y_1 y_2 y_3 \ldots y_i)) = x_0 y_0\}$$
$$= \mu(x_0 y_0)$$
$$\geq \min\{\mu(x_0), \mu(y_0)\}$$
$$\geq min\{[max\langle \mu(x_1 x_2 x_3 \ldots x_i)/\forall\, x_i \in G_1, f(x_1 x_2 x_3 \ldots x_i) = x_0)], [max\langle \mu(y_1 y_2 y_3 \ldots y_i)/\forall\, y_i \in G_1, f(y_1 y_2 y_3 \ldots y_i) = y_0)]\}$$
$$\geq min\{[f(\mu)(x_1 x_2 x_3 \ldots x_i)], [f(\mu)(y_1 y_2 y_3 \ldots y_i)]\}$$
i.e., $f(\mu)((x_1 x_2 x_3 \ldots x_i)(y_1 y_2 y_3 \ldots y_i)) \geq min\{[f(\mu)(x_1 x_2 x_3 \ldots x_i)], [f(\mu)(y_1 y_2 y_3 \ldots y_i)]\}$

(ii)　　Let, $f(\mu)((x_1 x_2 x_3 \ldots x_i)^{-1}) = max\{\mu((x_1 x_2 x_3 \ldots x_i)^{-1})/\forall x_i{}^{-1} \in G_1, f((x_1 x_2 x_3 \ldots x_i)^{-1}) = x_0\}$
$$= max\{\mu(x_1 x_2 x_3 \ldots x_i)/\forall x_i \in G_1, f(x_1 x_2 x_3 \ldots x_i) = x_0\} \quad [\because \text{By definition 2.7}]$$
$$= \mu(x_0)$$
$$= max\{\mu(x_1 x_2 x_3 \ldots x_i)/\forall x_i \in G_1, f(x_1 x_2 x_3 \ldots x_i) = x_0\}$$
i.e., $f(\mu)((x_1 x_2 x_3 \ldots x_i)^{-1}) = f(\mu)(x_1 x_2 x_3 \ldots x_i)$

(b). To prove that $f(\gamma)$ be an IMLFSG of G_2.
(i)　　　Let, $f(\gamma)((x_1 x_2 x_3 \ldots x_i)(y_1 y_2 y_3 \ldots y_i)) = min\{\gamma((x_1 x_2 x_3 \ldots x_i)(y_1 y_2 y_3 \ldots y_i))/\forall x_i y_i \in G_1,$
$$f((x_1 x_2 x_3 \ldots x_i)(y_1 y_2 y_3 \ldots y_i)) = x_0 y_0\}$$
$$= \gamma(x_0 y_0)$$

Gowrishankar and Akilesh

$$\leq \max\{\gamma(x_0),\gamma(y_0)\}$$
$$\leq max\{[min\langle\gamma(x_1x_2x_3\ldots\ldots x_i)/\ \forall x_i \in G_1, f(x_1x_2x_3\ldots\ldots x_i) = x_0)], [min\langle\gamma(y_1y_2y_3\ldots\ldots y_i)/\ \forall y_i$$
$$\in G_1, f(y_1y_2y_3\ldots\ldots y_i) = y_0)]\}$$
$$\leq max\{[f(\gamma)(x_1x_2x_3\ldots\ldots x_i)], [f(\gamma)(y_1y_2y_3\ldots\ldots y_i)]\}$$

i.e., $f(\gamma)\big((x_1x_2x_3\ldots\ldots x_i)(y_1y_2y_3\ldots\ldots y_i)\big) \leq max\{[f(\gamma)(x_1x_2x_3\ldots\ldots x_i)], [f(\gamma)(y_1y_2y_3\ldots\ldots y_i)]\}$

(ii)   Let, $f(\gamma)\big((x_1x_2x_3\ldots\ldots x_i)^{-1}\big) = min\{\gamma((x_1x_2x_3\ldots\ldots x_i)^{-1})/\forall x_i^{-1} \in G_1, f((x_1x_2x_3\ldots\ldots x_i)^{-1}) = x_0\}$
$$= min\{\gamma(x_1x_2x_3\ldots\ldots x_i)/\forall x_i \in G_1,\ f(x_1x_2x_3\ldots\ldots x_i) = x_0\}   [\because \text{By definition 2.7}]$$
$$= \gamma(x_0)$$
$$= min\{\gamma(x_1x_2x_3\ldots\ldots x_i)/\forall x_i \in G_1,\ f(x_1x_2x_3\ldots\ldots x_i) = x_0\}$$

i.e., $f(\gamma)\big((x_1x_2x_3\ldots\ldots x_i)^{-1}\big) = f(\gamma)(x_1x_2x_3\ldots\ldots x_i)$

Hence, from (a) & (b) we conclude that $f(\mu)$ and $f(\gamma)$ are the IMLFSG's of a group G_2.

Theorem

Let $G_1\ and\ G_2$ be any two groups. Let $f: G_1 \to G_2$ be a multi homomorphism and onto. Let $\mu: G_2 \to L$ and $\gamma: G_2 \to L$ be an Intuitionistic Multi L-fuzzy subgroups of a group G_2. Then prove that $f^{-1}(\mu)$ and $f^{-1}(\gamma)$ are the Intuitionistic Multi L-fuzzy subgroups of a group G_1.

Proof

Given $G_1\ and\ G_2$ be any two groups. Let $f: G_1 \to G_2$ be a multi homomorphism and onto.
Let $\mu: G_2 \to L$ and $\gamma: G_2 \to L$ be an Intuitionistic Multi L-fuzzy subgroups of G_2.
(a). To prove that $f^{-1}(\mu)$ be an IMLFSG of G_1.

(i)   Let, $f^{-1}(\mu)\big((x_1x_2x_3\ldots\ldots x_i)(y_1y_2y_3\ldots\ldots y_i)\big) = \mu\big(f((x_1x_2x_3\ldots\ldots x_i)(y_1y_2y_3\ldots\ldots y_i))\big)$
$$= \mu\big(f(x_1x_2x_3\ldots\ldots x_i)f(y_1y_2y_3\ldots\ldots y_i)\big)   [\because \text{By definition 3.1}]$$
$$\geq min\{\mu(f(x_1x_2x_3\ldots\ldots x_i)),\mu(f(y_1y_2y_3\ldots\ldots y_i))\}   [\because \text{By definition 2.7}]$$
$$\geq min\{f^{-1}(\mu)(x_1x_2x_3\ldots\ldots x_i), f^{-1}(\mu)(y_1y_2y_3\ldots\ldots y_i)\}$$

i.e., $f^{-1}(\mu)\big((x_1x_2x_3\ldots\ldots x_i)(y_1y_2y_3\ldots\ldots y_i)\big) \geq min\{f^{-1}(\mu)(x_1x_2x_3\ldots\ldots x_i), f^{-1}(\mu)(y_1y_2y_3\ldots\ldots y_i)\}$

(ii)   Let, $f^{-1}(\mu)\big((x_1x_2x_3\ldots\ldots x_i)^{-1}\big) = \mu(f((x_1x_2x_3\ldots\ldots x_i)^{-1}))$
$$= \mu(f(x_1x_2x_3\ldots\ldots x_i))   [\because \text{By definition 2.7}]$$
$$= f^{-1}(\mu)(x_1x_2x_3\ldots\ldots x_i)$$

i.e., $f^{-1}(\mu)\big((x_1x_2x_3\ldots\ldots x_i)^{-1}\big) = f^{-1}(\mu)(x_1x_2x_3\ldots\ldots x_i)$

(b). To prove that $f^{-1}(\gamma)$ be an IMLFSG of G_1.

(i)   Let, $f^{-1}(\gamma)\big((x_1x_2x_3\ldots\ldots x_i)(y_1y_2y_3\ldots\ldots y_i)\big) = \gamma\big(f((x_1x_2x_3\ldots\ldots x_i)(y_1y_2y_3\ldots\ldots y_i))\big)$
$$= \gamma(f(x_1x_2x_3\ldots\ldots x_i)f(y_1y_2y_3\ldots\ldots y_i))   [\because \text{f is a multi homomorphism}]$$
$$\leq max\{\gamma(f(x_1x_2x_3\ldots\ldots x_i)),\gamma(f(y_1y_2y_3\ldots\ldots y_i))\}$$
$$\leq max\{f^{-1}(\gamma)(x_1x_2x_3\ldots\ldots x_i), f^{-1}(\gamma)(y_1y_2y_3\ldots\ldots y_i)\}$$

i.e., $f^{-1}(\gamma)\big((x_1x_2x_3\ldots\ldots x_i)(y_1y_2y_3\ldots\ldots y_i)\big) \leq max\{f^{-1}(\gamma)(x_1x_2x_3\ldots\ldots x_i), f^{-1}(\gamma)(y_1y_2y_3\ldots\ldots y_i)\}$

(ii)   Let, $f^{-1}(\gamma)\big((x_1x_2x_3\ldots\ldots x_i)^{-1}\big) = \gamma(f((x_1x_2x_3\ldots\ldots x_i)^{-1}))$
$$= \gamma(f(x_1x_2x_3\ldots\ldots x_i))   [\because \text{By definition 2.7}]$$
$$= f^{-1}(\gamma)(x_1x_2x_3\ldots\ldots x_i)$$

i.e., $f^{-1}(\gamma)\big((x_1x_2x_3\ldots\ldots x_i)^{-1}\big) = f^{-1}(\gamma)(x_1x_2x_3\ldots\ldots x_i)$

Hence, from (a) & (b) we conclude that $f^{-1}(\mu)$ and $f^{-1}(\gamma)$ are the IMLFSG's of a group G_1.

Theorem

Let $G_1\ and\ G_2$ be any two groups. Let $f: G_1 \to G_2$ be an multi anti-homomorphism and onto. Let $\mu: G_1 \to L$ and $\gamma: G_1 \to L$ be an Intuitionistic Multi L-fuzzy subgroups of G_1. Then prove that

(a) $f(\mu)$ be an Intuitionistic Multi L-fuzzy subgroups of a group G_2, if μ has a sup property and μ is $f-invariant$,

(b) $f(\gamma)$ be an Intuitionistic Multi L-fuzzy subgroups of a group G_2, if γ has a inf property and γ is $f-invariant$.

Proof

Let $\mu: G_1 \to L$ and $\gamma: G_1 \to L$ be an Intuitionistic Multi L-fuzzy subgroups of G_1. Also $f: G_1 \to G_2$ be an multi anti-homomorphism and onto.

(a). To prove that $f(\mu)$ be an IMLFSG of G_2.

(i)   Let, $f(\mu)\big((x_1x_2x_3\ldots\ldots x_i)(y_1y_2y_3\ldots\ldots y_i)\big) = \min\{\mu\big((x_1x_2x_3\ldots\ldots x_i)(y_1y_2y_3\ldots\ldots y_i)\big)/\forall x_iy_i \in G_1,$
$f\big((x_1x_2x_3\ldots\ldots x_i)(y_1y_2y_3\ldots\ldots y_i)\big) = x_0y_0\}$
$\qquad = \mu(x_0y_0)$
$\qquad \leq \max\{\mu(x_0), \mu(y_0)\}$

$\leq \max\{[\min\langle\mu(x_1x_2x_3\ldots\ldots x_i)/\forall x_i \in G_1, f(x_1x_2x_3\ldots\ldots x_i) = x_0)], [\min\langle\mu(y_1y_2y_3\ldots\ldots y_i)/\forall y_i \in G_1, f(y_1y_2y_3\ldots\ldots y_i) = y_0)]\}$
$\qquad\qquad \leq \max\{[f(\mu)(x_1x_2x_3\ldots\ldots x_i)], [f(\mu)(y_1y_2y_3\ldots\ldots y_i)]\}$

i.e., $f(\mu)\big((x_1x_2x_3\ldots\ldots x_i)(y_1y_2y_3\ldots\ldots y_i)\big) \leq \max\{[f(\mu)(x_1x_2x_3\ldots\ldots x_i)], [f(\mu)(y_1y_2y_3\ldots\ldots y_i)]\}$

(ii)   Let, $f(\mu)\big((x_1x_2x_3\ldots\ldots x_i)^{-1}\big) = \min\{\mu\big((x_1x_2x_3\ldots\ldots x_i)^{-1}\big)/\forall x_i^{-1} \in G_1, f\big((x_1x_2x_3\ldots\ldots x_i)^{-1}\big) = x_0^{-1}\}$
$\qquad\qquad = \mu(x_0^{-1})$
$\qquad\qquad = \mu(x_0)$ [∵ By definition 2.7]
$\qquad\qquad = \min\{\mu(x_0)/x_0 \in G_2, f(x_0) = (x_1x_2x_3\ldots\ldots x_i)\}$
$\qquad\qquad = f(\mu)(x_1x_2x_3\ldots\ldots x_i)$

i.e., $f(\mu)\big((x_1x_2x_3\ldots\ldots x_i)^{-1}\big) = f(\mu)(x_1x_2x_3\ldots\ldots x_i)$

Hence, $f(\mu)$ be an Intuitionistic Multi L-fuzzy subgroups of a group G_2.

(b). To prove that $f(\gamma)$ be an IMLFSG of G_2.

(i)   Let, $f(\gamma)\big((x_1x_2x_3\ldots\ldots x_i)(y_1y_2y_3\ldots\ldots y_i)\big) = \max\{\gamma\big((x_1x_2x_3\ldots\ldots x_i)(y_1y_2y_3\ldots\ldots y_i)\big)/\forall x_iy_i \in G_1,$
$f\big((x_1x_2x_3\ldots\ldots x_i)(y_1y_2y_3\ldots\ldots y_i)\big) = x_0y_0\}$
$\qquad = \gamma(x_0y_0)$
$\qquad \geq \min\{\gamma(x_0), \gamma(y_0)\}$
$\qquad \geq \min\{[\max\langle\gamma(x_1x_2x_3\ldots\ldots x_i)/\forall x_i \in G_1, f(x_1x_2x_3\ldots\ldots x_i) = x_0)], [\max\langle\gamma(y_1y_2y_3\ldots\ldots y_i)/$
$\forall y_i \in G_1, f(y_1y_2y_3\ldots\ldots y_i) = y_0)]\}$
$\qquad \geq \min\{[f(\gamma)(x_1x_2x_3\ldots\ldots x_i)], [f(\gamma)(y_1y_2y_3\ldots\ldots y_i)]\}$

i.e., $f(\gamma)\big((x_1x_2x_3\ldots\ldots x_i)(y_1y_2y_3\ldots\ldots y_i)\big) \geq \min\{[f(\gamma)(x_1x_2x_3\ldots\ldots x_i)], [f(\gamma)(y_1y_2y_3\ldots\ldots y_i)]\}$

(ii)   Let, $f(\gamma)\big((x_1x_2x_3\ldots\ldots x_i)^{-1}\big) = \max\{\gamma\big((x_1x_2x_3\ldots\ldots x_i)^{-1}\big)/\forall x_i^{-1} \in G_1, f\big((x_1x_2x_3\ldots\ldots x_i)^{-1}\big) = x_0^{-1}\}$
$\qquad\qquad = \gamma(x_0^{-1})$
$\qquad\qquad = \gamma(x_0)$ [∵ By definition 2.7]
$\qquad\qquad = \max\{\gamma(x_0)/x_0 \in G_2, f(x_0) = (x_1x_2x_3\ldots\ldots x_i)\}$
$\qquad\qquad = f(\gamma)(x_1x_2x_3\ldots\ldots x_i)$

i.e., $f(\gamma)\big((x_1x_2x_3\ldots\ldots x_i)^{-1}\big) = f(\gamma)(x_1x_2x_3\ldots\ldots x_i)$

Hence, $f(\gamma)$ be an Intuitionistic Multi L-fuzzy subgroups of a group G_2.

Theorem

Let $G_1 \text{ and } G_2$ be any two groups. Let $f: G_1 \to G_2$ be an multi anti-homomorphism and onto. Let $\mu: G_2 \to L$ and $\gamma: G_2 \to L$ be an Intuitionistic Multi L-fuzzy subgroups of G_2. Then prove that

(a) $f^{-1}(\mu)$ is an Intuitionistic Multi L-fuzzy subgroups of a group G_1.

(b) $f^{-1}(\gamma)$ is an Intuitionistic Multi L-fuzzy subgroups of a group G_1.

Proof

Given $G_1 \text{ and } G_2$ be any two groups and let $f: G_1 \to G_2$ be an multi anti-homomorphism and onto.

Let $\mu: G_2 \to L$ and $\gamma: G_2 \to L$ be an Intuitionistic Multi L-fuzzy subgroups of G_2.

(a). To prove that $f^{-1}(\mu)$ be an IMLFSG of G_1.

(i)   Let, $f^{-1}(\mu)\big((x_1x_2x_3\ldots\ldots x_i)(y_1y_2y_3\ldots\ldots y_i)\big) = \mu\big(f\big((x_1x_2x_3\ldots\ldots x_i)(y_1y_2y_3\ldots\ldots y_i)\big)\big)$
$\qquad = \mu\big(f(x_1x_2x_3\ldots\ldots x_i)f(y_1y_2y_3\ldots\ldots y_i)\big)$ [∵ By definition 3.1]
$\qquad \leq \max\{\mu\big(f(x_1x_2x_3\ldots\ldots x_i)\big), \mu\big(f(y_1y_2y_3\ldots\ldots y_i)\big)\}$ [∵ By definition 2.7]
$\qquad \leq \max\{f^{-1}(\mu)(x_1x_2x_3\ldots\ldots x_i), f^{-1}(\mu)(y_1y_2y_3\ldots\ldots y_i)\}$

64139

Gowrishankar and Akilesh

i.e., $f^{-1}(\mu)\big((x_1x_2x_3\ldots\ldots x_i)(y_1y_2y_3\ldots\ldots y_i)\big) \leq max\{f^{-1}(\mu)(x_1x_2x_3\ldots\ldots x_i), f^{-1}(\mu)(y_1y_2y_3\ldots\ldots y_i)\}$

(ii)   Let, $f^{-1}(\mu)\big((x_1x_2x_3\ldots\ldots x_i)^{-1}\big) = \mu\big(f((x_1x_2x_3\ldots\ldots x_i)^{-1})\big)$

$= \mu(f(x_1x_2x_3\ldots\ldots x_i))$ [∵ By definition 2.7]

$= f^{-1}(\mu)(x_1x_2x_3\ldots\ldots x_i)$

i.e., $f^{-1}(\mu)\big((x_1x_2x_3\ldots\ldots x_i)^{-1}\big) = f^{-1}(\mu)(x_1x_2x_3\ldots\ldots x_i)$

Hence, $f^{-1}(\mu)$ is an Intuitionistic Multi L-fuzzy subgroups of a group G_1.

(b). To prove that $f^{-1}(\gamma)$ be an IMLFSG of G_1.

(i)   Let, $f^{-1}(\gamma)\big((x_1x_2x_3\ldots\ldots x_i)(y_1y_2y_3\ldots\ldots y_i)\big) = \gamma\left(f\big((x_1x_2x_3\ldots\ldots x_i)(y_1y_2y_3\ldots\ldots y_i)\big)\right)$

$= \gamma(f(x_1x_2x_3\ldots\ldots x_i)f(y_1y_2y_3\ldots\ldots y_i))$ [∵ f is a multi homomorphism]

$\geq \min\{\gamma(f(x_1x_2x_3\ldots\ldots x_i)), \gamma(f(y_1y_2y_3\ldots\ldots y_i))\}$

$\geq min\{f^{-1}(\gamma)(x_1x_2x_3\ldots\ldots x_i), f^{-1}(\gamma)(y_1y_2y_3\ldots\ldots y_i)\}$

i.e.,$f^{-1}(\gamma)\big((x_1x_2x_3\ldots\ldots x_i)(y_1y_2y_3\ldots\ldots y_i)\big) \geq min\{f^{-1}(\gamma)(x_1x_2x_3\ldots\ldots x_i), f^{-1}(\gamma)(y_1y_2y_3\ldots\ldots y_i)\}$

(ii)   Let, $f^{-1}(\gamma)\big((x_1x_2x_3\ldots\ldots x_i)^{-1}\big) = \gamma\big(f((x_1x_2x_3\ldots\ldots x_i)^{-1})\big)$

$= \gamma(f(x_1x_2x_3\ldots\ldots x_i))$ [∵ By definition 2.7]

$= f^{-1}(\gamma)(x_1x_2x_3\ldots\ldots x_i)$

i.e., $f^{-1}(\gamma)\big((x_1x_2x_3\ldots\ldots x_i)^{-1}\big) = f^{-1}(\gamma)(x_1x_2x_3\ldots\ldots x_i)$

Hence, $f^{-1}(\gamma)$ is an Intuitionistic Multi L-fuzzy subgroups of a group G_1.

Hence the theorem.

Theorem

Let $(G_1,.)$ and $(G_2,.)$ be any two groups. The multi homomorphic image(pre-image) of an Intuitionistic Multi L-fuzzy subgroup of G_1 is an Intuitionistic Multi L-fuzzy subgroup of a group G_2.

Proof

Given $(G_1,.)$ and $(G_2,.)$ be any two groups and let $f:G_1 \to G_2$ be a multi homomorphism map.

i.e., $f\big((x_1x_2x_3\ldots\ldots x_i)(y_1y_2y_3\ldots\ldots y_i)\big) = f(x_1x_2x_3\ldots\ldots x_i)f(y_1y_2y_3\ldots\ldots y_i)$, for all $x_i, y_i \in G_1$.

Let A be an IMLFSG of a group G_1.

To prove that $f(A)$ is an IMLFSG of a group G_2.

Now, for $f(x)$ and $f(y)$ in G_2, we have

(a). Let μ_A be a degree of membership function, then

(i)   Let, $\mu_A(f(x_1x_2x_3\ldots\ldots x_i)f(y_1y_2y_3\ldots\ldots y_i)) = \mu_A(f((x_1x_2x_3\ldots\ldots x_i)(y_1y_2y_3\ldots\ldots y_i)))$

[∵ f is a multi homomorphism]

$\geq \min\{\mu_A(f(x_1x_2x_3\ldots\ldots x_i)), \mu_A(f(y_1y_2y_3\ldots\ldots y_i))\}$

i.e., $\mu_A(f(x_1x_2x_3\ldots\ldots x_i)f(y_1y_2y_3\ldots\ldots y_i)) \geq \min\{\mu_A(f(x_1x_2x_3\ldots\ldots x_i)), \mu_A(f(y_1y_2y_3\ldots\ldots y_i))\}$

(ii)   Let, $\mu_A[f(x_1x_2x_3\ldots\ldots x_i)]^{-1} = \mu_A[f((x_1x_2x_3\ldots\ldots x_i)^{-1})]$

$= \mu_A[f(x_1x_2x_3\ldots\ldots x_i)]$ [∵ A is an IMLFSG]

i.e., $\mu_A[f(x_1x_2x_3\ldots\ldots x_i)]^{-1} = \mu_A[f(x_1x_2x_3\ldots\ldots x_i)]$

(b) . Let γ_A be a degree of non-membership function, then

(i)   Let, $\gamma_A(f(x_1x_2x_3\ldots\ldots x_i)f(y_1y_2y_3\ldots\ldots y_i)) = \gamma_A(f((x_1x_2x_3\ldots\ldots x_i)(y_1y_2y_3\ldots\ldots y_i)))$

[∵ f is a multi homomorphism]

$\leq \max\{\gamma_A(f(x_1x_2x_3\ldots\ldots x_i)), \gamma_A(f(y_1y_2y_3\ldots\ldots y_i))\}$

i.e., $\gamma_A(f(x_1x_2x_3\ldots\ldots x_i)f(y_1y_2y_3\ldots\ldots y_i)) \leq \max\{\gamma_A(f(x_1x_2x_3\ldots\ldots x_i)), \gamma_A(f(y_1y_2y_3\ldots\ldots y_i))\}$

(ii)   Let, $\gamma_A[f(x_1x_2x_3\ldots\ldots x_i)]^{-1} = \gamma_A[f((x_1x_2x_3\ldots\ldots x_i)^{-1})]$

$= \gamma_A[f(x_1x_2x_3\ldots\ldots x_i)]$ [∵ A is an IMLFSG]

i.e., $\gamma_A[f(x_1x_2x_3\ldots\ldots x_i)]^{-1} = \gamma_A[f(x_1x_2x_3\ldots\ldots x_i)]$

Hence, f(A) is an IMLFSG of a group G_2.

Hence the proof.

Theorem

Let $f:G_1 \to G_2$ be surjective multi homomorphism and A be an Intuitionistic Multi L-fuzzy subgroups of G_1. Then prove that $f(A)$ is an Intuitionistic Multi L-fuzzy subgroups of a group G_2.

Proof

Since A is an IMLFSG of a group G_1.

Let y_1 and y_2 be any elements of G_2.

Then there exists some $x_1, x_2, x_3, \ldots, x_i \in G_1$ s.t. $f(x_1) = y_1, f(x_2) = y_2, f(x_3) = y_3, \ldots, f(x_i) = y_i$.

[Note that $x_1, x_2, x_3, \ldots, x_i$ need not be unique]

Let, $f(A)(y_1 y_2 y_3 \ldots y_i) = \{\mu_{f(A)}(y_1 y_2 y_3 \ldots y_i), \gamma_{f(A)}(y_1 y_2 y_3 \ldots y_i)\}$ .... (1)

and $f(A)(y_1 y_2 y_3 \ldots y_i)^{-1}) = \{\mu_{f(A)}(y_1 y_2 y_3 \ldots y_i)^{-1}), \gamma_{f(A)}(y_1 y_2 y_3 \ldots y_i)^{-1})\}$ .... (2)

To prove that $f(A)$ is an IMLFSG of G_2.

(a). Let $\mu_{f(A)}$ be a degree of membership function in G_2, then

(i) Let, $\mu_{f(A)}(y_1 y_2 y_3 \ldots y_i) = \min \{\mu_{f(A)}(f(x_1)f(x_2)f(x_3) \ldots f(x_i))/y_1 = f(x_1), y_2 = f(x_2), y_3 = f(x_3), \ldots, y_i = f(x_i)\}$

$= \min \{\mu_{f(A)}(f(x_1 x_2 x_3 \ldots x_i))/x_1, x_2, x_3, \ldots, x_i \in G_1\}$ [∵ f is multi homomorphism]

$= \min \{\mu_A(x_1 x_2 x_3 \ldots x_i)/x_1, x_2, x_3, \ldots, x_i \in G_1\}$ [∵ f is surjective]

$\geq \min\{\mu_A(x_1), \mu_A(x_2), \mu_A(x_3), \ldots, \mu_A(x_i)/x_1, x_2, x_3, \ldots, x_i \in G_1$ and $f(x_1) = y_1, f(x_2) = y_2, f(x_3) = y_3, \ldots, f(x_i) = y_i\}$

$= \min\{\max [\mu_A(x_1)/f(x_1) = y_1], \max [\mu_A(x_2)/f(x_2) = y_2], \max [\mu_A(x_3)/f(x_3) = y_3], \ldots, \max [\mu_A(x_i)/f(x_i) = y_i]\}$

$= \min\{\mu_{f(A)}(y_1), \mu_{f(A)}(y_2), \mu_{f(A)}(y_3), \ldots, \mu_{f(A)}(y_i)\}$

i.e., $\mu_{f(A)}(y_1 y_2 y_3 \ldots y_i) \geq \min\{\mu_{f(A)}(y_1), \mu_{f(A)}(y_2), \mu_{f(A)}(y_3), \ldots, \mu_{f(A)}(y_i)\}$

(ii) Also,

$\mu_{f(A)}((y_1 y_2 y_3 \ldots y_i)^{-1}) = \max \{\mu_A((x_1 x_2 x_3 \ldots x_i)^{-1})/f((x_1 x_2 x_3 \ldots x_i)^{-1}) = (y_1 y_2 y_3 \ldots y_i)^{-1}\}$

$= \max \{\mu_A(x_1 x_2 x_3 \ldots x_i)/f(x_1 x_2 x_3 \ldots x_i) = y_1 y_2 y_3 \ldots y_i\}$ [∵ f is IMLFSG]

$= \mu_{f(A)}(y_1 y_2 y_3 \ldots y_i)$

i.e., $\mu_{f(A)}((y_1 y_2 y_3 \ldots y_i)^{-1}) = \mu_{f(A)}(y_1 y_2 y_3 \ldots y_i)$

(b). Let $\gamma_{f(A)}$ be a degree of non-membership function in G_2, then

(i) Let, $\gamma_{f(A)}(y_1 y_2 y_3 \ldots y_i) = \max \{\gamma_{f(A)}(f(x_1)f(x_2)(f(x_3) \ldots f(x_i))/y_1 = f(x_1), y_2 = f(x_2), y_3 = f(x_3), \ldots, y_i = f(x_i)\}$

$= \max \{\gamma_{f(A)}(f(x_1 x_2 x_3 \ldots x_i))/x_1, x_2, x_3, \ldots, x_i \in G_1\}$ [∵ f is multi homomorphism]

$= \max \{\gamma_A(x_1 x_2 x_3 \ldots x_i)/x_1, x_2, x_3, \ldots, x_i \in G_1\}$ [∵ f is surjective]

$\leq \max\{\gamma_A(x_1), \gamma_A(x_2), \gamma_A(x_3), \ldots, \gamma_A(x_i)/x_1, x_2, x_3, \ldots, x_i \in G_1$ and $f(x_1) = y_1, f(x_2) = y_2, f(x_3) = y_3, \ldots, f(x_i) = y_i\}$

$= \max\{\min [\gamma_A(x_1)/f(x_1) = y_1], \min[\gamma_A(x_2)/f(x_2) = y_2], \min[\gamma_A(x_3)/f(x_3) = y_3], \ldots, \min[\gamma_A(x_i)/f(x_i) = y_i]\}$

$= \max\{\gamma_{f(A)}(y_1), \gamma_{f(A)}(y_2), \gamma_{f(A)}(y_3), \ldots, \gamma_{f(A)}(y_i)\}$

i.e., $\gamma_{f(A)}(y_1 y_2 y_3 \ldots y_i) \leq \max\{\gamma_{f(A)}(y_1), \gamma_{f(A)}(y_2), \gamma_{f(A)}(y_3), \ldots, \gamma_{f(A)}(y_i)\}$,

(ii) Also, $\gamma_{f(A)}((y_1 y_2 y_3 \ldots y_i)^{-1}) = \min \{\gamma_A((x_1 x_2 x_3 \ldots x_i)^{-1})/f((x_1 x_2 x_3 \ldots x_i)^{-1}) = (y_1 y_2 y_3 \ldots y_i)^{-1}\}$

$= \min \{\gamma_A(x_1 x_2 x_3 \ldots x_i)/f(x_1 x_2 x_3 \ldots x_i) = y_1 y_2 y_3 \ldots y_i\}$ [∵ f is IMLFSG]

$= \gamma_{f(A)}(y_1 y_2 y_3 \ldots y_i)$

i.e. $\gamma_{f(A)}((y_1 y_2 y_3 \ldots y_i)^{-1}) = \gamma_{f(A)}(y_1 y_2 y_3 \ldots y_i)$

Hence $f(A)$ is an IMLFSG of G_2.

Hence the proof.

CONCLUSION

In this paper, we have seen some fundamental definitions related on Intuitionistic Multi L-fuzzy subgroups (IMLFSG). In the studies, we have also studied the concept of homomorphism and anti homomorphism in Intuitionistic Multi L-fuzzy subgroups are discussed. Additionally, we have looked into a few theorems and characteristics based on the homomorphism of an IMLFSG. Further work is in progress in order to develop the Homomorphism of an Intuitionistic Multi L-fuzzy subgroup (HIMLFSG) in to Non-Homomorphism of an Intuitionistic Multi L-fuzzy subgroup (NHIMLFSG).

REFERENCES

1. Anthony.J.M and Sherwood.H, "A Characterization of fuzzy subgroups", Fuzzy sets and system, Vol.7, 297-305, (1982).
2. Atanassov. K.T, "Intuitionistic fuzzy sets", Fuzzy Sets and Systems, 20(1986), no.1, 87-96.
3. Balasubramanian..K.R and Rajangam..R, "t- intuitionistic multi fuzzy subgroup of a group", Journal of Applied Science and Computations, Volume 5, Issue 11, ISSN: 1076- 5131 (2018).
4. Balasubramanian.K.R and .Revathy.R, "Product of (λ, μ) - Multi fuzzy Subgroups of A Group", Annals of R.S.C.B., ISSN:1583-6258, Vol. 25, Issue 6, 2021, 2448-2460.
5. Balasubramaniyan.K.R and Revathy.R, "Some Theorems on Intuitionistic Multi L-Fuzzy Subgroups", International Journal of Scientific and Research Publications, Vol.10, Issue 1 (2020), 653-655.
6. Balasubramanian.K.R, Revathy.R and Rajangam.R, "(Λ,M)-Multi Fuzzy Subgroup Of A Group", Turkish Journal of Computer and Mathematics Education, Vol.12, No.11 (2021), 6148 – 6160.
7. Choudhury. F.P, Chakraborty. A.B and Khare .S.S, " A note on fuzzy subgroups and fuzzy homomorphism", Journal of mathematical analysis and applications 131, 537-553 (1988).
8. Das.P.S, "Fuzzy groups and level subgroups", J. Math. Anal. and Appl. 84, 264-269, 1981.
9. Mary Jansi Rani.M , Alponse Anita.A, Rexiline Jayakumari.S and Shiny Bridjet, "N-Generated T-Intuitionistic Fuzzy Subgroups", Palarch's Journal Of Archaeology Of Egypt/Egyptology 17(12) (2020), ISSN 1567-214x , 981-987.
10. Muthuraj.R and Balamurugan.S, " A Study on Intuitionistic Multi-Fuzzy Subgroups", International Journal of Applications of Fuzzy sets and Artificial Intelligence, Vol.4, 153-172 (2014).
11. Muthuraj.R and Balamurugan.S, "Multi-Fuzzy Group and its level Subgroup", Gen. Math. Notes, Vol.17, No.1, 74-81 (2013).
12. Palaniappan.N and Muthuraj.R, "The homomorphism, anti-homomorphism of a fuzzy and an anti-fuzzy groups, Varahmihir Journal of Mathematics Sciences, Vol. 4 No. 2 (2004), 387-399.
13. Palaniappan.N , Naganathan.S and Arjunan.K, "A Study on Intuitionistic L-Fuzzy Subgroups", Applied mathematical Sciences, 3 (53) (2009), 2619-2624.
14. Pandiammal.P, Natarajan.R. and Palaniappan.N , "Anti L- fuzzy M-subgroups", Antarctica J. Math., Vol. 7, number 6, 683-691, (2010).
15. Prabir Bhattacharya, "Fuzzy subgroups", Some characterizations, J. Math. Anal. Appl. 128 (1981), 241-252.
16. Rosenfeld.A, "Fuzzy groups", J. Math. Anal. Appl, Vol. 35, 512 – 517, 1971.
17. Roventa.A and Spircu.T., "Groups operating on fuzzy sets", Fuzzy sets and systems, Vol.120 , 543 – 548,2001.
18. Sabu.S, Ramakrishnan.T.V, "Multi Fuzzy Sub Groups", Int.J. Contemp. Math. Sciences, Vol.6,No.8, 365- 372 (2011) .
19. Sharma.P.K., "Homomorphism of Intuitionistic fuzzy groups", International Mathematics Forum , Vol. 6, 2011, no. 64, 3169-3178.
20. Sharma.P.K.,"Intuitionistic Fuzzy Groups", ifrsa International Journal of Data warehousing and Mining, vol.1, 2011, issue 1, 86-94.
21. Sharma.P.K., "t- Intuitionistic Fuzzy Subgroups", International Journal of Fuzzy Mathematics and Systems. ISSN: 2248-9940 , Volume 2, Number 3 (2012), 233-243.

22. Sinoj.T.K and Sunil.J.J, "Intuitionistic Fuzzy Multi-Sets", International Journal of Engineering Sciences and Innovaive Technology, Vol.2, No.6, 1-24 (2013).

23. Souriar Sebastian and Babu Sundar.S , "Commutative L-Fuzzy Subgroups Fuzzy Sets and Systems", 68 (1994), 115-121.

24. Sunderrajan.K and Suresh.M , "Homomorphism of Multi L-Fuzzy Subgroup", Gen. Math. Notes, ISSN 2219-7184, Vol. 22, No. 1 (2014), 86-92.

25. Tarnauceanu.M and Bentea.L, " On the number of fuzzy subgroup of finite abelian groups", Fuzzy sets and systems, Vol. 159, 1084 – 1096, 2008.

26. Yuying Li, Xuzhu Wang and Liqiong Yang, "A Study of (λ, μ)-Fuzzy Subgroups", Journal of Applied Mathematics Volume 2013.

27. Zadeh.L.A, "Fuzzy sets", Information and control, 8, (1965), 338-353.

28. Zhan J and Tan Z , " Intuitionistic fuzzy M- groups" Soochow Journal of Mathematics , Vol. 30 , no.,1 2004 , 85-90.

RESEARCH ARTICLE

Ranking Measures of Fuzzy Multi Numbers

E. Vivek[1], N. Uma[1] and M. Keerthika[2]*

[1]Department of Mathematics, Sri Ramakrishna College of Arts and Science (Formerly SNR Sons College), Coimbatore, Tamil Nadu, India
[2]Research Scholar, Department of Mathematics, Sri Ramakrishna College of Arts and Science (Formerly SNR Sons College), Coimbatore, Tamil Nadu, India

*Address for Correspondence
M. Keerthika
Research Scholar,
Department of Mathematics,
Sri Ramakrishna College of Arts and Science (Formerly SNR Sons College),
Coimbatore, Tamil Nadu, India
E.Mail: vivek@srcas.ac.in

ABSTRACT

In this paper, we have introduced and compared three ranking techniques of Fuzzy Multi Numbers. Here, we have considered the Triangular, Trapezoidal, Pentagonal, Hexagonal and Octagonal Fuzzy Multi Numbers with its membership function. The Fuzzy Multi Numbers are transformed to crisp data by the introduced ranking techniques. Also, the efficiency of the Ranking Techniques is analyzed and compared with the numerical examples.

Keywords: Fuzzy Set, Multi Set, Fuzzy Multi Set, Triangular Fuzzy Multi Number, Trapezoidal Fuzzy Multi Number, Pentagonal Fuzzy Multi Number, Hexagonal Fuzzy Multi Number, Octagonal Fuzzy Multi Number, Ranking Function.

INTRODUCTION

The Fuzzy Set (FS) was introduced by Zadeh [17], it is a class of objects with a of membership between 0 and 1. Zimmermann [18] proposed the basic definitions of fuzzy sets and algebraic operations. And for further considerations, the Fuzzy Number [6], [8] and [10] was defined, which is a fuzzy subset of the real line whose highest membership values are clustered around the membership function which is monotonic on both sides of a given real number known as the mean value.Yager [16] first discussed fuzzy multisets, he uses the term of fuzzy bag; an element of X may occur more than once with possibly of the same or different membership values. Ranking the fuzzy numbers is an important aspect of decision making in a fuzzy environment for practical applications. Buckley

64144

[4] use fuzzy numbers to express their preferences and Li & Lee [11] proposed the order of fuzzy numbers based on the concept of probability measure of fuzzy events.

In ranking of fuzzy number, Triangular, Trapezoidal, Pentagonal, Hexagonal and Octagonal Fuzzy numbers with its membership function plays an important role to find the efficiency. Chen [6] suggested the concept of maximizing set and minimizing set to decide the ordering value of each fuzzy number and uses these values to determine the order of the *n* fuzzy numbers.Nagoor Gani & Mohamed Assarudeen [13] introduced a new method to find the fuzzy optimal solution of fully fuzzy linear programming problems with triangular fuzzy numbers and Amit Kumar, et.all[2], BongJu Lee and Yong Sik Yun[3] proposed the method to generalize the results of four operations for two generalized trapezoidal fuzzy sets. Helen & Uma [9], defined some operations and ranking function of a Pentagonal Fuzzy Number. The pentagonal fuzzy set was defined and the results of addition, subtraction, multiplication, and division based are generalized on the Zadeh's extension principle for two pentagonal fuzzy sets by Lee & Yun [12]. A fuzzy transportation problem with hexagonal fuzzy numbers was introduced by Thamaraiselvi & Santhi [15]. Arora et.all [1] introduced a fuzzy linear programming problem with hexagonal fuzzy numbers. Chandrasekaran. et.all [5] proposed a ranking procedure based on Octagonal Fuzzy numbers was applied to a Multi-objective Linear Programming Problem (MOLPP) with fuzzy coefficients.

PRELIMINARIES
The basis notions, concepts and definitions are reviewed in this section.

Definition: 2.1
Let X be a nonempty set. A fuzzy setA of X is defined as A= { < x, $\mu_A(x)$> / x∈ X }, where $\mu_A(x)$ is called membership function and it maps each element of X to a value between 0 and 1.

Definition: 2.2
A Multi Set(MS)is an unordered collection of objects in which, unlike an ordinary set, objects are allowed to repeat. Each individual occurrence of an object is a multi-set which is called its element.

Definition: 2.3
Let X be a nonempty set. The count membership function of a Fuzzy Multi Set (FMS) A in X has the form Mc : $X \rightarrow$ Q where Q is the set of all crisp multi sets in [0,1]. Hence, for any $x \in X$, Mc(x) is the crisp multi set from [0, 1]. The membership sequence is defined as $(\mu_A^1(x), \mu_A^2(x), \dots \dots \mu_A^p(x))$ where$\mu_A^1(x) \geq \mu_A^2(x) \geq \cdots \geq \mu_A^p(x)$.
Therefore, FMS Ais given by $A = \{\langle x, (\mu_A^1(x), \mu_A^2(x), \dots \dots \mu_A^p(x)) \rangle / x \in X \}$

Definition: 2.4
A regular real number is a generalization of a fuzzy number. It does not refer to a single value but rather to a connected set of possible values, where each possible value has its weight between 0 and 1. The weight is called the membership function. A fuzzy number Ais a convex normalized fuzzy set on the real line R such that there exist at least one x ∈ R with $\mu_A(x)$= 1 and $\mu_A(x)$is piecewise continuous.

Definition: 2.5
A Triangular fuzzy numberA is denoted by 3 – tuples (a, b, c), where a, b and c are real numbers and $a \leq b \leq c$with membership function defined as

$$\mu_A(x) = \begin{cases} 0 & for \quad x \leq a \\ \dfrac{x-a}{b-a} & for \, a \leq x \leq b \\ \dfrac{c-x}{c-b} & for \; b \leq x \leq c \\ 0 & for \quad x \geq c \end{cases}$$

Vivek *et al.*,

Definition: 2.6

A Trapezoidal fuzzy number A is denoted by 4 – tuples (a, b, c, d) where $a, b, c, and\ d$ are real numbers and $a \le b \le c \le d$ with membership function defined as

$$\mu_A(x) = \begin{cases} 0 & for\ \ x \le a \\ \dfrac{x-a}{b-a} & for\ a \le x \le b \\ 1 & for\ \ b \le x \le c \\ \dfrac{d-x}{d-c} & for\ \ c \le x \le d \\ 0 & for\ \ x \ge d \end{cases}$$

Definition: 2.7

A Pentagonal fuzzy number A is denoted by 5 – tuples (a, b, c, d, e), where $a, b, c, d\ and\ e$ are real numbers and $a \le b \le c \le d \le e$ with membership function defined a

$$\mu_A(x) = \begin{cases} 0 & for\ \ x \le a \\ \dfrac{x-a}{b-a} & for\ a \le x \le b \\ \dfrac{x-b}{c-b} & for\ b \le x \le c \\ 1 & for\ x = c \\ \dfrac{d-x}{d-c} & for\ c \le x \le d \\ \dfrac{e-x}{e-d} & for\ d \le x \le e \\ 0 & for\ \ x \ge e \end{cases}$$

Definition : 2.8

A hexagonal fuzzy number A_H is specified by 6 tuples $A_H = (a, b, c, d, e, f)$ where, $a, b, c, d, e\ and\ f$ are real number and $a \le b \le c \le d \le e \le f$ with membership function are given below

$$\mu_A(x) = \begin{cases} 0 & for\ x \le a \\ \dfrac{1}{2}\left(\dfrac{x-a}{b-a}\right) & for\ a \le x \le b \\ \dfrac{1}{2} + \dfrac{1}{2}\left(\dfrac{x-b}{c-b}\right) & for\ b \le x \le c \\ 1 & for\ c \le x \le d \\ 1 - \dfrac{1}{2}\left(\dfrac{x-d}{e-d}\right) & for\ d \le x \le e \\ \dfrac{1}{2}\left(\dfrac{f-x}{f-e}\right) & for\ e \le x \le f \\ 0 & for\ x \ge f \end{cases}$$

Definition: 2.9

A Fuzzy number A_{oct} is a normal octagonal fuzzy number denoted by $A_{oct} = (a, b, c, d, e, f, g, h)$ where $a, b, c, d, e, f, g\ and\ h$ are real number and $a \le b \le c \le d \le e \le f \le g \le h$ with its membership function is given below.

$$\mu_A(x) = \begin{cases} 0 & \text{for } x < a \\ \frac{1}{2}\left(\frac{x-a}{b-a}\right) & \text{for } a \leq x \leq b \\ 0.5 & \text{for } b \leq x \leq c \\ \frac{1}{2} + \frac{1}{2}\left(\frac{x-c}{d-c}\right) & \text{for } c \leq x \leq d \\ 1 & \text{for } d \leq x \leq e \\ \frac{1}{2} + \frac{1}{2}\left(\frac{f-x}{f-e}\right) & \text{for } e \leq x \leq f \\ 0.5 & \text{for } f \leq x \leq g \\ \frac{1}{2}\left(\frac{h-x}{h-g}\right) & \text{for } g \leq x \leq h \\ 0 & \text{for } x \geq h \end{cases}$$

Definition: 2.10

A fuzzy multi number is a generalization of a regular real number. It does not refer to a single value but rather to a connected set of possible values, where each possible value has its weight between 0 and 1. The weight is called the membership function. The membership sequence is in the form $(\mu_A^1(x), \mu_A^2(x), \ldots \ldots \mu_A^p(x))$ where $\mu_A^1(x) \geq \mu_A^2(x) \geq \cdots \geq \mu_A^p(x)$

Definition: 2.11

The Cardinality of the membership function Mc(x) is the length of an element x in the Fuzzy Multi Set *A* denoted as η, defined as $\eta = Mc(x)$. If A, B, C are the *FMS* defined on *X*, then their cardinality $\eta = \text{Max } \{ \eta(A), \eta(B), \eta(C) \}$.

Definition: 2.12

A Triangular fuzzy multi number A_i is denoted by 3 – tuples (a_i, b_i, c_i), where $a_i, b_i \text{ and } c_i$ are real numbers and $a_i \leq b_i \leq c_i$ with membership function defined as

$$\mu_{A_i}(x) = \begin{cases} 0 & for \quad x \leq a_i \\ \frac{x - a_i}{b_i - a_i} & for \, a_i \leq x \leq b_i \\ \frac{c_i - x}{c_i - b_i} & for \, b_i \leq x \leq c_i \\ 0 & for \quad x \geq c_i \end{cases}$$

Definition: 2.13

A Trapezoidal fuzzy multi number A_i is denoted by 4 – tuples (a_i, b_i, c_i, d_i), where $a_i, b_i, c_i \text{ and } d_i$ are real numbers and $a_i \leq b_i \leq c_i \leq d_i$ with membership function defined as

$$\mu_{A_i}(x) = \begin{cases} 0 & for \quad x \leq a_i \\ \frac{x - a_i}{b_i - a_i} & for \, a_i \leq x \leq b_i \\ 1 & for \, b_i \leq x \leq c_i \\ \frac{d_i - x}{d_i - c_i} & for \, c_i \leq x \leq d_i \\ 0 & for \quad x \geq d_i \end{cases}$$

Definition: 2.14

A Pentagonal fuzzy multi number A_i is denoted by 5 – tuples $(a_i, b_i, c_i, d_i, e_i)$, where $a_i, b_i, c_i, d_i \text{ and } e_i$ are real numbers and $a_i \leq b_i \leq c_i \leq d_i \leq e_i$ with membership function defined as

Vivek *et al.*,

$$\mu_{A_i}(x) = \begin{cases} 0 & for \quad x \le a_i \\ \frac{x-a_i}{b_i-a_i} & for\ a_i \le x \le b_i \\ \frac{x-b_i}{c_i-b_i} & for\ b_i \le x \le c_i \\ 1 & for\ x = c_i \\ \frac{d_i-x}{d_i-c_i} & for\ c_i \le x \le d_i \\ \frac{e_i-x}{e_i-d_i} & for\ d_i \le x \le e_i \\ 0 & for\quad x \ge e_i \end{cases}$$

Definition : 2.15

A hexagonal fuzzy multi number A_i is specified by 6 tuples $A_H = (a_i, b_i, c_i, d_i, e_i, f_i)$ where $a_i, b_i, c_i, d_i, e_i, and\ f_i$ are real number and $a_i \le b_i \le c_i \le d_i \le e_i \le f_i$ with membership function are given below

$$\mu_{A_i}(x) = \begin{cases} 0 & for\ x \le a_i \\ \frac{1}{2}\left(\frac{x-a_i}{b_i-a_i}\right) & for\ a_i \le x \le b_i \\ \frac{1}{2}+\frac{1}{2}\left(\frac{x-b_i}{c_i-b_i}\right) & for\ b_i \le x \le c_i \\ 1 & for\ c_i \le x \le d_i \\ 1-\frac{1}{2}\left(\frac{x-d_i}{e_i-d_i}\right) & for\ d_i \le x \le e_i \\ \frac{1}{2}\left(\frac{f_i-x}{f_i-e_i}\right) & for\ e_i \le x \le f_i \\ 0 & for\ x \ge f_i \end{cases}$$

Definition: 2.16

A Fuzzy number A_i is a normal octagonal fuzzy multi number denoted by $A_i = (a_i, b_i, c_i, d_i, e_i, f_i, g_i, h_i)$ where $a_i, b_i, c_i, d_i, e_i, f_i, g_i$ and h_i are real number and $a_i \le b_i \le c_i \le d_i \le e_i \le f_i \le g_i \le h_i$ with its membership function is given below.

$$\mu_{A_i}(x) = \begin{cases} 0 & for\ x < a_i \\ \frac{1}{2}\left(\frac{x-a_i}{b_i-a_i}\right) & for\ a_i \le x \le b_i \\ 0.5 & for\ b_i \le x \le c_i \\ \frac{1}{2}+\frac{1}{2}\left(\frac{x-c_i}{d_i-c_i}\right) & for\ c_i \le x \le d_i \\ 1 & for\ d_i \le x \le e_i \\ \frac{1}{2}+\frac{1}{2}\left(\frac{f_i-x}{f_i-e_i}\right) & for\ e_i \le x \le f_i \\ 0.5 & for\ f_i \le x \le g_i \\ \frac{1}{2}\left(\frac{h_i-x}{h_i-g_i}\right) & for\ g_i \le x \le h_i \\ 0 & for\ x \ge h_i \end{cases}$$

Definition: 2.17

The ranking function is an effective method of arranging fuzzy numbers. The ranking function is denoted by F ($\mathbb{R}$), where $\mathbb{R}$: F($\mathbb{R}$) →$\mathbb{R}$, and F ($\mathbb{R}$) is the collection of fuzzily specified numbers on a real line with a natural order. Let $a, b \in \mathbb{R}$, then ranking function for real numbers a, b is defined as

    (i) $D(a,b) > 0 \iff D(a,0) > D(b,0) \iff a > b$
    (ii) $D(a,b) < 0 \iff D(a,0) < D(b,0) \iff b < a$
    (iii) $D(a,b) = 0 \iff D(a,0) = D(b,0) \iff b = a$

Vivek *et al.*,

RANKING MEASURES OF FUZZY NUMBERS

In general, a fuzzy number A is described as any fuzzy subset of real line R, whose membership function μ_A satisfies the condition that μ_A is a continuous mapping from R to the closed interval [0,1]. Then the Ranking Measure of Graded Mean Integration Representation proposed by Chen and Hsieh [7] is as follows for the

- Triangular fuzzy number (a, b, c) is $\frac{(a+4b+c)}{6}$
- Trapezoidal fuzzy number (a, b, c, d) is $\frac{(a+2b+2c+d)}{6}$
- Pentagonal fuzzy number (a, b, c, d, e) is $\frac{(a+b+4c+d+e)}{8}$
- Hexagonal fuzzy number (a, b, c, d, e, f) is $\frac{(a+b+4c+4d+e+f)}{12}$
- Octagonal fuzzy number (a, b, c, d, e, f, g, h) is $\frac{(a+b+c+4d+4e+f+g+h)}{14}$

Later Helipern [10] proposed the Ranking Measure for the fuzzy number based on the expected value as

- Triangular fuzzy number (a, b, c) is $\frac{(a+2b+c)}{4}$
- Trapezoidal Fuzzy Set (a, b, c, d) is $\frac{(a+b+c+d)}{4}$
- Pentagonal Fuzzy Set (a, b, c, d, e) is $\frac{(a+b+2c+d+e)}{6}$
- Hexagonal Fuzzy Set (a, b, c, d, e, f) is $\frac{(a+b+2c+2d+e+f)}{8}$
- Octagonal Fuzzy Set (a, b, c, d, e, f ,g, h) is $\frac{(a+b+c+2d+2e+f+g+h)}{10}$

Recently, using the Sub Interval Average Method, the Ranking Measure of linear fuzzy numbers was defined by Stephen Dinagaret.all [14] as

- $\frac{(a+b+c)}{3}$ for the Triangular fuzzy number (a, b, c)
- $\frac{(a+b+c+d)}{4}$ for the Trapezoidal fuzzy number (a, b, c, d)
- $\frac{(a+b+c+d+e)}{5}$ for the Pentagonal fuzzy number (a, b, c, d, e)
- $\frac{(a+b+c+d+e+f)}{6}$ for Hexagonal fuzzy number (a, b, c, d, e, f)
- $\frac{(a+b+c+d+e+f+g+h)}{8}$ for Octagonal fuzzy number (a, b, c, d, e, f, g, h)

Analytical Evaluation of the Fuzzy Ranking Measures

Example 1 : The Ranking Measure of the given triangular fuzzy numbers of A = { (3,4,5)}, B = { (8,10, 12)}, C = {(2,3,5)}, D = {(4,5,6)}, E = {(1,1,3)}, F = { (4,8,9)} is represented in the following tabular form for the three defined methods of Graded Mean Integration Representation Method by Chen & Hsieh, Expected Value Method by Helipern and Sub Interval Average Method by Stephen Dinagarshows that, these measures are well suited to use for any linguistic variables.

Example 2 : The determination of the Ranking Measure of the **trapezoidal fuzzy numbers** of A = {(3,5,6,8)}, B = {(4,5,7,10)}, C = {(3,4,5,7)} and D = {(2,4,8,10)} is in the following table using the three defined methods of Graded Mean Integration Representation Method, Expected Value Method and Sub Interval Average Method shows that, these measures are well suited for any decision making real time applications.

Example 3 : The **pentagonal fuzzy numbers** Ranking Measure of A = {(2,4,5,7,8)},   B = {(7,8,9,10,12)}, C = {(3,4,5,6,8)} and D = {(8,9,10,12,13) is illustrated in the following tabular column for the three defined methods by Graded Mean Integration Representation Method of **Chen & Hsieh**, Expected Value Method of **Helipern** and Sub Interval Average Method of **Stephen Dinagar**shows that these measures are well suited for any real tie applications.

Example 4 : The Ranking Measure of the given **hexagonal fuzzy numbers** of
A = {(1,2,3,4,4,5)}, B = {(8,7,9,10,12,13)}, C = {(3, 5,7,8,9,10)} and

Vivek *et al.,*

D = {(14,15,17,19,20,24) } is defined in the following tabular column for the methods of Graded Mean Integration Representation Method, Expected Value Method and Sub Interval Average Method which shows that the these measures are efficient.

Example 5 : The three defined methods of Graded Mean Integration Representation Method by Chen & Hsieh, Expected Value Method by Helipern and Sub Interval Average Method by Stephen Dinagarofthe octagonal fuzzy numbers, A = {(8,9,10,12,15,16,18,20) },

B = {(2, 5,9,12,15,18,20,24) }, C = {(3,4,6,8,10,13,15,19) }, D = {(3,4,5,7,8,9,11,12) } isrepresented in the following tableshows that the these measures are well suited for any decision making applications

RANKING MEASURES OF FUZZY MULTI NUMBERS

The membership sequence is in the form $(\mu_A^1(x), \mu_A^2(x) , \ldots \ldots \mu_A^p(x))$ where $\mu_A^1(x) \geq \mu_A^2(x) \geq \cdots \geq \mu_A^p(x)$ with the Cardinality, the length of an element x in the Fuzzy Multi Set A denoted as η. Here, we have introduced the ranking measure for the Triangular, Trapezoidal, Pentagonal, Hexagonal and Octagonal of Graded Mean Representation Method,Helipern's Expected Value Method and Sub Interval Average Method

Method I
We have defined the Ranking Measure by the Graded Mean Integration Representation of fuzzy multi numberA_i.

- Triangular fuzzy multi numbers (a$_i$, b$_i$, c$_i$) is$\frac{1}{\eta}\sum_{i=1}^{\eta}\frac{(a_i+4b_i+c_i)}{6}$

- Trapezoidal fuzzymulti numbers (a$_i$, b$_i$, c$_i$, d$_i$) is $\frac{1}{\eta}\sum_{i=1}^{\eta}\frac{(a_i+2b_i+2c_i+d_i)}{6}$

- Pentagonal fuzzy multi numbers (a$_i$, b$_i$, c$_i$, d$_i$, e$_i$) is $\frac{1}{\eta}\sum_{i=1}^{\eta}\frac{(a_i+b_i+4c_i+d_i+e_i)}{8}$

- Hexagonal fuzzy multi numbers (a$_i$, b$_i$, c$_i$, d$_i$, e$_i$, f$_i$)   is$\frac{1}{\eta}\sum_{i=1}^{\eta}\frac{(a_i+b_i+4c_i+4d_i+e_i+f_i)}{12}$

- Octagonal fuzzy multi numbers($a_i b_i c_i \ d_i e_i \ f_i \ g_i \ h_i$) is

$$\frac{1}{\eta}\sum_{i=1}^{\eta}\frac{(a_i + b_i + c_i + 4d_i + 4e_i + f_i + g_i + h_i)}{14}$$

Method II
We have presented a new techniquethat make use of**Helipern's Expected Value.** Here, the notions of the expected value are based on the lower and upper expected values of A_i,fuzzy multi number.

- Triangular fuzzy multi numbers (a$_i$, b$_i$, c$_i$) is $\frac{1}{\eta}\sum_{i=1}^{\eta}\frac{(a_i+2b_i+c_i)}{4}$

- Trapezoidal fuzzy multi numbers (a$_i$, b$_i$, c$_i$, d$_i$) is $\frac{1}{\eta}\sum_{i=1}^{\eta}\frac{(a_i+b_i+c_i+d_i)}{4}$

- Pentagonal fuzzy multi numbers (a$_i$, b$_i$, c$_i$, d$_i$, e$_i$) is $\frac{1}{\eta}\sum_{i=1}^{\eta}\frac{(a_i+b_i+2c_i+d_i+e_i)}{6}$

- Hexagonal fuzzy multi numbers (a$_i$, b$_i$, c$_i$, d$_i$, e$_i$, f$_i$) is$\frac{1}{\eta}\sum_{i=1}^{\eta}\frac{(a_i+b_i+2c_i+2d_i+e_i+f_i)}{8}$

- Octagonal fuzzy multi numbers($a_i b_i c_i \ d_i e_i \ f_i \ g_i \ h_i$)is

$$\frac{1}{\eta}\sum_{i=1}^{\eta}\frac{(a_i + b_i + c_i + 2d_i + 2e_i + f_i + g_i + h_i)}{10}$$

Method III
Another Ranking Measure based on**Sub Interval Average** for Ranking of Linear Fuzzy Multi Number$A_i$is also proposedas follows:

- $\frac{1}{\eta}\sum_{i=1}^{\eta}\frac{(a_i+b_i+c_i)}{3}$ for the Triangular fuzzy multi numbers (a$_i$, b$_i$, c$_i$,)

- $\frac{1}{\eta}\sum_{i=1}^{\eta}\frac{(a_i+b_i+c_i+d_i)}{4}$ for the Trapezoidal fuzzy multi numbers (a$_i$, b$_i$, c$_i$, d$_i$)

- $\frac{1}{\eta}\sum_{i=1}^{\eta}\frac{(a_i+b_i+c_i+d_i+e_i)}{5}$for the Pentagonal fuzzy multi numbers (a$_i$, b$_i$, c$_i$, d$_i$, e$_i$)

- $\frac{1}{\eta}\sum_{i=1}^{\eta}\frac{(a_i+b_i+c_i+d_i+e_i+f_i)}{6}$for Hexagonal fuzzy multi numbers (a$_i$, b$_i$, c$_i$, d$_i$, e$_i$, f$_i$)

Vivek *et al.,*

- $\frac{1}{\eta}\sum_{i=1}^{\eta}\frac{(a_i + b_i + c_i + d_i + e_i + f_i + g_i + h_i)}{8}$ for Octagonal fuzzy multi numbers
  $(a_i b_i c_i \ d_i e_i \ f_i \ g_i \ h_i)$

Analytical Evaluation of the Fuzzy Multi Ranking Measures
Example 1 : The Ranking Measure of the triangular fuzzy multi numbers of cardinality η = 4
A = { (3,4,5) (4,5,6) (3,4,4) (2,3,6)}, B = { (8,10, 12) (7,9,11) (6,8,9) (11,12,13)},
C = {(2,3,5) (4,7,7) (3,5,6) (1,2,3)}, D = {(4,5,6) (3,4,7) (2,5,8) (7,8,9)},
E = {(1,1,3) (2,4,5) (3,7,9) (5,7,8)},F = { (4,8,9) (5,5,5) (6,7,8) (7,10,12)}
is represented in the following tabular column for the three defined methods of Graded Mean Integration Representation Method by Chen & Hsieh, Expected Value Method by Helipern and Sub Interval Average Method by Stephen Dinagar which shows that these measures are well suited to use for any multi linguistic variables.

Example 2 : The determination of the Ranking Measure of the **trapezoidal fuzzy multi numbers** of cardinality η = 3
A = {(3,5,6,8) (7, 9,10,11) (2,4,5,7) }, B = {(4,5,7,10) (8,10,13,14) (2,8,13,16)},
C = {(3,4,5,7) (6,7,12,14) (5,4,7,8)}, D = {(2,4,8,10) (3,7,11,15) (2,7,10,14)} is in the following table using the three defined methods of Graded Mean Integration Representation Method, Expected Value Method and Sub Interval Average Method which shows that these measures are well suited for any multi decision making real time applications.

Example 3 : The **pentagonal fuzzy multi numbers** Ranking Measure of cardinality η = 3
A = {(2,4,5,7,8) (3,5,7,9,11) (4,8,9,13,14)}, B = {(7,8,9,10,12) (10,12,14,16,18) (2,5,7,9,13)}, C={(3,4,5,6,8)(5,7,8,,9,11) (2,5,7,9,15)}, D = {(8,9,10,12,13) (10,12,14,15,17) (7, 8,9,10,11)} is illustrated in the following tabular column for the three defined methods of **Chen & Hsieh**, **Helipern** and **Stephen Dinagar.** It is clearthat,these measures are well suited for any real time applications with multiple criteria

Example 4 : The Ranking Measure of the **hexagonal fuzzy multi numbers** of cardinality η = 3
A = {(1,2,3,4,4,5) (2,5,7,8,9,10) (4,5,6,7,8,10)},
B = {(8,7,9,10,12,13) (10,12,13,15,16,18) (9,10,14,15,18,20)},
C = {(3, 5,7,8,9,10) (9,10,12,14,18,19) (2,5,7,8,10,13),
D = {(14,15,17,19,20,24) (5,8,10,12,14,16) (6,8,9,11,14,18)} is defined in the following tabular column for the methods of Graded Mean Integration Representation Method, Expected Value Method and Sub Interval Average Method which shows that the these measures are efficient.

Example 5 : The three defined methods of Graded Mean Integration Representation Method by **Chen & Hsieh**, Expected Value Method by **Helipern** and Sub Interval Average Method by **Stephen Dinagar**ofthe **octagonal fuzzy multi numbers**of cardinality of η = 2,
A = {(8,9,10,12,15,16,18,20) (10,12,14,16,19,21,25,28)},
B = {(2, 5,9,12,15,18,20,24) (1,2,3,6,7,8,10,14)},
C = {(3,4,6,8,10,13,15,19) (1,2,3,4,5,6,7,8)},
D = {(3,4,5,7,8,9,11,12) (2,5,7,9,12,13,14,17)}is explained in the following tableshows that, these measures are well suited for any multi criteria decision making applications

SIGNIFICANCE OF THE STUDY
There are many ranking measures available to the Fuzzy Environments, but still the percentage of verification varies. In Fuzzy Environments, we deal with the membership functions once (single data), whereas in Fuzzy Multi Environments, we deal with repeated (multi) membership functions. The new ranking measures of Fuzzy Multi Environment analyses the options in a more intuitively, appealing and consistent way than the other specified measures. Hence, we have introduced the Ranking Measure of Fuzzy Multi Numbers of Triangular, Trapezoidal, Pentagonal, Hexagonal and Octagonal categories. This concept of Ranking Measures for the Fuzzy Multi Numbers

Vivek *et al.,*

can be applicable in any multi criteria decision making analysis which is found to be aunique, advanced, new application-oriented approach.

CONCLUSION

We have studied three ranking measures of fuzzy numbers of Graded Mean Integration Representation Method by Chen & Hsieh, Expected Value Method by Helipern and Sub Interval Average Method by Stephen Dinagar and in this paper, we have extended those measures to Fuzzy Multi Numbers. The introduced ranking techniques of Fuzzy Multi Numbers are compared by considering the Triangular, Trapezoidal, Pentagonal, Hexagonal and Octagonal Fuzzy Multi Numbers with its membership function. The Fuzzy Multi Numbers are transformed to crisp data by the introduced ranking techniques. The efficiency of the Ranking Techniques is analyzed with the numerical examples, and it is clear that all three methods are well suited for any multi criteria decision making problemsas their ranking measures are closer to one another.

ACKNOWLEDGEMENT

REFERENCES

1. Arora, Sudha & Revathi . M. (2016). A new ranking on hexagonal fuzzy numbers, International Journal of Fuzzy Logic Systems. 6. 1-8. 10.5121/ijfls.2016.6401.
2. Amit Kumar, Pushpinder Singh, Amarpreet Kaur, Parmpreet Kaur, Ranking of Generalized Trapezoidal Fuzzy Numbers Based on Rank, Mode, Divergence and Spread, Turkish Journal of Fuzzy Systems (ISSN: 1309–1190), Vol.1, No.2, pp. 141-152, 2010.
3. BongJu Lee and Yong Sik Yun, The Generalized Trapezoidal Fuzzy Sets, Journal of the Chungcheong Mathematical Society, Volume 24, No. 2, June 2011.
4. Buckley . J.J, A fuzzy ranking of fuzzy numbers, Fuzzy Sets and Systems 33, 119—121 (1989).
5. Chandrasekaran . S, G. Gokila and Juno Saju, Ranking of octagonal fuzzy numbers for solving multi objective fuzzy linear programming problem with simplex method and graphical Method, (IJSEAS), 1(2015), 504–515.
6. Chen . S. H, Ranking fuzzy numbers with maximizing set and minimizing set, Fuzzy Sets and Systems 17, 113-129 (1985).
7. Chen, S. H. and Hsieh, C. H. , "Graded Mean Integration Representation of Generalized Fuzzy Number" Journal of the Chinese Fuzzy System Association, Vol. 5, No. 2, pp. 1-7, 1999.
8. Dubois, D., and Prade, H., "Operations on Fuzzy Numbers", International Journal of System Sciences, Vol. 9, pp. 613-626, (1978).
9. Helen, R., and Uma, G., "A New Operation and Ranking on Pentagon Fuzzy Number", IJMSA, Vol. 5, No. 2, pp. 341346, (2015).
10. Heilpern, S.,"Representation and application of fuzzy numbers", Fuzzy sets and Systems, vol. 91, pp.259-268, 1997.
11. Lee .E.S and Li. R.J.,"Comparison of fuzzy numbers based on the probability measure of fuzzy events", Computational Mathematical Application, Volume 15, No. 10, pp. 887-896, (1988).
12. Lee . B. J and Yun . Y. S, The Pentagonal Fuzzy Numbers, Journal of Chungcheong Mathematical Society, 27(2) (2014) 277 - 286.
13. Nagoor Gani A and Mohamed Assarudeen S N, " A New operation on Triangular fuzzy number for solving FLPP", Applied Mathematical Sciences 2011 6(11) pp525 -532

Vivek *et al.,*

14. Stephen Dinagar, Kamalanathan, Rameshan, "Sub Interval Average Method for Ranking of Linear Fuzzy Numbers", International Journal of Pure and Applied Mathematics, Volume 114 No. 6 2017, 119 – 130
15. Thamaraiselvi . A and Santhi. R, (2015) "Optimal solution of FTP Using Hexagonal Fuzzy Numbers", International Journal of Scientific & Engineering Research, 6, pp. 4045.
16. Yager . R. R, ON THE THEORY OF BAGS, Int. J. General Systems, Vol. 13, pp 23–37, 1986.
17. Zadeh, L.A. Fuzzy sets. Information and Control, 8(3), 338-356,1965.
18. Zimmermann . H. J, Fuzzy Set Theory and Its Applications, Kluwer Academic Publishers, Boston, Mass, USA, Second edition, 1996.

Table 1. Triangular Fuzzy Ranking

Triangular Fuzzy Ranking	A	B	C	D	E	F
Method 1	4	10	3.1667	5	1.3333	7.5
Method 2	4	10	3.25	5	1.5	7.25
Method 3	4	10	3.3333	5	1.6667	7

Table 2. Trapezoidal Fuzzy Ranking

Trapezoidal Fuzzy Ranking	A	B	C	D
Method 1	5.5	6.33333	4.6667	6
Method 2	5.5	6.5	4.75	6
Method 3	5.5	6.5	4.75	6

Table 3. Pentagonal Fuzzy Ranking

Pentagonal Fuzzy Ranking	A	B	C	D
Method 1	5.125	9.125	5.125	10.25
Method 2	5.1667	9.1667	5.1667	10.3333
Method 3	5.2	9.2	5.2	10.4

Table 4. Hexagonal Fuzzy Ranking

Hexagonal Fuzzy Ranking	A	B	C	D
Method 1	3.3333	9.6667	7.25	18.0833
Method 2	3.25	9.75	7.125	18.125
Method 3	3.1667	9.8333	7	18.1667

Table 5. Octagonal Fuzzy Ranking

Octagonal Fuzzy Ranking	A	B	C	D
Method 1	13.5	13.2857	9.4286	7.4286
Method 2	13.5	13.2	9.6	7.4
Method 3	13.5	13.125	9.75	7.375

Table 6. Triangular Fuzzy Multi Ranking

Triangular Fuzzy Multi Ranking	A	B	C	D	E	F
Method 1	4.0416	9.7083	4.125	5.5833	4.6667	7.3333
Method 2	4.0625	9.6875	4.0625	5.625	4.625	7.25
Method 3	4.0833	9.6667	4	5.6667	4.5833	7.1667

Vivek *et al*.,

Table 7. Trapezoidal Fuzzy Multi Ranking

Trapezoidal Fuzzy Multi Ranking	A	B	C	D
Method 1	6.4444	9.3333	6.7222	7.7778
Method 2	6.4167	9.3333	6.8333	7.75
Method 3	6.4167	9.3333	6.8333	7.75

Table 8. Hexagonal Fuzzy Multi Ranking

Hexagonal Fuzzy Multi Ranking	A	B	C	D
Method 1	5.6944	12.6945	9.3611	13.1667
Method 2	5.625	12.7083	9.375	13.25
Method 3	5.5556	12.7222	9.3889	13.3333

Table 9. Octagonal Fuzzy Multi Ranking

Octagonal Fuzzy Multi Ranking	A	B	C	D
Method 1	15.6786	9.8571	6.9643	8.7857
Method 2	15.75	9.8	7.05	8.7
Method 3	15.8125	9.75	7.125	8.625

RESEARCH ARTICLE

Antischizophrenic-Active Medicinal Herbs and Complementary Therapies for the Treatment of Schizophrenia

Vasudha Negi[1]*, Chandra Shekhar Tailor [2] and Bhawana Bhatt[3]

[1]PG Research Scholar, School of Pharmaceutical Sciences, SGRR University, Patel Nagar, Dehradun – 248001, Uttarakhand, India.
[2]Associate Professor and Head Department of Pharmacogony, School of Pharmaceutical Sciences, SGRR University, Patel Nagar, Dehradun – 248001, Uttarakhand, India.
[3]Assistant Professor, School of Pharmaceutical Sciences, SGRR University, Patel Nagar, Dehradun – 248001, Uttarakhand, India.

*Address for Correspondence
Vasudha Negi
PG Research Scholar,
School of Pharmaceutical Sciences,
SGRR University, Patel Nagar,
Dehradun – 248001, Uttarakhand, India.
E.Mail: vasudhanegi956@gmail.com

ABSTRACT

Mental problems are becoming more and more common as a result of ambitious lifestyle, urbanisation, and stressful surroundings. Schizophrenia is a chronic psychiatric condition that affects people all over the world, with a lifetime prevalence of 1% and significant long-term mortality and morbidity. A devastating, inherited brain condition called schizophrenia is caused by defects that appear early in infancy and disrupt the brain's natural development. There are now a number of dietary supplements and herbal medicines that can be used alone by people with mild to severe symptoms of schizophrenia. Ayurvedic medications and dietary supplements can be used as adjuvant therapy with current medications for schizophrenic patients who have severe symptoms in order to maximise the therapeutic efficacy while minimising the side-effect load. This article provides information on some typical complementary treatments as well as specific medicinal plants that are used to treat various ailments, including schizophrenia.

Keywords: Medicinal, herbal, urbanisation, schizophrenia, dietary supplements.

INTRODUCTION

India has a long history of learning about using plant-based medicines for both therapeutic and preventive purposes. These plants are widely grown in the wild and are specifically used in local pharmaceutical factories. Some of these plants yield high-potential pharmaceuticals with a high value for export [1]. The history of using plants and plant-based products as medicines dates back to the dawn of human civilization. The Rig Veda, which is regarded as the oldest collection of human knowledge and is thought to have been composed between 4500 and 1600 B.C., has the earliest reference of the medical usage of plants in Hindu culture [2]. Ambitious living, urbanisation, and stressful environments have all contributed to the rise in the prevalence of mental illnesses [3]. It has been discovered that the Indian system of complementary medicine (herbal medications) has drawn interest from all around the world due to its efficacy and security. Therefore, with a remarkable rate of success, these traditional herbal medicines are being tried for a variety of medical conditions such as arthritis, jaundice, respiratory illness, hyperlipidaemia, diabetes mellitus, hypertension, obesity, schizophrenia, and coronary artery disease, among others [4]. India is a country where Ayurveda has been used quite successfully since the Vedic era. Although various plant sources that are known to have CNS function have been investigated [5].One of the most exhausting, expensive, and complicated illnesses is psychosis. The Greek word "-osis" denotes an abnormal state, and the word "psyche" is often used to refer to the mind or soul. Thus, a loss of connection to reality is a common description of psychosis. These conditions affect a person's capacity to think clearly, make sound decisions, react emotionally, communicate clearly, assess reality, and conduct appropriately [3].

Due to the fact that there is no cure for incurable psychotic diseases, only symptomatic treatment is available, there is an increasing need for medications with minimal side effects, particularly when administered for an extended period of time.Herbal medications are recognised to have extremely little side effects, making them a promising treatment option for chronic CNS illnesses that are essentially incurable [6].Due to its affordability, environmental friendliness, and ability to effectively treat illness condition, herbal medicines are attracting more and more attention [7]. A crucial organ system is the central nervous system (CNS). Drugs that affect the central nervous system are therefore crucial from both perspectives. It's not always been evident how specific medications affect the CNS or how they work. Since many of the ailments for which these medications are prescribed (schizophrenia, anxiety, etc.) have poorly known root causes [8].it is still unclear what exactly causes the illness. There are many subgroups of people who have schizophrenia; for instance, drug-resistant illnesses may represent a separate subtype of schizophrenia rather than just a more severe variety. The present antipsychotic regimen is efficient in treating the disease's positive symptoms, but there are few options for addressing the disease's negative symptoms and cognitive issues [9].

It is frequently a chronic, debilitating illness that affects numerous functional domains. The typical course of treatment for schizophrenia is based on the biopsychosocial model and includes prescribing antipsychotic medications, as well as patient and family counselling[10]. The majority of schizophrenia patients may experience a chronic course and require long-term maintenance therapy. Even though antipsychotic therapy is a mainstay of schizophrenia maintenance therapy, patients nevertheless frequently experience relapse and other side effects from antipsychotic medication. Herbal medicine and other alternative therapies are being used more frequently to treat schizophrenia in order to increase therapeutic efficacy and lessen unfavourable side effects associated with antipsychotic therapy [11]. Antipsychotic medications are used to treat psychosis. The first generation of antipsychotics, also known as neuroleptics, are known as antipsychotics, whereas the second generation are known as atypical antipsychotics.The effectiveness and side effects of atypical antipsychotics are usually thought to be superior than those of typical antipsychotics [12].

MEDICINAL PLANTS HAVING ANTISCHIZOPHRENIC ACTIVITY
Maidenhair tree (*Ginkgo biloba*): The primary constituents of ginkgo biloba extract include terpenoids, flavonol glycosides and proanthocyanidin [13,14]. Ginkgo biloba extracts contains anti-oxidant and anti-inflammatory properties . They have been linked to terpene and flavone lactone actions, as well as increased cerebral blood flow

and antiplatelet effects [15].Together with clozapine, they are promising treatments for schizophrenia since they considerably lessen the negative symptoms that people with schizophrenia experience. [16].

Ashwagandha (*Withania somnifera*): It consists of dried root and stem bases from the Solanaceae plant *Withania somnifera*. In subtropical India and all other arid regions, this plant thrives freely. Ashwagandha is also referred to as Indian ginseng, poison gooseberry, and winter cherry. Alkaloids and steroidal lactone are the main chemical components. The alkaloids in ashwagandha include somniferinine, somnine, somniferinine, withananine, pseudo-withanine, tropine, pseudo-tropine, 3-a-gloyloxytropane, cuscohygrine, and anaferine, with withanine being the main one [17].

St. John's Wort (*Hypericum perforatum*): This herb can be utilised to treat various positive, negative, and cognitive symptoms of schizophrenia since it also inhibits serotonin receptors, whose activity has been discovered to be increased in schizophrenia [18].

Spinach (*Spinacia oleracea*): Spinach, a member of the family Chenopodiaceae, has a multitude of therapeutic benefits. It is an excellent package of unique phytoconstituents such as ascorbic acid, apigenin, astragalin, caffeic, lutein, β-carotene, ferulic acid, kampeferol, rutin, querecetin, myricetin, luteolin, ortho-coumaric acid, para-coumaric acid, stigmasterol, protocatechuic acids, methylenedioxyflavonol, glycoglycerolipids, 20- hydroxyecdysone, vitamins, spirasaponins violaxanthin etc., which are responsible for its biomedicinal& pharmacotherapeutic effects[19].

Kava(*Piper methysticum*): One of the few herbal treatments with a known pharmacologically active component is kava. A biologically active substance known as kavain and kavapyrone is derived from the kava plant, Piper methysticum. It is unknown how exactly the kavapyrones cause these effects because they operate in a number of different ways, including by inhibiting voltage-dependent sodium channels, raising GABAA (-aminobutyric acid) receptor densities, blocking norepinephrine reuptake, and inhibiting glutamate release [20, 21,22].

Brahmi (*Bacopa monnieri*): Brahmi (Bacopa monnieri; family: Scrophulariaceae), an Ayurvedic herb, has been used extensively to enhance cognition, memory, and learning skills. The addition of 500 mg/day of Brahmi extract over the course of a month reduced psychopathology in a case study of schizophrenia without resulting in any treatment-emergent negative effects [23]. Brahmi, a herb with nervine and revitalising properties, soothes nervous excitement and has sedative-like effects [24].

Tulsi (*Ocimumbasilicum*) : The scientific name for sweet basil, also known as Reihan, is Ocimumbasilicum L. (Family Lamiaceae) [25].Ocimumbasilicum leaves have antioxidant qualities that may be used to treat schizophrenia and other brain illnesses. Regularly consuming tea made from O. basilicum leaves can improve brain function and, as a result, help to moderate schizophrenia symptoms. For best effects, try to consume this herb tea twice daily [26,27,28,29].

Ginseng(*Panax ginseng*): The dried roots of several species of panax, including P. ginseng, P. japonica, P. notoginseng, and P. quinquefolium, are used to make ginseng. A variety of saponin glycosides from the triterpenoid family are found in ginseng. Ginsenosides, panaxosides, and chikusetsusaponin are the names given to them. The majority of ginseng species contain ginsenosides, polysaccharides, peptides, polyacetylenic alcohols, and fatty acids among their constituents [30]. It strengthens the ability to fight off sickness and increases natural resistance. It has calming and stimulating effects [31].

Ziziphus jujube(*Ziziphus mauritiana*):A species of Ziziphus in the buckthorn family Rhamnaceae, Ziziphus zizyphus is also known as jujube (or jujuba), red date, or Chinese date. It is mostly utilised as a fruiting shade tree. The fruits are utilised in traditional Chinese and Korean medicine, where they are thought to reduce stress,[32] and traditionally for sedative[33] antioxidant, immunostimulant, and wound healing properties[34].

Vasudha Negi *et al.,*

Cardamom (*Elettaria cardamomum***):** The numerous symptoms of schizophrenia may also be managed with the use of Elettaria cardamomum seeds. The neurological system benefits greatly from the therapeutic qualities of E. cardamomum seeds. Making herbal tea is the simplest way to use *E. cardamomum* seeds. This tea should be consumed twice per day to aid with schizophrenia symptoms.

Liquorice (*Glycyrrhiza glabra***):** Compounds and minerals included in *Glycyrrhiza glabra* may help to manage and control the healthy status of the brain. This herb is very effective at reducing stress and anxiety. Schizophrenia could be successfully treated with *G. glabra's* healing abilities. For this remedy, morning consumption on an empty stomach yields the finest benefits. Breakfast should be consumed after an hour has passed so that the herb can be thoroughly digested and absorbed into the bloodstream [26,27,28,29].

Saffron(*Crocus sativus***):** The perennial herb *Crocus sativus* L. (*C. sativus*) belongs to the Liliaceae branch of the Iridaceae family [35,36]. Saffron extract or its components have antidepressant properties, according to recent pharmacological studies[37], anti-inflammatory, anti-tumor effects, radical-scavenging, learning and memory improving properties [38,39,40].

Amla (*Phyllanthus emblica***):** *Phyllanthus emblica* is a sort of natural antioxidant. Additionally, it boosts the immune system, giving a much-needed boost the body to fight against psychological disorders like schizophrenia. One way of consuming the herb would be to bring the dried leaves of *P. emblica* and grind them all to create a smooth powder. Take one teaspoonful of the powder with hot water two times each day [26,27,28,29].

COMPLIMENTARY METHODS USED IN THE TREATMENT OF SCHIZOPHRENIA

Multivitamin products: Due to their inadequate diets, multivitamin products are advised for the vast majority of schizophrenia patients. Vitamins must be obtained from an outside source in order to adequately nourish the brain and other organs because humans cannot make them, with the exception of vitamin D[41].

EPA omega-3 fish oils: Early scientific research suggests that taking fish oil capsules that are high in the EPA (a type of Omega-3 fatty acid) form of oil may help people with schizophrenia by reducing their symptoms, despite the fact that the research is somewhat contradictory (there are some positive studies and some negative studies) [42].

Glycine: Numerous studies demonstrate that the non-essential amino acid glycine, especially when combined with the antipsychotic drugs haloperidol, thioridazine, and perphenazine, improves neurotransmitter activity and lessens negative symptoms of schizophrenia [43,44,45].

BENEFITS OF USING HERBS FOR SCHIZOPHRENIA [46,47]
1. Less risk on health
2. 2.Provides a wide range of noteworthy development
3. Increase energy level
4. Enhanced overall perception of health
5. Reduced level of pain
6. Increasing emotional stability
7. Alleviating anxiety
8. Reducing social isolation

CONCLUSION

Since the dawn of civilisation, plants have been used all across the world to treat illnesses. Plants are generally safe, free of adverse effects, widely available nearby, and environmentally good because they are natural items. Some

plants that have previously been investigated for their anti-schizophrenic effects by various researchers have been mentioned in this overview. Psychiatrists find it challenging to suggest nutritional supplements and natural cures instead of tested conventional therapies. Studies comparing the efficacy of herbal supplements and conventional therapies have been conducted. Herbal supplements and conventional therapies were not shown to be highly successful when used separately, but when combined, improved outcomes were obtained. Clinical investigations should consider further examining herbal extracts and elements with proven psychotherapy effects in animal models. Some nutritional supplements, such as anti-oxidant vitamins and EPA omega-3 fish oils, aid in reducing schizophrenia symptoms. As a result, using herbal therapy in conjunction with dietary supplements can produce superior effects. On the other side, our lifestyle choices have an impact on our health.

REFERENCES

1. Rathish R. Nair and Sumitra V. Chandra, 2005. Pucinia granatum – A potential source as antibacterial drug. Asian Journal of Microbiology, Biotechnology and Environmental Science, 7: 625- 628.
2. Rastogi, R.P and B.N. Mehrotra, 2002. Glossary of Indian Medicinal Plants. National Institute of Science Communication, New Delhi, India.
3. Siddique N, Hussain S, Yadav S, Gupta A. Psychosis and antipsychotic plants an: overview. Int J Indig Herb Drug . 2022Feb.12 [cited 2023Mar.8];7(1):22-9.
4. Suresh V, Lakhani JD, Balaraman R. A Review on the Possible Therapeutic Intervention by Herbal Remedies on Antipsychotic Drugs Induced Metabolic Disorder. Journal of Natural Remedies. 2022.
5. Wall PM, Messier C: Ethological confirmatory factor analysis of anxiety - like behaviour in the murine elevated plus - maze. Behav Brain Res; 2000 Sep; 114 (1 - 2): 199 - 212.
6. Reddy, K. S. Psychopharmacological studies of hydro alcoholic extractof whole plant of Marsilea quadrifolia. J. Sci. Res.2012; 4 (1): 279 - 285.
7. Horacek, J., Bubenikova - Valesova, V., Kopecek, M., Palenicek, T., Dockery, C., Mohr, P. Mechanism of action of atypical antipsychotic drugs and the neurobiology of schizophrenia. CNS Drugs.2006; 20, 389–409.
8. KatzungBG.In Basic and Clinical Pharmacology, Ninth edition, Lange Medical Publications, California.2010; 175, 489 - 492
9. Shi XJ, Fan FC, Liu H, Ai YW, Liu QS, Jiao YG, Cheng Y. Traditional Chinese medicine decoction combined with antipsychotic for chronic schizophrenia treatment: a systematic review and meta-analysis. Frontiers in Pharmacology. 2021 Jan 20;11:616088.
10. Grover S, Davuluri T, Chakrabarti S. Religion, spirituality, and schizophrenia: A review. Indian journal of psychological medicine. 2014 Apr;36(2):119-24.
11. Brothers Zhang ZJ, Tan QR, Tong Y, Wang XY, Wang HH, Ho LM, Wong HK, Feng YB, Wang D, Ng R, McAlonan GM. An epidemiological study of concomitant use of Chinese medicine and antipsychotics in schizophrenic patients: implication for herb-drug interaction. PloS one. 2011 Feb 16;6(2):e17239.
12. K D Tripathi, Essential of Medicinal Pharmacology, Jaypee Medicinal Publisher Ltd. 6th Edition, 2008, 423 – 428.
13. Natascia Brondino, Annalisa De Silvestri, Simona Re, Niccolò Lanati, Pia Thiemann, Anna Verna, Enzo Emanuele, and Pierluigi Politi. A Systematic Review and MetaAnalysis of Ginkgo biloba in Neuropsychiatric Disorders: From Ancient Tradition to Modern-Day Medicine. Evidence based complementary and alternative medicine, 2013; ID 915691: 11
14. Hongyong Deng, Ji Xu, and Wing-Fai Yeung. Ginkgo biloba versus placebo for schizophrenia. Cochrane Database of Systematic Reviews, 2017; (1): CD012524.
15. Tulsulkar J, Shah ZA. Ginkgo biloba prevents transient global ischemia-induced delayed hippocampal neuronal death through antioxidant and anti-inflammatory mechanism. Neurochemistry International. 2013;62(2):189-97.
16. Mishra A, Mishra AK, Jha S. Effect of traditional medicine brahmivati and bacoside A-rich fraction of Bacopa monnieri on acute pentylenetetrzole-induced seizures, amphetamine-induced model of schizophrenia, and scopolamine induced memory loss in laboratory animals. Epilepsy and Behavior. 2018;80:144- 51.

17. Sultan Zahiruddin, ParakhBasist, Abida Parveen, Rabea Parveen, Washim Khan, Gaurav, Sayeed Ahmad . Ashwagandha in Brain Disorders: A Review of Recent Developments. Journal of Ethnopharmacology, 2020; 15; 257: 112876

18. Reena kumari, madhukaundal, zaheerahmad, ashwalayan VD. Herbal and dietary supplements in treatment of schizophrenia: an approach to improve therapeutics. International journal of pharmaceutical sciences review and research, 2011; 10(1): 217-224.

19. Monu Yadav, Milind Parle, Nidhi Sharma, Deepak Kumar Jindal, Aryan Bhidhasra, Mamta Sachdeva Dhingra, AnilKumar, Sameer Dhingra. Protective effects of Spinacia oleracea seeds extract in an experimental model of schizophrenia: Possible behavior, biochemical, neurochemical and cellular alterations. Biomedicine & Pharmacotherapy, 2018; 105: 1015-1025.

20. Magura EI, Kopanitsa MV, Gleitz J. Kava extract ingredients, (+)-methysticin and (+/-)- kavain inhibit voltage-operated Na (+)-channels in rat CA1 hippocampal neurons. Neuroscience, 1997; 81: 345-351

21. Jussofie A, Schmiz A, Hiemke C, Kavapyrone enriched extract from Piper methysticum as modulator of the GABA binding site in different regions of rat brain. Psychopharmacology, 1997; 116: 469-474.

22. Seitz U, Schule A, Gleitz J. Monoamine uptake inhibition properties of kava pyrones, Planta Medica, 1997; 63: 548-549.

23. Sukanto Sarkar, Biswa Ranjan Mishra, Samir Kumar Praharaj, S Haque Nizamie. Add-on Effect of Brahmi in the Management of Schizophrenia. Journal of Ayurveda Integrative Medicine, 2012; 3(4): 223-5

24. Agrawal A, Pandey MN, Dubey GP. Management of mental deficiency by an indigenous drug, *Brahmi*(*Bacopa monnieri*) *Pharmacopsychoecologia.* 1993;6:1–5.

25. Ayuob NN, Firgany AE, El-Mansy AA, Ali S. Can Ocimumbasilicum relieve chronic unpredictable mild stress-induced depression in mice?. Experimental and molecular pathology. 2017 Oct 1;103(2):153-61

26. Rathbone J, Zhang L, Zhang M, Xia J, Liu X and Yang Y. Chinese herbal medicine for schizophrenia. Cochrane Database Systematic Rev. 2005; 19 (4): CD003444.

27. Rathbone J, Zhang L, Zhang M, Xia J, Liu X, Yang Y and Adams CE. Chinese herbal medicine for schizophrenia: cochrane systematic review of randomised trials. British Journal of Psychiatry 2007; 190: 379-84.

28. Xiao SF, Xue HB, Li X, Chen C, Li GJ, Yuan CM and Zhang MY. A double-blind, placebocontrolled study of traditional Chinese medicine sarsasapogenin added to risperidone in patients with negative symptoms dominated schizophrenia. Neuroscience Bulletin 2011; 27 (4): 258-68.

29. Deng H and Adams CE. Traditional Chinese medicine for schizophrenia: A survey of randomized trials. Asia Pacific Psychiatry 2017; 9 .

30. Hak-Jae Kim, Hansol Won, JiyunIm, Hwayoung Lee, Jiwoo Park, Sanghyun Lee, Young-Ock Kim, Hyung-Ki Kim, and Jun-Tack Kwon. Effects of Panax ginseng C.A. Meyer extract on the offspring of adult mice with maternal immune activation. Molecular Medicine Report, 2018; 18(4): 3834–3842.

31. Chatterjee M, Ganguly S, Srivastava M, Palit G, Effect of 'chronic' versus 'acute' ketamine administration and its 'withdrawal' effect on behavioural alterations in mice: implications for experimental psychosis, Behav Brain Res, 216, 2011, 247-254.

32. Sultan Zahiruddin, ParakhBasist, Abida Parveen, Rabea Parveen, Washim Khan, Gaurav, Sayeed Ahmad . Ashwagandha in Brain Disorders: A Review of Recent Developments. Journal of Ethnopharmacology, 2020; 15; 257: 112876.

33. Mill Goetz P, "Demonstration of the psychotropic effect of mother tincture of Zizyphus jujuba", Phytotherapie, 7, 2009, 1 (31-36).

34. Jiang J.-G, Huang X.-J, Chen J, Lin Q.-S, "Comparison of the sedative and hypnotic effects of flavonoids, saponins, and polysaccharides extracted from Semen Ziziphus jujube", Natural Product Research,21, 2007, 4 (310-320).

35. Nikolaos Pitsikas. Constituents of Saffron (Crocus sativus L.) as Potential Candidates for the Treatment of Anxiety Disorders and Schizophrenia. Molecules, 2016; 21(3): 303.

36. MortezaZare, Azam Bazrafshan, Reza Malekpour Afshar, and Seyed Mohammad Mazloomi. Saffron (adjunct) for people with schizophrenia who have antipsychotic-induced metabolic syndrome. Cochrane Database of Systematic Reviews, 2018; (3): CD012950.

Vasudha Negi *et al.*,

37. Hosseinzadeh H, Karimi GH, Niapoor M, Antidepressant effects of Crocus sativus stigma extracts and its constituents, crocin and safranal, in mice, Acta Hort, 650, 2004, 435-45.

38. Abdullaev FJ, Biological effects of saffron, Biofactors, 4, 1993, 83-6.

39. Zhang Y, Sugiura M, Saito H, Shoyama Y, Acute effects of Crocus sativus L. on passive avoidance performance in mice, BiolPharmacol Bull, 17,1994, 217-21.

40. Abe K, Sugiura M. Ymaguchi S, Shoyama Y, Saito H, Saffron extract prevents acetaldehyde-induced inhibition of long-term potentiation in the rat dentate gyrus in vivo, Brain Res, 851, 1999, 287-9.

41. Devi U Chinnaswamy. Oxidative injury and enzymic antioxidant misbalancein schizophrenics with positive, negative and cognitive symptoms. African Journal of Biochemistry Research, 2008; 2(4): 92-97.

42. Guochuan T, Glycine Trnasporter 1 Inhibitor, NMethylglycine [sarcosine], Added to Antipsychotics for the Treatment of Schizophrenia, Biological Psychiatry 55, 2004, 452-456.

43. Waziri R: Glycine therapy of schizophrenia: some caveatus. Biological Psychiatry, 1996; 39(3): 155-6.

44. Heresco Levy-U, Javitt DC, Ermilov M et al. Efficacy of high-dose glycine in the treatment of enduring negative symptoms of schizophrenia. Archives of General Psychiatry, 1999; 56: 29-36.

45. Javitt DC, Zilberman I, Zukin SR et al. Amelioration of negative symptoms in schizophrenia by glycine. The American Journal of Psychiatry, 1994; 151: 1234-6

46. Saki K, Hassanzad-Azar H, Naghdi N, Bahmani M. Ginkgo biloba: An effective medicinal plant on neurological disorders. J Prev Epidemiol. 2016;1:e03.

47. Barrios M, Gómez-Benito J, Pino O, Rojo E, Guilera G. Functioning in patients with schizophrenia: A multicentre study evaluating the clinical perspective. Psychiatry Research. 2018;270:1092-8.

RESEARCH ARTICLE

Fuzzy Proposed MCDM Method to Analyze the Risk Factors in Breast Cancer

Iswariya S[1]* and Sahaya Sudha A[2]

[1]Research Scholar, PG and Research Department of Mathematics, Nirmala College for Women, Coimbatore, Tamil Nadu, India.
[2]Associate Professor, PG and Research Department of Mathematics, Nirmala College for Women, Coimbatore, Tamil Nadu, India

*Address for Correspondence
Iswariya S
Research Scholar,
PG and Research Department of Mathematics,
Nirmala College for Women,
Coimbatore, Tamil Nadu, India.
E.Mail: iswariya25041999@gmail.com

ABSTRACT

Breast cancer ranks as one of the most prevalent cancers in women, with a higher incidence among those aged 50 and older. It stands as the second leading cause of cancer-related fatalities among women. In the year 2023, projections anticipate approximately 297,790 new cases of invasive breast cancer and 55,720 new cases of non-invasive breast cancer among women. So, it is our utmost interest is to analyze the risk factors of Breast cancer. Therefore, this present study is intended a propose an MCDM method under a fuzzy environment to analyze the risk factors in Breast Cancer. To illustrate the implementation process of this methodology, we'll delve into a numerical example.

Keywords: Breast Cancer, Risk Factors, Fuzzy logic, MCDM method

INTRODUCTION

Breast Cancer creates a significant global health concern, affecting millions of women every year[1]. With advancements in medical research and treatment modalities, there has been significant progress in understanding the molecular mechanisms of breast cancer development, early detection, diagnosis, and targeted therapies. This comprehensive review highlights recent breakthroughs in breast cancer research and treatment, shedding light on emerging strategies to combat this devastating disease. Understanding the risk factors associated with breast cancer can help identify individuals who may have a higher likelihood of developing the disease. While having one or more

64162

of these risk factors does not guarantee the development of breast cancer, they can increase the overall risk[6]. Zadeh [9] put forward the concept of fuzzy sets in 1965. In subsequent years, the theory of fuzzy sets continued to evolve and mature. Multiple Criteria Decision Making (MCDM), which is a field of study that deals with decision-making problems involving multiple and often conflicting criteria. In many real-world situations, decision-makers need to evaluate and compare alternatives based on multiple attributes or criteria before making a final decision. Fuzzy MCDM methods handle decision-making problems with fuzzy or uncertain data[8]. They extend traditional MCDM methods to deal with imprecise information. MCDM methods play a crucial role in fields like management, engineering, finance, environmental planning, and many other areas where complex decisions need to be made considering multiple conflicting criteria [20]. These methods help decision-makers consider different perspectives, weigh the importance of various criteria, and arrive at a well-informed decision. The researcher determined the most significant risk factors of breast cancer by applying the MCDM statistical model.

The main purpose is to identify the significant risk factors for Breast cancer and to raise awareness and prevent the spread of the disease. High-risk factors are sorted using fuzzy MCDM models. Here a new MCDM method is proposed to find the utmost influencing risk factors of Breast cancer so that we can bring awareness among the public.

PRELIMINARIES

Fuzzy set [10]
Fuzzy set was first introduced by Lotfi A. Zadeh in 1965. Let X be a non-empty set. A fuzzy set $\tilde{A}$ in X is represented by its membership function $\mu_{\tilde{A}} : X \rightarrow [0,1]$ and $\mu_{\tilde{A}}(x)$ is interpreted as the degree of membership of element x in fuzzy set $\tilde{A}$ for each $x \in X$.

Fuzzy number [10]
A fuzzy set $\tilde{A}$ on R must possess at least the following 3 properties to qualify as a fuzzy number,
　　i.　　The set $\tilde{A}$ must satisfy the criteria of being a normal fuzzy set.
　　ii.　　$^{\alpha}\tilde{A}$ must be closed interval for every $\alpha \in [0,1]$
　　iii.　　The support of $\tilde{A}$, should be bounded.

Trapezoidal fuzzy number [10]
A trapezoidal fuzzy number $\tilde{A} = (a_1, a_2, a_3, a_4)$ is a fuzzy number with a membership function $\mu_{\tilde{A}}(x)$ is described as

$$\mu_{\tilde{A}}(x) = \begin{cases} \dfrac{x - a_1}{a_2 - a_1}, & a_1 \leq x \leq a_2 \\ 1, & a_2 \leq x \leq a_3 \\ \dfrac{a_3 - x}{a_4 - a_3}, & a_3 \leq x \leq a_4 \\ 0, & otherwise \end{cases}$$

PROPOSED MCDM METHOD:
Step I: Frame the alternatives and criteria based on the risk factors of breast cancer.
Let A = {A_1, A_2, ..., A_m} be the set of alternatives and C = {C_1, C_2, ... C_n} be the set of criteria and decision-makers are D = {D_1, D_2, ..., D_n}.

Step II: Construct the decision matrices using linguistic terms with aid of decision makers
Step III: Transform the linguistic matrices into trapezoidal fuzzy matrices. Then construct the aggregated trapezoidal decision matrix D.

Iswariya and Sahaya Sudha

$$D = \begin{array}{c} \\ A_1 \\ A_2 \\ A_3 \\ A_4 \end{array} \begin{bmatrix} (a_{11},b_{11},c_{11},d_{11}) & (a_{12},b_{12},c_{12},d_{12}) & \cdots & (a_{1n},b_{1n},c_{1n},d_{1n}) \\ (a_{21},b_{21},c_{21},d_{21}) & (a_{22},b_{22},c_{22},d_{22}) & \cdots & (a_{2n},b_{2n},c_{2n},d_{2n}) \\ \vdots & \vdots & \vdots & \vdots \\ \vdots & \vdots & \vdots & \vdots \\ (a_{m1},b_{m1},c_{m1},d_{m1}) & (a_{m2},b_{m2},c_{m2},d_{m2}) & \cdots & (a_{mn},b_{mn},c_{mn},d_{mn}) \end{bmatrix}$$

with column headers $C_1 \quad C_2 \quad \cdots \quad C_n$

Step IV: The trapezoidal fuzzy matrix D is converted into crisp value matrix T using the ranking function

$R(A) = \frac{1}{4}\big[a_1 + a_2 + a_3 + a_4\big]$. Then the defuzzified matrix is $T = \begin{bmatrix} u_{11} & u_{12} & \cdots & u_{1n} \\ u_{21} & u_{22} & \cdots & u_{2n} \\ \vdots & \vdots & \ddots & \vdots \\ u_{m1} & u_{m2} & \cdots & u_{mn} \end{bmatrix}$

Step V: Normalize the defuzzified matrix:

The defuzzified matrix is normalized by $r_{ij} = \dfrac{u_{ij}}{\sqrt{\sum\limits_{i=1}^{n} u_{ij}^{2}}}$ to get the normalized matrix U

$$U = \begin{bmatrix} r_{11} & r_{12} & \cdots & r_{1n} \\ r_{21} & r_{22} & \cdots & r_{2n} \\ \vdots & \vdots & \ddots & \vdots \\ r_{m1} & r_{m2} & \cdots & r_{mn} \end{bmatrix}$$

Step VI: Weight Calculation

From the normalized matrix U, determine the nxn symmetric matrix with the element h_{jk}, which is the linear correlation coefficient between the criteria.

$$H = \begin{array}{c} \\ C_1 \\ C_2 \\ \vdots \\ C_n \end{array} \begin{bmatrix} h_{11} & h_{12} & \cdots & h_{1n} \\ h_{21} & h_{22} & \cdots & h_{21} \\ \vdots & \vdots & \ddots & \vdots \\ h_{n1} & h_{n2} & \cdots & h_{nn} \end{bmatrix}$$

with column headers $C_1 \quad C_2 \quad \cdots \quad C_n$ where h_{jk} = linear correlation coefficient between the criteria

Then the weight W=(w_1,w_2, …, w_n) can be calculated using the formula $W = \dfrac{h_{jk}}{\sum\limits_{k=1}^{n}(1 - h_{jk})}$

Step VII: Construct the weighted normalized matrix W.

$$W = \begin{bmatrix} w_1 r_{11} & w_2 r_{12} & \cdots & w_n r_{1n} \\ w_1 r_{21} & w_2 r_{22} & \cdots & w_n r_{2n} \\ \vdots & \vdots & \ddots & \vdots \\ w_1 r_{m1} & w_2 r_{m2} & \cdots & w_n r_{mn} \end{bmatrix} = \begin{bmatrix} m_{11} & m_{12} & \cdots & m_{1n} \\ m_{21} & m_{22} & \cdots & m_{2n} \\ \vdots & \vdots & \ddots & \vdots \\ m_{m1} & m_{m2} & \cdots & m_{mn} \end{bmatrix}$$

Step VIII:

Iswariya and Sahaya Sudha

Calculate the Best and Worst value from the weighted normalized matrix W

$$Best\,M^{+} = \{(\max_i W_{ij} / j \in J), (\min_i W_{ij} / j \in J') / i = 1,2,\cdots m\}$$

$$Worst\,M^{-} = \{(\min_i W_{ij} / j \in J), (\max_i W_{ij} / j \in J') / i = 1,2,\cdots m\}$$

$$where\ J = 1,2,\cdots n \ and \ J' = 1,2,\cdots n$$

Step IX: Best Distance Calculation (BD)

Non Beneficial criteria : $BD = \dfrac{1}{n}\sum_{i=1}^{n}\left[\dfrac{m_{ij} - m_{ij}^{+}}{A_j}\right]$ where n= number of criteria

Beneficial criteria : $BD = \dfrac{1}{n}\sum_{i=1}^{n}\left[\dfrac{m_{ij}^{+} - m_{ij}}{A_j}\right]$ where n= number of criteria

where $A_j = \dfrac{1}{n}\sum_{i=1}^{n}\left[m_{ij}\right]$, n= number of criteria

Step X: Worst Distance Calculation (WD)

Non Beneficial criteria : $WD = \dfrac{1}{n}\sum_{i=1}^{n}\left[\dfrac{m_{ij}^{-} - m_{ij}}{A_j}\right]$ where n= number of criteria

Beneficial criteria : $WD = \dfrac{1}{n}\sum_{i=1}^{n}\left[\dfrac{m_{ij} - m_{ij}^{-}}{A_j}\right]$ where n= number of criteria

where $A_j = \dfrac{1}{n}\sum_{i=1}^{n}\left[m_{ij}\right]$, n= number of criteria

Step XI: Normalize the BD and WD $N_i = \dfrac{1}{2}\left[BD_i + WD_i\right]$

Step XII:
Rank all alternatives and select the most desirable one in accordance with N$_i$. The alternative with minimum value is the best one.

CASE ANALYSIS
The main aim of this work is to analyze the topmost risk factor of Breast cancer from its symptoms. Based on the three decision-makers opinions, the risk factors are analyzed. In the operation of proposed MCDM method, 10 risk factors and 5 criteria are chosen to analyze the most threatening risk factors of Breast cancer.

Applying the proposed MCDM method
Step I: Frame the alternatives and criteria
Step II: Setup the linguistic direct relation matrices
Step III: Transform the linguistic matrices into trapezoidal fuzzy matrices. Then, construct the aggregated triangular decision matrix D. This analysis incorporates the perspectives of three decision-makers. The fuzzy linguistic values are utilized to provide the relationship between alternatives and criteria with the opinion of the decision-maker.
Step IV: Convert trapezoidal fuzzy values into crisp values
Step V: Normalize the defuzzified matrix
Step VI: Weight Calculation From the normalized matrix U, determine the nxn symmetric matrix with the element h$_{jk}$, which is the linear correlation coefficient between the criteria.

The weight W=(w₁,w₂, …, wₙ) can be calculated using the formula $W = \dfrac{h_{jk}}{\displaystyle\sum_{k=1}^{n}(1 - h_{jk})}$

Then the weights are W=(0.466504, 0.100959, 0.122754, 0.117708, 0.192075).
Step VII: Construct the weighted normalized matrix W.

Step VIII: Calculate the Best and Worst value from the weighted normalized matrix W

Best ={0.109956, 0.010198, 0.007021, 0.012877, 0.019089}
Worst = {0.329868, 0.050992, 0.063187, 0.050388, 0.074696}

Step IX: Best Distance Calculation (BD)
Step X: Worst Distance Calculation (WD)
Step XI&XII : Normalize BD and WD and rank the alternatives with minimum value.
According to the ranking, the most important risk factor of Breast cancer A4 Personal History of Breast cancer. The top five risk factors are A4 < A3 < A5 < A10 < A8.

CONCLUSION

In this paper, the risk factors for breast cancer have been investigated. Despite the outbreak of various types of cancers in the world. Recently, the death rate in the world has increased due to infection with this dangerous disease. Numerous risk factors have been recognized for this condition. MCDM techniques were adapted to evaluate the risk factors using fuzzy logic combined with the proposed method to calculate the weights of criteria based on the preferences of the experts. Comparing other method, this proposed method is easily understandable and accessible by all. Also, the problem focuses on finding the high-level risk factor of Breast Cancer and will bring awareness and knowledge about Breast cancer among people.

REFERENCES

1. World Health Organization (WHO), Breast cancer report 2020.
2. Monika LambaGeetika Munjaland Yogita Gigras 2022, A MCDM-based performance of classification algorithms in breast cancer prediction for imbalanced datasets
3. Mostafa Hasan, I. Esra Büyüktahtakın, and Elshami Elamin 2017, A Multi-Criteria Ranking Algorithm (MCRA) for Determining Breast Cancer Therapy
4. Mubarak Taiwo Mustapha, Dilber Uzun Ozsahin , Ilker Ozsahin and Berna Uzun 2022, Breast Cancer Screening Based on Supervised Learning and Multi-Criteria Decision-Making.
5. Hatice Camgöz-Akdağ, Aziz Kemal Konyalıoğlu, Tuğçe Beldek, Prioritization of Factors of Breast Cancer Treatment Using Fuzzy AHP, 2020.
6. Priyanka Majumder, Apu Kumar Saha and Mrinmoy Majumder, 2018, A Mathematical Approach Of Exploration Towards Extreme Risk Factor In Cancer Of Optimal Condition.
7. Fei L, Xia J, Feng Y and Liu L 2019 An ELECTRE-Based Multiple Criteria Decision-Making Method for Supplier Selection Using Dempster-Shafer Theory IEEE Access 7 84701-16
8. Liang GS 1999, Fuzzy MCDM based on ideal and anti-ideal concepts European Journal of Operational Research 112 682-691
9. "In 1965, Lotfi A. Zadeh introduced the concept of fuzzy sets in his influential paper titled 'Fuzzy Sets,' published in 'Information and Control.', Volume 8, spanning pages 338 to 353."

10. Sanhita Banerjee and Tapan Kumar Roy, Arithmetic Operations on Generalized Trapezoidal Fuzzy Number and its Applications,2012.
11. Zhang Yong, Analysis of Breast Cancer using Weighted Sum Method (WSM), 2022.
12. Priyanka Majumdera, Apu Kumar Sahab ,Mrinmoy Majumder, Selection of Significant Lifestyle Risk Factor of Cancer by Hybrid X- Bar – DEMATEL-TOPSIS Method, 2017.
13. MadhusreeKuanr and Puspanjali Mohapatra, Outranking Relations based Multi-criteria Recommender System for Analysis of Health Risk using Multi-objective Feature Selection Approach, 2023.
14. Zhang Yong, Evaluation of Cancer Using Weighted aggregate product assessment (WASPAS) Method, 2022.
15. QahtanM.Yas, Emad Majeed Hameed, AymenMudheherBadr, Baidaa Al-Bander, Multi Risk Factors Evaluation for Lung Cancer Incidence Based Decision Support Systems, 2021.
16. A. Sahaya Sudha, Luiz Flavio Autran Monteiro Gomes, K. R. Vijayalakshmi, Assessment of MCDM problems by TODIM using aggregated weights, 2020.
17. Tevfik Bulut, A New Multi Criteria Decision Making Method : Approach Of Logarithmic Concept (APLOCO), 2018.
18. Melih Yucesanand Muhammet Gul, Failure prioritization and control using the neutrosophic best and worst method, 2019.
19. Ram Kumar Dhurkari, MCDM Methods: Practical Difficulties And Future Directions For Improvement, 2022.
20. Girish P Bhole, Dr. Tushar Deshmukh, Multi Criteria Decision Making (MCDM) Methods and its applications, 2018.

Table 1: Risk factors of Breast Cancer

Risk Factors	Notation
Gender	A1
Age	A2
Family History	A3
Personal History of Breast Cancer	A4
Inherited Genetic Mutations	A5
Hormone Replacement Therapy	A6
Dense Breast Tissue	A7
Alcohol	A8
Obesity	A9
Early Menstruation and Late Menopause	A10

Table 2: Stages of Breast cancer

Criteria	Notation
Preclinical stage	C1
Early stage	C2
Early primary progressive	C3
Late primary progressive	C4
Latent	C5

Table 3: Linguistic variables

Linguistic variables	Trapezoidal membership function
Very Low Risk (VLR)	(-1,0,2,3)
Low Risk (LR)	(1,2,4,5)
Medium Risk (MR)	(3,4,6,7)
High Risk (HR)	(5,6,8,9)
Very High Risk (VHR)	(7,8,10,11)

Table 4. First decision maker opinion

	C1	C2	C3	C4	C5
A1	VLR	VLR	VLR	LR	LR
A2	VLR	LR	LR	HR	HR
A3	VLR	LR	HR	HR	HR
A4	LR	MR	VHR	VHR	VHR
A5	VLR	LR	HR	HR	HR
A6	VLR	LR	MR	MR	MR
A7	VLR	LR	MR	MR	MR
A8	VLR	LR	HR	HR	HR
A9	VLR	LR	MR	HR	HR
A10	VLR	LR	MR	HR	HR

	C1	C2	C3	C4	C5
A1	(-1,0,2,3)	(-1,0,2,3)	(-1,0,2,3)	(-1,0,2,3)	(-1,0,2,3)
A2	(-1,0,2,3)	(1,2,4,5)	(1,2,4,5)	(5,6,8,9)	(5,6,8,9)
A3	(-1,0,2,3)	(1,2,4,5)	(5,6,8,9)	(5,6,8,9)	(5,6,8,9)
A4	(1,2,4,5)	(3,4,6,7)	(7,8,10,11)	(7,8,10,11)	(7,8,10,11)
A5	(-1,0,2,3)	(1,2,4,5)	(5,6,8,9)	(5,6,8,9)	(5,6,8,9)
A6	(-1,0,2,3)	(1,2,4,5)	(3,4,6,7)	(3,4,6,7)	(3,4,6,7)
A7	(-1,0,2,3)	(1,2,4,5)	(3,4,6,7)	(3,4,6,7)	(3,4,6,7)
A8	(-1,0,2,3)	(1,2,4,5)	(5,6,8,9)	(5,6,8,9)	(5,6,8,9)
A9	(-1,0,2,3)	(1,2,4,5)	(3,4,6,7)	(5,6,8,9)	(5,6,8,9)
A10	(-1,0,2,3)	(1,2,4,5)	(3,4,6,7)	(5,6,8,9)	(5,6,8,9)

Table 5. Second decision maker opinion

	C1	C2	C3	C4	C5
A1	VLR	VLR	VLR	LR	LR
A2	VLR	LR	MR	HR	VHR
A3	VLR	LR	MR	HR	VHR
A4	LR	MR	VHR	VHR	VHR
A5	VLR	LR	MR	HR	VHR
A6	VLR	LR	MR	HR	VHR
A7	VLR	LR	MR	HR	VHR
A8	VLR	LR	MR	HR	HR
A9	VLR	LR	MR	HR	HR
A10	VLR	LR	MR	HR	VHR

	C1	C2	C3	C4	C5
A1	(-1,0,2,3)	(-1,0,2,3)	(-1,0,2,3)	(1,2,4,5)	(1,2,4,5)
A2	(-1,0,2,3)	(1,2,4,5)	(3,4,6,7)	(5,6,8,9)	(7,8,10,11)
A3	(-1,0,2,3)	(1,2,4,5)	(3,4,6,7)	(5,6,8,9)	(7,8,10,11)
A4	(1,2,4,5)	(3,4,6,7)	(7,8,10,11)	(7,8,10,11)	(7,8,10,11)
A5	(-1,0,2,3)	(1,2,4,5)	(3,4,6,7)	(5,6,8,9)	(7,8,10,11)
A6	(-1,0,2,3)	(1,2,4,5)	(3,4,6,7)	(5,6,8,9)	(7,8,10,11)
A7	(-1,0,2,3)	(1,2,4,5)	(3,4,6,7)	(5,6,8,9)	(7,8,10,11)
A8	(-1,0,2,3)	(1,2,4,5)	(3,4,6,7)	(5,6,8,9)	(5,6,8,9)
A9	(-1,0,2,3)	(1,2,4,5)	(3,4,6,7)	(5,6,8,9)	(5,6,8,9)
A10	(-1,0,2,3)	(1,2,4,5)	(3,4,6,7)	(5,6,8,9)	(7,8,10,11)

Table 6. Third decision maker opinion

	C1	C2	C3	C4	C5
A1	VLR	VLR	VLR	LR	LR
A2	VLR	LR	LR	MR	HR
A3	VLR	LR	MR	HR	VHR
A4	LR	MR	VHR	VHR	VHR
A5	VLR	LR	HR	HR	HR
A6	VLR	LR	MR	MR	HR
A7	VLR	LR	MR	HR	VHR
A8	VLR	LR	HR	HR	HR
A9	VLR	LR	MR	HR	HR
A10	VLR	LR	MR	HR	VHR

	C1	C2	C3	C4	C5
A1	(-1,0,2,3)	(-1,0,2,3)	(-1,0,2,3)	(1,2,4,5)	(1,2,4,5)
A2	(-1,0,2,3)	(1,2,4,5)	(1,2,4,5)	(3,4,6,7)	(3,4,6,7)
A3	(-1,0,2,3)	(1,2,4,5)	(3,4,6,7)	(5,6,8,9)	(7,8,10,11)
A4	(1,2,4,5)	(3,4,6,7)	(7,8,10,11)	(7,8,10,11)	(7,8,10,11)
A5	(-1,0,2,3)	(1,2,4,5)	(5,6,8,9)	(5,6,8,9)	(5,6,8,9)
A6	(-1,0,2,3)	(1,2,4,5)	(3,4,6,7)	(3,4,6,7)	(5,6,8,9)
A7	(-1,0,2,3)	(1,2,4,5)	(3,4,6,7)	(5,6,8,9)	(7,8,10,11)
A8	(-1,0,2,3)	(1,2,4,5)	(5,6,8,9)	(5,6,8,9)	(5,6,8,9)
A9	(-1,0,2,3)	(1,2,4,5)	(3,4,6,7)	(5,6,8,9)	(5,6,8,9)
A10	(-1,0,2,3)	(1,2,4,5)	(3,4,6,7)	(5,6,8,9)	(7,8,10,11)

Iswariya and Sahaya Sudha

Table 7. Aggregated trapezoidal fuzzy matrix

	C1	C2	C3	C4	C5
A1	(-1,0,2,3)	(-1,0,2,3)	(-1,0,2,3)	(0.3, 1.3,3.3, 4.3)	(0.3, 1.3,3.3, 4.3)
A2	(-1,0,2,3)	(1,2,4,5)	(1.6, 2.6, 4.6, 5.6)	(4.3, 5.3, 7.3, 8.3)	(5,6,8,9)
A3	(-1,0,2,3)	(1,2,4,5)	(3.6, 4.6,6.6,7.6)	(5,6,8,9)	(6.3,7.3,9.3,10.3)
A4	(1,2,4,5)	(3,4,6,7)	(7,8,10,11)	(7,8,10,11)	(7,8,10,11)
A5	(-1,0,2,3)	(1,2,4,5)	(4.3,5.3, 7.3, 8.3)	(5,6,8,9)	(5.6, 6.6,8.6,9.6)
A6	(-1,0,2,3)	(1,2,4,5)	(3,4,6,7)	(3.6, 4.6,6.6,7.6)	(5,6,8,9)
A7	(-1,0,2,3)	(1,2,4,5)	(3,4,6,7)	(4.3,5.3, 7.3, 8.3)	(5.6, 6.6,8.6,9.6)
A8	(-1,0,2,3)	(1,2,4,5)	(4.3,5.3, 7.3, 8.3)	(5,6,8,9)	(5,6,8,9)
A9	(-1,0,2,3)	(1,2,4,5)	(3,4,6,7)	(5,6,8,9)	(5,6,8,9)
A10	(-1,0,2,3)	(1,2,4,5)	(3,4,6,7)	(5,6,8,9)	(6.3,7.3,9.3,10.3)

Table 8. Defuzzified matrix T

	C1	C2	C3	C4	C5
A1	1	1	1	2.3	2.3
A2	1	3	3.6	6.3	7
A3	1	3	5.6	7	8.3
A4	3	5	9	9	9
A5	1	3	6.3	7	7.6
A6	1	3	5	5.6	7
A7	1	3	5	6.3	7.6
A8	1	3	6.3	7	7
A9	1	3	5	7	7
A10	1	3	5	7	8.3

Table 9. Normalized decision matrix U

	C1	C2	C3	C4	C5
A1	0.235702	0.101015	0.057194	0.109396	0.099383
A2	0.235702	0.303046	0.205899	0.29965	0.30247
A3	0.235702	0.303046	0.320288	0.332945	0.358643
A4	0.707107	0.505076	0.514748	0.428072	0.38889
A5	0.235702	0.303046	0.360324	0.332945	0.328396
A6	0.235702	0.303046	0.285971	0.266356	0.30247
A7	0.235702	0.303046	0.285971	0.29965	0.328396
A8	0.235702	0.303046	0.360324	0.332945	0.30247
A9	0.235702	0.303046	0.285971	0.332945	0.30247
A10	0.235702	0.303046	0.285971	0.332945	0.358643

Iswariya and Sahaya Sudha

Table 10. Weight Calculation

	C1	C2	C3	C4	C5
C1	1	0.74536	0.65864	0.5271	0.36331
C2	0.74536	1	0.92529	0.92903	0.86397
C3	0.65864	0.92529	1	0.92282	0.84005
C4	0.5271	0.92903	0.92282	1	0.93963
C5	0.36331	0.86397	0.84005	0.93963	1

The weight W=($w_1,w_2, …, w_n$) can be calculated using the formula $W = \dfrac{h_{jk}}{\displaystyle\sum_{k=1}^{n}(1 - h_{jk})}$

Table 11. Weighted Normalized matrix W

	C1	C2	C3	C4	C5
A1	0.10996	0.0102	0.00702	0.01288	0.01909
A2	0.10996	0.0306	0.02527	0.03527	0.0581
A3	0.10996	0.0306	0.03932	0.03919	0.06889
A4	0.32987	0.05099	0.06319	0.05039	0.0747
A5	0.10996	0.0306	0.04423	0.03919	0.06308
A6	0.10996	0.0306	0.0351	0.03135	0.0581
A7	0.10996	0.0306	0.0351	0.03527	0.06308
A8	0.10996	0.0306	0.04423	0.03919	0.0581
A9	0.10996	0.0306	0.0351	0.03919	0.0581
A10	0.10996	0.0306	0.0351	0.03919	0.06889

Table 12. Best Distance

	C1	C2	C3	C4	C5	BD
A1	0	0	0	0	0	**0**
A2	0	0.39347	0.35213	0.432	0.75248	**0.38602**
A3	0	0.35419	0.5608	0.45692	0.8647	**0.44732**
A4	1.932	0.35839	0.49344	0.32954	0.48852	**0.72038**
A5	0	0.35529	0.64815	0.45834	0.7662	**0.4456**
A6	0	0.3847	0.52966	0.34845	0.73571	**0.3997**
A7	0	0.37221	0.51246	0.40865	0.80268	**0.4192**
A8	0	0.36156	0.65959	0.46643	0.69146	**0.43581**
A9	0	0.37366	0.51445	0.48203	0.71458	**0.41694**
A10	0	0.35945	0.49489	0.4637	0.87754	**0.43911**

Iswariya and Sahaya Sudha

Table 13. Worst Distance

	C1	C2	C3	C4	C5	WD
A1	6.90935	1.28168	1.76467	1.17855	1.7471	**2.57627**
A2	4.24222	0.39346	0.73134	0.29161	0.32021	**1.19577**
A3	3.81866	0.35418	0.4145	0.19444	0.10088	**0.97653**
A4	0	0	0	0	0	**0**
A5	3.83056	0.35528	0.33018	0.19505	0.2024	**0.98269**
A6	4.14765	0.38469	0.52966	0.35902	0.31307	**1.14682**
A7	4.01295	0.3722	0.51246	0.27585	0.21203	**1.0771**
A8	3.89819	0.36155	0.33601	0.19849	0.29424	**1.0177**
A9	4.02854	0.37364	0.51445	0.20513	0.30408	**1.08517**
A10	3.87535	0.35944	0.49488	0.19733	0.10238	**1.00588**

Table 14. Normalize BD and WD and rank the alternatives with minimum value

	Normalize	Rank
A1	1.2881347	10
A2	0.7908933	9
A3	0.7119258	2
A4	0.3601894	1
A5	0.7141458	3
A6	0.7732615	8
A7	0.7481484	6
A8	0.7267535	5
A9	0.7510558	7
A10	0.7224956	4

RESEARCH ARTICLE

Triangular Decomposition of Some Special Graphs

M.Subbulakshmi[1] and S.Chitra Devi[2]*

[1]Associate Professor, PG and Research Department of Mathematics, G .Venkataswamy Naidu College, Kovilpatti. Affiliated to Manonmaniam Sundaranar University, Tirunelveli, Tamil Nadu, India.
[2]Research Scholar, Reg. No. 19222052092002, PG and Research Department of Mathematics, G .Venkataswamy Naidu College, Kovilpatti. Affiliated to Manonmaniam Sundaranar University, Tirunelveli, Tamil Nadu, India.

*Address for Correspondence
S.Chitra Devi
Research Scholar, Reg. No. 19222052092002,
PG and Research Department of Mathematics,
G .Venkataswamy Naidu College, Kovilpatti.
Affiliated to Manonmaniam Sundaranar University,
Tirunelveli, Tamil Nadu, India.
E.Mail: schitradevimaths2016@gmail.com

ABSTRACT

Let G = (V, E) be a simple connected graph of order p and size q. If $G_1, G_2, G_3, \ldots, G_n$ are edge disjoint subgraphs of G such that $E(G) = E(G_1) \cup E(G_2) \cup \ldots \ldots \cup E(G_n)$, then $(G_1, G_2, G_3, \ldots, G_n)$ is said to be a Decomposition of a graph G. A graph of size $q = \binom{n+2}{3}$ is said to have a Triangular decomposition (TD) if G can be decomposed into n - subgraphs $G_1, G_2, G_3, \ldots, G_n$ such that each G_i is connected and $|E(G_i)| = \binom{i+1}{2}$ for $1 \leq i \leq n$. In this paper, we investigate Triangular decomposition of some special graphs.

Keywords – Decomposition, Triangular decomposition, Bistar graph, Friendship graph.

INTRODUCTION

A graph G, referred to here is an undirected connected graph without loops or multiple edges. Different types of decomposition of a graph G have been studied in the literature by imposing suitable conditions on the sub graphs G_i. In this paper we discuss about Triangular decomposition of some special graphs.

Definition 1.1

Let G = (V, E) be a simple graph of order p and q. If $G_1, G_2, G_3, \ldots\ldots G_n$ are edge disjoint subgraphs of G such that $E(G) = E(G_1) \cup E(G_2) \cup E(G_3) \cup \ldots\ldots\ldots \cup E(G_n)$, then ($G_1, G_2, G_3, \ldots\ldots G_n$) is said to be decomposition of G.
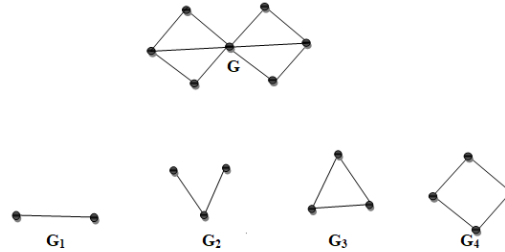
Decomposition (G_1, G_2, G_3, G_4) of G

Definition:1.2

A decomposition ($G_1, G_2, G_3, \ldots\ldots G_n$) of G is said to be Triangular decomposition if each G_i is connected and $|E(G_i)|$ = $\frac{i(i+1)}{2}$ for $1 \leq i \leq n$.
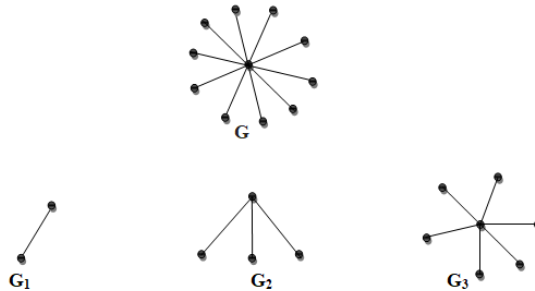
Triangular Decomposition (G_1, G_2, G_3) of G

Triangular Decomposition of some special Graphs

Theorem: 2.1

The Bistar graph $B_{k,k}$ admits Triangular decomposition $G_1, G_2, \ldots\ldots, G_{4n+1}$ if and only if $k = \frac{16n^3 + 24n^2 + 11n}{3}$ for all $n \in N$.

Proof:

Let V = {$v_j / 0 \leq j \leq k$} $\cup$ {$u_j / 0 \leq j \leq k$} be the vertex set and E = {$u_0 u_j / 1 \leq j \leq k$} $\cup$ {$v_0 v_j / 1 \leq j \leq k$} $\cup$ {$v_0 u_0$} be the edge set.

Suppose a Bistar graph $B_{k,k}$ admits triangular decomposition ($G_1, G_2, \ldots\ldots, G_{4n+1}$). We know that G admits Triangular Decomposition of $G_1, G_2, \ldots\ldots, G_n$ iff q(G) = $\frac{n(n+1)(n+2)}{6}$ where $n \in N$. That is a graph $B_{k,k}$ admits triangular decomposition ($G_1, G_2, \ldots\ldots\ldots\ldots, G_{4n+1}$) $\Leftrightarrow$ q($B_{k,k}$) = $\frac{(4n+1)(4n+2)(4n+3)}{6}$ for some $k \in N$. We have q($B_{k,k}$) = 2k+1.

This implies 2k+1 = $\frac{(4n+1)(4n+2)(4n+3)}{6}$.

That is 2k = $\frac{32n^3 + 48n^2 + 22n + 3}{3}$ -1

That is k = $\frac{32n^3 + 48n^2 + 22n}{6}$

This is k = $\frac{16n^3 + 24n^2 + 11n}{3}$ for all $n \in N$

Conversely assume that Bistar graph $B_{k,k}$ with k = $\frac{16n^3 + 24n^2 + 11n}{3}$ for all $n \in N$

$\Rightarrow$ q($B_{k,k}$) = 2k+1

Subbulakshmi and Chitra Devi

$\Rightarrow$ $q(B_{k,k}) = 2(\frac{16n^3 + 24n^2 + 11n}{3}) + 1$

$\Rightarrow$ $q(B_{k,k}) = \frac{32n^3 + 48n^2 + 22n + 3}{3}$

$\Rightarrow$ $q(B_{k,k}) = \frac{(4n+1)(4n+2)(4n+3)}{6}$

This implies the Bistar graph $B_{k,k}$ admits Triangular decomposition $G_1, G_2, \ldots\ldots, G_{4n+1}$.

The following table gives the Triangular Decomposition of $B_{k,k,m}$'s for different values of m.

k	$q(B_{k,k})$	Triangular Decomposition
17	35	$G_1, G_2, \ldots\ldots, G_5$
82	165	$G_1, G_2, \ldots\ldots, G_9$
227	455	$G_1, G_2, \ldots\ldots, G_{13}$
484	969	$G_1, G_2, \ldots\ldots, G_{17}$
885	1771	$G_1, G_2, \ldots\ldots, G_{21}$
1462	2925	$G_1, G_2, \ldots\ldots, G_{25}$
2247	4495	$G_1, G_2, \ldots\ldots, G_{29}$
3272	6545	$G_1, G_2, \ldots\ldots, G_{33}$
4569	9139	$G_1, G_2, \ldots\ldots, G_{37}$
6170	12341	$G_1, G_2, \ldots\ldots, G_{41}$

Illustraion:2.2
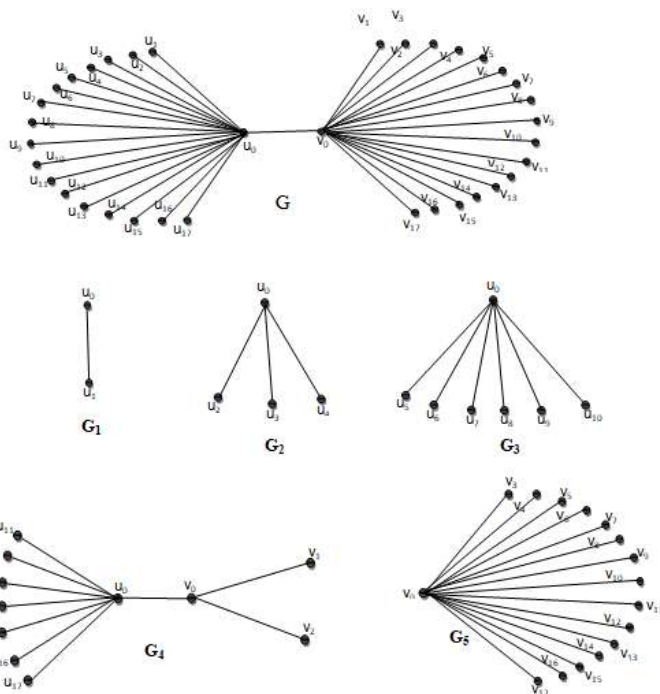
Triangular Decomposition ($G_1, G_2, \ldots\ldots, G_5$) of G.

Theorem:2.3

The friendship graph F_s admits Triangular decomposition $G_1, G_2, \ldots\ldots, G_{9m+7}$ if and only if s = $\frac{81m^3 + 216m^2 + 191m + 56}{2}$ for all m∈N.

Subbulakshmi and Chitra Devi

Proof:

Assume that a friendship graph F_s admits Triangular decomposition $(G_1, G_2,\ldots\ldots,G_{9m+7})$. We know that G accepts Triangular Decomposition of $G_1, G_2,\ldots\ldots,G_n$ iff $q(G) = \frac{n(n+1)(n+2)}{6}$, $n \in N$. That is the graph F_s admits Triangular decomposition $(G_1,G_2,\ldots,G_{9m+7}) \Leftrightarrow q(F_s) = \frac{(9m+7)(9m+8)(9m+9)}{6}$ for some $m \in N$. We have $q(F_s) = 3s$

Implies $3s = \frac{(9m+7)(9m+8)(9m+9)}{6}$.

That is $3s = \frac{9(81m^2+135m+56)(m+1)}{6}$

This is $s = \frac{81m^3+216m^2+191m+56}{2}$ for all $m \in N$.

Conversely assume that a friendship graph F_s with $s = \frac{81m^3+216m^2+191m+56}{2}$ for all $m \in N$.

$\Rightarrow$ $q(F_s) = 3s$

$\Rightarrow$ $q(F_s) = 3(\frac{81m^3+216m^2+191m+56}{2})$

$\Rightarrow$ $q(F_s) = \frac{729m^3+486m^2+99m+6}{6}$

$\Rightarrow$ $q(F_s) = \frac{(9m+7)(9m+8)(9m+9)}{6}$

This implies F_s can be decomposed into $G_1, G_2,\ldots\ldots,G_{9m+7}$.

The following table gives the Triangular Decomposition of F_s's for different values of m.

S	$q(F_s)$	Triangular Decomposition
272	816	$G_1, G_2,\ldots\ldots,G_{16}$
975	2925	$G_1, G_2,\ldots\ldots,G_{25}$
2380	7140	$G_1, G_2,\ldots\ldots,G_{34}$
4730	14190	$G_1, G_2,\ldots\ldots,G_{43}$
8268	24804	$G_1, G_2,\ldots\ldots,G_{52}$
13237	39711	$G_1, G_2,\ldots\ldots,G_{61}$
19880	59640	$G_1, G_2,\ldots\ldots,G_{70}$
28440	85320	$G_1, G_2,\ldots\ldots,G_{79}$
39160	117480	$G_1, G_2,\ldots\ldots,G_{88}$
52283	156849	$G_1, G_2,\ldots\ldots,G_{97}$

Illustration: 2.4

G
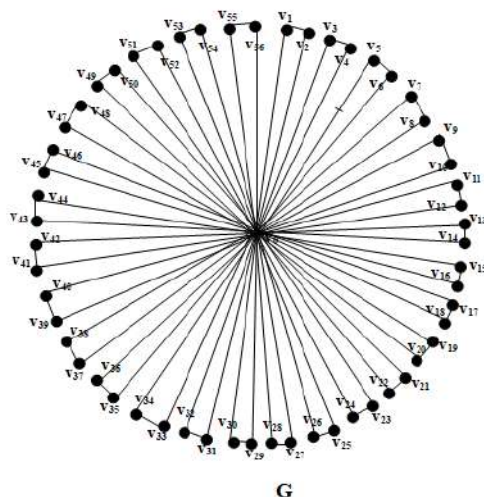
Subbulakshmi and Chitra Devi
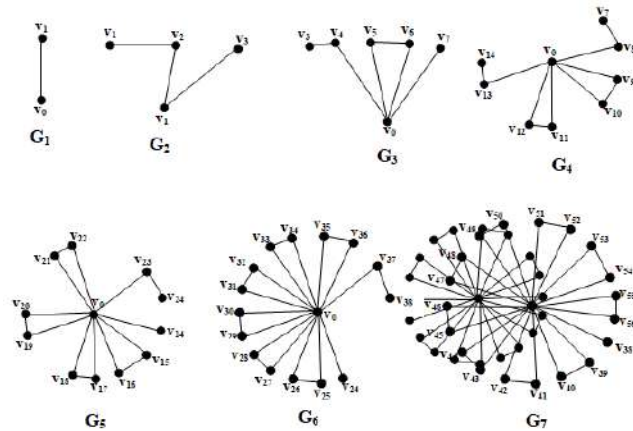
Triangular Decomposition (G₁,G₂,G₃,G₄,……..,G₇) of G

Theorem: 2.5

A complete tripartite graph $K_{1,3,m}$ admits Triangular Decomposition of G_1, G_2,………..,G_{8n+5} if and only if m= $\frac{64n^3+144n^2+107n+24}{3}$ for all n∈N.

Proof:

We have q($K_{1,3,m}$) = $\frac{1(3+m)+3(m+1)+m(1+3)}{2}$

$\qquad\qquad$ = 4m+3 for all m∈N

Suppose a complete tripartite graph $K_{1,3,m}$ admits Triangular Decomposition of G_1,G_2,………..,G_{8n+5} for all n ≥ 0. We know that G admits Triangular Decomposition of G_1,G_2,…………,G_n if and only if q(G) = $\frac{n(n+1)(n+2)}{6}$, n∈N. That is a graph $K_{1,3,m}$ admits Triangular Decomposition of G_1,G_2,………..,G_{8n+5} if and only if q($K_{1,3,m}$) = $\frac{(8n+5)(8n+6)(8n+7)}{6}$ for all n∈N.

$\qquad$ That is 4m+3 = $\frac{k(k+1)(k+2)}{6}$ for some k∈N.

$\qquad$ That is 4m+3 = $\frac{(8n+5)(8n+6)(8n+7)}{6}$

$\qquad$ That is 4m = $\frac{256n^3+576n^2+428n+105}{3}$ -3 for all n∈N

$\qquad$ That is m = $\frac{64n^3+144n^2+107n+24}{3}$ for all n∈N

The values of m are 8, 113, 442, …………

Conversely, assume that a graph $K_{1,3,m}$ with m = $\frac{64n^3+144n^2+107n+24}{3}$ for all n∈N. We know that

q($K_{1,3,m}$) = 4m + 3

$\qquad\qquad$ = $4(\frac{64n^3+144n^2+107n+24}{3})$ + 3

$\qquad\qquad$ = $\frac{256n^3+576n^2+428n+105}{3}$

$\qquad\qquad$ = $\frac{(8n+5)(8n+6)(8n+7)}{6}$

This implies that G_1,G_2,………..,G_{8n+5} for all n∈N.

The following table gives the Triangular Decomposition of $K_{1,3,m}$'s for different values of m.

m	q($K_{1,3,m}$)	Triangular Decomposition
8	35	G_1, G_2,…………,G_5
113	455	G_1, G_2,…………,G_{13}
442	1771	G_1, G_2,…………,G_{21}

1123	4495	$G_1, G_2,\ldots\ldots,G_{29}$
2284	9139	$G_1, G_2,\ldots\ldots,G_{37}$
4053	16215	$G_1, G_2,\ldots\ldots,G_{45}$
6558	26235	$G_1, G_2,\ldots\ldots,G_{53}$
9927	39711	$G_1, G_2,\ldots\ldots,G_{61}$
14288	57155	$G_1, G_2,\ldots\ldots,G_{69}$
19769	79079	$G_1, G_2,\ldots\ldots,G_{77}$

Illustraion: 2.6

$K_{1,3,8}$
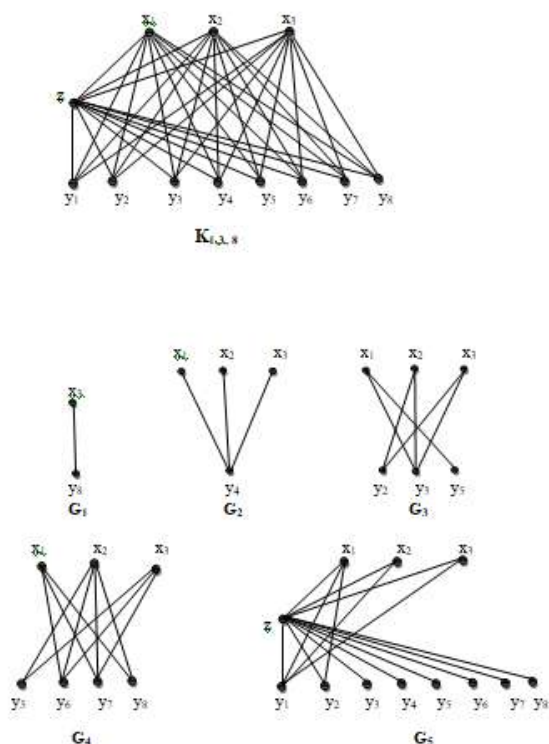
Triangular Decomposition ($G_1,G_2,\ldots\ldots,G_5$) of G

REFERENCES

1. J.REMYA, M.SUDHA : Geometric Decomposition of graph with various common ratio, Advanced in Mathematics: Scientific journal 9(2020), no **7**, 5225–5229.
2. E. EBIN RAJA MERLY, D. SUBITHA: Geometric Decomposition of Spider Tree, International Journal of Science and Research (IJSR)., 56 (2014), 2319–7064.
3. E. EBIN RAJA MERLY, D. SUBITHA: Geometric Decomposition of Complete Tripartite Graphs, International Journal of Research Foundation., 5 (2016), 23–26.
4. N. GNANA DHAS, J. PAULRAJ JOSEPH: Continuous Monotonic Decomposition of Graphs, International Journal of Management and Systems, 16(3) (2000), ID: 145814836.
5. F. HARARY: Graph Theory, Addison-Wesley, Reading, Mass., 1969.
6. M. BHANUMATHI , S. SANTHIYA: Geometric Star Decomposition Of Some Trees, Advances in Theoretical and Applied Mathematics.,11(3) (2016), 189 – 198.

RESEARCH ARTICLE

A New Approach for Finding IBFS of Interval Valued Picture Fuzzy Transportation Problems

P.Rajarajeswari[1]*, K.Vanithamani[2] and D.Maheswari[3]

[1]Associate Professor, Department of Mathematics, Chikkanna Govt. Arts College, Tirupur-02, Tamil Nadu, India
[2]Research Scholar, Department of Mathematics, Chikkanna Govt. Arts College, Tirupur-02, Tamil Nadu, India
[3]Assistant Professor, Department of Mathematics, Sri Krishna Arts and College, Coimbatore, Tamil Nadu, India.

*Address for Correspondence
P.Rajarajeswari,
Associate Professor,
Department of Mathematics,
Chikkanna Govt. Arts College, Tirupur-02,
Tamil Nadu, India

ABSTRACT

In order to handle uncertainty and hesitancy in real-world problems,Researchers and businesspeople are becoming more interested in Picture Fuzzy Sets(PFS).Interval Valued Picture Fuzzy Set (IVPFS) is more effective tool for dealing with uncertainty and impressions.The transportation problem offers practical solutions to the problem of how to deliver goods to customers in a more expert way.Real-world problems, such as traffic restrictions and weather conditions, frequently involve unpredictable events.In this study, we introduced the three different types of formulae namely WIDTH, GM and PERT are used to convert the IVPFS into crisp values and RANGE method was used to find IBFS of IVPFTP. Three types of Interval Valued Picture Fuzzy Transportation Problem(IVPFTP) are considered namely Type1(supply, demand),Type 2(cost only) and Type 3(supply, demand and cost) in which above parameters represented as IVPFS. Finally the results obtained from Type 1, Type2 and Type3 IVPFTP compared with each other.

Keywords: Picture Fuzzy Sets, Interval Valued Picture Fuzzy Sets, RANGE method

Rajarajeswari *et al*.,

INTRODUCTION

Fuzzy sets were introduced by Lotfi A. Zadeh[15] in1965 as a way to represent uncertainty and vagueness. Fuzzy sets assign a degree of membership between 0 and 1, indicating the extent to which an element belongs to the set. IVFS, which are a generalization of FSs, were also proposed by Zadeh[14]. As a alternative generalization of FS, Atanassov[3] introduced Intuitionistic Fuzzy Sets. IFSs have two functions called the membership function and non-membership function, both of which must be added under a closed unit interval. Interval Valued Intuitionistic Fuzzy Set (IVIFS), developed by Atanassov and Gargov [3]. IVIFS continues to maintain the constraint that the sum of the supremum for these intervals must fall within the range of [0, 1]. Coung[5] generalized the concept of PFS, stating that the three PFS components are membership, neutral, and non-membership functions, and that the total of these three values must lie inside the closed unit interval. Picture fuzzy sets(PFS) extend the concept of intuitionistic fuzzy sets by allowing membership degrees to be represented not only as scalar values but also as intervals. In other words, instead of assigning a single membership value to an element, you assign a range of possible membership values.IVPFS combine the notions of IVFS and PFS. In an IVPFS, membership degrees are represented not only as intervals but also as PFS. This adds another layer of flexibility in representing uncertainty. Transportation problems often deal with the optimal distribution of goods from multiple suppliers to multiple consumers while minimizing transportation costs or maximizing profits. Over the years, researchers have extended the traditional transportation problem to encompass more complex and uncertain environments. In the context of transportation problems, uncertainties can arise from various sources such as imprecise data, ambiguous preferences, and fluctuating market conditions. The primary objective of TP is to find the most effective solution at the lowest possible overall transportation cost.The ideal TP solution requires two steps: finding an Initial Basic Feasible Solution (IBFS) and determining the optimal solution using the Northwest Corner Method, Least Cost Method, or Vogel's Approximation Method[13]. Nagoorgani A andS.Abbas[9] introduced a new method for solving Intuitionistic fuzzy transportation problem Sathya Geetha and Selva Nayaki[11] used picture fuzzy numbers as a cost of transportation problem and used some techniques for convert the Picture fuzzy numbers into crisp values and find the IBFS of that picture fuzzy numbers.IVPFTPemerges as a powerful model to address these uncertainties. In this problem, not only are the supply and demand values represented as IVPFN, but the transportation costs between sources and destinations are also subject to imprecision and ambiguity.

Basic definitions
In this section we define a few fundamental terms to make the following sections easier to understand for readers. The universal set is called X.

Definition 2.1. A FS on X is defined as:

$T = \{x, \omega(x) \mid x \in X\},$ (1)

where the term $\omega(x)$ refers to"membership function",ω: X → [0, 1] that expresses the degree to which an object is a member of a non-empty set.Each $\omega(x)$ is known as a fuzzy number.

Definition 2.2. An IVFS on X is defined as:

$T = \{x, \omega_T(x) \mid x \in X\},$ (2)

where $\omega_T = [\omega_{TL}, \omega_{TU}]$ is subinterval of [0, 1] and it expresses the degree of membership by sub-interval and each $\omega(x)$ is called IVFN.

Definition 2.3. An IFS on X is defined as:

$T = \{x, \omega(x), \varpi(x) \mid x \in X\},$ (3)

where $\omega, \varpi: X \to [0,1]$ are called membership and non-membership functions. An IFS has a condition that the sum of both functions must lie in unit interval and the degree of refusal is defined as $r(x) = 1 - (\omega(x) + \varpi(x))$. A duplet ($\omega(x), \varpi(x)$) is called an intuitionistic fuzzy number (IFN).

Rajarajeswari *et al*.,

Definition 2.4. An IVIFS on a universal set X is defined as:

$T = \{x,\ \omega_T(x),\ \varpi_T(x)\ |\ x \in X\}$, \hfill (4)

where $\omega_T = [\omega_{TL},\ \omega_{TU}]$, $\varpi_T = [\varpi_{TL},\ \varpi_{TU}]$ and $\omega_T, \varpi_T : X \to [0,1]$. An IVIFS has a condition that the sum of supremum of membership and non-membership functions must lie in unit interval. A duplet $(\omega(x),\ \varpi(x))$ is called interval-valued intuitionistic fuzzy number (IVIFN).

Definition 2.5. A PFS on X is defined as:

$T = \{x,\ \omega(x),\ \vartheta(x),\ \varpi(x)\ |\ x \in X\}$, \hfill (5)

where $\omega, \vartheta, \varpi : X \to [0,1]$ are called membership, abstinence, and non-membership functions. A PFS has a condition that the sum of all three functions must lie in unit interval and the degree of refusal is defined as $r(x) = 1 - (\omega(x) + \vartheta(x) + \varpi(x))$. A triplet $(\omega(x),\ \vartheta(x),\ \varpi(x))$ is called a PFN.

Definition 2.6. An IVPFS on a universal set X is defined as:

$T = \{x,\ \omega_T(x),\ \vartheta(x),\ \varpi(x)\ |\ x \in X\}$, \hfill (6)

where $\omega_T = [\omega_{TL},\ \omega_{TU}]$, $\vartheta_T = [\vartheta_{TL},\ \vartheta_{TU}]$, $\varpi_T = [\varpi_{TL},\varpi_{TU}]$ and $\omega_T, \vartheta_T, \varpi_T : X \to [0,1]$. An IVPFS has a condition that the sum of supremum of all three functions must lie in unit interval. A triplet $(\omega(x),\ \vartheta(x),\ \varpi(x))$ is called interval-valued picture fuzzy number (IVPFN).

Definition 2.7:Type 1 IVPFTP

In this type of interval valued picture fuzzy transportation problem, the transportation costs are crisp values and the supply, demand are interval valued picture fuzzy numbers.

In the below IVPFTP table1where

C_{ij} – be the costs,

$[a_{d\omega_j}, b_{d\omega_j}]$, $[a_{d\vartheta_j}, b_{d\vartheta_j}]$, $[a_{d\varpi_j}, b_{d\varpi_j}]$)- be the demands,

$[a_{s\omega_i}, b_{s\omega_i}]$, $[a_{s\vartheta_i}, b_{s\vartheta_i}]$, $[a_{s\varpi_i}, b_{s\varpi_i}]$)-be the supply.

Definition 2.7. Type 2 IVPFTP

In the IVPFTP type 2,the transportation costs are interval valued picture fuzzy numbers and the supply, demands are crisp values.

The Type 2 IVPFTP from the below IVPFTP Table 2, where

$[a_{\omega_{ij}}, b_{\omega_{ij}}, a_{\vartheta_{ij}}, b_{\xi_{ij}}, a_{\varpi_{ij}}, b_{\varpi_{ij}}]$ are costs,

C_{dj} be the demand,

C_{si} be the supply.

Type 3 IVPFTP

This type of IVPFTP have transportation costs, supply and demands are interval valued picture fuzzysets. The following table represents IVPFTP Type 3.

In Type 3,IVPFTP Table 3

$C_{ij} = ([a_{\omega_{ij}}, b_{\omega_{ij}}],\ [a_{\vartheta_{ij}}, b_{\vartheta_{ij}}],\ [a_{\varpi_{ij}}, b_{\varpi_{ij}}])$ for $i = 1,2,3\ldots m$ and $j = 1,2,3\ldots n$ represents the transportation cost for transporting one unit from the ith origin to j^{th} destination ,where $[a_{\omega_{ij}}, b_{\omega_{ij}}]$ represents the membership,$[a_{\vartheta_{ij}}, b_{\vartheta_{ij}}]$ represents abstinence and $[a_{\varpi_{ij}}, b_{\varpi_{ij}}]$ represents non-membership values which are Interval Valued Picture Fuzzy Sets.

Algorithm to IBFS for IVPFTP

RANGE method for IBFS of IVPFTP. The following algorithm is used to find IBFS for IVPTP.

Rajarajeswari *et al.*,

Step 1: Find width by using the following formulae

$d_{\omega_{ij}}=(b_{\omega_{ij}}-a_{\omega_{ij}})/2,$ $\qquad$ $d_{\vartheta_{ij}}=(b_{\vartheta_{ij}}-a_{\vartheta_{ij}})/2$ and

$d_{\varpi_{ij}}=(b_{\varpi_{ij}}-a_{\varpi_{ij}})/2$ and we get the values of $d_{\omega_{ij}},d_{\vartheta_{ij}},d_{\varpi_{ij}},$

where i =1,2,3…m and j =1,2,3…n

Step 2: Find the number between the interval $([a_{\omega_{ij}},b_{\omega_{ij}}],[a_{\vartheta_{ij}},b_{\vartheta_{ij}}],[a_{\varpi_{ij}},b_{\varpi_{ij}}])$ by using following.

$e_{\omega_{ij}}=a_{\omega_{ij}}+d_{\omega_{ij}};$ $\;\;$ $e_{\vartheta_{ij}}=a_{\vartheta_{ij}}+d_{\vartheta_{ij}}$ and $\qquad$ $e_{\varpi_{ij}}=a_{\varpi_{ij}}+d_{\varpi_{ij}},$

where i =1,2,3…m and j =1,2,3…n

Form,

$T_{\omega_{ij}}=(a_{\omega_{ij}},e_{\omega_{ij}},b_{\omega_{ij}});$ $\qquad$ $T_{\vartheta_{ij}}=(a_{\vartheta_{ij}},e_{\vartheta_{ij}},b_{\vartheta_{ij}}),$ and $\quad$ $T_{\varpi_{ij}}=(a_{\varpi_{ij}},e_{\varpi_{ij}},b_{\varpi_{ij}}),$

where i =1,2,3…m and j =1,2,3…n

Step 3: Use the GM formula and find the value of triangular values. After that, get Picture Fuzzy Sets are following.

$C_{\omega_{ij}}=(a_{\omega_{ij}}*e_{\omega_{ij}}*b_{\omega_{ij}})^{1/3}$ $;C_{\vartheta_{ij}}=(a_{\vartheta_{ij}}*e_{\vartheta_{ij}}*b_{\vartheta_{ij}})^{1/3}$and

$C_{\varpi_{ij}}=(a_{\varpi_{ij}}*e_{\varpi_{ij}}*b_{\varpi_{ij}})^{1/3},$ where i =1,2,3…m and j =1,2,3…n

Step 4: Use the ranking formula namely PERT formula and change the PFS into crisp values in the IVPFTP.

$C_{ij}=(C_{\omega_{ij}}+(4xC_{\vartheta_{ij}})+C_{\varpi_{ij}})/6,$ where i =1,2,3…m and j =1,2,3…n

Step 5.Find the range for each row and each column,

where range = largest cost- smallest cost.

Step 6. Find the row or column with the largest range. For the minimum cost in the selected row or column assign the corresponding demand or supply, whichever is minimum. Supply and demand in related to the value that was assigned to the cell. Once you have crossed the fully satisfied row or column, continue.

Step 7. Steps 5 and 6 should be repeated until all conditions are fulfilled.

Step 8. Calculate the Transportation Cost.

Example 1

Example1 represent the Type 1 IVPFTP.

Use the steps 1-5 from the algorithm and get the following table values.

The IBFS table is given below by the steps 6-8 from the proposed algorithm

z=(0*0.2)+(0.1*0.1)+(0.1*0.1)+(0.4*0.2)+(0.2*0.1)+(0*0.1)+(0.2*0.3)=0.18

Example 2

This example represent the Type 2 model and it has the costs are IVPFS and the supply ,demands are crisp values.

We use the steps 6-8 from the proposed algorithm after converting the crisp value of example 3 and we get the IBFS of example 3 as given below.

z=(0.3*0.12)+(0*0.24)+(0.2*0.26)+(0.1*0.22)+(0.1*0.12)+(0.5*0.12)=0.29

Example 3.

In this example all costs, supply and demands are IVPFS

Use the RANGE method to find the minimum cost for IBFS table 11 values.

Minimum cost =(0.24*0.14)+(0.017*0.26)+(0.12*0.12)+

(0.12*0.27)+(0.11*0.27)+(0.13*0.22)+(0.12*0.12)

=0.16

Comparing the results with the Type 1,Type 2 and Type 3 of IVPFN by using proposed algorithm.

From the above IVPFTP Table 13, Type 3 IVPFTP given the better result.

64181

Rajarajeswari *et al.*,

CONCLUSION

In this paper applied the new ranking formulae for converting the IVPFN into crisp values in the Type1,Type 2 and Type 3 IVPFTP. Then used a RANGE method for find IBFS of that three types of IVPFTP.From the above table it is observed that Type 3 IVPFTP gives the better solution than the Type1 and Type2 IVPFTP.

REFERENCES

1. Ahmed MM, Khan AR, Uddin S, Ahmed F. A new approach to solve transportation problems. Open J Optim2016;5(March):22–30.
2. Atanassov, K.; Gargov, G. Interval valued intuitionistic fuzzy sets. Fuzzy Sets Syst. 1989, 31, 343–349.
3. Atanassov, K.T. Intuitionistic fuzzy sets. Fuzzy Sets Syst. 1986, 20, 87–96.
4. Coung, B.C. Picture fuzzy sets. J. Comput. Sci. Cybern. 2014, 30, 409–420. 8. Dengfeng L.; Chuntian, C. New similarity measures of intuitionistic fuzzy sets and application to pattern recognitions. Pattern Recognit. Lett. 2002, 23, 221–225.
5. Cuong, B.C. Picture Fuzzy Sets-First Results. Part 1, Seminar Neuro-Fuzzy Systems with Applications; Instiute of Mathematics: Hanoi, Vietnam, 2013.
6. Cuong, B.C. Picture Fuzzy Sets-First Results. Part 2, Seminar Neuro-Fuzzy Systems with Applications; Instiute of Mathematics: Hanoi, Vietnam, 2013.
7. Deshmukh NM. An Innovative Method for Solving Transportation. Int J Phys Math Sci 2012;2(3):86–91.
8. Muhammad Athar Mehmood and Shahida Bashir, Extended transportation models based on picture fuzzy sets(2022).
9. Nagoorgani A andS.Abbas,AnewmethodforsolvingIntuitionisticfuzzytransportationproblem.*Applied MathematicalSciences,*7(28),(2013): 1357-1365.
10. Rajarajeswari and Vanithamani introduced a new approach for finding ibfs to interval valued picture fuzzy transportation problem. Volume:96,2023,ISSN:0972-0766,159-169.
11. Sathya Geetha S, Seelvakumari K A Picture Fuzzy Approach to Solving Transportation Problem. European Journal of Molecular & Clinical Medicine. ISSN: 2515-8260 Volume 07, Issue 02,2020.
12. Soomro AS et al. Modified Vogel's approximation method for solving transportation problem. Math Theory Model 2015;5(4):32–43.
13. Vogel and N.V., W.R. Mathematical Programming Englewood Cliffs. NJ: Prentice -Hall (1958)
14. Zadeh, L.A. Fuzzy Sets. Inf. control 1965, 8, 338–353.
15. Zadeh, L.A. The concept of a linguistic variable and its application to approximate reasoning. Inf. Sci. 1975, 8, 199–249.

Table 1 IVPFTP

	D_1	D_2	D_3	...	D_n	Supply
S_1	C_{11}	C_{12}	C_{13}	...	C_{1n}	$([a_{s\alpha\sigma_1}, b_{s\alpha\sigma_1}],$ $[a_{s\beta_1}, b_{s\beta_1}],$ $[a_{s\alpha\gamma_1}, b_{s\alpha\gamma_1}]),$
S_2	C_{21}	C_{22}	C_{23}	...	C_{2n}	$([a_{s\alpha\sigma_2}, b_{s\alpha\sigma_2}],$ $[a_{s\beta_2}, b_{s\beta_2}],$ $[a_{s\alpha\gamma_2}, b_{s\alpha\gamma_2}]),$
S_3	C_{31}	C_{32}	C_{33}	...	C_{3n}	$([a_{s\alpha\sigma_3}, b_{s\alpha\sigma_3}],$ $[a_{s\beta_3}, b_{s\beta_3}],$ $[a_{s\alpha\gamma_3}, b_{s\alpha\gamma_3}]),$
⋮	⋮	⋮	⋮	...	⋮	⋮
S_m	C_{m1}	C_{m2}	C_{m3}	...	C_{mn}	$([a_{s\alpha\sigma_m}, b_{s\alpha\sigma_m}],$ $[a_{s\beta_m}, b_{s\beta_m}],$ $[a_{s\alpha\gamma_m}, b_{s\alpha\gamma_m}]),$
Demand	$([a_{d\alpha\sigma_1}, b_{d\alpha\sigma_1}],$ $[a_{d\beta_1}, b_{d\beta_1}],$ $[a_{d\alpha\gamma_1}, b_{d\alpha\gamma_1}]),$	$([a_{d\alpha\sigma_2}, b_{d\alpha\sigma_2}],$ $[a_{d\beta_2}, b_{d\beta_2}],$ $[a_{d\alpha\gamma_2}, b_{d\alpha\gamma_2}]),$	$([a_{d\alpha\sigma_3}, b_{d\alpha\sigma_3}],$ $[a_{d\beta_3}, b_{d\beta_3}],$ $[a_{d\alpha\gamma_3}, b_{d\alpha\gamma_3}]),$	...	$([a_{d\alpha\sigma_n}, b_{d\alpha\sigma_n}],$ $[a_{d\beta_n}, b_{d\beta_n}],$ $[a_{d\alpha\gamma_n}, b_{d\alpha\gamma_n}]),$	

Table 2. IVPFTP

	D_1	D_2	D_3	...	D_n	Supply
S_1	$([a_{\omega_{11}}, b_{\omega_{11}}], [a_{\vartheta_{11}}, b_{\xi_{11}}], [a_{\varpi_{11}}, b_{\varpi_1}])$	$([a_{\omega_{12}}, b_{\omega_{12}}], [a_{\vartheta_{12}}, b_{\xi_{12}}], [a_{\varpi_{12}}, b_{\varpi_{12}}])$,	$([a_{\omega_{13}}, b_{\omega_{13}}], [a_{\vartheta_{13}}, b_{\xi_{13}}], [a_{\varpi_{13}}, b_{\varpi_{13}}])$,	...	$([a_{\omega_{1n}}, b_{\omega_{1n}}], [a_{\vartheta_{1n}}, b_{\xi_{1n}}], [a_{\varpi_{1n}}, b_{\varpi_{1n}}])$,	C_{s1}
S_2	$([a_{\omega_{21}}, b_{\omega_{21}}], [a_{\vartheta_{21}}, b_{\xi_{21}}], [a_{\varpi_{21}}, b_{\varpi_2}])$	$([a_{\omega_{22}}, b_{\omega_{22}}], [a_{\vartheta_{22}}, b_{\xi_{22}}], [a_{\varpi_{22}}, b_{\varpi_{22}}])$,	$([a_{\omega_{23}}, b_{\omega_{23}}], [a_{\vartheta_{23}}, b_{\xi_{23}}], [a_{\varpi_{23}}, b_{\varpi_{23}}])$,	...	$([a_{\omega_{2n}}, b_{\omega_{2n}}], [a_{\vartheta_{2n}}, b_{\xi_{2n}}], [a_{\varpi_{2n}}, b_{\varpi_{2n}}])$,	C_{s2}
S_3	$([a_{\omega_{31}}, b_{\omega_{31}}], [a_{\vartheta_{31}}, b_{\vartheta_{31}}], [a_{\varpi_{31}}, b_{\varpi_{31}}])$,	$([a_{\omega_{32}}, b_{\omega_{32}}], [a_{\vartheta_{32}}, b_{\vartheta_{32}}], [a_{\varpi_{32}}, b_{\varpi_{32}}])$,	$([a_{\omega_{33}}, b_{\omega_{33}}], [a_{\vartheta_{33}}, b_{\vartheta_{33}}], [a_{\varpi_{33}}, b_{\varpi_{33}}])$,	...	$([a_{\omega_{3n}}, b_{\omega_{3n}}], [a_{\vartheta_{3n}}, b_{\vartheta_{3n}}], [a_{\varpi_{3n}}, b_{\varpi_{3n}}])$,	C_{s3}
⋮	⋮	⋮	⋮	⋮	⋮	⋮
S_m	$([a_{\omega_{m1}}, b_{\omega_{m1}}], [a_{\vartheta_{m1}}, b_{\xi_{m1}}], [a_{\varpi_{m1}}, b_{\varpi_{m1}}])$,	$([a_{\omega_{m2}}, b_{\omega_{m2}}], [a_{\vartheta_{m2}}, b_{\vartheta_{m2}}], [a_{\varpi_{m2}}, b_{\varpi_{m2}}])$,	$([a_{\omega_{m3}}, b_{\omega_{m3}}], [a_{\vartheta_{m3}}, b_{\vartheta_{m3}}], [a_{\varpi_{m3}}, b_{\varpi_{m3}}])$,	...	$([a_{\omega_{mn}}, b_{\omega_{mn}}], [a_{\vartheta_{mn}}, b_{\vartheta_{mn}}], [a_{\varpi_{mn}}, b_{\varpi_{mn}}])$,	C_{sm}
Demand	C_{d1}	C_{d2}	C_{d3}	...	C_{dn}	

Table 3IVPFTP

	D_1	D_2	D_3	...	D_n	Supply
S_1	$([a_{\omega_{11}}, b_{\omega_{11}}], [a_{\vartheta_{11}}, b_{\xi_{11}}], [a_{\varpi_{11}}, b_{\varpi_{11}}])$	$([a_{\omega_{12}}, b_{\omega_{12}}], [a_{\vartheta_{12}}, b_{\xi_{12}}], [a_{\varpi_{12}}, b_{\varpi_{12}}])$	$([a_{\omega_{13}}, b_{\omega_{13}}], [a_{\vartheta_{13}}, b_{\xi_{13}}], [a_{\varpi_{13}}, b_{\varpi_{13}}])$	...	$([a_{\omega_{1n}}, b_{\omega_{1n}}], [a_{\vartheta_{1n}}, b_{\xi_{1n}}], [a_{\varpi_{1n}}, b_{\varpi_{1n}}])$,	$([a_{s\omega_1}, b_{s\omega_1}], [a_{s\vartheta_1}, b_{s\vartheta_1}], [a_{s\varpi_1}, b_{s\varpi_1}])$
S_2	$([a_{\omega_{21}}, b_{\omega_{21}}], [a_{\vartheta_{21}}, b_{\xi_{21}}], [a_{\varpi_{21}}, b_{\varpi_{21}}])$	$([a_{\omega_{22}}, b_{\omega_{22}}], [a_{\vartheta_{22}}, b_{\xi_{22}}], [a_{\varpi_{22}}, b_{\varpi_{22}}])$	$([a_{\omega_{23}}, b_{\omega_{23}}], [a_{\vartheta_{23}}, b_{\xi_{23}}], [a_{\varpi_{23}}, b_{\varpi_{23}}])$	...	$([a_{\omega_{2n}}, b_{\omega_{2n}}], [a_{\vartheta_{2n}}, b_{\xi_{2n}}], [a_{\varpi_{2n}}, b_{\varpi_{2n}}])$,	$([a_{s\omega_2}, b_{s\omega_2}], [a_{s\vartheta_2}, b_{s\vartheta_2}], [a_{s\varpi_2}, b_{s\varpi_2}])$
S_3	$([a_{\omega_{31}}, b_{\omega_{31}}], [a_{\vartheta_{31}}, b_{\vartheta_{31}}],$	$([a_{\omega_{32}}, b_{\omega_{32}}], [a_{\vartheta_{32}}, b_{\vartheta_{32}}],$	$([a_{\omega_{33}}, b_{\omega_{33}}], [a_{\vartheta_{33}}, b_{\vartheta_{33}}],$	...	$([a_{\omega_{3n}}, b_{\omega_{3n}}], [a_{\vartheta_{3n}}, b_{\vartheta_{3n}}],$	$([a_{s\omega_3}, b_{s\omega_3}], [a_{s\vartheta_3}, b_{s\vartheta_3}],$
⋮	⋮	⋮	⋮	⋮	⋮	⋮
S_m	$([a_{\omega_{m1}}, b_{\omega_{m1}}], [a_{\vartheta_{m1}}, b_{\xi_{m1}}], [a_{\varpi_{m1}}, b_{\varpi_{m1}}])$	$([a_{\omega_{m2}}, b_{\omega_{m2}}], [a_{\vartheta_{m2}}, b_{\vartheta_{m2}}], [a_{\varpi_{m2}}, b_{\varpi_{m2}}])$	$([a_{\omega_{m3}}, b_{\omega_{m3}}], [a_{\vartheta_{m3}}, b_{\vartheta_{m3}}], [a_{\varpi_{m3}}, b_{\varpi_{m3}}])$	...	$([a_{\omega_{mn}}, b_{\omega_{mn}}], [a_{\vartheta_{mn}}, b_{\vartheta_{mn}}], [a_{\varpi_{mn}}, b_{\varpi_{mn}}])$	$([a_{s\omega_m}, b_{s\omega_m}], [a_{s\vartheta_m}, b_{s\vartheta_m}], [a_{s\varpi_m}, b_{s\varpi_m}])$
Demand	$([a_{d\omega_1}, b_{d\omega_1}], [a_{d\vartheta_1}, b_{d\vartheta_1}], [a_{d\varpi_1}, b_{d\varpi_1}])$	$([a_{d\omega_2}, b_{d\omega_2}], [a_{d\vartheta_2}, b_{d\vartheta_2}], [a_{d\varpi_2}, b_{d\varpi_2}])$	$([a_{d\omega_3}, b_{d\omega_3}], [a_{d\vartheta_3}, b_{d\vartheta_3}], [a_{d\varpi_3}, b_{d\varpi_3}])$	...	$([a_{d\omega_n}, b_{d\omega_n}], [a_{d\vartheta_n}, b_{d\vartheta_n}], [a_{d\varpi_n}, b_{d\varpi_n}])$	

Rajarajeswari *et al.*,

Table 4 IVPFTP

	D_1	D_2	D_3	D_4	Supply
S_1	0.3	0.2	0.6	0.1	([0.7,0.8], [0,0.1], [0.05,0.1])
S_2	0.7	0.9	0.1	0.3	([0.5,0.6], [0.2,0.3], [0,0.1])
S_3	0.2	0.4	0.7	0.1	([0.1,0.2], [0.5,0.6], [0,0.1])
S_4	0.3	0.1	0.4	0.2	([0.3,0.4], [0.1,0.3], [0.2,0.3])
Demand	([0.1,0.2], [0.5,0.6],[0,0.1])	([0.3,0.4], [0.1,0.3],[0.2,0.3])	([0.7,0.8], [0,0.1],[0.05,0.1])	([0.5,0.6],[0.2,0.3], [0,0.1])	

Table 5 IVPFTP

	D_1	D_2	D_3	D_4	Supply
S_1	0.3	0.2	0.6	0.1	0.1
S_2	0.7	0.9	0.1	0.3	0.3
S_3	0.2	0.4	0.7	0.1	0.4
S_4	0.3	0.1	0.4	0.2	0.2
Demand	0.4	0.2	0.1	0.3	

Table 6 IVPFTP

	D_1	D_2	D_3	D_4	Supply
S_1	0.3	0 0.2	0.6	0.1 0.1	0.1
S_2	0.7	0.9	0.1 0.1	0.2 0.3	0.3
S_3	0.4 0.2	0.4	0.7	0 0.1	0.4
S_4	0.3	0.2 0.1	0.4	0.2	0.2
Demand	0.4	0.2	0.1	0.3	

Table 7 IVPFTP

	D_1	D_2	D_3	D_4	Supply
S_1	([0.5,0.6],[0.2,0.3],[0,0.1])	([0.3,0.4],[0.4,0.5],[0,0.1])	([0,0.1],[0.1,0.1],[0.7,0.8])	([0,0.2],[0.1,0.2],[0.5,0.6])	0.3
S_2	([0,0.1],[0.2,0.3],[0.4,0.5])	([0.5,0.6],[0.2,0.3],[0,0.1])	([0.4,0.5],[0.2,0.3],[0.1,0.2])	([0.3,0.4],[0.1,0.3],[0.2,0.3])	0.7
S_3	([0,0.1],[0.5,0.6],[0.1,0.2])	([0.0,0.1],[0,0.1],[0.6,0.7])	([0.3,0.4],[0.5,0.6],[0,0])	([0.1,0.2],[0.5,0.6],[0,0.1])	0.1
S_4	([0,0.1],[0,0.1],[0.7,0.8])	([0.2,0.3],[0.3,0.4],[0,0.1])	([0.3,0.4],[0.1,0.3],[0.2,0.3])	([0.4,0.5],[0.2,0.3],[0,0.1])	0.5
Demand	0.5	0.3	0.7	0.1	

Table 8 IVPFTP

	D₁	D₂	D₃	D₄	Supply
S₁	0.26	0.19	0.12	0.12	0.3
S₂	0.24	0.26	0.26	0.22	0.7
S₃	0.39	0.12	0.42	0.40	0.1
S₄	0.12	0.27	0.24	0.24	0.5
Demand	0.5	0.3	0.7	0.1	

Table 9 IVPFTP

	D₁	D₂	D₃	D₄	Supply
S₁	0.26	0.19	0.3 0.12	0.12	0.3
S₂	0 0.24	0.2 0.26	0.4 0.26	0.1 0.22	0.7
S₃	0.39	0.1 0.12	0.42	0.40	0.1
S₄	0.5 0.12	0.27	0.24	0.24	0.5
Demand	0.5	0.3	0.7	0.1	

Table 10 IVPFTP

	D₁	D₂	D₃	D₄	Supply
S₁	([0.7,0.8], [0,0.1],[0.05,0.1])	([0.3,0.4],[0.1,0.3],[0.2,0.3])	([0.4,0.5],[0.2,0.3],[0.1,0.2])	([0.6,0.7],[0,0.1],[0.05,0.1])	([0.5,0.6],[0.2,0.3],[0,0.1])
S₂	([0.1,0.2],[0.5,0.6],[0,0.1])	([0.4,0.5],[0.2,0.3],[0,0.1])	([0.7,0.8],[0,0.1],[0,0])	([0.3,0.4],[0.4,0.5],[0,0.1])	([0.7,0.8],[0,0.1],[0,0.1])
S₃	([0.5,0.6],[0.2,0.3],[0,0.1])	([0.6,0.7],[0.2,0.3],[0,0])	([0.2,0.3],[0.3,0.4],[0,0.1])	([0.5,0.6],[0.1,0.2],[0,0.2])	([0.4,0.5],[0.2,0.3],[0,0.1])
S₄	([0.3,0.4],[0.2,0.4],[0.1,0.2])	([0.7,0.8],[0.1,0.2],[0,0])	([0.3,0.4],[0.5,0.6],[0,0])	([0.6,0.7],[0,0.1],[0.05,0.1])	([0.3,0.4],[0.2,0.4],[0,0.1])
Demand	([0.4,0.5],[0.2,0.3],[0,0.1])	([0.3,0.4],[0.2,0.4],[0,0.1])	([0.5,0.6],[0.2,0.3],[0,0.1])	([0.7,0.8],[0,0.1],[0,0.1])	

Table 11 IVPFTP

	D₁	D₂	D₃	D₄	Supply
S₁	0.14	0.22	0.26	0.12	0.26
S₂	0.39	0.24	0.12	0.36	0.12
S₃	0.26	0.27	0.28	0.19	0.24
S₄	0.27	0.22	0.42	0.12	0.25
Demand	0.24	0.25	0.26	0.12	

Table 12 IVPFTP

	D_1	D_2	D_3	D_4	Supply
S_1	0.24 0.14	0.22	0.017 0.26	0.12	0.26
S_2	0.39	0.24	0.12	0.36	0.12
S_3	0.26	0.12 0.27	0.11 0.28	0.19	0.24
S_4	0.27	0.13 0.22	0.42	0.12 0.12	0.25
Demand	0.24	0.25	0.26	0.12	

Table 13 IVPFTP

IVPFTP	Type 1	Type 2	Type 3
	0.18	0.29	0.16

RESEARCH ARTICLE

On Selje Topological Spaces

V.Jeyanthi[1] and N.Selvanandhini[2]*

[1]Assistant Professor, Department of Mathematics, Sri Krishna Arts and Science College, Kuniamuthur, Coimbatore,-Tamil Nadu, India - 641008.
[2]Research Scholar, Department of Mathematics, Sri Krishna Arts and Science College, Kuniamuthur, Coimbatore,-Tamil Nadu, India - 641008.

*Address for Correspondence
N.Selvanandhini
Research Scholar,
Department of Mathematics,
Sri Krishna Arts and Science College,
Kuniamuthur, Coimbatore,
Tamil Nadu, India - 641008.
E.Mail: nandhininagaraj230@gmail.com

ABSTRACT

In 2019, S. Chandrasekar introduced microtopology from nanotopology. In this paper, we introduce Selje topological spaces and some new classes of weak open sets, such as Selje Semi-open sets and Selje Semi-open sets.

Keywords: Selje topological spaces, Selje-Semi-open sets, Selje-continuous function.

INTRODUCTION

Various types of topological spaces such as fuzzy topology, hypertopology, nanotopol- ogy and microtopology are introduced. In 2013, L. Thivagar et al. [5] introduced nanotopology in 2019 and introduced microtopology as an extension of nanotopology using Levine's simple extension steps. The concepts of *Semi*-open set and *Semi*-open set have been proposed by Mashour et al. [3] and Levine [6] respectively. This article introduces a new type of topological space, the selje topological space. Its main prod- ucts and relations with other classes are education. continuous operations are defined such as continuous operation of Selje, continuous operation of Selje and intermittent operation of Selje.

Definition 2.1. In the topological space (E, T), the subset G is characterized as:
- *Semi*-open is called set , if the condition if met: G is part of the closed interior of G. Section
- If the condition is met: G is a subset of the closed set G, called the pre-open set.

64187

The addition of a *Semi*-open set (called a *Semi*-closed set) in space E is called a pre-closed set (*Semi*-closed set).

Definition 2.2. Let us define the universal set V as nonempty and consider the equivalence relation R on V , also known as the indistinguishability relation. The pair (V, R) is referred to as the approximation space. For the subset E ⊆ V:

1. The lower approximation of E concerning R is symbolized as $L_R(E)$, defined by:
$B_R(E) = x \in V$: For all equivalence classes $G(x) \subseteq E$
2. The upper approximation of E concerning R is denoted as $U_R(E)$, given by:
$B_R(E) = x \in V$: There exists an equivalence class $G(x)$ that intersects withE 3.The boundary region of E with respect to R is represented as $B_R(E)$, calculated as: $B_R(E) = U_R(E) - L_R(E)$

Definition 2.3. Let V represent a universal set, and letR denote an equivalence relation on V. We define $T_R(E)$ as the set {V, Φ, $L_R(E)$, $U_R(E)$, $B_R(E)$}, where E is a subset of V that adheres to the following axioms:
*   Both V and Φ belong to $T_R(E)$.
*   The union of elements from any subcollection of $T_R(E)$is an element of $T_R(E)$.
*   The intersection of elements from any finite subcollection of $T_R(E)$ is an element of $T_R(E)$

In this context, $T_R(E)$ is termed the Nanotopology [5] of the universal setV with respect to the subset E. The pair (V, $T_R(E)$)) constitutes a nano topological space, and its constituent elements are referred to as nano-open sets.

Definition 2.4. (V, $T_R(E)$)) creates a nanotopological space. In this case, the set $Y_R(E)$ consists of two groups, namely {N ∪ (N ′ ∩): N , N ′ ∈$T_R(E)$}. The com- bination $T_R(E)$ is expressed as the microtopology Y; where Y is not nanotopology elements of $T_R(E)$.

Definition 2.5. Microtopology [7] $Y_R(E)$ satisfies the following axioms.
1   V,$\varphi \in T_R(E)$
2   The union of the elements of the subset$Y_R(E)$, is in $Y_R(E)$.
The intersection of the elements of a finite subset of $Y_R(E)$ is in $Y_R(E)$. Next, $Y_R(E)$ is called the microtopology of E and V. Triple (E, $T_R(E)$,$Y_R(E)$)) called microtopological space. Elements in $Y_R(E)$ are slightly open and their complements are slightly off.

Selje Topological Space
Definition 3.1. Let (V, $Y_R(E)$)) be a microtopological space and let the Selje topol ogy be defined as $SJ_k(E)$ = {(S-J)∪(S-J'): S∈ $Y_R(E)$ and for fixed J,J' ∈/),J∪J =V}

Definition 3.2. The Selje topology $SJ_k(E)$ satisfies the following axioms 1.V, Φ ∈ $T_R(E)$
The Union of the elements of any subcollection of $SJ_k(E)$ is in $SJ_k(E)$.Y_R(E
The intersection of the elements of any finite subcollection of $SJ_k(E)$ is in$SJ_k(E)$.

The triplet (E, $Y_R(E)$,$SJ_k(E)$)) is called selje topological space. Then, the elements of selje topology are selje-open(SJ-open) sets and their complements are selje-closed(SJ- closed) sets. The collection of selje closed sets of selje topology is denoted as SJCL(E).

Definition 3.3. Selje closure and interior Selje of G are defined as follows:
$SJ_k(G)$ = ∩ {H: H is a closed set and G ⊆ H }
$SJ_{int}(G)$ = ∪ {H : H is selje-open and H ⊆ G }

Definition 3.4. In a selje topological space (E, $Y_R(E)$,$SJ_k(E)$)), for any two selje sets G and H

i G is selje closed if and only if $SJ_{cl}(G)$ = G.

ii G is selje open if and only if $SJ_{int}(G)$ = G.

iii G ⊆ H =⇒ $SJ_{cl}(G)$ ⊆ $SJ_{cl}(H)$ and $SJ_{int}(G)$ ⊆ $SJ_{int}(H)$

iv $SJ_{cl}(G)$ = $SJ_{cl}(SJ_{cl}(G))$ and $SJ_{int}(G)$ = $SJ_{int}(SJ_{int}(G))$

v $SJ_{cl}(G \cup H) \supseteq SJ_{cl}(G) \cup SJ_{cl}(H)$

vi $SJ_{int}(G \cup H) \supseteq SJ_{int}(G) \cup SJ_{int}(H)$

vii $SJ_{cl}(G \cap H) \subseteq SJ_{cl}(G) \cap SJ_{cl}(H)$

viii $SJ_{int}(G \cap H) \subseteq SJ_{int}(G) \cap SJ_{int}(H)$

ix $SJ_{cl}(G^c) = [SJ_{int}(G)]^c$ x $SJ_{int}(G^c) = [SJ_{cl}(G)]^c$

Example 3.1. Let V={Ψ, Θ, Γ, Δ} with V/R= {{Ψ}, {Γ}, {Θ, Δ}} and E={Ψ, Θ}⊂V.

Then $Y_R(E)$={V,φ,{Ψ},{Ψ, Θ, Δ},{Θ, Δ}}. If Y={Γ} then

$Y_R(E)$={V,φ,{Ψ},{Θ},{Δ},{Ψ,Θ},{Ψ,Γ},{Ψ,Δ},{Θ,Γ},{Θ,Δ},{Γ,Δ},{Ψ,Θ,Γ},{Ψ,Θ,Δ},{Ψ,Γ,Δ},{Θ,

$SJ_k(E)$={V,φ,{Θ},{Q},{Θ,Q},{Γ,Δ},{Ψ,Γ,Δ},{Θ,Γ,Δ},{Γ,Δ,Q},{Ψ,Θ,Γ,Δ},{Ψ,Γ,Δ,Q},{Θ,Γ,Δ,Q}}

Selje-Pre-Open Sets

Definition 4.1. Let (E, $Y_R(E)$,$SJ_k(E)$) be a selje topological space. If G ⊆ V,then G is selje-pre open if G ⊆ $SJ_{int}(SJ_{cl}(G))$ and G is selje-pre-closed if G ⊇ $SJ_{cl}(SJ_{int}(G))$. All the elements in Selje-Pre open sets and Selje-Pre closed sets are denoted by SJPO(E) and SJPCL(E) respectively.

Example 4.1. Let V = {Ψ,Θ,Γ,Δ,Q} with V/R={{Ψ},{Θ,Γ,Δ},{Q}}, E={Δ,Q} ⊂

V. Then $Y_R(E)$={V,φ,{Q},{Θ,Γ,Δ,Q}. If Y={Ψ} then $Y_R(E)$={V,φ,{Q},{Ψ},{Q,Ψ},{Θ,Γ,Δ,Q},{Θ,Γ,Δ},{Ψ,Θ,Γ,Δ}} If J={Ψ,Γ,Δ},J' ={Θ,Q} then,

$SJ_k(E)$={V,φ,{Θ},{Q},{Θ,Q},{Γ,Δ},{Ψ,Γ,Δ},{Θ,Γ,Δ},{Γ,Δ,Q},{Ψ,Θ,Γ,Δ},{Ψ,Γ,Δ,Q},{Θ,Γ,Δ,Q}}

SJPO(E)={V,φ,{Θ},{Γ},{Δ},{Q},{Ψ,Γ},{Ψ,Δ},{Θ,Γ},{Θ,Δ},{Θ,Q},{Γ,Δ},{Γ,Q},{Δ,Q},{Ψ,Θ,Γ},{Ψ,Θ

{Ψ,Θ,Q},{Ψ,Γ,Δ},{Ψ,Γ,Q},{Ψ,Δ,Q},{Θ,Γ,Δ},{Θ,Γ,Q},{Θ,Δ,Q},{Γ,Δ,Q},{Ψ,Θ,Γ,Δ},{Ψ,Γ,Δ,Q},{Θ,Γ,Δ,

Theorem 4.1. $SJ_k(E) \subseteq SJPO(E)$

Proof. Consider G belongs to $SJ_k(E)$. Then,

G ⊆ $SJ_{int}(SJ_{cl}(G))$ (1)

Here, $SJ_{int}(SJ_{int}(G)) \subseteq SJ_{int}(SJ_{cl}(G))$. From(1), we have G ⊆ $SJ_{int}(SJ_{cl}(G))$. There- fore,

G belongs to SJPO(E)

Example 4.2. From Example 4.1, it is recognizable that G = {Ψ, Θ, Δ} belongs to the set SJPO(E) but it does not belong to set $SJ_k(E)$.

Remark 4.1. In Common, SJPO(E) ⊄ $SJ_k(E)$, from the example 3.2, it is seen that

G = {Ψ, Δ, Q} ∈/ $SJ_k(E)$

Theorem 4.2. $SJCL(E) \subseteq SJPCL(E)$

Proof. Consider G ∈ SJCL(E), then G=SJCL(G) from which we have G ⊇ $SJ_{cl}(SJ_{cl}(G))$. We know

G ⊇ $SJ_{cl}(G)$ (2)

$SJ_{cl}(SJ_{cl}(G)) \supseteq SJ_{cl}(SJ_{int}(G))$ (3)

From (2) and (3), G ⊇ $SJ_{cl}(SJ_{int}(G))$

Remark 4.2. In Common,SJPCL(E) ⊄ SJCL(E). From the example 3.2, we have $SJCL(E)$=
{V,φ,{Ψ},{Θ},{Q},{Ψ,Θ},{Ψ,Q},{Θ,Q},{Ψ,Θ,Q},{Ψ,Γ, Δ},{Ψ,Θ,Γ,Δ},{Ψ,Γ,Δ,Q}} SJPCL(E)={V,φ,{Ψ},{Θ},{Q},{Ψ,
Θ},{Ψ,Γ},{Ψ,Δ},{Ψ,Q},

Jeyanthi and Selvanandhini

{Θ,Γ},{Θ,Δ},{Θ,Q},{Γ,Δ},{Γ,Q},{Δ,Q},{Ψ,Θ,Γ},{Ψ,Θ,Δ},{Ψ,Θ,Q}, {Ψ,Γ,Δ},{Ψ,Γ,Q},
{Ψ,Δ,Q},{Θ,Γ,Q},{Θ,Δ,Q},{Ψ,Θ,Γ,Δ},{Ψ,Θ,Γ,Q},{Ψ,Θ,Δ,Q},{Ψ,Γ,Δ,Q}}.
Here, G ={Ψ, Θ, Δ} belongs to SJPCL(E) But G does not belong to *SJCL*(E).

Definition 4.2. *SJ− Pre$_d$*(G) and *SJ− Pre$_{int}$*(G) is denoted as selje-pre closed sets and selje-Pre-open sets respectively.
Selje-Pre-closed is defined as
*SJ− Pre$_d$*G = ∩{H: G ⊆ H,H is selje-pre-closed} Similarly, Selje-Pre-Open is defined as
*SJ− Pre$_{int}$*G = ∪{H: G ⊇ H,H is selje-pre-open}

Remark 4.3. The following remark is derived from the above results
1.   The smallest Selje-Pre-Open set containing G is *SJ− Pre$_d$*(G).
2.   The largest Selje-Pre-Closed set contained in G is *SJ− Pre$_{int}$*(G).

Theorem 4.3.
1. If ς is an index set, then $\cap_{\delta \in \varsigma}$ G$_\delta$ ∈ SJPCL(E) whenever G$_\delta$ ∈ *SJPCL*(E*)*
2.If ς is an index set, then $\cup_{\delta \in \varsigma}$ G$_\delta$ ∈ SJPO(E) whenever G$_\delta$ ∈ *SJPO*(E*)*

Proof.
Consider {G$_\delta$: δ ∈ *I*} is a subset of SJPCL(E). From the definition, for each δ

SJ$_d$(*SJ$_{int}$*(G$_\delta$)) ⊆ G$_\delta$. Here,
SJ$_d$(*SJ$_{int}$*(∩$_\delta$(G$_\delta$))) ⊆ *SJ$_d$*(∩$_\delta$(*SJ$_{int}$*(G$_\delta$))
⊆ ∩$_\delta$(*SJ$_d$*(*SJ$_{int}$*(G$_\delta$))
⊆ ∩$_\delta$G$_\delta$

Therefore,∩$_\delta$G$_\delta$ ∈ SJPO(E)
1.   Consider {G$_\delta$: δ ∈ *I*} is a subset of SJPO(E). From the definition, for each δ *SJ$_{int}$*(*SJ$_d$*(G$_\delta$)) ⊇ G$_\delta$. Here,
(∪$_\delta$(G$_\delta$))) ⊆ ∪$_\delta$(*SJ$_{int}$*(*SJ$_d$*(G$_\delta$)))
⊆ *SJ$_{int}$*(∪$_\delta$*SJ$_d$*(G$_\delta$))
⊆ *SJ$_{int}$*(*SJ$_d$*(∪$_\delta$(G$_\delta$)))
Therefore,∪$_\delta$G$_\delta$ ∈ SJPO(E)

Remark 4.4. Finite intersection of Selje-Pre-Open set need not to be Selje-Pre-Open.

Example 4.3. In Example 3.2, V = {Ψ,Θ,Γ,Δ,Q} with V/R={{Ψ},{Θ,Γ,Δ},{Q}}, E={Δ,Q} ⊂ V. If J={Ψ,Γ,Δ},J={Θ,Q}
SJPO(E)={V,φ,{Θ},{Γ},{Δ},{Q},{Ψ,Γ},{Ψ,Δ},{Θ,Γ},{Θ,Δ},{Θ,Q},{Γ,Δ},{Γ,Q},{Δ,Q},{Ψ,Θ,Γ},{Ψ,Θ
{Ψ,Θ,Q},{Ψ,Γ,Δ},{Ψ,Γ,Q},{Ψ,Δ,Q},{Θ,Γ,Δ},{Θ,Γ,Q},{Θ,Δ,Q},{Γ,Δ,Q},{Ψ,Θ,Γ,Δ},{Ψ,Γ,Δ,Q},{Θ,Γ,Δ,
Here, {Ψ, Δ, Q} and {Ψ, Θ, Q} belongs to SJPO(E) but their intersection (i.e.,) {Ψ, Δ, Q} {Ψ, Θ, Q} = {Ψ, Q} does not
belong to SJPO(E).T

Theorem 4.4. G *= SJ− Pre$_d$*(G*) iff* G ∈ *SJPCL*(E*)*
Proof. Assume that G ∈ SJPCL(E). G ⊆ *SJ− Pre$_d$*(E) and then
SJ− Pre$_d$(G) = ∩{H: G ⊆ H, H*isSJ− Pre−closedset*} (4) Since G ∈ SJPCL(E). G is an element from (4).
Therefore, G = ∩{H: G ⊆ H, H is SJ-Pre-closed set} Hence, G = *SJ− Pre$_d$*(G).

Selje-Semi-Open Sets
Definition 5.1. Let (E, Y$_R$(E),*SJ$_k$*(E)) be an selje topological space. If G ⊆ V,then G is selje-pre open if G ⊆
SJ$_d$(*SJ$_{int}$*(G)) and G is selje-pre-closed if G ⊇ *SJ$_{int}$*(*SJ$_d$*(G)). Then, all the elements in Selje-Pre open sets [Selje-Pre closed
sets] are denoted by SJPO(E) [SJPL(E)] respectively.

Theorem 5.1. $SJ_k(E) \subseteq SJSO(E)$

Proof. Consider G belongs to $SJ_k(E)$ (i.e.,) G = $SJ_{int}(G)$. For all subset G of V and G $\subseteq SJ_{cl}(G)$, we have G $\subseteq SJ_{cl}(SJ_{int}(G))$. Hence, G belongs to $SJSO(E)$.

Remark 5.1. In some cases, $SJ_k(E)$ = SJSO(E)(From Example 5.1)

Example 5.1. Consider V = $\{\Psi,\Theta,\Gamma,\Delta,Q\}$ with V/R=$\{\{\Psi\},\{\Theta,\Gamma,\Delta\},\{Q\}\}$, E=$\{\Delta,Q\}\subset$ V. If J=$\{\Psi,\Gamma,\Delta\}$,J=$\{\Theta,Q\}$

SJSO(E) = $\{V,\varphi,\{\Theta\},\{Q\},\{\Theta,Q\},\{\Gamma,\Delta\},\{\Psi,\Gamma,\Delta\},\{\Theta,\Gamma,\Delta\},\{\Gamma,\Delta,Q\},\{\Psi,\Theta,\Gamma,\Delta\},\{\Psi,\Gamma,\Delta,Q\},\{\Theta,\Gamma,\Delta,Q\}\}$.

Here, all the elements from $SJ_k(E)$ belongs to SJSO(E)

Theorem 5.2. $SJCL(E) \subseteq SJSCL(E)$

Proof. Consider G belongs to SJCL(E), then G=$SJ_{cl}G$. Here,

G $\supseteq SJ_{cl}(SJ_{int}(G))$ (5)

It is known that $SJ_{int}(G) \subseteq$ G   (6)

$SJ_{int}(SJ_{cl}(G)) \subseteq SJ_{cl}(SJ_{int}(G))$ (7)

From (5),(6),(7) we have, $SJ_{int}(SJ_{cl}(G)) \subseteq SJ_{cl}(SJ_{int}(G)) \subseteq$ G

Therefore, G belong to SJSCL(E).

Remark 5.2. In some exceptional cases SJCL(G) = SJSCL(G) (see example 5.1)

Definition 5.2. $SJ - Semi_{cl}(G)$ is denoted as selje-*Semi* closed sets and and $SJ Semi_{int}(G)$is denoted as selje-*Semi*-open sets. Selje-*Semi*-closed is defined as

$SJ - Semi_{cl}(G)$= $\cap\{H: G \subseteq H, H$ is selje-*Semi*-closed} Similarly, Selje-Pre-Open is defined as

$SJ - Pre_{int}(G)$ = $\cup\{H: G \supseteq H, H$ is selje-*Semi*-open}

Remark 5.3. The following remark is derived from the above results 1.The largest SJ-*Semi* open set contained in G is $SJ - Semi_{int}(G)$ 2.The smallest SJ-*Semi* closed set containing G is $SJ - Semi_{cl}(G)$

Theorem 5.3. *1. If ς is an index set, whenever* $G_\delta \in SJSO(E)$ *then* $\cap_{\delta \in \varsigma} G_\delta \in SJSO(E)$

2.If ς is an index set, whenever $G_\delta \in SJSO(E)$ *then* $\cup_{\delta \in \varsigma} G_\delta \in SJSO(E)$

Proof.

Consider $\{G_\delta : \delta \in I\}$ is a subset of SJSO(E). From the definition, for each δ $G_\delta \subseteq SJ_{cl}(SJ_{int}(G_\delta))$. Here,

$\cup_\delta G_\delta \subseteq \cup_\delta SJ_{cl}((SJ_{int}(G_\delta))$

$\subseteq (SJ_{cl}(SJ_{int}(\cup_\delta(G_\delta)))$

Therefore, $\cup_\delta G_\delta \in$ SJPO(E)

Consider $\{G_\delta : \delta \in I\}$ is a subset of SJSCL(E). From the definition, for each δ

$G_\delta \supseteq SJ_{int}(SJ_{cl}(G_\delta))$. Here,

$SJ_{int}(SJ_{cl}(\cap_\delta(G_\delta))) \in SJ_{int}(\cap_\delta(SJ_{cl}(G_\delta)))$

$\in \cap_\delta G_\delta$

Therefore, $\cap_\delta G_\delta \in$ SJSCL(E)

Theorem 5.4. G= $SJ_{int}(G)$ *if and only if* G $\in SJSO(E)$

Proof.

Neccessary

Assume that G $\in$ SJSO(E), then G $\subseteq \cup\{H$ is SJ-*Semi*-Open}

then G = SJ-*Semi*-Open set. So, G $\subseteq SJ - Semi_{int}(G)$. As G belongs to SJSO(G),

$SJ - Semi_{int}(G) \subseteq$ G. Therefore, G=$SJ - Semi_{int}(G)$.

Sufficient

Consider G = $SJ-Semi_{int}$(G). Then from Remark 5.3 it is shown that the largest SJ-*Semi* open set contained in G is $SJ-Semi_{int}$(G). Hence,G ∈ SJSO(E).

Example 5.2. Consider V = {Ψ,Θ,Γ,Δ,Q} with V∕R={{Ψ},{Θ,Γ,Δ},{Q}}, E={Δ,Q}⊂V. If J={Ψ,Γ,Δ},*J*={Θ,Q}
SJPO(E)={V,φ,{Θ},{Γ},{Δ},{Q},{Ψ,Γ},{Ψ,Δ},{Θ,Γ},{Θ,Δ},{Θ,Q},{Γ,Δ},{Γ,Q},{Δ,Q},{Ψ,Θ,Γ},{Ψ,Θ
{Ψ,Θ,Q},{Ψ,Γ,Δ},{Ψ,Γ,Q},{Ψ,Δ,Q},{Θ,Γ,Δ},{Θ,Γ,Q},{Γ,Δ,Q},{Ψ,Θ,Γ,Δ},{Ψ,Γ,Δ,Q},{Θ,Γ,Δ,Q}}
SJSO(E) = {V,φ,{Θ},{Q},{Θ,Q},{Γ,Δ},{Ψ,Γ,Δ},{Θ,Γ,Δ},{Γ,Δ,Q},{Ψ,Θ,Γ,Δ},{Ψ,Γ,Δ,Q},{Θ,Γ,Δ,Q}}.

Remark 5.4. {Γ} is in SJPO(E) but not in SJSO(E)
SPSO(G) ⊄ SJPO(G)
Similarly, {Θ} is in SJSO(E) but not in SJPO(E)
SJPO(G) ⊄ SJSO(G).

Selje-Continuous function
The definition of Selje continuous function(SJ-continuous function) is given as

Definition 6.1. Consider two topological space (V, Y_R(E), SJ_R(E)) and (U, ZR′ (F), $SJR′$ (F)) and E ⊆ V and F ⊆ U. Then a function k : V → U is Selje continuous (SJ-continuous) function if k^{-1}(x) ∈ SJ_R(E) whenever x ∈ SJ_R(E).

Theorem 6.1. *Let* (V, Y_R(E), SJ_R(E)) *and* (U, ZR′ (F), $SJR′$ (F)) *and* E ⊆ V *and* F ⊆ U. *Then a function* k : V → U *is SJ-continuous function if and only if* k^{-1}(x) ∈ $SJCL$(E*) whenever* x ∈ $SJCL$(E*).*

Proof.
Neccessity
Consider k: V → U is SJ-continuous function and x ∈ SJCL(F) then the complement belongs to SJ_R(F) then k^{-1}(x$_c$) ∈ SJ_R(E) (i.e.,)(k^{-1}(x))$_c$ belongs to SJ_R(E).Therefore, (k^{-1}(x)) ∈ SJCL(E) whenever x ∈ SJCL(F)

Sufficient
Consider (k^{-1}(x))$_c$ belongs to SJ_R(E) whenever x ∈ SJCL(F). If whenever x ∈ SJCL(F) then whenever x$_c$ ∈ SJCL(E). By assumption k^{-1}(x$_c$) ∈ $SJCL$(E) where k^{-1}(x) belongs to SJ_R(E). Therefore k is SJ-continuous.

Definition 6.2. Consider two topological space (V, Y_R(E), SJ_R(E)) and (U, ZR′ (F), $SJR′$ (F)) and E ⊆ V and F ⊆ U. Then a function k : V → U is Selje-Pre-continuous function
if k^{-1}(x) ∈ $SJPCL$(E) whenever x ∈ $SJCL$(E).

Theorem 6.2. *Every SJ-continuous function is SJ-Pre-continuous function*
Proof.
Let k : V → U be a SJ-continuous function. k^{-1}(x) ∈ $SJCL$(F). From theorem 4.1 it is given that for every x ∈ $SJCL$(F), we have k^{-1}(x) ∈ $SJPCL$(E). Hence, k is SJ-Pre-continuous function.

Definition 6.3. Consider two topological space (V, Y_R(E), SJ_R(E)) and (U, ZR′ (F), $SJR′$ (F)) and E ⊆ V and F ⊆ U. Then a function k : V → U is Selje-*Semi*-continuous function
if k^{-1}(x) ∈ $SJSCL$(E) whenever x ∈ $SJCL$(E).

Theorem 6.3. Every SJ-continuous function is an SJ-Semi-continuous function

Jeyanthi and Selvanandhini

Proof.

Consider a function $k : V \rightarrow U$ be a SJ-continuous function. Whenever x ∈ *SJCL*(F), k^{-1}(x) ∈ *SJCL*(E). From theorem 5.1 it is given that for every x ∈ *SJCL*(F), we have k^{-1}(x) ∈ *SJSCL*(E). Hence, k is SJ-*Semi*-continuous function.

CONCLUSION

Throughout this paper, the properties of SJ_k(E) are discussed and we have arrived at a conclusion that SJ_k(E) + SJPO(E) but in some rare cases there were some results like SJ_k(E)=SJSO(E) from some of the worked examples. This results can be extended for the further research on homeomorphism and other strong sets in topo- logical space and can be used for some real time application in other fields.

ACKNOWLEDGEMENTS

REFERENCES

1. A.S.Mashhour, M.E.Abd El-Monsef, S.N.El-Deep, *"On Pre continuous map- pings and weak pre continuous mappings,"* Proc.Math. and Phys. Soc. Egypt, 53(1982),47-53.
2. D.A.Mary and A.Arokia Rani, *"On Semi pre open sets in nanotopological spaces,"* Math.Sci.Int.Res.J,3(2014),771-773.
3. D.Andrijevic, *"On the topology generated by pre-open sets,"* Mat.Vesnik,39(1987)367-376.
4. Kashyap G.Rachchh and Sajeed I.Ghanchi, *"On Kasaj topological spaces,"* Malaya Journal of Mathematik,8(2020),1776-1770.
5. M.L.Thivagar and C.Richard, *"On Nano forms of weakly open sets"*,International Journal of Mathematics and Stastic Invention, 1/1(2023),31- 37.
6. N.Levine, *"Semi open sets and Semi continuity in Topological spaces"*,Amer.Math.Monthly, 70(1963),36-41. S.Chandrasekar, *"On Micro Topological Spaces"*,Journal of New Theory, 26(2019)23-31.

RESEARCH ARTICLE

B-Hψ-Open Sets in HGTS

R. Ramesh*, L. Senthil Kumar and T. Muthukumar

Assistant Professor, Department of Science and Humanities, Dr. Mahalingam College of Engineering and Technology, Pollachi, Coimbatore , Tamil Nadu, India.

*Address for Correspondence
R. Ramesh,
Assistant Professor,
Department of Science and Humanities,
Dr. Mahalingam College of Engineering and Technology,
Pollachi, Coimbatore , Tamil Nadu, India.
E.Mail: rameshwaran141@gmail.com

ABSTRACT

In this work, we present and look into the new kind of open sets namely Δ-$\mathcal{H}_\psi$-ópen, Σ-$\mathcal{H}_\psi$- ópen, Φ-$\mathcal{H}_\psi$-ópen, Ω-$\mathcal{H}_\psi$-ópen and $\mathcal{B}$-$\mathcal{H}_\psi$-o´pen sets. Additionally, we find decomposition of $(\Delta$-$H_\psi,\lambda)$-continuous.

Keywords: Hereditary generalized topology, Δ-$\mathcal{H}\psi$-o´pen, Σ-$\mathcal{H}\psi$-o´pen and Φ- $\mathcal{H}O(A)$ sets, $\mathcal{B}$-$\mathcal{H}\psi$-o´pen sets.
2000 Mathematics Subject Classification: 54A05.

INTRODUCTION

Let ϑ be a collection from A, which is a nonempty set. Then ϑ is called a generalized topology (briefly GT)[2], iff $\emptyset \in \vartheta$ and $\mathscr{L}j \in \vartheta$ for j∈J implies $\mathscr{L} = \text{J}j \in \text{Y } \mathscr{L}j \in \vartheta$. The ϑ-closure (σ-closure) of $\mathscr{L}$ is denoted by c ϑ ($\mathscr{L}$) (resp. c σ ($\mathscr{L}$)) is the smallest ϑ - c´losed (resp. ϑ- σ- c´losed) sets containing $\mathscr{L}$ and the ϑ-interior (resp. σ-interior) of $\mathscr{L}$, denoted by i ϑ ($\mathscr{L}$) (resp. i σ ($\mathscr{L}$)) is the largest ϑ-o´pen (resp. ϑ-σ-o´pen) sets contained in $\mathscr{L}$.

Definition 1.1. A subset $\mathscr{L} \subset$ A is called
1. ϑ - α- o´pen [3], if $\mathscr{L} \subset$ i ϑ c ϑ i ϑ ($\mathscr{L}$).
2. ϑ - σ- o´pen [3], if $\mathscr{L} \subset$ c ϑ i ϑ ($\mathscr{L}$).
3. ϑ - π- o´pen [3], if $\mathscr{L} \subset$ i ϑ c ϑ ($\mathscr{L}$).
4. ϑ - β- o´pen [3], if $\mathscr{L} \subset$ c ϑ i ϑ c ϑ ($\mathscr{L}$).
5. ϑ - b- o´pen [12], if $\mathscr{L} \subset$ c ϑ i ϑ ($\mathscr{L}$) $\cup$ i ϑ c ϑ ($\mathscr{L}$).

Ramesh *et al.*,

Definition 1.2. A hereditary class [4], is defined as $\mathcal{H}$ of subsets of $\mathbb{Z}$, if $\mathscr{L} \in \mathcal{H}$ and $V \subset \mathcal{L}$, then $V \in \mathcal{H}$.

Definition 1.3. For a hereditary class $\mathcal{H}$ on $\mathscr{L}$ and $\mathscr{L} \subset \mathbb{Z}$, we define $\mathscr{L}^*(\mathcal{H}, \vartheta) = \{a \in \mathbb{Z}: \mathscr{L} \cap V \notin \mathcal{H}$ for all $V \in \vartheta$ such that $a \in V\}$ [4].

Definition 1.4. [5] Let $\mathscr{L} \subset \mathbb{Z}$. Then $\mathscr{L}^*\sigma(\mathcal{H}, \vartheta) = \{z \in \mathbb{Z}: \mathscr{L} \cap V \notin \mathcal{H}$ for all $V \in \vartheta$ - σ - o´pen such that $z \in V\}$ and $c^*\sigma(\mathscr{L}) = \mathscr{L} \cup \mathscr{L}\sigma*$.

Definition 1.5. A subset $\mathscr{L} \subset \mathbb{Z}$ is called
1. α - H - o´pen [4], if $\mathscr{L} \subseteq i \vartheta \ c^*\vartheta i \vartheta (\mathscr{L})$,
2. σ - H - o´pen [4], if $\mathscr{L} \subseteq c^*\vartheta i \vartheta (\mathscr{L})$,
3. π - H - o´pen [4], if $\mathscr{L} \subseteq i \vartheta \ c^*\vartheta (\mathscr{L})$,
4. β - H - o´pen [4], if $\mathscr{L} \subseteq c \vartheta i \vartheta \ c^*\vartheta(\mathscr{L})$,
5. $\vartheta *$ - c´losed [4], if $c^*\vartheta(\mathscr{L}) \subset \mathscr{L}$.
6. b - H - o´pen [8], if $\mathscr{L} \subseteq i \vartheta \ c^*\vartheta \ \mathscr{L}) \cup c^*\vartheta \ i \vartheta (\mathscr{L})$,
7. $\sigma\vartheta$ *- c´losed [5], if $\mathscr{L}\sigma * \subseteq \mathscr{L}$

Definition 1.6. A subset $\mathscr{L} \subset \mathbb{Z}$ is said to be
1. α - H σ - o´pen [10], if $\mathscr{L} \subseteq i \vartheta \ c^*\sigma i \vartheta (\mathscr{L})$,
2. σ - H σ - o´pen [10], if $\mathscr{L} \subseteq c^*\sigma i \vartheta (\mathscr{L})$,
3. π - H σ - o´pen [10], if $\mathscr{L} \subseteq i \vartheta \ c^*\sigma (\mathscr{L})$,
4. β - H σ - o´pen [10], if $\mathscr{L} \subseteq c \vartheta i \vartheta \ c^*\sigma (\mathscr{L})$.
5. b - H σ - o´pen [9], if $\mathscr{L} \subseteq i \vartheta \ c^*\sigma (\mathscr{L}) \cup c^*\sigma i \vartheta (\mathscr{L})$.

$\mathscr{B}$ - $\mathcal{H} \ \Psi$ - O´PEN SETS
Definition 2.1. A subset $\mathscr{L} \subset \mathbb{Z}$ is called
1. Δ- $\mathcal{H}\psi$ - o´pen, if $\mathcal{L} \subseteq i \ \sigma \ c * \sigma i \sigma (\mathcal{L})$.
2. Σ- $\mathcal{H}\psi$ - o´pen, if $\mathscr{L} \subseteq c^*\sigma i \sigma(\mathscr{L})$.
3. Φ- $\mathcal{H}O(\mathbb{Z})$, if $\mathscr{L} \subseteq i \ \sigma \ c^*\sigma (\mathscr{L})$.
4. Ω- $\mathcal{H}\psi$ - o´pen, if $\mathscr{L} \subseteq c \vartheta i \sigma \ c^*\sigma (\mathscr{L})$.
5. $\mathscr{B}$ - $\mathcal{H} \ \psi$ - o´pen, if $\mathscr{L} \subseteq c^*\sigma i \sigma \cup i \ \sigma \ c^*\sigma (\mathscr{L})$.

The set of all Δ-$\mathcal{H}\psi$ -o´pen (resp. Σ-$\mathcal{H}\psi$ -o´pen, Φ-$\mathcal{H}O(\mathbb{Z})$, Ω-$\mathcal{H}\psi$ - o´pen and $\mathscr{B}$-$\mathcal{H}\psi$ - o´pen , λ-o´pen) is denoted by Δ-$\mathcal{H}O(\mathbb{Z})$ (resp. Σ-$\mathcal{H}O(\mathbb{Z})$, Φ-$\mathcal{H}O(\mathbb{Z})$, Ω-$\mathcal{H}O(\mathbb{Z})$, $\mathscr{B}$-$\mathcal{H}O(\mathbb{Z})$, $\lambda O(\mathbb{Z})$).

Proposition 2.2. In $\mathcal{H}$ -GTS $(\mathbb{Z}, \vartheta, \mathcal{H})$,
1. Any $\vartheta O(\mathbb{Z})$ set is Δ-$\mathcal{H}O(\mathbb{Z})$.
2. Any $\vartheta O(\mathbb{Z})$ set is Σ-$\mathcal{H}O(\mathbb{Z})$.
3. Any $\vartheta O(\mathbb{Z})$ set is Φ-$\mathcal{H}O(\mathbb{Z})$.
4. Any $\vartheta O(\mathbb{Z})$ set is Ω-$\mathcal{H}O(\mathbb{Z})$.
5. Any $\vartheta O(\mathbb{Z})$ set is $\mathscr{B}$-$\mathcal{H}O(\mathbb{Z})$.

Proof. (1). Consider $\mathscr{L} \subset \mathbb{Z}$ is ϑ-o´pen. Then, $\mathscr{L} \subseteq i \vartheta (\mathscr{L}) \subseteq i \vartheta \ c^*\sigma(\mathscr{L}) \subseteq i \ \sigma \ c^*\sigma i \vartheta (\mathscr{L}) \subseteq i \ \sigma \ c^*\sigma i \sigma (\mathscr{L})$. Hence $\mathscr{L}$ is Δ- $\mathcal{H}O(\mathbb{Z})$.
(2). Consider $\mathscr{L} \subset \mathbb{Z}$ is ϑ- o´pen. Then, $\mathscr{L} \subseteq i \vartheta (\mathscr{L}) \subseteq c\sigma * i \vartheta (\mathscr{L}) \subseteq c^*\sigma i \sigma (\mathscr{L})$. Hence $\mathscr{L}$ is Σ - $\mathcal{H}O(\mathbb{Z})$.
(3). Consider $\mathscr{L} \subset \mathbb{Z}$ is ϑ-o´pen. Then, $\mathscr{L} \subseteq i \vartheta (\mathscr{L}) \subseteq i \vartheta \ c\sigma * (\mathscr{L}) \subseteq i \ \sigma \ c\sigma * (\mathscr{L})$. Hence $\mathscr{L}$ is Φ - $\mathcal{H}O(\mathbb{Z})$.
(4). Consider $\mathscr{L} \subset \mathbb{Z}$ is ϑ-o´pen. Then $\mathscr{L} = i \vartheta (\mathscr{L})$. Now $\mathscr{L} \subseteq c \vartheta (\mathscr{L}) \subseteq c \vartheta i \vartheta (\mathscr{L}) \subseteq c \vartheta i \sigma \ c\sigma * (\mathscr{L})$. Hence $\mathscr{L}$ is Ω - $\mathcal{H}O(\mathbb{Z})$.
(5). Consider $\mathscr{L} \subset \mathbb{Z}$ is ϑ-o´pen. Then $\mathscr{L} = i \vartheta (\mathscr{L})$. Now $\mathscr{L} \subseteq i \vartheta (\mathscr{L}) \subseteq i \vartheta \ c\sigma * (\mathscr{L}) \subseteq i \ \sigma \ c\sigma * (\mathscr{L}) \subseteq i \ \sigma \ c\sigma * (\mathscr{L}) \cup c\sigma * i \ \sigma (\mathscr{L})$. Hence $\mathscr{L}$ is $\mathscr{B}$ - $\mathcal{H}O(\mathbb{Z})$.

Ramesh *et al.,*

Example 2.3. Consider $\mathbb{Z}$={1, 2, 3, 4, 5} ϑ={∅, {1}, {3}, {1, 3}, {3, 4, 5},{1, 3, 4, 5}, {1, 2, 3}, $\mathbb{Z}$}, ℋ={∅, {1}}. Then $\mathscr{L}$={1, 4, 5} is Δ-ℋO($\mathbb{Z}$) (resp. Σ-ℋO($\mathbb{Z}$) , Φ-ℋO($\mathbb{Z}$), Ω-ℋO($\mathbb{Z}$), $\mathscr{B}$ -ℋO($\mathbb{Z}$)) but not ϑ-oʹpen.

Proposition 2.4. In ℋ -GTS ($\mathbb{Z}$, ϑ, ℋ),
1. Any α-ℋ σ -oʹpen is Δ-ℋO($\mathbb{Z}$).
2. Any σ-ℋ σ -oʹpen is Σ-ℋO($\mathbb{Z}$).
3. Any π-ℋ σ -oʹpen is Φ-ℋO($\mathbb{Z}$).
4. Any β-ℋ σ -oʹpen is Ω - ℋO($\mathbb{Z}$).
5. Any b-ℋ σ - oʹpen is $\mathscr{B}$ - ℋO($\mathbb{Z}$).

Proof.
1. Consider $\mathscr{L}$⊂ $\mathbb{Z}$ is α-ℋ σ -oʹpen set. Then $\mathscr{L}$⊆ i ϑ c⊛∗ i ϑ ($\mathscr{L}$)⊆ i σ c⊛∗ i σ ($\mathscr{L}$). Hence $\mathscr{L}$ is Δ-ℋO($\mathbb{Z}$).
2. Consider $\mathscr{L}$⊂$\mathbb{Z}$ is σ-ℋ σ - oʹpen set. Then $\mathscr{L}$⊆c ∗ σi ϑ ($\mathscr{L}$)⊆c⊛∗ i σ ($\mathscr{L}$). Hence $\mathscr{L}$ is Σ- ℋO($\mathbb{Z}$).
3. Consider $\mathscr{L}$⊂$\mathbb{Z}$ is π-ℋ σ - oʹpen set. Then $\mathscr{L}$⊆i ϑ c⊛∗ ($\mathscr{L}$) ⊆i σ c⊛∗ ($\mathscr{L}$). Hence $\mathscr{L}$ is Φ- ℋO($\mathbb{Z}$).
4. Consider $\mathscr{L}$⊂ $\mathbb{Z}$ is β-ℋ σ - oʹpen set. Then $\mathscr{L}$⊆ c ϑ i ϑ c⊛∗ ($\mathscr{L}$)⊆ c ϑ i σ c*σ ($\mathscr{L}$). Hence $\mathscr{L}$ is Ω-ℋO($\mathbb{Z}$) .
5. Consider $\mathscr{L}$⊂$\mathbb{Z}$ is b-ℋ σ -oʹpen . Then $\mathscr{L}$⊆ i ϑ c ∗ σ ($\mathscr{L}$) ∪c⊛∗ i ϑ ($\mathscr{L}$) ⊆ i σ c*σ ($\mathscr{L}$) ∪c ∗ σi σ ($\mathscr{L}$).
Hence $\mathscr{L}$ is $\mathscr{B}$ - ℋO($\mathbb{Z}$) .

Example 2.5. Consider $\mathbb{Z}$ = {1, 2, 3, 4, 5} ϑ = {∅, {1}, {2}, {3}, {1, 2}, {1,3,{2,3}, {1,2,3}, {1,3,4},{2,3,4}, {1,2,3,4}}, ℋ = {∅, {1}}.Then $\mathscr{L}$ ={5} is Δ -ℋO($\mathbb{Z}$) (resp. Σ- ℋO($\mathbb{Z}$), Φ-ℋO($\mathbb{Z}$), Ω-ℋO($\mathbb{Z}$), $\mathscr{B}$-ℋO($\mathbb{Z}$)) but not α-ℋ σ -oʹpen (resp. σ-ℋ σ -oʹpen , π-ℋ σ - oʹpen , β-ℋ σ -oʹpen , b-ℋ σ -oʹpen).

Proposition 2.6. Every Δ-ℋO($\mathbb{Z}$) is Σ-ℋO($\mathbb{Z}$) but not conversely.

Proof. Consider $\mathscr{L}$⊂$\mathbb{Z}$ is Δ-ℋO($\mathbb{Z}$). Then $\mathscr{L}$⊆i σ c ∗ *i σ ($\mathscr{L}$)⊆c*σ i σ ($\mathscr{L}$). Hence $\mathscr{L}$ is Σ-ℋO($\mathbb{Z}$).

Example 2.7. Consider Z={1,2,3,4,5}, ϑ={∅,{1}{2}{3}{1, 2}, {1, 3}, {2, 3}, {1,2,3}, {1,3,4}, {1,2,3}, {1,2,3,4}}, ℋ={∅, {1}}. Then $\mathscr{L}$={1, 5} is Σ-ℋO($\mathbb{Z}$) but not Δ-ℋO($\mathbb{Z}$).

Proposition 2.8. Every Δ-ℋO($\mathbb{Z}$) is Φ-ℋO($\mathbb{Z}$) but not conversely.
Proof. Consider $\mathscr{L}$⊂$\mathbb{Z}$ is Δ- ℋO($\mathbb{Z}$). Then $\mathscr{L}$⊆i σ c*σ i σ ($\mathscr{L}$)⊆i σ c*σ ($\mathscr{L}$). Hence $\mathscr{L}$ is Φ-ℋO($\mathbb{Z}$).

Example 2.9. Consider $\mathbb{Z}$={1,2,3,4}, ϑ={∅,{1, 3}{4}{1,3,4}, $\mathbb{Z}$}, ℋ={∅, {3}}. Then $\mathscr{L}$= {1, 2, 4} is Φ-ℋO($\mathbb{Z}$) but not Δ-ℋO($\mathbb{Z}$).
Theorem 2.10. In ℋ -GTS ($\mathbb{Z}$, ϑ, ℋ), the following are equivalent.
1. $\mathscr{L}$ is Δ - ℋO($\mathbb{Z}$).
2. $\mathscr{L}$ is Σ - ℋO($\mathbb{Z}$) and Φ - ℋO($\mathbb{Z}$) .

PROOF. (1) ⇒ (2). Consider $\mathscr{L}$ is Δ-ℋO($\mathbb{Z}$). Then by Proposition 2.4 and 2.6, $\mathscr{L}$ is Σ-ℋO($\mathbb{Z}$) and Φ-ℋO($\mathbb{Z}$) .
(2) ⇒ (1). Consider $\mathscr{L}$ is both Σ - ℋO($\mathbb{Z}$) and Φ-ℋO($\mathbb{Z}$). Then $\mathscr{L}$ ⊆ i σ c*σ ($\mathscr{L}$) ⊆ i σ c*σ
c*σ i σ ($\mathscr{L}$) ⊆ i σ c*σ i σ ($\mathscr{L}$). Hence $\mathscr{L}$ is Δ-ℋO($\mathbb{Z}$).

Remark 2.11. The notions of Σ-ℋO($\mathbb{Z}$) and Φ-ℋO($\mathbb{Z}$) are independent.
Example 2.12. Consider $\mathbb{Z}$={1,2,3,4,5} , ϑ={∅,{1}{2}{3}{1,2}{1,3}{2,3}{1,2,3}{1,3,4}{2,3,4}{1,2,3,4}}, ℋ={∅,{1}}. Then $\mathscr{L}$={1,3}is Σ-ℋO($\mathbb{Z}$) but not Φ-ℋO($\mathbb{Z}$) .

Example 2.13. Consider $\mathbb{Z}$={1,2,3,4}, ϑ={∅,{1,3}{4}{1,3,4}, $\mathbb{Z}$}, ℋ={∅,{3}}. Then $\mathscr{L}$={1,3,4} is Φ-ℋO($\mathbb{Z}$) but not Σ-ℋO($\mathbb{Z}$).
Proposition 2.14. Every Φ-ℋO($\mathbb{Z}$) set is Ω-ℋO($\mathbb{Z}$) but converse need not be true.
Proof. Consider $\mathscr{L}$⊂$\mathbb{Z}$ is Φ-ℋO($\mathbb{Z}$). Then $\mathscr{L}$ ⊆ i σ c*σ ($\mathscr{L}$) ⊆ c ϑ i σ c*σ ($\mathscr{L}$). Hence $\mathscr{L}$ is Ω-ℋO($\mathbb{Z}$) set.

Proposition 2.15. Every Δ-ℋO($\mathbb{Z}$) (resp. Σ-ℋO($\mathbb{Z}$) , Φ-ℋO($\mathbb{Z}$))is $\mathscr{B}$ -ℋO($\mathbb{Z}$) but not conversely.

Ramesh *et al.,*

Proof.
1. Let $\mathscr{L}$ be Δ-ℋO($\mathbb{Z}$). Then $\mathscr{L}$⊆ i σ c*σ i σ ($\mathscr{L}$)⊆c*σ i σ ($\mathscr{L}$)∪i σ c*σ ($\mathscr{L}$). Hence $\mathscr{L}$ is $\mathscr{B}$- ℋO($\mathbb{Z}$) .
2. Let $\mathscr{L}$ be Σ - ℋO($\mathbb{Z}$). Then $\mathscr{L}$⊆ c*σ i σ ($\mathscr{L}$)⊆c*σ i σ ($\mathscr{L}$)∪ i σ c*σ ($\mathscr{L}$). Hence $\mathscr{L}$ is $\mathscr{B}$-ℋO($\mathbb{Z}$) .
3. Let $\mathscr{L}$ be Φ-ℋO($\mathbb{Z}$) . Then $\mathscr{L}$⊆i σ c*σ ($\mathscr{L}$)⊆c*σ i σ ($\mathscr{L}$)∪ i σ c*σ ($\mathscr{L}$). Hence $\mathscr{L}$ is $\mathscr{B}$-ℋO($\mathbb{Z}$) .

Example 2.16. Consider $\mathbb{Z}$={1,2,3,4,5} ϑ={∅,{1},{3},{1,3},{3,4,5}, {1,3,4,5},{1,2,3, }, $\mathbb{Z}$}, ℋ={∅,{1}}. Then $\mathscr{L}$={1,4,5} is $\mathscr{B}$-ℋO($\mathbb{Z}$) but not Δ-ℋO($\mathbb{Z}$) (resp. Σ-ℋO($\mathbb{Z}$) , Φ-ℋO($\mathbb{Z}$)).

Theorem 2.17. If $\mathscr{L}$⊂ $\mathbb{Z}$ is $\mathscr{B}$ -ℋO($\mathbb{Z}$) and ϑ-σ-o´pen, then it is Σ-ℋO($\mathbb{Z}$).
Proof. Let $\mathscr{L}$ be both $\mathscr{B}$ -ℋO($\mathbb{Z}$) and μ-σ-o´pen . Then $\mathscr{L}$ ⊆ i σ c*σ ($\mathscr{L}$)∪ c*σ i σ ($\mathscr{L}$) and $\mathscr{L}$=i σ ($\mathscr{L}$). Now $\mathscr{L}$⊆i σ c*σ ($\mathscr{L}$)∪c*σ i σ ($\mathscr{L}$)⊆c*σ ($\mathscr{L}$), which implies $\mathscr{L}$⊆c*σ i σ ($\mathscr{L}$). Hence $\mathscr{L}$ is Σ-ℋO($\mathbb{Z}$).

Theorem 2.18. If $\mathscr{L}$⊂$\mathbb{Z}$ is $\mathscr{B}$-ℋO($\mathbb{Z}$) and ϑ-σ-o´pen, then it is Φ -ℋO($\mathbb{Z}$) .
Proof. Let $\mathscr{L}$ be both $\mathscr{B}$ -ℋO($\mathbb{Z}$) and μ- σ- o´pen . Then $\mathscr{L}$ ⊆ i σ c*σ ($\mathscr{L}$)∪ c*σ i σ ($\mathscr{L}$) and $\mathscr{L}$=i σ ($\mathscr{L}$). Now $\mathscr{L}$ ⊆ i σ c*σ ($\mathscr{L}$)∪c*σ i σ ($\mathscr{L}$)⊆c*σ ($\mathscr{L}$), which implies $\mathscr{L}$ ⊆ i σ ($\mathscr{L}$) ⊆ i σ cσ∗ ($\mathscr{L}$). Hence $\mathscr{L}$ is Φ - ℋO($\mathbb{Z}$).

Theorem 2.19. If $\mathscr{L}$⊂$\mathbb{Z}$ is $\mathscr{B}$ -ℋO($\mathbb{Z}$) and ϑ-σ-o´pen, then it is Δ-ℋO($\mathbb{Z}$).

Proof. Let $\mathscr{L}$ be both $\mathscr{B}$ - ℋO($\mathbb{Z}$) and μ - σ - o´pen . Then $\mathscr{L}$ ⊆ i σ c*σ ($\mathscr{L}$)∪ c*σ i σ ($\mathscr{L}$) and $\mathscr{L}$ = i σ ($\mathscr{L}$). Now $\mathscr{L}$ ⊆ i σ c*σ ($\mathscr{L}$)∪ c*σ i σ ($\mathscr{L}$)⊆c*σ ($\mathscr{L}$), which implies $\mathscr{L}$ ⊆ i σ c*σ i σ ($\mathscr{L}$). Hence $\mathscr{L}$ is Δ-ℋO($\mathbb{Z}$).

Theorem 2.20. If $\mathscr{L}$⊂$\mathbb{Z}$ is $\mathscr{B}$ -ℋO($\mathbb{Z}$) and ϑ*-c´losed, then it is Σ-ℋO($\mathbb{Z}$).

Proof. Let $\mathscr{L}$ is both $\mathscr{B}$ - ℋO($\mathbb{Z}$) and ϑ*-c´losed . Then $\mathscr{L}$ ⊆ i σ c*σ ($\mathscr{L}$)∪c*σ i σ ($\mathscr{L}$) and c*σ ($\mathscr{L}$) ⊆ c*ϑ ($\mathscr{L}$) ⊆ $\mathscr{L}$. Now $\mathscr{L}$ ⊆ i σ c*σ ($\mathscr{L}$)∪c*σ i σ ($\mathscr{L}$)⊆c*σ i σ ($\mathscr{L}$) ∪ i σ ($\mathscr{L}$) = c*σ i σ ($\mathscr{L}$). Hence $\mathscr{L}$ is Σ-ℋO($\mathbb{Z}$).

Theorem 2.21. If $\mathscr{L}$⊂$\mathbb{Z}$ is $\mathscr{B}$ -ℋO($\mathbb{Z}$) and σϑ*-c´losed, then it is Σ-ℋO($\mathbb{Z}$).

Proof. Let $\mathscr{L}$ is $\mathscr{B}$ - ℋO($\mathbb{Z}$) and σϑ*-c´losed. Then $\mathscr{L}$ ⊆i σ c*σ ($\mathscr{L}$)∪c*σ i σ ($\mathscr{L}$) and c*σ ($\mathscr{L}$) ⊆$\mathbb{Z}$, which implies i σ c*σ ($\mathscr{L}$)⊆i σ ($\mathscr{L}$). Now $\mathscr{L}$ ⊆ i σ cσ∗ ($\mathscr{L}$)∪c*σ i σ ($\mathscr{L}$)⊆ c*σ i σ ($\mathscr{L}$)∪ i σ ($\mathscr{L}$)= c*σ i σ ($\mathscr{L}$). Hence Σ- ℋO($\mathbb{Z}$).

Theorem 2.22. If $\mathscr{L}$⊂$\mathbb{Z}$ is$\mathscr{B}$ -ℋO($\mathbb{Z}$) and ϑ-σ- c´losed, then it is Σ-ℋO($\mathbb{Z}$).

Proof. Let $\mathscr{L}$ is both $\mathscr{B}$ - ℋO($\mathbb{Z}$) and ϑ- σ - c´losed. Then $\mathscr{L}$ ⊆ i σ c*σ ($\mathscr{L}$)∪ c*σ i σ ($\mathscr{L}$) and c*σ ($\mathscr{L}$) ⊆$\mathcal{L}$ by Proposition 2.9 of [5]. Which implies iσ c*σ ($\mathscr{L}$) ⊆i σ ($\mathscr{L}$). Now $\mathscr{L}$ ⊆ i σ c*σ ($\mathscr{L}$)∪c*σ i σ ($\mathscr{L}$)⊆c*σ i σ ($\mathscr{L}$) ∪ i σ ($\mathscr{L}$)=c*σ i σ ($\mathscr{L}$). Hence Σ-ℋO($\mathbb{Z}$).

Theorem 2.23. If $\mathscr{L}$⊂$\mathbb{Z}$ is $\mathscr{B}$ - ℋO($\mathbb{Z}$) such that i σ ($\mathscr{L}$)=∅ , then it is Φ-ℋO($\mathbb{Z}$) .
Proof. Let $\mathscr{L}$ be $\mathscr{B}$ - ℋO($\mathbb{Z}$) and i σ ($\mathscr{L}$) =φ. Then $\mathscr{L}$⊆i σ c*σ ($\mathscr{L}$)∪c*σ i σ ($\mathscr{L}$) =i σ cσ∗ ($\mathscr{L}$). Hence $\mathscr{L}$ is Φ - ℋO($\mathbb{Z}$).

Theorem 2.24. If $\mathscr{L}$⊂$\mathbb{Z}$ is $\mathscr{B}$-ℋO($\mathbb{Z}$) and $\mathscr{L}$∈ ℋ, then it is Σ - ℋO($\mathbb{Z}$).
Proof. Let $\mathscr{L}$ is $\mathscr{B}$ - ℋO($\mathbb{Z}$) and $\mathscr{L}$∈ℌ. Then $\mathscr{L}$ ⊆ i σ c*σ ($\mathscr{L}$)∪c*σ i σ ($\mathscr{L}$) and c*σ ($\mathscr{L}$)=$\mathscr{L}$ by Remark 2.10 of [5]. Now $\mathscr{L}$ ⊆ i σ c*σ ($\mathscr{L}$) ∪ c*σ i σ ($\mathscr{L}$) = i σ ($\mathscr{L}$) ∪ c*σ i σ ($\mathscr{L}$) = c*σ i σ ($\mathscr{L}$). Hence $\mathscr{L}$ is Σ-ℋO($\mathbb{Z}$).

Theorem 2.25. If $\mathscr{L}$⊂$\mathbb{Z}$ is $\mathscr{B}$-ℋO($\mathbb{Z}$) and ℋ=P($\mathscr{L}$) then it is $\mathscr{L}$ is Σ-ℋO($\mathbb{Z}$).
Proof. Let $\mathscr{L}$ is $\mathscr{B}$ - ℋO($\mathbb{Z}$) and ℋ = P ($\mathscr{L}$). Then $\mathscr{L}$ ⊆ i σ c*σ ($\mathscr{L}$) ∪c*σ i σ ($\mathscr{L}$) and c*σ ($\mathscr{L}$)=$\mathscr{L}$ by Remark 2.10 of [5]. Now $\mathscr{L}$ ⊆ i σ c*σ ($\mathscr{L}$) ∪ c*σ i σ ($\mathscr{L}$)=i σ ($\mathscr{L}$) ∪ c ∗ σi σ ($\mathscr{L}$) = c ∗ σi σ ($\mathscr{L}$). Hence $\mathscr{L}$ is Σ- ℋO($\mathbb{Z}$).

Theorem 2.26. If $\mathscr{L}$⊂$\mathbb{Z}$ is $\mathscr{B}$-ℋO($\mathbb{Z}$) and $\mathscr{L}$⊂$\mathcal{L}$ σ *, then it is $\mathscr{L}$ is Ω-ℋO($\mathbb{Z}$).

Ramesh *et al.*,

Proof. Let $\mathscr{L}$ is $\mathscr{B}$ -ℋO($\mathbb{Z}$) and $\mathscr{L}\subset \mathscr{L}\sigma$ *. Then $\mathscr{L}\subseteq$ i σ co∗ ($\mathscr{L}$) ∪c*σ i σ ($\mathscr{L}$) and c*σ i σ ($\mathscr{L}$)⊂c*σ i σ c*σ ($\mathscr{L}$). Now $\mathscr{L}\subseteq$ i σ c*σ ($\mathscr{L}$)∪c*σ i σ ($\mathscr{L}$) ⊆i σ c ∗ σ ($\mathscr{L}$) ∪ co∗ i σ co∗ ($\mathscr{L}$) ⊆ c ∗ σi σ c ∗ σ ($\mathscr{L}$) ⊆ cϑ∗ i σ co∗ ($\mathscr{L}$). Hence $\mathscr{L}$ is Ω-ℋO($\mathbb{Z}$).

DECOMPOSITION OF (Δ- ℋ Ψ , λ) -CONTINUITY

Definition 3.1. A map j:($\mathbb{Z}$, ϑ, ℋ)→($\mathscr{B}$, λ) is (Δ-ℋ ψ , λ) -continuous ((Δ -ℋ ψ , λ)-C), if j −1 (V) is Δ- ℋO($\mathbb{Z}$) for each λO($\mathbb{Z}$) set V in (W, λ, ℋ).

Definition 3.2. A map j:($\mathbb{Z}$, ϑ, ℋ)→ ($\mathscr{B}$, λ) is (Σ- ℋ ψ , λ) -continuous ((Σ -ℋ ψ , λ) - C), if j −1 (V) is Σ- ℋO($\mathbb{Z}$) for each λO($\mathbb{Z}$) set V in (W, λ, ℋ).

Definition 3.3. A map j:($\mathbb{Z}$, ϑ, ℋ)→ ($\mathscr{B}$, λ) is (Φ-ℋ ψ , λ) -continuous ((Φ-ℋ ψ , λ)-C), if j −1 (V) is Φ-ℋO($\mathbb{Z}$) for each λO($\mathbb{Z}$) set V in (W, λ, ℋ).

Proposition 3.4. Every (Δ-ℋ ψ , λ)-C is (Σ-ℋ ψ , λ)- C but not conversely.

Proof. Consider the map j:($\mathbb{Z}$,ϑ,ℋ)→($\mathscr{B}$,λ) be a (Δ-ℋ ψ , λ)-C. Then j −1 (V) is Δ-ℋO($\mathbb{Z}$) for each λO($\mathbb{Z}$) set V in ($\mathscr{B}$, λ, ℋ). By Proposition 2.6, j −1 (V) is Σ-ℋO($\mathbb{Z}$). Hence, j is (Σ-ℋ ψ , λ)-C.

Example 3.5. Consider $\mathbb{Z}$={1,2,3,4,5}, ϑ={∅,{1},{2},{3},{1,2},{1, 3,{2,3,{1,2,3,{1,3,4, {2, 3, 4}, {1, 2, 3, 4}}, λ={∅,{1,2}}and ℋ={∅,{1}}. Then, the identity map j:($\mathbb{Z}$,ϑ,ℋ)→($\mathscr{B}$, λ) is (Σ-ℋ ψ , λ)-C and but not (Δ-ℋ ψ , λ)-C .

Proposition 3.6. Every (Δ-ℋ ψ , λ)-C is (Φ-ℋ ψ , λ)-C but not conversely.

Proof. Consider the map j:($\mathbb{Z}$,ϑ,ℋ)→($\mathscr{B}$,λ,ℋ) be a (Δ-ℋ ψ , λ)-C. Then j −1 (V) is Δ- ℋO($\mathbb{Z}$) for each λO($\mathbb{Z}$) set V in ($\mathscr{B}$, λ, ℋ). By Proposition 2.8, j −1 (V) is Φ - ℋO($\mathbb{Z}$) . Hence, j is (Φ-ℋ ψ , λ)-C.

Example 3.7. Consider $\mathbb{Z}$={1,2,3,4}, ϑ={∅, {1,3}, {4}, {1,3,4}, $\mathbb{Z}$}, λ={∅, {1,3,4}}, ℋ={∅,{3}}. Then the identity map j:($\mathbb{Z}$, ϑ, ℋ)→($\mathscr{B}$, λ) is (Φ-ℋ ψ , λ)-C but not (Δ-ℋ ψ , λ)-C .

Remark 3.8. The notions of (Σ-ℋ ψ , λ)-C and (Φ-ℋ ψ , λ)-C are independent.

Example 3.9. Consider $\mathbb{Z}$={1,2,3,4,5}, ϑ={∅,{1},{2},{3},{1,2},{1,3}, {2,3},{1,2,3},{1,3,4}, {2,3,4}, {2,3,4,5}}, λ={∅, {2,3}} and ℋ={∅,{5}}. Then, the identity map j:($\mathbb{Z}$,ϑ,ℋ)→($\mathscr{B}$, λ) is (Σ-ℋ ψ , λ)-C but not (Φ-ℋ ψ , λ)-C .

Example 3.10. Consider $\mathbb{Z}$={1,2,3,4}, ϑ={∅,{1, 3},{3},{1,3,4}, $\mathbb{Z}$} , λ={∅,{1,3,4}}, ℋ={∅,{3}}. Then, the identity map j :($\mathbb{Z}$, ϑ, ℋ)→($\mathscr{B}$, λ) is (Φ-ℋ ψ , λ)-C but not (Σ-ℋ ψ , λ)-C.

Theorem 3.11. For a map j: ($\mathbb{Z}$, ϑ, ℋ)→($\mathscr{B}$, λ, ℋ), the following results are equivalent.
1. j is (Δ- ℋ ψ , λ)-C .
2. j is (Σ-ℋ ψ , λ)-C and (Φ-ℋ ψ , λ)-C .

Proof. (1)⇒(2): Follows from the Proposition 3.4 and Proposition 3.6.
(2)⇒(1): Consider the map j:($\mathbb{Z}$, ϑ, ℋ)→($\mathscr{B}$, λ, ℋ) be (Σ-ℋ ψ , λ)-C and (Φ-ℋ ψ , λ) - C. Then
j −1 (V) is Σ-ℋO($\mathbb{Z}$) and Φ-ℋO($\mathbb{Z}$) for each λO($\mathbb{Z}$). By Theorem 2.10, j −1 (V) is Δ-ℋO($\mathbb{Z}$). Hence, j is (Δ-ℋ ψ , λ)-C.

CONCLUSION

In this paper, we introduced Δ-ℋO($\mathbb{Z}$), Σ-ℋO($\mathbb{Z}$), Φ-ℋO($\mathbb{Z}$), Ω- ℋO($\mathbb{Z}$) and $\mathscr{B}$-ℋO($\mathbb{Z}$) sets and obtained decomposition of (Δ-ℋ ψ , λ)-C. In future work we will introduce new types of generalized open sets related to these sets and obtain new decomposition of (ϑ, λ)-C .

REFERENCES

1. Ahmad AI-Omari and Mohd. Salmi Md. Noorani, Decomposition of continuity via b-open set, Bol. Soc. Paran. Mat., 26(1-2)(2008), 53-64.
2. A. Csaszar, Generalized topology, generalized continuity, Acta Math. Hungar., 96(2002), 351-357.
3. A. Csaszar, Generalized open sets in generalized topologies, Acta Mathematica Hungarica., 106(2005), 53-56.
4. A. Csaszar, Modification of generalized topologies via hereditary classes, Acta Mathematica Hungarica., 115, (2007), 29-36.
5. M. Rajamani, V. Inthumathi and R. Ramesh, Some new generalized topologies via hereditary classes, Bol. Soc. Paran. Mat., 30(2) (2012), 71-77.
6. M. Rajamani, V. Inthumathi and R. Ramesh, A decomposition of (μ, λ) – continuity in generalized topological spaces, Jordan Journal of Mathematics and Statistics, 6(1)(2013), 15 - 27.
7. A. AI-Omari, M. Rajamani and R. Ramesh, A - Expansion continuous maps and (A, B) -weakly continuous maps in hereditary generalized topological spaces, Scientific Studies and Research, 23(2) (2013), 13-22.
8. R. Ramesh and R. Mariappan Generalized open sets in hereditary generalized topological spaces, J. Math. Comput. Sci., 5(2) (2015), 149-159.
9. R. Ramesh and Ahmad AI-Omari, b - H σ -open sets in HGTS, Poincare Journal of Analysis and Applications 9(1) (2022), 31-40.
10. R. Ramesh and Ahmad AI-Omari Decomposition of $(\alpha$ - H σ , $\lambda)$ -continuity, Poincare Journal of Analysis and Applications 10(1) (2023), 155-163.
11. R. Ramesh, Decomposition of $(\kappa\mu *$, $\lambda)$ - continuity, Journal of Xi'an University of Architecture and Technology, 11(VI), (2020), 2095-2101.
12. M.S. Sarsak, On some properties of Generalized open sets in Generalized topological spaces, Demonstratio Math. (2013).

RESEARCH ARTICLE

Metric Dimension of BG₂(G) in an Algorithmic Aspect

Sameerali C.P [1]* and Sameena K[2]

[1]Research Scholar, PG and Research Department of Mathematics, MES Mampad College, Mampad, Kerala, India.
[2]PG and Research Department of Mathematics, MES Mampad College, Mampad, Kerala, India.

*Address for Correspondence
Sameerali C.P
Research Scholar,
PG and Research Department of Mathematics,
MES Mampad College,
Mampad, Kerala, India.
E.Mail: sameercup@yahoo.com

ABSTRACT

Let G be a simple connected graph with V as its vertex set and E as its edge set. Boolean graph $BG_2(G)$ is the graph with vertex set $V \cup E$ and two vertices of $BG_2(G)$ are adjacent if and only if they are adjacent vertices of G or represent an edge incident with the vertex in G or represent two non-adjacent edges of G. In this paper, a theorem and an algorithm based on that theorem is set to obtain the metric dimension of $BG_2(G)$, a metric base, the adjacency matrix and the distance matrix of $BG_2(G)$

Keywords: Boolean graph $BG_2(G)$algorithms, metric base ,metric dimension,

INTRODUCTION

In today's fast-paced world, it is important to study the development of networks and hence the study of graphs like $BG_2(G)$ is trending. A graph G and $BG_2(G)$ are given below.
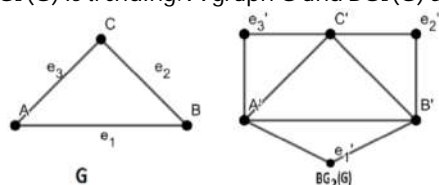
A vertex g is said to resolve another vertices h and k If $d(h, g) \neq d(k, g)$.If $W \subseteq V$ contains a resolving vertex for every pair of vertices of G then W is said to be a resolving set. If $W=\{W_1,W_2,…W_K\}$ is a resolving set then every vertex can be uniquely identified by a code,

64200

$C_W(u) = (d(u_1, w_1)...., d(u_2, w_2), \cdots, d(u, w_k))$. $C_W(u)$ is known as the metric code or location code of u [5].Codes of W_i's are all different since the i th component is zero and others are non zeros. Every superset of a resolving set is a resolving set so a graph can have more than one resolving set.

A metric base is a resolving set with minimum cardinality. Cardinality of a metric base is called the metric dimension of G, denoted by $\beta(G)$ [5]. The vertices of $BG_2(G)$ corresponding to vertices of G are known as point vertices and that correspond to edges of G are called line vertices. "If the number of vertices of G is more than four then the distance between two point vertices is either one or two or three, distance between two line vertices is one or two and the distance between a point vertex and a line vertex is either one or two" [1].

RESULTS AND DISCUSSION

Theorem 1: Collection of point vertices is a resolving set for $BG_2(G)$

Proof:- let $S = \{P_1, P_2 \ldots\ldots P_\alpha\}$ be the set of point vertices and $T = \{Q_1, Q_2 \ldots, Q_Q\}$ be the set of line vertices. The metric codes, $C_S(P_i)$, are all different since i th component of the code is zero and the rest are non-zero. Metric code of Q_j, $C_S(Q_j)$, are also different because in every code 1's occur exactly at two positions and the remaining positions are numbers other than 1. Positions of these 1's will vary from line vertex to line vertex as they appear in places of vertices corresponding to that line vertex. Hence all vertices have different codes.

The algorithm

Algorithms play a vital role in modern computing. In this section, using the fact in theorem 1, an algorithm is established to obtain metric dimension of $BG_2(G)$a metric base for $BG_2(G)$, adjacency matrix of $BG_2(G)$ and the distance matrix of $BG_2(G)$. The graph considered in the algorithm is a simple connected undirected graph with more than two vertices. Number of vertices and upper triangular part of the adjacency matrix are to be given as inputs. Theorem 1 plays a crucial in the algorithm.

Step 1: Start.
Step 2: Declare two dimensional arrays; a ,b and d
Declare the integer variables; e=0, n, r, i , j, k, flag=0.
Step 3: Read n>1; 1, the number of vertices in G.
Step 4: For i and j from 0 to n-1, read a ij for i>j "if aij=1" is to be deleted from the end of the line , the upper triangular part of adjacency Matrix of G. If a ij =1,

If $a_{ij}=1$,
{
$e=e+1, d_{ij}=1, b_{ij}=1$,
$b_{i,n+e-1}=1, b_{j,n+e-1}=1$,
$d_{i,n+e-1}=1, d_{j,n+e-1}=1$.
For k= 0to k= n-1,
If k is different from i and j,
then, set $b_{k,n+e-1}=0, d_{k,n+e-1}=2$.
For g=n tog=n+e-1,
If $b_{ig}=0$ and $b_{jg}=0$,
Then set $b_{n+e-1,g}=1$ and $d_{n+e-1,g}=1$.
else,
$b_{n+e-1,g}=0$ and $d_{n+e-1,g}=2$.
}
If $a_{ij}=0$, then set $b_{ij}=0$.

Sameerali and Sameena

Step 5: for i from 1 to n-1…. to n-1,
If $a_{ij}=0$
For K=0 to n-1
{
If $b_{ik}=1$ and $b_{jk}=1$, then set $d_{ij}=2$, break.
If k=n-1 then set $d_{ij}=3$.
}

Step 6: For i from 0 to n+e-1 and j from i to n+e-1
Set $a_{ii}=0, b_{ii}=0, d_{ii}=0. a_{ji}=a_{ij}, b_{ji}=b_{ij}, d_{ji}=d_{ij}$.

Step 7: For r=2 to r=n,
{
For k=1 to $n+eC_r$
{

Consider each $^{n+e}C_r$ combinations of vertices of $BG_2(G)$. Let the kth combination

be $(v_{\alpha_1}, v_{\alpha_2}, \cdots, v_{\alpha_r})$

Let $v_{\beta_1}, v_{\beta_2} \ldots, v_{\beta_{n+e-r}}$ be the vertices out side the current combination.
If r=n-1 then go to Step 8
ag=0
For i=1 to n+e-r
{
If flag =1, break;
For j=i+1 to n+e-r
{
if $(d_{\beta i\alpha_1}, d_{\beta i\alpha_2}, \ldots, d_{\beta i\alpha_r}) = (d_{\beta j\alpha_1}, d_{\beta j\alpha_2}, \ldots, d_{\beta j\alpha_r})$
{flag=1, break}
if(j=n+e-r) goto Step8
}
}
}
}
Step 8: Print $[b_{ij}]$-Adjacency matrix of $BG_2(G)$.
Print $[d_{ij}]$-Distance matrix of $BG_2(G)$.
Print r-Metric Dimension of $BG_2(G)$.
Print $\{v_{\alpha_1}, v_{\alpha_2}, \cdots, v_{\alpha_r}\}$ - Metricbase of $BG_2(G)$.

Step 9: Stop

Example: Let $G=P_3$

Input
Enter the number of vertices of the simple connected Graph G with more than 2 vertices 3
Enter the upper triangular part of the adjacency matrix of G excluding the diagonal elements.

1
0
1

Output

Adjacency matrix of $BG_2(G)$

	V0	V1	V2	V3	V4
V0	0	1	0	1	0
V1	1	0	1	1	1
V2	0	1	0	0	1
V3	1	1	0	0	0
V4	0	1	1	0	0

Distance matrix of $BG_2(G)$

	V0	V1	V2	V3	V4
V0	0	1	2	1	2
V1	1	0	1	1	1
V2	2	1	0	2	1
V3	1	1	2	0	2
V4	2	1	1	2	0

Metric dimension=2
A resolving set is { v0, v2 }

REFERENCES

1. T N Janakiraman, M Bhanumathi and S Muthamai, Eccentric proper- ties of the Boolean graphs **B**$G_2(G)$ and $BG_3(G)$ International Journal of Engineering Science , Advanced computing and Bio technology, (Vol 4 No. 2 ,January March 2013, pp 32 - 42)
2. C.P Sameerali and K. Sameena ,On properties of Boolean graph $BG_2(G)$ Advances in Mathematics: Scientific journal , (9-2020, pp 1845 - 1850)
3. Buckley F and Harary F , Distance in Graphs, Addition Wesley publishing company(1990)
4. Harary F, Graph theory, Addition Wesley publishing company Reading, Mass(1972)
5. Harary, F., and Melter, R. A. (1976) On the Metric dimension of a Graph, Ars Combinatoria, 2, 191 to 195.

RESEARCH ARTICLE

Decomposition of (αH b , δ) -Continuity

R.Ramesh[1] and R.Uma[2]*

[1]Department of Science and Humanities, Dr.Mahalingam College of Engineering and Technology Pollachi, Coimbatore, Tamil Nadu,
[2]Department of Mathematics, Sree Saraswathi Thyagaraja College, Pollachi, Coimbatore, TamilNadu, India.

*Address for Correspondence
R.Uma
Department of Mathematics,
Sree Saraswathi Thyagaraja College,
Pollachi, Coimbatore, Tamil Nadu, India.
E.Mail: ramumaraj@gmail.com

ABSTRACT

This article, explores and introduces the variety of H - GT S –open sets in H-GTS. Additionally, the following is obtained: The decomposition of $(\alpha\ H_b,\delta)$-C.

Keywords: ℋ-GTS, α- H$_b$-open, π- H$_b$-open and π- H$_b$-open sets.

2000 Mathematics Subject Classification: 54A05.

INTRODUCTION

Let ϑ be the collection of all the subsets of $\mathbb{Z}$, which is an on empty set $\mathbb{Z}$. Then ϑ is called a generaliZed topology (briefly GT)[1], if f∅∈ϑ and U$_J$∈ϑ for j ∈**J** implies U =$\bigcup_{j\in J}$ U$_J$∈ϑ.. The closure of a subset B of $\mathbb{Z}$ is shown by the symbolc $_\vartheta$(B)is the smallest closed set counting B and i$_\vartheta$(B)is the interior of B are called the greatest ϑ-ópen sets in are included in B.

Definition1.1. AsubsetB⊂$\mathbb{Z}$iscalled

1. ϑ-α-ópen[2], if B⊂i$_\vartheta$c$_\vartheta$i$_\vartheta$(B).
2. ϑ-σ-ópen[2], if B⊂c$_\vartheta$i$_\vartheta$(B).
3. ϑ-π-ópen[2], if B⊂i$_\vartheta$c$_\vartheta$(B).
4. ϑ-β-ópen[2], if B⊂c$_\vartheta$i$_\vartheta$c$_\vartheta$(B).
5. ϑ-b-ópen[12],ifB⊂c$_\vartheta$i$_\vartheta$(B)∪i$_\vartheta$c$_\vartheta$(B).

Definition 1.2.A hereditary class [4] is described as ℋ of subsets of $\mathbb{Z}$, where L∈ ℋ and V⊂ L, and where V ∈ ℋ otherwise.

64204

Definition 1.3. Regarding a hereditary class $\mathcal{H}$ on $\mathscr{L}$ and $\mathscr{L}\subset\mathbb{Z}$, we define $\mathscr{L}^{*}(\mathcal{H},\vartheta)=\{z\in\mathbb{Z}:\mathscr{L}\cap V\notin\mathcal{H}$ for all $V\in\vartheta$ such that $a\in V\}$ [4].

Definition 1.4.[5] Let $\mathscr{L}\subset\mathbb{Z}$. Then $\mathscr{L}^{*}{}_{\sigma}(\mathcal{H},\vartheta)=\{z\in\mathbb{Z}:\ \mathscr{L}\cap V\notin\mathcal{H}$ for all $V\in\vartheta$-σ-ópen such that $\mathbb{Z}\in V\}$ and $c^{*}{}_{\sigma}(\mathscr{L})=\mathscr{L}\cup\mathscr{L}^{*}_{\sigma}.$

Definition1.5. A subset $\mathscr{L}\subset\mathbb{Z}$ is called

1. α-H-ópen[4], if$\mathscr{L}\subseteq$ i$_\vartheta$c$^{*}_\vartheta$ i$_\vartheta(\mathscr{L})$,
2. σ-H-ópen[4], if$\mathscr{L}\subseteq$c$^{*}_\vartheta$ i$_\vartheta(\mathscr{L})$,
3. π-H-ópen[4], if$\mathscr{L}\subseteq$ i$_\vartheta$c$^{*}_\vartheta(\mathscr{L})$,
4. β-H-ópen[4], if$\mathscr{L}\subseteq$c$_\vartheta$ i$_\vartheta$c$^{*}_\vartheta(\mathscr{L})$,
5. ϑ-ćlosed[4], ifc$^{*}_\vartheta(\mathscr{L})\subset\mathscr{L}$.
6. b-H-ópen[8], if$\mathscr{L}\subseteq$ i$_\vartheta$ c$^{*}_\vartheta$ $\mathscr{L})\cup$c$^{*}_\vartheta$ i$_\vartheta(\mathscr{L})$,
7. $\sigma\vartheta^{*}$-ćlosed[5], if$\mathscr{L}^{*}_\sigma\subseteq\mathscr{L}$

Definition1.6. A sub set $\mathscr{L}\subset\mathbb{Z}$ is said to be

1. α-H$_\sigma$-ópen[10], if$\mathscr{L}\subseteq$ i$_\vartheta$c$^{*}_\sigma$ i$_\vartheta(\mathscr{L})$,
2. σ-H$_\sigma$-ópen[10], if$\mathscr{L}\subseteq$c$^{*}_\sigma$ i$_\vartheta(\mathscr{L})$,
3. π-H$_\sigma$-ópen[10], if$\mathscr{L}\subseteq$ i$_\vartheta$c$^{*}_\sigma(\mathscr{L})$,
4. β-H$_\sigma$-ópen[10], if$\mathscr{L}\subseteq$c$_\vartheta$ i$_\vartheta$c$^{*}_\sigma(\mathscr{L})$.
5. b-H$_\sigma$-ópen[9], if$\mathscr{L}\subseteq$ i$_\vartheta$c$^{*}_\sigma(\mathscr{L})\cup$c$^{*}_\sigma$i$_\vartheta(\mathscr{L})$.

Definition 1.6. Consider B to be a part of $\mathcal{H}$-GTS$(\mathbb{Z},\vartheta,\mathcal{H})$. Then B$^{*}_b(\mathcal{H},\vartheta)=\{\mathbb{Z}\in\mathbb{Z}:$ B$\cap V\notin\mathcal{H}$ for all $V\in\vartheta$-b-open such that $\mathbb{Z}\in V\}$.

Consider$(\mathbb{Z},\vartheta,\mathcal{H})$ be a $\mathcal{H}$ -GTS for B$\subset\mathbb{Z}$, define c$^{*}_b$(B)=B$\cup$B$^{*}_b(\mathcal{H},\vartheta)$ and c$_b$ (B) is enlarging, monotone an didempotent.

Generalized $\mathcal{H}_b$- open sets
Definition 2.1. A subset B of $\mathcal{H}$-GTS $(\mathbb{Z},\vartheta,\mathcal{H})$ is called as

6. α-$\mathcal{H}_b$-open, ifB$\subseteq$i$_\vartheta$c$^{*}_b$i$_\vartheta$(B)
7. σ-$\mathcal{H}$b-open, ifB$\subseteq$c$^{*}_b$(i$_\vartheta$(B)
8. π-$\mathcal{H}_b$-open, ifB$\subseteq$i$_\vartheta$c$^{*}_b$(B)
9. β-$\mathcal{H}_b$-open, ifB$\subseteq$c$_\vartheta$i$_\vartheta$c$^{*}_b$($_b$(B)
10. b-$\mathcal{H}_b$-open, ifA$\subseteq$i$_\vartheta$c$^{*}_b$(A)$\cup$c$^{*}_b$i$_\vartheta$(A).

The sets α-$\mathcal{H}$ b-pen (resp. σ-$\mathcal{H}$ b-open, π-$\mathcal{H}_b$-open, β-$\mathcal{H}_b$-open, b-$\mathcal{H}_b$-open, ϑ-open) denoted by α-$\mathcal{H}_b$ O$(\mathbb{Z})$ (resp.σ-$\mathcal{H}_b$O$(\mathbb{Z})$,π-$\mathcal{H}_b$O$(\mathbb{Z})$,β-$\mathcal{H}_b$O$(\mathbb{Z})$,b-$\mathcal{H}_b$O$(\mathbb{Z})$,ϑO$(\mathbb{Z})$)).

Theorem2.2. In $\mathcal{H}$-GTS $(\mathbb{Z},\vartheta,\mathcal{H})$:

1. Any $\vartheta O(\mathbb{Z})$ set is α-$\mathcal{H}_bO(\mathbb{Z})$.
2. Any $\vartheta O(\mathbb{Z})$ set is σ-$\mathcal{H}_bO(\mathbb{Z})$.
3. Any $\vartheta O(\mathbb{Z})$ set is π-$\mathcal{H}_bO(\mathbb{Z})$.
4. Any $\vartheta O(\mathbb{Z})$ set is β-$\mathcal{H}_bO(\mathbb{Z})$.
5. Any $\vartheta O(\mathbb{Z})$ set is b-$\mathcal{H}_bO(\mathbb{Z})$.

Proof.(1). Consider a subset B of$\mathcal{H}$-GTS $(\mathbb{Z},\vartheta,\mathcal{H})$ is $\vartheta O(\mathbb{Z})$. Then $B \subseteq i_\vartheta(B) \subseteq i_\vartheta c_b^*(B) \subseteq i_\vartheta c_b i_\vartheta(B)$. Hence B is α-$\mathcal{H}_bO(\mathbb{Z})$.

(2).   Consider a subset B of $\mathcal{H}$-GTS $(\mathbb{Z},\vartheta,\mathcal{H})$ is $\vartheta O(\mathbb{Z})$. Then, $B \subseteq i_\vartheta(B) \subseteq c_b^* i_\vartheta(B)$. Hence B is σ-$\mathcal{H}_bO(\mathbb{Z})$.

(3).   Consider a subset B of $\mathcal{H}$-GTS $(\mathbb{Z},\vartheta,\mathcal{H})$ is $\vartheta O(\mathbb{Z})$. Then, $B \subseteq i_\vartheta(B) \subseteq i_\vartheta c_b^*(B)$. Hence B is π-$\mathcal{H}_bO(\mathbb{Z})$.

(4).   Consider a subset B of $\mathcal{H}$-GTS $(\mathbb{Z},\vartheta,\mathcal{H})$ is $\vartheta O(\mathbb{Z})$. Then, $B \subseteq i_\vartheta(B) \subseteq c_\vartheta i_\vartheta c_b^*(B)$. Hence B is β-$\mathcal{H}_bO(\mathbb{Z})$.

(5).   Consider a subset B of $\mathcal{H}$-GTS $(\mathbb{Z},\vartheta,\mathcal{H})$ is $\vartheta O(\mathbb{Z})$. Then, $B \subseteq i_\vartheta(B) \subseteq i_\vartheta c_b(B) \subseteq i_\vartheta c_b(B) \cup c_b^* i_\vartheta(B)$. Hence, B is b-$\mathcal{H}_bO(\mathbb{Z})$.

Example2.3. Consider $\mathbb{Z}=\{1,2,3,4\}$ $\vartheta=\{\emptyset,\{1\},\{2\},\{1,2\},\{2,3,4\},\mathbb{Z}\}$, $\mathcal{H}=\{\emptyset,\{1\}\{3\}\}$. Then $\mathscr{B}=\{1,2,3\}$ is $\mathscr{B}$ is α-$\mathcal{H}_bO(\mathbb{Z})$. (resp. β-$\mathcal{H}_bO(\mathbb{Z})$, σ-$\mathcal{H}_bO(\mathbb{Z})$, π-$\mathcal{H}_bO(\mathbb{Z})$, β-$\mathcal{H}_bO(\mathbb{Z})$, b-$\mathcal{H}_bO(\mathbb{Z})$)
But not$\vartheta O(\mathbb{Z})$.

Theorem2.4. In$\mathcal{H}$-GTS $(\mathbb{Z},\vartheta,\mathcal{H})$:

1. Any α-$\mathcal{H}_bO(\mathbb{Z})$ is ϑ-α-open.
2. Any σ-$\mathcal{H}_bO(\mathbb{Z})$ is ϑ-σ-open.
3. Any π-$\mathcal{H}_bO(\mathbb{Z})$ is ϑ-π-open.
4. Any β-$\mathcal{H}_bO(\mathbb{Z})$ is ϑ-β-open.
5. Any b-$\mathcal{H}_bO(\mathbb{Z})$ is ϑ-b-open.

Proof.

1.   Consider $\mathscr{B}$ be α-$\mathcal{H}_bO(\mathbb{Z})$. Then we have, $\mathscr{B} \subseteq i_\vartheta c_b^* i_\vartheta(\mathscr{B}) \subseteq i_\vartheta c^*_\vartheta i_\vartheta(\mathscr{B}) \subseteq i_\vartheta c_\vartheta i_\vartheta(\mathscr{B})$. Hence, $\mathscr{B}$ is ϑ-α-open.

2.   Consider $\mathscr{B}$ beσ-$\mathcal{H}_bO(\mathbb{Z})$. Then, $\mathscr{B} \subseteq c_b^* i_\vartheta(\mathscr{B}) \subseteq c^*_\vartheta i_\vartheta(\mathscr{B}) \subseteq c_\vartheta i_\vartheta(\mathscr{B})$. Hence, $\mathscr{B}$ isϑ-σ-open.

3.   Consider $\mathscr{B}$ be π-$\mathcal{H}_bO(\mathbb{Z})$. Then we have, $\mathscr{B} \subseteq i_\vartheta c_b^*(\mathscr{B}) \subseteq i_\vartheta c^*_\vartheta(\mathscr{B}) \subseteq i_\vartheta c_\vartheta(\mathscr{B})$. Hence, $\mathscr{B}$ isϑ-π-open.

4.   Consider $\mathscr{B}$ be β-$\mathcal{H}_bO(\mathbb{Z})$. Then we have, $\mathscr{B} \subseteq c_\vartheta i_\vartheta c_b^*(\mathscr{B}) \subseteq c_\vartheta i_\vartheta c^*_\vartheta(\mathscr{B}) \subseteq c_\vartheta i_\vartheta c_\vartheta(\mathscr{B})$. Hence $\mathscr{B}$ is ϑ-β-open.

5.   Consider $\mathscr{B}$ be b-$\mathcal{H}_b O(\mathbb{Z})$. Then we have, $\mathscr{B} \subseteq i_\vartheta c_b^*(\mathscr{B}) \cup c_b^* i_\vartheta(\mathscr{B}) \subseteq i_\vartheta c^*_\vartheta(\mathscr{B}) \cup c^*_\vartheta i_\vartheta(\mathscr{B}) \subseteq i_\vartheta c_\vartheta(\mathscr{B}) \cup c_\vartheta i_\vartheta(\mathscr{B})$. Hence, $\mathscr{B}$ isϑ-b-open.

Example 2.5. Consider $\mathbb{Z}=1,2,3,4,5$, $\vartheta=\{\emptyset,\{1\},\{2\},\{3\},\{1,2\},\{1,3\},\{2,3\},\{1,2,3\},\{1,2,4\},\{2,3,4\},\{1,2,3,4\}\}$, $\mathcal{H}=\{\emptyset,\{1\}\}$. Then $\mathscr{B}=\{1,2,4\}$ is ϑ-α-open(resp. ϑ-σ-open)but not α-$\mathcal{H}_bO(\mathbb{Z})$. (resp.$\sigma$-$\mathcal{H}_bO(\mathbb{Z})$.)and $C=\{3,4\}$ is ϑ-π-open but not π-$\mathcal{H}_bO(\mathbb{Z})$.

Example 2.6. Consider $\mathbb{Z}=\{1,2,3,4,5\}$ $\vartheta=\{\emptyset,\{1\},\{3\},\{1,2\},\{1,3\},\{1,2,3\},\{1,3,4,5\},\{2,3,4,5\},\mathbb{Z}\}$, $\mathcal{H}=\{\emptyset,\{1\},\{4\}\}$. Then $\mathscr{B}=\{1,4\}$ is ϑ-β-open but not β-$\mathcal{H}_bO(\mathbb{Z})$.

Example2.7. Consider $\mathbb{Z}=\{1,2,3,4,5\}$
$\vartheta=\{\emptyset,\{1\},\{2\},\{3\},\{1,2\},\{1,3\},\{2,3\},\{1,2,3\},\{1,3,4\},\{2,3,4\},\{1,2,3,4\}\}$,$\mathcal{H}=\{\emptyset,\{1\}\}$.Then $\mathcal{B}=\{5\}$is ϑ-b-open(resp. b-$\mathcal{H}$-open) but not b-$\mathcal{H}_bO(\mathbb{Z})$.

Theorem2.8. In$\mathcal{H}$-GTS $(\mathbb{Z},\vartheta,\mathcal{H})$:
1.　　　Any α-$\mathcal{H}_bO(\mathbb{Z})$is α-$\mathcal{H}_\sigma$-ópen.
2.　　　Any σ-$\mathcal{H}_bO(\mathbb{Z})$is σ-$\mathcal{H}_\sigma$-ópen.
3.　　　Any π-$\mathcal{H}_bO(\mathbb{Z})$is π-$\mathcal{H}_\sigma$-ópen.
4.　　　Any β-$\mathcal{H}_bO(\mathbb{Z})$is β-$\mathcal{H}_\sigma$-ópen.
5.　　　Any b-$\mathcal{H}_bO(\mathbb{Z})$is b-$\mathcal{H}_\sigma$-ópen.

Proof.

1.　　　Consider $\mathcal{B}$ be α-$\mathcal{H}_bO(\mathbb{Z})$.Then we have, $\mathcal{B}$i$_\mathcal{s}$c$_b^*$i$_\mathcal{s}(\mathcal{B})\subseteq$i$_\mathcal{s}c_\sigma^*i_\mathcal{s}(\mathcal{B})$.Hence α-$\mathcal{H}_\sigma$-ópen.

2.　　　Consider $\mathcal{B}$ be σ-$\mathcal{H}bO(\mathbb{Z})$.Then we have, $\mathcal{B}\subseteq$c$_b^*$i$_\mathcal{s}(\mathcal{B})\subseteq$c$_\sigma^*i_\mathcal{s}(\mathcal{B})$.Hence $\mathcal{B}$ isσ-$\mathcal{H}_\sigma$-ópen.

3.　　　Consider $\mathcal{B}$ be π-$\mathcal{H}bO(\mathbb{Z})$.Then we have ,$\mathcal{B}\subseteq$i$_\mathcal{s}c_b^*(\mathcal{B})\subseteq$i$_\mathcal{s}c_\sigma^*(\mathcal{B})$.Hence $\mathcal{B}$ isπ-$\mathcal{H}_\sigma$-ópen.

4.　　　Consider $\mathcal{B}$ be β-$\mathcal{H}bO(\mathbb{Z})$.Then we have, $\mathcal{B}\subseteq$c$_\mathcal{s}$i$_\mathcal{s}$c$_b^*$(B)$\subseteq$c$_\mathcal{s}$i$_\mathcal{s}$c$_\sigma^*(\mathcal{B})$.Hence$\mathcal{B}$ is　β-$\mathcal{H}_\sigma$-ópen.

5.　　　Consider $\mathcal{B}$ be b-$\mathcal{H}bO(\mathbb{Z})$.Then we have, $\mathcal{B}\subseteq$i$_\mathcal{s}$c$_b^*(\mathcal{B})\cup$c$_b$i$_\mathcal{s}(\mathcal{B})\subseteq$i$_\mathcal{s}c_\sigma^*(\mathcal{B})\cup$c$_\sigma^*i_\mathcal{s}(\mathcal{B})$.Hence $\mathcal{B}$isb-$\mathcal{H}_\sigma$-ópen.

Theorem2.9. In $\mathcal{H}$-GTS $(\mathbb{Z},\vartheta,\mathcal{H})$:

1.　　　Any α-$\mathcal{H}_bO(\mathbb{Z})$ is α-$\mathcal{H}$-open.
2.　　　Any σ-$\mathcal{H}_bO(\mathbb{Z})$ is σ-$\mathcal{H}$-open.
3.　　　Any π-$\mathcal{H}_bO(\mathbb{Z})$ is π-$\mathcal{H}$-open.
4.　　　Any β-$\mathcal{H}_bO(\mathbb{Z})$ is β-$\mathcal{H}$-open.
5.　　　Any b-$\mathcal{H}_bO(\mathbb{Z})$ is b-$\mathcal{H}$-open.

Proof.

1.　　　Consider $\mathcal{B}$be aα-$\mathcal{H}_bO(\mathbb{Z})$set. Then wehave,$\mathcal{B}\subseteq$i$_\mathcal{s}c_b^*i_\mathcal{s}(\mathcal{B})\subseteq$i$_\mathcal{s}c_\mathcal{S}i_\mathcal{s}(\mathcal{B})$.Hence $\mathcal{B}$ is α-$\mathcal{H}$-open.

2.　　　Consider $\mathcal{B}$ be a α-$\mathcal{H}_bO(\mathbb{Z})$set. Then we have, $\mathcal{B}\subseteq$c$_b^*$i$_\mathcal{s}(\mathcal{B})\subseteq$c$_\mathcal{S}^*i_\mathcal{s}(\mathcal{B})$.Hence $\mathcal{B}$ is σ-$\mathcal{H}$-open.

3.　　　Consider $\mathcal{B}$ be a α-$\mathcal{H}bO(\mathbb{Z})$set. Then we have, $\mathcal{B}\subseteq$i$_\mathcal{s}$c$_b^*(\mathcal{B})\subseteq$i$_\mathcal{s}c_\mathcal{S}(\mathcal{B})$.Hence $\mathcal{B}$ is π-$\mathcal{H}$-open.

4.　　　Consider $\mathcal{B}$ be a α-$\mathcal{H}_bO(\mathbb{Z})$set. Then wehave, $\mathcal{B}\subseteq$c$_\mathcal{s}$i$_\mathcal{s}$c$_b^*(\mathcal{B})\subseteq$c$_\mathcal{s}i_\mathcal{s}c_\mathcal{S}(\mathcal{B})$.Hence $\mathcal{B}$ is α-$\mathcal{H}$-open.

5.　　　Consider $\mathcal{B}$ be a b-$\mathcal{H}bO(\mathbb{Z})$set. Then we have, $\mathcal{B}\subseteq$i$_\mathcal{s}$c$_b^*(\mathcal{B})\cup$c$_b$i$_\mathcal{s}(\mathcal{B})\subseteq$i$_\mathcal{s}c_\mathcal{S}(\mathcal{B})\cup$c$_\mathcal{S}i_\mathcal{s}(\mathcal{B})$.Hence $\mathcal{B}$ is b-$\mathcal{H}$-open.

Example2.10. Consider$\mathbb{Z}=\{1,2,3,4,5\}$$\vartheta=\{\emptyset,\{1\},\{2\},\{3\},\{1,2\},\{1,3\},\{2,3\},\{1,2,3\},\{1,3,4\},\{2,3,4\},\{1,2,3,4\}\}$,$\mathcal{H}=\{\emptyset,\{1\}\}$.Then$\mathcal{B}=\{2,3,4,5\}$is σ-$\mathcal{H}$-open but not σ-$\mathcal{H}_bO(\mathbb{Z})$.

Example 2.11. Consider $\mathbb{Z}=\{1,2,3,4,5\}$$\vartheta=\{\emptyset,\{1\},\{3\},\{1,3\},\{3,4,5\},\{1,2,3\},\{1,3,4,5\},\mathbb{Z}\}$, $\mathcal{H}=\{\emptyset,\{1\},\{2\}\}$. Then $\mathcal{B}=\{3,4\}$ is π-$\mathcal{H}$-open but not π-$\mathcal{H}_bO(\mathbb{Z})$

Example2.12. Consider $\mathbb{Z}=\{1,2,3,4,5\}$$\vartheta=\{\emptyset,\{1\},\{2\},\{3\},\{1,2\},\{1,3\},\{2,3\},\{1,2,3\},\{1,3,4\},\{2,3,4\},\{1,2,3,4\}\}$, $\mathcal{H}=\{\emptyset,\{1\}\}$.Then $\mathcal{B}=\{5\}$is ϑ-b-open(resp. b-$\mathcal{H}$-open)but not b-$\mathcal{H}_bO(\mathbb{Z})$.

Ramesh and Uma

Theorem 2.13. In $\mathcal{H}$-GTS $(\mathbb{Z},\vartheta,\mathcal{H})$, any α-$\mathcal{H}_bO(\mathbb{Z})$ is σ-$\mathcal{H}_bO(\mathbb{Z})$.
Proof. Consider a subset $\mathcal{B}$ of $\mathcal{H}$-GTS $(\mathbb{Z},\vartheta,\mathcal{H})$ is α-$\mathcal{H}_bO(\mathbb{Z})$. Then,

$\mathcal{B}\subseteq i_\vartheta c_b^* i_\vartheta(\mathcal{B})\subseteq c_b^* i_\vartheta(\mathcal{B})$. Hence σ-$\mathcal{H}_bO(\mathbb{Z})$.

Theorem 2.14. In $\mathcal{H}$-GTS $(\mathbb{Z},\vartheta,\mathcal{H})$, any α-$\mathcal{H}_bO(\mathbb{Z})$ is π-$\mathcal{H}_bO(\mathbb{Z})$.
Proof. Consider a subset $\mathcal{B}$ of $\mathcal{H}$-GTS $(\mathbb{Z},\vartheta,\mathcal{H})$ is α-$\mathcal{H}_bO(\mathbb{Z})$. Then,

$\mathcal{B}\subseteq i_\vartheta c_b^* i_\vartheta(\mathcal{B})\subseteq i_\vartheta c_b^*(\mathcal{B})$. Hence π-$\mathcal{H}_bO(\mathbb{Z})$.

Theorem 2.15. A subset $\mathcal{B}$ of a $\mathcal{H}$-GTS $(\mathbb{Z},\vartheta,\mathcal{H})$, the following results are equivalent.

1. α-$\mathcal{H}_bO(\mathbb{Z})$
2. σ-$\mathcal{H}_bO(\mathbb{Z})$ and π-$\mathcal{H}_bO(\mathbb{Z})$.

Proof. (1)⇒(2). Consider β-$\mathcal{H}_bO(\mathbb{Z})$. Then by Theorem 2.12 and 2.13, σ-$\mathcal{H}_bO(\mathbb{Z})$ and π-$\mathcal{H}_bO(\mathbb{Z})$.
(2)⇒(1). Consider $\mathcal{B}$ is both σ-$\mathcal{H}_bO(\mathbb{Z})$ and π-$\mathcal{H}_bO(\mathbb{Z})$. Then $\mathcal{B}\subseteq i_\vartheta c_b^*(\mathcal{B})\subseteq i_\vartheta c_b c_b i_\vartheta(\mathcal{B})\subseteq i_\vartheta c_b^* i_\vartheta(\mathcal{B})$. Hence α-$\mathcal{H}_bO(\mathbb{Z})$.

Example 2.16. Consider $\mathbb{Z}=\{1,2,3,4,5\}$, $\vartheta=\{\emptyset,\{1\},\{2\},\{3\},\{1,2\},\{1,3\},\{2,3\},\{1,2,3\},\{1,3,4\},\{1,2,3\},\{1,2,3,4\}\}$, $\mathcal{H}=\{\emptyset,\{1\}\}$.
Then $\mathcal{B}=\{1\},\{5\}\}$ is σ-$\mathcal{H}_bO(\mathbb{Z})$ but not α-$\mathcal{H}_bO(\mathbb{Z})$.

Example 2.17. Consider $\mathbb{Z}=\{1,2,3,4\}$, $\vartheta=\{\emptyset,\{1,3\},\{4\},\{1,3,4\},\mathbb{Z}\}$, $\mathcal{H}=\{\emptyset,\{3\}\}$. Then $\mathcal{B}=\{1,2,4\}$ is π-$\mathcal{H}_bO(\mathbb{Z})$ but not α-$\mathcal{H}_bO(\mathbb{Z})$.

Remark 2.18. The notions of σ-$\mathcal{H}_bO(\mathbb{Z})$ and π-$\mathcal{H}_bO(\mathbb{Z})$ are independent.
Example 2.19. Consider $\mathbb{Z}=\{1,2,3,4,5\}$ $\vartheta=\{\emptyset,\{1\},\{2\},\{3\},\{1,2\},\{1,3\},\{2,3\},\{1,2,3\},\{1,3,4\},\{2,3,4\},\{1,2,3,4\}\}$, $\mathcal{H}=\{\emptyset,\{1\}\}$.
Then $\mathcal{B}=\{1,3\}$ is σ-$\mathcal{H}_bO(\mathbb{Z})$ but not π-$\mathcal{H}_bO(\mathbb{Z})$.

Example 2.20. Consider $\mathbb{Z}=\{1,2,3,4\}$ $\vartheta=\{\emptyset,\{1,3\},\{4\},\{1,3,4\},\mathbb{Z}\}$, $\mathcal{H}=\{\emptyset,\{3\}\}$. Then $\mathcal{B}=\{1,3,4\}$ is π-$\mathcal{H}_bO(\mathbb{Z})$ but not σ-$\mathcal{H}_bO(\mathbb{Z})$.

Theorem 2.21. Any π-$\mathcal{H}_bO(\mathbb{Z})$ set is β-$\mathcal{H}_bO(\mathbb{Z})$ but not conversely.

Proof. Consider a subset $\mathcal{B}$ of $\mathcal{H}$-GTS $(\mathbb{Z},\vartheta,\mathcal{H})$ is π-$\mathcal{H}_bO(\mathbb{Z})$. Then

$\mathcal{B}\subseteq i_\vartheta c_b^*(\mathcal{B})$. Now, $\mathcal{B}\subseteq i_\vartheta c_b(\mathcal{B})\subseteq c_\vartheta i_\vartheta c_b^*(\mathcal{B})$. Hence β-$\mathcal{H}_bO(\mathbb{Z})$ set.

Theorem 2.22. If a subset $\mathcal{B}$ of $\mathcal{H}$-GTS $(\mathbb{Z},\vartheta,\mathcal{H})$ is both σ-$\mathcal{H}_bO(\mathbb{Z})$ and ϑ-σ-open, then β-$\mathcal{H}_bO(\mathbb{Z})$.
Proof. Consider a subset $\mathcal{B}$ of $\mathcal{H}$-GTS $(\mathbb{Z},\vartheta,\mathcal{H})$ is both σ-$\mathcal{H}_bO(\mathbb{Z})$ and ϑ-σ-open. Then, $\mathcal{B}\subseteq c_b i_\vartheta(\mathcal{B})\subseteq c_b^*(\mathcal{B})$ which implies $c_\vartheta i_\vartheta(\mathcal{B})\subseteq c_\vartheta i_\vartheta c_b^*(\mathcal{B})$, so $\mathcal{B}\subseteq c_\vartheta i_\vartheta c_b^*(\mathcal{B})$ since $\mathcal{B}$ is ϑ-σ-open. Hence β-$\mathcal{H}_bO(\mathbb{Z})$.
Theorem 2.23. If $\mathcal{B}\subset\mathbb{Z}$ is both b-$\mathcal{H}_bO(\mathbb{Z})$ and ϑ-σ-open, then it is β-$\mathcal{H}$-open.

Proof. Let $\mathcal{B}$ is both b-$\mathcal{H}_bO(\mathbb{Z})$ and ϑ-σ-open. Then $\mathcal{B}\subseteq i_\vartheta c_b^*(\mathcal{B})\cup c_b i_\vartheta(\mathcal{B})$ and

$\mathcal{B}\subseteq c_\vartheta i_\vartheta(\mathcal{B})$. Now $\mathcal{B}\subseteq i_\vartheta c_b^*(\mathcal{B})\cup c_b i_\vartheta(\mathcal{B})\subseteq c_b^*(\mathcal{B})$, which implies

$i_\vartheta(\mathcal{B})\subseteq c_\vartheta i_\vartheta c_b^*(\mathcal{B})\subseteq c_\vartheta i_\vartheta c_\vartheta^*(\mathcal{B})$ So $\mathcal{B}\subseteq c_\vartheta i_\vartheta(\mathcal{B})\subseteq c_\vartheta i_\vartheta c_\vartheta(\mathcal{B})$. Hence $\mathcal{B}$ is β-$\mathcal{H}$-open.

Theorem 2.24. If $\mathscr{B} \subset \mathbb{Z}$ is both b-$\vartheta\ell_bO(\mathbb{Z})$ and ϑ-σ-open, then it is ϑ-β -open.

Proof. Let $\mathscr{B}$ is both b-$\vartheta\ell bO(\mathbb{Z})$ and ϑ-σ-open. Then $\mathscr{B} \subseteq i\vartheta cb*(\mathscr{B}) \cup c*bi\vartheta(\mathscr{B})$ and $\mathscr{B} \subseteq c\vartheta i\vartheta(\mathscr{B})$. Now $\mathscr{B} \subseteq i\vartheta cb*(\mathscr{B}) \cup c*bi\vartheta(\mathscr{B}) \subseteq cb*(\mathscr{B})$, which implies $c\vartheta i\vartheta(\mathscr{B}) \subseteq c\vartheta i\vartheta c*b(\mathscr{B}) \subseteq c\vartheta i\vartheta c*(\mathscr{B}) \subseteq c\vartheta i\vartheta c\vartheta (\mathscr{B})$ So $\mathscr{B} \subseteq c\vartheta i\vartheta(\mathscr{B}) \subseteq c\vartheta i\vartheta c\vartheta(\mathscr{B})$. Hence $\mathscr{B}$ is ϑ-β-open.

Theorem 2.25. If $\mathscr{B} \subset \mathbb{Z}$ is both b-$\vartheta\ell bO(\mathbb{Z})$ and $\vartheta*$-closed, then it is σ- $\vartheta\ell bO(\mathbb{Z})$.

Proof. Let $\mathscr{B}$ is both b-$\vartheta\ell bO(\mathbb{Z})$ and $\vartheta*$-closed. Then $\mathscr{B} \subseteq i\vartheta c_b^*(\mathscr{B}) \cup c_b i\vartheta(\mathscr{B})$ and $c_b(\mathscr{B}) \subseteq \mathscr{B}$. Now $\mathscr{B} \subseteq i\vartheta c_b^*(\mathscr{B}) \cup c_b^* i\vartheta(\mathscr{B}) \subseteq c_b^* i\vartheta(\mathscr{B}) \cup i\vartheta(\mathscr{B}) = c_b^* i\vartheta(\mathscr{B}) \subseteq c_\sigma^* i\vartheta(\mathscr{B})$. Hence $\mathscr{B}$ is σ-$\vartheta\ell bO(\mathbb{Z})$.

Theorem 2.26. If $\mathscr{B} \subset \mathbb{Z}$ is both b-$\vartheta\ell bO(\mathbb{Z})$ and b$\vartheta*$-closed, then it is σ-$\vartheta\ell bO(\mathbb{Z})$.

Proof. Let $\mathscr{B}$ is both b-$\vartheta\ell bO(\mathbb{Z})$ and b$\vartheta*$-closed. Then $\mathscr{B} \subseteq i\vartheta cb*(\mathscr{B}) \cup c*bi\vartheta(\mathscr{B})$ and $c*b(\mathscr{B}) \subseteq \mathscr{B}$, which implies $i\vartheta cb*(\mathscr{B}) \subseteq i\vartheta(\mathscr{B})$. Now $\mathscr{B} \subseteq i\vartheta cb*(\mathscr{B}) \cup cb*i\vartheta(\mathscr{B}) \subseteq c*bi\vartheta(\mathscr{B}) \cup i\vartheta(\mathscr{B}) = c*bi\vartheta(\mathscr{B}) \subseteq c\vartheta*i\vartheta(\mathscr{B})$. Hence σ-$\vartheta\ell bO(\mathbb{Z})$.

Theorem 2.27. If $\mathscr{B} \subset \mathbb{Z}$ is b - $\vartheta\ell bO(\mathbb{Z})$ such that $i\vartheta(\mathscr{B}) = \emptyset$, then it is π - $\vartheta\ell$-open.

Proof. Let $\mathscr{B}$ be a b-$\vartheta\ell bO(\mathbb{Z})$ and $i\vartheta(\mathscr{B}) = \emptyset$. Then $\mathscr{B} \subseteq i\vartheta cb*(\mathscr{B}) \cup cb*i\vartheta(\mathscr{B}) = i\vartheta c*b(\mathscr{B}) \subseteq i\vartheta c\vartheta*(\mathscr{B})$. Hence π-$\vartheta\ell$-open.

Decomposition of $(\alpha\vartheta\ell b, \vartheta)$-Continuity

Definition 3.1. A map $j:(\mathbb{Z}, \vartheta, \vartheta\ell) \rightarrow (W, \delta)$ is $(\alpha\vartheta\ell b, \delta)$-continuous $((\alpha\vartheta\ell b, \vartheta)$-C), if $j^{-1}(V)$ is α-$\vartheta\ell bO(\mathbb{Z})$ for each $\delta O(\mathbb{Z})$ set V in (W, δ).

Definition 3.2. A map $j:(\mathbb{Z}, \vartheta, \vartheta\ell) \rightarrow (W, \delta)$ is $(\sigma\vartheta\ell b, \delta)$-continuous $((\sigma\vartheta\ell b, \vartheta)$-C), if $j^{-1}(V)$ is σ-$\vartheta\ell bO(\mathbb{Z})$ for each $\delta O(\mathbb{Z})$ set V in (W, δ).

Definition 3.3. A map $j:(\mathbb{Z}, \vartheta, \vartheta\ell) \rightarrow (W, \delta)$ is $(\pi\vartheta\ell b, \delta)$-continuous $((\pi\vartheta\ell b, \vartheta)$-C), if $j^{-1}(V)$ is π-$\vartheta\ell bO(\mathbb{Z})$ for each $\delta O(\mathbb{Z})$ set V in (W, δ).

Theorem 3.4. For a map $j:(\mathbb{Z}, \vartheta, \vartheta\ell) \rightarrow (W, \delta)$ the following results are equivalent.

j is $(\alpha\vartheta\ell_b, \vartheta)$-C.
j is $(\sigma\vartheta\ell_b, \vartheta)$-C and $(\pi\vartheta\ell_b, \vartheta)$-C.

PROOF
Proof is trivial from Theorem 2.17.

CONCLUSION

In this paper, we introduced α-$\vartheta\ell bO(\mathbb{Z})$, σ-$\vartheta\ell bO(\mathbb{Z})$, π-$\vartheta\ell bO(\mathbb{Z})$, β - $\vartheta\ell bO(\mathbb{Z})$, and b - $\vartheta\ell bO(\mathbb{Z})$ sets and obtained decomposition of $(\alpha\vartheta\ell b, \vartheta)$ - C. In future work we will introduce new types of generalized open sets related to these sets and obtain new decomposition of (ϑ, δ)-C.

REFERENCES

1. A. Csas$\mathbb{Z}$ar, Generalized topology generalized continuity Act a Mathematic a Hungaric a **96**(2002),351-357.
2. A. Csas$\mathbb{Z}$ar, Generalized open sets in generalized topologies Act a Mathematic a Hungarica 106(2005),53-56.
3. A. Csas$\mathbb{Z}$ar, Modification of generalized topologies via hereditary classes Act a Mathematic a Hungarica

115 (2007), 29-36.

4. W. K. Min, Generalized Continuity maps defined by generalized open sets ongeneralized topological spaces Acta Mathematica Hungarica128(4) (2010)pp299-306.

5. M. Rajamani, V. Inthumathi and R. Ramesh, Some new generalized topologies via hereditary classes Bol.Soc.Paran.Mat.30(2)(2012),71-77.

6. M.Rajamani, V.Inthumathi and R.Ramesh,A de composition of(μ, λ) –continuity in generalized topological spaces, Jordan Journal of Mathematics and Statistics,6(1)(2013),15-27.

7. A. Al-Omari, M. Rajamani and R. Ramesh,A - Expansion continuous mapsand(A, B) -weakly continuous maps in hereditary generalized topological spaces,ScientificStudiesandResearch,23(2)(2013),13-22.

8. R. Ramesh and R. Mariappan Generalized open sets in hereditary generalized topological spaces, J.Math.Comput.Sci.,5(2)(2015),149-159.

9. R.Ramesh and Ahmad Al-Omari,b-H$_\sigma$-open sets in HGTS, Poincare Journal of Analysis and Applications 9(1)(2022),31-40.

10. R.Ramesh and Ahmad Al-Omari Decomposition of$(\alpha$-H$_\sigma,\lambda)$-continuity, Poincare Journal of Analysis and Applications 10(1)(2023),155-163.

11. R.Ramesh, Decomposition of $(\kappa\mu^*,\lambda)$-continuity, Journal of Xi'an University of Architecture and Technology, **11**(VI),(2020),2095-2101.

12. M.S.Sarsak, On some properties of Generali$\mathbb{Z}$ed open sets in Generali$\mathbb{Z}$ed topological spaces, Demonstration Math.(2013).

RESEARCH ARTICLE

An Extension of Some Products in Fermatean Neutrosophic Dombi Fuzzy Graphs

D. Sasikala[1]* and B.Divya[2]

[1]Assistant Professor, PSGR Krishnammal College for Women, Coimbatore, Tamil Nadu, India
[2]Research Scholar, PSGR Krishnammal College for Women, Coimbatore, Tamil Nadu, India

*Address for Correspondence
D. Sasikala
Assistant Professor,
PSGR Krishnammal College for Women,
Coimbatore, Tamil Nadu, India
E.Mail: 22phdma02@ psgrkcw.ac.in

ABSTRACT

The aggregation operators of dombi have some great effectiveness and flexibility to work with multi criteria decision making problems. By applying this concept, we have established fermatean neutrosophic dombi fuzzy graphs, an extension of Pythagorean neutrosophic dombi fuzzy graphs and pythogorean dombi fuzzy graphs. As well, we define semi- strong, strong and boxdot and modular product of fermatean neutrosophic dombi fuzzy graphs. Likewise, we explored proposition with suitable illustrations with graphs.

Keywords: Dombi fuzzy graph, neutrosophic dombi fuzzy graph, neutrosophic fuzzy edge graph, fermatean neutrosophic dombi fuzzy graph, fermatean neutrosophic fuzzy edge graph.

INTRODUCTION

The fuzzy logic is upgrade to classical logic. It has varying grade of membership. Fuzzy set was introduced by zadeh[18] in 1965.Atanassov (1983)[5] and (1989) has explored the idea of intuitionistic fuzzy set, in this set each element has membership and non-membership function. Smarandache (2005)[15] has presented the main concept of neutrosophic set, by an extension of the IFS. Each element of neutrosophic set has three membership grade of truth,indeterminacy and falsehood. Mohana,R.Jansi and F.Smarandache[16] introduced pythogorean neutrosophic set, based on the total squares of membership, indeterminacy and falsehood lies between 0 and 2. C.Antony and jansi[16]defined the sum of cubes of three membership functions lies between 0 and 2 is fermatean neutrosophic sets. A graph is made up of nodes and arcs. The main concept of classical graph theory is based on crisp logic / set which was proposed by cantor. The aim of fuzzy graph has been first time presented by Kaufmann(1975)[10] based on

64211

fuzzy relation. Atanassov(1983)[14] has described the concept of IF graphs. Ghori and paul (2017)[8] introduced neutrosophic graphs. The concept of fuzzy graph was advanced to neutrosophic fuzzy graphs was introduced by S.Naz and S.Ashraf[12]. The Dombi operator with relevant parameter was inaugurated by Dombi[7] in 1982, and the concept of the Dombi fuzzy graph was developed by Ashraf et al. (2018)[4]. The dombi operator is crucial in simulating and resolving numerous problems encountered in everyday life. In order to take use of this advantage, Mijanur Rahman Seikh and Utpal Mandal(2021)[11] applied dombi operations to intuitionistic fuzzy graphs and created a multiple attribute group decision-making problem.The neutrosophic dombi graph was invented and refined by Tejindarsingh lakhwani, Karthick[16].In addition to proposing Pythogorean neutrosophic fuzzygraphs using the dombi operator,Ajay et al.[1] presented an innovative concept of pythogoreanneutr [1] presented an innovative concept of pythogorean neutrosophic fuzzy graph.

In this research, we introduced a new emergent notion of fermatean neutrosophic dombi fuzzy graph using dombi operator. The primary consideration, In Section2, we developed and remembered the fundamental concepts and notions used in this part. In Section 3, we described the new concepts and products of fermatean neutrosophic dombi fuzzy graphs and establish their proposition with relatable illustration and graphs.

Preliminaries

Definition

Let ϑ_D be a non-empty set. A fuzzy set A^μ in ϑ_D is distinguished by its membership function $\alpha_{\mu_D}(\vartheta_D){:}\rightarrow[0,1]$ and $\mu_D(n)$ is interpreted as the degree of member of element n^μ in a fuzzy set N^μ, for each $n^\mu \in \vartheta_D$.It is clear that N^μ is determined by the set of tuples of $N^\mu = \{(n^\mu, \alpha_{\mu_D}(\vartheta_D), n^\mu \in \vartheta_D\}$.

Definition

An intuitionistic fuzzy set (briefly IFS) N^μ is an object of having the form $A^\mu = \{<n^{\mu*}, \alpha_{\mu_D}(\vartheta_D), \beta_{\mu_D}(\vartheta_D)> : n^\mu \in R_{N^\mu}\}$ where the functions $\alpha_{\mu_D}(\vartheta_D){:}\rightarrow[0,1]$ and $\beta_{\mu_D}(\vartheta_D){:}\rightarrow[0,1]$ denote the degree of membership and the degree non-membership of each element $n^\mu \in \vartheta_D$ to the set G^* respectively, and $0 \le \alpha_{\mu_D}(\vartheta_D) + \beta_{\mu_D}(\vartheta_D) \le 1$ for each $n^\mu \in \vartheta_D$. Denote by IFS(R_{N^μ}), The set of all intuitionistic fuzzy sets in ϑ_D. An intuitionistic fuzzy set G^* in ϑ_D is simply denoted by $N^\mu = <n^\mu, \alpha_{\mu_D}(\vartheta_D), \beta_{\mu_D}(\vartheta_D)>$ instead of denoting $A^\mu = \{(n^\mu, \alpha_{\mu_D}(\vartheta_D), \beta_{\mu_D}(\vartheta_D)) : n^\mu \in \vartheta_D\}$.

Definition

Let ϑ_D be a non-empty set. A Neutrosophic set (NS) A^μ in ϑ_D is characterized by a truth-membership function α_{μ_D}, an indeterminacy-membership function β_{μ_D}, and a falsity - membership function γ_{μ_D} is $\alpha_{\mu_D}(\vartheta_D), \beta_{\mu_D}(\vartheta_D), \gamma_{\mu_D}(\vartheta_D)$ are real or non-standard subsets of $]0^-, 1^+[$ on ϑ_D.
i.e.) $\alpha_{\mu_D}(\vartheta_D){:}\vartheta_D \rightarrow]0^-, 1^+[\quad ; \beta_{\mu_D}(\vartheta_D){:}\vartheta_D \rightarrow]0^-, 1^+[\quad ; \gamma_{\mu_D}(\vartheta_D){:}\vartheta_D \rightarrow]0^-, 1^+[$

Definition

A fuzzy graph of the graph $D^* = (\varphi_D, \varsigma_D)$ is a pair of $D = (\mu_D, \nu_D)$, Where $\mu_D \rightarrow [0,1]$ is a fuzzy set on φ_D and $\nu_D{:}\varphi_D X \varphi_D \rightarrow [0,1]$ is a fuzzy relation on φ_D such that
$\nu_D(n,t) \le \mu_D(n) \wedge \mu_D(t), \forall (n,t) \in \varphi_D X \varphi_D$.

Definition

A binary function $\mathbb{F}{:}[0,1]X[0,1] \rightarrow [0,1]$ is known as triangular norm (t-norm) if for all n,t,s ∈ [0,1], it satisfied the following conditions
1. (Neutral property or boundary condition) $\mathbb{F}(n,1) = n$
2. (commutativity) $\mathbb{F}(n,t) = \mathbb{F}(t,n)$
3. (associativity) $\mathbb{F}(n,(t,s)) = \mathbb{F}((n,t),s)$
4. (monotonicity) $\mathbb{F}(n,t) \le \mathbb{F}(s,d)$ if $n \le s$ and $t \le d$

Definition

Abinary function $\mathcal{M}:[0,1]X[0,1] \to [0,1]$ is known as triangular conorm (t-conorm) if and only if there exists a t-norm $\mathcal{F}$ for all $\mathcal{F}(n,t)\in [0,1]X[0,1]$; $\mathcal{M}($ n,t)=1-$\mathcal{F}$(1-n,1-t)

Preferred options for t-norms are:

o　　　　The minimum operator $\mathcal{M}$ *(n,t)=MIN(n,t)*

o　　　　The product operator $\mathcal{P}(n,t)=nt$

o　　　　The dombi's t-norm, $\frac{1}{1+([(\frac{1-n}{n})]^{\delta}+[(\frac{1-t}{t})]^{\delta})^{\frac{1}{\delta}}}$, $\delta > 0$

Preferred options for related t-conorms are:

o　　　　The maximum operator $\mathcal{M}^*(n,t)=MAX$ *(n,t)*

o　　　　The Probabilistic sum $\mathcal{P}^*(n,t)$ *=n+t-nt*

o　　　　The Dombi's t-conorm $\frac{1}{1+([(\frac{1-n}{n})]^{-\delta}+[(\frac{1-t}{t})]^{-\delta})-\frac{1}{\delta}}$, $\delta > 0$ One more pair of $\mathcal{F}$-operator is $\mathcal{F}(n,t)=\frac{nt}{n+t-nt}$

$\mathcal{P}(n,t)=\frac{n+t-2nt}{1-nt}$,which is obtained by substituting δ = 1 in dombi's t-norm and t-conorm. Also $\mathcal{P}(n,t)\le \frac{nt}{n+t-nt} \le \mathcal{M}(n,t)$ and $\mathcal{M}^*(n,t)\le \frac{n+t-2nt}{1-nt} \le \mathcal{P}^*(n,t)$.

Definition

A dombi fuzzy graph with a countable set φ_D as the elementary set is a pair $D=(\mu_D,\nu_D)$,where $\mu_D \to [0,1]$ is a symmetric fuzzy on φ_D such that $\varsigma_D(nt) \le \frac{\varphi_D(n)\varphi_D(t)}{\varphi_D(n)+\varphi_D(t)-\varphi_D(n)\varphi_D(t)}$, $\forall n,t \in \varphi_D$.

Definition

Let $D^*= (\varphi_D,\varsigma_D)$ be a crisp undirected graph contain no self loop and parallel edges. Let $\mu_D = (\alpha_{\mu_D},\beta_{\mu_D}\gamma_{\mu_D})$such that $\alpha_{\mu_D}:\vartheta_D \to [0,1],\beta_{\mu_D}:\vartheta_D \to [0,1],\gamma_{\mu_D}:\vartheta_D \to [0,1]$ $\alpha_{\nu_D}: \vartheta_D \to [0,1]$, $\beta_{\nu_D}: \vartheta_D \to [0,1]$,$\gamma_{\nu_D}: \vartheta_D \to [0,1]$ .Here $\alpha_{\mu_D},\alpha_{\nu_D} \to$ The membership function, $\beta_{\mu_D},\beta_{\nu_D} \to$ The indeterminacy function, $\gamma_{\mu_D},\gamma_{\nu_D} \to$ The falsity function in the neutrosophic dombi fuzzy graph, $\varsigma_F \subset \vartheta_D X\vartheta_D$ Then the neutrosophic dombi fuzzy graph, $D = (\varphi_D,\mu_D,\nu_D)$

$\alpha_{\varsigma_D}(nt) \le \frac{\alpha_{\varphi_D}(n)\alpha_{\varphi_D}(t)}{\alpha_{\varphi_D}(n)+\alpha_{\varphi_D}(t)-\alpha_{\varphi_D}(n)\alpha_{\varphi_D}(t)}$, $\forall nt \in \varsigma_D$

$\beta_{\varsigma_D}(nt) \le \frac{\beta_{\mu_D}(n)\beta_{\mu_D}(t)}{\beta_{\mu_D}(n)+\beta_{\mu_D}(t)-\beta_{\mu_D}(n)\beta_{\mu_D}(t)}$, $\forall nt \in \varsigma_D$

$\gamma_{\varsigma_D}(nt) \le \frac{\gamma_{\nu_D}(n)+\gamma_{\nu_D}(t)-2\gamma_{\nu_D}(n)\gamma_{\nu_D}(t)}{1-\gamma_{\nu_D}(n)\gamma_{\nu_D}(t)}$, $\forall nt \in \varsigma_D$

Definition

A fermatean neutrosophic dombi fuzzy graph is defined [its indicated by *FNDFG*] with a finite elementary set ϑ_D of its order pair $D = (\varphi_D,\varsigma_D)$ where $\varphi_D:\vartheta_D \to [0,1]$.Here we consider, $\mu_D = (\alpha_{\varphi_D},\beta_{\mu_D}\gamma_{\nu_D})$ such that $\alpha_{\varphi_D}: \vartheta_D \to [0,1]$, $\beta_{\mu_D}: \vartheta_D \to [0,1]$,$\gamma_{\nu_D}: \vartheta_D \to [0,1]$, $\alpha_{\mu_D}:\vartheta_D \to [0,1]$, $\beta_{\mu_D}: \vartheta_D \to [0,1]$,$\gamma_{\nu_D}: \vartheta_D \to [0,1]$ .Here $\alpha_{\mu_D},\alpha_{\nu_D} \to$ The membership function, $\beta_{\mu_D},\beta_{\nu_D} \to$ The indeterminacy function, $\gamma_{\mu_D},\gamma_{\nu_D} \to$ The falsity function in the Fermatean neutrosophic dombi fuzzy graph, $\varsigma_F \subset \vartheta_D X\vartheta_D$ Then the fermateanneutrosophicdombi fuzzy graph, $d = (\varphi_D,\mu_D,\nu_D)$

$\alpha_{\varsigma_D}(nt) \le \frac{\alpha_{\varphi_D}(n)\alpha_{\varphi_D}(t)}{\alpha_{\varphi_D}(n)+\alpha_{\varphi_D}(t)-\alpha_{\varphi_D}(n)\alpha_{\varphi_D}(t)}$, $\forall nt \in \varsigma_D$

$\beta_{\varsigma_D}(nt) \le \frac{\beta_{\mu_D}(n)\beta_{\mu_D}(t)}{\beta_{\mu_D}(n)+\beta_{\mu_D}(t)-\beta_{\mu_D}(n)\beta_{\mu_D}(t)}$, $\forall nt \in \varsigma_D$

$\gamma_{\varsigma_D}(nt) \le \frac{\gamma_{\nu_D}(n)+\gamma_{\nu_D}(t)-2\gamma_{\nu_D}(n)\gamma_{\nu_D}(t)}{1-\gamma_{\nu_D}(n)\gamma_{\nu_D}(t)}$, $\forall nt \in \varsigma_D$

And $0\le \alpha_{\nu_D}{}^3(nt)+\beta_{\nu_D}{}^3(nt)+\gamma_{\nu_D}{}^3(nt) \le 2$; $0\le \alpha_{\nu_D}{}^3(nt)+\gamma_{\nu_D}{}^3(nt) \le 1$; $0\le \beta_{\nu_D}{}^3(nt)\le 1$.

Some Products of Fermatean Neutrosophic Dombi Fuzzy Graphs
Definition: (Semi-Strong Product)

Let $\emptyset_i$ be a fermatean neutrosophic fuzzy subset of φ_D and ς_i be a neutrosophic fuzzy subset ς_D of ς_i =1, 2 define the semi strong product of fermatean neutrosophic dombi fuzzy graph. $D = (\emptyset_D, \mu_D, \nu_D)$ and $F = (\emptyset_F, \mu_F, \nu_F)$ $D^* = (\varphi_D, \varsigma_D)$ and $F^* = (\varphi_F, \varsigma_F)$ separately is established by $D \bullet F$ is $D \bullet F = (\emptyset_D \bullet \emptyset_F, \mu_D \bullet \mu_F, \nu_D \bullet \nu_F)$. (i.e) $\emptyset_D \bullet \emptyset_F = [\alpha_{\emptyset_D \bullet \emptyset_F}, \beta_{\emptyset_D \bullet \emptyset_F}, \gamma_{\emptyset_D \bullet \emptyset_F}] \mu_D \bullet \mu_F = [\alpha_{\mu_D \bullet \mu_F}, \beta_{\mu_D \bullet \mu_F}, \gamma_{\mu_D \bullet \mu_F}]; \nu_D \bullet \nu_F = [\alpha_{\nu_D \bullet \nu_F}, \beta_{\nu_D \bullet \nu_F}, \gamma_{\nu_D \bullet \nu_F}]$ such that $\xi_{D \bullet F} = \{(n, n_2), (n, t_2) : n \in \varphi_D, n_2 t_2 \in \varsigma_F\} \cup \{(z, n_2), (z, t_2) : z \in \varphi_D, n_2 t_2 \in \varsigma_F\} \cup \{(n_1, n_2), (t_1, t_2) : n_1 n_2 \in \varsigma_D, z \in \varphi_F\}$ such that, For all $(n_1, n_2) \in \varphi_D \times \varphi_F$,

- $\alpha_{\emptyset_D \bullet \emptyset_F}(n_1, n_2) = \dfrac{\alpha_{\emptyset_D}(n_1)\alpha_{\emptyset_F}(n_2)}{\alpha_{\emptyset_D}(n_1) + \alpha_{\emptyset_F}(n_2) - \alpha_{\emptyset_D}(n_1)\alpha_{\emptyset_F}(n_2)}$

$\beta_{\mu_D \bullet \mu_F}(n_1, n_2) = \dfrac{\beta_{\mu_D}(n_1)\beta_{\mu_F}(n_2)}{\beta_{\mu_D}(n_1) + \beta_{\mu_F}(n_2) - \beta_{\mu_D}(n_1)\beta_{\mu_F}(n_2)}; \gamma_{\nu_D \bullet \nu_F}(n_1, n_2) = \dfrac{\gamma_{\nu_D}(n_1) + \gamma_{\nu_F}(n_2) - 2\gamma_{\nu_D}(n_1)\gamma_{\nu_F}(n_2)}{1 - \gamma_{\nu_D}(n_1)\gamma_{\nu_F}(n_2)}$.

$(\varsigma_D \bullet \varsigma_F)(z, n_2), (z, t_2) = \dfrac{\alpha_{\emptyset_D}(z)\varsigma_{\alpha_{\emptyset_F}}(n_2 t_2)}{\alpha_{\emptyset_D}(z) + \varsigma_{\alpha_{\emptyset_F}}(n_2 t_2) - \alpha_{\emptyset_D}(z)\varsigma_{\alpha_{\emptyset_F}}(n_2 t_2)}$,

$\dfrac{\beta_{\mu_D}(z)\varsigma_{\beta_{\mu_F}}(n_2 t_2)}{\beta_{\mu_D}(z) + \varsigma_{\beta_{\mu_F}}(n_2 t_2) - \beta_{\mu_D}(z)\varsigma_{\beta_{\mu_F}}(n_2 t_2)}, \dfrac{\gamma_{\nu_D}(z)\varsigma_{\gamma_{\nu_F}}(n_2 t_2) - 2\gamma_{\nu_D}(z)\varsigma_{\gamma_{\nu_F}}(n_2 t_2)}{1 - \gamma_{\nu_D}(z)\varsigma_{\gamma_{\nu_F}}(n_2 t_2)}$.

For all $z \in \varphi_D, n_2 t_2 \in \varsigma_F (\varsigma_D \bullet \varsigma_F)(n_1, n_2)(t_1, t_2) = \dfrac{\varsigma_{\alpha_{\emptyset_D}}(n_1 t_1)\varsigma_{\alpha_{\emptyset_F}}(n_2 t_2)}{\varsigma_{\alpha_{\emptyset_D}}(n_1 t_1) + \varsigma_{\alpha_{\emptyset_F}}(n_2 t_2) - \varsigma_{\alpha_{\emptyset_D}}(n_1 t_1)\varsigma_{\alpha_{\emptyset_F}}(n_2 t_2)}$,

$\dfrac{\varsigma_{\beta_{\mu_D}}(n_1 t_1)\varsigma_{\beta_{\mu_F}}(n_2 t_2)}{\varsigma_{\beta_{\mu_D}}(n_1 t_1) + \varsigma_{\beta_{\mu_F}}(n_2 t_2) - \varsigma_{\beta_{\mu_D}}(n_1 t_1)\varsigma_{\beta_{\mu_F}}(n_2 t_2)}, \dfrac{\varsigma_{\gamma_{\nu_D}}(n_1 t_1) + \varsigma_{\gamma_{\nu_F}}(n_2 t_2) - 2\varsigma_{\gamma_{\nu_D}}(n_1 t_1)\varsigma_{\gamma_{\nu_F}}(n_2 t_2)}{1 - \varsigma_{\gamma_{\nu_D}}(n_1 t_1)\varsigma_{\gamma_{\nu_F}}(n_2 t_2)}$.

For all $n_1 t_1 \in \varsigma_D, n_2 t_2 \in \varsigma_F$

Example

Consider two neutrosophic dombi fuzzy graphs $d = (\emptyset_D, \mu_D, \nu_D)$ and $F = (\emptyset_F, \mu_F, \nu_F)$. Here $\varphi_D = \{a, b\}, \varphi_F = \{x, y, z\}, \varsigma_D = \{ab\}, \varsigma_F = \{xy, yz\}$ where $\varphi_D = \left\{\dfrac{a}{(0.5, 0.7, 0.9)}, \dfrac{b}{(0.7, 0.6, 0.8)}\right\} \varsigma_D = \left\{\dfrac{ab}{(0.4, 0.4, 0.9)}\right\}, \varphi_F = \left\{\dfrac{x}{(0.5, 0.7, 0.8)}, \dfrac{y}{(0.9, 0.7, 0.6)}, \dfrac{z}{(0.6, 0.7, 0.8)}\right\}, \varsigma_F = \left\{\dfrac{xy}{(0.4, 0.5, 0.8)}, \dfrac{yz}{(0.5, 0.5, 0.8)}\right\}$. Then we have

$(\varphi_D \bullet \varphi_F)(a, b) = (0.4, 0.4, 0.9), (\varphi_D \bullet \varphi_F)(x, y) = (0.4, 0.5, 0.8), (\varphi_D \bullet \varphi_F)(y, z) = (0.5, 0.5, 0.8), (\varphi_D \bullet \varphi_F)(a, x) = (0.3, 0.5, 0.9), (\varphi_D \bullet \varphi_F)(a, y) = (0.4, 0.5, 0.9), (\varphi_D \bullet \varphi_F)(a, z) = (0.3, 0.5, 0.9)$ $(\varphi_D \bullet \varphi_F)(b, x) = (0.4, 0.4, 0.8), (\varphi_D \bullet \varphi_F)(b, y) = (0.6, 0.4, 0.8), (\varphi_D \bullet \varphi_F)(b, z) = (0.4, 0.4, 0.9)(\varsigma_D \bullet \varsigma_F)(a, x)(b, y) = (0.21, 0.25, 0.85), (\varsigma_D \bullet \varsigma_F)(a, y)(b, z) = (0.21, 0.25, 0.84), (\varsigma_D \bullet \varsigma_F)(b, x)(a, y) = (0.21, 0.28, 0.85), (\varsigma_D \bullet \varsigma_F)(b, y)(a, z) = (0.21, 0.28, 0.85)$.

Theorem

Let D^* and F^* be the fermatean neutrosophic dombi fuzzy graphs of the graphs D and F, respectively. The semi-strong product $D \bullet F$ of D^* and F^* is the fermatean neutrosophic dombi fuzzy edge graph of $D \bullet F$.

Proof:

Let D and F be the fermatean neutrosophic dombi fuzzy graphs $D = (\emptyset_D, \mu_D, \nu_D)$ and $F = (\emptyset_F, \mu_F, \nu_F)$ respectively. Consider, i) For all $n \in \varsigma_D, n_2 t_2 \in \varsigma_F$ such that $(\varsigma_D \bullet \varsigma_F)(n, n_2)(n, t_2) = T[\varphi_D(n), \varsigma_F(n_2 t_2)] = T[1, \varsigma_F(n_2 t_2)](\varsigma_D \bullet \varsigma_F)(n, n_2)(n, t_2)$

Sasikala and Divya

$$\leq T\left[\frac{\frac{\alpha_{\emptyset_D}\,\varphi(n)\alpha_{\emptyset_F}\varsigma(n_2 t_2)}{\alpha_{\emptyset_D}\,\varphi(n)+\alpha_{\emptyset_F}\varsigma(n_2 t_2)-\alpha_{\emptyset_D}\,\varphi(n)\alpha_{\emptyset_F}\varsigma(n_2 t_2)}}{\frac{\beta_{\mu_D}\,\varphi(n)\beta_{\mu_F}\varsigma(n_2 t_2)}{\beta_{\mu_D}\,\varphi(n)+\beta_{\mu_F}\varsigma(n_2 t_2)-\beta_{\mu_D}\,\varphi(n)\beta_{\mu_F}\varsigma(n_2 t_2)}},\frac{\gamma_{\nu_D}\,\varphi(n)+\gamma_{\nu_F}\varsigma(n_2 t_2)-2\gamma_{\nu_D}\,\varphi(n)\gamma_{\nu_F}\varsigma(n_2 t_2)}{\gamma_{\nu_D}\,\varphi(n)\gamma_{\nu_F}\varsigma(n_2 t_2)}\right]$$

$$\varsigma_F(n_2 t_2)=\begin{cases}\frac{\alpha_{\emptyset_D}\,(n_2)\alpha_{\emptyset_F}(t_2)}{\alpha_{\emptyset_D}\,(n_2)+\alpha_{\emptyset_F}(t_2)-\alpha_{\emptyset_D}\,(n_2)\alpha_{\emptyset_F}(t_2)},\\\frac{\beta_{\mu_D}\,(n_2)\beta_{\mu_F}\,(t_2)}{\beta_{\mu_D}\,(n_2)+\beta_{\mu_F}\,(t_2)-\beta_{\mu_D}\,(n_2)\beta_{\mu_F}\,(t_2)},\\\frac{\gamma_{\nu_D}\,(n_2)+\gamma_{\nu_F}(t_2)-2\gamma_{\nu_D}\,(n_2)\gamma_{\nu_F}(t_2)}{\gamma_{\nu_D}\,(n_2)\gamma_{\nu_F}(t_2)}\end{cases}$$

$$=\begin{cases}\frac{(\varphi_D\bullet\varphi_F)\alpha_{\emptyset_D}\,(n,n_2)(\varphi_D\bullet\varphi_F)\alpha_{\emptyset_F}(n,t_2)}{(\varphi_D\bullet\varphi_F)\alpha_{\emptyset_D}\,(n,n_2)+(\varphi_D\bullet\varphi_F)\alpha_{\emptyset_F}(n,t_2)-(\varphi_D\bullet\varphi_F)\alpha_{\emptyset_D}\,(n,n_2)(\varphi_D\bullet\varphi_F)\alpha_{\emptyset_F}(n,t_2)},\\\frac{(\varphi_D\bullet\varphi_F)\beta_{\mu_D}\,(n,n_2)(\varphi_D\bullet\varphi_F)\beta_{\mu_F}(n,t_2)}{(\varphi_D\bullet\varphi_F)\beta_{\mu_D}\,(n,n_2)+(\varphi_D\bullet\varphi_F)\beta_{\mu_F}(n,t_2)-(\varphi_D\bullet\varphi_F)\beta_{\mu_D}\,(n,n_2)(\varphi_D\bullet\varphi_F)\beta_{\mu_F}(n,t_2)},\\\frac{(\varphi_D\bullet\varphi_F)\gamma_{\nu_D}\,(n,n_2)+(\varphi_D\bullet\varphi_F)\gamma_{\nu_F}(n,t_2)-2(\varphi_D\bullet\varphi_F)\gamma_{\nu_D}\,(n,n_2)(\varphi_D\bullet\varphi_F)\alpha_{\emptyset_F}(n,t_2)}{1-(\varphi_D\bullet\varphi_F)\gamma_{\nu_D}\,(n,n_2)(\varphi_D\bullet\varphi_F)\alpha_{\emptyset_F}(n,t_2)}\end{cases}$$

ii) Consider, for all $n_1 t_1 \in \varsigma_D, n_2 t_2 \in \varsigma_F$ such that
$(\varsigma_D\bullet\varsigma_F)(n_1,n_2)(t_1,t_2)$;The semi-strong product of $D\bullet F = T[\varsigma_D(n_1 t_1),\varsigma_F(n_2 t_2)]$

$$\leq T\left[\frac{\frac{\alpha_{\emptyset_D}\,(n_1)\alpha_{\emptyset_D}\,(n_2)}{\alpha_{\emptyset_D}\,(n_1)+\alpha_{\emptyset_D}\,(n_2)-\alpha_{\emptyset_D}\,(n_1)\alpha_{\emptyset_D}\,(n_2)}}{\frac{\beta_{\mu_D}\,(n_1)\beta_{\mu_D}\,(n_2)}{\beta_{\mu_D}\,(n_1)+\beta_{\mu_D}\,(n_2)-\beta_{\mu_D}\,(n_2)\beta_{\mu_D}\,(n_2)}},\frac{\gamma_{\nu_D}\,(n_1)+\gamma_{\nu_D}\,(n_2)-2\gamma_{\nu_D}\,(n_1)\gamma_{\nu_D}\,(n_2)}{\gamma_{\nu_D}\,(n_1)\gamma_{\nu_D}\,(n_2)}\right]$$

$(\varsigma_D\times\varsigma_F)(n_1,n_2)(t_1,t_2)$

$$\leq\begin{cases}\frac{(\varphi_D\bullet\varphi_F)\alpha_{\emptyset_D}\,(n_1 n_2)(\varphi_D\bullet\varphi_F)\alpha_{\emptyset_F}(t_1 t_2)}{(\varphi_D\bullet\varphi_F)\alpha_{\emptyset_D}\,(n_1 n_2)+(\varphi_D\bullet\varphi_F)\alpha_{\emptyset_F}(t_1 t_2)-(\varphi_D\bullet\varphi_F)\alpha_{\emptyset_D}\,(n_1 n_2)(\varphi_D\bullet\varphi_F)\alpha_{\emptyset_F}(t_1 t_2)},\\\frac{(\varphi_D\bullet\varphi_F)\beta_{\mu_D}\,(n_1 n_2)(\varphi_D\bullet\varphi_F)\beta_{\mu_F}(t_1 t_2)}{(\varphi_D\bullet\varphi_F\beta_{\mu_D}\,(n_1 n_2)+(\varphi_D\bullet\varphi_F)\beta_{\mu_F}(t_1 t_2)-(\varphi_D\bullet\varphi_F)\beta_{\mu_D}\,(n_1 n_2)(\varphi_D\bullet\varphi_F)\beta_{\mu_F}(t_1 t_2)},\\\frac{(\varphi_D\bullet\varphi_F)\gamma_{\nu_D}\,(n_1 n_2)(+\varphi_D\bullet\varphi_F)\gamma_{\nu_F}(t_1 t_2)-2(\varphi_D\bullet\varphi_F)\gamma_{\nu_D}\,(n_1 n_2)(\varphi_D\bullet\varphi_F)\alpha_{\emptyset_F}(t_1 t_2)}{1-(\varphi_D\bullet\varphi_F)\gamma_{\nu_D}\,(n_1 n_2)(\varphi_D\bullet\varphi_F)\alpha_{\emptyset_F}(t_1 t_2)}\end{cases}$$

Corollary

The semi-strong fermatean neutrosophic dombi fuzzy graph is not necessiarily to a fermate an neutrosophic dombi fuzzy graph.$(\varsigma_D\bullet\varsigma_F)(a,x)(b,y) = (0.21,0.25,0.85)$Edge product of (a,x) and (b,y) is$(\varsigma_D\bullet\varsigma_F)(a,x)(b,y) = (0.25,0.28,0.9)(0.25,0.28,0.9)\nleqq(0.21,0.25,0.85)$

Definition: (Strong Product)

Let $\emptyset_i$ be a fermatean neutrosophic fuzzy subset of φ_D and ς_i be a neutrosophic fuzzy subset $\varsigma_D$of $\varsigma_i=1,2$ define the strong product of fermateanneutrosophicdombi fuzzy graph. $D = (\emptyset_D,\mu_D,\nu_D)$ and $F = (\emptyset_F,\mu_F,\nu_F)$ $D^*= (\varphi_D,\varsigma_D)$ and $F^*=(\varphi_F,\varsigma_F)$ separately is established by $D⊞F$ is $D ⊞ F = (\emptyset_D ⊞ \emptyset_F,\mu_D ⊞ \mu_F,\nu_D ⊞ \nu_F)$. (i.e) $\emptyset_D ⊞ \emptyset_F=[\alpha_{\emptyset_D ⊞\emptyset_F},\beta_{\emptyset_D ⊞\emptyset_F},\gamma_{\emptyset_D ⊞\emptyset_F}];\mu_D ⊞ \mu_F=[\alpha_{\mu_D ⊞\mu_F},\beta_{\mu_D ⊞\mu_F},\gamma_{\mu_D ⊞\mu_F}]\nu_D ⊞ \nu_F=[\alpha_{\nu_D ⊞\nu_F},\beta_{\nu_D ⊞\nu_F},\gamma_{\nu_D ⊞\nu_F}]$ suchthat $\xi_{D ⊞F}=\{(n_1,n_2)(t_1,t_2):n_1 t_1\in\varsigma_D,n_2 t_2\in\varsigma_F\}\cup\{(z,n_2),(z,t_2):z\in\varphi_D,n_2 t_2\in\varsigma_F\}\cup\{(n_1,z),(t_1,z) : n_1 t_1\in\varsigma_D,z\in\varphi_F\}$ such that,For all $(n_1,n_2)\in\varphi_D\times\varphi_F$,

- $\alpha_{\emptyset_D ⊞\emptyset_F}\,(n_1,n_2)=\frac{\alpha_{\emptyset_D}\,(n_1)\alpha_{\emptyset_F}\,(n_2)}{\alpha_{\emptyset_D}\,(n_1)+\alpha_{\emptyset_F}\,(n_2)-\alpha_{\emptyset_D}\,(n_1)\alpha_{\emptyset_F}\,(n_2)}$

$\beta_{\mu_D ⊞\mu_F},\gamma_{\nu_D ⊞\nu_F}\,(n_1,n_2)=\frac{\beta_{\mu_D}\,(n_1)\beta_{\mu_F}(n_2)}{\beta_{\mu_D}\,(n_1)+\beta_{\mu_F}(n_2)-\beta_{\mu_D}\,(n_1)\beta_{\mu_F}(n_2)},\frac{\gamma_{\nu_D}\,(n_1)+\gamma_{\nu_F}\,(n_2)-2\gamma_{\nu_D}\,(n_1)\gamma_{\nu_F}\,(n_2)}{1-\gamma_{\nu_D}\,(n_1)\gamma_{\nu_F}\,(n_2)}$

$(\varsigma_D ⊞ \varsigma_F)\,(z,n_2),(z,t_2)=\frac{\alpha_{\emptyset_D}\,(Z)(n_1 t_1)\varsigma_{\alpha_{\emptyset_F}}\,(n_2 t_2)}{\alpha_{\emptyset_D}\,(Z)+\varsigma_{\alpha_{\emptyset_F}}\,(n_2 t_2)-\alpha_{\emptyset_D}\,(Z)\varsigma_{\alpha_{\emptyset_F}}\,(n_2 t_2)}$,

$\frac{\beta_{\mu_D}\,(Z)\varsigma_{\beta_{\mu_F}}\,(n_2 t_2)}{\beta_{\mu_D}\,(Z)+\varsigma_{\beta_{\mu_F}}\,(n_2 t_2)-\beta_{\mu_D}\,(Z)\varsigma_{\beta_{\mu_F}}\,(n_2 t_2)},\frac{\gamma_{\nu_D}\,(Z)\varsigma_{\gamma_{\nu_F}}\,(n_2 t_2)-2\gamma_{\nu_D}\,(Z)\varsigma_{\gamma_{\nu_F}}\,(n_2 t_2)}{1-\gamma_{\nu_D}\,(Z)\varsigma_{\gamma_{\nu_F}}\,(n_2 t_2)}$.

For all $z\in\varphi_D, n_2 t_2\in\varsigma_F$$(\varsigma_D ⊞ \varsigma_F)\,(n_1,z),(t_1,z)=\frac{\alpha_{\emptyset_F}\,(Z)(n_1 t_1)\varsigma_{\alpha_{\emptyset_D}}\,(n_2 t_2)}{\alpha_{\emptyset_F}\,(Z)+\varsigma_{\alpha_{\emptyset_D}}\,(n_2 t_2)-\alpha_{\emptyset_F}\,(Z)\varsigma_{\alpha_{\emptyset_D}}\,(n_2 t_2)}$

$\frac{\beta_{\mu_F}\,(Z)\varsigma_{\beta_{\mu_D}}\,(n_2 t_2)}{\beta_{\mu_F}\,(Z)+\varsigma_{\beta_{\mu_D}}\,(n_2 t_2)-\beta_{\mu_F}\,(Z)\varsigma_{\beta_{\mu_D}}\,(n_2 t_2)},\frac{\gamma_{\nu_F}\,(Z)\varsigma_{\gamma_{\nu_D}}\,(n_2 t_2)-2\gamma_{\nu_F}\,(Z)\varsigma_{\gamma_{\nu_D}}\,(n_2 t_2)}{1-\gamma_{\nu_F}\,(Z)\varsigma_{\gamma_{\nu_D}}\,(n_2 t_2)}$

$(\varsigma_D ⊞ \varsigma_F)(n_1,n_2)(t_1,t_2)=\frac{\varsigma_{\alpha_{\emptyset_D}}\,(n_1 t_1)\varsigma_{\alpha_{\emptyset_F}}\,(n_2 t_2)}{\varsigma_{\alpha_{\emptyset_D}}\,(n_1 t_1)+\varsigma_{\alpha_{\emptyset_F}}\,(n_2 t_2)-\varsigma_{\alpha_{\emptyset_D}}\,(n_1 t_1)\varsigma_{\alpha_{\emptyset_F}}\,(n_2 t_2)}$,

$$\frac{\varsigma_{\beta_{\mu_D}}(n_1t_1)\,\varsigma_{\beta_{\mu_F}}(n_2t_2)}{\varsigma_{\beta_{\mu_D}}(n_1t_1)+\varsigma_{\beta_{\mu_F}}(n_2t_2)-\varsigma_{\beta_{\mu_D}}(n_1t_1)\,\varsigma_{\beta_{\mu_F}}(n_2t_2)},\frac{\varsigma_{\gamma_{\nu_D}}(n_1t_1)\,\varsigma_{\gamma_{\nu_F}}(n_2t_2)-2\varsigma_{\gamma_{\nu_D}}(n_1t_1)\,\varsigma_{\gamma_{\nu_F}}(n_2t_2)}{1-\varsigma_{\gamma_{\nu_D}}(n_1t_1)\,\varsigma_{\gamma_{\nu_F}}(n_2t_2)}.$$

For all $n_1t_1 \in \varsigma_D, n_2t_2 \in \varsigma_F$

Example

Consider two neutrosophicdombi fuzzy graphs $d = (\emptyset_D, \mu_{D,}\nu_D)$ and $F = (\emptyset_F, \mu_{F,}\nu_F)$. Here $\varphi_D=\{a,b\}, \varphi_F=\{x,y,z\}, \varsigma_D = \{ab\}, \varsigma_F=\{xy,yz\}$ where $\varphi_D = \left\{\frac{a}{(0.8,0.5,0.7)}, \frac{b}{(0.6,0.5,0.8)}\right\}$, and $\varphi_F=\{\frac{x}{(0.9,0.6,0.4)}, \frac{y}{(0.8,1,0.4)}, \frac{z}{(0.6,1,0.7)}\}, \varsigma_D = \left\{\frac{ab}{(0.5,0.4,0.8)}\right\}$, $\varsigma_F=\{\frac{xy}{(0.7,0.6,0.5)}, \frac{yz}{(0.5,1,0.7)}\}$. Then we have $(\varphi_D \boxplus \varphi_F)(a,b)$ $=(0.5,0.4,0.8),(\varphi_D \boxplus \varphi_F)(x,y)=(0.7,0.6,0.5)$, $(\varphi_D \boxplus \varphi_F)(y,z)=(0.5,1,0.7),(\varphi_D \boxplus \varphi_F)(a,x)=(0.7,0.3,0.7),(\varphi_D \boxplus \varphi_F)(a,y)=(0.6,0.5,0.7),(\varphi_D \boxplus \varphi_F)(a,z)=(0.5,0.5,0.8)$ $(\varphi_D \boxplus \varphi_F)(b,x)=(0.5,0.3,0.8),(\varphi_D \boxplus \varphi_F)(b,y)=(0.5,0.5,0.8),(\varphi_D \boxplus \varphi_F)(b,z)=(0.4,0.5,0.8)(\varsigma_D \boxplus \varsigma_F)(a,x)(b,y)=(0.41,0.31,0.82),(\varsigma_D \boxplus \varsigma_F)(a,y)(b,x) = (0.41,0.31,0.82),(\varsigma_D \boxplus \varsigma_F)(a,z)(b,y)=(0.33,0.4,0.6),(\varsigma_D \boxplus \varsigma_F)(a,y)(b,z)=(0.33,0.4,0.6)$.

$(\varsigma_D \boxplus \varsigma_F)(a,x)(a,y)=(0.5,0.4,0.8),(\varsigma_D \boxplus \varsigma_F)(a,y)(a,z) = (0.4,0.5,0.5)$, $(\varsigma_D \boxplus \varsigma_F)(b,x)(b,y)=(0.5,0.4,0.8),(\varsigma_D \boxplus \varsigma_F)(b,y)(b,z)=(0.3,0.5,0.6)$.

Corollary

The strong product of two fermatean neutrosophic dombi fuzzy graph is not necessarily to a to a fermatean neutrosophic dombi fuzzy graph. $(\varsigma_D \boxplus \varsigma_F)(a,z)(b,y) = (0.33,0.4,0.6)$. Edge product of $(a,z)\ and\ (b,y)$ is $(\varsigma_D \boxplus \varsigma_F)(a,z)(b,y) = (0.35,0.33,0.9)$ $(0.35,0.33,0.9) \nleq (0.33,0.4,0.6)$

Theorem

Let D^* and F^* be the fermatean neutrosophic dombi fuzzy graphs of the graphs D and F, respectively. The Strong product $D\boxplus F$ of D^* and F^* is the fermateanneutrosophicdombi fuzzy edge graph of $D\boxplus F$.

Proof

Let D and F be the fermate an neutrosophic dombi fuzzy graphs $D = (\emptyset_D, \mu_{D,}\nu_D)$ and $F = (\emptyset_F, \mu_{F,}\nu_F)$ respectively. Consider,

i)For all $n \in \varsigma_D, n_2t_2 \in \varsigma_F$ such that $(\varsigma_D \boxplus \varsigma_F)(n,n_2)(n,t_2)= T[\varphi_D(n), \varsigma_F(n_2t_2)]=T[1,\varsigma_F(n_2t_2)]$ $(\varsigma_D \boxplus \varsigma_F)(n,n_2)(n,t_2)$

$$\leq T\begin{bmatrix}\frac{\alpha_{\emptyset_D}\,\varphi(n)\alpha_{\emptyset_F}\varsigma(n_2t_2)}{\alpha_{\emptyset_D}\,\varphi(n)+\alpha_{\emptyset_F}\varsigma(n_2t_2)-\alpha_{\emptyset_D}\,\varphi(n)\alpha_{\emptyset_F}\varsigma(n_2t_2)},\\\frac{\beta_{\mu_D}\,\varphi(n)\beta_{\mu_F}\,\varsigma(n_2t_2)}{\beta_{\mu_D}\,\varphi(n)+\beta_{\mu_F}\,\varsigma(n_2t_2)-\beta_{\mu_D}\,\varphi(n)\beta_{\mu_F}\,\varsigma(n_2t_2)},\\\frac{\gamma_{\nu_D}\,\varphi(n)+\gamma_{\nu_F}\,\varsigma(n_2t_2)-2\gamma_{\nu_D}\,\varphi(n)\gamma_{\nu_F}\,\varsigma(n_2t_2)}{1-\gamma_{\nu_D}\,\varphi(n)\gamma_{\nu_F}\,\varsigma(n_2t_2)}\end{bmatrix}\varsigma_F(n_2t_2)=\begin{cases}\frac{\alpha_{\emptyset_D}(n_2)\alpha_{\emptyset_F}(t_2)}{\alpha_{\emptyset_D}(n_2)+\alpha_{\emptyset_F}(t_2)-\alpha_{\emptyset_D}(n_2)\alpha_{\emptyset_F}(t_2)},\\\frac{\beta_{\mu_D}(n_2)\beta_{\mu_F}(t_2)}{\beta_{\mu_D}(n_2)+\beta_{\mu_F}(t_2)-\beta_{\mu_D}(n_2)\beta_{\mu_F}(t_2)},\\\frac{\gamma_{\nu_D}(n_2)+\gamma_{\nu_F}(t_2)-2\gamma_{\nu_D}(n_2)\gamma_{\nu_F}(t_2)}{1-\gamma_{\nu_D}(n_2)\gamma_{\nu_F}(t_2)}\end{cases}$$

$$=\begin{cases}\frac{(\varphi_D\boxplus\varphi_F)\alpha_{\emptyset_D}(n,n_2)(\varphi_D\boxplus\varphi_F)\alpha_{\emptyset_F}(n,t_2)}{(\varphi_D\boxplus\varphi_F)\alpha_{\emptyset_D}(n,n_2)+(\varphi_D\boxplus\varphi_F)\alpha_{\emptyset_F}(n,t_2)-(\varphi_D\boxplus\varphi_F)\alpha_{\emptyset_D}(n,n_2)(\varphi_D\boxplus\varphi_F)\alpha_{\emptyset_F}(n,t_2)},\\\frac{(\varphi_D\boxplus\varphi_F)\beta_{\mu_D}(n,n_2)(\varphi_D\boxplus\varphi_F)\beta_{\mu_F}(n,t_2)}{(\varphi_D\boxplus\varphi_F)\beta_{\mu_D}(n,n_2)+(\varphi_D\boxplus\varphi_F)\beta_{\mu_F}(n,t_2)-(\varphi_D\boxplus\varphi_F)\beta_{\mu_D}(n,n_2)(\varphi_D\boxplus\varphi_F)\beta_{\mu_F}(n,t_2)},\\\frac{(\varphi_D\boxplus\varphi_F)\gamma_{\nu_D}(n,n_2)+(\varphi_D\boxplus\varphi_F)\gamma_{\nu_F}(n,t_2)-2(\varphi_D\boxplus\varphi_F)\gamma_{\nu_D}(n,n_2)(\varphi_D\boxplus\varphi_F)\alpha_{\emptyset_F}(n,t_2)}{1-(\varphi_D\boxplus\varphi_F)\gamma_{\nu_D}(n,n_2)(\varphi_D\boxplus\varphi_F)\alpha_{\emptyset_F}(n,t_2)}\end{cases}$$

For all $n \in \varsigma_D, n_2t_2 \in \varsigma_F$ i)Now consider $n_1t_1 \in \varsigma_D, z \in \varphi_F (\varsigma_D \boxplus \varsigma_F)(n_1,z)(t_1,z)$ $= T[\varsigma_D(n_1t_1), \varphi_F(z)]$

$$\backslash\varsigma_D(n_1t_1) \leq \begin{cases}\frac{\alpha_{\emptyset_D}(n_1)\alpha_{\emptyset_D}(t_1)}{\alpha_{\emptyset_D}(n_1)+\alpha_{\emptyset_D}(t_1)-\alpha_{\emptyset_D}(n_1)\alpha_{\emptyset_D}(t_1)},\\\frac{\beta_{\mu_D}(n_1)\beta_{\mu_D}(t_1)}{\beta_{\mu_D}(n_1)+\beta_{\mu_D}(t_1)-\beta_{\mu_D}(n_1)\beta_{\mu_D}(t_1)},\\\frac{\gamma_{\nu_D}(n_1)+\gamma_{\nu_D}(t_1)-2\gamma_{\nu_D}(n_1)\gamma_{\nu_D}(t_1)}{1-\gamma_{\nu_D}(n_1)\gamma_{\nu_D}(t_1)}\end{cases}$$

Sasikala and Divya

$$= \begin{cases} \dfrac{(\varphi_D \boxplus \varphi_F)\alpha_{\emptyset_D}(n_1,z)(\varphi_D \boxplus \varphi_F)\alpha_{\emptyset_F}(t_1,z)}{(\varphi_D \boxplus \varphi_F)\alpha_{\emptyset_D}(n_1,z)+(\varphi_D \boxplus \varphi_F)\alpha_{\emptyset_F}(t_1,z)-(\varphi_D \boxplus \varphi_F)\alpha_{\emptyset_D}(n_1,z)(\varphi_D \boxplus \varphi_F)\alpha_{\emptyset_F}(t_1,z)}, \\[2mm] \dfrac{(\varphi_D \boxplus \varphi_F)\beta_{\mu_D}(n_1,z)(\varphi_D \boxplus \varphi_F)\beta_{\mu_F}(t_1,z)}{(\varphi_D \boxplus \varphi_F)\beta_{\mu_D}(n_1,z)+(\varphi_D \boxplus \varphi_F)\beta_{\mu_F}(t_1,z)-(\varphi_D \boxplus \varphi_F)\beta_{\mu_D}(n_1,z)(\varphi_D \boxplus \varphi_F)\beta_{\mu_F}(t_1,z)}, \\[2mm] \dfrac{(\varphi_D \boxplus \varphi_F)\gamma_{\nu_D}(n_1,z)+(\varphi_D \boxplus \varphi_F)\gamma_{\nu_F}(t_1,z)-2(\varphi_D \boxplus \varphi_F)\gamma_{\nu_D}(n_1,z)(\varphi_D \boxplus \varphi_F)\alpha_{\emptyset_F}(t_1,z)}{1-(\varphi_D \boxplus \varphi_F)\gamma_{\nu_D}(n_1,z)(\varphi_D \boxplus \varphi_F)\alpha_{\emptyset_F}(t_1,z)} \end{cases}$$

ii) Consider, for all $n_1 t_1 \in \varsigma_D, n_2 t_2 \in \varsigma_F$ such that $(\varsigma_D \boxplus \varsigma_F)(n_1,n_2)(t_1,t_2)$ The strong product of $D \boxplus F$ = T $[\varsigma_D(n_1 t_1),\varsigma_F(n_2 t_2)]$

$$\leq T \begin{bmatrix} \dfrac{\alpha_{\emptyset_D}(n_1)\alpha_{\emptyset_D}(n_2)}{\alpha_{\emptyset_D}(n_1)+\alpha_{\emptyset_D}(n_2)-\alpha_{\emptyset_D}(n_1)\alpha_{\emptyset_D}(n_2)}, \\[2mm] \dfrac{\beta_{\mu_D}(n_1)\beta_{\mu_D}(n_2)}{\beta_{\mu_D}(n_1)+\beta_{\mu_D}(n_2)-\beta_{\mu_D}(n_2)\beta_{\mu_D}(n_2)}, \\[2mm] \dfrac{\gamma_{\nu_D}(n_1)+\gamma_{\nu_D}(n_2)-2\gamma_{\nu_D}(n_1)\gamma_{\nu_D}(n_2)}{1-\gamma_{\nu_D}(n_1)\gamma_{\nu_D}(n_2)} \end{bmatrix} (\varsigma_D \boxplus \varsigma_F)(n_1,n_2)(t_1,t_2)$$

$$\leq \begin{cases} \dfrac{(\varphi_D \boxplus \varphi_F)\alpha_{\emptyset_D}(n_1 n_2)(\varphi_D \boxplus \varphi_F)\alpha_{\emptyset_F}(t_1 t_2)}{(\varphi_D \boxplus \varphi_F)\alpha_{\emptyset_D}(n_1 n_2)+(\varphi_D \boxplus \varphi_F)\alpha_{\emptyset_F}(t_1 t_2)-(\varphi_D \boxplus \varphi_F)\alpha_{\emptyset_D}(n_1 n_2)(\varphi_D \boxplus \varphi_F)\alpha_{\emptyset_F}(t_1 t_2)}, \\[2mm] \dfrac{(\varphi_D \boxplus \varphi_F)\beta_{\mu_D}(n_1 n_2)(\varphi_D \boxplus \varphi_F)\beta_{\mu_F}(t_1 t_2)}{(\varphi_D \boxplus \varphi_F \beta_{\mu_D}(n_1 n_2)+(\varphi_D \boxplus \varphi_F)\beta_{\mu_F}(t_1 t_2)-(\varphi_D \boxplus \varphi_F)\beta_{\mu_D}(n_1 n_2)(\varphi_D \boxplus \varphi_F)\beta_{\mu_F}(t_1 t_2)}, \\[2mm] \dfrac{(\varphi_D \boxplus \varphi_F)\gamma_{\nu_D}(n_1 n_2)(+\varphi_D \boxplus \varphi_F)\gamma_{\nu_F}(t_1 t_2)-2(\varphi_D \boxplus \varphi_F)\gamma_{\nu_D}(n_1 n_2)(\varphi_D \boxplus \varphi_F)\alpha_{\emptyset_F}(t_1 t_2)}{1-(\varphi_D \boxplus \varphi_F)\gamma_{\nu_D}(n_1 n_2)(\varphi_D \boxplus \varphi_F)\alpha_{\emptyset_F}(t_1 t_2)} \end{cases}$$

Definition: (Boxdot Product)

Let $\emptyset_i$ be a fermatean neutrosophic fuzzy subset of φ_D and ς_i be a neutrosophic fuzzy subset ς_D of $\varsigma_i=1,2$ define the boxdot product of fermatean neutrosophicdombi fuzzy graph. $D = (\emptyset_D, \mu_D, \nu_D)$ and $F = (\emptyset_F, \mu_F, \nu_F)$ $D^* = (\varphi_D, \varsigma_D)$ and $F^* = (\varphi_F, \varsigma_F)$ separately is established by $D \boxdot F$ is $D \boxdot F = (\emptyset_D \boxdot \emptyset_F, \mu_D \boxdot \mu_F, \nu_D \boxdot \nu_F)$.(i.e.) $\emptyset_D \boxdot \emptyset_F = [\alpha_{\emptyset_D \boxdot \emptyset_F}, \beta_{\emptyset_D \boxdot \emptyset_F}, \gamma_{\emptyset_D \boxdot \emptyset_F}] \mu_D \boxdot \mu_F = [\alpha_{\mu_D \boxdot \mu_F}, \beta_{\mu_D \boxdot \mu_F}, \gamma_{\mu_D \boxdot \mu_F}] \nu_D \boxdot \nu_F = [\alpha_{\nu_D \boxdot \nu_F}, \beta_{\nu_D \boxdot \nu_F}, \gamma_{\nu_D \boxdot \nu_F}]$ such that $\xi_{D \boxdot F} = \{(n_1, t_1), (n_2, t_2): \forall (n_1 n_2 \in \varsigma_D) \text{ and } t_1 t_2 \notin \varsigma_F\} \cup \{(n_1 = n_2) \text{ and } t_1 t_2 \notin \varsigma_F\}$ such that,

For all $(n_1, n_2) \in \varphi_D \times \varphi_F$,

- $\alpha_{\emptyset_D \boxdot \emptyset_F}(n_1, n_2) = \dfrac{\alpha_{\emptyset_D}(n_1)\alpha_{\emptyset_F}(n_2)}{\alpha_{\emptyset_D}(n_1)+\alpha_{\emptyset_F}(n_2)-\alpha_{\emptyset_D}(n_1)\alpha_{\emptyset_F}(n_2)}$

$\beta_{\mu_D \boxdot \mu_F}(n_1, n_2) = \dfrac{\beta_{\mu_D}(n_1)\beta_{\mu_F}(n_2)}{\beta_{\mu_D}(n_1)+\beta_{\mu_F}(n_2)-\beta_{\mu_D}(\chi)\beta_{\mu_F}(n_2)}; \gamma_{\nu_D \boxdot \nu_F}(n_1, n_2) = \dfrac{\gamma_{\nu_D}(n_1)+\gamma_{\nu_F}(n_2)-2\gamma_{\nu_D}(n_1)\gamma_{\nu_F}(n_2)}{1-\gamma_{\nu_D}(n_1)\gamma_{\nu_F}(n_2)}$

For all $(n_1 n_2 \in \varsigma_D)$ and $t_1 t_2 \notin \varsigma_F (\varsigma_D \boxdot \varsigma_F) (n_1, t_1), (n_2, t_2)$

$$= \dfrac{\alpha_{\emptyset_F}(t_1)\varsigma_{\alpha_{\emptyset_D}}(n_1 n_2)\alpha_{\emptyset_F}(t_2)}{\alpha_{\emptyset_F}(t_1)\varsigma_{\alpha_{\emptyset_D}}(n_1 n_2)+\varsigma_{\alpha_{\emptyset_D}}(n_1 n_2)\alpha_{\emptyset_F}(t_2)+\alpha_{\emptyset_F}(t_1)\alpha_{\emptyset_F}(t_2)+\varsigma_{\alpha_{\emptyset_F}}(n_2 t_2)-2\alpha_{\emptyset_F}(t_1)\varsigma_{\alpha_{\emptyset_D}}(n_1 n_2)\alpha_{\emptyset_F}(t_2)},$$

$$\dfrac{\beta_{\mu_F}(t_1)\varsigma_{\beta_{\mu_D}}(n_1 n_2)\beta_{\mu_F}(t_2)}{\beta_{\mu_F}(t_1)\varsigma_{\alpha_{\emptyset_D}}(n_1 n_2)+\varsigma_{\beta_{\mu_D}}(n_1 n_2)\beta_{\mu_F}(t_2)+\beta_{\mu_F}(t_1)\beta_{\mu_F}(t_2)+\varsigma_{\beta_{\mu_D}}(n_2 t_2)-2\beta_{\mu_F}(t_1)\varsigma_{\beta_{\mu_D}}(n_1 n_2)\beta_{\mu_F}(t_2)}$$

$$\dfrac{\gamma_{\nu_F}(t_1)\varsigma_{\gamma_{\nu_D}}(n_1 n_2)\gamma_{\nu_F}(t_2)}{\gamma_{\nu_F}(t_1)\varsigma_{\gamma_{\nu_D}}(n_1 n_2)+\varsigma_{\gamma_{\nu_D}}(n_1 n_2)\gamma_{\nu_F}(t_2)+\gamma_{\nu_F}(t_1)\gamma_{\nu_F}(t_2)+\varsigma_{\gamma_{\nu_D}}(n_2 t_2)-2\gamma_{\nu_F}(t_1)\varsigma_{\gamma_{\nu_D}}(n_1 n_2)\gamma_{\nu_F}(t_2)}.$$

For all $(n_1 = n_2)$ and $t_1 t_2 \notin \varsigma_F (\varsigma_D \boxdot \varsigma_F) (n_1, t_1), (n_2, t_2)$

$$= \dfrac{\alpha_{\emptyset_F}(t_1)\alpha_{\emptyset_D}(n_1)\alpha_{\emptyset_F}(t_2)}{\alpha_{\emptyset_F}(t_1)\alpha_{\emptyset_D}(n_1)+\alpha_{\emptyset_D}(n_1)\alpha_{\emptyset_F}(t_2)+\alpha_{\emptyset_F}(t_1)\alpha_{\emptyset_F}(t_2)-2\alpha_{\emptyset_F}(t_1)\alpha_{\emptyset_D}(n_1)\alpha_{\emptyset_F}(t_2)}, \dfrac{\beta_{\mu_F}(t_1)\beta_{\mu_D}(n_1)\beta_{\mu_F}(t_2)}{\beta_{\mu_F}(t_1)\beta_{\mu_D}(n_1)+\beta_{\mu_D}(n_1)\beta_{\mu_F}(t_2)+\beta_{\mu_F}(t_1)\beta_{\mu_F}(t_2)-2\beta_{\mu_F}(t_1)\beta_{\mu_D}(n_1)\beta_{\mu_F}(t_2)},$$

$$\dfrac{\gamma_{\nu_F}(t_1)\gamma_{\nu_D}(n_1)\gamma_{\nu_F}(t_2)}{\gamma_{\nu_F}(t_1)\gamma_{\nu_D}(n_1)+\gamma_{\nu_D}(n_1)\gamma_{\nu_F}(t_2)+\gamma_{\nu_F}(t_1)\gamma_{\nu_F}(t_2)-2\gamma_{\nu_F}(t_1)\varsigma_{\gamma_{\nu_D}}(n_1 n_2)\gamma_{\nu_F}(t_2)}.$$

Example

Consider two neutrosophicdombi fuzzy graphs $d = (\emptyset_D, \mu_D, \nu_D)$ and $F = (\emptyset_F, \mu_F, \nu_F)$. Here $\varphi_D = \{a,b,c\}, \varphi_F = \{x,y\}, \varsigma_D = \{ab, bc\}, \varsigma_F = \{xy\}$, where $\varphi_D = \left\{\dfrac{x}{(0.7,0.6,0.8)}, \dfrac{y}{(0.5,0.7,0.9)}\right\}, \varphi_F = \left\{\dfrac{a}{(0.6,0.7,0.8)}, \dfrac{b}{(0.9,0.7,0.6)}, \dfrac{c}{(0.5,0.7,0.8)}\right\}, \varsigma_D =$

$\left\{\frac{xy}{(0.4,0.4,0.9)}\right\}$, $\varsigma_F = \left\{\frac{ab}{(0.5,0.5,0.8)}, \frac{bc}{(0.4,0.5,0.8)}\right\}$. Then we have $(\varphi_D \boxdot \varphi_F)$(a,b) =(0.5,0.5,0.8), $(\varphi_D \boxdot \varphi_F)$(b,c)=(0.4,0.5,0.8) ,$(\varphi_D \boxdot \varphi_F)$(x,y)=(0.4,0.4,0.9),$(\varphi_D \boxdot \varphi_F)$(a,x)=(0.4,0.4,0.8),$(\varphi_D \boxdot \varphi_F)$(a,y)=(0.3,0.5,0.9),$(\varphi_D \boxdot \varphi_F)$(b,x)=(0.6,0.4,0.8) $(\varphi_D \boxdot \varphi_F)$(b,y)=(0.4,0.5,0.9),$(\varphi_D \boxdot \varphi_F)$(c,x)=(0.4,0.4,0.8),$(\varphi_D \boxdot \varphi_F)$(c,y)=(0.3,0.5,0.9)$(\varsigma_D \boxdot \varsigma_F)(a,x)(a,y)$=(0.32,0.39,0.62),$(\varsigma_D \boxdot \varsigma_F)(b,x)(b,y)$ = (0.41,0.31,0.82),$(\varsigma_D \boxdot \varsigma_F)(c,x)(c,y)$=(0.29,0.39,0.62),$(\varsigma_D \boxdot \varsigma_F)(a,x)(b,y)$=(0.29,0.33,0.62) $(\varsigma_D \boxdot \varsigma_F)(a,y)(c,x)$=(0.25,0.33,0.62),$(\varsigma_D \boxdot \varsigma_F)(b,x)(c,y)$ = (0.25,0.33,0.62),$(\varsigma_D \boxdot \varsigma_F)(a,x)(c,y)$=(0.25,0.33,0.62),$(\varsigma_D \boxdot \varsigma_F)(b,y)(c,x)$=(0.29,0.33,0.62).$(\varsigma_D \boxdot \varsigma_F)(a,y)(b,x)$= (0.29,0.33,0.62).

Corollary

The box dot product of two fermate an neutrosophic dombi fuzzy graph is not necessarily to a fermate an neutrosophic dombi fuzzy graph.$(\varsigma_D \boxdot \varsigma_F)(a,x)(a,y)$ =(0.20,0.28,0.9) Edge product of (a,x) and (a,y) is$(\varsigma_D \boxdot \varsigma_F)(a,x)(a,y)$ = (0.32,0.39,0.62).   (0.32,0.39,0.62 $\nleq$ (0.20,0.28,0.9)

Theorem

Let D* and F^* be the fermatean neutrosophic dombi fuzzy graphs of the graphs D and F , respectively. The boxdot product $D\boxdot F$ of D* and F^* is the fermatean neutrosophic dombi fuzzy edge graph of $D\boxdot F$.

Proof

Let D and F be the fermate an neutrosophic dombi fuzzy graphs $D = (\emptyset_D, \mu_{D,} \nu_D)$ and $F = (\emptyset_F, \mu_{F,} \nu_F)$ respectively. Consider,$n_1 t_1 \in \varsigma_D, n_2 = t_2$.$(\varsigma_D \circ \varsigma_F)[(n_1,n_2)(t_1,t_2)] = T[T(\varphi_F(n_2), \varphi_F(t_2), \varsigma_D(n_1t_1))] = T[(T(1,1),\varsigma_{\mu_D}(n_1t_1)),(T(0,0),\varsigma_{\nu_F}(n_1t_1)) = T[(T(1,0),T(1,0)),(T(\varsigma_{\mu_D}(n_1t_1),$

$$\varsigma_{\nu_F}(n_1t_1)) \leq \begin{cases} \frac{\alpha_{\emptyset_D}(n_1t_1)\alpha_{\emptyset_F}(n_2)\alpha_{\emptyset_F}(t_2)}{\alpha_{\emptyset_D}(n_1t_1)\alpha_{\emptyset_F}(n_2)+\alpha_{\emptyset_F}(n_2)\alpha_{\emptyset_F}(t_2)+\alpha_{\emptyset_D}(n_1t_1)\alpha_{\emptyset_F}(t_2)-2\alpha_{\emptyset_D}(n_1t_1)\alpha_{\emptyset_F}(n_2)\alpha_{\emptyset_F}(t_2)}, \\ \frac{\beta_{\mu_D}(n_1t_1)\beta_{\mu_F}(n_2)\beta_{\mu_F}(t_2)}{\beta_{\mu_D}(n_1t_1)\beta_{\mu_F}(n_2)+\beta_{\mu_F}(n_2)\beta_{\mu_F}(t_2)+\beta_{\mu_D}(n_1t_1)\beta_{\mu_F}(t_2)-2\beta_{\mu_D}(n_1t_1)\beta_{\mu_F}(n_2)\beta_{\mu_F}(t_2)}, \\ \frac{\gamma_{\nu_D}(n_1t_1)+\gamma_{\nu_F}(n_2)+\gamma_{\nu_F}(t_2)-2\gamma_{\nu_D}(n_1t_1)\gamma_{\nu_F}(n_2)-2\gamma_{\nu_F}(n_2)\gamma_{\nu_F}(t_2)-2\gamma_{\nu_D}(n_1t_1)\gamma_{\nu_F}(t_2)-2\gamma_{\nu_D}(n_1t_1)\gamma_{\nu_F}(n_2)\gamma_{\nu_F}(t_2)}{1-\gamma_{\nu_D}(n_1t_1)\gamma_{\nu_F}(n_2)-\gamma_{\nu_F}(n_2)\gamma_{\nu_F}(t_2)-\gamma_{\nu_D}(n_1t_1)\gamma_{\nu_F}(t_2)} \end{cases}$$

$$= \begin{cases} \alpha_{\emptyset_D}(n_1t_1) & [\because \alpha_{\emptyset_F}(t_1) = 1, \alpha_{\emptyset_F}(t_2) = 1] \\ \beta_{\mu_D}(n_1t_1) & [\because \beta_{\mu_F}(t_1) = 1, \alpha_{\emptyset_F}(t_2) = 1] \\ \gamma_{\nu_D}(n_1t_1) & [\because \gamma_{\nu_F}(t_1) = 0, \alpha_{\emptyset_F}(t_2) = 0] \end{cases} \leq \begin{cases} \frac{\alpha_{\emptyset_D}(n_1)\alpha_{\emptyset_D}(t_1)}{\alpha_{\emptyset_D}(n_1)+\alpha_{\emptyset_D}(t_1)-\alpha_{\emptyset_D}(n_1)\alpha_{\emptyset_D}(t_1)}, \\ \frac{\beta_{\mu_D}(n_1)\beta_{\mu_D}(t_1)}{\beta_{\mu_D}(n_1)+\beta_{\mu_D}(t_1)-\beta_{\mu_D}(n_1)\beta_{\mu_D}(t_1)}, \\ \frac{\gamma_{\nu_D}(n_1)+\gamma_{\nu_D}(t_1)-2\gamma_{\nu_D}(n_1)\gamma_{\nu_D}(t_1)}{1-\gamma_{\nu_D}(n_1)\gamma_{\nu_D}(t_1)} \end{cases}$$

$$\leq 0 = \begin{cases} \frac{(\varphi_D\boxdot\varphi_F)\alpha_{\emptyset_D}(n_1,n_2)(\varphi_D\boxdot\varphi_F)\alpha_{\emptyset_F}(t_1,t_2)}{(\varphi_D\boxdot\varphi_F)\alpha_{\emptyset_D}(n_1,n_2)+(\varphi_D\boxdot\varphi_F)\alpha_{\emptyset_F}(t_1,t_2)-(\varphi_D\boxdot\varphi_F)\alpha_{\emptyset_D}(n_1,n_2)(\varphi_D\boxdot\varphi_F)\alpha_{\emptyset_F}(t_1,t_2)}, \\ \frac{(\varphi_D\boxdot\varphi_F)\beta_{\mu_D}(n_1,n_2)(\varphi_D\boxdot\varphi_F)\beta_{\mu_F}(t_1,t_2)}{(\varphi_D\boxdot\varphi_F)\beta_{\mu_D}(n_1,n_2)+(\varphi_D\boxdot\varphi_F)\beta_{\mu_F}(t_1,t_2)-(\varphi_D\boxdot\varphi_F)\beta_{\mu_D}(n_1,n_2)(\varphi_D\boxdot\varphi_F)\beta_{\mu_F}(t_1,t_2)}, \\ \frac{(\varphi_D\boxdot\varphi_F)\gamma_{\nu_D}(n_1,n_2)+(\varphi_D\boxdot\varphi_F)\gamma_{\nu_F}(t_1,t_2)-2(\varphi_D\boxdot\varphi_F)\gamma_{\nu_D}(n_1,n_2)(\varphi_D\boxdot\varphi_F)\gamma_{\nu_F}(t_1,t_2)}{1-(\varphi_D\boxdot\varphi_F)\gamma_{\nu_D}(n_1,n_2)(\varphi_D\boxdot\varphi_F)\gamma_{\nu_F}(t_1,t_2)} \end{cases}$$

ii) For all $(n_1 = t_1)$ and $t_1 t_2 \varsigma_F$,

$(\varsigma_D \boxdot \varsigma_F) (n_1,t_1), (n_2,t_2)$

$= \frac{\alpha_{\emptyset_F}(t_1)\alpha_{\emptyset_D}(n_1)\alpha_{\emptyset_F}(t_2)}{\alpha_{\emptyset_F}(t_1)\alpha_{\emptyset_D}(n_1)+\alpha_{\emptyset_D}(n_1)\alpha_{\emptyset_F}(t_2)+\alpha_{\emptyset_F}(t_1)\alpha_{\emptyset_F}(t_2)-2\alpha_{\emptyset_D}(n_1)\alpha_{\emptyset_F}(t_2)}$,

$\frac{\beta_{\mu_F}(t_1)\beta_{\mu_D}(n_1)\beta_{\mu_F}(t_2)}{\beta_{\mu_F}(t_1)\beta_{\mu_D}(n_1)+\beta_{\mu_D}(n_1)\beta_{\mu_F}(t_2)+\beta_{\mu_F}(t_1)\beta_{\mu_F}(t_2)-2\beta_{\mu_F}(t_1)\beta_{\mu_D}(n_1)\beta_{\mu_F}(t_2)}$ $\frac{\gamma_{\nu_D}(n_1t_1)+\gamma_{\nu_F}(n_2)+\gamma_{\nu_F}(t_2)-2\gamma_{\nu_D}(n_1t_1)\gamma_{\nu_F}(n_2)-2\gamma_{\nu_F}(n_2)\gamma_{\nu_F}(t_2)-2\gamma_{\nu_D}(n_1t_1)\gamma_{\nu_F}(t_2)+4\gamma_{\nu_D}(n_1t_1)\gamma_{\nu_F}(n_2)\gamma_{\nu_F}(}{1-\gamma_{\nu_D}(n_1t_1)\gamma_{\nu_F}(n_2)-\gamma_{\nu_F}(n_2)\gamma_{\nu_F}(t_2)-\gamma_{\nu_D}(n_1t_1)\gamma_{\nu_F}(t_2)-2\gamma_{\nu_D}(n_1t_1)\gamma_{\nu_F}(n_2)\gamma_{\nu_F}(t_2)}$

$$= \begin{cases} \alpha_{\emptyset_D}(n_1t_1) & [\because \alpha_{\emptyset_F}(t_1) = 1, \alpha_{\emptyset_F}(t_2) = 1] \\ \beta_{\mu_D}(n_1t_1) & [\because \beta_{\mu_F}(t_1) = 1, \alpha_{\emptyset_F}(t_2) = 1] \\ \gamma_{\nu_D}(n_1t_1) & [\because \gamma_{\nu_F}(t_1) = 0, \alpha_{\emptyset_F}(t_2) = 0] \end{cases} \leq \begin{cases} \frac{\alpha_{\emptyset_D}(n_1)\alpha_{\emptyset_D}(t_1)}{\alpha_{\emptyset_D}(n_1)+\alpha_{\emptyset_D}(t_1)-\alpha_{\emptyset_D}(n_1)\alpha_{\emptyset_D}(t_1)}, \\ \frac{\beta_{\mu_D}(n_1)\beta_{\mu_D}(t_1)}{\beta_{\mu_D}(n_1)+\beta_{\mu_D}(t_1)-\beta_{\mu_D}(n_1)\beta_{\mu_D}(t_1)}, \\ \frac{\gamma_{\nu_D}(n_1)+\gamma_{\nu_D}(t_1)-2\gamma_{\nu_D}(n_1)\gamma_{\nu_D}(t_1)}{\gamma_{\nu_D}(n_1)\gamma_{\nu_D}(t_1)} \end{cases}$$

Sasikala and Divya

$$\leq 0 = \begin{cases} \dfrac{(\varphi_D \square \varphi_F)\alpha_{\emptyset_D}(n_1,n_2)(\varphi_D \square \varphi_F)\alpha_{\emptyset_F}(t_1,t_2)}{(\varphi_D \square \varphi_F)\alpha_{\emptyset_D}(n_1,n_2)+(\varphi_D \square \varphi_F)\alpha_{\emptyset_F}(t_1,t_2)-(\varphi_D \square \varphi_F)\alpha_{\emptyset_D}(n_1,n_2)(\varphi_D \square \varphi_F)\alpha_{\emptyset_F}(t_1,t_2)}, \\[2mm] \dfrac{(\varphi_D \square \varphi_F)\beta_{\mu_D}(n_1,n_2)(\varphi_D \square \varphi_F)\beta_{\mu_F}(t_1,t_2)}{(\varphi_D \square \varphi_F)\beta_{\mu_D}(n_1,n_2)+(\varphi_D \square \varphi_F)\beta_{\mu_F}(t_1,t_2)-(\varphi_D \square \varphi_F)\beta_{\mu_D}(n_1,n_2)(\varphi_D \square \varphi_F)\beta_{\mu_F}(t_1,t_2)}, \\[2mm] \dfrac{(\varphi_D \square \varphi_F)\gamma_{\nu_D}(n_1,n_2)+(\varphi_D \square \varphi_F)\gamma_{\nu_F}(t_1,t_2)-2(\varphi_D \square \varphi_F)\gamma_{\nu_D}(n_1,n_2)(\varphi_D \square \varphi_F)\gamma_{\nu_F}(t_1,t_2)}{1-(\varphi_D \square \varphi_F)\gamma_{\nu_D}(n_1,n_2)(\varphi_D \square \varphi_F)\gamma_{\nu_F}(t_1,t_2)} \end{cases}$$

Definition: (Modular Product)

Let $\emptyset_i$ be a fermatean neutrosophic fuzzy subset of φ_D and ς_i be a neutrosophic fuzzy subset ς_D of ς_i=1,2 define the modular product of fermatean neutrosophic dombi fuzzy graph. $D = (\emptyset_D, \mu_D, \nu_D)$ and $F = (\emptyset_F, \mu_F, \nu_F)$ $D^* = (\varphi_D, \varsigma_D)$ and $F^* = (\varphi_F, \varsigma_F)$ separately is established by $D \circledast F$ is $D \circledast F = (\emptyset_D \circledast \emptyset_F, \mu_D \circledast \mu_F, \nu_D \circledast \nu_F)$.(i.e) $\emptyset_D \circledast \emptyset_F = [\alpha_{\emptyset_D \circledcirc \emptyset_F}, \beta_{\emptyset_D \circledcirc \emptyset_F}, \gamma_{\emptyset_D \circledcirc \emptyset_F}]\mu_D \circledast \mu_F = [\alpha_{\mu_D \circledcirc \mu_F}, \beta_{\mu_D \circledcirc \mu_F}, \gamma_{\mu_D \circledcirc \mu_F}]\nu_D \circledast \nu_F = [\alpha_{\nu_D \circledcirc \nu_F}, \beta_{\nu_D \circledcirc \nu_F}, \gamma_{\nu_D \circledcirc \nu_F}]$ suchthat $\xi_{D \circledcirc F} = \{(n_1,n_2),(t_1,t_2): \forall n_1 t_1 \in \varsigma_D \& n_2 t_2 \in \varsigma_F\} \cup \{(n_1,n_2),(t_1,t_2): \forall n_1 t_1 \notin \varsigma_D \& n_2 t_2 \notin \varsigma_F\}$ such that, For all $(n_1,n_2) \in \varphi_D \times \varphi_F$,

- $\alpha_{\emptyset_D \circledcirc \emptyset_F}(n_1,n_2) = \dfrac{\alpha_{\emptyset_D}(n_1)\alpha_{\emptyset_F}(n_2)}{\alpha_{\emptyset_D}(n_1)+\alpha_{\emptyset_F}(n_2)-\alpha_{\emptyset_D}(n_1)\alpha_{\emptyset_F}(n_2)}$

$\beta_{\mu_D \circledcirc \mu_F}(n_1,n_2) = \dfrac{\beta_{\mu_D}(n_1)\beta_{\mu_F}(n_2)}{\beta_{\mu_D}(n_1)+\beta_{\mu_F}(n_2)-\beta_{\mu_D}(\chi)\beta_{\mu_F}(n_2)}, \gamma_{\nu_D \circledcirc \nu_F}(n_1,n_2) = \dfrac{\gamma_{\nu_D}(n_1)+\gamma_{\nu_F}(n_2)-2\gamma_{\nu_D}(n_1)\gamma_{\nu_F}(n_2)}{1-\gamma_{\nu_D}(n_1)\gamma_{\nu_F}(n_2)}$ For all $n_1 t_1 \in \varsigma_D$ and $n_2 t_2 \in \varsigma_F$

$\alpha_{\emptyset_D \circledcirc \emptyset_F}(n_1,n_2),(t_1,t_2) = \dfrac{\alpha_{\emptyset_D}(n_1 t_1)\alpha_{\emptyset_F}(n_2 t_2)}{\alpha_{\emptyset_D}(n_1 t_1)+\alpha_{\emptyset_F}(n_2 t_2)-\alpha_{\emptyset_D}(n_1 t_1)\alpha_{\emptyset_F}(n_2 t_2)}$

$\beta_{\mu_D \circledcirc \mu_F}(n_1,n_2),(t_1,t_2) = \dfrac{\beta_{\mu_D}(n_1 t_1)\beta_{\mu_F}(n_2 t_2)}{\beta_{\mu_D}(n_1 t_1)+\beta_{\mu_F}(n_2 t_2)-\beta_{\mu_D}(n_1 t_1)\beta_{\mu_F}(n_2 t_2)}$

$\gamma_{\nu_D \circledcirc \nu_F}(n_1,n_2),(t_1,t_2) = \dfrac{\gamma_{\nu_D}(n_1 t_1)+\gamma_{\nu_F}(n_2 t_2)-2\gamma_{\nu_D}(n_1 t_1)\gamma_{\nu_F}(n_2 t_2)}{1-\gamma_{\nu_D}(n_1 t_1)\gamma_{\nu_F}(n_2 t_2)}$

For all $n_1 t_1 \notin \varsigma_D$ and $n_2 t_2 \notin \varsigma_F$

- $\alpha_{\emptyset_D \circledcirc \emptyset_F}(n_1,n_2),(t_1,t_2) =$

$\dfrac{\alpha_{\emptyset_D}(n_1)\alpha_{\emptyset_D}(t_1)\alpha_{\emptyset_F}(n_2)\alpha_{\emptyset_F}(t_2)}{\alpha_{\emptyset_D}(n_1)\alpha_{\emptyset_D}(t_1)\alpha_{\emptyset_F}(n_2)+\alpha_{\emptyset_D}(n_1)\alpha_{\emptyset_D}(t_1)\alpha_{\emptyset_F}(t_2)+\alpha_{\emptyset_D}(t_1)\alpha_{\emptyset_F}(n_2)\alpha_{\emptyset_F}(t_2)-3\alpha_{\emptyset_D}(n_1)\alpha_{\emptyset_D}(t_1)\alpha_{\emptyset_F}(n_2)\alpha_{\emptyset_F}(t_2)}$

$\beta_{\mu_D \circledcirc \mu_F}(n_1,n_2),(t_1,t_2) = \dfrac{\beta_{\mu_D}(n_1)\beta_{\mu_D}(t_1)\beta_{\mu_F}(n_2)\beta_{\mu_F}(t_2)}{\beta_{\mu_D}(n_1)\beta_{\mu_D}(t_1)\beta_{\mu_F}(n_2)+\beta_{\mu_D}(n_1)\beta_{\mu_D}(t_1)\beta_{\mu_F}(t_2)+\beta_{\mu_D}(t_1)\beta_{\mu_F}(n_2)\beta_{\mu_F}(t_2)-3\beta_{\mu_D}(n_1)\beta_{\mu_D}(t_1)\beta_{\mu_F}(n_2)\beta_{\mu_F}(t_2)}$

$\gamma_{\nu_D \circledcirc \nu_F}(n_1,n_2),(t_1,t_2) = \dfrac{\gamma_{\nu_D}(n_1)\gamma_{\nu_D}(t_1)\gamma_{\nu_F}(n_2)\gamma_{\nu_F}(t_2)}{\gamma_{\nu_D}(n_1)\gamma_{\nu_D}(t_1)\gamma_{\nu_F}(n_2)+\gamma_{\nu_D}(n_1)\gamma_{\nu_D}(t_1)\gamma_{\nu_F}(t_2)+\gamma_{\nu_D}(t_1)\gamma_{\nu_F}(n_2)\gamma_{\nu_F}(t_2)-3\gamma_{\nu_D}(n_1)\gamma_{\nu_D}(t_1)\gamma_{\nu_F}(n_2)\gamma_{\nu_F}(t_2)}$

Example

Consider two neutrosophicdombi fuzzy graphs $d = (\emptyset_D, \mu_D, \nu_D)$ and $F = (\emptyset_F, \mu_F, \nu_F)$. Here φ_D={a,b,c}, φ_F={x,y}, ς_D = {ab, bc}, ς_F={xy} where $(\varphi_D \circledast \varphi_F)$(a,b)=(0.5,0.5,0.8), $(\varphi_D \circledast \varphi_F)$(x,y)=(0.4,0.4,0.9), $(\varphi_D \circledast \varphi_F)$(b,c)=(0.4,0.5,0.8), $(\varphi_D \circledast \varphi_F)$(a,x)=(0.4,0.4,0.8), $(\varphi_D \circledast \varphi_F)$(a,y)=(0.3,0.5,0.9), $(\varphi_D \circledast \varphi_F)$(b,x)=(0.6,0.4,0.8), $(\varphi_D \circledast \varphi_F)$(b,y)=(0.4,0.5,0.9), $(\varphi_D \circledast \varphi_F)$(c,x)=(0.4,0.4,0.8), $(\varphi_D \circledast \varphi_F)$(c,y)=(0.3,0.5,0.9), $(a,x)(a,y)$=(0.32,0.39,0.62), $(\varsigma_D \circledast \varsigma_F)(b,x)(b,y) = (0.41,0.31,0.82)$, $(\varsigma_D \circledast \varsigma_F)(c,x)(c,y)$=(0.29,0.39,0.62), $(\varsigma_D \circledast \varsigma_F)(a,x)(b,y)$=(0.29,0.33,0.62), $(\varsigma_D \circledast \varsigma_F)(a,y)(c,x)$=(0.25,0.33,0.62), $(\varsigma_D \circledast \varsigma_F)(b,x)(c,y) = (0.25,0.33,0.62)$, $(\varsigma_D \circledast \varsigma_F)(a,x)(c,y)$=(0.25,0.33,0.62), $(\varsigma_D \circledast \varsigma_F)(b,y)(c,x)$=(0.29,0.33,0.62), $(\varsigma_D \circledast \varsigma_F)(a,y)(b,x)$=(0.29,0.33,0.62).

CONCLUSION

We have observed the excellent flexibility of dombi operators with operational parameters in graph theoretical concept under fermatean neutrosophic dombi fuzzy environment. In this manuscript, the innovative concept of fermatean neutrosophic dombi fuzzy graph was introduced. As well, we described some different types of fermatean neutrosophic dombi fuzzy graph such as a products of semi-strong, strong, boxdot, modular fermatean neutrosophic dombi fuzzy graphs. Further work will be extended in the future to investigate the operations of isomorphic, homomorphic, complete, complement fermatean neutrosophic dombi fuzzy graphs along with applications and proposition with relatable illustrations.

REFERENCES

1. Ajay.D and P.Chellamani,"Pythogorean Neutrosophic fuzzy graphs",International journal of Neutrosophic science,vol.11,pp.108-1144,(2020).
2. Akram M,Akram R(2016) Operations on intuitionistic fuzzy graph structures,Fuzzy Inf Eng 8(4):389-410
3. M.Akram,and G.Shahzadi,"Decision-making approach based on Pythogorean dombi fuzzy soft graphs",Granular computing,pp.1-19,2020.
4. Ashraf S,Naz S,Kerre EE(2018) Dombi fuzzy graphs,Fuzzy Inf Eng 10(1):58-79
5. Atanassov.K.Intuitionistic fuzzy sets,In:Fuzzy sets and system.vol.20(1986)87-96.
6. Aydemir,S.B.,&Yilmaz Gunduz,S.(2020).Fermatean fuzzy TOPSIS method with Dombi Aggregation operators and its application in multi-criteria decision making.In journal of Intelligent&Fuzzysystems(Vol.39,Issue1,pp.851-869).IOSPress. https://doi.org/10.3233/jifs-191763
7. Dombi.J ,The Generalized Dombi operator family and the Multiplicative Utility function,Soft Computing Based Modeling in Intelligent systems.(2009).115-131.
8. Ghori G,Pal M(2017) Certain types of product bipolar fuzzy graphs.Int J Appl Comput Math 3(2):605-619
9. Hamacher H(1978) On logical aggregations of non-binar explicit decision Criteria.Rita G.Fischer Verlag.Frankfurt
10. Kaufmann A(1975) Introduction to the theory of fuzzy subsets,vol 2.Academic Press,Newyork.
11. Mijanur Rahman Seikh,Utpal Mandal(2021) Intuitionistic fuzzy Dombi aggregation operators and their application to multiple attribute decision-making,Granular computing 6:473-488, https://doi.org/10.1007/s41066-019-00209-y
12. Naz S.Rashmanlou H,Malik MA(2017) Operations on single valued neutrosophic graphs with application.J Intell fuzzy syst 32(3):2137-2151
13. Parvathi R.Karunambigai M(2006) Intuitionistic fuzzy graphs, Computational intelligence, theory and applications.Springer,Berlin,pp 139-150
14. Shannon A,Atanassov K(2006) On a generalization of Intuitionistic fuzzy graphs.NIFS 12(1):24-29.
15. Smarandache.F(2005) Neutrosophic set-A generalization of the intuitionistic fuzzy set.Int J Pure Applied mathematics 24(3):287
16. F.Smarandache ,R.Jansi,K.Mohana ," Correlation measure for pythogorean neutrosophic sets with t and f as dependent neutrosophic components," Neutrosophic sets and systems,vol 30,pp.202-212,2019.
17. Tejinder Singh Lakhwani,Karthick Mohanta(2020)Some operations on Dombi Neutrosophic graph,Journal of Ambient Intelligence and Humanaized Computing https://doi.org/10.1007/s12652-021-02909-3.
18. Zadeh LA(1965) Fuzzy sets,Inf Control 8(3):338-353

Sasikala and Divya
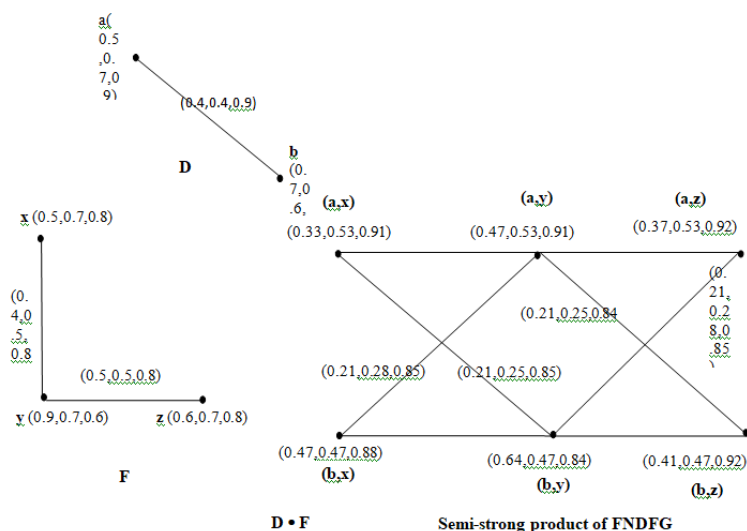
Fig. 1. Semi-Strong product of FNDFG
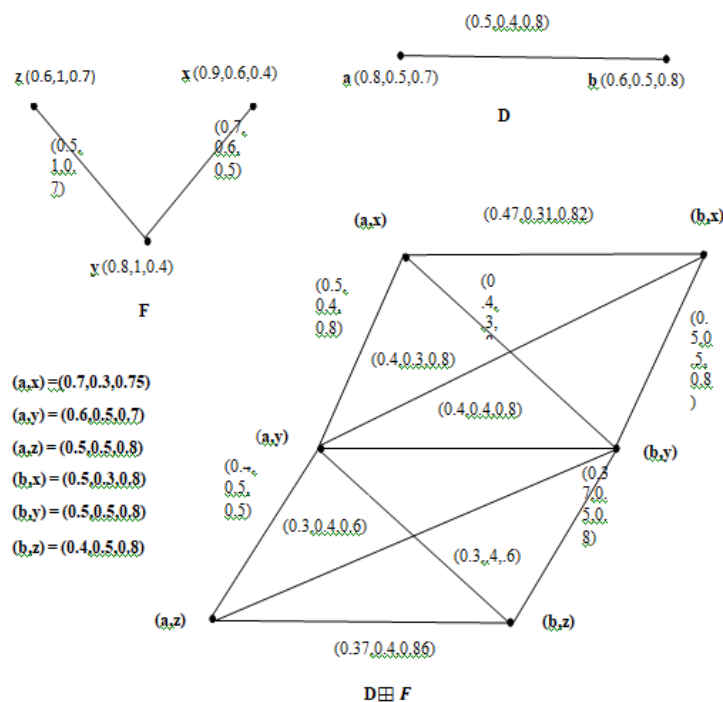
Fig. 2. Strong product of FNDFG
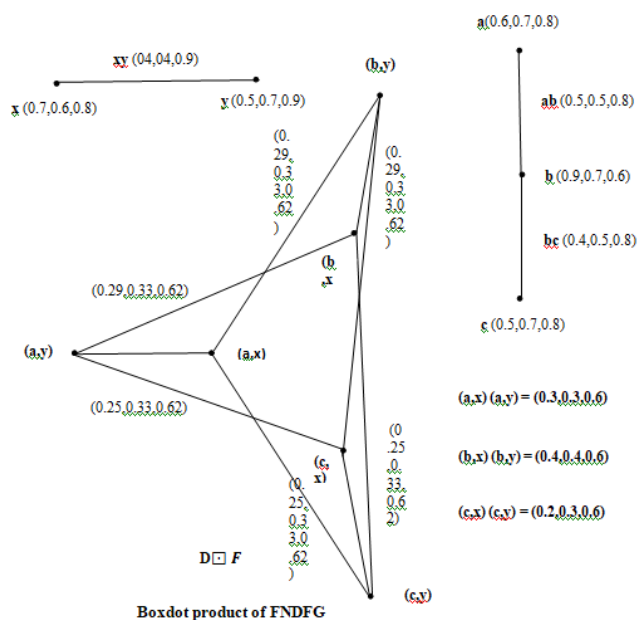
Fig. 3. Boxdot product of FNDFG
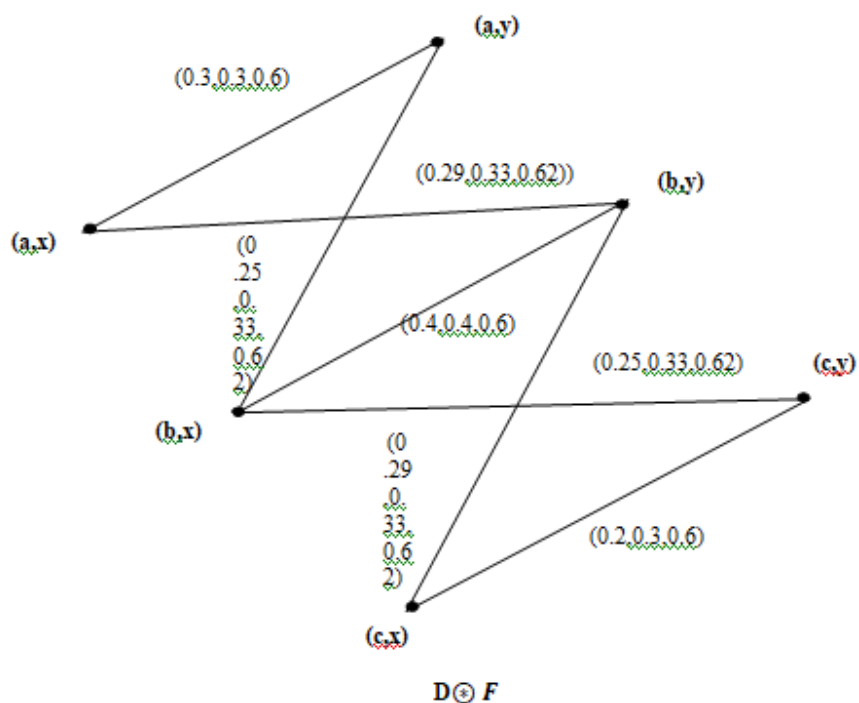
Fig. 4. Modular product of FNDFG

RESEARCH ARTICLE

Fuzzy Matroid from Fuzzy Graph

R.Buvaneswari and S.Saranya*

Department of Mathematics, Sri Krishna Arts and Science College, Coimbatore,Tamil Nadu, India.

***Address for Correspondence**
S.Saranya
Department of Mathematics,
Sri Krishna Arts and Science College,
Coimbatore,Tamil Nadu, India.
E.Mail: saranyashanmugavel96@gmail.com

ABSTRACT

Matroid theory deals with study of graphs in terms of its edges and circuits. The aim of this paper is to emphasis on the link between fuzzy matroids and fuzzy graphs Gˆ. The fuzzy matroids from fuzzy graphs, bases, Circuits, Dual defined and also analysed the properties.

Keywords: Fuzzy Graphs, Fuzzy Matroids, Circuits, Bases, Rank Function, Dual, Minor.
AMS Classification: 05C40, 05C62.

INTRODUCTION

Graph theory has proven to be the valuable instrument for modeling real-life is- sues. A Graph serves as a means to model the connections within a provided set of objects. Every object is depicted as a vertex, and the interconnections between them are illustrated with edges if the relationship is unordered, or with directed edges if there exists an ordered relationship between the objects. In 1965, L.A. Zadeh introduced a mathematical framework for the notion of uncertainty within real-world issues. Kauffman put forward the initial ideas of fuzzy graphs. A. Rosenfeld employed fuzzy relations in fuzzy graphs to depict the connections be- tween objects, signifying the degree of relationship existing among the elements within the provided set. If a theorem concerning graphs can be articulated using edges and circuits, it is likely to illustrate a broader concept of matroids. A matroid uses the concept of linear independence in vector spaces. Whitney in 1935 presented the concept of matroids. Matroids can be defined in several equiva-lent ways, with the most notable approaches. Matroid theory draws extensively from the terminology of both linear algebra and graph theory. The fuzzy matroids were introduced by Goetschal and Voxman. In this article a fuzzy matroid is con- structed from fuzzy graph.

The paper is organised as follows:
In section 2 the basic definition for matroids is given and in section 3 the definition of fuzzy matroid, bases, circuits, rank function and dual of fuzzy matroids are defined and analysed.

64223

Preliminaries:
Definition 2.1: A fuzzy graph is a pair of function **G = (σ, μ),** where the set V serves as the underlying domain. Here, $\sigma: V \to [0, 1]$ and $\mu: V \times V \to [0, 1]$. Furthermore, a fuzzy subset of a non-empty set S can be described as a mapping where in each element x belonging to S.

Definition 2.2: Let I be a family of be a non-empty family of a finite subset of E and satisfy the following properties:

i) $\varphi \in I$.
ii) If $X \in I, Y \subset X$, then $Y \in I$.
iii) If $X, Y \in I$; $|Y| \geq |X|$ then there exist an element $x \in Y \backslash X \; such \; that \; X \cup \{x\} \in I$.
The Pair (E, I) is called a Matroid.

Definition 2.3
In matroid M a basis (or base) refers to the largest independent set within M, while a circuit of the matroid corresponds to the smallest dependent set in M.

Definition 2.4
The Rank of a subset E in M is defined as the largest cardinality of an independent set within E, it is denoted as r(X).

Definition 2.5
The matroid dual involves a second matroid M * sharing the same underlying elements as the original matroid M. In this dual matroid, a set is considered independent iff M contains a disjoint basis set from it.

Definition 2.6
A matroid minor is formed by two operations, the restriction M\x deletes x from M without changing the independence or rank of the remaining set. The contraction M/x deletes x from M after subtracting one from the rank of every set it belongs to.

Properties of Fuzzy Matroids from Fuzzy Matroids:
Definition 3.1
Let F M = (X, A) is defined as a fuzzy matroid, if it satisfies the following conditions,
i) $\varphi \in A$
ii) $\Psi i \subset \Psi j$ and $\Psi j \in A$, where $\Psi i \subset \Psi j$, $\Psi i (x) \leq \Psi j (x)$ forall $x \in X$
iii) If $\Psi i , \Psi j \in A$ with $|supp (\Psi i)| \leq |supp (\Psi j)|$, there exists $\Psi k \in A$ such that

a) $\Psi i \subset \Psi k \subseteq \Psi i \cup \Psi j$, where $(\Psi i \cup \Psi j) x = \max \{\Psi i (x), \Psi j (x)\}$
b) $m(\Psi k) = \min \{m(\Psi i), m(\Psi j)\}$ where $m(\Psi i) = \min \{\Psi i (x); x \in supp (\Psi i)\}$; i, j, k = 1, 2, 3.

Definition 3.2:
The largest fuzzy subset of X that is independent is referred to as the basis or base of F M.

Lemma 3.3: If F_B and F_B' are the bases of F_M then $|F_B| = |F_B'|$.
Proof: Let $F_M = (X, A)$ and let F_B and $F_B' \in B(X)$. Suppose $|F_B| > |F_B'|$. Then F_B and F_B' are
in $A. x \in F_B - F_B'$ such tha t$F_B' - x \in A$. This contradicts maximal independence. Thus $|F_B| \leq F_B'$.
Similarly, $F_B' \leq |F_B|$. Hence $|F_B| =$
$|F_B'|$.

Buvaneswari and Saranya

Lemma 3.4: Let F_M is fuzzy matroid and F_B be family of its bases. The family F_B has the following properties

i) F_B is non empty

ii) If $F_{Bi}, F_{Bj} \in F_B$ and $x \in F_{Bi} \backslash F_{Bj}$ then there exists $y \in F_{Bj} \backslash F_{Bi}$ such that $(F_{Bi} - x) + y \in F_B$.

Proof: By the definition of Fuzzy Matroid A is non-empty then the family of bases F_B is also non-empty.
Consider two bases F_B and F_B' and an element $x \in F_{Bi} \backslash F_{Bj}$ Both $F_{Bi} - x$ and F_{Bj} are independent fuzzy subsets and $|F_{Bi} - x| < |F_{Bj}|$. Similarly, $y \in F_{Bj} \backslash F_{Bi} - x$ such that $(F_{Bi} - x) + y = |F_{Bi}|$, $(F_{Bi} - x) + y$ is a base of F_M.

Let A be the family of fuzzy subsets of X that contains some members of F B . Then the pair (X, A) is a fuzzy matroid from fuzzy graph Gˆ and F B are its bases.

Proof. Since $F_{B \neq \varphi}$ it also holds that $\varphi = A$. There are members Ψ i and Ψ j of A with $|\Psi$ i $|$ < $|\Psi$ j $|$ such that for each x $\in \Psi$ i /Ψ j . The fuzzy set Ψ i + x is dependent. By the definition of A, there are bases F B i and F B j such that Ψ i $\subseteq$ F B i and Ψ j $\subseteq$ F B i. Choose F B j then there is an element x, x $\in$ F B j\ (Ψ i $\cup$ F B i), then y $\in$ F B i \F B j by Lemma 3.5 (F B j − x)+ y $\in$ F B . Since
Since, $|(F_{Bj} - x) + y \backslash \psi_j \cup F_{Bi}| < |F_{Bj} \backslash (\psi_j \cup F_{Bi.})|$

This contradicts the choice of F B j. The choice of Ψ i and Ψ j implies that Ψ j \F B i = Ψ j \Ψ i .
Then F B j − F B i = Ψ j − Ψ i . To show that F B i \ (Ψ j $\cup$ Ψ i) is empty. If not x $\in$ F B i \ (Ψ i $\cup \Psi$ j). By Lemma 3.5 there exist y $\in$ F B j \F B i such that (F B i − x) + y $\in$ F B . Clearly, Ψ i + y $\subseteq$ (F B i − x) $\cup$ y is a contradiction. Since y $\in \Psi$ j \Ψ j .

Definition 3.7: The smallest fuzzy subset of X that is dependent is known as the circuits of F M .
Theorem 3.8: The family F C of F M from Gˆ has the following properties
i) $\varphi \in$/ F C.
ii) If F C 1 , F C 2 $\in$ F C and F C 1 $\subseteq$ F C 2 then F C 1 = F C 2.
iii) If F C 1 , F C 2 $\in$ F C , F C 1 /= F C 2 and x $\in$ F C 1 $\cap$ F C 2 , then there exists F C 3 $\in$ F C such that F C 3 $\subseteq$ (F C 1 $\cup$ F C 2) − x.

Proof. (i) and (ii) follows the definition of the circuit. Assume (F C 1 $\cup$ F C 2) − x does not contain any circuit and it is independent. By (ii), there is an element y $\in$ F C 2 − F C 1 and F C 2 − y is independent.
Let A be a maximal independent fuzzy subset of (F C 1 $\cup$ F C 2) containing F C 2 − y. Clearly y $\in$/ A, there exist z $\in$ F C 1 \A 1 since A Ç F C . The elements y and z are distinct.
$|A| \leq |(F_{C1} \cup F_{C2}) \backslash y, z| = |(F_{C1} \cup F_{C2})| - 2 < |(F_{C1} \cup F_{C2}) - x|$

Applying the property (iii) of Fuzzy Matroid to the fuzzy independent sets A and (F C 1 $\cup$ F C 2) − x; the resulting fuzzy independent set contradicts the maximality of A.

Definition 3.9: The Rank of F M is defined as the largest fuzzy subset of X that is independent.
Theorem 3.10: Let F M on a set X, then the rank function F r has the following properties
i) $0 \leq$ F r (Ψ i) $\leq$ |X| for every Ψ i $\in$ X
ii) F r (Ψ i) $\leq$ F r (Ψ j) for every Ψ j $\subseteq \Psi$ i , and
iii) F r (Ψ i $\cup \Psi$ j) + F r (Ψ i $\cap \Psi$ j) $\leq$ F r (Ψ i) + F r (Ψ j) for every Ψ i , Ψ j $\subseteq$ X.

Proof. (i) and (ii) follows the definition of the rank function.
consider the fuzzy subsets Ψ i and Ψ j of X. Let Sˆ$\cap$ be the inclusion wise maxi- mal
independent fuzzy subset of Ψ i $\cap \Psi$ j and Sˆ$\cup$ be the inclusion wise maximal

Buvaneswari and Saranya

independent fuzzy subset of $\Psi i \cup \Psi j$ such that $S \hat{\cap} \subseteq S \hat{\cup}$. $S' \cup \cap \Psi i$ and $S \cup \cap \Psi j$ are
independent fuzzy subsets of Ψi and Ψj. By the properties (i) and (ii)

$F r (\Psi i) + F r (\Psi j) \leq |S \hat{\cup} \cap \Psi i| + |S \hat{\cup} \cap \Psi j|$

$= |(S \cup \cap \Psi i) \cup (S \cup \cap \Psi j)| + |(S \cup \cap \Psi i) \cap (S \cup \cap \Psi j)|$

$= |S \hat{\cup} \cap (\Psi i \cup \Psi j)| + |S \hat{\cup} \cap (\Psi i \cap \Psi j)|$

$= |S \hat{\cup}| + |S' \hat{\cap}|$

$= F r (\Psi i \cup \Psi j) + F r (\Psi i \cap \Psi j)$

Definition 3.11 The dual of F M with respect to X is denoted as F M $*$, where the bases of F M $*$ consist of the complements of bases present in F M . The sub- bases F S of F M are the fuzzy sets containing a base. The hypobase F H of F M are the maximal fuzzy sets containing no base.
$F_B *$, $F_C *$ are the cobases and cocircuits of F M .

Lemma 3.12 If F M is a fuzzy matroid and F B i , F B j $\in$ F B , then for each
$x \in F_B i - F B j \exists y \in F B j$ then F B j $-$ x $+$ y is a base.
Proof. F B j is a base, F B j $+$ x contains exactly one circuit F C . F B i is independent, F C
contains an element y $\in$ F B j $-$ F B i . Then F B j $+$ x $-$ y contains no circuit and has size F r (X).

Theorem 3.13 The dual of a F M on X is a Fuzzy Matroid with rank function

$F r * (\Psi i) = |\Psi i| - F r (x) - F r (\Psi \bar{} i)$

Proof. F r $*$ is a fuzzy matroid. We prove the base exchange property for F M $*$.
$F \bar{} B, F \bar{} B \in F B *$ and x $\in F \bar{} B - F \bar{} B$ then F B , F B $\in$ F B with x $\in$ F B $-$ F B there exist y
$\in$ F B $-$ F B such that F B $+$ x $-$ y $\in$ F B . Now $F \bar{} B - x + y \in F B *$ is the desired exchange.
Let Ψj be the maximal coindependent subset of Ψi
$F r * (\Psi i) = F r * (\Psi j) = |\Psi j| |\Psi \bar{} j$ is a minimal super set of $\Psi \bar{} j$ that contains base of F M . Since $\Psi \bar{} j$ arises from $\Psi \bar{} i$
by agumenting a maximal independent subset of $\Psi \bar{} i$ to become a base.

$|\Psi \bar{} j| - |\Psi \bar{} i|$

$= F r (X) - F r (\Psi \bar{} i)$

$|\Psi \bar{} j| - |\Psi \bar{} i| = |\Psi i| - |\Psi j|$

$F r * (\Psi i) = |\Psi j|$

$= |\Psi i| - (|\Psi \bar{} j| - |\Psi \bar{} i|)$

$F r * (\Psi i) = |\Psi i| - F r (x) - F r (\Psi \bar{} i)$

CONCLUSION

In this article, the author constructed a F_M from $G \hat{}$. Furthermore, the examination of the largest independent fuzzy subsets and the smallest dependent fuzzy subsets among the edges of $G \hat{}$ constitutes the bases and circuits of the fuzzy matroid F_M . This aspect holds significance in the continued advancement of fuzzy matroids derived from fuzzy graphs. The author also suggests exploring the representation of F_M.

ACKNOWLEDGEMENTS

REFERENCES

1. Douglas B. West; Introduction to Graph Theory, Prentice-Hall, New Jersey, 2001.
2. Leonidas S. Pitsoulis; Topics in Matroid Theory, Springer-2014.
3. Muhammad Asif, Muhammad Akram and Ghous Ali; Pythagorean Fuzzy Matroids with Application, Symmetry 2020, 12, 423, 2020.
4. O.K. Shabna and K.Sameena; Matroids from Fuzzy Graphs, Malaya Journal of Matematik, Vol. S,No. 1,500-504,2019.
5. Oxley, J. G.,Matroid Theory; Oxford University Press, New York, 1992.
6. Roy Goetschel Jr., William Voxman; Fuzzy Matroids, Fuzzy Sets and Sys- tems, Volume 27, Issue 3, September 1988, Pages 291-302.
7. Sunil Mathew, John N. Mordeson, Davender S. Malik; Fuzzy Graph Theory, studies in fuzziness and soft computing, volume 363.
8. Sunil Mathew, John N. Mordeson; Advanced Topics in Fuzzy Graph Theory, studies in fuzziness and soft computing, volume 375.
9. Tutte, W. T.; Matroids ang Graphs, Trans, Amer. Math. Soc 90(1959), 527- 552.
10. Whitney, H.; On the abstract properties of linear dependence, Amer. J. Math. 57(1935), 509-533.
11. Wilson, R. J., An Introduction to Matroid Theory, Amer. Math. Monthly 80(1973), 500-525.
12. Zadeh,L.A.: Fuzzy Sets. Information Sciences and Control,1965; 338-353.
13. A. Kauffmann: Theory of Expertons and Fuzzy Logic Fuzzy sets and Systems, 1988; 3(28), 295-3

RESEARCH ARTICLE

An Uniqueness of Drug Delivery Methods Practised in Siddha System of Medicine

Jayalakshmi .J[1*], Thirunarayanan. G[2] and Sivakkumar .S[3]

[1]Professor, Dept of Gunapadam, Sivaraj Siddha Medical College, Salem, Tamil Nadu, India.
[2]Medical Officer, National Institute of Siddha, Chennai-47, Tamil Nadu, India.
[3]Associate professor, Dept of Gunapadam, National Institute of Siddha, Chennai-47, Tamil Nadu, India.

*Address for Correspondence
Jayalakshmi .J
Professor, Dept. of Gunapadam,
Sivaraj Siddha Medical College,
Salem, Tamil Nadu, India.
E.Mail: drjai@ymail.com

ABSTRACT

Drug delivery system is a formulation or a device that enables a therapeutic substance selectively to reach its site of action. *Siddha* system of medicine is an ancient traditional system which has different drug delivery systems other than oral route which include *Kalikkam* (Eye medicines) *Nasiyam* (Nasal drops), *Naasikaparanam* (Blowing dry powder into nostril), *Aakraanam* (Inhaling dry powder), *Peechu* (Instillation), *Oothal* (Blowing air by keeping medicated substances in mouth), *Patru* (Dense application), *Gargling*, *Varthi vaithal* (Suppositories), *Kudori Maruthuvam* (piercing the superficial layer of the scalp skin and keep medicines within that) etc.. These drug delivery systems work in an excellent manner without any side effects and resolve many ailments. Few examples are application of paste of tuberous root of *Gloriosa superba* in both palms enhances labour pain and facilitates normal labour. Keeping a small amount of *sanjeevakarani thylam*as *kudori sikitchai* in cases of snake bites, it acts as an antidote and become a lifesaving drug. And in psychiatric diseases cow dung used as *kudori marundhu* by piercing the scalp with paddy. These drug delivery methods were successfully practised by ancient *siddha* practitioners/traditional healers without any discomforts, complications and unwanted effects. Nowadays, in this fast pace of modern life, these drug delivery methods are vanished slowly due to inadequate knowledge, difficulty in practise and lack of availability of advanced modern instruments/devices. Hence this study creates awareness about the effective traditional drug delivery techniques available in *siddha* system and helps the researchers to establish technology based advanced instruments or devices to propagate the ancient drug delivery methods for the well-being of mankind.

Keywords: Drug delivery methods in *Siddha system* of medicine, Traditional techniques, Advanced instruments.

INTRODUCTION

Drug delivery system is a science in the field of pharmacokinetics describes the way in which a drug is carried into the living organism. An effective drug delivery can increase the efficacy and minimize the unknown side effects of that drug, hence *Siddha* system of medicine give more importance to *anubanam* (Vehicle that carries the drug). In other system of medicine, drug delivery is being well advanced only in the past few decades and greater innovations are being anticipated in the coming years[1], whereas the medicine which originated long back in Tamil region and believed to be an oldest system of medicine has a very clear view on drug delivery methods. Achievement or Perfection is the meaning of the word '*Siddha*' [2]. As its word means to perfection, Siddha system has a clear view in all aspects of the medicinal world. Siddha system not just focuses on treating the disease but it also takes into account of the patient's behaviour, age, habits, physical condition and environmental aspects. For this purpose *Siddhars* afforded different drug delivery systems other than oral route which include *Kalikkam* (Eye medicines), *Nasiyam* (Nasal drops), *Naasikaparanam* (Blowing dry powder into nostril), *Aakraanam* (Inhaling dry powder), *Peechu* (Instillation), *Oothal* (Blowing air by keeping medicated substances in mouth), *Patru* (Dense application), *Gargling*, *Varthi vaithal* (Suppositories), *Kudori maruthuvam* (piercing the superficial layer of the scalp skin and keep medicines within that) etc. This review study explains about these drug delivery techniques available in *Siddha* system.

MATERIALS AND METHODS

This study is carried out as the systematic quantitative review on various authenticated *Siddha* texts by organizing large volumes of raw information from various sources into an organized format.

RESULTS
DRUG DELIVERY SYSTEM
Drug delivery is the process of administering medication or other pharmaceutical compounds to achieve a therapeutic effect [3]. It is a formulation or a device that enables a therapeutic substance to selectively reach its site of action.

Types of Drug Delivery Routes
Oral route
Oral route of drug delivery is the most common. Many drugs can be administered orally as capsules, tablets, or liquids. The oral route is usually safe, convenient, and inexpensive.

Injection
Intravenously, intramuscularly, intrathecally or subcutaneously.

Inhalation
Breathed into the lungs through the mouth (inhaled) or mouth and nose (Nebulized).

Nasal
Sprayed into the nostril(s) and absorbed through the nasal membranes.
Topical
Applied to the skin for a local effect.

Transdermal
Delivered through the skin via a patch for a systemic effect.

Rectal
Inserted into the rectum to be absorbed into the bloodstream.

Sublingual
Placed underneath the tongue for rapid absorption into the bloodstream.

Drug Delivery Devices
Commonly used drug delivery devices are Prefilled syringes, Auto injectors, Infusion pumps, Metered dose inhalers (MDIs), Nebulizers, Nasal sprays, Eye droppers, Intrauterine devices (IUDs), Transdermal patches.

Ancient and Traditional Drug Delivery Methods in Siddha System of Medicine: [4]
Siddha system of medicine is an ancient traditional system which has different drug delivery methods other than oral route which include:

- *Kalikkam* (Liquid ophthalmic application)
- *Nasiyam* (Liquid nasal application)
- *Naasikaparanam* (Powder nasal application)
- *Aakraanam* (Inhaling dry powder)
- *Peechu* (Douche application)
- *Oothal* (Medicated aerosol)
- *Patru* (Semi solid poultice)
- *Kopalithal*(Gargling)
- *Varthi vaithal* (Medicated pessary)

These drug delivery systems work in an excellent manner without any side effects and resolve many ailments.

KATTU [Dense application]
Few examples are: Application of paste of tuberous root of *Gloriosa superba* in both palms enhances labour pain and facilitates normal labour [5]. Leaf and plumule paste of *Cajanus cajan* over the breasts as a thick package aid to reduce breast milk secretion [5].

PEECHU [Douche application]
Borax dissolved in water use as an instillation in cases of Leucorrhoea[4]. Seed peel of *Plantago ovata* soaked and boiled in water and use as douche application in Dysentry[5].

AAKRAANAM [Inhaling dry powder]
Navachara (Ammonium chloride) *aakraanam* act as a best remedy for headache, unconsciousness and sinusitis[4]. Dry powder of Root of *Anacyclus pyrethrum* acts as an anti convulsant and be a remedy for Epilepsy[5].

KALIKKAM [Liquid ophthalmic application]
Continuous application of Ash powder of *Lagenaria siceraria* with honey into eyes behave as a sight promotor for Night blindness[5]. Flower extract of *Tabernamontana divericata*[5] and *Sesbania grandiflora* reduces burning sensation in eyes and mitigates many eye diseases respectively[5].

PATRU [Semi solid poultice]
Dense application of *Chukku kali* over eye brows helps to improve vision in cases of hypermetropia and it act as a sight promotor[5]. Latex of *Ficus carica* has anti-inflammatory and astringent activity which shows its potent healing in Diabetic carbuncle and in Arthritis[5].

KOPALITHAL [Gargling]

64230

Jayalakshmi *et al.*,

Gargling with *Thiripala kashayam* is the best cure for Aphthus ulcer[5].

PODI [Medicated powder application]

Sprinkling dry powder of leaves of *Acalypha indica* on bed sores accord good heal[5]. *Poora podi-* an elixir for Syphilitic sore in male genitals[4].

NASIYAM [Liquid nasal application]

Few drops of *Sesbania grandiflora* leaf juice into nostril acts as an anti-pyretic and be a remedy in cases of fourth intermittent fever[5]. Flower extract of *Leucas aspera* as *nasiyam* give best results in Cephalalgia[5].

POOCHU [Liquid poultice]

Latex of *Euphorbia hirta* accord best heal in Paronychia[5]. Leaves of *Sida acuta* possess styptic action which stops the bleeding from incised wounds immediately[5].

POTTANAM [Bundle application]

Inhale the Bundle application of *Nigella sativa* for Rhinorrhea & Sinusitis[5]. Bundle application of Garlic & Onion into ears for Otalgia & Tinnitus[6].

PUGAI [Medicated fumigation]

Agasthiyar kuzhambu pugai for fistula, *Vanga pugai* for wound healing *(viranam)*[6].

VEDHU [Steaming]:

Steaming Lemon seeds into the hot water used for Sinusitis. Steaming Common Salt into the hot water used for Myalgia [6].

DISCUSSION

These drug delivery methods were successfully practiced by ancient *siddha* practitioners/traditional healers without any discomforts, complications and unwanted effects. In recent days, due to fast pace of modern life, these drug delivery methods are vanished slowly due to inadequate knowledge, difficulty to practice, lack of availability of advanced modern instruments/devices.

CONCLUSION

This study would have created awareness about the effective traditional drug delivery techniques available in *Siddha* system. It may help the researchers to establish technology based   advanced instruments or devices to propagate the ancient drug delivery methods for the well-being of mankind.

REFERENCES

1. Science Education, Science Topics, "Drug Delivery Systems"' https://www.nibib.nih.gov/science-education/science-topics/drug-delivery-systems-getting-drugs-their-targets-controlled-manner. 2022.
2. Ayush Systems, *Siddha*, "Introduction and Origin", https://main.ayush.gov.in/ayush-systems/siddha/introduction-and-origin/. 2021.
3. Tiwari G, Tiwari R, Sriwastawa B, Bhati L, Pandey S, Pandey P, Bannerjee SK. Drug delivery systems: An updated review. Int J Pharm Investig. 2012 Jan;2(1):2-11. doi: 10.4103/2230-973X.96920. PMID: 23071954; PMCID: PMC3465154.

Jayalakshmi *et al.*,

4. Thiyagarajain *Gunapadam Bagam – II (Thathu jeeva Vagupu),* Department of Indian Medicine and Homoepathy, Chennai - 106, PP : 77-86, 438,411, 287

5. Murugaesa Mudhaliyar(2013), *Gunapadam Bagam – I(Mooligai),* Department of Indian Medicine and Homoepathy, Chennai - 106, PP : 244, 530, 98, 8, 477, 557, 3 , 471, 19, 520, 361, 528, 260, 464.

6. Uthamarayan(2013), *Siddhar Aruvai Maruthuvam*, Department of Indian Medicine and Homoepathy, Chennai – 106, PP : 40-41,42, 46.

REVIEW ARTICLE

Brahmiyathi Pavanai Chooranam; A Novel Siddha Drug for Alzheimer's Disease – A Review

Rujitha D[1]*, Sivakkumar S[2] and R.Meenakumari [3]

[1]PG Scholar, Dept of Gunapadam, National Institute of Siddha,Ministry of Ayush, Govt of India, Chennai-600047 ,Tamil Nadu, India.
[2]Associate Professor, Dept of Gunapadam, National Institute of Siddha, Ministry of Ayush, Govt of India, Chennai-600047,Tamil Nadu, India.
[3]The Director, National Institute of Siddha, Ministry of Ayush, Govt of India, Chennai-600047, Tamil Nadu, India

*Address for Correspondence
Rujitha D
PG Scholar, Dept of Gunapadam,
National Institute of Siddha,
Ministry of Ayush, Govt of India,
Chennai-600047 ,Tamil Nadu, India.
E.Mail: rujirujitha481@gmail.com

ABSTRACT

Alzheimer's disease (AD) is a progressive, irreversible brain disorder that slowly destroys memory and thinking skills and eventually the ability to carry out a daily simple task. Alzheimer's Disease is the most common form of dementia. Worldwide, around 55 million people have dementia, with over 60% living in low- and middle-income countries, this number is expected to rise to 78 million in 2030 and 139 million in 2050. In India, more than 4 million people have dementia, making the disease a global health crisis that must be addressed. Cholinesterase Inhibitors and NMDA Receptor blockers are choices of drugs for AD which commonly cause side effects like nausea, diarrhea, vomiting, insomnia, skin lesion, muscle cramps, fatigue, sleep disturbances, headache and dizziness, bradycardia, hypertension, weight gain, hallucination, confusion, aggressive behavior, urinary incontinence. etc. In Siddha medicine, so many formulations are indicated for AD; *Brahmiyath Pavanai Chooranam*(BPC) is one among them which is indicated for Intelligence, Intellect, Focus, Strengthening the brain, Physical strength, increase memory and reducing forgetfulness. BPC prepared from *Amukkara* (*Withania somnifera*), *Kadugurohini* (*Picrorhiza scrophulariiflora*), *Ajamthaomam* (*Trachyspermum roxburghianum*), *Karupuppu* (Black salt), *Seeragam* (*Cuminum cyminum*), *Karunjeeragam* (*Nigella sataiva*), *Chukku* (*Zingiber officinale*), *Milagu*(*Piper nigrum*), *Thippili* (*Piper longum*), *Karisalai* (*Eclipta prostrata*), *Vellarugu* (*Enicostema axillare*), *Kadukaai* (*Terminalia chebula*), *Thandrikaai* (*Terminalia bellirica*), *Nellimulli* (*Phyllanthus embilica*), *Vasambu* (*Acorus calamus*) *Vallarai* (*Centella asiatica*). Most of the ingredients in BPC have been proven for their Neurological antioxidant, Neuromodulatory, Cognitive enhancement, Neuroprotective, enhancing neurite growth, enhance acetylcholine content and Acetylcholinesterase inhibitor actions. According to the Siddha fundamental and taste theory, the ingredients are favourable for the management of AD. This review study

Rujitha *et al.*,

concluded that the polyherbal Siddha preparation *Brahmiyathi Pavanai Chooranam*can be used a Novel drug for the management of Alzheimer's disease. Further clinical studies are to be conducted to confirm the clinical efficacy.

Keywords: Alzheimer's disease; *Brahmiyathi Pavanai Chooranam*; Siddha Medicine.

INTRODUCTION

Alzheimer's Disease (AD) is the most common type of dementia and can be defined as a slowly progressive neurodegenerative disease characterized by neuritic plaques and neurofibrillary tangles as a result of amyloid-beta peptide (Aβ) accumulation in the brain, the medial temporal lobe, and neocortical structures [1,2,3]. Brain cells inthe hippocampus, associated with learning, are the first to be damaged by Alzheimer's. The first symptom of the diseaseis memory loss, mainly difficulty remembering recently learned information[4]. There is no cure for Alzheimer's disease. Treatments are available that may only improve some symptoms. Cholinesterase Inhibitors (Donepezil, Rivastigmine, Galantamine)[5,6,7]and

NMDA (Memantine)[8] Receptor blockers are choices of drugs for AD which commonly cause side effects like nausea, diarrhea, vomiting, insomnia, and skin lesion, muscle cramps, fatigue, sleep disturbances, headache and dizziness, bradycardia, hypertension, weight gain, hallucination, confusion, aggressive behavior, urinary incontinence, etc. Worldwide, about 55 million people have dementia, 60% of them living in low- and middle-income countries. In every country's populationthe proportion of older people is increasing, so this number is expected to rise to 78 million in 2030 and 139 million in 2050[1]. In India, more than 4 million people have dementia, making the disease a global health crisis[2].In Siddha medicine, so many formulations are indicated for AD, *Brahmiyathi Pavanai Chooranam*(BPC) is one among them which is indicated for Intelligence, Intellect, Focus, Strengthening the brain, Physical strength, increase memory, and reducing forgetfulness[9].

MATERIALS AND METHODS

Preparation of BPC
The ingredients from s.no 1 to 14 in Table no 1 are purified and separately made into powder. The powders are mixed together and placed in *Kalvam* (stone mortar). The *Vallarai* juice is poured into *Kalvam* and ground well until attains dry powder then let dry in the shade. On the next day, the dried powder is collected and subjected to the same process 21 times. Finally, the dried powder is collected and stored in an air-tight container.
Dose: 2 – 4 grams

Adjuvant: Mixture of honey (8gm) and Cow's ghee (8gm) [9].

Amukkara – Withania somnifera(WS)
Alzheimer's disease on animal model
Bhattacharya et al. studied that, the effect of *Withania somnifera* (WS) in cognitive deficits induced in NMB-lesion ina rat modelthat was assessed by attenuation of a learned active avoidance task and a reduction in acetylcholine (ACh) concentrations in frontal cortical and hippocampal region, choline acetyltransferase activity and muscarinic cholinergic receptor (MCR) binding. IA-induced NBM lesioning in rats caused a marked cognitive deficit, assessed severe reduction of the learned task, anda significant decrease in the frontal cortex and hippocampal ach levels, chat activity, and MCR binding. In 2 weeks, treatment withWS reversedthe IA-induced cognitive deficit and the reduction in cholinergic markers [11].

Tohda et al, revealed that in human neuroblastoma SK-N-SH cells, the methanolic extract of roots of *Withania somnifera* notably increased the percentage of cells with neurites. The mRNA levels of the dendritic markers MAP2 and PSD-95 by RT-PCR were markedly increased by treatment with the extract [12].

Neuroprotective activity

Kurapati et al. tested the neuroprotective effects of methanol:Chloroform (3:1) extract of dried root of WS in a human neuronal SK-N-MC cell line, against β-amyloid induced toxicity and HIV-1Ba-L (clade B) infection.The neuroprotective effect of WS root extract was assessed by the MTT cell viability assays.The study results showed that the toxic effects were neutralized[13]. *Zhao J et al*, reported that the neurite outgrowth activities of WS derivatives showed significant neurite outgrowth activity at a concentration of 1 mm on a human neuroblastoma SH-SY5Y cell line[14].

Kadugurohini –Picrorhiza scrophulariiflora (PS)
Neuroprotective activity

Li Q et al, revealed that the Neuroprotective Properties of Picroside II, the main active constituent of *Picrorhiza scrophulariiflora* (Scrophulariaceae), which might reduce the expressions of Caspase-3 and PARP to inhibit the neuronal apoptosis caused by cerebral ischemia-reperfusion injury and promote the neurological function of rats[15].

Enhancement of nerve growth factor

Li P et al, studiedthe Enhancement of nerve growth factor-mediated neurite outgrowth from PC12D cells by Chinese and Paraguayan medicinal plants, and the results show that methanol extract of *Picrorhizascrophulariiflora*induced the longest neurites in PC12D cells[16].

NGF-potentiating

Ping Li et al, evaluated the isolated Picrosides I and II as NGF-potentiating substances from the dried underground parts of P. Picrosides alone, even at high concentrations, did not cause neurite elongation from PC12D cells but significantly increased the proportion of cells with neurites in cultures treated with NGF. It has been revealed that picrosides are marked NGF-potentiating compounds[17].

Ajamthaomam – Trachyspermum roxburghianum(TR)
Antioxidant activity

*Sunee Chansakaow et al.*reported the antioxidant and antibacterial activities of the essential oil *Trachyspermumroxburghianum*(DC.).Folin-Ciocalteu colorimetric method, DPPH, ABTS, and FRAP assays were used to determine total phenolic content and evaluate antioxidant potential. Sabinene and α-terpinolene including 3-n-butyl phthalide are the main compounds of *T. Roxburghinum*. The essential oils of *T. Roxburghinum* showed high total phenolic content (GEA= 3.0971 mg/ml) and exhibited potent antioxidant activities in DPPH (TEAC= 357.9297 mg/ml), ABTS (TEAC= 13.4242 mg/ml) and FRAP assays (TEAC= 27.4173 mg/ml)[18].

Seeragam - Cuminum cyminum (CC)
In - vitro acetylcholinesterase inhibitory activity

*Kumar et al,*the study showed that an aqueous extract of *C.cyminum* seed inhibited ache in *in-vitro* acetylcholinesterase inhibitory activity based on Ellman's method in a concentration-dependent manner. Also, lower concentrations and higher concentrations of *C. Cyminum* show competitive and mixed modes of inhibition respectively. So, *C. Cyminum*can act as an inhibitor of aches, which helps in enhancing memory and cognitive functions of the brain [19].

Antistress, anti-oxidant and memory-enhancing activities

Koppula et al evaluated the antistress, and memory-enhancing activities of cumin extract by stress-induced urinary biochemical changes in rats, and scopolamine-induced memory loss in rats respectively. And antioxidant activity by

Lipid peroxidation inhibition in the liver and brain of rats using TBARS assay the extract showed better activity in inhibiting lipid peroxides is more effective in brain homogenate compared with liver[20].

Ache inhibition and Activation of CE enzyme

Prabha et al, evaluated esterase properties of hot and cold extracts of Indian spices*Cuminum cyminum, Elettaria cardamomum, Cinnamomum verum, and Syzygiumaromaticum*for AD, by the *in-vitro* of homogenates prepared from hippocampal region dissected from control and non-transgenic AD rats made available from a laboratory using Ellman method, showed maximum AChEinhibition in striatum region at the same time activated CE enzyme in the hippocampus, i.e., region of learning and memory [21].

Karunjeeragam - Nigella sataiva (NS)
Recovers learning function in AD

Poorgholam et al revealed that hippocampal injection of Aβ could induce Alzheimer's disease in male Wistar rats, and administration of Thymoquinone the main active component of *Nigella sativa* could prevent learning dysfunction and improve initial latency. TQ also decreased plaque formation in the CA1 region of the hippocampus, increased the number of surviving neurons, and protected pyramidal cells against the neurotoxic effects of Aβ[22].

Antioxidant activity, Inhibition of AChE and BChE,and Inhibition of Aβ42 aggregation

Veerabomma Sreedhar et al revealed that Methanolicextract of *Nigella sativa*shows Maximum scavenging antioxidant activity by the DPPH method with 93.01% at 400 µg/mL concentration. Cholinesterase activity by Ellman's method shows Methonolic extract of *Nigella sativa* for both enzymes AChE and BChEwere 51.19% and 63.86% respectively, and was compared with standard galantamine (96.68% and 83.68%) at 100 µg/mL. This study results shows Methonolic extract of *Nigella sativa* has anti-amyloidogenic activity by using ThTfluroscence assay and Inhibition of Aβ42 aggregation by ThTassay[23].

Improves learning and memory impairments and oxidative damage

RahimehBargi et al, a study indicated that TQ improves learning and memory impairments induced by LPS in rats by Morris water maze apparatus and procedures. TQ attenuates hippocampal cytokine levels and improves oxidative damage biomarkers in the brain tissues[24].

Chukku - Zingiber officinale(ZO)
Antioxidant and acetylcholinesterase inhibitory activity

Tung et al,studied the Antioxidant and acetylcholinesterase inhibitory activity of *Zingiber officinale*by its extraction with ethanol 96 % and fractionated it with n-hexane, ethyl acetate (etoac)evaluated by 1,1-Diphenyl -2-picrylhydrazyl (DPPH) assay and Ellman's colorimetric method respectively. The results showed that the etoacfraction had the antioxidant activity strongestat IC50 was 8.89±1.37 µg/ml and ache inhibitory activity at IC50 value of 22.85±2.37 µg/ml in a dose-dependent manner[25].

Improves *β*-Amyloid-Induced Memory Impairment

Kim et al, revealed that WS-5, an ethanol extract derived from *Z. Officinale* Roscoe,*C.longa, and C.sinensis* significantly attenuated the A beta-induced memory impairment in mice that were evaluated by the passive avoidance test and the Morris water maze test and suppressed A beta plaque formation in the Abeta-inducedAD mice[26].

Antioxidant activity, cholinesterase inhibition, anti-amyloidogenic potential, and neuroprotective properties

Mathew et al., evaluated the antioxidant activity, cholinesterase inhibition, anti-amyloidogenic potential, and neuroprotective properties of dry ginger's methanolic extract. The methanolic extract contained 18+0.6 mg/g gallic acid equivalents of total phenolic content and 4.1840.69 mg quercetin equivalents/g of dry material. GE expressed high antioxidant activity with an IC value of 7040 304 µg/ml in DPPH assay and 845.4156.62 µm Fe(II) equivalents/g dry weight in FRAP assay respectively. In Ellman's assay for the cholinesterase inhibitory activity, GE had an

ICvalue of 41±12 pg/ml. And 52+2 µg/ml for inhibition of acetyl- and butyrylcholinesterase respectively. Also, GE increased the cell survival against amyloid B (AB) induced toxicity in primary adult rat hippocampal cell culture[27].

Milagu - Piper nigrum (PN)
Improves memory impairment and neurodegeneration

Chonpathompikunlert et al. revealed the effect of Piperine, a main active alkaloid in the fruit of *Piper nigrum*, on memory performance and neurodegeneration in an animal model of Alzheimer's disease. piperinewas orally given at various doses ranging from 5, 10, and 20 mg/kg BW at a period of 2 weeks before and 1-week toadult male Wistar rats after the intracerebroventricular administration of acetylcholine aziridinium ion (AF64A) bilaterally. Piperine at various dosage ranges, the results of this study showed significant improvement in memory impairment and neurodegeneration in the hippocampus[28].

Cognitive function

Wang et al, reported that piperineameliorates ICV-STZ-induced cognitive impairments via antioxidant and anti-inflammatory activities and its ability to restore hippocampal neurotransmission in the mouse[29]. *Subedee et al.* evaluated PN as a preventive drug for Alzheimer's associated histopathological, biochemical, and behavior changes in a rat model[30]. *Hirtu et al.*analyzedthe spatial memory formation following administration of the methanolic extract of *P. nigrum*fruits (50 and 100 mg/kg, orally, for 21 consecutive days) in rats subjected to intracerebroventricular injection of Ab (1–42). Intracerebroventricular injection of Ab(1–42) interferes with memory function and subsequently causes impairment of spatial memory within Y-maze and radial arm-maze tasks, hence the results showed the methanolic extract of *P. nigrum* fruits could effectively enhance memory processes and restore antioxidant brain status and may confer neuroprotection due to alleviation of oxidative damage induced by Ab(1–42)[31].

Thippili - Piper longum(PL)
Improves cognitive function

Jun Go et al, reported that one of the major chemical constituents of *Piper longum*Piperlongumine (PL), significantly activated the deacetylase ability of Sirt1 *in vitro*. Treatment with PL, regulated the gene transcription of antioxidant response elements in hippocampal neurons and attenuated the cytotoxicity induced by intraneuronal Aβ1-42 expression. The oral administration of PL, at a dose of 50 mg/kg/day for 2.5 months, significantly reduced the occupied area of beta-amyloid in the parietal cortex of APP/PS1 mice. Also improved the novel object recognition and working memory impairment[32].

Neuroprotective

Bi Y et al., evaluated that the alkaloid of *P. Longum* (PLA) has neuroprotective effects in an MPTP-induced chronic mouse model of Parkinson's disease[33].

MAO inhibitory activity and antidepressant-like activity

Lee SA et al. studied that an ethanol extract of the fruits of *P. Longum*showed strong inhibitory activity on mouse brain MAO (Monoamine oxidase (MAO) catalyzes the oxidative deamination of monoamine neurotransmitters like serotonin, dopamine, and norepinephrine, and plays important roles in several psychiatric and neurological disorders). Also, antidepressant-like activity by In Vivo Tail Suspension and Mismeasurement of Spontaneous Motor Activity[34].

Karisalai - Ecliptaprostrata(EP)

*Banji O et al.*studied that the aqueous extract obtained from leaves of *E. Prostrata* at the dose of 100 and 200 mg/kg was evaluated for its potential application on transfer latency as a parameter of acquisition and retrieval learning in rats using an elevated plus-maze. The administration of extract was reported to significantly improve retrieval memory[35]. *Kim D et al.* investigated the different concentrations of butanol fractions of the *E. Prostrata* aqueous extractin CD rats. The acetylcholine formation and oxidative stress inhibition in the brain and serum of rats were accessed before and after feeding the experimental diet. The acetylcholine level was increased by 9.6–12.1% in the fed

group as compared to the control. Monoamine oxidase-B activity and superoxide radical levels were decreased by 10.5% and 9.4%, respectively in the treated group[36]. *Xia X, Yu R, Wang X, et al.*investigated the role of *Ecliptaprostrata*extract reversed the spatial learning and memory deficits caused by D-galactose-induced aging in rats, particularly in the groups with higher treatment concentrations. Compared with the normal group, the levels of dopamine (DA), Norepinephrine (NE), and 5-HT were significantly lower in the D-galactose-treated model group. Spatial memory performance was evaluated using the Morris water maze[37].

*Jung WY et al.*used the passive avoidance, Y-maze, and Morris water maze tasksto evaluate the anti-amnesic effects of the ethanolic extract of *Ecliptaprostrata* (EEEP) in mice. In the passive avoidance task, EEEP significantly ameliorated the shortened step-through latency induced by scopolamine. In the Y-maze task, EEEP showed a significant increase in alternation behavior.From the results the scopolamine-induced decrease in the swimming time within the target zone and the number of crossings where the platform was significantly reversed by EEEP[38].

Vellalrugu – *Enicostema axillare*(EA)
Vaijanathappa et al., studied four successive extracts of the whole plant of *Enicostemma axillare* (*E. Axillare*), for antioxidant activity in *in-vitro* methods using nine different ways. All four extracts of *E. Axillare* showed potent antioxidant activityin the 2,2 -azino-bis (3-ethyl benzo-thiazoline-6-sulfonic acid) diammonium salt (ABTS) method. The chloroform extract also showed potent antioxidant activity in H_2O_2, nitric oxide, and hydroxyl radicals using the deoxyribose and lipid peroxidation methods [39].

Kadukkaai - *Terminalia chebula*(TC)
Learning memory
Seth et al. evaluated that ethanolic extracts of *T. Chebula*significantly improved learning memory in Chemical Induced Memory Impairments in Rats assessed by Morris water maze test [40].

Acetylcholinesterase inhibitory activity
Kim MS et al., reported that TCE treatment reversed scopolamine-induced learning and memory deficits in acquisition and retention in the Morris water maze task. TCE reduced hippocampal ache activities and increased chat and ach levels and also TCE treatment suppressed scopolamine-induced oxidative damage by ameliorating the increased levels of ROS, NO, and MDA [41].

Alzheimer's disease in rat
Lakshmi et al., evaluated that the Fruit extracts of *Terminalia chebula* exhibited significant learning and memory activity in Alzheimer's disease and neurodegenerative diseases in rats, which modulates oxidative stress and is involved in the protective effect against oxidative damage [42].

Thandrikaai - *Terminalia bellirica*(TB)
Dinesh Dhingra et al. evaluated the anti-depressant-like activity of aqueous and ethanolic extracts of *T. Bellirica*on depression in mice using the forced swim test (FST) and tail suspension test (TST) and its efficacy was found to be similar to fluoxetine and imipramine (antidepressant drugs) [43].

Waheed, revealed the antioxidant on neuroprotective activities of TB by Lipid Peroxidation (LPO) assay reduced Glutathione (GSH) assay catalase(CAT) Assay Superoxide Dismutase (SOD) Assay [44]. *Nirala*, reported that the Aqueous Extract of TB enhances the learning process and is comparable to the standard drug Piracetam at higher doses (36mg/kg). Also, it can oppose the alcohol-induced learning impairment at lower doses (9mg/kg) in the *invivo* rat model and assessed by Hebb- William Maze[45].

Nellimulli - *Phyllanthus embilica*(PE)
AChE & BuChEinhibitory activity

Biswas et al. evaluated that A crude methyl extract (CME) of dry fruit of *P. Emblica* for its acetylcholinesterase (AChE) and butyrylcholinesterase (BuChE) inhibitory activity using Ellman's method results shows that inhibiting AChEand BuChEwith IC50 of 53.88 μg/ml and 65.12 μg/ml respectively, which shows that the CME of *P. Emblica* is a source forAChEand BuChEinhibitors[46].

Vrish et al. investigated the methanolic fruit extract of *Phyllanthus emblica* Linn. for its reversal effect on Scopolamine and sodium nitrite-induced memory deficits in mice. Elevated plus maze (EPM) and Morris water maze (MWM) were used to evaluate short and long-term memory respectively. The administration of methanolic fruit extract from the plant significantly improved learning and memory, prevented scopolamine and sodium nitrite-induced experimental amnesia and may be a great potential in memory deficits[47]. *Uddin MS et al,* demonstrated that the Ethanolic extract of *P.embilica* fruits showed marked beneficial effects for improving learning, memory, and antioxidant activity. Among ripe and unripe fruits, significant cognitive enhancing effects were observed by unripe fruit which is comparable with the standard. Antioxidant activity was evaluated by measuring enzymes such as superoxide dismutase (SOD), reduced glutathione (GSH), catalase (CAT), glutathione peroxidase (GSH-Px), glutathione reductase, glutathione-S-transferase, and the contents of thiobarbituric acid reactive substances (TBARS) in entire brain tissue homogenates. Ache activity was determined using a colorimetric method[48].

Vasambu - *Acorus calamus*(AC)

*Mukherjee et al.*revealed the Acetylcholinesterase inhibitory activity of essential oil from the *Acorus calamus* and its main constituents, β -asarone and α-asarone by Ellman's method.In this study,Physostigmine was the standard inhibitor that showed inhibition with an IC_{50} value of 0.28 ± 0.015. From the resultsInhibitory activity of the hydroalcoholic extract of AC with IC_{50} value of 182.31 ± 16.78mL. AC rhizomes essential oil, β -asarone and α-asarone, IC $_{50}$values were 10.67 ± 0.81, 3.33 ± 0.02, and 46.38 ± 2.69 respectively. That shows β -asarone is the most active component in AC but weaker than the standard physostigmine[49].

Reddy et al, studied that AC treatment effectively prevented stress-induced cognitive dysfunction and anxious behavior by chronic stress-induced cognitive dysfunction and anxiety in rats. Also found antioxidant activities. This study shows the neuroprotective effect of AC against restraint stress-induced neuronal damage[50]. *C. Venkatramaniah et al,* observed the Neuroprotective role of Acorus calamus us and its active principle beta asarone in a Hippocampal (the hippocampus is the main organ for memory) lesion surgery rat model by analyzing the memory of the animals in 8 arms radial maze[51].

Vallarai - *Centella asiatica* (CA)

Gray et al. evaluated the cognitive-enhancing effects of *Centella asiatica* Water extract(CAW), These cognitive-enhancing effects appear independent of Aβ plaque reduction, CAW reduced the Aβ plaque burden in the hippocampus but it did not affect Aβ levels in the cortex and improvements were observed in both hippocampal and cortically mediated tasks. Hippocampal mitochondrial function was improved by CAW treatment and also induced the expression of mitochondrial as well as antioxidant response genes in the brains of mice [52]. *Jintanaporn et al.* reported in their trial the Positive modulation of cognition and mood-enhancing effect of *Centella asiatica* in the healthy elderly volunteer. Twenty-eight Healthy elder participants were treated with plant extract for 2 months with doses ranging from 250, 500, and 750 once daily. The computerized test battery and event-related potential were used to assess the cognitive function and Bond–Lader visual analog scales were used to assess the mood, before the trial and after single, 1, and 2 months. The results showed enhanced working memory and improvement in self-related mood with a high dose of plant extract [53].

Kumar et al. revealed in their study that the *Centella asiatica* extract significantly attenuated colchicine-induced memory impairment assessed by the Elevated plus maze test and Morris water maze oxidative damage assessed by attenuated the increase in MDA, nitrite levels, and restored decrease in reduced GSH [54].

Rujitha *et al.,*

DISCUSSION

This review has proven that the ingredients of *Brahmiyathi Pavanai Chooranam* have Neurological antioxidants, Neuromodulatory, Cognitive enhancement, Neuroprotective, enhancing neurite growth, Enhancing acetylcholine content, and Acetylcholinesterase inhibitor actions. According to the method are preparation soaking the drugs with *Centella asiatica* juice 21 times enhances the efficacy of the drug and preserves the concentration of phytoconstituents. According to the Siddha fundamental and taste theory, the ingredients are favorable for the management of Alzheimer's Disease.Finally, this review concludes that the drug *Brahmiyathi Pavanai Chooranam*is a novel drug for Alzheimer's Disease.

REFERENCES

1. Dementia (who.int)
2. Alzheimer's Disease | National Health Portal Of India (nhp.gov.in)
3. Alzheimer Disease - StatPearls - NCBI Bookshelf (nih.gov)
4. Alzheimer's & Dementia Help | INDIA | Alzheimer's Association
5. Galantamine - StatPearls - NCBI Bookshelf (nih.gov)
6. Rivastigmine - StatPearls - NCBI Bookshelf (nih.gov)
7. Donepezil - StatPearls - NCBI Bookshelf (nih.gov)
8. Memantine - StatPearls - NCBI Bookshelf (nih.gov)
9. Hakkim,Pa. Mohamad AbdhulaSayubu, *KadukkaaiVallaraiyin Thani Maanbu.*
10. Ka.sa.Murukesamudaliyar, Gunapadammooligai , 9th edition ,Indian medicine and homeopathy, the nadar press limited, sivakasi 2013
11. Bhattacharya, S.K., Kumar, A. and Ghosal, S. (1995), Effects of glycowithanolides from *Withania somnifera* on an animal model of Alzheimer's disease and perturbed central cholinergic markers of cognition in rats. Phytother. Res., 9: 110-113.
12. Tohda C, Kuboyama T, Komatsu K. Dendrite extension by methanol extract of Ashwagandha (roots of Withaniasomnifera) in SK-N-SH cells. *Neuroreport.* 2000;11(9):1981-1985. doi:10.1097/00001756-200006260-00035
13. Kurapati KR, Atluri VS, Samikkannu T, Nair MP. Ashwagandha (Withaniasomnifera) reverses β-amyloid1-42 induced toxicity in human neuronal cells: implications in HIV-associated neurocognitive disorders (HAND). *PLoS One.* 2013;8(10):e77624. Published 2013 Oct 16. doi:10.1371/journal.pone.0077624
14. Zhao J, Nakamura N, Hattori M, Kuboyama T, Tohda C, Komatsu K. Withanolide derivatives from the roots of Withaniasomnifera and their neurite outgrowth activities. *Chem Pharm Bull (Tokyo).* 2002;50(6):760-765. doi:10.1248/cpb.50.760
15. Li Q, Li Z, Xu XY, Guo YL, Du F. Neuroprotective properties of picroside II in a rat model of focal cerebral ischemia. *Int J Mol Sci.* 2010;11(11):4580-4590. Published 2010 Nov 16. doi:10.3390/ijms11114580
16. Li P, Matsunaga K, Ohizumi Y. Enhancement of the nerve growth factor-mediated neurite outgrowth from PC12D cells by Chinese and Paraguayan medicinal plants. Biol Pharm Bull. 1999 Jul;22(7) 752-755. doi:10.1248/bpb.22.752. PMID: 10443479.
17. Ping LI, Kimihiro MATSUNAGA, Yasushi OHIZUMI, Nerve Growth Factor-Potentiating Compounds from PicrorhizaeRhizoma, Biological and Pharmaceutical Bulletin, 2000, Volume 23, Issue 7, Pages 890-892, Released on J-STAGE April 10, 2008, Online ISSN 1347-5215, Print ISSN 0918-6158,
18. SuneeChansakaow et al. Chemical compositions, antioxidant and antibacterial activities of essential oils from *Anethum graveolens* L. and *Trachyspermumroxburghianum* (DC.) Craib grown in Thailand, Journal of Natural Sciences Research, Vol.4, No.12, (2014): 62-70.
19. Kumar, S., & Chowdhury, S. (2014). Kinetics of acetylcholinesterase inhibition by an aqueous extract of Cuminum cyminum seeds. *International Journal of Applied Sciensces and Biotechnology, 2*(1), 64-68.

Rujitha *et al.*,

20. Koppula, S., & Choi, D. K. (2011). Cuminum cyminum extract attenuates scopolamine-induced memory loss and stress-induced urinary biochemical changes in rats: a non-invasive biochemical approach. *Pharmaceutical biology, 49*(7), 702-708.

21. Prabha, M., & Anusha, T. S. (2015). Esterase's properties in commonly used Indian spices for Alzheimer's disease model. *Journal of biochemical technology, 6*(1), 875-882

22. Kanter M. Protective effects of thymoquinone on the neuronal injury in frontal cortex after chronic toluene exposure. *J Mol Histol.* 2011;42(1):39-46. doi:10.1007/s10735-010-9305-3

23. Poorgholam P, Yaghmaei P, Hajebrahimi Z. Thymoquinone recovers learning function in a rat model of Alzheimer's disease. *Avicenna J Phytomed.* 2018;8(3):188-197.

24. Veerabomma Sreedhar, LanguluriReddenna, ThamineniRajavardhana, JangamThippe Rudra, Bestha Chakrapani. Phytochemical Composition of Nigella sativa Extract as Potential Source for Inhibiting β-Amyloid Aggregation: Significance to Alzheimer's Disease. /J. Pharm. Sci. & Res. Vol. 14(1), 2022

25. RahimehBargi, Fereshteh Asgharzadeh, Farimah Beheshti, Mahmoud Hosseini, Hamid Reza Sadeghnia, Majid Khazaei, The effects of thymoquinone on hippocampal cytokine level, brain oxidative stress status and memory deficits induced by lipopolysaccharide in rats, Cytokine, Volume 96, 2017, Pages 173-184, ISSN 1043-4666

26. Tung BT, Thu DK, Thu NTK, Hai NT. Antioxidant and acetylcholinesterase inhibitory activities of ginger root (Zingiber officinale Roscoe) extract. *J Complement Integr Med.* 2017;14(4):/j/jcim.2017.14.issue-4/jcim-2016-0116/jcim-2016-0116.xml. Published 2017 May 4. doi:10.1515/jcim-2016-0116

27. Kim JE, Shrestha AC, Kim HS, et al. WS-5 Extract of *Curcuma longa, Chaenomeles sinensis,* and *Zingiber officinale* Contains Anti-AChE Compounds and Improves *β*-Amyloid-Induced Memory Impairment in Mice [published correction appears in Evid Based Complement Alternat Med. 2021 Aug 10;2021:5127585]. *Evid Based Complement Alternat Med.* 2019;2019:5160293. Published 2019 Apr 1. doi:10.1155/2019/5160293

28. Mathew M, Subramanian S. In vitro evaluation of anti-Alzheimer effects of dry ginger (Zingiber officinale Roscoe) extract. *Indian J Exp Biol.* 2014;52(6):606-612.

29. Chonpathompikunlert P, Wattanathorn J, Muchimapura S. Piperine, the main alkaloid of Thai black pepper, protects against neurodegeneration and cognitive impairment in animal model of cognitive deficit like condition of Alzheimer's disease. *Food Chem Toxicol.* 2010;48(3):798-802. doi:10.1016/j.fct.2009.12.009

30. Wang C, Cai Z, Wang W, et al. Piperine attenuates cognitive impairment in an experimental mouse model of sporadic Alzheimer's disease. *J NutrBiochem.* 2019;70:147-155. doi:10.1016/j.jnutbio.2019.05.009

31. Subedee L, Suresh RN, Mk J, HI K, Am S, Vh P. Preventive role of Indian black pepper in animal models of Alzheimer's disease. *J Clin Diagn Res.* 2015;9(4):FF01-FF4. doi:10.7860/JCDR/2015/8953.5767

32. Hritcu L, Noumedem JA, Cioanca O, Hancianu M, Kuete V, Mihasan M. Methanolic extract of Piper nigrum fruits improves memory impairment by decreasing brain oxidative stress in amyloid beta(1-42) rat model of Alzheimer's disease. *Cell Mol Neurobiol.* 2014;34(3):437-449. doi:10.1007/s10571-014-0028-y

33. Jun Go, Thi-Kim-Quy Ha, Ji Yeon Seo, Tae-Shin Park, Young-Kyoung Ryu, Hye-Yeon Park, Jung-Ran Noh, Yong-Hoon Kim, Jung Hwan Hwang, Dong-Hee Choi, Dae Youn Hwang, Sanghee Kim, Chul-Ho Lee, Won Keun Oh, Kyoung-Shim Kim, Piperlongumine activates Sirtuin1 and improves cognitive function in a murine model of Alzheimer's disease, Journal of Functional Foods, Volume 43, 2018, Pages 103-111, ISSN 1756-4646,

34. Bi Y, Qu PC, Wang QS, et al. Neuroprotective effects of alkaloids from Piper longum in an MPTP-induced mouse model of Parkinson's disease. *Pharm Biol.* 2015;53(10):1516-1524. doi:10.3109/13880209.2014.991835

35. Lee SA, Hong SS, Han XH, et al. Piperine from the fruits of Piper longum with inhibitory effect on monoamine oxidase and antidepressant-like activity. *Chem Pharm Bull (Tokyo).* 2005;53(7):832-835. doi:10.1248/cpb.53.832.

36. Banji O., Banji D., Annamalai A., Manavalan R. Investigation on the Effect of *Eclipta alba* on Animal Models of Learning and Memory. Indian J. Physiol. Pharmacol. 2007; 51:274–278.

37. Kim D.-I., Lee S.-H., Hong J.-H., Lillehoj H.S., Park H.-J., Rhie S.-G., Lee G.-S. The Butanol Fraction of *Ecliptaprostrata* (Linn) Increases the Formation of Brain Acetylcholine and Decreases Oxidative Stress in the Brain and Serum of Cesarean-Derived Rats. Nutr. Res. 2010; 30:579–584.

38. Xia X, Yu R, Wang X, et al. Role of *Ecliptaprostrata* extract in improving spatial learning and memory deficits in D-galactose-induced aging in rats. *J Tradit Chin Med.* 2019;39(5):649-657.

39. Jung WY, Kim H, Jeon SJ, et al. Eclalbasaponin II Ameliorates the Cognitive Impairment Induced by Cholinergic Blockade in Mice. *Neurochem Res.* 2018;43(2):351-362.

40. Vaijanathappa, Jaishree & Badami, Shrishailappa& Bhojraj, Suresh. (2008). In Vitro Antioxidant Activity of *Enicostemmaaxillare*. Journal of Health Science. 54. 524-528.

41. Seth, D., Khan, N., & Jain, N. K. (2020). Influence of Fruits Extract & Fractions of Terminalia Chebula on Chemical Induced Memory Impairments in Rats. *Annals of the Romanian Society for Cell Biology*, 2074-2090.

42. Kim MS, Lee DY, Lee J, et al. Terminalia chebula extract prevents scopolamine-induced amnesia via cholinergic modulation and anti-oxidative effects in mice. *BMC Complement Altern Med.* 2018;18(1):136. Published 2018 May 2. doi:10.1186/s12906-018-2212-y

43. Lakshmi, K. & Karishma, S. & Chandra Sekhar, Guduru& Babu, Ankem& Kumar, N.. (2018). Terminalia chebula Retz improve memory and learning in Alzheimer's Model: (Experimental Study in Rat). Research Journal of Pharmacy and Technology. 11. 4888. 10.5958/0974-360X.2018.00890.9.

44. Dhingra, Dinesh &Valecha, Rekha. (2007). Evaluation of the antidepressant-like activity of aqueous and ethanolic extracts of Terminalia belliricaRoxb. fruits in mice. Indian journal of experimental biology. 45. 610-6.

45. Waheed, Syed & Badoni, Himani. (2020). Anti-Parkinson's activity of Emblica officinalis and Terminalia bellirica.

46. Nirala, K. K., & Singh, R. K. Effect of Aqueous Extract of Terminalia Bellirica Fruit Pulp: An Animal Experimental Study

47. Biswas, Kushal & Islam, Md &Sharmin, Tahmida& Biswas, Pulak. (2015). In-vitro cholinesterase inhibitory activity of dry fruit extract of Phyllanthus emblica relevant to the treatment of Alzheimer's disease. The Journal of Phytopharmacology. 4. 5-8. 10.31254/phyto.2015.4102.

48. Vrish, Dhwaj&Ashwlayan, Vrish& Singh, Ranjit. (2011). Reversal effect of Phyllanthus emblica (Euphorbiaceae) rasayana on memory deficits in mice. International Journal of Applied Pharmaceutics. 3.

49. Uddin MS, Mamun AA, Hossain MS, Akter F, Iqbal MA, Asaduzzaman M. Exploring the Effect of *Phyllanthus emblica* L. on Cognitive Performance, Brain Antioxidant Markers and Acetylcholinesterase Activity in Rats: Promising Natural Gift for the Mitigation of Alzheimer's Disease. *Ann Neurosci.* 2016;23(4):218-229. doi:10.1159/000449482

50. Mukherjee PK, Kumar V, Mal M, Houghton PJ. In vitro acetylcholinesterase inhibitory activity of the essential oil from Acorus calamus and its main constituents. *Planta Med.* 2007;73(3):283-285. doi:10.1055/s-2007-967114

51. Reddy S, Rao G, Shetty B, Hn G. Effects of Acorus calamus Rhizome Extract on the Neuromodulatory System in Restraint Stress Male Rats. *Turk Neurosurg.* 2015;25(3):425-431. doi:10.5137/1019-5149.JTN.11405-14.1

52. C. Venkatramaniah, A. Mary Antony Praba, B. Mohammed Ismail. "NEUROPROTECTIVE ROLE OF ACORUS CALAMUS AND IT'S ACTIVE PRINCIPLE BETA ASARONE IN RETAINING THE MEMORY OF RATS USING 8 ARM RADIAL MAZE." International Journal of Anatomy and Research 4.2 (2016) 2238-2244

53. Gray NE, Zweig JA, Caruso M, et al. Centella asiatica attenuates hippocampal mitochondrial dysfunction and improves memory and executive function in β-amyloid overexpressing mice. *Mol Cell Neurosci.* 2018;93:1-9. doi:10.1016/j.mcn.2018.09.002

54. JintanapornWattanathorn, LugkanaMator, SupapornMuchimapura, TerdthaiTongun, OrapinPasuriwong, NawanantPiyawatkul, KwanchanokYimtae, BungornSripanidkulchai, JintanaSingkhoraard, Positive modulation of cognition and mood in the healthy elderly volunteer following the administration of Centella asiatica, Journal of Ethnopharmacology, Volume 116, Issue 2, 2008, Pages 325-332, ISSN 0378-8741,

55. Kumar A, Dogra S, Prakash A. Neuroprotective Effects of Centella asiatica against Intracerebroventricular Colchicine-Induced Cognitive Impairment and Oxidative Stress. *Int J Alzheimers Dis.* 2009;2009:972178. Published 2009 Sep 13. doi:10.4061/2009/972178

Table.1. The Ingredients and Their Characteristics of BPC are Listed [10].

S.No	Tamil / Siddha Name	Botanical Name	Parts used	Taste/Potency
1.	*Amukkara*	*Withaniasomnifera*	Root	Bitter/Hot
2.	*Kadugurohini*	*Picrorhizascrophulariiflora*	Root	Bitter, Acrid/Hot
3.	*Ajamthaomam*	*Trachyspermumroxburghianum*	Seed	Acrid/Hot
4.	*Seeragam*	*Cuminum cyminum*	Seed	Acrid, Sweet/ Cold
5.	*Karunjeeragam*	*Nigella sataiva*	Seed	Acrid/Hot
6.	*Chukku*	*Zingiber officinale*	Rhizome(Dried)	Acrid/Hot
7.	*Milagu*	*Piper nigrum*	Fruit	Acrid/Hot
8.	*Thippili*	*Piper longum*	Fruit	Acrid/Hot
9.	*Karisalai*	*Ecliptaprostrata*	Whole plant	
10.	*Vellarugu*	*Enicostemaaxillare*	Whole plant	Acrid/Hot
11.	*Kadukaai*	*Terminalia chebula*	Fruit	Astringent, Sweet, Acrid, Bitter, Sour/Cold
12.	*Thandrikaai*	*Terminalia bellirica*	Fruit	Astringent/Hot
13.	*Nellimulli*	*Phyllanthus embilica*	Fruit	Sour, Astringent/Cold
14.	*Vasambu*	*Acorus calamus*	Rhizome	Acird/Hot
15.	*Vallarai*	*Centellaasiatica*	Whole plant	Acrid/Hot

RESEARCH ARTICLE

A New Insights on Kadukkai (*Terminalia chebula*.Retz.) as a Prebiotic and its Effect on Gut Health

A.Aishwarya[1*], B. K. Priya[2] ,V.Elakkiyaa[3] and T. Lakshmikantham[4]

[1]Assistant Professor, Department of Maruthuvam, National Institute of Siddha, Tamabaram Sanatorium,Chennai-47, Tamil Nadu, India.
[2]Resident Medical Officer, National Institute of Siddha, Tamabaram Sanatorium,Chennai-47, Tamil Nadu, India.
[3]Research Associate -I, Siddha Clinical Research Unit,under Central Council for Research in Siddha, Bengaluru, Karnataka, India.
[4]Associate Professor, HoD (i/c), Department of Maruthuvam, National Institute of Siddha, Tambaram Sanatorium, Chennai, Tamil Nadu, India.

*Address for Correspondence
A.Aishwarya
Assistant Professor,
Department of Maruthuvam,
National Institute of Siddha,
Tamabaram Sanatorium,
Chennai-47, Tamil Nadu, India.
E.Mail: draishwaryabalan6@gmail.com

ABSTRACT

Most of the Siddha herbs plays a dominant role in modulating the gut microbiota. The gut microbiota is now considered a relevant therapeutic target for many chronic diseases. Kadukkai (*Terminalia Chebula*.Retz**.)**, which is referred to as "King of herb" alters the gut microbiota and promote human health. Gut microbiota release by-products in the intestine which are beneficial for human health with different physiological impacts including diabetes, hypertension, obesity, gastrointestinal diseases, hormonal brain axis, cancer, etc. Clinical studies on the effects of Kadukkai on human gut microbiome are lacking. The authors hypothesized that Kadukkai consumption may alter the gut microbiota composition and exerts differential effects on subsets of the gut microbiota. The present work provides new findings on the influence of extracts from Kadukkai that act like prebiotics and augment the probiotic activity.

Keywords: Gastrointestinal, Herb, Kadukkai, Microbiota, Prebiotic, Siddha medicine

INTRODUCTION

Siddha system of medicine places great importance on proper diet and digestion, as well as on all aspects of lifestyle. In future, most of the researchers will agree that the Siddha medicine to be an ancient science of epigenetics. The Siddha practitioners might not have understood the precise nutrigenomic mechanics of how food and herbs can affects gene expression , but they did recognize that each individual has their own unique psychophysiological constitution, which is affected by diet, lifestyle, and environmental factors.Siddha medicine describes the functioning of our mind and body in terms of three main *Uyir thathukkal*—the governing principles of the physiology—*Vatham, Pitham,* and *Kabam*[1]Siddha system of medicine, as well as integrative medicine practitioners, commonly prescribes these herbal medicines for a variety of gut- and skin-related conditions. However, insufficient data exist on the effects of Kadukkai on gut microbiota, and clinical investigations of this herbal medicines are lacking.

GENERAL DESCRIPTION OF KADUKKAI
Terminalia chebula (common name: Kadukkai), a widely studied Single herb is held in high esteem in Siddha for its properties to prevent and cure diseases. It has enjoyed the prime place among medicinal herbs in India since ancient times. It is called the 'King of Medicines' and is always listed first in traditional medicines because of its extraordinary therapeutic benefits.

SIDDHA PHARMACOLOGY OF KADUKKAI[2]
Siddha pharmacology describes the attributes of herbs. The *suvai* or veeriyam of Kadukkai is sweet, sour, pungent, bitter, and astringent; except salty taste. The veeriyam, or potency and action, is neutral, and the Vipagam, or post digestive effect is sweet. Kadukkai has a prabhavam, meaning special action or trophism, for all doshas (energetics and mind–body types) and thus is balancing for all doshas and constitutions. The gunam, or qualities of Kadukkai is considered light and dry.

GUT HEALTH, SIDDHA HERBS AND PREBIOTICS
Siddha medicine explains that most diseases are caused by an accumulation of undigested food (*Vishamakkini*) in gut. *Vishamakkini* literally means to digest the foods and drinks very slowly and digestion will not complete. Hence some toxic condition may prevail because of *Samana Vaayu* misses its proper place, the heat will be toxic. Generally *Samana vayu* helps us smoothening the food , liquids and makes softening the six tastes and helps in spreading them in the body. The *Vishamakkini* which caused the "undigested food," but it can be understood from a scientific perspective as endogenous toxins resulting from imbalanced or incomplete digestion. *Manthakkini* can be formed as a result of reduced Udal thee, or digestive power (*Manthakkini*-when *Samanavaayu* unites with *Kabam*,the heat produced will be dull). *Udal thee* has a number of different meanings and not only relates to digestive enzymes but also to the metabolic process in the different tissues or *Udal thathukkal* of the body. *Manthakkini* is initially formed in the digestive tract, but at a later stage of disease it can leak into the bodily tissues and turn into *Vishamakkini*, a reactive form of *Manthakkini*, that leads to tissue disruption and chronic inflammation and disease.[3] A disruption in the gut microbiome has been associated with problems in the gut barrier.

Although the body can withstand brief disruption of the intestinal barrier, due to ageing, persistent stress, and genetic predisposition which may contribute to the development of autoimmune, metabolic, and mental health disorders. Chronic breakdown of the intestinal barrier can cause microbial components to enter the bloodstream and that leads to low-grade, systemic inflammation. [4]. Most of the ingredients in Siddha medicine are derived from herbal origin .Major components, and their biosynthesis is influenced by various environmental factors. Recently, various biological activities of Siddha herbs, such as antitumor, anti-oxidation, hypolipidemic, and immunomodulatory have been investigated and have received increased attention. Human microbiota investigations by a study has revealed the significant prebiotic potential of medicinal herbs used in digestive health

and disease via the microbial metabolism of herb-provided substrates, e.g., polyphenols, sugars, glycans and amino acids [5].

BIOLOGICAL RHYTHMS AND GUT MICROBIOTA

Siddha system of medicine clearly identifies *Sirupozhuthugal* (daily), *Perumpozhuthugal* (seasonal) rhythms. Each day, for example, consists of a sequence of periods, which are characterized by *Vatham, Pitham,* or *Kabam*. [6]The day starts with a *Vatham* period from 6 am to 10 am, then a *Pitham* period from 10 am to 2 pm, and then a *Kabam* period from 2 pm to 6 pm. Next is another *Vatham* period from 6 pm to 10 pm, a *Pitham* from 10 pm to 2 am and finally a *Kabam* from 2 am to 6 am. Each season is represented by either one *thodam* or a combination of *thodangal* (Table 2).

The daily routine is called *Nithiya ozhukkam* and the seasonal routine is called *Kaala ozhukkam*[6] . In 2017, Nobel Prize in Physiology and Medicine was given for studies on the genetic foundation of biological rhythms, demonstrating how modern medicine also understands the significance of daily rhythms to your health. Almost all living things, including bacteria to humans, have an internal "biological clock" that keeps a roughly 24-hour rhythm. The master clock (biological clock) becomes confused when artificially introducing light and dark signals from the outside world, which has negative health effects. For instance, shift workers have been found to have a greater prevalence of cancer, cardiovascular disease, obesity, digestive issues, and mental and neurological illnesses. [7].

Siddha system of medicine recommendations of specific diets at specific times may relate to the seasonal rhythms of the microbiome. Due to the habits of diet, activities of the individual against nature and changes in the environment and seasonal changes affect the system and the seven Thathus are affected. Hence, the three Naadis deviate from their natural state and indicate through pulse and symptoms in the body. Since the three naadi derange from their natural state and indicate disease they are called mukkutram (making physical imperfection) [3]. Over the *Ilavenil kalam*, for example, Kabam was said to build up in the body. *Munpanikalam* is described as the ideal time to rebalance Kabam to prevent toxins and excess mucus from creating congestion and allergies. Foods that are primarily Kabam in nature—heavy, greasy, and mucus forming—tend to increase both Kabam. Siddha recommends reducing or eliminating Kabam foods during this time, which might help to heal the gut and reboot the microbiome.[6]. Seasonal differences in the gut microbiome, observed higher relative abundance of the phylum Bacteroidetes, one of the most common and prevalent groups of gut bacteria, during the summer compared to the winter months. Also found that Actinobacteria abundance increased in the winter compared to the summer months. A study showed that significant seasonal shifts in the abundance of quite a few other types of bacteria (for example, phyla Chloroflexi, Gemmatimonadetes, TM7, etc.).[8]

The Role of Prebiotics in various disease conditions:

Prebiotics are nondigestible dietary components that are said to have a positive impact on the host by promoting the growth and/or activity of bacteria in the digestive system in ways that are allegedly good for health.[9]
There are various types of prebiotics and majority of them are mostly oligosaccharide carbohydrates (OSCs),
- Fructans – oligofructose (FOS)
- Galacto-Oligosaccharides (GOS)
- Starch and Glucose-Derived Oligosaccharides
- pectic oligosaccharide (POS)
  Non Carbohydrate Oligosaccharide,
- cocoa-derived flavanols[10]

PHYTOCHEMICALS AS A MODIFIER OF GUT MICROBIOTA

Kadukkai likely interact with gut microbiota to induce gastrointestinal and systemic effects through its bioactive compounds. Kadukkai is enriched in diverse polyphenolic compounds such as tannins, phenolic carboxylic compounds, phenols,terpenoids and triterpene saponins,flavonoids, sterols,etc..[19]. The tannin content of *Terminalia chebula* ranges from 32% to 45% and consists of punicalagin, gallic acid, ellagic acid, chebulic acid, and chebulinic acid. There has been evidence of the flavonoids quercetin, catechin, and kaempferol.

Aishwarya *et al.*,

Monosaccharides/oligosaccharides (9%) detected are D-glucose, D-fructose, and saccharose. The fruit acids include quinic acid (1.5%), shikimic acid (2%), and fatty oil (from seeds; 40%). The high tannin content of myrobalan makes it popular for use as an astringent.[20]. Polyphenols are a diverse class of secondary plant metabolites found in most diets. Owing to their chemical structure, they are poorly absorbed and thus reach the colon, where they affect the resident microbiota. Specifically, (poly)phenols can stimulate several of keystone bacterial species such as *Akkermansia muciniphila, Bacteroides thetaiotaomicrom, Faecalibacterium prausnitzii*, Bifidobacteria, and Lactobacilli [21] . Recent studies have evaluated the biotransformation of polyphenolic compounds by gut microbiota that result in increased bio absorption and/or bioactivity. For instance, the biotransformation of chebulinic acid by gut microbes, which has been demonstrated to have direct impacts on COX-2 production, may eventually reduce oxidative damage. Most of the animal and human studies suggest that *Akkermansi muciniphila* is a highly promising probiotic, especially its potential for the prevention and treatment of diabetes, obesity, and their associated metabolic disorders. The positive modulation of *Akkermansia* was, it increases the mucus thickness and gut barrier integrity [22]. Polyphenols shows that the human gut microbiota also responds with a major shift in *Akkermansia* abundance when challenged with high polyphenol intake, as it also suggests that healthy individuals may also take advantage of the prebiotic effects of polyphenols on *Akkermansia.* [23]

CONCLUSION AND FUTURE PERSPECTIVES

This review article revealed the promising findings of current prebiotic activity of Kadukkai. This study is novel in highlighting the significant prebiotic potential of herbal medicine Kadukkai and suggest that the health benefits of this herb was due to their ability to modulate the gut microbiota in a manner predicted to improve colonic epithelium function, reduce inflammation, and promote protection from bacterial opportunistic pathogenic infection. Future research in human clinical trials will examine if the in vitro results and the predictions from genomic analysis agree.

REFERENCES

1. P.M.Venugopal Udal Thathuvam,3rd edition 1993, Department of Indian medicine and Homoeopathy. Chennai-10 pg no-214,215
2. K.S.Murugesa mudhaliyar ,Gunapadam mooligai vaguppu 7th edition 2003, , Department of Indian medicine and Homoeopathy. Chennai-10 pg no-314-329
3. Shanmughavelu, H.P.I.M., Noinaadal Noimudhal Naadal Thirattu Part 1, First Edition, Published by D I M& H , Chennai, Pg no-165,168,265-266
4. Martel J, Chang SH, Ko YF, Hwang TL, Young JD, Ojcius DM. Gut barrier disruption and chronic disease. Trends Endocrinol Metab. 2022 Apr;33(4):247-265. doi: 10.1016/j.tem.2022.01.002. Epub 2022 Feb 9. PMID: 35151560.
5. Peterson CT, Rodionov DA, Iablokov SN, Pung MA, Chopra D, Mills PJ, Peterson SN. Prebiotic Potential of Culinary Spices Used to Support Digestion and Bioabsorption. Evid Based Complement Alternat Med. 2019 Jun 2;2019:8973704. doi: 10.1155/2019/8973704. PMID: 31281405; PMCID: PMC6590564.
6. Dr.Ko.Dhurairasan., Noi illa neri,3rd edition-1993, , Department of Indian medicine and Homoeopathy 2005. Chennai-10 Pg no-55-59,120-121
7. Zarrinpar A, Chaix A, Panda S. Daily Eating Patterns and Their Impact on Health and Disease. Trends Endocrinol Metab. 2016 Feb;27(2):69-83. doi: 10.1016/j.tem.2015.11.007. Epub 2015 Dec 17. PMID: 26706567; PMCID: PMC5081399.
8. Davenport ER, Mizrahi-Man O, Michelini K, Barreiro LB, Ober C, Gilad Y. Seasonal variation in human gut microbiome composition. *PLoS One.* 2014;9(3):e90731. Published 2014 Mar 11. doi:10.1371/journal.pone.0090731
9. R.A. Hegazi, A. Seth, Chapter 37 - The Role of Prebiotics in Gastrointestinal and Liver Diseases, Editor(s): Ronald Ross Watson, Victor R. Preedy, Bioactive Food as Dietary Interventions for Liver and Gastrointestinal Disease, Academic Press, 2013, Pages 569-583, ISBN 9780123971548, https://doi.org/10.1016/B978-0-12-397154-8.00021-X

Aishwarya *et al.,*

10. Davani-Davari D, Negahdaripour M, Karimzadeh I, et al. Prebiotics: Definition, Types, Sources, Mechanisms, and Clinical Applications. *Foods.* 2019;8(3):92. Published 2019 Mar 9. doi:10.3390/foods8030092

11. Macfarlane S, Macfarlane GT, Cummings JH. Review article: prebiotics in the gastrointestinal tract. Aliment Pharmacol Ther. 2006 Sep 1;24(5):701-14. doi: 10.1111/j.1365-2036.2006.03042.x. PMID: 16918875.

12. Benjamin J.L., Hedin C.R., Koutsoumpas A., Ng S.C., McCarthy N.E., Hart A.L., Kamm M.A., Sanderson J.D., Knight S.C., Forbes A., et al. Randomised, double-blind, placebo-controlled trial of fructo-oligosaccharides in active crohn's disease. Gut. 2011;60:923–929. doi: 10.1136/gut.2010.232025.

13. Patel R.M., Denning P.W. Therapeutic use of prebiotics, probiotics, and postbiotics to prevent necrotizing enterocolitis: What is the current evidence? Clin. Perinatol. 2013;40:11–25. doi: 10.1016/j.clp.2012.12.002.

14. Candela M., Guidotti M., Fabbri A., Brigidi P., Franceschi C., Fiorentini C. Human intestinal microbiota: Cross-talk with the host and its potential role in colorectal cancer. Crit. Rev. Microbiol. 2011;37:1–14. doi: 10.3109/1040841X.2010.501760.

15. Grüber C., van Stuijvenberg M., Mosca F., Moro G., Chirico G., Braegger C.P., Riedler J., Boehm G., Wahn U., MIPS 1 Working Group Reduced occurrence of early atopic dermatitis because of immunoactive prebiotics among low-atopy-risk infants. J. Allergy Clin. Immunol. 2010;126:791–797.

16. Moro G., Arslanoglu S., Stahl B., Jelinek J., Wahn U., Boehm G. A mixture of prebiotic oligosaccharides reduces the incidence of atopic dermatitis during the first six months of age. Arch. Dis. Childhood. 2006;91:814–819. doi: 10.1136/adc.2006.098251.

17. Van Den Heuvel E.G., Muijs T., Van Dokkum W., Schaafsma G. Lactulose stimulates calcium absorption in postmenopausal women. J. Bone Miner. Res. 1999;14:1211–1216. doi: 10.1359/jbmr.1999.14.7.1211.

18. Vulevic J., Juric A., Tzortzis G., Gibson G.R. A mixture of trans-galactooligosaccharides reduces markers of metabolic syndrome and modulates the fecal microbiota and immune function of overweight adults. J. Nutr. 2013;143:324–331. doi: 10.3945/jn.112.166132.

19. Riaz M, Khan O, Sherkheli MA, et al. Chemical Constituents of Terminalia Chebula. Nat Prod Ind J. 2017;13(2):112

20. Assie Jokar et.al., Potential therapeutic applications for *Terminalia chebula* in Iranian traditional medicine, J Tradit Chin Med 2016 April 15; 36(2): 250-254

21. Maria Carolina Rodríguez-Daza et.al.,Polyphenol-Mediated Gut Microbiota Modulation: Toward Prebiotics and Further,Front. Nutr., 28 June 2021 Sec. Nutrition and Microbes Volume 8 - 2021 | https://doi.org/10.3389/fnut.2021.689456

22. Zhou K. Strategies to promote abundance of *Akkermansia muciniphila*, an emerging probiotics in the gut, evidence from dietary intervention studies. J Funct Foods. 2017 Jun;33:194-201. doi: 10.1016/j.jff.2017.03.045. Epub 2017 Mar 29. PMID: 30416539; PMCID: PMC6223323.

23. Anhê FF, Pilon G, Roy D, Desjardins Y, Levy E, Marette A. Triggering Akkermansia with dietary polyphenols: A new weapon to combat the metabolic syndrome, Gut Microbes. 2016;7(2):146-53. doi: 10.1080/19490976.2016.1142036. Erratum in: doi: 10.1136/gutjnl-2014-307142. PMID: 26900906; PMCID: PMC4856456.

24. Santhiravel S, Bekhit AEA, Mendis E, Jacobs JL, Dunshea FR, Rajapakse N, Ponnampalam EN. The Impact of Plant Phytochemicals on the Gut Microbiota of Humans for a Balanced Life. Int J Mol Sci. 2022 Jul 23;23(15):8124. doi: 10.3390/ijms23158124. PMID: 35897699; PMCID: PMC9332059.

25. Lippolis T, Cofano M, Caponio GR, De Nunzio V, Notarnicola M. Bioaccessibility and Bioavailability of Diet Polyphenols and Their Modulation of Gut Microbiota. Int J Mol Sci. 2023 Feb 14;24(4):3813. doi: 10.3390/ijms24043813. PMID: 36835225; PMCID: PMC9961503.

26. Wenxia Qin, et.al., Dietary ellagic acid supplementation attenuates intestinal damage and oxidative stress by regulating gut microbiota in weanling piglets, Animal Nutrition,Volume 11, 2022,Pages 322-333,ISSN 2405-6545,https://doi.org/10.1016/j.aninu.2022.08.004.

27. Aa LX, Fei F, Qi Q, Sun RB, Gu SH, Di ZZ, Aa JY, Wang GJ, Liu CX. Rebalancing of the gut flora and microbial metabolism is responsible for the anti-arthritis effect of kaempferol. Acta Pharmacol Sin. 2020 Jan;41(1):73-81. doi: 10.1038/s41401-019-0279-8. Epub 2019 Aug 19. PMID: 31427695; PMCID: PMC7468310.

28. Xu Y, Wang N, Tan HY, et al. *Panax notoginseng* saponins modulate the gut microbiota to promote thermogenesis and beige adipocyte reconstruction *via* leptin-mediated AMPKα/STAT3 signaling in diet-induced obesity. *Theranostics.* 2020;10(24):11302-11323. Published 2020 Sep 14. doi:10.7150/thno.47746

29. Lei Chen, William C.S. Tai, W.L. Wendy Hsiao, Dietary saponins from four popular herbal tea exert prebiotic-like effects on gut microbiota in C57BL/6 mice, Journal of Functional Foods, Volume 17, 2015, Pages 892-902, ISSN 1756-4646, https://doi.org/10.1016/j.jff.2015.06.050

30. Ruisong Pei, Xiaocao Liu, Bradley Bolling, Flavonoids and gut health, Current Opinion in Biotechnology, Volume 61, 2020, Pages 153-159, ISSN 0958-1669, https://doi.org/10.1016/j.copbio.2019.12.018.

31. Molino S, Lerma-Aguilera A, Jiménez-Hernández N, Rufián Henares JÁ, Francino MP. Evaluation of the Effects of a Short Supplementation With Tannins on the Gut Microbiota of Healthy Subjects. Front Microbiol. 2022 Apr 27;13:848611. doi: 10.3389/fmicb.2022.848611. PMID: 35572677; PMCID: PMC9093706.

32. Li X, Mo K, Tian G, Zhou J, Gong J, Li L, Huang X. Shikimic Acid Regulates the NF-κB/MAPK Signaling Pathway and Gut Microbiota to Ameliorate DSS-Induced Ulcerative Colitis. J Agric Food Chem. 2023 Jun 14;71(23):8906-8914. doi: 10.1021/acs.jafc.3c00283. Epub 2023 May 31. PMID: 37257042; PMCID: PMC10273308.

33. Yang K, Zhang L, Liao P, et al. Impact of Gallic Acid on Gut Health: Focus on the Gut Microbiome, Immune Response, and Mechanisms of Action. *Front Immunol.* 2020;11:580208. Published 2020 Sep 16. doi:10.3389/fimmu.2020.580208

Table 1 - General Description of Kadukkai [2]

Characteristics	Description
Colour	Colour of the fruit rind varies from yellowish brown, uniform brown to light black owing to the variety and place of origin
Taste	Astringent, sweet, sour, pungent, bitter.
Potency	Hot
Division	Sweet
Indications in Siddha Medicine	*Athithoolam* (obesity), *Pun* (ulcers), *Kamalai* (jaundice), *Silipatham* (filariasis), diseases of cheek, throat, tongue and male genitalia, *Pandu* (Anemia), *Moothrakireecharam* (Dysuria), *Moolam* (Hemorrhoids), *Thamaraganoi* (Cardiac diseases), *Kannnoikal* (Eye diseases), *Aanmaiinmai* (impotency), *Gunmam* (Gastro intestinal conditions) *Megharogam* (Sexually transmitted diseases), *Kuttam* (Skin diseases) etc

Table 2 - Derangement stages of *Thirithodangal* in respective season [3]

DERANGEMENT STAGES	*VATHAM*	*PITHAM*	*KABAM*
Thannilai	*Mudhuvenrikaalam* (Jun 16 - Aug 15)	*Kaarkaalam* (Aug 16 - Oct 15)	*Munpanikalam* (Dec 16 - Feb 15)
Thannilaivalarchi	*Kaarkaalam* (Aug 16 - Oct 15)	*Koothirkalam* (Oct 16 - Dec 15)	*Pinpanikalam* (Feb 16 - Apr 15)
Vetrunilaivalarchi	*Koothirkalam* (Oct 16 - Dec 15)	*Munpanikalam* (Dec 16 - Feb 15)	*Ilavenil kalam* (Apr 16 - Jun 15)

Aishwarya *et al.*,

Table 3: Role of Prebiotics in various disease conditions

Route of administration of prebiotic	Disease condition
Administration of some prebiotics in diarrhoea predominant irritable bowel syndrome	Increase numbers of lactobacilli and *Bifidobacteria* in faecal microbiota and thereby IBS symptoms improvement noted [11]
Supplementation with FOS 15 g/day for 3 weeks in Crohn's disease	Elevated *Bifidobacteria* population in the feces and improved the symptoms[12]
FOS and GOS administration Necrotizing enterocolitis (NEC) in premature infants	Stimulate the growth of *Bifidobacteria* and reduce the pathogenic bacteria in preterm infants. It is further claimed for the prevention of NEC.[13]
Symbiotic therapy – Administration of *Lactobacillus rhamnosus* and *Bifidobacterium Lactis* plus inulin	Reducing the proliferation rate in colorectal thereby reduce the risk of colorectal cancer, inducing colonic cells necrosis[14]
Administration of GOS in newborn infants.	Decrease the risk of some immune diseases and decrease the severity of allergic skin disease like atopic dermatitis.[15,16]
Administration of Lactulose in post-menopausal women for two 19 days.	The calcium absorption increased.[17]
Administration of GOS for 2 six weeks	Decreases the total cholesterol and triacylglycerol and total cholesterol:HDL cholesterol ratio[18]

Table 4: Phytochemicals of Kadukkai and gut microbita

S. NO	Phytochemicals present in *Terminalia chebula*	Main Findings
1	Gallic acid	↑ Lactobacillaceae, Prevotellaceae ↓ Firmicutes, Proteobacteria ↑ Lactiplantibacillus, Faecalibaculum ↓ Escherichia, Shigella, Clostridium[24]
2	Catechin	↓ *C. histolyticum* ↑ *Enterococcus,Bifidobacterium spp and Lactobacillus*[24]
3	Quercetin	↑ f_Porphyromonadaceae, f_ Oxalobacteraceae, g_ Oxalobacter, g_ Klebsiella ↓ p_Actinobacteria, c_ Actinobacteria ↓ Firmicutes, Lachnospiraceae, Ruminicoccaceae ↑ Bacteroidetes[25]
4	Ellagic acid	↓ Ruminococcaceae and *Clostridium ramosum*[26]
5	Kaempferol	↓ *Lachnospiraceae, Bacteroidales_S24-7_group, Prevotellaceae, Erysipelotrichaceae, Staphylococcaceae,* and *Alcaligenaceae*[27]
6	Saponins	↑ *Akkermansia muciniphila* and *Parabacteroides distasonis*[28] ↑ *Bacteroides, Lactobacillus, Firmicutes* and *Bifidobacterium* [29]
7	Flavonoids and flavonoid metabolites	↑ *Bifidobacterium* and *Lactobacillus, Akkermansia muciniphila*[30]
8	Tannins	↑ *Ruminococcus bicirculans, Faecalibacterium prausnitzii,* Lachnospiraceae UCG 010, Lachnospiraceae NK4A136, *Bacteroides thetaiotaomicron* and *B. uniformis.* ↓ Firmicutes and Proteobacteria [31]
9	Shikimic acid	↓ *Bacteroidetes* increased and *Proteobacteria* [32]
10	Gallic acid	↑ *Lactobacillus spp., Lactobacillus plantarum, Lactobacillus reuteri,* and *Lactobacillus lactis*[33]

64250

RESEARCH ARTICLE

Secured Routing and Data Communication in Wireless Sensor Network using Segmented Regressive Gradient Deep Artificial Neural Network BASED Algorithm

D.Sudhakar[1]* and V.S.Meenakshi[2]

[1]Research Scholar, PG and Research Department of Computer Science, Chikkanna Govt. Arts College, Tirupur-2, Tamil Nadu, India
[2]Associate Professor, PG and Research Department of Computer Science, Chikkanna Govt. Arts College, Tirupur-2, Tamil Nadu, India.

*Address for Correspondence
D.Sudhakar
Research Scholar,
PG and Research Department of Computer Science,
Chikkanna Govt. Arts College,
Tirupur-2, Tamil Nadu, India
E.Mail: sudhakar.dr@gmail.com

ABSTRACT

Wireless Sensor Networks (WSNs) are made up of small nodes with sensing, processing, and wireless communication capabilities. Routing is a critical activity in wireless sensor networks since it deals with data transmission to base stations. Routing attacks can cripple it easily and drastically affect the functionality of WSNs. In this paper, a novel technique called Segmented Regressive Gradient Deep Artificial Neural Learning Based algorithm (SRGDANL-DCS) is introduced for secure routing and data communication in WSN by detection of the different types of attacks. The Deep Artificial Neural Learning classifier is used in the proposed technique to determine the most energy-efficient neighboring node selection and to detect attackers. The Artificial Neural Learning classifier consists of three or more layers such as an input, and output with more than one hidden layer with sub-layers. The number of sensor nodes is given to the input layer. For each sensor node, attack characteristics such as energy level, and number of packets dropped are measured. The segmented regression is applied to analyze the characteristics of the node. Then, the Heaviside step activation function is employed to classify normal nodes and different types of attack nodes. After identifying the normal neighboring sensor nodes, the route paths are constructed between the source and destination based on the time of arrival method.

64251

D.Sudhakar and V.S.Meenakshi

Finally, along the route path, secure data transmission is accomplished by applying a Deterministic Schmidt-Samoa certificate less signcryption.

Keywords: WSN, Security, attack detection, Deep Artificial Neural Learning classifier, segmented regression, heaviside step activation function, Time of Flight method.

INTRODUCTION

WSNs are used in a wide range of applications.. These networks are susceptible to different unique security risks and risks in their data transmission processes. Attackers interfere and eavesdrop on transmission to modify the data. Data communication between nodes must be encrypted before transmission in order to ensure WSN security. Several methods have been developed for attack detection and secure communication.

LITERATURE REVIEW

A lightweight replica node identification mechanism with a three-step approach was presented in [1] to determine replica attacks with a lower false detection rate. However, greater security in data communication was not achieved. An automated, flexible, and lightweight encryption method called (FlexCrypt) was designed in [2] to establish a secure communication and data transmission with symmetric keys. But it was not efficient to enhance the performance of the packet delivery ratio in secure communication. A hybrid Elliptic Curve Cryptography (ECC) and Advanced Encryption Standard (AES) were developed in [3] for encryption and decryption of data to avoid a variety of security threats including side-channel attacks. But the deep learning techniques were not implemented to further enhance the attack detection accuracy. Deep learning (DL) based intrusion detection scheme was developed in [4] for detecting four types of DoS attacks that affect the communication of WSNs. But it failed to reduce the size of the training data for enhancing the performance. An intrusion detection method based on deep neural networks (DNN) was developed in [5] to efficiently identify the attacks. However, it was higher computational complexity and lesser classification accuracy. Fuzzy-based DDoS attack Detection and Recovery mechanism (FBDR) was developed in [6] to distinguish the occurrence of DDoS attacks. However, the accuracy of DDoS attack detection was not improved. An efficient asymmetric multi-recipient cryptographic method was introduced in [7] for secure multi-party communication. However, the communication cost was not minimized.

PROPOSAL METHODOLOGY

The proposed technique employs a Deep Artificial Neural Learning classifier to determine the most energy-efficient neighboring node selection and to detect attackers.. A Deep Artificial Neural Learning classifier is a feed-forward neural network that produces a set of outputs from a set of inputs. It means that the input is transferred from the input layer to the output layer in the forward direction. The input layer is given the number of sensor nodes. For each sensor node, attack characteristics such as energy level, and number of packets dropped are measured. The segmented regression is applied to analyze the characteristics of the node. Then, the Heaviside step activation function is employed to classify normal nodes and different types of attack nodes. After identifying the normal neighboring sensor nodes, the time of arrival approach is used to construct the route paths between the source and destination. Finally, secure data transmission is performed along the route path by applying a Deterministic Schmidt-Samoa certificateless signcryption. Figure 1 given abovedepicts structural design of the proposed technique SRGDANL-DCS technique for secure efficient routing and data transmission in WSN. The WSN includes a number of sensor nodes $Sn_i \in Sn_1, Sn_2, Sn_3 \dots Sn_n 'SN'$ or base station deployed. In WSN, sensor node transmits the collected data packets '$d_1, d_2, \dots, d_m$' to sink through the energy efficient neighboring nodes $Nn_1, Nn_2, Nn_3, \dots Nn_b$ in a secured manner. The above said different process of the proposed SRGDANL-DCSapproach is described in the following subsections.

Segmented regressive gradient deep artificial neural learning classifier based attack detection

First, the proposed SRGDANL-DCS technique finds the neighboring node using a deep artificial neural learning classifier. A deep artificial neural learning classifier is a class of machine learning algorithms that consists of multiple layers to perform certain tasks from the raw input. The proposed deep artificial neural learning classifier consists of one input layer, three hidden layers, and one output layer. Each layer comprises small individual units called nodes or neurons. Neurons within individual layers are fully connected to successive layers. The architecture is said to be deeper with respect to the number of layers used. The main advantage of a deep artificial neural learning classifier is to return accurate results when it uses large amounts of input.

The input layer receives the input (i.e. number of sensor nodes) to be processed. The required task such as analysis and classification is performed at the hidden layer. A random number of hidden layers are located between the input and output layers. Finally, the classification outcomes are obtained at the output layer. Let us consider the number of wireless sensor nodes $Sn_1, Sn_2, Sn_3, \ldots Sn_n$ are considered as input to the input layer. A neuron is a mathematical function that considered an input and assigns the weight, bias returns the output. Therefore, the activity of the neuron is formulated as given below, Figure 2 illustrates aactivity of neurons that considers the input of sensor nodes associated with a set of weight '$q_1, q_2, \ldots, q_n$' and summed with bias 'd'. As a result, the neuron output is as

Follows $y = [\sum_{i=1}^{n} Sn_i * q_i] + d$ $\qquad$ (1)

Where the output of neuron 'y' is obtained with the sensor nodes 'Sn_i' multiplied with the set of weights 'q_i' and bias 'd' stored the integer value '1'. The sensor node is transferred into the hidden layer where the energy level is measured for identifying the attack nodes. In order to launch a replica attack in WSN, replica nodes must use additional energy. For each fake identity created while distributing the replica node, energy consumption is doubled. As the number of attacker nodes grows, so does energy usage. Initially, all the sensor nodes deployed in WSN have similar energy levels. The residual energy level of sensor nodes is estimated based on the difference between the initial energy and consumed energy. Therefore, the residual energy of the sensor nodes is estimated as given below.

$E_{RL} = [E_{TT}] - [E_C]$ $\qquad$ (2)

Where, E_{RL} denotes a residual energy of the sensor nodes, E_{TT} shows total energy of sensor node and E_C represents the consumed energy of the nodes. The black hole node is identified based ondropping the data packets. The alicious node or black hole node drops the entire data packets received from the previous node rather than data forwarding to next node.

$BA_{Sn} = \left(\frac{dpd}{dps}\right)$ $\qquad$ (3)

Where, BA_{Sn} indicates a black hole node behavior, dpd denotes a data packets dropped by the particular sensor node and dps' indicates a data packets sent by previous node 'dps'. The gray hole attack is also called a selective forwarding attack. It did not drop all the packets received from the other node but only the part of the data packets gets dropped.

$GA_{Sn} = \left(\frac{spd}{dps}\right)$ $\qquad$ (4)

Where, 'GA_{Sn}' indicates a gray hole attacks characteristics of sensor nodes based on a selective number of packets dropped 'spd' and the data packets sent by previous node 'dps'. The above estimated node characteristics are sent to another hidden layer for identifying the attacks. Segmented regression is a machine learning technique in which the independent variable (i.e. sensor nodes) is classified by setting the threshold value.

$R = \{ (E_{RL} > t_E) \&\& (dpd > t_{dpd}) \&\& (spd > t_{spd}) \}$ $\quad$ (5)

64253

D.Sudhakar and V.S.Meenakshi

Where R indicates an output of the regression, t_E, t_{dpd}, t_{spd} indicates a threshold value of the energy, data packet drop threshold, and selective number of packets dropped, respectively. The regression results are sent into the Heaviside activation function, which permits the output neuron to create a '1' if the input reaches a threshold; otherwise, it returns a '0'.

$$A = \begin{cases} 1, & Attack\ node \\ 0, & normal\ node \end{cases} \qquad (6)$$

The activation function 'A' returns '1' indicates an estimated value is greater than the threshold. Otherwise, activation function 'A' returns '0'. The value '0' indicates that the sensor nodes are classified as a legitimate or normal node. The value '1' indicates that the sensor nodes are classified as a black hole, greyhole, replication attack nodes. In order to minimize the error rate of classification, weights gets updated by applying a gradient momentum method,

$$q_{t+1} \quad = q_t - \eta r_t \qquad (7)$$
$$Where,\ r_t = \ \alpha r_{t-1} + (1 - \alpha)\left[\frac{\partial er}{\partial q_t}\right] \qquad (8)$$

Where, q_{t+1} indicates an updated weight, q_t represents a current weight, η denotes a learning rate $(\eta < 1)$, r_t denotes a common default value $r_t = 0.9$. '$\left[\frac{\partial er}{\partial q_t}\right]$' denotes a partial derivative of the error 'er' with respect to current weight 'q_t'. This process gets repeated until finding the minimum classification error at the output layer. In this way, normal and attack neighboring nodes are identified.

In the proposed technique the process of sensor node classification is performed using deep learning techniques. The deep learning classifier includes numerous layers to analyze the sensor nodes' energy level and packet drop. The number of sensor nodes are given as input to the deep learning classifier. For each input, the weights and biases get assigned. Then the residual energy, packet drop, and selective packet drop of the nodes are computed. After that, segmented regression is applied, and set the threshold value. The heavy side step activation function analyzes the regression output and returns '1' if the node is classified as an attack. Otherwise, the activation function returns '0', if the node is classified as normal. After the classification, the weights get updated to minimize the error. Finally, the classification results are obtained at the output layer. This process enhances attack detection accuracy.

Route path construction
Once the normal node is identified, the neighbors are detected to establish a route for data transmission. The neighboring nodes are identified through the application of the time of flight method. It is used to measure the time difference between the arrival of the beacon reply message and the transmission of the beacon request message.
The source node transmits a beacon request message to the other normal nodes.

$$Sn \xrightarrow{M_{beacon\ request}} \sum_{i=1}^{m} Nn_i \xrightarrow{M_{beacon\ request}} Dn \qquad (9)$$

Where, source node 'Sn' sends the beacon request message '$M_{beacon\ request}$' to destination 'Dn' via other nodes Nn_i. Upon successful transmission of the beacon request message, the destination sensor node 'Dn' send response message back to the source via neighboring nodes.

$$Dn \xrightarrow{M_{beacon\ response}} \sum_{i=1}^{m} Nn_i \xrightarrow{M_{beacon\ response}} Sn \qquad (10)$$

Where, destination node 'Dn' reply the beacon response message '$M_{beacon\ response}$' to via other nodes Nn_i. Upon successful response of the beacon message, the time of arrival is computed as given below,

$$ToA_{M_{beacon}} = M_{beacon\ response}(T) - M_{beacon\ request}(T) \qquad (11)$$

64254

D.Sudhakar and V.S.Meenakshi

Where, $ToA_{M_{beacon}}$ indicates a time difference between the response arrival time $M_{beacon\ response}(T)$and the request message sent from the source node '$M_{beacon\ request}$'. The minimum time taken for message arrival is selected as an optimal route path for efficient data transmission. Figure 3 demonstrates the route paths establishment between the source and destination through the normal sensor nodes$Nn_1, Nn_2, Nn_3, Nn_4, Nn_5, Nn_6$. Among the numerous paths, the minimum distance is chosen for transmitting the data. If any route failure occurs, select an alternative route with minimum distance for delay minimized data transmission.

Deterministic Schmidt- Samoa Certificateless Signcryption based secure data transmission
After selecting the route path, secure communication between sensor nodes is performed by applying a Deterministic Schmidt-Samoa certificateless signcryption. It is a feasible cryptographic technique to offer data integrity and identity authentication, which removes the certificate-based signature system. The proposed cryptographic techniques consist of three processes namely key generation, signryption and unsigncryption. To do the secured data transmission between the sender and receiver, the sink node generates the private and public keys. The sender node performs data encryption and signature generation. The cipher text and signature are sent to the receiver sensor node. At the receiver end, the signature verification is performed. If the signature is valid, then the receiver gets the original data after the decryption process. This helps to improve the data packet delivery and minimize pack loss.

SIMULATION SETTINGS
In this section, the performance of the SRGDANL-DCS technique, Lightweight replica node detection mechanism [1], FlexCrypt [2], Hybrid ECC-AES model[3] are implemented in the NS3 network simulator. In order to conduct the simulation various simulation parameters are used which are listed in table 1.

RESULTS AND DISCUSSION

The comparative results of the SRGDANL-DCStechnique, Lightweight replica node detection mechanism [1], FlexCrypt [2], Hybrid ECC-AES model[3] are discussed with respect to various evaluation metrics such as attack detection accuracy, false-positive rate, packet delivery ratio, packet loss rate, and an end to end delay. These metrics are described as given below.

Impact of attack detection accuracy
The formula for calculating the attack detection accuracy is given below,

$$ACC = \left[\frac{n_{CD}}{n}\right] * 100 \qquad (12)$$

where,'n' denotes the number of sensor nodes, n_{CD} indicates the number of sensor nodes correctly classified as normal or attack.
Figure 4 graphical analysis of attack detection accuracy versus number of sensor nodes ranges from 50 to 500. From this result, the attack detection accuracy using SRGDANL-DCStechnique was observed to be comparatively higher than [1] and [2] [3]. The overall performance of attack detection accuracy of SRGDANL-DCStechnique is improved by 9% ,6% and 4% when compared to [1] [2] [3] respectively.

Impact of false-positive rate
The false-positive rate is mathematically calculated as given below,

$$FP_{rate} = \left[\frac{n_{ICD}}{n}\right] * 100 \qquad (13)$$

'n'denotes the number of sensor nodes, n_{ICD} indicates the number of sensor nodes incorrectly detected as normal or attack.

D.Sudhakar and V.S.Meenakshi

Figure 5 portrays the comparative performance analysis of false positive rateSimulations performed with 500sensor nodes, From this result, the false positive ratewas observed to be reduced using SRGDANL-DCS technique when compared to [1] and [2] [3]. The reason behind the improvement was due to the employment of gradient momentum method in the deep learning classifier. As a result, incorrect classification of normal or attack nodes are minimized. This in turn minimized the false positive rateusing SRGDANL-DCS technique by 61% compared to [1] , 51% compared to [2] and 42%compared to [3] respectively.

Impact of Packet delivery ratio:

$$R_{PD} = \left[\frac{Number\ of\ data\ packets\ correctly\ received}{Number\ of\ data\ packets} \right] * 100 \qquad (14)$$

Where, R_{PD} denotes a packet delivery ratio. The performance of packet delivery ratio is measured in terms of percentage (%). Figure 6 portrays the comparative performance analysis of packet delivery ratio using number of data packets from 25, 50 …250. With the selected route path, the secure data transmission is performed by applying Deterministic Schmidt-Samoa certificateless signcryption. This helps to enhance data transmission. This in turn improved the packet delivery ratio using SRGDANL-DCS technique by 11%, 9%, and 6%, whencompared to [1] [2] [3] respectively.

Impact of Packet loss rate

The Packet loss rate is measured as follows,

$$R_{PL} = \left[\frac{Number\ of\ data\ packets\ lost}{Number\ of\ data\ packets} \right] * 100 \qquad (15)$$

Where, R_{PL} indicates a packet loss rate and it is measured in terms of percentage (%).

Finally, figure 7 given above shows the graphical representation of packet loss rate. From the above figure it is observed that the packet loss rate was found to be comparatively reduced using SRGDANL-DCS.. The average of ten comparison results indicates that the packet loss rate of the SRGDANL-DCS technique is considerably reduced by 62%, 57% and 46% respectively.

Impact of End to end delay

The overall delay is measured as follows,
$$End-to-end\ delay = [T_{act}] - [T_{obs}] \qquad (16)$$

Where, T_{act} denotes an actual arrival time and 'T_{obs}' indicates an observed arrival time. The performance ofend to end delay is estimated in terms of milliseconds (ms). As shown in figure 8, the end to end delay of all the methods gets increased while increasing the number of data packets being sent from the source node. But comparatively, the proposed SRGDANL-DCS technique outperforms and significantly decreases the end to end delay. This is because of selecting the normal node and removes the attack nodes. These nodes perform efficient data transmission from sender to receiver with minimum delay. As a result, the comparison of four methods illustrates that the end to end delay is said to be considerably minimized by 33%,28% and 21% when compared to the [1] [2] and[3] respectively.

CONCLUSION

The rapid growth and large-scale deployment of the WSN have susceptible for a variety of attacks in the data communication. This directs to reduce the confidential data communication between the sensor nodes for different applications. In this paper, SRGDANL-DCS techniqueis introduced for WSNs to improve secure data transmission.

The simulation is conducted for proposed SRGDANL-DCS technique and existing methods with different performance metrics. The discussed result indicates that the SRGDANL-DCS technique has significantly improved the performance of the attack detection accuracy, packet delivery ratio and minimizes the false positive rate, delay as well as packet loss rate when compared to conventional methods.

REFERENCES

1. Mojtaba Jamshidi, Shokooh Sheikh Abooli Poor, Abbas Arghavani, Mehdi Esnaashari, Abdusalam Abdulla Shaltooki, Mohammad Reza Meybodi, "A simple, lightweight, and precise algorithm to defend against replica node attacks in mobile wireless networks using neighboring information", Ad Hoc Networks, Elsevier, Volume 100, 2020, Pages 1-16.https://doi.org/10.1016/j.adhoc.2020.102081

2. Osama A. Khashan,Rami Ahmad, Nour M. Khafajah,"An automated lightweight encryption scheme for secure and energy-efficient communication in wireless sensor networks", Ad Hoc Networks, Elsevier, Volume 115, 2021, Pages 1-14.https://doi.org/10.1016/j.adhoc.2021.102448

3. ShabanaUrooj, SonamLata, Shahnawaz Ahmad, ShabanaMehfuz, S Kalathil, "Cryptographic Data Security for Reliable Wireless Sensor Network", Alexandria Engineering Journal, Elsevier, Volume 72, 1 June 2023, Pages 37-50. https://doi.org/10.1016/j.aej.2023.03.061

4. SalimSalmi&LahcenOughdir, "Performance evaluation of deep learning techniques for DoS attacks detection in wireless sensor network", Journal of Big Data, Springer, Volume 10, 2023, Pages 1-25.https://doi.org/10.1186/s40537-023-00692-wn

5. V. Gowdhaman and R. Dhanapal, "An intrusion detection system for wireless sensor networks using deep neural network", Soft Computing, Springer,Volume 26, 2022, Pages 13059–13067 .https://doi.org/10.1007/s00500-021-06473-y

6. P. J. BeslinPajila, E. Golden Julie & Y. Harold Robinson, "FBDR-Fuzzy Based DDoS Attack Detection and Recovery Mechanism for Wireless Sensor Networks", Wireless Personal Communications, Springer, Volume 122, 2022, Pages3053–3083. https://doi.org/10.1007/s11277-021-09040-8

7. Ahmad Mansour, Khalid M. Malik,NikoKaso, "AMOUN: Asymmetric lightweight cryptographic scheme for wireless groupcommunication", Computer Communications, Elsevier, Volume 169, 2021, Pages 154-16. https://doi.org/10.1016/j.comcom.2021.01.019

8. DeokKyu Kwon, Sung Jin Yu , Joon Young Lee,Seung Hwan Son and Young Ho Park, "WSN-SLAP: Secure and Lightweight Mutual AuthenticationProtocol for Wireless Sensor Networks", Sensors, Volume 21, Issue 3, 2021, Pages 1-23.https://doi.org/10.3390/s21030936

9. Anuj Kumar Singh, Mohammed AlshehriShashiBhushan, Manoj Kumar, Osama Alfarraj and Kamal Raj Pardarshani, "Secure and Energy Efficient Data Transmission Model for WSN",Intelligent Automation & Soft Computing, Volume 27, Issue 3, 2021, Pages 761-769. https://doi.org/10.32604/iasc.2021.012806

10. HaythemHayouni and Mohamed Hamdi, "A novel energy-efcient encryption algorithm for securedata in WSNs", The Journal of Supercomputing, Springer, Volume 77, 2021,Pages 4754–4777.https://doi.org/10.1007/s11227-020-03465-x

Table 1. Simulation Parameters

Simulation Parameters	Values
Simulator	NS3
Network area	1100 m * 1100 m
Number of sensor nodes	50,100,150,200,250,300,350,400,450,500
Mobility model	Random Waypoint model
Number of data packets	25,50,75,100,125,150,175,200,225,250
Speed of node	0 – 20 m/s
Simulation time	300s
Number of runs	10
Protocol	Ad hoc on-demand distance vector routing protocol (AODV)

D.Sudhakar and V.S.Meenakshi

Table 2 comparison of attack detection accuracy

Number of sensor nodes	Attack detection accuracy (%)			
	Lightweight replica node detection mechanism	FlexCrypt	Hybrid ECC-AES model	SRGDANL-DCS
50	88	90	92	96
100	87	89	90	92
150	85	88	91	95
200	87	90	91	93
250	88	89	90	94
300	86	88	91	95
350	85	89	90	94
400	86	90	91	95
450	88	89	91	97
500	86	87	90	94

Table 3. comparison of false positive rate

Number of sensor nodes	False positive rate (%)			
	Lightweight replica node detection mechanism	FlexCrypt	Hybrid ECC-AES model	SRGDANL-DCS
50	12	10	8	4
100	13	11	10	8
150	14	12	9	5
200	15	10	9	7
250	16	13	10	6
300	13	12	9	5
350	15	11	10	6
400	14	10	10	5
450	16	12	9	3
500	15	13	10	6

Table 4 comparison packet delivery ratio

Number of data packets	Packet delivery ratio (%)			
	Lightweight replica node detection mechanism	FlexCrypt	Hybrid ECC-AES model	SRGDANL-DCS
25	84	84	88	96
50	86	88	90	94
75	85	87	89	92
100	87	89	91	94
125	86	87	90	94
150	85	86	88	95
175	84	85	89	96
200	85	86	90	94
225	84	88	91	95
250	86	86	88	94

D.Sudhakar and V.S.Meenakshi

Table 5 comparison of packet loss rate

Number of data packets	Packet loss rate (%)			
	Lightweight replica node detection mechanism	FlexCrypt	Hybrid ECC-AES model	SRGDANL-DCS
25	16	16	12	4
50	14	12	10	6
75	15	13	11	8
100	13	11	9	6
125	14	13	10	6
150	15	14	12	5
175	16	15	11	4
200	15	14	10	6
225	16	12	9	5
250	14	14	12	6

Table 6 comparison of end-to-end delay

Number of data packets	End-to-end delay(ms)			
	Lightweight replica node detection mechanism	FlexCrypt	Hybrid ECC-AES model	SRGDANL-DCS
25	12	12	10	6
50	14	13	11	9
75	15	14	12	10
100	17	15	14	11
125	19	17	16	12
150	21	20	18	14
175	23	22	21	16
200	25	23	22	18
225	26	24	23	20
250	28	25	24	21
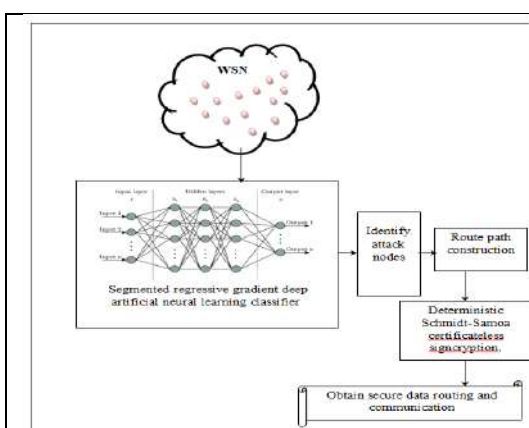
Figure 1 Architecture of Proposed SRGDANL-DCS technique	Figure 2 function of neurons
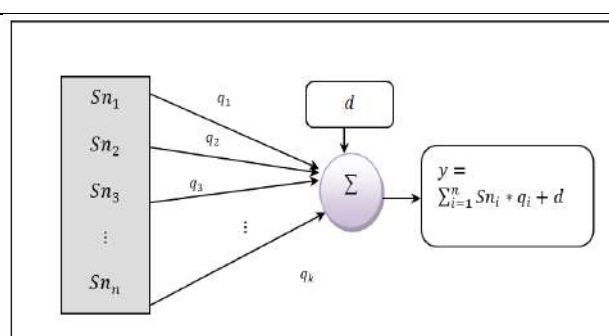
D.Sudhakar and V.S.Meenakshi
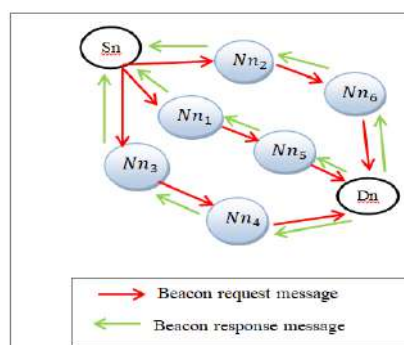
Figure 3 Construction of route paths
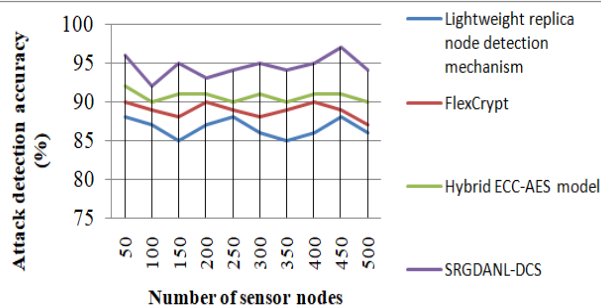
Figure 4 graphical analysis of attack detection accuracy
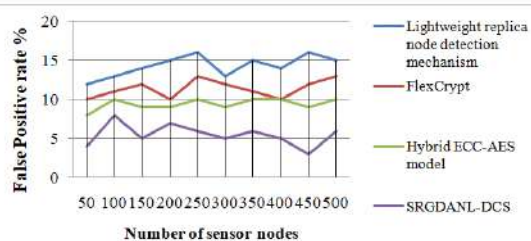
Figure 5 graphical analysis of false positive rate
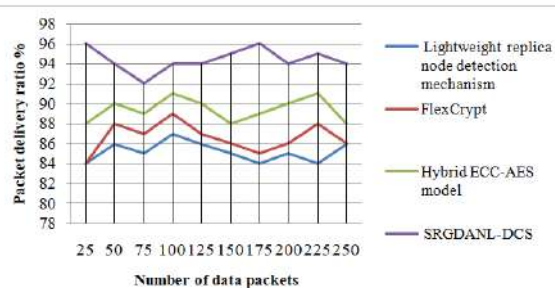
Figure 6 graphical analysis of packet delivery ratio
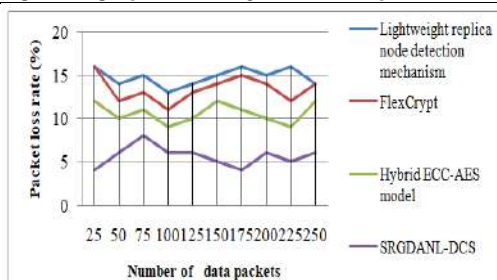
Figure 7 graphical analysis of packet loss rate
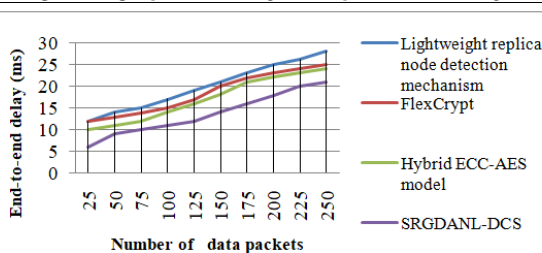
Figure 8 graphical analysis of end to end delay

RESEARCH ARTICLE

Compositions of Knots using Alexander Polynomial

G. Infant Gabriel[1] and N. Uma[2] *

[1]Assistant Professor, PG and Research Department of Mathematics, Sri Ramakrishna College of Arts and Science (Formerly SNR Sons College), Coimbatore, Tamil Nadu, India.
[2]Associate Professor and Head, PG and Research Department of Mathematics, Sri Ramakrishna College of Arts and Science (Formerly SNR Sons College), Coimbatore, Tamil Nadu, India.

*Address for Correspondence
N. Uma
Associate Professor and Head,
PG and Research Department of Mathematics,
Sri Ramakrishna College of Arts and Science (Formerly SNR Sons College),
Coimbatore, Tamil Nadu, India.
E.Mail: uma.n@srcas.ac.in

ABSTRACT

Knot theory is the Mathematical study of knots. In this paper we have studied theComposition of two knots. Knot theory belongs to Mathematical field of Topology, where the topological concepts such as topological spaces, homeomorphisms, and homology are considered. We have studied the basics of knot theory, with special focus on Composition of knots, and knot determinants using Alexander Polynomials. And we have introduced the techniques to generalize the solution of composition of knots to present how knot determinants behave when we compose two knots.

Keywords: Topology, Knot theory, Homeomorphisms, Reidemeister Moves, Alexander polynomials and Composition of Knots.

INTRODUCTION

Knot theory is a new kind of applicable Mathematics. Edward E. David, Jr. [3] referred that utility of Mathematics conceived symbolically. The history of Knot theory starts from 19th century physics, with the work of Gauss on computing linking numbers in a system of linked circular wires. D. Silver [7] also studied the knots and coined the word topology. In 1867, Kelvin's vortex model of atom by W.T Thompson [8] was presented. The American Mathematician J.W Alexander [1] (1888-1971) was the first to suggest that knot theory is extremely important in the study of 3-dimensional topology which was further underlined by the German mathematician H. Seifert. Later K. Murasugi [5] studied the relationship between algebraic geometry and the knot theory.

64261

Knot theory was first presented by the physicist and chemists William Thomson based on the study by Baron Kelvin who hypothesized that atoms of different elements can be defined by different knots. Through Thomson's theory was later proved incorrect, his work inspired Peter Trait, who developed many concepts that are used today in application of knots theory to biology, chemistry and physics. Colin Adams[2].suggested that the knot theory was used in modelling of DNA, the effects of enzymes and in statistical mechanics while examining the interaction between particles in a system. By using more theoretical models, Scientists and Mathematicians can make these concrete concepts to manipulate and work within.

And in this paper, we have studied knots that are embedded in S^3. A knot can be projected onto a plane (or simply drew it on a paper). These projections are called knots diagrams (Figure.1).

To avoid ambiguity the following restrictions are considered

1. At each crossing, the string segment passes over respectively under the other (this is usually done by drawing a gap in the bottom segment).

2. Each crossing involves exactly two segments of the string.

3. The segments must cross transversely.

4.At each crossing there is always one over strand and one understand.

5. An arc is a piece of the knot that passes from one undercrossing to another with only overcrossing in between (an unbroken line)

The Figure 1 & Figure 2 are projections of the knots.

PRELIMINARIES
Basic definitions and concepts are presented in this chapter

Definition[6]:

K is a knot for the embedding $h : S^1 \to S^3$ whose image is *K*. If $K \subseteq S^3$ then it is**homeomorphic** to the unit circle S^1. The actual knot is a smooth embedding of the unit circle in S^3 . A knot can only consist of one component; a link on the other hand is a finite union of disjoint knots.

Definition[6]:

Knots K_1 and K_2 in S^3 are **equivalent** if there exist a homeomorphism $h : S^3 \to S^3$ such that $h(K_1) = h(K_2)$.

Definition[6]:

If *H* is an isotopy between ambient spaces $H : S^3 \times I \to S^3$, then *H* is an **ambient isotopy**. The knot can be deformed to any expected manner. The arcs can be bent and moved through space without passing through one another (knot can be shrunk or grown). Also, it is not permitted to pull the knot so tight that it unknots itself by disappearing into a point.

Definition [4]
1.   **R1** allows to remove (or introduce) a twist in a diagram. The result is that the knot will have one fewer (or one more) crossing.
2.   **R2**lets separate two strings that lie on top of each other or vice versa. This will add or remove two crossings.
3.   **R3**allows moving a strand from one side of a crossing to the other. This also works if the strand is moved above the other two strands.

R3 does not affect the number of crossings in the current projection. If a deformation of the diagram uses *R2* and *R3*, referred as Regular Isotopy (or Planar Isotopy).The regular isotopy is an equivalence relation for the knot diagrams (Figure 3) and is not defined for the knot embedding. The Reidemeister moves describes the procedures performed on diagrams

Definition[4]:
The crossing number, *c(K)* of a knot *K*, is the **minimum number of crossings,** that occur in any diagram of *K*.

Definition[4]:
A knot is **oriented** if it has an orientation assigned and refered by arrows.
If a knot *K* has a given orientation, *−K* refers as reverse orientation (Figure 4).
A knot is called invertible if *K* and *−K* are equivalent. All knots in Figure 2 are invertible (Figure 4).

Definition [4]
The writhe of an oriented knot, *w(K)*, is the sum of the crossings with signs as shown in Figure 4.

Definition [4]
A knot *K* is called alternating if its diagram, the undercrossing and overcrossings alternate around *K.*

Definition[4]
The knot sum or connected sum $K_1 \# K_2$ is formed by placing two knots side by side, removing a small arc from each knot and then joining the knots together with two new arcs.

Definition[4]:
A knot is called composite if it can be written as the sum of K_1 and K_2, neither of which is the unknot and prime if it is not composite. Knot tables only show prime knots, see Figure 2.

COMPOSITION OF KNOTS

Given two projections of knots, a new knot obtained by removing a small arc from each knot projection and then connecting the four endpoints by two new arcs as in Figure 1.5. The resulting knot is the composition of the two knots. If we denote the two knots by the symbols K_{4_1} and K_{3_1}, then their composition is denoted by $K_{4_1} \# K_{3_1}$ (Figure 5).

The two projections should not overlap, and the two arcs are chosen to remove the outside of each projection to avoid any crossings i.e., they do not cross either the original knot projections or each other (Figure 6).

Definition
A knot a composite knotif it can be expressed as the composition of two knots, neither of which is the trivial knot. The knots that makeup the composite knot is called factor knots. The composition of a knot *K* with the unknot, the result is again *K*. (Figure 7).If a knot is not the composition of any two nontrivial knots, we call it a prime knot**.**

Definition
An orientation is defined by choosing a direction to travel around the knot. The orientation on K_{3_1} matches the orientation on K_{5_2} in $K_{3_1} \# K_{5_2}$, resulting in an orientation for $K_{3_1} \# K_{5_2}$, or the orientation on K_{3_1} and K_{5_2} do not match up in $K_{3_1} \# K_{5_2}$ .If the orientations do match up in all the compositions of the two knots then it will yield the same composite knot.If the orientations do match up in all the compositions of the two knots then it will yield the single composite knot.

THE ALEXANDER POLYNOMIAL OF COMPOSITION

In 1928, J.W Alexander [4] introduced polynomial invariant to compute the knot diagram entries of a matrix determinant called the Alexander polynomial. Alexander determined the entries of a matrix from the crossing and arcs of the diagram. The Alexander polynomial does not depend on the indexing of crossing and arcs. It does not also depend on the row and column eliminated from the crossing/arc matrix. The Skein relation discovered by John Conway in 1969 is to compute the Alexander polynomial. The Alexander polynomial is invariant up to multiplication by $\pm t^N$ where N is some integer.

Numerical Example

Composition of two knots $K_{3_1} \# K_{1_1}$ (Figure 9)

Applying the condition of Alexander polynomial in above composition knot knots $K_{3_1} \# K_{1_1}$ (Figure 10)we get,

$$M_{K_{3_1} \# K_{1_1}} = \begin{bmatrix} 1-t & 0 & -1 & t \\ t & 1-t & 0 & -1 \\ 0 & -1 & t-t^2 & 0 \\ -1 & t & 0 & 1-t \end{bmatrix}$$

The Alexander matrix A_k is defined as the matrix M by deleting row n and column n, where

$$A_{K_{3_1} \# K_{1_1}} = \begin{bmatrix} 1-t & 0 & -1 \\ t & 1-t & 0 \\ 0 & -1 & t-t^2 \end{bmatrix}$$

The Alexander polynomial $\Delta_k(t)$ of a Knot K is the determinant of its Alexander matrix, which is

$$\Delta_{K_{3_1} \# K_{1_1}} = 2t - 3t^2 + 3t^3 - t^4$$

Finally, the resulting determinant is multiplied by t^{-1} to normalize the Alexander polynomial in order to have a positive constant term.

Thus $2 - 3t + 3t^2 - t^3$ is the Alexander Polynomial of this Composition of Knot $K_{3_1} \# K_{1_1}$.

We observe that Alexander polynomial for compositions of K_{3_1} and K_{1_1} is $2 - 3t + 3t^2 - t^3$. Similarly the composition of K_{3_1} and K_{2_1} is $3 - t^{-1} - 5t + 5t^2 - t^3$.

  ➢ $K_{4_1} \to K_{1_1}, K_{2_1}$ are found to be $1 - 3t + 4t^2 - 2t^3$ and $2 + t - 8t^2 + 8t^3 - 4t^4 + t^5$ respectively.

  ➢ $K_{5_1} \to K_{1_1}, K_{2_1}$ together to form $2 - 5t + 2t^2 - 7t^3 + 5t^4 - t^5$ and
  $3 - t^{-1} - 9t + 12t^2 - 14t^3 + 10t^4 + 2t^5$.

  ➢ $K_{5_2} \to K_{1_1}, K_{2_1}$ are joined to be $2 - t^{-1} - 5t + 7t^2 - 6t^3 + 2t^4$ and
  $1 - t^{-1} - 2t + 7t^2 - 10.t^3 + 6t^4 - 2t^5$.

  ➢ $K_{6_1}, K_{6_2}, K_{6_3} \to K_{1_1}$ are found to be $4 - 10t + 4t^2 + 7t^3 - 8t^4$, $2 - 2t - 3t^2 + 3t^3 + 2t^4 - 2t^5$
  and $1 - 3t + 2t^2 + 2t^3 - 2t^4$.

CONCLUSION

Knots have always been an integral part of real life and have found Mathematical uses recently.As we can also visualize the application of compositions of knots in DNA replication, in this paper we have explained a brief about the composition of knots. Algebraic area is more important in knot theory and it involves drawing comparison between two knot compositions, hence we have applied the Alexander polynomial to get different polynomial for compositions of knots for $K_{3_1} \# K_{1_1}$, $K_{3_1} \# K_{2_1} ......etc.$. And in future we will extend the compositions of knots for

$K_{6_2} \# K_{2_1}$, $K_{7_1} \# K_{1_1} ......etc.$

REFERENCES

1. J.W Alexandar, "Topological invariants of knots and links", Transactions of the American Mathematical Society 30 (1928), 275-306.
2. Colin Adams, "An Elementary Introduction to the Theory of Knots", New York, WH Freeman, 1994.
3. David, E.E. Jr, Renewing US Mathematics: An agenda to begin the second century. Notices of the A.M.S. 35 (1988), 1119-1123.
4. Mari Ahlquist, "On Knots and DNA", Department of Mathematics, Linköping University, LiTH-MAT-EX–2017/17–SE, December 2017.
5. K. Murasugi, "knot theory and its Application", Birkhäuser Boston, (1993).
6. Richard H Crowell and Ralph H Fox,"Introduction to Knot theory". Springer-Verlag, 1977.
7. D. Silver, Knot Theory's odd origins. American Scientist 94 (2006), 158-165.
8. W.T Thompson, Mathematical and Physical papers, III Cambridge U. Press (1890).
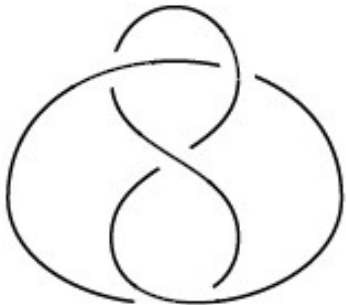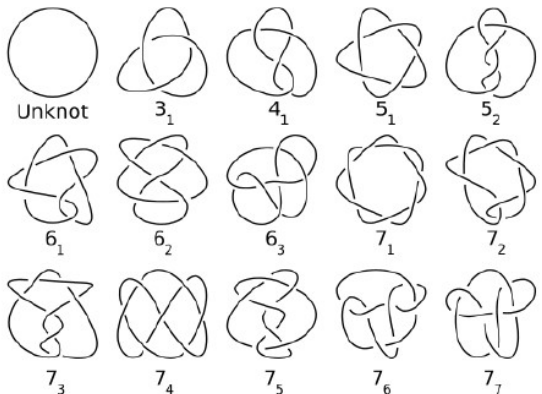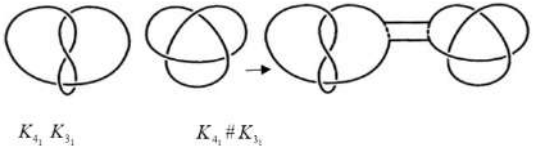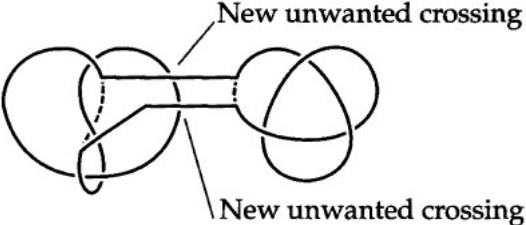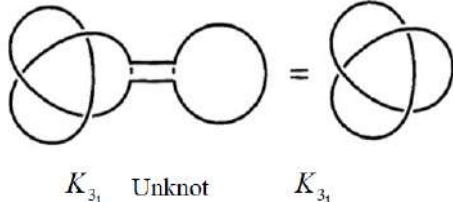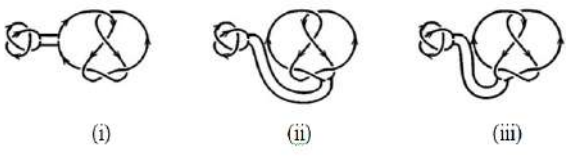
Table. 1. Composition of Knots

S.No	Composition of two Knot	Composition Solution using AP
1.	$K_{3_1} \# K_{1_1}$	$2 - 3t + 3t^2 - t^3$
2.	$K_{3_1} \# K_{2_1}$	$3 - t^{-1} - 5t + 5t^2 - t^3$
3.	$K_{4_1} \# K_{1_1}$	$1 - 3t + 4t^2 - 2t^3$
4.	$K_{4_1} \# K_{2_1}$	$2 + t - 8t^2 + 8t^3 - 4t^4 + t^5$
5.	$K_{5_1} \# K_{1_1}$	$2 - 5t + 2t^2 - 7t^3 + 5t^4 - t^5$
6.	$K_{5_1} \# K_{2_1}$	$3 - t^{-1} - 9t + 12t^2 - 14t^3 + 10t^4 + 2t^5$
7.	$K_{5_2} \# K_{1_1}$	$2 - t^{-1} - 5t + 7t^2 - 6t^3 + 2t^4$
8.	$K_{5_2} \# K_{2_1}$	$1 - t^{-1} - 2t + 7t^2 - 10.t^3 + 6t^4 - 2t^5$
9.	$K_{6_1} \# K_{1_1}$	$4 - 10t + 4t^2 + 7t^3 - 8t^4$
10.	$K_{6_2} \# K_{1_1}$	$2 - 2t - 3t^2 + 3t^3 + 2t^4 - 2t^5$
11.	$K_{6_3} \# K_{1_1}$	$1 - 3t + 2t^2 + 2t^3 - 2t^4$

Figure 1. Figure 8 knot	**Figure 2: Knot Diagram**
Figure 3: Reidemeister Moves Diagram	**Figure 4: Positive and Negative crossing**
Figure 5: $K_{4_1} \# K_{3_1}$ of two knots K_{4_1} and K_{3_1}	**Figure 6: Not the Composition of K_{4_1} and K_{3_1}**
Figure 7: K_{3_1} # Unknot gives K_{3_1}	**Figure 8: (i) & (ii) K_{3_1} # K_{5_2} Orientations match** (iii) K_{3_1} # K_{5_2} Orientations match differ

Figure 9. Numerical Example

Figure 10. Numerical Example

RESEARCH ARTICLE

Impact of Covid-19 on Digital Payments

N. Sivakumar*

Associate Professor, Department of Commerce, Sri Krishna Arts and Science College-641008, Coimbatore, Tamil Nadu, India.

*Address for Correspondence
N. Sivakumar
Associate Professor,
Department of Commerce,
Sri Krishna Arts and Science College-641008,
Coimbatore, Tamil Nadu, India.
E.Mail: sivakumarn@skasc.ac.in

ABSTRACT

A global coordinated effort is needed to stop the further spread of the virus. A pandemic is defined as "occurring over a wide geographic area and affecting an exceptionally high proportion of the population." The last pandemic that was reported in the world was the H1N1 flu pandemic in 2019. In the current COVID-19 situation, the digital payments sector witnessed a decline of ~30 per cent in the transaction value, and recent data made available from National Payments Corporation of India (NPCI) attest to a sharp decline observed in the months when lockdowns were initiated in impact of covid 19. The Covid-19 pandemic accelerated the digitalisation of payments. The latest Red Book Statistics from the BIS Committee on Payments and Market Infrastructures (CPMI) show that consumers have shifted from physical cash to digital and contactless payment instruments at a rate unprecedented since the start of the Red Book Statistics

Keywords: Covid-19, Electronic payment, National Payments Corporation of India (NPCI) & Red Book Statistics from the BIS Committee.

INTRODUCTION

The World Health Organisation (WHO) has declared the corona virus disease 2019 (COVID-19) a pandemic. A global coordinated effort is needed to stop the further spread of the virus. A pandemic is defined as "occurring over a wide geographic area and affecting an exceptionally high proportion of the population." The last pandemic that was reported in the world was the H1N1 flu pandemic in 2009.

Sivakumar

Digital payment is a form of payment that is made through electronic means. Both the payer and the payee use digital modes to send and receive money in digital payments. It is also called electronic payment. In recent months, all of us have heard extensively about the "war on cash", the move to make India and other countries "cashless economies" and the general trend among policymakers worldwide to move the economies of the world to a digital and information enabled paradigm. In this context, it is worth noting that the emphasis laid on digital payments and the digitalization of commerce has implications for individuals, businesspersons, governments, and anyone and everyone who is a participant in the economy.

It is important to understand what digital payments are and how they work and how they benefit the economy as well as the associated problems that occur from using such modes of transactions and commercial dealings. Digital Payments are payments that are conducted over the internet and mobile channels and hence, any payment that is sent online or through mobile computing and internet-enabled devices can be called such. This means that, for digital payments to take place, the sender of the payment must have a bank account, an online banking method, a device from which he or she can make the payment, and a medium of transmission meaning that either he or she should have signed up to a provider or an intermediary such as a bank or a service provider. Apart from the sender having such means, the receiver of the payment too must have these ways to accept payments.

REVIEW OF LITERATURE

Dr. Rajeshwari M (May-June 2019), This article explaining the operating cost of banks has been significantly decreased by Digital Banking. This has made it easier for banks to charge lower service fees and provide higher interest rates for depositors as well. The V. Achutamba1, et.al 4396 © 2021 JPPW. All rights reserved decrease in operational costs meant more benefit for the banks. This paper covers the role of digitization in Indian banking, factors that affect the scope of digital banking in India, and trends in digital banking in India. Data were derived from a number of sources, such as journal journals, government publications from India, and various RBI databases. The study also showed that the simple use of digital banking would drive the integration of the unbanked economy into the mainstream.

Jayalakshmi. S and Parvathi. S (July 2019) This article showed that digital payment is an effective means of doing business of all sectors to reach out to prospective clients and to examine the idea of digital banking, digital payment and digital payment methods. Digital payments have many benefits over cash, such as simplicity, security and clarity. In the next few years, there will be a whole new way of transferring capital in the Indian economy.

V. Sornagnesh (October 2020), titled "Impact of Covid-19 Outbreak in Digital Payments" had conveyed that "It is too early to conclude what the changes on the digital payments might look like in each cultural, demographic, and institutional context, but we can be sure that covid-19 is already reinforcing existing trends towards increased digitalisation of payments. The Reserve Bank of India said it aimed to increase digital payment transactions to about 15% of GDP by 2021, from nearly 10% during that time. The government is aiming for a billion digital transactions per day as the world is fast growing and smart phone market empowers consumers to transact at the click of a button. The Indian government has asked banks to encourage their customers to use digital payment methods as a precautionary measure against the Corona virus outbreak. RBI has also urged customers to use digital banking facilities amid the Corona virus outbreak."

M. Thangajesu Sathish, R. Sermakani, G.Sudha(May 2020) titled "A Study on the Customer's attitude towards the E-Wallet Payment system" had inferred that "E-wallets are rapidly growing and gaining importance, acceptance as a mainstream mode of payment and in near future it will hold a significant share as a mode of payment for sure going online as well as offline business. Their study indicated that main reasons for low preference of E-wallet as mode of payment are tendency of people to do not move out of comfort of using traditional mode of payments. E-wallet users give very high level of importance to attributes like security, privacy concerns and pricing (Fees). The major

Sivakumar

problems frequently encountered by the people while using E-wallet are long transaction time taken by E-wallet for processing the transaction, security breach and delayed payment. Therefore, people can adopt and use their mobile wallets for the payment transaction, fund transfer, purchasing groceries and paying bills etc."

V. Achutamba1, Dr. CH. Hymavathi (2021) tilted "Impact of Covid-19 on Digital Payments in India" COVID-19 brought change in the method of payment from traditional to digital payments. Though people have been facing few issues and might have a problem in trusting the digital payments but still they definitely will switch to digitalized payments once certain steps are taken. COVID-19 has definitely made us take a step forward towards digitalization due to people not wanting to use cash as much in any of the payment methods. There have been concerns over the transmission of the COVID19 through the exchange of cash.

OBJECTIVES OF THE STUDY
1. To analyse the preferred mode of payment by the respondents before lockdown and after lockdown.
2. To study the factors motivating the customers to use digital payments.
3. To interpret the satisfaction level of customers towards digital payments.

SCOPE OF THE STUDY
Before the pandemic struck, the payment industry has been quite dynamic over the past few years. The Corona Virus outbreak, and the subsequent global recession, will take forever to transform the way in which people are paid and the way they make payments as well. At a surface level, paper checks, which accounted for nearly half of all payments at the beginning of the pandemic are being replaced with digital payment options. But these changes run even farther. Post demonetization, people gradually begun embracing digital payments to an extent where small time merchants and shop owners too begun accepting payments through the digital mode. The covid-19 pandemic situation has had the ability to move the world more rapidly towards digital payments simply because it's more comfortable, easier and safer. The purpose of this study is to find out people preference of the mode of payments before and after the pandemic. Satisfaction level and the effectiveness of the current digital payment options are also assessed in this study. Impact of COVID19 on the digital payments is also studied. Every mode of transactions has its pros and cons, the issues faced by the general public is assessed and also interpreted in this study.

LIMITATIONS OF THE STUDY
1. The area of study is limited to cities (Coimbatore).
2. The information given by the respondents might be biased.
3. Today's findings may not hold true for the future
4. This study is only limited to 150 responses.

RESEARCH METHODOLOGY

Primary Data: The primary data for this study is collected by circulating a questionnaire among the general public to know the effects of the pandemic on digital payments.

Secondary Data: Research articles, Authenticated Websites, bulletins of RBI, and Daily's.
1. Sample size – 150 respondents.
2. Sample area – Coimbatore city
3. Sample technique –Convenience sampling.

Sivakumar

Statistical tools used
- Percentage
- Correlation
- Chi-square
- Annova

Interpretation

From the above, it is inferred that significant value is .009 which is more than 0.05, so null hypothesis is accepted. From this test it can derive that annual income is not associated with the preference of digital payments.

ANOVA

Table No. 2 Genders and Convenience of Digital Payment

Null Hypothesis (H0): There is no significant difference between gender and Convenience of Digital payments over Cash
Alternate Hypothesis (H1): There   is significant difference b between gender and Convenience of Digital payments over Cash

Interpretation

From the above table, it is concluded that the significant value falls to be .038, which is above 0.05.Hence, the null hypothesis is accepted. It can be concluded that there is no significant relationship between gender and Convenience of Digital payments over cash

Table No. 3 Age and Frequency of using Digital Payments during Covid -19

Null Hypothesis (H0): There is no significant difference between age and frequency of using digital payments during COVID -19

Alternate Hypothesis (H1): There is a significant difference between age and frequency of using digital payments during COVID -19

Interpretation

From the above table, it is concluded that the significant value falls to be .062, which is above 0.05.Hence, the null hypothesis is accepted. Thus, it can be concluded that there is no significant relationship between Age and frequency of using digital payments during COVID -19

CORRELATION

To test the correlation between the volume of transactions and employment status.

Interpretation

The correlation between the volume of transaction and employment status is 0.086, which is less than 1, which shows there is a significant relationship between the volume of transaction and employment status.
There is a relationship because, earnings of people play a role on their volume of transactions.

FINDINGS

➢ It can be concluded that the volume of transaction influences the respondent's choice towards making digital payments.
➢ It can be concluded that the majority of respondents are satisfied with working of internet banking.

Sivakumar

- ➢ It is inferred that that the majority of respondents are satisfied with working of mobile banking
- ➢ It is found that people's frequency of payments through digital payments have   increased during COVID-19
- ➢ It is inferred that the majority of respondents only use UPI the most followed by banking cards.
- ➢ It is inferred that the majority of respondents are satisfied with working of internet   banking.
- ➢ It can be concluded that annual income is not associated with the preference of digital payments (Chi Square Test).
- ➢ It can be concluded that there is no significant relationship between gender and Convenience of Digital payments over Cash (ANOVA).
- ➢ It can be concluded that there is no significant relationship between Age and frequency of using digital payments during COVID (ANOVA).
- ➢ It is inferred that there is a significant relationship between the volume of transaction and employment status (Correlation).

SUGGESTIONS

- ➢ Many consumers are still wary about using digital payments, but if companies can educate their customers on the security advantages of digital payments, more consumers will be comfortable with the new form of payment
- ➢ Companies and banks have to increase their security level and educate their customers about the digital payment options
- ➢ More consumers are willing to switch their primary cards if it means that they can receive higher return values, which is why a built-in rewards system can be so enticing. However, when it comes to earning and redeeming rewards, consumers desire simplicity. To make digital payments more effective, allow consumers to redeem rewards at the point-of-sale terminal so that they can benefit even faster.
- ➢ Companies have to standardize browser and device support. As with password management, different browsers and devices use different mechanisms for storing credit card information and automatically supplying that information when prompted by apps and Web pages. Some standardization would help.
- ➢ Redirects should be avoided and payments should be faster.

CONCLUSION

The negative consequences of the COVID-19 pandemic are trickling right down to major sectors of the Indian economy, this in turn has played a major role in affecting fast- growing digital payments which are closely linked to the aforementioned sectors. Shops shut, travel bans and reduced discretionary spent by consumers (on dining out, movies and entertainment then on) are further negatively impacting digital payments. These include online grocery shops, OTT (telecom and media) players, EdTech, online gaming, utility/bill recharges and payments.

Digital payment rates are also obtained mostly by government, which has pledged monetary support to the poor through direct transfers to the appropriate bank accounts. In these days, digital payments, once a convenience, have become a necessity. It is too early to assess the long-term effect of COVID-19 on digital payments, with many of the industries that relate to digital payments still in a state of flux. The effect was profound and substantial, but not irreparable. Elements on the payment ecosystem are most adaptable to disruption and least dependent on physical infrastructure have been able to withstand, mitigate and even so far as capitalize the crisis, turning an imminent threat into their advantage. So conclude that, the impact of Covid-19 on digital payments has been complex and multi faced. In a shorter run, there has been significant increase in the digital payments. The effect of longer run will take some time to assess and derive.

REFRENCES

1. M. Thangajesu Sathish, R. Sermakani, G.Sudha   A Study on the Customer's Attitude toward the E-Wallet Payment System , INTERNATIONAL JOURNAL OF INNOVATIVE RESEARCH IN TECHNOLOGYMay 2020 | IJIRT | Volume 6 Issue 12 | ISSN: 2349-6002 Page No 642 -645
2. V. Achutamba1 , Dr. CH. Hymavathi2, Impact of Covid-19 on Digital Payments in India Journal of Positive School Psychology http://journalppw.com 2022, Vol. 6, No. 3, 4394 – 4400
3. Gochhwal, R. (2017). Unified Payment Interface—An Advancement in Payment Systems. American Journal of Industrial and Business Management, 07(10), 1174–1191. https://doi.org/10.4236/ajibm.2017.710 084 9.
4. Goriparthi, R. K., & Tiwari, P. (n.d.). Demonetization in India an Era for Digital Payments.
5. https://www.thehindubusinesslin.com/
6. https://www.researchdive.com/
7. https://www.timesofindia.indiatimes.co m/
8. https://www.indiaexpress.com/
9. https://www.betterthancash.org/define-digital-payments
10. https://www.bankbazaar.com/ifsc/digital-payment.html
11. https://www.researchgate.net/publication/331112911_CUSTOMERS_PERCEPTION_IN_ONLINE_PAYMENT_SYSTEM_IN_INDIA
12. http://www.iosrjournals.org/iosr-jbm/papers/Conf.17037-2017/Volume-9/5.%2028-33.pdf https://www.semanticscholar.org/paper/Factors-Affecting-the-Adoption-of-Mobile-Payment-An-
13. Dastan-G%C3%BCrler/43eef340a2f351f4f26fd87c609320efc5c5fe07   https://www.semanticscholar.org/paper/UPI-%3A-The-Growth-of-Cashless-Economy-in-India-Rakesh-

Table 1. Chi-Square Tests

	Value	df	Asymp. Sig. (2-sided)
Pearson Chi-Square	30.912[a]	15	.009
Likelihood Ratio	36.575	15	.001
Linear-by-Linear Association	8.973	1	.003
N of Valid Cases	150		

Table 2. ANOVA

Age	Sum of Squares	df	Mean Square	F	Sig.
Between Groups	5.351	4	1.338	2.616	.038
Within Groups	74.149	145	.511		
Total	79.500	149			

Table 3. ANOVA

Age	Sum of Squares	df	Mean Square	F	Sig.
Between Groups	6.630	4	1.657	2.295	.062
Within Groups	104.703	145	.722		
Total	111.333	149			

Sivakumar

Table 4. Correlations				Volume plays a role	ES
Kendall's tau_b	Volume plays a role	Correlation Coefficient		1.000	.137
		Sig. (2-tailed)		.	.086
		N		150	150
	Employment Status	Correlation Coefficient		.137	1.000
		Sig. (2-tailed)		.086	.
		N		150	150
Spearman's rho	Volume plays a role	Correlation Coefficient		1.000	.141
		Sig. (2-tailed)		.	.086
		N		150	150
	Employment Status	Correlation Coefficient		.141	1.000
		Sig. (2-tailed)		.086	.
		N		150	150

RESEARCH ARTICLE

Anti-Anxiety and Anti-Depressant Activity of Methanolic Extract of *Chrysanthemum morifolium* Ramat in Swiss Albino Mice

Priyanka Manoharan[1], Sureh Velayutham[2] and Perumal Pandurangan[3]*

Assistant Professor, Spurthy College of Pharmacy, Marasur Gate, Anekal Taluk, Bangalore-562106, Karnataka, India
[2]Professor and HoD, Department of Pharmacology, JKK Munirajaa Medical Research Foundation College of Pharmacy, Tiruchengode, Tamil Nadu-638183, India.
[3]Dean, Sri Shanmugha College of Pharmacy, Sankari, Salem-637304,Tamil Nadu, India.

*Address for Correspondence
Perumal Pandurangan
Dean,
Sri Shanmugha College of Pharmacy,
Sankari, Salem-637304,
Tamil Nadu, India.
E.Mail: perupharma78@gmail.com

ABSTRACT

Objective: The current study was designed to explore antianxiety and antidepressant actions of *Crysanthemum morifolium* ramat flower (Methanolic extract) in mice. Procedures of anxiety and depression were assessed in swiss albino mice. CM(125, 250, and 500 mg/kg) was given once a daily for 7 days via i.p route and the efficacy was matched by those elicited by Diazepam (5 mg/kg, i.p.), imipramine (15 mg/kg, i.p.), for anxiolytic, antidepressant studies, respectively. Standard drugs were given 1 time, 30 min preceding the behavioral trials. One-way analysis of variance followed by Newman–Keuls multiple comparison test was employed to analyze the results. $P < 0.05$ was considered statistically significant as compared to control. CM at 500 mg/kg produced an antianxiety effect equivalent to Diazepam, in the elevated plus maze, open field, and social interaction tests among selected doses of the CM. CM at 500 mg/kg also induced an antidepressant activity similar to imipramine, in the behavioral despair, learned helplessness test, and tail suspension among selected doses of the CM. The study shows that among the different CM doses, CM at 500 mg/kg possesses significant anxiolytic, antidepressant and has therapeutic beneficial for the management of psychological ailments.

Keywords: Antidepressant; antianxiety; *Crysanthemum morifolium;* behavioral tests; diazepam; imipramine

Priyanka Manoharan *et al.*,

INTRODUCTION

Anxiety and depression and are the most predominant psychological diseases globally. The estimated range of their occurrence among adolescents across the globe is from 5%to 70%. [1] Implausibly, women are more affected by this unwellness rather than men. [2] *Chrysanthemum morifolium* Ramat is known to have antioxidant, antiinflammatory, antimutagenic, antimicrobial, antifungal, antiangiogenic and nematocidal properties .This plant is also known to produce flavonoids of medicinal value. The literature survey suggests that the neuropharmacological effects of CM were not studied at the time of conceptualization of this investigation. Therefore, we proposed to explore the antidepressant, antianxiety activity of the CM flower extract on rodent models and compared the efficacy to standard drugs.

MATERIALS AND METHODS

Animal
Swiss albino mice (male: 20-25g) were used in the present study. The animals were produced from disease free animal house, ultra-college of pharmacy, Madurai, Tamilnadu, India. They were provided normal diet and tap water and libitum and were exposed to 12-h light and 12-h dark cycle. The studies were conducted accordance with the ethical committee and all the animals were sacrificed by euthanasia method. The mice were placed in poly propylene cage and were allowed to acclimatize one week prior to treatments. All studies were carried out in accordance with the guidelines provided by the Committee for the Purpose ofControl and Supervision of Experiments on Animals, India. The Experimental protocol was approved by the Central Animal Ethical Committee.

Plant Material and Preparation of the Extract
A total of 125gm of powdered *Chrysanthemum morifolium* Ramat flower was collected from nursery garden Erode tamilnadu. The samples flowers were finely powdered without any impurities mixed in them. After collection they were stored at the laboratory at room temperature. The methanolic extracts were collected in the same way as the ethanolic extracts. 250g of powdered sample was weighed in the weighing machine and packed in the soxhlet apparatus with 250ml methanol. As the methanol boiled the extract was slowly collected in the flask below. The temperature here too was solvent was recovered. The final solution was evaporated to dryness. The colour, consistency and yield of Methanolic extract were noted.

Drugs
Imipramine is a standard antidepressant drug. This was a gift sample from Sun Pharmaceutical Industries Ltd., India. Lorazepam is reference standard for antianxiety effect it was provided by Intas Pharmaceutical Ltd., India, as a gift sample. All chemicals used in the present study were of analytical grade and were obtained from Sigma Chemical Co. and Merck.

Experimental Protocol
Swiss albino mice (male: 20-25g) were used in the present study. The animals were produced from disease free animal house, jkkm college of pharmacy, namakkal, Tamilnadu, India. They were provided normal diet and tap water and libitum and were exposed to 12-h light and 12-h dark cycle. The studies were conducted accordance with the ethical committee and all the animals were sacrificed by euthanasia method. The mice were placed in poly propylene cage and were allowed to acclimatize one week prior to treatments. They were grouped into five, containing six animals each group.
• Group I: Control (10 mL/kg/p.o.)
• Group II: Standard drugs (lorazepam 10 mg/kg, imipramine 15 mg/kg)
• Group III: CMME 125 mg/kg/i.p
• Group IV: CMME 250 mg/kg/i.p

• Group V: CMME 500 mg/kg/i.p

CM dose was selected on the basis of randomization and was administered in distilled water to Groups (III, IV, and V) at 125, 250, and 500 mg/kg orally, once in a day for 7 days. The control group (Group I) received an equal volume of distilled water. Standard drugs were also employed to Group II accordingly in each set of protocol and were dispensed orally to animals 1 h before the experiments. On day 7, animals were subjected to behavioral studies.

Behavioral Evaluation
Anxiolytic activity
Elevated plus maze
The elevated plus maze consist of two open and two enclosed arms of 50 x10 x 40cm dimensions, with an open roof arranged in such a manner that the two open arms are opposite to each other. The maze is elevated to a height of 50 cm. The mice weighing (20-30 kg) are housed in pairs for 10 days prior to testing During this period they are handled by the investigator on alternate days in order to acclimatize than reduce stress. Four mice are taken for each test group. The test drug and the standard are administered 30min prior experimentation by i.p. route. The mice are then placed in the centre of the maze facing one of the enclosed arms. During the next 5 minutes the number of entries into and the time spent in the open and enclosed arms and the total number of arm entries is recorded. The procedure should be conducted preferably in a arm sound-proof room. The values of treated groups are expressed as percentage of control groups in terms of motor activity and open arm exploratory time. Benzodiazepines have been shown to de decrease motor activity and increase open arm exploratory time. Though the method is time consuming considered as reliable measure of anxiolytic activity.

Light and dark model
The testing apparatus consists of a light and dark chamber divided by a photocell equipped zone. A polypropylene animal cage. 44x21x21cm, is darkened with black spray over one third of its surface.A partition containing a 13' cm long x 5 cm height opening separate the dark one third from the bright two third of edge . Extract / vehicle and standard drug is administered through per i.p. route. 30minutes after i.p. administration the mouse are placed individually on the light compartment and observe for a period of 5 min. Number of rearing, number of locomotion, time spent in light and dark zones and number entries in light zone are observed during this observation period

Open field test
The open field apparatus is made up plywood consist of 56x56 (1xb) cm. the entire apparatus is painted black and 6 mm thick white lines divided the floor in to 16 square of identical dimension. Open field is lightening by 40 w bulb focusing on to the field from the height of about 100cm. The entire room, except the open field is kept dark during the experiment. One hour after the drug treatment, each animal was placed at once corner of the apparatus and the following behavioral aspects were noted in the next 5min.
Latency: time taken by animal to leave square in which it was placed
Ambulation: Number of square passed by animal
Rearing: Number of times animal stood on its hind legs

Antidepressant activity
Forced swim test
Swiss albino mice weighing 20-30g are used. They are brought to the laboratory at least one day before the experiment and are housed separately in cages with free access to food and water. Swiss albino mice are individually forced to swim inside a vertical Plexiglas cylinder (height; 40 cm; diameter; 18 cm, containing 15 cm of water maintained at 25c. Mice placed in cylinder for the first time are initially highly active, vigorously swimming in circles, trying to climb the wall or diving to the bottom. After 2-3 min activity begins to subside and to be interspersed with phases of immobility or floating of increasing length. After 5-6 min immobility reaches a plateau where the mice immobile for approximately 80% of the time. After 15 min the water the mice are removed and allowed to dry in a heated enclosure (32 C) before being returned to their home cages. They are again placed in the cylinder 24 h later and the total duration of immobility is measured during a 5 min test. Floating behaviour during

this 5 min period has been found to be reproducible in different t group of mice. An animal is judged to be immobile whenever it remains floating passively in the water in a slightly hunched but up or standard are administered one hour prior testing. Duration of immobility is measured in controls and animals treated with various doses of a test drug or standard, anti-depressant drugs, but also stimulants like caffeine, reduced duration of immobility. The response can be evaluated.

Tail suspension test
Each rat in the group was hanged by the tail (50 cm above the floor) with an adhesive tape to a cord in an upside down position so that its nostrils touch the water surface in a vessel. After the early escape oriented actions, the rat rapidly turns out to be immobile, and the immobility period (the absence of initiating movements and includes passive swaying) was recorded during 5 min observation period. Results of this study were statistically analyzed by Graph Pad Prism 5 software. The data were expressed as a mean ± standard error of mean. The data from various groups were statistically analyzed using one-way analysis of variance, followed by *post hoc* Tukey's multiple comparisons test. *P* <0.05 was considered statistically significant.

RESULTS

The extract obtained were subjected to qualitative Phytochemical test to find out the active constituents is shown in table 1. Acute toxicity studies and evaluation of datas are studied as per the guideline of OECD (423). No toxicity or death was observed for these given dose levels, in selected and treated animals. So the LD_{50} of the Methanolic extract of flowers of *Chrysanthemum morifolium* was greater than 2000mg/kg (L_{50}>2000mg/kg).Hence the biological dose was fixed at three levels, 125,250 and 500mg/kg body weight for the extract. The effect of methanolic extract of CM on EPM test shows significant anxiolytic activity is shown in table 2and the comparative activity is shown in fig 1-4.

The effect of methanolic extract of *Chrysanthemum morifolium* on light and dark model shows in table 3 having potent anxiolytic activity as compared with standard and the comparative data shows in fig 5. The effect of methanolic extract of *Chrysanthemum morifolium* on immobility of mice in forced swim test shown in table 4 and comparative percentage of reduced immobility is shown in fig. 6. The effect of methanolic extract of *Chrysanthemum morifolium* on immobility of mice in tail suspension test shown in table 5 and comparative duration of immobility of tail suspension test is shown in fig. 7.

DISCUSSION

The EPM test
The methanolic flowers extract of *Chrysanthemum morifolium*, at 125mg, 250 and 500mg/kg, had increased the time spent and percent of entries in to the open arm with percent of entries in to the open arm with percent decrease the in the spent in closed arm.The dose methanolic extracts of *chrysanthemum morifolium*125mg, 250 and 500mg/kg had increase percent number of entries in to the open arm as compared with control group. In case of rearing there is no much significant difference has been control group with the dose 125, 250mg and 500mg, the time spent the neutral zone is also reduced compared to control groups'. This decrease in number of entry and time spent in dark zone and decrease in the time spent in neutral zone compared to control groups show anxiolytic activity of flowers extract of *Chrysanthemum morifoliumramat.(3)*

Diazepam 1mg/kg and shown significant effect with all four parameters. Number of entries in light zone and time spent in light zone increased as compared to control group with 125, 250mg/kg and 500mg/kg dose of both extract. There is increase in number of rearing and in total locomotion as compared to control group. An increase in locomotion and time spent in light zone indicates anxiolytic activity of the methanolic flowers extract of *Chrysanthemum morifoliumramat.(4)*

In the Open Field Model,

125, 250mg/kg and 500mg/kg to decrease the time spent in square where it where it was placed and time taken to enter in central compartment as compared to control group. Results obtained from all the doses showed increase the spent in central compartment and increase number of square crossed by the animal which shows decrease in fear of animals, indicates the anxiolytic activity of the methanolic flowers extract of *Chrysanthemum morifolium Ramat.(5)*

In the force swim test,

The methanolic extract 125, 250mg/kg and 500mg/kg showed the significant antidepressant activity in term of responding to the stress in experimental studies that they exposed in force swim test showed decreased the immobility, to the response indicate the antidepressant activity of the methanolic extract of flowers of *Chrysanthemum morifolium Ramat.*

Tail suspension test,

The methanolic extract 125, 250mg/kg and 500mg/kg showed the significant antidepressant activity in term responding to the stress in experimental studies they are exposed in tail suspension test showed the animal struggled to escape and the struggling time was increased, to the response indicate the antidepressant activity of methanolic extract of flowers of *Chrysanthemum morifoliumRamat.(6-7)*

CONCLUSION

The methanolic extract of *Chrysanthemum morifolium* flowers possess a combination of activities like produce anti-anxiety and anti-depressant. The extract is bind with highly affinity BZD site GABA –A receptor. From above observation, we can conclude that methanolic extract of *Chrysanthemum morifolium* possess the Antianxiety and Antidepressant activity for both dose level which comparable with the standard drugs (Benzodiazepine). The investigation demonstrated that CT at 500 mg/kg possesses significant anxiolytic and antidepressant effects and is therapeutically beneficial for the management of psychological ailments.

RERERENCES

1. Tripathi KD. Essential of medical pharmacology, 6th ed. JAYPEE brothers, medical publisher (P) Ltd, New Delhi. Pp. 439- 452.
2. Neil A. Rector PhD. Anxiety Disorders information guide. Library and archives Canada cataloguing in publication. Camh- centre for addiction and mental health centredetoxicomanie et de santé mentale. Pp. 3973/02-2011/PM 041.
3. Ki-Wan Oh et al., has reported Ethanol Extract of the Flower *Chrysanthemum morifolium* Augments Pentobarbital - Induced sleep Behaviours: Involvement of cl⁻ channel Activation On Evidence Based Complementary and Alternative Medicine 2011 Feb 10, 109164.
4. Saba Shafeen, Srinath Reddy T, Arafath S, Nagarjuna S, Padmanabha Reddy Y.Evaluation of Antianxiety and Antidepressant activity of *Cassia occidentalis*leaves. Asian Journal of Pharmaceutical and Clinical Research, Volume 5, Suppl 3, 2012, ISSN-0974-2441.
5. Poonam Mahendra, SharadhaBisht, Anti-anxiety activity of *Coriandrum sativum* assessed using different experimental anxiety models. An official Publication of the Indian Pharmacological society. Indian Journal Pharmacology, 2011, Pp.547-577.
6. F.Josef van der staay, Animal model of behaviour dysfunctions: Basic concept and an evaluation strategy. Brain Research Reviews. Science Direct, 2006 Pp.131-159.
7. R.J Rodger, B –J Cao, A. David, A, Holmes. Animal models of anxiety: an ethological Perspective. Brazilian Journal of Medical and Medical and Biological Research (1997)Pp.289-304.

Priyanka Manoharan *et al.,*

Table :1 Qualitative Phytochemical analysis of the extract

S. NO	PHYTOCHEMICALS	INFERENCE
1	Alkaloids	+
2	Steroids	–
3	Flavanoids	+
4	Phenol	+
5	Saponin	Trace
6	Tannins	Trace
7	Glycosides	+

Table No. 2 Effect of Methanolic extract of *Chrysanthemum morifolium* **on EPM Test**

GROUP	TREATMENT	DOSE	TIME SPENT INOPENARM(S)	NO ENTRIES INOPENARM
I	Saline	10ml/kg	40.3±2.1	10.1±1.5
II	Diazepam	5mg/kg	29.6±3.6**	8.3±1.8**
III	CMME	125mg/kg	22.8±2.4	5.5±2.3
IV	CMME	250mg/kg	23.7±3.2*	7.8±3.5*
V	CMME	500mg/kg	26.5±2.8**	9.4±1.3**

The data represent the mean ±S.D(n=6)*p<0.01.**p<0.001 significantly different compared to normal control and diazepam.

Table No. 2 Effect of Methanolic extract of *Chrysanthemum morifolium* **on open field Test**

GROUP	TREATMENT	DOSE	NUMBER OFSQUARECROSSED	NUMBEROFREARING
I	Saline	10ml/kg	40.3±2.1	10.1±1.5
II	Diazepam	5mg/kg	29.6±3.6**	8.3±1.8**
III	Plantextract	125mg/kg	22.8±2.4	5.5±2.3
IV	Plantextract	250mg/kg	23.7±3.2*	7.8±3.5*
V	Plantextract	500mg/kg	26.5±2.8**	9.4±1.3**

Table 3: Effect of Methanolic extract of *Chrysanthemum morifolium* **on light and dark model**

TREATMENT	LATENCY	TIME SPENT INDARKZONE(5 MIN/SEC)	TIME SPENT INLIGHTZONE (5MIN/SEC)	REARING	TOTALLOCOMOTIONTIME(SEC)	FECAL
Control(Vehicle)	6.34±1.01	236±8.78	63.17±8.54	2.34±0.75	55.4±9.35	1.5±0.22
Ethanolic extract of *C.morifolium* (200mg/kg)	8.16±0.88	92±12.50	142.34±20.43**	13.85±2.4	262±11.83***	0.17±0.17***
Ethanolic extract of *C.morifolium* (400mg/kg)	6.32±1.35	152.5±20.13*	169.17±20.25	10.16±2.5	271.34±6.17***	0.68±0.49
Standard anxiolytic drug (diazepam 0.5mg/kg)	11±0.35*	172.67±23.38	180.5±8.59**	6.35±1.22	247.67±14.88***	0.67±0.02

Priyanka Manoharan *et al.*,

Table: 4. Effect of Methanolic extract of *Chrysanthemum morifolium* on immobility of mice (FST)

S.NO	GROUPS	DOSE(MG/KG)	DURATION OFIMMOBILITY(SEC)	DURATION OFIMMOBILITY(%OF ACTIVITY)
1	Control	0.5%CMC	206.6±3.03	---------------
2	Positivecontrol	Imipramine15	33.67±3.04	85.66
3	CMME	125	154.4±3.88	22.6
4	CMME	250	115±3.46	35.19
5	CMME	500	52.6±2.47	77.43

Table: 5 Effect of Methanolic extract of *Chrysanthemum morifolium* on Immobility of mice (TST)

S.NO.	GROUPS	DOSE(MG/KG)	DURATION OFIMMOBILITY(SEC)
1	Control	0.5%CMC	125.6±1.03
2	Positivecontrol	Imipramine15	38.67±1.02
3	CMME	125	105.3±3.01
4	CMME	250	87.5±2.06
5	CMME	500	54.6±2.09
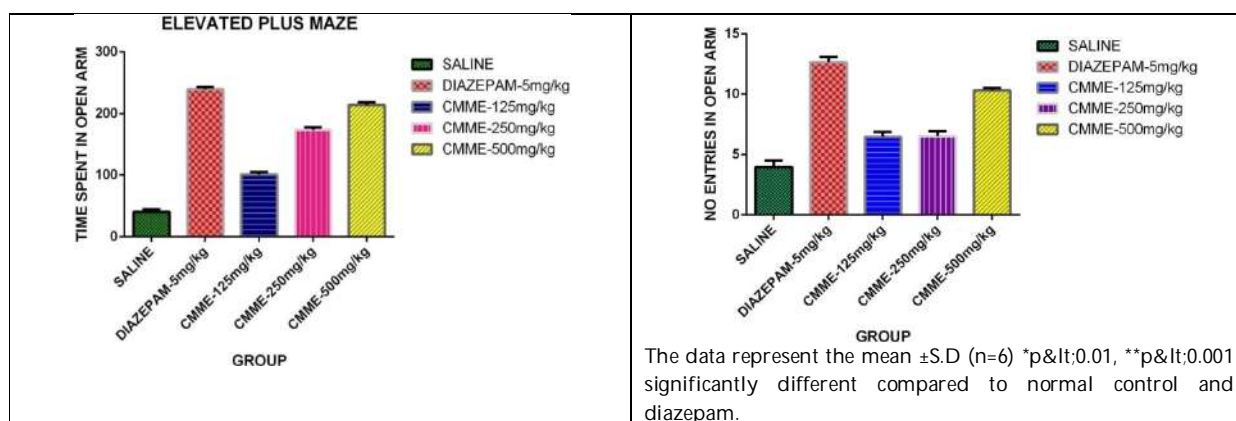
	The data represent the mean ±S.D (n=6) *p<0.01, **p<0.001 significantly different compared to normal control and diazepam.
Fig.1. Effect of Methanolic extract of *Chrysanthemum morifolium* On Time Spent in open arm in EPM Test	**Fig.2 Effect of Methanolic extract of *Chrysanthemum morifolium*, No of entries in Open arm on EPM Test**
Fig.3. Effect of Methanolic extract of *Chrysanthemum morifolium* on No of Square crossed in OPM Test in mice	**Fig.4. Effect of Methanolic extract of *Chrysanthemum morifolium* on Number of rearing in OPM Test in mice**
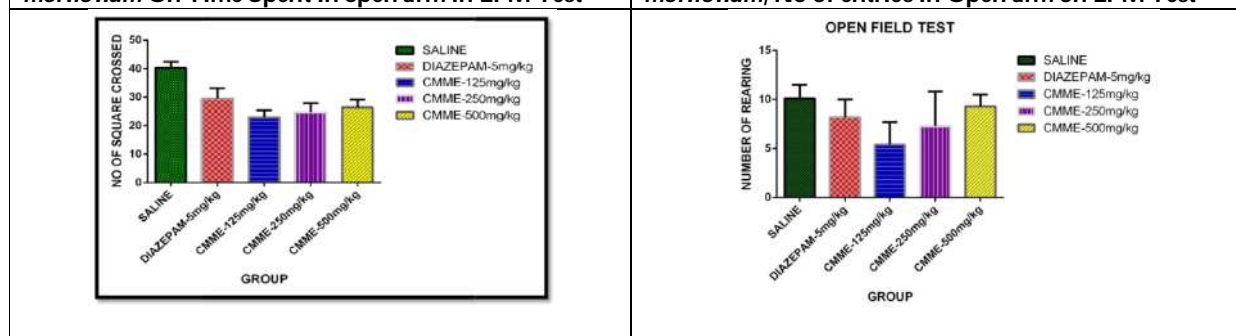
64281
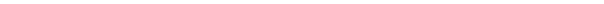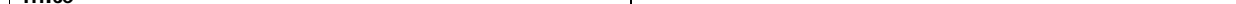
Priyanka Manoharan *et al.*,
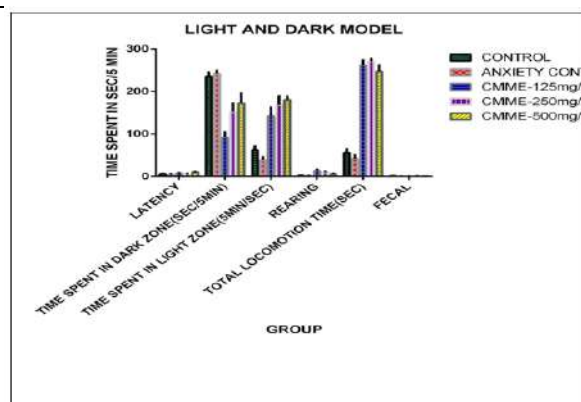
Value expressed by are mean SEM, n=6, p<0.05*, p<0.001 as compared to normal group**

Fig.5. Effect of Methanolic extract of *Chrysanthemum morifolium* On Time Spent in sec/5 Min Light and dark model Test
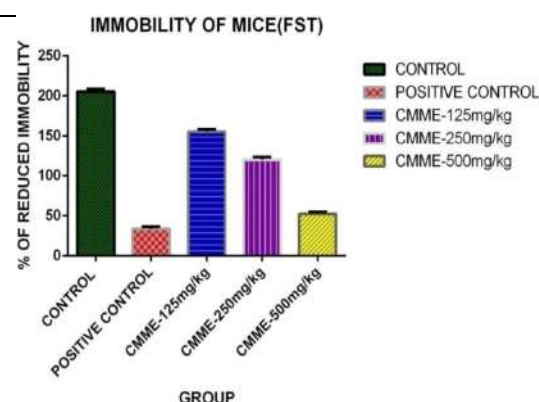
Fig .6 Effect of Methanolic extract of *Chrysanthemum morifolium* immobility of mice in forced swim test
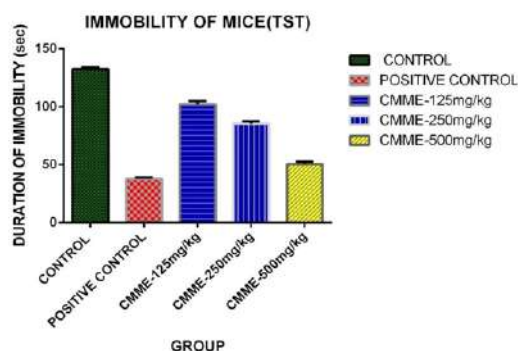
Fig.7 Effect of Methanolic extract of *Chrysanthemum morifolium*, Duration of immobility in tail suspension test

REVIEW ARTICLE

Nanoparticle Toxicity : A Review

Surajit Majumder[1]*, Dipankar Saha[2] and   Soumitra Kumar Choudhuri[3]

[1]Associate Professor, Dept. of Zoology, Bankura Sammilani College, Bankura- 722102, West Bengal, India.
[2]Part-Time Researcher, Dept. of Zoology, Bankura Sammilani College, Bankura-722102, West Bengal, India.
[3]Former HoD and Emeritus Medical Scientist, Chattaranjan National Cancer Institute (CNCI), 26, S.P. Mukherjee Road, Kolkata - 700026, West Bengal, India.

*Address for Correspondence
Surajit Majumder
Associate Professor,
Dept. of Zoology, Bankura Sammilani College,
Bankura- 722102, West Bengal, India.
E.Mail: surajitnajumder.sm@gmail.com

ABSTRACT

The particles having size 1-100 nm in length is considered as nanoparticles (NP) and the application of such particles is termed as Nanotechnology. Nanotechnology is developing very fast with applications in various industries and also in detection and treatment of diseases. Although showing beneficial results, nanotechnology is mingled with adverse effects and toxicity. Hence it is of utmost importance to undertake in depth studies dealing with NPs and undergo detailed toxicological studies before NPs enter into the market for human application. The present review describes various types of NPs and their methods of preparations and ways of detection through modern techniques. The present review describes the toxic properties of NPs in various parts and organs of human body.

Keywords: Nanoparticles, synthesis and types, toxicological effects, inorganic nano and organic nano, nano emulsions.

INTRODUCTION

Nanoparticles (NPs) are the particles having size 1-100 nm in length. NPs show variable properties depending on their size and surface functionalities (1). A small size and large surface area NPs have applications in various industries like, agriculture, cosmetics, electronics, medical therapeutics, diagnostics, and research appliances (2). Especially the polymeric NPs, nano emulsions, liposomes and solid NPs have potential clinical applications (3). The use of NPs escalated in last decade due to availability and development of so many techniques to detect its size.

64283

Surajit Majumder *et al.*,

Some of these techniques include scanning tunneling microscopy, scanning transmission electron microscopy, tandem electron microscopy (4-6). NPs can be prepared in the laboratory and may also be present as a biproduct in many events, e.g., engine exhaust (7, 8), cigarette smoke (9), e-cigarette fluid and aerosols (10), cooked food (11), and numerous spray products (12).

Despite potential uses in the clinical fields, a number of studies suggest that the NPs can be toxic too. Following exposure, NPs accumulate in the cells and induce organ specific toxicity; the most common exposure occurs through inhalation in the manufacturing workplace as well as the exhaust of fumes or spray (13,14). Other than these routes, NP exposer occurs through skin contact (e.g., creams and cosmetics), ingestion (e.g., food color, packet), and occasionally through intravenous (iv) pathway required for medicinal purposes (15-16. Considering the adversities, strict guidelines are required to ensure the proper designing of safe NPs having minimal toxicity. The present review briefly describes the types and uses of NPs in different industrial sectors and also summarizes its toxic effect in cellular level.

Different types of nanoparticles and their applications
On the basis of the composition NPs can classified into three major categories,

Organic NPs: The nanoparticles which are made of organic compounds, like carbohydrate, protein, lipids and polymers (17). The most common types of organic NPs are liposomes, micelles and ferritin. These organic NPs are bio-degradable, nontoxic and mostly used for the targeted drug delivery and cancer therapy (18, 19). Liposomes are the classical examples of organic NPs consisting an aquas core surrounded by phospholipids and cholesterol bilayer. Liposomes have high encapsulation capacity and high circulation time. Hence liposomes accumulate at specific site of diseases. For example, the outer layer in the tumors is composed of lipids having high cellular permeability where endothelial layer and lymphatic system is lacking. In recent era, liposomes are considered to be the most common drug delivery system for clinical trial of several FDA approved drug (20). Early developed liposomes had very short half-life and easily could remove by the reticule endothelial system. This limitation has been overcome by conjugation of the polymers like polyethylene glycol (PEG), saturated high-phase transition lipids and resulted in generation of stabilized long life 'Stealth liposomes' (21).

Inorganic NPs: These classes of NPs are made of metals and metal oxides. They are like, metal, ceramic and semiconductor NPs. The metallic NPs are formed from metal precursors and can be classified into mono metallic, bimetallic and polymetallic, based on the metallic precursor used (22, 23). These NPs possess unique optical, electrical, thermal, magnetic and biological properties; thus, they can be used in several physical, biological, chemical and pharmaceutical applications. The most common solid metallic NPs are gold NPs and silver NPs. Depending on the size, shape and surface properties of gold NPs; it can be used as cancer diagnostics and radiotherapy (24). Silver NPs have unique properties of absorbing and scattering light, thus this is used as biosensors. Silver NPs also used in electronic devices, textiles, wound dressings, antimicrobial coatings and biomedical devices (25, 26).

Ceramic NPs are made of carbonate, carbide, phosphate and oxides of metal and metalloids. These are found in different forms, like amorphous, polycrystalline, dense, porous or hollow (27). Ceramic NPs are stable and also have high load capacity (28) and therefore, can be used in biomedical applications, catalysis, degradation of dyes, protomorphic and optoelectronics applications (29). The most common example of this type of NPs is iron oxide. Iron oxide NPs are solid and have a superparamagnetic property, thus heavily used in the magnetic resonance imaging (MRI) (30). Iron oxide NPs also used in various diagnostics and imaging techniques as a biosensor due to their unique optical properties. Semiconductor NPs are made up of semiconductor materials and possesses unique wide bandgaps, which make it different from the other semiconductor materials (27). These NPs are commonly used in the photocatalysis, optic and electronic devices (31, 32).

Carbon based NPs: Carbon NPs are solely made up of carbon atoms which are bonded with sp^2 hybridized carbon bonds. The most common examples are Fullerenes, Carbon nanofibers, Graphene, Carbon nanotubes, Carbon black.

Surajit Majumder *et al.,*

Fullerene is made up of 60 carbon atom molecules arranged in a ball like structure. Carbon black are formed by aggregate of highly fused spherical particles. Carbon based NPs have their unique properties of high strength, electrical conductivity, electron affinity, optical and thermal properties (33,34). Due to such unique characteristics, carbon-based NPs are used for drug delivery, energy storage, bioimaging and tissue engineering applications (35-38). Other than these three major types, NPs can be categorized as polymer-based NPs, and nano emulsions based on their nature.

Polymer based Nanoparticles: Polymer based NPs are widely used as drug carrier for control and sustain release. In case of polymer-based NPs, encapsulated drug was incorporated into the matrix of the polymer (39). Commonly used polymer bases NPs are ploy lactic glycolic acid and chitosan. Due to their biocompatibility and biodegradable nature, both are being FDA approved for the clinical use (40, 41).

Nano-emulsions: Nano-emulsions (NEs) are the colloidal dispersions composed of either oil nanodroplets dispersed in water or water nanodroplets dispersed in oil. These are commonly used as a drug carrier molecule with limited water solubility, such as delivery of vaccine and anti-cancer agents (42). Thermodynamic stability of the NEs depends on the size and most stable size is 20-200 nm (43). To increase the stability, surfactants are incorporated into of the NEs.

Toxicological effect of NPs
The uses of the NPs have increased tremendously in last decade in different applications, like diagnosis of disease, medical imaging, targeted drug delivery, gene therapy and other industrial applications. The exponential increase of the use of NPs occurred due to its useful nature but still the toxicological effect of NPs following exposure remains unexplored. Hence, the lack of knowledge in this field invokes the ethical responsibility to take necessary precaution and minimize their exposure in both occupational and environmental (44) field.

The reminder of this review focused on the toxic effect of the NPs. The toxic effects of some NPs in use are fairly known and moreover, the toxic effects of most of the NPs are not completely understood. There is insufficient information correlating NP induced toxicity to exposure in humans. Many NPs can cause oxidative stress and interact with cellular macromolecules. On the other hand, a few NPs also cause high pulmonary inflammatory response (45, 46). The toxic effect of NPs is dependent on their size and surface area and also the route of uptake and accumulation.

Different routes of exposures
In case of human, the exposure of NPs can occur through ingestion, injection, inhalation and skin contact. The toxicity in different organs depends on the route of exposure. Some of the exposure is unintentional, such as the inhalation of the NPs in work places that leads to tissue damage in the lung (47, 48). On the other hand, some exposures are intentional, like application of the skin product topically and through injection.

Exposure through the skin
Skin is the largest organ of the human body and plays a barrier for many toxic materials. The skin is one of the major routes of administration and exposure of NPs present in different cosmetics, cream. The permeability of the skin to these NPs is still not clearly known (49). The vast use of the NPs based cosmetics resultant in high exposure through skin and ultimately reaches to the blood circulation. The penetration of the NPs can occur through the follicular cell, sweat gland (50, 51). For the example, Titanium dioxide nanoparticles are widely used in the dermatological applications. These can cause the cell death. Reports also disclose that the NPs can cause the organ damage due to its accumulation in the organ followed by the absorption through the skin (52). The skin is also a major route of NPs exposure which mostly occurs in welding fumes, during the natural gas and oil production, and also during the NPs manufacturing; such exposure can cause the DNA damage and cellular apoptosis (53, 54).

Surajit Majumder *et al.,*

Exposure through inhalation
The major route of insertion occurs through inhalation as NPs are present in air in abundance. Inhaled NPs directly enter into the lungs and penetrate the epithelium layer and invade the nearby lymph node resulting in the inflammation that ultimately leads to lung cancer (55-59). The effect of the NPs in the lung depends on various factors, viz., size, chemical properties of the NPs, quantity of the inhaled NPs, rate of deposition in the lungs, rate of elimination (60). Some reports disclose that the inhaled NPs cause asthma through inflammatory reactions occurring in the system (61). Evidences also show that exposure of carbon NPs cause the increased eosinophilic response in the mice lungs (62). Other NPs, like carbon nano-tubes, aluminum oxides, silver also cause pulmonary damage when exposed to these particles in the workplace.

Exposure through ingestion
The uses of NPs gradually increased in the agriculture and food industry (63). In food industry, NPs are used for making test, texture of food, improving packages (64). The oral ingestion of those food materials leads to NPs exposure and following ingestion, these NPs get absorbed through the digestive system leading to serious problem in human health.

Biodistribution and Toxic effect of NPs on target organs
Once the NPs enter into the circulation, they travel throughout the body and deposited in different organ and tissues, including kidney, spleen, heart, liver, bone marrow and nervous system (65). The absorption of NPs into the different tissues and organs depends on the physico-chemical properties of the NPs and also the diffusion rate from the capillaries to the organ (66). NPs are reached to the blood through the phagocytosis process and then filtered by the spleen (67, 68). Large size particles are accumulated into the liver, resulting liver narcosis (69, 70). NPs can penetrate the blood brain barrier and accumulated into the brain (71). The excretion of the NPs takes place through kidneys, feces, sweat and breast milk and also through saliva. The excretion through kidneys depends on the size of the NPs, as the kidney has fixed pore size of 70 nm (72). To summarize, the NPs accumulate into the organs like liver, spleen, lung, kidneys and cause the damage of these organ.

Toxic effect on the liver
Liver is the vital organ where metabolism of the exogenous chemicals takes place. Macrophages clear the NPs from the body but their fragmented parts remain encapsulated with the drugs and are metabolized through the liver (73,74). Evidences disclose that, silver NPs can cause mild liver damage through accumulation of the metal ions of the NPs in the liver cell (75). Intraperitoneal injection of zinc oxide NPs in mice causes the liver damage by increasing the level of alkaline phosphatase and glutamic transaminase. Following the use of gold NPs, the gold molecules are accumulated into the liver and activate the hepatic macrophage induced liver damage (76).

Toxic effect on the Spleen
Studies have shown that NPs are removed by the immune cells, and are accumulated in spleen (77, 78). Metal containing NPs induce the inflammatory response, especially iron containing NPs. These metal irons further accumulate in the liver and spleen and induce the oxidative stress in those organs (79). Evidences also show that nonmetallic NPs also accumulate in the macrophages (80). Use of NPs in different animals induces the level of different cytokines and chemokines, which further induce the immune response in the spleen (81).

Toxic effect on the lung
The respiratory exposure of the NPs causes the inflammatory response and fibrosis in rat lungs (82, 83). However, studies have also shown that, injection of NPs to the lung causes the inflammatory response only (84). Several in vivo studies show that the respiratory exposure of the NPs does not cause serious toxic effect to the lung (85).

Toxic effect on the kidneys
Kidneys play a major role in excretion of the metabolic wastes. Small size NPs are filtered through kidney and during filtration, depending upon the time it stays in kidney, leads to nephrotoxicity (86). Respiratory exposure of

Surajit Majumder *et al.,*

silica NPs causes the renal inflammation and fibrosis (87). Silica NPs also result in acute kidney damage in mice after single peritoneal injection indicating the translocation of NPs from the systematic circulation to the kidneys (88). The gold NPs can cause tubular dilation, inflammation and also mineralization in the rat kidney (82). The gold NPs associated kidney damage is two times higher in female rat than the male (74). The renal effect can persist up to 30 days of post administration.

Toxic effect on brain
Although most of the NPs can't reach the brain due to impermeability of blood brain barrier (BBB), a few small size NPs can penetrate the BBB by passive diffusion or by receptor mediated endocytosis and also accumulate inside the brain (89). Metal containing NPs can penetrate the BBB either by the transsynaptic transport mechanism or by the direct disruption of the BBB, resulting in the central nervous system toxicity (90-92). The most common example is Poly-n-butylcyano-acreylate NPs coated with polysorbate 80 that has been used for the drug delivery into the brain (86). Other metal containing NPs, such as silver NPs, titanium dioxide, zinc oxide, aluminum oxide are reported to induce oxidative stress in the brain (93). Furthermore, long tern respiratory exposure of the titanium dioxide results in hemorrhage in mice (94).

Toxic effect on other organs
Other than these target organs' toxic effect, NPs can also cause toxicity in other organs. For example, oral administration of zinc oxide for a long period causes the submucosal edema and inflammatory cell infiltration in the stomach (93). It also causes the inflammatory response and apoptosis in the pancreas (94). Dermal administration of the silver NPs reduces the thickness of the epidermis and papillary layer (95).

Mechanism of cytotoxic effects of NPs
The toxicity of the NPs on different target organs are well established. The toxicity is facilitated through different mechanism, such as by reactive oxygen species (ROS) generation, DNA damage, alteration of protein structure and by disruption of the membrane structure.

ROS generation
ROS are the oxygen containing chemically reactive substances, which play important role in cell signaling and cellular homeostasis. They are formed natural biproduct of oxygen metabolism. The pool of ROS establishes an oxidative stress in the cell. Several NPs have been reported to cause oxidative stress in the cell and inhibit the action of antioxidant. The increased level of ROS in the cell results in activation of the stress related cell signaling pathway, mitochondrial disfunction, DNA damage, which leads to the cell cycle arrest or apoptosis (96). Metal and metal oxides NPs induce the oxidative stress in liver, kidneys and spleen when accumulated in the organs (79,93,97). The large size NPs are not easily taken up by the cell than the small size NPs. Thus, the toxicity effect of small NPs is much higher than the large NPs. NP induced ROS production is due to mitochondrial dysfunction (97). Titanium dioxide NPs cause the oxidative stress by protein oxidation, alteration of catalases activities, increased release of glutamic acids and nitric acids (98). Other reports also indicate that NP induced oxidative stress occurs via p38-Nrf-2 signaling pathway (99).

DNA damage
NPs induce oxidative stress in the cell, which ultimately lead to mutagenesis due to the oxidation, hydrolysis and deamination of nucleic acid bases. Prolong oxidative stress can also lead to the gene alteration and carcinogenesis. Reports also disclose that following expose to silver NPs, cells release high amount of DNA damage marker protein, p-H2AX which leads to the DNA damage (100)

Protein structure alteration
Heavy metals NPs bind with the protein and amino acids and causes protein structure alteration, which leads to altered protein function. Such as serum albumin, hemoglobin and cytoskeletal proteins are easily bind with the NPs and result in protein damage (101). Similarly, silica NPs also significantly alters the function of RNase (102).

Inflammatory reaction
Reports substantiate that the NPs usually taken up by the macrophages in macrophage reach organs, like spleen and liver. NPs bind with the macrophages with specific macrophages receptor and in consequence release of various inflammatory cytokines occur (103-105). Earlier study also reports that titanium dioxide induces the inflammation response through c-Src, p38 MAP kinase, NF-κB pathways (106).

Epigenetic modifications
Other than the mechanisms mentioned, NPs can also alter the epigenetic modifications. Recent studies show the adverse effect of NPs on the DNA methylation, histone acetylation, RNA methylation, chromatin remodeling (107-109). Previous study has also reported that exposure to the carbon-based NPs; titanium dioxide and selenium dioxide can alter the DNA methyl transferase expression (110-112) and leads to the changes in the global DNA methylation. Studies also show that exposer of titanium dioxide NPs results hypermethylation at the promoter region of poly ADP ribose 1 in human lung carcinoma cells (113).

Factors affecting the toxicity of NPs
The toxicity of the NPs is depended on the several factors as follows:

Partial size and surface area
Particle size and surface area of NPs paly important role in different biological molecules. Small size NPs exhibit higher tissue distribution than the large size. The size of NPs is directly correlated with the ROS generation in the kidneys (114). Reports also show that 10 nm silver NPs had higher liver distribution and hepatobiliary toxicity as compared to the 40 and 100 nm NPs (115)

Surface charge
Surface charges of NPs also have important role in various interactions, such as plasma protein binding, permeability of BBB, selective absorption. Cell membrane possesses negative charges, so the positively charged particles can easily enter into the cells. Moreover, ionized form of zinc oxide NPs accumulation rate is much higher than the particulate form in different organ like kidneys, liver and lungs (116). Positively charged silica NPs induces more ROS production than the neutral and negatively charged partials (117).

Aggregation
Depending on the surface charges, size and composition, aggregation of NPs also plays important role in toxicity which is the most common occurrence with the carbon nanotubes. Aggregated carbon nanotubes show more cytotoxic effect than their dispersed form (118).

Surface coating
The surface property of NPs can be altered by using several coting materials. Such materials can change the physico-chemical properties of the NPs, e.g., charges, electric, magnetic, optic and chemical properties. This phenomenon can be employed for the reduction of the toxicity of NPs. For example, PEG has been used for the reduction of the toxicity of the gold NPs (119).

CONCLUSION

Nanotechnology is the fastest growing field with applications in disease diagnosis and treatment, biosensors, cosmetics, food industry and other technologies. However, the rapid growth in the application, many a times, overlooking the consequences of NPs toxicity. Thus, there is an urgent need for more toxicological study of the NPs before these particles enters into the market for human application. Utmost need is to understand the physico-chemical properties of the NPs and their cellular reactivity and interaction with several tissues and organs. Through

information may help to reduce the knowledge gap of the NPs toxicity and may also lead to the generation of biocompatible and less toxic NPs.

REFERENCES

1. Gwinn, M.R.; Vallyathan, V. Nanoparticles: Health effects–pros and cons. Environ. Health Perspect. 2006, 114: 1818–1825.
2. Missaoui,W.N.; Arnold, R.D.; Cummings, B.S. Toxicological status of nanoparticles: What we know and what we don't know.Chem. Biol. Interact. 2018, 295: 1–12.
3. Park, J.; Ham, S.; Jang, M.; Lee, J.; Kim, S.; Kim, S.; Lee, K.; Park, D.; Kwon, J.; Kim, H.; et al. Spatial-Temporal Dispersion ofAerosolized Nanoparticles during the Use of Consumer Spray Products and Estimates of Inhalation Exposure. Environ. Sci.Technol. 2017, 51: 7624–7638.
4. Sharma, S.; Jaiswal, S.; Duffy, B.; Jaiswal, A.K. Nanostructured Materials for Food Applications: Spectroscopy, Microscopy andPhysical Properties. Bioengineering (Basel) 2019, 6.
5. Jin, S.E.; Bae, J.W.; Hong, S. Multiscale observation of biological interactions of nanocarriers: From nano to macro. Microsc. Res.Tech. 2010, 73: 813–823.
6. Banerjee, R.; Katsenovich, Y.; Lagos, L.; McIntosh, M.; Zhang, X.; Li, C.Z. Nanomedicine: Magnetic nanoparticles and theirbiomedical applications. Curr. Med. Chem. 2010, 17:3120–3141.
7. Rönkkö, T.; Pirjola, L.; Ntziachristos, L.; Heikkilä, J.; Karjalainen, P.; Hillamo, R.; Keskinen, J. Vehicle engines produce exhaustnanoparticles even when not fueled. Environ. Sci. Technol. 2014, 48: 2043–2050.
8. Evelyn, A.; Mannick, S.; Sermon, P.A. Unusual carbon-based nanofibers and chains among diesel-emitted particles. Nano Lett.2003, 3:63–64.
9. Van Dijk,W.D.; Gopal, S.; Scheepers, P.T.J. Nanoparticles in cigarette smoke; Real-time undiluted measurements by a scanningmobility particle sizer. Anal. Bioanal. Chem. 2011, 399: 3573–3578.
10. Williams, M.; Villarreal, A.; Bozhilov, K.; Lin, S.; Talbot, P. Metal and Silicate Particles Including Nanoparticles Are Present in Electronic Cigarette Cartomizer Fluid and Aerosol. PLoS ONE 2013, 8: e57987.
11. Lai, B.; Cui, G.;Wang, H.; Song, Y.; Tan, M. Identification of fluorescent nanoparticles from roasted sweet potato (Ipomoea batatas)during normal cooking procedures. LWT 2020, 134: 109989.
12. Park, J.; Ham, S.; Jang, M.; Lee, J.; Kim, S.; Kim, S.; Lee, K.; Park, D.; Kwon, J.; Kim, H.; et al. Spatial-Temporal Dispersion ofAerosolized Nanoparticles during the Use of Consumer Spray Products and Estimates of Inhalation Exposure. Environ. Sci.Technol. 2017, 51: 7624–7638.
13. Hewitt, R.E.; Chappell, H.F.; Powell, J.J. Small and dangerous? Potential toxicity mechanisms of common exposure particles andnanoparticles. Curr. Opin. Toxicol. 2020, 19:93–98.
14. Park, J.; Kwak, B.K.; Bae, E.; Lee, J.; Kim, Y.; Choi, K.; Yi, J. Characterization of exposure to silver nanoparticles in a manufacturingfacility. J. Nanopart. Res. 2009, 11: 1705–1712.
15. Chenthamara, D.; Subramaniam, S.; Ramakrishnan, S.G.; Krishnaswamy, S.; Essa, M.M.; Lin, F.H.; Qoronfleh, M.W. Therapeuticefficacy of nanoparticles and routes of administration. Biomater. Res. 2019, 23: 1–29.
16. El-Sayed, A.; Kamel, M. Advances in nanomedical applications: Diagnostic, therapeutic, immunization, and vaccine production. Environ. Sci. Pollut. Res. 2020, 27: 19200–19213.
17. Pan K, Zhong Q. Organic nanoparticles in foods: fabrication, characterization, and utilization. Annu Rev Food Sci Technol. 2016;7: 245–66.
18. Ealia SAM, Saravanakumar MP. A review on the classification, characterisation,synthesis of nanoparticles and their application. In: IOP ConferenceSeries: Materials Science and Engineering. IOP Publishing; 2017. p.32019.
19. Gujrati M, Malamas A, Shin T, Jin E, Sun Y, Lu Z-R. Multifunctional cationiclipid-based nanoparticles facilitate endosomal escape and reduction-triggered cytosolic siRNA release. Mol Pharm. 2014;11(8):2734–44.
20. (PAK-1) inhibitor IPA-3 limits prostate tumor growth in vivo. Nanomedicine 2016, 12, 1231–1239.
21. Laverman, P.; Brouwers, A.H.; Dams, E.T.; Oyen, W.J.; Storm, G.; van Rooijen, N.; Corstens, F.H.; Boerman, O.C. Preclinical and clinical evidence for disappearance of long-circulating characteristics of polyethylene glycol liposomes at low lipid dose. J. Pharmacol. Exp. Ther. 2000, 293, 996–1001.

22. Toshima N, Yonezawa T. Bimetallic nanoparticles—novel materials for chemical and physical applications. New J Chem. 1998;22(11):1179–201.

23. Nascimento MA, Cruz JC, Rodrigues GD, de Oliveira AF, Lopes RP. Synthesis of polymetallic nanoparticles from spent lithium-ion batteries and application in the removal of reactive blue 4 dye. J Clean Prod. 2018; 202:264–72.

24. Stuchinskaya, T.; Moreno, M.; Cook, M.J.; Edwards, D.R.; Russell, D.A. Targeted photodynamic therapy of breast cancer cells using antibody-phthalocyanine-gold nanoparticle conjugates. Photochem. Photobiol. Sci. 2011, 10, 822–831.

25. Deshmukh, S.P.; Patil, S.M.; Mullani, S.B.; Delekar, S.D. Silver nanoparticles as an effective disinfectant: A review. Mater Sci. Eng. C Mater Biol. Appl. 2019, 97, 954–965.

26. Kaushik Banerjee, Satyajit Das, Pritha Choudhury, Sarbari Ghosh, Rathindranath Baral, Soumitra Kumar Choudhuri. A novel approach of synthesizing and evaluating the anticancer potential of silver oxide nanoparticles in vitro, Chemotherapy, 2017, 62, 279-289.

27. Khan I, Saeed K, Khan I. Nanoparticles: properties, applications and toxicities. Arab J Chem. 2019;12(7):908–31.

28. Moreno-Vega A-I, Gomez-Quintero T, Nunez-Anita R-E, Acosta-Torres L-S, Castaño V. Polymeric and ceramic nanoparticles in biomedical applications. J Nanotechnol. 2012.

29. D'Amato R, Falconieri M, Gagliardi S, Popovici E, Serra E, Terranova G, et al. Synthesis of ceramic nanoparticles by laser pyrolysis: from research to applications. J Anal Appl Pyrolysis. 2013,104:461–9.

30. Wu,W.;Wu, Z.; Yu, T.; Jiang, C.; Kim,W.S. Recent progress on magnetic iron oxide nanoparticles: Synthesis, surface functional strategies and biomedical applications. Sci. Technol. Adv. Mater 2015, 16: 023501.

31. Gupta SM, Tripathi M. An overview of commonly used semiconductor nanoparticles in photocatalysis. High Energy Chem. 2012,46(1):1–9.

32. Sun S, Murray CB, Weller D, Folks L, Moser A. Monodisperse FePt nanoparticles and ferromagnetic FePt nanocrystal superlattices. Science (80-). 2000;287(5460):1989–92.

33. Mauter MS, Elimelech M. Environmental applications of carbon-based nanomaterials. Environ Sci Technol. 2008,42(16):5843–59.

34. Oh W-K, Yoon H, Jang J. Size control of magnetic carbon nanoparticles for drug delivery. Biomaterials. 2010;31(6):1342–8.

35. Liu M, Zhao F, Zhu D, Duan H, Lv Y, Li L, et al. Ultra-microporous carbon nanoparticles derived from metal–organic framework nanoparticles for high-performance supercapacitors. Mater Chem Phys. 2018, 211:234–41.

36. Chandra S, Das P, Bag S, Laha D, Pramanik P. Synthesis, functionalization and bioimaging applications of highly fluorescent carbon nanoparticles. Nanoscale. 2011,3(4):1533–40.

37. Mochalin VN, Shenderova O, Ho D, Gogotsi Y. The properties and applications of nanodiamonds. Nat Nanotechnol. 2012,7(1):11–23.

38. Al-Azayzih A, Missaoui WN, Cummings BS, Somanath PR. Liposome-mediated delivery of the p21 activated kinase-1 (PAK-1) inhibitor IPA-3 limits prostate tumor growth in vivo. Nanomedicine. 2016,12(5):1231-1239.

39. Vauthier, C.; Bouchemal, K.Methods for the preparation andmanufacture of polymeric nanoparticles. Pharm. Res. 2009, 26: 1025–1058.

40. Wang, Y.; Li, P.; Truong-Dinh Tran, T.; Zhang, J.; Kong, L. Manufacturing Techniques and Surface Engineering of Polymer BasedNanoparticles for Targeted Drug Delivery to Cancer. Nanomaterials (Basel) 2016,6(2):26

41. Ahmed, T.A.; Aljaeid, B.M. Preparation, characterization, and potential application of chitosan, chitosan derivatives, and chitosanmetal nanoparticles in pharmaceutical drug delivery. Drug Des. Devel. Ther. 2016, 10: 483–507.

42. Ganta, S.; Talekar, M.; Singh, A.; Coleman, T.P.; Amiji, M.M. Nanoemulsions in translational research-opportunities and challengesin targeted cancer therapy. AAPS Pharm. Sci. Tech. 2014, 15: 694–708.

43. Rai, V.K.; Mishra, N.; Yadav, K.S.; Yadav, N.P. Nanoemulsion as pharmaceutical carrier for dermal and transdermal drug delivery: Formulation development, stability issues, basic considerations and applications. J. Control Release 2017, 270: 203–225.

44. Gwinn MR, Vallyathan V, Nanoparticles: health effects—pros and cons, Environ. Health Perspect 2006, 114:1818–1825.

45. Akhtar S, Cationic nanosystems for the delivery of small interfering ribonucleic acid therapeutics: a focus on toxicogenomics, ExpetOpin. Drug Metabol. Toxicol 2010,6: 1347–1362.

46. Dick CA, Brown DM, Donaldson K, Stone V, The role of free radicals in the toxic and inflammatory effects of four different ultrafine particle types, Inhal. Toxicol 2003, 15: 39–52.

47. Shi H, Magaye R, Castranova V, Zhao J, Titanium dioxide nanoparticles: a review of current toxicological data, Part. FibreToxicol 2013, 10: 15.

48. Inoue K, Takano H, Aggravating impact of nanoparticles on immune-mediated pulmonary inflammation, Sci. Wor. J 2011, 11:382–390.

49. Tang L, Zhang C, Song G, Jin X, Xu Z, In vivo skin penetration and metabolic path of quantum dots, Science China, Life Sciences 2013, 56:181–188.

50. Nangia S, Sureshkumar R, Effects of nanoparticle charge and shape anisotropy on translocation through cell membranes, Langmuir 2012,28: 17666–17671.

51. Tak YK, Pal S, Naoghare PK, Rangasamy S, Song JM, Shape-dependent skin penetration of silver nanoparticles: does it really matter?Sci. Rep 2015, 5:16908.

52. Nel A, Xia T, Madler L, Li N, Toxic potential of materials at the nanolevel, Science2006, 311:622–627.

53. Piao MJ, Kang KA, Lee IK, Kim HS, Kim S, Choi JY, Choi J, Hyun JW, Silver nanoparticles induce oxidative cell damage in human liver cells through inhibition of reduced glutathione and induction of mitochondria-involved apoptosis, Toxicol. Lett 2011,201:92–100.

54. Raj S, Jose S, Sumod US, Sabitha M, Nanotechnology in cosmetics: opportunities and challenges, J. Pharm. BioAllied Sci 2012,4:186–193.

55. Wan R, Mo Y, Zhang Z, Jiang M, Tang S, Zhang Q, Cobalt nanoparticles induce lung injury, DNA damage and mutations in mice, Part. FibreToxicol 2017, 14:38.

56. Sarfraz M, Roa W, Bou-Chacra N, Lobenberg R, Inflammation caused by nanosized delivery systems: is there a benefit? Mol. Pharm 2016, 13:3270–3278.

57. Nazarenko Y, Han TW, Lioy PJ, Mainelis G, Potential for exposure to engineered nanoparticles from nanotechnology-based consumer spray products, J. Expo. Sci. Environ. Epidemiol 2011, 21:515–528.

58. Risom L, Moller P, Loft S, Oxidative stress-induced DNA damage by particulate air pollution, Mutat. Res 2005,592, 119–137.

59. Mehta M, Chen LC, Gordon T, Rom W, Tang MS, Particulate matter inhibits DNA repair and enhances mutagenesis, Mutat. Res 2008,657, 116–121.

60. Rollerova E, Tulinska J, Liskova A, Kuricova M, Kovriznych J, Mlynarcikova A, Kiss A, Scsukova S, Titanium dioxide nanoparticles: some aspects of toxicity/focus on the development, Endocr. Regul 2015, 49:97–112.

61. Schulte P, Geraci C, Zumwalde R, Hoover M, Kuempel E, Occupational risk management of engineered nanoparticles, J. Occup. Environ. Hyg 2008,5:239–249.

62. Scown TM, Santos EM, Johnston BD, Gaiser B, Baalousha M, Mitov S, Lead JR, Stone V, Fernandes TF, Jepson M, van Aerle R, Tyler CR, Effects of aqueous exposure to silver nanoparticles of different sizes in rainbow trout, Toxicol. Sci.: An Official Journal of the Society of Toxicology1 2010,15:521–534.

63. Shang L, Nienhaus K, Nienhaus GU, engineered nanoparticles interacting with cells: size matters, J. Nanobiotechnol 2014, 12:5.

64. Iavicoli I, Leso V, Beezhold DH, Shvedova AA, Nanotechnology in agriculture: opportunities, toxicological implications, and occupational risks, Toxicol. Appl. Pharmacol 2017,329:96–111.

65. Oberdörster G, Maynard A, Donaldson K et al. Principles for characterizing the potential human health effects from exposure to nanomaterials: elements of a screening strategy. Part Fibre Toxicol 2005, 2:8.

66. Yang Y, Qin Z, Zeng W et al. Toxicity assessmentof nanoparticles in various systems and organs.Nanotechnol Rev 2017, 6(3):279–289.

67. Longmire M, Choyke PL, Kobayashi H. Clearance properties of nano-sized particles and molecules as imaging agents: considerations and caveats. Nanomedicine (Lond) 2008, 3(5):703–717

68. Blanco E, Shen H, Ferrari M. Principles ofnanoparticle design for overcoming biological barriers to drug delivery. Nat Biotechnol2015, 33(9):941–951.

69. Doudi M, Setorki M. The acute liver injuryin rat caused by gold nanoparticles. Nanomedicine J 2014, 1:248–257

70. Gaiser BK, Hirn S, Kermanizadeh A et al. Effects of silver nanoparticles on the liver and hepatocytesin vitro. Toxicol Sci2012, 131:537–547.

71. Tang J, Xiong L, Zhou G et al. Silver nanoparticles crossing through and distribution in the blood-brain barrier In vitro. J Nanosci Nanotechnol 2010, 10(10):6313–6317.

72. Choi HS, Liu W, Misra P et al. Renal clearance of nanoparticles. Nat Biotechnol2007, 25:1165–1170.

73. Tseng WK, Chieh JJ, Yang YF, Chiang CK, Chen YL, Yang SY, Horng HE, Yang HC, Wu CC, A noninvasive method to determine the fate of Fe(3)O(4) nanoparticles following intravenous injection using scanning SQUID biosusceptometry, PLoS One 2012,7: e48510.

74. Kim YS, Song MY, Park JD, Song KS, Ryu HR, Chung YH, Chang HK, Lee JH, Oh KH, Kelman BJ, Hwang IK, Yu IJ, Subchronic oral toxicity of silver nanoparticles, Part. FibreToxicol2010, 7:20.

75. Wang C, Cheng K, Zhou L, He J, Zheng X, Zhang L, Zhong X, Wang T, Evaluation of long-term toxicity of oral zinc oxide nanoparticles and zinc sulfate in mice, Biol. Trace Elem. Res 2017,178: 276–282.

76. Bartneck M, Ritz T, Keul HA, Wambach M, Bornemann J, Gbureck U, Ehling J, Lammers T, Heymann F, Gassler N, Ludde T, Trautwein C, Groll J, Tacke F, Peptide-functionalized gold nanorods increase liver injury in hepatitis, ACS Nano 2012,6: 8767–8777.

77. Dumkova J, Smutna T, Vrlikova L, Le Coustumer P, Vecera Z, Docekal B, Mikuska P, Capka L, Fictum P, Hampl A, Buchtova M, Sub-chronic inhalation of lead oxide nanoparticles revealedtheir broad distribution and tissue-specific subcellular localization in target organs, Part. FibreToxicol 2017,14: 55.

78. Wiemann M, Vennemann A, Blaske F, Sperling M, Karst U, Silver Nanoparticles in the Lung: Toxic Effects and Focal Accumulation of Silver in Remote Organs vol. 7, Nanomaterials, Basel, Switzerland), 2017,7(12):441.

79. Couto D, Freitas M, Costa VM, Chiste RC, Almeida A, Lopez-Quintela MA, Rivas J, Freitas P, Silva P, Carvalho F, Fernandes E, Biodistribution of polyacrylic acid-coated iron oxide nanoparticles is associated with proinflammatory activation and liver toxicity, J. Appl. Toxicol. : JAT (J. Appl. Toxicol.) 2016,36: 1321–1331.

80. Nahar M, Jain NK, Preparation, characterization and evaluation of targeting potential of amphotericin B-loaded engineered PLGA nanoparticles, Pharm. Res. (N. Y.) 2009,26 :2588–2598.

81. Park EJ, Kim SW, Yoon C, Kim Y, Kim JS, Disturbance of ion environment and immune regulation following biodistribution of magnetic iron oxide nanoparticles injected intravenously, Toxicol. Lett.2016,243: 67–77.

82. Sung JH, Ji JH, Park JD, Yoon JU, Kim DS, Jeon KS, Song MY, Jeong J, Han BS, Han JH, Chung YH, Chang HK, Lee JH, Cho MH, Kelman BJ, Yu IJ, Subchronic inhalation toxicity of silver nanoparticles, Toxicol. Sci.: Offic. J. Soc. Toxicol 2009,108: 452–461.

83. Warheit DB, Sayes CM, Frame SR, Reed KL, Pulmonary exposures to Sepiolite nanoclay particulates in rats: resolution following multinucleate giant cell formation, Toxicol. Lett 2010,192: 286–293.

84. Gosens I, Cassee FR, Zanella M, Manodori L, Brunelli A, Costa AL, Bokkers BG, de Jong WH, Brown D, Hristozov D, Stone V, Organ burden and pulmonary toxicity of nano-sized copper (II) oxide particles after short-term inhalation exposure, Nanotoxicology 2016, 10: 1084–1095.

85. Bhirde AA, Patel S, Sousa AA, Patel V, Molinolo AA, Ji Y, Leapman RD, Gutkind JS, Rusling JF, Distribution and clearance of PEG-single-walled carbon nanotube cancer drug delivery vehicles in mice, Nanomedicine 2010,5: 1535–1546.

86. Missaoui, Wided N et al. "Toxicological status of nanoparticles: What we know and what we don't know." Chemico-biological interactions 2018, 295: 1-12.

87. Coccini T, Barni S, Mustarelli P, Locatelli C, Roda E, One-month persistence of inflammation and alteration of fibrotic marker and cytoskeletal proteins in rat kidney after Cd-doped silica nanoparticle instillation, Toxicol. Lett 2015, 232: 449–457.

88. Chen X, Zhouhua W, Jie Z, Xinlu F, Jinqiang L, Yuwen Q, Zhiying H, Renal interstitial fibrosis induced by high-dose mesoporous silica nanoparticles via the NF-kappaB signaling pathway, Int. J. Nanomed 2015, 10: 1–22.

89. Hoet PH, Bruske-Hohlfeld I, Salata OV, Nanoparticles - known and unknown health risks, J. Nanobiotechno 2004, I2: 12.

90. Oberdorster E, Manufactured nanomaterials (fullerenes, C60) induce oxidative stress in the brain of juvenile largemouth bass, Environ. Health Perspect 2004,112: 1058–1062.

Surajit Majumder *et al.,*

91. Sharma HS, Sharma A, Nanoparticles aggravate heat stress induced cognitive deficits, blood-bloodbrain barrier disruption, edema formation and brain pathology, Prog. Brain Res 2007, 162: 245–273.

92. Yang Z, Liu ZW, Allaker RP, Reip P, Oxford J, Ahmad Z, Ren G, A review of nanoparticle functionality and toxicity on the central nervous system, J. R. Soc. Interface 2010,7 (4): S411–S422.

93. Shrivastava R, Raza S, Yadav A, Kushwaha P, Flora SJ, Effects of sub-acute exposure to TiO2, ZnO and Al2O3 nanoparticles on oxidative stress and histological changes in mouse liver and brain, Drug Chem. Toxicol 2014,37: 336–347.

94. Kim YR, Park SH, Lee JK, Jeong J, Kim JH, Meang EH, Yoon TH, Lim ST, Oh JM, An SS, Kim MK, Organization of research team for nano-associated safety assessment in effort to study nanotoxicology of zinc oxide and silica nanoparticles, Int. J. Nanomed 2014, 9 (2): 3–10.

95. Korani M, Rezayat SM, Gilani K, ArbabiBidgoli S, Adeli S, Acute and subchronic dermal toxicity of nanosilver in Guinea pig, Int. J. Nanomed 2011, 6: 855–862.

96. Khanna P, Ong C, Bay BH, Baeg GH, Nanotoxicity: an Interplay of Oxidative Stress, Inflammation and Cell Death, Nanomaterials, Basel, Switzerland, 2015, 5: 1163–1180.

97. Teodoro JS, Silva R, Varela AT, Duarte FV, Rolo AP, Hussain S, Palmeira CM, Low-dose, subchronic exposure to silver nanoparticles causes mitochondrial alterations in Sprague-Dawley rats, Nanomedicine 2016, 11: 1359–1375.

98. Wang J, Chen C, Liu Y, Jiao F, Li W, Lao F, Li Y, Li B, Ge C, Zhou G, Gao Y, Zhao Y, Chai Z, Potential neurological lesion after nasal instillation of TiO(2) nanoparticles in the anatase and rutile crystal phases, Toxicol. Lett 2008, 183: 72–80.

99. Ze Y, Zheng L, Zhao X, Gui S, Sang X, Su J, Guan N, Zhu L, Sheng L, Hu R, Cheng J, Cheng Z, Sun Q, Wang L, Hong F, Molecular mechanism of titanium dioxide nanoparticles-induced oxidative injury in the brain of mice, Chemosphere 2013, 92: 1183–1189.

100. Eom H-J, Choi J. p38 MAPK activation, DNA damage, cell cycle arrest and apoptosis as mechanisms of toxicity of silver nanoparticles in Jurkat T cells. Environ Sci Technol2010, 44:8337–8342.

101. Talkar, Swapnil et al. "Transmucosal Nanoparticles: Toxicological Overview." Advances in experimental medicine and biology 2018,1048: 37-57.

102. Shang W, Nuffer JH, Dordick JS et al. Unfolding of ribonuclease A on silica nanoparticle surfaces. Nano Lett2007, 7:1991–1995.

103. Manshian BB, Poelmans J, Saini S, Pokhrel S, Grez JJ, Himmelreich U, Mädler L, Soenen SJ, Nanoparticle-induced inflammation can increase tumor malignancy, Acta Biomater 2018, 68: 99–112.

104. Pandey RK, Prajapati VK, Molecular and immunological toxic effects ofnanoparticles, Int. J. Biol. Macromol. 2018,107 (Pt A) : 1278–1293,

105. Roy R, Kumar S, Tripathi A, Das M, Dwivedi PD, Interactive threats of nanoparticles to the biological system, Immunol. Lett 2014,158: 79–87.

106. Moon C, Park HJ, Choi YH, Park EM, Castranova V, Kang JL, Pulmonary inflammation after intraperitoneal administration of ultrafine titanium dioxide (TiO2) at rest or in lungs primed with lipopolysaccharide, J. Toxicol. Environ. Health Part 2010,a73: 396–409.

107. Sierra MI, Valdes A, Fernandez AF, Torrecillas R, Fraga MF, The effect of exposure to nanoparticles and nanomaterials on the mammalian epigenome, Int. J. Nanomed 2016, 11: 6297–6306.

108. Shyamasundar S, Ng CT, Yung LY, Dheen ST, Bay BH, Epigenetic mechanisms in nanomaterial-induced toxicity, Epigenomics 2015,7: 395–411.

109. Smolkova B, El Yamani N, Collins AR, Gutleb AC, Dusinska M, Nanoparticles in food. Epigenetic changes induced by nanomaterials and possible impact on health, Food Chem. Toxicol.: Int. J. Pub. Br. Ind. Biol. Res. Assoc 2015,77: 64–73.

110. Brown TA, Lee JW, Holian A, Porter V, Fredriksen H, Kim M, Cho YH, Alterations in DNA methylation corresponding with lung inflammation and as a biomarker for disease development after MWCNT exposure, Nanotoxicology 2016,10: 453–461.

111. Lu X, Miousse IR, Pirela SV, Melnyk S, Koturbash I, Demokritou P, Short-term exposure to engineered nanomaterials affects cellular epigenome, Nanotoxicology 2016,10: 140–150.

Surajit Majumder *et al.*,

112. Gong C, Tao G, Yang L, Liu J, Liu Q, Zhuang Z, SiO(2) nanoparticles induce global genomic hypomethylation in HaCaT cells, Biochem. Biophys. Res. Commun 2010,397: 397–400.

113. Bai W, Chen Y, Gao A, Cross talk between poly(ADP-ribose) polymerase 1 methylation and oxidative stress involved in the toxic effect of anatase titanium dioxide nanoparticles, Int. J. Nanomed 2015,10: 5561–5569.

114. Bai W, Chen Y, Gao A, Cross talk between poly (ADP-ribose) polymerase 1 methylation and oxidative stress involved in the toxic effect of anatase titanium dioxide nanoparticles, Int. J. Nanomed 2015,10: 5561–5569.

115. Recordati C, De Maglie M, Bianchessi S, Argentiere S, Cella C, Mattiello S, Cubadda F, Aureli F, D'Amato M, Raggi A, Lenardi C, Milani P, Scanziani E, Tissue distribution and acute toxicity of silver after single intravenous administration in mice: nano-specific and size- sizedependent effects, Part. FibreToxicol 2016,13: 12.

116. Paek HJ, Lee YJ, Chung HE, Yoo NH, Lee JA, Kim MK, Lee JK, Jeong J, Choi SJ, Modulation of the pharmacokinetics of zinc oxide nanoparticles and their fates in vivo, Nanoscale 2013,5: 11416–11427.

117. Bhattacharjee S, Haan LHJD, Evers NM et al. Role of surface charge and oxidative stress in cytotoxicity of organic monolayer-coated silicon nanoparticles towards macrophage NR8383 cells. Part Fibre Toxicol 2010, 7:25.

118. Wick P, Manser P, Limbach L et al The degreeand kind of agglomeration affect carbon nanotube cytotoxicity. Toxicol Lett 2007, 168:121–131.

119. Simpson CA, Salleng KJ, Cliffel DE, Feldheim DL, In vivo toxicity, biodistribution, and clearance of glutathione-coated gold nanoparticles, Nanomedicine. 2013,9: 257–263.

120. Dr. Surajit Majumder, Associate Professor, Dept. of Zoology, Bankura Sammilani College, Bankura- 722102, West Bengal, India; surajitnajumder.sm@gmail.com. * Communicating author.

121. Dr. Dipankar Saha, Part-time researcher, Dept. of Zoology, Bankura Sammilani College, Bankura-722102, West Bengal, India, dipankar275@gmail.com

122. Dr. Soumitra Kumar Choudhuri, Former HOD and Emeritus Medical Scientist, Chattaranjan National Cancer Institute, Calcutta-700 026, West Bengal, India; soumitrag10@gmail.com

www.tnsroindia.org.in ©IJONS

RESEARCH ARTICLE

Generalized Semi Operators in Soft Multi Topological Spaces

Inthumathi Velusamy [1], Gnanasoundari Arunagiri [2]* and Maheswari Marimuthu [2]

[1]Associate Professor, PG and Research Department of Mathematics, Nallamuthu Gounder Mahalingam College, Pollachi-642 001, Coimbatore, Tamil Nadu, India.
[2]Assistant Professor, PG and Research Department of Mathematics, Nallamuthu Gounder Mahalingam College, Pollachi-642 001, Coimbatore, Tamil Nadu, India.

*Address for Correspondence
Gnanasoundari Arunagiri
Assistant Professor,
PG and Research Department of Mathematics,
Nallamuthu Gounder Mahalingam College,
Pollachi-642 001, Coimbatore, Tamil Nadu, India.
E.Mail: gnana.ngm@gmail.com

ABSTRACT

This paper's major goal is to investigate the properties of generalized semi soft multi course and generalized semi soft multi interior with the help of generalized semi closed soft multiset and generalized semi open soft multiset notions and to acquaint the conception of generalized semi soft multi neighbor hoods.

INTRODUCTION

In 2013, Babitha and John [1] was acquainted the conception of soft multisets as a combination of soft sets and multisets. Then Deniz Tokat et al. [2,3] acquainted the concept of the soft multi topology and its basic properties. S. A. El-Sheikh et al. [4,5] acquainted the generalized closed soft multisets and generalization of open soft multisets and mappings in soft multi topological spaces. In 2022, Inthumathi et al. [6] acquainted the concept of generalized semi closed set in soft multi topological space. In this paper, we acquaint the conception of generalized semi soft multi closure, generalized semi soft multi interior and generalized semi soft multi neighbourhood and discuss few important attributes in detail.

Inthumathi Velusamy *et al.,*

PRELIMINARIES

Throughout this paper, SMTS denotes the soft multi topological spaces and smset denotes soft multi set.

Definition 2.1. [3] Let M be an universal mset, L be a set of parameters and $I \subseteq L$. Then, an ordered pair (S, I) is called a smset where S is a mapping given by $S : I \to P^*(M)$; $P^*(M)$ is the power set of a mset M. For all l ∈ I, S(l) mset represents by count function $C_{S(l)}: M^* \to N$ where N represents the set of non-negative integers and M^* represents the support set of M.

Definition 2.2. [3] For two soft msets(S, I) and (T, J) over M, we say that is a subs mset of if:

Definition 2.2. [3] For two soft m sets(S, I) and (T, J) over M, we say that (S, I) is a subsmsetof(T, J)if:
1.$I \subseteq J$,
2.$C_{S(l)}(v) \leq C_{T(l)}(v), \forall v \in M^*, \forall\ l \in I \cap J$.
We write $(S, I) \widetilde{\subseteq} (T, J)$.

Definition 2.3.[3] The union of two smsets(S, I) and (T, J)over $M$is the smset(H, C),where$C = I \cup J$and$C_{H(l)}(v) = \max\{C_{S(l)}(v), C_{T(l)}(v)\}, \forall l \in I \cup J, \forall\ v \in M^*$.We write$(S, I) \widetilde{\cup} (T, J)$.

Definition 2.4. [3] The intersection of two soft msets(S, I) and (T, J)over $M$is the smset(H, C),where$C = I \cap J$and$C_{H(l)}(v) = \min\{C_{S(l)}(v), C_{T(l)}(v)\}, \forall l \in I \cap J, \forall\ v \in M^*$.We write$(S, I) \widetilde{\cap} (T, J)$.

Definition2.5. [3] A soft mset (S, I) over M is said to be a null smset denoted $\widetilde{\phi}$ if for all $l \epsilon I, S(l) = \phi$.

Definition2.6. [3] A soft mset(S, I)over M is said to be an absolute smset denoted by $\widetilde{M}$ for all $l \epsilon I, S(l) = M$
Definition2.7.[3] The complement of a smset (S, I) is denoted by $(S, I)^c$ and is defined by $(S, I)^c = (S^c, I)$ where $S^c: I \to P^*(M)$ is mapping given by $S^c(l) = M \backslash S(l)$for all $l \epsilon I$ where $C_{S^c(l)}(v) = C_{U(l)}(v) - C_{S(l)}(v), \forall\ v \in M^*$.

Definition 2.8.[3] Let Mbe an universal mset and$L$be a set of parameters. Then, the collection of all smsets over M with parameters from$L$is called a soft multi class and is denoted as $SMS(M)_L$.

Definition 2.9. [3] Let$\tau \subseteq$ SMS(M)$_L$, then τ is said to be a soft multi topology on$M$if the following conditions hold:
1. $\widetilde{\phi}, \widetilde{M}$ belong to τ
2. The union of any number of smsets in τ belongs to τ,
3. The intersection of any two smsets in τ belongs to τ
τ is called a soft multi topology over M and the triple (M, τ, L) is called a soft multi topological space over M. Also, the member of τ are said to be open soft msets in M. A soft mset (S, L) in $SMS(M)_L$ is said to be a closed soft mset in M, if its complement$(S, L)^c$ belongs to τ.

Definition 2.10. Let (M, τ, L) be a SMTS over $M$and (S, L) be a smset over M.Then, the softmulti closure of(S, L), denoted by$cl(S, L)[\ or\ \overline{(S, L)}]$ is the intersection of all closed smset containing(S, L).

Definition 2.11. [2] Let (M, τ, L) be a SMTS over M and (S, L)be a smset over M. Then, the soft multi interior of (S, L), denoted by int (S,L) $[or\ (S, L)^o]$ is the union of all open soft multiset contained in(S,L).

Inthumathi Velusamy *et al.*,

Definition 2.12. Let (M, τ, L) be a SMTS over M and (G, L) be a smset over M and $v \in M$. Then, (G, L) is said to be a soft multi neighbourhood of v if there exists a soft multi open set (F, L) such that $v \in (F, L) \subseteq (G, L)$. The set of all soft multi neighbourhood of α, denoted by $\widetilde{N}(\alpha)$, is called the family of soft multi neighbourhoods of α,

i.e. $\widetilde{N}(\alpha) = \{(G, L) : (G, L) \in \tau, \alpha \in (G, L)\}$.

Definition 2.13. Let (M, τ, L) be a SMTS. A mapping $\gamma : SMS(M)_L \to SMS(M)_L$ is said to be an operation on $OSM(M)_L$, if $N_L \subseteq \gamma(N_L)$ for all $N_L \in OSM(M)_L$. The family of all γ-open soft multi sets is denoted by $OSM(\gamma) = \{N_L : N_L \subseteq \gamma(N_L), N_L \in SMS(M)_L\}$. Also, the complement of γ-open soft multiset is called a γ-closed soft multiset and the set of all γ-closed soft multisets denoted by $CSM(\gamma)$.

Definition 2.14. [5] Let(M, τ, L) be a SMTS. Different cases of -operations on SMS $(M)_L$ are as follows:

i.   If γ = int(cl),then γ is called a pre-open soft multi operator. The family of all pre-open soft multisets is denoted by POSM $(M)_L$ and the family of all pre-closed soft multisets is denoted by PCSM $(M)_L$.

ii. If γ = int(cl(int)),then γ is called an -open soft multi operator. The family of all - open soft multisets is denoted by αOSM $(M)_L$ and family fall-closed soft multisets is denoted by αCSM $(M)_L$

iii. If γ = cl(int),then is called a semi open soft multi operator. The family of all semi opensoft multisets is denoted by SOSM $(M)_L$ and the family of all semi closed soft multisets is denoted by SCSM (X)L.

iv. If γ = cl(int(cl)),then γ is called a-open soft multi operator. The family of all -open soft multisets is denoted by βOSM $(M)_L$ and family fall-closed soft multisets is denoted by βCSM $(M)_L$

Definition 2.15. A smset (S, L) in a SMTS (M, τ, L) is said to be a generalized closed (briefly g-closed) smset if $C_{cl(S)(l)}(v) \leq C_{B(l)}(v)$ whenever $C_{S(l)}(v) \leq C_{B(l)}(v)$ for all $v \in M^*, l \in L$ and (B, L) is open smset in M_L.

Definition 2.16. A soft mset S_L in a SMTS (M, τ, L) is said to be a generalized semi closed softmulti set (briefly $gscs$ mset) if $C_{scl(S)(l)}(v) \leq C_{U(l)}(v)$ whenever $C_{(S)(l)}(v) \leq C_{U(l)}(v)$ and $U_L \in OSM(M)_L$.

Definition 2.17.[6] Let f_L be a smset over M_L. f_L is called a smpoint over M, if there exists $l \in L$ and $n/v \in M, 1 \leq n \leq m$ such that

$$f(\varepsilon) = \begin{cases} \{n/v\} \ if \varepsilon = l, 1 \leq n \leq m \\ \varphi \ \ if \ \varepsilon \in L - \{l\} \end{cases}$$

We denote f_L by $[(n/v)_l]_L$. The family of all smpoints over M is denoted by $P(M, L)$ or P.

i.e. $P(M, L) = \{[(n/v_i)l_j]_L : v_i \in M, l_j \in L, 1 \leq n \leq m\}$.

GENERALIZED SEMI SOFT MULTI CLOSURE

Definition 3.1. Let S_L be a smset over M_L. Then the generalized semi soft multi closure of S_L, denoted by gssm-cl(S_L), is the intersection of all gsc smsets containing S_L.

Proposition 3.2. *For any* $C_{S(l)}(v) \leq C_{M(l)}(v)$,

1. $C_{S(l)}(v) \leq C_{gssm-cl(S)(l)}(v) \leq C_{scl(S)(l)}(v)$
2. $C_{S(l)}(v) \leq C_{gssm-cl(S)(l)}(v) \leq C_{\alpha cl(S)(l)}(v)$
3. $C_{S(l)}(v) \leq C_{gssm-cl(S)(l)}(v) \leq C_{gcl(S)(l)}(v)$

Proof. Since every semi closed (resp. α-closed, g-closed) smsts gsc smset.

Proposition 3.3. *For any two sub smsets* S_L *and* T_L *of* M_L. *The following hold,*

1. *If* S_L *is a gscs mset,then* $C_{gssm-cl(S)(l)}(v) = C_{S(l)}(v)$,
2. $C_{gssm-cl(\varphi)(l)}(v) = C_{\varphi(l)}(v)$, *and* $C_{gssm-cl(M)(l)}(v) = C_{M(l)}(v)$,

64297

Inthumathi Velusamy *et al.*,

3. If $C_{S(l)}(v) \leq C_{T(l)}(v)$, then $C_{gssm-cl(S)(l)}(v) \leq C_{gssm-cl(T)(l)}(v)$,

4. $C_{gssm-cl(S \cap T)(l)}(v) \leq C_{(gssm-cl(S) \cap gssm-cl(T))(l)}(v)$

5. $C_{gssm-cl(S \cup T)(l)}(v) \geq C_{(gssm-cl(S) \cup gssm-cl(T))(l)}(v)$

6. $C_{gssm-cl(gssm-cl(S))(l)}(v) \leq C_{gssm-cl(S)(l)}(v)$.

Proof.

1. If S_L is a gscs mset, then the smallest gsc smset containing S_L is itself. Therefore $C_{gssm-cl(S)}v = C_{S(l)}(v)$.

2. Since $\tilde{\varphi}$ and $\tilde{M}$ are *gscs* mset, $C_{gssm-cl(\varphi)(l)}(v) = C_{\varphi(l)}(v)$ *and* $C_{gssm-cl(M)(l)}(v) = C_{M(l)}(v)$ *by (1)*.

3. Let $C_{S(l)}(v) \leq C_{T(l)}(v)$. Then $C_{S(l)}(v) \leq C_{T(l)}(v) \leq C_{gssm-cl(T)(l)}(v)$. But $gssm-cl(S_L)$ is the smallest *gssm* closure of S_L. Therefore $C_{gssm-cl(S)(l)}(v) \leq C_{gssm-cl(T)(l)}(v)$.

4. Since $C_{S \cap T(l)}(v) \leq C_{S(l)}(v)$ and $C_{S \cap T(l)}(v) \leq C_{T(l)}(v)$, by (3) $C_{gssm-cl(S \cap T)(l)}(v) \leq C_{gssm-cl(S)(l)}(v)$ and $C_{gssm-cl(S \cap T)(l)}(v) \leq C_{gssm-cl(T)(l)}(v)$. Wherefore $C_{gssm-cl(S \cap T)(l)}(v) \leq C_{(gssm-cl(S) \cap gssm-cl(T))(l)}(v)$.

5. Since $C_{S(l)}(v) \leq C_{S \cup T(l)}(v)$ and $C_{T(l)}(v) \leq C_{S \cup T(l)}(v)$,

   $C_{gssm-cl(S)(l)}(v) \leq C_{gssm-cl(S \cup T)(l)}(v)$ and $C_{gssm-cl(T)(l)}(v) \leq C_{gssm-cl(S \cup T)(l)}(v)$. Thus $C_{gssm-cl(S \cup T)(l)}(v) \geq C_{(gssm-cl(S) \cup gssm-cl(T))(l)}(v)$.

6. Let $C_{S(l)}(v) \leq C_{F(l)}(v)$ and F_L be a *gscs* mset. Then by definition $C_{gssm-cl(S)(l)}(v) \leq C_{F(l)}(v)$ and $C_{gssm-cl(gssm-cl(S))(l)}(v) \leq C_{F(l)}(v)$. Since $C_{gssm-cl(gssm-cl(S))(l)}(v) \leq C_{\cap\{T_L / C_{S(l)}(v) \leq C_{T(l)}(v) \text{ and where } T_L \text{ be a } gscs \text{ mset}\}} = C_{gssm-cl(S)(l)}(v)$. Ergo $C_{gssm-cl(gssm-cl(S))(l)}(v) \leq C_{gssm-cl(S)(l)}(v)$ by Proposition3.2.

Note 3.1. Reverse implication of the above result (1) need not be true. Let (M, τ, L) be a SMTS with mset $M = \{2/v_1, 2/v_2\}$, parameter set $L = \{l_1, l_2\}$ and smtopology $\tau = \{\tilde{\varphi}, \tilde{M}, S_L\}$ where $S(l_1) = \{2/v_1\}, S(l_2) = \{2/v_2\}$ and let T_L be a sub smset of M_L such that $T(l_1) = \{\varphi\}, T(l_2) = \{1/v_1\}$. Then $C_{gssm-cl(T)(l)}(v) = C_{T(l)}(v)$ but T_L is not a *gscs* mset.

Definitions 3.4. A sub smset S_L in (M, τ, L) is called generalized semi open soft multi set (insummary *gsos* mset) if its complement is a *gscs* mset. The set of all *gsos* mset in (M, τ, L) is denoted by $gsosm(M)_L$.

Theorem 3.5. A sub smset S_L of (M, τ, L) is *gsos* mset iff $C_{F(l)}(v) \leq C_{sint(S)(l)}(v)$ whenever $C_{F(l)}(v) \leq C_{S(l)}(v)$ and F_L is a closed smset.

Proof. Suppose that $C_{F(l)}(v) \leq C_{sint(S)(l)}(v)$ whenever $C_{F(l)}(v) \leq C_{S(l)}(v)$ and F_L is a closed smset. Let $C_{S^c(l)}(v) \leq C_{U(l)}(v)$, where U_L is a open smset. Then $C_{U^c(l)}(v) \leq C_{S(l)}(v)$, where $U_L{}^c$ is a closed smset. By proposal $C_{U^c(l)}(v) \leq C_{sint(S)(l)}(v)$, which implies $C_{(sint(S))^c(l)}(v) \leq C_{U(l)}(v)$. That is $C_{scl(S^c)(l)}(v) \leq C_{U(l)}(v)$. Thus $S_L{}^c$ is a *gscs* mset. Consequently S_L is a *gsos* mset.

Conversely, suppose that S_L is a *gsos* mset such that $C_{F(l)}(v) \leq C_{S(l)}(v)$ and F_L is a closed smset. Then $F_L{}^c$ is a open smset and $C_{S^c(l)}(v) \leq C_{F^c(l)}(v)$. Ergo $C_{scl(S^c)(l)}(v) \leq C_{F^c(l)}(v)$ and so $C_{F(l)}(v) \leq C_{(scl(S^c))^c(l)}(v) = C_{sint(S)(l)}(v)$. Hence $C_{F(l)}(v) \leq C_{sint(S)(l)}(v)$.

.

Proposition 3.6. *For a SMTS* (M,τ,L), *the following hold*

i.   *Every open smset is a* gsos *mset.*

ii. *Every-open smset is a* gsos *mset.*

iii. *Every semi open smset is a* gsos *mset.*

iv. *Every* g-*open smset is a* gsos *mset.*

Inthumathi Velusamy *et al.*,

Proof.

(i)Let$S_L$be a open smset and $F_L$be a closed smset such that $C_{F(l)}(v) \leq C_{S(l)}(v)$. Then$F_L{}^c$is a open smset and$C_{S^c(l)}(v) \leq C_{F^c(l)}(v)$. Wherefore$C_{scl(S^c)(l)}(v) \leq C_{cl(S^c)(l)}(v) = C_{S^c(l)}(v) \leq C_{F^c(l)}(v)$. That is$C_{F(l)}(v) \leq C_{(scl(S^c))^c(l)}(v) = C_{sint(S)(l)}(v)$. Hence$C_{F(l)}(v) \leq C_{sint(S)(l)}(v)$. Therefore S_L is a *gsos* mset.

(ii) Let$S_L$be an α-open smset and $F_L \in CSM\ (M)_L$such that $C_{F(l)}(v) \leq C_{S(l)}(v)$. Then $F_L{}^c$is a open smset and$C_{S^c(l)}(v) \leq C_{F^c(l)}(v)$.Therefore$C_{scl(S^c)(l)}(v) \leq C_{\alpha cl(S^c)(l)}(v) = C_{S^c(l)}(v) \leq C_{F^c(l)}(v)$. That is$C_{F(l)}(v) \leq C_{(scl(S^c))^c(l)}(v) = C_{sint(S)(l)}(v)$. Hence$C_{F(l)}(v) \leq C_{sint(S)(l)}(v)$. Therefore$S_Lisagsos$mset.

(iii) Let $S_L$be a semi-open smset and $F_L \in CSM\ (M)_L$such that $C_{F(l)}(v) \leq C_{S(l)}(v)$.Then$F_L{}^c$is a open smset and$C_{S^c(l)}(v) \leq C_{F^c(l)}(v)$.Therefore $C_{scl(S^c)(l)}(v) = C_{S^c(l)}(v) \leq C_{F^c(l)}(v)$ .Hence$C_{F(l)}(v) \leq C_{sint(S)(l)}(v)$. Ergo S_L is a $gsos$mset.

(iv)Let$S_L$bea *g*-open smset and $F_L \in CSM\ (M\ )_L$suchthat $C_{F(l)}(v) \leq C_{S(l)}(v)$. Then $F_L{}^c$is a open smset and$C_{S^c(l)}(v) \leq C_{F^c(l)}(v)$. Therefore$C_{scl(S^c)(l)}(v) \leq C_{cl(S^c)(l)}(v) \leq C_{F^c(l)}(v)$. Hence$C_{F(l)}(v) \leq C_{sint(S)(l)}(v)$. Ergo S_L is a $gsos$ mset.

Remark 3.7.1.

1. The union of gsos msets need not be a gsosmset.

2.The intersection of gsos msets need not be a gsosmset.

The Intersection of gsos msets need not be a gsos mset.

Example 3.8. Let (M, τ, L)be a SMTSwith mset $M = \{1/v_1, 2/v_2, 1/v_3\}$, parameter set $L = \{l_1, l_2\}$ and smtopology $\tau = \{\widetilde{\varphi}, \widetilde{M}, (S_L)_1, (S_L)_2, (S_L)_3, (S_L)_4\}\ whereS_1(l_1) = \{1/v_1, 1/v_3\}$, $S_1(l_2) = \{1/v_1, 1/v_3\}$, $S_2(l_1) = \{1/v_1\}$, $S_2(l_2) = \{1/v_3\}$, $S_3(l_1) = \{2/v_2\}$, $S_3(l_2) = \{2/v_2\}, S_4(l_1) = \{1/v_1, 2/v_2\}$, $S_4(l_2) = \{2/v_2, 1/v_3\}$. Let $S_L$and $T_L$be two subsmsets of $M_L$such that $S(l_1) = \{1/v_3\}$, $S(l_2) = \{2/v_2, 1/v_3\}$and $T(l_1) = \{1/v_2\}$, $S(l_2) = \{1/v_1, 1/v_2, 1/v_3\}$. Then $S_L$and $T_L$are $gsos$msetsbut$S_L \widetilde{\cup} T_L$ is not a $gsos$ mset in (M, τ, L).

Example 3.9. Let (M, τ, L) be a SMTS with mset$M = \{2/v_1, 2/v_2, 2/v_3\}$, parameter set $L = \{l_1, l_2\}$andsmtopology$\tau = \{\widetilde{\varphi}, \widetilde{M}, (S_L)_1, (S_L)_2, (S_L)_3\}whereS_1(l_1) = \{2/v_2\}$, $S_1(l_2) = \{2/v_2\}, {\sim}\ S_2(l_1) = \{2/v_3\}$, $S_2(l_2) = \{2/v_3\}, S_3(l_1) = \{2/v_2, 2/v_3\}$, $S_3(l_2) = \{2/v_2, 2/v_3\}$. Let $S_L$and $T_L$betwosubsmsetsof $M_L$suchthat $S(l_1) = \{2/v_1, 2/v_3\}$, $S(l_2) = \{2/v_1, 2/v_3\}$and $T(l_1) = \{2/v_1, 2/v_2\}$, $S(l_2) = \{2/v_1, 2/v_2\}$..Then$S_L$and $T_L$are $gsos$msets but $S_L \widetilde{\cap} T_L$isnota$gsos$msetin(M, τ, L).

Definition 3.10. Let (M, τ, L)be a SMTS over$M_L$and$S_L$be a smset overM_L. Then the generalized semi soft multi Interior of S_L,,denoted by $gssm - int(S_L)$ is the union fall $gsos$msets contained in S_L

Proposition 3.11. *Forany* $C_{S(l)}(v) \leq C_{M(l)}(v), C_{int(S)(l)}(v) \leq C_{gssm-int(S)(l)}(v)$.

Proof. Since Every Opens Set a $gsos$mset..

Proposition 3.12. For any *Two subsmsets*$S_L$and T_L *of* (M,τ,L). *The following are hold,*

1. *If* S_L *is a gsos mset,then* $C_{gssm-int(S)(l)}(v) = C_{S(l)}(v)$,

2. $C_{gssm-int(\varphi)(l)}(v) = C_{\varphi(l)}(v)$, *and* $C_{gssm-int(M)(l)}(v) = C_{M(l)}(v)$,

3. *If* $C_{S(l)}(v) \leq C_{T(l)}(v)$,*then* $C_{gssm-int(S)(l)}(v) \ \leq^{\leq} C_{gssm-int(T)(l)}(v)$,

4. $C_{gssm-int(S \cap T)(l)}(v) \ \geq C_{(gssm-int(S) \cap gssm-int(T))(l)}(v)$,

5. $C_{gssm-int(S \cup T)(l)}(v) \ \leq C_{(gssm-int(S) \cup gssm-int(T))(l)}(v)$,

6. $C_{gssm-int(gssm-int(S))(l)}(v) \ =^{\leq} C_{gssm-int(S)(l)}(v)$.

Theorem 3.13. *For a subsmset*S_L *of a SMTS* (M,τ,L)*, the following are equivalent*

64299

Inthumathi Velusamy *et al.*,

(i) $cl(S_L) - S_L$ *isa gscs mset,*

(ii) $S_L \cap (cl(S_L))^c$ *isa gsos mset.*

Proof.(*i*)⇒(*ii*)　Let　$C_{V(l)}(v)$=C_{(cl(S)-S)(l)}(v).　Then　$C_{V^c(l)}(v) = C_{S \cap (cl(S))^c(l)}(v)$　and　$S_L \cap (cl(S_L))^c$isa *gsos*mset.

(*ii*) ⇒ (*i*) Let$C_{V(l)}(v) = C_{S \cap (cl(S))^c(l)}(v)$. Then $C_{U^c(l)}(v) = C_{(cl(S)-S)(l)}(v)$and $U_L{}^c$is a *gscs*mset and so $cl(S_L) - S_L$isa *gscs* mset.

Proposition 3.14. *If* S_L *is a gsos mset and* C_{sint(S)(l)}(v)≤C_{T(l)}(v)≤C_{S(l)}(v), *then* T_L*isa gsos mset.*

Proof.　Suppose　that　C_{sint(S)(l)}(v)≤C_{T(l)}(v)≤C_{S(l)}(v)　and　S_L　is　a　　*gsos*mset.　Then $C_{S^c(l)}(v) \le C_{T^c(l)}(v) \le C_{scl(S^c)(l)}(v)$andsince $S_L{}^c$isa *gscs* mset, byusing Proposition [6] it follows that $T_L{}^c$ is a gscs mset. Thus $T_L$is a gsosmset.

Proposition 3.15. *IfS$_L$ is a gscs msetthen* $scl(S_L) - S_L$*isa gsos mset*

Proof.　Suppose　that　$S_L$agscs mset.　Let　C_{F(l)}(v)≤C_{(scl-S)(l)}(v),　where　FLis　closeds mset.　It　follows　that $C_{F(l)}(v) =$ Therefore C_{F(l)}(v)≤C_{sint(scl-S)(l)}(v), by　Theorem 3.5 and hence,$scl(S_L) - S_L$isa *gsos mset*

Proposition　3.16.　For　any $[(n/v)_l]_L \in P(M, L)$,$[(n/v)_l]_L \le C_{gssm-cl(S)(l)}(v)iff\le C_{(U \cap S)(l)}(v) \ne C_{\varphi(l)}(v)$forevery *gsos*mset $U_L$containing $[(n/v)_l]_L$.

Proof. Let$[(n/v)_l]_L \le C_{gssm-cl(S)(l)}(v)$for any$[(n/v)_l]_L \in P(M, L)$.Suppose Subsists a*gsos* msetU_L containing $[(n/v)_l]_L$such that C_{U∩S}V=C_{φ(l)}(v). Then $C_{S(l)}(v) \le C_{U^c(l)}(v)$.Since U_L is a*gscs* mset containing S_L,$C_{gssm(S)(l)}(v) \le C_{U^c(l)}(v)$,which implies that $[(n/v)_l]_L \nleq C_{gssm(S)(l)}(v)$, acontradiction. Thus$C_{(U \cap S)(l)}(v) \ne C_{\varphi(l)}(v)$.

Conversely, Suppose that $[(n/v)_l]_L \nleq$.Thereby Definition, there subsists a *gscs* mset $F_L$containing $S_L$such that $[(n/v)_l]_L \nleq C_{F(l)}(v)$.Thus$[(n/v)_l]_L \le C_{F^c(l)}(v)$and $F_L{}^c$ is a*gsos* mset.Also$C_{(F^c \cap S)(l)}(v) = C_{\varphi(l)}(v)$ which is a contradiction. There fore $[(n/v)_l]_L \le C_{gssm-cl(S)(l)}(v)$.

Proposition 3.17. *Let* S_L *be a sub smset of* (M,τ,L),*then* C_{(M-gssm-int(S))l}V=C_{gssm-cl(M-S)(l)}(v).

Proof. Let $[(n/v)_l]_L \le C_{(M-gssm-int(S)(l)}(v)$.Then$[(n/v)_l]_L \nleq C_{gssm-cl(M-S)(l)}(v)$.That is every *gsos* mset T_L containing$[(n/v)_l]_L$ is that T_L is not contained in S_L. This implies every *gsos*mset T_L containing$[(n/v)_l]_L$is such

that $C_{(T \cap (M-S))(l)}(v) \ne C_{\varphi(l)}(v)$.Then$[(n/v)_l]_L \nleq C_{gssm-cl(M-S)(l)}(v)$.Hence$C_{(M-gssm-int(S)(l)}(v) \le C_{gssm-cl(M-S)(l)}(v)$.Conversely, Let $[(n/v)_l]_L \le C_{gssm-cl(M-S)(l)}(v)$. Then by above Proposition Every gsos mset T_L containing $[(n/v)_l]_L$is such that $C_{(T \cap (M-S))(l)}(v) \ne C_{\varphi(l)}(v)$.That is every *gsos*mset T_L containing $[(n/v)_l]_L$is such that T_L is not contained inS_L.This implies that $[(n/v)_l]_L \nleq C_{gssm-int(S)(l)}(v)$.Thus $[(n/v)_l]_L \le C_{(M-gssm-int(S)(l)}(v)$.

Hence $C_{gssm-cl(M-S)(l)}(v) \le C_{(M-gssm-int(S)(l)}(v)$. Ergo $C_{(M-gssm-int(S)(l)}(v) = C_{gssm-cl(M-S)(l)}(v)$.

Proposition　3.18.　*If*　　$gssm - cl(S_L) - S_L$　　*is*　　*a*　　*gscsmset, then* $C_{S(l)}(v) \le C_{gssm-int(S \cup gssm-cl(S^c))(l)}(v)$.

Proof. We know that $C_{S \cup (gssm-cl(S^c))(l)}(v)$=$C_{(gssm-cl(S)-S)^c(l)}(v)$ and by assumption$(gssm - cl(S_L) - S_L)^c$is a *gsos* mset and so $S_L \cup (gssm - cl(S_L))^c$ is *gsos* mset. Thus $C_{S \cup (gssm-cl(S^c))(l)}(v)$=$C_{gssm-int(S \cup gssm-cl(S^c))(l)}(v)$and 　hence $C_{S(l)}(v) \le C_{gssm-int(S \cup gssm-cl(S^c))(l)}(v)$.

Inthumathi Velusamy *et al*.,

GENERALIZED SEMI SOFT MULTI NEIGHBOURHOOD

Definition 4.1. A sub smset N_L in SMTS(M, τ, L)is said to be generalized semi soft multi neighborhood (in summary *gssm*-nbd) of a smpoint $[(n/v)_l]_L$ in M_L if there subsists an *gsos* mset U_L such that $[(n/v)_l]_L \leq C_{U(l)}(v) \leq C_{N(l)}(v)$.

If N_L is a *gsos* mset containing $[(n/v)_l]_L$, then N_L is called generalized semi soft multi open neighborhood (in summary *gssm*-opennbd) of $[(n/v)_l]_L$ and is denoted by $gssmN[(n/v)_l]_L$.

Example 4.2. Let (M, τ, L) be a SMTS with mset $M = \{2/v_1, 2/v_2\}$, parameter set $L = \{l_1, l_2\}$ and smtopology $\tau = \{\widetilde{\varphi}, \widetilde{M}, (S_L)_1\}$ where $S_1(l_1) = \{2/v_1\}, S_1(l_1) = \{2/v_2\}$. The *gssm*-nbd of $[(2/v_1)_{l_1}]_L$ is $\{\{(l_1, \{2/v_1\}), (l_2, \{\varphi\})\}, \{(l_1, \{2/v_1\}), (l_2, \{1/v_1\})\}, \{(l_1, \{2/v_1\}), (l_2, \{2/v_1\})\}, \{(l_1, \{2/v_1\}), (l_2, \{1/v_2\})\}, \{(l_1, \{2/v_1\}), (l_2, \{2/v_2\})\}, \{(l_1, \{2/v_1\}), (l_2, \{1/v_1, 1/v_2\})\}, \{(l_1, \{2/v_1\}), (l_2, \{1/v_1, 2/v_2\})\}, \{(l_1, \{2/v_1\}), (l_2\{2/v_1, 1/v_2\})\}, \{(l_1, \{2/v_1\}), (l_2, \{M\})\}, \{(l_1, \{2/v_1, 1/v_2\}), (l_2, \{\varphi\})\}, \{(l_1, \{2/v_1, 1/v_2\}), (l_2, \{1/v_1\})\}, \{(l_1, \{2/v_1, 1/v_2\}), (l_2, \{2/v_1\})\}, \{(l_1, \{2/v_1, 1/v_2\}), (l_2, \{1/v_2\})\}, \{(l_1, \{2/v_1, 1/v_2\}), (l_2, \{2/v_2\})\}, \{(l_1, \{2/v_1, 1/v_2\}), (l_2, \{1/v_1, 1/v_2\})\}, \{(l_1, \{2/v_1, 1/v_2\}), (l_2, \{1/v_1, 2/v_2\})\}, \{(l_1, \{2/v_1, 1/v_2\}), (l_2, \{2/v_1, 1/v_2\})\}, \{(l_1, \{2/v_1, 1/v_2\}), (l_2, \{M\})\}, \{(l_1, \{M\}), (l_2, \{\varphi\})\}, \{(l_1, \{M\}), (l_2, \{1/v_1\})\}, \{(l_1, \{M\}), (l_2, \{2/v_1\})\}, \{(l_1, \{M\}), (l_2, \{1/v_2\})\}, \{(l_1, \{M\}), (l_2, \{2/v_2\})\}, \{(l_1, \{M\}), (l_2, \{1/v_1, 1/v_2\})\}, \{(l_1, \{M\}), (l_2, \{1/v_1, 2/v_2\})\}, \{(l_1, \{M\}), (l_2, \{2/v_1, 1/v_2\})\}, \widetilde{M}\}$.

Definition 4.3. The family of all *gssm*-nbd of a point $[(n/v)_l]_L \leq C_{M(l)}(v)$ is called the *gssm*- neighbourhood system of $[(n/v)_l]_L$.

Proposition 4.4. *Every sm nbd of $[(n/v)l]L$ is a gssm-nbd of $[(n/v)_l]_L$*

Proof. Let N_L be a smnbd of $[(n/v)_l]_L \leq C_{M(l)}(v)$. Then there subsists an open smset U_L such that $[(n/v)_l]_L \leq C_{U(l)}(v) \leq C_{N(l)}(v)$. Since every open smset is a *gscs* mset, U_L

Remark 4.5. *The converse of the above proposition need not be true as seen from the following example.*

Example 4.6. In Example4.2, The smset $\{(l_1, \{2/v_1\}), (l_2, \{2/v_1, 2/v_2\})\}$ is *gssm*-nbd of $[(2/v_1)_{l_1}]_L$ but not a smnbd of $[(2/v_1)_{l_1}]_L$.

Proposition 4.7. *Every gsosmset is a gssm-nbd of each of its points.*

Proof. Let N_L be a *gsos* mset and $[(n/v)_l]_L \leq C_{N(l)}(v)$. Then $[(n/v)_l]_L \leq C_{N(l)}(v) \leq C_{N(l)}(v)$. Since $[(n/v)_l]_L$ is an arbitrary point of N_L it follows that N_L is *gssm*-nbd of each of its points.

Proposition 4.8. For a SMTS (M,τ,L), the following holds:
a. Every $[(n/v)_l]_L \in \widetilde{M}$ has atleast one *gssm*–nbd.
b. Every *gssm*-nbd of $[(n/v)_l]_L \in \widetilde{M}$ and $[(n/v)_l]_L$
c. Every super smset of a *gssm*-nbd of $[(n/v)_l]_L \in \widetilde{M}$ and $[(n/v)_l]_L$
d. If N_L is a *gssm*-nbd of $[(n/v)_l]_L \in \widetilde{M}$ then there subsists a *gssm*-nbd Z_L of $[(n/v)_l]_L$ such that $C_{Z(l)}(v) \leq C_{N(l)}(v)$ and Z_L is a *gssm*-nbd of each of its sm points.

Proof. (a)M being gsos-mset it is a gsm-nbd of each of its sm points. So each $[(n/v)l]$ LM has at least one gssm-nbd namely M.

(b) Let N_L be a *gssm*-nbd of $[(n/v)_l]_L$. Then there subsists a *gsos*-mset G_L such that $[(n/v)_l]_L \leq C_{G(l)}(v) \leq C_{N(l)}(v)$. Clearly $[(n/v)_l]_L \leq C_{N(l)}(v)$. So each *gssm*-nbd of $[(n/v)_l]_L$ contains $[(n/v)_l]_L$.

Inthumathi Velusamy *et al.,*

(c) Let N_L be a $gssm$-nbd of $[(n/v)_1]_L$ and let K_L be a super sm set of N_L. Then by Definition ofgssm-nbd of as m point, there subsists gsos-mset G_L such that$[(n/v)I]LC_{G(l)}(v) \leq C_{N(l)}(v) \leq C_{K(l)}(v)$.This shows that KL is also a gssm-nbdof$[(n/v)I]$ L. Let NL be a gssm-nbd of$[(n/v)I]L$. Then there subsists a gsos-mset ZL such that $[(n/v)I]LC_{Z(l)}(v) \leq C_{N(l)}(v)$.Now ZL being gsos-mset, it is a gssm-nbd of each of its sm points.

RESULTS AND DISCUSSION

In this work we have acquainted with the conception of generalized semi soft multi closure, generalized semi soft multi interior and generalized semi soft multi neighborhood and also some basic characteristics. In future we extend the conception of generalized semi soft multi continuous mappings, their respective open mappings and homeomorphisms.

REFERENCES

1. BabithaK. V. and JohnS. J., On soft multisets, Ann. fuzzy Math. Inform.,2013, 5(1), 35-44.
2. DenizTokat and Ismail Osmanoglu, On the soft multi topology and its some properties, NevsehirUniversitesiFenBilimleriEnstitusuDergisiCilt2,2013,109-118.
3. DenizTokatandIsmailOsmanoglu,Connectednessonsoftmultitopologicalspaces,JournalofNewResultsinScience,2013,2,8-18.
4. EI-SheikhS. A., Omar R. A-K. and RaafatM., Generalized closed soft multiset in soft multitopologicalspaces,AsianJournalofMathematicsandcomputerresearch,2015, 9,302-311.
5. EI-SheikhS. A., Omar R. A-K. and RaafatM., Some types of open soft multisets and sometypes of mappings in soft multi topological spaces, Annals of fuzzy Mathematics and Informatics,2016, 12(1),15-30.
6. InthumathiV., GnanasoundariA. and MaheswariM., Generalized semi closed soft multisets,JournalofXidianuniversity,2022,16(8),234-243.

RESEARCH ARTICLE

Heptapartitioned Neurtosophic Topological Spaces

V. Jeyanthi1 and T. Mythili2*

1Assistant Professor, Department of Mathematics, Sri Krishna Arts and Science College, Coimbatore, Tamil Nadu, India-614008
2Research Scholar Professor, Department of Mathematics Sri Krishna Arts and Science College, Coimbatore, Tamil Nadu, India-614008

*Address for Correspondence
T. Mythili
Research Scholar Professor,
Department of Mathematics,
Sri Krishna Arts and Science College,
Coimbatore, Tamil Nadu, India-614008.
E.Mail: mythilisridevk@gmail.com

ABSTRACT

The purpose of this paper is to propose a new notion of Heptapartitioned Neutrosophic topological space. The author examined some of the fundamental characteristics of Heptapartitioned Neutrosophic collections in Neutrosophic Topological Spaces and defined the concepts on closure & interior Further, the author describes Heptapartitioned-Ṇ-P-Ŏ-sets Heptapartitioned-Ṇ-Ś-Ŏ-sets, Heptapartitioned-Ṇ-Ᏻ-Ŏ-sets and Heptapartitioned-Ṇ-α-Ŏ-sets via Heptapartitioned Neutrosophic topological spaces. By defining these Heptapartitioned Neutrosophic open sets, the author provides few acceptable examples and develop few primary solutions on H-Ṇ-Ṭ-spaces.

Keywords: Heptapartitioned Neutrosophic Topology, H-Ṇ Sets, H-Ṇ-preopen, H-Ṇ -Semiopen, H-Ṇ- Ᏻ-open, H-Ṇ-α-open.

INTRODUCTION

In 1965 [1], Zadeh presented the fuzzy set. F. Smarandache further advanced this notion by formulating the conception of neutrosophic sets, whichever presents a mathematical approach as addressing issues implicating imprecision, indeterminacy and inconsistency in data. The notion of neutrosophic topological space was later formulated in 2012 by Salama and Alblowi [2]. In 2020, Rama Malik [3] established the idea of pentapartitioned set. The framework of Neutrosophic topological spaces have been then leveraged by Das and Tripathy [4] to define and analyze the idea of neutrosophic simply Ᏻ-open sets.

Recently, Das [5] et al. extended these ideas by introducing Quadripartitioned Neutrosophic Topological Spaces, applying topological principles to quadripartitioned neutrosophic sets. I have refined the symbols as follows: U, C, and G represent the refinement of U, C, and G respectively. In the same manner, T has been further defined as $\dot{T}_A$, representing absolute truth & $\dot{T}_R$, representing relative truth. Similarly, $\dot{F}$ has been delineated as $\dot{F}_A$, signifying absolute falsity & $\dot{F}_R$, signifying relative falsity. The introduction of Seven Symbol-Valued Neutrosophic Logic were initially undertaken by F. Smarandache [6] in 1995. According to this framework, we have the following relationships C = ($\dot{T}_A$ or $\dot{T}_R$) / ($\dot{F}_A$ or $\dot{F}_R$) denoting Contradiction, whichever incorporates Extenics principles; G = ($\dot{T}_A$ or $\dot{T}_R$) / ($\dot{F}_A$ or $\dot{F}_R$) representing Ignorance; and U = signifying a state where neither ($\dot{T}_A$ or $\dot{T}_R$) nor ($\dot{F}_A$ or $\dot{F}_R$) holds, rendering it unspecified. Each of these entities is symbolized.

However, when considering $\dot{T}_A$, $\dot{T}_R$, $\dot{F}_A$, $\dot{F}_R$, U, C, and G as subsets within the range [0, 1], a numerical logic system emerges, encompassing seven distinct numerical values. This numeric Fra ework enables the definition of the Heptapartitioned Neutrosophic set and facilitates the exploration of its inherent properties. The year 2021 marked the development of Heptapartitioned Neutrosophic Set by R. Radha & A. Stanis Arul Mary [7], building upon the foundations of Ṇ-Ṣ concepts. This article's main goal is to gather concepts of heptapartitioned neutrosophic topological space and examine various aspects of them.

PRELIMINARIES

The author provides some fundamental concepts and findings that are pertinent to the article's primary findings in this part.

Definition 2.1.

Consider R be an universe. Then G, a H-Ṇ-Ṣ over R :

G = {(ζ, $T_G(\zeta)$, $M_G(\zeta)$, $C_G(\zeta)$, $U_G(\zeta)$, $I_G(\zeta)$, $K_G(\zeta)$, $F_G(\zeta)$: $\zeta \in$R}

The values $T_G(\zeta)$, $M_G(\zeta)$, $C_G(\zeta)$, $U_G(\zeta)$, $I_G(\zeta)$, $K_G(\zeta)$, $F_G(\zeta)$ correspond to the absolute truth membership, relative truth membership, contradiction membership, unknown membership, ignorance membership, relative falsity membership & absolute falsity membership of ζ, where ζ is an element of the set R and belongs to the interval [0, 1]. So, $0 \leq$ $T_G(\zeta)$+$M_G(\zeta)$+$C_G(\zeta)$+$U_G(\zeta)$+$I_G(\zeta)$+$K_G(\zeta)$+$F_G(\zeta)$ ≤ 7, for all $\zeta \in$R.

Definition 2.2.

Let E = {(ζ, $T_E(\zeta)$, $M_E(\zeta)$, $C_E(\zeta)$, $U_E(\zeta)$, $I_E(\zeta)$, $K_E(\zeta)$, $F_E(\zeta)$):$\zeta \in$R} and

F= { ζ, $T_F(\zeta)$, $M_F(\zeta)$, $C_F(\zeta)$, $U_F(\zeta)$, $I_F(\zeta)$, $K_F(\zeta)$, $F_F(\zeta)$): $\zeta \in$R} be a two H-Ṇ-sets over a fixed sets R.

subsequently, E $\subseteq$ F iff T E (ζ) $\leq$ T F (ζ), M E (ζ) $\leq$ M F (ζ), C E (ζ) $\leq$ C F (ζ), U E (ζ) $\geq$ U F (ζ), I E (ζ) $\geq$ I F (ζ), K E (ζ) $\geq$ K F (ζ), F E (ζ) $\geq$ F F (ζ), for all $\zeta \in$R.

Example 2.3.

Let R = {a_1, a_2}. Consider two Heptapartitioned Neutrosophic sets

E = {(a_1,0.4,0.3,0.4,0.3,0.7,0.7,0.8), (a_2,0.2,0.5,0.5,0.7,0.8,0.7,0.8)} and

F = {(a_1,0.7,0.5,0.6,0.6,0.5,0.5,0.4), (a_2,0.8,0.7,0.5,0.7,0.5,0.4,0.3)} over R. Then, E $\subseteq$ F.

Definition 2.4.

The whole H-Ṇ-Ṣ ($1_{H_Ṇ}$) and empty H-Ṇ-Ṣ ($0_{H_Ṇ}$) over a immovanle set R are explained in this way:

(i) $1_{H_Ṇ}$ = {(ζ,1,1,1,0,0,0,0): $\zeta \in$R};

(ii) $0_{H_Ṇ}$ = {(ζ,0,0,0,1,1,1,1): $\zeta \in$R}.

Jeyanthi and Mythili

There is other nine types of representations for both the whole H-Ɲ-S 1_{H_N} and the empty H-Ɲ-S 0_{H_N}. Here are several examples:

1_{H_N} = {(ζ,1,1,1,0,0,0,1): ζ∈R};
1_{H_N} = {(ζ,1,1,1,0,0,1,0): ζ∈R};
1_{H_N} = {(ζ,1,1,1,0,1,0,0): ζ∈R};
1_{H_N} = {(ζ,1,1,1,1,0,0,0): ζ∈R};
1_{H_N} = {(ζ,1,1,1,0,1,1,1): ζ∈R};
1_{H_N} = {(ζ,1,1,1,1,0,1,1): ζ∈R};
1_{H_N} = {(ζ,1,1,1,1,1,0,1): ζ∈R};
1_{H_N} = {(ζ,1,1,1,1,1,1,0): ζ∈R};
1_{H_N} = {(ζ,1,1,1,1,1,1,1): ζ∈R};
0_{H_N} = {(ζ,0,0,0,1,1,1,0): ζ∈R};
0_{H_N} = {(ζ,0,0,0,1,1,0,1): ζ∈R};
0_{H_N} = {(ζ,0,0,0,1,0,1,1): ζ∈R};
0_{H_N} = {(ζ,0,0,0,0,1,1,1): ζ∈R};
0_{H_N} = {(ζ,0,0,0,1,0,0,0): ζ∈R};
0_{H_N} = {(ζ,0,0,0,0,1,0,0): ζ∈R};
0_{H_N} = {(ζ,0,0,0,0,0,1,0): ζ∈R};
0_{H_N} = {(ζ,0,0,0,0,0,0,1): ζ∈R};
0_{H_N} = {(ζ,0,0,0,0,0,0,0): ζ∈R}.

Remark 2.5.
The author will refer to 1_{H_N} = (ζ,1,1,1,0,0,0,0): ζ∈R and 0 HƝ = (ζ,0,0,0,1,1,1,1): ζ∈R throughout this article because the complements of 1 HƝ and 0 HƝ must be the same. However, it does not hold true for any of the other nine sorts of combinations that contain 1_{H_N} and 0 HƝ . For any H-Ɲ-S E over R, it is evident that 0 HƝ ⊆E ⊆ 1_{H_N} .

Definition 2.6.
Let E = {(ζ, T_E(ζ), M_E(ζ), C_E(ζ), U_E(ζ), I_E(ζ), K_E(ζ), F_E(ζ)): ζ∈R} be a Heptapartitioned Neutrosophic set over a immovable set R. Also, the complement of E or E^c is represented as follows:
E^c = {(ζ, F_E(ζ), K_E(ζ), I_E(ζ),1-U_E(ζ), C_E(ζ), M_E(ζ), T_E(ζ)): for all ζ∈ R}.

Definition 2.7.
The union of any two Heptapartitioned Neutrosophic collections E & F over R is indicated as E ∪ F and is referred to as E ∪ F = [ζ, (max((T_E(ζ), T_F(ζ)), max (M_E(ζ), M_F(ζ)), max(C_E(ζ), C_F(ζ)), min(U_E(ζ), U_F(ζ)), min(I_E(ζ), I_F(ζ)), min(K_E(ζ), K_F(ζ)), min(F_E(ζ), F_F(ζ)): ζ∈R]. and The intersection of any two Heptapartitioned Neutrosophic sets E & F over R is indicated as E ∩ F and is referred to as E ∩ F = [ζ, (min((T_E(ζ), T_F(ζ)), min (M_E(ζ), M_F(ζ)), min(C_E(ζ), C_F(ζ)), max(U_E(ζ), U_F(ζ)), max(I_E(ζ), I_F(ζ)), max(K_E(ζ), K_F(ζ)), max(F_E(ζ), F_F(ζ))):ζ∈R].

HEPTAPARTITIONED NEUTROSOPHIC TOPOLOGY

The concepts of Heptapartitioned neutrosophic topology on H-Ɲ-Ss are acquired in this section.
Then, using the perspective of a Heptapartitioned Ɲ -Ṭ- Ṣ, the author describes the interior & closure of an H-Ɲ-Ṣ and demonstrate some results.

Description 3.1.

A Heptapartitioned Neutrosophic Topology on a non-empty set R is a family $\Im$ of Heptapartitioned Neutrosophic subsets in R satisfies the following axioms:

(i) 0_{H_N}, $1_{H_N} \in \Im$;

(ii) $F_1, F_2 \in \Im \Rightarrow F_1 \cap F_2 \in \Im$;

(iii) $\{Fi: i \in \Delta\} \subseteq \Im \Rightarrow \cup Fi \in \Im$.

In this scenario, the pair $(R,\Im)$ is denoted as a Heptapartitioned- Ṇ-Ṭ- Ş. Every member of the set $\Im$ is referred to as a Heptapartitioned neutrosophic open sets (abbreviated as H-ṆŎŞ). Furthermore, If $F \in \Im$, then it's compliment F C is termed a Heptapartitioned neutrosophic closed set (abbreviated as H-ṆĊŞ).

Example 3.2.

Consider two H-Ṇ-Şs, denoted as Ṃ and Ṇ, defined over a immovable set R = $\{\zeta, \xi\}$, with the following compositions:

Ṃ = $\{(\zeta, 0.7, 0.4, 0.6, 0.7, 0.5, 0.4, 0.3)$, $(\xi, 0.5, 0.6, 0.7, 0.5, 0.1, 0.4, 0.1)$: $\zeta, \xi \in R\}$;

Ṇ = $\{(\zeta, 0.6, 0.4, 0.5, 0.8, 0.9, 0.5, 0.8)$, $(\xi, 0.5, 0.4, 0.6, 0.8, 0.3, 0.4, 0.1)$: $\zeta, \xi \in R\}$;

It follows that the collection $\Im$= $\{0_{H_N}, 1_{H_N}, Ṃ, Ṇ\}$ constitutes a Heptapartitioned-Ṇ-Ṭ structure over the set R.

Definition 3.3.

Let $(R, \Im)$ represent a heptapartitioned Neutrosophic topological space. Consider Φ as an H-Ň-Ş over R. The Heptapartitioned Neutronosophic Closure, denoted as H-N_{cl}, for Φ can be defined as the

intersection of all H-ṆĊŞs that encompass Φ. On the other hand, the Heptapartitioned Neutronosophic Interior, abbreviated as H-Ṇ int , of Φ can be defined as the union of all H-ṆŎŞs that are contained within Φ.

H-N_{int} $(\Phi) = \cup\{\Psi: \Psi \subseteq \Phi$ and Ψ is a H-ṆŎŞ in $(R,\Im)\}$, and H-Ṇ cl $(\Phi) = \cap\{\Omega: \Phi \subseteq \Omega$ and Ω is a H-ṆĊŞ in $(R,\Im)\}$.

Remark 3.4.

The largest H-ṆŎŞ in $(R,\Im)$ that contains Φ in H- Ṇ int (Φ) while the smallest H-ṆĊŞ in $(R,\Im)$ that contains Φ in H-Ṇ cl (Φ).

Theorem 3.5.

Let $(R,\Im)$ be a Heptapartitioned- Ṇ-Topological space. Consider any two H-Ṇ-Şs over R, denoted as Γ and Δ. In this context, the following statement is well founded:

(i) H- Ṇ int $(\Gamma) \subseteq \Gamma \subseteq$ H- Ṇ int (Γ);

(ii) $\Gamma \subseteq \Delta \Rightarrow$ H- Ṇ cl $(\Gamma) \subseteq$ H- Ṇ cl (Δ);

(iii) $\Gamma \subseteq \Delta \Rightarrow$ H- Ṇ cl $(\Gamma) \subseteq$ H- Ṇ cl (Δ);

(iv) H- Ṇ cl $(\Gamma \cup \Delta)$ = H- Ṇ cl $(\Gamma) \cup$ H- Ṇ cl (Δ);

(v) H- Ṇ cl $(\Gamma \cap \Delta) \subseteq$ H- Ṇ cl $(\Gamma) \cap$ H- Ṇ cl (Δ);

(vi) H- Ṇ int $(\Gamma \cup \Delta) \supseteq$ H- Ṇ int $(\Gamma) \cup$ H- Ṇ int (Δ);

(vii) H- Ṇ int $(\Gamma \cap \Delta) \subseteq$ H- Ṇ int $(\Gamma) \cap$ H- Ṇ int (Δ).

Proof.

(i) from definition 3.3., we obtain H-$N_{int}(\Gamma)$ = $\cup\{\Delta: \Delta$ is a H-ṆŎŞ in $(R,\Im)$ and $\Delta \subseteq \Gamma\}$. Since, every $\Delta \subseteq \Gamma$, so $\cup\{\Delta: \Delta$ is a H-ṆŎŞ in $(R,\Im)$ and $\Delta \subseteq \Gamma\} \subseteq \Gamma$, i.e., H-$N_{int}(\Gamma) \subseteq \Gamma$. Again, H-$N_{cl}(\Gamma)$ = $\cap\{\Omega: \Omega$ is a H-ṆĊŞ in $(R,\Im)$ and $\Gamma \subseteq \Omega\}$. Since, each $\Omega \supseteq \Gamma$, so $\cap\{\Omega: \Omega$ is a H-ṆĊŞ in $(R,\Im)$ and $\Gamma \subseteq \Omega\} \supseteq \Gamma$, i.e., H-$N_{cl}(\Gamma) \supseteq \Gamma$.

Therefore, H-$N_{int}(\Gamma) \subseteq \Gamma \subseteq$ H-$N_{cl}(\Gamma)$.

Jeyanthi and Mythili

(ii) Suppose (R,ℑ) constitutes a Heptapartitioned- Ɲ-Ṭ-Ş. Consider Γ and Δ as arbitrary H-Ɲ-Şs over R, with the additional condition that Γ is a subset of Δ. here, H-Ɲ$_{cl}$(Γ) = ∩{ Ω: Ω is a H-ƝĊŞ in (R,ℑ) and Γ⊆ Ω }

⊆∩{ Ω: Ω is a H-ƝĊŞ in (R,ℑ) and Δ ⊆ Ω}   [Since Γ⊆Δ]   = H-Ɲ$_{cl}$(Δ)

⇒H-Ɲ$_{cl}$(Γ) ⊆H-Ɲ$_{cl}$(Δ). Therefore, Γ ⊆ Δ⇒H-Ɲ$_{cl}$(Γ)⊆H-Ɲ$_{cl}$(Δ).

(iii) Consider a Heptapartitioned- Ɲ-Ṭ-Ş (R, ℑ). Consider Γ & Δ as two H-Ɲ-Şs over R, where it is given that Γ is a subset of Δ.Then, H-Ɲ$_{cl}$(Γ) = ∩{ Ω: Ω is a H-ƝŎŞ in (R,ℑ) and Γ⊆ Ω }

⊆∩{ Ω: Ω is a H-ƝŎŞ in (R,ℑ) and Δ⊆ Ω }   [Since Γ⊆Δ]   = H-Ɲ$_{int}$(Δ)

⇒H-Ɲ$_{int}$ (Γ) ⊆H-Ɲ$_{int}$(Δ).

Therefore, Γ⊆Δ⇒H-Ɲ$_{int}$(Γ)⊆H-Ɲ$_{int}$(Δ).

(iv) Let Γ and Δdenote two Heptapartitioned-Ɲ subsets of a Heptapartitioned- Ɲ-Ṭ-Ş (R,ℑ). As we knowΓ ⊆Γ∪Δ,Δ ⊆ Γ∪Δ. here, Γ⊆Γ∪ Δ⇒H-Ɲ$_{cl}$(Γ) ⊆H-Ɲ$_{cl}$(Γ∪Δ); and Δ⊆Γ∪ Δ⇒H-Ɲ$_{cl}$(Δ) ⊆H-Ɲ$_{cl}$(Γ∪ Δ).

Therefore, H-Ɲ$_{cl}$ (Γ)∪H-Ɲ$_{cl}$(Δ) ⊆H-Ɲ$_{cl}$(Γ∪Δ) (1)

We have, Γ⊆H-Ɲ$_{cl}$(Γ), Δ ⊆H-Ɲ$_{cl}$(Δ). Therefore, Γ∪ Δ⊆H-Ɲ$_{cl}$(Γ)∪H-Ɲ$_{cl}$(Δ). additionally, w.k.tH-Ɲ$_{cl}$(Γ)∪H-Ɲ$_{cl}$(Δ) is a H-ƝĊŞ in (R,ℑ). As a result, H-Ɲ$_{cl}$(Γ)∪H-Ɲ$_{cl}$(Δ) is a H-ƝĊŞ in (R,ℑ), this holdsΓ∪ Δ. But it emerges that H-Ɲ$_{cl}$(Γ∪Δ) is the lowest H-ƝĊŞ in (R,ℑ), which involvesΓ∪ Δ.

Consequently, H-Ɲ$_{cl}$(Γ∪Δ) ⊆H-Ɲ$_{cl}$(Γ)∪H-Ɲ$_{cl}$(Δ)   (2)

Combining equations (1) and (2) we can conclude that: H-Ɲ$_{cl}$(Γ∪ Δ) = H-Ɲ$_{cl}$(Γ)∪H-Ɲ$_{cl}$(Δ).

(v)Consider Γ and Δ as two Heptapartitionedneutrosophic subsets of a H-ƝṬŞ (R, ℑ).

As we know Γ∩Δ⊆ Γ, Γ∩Δ⊆Δ. Now, Γ∩Δ⊆ Γ⇒H-Ɲ$_{cl}$(Γ∩Δ) ⊆H-Ɲ$_{cl}$(Γ);

and Γ∩Δ⊆Δ⇒H-Ɲ$_{cl}$(Γ∩Δ) ⊆H-Ɲ$_{cl}$(Δ).

Therefore, H-Ɲ$_{cl}$(Γ∩Δ) ⊆H-Ɲ$_{cl}$(Γ)∩H-Ɲ$_{cl}$(Δ).

(vi) Consider Γ and Δ as two Heptapartitionedneutrosophic subsets of a H-ƝṬŞ (R, ℑ).

As we knowΓ⊆Γ∪Δ,Δ ⊆ Γ∪Δ. so, we obtain

Γ⊆Γ∪Δ⇒H-Ɲ$_{int}$(Γ) ⊆H-Ɲ$_{int}$(Γ∪Δ); and Ɲ⊆ Γ∪Δ⇒H-Ɲ$_{int}$(Δ) ⊆H-Ɲ$_{int}$(Γ∪Δ).

Therefore, H-Ɲ$_{int}$(Γ)∪H-Ɲ$_{int}$(Δ) ⊆H-Ɲ$_{int}$(Γ∪Δ).

(vii) Consider Γ and Δ as two Heptapartitionedneutrosophic subsets of a H-ƝṬŞ (R, ℑ).

As we knowΓ∩Δ⊆ Γ, Γ∩Δ⊆Δ.

Now, Γ∩Δ⊆ Γ⇒H-Ɲ$_{int}$(Γ∩Δ) ⊆H-Ɲ$_{int}$(Γ); and Γ∩Δ⊆Δ⇒H-Ɲ$_{int}$(Γ∩Δ) ⊆H-Ɲ$_{int}$(Δ).

Therefore, H-Ɲ$_{int}$(Γ∩Δ) ⊆H-Ɲ$_{int}$(Γ)∩H-Ɲ$_{int}$(Δ).

Theorem 3.6. Consider Γ as a Heptapartitioned neutrosophic subset of a Heptapartitioned- Ɲ-Ṭ-Ş denoted by (R, ℑ). In this context, the following assertion is valid:
(i) Γ is a H-Ɲ-open sets iffH-Ɲ$_{int}$(Γ) = Γ;
(ii) Γ is a H-Ɲ-closed sets iffH-Ɲ$_{cl}$(Γ) = Γ.

Proof:(i) Let Γ be a H-Ɲ-open sets on a Heptapartitioned- Ɲ-Ṭ-Ş (R,ℑ). Here, H-Ɲ$_{int}$(Γ) = ∪{ Ω: Ω is a H-Ɲ-open sets in (R,ℑ) and Ω⊆ Γ}. Since, Γ is a H-Ɲ-open sets in (R,ℑ), so Γ is the biggestH-Ɲ-open sets, which is included in Γ. ⇒∪{Ω: Ω is a H-Ɲ-open sets in (R,ℑ) and Ω⊆ Γ} = Γ. Therefore, H-Ɲ$_{int}$(Γ) = Γ.
(ii) Consider Γ as a Heptapartitionedneutrosophic subsets of a H-ƝṬŞ (R, ℑ). Here, H-Ɲ$_{cl}$(Γ) = ∩{ Ω: Ω is a H-Ɲ-closed sets in (R,ℑ) and Γ ⊆ Ω}. Since, Γ is a H-Ɲ-closed sets in (R,ℑ), so Γ is the tiniest H-Ɲ-closed sets, which carriesΓ.⇒∩{ Ω: Ω is a H-Ɲ-closed sets in (R,ℑ) and Γ ⊆ Ω} = Γ. Therefore, H-Ɲ$_{cl}$(Γ) = Γ.

Definition 3.7. Consider the Heptapartitioned- Ɲ-Ṭ-Ş denoted as (R, ℑ). Within this context, a H-Ɲ-S namedŞ is labeled as:

Jeyanthi and Mythili

(i) A Heptapartitioned-ṆŚǑ set iffꞫ a subset of the H-Ṇ-complement of the H-Ṇ-accumulation of Q, i.e., Ɜ⊆H-Ṇcl(H-Ṇint(Ɜ));   .

(ii) A Heptapartitioned-ṆPǑ set iffꞫis a subset of the H-Ṇ-accumulation of the H-Ṇ-complement of Q, i.e., Ɜ⊆H-Ṇint(H-Ṇcl(Ɜ)).

Theorem 3.8. Let (R,ℑ) is a Heptapartitioned- Ṇ-Ṭ-Ṣ. Then,   (i)
every H-Ṇ-open set is a H-Ṇ-semi-open set.   (ii)
every H-Ṇ-open set is a H-Ṇ-pre-open set. But conversely not true

Proof.
(i) Let (R,ℑ) be a Heptapartitioned- Ṇ-Ṭ-Ṣ. LetꞪ be a H-ṆŎṢ. Therefore, Ɜ=H-Ṇint(Ɜ). As we knowꞪ⊆H-Ṇcl(Ɜ). ⇒Ɜ⊆H-Ṇcl(H-Ṇint(Ɜ)). Consequently,Ɜ is a H-ṆŚǑ set in (R,ℑ).
(ii) Consider Γ as a Heptapartitionedneutrosophic subsets of a H-ṆṬṢ (R,ℑ). Consequently, Ɜ=H-Ṇint(Ɜ). As we know, Ɜ⊆H-Ṇcl(Ɜ). ⇒H-Ṇint(Ɜ)⊆H-Ṇint(H-Ṇcl(Ɜ)) i.e., Ɜ= H-Ṇint(Ɜ) ⊆H-Ṇint(H-Ṇcl(Ɜ)). Consequently, Ɜ⊆H-Ṇint(H-Ṇcl(Ɜ)). Hence, Ɜ is a H-ṆPǑ set in (R,ℑ).

Example 3.9. Consider a Heptapartitioned-Ṇ-Ṭ-Ṣ (R,ℑ), ℑ= {0$_{H_N}$, 1$_{H_N}$, {(a,0.4,0.5,0.6,0.3,0.2,0.1,0)}, {(a,0.5,0.6,0.6,0.2,0.2,0.1,0)}}. Then,
(i) S={(a,0,0.1,0.2,0.8,0.6,0.5,0.5)}is categorized as a H-ṆŚǑ set andwhich is not qualify as a H-ṆŎṢ in (R,ℑ).
(ii) L={(a,0.7,0.6,0.6,0.2,0.2,0.1,0)} is classifies as a H-ṆPǑ set although it does not satisfy criteria for being a H-ṆŎṢ in (R,ℑ).

Theorem 3.10. ForHeptapartitioned- Ṇ-Ṭ-Ṣ (R,ℑ), the union of two H-ṆŚǑcollections is a H-ṆŚǑ set.

Proof.
ConsiderΘ&Λas two H-ṆŚǑ sets in a HeptapartitionedNeutrosophicTopological spaces(R,ℑ). consequently, Θ⊆H-Ṇcl (H-Ṇint(Θ)) (3)
and Λ⊆H-Ṇcl(H-Ṇint(Λ)) (4)
From eq. (3) and eq. (4), we obtain Θ∪Λ⊆H-Ṇcl(H-Ṇint(Θ))∪H-Ṇcl (H-Ṇint(Λ))
= H-Ṇcl(H-Ṇint(Θ)∪H-Ṇint(Λ)) ⊆H-Ṇcl(H-Ṇint(Θ∪Λ)).
Therefore, Θ∪Λ⊆ H-Ṇcl(H-Ṇint(Θ∪Λ)). Hence, Θ∪Λ is a H-ṆŚǑ set in (R,ℑ).

Theorem 3.11. ForHeptapartitioned- Ṇ-Ṭ-Ṣ (R,ℑ), the union of two H-ṆPǑ sets additionally a H-ṆPǑ set.
Proof. ConsiderΘ&Λas two H-ṆPǑ sets in a Heptapartitioned- Ṇ-Ṭ-Ṣ (R,ℑ). Consequently,
Θ ⊆H-Ṇint (H-Ṇcl(Θ))   (5)   and Λ ⊆H-Ṇint(H-Ṇcl(Λ)) (6) Combining equations (5) and (6), we obtain,
Θ ∪D⊆H-Ṇint(H-Ṇcl(Θ))∪H-Ṇint(H-Ṇcl(Λ)) ⊆H-Ṇint(H-Ṇcl(Θ)∪H-Ṇcl(Λ))
= H-Ṇint(H-Ṇcl(Θ∪Λ)).
 Therefore, Θ∪Λ⊆H-Ṇint(H-Ṇcl(Θ∪Λ)). Hence, Θ∪Λ is a H-ṆPǑ set in (R,ℑ).

Example 3.12. Examine a Heptapartitioned-Ṇ-Ṭ-Ṣ (R, ℑ) as demonstrated in Example 3.9. It is evident that the Heptapartitioned neutrosophic set L = {(a, 0.7, 0.6, 0.6, 0.2, 0.2, 0.1, 0)} qualifies as a H-ṆάǑ set, but it does not meet the criteria to be classified as a H-ṆŎṢ set within the confines of the space (R, ℑ).
Proposition 3.13. For a Heptapartitioned- Ṇ-Ṭ-Ṣ (R,ℑ), eachH-ṆάǑ set is a H-ṆŚǑ set but conversely not true.
Proof. Consider a Heptapartitioned- Ṇ-Ṭ-Ṣ (R, ℑ). ConsiderΘis a H-ṆάǑ set in (R,ℑ). consequently, Θ ⊆H-Ṇint(H-Ṇcl(H-Ṇint(Θ))). It emerges that H-Ṇint (H-Ṇcl(H-Ṇint(Θ))) ⊆H-Ṇcl(H-Ṇint(Θ)). Thus, we obtain Θ ⊆H-Ṇcl(H-Ṇint(Θ)). Hence, Θ is a H-ṆŚǑ set. consequently, every H-ṆάǑ set is a H-ṆŚǑ set.
Example 3.14. Consider a Heptapartitioned- Ṇ-Ṭ-Ṣ (R,ℑ), ℑ={0$_{H_N}$, 1$_{H_N}$, {(a,0.5,0.6,0.6,0.5,0.7,0.8,0.5), (b,0.5,0.5,0.8,0.5,0.5,0.6,0.6)}, {(a,0.4,0.4,0.5,0.8,0.8,0.8,0.6), (b,0.5,0.5,0.6,0.8,0.8,0.8,0.6)}}. Then, it can be easily verified that A={(a,0.6,0.6,0.7,0.5,0.3,0.3,0.3), (b,0.5,0.5,0.8,0.5,0.4,0.4,0.4)} Represents an H-ṆŚǑ set within (R, ℑ), yet does not qualify as an H-ṆάǑ set within the same (R, ℑ) context.

64308

Jeyanthi and Mythili

Theorem 3.15. For a Heptapartitioned- Ɲ-Ṭ-Ṣ (R,ℑ), every H-ƝáǑ collection is a H-ƝPǑ set.Conversely not true.

Proof. Let (R,ℑ) be a Heptapartitioned- Ɲ-Ṭ-Ṣ. Let Θ be a H-ƝáǑ set in (R,ℑ). Therefore, Θ ⊆H-Ɲint(H- Ɲcl (H-Ɲint(Θ))). It is known that H-Ɲint(Θ)⊆ Θ. This implies, H-Ɲcl(H- Ɲint(Θ))⊆H-Ɲcl(Θ). Which implies H-Ɲint (H- Ɲcl(H-Ɲint(Θ))) ⊆H-Ɲint(H-Ɲcl(Θ). Therefore, Θ ⊆H-Ɲint(H-Ɲcl(Θ). Hence, Θ is a H-ƝPǑset. consequently, every H-ƝáǑ set is a H-ƝPǑ set in (R,ℑ).

Example 3.16. Let's examine a Heptapartitioned-Ɲ-Ṭ-Ṣ space (R, ℑ) as depicted in Example 3.9. In this context, the Heptapartitionedneutrosophic set S = {(a, 0, 0.1, 0.2, 0.8, 0.6, 0.5, 0.5)} qualifies as a H-ƝPǑ set within the space (R, ℑ). However, it does not meet the criteria to be categorized as a H-ƝáǑ set within the same space (R, ℑ).

Remark 3.17.A Heptapartitioned- Ɲ set Θ is referred to as a Heptapartitioned- Ɲ-б-closed set (abbreviated as H-Ɲ-б-Ċ set) iff the succeding condition holds: Θ is a Heptapartitionedneutrosophic б-Ǒ set, this means that the intersection of the Heptapartitionedneutrosophic closure of the neutrosophic interior of Θ (denoted as H-Ɲint (H-Ɲcl (Θ))) with the Heptapartitionedneutrosophic closure of the neutrosophic interior of Θ (denoted as H-Ɲcl (H-Ɲint (Θ))) is a subset of Θ.

Theorem 3.18. For a H-ƝṬṢ (R,ℑ), every H-ƝPǑ (H-ƝŚǑ) collection is a H-Ɲ-б-Ǒ set.

Proof. Straight forward from definition.

Proposition 3.19. For H-ƝṬṢ (R,ℑ) the union of two H-Ɲ-б-Ǒ set is a H-Ɲ-б-Ǒ set.

Proof. Consider Θ & Λ as two H-Ɲ-б-Ǒ sets in a H-ƝṬṢ (R,ℑ).

consequently, Θ⊆H-Ɲint(H-Ɲcl(Θ)) ∪H-Ɲcl(H-Ɲint(Θ))(7)

and Λ⊆H-Ɲint(H-Ɲcl(Λ)) ∪H-Ɲcl(H-Ɲint(Λ))(8) It emerges that, Θ⊆Θ ∪ Λ and Λ⊆Θ ∪ Λ.

Now, Θ⊆Θ∪ Λ⇒H-Ɲint(Θ) ⊆H-Ɲint(Θ ∪ Λ)

⇒H-Ɲcl(H-Ɲint(Θ)) ⊆H-Ɲcl(H-Ɲint(Θ ∪ Λ))(9)

and Θ⊆Θ∪ Λ⇒H-Ɲcl(Θ) ⊆H-Ɲcl(Θ ∪ Λ)

⇒H-Ɲint(H-Ɲcl(Θ)) ⊆H-Ɲint(H-Ɲcl(Θ ∪ Λ)) (10)

Similarly, demonstrablyH-Ɲcl(H-Ɲint(Λ)) ⊆H-Ɲcl(H-Ɲint(Θ ∪ Λ))(11)

 H-Ɲint(H-Ɲcl(Λ)) ⊆H-Ɲint(H-Ɲcl(Θ ∪ Λ)) (12)

Combining equations (7) and (8) we obtain,

Θ ∪ Λ⊆H-Ɲcl(H-Ɲint(Θ)) ∪H-Ɲint(H-Ɲcl (Θ)) ∪H-Ɲcl(H-Ɲint (Λ)) ∪H-Ɲint (H-Ɲcl(Λ))

⊆H-Ɲcl(H-Ɲint(Θ ∪ Λ)) ∪H-Ɲint(H-Ɲcl(Θ ∪ Λ)) ∪H-Ɲcl(H-Ɲint (Θ ∪ Λ)) ∪H-Ɲint (H-Ɲcl(Θ∪Λ))

[Fom equations (9), (10), (11) and (12)]

= H-Ɲcl(H-Ɲint (Θ ∪ Λ)) ∪H-Ɲint(H-Ɲcl(Θ ∪ Λ))

⇒Θ ∪ Λ⊆H-Ɲcl(H-Ɲint(Θ ∪ Λ)) ∪H-Ɲint(H-Ɲcl(Θ ∪ Λ)).

Therefore, Θ ∪ Λbe a H-Ɲ-б-Ǒ set.

As a result, combining two H-Ɲ-б-Ǒ collections yields an H-Ɲ-б-Ǒ set.

Proposition 3.20. For H-ƝṬṢ (R,ℑ), the intersection of two H-Ɲ-б-Ċ sets is a H-Ɲ-б-Ċ set.

Proof.

Consider a H-ƝṬṢ(R,ℑ). ConsiderΘ&Λ be two H-Ɲ-б-Ċ sets in (R,ℑ). Consequently,

H-Ɲint (H-Ɲcl (Θ)) ∩H-Ɲcl (H-Ɲint (Θ)) ⊆Θ(13) H-Ɲint (H-Ɲcl (Λ)) ∩H-Ɲcl (H-Ɲint (Λ) ⊆Λ(14)

As, Θ ∩ Λ⊆Θ,Θ ∩ Λ⊆ Λ, so we obtain H-Ɲint (Θ∩ Λ)⊆H-Ɲint (Θ) ⇒H-Ɲcl (H-Ɲint (Θ ∩ Λ))⊆H-Ɲcl (H-Ɲint (Θ)); (15)

H-Ɲcl (Θ ∩ Λ) ⊆H-Ɲcl (Θ) ⇒H-Ɲint (H-Ɲcl (Θ ∩ Λ)) ⊆H-Ɲint (H-Ɲcl (Θ)) (16)   H-Ɲint (Θ ∩ Λ)⊆ H-Ɲint (Λ) ⇒H-Ɲcl (H-

Jeyanthi and Mythili

$Ɲ_{int}$ (Θ ∩ Λ))⊆H-$Ɲ_{cl}$ (H-$Ɲ_{int}$ (Λ)) (17)   and H-$Ɲ_{cl}$ (Θ ∩ Λ) ⊆H-$Ɲ_{cl}$ (Λ) ⇒H-$Ɲ_{int}$ (H-$Ɲ_{cl}$ (Θ ∩ Λ))⊆H-$Ɲ_{int}$ (H-$Ɲ_{cl}$ (Λ)) (18)
Combining equations (13) and (14) we obtain Θ∩ Λ⊇H-$Ɲ_{int}$ (H-$Ɲ_{cl}$ (Θ)) ∩H-$Ɲ_{cl}$ (H-$Ɲ_{int}$ (Θ)) ∩H-$Ɲ_{int}$ (H-$Ɲ_{cl}$ (Θ)) ∩H-$Ɲ_{cl}$
(H-$Ɲ_{int}$ (Λ)) ⊇H-$Ɲ_{int}$ (H-$Ɲ_{cl}$ (Θ ∩ Λ)) ∩H-$Ɲ_{cl}$ (H-$Ɲ_{int}$ (Θ ∩ Λ)) ∩H-$Ɲ_{int}$ (H-$Ɲ_{cl}$ (Θ ∩ Λ)) ∩H-$Ɲ_{cl}$ (H-$Ɲ_{int}$(Θ∩Λ)) [from
equations (15), (16), (17) and (18)]
= H-$Ɲ_{int}$ (H-$Ɲ_{cl}$ (Θ ∩ Λ)) ∩H-$Ɲ_{d}$ (H-$Ɲ_{int}$ (Θ ∩ Λ))
⇒Θ ∩ Λ⊇H-$Ɲ_{cl}$ (H-$Ɲ_{int}$ (Θ ∩ Λ)) ∩H-$Ɲ_{int}$ (H-$Ɲ_{d}$ (Θ ∩ Λ)).
Hence, Θ ∩ Λbe a H-Ɲ-б-Ċ set in (R,ℑ).
consequently, combining two H-Ɲ-б-Ŏ collections yields an H-Ɲ-б-Ŏ set.

CONCLUSION

According to this paper, the author introduces the concept of an H-Ɲ-Ṭ-space and extensively explores different types of open sets, namely H-Ɲ-preopen sets, H-Ɲ-semiopen sets, H-Ɲ-b-open sets, and H-Ɲ-ά-open sets. The author establishes significant implications for Heptapartitioned-Ɲ- Ṭ-Sets through the formulation of theorems, propositions, and similar constructs. By precisely defining the characteristics of H-Ɲ-preopen sets, H-Ɲ-semiopen sets, H-Ɲ-б-open sets, and H-Ɲ-ά- open sets, the author presents concrete examples that demonstrate instances where the results do not hold, serving as illustrative counter examples. Anticipating further exploration and inquiry, the author envisions that these ideas, along with the various open sets on Heptapartitioned-Ň-Ṭ-Ş, will be subject to more in-depth study in the future. The practical applicability of Heptapartitioned Neutrosophic topological space extends to decision-making, data mining, and other related fields.

ACKNOWLEDGEMENT

REFERENCES

1. Xindong Peng, Yong Yang: Some results for pythagorean fuzzy sets, International Journal of Intelligent systems; 30(2015),1133-1160.
2. Suman Das and Binod Chandra Tripathy : Pentapartitioned Neutrosophic Topological Space. Neutrosophic Sets and Systems; (2021),Vol. 45.
3. Rama Mallick,Surapati Pramanik: Pentapartitioned neutrosophic set and its properties,Neutrosophic sets and systems;Vol36,2020.
4. Das, S., & Tripathy, B. C : Neutrosophic simply b-open set in neutrosophic topological space;(2021) Iraqi Journal of Science, In Press.
5. Das, S., Das, R., & Granados, C: Topology on Quadripartitioned Neutrosophic Sets. Neutrosophic Sets and Systems; In Press.
6. F,Smarandache, n-Valued Refined :Neutrosophic Logic and Its Applications to Physics Progress in Physics; Vol. 4, 2013,143-146.
7. R. Radha, A. Stanis Arul Mary: Heptapartitioned Neutrosophic Set. International Journal of Creative Research Thoughts;(2021) Vol 9, 2320-2882.
8. Ebenanjar, E., Immaculate, J., & Wilfred, C. B: On neutrosophic b-open sets in neutrosophic topological space. Journal of Physics Conference Series; (2018) 1139 (1), 012062.
9. Iswarya, P., & Bageerathi, K.: On neutrosophic semi-open sets in neutrosophic topological spaces. International Journal of Mathematical Trends and Technology; (2016) 37 (3), 214-223
10. Salama, A. A., & Alblowi, S. A: Neutrosophic set and neutrosophic topological space. ISOR Journal of Mathematics; (2012) 3 (4), 31-35.

RESEARCH ARTICLE

Interval-Valued Intuitionistic Fuzzy Convex Optimization Techniques

R. Santhi[1] and N. Udhayarani[2]*

[1]PG and Research Department of Mathematics, Nallamuthu Gounder Mahalingam College, Pollachi-642001, Coimbatore, Tamil Nadu, India.
[2]Department of Mathematics, Sri GVG Vishalakshi College for Women, Udumalpet- 642128, Tiruppur, Tamil Nadu, India

*Address for Correspondence
N. Udhayarani
Department of Mathematics,
Sri GVG Vishalakshi College for Women,
Udumalpet- 642128, Tiruppur,
Tamil Nadu, India
E.Mail: udhayaranin@gmail.com

ABSTRACT

Optimization is a procedure of finding and comparing feasible solutions. Convex optimization is one of the fields among several fields of Optimization techniques. This article presents the definition of interval-valued intuitionistic fuzzy local maximum point and interval-valued intuitionistic fuzzy global maximum point and its characterizations.

Keywords: IVIF-convex set, TOPSIS, IVIF-convex objective function, IVIF-convex constraints

INTRODUCTION

In this paper, we introduced the interval-valued intuitive fuzzy local maximum point. (abbreviated *IVIF* [LM] point) and the interval-valued intuitionistic fuzzy global maximum point (abbreviated *IVIF* [GM] point) of *convex IVIF* sets and its properties. Throughout this paper U as universal crisp set, *I* is the collection of all subintervals of the closed interval [0,1] and I^U represents the family of all closed subintervals of [0,1]. with respect to the specified set U

Convex IVIF-sets: Characteristics

Definition 2.1.
Let A be an on empty sub set of I^U. An element $x_P \in$ *supp* (A)is called an *IVIF* [LM] point of A if there exists $\epsilon > 0$ such that $[\underline{\mu}, \overline{\mu}]_A(x_P) \geq [\underline{\mu}, \overline{\mu}]_A(x)$ and $[\underline{v}, v]_A(x) \leq [\underline{v}, v]_A(x_P)$ for all $x \in B(x,r)$

64311

Definition 2.2.
An element $x_\rho \in supp$(A) is called an *IVIF* GM point of an interval-valued intuitionistic fuzzy set A if $[\underline{\mu},\overline{\mu}]_A(x) \leq [\underline{\mu},\overline{\mu}]_A(x^\rho)$ and $[\underline{\nu}, \nu]_A(x^\rho) \geq [\underline{\nu},\nu]_A(x), \forall x \in U$.

Definition 2.3.
Let A be a *convex IVIF* subset of I^U. An element $x_\rho \in supp$(A) is called a strictly *IVIF* LM point of A if there exists $\epsilon > 0$ such that $[\underline{\mu},\overline{\mu}]_A(x^\rho) > [\underline{\mu},\mu]_A(x)$ and $[\underline{\nu},\nu]_A(x) < [\underline{\nu},\nu]_A(x^\rho)$ for all $x \in B(x,r)$ and $x /= x^\rho$.

Proposition 2.4. *Let* A *be a convex* IVIF *set and* $x_\rho \in supp$(A) *be a IVIF* LM
Point of A. *Then* x_ρ *be a IVIF* GM *of* A *over supp*(A).
Proof : Given that, A *is a convex* IVIF *set and* $x_\rho \in supp$(A) *is a IV IF* LM *point, implies*
$[\underline{\mu},\overline{\mu}]_A(x^\rho) \geq [\underline{\mu},\overline{\mu}]_A(x)$ and $[\underline{\nu},\nu]_A(x^\rho) \leq [\underline{\nu},\nu]_A(x)$

We have to prove, $x_\rho \in supp$(A) is a IVIF GM point, that is,
$[\underline{\mu},\overline{\mu}]_A(x) \leq [\underline{\mu},\overline{\mu}]_A(x^\rho)$ and $[\underline{\nu},\nu]_A(x) \geq [\underline{\nu},\nu]_A(x^\rho)$

Suppose that x^ρ *is not a IV IF* GM *point then there exists another point* $x^{\rho\prime} \in supp$(A)
such that, $x^\rho \leq x^{\rho\prime}$ *implies,* $[\underline{\mu},\mu]_A(x) \leq [\underline{\mu},\mu]_A(x^{\rho\prime})$ *and* $[\underline{\nu},\nu]_A(x) \geq [\underline{\nu},\nu]_A(x^{\rho\prime})$
Since A *is a convex* IV IF *set, then*

$$\lambda[\underline{\mu},\mu]_A(x^{\rho\prime}) + (1 - \lambda)[\underline{\mu},\mu]_A(x^\rho) \geq min\{[\underline{\mu},\mu]_A(x^{\rho\prime}), [\underline{\mu},\mu]_A(x^\rho)\}$$
$$\geq min\{[\underline{\mu},\mu]_A(x), [\underline{\mu},\mu]_A(x)\}$$
$$= [\underline{\mu},\mu]_A x^\rho$$

But this is not possible, by the definition of IVIF LM *point. Therefore* $x^\rho = x^{\rho\prime}$. *Next, for nonmembership degree, we have,*

$$\lambda[\underline{\nu},\nu]_A(x^{\rho\prime}) + (1 - \lambda)[\underline{\nu},\nu]_A(x^\rho) \leq max\{[\underline{\nu},\nu]_A(x^{\rho\prime}), [\underline{\nu},\nu]_A(x^\rho)\}$$
$$\leq max\{[\underline{\nu},\nu]_A(x), [\underline{\nu},\nu]_A(x)\}$$
$$= [\underline{\nu},\nu]_A(x^\rho)$$

which is a contradiction to the definition of IVIF LM. Therefore, x_ρ is a IV IF GM point.

Proposition 2.5. If A is a strictly convex IVIF set then x_ρ is the unique IVIF GM point.

Proof: *Here, we have to prove* x^ρ *is a unique IVIF global maximum point.*
Assume that A *is a strictly convex* IVIF *set, and* x^ρ *is a strictly IV IF* GM *point, implies,* $[\underline{\mu},\mu]_A(x) < [\underline{\mu},\mu]_A(x^\rho)$ *and* $[\underline{\nu},\nu]_A(x) > [\underline{\nu},\nu]_A(x^\rho)$
Suppose that $x^{\rho*}$ *is another IVIF* GM *point,* $\Rightarrow$ $[\underline{\mu},\overline{\mu}]_A(x) < [\underline{\mu},\overline{\mu}]_A(x^{\rho*})$ *and* $[\underline{\nu},\nu]_A(x) > [\underline{\nu},\nu]_A(x^{\rho*})$
Since A *is a strictly convex* IVIF *set, then*

Santhi and Udhayarani

$$\lambda[\underline{\mu}, \mu]_A(x^{\rho}*) + (1-\lambda)[\underline{\mu}, \mu]_A(x^{\rho}) > min\{[\underline{\mu}, \overline{\mu}]_A(x^{\rho}*), [\underline{\mu}, \overline{\mu}]_A(x^{\rho})\}$$

$$> min\{[\underline{\mu}, \mu]_A(x^{\rho}), [\underline{\mu}, \mu]_A(x^{\rho})\}$$

$$= [\underline{\mu}, \mu]_A(x^{\rho})$$

$[\underline{\mu}, \mu]_A(x^{\rho}) < [\underline{\mu}, \mu]_A(x^{\rho}*)$. *Also we have* $[\underline{\mu}, \mu]_A(x^{\rho}) > [\underline{\mu}, \mu]_A(x^{\rho}*)$. *Thus* $[\underline{\mu}, \mu]_A(x^{\rho}) = [\underline{\mu}, \mu]_A(x^{\rho}*)$.

Similarly for nonmembership interval,

$$\lambda[\underline{v}, v]_A(x^{\rho}*) + (1-\lambda)[\underline{v}, v]_A(x^{\rho}) < max\{[\underline{v}, \overline{v}]_A(x^{\rho}*), [\underline{v}, \overline{v}]_A(x^{\rho})\}$$

$$< max\{[\underline{v}, v]_A(x^{\rho}), [\underline{v}, v]_A(x^{\rho})\}$$

$$= [\underline{v}, \underline{v}]_A(x^{\rho})$$

$[\underline{v}, v]_A(x^{\rho}) > [\underline{v}, v]_A(x^{\rho}*)$. *And* $[\underline{v}, v]_A(x^{\rho}) < [\underline{v}, v]_A(x^{\rho}*)$. *Thus* $[\underline{v}, v]_A(x^{\rho}) = [\underline{v}, v]_A(x^{\rho}*)$.

Hence x^{ρ} *is a unique IVIF^{GM} point.*

Proposition 2.6.
Let A $\in$ I^U be a strictly convex IVIF set. The set of IVIF points at which A attains its IV IF^{GM} over supp(A) is a convex(crisp) set.

Proof: *Assume that* A *is a convex$_{IVIF}$ set. Let* $\{[\underline{\mu}, \mu]_A(x_T), ...[\underline{\mu}, \mu]_A(x^{\rho}), ...[\underline{\mu}, \mu]_A(x_n)\}$
and $\{[\underline{v}, v]_A(x_1), ...[\underline{v}, v]_A(x^{\rho}), ...[\underline{v}, v]_A(x_n)\}$ *be the set of all membership and non-membership intervals of IF points contained in* supp(A). *If* $x^{\rho} \in$ supp(A) *is an IV IF^{LM} point of* A *then* x^{ρ} *is also an IV IF^{GM} of* A *over* supp(A). *By definition,* supp(A) $= \{x : [\underline{\mu}, \mu]_A(x) > 0, [\underline{v}, v]_A(x) > 0\}$. *This implies, IV IF^{GM} point is in convex(crisp) set.*

Proposition 2.7. *Let* A $\in I^U$ *be a strictly convex$_{IVIF}$ set, then the following conditions hold:*

1. *If* $x^{\rho} \in$ supp(A) *is a IVIF^{LM} of* A, *then it is a unique IVIF^{GM} point.*

2. A *attains its IVIF^{GM} point over* supp(A) *at only one point.*

Proof: *Let us assume that* $x^{\rho} \in$ supp(A) *be a strictly IV IF^{LM} point. Then there exists* $\epsilon > 0$, *such that* $x \in$ supp(A), $[\underline{\mu}, \mu]_A(x) \neq [\underline{\mu}, \mu]_A(x^{\rho})$, $[\underline{v}, v]_A(x)$ $[\underline{v}, v]_A(x^{\rho})$
and $\|(x) - x^{\rho}\| < \epsilon$, $\implies$ $[\underline{\mu}, \mu]_A(x^{\rho}) > [\underline{\mu}, \mu]_A(x)$ *and* $[\underline{v}, v]_A(x^{\rho}) < [\underline{v}, v]_A(x)$
Suppose x^{ρ} *is not a strictly IVIF^{GM} over its* supp(A), *then* $x^{\rho}* \in$ supp(A) *and*
$x^{\rho}*$ x^{ρ} *such that* $[\underline{\mu}, \mu]_A(x^{\rho}*) > [\underline{\mu}, \mu]_A(x^{\rho})$ *and* $[\underline{v}, v]_A(x^{\rho}*) < [\underline{v}, v]_A(x^{\rho})$. *Since* A *is a strictly convex$_{IV IF}$ set. For all* $\lambda \in [0, 1]$, *we have*

$$[\underline{\mu}, \mu]_A(x^{\rho*}) = \lambda[\underline{\mu}, \mu]_A(x) + (1-\lambda)[\underline{\mu}, \mu]_A(x^\rho)$$

$$\leq \lambda[\underline{\mu}, \mu]_A(x) + [\underline{\mu}, \mu]_A(x\_) - \lambda[\underline{\mu}, \mu]_A(x\_) \quad {}_\rho$$

$$< \lambda[\underline{\mu}, \mu]_A(x^\rho) + [\underline{\mu}, \mu]_A(x^\rho) - \lambda[\underline{\mu}, \mu]_A(x^\rho)$$

$$= [\underline{\mu}, \mu]_A(x^\rho)$$

Similarly, we can prove for nonmembership intervals. Hence x^ρ *is a only one strictly*

IVIF^{GM} point.

Proposition 2.8. Let A be a convex IVIF set with supp (A)φ . If A has a unique IVIF LM point on every closed interval [x, y] in its support then A is a strictly convex IVIF set.

Definition 2.9. Let $f_A : U^n \rightarrow U$ be a convex function and $f_A : U \rightarrow D[0, 1]$ be a nonincreasing interval-valued IF set. The composition is denoted by $f_A \circ f_A = A$, then the membership composite interval function, $[\underline{\mu}, \mu]_A : U^n \rightarrow D[0, 1]$ defined by

$$[\underline{\mu}, \mu]_A(x) = \begin{cases} f_A(f_A(x)) \text{ if } f_A \in supp(f_A) \\ \qquad\qquad \text{if } f_A \notin supp(f_A) \end{cases}$$

and nonmembership composite interval function $[v^L, v^U]_A : U^n \rightarrow D[0, 1]$ defined by

$$[\underline{v}, v]A(x) = \begin{cases} f_A(f_A(x)) & \text{if } f_A \in supp(f_A) \\ \qquad\varphi & \text{if } f_A \notin supp(f_A) \end{cases}$$

Definition 2.10. Let $A : I^U \rightarrow D[0, 1]$ be a *convex$_{IVIF}$* set and $B : I^U \rightarrow D[0, 1]$ be an another *convex$_{IVIF}$* set. Then the membership composite interval sets of $(A \circ B)(x) = A(B(x))$ defined by $([\underline{\mu}, \mu]_A \circ [\underline{\mu}, \mu]_B)(x) = \vee\{\wedge([\underline{\mu}, \mu]_A, [\underline{\mu}, \mu]_B)(x)\}$, and the nonmembership composite interval sets of $(A \circ B)(x) = A(B(x))$ defined by $([\underline{v}, v]_A \circ [\underline{v}, v]_B)(x) = \wedge\{\vee([\underline{v}, v]_A, [\underline{v}, v]_B)(x)\}$

Multitask *convex$_{IVIF}$* -Optimization Problems

In this part we introduce the general approach of decision making problems under *convex$_{IVIF}$* sets. A decision maker wants to evaluate n-number of goals as convex functions $G_1, G_2, ...G_n$ and m-number of IVIF-constraints $C_1, C_2, ...C_m$ defined the solution space $U \subseteq U^n$ are assumed to be given. An IVIF-decision D in U is defined by,

$$[\underline{\mu}, \mu]^D(x) = max\{[\underline{\mu}, \mu]_G *[\underline{\mu}, \mu]_G *..._2*[\underline{\mu}, \mu]_G *[\underline{\mu}_n\mu]_C *[\underline{\mu}_1\mu]_C *... \,^*_2 [\underline{\mu}, \mu]_C \}(x)\,_n$$

$$[\underline{v}, v]^D(x) = min\{[\underline{v}, v]_G *... *[\underline{v}, v]_G *[\underline{v}, v]_C *[\underline{v}, v]_C *... *[\underline{v}, v]_C (x)$$

where $x \in U$ and $*$ denotes an aggregation operator. Many different aggregation operators have been proposed. Here we desired to use min operator to aggregate the convex combination of goals and constraints. Due to computational simplicity, D might be expressed as a convex combination of the goals and constraints with weighting co-efficient reflecting the relative importance of the various terms. If thereexists a subset $M \subseteq U$ for which $A(x)$ reaches its maximum, then M is called the set of maximizing decisions.

CONCLUSION

In further we can work towards the problem of assigning location centers in convex sets with interval-valued intuitionistic fuzzy sets. That is, a convex set is characterized by an interval-valued intuitionistic fuzzy convex-objective function and interval-valued intuitionistic fuzzy convex constraint functions over a convex set which is the set of the decision variables. Also, assign a new location with the given convex sets using a TOPSIS-based computational procedure.

REFERENCES

1. I. Aguirre-cipe, R. Lopez, E. Mallea-zepeda, and Lautaro Vasquez, A study of interval optimization problems, Optim Lett 15(2021), 859-877.
2. E. Ammar and J. Metz, On fuzzy convexity and parametric fuzzy optimization, Fuzzy Sets and systems, 49(1992) 135-141.
3. K.T. Atanassov and G. Gargov, Interval-valued intuitionistic fuzzy sets, Fuzzy sets and Systems, 31(1989), 343-349.
4. Omar salazar and Jairo soriano, Convex combination and its application to fuzzy sets and interval-valued fuzzy sets - I, App. Math. Sci., 9(22)(2015), 1061-1068.
5. Sangeetha saha and Pradip Debnath, Intuitionistic fuzzy ' - convexity and intuitionistic fuzzy decision making, Int. J. Eng. Sci. Tech., 10(2)(2018).
6. Susana Diaz, Esteban Indurain, Vladimir Jamis and Susana Montes, Aggregation of Convex Intuitionistic Fuzzy sets, Information Sci., 308(2015), 61-71.
7. Xinmin Yang, Short Communication: Some Properties of Convex Fuzzy sets, Fuzzy Sets and Systems, 72(1995), 129-132.
8. Ying-Ming Liu, Some properties of convex fuzzy sets, J. Math. Ana. App., 111(1985), 119-129.
9. Yu-Ru Syau and E. Stanley Lee, Fuzzy Convexity and Multiobjective convex Optimization Problems, An Int. J. Computers and Math. App., 52(2006), 351-362.
10. L.A. Zadeh, Fuzzy Sets, Information and Control, 8(1965), 338-353.
11. Ze-Shui Xu and Jian Chen, Approach to Group Decision Making Based on Interval-Valued Intuitionistic Judgement Matrices, Systems Engineering: Theory and Practices, 27(2007), 126-133.